

Introduction: Frontiers in Polymer Chemistry

The word polymer was introduced by Berzelius in 1833. About 100 years later, during the classic period of polymer science, Wallace Carothers reviewed the entire field of polymer chemistry including that of biological polymers and of polymer physics in a single article in *Chemical Reviews* (Carothers, W. H. Polymerization. *Chem. Rev.* **1931**, *8*, 353). Today, the field of synthetic and biological polymers is impacting extensively various areas of chemistry, biochemistry, molecular biology, nanotechnology, electronics, medicine, life sciences, materials, etc., and is reviewed in almost every individual and thematic issue of *Chemical Reviews*. The present thematic issue is focused only on a very selected series of subjects in an attempt to avoid overlap with very recent thematic issues such as "Nanostructures" (Vol. 99, No. 7, 1999), "Frontiers in Metal-Catalyzed Polymerization" (Vol. 100, No. 4, 2000), "Chemical Sensors" (Vol. 100, No. 7), and "Protein Design" (Vol. 101, No. 10, 2001).

Living polymerizations and iterative synthesis are the two most advanced synthetic methods in the field of polymer synthesis. Anionic, cationic, and metathesis living polymerizations are already well-established methods for the synthesis of well-defined and monodisperse polymers that have a narrow molecular weight distribution and complex topology and architecture. Their mechanisms have been relatively well elucidated both in the case of ring opening and of vinyl polymerization reactions and therefore will not be reviewed in this thematic issue. However, living radical polymerization and other methods to produce well-defined polymers by radical reactions are currently being developed and are investigated extensively in many laboratories, in spite of the fact that this is a topic of old concern (Otsu, T. Iniferter Concept and Living Radical Polymerization. *J. Polym. Sci., Part A: Polym. Chem.* **2000**, *38*, 2121). This issue begins with an article by Fischer, who discusses the concept of the persistent radical effect and explains the mechanism via which this concept provides access both to selective radical organic reactions and to various methods used to accomplish living radical polymerization. Gridnev and Ittel follow with an analysis of the catalytic chain transfer in free-radical polymerization and its application to the design of various classes of well-defined polymers. Hawker, Bosman, and Harth review the synthesis of new poly-

mers by nitroxide-mediated living radical polymerization. The contribution by Kamigaito, Ando, and Sawamoto provides an extensive review of metal-catalyzed living radical polymerization. Today, the most versatile method for the synthesis of polymers with complex architecture is based on living anionic polymerization. A very comprehensive review on this topic is presented by Hadjichristidis, Pitsikalis, Pispas, and Iatrou.

Synthetic methods that are borrowing the tools of biology are being actively developed for the synthesis of nonbiological and biological macromolecules. Enzymatic polymerization is one of the most recent entries to this field and is reviewed by Kobayashi, Uyama, and Kimura.

Iterative synthesis is the only synthetic method available for the preparation of biological (peptides, nucleic acids, and polysaccharides) and nonbiological oligomers with well-defined sequences and molecular weight free of chain length distribution. One of the most powerful illustrations of the utility of this synthetic strategy is in the preparation of dendrimers. They represent a class of synthetic macromolecules that have impacted dramatically the field of organic and polymer chemistry in the past decade. A contribution by Grayson and Fréchet details the convergent iterative synthesis and the applications of dendrons and dendrimers. Another relevant example, the preparation of rod-coil block copolymers, relies on a combination of iterative synthesis and living polymerizations. The self-assembly of supramolecular structures from rod-coil block copolymers is analyzed by Lee, Cho, and Zin.

Folding and chirality (including its transfer and amplification) are two of the most important events that determine the correlation between the primary structure of biological macromolecules and their tertiary and quaternary structures that ultimately are responsible for their functions and properties. Biological macromolecules know how to fold in very specific secondary structures that determine their 3-dimensional architecture and their large diversity of functions. While the understanding of folding processes in biological macromolecules is still incomplete, it is believed that its complete elucidation relies on the ability to produce synthetic nonbiological macromolecules that will exhibit the same mecha-

nism of folding, formation of 3-dimensional structure, functions, and properties at the level of sophistication displayed by the natural compounds. Hill, Mio, Prince, Hughes, and Moore provide a very comprehensive review that discusses for the first time all classes of biological and nonbiological foldamers. On related topics, Nakano and Okamoto detail the synthesis and properties of helical polymers. This theme is further developed by Cornelissen, Rowan, Nolte, and Sommerdijk in their analysis of chiral architectures from macromolecular building blocks.

Both in biological and nonbiological macromolecules the intramolecular folding process is determined by a combination of primary structure and noncovalent directional and nondirectional interactions. Most recently, combinations of various noncovalent interactions were also used to self-assemble supramolecular polymers in which the repeat units are interconnected via noncovalent rather than covalent bonds. The field of supramolecular polymers is reviewed by Brunsveld, Folmer, Meijer, and Sijbesma.

Progress in the field of chemical and biological sciences is continually impacted by the development of novel methods of structural analysis. Sheiko and Möller review a field that started to develop only in the past several years, i.e., visualization of biological and synthetic macromolecules including individual macromolecules and their motion on surfaces with the aid of scanning force microscopy (SFM). Brown and Spiess analyze the most recent advances in solid-state NMR methods for the elucidation of the struc-

ture and dynamics of molecular, macromolecular, and supramolecular systems. Finally, Ungar and Zeng discuss the use of linear, branched, and cyclic model compounds prepared mostly by iterative methods in the elucidation of the polymer crystallization mechanism by using the most advanced X-ray diffraction methods.

Although I completely agree with the following statement made by one of the pioneers of the field of polymer science: "...*there is no substitute for reading every reference, cited-second-hand citations are incredibly unreliable...*" (Morawetz, H. *Polymers. The Origins and Growth of a Science*; Wiley: New York, 1985), I hope that our readers will find that the outstanding work done by the authors mentioned above will provide an excellent and state of the art report for the *Frontiers in Polymer Chemistry* at the beginning of the 21st century. The field of polymer chemistry was born at the interface between many disciplines and today is more interdisciplinary than ever.

Finally, I express my great appreciation for the cooperation on this thematic issue to all contributing authors and reviewers and to the Editorial Office of *Chemical Reviews*.

Virgil Percec
Roy & Diana Laboratories,
Department of Chemistry,
University of Pennsylvania,
Philadelphia, Pennsylvania 19104-6323

CR000885X

Synthetic Helical Polymers: Conformation and Function

Tamaki Nakano[†] and Yoshio Okamoto^{*,‡}

Graduate School of Materials Science, Nara Institute of Science and Technology (NAIST), Takayama-cho 8916-5, Ikoma, Nara 630-0101, Japan, and Department of Applied Chemistry, Graduate School of Engineering, Nagoya University, Furo-cho, Chikusa-ku, Nagoya 464-8603, Japan

Received February 5, 2001

Contents

I. Introduction	4013
II. Helical Polymers	4015
A. Polyolefins	4015
B. Polymethacrylate and Related Polymers	4016
1. Poly(triphenylmethyl methacrylate)	4016
2. Poly(triphenylmethyl methacrylate) Analogues: Anionic Polymerization	4017
3. Poly(triphenylmethyl methacrylate) Analogues: Free-Radical Polymerization	4018
4. Polymers of Other Acrylic Monomers	4022
C. Miscellaneous Vinyl Polymers	4023
D. Polyaldehydes	4023
1. Polychloral and Related Polymers	4023
2. Other Polyaldehydes	4024
E. Polyisocyanides	4024
1. Polymers of Monoisocyanides	4024
2. Polymers of Diisocyanides	4025
F. Polyisocyanates and Related Polymers	4025
1. Polyisocyanates	4025
2. Polycarbodiimides	4027
G. Polyacetylene Derivatives and Related Polymers	4027
1. Polyacetylene Derivatives	4027
2. Polyphosphazene	4029
H. Poly(aryleneethynylene)s	4029
I. Polyarylenes	4030
J. Si-Containing Polymers	4031
1. Polysilanes	4031
2. Polysiloxane	4032
K. Other Types of Polymers	4032
1. Miscellaneous Examples	4032
2. Mimics and Analogues of Biopolymers	4033
III. Helical Polymeric Complexes and Aggregates	4033
A. Helicates	4033
B. Helical Aggregates	4033
IV. Summary and Outlook	4034
V. Acknowledgments	4034
VI. References	4034

I. Introduction

The high functionalities of naturally occurring macromolecules such as proteins and genes arise

* To whom correspondence should be addressed. Phone: +81-52-789-4600. Fax: +81-52-789-3188. E-mail: okamoto@apchem.nagoya-u.ac.jp.

[†] NAIST.

[‡] Nagoya University.

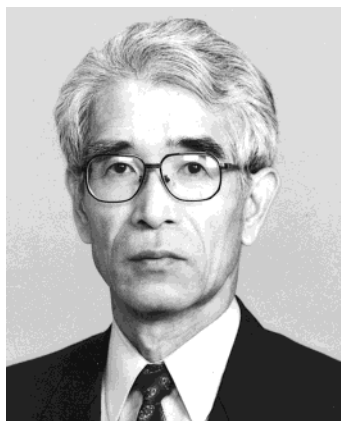
from their precisely ordered stereostructures.¹ In such systems, the helix is often found among the most fundamental structures of the polymer chain and plays important roles in realizing biological activities. On the other hand, the helix also attracts the particular interest of synthetic polymer scientists, because broad applications and characteristic features are expected for synthetic helical polymers. The potential applications include molecular recognition (separation, catalysis, sensory functions), a molecular scaffold function for controlled special alignment of functional groups or chromophores, and ordered molecular alignment in the solid phase such as that in liquid crystalline materials.

The history of helical macromolecules is traced back to the finding of the conformation for some natural polymers. The progress in this field is summarized in Chart 1 with selected topics. The helical structure of α -amylose was proposed by Hanes in 1937^{2a} and was extended by Freudenberg.^{2b} Pauling proposed the α -helical structure for natural polypeptides,³ and then Watson and Crick found the double-helical structure for DNA⁴ in the early 1950s. These two findings were major breakthroughs in the field of molecular biology. Regarding the helix of polypeptides, in 1956, Doty demonstrated helix formation for poly(γ -benzyl-L-glutamate) arising from the polymerization of the *N*-carboxyanhydride of the corresponding α -amino acid, where a random-coil conformation changes into an α -helix as the chain grows.⁵ As a family of amino acid polymers, the conformation of poly(β -amino acid)s was investigated.^{6–8} Although β -structures were proposed for poly[(*S*)- β -aminobutyric acid] by Schmidt in 1970^{6a} and by Goodman in 1974^{6b} and for poly(α -isobutyl L-aspartate) by Yuki in 1978,⁷ experimental results suggesting a helical conformation for poly(α -isobutyl L-aspartate) were obtained by Subirana in 1984.⁸ Later, in 1996, Seebach⁹ and Gellman¹⁰ independently proved that β -peptide oligomers take a helical conformation that is different from the α -helical structure of the α -peptide polymers. In 1955, Natta found that stereoregular isotactic polypropylene has a helical structure in the solid state.¹¹ This was the beginning of the field of synthetic helical macromolecules, leading to the wide variety of helical polymers available today.

A helical structure for vinyl polymers with an excess helicity in solution was realized for isotactic poly(3-methyl-1-pentene) by Pino in 1960.¹² Although the chiral side groups affect the helical conformation in the polyolefin, the single-handed helix of poly-



Tamaki Nakano was born in Shizuoka, Japan, on Aug 24, 1962. He received his B.S. degree in 1986, M.S. degree in 1988, and Ph.D. degree in 1991 from Osaka University. At Osaka University, he worked with Professors Yoshio Okamoto and Koichi Hatada on helix-sense-selective polymerization of bulky methacrylates. He joined the faculty at Nagoya University as Assistant Professor in the Department of Applied Chemistry, Graduate School of Engineering, in 1990 and was promoted to Associate Professor in 1998. At Nagoya University, he worked on the asymmetric polymerization systems and also on the stereoregulation of free-radical polymerization of vinyl monomers with Professor Yoshio Okamoto. He was a visiting scientist with Professor Dotsevi Y. Sogah at Cornell University (1993–1994), where he studied group-transfer polymerization (GTP) of methacrylates and synthesis of novel peptide-based polymers. In 1999, he moved to NAIST as Associate Professor. His current research interest is in the areas of chiral polymers, stereocontrol of polymerization, and photophysics of polymers. A research topic of his group on the synthesis and photophysics of π -stacked polymers has been a Precursory Research for Embryonic Science and Technology (PRESTO) project (2000–2003) supported by Japan Science and Technology Corp. (JST). He lives with his wife and daughter in the city of Nara.



Yoshio Okamoto was born in Osaka, Japan, in 1941. He received his bachelor (1964), master (1966), and doctorate (1969) degrees from Osaka University, Faculty of Science. He joined Osaka University, Faculty of Engineering Science, as an assistant in 1969, and spent two years (1970–1972) at the University of Michigan as a postdoctoral fellow with Professor C. G. Overberger. In 1983, he was promoted to Associate Professor, and in 1990 moved to Nagoya University as a professor. His research interest includes stereocontrol in polymerization, asymmetric polymerization, optically active polymers, and enantiomer separation by HPLC. He received the Award of the Society of Polymer Science, Japan, in 1982, the Chemical Society of Japan Award for Technical Development in 1991, the Award of The Chemical Society of Japan (1999), and the Chirality Medal (2001), among others.

(triphenylmethyl methacrylate) synthesized by Okamoto and Yuki in 1979 did not require chiral side chains.¹³ This was the first vinyl polymer prepared from an achiral (prochiral) monomer having a single-handed helical structure stable even in solution. In

Chart 1. Historical Aspect of Helical Polymers

- 1937 α -Amylose (Hanes [Freudenberg 1939])
- 1951 Polypeptide (α -Helix) (Pauling)
- 1953 DNA (Watson, Crick)
- 1955 Isotactic polypropylene (Natta)
- 1956 Poly(γ -benzyl-L-glutamate) (Doty)
- 1960 Isotactic poly(3-methyl-1-pentene) (Pino)
- 1969 Poly((+)-1-phenylethyl isocyanide) (Millich)
- 1970 Poly(isocyanate) (Goodman)
- 1974 Poly(*t*-butyl isocyanide) (Drenth, Nolte)
- 1974 Polyacetylene derivatives (Ciardelli [Sinionescu, Percec 1977; Grubbs 1991; Yashima, Okamoto 1995])
- 1979 Poly(triphenylmethyl methacrylate) (Okamoto, Yuki)
- 1980 Polychloral (Vogl) [Ute, Hatada, Vogl 1991])
- 1984 Poly(α -isobutyl L-aspartate) (Subirana [Yuki 1978])
- 1987 Helicates (Lehn)
- 1988 Poly(alkyl isocyanate) with isotopic chirality (the uniform chiral field concept) (Green)
- 1994 Polysilane (Fujiki, Möller [Matyjaszewski 1992])
- 1995 Induced helix of poly(phenylacetylene) derivatives (Yashima, Okamoto)
- 1995 Oligoarylene (Lehn)
- 1996 β -Peptide oligomers (Seebach, Gellman)
- 1997 Oligoaryleneethynylene (Moore)

addition, the polymer exhibits high chiral recognition and has been successfully commercialized, clearly demonstrating the practical use of synthetic helical structures.^{14–16}

The helical conformation of polyisocyanides having bulky side-chain groups was first postulated by Millich¹⁷ in 1969 and confirmed by Drenth and Nolte in 1974.¹⁸ This aspect was later studied by Green,¹⁹ Hoffman,²⁰ and Salvadori.²¹ Goodman synthesized helical polyisocyanates having chiral side groups in 1970.²² Green further studied the helix of polyisocyanates with chirality only by virtue of a deuterium substitution and in other ways introduced extreme amplification of chirality that can be associated with helical structures in 1988.²³

The helical conformation of polyacetylene derivatives bearing chiral side chains was first pointed out by Ciardelli in 1974²⁴ and later extended and more clearly demonstrated by Grubbs in 1991²⁵ and by Yashima and Okamoto in 1994.^{26a} For poly(phenylacetylene) derivatives bearing no chiral side groups, Yashima and Okamoto showed that a helical conformation can be induced by interaction with added chiral small molecules.^{26b} Apart from optical activity, a helical conformation of *cis*-*cisoidal* poly(phenylacetylene) in the solid state was pointed out by Sinionescu and Percec.²⁷

The helical structure of polychloral was proposed by Vogl in 1980²⁸ and was demonstrated by Ute, Hatada, and Vogl via a detailed conformational analysis of chloral oligomers.²⁹ As an example of a helical polymer with an inorganic backbone, polysilanes bearing a chiral side chain were synthesized and their conformational aspects were studied. A helical conformation with an excess screw sense for this class of polymers in solution was found in 1994 independently by Fujiki^{30a} and by Möller.^{30b} Matyjaszewski had pointed out such a conformation for chiral polysilanes in the solid state in 1992.^{30c}

In addition to these examples, and as notable progress in this field, helical conformations were found for "helicates (helical complexes of oligomeric ligands and metals)" by Lehn in 1987,³¹ oligoarylenes by Lehn in 1995,³² and oligo(aryleneethynylene)s by Moore in 1997,³³ although these helices may be

regarded as only oligomers by synthetic polymer scientists.

A helix is a chiral structure; that is, right- and left-handed helices are nonidentical mirror images. Hence, if one of the two helices is selectively synthesized or induced for a polymer, the polymer may be optically active even if it contains no configurationally chiral group in the side chain or the main chain.

There are basically two types of helical structures. One is a rigid helix having a stable existence at room temperature, while the other is a dynamic helix in which helix reversals can readily move along a polymer chain at room temperature. The average length of a one-handed helical sequence can be very long for some polymers. In the former case, one may expect to obtain an optically active polymer with an excess of a screw sense through the polymerization process using a chiral initiator or catalyst. This kind of polymerization is interesting and important in the field of polymer synthesis and has been called helix-sense-selective polymerization. The first helix-sense-selective polymerization was achieved from the monomer triphenylmethyl methacrylate, leading to a nearly 100% one-handed helical polymer during polymerization with a chiral anionic initiator.¹³

We published a review paper in this journal entitled "Asymmetric Polymerization" in 1994 which encompassed this aspect of helical polymer synthesis in addition to the other types of polymerization in which chirality is introduced during the polymerization process.³⁴ There have been several other review papers on asymmetric polymerization and chiral polymers.^{35–40} On the other hand, if the energy barrier is low enough to allow rapid helix inversion at room temperature, one cannot expect to obtain a stable one-handed helical polymer but may expect to induce a prevailing helical sense with a small amount of chiral residue or stimulant. The existence of this type of polymer was most clearly demonstrated with poly(alkyl isocyanate)s.^{23,41}

In the present paper, in addition to the helical polymers with a screw-sense excess, those in a completely racemic form will also be discussed. Following up on the types of polymers discussed in our last review, newer publications that appeared since 1994 will be mainly reviewed here. Moreover, in addition to the "classical" helical polymers consisting of monomeric units connected to each other through covalent bonds, polymeric aggregates having a helical form in which their constituent units interact through weaker forces have been reported lately. This type of aggregate will also be covered. Furthermore, although a helical conformation stable in solution was the theme of our last review, some newer polymers and aggregates whose helical structures were proposed in the solid phase (liquid crystals, suspensions) are also included this time.

The method and accuracy of proving the presence of a helical structure varies depending on the type of study and the structure of the polymer. Structural questions can be addressed by (1) various methods based on computer calculations or observations of molecular models, (2) achiral spectroscopic evidence (NMR spectra, absorption spectra, X-ray diffraction),

(3) viscosity or light scattering data giving information on the shape and size of an entire molecule, (4) chiroptical properties [optical activity, circular dichroism (CD)] when the helix has an excess screw sense, (5) X-ray diffraction data for fiber samples of polymers, (6) microscopic observation, or (7) single-crystal X-ray analysis.

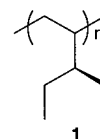
Although the last method generally gives the surest information on molecular conformation, it has limitations in that it is only applicable to oligomers and polymers uniform in terms of molecular weight including proteins but not to polydisperse real polymers and that it reveals only the structure in the solid state. In most cases, one or more of these methods (1–7) have been chosen to support the presence of helical structures. Hence, the structural proof in the studies reviewed in this paper may not be necessarily perfect in establishing helical structures. In the following sections, the topics are classified in terms of the chemical structure of the polymers.

II. Helical Polymers

A. Polyolefins

The isotactic polyolefins prepared using a Ziegler–Natta catalyst form a helical conformation in the solid state (crystalline regions).^{11,38,42} This helical structure persists in solution, but because of fast conformational dynamics, only short segments of the helix exist among disordered conformations. When an isotactic polyolefin is prepared from an optically active monomer having a chiral side group, the polymer shows the characteristic chiroptical properties which can be ascribed to a helical conformation with an excess helicity.^{12,43–46} The chiroptical properties arise in this case predominantly from the helical conformation of the backbone.

Because polyolefins do not absorb light in the accessible UV range, CD spectroscopy, which is a powerful tool for studying the chiral structure of polymers, could not be used for these vinyl-derived polymers. Hence, the chiral structures were elucidated in terms of optical rotatory dispersion. For example, isotactic poly[(S)-3-methyl-1-pentene] (1)



shows a larger specific rotation than the corresponding monomer.^{12,43–46} The optical activity of the polymer increased with its decreasing solubility and increasing melting point, which are related to the isotacticity of the polymer, but decreased as the temperature of the measurement increased (Table 1).⁴⁴ This relation between isotacticity and optical rotation means that the helical conformation may become imperfect when configurational disorders take place in the main chain. In addition, in the conformation of the polyolefin, right- and left-handed helical segments are considered to be separated

Table 1. Physical Properties of Poly[(S)-3-methyl-1-pentene] Fractions Having Different Stereoregularities^a

fraction	sample A, ⁱ catalyst Al(<i>i</i> -C ₄ H ₉) ₃ /TiCl ₄					sample B, ^l catalyst Al(<i>i</i> -C ₄ H ₉) ₃ /TiCl ₃				
	%	[η] ²⁵ _D ^{a,b} (deg)	[η] ^b (dL/g)	mp (°C)	Δ[η] _D ^{a/l} Δ <i>T</i>	%	[η] ²⁵ _D ^{c,h} (deg)	[η] ^b (dL/g)	mp (°C)	Δ[η] _D ^{c/l} Δ <i>T</i>
acetone-soluble	6.3	+29.4	d	nd	-0.08	2.4	+75.8	nd	nd	nd
acetone-insoluble, diethyl ether-soluble	2.6	+96.4	0.08	65–75 ^e	-0.23	4.8	+127	0.13	93–96 ^f	nd
diethyl ether-insoluble, benzene-soluble	0.9	+120	0.10	135–140 ^e	-0.26	1.5	+146	0.13	187–193 ^f	-0.31
isooctane-insoluble, benzene-soluble	0.4	+158	0.11	175–180 ^e	-0.34	0.5	+157	nd	200–210 ^e	-0.39
benzene-insoluble, decalin-soluble	2.0	+161 ^m	0.50	228–232 ^e	-0.36	1.7	+158 ^m	0.60	200–210 ^e	-0.40
residue	87.8	nd	nd	271–273 ^g	nd	89.1	nd	nd	265–275 ^e	nd

^a In tetralin solution. ^b Determined in tetralin at 120 °C. ^c In toluene solution. ^d Molecular weight determined by cryoscopy in benzene 1200 ± 100. ^e Determined by a Kofler melting point apparatus. ^f Determined by the X-ray method. ^g Determined by the capillary method. ^h Referred to one monomeric unit. ⁱ Monomer optical purity 91%. ^l Monomer optical purity 89%. ^m ±10%. ⁿ Reprinted with permission from ref 44. Copyright 1963 Wiley-VCH.

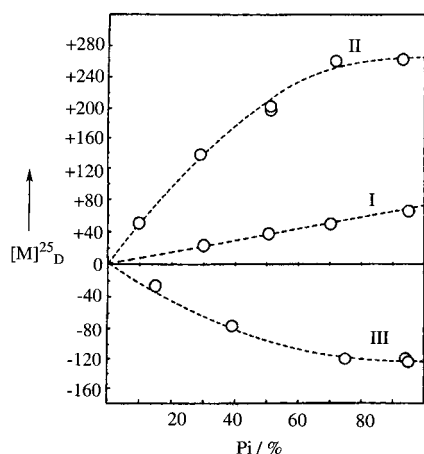
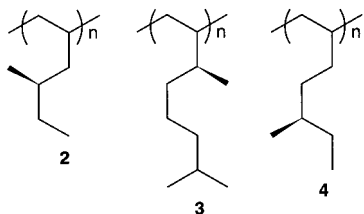


Figure 1. Relation between molecular rotation in a hydrocarbon solvent (referred to the monomeric unit) of the unfractionated methanol-insoluble **4** (I), **2** (II), and **3** (III) samples and the optical purity of the monomers used for polymerization. (Reprinted with permission from ref 47. Copyright 1967 Wiley.)

dynamically by helical reversals. This model is consistent with the temperature dependence of the optical activity of the polymer in which an increase in temperature increased the population of the helical reversals.

In these isotactic polymers, the optical purity of the monomer affected the optical activity via the relationship to the excess helical sense of the polymer (Figure 1).⁴⁷ In the case of isotactic poly[(S)-4-methyl-1-hexene] (**2**) and poly[(R)-3,7-dimethyl-1-octene] (**3**), an increase in the optical purity of the monomers resulted in an increase in the optical activity of the polymers in a nonlinear fashion: the optical activity of the polymers leveled off when the optical purity of the monomer reached ca. 80%. In contrast, in the case of isotactic poly[(S)-5-methyl-1-heptene] (**4**), the



relation was linear. These findings imply that the side-chain chiral centers of poly[(S)-5-methyl-1-hep-

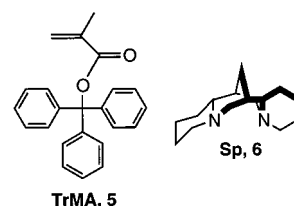
tene], which are separated from the main chain by three covalent bonds, may be too far from the main chain to affect the helical conformation.

Helical conformations were also proposed for the isotactic copolymer derived from (*R*)-3,7-dimethyl-1-octene and styrene.^{48,49} The copolymer showed intense CD bands based on the styrene units incorporated into the polymer chain. The CD intensity was much larger than that of a model compound of an adduct of the chiral olefin and styrene. The helical structure of polyolefins has also been supported by force field calculations.⁵⁰ The relationship of these considerations to isotactic vinyl polymers and more recent studies have recently been reviewed.⁴¹

B. Polymethacrylate and Related Polymers

1. Poly(triphenylmethyl methacrylate)

Vinyl polymers with a stable helical conformation are obtained from methacrylates with a bulky side group by isotactic specific anionic or radical polymerization.^{13,34} This type of polymer was first synthesized by asymmetric anionic polymerization (helix-sense-selective polymerization) of triphenylmethyl methacrylate (TrMA, **5**) using a complex of *n*-BuLi with (-)-sparteine (Sp, **6**).¹³ Although, as discussed



in the preceding section, a chiral side group was necessary in realizing a helical conformation with an excess helical sense in solution for stereoregular polyolefins, helical poly(TrMA) is prepared from the achiral (prochiral) vinyl monomer. The poly(TrMA) possesses a nearly completely isotactic configuration and a single-handed helical conformation of the main chain, which is stabilized by steric repulsion of the bulky side groups, and shows high optical activity based on the conformation.^{13,51–53} The helical conformation is lost when the triphenylmethyl group is removed from the polymer chain. Thus, the PMMA derived from the poly(TrMA) shows only a small optical activity based on the configurational chirality

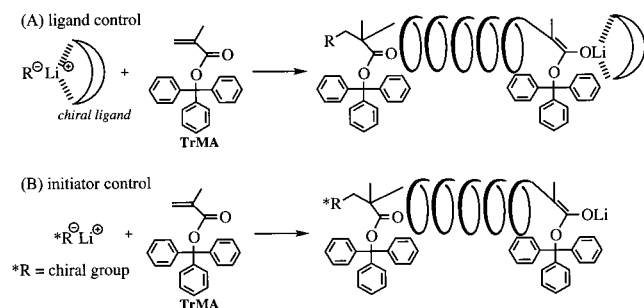


Figure 2. Helix-sense-selective anionic polymerization of TrMA: ligand (A) and initiator (B) control.

Table 2. Optical Activity of Poly(TrMA) in the Polymerization at $-78\text{ }^{\circ}\text{C}^a$

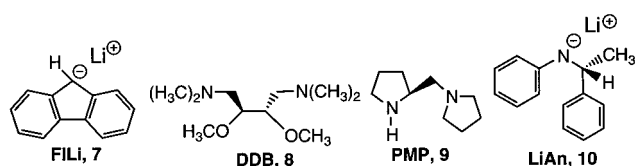
control method	initiator	solvent	yield (%)	$[\alpha]_D$ (deg)
ligand control	FILi-($-$)-Sp	toluene	99	+383
ligand control	FILi-($+$)-DDB	toulene	100	+344
ligand control	FILi-($+$)-PMP	toulene	100	+334
ligand control	<i>n</i> -BuLi-($-$)-Sp	THF	100	+7
initiator control	LiAn	toulene	73	-70
initiator control	LiAn	THF	93	-82

^a Conditions: [monomer]/[initiator] = 20. Data cited from refs 13 and 52.

of the stereogenic centers in the vicinity of the chain terminals.⁵³

The helical-sense excess in polymethacrylates is estimated, in principle, by comparing their optical activity and CD band intensity with those of the corresponding single-handed helical specimen having the same side group. A polymer is expected to have a single-handed helical structure if it has a completely isotactic configuration, except for minor configurational errors in the vicinity of the chain terminals, and has no clear dependence of optical activity on molecular weight. In the case of poly(TrMA), a nearly completely isotactic sample which is a mixture of right- and left-handed helices was resolved into several fractions showing different specific rotations with different helical-sense excesses by chiral chromatography.⁵⁴ The polymer contained in the fraction showing the highest optical activity obtained through resolution was taken as a single-handed one.

Asymmetric anionic polymerization is carried out using a complex of an organolithium with a chiral ligand or using a chiral organolithium (Figure 2).^{13,51,52} The helix-sense selection takes place on the basis of the chirality of the ligand or the initiator. The chiral ligand is assumed to coordinate to the counteranion (Li^+) at the living growing end and to create a chiral reaction environment (path A), while the chiral initiator will affect the initial stages of helix formation (path B). Table 2 shows the results of polymerization using the complexes of 9-fluorenyllithium (FILi, **7**) or *n*-BuLi with ($-$)-Sp, ($+$)- and ($-$)-2,3-dimethoxy-1,4-bis(dimethylamino)butane (DDB, **8**), and ($+$)-(1-pyrrolidinylmethyl)pyrrolidine (PMP, **9**) as chiral ligands and lithium (*R*)-*N*-(1-phenylethyl)-anilide (LiAn, **10**), a chiral initiator, to compare the effectiveness of the two methods. Ligand control has been shown to lead to a higher helix-sense excess, i.e., higher optical activity of the product, in the polymerization in toluene than in THF. This is



because the coordination of the ligand is inhibited by the coordination of the solvent in THF, removing the chiral ligand from the chain end and therefore reducing its influence. The initiator control gives relatively low selectivity independent of the solvent polarity.

In the asymmetric polymerization of TrMA using a complex of an organolithium and a chiral ligand, the chiral ligand controls the main-chain configuration in addition to the conformation. ($-$)-Sp, ($+$)-PMP, and ($+$)-DDB convert TrMA into the ($+$)-polymers having the same helical sense; however, the one synthesized using Sp has an $---RRR---$ configuration, while those prepared using the other two ligands have an $---SSS---$ configuration.⁵²

Helical block copolymers of TrMA with other monomers have been prepared, and their properties have been studied.⁵⁵⁻⁵⁷

Poly(TrMA) exhibits chiral recognition ability toward various types of racemic compounds when used as a chiral stationary phase for high-performance liquid chromatography (HPLC).¹⁴⁻¹⁶

Helical poly(TrMA) and its analogues can be used as chiral template molecules in molecular-imprint synthesis of a chiral cross-linked gel.⁵⁸ The chirality of the helical polymer may be transferred to the cross-linked material.

2. Poly(triphenylmethyl methacrylate) Analogues: Anionic Polymerization

Since the finding of the helix-sense-selective polymerization of TrMA, various other bulky monomers have been designed to find parallels to this behavior. The examples that appeared after our last review³⁴ are discussed in this section.

Some monomers having a pyridyl group in the side chain including diphenyl-3-pyridylmethyl methacrylate (D3PyMA, **11**),⁵⁹ phenylbis(2-pyridyl)methyl methacrylate (PB2PyMA, **12**),⁶⁰ 1-(2-pyridyl)dibenzosuberyl methacrylate (2PyDBSMA, **13**),⁶¹ and 1-(3-pyridyl)dibenzosuberyl methacrylate (3PyDBSMA, **14**)⁶² were prepared and polymerized. These mono-

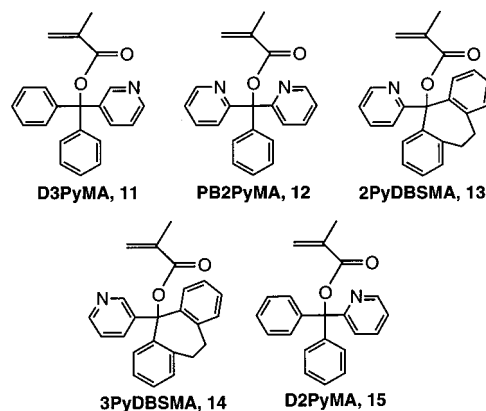


Table 3. Methanolysis of Bulky Methacrylates^a

monomer	k^b (h ⁻¹)	half-life (min)	monomer	k^b (h ⁻¹)	half-life (min)
TrMA	2.86	14.5	PB2PyMA	1.24×10^{-5}	335×10^4
D2PyMA	0.0256	1620	2PyDBSMA	0.0165	2520
D3PyMA	0.0291	1439	3PyDBSMA	0.0444	936

^a Measured by monitoring the monomer decomposition (methanolysis) in a CDCl₃/CD₃OD (1/1) mixture at 35 °C by means of ¹H NMR spectroscopy. Data cited from refs 60 and 61. ^b Pseudo-first-order rate constant.

mers were designed so that their ester linkage is more durable toward methanolysis than that of poly-(TrMA). This design had been introduced for diphenyl-2-pyridylmethyl methacrylate (D2PyMA, **15**).^{63–65} The durability of the ester linkage is an important feature of the helical polymethacrylates when they are used as chiral packing materials for HPLC. Poly-(TrMA) is known to slowly decompose and lose its helical structure by reaction with methanol, which is a good solvent for a chiral separation experiment.^{14–16} The methanolysis rates of these monomers are shown in Table 3 with the data for TrMA. The results indicate that the pyridyl-group-containing monomers are more durable than TrMA, suggesting that the monomers will afford helical polymers more resistant to methanolysis than poly(TrMA).

Stereoregulation in the anionic polymerization of D3PyMA and PB2PyMA using organolithium–chiral ligand complexes was more difficult than that of TrMA reasonably because the coordination of the pyridyl group to Li⁺ cation competes with the effective complexation of a chiral ligand to Li⁺ cation. Sp and DDB that are effective in controlling the TrMA polymerization^{13,52} resulted in rather low specific rotation values, and only PMP led to the polymers showing a relatively high optical activity [poly-(D3PyMA),⁵⁹ $[\alpha]_{365} +708^\circ$; poly(PB2PyMA),⁶⁰ $[\alpha]_{365} +1355^\circ$]. However, in contrast, the polymerization of 2PyDBSMA⁶¹ and 3PyDBSMA⁶² was much more readily controlled using Sp, DDB, and PMP as ligands. The bulky and rigid fused ring systems in these monomers may prevent the side-chain–Li⁺ coordination.

The polymers obtained from D3PyMA and P2BPYMA have a less stable helix than that of poly-(TrMA).^{59,60} Their helical conformation undergoes helix–helix transition, leading to a decrease in the screw-sense excess as observed for the single-handed helical poly(D2PyMA).⁶⁶

Helical copolymers of some of the monomers discussed in this section with TrMA have been synthesized.⁶⁷

The optically active polymers obtained from D3PyMA, PB2PyMA, 2PyDBSMA, and 3PyDBSMA show chiral recognition ability toward some racemic compounds in chiral HPLC or chiral adsorption experiments, though the ability was generally lower than that of poly(TrMA).^{16,59–62}

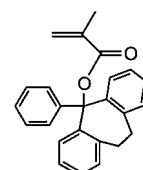
Quaternary salt formation with alkyl iodides was studied using the optically active poly(D3PyMA) and poly(3PyDBSMA).⁶⁸ The polymers were found to form a quaternary salt by reaction with CH₃I in CHCl₃. Upon salt formation, poly(D3PyMA) lost its helical conformation and optical activity probably due to electrostatic repulsion between the charged side groups, whereas poly(3PyDBSMA) maintained the

helical conformation, with the polymer still exhibiting optical activity in the salt form. Poly(3PyDBSMA) also formed a salt with *n*-butyl iodide.

3. Poly(triphenylmethyl methacrylate) Analogues: Free-Radical Polymerization

As discussed so far in this section, the helical polymethacrylates are synthesized predominantly using anionic polymerization techniques. However, recently, more versatile, inexpensive, and experimentally simple free-radical polymerization has been proved to be an alternative, effective way to prepare helical polymethacrylates from some monomers. Although the stereochemical control of radical polymerization is generally more difficult compared with that in other types of polymerization,⁶⁹ an efficient method would make it possible to synthesize helical, optically active polymers having functional side chains by direct radical polymerization without using protective groups. In the radical polymerization of bulky methacrylates, helix-sense selection is governed by the chirality of a monomer itself or an additive.

Although most of the bulky methacrylates described so far give isotactic polymers by radical polymerization as well as by anionic polymerization at low temperatures, the isotactic specificity of the radical polymerization is generally lower than that in the anionic polymerization.⁷⁰ However, 1-phenyldibenzosuberlyl methacrylate (PDBSMA, **16**)^{71–73}

PDBSMA, **16**

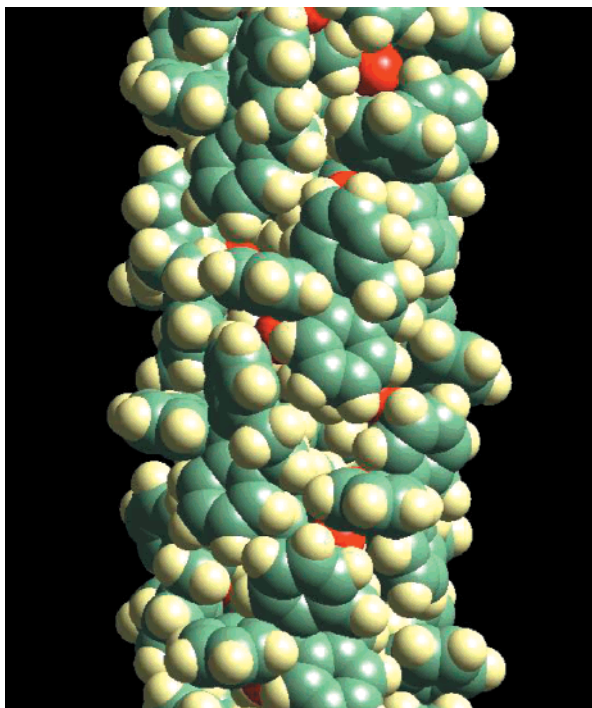
and its derivatives, 2PyDBSMA⁶¹ and 3PyDBSMA,⁶² afford nearly completely isotactic polymers by radical polymerization regardless of the reaction conditions. A possible polymer structure of isotactic poly(PDBSMA) is shown in Figure 3 in which the polymer has an approximately 7/2-helical conformation. The high isotactic specificity implies that the obtained polymer is an equimolar mixture of completely right- and left-handed helical molecules, suggesting that introduction of a nonracemic chiral influence to the polymerization reaction could result in the production of a single-handed helical, optically active polymer with an almost complete isotactic structure.

This concept was realized in the radical polymerization of PDBSMA using optically active initiators DMP (**17**) and CMBP (**18**), chain-transfer agents NMT (**19**) and MT (**20**), and solvents including

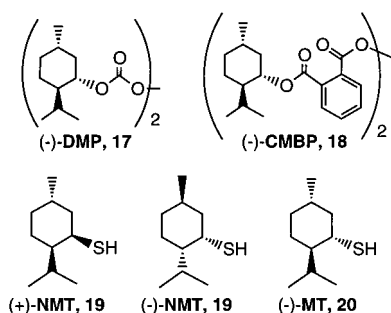
Table 4. Radical Polymerization of PDBSMA^a

initiator	chain-transfer agent or solvent	[M] ₀ (M)	[I] ₀ (M)	yield ^c (%)	THF-soluble part ^b		
					yield (%)	[α] ₃₆₅ ^d (deg)	DP
(-)-DMP	none	0.16	0.16	75	3	+40	44
(<i>i</i> -PrOCOO) ₂	(+)-NMT (0.032 M)	0.16	0.003	71	5	-140	42
(<i>i</i> -PrOCOO) ₂	(-)-menthol (4.6 M)/toluene	0.05	0.0017	45	1	+180	50

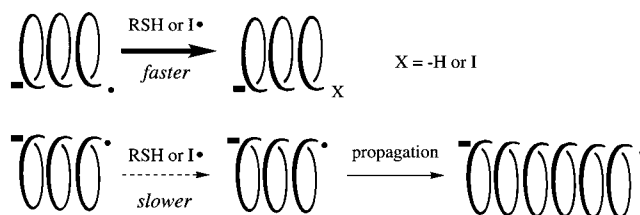
^a Data cited from ref 72. Polymerization in toluene at 40 or 50 °C. ^b Washed with a benzene/hexane (1/1) mixture. ^c Hexane-insoluble products. ^d In THF.

**Figure 3.** A possible 7/2 helix of isotactic poly(PDBSMA).

menthol (Table 4).^{72,73} The reaction using DMP as chiral initiator gave an optically active polymer

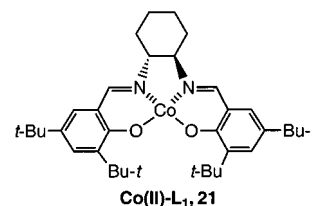


whose chirality appeared to be based on excess single-handed helicity, while CMBP failed in the helix-sense selection. Helix-sense selection was also possible by polymerization in the presence of the chiral thiols NMT and MT. The optical activity of the products obtained using the chiral initiator or the chiral chain-transfer agents depended on the molecular weight as revealed by an SEC experiment with simultaneous UV (concentration) and polarimetric (optical activity) detections. For example, the polymer prepared with (+)-NMT (Table 4, third row) consisted of levorotatory fractions of higher molecular weight and dextrorotatory fractions of lower molecular weight. These results strongly suggest that helix-sense selection

**Figure 4.** Helix-sense-selective radical polymerization using optically active thiol as a chain-transfer agent or initiator.

took place at the step of the termination reaction, that is, primary radical termination in the polymerization using DMP and hydrogen abstraction from the thiol by a growing radical in the polymerization using NMT or MT (Figure 4). The highest specific rotation of the poly(PDBSMA) prepared using (+)-NMT was [α]₃₆₅ -750° after SEC fractionation. This specific rotation corresponds to a ratio of enantiomeric helices of 3/7 as estimated by comparison with the optical activity of the anionically synthesized, single-handed helical poly(PDBSMA) ([α]₃₆₅ +1780°). The polymerization in a mixture of toluene and menthol was also effective in synthesizing optically active poly(PDBSMA)s. The mechanism of helix-sense selection in this case seemed to be the same as that for the polymerization using the thiols.

Helix-sense-selective radical polymerization of PDBSMA was also performed using a chiral Co(II) complex, Co(II)-L₁ (**21**).⁷⁴ Complex Co(II)-L₁ can possibly interact with the growing radical in the



polymerization system because Co(II)-L₁ is a d⁷ species. Regarding the interaction of a Co(II) species with a growing radical, several examples of catalytic chain transfer in methacrylate polymerization by the use of Co(II) have been published.^{75,76} The polymerization was carried out in the presence of Co(II)-L₁ in a CHCl₃/pyridine mixture at 60 °C. Although the polymer yield and the molecular weight of the products became lower by the effect of Co(II)-L₁, the polymerization led to optically active polymers whose specific rotation was [α]₃₆₅ +160° to +550° depending on the reaction conditions (Table 5). The CD spectrum of the polymer showing [α]₃₆₅ +550° had a pattern very similar to that of the spectrum of a single-handed helical polymer synthesized by anionic

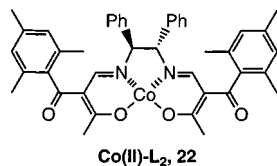
Table 5. Free-Radical Polymerization of PDBSMA with AIBN in the Presence of Co(II)-L₁ in a Chloroform/Pyridine Mixture at 60 °C for 24 h^a

[Co(II)-L ₁] ₀ (M)	[pyridine] ₀ (M)	yield ^b (%)	THF-soluble part			
			yield (%)	DP ^c	M _w /M _n ^c	[α] ₃₆₅ ^d (deg)
0	0	74 ^e	4	22	1.24	
0	0.51	86 ^f	3	19	1.27	+270
0.011	0.54	59	2	19	1.20	+550
0.039	0.50	39 ^g	3	19 ^h	1.18	+160
0.057	0.54	16	4	19	1.19	

^a Data cited from ref 74. Conditions: monomer 0.5 g, [monomer]₀ = 0.44–0.45 M, [AIBN]₀ = 0.029–0.031 M. ^b MeOH-insoluble part of the products. ^c Determined by GPC of poly(PDBSMA). ^d Estimated on the basis of GPC curves obtained by UV and polarimetric detections (see the text). ^e DP = 155 (M_w/M_n = 3.72) as determined by GPC of PMMA. ^f DP = 170 (M_w/M_n = 2.78) as determined by GPC of PMMA. ^g DP = 78 (M_w/M_n = 1.60) as determined by GPC of PMMA. ^h DP = 20 (M_w/M_n = 1.14) as determined by GPC of PMMA.

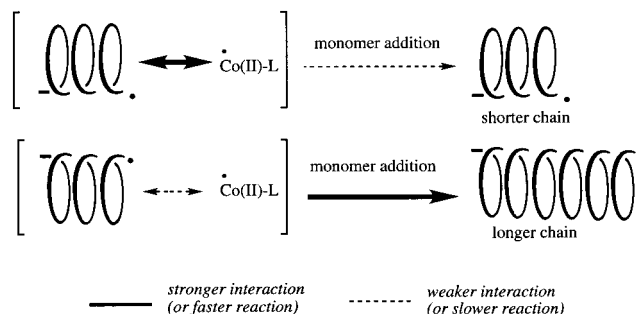
polymerization, indicating that the chiroptical properties of the radically obtained polymer arise from an excess of one helical sense. The SEC separation of the polymer revealed that the higher-molecular-weight fractions had higher optical activity. SEC fractionation of the high-molecular-weight part of the THF-soluble product gave ca. 8 wt % polymer: this fraction was found to have a completely single-handed helical structure (total yield 0.24%). Thus, the Co(II)-L₁-mediated method was demonstrated to be effective for helix-sense selection though the yield of the single-handed helical polymer was low.

Through a search for a better Co(II) complex, Co(II)-L₂ (**22**)⁷⁷ was recently found to be more effective than Co(II)-L₁ in the PDBSMA polymerization.⁷⁸ The polymerization in the presence of Co(II)-L₂ afforded a polymer showing [α]₃₆₅ +1379° before GPC separation in a higher yield compared with the reaction using Co(II)-L₁.

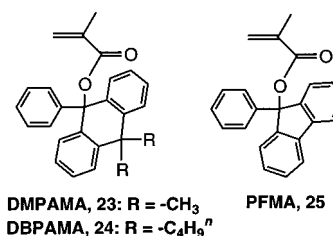


The mechanism of the helix-sense selection most probably involves the interaction of the Co(II) species with the growing polymer radical. It is assumed that the polymerization of PDBSMA proceeds only through the right- and left-handed helical radicals and that the two chiral radicals have different interactions with the chiral Co(II) species or different constants of binding with the chiral Co(II) species (Figure 5), leading to a difference in the apparent propagation rate of the two radicals, giving different molecular weights of the products derived therefrom. The dependence of optical activity on the degree of polymerization (DP) is indicative of a mechanism in which both helical senses are formed at a low DP of the growing species and one of the two has stronger interaction with the chiral Co(II) species, resulting in a lower apparent propagation rate.

In addition to PDBSMA, two novel monomers, DMPAMA (**23**) and DBPAMA (**24**), give highly iso-

**Figure 5. Helix-sense-selective radical polymerization using an optically active Co(II) complex.**

tactic polymers by radical polymerization as well as anionic polymerization.^{79,80} This means that a fused ring system may be important in realizing a high stereospecificity in radical polymerization, though it should be noted that PFMA (**25**) leads to a relatively



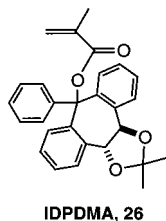
low isotactic specificity by radical and anionic polymerization.⁵³ DMPAMA results in mm selectivity of >99%, whereas DBPAMA affords polymers with slightly lower mm contents (mm 91–99%). An important result was that the isotactic poly(DBPAMA)s with relatively high DPs (up to 974) obtained by the radical polymerization were completely soluble in THF and chloroform, suggesting that the two butyl groups per unit prevent aggregation of the helical molecules. This is interesting because helical polymethacrylates with high DPs generally have a tendency to form aggregates and become quite insoluble.^{13,52,65,72} The good solubility of the poly-(DBPAMA)s would make it possible to clarify the solution properties of the high-molecular-weight, helical vinyl polymers.

The two monomers gave nearly completely isotactic, single-handed helical polymers by the anionic polymerization using the complex of *N,N*-diphenylethylenediamine monolithium amide (DPEDA-Li) with DDB or PMP.^{79,80} The single-handed helical polymers showed much lower optical activity [poly(DMPAMA), [α]₃₆₅ +125°; poly(DBPAMA), [α]₃₆₅ +183°] than the single-handed helical poly(TrMA) ([α]₃₆₅ ≈ +1500°). The relatively low specific rotation values for a single-handed helix suggest that the reported high optical activity of poly(TrMA) and its analogues is partly based on the single-handed propeller conformation^{14,15,81,82} of the triarylmethyl group in the side chain in addition to the helical arrangement of the entire polymer chain. Such a propeller conformation would be difficult for poly-(DMPAMA) and poly(DBPAMA) because the anthracene moiety in the side chain should have a planar structure.

Helix-sense selection was also realized during the radical polymerization of DBPAMA at 0 °C using

optically active NMT as the chain-transfer agent.^{79,80} Optically active poly(DBPAMA) $[\alpha]_{365} +74^\circ$ using (+)-NMT; $[\alpha]_{365} -53^\circ$ using (-)-NMT was obtained. The specific rotation values suggest that the helical sense excess (ee) may be ca. 30–40%. In contrast to the asymmetric radical polymerization of PDBSMA, the optically active product was completely soluble in this case.

A chiral PDBSMA derivative, IDPDMA (**26**), was designed to form a single-handed helical polymer through radical polymerization due to the effect of the chirality in the side chain.⁸³ The anionic polym-



erization of (+)-IDPDMA with 100% ee ($[\alpha]_{365} +548^\circ$) was performed using achiral DPEDA-Li in THF, resulting in an optically active polymer whose specific rotation ($[\alpha]_{365} +1540^\circ$) was comparable to those of other single-handed helical polymethacrylates. Hence, the chiral side chain can induce an excess helicity in the anionic polymerization. The radical polymerization of (+)-IDPDMA led to polymers with an almost completely isotactic structure regardless of the ee of the monomers. The polymer obtained by the radical polymerization of the (+)-IDPDMA with 100% ee showed a CD spectrum with the features of both that of (+)-IDPDMA and that of the highly optically active poly[(+)-IDPDMA] obtained by the anionic polymerization. This suggests that the radically obtained poly[(+)-IDPDMA] has a prevailing helicity, though the helical sense in excess appeared to be lower than that of the anionically obtained polymer. In the radical polymerization of IDPDMA having various ee's, the ee of the monomeric units of the polymer was always higher than that of the starting monomer, indicating the enantiomer in excess was preferentially incorporated into the polymer chain (enantiomer-selective polymerization). The enantiomer selection may be governed by the excess helicity of the growing radical. The growing species consisting of an excess enantiomeric component of monomeric units probably takes a helical conformation with an excess helical sense which can choose one enantiomer of IDPDMA over the other.

Phenyl-2-pyridyl-*o*-tolylmethyl methacrylate (PPyoTMA, **27**) having a chiral ester group is known to lead to highly enantiomer-selective and helix-sense-selective polymerization by anionic catalysis.^{84–86} The selection was also found in the radical polymerization of optically active PPyoTMA having various ee's,

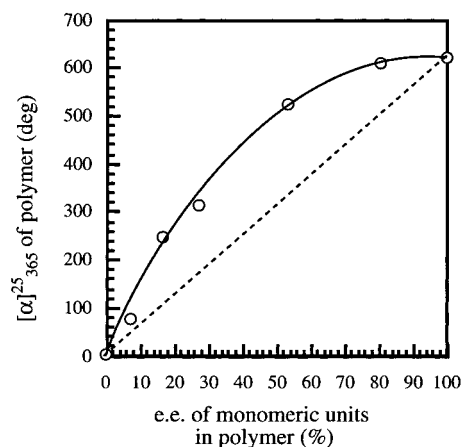
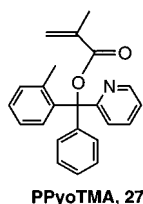
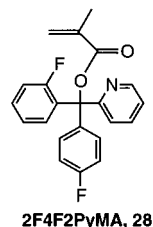


Figure 6. Relation between the optical activity of poly(PPyoTMA) obtained by radical polymerization and the optical purity of the monomeric units. (Reprinted with permission from ref 87. Copyright 1996 American Chemical Society.)

although the isotactic specificity in the radical polymerization was moderate (mm 72–75%) [polymerization in toluene at 40 °C using (*i*-PrOCOO)₂].⁸⁷ The polymer obtained from optically pure (+)-PPyoTMA ($[\alpha]_{365} +190^\circ$) showed a large levorotation ($[\alpha]_{365} -617^\circ$), suggesting that the polymer has a helical conformation with an excess helical sense. The anionic polymerization of the same monomer using *n*-BuLi at -78 °C produces a polymer with an mm content of 98% and a higher specific rotation ($[\alpha]_{365} -1280^\circ$), which is comparable to the rotation values for the single-handed helical poly(TrMA). The radically obtained polymer may have a shorter single-handed helical sequence based on the lower isotacticity of the main chain.

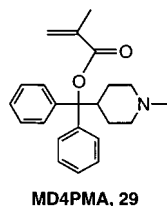
In the polymerization of the (-)-monomers with various ee's, enantiomer selection was observed though the selectivity was lower compared with that of the polymerization of IDPDMA.^{83,87} In this experiment, a nonlinear relation was observed between the ee of the monomer in the feed and the optical activity of the obtained polymer (Figure 6). This indicates that the optical activity of the polymer is not based only on the side chain chirality. Furthermore, the chirality of a one-handed helical part induced by a successive sequence of the (-)-monomeric units (monomeric units derived from a (-)-monomer) can overcome the opposite chiral induction by the sporadic (+)-monomeric units. In other words, once a one-handed helical radical comes under the influence of the (-)-monomeric units, an entering (+)-monomer becomes a part of the one-handed helix whose direction may be unfavorable to the chiral nature of the (+)-monomer.

The stereochemistry of 2F4F2PyMA (**28**) polymerization was also investigated.^{88,89} The optically pure



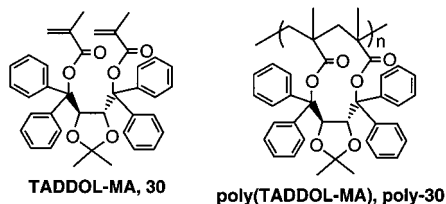
(+)-2F4F2PyMA ($[\alpha]_{365} +28^\circ$) afforded polymers with a relatively low mm content and a low optical activity either by the anionic polymerization with DPEDA–Li in THF at -78°C (mm/mr/rr = 70/30/~0, $[\alpha]_{365} -82^\circ$) or by the radical polymerization in toluene using (*i*-PrOCOO)₂ at 40°C (mm/mr/rr = 54/27/19, $[\alpha]_{365} -2^\circ$).⁸⁹ The monomer design of 2F4F2PyMA was not as effective as that of PPyoTMA in controlling the polymerization stereochemistry.

(1-Methylpiperidin-4-yl)diphenylmethyl methacrylate (MP4DMA, **29**) has been revealed to afford highly isotactic, helical polymers by radical polym-



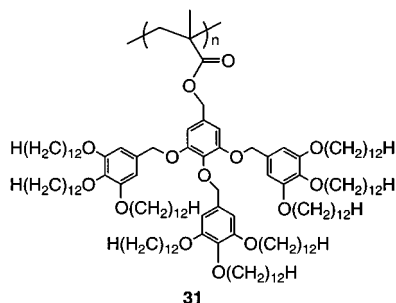
erization (mm 94–97%).⁹⁰ This is in contrast to the moderate mm specificity in the radical polymerization of cyclohexyldiphenylmethyl methacrylate.⁹¹ MP4DMA was polymerized using a free-radical initiator in the presence of (–)-menthol to afford an optically active polymer with an excess helical sense. Because the *N*-substituent of the monomer can be replaced with other functional groups, the design of MP4DMA may be extended to the synthesis of a variety of helical polymers having functional groups attached to the side chain.

Free-radical and anionic polymerizations of TADDOL–MA (**30**) proceed exclusively via a cyclization mechanism, and the obtained polymer seems to have a helical conformation with an excess helicity.^{92–94} The main chain structure of poly(TADDOL–MA) with cyclized units (poly-**30**) is different from that of all other polymethacrylates discussed here. Similar monomers have been synthesized and polymerized.⁹⁵



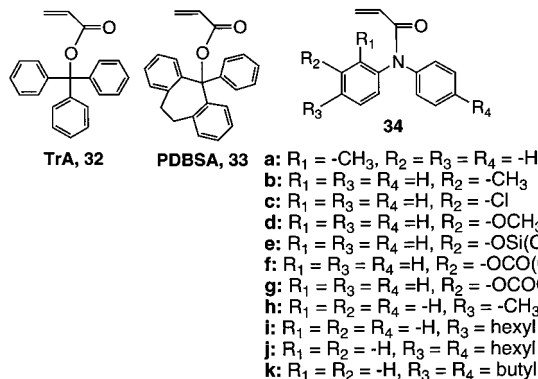
4. Polymers of Other Acrylic Monomers

There is a class of helical polymethacrylates whose conformation is induced by the assembly of their side groups.⁹⁶ The polymer **31**, having a dendritic side



group, is an example. The helical conformation was first found in the solid state by the X-ray analysis of oriented fiber samples. The conformation was then confirmed visually by scanning force micrography. In contrast to the polymethacrylates discussed in the preceding section, the polymers are likely to form a helical conformation regardless of the main chain configuration. A similar conformational control has been realized also with polystyrene derivatives having a dendritic side group.

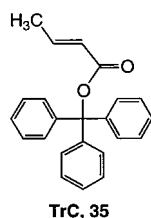
Helix-sense-selective anionic polymerization of acrylates TrA (**32**) and PDBSA (**33**)^{97,98} and acrylamides including the series of *N,N*-diphenylacrylamides^{99–104} (**34**) have been investigated using (+)-PMP, (–)-Sp,



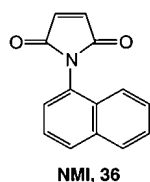
and (+)-DDB as chiral ligands. The stereocontrol in the polymerization of the acrylates and acrylamides was more difficult compared with that in the methacrylate polymerization. The specific rotations ($[\alpha]_{25}^{365}$) of poly(TrA) and poly(PDBSA) obtained by the asymmetric polymerization were much smaller than those of the corresponding polymethacrylates prepared under similar conditions and were up to $+102^\circ$ (ligand PMP, diad isotacticity 70%) and -94° (ligand DDB, diad isotacticity 61%), respectively. The isotactic part of the polymers is considered to have a helical conformation with an excess helicity. For the polymerization of the bulky acrylamides, (–)-Sp has been mainly used as the chiral ligand. Sp was also a better ligand compared with DDB and PMP in the polymerization of **34d**. The highest isotacticity (mm 87%) and optical activity ($[\alpha]_{25}^{365} -657^\circ$) in the asymmetric polymerization of acrylamides were achieved in the polymerization of **34h** using the (–)-Sp–FILI complex as an initiator at -98°C .¹⁰² The stereostructure of poly-**34h** depended on the molecular weight, and the high-molecular-weight fractions separated by GPC fractionation exhibited large levorotation, $[\alpha]_{25}^{365} -1122^\circ$ (mm 94%), which is comparable to the optical activity of the single-handed helical polymethacrylates.¹⁰²

Helix-sense-selective polymerization has also been attempted for several bulky monomers including an acrylonitrile derivative¹⁰⁵ and α -substituted acrylates.^{106,107} Triphenylmethyl crotonate (TrC, **35**) affords optically active, helical polymers by the polymerization using DDB–FILI and PMP–FILI complexes.^{108,109} The polymers possess a nearly completely threo-diisotactic structure. Although the polymers indicate relatively small specific rotation ($[\alpha]_{\text{D}} +5.6^\circ$ and $+7.4^\circ$ for the samples with DP = 15 and

36, respectively), the optical activity is considered to be based on an excess helicity because the rotation was lost when the polymers were converted to the methyl esters.

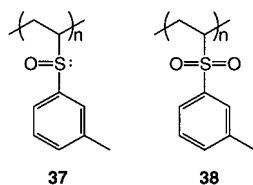


N-1-Naphthylmaleimide (NMI, **36**) affords an optically active polymer ($[\alpha]_{435} +152^\circ$ to 296°) by polymerization using an Et_2Zn – Bnbox complex.¹¹⁰ The obtained polymer resolves 1,1'-bi-2-naphthol when used as an HPLC packing material. Although the tacticity of the polymer is not clear, the polymer may have a helical conformation with an excess screw sense in this case.



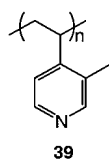
C. Miscellaneous Vinyl Polymers

The anionic polymerization of optically active (+)- or (–)-*m*-tolyl vinyl sulfoxide ($[\alpha]_{\text{D}} +486^\circ$, -486°) using BuLi or BuLi –(–)-*Sp* leads to an optically active polymer, **37** [$[\alpha]_{\text{D}} +274^\circ$ to $+311^\circ$ (from (+)-monomer); $[\alpha]_{\text{D}} -272^\circ$ to -310° (from (–)-monomer)]. Oxidation of **37** afforded polymer **38** with an achiral



side group that was still optically active [$[\alpha]_{\text{D}} +19^\circ$ to $+42^\circ$ starting from the (+)-monomer, -16° to $<41^\circ$ starting from the (–)-monomer]. Polymer **38** may have a helical conformation with a prevailing helicity of the main chain.¹¹¹

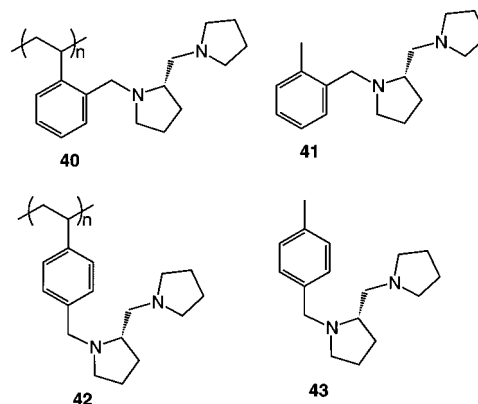
Optically active poly(3-methyl-4-vinylpyridine) ($[\alpha]_{589}^{-4} +14.2^\circ$) (**39**) has been prepared by anionic polymerization of the corresponding monomer using the (–)-DDB–DPEDA– Li complex in toluene at -78



$^\circ\text{C}$.¹¹² The optical activity has been ascribed to a helical conformation, although the tacticity of the polymer is not yet clear. The optical activity was lost in solution at -4°C within 30 min of dissolution. This

is reasonably due to a conformational transition allowed only in solution.

An optically active polystyrene derivative, **40** ($[\alpha]_{365}^{25} -224^\circ$ to -283°), was prepared by anionic and radical catalyses.¹¹³ The one synthesized through the anionic polymerization of the corresponding styrene derivative using BuLi in toluene seemed to have a high stereoregularity and showed an intense CD spectrum whose pattern was different from those of the monomer and a model compound of monomeric unit **41**. In contrast, polymer **42** and a model compound, **43**,

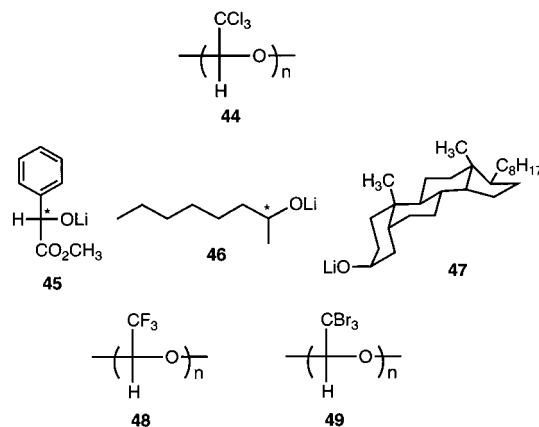


for the polymer indicated very similar CD spectra. These results suggest that polymer **40** may have a regular conformation, probably a helix, while the chiroptical properties of polymer **42** are mainly due to the chiral side-chain group. Together with the results on **40**, a substituent at the 2-position of the aromatic ring may be important in realizing a helical conformation for polystyrene derivatives and related polymers.

D. Polyaldehydes

1. Polychloral and Related Polymers

Asymmetric anionic polymerization can convert trichloroacetaldehyde (chloral) to a one-handed helical, isotactic polymer (**44**) having a 4/1-helical conformation with high optical activity ($[\alpha]_{\text{D}} +4000^\circ$ in film).^{28,114–118} Anionic initiators such as **45**,¹¹⁵ **46**,¹¹⁵ and **47**¹¹⁷ and Li salts of optically active carboxylic acids or alcohols are used for the polymerization. Although the polymers are insoluble in solvents and their conformation in solution cannot be directly

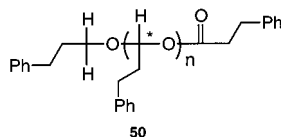


elucidated, a helical structure has been verified by NMR and crystallographic analyses of the uniform oligomers separated by chromatographic techniques.^{29,118} A helical conformation has also been proposed for poly(trifluoroacetaldehyde) (**48**) and poly(tribromoacetaldehyde) (**49**).^{119,120}

Optically active **44** partially resolves *trans*-stilbene oxide¹²¹ and separates several aromatic compounds¹²² when used as an HPLC stationary phase. **44** also partially resolves isotactic polymers of (*R*)-(+)- and (*S*)-(–)- α -methylbenzyl methacrylate.¹²³

2. Other Polyaldehydes

Optically active poly(3-phenylpropanal) ($[\alpha]_D^{25,365}$ -33° to -56°) (**50**) is obtained by the anionic polymerization of 3-phenylpropanal (**51**) using the complexes of Sp with ethylmagnesium bromide (EtMgBr)



and *n*-octylmagnesium bromide (OctMgBr).¹²⁴ The optical activity may be based on a predominant single-handed helical conformation. Reaction of the initiator with **51** gives an ester (**52**) and the (3-phenylpropoxy)magnesium bromide–Sp complex through the Tishchenko reaction (Figure 7). The

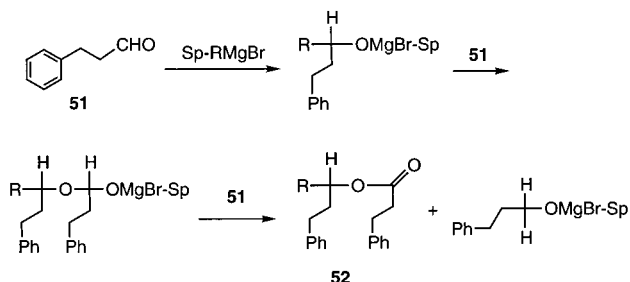
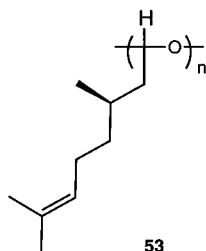


Figure 7. Polymerization of **51** using an Sp–Grignard reagent complex.

complex initiates the polymerization of **51**, and the termination reaction takes place through the Tishchenko reaction, resulting in the polymer structure **50**.

The major diastereomer of dimer **50** ($n = 2$) (diastereomeric stereostructure not identified) prepared by oligomerization using Sp as a chiral ligand was found to be rich in the (+)-isomer with 70% ee. This suggests that oligomer anions with a certain configuration, for instance, (*S,S*) or (*R,R*), may propagate preferentially to the polymers.

An optically active aldehyde is also considered to afford a polymer having a helical conformation.¹²⁵

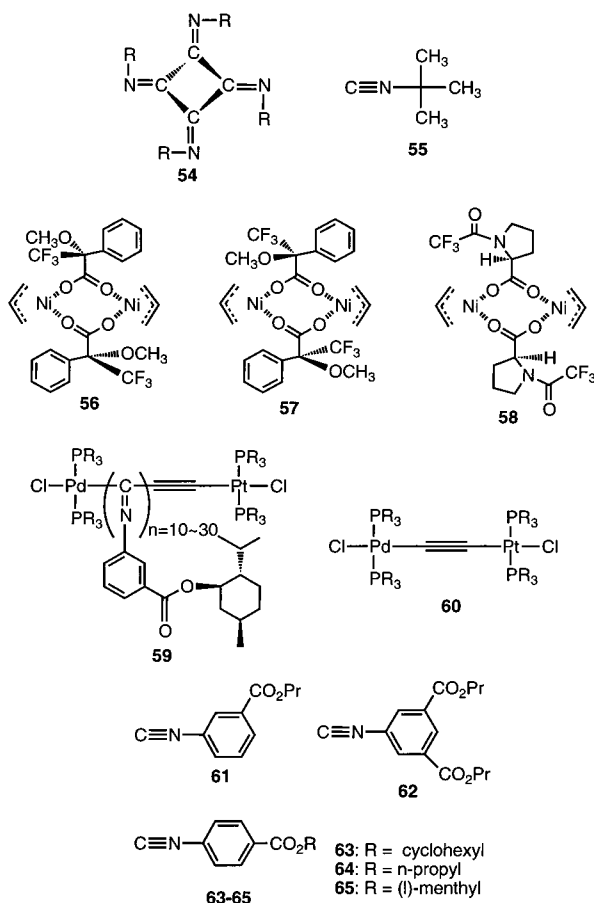


The polymer **53**, bearing a chiral side group, showed much larger optical activity ($[\alpha]_D -81^\circ$ to -94°) than a model compound of the monomeric unit.^{125a,b}

E. Polyisocyanides

1. Polymers of Monoisocyanides

Polyisocyanides having a 4/1-helical conformation (**54**) are obtained by the polymerization of chiral isocyanide monomers.^{17,126} An optically active polyisocyanide having a chirality due to the helicity was first obtained by chromatographic resolution of poly(*tert*-butyl isocyanide) (poly-**55**) using optically active poly[(*S*)-*sec*-butyl isocyanide] as a stationary phase, and the polymer showing positive rotation was found to possess an M-helical conformation on the basis of CD spectral analysis.^{127,128} Details of the helical structure of polyisocyanides have been discussed on the basis of theoretical and experimental analyses.^{19–21} Optically active polymers having an excess helicity can be prepared by the polymerization of bulky isocyanides using chiral catalysts. Catalysts effective for helix-sense-selective polymerization include Ni(CNR)₄(ClO₄)/optically active amine systems,¹²⁸ the Ni(II) complexes **56–58**,¹²⁹ and the dinuclear complex containing Pd and Pt which has a single-handed oligomeric isocyanide chain (**59**).¹³⁰ By the polymerization of **55** using Ni(CN–Bu^t)₄(ClO₄)/(*R*)-(+)-C₆H₅–CH(CH₃)NH₂, an M-helical polymer with an ee of 62% can be synthesized,¹²⁸ and complex **58** converts **55** to a levorotatory polymer with 69% ee.¹²⁹ The complex **59** is obtained by oligomerization of *m*-(*l*)-menthoxy-carbonylphenyl isocyanide with Pt–Pd di-



nuclear complex **60**. **59** can smoothly polymerize bulky monomers **61** and **62** in a helix-sense-selective manner. For example, the polymerization of **62** with **59** ($n = 10$, $M_n = 3720$, $[\alpha]_D +22^\circ$) affords a polymer with $M_w = 13.5 \times 10^3$ and $[\alpha]_D +126^\circ$.¹³⁰ An excess helicity is also induced in the copolymerization of achiral **63** or **64** with optically active **65** using complex **60**. A nonlinear relationship exists between optical rotation and the content of the chiral monomer: the optical activity of a copolymer containing 70% chiral monomeric unit is almost the same as the optical activity of the homopolymer of the chiral monomer.^{131,132} The effect of the ee of the monomer on the optical activity of the monomer in the homopolymerization of **65** using **60** has been studied; a nonlinear effect was also found in this case.^{132,133}

A helical polyisocyanide bearing a porphyrin residue in the side chain has been prepared.¹³⁴ The special alignment of the porphyrin chromophores was controlled using the helical main chain as established by an absorption spectrum. In addition, helical polyisocyanides having a saccharide residue in the side chain have been designed, and the molecular recognition of the polymers by lectin was investigated.^{135,136} Furthermore, block copolymers of styrene with isocyanides having L-alanine-L-alanine and L-alanine-L-histidine side chains have been synthesized; the copolymers consist of a flexible polystyrene chain and a rigid, helical, and charged isocyanide chain.¹³⁷ The copolymers were found to form rodlike aggregates having a nanometer-scale helical shape.

Optically active poly-**55** shows chiral recognition ability toward several racemates including $\text{Co}(\text{acac})_3$.¹³⁸

2. Polymers of Diisocyanides

1,2-Diisocyanobenzene derivatives yield helical polymers via a cyclopolymerization mechanism by the polymerization with Pd and Ni complexes. Optically active polymers were initially obtained by the method illustrated in Figure 8.^{139–143} Monomer **66** was reacted with an optically active Pd complex to form diastereomeric pentamers **67**, which were separated into (+)- and (-)-forms by HPLC. The polymerization of **68** using the separated **69** led to a one-handed helical polymer.¹³⁹ The polymerization of **68** using the initiators having chiral binaphthyl groups, **69–71**, also produced optically active polymers.¹⁴² The helix-sense selectivity in the polymerization using **69**

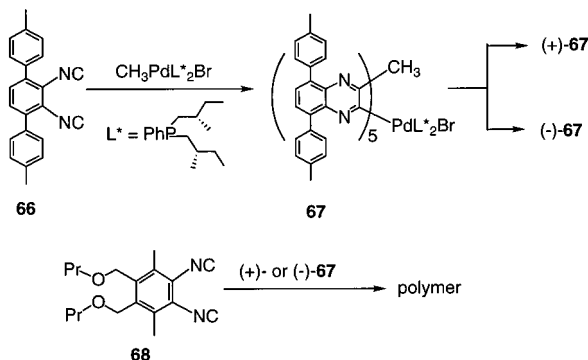
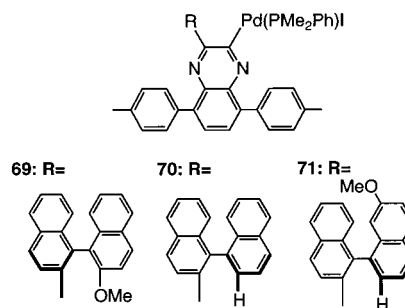


Figure 8. Helix-sense-selective polymerization of 1,2-diisocyanobenzene derivatives.



depended on the polymerization procedure. The polymer obtained by direct polymerization with **69** had a much lower helix-sense excess compared with the polymer prepared using a pentamer synthesized using **69** and purified into a single-handed helical form which led to a single-handed helical structure of the obtained polymer. In contrast to **69**, **70** without purification of the intermediate oligomeric species yields poly-**68** with high helix-sense selectivity (79%). The helix-sense selectivity in the polymerization of **68** using **71** as the initiator was estimated to be over 95%.^{143,144} Block copolymerization of different diisocyanide monomers was carried out, and helical tri-block copolymers were synthesized.¹⁴⁵

F. Polyisocyanates and Related Polymers

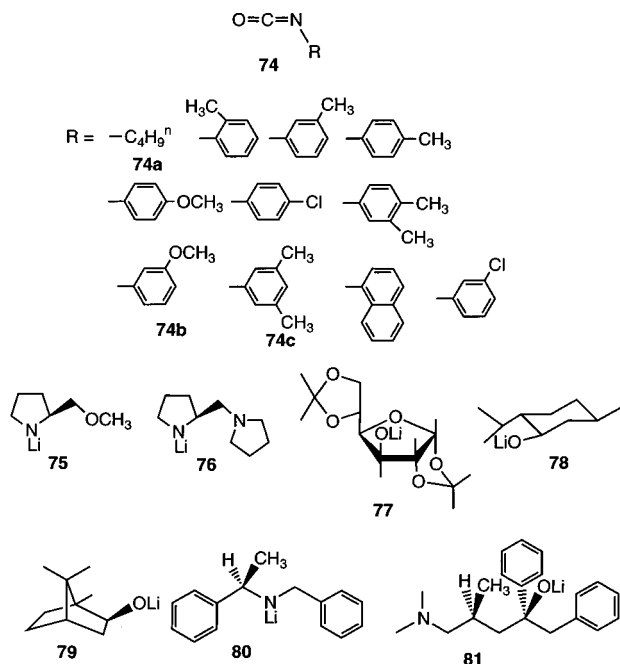
1. Polyisocyanates

Polyisocyanates are obtained by anionic polymerization using initiators such as NaCN and organolithiums and have the structure of 1-nylon (**72**).^{146,147} Polymerization of hexyl isocyanate with a half-metallocene complex (**73**) leads to a living polymer,¹⁴⁸



and this catalyst can be applied to the polymerization of functionalized monomers.¹⁴⁹ Polyisocyanates possess a dynamic helical conformation in which right-handed helical and left-handed helical parts coexist in the chain and are separated by helix-reversal points.^{23,41,146,147} Hence, if a polymer is made from an achiral monomer using an achiral initiator, the polymer is optically inactive; i.e., the amounts of right- and left-handed helices are equal, although the energy barrier for the movement of the helix reversals depends on the kind of side chain.^{150,151} Optically active polyisocyanates having an excess helicity are obtained by (1) polymerization of achiral isocyanates using optically active anionic initiators, (2) polymerization of optically active monomers, and (3) the interaction of a polymer chain with an optically active solvent.

The polymerization of butyl isocyanate and other achiral monomers (**74**) using optically active anionic initiators **75–81** affords optically active polymers.^{152–156} The poly-**74a** ($M_n = 9000$) obtained using **75** exhibits $[\alpha]_{435} +416^\circ$. The optical activity of the polymers arises from the helical part extending from the chain terminal bearing the chiral group originat-



ing from the initiator to a certain length (persistence length) that has a single-screw sense due to the influence of the terminal chiral group. The relation between the DP and optical activity was investigated for the oligomers obtained from **74b** and **74c** using **75** as initiator (Figure 9). For this purpose, the oligomers in the DP range of 1–20 were isolated using supercritical fluid chromatography (SFC). In the figure, the optical activity of oligo-**74b** and oligo-**74c** increased with an increase in DP in the range of DP < 13 and DP < 15, respectively. This is probably because, in this DP range, the oligomers have no helix-reversal point and the helical structure becomes stiffer as the DP increases. In the higher DP range, the optical activity of the oligomers gradually decreased due to the generation of helix-reversal points, indicating that the reversal points start to be generated at the DPs mentioned above for the two oligomers.¹⁵⁵

A helix-sense excess can also be realized based on the effects of a chiral side chain.^{22,23,41,157–166} For example, optically active monomer (*R*)-**82**, whose chirality is based only on the difference between –H

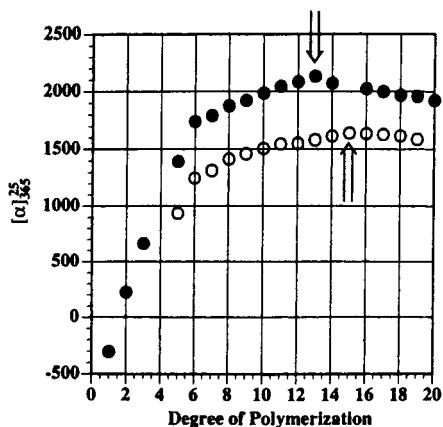


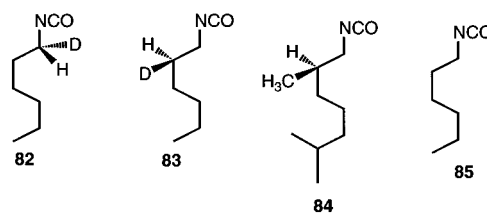
Figure 9. Specific rotation of oligomers of **74b** (upper) and **74c** (lower). Reprinted with permission from ref 155. Copyright 1998 The Society of Polymer Science, Japan.

Table 6. Specific Rotation of Copolymers of **84** and **85**^a

[85] (%) ^b	[84] (%) ^b	[α] ⁻²⁰ _D (deg)	[α] ⁺²⁰ _D (deg)
100	0	0	0
99.5	0.5	-140	-66
97.7	2.3	-379	-231
85	15	-532	-480
0	100	-514	-500

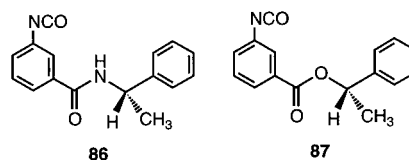
^a Measured in CHCl₃ (*c* = 0.5 mg mL⁻¹). Reprinted with permission from ref 41. Copyright 1999 Wiley-VCH. ^b Mole percent.

and –D ([α]_D < 1°), gives a polymer showing [α]_D –367° by anionic polymerization with NaCN.^{23,157} The preferential helical sense is sensitive to the side-chain structure; **82** and **83** with the same absolute configuration and very similar structures result in an opposite helical sense of the polymers.¹⁶¹ A screw-sense excess is also realized in copolymers of chiral and achiral monomers. Only a small amount of chiral **84** randomly incorporated into a polymer chain consisting mainly of achiral monomeric units based on **85** effectively induces a helical-sense excess (“ser-



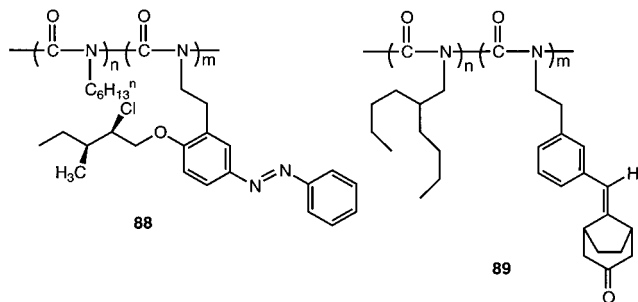
geants and soldiers” effect) (Table 6). The data shown in Table 6 indicate that only 0.5% **84** units can induce an excess helical sense and that 15% **84** units induces the excess helicity essentially the same as that of the homopolymer of **84**. Using structurally different enantiomers along one chain gives rise to an unusual relationship of optical activity and temperature in the polyisocyanates.¹⁶⁴ Optically active block copolymers have been created using the living polymerization catalyst **73** mentioned earlier.¹⁶⁵

Optically active aromatic isocyanates have been synthesized and polymerized.^{152–156,166–169} Poly-(*S*)-**86** prepared by the polymerization using the lithium amide of piperidine showed a very large levorotation ([α]₃₆₅ –1969° to –2014°) which was only slightly affected by temperature.¹⁶⁷ This is in contrast to the fact that the optical activity of polyisocyanates with chiral side chains is often greatly dependent on temperature and may suggest that the poly-(*S*)-**86** has a perfectly single-handed helical conformation. The polymer showed chiral discrimination ability toward 1,1'-bi-2-naphthol and mandelic acid.¹⁶⁷ In the copolymers of **87** with **74b**, the predominant helicity was reversed depending on the ratio of the monomeric units.¹⁶⁹ The polymer having 10% chiral **87**



units showed $[\alpha]_{365}^{25} +733^\circ$, while the one having 80% **87** units showed $[\alpha]_{365}^{25} -1278^\circ$.

The helical sense of polyisocyanates **88** and **89** can be controlled in terms of photoinduced isomerization of the side chain chromophores.^{165,170} For **88**, photoirradiation causes the *cis*–*trans* isomerization of the azo moiety, which induces a change in the helix population of the main chain.¹⁶⁵ In the case of **89** having a chiral bicyclo[3.2.1]octan-3-one group in the side chain, photoirradiation results in rotation around the styryl double bond in the side chain. When (+)- or (–)-circularly-polarized light is used for irradiation, the chirality of the bicyclo[3.2.1]octan-3-one is controlled, leading to a change in the predominant helicity.¹⁷⁰



An excess helicity is induced by the effect of a chiral solvent or additive.^{41,161,171,172} In the case of poly(*n*-hexyl isocyanate), a CD spectrum based on an excess helicity was observed in chiral chloroalkane solvents (Figure 10), and the sign and intensity of the CD

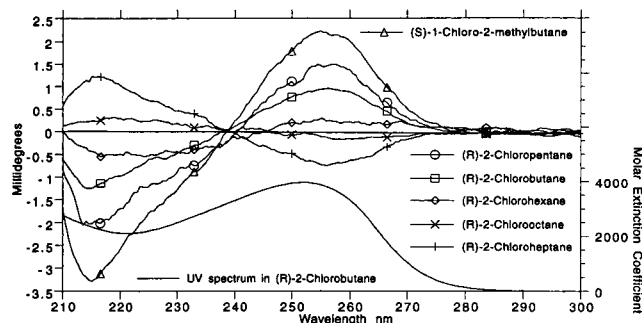
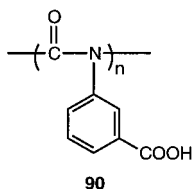


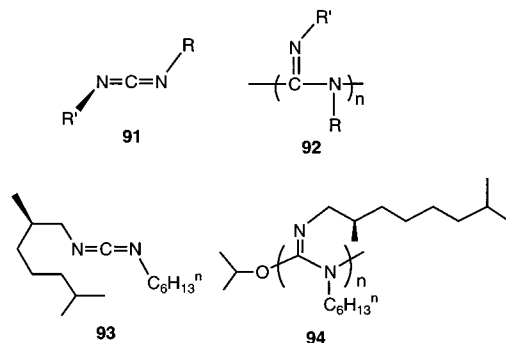
Figure 10. CD spectra of poly(*n*-hexylisocyanate) (poly-**85**) dissolved in optically active solvents at 20 °C. Ultraviolet spectrum (bottom) shown only for (*R*)-2-chlorobutane (polymer concentration 1.9 mg/mL). (Reprinted with permission from ref 171. Copyright 1993 American Chemical Society.)

absorptions changed depending on the kind of solvent.¹⁷¹ A minute difference in the solvation energy for right- and left-handed helical parts is considered to cause the screw-sense excess. The addition of chiral amino alcohols and amines to polymer **90** having a carboxylic acid residue induced an excess screw sense probably through an acid–base interaction.¹⁷²



2. Polycarbodiimides

Carbodiimide **91** gives helical polymer **92** through living polymerization with titanium and copper catalysts.^{173,174} The conformation of a polycarbodiimide has been studied by means of NMR.¹⁷⁵ An optically active carbodiimide, (*R*)-**93** ($[\alpha]_{365} +7.6^\circ$), gives polymer **94** by the polymerization using a titanium



catalyst.¹⁷⁶ The polymer showed optical activity essentially identical to that of the monomer; however, on heating, the polymer indicated mutarotation and the specific rotation reached a plateau value of $[\alpha]_{365} -157.5^\circ$ probably based on the excess helical sense of the main chain. The mutarotation has been ascribed to a conformational transition from a kinetically controlled one to a thermodynamically controlled one. An excess single-handed helical conformation can be induced for poly(di-*n*-hexylcarbodiimide) (**95**) by protonating the polymer with (*R*)- or (*S*)-camphorsulfonic acid (**96**) (Figure 11).¹⁷⁶

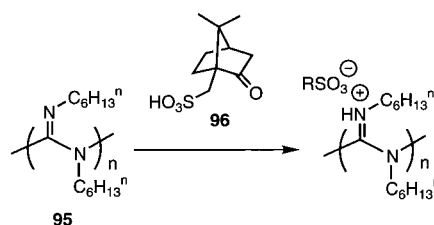


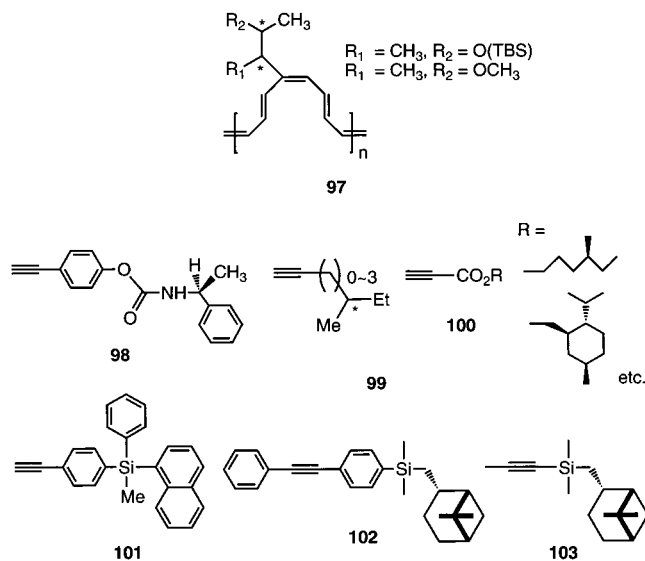
Figure 11. Induction of an excess helix sense for carbodiimide polymer by complexation with camphorsulfonic acid.

G. Polyacetylene Derivatives and Related Polymers

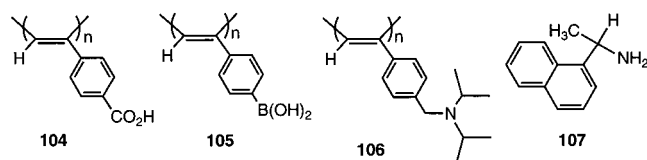
1. Polyacetylene Derivatives

Optically active polyacetylene derivatives **97** were synthesized through ring-opening polymerization of the corresponding cyclooctatetraene derivatives.²⁵ A twisted conformation of the main chain was proposed on the basis of CD and UV absorptions. Various optically active polyacetylenes have also been prepared from chiral monomers.^{24,25,26a,177–183} The examples include a phenylacetylene derivative (**98**),^{26a} alkylacetylenes **99**,²⁴ propionic esters such as **100**,^{177,178} a Si-containing monomer (**101**),¹⁷⁹ and disubstituted monomers such as **102**.¹⁸⁰ Poly-(*R*)-**98** synthesized using a $[\text{RhCl}(\text{norbornadiene})_2]$ catalyst shows intense CD bands in the UV–vis region, probably based on a predominant helical sense of the main chain.^{26a} This polymer effectively resolves several racemic

compounds including Tröger's base, *trans*-stilbene oxide, and methyl phenyl sulfoxide when coated on silica gel and used as chiral packing material for HPLC.¹⁸¹ More examples of chiral recognition by optically active poly(phenylacetylene) derivatives are known.¹⁸² Chiral recognition by a membrane prepared from optically active poly-**103** has been reported.¹⁸³



Poly(phenylacetylene) derivatives **104**–**106** bearing achiral functional side groups have been synthesized. The polymers possess a stereoregular *cis*-*trans*oidal structure. Excess single-handed helicity of the main chain can be induced for the polymers by the interaction with chiral molecules.^{26b,184–188} For example, **104** shows intense CD bands in the presence of optically active amines and amino alcohols including **107**



(Figure 12).^{26b,184} In Figure 12, mirror images of CD spectra were obtained in the presence of the (*R*)- and (*S*)-amine. The CD absorptions are not based on the chiral amine but on the excess helicity of the main chain of **104** as clearly understood from the wave-

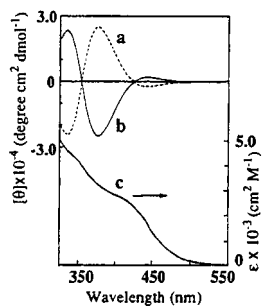


Figure 12. CD spectra of **104** in the presence of (*R*)-**107** (a) and (*S*)-**107** (b) and absorption spectrum (c) in the presence of (*R*)-**107** in DMSO (the molar ratio of **107** to **104** is 50). (Reprinted with permission from ref 26b. Copyright 1995 American Chemical Society.)

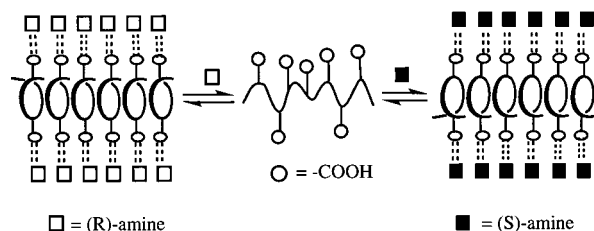


Figure 13. Helix formation of poly(phenylacetylene) derivatives through the interaction with added chiral amine.

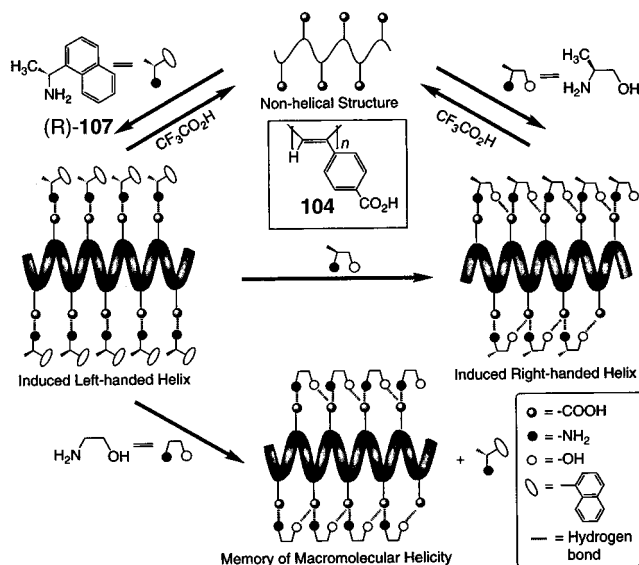


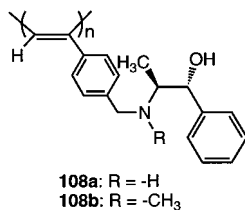
Figure 14. Concept of memory of macromolecular helicity. (Reprinted with permission from Nature (<http://www.nature.com>), ref 186. Copyright 1999 Macmillan Magazines.)

length range. These results indicate that **104** originally having a rather irregular twist of the adjacent double bonds around a single bond may be transformed into the helical conformation with an excess screw sense by the interaction with the chiral amines (Figure 13). Helicity induction was also found for the Na salt of **104** by the interaction of a natural amino acid including L- and D-methionine.¹⁸⁵

The concept of "memory of macromolecular helicity" has been introduced for **104** (Figure 14).¹⁸⁶ As discussed above, a right- or left-handed helical conformation is induced for **104** with the interaction with chiral additives. For this system, it was found that the helical conformation is not lost even after the chiral additives are replaced with achiral additives. In the case shown in Figure 14, chiral **107** is replaced with achiral 2-aminoethanol. Hence, the helicity is memorized. The effectiveness of the memory depends sensitively on the structure of the achiral additive replacing the chiral additive. It should be noted that the memorized helical-sense excess increased on storage with *achiral* 2-aminoethanol complexed to **104**.

In the case of **105**, carbohydrates and steroids induced the helicity.¹⁸⁷ A reverse combination of acid and base compared to the helix induction using **104** was achieved using **106**, whose interaction with various chiral carboxylic acids led to an excess screw sense of the main chain.^{188,189}

Polymer **108** having a chiral side chain possesses a helical conformation with a predominant helicity due to the effect of the side groups. The predominant helicity was reversed by the interaction with (*R*)-



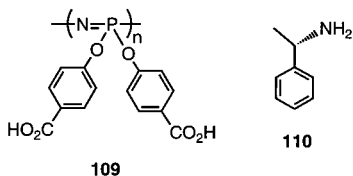
mandelic acid (helix-helix transition), while (*S*)-mandelic acid only slightly affected the conformation of the polymer. The diastereomeric acid-base interaction causes the conformational transition.¹⁹⁰ Complexes of **108** with R₂Zn effectively catalyze the asymmetric alkylation of benzaldehyde.¹⁹¹

The poly(phenylacetylene) derivatives discussed here are considered to be molecular probes for chirality detection of various chiral molecules.

As another example of a helical polyacetylene, the single-handed helical polyacetylene fibril, whose structure was studied by SEM, was prepared by the polymerization of acetylene within a chiral nematic liquid crystalline phase.¹⁹²

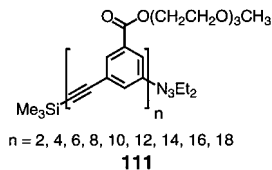
2. Polyphosphazene

Helicity induction was also realized for polyphosphazene derivative **109** using (*R*)-1-phenethylamine (**110**) as the chiral additive.¹⁹³



H. Poly(aryleneethynylene)s

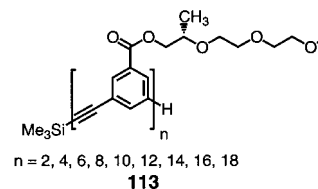
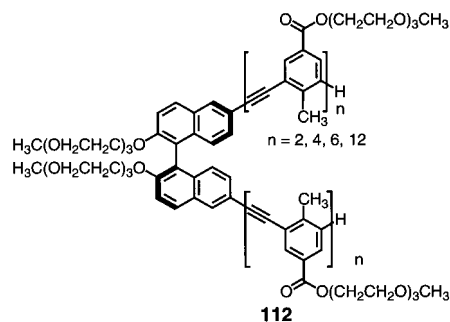
Oligo(*m*-phenyleneethynylene)s **111** have been shown to adopt a helical conformation in acetonitrile, although they do not in chloroform.^{33,194} The helix



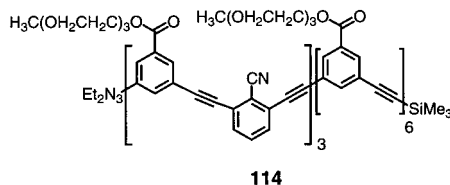
formation is thought to be a result of the solvatophobic effect: the oligomers fold into a compact, helical structure in a poorer solvent such as acetonitrile. The conformation was proposed on the basis of the hypochromic effect. In acetonitrile and chloroform, the oligomers show a different dependence of the molar extinction coefficient (ϵ) on the DP. In the range of DP = 2–8, ϵ values in acetonitrile are close to those in chloroform in which the ϵ -DP plot is linear. However, in the DP range larger than 8, the slope of the ϵ -DP plot in acetonitrile becomes smaller than that in chloroform, indicating that the overlap of phenylene groups driven by the helix formation

(folding of the molecule) causes the hypochromicity in acetonitrile. The absorption spectral pattern also differs depending on the solvent. Intermolecular interaction was ruled out by the spectral studies at various concentrations, and the helical structure was supported by the ¹H NMR measurement, which showed a remarkable upfield shift of the aromatic protons, an indication of overlap of the phenylene groups.

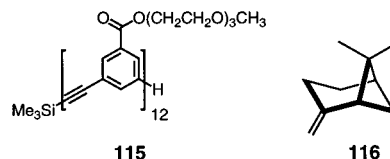
Oligomers **112**¹⁹⁵ and **113**¹⁹⁶ having chiral groups in the main or side chain have an excess helicity. A **112** analogue having a flexible chiral group in place of the binaphthyl group has also been reported.¹⁹⁷ Although the exact values of the helical-sense excess are not known, the chiral oligomers show the characteristic CD bands in acetonitrile, which are not seen in chloroform.



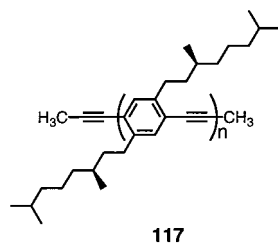
In the case of oligomer **114**, Ag⁺ ions are taken into the interior part of the helix and stabilize the helical conformation.¹⁹⁸



Chiral monoterpenes including (+)- β -pinene (**116**) can induce an excess helicity to achiral **115**. The chiral terpene forms a complex preferentially with right- or left-handed helical **115**, which exists in a dynamic racemic form. This can be regarded as chiral recognition by the helical oligo(phenyleneethynylene).¹⁹⁹

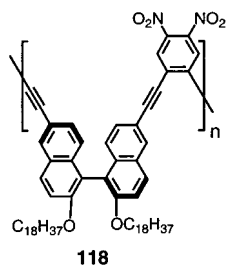


Poly(*p*-phenyleneethynylene) (DP \approx 500) (**117**) having two chiral side chains per *p*-phenylene unit



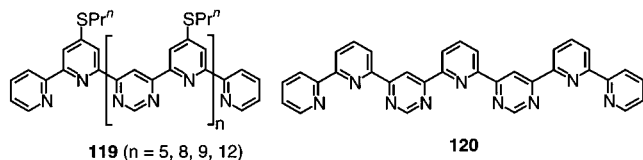
has been synthesized by alkyne metathesis of the corresponding monomer having two acetylene moieties.²⁰⁰ The polymer forms aggregates in a poor solvent such as decanol and shows a characteristic bisignate CD spectrum, which is not seen in a solution of chloroform, a good solvent. The contribution of a chiral conformation including the helix of the aggregate to the CD absorptions has been proposed.

Several poly(aryleneethynylene)s having chiral binaphthylene moieties in the main chain have been prepared.^{40,201,202} A propeller-like conformation has been proposed for **118** as one of the possible structures.²⁰¹



I. Polyarylenes

Conformations of oligo(pyridine-*alt*-pyrimidine)s **119** have been studied. On the basis of NMR analysis and the fluorescence spectrum in solution, the oligomers were found to take a helical conformation.²⁰³ The conformation was characterized by distinct chemical shifts (upfield shift), NOE effects, and excimer emission arising from the overlap of aromatic groups. The helical structure was confirmed for **120** in the



solid state by X-ray single-crystal analysis.³² By variable-temperature NMR analyses of **119** ($n = 5, 8, 12$), the oligomers were found to be in an equilibrium of the right- and left-handed helical conformations in solution and the barrier for helix reversal was revealed to be independent of the chain length. This suggests that the helix reversal may take place not through a helix-to-random-to-helix transition including an unwrapping process of the entire chain (a global wrap-unwrap process) but through a step-wise folding mechanism where the transition state is common to **119** with different chain lengths. In the proposed transition state, the right- and left-handed helical parts are connected through a perpendicularly

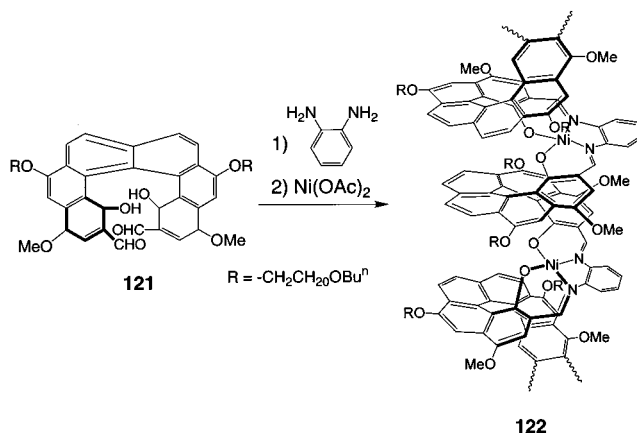
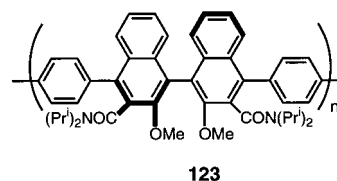


Figure 15. Synthesis of a Schiff-base-type helical polymer.

twisted 2,2'-bipyridine moiety. Shorter oligomeric chains were also shown to adopt a helical conformation.²⁰⁴ Several oligomers with structures similar to those discussed here form polymeric aggregates as described later. A helical structure has also been proposed for poly(*m*-phenylene) on the basis of X-ray diffraction data.²⁰⁵

The reaction of optically active, helicene derivative **121** first with *o*-phenylenediamine and then with Ni(OAc)₂ led to a helical polymer ($M_n \approx 7000$) (**122**) having a unique ladder-type structure with Schiff base moieties immersed in the main chain (Figure 15).²⁰⁶ The polymer showed red-shifted absorptions with respect to nickel salophene, the parent compound for the polymer, supporting the formation of a long conjugation system. Intense CD bands were reported for the polymer.

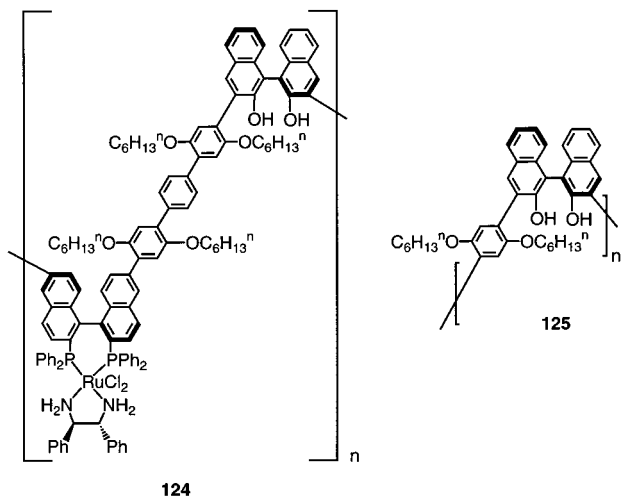
A polyarylene, **123**, containing a chiral binaphthyl group has been synthesized via the Suzuki coupling reaction.²⁰⁷ The polymer may have a helical structure segmented by a phenylene group. Another optically active polyarylene has been synthesized and its conformation has been considered.²⁰⁸



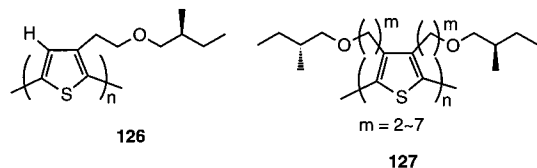
Binaphthyl-based polyarylene **124** bearing the Ru-Binaph sites has been synthesized. This polymer has a structural similarity to poly(aryleneethynylene) **118** discussed above and therefore may have a similar propeller-like conformation. **124** complexed with Et₂Z catalyzes a tandem asymmetric reaction involving Et₂N addition and hydrogenation that converts *p*-acetylbenzaldehyde into chiral 1-(1-hydroxypropyl)-4-(1-hydroxyethyl)benzene.²⁰⁹ Polyarylene **125** bearing a binaphthol unit was also prepared as a polymer ligand. **125** catalyzed the asymmetric reaction of aldehydes with Et₂N. Related binaphthyl-based polyarylenes have been reported.²¹⁰ Some more examples using similar polymers are known.^{211,212}

A helical structure has been proposed for an oligo(β -pyrrole) on the basis of NMR data and conforma-

tional calculation.²¹³ The NMR analysis of a trimer having a chiral group at the chain terminal suggested that two diastereomeric conformers existed, which may be right- and left-handed helical ones.



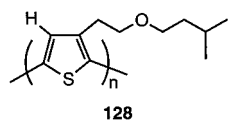
Polythiophenes **126** and **127** having chiral side groups have been synthesized, and their conformation has been studied by means of CD absorption and fluorescent spectra.^{214,215} For example, polymer **126**



shows a characteristic CD spectrum in a methanol/chloroform mixture, a poor solvent, while no CD absorption is seen in chloroform, a good solvent. In a poor solvent, the polymer forms an aggregate (microcrystalline) in which the polymer chains are stacked on top of each other to have a single-handed helical conformation. The conformation has been reported to be as rigid as that in the solid phase (crystalline phase). In a good solvent, such an aggregate does not form. In addition, the dominant helicity for **126** depends on the solvent. The chiroptical properties of **126** also depended on the ee of the monomeric units, and the dependence was nonlinear. This effect may be based on a cooperative effect of the chiral side chain and may be explained by the "majority rules" concept originally introduced for polyisocyanates.⁴¹

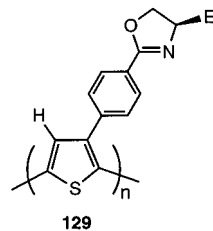
For polymer **127** with two chiral side chains per monomeric unit, a right-handed helical order of the aggregates has been proposed by interpreting their CD spectra on the basis of the exciton theory and model studies.^{216,217}

For the mixed aggregates of **126** and **128**, the CD intensity showed a nonlinear relation with the content of **128**.²¹⁸ This behavior has a similarity to the optical activity of a copolymer of chiral and achiral



isocyanates, which has been interpreted by the sergeants and soldiers theory.⁴¹

A regioregular polymer, **129**, having chiral monomeric units has been synthesized. This polymer does not show CD absorption in chloroform, a good solvent.

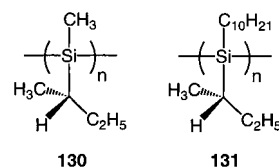


However, on addition of $\text{Cu}(\text{OTf})_2$ to the solution, the resulting suspension showed strong CD bands.²¹⁹ Because no gelling effect was observed and the absorption position did not change on addition of $\text{Cu}(\text{OTf})_2$, the CD bands which appeared due to the effect of Cu^{2+} are not based on the π -stacked aggregate suggested for **126**–**128** but on a helical conformation of a single molecule induced by the complexation with Cu^{2+} .

J. Si-Containing Polymers

1. Polysilanes

Polysilanes adopt a helical conformation. This class of polymers has the Si σ conjugating backbone, which allows the conformational study by means of photophysical analysis of the polymers.^{30,220–226} Two polysilanes, **130** and **131**, were synthesized by the Na-

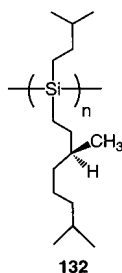


mediated condensation reaction of the corresponding chiral dichlorosilanes in the presence of 15-crown-5. **130** consists of right- and left-handed helical parts coexisting in one polymer chain, while **131** is a single-handed helix.^{30a,221} **130** showed a positive and a negative peak in the CD spectra corresponding to P-helical and M-helical segments, respectively (the P- and M-notations do not mean the absolute conformation), a rather broad absorption band, and a fluorescent peak whose half-peak width was close to that of the negative peak in the CD spectrum. In addition, the fluorescent anisotropy depended greatly on the wavelength. These features support the belief that a polymer chain of **130** has energetically different P- and M-helical parts. In contrast, **131** exhibited a narrow absorption peak, a CD peak whose spectral profiles match, and a fluorescent peak which is an mirror image of the absorption peak. A slight dependence of the fluorescent anisotropy on the wavelength indicates the presence of an ordered, single-handed helical conformation of **131** with a homogeneous photophysical profile along the chain. Although the tacticity of these polymers is not known, the molecular mechanics calculation on iso- and syndiotactic

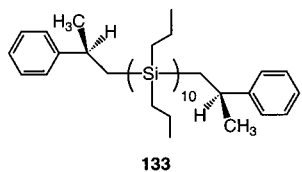
models indicated that either configuration can yield a similar helical structure.

In addition to the polymers described above, the polysilanes having aromatic side groups^{222,225} and the copolymers of a chiral monomer and an achiral monomer^{224–228} have been shown to adopt a helical conformation. A water-soluble, helical polysilane having an ammonium moiety has also been prepared.²²⁹

Furthermore, a helix–helix transition was found for polysilane **132** and some copolymers having a 3,7-dimethyloctyl group as a chiral group.²³⁰ In the stereomutation of **132** in an isoctane solution, the ratio of right- and left-handed helices depends on temperature and is 1/1 at $-20\text{ }^{\circ}\text{C}$.

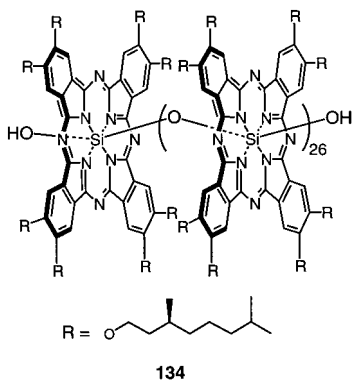


An excess helicity was induced not only by the chirality of the side chain but also by the terminal group. **133** shows the CD absorptions based on an excess helicity at 85K in an isopentane/methylcyclohexane matrix.²³¹



2. Polysiloxane

Polysiloxane **134** having chiral phthalocyanine moieties as repeating constituents takes a helical conformation in a chloroform solution.²³² The helical structure was indicated to be stable at up to $120\text{ }^{\circ}\text{C}$ in a dodecane solution. On the basis of the CD spectra, the helix was found to be left-handed.



K. Other Types of Polymers

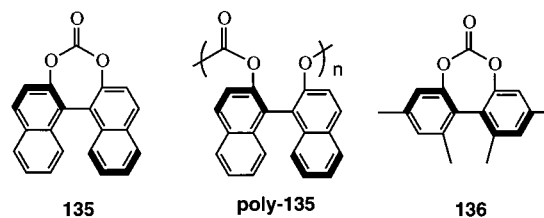
1. Miscellaneous Examples

The electropolymerization of *o*-methoxyaniline in the presence of (+)-(1*S*)- or (–)-(1*R*)-camphorsulfonic

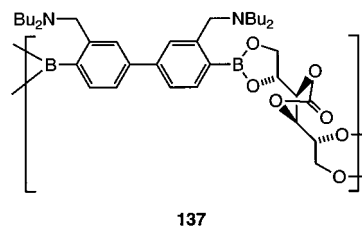
acid yields an optically active polyaniline derivative. The polymer shows intense CD bands as a film deposited on an electrode.²³³ The polymer is soluble in NMP, CHCl_3 , DMF, DMSO, and MeOH, and the polymer also showed a CD absorption in solution probably based on a chiral main chain conformation such as a helix. A film made by spin-coating a mixture of polyaniline with camphorsulfonic acid also showed strong CD absorptions that may be based on a helical conformation of the main chain.^{233c} The electropolymerization method has been applied to the synthesis of an optically active polypyrrole which may have a helical conformation.²³⁴

A polyaniline film prepared by doping an emeraldine base with optically active CSA showed a CD spectrum. Even after dedoping, the film exhibited CD bands which were different in pattern from those of the original dedoped film, suggesting that a chiral conformation such as a helix remains in the polymer chain. The dedoped film exhibited chiral recognition ability toward phenylalanine.²³⁵

By anionic polymerization using *t*-BuOK, an optically active, binaphthyl-based carbonate monomer (**135**) gives polymer poly-**135**, which has a single-handed 4_1 -helical conformation.²³⁶ An analogous polymer has been synthesized from a biphenyl-based monomer, **136**.^{237,238}



Polycondensation of a corresponding tetraol compound derived from D-mannitol with a bisboric acid compound produces polymer **137**.²³⁹ The M_w of the

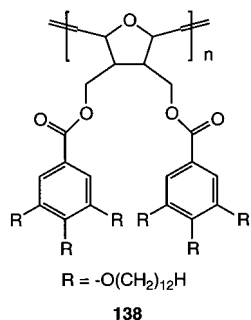


polymer was estimated to be 14000 by a light scattering method. The CD spectrum of the polymer had a pattern clearly different from that of the model compound for the monomeric unit and was indicative of a single-handed helical structure. The conformation was supported by MO calculation.

A poly(7-oxabicyclo[2.2.1]hept-2-ene) derivative (polymerization using RuCl_3), **138**, and a poly(*N*-phenylmaleimide) derivative (radical polymerization) bearing phenyl groups having long alkyl chains form a hexagonal columnar liquid crystalline phase.²⁴⁰ The polymers are proposed to take a helical conformation that may be stabilized by the intra- and intermolecular interaction of the side chains.

There are some examples of polyamides, poly(arylene ether)s,²⁴¹ polyimides,^{242,243} and poly-

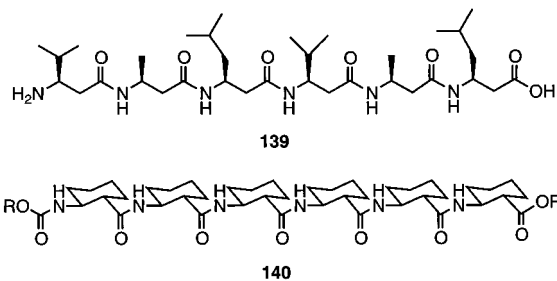
amides^{244,245} having 1,1'-binaphthylene-2,2'-diyl or biphenylene units that introduce chiral twists in the polymer chain. The chiral groups are expected to make the entire chain take a helical conformation. Earlier studies based on similar molecular designs are referenced in ref 243.



Support for a helical structure of polyketones arose from chiroptical studies as a function of temperature in the glassy state.²⁴⁶

2. Mimics and Analogues of Biopolymers

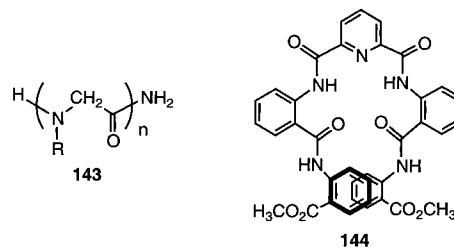
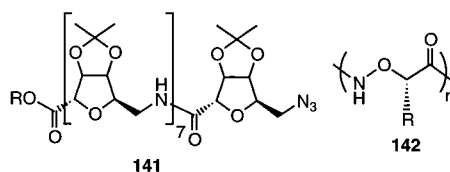
β -Peptides form well-defined, stable secondary structures including a helical structure as well as α -peptides.^{7-10,247} A helical structure was proved for β -peptide **139** in solution by NMR studies.^{9,248-251} The fact that **139** consisting of only six monomeric units has a stable helical conformation is interesting because a longer monomeric sequence (10-15-mer) is generally needed for α -peptides except for those containing proline or a 2-amino-2-methylpropanoic acid residue. A similar helical structure has been found for β -peptide **140** in the solid state and in



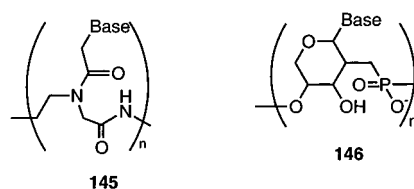
solution.^{10,252,253} These two β -peptides form a 3/1-helix, while an α -helix for α -peptides is a 3.6/1-helix. A series of **140** analogues having different cyclic structures in the main chain have been synthesized; the helical pitch depends on the ring structures.^{253,254}

Helical conformations have also been found or postulated for peptide analogues including γ -peptides,²⁵⁵ an octameric 5-(aminomethyl)tetrahydrofuran-2-carboxylate (**141**),²⁵⁶ a vinylogous peptide,²⁵⁷ vinylogous sulfonamidopeptides,²⁵⁸ peptides of α -amino acids (**142**),²⁵⁹ and polypeptoids (*N*-substituted glycine oligomers) **143**.²⁶⁰ The oligoanthranilamide **144** was found to have a helical conformation in the solid state by X-ray analysis.^{261,262} **144** also takes a helical conformation in solution as proved by NMR analysis. An analogous oligomer has been studied.²⁶³

Gene analogues have been synthesized, and their conformational aspects have been studied.²⁶⁴ Peptide nucleic acid (PNA) **145** and pentopyranosyl-(2'→4')



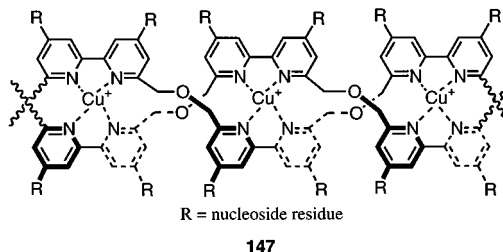
oligonucleotides **146** and their analogues form DNA- or RNA-like double-helical strands.²⁶⁵



III. Helical Polymeric Complexes and Aggregates

A. Helicates

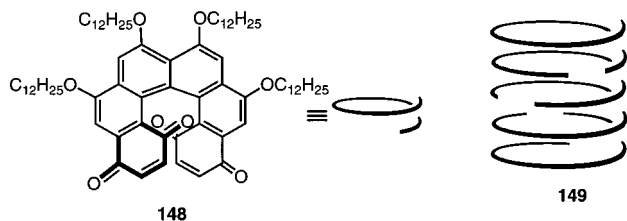
There is a class of metallic complexes called helicates.^{31,266-271} Such complexes typically consist of two or three oligomeric chains containing bipyridine moieties and transition metals. The oligomeric chains form a double- or triple-helical complex with the metallic species inside the complex coordinated by the pyridyl moieties. Intensive studies have been performed in this area, and there are comprehensive reviews covering various aspects.^{31,266-270} As an interesting example, the helicates with a generic structure, **147**, have been synthesized: the helicates have nucleoside residues in the positions of R and may be regarded as an artificial system mimicking the double-helical structure of DNA.²⁷¹



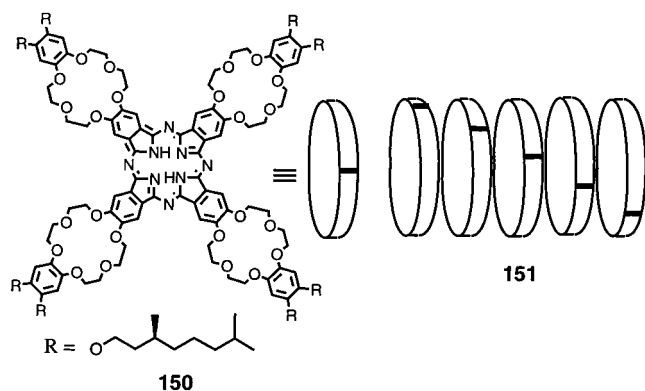
B. Helical Aggregates

Polymeric aggregates having a helical structure are known though they are not in the category of conventional polymers. Hexahelicenequinone **148** (ee 98-99.5%) and its analogues cause aggregation in a concentrated solution in *n*-dodecane and show intense CD absorptions.²⁷²⁻²⁷⁴ The aggregate formation was studied by NMR, UV-vis spectra, light scattering, and viscosity. A polymeric columnar aggregate

(149) in which the molecules are stacked along their helix axes has been proposed.



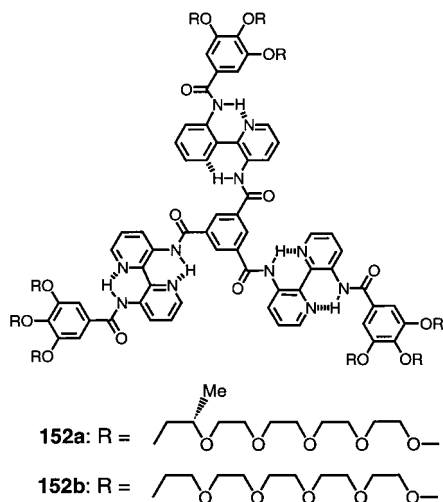
A chiral crown ether compound based on phthalocyanine (150) forms a linear polymeric aggregate (151) in which the π -electron systems are stacked on top of each other in a mixture of chloroform and



methanol.²⁷⁵ The addition of excess K^+ ion to the aggregate destroys the helical structure; the complexation between the crown ether moiety and K^+ weakens the interaction between the chromophores.

Similar helical aggregates have been constructed for oligo(pyridine–pyrimidine)s and a oligo(pyridine–pyridazine) in a solution of chloroform, dichloromethane, or pyridine.^{276,277} The helical structure was elucidated by NMR spectroscopy, vapor pressure osmometry, and freeze-fracture electron micrography and was supported by molecular modeling.

Compounds **152a,b** having a planar structure stabilized by intramolecular hydrogen bonds form rodlike aggregates in which **152a** or **152b** molecules are densely stacked.^{278,279} The aggregate of **152a** in water showed a CD spectrum which suggested a



helical chirality within the aggregate. Moreover, an aggregate consisting of 8% chiral **152a** and 92% achiral **152b** also showed CD absorptions whose intensity was comparable with that of the spectrum of the **152a** aggregate. This means that a small amount of **152a** incorporated into an aggregate consisting mostly of **152b** can induce an excess helicity in the aggregate.

IV. Summary and Outlook

A wide spectrum of synthetic polymers, polymeric complexes, and aggregates that have or may have a helical conformation were reviewed. The synthetic method varies from the addition polymerization methods for the vinyl and related polymers to the simple mixing methods for the aggregates. Some of the polymers exhibited functions based on the helical structure such as chiral recognition and asymmetric catalyses.

Since our last review was published in 1994, a large volume of research work has been published in this field, and the structural variation of helical polymers has been significantly broadened. The relatively new examples include polyacetylene derivatives, poly(aryleneethynylene)s, polyarylenes, silane-containing polymers, polycarbonates, biopolymer-mimicking oligomers, and some aggregates and complexes. Apart from the structural variation, notable progress lies in the introduction of the concept of dynamic helices through the studies on the polyacetylene derivatives, which are not helical themselves but become helical on the basis of relatively weak interaction with chiral additives. This finding implies that basically any flexible polymer such as PMMA or polystyrene may take a dynamic helical conformation in solution if an adequate additive is chosen, though the configurational control of the polymer chain may be prerequisite.

Knowing that the field of synthetic chemistry is always expanding and that so many new variations of chemical reactions are being made possible using new catalyses, newer helical polymers may be introduced by incorporating the advanced synthetic techniques into polymer synthesis in the future.²⁸⁰ In addition, by taking full advantage of the structural variation of helical polymers so far realized and the sophisticated functions of natural macromolecules with a helical conformation, the spectrum of their applications will also be broadened.

V. Acknowledgments

We are grateful to Ms. Kiyoko Ueda (Nagoya University) and Mr. Toru Yade (NAIST) for their assistance in preparing the manuscript.

VI. References

- (1) (a) Branden, C.; Tooze, J. *Introduction to Protein Structure*, 2nd ed.; Garland Publishing: New York, 1999. (b) Voet, D.; Voet, J. G.; Pratt, C. W. *Fundamentals of Biochemistry*; Wiley: New York, 1999.
- (2) (a) Hanes, C. S. *New Phytol.* **1937**, *36*, 101, 189. (b) Freudenberg, K.; Schaaf, E.; Dumpert, G.; Ploetz, T. *Naturwissenschaften* **1939**, *27*, 850.
- (3) Pauling, L.; Corey, R. B.; Branson, H. R. *Proc. Natl. Acad. Sci. U.S.A.* **1951**, *378*, 205.

- (4) Watson, J. D.; Crick, F. H. C. *Nature* **1953**, *171*, 737.
- (5) (a) Doty, P.; Lundberg, R. D. *J. Am. Chem. Soc.* **1956**, *78*, 4801. (b) Lundberg, R. D.; Doty, P. *J. Am. Chem. Soc.* **1957**, *79*, 3961. (c) Doty, P.; Lundberg, R. D. *J. Am. Chem. Soc.* **1957**, *79*, 2338.
- (6) (a) Schmidt, E. *Angew. Makromol. Chem.* **1970**, *14*, 185. (b) Chen, F.; Lepore, G.; Goodman, M. *Macromolecules* **1974**, *7*, 779.
- (7) (a) Yuki, H.; Okamoto, Y.; Taketani, Y.; Tsubota, T.; Marubayashi, Y. *J. Polym. Sci., Polym. Chem. Ed.* **1978**, *16*, 2237. (b) Yuki, H.; Okamoto, Y.; Doi, Y. *J. Polym. Sci., Polym. Chem. Ed.* **1979**, *17*, 1911.
- (8) Fernandez-Santin, J. M.; Aymami, J.; Rodriguez-Galan, A.; Munoz-Guerra, S.; Subirana, J. A. *Nature* **1984**, *311*, 53.
- (9) Seebach, D.; Overhand, M.; Kühnle, F. N. M.; Martinoni, B.; Oberer, L.; Hommel, H.; Widmer, H. *Helv. Chim. Acta* **1996**, *79*, 913.
- (10) Appella, D. H.; Christianson, L. A.; Karle, I. L.; Powell, D. R.; Gellman, S. H. *J. Am. Chem. Soc.* **1996**, *118*, 13071.
- (11) Natta, G.; Pino, P.; Corradini, P.; Danusso, F.; Mantica, E.; Nazzanti, G.; Moraglio, G. *J. Am. Chem. Soc.* **1955**, *77*, 1708.
- (12) (a) Pino, P.; Lorenzi, G. P. *J. Am. Chem. Soc.* **1960**, *82*, 4745. (b) Pino, P.; Lorenzi, G. P.; Lardicci, L. *Chim. Ind. (Milan)* **1960**, *42*, 712.
- (13) Okamoto, Y.; Suzuki, K.; Ohta, K.; Hatada, K.; Yuki, H. *J. Am. Chem. Soc.* **1979**, *101*, 4763.
- (14) (a) Okamoto, Y.; Honda, S.; Okamoto, I.; Yuki, H.; Murata, S.; Noyori, R.; Takaya, H. *J. Am. Chem. Soc.* **1981**, *103*, 6971. (b) Yuki, H.; Okamoto, Y.; Okamoto, I. *J. Am. Chem. Soc.* **1980**, *102*, 6358.
- (15) (a) Okamoto, Y. *CHEMTECH* **1987**, *144*. (b) Okamoto, Y.; Hatada, K. *J. Liq. Chromatogr.* **1986**, *9*, 369.
- (16) A review: Nakano, T. *J. Chromatogr., A* **2001**, *906*, 205.
- (17) Millich, F.; Baker, G. K. *Macromolecules* **1969**, *2*, 122.
- (18) Nolte, R. J. M.; van Beijnen, A. J. M.; Drenth, W. *J. Am. Chem. Soc.* **1974**, *96*, 5932.
- (19) (a) Green, M. M.; Gross, R. A.; Schilling, F. C.; Zero, K.; Crosby, C., III. *Macromolecules* **1988**, *21*, 1839. (b) Green, M. M.; Gross, R. A.; Crosby, C., III.; Schilling, F. C. *Macromolecules* **1987**, *20*, 992. (c) Green, M. M.; Gross, R. A.; Cook, R.; Schilling, F. C. *Macromolecules* **1987**, *20*, 2638.
- (20) Kollmar, C.; Hoffmann, R. *J. Am. Chem. Soc.* **1990**, *112*, 8230.
- (21) (a) Pini, D.; Inuliano, A.; Salvadori, P. *Macromolecules* **1992**, *25*, 6054. (b) Clericuzio, M.; Alagone, G.; Ghio, C.; Salvadori, P. *J. Am. Chem. Soc.* **1997**, *119*, 1059.
- (22) (a) Goodman, M.; Chen, S.-C. *Macromolecules* **1970**, *3*, 398. (b) Goodman, M.; Chen, S.-C. *Macromolecules* **1971**, *4*, 625.
- (23) Green, M. M.; Andreola, C.; Munoz, B.; Reidy, M. P.; Zero, K. *J. Am. Chem. Soc.* **1988**, *110*, 4063.
- (24) Ciardelli, F.; Lanzillo, S.; Pieroni, O. *Macromolecules* **1974**, *7*, 174.
- (25) Moore, J. S.; Gorman, C. B.; Grubbs, R. H. *J. Am. Chem. Soc.* **1991**, *113*, 1704.
- (26) (a) Yashima, E.; Huang, S.; Matsushima, T.; Okamoto, Y. *Macromolecules* **1995**, *28*, 4184. (b) Yashima, E.; Matsushima, T.; Okamoto, Y. *J. Am. Chem. Soc.* **1995**, *117*, 11596.
- (27) (a) Simionescu, C. I.; Percec, V.; Dumitrescu, S. *J. Polym. Sci., Polym. Chem. Ed.* **1977**, *15*, 2497. (b) Simionescu, C. I.; Percec, V. *Prog. Polym. Sci.* **1982**, *8*, 133.
- (28) Corley, L. S.; Vogl, O. *Polym. Bull.* **1980**, *3*, 211.
- (29) Ute, K.; Hirose, K.; Kashimoto, H.; Hatada, K.; Vogl, O. *J. Am. Chem. Soc.* **1991**, *113*, 6305.
- (30) (a) Fujiki, M. *J. Am. Chem. Soc.* **1994**, *116*, 6017. (b) Frey, H.; Möller, M.; Matyjaszewski, K. *Macromolecules* **1994**, *27*, 1814. (c) Matyjaszewski, K. *J. Inorg. Organomet. Polym.* **1992**, *2*, 5.
- (31) Lehn, J.-M.; Rigault, A.; Siegel, J.; Harrowfield, J.; Chevrier, B.; Moras, D. *Proc. Natl. Acad. Sci. U.S.A.* **1987**, *84*, 2565.
- (32) Hanan, G. S.; Lehn, J.-M.; Kyritsakas, N.; Fischre, J. *J. Chem. Soc., Chem. Commun.* **1995**, 765.
- (33) Nelson, J. C.; Saven, J. G.; Moore, J. S.; Wolynes, P. G. *Science* **1997**, *277*, 1793.
- (34) Okamoto, Y.; Nakano, T. *Chem. Rev.* **1994**, *94*, 349.
- (35) (a) Okamoto, Y.; Yashima, E. *Prog. Polym. Sci.* **1990**, *15*, 263. (b) Okamoto, Y.; Nakano, T.; Habaue, S.; Shiohara, K.; Maeda, K. *J. Macromol. Sci., Pure Appl. Chem.* **1997**, *A34*, 1771. (c) Nakano, T.; Okamoto, Y. *Macromol. Rapid Commun.* **2000**, *21*, 603. (d) Okamoto, Y.; Nakano, T. *Catalytic Asymmetric Synthesis*, 2nd ed.; Wiley: New York, 2000; pp 757–796.
- (36) (a) Wulff, G. *Angew. Chem., Int. Ed. Engl.* **1989**, *28*, 21. (b) Wulff, G. *CHEMTECH* **1991**, 364.
- (37) Tsuruta, T. *J. Polym. Sci., Part D: Macromol. Rev.* **1972**, *6*, 179.
- (38) Farina, M. *Top. Stereochem.* **1987**, *17*, 1.
- (39) Vogl, O.; Jaycox, G. D. *Polymer* **1987**, *28*, 2179.
- (40) Pu, L. *Acta Polym.* **1997**, *48*, 116.
- (41) Green, M. M.; Park, J.-W.; Sato, T.; Teramoto, A.; Lifson, S.; Selinger, R. L. B.; Selinger, J. V. *Angew. Chem., Int. Ed.* **1999**, *39*, 3138.
- (42) Tadokoro, H. *Structure of Crystalline Polymers*; Wiley: New York, 1979.
- (43) Pino, P. *Adv. Polym. Sci.* **1965**, *4*, 393.
- (44) Pino, P.; Ciradelli, F.; Lorenzi, G. *Makromol. Chem.* **1963**, *61*, 207.
- (45) Luisi, P. L.; Pino, P. *J. Phys. Chem.* **1968**, *72*, 2400.
- (46) (a) Luisi, P. L.; Bionsignori, O. *J. Chem. Phys.* **1972**, *56*, 4298. (b) Bailey, W. J.; Yates, E. T. *J. Org. Chem.* **1960**, *25*, 1800.
- (47) Pino, P.; Ciardelli, F.; Motagnoli, G.; Pieroni, O. *J. Polym. Sci., Part B: Polym. Lett.* **1967**, *5*, 307.
- (48) Pino, P.; Carlini, C.; Chielline, E.; Ciardelli, F.; Salvadori, P. *J. Am. Chem. Soc.* **1968**, *90*, 5025.
- (49) Bassi, I. W.; Bionsignori, O.; Lorenzi, G. P.; Pino, P.; Corradini, P.; Temussi, P. A. *J. Polym. Sci., Part A-2* **1971**, *9*, 193.
- (50) (a) Allegera, G.; Corradini, P.; Ganis, P. *Makromol. Chem.* **1966**, *90*, 60. (b) Pino, P. *Polym. Prepr.* **1989**, *30*, 433. (c) Nueenschwander, P.; Pino, P. *Eur. Polym. J.* **1983**, *19*, 1075. (d) Hug, W.; Ciardelli, I.; Tinoco, I., Jr. *J. Am. Chem. Soc.* **1974**, *96*, 3407.
- (51) (a) Okamoto, Y.; Suzuki, K.; Yuki, H. *J. Polym. Sci., Polym. Chem. Ed.* **1980**, *18*, 3043. (b) Okamoto, Y.; Shohi, H.; Yuki, H. *J. Polym. Sci., Polym. Lett. Ed.* **1983**, *21*, 601.
- (52) Nakano, T.; Okamoto, Y.; Hatada, K. *J. Am. Chem. Soc.* **1992**, *114*, 1318.
- (53) Nakano, T.; Hidaka, Y.; Okamoto, Y. *Polym. J.* **1998**, *30*, 596.
- (54) Okamoto, Y.; Okamoto, I.; Yuki, H. *J. Polym. Sci., Polym. Lett. Ed.* **1981**, *19*, 451.
- (55) Liu, W.; Yang, Y.; Chen, C.; Chen, Y.; Xi, F. *Macromol. Chem. Phys.* **1997**, *198*, 279.
- (56) Chen, J. P.; Gao, J. P.; Wang, Z. Y. *J. Polym. Sci., Part A: Polym. Chem.* **1997**, *35*, 9.
- (57) Chen, J. P.; Gao, J. P.; Wang, Z. Y. *J. Am. Chem. Soc.* **1995**, *117*, 5377.
- (58) Nakano, T.; Satoh, Y.; Okamoto, Y. *Macromolecules* **2001**, *34*, 2405.
- (59) Nakano, T.; Taniguchi, K.; Okamoto, Y. *Polym. J.* **1997**, *29*, 540.
- (60) Ren, C.; Chen, F.; Xi, F.; Nakano, T.; Okamoto, Y. *J. Polym. Sci., Part A: Polym. Chem.* **1993**, *31*, 2721.
- (61) Nakano, T.; Matsuda, A.; Mori, M.; Okamoto, Y. *Polym. J.* **1996**, *28*, 300.
- (62) Nakano, T.; Satoh, Y.; Okamoto, Y. *Polym. J.* **1998**, *30*, 635.
- (63) Okamoto, Y.; Ishikura, M.; Hatada, K.; Yuki, H. *Polym. J.* **1983**, *15*, 851.
- (64) Okamoto, Y.; Mohri, H.; Hatada, K. *Chem. Lett.* **1988**, 1879.
- (65) Okamoto, Y.; Mohri, H.; Nakano, T.; Hatada, K. *Chirality* **1991**, *3*, 277.
- (66) Okamoto, Y.; Mohri, H.; Nakano, T.; Hatada, K. *J. Am. Chem. Soc.* **1989**, *111*, 5952.
- (67) Ren, C.; Chen, C.; Xi, F. *J. Polym. Sci., Part A: Polym. Chem.* **1998**, *36*, 2127.
- (68) Nakano, T.; Sato, Y.; Okamoto, Y. *React. Funct. Polym.* **1999**, *40*, 135.
- (69) Nakano, T.; Okamoto, Y. *Controlled Radical Polymerization*; ACS Symposium Series 685; American Chemical Society: Washington DC, 1998; p 451.
- (70) Nakano, T.; Matsuda, A.; Okamoto, Y. *Polym. J.* **1996**, *28*, 556.
- (71) Nakano, T.; Mori, M.; Okamoto, Y. *Macromolecules* **1993**, *26*, 867.
- (72) Nakano, T.; Shikisai, Y.; Okamoto, Y. *Polym. J.* **1996**, *28*, 51.
- (73) Nakano, T.; Shikisai, Y.; Okamoto, Y. *Proc. Jpn. Acad.* **1995**, *71B*, 251.
- (74) Nakano, T.; Okamoto, Y. *Macromolecules* **1999**, *32*, 2391.
- (75) (a) Enikolopyan, N. S.; Smirnov, B. R.; Ponomarev, G. V.; Belgovski, I. M. *J. Polym. Sci., Polym. Chem. Ed.* **1981**, *19*, 879. (b) Burczyk, A. F.; O'driscoll, K. F.; Rempel, G. L. *J. Polym. Sci., Polym. Chem. Ed.* **1984**, *22*, 3255. (c) Haddelton, D. M.; Maloney, D. R.; Suddaby, K. G. *Macromolecules* **1996**, *29*, 481.
- (76) Gridnev, A. A.; Ittel, S. D.; Fryd, M. *J. Polym. Sci., Part A: Polym. Chem.* **1995**, *3*, 1185.
- (77) Nagata, T.; Yorozu, K.; Yamada, T.; Mukaiyama, T. *Angew. Chem., Int. Ed. Engl.* **1995**, *34*, 2145.
- (78) Tsunematsu, K.; Nakano, T.; Okamoto, Y. *Polym. Prepr. Jpn.* **2000**, *49* (2), 283. Nakano, T.; Tsunematsu, K.; Okamoto, Y. *Chem. Lett.*, in press.
- (79) Nakano, T.; Kinjo, N.; Hidaka, Y.; Okamoto, Y. *Polym. J.* **2001**, *33*, 360.
- (80) Okamoto, Y.; Ueda, K.; Kinjo, N.; Nakano, T. *Polym. Prepr.* **2000**, *41* (1), 887.
- (81) Wang, Y.; Ding, M.; Wang, F. *Makromol. Chem.* **1991**, *192*, 1769.
- (82) Andose, J. D.; Mislow, K. *J. Am. Chem. Soc.* **1974**, *96*, 2168.
- (83) Nakano, T.; Kinjo, N.; Hidaka, Y.; Okamoto, Y. *Polym. J.* **1999**, *31*, 464.
- (84) Yashima, E.; Okamoto, Y.; Hatada, K. *Polym. J.* **1987**, *19*, 897.
- (85) Yashima, E.; Okamoto, Y.; Hatada, K. *Macromolecules* **1988**, *21*, 854.
- (86) Okamoto, Y.; Yashima, E.; Hatada, K. *J. Polym. Sci., Part C: Polym. Lett.* **1987**, *25*, 297.
- (87) Okamoto, Y.; Nishikawa, M.; Nakano, T.; Yashima, E.; Hatada, K. *Macromolecules* **1995**, *28*, 5135.
- (88) Wu, J.; Nakano, T.; Okamoto, Y. *J. Polym. Sci., Part A: Polym. Chem.* **1998**, *36*, 2013.
- (89) Wu, J.; Nakano, T.; Okamoto, Y. *J. Polym. Sci., Part A: Polym. Chem.* **1999**, *37*, 2645.

- (90) Nakano, T.; Ueda, K.; Okamoto, Y. *J. Polym. Sci., Part A: Polym. Chem.* **2001**, *39*, 1610.
- (91) Okamoto, Y.; Nakano, T.; Fukuoka, T.; Hatada, K. *Polym. Bull.* **1991**, *26*, 259.
- (92) Nakano, T.; Okamoto, Y.; Sogah, D. Y.; Zheng, S. *Macromolecules* **1995**, *28*, 8705.
- (93) Wulff, G.; Gladow, S.; Kühneweg, B.; Krieger, S. *Macromol. Symp.* **1996**, *101*, 335.
- (94) Wulff, G.; Matuseek, A.; Hanf, C.; Gladow, S.; Lehmann, C.; Goddard, R. *Angew. Chem., Int. Ed.* **2000**, *39*, 2275.
- (95) Zheng, S.; Sogah, D. Y. *Tetrahedron* **1997**, *53*, 15469.
- (96) (a) Kwon, Y. K.; Chvalun, S.; Scheider, A.-I.; Backwell, J.; Percec, V.; Heck, J. A. *Macromolecules* **1994**, *27*, 6129. (b) Kwon, Y. K.; Danko, C.; Chvalun, S.; Backwell, J.; Heck, J. A.; Percec, V. *Macromol. Symp.* **1994**, *87*, 103. (c) Kwon, Y. K.; Chvalun, S.; Backwell, J.; Percec, V.; Heck, J. A. *Macromolecules* **1995**, *28*, 1552. (d) Chvalun, S. N.; Blackwell, J.; Cho, J. D.; Kwon, Y. K.; Percec, V.; Heck, J. A. *Polymer* **1998**, *39*, 4515. (e) Chvalun, S. N.; Blackwell, J.; Kwon, Y. K.; Percec, V. *Macromol. Symp.* **1997**, *118*, 663. (f) Chvalun, S. N.; Blackwell, J.; Cho, J. D.; Bykova, I. V.; Percec, V. *Acta Polym.* **1999**, *50*, 51. (g) Percec, V.; Ahn, C.-H.; Ungar, G.; Yearley, D. J. P.; Möller, M.; Sheiko, S. *Nature* **1998**, *391*, 161. (h) Percec, V.; Ahn, C.-H.; Cho, W.-D.; Jamieson, A. M.; Kim, J.; Leman, T.; Schmidt, M.; Gerle, M.; Möller, M.; Prokhorova, S. A.; Sheiko, S. S.; Cheng, S. Z. D.; Zhang, A.; Ungar, G.; Yearley, D. J. P. *J. Am. Chem. Soc.* **1998**, *120*, 8619.
- (97) Tanaka, T.; Habaue, S.; Okamoto, Y. *Macromolecules* **1995**, *28*, 5973.
- (98) Tanaka, T.; Habaue, S.; Okamoto, Y. *Polym. J.* **1995**, *27*, 1202.
- (99) Okamoto, Y.; Adachi, M.; Shohi, H.; Yuki, H. *Polym. J.* **1981**, *13*, 175.
- (100) Okamoto, Y.; Hayashida, H.; Hatada, K. *Polym. J.* **1989**, *21*, 543.
- (101) Shiohara, K.; Habaue, S.; Okamoto, Y. *Polym. J.* **1996**, *28*, 682.
- (102) Shiohara, K.; Habaue, S.; Okamoto, Y. *Polym. J.* **1998**, *30*, 249.
- (103) Habaue, S.; Shiohara, K.; Uno, T.; Okamoto, Y. *Enantiomer* **1996**, *1*, 55.
- (104) Uno, T.; Shiohara, K.; Habaue, S.; Okamoto, Y. *Polym. J.* **1998**, *30*, 352.
- (105) Wulff, G.; Wu, Y. *Makromol. Chem.* **1990**, *191*, 2993.
- (106) Wulff, G.; Wu, Y. *Makromol. Chem.* **1990**, *191*, 3005.
- (107) Okamoto, Y.; et al. Unpublished data.
- (108) Ute, K.; Asada, T.; Nabeshima, Y.; Hatada, K. *Acta Polym.* **1995**, *46*, 458.
- (109) Ute, K.; Asada, T.; Nabeshima, Y.; Hatada, K. *Macromolecules* **1993**, *26*, 7086.
- (110) Oishi, T.; Isobe, Y.H.; Onimura, K.; Tsutsumi, H. *Polym. Prepr. Jpn.* **1999**, *48* (8), 1850.
- (111) Toda, F.; Mori, K. *J. Chem. Soc., Chem. Commun.* **1986**, 1059.
- (112) Oriz, L. J.; Khan, I. M. *Macromolecules* **1998**, *31*, 5927.
- (113) Habaue, S.; Ajiro, H.; Okamoto, Y. *J. Polym. Sci., Part A: Polym. Chem.* **2000**, *38*, 4088.
- (114) Vogl, O.; Miller, H. C.; Sharkey, W. H. *Macromolecules* **1972**, *5*, 658.
- (115) Vogl, O.; Corley, L. S.; Harris, W. J.; Jaycox, G. D.; Zhang, J. *Makromol. Chem. Suppl.* **1985**, *13*, 1.
- (116) Zhang, J.; Jaycox, G. D.; Vogl, O. *Polym. J.* **1987**, *19*, 603.
- (117) Jaycox, G. D.; Vogl, O. *Makromol. Chem., Rapid Commun.* **1990**, *11*, 61.
- (118) (a) Ute, K.; Hirose, K.; Kashimoto, H.; Nakayama, K.; Hatada, K.; Vogl, O. *Polym. J.* **1993**, *25*, 1175. (b) Vogl, O.; Xi, F.; Vass, F.; Ute, K.; Nishimura, T.; Hatada, K. *Macromolecules* **1989**, *22*, 4660. (c) Ute, K.; Oka, K.; Okamoto, Y.; Hatada, K.; Xi, F.; Vogl, O. *Polym. J.* **1991**, *23*, 142.
- (119) (a) Qin, M.; Bartus, J.; Vogl, O. *Macromol. Symp.* **1995**, *98*, 387. (b) Vogl, O. *J. Polym. Sci., Part A: Polym. Chem.* **2000**, *38*, 2623.
- (120) Sikorski, P.; Cooper, S. J.; Atkins, E. D. T.; Jaycox, G. D.; Vogl, O. *J. Polym. Sci., Part A: Polym. Chem.* **1988**, *36*, 1855.
- (121) Ute, K.; Hirose, K.; Hatada, K.; Vogl, O. *Polym. Prepr. Jpn.* **1992**, *41*, 1358.
- (122) Hatada, K.; Kitayama, T.; Shimizu, S.-I.; Yuki, H.; Harris, W.; Vogl, O. *J. Chromatogr.* **1982**, *248*, 63.
- (123) Hatada, K.; Shimizu, S.-I.; Yuki, H.; Harris, W.; Vogl, O. *Polym. Bull.* **1981**, *4*, 179.
- (124) Choi, S.-H.; Yashima, E.; Okamoto, Y. *Macromolecules* **1996**, *29*, 1880.
- (125) (a) Goodman, M.; Abe, A. *J. Polym. Sci.* **1962**, *59*, S37. (b) Abe, A.; Goodman, M. *J. Polym. Sci., Part A: Polym. Chem.* **1963**, *1*, 2193. (c) Goodman, M.; Clark, K. J.; Stake, M. A.; Abe, A. *Makromol. Chem.* **1964**, *72*, 131. (d) Goodman, M.; Abe, A.; Fan, Y.-L. *Makromol. Rev.* **1966**, *1*, 1.
- (126) (a) Millich, F. *Chem. Rev.* **1972**, *72*, 101. (b) Millich, F. *Adv. Polym. Sci.* **1975**, *19*, 117. (c) Millich, F. *Macromol. Rev.* **1980**, *15*, 207.
- (127) van Beijnen, A. J. M.; Nolte, R. J. M.; Drenth, W.; Hezemans A. M. F. *Tetrahedron* **1976**, *32*, 2017.
- (128) Kamer, P. C. J.; Nolte, R. J. M.; Drenth, W. *J. Am. Chem. Soc.* **1988**, *110*, 6818.
- (129) Deming, T. J.; Novak, B. M. *J. Am. Chem. Soc.* **1992**, *114*, 7926.
- (130) (a) Takei, F.; Yanai, K.; Onitsuka, K.; Takahashi, S. *Angew. Chem., Int. Ed. Engl.* **1996**, *35*, 1554. (b) Takahashi, S.; Onitsuka, K.; Takei, F. *Proc. Jpn. Acad., Ser. B* **1998**, *74B*, 25.
- (131) Takei, F.; Onitsuka, K.; Takahashi, S. *Polym. J.* **2000**, *32*, 524.
- (132) Takei, F.; Yanai, K.; Onitsuka, K.; Takahashi, S. *Chem.-Eur. J.* **2000**, *6*, 983.
- (133) Takei, F.; Onitsuka, K.; Takahashi, S. *Polym. J.* **1999**, *31*, 1029.
- (134) Takei, F.; Onitsuka, K.; Kobayashi, N.; Takahashi, S. *Chem. Lett.* **2000**, 914.
- (135) Hasegawa, T.; Kondoh, S.; Matsuura, K.; Kobayashi, K. *Macromolecules* **1999**, *32*, 6595.
- (136) Hasegawa, T.; Matsuura, K.; Ariga, K.; Kobayashi, K. *Macromolecules* **2000**, *33*, 2772.
- (137) Cornelissen, J. J. L. M.; Fischer, M.; Sommerdijk, N. A. J. M.; Nolte, R. J. M. *Science* **1998**, *280*, 1427.
- (138) Yamagishi, A.; Tanaka, I.; Taniguchi, M.; Takahashi, M. *J. Chem. Soc., Chem. Commun.* **1994**, 1113.
- (139) Ito, Y.; Ihara, E.; Murakami, M. *Angew. Chem., Int. Ed. Engl.* **1992**, *31*, 1509.
- (140) Ito, Y.; Ihara, E.; Murakami, Y.; Sisido, M. *Macromolecules* **1992**, *25*, 6810.
- (141) Itoh, Y.; Kojima, Y.; Murakami, M. *Tetrahedron Lett.* **1993**, *34*, 8279.
- (142) Itoh, Y.; Ohara, T.; Shima, R.; Suginome, M. *J. Am. Chem. Soc.* **1996**, *118*, 9188.
- (143) Itoh, Y.; Miyake, T.; Ohara, T.; Suginome, M. *Macromolecules* **1998**, *31*, 1697.
- (144) Itoh, Y.; Miyake, T.; Hatano, S.; Shima, R.; Ohara, T.; Suginome, M. *J. Am. Chem. Soc.* **1998**, *120*, 11880.
- (145) Itoh, Y.; Miyake, T.; Suginome, M. *Macromolecules* **2000**, *33*, 4034.
- (146) Bur, A.; Fetters, L. J. *Chem. Rev.* **1976**, *76*, 727.
- (147) Shashoua, V. E.; Sweeny, W.; Tietz, R. F. *J. Am. Chem. Soc.* **1960**, *82*, 866.
- (148) Patten, T.; Novak, B. M. *J. Am. Chem. Soc.* **1991**, *113*, 5065.
- (149) Patten, T.; Novak, B. M. *Macromolecules* **1994**, *26*, 436.
- (150) Ute, K.; Fukunishi, Y.; Jha, S. K.; Cheon, K.-S.; Munoz, B.; Hatada, K.; Green, M. M. *Macromolecules* **1999**, *32*, 1304.
- (151) Ute, K.; Asai, T.; Fukunishi, Y.; Hatada, K. *Polym. J.* **1995**, *27*, 445.
- (152) Okamoto, Y.; Matsuda, M.; Nakano, T.; Yashima, E. *Polym. J.* **1993**, *25*, 391.
- (153) Okamoto, Y.; Matsuda, M.; Nakano, T.; Yashima, E. *J. Polym. Sci., Part A: Polym. Chem.* **1994**, *32*, 309.
- (154) Maeda, K.; Matsuda, M.; Nakano, T.; Okamoto, Y. *Polym. J.* **1995**, *27*, 141.
- (155) Maeda, K.; Okamoto, Y. *Polym. J.* **1998**, *30*, 100.
- (156) Maeda, K.; Okamoto, Y. *Kobunshi Ronbunshu* **1997**, *54*, 608.
- (157) Green, M. M.; Gross, R. A.; Crosby, C., III; Schilling, R. C. *Macromolecules* **1987**, *20*, 992.
- (158) Green, M. M.; Gross, R. A.; Cook, R.; Schilling, R. C. *Macromolecules* **1987**, *20*, 2638.
- (159) Green, M. M.; Andreola, C.; Munoz, B.; Reidy, M. P.; Zero, K. *J. Am. Chem. Soc.* **1988**, *110*, 4063.
- (160) Green, M. M.; Reidy, M. P.; Johnson, R. J.; Darling, G.; O'Leary, D. J.; Willson, G. *J. Am. Chem. Soc.* **1989**, *111*, 6452.
- (161) Green, M. M.; Peterson, N. C.; Sato, T.; Teramoto, A.; Cook, R.; Lifson, S. *Science* **1995**, *268*, 1860.
- (162) Green, M. M.; Garetz, B. A.; Munoz, B.; Chang, S.; Hoke, S.; Cook, R. G. *J. Am. Chem. Soc.* **1995**, *117*, 4182.
- (163) Jha, S. K.; Cheon, K.-S.; Green, M. M.; Selinger, J. V. *J. Am. Chem. Soc.* **1999**, *121*, 1665.
- (164) Cheon, K. S.; Selinger, J. V.; Green, M. M. *Angew. Chem., Int. Ed.* **2000**, *39*, 1482.
- (165) Maxein, G.; Mayer, S.; Zentel, R. *Macromolecules* **1999**, *32*, 5747.
- (166) Sanda, F.; Takata, T.; Endo, T. *J. Polym. Sci., Part A: Polym. Chem.* **1995**, *33*, 2353.
- (167) Maeda, K.; Okamoto, Y. *Macromolecules* **1998**, *31*, 1046.
- (168) Maeda, K.; Matsunaga, M.; Yamada, H.; Okamoto, Y. *Polym. J.* **1997**, *29*, 333.
- (169) Maeda, K.; Okamoto, Y. *Macromolecules* **1999**, *32*, 974.
- (170) Li, J.; Schuster, G. B.; Cheon, K.-S.; Green, M. M.; Selinger, J. V. *J. Am. Chem. Soc.* **2000**, *122*, 2603.
- (171) Green, M. M.; Khatri, C.; Peterson, N. C. *J. Am. Chem. Soc.* **1993**, *115*, 4941.
- (172) Maeda, K.; Yamamoto, N.; Okamoto, Y. *Macromolecules* **1998**, *31*, 5924.
- (173) Goodwin, A.; Novak, B. M. *Macromolecules* **1994**, *27*, 5520.
- (174) Shibayama, K.; Seidel, S. W.; Novak, B. M. *Macromolecules* **1997**, *30*, 3159.
- (175) Lim, A. R.; Novak, B. M. *Solid State Commun.* **1999**, *112*, 459.
- (176) Schlitzer, D. S.; Novak, B. M. *J. Am. Chem. Soc.* **1998**, *120*, 2196.
- (177) Nakako, H.; Mayahara, Y.; Nomura, R.; Tabata, M.; Masuda, T. *Macromolecules* **2000**, *33*, 3978.
- (178) Nakako, H.; Nomura, R.; Tabata, M.; Masuda, T. *Macromolecules* **1999**, *32*, 2861.
- (179) Kwak, G.; Masuda, T. *Macromolecules* **2000**, *33*, 6633.

- (180) Aoki, T.; Kobayashi, Y.; Kaneko, T.; Oikawa, E.; Yamamura, Y.; Fujita, Y.; Teraguchi, M.; Nomura, R.; Masuda, T. *Macromolecules* **1999**, *32*, 79.
- (181) Yashima, E.; Huang, S.; Okamoto, Y. *J. Chem. Soc., Chem. Commun.* **1994**, 1811.
- (182) Yashima, E.; Matsushima, T.; Nimura, T.; Okamoto, Y. *Korea Polym. J.* **1996**, *4*, 139.
- (183) Aoki, T.; Shinohara, K.-I.; Kaneko, T.; Oikawa, E. *Macromolecules* **1996**, *29*, 4192.
- (184) Yashima, E.; Matsushima, T.; Okamoto, Y. *J. Am. Chem. Soc.* **1997**, *119*, 6345.
- (185) Saito, M. A.; Maeda, K.; Onouchi, H.; Yashima, E. *Macromolecules* **2000**, *33*, 4616.
- (186) Yashima, E.; Maeda, K.; Okamoto, Y. *Nature* **1999**, *399*, 449.
- (187) Yashima, E.; Nimura, T.; Matsushima, T.; Okamoto, Y. *J. Am. Chem. Soc.* **1996**, *118*, 9800.
- (188) Yashima, E.; Maeda, Y.; Okamoto, Y. *Chem. Lett.* **1996**, 955.
- (189) Yashima, E.; Maeda, Y.; Matsushima, T.; Okamoto, Y. *Chirality* **1997**, *9*, 593.
- (190) Yashima, E.; Maeda, Y.; Okamoto, Y. *J. Am. Chem. Soc.* **1998**, *120*, 8895.
- (191) Yashima, E.; Maeda, Y.; Okamoto, Y. *Polym. J.* **1999**, *31*, 1033.
- (192) Akagi, K.; Piao, G.; Kaneko, S.; Sakamaki, K.; Shirakawa, H.; Kyotani, M. *Science* **1998**, *282*, 1683.
- (193) Yashima, E.; Maeda, K.; Yamanaka, T. *J. Am. Chem. Soc.* **2000**, *122*, 7813.
- (194) Prince, R. B.; Saven, J. G.; Wolynes, P. G.; Moore, J. S. *J. Am. Chem. Soc.* **1999**, *121*, 3144.
- (195) Gin, M. S.; Yokozawa, T.; Prince, R. B.; Moore, J. S. *J. Am. Chem. Soc.* **1999**, *121*, 2643.
- (196) Prince, R. B.; Brunsfeld, L.; Meijer, E. W.; Moore, J. S. *Angew. Chem., Int. Ed.* **2000**, *39*, 228.
- (197) Gin, M. S.; Moore, J. S. *Org. Lett.* **2000**, *2*, 135.
- (198) Prince, R. B.; Okada, T.; Moore, J. S. *Angew. Chem., Int. Ed.* **1999**, *38*, 233.
- (199) Prince, R. B.; Barnes, S. A.; Moore, J. S. *J. Am. Chem. Soc.* **2000**, *122*, 2758.
- (200) Fiesel, R.; Halkyard, C. E.; Rampey, M. E.; Kloppenburg, L.; Studer-Martinez, S. L.; Scherf, U.; Bunz, U. H. F. *Macromol. Rapid Commun.* **1999**, *20*, 107.
- (201) Ma, L.; Hu, Q.-S.; Vitharanak D.; Wu, C.; Kwan, C. M. S.; Pu, L. *Macromolecules* **1997**, *30*, 204.
- (202) Cheng, H.; Pu, L. *Macromol. Chem. Phys.* **1999**, *200*, 1274.
- (203) Ohkita, M.; Lehn, J.-M.; Baum, G.; Fenske, D. *Chem.—Eur. J.* **1999**, *12*, 3471.
- (204) Bassani, D. M.; Lehn, J.-M.; Baum, G.; Fenske, D. *Angew. Chem., Int. Ed. Engl.* **1997**, *36*, 1845.
- (205) Williams, D. J.; Colquhoun, H. M.; O'Mahoney, C. A. *J. Chem. Soc., Chem. Commun.* **1994**, 1643.
- (206) Dai, Y.; Katz, T. J.; Nichols, D. A. *Angew. Chem., Int. Ed. Engl.* **1996**, *35*, 2109.
- (207) Bedworth, P. V.; Tour, J. M. *Macromolecules* **1994**, *27*, 622.
- (208) Fiesel, R.; Huber, J.; Scherf, U. *Angew. Chem., Int. Ed. Engl.* **1996**, *35*, 2111.
- (209) Yu, H.-B.; Hu, Q.-S.; Pu, L. *J. Am. Chem. Soc.* **2000**, *122*, 6500.
- (210) Huang, W.-S.; Hu, Q.-S.; Zheng, X.-F.; Anderson, J.; Pu, L. *J. Am. Chem. Soc.* **1997**, *119*, 4313.
- (211) Hu, Q.-S.; Zhang, X.-F.; Pu, L. *J. Org. Chem.* **1996**, *61*, 5200.
- (212) Hu, Q. S.; Vitharana, D.; Liu, G.; Jain, V.; Pu, L. *Macromolecules* **1996**, *29*, 5075.
- (213) Magnus, P.; Danikiewicz, W.; Katoh, T.; Huffman, J. C.; Folting, K. *J. Am. Chem. Soc.* **1990**, *112*, 2465.
- (214) Bouman, M. M.; Havinga, E. E.; Janssens, R. A. J.; Meijer, E. W. *Mol. Cryst. Liq. Cryst.* **1994**, *256*, 439.
- (215) Langeveld-Voss, B. M. W.; Christiaans, M. P. T.; Janssens, R. A. J.; Meijer, E. W. *Macromolecules* **1998**, *31*, 6702.
- (216) Langeveld-Voss, B. M. W.; Janssens, R. A. J.; Christiaans, M. P. T.; Meskers, S. C. J.; Dekkers, H. P. J. M.; Meijer, E. W. *J. Am. Chem. Soc.* **1996**, *118*, 4908.
- (217) Lremo, E. R.; Langeveld-Voss, B. M. W.; Janssens, R. A. J.; Meijer, E. W. *Chem. Commun.* **1999**, 791.
- (218) Langeveld-Voss, B. M. W.; Waterval, R. J. M.; Janssens, R. A. J.; Meijer, E. W. *Macromolecules* **1999**, *32*, 227.
- (219) Yashima, E.; Goto, H.; Okamoto, Y. *Macromolecules* **1999**, *32*, 7942.
- (220) Miller, R. D.; Michl, J. *Chem. Rev.* **1989**, *89*, 1359.
- (221) Fujiki, M. *J. Am. Chem. Soc.* **1994**, *116*, 11976.
- (222) Fujiki, M. *Appl. Phys. Lett.* **1994**, *65*, 3251.
- (223) Fujiki, M. *J. Am. Chem. Soc.* **1996**, *118*, 7424.
- (224) Toyoda, S.; Fujiki, M. *Chem. Lett.* **1999**, 699.
- (225) Koe, J. R.; Fujiki, M.; Nakashima, H. *J. Am. Chem. Soc.* **1999**, *121*, 9743.
- (226) Nakashima, H.; Fujiki, M.; Koe, J. R. *Macromolecules* **1999**, *32*, 7707.
- (227) Koe, J. R.; Fujiki, M.; Motonaga, M.; Nakashima, H. *Chem. Commun.* **2000**, 389.
- (228) Frey, H.; Möller, M.; Turetskii, A.; Lotz, B.; Matyjaszewski, K. *Macromolecules* **1995**, *28*, 5498.
- (229) Terunuma, D.; Nagumo, K.; Kamata, N.; Matsuoka, K.; Kuzuhara, H. *Polym. J.* **2000**, *32*, 113.
- (230) Fujiki, M. *J. Am. Chem. Soc.* **2000**, *122*, 3336.
- (231) Obata, K.; Kabuto, C.; Kira, M. *J. Am. Chem. Soc.* **1997**, *119*, 11345.
- (232) Engelkamp, H.; van Nostrum, C. F.; Picken, S. J.; Nolte, R. J. M. *Chem. Commun.* **1998**, 979.
- (233) (a) Norris, I. D.; Kane-Maguire, L. A. P.; Wallece, G. G. *Macromolecules* **2000**, *33*, 2327. (b) Strounina, E. V.; Kane-Maguire, L. A. P.; Wallece, G. G. *Synth. Met.* **1999**, *106*, 129. (c) Havinga, E. E.; Bouman, E. E.; Meijer, M. M.; Pomp, A.; Simenon, M. M. J. *Synth. Met.* **1994**, *66*, 93.
- (234) Zhou, Y.; Zhu, G. *Polymer* **1997**, *38*, 5493.
- (235) Guo, H.; Knobler, C. M.; Kaner, R. B. *Synth. Met.* **1999**, *101*, 44.
- (236) Takata, T.; Furusho, Y.; Murakawa, K.-i.; Endo, T.; Matsuoka, H.; Hirasa, T.; Matsuo, J.; Sisido, M. *J. Am. Chem. Soc.* **1998**, *120*, 4530.
- (237) Murakawa, K.-i.; Furusho, Y.; Takata, K. *Chem. Lett.* **1999**, 93.
- (238) Takata, T.; Murakawa, K.-i.; Furusho, Y. *Polym. J.* **1999**, *31*, 1051.
- (239) Mikami, M.; Shinkai, S. *Chem. Lett.* **1995**, 603.
- (240) Percec, V.; Schlueter, D.; Ronda, J. C.; Johansson, G.; Ungar, G.; Zhou, J. P. *Macromolecules* **1996**, *29*, 1464.
- (241) Wang, Z. Y.; Douglas, J. E. *Macromolecules* **1997**, *30*, 8091.
- (242) Mi, Q.; Ma, Y.; Gao, L.; Ding, M. *J. Polym. Sci., Part A: Polym. Chem.* **1999**, *37*, 4536.
- (243) Mi, Q.; Gao, L.; Ding, M. *Macromolecules* **1996**, *29*, 5758.
- (244) Kondo, F.; Takahashi, D.; Kimura, H.; Takeishi, M. *Polym. J.* **1998**, *30*, 161.
- (245) Kondo, F.; Kakimi, S.; Kimura, H.; Takeishi, M. *Polym. Int.* **1998**, *46*, 339.
- (246) B. T. Muellers, B. T.; Park, J.-W.; Brookhart, M. S.; Green, M. M. *Macromolecules* **2001**, *34*, 572.
- (247) (a) Koert, U. *Angew. Chem., Int. Ed. Engl.* **1997**, *36*, 1836. (b) Gellman, S. H. *Acc. Chem. Res.* **1998**, *31*, 173. (c) Seebach, D.; Matthews, J. L. *Chem. Commun.* **1997**, 2015. (d) Lverson, B. L. *Nature* **1997**, *385*, 113. For earlier publications, see the references cited in these papers.
- (248) Seebach, D.; Overhand, M.; Kühnle, F. N. M.; Marinoni, B.; Oberer, L.; Hommel, U.; Widmer, H. *Helv. Chim. Acta* **1996**, *79*, 913.
- (249) Seebach, D.; Ciceri, P. E.; Overhand, M.; Jaun, B.; Rigo, D.; Oberer, L.; Hommel, U.; Amstutz, R.; Widmer, H. *Helv. Chim. Acta* **1996**, *79*, 2043.
- (250) Seebach, D.; Abele, S.; Gademann, K.; Guichard, G.; Hintermann, T.; Jaun, B.; Matthews, J. L.; Schreiber, J. V.; Oberer, L.; Hommel, U.; Widmer, H. *Helv. Chim. Acta* **1998**, *81*, 932.
- (251) Seebach, D.; Abele, S.; Sifferlen, T.; Hänngli, M.; Gruner, S.; Seiler, P. *Helv. Chim. Acta* **1998**, *81*, 2218.
- (252) Appella, D. H.; Christianson, L. A.; Karle, I. L.; Powell, D. R.; Huang, X.; Barchi, J.; Gellman, S. H. *Nature* **1997**, *387*, 381.
- (253) Barchi, J. J., Jr.; Huang, X.; Appella, D. H.; Christianson, L. A.; Durell, S. R.; Gellman, S. H. *J. Am. Chem. Soc.* **2000**, *122*, 2177.
- (254) (a) Appella, D. H.; Christianson, L. A.; Karle, I. L.; Powell, D. R.; Gellman, S. H. *J. Am. Chem. Soc.* **1996**, *118*, 13071. (b) Huck, B. R.; Langenhan, J. M.; Gellman, S. H. *Org. Lett.* **1999**, *1*, 1717. (c) Appella, D. H.; Christianson, L. A.; Karle, I. L.; Powell, D. R.; Gellman, S. H. *J. Am. Chem. Soc.* **1999**, *121*, 6206. (d) Appella, D.; Christianson, L. A.; Klein, D. A.; Richards, M. R.; Powell, D. R.; Gellman, S. H. *J. Am. Chem. Soc.* **1999**, *121*, 7545. (e) Appella, D. H.; Barchi, J. J., Jr.; Durell, S. R.; Gellman, S. H. *J. Am. Chem. Soc.* **1999**, *121*, 2309. (f) Wang, X.; Espinosa, J. F.; Gellman, S. H. *J. Am. Chem. Soc.* **2000**, *122*, 4821.
- (255) Hanessian, S.; Luo, X.; Shaum, R. *Tetrahedron Lett.* **1999**, *40*, 4925.
- (256) Claridge, T. D. W.; Long, D. D.; Hugerford, N. L.; Aplin, R. T.; Smith, M. D.; Marquess, D. G.; Fleet, W. J. *Tetrahedron Lett.* **1999**, *40*, 2199.
- (257) Hagahara, M.; Anthony, N. J.; Stout, T. J.; Clardy, J.; Schreiber, S. L. *J. Am. Chem. Soc.* **1992**, *114*, 6568.
- (258) Gennari, C.; Salom, B.; Potenza, D.; Longari, C.; Fioravanzo, E.; Carugo, O.; Sardone, N. *Chem.—Eur. J.* **1996**, *2*, 644.
- (259) Yang, D.; Qu, J.; Li, B.; Ng, F.-F.; Qng, X.-C.; Cheung, K.-K.; Wang, D.-P.; Wu, Y.-D. *J. Am. Chem. Soc.* **1999**, *121*, 589.
- (260) Kirshenbaum, K.; Barron, A. E.; Coldsmith, R. A.; Armand, P.; Zukermann, R. N. *Proc. Natl. Acad. Sci. U.S.A.* **1998**, *95*, 4303.
- (261) Hamuro, Y.; Geib, S. J.; Hamilton, A. D. *J. Am. Chem. Soc.* **1996**, *118*, 7529.
- (262) Hamuro, Y.; Geib, S.; Hamilton, A. D. *J. Am. Chem. Soc.* **1997**, *119*, 10587.
- (263) Zhu, J.; Parra, R. D.; Zeng, H.; Skrzypczak-Jankun, E.; Zeng, X. C.; Gong, B. *J. Am. Chem. Soc.* **2000**, *122*, 4219.
- (264) Wittung, P.; Nielsen, P. E.; Buchardt, O.; Egholm, M.; Norden, B. *Nature* **1994**, *368*, 561.
- (265) Beier, M.; Reck, F.; Wagner, T.; Krishnamurthy, R.; Eshenmoser, A. *Science* **1999**, *283*, 699.
- (266) Piquet, C.; Bernardinelli, G.; Hophgartner, G. *Chem. Rev.* **1997**, *97*, 2005.

- (267) Constable, E. C. *Tetrahedron* **1992**, *48*, 10013.
(268) Constable, E. C. *Angew. Chem., Int. Ed. Engl.* **1991**, *30*, 1450.
(269) Williams, A. *Chem.—Eur. J.* **1997**, *3*, 15.
(270) Lehn, J.-M. *Supramolecular Chemistry*; VCH: Weinheim, Germany, 1995.
(271) Koert, U.; Harding M. M.; Lehn, J.-M. *Nature* **1990**, *346*, 339.
(272) Nuckolls, C.; Katz, T. J.; Katz, G.; Collings, P. J.; Castellanos, L. *J. Am. Chem. Soc.* **1999**, *121*, 79.
(273) Lovinger, A.; Nuckolls, C.; Katz, T. J. *J. Am. Chem. Soc.* **1998**, *120*, 264.
(274) Nuckolls, C.; Katz, T. J.; Katz, G.; Castellanos, L. *J. Am. Chem. Soc.* **1996**, *118*, 3767.
(275) Engelkamp, H.; Middlebeek, S.; Nolte, R. J. M. *Science* **1999**, *284*, 785.
(276) Cuccia, L. A.; Lehn, J.-M.; Homo, J.-C.; Schmutz, M. *Angew. Chem., Int. Ed.* **2000**, *39*, 233.
(277) Bassani, M.; Lehn, J.-M. *Bull. Soc. Chim. Fr.* **1997**, *134*, 897.
(278) Brunsveld, L.; Lohmeijer, B. G. G.; Vekemas, J. A. J. M.; Meijer, E. W. *Chem. Commun.* **2000**, 2305.
(279) Brunsveld, L.; Zhang, H.; Glasbeek, M.; Vekemas, J. A. J. M.; Meijer, E. W. *J. Am. Chem. Soc.* **2000**, *122*, 6175.
(280) Okamoto, Y. *Prog. Polym. Sci.* **2000**, *25*, 159.

CR0000978

Supramolecular Structures from Rod–Coil Block Copolymers

Myongsoo Lee,^{*,†} Byoung-Ki Cho,[†] and Wang-Cheol Zin[‡]

Department of Chemistry, Yonsei University, Shinchon 134, Seoul 120-749, Korea, and Department of Materials Science and Engineering and Polymer Research Institute, Pohang University of Science and Technology, Pohang 790-784, Korea

Received February 22, 2001

Contents

I. Introduction	3869
II. Rod–Coil Block Copolymer Theories	3869
III. Rod–Coil Copolymers Based on Helical Rods	3872
IV. Rod–Coil Copolymers Based on Mesogenic Rods	3875
A. Bulk-State Supramolecular Structures	3875
B. Supramolecular Structures from Binary Mixtures	3882
V. Rod–Coil Copolymers Based on Conjugated Rods	3884
VI. Conclusions	3890
VII. Acknowledgments	3891
VIII. References	3891

I. Introduction

One of the fascinating subjects in areas such as materials science, nanochemistry, and biomimetic chemistry is concerned with the creation of supramolecular architectures with well-defined shapes and functions. Self-assembly of molecules through non-covalent forces including hydrophobic and hydrophilic effects, electrostatic interactions, hydrogen bonding, microphase segregation, and shape effects has the great potential for creating such supramolecular structures.^{1–5} An example is provided by rodlike macromolecules whose solutions and melts exhibit liquid crystalline phases such as nematic and/or layered smectic structures with the molecules arranged with their long axes nearly parallel to each other.^{6,7} The main factor governing the geometry of the supramolecular structures in the liquid crystalline phase is the anisotropic aggregation of the molecules. In contrast, coil–coil diblock molecules consisting of different immiscible segments exhibit a wide range of microphase-separated supramolecular structures with curved interfaces in addition to layered structures.^{8–11} This phase behavior is mainly due to the mutual repulsion of the dissimilar blocks and the packing constraints imposed by the connectivity of each block.

The covalent linkage of these different classes of molecules to a single linear polymer chain (rod–coil copolymer) can produce a novel class of self-assembling materials since the molecules share certain general characteristics of diblock molecules and rodlike liquid crystalline molecules.^{12–15} The difference

in chain rigidity of stiff rodlike and flexible coillike block is expected to greatly affect the details of molecular packing and thus the nature of thermodynamically stable supramolecular structures. This rod–coil molecular architecture imparts microphase separation of the rod and coil blocks into ordered periodic structures even at very low molecular weights relative to flexible block copolymers due to the high stiffness difference between the blocks. As a consequence, the rod–coil copolymer forms supramolecular structures with dimensions as small as few nanometers, which are not common in microphase-separated flexible block copolymers.¹⁶ The supramolecular structures of rod–coil polymers arise from a combination of organizing forces including the mutual repulsion of the dissimilar blocks and the packing constraints imposed by the connectivity of each block, and the tendency of the rod block to form orientational order. Apart from the wide range of different supramolecular structures in nanoscale dimensions, another unique characteristic is that rod segments can endow various functionalities such as photophysical and electrochemical properties to the supramolecular materials.

Many of the syntheses of rod–coil diblock and triblock copolymers as well as their interesting supramolecular structures and the intriguing properties of rod–coil copolymers are discussed in excellent books and reviews that have been published by several experts in the field.^{16–19} Here, we do not want to present a complete overview on reported rod–coil copolymers. Instead, we have highlighted the most recently synthesized rod–coil copolymers and their supramolecular structures.

II. Rod–Coil Block Copolymer Theories

In A-B diblock copolymers with well-defined molecular architectures, microphase separation occurs, and microdomains rich in monomer A and in monomer B are formed. When microphase separation occurs, the microdomains are not dispersed randomly but form a rather regular arrangement giving rise to a periodic structure. The geometry of the microdomain is largely dictated by the relative volume fraction of the A block to that of the B block.^{8–11,20–23} Conformational asymmetry between A and B blocks also plays a significant role in determining the geometry of the lattice. Several theoretical attempts have been made to deal with this conformational asymmetry and study its effects on the microphase-separated morphologies.^{24–27} Increasing the chain stiffness of a polymer chain eventually results in a rodlike block that can be characterized by a persis-

* To whom correspondence should be addressed. FAX: 82-2-364-7050. E-mail: mslee@yonsei.ac.kr.

[†] Yonsei University.

[‡] Pohang University of Science and Technology.



Myongsoo Lee, born in 1960, received a bachelor degree in Chemistry from Chungnam National University, Korea, in 1982 and his Ph.D. degree in Macromolecular Science from Case Western Reserve University, Cleveland, in 1992. In the same year, he became a postdoctoral fellow at University of Illinois, Urbana-Champaign. In 1993, he was a senior research scientist at Korea Research Institute of Chemical Technology where he worked in the field of π -conjugated systems. In 1994, he joined the Faculty of Chemistry at Yonsei University, Korea, where he is presently Associate Professor of Chemistry. His current research interests include synthetic self-organizing macromolecules, controlled supramolecular architectures, and organic nanostructured materials.



Byoung-Ki Cho was born in Daejeon, Korea, in 1971 and studied Chemistry at Yonsei University, Korea. After receiving his B.S. degree in 1996, he joined the research group of Professor Myongsoo Lee, Yonsei University, where he received his Ph.D. degree in 2001. His graduate research focused on supramolecular organization based on organic rod building blocks. During his graduate study, he received research excellence award in Yonsei University and graduate fellowship granted by Seo-Am Foundation. Dr. Cho is currently a postdoctoral associate at Cornell University, Ithaca.

tent length and whose end to end distance scales linearly with the number of monomer units.

Rod-coil block copolymers have both rigid rod and block copolymer characteristics. The formation of liquid crystalline nematic phase is characteristic of rigid rod, and the formation of various nanosized structures is a block copolymer characteristic. A theory for the nematic ordering of rigid rods in a solution has been initiated by Onsager and Flory,^{28,29} and the fundamentals of liquid crystals have been reviewed in books.^{30,31} The theoretical study of coil-coil block copolymer was initiated by Meier,³² and the various geometries of microdomains and micro phase transitions are now fully understood. A phase diagram for a structurally symmetric coil-coil block copolymer has been theoretically predicted as a



Wang-Cheol Zin received his Ph.D. degree from the University of Cincinnati in 1983 and did postdoctoral work at Stanford University before joining the Korea Research Institute of Chemical Technology as a senior researcher. He is Professor of Materials Science and Engineering at the Pohang University of Science and Technology since 1986. His research focuses on the self-organization of rod-coil block molecules and phase relationship in block copolymers and polymer blends.

function of the volume fraction of one component f and the product χN , where χ is the Flory-Huggins interaction parameter and N is the degree of polymerization.³³ A predicted stable microstructure includes lamellae, hexagonally packed cylinders, body-centered cubic spheres, close-packed spheres, and bicontinuous cubic network phases with $Ia\bar{3}d$ symmetry (Figure 1).

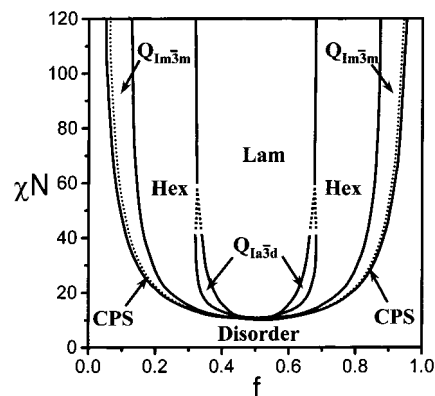


Figure 1. Phase diagram for a structurally symmetric coil-coil block copolymer (Lam = lamellae, Hex = hexagonally packed cylinders, $Q_{Ia\bar{3}d}$ = bicontinuous cubic with $Ia\bar{3}d$ symmetry, $Q_{Im\bar{3}m}$ = body-centered cubic, CPS = close packed sphere).

Including both rod and block characters, Semenov and Vasilenko (SV) have initiated a theoretical study on the phase behavior of rod-coil block copolymers.¹² In their study, SV only considered the nematic phase and smectic A lamellar phases where rods remain perpendicular to the lamellae. The smectic phase has either a monolayer or bilayer structure. In the following study, Semenov included the smectic C phases, where the rods are tilted by an angle θ to the lamellar normal.^{13,14} The model also included a weak phase in which lamellar sheets containing the rigid rod were partly filled by flexible coil. For free energy calculations, SV introduced four main terms: ideal gas entropy of mixing, steric interaction among rods, coil stretching, and unfavorable rod-coil interactions. The ideal gas entropy of the mixing term is

associated with the spatial placement of the junction point of rod–coil molecules. To find the steric interaction energy term of the rods SV used the lattice packing model (Flory lattice approach). Coil stretching arises from the constraint of the density uniformity, and it restricts the number of possible conformations of flexible coil in the structured system. The Flory–Huggins interaction parameter measures unfavorable rod–coil interaction energy. The schematic phase diagram calculated shows various phases as a function of the volume fraction of the flexible component f , the product χN and the ratio ν of the characteristic coil to rod dimensions. In rod–coil block copolymers, the shape of the phase diagram is affected by the ratio ν . It was also shown that the nematic–smectic transition is a first-order transition, while the smectic A–smectic C transition is a continuous second-order transition.

Williams and Fredrickson proposed the hockey puck micelle (one of the nonlamellar structure) where the rods are packed axially to form finite-sized cylindrical disk covered by coils (Figure 2).¹⁵ They

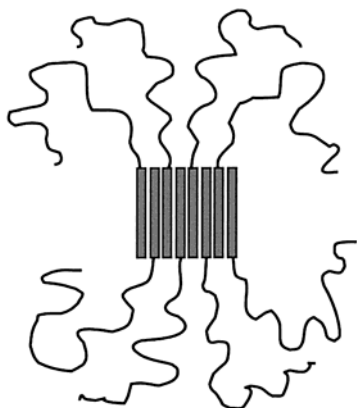


Figure 2. Schematic representation of a monolayer puck.

predicted that the hockey puck structure should be stable at large coil fractions ($f > 0.9$). The main advantage of micelle formation relative to lamellae is the reduction of the stretching penalty of coils; because in a rod–coil block copolymer the coils are permanently attached to the rods, complete separation is never possible, and there is always some interface between the two. In general, the sharper the interface, the more the coils have to stretch and the greater the stretching free energy. At high χ values, the system can be modeled as a set of chains grafted to a wall. In the lamellae structure, the highly grafted chains pay a large stretching penalty. This penalty is governed by how rapidly the volume away from the interface increases. In a micellar puck, the rods are assumed to be well aligned to get rid of the strong steric problems, and the chains are assumed to form a hemispherical shell at a radius of R from the disk with a constant surface density on this shell. The coils are strongly stretched inside the hemisphere. The model assumed that coils travel in straight line trajectories, consistent with constant density constraints. After the chains have passed this hemisphere, they are assumed to have radial trajectories as if they emanated from the center of the puck. This model has only one free parameter R to

minimize free energy. The main disadvantage of forming the hockey puck relative to lamellae is the creation of an extra surface, for which they pay a surface energy penalty. WF, following the SV approach, included the hockey puck micelle phase in the phase diagram by comparing the free energy of micelle to that of the lamellar structures (Figure 3).

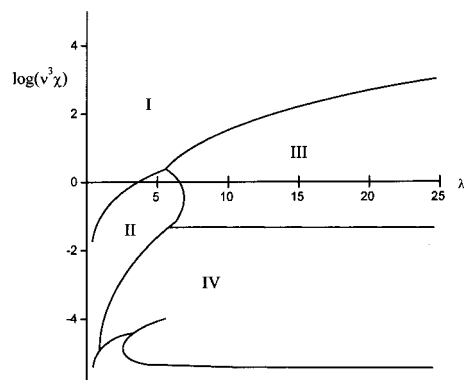
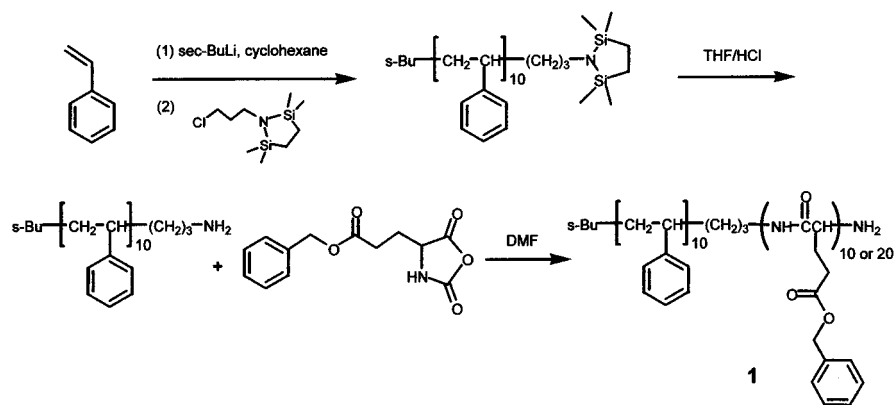


Figure 3. Phase diagram including the hockey puck and lamellae phases. The phases are (I) bilayer lamellae, (II) monolayer lamellae, (III) bilayer hockey pucks, (IV) monolayer hockey pucks, and (V) incomplete monolayer lamellae. $\log(v^3\chi)$ is plotted against λ . $\lambda = \phi/(1 - \phi)$ where ϕ is the volume fraction of the coil. $\nu = \kappa/\lambda$ and $\kappa = Na^2/L^2$ where the coil part is assumed to consist of N segments with a mean-square separation between adjacent segments of $6a^2$, and L is the rod length. χ is the Flory–Huggins interaction parameter.

Müller and Schick (MS) studied the phase behavior of rod–coil molecules by applying the numerical self-consistent field theory within the weak segregation limit.³⁴ In the strong segregation limit at high incompatibilities, MS used a brush-like approximation to determine the phase boundaries. Their most interesting finding was that in stable morphologies the coils are on the convex side of the rod–coil interface. This result emphasizes the importance of the conformational entropy of the flexible component, which is increased when the coil occupies the larger space on the convex side of the interface. They also found that the extreme structural asymmetry in rod–coil blocks has a pronounced influence on the phase diagram. The wide region encompassing cylinder phase was also predicted in the phase diagram of a rod–coil block copolymer in the weak segregation limit. Matsen and Barrett also applied the self-consistent field techniques to the SV model for lamellar structures.³⁵ Their theory predicts a nematic phase composed by the mixing of rods and coils when $\chi N < 5$. By increasing χN , the various lamellar phases appear as a stable phase.

Scaling approaches have been used to theoretically predict the structures of rod–coil block molecules in a selective solvent.^{36–38} Halperin investigated the transition between smectic A and smectic C by comparing interfacial and coil deformation free energy. Since the tilt increases the surface area per coil, tilting is favored when the stretching penalty of the coil is dominant. At high f , the suggested shape of the stable micelle was similar to hockey puck structure presented by WF. In addition, Raphael and de Gennes suggested “needles” and “fence” morphologies

Scheme 1



of coil–rod–coil triblock copolymers in a selective solvent of low molecular weight.

III. Rod–Coil Copolymers Based on Helical Rods

Polymers with a stiff helical rodlike structure have many advantages over other synthetic polymers because they possess stable secondary structures due to cooperative intermolecular interactions. An example of polymers with helical conformation is polypeptides in which the two major structures include α -helices and β -sheets. The α -helical secondary structure enforces a rodlike structure, in which the polypeptide main chain is coiled and forms the inner part of the rod.¹⁸ This rodlike feature is responsible for the formation of the thermotropic and lyotropic liquid crystalline phases. Polypeptide molecules with α -helical conformation in the solution are arranged with their long axes parallel to each other to give rise to a nematic liquid crystalline phase. However, even long chain polypeptides can exhibit a layered supramolecular structure, when they have a well-defined chain length. For example, the monodisperse poly(α ,L-glutamic acid) prepared by the bacterial synthetic method assembles into smectic ordering on length scales of tens of nanometers.^{39,40}

Incorporation of an elongated coillike block to this helical rod system in a single molecular architecture may be an attractive way of creating new supramolecular structures due to its ability to segregate incompatible segment of individual molecules. The resulting rod–coil copolymers based on a polypeptide segment may also serve as models providing insight into the ordering of complicated biological systems. High molecular weight rod–coil block copolymers consisting of a polypeptide connected to either a polystyrene or a polybutadiene were thoroughly studied by Gallot et al.^{18,41–43} These rod–coil copolymers were observed to self-assemble into lamellar structures with a uniform thickness even though the polypeptide blocks are not monodisperse. Furthermore, one of these studies that involved hydrophobic–hydrophilic polypeptide rod–coil copolymers with coil volume fractions ranging between approximately 25 and 45% showed that the rods are tilted 15–70° in the lamellae and that the tilt angle increased with water content.⁴³ In all these studies, the polypeptide segments in these block copolymers have an α -helix conformation.

Very recently, low molecular weight block copolymers consisting of poly(γ -benzyl-L-glutamate) with degrees of polymerization of 10 or 20 and polystyrene with degree of polymerization of 10 were synthesized by Klok, Lecommandoux, and a co-worker (Scheme 1).⁴⁴ The coil block was synthesized by conventional living anionic polymerization initiated by *sec*-butyllithium followed by end capping with 1-(3-chloropropyl)-2,2,5,5-tetramethyl-1-aza-2,5-disilacyclopentane. Acid-catalyzed hydrolysis produced a primary amine functionalized oligostyrene with a degree of polymerization of 10. The resulting primary amine functionalized polystyrene was then used as a macroinitiator for the polymerization of γ -benzyl-L-glutamate *N*-carboxyanhydride to produce the polypeptide block. The length of the polypeptide segment was controlled by the molar ratio of the *N*-carboxyanhydride monomer to the primary amine macroinitiator. In this way, two different rod–coil copolymers consisting of polystyrene with the degree of polymerization of 10 and polypeptide containing either 10 or 20 γ -benzyl-L-glutamate repeating units were prepared.

Both the rod–coil polymers were observed to exhibit thermotropic liquid–crystalline phases with assembled structures that differ from the lamellar structures. Incorporation of a polypeptide segment into a polystyrene segment was observed to induce a significant stabilization of the α -helical secondary structure as confirmed by FT-IR spectra. However, small-angle X-ray diffraction patterns indicated that α -helical polypeptides do not seem to assemble into hexagonal packing for the rod–coil copolymer with 10 γ -benzyl-L-glutamate repeating units. The amorphous character of the polystyrene coil is thought to frustrate a regular packing of the α -helical fraction of the short polypeptide segments. Increasing the length of the polypeptide segment to a DP of 20 gives rise to a strong increase in the fraction of diblock copolymers with α -helical polypeptide segment. By studying this block copolymer with small-angle X-ray analysis, a 2-D hexagonal columnar supramolecular structure was observed with a hexagonal packing of the polypeptide segments adopting an 18/5 α -helical conformation with a lattice constant of 16 Å. The authors proposed a packing model for the formation of the “double-hexagonal” organization (Figure 4). In this model, the rod–coil copolymers are assembled

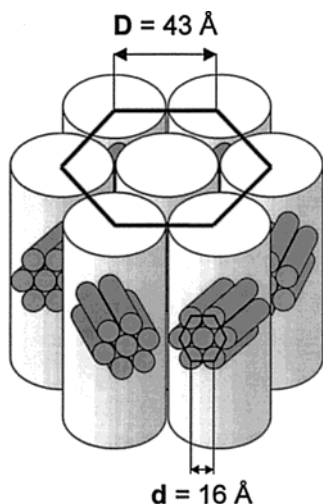


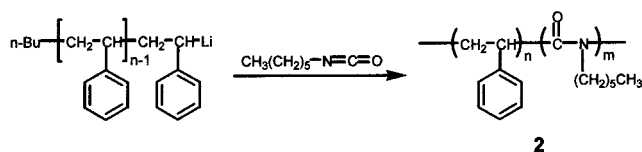
Figure 4. Packing model for the formation of “double-hexagonal” organization. (Reprinted with permission from ref 44. Copyright 2000 American Chemical Society).

in a hexagonal fashion into infinitely long columns, with the polypeptide segments oriented perpendicularly to the director of the columns. The subsequent supramolecular columns are packed in a superlattice with hexagonal periodicity parallel to the α -helical polypeptide segments with a lattice constant of 43 Å.

In contrast to polypeptides that have many possible conformations, poly(hexyl isocyanate) is known to have a stiff rodlike helical conformation in the solid state and in a wide range of solvents, which is responsible for the formation of a nematic liquid crystalline phase.^{45–47} The inherent chain stiffness of this polymer is primarily determined by chemical structure rather than by intramolecular hydrogen bonding. This results in a greater stability in the stiff rodlike characteristics in the solution as compared to polypeptides. The lyotropic liquid crystalline behavior in a number of different solvents was extensively studied by Aharoni et al.^{48–50} In contrast to homopolymers, interesting new supramolecular structures can be expected if a flexible block is connected to the rigid polyisocyanate block (rod–coil copolymers) because the molecule imparts both microphase separation characteristics of the blocks and a tendency of rod segments to form anisotropic order.

Ober and Thomas et al. reported on rod–coil diblock copolymers consisting of poly(hexyl isocyanate) as the rod block and polystyrene as the coil block (Scheme 2).^{51–53} The polymers (**2**) were synthesized

Scheme 2



by sequential living anionic polymerization initiated by *n*-butyllithium. A block copolymer consisting of poly(hexyl isocyanate) with DP of 900 and polystyrene with DP of 300 displays liquid crystalline behavior in concentrated solutions, suggestive of an anisotropic order of rod segments.⁵¹ Transmission electron mi-

croscopy of bulk and thin film samples cast from toluene solutions showed the existence of a zigzag morphology with high degree of smectic-like long-range order. The average domain spacings of the poly(hexyl isocyanate) block are approximately 180 nm and of the polystyrene block approximately 25 nm. Wide-angle electron diffraction pattern showed that the rod domains are highly crystalline with an orientational order. In addition, electron diffraction patterns that showed the orientation of the rod blocks with respect to the zigzags confirmed that the rods are tilted with respect to the interface separating the rod and coil domains. On the basis of these data, the authors proposed a packing model either as an interdigitated model or as a bilayer model (Figure 5). Of the two proposed models for zigzag morphology,

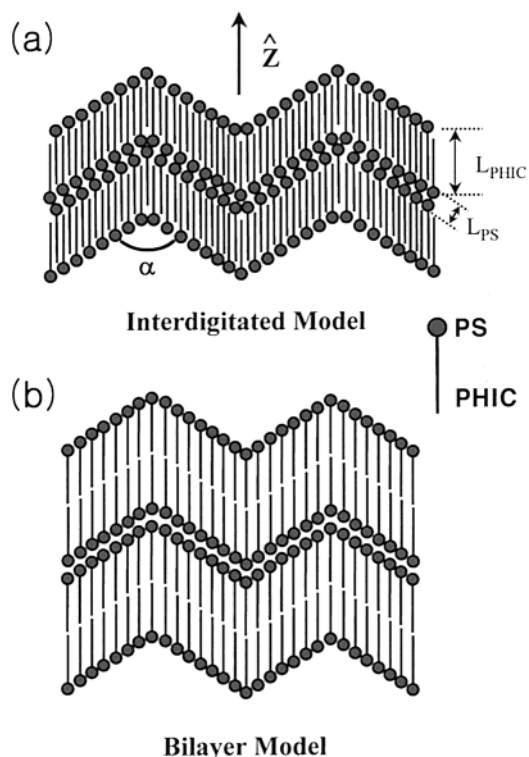


Figure 5. Schematic representation of (a) interdigitated model and (b) bilayer model in the zigzag morphology.

the interdigitated model was suggested to be more consistent with domain spacing predictions based on molecular weight data.

With additional research into the influence of the rod volume fraction on the phase behavior, the authors studied the rod–coil copolymers with varying compositions of rod blocks.⁵² Transmission electron microscopy revealed phase-separated morphologies with rod-rich regions and coil-rich regions in which rod segments are organized into tilted layers analogous to those observed in smectic phases. In these layers, the polymer backbone axis is tilted at an angle relative to the layer normal. It was suggested that the tilting of rod segments might produce a greater volume for coil segments to explore conformational space. This would be particularly important as the molar mass of the coil segment increases due to the proportional increase in the average equilibrium

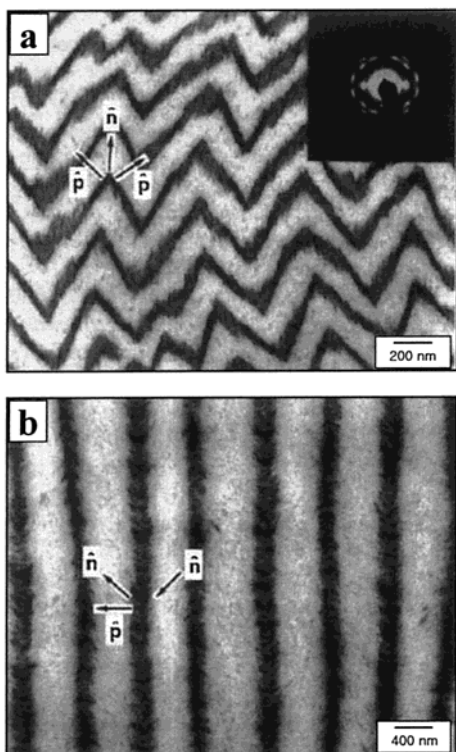


Figure 6. TEM images for (a) zigzag lamellar morphology of rod-coil copolymer with $f_{\text{rod}} = 0.90$ and (b) arrowhead morphology of rod-coil copolymer with $f_{\text{rod}} = 0.98$. (Reprinted with permission from ref 52. Copyright 1996 American Association for the Advancement of Science).

cross section with respect to the degree of polymerization. A rod-coil copolymer with a rod volume fraction $f_{\text{rod}} = 0.42$ organizes into a wavy lamellar morphology, in which the rod blocks are tilted with respect to the lamellar normal by approximately 60° . Small-angle electron diffraction patterns revealed that the rod domains are crystalline and that the local orientation of the stiff rod blocks extends up to $1 \mu\text{m}$.

Rod-coil copolymers with rod volume fractions $f_{\text{rod}} = 0.73$ and $f_{\text{rod}} = 0.90$ were observed to form a zigzag morphology consisting of alternating rod and coil layers arranged in a zigzag fashion. The rod axis is tilted with respect to the layer normal by approximately 45° , and the rod blocks are crystalline as confirmed by the small-angle electron diffraction. The formation of two distinct sets of lamellar with equal that opposite orientations from the local rod directors was suggested to be a consequence of the nucleation of the smectic C phase in a thin film. The rod-coil copolymers with a short polystyrene coil and a very long rod block ($f_{\text{rod}} = 0.96$ and $f_{\text{rod}} = 0.98$) form an interesting different morphology as evidenced by transmission electron microscopy. The authors described this morphology as the *arrowhead* morphology because tilted layers in a chevron pattern are spaced by arrowhead shaped domains of polystyrene which alternatively flip by 180° . Presumably, the alternating direction of the arrowheads reflects the deformation experienced by polystyrene coils as the layer normal in adjacent layers alternate between 45° and -45° . In terms of rod packing with the rod

domains, a bilayer and an interdigitated model were suggested to be most consistent for the polymers with $f_{\text{rod}} = 0.96$ and $f_{\text{rod}} = 0.98$. A series of morphologies including zigzag lamellar to arrowhead microdomain structures observed by transmission electron microscopy is shown in Figure 6 and the structural packing model is shown in Figure 7. A preliminary morphol-

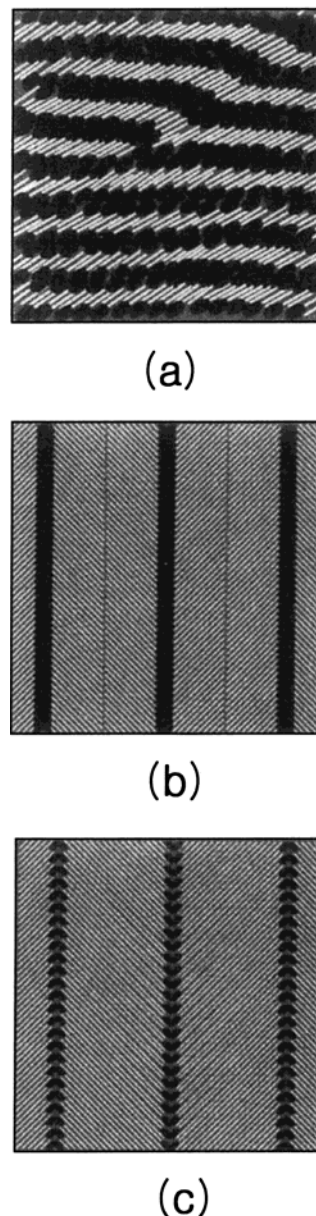


Figure 7. Structural packing models for (a) wavy lamellar, (b) bilayer arrowhead, and (c) interdigitated arrowhead morphologies in rod-coil copolymers **2**. (Reprinted with permission from ref 52. Copyright 1996 American Association for the Advancement of Science).

ogy diagram for this rod-coil system was suggested as shown in Figure 8, based on these experimental results.⁵³ As solvent is evaporated, the rod-coil solutions are predicted to form a homogeneous lyotropic nematic liquid crystal phase prior to microphase separation which supports rod-coil theories.^{12,36–38} Further evaporation of solvent causes microphase separation into various lamellar structures depending on the rod volume fraction of the molecule.

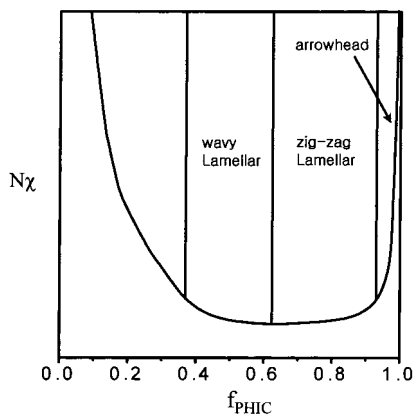
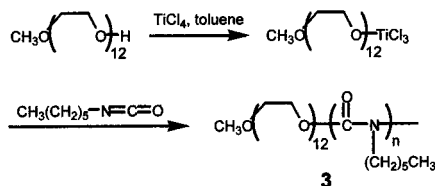


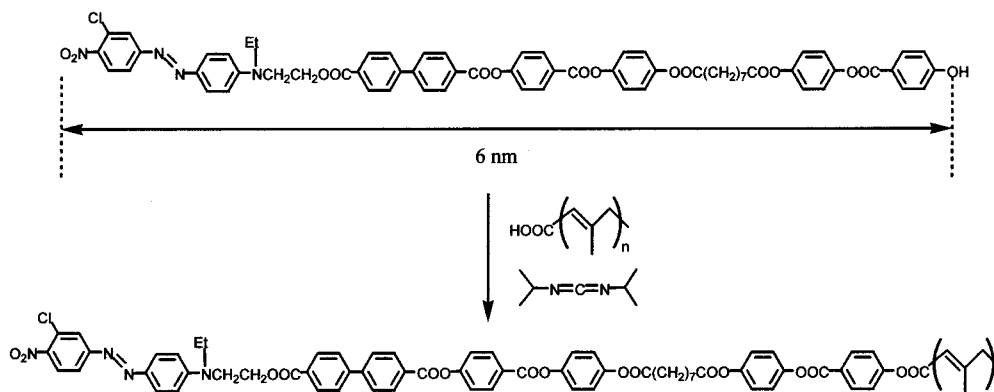
Figure 8. Morphology diagram for rod-coil diblock copolymers (**2**).

Scheme 3



Recently, Pearce et al. reported on rod-coil copolymers consisting of poly(hexyl isocyanate) as the rod block and poly(ethylene oxide) as the coil block (Scheme 3).⁵⁴ The copolymers (**3**) were obtained by coordination polymerization of *n*-hexyl isocyanate initiated by TiCl_3 end functionalized poly(ethylene oxide). A block copolymer with poly(ethylene oxide) with 12 repeating units and poly(hexyl isocyanate) with 50 repeating units exhibits lyotropic liquid crystalline phases in concentrated toluene solution (above 20 wt %) as determined by optical polarized microscopy. When the block copolymer film was cast from the dilute toluene solution, a nematic-like domain texture was observed. However, when cast from a mixture of toluene and pentafluorophenol, where the poly(hexyl isocyanate) block is converted from rod to coil configuration, the liquid crystalline phase behavior disappears. The tendency of the rod segments to be arranged into anisotropic order along their axes seems to play an important role in liquid crystalline behavior of the polymer.

Scheme 4



IV. Rod-Coil Copolymers Based on Mesogenic Rods

A. Bulk-State Supramolecular Structures

It is well-known that classical rodlike mesogenic molecules arrange themselves with their long axes parallel to each other to give rise to nematic and/or layered smectic types of supramolecular structures.^{6,7} Because of the preferred parallel arrangement of the rigid, rodlike units, the formation of curved interfaces is strongly hindered in the mesogenic rods. On the contrary, rod-coil block systems based on mesogenic rods can provide a variety of supramolecular structures due to the effect of microphase separation and the molecular anisotropy of rod block. Even though the molecular weight is very small, microphase separated structures can form due to large chemical differences between each block. In addition to various layered structures as described in Ober's rod-coil copolymers,^{51,52} the stiff rod blocks might assemble into finite nanostructures at higher coil volume fractions as predicted by rod-coil theories.^{15,36-38}

Stupp et al. reported on rod-coil copolymers consisting of an elongated mesogenic rod and a monodisperse polyisoprene (Scheme 4).⁵⁵⁻⁵⁷ The living polyisoprene was converted to a carboxylic acid group with CO_2 , and the rod having a well-defined structure with a fully extended rod length of 6 nm was synthesized by conventional synthetic methods. The final rod-coil polymers (**4**) with the rod volume fractions range from 0.19 to 0.36 were prepared by esterification of an acid functionalized polyisoprene and a hydroxy functionalized rod block in the presence of diisopropylcarbodiimide (DIPC).

These rod-coil copolymers organize into ordered structures that differ in terms of varying the rod volume fraction as monitored by transmission electron microscopy and electron tomography. The rod-coil copolymer with rod volume fraction $f_{\text{rod}} = 0.36$ forms alternating rod- and coil-rich strips 6–7 and 5–6 nm wide, respectively. Electron tomography revealed that the copolymers self-assemble into layered 2-D superlattices and ordered 3-D morphology. Slices orthogonal to the plane of the film showed that the rod-domains are not lamellae but discrete channel-like long objects, 6–7 nm in diameter. In strip

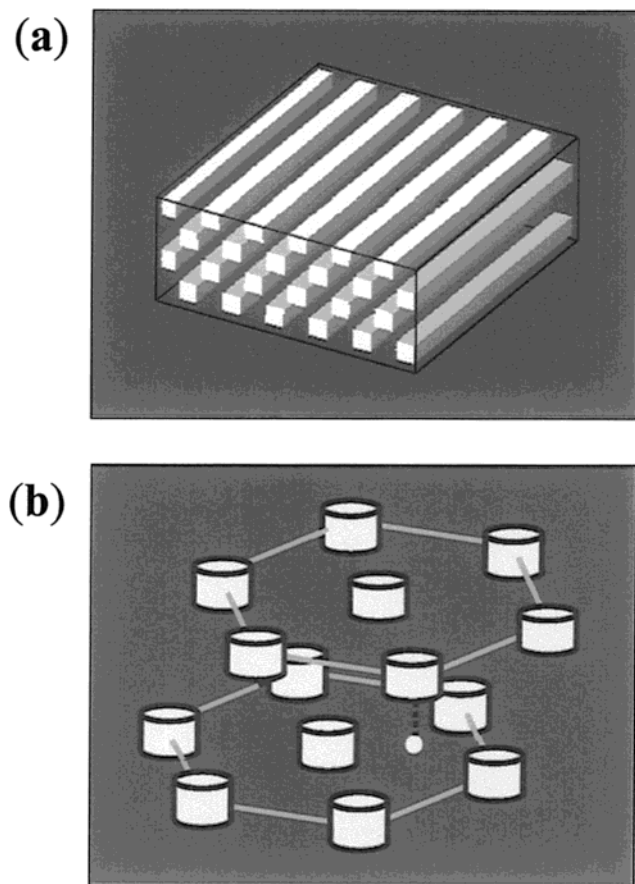
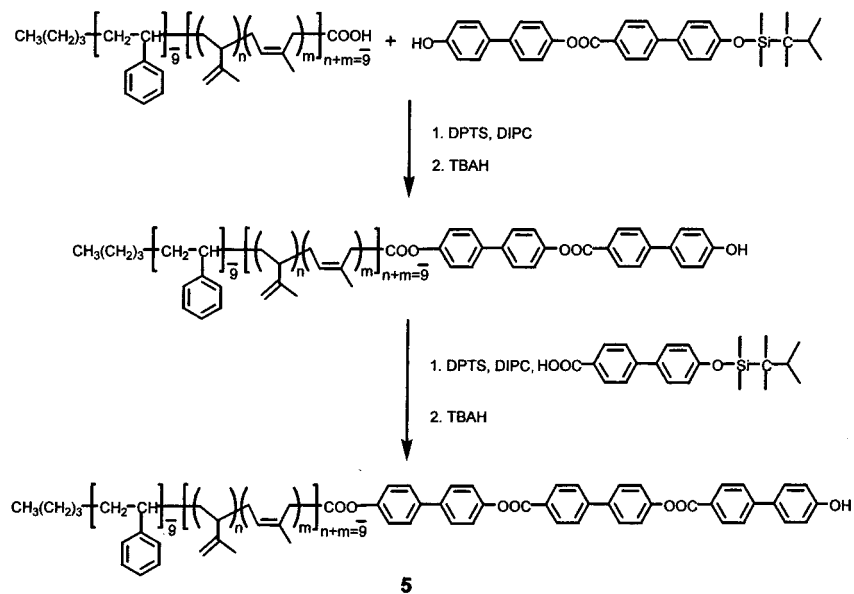


Figure 9. Schematic diagrams of (a) strip morphology of rod-coil copolymer with $f_{\text{rod}} = 0.36$ and (b) hexagonal superlattice of rod-coil copolymer with $f_{\text{rod}} = 0.25$. (Reprinted with permission from ref 57. Copyright 1997 American Chemical Society).

morphology, layers are correlated such that each strip resides over a coil region of the adjacent layer and that the direction of its long axis remains constant through the layers as illustrated in Figure 9a. The rod segments are thought to assemble into interdigitated bilayer or monolayer.

Scheme 5



The rod-coil copolymer with $f_{\text{rod}} = 0.25$ forms a hexagonal superlattice of rod aggregates measuring approximately 7 nm in diameter and a domain spacing of 15 nm as evidenced by transmission electron micrograph. By studying the films by electron tomography, the authors observed that each layer contains a hexagonal superlattice. Slices orthogonal to the film plane showed that the rod aggregates are discrete objects with roughly the same dimensions in all directions as schematically illustrated in Figure 9b. The rod-coil copolymer with $f_{\text{rod}} = 0.19$ does not show phase separated morphology in the as-cast state. Interestingly, annealing the film near 100 °C produced a hexagonal superlattice with long-range order comparable to $f_{\text{rod}} = 0.25$. These works clearly show that the supramolecular structure formed by self-assembly of rod segments can be controlled by simple variation of rod to coil volume ratio.

The authors also synthesized triblock rod-coil copolymers containing oligostyrene-*block*-oligoisoprene as the coil block and three biphenyl units connected by ester linkages as the rod block (Scheme 5).^{58,59} Carboxylic acid functionalized coil block was prepared by anionic sequential living polymerization of styrene and then isoprene, followed by end capping with CO₂. The resulting coil block was then connected to a rigid block made up of two biphenyl units through an ester bond, followed by deprotection at the phenolic terminus. The final rod-coil copolymers were synthesized by following the same sequence of reactions, i.e., esterification and then subsequent deprotection of a protecting silyl group.

The rod-coil copolymer containing a (styrene)₉-(isoprene)₉ block oligomer (5) as coil segment was observed to self-assemble into uniform narrow-sized aggregates and to subsequently organize into a superlattice with periodicities of 70 and 66 Å as evidenced by transmission electron microscopy (Figure 10a) and small-angle electron diffraction.⁵⁸ The wide-angle electron diffraction pattern revealed an a^*b^* reciprocal lattice plane, suggesting that the rod

Chart 1

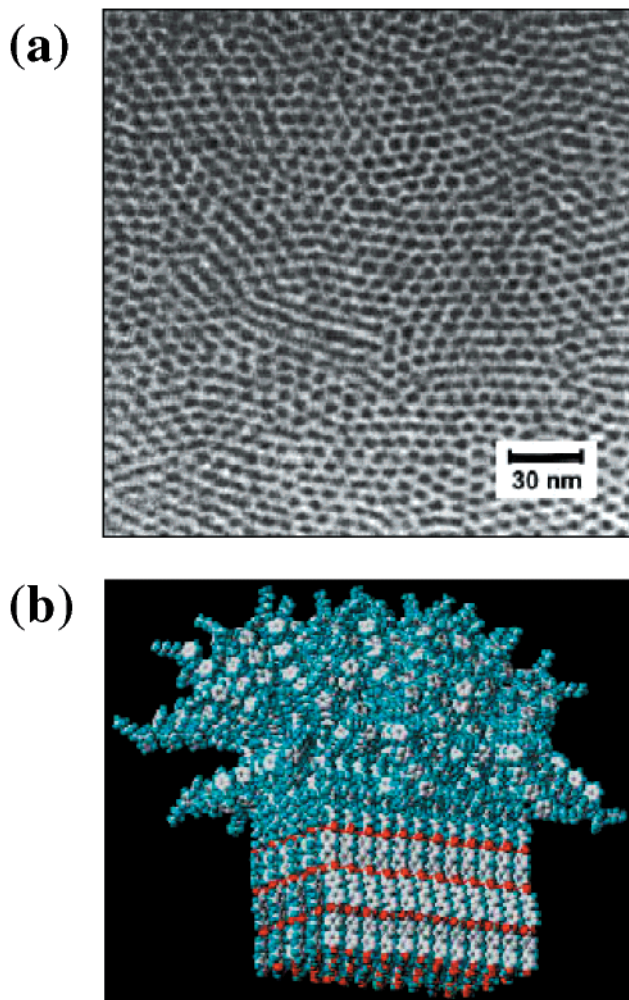
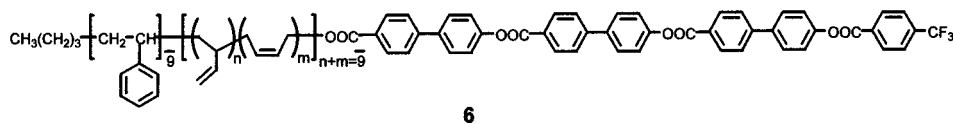


Figure 10. (a) TEM image (Reprinted with permission from ref 59. Copyright 2000 American Chemical Society) and (b) schematic packing structure of rod–coil copolymer (5) (Reprinted with permission from ref 58. Copyright 1997 American Association for the Advancement of Science).

segments are aligned axially with their preferred direction with respect to the plane normal of the layer with long-range order. Transmission electron microscopy of the microtomed sections revealed a layered structure with characteristic periods of the 70 Å layers consisting of one dark and one light band with thicknesses of 30 and 40 Å, respectively. On the basis of these experimental data together with molecular modeling calculations, the authors proposed that these rod–coil copolymers self-assemble into fascinating mushroom-shaped supramolecular structures containing 100 rod–coil molecules with a molar mass about 200 kD, which assemble in a “cap to stem” arrangement (Figure 10b). Spontaneous polar organization in this system was reported and was presumably due to the nature of the supramolecular units of molecule preformed in solution. Both microphase separation between the two coil blocks and the crystallization of the rod segments are likely to

play important roles in the formation of the unusual mushroom-shaped aggregate. This leads to the asymmetrical packing of the nanostructures that form micrometer-sized platelike objects exhibiting tape-like characteristics with nonadhesive-hydrophobic and hydrophilic-sticky opposite surfaces.

Molecular object polymers have distinct and permanent shapes similar to proteins with a well-defined folded shape. Stupp et al. presented an elegant approach to produce well-defined macromolecular objects converting supramolecular clusters by polymerization of cross-linkable group within a discrete supramolecular unit.⁶⁰ The rod–coil triblock molecule (6) synthesized by the authors is composed of a block of oligostyrene, a block of polymerizable oligobutadiene, and a rodlike block containing CF₃ end group which has a large dipole moment (Chart 1).

Transmission electron microscopy revealed that the triblock molecules self-assemble into a solid-state structure consisting of aggregates ~2 nm in diameter. The thickness of layers revealed by small-angle X-ray scattering appears to be 8 nm. The rod axes in the cluster were observed to be normal to the layers and be perpendicular to the plane of the TEM micrographs as confirmed by wide-angle electron diffraction patterns. On the basis of these data, the rod–coil triblock molecules were suggested to pack into the mushroom-shaped nanostructure with a height of 8 nm and a diameter of 2 nm. Each supramolecular nanostructure was estimated to contain approximately 23 molecules. Most important, this nanostructure was proposed to impart the spatial isolation of cross-linkable oligobutadiene blocks required to form a well-defined object. Therefore, polymerization might be confined to the volume of the supramolecular cluster. Thermal polymerization of rod–coil triblock molecules in liquid crystalline state produced high molar-mass products with a very narrow polydispersity within a range from 1.15 to 1.25 and molecular weight of approximately 70 000 as confirmed by GPC (Figure 11). The macromolecular objects obtained reveal an anisotropic shape (2 by 8 nm) similar to that of supramolecular clusters, as determined by electron microscopy and small-angle X-ray scattering. Polarized optical microscopy showed that polymerization of the triblock molecules into macromolecular objects results in a strong stabilization of the ordered structure that remains up to a chemical decomposition temperature of 430 °C. This result is interesting because the self-assembly process provides a direct pathway to prepare well-defined molecular nano-objects with distinct and permanent shape through polymerization within supramolecular structures.

A strategy to manipulate the nanostructure assembled by rod building blocks may be accessible by attaching a bulky dendritic wedge to a rod end. As the cross-sectional area of rod segment increases

Chart 2

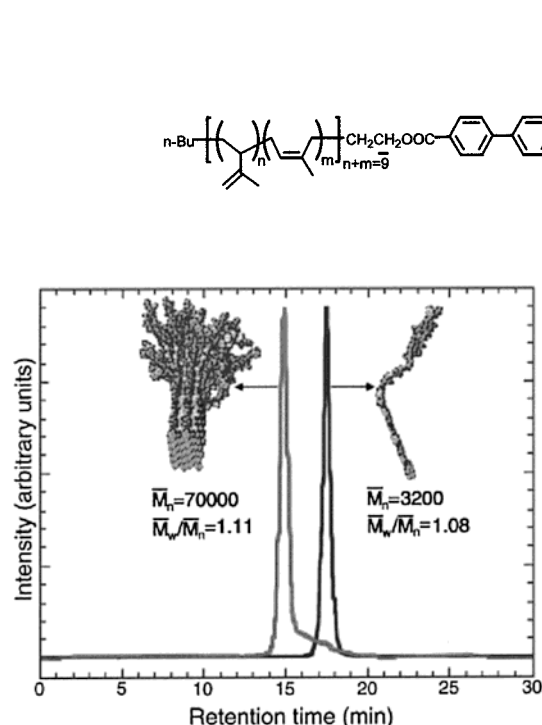


Figure 11. GPC traces of rod-coil triblock molecule (**6**) and macromolecular object. (Reprinted with permission from ref 60. Copyright 1999 American Association for the Advancement of Science).

while maintaining anisotropic order of rod segments, greater steric repulsion between rod segments could possibly frustrate the formation of two-dimensional assemblies. An interesting example of dendron rod-coil molecules synthesized recently by Stupp and co-workers is depicted in Chart 2.⁶¹

In contrast to previously described structurally simple rod-coil molecules, these dendron rod-coil molecules (**7**) form well-defined ribbonlike 1-D nano-

structure. When cast from a 0.004 wt % solution of the CH_2Cl_2 solution onto a carbon support film, one-dimensional objects with a uniform width of 10 nm were observed by the transmission electron microscopy (TEM), in which the objects build networks that cause the dilute CH_2Cl_2 solution (as low as 0.2 wt %) to undergo gelation (Figure 12a). Atomic force microscopy (AFM) revealed their thickness of 2 nm, indicative of a ribbonlike shape. The crystal structure of the model compound made up of a dendron identical to that presented in **7** but covalently attached to only one biphenyl revealed 8 hydrogen bonds that connect the tetramers along the axis of the ribbon. The thickness of the tetrameric cycles was measured to be 2 nm, which is in good agreement with the thickness of the nanoribbons as determined by AFM. On the basis of these results as well as the crystal structure of the model compound, the supramolecular structure was proposed to be a ribbonlike structure with a width of 10 nm and a thickness of 2 nm (Figure 12b). π - π stacking interactions between aromatic segments and directional hydrogen bonding seem to play important roles in the formation of this well-defined novel nanostructure.

Lee et al. also reported on small rod-coil systems with a mesogenic rod segment. Their molecules are based on flexible poly(ethylene oxide) or poly(propylene oxide) as a coil block.^{62,63} The rod-coil molecule based on poly(ethylene oxide) coil (**8**) exhibits a

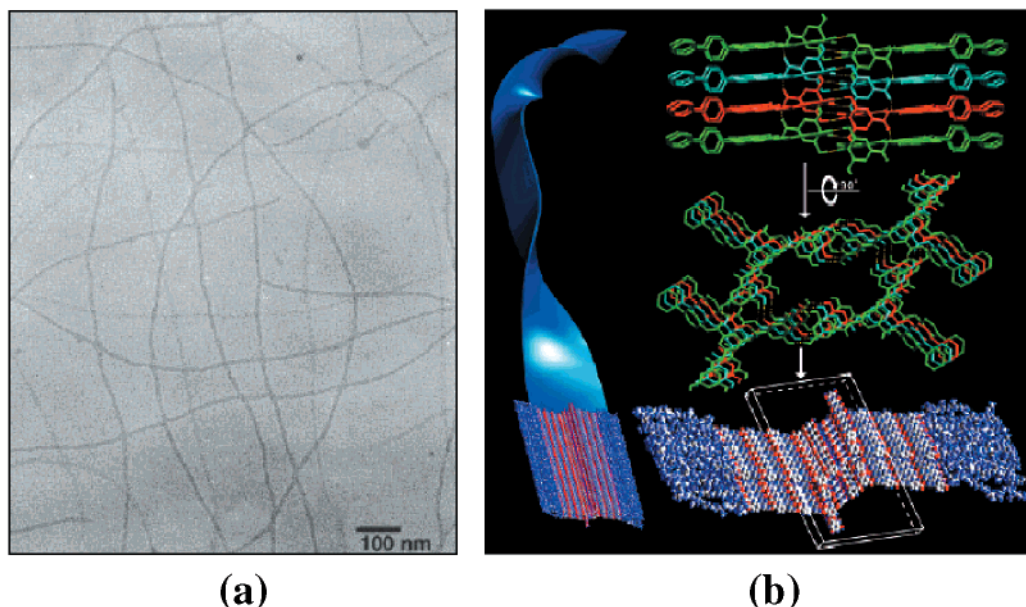
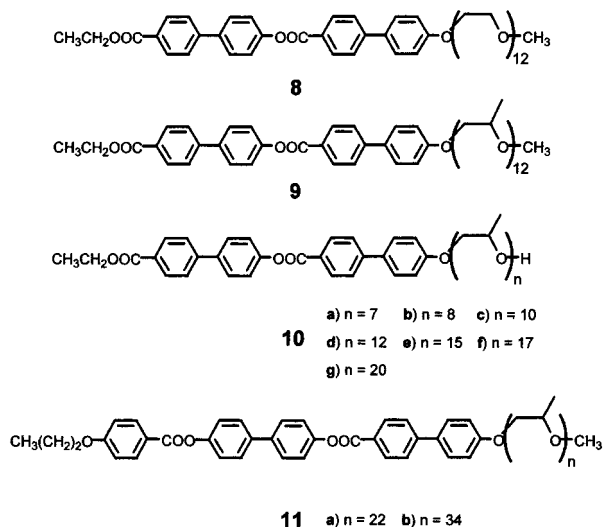


Figure 12. (a) TEM image of nanoribbons formed in dichloromethane. (b) Schematic representation of supramolecular nanoribbon by self-assembly of dendron rod-coil molecules. (Reprinted with permission from ref 61. Copyright 2001 American Chemical Society).

smectic A phase, whereas the latter molecule (**9**) shows a hexagonal columnar structure.⁶³ This large structural variation between the molecularly similar systems should be caused by the larger spatial requirement of the bulkier poly(propylene oxide) coil in comparison with the poly(ethylene oxide).

In a more systematic work on the influence of the coil length on phase behavior, the authors studied rod–coil molecules (**10**) with poly(propylene oxide) having different degrees of polymerization but the identical rod segment (Chart 3).^{64,65} A dramatic

Chart 3



structural change in the melt state of this rod–coil system was observed with variation in the coil length as determined by a combination of techniques consisting of differential scanning calorimetry (DSC), optical polarized microscopy, and X-ray scattering. Rod–coil molecules with 7 and 8 propylene oxide units exhibit layered smectic C and smectic A phases, while rod–coil molecules with 10 to 15 repeating units exhibit an optically isotropic cubic phase. This structure was identified by the X-ray scattering method to be a bicontinuous cubic phase with $Ia3d$ symmetry. Further increasing the coil length induces a hexagonal columnar mesophase as in the case of the molecules with 15 to 20 repeating units (Figure 13). Organization of the rod–coil molecules into a cross sectional slice of a cylinder for cubic and columnar phases is thought to give rise to a aromatic core with approximately square cross section taking into account the calculation based on the lattice parameters and densities. The sizes and periods of these supramolecular structures are typically in a range of less than 10 nm.

Supramolecular structures of rod–coil diblock molecules consisting of more elongated rod segment and PPO coil segment (**11**) were also investigated by the authors (Chart 3).⁶⁶ In these rod–coil molecules, the rod segment consists of two biphenyl and a phenyl group connected through ester linkages. Thus, the tendency of this system to self-organize into layered structures at a given rod volume fraction was expected to be stronger than that of the rod–coil system containing only two biphenyl units as the rod block. These rod–coil molecules with 22 (**11a**) and 34 (**11b**)

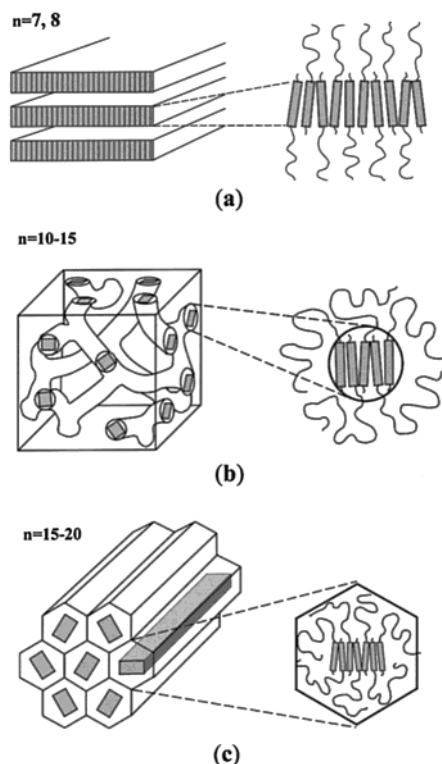


Figure 13. Schematic representation of supramolecular structures of rod-coil molecules **10**. (a) Smectic A, (b) bicontinuous cubic, and (c) hexagonal columnar phases. (Reprinted with permission from ref 64. Copyright 1998 American Chemical Society).

PPO repeating units self-assemble into a supramolecular honeycomb-like layered structure, in which perforations are filled by coil segments. When cast from dilute CHCl_3 solution onto a carbon support film, honeycomb-like supramolecular structure was observed, as revealed by transmission electron microscopy (TEM), in which coil perforations are packed on a hexagonal symmetry with distances between perforations of approximately 10 nm (Figure 14a).

Electron diffraction patterns revealed very well-oriented, single crystal-like reflections associated with the a^*b^* reciprocal plane of a rectangular lattice, indicating that the rod segments are aligned axially with their preferred direction with respect to the plane normal of the layer. Small-angle X-ray diffraction pattern showed a number of sharp reflections that are indexed as a 3-dimensional hexagonal structure (Figure 14b). On the basis of these results as well as density measurements, the supramolecular structure was proposed to be a honeycomb-like crystalline layer of the rod segments with in-plane hexagonal packing of coil perforation as illustrated in Figure 15. The consequent layers were suggested to be stacked in ABAB arrangement to generate 3-dimensional order. The diameters of perforation sizes were estimated to be approximately 6.5 nm as confirmed by TEM, SAXS, and density measurements. These dimensions are comparable to those to Bacillaceae in which pores with regular size are organized predominantly into a hexagonal lattice. Thus, this system might provide access to an excellent model for exploring biological processes in supramolecular materials.

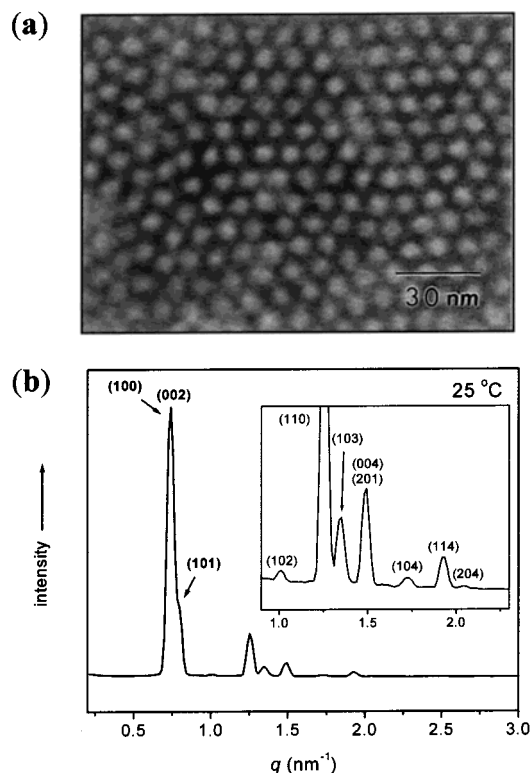
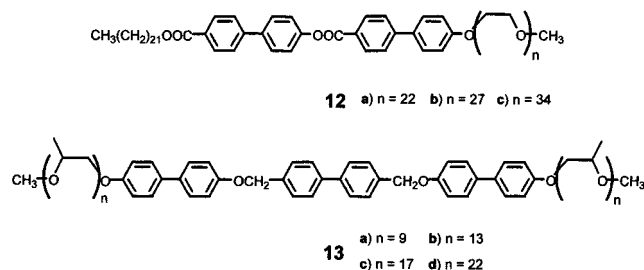


Figure 14. (a) TEM image and (b) small-angle X-ray diffraction pattern of rod-coil molecule **11b**. (Reprinted with permission from ref 65. Copyright 2001 American Chemical Society).

Lee et al. also reported the assembling behavior of coil-rod-coil ABC triblock molecules where the rod block is connected as the middle block, consisting of poly(ethylene oxide) with different degrees of polymerization, two biphenyl unit as rod and docosyl coil (Chart 4).⁶⁷ All of the coil-rod-coil ABC triblock molecules (**12**) exhibit three different crystalline melting transitions associated with poly(ethylene oxide), docosyl, and rod blocks, respectively, as determined by DSC, indicative of phase separation among blocks.

Interestingly, molecules with 22 to 34 ethylene oxide repeating units exhibit a hexagonal columnar

Chart 4



mesophase which, in turn, undergoes transformation into discrete spherical micellar structure with a lack of symmetry (Figure 16). Small-angle X-ray diffraction in the optically isotropic state revealed a strong primary peak together with a broad peak of weak intensity at about 1.8 relative to the primary peak position, indicating that the spatial distribution of centers of the spherical micelles has only liquidlike short range order, most probably due to random thermal motion of spherical micelles. From the observed primary peak of X-ray diffraction, the diameter (d) of spheres was estimated to be approximately 13 nm. It is likely that hydrophobic force plays an important role in the self-assembly of the molecules into discrete nanostructures.

In a separated work, the authors reported on supramolecular structural behavior of symmetric coil-rod-coil molecules (**13**) consisting of three biphenyl units with ether linkages as the rod segment and poly(propylene oxide) with different degrees of polymerization (Chart 4).⁶⁸ Molecules with a certain length of coil (DP of PPO = 9 to 22) assemble into discrete supramolecular aggregates that spontaneously organize into a novel 3-D tetragonal phase with a body-centered symmetry in the solid and melt states as determined by small-angle X-ray scattering (Figure 17).

On the basis of X-ray data and density measurements, the authors proposed that the inner core of the supramolecular aggregate is constituted by the discrete rod bundle with a cylindrical shape with 5 nm in diameter and 3 nm in length that is encapsu-

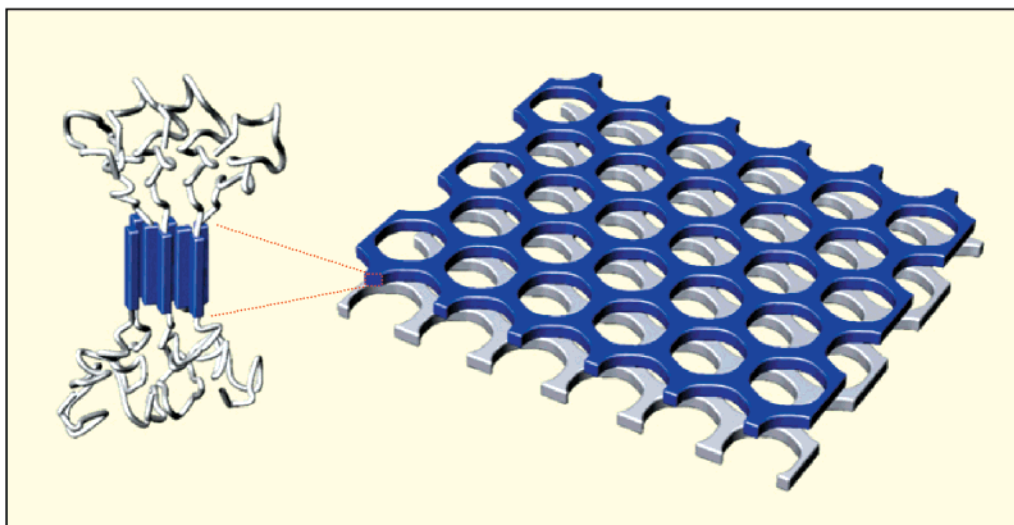


Figure 15. Schematic diagram for the honeycomb-like layer formed by the rod segments of rod-coil molecule **11b**. (Reprinted with permission from ref 65. Copyright 2001 American Chemical Society).

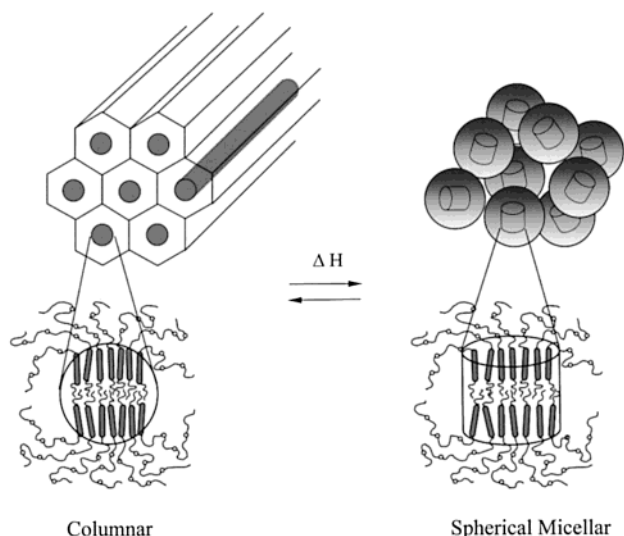


Figure 16. Schematic representation for the organization of the hexagonal columnar and spherical micellar phases of rod-coil molecules **12a–c**. (Reprinted with permission from ref 66. Copyright 1998 American Chemical Society).

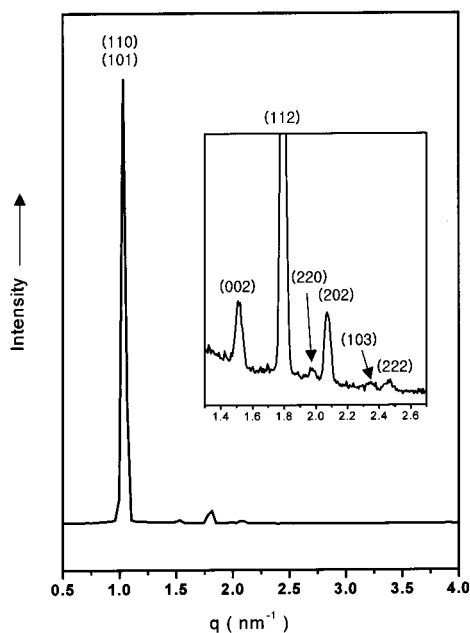


Figure 17. Small-angle X-ray scattering pattern of rod-coil molecule **13c**. (Reprinted with permission from ref 67. Copyright 2000 American Chemical Society).

lated with phase-separated poly(propylene oxide) coils, which gives rise to the formation of nonspherical oblate aggregate as illustrated schematically in Figure 18. The supramolecular rod bundles subse-

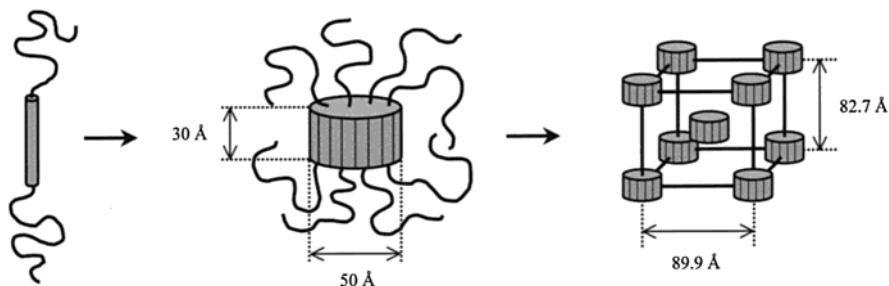
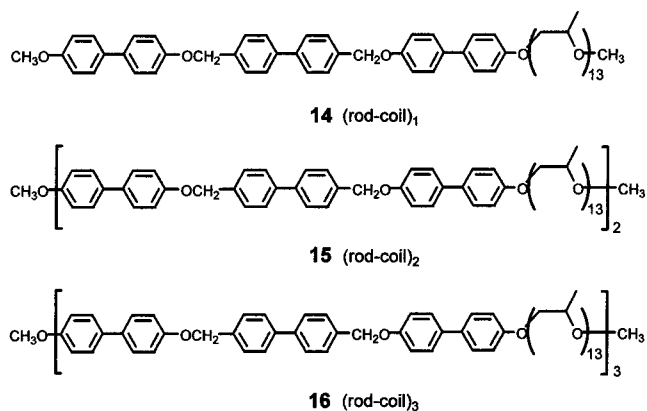


Figure 18. Schematic diagram of self-assembly of **13c** into a supramolecular bundle and the subsequent formation of the body-centered tetragonal lattice. (Reprinted with permission from ref 67. Copyright 2000 American Chemical Society).

Chart 5



quently organize into a 3-D body-centered tetragonal symmetry. The oblate shape of supramolecular aggregates is believed to be responsible for the formation of unusual 3-D tetragonal phase. The authors suggested that this unique phase behavior is mostly originated from the anisotropic aggregation of rod segments with their long axes within microphase separated aromatic domains. Consequently, rod bundles with a puck-like cylindrical shape would give rise to oblate micelles that can pack more densely into an optically anisotropic 3-dimensional tetragonal lattice, rather than an optically isotropic cubic lattice.

The rod-coil approach as a means to manipulate supramolecular structure as a function of rod volume fraction was reported to be extended to main chain multiblock copolymer systems.⁶⁹ In contrast to this, another strategy to manipulate the supramolecular structure at constant rod-to-coil volume ratio can also be accessible by varying the number of grafting sites per rod which might be closely related to the grafting density at the interface separating rod and coil segments.⁷⁰ For this reason, Lee et al. synthesized (rod-coil)₁ (**14**), (rod-coil)₂ (**15**), and (rod-coil)₃ (**16**) with rod-coil repeating units consisting of three biphenyl units connected by methylene ether linkages as the rod block and poly(propylene oxide) with DP of 13 as the coil block (Chart 5).

All of the oligomers are self-organized into ordered supramolecular structures that differ significantly on variation of the number of repeating units as confirmed by X-ray scattering. The (rod-coil)₁ shows a lamellar crystalline and a bicontinuous cubic liquid crystalline structures. In contrast, the (rod-coil)₂ shows a 2-D rectangular crystalline and a tetragonal columnar liquid crystalline structure, while the (rod-coil)₃ displays a hexagonal columnar structure in both

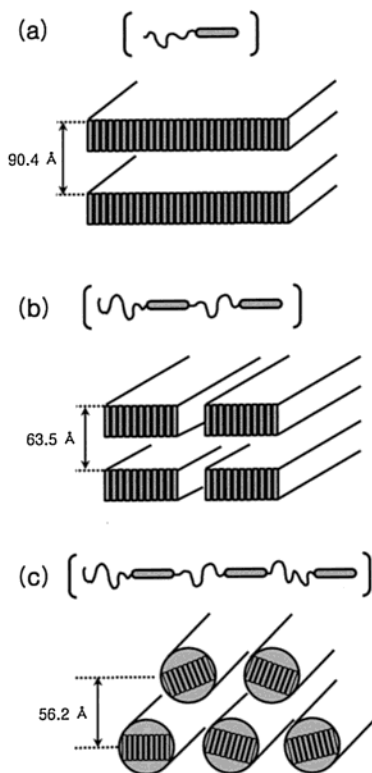


Figure 19. Schematic representation for the formation of (a) lamellar of the (rod-coil)₁, (b) 2-D rectangular of the (rod-coil)₂, and (c) hexagonal columnar of the (rod-coil)₃. (Reprinted with permission from ref 70. Copyright 2001 American Chemical Society).

their solid and melt states (Figure 19). These results represent that self-assembled solid state structure, from 1-D lamellar, 2-D rectangular to 2-D hexagonal lattices are formed by rod-coil structures that differ only in the number of repeating units. This interesting variation of self-assembled structures, at an identical rod to coil volume ratio, was explained by considering the density of grafting sites at the interface separated by rod and coil segments as shown in Figure 20.

B. Supramolecular Structures from Binary Mixtures

Rod-coil copolymers are a type of amphiphile that can self-assemble into a variety of ordered nanostructures in a selective solvent.^{36,37,71} In solvents that selectively dissolve only coil blocks, rod-coil copolymers can form well-defined nanostructures with rod domain consisting of the insoluble block. This results in an increase of the relative volume fraction of the coil segments relative to the rod segments, which gives rise to various supramolecular structures. Particularly, poly(alkylene oxide) as the coil block of rod-coil molecule has additional advantages due to complexation capability with alkali metal cation, which can provide an application potential for solid polyelectrolytes and induce various supramolecular structures.^{72–75}

Lee et al. showed that control of the supramolecular structure in rod-coil molecular systems containing either poly(ethylene oxide) (**8**) or poly(propylene oxide) (**17**) coils and induction of ordered structures

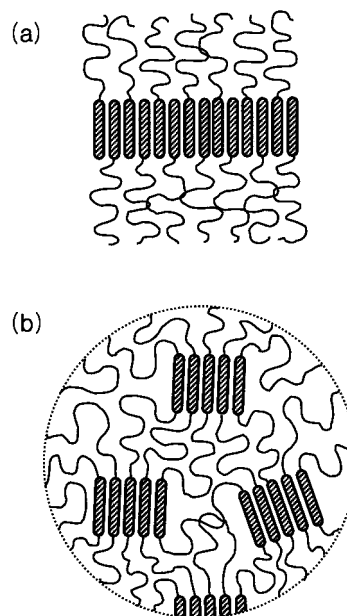
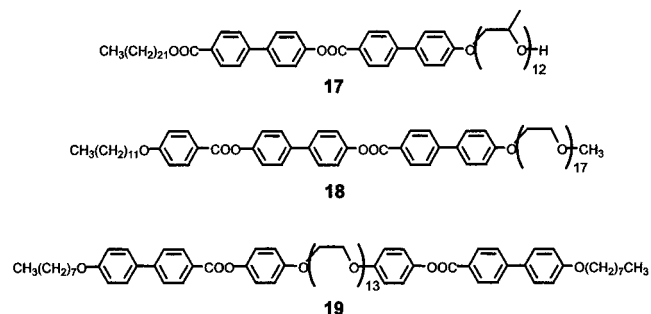


Figure 20. Schematic representation of the molecular arrangement of rod-coil units in (a) (rod-coil)₁ and (b) rod-coil multiblock copolymer. (Reprinted with permission from ref 70. Copyright 2001 American Chemical Society).

Chart 6



are possible through complexation with lithium ion (Chart 6).^{76–79}

First of all, the authors investigated the influence of complexation with LiCF₃SO₃ on the phase behavior of rod-coil diblock molecule containing poly(ethylene oxide) with DP of 12 as the coil block (**8**).⁷⁷ The complexes with 0.0–0.15 mol of LiCF₃SO₃/ethylene oxide unit ([Li⁺]/[EO]) were observed to exhibit only a smectic A mesophase, while the complex with [Li⁺]/[EO] = 0.20 shows an optical isotropic cubic phase in addition to a high-temperature smectic A phase. The complex with [Li⁺]/[EO] = 0.25 exhibits only a bicontinuous cubic phase, and the smectic A phase is suppressed for this complex. On melting of complexes with [Li⁺]/[EO] = 0.30 and 0.35, a cubic phase is also formed; however, further heating gives rise to a 2-D hexagonal columnar mesophase as evidenced by X-ray scattering. Complexes with [Li⁺]/[EO] = 0.40–0.70 exhibit only a columnar phase. As shown in the binary phase diagram of Figure 21, the supramolecular structure in the melt state of the rod-coil molecule changes successively from smectic A through bicontinuous cubic to hexagonal columnar structures as the salt concentration increases.

Complexation of rod-coil molecules with LiCF₃SO₃ also induces an ordered supramolecular structure.⁷⁸

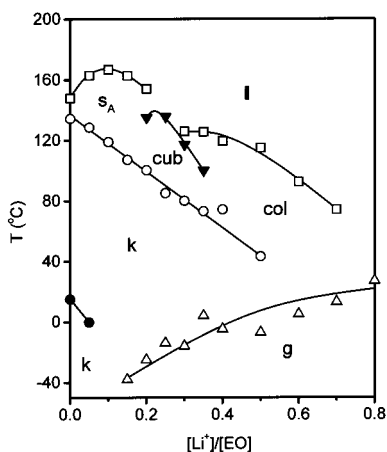


Figure 21. Phase diagram of the complexes of **8** with lithium triflate (g = glassy, k = crystalline, s_A = smectic A, cub = cubic, col = columnar, i = isotropic).

The coil-rod-coil triblock molecule (**17**) based on poly(propylene oxide) (PPO) coil segment was observed to show only an isotropic liquid upon melting. In contrast, the addition of greater than 0.10 mol of lithium salt/propylene oxide (PO) unit induces the formation of a liquid crystalline order (Figure 22).

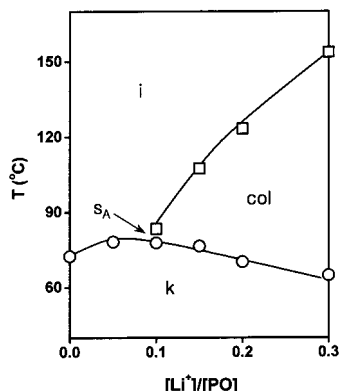


Figure 22. Phase diagram of the complexes of **17** with lithium triflate (k = crystalline, s_A = smectic A, col = hexagonal columnar, i = isotropic).

The complex with $[Li^+]/[PO] = 0.10$ exhibits a crystalline melting transition followed by a smectic A mesophase. By increasing the salt concentration as in the case of complexes with $[Li^+]/[PO] = 0.15 \sim 0.30$, the smectic A phase is suppressed; instead, they exhibit a hexagonal columnar mesophase as evidenced by X-ray scattering. The induction of ordered structure in the melt state of the rod-coil molecule by complexation is most probably due to enhanced microphase separation between hydrophobic blocks and poly(propylene oxide) block caused by transformation from a dipolar medium to an ionic medium in poly(propylene oxide) coil.

Rod-coil molecular architecture containing poly(ethylene oxide) endows an amphiphilic character as discussed earlier, and thus hydrophilic solvents such as acryl amide would be selectively dissolved in the microphase-separated coil domains, which gives rise to a variety of supramolecular structures. Polymerization of acryl amide solution in ordered state can give rise to ordered nanocomposite materials. Similar

to rod-coil complexes with $LiCF_3SO_3$,⁷⁷ the acryl amide solution of a rod-coil molecule (**18**) was reported to show a phase transition from layered smectic to columnar phase with a bicontinuous cubic phase as the intermediate regime with increasing acryl amide content (Figure 23).⁸⁰ More importantly,

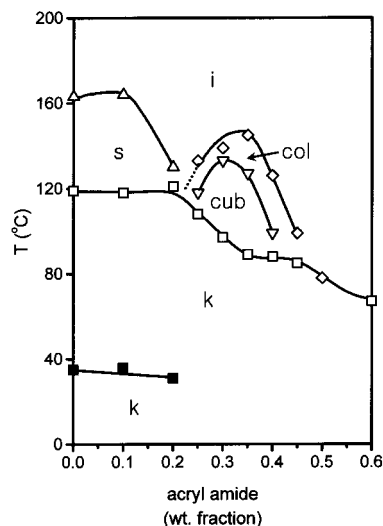


Figure 23. Phase diagram of **18** with acryl amide (k = crystalline, s = smectic, cub = bicontinuous cubic, col = hexagonal columnar, i = isotropic).

this organized polymerizable solution can be used for construction of ordered aromatic-aliphatic nanocomposite materials. Thermal polymerization of the hexagonally ordered solution containing acryl amide and 0.5 mol % of 2,2'-azobisisobutyronitrile with respect to acryl amide at 130 °C for 24 h was observed to produce a hexagonally ordered nanocomposite material with a primary spacing of 4.8 nm as monitored by FT-IR and small-angle X-ray scattering. As illustrated in Figure 24, the acryl amide would be selectively dissolved by hydrophilic PEO coil

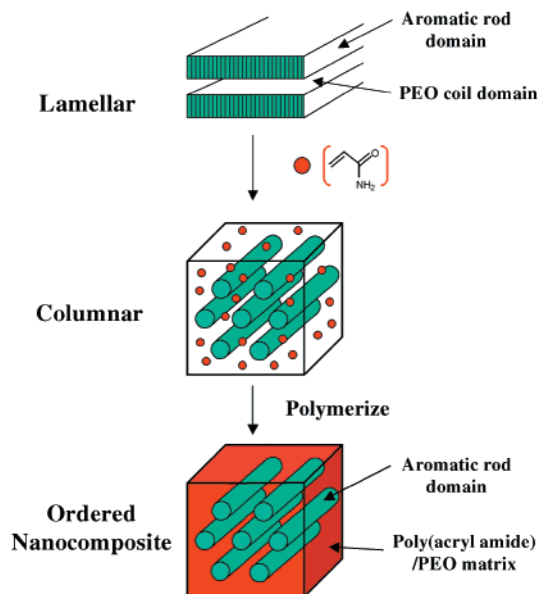


Figure 24. Schematic diagram for the induction of a hexagonal columnar structure by addition of acryl amide and subsequent formation of ordered nanocomposite through polymerization.

domains in a lamellar structure, creating a spontaneous interfacial curvature between the rod and PEO/acryl amide which induces a hexagonal columnar structure. Upon polymerization, the system retains the hexagonally ordered nanostructure consisting of aromatic rod domains in a poly(acryl amide)/PEO matrix to construct ordered aromatic–aliphatic nanocomposite.

Kato et al. reported on rod–coil–rod molecules consisting of rigid mesogenic cores and flexible poly(ethylene oxide) coils.⁸¹ The small triblock molecule (**19**) (Chart 6) was observed to exhibit smectic A liquid crystalline phase as determined by a combination of optical polarized microscopy and differential scanning calorimetry. The incorporation of LiCF_3SO_3 into the rod–coil–rod molecules shows significant mesophase stabilization. X-ray diffraction patterns revealed that complexation of **19** ($[\text{Li}^+]/[\text{EO}] = 0.05$) drastically reduces the layer spacing from 44 to 23 Å. This decrease is thought to be due to the interaction of the lithium salt with the ether oxygen which results in a more coiled conformation of the poly(ethylene oxide) coil. Ion conductivities were also measured for complexes forming homeotropically aligned molecular orientation of the smectic phase. Interestingly, the highest conductivity was observed for the direction parallel to the layer (Figure 25).

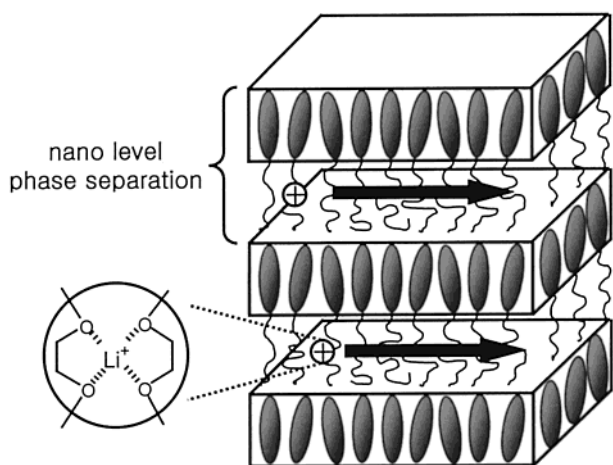
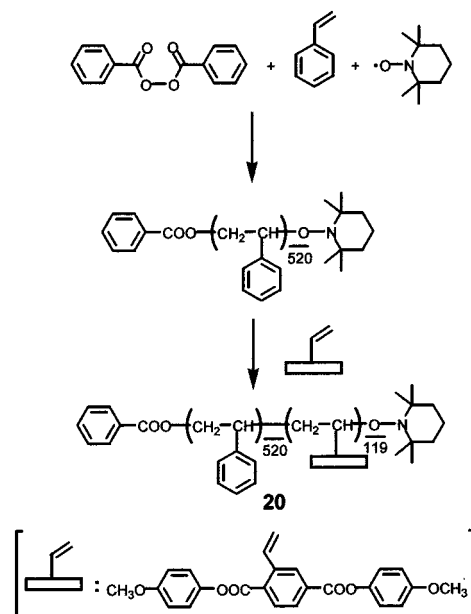


Figure 25. Schematic representation of Li^+ ion conduction for the complex of **19** with $[\text{Li}^+]/[\text{EO}] = 0.05$ in smectic A phase.

However, the conductivities decrease in the polydomain sample which disturbs the arrangement of ion paths. These results suggest that the self-organized rod–coil salt complexes can provide access to a novel strategy to construct ordered nanocomposite materials exhibiting low dimensional ionic conductivity.

Wu et al. reported on a rod–coil diblock copolymers based on mesogen-jacketed liquid crystalline polymer as the rod block and polystyrene as the coil block (Scheme 6).⁸² Styrene was polymerized by TEMPO mediated radical polymerization, followed by sequential polymerization of 2,5-bis[4-methoxyphenyl]oxycarbonylstyrene (MPCS) to produce the rod–coil diblock copolymer (**20**) containing 520 styrene and 119 MPCS repeating units. The rod–coil copolymer was observed to self-assemble into a core–shell nanostructure in a selective solvent for polystyrene

Scheme 6



block when the solution was cooled from 110 °C to room temperature as determined by a combination of static and dynamic laser light scattering studies. Interestingly, the average number of chains assembled in each nanostructure increases with the copolymer concentration in a selective solvent, different from the self-assembly of conventional diblock copolymers, whereas the size of the core remains a constant, very close to the contour length of the mesogen-jacketed rod block, but the shell becomes thicker (Figure 26). This observation may indicate

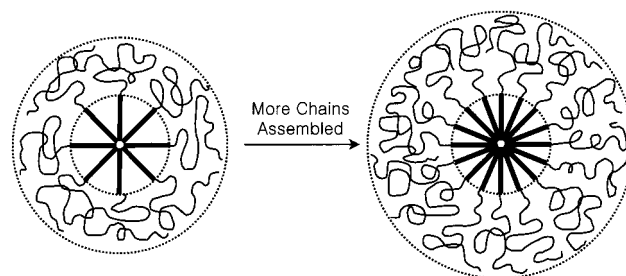


Figure 26. Schematic representation of a core–shell nanostructure formed by a self-assembly of **20** in a selective solvent.

that the attraction between the insoluble rigid-like mesogen-jacketed polymer blocks lead to their insertion into the core, while the repulsion between the soluble coil-like polystyrene blocks forces them to stretch at the interface.

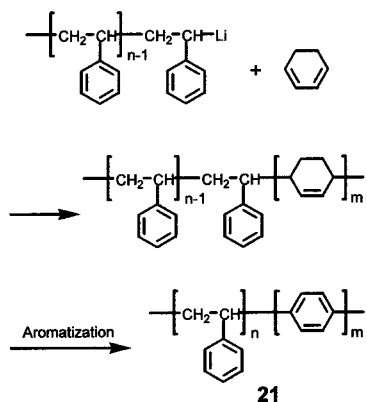
V. Rod–Coil Copolymers Based on Conjugated Rods

As a result of great interest in the optically and electronically active properties of highly conjugated and stiff rodlike molecules, a variety of oligomers and polymers have been synthesized to establish the molecular structure and property relationship.^{83,84} In addition to molecular structure, supramolecular structure was reported to have a dramatic effect on the

physical properties of conjugated rodlike molecules.^{85,86} Thus, manipulation of supramolecular structure in conjugated rods is of paramount importance to achieving efficient optophysical properties in solid-state molecular materials. One way to manipulate the supramolecular structure might be incorporation of the conjugated rod into a rod-coil molecular architecture which would allow formation of well-defined one-, two-, or three-dimensional conjugated domains in nanoscale dimensions. In this section, we will discuss on the studies of rod-coil systems based on well-defined conjugated rods. Synthetic strategies toward rod-coil copolymers involve either polymerization using a macroinitiator or grafting of two preformed conjugated blocks.

A monofunctionized segment may be used as macroinitiator to prepare rod-coil polymeric architecture as described Francois et al. (Scheme 7).⁸⁷⁻⁹³ The

Scheme 7



authors prepared polystyrene macroinitiator by living anionic polymerization. After sequential polymerization of styrene and then cyclohexadiene, a polystyrene-*block*-poly(cyclohexa-1,3-diene) was obtained and subsequently aromatized with *p*-chloranil to yield the corresponding oligo(*p*-phenylene) grafted to a polystyrene chain. Although the aromatization was not complete, the authors discovered special non-equilibrium honeycomb morphologies in which monodispersed pores arrange in a hexagonal array by evaporating the solvent from CS₂ solution in moist air (Figure 27). This novel morphology was proposed to be due to micelle formation. Interestingly, the presence of defects in the oligo(*p*-phenylene) sequence does not have a significant effect on honeycomb morphology. The authors also reported on the synthesis of polystyrene-polythiophene block and graft copolymers.⁹⁴⁻⁹⁷ These polymers incorporate the unique properties of polythiophene with processability. The reported block copolymers showed nearly the same spectral characteristics as pure polythiophene, and the authors proved that their block copolymers are still soluble after doping.

Rod-coil molecules containing structurally perfect conjugated rods were synthesized by using α -(phenyl)- ω -(hydroxymethyl phenyl)-poly(fluoren-2,7-ylene) as macroinitiator (Scheme 8).⁹⁸ Anionic polymerization of ethylene oxide by using the macroinitiator produced a corresponding rod-coil block copolymer (**22**). The absorption and emission measurements of

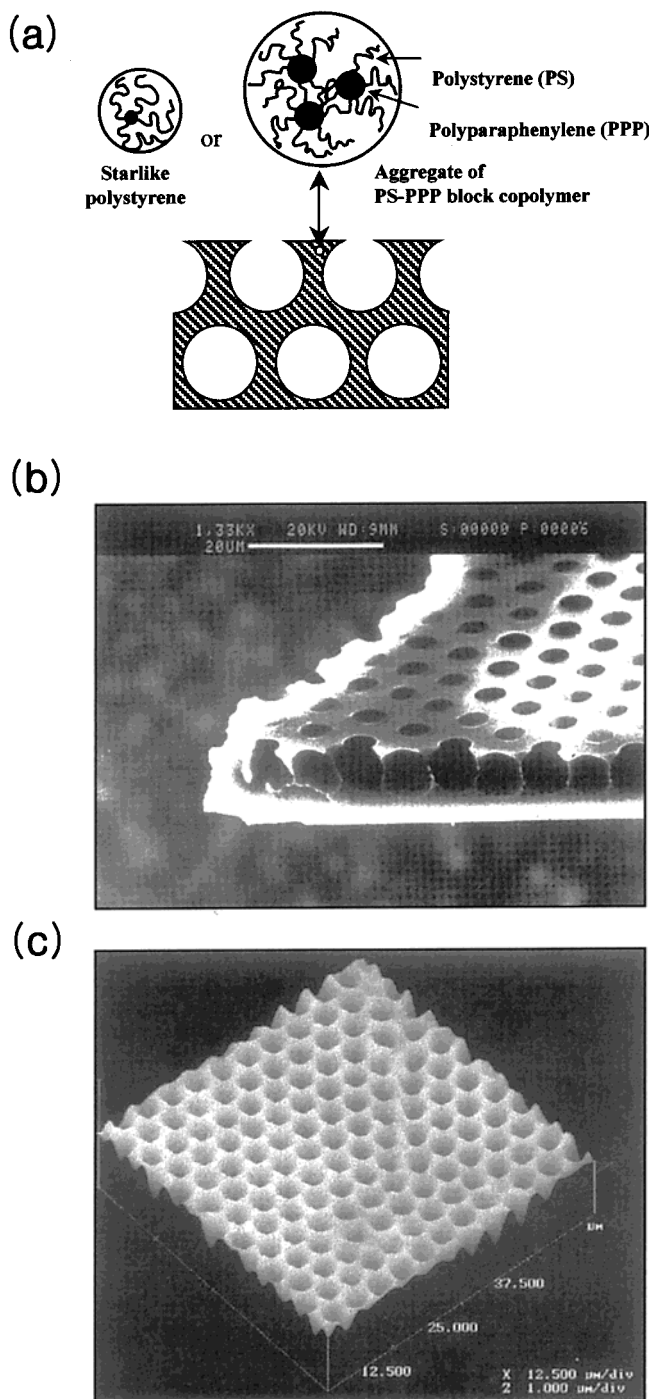
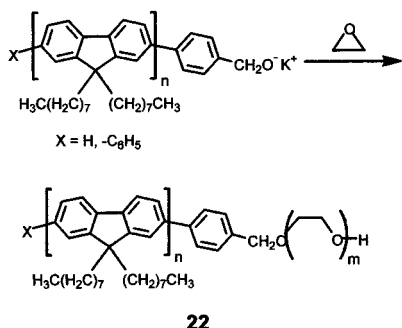


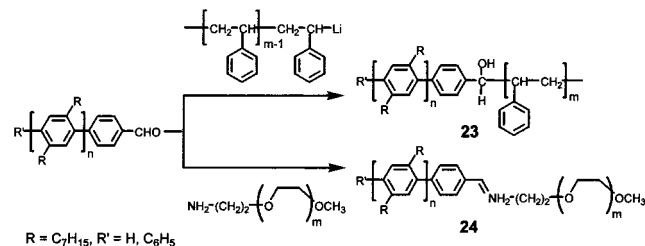
Figure 27. (a) Schematic representation for the cross section, (b) SEM image, and (c) AFM image of a honeycomb structure with a regular micropore in rod-coil copolymer **21**. (Reprinted with permission from Nature (<http://www.nature.com>), ref 93. Copyright 1994 Macmillan Magazines Ltd.).

this rod-coil copolymer revealed the influence of the coil blocks on the optoelectronic properties of the rod segments. The coupling reaction of preformed rod and coil blocks was also used to prepare a rod-coil block copolymer. Müllen et al. prepared perfectly end-functionalized oligo(2,5-diheptyl-*p*-phenylenes) (Scheme 9).⁹⁹ Further reaction of the end functionalized rod with either polystyrene or poly(ethylene oxide) yielded corresponding luminescent rod-coil block copolymers (**23** and **24**, respectively). Rod-coil copolymers consisting of poly(*p*-phenyleneethynylene) as the rod

Scheme 8



Scheme 9



block and poly(ethylene oxide) as the coil block (**25**) were also synthesized by coupling reaction of mono-functionalized rod to poly(ethylene oxide) (Chart 7).¹⁰⁰ More recently, the synthesis of triblock poly(isoprene-*block-p*-phenyleneethynylene-*block*-isoprene) (**26**) was reported by Godt et al. by using hydroxy functionalized polyisoprene (Chart 7).¹⁰¹

Lazzaroni et al. showed that rod-coil copolymers containing poly(*p*-phenylene) or poly(*p*-phenylene-ethynylene) as the rod segments have a strong tendency to spontaneously assemble into stable ribbonlike fibrillar morphology when coated on mica substrate as evidenced by AFM images.¹⁰² The ribbonlike supramolecular structure was proposed that in the first observed layer, the conjugated segments are packed according to a head-to-tail arrangement with their conjugated system parallel to each other surrounded by coil segments (Figure 28). A similar ribbonlike morphology was also observed from rod-coil copolymers consisting of poly(*p*-phenylene) as the rod block and poly(methyl methacrylate) as the coil block.¹⁰³

Hempenius et al. reported on a polystyrene-oligothiophene-polystyrene triblock rod-coil copolymer (Scheme 10).¹⁰⁴ The authors employed a polystyrene with a phenolic terminus that was modified

Chart 7

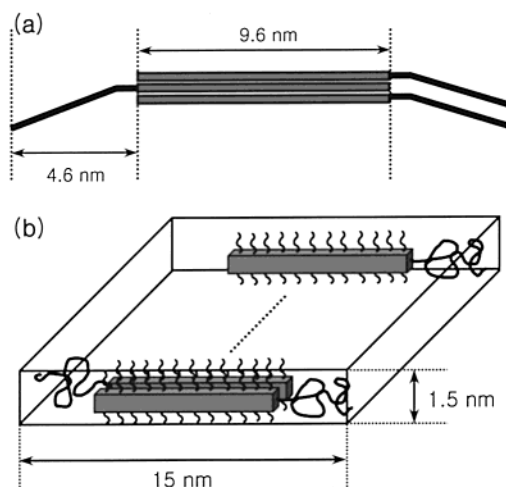
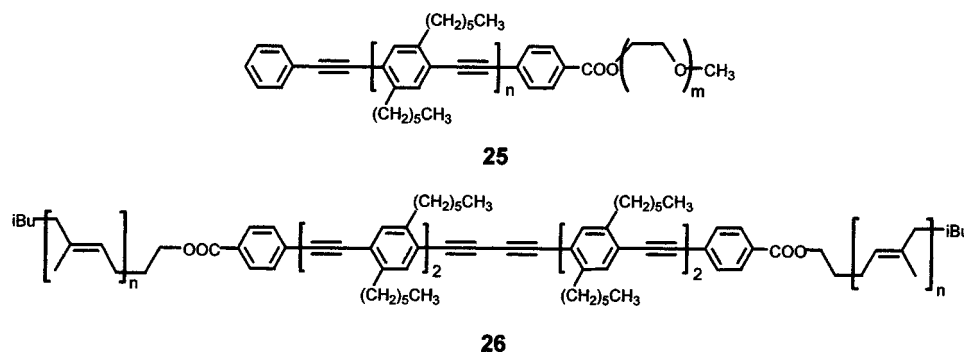


Figure 28. (a) Schematic molecular arrangement of three head-to-tail PPE-*block*-PDMS. (b) Schematic representation of the ribbonlike supramolecular structure formed by PPE-*block*-PDMS.

by an α -terthiophene unit, followed by a coupling reaction to yield a well-defined rod-coil triblock copolymer (**27**). Scanning force microscopy (SFM) revealed the formation of nonspherical micelles with axes of about 10 and 14 nm, corresponding to an aggregate of about 60 rod-coil molecules, consistent with the results determined from GPC (Figure 29). The optical properties were shown to be consistent with those of corresponding unsubstituted oligothiophenes.

Yu et al. reported on the synthesis of rod-coil block copolymers containing oligo(phenylene vinylene)s coupled to either polyisoprene (**28**) or poly(ethylene glycol) (**29**) (Chart 8).^{105,106} The first one was obtained by reaction of a living anionic polyisoprene derivative with oligo(phenylene vinylene)s containing an aldehyde group.¹⁰⁵ Four copolymers that have the same oligo(phenylene vinylene) block with different polyisoprene volume fractions were synthesized. TEM and small-angle X-ray scattering revealed alternating strips of rod-rich and coil-rich and coil-rich domains, and the domain sizes of the strips suggested that the supramolecular structures could be bilayer lamellar structure (Figure 30). On the other hand, it could be observed that as the conjugation length increases, the processability of the molecule decreases dramatically, thus limiting the length of the conjugated segment to be used in the coupling reaction. To solve the solubility problem, the authors modified the synthetic

Scheme 10

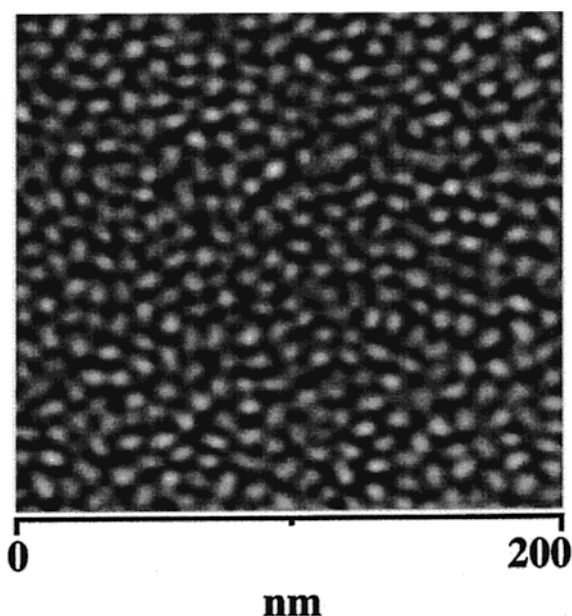
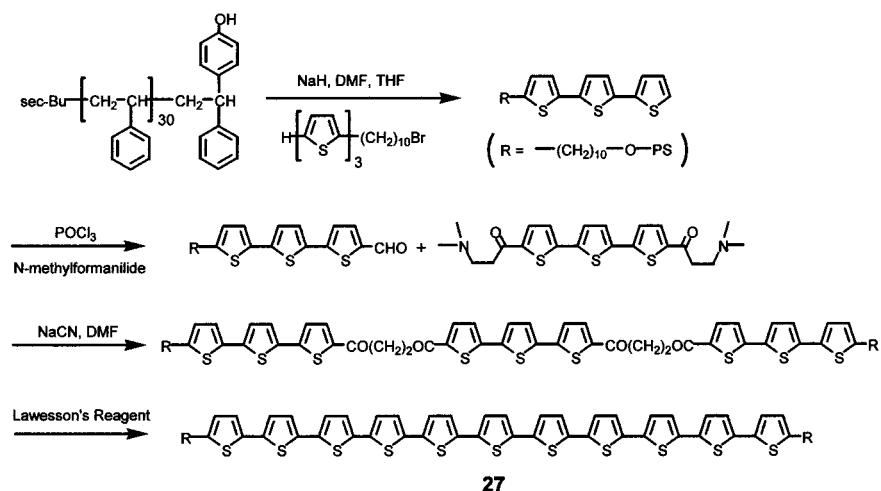
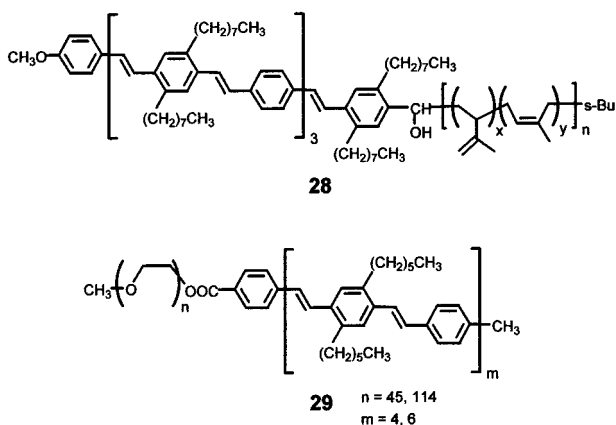


Figure 29. SFM image of nonspherical micelles formed by rod-coil triblock copolymer **27**. (Reprinted with permission from ref 104. Copyright 1998 American Chemical Society).

Chart 8



strategy by first coupling with poly(ethylene oxide) coil block with a oligo(phenylene vinylene) followed by coupling of the functionalized rod-coil copolymer.¹⁰⁶ The resulting block copolymer was subse-

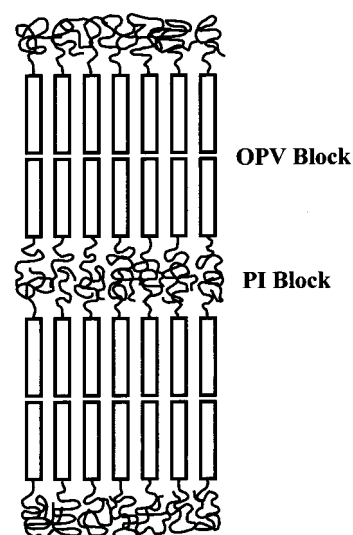


Figure 30. Proposed model for the bilayer structure of **28**.

quently coupled with oligo(phenylene vinylene) containing a vinyl end functional group to yield final rod-coil copolymers (**29**) with larger conjugated block (Chart 8). These rod-coil copolymers were observed to have remarkable self-assembling properties, and long cylindrical micelles are formed. TEM and AFM studies showed that the core of the micelles formed by **29** with $n = 45$ and $m = 6$ has a diameter of about 8–10 nm and is composed of a conjugated block surrounded by a poly(ethylene oxide) coil block (Figure 31).

Jenekhe et al. reported on the self-assembling behavior of rod-coil diblock copolymers consisting of poly(phenylquinoline) as the rod block and polystyrene as the coil block (Scheme 11).^{107,108} The rod-coil copolymers (**30**) were prepared by condensation reaction of ketone methylene-terminated polystyrene and 5-acetyl-2-aminobenzophenone in the presence of diphenyl phosphate. The degree of polymerization of the conjugated rod block in the rod-coil copolymers was controlled by the stoichiometric method. These block copolymers were found to self-assemble into fascinating supramolecular structures, although the rod block might not be monodisperse. For example, a rod-coil copolymer consisting of poly(phenylquino-

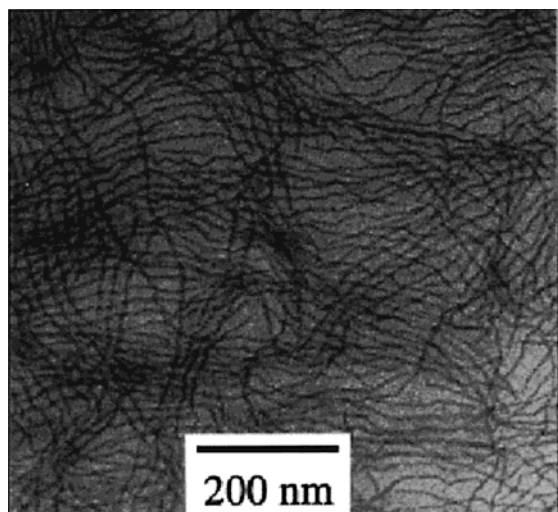
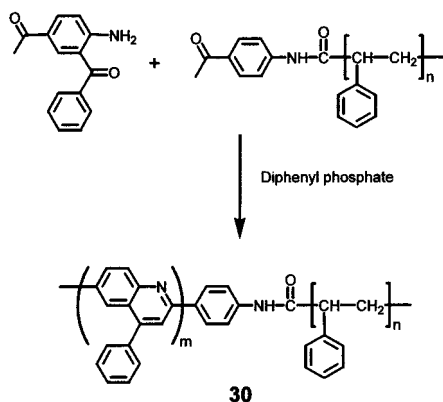


Figure 31. TEM image of long cylindrical micelles formed by **29** with $n = 45$ and $m = 6$. (Reprinted with permission from ref 106. Copyright 2000 American Chemical Society).

Scheme 11



line) with a degree of polymerization of 50 of polystyrene with degree of polymerization of 300 was observed to aggregate in the form of hollow spheres, lamellar, hollow cylinders, and vesicles in a selective solvent for the rod segment. The observed shape of supramolecular structures was dependent on the type of solvent mixture and drying rate. Photoluminescence emission and excitation studies showed that the photophysical properties strongly depend on the supramolecular structure of π -conjugated rod segments. Interestingly, their rod-coil systems proved to be possible for encapsulating fullerenes into the spherical cavities. As compared to conventional solvent for C_{60} , such as dichloromethane or toluene, the solubility is enhanced by up to 300 times when the molecules are encapsulated into micelles. In a further study, the authors observed that these rod-coil copolymers in a selective solvent for the coil segment self-assemble into hollow spherical micelles with diameters of a few micrometers, which subsequently self-organize into a 2-dimensional hexagonal superlattice (Figure 32).¹⁰⁹ Solution-cast micellar films were found to consist of multilayers of hexagonally ordered arrays of spherical holes whose diameter, periodicity, and wall thickness depend on copolymer molecular weight and block composition.

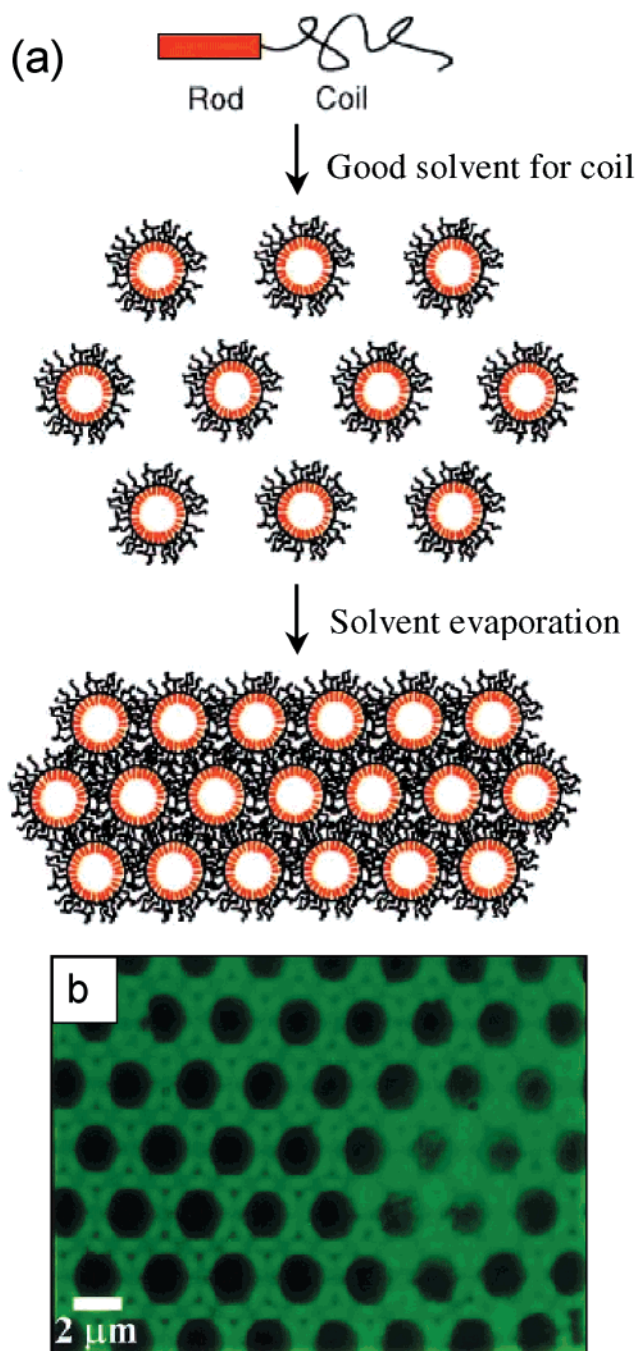


Figure 32. (a) Schematic representation of hierarchical self-organization of **30** into ordered microporous structure. (b) Fluorescence photomicrograph of solution-cast micellar film of **30** with $m = 10$ and $n = 300$. (Reprinted with permission from ref 109. Copyright 1999 American Association for the Advancement of Science).

The authors also reported on the supramolecular self-assembly from rod-coil-rod triblock copolymers prepared by copolymerization of 5-acetyl-2-aminobenzophenone with diacetyl functionalized polystyrene with low polydispersity (Scheme 12).¹¹⁰ In contrast to the rod-coil diblock copolymers which exhibit multiple morphologies, the triblock copolymers were found to spontaneously form only microcapsules or spherical vesicles in solution as evidenced by optical polarized, fluorescence optical, and scanning electron microscopies (Figure 33).

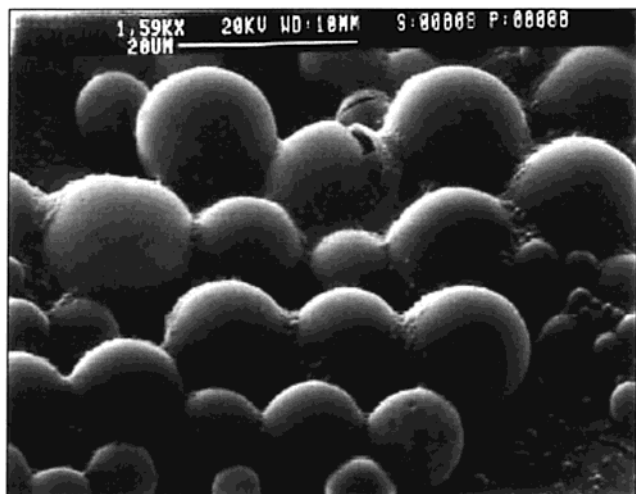
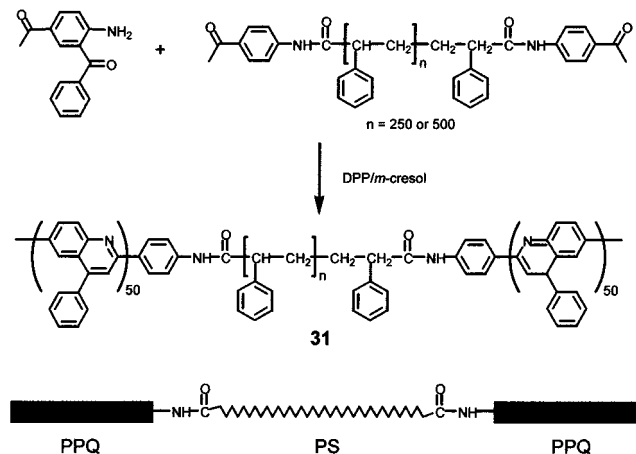


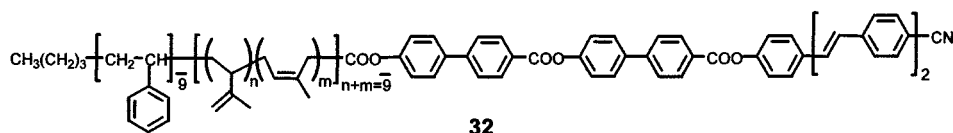
Figure 33. SEM image of microcapsules formed by **31** with $n = 250$. (Reprinted with permission from ref 110. Copyright 2000 American Chemical Society).

Scheme 12



As previously described, Stupp et al. reported on supramolecular materials formed by molecules with triblock architecture that self-organize into discrete mushroom-shaped nanostructures.^{58–60} To introduce optical functionalities, they synthesized rod–coil triblock molecules containing oligo(phenylene vinylene) (**32**) by reaction of functionalized rod–coil triblock molecules with hydroxy functionalized oligo(phenylene vinylene) building blocks (Chart 9).^{111,112} The cyano-substituted phenylene vinylene building block imparts fluorescence properties to these molecules and increases drastically their dipole moment. The nanostructured materials obtained contain thousands of molecular layers organized with polar ordering and give rise to strong photoluminescence. The authors also showed that supramolecular films composed of these dipolar rod–coil molecules self-organize into polar macroscopic materials showing piezoelectric activity.¹¹³

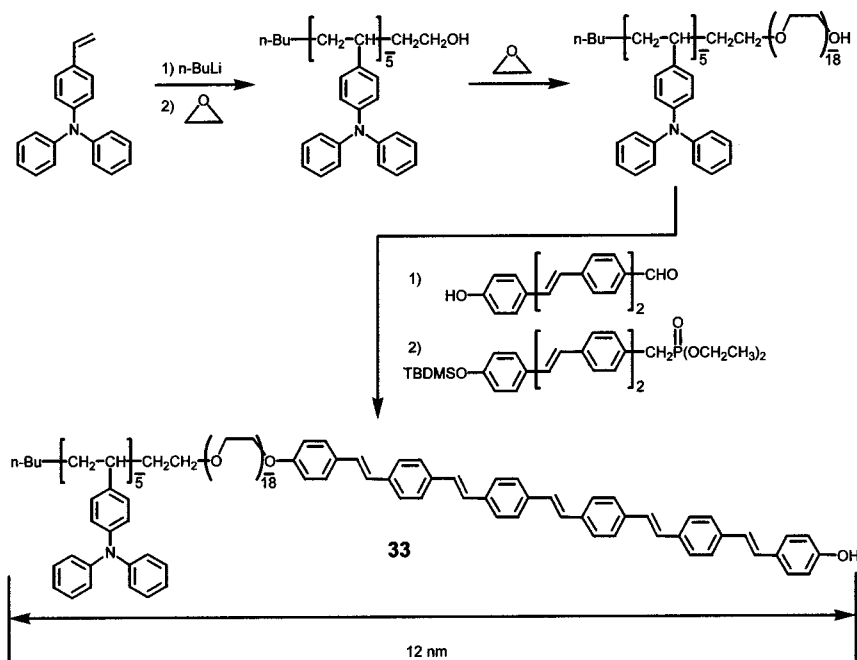
Chart 9



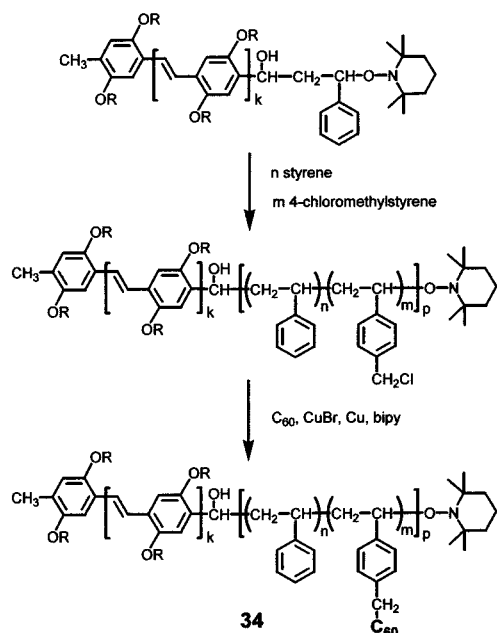
In addition, they have incorporated these supramolecular materials into triphenylamine moieties that are of interest as hole transport layers in light emitting devices.¹¹⁴ As shown in Scheme 13, living anionic polymerization of triphenylamine derivative followed by quenching with ethylene oxide afforded a hydroxy functionalized triphenylamine oligomer. The subsequent polymerization of this oligomer with ethylene oxide produced the diblock copolymer. Reaction of the resulting hydroxy terminated polymer with difunctionalized oligo(phenylene vinylene) produced a triblock copolymer endowed with an aldehyde functionality, which was further reacted with another oligo(phenylene vinylene) derivative with a Wittig–Horner reaction. Deprotection of the *tert*-butyl dimethylsilyl group yielded a triblock rod–coil copolymer containing a terminal hydroxy polar group (**33**). TEM revealed that these block molecules self-assemble into discrete nanostructures and electron diffraction indicated that this material contains crystalline domains with rod segments oriented perpendicular to the plane of the film, being both ethylene oxide segments and TPA segments contained in amorphous matrix. The emission spectra of **33** using 302 nm as the excitation wavelength showed substantial emission from conjugated rod segments and additional optical studies suggested that energy transfer occurs between the coil-like triphenylamine and rod-like conjugated segments of these molecules.

Hadziioannou et al. reported on the synthesis of a donor–acceptor, rod–coil diblock copolymer with the objective of enhancing the photovoltaic efficiency of the poly(phenylenevinylene)-C₆₀ system by incorporation of both components in a rod–coil molecular architecture that is self-assembling through microphase separation (Scheme 14).¹¹⁵ These rod–coil copolymers were obtained by using an end-functionalized rigid-rod block of poly(2,5-dioctyloxy-1,4-phenylene vinylene) as a macroinitiator for the nitroxide-mediated controlled radical polymerization of a flexible poly(styrene-stat-chloromethylstyrene) block. The chloromethyl group in the polystyrene block was subsequently transformed into C₆₀ onto the flexible polystyrene segment through atom transfer radical addition to yield the final rod–coil polymer (**34**) based on poly(phenylene vinylene) and C₆₀. Photoluminescence decay studies indicated that the luminescence from conjugated poly(phenylene vinylene) is quenched vigorously, suggesting efficient electron transfer as the donor–acceptor interface occurs. Films obtained through a coating process from CS₂ solution exhibit micrometer-scale, honeycomb-like aggregation structure (Figure 34). The porous character of the rod–coil materials was reported to be used as a template for the formation of a two-dimensional hexagonal array of functional dots.^{116,117}

Scheme 13



Scheme 14



VI. Conclusions

There is no doubt that manipulation of supramolecular architectures of rodlike polymers and their low molar mass homologues is of critical importance to achieving desired functions and properties in molecular materials. The incorporation of different rodlike segments such as helical rods, low molar mass mesogenic rods and conjugated rods as a part of the main chain in rod-coil molecular architecture has already proven to be an effective way to manipulate supramolecular structures in nanoscale dimensions. Depending on the relative volume fraction of rigid and flexible segments, and the chemical structure of these segments, rod-coil copolymers and their low molar mass homologues self-assemble into a variety of supramolecular structures through the combina-

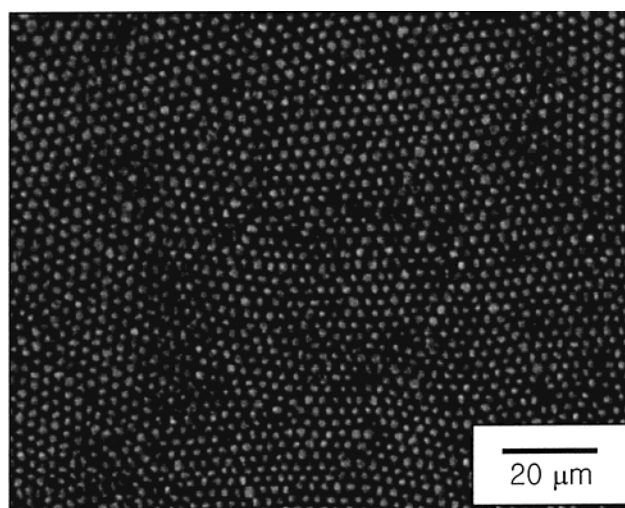


Figure 34. Optical transmission micrograph of honeycomb structures formed by **34**. (Reprinted with permission from ref 115. Copyright 2000 American Chemical Society).

tion of shape complementarity and microphase separation of rod and coil segments as an organizing force. The supramolecular structures assembled by rod segments in rod-coil systems include sheets, cylinders, finite nanostructures, and even perforated sheets that organize into 1-D, 2-D, and 3-D superlattices, respectively. It should be noted that self-assembly can be used to prepare well-defined macromolecular nano-objects that are not possible to prepare by conventional synthetic methodologies, when the rod-coil copolymers self-assemble into discrete supramolecular structures.

Another remarkable feature of rod-coil copolymers is their amphiphilic characteristics that show the tendency of their lipophilic and lipophobic parts to segregate in space into distinct microdomains. Depending on the solvent content and polarity, rod-coil copolymers self-assemble into a wide variety of different supramolecular structures. Because of the

covalent linkage of the amphiphilic segments, segregation does not lead to macroscopic separation. Instead, it results in the formation of different regions which are separated by interfaces at a molecular scale. This amphiphilic feature allows rod-coil copolymers to construct low dimensional ionic conductive nanomaterials as well as ordered nanocomposite materials.

It would be of interest to synthesize rod-coil copolymers based on conjugated rods that can self-assemble into a variety of supramolecular structures with unique optical and electronic properties because manipulation of supramolecular structures with different functionalities is of paramount importance to achieving desired physical properties of molecular materials. In this respect, many synthetic strategies have been developed that allow the incorporation of functional rod segments in well-defined rod-coil architectures for specific properties. Electron transfer, second harmonic generation, and piezoelectricity have been reported for supramolecular structures of rod-coil copolymers containing conjugated rods or highly polar end groups.^{59,111,113-115} Many more rod-coil systems are expected to be developed soon for possible applications as diverse as molecular materials for nanotechnology, supramolecular reactor, periodic porous materials, transport membrane, and biomimic materials.

VII. Acknowledgments

We gratefully acknowledge the financial support by CRM-KOSEF (2001), Korea Science and Engineering Foundation (R03-2001-00034), and the BK 21 fellowship (CBK).

VIII. References

- Whitesides, G. M.; Mathias, J. P.; Seto, C. P. *Science* **1991**, *254*, 1312.
- Lehn, J. M. *Supramolecular Chemistry*; VCH: Weinheim, Germany, 1995.
- Muthukumar, M.; Ober, C. K.; Thamas, E. L. *Science* **1997**, *277*, 1225.
- Föster, S.; Antonietti, M. *Adv. Mater.* **1998**, *10*, 195.
- Israelachvili, J. N. *Intermolecular and Surface Forces*; Academic Press: London, 1992.
- Collings, P. J.; Hird, M. *Introduction to Liquid Crystals*; Taylor & Francis: London, 1997.
- Stegemeyer, H. *Liquid Crystals*; Springer: New York, 1994.
- Bates, F. S.; Fredrickson, G. H. *Annu. Rev. Phys. Chem.* **1990**, *41*, 525.
- Hashimoto, T.; Shibayama, M.; Kawai, H. *Macromolecules* **1983**, *16*, 1093.
- Helfand, E.; Wasserman, Z. R. *Macromolecules* **1980**, *13*, 994.
- Leibler, L. *Macromolecules* **1980**, *13*, 1602.
- Semenov, A. N.; Vasilenko, S. V. *Sov. Phys. JETP S. V.* **1986**, *63* (1), 70.
- Semenov, A. N. *Mol. Cryst. Liq. Cryst.* **1991**, *209*, 191.
- Semenov, A. N.; Subbotin, A. V. *Sov. Phys. JETP A. V.* **1992**, *74* (4), 690.
- Williams, D. R. M.; Fredrickson, G. H. *Macromolecules* **1992**, *25*, 3561.
- Stupp, S. I. *Curr. Opin. Colloid Interface Sci.* **1998**, *3*, 20.
- Mao, G.; Ober, C. K. *Handbook of Liquid Crystals-Vol. 3: High Molecular Weight Liquid Crystals*; Wiley-VCH: Weinheim, 1998.
- Gallot, B. *Prog. Polym. Sci.* **1996**, *21*, 1035.
- Loos, K.; Munoz-Guerra, S. *Supramolecular Polymers-Chapter 7: Microstructure and Crystallization of Rigid-Coil Comblike Polymers and Block Copolymers*; Marcel Dekker: New York, 2000.
- Hamley, I. W.; Koppi, K. A.; Rosedale, J. H.; Bates, F. S.; Almdal, K.; Mortensen, K. *Macromolecules* **1993**, *26*, 5959.
- Hajduk, D. A.; Harper, P. E.; Gruner, S. M.; Honecker, C. C.; Kim, G.; Thomas, E. L.; Fetters, L. J. *Macromolecules* **1994**, *27*, 4063.
- Bates, F. S.; Schulz, M. F.; Khandpur, A. K.; Förster, S.; Rosedale, J. H.; Almdal, K.; Mortensen, K. *Faraday Discuss., Chem. Soc.* **1994**, *98*, 7.
- Khandpur, A. K.; Förster, S.; Bates, F. K.; Hamley, I. W.; Ryan, A. J.; Bras, W.; Almdal, K.; Mortensen, K. *Macromolecules* **1995**, *28*, 8796.
- Fredrickson, G. H.; Liu, A. J.; Bates, F. S. *Macromolecules* **1994**, *27*, 2503.
- (a) Matsen, M. W.; Schick, M. *Macromolecules* **1994**, *27*, 4014. (b) Milner, S. T. *Macromolecules* **1994**, *27*, 2333.
- Vavasour, J. D.; Whitmore, M. D. *Macromolecules* **1993**, *26*, 7070.
- Matsen, M. W.; Bates, F. S. *J. Polym. Sci. B: Polym. Phys.* **1997**, *35*, 945.
- Onsager, L. *Ann. N. Y. Acad. Sci.* **1949**, *51*, 627.
- Flory, P. J. *J. Chem. Phys.* **1949**, *17*, 303.
- de Gennes, P. G.; Prost, J. *The Physics of Liquid Crystals*, 2nd ed.; Oxford University Press: New York, 1993.
- Demus, D.; Goodby, J.; Gray, G. W.; Spiess, H. W.; Vill, V. *Handbook of Liquid Crystals, Vol. 1: Fundamentals*; Wiley-VCH: New York, 1998.
- Meier, D. J. *J. Polym. Sci.* **1969**, *C26*, 81.
- Matsen M. W.; Bates F. S. *Macromolecules* **1996**, *29*, 1091.
- Müller, M.; Schick, M. *Macromolecules* **1996**, *29*, 8900.
- Matsen, M. W.; Barrett, C. J. *Chem. Phys.* **1998**, *109*, 4108.
- Halperin, A. *Europhys. Lett.* **1989**, *10*, 549.
- Halperin, A. *Macromolecules* **1990**, *23*, 2724.
- Raphael, E.; de Gennes, P. G. *Makromol. Symp.* **1992**, *62*, 1.
- Zhang, G.; Fournier, M. J.; Mason, T. L.; Tirrell, D. A. *Macromolecules* **1992**, *25*, 3601.
- Yu, S. M.; Conticello, V. P.; Zhang, G.; Kayser, C.; Fournier, M. J.; Mason, T. L.; Tirrell, D. A. *Nature* **1997**, *389*, 167.
- Perly, B.; Douy, A.; Gallot, B. *Makromol. Chem.* **1976**, *177*, 2569.
- Billot, J.-P.; Douy, A.; Gallot, B. *Makromol. Chem.* **1977**, *178*, 1641.
- Douy, A.; Gallot, B. *Polymer* **1987**, *28*, 147.
- Klok, H.-A.; Langenwalter, J. F.; Lecommandoux, S. *Macromolecules* **2000**, *33*, 7819.
- Berger, M. N. *J. Macromol. Sci. Rev. Macromol. Chem.* **1973**, *C9* (2), 269.
- Bur, A. J.; Fetters, L. J. *Chem. Rev.* **1976**, *76* (6), 727.
- Fetters, L. J.; Yu, H. *Macromolecules* **1971**, *4*, 385.
- Aharoni, S. M. *Macromolecules* **1979**, *12*, 94.
- Aharoni, S. M.; Walsh, E. K. *Macromolecules* **1979**, *12*, 271.
- Aharoni, S. M. *J. Polym. Sci., Polym. Phys. Ed.* **1980**, *18*, 1439.
- Chen, J. T.; Thomas, E. L.; Ober, C. K.; Hwang, S. S. *Macromolecules* **1995**, *28*, 1688.
- Chen, J. T.; Thomas, E. L.; Ober, C. K.; Mao, G. *Science* **1996**, *273*, 343.
- Thomas, E. L.; Chen, J. T.; O'Rourke, M. J.; Ober, C. K.; Mao, G. *Macromol. Symp.* **1997**, *117*, 241.
- Wu, J.; Pearce, E. M.; Kwei, T. K. *Macromolecules* **2001**, *34*, 1828.
- Radzilowski, J. L.; Wu, J. L.; Stupp, S. I. *Macromolecules* **1993**, *26*, 879.
- Radzilowski, J. L.; Stupp, S. I. *Macromolecules* **1994**, *27*, 7747.
- Radzilowski, J. L.; Carragher, B. O.; Stupp, S. I. *Macromolecules* **1997**, *30*, 2110.
- Stupp, S. I.; Lebonheur, V.; Walker, K.; Li, L. S.; Huggins, K. E.; Keser, M.; Amstutz, A. *Science* **1997**, *276*, 384.
- Pralle, M. U.; Whitaker, C. M.; Braun, P. V.; Stupp, S. I. *Macromolecules* **2000**, *33*, 3550.
- Zubarev, E. R.; Pralle, M. U.; Li, L.; Stupp, S. I. *Science* **1999**, *283*, 523.
- Zubarev, E. R.; Pralle, M. U.; Sone, E. D.; Stupp, S. I. *J. Am. Chem. Soc.* **2001**, *123*, 4105.
- Lee, M.; Oh, N.-K. *J. Mater. Chem.* **1996**, *6*, 1079.
- Lee, M.; Oh, N.-K.; Zin, W.-C. *Chem. Commun.* **1996**, 1788.
- Lee, M.; Cho, B.-K.; Kim, H.; Zin, W.-C. *Angew. Chem., Int. Ed.* **1998**, *37*, 638.
- Lee, M.; Cho, B.-K.; Kim, H.; Yoon, J.-Y.; Zin, W.-C. *J. Am. Chem. Soc.* **1998**, *120*, 9168.
- Lee, M.; Cho, B.-K.; Ihn, K.-J.; Oh, N.-K.; Zin, W.-C. *J. Am. Chem. Soc.* **2001**, *123*, 4647.
- Lee, M.; Lee, D.-W.; Cho, B.-K.; Yoon, J.-Y.; Zin, W.-C. *J. Am. Chem. Soc.* **1998**, *120*, 13258.
- Lee, M.; Cho, B.-K.; Jang, Y.-G.; Zin, W.-C. *J. Am. Chem. Soc.* **2000**, *122*, 7449.
- (a) Lee, M.; Cho, B.-K.; Kang, Y.-S.; Zin, W.-C. *Macromolecules* **1999**, *32*, 7688. (b) Lee, M.; Cho, B.-K.; Kang, Y.-S.; Zin, W.-C. *Macromolecules* **1999**, *32*, 8531.
- Lee, M.; Cho, B.-K.; Oh, N.-K.; Zin, W.-C. *Macromolecules* **2001**, *34*, 1987.
- (a) Vilgis, T.; Halperin, A. *Macromolecules* **1991**, *24*, 2090. (b) Ji, S.-H.; Oh, N.-K.; Lee, M.; Zin, W.-C. *Polymer* **1997**, *38*, 4377.
- Thatcher, J. H.; Thanappapras, K.; Nagae, S.; Mai, S.-M.; Booth, C.; Owen, J. R. *J. Mater. Chem.* **1994**, *4*, 591.
- Le Nest, J. F.; Ghandini, A.; Schönenberger, C. *Trends Polym. Sci.* **1994**, *2*, 32.

- (74) Dias, F. B.; Voss, T. P.; Batty, S. V.; Wright, P. V.; Ungas, G. *Macromol. Rapid Commun.* **1994**, *15*, 961.
- (75) Percec, V.; Heck, J.; Johansson, G.; Tomazos, D.; Ungar, G. *Macromol. Symp.* **1994**, *77*, 237.
- (76) Lee, M.; Oh, N.-K.; Choi, M.-G. *Polym. Bull.* **1996**, *37*, 511.
- (77) Lee, M.; Oh, N.-K.; Lee, H.-K.; Zin, W.-C. *Macromolecules* **1996**, *29*, 5567.
- (78) Lee, M.; Cho, B.-K. *Chem. Mater.* **1998**, *10*, 1894.
- (79) Kang, Y. S.; Zin, W.-C.; Lee, D. W.; Lee, M. *Liq. Cryst.* **2000**, *27*, 2543.
- (80) Lee, M.; Jang, D.-W.; Kang, Y.-S.; Zin, W.-C. *Adv. Mater.* **1999**, *11*, 1018.
- (81) Ohtake, T.; Ogasawara, M.; Ito-Akita, K.; Nishina, N.; Ujie, S.; Ohno, H.; Kato, T. *Chem. Mater.* **2000**, *12*, 782.
- (82) Tu, Y.; Wan, X.; Zhang, D.; Zhou, Q.; Wu, C. *J. Am. Chem. Soc.* **2000**, *122*, 10201.
- (83) Kraft, A.; Grimsdale, A. C.; Holmes, A. B. *Angew. Chem., Int. Ed.* **1998**, *37*, 402.
- (84) Segura, J. L.; Martin, N. *J. Mater. Chem.* **2000**, *10*, 2403.
- (85) Osaheni, J. A.; Jenekhe, S. A. *J. Am. Chem. Soc.* **1995**, *117*, 7389.
- (86) Berresheim, A. J.; Müller, M.; Müllen, K. *Chem. Rev.* **1999**, *99*, 1747.
- (87) Zhong, X. F.; Francois, B. *Macromol. Chem. Rapid Commun.* **1998**, *9*, 411.
- (88) Zhong, X. F.; Francois, B. *Synth. Met.* **1989**, *29*, E35.
- (89) Zhong, X. F.; Francois, B. *Macromol. Chem.* **1990**, *191*, 2735.
- (90) Zhong, X. F.; Francois, B. *Macromol. Chem.* **1990**, *191*, 2743.
- (91) Zhong, X. F.; Francois, B. *Macromol. Chem.* **1991**, *192*, 2277.
- (92) Zhong, X. F.; Francois, B. *Synth. Met.* **1991**, *41*, 955.
- (93) Widawski, G.; Rawiso, M.; Francois, B. *Nature* **1994**, *369*, 387.
- (94) Francois, B.; Pitois, O.; Francois, J. *Adv. Mater.* **1995**, *7*, 1041.
- (95) Olinga, T.; Francois, B. *Macromol. Chem. Rapid Commun.* **1991**, *12*, 575.
- (96) Olinga, T.; Francois, B. *J. Chim. Phys., Phys. Chim. Biol.* **1992**, *89*, 1079.
- (97) Francois, B.; Olinga, T. *Synth. Met.* **1993**, *57*, 3489.
- (98) Marsitzky, D.; Klapper, M.; Müllen, K. *Macromolecules* **1999**, *32*, 8685.
- (99) Marsitzky, D.; Brand, T.; Geerts, Y.; Klapper, M.; Müllen, K. *Macromol. Rapid Commun.* **1998**, *19*, 385.
- (100) Francke, V.; Räder, H. J.; Müllen, K. *Macromol. Rapid Commun.* **1998**, *19*, 275.
- (101) KuKula, H.; Ziener, U.; Shöps, M.; Godt, A. *Macromolecules* **1998**, *31*, 5160.
- (102) Leclere, P.; Calderone, A.; Marsitzky, D.; Francke, V.; Geerts, Y.; Müllen, K.; Bredas, J. L.; Lazzaroni, R. *Adv. Mater.* **2000**, *12*, 1042.
- (103) Leclere, P.; Parente, V.; Bredas, J. L.; Francois, B.; Lazzaroni, R. *Chem. Mater.* **1998**, *10*, 4010.
- (104) Hempenius, M. A.; Langeveld-Voss, B. M. W.; van Haar, J. A. E. H.; Janssen, R. A. J.; Sheiko, S. S.; Spatz, J. P.; Möller, M.; Meijer, E. W. *J. Am. Chem. Soc.* **1998**, *120*, 2798.
- (105) Li, W.; Wang, H.; Yu, L.; Morkved, T. L.; Jaeger, H. M. *Macromolecules* **1999**, *32*, 3034.
- (106) Wang, H.; Wang, H. H.; Urban, V. S.; Littrell, K. C.; Thiyagarajan, P.; Yu, L. *J. Am. Chem. Soc.* **2000**, *122*, 6855.
- (107) Jenekhe, S. A.; Chen, X. L. *Science* **1998**, *279*, 1903.
- (108) Chen, X. L.; Jenekhe, S. A. *Langmuir* **1999**, *15*, 8007.
- (109) Jenekhe, S. A.; Chen, X. L. *Science* **1999**, *283*, 372.
- (110) Chen, X. L.; Jenekhe, S. A. *Macromolecules* **2000**, *33*, 4610.
- (111) Tew, G. N.; Li, L.; Stupp, S. I. *J. Am. Chem. Soc.* **1998**, *120*, 5601.
- (112) Tew, G. N.; Pralle, M. U.; Stupp, S. I. *J. Am. Chem. Soc.* **1999**, *121*, 9852.
- (113) Pralle, M. U.; Urayama, K.; Tew, G. N.; Neher, D.; Wegner, G.; Stupp, S. I. *Angew. Chem., Int. Ed.* **2000**, *39*, 1486.
- (114) Tew, G. N.; Pralle, M. U.; Stupp, S. I. *Angew. Chem., Int. Ed.* **2000**, *39*, 517.
- (115) Stalmach, U.; de Boer, B.; Videlot, C.; van Hutten, P. F.; Hadziioannou, G. *J. Am. Chem. Soc.* **2000**, *122*, 5464.
- (116) de Boer, B.; Stalmach, U.; Nijland, H.; Hadziioannou, G. *Adv. Mater.* **2000**, *12*, 1581.
- (117) de Boer, B.; Stalmach, U.; Melzer, C.; Hadziioannou, G. *Synth. Met.* **2001**, *121*, 1541.

CR0001131

Convergent Dendrons and Dendrimers: from Synthesis to Applications

Scott M. Grayson and Jean M. J. Fréchet*

Department of Chemistry, University of California, Berkeley, California 94720-1460

Received March 5, 2001

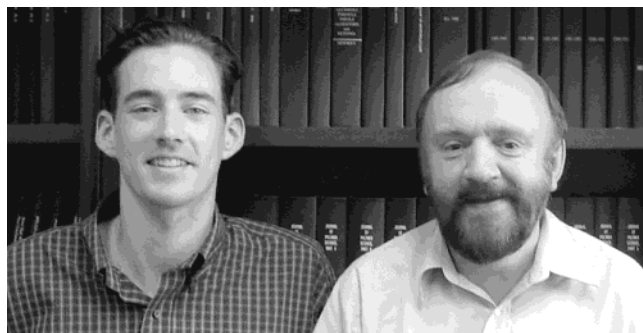
Contents

I. Introduction	3819	C. Applications of Peripheral Modification	3850
A. Structure	3820	V. Modification of Repeat Unit	3854
B. Applications	3821	A. Incorporating Monomer with Functionality.	3854
C. Synthetic Approaches	3821	B. Postsynthetic Modification of Repeat Unit	3855
1. Divergent Approach	3821	Functionality	
2. Convergent Approach	3822	VI. Dendritic Copolymers	3855
D. Features of the Convergent Synthesis	3823	A. Layered Copolymers	3856
1. Structural Purity	3823	B. Segmented Copolymers	3857
2. Synthetic Versatility	3823	C. Tailored Copolymers	3858
II. Convergent Synthesis of Dendrons and Dendrimers	3824	VII. Conclusion	3860
A. Single-Stage Convergent Syntheses	3824	VIII. Acknowledgments	3861
1. Poly(aryl ether) Dendrimers	3824	IX. Glossary	3861
2. Poly(aryl alkyne) Dendrimers	3826	X. References	3862
3. Poly(phenylene) Dendrimers	3827		
4. Poly(alkyl ester) Dendrimers	3827		
5. Poly(aryl alkene) Dendrimers	3828		
6. Poly(alkyl ether) Dendrimers	3828		
7. Other Convergent Dendrimer Syntheses	3829		
B. Accelerated Approaches	3829		
1. Multigenerational Coupling: Hypercores, Hypermonomers, and Double Exponential Growth	3830		
2. Orthogonal Syntheses	3832		
III. Modification of the Focal Functionality	3835		
A. Traditional Covalently Bound Cores	3835		
1. Environmentally Responsive Cores: Dendritic Probes	3837		
2. Chiral Cores	3838		
3. Host–Guest Core Binding Sites	3839		
4. Core Catalytic Sites	3840		
5. Photochemically Responsive Cores	3841		
6. Fluorescent Cores	3842		
7. Redox-Active Cores	3842		
8. Other Core Functionalities	3843		
B. Linear–Dendritic Copolymers	3843		
C. Dendronized Linear Polymers	3844		
1. Macromonomer Approach	3844		
2. “Coupling to” Approach	3846		
D. Self-Assembly of Dendritic Cores	3847		
E. Surface-Bound Dendrons	3848		
IV. Modification of the Periphery	3849		
A. Introduction of End Groups Prior to Dendritic Growth	3849		
B. Introduction of End Groups after Completion of Dendritic Growth	3849		

I. Introduction

Dendrimers represent a key stage in the ongoing evolution of macromolecular chemistry. From the origins of polymer chemistry until 20 years ago, a major focus had been the synthesis and characterization of linear polymers. Although the molecular interactions and the many conformations of linear polymers involve three dimensions, their covalent assembly is strictly a one-dimensional process. Half a century ago, in theoretical studies, Flory was among the first to examine the potential role of branched units in macromolecular architectures,^{1,2} but it was not until the mid-1980s that methods for the orderly preparation of these polymers had been sufficiently developed to enable their practical study. In 1978, Vögtle developed an iterative cascade method for the synthesis of low molecular weight branched amines.³ Using chemistry and conditions less prone to cyclization side-reactions and therefore more suitable for repetitive growth, Tomalia et al. disclosed the synthesis and characterization of the first family of dendrimers in 1984–1985.^{4,5} The synthesis was initiated by Michael addition of a “core” molecule of ammonia to three molecules of methyl acrylate, followed by exhaustive amidation of the triester adduct using a large excess of ethylenediamine, a process that generates a molecule with six terminal amine groups. Iterative growth is then continued using alternating Michael addition and amidation steps with the appropriate excess of reagents. Optimization of this procedure enabled the synthesis of globular poly(amidoamine) (PAMAM) dendrimers on a commercial scale with molecular weights well above 25 000. Shortly thereafter, in 1985, Newkome reported preliminary results toward another family of trisbranched polyamide dendrimers,⁶ and in 1993,

* Corresponding author. E-mail: frechet@cchem.berkeley.edu.



Scott M. Grayson (left) was born in 1974 in St. Louis, Missouri. He studied at Tulane University in New Orleans and graduated summa cum laude with a BS in Chemistry in 1996. After completing his M.Phil. in Archaeological Chemistry at the University of Bradford (Bradford, U.K.), under the guidance of Prof. Carl Heron, he returned to the US to pursue doctoral studies in chemistry. He is presently researching the applications of dendritic architectures with Professor Jean M. J. Fréchet at the University of California, Berkeley.

Jean M. J. Fréchet (right) obtained his first degree at the Institut de Chimie et Physique Industrielles (now CPE) in Lyon, France, and Ph.D. degrees at SUNY-CESF and Syracuse University. Following academic appointments at the University of Ottawa (1973–1986) and Cornell University (1987–1996), he joined the department of chemistry at the University of California, Berkeley. Fréchet is a member of the National Academy of Science, the National Academy of Engineering, and the American Academy of Arts and Sciences. His research is concerned with functional polymers from their design and synthesis to their applications.

improvements on Vögtle's original synthesis were disclosed by Meijer and Mülhaupt that enabled the production of poly(propylene imine) (PPI) dendrimers.^{7,8} In 1989–1990, Hawker and Fréchet introduced the convergent growth approach to dendrimers,^{9,10} the second general route to dendritic structures, and the primary subject of this review. Since these seminal reports, thousands of papers have been written about the synthesis, properties, and applications of dendrimers, and a diverse range of complex macromolecules have been assembled, capitalizing on the unique architecture of dendritic molecules and the properties they confer.^{11–28}

A. Structure

There are two basic types of polymers that consist entirely of branched repeat units: dendrimers and hyperbranched polymers. Hyperbranched polymers are usually the product of a noniterative polymerization procedure^{29–31} and therefore exhibit an irregular architecture (Figure 1a) with incompletely reacted branch points throughout the structure.^{17,32,33} Dendrimers, on the other hand, are highly ordered, regularly branched, globular macromolecules prepared by a stepwise iterative approach. Their structure is divided into three distinct architectural regions: (i) a core or focal moiety, (ii) layers of branched repeat units emanating from this core, and (iii) end groups on the outer layer of repeat units (Figure 1b). Dendrimers are differentiated from hyperbranched polymers by their structural perfection, leading to an exact number of concentric layers of branching points, or generations.

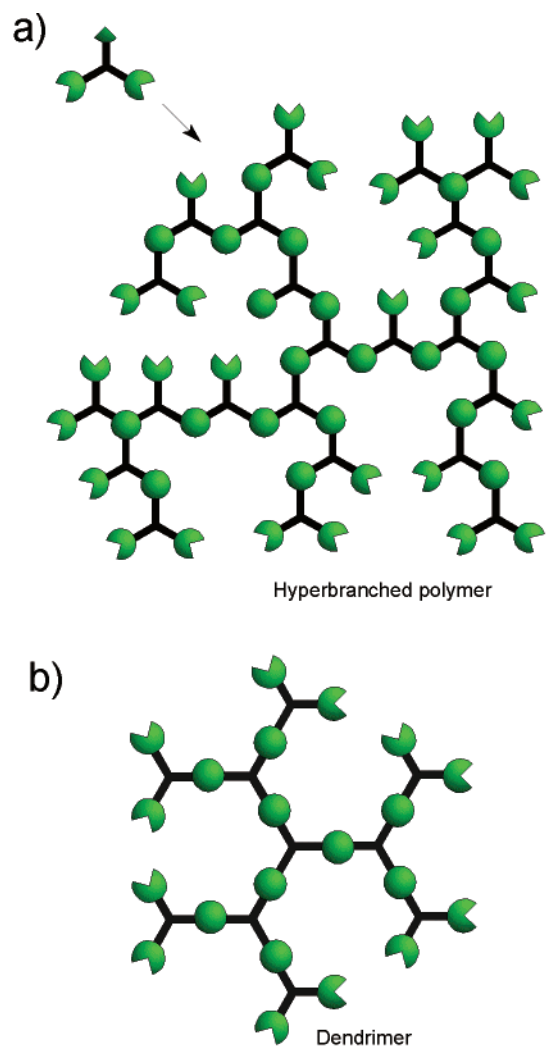


Figure 1.

At least three characteristic features of dendrimers are in sharp contrast to those of traditional linear polymers.

(i) A dendrimer can be isolated as an essentially monodisperse single compound, unlike most linear polymers whose synthesis affords a range of molecular species differing in molecular weight (MW). Size monodispersity results from a well-designed iterative synthesis that allows reactions to be driven to completion, side-reactions to be avoided, and in some cases, the dendritic products to be purified at intermediate steps during their growth.

(ii) As their molecular weight increases, the properties of dendrimers (e.g., solubility, chemical reactivity, glass transition temperature) are dominated by the nature of the end groups. Unlike linear polymers that contain only two end groups, the number of dendrimer end groups increases exponentially with generation, and therefore the end-groups frequently become the primary interface between the dendrimer and its environment.

(iii) In contrast to linear polymer growth that, theoretically, can continue ad infinitum barring solubility issues, dendritic growth is mathematically limited. During growth of a dendrimer, the number of monomer units increases exponentially with gen-

eration, while the volume available to the dendrimer only grows proportionally to the cube of its radius. As a result of this physical limitation, dendritic molecules develop a more globular conformation as generation increases. At a certain generation a steric limit to regular growth, known as the De Gennes dense packing³⁴ is reached. Growth may be continued beyond de Gennes dense packing but this leads to irregular dendrimers incorporating structural flaws.

B. Applications

Because of their well-defined, unique macromolecular structure, dendrimers are attractive scaffolds for a variety of high-end applications. Their highly branched, globular architecture gives rise to a number of interesting properties that contrast those of linear polymers of analogous molecular weight.^{35–39} When compared to linear analogues, dendrimers demonstrate significantly increased solubility^{35,36} that can be readily tuned by derivatizing the periphery,⁴⁰ and they also exhibit very low intrinsic viscosities.^{11,37} Unlike linear polymers, properly designed high generation dendrimers exhibit a distinct “interior” that is sterically encapsulated within the dendrimer, enabling applications as unimolecular container molecules.⁴¹ For example, Meijer et al. have described an elegant “dendritic box” that can encapsulate various small organic molecules and control their release by modifying the steric crowding of the dendritic periphery.⁴² Synthetic approaches have been developed that allow the functionalization of both the interior and exterior of these versatile macromolecules enabling them to operate as transition state catalysts with high turnover.⁴³ The encapsulation of function²⁸ provided by dendrimers has been utilized in a variety of light-harvesting,⁴⁴ emission,⁴⁴ and amplification⁴⁵ functions. Among many other applications under consideration, the use of dendrimers as components in drug or gene delivery is the object of numerous current studies.^{46–54}

C. Synthetic Approaches

Two complementary general approaches, the divergent and the convergent, have been used for the synthesis of dendrimers.^{15,17}

1. Divergent Approach

The divergent approach, arising from the seminal work of Tomalia and Newkome, as well as the branched model work of Vögtle, initiates growth at what will become the core of the dendrimer and continues outward by the repetition of coupling and activation steps (Figure 2). Reaction of the peripheral functionalities of the core with the complementary reactive group of the monomer introduces a new latent branch point at each coupling site and results in an increase in the number of peripheral functionalities (Figure 2: coupling step). The peripheral functionalities on each monomer are designed to be inert to focal monomer functionality, thereby pre-

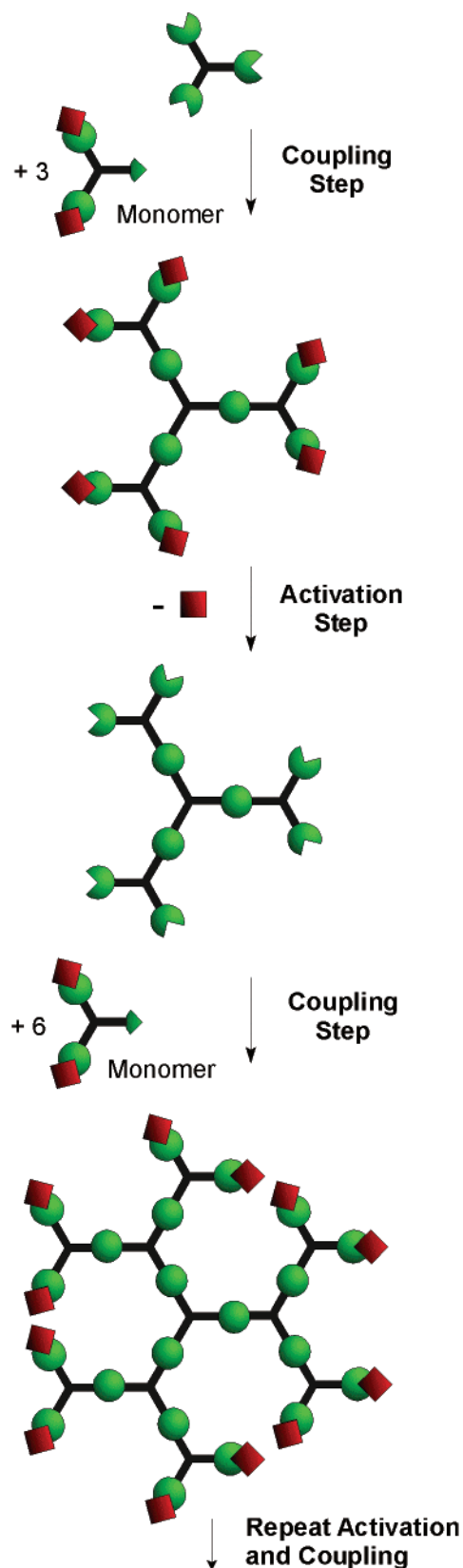


Figure 2.

venting uncontrolled hyperbranched polymerization. After driving the first coupling reaction to completion, these latent functionalities can be activated to afford a new layer of peripheral groups capable of coupling to additional monomer (Figure 2: activation step).

The activation of the peripheral group may involve its conversion to a reactive functionality, its coupling with a second molecule, or the removal of a protecting group. Repetition of the coupling and activation steps leads to an exponential increase in the number of reactions at the periphery; therefore, a large excess of reagents is required to drive both reactions to completion. Because of the difference in molecular weight, it may be possible to separate the macromolecule from the excess reagents by a simple distillation, precipitation, or ultrafiltration.

Given an appropriate choice of coupling and activation steps, reagents, and reaction conditions, the divergent approach is ideally suited for the large-scale preparation of dendrimers as the quantity of dendrimer sample essentially doubles with each generation increment. However, because the number of coupling reactions increases exponentially with each generation, the likelihood of incomplete functionalization or side reaction increases exponentially as well. Although removal of the monomer may be straightforward, any flawed molecules resulting from cyclizations or incomplete reactions cannot easily be removed because of their structural similarity to the intended product. In addition, if the activating agent itself is capable of initiating new growth, rigorous measures must be taken to ensure its complete removal in order to prevent the growth of smaller dendritic impurities. Because of this and the onset of De Gennes dense packing, high generation dendrimers produced using the divergent method, though quite monodisperse when compared to the narrowest polydispersity linear polymers, still contain an appreciable number of structural flaws. Of the many divergent syntheses studied to date, a few appear to be particularly noteworthy. These include Dow's PAMAM^{5,55} and DSM's poly(propylene imine)^{8,56} dendrimers, Newkome's arborols,^{6,57-61} and Majoral's phosphorus-based dendrimers.⁶²⁻⁶⁴

2. Convergent Approach

The convergent method, first reported by Hawker and Fréchet in 1989–1990,^{9,10,65} initiates growth from what will eventually become the exterior of the molecule (Figure 3), and progresses inward by coupling end groups to each branch of the monomer (Figure 3: coupling step). After completion of the coupling, the single functional group located at the focal point of the wedge-shaped dendritic fragment, or dendron, can be activated (Figure 3: activation step). Coupling of this activated dendron to each of the complementary functionalities on an additional monomer unit affords a higher generation dendron. After sufficient repetition of this process, these dendrons can be attached to a polyfunctional core through their focal point to form a globular multidendron dendrimer. Although again an iterative synthesis, the convergent route strongly contrasts its divergent counterpart since it involves only a small number of reactions per molecule during the coupling and activation steps.

Although the molecular weight of the dendron is effectively doubled at each coupling step, the contribution of the monomer to the mass of the product

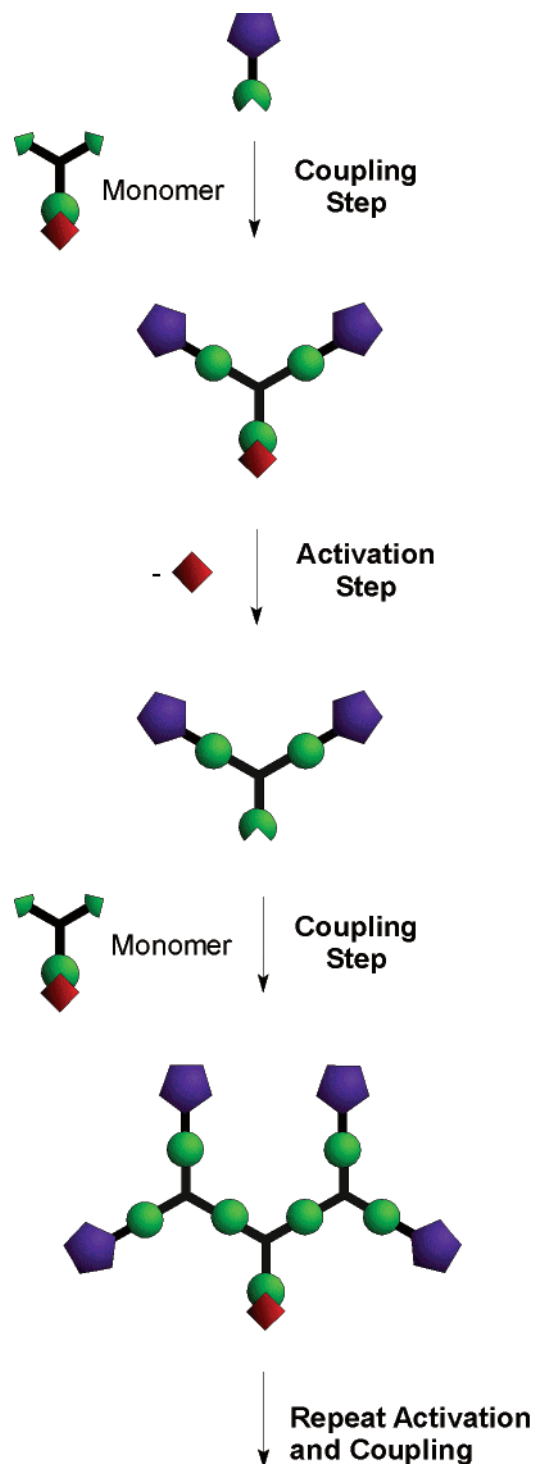


Figure 3.

decreases exponentially as the generation number increases. Since coupling yields are not quantitative and purification results in some losses, the mass of the sample decreases with each additional generation. In addition, because the coupling reaction occurs at the focal point of the growing dendron, the preparation of very large dendrimers (typically above the sixth generation) is complicated by steric inhibition, resulting in decreased yields.

As mentioned earlier, each activation and coupling step in the convergent synthesis requires only a very

small number of transformations per molecule. As a result, the reactions can be driven to completion with only a slight excess of reagent, in contrast to the massive excess of reagent required for the divergent synthesis of high generation dendrimers. Product purification after the coupling step is also facilitated by the very small number of components in the reaction mixture. The dissimilarity between these components enables the effective use of chromatographic purification, ensuring that convergent dendrons are probably the purest synthetic macromolecules prepared to date.

This review will focus on the development of the convergent approach to dendrimers since its conception over a decade ago. In addition to discussing a number of noteworthy convergent syntheses, it will also cover their chemical modification for incorporation of function. The divergent approach, which has provided numerous valuable contributions to the field of functional macromolecules, is beyond the scope of this review and has been covered elsewhere.^{20,22,24,26,28}

D. Features of the Convergent Synthesis

The convergent synthesis with its stepwise assembly of building blocks can be described as the "organic chemist's approach" to dendrimers. It provides greater structural control than the divergent approach due to its relatively low number of coupling reactions at each growth step, allowing access to dendritic products of unmatched purity and functional versatility. The ability to precisely place functional groups throughout the structure, to selectively modify the focal point or the chain ends, and to prepare well-defined unsymmetrical dendrimers are among the most attractive features of the convergent synthesis. Yet because it is less readily scaled up than the divergent synthesis, its commercialization is presently limited to one family of polyether dendrons by Tokyo Kasei Co., Ltd. in Japan.¹⁰

1. Structural Purity

A convenient way to examine sample purity involves the use of matrix-assisted laser desorption ionization time-of-flight mass spectroscopy (MALDI-TOF MS). Figure 4 shows the mass spectrum of a convergently synthesized fifth generation aliphatic polyether dendron. In the mass spectrum, only one peak is observed, corresponding to the mass of the dendron plus a silver cation. The mass spectrum of a purchased sample of divergently prepared fourth generation poly(propylene imine) dendrimer, also displayed in Figure 4, exhibits a measurable amount of defective molecules as the sample could not be purified by chromatography. Detailed mass spectral studies by Meijer and co-workers have identified a number of recurring flaws within the PPI dendrimer synthesis including cyclizations and incomplete couplings. From mass spectral analysis, they approximate the purity of a fourth generation PPI dendrimer to be only 41%.⁶⁶ Although the structural purity obtained from the two approaches varies significantly, depending on the specific conditions employed

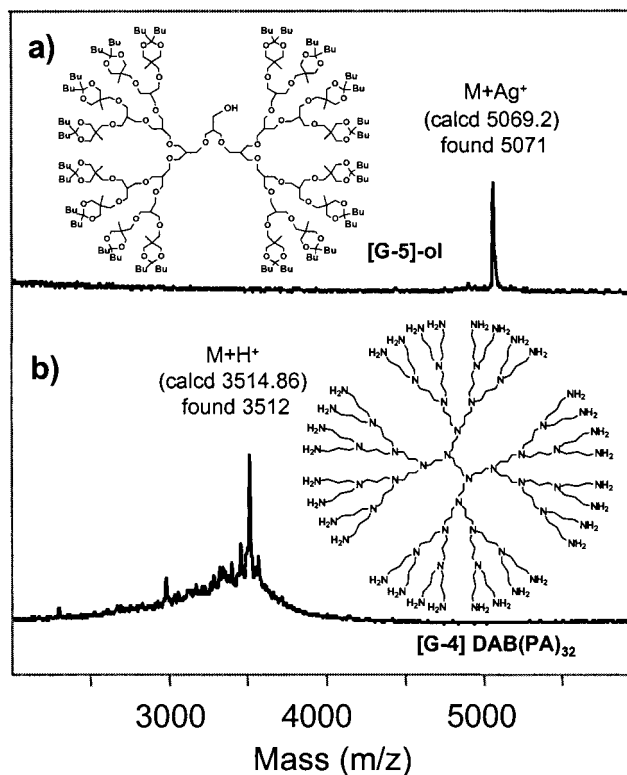


Figure 4.

during synthesis, the divergently prepared samples are generally mixtures of several closely related compounds with an extremely low overall polydispersity,⁶⁷⁻⁶⁹ whereas the convergently prepared materials, with appropriate chromatographic purification, can be isolated essentially as a single molecular species of precise molecular weight and structure.^{70,71}

2. Synthetic Versatility

The convergent approach has seen extensive use in the construction of functional macromolecules because of its ability to modify dendrons at both the focal point and the chain ends. This modularity is especially helpful in design optimization because the same dendritic structure can be modified, after the dendron synthesis, to vary the number and chemistry of functional moieties in the resultant dendrimer.⁷²

In addition, structural variations involving the attachment of chemically different dendrons to a single monomer unit are possible. For example, it is possible to carry out a coupling reaction involving only one of the active functionalities of the monomer (Figure 5). The remaining site may then be coupled with an alternative dendron, affording a dendritic "copolymer." Appropriate variations of the chemistry and sequencing of such unsymmetrical growth enables accurate control over the exact number and placement of different peripheral groups, as well as different monomer units, throughout the dendritic structure. We first demonstrated this capability in 1990 with the preparation of unsymmetrically end-functionalized dendrimers and in 1991 with new types of dendritic copolymers that are not readily obtainable by other approaches.^{73,74}

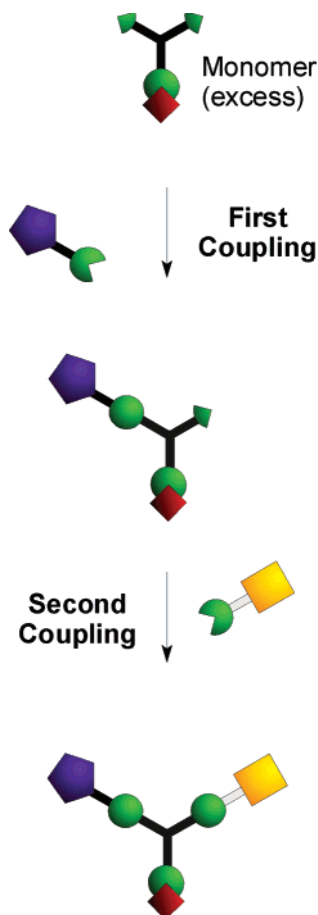


Figure 5.

II. Convergent Synthesis of Dendrons and Dendrimers

In the past decade, a variety of convergent syntheses have been developed, incorporating a wide range of functionalities. While many are imaginative, only a few have proven sufficiently versatile and efficient to see consistent use since they were first reported. By far the most widely used convergent syntheses are the poly(aryl ether), developed by Fréchet and co-workers, and the poly(aryl alkyne) developed by Moore and co-workers. Other noteworthy syntheses include those of the poly(phenylene), the poly(alkyl ester), the poly(aryl alkene), and the poly(alkyl ether) dendrimers. All of these syntheses will be described in more detail below.

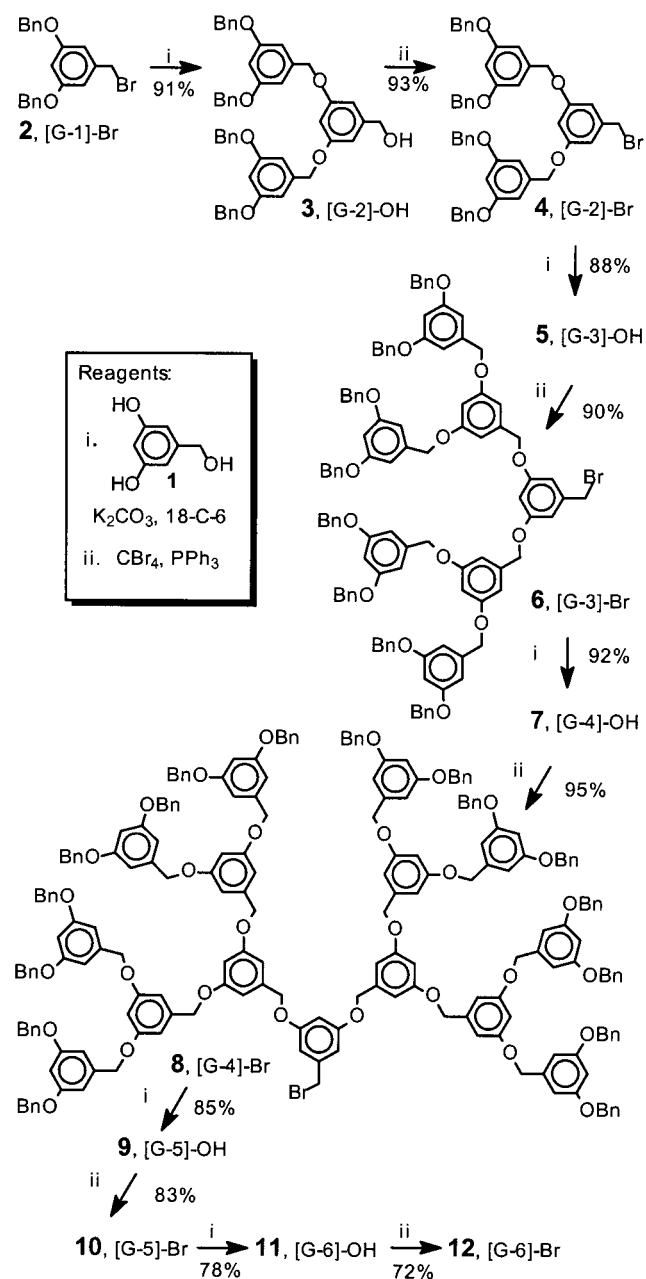
A. Single-Stage Convergent Syntheses

An effective convergent synthesis requires a monomer that can undergo the activation and coupling steps in high yield and whose products can be readily isolated from excess starting material and byproducts. In addition, the coupling step must be very efficient to enable complete reaction even when involving sterically demanding high generation dendrons.

1. Poly(aryl ether) Dendrimers

Developed by Hawker and Fréchet in 1989–1990, the poly(benzyl ether) synthesis^{10,65,75} makes use of 3,5-dihydroxybenzyl alcohol (Scheme 1) as the mono-

Scheme 1

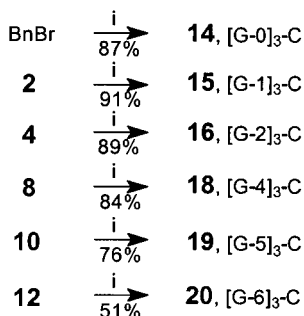
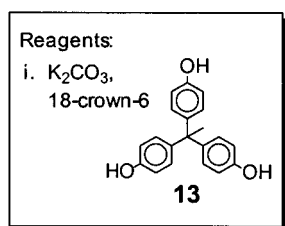
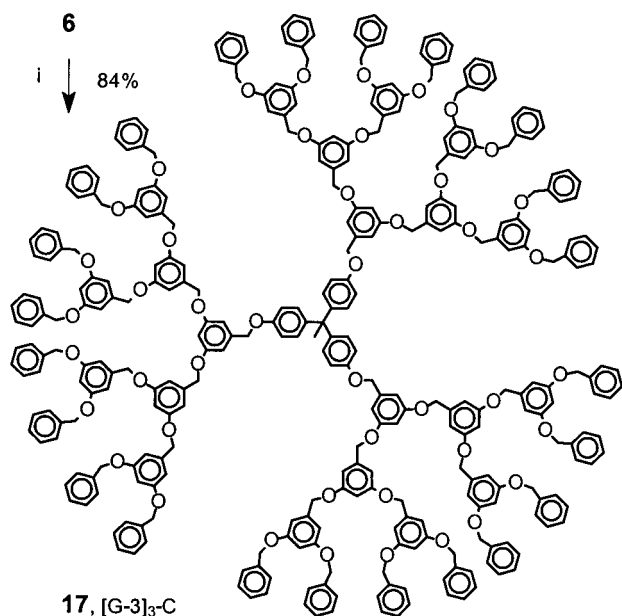


mer **1**. The two phenolic groups of this monomer were coupled to the benzylic bromide **2**, in the presence of potassium carbonate and 18-crown-6, producing the two new ether linkages of the second generation benzylic alcohol **3**. The focal benzylic alcohol functionality was then activated for the next coupling step by reaction with carbon tetrabromide and triphenyl phosphine affording brominated dendron **4**. The coupling step was then repeated using 2 equiv of activated dendron **4** and 1 equiv of the monomer, yielding the third generation benzylic alcohol, **5**. Subsequent repetitions of the Williamson coupling and bromination steps enabled the production of the sixth generation dendrons **11** and **12**. This effective synthesis was designed to incorporate the efficient Williamson coupling reaction between a highly nucleophilic phenolate, and a highly activated benzylic bromide, ensuring exceptional yields during all the generation growth steps. The benzylic substrate also

prevented elimination side reactions that frequently accompany nucleophilic displacements. Similarly, optimization of the activation step from a benzylic alcohol to the benzylic bromide ensured that this reaction could be achieved with consistently high yields. These considerations mandated our initial choice of monomer **1** in order to provide excellent yields and regioselectivity during its activation and coupling reactions.

A clear limitation of the convergent growth is observed when pursuing the synthesis at very high generation number, as steric constraints begin to hinder the coupling step. For example, in the poly(benzyl ether) synthesis depicted in Scheme 1, the yields obtained during the coupling reactions for the first four generations are consistently near 90%, but drop to 85% at the fifth generation coupling step and to 78% at the sixth. All of the dendrons from generation one through six can also be effectively coupled to a tris(phenolic) core **13** to form tridendron dendrimers **14–20**, though an analogous steric effect causes a slight reduction in yields for the larger dendrimers (Scheme 2).

Scheme 2



The poly(benzyl ether) dendrimer synthesis is one of only a few convergent syntheses that can produce dendrons and dendrimers in reasonable yields up to the sixth generation. These dendrons, now frequently referred to as “Fréchet-type” dendrons, have been utilized by a number of groups because they are

relatively readily accessed and exhibit the chemical stability associated with ether linkages.

The versatility of this Williamson type convergent dendritic synthesis can be witnessed by the number of variations (Figure 6) reported on the original

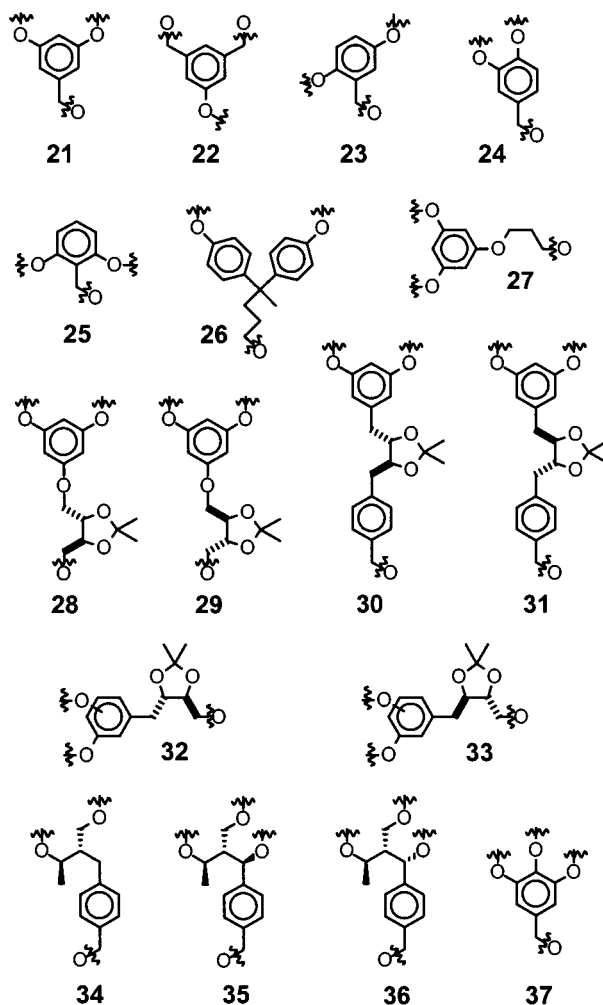


Figure 6.

repeat unit **21**. Tyler et al. reported the use of “reversed” monomer **22**, where the building block instead consists of two benzylic alcohols as the latent electrophiles, and one nucleophilic phenol.^{76,77} Both the Fréchet-type dendrons and these “reversed” dendrons have proven to be of particular interest in light amplification⁴⁵ and light-harvesting systems,^{78–81} because of their complementary behavior in energy transfer through their molecular frameworks. A number of structural variations have been reported on the original 3,5-branching geometry of repeat unit **21**, including 2,5-substitution,⁴⁵ **23**, 3,4-substitution,^{82–85} **24**, and the “backfolded” system⁸⁶ which incorporates monomer **25**. As was the case with the “reversed” dendrons these structural variations lead to significant changes in properties of the resultant dendrons.^{45,82,86} In addition, a range of different leaving groups (chloride, tosylate, and mesylate, as well as bromide) and masked focal functionalities (aldehyde and ester, as well as benzyl alcohol) has enabled further flexibility in the synthesis.

The poly(aryl ether) system can also be easily adapted to incorporate spacer groups. Wooley et al.

first reported the use of the 4,4-bis(4'-hydroxyphenyl)pentanol monomer **26** with identical Williamson coupling and bromination activation procedures, as a more extended, flexible repeat unit designed to reduce problematic steric interaction during the synthesis of large poly(aryl ether) dendrimers.⁸⁷ This goal was realized, as the new dendrons, in conjunction with the traditional poly(benzyl ether) dendrons, led to the first reported convergent synthesis of a seventh generation dendrimer. Chow et al. later reported the synthesis of similar poly(aryl ether) dendrons utilizing a 3-(3,5-dihydroxyphenoxy)propanol as a more extended repeat unit,^{88–90} **27**. Because both of these poly(aryl ether) dendritic structures lack the benzylic ether functionality of the original synthesis, their stability to redox and acidic conditions is believed to be improved. For this reason, the Gorman and Chow groups have used these elongated dendritic structures extensively for the encapsulation of redox-active cores.^{91–95}

To investigate the effect of chirality in dendrimers, a number of groups have incorporated chiral spacers into the poly(aryl ether) repeat unit. Chow et al.^{96–100} modified their dihydroxyphenoxypropanol repeat unit **27** to include the acetonide protected diol spacers: (2*R*,3*R*)- or (2*S*,3*S*)-threitol, **28** and **29**. McGrath and co-workers incorporated similar chiral protected diols **30–33** into their studies,^{101–105} whereas Seebach and co-workers^{106–109} investigated the di- and tribranched chiral monomers **34–36**.

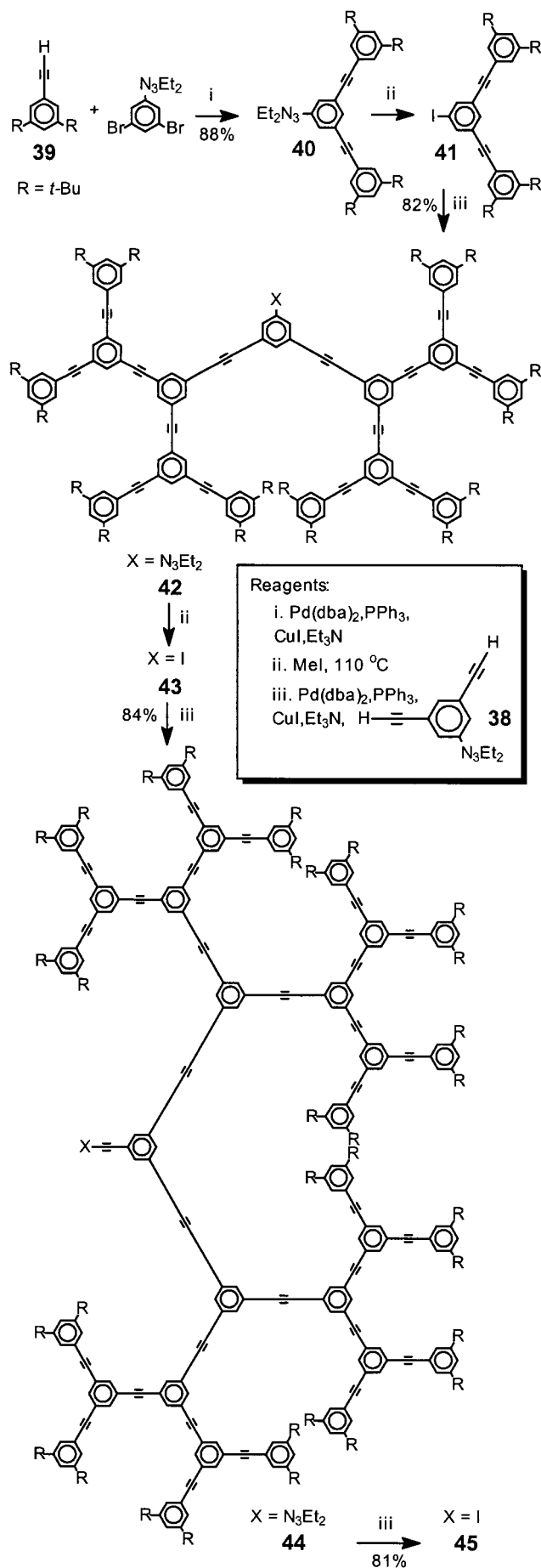
To expedite the synthesis of densely packed dendrons, Percec and co-workers¹¹⁰ have utilized the triply branched monomer **37**, methyl 3,4,5-trihydroxybenzoate.^{84,85,111–113} The materials were synthesized by coupling the phenolic groups of the monomer to 3 equiv of a benzylic chloride, followed by transformation of the focal ester functionality to a chloromethyl group, via LiAlH₄ reduction and SOCl₂ chlorination. This procedure could be repeated up to the fourth generation.

2. Poly(aryl alkyne) Dendrimers

Moore and co-workers have used aryl alkyne, or "phenylacetylene," building blocks to explore a variety of well-defined macromolecular architectures ranging from linear oligomers and complex macrocycles, to dendritic compounds.¹¹⁴ Because of their poor intrinsic solubility, the poly(phenylacetylene) dendrons required solubilizing end groups. The 4-*tert*-butylphenyl peripheral units initially incorporated proved useful as solubilizing groups only to the third generation dendron; however, their replacement with the 3,5-di-*tert*-butylphenyl peripheral groups provided sufficient solubility to access fourth generation dendrons.¹¹⁵ Initial modifications to enable the synthesis of larger dendrimers included the use of elongated monomer units designed to counteract steric hindrance.¹¹⁶

More recently, the synthesis has been optimized, to eliminate the necessity of extended monomer units by simply reversing the functionalities on the monomer while using a dialkyltriazene precursor for the focal iodo functionality.¹¹⁷ The dendritic compounds (Scheme 3) were synthesized using the diethynyl

Scheme 3

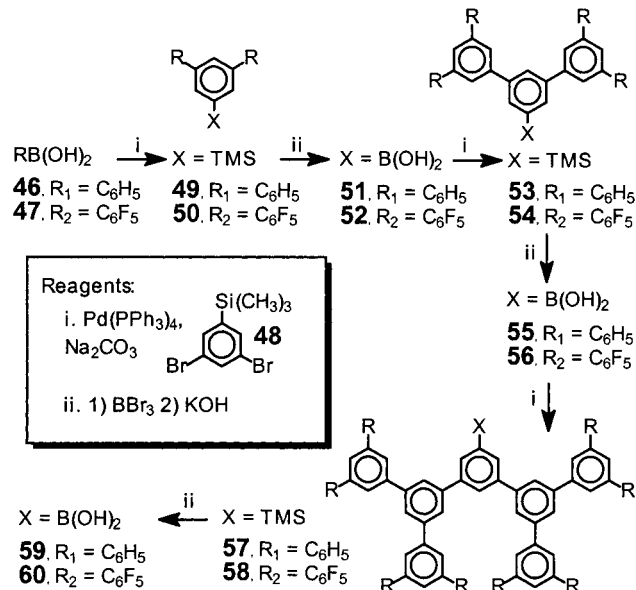


monomer **38** with a triazine protecting group. The terminal alkyne functionalities of the monomer are capable of two efficient palladium-catalyzed cross-couplings with the first generation aryl halide dendron **41**, producing the second generation dendron **42**. The nearly quantitative halogenation of the triazine group produces an aryl halide, **43**, activated toward further coupling with the monomer.¹¹⁷ In addition to improving the yields significantly, this reversed approach enabled the synthesis of fifth generation dendrons, and allowed these compounds to be synthesized via a solid supported technique.¹¹⁷ The notable features of these phenylacetylene dendritic structures are the rigid repeat units that lead to shape persistent dendrimers,¹¹⁸ and the conjugated segments within the structure, which impart interesting photophysical properties.^{119–131}

3. Poly(phenylene) Dendrimers

Two other convergent syntheses including that of a family poly(1,3,5-phenylene) dendrimers^{132,133} were reported by Miller and Neenan shortly after that of the poly(benzyl ether) dendrimer.¹⁰ Preparation of these polyphenylenes (Scheme 4) and their fluori-

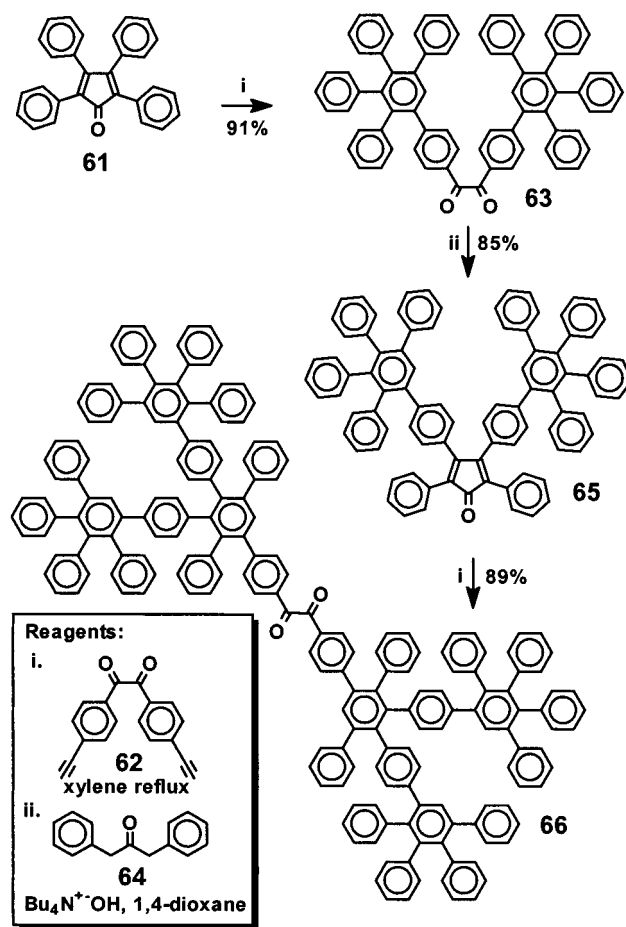
Scheme 4



nated analogues involved the Suzuki coupling of aryl boronic acids **46** or **47** with monomer **48**, 3,5-dibromo-1-(trimethylsilyl)benzene. Conversion of the trimethylsilyl (TMS) protecting group of products **49** and **50** to the boronic acid functionality in **51** and **52** enabled further coupling to the monomer. This procedure enabled the preparation of dendrons up to the third generation **57–60**. The rigid repeat units of these molecules lead to dendritic structures with well-defined shapes and diameters.

Recently, Müllen et al. have reported a convergent approach¹³⁴ to poly(phenylene) dendrimers (Scheme 5) similar to the divergent [4 + 2] cycloaddition route they had previously developed.¹³⁵ The process was initiated by a Diels–Alder reaction between tetrasubstituted cyclopentadienone **61** and dialkynyl mono-

Scheme 5

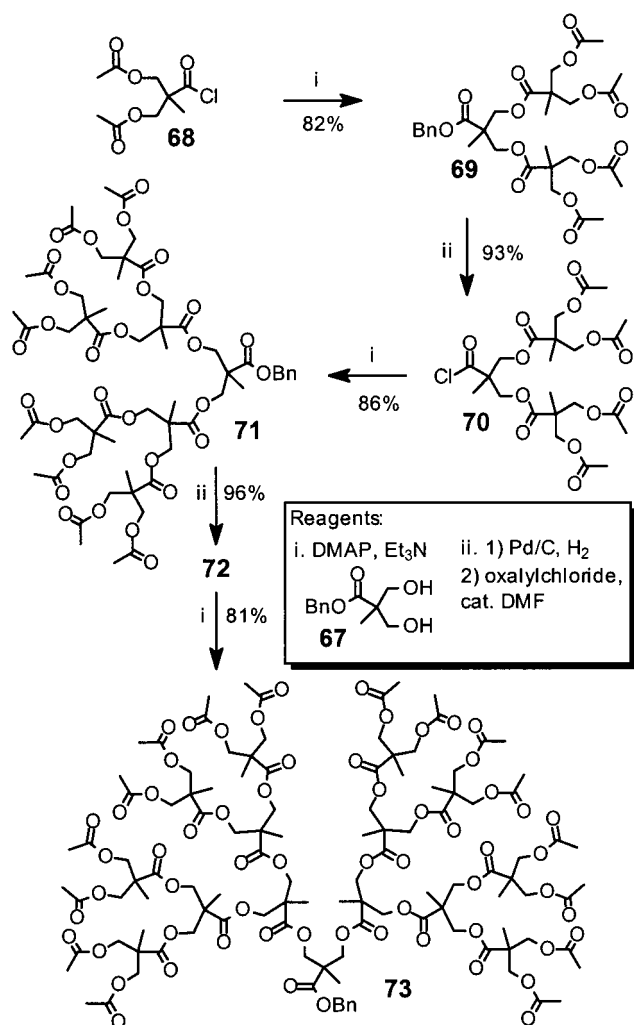


mer **62**, to yield the corresponding dione **63**. The Knoevenagel condensation of dione **63** and 1,3-diphenylacetone, **64**, then afforded the substituted cyclopentadienone **65**. This synthesis is of particular interest because it illustrates a potential steric complication involved in some convergent syntheses. Dendritic growth is not practical beyond the second generation, because the enormous steric interactions between the two poly(phenylene) wedges of **66** prevent them from adopting the conformation required for the subsequent Knoevenagel condensation. In contrast, the divergent synthesis using a Diels–Alder cycloaddition and a less conformationally demanding TMS deprotection step could be driven effectively to the fourth generation.

4. Poly(alkyl ester) Dendrimers

One of the more efficient convergent dendrimer syntheses was reported by Hult and co-workers (Scheme 6) utilizing a repeat unit based on 2,2-bis-(hydroxymethyl)propanoic acid.¹³⁶ The two alcohol moieties of the benzyl 2,2-bis(hydroxymethyl)propanoate monomer, **67**, could be coupled efficiently with an activated acid chloride end-group, **68**. Following removal of the focal benzyl ester by hydrolysis, the carboxylic acid could be transformed to the corresponding acid chloride **70**, in nearly quantitative yields using oxalyl chloride. The coupling-deprotection procedure was then repeated to the fourth generation dendron **73**. Although these poly-

Scheme 6

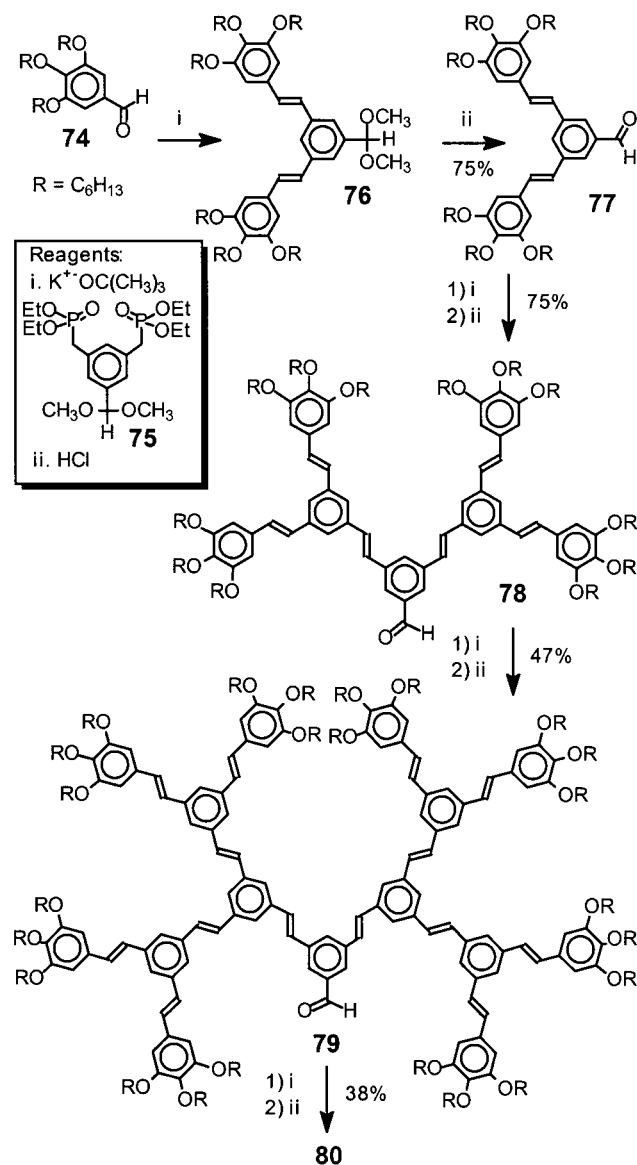


esters do not exhibit the chemical stability of other dendritic macromolecules based on ether or hydrocarbon linkages, the dendrons show rather high stability to acidic conditions because their ester functionalities are shielded from nucleophilic attack by the neighboring quaternary carbon. Recently, Ihre et al. reported a remarkably efficient¹³⁷ and versatile¹³⁸ divergent synthesis of analogous dendrimers.

5. Poly(aryl alkene) Dendrimers

The Meier and Burn groups both developed a convergent approach to conjugated poly(aryl alkene) dendrimers using coupling chemistry similar to the orthogonal synthesis first reported by Deb et al.¹³⁹ Meier and co-workers reported the synthesis of these compounds^{140–142} using the Horner–Wadsworth–Emmons coupling of aldehyde **74** with the bis(phosphite) monomer **75**, (Scheme 7). The dimethoxyacetal focal point of product **76** could be readily hydrolyzed to regenerate the active aldehyde **77**. However, the synthesis suffered from low yields and prohibitively long reaction times above the fourth generation **80**. Burn and co-workers^{143,144} reported the synthesis of an identical dendritic framework (Scheme 8), via the Heck coupling of a derivatized styrene **81** with the monomer 3,5-dibromobenzaldehyde, **82**,

Scheme 7

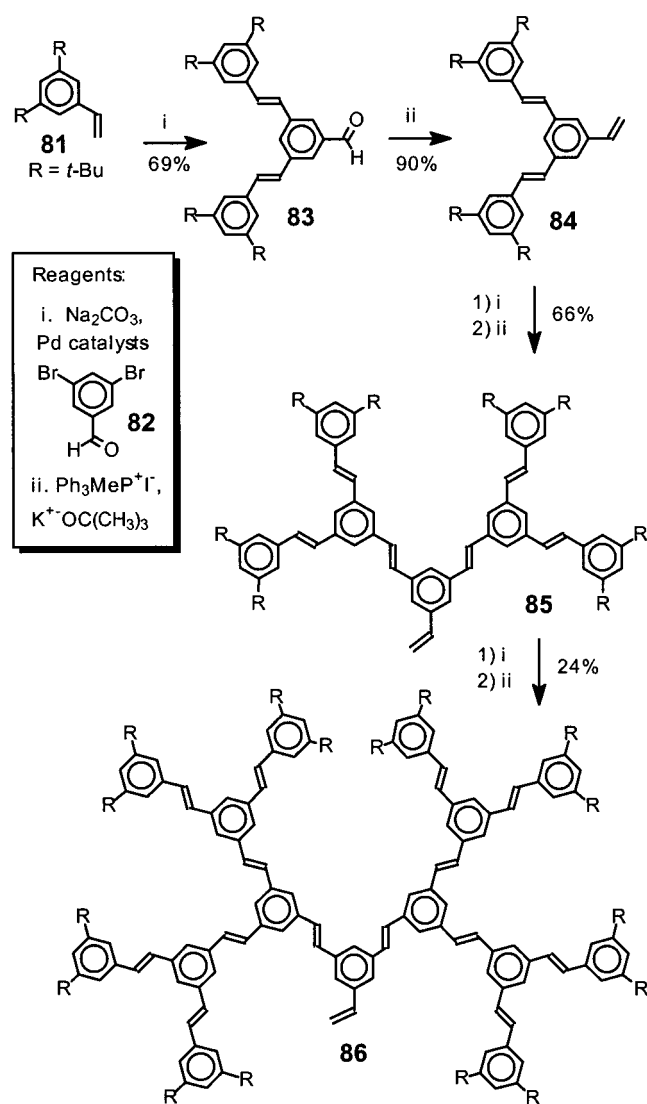


followed by a Wittig reaction with methyltriphenylphosphonium iodide to produce the activated dendritic styrene **84**. With this procedure, dendritic materials could be prepared up to the third generation **86**. Halim et al. have studied the photophysical properties of these materials, in particular their application toward light-emitting diode devices.^{145–148}

6. Poly(alkyl ether) Dendrimers

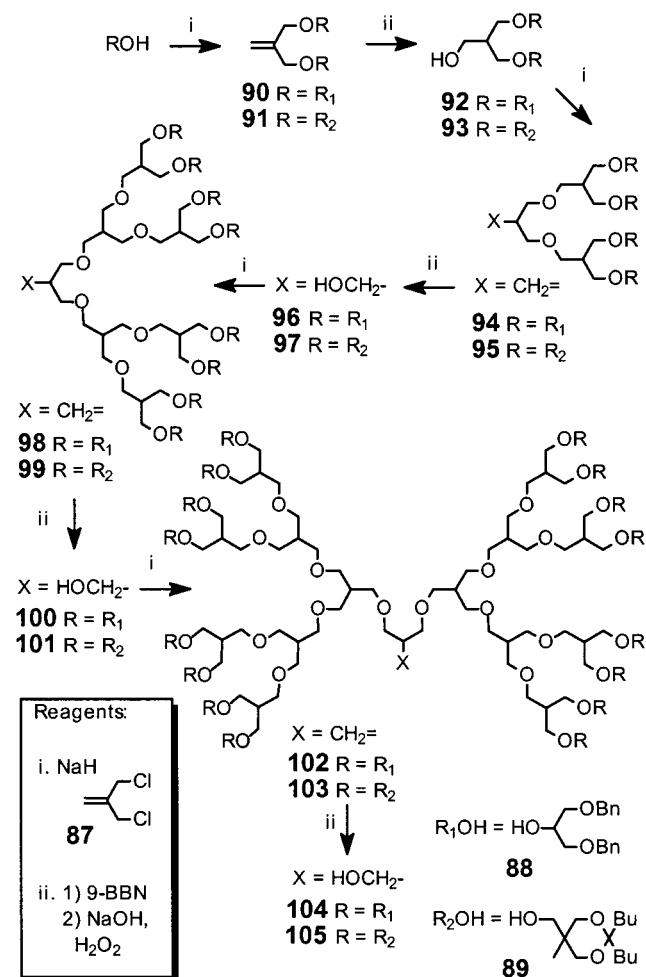
An aliphatic analogue of the poly(benzyl ether) dendrimer was recently developed by Fréchet and co-workers (Scheme 9). Based on monomer **87**, 3-chloro-2-chloromethyl-propene, the synthesis was initiated by coupling the end groups to the monomer using the Williamson ether coupling of a bis-protected triol, **88**, or **89**, with the allylic chloride functionalities of the monomer.^{149,150} The double bond of the monomer serves three distinct functions: (i) it activates the allylic halide moieties for Williamson coupling, (ii) it prevents elimination side reactions, and (iii) it serves as a latent hydroxyl group for growth of the next generation. The double bond of the resulting

Scheme 8



product **90** or **91** was converted to the corresponding primary alcohol **92** or **93** via hydroboration/oxidation, thereby enabling further coupling. This procedure could be repeated in high yields (85% or greater for **88** and 69% or greater for **89**) through fifth generation dendrons **102**–**105**. Although the more demanding purification of these compounds will likely prevent them from supplanting the poly(benzyl ether) family for many applications, they offer a significantly more rugged backbone allowing a wider range of chemical modification. For example, the peripheral ketal and benzyl ether protecting groups can be quantitatively removed by acid-catalyzed hydrolysis or palladium-catalyzed hydrogenolysis exposing multiple peripheral hydroxyl groups capable of further modification by alkylation or esterification.⁴⁰ The poly(alkyl ether) dendrons were selected as solubilizing scaffolds for otherwise intractable oligothiophenes because they did not interfere with the N-bromosuccinimide bromination of the pendant oligothiophene or subsequent Stille couplings.^{151,152} In addition, these compounds exhibit a significantly more polar backbone, similar to poly(ethylene glycol), which may prove useful in macromolecular catalysts or biomedical applications.

Scheme 9



7. Other Convergent Dendrimer Syntheses

A wide variety of other convergent syntheses have been developed for the preparation of dendritic poly(amides),^{132,153–160} poly(esters),^{161,162} poly(urethanes),^{163,164} poly(carbonates),¹⁶⁵ poly(aryl ethers),^{166–169} poly(arylamines),^{170–173} poly(aryl ketones),¹⁷⁴ poly(aryl alkynes),¹⁷⁵ poly(aryl methanes),¹⁷⁶ poly(aryl ammonium) salts,¹⁷⁷ poly(ethers),¹⁷⁸ poly(ether imides),¹⁷⁹ poly(keto esters),^{180–182} poly(amine ethers),¹⁸³ poly(amino esters),¹⁸⁴ poly(amide ethers),^{185–189} poly(pyridyl amides),¹⁹⁰ poly(uracils),¹⁹¹ poly(triazenes),^{192,193} poly(saccharides),¹⁹⁴ poly(glycopeptides),¹⁹⁵ and poly(nucleic acids).¹⁹⁶ In addition, chiral dendrimers^{197,198} including amide,^{199–201} ether,^{96–108} and ester²⁰² linkages, and organometallic dendrimers,^{203–207} including silicon,²⁰⁸ germanium,²⁰⁹ palladium,²¹⁰ and platinum^{211–214} containing repeat units have been reported. Syntheses that incorporate specific functional moieties within the monomer will be addressed in section 6.

B. Accelerated Approaches

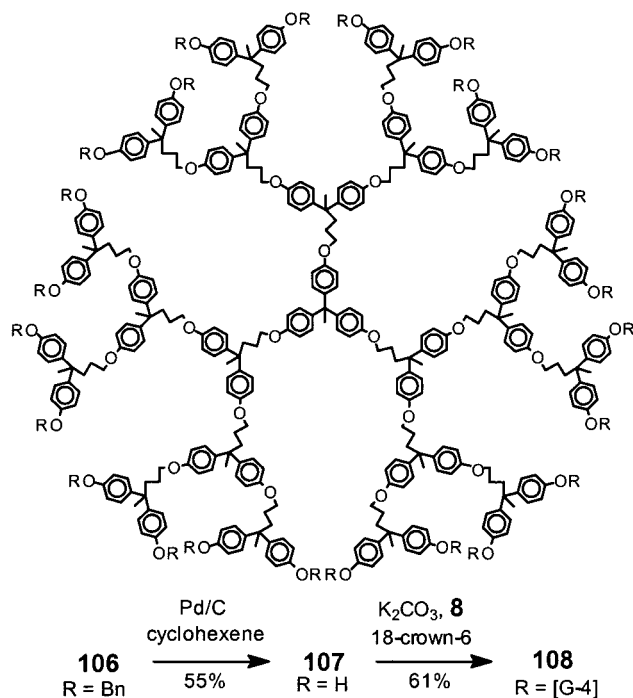
In response to the often tedious and purification intensive iterative dendrimer syntheses, many researchers have sought accelerated approaches that combine the convergent and divergent strategies.

These procedures generally maintain the versatility and product monodispersity offered by the traditional convergent method, but reduce the number of linear synthetic steps required to access larger dendritic materials.

1. Multigenerational Coupling: Hypercores, Hypermonomers, and Double Exponential Growth

Fréchet and co-workers developed the "hypercore" approach in order to improve the yields of sterically inhibited high-generation coupling reactions. The goal of this approach is to couple convergently synthesized dendrons to the periphery of a dendritic core that already contained layers of branching units. Using the standard convergent approach, first, second, and third generation dendrimers were constructed with 4,4-bis(4'-hydroxyphenyl)pentanol as the flexible repeat unit.⁸⁷ The benzyl ether periphery of these dendrimers could be removed via hydrogenolysis (Scheme 10) to expose 6, 12, or 24 phenolic

Scheme 10



groups. In a second stage of growth the dendritic polyols were utilized as multigenerational "hypercores" capable of coupling with the benzylic bromide functionalities of Fréchet-type dendrons. As a result, coupling of the third generation hypercore **107** with 24 fourth generation dendritic bromides **8** afforded the seventh generation dendrimers **108** in a 61% yield. This so-called "double stage convergent" approach not only provides access to dendrimers with chemically differentiated internal and external repeat units, but it also provides a more rapid and less demanding route to very large dendritic molecules. This approach has also been employed by Neenan and Miller, to enable the synthesis of a third generation poly(phenylene) dendrimer,¹³³ and by Xu et al. in the synthesis of a fourth generation phenylacetylene dendrimer.²¹⁵

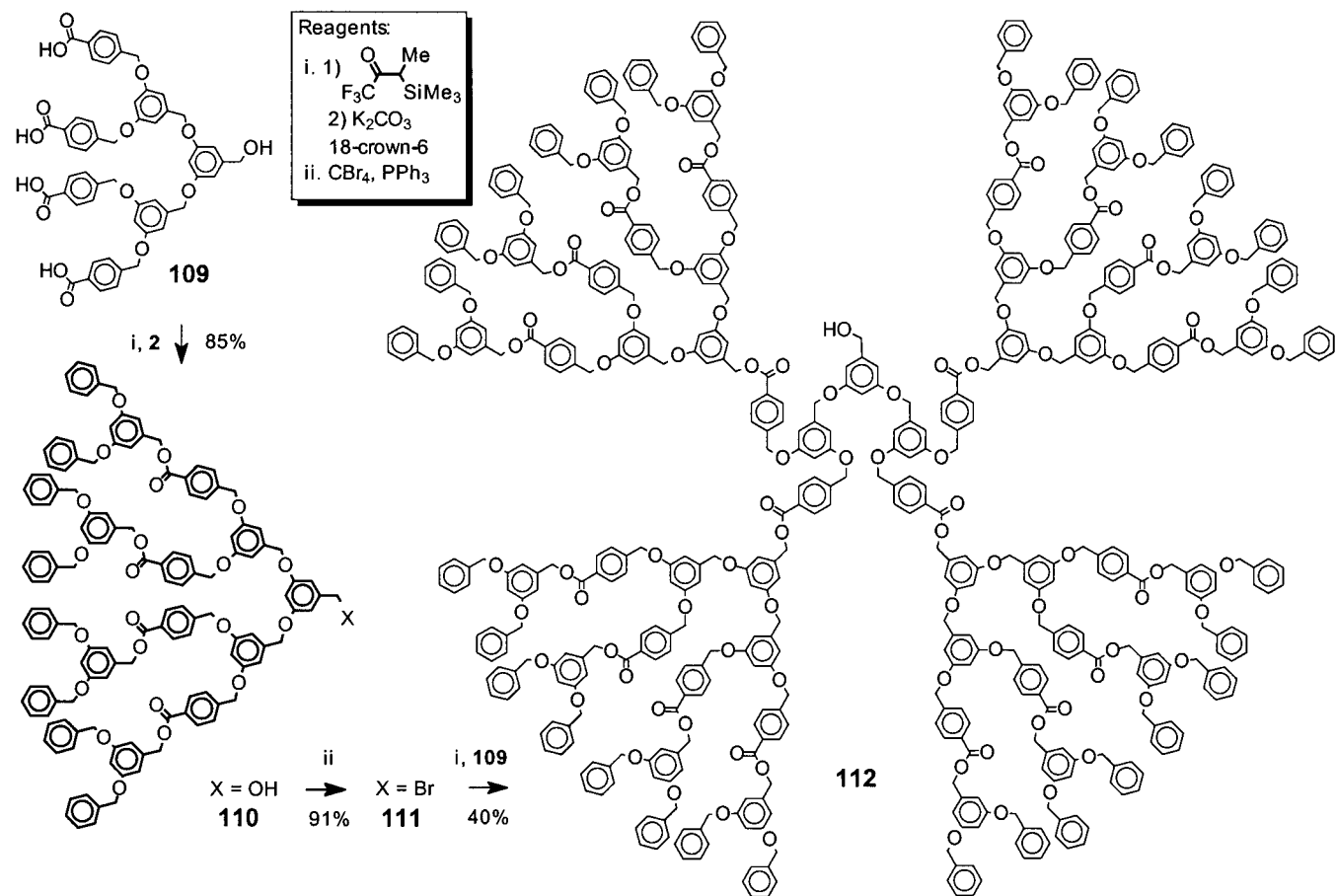
The "hypermonomer" approach, applies the concept of multistage growth to the monomer itself. Instead of assembling dendrons one generation at a time, hypermonomers contain two or more layers of branching units, enabling the addition of multiple generations during each coupling step. Although the coupling and activation steps may involve reactions identical to those used with traditional monomers, the number of individual coupling reactions per growth step increases exponentially with the generation of the hypermonomer, requiring the use of very efficient coupling chemistry.

Wooley et al. first demonstrated this approach (Scheme 11) by utilizing a second generation hypermonomer, **109**, consisting of two layers of branch points.²¹⁶ The carboxylic acid terminated hypermonomer allowed the facile synthesis of the fifth generation dendron **112** from the first generation benzyl bromide **2** in just three reaction steps. L'abbé and co-workers^{217,218} later introduced silyl-protected second and third generation hypermonomers **113** and **114**, to enable the accelerated synthesis of the poly-(benzyl ether) dendrons initially reported by Hawker and Fréchet (Scheme 12). *tert*-Butyldiphenylsilyl protecting groups were selected for the periphery because they could withstand the conditions required for hypermonomer synthesis, yet could be readily cleaved with fluoride ions. The deprotection step is followed by an immediate in situ coupling to dendritic benzylic bromides to produce dendrons up to the fifth generation in greater than 80% yield.

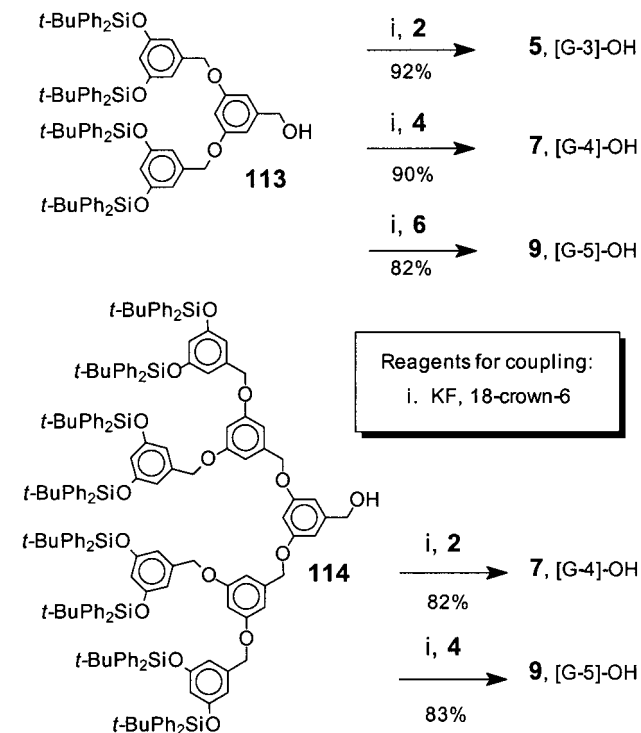
The final development in multigeneration growth was proposed by Moore and co-workers in 1995 and takes direct advantage of both divergent and convergent techniques.²¹⁹ Dubbed "double exponential dendrimer growth", this procedure requires a monomer with orthogonally masked focal and peripheral functionalities. The first generation dendron can be modified either at the focal point, to obtain the activated dendron, or at the periphery, to yield the first generation monomer. Coupling of the monomer and activated dendron yields a second generation dendron, which may likewise be activated at either the focal point or the periphery. Coupling of the resultant activated second generation dendrons to the second generation hypermonomer affords a fourth generation dendron. Each successive repetition of these three steps (dendron activation, monomer activation, and coupling) leads to a doubling of the generation number.

To demonstrate this approach (Scheme 13), Moore and co-workers selected compound **115**, containing the orthogonal focal triazine protecting group and two TMS-protected alkynes, to initiate their synthesis. Conversion of its focal point to an iodo functionality afforded the activated first generation dendron **116**, while removal of the TMS protecting groups yielded the activated first generation monomer **117**. Coupling of monomer **116** with 2 equiv of dendron **117** yielded the second generation dendron **118**. Subsequent halogenation of its focal point or deprotection of its periphery yielded **119** and **120** respectively, the two reactants necessary to produce the fourth generation dendron **121**. Attempts to continue

Scheme 11



Scheme 12



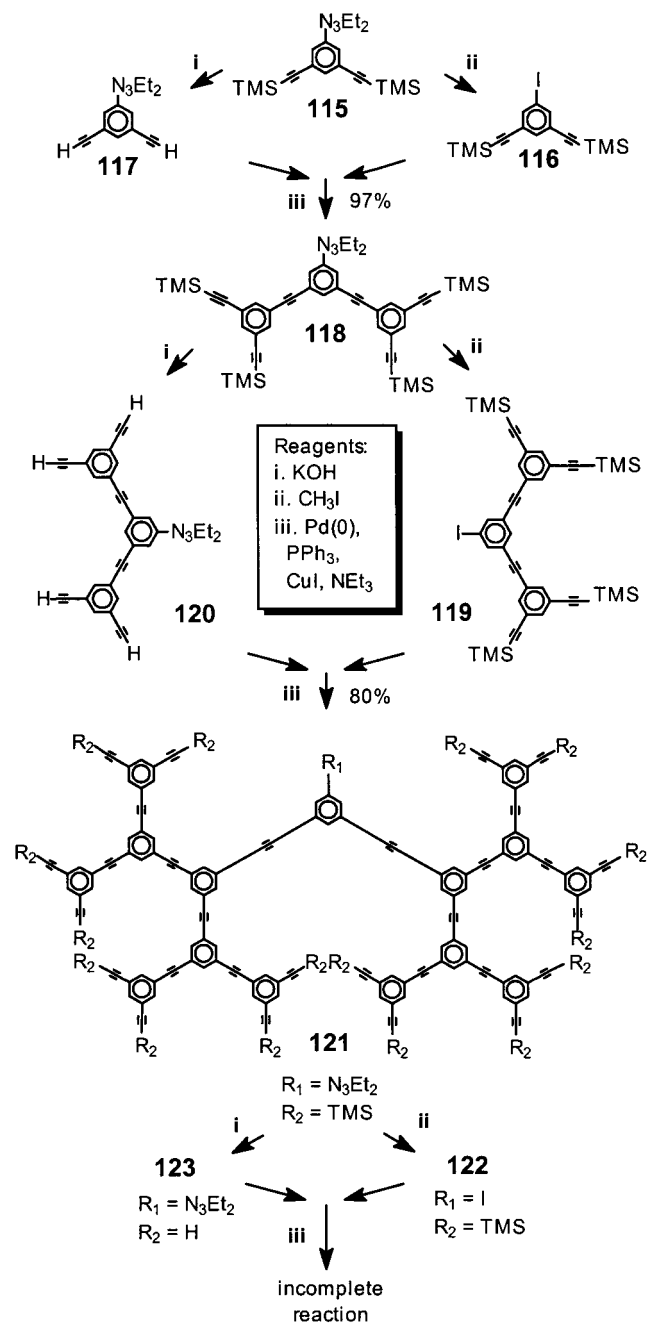
the synthesis to the eighth generation dendron proved problematic, however, as all 16 simultaneous couplings of **122** to **123** could not be completed.²¹⁹ Chi

et al. recently utilized this approach to synthesize a closely related poly(phenylacetylene) structure.²²⁰

Thre et al. utilized the double exponential growth approach (Scheme 14) to develop an efficient synthesis of aliphatic polyester dendrimers.²²¹ Similar to Moore's approach, the synthesis utilized orthogonal protecting groups for the focal and peripheral functionalities of the growing dendron. The 2,2-bis(hydroxymethyl)propanoic acid starting material was protected either with a cyclic acetonide group to mask the hydroxyl groups of **124**, or with a benzyl ester at its focal point, **125**. The two complementary dendrons **124** and **125** were coupled efficiently using DCC and catalytic amounts of DPTS to afford the second generation dendron **126**. The peripheral ketal of **126** could be hydrolyzed using an acidic polymer resin, to afford the second generation hypermonomer **127**. Alternatively, catalytic hydrogenolysis of dendron **126** produced the activated carboxylic acid dendron **128**. Finally, DCC coupling of **127** and **128** produced the fourth generation dendron **129**, in 91% yield.

These accelerated growth procedures have been used by a number of groups to synthesize dendritic poly(amides),^{222–224} poly(esters),²²⁵ poly(ether urethanes),²²⁶ and chiral poly(ethers).²²⁷ The orthogonality of the focal and peripheral protecting groups required for double exponential growth also enables facile modification at either the periphery or focal point. Although this approach is one of the most rapid methods yet reported for the synthesis of well-

Scheme 13

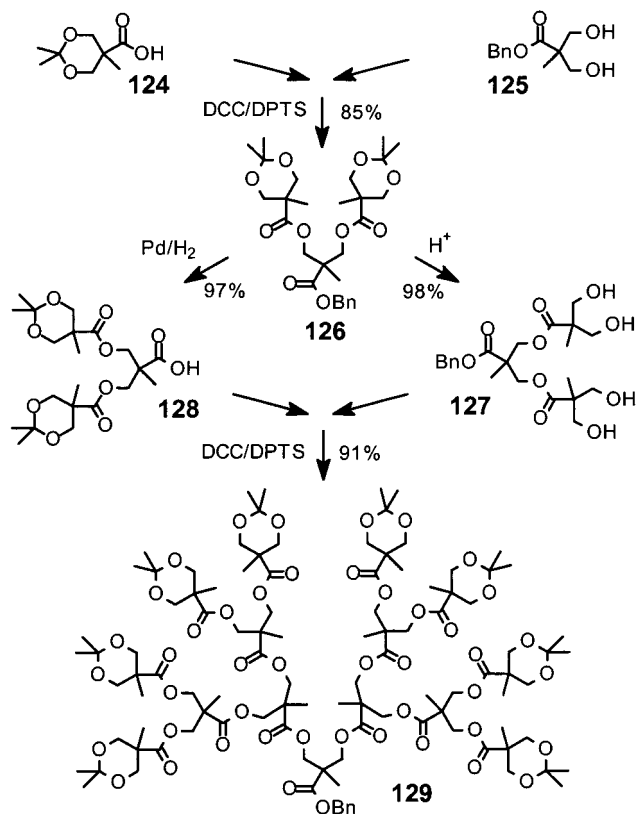


defined, large dendrimers, the number of coupling reactions required during each growth step increases exponentially each time the iteration is repeated, requiring high-yielding coupling chemistry. In this way, double exponential growth incorporates the advantages, and the disadvantages of both the convergent and divergent approaches.

2. Orthogonal Syntheses

The other accelerated approach for dendrimer synthesis, the orthogonal approach, involves convergent growth with two different monomers. The monomers, an AB₂ and a CD₂ must be carefully selected such that the focal functionalities of each individual monomer will only react with the periphery of the other monomer (B couples only with C and D only with A) thus removing the need for activation reactions. As

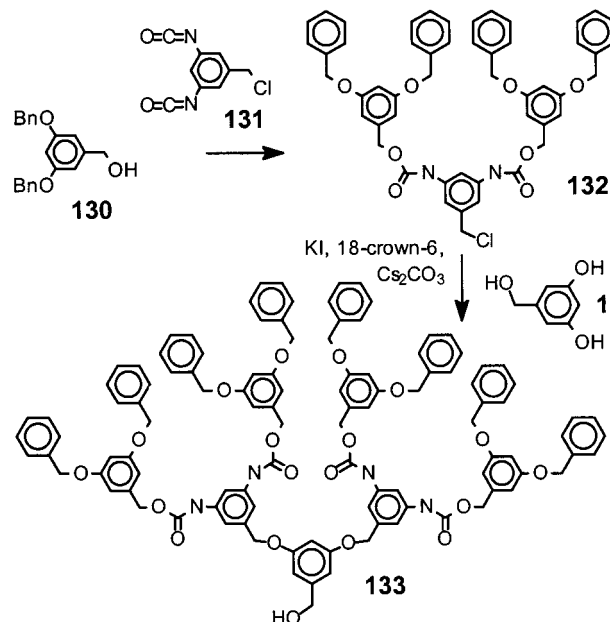
Scheme 14



a result of this synthetic design, each reaction in the synthesis adds a single generation to the dendron.

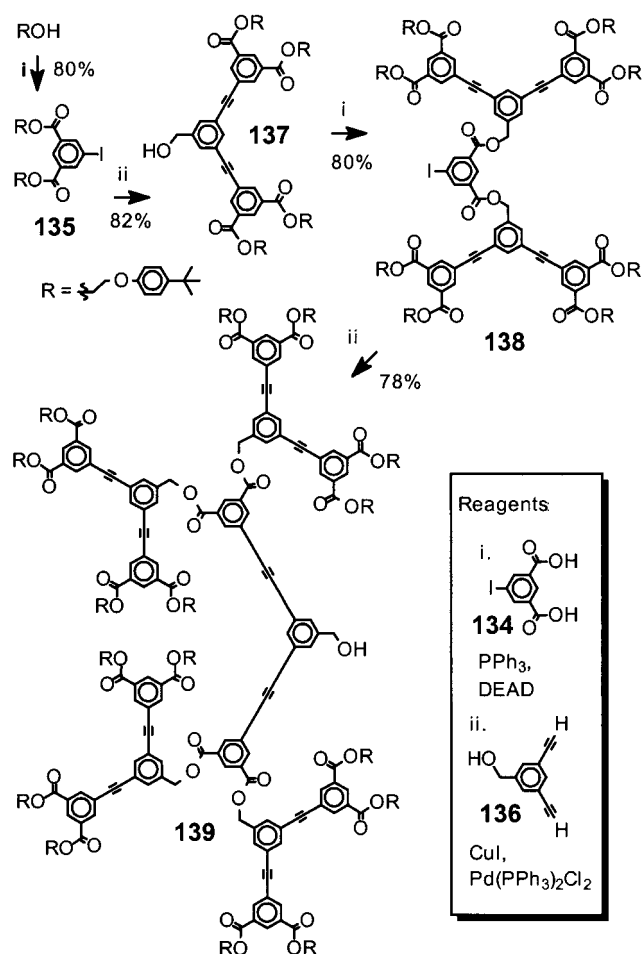
Spindler and Fréchet²²⁸ reported the first orthogonal synthesis (Scheme 15) using the alternating

Scheme 15



monomers 3,5-diiocyanatobenzyl chloride, **131**, and 3,5-dihydroxybenzyl alcohol, **1**. Although this approach enabled a one-pot, two-step synthesis of the third generation poly(ether carbamate) dendron **133**, difficulties in purification prohibited further growth. Zimmerman and co-workers were the first to report

Scheme 16



the orthogonal synthesis of high generation dendrimers,²²⁹ producing dendrimers with alternating benzyl ester and alkynyl linkages (Scheme 16). The synthesis utilized the Mitsunobu esterification of the carboxylic acid end groups of monomer **134**, followed by the Sonogashira coupling of the resultant aryl iodide **135**, with the terminal alkyne units of a second monomer, **136**. The focal alcohol functionality of **137** is appropriately functionalized to continue iterative couplings to the diacid monomer **134** and the dialkynyl monomer **136** yielding the fourth generation dendrimer **139**. Both coupling reactions afforded product in nearly 80% yield, through the fourth generation, demonstrating the efficiency of this route to high generation dendrons. To further accelerate the synthesis, the authors also investigated the use of the AB_4 hypermonomers **140** and **141** (Figure 7),

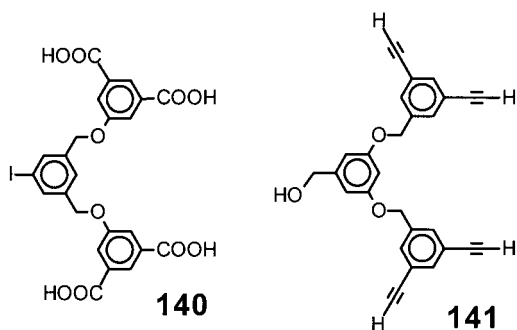
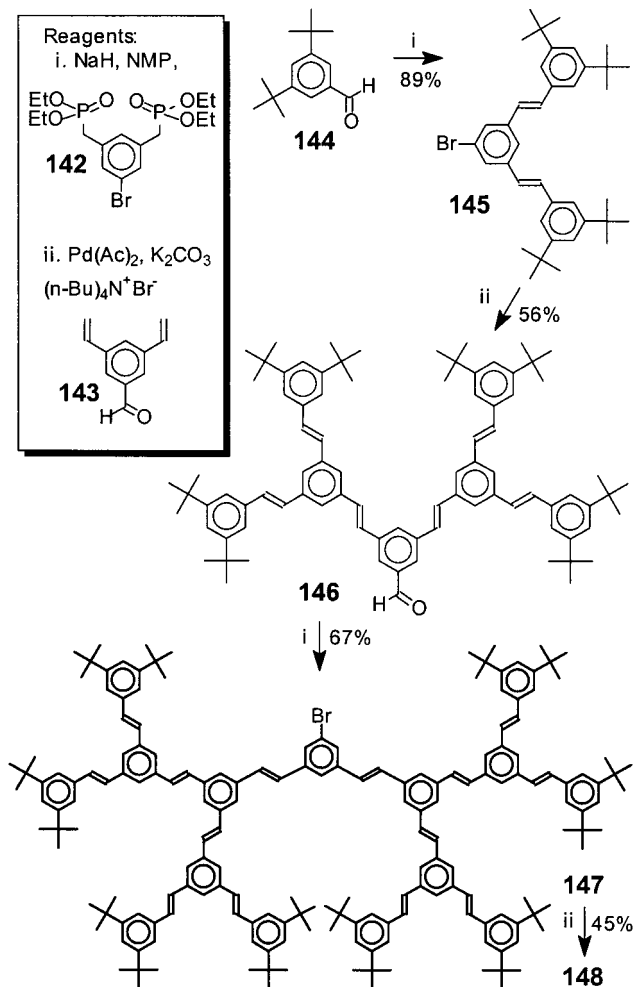


Figure 7.

utilizing the same two orthogonal coupling reactions. Although the yields for the higher generation reactions were reduced to less than 50%, a sixth generation dendrimer could be accessed in three synthetic steps with only two purifications.

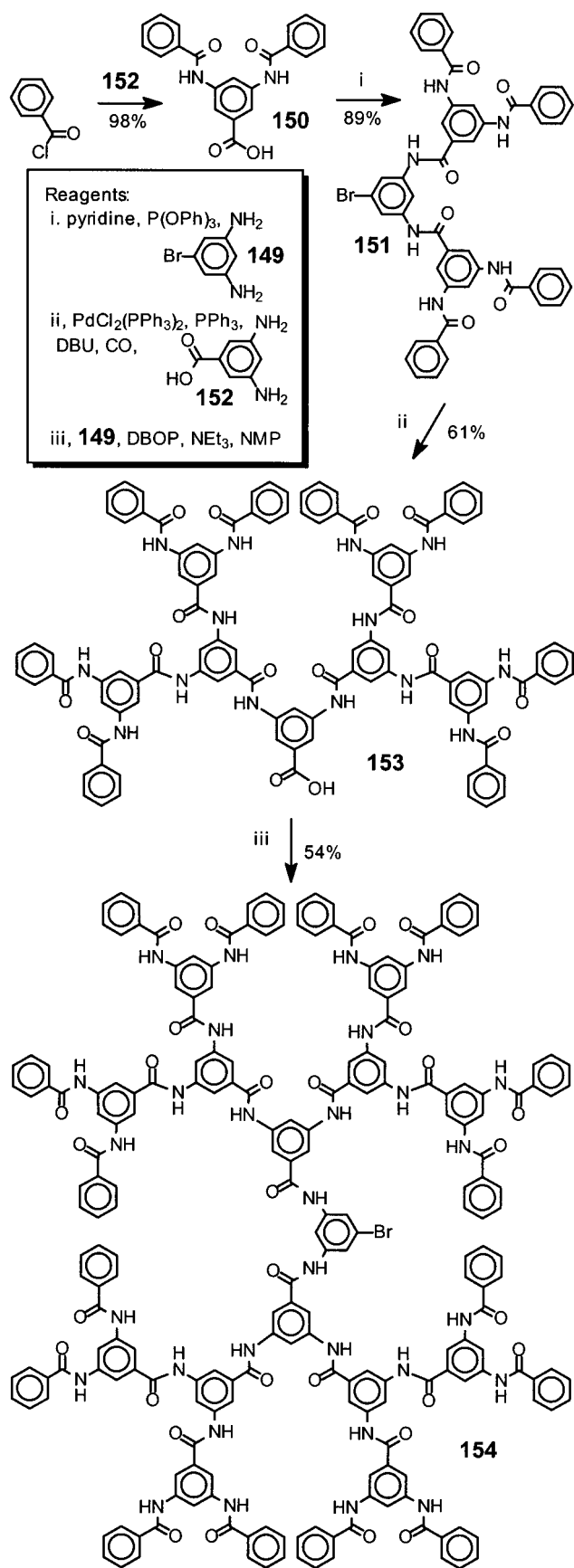
Yu and co-workers demonstrated the first orthogonal synthesis of chemically homogeneous dendrons (Scheme 17) with identical chemical connectivities,

Scheme 17



alkenyl linkages, between each generation.¹³⁹ Combining the coupling strategies from the two previously discussed convergent approaches^{140–144} their clever synthesis utilized a repetition of the Horner–Wadsworth–Emmons and the Heck coupling reactions. Monomers **142** and **143** could be used to access the fourth generation poly(aryl alkene) dendron **148** in an overall 15% yield in just four steps. Kakimoto and co-workers²²⁴ also developed an orthogonal synthesis to poly(aryl amide) dendrimers (Scheme 18). Condensation of the monomer 3,5-diaminobromobenzene, **149**, and the carboxylic acid **150** yielded the dendritic bromide **151**. Dendrion **151** could then be activated by a palladium-catalyzed insertion of carbon monoxide, enabling reaction with the second monomer, **152**, to yield a dendritic carboxylic acid, **153**. All of the poly(aryl amide) dendrons exhibited solubility in THF and dimethylacetamide (DMAc),

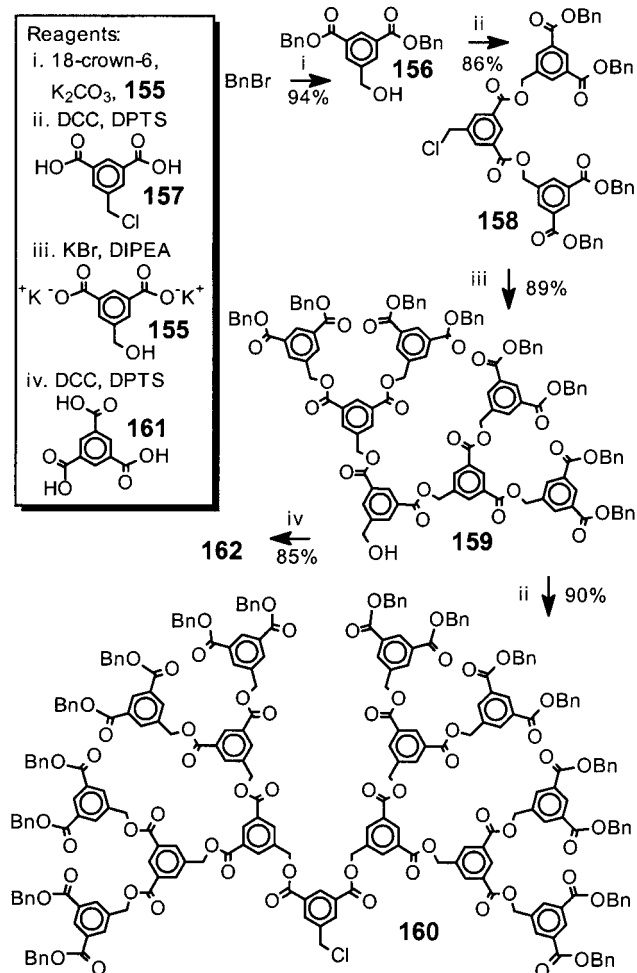
Scheme 18



but isolation of the third and fourth generation dendrons **153** and **154** required the use of preparative GPC.

The only chemically homogeneous orthogonal synthesis capable of efficiently producing high generation dendrimers (Scheme 19) was reported by Free-

Scheme 19



man and Fréchet.²³⁰ Two complementary monomers **155** and **157** are used for this synthesis. Introducing benzyl ester end groups onto monomer **155** via nucleophilic displacement is followed by a DCC coupling with the second monomer to afford the second generation dendron **158**. The reactive benzylic chloride focal point of **158** allows its direct coupling with monomer **155**, and the process can be continued up to the fourth generation dendron **160**. The monomer sequence can also be readily reversed, by starting with the DCC coupling of benzyl alcohol to **157**, followed by the nucleophilic displacement reaction with monomer **155**. Both approaches afforded isolated yields of above 80% per coupling reaction through the fourth generation. The attachment of dendron **159** to the tricarboxylate core **161** produced the third generation dendrimer **162**, further demonstrating the high efficiency of the DCC-mediated esterification.

Although the orthogonal approach allows the rapid synthesis of dendrimers, and reduces the number of purification steps, few syntheses of this type have

been reported because of the complex synthetic parameters. In addition to requiring highly efficient coupling reactions, orthogonal syntheses require two pairs of coupling functionalities that are strictly orthogonal. This orthogonality also places a greater limitation on which functionalities may be incorporated into the dendritic structure without interfering with the synthesis.

III. Modification of the Focal Functionality

The inward growth employed by the convergent synthesis is ideally suited for the attachment of diverse core moieties. In the divergent method, since the core is used to initiate dendritic growth, it must be stable to the subsequent activation and coupling conditions. The convergent synthesis, on the other hand, installs the core in the final step, enabling the incorporation of functionalities that may not withstand the conditions required for dendrimer growth. As a result, the convergent synthesis has been exploited for the construction of a wide variety of functional dendrimers.

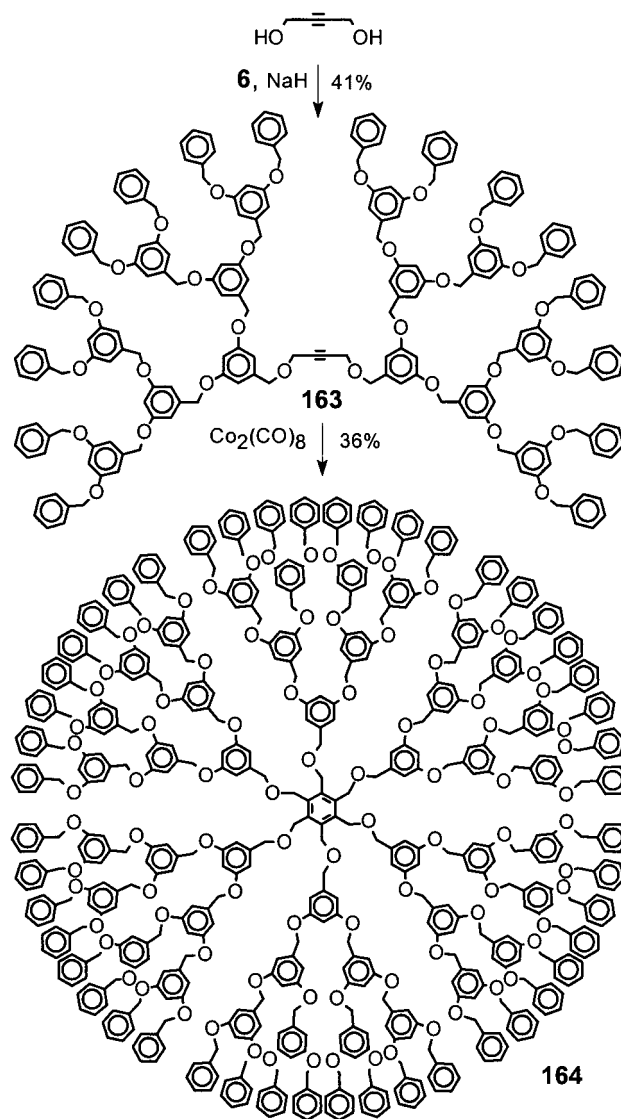
A. Traditional Covalently Bound Cores

For the purpose of this article, a traditional covalently bound core will be defined as a low molecular weight molecule with one or more functionalities capable of covalently coupling to the focal point of a dendron. This distinction is made to differentiate these cores from polymeric or self-assembled cores. The first dendrimer cores reported were simple di- or trifunctional molecules capable of coupling with dendrons utilizing identical chemistry as that repeated during dendron growth. For example, the earliest dendrimer cores (Scheme 2) include the trisphenolic core, **13**, reported by Hawker and Fréchet,¹⁰ and the 1,3,5-triiodobenzene core reported by Moore and co-workers.²³¹

Since then, a variety of methods for core attachment have been explored. Hecht and Fréchet²³² utilized the cobalt-catalyzed [2 + 2] cycloaddition (Scheme 20) of dendritically substituted alkynes **163** to produce a hexasubstituted benzene core dendrimer, **164**. Although the steric demand of higher generation substrates slowed the cyclization reaction, this approach successfully yielded highly functionalized, compact cores through the third generation. A similar cyclization approach has been reported by Van Wuytswinkel et al. utilizing the 1,3-dipolar cycloaddition reaction between a poly-azide core and dendritically di-substituted acetylene dicarboxylates.²³³ Because of steric constraints, the reaction yields were significantly reduced with larger dendrons, preventing the preparation of the third generation dendrimer.

Within the past decade, a significant focus of dendrimer research has been the incorporation of "functional" core molecules that, by their very nature, contribute clearly to the properties of the dendrimers. A number of groups have investigated the feasibility of coupling dendrons to a buckminsterfullerene core.

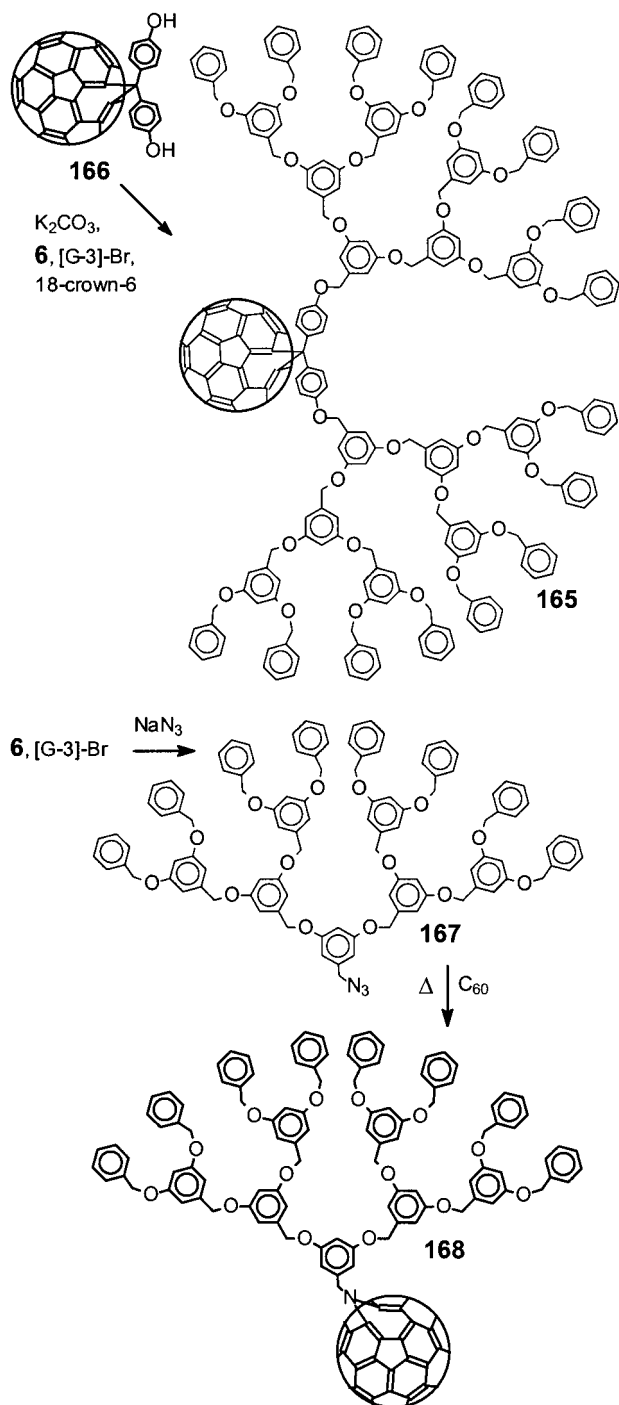
Scheme 20



Wooley et al.²³⁴ reported the first dendrimer–fullerene hybrid, **165** (Scheme 21), via the alkylation of a prederivatized fullerene diphenol, **166**, with the dendritic bromide **6**. Because of purification problems related to impure fullerene starting material, Hawker et al. later investigated the direct cycloaddition²³⁵ of a fourth generation azide-functionalized Fréchet-type dendron, **167**, with C₆₀. This dendritic fullerene, **168**, could be easily isolated by flash chromatography and showed a significant increase in solubility over the parent fullerene. Avent et al. reported a similar cycloaddition of poly(phenylacetylene) dendrons bearing a focal tosylhydrazone functionality.²³⁶

More recently Hirsch and co-workers have pursued the controlled attachment of multiple dendrons to C₆₀ cores (Scheme 22) via the cyclopropanation of bis-dendritic malonates.^{237–239} The versatility of the cyclopropanation coupling approach has been utilized by others to attach complex multifunctional dendrons.²⁴⁰ Cyclopropanation could be achieved with less than a 2-fold excess of the bis-dendritic malonates per coupling site, enabling the attachment of six-third generation dendrons in 28% yield, or eight

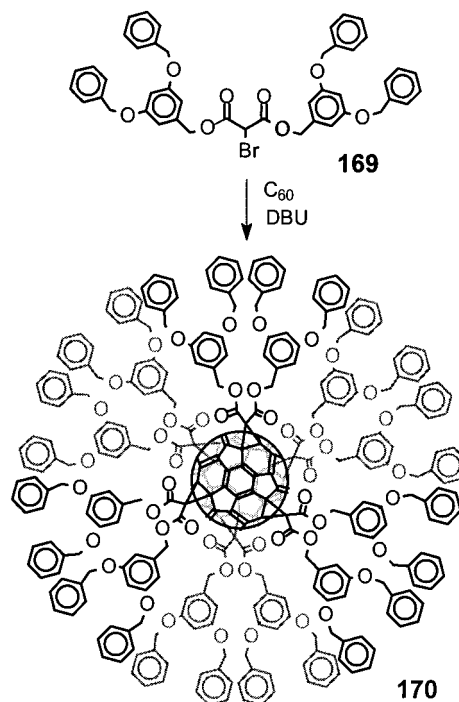
Scheme 21



second generation dendrons in a 73% yield.²³⁷ Attachment of additional dendrons to the fullerene core appeared to be sterically disfavored,²³⁹ as attempts to synthesize a fullerene with 12 first generation dendrons only proceeded in a 5.4% yield, **170**, and the analogous second generation molecule could not be synthesized.²³⁸

Dendrons have also been used as the capping moieties for rotaxane cores (Figure 8). Amabilino et al. reported the Williamson coupling of the third generation Fréchet-type dendrons **6** to cap polyether macrocycles threaded around linear bipyridinium oligomers.²⁴¹ When the linear component consisted of multiple viologen units, **171**, shuttling of the

Scheme 22



macrocycles could be observed between the different bipyridinium sites. Because the dendrons imparted enhanced solubility in organic solvents, the rate of shuttling as a function of solvent polarity could be determined and exhibited a dramatic increase in more polar solvents. Dendrimers have also been reported that incorporate a pseudo-rotaxane linkage between each of the dendrons and the core.²⁴² Gibson and co-workers assembled these pseudorotaxanes by threading Fréchet-type dendrons with a crown ether focal point onto a tris-ammonium salt core. Because these pseudorotaxanes lack one blocking group along the linear portion, the threading and dethreading equilibrium is subject to environmental conditions.

Porphyrins^{72,143,146,164,243–259} and the closely related phthalocyanines^{260–267} have been utilized extensively as dendrimer cores because of their interesting electrical, optical, and catalytic properties. Inoue and co-workers reported the first convergent synthesis of a porphyrin-core dendrimer²⁴⁸ by attaching poly(aryl ether) dendrons onto the preformed porphyrin **172**. Fréchet and co-workers later compared the utility of this approach to the Lindsey condensation (Scheme 23) of dendritic aldehyde **173** and pyrrole.²⁴³ The two methods offered complementary routes toward the synthesis of porphyrin-core dendrimer **174**, as the Lindsey condensation is acid catalyzed, while the Williamson route required prolonged reactions under basic conditions. Though the “Lindsey products” were easier to purify, the Williamson coupling appeared to be more suitable for the synthesis of larger dendrimers, since this approach was less sensitive to steric constraints. Similar complementary approaches have been reported for the synthesis of dendritic phthalocyanines.^{265,268} The attachment of dendrons to the porphyrin and phthalocyanine cores enabled modification of their solubility,^{245,246,265,266} improvement of their processibility,^{260,263,264} and steric

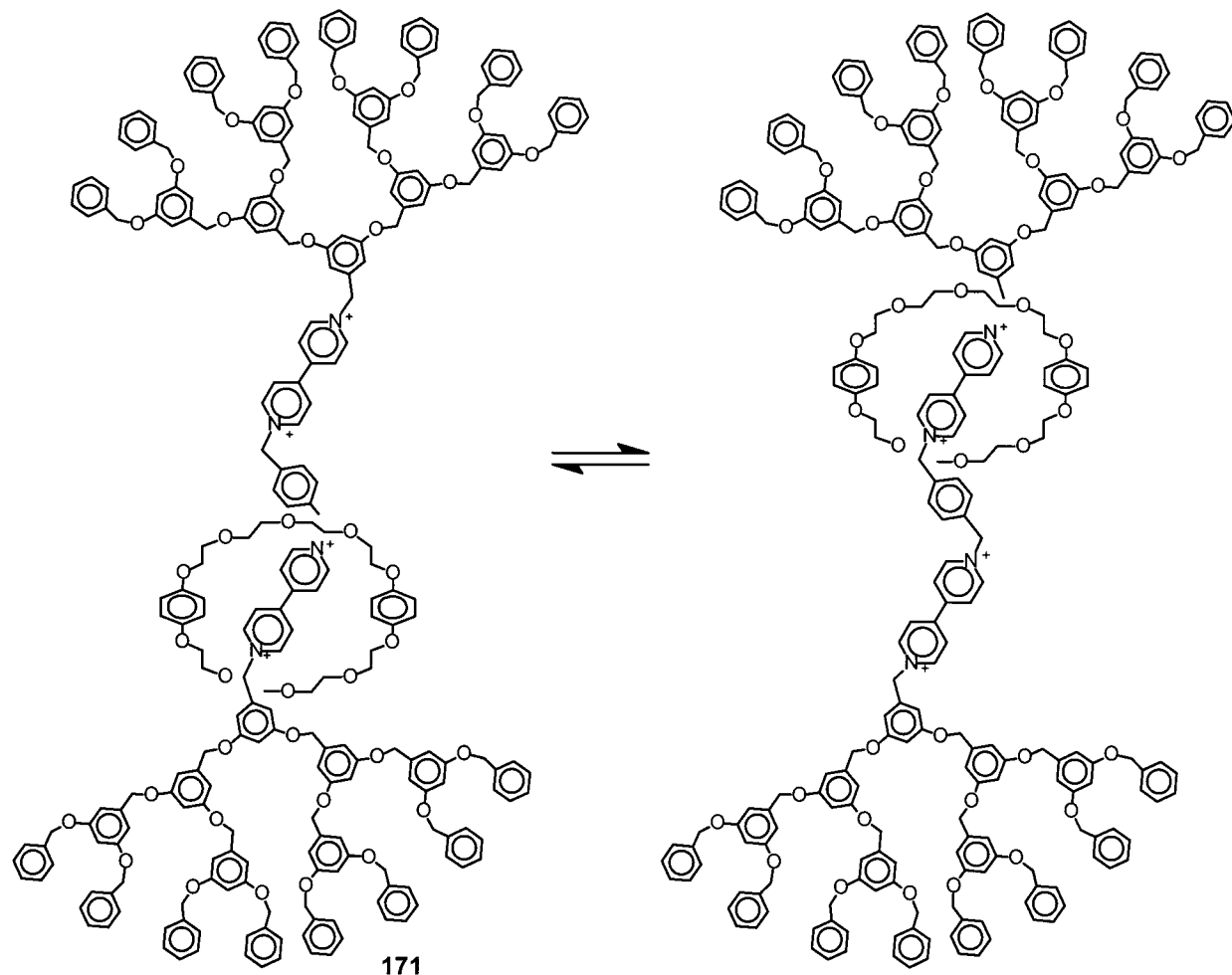


Figure 8.

encapsulation of their reactive sites.^{253,254,259,263} A substantial contribution to the field of dendritic porphyrins and phthalocyanines has also been made by the groups of Diederich^{269–272} and Koboyashi^{268,273} using the divergent approach.

In the following section, a variety of convergently prepared dendrimers will be discussed in the general context of their applications. Given the focus of this review, such a classification is quite appropriate since it is the application that dictates the design of the dendrimer and hence its synthesis.

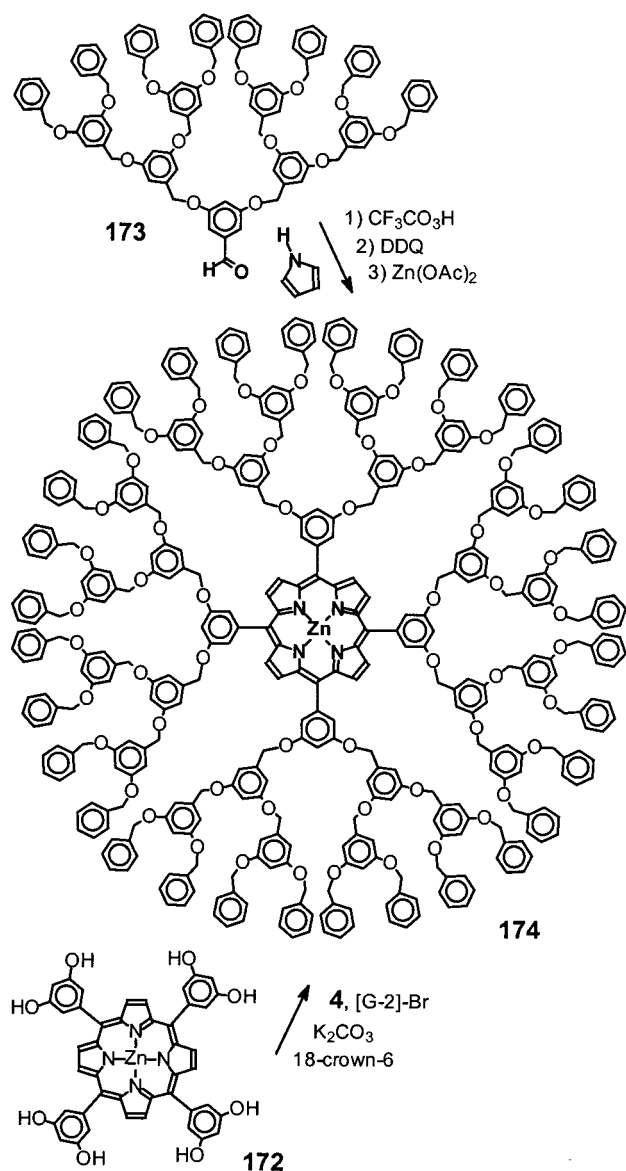
1. Environmentally Responsive Cores: Dendritic Probes

Because high generation dendrimers can sterically encapsulate the core from the external environment, the interior is expected to exhibit a unique microenvironment. The ability to tune this environment may eventually provide a synthetic mimic of enzymatic catalysis or biological binding events, but initial investigations have focused on the incorporation of responsive core moieties designed to help elucidate the complex nature of the dendritic molecules themselves. For example, Hawker et al. coupled the anion of 4-(*N*-methylamino)-1-nitrobenzene to Fréchet-type dendritic bromides (Figure 9) yielding **175**, a solvatochromic probe to elucidate the internal polarity of the dendrimer.²⁷⁴ When measured in nonpolar sol-

vents, the solvatochromic shift in the absorption spectra appeared to change drastically between the third and fourth generations, confirming that only large dendrimers are capable of efficiently shielding their core from the exterior environment. Devadoss et al. reported a similar shift in the fluorescence spectra between the fourth and fifth generations, utilizing the characteristic charge transfer in poly(phenylacetylene) dendrimers having a 2,5-dimethoxyphenylethyne focal point.²⁷⁵ In other studies, tryptophan cores were used to evaluate the nature of hydrogen bonding within the interior of the dendrimer,²⁷⁶ rubicene cores were incorporated to determine the hydrodynamic volume of dendrimers in different solvents,²⁷⁷ and paramagnetic,²⁷⁸ or isotope labeled²⁷⁹ cores were utilized in conjunction with nuclear magnetic resonance to probe dendritic conformation.

Vögtle and co-workers have also explored the steric demands and flexibility of the Fréchet-type dendrons by comparing the rate of rotaxane dethreading between the dendritic stoppers and traditional rigid stoppers.²⁸⁰ The dendritic rotaxanes were prepared by Williamson ether coupling reaction between a bulky alkoxide and a dendritic bromide. Dethreading rates and computer modeling suggested that the steric requirements of the second generation dendron

Scheme 23



exceeded those of a trityl group, whereas the third generation appeared to be larger than the *tert*-butyl trityl group.

2. Chiral Cores

The structural purity of convergent dendrimers has provided a unique opportunity to study chirality in synthetic macromolecules.^{197,198,281} A wide variety of poly(aryl ether) dendrimers have been prepared with chiral cores, using the Williamson ether coupling reaction. The effect of dendritic substitution on the chiral properties of a core molecule depend primarily on the origin of its chirality. Dendritic analogues of the axially chiral molecule binaphthol **176** were prepared by the Williamson ether coupling of Fréchet-type dendritic bromides to the phenols of 1,1'-bi-2-naphthol (Figure 10). Increasing the size of dendritic substituents produces an increasingly negative value for the molar optical rotation.^{282–284} Circular dichroism has determined that this effect results from an expansion of the dihedral angle

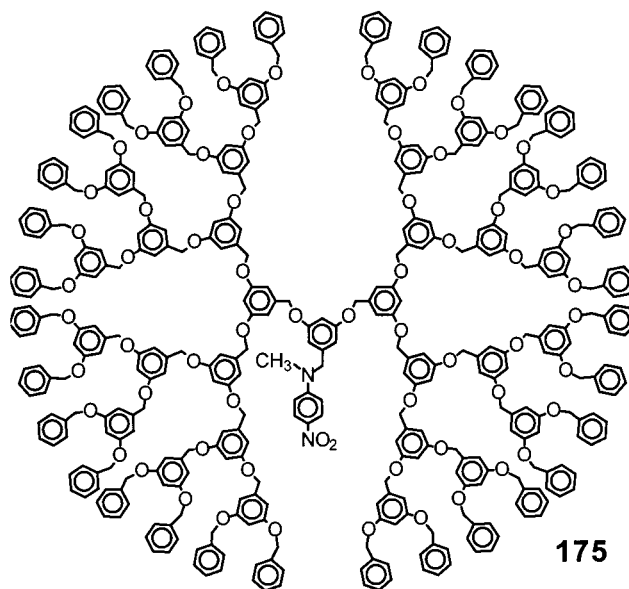


Figure 9.

between the naphthyl units caused by steric repulsion between the dendrons. The attachment of two Fréchet-type dendrons in the 6 and 6' positions²⁸⁵ or four Moore-type dendrons to the 4, 4', 6, and 6' positions appeared to have a less drastic effect on the dihedral angle.²⁸⁶ With the rigid spirobifluorene²⁸⁷ core, less susceptible to sterically induced rotation, it was found that dendritic substitution had little effect on the optical rotation of these chiral molecules.

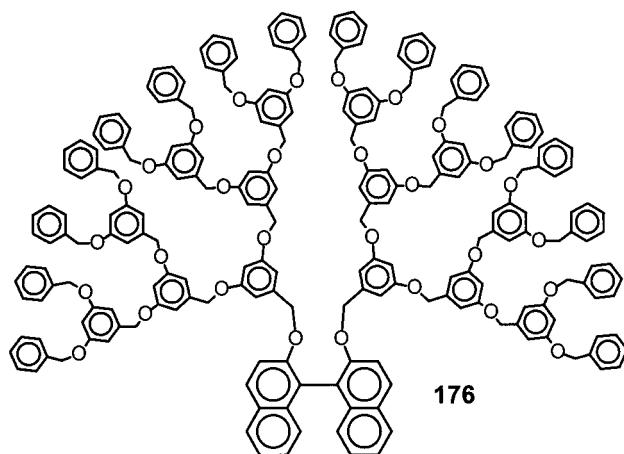


Figure 10.

The inclusion of Fréchet-type dendrons around stereogenic cores such as (3*R*,4*S*,5*R*)-3,5-dihydroxy-4-hydroxymethyl-2,2-dimethylhexane,^{288,289} (1*R*,2*S*)-2-amino-1-phenyl-1,3-propanediol,²⁹⁰ 2,5-anhydro-D-mannitol,²⁹¹ and TADDOL²⁹² produced the opposite effect. As the generation number of the attached dendrons increased, the molar optical rotation of these materials generally decreased. This trend is believed to result from perturbation of the chiral conformation by the bulky dendrons.⁸⁶

Meijer and co-workers have prepared an interesting set of molecules with chirality that originates from dendrons of different generation radiating from an otherwise achiral pentaerythritol core.^{293–295} Unfortunately, attempts to resolve the racemic products

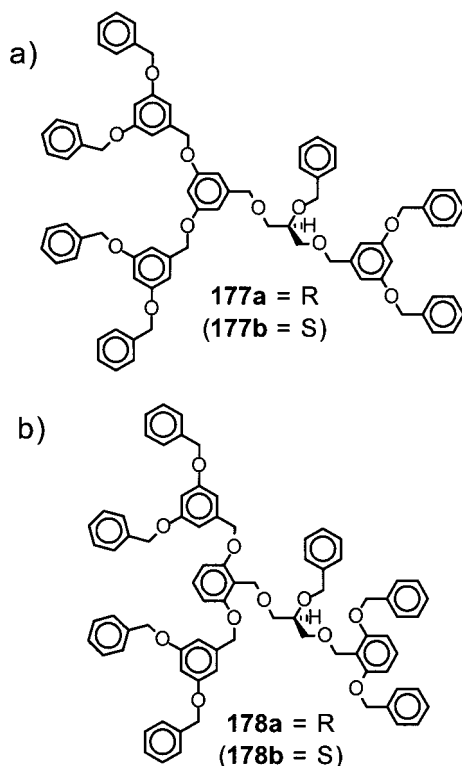


Figure 11.

were unsuccessful, and the chirotopic properties of the materials could not be studied. However, the same group later reported the successful preparation (Figure 11) of the optically pure (*R*) and (*S*) enantiomers **177a** and **177b**, by Williamson coupling of Fréchet-type dendrons to a chiral glycerol derivative using a series of protection and deprotection steps.²⁹⁶ These compounds were found to be “cryptochiral,” having no measurable chiral properties, presumably because of the flexibility of the molecule and the electronic similarity of the three poly(benzyl ether) dendritic substituents. When “backfolding” dendritic wedges were introduced in the preparation of **178a** and **178b**, the more rigid structure did exhibit optical activity.⁸⁶

3. Host–Guest Core Binding Sites

The nature of dendritic architecture with its lack of congestion near the core and increased crowding near the chain-ends makes dendrimers attractive candidates for guest encapsulation. The coordination of fullerenes to Fréchet-type dendritic hosts has been achieved using cores consisting of an iridium complex,²⁹⁷ cyclotrimeratrylene,²⁹⁸ and a porphyrin.²⁴⁹ The iridium-containing macromolecule was prepared by reacting two diphenyl phosphine derivatized dendrons with an iridium core. In all of these studies, the association constants appear to be higher for the larger dendrimers, presumably because the π – π interactions between the dendrons and the bound fullerene slow the disassociation process. Shinkai and co-workers have provided support for this hypothesis by observing that Fréchet-type dendrimers can, by themselves, act as fullerene hosts.^{249,299}

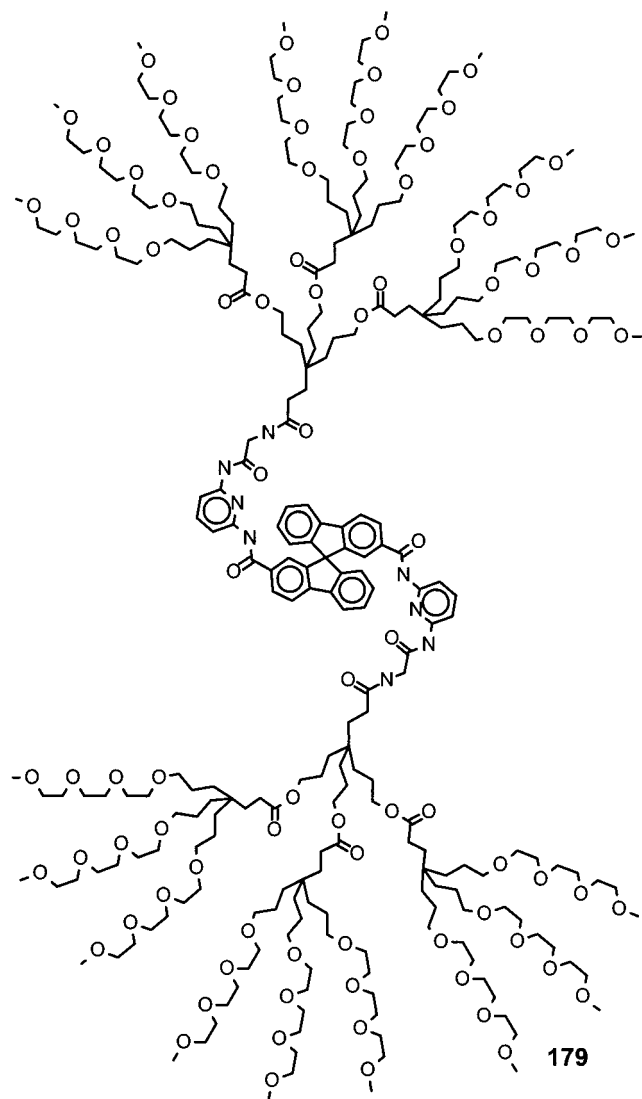
Zimmerman et al. have reported evidence that the binding constants between a dendritic naphthyridine

host and a benzamidine guest molecule are dependent upon both the size of the guest and the steric congestion of the host.³⁰⁰ The macromolecular hosts were prepared by attaching the first through fourth generation dendrons of both the poly(phenylacetylene) and the poly(benzyl ether) families to a naphthyridine core via a Sonogashira coupling. In addition, two different benzamidine guests were investigated, a smaller one with a 3,5-*tert*-butylphenyl substituent and a larger one with a first generation poly(phenylacetylene) dendron attached. The difference in binding free energy values between the smaller guest and the eight different dendritic hosts was sufficiently small to conclude that the steric bulk of the dendrimer, up to the fourth generation, does not seriously impede access of small guests to the binding site. In contrast, the larger benzamidine guest exhibited an appreciable drop in binding free energy when interacting with the largest naphthyridine dendrimers.

The groups of Aida and Suslick have reported similar results with dendrimers having zinc porphyrin cores. Using computer modeling,²⁵⁰ Aida determined that the porphyrin core of the dendrimers was accessible for the first three generations, partly accessible at the fourth and fully hindered at the fifth. Experimental measurements of the binding between dendritic zinc porphyrins and dendritic imidazoles confirmed the theoretical predictions, exhibiting a significant decrease in relative binding constants at the fifth generation.²⁵⁰ Suslick observed similar results with aryl ester and aryl amide zinc porphyrin-core dendrimers, but noticed enhanced binding selectivities toward less hindered amines when incorporating backfolding benzyl ester dendritic wedges.²⁵¹

Through fluorescence studies, Kaifer and co-workers documented a drastic decrease in binding efficiency between cyclodextrins and dansyl modified dendrons as the dendrimer size increases.³⁰¹ Yet, surprisingly, quantification of the binding efficiency with significantly larger anti-dansyl antibodies exhibited a less substantial decrease in binding stability between the first and third generations.

Diederich and co-workers have systematically investigated the effect of dendritic size on the stereoselective binding (Figure 12) between 9,9'-spiro[9-*H*-fluorene] chiral cores and glucosides.^{287,302} The dendrimers **179** were synthesized by reaction between the focal carboxylic acid functionality of the dendrons and glycine spacers attached to the spirobifluorene core. As the generation number of the dendritic host is increased from zero to two, the enantioselectivity of the macromolecular host appeared to be reduced while the diastereoselectivity was increased. A more recent study by Diederich and co-workers using Fréchet-type dendrons and derivatives of binaphthol as binding sites yielded less striking results.³⁰³ This inconsistency is believed to result from the perturbation of the binding site by dendritic substitution. This result highlights the fact that although the steric bulk of the dendritic structure may not inhibit substrate access, it may adversely affect binding in other ways.

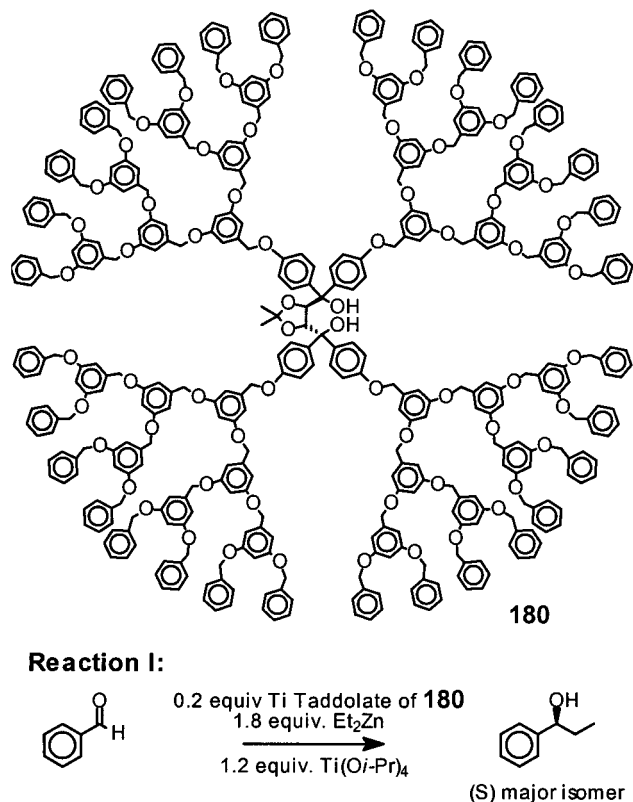
**Figure 12.**

Although the steric bulk of larger dendritic systems has been shown to suppress host–guest binding, the studies above suggest that smaller molecules can easily permeate into moderately sized dendritic structures—typically up to the fourth generation—and interact with the core moiety. This result provides encouraging evidence for substrate accessibility in appropriately designed dendrimers with catalytic cores.

4. Core Catalytic Sites

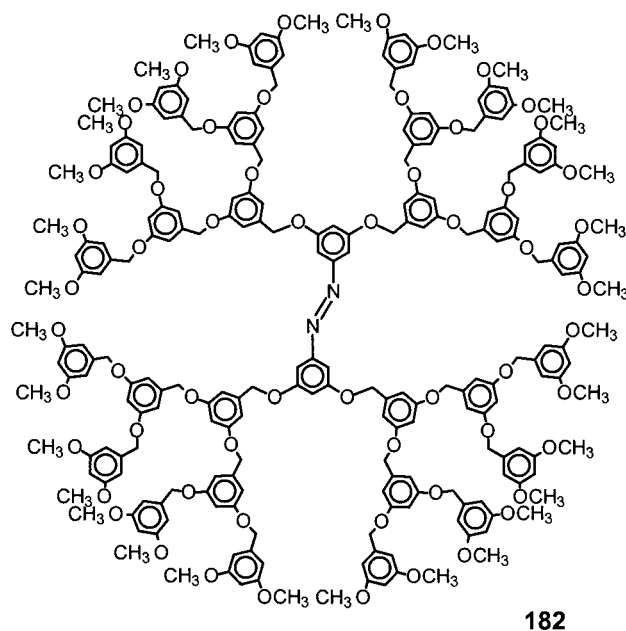
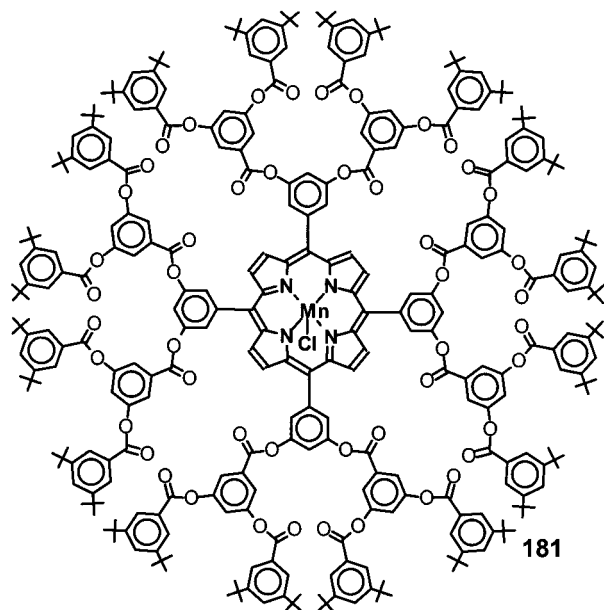
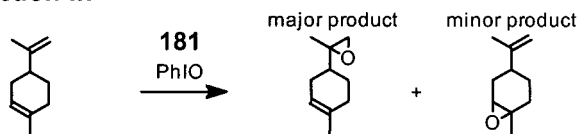
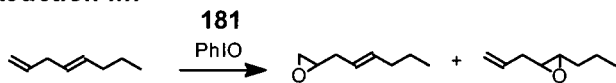
Convergent dendrimers, with their versatile three-dimensional scaffold, may be tailored to mimic, perhaps crudely, some elements of enzymatic structures. Numerous catalytic moieties, including manganese porphyrins,^{253,254} bis(oxazoline) copper complexes,^{304,305} tertiary amines,³⁰⁶ binaphthol titanium complexes,^{285,307} titanium taddolates,^{292,308} thiazolium-cyclophanes,³⁰⁹ and fullerene-bound bisoxazoline copper complexes,³¹⁰ have been incorporated at the core of dendritic molecules to determine the effect of dendritic encapsulation on their catalytic activity.

Not unexpectedly, a chiral TADDOL dendritic catalyst²⁹² demonstrated a slight reduction in enan-

**Figure 13.**

tioselectivity as the generation number of the dendrimer increased (Figure 13). These dendrimers were prepared by the Williamson ether coupling between the four phenolic groups of a TADDOL derivative and Fréchet-type dendritic bromides. During the nucleophilic addition of ethyl zinc to benzaldehyde, Seebach and co-workers showed a only a slight decrease from 99% stereoselectivity with the unsubstituted titanium taddolate ligand, to 94.5% with the fourth generation dendrimer **180**. Similar results were observed when using a binaphthol core.²⁸⁵ Dendritic size did, however, exhibit a profound effect on the rate of the reaction. For both of the dendrimer-catalyzed chiral reactions, as well as achiral Diels–Alder³¹⁰ and Henry reactions,³⁰⁶ rates of conversion fell sharply by the third or fourth generation, suggesting that the dendritic bulk was preventing substrate access to the active site.

Bhyrappa et al. have investigated the effect of dendritic substitution on the regioselectivity afforded by a porphyrin core during the epoxidation of substituted alkenes.^{253,254} The attachment of first and second generation poly(aryl ester) dendrons to a manganese porphyrin core (Figure 14) through a DCC-mediated esterification yielded **181**. The dendritic substitution blocked the catalytic site from the top and bottom faces, thereby improving the oxidative stability of the catalysts and increasing catalyst lifetime. The reaction of the dendritic catalyst with unconjugated dienes, consisting of one more and one less hindered double bond, revealed that the second generation dendritic catalyst was significantly more regioselective than the parent porphyrin (2-fold for reaction II and nearly 4-fold for reaction III). However, the regioselectivities were not as high as those

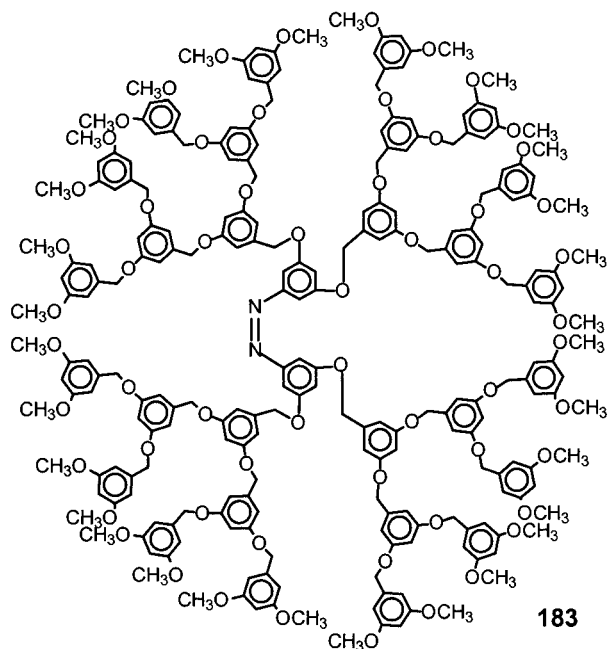
**Reaction II:****Reaction III:****Figure 14.**

reported for the bis(pocket porphyrin)^{311,312} (5,10,15,-20-tetrakis(2',4',6'-triphenylphenylporphyrin)) that, according to computer modeling, exhibits an opening above and below the face of the porphyrin.

Because the increasing steric environment of high generation dendrimer reduces substrate accessibility, the larger dendritic system must be designed to address mass transport problems. In addition to providing some sterically induced regioselectivity, the dendritic scaffold appears capable of maintaining the stereoselectivity of analogous nondendritic systems. Currently, the most significant advantages of incorporating catalytic sites into dendritic structure are the ability to tune their solubility and facilitate catalyst recycling via precipitation or ultrafiltration.

5. Photochemically Responsive Cores

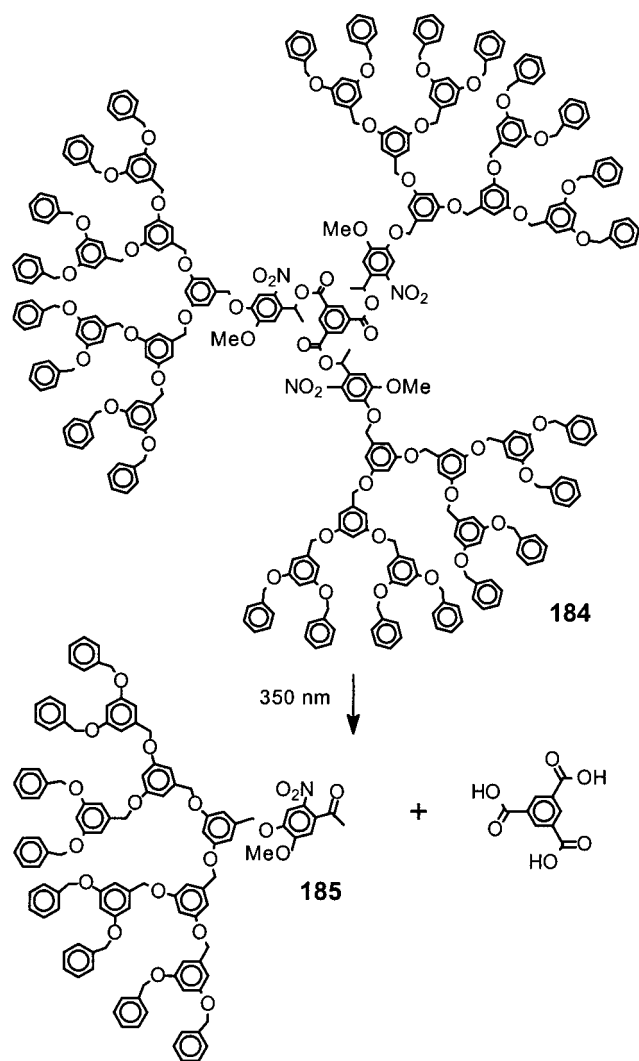
Molecules that can respond to external stimuli are of particular interest for macromolecular devices, and may potentially serve as molecular switches. A number of groups have examined the incorporation of photochemically responsive cores into dendritic structures. Azobenzene moieties, which are capable of undergoing a photochemical cis–trans isomerization, were first incorporated into the core of poly(aryl ether) dendrimers (Figure 15) via a Williamson ether coupling by Aida and co-workers^{313–315} and shortly thereafter, by Junge and McGrath.³¹⁶ UV irradiation of the samples converted the more stable trans

**Figure 15.**

isomer **182** to the cis isomer **183**. It is interesting to note that the activation energy for this transformation is only marginally affected when the size of the dendron substituents is increased from the first to the fourth generation.³¹⁷ In addition, Jiang and Aida noted that IR irradiation could accelerate the conversion back to the trans conformation for sufficiently larger dendrimers. In detailed studies, they deduced that this process resulted from the absorption of multiple IR photons (1597 cm⁻¹) by the aromatic rings of the dendritic framework, and subsequent transfer of the absorbed energy to the azobenzene core.³¹³

In addition, Junge and McGrath have designed a trifunctional core moiety in which each dendron is attached via an azo linker, enabling three such isomerizations per macromolecule.³¹⁸ The physical properties of these dendrimers can be noticeably modified by this isomerization, and have been documented by a change of polarity during thin-layer chromatography and a change in hydrodynamic volume as measured by size exclusion chromatography.³¹⁹ McGrath also reported a photodegradable dendrimer, **184**, containing *o*-nitrobenzyl ester linkages (Scheme 24) that could be quantitatively cleaved by irradiation to strip the dendrons **185** from their core.³²⁰

Scheme 24



Photoresponsive dendrimers are of interest because the properties of these materials can be readily modified by an external stimulus. These initial studies have verified that the inclusion of photoactive moieties into dendritic systems does not adversely affect their photochemical response and can enable changes in the overall macromolecular structure.

6. Fluorescent Cores

Dendrimers have also been attached to fluorescent cores in order to modify the properties of the dye. The

attachment of dendrons to oligothiophenes^{152,321–324} improved the solubility of the oligothiophenes in organic solvents, whereas the placement of appropriate dendritic substituents on porphyrin chromophores yielded water solubility dyes.^{245,246,266} In addition, the attachment of dendrons to chromophore cores can improve the processibility of the core¹⁵¹ for incorporation in monolayers³²⁵ and films.³²⁶ However, by far the most useful advantage to dendritic chromophores is the site isolation²⁸ provided by large dendritic substituents. With sufficiently large dendritic shielding, intermolecular quenching between the encapsulated dyes can be significantly decreased leading to an enhanced luminescence efficiency,^{45,250,327,328} and in some instances, the penetration of small molecule quenchers, such as triplet oxygen, can be reduced.³²⁹ However, even in the case of fourth generation porphyrin core dendrimers, steric shielding may not be sufficient to prevent the penetration of small quenchers, such as vitamin K₃. At least two groups have reported that the porphyrin at the core of a fourth generation poly(aryl ether) dendrimer was more efficiently quenched than the first generation analogue because the quencher was not only sufficiently small to penetrate the steric shielding, but also had a greater affinity for the dendritic structure than for the surrounding solvent.^{248,252}

Dendrimers have also been used as scaffold for light-harvesting and light-emitting diode devices by controlling the spatial interaction between focal and peripheral functionalities, these will be discussed in detail in a later section.

7. Redox-Active Cores

As with chromophores, the steric encapsulation of a dendrimer core can be utilized to prevent intermolecular interactions between redox active sites. A number of different redox active core moieties have been investigated, including, iron–sulfide clusters,^{93,94} bis(terpyridine)iron(II) complexes,⁹² tris(bipyridine)ruthenium(II) complexes,³³⁰ zinc porphyrins,²⁵² oligothiophenevinylenes,³³¹ fullerenes,^{236,332} ferrocenes,^{333–336} oligothiophenes,³²² oligonaphthalenes,³³⁷ and 4,4'-bipyridinium.³³⁸

Following the early cyclic voltammetry (CV) studies by Fréchet and co-workers with dendrimer-encapsulated fullerenes²³⁵ **168** and Chow et al. with dendritic bis(terpyridine)iron(II) complexes **186** (Figure 16),⁹² a number of groups have reported the insulating effect of dendritic structures on redox active sites.^{93,236,252,322,330–333,339} Gorman et al. were the first to report the dendritic encapsulation (Figure 17) of inorganic clusters **187**. These molecules were synthesized by a ligand exchange reaction where alkanethiols on a (Fe₄S₄(S-*t*-Bu)₄)²⁻ cluster were replaced by dendritic aromatic thiols.⁹³ As demonstrated with other encapsulated redox sites, the irreversibility of electron transfer increases with dendrimer size because the active core moiety becomes more insulated from the electrodes and other redox sites. Comparison of the CV data of the poly(phenylacetylene) and the poly(benzyl ether) dendrimers suggested that more rigid poly(phenylacetylene) structure led to more efficient redox site encapsula-

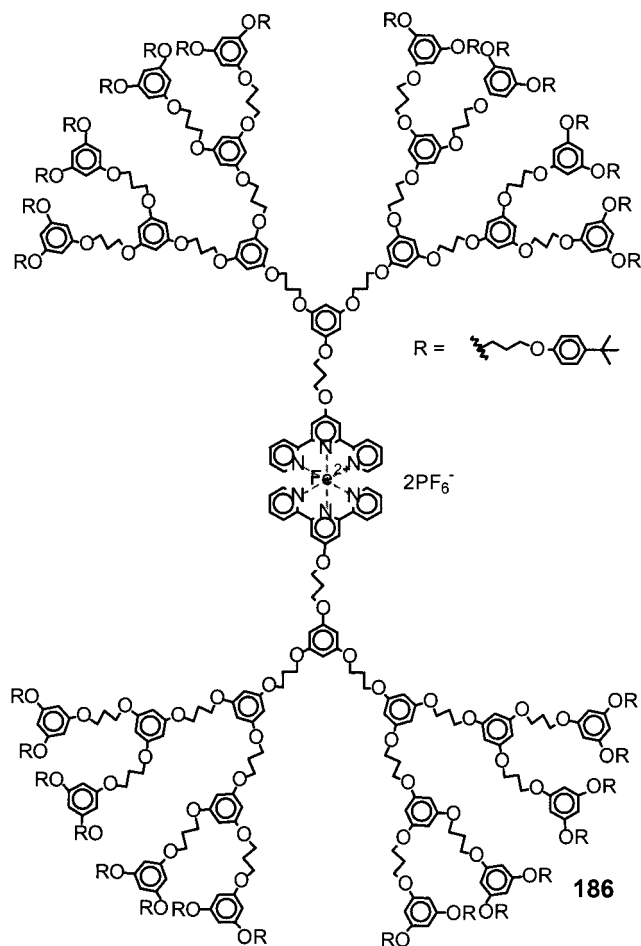


Figure 16.

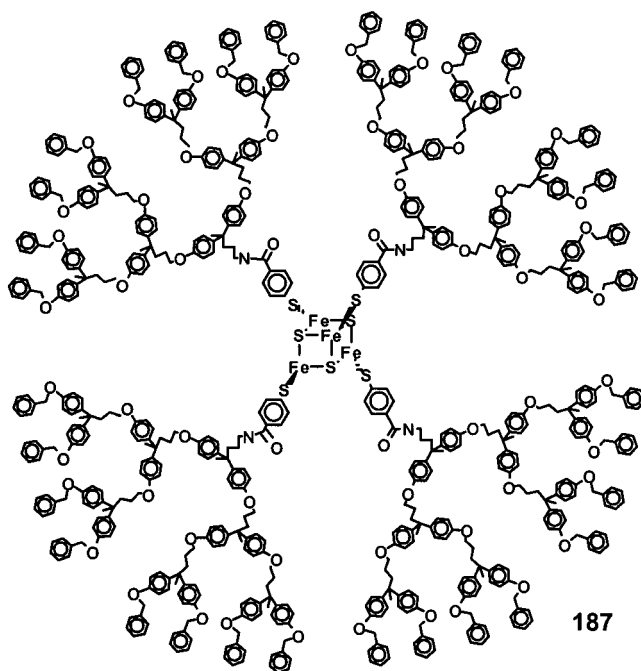


Figure 17.

tion.³⁴⁰ Noteworthy redox active dendrimers prepared via the divergent approach have been reported by Diederich^{269–272} and Newkome.³⁴¹

Kaifer and co-workers designed an interesting molecular device that exhibits a pH dependency on

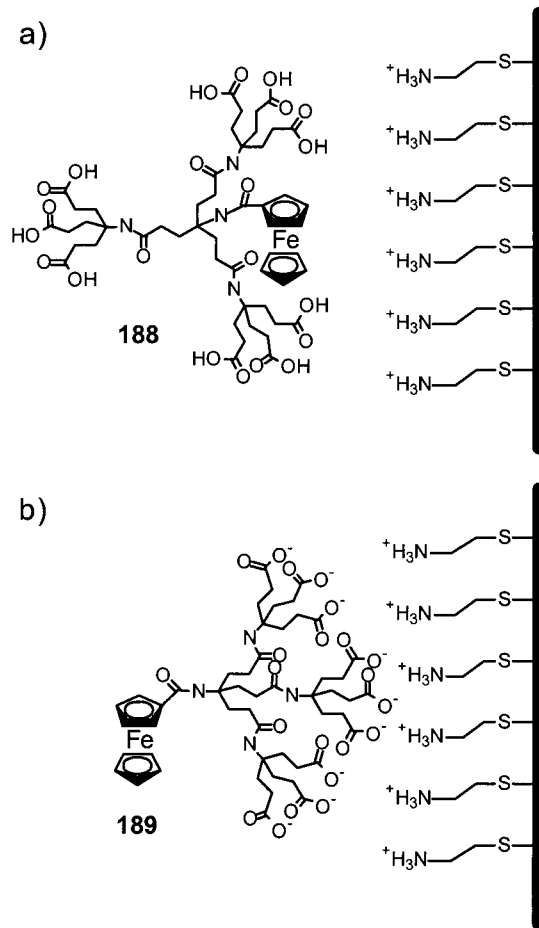


Figure 18.

electron transfer.³³⁵ They coupled a chlorocarbonyl-ferrocene core to first, second, or third generation amine functionalized convergently prepared Newkome-type dendrons,³³³ and studied their conductivity on cystamine derivatized gold electrodes. At low pH, the peripheral carboxylic acid units of **188** were protonated, enabling the ferrocene units to freely interact with the electrodes, but at neutral pH, the carboxylates of **189** would bind to the ammonium surface of the electrode, insulating the ferrocene unit (Figure 18).

8. Other Core Functionalities

Other functional core moieties include: stable TEMPO-based radicals for controlled radical polymerization,³⁴² crown ethers,^{343,344} hexacyclenes,¹⁷⁰ poly-(quarternary ammonium) cations,³⁴⁵ ethylene thioates,^{346,347} calixarenes,^{348–352} cyclodextrins,¹⁷⁸ inorganic clusters,^{93–95,340,353,354} dichalcogenides,³⁵⁵ and silsesquioxanes.³⁵⁶

B. Linear–Dendritic Copolymers

Because linear and dendritic polymers have very different physical properties and intermolecular interactions, copolymers of these two macromolecular architectures are expected to exhibit interesting behavior. Gitsov et al. first synthesized these polymeric hybrids by reacting one or both hydroxyl

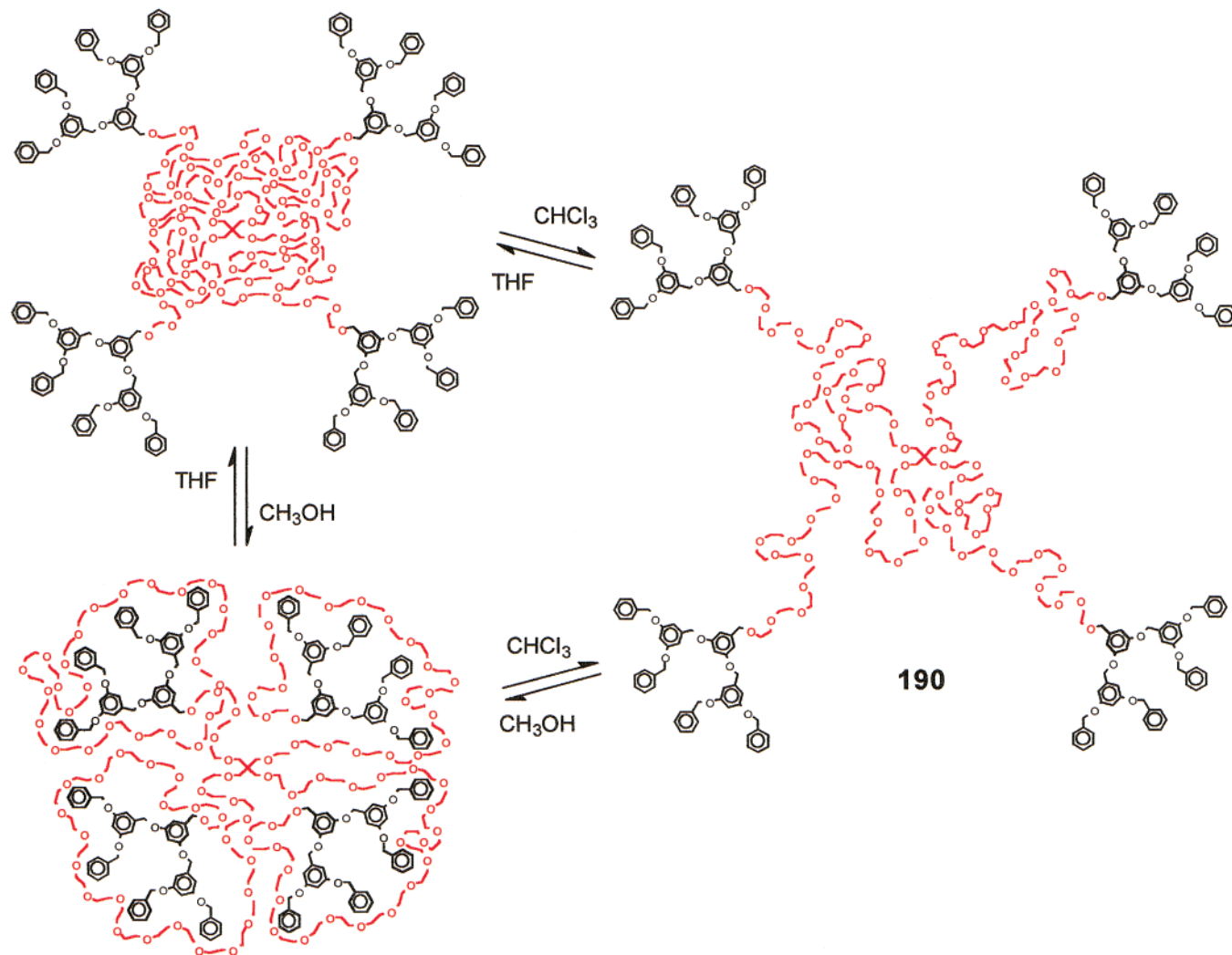


Figure 19.

termini of poly(ethylene glycol) (PEG) chains with dendritic bromides.^{357,358} Subsequent studies of PEG with one and two terminal dendrons, as well as a four armed-star PEG with four dendritic end groups, **190**,^{359,360} revealed that these materials change conformation depending on their interactions with solvent (Figure 19). ¹H NMR verified that in nonpolar solvents the linear PEG chains collapse, enabling the nonpolar dendritic blocks to shield them from energetically unfavorable interactions with solvent. In polar solvents, the system minimizes its free energy by “inverting” so that the collapsed nonpolar dendrons are shielded from solvent allowing the surrounding PEG chains to form the interface between the molecule and the solvent.^{359,361,362} In addition, these amphiphilic materials exhibited the ability to solubilize polyaromatic compounds, including fullerenes, without a critical micelle concentration (CMC).³⁶³ Amphiphilic linear–dendritic block copolymers can also be utilized to modify surface properties. When used with a cellulose substrate or even a more hydrophobic poly(ethylene terephthalate) film, the PEG–poly(benzyl ether) dendron copolymers self-assemble at the surface, increasing its hydrophilicity.³⁶⁴

Linear–dendritic copolymers have also been synthesized by capping a “living” polystyrene dianion

with two poly(benzyl ether) benzyl bromides,³⁶⁵ by atom transfer radical polymerization (ATRP) of styrene initiated by a dendritic benzyl bromide,^{366,367} by a nitroxide mediated “living” radical polymerization,^{367,368} and by ring opening polymerization of lactones with a dendritic alcohol.^{369,370}

C. Dendronized Linear Polymers

Dendronized, or dendritic-grafted linear polymers, are linear polymers that bear pendant dendrons along the repeat units. Although there have been a few reports of divergently prepared dendronized materials,^{138,371,372} the majority of the research in this field has focused on the convergent approach. Recently, the convergent synthesis of these materials has been optimized, and their preparation has been reviewed extensively elsewhere.^{373–375} The salient examples are, however, briefly mentioned below.

1. Macromonomer Approach

The “macromonomer approach” refers to the polymerization of a monomer that is functionalized with a dendron. The first attempts to make these compounds via the convergent approach were reported by Hawker and Fréchet and utilized a fourth genera-

tion poly(benzyl ether) dendron having a styrene³⁷⁶ or methacrylate³⁶² focal point functionality. Attempts to homopolymerize these materials led to the formation of oligomers in very low yields,³⁶² but these dendrons could be successfully copolymerized with styrene.³⁷⁶

In the last six years, a number of groups, most notably those of Schlüter and Percec, have developed the synthesis of dendritic grafted materials by utilizing a wide variety of polymerization techniques including: radical polymerization of methacrylates,^{84,377–382} Suzuki polycondensation,^{383–385} rhodium-catalyzed insertion,³⁸⁶ ring-opening metathesis,^{387–389} polyurethane condensation,^{390,391} Heck coupling,³⁹² oxidative Hay coupling,³⁹³ polyamide condensation,^{394,395} polyimide condensation,³⁹⁵ palladium-catalyzed polycondensation of poly(aryl alkynes),³²⁸ Stille coupling of poly(thiophene),¹⁵² and radical polymerization of styrenes.^{396–398}

Because the steric bulk of the monomer shields the reactive functionality, higher generation macromonomers tend to produce materials with a low degree of polymerization, and only moderately controlled polydispersity. Examples with average degrees of polymerization above 100 repeat units usually involve small first or second generation dendrons.^{112,386,399,400} Recently fourth generation dendrons have been incorporated into dendronized linear polymers, such as **192**, using a Suzuki polycondensation of macromonomer **191**, (Scheme 25), but with average degrees of polymerization near 10 and an average PDI of about 2.^{401,402}

Scheme 25

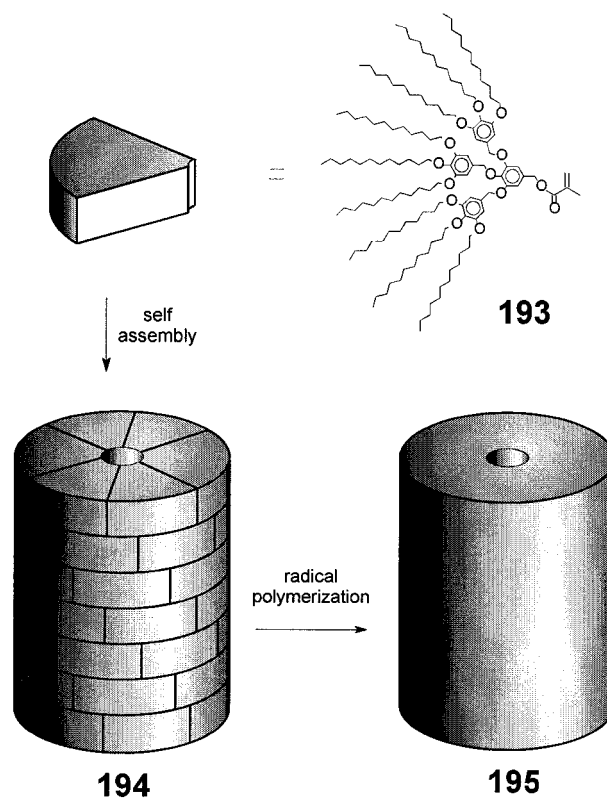
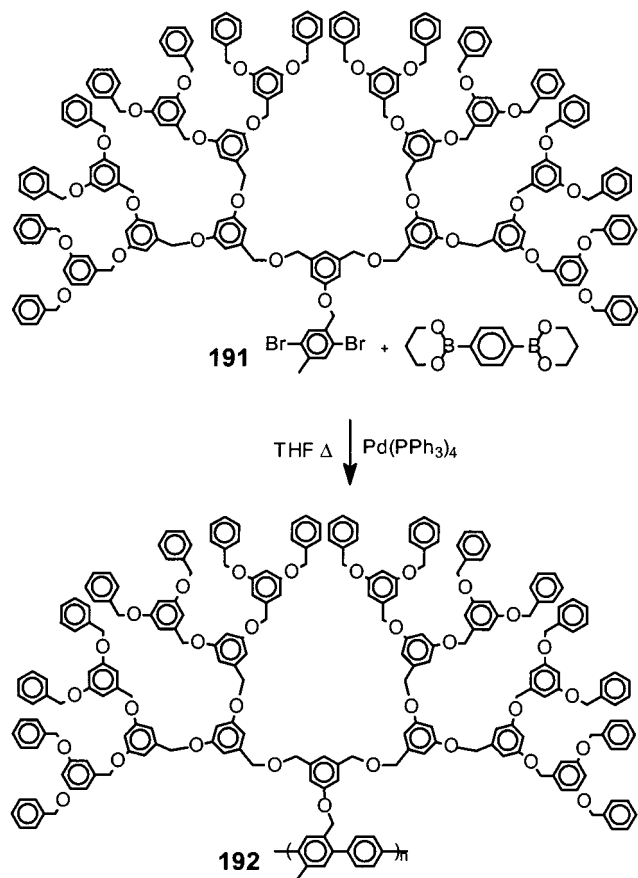


Figure 20.

Investigation with scanning force microscopy (SFM)³⁸⁵ and small angle neutron scattering (SANS)³⁹⁷ reveal that dendronized linear polymers exhibit a cylindrical conformation with a well-defined diameter, close to the predictions of molecular dynamics studies.⁴⁰³ Schlüter's polymers exhibit a unique degree of structural control: as the degree of polymerization increases, the conformation of the polymers changes from a spherical to a tubular shape.⁴⁰³

Percec and co-workers developed a unique approach toward dendronized polymers,^{343,404} making use of the tendencies of tapered dendrons with lipophilic chain ends **193** to self-assemble into columnar aggregates **194**. By incorporating styrene or methacrylate functionalities at the focal point (Figure 20), these dendritic macromonomers could be polymerized⁴⁰⁵ after forming tubular aggregates.^{84,112,406–408} Because of the proximity of the reactive monomer units in the shaft of the columnar aggregate, this approach exhibited an enhanced rate of polymerization.⁴⁰⁷ During subsequent SFM studies, it was determined that as the size of the dendritic side chain increases, the steric bulk forces the molecule to adopt a more extended, rigidity conformation.^{408,409}

Dendronized amphiphilic polymers have been synthesized with lengthwise segregation of the hydrophobic and hydrophilic domains (Figure 21). Bo et al. prepared these materials by polymerization of monomers that carried two domains of contrasting polarity,^{410,411} affording polymers, such as **196**, capable of forming monolayers at the air/water interface.

In addition, luminescent linear backbones have been encapsulated in dendritic shells through this technique,^{152,328} while the increased solubility im-

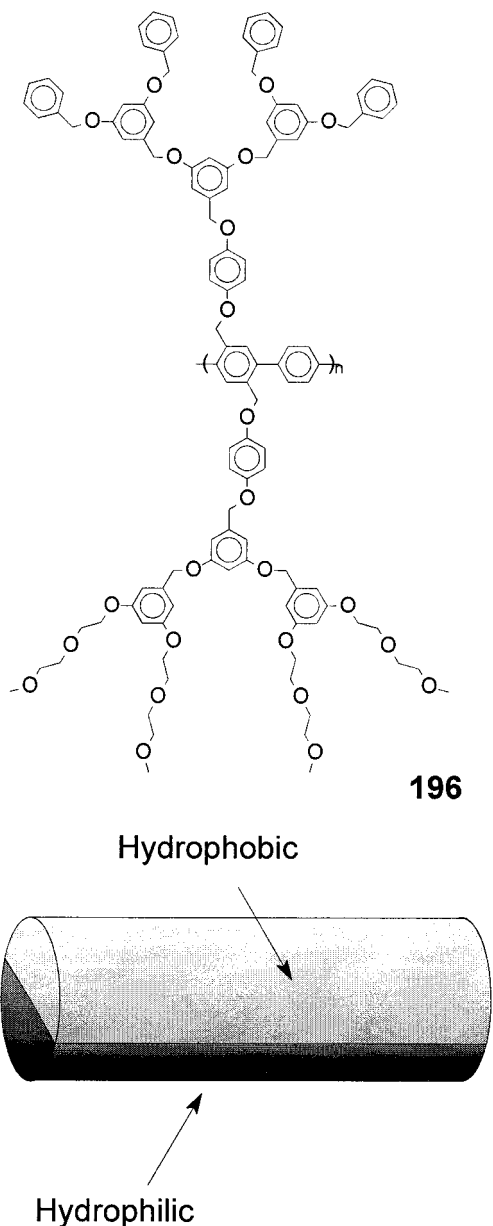


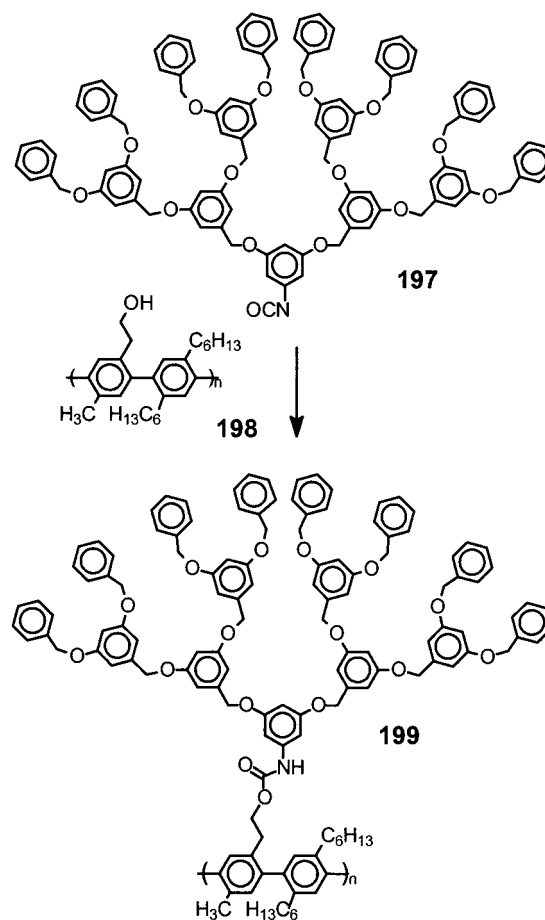
Figure 21.

parted by the dendrons has enabled the synthesis of elongated polymer chains.¹⁵² Sato et al. reported poly(phenylene ethynylene) cores encapsulated with Fréchet-type dendrons that exhibited enhanced luminescence from both dendritic antenna effects and reduced intermolecular quenching through steric encapsulation.³²⁸ Bao et al. also demonstrated that the encapsulation of poly(phenylenevinylene) cores with tris-branched poly(aryl ether) dendrons prevents the type of intermolecular π - π stacking that frequently occurs with smaller side chains.³⁹²

2. "Coupling to" Approach

An alternative approach developed by Schlüter and co-workers involves the attachment of convergently prepared dendrons onto a preformed, functional linear polymer. This was first attempted by the Williamson ether couplings between dendritic bromides and pendant hydroxyl groups on poly([1.1.1]-propellane)⁴¹² and poly(*p*-phenylene).⁴¹³ Nearly quan-

Scheme 26



titative coverage was obtained using the first and second generation Fréchet-type dendrons, while the more sterically demanding third generation dendron still achieved an impressive 70% coverage. A more efficient procedure (Scheme 26) involving the coupling of a third generation isocyanate functionalized dendron, **197**, with the pendant hydroxyl groups of the poly(*p*-phenylene) polymer **198**, led to a very high 92% coverage.³⁸⁴

Hawker et al. recently reported the synthesis of a low polydispersity, partly dendronized polymer that carried a statistical distribution of dendrons on one-fifth of the repeat units.⁴¹⁴ A random copolymer containing 80% styrene and 20% of a styrenic monomer (*N*-oxysuccinimide 4-vinylbenzoate) bearing the activated ester was produced with polydispersities below 1.2 using the living free radical approach. Because of the relatively large statistical spacing between the activated esters, amine functionalized Fréchet-type dendrons could be coupled with a high degree of incorporation. For the first three generations, the coupling reaction appeared to be quantitative, but in the fourth and fifth generation materials, a small percentage of the activated ester remained unreacted.⁴¹⁴

The two convergent approaches toward dendronized polymers offer complementary control over structural parameters. The macromonomer route ensures well-defined connectivity between the dendron and the polymer, but affords polymers with broad dispersity and generally low degrees of polymerization. In the

"coupling to" approach, on the other hand, the initial linear polymer may be prepared with a well-defined length and polydispersity, but the attachment of dendrons is prone to incomplete reaction.

D. Self-Assembly of Dendritic Cores

Self-assembled macromolecular structures are of particular interest because of their ability to reorganize in response to changes in their environment (concentration, solvent, pH, etc.)^{415,416} Zimmerman and co-workers^{417,418} first demonstrated the hydrogen-bond mediated self-assembly of dendritic cores (Figure 22) in 1996. The rigid bis(isophthalic acid)

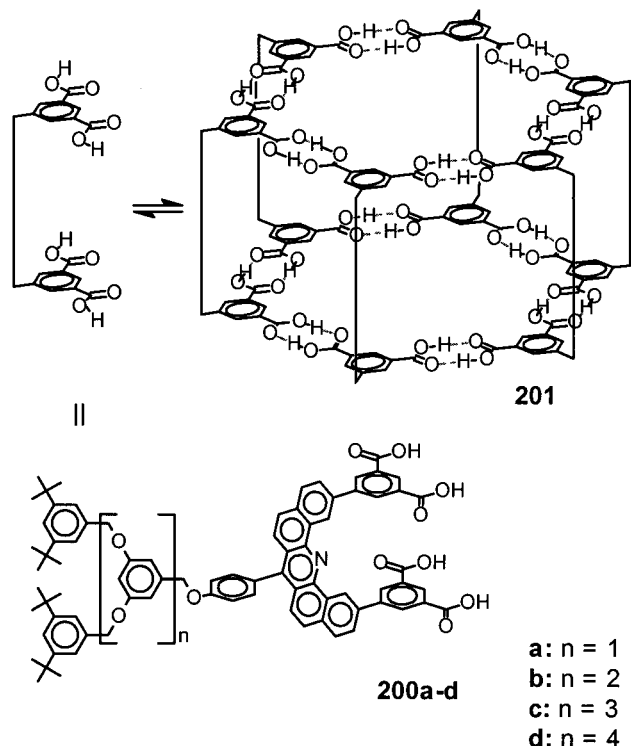


Figure 22.

component **200** was designed to form a hexameric aggregate **201**. A number of Fréchet-type dendrons of different generations were attached to **200** to elucidate the aggregation behavior of the resulting compounds. Size exclusion chromatography studies revealed that the nature of aggregation was very dependent upon the size of the pendant dendrons, as the second through fourth generation compounds, **200b–d**, formed strongly associated hexamers, regardless of concentration, whereas the aggregation behavior of the first generation dendrimer, **190a**, appeared very sensitive to concentration. This approach has since been used to assemble dendritic hexamers,⁴¹⁹ trimers, and dimers⁴²⁰ of hydrogen-bonded donor and acceptor moieties.

Shinkai and co-workers reported a spherical self-assembled system based upon a focal maltonolactone moiety.⁴²¹ The strong hydrogen bonding between focal saccharide moieties led to aggregation when placed in nonpolar solvents. Unlike previous examples, the number of dendrons aggregating was not due to a pre-designed core geometry or charge ratio and therefore was primarily influenced by the size of the

dendron attached. Dynamic light scattering data suggested that the sterically bulky high generation Fréchet-type dendrons produced small aggregates, while the smaller dendrons led to larger aggregates.⁴²²

Columnar aggregation was investigated by Aida and co-workers, who attached Fréchet-type dendrons to a *tert*-butoxycarbonyl-(L)-tyrosinyl-(L)-alanine focal group.⁴²³ In moderately nonpolar organic solvents, hydrogen-bonding interactions between the peptide segments led to the formation of a gel for dendrons of the second and third generations. Cross-polarized microscopy and scanning electron microscopy revealed the presence of fibril bundles, on the order of 1 μm . Such ordering was not seen in the parent peptide or the first generation dendron. The gel could be rapidly dissolved by addition of a small percentage of DMSO into the solvent.

Dendritic self-assembly has also been reported in a number of inorganic systems.^{45,92,327,329,353,424–426} Seminal studies in this area were carried out by Balzani and co-workers utilizing the self-assembly of polypyridine-type ligands around transition metals.^{427–430} These materials are considered beyond the scope of this review, as their preparation does not follow a strictly convergent methodology. However, more recently, convergent self-assembly utilizing polypyridine ligands around a transition metal core has been reported by the Chow,⁹² Balzani, De Cola, and Vögtle groups.³²⁹ Plevoets et al. designed a dendrimer consisting of three Fréchet-type dendrons bearing focal bipyridine units arranged around a ruthenium core.^{329,330} In aerated solution the ruthenium core with higher generation dendrons exhibited longer luminescence lifetime because the dendritic wedges protected the core from dioxygen quenching. The self-assembly of Fréchet-type dendrons bearing a focal carboxylate group (Figure 23) around a series of lanthanide metals, **202–204**, was

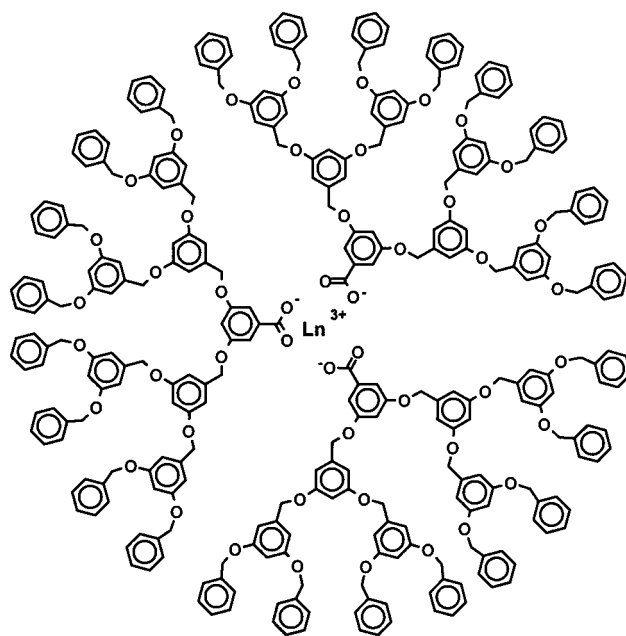


Figure 23.

reported by Kawa and Fréchet.^{45,327} The product exhibited a generation dependent increase in luminescence, suggesting the larger dendrimers can more effectively isolate their lanthanide cores from each other, reducing the rate of self-quenching.⁴⁵ Enomoto et al. noted a similar dendritic stabilizing effect with bis(μ -oxo-bridged)copper complexes.³⁵³ Triazacyclononanes with Fréchet-type dendron substituents were first metalated with copper and then oxygenated to form dimers. The half-lives of these compounds toward oxidative degradation were increased from 24 s for the second generation dendrimer to nearly an hour for the third.

The ability to construct and optimize self-assembled structures requires versatile substrates such as dendrons whose steric bulk, polarity and shape can be easily modified. Unfortunately relatively few systems are capable of producing large self-assembled structures with sufficient cohesive strength to withstand significant environmental changes.

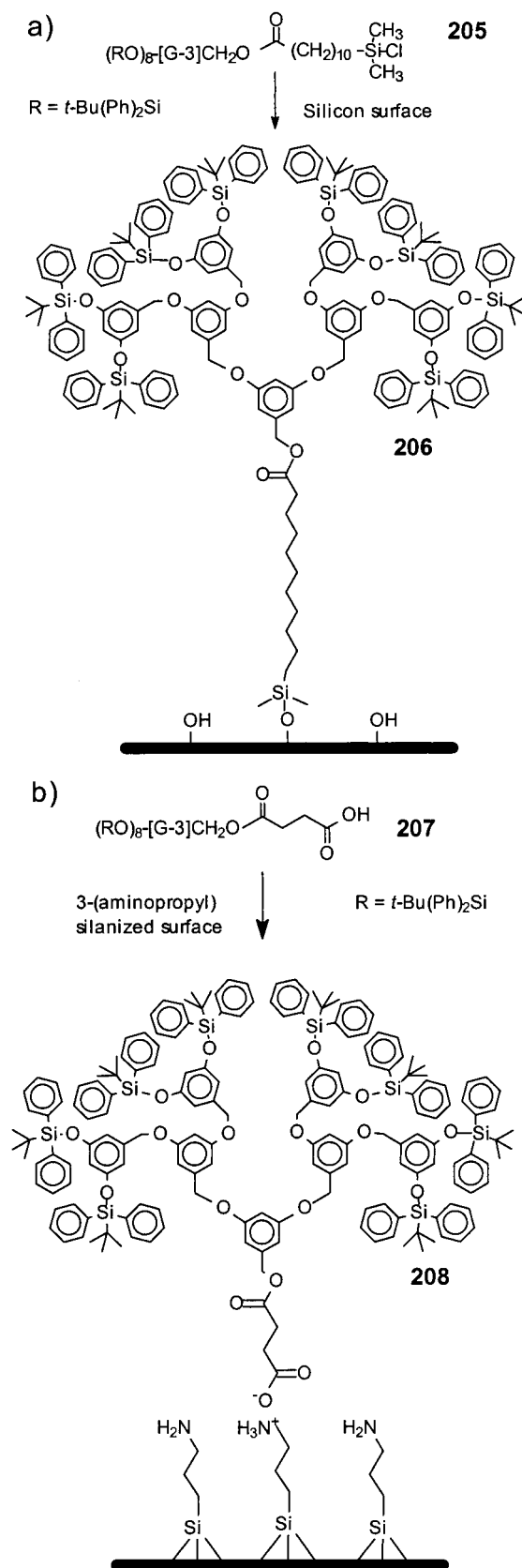
E. Surface-Bound Dendrons

The control of surface chemistry has become increasingly important as numerous device and material properties are controlled by surfaces and interfaces. For example, surface patterning is the foundation of lithography, and its implications in fields such as microelectronics or microfluidics are profound.

The synthetic and functional versatility of dendrimers as well as their defined shape has made them attractive molecules for surface modification.⁴³¹ Gorman and co-workers first reported the attachment of dendrons to a solid surface. Using dendrons with a focal thiol substituent⁹¹ they were able to assemble monolayers of first, second, or third generation dendrons on a gold surface.⁴³² Zhang and co-workers prepared similar monolayers of thiol substituted dendrons adsorbed onto silver and gold films and studied the modified surfaces in detail with scanning tunneling microscopy.^{433,434} Light-harvesting dendritic antennas can also be self-assembled onto the surface of silicon wafers providing a synthetically less demanding approach toward constructing chromophore arrays for energy transfer applications.⁴³⁵

Recently, Tully et al. demonstrated that dendrons could be applied onto surfaces as single, uniform layers with potential for high-resolution nanolithography through molecular level addressing. Both covalent and ionic (Scheme 27) approaches were investigated for the attachment of poly(aryl ether) dendrons onto the surface of a silicon wafer. The covalent dendritic monolayers were attached via a silyl chloride functionalized linker, **205**, capable of reacting with the surface silanol groups of the wafer.⁴³⁶ Ionically bound monolayers could also be prepared by treating an aminopropyl functionalized silicon surface with a dendron bearing a single carboxylic acid functionality at its focal point, **207**, while stronger surface attachment was achieved using dendrons bearing multiple carboxylate functionalities.⁴³⁷ Both the covalently and the ionically bound dendritic monolayers could be patterned using scanning probe lithographic techniques, affording raised SiO₂ features in the patterned areas. The

Scheme 27



homogeneous thin dendrimer monolayer remaining in unpatterned areas of the wafer surface proved resistant to etching with aqueous HF, which removed the oxidized pattern and etched a positive tone trench into the underlying silicon. At present, this approach

to nanolithography is not limited by the properties of the dendritic materials but rather by the imaging tools available. Both the size of the tip, which far exceeds that of a dendrimer, and the very low throughput of the single-tip scanning probe instrument prevent this approach from realizing its ultimate single-molecule addressing potential.

IV. Modification of the Periphery

Modification of the dendritic periphery is of particular interest because this portion of the dendrimer acts as the primary interface with the external environment. As might be expected, the functionalities at the periphery dominate the solubility properties of the molecule as the generation of the dendrimer increases.^{35,40} Although both NMR⁴³⁸ and molecular dynamic⁴³⁹ studies have suggested that the end groups of some dendritic systems are capable of "backfolding" toward the core, other studies clearly indicate that backfolding is not predominant in many dendritic systems.^{13,440} Being related to free-energy that controls interactions between chain-ends, repeat unit, and general environment (solvent), backfolding can be controlled by changing the design of the dendrimer.^{13,440} In fact, in a systematic comparison between analogous linear, hyperbranched, and dendritic polymers, Wooley et al. demonstrated that the chain ends of the poly(aryl ester) dendrimers were sufficiently accessible to be quantitatively modified, unlike the analogous functionalities of linear or hyperbranched structures.³⁵

There are two possible approaches toward incorporation of functionality at the periphery: the attachment of the desired end group before initiating the dendritic synthesis, or modification of the existing peripheral groups after completion of the synthesis.

A. Introduction of End Groups Prior to Dendritic Growth

Because the convergent route begins with the attachment of the end groups to the monomer, initial incorporation of a functional end group involves only a few coupling reactions that can be easily driven to completion. However, these peripheral moieties must possess the appropriate stability and solubility to permit dendritic growth through the repetition of coupling and activation steps without side reaction or degradation of the end groups.

The first examples of convergent end group modification were carried out by initiating the poly(benzyl ether) synthesis with para-substituted benzyl bromide end groups.^{73,74} A wide range of functional end groups proved compatible with the halogenation and Williamson coupling conditions required during iterative dendritic growth, including cyano,^{73,74,441,442} bromo,^{74,443,444} alkyl ester,^{41,442,445,446} alkyl ether,^{43,110,447,448} perfluoro alkyl ether,^{110,448–450} and oligo(ethylene glycol) ether.^{46,451} These simple variations enabled the solubility of the resulting dendrimers to be readily tuned. Fréchet-type dendrons have also been synthesized with end groups

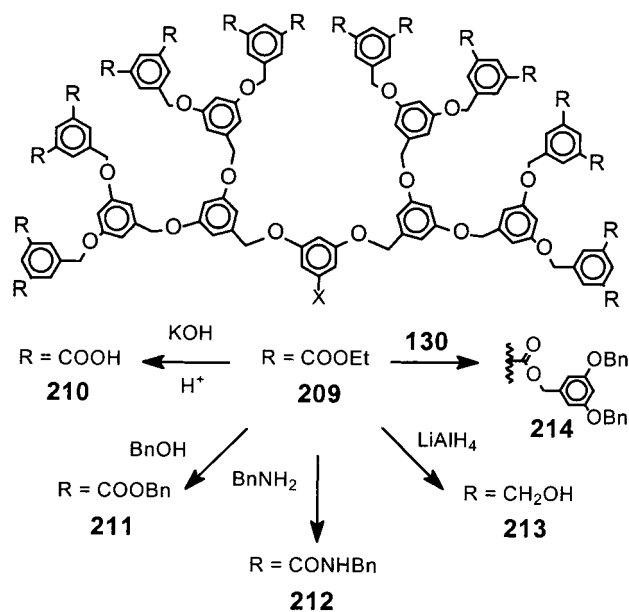
containing vinyl groups,^{308,452} organoruthenium moieties,^{453–455} ferrocenyl groups,⁴⁵⁶ TADDOL catalytic sites,⁴⁵⁷ concave pyridine units,^{458,459} liquid crystalline end groups,²⁴⁰ and chromophores.^{44,79–81,329,460,461} Similar approaches have been employed to incorporate triarylamine,¹²⁰ oligo(ethylene glycol),^{462,463} tetrathiafulvalene (TTF),^{464–466} saccharide,^{467–469} fullerene,^{426,470,471} and ferrocene^{169,472} moieties onto the periphery of other dendritic backbones.

B. Introduction of End Groups after Completion of Dendritic Growth

In the post modification route, the peripheral functionality is masked or remains unreactive during convergent growth, to be modified in a subsequent reaction. This approach allows the eventual incorporation of end groups that may be incompatible with the generation growth steps. However, these transformations suffer from the same complications as the divergent synthesis; in the case of larger dendrimers, the multiplicity of end group transformations requires the careful optimization of synthetic and purification techniques.

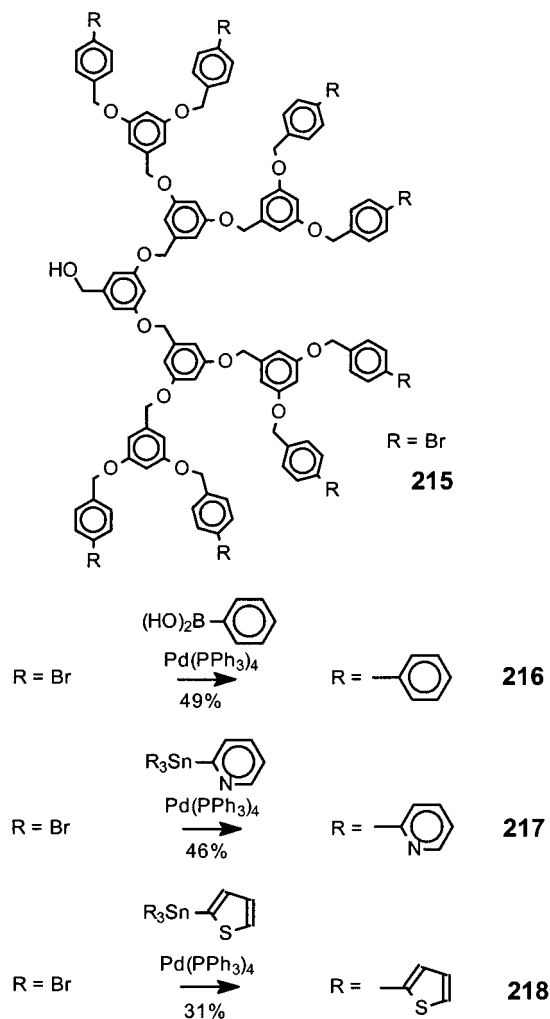
Numerous examples of postsynthetic modifications at the dendritic periphery have been explored. In early work, Hawker et al. investigated the hydrogenolysis and subsequent modification of benzyl-protected poly(aryl ester) dendrimers⁴⁷³ and later the saponification of Fréchet-type dendrimers with *p*-methyl benzoate end groups to afford an anionic carboxylated periphery.⁴¹ The isophthalate ester end groups proved to be especially versatile (Scheme 28)

Scheme 28



during the post modification of poly(benzyl ether) dendrimer **209**. Hydrolysis of the esters of **209** afforded poly-acid **210**,⁴⁴⁶ while reduction produced the polyol **213**.³⁶⁶ In addition, the isophthalate ester **209** could undergo transesterification or amidation reactions to yield **211** and **212**.⁴⁴⁶ The efficiency of the transesterification reaction enabled the divergent

Scheme 29

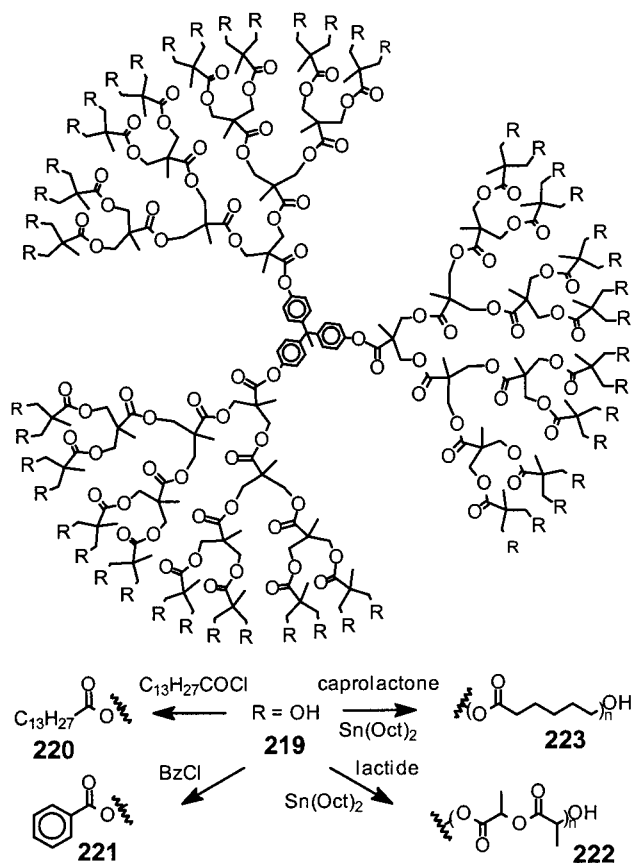


growth of an additional generation, **214**, by the attachment of first generation benzylic alcohols **130** to the periphery.

Groenendaal et al. have investigated the efficiency of palladium-catalyzed coupling reactions (Scheme 29) involving Fréchet-type dendrons with *p*-bromobenzyl end groups, **215**.⁴⁴⁴ The yields for the Suzuki coupling of a phenyl group, **216**, and the Stille coupling of thienyl, **217**, and pyridinyl groups, **218**, remained consistently near 90% per coupling reaction. However, the multiplicity of end groups on the third generation dendron reduced the overall yield to below 50% demonstrating the importance of using highly efficient transformations during modification of the periphery. The poly(alkyl ether) dendrons reported by Grayson et al. could withstand a wide range of postsynthetic modification because of their chemically rugged backbone.⁴⁰ Quantitative hydrogenolysis of the benzyl ether end groups of **98** or hydrolysis of the ketal end groups of **99** yielded a poly-hydroxylated periphery that could be efficiently modified through a variety of high-yielding esterification or etherification reactions.

Because the double exponential growth approach requires orthogonal focal and peripheral functionalities, it is inherently suited for peripheral modification. Zanini and Roy reported the peripheral glycolation of poly(alkyl amide) dendrons by treating the

Scheme 30

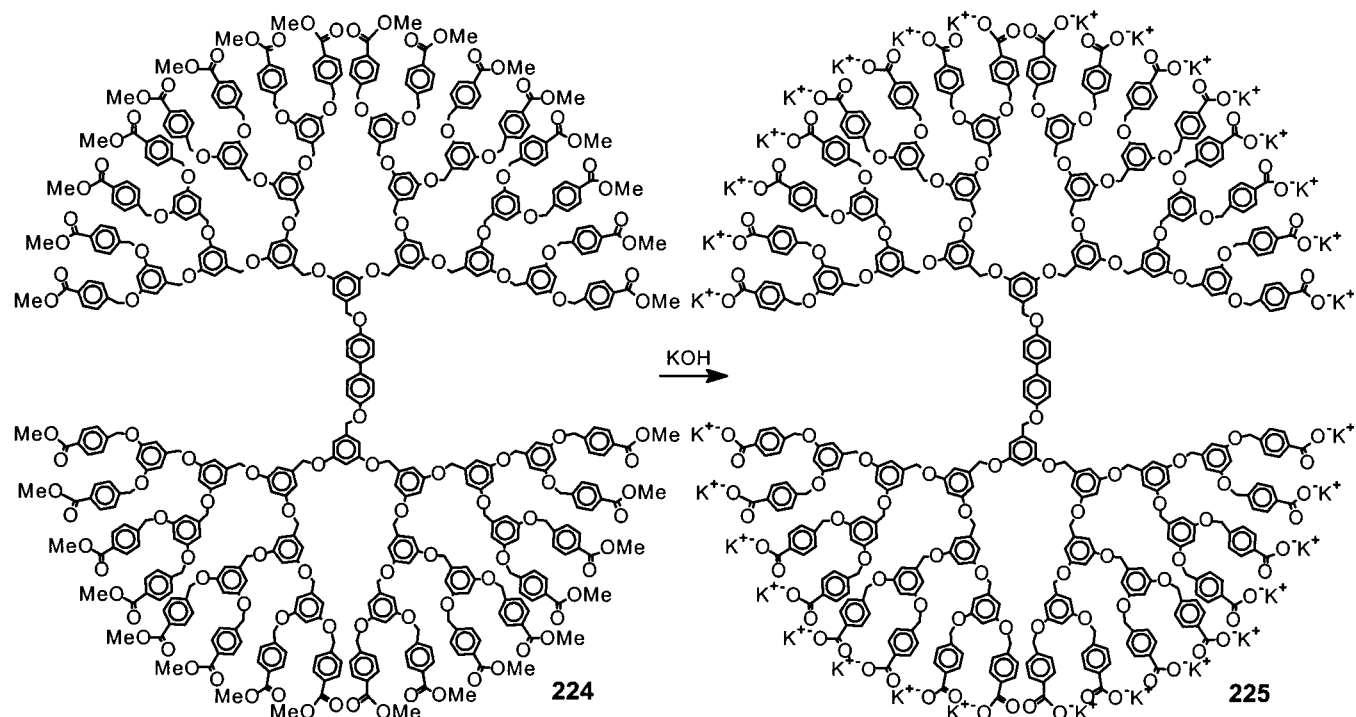


peripheral amine groups with chloroacetic anhydride and then coupling them to the desired sialic acid derivative.²²² Ihre et al. also demonstrated the facile peripheral functionalization (Scheme 30) of poly(alkyl ester) dendrimers prepared by both the double exponential growth and the single-stage convergent procedures. The poly-hydroxyl dendrimer **219** could be accessed by the hydrolysis of the acetonide protecting groups and esterified by reaction with the appropriate acid chloride²²¹ to afford a dendrimer with octanoate, palmitoate, **220**, benzoate, **221**, or even liquid crystalline peripheral units.⁴⁷⁴ Hedrick and co-workers have also explored the assembly of star-polymer structures that incorporate both linear and dendritic polyester units into the polymeric architecture. Their investigation included the use of the hydroxyl-terminated dendrimers as initiators^{475–477} for lactide, **222**, and caprolactone, **223**, ring opening polymerizations and the synthesis of dendrimers with a tertiary alkylbromide periphery for ATRP of methacrylate monomers,⁴⁷⁸ as well as the incorporation of linear poly(ester) chains between dendritic branch points.^{479,480} A similar approach was used by Hecht et al. to grow poly(caprolactone) from the multiple sites of a porphyrin core to insulate it from neighboring species.^{481,482}

C. Applications of Peripheral Modification

The simplest application of peripheral alteration is the modification of a dendrimer's solubility. For example, a number of groups have reported the use of terminal groups such as carboxylates^{41,265} or oligo-

Scheme 31



ethylene glycol chains^{261,262,303,334,483} to impart water solubility on the corresponding dendrimers. Hawker et al. demonstrated the first convergent synthesis of dendritic unimolecular micelles,⁴¹ using molecules with a spherical amphiphilic architecture (Scheme 31) analogous to that reported by Newkome in divergent systems.⁵⁷ Saponification of ester-terminated Fréchet-type dendrimer **224**, afforded a dendrimer with a polycarboxylate periphery and pH-dependent solubility.⁴¹ The polycarboxylate **225** also exhibited micellelike solubilization of polycyclic aromatic hosts (e.g., pyrene). These structures have been dubbed “unimolecular micelles” because, unlike traditional micelles, their covalently bound structure is not subject to disaggregation below a certain concentration threshold. Piotti et al. later utilized these micellar properties to design efficient macromolecular nanoreactors **226** and **227** (Scheme 32), that used the polarity difference between the dendrimers’ interior and exterior to drive the reactants toward the internal catalytic sites while simultaneously expelling the products to prevent catalyst inhibition.⁴³

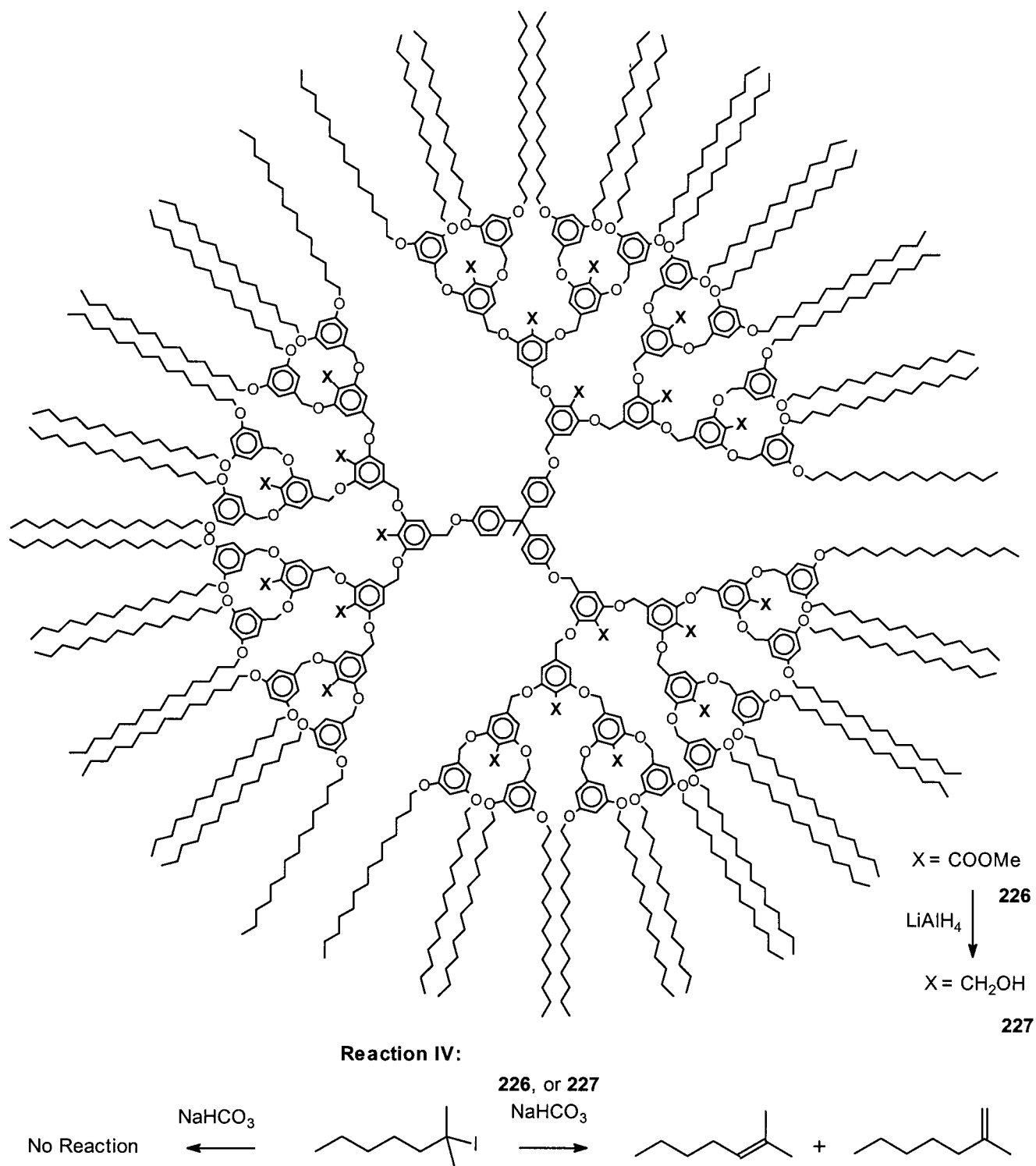
Because convergent dendrons exhibit a multiplicity of peripheral groups together with a single reactive focal point, providing for easy orthogonal functionalization and control of solubility, they represent an ideal scaffold for drug delivery applications.⁵³ Fréchet and co-workers recently investigated the incorporation of drug moieties by both encapsulation and covalent attachment. Liu et al. designed a water-soluble “unimolecular micelle” consisting of a dendritic polyether structure fitted with peripheral oligo(ethylene glycol) chains. The macromolecule could encapsulate 11 wt % of the model drug indomethacin and exhibited a slow sustained release of this drug when placed in an aqueous environ-

ment.⁴⁶ Kono et al. studied the concepts of covalent drug loading and targeting by attaching folate or methotrexate residues to Fréchet-type dendrons via diacylhydrazine linkages.⁴⁸⁴ The water solubility of these materials could be improved by attachment of a poly(ethylene glycol) chain to the focal point of the dendron.

The ability to drastically alter dendritic solubility by modification of the end groups also makes convergent dendrons attractive materials for nanolithography. As photolithographic resolution approaches the size regime of linear polymers, the compact, “pixellike,” globular conformation of the dendrimer is expected to provide better resolution than longer linear polymer chains. Tully et al. have reported the preparation of *tert*-butyloxycarbonyloxy (*t*-BOC) protected dendrimers **228**, spun cast onto silicon wafers for use as dendritic photoresists (Scheme 33).⁴⁸⁵ Imaging was achieved by activation of a photoacid generator where the polymeric film was exposed to e-beam lithography, leading to removal of the *t*-BOC protecting groups and producing the base-soluble poly-phenol dendrimer **229**. Developing with aqueous base removed the exposed regions of the resist, while development with organic solvents remove the unexposed polymer, enabling access to complementary images with feature sizes well below 100 nm.

Dendrimers can also serve as a scaffold for energy transfer between chromophores,⁴⁴ a useful step toward the goal of efficient light-harvesting and artificial photosynthesis. Although a number of studies have demonstrated the ability of dendritic repeat units to act as an antenna,^{119,257,428,429,486,487} funneling energy toward the core, attachment of dye groups to the periphery of an “insulating” dendritic structure (Figure 24) has enabled Fréchet and co-workers to carry out a more systematic study of the energy

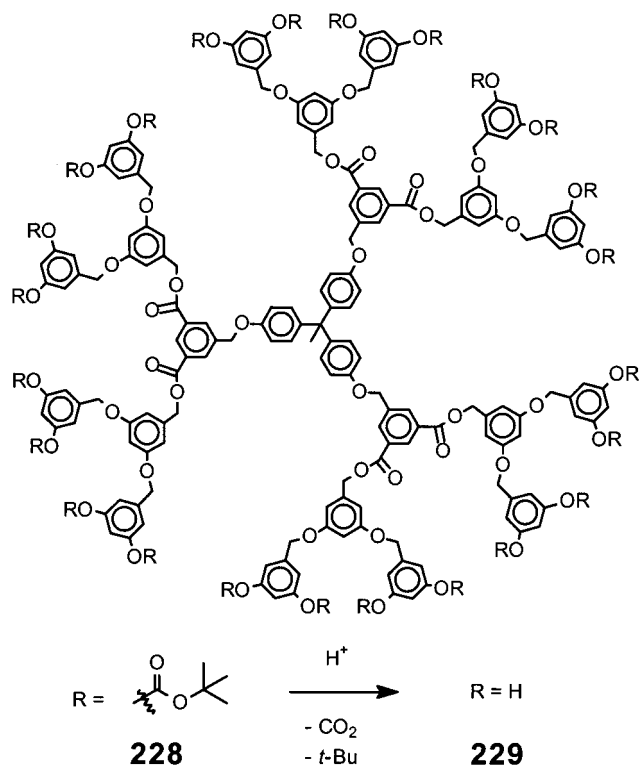
Scheme 32



transfer in these dendritic systems.^{80,488,489} The well-defined dendrimer architecture enables a multiplicity of donating chromophores at the periphery and an acceptor chromophore at the focal point to be fixed within the distance range required for efficient Förster energy transfer. In addition, the irradiation of multiple donating chromophores around a single acceptor amplifies the emission of the focal acceptor due to the highly efficient energy transfer that occurs within these molecules.⁴⁸⁸ A variety of systems with different chromophores, including coumarin dyes **230**

and oligothiophenes have been investigated,⁸¹ verifying the generality of this approach. In addition, Christoffels et al. have investigated the energy transfer between dye-labeled dendrons assembled onto a silicon substrate, and verified that the energy transfer and amplification phenomena could also be observed within monolayers.⁴³⁵ Pioneering work by Moore and co-workers on a different approach utilizing a layered convergent structure^{119,486} rather than end-functionalized dendrons is discussed in a later section.

Scheme 33



Dendritic LEDs (light-emitting diodes) can also be prepared by attaching hole transporting triaryl-amines to the periphery of dendrimers bearing fluorescent cores.^{120,145–147,461} Moore and co-workers¹²⁰

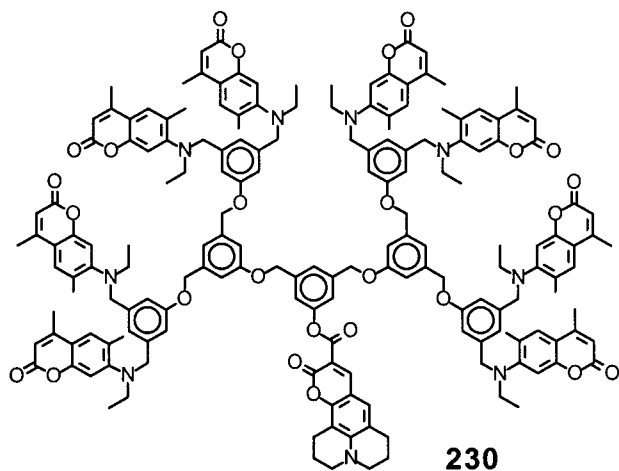


Figure 24.

first reported the design and synthesis of a dendritic LED (Figure 25) in 1996. The incorporation of triarylamine groups on the periphery **231** improved the hole injection process, lowering the onset voltage required to operate the devices. In separate work, Freeman et al. showed that if the dendrimers are designed to provide sufficient site isolation of their core, intermolecular energy transfer is inhibited enabling simultaneous emission from different core chromophores.^{461,490} As a result, the color of emission from the device may be tuned by simply adjusting the ratio between different “site-isolated” dendritic chromophores.

The nature of dendritic self-assembly processes, and therefore the resulting overall architecture, can

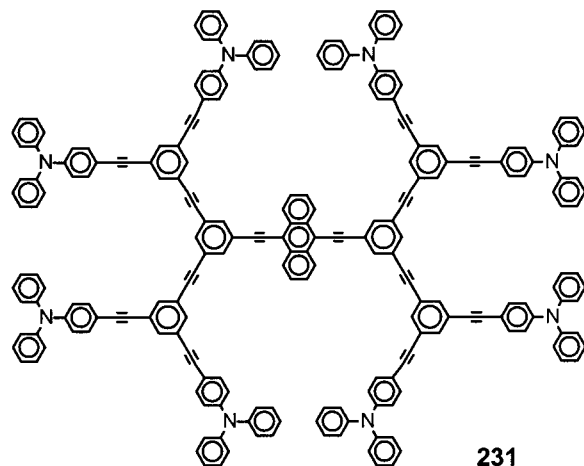


Figure 25.

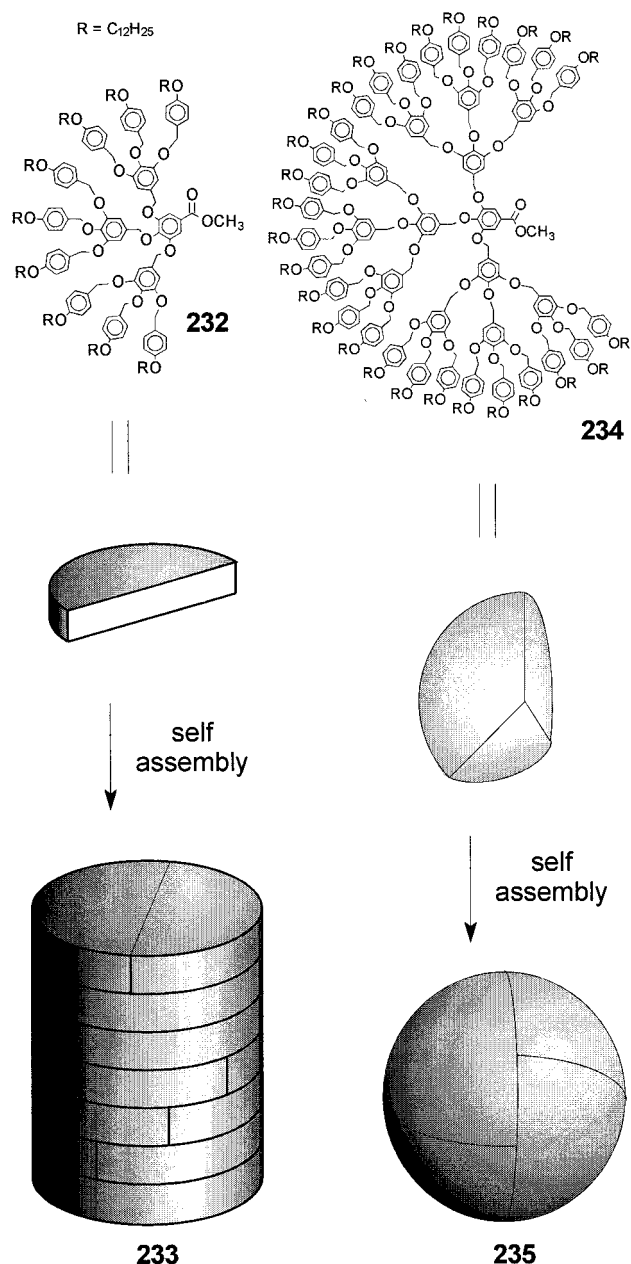


Figure 26.

also be tuned by modification of the periphery. After investigating the tubular self-assembly of first gen-

eration dendrons bearing lipophilic chains at the periphery,^{343,404,491} Percec and co-workers systematically studied the effect of generation number on the self-assembly of dendrons.^{82,83,85,110–113,492,493} X-ray diffraction of a representative system¹¹¹ (Figure 26) showed that the first and second generation dendrons exhibited disklike shapes **232** that self-assembled into cylindrical columns **233** while the third generation dendrons resembled a fragment of a sphere, **234**, and formed spherical aggregates **235**, within a cubic lattice.

The periphery of convergently synthesized dendrimers has also been modified to allow the assembly of monolayers,⁴⁹⁴ to support dendritic catalysts,⁴⁹⁵ to control the intermolecular assembly of porphyrin dendrimers,²⁴⁶ to probe the effect of photoisomerization,³¹⁹ and to enable cross-linking of the periphery followed by removal of the core.⁴⁹⁶ These studies in peripheral modification highlight the versatility of the convergent synthesis. In particular, the ability to selectively modify the periphery and focal functionalities of a dendron enables the design of complex macromolecules that involve the interaction between multiple functional components.

V. Modification of Repeat Unit

The convergent approach also permits the incorporation of functional repeat units. Because the repeat units comprise the majority of the dendritic structure, they represent an ideal location for multiple functional moieties. In addition to the numerous examples of conjugated dendrimers previously discussed,^{115,116,119–122,124–130,132–134,140–148,497} the convergent approach has been demonstrated as a viable route toward the preparation of dendrimers with a range of repeat units including: fullerene,^{498,499} quaternary ammonium salt,¹⁷⁷ pyridine,^{382,500–502} TTF,^{503–506} triarylamine,^{171–173,507,508} carbazole,^{509,510} azobenzene,^{351,511–513} liquid crystalline,^{514–516} and chiral repeat units.^{96–108,199,202}

A. Incorporating Monomer with Functionality

Because of the sheer multiplicity of repeat units, the incorporation of functional moieties into the monomer can have a profound effect on macromolecular properties. For example, Nagasaki et al. reported the synthesis of photoresponsive dendrimers containing an azobenzene functionality in each repeat unit.³⁵¹ Exposure to UV light induced an isomerization of the azobenzene units, leading to a significant molecular contraction observed by both dynamic light scattering and size exclusion chromatography.³⁵⁰ In the poly(TTF) dendrimers reported by Christensen et al., each of the 21 TTF units is capable of two single electron oxidations. All of the repeat units in the second generation dendrimer can be oxidized concurrently, affording a macromolecule exhibiting a 42⁺ oxidation state.⁵⁰⁶

Modification of the repeat units can also provide conformational control in dendritic structures. Huang et al. reported the synthesis of a family of dendrons,

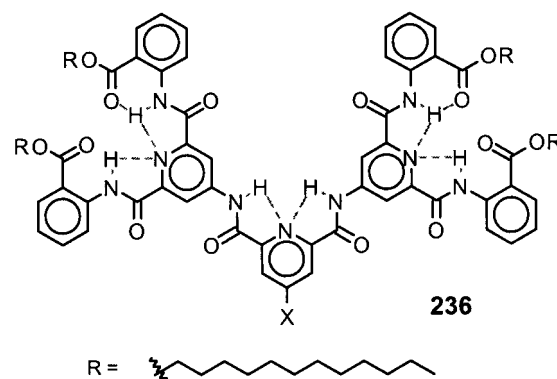


Figure 27.

236, that incorporate hydrogen bond donor and acceptor moieties within the repeat units (Figure 27) to rigidify dendritic structure.^{190,517} ¹H NMR and IR characterization suggest that each of the expected hydrogen bonding interactions occurs in solution, affording a more conformationally rigid structure than the analogous Fréchet-type dendron. Pursuing the goal of controlled encapsulation and release of guest molecules, Tominaga et al. reported the synthesis of a dendron, **237**, with cross-linkable (Figure 28) uracil repeat units.⁵¹⁸ Upon irradiation at 280 nm,

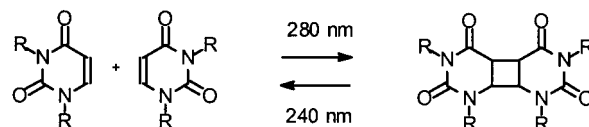
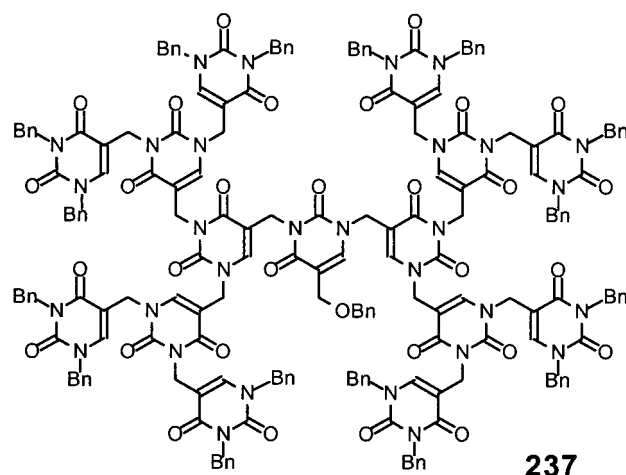


Figure 28.

the conformation could be “locked” through the incorporation of intramolecular cross-linking. The cyclization reaction could be readily reversed by irradiation at 240 nm reverting back to an “open” dendritic configuration. Recently, Thayumanavan and co-workers have synthesized dendrons based on an amphiphilic analogue of the Fréchet-type repeat unit that are expected to undergo drastic conformational transformations in response to changes in solvent polarity.⁵¹⁹

Dendrimers containing chiral repeat units have also been investigated in the context of chiral recognition. While the coupling reaction between a tri-

functional chiral core and a dendron composed entirely of *S* repeat units, **35**, could be driven to completion, the coupling with the corresponding *R* enantiomer, **36**, could not proceed past the second coupling.¹⁰⁷

B. Postsynthetic Modification of Repeat Unit Functionality

Postsynthetic transformations of dendritic repeat units have been largely ignored until recently. In early work, Lochmann et al. had investigated the deprotonation, metalation, and functionalization of generation four Fréchet-type dendrons with super-bases. The majority of the benzylic sites, as well as some aromatic sites, could be deprotonated and up to 34 atoms of potassium introduced without degradation of the dendrimer framework. Subsequent quenching and modification was carried out using D₂O, carbon dioxide, or octadecylbromide.⁵²⁰ At about the same time, Rajca et al. synthesized a dendritic polyradical by lithium metalation and iodine oxidation of a triarylmethyl alcohol repeat unit.¹⁷⁶ Matsuda et al. also reported the synthesis of a dendritic polycarbene from a poly(aryl ketone).¹⁷⁴ The ketone repeat unit was converted to the corresponding hydrazone, oxidized to the poly-azo compound, and then photolyzed to produce a polycarbene dendrimer. Although the later two dendrimers were prepared to study their magnetic properties, both proved to be unstable, likely due to flexibility in their structure that enabled cross-linking.

Recently Piotti et al. reported the modification of repeat units as a means of tuning the interior polarity of a dendrimer catalyst (Scheme 32). The relatively polar dendritic interior of **226** helped to catalyze the formation of the ionic intermediate in a unimolecular elimination reaction. (reaction IV) The product outflow is driven by a "free energy pump," resulting from the inverse micellar character of the dendrimer. Due to solvation effects, the relatively polar halide substrate is driven toward the dendritic interior from the nonpolar solvent pool, while the alkene product is readily expelled, giving rise to high turnover. If the ester group on the 4-position of each Fréchet-type repeat units of dendrimer **226** is reduced⁴³ to the alcohol **227**, the increased internal polarity leads to an increase in both conversion and turnover for the corresponding elimination reaction.

Since this study, the addition of repeat units capable of a postsynthetic transformation have been investigated. Bo et al. investigated the incorporation of an aryl bromide functionality on the Fréchet-type repeat unit, which could be modified by a Suzuki cross-coupling with an aryl boronic acid.⁵²¹ Freeman et al. explored the attachment of an allyl ether functionality on the same repeat unit,⁵²² while Schultz et al. incorporated an aromatic spacer with two allyl groups to enable internal cross-linking via olefin metathesis.⁵²³

VI. Dendritic Copolymers

One of the primary advantages of the convergent synthesis is its unparalleled synthetic control that

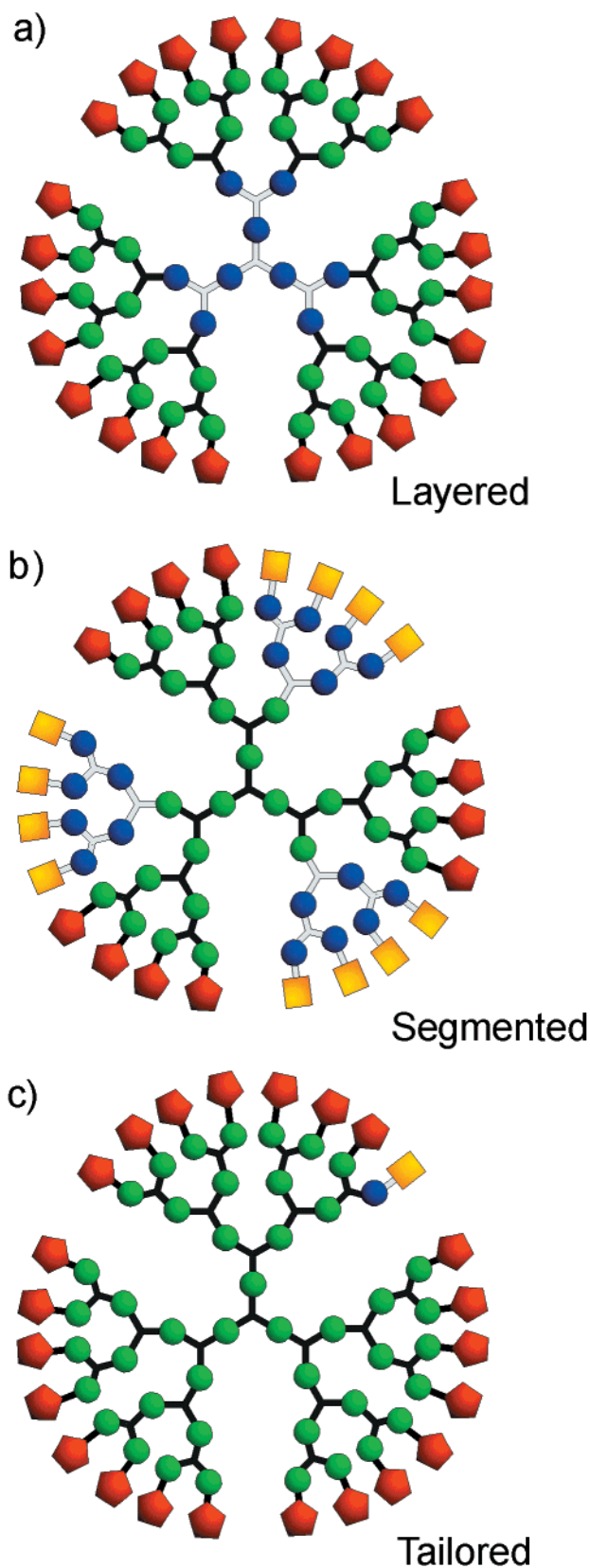


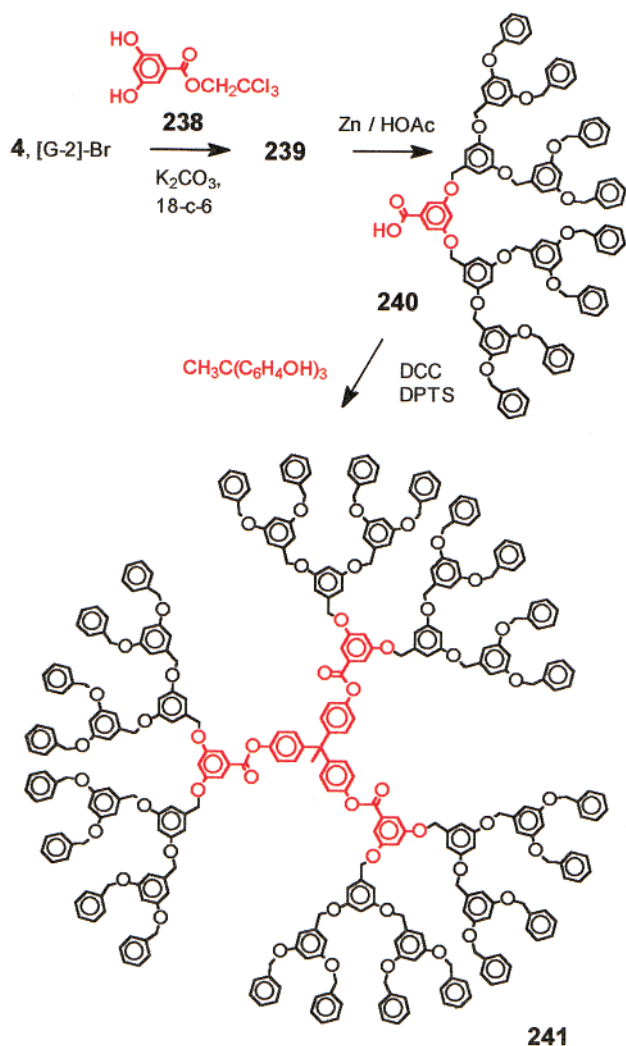
Figure 29.

enables the synthesis of well-defined dendritic copolymers. The wide range of possible dendritic copolymers can be divided into three basic structural categories (Figure 29): layered, segmented, and tailored copolymers.⁴⁴³

A. Layered Copolymers

Layered copolymers contain two or more types of repeat units that are segregated in a layerwise fashion in the final dendritic product (Figure 29a). Since both the divergent and convergent syntheses progress by the stepwise addition of layers, both procedures can theoretically access these hybrid structures. However, with the notable exception of Balzani and co-workers, who have divergently prepared dendrimers containing concentric layers of transition metals connected through multidentate oligopyridine ligands,^{427,430} and preliminary studies by Dvornic et al.,⁵²⁴ layer copolymers have been predominantly investigated through the convergent growth approach. The first synthesis of a layered dendritic copolymer (Scheme 34) was reported by

Scheme 34



Hawker and Fréchet⁵²⁵ via convergent attachment of preformed poly(benzyl ether) dendrons **4** to a poly(benzyl ester) monomer, **238**. Continuation of the poly(benzyl ester) synthesis followed by coupling to a triphenolic core afforded the layered dendrimer **241**. The primary synthetic requirement for the two different monomers is that the outermost dendritic layers must be chemically inert to the coupling and

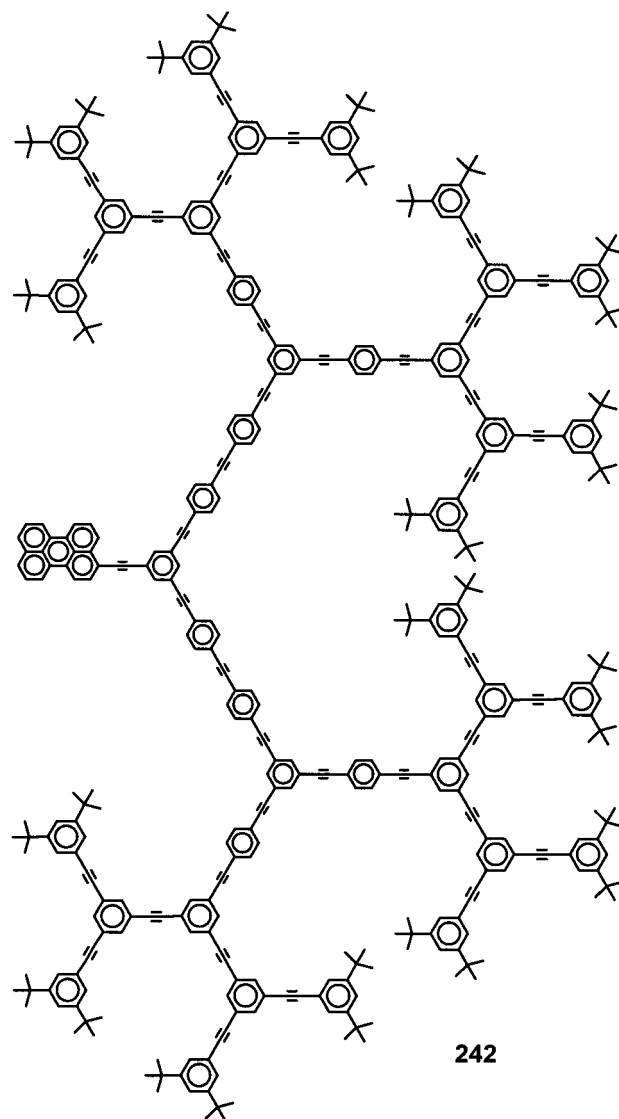


Figure 30.

activation conditions required during the dendritic growth of the inner repeat units.

The most noteworthy application of layered dendrimers to date has been their use in light-harvesting devices (Figure 30). Moore and co-workers reported an interesting gradient effect when using a poly(phenylacetylene) dendrimer, **242**, with repeat unit conjugation length that increases with generation from the periphery to the core.^{119,486} As a result, the HOMO–LUMO gaps of the conjugated repeat units decrease from the exterior to the interior, causing a directional energy flow toward the core. A similar approach has been used by Morikawa et al. in the synthesis of graded poly(ether ketone) dendrons,¹⁸¹ and van Manen et al. in the synthesis of layered metallodendrimers²¹⁰

Dendritic layer copolymers have also been prepared via the hypercore approach,⁸⁷ and by divergent growth from the periphery of convergently prepared dendrimers,⁴⁴⁶ or dendronized polymers.³⁹⁸ This layered dendritic architecture has been used by a number of groups to probe the nature of chirality.

Mak and Chow^{99,100,526} and Murer et al.¹⁰⁷ investigated the chiroptical properties of dendrimers consisting of alternating layers of chiral repeat units, whereas McGrath and co-workers examined a series of dendrons that contained a single chiral generational shell within an otherwise achiral fourth generation dendron.⁵²⁷

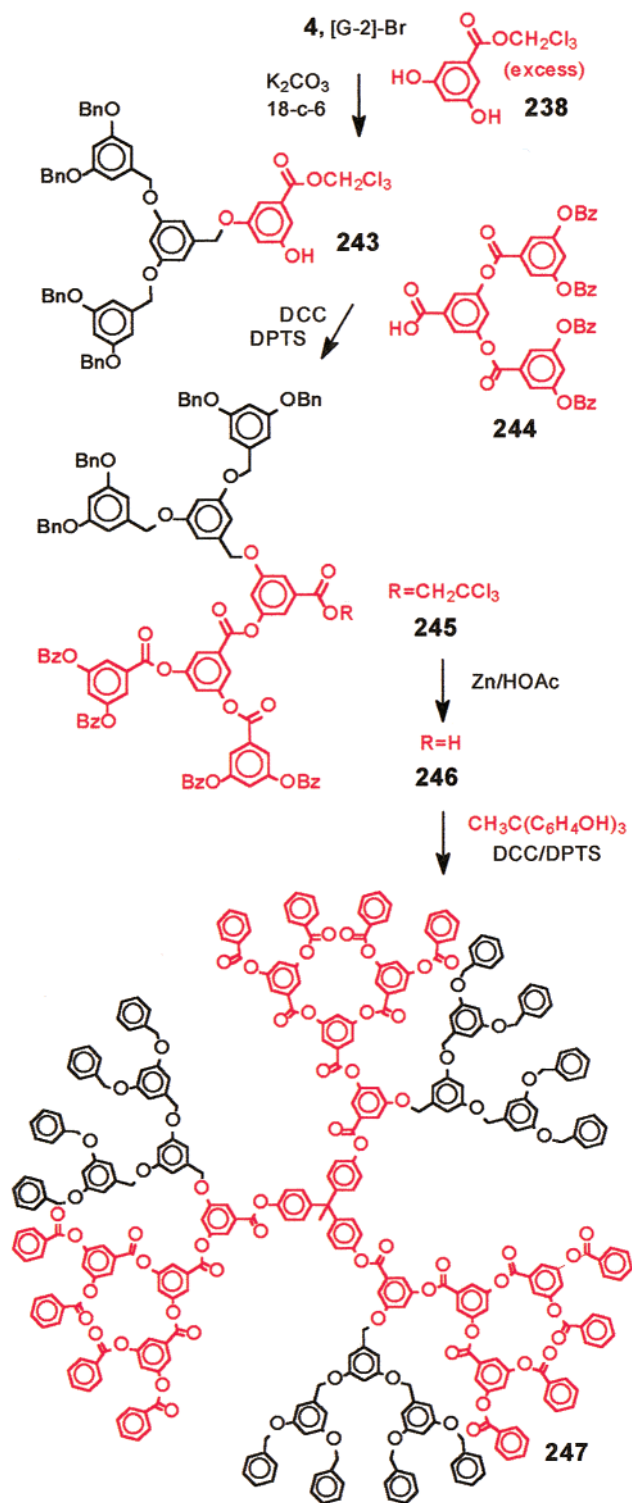
B. Segmented Copolymers

Segmented copolymers are hybrids in which contrasting repeat units are segregated into wedge-shaped regions (Figure 29b). The convergent approach is ideally suited to create these structures because each growth reaction may be stopped after the first of two possible coupling reactions by using an excess of monomer. After isolating the singly coupled product, the remaining active functionality of the monomer may be coupled to a dendron with a chemically different backbone (Figure 5). This hybrid coupling strategy produces a dendron composed of two contrasting wedges. Because growth in the divergent synthesis proceeds outward from the core, it is difficult to control the multiple reactions of the surface groups with enough precision to access these architectures. Only through the application of protecting group chemistry have representative molecules of this type been accessed via the divergent methodology, but these approaches are not generally applicable.^{528–530}

The first report of such architectures by Hawker and Fréchet, was again based on the poly(benzyl ether) and poly(benzyl ester) repeat units as contrasting dendritic components⁵²⁵ (Scheme 35). The second generation Fréchet-type dendritic bromide **4** reacted with an excess of the poly(benzyl ester) monomer **238** to afford the singly coupled product **243**. The remaining phenol of **243** was coupled by a DCC-mediated esterification to the second generation poly(benzyl ester) carboxylic acid **244**, yielding the unsymmetrical hybrid dendron **245**. After activation of the focal point, three of these dendrons could be coupled to a trisphenolic core to yield dendrimer **247** with three pairs of hybrid ester–ether dendritic wedges. An analogous approach was utilized by Chow and co-workers during the preparation of dendritic copolymers with alternating D and L chiral segments.^{99,100,526} Although the structures of the segmented block copolymers are often represented in two dimensions, implying C_n symmetry, the flexibility within the repeat units enables considerable conformational variations.

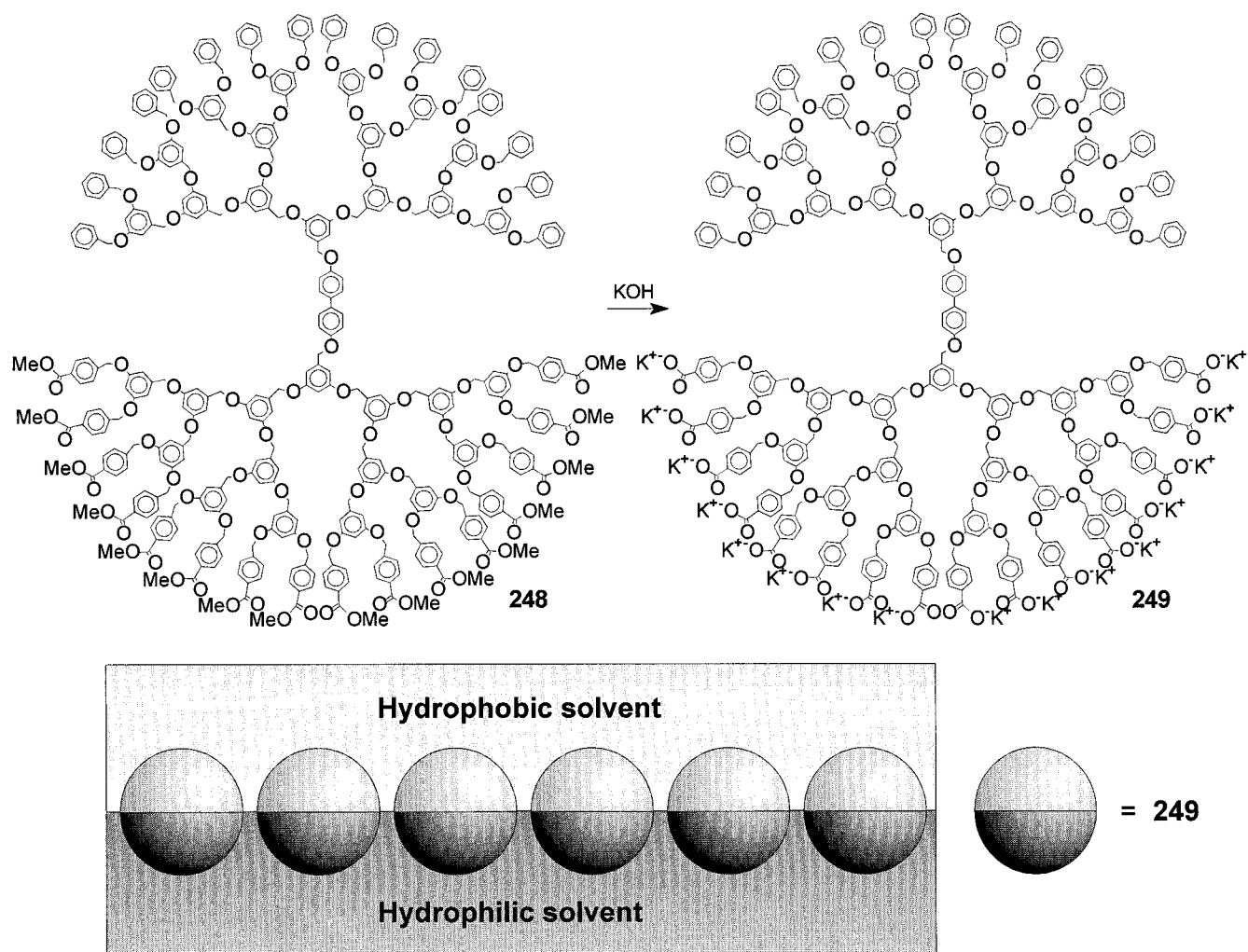
The synthesis of surface copolymers entails the same methodology as the segment copolymers, except the two contrasting dendrons differ only in the identity of their end groups.⁴⁴³ This technique was developed to access hemispherically segregated surface copolymers. Wooley et al. described the preparation of dendrimers in which one of the hemispheres contained *p*-cyanophenyl electron-withdrawing groups, and the other traditional 3,5-bis(benzyloxy)phenyl electron-donating groups. The resulting dendrimer was shown to have a strong dipole due to its globular shape and the structural segregation of different end

Scheme 35



groups.⁴⁴¹ Dendrimers were also synthesized that contained benzyl ether end groups in one hemisphere and methyl esters in the other. Saponification of the esters produced the dendritic amphiphile **249** that demonstrated micellar properties (Scheme 36). Because of the well-segregated polar and nonpolar regions within the dendrimer, these structures are believed to orient themselves at the interface between hydrophilic and hydrophobic solvents.⁴¹ Pesak and Moore used a similar approach to investigate the

Scheme 36



aggregation behavior of poly(phenylacetylene) dendrimers with a periphery made of lipophilic *tert*-butyl end groups, and blocks of 4, 8, 16, or 32 carboxylic acid groups,⁵³¹ and Bryce et al. used this approach to control the number of π -donor and π -acceptor groups on the periphery of polyester dendrimers.⁴⁶⁵

The chemically robust backbone of the poly(alkyl ether) dendrons enabled a unique opportunity to demonstrate the orthogonal functionalization of surface copolymers.⁴⁰ The benzyl and ketal protected dendrons reported by Grayson et al. were incorporated into two different copolymer architectures: a block and an alternating surface copolymer. The block copolymer (Scheme 37a) was synthesized by coupling a single allylic functionality of monomer **87** with the third generation ketal protected dendritic alcohol **97**. After isolation of **250**, displacement of the remaining allylic chloride by the third generation benzyl-protected dendron **96** afforded **251**. The fourth generation alternating copolymer (Scheme 37b) was prepared by using an identical hybrid coupling strategy to produce the second generation hybrid dendron **253** and then by repeating the activation and coupling steps until the fourth generation, **257**. Both copolymer structures exhibited a quantitative, selective deprotection of either the eight benzyl ethers

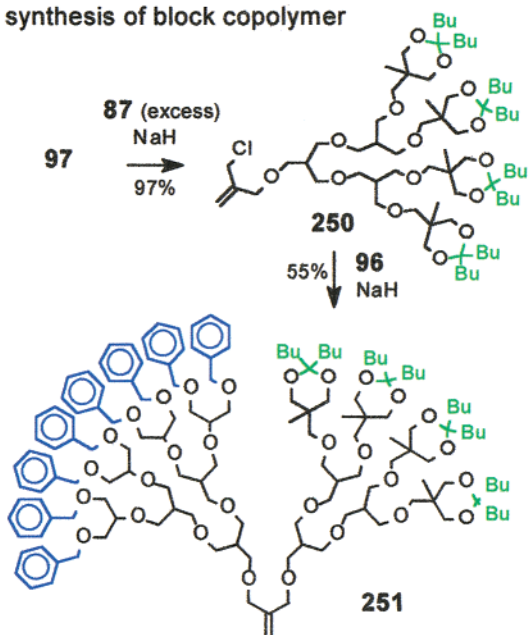
by palladium-catalyzed hydrogenation, **258**, or the four cyclic ketals by acid-catalyzed hydrolysis, **259** (Scheme 38). The periphery of these molecules could be selectively functionalized to replace the eight ketal-protected alcohols with oligoethylene glycol chains and the eight benzyl ethers with benzoate esters.⁴⁰

C. Tailored Copolymers

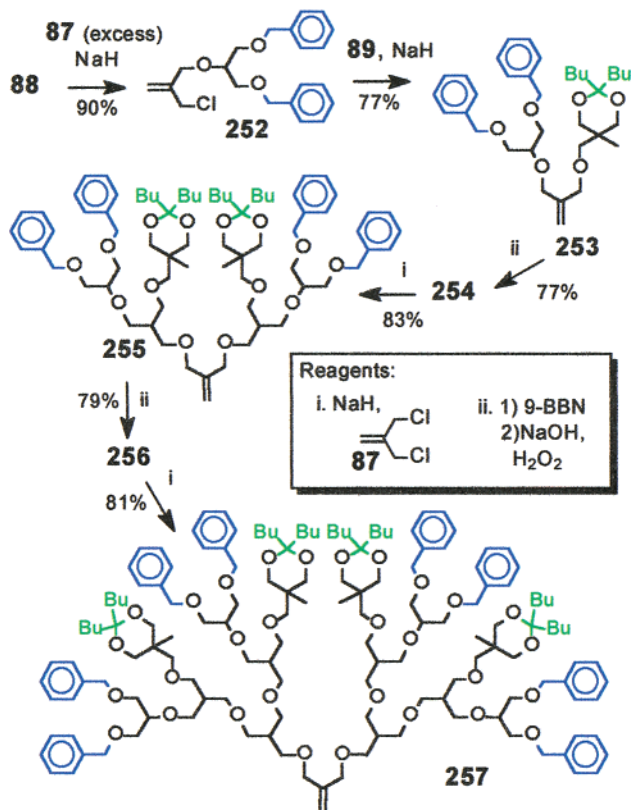
Tailored copolymers can only be accessed by the convergent approach and utilize the hybrid coupling strategy during a series of coupling steps to control the exact number and placement of functional moieties within the dendritic structure (Figure 29c). Control over the peripheral functionalities is best exemplified by the synthesis of the fourth generation Fréchet-type dendron **260**, bearing a single *p*-cyano-benzyl group at the periphery⁷³ (Figure 31). This architecture is achieved (Scheme 39) by coupling one of the two phenolic groups of the monomer with benzyl bromide by using an excess of monomer **1**. After isolating **261**, the remaining phenolic group can be coupled with the *p*-cyanobenzyl bromide, yielding the hybrid dendron **262**. Activation of the focal functionality affords **263**, which can be coupled with

Scheme 37

a) synthesis of block copolymer



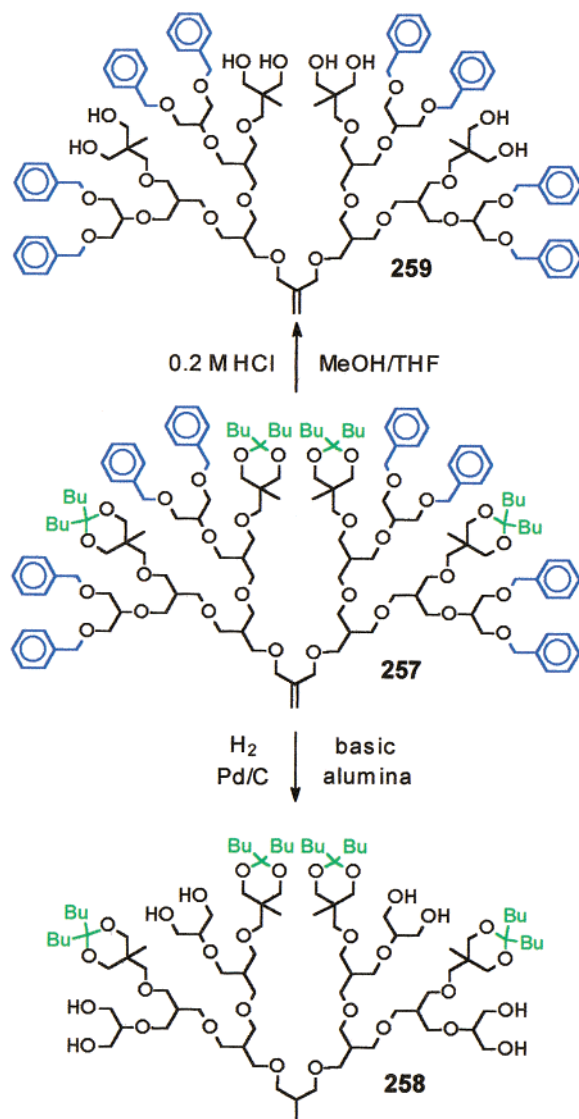
b) synthesis of alternating copolymer



dendron **264** to produce the second generation dendron **265**, with a single peripheral nitrile group. Repetition of this process affords the fourth generation dendron **260**, bearing a single cyano substituent on its periphery. Though tedious, this procedure enables the synthesis of dendrons bearing any number of modified peripheral groups.

This technique can also be used to control the placement of a specific functionality on any repeat

Scheme 38



unit within the interior of the dendrimer. Schlüter elegantly demonstrated this concept by preparing a third generation Fréchet-type dendrimer bearing a single *p*-bromo functionalized monomer unit at the first, second, or third generation branching points⁵²¹ (Scheme 40). These dendrons could then be incorporated into a dendrimer with two unfunctionalized

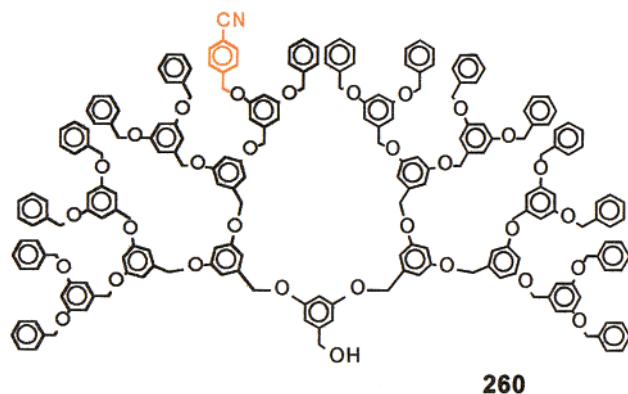
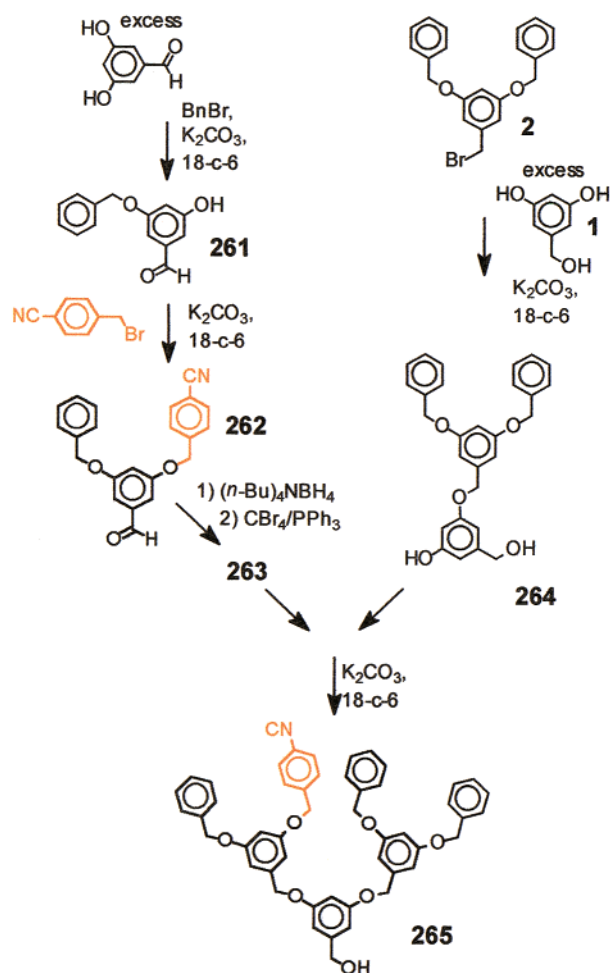


Figure 31.

Scheme 39



third generation dendrons. The single aryl bromide functionality of each dendrimer can be modified by a Suzuki cross-coupling reaction. The palladium-catalyzed coupling of *tert*-butylphenylboronic acid afforded the derivatized dendrimers in 88, 95, and 97% isolated yields for the dendrimers incorporating **267**, **269**, and **273**, respectively.

VII. Conclusion

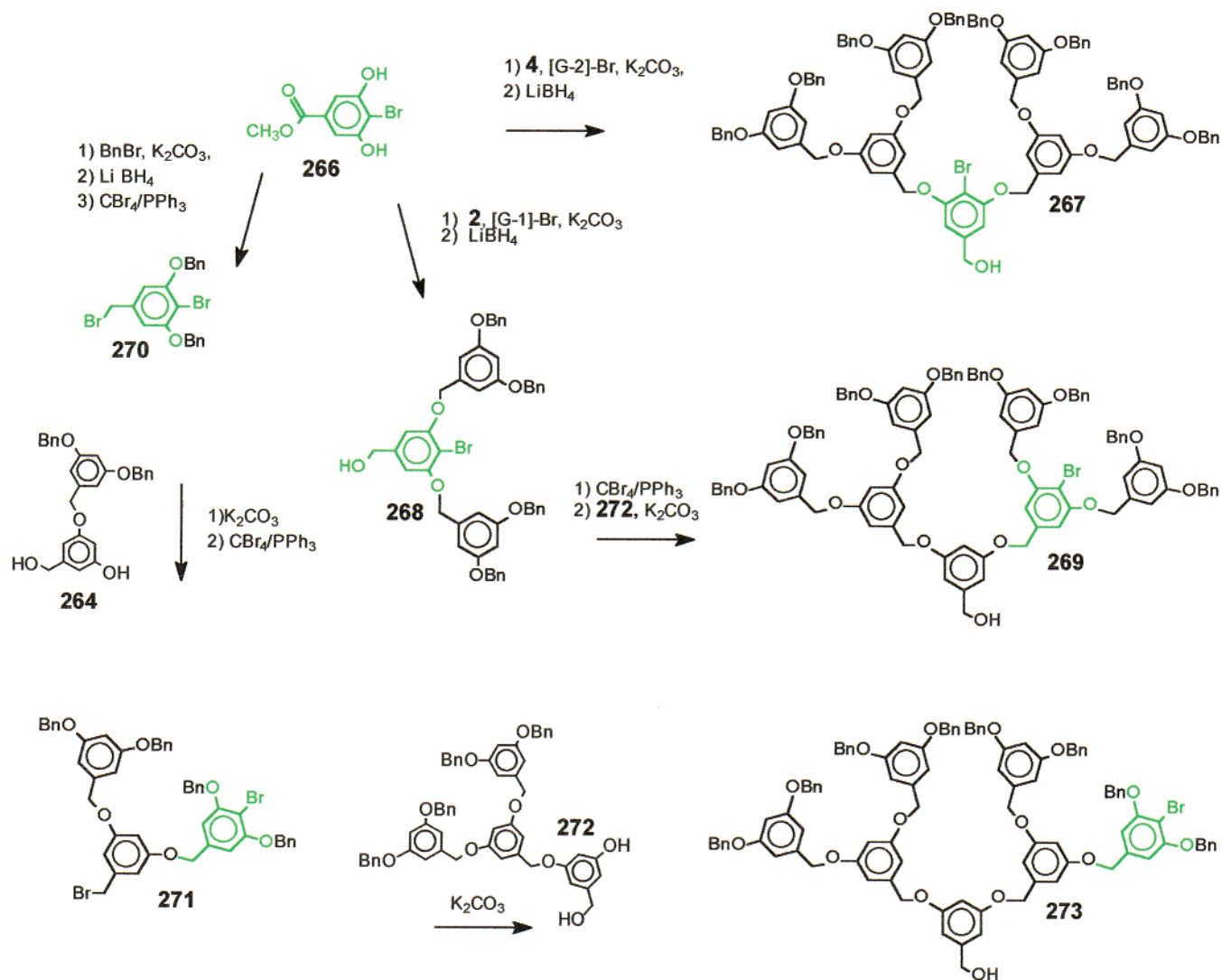
Many synthetic chemists appreciate the beauty of natural product synthesis where practical skill and creativity are cleverly combined to mimic nature's feats. The authors and many practitioners in the emerging field of nanotechnology derive much scientific fulfillment from designing targets such as molecular devices that are not specified by nature but for which function is the objective. Unlike natural product synthesis for which a very specific molecular target is provided by nature, the "materials" chemist makes use of elements of biomimetics, macroscopic analogies, and intuition to define the target. When nanometer scale assemblies are the target, this leads to unusual building blocks that today include elements such as fullerenes, clusters, nanocrystals, nanotubes, molecular wires, cage compounds, dendrons, dendrimers, etc. As a result of the countless

structural variations that can be implemented during their preparation, dendrimers are especially attractive to the materials chemist.

The convergent approach to dendrimer growth takes its place alongside the now well-established divergent synthesis providing an alternative approach from which the synthetic chemist can choose in order to construct a particular target molecule. Because of its modular design, great flexibility, and compatibility with the standard purification procedures of organic chemistry, the convergent approach offers a number of unique opportunities for the precise construction of nanoscale structures. Although high yield reactions always afford best results, the convergent synthesis is more tolerant of reactions that proceed in somewhat lower than ideal yields as only a few simultaneous reactions are required for growth of the convergent dendron and therefore a pure product can still be isolated and purified. This is clearly not the case with a divergent synthesis for which structural flaws resulting from lower yield reactions would quickly overwhelm the entire process and lead to a reaction mixture in which the desired product, if at all present, is only a minor component. Despite such realities, the fact remains that, in many instances, the presence of impurities that are structurally closely related to the desired product does not detract from the usefulness of dendrimers. Therefore the significance of the convergent approach will mirror its synthetic and functional versatility and not just its ability to afford some of the purest synthetic macromolecules known today. The presence of orthogonal functionalities at the focal point and the periphery of a dendron remains a very attractive feature for the molecule builder trying to assemble complex functional structures from a limited set of building blocks. There is no doubt that when issues of product availability—as translated into kilograms of materials—are taken into consideration, the divergent route will nearly always be superior to the convergent approach. When issues such as functional control, structural precision, building block versatility, the ability to perform custom encapsulation, and the like come to the fore, the convergent dendrimers will nearly always have an edge. Clearly, the synthetic requirements of the convergent method are such that all but the smaller dendrons can only be used for high added value applications or fundamental studies. With the convergent tool at their disposal, synthetic chemist can fashion large molecular assemblies that are structurally perfect and therefore provide ideal tools for fundamental studies. In many cases, when the ultimate properties of a molecule or material are known or when the mechanism of a phenomenon has been elucidated, it is possible to simplify the structure of the molecule or material. In such instances the convergently built molecules may well serve the role of model compounds or prototype leading to less perfect and simplified structures that perhaps perform a lesser function but benefit from increased accessibility.

In the age of nanotechnology, few nanoscale building blocks have the structural and functional versa-

Scheme 40



tility exhibited by convergent dendrons. There is little doubt that these versatile building blocks that can be used to prepare not only highly symmetrical, but also anisotropic structures will continue to stimulate our creativity leading us to fundamental discoveries while seeding very real applications. For example, it may be expected that dendrimers will be used in a variety of energy harvesting and conversion functions, as nanoreactors or catalytic enzyme mimics, as highly targeted drugs capable of penetrating a variety of biological barriers, as carriers of genetic material, as shape-persistent or functional components for nanoscale electronics or microfluidics, as memory, storage, encoding, or logic devices, etc.

VIII. Acknowledgments

Financial support of our work on convergent dendrimers by the National Science Foundation (DMR #9816166) and the US Department of Energy (Basic Energy Sciences, Polymer Program of the Center for Advanced Materials, Lawrence Berkeley National Laboratory) is gratefully acknowledged. The authors also thank Dr. Stefan Hecht and Prof. Alex Adronov for invaluable discussions.

IX. Glossary

ATRP	atom transfer radical polymerization
9-BBN	9-borabicyclo[3.3.1]nonane
CMC	critical micelle concentration
CV	cyclic voltammetry
DBOP	(2,3-dihydro-2-thioxo-3-benzoxazolyl)phosphonic acid diphenyl ester
DBU	diazabicyclo[5.4.0]-7-undecene
DCC	<i>N,N</i> -dicyclohexylcarbodiimide
DDQ	2,3-dichloro-5,6-dicyano-1,4-benzoquinone
DEAD	diethyl azodicarboxylate
DIPEA	<i>N,N</i> -diisopropylethylamine
DMAc	dimethyl acetamide
DPTS	4-(dimethylamino)pyridinium <i>p</i> -toluenesulfonate
DSM	Dutch State Mines
GPC	gel permeation chromatography
LED	light-emitting diode
MALDI-TOF	matrix-assisted laser desorption ionization time-of-flight mass spectrometry
MS	time-of-flight mass spectrometry
MW	molecular weight
NMP	<i>N</i> -methyl-2-pyrrolidone
PAMAM	poly(amidoamine)
PEG	poly(ethylene glycol)
PPI	poly(propyleneimine)
SFM	scanning force microscopy

SANS	small angle neutron scattering
TADDOL	(<i>R,R</i>)- $\alpha,\alpha,\alpha',\alpha'$ -tetraaryl-1,3-dioxolane-4,5-dimethanol
<i>t</i> -BOC	<i>tert</i> -butyloxycarbonyloxy
TEMPO	2,2,6,6-tetramethyl-1-oxylpiperidine
TMS	trimethylsilyl
TTF	tetrathiafulvalene

X. References

- Flory, P. J. *J. Am. Chem. Soc.* **1952**, *74*, 2718.
- Flory, P. J. *Principles of Polymer Chemistry*; Cornell University Press: Ithaca, NY, 1953; p 361.
- Buhleier, E.; Wehner, W.; Vögtle, F. *Synthesis* **1978**, 155–158.
- Tomalia, D. A.; Dewald, J.; Hall, M.; Martin, S.; Smith, P. *Prepr. 1st SPSJ Int. Polym. Conf., Soc. Polym. Sci. Jpn. (Kyoto)* **1984**, 65.
- Tomalia, D. A.; Baker, H.; Dewald, J.; Hall, M.; Kallos, G.; Martin, S.; Roeck, J.; Ryder, J.; Smith, P. *Polym. J.* **1985**, *17*, 117–132.
- Newkome, G. R.; Yao, Z.; Baker, G. R.; Gupta, V. K. *J. Org. Chem.* **1985**, *50*, 2003–2004.
- Wörner, C.; Mülhaupt, R. *Angew. Chem., Int. Ed. Engl.* **1993**, *32*, 1306–1308.
- Brabander-van den Berg, E. M. M.; Meijer, E. W. *Angew. Chem., Int. Ed.* **1993**, *32*, 1308–1310.
- Fréchet, J. M. J.; Jiang, Y.; Hawker, C. J.; Philippides, A. E. *Proc. IUPAC Int. Symp., Macromol. (Seoul)* **1989**, 19–20.
- Hawker, C. J.; Fréchet, J. M. J. *J. Am. Chem. Soc.* **1990**, *112*, 7638–7647.
- Tomalia, D. A.; Naylor, A. M.; Goddard, W. A., III. *Angew. Chem., Int. Ed. Engl.* **1990**, *29*, 138–175.
- Mekelburger, H. B.; Jaworek, W.; Vögtle, F. *Angew. Chem.* **1992**, *104*, 1609–1614.
- Fréchet, J. M. J. *Science* **1994**, *263*, 1710–1715.
- Issberner, J.; Moors, R.; Vögtle, F. *Angew. Chem.* **1994**, *106*, 2507–2514.
- Newkome, G. R.; Moorefield, C. N.; Vögtle, F. *Dendritic Molecules: Concepts, Syntheses, Perspectives*; VCH: Weinheim, Germany, 1996.
- Vögtle, F., Vol. Ed. *Dendrimers. Top. Curr. Chem.* **1998**, *197*.
- Fréchet, J. M. J.; Hawker, C. J. *Comprehensive Polymer Science, 2nd Supplement*; Pergamon: Oxford, England, 1996; pp 140–206.
- Matthews, O. A.; Shipway, A. N.; Stoddart, J. F. *Prog. Polym. Sci.* **1998**, *23*, 1–56.
- Frey, H.; Lach, C.; Lorenz, K. *Adv. Mater.* **1998**, *10*, 279–293.
- Chow, H. F.; Mong, T. K.; Nongrum, M. F.; Wan, C. W. *Tetrahedron* **1998**, *54*, 8543–8660.
- Smith, D. K.; Diederich, F. *Chem.—Eur. J.* **1998**, *4*, 1353–1361.
- Fischer, M.; Vögtle, F. *Angew. Chem., Int. Ed. Engl.* **1999**, *38*, 885–905.
- Bosman, A. W.; Janssen, H. M.; Meijer, E. W. *Chem. Rev.* **1999**, *99*, 1665–1688.
- Inoue, K. *Prog. Polym. Sci.* **2000**, *25*, 453–571.
- Vögtle, F., Vol. Ed. *Dendrimers II: Architecture Nanostructure and Supramolecular Chemistry. Top. Curr. Chem.* **2000**, *210*.
- Vögtle, F.; Gestermann, S.; Hesse, R.; Schwierz, H.; Windisch, B. *Prog. Polym. Sci.* **2000**, *25*, 987–1041.
- Vögtle, F., Vol. Ed. *Dendrimers III: Design Dimension Function. Top. Curr. Chem.* **2001**, *212*.
- Hecht, S.; Fréchet, J. M. J. *Angew. Chem., Int. Ed.* **2001**, *40*, 74–91.
- Kim, Y. H.; Webster, O. *Plast. Eng.* **1999**, *53*, 201–238.
- Kim, Y. H.; Webster, O. W. *J. Am. Chem. Soc.* **1990**, *112*, 4592–4593.
- Hawker, C. J.; Lee, R.; Fréchet, J. M. J. *J. Am. Chem. Soc.* **1991**, *113*, 4583–4588.
- Hawker, C. J. *Adv. Polym. Sci.* **1999**, *147*, 113–160.
- Fréchet, J. M. J.; Hawker, C. J.; Gitsov, I.; Leon, J. W. *J. Macromol. Sci., Pure Appl. Chem.* **1996**, *A33*, 1399–1425.
- De Gennes, P. G.; Hervet, H. *J. Phys. Lett.* **1983**, *44*, 351–360.
- Wooley, K. L.; Fréchet, J. M. J.; Hawker, C. J. *Polymer* **1994**, *35*, 4489–4495.
- Hawker, C. J.; Malmström, E.; Frank, C. W.; Kampf, J. P. *J. Am. Chem. Soc.* **1997**, *119*, 9903–9904.
- Mourey, T. H.; Turner, S. R.; Rubinstein, M.; Fréchet, J. M. J.; Hawker, C. J.; Wooley, K. L. *Macromolecules* **1992**, *25*, 2401–2406.
- Wooley, K. L.; Hawker, C. J.; Pochan, J. M.; Fréchet, J. M. J. *Macromolecules* **1993**, *26*, 1514–1519.
- Hawker, C. J.; Farrington, P. J.; Mackay, M. E.; Wooley, K. L.; Fréchet, J. M. J. *J. Am. Chem. Soc.* **1995**, *117*, 4409–4410.
- Grayson, S. M.; Fréchet, J. M. J. *J. Am. Chem. Soc.* **2000**, *122*, 10335–10344.
- Hawker, C. J.; Wooley, K. L.; Fréchet, J. M. J. *J. Chem. Soc., Perkin Trans. 1* **1993**, 1287–1297.
- Jansen, J. F. G. A.; de Brabander van den Berg, E.; Meijer, E. W. *Science* **1994**, *266*, 1226–1229.
- Piotti, M. E.; Rivera, F.; Bond, R.; Hawker, C. J.; Fréchet, J. M. J. *J. Am. Chem. Soc.* **1999**, *121*, 9471–9472.
- Adronov, A.; Fréchet, J. M. J. *J. Chem. Commun.* **2000**, 1701–1710.
- Kawa, M.; Fréchet, J. M. J. *J. Chem. Mater.* **1998**, *10*, 286–296.
- Liu, M.; Kono, K.; Fréchet, J. M. J. *J. Controlled Release* **2000**, *65*, 121–131.
- Haensler, J.; Szoka, F. C. Jr. *Bioconjugate Chem.* **1993**, *4*, 372–379.
- Tang, M.; Redemann, C. T.; Szoka, F. C. Jr. *Bioconjugate Chem.* **1996**, *7*, 703–714.
- Tang, M. X.; Szoka, F. C. *Gene Ther.* **1997**, *4*, 823–832.
- Bielinska, A.; Kukowska-Latallo, J. F.; Johnson, J.; Tomalia, D. A.; Baker, J. R. Jr. *Nucleic Acids Res.* **1996**, *24*, 2176–2182.
- Reuter, J. D.; Myc, A.; Hayes, M. M.; Gan, Z.; Roy, R.; Qin, D.; Yin, R.; Piehler, L. T.; Esfand, R.; Tomalia, D. A.; Baker, J. R. Jr. *Bioconjugate Chem.* **1999**, *10*, 271–278.
- Malik, N.; Wiwattanapatapee, R.; Klopsch, R.; Lorenz, K.; Frey, H.; Weener, J. W.; Meijer, E. W.; Paulus, W.; Duncan, R. *J. Controlled Release* **2000**, *65*, 133–148.
- Liu, M.; Fréchet, J. M. J. *Pharm. Sci. Technol. Today* **1999**, *2*, 393–401.
- Wiwattanapatapee, R.; Carreno-Gomez, B.; Malik, N.; Duncan, R. *Pharm. Res.* **2000**, *17*, 991–998.
- Tomalia, D. A.; Baker, H.; Dewald, J.; Hall, M.; Kallos, G.; Martin, S.; Roeck, J.; Ryder, J.; Smith, P. *Macromolecules* **1986**, *19*, 2466–2468.
- O'Sullivan, D. A. *Chem. Eng. News* **1993**, 20–24.
- Newkome, G. R.; Moorefield, C. N.; Baker, G. R.; Johnson, A. L.; Behera, R. K. *Angew. Chem., Int. Ed. Engl.* **1991**, *30*, 1176–1178.
- Newkome, G. R.; Moorefield, C. N.; Baker, G. R.; Saunders, M. J.; Grossman, S. H. *Angew. Chem., Int. Ed. Engl.* **1991**, *30*, 1178–1180.
- Newkome, G. R.; Behera, R. K.; Moorefield, C. N.; Baker, G. R. *J. Org. Chem.* **1991**, *56*, 7162–7167.
- Newkome, G. R.; Nayak, A.; Behera, R. K.; Moorefield, C. N.; Baker, G. R. *J. Org. Chem.* **1992**, *57*, 358–362.
- Newkome, G. R.; Young, J. K.; Baker, G. R.; Potter, R. L.; Audoly, L.; Cooper, D.; Weis, C. D.; Morris, K.; Johnson, C. S. Jr. *Macromolecules* **1993**, *26*, 2394–2396.
- Launay, N.; Caminade, A. M.; Lahana, R.; Majoral, J. P. *Angew. Chem.* **1994**, *33*, 1589–1592.
- Launay, N.; Caminade, A. M.; Majoral, J. P. *J. Am. Chem. Soc.* **1995**, *117*, 3282–3283.
- Majoral, J. P.; Caminade, A. M. *Top. Curr. Chem.* **1998**, *197*, 79–124.
- Hawker, C.; Fréchet, J. M. J. *J. Chem. Soc., Chem. Commun.* **1990**, 1010–1013.
- Hummelen, J. C.; Van Dongen, J. L. J.; Meijer, E. W. *Chem.—Eur. J.* **1997**, *3*, 1489–1493.
- Liu, M.; Fréchet, J. M. J. *Polym. Bull.* **1999**, *43*, 379–386.
- Bu, L.; Nonidez, W. K.; Mays, J. W.; Tan, N. B. *Macromolecules* **2000**, *33*, 4445–4452.
- Haag, R.; Sunder, A.; Stumbe, J. F. *J. Am. Chem. Soc.* **2000**, *122*, 2954–2955.
- Sahota, H.; Lloyd, P. M.; Yeates, S. G.; Derrick, P. J.; Taylor, P. C.; Haddleton, D. M. *J. Chem. Soc., Chem. Commun.* **1994**, 2445–2446.
- Leon, J. W.; Fréchet, J. M. J. *Polym. Bull.* **1995**, *35*, 449–455.
- Jiang, D. L.; Aida, T. *J. Am. Chem. Soc.* **1998**, *120*, 10895–10901.
- Hawker, C. J.; Fréchet, J. M. J. *Macromolecules* **1990**, *23*, 4726–4729.
- Wooley, K. L.; Hawker, C. J.; Fréchet, J. M. J. *J. Chem. Soc., Perkin Trans. 1* **1991**, 1059–1076.
- Fréchet, J. M. J.; Hawker, C. J.; Philippides, A. E. US Patent 5 041 516, 1991.
- Tyler, T. L.; Hanson, J. E. *Polym. Mater. Sci. Eng.* **1995**, *73*, 356–357.
- Tyler, T. L.; Hanson, J. E. *Chem. Mater.* **1999**, *11*, 3452–3459.
- Gilat, S. L.; Adronov, A.; Fréchet, J. M. J. *Polym. Mater. Sci. Eng.* **1997**, *77*, 91–92.
- Gilat, S. L.; Adronov, A.; Fréchet, J. M. J. *J. Org. Chem.* **1999**, *64*, 7474–7484.
- Gilat, S. L.; Adronov, A.; Fréchet, J. M. J. *Angew. Chem., Int. Ed.* **1999**, *38*, 1422–1427.
- Adronov, A.; Malenfant, P. R. L.; Fréchet, J. M. J. *J. Chem. Mater.* **2000**, *12*, 1463–1472.
- Percec, V.; Cho, W. D.; Ungar, G.; Yearley, D. J. P. *J. Am. Chem. Soc.* **2001**, *123*, 1302–1315.
- Percec, V.; Cho, W. D.; Moeller, M.; Prokhorova, S. A.; Ungar, G.; Yearley, D. J. P. *J. Am. Chem. Soc.* **2000**, *122*, 4249–4250.
- Percec, V.; Ahn, C. H.; Cho, W. D.; Jamieson, A. M.; Kim, J.; Leman, T.; Schmidt, M.; Gerle, M.; Moeller, M.; Prokhorova, S. A.; Sheiko, S. S.; Cheng, S. Z. D.; Zhang, A.; Ungar, G.; Yearley, D. J. P. *J. Am. Chem. Soc.* **1998**, *120*, 8619–8631.

- (85) Percec, V.; Cho, W. D.; Ungar, G. *J. Am. Chem. Soc.* **2000**, *122*, 10273–10281.
- (86) Peerlings, H. W. I.; Trimbach, D. C.; Meijer, E. W. *Chem. Commun.* **1998**, 497–498.
- (87) Wooley, K. L.; Hawker, C. J.; Fréchet, J. M. J. *J. Am. Chem. Soc.* **1991**, *113*, 4252–4261.
- (88) Chow, H. F.; Chan, I. Y.-K.; Mak, C. C. *Tetrahedron Lett.* **1995**, *36*, 8633–8636.
- (89) Chow, H. F.; Chan, I. Y.-K.; Mak, C. C.; Ng, M. K. *Tetrahedron* **1996**, *52*, 4277–4290.
- (90) Chow, H. F.; Wang, Z. Y.; Lau, Y. F. *Tetrahedron* **1998**, *54*, 13813–13824.
- (91) Chen, K. Y.; Gorman, C. B. *J. Org. Chem.* **1996**, *61*, 9229–9235.
- (92) Chow, H. F.; Chan, I. Y. K.; Chan, D. T. W.; Kwok, R. W. M. *Chem.—Eur. J.* **1996**, *2*, 1085–1091.
- (93) Gorman, C. B.; Parkhurst, B. L.; Su, W. Y.; Chen, K. Y. *J. Am. Chem. Soc.* **1997**, *119*, 1141–1142.
- (94) Gorman, C. B. *Adv. Mater.* **1997**, *9*, 1117–1119.
- (95) Gorman, C. B.; Su, W. Y.; Jiang, H.; Watson, C. M.; Boyle, P. *Chem. Commun.* **1999**, 877–878.
- (96) Chow, H. F.; Mak, C. C. *J. Chem. Soc., Perkin Trans. 1* **1994**, 2223–2228.
- (97) Chow, H. F.; Fok, L. F.; Mak, C. C. *Tetrahedron Lett.* **1994**, *35*, 3547–3550.
- (98) Chow, H. F.; Mak, C. C. *Tetrahedron Lett.* **1996**, *37*, 5935–5938.
- (99) Chow, H. F.; Mak, C. C. *J. Chem. Soc., Perkin Trans. 1* **1997**, 91–95.
- (100) Chow, H. F.; Mak, C. C. *Pure Appl. Chem.* **1997**, *69*, 483–488.
- (101) McGrath, D. V.; Wu, M. J.; Chaudhry, U. *Tetrahedron Lett.* **1996**, *37*, 6077–6080.
- (102) McElhanon, J. R.; Wu, M. J.; Escobar, M.; McGrath, D. V. *Macromolecules* **1996**, *29*, 8979–8982.
- (103) McElhanon, J. R.; Wu, M. J.; Escobar, M.; Chaudhry, U.; Hu, C. L.; McGrath, D. V. *J. Org. Chem.* **1997**, *62*, 908–915.
- (104) McElhanon, J. R.; McGrath, D. V. *J. Am. Chem. Soc.* **1998**, *120*, 1647–1656.
- (105) Junge, D. M.; McGrath, D. V. *Tetrahedron Lett.* **1998**, *39*, 1701–1704.
- (106) Murer, P.; Seebach, D. *Angew. Chem., Int. Ed. Engl.* **1995**, *34*, 2116–2119.
- (107) Murer, P. K.; Lapiere, J. M.; Greiveldinger, G.; Seebach, D. *Helv. Chim. Acta* **1997**, *80*, 1648–1681.
- (108) Murer, P.; Seebach, D. *Helv. Chim. Acta* **1998**, *81*, 603–631.
- (109) Greiveldinger, G.; Seebach, D. *Helv. Chim. Acta* **1998**, *81*, 1003–1022.
- (110) Hudson, S. D.; Jung, H. T.; Percec, V.; Cho, W. D.; Johansson, G.; Ungar, G.; Balagurusamy, V. S. K. *Science* **1997**, *278*, 449–452.
- (111) Percec, V.; Cho, W. D.; Mosier, P. E.; Ungar, G.; Yeardley, D. J. P. *J. Am. Chem. Soc.* **1998**, *120*, 11061–11070.
- (112) Percec, V.; Ahn, C. H.; Ungar, G.; Yeardley, D. J. P.; Moller, M.; Sheiko, S. S. *Nature* **1998**, *391*, 161–164.
- (113) Ungar, G.; Percec, V.; Holerca, M. N.; Johansson, G.; Heck, J. A. *Chem.—Eur. J.* **2000**, *6*, 1258–1266.
- (114) Moore, J. S. *Acc. Chem. Res.* **1997**, *30*, 402–413.
- (115) Xu, Z.; Moore, J. S. *Angew. Chem., Int. Ed. Engl.* **1993**, *32*, 246.
- (116) Moore, J. S.; Xu, Z. *Macromolecules* **1991**, *24*, 5893–5894.
- (117) Bharathi, P.; Patel, U.; Kawaguchi, T.; Pesak, D. J.; Moore, J. S. *Macromolecules* **1995**, *28*, 5955–5963.
- (118) Gorman, C. B.; Smith, J. C. *Polymer* **1999**, *41*, 675–683.
- (119) Devadoss, C.; Bharathi, P.; Moore, J. S. *J. Am. Chem. Soc.* **1996**, *118*, 9635–9644.
- (120) Wang, P. W.; Liu, Y. J.; Devadoss, C.; Bharathi, P.; Moore, J. S. *Adv. Mater.* **1996**, *8*, 237–241.
- (121) Shortreed, M. R.; Swallen, S. F.; Shi, Z. Y.; Tan, W.; Xu, Z.; Devadoss, C.; Moore, J. S.; Kopelman, R. *J. Phys. Chem. B* **1997**, *101*, 6318–6322.
- (122) Tretiakov, S.; Chernyak, V.; Mukamel, S. *J. Phys. Chem. B* **1998**, *102*, 3310–3315.
- (123) Devadoss, C.; Bharathi, P.; Moore, J. S. *Macromolecules* **1998**, *31*, 8091–8099.
- (124) Swallen, S. F.; Shi, Z. Y.; Tan, W.; Xu, Z.; Moore, J. S.; Kopelman, R. *J. Lumin.* **1998**, *76 & 77*, 193–196.
- (125) Harigaya, K. *Chem. Phys. Lett.* **1999**, *300*, 33–36.
- (126) Harigaya, K. *Phys. Chem. Chem. Phys.* **1999**, *1*, 1687–1689.
- (127) Poliakov, E. Y.; Chernyak, V.; Tretiakov, S.; Mukamel, S. *J. Chem. Phys.* **1999**, *110*, 8161–8175.
- (128) Chernyak, V.; Poliakov, E. Y.; Tretiakov, S.; Mukamel, S. *J. Chem. Phys.* **1999**, *111*, 4158–4168.
- (129) Swallen, S. F.; Kopelman, R.; Moore, J. S.; Devadoss, C. *J. Mol. Struct.* **1999**, *485–486*, 585–597.
- (130) Raychaudhuri, S.; Shapir, Y.; Chernyak, V.; Mukamel, S. *Phys. Rev. Lett.* **2000**, *85*, 282–285.
- (131) Swallen, S. F.; Zhu, Z.; Moore, J. S.; Kopelman, R. *J. Phys. Chem. B* **2000**, *104*, 3988–3995.
- (132) Miller, T. M.; Neenan, T. X. *Chem. Mater.* **1990**, *2*, 346–349.
- (133) Miller, T. M.; Neenan, T. X.; Zayas, R.; Bair, H. E. *J. Am. Chem. Soc.* **1992**, *114*, 1018–1025.
- (134) Wiesler, U. M.; Müllen, K. *Chem. Commun.* **1999**, 2293–2294.
- (135) Morgenroth, F.; Reuther, E.; Müllen, K. *Angew. Chem., Int. Ed. Engl.* **1997**, *36*, 631–634.
- (136) Ihre, H.; Hult, A.; Söderlind, E. *J. Am. Chem. Soc.* **1996**, *118*, 6388–6395.
- (137) Ihre, H.; Padilla de Jesus, O. L.; Fréchet, J. M. J. *J. Am. Chem. Soc.* **2001**, *123*, 5908–5917.
- (138) Grayson, S. M.; Fréchet, J. M. J. *Macromolecules* **2001**, *34*, 6542–6544.
- (139) Deb, S. K.; Maddux, T. M.; Yu, L. *J. Am. Chem. Soc.* **1997**, *119*, 9079–9080.
- (140) Meier, H.; Lehmann, M. *Angew. Chem., Int. Ed. Engl.* **1998**, *37*, 643–645.
- (141) Lehmann, M.; Schartel, B.; Hennecke, M.; Meier, H. *Tetrahedron* **1999**, *55*, 13377–13394.
- (142) Meier, H.; Lehmann, M.; Kolb, U. *Chem.—Eur. J.* **2000**, *6*, 2462–2469.
- (143) Pillow, J. N. G.; Halim, M.; Lupton, J. M.; Burn, P. L.; Samuel, I. D. W. *Macromolecules* **1999**, *32*, 5985–5993.
- (144) Pillow, J. N. G.; Burn, P. L.; Samuel, I. D. W.; Halim, M. *Synth. Met.* **1999**, *102*, 1468–1469.
- (145) Halim, M.; Samuel, I. D. W.; Pillow, J. N. G.; Monkman, A. P.; Burn, P. L. *Synth. Met.* **1999**, *102*, 1571–1574.
- (146) Halim, M.; Samuel, I. D. W.; Pillow, J. N. G.; Burn, P. L. *Synth. Met.* **1999**, *102*, 1113–1114.
- (147) Halim, M.; Pillow, J. N. G.; Samuel, I. D. W.; Burn, P. L. *Adv. Mater.* **1999**, *11*, 371–374.
- (148) Halim, M.; Pillow, J. N. G.; Samuel, I. D. W.; Burn, P. L. *Synth. Met.* **1999**, *102*, 922–923.
- (149) Jayaraman, M.; Fréchet, J. M. J. *J. Am. Chem. Soc.* **1998**, *120*, 12996–12997.
- (150) Grayson, S. M.; Jayaraman, M.; Fréchet, J. M. J. *Chem. Commun.* **1999**, 1329–1330.
- (151) Malenfant, P. R. L.; Jayaraman, M.; Fréchet, J. M. J. *Chem. Mater.* **1999**, *11*, 3420–3422.
- (152) Malenfant, P. R. L.; Fréchet, J. M. J. *Macromolecules* **2000**, *33*, 3634–3640.
- (153) Brouwer, A. J.; Mulders, S. J. E.; Liskamp, R. M. J. *Eur. J. Org. Chem.* **2001**, 1903–1915.
- (154) Uhrich, K. E.; Fréchet, J. M. J. *J. Chem. Soc., Perkin Trans. 1* **1992**, 1623–1630.
- (155) Bayliff, P. M.; Feast, W. J.; Parker, D. *Polym. Bull.* **1992**, *29*, 265–270.
- (156) Mulders, S. J. E.; Brouwer, A. J.; Liskamp, R. M. J. *Tetrahedron Lett.* **1997**, *38*, 3085–3088.
- (157) Mulders, S. J. E.; Brouwer, A. J.; van der Meer, P. G. J.; Liskamp, R. M. J. *Tetrahedron Lett.* **1997**, *38*, 631–634.
- (158) Mulders, S. J. E.; Brouwer, A. J.; Kimkes, P.; Sudholter, E. J. R.; Liskamp, R. M. J. *J. Chem. Soc., Perkin Trans. 2* **1998**, 1535–1538.
- (159) Voit, B. I.; Wolf, D. *Tetrahedron* **1997**, *53*, 15535–15551.
- (160) Brettreich, M.; Hirsch, A. *Synlett* **1998**, 1396–1398.
- (161) Miller, T. M.; Kwock, E. W.; Neenan, T. X. *Macromolecules* **1992**, *25*, 3143–3148.
- (162) Kwock, E. W.; Neenan, T. X.; Miller, T. M. *Chem. Mater.* **1991**, *3*, 775–777.
- (163) Taylor, R. T.; Puapaiboon, U. *Tetrahedron Lett.* **1998**, *39*, 8005–8008.
- (164) Puapaiboon, U.; Taylor, R. T. *Rapid Commun. Mass Spectrom.* **1999**, *13*, 508–515.
- (165) Rannard, S. P.; Davis, N. J. *J. Am. Chem. Soc.* **2000**, *122*, 11729–11730.
- (166) Chen, Y.-M.; Chen, C.-F.; Liu, W. H.; Xi, F. *Polym. Bull.* **1996**, *37*, 557–563.
- (167) Höger, S. *Synthesis* **1997**, 20–22.
- (168) Sartor, V.; Djakovitch, L.; Fillaut, J. L.; Moulines, F.; Neveu, F.; Marvaud, V.; Guittard, J.; Blais, J. C.; Astruc, D. *J. Am. Chem. Soc.* **1999**, *121*, 2929–2930.
- (169) Nlate, S.; Ruiz, J.; Sartor, V.; Navarro, R.; Blais, J. C.; Astruc, D. *Chem.—Eur. J.* **2000**, *6*, 2544–2553.
- (170) Kadei, K.; Moors, R.; Vögtle, F. *Chem. Ber.* **1994**, *127*, 897–903.
- (171) Louie, J.; Hartwig, J. F.; Fry, A. J. *J. Am. Chem. Soc.* **1997**, *119*, 11695–11696.
- (172) Elandaloussi, E. H.; Spangler, C. W.; Dirk, C.; Casstevens, M.; Kumar, D.; Burzynski, R. *Mater. Res. Soc. Symp. Proc.* **1999**, *561*, 63–68.
- (173) Bronk, K.; Thayumanavan, S. *Org. Lett.* **2001**, *3*, 2057–2060.
- (174) Matsuda, K.; Nakamura, N.; Inoue, K.; Koga, N.; Iwamura, H. *Bull. Chem. Soc. Jpn.* **1996**, *69*, 1483–1494.
- (175) Peng, Z.; Pan, Y.; Xu, B.; Zhang, J. *J. Am. Chem. Soc.* **2000**, *122*, 6619–6623.
- (176) Rajca, A.; Utamapanya, S. *J. Am. Chem. Soc.* **1993**, *115*, 10688–10694.
- (177) Ashton, P. R.; Shibata, K.; Shipway, A. N.; Stoddart, J. F. *Angew. Chem., Int. Ed. Engl.* **1997**, *36*, 2781–2783.
- (178) Baussanne, I.; Law, H.; Defaye, J.; Benito, J. M.; Mellet, C. O.; Garcia Fernandez, J. M. *Chem. Commun.* **2000**, 1489–1490.
- (179) Leu, C. M.; Chang, Y. T.; Shu, C. F.; Teng, C. F.; Shiea, J. *Macromolecules* **2000**, *33*, 2855–2861.

- (180) Morikawa, A.; Kakimoto, M.; Imai, Y. *Macromolecules* **1993**, *26*, 6324–6329.
- (181) Morikawa, A.; Ono, K. *Macromolecules* **1999**, *32*, 1062–1068.
- (182) Morikawa, A.; Ono, K. *Polym. J.* **2000**, *32*, 255–262.
- (183) Pan, Y.; Ford, W. T. *J. Org. Chem.* **1999**, *64*, 8588–8593.
- (184) Twyman, L. J.; Beezer, A. E.; Mitchell, J. C. *J. Chem. Soc., Perkin Trans. 1* **1994**, 407–411.
- (185) Ohta, M.; Fréchet, J. M. J. *Macromol. Sci., Pure Appl. Chem.* **1997**, *A34*, 2025–2046.
- (186) Appelhans, D.; Komber, H.; Voigt, D.; Haeussler, L.; Voit, B. I. *Macromolecules* **2000**, *33*, 9494–9503.
- (187) Pan, Y.; Ford, W. T. *J. Polym. Sci., Part A: Polym. Chem.* **2000**, *38*, 1533–1543.
- (188) Ingerl, A.; Neubert, I.; Klopsch, R.; Schlüter, A. D. *Eur. J. Org. Chem.* **1998**, 2551–2556.
- (189) Klopsch, R.; Koch, S.; Schlüter, A. D. *Eur. J. Org. Chem.* **1998**, *1275*, 5–1283.
- (190) Huang, B.; Parquette, J. R. *Org. Lett.* **2000**, *2*, 239–242.
- (191) Tominaga, M.; Hosogi, J.; Konishi, K.; Aida, T. *Chem. Commun.* **2000**, 719–720.
- (192) Zhang, W.; Simanek, E. E. *Org. Lett.* **2000**, *2*, 843–845.
- (193) Zhang, W.; Simanek, E. E. *Tetrahedron Lett.* **2001**, *42*, 5355–5357.
- (194) Colonna, B.; Harding, V. D.; Nepogodiev, S. A.; Raymo, F. M.; Spencer, N.; Stoddart, J. F. *Chem.—Eur. J.* **1998**, *4*, 1244–1254.
- (195) Sadalpure, K.; Lindhorst, T. K. *Angew. Chem., Int. Ed.* **2000**, *39*, 2010–2013.
- (196) Hudson, R. H. E.; Damha, M. J. *J. Am. Chem. Soc.* **1993**, *115*, 2119–2124.
- (197) Peerlings, H. W. I.; Meijer, E. W. *Chem.—Eur. J.* **1997**, *3*, 1563–1570.
- (198) Thomas, C. W.; Tor, Y. *Chirality* **1998**, *10*, 53–59.
- (199) Twyman, L. J.; Beezer, A. E.; Mitchell, J. C. *Tetrahedron Lett.* **1994**, *35*, 4423–4424.
- (200) Ritzén, A.; Frejd, T. *Chem. Commun.* **1999**, 207–208.
- (201) Kress, J.; Rosner, A.; Hirsch, A. *Chem.—Eur. J.* **2000**, *6*, 247–257.
- (202) Seebach, D.; Herrmann, G. F.; Lengweiler, U. D.; Amrein, W. *Helv. Chim. Acta* **1997**, *80*, 989–1026.
- (203) Gorman, C. *Adv. Mater. (Weinheim, Ger)* **1998**, *10*, 295–309.
- (204) Majoral, J. P.; Caminade, A. M. *Chem. Rev.* **1999**, *99*, 845–880.
- (205) Hearshaw, M. A.; Hutton, A. T.; Moss, J. R.; Naidoo, K. J. *Adv. Dendritic Macromol.* **1999**, *4*, 1–60.
- (206) Hearshaw, M. A.; Moss, J. R. *Chem. Commun.* **1999**, 1–8.
- (207) Cuadrado, I.; Morán, M.; Casado, C. M.; Alonso, B.; Losada, J. *Coord. Chem. Rev.* **1999**, *193–195*, 395–445.
- (208) Morikawa, A.; Kakimoto, M.; Imai, Y. *Macromolecules* **1992**, *25*, 3247–3253.
- (209) Huc, V.; Boussaguet, P.; Mazerolles, P. *J. Organomet. Chem.* **1996**, *521*, 253–260.
- (210) Van Manen, H. J.; Fokkens, R. H.; Nibbering, N. M. M.; van Veggel, F. C. J. M.; Reinhoudt, D. N. *J. Org. Chem.* **2001**, *66*, 4643–4650.
- (211) Achar, S.; Puddephatt, R. J. *J. Chem. Soc., Chem. Commun.* **1994**, 1895–1896.
- (212) Achar, S.; Puddephatt, R. J. *Angew. Chem., Int. Ed. Engl.* **1994**, *33*, 847–849.
- (213) Achar, S.; Vittal, J. J.; Puddephatt, R. J. *Organometallics* **1996**, *15*, 43–50.
- (214) Onitsuka, K.; Fujimoto, M.; Ohshiro, N.; Takahashi, S. *Angew. Chem., Int. Ed. Engl.* **1999**, *38*, 689–692.
- (215) Xu, Z.; Kahr, M.; Walker, K. L.; Wilkins, C. L.; Moore, J. S. *J. Am. Chem. Soc.* **1994**, *116*, 4537–4550.
- (216) Wooley, K. L.; Hawker, C. J.; Fréchet, J. M. J. *Angew. Chem., Int. Ed.* **1994**, *33*, 82–85.
- (217) L'abbé, G.; Forier, B.; Dehaen, W. *Chem. Commun.* **1996**, 2143–2144.
- (218) Forier, B.; Dehaen, W. *Tetrahedron* **1999**, *55*, 9829–9846.
- (219) Kawaguchi, T.; Walker, K. L.; Wilkins, C. L.; Moore, J. S. *J. Am. Chem. Soc.* **1995**, *117*, 2159–2165.
- (220) Chi, C.; Wu, J.; Wang, X.; Zhao, X.; Li, J.; Wang, F. *Tetrahedron Lett.* **2001**, *42*, 2181–2184.
- (221) Ihre, H.; Hult, A.; Fréchet, J. M. J.; Gitsov, I. *Macromolecules* **1998**, *31*, 4061–4068.
- (222) Zanini, D.; Roy, R. *J. Org. Chem.* **1996**, *61*, 7348–7354.
- (223) Ashton, P. R.; Anderson, D. W.; Brown, C. L.; Shipway, A. N.; Stoddart, J. F.; Tolley, M. S. *Chem.—Eur. J.* **1998**, *4*, 781–795.
- (224) Ishida, Y.; Jikei, M.; Kakimoto, M. *Macromolecules* **2000**, *33*, 3202–3211.
- (225) Bo, Z.; Zhang, X.; Zhang, C.; Wang, Z.; Yang, M.; Shen, J.; Ji, Y. *J. Chem. Soc., Perkin Trans. 1* **1997**, 2931–2935.
- (226) Klopsch, R.; Franke, P.; Schlüter, A. D. *Chem.—Eur. J.* **1996**, *2*, 1330–1334.
- (227) Chang, H. T.; Chen, C. T.; Kondo, T.; Siuzdak, G.; Sharpless, K. B. *Angew. Chem., Int. Ed. Engl.* **1996**, *35*, 182–186.
- (228) Spindler, R.; Fréchet, J. M. J. *J. Chem. Soc., Perkin Trans. 1* **1993**, 913–918.
- (229) Zeng, F.; Zimmerman, S. C. *J. Am. Chem. Soc.* **1996**, *118*, 5326–5327.
- (230) Freeman, A. W.; Fréchet, J. M. J. *Org. Lett.* **1999**, *1*, 685–687.
- (231) Xu, Z.; Moore, J. S. *Angew. Chem., Int. Ed. Engl.* **1993**, *32*, 246–248.
- (232) Hecht, S.; Fréchet, J. M. J. *J. Am. Chem. Soc.* **1999**, *121*, 4084–4085.
- (233) Van Wuytswinkel, G.; Verheyde, B.; Compennolle, F.; Toppet, S.; Dehaen, W. *J. Chem. Soc., Perkin Trans. 1* **2000**, 1337–1340.
- (234) Wooley, K. L.; Hawker, C. J.; Fréchet, J. M. J.; Wudl, F.; Srdanov, G.; Shi, S.; Li, C.; Kao, M. *J. Am. Chem. Soc.* **1993**, *115*, 9836–9837.
- (235) Hawker, C. J.; Wooley, K. L.; Fréchet, J. M. J. *J. Chem. Soc., Chem. Commun.* **1994**, 925–926.
- (236) Avent, A. G.; Birkett, P. R.; Paolucci, F.; Roffia, S.; Taylor, R.; Wachter, N. K. *J. Chem. Soc., Perkin Trans. 2* **2000**, 1409–1414.
- (237) Herzog, A.; Hirsch, A.; Vostrowsky, O. *Eur. J. Org. Chem.* **2000**, 171–180.
- (238) Camps, X.; Schonberger, H.; Hirsch, A. *Chem.—Eur. J.* **1997**, *3*, 561–567.
- (239) Schönberger, H.; Schwab, C. H.; Hirsch, A.; Gasteiger, J. *J. Mol. Model.* **2000**, *6*, 379–395.
- (240) Dardel, B.; Deschenaux, R.; Even, M.; Serrano, E. *Macromolecules* **1999**, *32*, 5193–5198.
- (241) Amabilino, D. B.; Ashton, P. R.; Balzani, V.; Brown, C. L.; Credi, A.; Fréchet, J. M. J.; Leon, J. W.; Raymo, F. M.; Spencer, N.; Stoddart, J. F.; Venturi, M. *J. Am. Chem. Soc.* **1996**, *118*, 12012–12020.
- (242) Yamaguchi, N.; Hamilton, L. M.; Gibson, H. W. *Angew. Chem., Int. Ed.* **1998**, *37*, 3275–3279.
- (243) Pollak, K. W.; Sanford, E. M.; Fréchet, J. M. J. *J. Mater. Chem.* **1998**, *8*, 519–527.
- (244) Jiang, D. L.; Aida, T. *Chem. Commun.* **1996**, 1523–1524.
- (245) Sadamoto, R.; Tomioka, N.; Aida, T. *J. Am. Chem. Soc.* **1996**, *118*, 3978–3979.
- (246) Tomioka, N.; Takasu, D.; Takahashi, T.; Aida, T. *Angew. Chem., Int. Ed.* **1998**, *37*, 1531–1534.
- (247) Stapert, H. R.; Nishiyama, N.; Jiang, D. L.; Aida, T.; Kataoka, K. *Langmuir* **2000**, *16*, 8182–8188.
- (248) Jin, R. H.; Aida, T.; Inoue, S. *J. Chem. Soc., Chem. Commun.* **1993**, 1260–1262.
- (249) Numata, M.; Ikeda, A.; Fukuhara, C.; Shinkai, S. *Tetrahedron Lett.* **1999**, *40*, 6945–6948.
- (250) Tomoyose, Y.; Jiang, D. L.; Jin, R. H.; Aida, T.; Yamashita, T.; Horie, K.; Yashima, E.; Okamoto, Y. *Macromolecules* **1996**, *29*, 5236–5238.
- (251) Bhyrappa, P.; Vaijayanthimala, G.; Suslick, K. S. *J. Am. Chem. Soc.* **1999**, *121*, 262–263.
- (252) Pollak, K. W.; Leon, J. W.; Fréchet, J. M. J.; Maskus, M.; Abruña, H. *Chem. Mater.* **1998**, *10*, 30–38.
- (253) Bhyrappa, P.; Young, J. K.; Moore, J. S.; Suslick, K. S. *J. Am. Chem. Soc.* **1996**, *118*, 5708–5711.
- (254) Bhyrappa, P.; Young, J. K.; Moore, J. S.; Suslick, K. S. *J. Mol. Catal. A: Chem.* **1996**, *113*, 109–116.
- (255) Jiang, D. L.; Aida, T. *J. Macromol. Sci., Pure Appl. Chem.* **1997**, *A34*, 2047–2055.
- (256) Mak, C. C.; Bampos, N.; Sanders, J. K. M. *Angew. Chem., Int. Ed.* **1998**, *37*, 3020–3023.
- (257) Kimura, M.; Shiba, T.; Muto, T.; Hanabusa, K.; Shirai, H. *Macromolecules* **1999**, *32*, 8237–8239.
- (258) Darling, S. L.; Mak, C. C.; Bampos, N.; Feeder, N.; Teat, S. J.; Sanders, J. K. M. *New J. Chem.* **1999**, *23*, 359–364.
- (259) Matos, M. S.; Hofkens, J.; Verheijen, W.; De Schryver, F. C.; Hecht, S.; Pollak, K. W.; Fréchet, J. M. J.; Forier, B.; Dehaen, W. *Macromolecules* **2000**, *33*, 2967–2973.
- (260) Brewis, M.; Clarkson, G. J. *Chem. Commun.* **1998**, 969–970.
- (261) Brewis, M.; Hassan, B. M.; Li, H.; Makhseed, S.; McKeown, N. B.; Thompson, N. *J. Porphyrins Phthalocyanines* **2000**, *4*, 460–464.
- (262) Brewis, M.; Helliwell, M.; McKeown, N. B.; Reynolds, S.; Shawcross, A. *Tetrahedron Lett.* **2001**, *42*, 813–816.
- (263) Brewis, M.; Clarkson, G. J.; Goddard, V.; Helliwell, M.; Holder, A. M.; McKeown, N. *Angew. Chem., Int. Ed. Engl.* **1998**, *37*, 1092–1094.
- (264) McKeown, N. B. *Adv. Mater.* **1999**, *11*, 67–69.
- (265) Ng, A. C. H.; Li, X.; Ng, D. K. P. *Macromolecules* **1999**, *32*, 5292–5298.
- (266) Li, X.; He, X.; Ng, A. C. H.; Wu, C.; Ng, D. K. P. *Macromolecules* **2000**, *33*, 2119–2123.
- (267) Brewis, M.; Clarkson, G. J.; Helliwell, M.; Holder, A. M.; McKeown, N. B. *Chem.—Eur. J.* **2000**, *6*, 4630–4636.
- (268) Kimura, M.; Sugihara, Y.; Muto, T.; Hanabusa, K.; Shirai, H.; Kobayashi, N. *Chem.—Eur. J.* **1999**, *5*, 3495–3500.
- (269) Dandliker, P. J.; Diederich, F.; Gross, M.; Knobler, C. B.; Louati, A.; Sanford, E. M. *Angew. Chem., Int. Ed. Engl.* **1994**, *33*, 1739–1742.
- (270) Dandliker, P. J.; Diederich, F.; Gisselbrecht, J. P.; Louati, A.; Gross, M. *Angew. Chem., Int. Ed. Engl.* **1996**, *34*, 2725–2728.
- (271) Dandliker, P. J.; Diederich, F.; Zingg, A.; Gisselbrecht, J. P.; Gross, M.; Louati, A.; Sanford, E. *Helv. Chim. Acta* **1997**, *80*, 1773–1801.

- (272) Weyermann, P.; Gisselbrecht, J. P.; Boudon, C.; Diederich, F.; Gross, M. *Angew. Chem., Int. Ed. Engl.* **1999**, *38*, 3215–3219.
- (273) Kimura, M.; Nakada, K.; Yamaguchi, Y.; Hanabusa, K.; Shirai, H.; Kobayashi, N. *Chem. Commun.* **1997**, 1215–1216.
- (274) Hawker, C. J.; Wooley, K. L.; Fréchet, J. M. J. *J. Am. Chem. Soc.* **1993**, *115*, 4375–4376.
- (275) Devadoss, C.; Bharathi, P.; Moore, J. S. *Angew. Chem., Int. Ed. Engl.* **1997**, *36*, 1633–1635.
- (276) Smith, D. K.; Müller, L. *Chem. Commun.* **1999**, 1915–1916.
- (277) De Backer, S.; Prinzie, Y.; Verheijen, W.; Smet, M.; Desmedt, K.; Dehaen, W.; De Schryver, F. C. *J. Phys. Chem. A* **1998**, *102*, 5451–5455.
- (278) Gorman, C. B.; Hager, M. W.; Parkhurst, B. L.; Smith, J. C. *Macromolecules* **1998**, *31*, 815–822.
- (279) Wooley, K. L.; Klug, C. A.; Tasaki, K.; Schaefer, J. *J. Am. Chem. Soc.* **1997**, *119*, 53–58.
- (280) Hübner, G. M.; Nachtsheim, G.; Li, Q. Y.; Seel, C.; Vögtle, F. *Angew. Chem., Int. Ed.* **2000**, *39*, 1269–1272.
- (281) Seebach, D.; Rheiner, P. B.; Greiveldinger, G.; Butz, T.; Sellner, H. *Top. Curr. Chem.* **1998**, *197*, 125–164.
- (282) Rosini, C.; Superchi, S.; Peerlings, H. W. I.; Meijer, E. W. *Eur. J. Org. Chem.* **2000**, 61–71.
- (283) Chen, Y.-M.; Chen, C.-F.; Xi, F. *Chirality* **1998**, *10*, 661–666.
- (284) Peerlings, H. W. I.; Meijer, E. W. *Eur. J. Org. Chem.* **1998**, 573, 3–577.
- (285) Yamago, S.; Furukawa, M.; Azuma, A.; Yoshida, J. *Tetrahedron Lett.* **1998**, *39*, 3783–3786.
- (286) Pu, L. *Macromol. Rapid Commun.* **2000**, *21*, 795–809.
- (287) Smith, D. K.; Diederich, F. *Chem. Commun.* **1998**, 2501–2502.
- (288) Seebach, D.; Lapierre, J. M.; Skobridis, K.; Greiveldinger, G. *Angew. Chem., Int. Ed. Engl.* **1994**, *33*, 440–444.
- (289) Seebach, D.; Lapierre, J. M.; Greiveldinger, G.; Skobridis, K. *Helv. Chim. Acta* **1994**, *77*, 1673–1688.
- (290) Chaumette, J. L.; Laufersweiler, M. J.; Parquette, J. R. *J. Org. Chem.* **1998**, *63*, 9399–9405.
- (291) Rohde, J. M.; Parquette, J. R. *Tetrahedron Lett.* **1998**, *39*, 9161–9164.
- (292) Rheiner, P. B.; Seebach, D. *Chem.—Eur. J.* **1999**, *5*, 3221–3236.
- (293) Kremers, J. A.; Meijer, E. W. *J. Org. Chem.* **1994**, *59*, 4262–4266.
- (294) Kremers, J. A.; Meijer, E. W. *React. Funct. Polym.* **1995**, *26*, 137–144.
- (295) Kremers, J. A.; Meijer, E. W. *Macromol. Symp.* **1995**, *98*, 491–499.
- (296) Peerlings, H. W. I.; Struijk, M. P.; Meijer, E. W. *Chirality* **1998**, *10*, 46–52.
- (297) Catalano, V. J.; Parodi, N. *Inorg. Chem.* **1997**, *36*, 537–541.
- (298) Nierengarten, J. F.; Oswald, L.; Eckert, J. F.; Nicoud, J. F.; Armaroli, N. *Tetrahedron Lett.* **1999**, *40*, 5681–5684.
- (299) Eckert, J. F.; Byrne, D.; Nicoud, J. F.; Oswald, L.; Nierengarten, J. F.; Numata, M.; Ikeda, A.; Shinkai, S.; Armaroli, N. *New J. Chem.* **2000**, *24*, 749–758.
- (300) Zimmerman, S. C.; Wang, Y.; Bharathi, P.; Moore, J. S. *J. Am. Chem. Soc.* **1998**, *120*, 2172–2173.
- (301) Cardona, C. M.; Alvarez, J.; Kaifer, A. E.; McCarley, T. D.; Pandey, S.; Baker, G. A.; Bonzagni, N. J.; Bright, F. V. *J. Am. Chem. Soc.* **2000**, *122*, 6139–6144.
- (302) Smith, D. K.; Zingg, A.; Diederich, F. *Helv. Chim. Acta* **1999**, *82*, 1225–1241.
- (303) Bahr, A.; Felber, B.; Schneider, K.; Diederich, F. *Helv. Chim. Acta* **2000**, *83*, 1346–1376.
- (304) Chow, H. F.; Mak, C. C. *J. Org. Chem.* **1997**, *62*, 5116–5127.
- (305) Mak, C. C.; Chow, H. F. *Macromolecules* **1997**, *30*, 1228–1230.
- (306) Morao, I.; Cossio, F. P. *Tetrahedron Lett.* **1997**, *38*, 6461–6464.
- (307) Hu, Q. S.; Pugh, V.; Sabat, M.; Pu, L. *J. Org. Chem.* **1999**, *64*, 7528–7536.
- (308) Rheiner, P. B.; Sellner, H.; Seebach, D. *Helv. Chim. Acta* **1997**, *80*, 2027–2032.
- (309) Habicher, T.; Diederich, F.; Gramlich, V. *Helv. Chim. Acta* **1999**, *82*, 1066–1095.
- (310) Djojo, F.; Ravanelli, E.; Vostrowsky, O.; Hirsch, A. *Eur. J. Org. Chem.* **2000**, 1051–1059.
- (311) Cook, B. R.; Reinert, T. J.; Suslick, K. S. *J. Am. Chem. Soc.* **1986**, *108*, 7281–7286.
- (312) Suslick, K. S.; Cook, B. R. *J. Chem. Soc., Chem. Commun.* **1987**, 200–202.
- (313) Jiang, D. L.; Aida, T. *Nature* **1997**, *388*, 454–456.
- (314) Aida, T.; Jiang, D. L.; Yashima, E.; Okamoto, Y. *Thin Solid Films* **1998**, *331*, 254–258.
- (315) Wakabayashi, Y.; Tokeshi, M.; Jiang, D. L.; Aida, T.; Kitamori, T. *J. Lumin.* **1999**, *83&84*, 313–315.
- (316) Junge, D. M.; McGrath, D. V. *Chem. Commun.* **1997**, 857–858.
- (317) McGrath, D. V.; Junge, D. M. *Macromol. Symp.* **1999**, *137*, 57–65.
- (318) Junge, D. M.; McGrath, D. V. *J. Am. Chem. Soc.* **1999**, *121*, 4912–4913.
- (319) Li, S.; McGrath, D. V. *J. Am. Chem. Soc.* **2000**, *122*, 6795–6796.
- (320) Smet, M.; Liao, L. X.; Dehaen, W.; McGrath, D. V. *Org. Lett.* **2000**, *2*, 511–513.
- (321) Malenfant, P. R. L.; Groenendaal, L.; Fréchet, J. M. J. *J. Am. Chem. Soc.* **1998**, *120*, 10990–10991.
- (322) Apperloo, J. J.; Janssen, R. A. J.; Malenfant, P. R. L.; Groenendaal, L.; Fréchet, J. M. J. *J. Am. Chem. Soc.* **2000**, *122*, 7042–7051.
- (323) Apperloo, J. J.; Malenfant, P. R. L.; Fréchet, J. M. J.; Janssen, R. A. J. *Synth. Met.* **2001**, *121*, 1259–1260.
- (324) Apperloo, J. J.; Janssen, R. A. J.; Malenfant, P. R. L.; Fréchet, J. M. J. *J. Am. Chem. Soc.* **2001**, *123*, 6916–6924.
- (325) Karthaus, O.; Ijro, K.; Shimomura, M.; Hellmann, J.; Irie, M. *Langmuir* **1996**, *12*, 6714–6716.
- (326) Hofkens, J.; Verheijen, W.; Shukla, R.; Dehaen, W.; De Schryver, F. C. *Macromolecules* **1998**, *31*, 4493–4497.
- (327) Kawa, M.; Fréchet, J. M. J. *Thin Solid Films* **1998**, *331*, 259–263.
- (328) Sato, T.; Jiang, D. L.; Aida, T. *J. Am. Chem. Soc.* **1999**, *121*, 10658–10659.
- (329) Plevoets, M.; Vögtle, F.; De Cola, L.; Balzani, V. *New J. Chem.* **1999**, *23*, 63–69.
- (330) Vögtle, F.; Plevoets, M.; Nieger, M.; Azzellini, G. C.; Credi, A.; Cola, L. D.; De Marchis, V.; Venturi, M.; Balzani, V. *J. Am. Chem. Soc.* **1999**, *121*, 6290–6298.
- (331) Jestin, I.; Levillain, E.; Roncali, J. *Chem. Commun.* **1998**, 2655–2656.
- (332) Camps, X.; Dietel, E.; Hirsch, A.; Pyo, S.; Echegoyen, L.; Hackbarth, S.; Roder, B. *Chem.—Eur. J.* **1999**, *5*, 2362–2373.
- (333) Cardona, C. M.; Kaifer, A. E. *J. Am. Chem. Soc.* **1998**, *120*, 4023–4024.
- (334) Smith, D. K. *J. Chem. Soc., Perkin Trans. 2* **1999**, 1563–1565.
- (335) Wang, Y.; Cardona, C. M.; Kaifer, A. E. *J. Am. Chem. Soc.* **1999**, *121*, 9756–9757.
- (336) Cardona, C. M.; McCarley, T. D.; Kaifer, A. E. *J. Org. Chem.* **2000**, *65*, 1857–1864.
- (337) Miller, L. L.; Zinger, B.; Schlechte, J. S. *Chem. Mater.* **1999**, *11*, 2313–2315.
- (338) Toba, R.; Maria Quintela, J.; Peinador, C.; Roman, E.; Kaifer, A. E. *Chem. Commun.* **2001**, 857–858.
- (339) Gorman, C. B.; Smith, J. C. *Acc. Chem. Res.* **2001**, *34*, 60–71.
- (340) Gorman, C. B.; Smith, J. C.; Hager, M. W.; Parkhurst, B. L.; Sierzputowska-Gracz, H.; Haney, C. A. *J. Am. Chem. Soc.* **1999**, *121*, 9958–9966.
- (341) Newkome, G. R.; Güther, R.; Moorefield, C. N.; Cardullo, F.; Echegoyen, L.; Pérez-Cordero, E.; Luftmann, H. *Angew. Chem., Int. Ed.* **1995**, *34*, 2023–2026.
- (342) Matyjaszewski, K.; Shigemoto, T.; Fréchet, J. M. J.; Leduc, M. *Macromolecules* **1996**, *29*, 4167–4171.
- (343) Percec, V.; Johansson, G.; Heck, J.; Ungar, G.; Batty, S. V. *J. Chem. Soc., Perkin Trans. 1* **1993**, 1411–1420.
- (344) Gitsov, I.; Ivanova, P. T. *Chem. Commun.* **2000**, 269–270.
- (345) Kleij, A. W.; Van de Coevering, R.; Gebbink, R. J. M. K.; Noordman, A. M.; Spek, A. L.; Van Koten, G. *Chem.—Eur. J.* **2001**, *7*, 181–192.
- (346) L'abbé, G.; Haelterman, B.; Dehaen, W. *J. Chem. Soc., Perkin Trans. 1* **1994**, 2203–2204.
- (347) L'abbé, G.; Haelterman, B.; Dehaen, W. *Bull. Soc. Chim. Belg.* **1996**, *105*, 419–420.
- (348) Ferguson, G.; Gallagher, J. F.; McKervey, M. A.; Madigan, E. *J. Chem. Soc., Perkin Trans. 1* **1996**, 599–602.
- (349) Evmenenko, G.; Bauer, B. J.; Kleppinger, R.; Forier, B.; Dehaen, W.; Amis, E. J.; Mischenko, N.; Reynaers, H. *Macromol. Chem. Phys.* **2001**, *202*, 891–899.
- (350) Nagasaki, T.; Noguchi, A.; Matsumoto, T.; Tamagaki, S.; Ogino, K. *An. Quim. Int. Ed.* **1997**, *93*, 341–346.
- (351) Nagasaki, T.; Tamagaki, S.; Ogino, K. *Chem. Lett.* **1997**, 717–718.
- (352) Kleppinger, R.; Reynaers, H.; Desmedt, K.; Forier, B.; Dehaen, W.; Koch, M.; Verhaert, P. *Macromol. Rapid Commun.* **1998**, *19*, 111–114.
- (353) Enomoto, M.; Aida, T. *J. Am. Chem. Soc.* **1999**, *121*, 874–875.
- (354) Gorman, C. B.; Smith, J. C. *J. Am. Chem. Soc.* **2000**, *122*, 9342–9343.
- (355) Takaguchi, Y.; Suzuki, S.; Mori, T.; Motoyoshiya, J.; Aoyama, H. *Bull. Chem. Soc. Jpn.* **2000**, *73*, 1857–1860.
- (356) Hong, B.; Thoms, T. P. S.; Murfee, H. J.; Lebrun, M. J. *Inorg. Chem.* **1997**, *36*, 6146–6147.
- (357) Gitsov, I.; Wooley, K. L.; Fréchet, J. M. J. *Angew. Chem., Int. Ed.* **1992**, *31*, 1200–1202.
- (358) Gitsov, I.; Wooley, K. L.; Hawker, C. J.; Ivanova, P. T.; Fréchet, J. M. J. *Macromolecules* **1993**, *26*, 5621–5627.
- (359) Gitsov, I.; Fréchet, J. M. J. *J. Am. Chem. Soc.* **1996**, *118*, 3785–3786.
- (360) Yu, D.; Vladimirov, N.; Fréchet, J. M. J. *Macromolecules* **1999**, *32*, 5186–5192.
- (361) Gitsov, I.; Fréchet, J. M. J. *Macromolecules* **1993**, *26*, 6536–6546.
- (362) Fréchet, J. M. J.; Gitsov, I. *Macromol. Symp.* **1995**, *98*, 441–465.
- (363) Gitsov, I.; Lambrych, K. R.; Remnant, V. A.; Pracitto, R. *J. Polym. Sci., Part A: Polym. Chem.* **2000**, *38*, 2711–2727.

- (364) Fréchet, J. M. J.; Gitsov, I.; Monteil, T.; Rochat, S.; Sassi, J. F.; Vergelati, C.; Yu, D. *Chem. Mater.* **1999**, *11*, 1267–1274.
- (365) Gitsov, I.; Fréchet, J. M. J. *Macromolecules* **1994**, *27*, 7309–7315.
- (366) Leduc, M. R.; Hayes, W.; Fréchet, J. M. J. *J. Polym. Sci., Part A: Polym. Chem.* **1998**, *36*, 1–10.
- (367) Leduc, M. R.; Hawker, C. J. J.; Dao, J.; Fréchet, J. M. J. *J. Am. Chem. Soc.* **1996**, *118*, 11111–11118.
- (368) Emrick, T.; Hayes, W.; Fréchet, J. M. J. *J. Polym. Sci., Part A: Polym. Chem.* **1999**, *37*, 3748–3755.
- (369) Gitsov, I.; Ivanova, P. T.; Fréchet, J. M. J. *Macromol. Rapid Commun.* **1994**, *15*, 387–393.
- (370) Mecerreyes, D.; Dubois, P.; Jérôme, R.; Hedrick, J. L.; Hawker, C. J. *J. Polym. Sci., Part A: Polym. Chem.* **1999**, *37*, 1923–1930.
- (371) Tomalia, D. A.; Stahlbush, J. R. US Patent 4 857 599, 1988.
- (372) Yin, R.; Zhu, Y.; Tomalia, D. A.; Ibuki, H. *J. Am. Chem. Soc.* **1998**, *120*, 2678–2679.
- (373) Schlüter, A. D.; Rabe, J. P. *Angew. Chem., Int. Ed.* **2000**, *39*, 864–883.
- (374) Frey, H. *Angew. Chem., Int. Ed. Engl.* **1998**, *37*, 2193–2197.
- (375) Schlüter, A. D. *Top. Curr. Chem.* **1998**, *197*, 165–191.
- (376) Hawker, C. J.; Fréchet, J. M. J. *Polymer* **1992**, *33*, 1507–1511.
- (377) Draheim, G.; Ritter, H. *Macromol. Chem. Phys.* **1995**, *196*, 2211–2222.
- (378) Chen, Y.-M.; Chen, C.-F.; Liu, W. H.; Li, Y. F.; Xi, F. *Macromol. Rapid Commun.* **1996**, *17*, 401–407.
- (379) Niggemann, M.; Ritter, H. *Acta Polym.* **1996**, *47*, 351–356.
- (380) Niggemann, M.; Ritter, H. *J. Macromol. Sci., Pure Appl. Chem.* **1997**, *A34*, 1325–1338.
- (381) Chen, Y.-M.; Liu, Y. F.; Gao, J. G.; Chen, C.-F.; Xi, F. *Macromol. Chem. Phys.* **1999**, *200*, 2240–2244.
- (382) Scrivanti, A.; Fasan, S.; Matteoli, U.; Seraglia, R.; Chessa, G. *Macromol. Chem. Phys.* **2000**, *201*, 326–329.
- (383) Claussen, W.; Schulte, N.; Schlüter, A. D. *Macromol. Rapid Commun.* **1995**, *16*, 89–94.
- (384) Karakaya, B.; Claussen, W.; Gessler, K.; Saenger, W.; Schlüter, A. D. *J. Am. Chem. Soc.* **1997**, *119*, 3296–3301.
- (385) Stocker, W.; Karakaya, B.; Schürmann, B. L.; Rabe, J. P.; Schlüter, A. D. *J. Am. Chem. Soc.* **1998**, *120*, 7691–7695.
- (386) Kaneko, T.; Horie, T.; Asano, M.; Aoki, T.; Oikawa, E. *Macromolecules* **1997**, *30*, 3118–3121.
- (387) Percec, V.; Schlüter, A. D.; Ronda, J. C.; Johansson, G.; Ungar, G.; Zhou, J. P. *Macromolecules* **1996**, *29*, 1464–1472.
- (388) Percec, V.; Schlüter, A. D. *Macromolecules* **1997**, *30*, 5783–5790.
- (389) Stewart, G. M.; Fox, M. A. *Chem. Mater.* **1998**, *10*, 860–863.
- (390) Jahromi, S.; Coussens, B.; Meijerink, N.; Braam, A. W. M. *J. Am. Chem. Soc.* **1998**, *120*, 9753–9762.
- (391) Jahromi, S.; Palmen, J. H. M.; Steeman, P. A. M. *Macromolecules* **2000**, *33*, 577–581.
- (392) Bao, Z.; Amundson, K. R.; Lovinger, A. J. *Macromolecules* **1998**, *31*, 8647–8649.
- (393) Schenning, A. P. H. J.; Martin, R. E.; Ito, M.; Diederich, F.; Boudon, C.; Gisselbrecht, J. P.; Gross, M. *Chem. Commun.* **1998**, 1013–1014.
- (394) Ji, T.; Zhang, J.; Cui, G. G.; Li, Y. F. *Polym. Bull.* **1999**, *42*, 379–386.
- (395) Li, Y.; Ji, T.; Zhang, J. *J. Polym. Sci., Part A: Polym. Chem.* **2000**, *38*, 189–197.
- (396) Neubert, I.; Amoulong-Kirstein, E.; Schlüter, A. D.; Dautzenberg, H. *Macromol. Rapid Commun.* **1996**, *17*, 517–527.
- (397) Förster, S.; Neubert, I.; Schlüter, A. D.; Lindner, P. *Macromolecules* **1999**, *32*, 4043–4049.
- (398) Shu, L.; Schäfer, A.; Schlüter, A. D. *Macromolecules* **2000**, *33*, 4321–4328.
- (399) Neubert, I.; Klopsch, R.; Claussen, W.; Schlüter, A. D. *Acta Polym.* **1996**, *47*, 455–459.
- (400) Neubert, I.; Schlüter, A. D. *Macromolecules* **1998**, *31*, 9372–9378.
- (401) Bo, Z.; Schlüter, A. D. *Macromol. Rapid Commun.* **1999**, *20*, 21–25.
- (402) Bo, Z.; Schlüter, A. D. *Chem.—Eur. J.* **2000**, *6*, 3235–3241.
- (403) Stocker, W.; Schürmann, B. L.; Rabe, J. P.; Förster, S.; Lindner, P.; Neubert, I.; Schlüter, A. D. *Adv. Mater.* **1998**, *10*, 793–797.
- (404) Percec, V.; Heck, J.; Tomazos, D.; Falkenberg, F.; Blackwell, H.; Ungar, G. *J. Chem. Soc., Perkin Trans. 1* **1993**, 2799–2811.
- (405) Percec, V.; Heck, J. A.; Tomazos, D.; Ungar, G. *J. Chem. Soc., Perkin Trans. 2* **1993**, 2381–2388.
- (406) Kwon, Y. K.; Chvalun, S.; Schneider, A. I.; Blackwell, J.; Percec, V.; Heck, J. A. *Macromolecules* **1994**, *27*, 6129–6132.
- (407) Percec, V.; Ahn, C. H.; Barboiu, B. *J. Am. Chem. Soc.* **1997**, *119*, 12978–12979.
- (408) Prokhorova, S. A.; Sheiko, S. S.; Ahn, C. H.; Percec, V.; Möller, M. *Macromolecules* **1999**, *32*, 2653–2660.
- (409) Prokhorova, S. A.; Sheiko, S. S.; Möller, M.; Ahn, C. H.; Percec, V. *Macromol. Rapid Commun.* **1998**, *19*, 359–366.
- (410) Bo, Z.; Rabe, J. P.; Schlüter, A. D. *Angew. Chem., Int. Ed. Engl.* **1999**, *38*, 2370–2372.
- (411) Bo, Z.; Zhang, C.; Severin, N.; Rabe, J. P.; Schlüter, A. D. *Macromolecules* **2000**, *33*, 2688–2694.
- (412) Schlüter, A. D.; Claussen, W.; Freudenberger, R. *Macromol. Symp.* **1995**, *98*, 475–482.
- (413) Karakaya, B.; Claussen, W.; Schäfer, A.; Lehmann, A.; Schlüter, A. D. *Acta Polym.* **1996**, *47*, 79–84.
- (414) Desai, A.; Atkinson, N.; Rivera, F. Jr.; Devonport, W.; Rees, I.; Branz, S. E.; Hawker, C. J. *J. Polym. Sci., Part A: Polym. Chem.* **2000**, *38*, 1033–1044.
- (415) Zeng, F.; Zimmerman, S. C. *Chem. Rev.* **1997**, *97*, 1681–1712.
- (416) Emrick, T.; Fréchet, J. M. J. *Curr. Opin. Colloid Interface Sci.* **1999**, *4*, 15–23.
- (417) Zimmerman, S. C.; Zeng, F.; Reichert, D. E. C.; Kolotuchin, S. V. *Science* **1996**, *271*, 1095–1098.
- (418) Thiagarajan, P.; Zeng, F.; Ku, C. Y.; Zimmerman, S. C. *J. Mater. Chem.* **1997**, *7*, 1221–1226.
- (419) Freeman, A. W.; Vreekamp, R. H.; Fréchet, J. M. J. *Polym. Mater. Sci. Eng.* **1997**, *77*, 138–139.
- (420) Wang, Y.; Zeng, F.; Zimmerman, S. C. *Tetrahedron Lett.* **1997**, *38*, 5459–5462.
- (421) Ikeda, A.; Numata, M.; Shinkai, S. *Chem. Lett.* **1999**, 929–930.
- (422) Numata, M.; Ikeda, A.; Shinkai, S. *Chem. Lett.* **2000**, 370–371.
- (423) Jang, W. D.; Jiang, D. L.; Aida, T. *J. Am. Chem. Soc.* **2000**, *122*, 3232–3233.
- (424) Serroni, S.; Campagna, S.; Juris, A.; Venturi, M.; Balzani, V.; Denti, G. *Gazz. Chim. Ital.* **1994**, *124*, 423–427.
- (425) Nierengarten, J. F.; Felder, D.; Nicoud, J. F. *Tetrahedron Lett.* **1999**, *40*, 273–276.
- (426) Armaroli, N.; Boudon, C.; Felder, D.; Gisselbrecht, J. P.; Gross, M.; Marconi, G.; Nicoud, J. F.; Nierengarten, J. F.; Vicinelli, V. *Angew. Chem., Int. Ed. Engl.* **1999**, *38*, 3730–3733.
- (427) Balzani, V.; Juris, A.; Venturi, M.; Campagna, S.; Serroni, S. *Chem. Rev.* **1996**, *96*, 759–833.
- (428) Denti, G.; Campagna, S.; Serroni, S.; Ciano, M.; Balzani, V. *J. Am. Chem. Soc.* **1992**, *114*, 2944–2950.
- (429) Campagna, S.; Denti, G.; Serroni, S.; Ciano, M.; Juris, A.; Balzani, V. *Inorg. Chem.* **1992**, *31*, 2982–2984.
- (430) Balzani, V.; Campagna, S.; Denti, G.; Juris, A.; Serroni, S.; Venturi, M. *Acc. Chem. Res.* **1998**, *31*, 26–34.
- (431) Tully, D. C.; Fréchet, J. M. J. *Chem. Commun.* **2001**, 1229–1239.
- (432) Gorman, C. B.; Miller, R. L.; Chen, K. Y.; Bishop, A. R.; Haasch, R. T.; Nuzzo, R. G. *Langmuir* **1998**, *14*, 3312–3319.
- (433) Bo, Z.; Zhang, L.; Zhang, X.; Chen, J.; Höppener, S.; Shi, L.; Fuchs, H. *Chem. Lett.* **1998**, 1197–1198.
- (434) Zhang, L.; Huo, F.; Wang, Z.; Wu, L.; Zhang, X.; Höppener, S.; Chi, L.; Fuchs, H.; Zhao, J.; Niu, L.; Dong, S. *Langmuir* **2000**, *16*, 3813–3817.
- (435) Chrisstoffels, L. A. J.; Adronov, A.; Fréchet, J. M. J. *Angew. Chem., Int. Ed.* **2000**, *39*, 2163–2167.
- (436) Tully, D. C.; Wilder, K.; Fréchet, J. M. J.; Trimble, A. R.; Quate, C. F. *Adv. Mater.* **1999**, *11*, 314–318.
- (437) Tully, D. C.; Trimble, A. R.; Fréchet, J. M. J.; Wilder, K.; Quate, C. F. *Chem. Mater.* **1999**, *11*, 2892–2898.
- (438) Kao, H. M.; Stefanescu, A. D.; Wooley, K. L.; Schaefer, J. *Macromolecules* **2000**, *33*, 6214–6216.
- (439) Naidoo, K. J.; Hughes, S. J.; Moss, J. R. *Macromolecules* **1999**, *32*, 331–341.
- (440) Topp, A.; Bauer, B. J.; Klimash, J. W.; Spindler, R.; Tomalia, D. A.; Amis, E. J. *Macromolecules* **1999**, *32*, 7226–7231.
- (441) Wooley, K. L.; Hawker, C. J.; Fréchet, J. M. J. *J. Am. Chem. Soc.* **1993**, *115*, 11496–11505.
- (442) Kirton, G. F.; Brown, A. S.; Hawker, C. J.; Reynolds, P. A.; White, J. W. *Physica B* **1998**, *248*, 184–190.
- (443) Hawker, C. J.; Wooley, K. L.; Fréchet, J. M. J. *Macromol. Symp.* **1994**, *77*, 11–20.
- (444) Groenendaal, L.; Fréchet, J. M. J. *J. Org. Chem.* **1998**, *63*, 5675–5679.
- (445) Fréchet, J. M. J.; Hawker, C. J.; Wooley, K. L. *J. Macromol. Sci., Pure Appl. Chem.* **1994**, *A31*, 1627–1645.
- (446) Leon, J. W.; Kawa, M.; Fréchet, J. M. J. *J. Am. Chem. Soc.* **1996**, *118*, 8847–8859.
- (447) Bo, Z. S.; Zhang, X.; Yi, X. B.; Yang, M. L.; Shen, J. C.; Rehn, Y. Z.; Xi, S. Q. *Polym. Bull.* **1997**, *38*, 257–264.
- (448) Mio, C.; Kiritsov, S.; Thio, Y.; Brafman, R.; Prausnitz, J.; Hawker, C.; Malmström, E. *J. Chem. Eng. Data* **1998**, *43*, 541–550.
- (449) Johansson, G.; Percec, V.; Ungar, G.; Zhou, J. P. *Macromolecules* **1996**, *29*, 646–660.
- (450) Percec, V.; Johansson, G.; Ungar, G.; Zhou, J. *J. Am. Chem. Soc.* **1996**, *118*, 9855–9866.
- (451) Liu, M.; Kono, K.; Fréchet, J. M. J. *J. Polym. Sci., Part A: Polym. Chem.* **1999**, *37*, 3492–3503.
- (452) Sellner, H.; Seebach, D. *Angew. Chem., Int. Ed. Engl.* **1999**, *38*, 1918–1920.
- (453) Liao, Y. H.; Moss, J. R. *J. Chem. Soc., Chem. Commun.* **1993**, 1774–1777.
- (454) Liao, Y. H.; Moss, J. R. *Organometallics* **1995**, *14*, 2130–2132.
- (455) Liao, Y. H.; Moss, J. R. *Organometallics* **1996**, *15*, 4307–4316.
- (456) Shu, C. F.; Shen, H. M. *J. Mater. Chem.* **1997**, *7*, 47–52.

- (457) Seebach, D.; Marti, R. E.; Hintermann, T. *Helv. Chim. Acta* **1996**, *79*, 1710–1740.
- (458) Marquardt, T.; Lüning, U. *Chem. Commun.* **1997**, 1681–1682.
- (459) Lüning, U.; Marquardt, T. *J. Prakt. Chem./Chem.-Ztg.* **1999**, *341*, 222–227.
- (460) Stewart, G. M.; Fox, M. A. *J. Am. Chem. Soc.* **1996**, *118*, 4354–4360.
- (461) Freeman, A.; Fréchet, J. M. J.; Koene, S.; Thompson, M. *Macromol. Symp.* **2000**, *154*, 163–169.
- (462) Pesak, D. J.; Moore, J. S. *Angew. Chem., Int. Ed. Engl.* **1997**, *36*, 1636–1639.
- (463) Pesak, D. J.; Moore, J. S.; Wheat, T. E. *Macromolecules* **1997**, *30*, 6467–6482.
- (464) Bryce, M. R.; Devonport, W.; Moore, A. J. *Angew. Chem., Int. Ed.* **1994**, *33*, 1761–1763.
- (465) Bryce, M. R.; de Miguel, P.; Devonport, W. *Chem. Commun.* **1998**, 2565–2566.
- (466) Devonport, W.; Bryce, M. R.; Marshallsay, G. J.; Moore, A. J.; Goldenberg, L. M. *J. Mater. Chem.* **1998**, *8*, 1361–1372.
- (467) Ashton, P. R.; Boyd, S. E.; Brown, C. L.; Jayaraman, N.; Nepogodiev, S. A.; Stoddart, J. F. *Chem.–Eur. J.* **1996**, *2*, 1115–1128.
- (468) Ashton, P. R.; Boyd, S. E.; Brown, C. L.; Jayaraman, N.; Stoddart, J. F. *Angew. Chem., Int. Ed. Engl.* **1997**, *36*, 732–735.
- (469) Ashton, P. R.; Hounsell, E. F.; Jayaraman, N.; Nilsen, T. M.; Spencer, N.; Stoddart, J. F.; Young, M. *J. Org. Chem.* **1998**, *63*, 3429–3437.
- (470) Nierengarten, J. F.; Felder, D.; Nicoud, J. F. *Tetrahedron Lett.* **1999**, *40*, 269–272.
- (471) Felder, D.; Gallani, J. L.; Guillon, D.; Heinrich, B.; Nicoud, J. F.; Nierengarten, J. F. *Angew. Chem., Int. Ed.* **2000**, *39*, 201–204.
- (472) Nlate, S.; Ruiz, J.; Astruc, D.; Blais, J. C. *Chem. Commun.* **2000**, 417–418.
- (473) Hawker, C. J.; Fréchet, J. M. J. *J. Chem. Soc., Perkin Trans. 1* **1992**, 2459–2469.
- (474) Bussion, P.; Ihre, H.; Hult, A. *J. Am. Chem. Soc.* **1998**, *120*, 9070–9071.
- (475) Atthoff, B.; Trollsås, M.; Claesson, H.; Hedrick, J. L. *Macromol. Chem. Phys.* **1999**, *200*, 1333–1339.
- (476) Trollsås, M.; Hawker, C. J.; Remenar, J. F.; Hedrick, J. L.; Johansson, M.; Ihre, H.; Hult, A. *J. Polym. Sci., Part A: Polym. Chem.* **1998**, *36*, 2793–2798.
- (477) Trollsås, M.; Claesson, H.; Atthoff, B.; Hedrick, J. L.; Pople, J. A.; Gast, A. P. *Macromol. Symp.* **2000**, *153*, 87–108.
- (478) Hedrick, J. L.; Trollsås, M.; Hawker, C. J.; Atthoff, B.; Claesson, H.; Heise, A.; Miller, R. D.; Mecerreyes, D.; Jérôme, R.; Dubois, P. *Macromolecules* **1998**, *31*, 8691–8705.
- (479) Trollsås, M.; Claesson, H.; Atthoff, B.; Hedrick, J. L. *Angew. Chem., Int. Ed. Engl.* **1998**, *37*, 3132–3136.
- (480) Trollsås, M.; Atthoff, B.; Würsch, A.; Hedrick, J. L.; Pople, J. A.; Gast, A. P. *Macromolecules* **2000**, *33*, 6423–6438.
- (481) Hecht, S.; Ihre, H.; Fréchet, J. M. J. *J. Am. Chem. Soc.* **1999**, *121*, 9239–9240.
- (482) Hecht, S.; Vladimirov, N.; Fréchet, J. M. J. *J. Am. Chem. Soc.* **2001**, *123*, 18–25.
- (483) Hannon, M. J.; Mayers, P. C.; Taylor, P. C. *J. Chem. Soc., Perkin Trans. 1* **2000**, 1881–1889.
- (484) Kono, K.; Liu, M.; Fréchet, J. M. J. *Bioconjugate Chem.* **1999**, *10*, 1115–1121.
- (485) Tully, D. C.; Trimble, A. R.; Fréchet, J. M. J. *Adv. Mater.* **2000**, *12*, 1118–1122.
- (486) Xu, Z.; Moore, J. S. *Acta Polym.* **1994**, *45*, 83–87.
- (487) Kimura, M.; Shiba, T.; Muto, T.; Hanabusa, K.; Shirai, H. *Tetrahedron Lett.* **2000**, *41*, 6809–6813.
- (488) Adronov, A.; Gilat, S. L.; Fréchet, J. M. J.; Ohta, K.; Neuwahl, F. V. R.; Fleming, G. R. *J. Am. Chem. Soc.* **2000**, *122*, 1175–1185.
- (489) Neuwahl, F. V. R.; Righini, R.; Adronov, A.; Malenfant, P. R. L.; Fréchet, J. M. J. *J. Phys. Chem. B* **2001**, *105*, 1307–1312.
- (490) Freeman, A. W.; Koene, S. C.; Malenfant, P. R. L.; Thompson, M. E.; Fréchet, J. M. J. *J. Am. Chem. Soc.* **2000**, *122*, 12385–12386.
- (491) Percec, V.; Johansson, G.; Schlueter, D.; Ronda, J. C.; Ungar, G. *Macromol. Symp.* **1996**, *101*, 43–60.
- (492) Balagurusamy, V. S. K.; Ungar, G.; Percec, V.; Johansson, G. *J. Am. Chem. Soc.* **1997**, *119*, 1539–1555.
- (493) Percec, V.; Cho, W. D.; Ungar, G.; Yeardley, D. J. P. *Angew. Chem., Int. Ed.* **2000**, *39*, 1598–1602.
- (494) Cui, G. L.; Xu, Y.; Liu, M. Z.; Fang, F.; Ji, T.; Chen, Y.-M.; Li, Y. F. *Macromol. Rapid Commun.* **1999**, *20*, 71–76.
- (495) Gossage, R. A.; Jastrzebski, J. T. B. H.; Van Ameijde, J.; Mulders, S. J. E.; Brouwer, A. J.; Liskamp, R. M. J.; Van Koten, G. *Tetrahedron Lett.* **1999**, *40*, 1413–1416.
- (496) Wendland, M. S.; Zimmerman, S. C. *J. Am. Chem. Soc.* **1999**, *121*, 1389–1390.
- (497) Xu, Z.; Moore, J. S. *Angew. Chem., Int. Ed. Engl.* **1993**, *32*, 1354–1357.
- (498) Nierengarten, J. F.; Felder, D.; Nicoud, J. F. *Tetrahedron Lett.* **2000**, *41*, 41–44.
- (499) Felder, D.; Nierengarten, H.; Gisselbrecht, J. P.; Boudon, C.; Leize, E.; Nicoud, J. F.; Gross, M.; Van Dorsselaer, A.; Nierengarten, J. F. *New J. Chem.* **2000**, *24*, 687–695.
- (500) Chessa, G.; Scrivanti, A. *J. Chem. Soc., Perkin Trans. 1* **1996**, 307–311.
- (501) Chessa, G.; Scrivanti, A.; Seraglia, R.; Traldi, P. *Rapid Commun. Mass Spectrom.* **1998**, *12*, 1533–1537.
- (502) Chessa, G.; Scrivanti, A.; Canovese, L.; Visentin, F.; Uguagliati, P. *Chem. Commun.* **1999**, 959–960.
- (503) Bryce, M. R.; Devonport, W.; Goldenberg, L. M.; Wang, C. *Chem. Commun.* **1998**, 945–952.
- (504) Christensen, C. A.; Bryce, M. R.; Becher, J. *Synthesis* **2000**, 1695–1704.
- (505) Wang, C.; Bryce, M. R.; Batsanov, A. S.; Goldenberg, L. M.; Howard, J. A. K. *J. Mater. Chem.* **1997**, *7*, 1189–1197.
- (506) Christensen, C. A.; Goldenberg, L. M.; Bryce, M. R.; Becher, J. *Chem. Commun.* **1998**, 509–510.
- (507) Drobizhev, M.; Rebane, A.; Sigel, C.; Elandaloussi, E. H.; Spangler, C. W. *Chem. Phys. Lett.* **2000**, *325*, 375–382.
- (508) Spangler, C. W.; Elandaloussi, E. H.; Reeves, B. *Polym. Prepr. (Am. Chem. Soc., Div. Polym. Chem)* **2000**, *41*, 789–790.
- (509) Zhu, Z.; Moore, J. S. *J. Org. Chem.* **2000**, *65*, 116–123.
- (510) Zhu, Z.; Moore, J. S. *Macromolecules* **2000**, *33*, 801–807.
- (511) Yokoyama, S.; Nakahama, T.; Otomo, A.; Mashiko, S. *Chem. Lett.* **1997**, 1137–1138.
- (512) Yokoyama, S.; Nakahama, T.; Otomo, A.; Mashiko, S. *Thin Solid Films* **1998**, *331*, 248–253.
- (513) Yokoyama, S.; Nakahama, T.; Otomo, A.; Mashiko, S. *J. Am. Chem. Soc.* **2000**, *122*, 3174–3181.
- (514) Percec, V.; Chu, P.; Ungar, G.; Zhou, J. *J. Am. Chem. Soc.* **1995**, *117*, 11441–11454.
- (515) Li, J. F.; Crandall, K. A.; Chu, P.; Percec, V.; Petschek, R. G.; Rosenblatt, C. *Macromolecules* **1996**, *29*, 7813–7819.
- (516) Percec, V. *Pure Appl. Chem.* **1995**, *67*, 2031–2038.
- (517) Recker, J.; Tomcik, D. J.; Parquette, J. R. *J. Am. Chem. Soc.* **2000**, *122*, 10298–10307.
- (518) Tominaga, M.; Konishi, K.; Aida, T. *Chem. Lett.* **2000**, 374–375.
- (519) Bharathi, P.; Zhao, H.; Thayumanavan, S. *Org. Lett.* **2001**, *3*, 1961–1964.
- (520) Lochmann, L.; Wooley, K. L.; Ivanova, P. T.; Fréchet, J. M. J. *J. Am. Chem. Soc.* **1993**, *115*, 7043–7044.
- (521) Bo, Z.; Schäfer, A.; Franke, P.; Schlüter, A. D. *Org. Lett.* **2000**, *2*, 1645–1648.
- (522) Freeman, A. W.; Chrisstoffels, L. A. J.; Fréchet, J. M. J. *J. Org. Chem.* **2000**, *65*, 7612–7617.
- (523) Schultz, L. G.; Zhao, Y.; Zimmerman, S. C. *Angew. Chem., Int. Ed.* **2001**, *40*, 1962–1966.
- (524) Dvornic, P. R.; Leuze-Jallouli, A. M.; Owen, M. J.; Perz, S. V. *Macromolecules* **2000**, *33*, 5366–5378.
- (525) Hawker, C. J.; Fréchet, J. M. J. *J. Am. Chem. Soc.* **1992**, *114*, 8405–8413.
- (526) Mak, C. C.; Chow, H. F. *Chem. Commun.* **1996**, 1185–1186.
- (527) Junge, D. M.; Wu, M. J.; McElhanon, J. R.; McGrath, D. V. *J. Org. Chem.* **2000**, *65*, 5306–5314.
- (528) Aoi, K.; Itoh, K.; Okada, M. *Macromolecules* **1997**, *30*, 8072–8074.
- (529) Maruo, N.; Uchiyama, M.; Kato, T.; Arai, T.; Nishino, N.; Akisada, H. *Chem. Commun.* **1999**, 2057–2058.
- (530) Pan, Y.; Ford, W. T. *Macromolecules* **1999**, *32*, 5468–5470.
- (531) Pesak, D. J.; Moore, J. S. *Tetrahedron* **1997**, *53*, 15331–15347.

CR990116H

New Polymer Synthesis by Nitroxide Mediated Living Radical Polymerizations

Craig J. Hawker,* Anton W. Bosman, and Eva Harth

IBM Almaden Research Center, 650 Harry Road, San Jose, California 95120-6099

Received April 9, 2001

Contents

I. Introduction	3661
A. Background	3661
B. Scope of Review	3662
II. Historical Perspective	3662
III. Nitroxide-Mediated Living Free Radical Polymerizations	3663
A. Bimolecular Process	3664
B. Unimolecular Initiators	3664
IV. Nitroxides Development	3665
V. Approaches to Alkoxyamines	3667
VI. Mechanistic and Kinetic Features	3669
A. Nitroxide Exchange	3669
B. Additives	3671
C. Chain End Degradation	3671
D. Elucidation of Living Nature	3672
E. Emulsion and Related Processes	3673
VII. Toward New Materials	3673
A. Molecular Weight Control	3673
B. Telechelic Polymers	3673
C. Block Copolymers	3674
D. Random Copolymers	3678
VIII. Complex Macromolecular Architectures	3680
A. Star and Graft Polymers	3680
B. Hyperbranched and Dendritic Structures	3681
IX. Surface-Initiated Polymerizations	3683
X. Outlook	3685
XI. Acknowledgments	3686
XII. Note Added after ASAP	3686
XIII. References	3686

I. Introduction

A. Background

At first glance, radical polymerization may be considered a mature technology with millions of tons of vinyl based homo- and copolymers being produced annually. This perception of maturity is based on the fact that free radical polymerization is so widely used industrially and in research laboratories for the synthesis of a wide variety of polymeric materials. This widespread adoption is due to its versatility, synthetic ease, and compatibility with a wide variety of functional groups, coupled with its tolerance to water and protic media. These features make possible the development of emulsion and suspension techniques, which greatly simplifies the experimental set up and has led to wide commercial adoption.



Tonny Bosman (left) was born in Nijmegen, The Netherlands, in 1970 and studied chemistry at the University of Nijmegen. His undergraduate research (1994) was done in the group of Roeland Nolte concerning chiral mesogenic phthalocyanines after which he undertook his Ph.D. with Bert Meijer at Eindhoven University of Technology (1999) in the area of dendritic molecules and functional materials. He is currently undertaking postdoctoral research at the IBM Almaden Research Center with Jean Fréchet and Craig Hawker on combinatorial/high-throughput chemistry and its application to developing new methods in living free radical procedures.

Eva Harth (center) was born in Cologne, Germany and studied chemistry at the University of Bonn and the University of Zurich, Switzerland under the supervision of Prof. A. Vasella, ETH Zurich, where she worked on the synthesis and application of glycosylidene fullerenes derivatives. In 1994 she joined the group of Prof. K. Muellen at the MPI for Polymer Research in Mainz, obtaining her Ph.D. in 1998 for work in the area of fullerene adducts and polymers. She is currently undertaking postdoctoral research at the IBM Almaden Research Center focusing on the development of new living free polymerization techniques and novel approaches to nanoscopic materials.

Craig Hawker (right) was born in Toowoomba, Australia, in 1964. He received a B.Sc. degree in chemistry from the University of Queensland in 1984 and a Ph.D. degree in bio-organic chemistry from the University of Cambridge in 1988 under the supervision of Prof. Sir Alan Battersby. Jumping into the world of polymer chemistry, he undertook a postdoctoral fellowship with Prof. Jean Fréchet at Cornell University from 1988 to 1990 and then returned to the University of Queensland as a Queen Elizabeth II Fellow from 1991 to 1993. He is currently a Research Staff Member at the IBM Almaden Research Center and an investigator in the NSF Center for Polymer Interfaces and Macromolecular Assemblies and was recently awarded the 2001 Carl S. Marvel Award in Creative Polymer Science. His research has focused on the interface between organic and polymer chemistry with emphasis on the design, synthesis, and application of unusual macromolecular structures in microelectronics and nanotechnology.

It is therefore surprising that the study of radical polymerization has witnessed a renaissance in terms of both synthetic possibilities and mechanistic understanding in recent years. One of the driving forces for this renaissance has been the growing demand for functionalized, well-defined materials as building blocks in nanotechnology applications. In the preparation of well-defined macromolecules, traditional

free radical procedures have a significant drawback, which is related to the reactivity of the propagating free radical chain end and its propensity to undergo a variety of different termination reactions. The materials obtained are therefore polydisperse with very limited control over macromolecular weight and architecture.¹ Until recently, ionic polymerizations (anionic or cationic) were the only "living" techniques available that efficiently controlled the structure and architecture of vinyl polymers. Although these techniques ensure low polydispersity materials, controlled molecular weight and defined chain ends, they are not useful for the polymerization and copolymerization of a wide range of functionalized vinylic monomers. This limitation is due to the incompatibility of the growing polymer chain end (anion or cation) with numerous functional groups and certain monomer families.² In addition, these polymerization techniques require stringent reaction conditions including the use of ultrapure reagents and the total exclusion of water and oxygen. The necessity to overcome all these limitations emboldened synthetic polymer chemists to develop new concepts, which would permit the development of a free-radical polymerization procedure possessing the characteristics of a living process. This field has witnessed explosive growth in recent years and a number of specialized reviews have been published in this general area.^{3–6}

B. Scope of Review

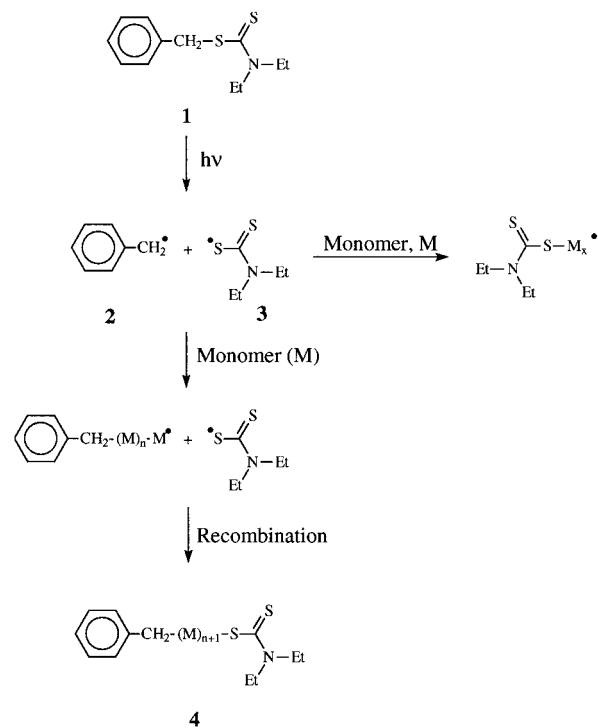
This review covers the scientific literature from 1980 to the present concerning nitroxide-mediated living free radical polymerization. Strategies for controlling polymeric structure and macromolecular architecture will be discussed in detail with special emphasis placed on the synthesis of functionalized polymers. Other important synthetic considerations such as the design of nitroxides with improved performance and the development of new synthetic approaches to alkoxyamine initiators will be examined in an effort to provide a basis for future development in the field. While mechanistic and kinetic details of the polymerization process will be examined, for a more detailed treatment the reader is directed to the review article by Fischer in this issue.⁷ Similarly, the relationship between nitroxide-mediated and other living free radical techniques, such as atom transfer radical polymerization (ATRP) and radical addition, fragmentation and transfer (RAFT) will be discussed and examples given for each of these novel techniques; however, for an in depth analysis, the reader is directed to the review by Sawamoto in this thematic issue.⁸

II. Historical Perspective

The first detailed attempt to use initiators that control radical polymerization of styrene and methyl methacrylate was reported by Werrington and Tobolsky in 1955.⁹ However, the specific dithiuram disulfides that were employed lead to high transfer constants, which resulted in retardation of the polymerization. This promising concept was subsequently overlooked for close to 30 years until the use

of "iniferters" (*initiator-transfer agent-terminator*) was introduced by Otsu in 1982 which is arguably the first attempt to develop a true LFRP technique.¹⁰ In this case, disulfides, **1**, including diaryl and dithiuram disulfides, were proposed as photochemical initiators where cleavage can occur at the C–S bond to give a carbon-based propagating radical, **2**, and the mediating thio radical **3** (Scheme 1). While the

Scheme 1



propagating radical **2** can undergo monomer addition followed by recombination with a primary sulfur radical, **3**, to give a dormant species, **4**, it may also undergo chain transfer to the initiator itself. As opposed to conventional free-radical polymerization, which results in chain termination, even at low conversion, this technique provides rudimentary characteristics of typical living systems, such as a linear increase in molecular weight with conversion. In addition, the monofunctional, or α,ω -bifunctional chains, can be considered as telechelic polymers, giving the possibility to prepare block copolymers. Nevertheless, other features of a true living system such as accurately controlled molecular weights and low polydispersities could not be obtained since a thio radical, **3**, can also initiate polymerization. As will be discussed below, one of the primary requirements for a mediating radical is that it undergoes reversible termination of the propagating chain end *without* acting as an initiator. Subsequently, a wide range of stabilized radicals has been examined as mediating radicals for the development of a living free radical system.^{11–13} As with the preliminary iniferter work of Otsu, they suffer from incomplete control over both the initiation and reversible termination steps and lead to poorly controlled polymerizations; however, their structures do point to interesting features that may be relevant in the future development of this technology (Figure 1). Delocalized systems, the pres-

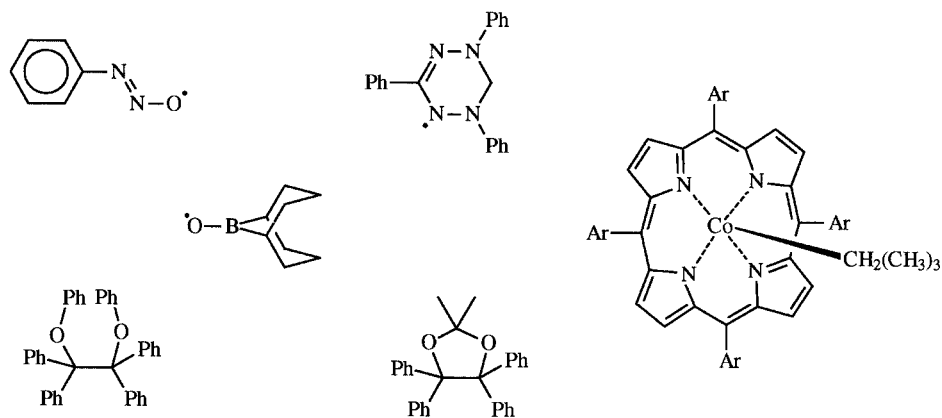


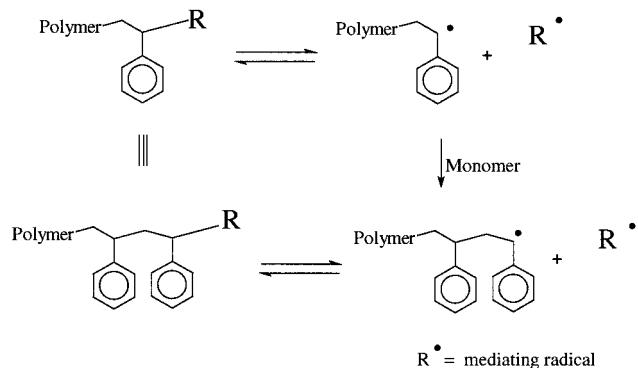
Figure 1.

ence of heteroatoms and in many examples, steric hindrance all play key roles in determining the success of the mediating radical. Of particular note to the nitroxide work described below, is the ability of radicals such as the verdazyl and borinate derivatives to control the polymerization of methacrylates. The tendency of the radical species in these examples to abstract α -hydrogens is obviously decreased for methacrylate polymerizations when compared to nitroxides and an understanding of the difference between these systems may permit the design of improved nitroxides for methacrylate polymerization.

III. Nitroxide-Mediated Living Free Radical Polymerizations

The pioneering iniferter work provided the basis for the development of LFRP and it is interesting to note the similarity between the iniferter mechanism outlined in Scheme 1 and the general outline of a **successful** living free radical mechanism (Scheme 2). In this general mechanism, the reversible termi-

Scheme 2

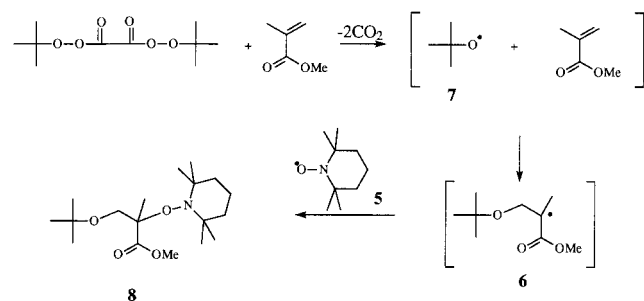


nation of the growing polymeric chain is the key step for reducing the overall concentration of the propagating radical chain end. In the absence of other reactions leading to initiation of new polymer chains (i.e., no reaction of the mediating radical with the vinylic monomer), the concentration of reactive chain ends is extremely low, minimizing irreversible termination reactions, such as combination or disproportionation. All chains would be initiated only from

the desired initiating species and growth should occur in a living fashion, allowing a high degree of control over the entire polymerization process with well-defined polymers being obtained.

The identity of the mediating radical, R^\bullet , is critical to the success of living free radical procedures and a variety of different persistent, or stabilized radicals have been employed. These range from (aryloxy)oxy,¹⁴ substituted triphenyls,¹⁵ verdazyl,¹⁶ triazolyl,¹⁷ nitroxides,¹⁸ etc. with the most widely studied and certainly most successful class of compounds being the nitroxides and their associated alkylated derivatives, alkoxyamines. Interestingly, the development of nitroxides as mediators for radical polymerization stems from pioneering work into the nature of standard free radical initiation mechanisms and the desire to efficiently trap carbon-centered free radicals. Solomon, Rizzardo, and Moad were able to demonstrate that at the low temperatures typically associated with standard free radical polymerizations, 40–60 °C, nitroxides such as 2,2,6,6-tetramethylpiperidinyloxy (TEMPO), **5**, reacted at near diffusion controlled rates with carbon-centered free radicals, **6**, generated from the addition of initiating radicals, **7**, to vinyl monomers.¹⁹ The resulting alkoxyamine derivatives, **8**, were essentially stable at these temperatures and did not participate in the reaction further, thus acting as radical traps (Scheme 3).

Scheme 3



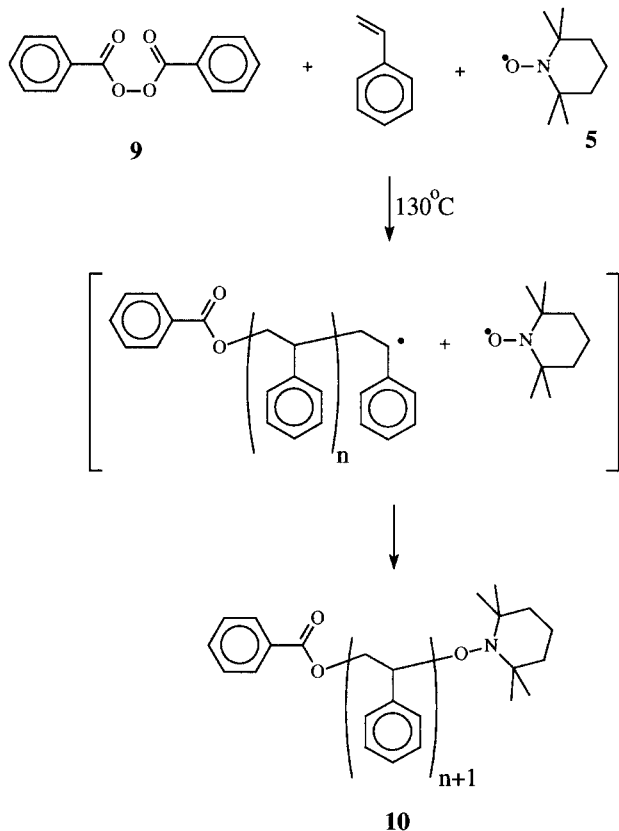
The same workers then applied a similar concept, albeit at increased temperatures (80–100 °C) to the synthesis of low molecular weight polymers and oligomers, primarily with acrylates and hindered

nitroxides.²⁰ While the polymerization of acrylates cannot be considered living at these low temperatures, this seminal piece of work did provide the foundation for many of the ensuing studies in the whole field of living free radical polymerization.

A. Bimolecular Process

The second seminal contribution which demonstrated to a wide audience that living free radical polymerizations are a viable synthetic methodology was a report from the group of Georges at XEROX describing the preparation of low polydispersity polystyrene.²¹ The key feature of this work was the preparation of high molecular weight, low polydispersity materials. By increasing the temperature to 130 °C and conducting the polymerizations in bulk, a system comprising benzoyl peroxide, **9**, and a stable nitroxide, TEMPO (**5**), in a molar ratio of 1.3:1, gave polystyrene derivatives, **10**, by a living process in which the molecular weight increased in a linear fashion with conversion (Scheme 4). Even more

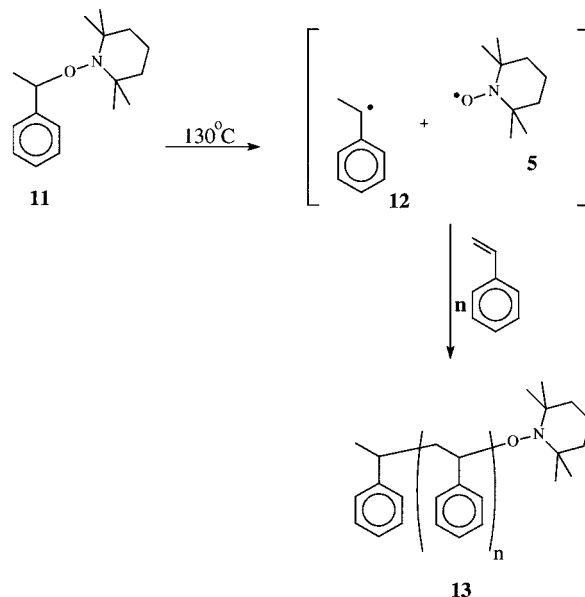
Scheme 4



startling were the polydispersity values for **10** (PDI = 1.2–1.3), which were significantly lower than the theoretical lower limit for a free radical process of 1.5 and the typical values of ca. 2.0 for free radical systems. At these elevated temperatures the C–ON bond becomes unstable, releasing the nitroxide which can now act as a polymerization mediator, not as an inhibitor as they are low temperatures, hence their use by Solomon to trap polymerization intermediates.

While this original work by the XEROX group displays many of the fundamental aspects of a living

Scheme 5

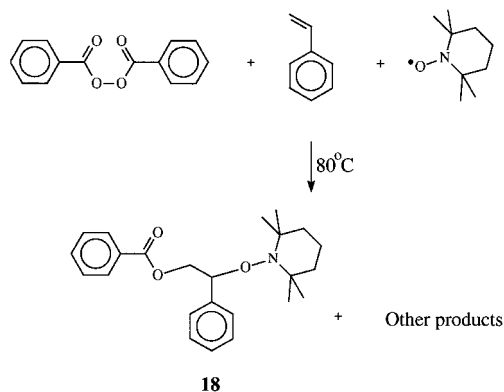


polymerization process, and subsequent studies have confirmed and reinforced these original observations, it must be emphasized that these are not *true* living systems.^{22–26} While the concentration and reactivity of radicals at the propagating chain end have been significantly reduced, it is still not negligible and therefore termination reactions can still occur. By the strictest definition, nitroxide-mediated and in fact all versions of LFRP are not living polymerizations; however, the best systems do display all of the characteristics of a living system and so the term, *living* will be used throughout this chapter. For an excellent discussion of the many varied opinions on the correct terminology for living free radical polymerizations the reader is directed to a special, “living or controlled” thematic issue of *J. Polym. Sci.*²⁷

B. Unimolecular Initiators

While successful, the poorly defined nature and unknown concentration of the initiating species in the bimolecular process prompted the development of a single molecule initiating system which would permit control over molecular weight, architecture, etc. Borrowing the concept of well-defined initiators from living anionic and cationic procedures, unimolecular initiators for nitroxide-mediated living free radical polymerizations have been developed.^{28,29} The structure of these initiators was based on the alkoxyamine functionality that is present at the chain end of the growing polymer during its dormant phase. The C–O bond of the small molecule alkoxyamine derivative **11** is therefore expected to be thermolytically unstable and decompose on heating to give an initiating radical, i.e., the α -methylbenzyl radical **12** as well as the mediating nitroxide radical **5** in the correct 1:1 stoichiometry (Scheme 5). Following initiation the polymerization would proceed as described previous for the bimolecular case to give the polystyrene derivative **13**.

Scheme 6



IV. Nitroxides Development

While the above strategies proved that the concept of a living free radical procedure was a viable process there were a large number of problems with the use of TEMPO, as the mediating radical.²⁹ In addition, the available synthetic methods for the preparation of alkoxyamines were poor and not amenable to the preparation of functionalized initiators in high yield.³⁰ These included the necessity to use high polymerization temperature (125–145 °C), long reaction times (24–72 h) and an incompatibility with many important monomer families. While it was shown that random copolymers of styrene and either butyl acrylate or methyl methacrylate could be readily prepared with TEMPO,³¹ at high incorporations of the comonomer (ca. 50%+) the copolymerization and homopolymerization of (meth)acrylates are no longer living. Before becoming a routine synthetic procedure for the preparation of well-defined polymers, these issues needed to be addressed.

To overcome these deficiencies it was apparent that changes in the structure of the nitroxide were needed. Unlike the initiating radical, which is involved only at the beginning of the polymerization, the mediating radical is involved in numerous reversible termination and activation steps and so changes in its structure would be expected to have a substantial effect on the polymerization. Initial efforts to develop new mediating nitroxides relied on TEMPO based derivatives. The XEROX group were able to polymerize acrylates at elevated temperatures (145–155 °C) in the presence of 4-oxo-TEMPO, **14**, as the mediating nitroxide, and while this is a significant improvement when compared to TEMPO, polydispersities were still between 1.40 and 1.67 and the living nature of the polymerization was questionable.³² Similarly, Matyjaszewski observed that the rate of polymerization of styrene could be significantly enhanced by the use of a TEMPO derivative, **15**, substituted in the 4-position with a phosphonic acid group (Figure 2). Presumably the ability to form an intramolecular H-bond in **15** leads to a change in mediating ability.³³ This prompted the investigation of a wide range of other TEMPO-like structures, such as di-*tert*-butyl nitroxides, and in the use of additives.³⁴ All of these approaches lead to an increase in the rate of polymerization, especially for

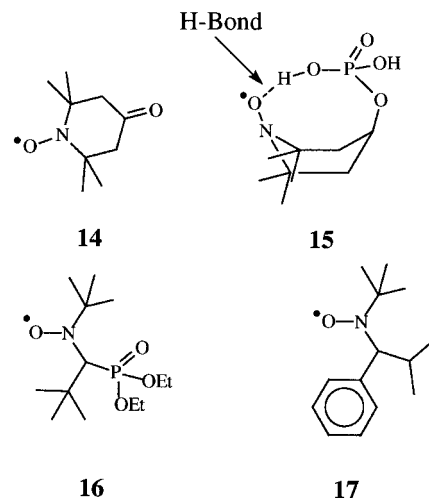


Figure 2.

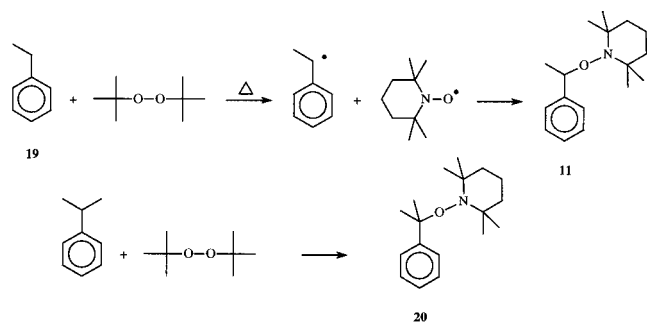
additives such as camphorsulfonic acid³⁵ or acetic anhydride,³⁶ however, the improvements were not significant enough to make nitroxide-mediated polymerizations a viable competitor to other living techniques.

The most significant breakthrough in the design of improved nitroxides was the use of alicyclic nitroxides, which bear no structural resemblance to TEMPO. In fact, their most striking difference was the presence of a hydrogen atom on one of the α -carbons, in contrast to the two quaternary α -carbons present in TEMPO and all the nitroxides discussed above. Interestingly this feature is traditionally associated with unstable nitroxide derivatives and may have some bearing on the success of these compounds. The best examples of these new materials are the phosphonate derivative, **16**, introduced by Gnanou and Tordo³⁷ and the family of arenes, **17**, introduced by Hawker (Figure 2).³⁸ These nitroxides have subsequently been shown to be vastly superior to the original TEMPO derivatives, delegating the latter to a niche role for select styrenic polymerizations. The use of nitroxides such as **16** and **17** now permits the polymerization of a wide variety of monomer families. Acrylates, acrylamides, 1,3-dienes and acrylonitrile based monomers can now be polymerized with accurate control of molecular weights and polydispersities as low as 1.05.³⁹ The versatile nature of these initiators can also be used to control the formation of random and block copolymers from a wide selection of monomer units containing reactive functional groups, such as amino, carboxylic acid, glycidyl. The universal nature of these initiators overcomes many of the limitations typically associated with nitroxide-mediated systems and leads to a level of versatility approaching atom transfer radical polymerization (ATRP) and radical addition fragmentation and transfer (RAFT) based systems.^{40–42} The applicability of these systems to other monomer families will be described and demonstrated in the following sections on block copolymers and macromolecular architectures. A list of nitroxides that have been employed as mediators in living free radical polymerizations are included in Table 1 with accompanying references.^{43–76}

Table 1. Structure of Nitroxides Employed in Living Free Radical Polymerizations

Structure	Reference	Structure	Reference	Structure	Reference	Structure	Reference
	43 51 52 57-59 67		47 48 50		38 54		38 54
	44 49 53 56 66		38		38 54		38 54
	72		38		38 54		38 54
	38 39 54 73		38 71		38 54		38 54
	37 38 55		38		38 54		38 54
	38 61 62		38 58		38 54		63 69
	69		46		65		67
			76		67		67
	73		64		67		68
	76		74 75		67		68
	76		65		67		70 71

Scheme 7



V. Approaches to Alkoxyamines

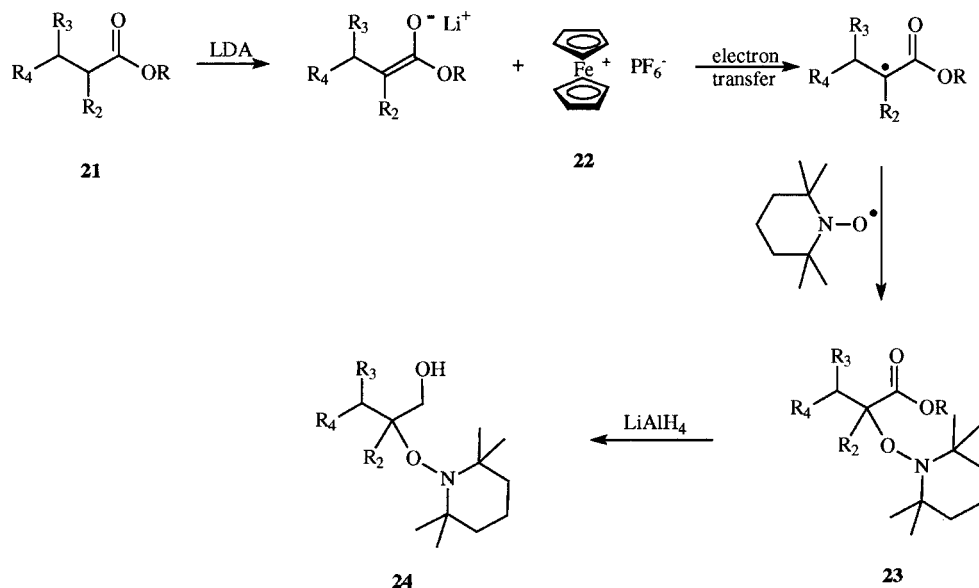
The development of stable, readily functionalized initiators, which mimic the growing chain end for living free radical systems, is one of the significant achievements and advantages of LFRP. Not only does it allow the greatest degree of control over the final polymeric structure, but also the ready functionalization permits the development of new areas of research in polymer science and nanotechnology. In the case of nitroxide-mediated systems, the dormant chain end is an alkylated nitroxide derivative, also termed an alkoxyamine. Unfortunately, as a class of compounds, alkoxyamines are poorly studied and the initial exploitation of their potential was limited by the lack of versatile and efficient synthetic procedures for their preparation.^{77–79}

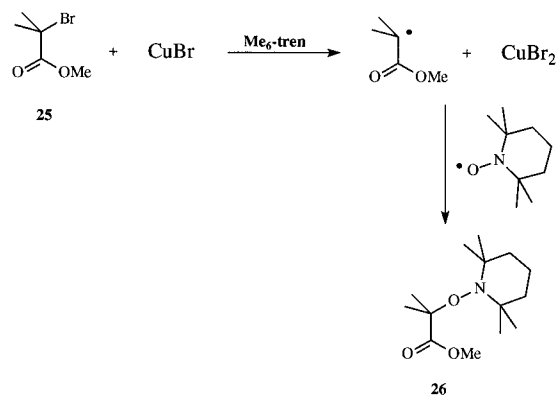
The growing importance of alkoxyamines for LFRP has motivated organic chemists to pursue new and more versatile synthetic approaches for their preparation. Initially the majority of synthetic approaches to alkoxyamines relied on the generation of carbon-centered radicals followed by the trapping of these radicals by a nitroxide derivative. Initial examples include the reaction of benzoyl peroxide with an excess of styrene to give a benzylic radical followed by trapping of the radical intermediate with TEMPO to give the benzoyl peroxide adduct, **18**. Problems with this synthesis include the relative poor yield (30–40% yield) and the wide range of byproducts,

which complicated purification (Scheme 6).²⁸ In an effort to both improve the yield of the desired alkoxyamine and simplify purification, a variety of other strategies for generation of the radical intermediate have been studied. Howell has taken advantage of the low reactivity of nitroxides with oxygen-based radicals to prepare benzylic alkoxyamines, **11**, by hydrogen abstraction from ethyl benzene, **19**, followed by nitroxide trapping (Scheme 7).^{80,81} Generation of the intermediate radical has also been accomplished photochemically using a di-*tert*-butyl peroxide reaction system and irradiation with 300 nm light. In this case, the mild nature of the reaction conditions allows the yields to be increased to over 90% and more importantly permits thermally unstable alkoxyamines such as the α,α -dimethyl-substituted derivative **20** to be isolated. Under traditional thermal conditions, **20** would decompose on formation due to the inherent instability of the quaternary C–ON bond.⁸²

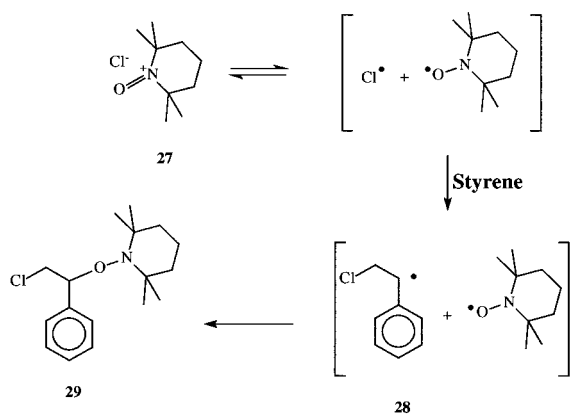
Alternative approaches have also been recently developed which rely on the controlled generation of carbon-centered radicals followed by trapping of the radical-like intermediates. Jahn⁸³ has employed single electron transfer in the highly efficient generation of radicals from ester enolates, **21**, by treatment of lithium salts with ferrocenium ions, **22**, at -78°C . These radicals are then trapped by nitroxides to provide functionalized alkoxyamines, **23**, in moderate to high yields. Reduction with LiAlH_4 gives the hydroxy derivative **24** in good yield with no attack at the alkoxyamine group, demonstrating the stability of alkoxyamines to a variety of reaction conditions (Scheme 8). Similarly, Braslau has employed Cu^{2+} -promoted single electron-transfer reactions with enolate anions to provide carbon-centered free radicals which can be trapped by nitroxides at low temperatures.⁸⁴ Matyjaszewski has applied techniques from atom transfer radical procedures to develop a facile, low-temperature approach to alkoxyamines involving the treatment of suitable ATRP-based initiators, **25**, with copper complexes in the presence of a nitroxide,

Scheme 8



Scheme 9

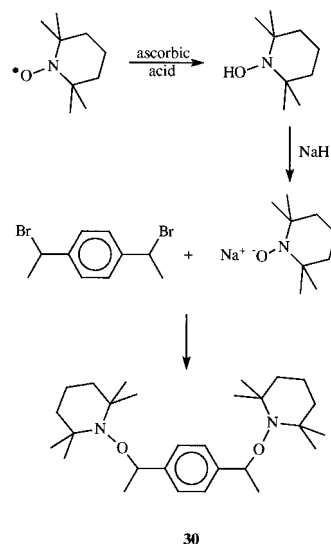
the resulting alkoxyamine **26** being obtained in very high yields (Scheme 9).⁸⁵ The use of lead oxide for the oxidation of alkyl hydrazides has also been shown to be an efficient method for the synthesis of alkoxyamines and if chiral nitroxyl radicals are employed a degree of stereochemical control can be obtained.⁸⁶ Finally in a novel application of single electron-transfer chemistry, Priddy⁸⁷ has employed oxoammonium salts to add across the double bond of styrenic derivatives leading to functionalized alkoxyamine initiators. In the proposed mechanism, the oxoammonium salt **27** undergoes a disproportionation reaction with associated electron transfer to give the corresponding nitroxide, TEMPO, and a chlorine radical. The chlorine radical then adds across the styrenic double bond to give the carbon center radical **28** which is then efficiently trapped by TEMPO to give the chloromethyl-substituted alkoxyamine **29** (Scheme 10). The advantage of this strategy is the facile

Scheme 10

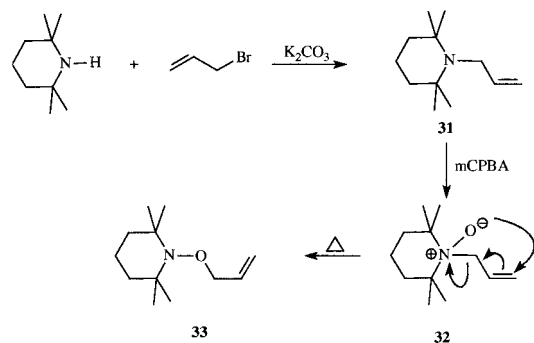
preparation of the alkoxyamine **29**, which can be subsequently transformed into a myriad of functionalized initiators.

Alternate strategies to the trapping of carbon-centered radicals has been developed by a variety of groups in an effort to extend the range of functionalities that can be incorporated into the alkoxyamine structure. Taking advantage of the rich oxidation chemistry of nitroxides, Catala⁸⁸ has demonstrated that oxidation to the hydroxyamine followed by proton abstraction with sodium hydride gives the anion which can nucleophilically displace alkyl halides to give the desired alkoxyamine. This is espe-

cially useful for multifunctional alkoxyamines such as **30**, whose synthesis from the corresponding diradical by trapping strategies is not practical (Scheme 11).

Scheme 11

In an interesting application of classical organic chemistry, Bergbreiter employed a Meisenheimer rearrangement of allyl *N*-oxides as a route to alkoxyamines.⁸⁹ As shown in Scheme 12, 2,2,6,6-

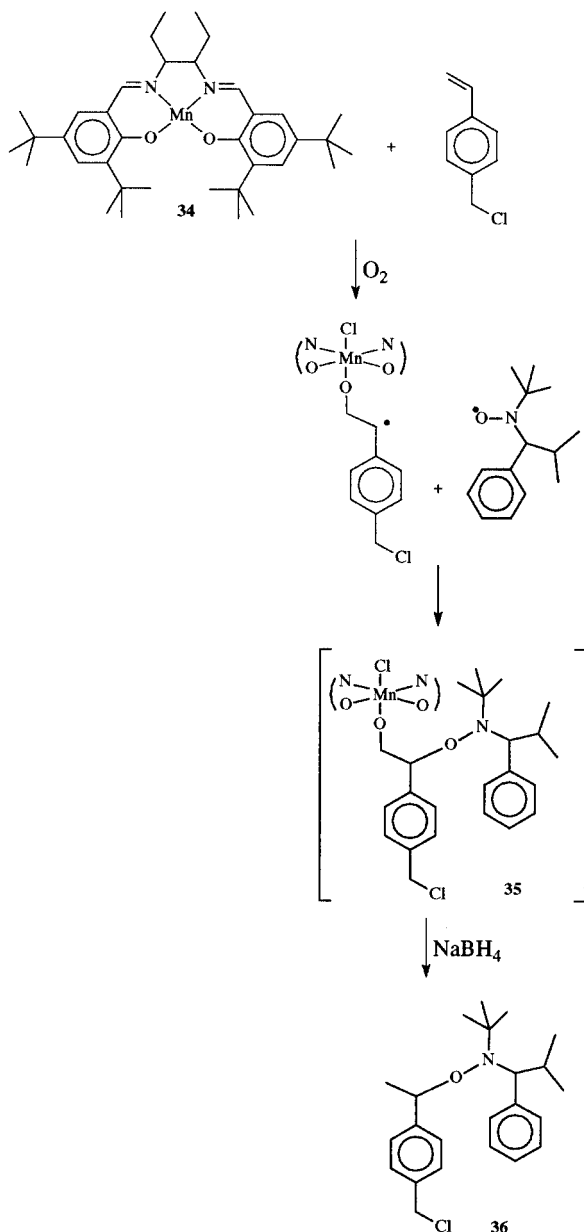
Scheme 12

tetramethylpiperidine is initially alkylated with allyl bromide to give the tertiary amine, **31**, which can be oxidized at low temperatures with *m*-chloroperbenzoic acid. The resulting *N*-oxide **32** is not isolated but allowed to undergo rearrangement on warming to give the allyl-TEMPO derivative **33** in moderate yield (Scheme 12). An attractive feature of this synthetic approach to alkoxyamines is the ready availability and low cost of starting materials which is in contrast to the high cost of many nitroxides. In addition, the controlled nature of polymerizations initiated with **33** demonstrates that an α -methylbenzyl group is not necessary for efficient initiation in these systems and a simple allyl group can be used in its place without any detrimental performance.

The use of transition metal complexes for the synthesis of alkoxyamines has also been exploited by Dao.⁹⁰ In this case, Jacobsen's reagent, manganese(III) salen, **34**, is employed to promote the addition of nitroxides across the double bond of olefinic derivatives, specifically activated double bonds such

as styrenics, leading to alkoxyamines suitable for use as initiators in living free radical procedures. While the mechanism for the Jacobsen epoxidation of olefins is still controversial, a substantial body of evidence has been accumulated that supports direct attack of the olefin at the oxomanganese center to generate a radical intermediate followed by collapse to give the desired epoxide.⁹¹ It is anticipated that a similar mechanism is involved during the synthesis of alkoxyamines with evidence suggesting that an intermediate organomanganese derivative, **35**, is involved, which on reduction with sodium borohydride gives the alkoxyamine **36** (Scheme 13). The advan-

Scheme 13



tages of these methods are that a variety of functional groups can be readily introduced, large excesses of reagents are not required to trap the extremely reactive free radical intermediates and near stoichiometric amounts of the alkene and nitroxide are required. Finally, the reactions are high yielding and

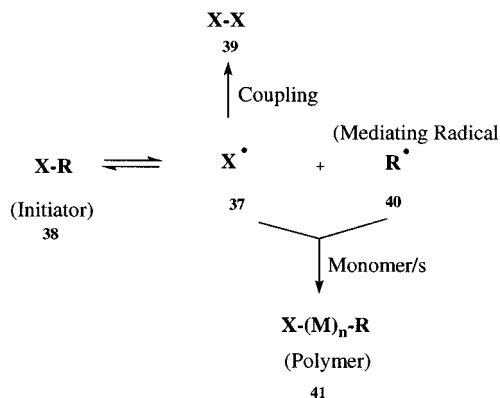
produce very few unwanted side products, which greatly facilitates isolation and purification.

VI. Mechanistic and Kinetic Features

A. Nitroxide Exchange

The key kinetic feature of nitroxide-mediated living free radical polymerization is the operation of a special kinetic phenomenon, termed the persistent radical effect. Fischer has developed the equations for the polymerization rates and for the polydispersities of the resulting polymers that have been shown to effectively model LFRP.^{92,93} In the initial stages of the polymerization, a small fraction of the initiating radicals **37** formed from decomposition of the unimolecular initiator **38** undergo radical-radical coupling. This leads to a terminated small molecule or oligomer, **39**, and the resulting elimination of two initiating radicals. At this early stage of the polymerization, this is a facile reaction since the diffusing radicals are sterically not congested and the reaction medium is not viscous. However, by its nature, the mediating radical, or persistent radical, **40** does not undergo coupling and so a small increase in the overall concentration of **40** relative to the propagating/initiating radical **37** occurs. This increased level of **40** is self-limiting since a higher concentration leads to more efficient formation of the dormant chain end **41** and a decrease in the amount of radical-radical coupling (Scheme 14). This interplay between

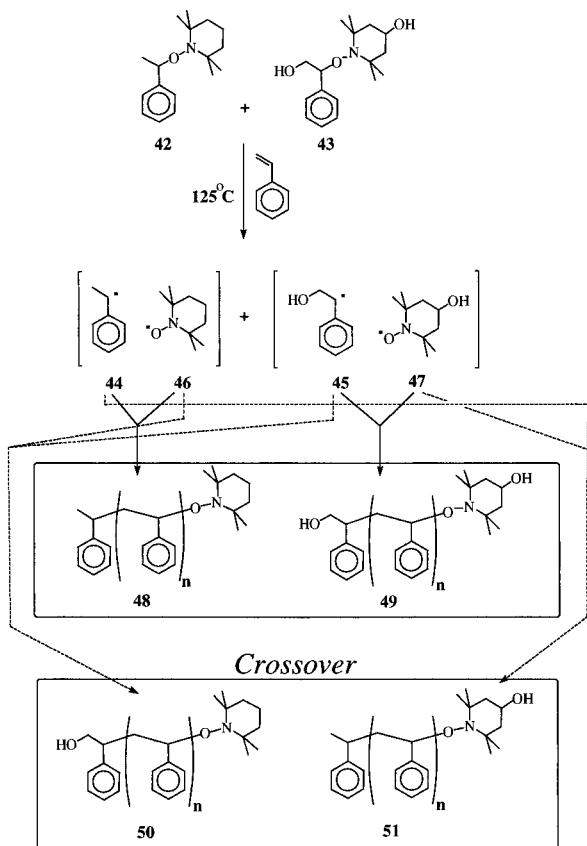
Scheme 14



termination and mediation leads to a small amount of excess mediating free radical, giving rise to the persistent radical effect (PRE) and to eventual control over the polymerization process.

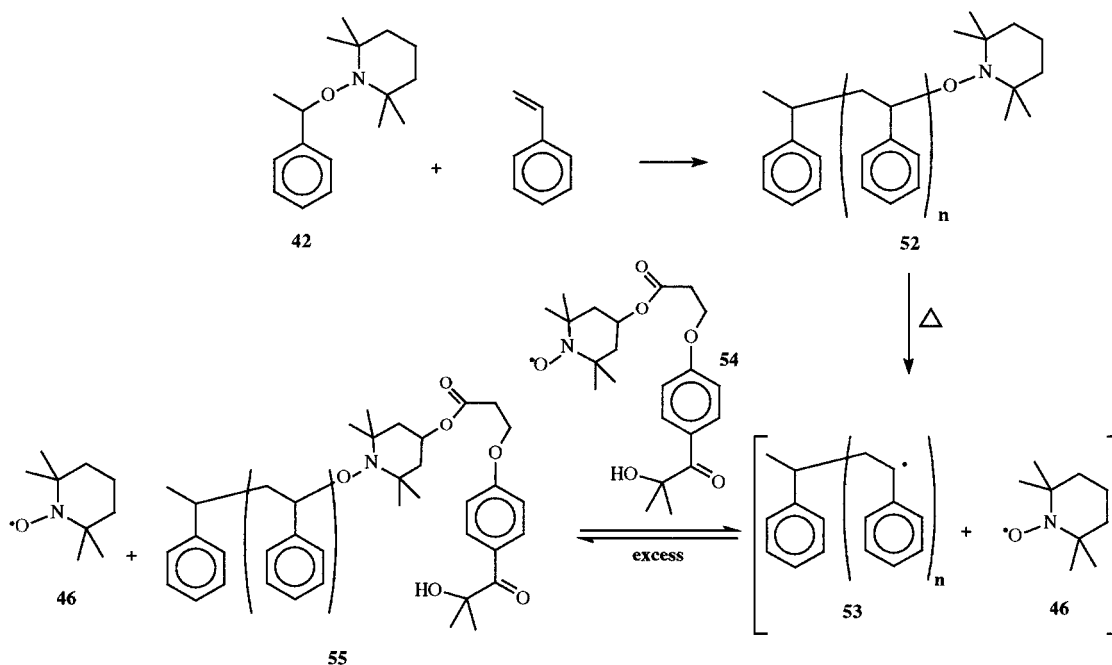
The nature of the equilibrium between the dormant system **41** and the pair of radicals **37** and **40** has been probed and exploited by a number of groups. The exact nature of the radical pair, caged pair of radicals, or freely diffusing radicals was probed by a series of crossover experiments.⁹⁴ This is an important synthetic issue: the nitroxide counter-radicals are associated with the same polymeric chain end during the course of the polymerization, or do they diffuse freely to the reaction medium, which affects the ability to insert functional groups at the chain ends. In these experiments, the potential diffusion of the mediating radical from the propagating chain end

Scheme 15



was probed by the use of two structurally similar alkoxyamines, which differ in the presence or absence of functional groups. One derivative is unfunctionalized, **42**, while the other alkoxyamine, **43**, contains two hydroxy groups, one attached to the TEMPO unit while the second is located at the beta-carbon atom of the ethylbenzene unit. If a 1:1 mixture of **42** and **43** is used to initiate the “living” free radical polymerization of styrene, homolysis of the carbon–oxygen

Scheme 16



bond of **42** and **43** will lead to four radical species. Each of the radicals produced are chemically different and comprise a pair of initiating, or propagating radicals, **44** and **45**, and a pair of structurally similar mediating nitroxide radicals are produced, TEMPO, **46**, and 4-hydroxy-TEMPO, **47**. If no escape of the mediating nitroxide radical from propagating chain end occurs, only two polystyrene derivatives will therefore be formed, **48** and **49**. In contrast, if radical crossover does occur and the mediating nitroxide radicals are free to diffuse to the polymerization medium, four polystyrenes having different substitution patterns, **48**–**51**, will be obtained. Significantly, the experimental result from these crossover experiments revealed a statistical mixture of all four products, even at low conversions (ca. 5%), implying freely diffusing radicals (Scheme 15).

Moreover, this crossover or exchange of mediating radical can be exploited as a synthetic tool to introduce functional groups at the polymer chain end/s. Turro⁹⁵ has elegantly taken advantage of this feature of nitroxide-mediated living free radical procedures to develop a strategy for the facile preparation of chain end functionalized macromolecules. In this approach a precursor polymer, **52**, is prepared from a standard unfunctionalized initiator, such as **42**, purified, and then redissolved in a high boiling point solvent such as chlorobenzene and heated at 125 °C in the presence of a large excess of functionalized nitroxide, **54**. At this temperature the equilibrium between **53** and the two radicals is established and since the released nitroxide, **46**, is free to diffuse into the solution, exchange with the functionalized nitroxide, **54**, can occur leading to the desired chain end functionalized macromolecule, **55** (Scheme 16). This strategy presents a number of advantages, reactive functional groups can be introduced under mild conditions, from the same precursor polymer a variety of differently tagged macromolecules can be prepared, and the same strategy can be applied to

macromolecules of different architectures. It should however, be noted that the primary driving force for this functional interconversion is statistics and so under normal laboratory conditions with nitroxide excesses of 10–20 equiv complete exchange of the chain end does not occur.

B. Additives

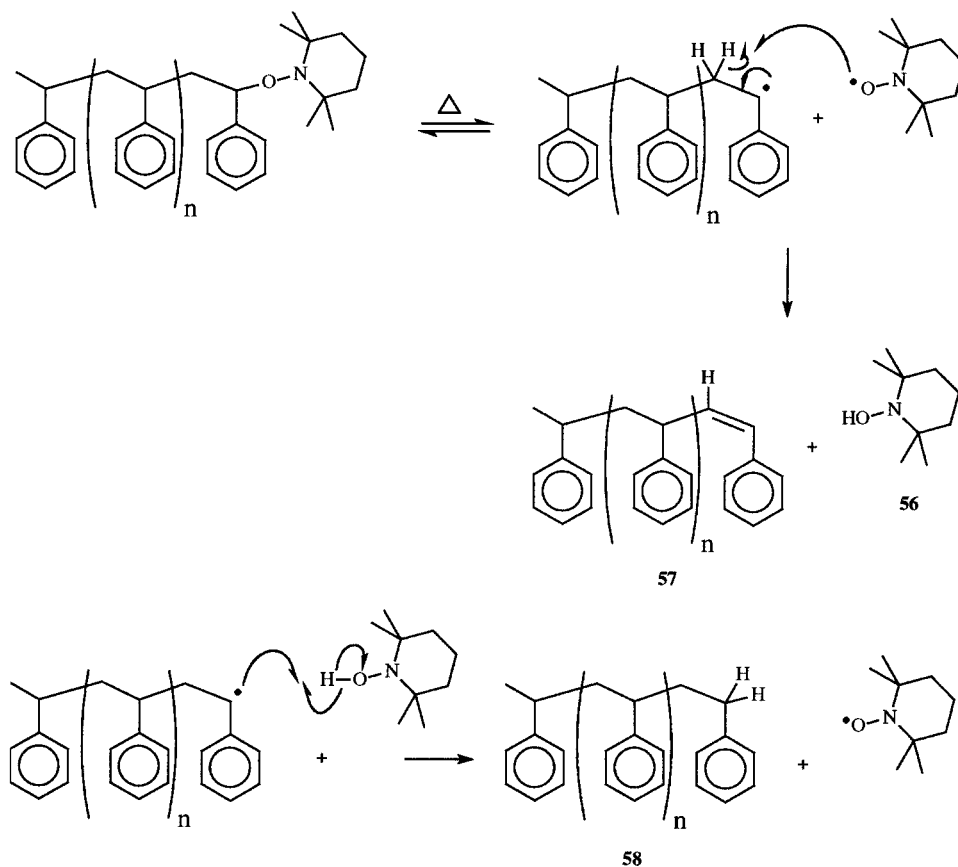
From the above discussion it is obvious that the persistent radical effect relies on a subtle interplay between the mediating nitroxide radicals and propagating radical chain ends. The rate of polymerization and extent of termination reactions such as radical coupling can however, be manipulated by changing the balance between all of these competing reactions and kinetic equations which are present during the persistent radical effect. This has been accomplished by a number of groups in different ways. One of the most well-studied strategies is to continuously add initiator or have a very slowly decomposing initiator also present in the polymerization mixture.⁹⁶ This continuously supplies initiating radicals to the system and results in the reaction continuously trying to obtain a steady state, persistent radical effect situation. The stationary concentration of the nitroxide is therefore reduced and correspondingly, the rate of deactivation is decreased. This should lead to an increase in the rate of polymerization with a concomitant increase in the polydispersity of the polymers obtained. Indeed this has been shown to be the case in a number of studies. The addition of either dicumyl peroxide and *tert*-butyl hydroperoxide has been shown to lead to rate enhancements of up to 300% with only moderate increases in polydispersity. In a related study, continuous slow addition of a standard low-temperature free radical initiator, AIBN, was also shown to give similar results.⁹⁷ These findings are important from a commercial viewpoint since they may allow the long reactions times and high temperatures normally associated with nitroxide-mediated polymerizations, especially those involving TEMPO, to be alleviated without compromising the gross characteristics of the product.

These experiments are also relevant to the polymerization of styrenic derivatives. As discussed above, styrenics were the first and still arguably the easiest monomer family to polymerize under living conditions using nitroxides. One of the primary reasons for the facile polymerization of styrenics is thermal polymerization. Unlike acrylates and other vinyl monomers, which do not readily undergo self-initiation to generate radicals, it has been shown that thermal self-initiation of styrene provides a low concentration of propagating radicals.^{98,99} This is sufficient for obtaining a rate enhancement similar to the addition of excess initiator and allows a reasonable rate of polymerization under the persistent radical effect. Another consequence of autopolymerization is that the rate of polymerization of styrene in the presence of nitroxides is independent of the concentration of the alkoxyamine and remarkably close to the rate of thermal polymerization under the same conditions.¹⁰⁰

C. Chain End Degradation

Another side reaction in nitroxide-mediated living free radical polymerization that affects the kinetics and structural integrity of the products is decomposition of the alkoxyamine chain ends. One potential pathway that has been studied in detail is the facile reduction of the mediating nitroxide radical to give the corresponding hydroxyamine **56** by H-transfer. As illustrated in Scheme 17 for polystyrene, this results in a dead polymer chain, **57**, containing an unsaturated chain end. Hydroxylamine **56** can then be involved in H-transfer back to a growing radical chain end to regenerate the nitroxide while at the same time leading to a second H-terminated dead polymer chain, **58**. These termination reactions decrease the living character of the polymerization and if they are significant enough will alter the overall kinetics and lead to a nonlinear system. To understand the system in more detail, Priddy has investigated the decomposition of alkoxyamine initiators in a variety of solvents.¹⁰¹ The results clearly show that alkoxyamines undergo significant decomposition at the temperatures normally associated with living free radical polymerization. In 1,2,4-trichlorobenzene, ca. 50% decomposition has occurred after 2 h leading to H-abstraction and the identification of styrene as a major decomposition product (cf. Scheme 17). The authors conclude that significant decomposition of the alkoxyamine chain ends should occur during polymerization due to the competitive rates of polymerization and decomposition. However, significant decomposition is not observed experimentally and may be due to the absence of monomer in the model studies coupled with the decreased rate of H-abstraction from a polymer chain end compared to a small molecule. While reduced, this reaction is not completely absent from nitroxide-mediated polymerizations and simulations and theoretical treatments have shown that its effect on the polymerization kinetics is slight but does result in an increase in molecular weights distribution.¹⁰² This also explains the lower polydispersities observed for the second-generation nitroxides **17** (ca. 1.05–1.10) compared to TEMPO (1.15–1.25) for polystyrene polymerizations. The shorter reaction times and lower temperatures associated with **17** leads to a decreased amount of alkoxyamine decomposition and associated broadening of the molecular weight distribution. This feature also explains the observed difference in the polymerization of styrenics and methacrylates under nitroxide-mediated conditions. Styrenics are able to undergo living polymerization under the influence of minor amounts of thermal initiation/hydrogen transfer reactions and the effect of these side reactions on the “livingness” of the system and the structure of the final products is not significant and cannot be detected in most cases. In contrast, for methacrylates there is no thermal initiation and the contribution from hydrogen transfer is significantly greater. The majority of chains therefore undergo termination reactions and effectively “die” leading to an uncontrolled, nonliving system. This has been observed experimentally with significant amounts of

Scheme 17



alkene-terminated polymer chains detected by MALDI mass spectrometry as well as NMR and UV-vis studies.^{103,104}

D. Elucidation of Living Nature

For monomer families other than methacrylates, the low occurrence of these side reactions and the essentially living nature of these polymerizations can be demonstrated by a variety of different techniques. A preliminary guide to the "livingness" can be obtained by examining the relationship between the evolution of molecular weight and conversion. As shown in Figure 3, the polymerization of *n*-butyl acrylate (250 equiv) in the presence of **59** (X = Y = H) (1.0 equiv) and **17** (0.05 equiv) at 123 °C for 16 h results in a linear relationship.³⁸ This demonstrates that all of the chains are initiated at the same time and grow at approximately the same rate. Following this initial screening, the efficiency of initiation and the degree of control during the polymerization can be accurately gauged by determining the correlation between the experimental molecular weight and the theoretical molecular weight. As for all living polymerizations, the theoretical molecular weight is determined by the molar ratio of monomer to initiator, taking into account the conversion of the polymerization. For an initiation efficiency of 100%, the relationship between experimental molecular weight and theoretical molecular weight should be a straight line with a slope of 1.0. Indeed, evolution of experimental molecular weight, M_n , with theoretical MW

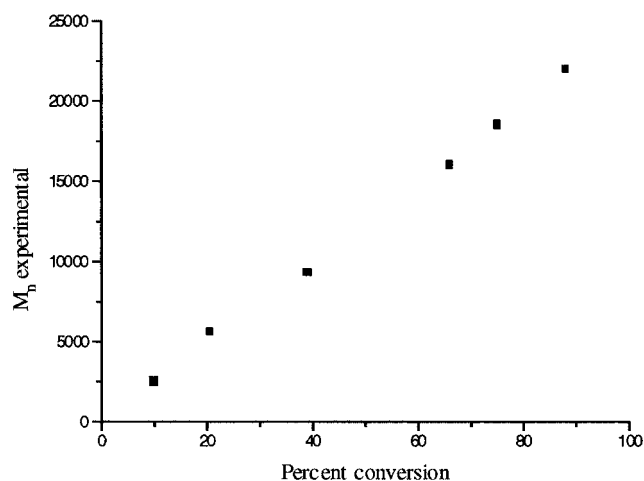


Figure 3. Evolution of molecular weight, M_n , with percent conversion for the polymerization of *n*-butyl acrylate (250 equiv) in the presence of **42** (X, Y = H) (1.0 equiv) and **17** (0.05 equiv) at 123 °C for 16 h.

for the polymerization of styrene and **59** (X = Y = H) at 123 °C for 8 h with no degassing or purification is a straight line. This suggests that initiating efficiencies are 95% or greater (Figure 4). The ability to obtain polydispersities of between 1.10 and 1.20 for these polymerization is further support for a controlled/living process. Figure 4 also demonstrates a critically important feature of nitroxide-mediated living free radical polymerizations that is also true for ATRP and RAFT, no purification of monomers or rigorous polymerization conditions are required to obtain very well-defined polymers, thereby opening

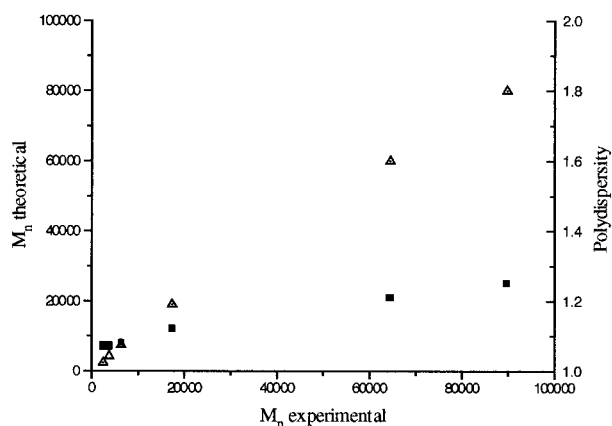


Figure 4. Evolution of experimental molecular weight, M_n , and polydispersity with theoretical MW for the polymerization of styrene and **42** at 123 °C for 8 h with no degassing or purification.

these synthetic techniques up to a much wider range of researchers.

As will be discussed below, the final piece of evidence that is needed to conclusively prove the living nature of a nitroxide-mediated process is to use the alkoxyamine chain end to prepare a block copolymer. Again if the polymerization is living, efficient reinitiation of the second block should be observed to give a block copolymer with no homopolymer contamination (care should be taken in analyzing homopolymer content by GPC, especially using RI detection). While this is a desired goal, it should be realized that the efficiency of reinitiation for the second block is monomer dependent and in select circumstances inefficient reinitiation may be obtained even though ca. 100% of the starting blocks contain an alkoxyamine chain end. This feature will be further discussed in the following section on structural control.

E. Emulsion and Related Processes

Until recently, living radical polymerizations have been predominantly studied in homogeneous systems, i.e., bulk or solution polymerizations. While simplified systems, they are less attractive to industry, which prefers to employ aqueous dispersed media and emulsion procedures in particular. A considerable amount of effort has therefore been directed to the development of nitroxide-mediated polymerizations under heterogeneous conditions such as suspension, dispersion, seeded emulsion, batch emulsion, and miniemulsion.^{105–108} The difficulty with many of these studies is that TEMPO or similar derivatives were employed as the mediating radical. This necessitated the use of temperatures greater than the boiling point of water and so high-pressure reaction setups were required and stabilization of the latex/emulsion particles at these elevated temperatures was problematic. Even with these difficulties a basic understanding of the process is starting to emerge. The choice of the nitroxide is critical and the compatibility of the nitroxide with water and the partition coefficients between the various phases are all critical factors.¹⁰⁹ Recent work by Charleux¹¹⁰ has also shown that the choice of second-generation nitroxides, which

operate at lower temperatures (<100 °C), may alleviate many of these difficulties and permit a viable emulsion process to be developed.

VII. Toward New Materials

It is obvious from the above discussion that under the correct conditions and with the appropriate mediating nitroxide free radical, living polymerization conditions can be achieved. On the basis of this realization, numerous groups have demonstrated that the degree of structural control normally associated with more traditional living processes, such as anionic procedures, can be equally applied to nitroxide-mediated living free radical polymerizations.

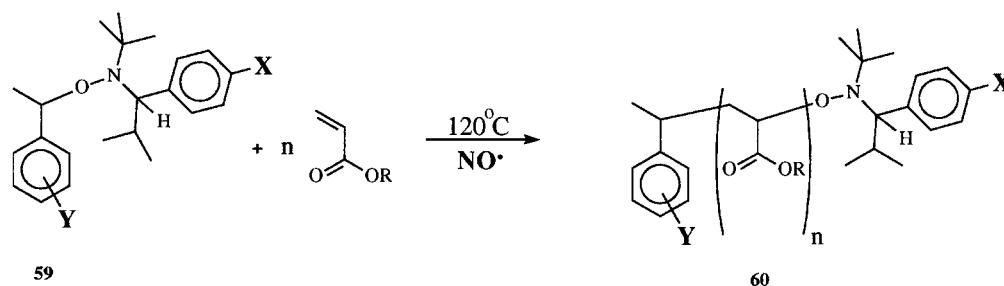
A. Molecular Weight Control

The initial work of Hawker²⁸ on the use of alkoxyamines as unimolecular initiators demonstrated that the molecular weight of polystyrene could be accurately controlled up to M_n values of ca. 75 000 using the assumption that one molecule of the TEMPO-based alkoxyamine **11** initiates the growth of one polymer chain and the length, or degree of polymerization, of that chain is governed by the molar ratio of styrene to **11**. Subsequent work by others, especially with the second-generation alkoxyamines, such as **59**, have conclusively proved this ability and, especially in the case of **59**, the upper molecular weight limit (M_n) for controlled molecular weights has been increased to between 150 000 and 200 000.³⁸ For typical monomers and polymerization conditions, values of ca. 200 000 may represent an upper limit for nitroxide-mediated, ATRP, and RAFT-based living free radical systems. At higher molecular weights the small amount of extraneous radicals and terminating species quickly become significant when compared to the low concentration of initiating and propagating radicals present in the system. This leads to a loss of control and an increasingly nonliving process.

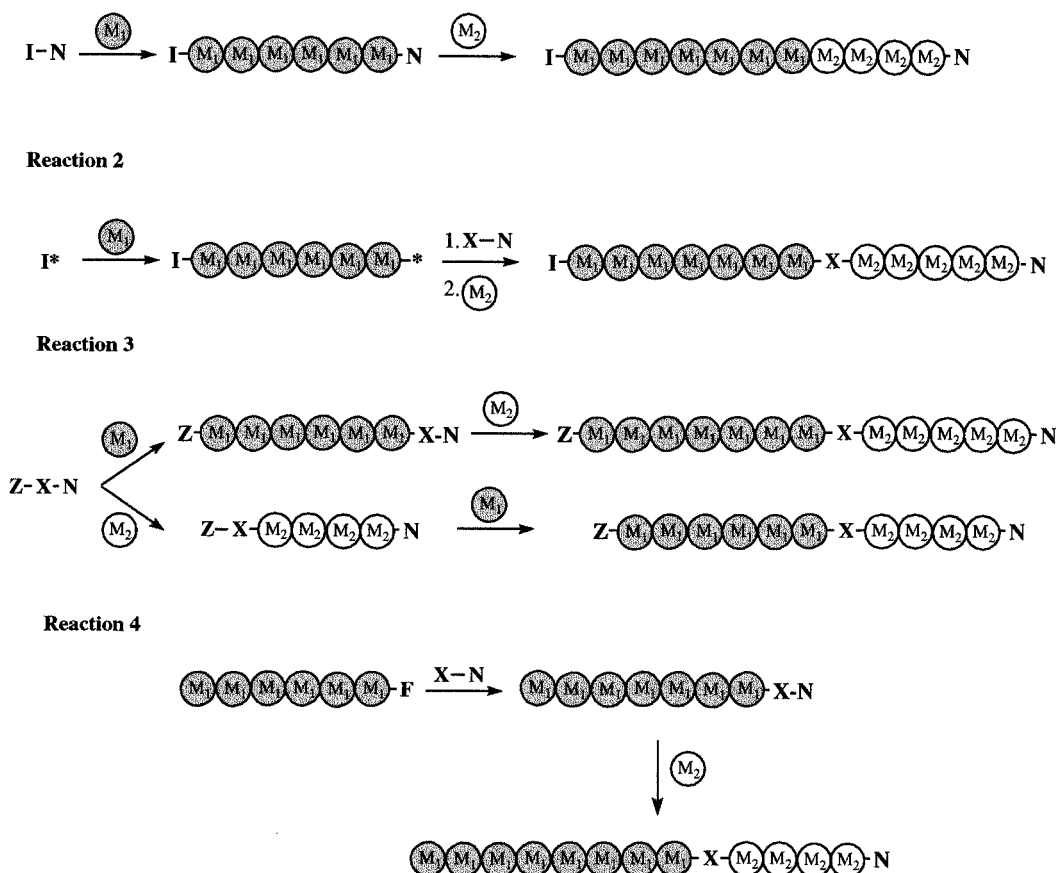
B. Telechelic Polymers

The ability to control molecular weights provides good evidence that the basic reaction scheme for alkoxyamine initiated polymerizations does operate. By analogy, it should therefore be possible to prepare telechelic polymers in a fashion similar to living anionic procedures. However, a major difference is that elaborate schemes for the efficient transformation of the anionic chain ends to the desired functionality does not need to be developed since living free radical procedures can tolerate a wide variety of functional groups. The ability exists to prepare functionalized alkoxyamines such as **59**, in which functional groups can be placed at either the initiating chain end, **Y**, or the nitroxide-mediating chain end, **X** (Scheme 18). The range of functional groups that have been introduced into telechelic polymers such as **60** is wide and include many useful reactive groups, e.g., CO₂H, NH₂, etc. A recent study has shown that at molecular weights of up to 50 000–75 000 the level of incorporation is very high, i.e., greater than 95%.^{73,111} This high level of incorpora-

Scheme 18



Scheme 19



tion is a direct result of having the functional groups built into the initiator, coupled with the necessity for no functional group transformations at the chain ends. It should also be realized that functional group interconversions are possible based at the propagating chain end on alkoxyamine chemistry and a number of groups have exploited this in the design of telechelic systems.^{112–115}

C. Block Copolymers

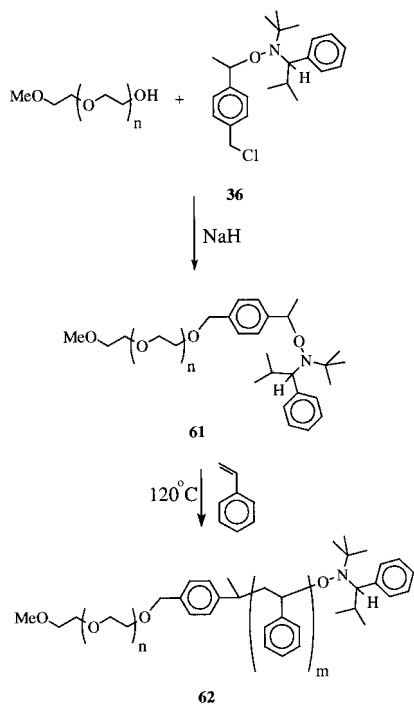
One of the primary driving forces behind the interest that living radical procedures have received in recent years is the ability to prepare block copolymers. Not only may existing block copolymers be prepared more efficiently and in some case with a greater degree of control, but also novel block copolymers, which were not accessible using existing techniques, may also be prepared. The synthetic versatility associated with alkoxyamine initiators and the ability to introduce a wide variety of functional

groups allows block copolymers to be prepared in at least four different ways. As shown in Scheme 19, vinyl block copolymers can be prepared in a traditional sequential fashion by the polymerization of one monomer followed by a second monomer (reaction 1). Alternatively, a functionalized alkoxyamine can be used to terminate polymerization of an initial monomer under conditions other than living free radical. The alkoxyamine-terminated macromolecule can then be used as a macroinitiator to prepare block copolymers. The interesting feature of this process is that it permits the facile introduction of a functional group or chromophore at the junction point between the two blocks (reaction 2). In reaction 3, a dual, or double-headed, initiator is prepared which has both an alkoxyamine initiating fragment and an initiating group for a different polymerization contained in the same molecule. Depending on the compatibility of the initiating groups, the polymerization processes and the desired structure of the block copolymer, the

order of polymerization can be varied to give the desired block copolymer. Finally, a preexisting telechelic polymer can be mono- or difunctionalized with the appropriate alkoxyamine to give a macroinitiator from which a vinyl block can be grown under living radical conditions. While not an extensive list of all possible procedures, the multitude of synthetic strategies that have currently been explored for nitroxide-mediated living radical procedures does give an indication of the extreme versatility in block copolymer formation which is possible using this novel technique. To give a greater insight into the myriad possibilities, a list of linear block copolymers that have been prepared using nitroxide-mediated processes is detailed in Table 2 and a number of actual examples discussed below.^{116–172}

As discussed above, one synthetic strategy relies on the coupling of a functionalized alkoxyamine with a telechelic or mono-functional nonvinylic polymer to give a macroinitiator. This macroinitiator can then be used in standard living free radical procedures. Such an approach is best illustrated by the preparation of poly(ethylene glycol)-based block copolymers^{129,136,150,167} by initial reaction of a mono-hydroxy terminated poly(ethylene glycol) with sodium hydride followed by the chloromethyl-substituted alkoxyamine **36**. The PEG-based macroinitiator (PDI = 1.05–1.10) **61** can then be used to polymerize a variety of vinyl monomers, such as styrene, to give amphiphilic block copolymers, **62**, which have accurately controlled molecular weights and very low polydispersities, 1.05–1.10 (Scheme 20).¹⁶⁷ The extremely low poly-

Scheme 20



dispersities may be due to the use of a macroinitiator in contrast to typical small molecule initiators. In the latter case, mobility and reactivity of the initiating radicals is high leading to radical–radical coupling. For the macroinitiator, diffusion and reactivity is


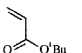
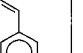
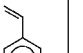
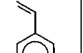
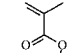
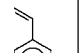

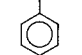
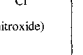

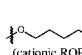
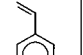
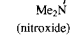

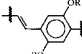
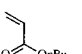
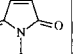
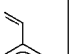
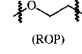
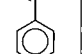
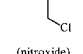
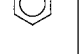
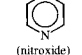
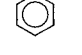
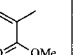
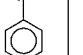
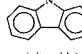
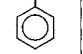
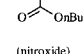
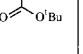
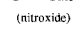
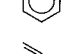
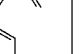
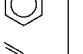
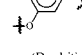
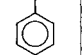
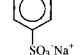
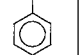
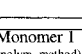
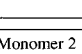
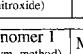
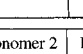
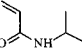
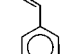
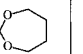
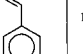
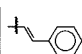
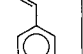
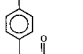
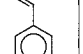
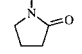
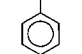
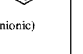
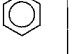
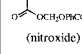
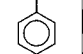
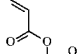
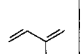
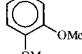
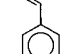
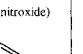
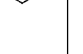
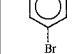
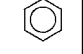
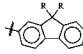
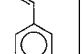
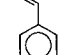
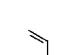
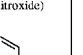

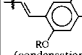
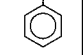
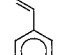
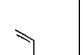
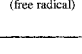

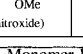

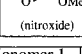
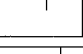
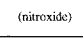

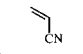
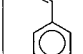
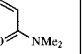
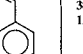




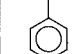
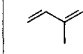
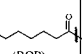
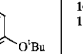




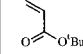
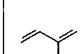
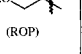
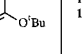




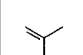
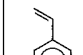
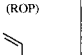
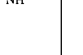




decreased, leading to reduced radical coupling and a more controlled polymerization.

The second strategy for nonvinylic block copolymer formation involves the combination of living free radical techniques with other polymerization processes either to form linear block copolymers or graft systems. All of these processes take advantage of the compatibility and stability of alkoxyamines and their associated nitroxide-mediated polymerization procedures with a wide range of reaction conditions. For example, this permits the alkoxyamine initiating group to be copolymerized into a poly(olefin) backbone under metallocene conditions¹⁶⁹ or into a vinyl backbone under anionic¹⁷⁰ or normal free radical conditions.¹⁷¹ The latter is an interesting application of the specificity of nitroxide-mediated living free radical polymerizations. Since the cleavage of the C–ON bond is thermally activated, reactions at lower temperatures (ca. <80 °C) can be performed without any initiation occurring from the alkoxyamine group/s. Therefore normal free radical polymerizations, ATRP, and RAFT procedures can be performed in the presence of alkoxyamines. Subsequent activation of the alkoxyamine permits the facile synthesis of graft and block copolymers.

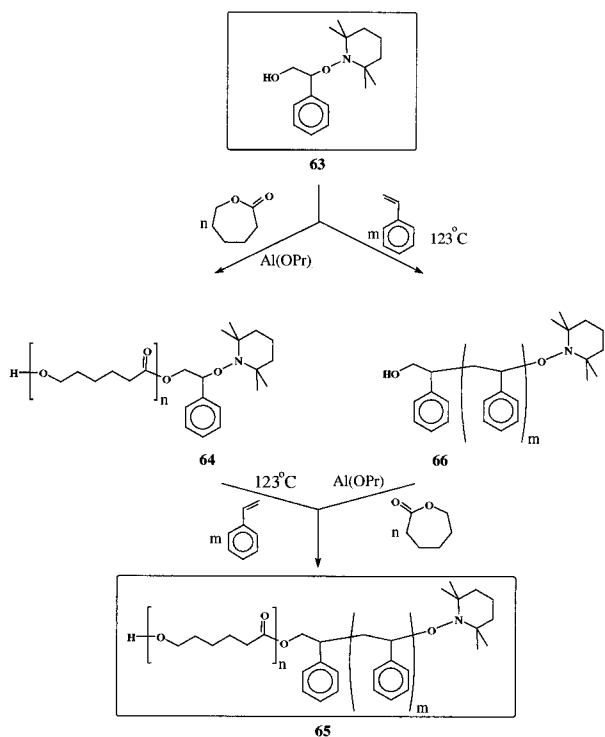
The synthetic versatility associated with combining different polymerization techniques can also be demonstrated by the preparation of poly(caprolactone)-*b*-(styrene) copolymers by a combination of living ring opening polymerization with nitroxide-mediated free radical procedures using a hydroxy-substituted alkoxyamine as a dual, or double-headed, initiator, **63**.¹⁷³ The primary alcohol is used as the initiating group for the ring opening polymerization of caprolactone to give the alkoxyamine-terminated macroinitiator **64**, which can then be used to initiate the living polymerization of styrene to afford the well-defined block copolymer **65**. Alternatively, the alkoxyamine group of **63** can be used to initiate the polymerization of styrene, and in turn, the hydroxy-terminated polystyrene **66** allows the ring opening polymerization to be initiated from the hydroxy group to give the analogous block copolymer **65** (Scheme 21). The significant feature of this approach is that either sequence of living polymerizations gives the same polymeric structure, the ultimate choice being dictated primarily by the block copolymer composition. In a similar vein, Sogah has combined living free radical polymerization with the cationic ring opening of oxazolines, and anionic ring opening into the same multifunctional initiator. This trifunctional system has been shown to be highly effective leading to well-defined block copolymers and can even be combined into a one-pot, one-step block copolymerization by simultaneous free radical and either cationic ring opening or anionic ring opening procedures.¹⁷⁴

The advantages of living free radical polymerizations are not restricted to the synthesis of block copolymers, which contain a nonvinylic block/s, i.e., caprolactone. The compatibility with functional groups and the inherent radical nature of the process also permits significant progress to be made in the synthesis of block copolymers based solely on vinyl monomers. While a number of these structures can

Table 2. Structure of Monomer Employed in the Synthesis of Block Copolymers by Nitroxide Mediated Living Free Radical Procedures

Monomer 1 (polym. method)	Monomer 2	Ref.	Monomer 1 (polym. method)	Monomer 2	Ref.	Monomer 1 (polym. method)	Monomer 2	Ref.	Monomer 1 (polym. method)	Monomer 2	Ref.
 (metalocene)		116	 (nitroxide)		153	C ₆₀		152 162	 (nitroxide)		147
 (metalocene)		116	 (nitroxide)		154	 (cationic ROP)		148 151	 (nitroxide)		38 118 142 149
 (condensation)		117	 (nitroxide)		130 155	 (ROP)		129 136 150	 (nitroxide)		38
 (nitroxide)		144 166	 (free radical)		120 130	 (nitroxide)		146	 (nitroxide)		38
 (nitroxide)		119	 (nitroxide)		131 156	 (Dendritic)		56 161	 (nitroxide)		135 145
 (ROP)		125 132 157	 (nitroxide)								
 (free radical)		141 172	 (nitroxide)		137	 (step-wise)		154	 (nitroxide)		123
 (free radical)		141	 (anionic)		134	 (nitroxide)		168	 (nitroxide)		124
 (free radical)		141	 (nitroxide)		139	 (nitroxide)		133	 (nitroxide)		123
 (free radical)		141	 (nitroxide)		38 164	 (nitroxide)		126	 (nitroxide)		122
 (free radical)		141	 (nitroxide)		164	 (nitroxide)		38 128	 (nitroxide)		
 (nitroxide)		38 165	 (nitroxide)		38 121	 (nitroxide)		165 172	 (nitroxide)		
 (nitroxide)		38 120	 (nitroxide)		38 121	 (nitroxide)		166 172	 (nitroxide)		
 (nitroxide)		38 138 158	 (nitroxide)		38 159 160 181	 (nitroxide)		167 172	 (nitroxide)		
 (nitroxide)		159 160 181	 (nitroxide)		163	 (nitroxide)			 (nitroxide)		

Scheme 21



be obtained from other living processes, such as anionic procedures, in many cases they can be prepared more readily by living free radical techniques and the special attributes of living free radical chemistry do allow a range of new materials to be prepared. For example, Bignozzi and Ober have reported the synthesis of a series of side chain LC-coil diblock copolymers by living free radical polymerization. Interestingly these materials were shown to possess a smectic mesophase and a lamellar microstructure by X-ray diffraction.¹⁶⁸

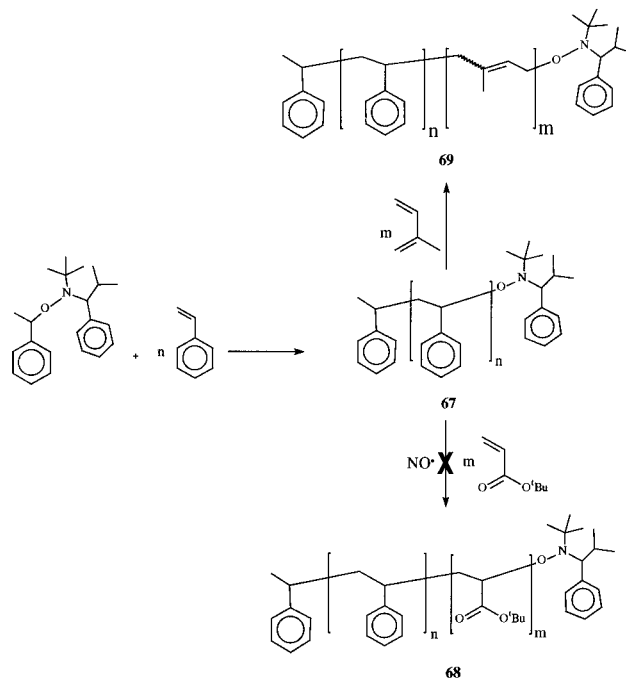
While the block copolymers available from "living" free radical procedures may not be as well defined as the best examples available from anionic techniques, they have the advantage of greater availability and a significantly enhanced tolerance of functional groups. Technological applications that have been examined for these block copolymer include dispersants for pigments,¹⁷⁵ precursors to shell cross-linked nanoparticles for drug delivery,^{176,177} supports for combinatorial chemistry,¹⁷⁸ and resist materials for photolithography.¹⁷⁹

The advent of second-generation alkoxyamines, which are suitable for the polymerization of a range of monomer families, has significantly enlarged the range of block copolymers that can be prepared using nitroxide-mediated processes. For example, block copolymers such as poly(styrene-*b*-isoprene), poly(*tert*-butyl acrylate-*b*-*N,N*-dimethylacrylamide), etc. can be readily obtained by polymerization of the first monomer to give the starting block, which is either isolated or used in situ.³⁸ The second monomer is then added, with or without the presence of a solvent to aid solubility, and on heating the second block is grown. One of the interesting features of preparing block copolymers by nitroxide-mediated, ATRP, or RAFT procedures is that initial block can be char-

acterized and stored before proceeding to the second block. This is totally unlike anionic procedures and is extremely useful from a synthetic viewpoint. In many respects, it is actually fortuitous since the conversions obtained in living free radical procedures do not typically reach 100%; therefore, the in situ approach actually affords an impure second block, which is contaminated with the first monomer.

One drawback that nitroxide-mediated polymerizations have in common with anionic procedures is that they both suffer from a monomer sequence issue when preparing specific block copolymers. The classic example for living free radical systems is the preparation of styrene-acrylate block copolymers. If a starting polystyrene macroinitiator, **67**, is used to polymerize *n*-butyl acrylate to give the block copolymer **68**, a significant amount of a low molecular weight shoulder is observed.³⁸ The exact nature of this shoulder, whether it is unreacted, or terminated starting polystyrene block is unknown. Attempts to overcome this unexpected lack of reactivity by the addition of solvent, etc., have been unsuccessful and are related to the relative rates of polymerization and initiation for styrene and acrylates. The initiating ability of the starting polystyrene block is however, not an issue since it can be used to initiate the polymerization of isoprene extremely efficiently leading to well-defined block copolymers, **69**, with no homopolymer or lower molecular weight contamination (Scheme 22).

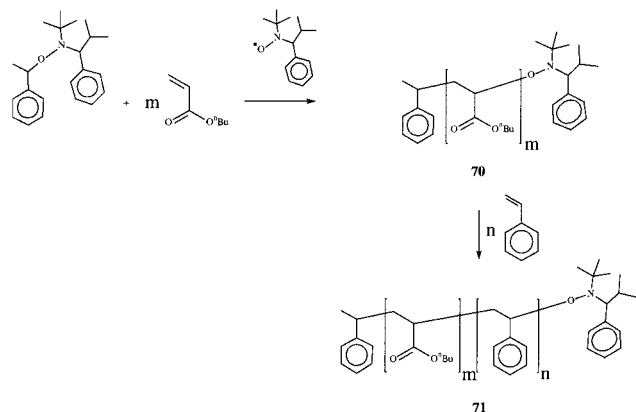
Scheme 22



The reverse strategy, polymerization of the acrylate block followed by styrene, has been successful and has allowed the preparation of well-defined block copolymers with levels of control comparable to ATRP procedures. In this strategy, an alkoxyamine functionalized (*n*-butyl acrylate) block, **70**, is initially grown and then used to polymerize styrene at 123 °C under argon for 8 h. This results in 92% conver-

sion to give the block copolymer **71**, analysis of which revealed the expected increase in molecular weight, while the polydispersity remained very low (PD. = 1.06–1.19) and there were no detectable amount of unreacted starting poly(acrylate) block (Scheme 23).

Scheme 23



The radical nature of nitroxide-mediated processes also allows novel types of block copolymers to be prepared in which copolymers, not homopolymer, are employed as one of the blocks. One of the simplest examples incorporate random copolymers¹²⁴ and the novelty of these structures is based on the inability to prepare random copolymers by living anionic or cationic procedures. This is in direct contrast to the facile synthesis of well-defined random copolymers by nitroxide-mediated systems. While similar in concept, random block copolymers are more like traditional block copolymers than random copolymers in that there are two discrete blocks, the main difference being one or more of these blocks is composed of a random copolymer segment. For example, homopolystyrene starting blocks can be used to initiate the copolymerization of styrene and 4-vinylpyridine to give a block copolymer consisting of a polystyrene block and a random copolymer of styrene and 4-vinylpyridine as the second block.¹⁶⁶

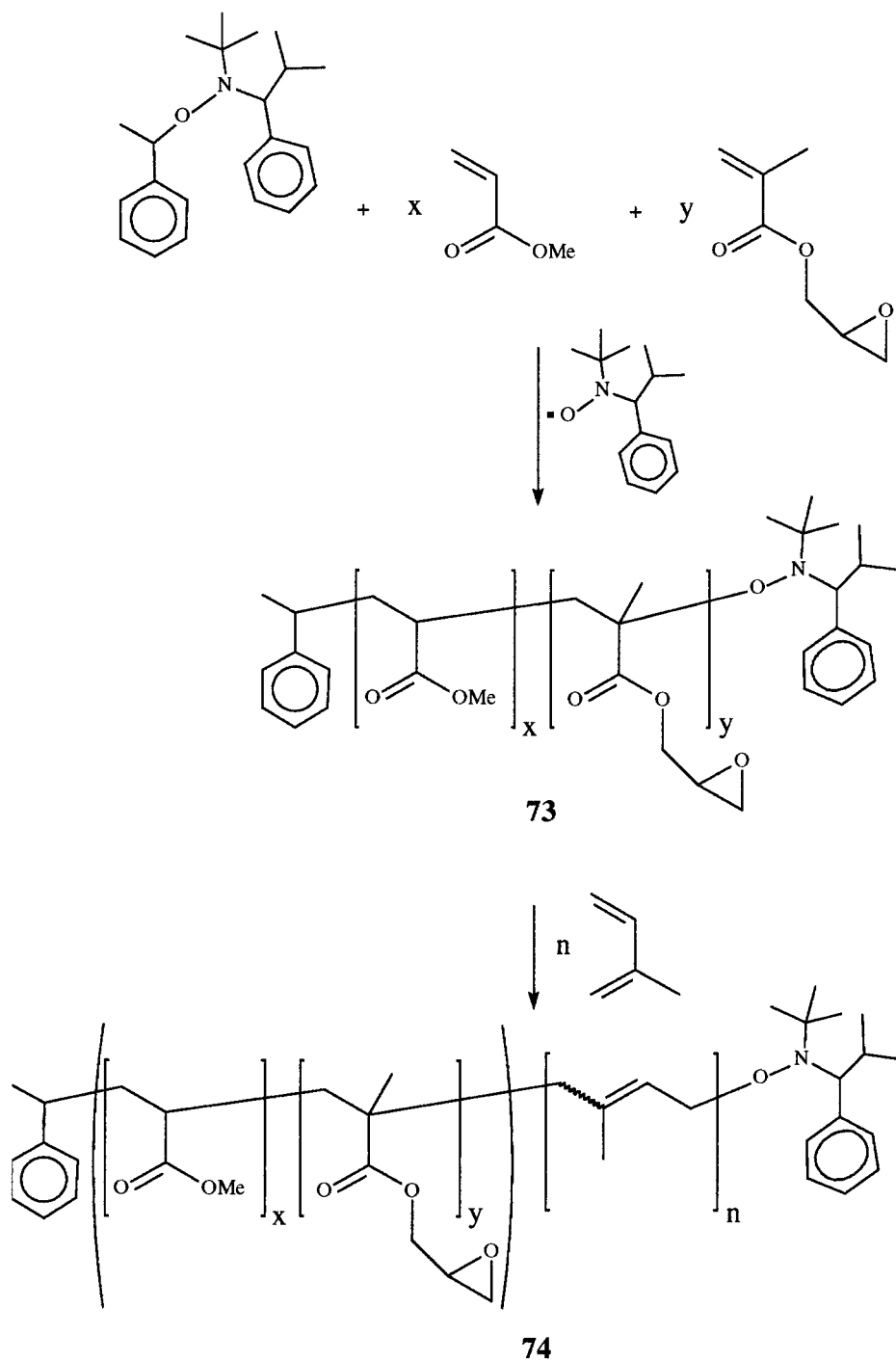
The potential for these materials can be better appreciated if the synthesis and application of the functionalized block copolymer **72** is considered. An initial random copolymer of methyl acrylate and glycidyl methacrylate, **73**, is prepared by nitroxide-mediated living free radical polymerization and then used to initiate the polymerization of isoprene leading to the random block copolymer **72** (Scheme 24). The design of these macromolecules incorporates a random block which is not only miscible with thermosetting epoxies, but also can undergo reaction leading to covalent linking between the copolymer microstructure and the cross-linked epoxy resin. The polyisoprene block is immiscible and so drives the formation of a nanoscopic phase separated structure and leads to modification of the physical and mechanical properties of the thermosetting epoxy. The facile synthesis of **72**, which combines reactive epoxy functionalities with both a block and random copolymer structure, demonstrates the far reaching potential of living radical procedures.

D. Random Copolymers

One of the major advantages of living radical procedures compared to living anionic or cationic polymerizations is the ability to prepare well-defined random copolymers. In traditional anionic or cationic procedures, there are numerous problems which normally preclude the successful synthesis of random copolymers. For example, reactivity ratios can be extremely large in anionic systems, and so true random copolymerizations do not occur and blocky structures are obtained. Alternatively, the polymerization conditions for one monomer or functional group are not compatible with the second monomer and an uncontrolled polymerization is obtained. This lack of synthetic versatility has prompted numerous groups to examine the synthesis of well-defined random copolymers via living radical techniques. While early work with TEMPO did demonstrate that random copolymers can be prepared under nitroxide-mediated conditions the inability to control the homopolymerization of monomers other than styrene limited the range of monomer units and possible random copolymer structures.^{31,174,180} With the advent of second-generation nitroxides, such as **17**, the realm of well-defined random copolymers have been dramatically opened. For example, while the homopolymerization of methacrylates does not give controlled polymers, random copolymers of methacrylates with up to 90 mol % of methacrylate incorporation can be prepared in a living fashion.³⁸ The actual rationale for this stark contrast is not known at the moment and deserves further study since it may provide insights into controlling H-abstraction and in turn methacrylate polymerization in these systems. The ultimate aim of these studies would be to develop a living polymerization of methacrylates that leads to well-defined materials, one of the major challenges in this general area.

The finding that the reactivity ratios for monomers under living free radical conditions are essentially the same as under normal free radical conditions is also fundamentally important. As a consequence of this, random copolymers prepared by living free radical processes are different on a molecular level to those prepared by normal free radical methods, even though they may appear the same on the macroscopic level (Scheme 25). In the case of traditional free radical polymerization, continuous initiation leads to chains initiating and terminating at different stages of the polymerization. Therefore, chains that are initiated and terminated at low conversion experience a different monomer feed ratio compared to chains initiated later in the polymerization. The polymerization product is therefore a complex mixture of random copolymers with different monomer compositions and different molecular weights. For living radical systems, all chains are initiated at the same time and grow at approximately the same rate, as a consequence all of the growing chains experience the same change in monomer concentrations. As a result the random copolymers have approximately the same composition coupled with a low dispersity of molecular weights. This is depicted graphically in Scheme 25; however, it should

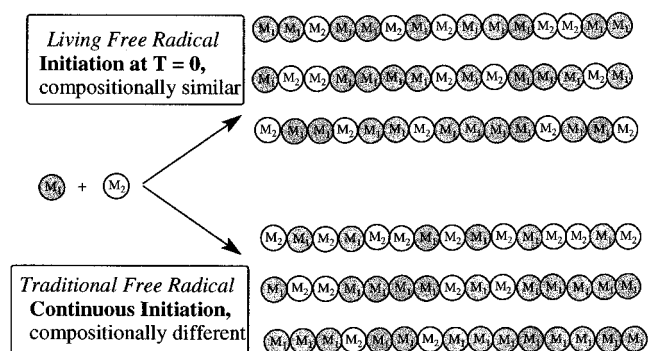
Scheme 24



also be pointed out that while the graphical representation suggests that all the chains are the same length, this is not the case especially for the traditional free radical case where polydispersities of 2.0 are typically obtained (cf. 1.1 for nitroxide systems). The structural variation between chains is therefore further exacerbated in traditional systems.

An excellent example of using reactivity ratios and the synthetic versatility of nitroxide systems to prepare unusual block copolymers is the copolymerization of styrene/maleic anhydride mixtures.¹⁸¹ When an excess of styrene is used, the copolymerization leads to preferential and finally total consumption of maleic anhydride at conversions of styrene signifi-

Scheme 25



cantly less than 100%. As a result, the growing polymer chains experience an initial monomer feed of styrene and maleic anhydride which gradually changes during the course of the polymerization to a monomer feed of neat styrene. This has been experimentally demonstrated, and as can be seen in Figure 5, after 1.5 h, no detectable amounts of maleic

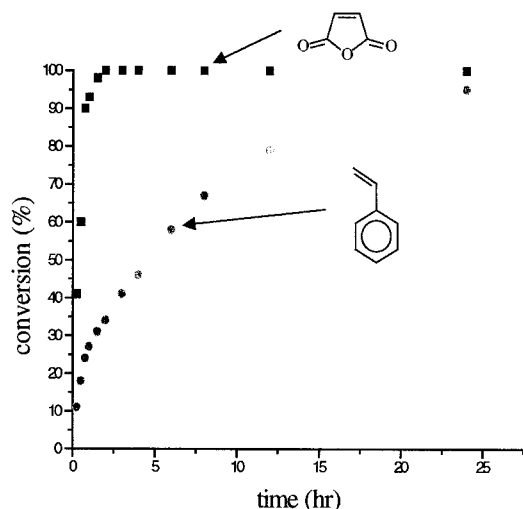


Figure 5. Evolution of conversion with time for the polymerization of a 9:1 mixture of styrene and maleic anhydride mediated by **42** and 0.05 equiv of **17** at 123 °C.

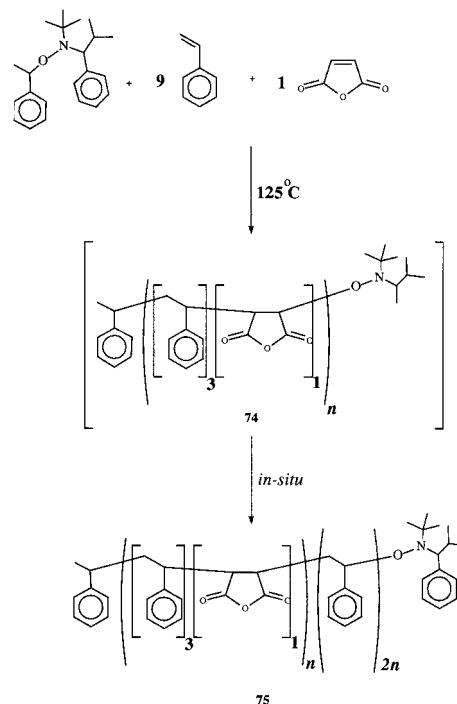
anhydride could be observed in the polymerization of a 9:1 mixture of styrene and maleic anhydride. Significantly, the conversion of styrene at this stage was only ca. 25–30% and the random copolymer of styrene and maleic anhydride **74** that is formed in situ now experiences a monomer feed that is neat styrene. Further polymerization now involves growth of a homopolystyrene block. This results in the formation of a functionalized block copolymer, **75**, in a single step, consisting of an initial ca. 1:3 copolymer of maleic anhydride and styrene, respectively, followed by a block of polystyrene which is roughly twice the molecular weight of the initial anhydride functionalized block (Scheme 26). These materials can be considered to be a limiting example of gradient copolymers and by carefully choosing reactivity ratios, structures intermediate between statistically random copolymers and one-step block copolymers can be prepared by living free radical techniques.¹⁸² Other examples include the controlled polymerization of termonomer mixtures of styrene, maleimides, *n*-butyl methacrylate, though in this example the polydispersity is moderate (i.e. 1.5–1.6) due to the use of TEMPO as the mediating radical.¹⁸³

VIII. Complex Macromolecular Architectures

A. Star and Graft Polymers

The reduced concentration of radical centers at the chain ends of living radical polymerizations opens up a number of possibilities in the synthesis of complex macromolecular architectures due to the very low

Scheme 26

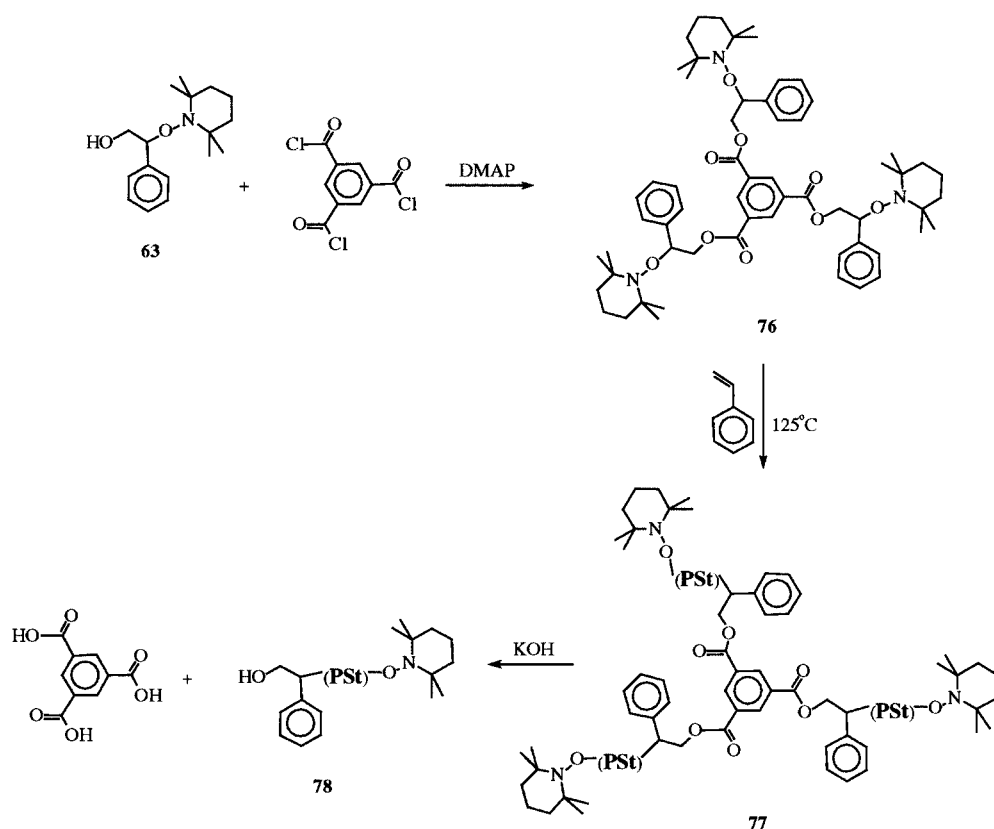


occurrence of side reactions such as radical–radical chain coupling. While the use of polyfunctional initiators under normal free radical conditions gives cross-linked networks due to radical coupling reactions, under living radical conditions a polyfunctional initiator may be expected to lead to the desired graft, or star polymer with little, or no, unwanted coupling products, provided the number of grafts/arms is not too high (less than 10–20). When compared to ATRP, this is one area in which nitroxides systems do suffer from a drawback. The actual concentration of radicals is dictated by the nitroxide systems and cannot be readily controlled by external means. This is in direct contrast to ATRP where the radical concentration can be varied by the level of catalyst added.

This principal was first tested by the synthesis and polymerization of the trifunctional unimolecular initiator **76**.¹⁸⁴ Interestingly, no detectable amounts of cross-linked or insoluble material was observed, and degradation of the 3-arm polystyrene star **77** by hydrolysis of the ester links was found to give the individual polystyrene arms **78** (Scheme 27). Analysis of **78** revealed a molecular weight comparable to that expected from the initiator-to-monomer ratio and a narrow polydispersity (ca. 1.10–1.15). These results demonstrate that each of the initiating units in the tris-alkoxyamine is “active” and the individual polystyrene arms grow at approximately the same rate with little or no cross-linking due to radical coupling reactions.

Subsequently, this concept has been extended to more highly functionalized star-initiators as well as polymeric initiators for the synthesis of graft structures. It should however, be appreciated that the polymerization process is still radical in nature and while radical–radical coupling reactions are decreased they are not eliminated and so as the number of initiating sites per molecule increase, the prob-

Scheme 27



ability of coupling also increases. For example, a mixture of styrene and *p*-chloromethylstyrene can be polymerized under “living” free radical conditions to give a well-defined linear copolymer, **79**, with controlled molecular weight and low polydispersity (ca. 1.10–1.25). Reaction of **79** with the sodium salt of the hydroxy functionalized unimolecular initiator then gives the desired polymeric initiator **80** which is a precursor to a variety of graft copolymers, **81**.¹⁸⁵ At average grafting densities of greater than six initiating sites per backbone, chain–chain coupling becomes apparent by GPC, and at densities greater than 15, it is a major process (Scheme 28).

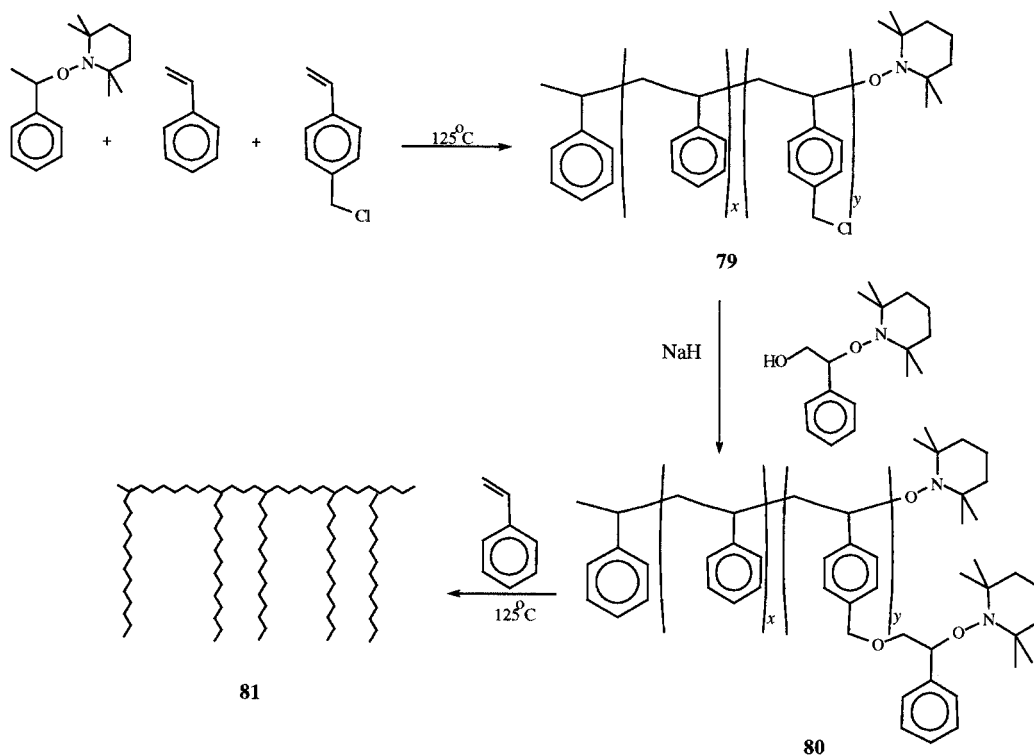
B. Hyperbranched and Dendritic Structures

As demonstrated by Fréchet¹⁸⁶ in the development of self-condensing polymerizations, the ability to form reactive unimolecular initiators, such as **82**, opens up a number of avenues to unusual macromolecular architectures that are either difficult, or impossible, to prepare using traditional free radical chemistry or living anionic procedures. In the case of the styrenic derivative **82**, a propagating center and an initiating center are combined in the same molecule to effectively create a self-condensing monomer, which is similar to AB₂ monomers used for the preparation of hyperbranched and dendritic macromolecules by condensation chemistry. Homopolymerization of **82** under “living” free radical conditions was shown to lead to initial formation of dimers, trimers, etc. and eventually hyperbranched macromolecules, **83**, with the kinetics of growth resembling a step-growth polymerization even though the polymerization occurs by a free radical mechanism

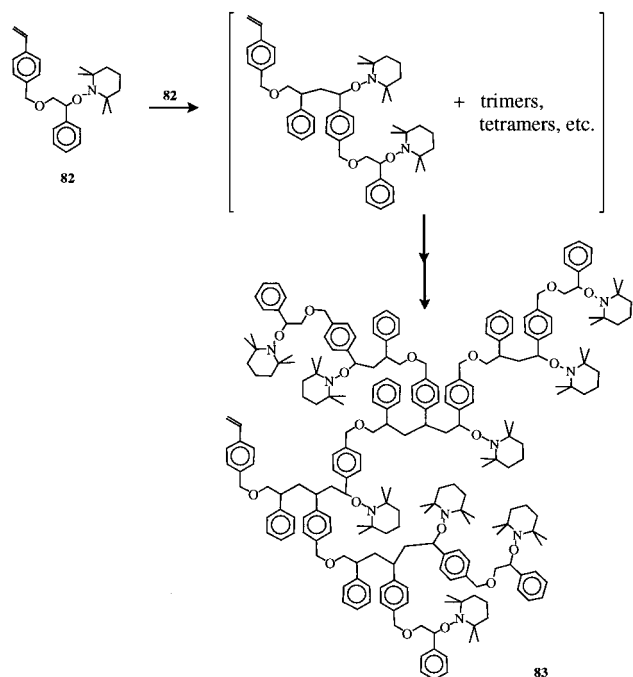
(Scheme 29).^{187a} One interesting facet of this polymerization is that the hyperbranched polystyrene derivatives contain numerous initiating centers. These numerous initiating centers have been used to form a unique class of star macromolecules in which the central core is a highly functionalized hyperbranched polymer. Subsequently, Fréchet^{187b} and Matyjaszewski¹⁸⁸ have applied a similar technique to the preparation of hyperbranched polystyrene derivatives by the homopolymerization of *p*-chloromethylstyrene using ATRP conditions, though the actual structure of the materials obtained seems to be variable.¹⁸⁹

The synthesis of these highly branched star polymers has recently attracted much interest and a variety of simplified approaches have been reported. While Yang¹⁹⁰ has discussed the use of mediating nitroxides, which contain a polymerizable double bond and therefore lead to branch points, the majority of work has centered on the coupling, or knitting together, of preformed linear chains by reaction with cross-linkable monomers, a technique which has been extensively used in anionic and cationic procedures. One of the attractive features of this approach, which is unique to living radical systems, is that the starting linear chains, **85**, can be isolated, characterized and stored before subsequent coupling. Additionally, a variety of different chains in terms of molecular weight, composition, etc. can be copolymerized together to give heterogeneous star-block copolymers.^{191,192} The basic strategy is outlined in Scheme 30, and involves the preparation of alkoxyamine terminated linear chains **84** and subsequent coupling of these dormant chains with cross-linking agents such as divinylbenzene or a bis(maleimide) deriva-

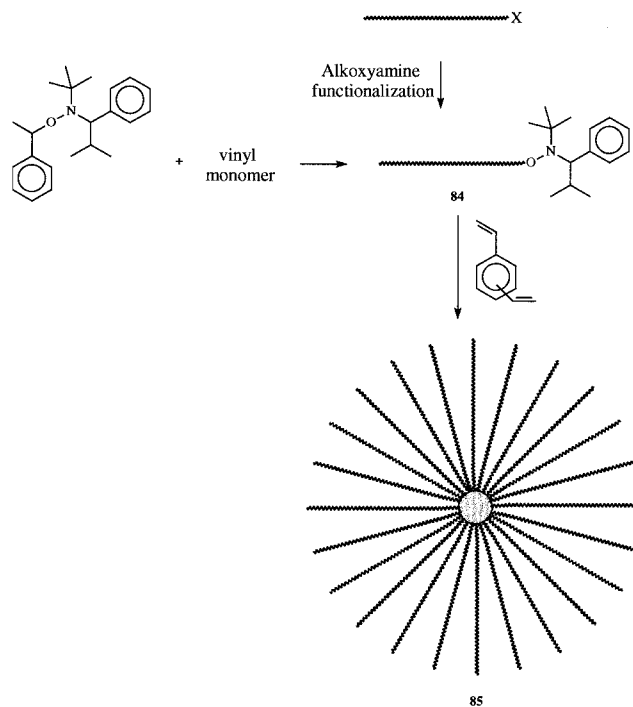
Scheme 28



Scheme 29



Scheme 30



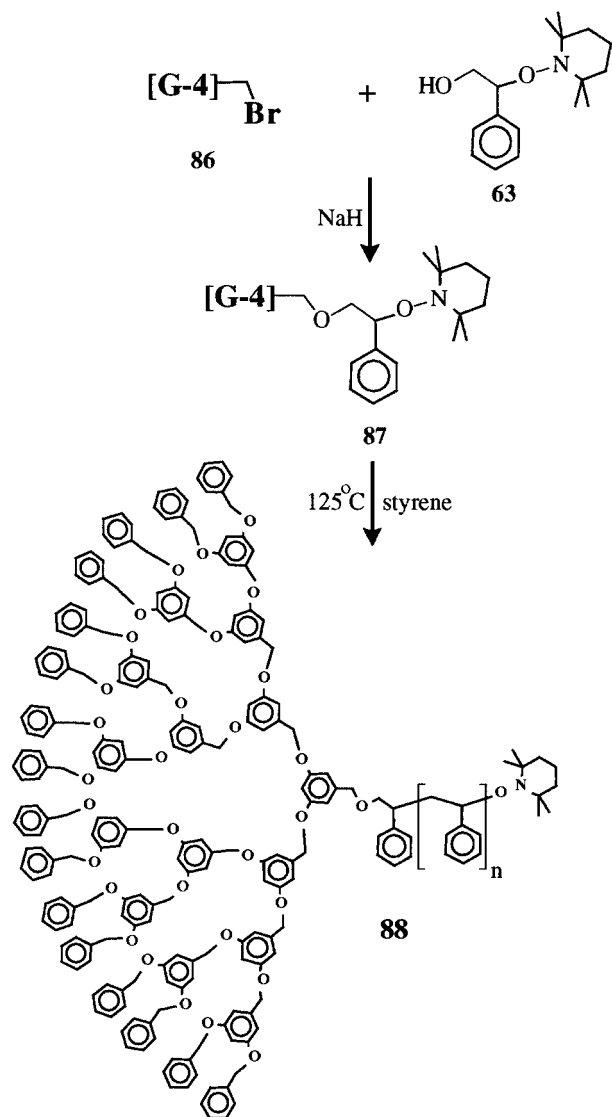
tive. Since the only requirement is an alkoxyamine chain end, the range of starting linear polymers is immense and is not restricted to vinyl polymers or homopolymers. Microgels have also been extensively studied by Solomon using living free radical procedures and their structure has been shown to be subtly different to that obtained using traditional free radical procedures.¹⁹³

Unique dendritic-linear block copolymers have also been prepared by the coupling of functionalized initiators with dendritic macromolecules prepared by the convergent growth approach.¹⁹⁴ In these ap-

proaches, the dendrimer can be attached to either the initiating fragment of the alkoxyamine or the mediating nitroxide and the dendritic initiator used to initiate the growth of linear vinyl blocks under controlled conditions. As demonstrated in the work of Fréchet and Hawker,¹⁹⁵ these monodisperse dendritic initiators are perfectly suited for the preparation of well-defined block copolymers, for example coupling of the dendrimer **86**, which contains a single bromomethyl group at its focal point with the hydroxy functionalized unimolecular initiators gives the

dendritic initiator **87**. Hybrid dendritic–linear block copolymers, **88**, with well-controlled molecular weights and low polydispersities are then obtained by the reaction of **87** with a variety of styrenic monomers or comonomer mixtures under living free radical polymerization conditions (Scheme 31).^{161,195,196} Simi-

Scheme 31



lar structures can also be prepared using ATRP chemistry and in this case the initiating group is simply a focal point chloromethyl, or bromomethyl functionality.¹⁹⁷ While the majority of examples involve the dendrimer being attached to the initiator, there is a single instance where it is attached to the mediating radical. Interestingly, in the case¹⁹⁸ where the dendritic block is attached to the nitroxide, the molecular weights and polydispersities for the block copolymers are not as well controlled as in the case where the dendrimer is attached to the initiating fragment. This difference may be due to the increased steric bulk of the dendritic nitroxide which would be expected to decrease its mobility and hence ability to control the polymerization. While a detailed study has not been performed this result may have important implications especially for complex, functionalized nitroxides whose diffusion characteristics may

be different to the more traditional small molecule nitroxides.

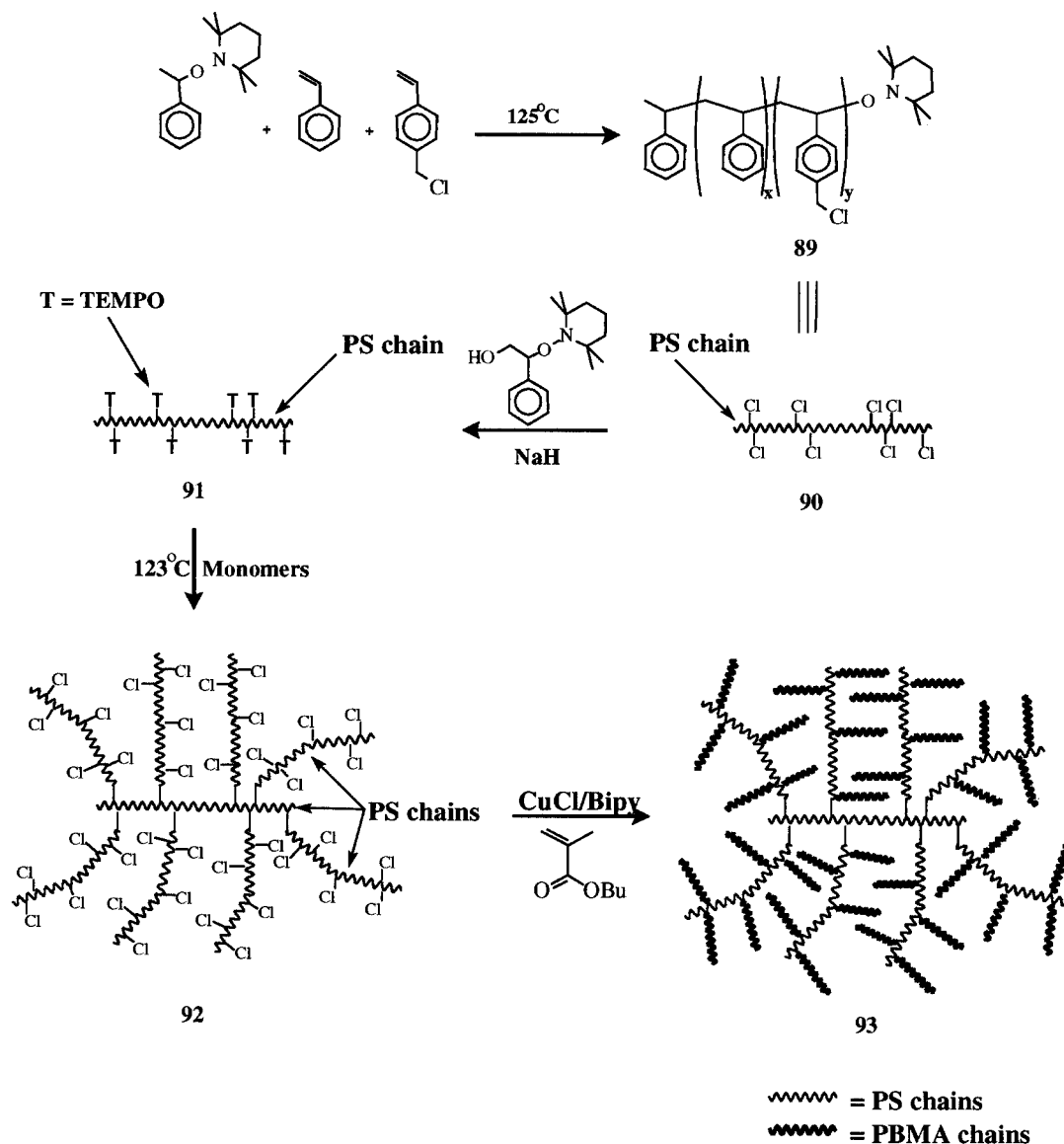
This building block, or modular approach to the synthesis of complex macromolecular architectures can be taken a step further in the rapid synthesis of combburst, or dendritic graft copolymers by a tandem “living” free radical approach.^{185,199,200} The underlying strategy in this novel approach to highly branched linear polymers is that each layer, or generation, of linear polymers is prepared by “living” free radical procedures and the initiating groups are either present during the polymerization or introduced in a post-polymerization functionalization step. In this way very large, highly branched combburst copolymers can be prepared in a limited number of steps using mild reaction conditions. As shown in Scheme 32 the initial linear backbone **89** is prepared by nitroxide-mediated “living” free radical polymerization of a mixture of styrene and *p*-chloromethyl styrene. At this stage the polymerization mechanism can be switched from nitroxide mediated to atom transfer “living” free radical conditions to give graft copolymers or TEMPO based initiating groups can be introduced by reaction of the numerous chloromethyl groups with the sodium salt of **63** to give the polymeric initiator **91**. A second layer, or generation, of reactive chloromethyl groups can be introduced on the grafted arms **92** by a second copolymerization of styrene and *p*-chloromethylstyrene. This functionalized graft copolymer can again be used as a complex polymeric initiator for ATRP polymerization that introduces a third layer of linear polymer chains, **93**. In analogy with the divergent growth approach to dendritic macromolecules, this stepwise functionalization/growth strategy can be continued to give larger and larger combburst macromolecules and the mild reaction conditions permit a wide variety of monomer units and functional groups to be used.

The versatility associated with nitroxide-mediated polymerizations, in terms of both monomer choice and initiator structure, also permits a wide variety of other complex macromolecular structures to be prepared. Sherrington²⁰¹ and Fukuda²⁰² have examined the preparation of branched and cross-linked structures by nitroxide-mediated processes, significantly the living nature of the polymerization permits subtly different structures to be obtained when compared to traditional free radical processes. In addition, a versatile approach to cyclic polymers has been developed by Hemery²⁰³ that relies on the synthesis of nonsymmetrical telechelic macromolecules followed by cyclization of the mutually reactive chain ends. In a similar approach, Chaumont has prepared well-defined polymer networks by the cross-linking of telechelic macromolecules prepared by nitroxide-mediated processes with bifunctional small molecules.²⁰⁴

IX. Surface-Initiated Polymerizations

The stability of alkoxyamine initiators is not only a major synthetic advantage when compared to more traditional living polymerization procedures but it also permits opportunities in the area of surface modification. In analogy with the work that has

Scheme 32



subsequently been done in the area of ATRP, functionalized alkoxyamines were the first example of living radical initiators, prepared and attached to a variety of surfaces and subsequently used to grow covalently attached polymer chains. The living nature of the polymerization provides an unprecedented ability to control the structure, density, functionality, etc. of the surface attached polymer chains and has rapidly become an area of significant importance and growth.²⁰⁵ Numerous studies have appeared demonstrating the ability to control the degree of polymerization or thickness of the grafted polymer chains, achieve low polydispersities and prepare block copolymers. The covalent nature of the surface attachment also allows either the living free radical initiators themselves to be patterned or the resulting polymer brushes to be patterned (Figure 6).^{206,207} This allows the surface chemistry and topology of the polymer brush to be controlled and this ability to control the placement and structure of vinyl polymer chains is an indication of the tremendous potential that both nitroxide-mediated and atom transfer living free radical polymerizations show in the general area

of nanotechnology. Two examples that capture this promise are the preparation of functionalized macroporous monoliths for advanced chromatographic separations and the design of "Rasta-resins". The latter are especially interesting as ultrahigh capacity supports for combinatorial chemistry which not only utilize the increased functionality or amplification afforded by the surface-initiated polymerization concept (one initiating site leads to numerous reactive functional groups) but takes advantage of the more "solution-like" environment of the functional groups attached to the solvated polymer chains when compared to functionalities at a solid-liquid interface or in a cross-linked resin.^{208,209} Similar strategies can be performed on alternate particulate substrates such as silica²⁰⁵ or carbon black²¹⁰ or via ATRP techniques.²¹¹

The potential for surface-initiated polymerizations using nitroxide-mediated living free radical procedures is perhaps best illustrated by the direct synthesis of dispersed nanocomposites by Sogah and Giannelis.²¹² In this approach the synthetic versatility of the alkoxyamine group is again exploited to

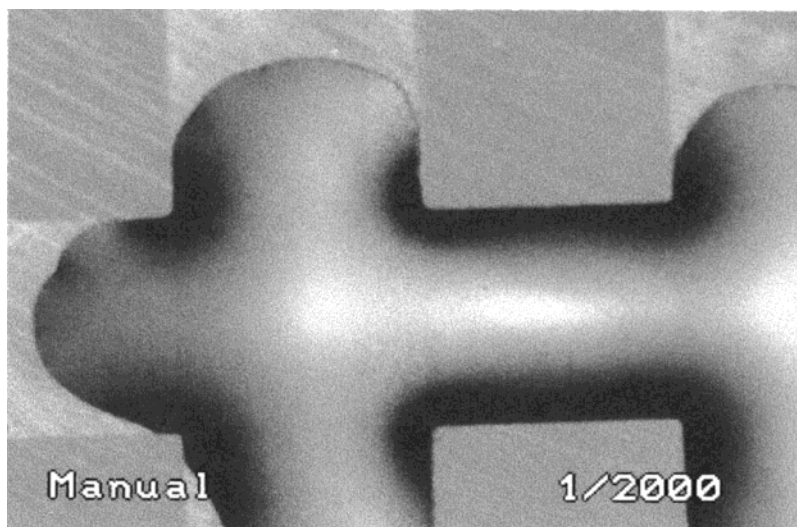


Figure 6. Interaction of a water droplet with 200 micron features of a patterned polymer brush prepared by surface-initiated polymerization. The unusual wetting profile is due to preferential interaction of the water droplet with the poly-(acrylic acid) brush domains (light) and complete non-wetting of the hydrophobic poly(*tert*-butyl acrylate) domains (dark).

prepare the quaternary amine salt **94** which due to its chemistry can intercalate readily into the inter-gallery spaces of a silicate or inorganic matrix. These “anchored” alkoxyamine groups can now be used to initiate the polymerization of a vinyl monomer such as styrene leading to a dispersed silicate nanocomposite. The advantages of this novel approach are that the intercalation of small initiating species such as **94** is orders of magnitude faster than for similar chain end functionalized polystyrene derivatives. In addition, critical polymer characteristics such as molecular weight and polydispersity are controlled while block or random copolymer formation is possible (Scheme 33).

X. Outlook

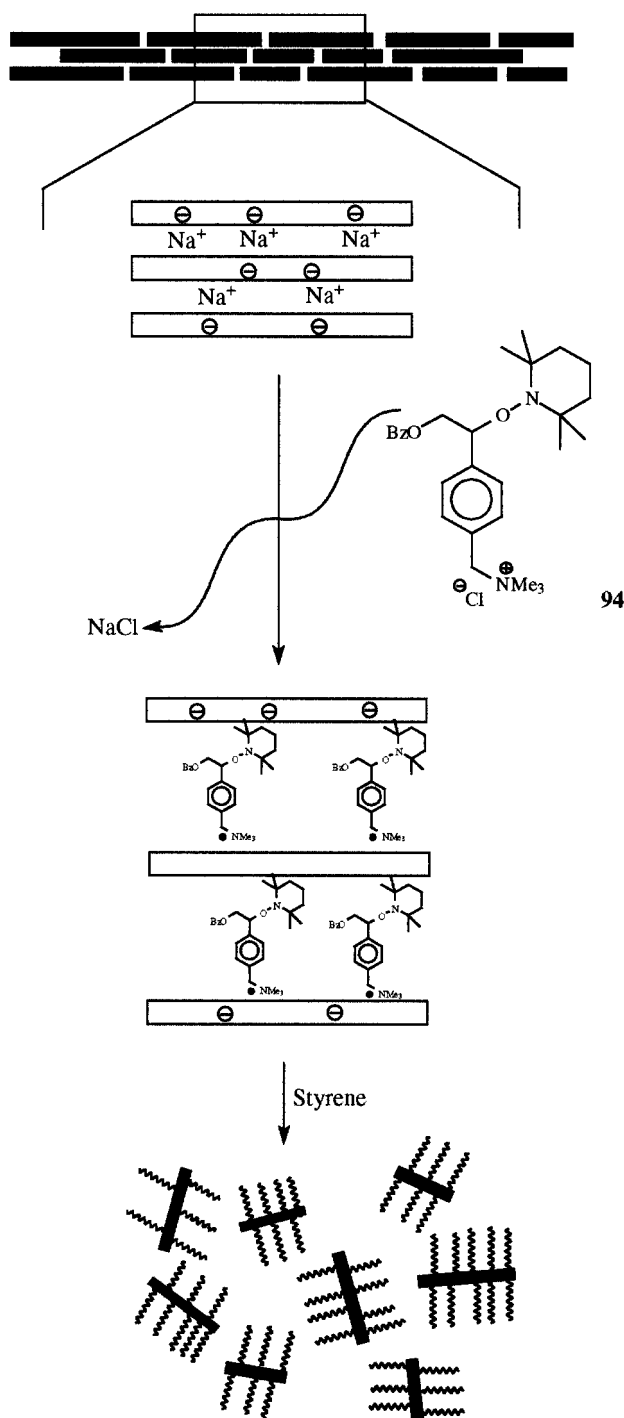
Even though the first reports of a successful living radical process leading to high molecular weight (>30 000), low polydispersity (1.1–1.2) materials were published in 1993 the impact on the field of polymer chemistry has been immense, opening up possibilities in both polymer synthesis and polymer physics that until recently were either prohibitively difficult or impossible. The development of nitroxide-mediated living free radical polymerizations as an important synthetic tool has been extremely rapid and poses exciting possibilities for the future. However, there are a number of issues that must be addressed to enable the continued evolution of this new technique. A greater understanding of the relationship between nitroxide/alkoxyamine structure and polymerization efficiency needs to be developed. Specifically, mediating nitroxides or strategies must be developed which allow the polymerizations to be conducted at lower temperatures (ca. 60–80 °C) in shorter time periods (2–5 h) and with higher conversions (ca. 99%+). It is also highly desirable to further increase the range of monomers that can be polymerized under living conditions, prime candidates are methacrylates and vinyl acetate based monomers. Finally a complete understanding of block copolymer formation, reinitiation efficiency, etc. needs

to be developed in order to make block copolymer formation a routine procedure for the nonexpert. If these challenges can be overcome the industrial appeal of nitroxide-mediated living free radical procedures will increase significantly, while also providing an extremely powerful synthetic technique for the synthesis of vinyl based polymers.

The power of living free radical procedures as synthetic tools in polymer science can be better appreciated by considering the potential advantages when compared to traditional techniques such as anionic polymerization. The ability to accommodate functional groups and diverse families of monomers permit block, random, and gradient copolymers to be prepared without complicated, multistep reaction schemes. Complex macromolecular architectures can also be prepared, however, the low occurrence of radical–radical coupling reactions does place restrictions on the number of propagating arms per macromolecule. The radical nature of the polymerization process does limit the ability to control the stereochemistry; no evidence has been currently presented to indicate that living free radical processes can lead to tacticity control. Presumably the generation of a planar radical at the propagating chain end during each monomer addition step is the key step in this loss of stereochemical control.

Another significant advantage of living free radical procedures is the stability of the initiating species. In the case of nitroxide-mediated processes, the above discussion clearly demonstrates that a variety of chemical transformations can be performed with no deleterious effect on the initiating ability of the alkoxyamine initiator. Not only does this significantly improve the ability to prepare chain end labeled macromolecules but also permits initiating fragments to be introduced at various surfaces, interfaces, chain ends of dendrimers, along the backbone of a linear polymer chain, etc. As more and more effort is devoted to controlling structure and function on the nanometer scale, the role of well-defined polymeric materials with controlled size, dispersity and func-

Scheme 33



tional group placement will become critical. The further development of nitroxide-mediated, ATRP, and RAFT processes is therefore critical for the preparation of these materials and for the continued evolution of nanotechnology.

XI. Acknowledgments

Financial support from the MRSEC Program of the National Science Foundation under Award Number DMR-9808677 for the Center for Polymeric Interfaces and Macromolecular Assemblies and the IBM Corp. is gratefully acknowledged.

XII. Note Added after ASAP

References to the paper by Chiefari and Rizzardo have been removed.

XIII. References

- (1) Moad G.; Solomon D. H. *The Chemistry of Free Radical Polymerization*, Pergamon: Oxford, England, 1995.
- (2) Quirk, R. P.; Kinning, D. J.; Fetters, L. J. *Comprehensive Polymer Science*; Aggarwal, S. L. Ed.; Pergamon Press: London, 1989; Vol. 7, p 1.
- (3) Sawamoto M.; Kamigaito M. *CHEMTECH* **1999**, *29*, 30–38.
- (4) Malmstrom, E. E.; Hawker, C. J. *Macromol. Chem. Phys.* **1998**, *199*, 923.
- (5) Matyjaszewski, K. *Controlled radical polymerization*; Matyjaszewski, K, Ed.; ACS Symposium Series 685; American Chemical Society: Washington, DC, 1998; pp 1–25.
- (6) Colombani, D. *Prog. Polym. Sci.* **1997**, *22*, 1649.
- (7) Fischer, H. *Chem. Rev.* **2001**, *101*, 3581–3610.
- (8) Kamigaito, M.; Ando, T.; Sawamoto, M. *Chem. Rev.* **2001**, *101*, 3689–3746.
- (9) Werrington, T. E.; Tobolsky, A. V. *J. Am. Chem. Soc.* **1955**, *77*, 4510.
- (10) Otsu, T.; Yoshida, M. *Makromol. Chem. Rapid Commun.* **1982**, *3*, 127–32; Otsu, T. *J. Polym. Sci., Polym. Chem.* **2000**, *38*, 2121.
- (11) Bledzki, A.; Braun, D.; Titzschkau, K. *Makromol. Chem.* **1983**, *184*, 745.
- (12) Crivello, J. V.; Lee, J. L.; Conlon, D. A. *J. Polym. Sci., Polym. Chem.* **1986**, *24*, 1251.
- (13) Chung, T. C.; Janvikul, W.; Lu, H. L. *J. Am. Chem. Soc.* **1996**, *118*, 705.
- (14) Druliner, J. D. *Macromolecules* **1991**, *24*, 6079.
- (15) Leon-Saenz, E. D.; Morales, G.; Guerrero-santos, R.; Gnanou, Y. *Macromol. Chem. Phys.* **2000**, *201*, 74–83.
- (16) Yamada, B.; Nobukane, Y.; Miura, Y. *Polym. Bull.* **1998**, *41*, 539–544.
- (17) Steenbock, M.; Klapper, M.; Mullen, K. *Macromol. Chem. Phys.* **1998**, *199*, 763–769.
- (18) Puts, R. D.; Sogah, D. Y. *Macromolecules* **1996**, *29*, 3323.
- (19) Rizzardo, E.; Solomon, D. H. *Polym. Bull.* **1979**, *1*, 529; Moad, G.; Rizzardo, E.; Solomon, D. H. *Macromolecules* **1982**, *15*, 909–14.
- (20) Solomon, D. H.; Rizzardo, E.; Cacioli, P. U.S. Patent, 4,581,429, 1986.
- (21) Georges, M. K.; Veregin, R. P. N.; Kazmaier, P. M.; Hamer, G. K. *Macromolecules* **1993**, *26*, 2987–8.
- (22) Hammouch, S. O.; Catala, J. M. *Macromol. Rapid Commun.* **1996**, *17*, 149.
- (23) Li, I. Q.; Howell, B. A.; Koster, R. A.; Priddy, D. B. *Macromolecules* **1996**, *29*, 8554.
- (24) Fukuda, T.; Terauchi, T.; Goto, A.; Ohno, K.; Tsujii, Y.; Yamada, B. *Macromolecules* **1996**, *29*, 6393.
- (25) Moad, G.; Rizzardo, E. *Macromolecules* **1995**, *28*, 8722.
- (26) Odell, P. G.; Veregin, R. P. N.; Michalak, L. M.; Georges, M. K. *Macromolecules* **1997**, *30*, 2232.
- (27) Percec, V.; Tirrell, D. A. *J. Polym. Sci., Polym. Chem.* **2000**, *38*, 1705.
- (28) Hawker, C. J. *J. Am. Chem. Soc.* **1994**, *116*, 11185–6.
- (29) Hawker, C. J.; Barclay, G. G.; Orellana, A.; Dao, J.; Devonport W. *Macromolecules* **1996**, *29*, 5245.
- (30) Zink, M. O.; Kramer, A.; Nesvadba, P. *Macromolecules* **2000**, *33*, 8106–8108.
- (31) Hawker, C. J.; Elce, E.; Dao, J.; Volksen, W.; Russell, T. P.; Barclay, G. G. *Macromolecules* **1996**, *29*, 4167.
- (32) Keoshkerian, B.; Georges, M. K.; Quinlan, M.; Veregin, R.; Goodbrand R. *Macromolecules* **1998**, *31*, 7559.
- (33) Matyjaszewski, K.; Gaynor, S.; Greszta, D.; Mardare, D.; Shigemoto, T. *Macromol. Symp.* **1995**, *95*, 217.
- (34) Chong, Y. K.; Ercole, F.; Moad, G.; Rizzardo, E.; Thang, S. H. *Macromolecules* **1999**, *32*, 6895.
- (35) Georges, M. K.; Veregin, R. P. N.; Kazmaier, P. M.; Hamer, G. K.; Saban, M. *Macromolecules* **1994**, *27*, 7228.
- (36) Malmstrom, E. E.; Hawker, C. J.; Miller, R. D. *Tetrahedron* **1997**, *53*, 15225.
- (37) Benoit, D.; Grimaldi, S.; Robin, S.; Finet, J. P.; Tordo, P.; Gnanou, Y. *J. Am. Chem. Soc.* **2000**, *122*, 5929.
- (38) Benoit, D.; Chaplinski, V.; Braslau, R.; Hawker, C. J. *J. Am. Chem. Soc.* **1999**, *121*, 3904.
- (39) Benoit, D.; Harth, E.; Fox, P.; Waymouth, R. M.; Hawker, C. J. *Macromolecules* **2000**, *33*, 363.
- (40) Kato, M.; Kamigaito, M.; Sawamoto, M.; Higashimura, T. *Macromolecules* **1995**, *28*, 1721.
- (41) Wang, J. S.; Matyjaszewski, K. *J. Am. Chem. Soc.* **1995**, *117*, 5614.
- (42) Mayadunne, R. T. A.; Rizzardo, E.; Chiefari, J.; Krstina, J.; Moad G.; Postma, A.; Thang, S. H. *Macromolecules* **2000**, *33*, 243.

- (43) Moroni, M.; Hilberer, A.; Hadziioannou, G. *Macromol. Rapid Commun.* **1996**, *17*, 693.
- (44) Yoshida, E.; Fujii, T. *J. Polym. Sci., Polym. Chem.* **1998**, *36*, 269.
- (45) Marque, S.; Le Mercier, C.; Tordo, P.; Fischer, H. *Macromolecules* **2000**, *33*, 4403.
- (46) Aldabbagh, F.; Busfield, W. K.; Jenkins, I. D.; Thang, S. H. *Tetrahedron Lett.* **2000**, *41*, 3673.
- (47) Greszta, D.; Matyjaszewski, K. *Macromolecules* **1996**, *29*, 7661.
- (48) Jousset, S.; Hammouch, S. O.; Catala, J. M.; *Macromolecules* **1997**, *30*, 6685.
- (49) Skene, W. G.; Belt, S. T.; Connolly, T. J.; Hahn, P.; Scaiano, J. C. *Macromolecules* **1998**, *31*, 9103.
- (50) Hammouch, S. O.; Catala, J. M.; *Macromol. Rapid Commun.* **1996**, *17*, 683.
- (51) Georges, M. K.; Veregin, R. P. N.; Kazmaier, P. M.; Hamer, G. K.; Saban, M. *Macromolecules* **1994**, *27*, 7228.
- (52) Baldovi, M. V.; Mohtat, N.; Scaiano, J. C. *Macromolecules* **1996**, *29*, 5497.
- (53) Hawker, C. J.; Barclay, G. G.; Dao, J. *J. Am. Chem. Soc.* **1996**, *118*, 11467.
- (54) Davey, M.; Hawker, C. J. Unpublished results.
- (55) Farcet, C.; Lansalot, M.; Charleux, B.; Pirri, R.; Vairon, J. P. *Macromolecules* **2000**, *33*, 8559.
- (56) Yoshida, E.; Sugita, A. *J. Polym. Sci., Polym. Chem.* **1998**, *36*, 2059.
- (57) Pradel, J. L.; Boutevin, B.; Ameduri, B. *J. Polym. Sci., Polym. Chem.* **2000**, *38*, 3293.
- (58) Braslau, R.; Burrill, L. C.; Siano, M.; Naik, N.; Howden, R. K.; Mahal, L. K. *Macromolecules* **1997**, *30*, 6445.
- (59) Ciriano, M. V.; Korth, H. G.; van Scheppingen, W. B.; Milder, P. *J. Am. Chem. Soc.* **1999**, *121*, 6375.
- (60) Benoit, D.; Grimaldi, S.; Robin, S.; Finet, J. P.; Tordo, P.; Gnanou, Y. *J. Am. Chem. Soc.* **2000**, *122*, 5929.
- (61) Einhorn, J.; Einhorn, C.; Ratajczak, F.; Gautier-Luneau, I.; Pierre, J. L.; *J. Org. Chem.* **1997**, *62*, 9385.
- (62) Moad, G.; Shipp, D. A.; Smith, T. A.; Solomon, D. H. *Macromolecules* **1997**, *30*, 7627.
- (63) Shigemoto, T.; Matyjaszewski, K. *Macromol. Rapid Commun.* **1996**, *17*, 347.
- (64) Jousset, S.; Catala, J. M. *Macromolecules* **2000**, *33*, 4705.
- (65) Yoshida, E.; Okada, Y. *Bull. Chem. Soc. Jpn.* **1997**, *70*, 275.
- (66) Skene, W. G.; Sciaiano, J. C.; Listigovers, N.; Kazmaier, P. M.; Georges, M. K. *Macromolecules* **2000**, *33*, 5065.
- (67) Miura, Y.; Nakamura, N.; Taniguchi, I. *Macromolecules* **2001**, *34*, 447.
- (68) Zink, M. O.; Kramer, A.; Nesvadba, P. *Macromolecules* **2000**, *33*, 8106.
- (69) Turro, N. J.; Lem, G.; Zavarine, I. S. *Macromolecules* **2000**, *33*, 9782.
- (70) Marque, S.; Fischer, H.; Baier, E.; Studer, A. *J. Org. Chem.* **2001**, *66*, 1146.
- (71) Harth, E.; van Horn B.; Hawker, C. J. *Chem. Commun.* **2001**, 823.
- (72) Matyjaszewski, K.; Gaynor, S. G.; Greszta, D.; Mardare, D.; Shigemoto T.; Wang, J. S. *Macromol. Symp.* **1995**, *95*, 217.
- (73) Rodlert, M.; Harth, E.; Rees, I.; Hawker, C. J. *J. Polym. Sci. Polym. Chem.* **2000**, *38*, 4749.
- (74) Han, C. H.; Drache, M.; Baethge, H.; Schmidt-Naake, G. *Macromol. Chem.* **1999**, *200*, 1779.
- (75) Veregin, R. P. N.; Georges, M. K.; Kazmaier, P. M.; Hamer, G. K. *Macromolecules* **1993**, *26*, 5316.
- (76) Chong, Y. K.; Ercole, F.; Moad, G.; Rizzardo, E.; Thang, S. H.; Anderson, A. G. *Macromolecules* **1999**, *32*, 6895.
- (77) Brown, T. M.; Cooksey, C. J.; Crich, D.; Dronsfield, A. T.; Ellis, R. *J. Chem. Soc., Perkin Trans 1* **1993**, 2131.
- (78) Patel, V. F.; Pattenden, G. *J. Chem. Soc., Perkin Trans 1* **1990**, 2703.
- (79) Kim, T. H.; Dokolas, P.; Feeder, N.; Giles, M.; Holmes, A. B.; Walther, M. *Chem. Commun.* **2000**, 2419.
- (80) Li, I. Q.; Howell, B. A.; Dineen, M. T.; Kastl, P. E.; Lyons, J. W.; Meunier, D. M.; Smith, P. B.; Priddy, D. B. *Macromolecules* **1997**, *30*, 5194.
- (81) Miura, Y.; Hirota, K.; Moto, H.; Yamada, B. *Macromolecules* **1999**, *32*, 8356–8362.
- (82) Connolly, T. J.; Baldovf, M. V.; Mohtat, N.; Scaiano, J. C. *Tetrahedron Lett.* **1996**, *37*, 4919.
- (83) Jahn, U. *J. Org. Chem.* **1998**, *63*, 7130.
- (84) Braslau, R.; Burrill, L. C.; Siano, M.; Naik, N.; Howden, R. K.; Mahal, L. K. *Macromolecules* **1997**, *30*, 6445.
- (85) Matyjaszewski, K.; Gaynor, S.; Greszta, D.; Mardare, D.; Shigemoto, T. *Macromol. Symp.* **1995**, *98*, 73.
- (86) Braslau, R.; Burrill, L. C.; Mahal, L. K.; Wedeking, T. *Angew. Chem., Int. Ed. Engl.* **1997**, *36*, 237.
- (87) Kobatake, S.; Harwood, H. J.; Quirk, R. P.; Priddy, D. B. *J. Polym. Sci. Part A: Polym. Chem.* **1998**, *36*, 2555.
- (88) Hammouch, S. O.; Catala, J. M. *Macromol. Rapid Commun.* **1996**, *17*, 149.
- (89) Bergbreiter, D. E.; Walchuk, B. *Macromolecules* **1998**, *31*, 6380.
- (90) Dao, J.; Benoit, D.; Hawker, C. J. *J. Polym. Sci. Part A: Polym. Chem.* **1998**, *36*, 2161–67.
- (91) Linker, T. *Angew. Chem., Int. Ed. Engl.* **1997**, *36*, 2060.
- (92) Fischer, H. *Macromolecules* **1997**, *30*, 5666–5672.
- (93) Fischer, H. *J. Polym. Sci. Part A: Polym. Chem.* **1999**, *37*, 1885–1901.
- (94) Hawker, C. J.; Barclay, G. G.; Dao, J. *J. Am. Chem. Soc.* **1996**, *118*, 11467.
- (95) Turro, N. J.; Lem, G.; Zavarine, I. S. *Macromolecules* **2000**, *33*, 9782–9785.
- (96) Greszta, D.; Matyjaszewski, K. *Macromolecules* **1996**, *29*, 5239–5240.
- (97) He, J.; Chen, J.; Li, L.; Pan, J.; Li, C.; Cao, J.; Tao, Y.; Hua, F.; Yang, Y.; McKee, G.; Brinkmann, S. *Polymer* **2000**, *41*, 4573–4577.
- (98) Georges, M. K.; Kee, R. A.; Veregin, R. P. N.; Hamer, G. K.; Kazmaier, P. M. *J. Phys. Org. Chem.* **1995**, *8*, 301.
- (99) Devonport, W.; Michalak, L.; Malmstrom, E.; Mate, M.; Kurdi, B.; Hawker, C. J.; Barclay, G. G.; Sinta, R. *Macromolecules* **1997**, *30*, 1929.
- (100) Greszta, D.; Matyjaszewski, K. *J. Polym. Sci. Part A: Polym. Chem.* **1997**, *35*, 1857–1861.
- (101) Li, I. Q.; Howell, B. A.; Matyjaszewski, K.; Shigemoto, T.; Smith, P. B.; Priddy, D. B. *Macromolecules* **1995**, *28*, 6692–6693.
- (102) He, J.; Li, L.; Yang, Y. *Macromolecules* **2000**, *33*, 2286–2289.
- (103) Dourges, M. A.; Charleux, B.; Varion, J. P.; Blais, J. C.; Bolbach, G.; Tabet, J. C. *Macromolecules* **1999**, *32*, 2495–2502.
- (104) Burguiere, C.; Dourges, M. A.; Charleux, B.; Varion, J. P. *Macromolecules* **1999**, *32*, 3883–3890.
- (105) Gabaston, L. I.; Jackson, R. A.; Armes, S. P. *Macromolecules* **1998**, *31*, 2883; Marestin, C.; Noel, C.; Guyot, A.; Claverie, J. *Macromolecules* **1998**, *31*, 4041.
- (106) MacLeod, P. J.; Barber, R.; Odell, P. G.; Keoshkerian, B.; Georges, M. K. *Macromol. Symp.* **2000**, *155*, 31.
- (107) Pan, G.; Sudol, E. D.; Dimonie, V. L.; El-Aasser, M. S. *Macromolecules* **2001**, *34*, 481.
- (108) Butte, A.; Storti, G.; Morbidelli, M. *Macromolecules* **2000**, *33*, 3485.
- (109) Ma, J. W.; Cunningham, M. F.; McAuley, K. B.; Keoshkerian, B.; Georges, M. K. *J. Polym. Sci. Polym. Chem.* **2001**, *39*, 1081.
- (110) Charleux, B. *Macromolecules* **2000**, *33*, 5358.
- (111) Rodlert, M.; Bosman, A.; Harth, E.; Rees, I.; Hawker, C. J. *Macromol. Symp.* **2001**, in press.
- (112) Hawker, C. J.; Hedrick, J. L. *Macromolecules* **1995**, *28*, 2993.
- (113) Baumert, M.; Mulhaupt, R. *Macromol. Rapid Commun.* **1997**, *18*, 787.
- (114) Kim, C. S.; Oh, S. M.; Kim, S.; Cho, C. G. *Macromol. Rapid Commun.* **1998**, *19*, 191.
- (115) Harth, E.; Hawker, C. J.; Fan, W.; Waymouth, R. M. *Macromolecules* **2001**, *34*, 3856.
- (116) Stehling, U. M.; Malmstrom, E. E.; Waymouth, R. M.; Hawker, C. J. *Macromolecules* **1998**, *31*, 4396.
- (117) Stalmach, U.; de Boer, B.; Post, A. D.; van Hutten, P. F.; Hadziioannou, G. *Angew. Chem., Int. Ed. Engl.* **2001**, *40*, 428.
- (118) Lacroix-Desmazes, P.; Delair, T.; Pichot, C.; Boutevin, B. *J. Polym. Sci., Polym. Chem.* **2000**, *38*, 3845.
- (119) Yousi, Z.; Jian, L.; Rongchuan, Z.; Jianliang, Y.; Lizong, D.; Lansun, Z. *Macromolecules* **2000**, *33*, 4745.
- (120) Benoit, D.; Harth, E.; Fox, P.; Waymouth, R. M.; Hawker, C. J. *Macromolecules* **2000**, *33*, 363.
- (121) Li, D.; Brittain, W. J. *Macromolecules* **1998**, *31*, 3852.
- (122) Ohno, K.; Ejaz, M.; Fukuda, T.; Miyamoto, T.; Shimizu, Y. *Macromol. Chem. Phys.* **1998**, *199*, 291.
- (123) Klaerner, G.; Trollsås, M.; Heise, A.; Husemann, M.; Athoff, B.; Hawker, C. J.; Hedrick, J. L.; Miller, R. D. *Macromolecules* **1999**, *32*, 8227.
- (124) Grubbs, R. B.; Dean, J. M.; Broz, M. E.; Bates, F. S. *Macromolecules* **2000**, *33*, 9522.
- (125) Hawker, C. J.; Hedrick, J. L.; Malmstrom, E. E.; Trollsås, M.; Mecerreys, D.; Dubois, Ph.; Jerome, R. *Macromolecules* **1998**, *31*, 213.
- (126) de Boer, B.; Stalmach, U.; Nijland, H.; Hadziioannou, G. *Adv. Mater.* **2000**, *12*, 1581.
- (127) Mariani, M.; Lelli, M.; Sparnacci, K.; Laus, M. *J. Polym. Sci., Polym. Chem.* **1999**, *37*, 1237.
- (128) Barbosa, C. A.; Gomes, A. S. *Polym. Bull.* **1998**, *41*, 15.
- (129) Chen, X.; Gao, B.; Kops, J.; Batsberg, W. *Polymer* **1998**, *39*, 911.
- (130) Li, I. Q.; Howell, B. A.; Dineen, M. T.; Kastl, P. E.; Lyons, J. W.; Meunier, D. M.; Smith, P. B.; Priddy, D. B. *Macromolecules* **1997**, *30*, 5196.
- (131) Barclay, G. G.; King, M.; Sinta, R.; Malmstrom, E. E.; Ito, H.; Hawker, C. J. *Polym. Prepr.* **1997**, *38* (1), 902.
- (132) Yoshida, E.; Osagawa, Y. *Macromolecules* **1998**, *31*, 1446.
- (133) Yoshida, E. *J. Polym. Sci., Polym. Chem.* **1996**, *34*, 2937.
- (134) Kobatake, S.; Harwood, H. J.; Quirk, R. P.; Priddy, D. B. *Macromolecules* **1997**, *30*, 4238.
- (135) Bouix, M.; Gouzi, J.; Charleux, B.; Vairon, J. P.; Guinot, P. *Macromol. Rapid Commun.* **1998**, *19*, 209.
- (136) Wang, Y.; Chen, S.; Huang, J. *Macromolecules* **1999**, *32*, 2480.

- (137) Ei, Y.; Connors, E. J.; Jia, X.; Wang, C. *J. Polym. Sci. Polym. Chem.* **1998**, *36*, 761.
- (138) Butz, S.; Baethge, H.; Schmidt-Naake, G. *Macromol. Rapid Commun.* **1997**, *18*, 1049.
- (139) Baumert, M.; Frohlich, J.; Stieger, M.; Frey, H.; Mulhaupt, R.; Plenio, H. *Macromol. Rapid Commun.* **1999**, *20*, 203.
- (140) Yoshida, E.; Tanimoto, S. *Macromolecules* **1997**, *30*, 4018.
- (141) Gravert, D.; Datta, A.; Wentworth, P.; Janda, K. D. *J. Am. Chem. Soc.* **1998**, *120*, 9481.
- (142) Bertin, D.; Boutevin, B. *Polym. Bull.* **1996**, *37*, 337.
- (143) Listigovers, N. A.; Georges, M. K.; Odell, P. G.; Keoshkerian, B. *Macromolecules* **1996**, *29*, 8992.
- (144) Bohrisch, J.; Wendler, U.; Jaeger, W. *Macromol. Rapid Commun.* **1997**, *18*, 975.
- (145) Keoshkerian, B.; Georges, M. K.; Boils-Boissier, D. *Macromolecules* **1995**, *28*, 6381.
- (146) Baethge, H.; Butz, S.; Schmidt-Naake, G. *Macromol. Rapid Commun.* **1997**, *18*, 911.
- (147) Lokaj, J.; Vlcek, P.; Kriz, J. *Macromolecules* **1997**, *30*, 7644.
- (148) Yoshida, E.; Sugita, A. *Macromolecules* **1996**, *29*, 6422.
- (149) Wendler, U.; Bohrisch, J.; Jaeger, W.; Rother, G.; Dautzberg, H. *Macromol. Rapid Commun.* **1998**, *19*, 185.
- (150) Wang, Y.; Huang, J. *Macromolecules* **1998**, *31*, 4058.
- (151) Yagci, Y.; Baskan Duz, A.; Onen, A. *Polymer* **1997**, *38*, 2861.
- (152) Okamura, H.; Terauchi, T.; Minoda, M.; Fukuda, T.; Komatsu, K. *Macromolecules* **1997**, *30*, 5279.
- (153) Yoshida, E.; Fujii, T. *J. Polym. Sci., Polym. Chem.* **1997**, *35*, 2371.
- (154) Schmidt-Naake, G.; Butz, S. *Macromol. Rapid Commun.* **1996**, *17*, 661.
- (155) Sun, Y.; Wan, D.; Huang, J. *J. Polym. Sci., Polym. Chem.* **2001**, *39*, 604.
- (156) Barclay, G. G.; Hawker, C. J.; Ito, H.; Orellana, A.; Malenfant, P. R. L.; Sinta, R. F. *Macromolecules* **1998**, *31*, 1024.
- (157) Burguiere, C.; Dourges, M. A.; Charleux, B.; Vairon, J. P. *Macromolecules* **1999**, *32*, 3883.
- (158) Miwa, Y.; Yamamoto, K.; Sakaguchi, M.; Shimada, S. *Macromolecules* **2001**, *34*, 2089.
- (159) Zhu, M. Q.; Wei, L. H.; Li, M.; Jiang, L.; Du, F. S.; Li, Z. C.; Li, F. M. *J. Chem. Soc., Chem. Commun.* **2001**, 365.
- (160) Lokaj, J.; Holler, P.; Kriz, J. *J. Appl. Polym. Sci.* **2000**, *76*, 1093.
- (161) Emrick, T.; Hayes, W.; Fréchet, J. M. J. *J. Polym. Sci., Polym. Chem.* **1999**, *37*, 3748.
- (162) Wang, C.; He, J.; Fu, S.; Jiang, K.; Cheng, H.; Wang, M. *Polym. Bull.* **1996**, *37*, 305.
- (163) Jones, R. G.; Yoon, S.; Nagasaki, Y. *Polymer* **1999**, *40*, 2411.
- (164) Yoshida, E.; Okada, Y. *J. Polym. Sci., Polym. Chem.* **1996**, *34*, 3631.
- (165) Baumann, M.; Roland, A. I.; Schmidt-Naake, G.; Fischer, H. *Macromol. Mater. Eng.* **2000**, *280*, 1.
- (166) Baumann, M.; Schmidt-Naake, G. *Macromol. Chem. Phys.* **2000**, *201*, 2751.
- (167) Bosman, A. W.; Fréchet, J. M. J.; Hawker, C. J. *Polym. Mater. Sci. Eng.* **2001**, *84*, 376.
- (168) Bignozzi, M. C.; Ober, C. K.; Laus, M. *Macromol. Rapid Commun.* **1999**, *20*, 622.
- (169) Stehling, U. M.; Malmstrom, E. E.; Waymouth, R. M.; Hawker, C. J. *Macromolecules* **1998**, *31*, 4396.
- (170) Tsoukatos, T.; Pispas, S.; Hadjichristidis, N. *Macromolecules* **2000**, *33*, 9504.
- (171) Grubbs, R. B.; Hawker, C. J.; Dao, J.; Fréchet, J. M. J. *Angew. Chem., Int. Ed. Engl.* **1997**, *36*, 270.
- (172) Bosman, A. W.; Fréchet, J. M. J.; Hawker, C. J. *Polym. Mater. Sci. Eng.* **84**, 376, 2001.
- (173) Hawker, C. J.; Hedrick, J. L.; Malmstrom, E. E.; Trollsas, M.; Mecerreyes, D.; Dubois, Ph.; Jerome, R. *Macromolecules* **1998**, *31*, 213.
- (174) Puts, R. D.; Sogah, D. Y. *Macromolecules* **1997**, *30*, 7050; Weimer, M. W.; Scherman, O. A.; Sogah, D. Y. *Macromolecules* **1998**, *31*, 8425.
- (175) Kazmaier, P. M.; Daimon, K.; Georges, M. K.; Hamer, G. K.; Veregin, R. P. N. *Macromolecules* **1997**, *30*, 2228; Bouix, M.; Gouzi, J.; Charleux, Vairon, J. P.; Guinot, P. *Macromol. Rapid Commun.* **1998**, *19*, 209.
- (176) Huang, H.; Remsen, E. E.; Wooley, K. L. *J. Chem. Soc., Chem. Commun.* **1998**, 1415.
- (177) Huang, H.; Kowalewski, T.; Remsen, E. E.; Gertzmann, R. Wooley, K. L. *J. Am. Chem. Soc.* **1997**, *119*, 11653.
- (178) Gravert, D. J.; P.; Janda, K. D. *Tetrahedron Lett.* **1998**, *39*, 1513.
- (179) Barclay, G. G.; King, M.; Orellana, A.; Malenfant, P. R. F.; Sinta, R. F.; Malmstrom, E. E.; Ito, H.; Hawker, C. J. *Organic Thin Films: Structure and Applications*; Frank, C. W., Ed.; ACS Symposium Series 695; American Chemical Society: Washington, DC, 1998; p 360.
- (180) Schmidt-Naake, G.; Butz, S. *Macromol. Rapid Commun.* **1996**, *17*, 661.
- (181) Benoit, D.; Hawker, C. J.; Huang, E. E.; Lin, Z.; Russell, T. P. *Macromolecules* **2000**, *33*, 1505.
- (182) Annighofer, F.; Gronski, W. *Colloid Polym. Sci.* **1983**, *263*, 15; Arehart, S.; Greszta, D.; Matyjaszewski, K. *Polym. Prepr.* **1997**, *38*, 705.
- (183) Butz, S.; Baethge, H.; Schmidt-Naake, G. *Macro. Chem. Phys.* **2000**, *16*, 2143.
- (184) Hawker, C. J. *Angew. Chem., Int. Ed. Engl.* **1995**, *34*, 1456.
- (185) Grubbs, R. B.; Hawker, C. J.; Dao J.; Fréchet, J. M. J. *Angew. Chem., Int. Ed. Engl.* **1997**, *36*, 270.
- (186) Voit, B. *J. Polym. Sci. Polym. Chem.* **2000**, *38*, 2505; Emrick, T.; Chang, H. T.; Fréchet, J. M. J. *J. Polym. Sci. Polym. Chem.* **2000**, *38*, 4805 and references therein.
- (187) (a) Hawker, C. J.; Fréchet, J. M. J.; Grubbs, R. B.; Dao J. *J. Am. Chem. Soc.* **1995**, *117*, 10763. (b) Fréchet, J. M. J.; Henmi, M.; Gitsov, I.; Aoshima, S.; Leduc, M.; Grubbs, R. B. *Science* **1995**, *269*, 1080–1083.
- (188) Gaynor, S. G.; Edelman G.; Matyjaszewski, K. *Macromolecules* **1996**, *29*, 1079.
- (189) Weimer, M. W.; Gitsov, I.; Fréchet, J. M. J. *J. Polym. Sci. Polym. Chem.* **1998**, *36*, 955–970.
- (190) Li, C.; He, J.; Li, L.; Cao, J.; Yang, Y. *Macromolecules* **1999**, *32*, 7012; Niu, A.; Li, C.; Zhao, J.; Yang, Y.; Wu, C. *Macromolecules* **2001**, *34*, 460.
- (191) Benoit, D.; Harth, E.; Hawker, C. J.; Helms, B. *Polym. Prepr.* **2000**, *41* (1), 42.
- (192) Bosman, A. W.; Heumann, A.; Klaerner, G. G.; Benoit, D. G.; Fréchet, J. M. J.; Hawker, C. J. *J. Am. Chem. Soc.* **2001**, *123*, 6461; Pasquale, A. J.; Long, T. E. *J. Polym. Sci. Polym. Chem.* **2001**, *39*, 216; Tsoukatos, T.; Pispas, S.; Hadjichristidis, N. *J. Polym. Sci. Polym. Chem.* **2001**, *39*, 320.
- (193) Abrol, S.; Kambouris, P. A.; Looney, M. G.; Solomon, D. H. *Macromol. Rapid Commun.* **1997**, *18*, 755.
- (194) Hawker, C. J.; Fréchet, J. M. J. *J. Am. Chem. Soc.* **1990**, *112*, 7638.
- (195) Leduc, M. R.; Hawker, C. J.; Dao, J.; Fréchet, J. M. J. *J. Am. Chem. Soc.* **1996**, *118*, 11111.
- (196) Vestberg, R.; Hawker, C. J. Unpublished work.
- (197) Leduc, M. R.; Hayes, W.; Fréchet, J. M. J. *J. Polym. Sci. Polym. Chem.* **1998**, *36*, 1–10.
- (198) Matyjaszewski, K.; Shigemoto, T.; Fréchet, J. M. J.; Leduc, M. *Macromolecules* **1996**, *29*, 4167–4171.
- (199) Percec, V.; Barboiu, B.; Bera, T. K.; van der Sluis, M.; Grubbs, R. B.; Fréchet, J. M. J. *J. Polym. Sci., Polym. Chem.* **2000**, *38*, 4776–4791
- (200) Tsoukatos, T.; Pispas, S.; Hadjichristidis, N. *Macromolecules* **2000**, *33*, 9504.
- (201) O'Brien, N.; McKee, A.; Sherrington, D. C.; Slark, A. T.; Titterton, A. *Polymer* **2000**, *41*, 6027.
- (202) Ide, N.; Fukuda, T. *Macromolecules* **1999**, *32*, 95.
- (203) Lepoittevin, B.; Perrot, X.; Masure, M.; Hemery, P. *Macromolecules* **2001**, *34*, 425.
- (204) Asgarzadeh, F.; Ourdouillie, P.; Beyou, E.; Chaumont, P. *Macromolecules* **1999**, *32*, 6996.
- (205) Husseman, M.; Malmström, E. E.; McNamara, M.; Mate, M.; Mecerreyes, D.; Benoit, D. G.; Hedrick, J. L.; Mansky, P.; Huang, E.; Russell, T. P.; Hawker, C. J. *Macromolecules* **1999**, *32*, 1424.
- (206) Husemann, M.; Morrison, M.; Benoit, D.; Frommer, J.; Mate, C. M.; Hinsberg, W. D.; Hedrick, J. L.; Hawker, C. J. *J. Am. Chem. Soc.* **2000**, *122*, 1844.
- (207) Meyer, U.; Svec, F.; Fréchet, J. M. J.; Hawker, C. J.; Irgum K. *Macromolecules* **2000**, *33*, 7769.
- (208) McAlpine, S. R.; Lindsley, C. W.; Hodges, J. C.; Leonard, D. M.; Filzen, G. F. *J. Comb. Chem.* **2001**, *3*, 1.
- (209) Lindsley, C. W.; Hodges, J. C.; Filzen, G. F.; Watson, B. M.; Geyer, A. G. *J. Comb. Chem.* **2000**, *2*, 550–559.
- (210) Yoshikawa, S.; Machida, S.; Tsubokawa, N. *J. Polym. Sci., Polym. Chem.* **1998**, *36*, 3165.
- (211) Angot, S.; Ayres, N.; Bon, S. A. F.; Haddleton, D. M. *Macromolecules* **2001**, *34*, 768.
- (212) Weimer, M. W.; Chen, H.; Giannelis, E. P.; Sogah, D. Y. *J. Am. Chem. Soc.* **1999**, *121*, 1615.

A Field Guide to Foldamers

David J. Hill,[†] Matthew J. Mio,[‡] Ryan B. Prince,[§] Thomas S. Hughes,[†] and Jeffrey S. Moore^{*,†}

Roger Adams Laboratory, Departments of Chemistry and Materials Science & Engineering, The Beckman Institute for Advanced Science and Technology, University of Illinois at Urbana–Champaign, Urbana, Illinois 61801; Department of Chemistry, Macalester College, 1600 Grand Avenue, St. Paul, Minnesota 55105; and 3M Adhesive Technology Center, 3M Center, 201-3N-04, St. Paul, Minnesota 55144

Received September 5, 2001

Contents

I. Introduction—Definition, Scope, and Relevance	3894	2. Pyridine–Pyrimidines with Hydrazal Linkers	3945
II. Generating Foldamers—Design, Synthesis, Purification, and Characterization	3897	3. Pyridine–Pyridazines	3946
A. Foldamer Design	3897	C. Backbones Utilizing Solvophobic Interactions	3947
1. The General Folding Problem	3897	1. Qualification	3947
2. Foldamers: Secondary Structure	3902	2. Guanidines	3947
3. Tyligomers: Secondary and Tertiary Structure	3904	3. Aedamers	3947
4. Designing Folding Molecules: Toward Tyligomers	3907	4. Cyclophanes	3949
B. Foldamer Synthesis and Purification—The Chemistry of Oligomers	3909	5. Side Chain–Backbone Interactions	3949
C. Foldamer Characterization—Experimental and Instrumental Methods	3910	D. Backbones Utilizing Hydrogen-Bonding Interactions	3961
III. Foldamer Research	3910	1. Aromatic Amide Backbones	3961
A. Overview	3910	2. Receptor Motif Backbones	3962
B. Motivation	3910	E. Backbones Utilizing Metal Coordination	3963
C. Methods	3910	1. Overview	3963
D. General Scope	3912	2. Metal-Binding Backbones	3964
IV. Peptidomimetic Foldamers	3912	3. Anionic-Binding Backbones—Hexapyrrins	3966
A. The α -Peptide Family	3913	VI. Nucleotidomimetic Foldamers	3967
1. Peptoids	3913	A. Overview	3967
2. <i>N,N</i> -Linked Oligoureas	3914	B. Isomeric Oligonucleotides	3968
3. Oligopyrrolinones	3915	1. Iso-RNA and Iso-DNA	3968
4. Oxazolidin-2-ones	3916	2. α -DNA, <i>alt</i> -DNA, and L-DNA	3969
5. Azatides and Azapeptides	3916	C. Carbohydrate Modifications	3969
B. The β -Peptide Family	3917	1. Backbones with C1'-Base Connectivities	3969
1. β -Peptide Foldamers	3917	2. Backbones with C2'-Base Connectivities	3973
2. α -Aminoxy Acids	3937	3. Torsionally Restricted Oligonucleotides	3975
3. Sulfur-Containing β -Peptide Analogues	3937	4. Torsionally Flexible Oligonucleotides	3977
4. Hydrazino Peptides	3938	D. Modifications of the Nucleotide Linkage	3977
C. The γ -Peptide Family	3938	1. PNAs	3978
1. γ -Peptide Foldamers	3938	2. NDPs	3980
2. Other Members of the γ -Peptide Family	3941	3. Fused Sugar–Base Backbones	3980
D. The δ -Peptide Family	3941	4. Cationic Linkages	3980
1. Alkene-Based δ -Amino Acids	3941	E. Alternative Nucleobases	3981
2. Carbopeptoids	3941	VII. Multi stranded Abiotic Foldamers	3982
V. Single-Stranded Abiotic Foldamers	3944	A. Hydrogen-Bonding-Stabilized Foldamer Multiplexes	3982
A. Overview	3944	B. Duplexes Stabilized by Hydrogen-Bonding and Aromatic–Aromatic Interactions	3986
B. Backbones Utilizing Bipyridine Segments	3944	1. Zipper Duplexes	3986
1. Pyridine–Pyrimidines	3944	2. Pyridylamide Oligomers	3986
		C. Helicates: Metal-Coordinating Foldamer Duplexes	3988
		1. Oligopyridines	3988
		2. Linked Oligopyridines	3990
		3. Pyridine Analogues	3994
		4. Catecholates	3995

[†] University of Illinois at Urbana–Champaign.

[‡] Macalester College.

[§] 3M and Company.

D. Multistranded Receptors	3995
E. Foldamer–Oligomer Interactions	3997
1. Minor Groove Binding Oligomers	3998
2. Peptide–Oligomer Complexes	3999
VIII. Conclusion	4000
IX. Acknowledgments	4000
X. References	4000



David J. Hill (second from left) was born in Monterey, CA, in 1973. He attended Point Loma Nazarene University in San Diego, CA, where he worked with Professor Victor L. Heasley on the halogenation of unsaturated carbonyl compounds. After receiving his B.A. degree in Chemistry in 1997, he began his graduate career at the University of Illinois with Professor Jeffrey S. Moore. Currently he is in his fifth year investigating solvent effects on the helix–coil transition in oligo(*m*-phenylene ethynylene) foldamers.

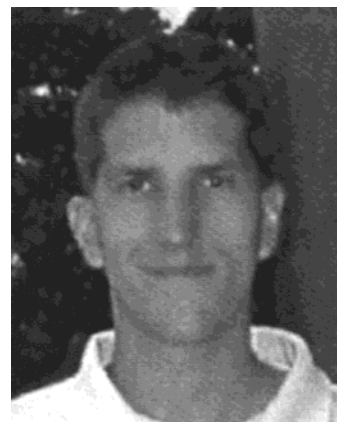
Matthew J. Mio (left) was born in Michigan in 1974. He attended the University of Detroit Mercy, where he worked with Professor Kevin D. Belfield (now at the University of Central Florida) on the synthesis of nonlinear optical chromophores for use in polymeric systems. He graduated with his B.S. degree in Chemistry in 1997. Later that year, he began his graduate career at the University of Illinois at Urbana–Champaign with Professor Jeffrey S. Moore. There, Matt studied the synthesis and solution/solid-state properties of oligo(*m*-phenylene ethynylene) foldamers and graduated with his Ph.D. degree in 2001. He then went to the Chemistry Department at Macalester College (St. Paul, MN) as a Mellon Postdoctoral Fellow to study the synthesis of novel CpCo–cyclobutadienyl-bridged cyclophanes with Professor Ronald G. Brisbois.

Thomas S. Hughes (right) is currently a postdoctoral fellow in the research group of Professor Jeff Moore at the University of Illinois. He was born in 1970 in Philadelphia, PA, and received his B.S. degree from Temple University in 1991. In 1999 he received his Ph.D. degree from Cornell University, where he worked in the laboratories of Professor Barry Carpenter. He is currently studying the association kinetics of the binding of a helical oligomer to a rodlike guest. He is also investigating the thermodynamics of oligo(phenylene ethynylene) folding using molecular mechanics.

Jeffrey S. Moore (second from right) was born in Illinois in 1962. After receiving his B.S. degree in Chemistry from the University of Illinois in 1984, he completed his Ph.D. degree in Materials Science and Engineering, also at the University of Illinois, with Samuel Stupp (1989). He then went to the California Institute of Technology as an NSF postdoctoral fellow to study with Robert Grubbs. In 1990 he joined the chemistry faculty at the University of Michigan in Ann Arbor. He returned to the University of Illinois in 1993, where he is currently a Professor of Chemistry and Materials Science and Engineering. In 1995 he became a part-time faculty member of the Beckman Institute for Advanced Science and Technology, where he now serves as co-chairman of the Molecular and Electronic Nanostructures Main Research Theme.

1. Introduction—Definition, Scope, and Relevance

The breadth of structure and function displayed by the molecules of biology is remarkable. Considering



Ryan B. Prince was born in Robbinsdale, MN, in 1972. He graduated from Southeast Missouri State University in 1995 with his B.S. degree in Chemistry, where he worked for Professor Jin K. Gong on the synthesis and characterization of transition-metal complexes that bind and activate carbon dioxide. He then went to the University of Illinois and worked with Professor Jeffrey S. Moore on the synthesis and study of oligo(*m*-phenylene ethynylene) foldamers. He completed his Ph.D. degree in Organic Chemistry in 2000 and is currently a senior research chemist at 3M Company in St. Paul, MN.

that there are only three major biopolymer backbones (proteins, ribonucleic acids, and polysaccharides), nature vividly teaches that copolymer sequence is a powerful way to meet diverse chemical challenges. It is logical then to ask are biomacromolecule building blocks are *matchless* in their suitability for life? Systematic studies on alternative monomers closely related to those found in nature have provided clues about the fitness of α -amino acids, ribofuranosyl (5'–3') nucleic acids, and phosphodiester linkages. Yet “why nature is such, and not otherwise”¹ is a question that continues to be asked. Looking beyond the biopolymers and their related derivatives however, it is possible to imagine that other chain molecules are capable of similar functions. This prediction has only recently begun to be tested, raising questions of great fundamental interest. On a more practical level, the discovery of new functional polymers clearly has widespread potential for both chemistry and biology.

Most of the interesting functions carried out by biomacromolecules, such as molecular recognition, information storage, and catalysis, involve stable, compact solution structures that approach conformational uniqueness. These high molecular weight macromolecules might be described as glassy-like, nanometer-sized particles² that are suspended in solution and consist of one to, at most, a few chains. The spatial position of most of the backbone atoms is fixed, except for minor fluctuations about their equilibrium coordinates. There is also a congruency between particles having identical or even similar sequences. The surface of these particles includes three-dimensional, molecular-sized crevices lined with information-rich surfaces, and it is from here that affinity, specificity, and catalytic activity spring forth. Reasoning by analogy, the quest for function in synthetic chains should thus be closely tied to the invention of new polymer molecules that acquire ordered solution structures.

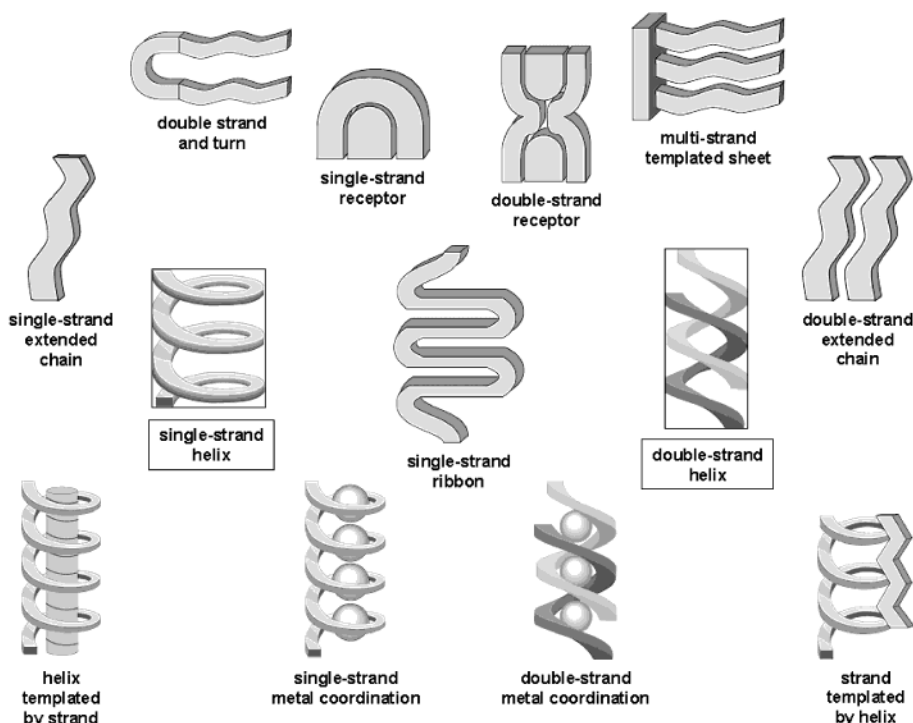


Figure 1. Illustrations depicting the different types of foldamer secondary structures.

Thus, the motivation for developing new chain molecules that adopt ordered solution conformations can be stated as an attempt to gain deeper insight into the fitness of nature's biomacromolecules and to identify new polymers that perform functions that are, at least in part, outside of those seen in nature. Toward these goals, chemists have endeavored to intentionally generate unnatural oligomeric sequences that take on well-defined conformations in solution. This subject has come to be known as the field of foldamers.³ This review covers the literature relevant to foldamers, as specified below, through July 2001. Progress to date has been encouraging, and the field is developing rapidly as demonstrated by the various architectures that have been generated, schematically represented in Figure 1. Yet, today we are still far from producing high molecular weight polymers that mimic the sophistication of biomacromolecules, either in form or function.

A foldamer has previously been defined as "any polymer with a strong tendency to adopt a specific, compact conformation".⁴ Upon inspection of the literature, we thought this definition was in need of clarification. First, the "foldamers" described in the literature are not polymers; they are oligomers. Second, the word "compact" is ambiguous and invokes high molecular weight globular proteins, unlike the smaller segments of secondary structure typical of this area. Third, a crucial aspect of chain conformation is its dynamic character, which in the case of foldamers is manifested in the context of folding and unfolding. Specifically, the "folding reaction" is the process that transforms the conformationally disordered oligomer into a conformationally ordered state, which corresponds to a small set of nearly congruent conformations.

Our definition of a foldamer is any oligomer that folds into a conformationally ordered state

in solution, the structures of which are stabilized by a collection of noncovalent interactions between nonadjacent monomer units. There are two major classes of foldamers: single-stranded foldamers that only fold (peptidomimetics and their abiotic analogues) and multiple-stranded foldamers that both associate and fold (nucleotidomimetics and their abiotic analogues). Before discussing this definition in detail, let us briefly reconsider high molecular weight biomacromolecules. We imagine that a foldamer will not be a very good mimic of a biomacromolecule. In other words, there is something beyond foldamers. This "something" is perhaps a high molecular weight polymer that consists of a collection of foldamers, just as proteins can be viewed as a collection of secondary structures. To clearly distinguish a foldamer, as defined above, from this higher molecular weight "something", we suggest the term *tyliger*. Tyliger is derived from *tyligos*, meaning "to fold", and *meros*, meaning "part" (i.e., a structure consisting of folded parts). Thus, foldamer relates to an element of secondary structure, in the same way that tyliger relates to a tertiary or quaternary conformation.

Let us now examine our definition in detail, since this has been used to limit the scope of this review. First, a foldamer is a chain molecule, meaning that there will almost certainly be a regularly repeating motif within the backbone. Second, foldamers are of oligomeric (not polymeric) size, consistent with the recent literature. Third, the verb in our definition is "to fold", which conveys the dynamic character of conformation, i.e., the folding reaction. Oligomers where no folding reaction can occur, such as helixes,^{5,6} cannot be considered foldamers (Figure 2a). The folding reaction also assumes that the *association* of multiple foldamer strands involves a similar type of entropy loss as folding. Fourth, when folded,

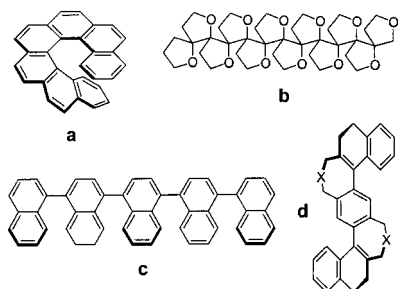


Figure 2. Oligomers not classified as foldamers: (a) helicenes,^{5,6} (b) polyoxapolyspiroalkanones,¹² (c) oligo(naphthalene)s,¹⁴ and (d) “gelander” molecules.¹³

the chain molecules populate a small set of nearly superimposable conformations, meaning that in the folded form all molecules can be described by a unique set of atomic coordinates (or at most a few different sets). Fifth, the folded form is of interest in solution, implying that the solvent is both a fundamental part of the folded state and that the dynamic character of the liquid environment will result in fluctuations about the chain's equilibrium set of atomic coordinates. Sixth, the chain's conformation is defined by noncovalent interactions between non-adjacent monomer units. This point requires special clarification. Many synthetic oligomers adopt stable, extended helical conformations in solution. Examples include poly(isocyanate)s,⁷ poly(proline)s,⁸ poly(aldehyde)s,⁹ poly[(triarylmethyl) methacrylates],¹⁰ and some oligo(saccharide)s.¹¹ However, in these cases, the chain's conformation is determined by the repeat unit's torsional potential energy surface. To distinguish a foldamer from a chain that adopts a regular conformation based on the repeat unit's torsional potential energy surface, we specify that the defining noncovalent interactions must be between atoms that are not contained within adjacent repeat units. By insisting on the role of these interactions in our definition, we are simply being consistent with the notion that foldamers are the synthetic analogues of secondary structure elements, as secondary structure fits this description. Oligomers where conformations are “predetermined” such as polyoxapolyspiroalkanones,¹² “gelander” molecules,¹³ and oligonaphthalenes¹⁴ will not be considered as foldamers (Figure 2b–d).

The accumulation of noncovalent interactions that dictate conformation has no direct counterpart in small molecule chemistry. These interactions arise from the simple reason that the chain segments are either all connected by covalent bonds or form through interstrand complementarity, both of which give rise to a high probability for various monomer pairs to encounter one another. Although the strength of the interaction between monomer pairs is generally weak, the *number of possible interactions* is high and is, presumably, chain-length dependent. A consequence of these collective interactions is that oligomers are apt to undergo cooperative conformational transitions.¹⁵ Thus, although an ordered solution conformation is a necessary criterion of what constitutes a foldamer, it is not sufficient. In addition, noncovalent interactions between nonadjacent monomer units, on some level, play a deciding role in

setting the chain's conformation. In other words, conformational order is stabilized by a collection of interactions acting within or between chains, reminiscent of some supramolecular assemblies.¹⁶

One additional point of distinction between intrinsically preset conformations and those derived primarily from the noncovalent interactions described above centers on environmental responsiveness. Given the weak nature of noncovalent forces, solvent can modulate their strength in a very significant way. It is thus possible to go from a state in which monomers repel one another to one in which the monomer interactions are attractive simply by changing the temperature, pH, or quality of the solvent. In contrast, the torsional potential energy surface is virtually independent of extrinsic variables and therefore is an invariant force to a chain's structure and dynamics. Consequently, the contribution of a monomer's local potential energy surface to an oligomer's conformation can be calculated by statistical mechanical methods such as the rotational isomeric state model.¹¹ Because conformational ordering in foldamers depends on interactions whose strength varies with the environment, these chains can undergo abrupt order-disorder transitions—the folding reaction. Oligomers that have intrinsically stable conformations will be less likely to exhibit this cooperative behavior. This is more than an academic distinction, since there are many potential functions of foldamers that may depend on the reversibility of the folding reaction.

Hopefully, this discussion has helped to shape the reader's view of the term foldamer and accordingly serves to define the scope and relevancy of this review. We note that as chemists have begun to tackle the challenging problem of conformational control in flexible organic molecules, it is becoming fashionable to abuse terms that incorporate the root “fold” (e.g., “folding molecule”, “self-folding”, “folded”). In this review we restrict our coverage to chain molecules (i.e., structures that have a repetitive structure) that have been experimentally demonstrated to exhibit a high degree of conformational order in solution, predominantly derived from noncovalent, intra- and interchain segmental interactions. The emphasis will be on unnatural backbones, although biological oligomers will be discussed as prototypical examples of foldamers.¹⁷ (For example, we have discerned that bilirubins are an excellent model of nature's minimal foldamer. Although the conformation of these molecules has been studied since the late 1980s,^{18,19} investigations into bilirubins' solution conformation continue to the present day.^{20–24}) This review is constrained to the size regime of oligomers, since there are as yet no high polymer tylogomers. We do not cover small molecule fragments that are described in the literature as “folded”,²⁵ although in some cases²⁶ extension of these structures to chain molecules may be obvious. We do not review here polymers that are a mixture of chemical structures or are conformationally incongruent, even if they are referred to in the literature as being “folded.”^{27–29} By analogy to its well-established usage in protein chemistry,³⁰ we

suggest that descriptions involving the verb “fold” should be reserved for conformationally defined chain molecules and not be used for polymeric mixtures. For example, a compact polymeric micelle certainly exists in multiple lowest energy conformations but should not be considered to adopt folded conformations.

Overall, it is the purpose of this article to present a thorough review of foldamer research contained within our definition. A survey of what is involved in the generation of foldamers is in order first, followed by a discussion of specific contributions to the field of foldamers.

II. Generating Foldamers—Design, Synthesis, Purification, and Characterization

The foundation for foldamer research was laid in the early 20th century, during the rise of modern synthetic polymer chemistry,³¹ molecular biology, and more recently through supramolecular chemistry.¹⁶ Upon examination of these disciplines, it becomes clear why and how modern foldamer research has evolved into a stimulating scientific field. It is hoped that the lessons learned in the roots of the foldamer field can be brought to bear upon the problems of designing, creating, and evaluating foldamers and, eventually, biomimetic tyligomers. Before reviewing the current state of the field of foldamers, a summary of various aspects impacting foldamer design will be presented.

A. Foldamer Design

Since the initial use of the term “foldamer” in 1996,³² the field has witnessed several design approaches. We begin by clarifying the context in which we use the word “design”. Our use of this word will be in the same sense as “building a house”—choosing raw materials, mapping out the blueprint for the structure, constructing the necessary subunits into the final framework, and performing interior decoration. Gellman’s daunting steps⁴ to generate useful foldamers echoes this analogy: determining novel backbones that can fold, developing efficient synthetic methods and integrating chemical function. Of course, it is presumptuous for the authors to profess knowledge of how published foldamers were initially conceived. Rather, we intend to detail the logical thought processes that must necessarily be considered in the generation of a successful foldamer.³³

The broad philosophical foundations of foldamer design draw on concepts developed over the past decades in the fields of polymer physics, condensed matter physics, and, in particular, biophysics. It is evident that oligomeric foldamers are not large or complex enough to form anything other than simple, secondary structures such as helices or sheets. A clear logical next step in the field would be to design larger, more complex chain molecules capable of folding into truly tertiary structures or structures having long-range intrachain energetic interactions.⁴ The designs of both simple and complex systems share many features, and much of the discussion below will be general whether tertiary structure is

present in the folded state or not. There are, however, several issues unique to tyligomers which mirror the more complex issues of the long-standing protein folding problem³⁴ and which will be treated below. Since a goal of the field is to endow synthetic foldamers, and eventually tyligomers, with the structural (and functional) specificity reminiscent of folding biopolymers, the theoretical models that describe these phenomena should be considered.

To rationally design a foldamer, it will be necessary to understand the properties of known foldamers, which are those secondary-structure domains of sequence-specific biopolymers that have been metabolically synthesized by living organisms, i.e., proteins, nucleic acids, and oligosaccharides. Each of these biopolymers derives its function from a conformationally well-defined folded state, which for proteins is usually called the “native state”.³⁰ The process of going from a large ensemble of extended conformations to this folded state is called the folding reaction,³⁵ and elucidating the general mechanism of this reaction involves the identification of the critical thermodynamic and kinetic parameters. It will then be instructive to relate these parameters to the properties of unnatural synthetic oligomers that can be adjusted by the synthetic chemist.

Three issues shared with the field of protein folding must be dealt with to make the design of foldamers possible: foldability, structure prediction (reverse engineering), and designability (forward engineering). The first of these refers to an individual chain’s ability to fold to a unique structure or a set of closely related structures; a chain that does so efficiently is said to have a high foldability. The second issue deals with the *ab initio* determination of the folded state structure given the primary sequence structure. The third issue, designability, refers to the number of these chains that will fold to a particular structure of interest; a folded structure that can be formed by many different, highly foldable sequences is said to have a high designability. By the very nature of their length, short oligomeric chains participate in relatively short-range intrachain contacts and as a result usually form structurally simple folded states that are straightforward to design. Longer chains are capable of folding into structures with very long-range interactions, making design more difficult because of the large number of potential contacts. The foldability of tyligomers has been treated analytically and by simulations of simple models. Although some progress has been made, the best methods for *ab initio* determination of a long sequence’s folded structure have been worked out in essentially taxonomic ways for the most well-studied biopolymer, proteins.^{36,37} Designability has been investigated but only for very simple systems. The fundamental idea that emerges from these models is that some structures are much more designable than others.

1. The General Folding Problem

Consider an oligomer or polymer chain consisting of N monomer units, each having ω torsionally accessible conformations. The parameter ω is dependent on the rigidity of the chain backbone and is

equivalent to the number of minima on a Ramachandran-like surface for the backbone repeat unit. This chain has ω^N accessible conformations, neglecting those conformations that are inaccessible as a consequence of the chain folding back upon itself in a sterically prohibitive manner (the so-called excluded-volume conformers). This simple calculation gives an overestimation of the total number of conformations but does accurately reflect the magnitude of the number of states. For polypeptides, ω has been determined to be between 2 and 3.³⁸ The exponential ω^N rapidly becomes very large with increasing chain length, to the point of being unimaginably large for a chain that would be capable of performing any sort of chemically or biologically significant function. As mentioned previously (Figure 2), oligomers may appear to be folded but in fact lack a folding reaction because ω is roughly equal to 1. Such oligomers have very few minima on their overall potential energy surface, since ω^N is very small for all values of N .

For an oligomer to populate a small subset of the ω^N conformations, this folded state, **F**, must have an energy that is much lower than the unfolded state, **U**. This must be the case if the lowest energy conformations are able to dominate the equilibrium mixture of conformers. The thermodynamics of the folding reaction are controlled by two main factors. The unfolded state must lose the *conformational entropy* present in its much larger conformational ensemble in order to realize the *enthalpic gain* present in the folded state. Multistranded systems are more complex since they must also lose some translational and rotational entropy upon association as well as chain conformational entropy. Yet, their thermodynamics are similar. The thermodynamic properties observed in biological folding reactions can be reproduced by a simple model having a single folded structure separated from **U** by an energy gap, illustrated in more detail below. To reach its lowest energy state, an oligomer will have to maximize its favorable energetic interactions and minimize those that are unfavorable, including both intrachain and chain-solvent interactions. The existence of an optimized set of unfavorable and favorable contacts in the folded state has been called the "minimally frustrated" state.³⁹

Noncovalent interactions involve much weaker and reversible interactions than covalent linkages, which allows for the exploration of many chain conformations during the folding reaction. The net strength of the nonadjacent contacts that determine the thermodynamics of folding are essentially the differences between the strengths of the chain-chain and the solvent-chain interactions. Undoubtedly, if solvent-chain contacts are stronger than chain-chain contacts, the molecule will not fold; such is the case in denaturing solvents. A subtle balance then exists in solvent-foldamer interactions; the solvent must solvate the molecule without competing for nonadjacent contacts while providing the chain with an environment in which to undergo the folding reaction.

The formation of unique, folded structures requires the presence of favorable nonadjacent chain-chain

contacts or unfavorable chain-solvent forces. For oligomers containing residues that are poorly solvated, collapse to a set of compact conformations can occur before the folded state is populated. In a protein, the minimization of the solvophobic force between apolar residues and polar solvent, namely, water, lowers the free energy of the protein-solvent system and is the primary driving force for collapse.^{40,41} This collapse minimizes the unfavorable solvation interactions and maximizes whatever favorable intrachain interactions exist, typically involving electrostatic and van der Waals forces. There is usually a gain in entropy for the solvent, since a higher degree of solvent ordering around the chain segment is required to solvate solvophobic segments than would be required to solvate solvophilic segments. The solvophobic collapse is then caused by a free energy gradient—having both entropic and enthalpic origins—toward states whose structures have a minimum of solvophobic segment-solvent contacts.

In the absence of any bias toward an energetically preferred folded state, this collapse will result in a random ensemble of compact conformations. For a chain that is able to fold reliably to a single folded state, the mechanism of folding is essentially a question of how the system loses entropy en route to the folded state. Two mechanisms of efficient overall entropy loss can be imagined. Initial collapse to the ensemble of compact conformations could be followed by a search through that ensemble to find the folded state or the collapse could take place concurrently with the formation of folded structure. Both types of behavior are observed for real biopolymers,⁴² and a general picture of oligomer folding must take both scenarios into account.

Especially for long chains capable of tertiary structure formation, it should also be noted that not every sequence that has a nondegenerate global minimum spontaneously folds to a unique state. A parallel can be drawn between the folding process and the condensation of individual molecules during crystallization or the condensation of atoms to form clusters. Just as there are some solid materials that crystallize quite efficiently, there are those that do not relax to their global thermodynamic minimum but form glasses instead.^{43,44} These glasses are formed when the entropy loss occurs faster than the loss of energy or equivalently when the barriers to interconversion between different conformations begin to dominate the kinetics of relaxation. Likewise, well-designed tylogomers efficiently find their folded state, while most random sequences do not fold to a unique structure but rather merely collapse to a 'molten globule' state or a unimolecular glass.

What then is required of a chain to fold reliably? Does the chain have a minimum energy state that is much lower in energy than the rest of the unfolded conformations **U**? If so, is this folded state thermodynamically accessible from **U** at temperatures and other conditions that allow characterization and perhaps function? For longer chains capable of many more contacts and potentially tertiary structure, is this transition kinetically accessible? Beyond predicting the existence of a folding reaction, what do the

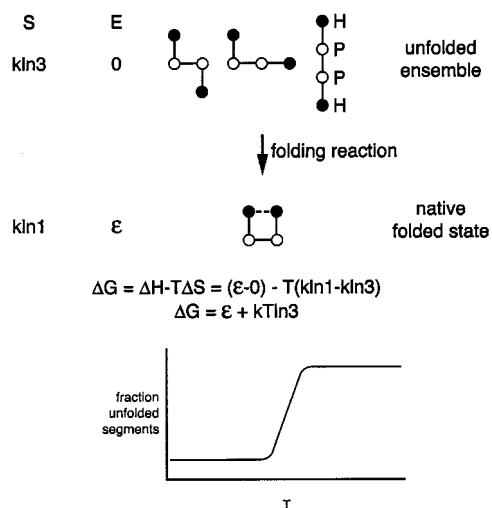


Figure 3. 2-D lattice tetramer toy model. Black circles represent solvophobic repeat units (H) and open circles polar repeat units (P). The sigmoidal plot shows the fraction of folded molecules as a function of temperature.

folded structures look like? Prediction of structure from sequence and prediction of sequence from structure are currently difficult for much studied polypeptides, let alone for any arbitrary monomer type that may be of interest to the foldamer chemist. Insight into these questions has been provided by simplified folding models.

a. Lattice Models of Folding. Minimalist models of biopolymers have been used for many years to analyze the general mechanism of folding and have proved fruitful toward understanding the folding mechanisms of proteins. These models provide computational accessibility, facile visualization, and easy conceptualization of the folding reactions known for proteins. Since the models do not rely on any properties specific to polypeptides, they are useful to chemists designing nonbiological folding systems. Go and co-workers⁴⁵ developed a widely used model that consists of a chain of different residue types that are constrained to the points of a lattice. Nonadjacent interactions are accounted for by assigning energies to neighboring lattice points occupied by residues that are not adjacent in the sequence.

Varying degrees of heterogeneity can be modeled by including any number of residue types and assigning energy values to the different pairs of neighboring nonbonded residues. In the simplest version of the model (the so-called HP model) a two-letter alphabet is employed, where H represents a solvophobic monomer and P represents a polar, or solvophilic, residue. The choice of a two-letter code reflects and models the importance of the solvophobic collapse of proteins as a key step in the folding process. Lattices with 2-D square, 3-D cubic, and even 2-D hexagonal geometries have been employed by different groups; some of this work will be described in later sections. An excellent review of these models by Chan and Dill⁴⁶ describes the picture they have provided of biopolymer folding.

Consider the tetramer toy model (TTM),⁴⁶ which is a 2-D square lattice chain consisting of two types of monomers, H and P (Figure 3). This is perhaps the simplest model that still captures many of the

key features of the folding reaction. A favorable interaction of magnitude ϵ exists between neighboring nonbonded H monomers. The exact nature of this interaction need not be defined to demonstrate the concepts involved. There are four possible conformations, one of which has energy ϵ lower than the other three (Figure 3). The three unfolded conformations make up the unfolded ensemble, and the single collapsed structure is the folded state. Note that there are fewer than ω^N (3^4) conformations for this system. This number is not reduced by excluded volume effects but by symmetry and the fact that only nonterminal monomer units have ω available conformations. Much of the thermodynamics of simple foldamers can be predicted by this model.

b. Thermodynamics of Folding. The size of the unfolded ensemble and the large number of potential folding pathways connecting this ensemble to the folded state suggest a statistical approach to the problem of folding. The thermodynamics of the folding reaction can be examined using statistical mechanics. This requires evaluating the partition function Z , which is given by eq 1 where $n(E)$ is the number of states that have an energy of E , and kT refers to the product of Boltzmann's constant and the temperature. The partition function is the Boltzmann-weighted sum of all the states, which for the TTM is given by the last term of eq 1.

$$Z = \sum_i e^{-E_i/kT} = \sum n(E) e^{-E/kT} = 3 + e^{-\epsilon/kT} \quad (1)$$

The fractions of the population in the unfolded and folded states at equilibrium for the TTM are given by eq 2, and the free energy of folding is given by eq 3 (the last term is specific to the TTM).

$$P(F) = \frac{e^{-\epsilon/kT}}{3 + e^{-\epsilon/kT}} \quad P(U) = \frac{3}{3 + e^{-\epsilon/kT}} \quad (2)$$

$$\Delta G_{\text{folding}} = -kT \ln K_{\text{eq}} = -kT \ln \left(\frac{P(F)}{P(U)} \right) = \epsilon + kT \ln 3 \quad (3)$$

Alternatively, the free energy of folding can be derived by considering the ΔH and ΔS of the reaction. The enthalpy change is clearly ϵ . The loss of entropy can be calculated by taking the sum of the loss of entropy of each chain segment. As each segment has ω conformations available, the sum of the entropy lost over the whole N -long chain is approximately $-k \ln(\omega^N)$ or $-kN \ln \omega$. At constant pressure and volume, it then follows that the free energy change is given by eq 4.

$$\Delta G = \Delta H - T\Delta S$$

$$\Delta G = \epsilon + kTN \ln \omega \quad (4)$$

It should be noted that this formulation has been used to experimentally estimate the entropy lost per chain segment and thus the average number of conformations available to each residue. Eq 4 suggests that there exists a folding temperature at which the population is evenly divided between

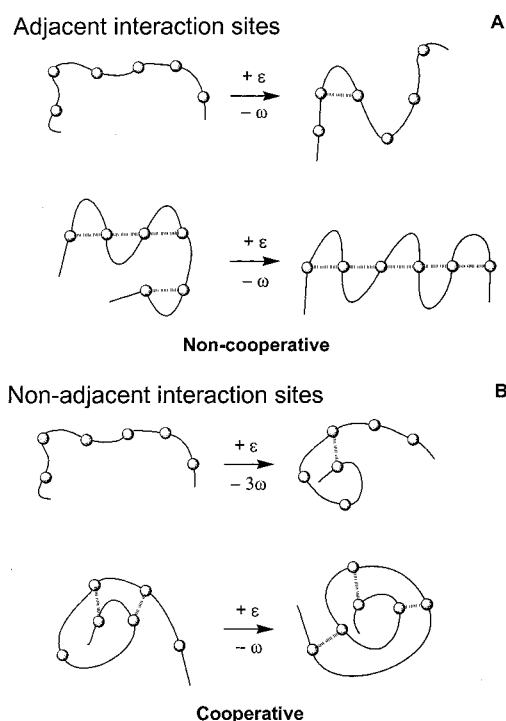


Figure 4. Origin of cooperativity. (A) Formation of a "trivial sheet", and (B) formation of a "trivial helix." Enthalpy change is shown above each reaction arrow and entropy change below. Trivial sheets do not require nucleation.

unfolded and folded states or at which $\Delta G = 0$, called the folding (or melting) temperature (eq 5).

$$T_{\text{fold}} = \frac{-\epsilon}{kN \ln \omega} \quad (5)$$

Thus, the TTM free energy of folding becomes negative at a temperature where $kT \ln 3$, the entropy of the chain lost during folding, equals the enthalpic gain of folding, the energy gap between the folded state and all other states. A plot of the fraction of the population that is in the unfolded state as a function of temperature shows a sigmoidal curve that is indicative of the cooperative nature of this transition (Figure 3). Although the very term indicates the cooperation of two or more interactions, the transition of this small single-interaction system is cooperative in the sense that the system has a tendency to be either completely unfolded or completely folded. Such transitions are observed for biopolymers, especially small, rapidly folding globular proteins.⁴⁷

Cooperativity cannot be achieved for systems that fold exclusively from noncovalent interactions between repeat units held adjacent by covalent bonds or more specifically interacting sites held adjacent by covalent bonds. Such chains fold to "trivial sheets". Conformations that result exclusively from adjacent interacting sites such as that schematically depicted in Figure 4A will not exhibit cooperative folding. As the trivial sheet folds, the ΔH and ΔS of each contact formation is the same. In other words, making the last contact is no easier than making the first. The situation for nonadjacent interacting sites is different (Figure 4B). Folded states stabilized by nonadjacent interacting sites can exhibit cooperativity. For the

model system here, forming the last contact is easier than forming the first. For simplicity throughout the rest of the review, "nonadjacent interacting sites" will be referred to as simply "nonadjacent repeat units", since for many foldamers each repeat unit has the potential to form a favorable chain-chain interaction.

The simple TTM model captures some of the essential features of the folding reaction and a key requirement of the folding system, namely, the large energy gap between the folded and unfolded states. Notice that the larger (and more negative) the value of ϵ , the more negative the free energy of folding will be. More detailed studies of a 27-mer on a 3-D lattice led Sali et al.⁴⁸ to propose that this energy gap was the definitive parameter for determining foldability. Again, further considerations of the kinetics involved in tyligomer folding suggest that this parameter is necessary but not sufficient to determine general foldability.

This is clearly only a gross view of the folding reaction, which despite its complexity is just the process of going from a large number of relatively high-energy conformers to a very small number of low-energy conformers. This model assumes that each state has equal accessibility from every other, implying that the kinetic barriers between each of the states are equal. Further consideration of the kinetics of this model is described below and obviates the need for a more complex description.

Given the requirement of a large energy gap, it then becomes important to determine the structure of the global minimum energy conformation and if its energy is sufficiently lower than the unfolded ensemble to be highly populated under some set of environmental conditions. The design of any foldamer will have to begin with the answer to these questions, which may be provided by intuition or by various computational techniques that can determine the global minimum energy structure efficiently.

c. Folding Reaction Free Energy Surfaces.

The folding reaction, in which the members of the unfolded ensemble converge to the folded state ensemble, is difficult to describe in the detail usually afforded to small molecule reactions. The reactant, product, and transition structures in small molecule reactions are often unique, structurally defined points in a space defined by the $3n - 6$ degrees of molecular freedom, where n is the number of atoms in the system. Because of the relatively small number of relevant structural parameters usually involved for small molecules, the potential energy can be represented as a function of those parameters—a potential energy surface (PES). Given a complete description of the potential energy surface along the degrees of freedom relevant to the reaction, the kinetics and thermodynamics of the reaction, and indeed its mechanism, are described by the set of trajectories along that surface connecting the reactant and product. The average path of these trajectories then suggests a reaction progress variable known as the reaction coordinate.

Such an analysis is impractical, indeed impossible, for the folding reaction because many more degrees of freedom are involved and because the folding

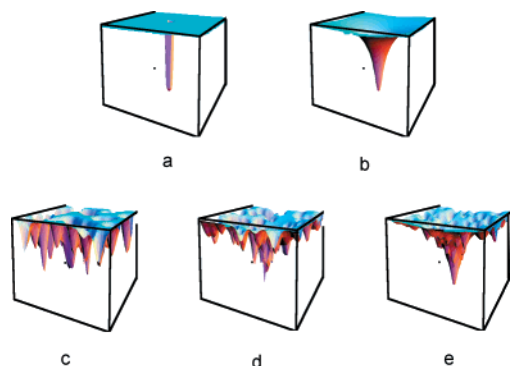


Figure 5. Free energy surfaces or “landscapes”. (a) The “golf-course” energy landscape, (b) the smooth funnel, and (c–e) rugged surfaces where c has no energy gap and e has a large energy gap.

reaction generally involves reactants, transition states, and products that are not single, well-defined structures. It is therefore much more difficult to define a reaction coordinate in terms of the internal coordinates of the chain. The situation is also more complex because a very large number of trajectories connect the many members of the unfolded ensemble with the folded state, often through an ensemble of transition structures. Because of these extra degrees of freedom in the reactant and transition-state ensembles, consideration must be given to the system's entropy, which is comparatively unimportant or easily deconvoluted in small molecule reactions. In addition, the role of the solvent is often significant in determining the energy of any given conformation; the exact structure of the solvent shell constitutes another large number of degrees of freedom, or structural variations, that must be taken into account.

For these reasons, the folding reaction is often described with a free energy surface (FES), or landscape. The FES is analogous to the PES drawn for small molecule reactions but includes a summation over the extra degrees of freedom, including those of the solvent, as a function of the internal coordinates of the oligomer. The effect of this summation at each point on the surface is the inclusion of the entropy at that point; the more degrees of freedom at that point, the larger the number of states at that point and the larger the entropy. Usually, the enthalpy and the entropy are evaluated over one or more progress variables, which are usually measures of structural similarity to the folded state, such as the degree of collapse or the fraction of interresidue ‘contacts’ that are present in the folded structure. Since FESs incorporate entropy, their shapes are very temperature dependent, unlike their PES counterparts.

Some examples of representative FESs are shown in Figure 5, including that for the lattice model (Figure 5a) examined above. This particular surface, consisting of a single, low-energy conformer distinct from the ensemble of nearly isoenergetic unfolded conformers is often referred to as the ‘golf-course’ landscape. If a more realistic description is used in which the unfolded conformers start taking on different energies, barriers between different minima

can become large enough such that examination of the kinetics across this surface is required.

Each accessible conformation lies at the bottom of local vibrational and torsional energy wells, and their energies will also be dependent on nonadjacent interactions such as electrostatic and van der Waals forces between nonneighboring chain segments and side chains. These nonadjacent interactions can be both energetically favorable and unfavorable. The folded state of a well-designed foldamer minimizes the unfavorable interactions and maximizes the favorable ones. Because small changes in local structural parameters, such as rotation around a bond, can bring previously separated parts of the molecule together, thereby introducing many new contact energies, the FES can be very rugged. This is not usually the case for small homooligomeric systems because of the relatively small number (compared to a biopolymer) of random intrachain interactions that generate the ruggedness. These systems have FESs such as that in Figure 5b, a smooth funnel. Longer chains, however, are capable of great ruggedness. Figure 5c depicts a completely rugged landscape with no single conformation dominating the thermal equilibrium mixture. Such rugged surfaces are typical of random heteropolymers, and an extremely poorly designed polypeptide would be expected to exhibit such an FES. Figure 5d shows a very rugged funnel, while Figure 5e depicts a classical rugged funnel typical of good folders having tertiary structure, such as globular proteins. Those systems having FESs such as Figure 5d might be expected to fold but more slowly than those having funnels such as Figure 5e since the greater depth of nonnative wells slows eventual escape to the folded state.

d. Kinetics of Folding. While the thermodynamics of some simple proteins and secondary structure domains are well modeled by the simple picture described above, the folding kinetics of chains can be more complex. The simple golf-course model (Figure 5a) grossly overestimates the amount of time necessary to reach the folded state, and this overestimation is often referred to as Levinthal's paradox.⁴⁹ For example, a protein containing 100 residues, each able to access only two local minima on the Ramachandran plot, has 2^{100} conformations. If it only took a picosecond to interconvert between conformers, it would take 10^{11} years to randomly search through all 2^{100} conformations before the system arrived at the folded state. This argument has been called a paradox because a concrete mathematical analysis gives an obviously erroneous result; the majority of globular proteins that exhibit simple two-state behavior fold on the timescale of a second or less.⁴⁷ However, the initial assumption that all 2^{100} conformers are equally thermally weighted is unfounded, despite the fitness of the model in describing the thermodynamics of folding. To accurately model the kinetics then, the loss of entropy that accompanies folding must be dealt with. Clearly, the FES of a foldamer cannot be described by a golf-course landscape if it is to fold reliably in a way that reproduces observation. It also suggests that more is required than simply the existence of a large energy gap for

the folded structure if the system is to fold on a reasonable time scale.

It is conceivable that the unreasonably long search time predicted by Levinthal could be reduced by decreasing the number of conformations involved in the random search. Discarding the conformations whose chains fold back on themselves and are therefore sterically disallowed reduces the number of conformers from 10^{60} to 10^{43} for a 2-D square lattice 100-mer,^{50,51} a number that still requires an unrealistic amount of search time.⁵²

If, however, the number of compact structures (those present after a solvophobic collapse) is considered, the size of the search drops further to 10^{17} conformers,⁵³ a much smaller number but one that is still too large for a truly random search to approximate real folding times. While the collapsed ensemble is still too large, it should be noted that the process of collapse reduces both the entropy and enthalpy of the system. This suggests a possible solution to Levinthal's paradox. Certain FESs can be described as funnels in which the energy generally decreases as the structure more closely resembles that of the folded state. Just as importantly, this lowering of the energy is accompanied by a concurrent loss of entropy. That is, the width of the funnel narrows and the energy goes down as the folded state is approached. Tyligomers must have FESs that are funnel-like, such that the overall free energy gradient favors movement of the system toward the folded state from any starting geometry or point of the multidimensional FES.

e. The Funnel Picture. For those systems with FESs resembling that in Figure 5c, that is, rugged surfaces with many deep minima and no single dominant folded state, any cooling will simply result in relaxation to the nearest well. If the temperature becomes low enough, the interconversion between these traps, or other deep minima structurally distinct from the folded state, will become very slow, even if one state is lower in energy than all the rest. Such conditions would lead to the observation of non-Arrhenius kinetics, as is observed for some polypeptides.⁵⁴ When this interconversion is slowed to the point that it is effectively nonexistent, a glass transition has taken place. At this point, it becomes very unlikely that the folding reaction, or indeed any further progress toward a global minimum structure, will proceed any further. Most folding biopolymers lie between the two extremes of the flat, rugged landscape and the smooth funnel, thereby exhibiting a range of thermodynamic and kinetic behaviors.

For systems with smooth funnel FESs such as that in Figure 5b, a cooling of the system will lead smoothly and rapidly to a relaxation to the bottom of the funnel. Such is the case for reliably folding helical oligomers. Again, small oligomers are more likely to have smooth funnels because shorter chains have fewer nonadjacent interactions that can contribute to ruggedness. The FES of an oligomer can be considered as a small section of a polymer's FES that immediately surrounds the folded state. Thus, the only ruggedness present in the oligomer FES will be that present near the folded state. Additionally,

the energy gap is already enhanced by the high symmetry of secondary structures. For instance, helices offer a minimally frustrated way of packing side chains to avoid unfavorable van der Waals forces while maximizing some favorable intrachain contacts, often hydrogen bonds. Small helices and sheets are thus well-designed folders, because of the smoothness of the FES and their energy gaps. Their thermodynamics are very similar to those for the golf-course model, as reflected in the similarity in the overall topology of the two funnels.

2. Foldamers: Secondary Structure

Since many of the foldamers described in this review have helical folded structures, the FES as well as the thermodynamics and kinetics of folding to a helical geometry will be considered in some detail. It should be noted that sheets, having regions of segments of the same dihedral angles, are themselves helices or bundles of two or more interacting helices. As a result, the mechanism of sheet folding is related to that for helices. It involves potential cooperativity in two dimensions, both along the strand and between strands.^{55,56} As it is slightly more complicated, it will not be treated in detail.

a. Folding of Helices: Thermodynamics of the Helix-Coil Model. Since the FES that describes helix folding, the smooth funnel, is topographically similar to that of the golf-course landscape, it represents a cooperative transition. There exists one transition between the higher energy unfolded state and the lower energy folded state. The statistical thermodynamics of the helix-coil transition were first described by Zimm and Bragg⁵⁷ as a one-dimensional problem. Cooperative phase transitions can be described in terms of a nucleation/propagation model,⁵⁸ a description of which follows.

Consider an oligomer that forms a helix with N_i segments per turn, again with ω conformations available to each chain segment. If the favorable intrachain contacts each contribute an energy ϵ to the system (usually called ϵ_H because a hydrogen bond is often responsible), the change in entropy and energy for each step of helix formation can be considered. Since each conformational choice along the chain—helical or nonhelical—is dependent only on the immediately previous step, the problem is essentially one-dimensional. That is, the free energy change of a residue as it progresses from a random-coil geometry to that of the helix is dependent only on the state of its neighbors. Figure 6 shows ΔH (ΔE) and ΔS for the coil-to-helix change for a segment adjacent to a helical segment and to a coil segment. Each situation involves the loss of $k_B \ln(\omega)$ conformational entropy. Only when $N_i + 1$ adjacent helix segments are formed does the system gain the ϵ interaction energy. Thus, for the first N_i coil-to-helix steps, there is a total loss of entropy of $N_i k_B \ln(\omega)$ but no gain in energy; this is called the nucleation of helix formation. Once this helix nucleation has occurred, each subsequent conversion of a segment from coil to helix geometry, i.e., propagation, involves the loss of $k_B \ln(\omega)$ entropy and a gain of energy ϵ .

The free energy change in going from a random coil to a helix where n is the number of segments in the

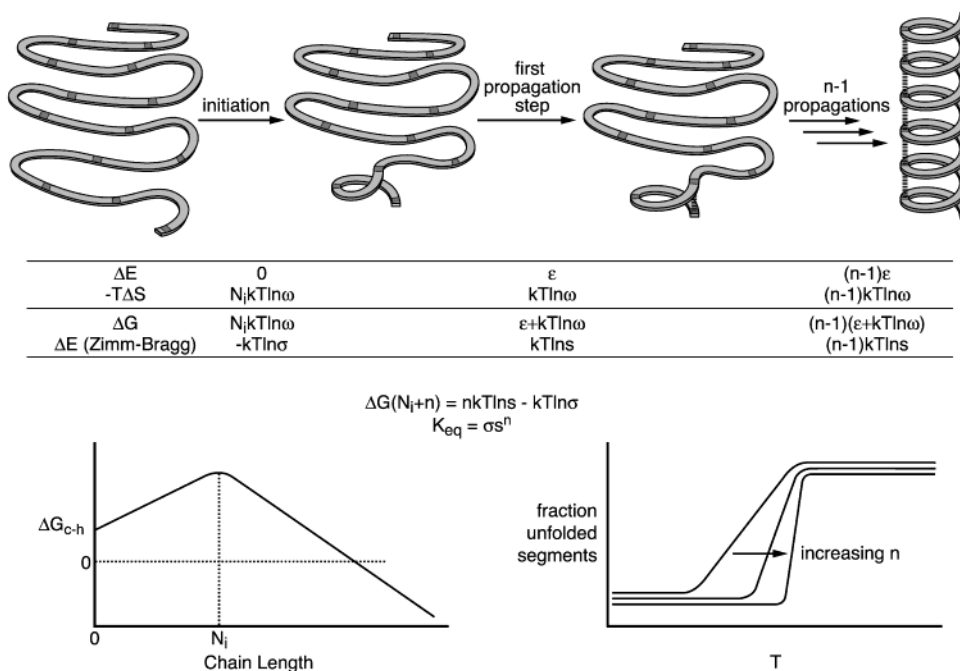


Figure 6. Helix–coil transition. (top) The initiation and propagation steps and their attendant changes in enthalpy and entropy. (lower left) The free energy of folding as a function of chain length, and (lower right) the sharpness of the transition as a function of chain length.

helix minus the number required to form the first turn is given by eq 6 and is plotted in the lower left of Figure 5.

$$\Delta G_n = \Delta G_{\text{nuc}} + n(\Delta G_{\text{prop}}) = N_i kT \ln \omega + n(kT \ln \omega - \epsilon) \quad (6)$$

There is a free energy cost upon folding until the chain reaches a length at which the enthalpic gain of the intrachain interactions outweighs the entropic cost of constraining the chain in the folded conformation. It can then be seen that a cooperative transition takes place when the change in free energy between helix and coil states becomes negative at the folding temperature, T_f (eq 7). The sharpness of this transition is dependent on the number of residues required for initiation, as can be seen from eq 2 and is shown in the lower right of Figure 6.

$$T_f = \frac{n\epsilon}{(N_i + n)k \ln \omega} \quad (7)$$

These quantities are often cast in the form of an equilibrium constant, with σ and s representing the equilibrium constants for the nucleation and propagation steps, respectively (eq 8)

$$K_{\text{eq}} = e^{-\Delta G/kT} = e^{-N_i \ln \omega} (e^{\epsilon/kT} e^{-\ln \omega})^n = \sigma s^n \quad (8)$$

where $\sigma = \omega^{-N_i}$ and $s = e^{\epsilon/kT} \omega^{-1}$.

Zimm and Bragg showed that the fraction of segments in a helical conformation exhibits a sharp cooperative transition as s is increased, which is equivalent to increasing the interaction energy ϵ or decreasing the temperature. The interaction energy is designed into the system based on the chemical

structure of the segments, but since it is a free energy it may also be changed by the environmental factors over which the free energy is evaluated. For instance, if the interaction arises from a solvophobic force, it can be made stronger by making the solvent more polar. Likewise, a hydrogen bond interaction can be made stronger by making the solvent less polar or weaker by adding competitive, protic solvents. Changing the net strength of the intrachain interactions shifts the folding temperature; this is the principal underlying solvent denaturation experiments. Rather than changing the temperature while keeping ϵ constant, the reverse may be done in order to see the transition.

Foldamers that adopt helical conformations are reliable folders because they lie on a smooth funnel FES. The folding to these highly symmetrical structures can be described by the two parameters ϵ and ω , both of which can be controlled by the foldamer chemist in the design of the oligomer.

b. Folding of Helices: Kinetics. Since helices have experimentally been shown to fold on a time scale in the milliseconds to microseconds,^{59,60} there do not seem to be serious kinetic issues that must be considered in their design. This is consistent with a smooth-funnel FES, with little ruggedness to slow the progress of the system down the funnel to the folded state. There is some evidence that the little ruggedness present does lead to the presence of folding intermediates for some helices,^{61,62} and in some cases the pathways between these intermediates can be enumerated,⁶³ but in general the folding should be rapid enough that (a) changes in the design will make only small differences in the absolute folding rates and (b) small helices with a thermodynamic propensity to fold will do so rapidly enough to demonstrate ideal foldamer properties.

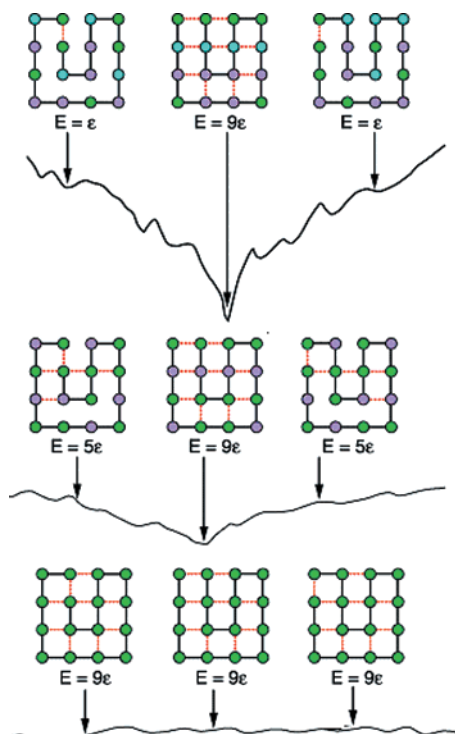


Figure 7. Effect of heterogeneity on energy gap. Homopolymers have degenerate folded structures, but increased heterogeneity leads to a larger energy gap between the lowest energy structure and the rest. (Adapted from ref 65.)

3. Tylligomers: Secondary and Tertiary Structure

This review covers the topic of foldamers, those oligomers that can fold, but since it is a natural goal of this field to be able to design and construct larger, more complicated molecules capable of folding to a greater variety of more complex structures, the issues of design of these tylligomers should be considered. Many of the aspects of folding are the same as those described above, but there are additional design issues that arise for tylligomers. Because such molecules have many more possible nonadjacent contacts and exponentially more conformations available, the FES can become much more rugged. There is also the need to construct heteropolymers of specific sequence to break the symmetry of the homopolymer.

a. Homopolymers vs Heteropolymers: Widening the Energy Gap. The high symmetry of helices is responsible for making them the lowest energy structures available to many of the short foldamers discussed below. Their existence belies the fact that homopolymers do not, in general, have unique low-energy folded states. This can be illustrated with a 2-D square lattice model in Figure 7. All of the compact homooligomers have the same energy. One way to reduce this degeneracy, and the way that has been employed by nature in the case of proteins, is to use several different residues in the chain. These different residues can have different interaction energies with each other and thus reduce the symmetry of the FES. For instance, using two different monomers in the oligomer, both of which interact with alike monomers much more strongly than with dissimilar monomers, will lower the relative energy

of some conformations as in Figure 7. The use of a three-letter code provides an even greater energy difference; the more information-rich the sequence, the more information-rich the FES.

While proteins are able to form very specific structures and perform very specific functions by employing 20 different types of monomers, or a 20-letter code, it is of great interest whether such a large number, and indeed such a large and complex set of sequences, is necessary for such specificity. Since the design and perhaps even synthesis of a foldamer with specific structure and function will be simpler with a smaller set of structural units, it would be advantageous to determine how small a set of these monomers can give rise to specificity of structure and, ideally, function.

Screening of combinatorial libraries of simplified proteins has recently revealed that as few as five amino acids can be necessary to generate a specific structure.⁶⁴ These same experiments suggested that when only three different residues are included, reliable folders are not made. The folding funnel can be used to interpret these results, as demonstrated in Figure 7.⁶⁵ Assuming a model in which interactions between similar residues are more stabilizing than those between different residues, it can easily be seen how a folded state with a large energy gap can be designed.

Simulations on a 2-D square lattice with a two-letter alphabet have been performed to determine what fraction of possible sequences have a unique ground state and how this fraction changes as a function of the number of residue types along the chain. Chan and Dill⁶⁶ enumerated all of the conformations of each possible HP heteropolymer of length less than 18, while Thirumalai and Camacho⁵³ did the same for $N < 23$. They reported that the average number of lowest energy conformations for a chain of length N converged to approximately 13 as N increased. They also reported that the average number of lowest energy structures had a minimum when the fraction of nonpolar monomers in the chain was around 0.6, which is approximately the same ratio as that found in proteins.⁶⁷ Chan and Dill earlier reported similar results and further calculated the percentage of sequences with unique ground states to be between 2.1% and 2.6% for sequences with $N = 12$ to $N = 17$. While they were not able to extrapolate this percentage to longer chains, they did estimate that the fraction of 100-mer sequences with a ground-state degeneracy of 5 or less to be on the order of 10^{-3} to 10^{-5} . Both of these studies suggest that even a very simple set of monomers may have a very good chance of exhibiting protein-like behavior by virtue of having a natively unique ground state.

Chan and Dill also evaluated the percentage of residues that existed in a secondary structure, either helix-like, sheet-like, or turn-like. They found that an average of ca. 40% of all monomers were part of a secondary structure over all conformations, a number that is in good agreement with the experimental observation that random heteropolypeptides exhibit 46% helicity, as measured by circular dichroism.⁶⁸ This percentage increased to over 60% for

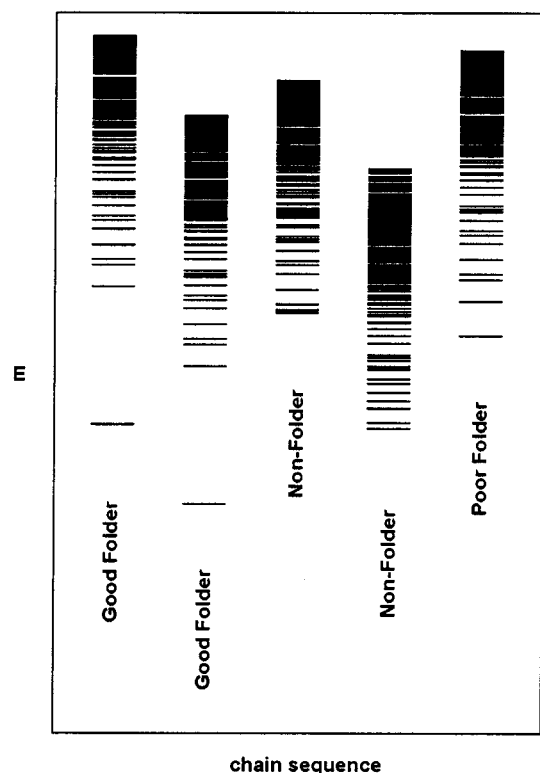


Figure 8. Energy spectra (density of states) for several 3-D 27-mer HP heteropolymers and the fraction of MC runs which resulted in folding. Larger energy gaps lead to greater foldability. (Adapted from ref 48.)

compact homopolymer conformations⁶⁹ and suggests that the formation of highly symmetric secondary structures is not sequence-specific nor only a property of reliable folders. The existence of these locally organized low-energy structures suggests a self-similarity of the FES that enhances its funnel-like shape even if helices or sheets that are not present in the folded state are formed during folding.

Similar studies were performed on 3-D 27-mer HP heteropolymers,⁴⁸ but because of the much larger number of possible conformations, the sequence space was sampled randomly. The likelihood of folding for several randomly generated sequences was evaluated by measuring the number of random Monte Carlo steps required for the sequence to find the folded state.^{70–72} Figure 8 represents the energy spectra of several of these sequences and the folding efficiency, which was measured as the fraction of MC runs that led to folding. Each individual line represents an individual conformation and its height the energy of that structure. Degeneracy of conformations is represented by the dense packing of states, which appear as regions of solid continuum. It can be seen that although each of the sequences had a nondegenerate ground state, only those with a large energy gap were reliable folders. Again, this indicates that a large energy gap, which will be referred to below as δE_s , between the native state and the rest of the non-native states is at least necessary if a chain is to fold.

b. The REM Analysis of the Rugged Funnel. It has been noted that the stability gap alone does not indicate whether a polymer will fold. If the barriers to interconversion between the states shown

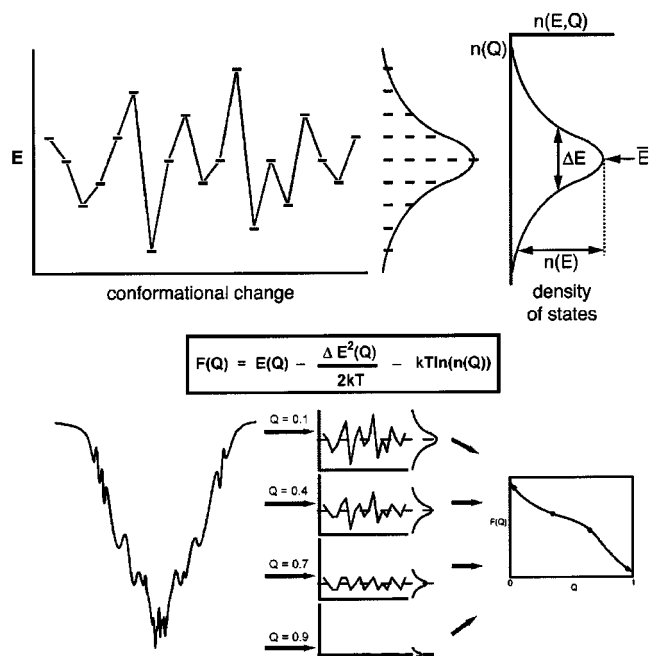


Figure 9. REM analysis of the rugged funnel. Free energy diagrams can be generated by examining the density of states at every level of the funnel.

in Figure 8 are taken into account, it is possible to imagine a system that becomes trapped in a non-native state, below the glass transition temperature, even if the folded state lies far below the trap. The kinetics and thermodynamics of rugged folding funnels have been analyzed by Wolynes and co-workers⁷³ using a random energy model (REM) developed by Derrida.⁷⁴ The large number of states and pathways between the states complicates a complete, explicit analysis of the free energy surface but is well-suited to a statistical description.

The key assumption of the generalized random energy model is that the energies of any two conformations are independent of each other. This leads to a distribution of states that can be described as a Gaussian function. This approximation can be made less stringent by assuming that there will be some correlation of energies, which will be dependent on the proximity of the two conformations to the folded structure. This similarity measure, called Q , is a function of certain internal geometrical coordinates of the foldamer that describe the folded state, such as those between nonbonded residues that become proximate after folding. The rugged funnel, shown in Figure 5e, is intermediate between the completely rugged surface, shown in Figure 5c, and the smooth funnel, shown in Figure 5b. The parameter Q on the rugged funnel roughly indicates the energy of a conformation arising from the smooth funnel component. The closer Q is to 1, the more the conformation resembles the folded state and the lower the energy will be in general. Within each strata of Q on the funnel, however, the energy level distribution will be given by a Gaussian function, in that it represents the smooth funnel component of the FES (Figure 9). This density of states, or the probability that a given state will have a structure parameter Q and an energy E , is given by eq 9. Here $\overline{E(Q)}$ is the average

energy of all structures having a structure parameter of Q . $\Delta E^2(Q)$ corresponds to the width of the Gaussian distribution for all of the structures at Q ; this value is a measure of the roughness of a section of the FES that contains all of the structures at Q .

$$P(Q, E) = \frac{1}{\sqrt{2\pi\Delta E^2(Q)}} \exp\left\{-\frac{[E - \overline{E(Q)}]^2}{2\Delta E^2(Q)}\right\} \quad (9)$$

To describe the thermodynamics, the free energy can be evaluated. Assuming that the folding reaction is taking place at constant temperature and pressure, the free energy is given by eq 10, where E_{mp} is the thermally most probable energy and S the entropy.

$$F(Q) = E_{mp}(Q) - TS(E_{mp}, Q) \quad (10)$$

The entropy can be calculated by taking the logarithm of the amplitude of the density of states (the height of the Gaussian distribution). The energy can then be evaluated by determining the value at which the density of states function reaches its maximum value.

Substitution and simplification gives the following expression for the free energy of the system as a function of Q in terms of the average energy along the funnel (equivalent to its slope) and the ruggedness or width of the Gaussian probability distributions at each strata of the funnel (eq 11). The derivation of this result is depicted graphically in Figure 9.

$$F(Q) = \overline{E}(Q) - \frac{\Delta E^2(Q)}{2kT} - TS_0(Q) \quad (11)$$

A significant feature of this model is that it predicts a glass transition, that is, a point below which the entropy of the system goes to zero. The entropic part of the free energy expressed in eq 11 is clearly given by the last two terms divided by the temperature (eq 12).

$$S(Q) = S_0(Q) - \frac{\Delta E^2(Q)}{2kT^2} \quad (12)$$

The temperature at which the entropy becomes zero and therefore at which no other structures are kinetically accessible is then given by eq 13 and is called the glass transition temperature.

$$T_g(Q) = \sqrt{\frac{\Delta E^2(Q)}{2kS_0(Q)}} \quad (13)$$

Below this temperature, the system becomes trapped as the barriers to interconversion between states become thermodynamically insurmountable. The larger the roughness of the surface, represented by the width of the Gaussian that describes the energy distribution function, the higher this T_g occurs. Thus, the roughness of the surface can be identified as another parameter that determines the foldability of a chain because it is this roughness that determines how likely the chain is to become frozen

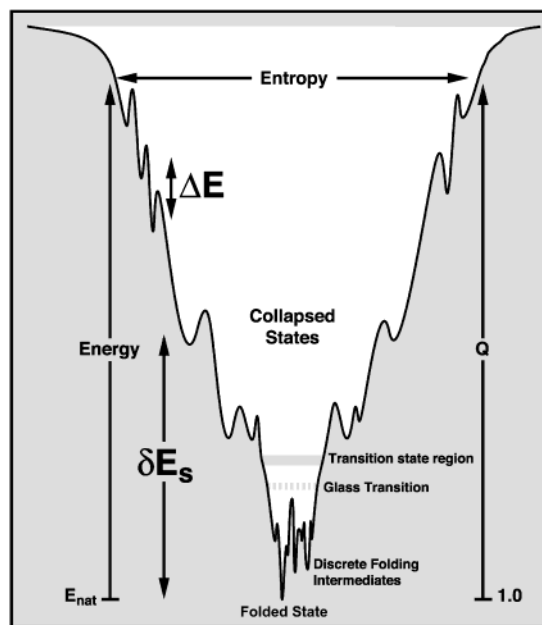


Figure 10. Folding funnel.

into a nonnative state before it can reach the global minimum. While T_g is the primary kinetic parameter of this analysis, T_f , or the folding temperature, is the primary thermodynamic one and has the same meaning and derivation as that discussed previously. It can be shown that $T_f \approx \delta E_s/S_0$, which describes the slope of the folding funnel in terms of the energy gap between the folded and unfolded populations, δE_s . As would be expected, the larger the energy gap, the higher the folding temperature will be.

These parameters can be illustrated on a more detailed schematic of the folding funnel (Figure 10). The height of the funnel FES corresponds not only to the energy but also approximately to Q , the folding reaction coordinate. These are E_{nat} (the energy of the folded state) and 1 at the bottom of the funnel, respectively. The width of the funnel is approximately the entropy or the density of states at that level of the funnel. As the system progresses down the funnel, it has the possibility of passing through a collapsed state, a transition state, and a glass transition. The degree of ruggedness also changes as the system progresses down the funnel.

It has been shown by Wolynes and co-workers^{75,76} that maximizing the ratio of T_f to T_g produces the most reliable folders, and this ratio is related to the ratio of the energy gap to the ruggedness (eq 14).

$$\frac{T_f}{T_g} \approx \frac{\delta E_s}{\Delta E} \sqrt{\frac{2k}{S_0}} \quad (14)$$

It should be noted that reducing the ruggedness measure $(\Delta E)^2$ to zero gives the same result as that obtained for the smooth funnel that models the folding of a helix. The possibility of another transition, the glass transition, reveals the complexity possible in the tylogomer folding mechanism. Tylogomers with particularly smooth FESs may never encounter this second-order phase transition and exhibit simple and cooperative Arrhenius kinetics. As the ruggedness is increased, the likelihood of encoun-

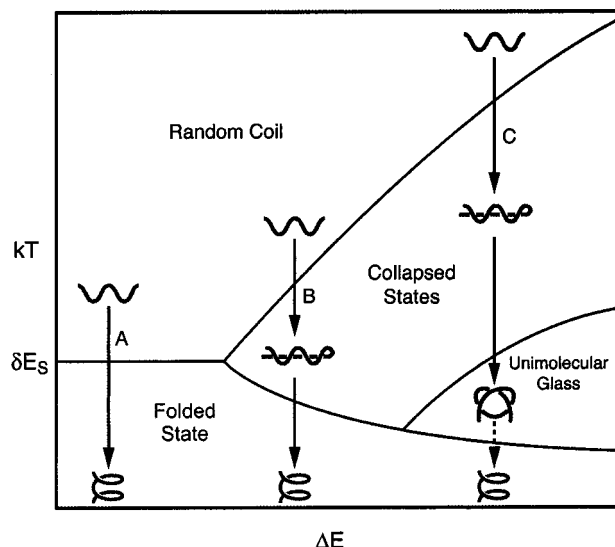


Figure 11. Phase diagram of foldamers. The ruggedness of the FES is ΔE . Small, two-state foldamers exhibit only a single cooperative transition (A). Tylligomers, both longer and having more rugged FESs, undergo a preliminary collapse transition which then folds to the folded state (B). Increasing the ruggedness further leads to a glass transition (C) where subsequent formation of the folded state may be extremely slow.

tering a second transition and complex dynamics increases. This is illustrated in the folding “phase diagram” (Figure 11), which has been generated by enumeration of a 2-D lattice model⁷⁷ and corroborated by other theoretical and experimental results. Along the x -axis is the ruggedness, and the y -axis represents the temperature. The smoothest funnels will undergo collapse and folded structure formation at the same time in a very cooperative process (pathway A), which is reminiscent of a two-state cooperative system. As the $(\Delta E)^2$ increases, a transition to the collapsed state may be observed (pathway B), followed by folding to the folded state. This collapse transition has been observed in homo-⁷⁸ and heteropolymer⁷⁹ lattice simulations. In both studies, the collapse transition was sometimes accompanied by folding fully to the folded state, especially when the intrachain contact energies were large. Of course, increasing these energies raises the folding temperature and in effect decreases the relative ruggedness. When the ruggedness is increased still further, the possibility of a glass transition (pathway C) exists.

A ratio of T_f/T_g of greater than 1 is required for a polymer to be a reliable foldamer, and this analysis provides some parameters that must be considered in the molecular design. Just as lattice simulations and simpler thermodynamic models suggested, maximizing the energy gap produces a more reliable folder. Minimizing the ruggedness to avoid the slowing of interconversion of conformers on the way down the funnel also gives a better folder. The last parameter, S_0 , is related only to the number of possible conformations available to the system. It is shown that the smaller this number, the better the folder will be. Thus, the conformational flexibility of each residue must be taken into account when designing a tylligomer and is possibly the most easily controlled of the parameters generated by the REM funnel

analysis. The readers are directed to excellent reviews^{39,80} of the folding funnel for further details.

4. Designing Folding Molecules: Toward Tylligomers

a. Designing Foldamers: Helices and Sheets.

The design of helical oligomers, then, is a fairly simple task, compared to the design of tertiary folds. Of course, any design must take into account the synthetic feasibility of the chain, and this is addressed in the next section. Since helices appear to fold on a very small time scale along a smooth funnel, an oligomer that folds to a helix or a small sheet (usually called a turn) must meet only thermodynamic criteria, namely, the δE_s and S_0 parameters discussed in the rugged funnel analysis above. Since the funnel is indeed smooth, we can consider the ruggedness ΔE for oligomeric systems to be negligible.

The simpler of these parameters is the conformational entropy, S_0 , which is a function of the chain length and conformational entropy of each chain segment. The chain length may be tuned by the synthetic chemist, either by the traditional methods available for polymerizations or by the synthesis of discrete oligomer lengths. As discussed above, the conformational entropy of the chain segments can be determined by a simple Ramachandran-like analysis of the segment’s potential energy surface. A greater number of conformations available to each segment will tend to reduce the foldability simply by increasing the conformational phase space through which the ‘search’ for the folded state takes place. In other words, increasing ω increases the entropy that must be lost to achieve folding, thereby lowering the folding temperature. Of course, lowering ω too far can result in raising the folding temperature to the point that the unfolded state will never be observed at relevant temperatures. This is problematic for foldamers whose function depends on the reversibility of folding.

Chemically, of course, the segments must be joined in such a way that a helix or a turn is at least a plausible sterically allowed structure among many nonordered conformations. Simple chemists’ intuition or molecular modeling should be adequate to determine this criterion. Second, the turns of the helix or the strand-to-strand contact must be stabilized by some interaction that is long range or not on adjacent monomer units. Several analyses have indicated that the energy gap δE_s must be maximized for a reliable folder, but how is this related to the actual physical parameters of oligomers? Larger intrachain interaction energies and greater heterogeneity of residues (and thus interaction energies) tend to maximize the energy gap, as does the minimization of geometrical frustrations arising from sterically unfavorable backbone or side-chain interactions in the folded state. (Adjacent contacts may result in noncooperativity.) The orientation and strength of these interactions is the key factor that will stabilize the folded state. The strength of the interactions may be difficult to predict since they will be dependent on extrinsic factors such as the solvent and may be enhanced or diminished by nonspecific, nondirectional forces in the molecule, such as the solvophobic force. It could be considered

that the stronger these interactions are, the “better” the foldamer would be. However, this may not be the case; one must always consider the strength of all of the interactions in the folded state relative to the entropy of the chain that is lost upon folding. Again, interactions that are too strong will lead to a structure that will never unfold. It should be noted that stronger interactions may be required for the folding of multistranded systems to overcome the greater entropy loss that must occur from bringing two noncovalently connected pieces of the foldamer together.

Ideally, to be able to observe a folding reaction, the entropy must be balanced with the enthalpy of the intrachain interactions over some reasonable temperature range that allows observation, characterization, and utilization of the two states.

b. Toward Designing Tyligomers. The analysis of the rugged funnel landscape indicates the properties the FES of a chain should have in order to be a reliable folder. Rational design of a foldable tyligomer, then, depends on being able to control not only the thermodynamic parameters discussed above, δE_s , and S_0 , but also the kinetic parameter, ΔE , or FES ruggedness.

It has been noted that while in general homopolymers do not exhibit unique ground-state structures, many of the homopolymers described in this review do exhibit structurally unique folded states reminiscent of small proteins or at least of highly symmetrical secondary substructures of protein segments. The apparent contradiction results from the symmetry of the folded conformations of these relatively short homopolymers and of the smoothness of their funnels. Just as atomic clusters exhibit magic numbers,⁸¹ that is, structures of certain sizes which possess a high symmetry exhibit larger than expected stabilities, so too do proteins. It has been found that certain numbers of residues⁸² and secondary structures⁸³ occur more frequently than others in the set of known proteins. There is no reason to suppose that the high symmetry of helices should not also reduce the degeneracy of homopolymers as well.^{84–86} This does point to the need for further heterogeneity in future tyligomers if less symmetric folded structures are to be realized. It also suggests that the inclusion of these symmetric domains in a complex tyligomer may result in a smoother, steeper funnel.⁸⁷ Nature has made full use of these symmetric domains in biopolymers, not only as structural motifs, but also as easily foldable, funneled domains in the overall folding funnel.^{88,89} While such secondary domains may not be necessary to ensure a foldable oligomer, they may provide a simplifying shortcut from the design perspective. Lattice model tertiary structures containing high helical content have been shown to be highly foldable.⁹⁰ Indeed, the *de novo* protein designs to date rely heavily on the presence of secondary structures.⁹¹ Lattice model studies have shown that strong short-range chain–chain interactions provide a large energy gap with cooperativity.^{92,93} On the other hand, tyligomer designers must also take care to include a sufficient number of longer range chain–chain interactions. Lattice model stud-

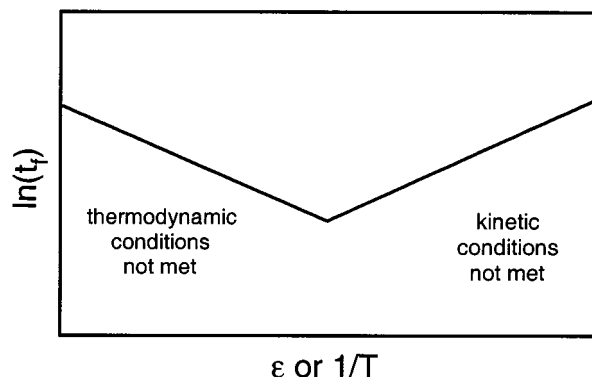


Figure 12. Non-Arrhenius folding kinetics. The folding time as a function of the intrachain interaction energy or equivalently temperature.

ies⁹⁴ indicate that longer range interactions speed up the folding reaction as well as make it more cooperative.⁹⁵

The heterogeneity of the chain can be controlled completely by discrete synthesis, and the strength of the intrachain interactions can be controlled by the choice of chemical moieties present in each monomer. It should be noted that increasing the strength of the interactions that hold the compact folded state together is equivalent to raising the folding temperature or lowering the ambient temperature. All of these serve to increase the thermodynamic likelihood of folding. However, it should also be noted that increasing the interaction magnitudes too much could lead to a decrease in the folding rate, even for homooligomers. This leads to a consideration of the ruggedness parameter, ΔE .²

Ruggedness is a property of the FES that should be minimized in a reliably folding tyligomer. If the favorable interaction energies that keep the chain in a compact conformation become too large, then interconversion among these compact states will become too slow. Deep energy wells will have large barriers to interconversion. In fact, the incorporation of secondary structures that are too strongly stabilized may increase the ruggedness and slow the folding rather than facilitate it.

Thus, increasing the magnitude of this intrachain interaction energy will potentially increase the energy gap by deepening the funnel, but it can also increase the ruggedness. A plot of the folding rate versus the interaction energy, or equivalently the temperature, has a shape such as that in Figure 12. This non-Arrhenius dependence of the rate on the temperature has been observed in experimental measurements of the folding rate⁹⁶ as well as several lattice simulations,^{97–99} where the rate measured by the number of MC steps before the simulation arrives at the folded state. The reason for this behavior is that at temperatures higher than ideal or interaction energies lower than ideal, folding is not favored enthalpically, whereas at temperatures lower than or interaction energies higher than ideal, folding is slow because of slow passage over the barriers between local minima.

c. Predicting Foldability. It is relatively straightforward to determine if a certain tyligomer sequence will indeed possess a unique folded state that is

kinetically accessible from the unfolded ensemble. The rigorous approach is to simulate the folding funnel, which involves determining the energy gap and the ruggedness. Finding the magnitude of the energy gap requires the identification of the global minimum, the folded structure, which has been proven in information theory to be an NP-hard problem. That is, there does not exist an algorithm with a difficulty and average time of completion that scales polynomially with the size of the problem. Thus, essentially the only way to ensure location of the global minimum is to exhaustively search all of phase space, a prohibitively long procedure for the reasons that Levinthal illustrated. However, algorithms have been developed that stand a very good chance of locating the global minimum, often taking advantage of the properties of funnels just as real biopolymers do. Once the global minimum has been found as a likely candidate for the folded structure, the gap can be measured by comparing its energy to the energies of the next lowest lying states. While the presence of a sizable gap does not guarantee folding behavior, it does favor it, and the presence of degenerate states that are not similar in structure would be sufficient to screen out a polymer sequence as a folding candidate.

The characteristics of the funnel can also be measured, and given a knowledge of the ruggedness and slope as a function of Q , the free energy can be determined for each strata of the funnel by the equations given above.^{100,101} This can be accomplished by sampling the FES using Monte Carlo algorithms or by sampling during molecular dynamics simulations. Once enough structures are sampled for each strata of the funnel, a plot of the free energy as a function of Q can be made, which is very reminiscent of a potential energy diagram of the type used to picture the mechanisms of small molecule reactions. T_f and T_g can also be determined from this simulation data and the likelihood of folding evaluated.

d. Designing Tylogomeric Folded Structures.

It may be enough to simply show that a single structure can be obtained; if the goal is simply to design a chain that folds, this is sufficient. However, designing tylogomers that are capable of carrying out certain functions such as binding or catalysis will involve the much more complicated task of designing heteropolymers that fold to specific folded structures. Forward engineering is much easier if one knows the rules of design, which can be learned from extensive reverse engineering. There has been some progress made on the reverse engineering of proteins, that is, the *ab initio* prediction of protein structure given the amino acid sequence. Unfortunately, most of this progress has been specific to the polypeptide chemical system and, as such, is parametrized for these particular biopolymers. Some theoretical work on this problem has been done, as well as lattice simulations, but there are few results that can guide the foldamer designer at present.

The forward engineering problem may be even more difficult for real systems, but there has been some illuminating work done using lattice models that helps to identify the challenges involved. Lattice

simulations have demonstrated that not all structures are equally designable. An exhaustive enumeration of all of the possible 3×3 3-D lattice two-letter alphabet structures and sequences was performed.¹⁰² All of the sequences that had a high foldability were considered, and it was found that there were some structures to which many sequences folded and some structures to which no sequences folded. Earlier studies of 2-D lattices revealed the same result.¹⁰³ These structures that kept turning up were considered to have a high "designability". If one were to try to design a sequence that would fold to such a structure, one's chances of success would be relatively high. Additionally, such structures are more stable to mutations of the sequence and can be considered more evolutionarily robust.

Since there are some structures that are easier to design than others, their nature and structural properties should be considered. These highly designable 3-D lattice structures have high symmetry and often have high proportions of secondary structure-like motifs.^{104,105} Thus, there seems to be a correlation between those structures that are highly designable and the highly foldable sequences that fold into them. These design principals must be tested for the backbones and structural motifs that are described below. We must first learn to design synthetic foldamers that will simply fold before we can learn to design tylogomers that are endowed with the same specific functionality found among the biopolymers.

B. Foldamer Synthesis and Purification—The Chemistry of Oligomers

As discussed in the Introduction, one goal is the generation of high molecular weight tylogomers with discrete chain lengths and primary sequences. Yet, chemists' inability to prepare high molecular weight substances in pure, monodisperse form precludes their current study. Thus, the field is currently restricted to the size regime of oligomers. Even here the synthetic challenges are significant. It has been stated, "despite much methodological progress, the synthesis and purification of monodisperse oligomers often remains quite tedious."¹⁰⁶ Three approaches to heteromeric chain molecules have been developed: step-by-step, iterative, and polymeric growth. Step-by-step growth is the extension of a chain one monomer at a time and allows for high sequence control at the cost of slow chain growth. Iterative approaches permit more rapid chain lengthening, especially through split pool divergent/convergent methods, while imposing some limits on sequence control.¹⁰⁷ For instance, an orthogonally diprotected dimer, A–B, can be coupled to a tetramer, A–B–A–B, doubling chain length but limiting sequence variability. Solid-phase methodologies in foldamer synthesis have utilized both step-by-step and iterative growth.^{107–111} The third approach, polymeric growth, provides rapid but statistical chain lengthening to a heteropolymeric mixture with minimal control over length or sequence and, therefore, has been avoided for the generation of foldamers. Though modifications of polymeric growth methodologies to narrow chain-length distribution have been proposed, a reliable

approach to generation of heteromeric tylogomers remains unidentified. Furthermore, while methodologies for the separation and purification of polymers exist, strategies for isolating one component from a high molecular weight heteropolymeric mixture are lacking and may limit this approach toward the generation of sequence-specific chains.

C. Foldamer Characterization—Experimental and Instrumental Methods

Foldamer characterization is approached in two stages: determining the properties of covalent synthesis (structure and purity) and conformational analysis of the folded state. Although established methods for organic synthesis, such as NMR, HPLC, and mass spectrometry, are employed in foldamer research routinely, various techniques must be drawn upon in order to *infer* the state of aggregation and the solution conformation of a chain molecule. This first aspect mostly involves using conventional methods of organic and polymer analysis while the second is much more difficult, since most new foldamer backbones do not have established spectroscopic signatures of secondary structure. Table 1 shows representative examples of common approaches to foldamer characterization. In addition, there are three powerful approaches to ascertain the stabilizing forces responsible for the folded state: variation in oligomer length, stoichiometry (and concentration), and environmental conditions. Through the use of chain-length studies, information about the critical chain length in cooperative folding and the Zimm–Bragg equilibria, σ and s , can be determined.¹¹² Concentration effects are known to impact foldamer architectures¹¹³ and require scrutiny when attempting to characterize the folding transition of a particular foldamer. In a single-stranded chain, the folding process is driven by intramolecular association and, therefore, concentration must be kept low enough to avoid aggregation, which can disrupt the ability of the oligomer to fold into the most thermodynamically stable conformation. In multistranded foldamers, both concentration and stoichiometry must be controlled since subtle changes in either can promote the formation of deleterious assemblies. Additionally, titrations of multicomponent systems allow for the determination of the stoichiometric ratios of the assembly. Elucidation of specific interactions by investigating solvent, temperature, and pressure effects can reveal driving forces present in the folding reaction.

III. Foldamer Research

A. Overview

As implied in the Introduction, both proteins and (deoxy)ribonucleic acids can be viewed as ideal tylogomers—that is, the archetypal biological examples of discrete, high molecular weight macromolecules of mixed sequences with compact solution conformations assembled from many subunits of secondary structure. In our assessment of the literature, we have organized foldamer systems into four

categories: peptidomimetics, single-stranded abiotics, nucleotidomimetics, and multistranded abiotics. In general, single-stranded abiotics are unnatural backbones that mimic secondary structures, such as helices and sheets, while multistranded abiotics commonly emulate double- and triple-helical conformations seen in oligomeric nucleic acids. When examining those systems that fit within our definition of a foldamer, a subtle disparity in *motivation* and *method* for mimicking biomacromolecules is uncovered. This disparity has dictated the inclusion and exclusion of specific examples of foldamers in past reviews, with the single-stranded abiotics being predominantly identified as foldamers. Therefore, a short discussion of these distinctions is helpful to understand our delineation of the literature.

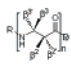
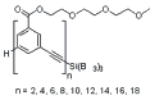
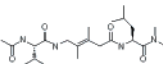
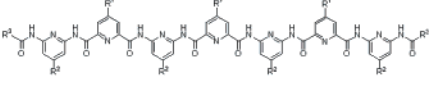
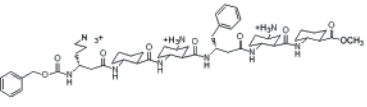
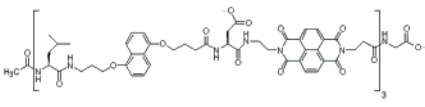
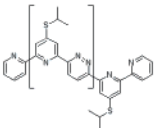
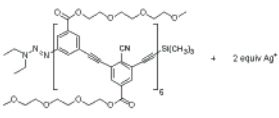
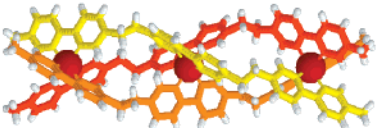
B. Motivation

The motivation for foldamer research will function as our first classification for this article. Specifically, we wish to call attention to the difference between “foldamer research” (the purposeful development of chain molecules that exhibit ordered conformations in solution predominantly determined by noncovalent interactions within or between nonadjacent monomer units) and “research on molecules that are foldamers” (the study of such molecules predominantly for their functional attributes). A myriad of functions have been sought in the study of foldamers, from information storage and antibiotic properties to gene therapy and materials applications. However, no matter what the final aim, there exists a clear disproportionality between the *basic* research of designing, synthesizing, and characterizing the secondary structures of unnatural oligomers and the *targeted* research of generating such molecules purely for their functional properties. More for historical than conceptual reasons, these motivations led to our first division of the literature into single- and multistranded foldamers, where single-stranded systems have predominantly been identified in the literature as foldamers.

C. Methods

Additionally, these two research motivations can be further categorized as being a part of either “top-down” or “bottom-up” foldamer design methods. Considerable progress has been made in the modifications of biological systems whose design is primarily based on a top-down approach, where logical extensions of either peptidic or nucleic backbones to enhance, elucidate, or mimic their structure and properties have led to related families of backbones, referred to here as peptidomimetics and nucleotidomimetics. Alternatively, supramolecular chemists have been interested in mimicking biological structures and properties from a bottom-up design, where analogous architectures to biomacromolecules are obtained by backbones that bear little resemblance to natural chains. Both design methods aim to develop unique structures that exhibit similarity to the components and the mechanisms of biochemical systems. Overall, we have chosen to arrange our specific examples not by application, but by the

Table 1. Foldamer-Specific Characterization Techniques, Possible Secondary Structure Data Thereof, General References Regarding Their Usage, and a Representative Reference, Structure, and Type of Foldamer from Each Field

Technique	Structural Information	General Reference	Representative Oligomer Reference	Structure and Type of Representative Oligomer
<i>Spectroscopic Methods</i>				
Circular dichroism (CD)	Chromophore interactions; local conformation of chromophore	902	223	 helical β -peptides
Fluorescence	Chromophore interactions; local conformation of chromophore	903	112	 helical oligo(<i>m</i> -phenylene ethynylene)
Infrared (IR)	Aggregation; H-bonding	904	342	 <i>trans</i> -5-amino-3,4-dimethylpent-3-enoic acid (ADPA) β -turn mimic
NMR (1D)	Aggregation; H-bonding; aromatic interactions	905	448	 helical oligo(2'-pyridyl-2-pyridinecarboximide)
NMR (2D)	3D arrangement of structured backbone in solution	905	239	 helical <i>trans</i> -2-amniocyclohexane-carboxylic acid (ACHC) β -peptide
Ultraviolet-Visible (UV-vis)	Chromophore interactions; local conformation of chromophore	906	391	 donor-acceptor stacked aedamer
<i>Non-Spectroscopic Methods</i>				
Electron Microscopy	Real-space visulation of morphology and chain packing in the solid state	907	382	 helical oligo(pyridine-pyridazine)
Microcalorimetry (μ -cal)	Thermodynamics of folding and association	908	476	 helical oligo(<i>m</i> -phenylene ethynylene)
X-ray crystallography	3D arrangement of atoms in the solid state	909	815	 Helicate triplex

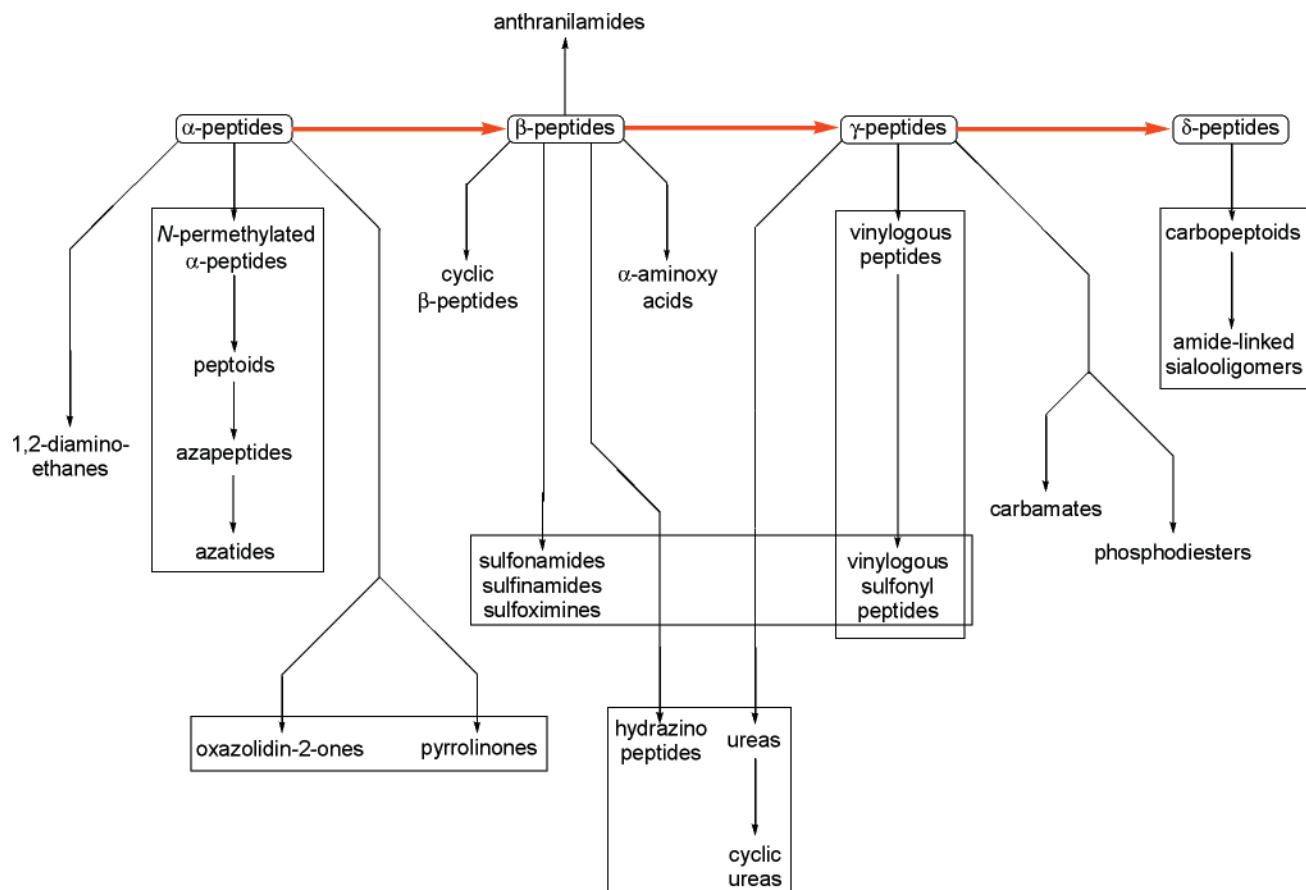


Figure 13. Structural lineage of peptidomimetic backbones.

structure of the backbone repeat unit, thereby casting a reasonably wide net of coverage. For these reasons, we partitioned the literature into peptidomimetics, nucleotidomimetics, and abiotic variations of each.

D. General Scope

Our foremost criterion for inclusion of specific examples from foldamer research in this section is as follows: was conformational analysis performed on the molecules in question through studies on discrete oligomers? We chose “interesting examples” from the literature to demonstrate the basic character of foldamer research and have been as exhaustive as possible within this definition of the field. Additionally, we limited our treatment of more extensive areas to suit the length of this review. While many of the following might technically fit our definition of foldamers, they will not be covered here: oligo(α -amino acid)s, oligo(deoxy)ribonucleotides, simple ligand–metal complexes, non-oligomeric synthetic receptors,^{114–119} non-oligomeric chemosensors,^{120–123} transition-metal-assembled three-dimensional cyclic nanostructures¹²⁴ and two-dimensional grids,¹²⁵ hydrogen-bonded networks and tapes,¹¹⁸ supramolecular polymers,^{33,126} dendrimers,¹²⁷ and oligomers mentioned in the Introduction. We will also not be inspecting the abundance of molecules that adopt helical conformations *only* in the solid state, as this defies our definition of having discrete solution structure.

IV. Peptidomimetic Foldamers

The field of peptidomimetics aims at mimicking peptide structure through substances having controlled spatial disposition of functional groups. Peptidomimetics have general features analogous to their parent structure, polypeptides, such as amphiphilicity. They have been developed, to a large extent, for the purpose of replacing peptide substrates of enzymes or peptide ligands of protein receptors.^{128–133} Peptidomimetic strategies include the modification of amino acid side chains, the introduction of constraints to fix the location of different parts of the molecule,¹³⁴ the development of templates that induce or stabilize secondary structures of short chains,^{135,136} the creation of scaffolds that direct side-chain elements to specific locations, and the modification of the peptide backbone. Of these strategies, systematic backbone modifications—structural alterations of the repeat unit—are most relevant to the field of foldamers. Backbone modifications may involve isosteric or isoelectronic exchange of units or the introduction of additional fragments. Efficient monomer preparations and repetitive synthetic methods for oligomer constructions have recently been developed for many biologically inspired, unnatural chain molecules.¹³⁷ To summarize progress to date on these systems and structurally organize them, a family tree of peptidomimetic backbones is shown in Figure 13, organized from left-to-right by the number of atoms separating peptide (or peptide-like) units and top-to-bottom by the functional group classes.

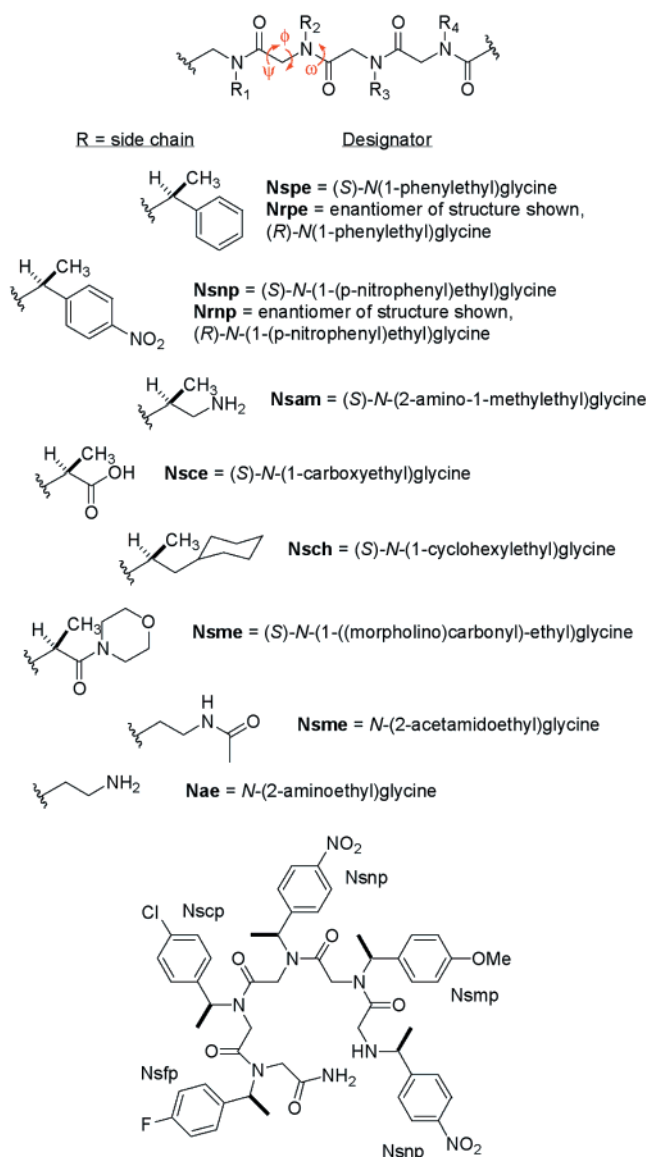


Figure 14. General peptoid backbone, representative chiral side chains, and a peptoid pentamer that adopts a helical secondary structure.

Our focus here is on peptidomimetic oligomers whose secondary structure has been well characterized. For some of these backbones, monomers and sequences giving rise to helical, extended (i.e., “strand”), and turn conformations have been identified. These will be discussed in greatest detail. Other systems included in this section are considered either as potential foldamers or systems that have been discussed within the context of foldamer research but for which only limited information about their secondary structures is presently available. In these cases we will restrict our discussion to brief summaries.

A. The α -Peptide Family

1. Peptoids

Poly-N-substituted glycines or “peptoids”¹³⁸ belong to the α -amino acid lineage, differing from their genitor in that the pendant groups are attached to the amide nitrogen rather than C_{α} (Figure 14).

Although these peptidomimetic oligomers lack stereochemistry in the backbone, their side chains are spaced apart by a distance similar to that of the natural backbone. The absence of amide hydrogens precludes the possibility of intramolecular $CO\cdots H-N$ H-bonds. Moreover, low energy conformations for tertiary amides include both *cis* and *trans* states about the peptide bond (*cis* amide refers to geometries where the main-chain C_{α} atoms are *cis* to one another). Calculations on dipeptoids^{138,139} reveal significant twisting about the peptide bond owing to steric interactions that involve the nitrogen substituents. These steric interactions limit the set of energetically accessible conformations about the other two backbone torsions. The lack of H-bond constraints and the presence of both *cis* and *trans* peptide bonds are reasons to expect the conformational diversity of peptoids to be greater than α -peptides. However, peptoid sequences as short as five residues adopt stable helical secondary structures in a variety of solvents, and the unfolding process is both reversible and cooperative.¹⁴⁰

Calculations predicted that peptoids bearing side chains with stereocenters adjacent to the main-chain nitrogen have a limited number of energetically accessible conformations.¹⁴¹ On the basis of this prediction, longer oligomers were postulated to adopt a helical conformation with *cis* amide bonds, similar to the polyproline type I helix. To test this idea, a series of peptoid sequences were prepared from monomers bearing chiral, nonracemic side chains (Figure 14).¹⁴⁰ The shape of the CD band changed from the monomer up to the pentamer, beyond which the CD band shape remained constant with increasing chain length, resembling the α -helical conformation of the α -peptide backbone. Moreover, beyond the pentamer, the intensity of the CD signal, on a per-residue basis, did not increase.^{140,142}

A pentamer sequence that exhibited good dispersion and sharp 1H NMR signals was used in a detailed conformational study.¹⁴³ On the basis of ROE cross-peak data obtained in methanol, all of the amide bonds of the major species were of *cis* geometry. Although multiple species in slow exchange were apparent from the NMR spectra, the major species was determined to be a regular helix with three residues per turn and a pitch of ca. 6 Å, in good agreement with molecular modeling predictions. The minor species were postulated as resulting from slow exchange of *cis* and *trans* isomers.

The conformation of the major species identified by 1H NMR was presumed to give rise to the observed CD signal. To verify this, the conformational transition was studied by CD as a function of both pH and temperature for peptoids bearing ionizable carboxylic acid side chains.¹⁴⁰ Over the pH range of 7–3, the CD signal intensity of a 30-mer changed very little. At pH 2, the CD signal was greatly diminished and interpreted to signify complete unfolding. At pH 4.1, this oligomer exhibits a complete, reversible loss of the helix-like CD signal over a 40 °C temperature range. Although it is not clear what causes helix destabilization at low pH, the behavior was characterized as highly cooperative as compared to α -peptides of similar length.

Recent studies by Barron et al. helped refine details on the sequence¹⁴⁴ and chain-length¹⁴² requirements for stable peptoid helices. A systematic study using a series of discrete homooligomers of (*R*)-*N*-(1-phenylethyl)glycine ranging from 3 to 20 residues in length showed that there is a length-dependent shift in the relative population of *cis*-amide helices. The spectrum of the nonamer is unlike any of the other members in the series, suggesting that this sequence adopts a different conformation. However, the unusual behavior of this particular chain length is presently unexplained. When the oligomer length exceeds 12 residues, a helix with *cis* amide bonds becomes the most favored conformation by a significant degree, and no changes are noted in the CD of longer chains up to the 20-mer. In an effort to better understand factors that contribute to helix stability, a series of 30 heterooligomers was prepared and their solution conformation studied by CD and NMR.¹⁴⁴ On the basis of these results, it was concluded that a stable helix results from (1) a monomer composition in which at least 50% side chains bear *N*- α -stereocenters and aromatic substituents, (2) placement of one or more α -chiral substituents on the carboxy-terminus to prevent helix fraying, and (3) a sequence that maximizes the number of aromatic–aromatic interactions along the direction of the helix axis. While these factors contribute significantly to the stability of short peptoid helices, they are less important for peptoids containing more than 12–15 monomers, as the chain length itself contributes significantly to helix stability.

Protease enzymes do not degrade *N*-substituted glycine oligomers.¹⁴⁵ This observation together with the fact that peptoids are readily synthesized¹⁴⁶ by standard solid-phase methods and the fact that many display good solubility in water make them prime candidates for pharmaceutical and agrochemical research. Peptoid analogues of peptide ligands were identified in the initial studies supporting the feasibility of this idea.¹³⁸ More recently, cationic peptoid sequences were shown to be efficient reagents for gene delivery.¹⁴⁷ A combinatorial approach that varied chain length, frequency of cationic side chain, hydrophobicity, and shape of side chain produced a small subset of sequences that were active at condensing DNA and offering nuclease protection. One member of the peptoid library, a 36-mer, was found to have good transfection activity for many cell lines, apparently as the result of a spherical nanostructure complex that it formed with DNA.

2. *N,N*-Linked Oligoureas

In 1992, Nowick and co-workers began a program of study on acyclic oligomers whose conformations are stabilized by intramolecular H-bonds. As part of this effort, they investigated the solution and solid-state structures of a family of *N,N*-linked oligoureas having the repeat unit $[-N(\text{CONHR})-(\text{CH}_2)_m^-]_n$,¹⁴⁸ the $m = 2$ member of this family belongs to the α -peptide family of peptidomimetics (Figure 15). This particular chain molecule has interesting conformational characteristics in solution, in part owing to the **S(9)** H-bond between side chains of adjacent units. (Throughout this review we use Etter's graph set convention to describe H-bond interactions:^{149–151}

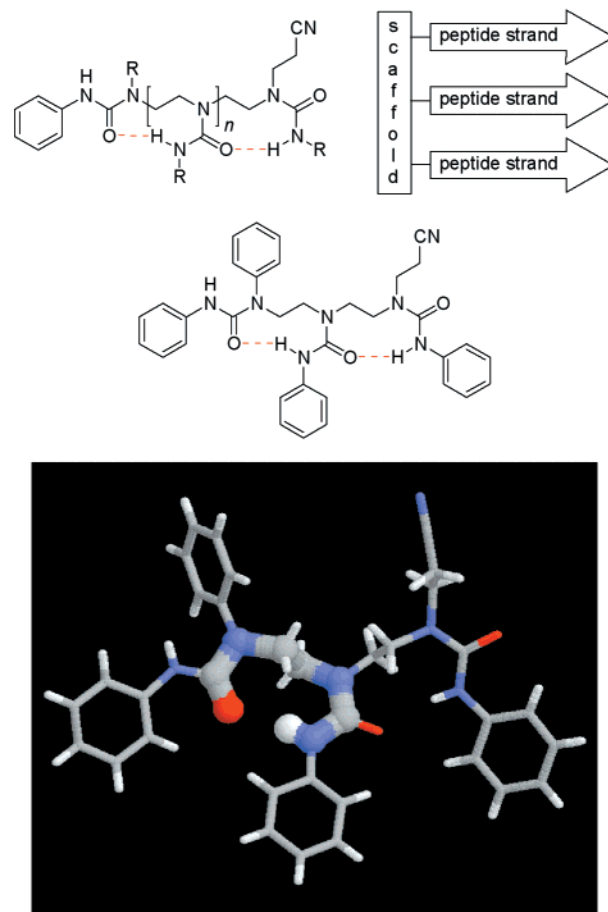


Figure 15. *N,N*-Linked oligoureas. X-ray crystal structure of a triurea derivative.¹⁵³

S(*n*) stands for “self” and denotes an intramolecular hydrogen bond involving *n* atoms; **C(*n*)** stands for “chain” and denotes a repetitive motif whose repeat unit contains *n* atoms). Detailed infrared and ¹H NMR studies have indicated that the dimer and trimer are fully hydrogen bonded in CHCl₃ solution.^{152,153} The ¹H NMR chemical shifts of the NH groups did not vary with concentration over the range from 1 to 10 mM, suggestive of intramolecular H-bonding.

The crystal structure of a triurea derivative revealed a conformation in which **S(9)** H-bonds orient the side-chain residues in roughly parallel directions, thus resembling peptide β -turns (Figure 15).¹⁵³ Thus, as originally envisioned,^{148,152} these peptidomimetics are well-suited as molecular scaffolds to template multistrand artificial β -sheets.^{154–157} It should be noted that if only simple urea pendant groups were attached to the oligomeric backbone, the nonadjacency criterion would place these structures outside of our foldamer definition. Given the collection of H-bonding interactions that comes with pendant β -strands, the conformation of these more complex *N,N*-linked oligoureas are stabilized by long-range noncovalent interactions, and therefore, they likely possess cooperativity and other characteristics expected of foldamers. We return to some of these aspects in the section of this review on multistranded abiotic foldamers.

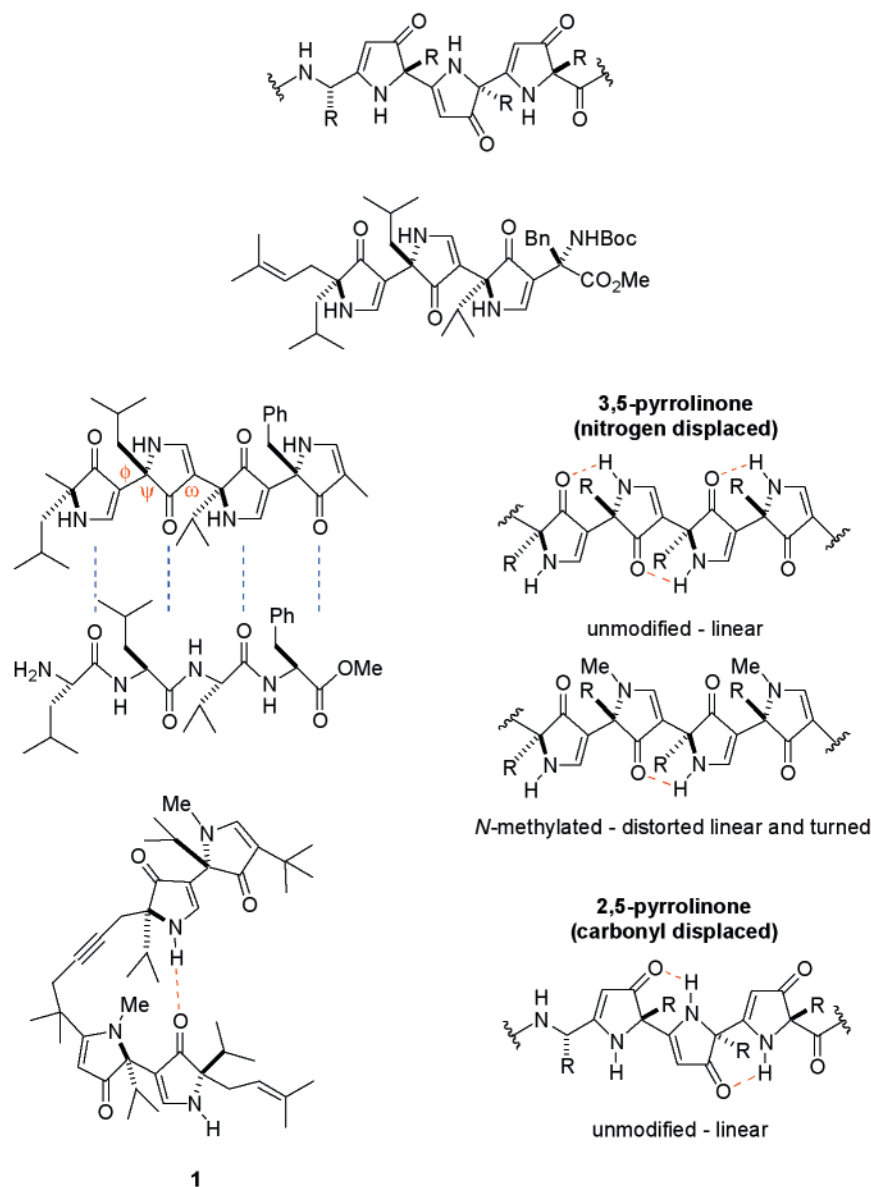


Figure 16. Oligo(pyrrolinone) backbones linked through the 2,5- and 3,5-positions. The correlation between the 3,5-linked pyrrolin-4-ones and α -peptide β -strands. The **S(6)** hydrogen-bonding interaction is indicated in red. *N*-Methylated 3,5-linked pyrrolin-4-one sequence **1** adopts a helical conformation in the solid state and in solution.

3. Oligopyrrolinones

Oligopyrrolinones (Figure 16) are best classified as members of the α -peptide backbone, even though their vinylogous amide bond is not a part of the primary chain. With the initial intention of creating a non-peptide β -strand mimic,¹⁵⁸ Smith and Hirschmann originally conceived two backbone types (Figure 16).¹⁵⁹ The first is based on 3,5-linked pyrrolin-4-ones having an all carbon primary backbone in which the nitrogen is displaced relative to the α -peptide chain. The second is based on 2,5-linked pyrrolin-4-ones in which the primary backbone contains a nitrogen atom and the carbonyl is considered displaced relative to the α -peptide chain. Thus far, only the nitrogen-displaced backbone has been reported, although the other scaffolds still appear to be under consideration.¹⁶⁰

Peptidomimetics based on 3,5-linked, 5-substituted pyrrolin-4-ones have many structural features common to α -peptide chains (Figure 16). The carbonyl

group is spaced every three atoms with an orientation similar to that of carbonyl groups in β -pleated strands,¹⁶¹ while the nitrogen is displaced with respect to its usual location in the α -peptidic backbone. Incorporation of the nitrogen atom as a vinylogous amide into the pyrrolinone ring provides rigidity and constrains the ψ and ω angles of the corresponding α -peptide chain. An **S(6)** intramolecular hydrogen bond between the $\text{C}=\text{O}\cdots\text{H}-\text{N}$ groups of adjacent residues helps to constrain the ϕ dihedral and ensure an extended conformation. By the non-adjacency criterion in our definition, this example is technically not a foldamer; it is simply an oligomer whose conformation is fixed by intramolecular non-covalent interactions. In other words, the chain's conformation can probably be described as a collection of independent units rather than as a cooperative group. Nonetheless, the oligomer is interesting because side chains added to the ring's 5-position are oriented similarly to those of an α -peptide chain that

adopts an extended β -strand conformation. A drawback to this design, however, is the difficulty of monomer and oligomer syntheses, which has been improved with a more general synthetic scheme, allowing the incorporation of functionalized side chains.¹⁶²

Molecular modeling and X-ray crystallographic studies¹⁵⁹ showed that side chains in the 5-position take on the alternating above-plane, below-plane orientations as found in β -pleated sheets. The pyrrolinone NH protons were observed to form hydrogen bonds both intramolecularly to stabilize the β -strand and intermolecularly to produce sheets. These observations suggest that the disposition of vinylogous amide carbonyls retain H-bond acceptor characteristics and closely correspond to the α -peptide chain. Furthermore, the pyrrolinone NH groups, while vinylogously displaced from the backbone, engage in H-bonding, presumably owing to their comparable basicity (pK_a ca. 2–3)¹⁶³ with amide NH groups (pK_a ca. 0–1).¹⁶⁴ Parallel and antiparallel strand orientations were observed in the solid state, depending on the presence or absence of protecting groups on the terminal nitrogen.

The oligopyrrolinone scaffold has been used as a protease inhibitor and a ligand for hormone and other protein receptors. The main idea is that these sequences can adopt bioactive conformations of endogenous peptide ligands while exhibiting good pharmacokinetic properties. This strategy was used to design pyrrolinone-based inhibitors of renin¹⁶¹ and HIV-1¹⁶⁵ proteases that are known to bind their substrates in an extended β -strand conformation. Similarly, this strategy was used¹⁶⁶ to design a bispyrrolinone–peptide hybrid ligand that binds class II MHC receptors, where the antigenic peptide ligands adopt extended, polyproline type II conformations with twisted backbones projecting side chains every 120° . The crystal structure of this complex shows that the bispyrrolinone unit adopts a polyproline type II-like conformation with the side chains projecting into the same places as the peptide side chains they replace. Moreover, the bispyrrolinone backbone forms H-bond contacts with the receptor in much the same way as the natural ligand.

N-Methylated bispyrrolinones adopt a twisted dihedral about ϕ which opens the way to helical conformations in longer oligomers.¹⁶⁰ This idea was supported by crystallographic observations that revealed an extended helical array in the solid state, based on intermolecular hydrogen bonding from O(1) of one molecule to the hydrogen on N(2) of a second. This led to the design of 3,5-linked pyrrolinone sequence **1** in which an alkynyl tether was used to join a pair of bispyrrolinone units (Figure 16), designed from the geometry of the solid-state helical array. The crystal structure of this tetrapyrrolinone shows a twisted conformation that resembles a short helical stretch, stabilized by an **S(14)** intramolecular H-bond. In chloroform solution, ¹H NMR and IR data indicate that this H-bond is maintained, suggesting that a similar conformation exists in solution and the solid state. These results show that the pyrrolin-4-one unit is a versatile building block that may be used to generate both extended and helical secondary structures.¹⁶⁰

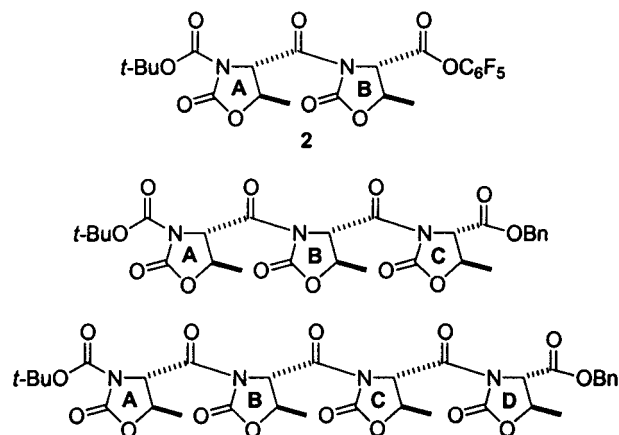


Figure 17. Oligomeric oxazolidin-2-ones synthesized and studied as possible foldamers.¹⁶⁷

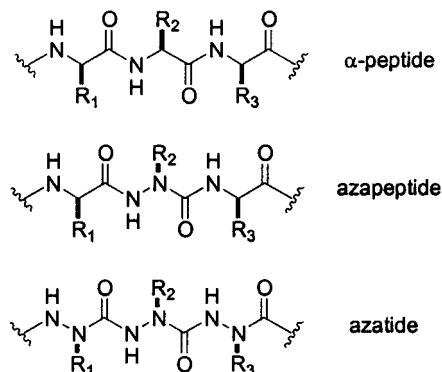


Figure 18. Comparison of the α -peptide, azapeptide, and azatide peptidomimetic backbones.

4. Oxazolidin-2-ones

Oligomers based on oxazolidin-2-ones (Figure 17) belong to the α -peptide genre and recently have been discussed in the context of foldamers.¹⁶⁷ This backbone can be considered as a pseudoproline structure. On the basis of ¹H NMR chemical shift data, shifts, and AM1 calculations, the bisoxazolidinone **2** was believed to adopt a conformation in which the two rings are approximately orthogonal to one another. A trimer and tetramer exhibited similar ¹H NMR behavior that led the authors to conclude that both oligomers fold into ordered structures. However, given the lack of supporting evidence and the apparent noninvolvement of conformationally stabilizing intrastrand noncovalent interactions, we hesitate to categorize these oligomers as foldamers at present.

5. Azatides and Azapeptides

Azatides and azapeptides are α -peptide relatives in which one or more of the α -carbons have been replaced by a trivalent nitrogen atom (Figure 18). While azapeptides (α -peptides in which only a portion of the C_α atoms are substituted with nitrogen) have long been known,¹⁶⁸ only recently have all-aza chains, or what has been termed azatides,¹⁶⁹ been synthesized.¹⁷⁰ The conformational properties of these oligomers have not yet been thoroughly explored, although they have interesting characteristics, which makes them appropriate for discussion here. Until more definitive studies are completed, we consider them as potential foldamers.

High-level *ab initio* calculations show that diacylhydrazines are intrinsically nonplanar with respect to the CO–N–N–CO torsion, and the corresponding rotational barriers are high.¹⁷¹ The global minimum finds the nitrogen lone pairs approximately perpendicular to one another. Thus, their conformational properties are essentially determined by the conformation of their hydrazine and urea constituents. As a result of restricted rotation about the N–N bond, azapeptides cannot adopt extended conformations. This is likely the reason that they are resistant¹⁷² to chymotrypsin-like proteases, which bind their substrates in extended forms.

X-ray data on azapeptides confirm their tendency to adopt turn conformations.^{170,173} For a variety of proteinogenic side chains, the most stable conformation is nearly identical to the calculated one. Although no azapeptides foldamers are presently known, they have been suggested as being strong inducers of secondary structure.¹⁷⁴ However, as their conformation is dominated by the intrinsic torsional characteristics of the hydrazine and urea constituents, it is unclear what role intrastrand noncovalent interactions will play in determining chain conformation. Consequently, the suitability of this unit as an ideal building block for foldamer research is called into question. More work is needed to determine the aptness of this subunit.

B. The β -Peptide Family

1. β -Peptide Foldamers

a. Introduction and General Considerations.

Considerable effort has been invested into studies on β -peptide backbones, a sensible starting point for foldamer research given the close relationship to the ubiquitous α -peptide^{175–178} chain. On the basis of the known high flexibility of glycine-rich peptides, one might expect β -peptides to possess greater conformational flexibility and, therefore, to be entropically disfavored from acquiring ordered solution conformations (Figure 19).^{179,180} In contrast to this intuitive view, certain substitution patterns in the β -amino acid family^{181,182} impart a strong bias to the torsional potential energy surface, enabling the formation of a rich variety of regular conformations.^{183–186}

b. β -Peptide Homopolymers. For more than 40 years, systematic studies on β -amino acid homopolymers in solution and the solid state have been conducted, revealing their potential to adopt well-defined conformational states (Figure 20).^{187–190} The first suggestion that poly(β -amino acids) take on helical conformations in solution appears to have been put forth in 1965 by Kovacs et al.¹⁸⁸ based on studies with poly(β -L-aspartic acid) [poly(β Asp)]. They proposed a 14-helix consisting of 3.4 residues per turn with H-bonding between each C=O and the third N–H group toward the N-terminus (i.e., a repetitive **S(14)** motif). Subsequent investigations^{191,192} raised doubts about this initial claim since it was found that poly(β Asp) is synthesized as a mixture of α - and β -linkages. These and studies with other poly(β -amino acids) suggested that β -peptides adopted disordered solution conformations^{179,193} or extended β -sheet structures^{189,194} rather than helical conformations.

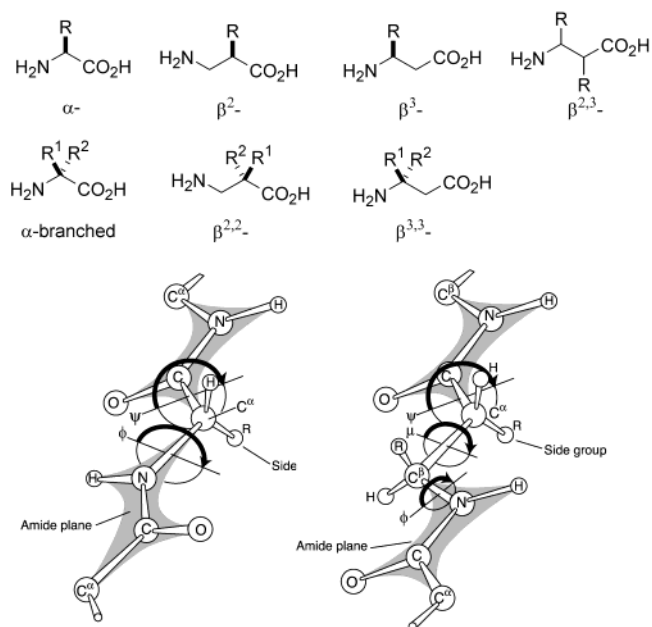


Figure 19. Labeling of atoms and dihedral angles in the α -peptide backbone according to the 1969 IUPAC–IUB Commission on Biochemical Nomenclature⁸⁹⁹ and the analogous scheme for β -peptides. In the text that follows, the abbreviated nomenclature introduced by Seebach is adopted,²²⁸ referring to β -amino acids as homologues of the natural α -amino acids bearing the same side chain by adding the letter “H” preceding the three-letter code of the natural amino acid. Thus, β^2 -HXaa and β^3 -HXaa are used to designate a homologue of the α -amino acid Xaa with the “natural” side chains in the 2- or 3-position, respectively.

Over the next decade, however, further work on poly(β -amino acids) continued to reveal evidence for ordered conformations in solution and the solid state. In 1972, on the basis of chiroptical data, viscosity, and NMR spectroscopy, Yuki et al. asserted that the poly- β -peptide poly- β -(α -isobutyl-L-aspartate) [i.e., poly(*S*- β AspOiBu)] adopts a helical conformation in solution and exhibits a helix–coil transition analogous to poly- α -(γ -benzyl-L-glutamate).¹⁹⁵ However, on the basis of X-ray diffraction and polarized IR spectroscopy of the stretched film, these authors reinterpreted the conformation as a type of β -sheet structure.¹⁹⁶ In solution, they proposed that the ordered state consisted of intramolecularly H-bonded β -sheets. Systematic studies with discrete β -peptide oligomers¹⁹⁷ determined the critical chain length for the putative β -sheet formation to be eight units.¹⁹⁸ In due course, however, the conformational structure of this polymer was once again reinterpreted as helical both in the solid state and in solution.¹⁹⁹ The uncertainty in being able to definitively establish the solution conformation of poly(β -amino acids) is characteristic of the field in decades past and illustrates the difficulties of determining the solution conformation of chain molecules.

It is interesting to note that as early as 1968, Bestian¹⁸⁹ and Schmidt¹⁹⁰ showed that the substitution pattern at the α - and β -carbons can dramatically influence the properties of the resulting polymers (Figure 20). Even though Bestian’s studies were conducted on polymers derived from racemic β -lactams, the observations foreshadowed many of the findings made recently.^{200,201} For example, the *threo*-

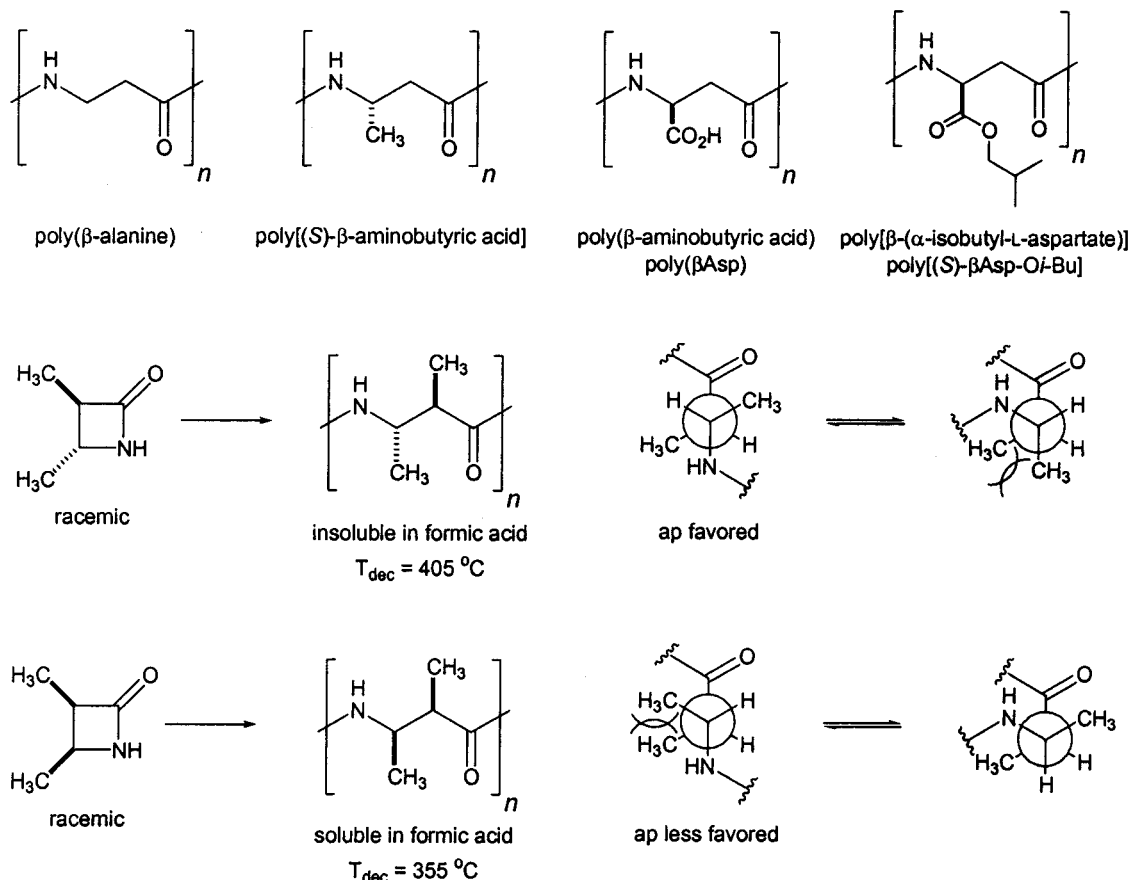


Figure 20. Examples of β -amino acid homopolymers from racemic lactams and the conformational preferences as rationalized in 1968 by Bestian.¹⁸⁹

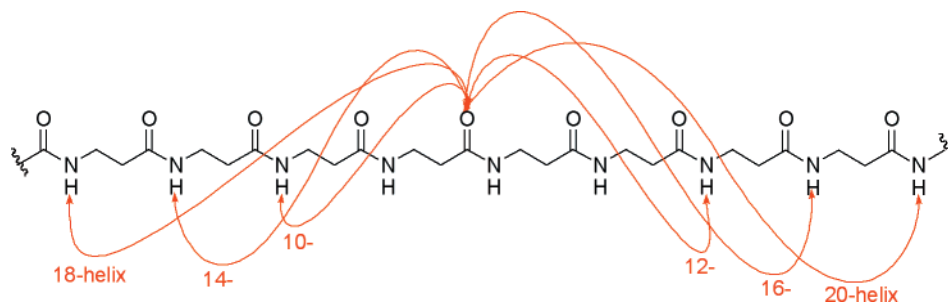


Figure 21. Possible intramolecular H-bond arrangements in β -peptides.

disubstituted monomer produced a highly stable, insoluble backbone, while the corresponding *erythro*-disubstituted monomer resulted in a polymer that was much more soluble and had lower thermal decomposition. This was explained¹⁸⁹ by the preference for antiperiplanar (*ap*) torsion angles with the *threo* isomer and hence extended chains in this case, while the *erythro* isomer was more prone to adopt synclinal (*sc*) torsion angles. Although detailed structural studies were not performed, powder X-ray diffraction and IR spectroscopic studies supported these assertions. Solubility was a serious problem that hampered these early investigations.

In 1984, Fernández-Santín et al. reported¹⁹⁹ that poly(*S*- β AspOiBu), the poly- β -peptide first described by Yuki,¹⁹⁵ does indeed exist in helical conformations when fibers are spun or films are cast from chloroform solutions. This work claimed to be the first report of helical conformations in a polyamide backbone other than chains of α -amino acids. Depending

on sample preparation, two types of helical structures were found in the solid state. Fibers pulled from a concentrated solution of chloroform showed hexagonal packing, while chloroform solutions precipitated with ethanol produced a tetragonal crystal habit. Systematic consideration of the possible helical conformations (Figure 21) led to four models. The tetragonal crystal was initially thought to consist of a right-handed helix in which 4 residues are present in one turn and hydrogen bonding involves a 20-membered ring. On the other hand, the hexagonal crystal was initially thought to consist of a left-handed helix in which 13 residues are present in 4 turns and H-bonding occurs through a 16-membered ring. Helical conformations were also believed to be stable in helicogenic solvents. Solvent denaturation experiments followed by ¹H NMR and solution viscosity showed evidence²⁰² of a helix-coil transition similar to that seen in helical poly(γ -benzyl-L-glutamate).²⁰³ However, experimental evidence²⁰⁴ and

molecular modeling studies^{205–207} now strongly support a right-handed 14-helix (similar to that originally proposed by Applequist¹⁸⁸) in the hexagonal crystal and a right-handed 18-helix in the tetragonal crystal. Predictions based on matching calculated and observed CD spectra, however, while qualitatively consistent with helical conformations, are unable to distinguish between the possible helical conformations.²⁰⁸

Studies with other poly(β -L-aspartate)s demonstrate that these polymers not only adopt conformational patterns that are similar to poly(α -amino acids), but that they exhibit greater conformational versatility. The range of conformations now include extended chain structures, arranged as antiparallel packings that come about by stretching poly(α -methyl- β -L-aspartate) films in boiling water.²⁰⁹ In solution, the helix-coil conformational transition is a phenomenon common to the whole family of poly(α -alkyl- β -L-aspartates).²¹⁰ The ordered conformation is responsive to environmental factors such as temperature and solvent in much the same way as for poly(α -peptides).

Methods for the facile preparation of high molecular weight poly(β -homopeptides) are not common and limited to specific cases such as poly(α -alkyl- β -aspartates). By analogy to the preparation of poly(α -homopeptides) by ring opening polymerization of α -amino acid-*N*-carboxyanhydrides, Cheng and Deming recently attempted to polymerize β -amino acid-*N*-carboxyanhydrides using either NaO^tBu or a nickel amido amidate complex as the initiator.²¹¹ The molecular weights achieved were generally low ($8 \leq$ degree of polymerization ≤ 20) due to precipitation of these poorly soluble macromolecules. The benzyl carbamate-protected oligo(β -homolysine) adopted a helical conformation in hexafluoro-2-propanol (HFIP). In direct analogy to poly(α -homolysine),²¹² the deprotected oligo(β -homolysine) exists in a disordered conformation at low pH due to electrostatic repulsion. As the pH was raised from 10 to 11.2, a strong Cotton effect was observed, suggesting a transition to a helical conformation. This transition was shown to be reversible. A similar pH-induced transition was found for oligo(β -homoglutamate) in aqueous solution. These examples show that polymerizations can be used as a rapid screening method to bypass the slow and tedious step-by-step preparation of oligomers.

c. β -Peptide Oligomers. Systematic studies on cyclic oligomers and small β -peptides have provided valuable insight into the conformational preferences of their long-chain linear counterparts. This approach has been extensively used to study conformations in α -peptides,²¹³ where a wide variety of folded forms has been observed. The geometric constraints in cyclic structures greatly reduce the conformational degrees of freedom, thus making it possible to observe turns and noncovalent interactions that may otherwise not be present in small linear analogues. The shapes of α -peptides have been described as sinusoidal, saddle, elongated loop, disk, pleated sheet, and helical. The general conclusion from crystallographic studies with small α -peptides is that the folding

resembles aspects of protein secondary structure, but overall it is quite unpredictable.²¹³

Although many fewer cyclic β -peptides have been crystallographically examined in comparison to α -peptides, a similar conclusion can be made: many of the observed conformations hint at features found in β -peptide oligomers and polymers. For example, systematic studies on cyclic oligomers that incorporated β -amino acids have revealed that these units readily adopt turned motifs.^{214–218} Using molecular models, Pavone et al. hypothesized²¹⁴ that cyclic peptide oligomers containing the β -HGly dipeptide sequence are able to adopt conformations that permit transannular H-bonds between the amide groups of the β -HGly residue. To test this idea and its generality, a variety of cyclic peptides were synthesized and their crystal structures obtained. Indeed, many turn types were observed depending on the number of β -peptide residues, their placement in the sequence, and the total number of residues in the cyclic structure. As a representative example, the structure of the **S(13)S(10)**²¹⁹ containing *cyclo*-(L-Pro-L-Pro-L-Phe- β -HGly- β -HGly) is shown in Figure 22.²¹⁵ A transannular H-bond between the carbonyl of the β -HGly and the N-H of Phe is clearly evident. Starting from the H-bond donor and tracing through the β -HGly dipeptide segment to the H-bond acceptor (i.e., the thick bonds in Figure 22), it can be seen that 13 atoms are involved in the H-bond circuit. The second hydrogen bond circuit involves 10 atoms tracing from donor to acceptor through the L-Pro-L-Pro segment. It can be seen from Figure 14 that the C $_{\alpha}$ -C $_{\beta}$ bonds of both β -HGly units adopt a gauche (i.e., *sc*) dihedral angle to form corners of the covalent ring and to orient the H-bond donor and acceptor for transannular interaction. An example of a crystallographically characterized macrocycle that incorporates a β^3 -substituted residue is also shown in Figure 22.²²⁰ The interesting features of this pentapeptide are the **S(12)S(10)** transannular H-bond interaction, the *cis* amide conformation, and the *sc* torsion about the C $_{\alpha}$ -C $_{\beta}$ bond (Figure 22). A similar dihedral arrangement is found in many of the β^3 -peptide oligomers as noted below.

Seebach and co-workers studied macrocycles composed entirely of β -amino acid residues.^{221,222} Three different stereoisomeric tetracycles of β -HALa were synthesized by cyclization of their pentafluorophenyl esters. The ease with which β -cyclopeptides were formed relative to α -cyclopeptides of similar size was noted as a tendency for the β -peptide backbone to favorably adopt turn structures.^{221,223} Poor solubility and high melting points characterized the physical properties of these compounds. Their solid-state structures, as shown in Figure 23, were determined by refinement of powder X-ray data.²²² It can be seen that the C=O and N-H bonds are approximately oriented in a direction perpendicular to the average macrocyclic plane (Figure 23). This in turn leads to tubular stacks held strongly together by intermolecular **C(4)** H-bond chains. These H-bond arrangements qualitatively resemble the intramolecular H-bonding motifs in helical β -peptide oligomers.

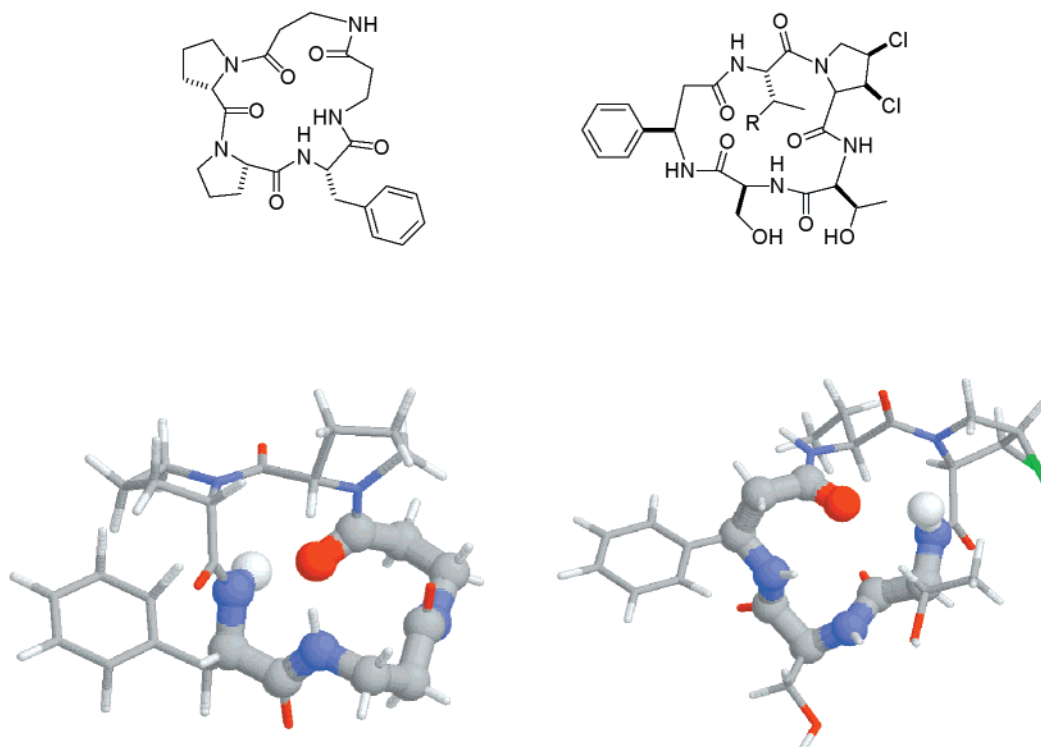


Figure 22. Crystal structures of *cyclo*(L-Pro-L-Pro-L-Phe- β -HGly- β -HGly)²¹⁵ showing H-bond patterns and another cyclopentapeptide.²²⁰ The β -peptide segments involved in **S(13)S(10)** and **S(12)S(10)** transannular H-bonds are rendered as thick cylinders. Newman projections about the C_{α} - C_{β} bonds of the β -amino acid residues show a *sc* conformational preference.

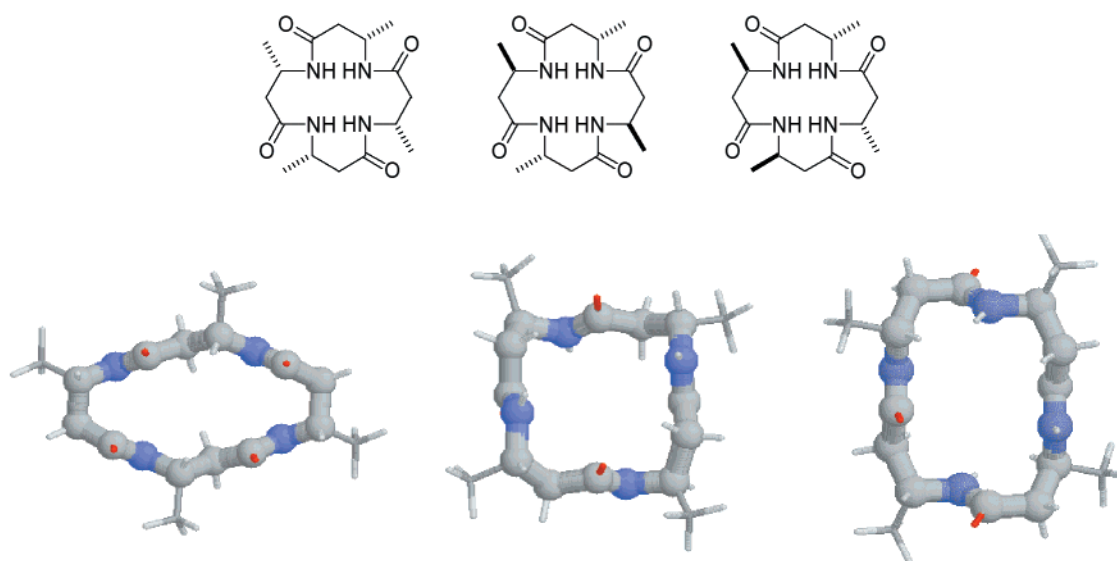


Figure 23. Chemical and crystal structures of three different stereoisomeric tetracycles of β -HAla.²²²

While the studies of Pavone and others with cyclic peptide oligomers showed that next-nearest-neighbor amides can engage in H-bonding interactions, the contribution of cyclic constraints raises the question of whether such interactions could readily occur in acyclic systems. In 1992, the crystal structure of the linear tripeptide *t*-Boc-Aib-Aib- β -HGly-NHMe (where Aib is α -aminoisobutyric acid) was reported, showing that intramolecular H-bonding interactions form even in short chains void of macrocyclic constraints.²²⁴ The *sc* dihedral about the C_{α} - C_{β} bond together with the sharp bend at the Aib C_{α} carbon form corners that

contribute to a next-nearest-neighbor **S(11)** H-bonding motif (Figure 24).

It is interesting to consider whether intramolecular H-bonding interactions or the dihedral preferences of the β -peptides dictate the conformations of these short β -peptides. Although this is difficult to deconvolute from X-ray structures, the importance of torsional bias can be inferred from the crystal structure of the β -tripeptide *t*-Boc- β^3 -HVal- β^3 -HAla- β^3 -HLeuOMe reported by Seebach in 1996 (Figure 25).²²³ No intramolecular H-bonds were observed in **3**; yet, it is apparent that one of the β -peptide

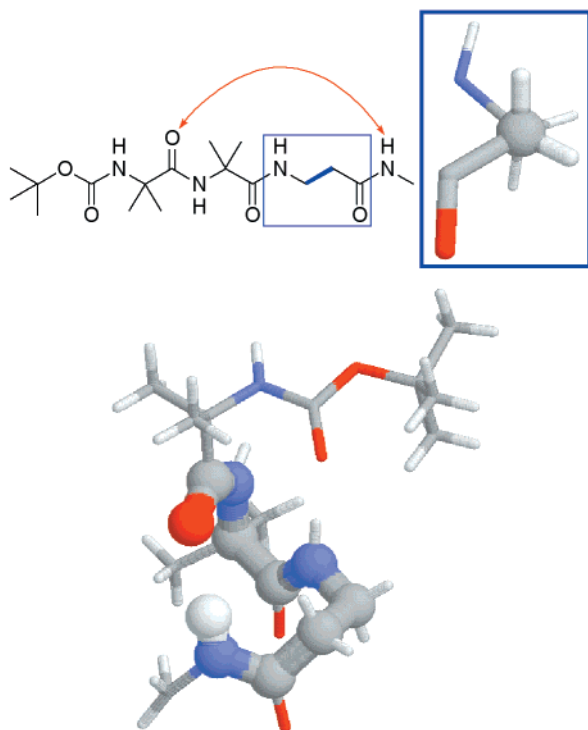


Figure 24. Crystal structure of the linear tripeptide *t*-Boc-Aib- β -HGly-NHMe (where Aib is α -aminoisobutyric acid).²²⁴ The **S(11)** H-bond segment is rendered in thick cylinders. The *sc* dihedral angle about the C_{α} - C_{β} bond of the β -peptide residue is also indicated.

residues makes a tight turn due to a *sc* C_{α} - C_{β} torsion. It is noteworthy that the *sc* dihedral angle is located in the residue bearing the largest substituent, possibly hinting that β -peptides, especially those

with bulky substituents, have a torsional potential energy surface that can easily accommodate turned conformations. On the basis of quantum mechanical calculations, Wu and Wang argued that an internal electrostatic interaction causes this *sc* C_{α} - C_{β} dihedral preference.¹⁸⁴

Dado and Gellman addressed the possibility of nearest-neighbor interactions between amides in β - and γ -peptides.²²⁵ Nearest-neighbor interactions, should they be common, could dominate the potential energy surface and work against the formation of long-range conformational order in β -peptides. To address this issue, the folding behavior of β -alanine and γ -amino butyric acid derivatives **4–9** were studied in solution by IR spectroscopy in methylene chloride (Figure 26). These studies concluded that nearest-neighbor H-bond formation in β -peptides is not a favorable process. The absence of intramolecular H-bond formation in **4** and **6** indicates that neither the six- nor the eight-membered cyclic H-bond is favorable. However, tertiary amide **5** did adopt an intramolecular H-bonded conformation. This observation with **5** is believed to result from at least two effects: first, an $A^{1,3}$ -like interaction between nitrogen substituents and, second, the stronger H-bond acceptor ability of tertiary amides over secondary amides. The important conclusion from Gellman's study was the recognition that since H-bonds between nearest-neighbor amides are not favorable in β -peptides, this backbone could likely be an unnatural amide-based polymer that is able to adopt compact and specific folding patterns. γ -Peptides **7–9**, on the other hand, which were also studied, were suggested to be less suitable since they

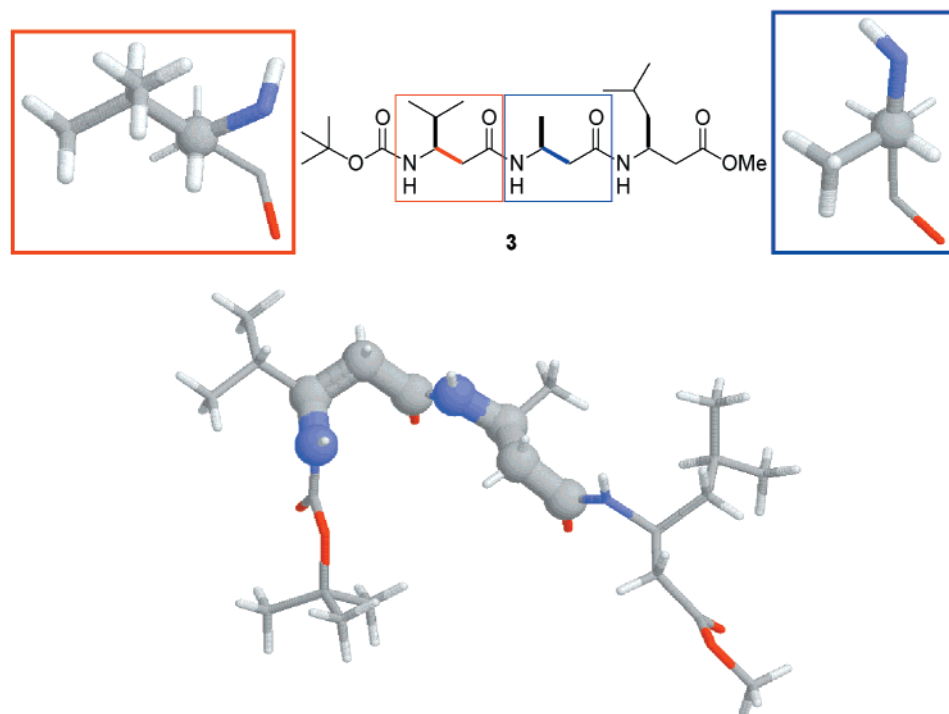


Figure 25. Crystal structure of the β -tripeptide *t*-Boc- β^3 -HVal- β^3 -HAla- β^3 -HLeuOMe (**3**) reported by Seebach²²³ showing an intrinsic preference for a turned conformation. Two of the β -peptide residues are rendered as thick cylinders. The Newman projections about the C_{α} - C_{β} bonds for these residues are shown, indicating the apparent preference of the β^3 -substituted residue bearing the bulky substituents to adopt a *sc* conformation while the residue with the smaller methyl substituents takes on an *ap* conformation.

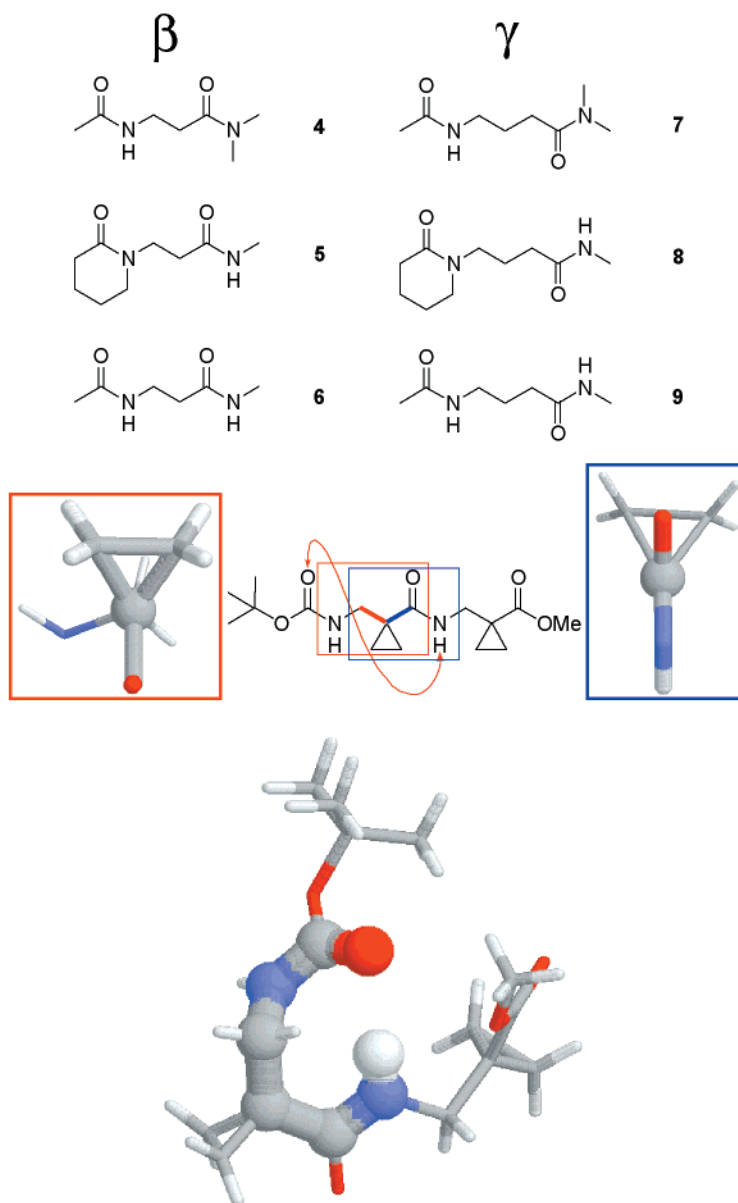


Figure 26. Nearest-neighbor H-bonds observed in β -peptides synthesized from 1-(aminomethyl)cyclopropanecarboxylic acids.²²⁶ This **S(8)** pattern is an example of residue-induced turn formation, resulting from the dihedral and bond angle constraints introduced into the $\beta^{2,2}$ -backbone by the cyclopropyl substituents. The crystal structures show a dipeptide and tripeptide in which the **S(8)** H-bond segments are rendered in thick cylinders. For the dipeptide, Newman projections are shown looking down the $C_\alpha-C_\beta$ bond and the $C(O)-C_\alpha$ bond.

were conducive to nearest-neighbor hydrogen bonding. It should be noted that following Gellman's studies, the special case of β -peptides synthesized from 1-(aminomethyl)cyclopropanecarboxylic acids was reported in which nearest-neighbor H-bonding interactions are observed.²²⁶ Hyperconjugation between the cyclopropane σ orbitals and the π^* orbital of the $C=O$ bond impart preference for the bisected or *s-cis* conformation. This together with bond angle deformations caused by the cyclopropyl substituent provide sufficient backbone constraints to induce nearest-neighbor **S(8)** H-bonding, as seen in the crystal structures of the β -peptide dimer and trimer (Figure 26).

d. Helical Secondary Structures in Oligomeric β -Peptides. *i. Background and General Considerations.* At least 15 α -amino acid residues are required for formation of stable α -helix secondary

structures in protic solvents.²²⁷ Given the seemingly greater flexibility of β -peptides, one might expect that even longer stretches of β -peptide oligomers would be required before stable helices form. However, this turns out not to be the case. As hinted from the observations highlighted above, short β -peptide backbones are poised to adopt ordered conformations. In 1996, two groups independently reached this conclusion: short β -peptide oligomers form surprisingly stable helices in solution and the solid state.^{32,223} Seebach^{221,228,229} approached the problem from the context of amide analogues of oligo-(*R*)-3-hydroxybutanoates (i.e., oligo-HBs) to address the question of whether replacing the oxygen in the HB backbone with the N-H hydrogen bond donor would stabilize helical conformations analogous to those observed for oligo-HBs.^{230,231} Gellman⁴ studied hydrogen bonding in model amides and on the basis of their previous

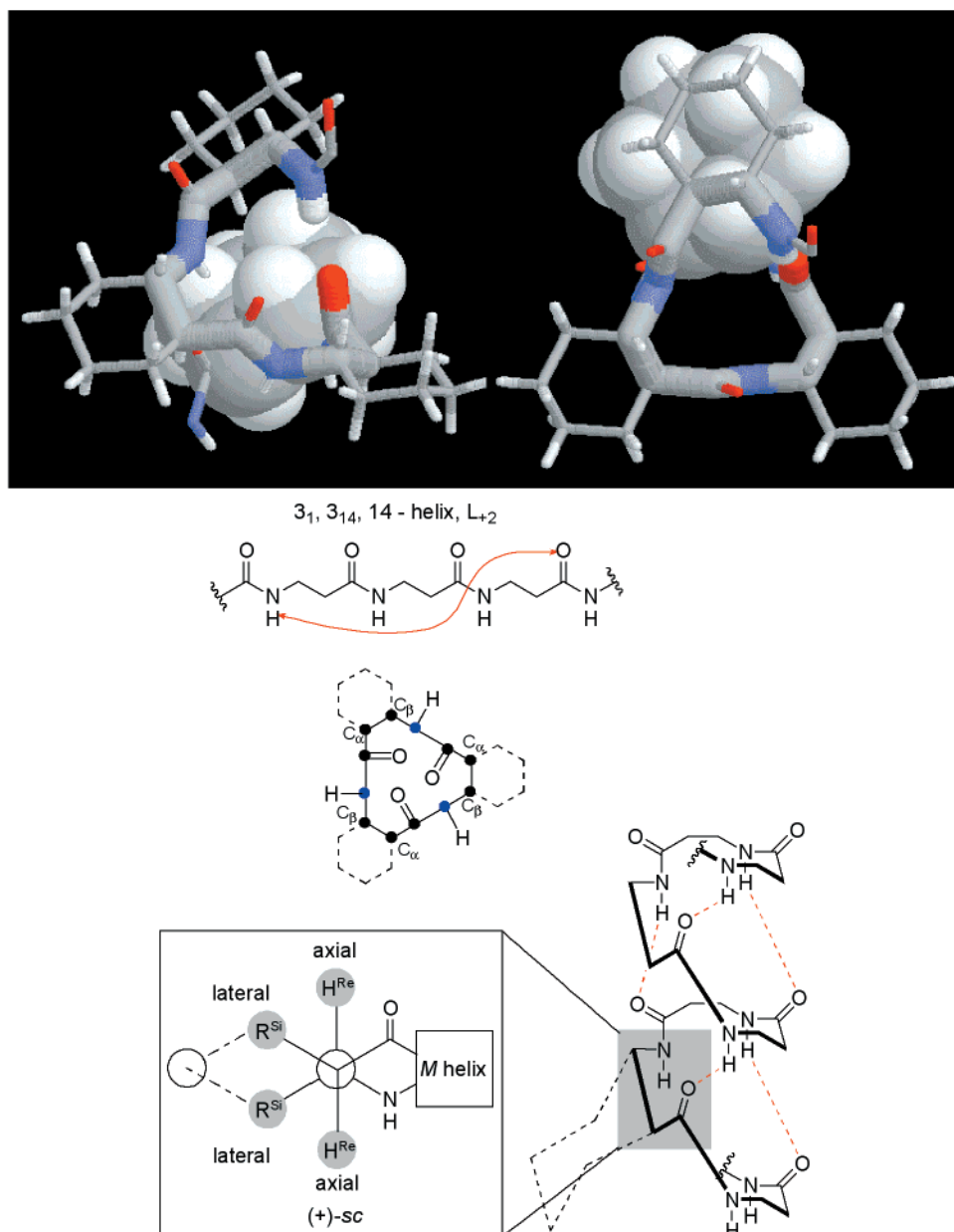


Figure 27. Side and top views of ca. one turn of the 14-helix extracted from the crystal structure of Gellman's *trans*-ACHC hexamer.²³⁹ A single **S(14)** H-bond circuit in the peptide backbone has been rendered as thick cylinders. Additionally, one residue has been rendered as a space-filling model to provide a frame of reference between the two views and to more clearly show the spatial relationship between cyclohexyl groups.

results predicted²²⁵ that β -peptide oligomers could adopt long-range conformational order.

Prompted by questions that arose from structural modification of oligo-HBs,^{221,229} Seebach's group investigated homologues of natural L-amino acids, beginning with a hexapeptide H-(β^3 -HVal- β^3 -HAla- β^3 -HLeu)₂-OH. The above-mentioned hexamer is considered as a β^3 -peptide since all of the side chains are in the 3-position. The particular sequence selected is reminiscent of the arrangements observed in the dimer-forming leucine zipper region of DNA binding proteins,²³² and the fragment Val-Ala-Leu has previously been used as a building block to study the influence of α,α -disubstituted amino acids on peptide conformation.²³³ The apolar side chains afforded β -peptide sequences that were soluble in organic solvents. In subsequent studies, functional-

ized sequences were also investigated.²³⁴ It is increasingly clear that functionalization with polar appendages can have a dramatic impact on the secondary structure.²³⁵ Extension to γ -peptides (see below),^{236,237} which were shown to adopt a stable right-handed helix, gave the surprising result that of the three backbones, the α -peptides are the least prone to adopt stable secondary structures.

Gellman's approach focused on conformationally rigidified residues that limited the degrees of freedom about the C $_{\alpha}$ -C $_{\beta}$ bond, with the intention of observing ordered conformations from the fewest possible residues. They approached the design of helical oligomeric β -peptides with the aid of systematic molecular modeling studies.³² The candidates were selected from β -amino acids in which the backbone carbons were embedded into carbocycles containing

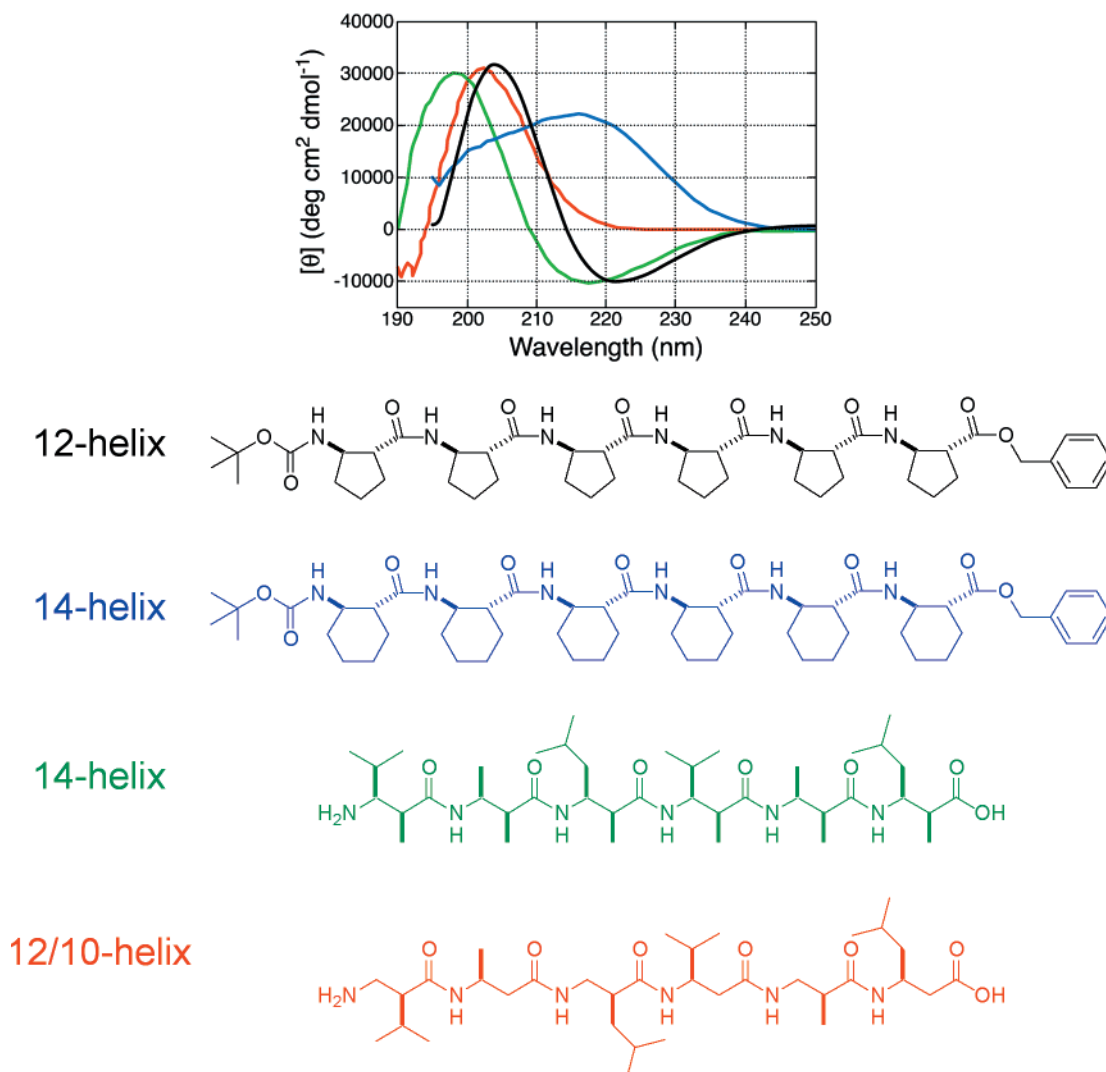


Figure 28. Circular dichroism spectra of four different β -peptide sequences in methanol: black,²⁴¹ blue,²³⁹ green,²⁷³ and red.²⁴⁹

three, four, five, or six atoms. Both *cis* and *trans* ring stereochemistries were considered, and for the *cis*-containing peptides, both orientations of the ring with respect to the helix were examined. Helical conformations were modeled for each of these 12 different sequences using the six smallest H-bonded cyclic patterns: the 12-, 16-, and 20-helix corresponding to H-bonds from carbonyls to N–H groups in the C-terminal direction and the 10-, 14-, and 18-helices corresponding to H-bonds from carbonyls to N–H in the N-terminal direction (Figure 21). Molecular mechanics studies of the resulting 72 structures led to the conclusion that the 14-helical form of *trans*-2-aminocyclohexanecarboxylic acid (*trans*-ACHC) would be the most stable among these hypothetical helices. These studies also predicted that *trans*-2-aminocyclopentanecarboxylic acid (*trans*-ACPC) would adopt the 12-helix,²³⁸ a surprising result in that there had been no example of this conformation in the β -peptide field. As mentioned below, both of these structure types were observed as predicted.

The helical conformations of Gellman's oligomers were firmly established by a battery of experimental techniques. The crystal structure of the *trans*-ACHC hexamer (Figure 27) revealed that all four of the

possible 14-membered ring H-bonds were present in the solid state.^{32,239} In solution, the β -peptides were established to be monomeric under the conditions used for NMR and CD studies.²⁴⁰ Amide proton NH/ND exchange experiments suggested that in methanol the hexamer adopts a very stable intramolecularly hydrogen-bonded conformation, presumably the 14-helix. A solution structure for the *trans*-ACHC hexamer based on NMR-derived constraints was hampered by severe overlap of signals in the $C_{\alpha}H$ and $C_{\beta}H$ regions in this case.²⁴⁰ The CD spectrum in methanol shows a single peak above 200 nm with a maximum at 217 nm (Figure 28). The intensity at the maximum increased as the chain lengthened, presumably the result of a growing population of the 14-helical state.²³⁹ This behavior was suggested to be an indication that the 14-helix formation involves a cooperative process (see below).

As predicted computationally, the *trans*-ACPC oligomers revealed a different type of helical conformation in both solution and the solid state. Crystal structures of the *trans*-ACPC hexamer and octamer displayed the 12-helical conformation (Figure 29).^{238,241} The spectral data of the ACPC oligomers in solution are consistent with the crystallographic observations.

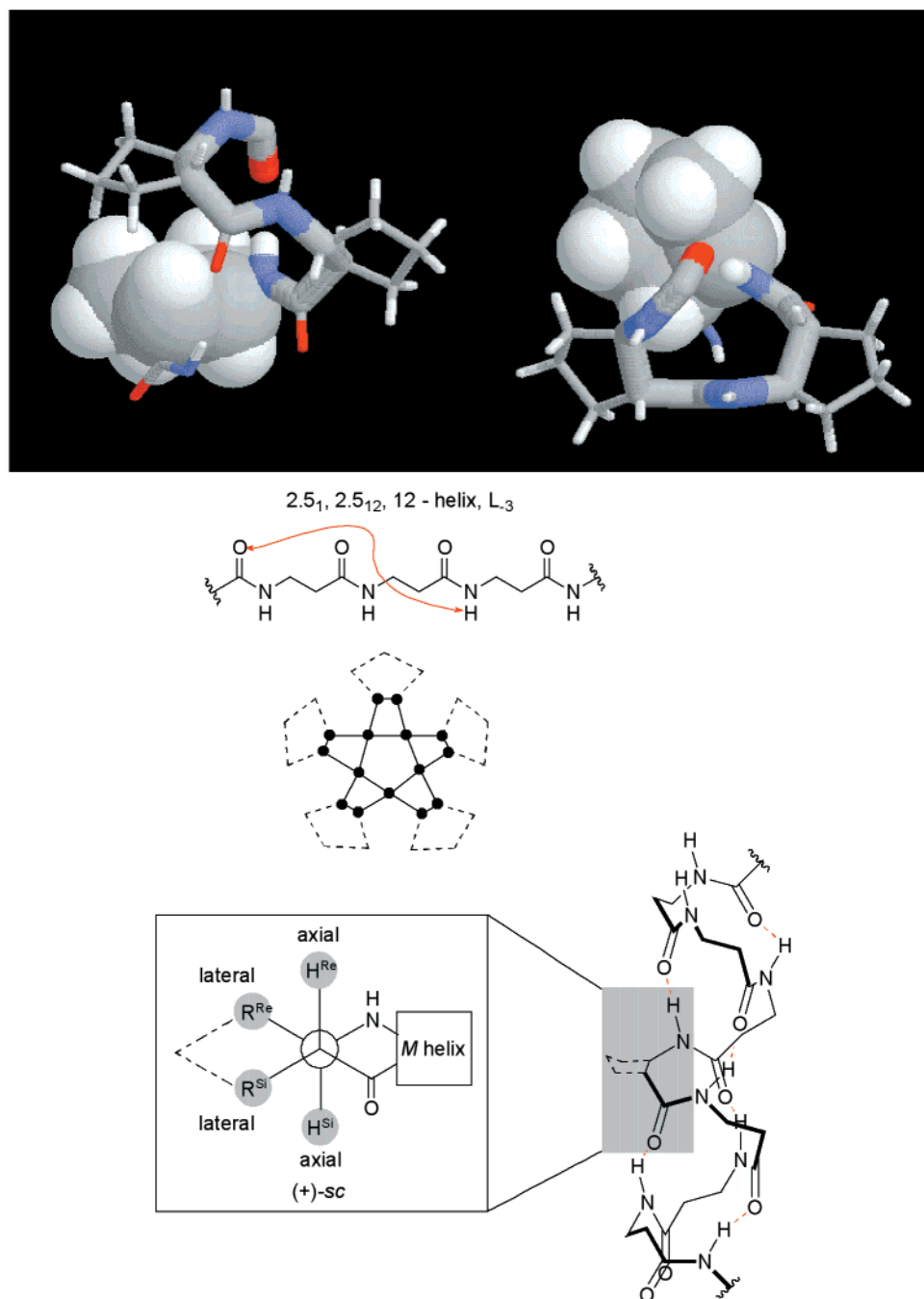


Figure 29. Side and top views of ca. one turn of the 12-helix extracted from the crystal structure of Gellman's *trans*-ACPC hexamer.²⁴¹ A single **S(12)** H-bond circuit in the peptide backbone has been rendered as thick cylinders. Additionally, a residue has been rendered as a space-filling model to provide a frame of reference between the two views and to more clearly show the spatial relationship between cyclopentyl groups.

Circular dichroism spectra of the ACPC oligomer series in CH_3OH vary significantly with chain length. While the trimer and tetramer show no maxima above 200 nm, the CD pattern of the pentamer and hexamer begin to converge and the magnitude of the Cotton effect increases as the chain lengthens. This behavior is interpreted as an increasing population of the 12-helical conformation with increasing chain length, reflecting cooperativity in the 12-helix formation. The CD spectrum of the ACPC hexamer is clearly distinct from the 14-helical β -peptides (Figure 28), displaying a maximum around 207 nm and a minimum at 222 nm. The observed CD spectrum agrees well with theoretical spectral predictions for

the 12-helical conformation.²⁴² In pyridine- d_5 , the ACPC hexamer and octamer displayed sufficient ^1H NMR dispersion to afford solution structures calculated from NMR-derived distance constraints.²⁴⁰ The NMR-determined conformations of these oligomers were similar to the conformations found from crystallography. Correlations established by NOE data were observed for all $\text{C}_\beta\text{H}(i)\text{-NH}(i+2)$ proton pairs along the backbone as expected for a fully formed 12-helix. However, the data suggested the lack of a high degree of conformational order in the chain ends, indicative of fraying.

The switch in H-bonded patterns for the ACHC and ACPC β -peptides teaches that foldamer conforma-

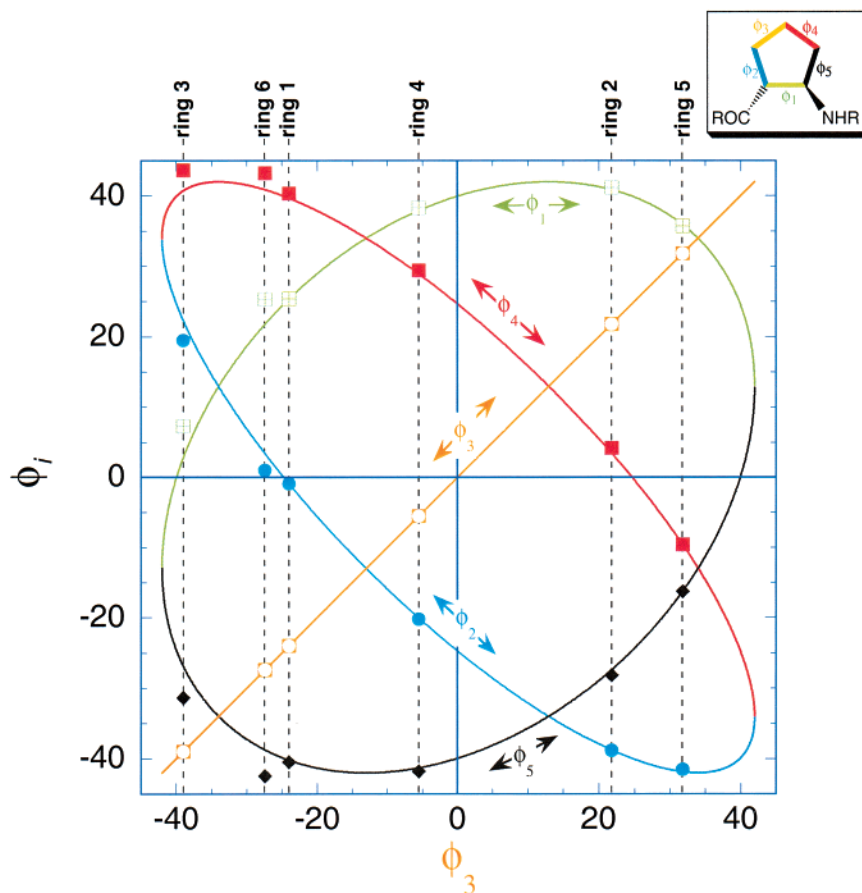


Figure 30. Data from the crystal structure of the ACPC hexamer show that the five internal torsions within each of the six cyclopentyl residues are superimposed on the cyclopentyl pseudorotation circuit as revealed in a correlation plot of ϕ_i vs ϕ_3 .

tions can be controlled by small residue changes, a concept not common to α -peptides. It is interesting to understand what specific residue-based changes bring about this conformational switch. The internal ring torsion across the C_α - C_β bond in the ACHC hexamer varies little among the six residues, spanning the range from -55.0° to -58.8° . In contrast to cyclohexyl rings, five-membered carbocyclics are considerably more flexible. The coupling of small bond angle deformations to internal rotational angles gives rise to an equipotential energy surface known as the pseudorotation circuit.^{243,244} The five internal dihedral angles, ϕ_i , are highly correlated to one another because of geometric restrictions from ring constraints. This correlation is apparent in a plot of ϕ_i vs any one of the internal angles (e.g., ϕ_3), whereby elliptical paths of the pseudorotation circuit connect equipotential points between torsional extremes of $\pm 42^\circ$ (Figure 30).^{245,246} From the crystal structure of ACPC hexamer, the five internal torsions within each of the six cyclopentyl residues are superimposed on the cyclopentyl pseudorotation circuit in Figure 30. It can be seen that nearly all of the ring dihedrals conform very well to the cyclopentane pseudorotation circuit. Only rings 3 and 6 show minor deviations from the expected correlations, suggesting either a slight deformation away from ideality or possibly limitations in the X-ray refinement of these two rings. In great contrast to the ACHC case, the C_α - C_β torsional angles (ϕ_1) in ACPC are significantly more

variable, taking on a range of values from 7.3° to 41.2° . Traversing along the helical backbone from one ring to the next, no obvious pattern in dihedral values emerges, which is somewhat surprising given the regular backbone conformation. In addition to the noted variability in ϕ_1 , the ring substituents deviate significantly from the nearly ideal gauche conformation of ACHC. The greater flexibility about ϕ_1 and the deviation from gauche geometry are apparently the major factors responsible for the tighter 12-helix in ACPC oligomers.

Recently, β -peptide oligomers from *cis*-substituted oxetane rings have been synthesized and studied.²⁴⁷ Molecular modeling and NMR NOE data in $CDCl_3$ and C_6D_6 on the hexamer have identified a helical secondary structure stabilized by four **S(10)** H-bonding interactions. Although **S(10)**-stabilized turns are known in β -peptides,^{248,249} this is the first example of the repetition of this pattern to generate a 10-helix. Thus, while the cyclopentane and cyclohexane β -amino acid oligomers adopt the 12- and 14-helix, respectively, and **S(8)** interactions produce a ribbon structure in cyclopropane-based β -peptides,²²⁶ the *cis*-oxetanes take on the intermediate **S(10)** H-bond ring size, giving a consistent trend. These latest results build on the general theme, previously mentioned, that foldamer conformations are sensitive to small residue changes. Finally, it should be mentioned that furanose²⁵⁰ and pyranose²⁵¹ carbopeptides having a β -amino acid repeating unit are under development,

but thus far, no information is available on the secondary structures of these presumably water-soluble backbones.

The 14-helix conformation of the β -peptide oligomers prepared by the Seebach group was also rigorously established in solution and the solid state. The first clues about solution structure for these β -peptides were revealed by the dramatic changes in CD spectra that accompanied an increase in chain length. The β -dipeptide and β -tripeptide showed CD traces that resembled that of the unstructured α -hexapeptide Val-Ala-Leu-Val-Ala-Leu-OMe in MeOH. In contrast to the CD spectrum of the unstructured α -hexapeptide, the corresponding β -hexapeptide exhibited a strong, broad minimum at 216 nm, a zero crossover at 207 nm, and a maximum at 198 nm (Figure 28).²²³ The spectrum of the β -hexapeptide was independent of concentration and, with the exception of sulfuric acid, independent of solvent. As noted above, the crystal structure of Boc- β -tripeptide **3** shows a turn-like conformation as a consequence of adopting a *sc* dihedral angle about one of the C_{α} - C_{β} bonds (Figure 25). This turn was envisioned as the starting point of a helix that could arise in longer sequences. ¹H NMR data was used to study the solution structure of the β -hexapeptide in pyridine-*d*₅ (a NMR structure in MeOH was later elucidated to corroborate the pyridine-*d*₅ NMR solution structure and CD data).²⁵² An analysis of coupling constants revealed hindered rotation around the C_{α} - C_{β} bond on the NMR time scale, while prevalent NOE's were observed between $NH^i-C_{\beta}H^{i+2}$ and $NH^i-C_{\beta}H^{i+3}$. The corresponding distance and bond angle restraints from coupling constants were used to compute a set of solution structures. The spiraling conformation of this β -hexapeptide is a 14-helix, similar to that identified for *trans*-ACHC. This finding was rather surprising given the short, hexameric chain length and the intuition that β -peptide backbones without rigidification are more flexible than α -peptides, which are typically unstructured if they possess less than 15–20 residues.

The CD data of Seebach's β -peptides differ somewhat from the 14-helix ACHC hexamer of Gellman (Figure 28). Although ¹H NMR data establish that the 14-helix conformation is adopted by H-(β^3 -HVal- β^3 -HAla- β^3 -HLeu)₂-OH, the differences at lower wavelengths are not easily explained. Gellman interpreted this to mean that the Seebach β -peptides and the *trans*-ACHC oligomers equilibrate between the 14-helix and other conformations in solution.²³⁹ The recorded CD may thus reflect averages of the various conformations, and therefore, the observed variations could indicate different populations of the 14-helix by these two classes of β -peptides. Longer β^3 -peptides, up to 15-mer, exhibited a very similar CD pattern, although the signal intensity increased significantly.²⁵³ It can be assumed, based on the magnitude of the Cotton effect, that longer chains contribute to greater conformational stability by increasing the set of ordered conformations relative to the ensemble of disordered conformations. However, the consistent CD pattern suggests that the distribution of conformations among those in the set

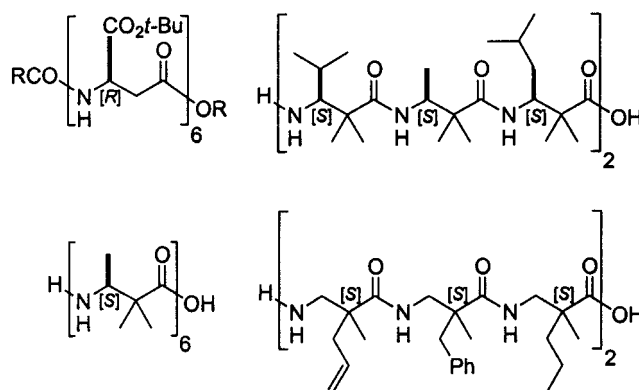


Figure 31. Examples of β -peptides that exhibit strong Cotton effects but whose structures are presumably incompatible with 14-helix conformation.

of ordered structures does not depend on chain length. An even greater mystery with regard to the CD spectra has emerged recently following studies of β -peptides that are presumably (vide infra) unable to adopt the 14-helix conformation (Figure 31).²⁵⁴ Surprisingly, these oligomers still exhibited strong Cotton effects with CD spectra matching that of the 14-helix. A compilation of CD data for a large number of β -peptides showed little variation despite putative differences in their secondary structures.²⁵⁴ The authors concluded that an interpretation of the CD spectra will have to wait until NMR solution structures become available. They went on to claim that at the present stage of knowledge, there is little structural information in CD spectra and CD is not a conclusive tool for determining β -peptide structures.

ii. Systematic Backbone and Sequence Variations in β -Peptides. Systematic backbone and sequence modification constitutes a powerful approach to learn about the fundamental interactions that contribute to the stability of secondary structure. For example, disulfide linkages have proven to be a valuable tool in the study of α -peptides by introducing conformational restrictions in order to verify the spatial relationships of side-chain positions. Jacobi et al. applied this technique to β -peptides to demonstrate the relationship of side chains in sequences prone to adopt the 14-helix conformation (Figure 32).²⁵⁵ For the 14-helix, a disulfide bridge is possible between lateral positions *i* and *i*+3 but not between *i* and *i*+4. In the former case, disulfide formation will prevent the helix from unwinding, while in the latter case, macrocycle formation can only occur if the helix unwinds. Air oxidation of β^3 -peptides with cysteine (CH_2SH) and homocysteine (CH_2CH_2SH) side chains gave the corresponding disulfide-containing macrocycles. Macrocycles from the *i* and *i*+3 positioned cysteine residues give CD spectra characteristic of the 14-helix in MeOH and H₂O. The ¹H NMR solution structure of this macrocycle has been determined to be that of the expected helical conformation.²⁵⁶ The corresponding macrocycles that result from linking the *i* and *i*+3 homocysteine units give weaker CD spectra in MeOH, while in H₂O, all evidence of helical secondary structure was absent. As expected, macrocycles from the joining of *i* and *i*+4 cysteine or homocysteine units gave CD spectra that do not match the 14-helix.

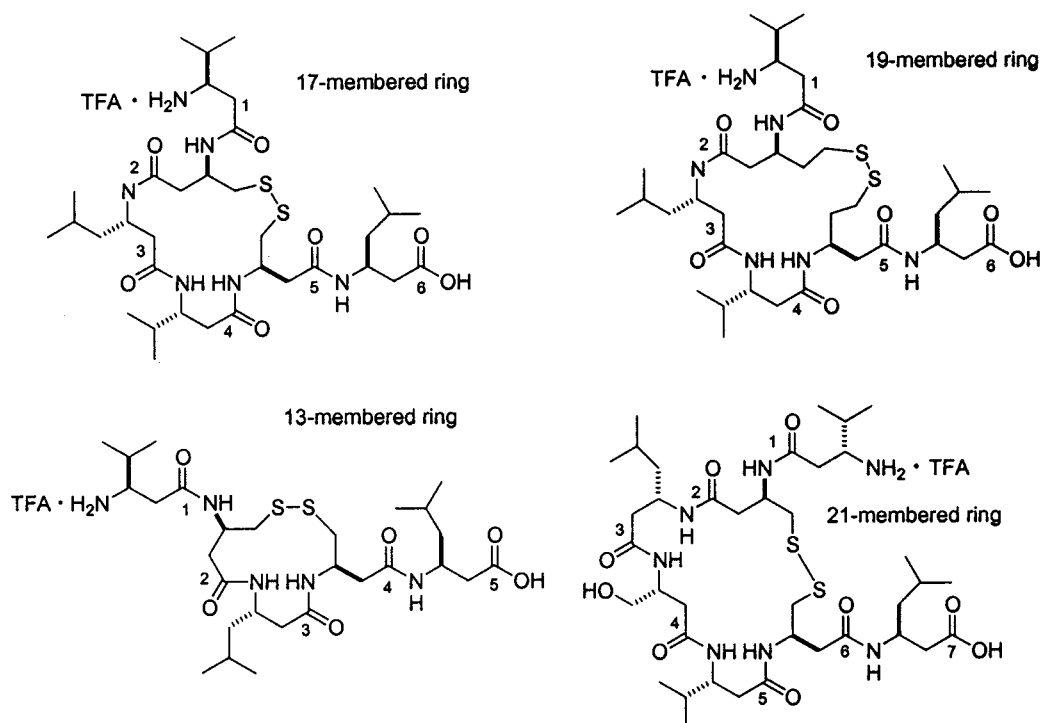


Figure 32. β -Peptides with β -HCys residues to demonstrate the side-chain relationship in sequences prone to adopt the 14-helix conformation through disulfide formation.

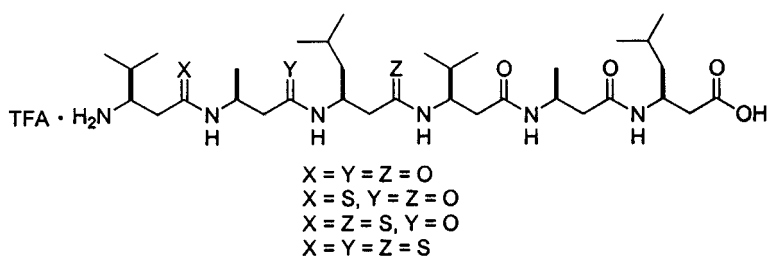


Figure 33. Backbones of monothio-, dithio-, and trithio- β -hexapeptides.

Thioamide replacement (i.e., thionation) introduces the C=S function as an isosteric substitution for C=O, perturbing H-bond donor and acceptor tendencies, and altering the geometry through a longer C=S bond length and a higher torsional barrier in the thioamide bond. Systematic studies on β -thiopeptides, while interesting, have yet to shed much light on the role of H-bonding or backbone rigidity on secondary structure stability in β -peptides.²⁵⁷ Monothio-, dithio-, and trithio- β -hexapeptides were prepared and studied (Figure 33). The solubility of the hexapeptides in organic solvents increased dramatically with the introduction of each C=S group. The CD spectra of these derivatives were difficult to interpret, but they suggest the presence of more than one secondary structure under various conditions. The β -trithiohexapeptide exhibited a pronounced exciton splitting of the $\pi \rightarrow \pi^*_{C=S}$ band, and the ^1H NMR solution structure in MeOH revealed the 14-helix to be the dominant conformation.

Although H-bonding interactions are typically invoked as a major contribution to secondary structure formation in β -peptides, the extent to which these interactions contribute to conformational stability is unclear.²⁵⁸ Should the monomer's torsional potential energy surface be sufficiently biased or solvophobic

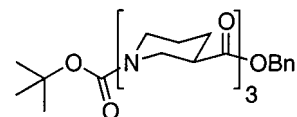
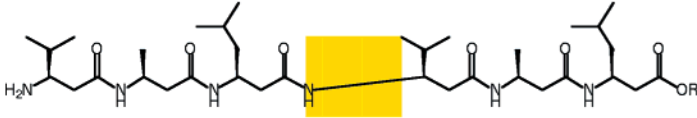
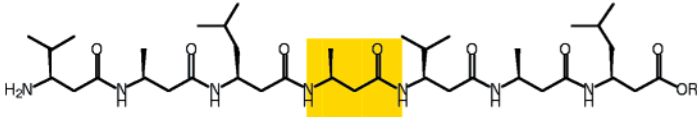
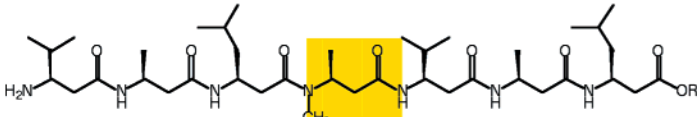
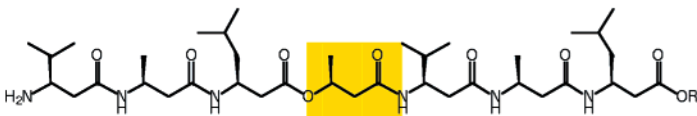
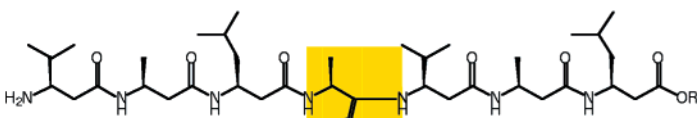
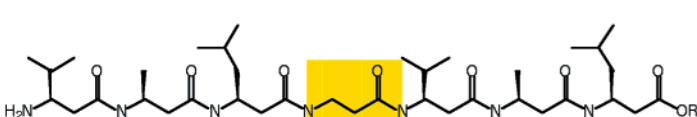


Figure 34. Structure of the β -tripeptide from β -HPro.

forces dominate secondary structure formation, one might expect that H-bond interactions could be eliminated without significant consequence. Surely in a solvent like MeOH, there is only a small energy difference between an intramolecular H-bond and a MeOH-amide H-bond. The fact that oligomers and polymers of proline²⁵⁹ as well as peptoids¹⁴⁰ adopt discrete secondary structures is clear evidence that H-bonds are not essential to ordered solution conformations of amide backbones.²⁵⁸ In 1999, Gellman²⁶⁰ and Seebach²⁶¹ both reported non-hydrogen-bonded secondary structure formation in β -peptides by preparing and studying analogues of proline (Figure 34). Complex mixtures of *cis* and *trans* amide rotamers were detected by ^1H NMR spectroscopy,²⁶¹ and this complexity has hampered conformational studies in solution. Nonetheless, CD spectra of these oligomers display intense and distinct patterns. Systematic studies of CD spectra as a function of chain length provided clues that these oligoproline analogues

Table 2. Single Residue Mutants Used To Probe the Structure of β -Peptides²⁵²

Sequence	Mutant	CD
	Original sequence	14-helix
	Original sequence extended by one internal β^3 -HAla	14-helix
	N-methylation (steric and H-bond perturbations)	Loss of CD pattern corresponding to 14-helix
	Replacement of NH by O (H-bond perturbation)	Loss of CD pattern corresponding to 14-helix
	Removal of one methylene group	Loss of CD pattern corresponding to 14-helix
	Omission of substituents.	Solvent dependent CD. MeOH: 14-helix H ₂ O/MeOH: loss of CD pattern corresponding to 14-helix

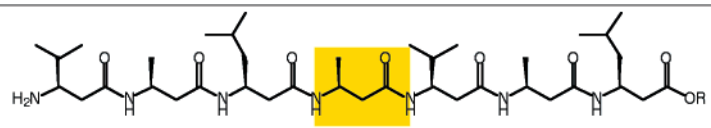
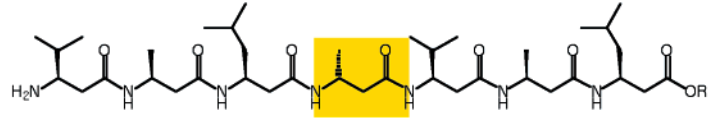
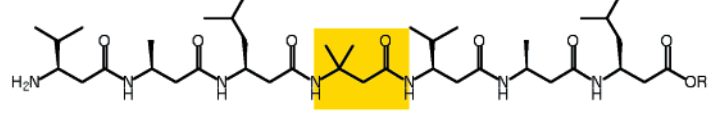
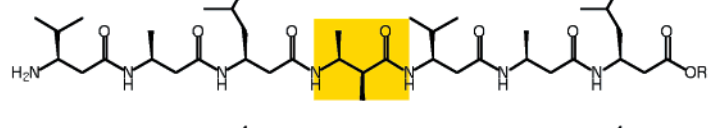
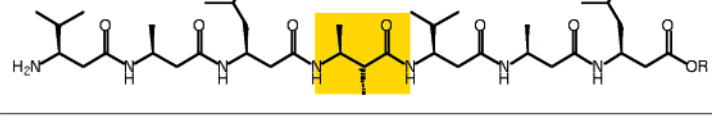
adopt regular secondary structure in MeOH and that the extent of secondary structure formation is maximal once four residues are in place.²⁶⁰ On the basis of the β -tripeptide crystal structure, ¹H NMR coupling constants, and assumptions based on conformational analysis, Seebach proposed a 10₃ right-handed helix for the (*S*)- β^3 -homoproline chain. This extended conformation is a further example that illustrates how the preferred backbone conformation around the central C _{α} -C _{β} bond dominates the secondary structure of β -peptides.

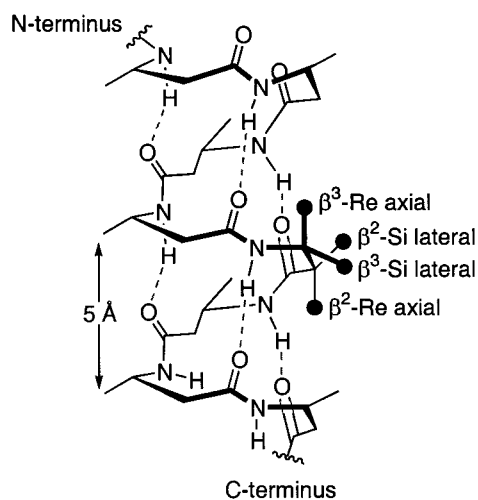
Seebach's helical molecular model led his group to test how variations in backbone constitution and stereochemical modifications stabilized or destabilized the secondary structure.²⁵² Incorporation of a single amino acid residue into the center of the original β^3 -hexapeptide HVal-HAla-HLeu-HVal-HAla-HLeu-OMe sequence generated a series of single point mutations (Table 2). As predicted by Seebach's model,²²³ many relatively minor structural changes to the central residue were incompatible with the 14-helix, resulting in sequences that did not show the characteristic CD pattern of the 14-helix. These included *N*-methylation (i.e., an *N*-Me β -amino acid), replacement of NH by O (i.e., a β -depsipeptide), and removal of the CH₂ group (an α -amino acid). These observations suggested that proper dihedral angles, H-bonding, and a periodic backbone are necessary in order to maintain conformational integrity. The absence of side-chain substituents on the central β -amino acid residue also destabilized the helical

secondary structure. Specifically, a sequence containing the 3-aminopropanoyl unit (β -HGly, i.e., loss of single methyl side chain) gave a CD spectrum that became highly dependent on solvent. In MeOH the CD spectrum of the β -HGly mutant was characteristic of the 14-helix, while in 1:1 MeOH:H₂O an entirely different and yet uncharacterized pattern emerged. These results pointed to a strongly biased torsional potential energy surface for β -peptides bearing side chains in the 2 or 3 position.²⁵² This is consistent with the subsequent observation that the helix to random conformation transition in β -peptides is a noncooperative process.²³⁴

A series of mutants having stereochemical variations in the central β -amino acid position revealed additional information (Table 3). According to Seebach's original model,²²³ the short pitch of the β -peptide helix and the equatorial orientation of the side chains with respect to the helical axis both place limits on substitution patterns that can sustain the helical secondary structure (Figure 35). Thus, lateral non-H-substituents in the 2- and 3-positions on the 3-amino acid residues of the helix were predicted not to interfere with the secondary structure, while axial ones were expected to disrupt the helix. This is borne out by the data in Table 3.²⁵² Incorporating a single mismatched residue in the central position of the β -heptadepsipeptide caused the CD pattern to disappear, while detailed NMR and CD data confirm the helical structure in mutants that have lateral substituents. The geminal dimethyl mutant is also

Table 3. Single Residue Mutants Used To Probe How Substituents on the β -Peptide Effect the 14-Helix Conformation²⁵²

Sequence	Mutant	CD
	Original sequence	14-helix
	Inversion of configuration at β^3	Loss of CD pattern corresponding to 14-helix
	Geminal dimethyl substitution at β^3	Loss of CD pattern corresponding to 14-helix
	<i>like</i> - $\beta^{2,3}$ -dimethyl substitution (methyl groups occupy lateral positions in the 14-helix)	Strong 14-helix signal
	<i>unlike</i> - $\beta^{2,3}$ substitution (methyl groups occupy a lateral and an axial position in the 14-helix)	Loss of CD pattern corresponding to 14-helix

**Figure 35.** Side view of the β -peptide 14-helix with 5 Å pitch. The black circles correspond to unspecified side chains.

consistent with this prediction since one of the methyl groups would be in the axial position. Here, the behavior is in contrast to α,α -disubstituted α -amino acids that are known to stabilize helical structures. Results based on NMR and CD data fully confirmed the predictions.

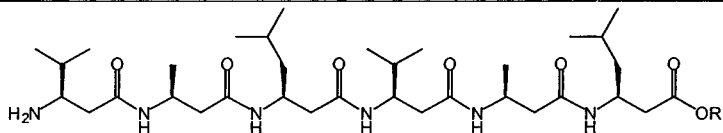
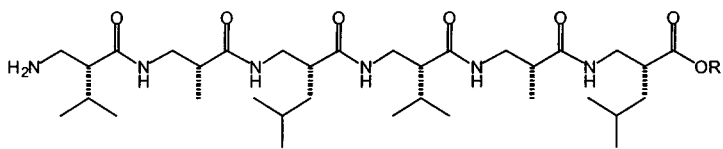
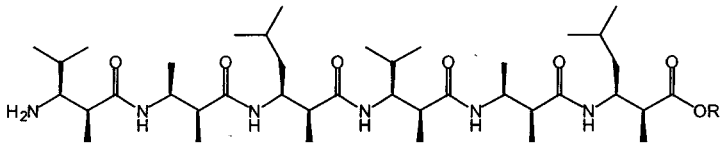
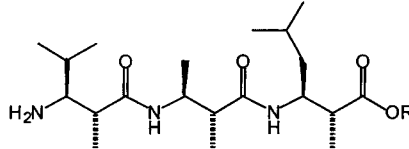
Noticeably absent from Table 3 are β -peptides from β -amino acids with side chains only in the 2-position (β^2 -amino acids). The isomeric β -peptide carrying the same side chains in the α - rather than β - position was predicted to also give the 14-helix secondary structure, but for the particular stereochemistry, shown in Table 4, the handedness was expected to be opposite of the previously studied β^3 -peptide. CD measurements on various β^2 peptide oligomers supported this prediction.^{253,262} Curiously, the magnitude

of the Cotton effect was relatively weak and strongly dependent on solvent and temperature, suggesting a less stable secondary structure for the β^2 vs β^3 sequence. This notion is consistent with calculations of the conformational potential energy surface of β -peptides.¹⁸⁵ These calculations show that β -substitution is more efficient than α -substitution in reducing the flexibility of the β -peptide backbone.

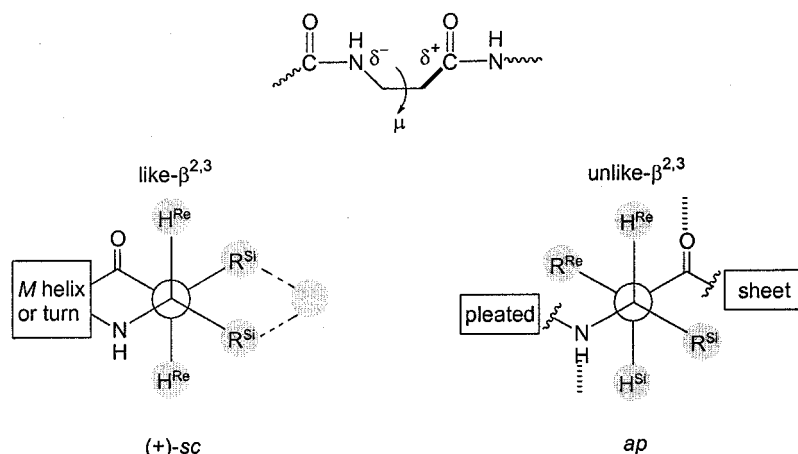
The strong CD signal from the stereochemical mutant carrying substituents in both the 2- and 3-positions (Table 3) suggested that this stereochemistry should favor the 14-helix. Indeed, a hexameric sequence made entirely from *like*- $\beta^{2,3}$ residues (Table 4) exhibited the characteristic CD pattern of the 14-helix, although the spectra recorded were not independent of concentration, suggestive of an aggregation phenomenon.²⁴⁹ Interestingly, the ¹H NMR solution structure and NH proton exchange studies on this sequence revealed that the peptide backbone is sterically protected by the many hydrophobic substituents, possibly to such a degree that crowding destabilizes the helix and causes it to unwind.

The simple “at-a-glance” predictive correlation that emerges from Tables 3 and 4 is as follows: with the peptide backbone drawn in the plane of paper, substituents in the same “half space” (i.e., *like*-configuration) are all matched to the same helical handedness. This correlation can be rationalized by analyzing the basic conformers in β -amino acids.^{183,184,263,264} Such an analysis reveals a strongly preferred backbone torsion around the C_α - C_β bond, driven in part by the tendency to minimize repulsive vicinal interactions (Figure 36)²⁴⁹ and possibly by internal electrostatic considerations.¹⁸⁴ The *sc* conformation, favored for monosubstituted β^2 - or β^3 -residues (especially if the substituents are bulky)²⁶³

Table 4. β -Peptide Amino Acid Sequences Probing the Effects of Stereochemistry and Substitution of the 14-Helix Conformation

Sequence	Sequence description	Assigned Structure
	Original sequence – a β^3 -amino acid	14-helix (<i>M</i>) ^a
	A β^2 amino acid sequence	14-helix (<i>P</i>) ^b
	A <i>like</i> - $\beta^{2,3}$ -amino acid sequence	14-helix; forms aggregates ^c
	An <i>unlike</i> - $\beta^{2,3}$ amino acid sequence	Extended strand ^d

^a Reference 223. ^b Reference 262. ^c Reference 249. ^d Reference 201.

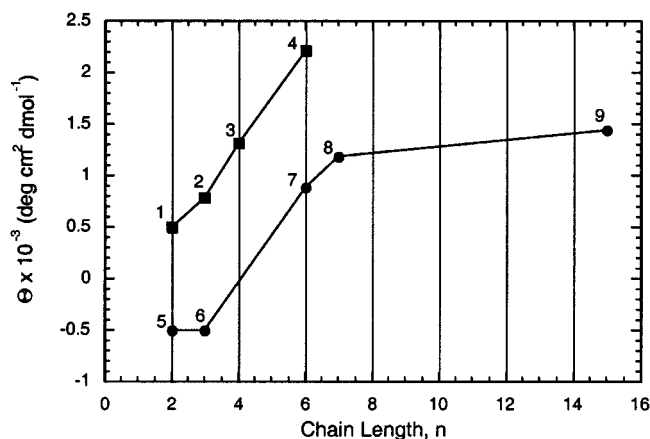
**Figure 36.** *sc* and *ap* conformations about the C_α – C_β bond of β -amino acid residues. Schematic depiction of the electrostatic considerations that favor the *sp* conformation.

and *like*- $\beta^{2,3}$ disubstituted residues, promotes helical or turn conformations. The *ap* conformation, favored for *unlike*- $\beta^{2,3}$ disubstituted residues, promotes an extended, strand-like structure (vide infra). Geminally disubstituted residues have no preferred conformation about the C_α – C_β bond, although axial positions in a helical conformation would destabilize a 14-helix (Figure 35).

iii. Cooperativity. Cooperative conformational order results from multiple noncovalent interactions between nonadjacent chain segments. A critical chain length and sigmoidal transitions are the hallmarks of cooperative ordering mechanisms. In the specific case of helical conformations, this behavior can be understood^{265–267} as resulting from a minimum number of residues required to nucleate stable helix propagation. Since the propagating helix is stabilized by noncovalent interactions between nonadjacent

repeat units, the critical nucleus size generally corresponds to a chain length of at least one turn. Experimental observations^{268,269} on helix-forming α -peptides are in good agreement with theory, although a deeper understanding of the specific interactions responsible for this cooperativity is still developing.^{258,270,271}

For β -peptide secondary structures, cooperative formation has been investigated in various ways. One test of cooperativity involves examining the onset of conformational order as a function of chain length. The earliest study of this sort for discrete β -peptide oligomer appears to date back to 1979 on poly(*S*- β AspOiBu).¹⁹⁸ However, at that time the structure of the ordered conformation was not understood. Clues about cooperativity in forming the 14-helix with β -peptides can be found from CD studies. Figure 37 shows a plot of CD intensity (normalized per



Data Point	Sequence	Conc.	Ref.
1	Boc-(ACHC) ₂ -Bn	0.3 – 1.0 mM	239
2	Boc-(ACHC) ₃ -Bn	0.3 – 1.0 mM	239
3	Boc-(ACHC) ₄ -Bn	0.3 – 1.0 mM	239
4	Boc-(ACHC) ₆ -Bn	0.3 – 1.0 mM	239
5	Boc-β ³ -HAla-β ³ -HLeu-OMe	0.2 mM	223
6	Boc-β ³ -HVal-β ³ -HAla-β ³ -HLeu-OMe	0.2 mM	223
7	CF ₃ CO ₂ H-(H(β ³ -HVal-β ³ -HAla-β ³ -HLeu) ₂ -OMe	0.2 mM	223
8	CF ₃ CO ₂ H-H-β ³ -HVal-β ³ -HAla-β ³ -HLeu-β ³ -HAla-β ³ -HVal-β ³ -HAla-β ³ -HLeu-OH	0.2 mM	254
9	CF ₃ CO ₂ H-H-β ³ -HLeu-β ³ -HAla-β ³ -HVal-β ³ -HPhe-β ³ -HVal-β ³ -HAla-β ³ -HLeu-β ³ -HPhe-β ³ -HLeu-β ³ -HAla-β ³ -HVal-β ³ -HPhe-β ³ -HVal-β ³ -HAla-β ³ -HLeu-OH	0.02 mM	253

Figure 37. Intensity of the CD maximum in the vicinity of 215 nm normalized per backbone amide bond as a function of the chain length. All of the spectra were taken in methanol. The sequence and concentration of the individual points are listed in the table. The signs of the CD signals were chosen such that all sequences have the same stereochemical configuration in the β³-position.

amide) vs the number of residues for Gellman's and Seebach's 14-helix forming β-peptides. In the Gellman series,²³⁹ a significant CD intensity is already present in the dimer, even though such a chain is too short to form a complete turn. The steady rise in CD intensity from dimer to hexamer suggests a continuous growth in 14-helix population, which presumably in the long chain limit will reach an asymptotic value. On the basis of this behavior, the backbone appears to be highly preorganized for the helical conformation and is reminiscent of helically templated polypeptides.²⁷² Although the steady rise of CD intensity was claimed by Gellman to be evidence that formation of the 14-helix involves a cooperative process,²³⁹ the dihedral angles of these β-peptides are highly constrained, possibly precluding this backbone from exhibiting cooperative conformational transitions.

In comparison to Gellman's conformationally constrained β-peptides, the Seebach β³-peptides display chain-length dependence^{223,253,273} more typical of α-peptides (Figure 37). The dimer and trimer show weak Cotton effects, uncharacteristic of the 14-helix. Beyond the trimer, a rapid rise in CD intensity is observed, and a plateau is reached for chains of sufficient length. Thus, a threshold chain length seems necessary to initiate conformational order and an asymptotic limit appears to exist. Although the behavior of Seebach's β-peptides shown in Figure 37 appears characteristic of cooperative helix formation,

temperature-dependent CD and ¹H NMR studies reveal that the dominant contribution to helix stability in these β-peptides is related to the preferred conformation about the C_α-C_β bond.²⁷⁴ The intensity of CD signals and ¹H NMR chemical shifts changed linearly with temperature over the range from 100 K up to 393 K. This temperature spans the theoretically predicted melting temperature of ca. 340 K.²⁷⁵ A cooperative melting transition in which the whole structure is lost all at once would be expected to show a sigmoidal rather than linear temperature dependence. Thus, rather than displaying all-or-none behavior characteristic of two-state phenomena, the 14-helix gradually populates nonhelical conformations as the temperature is raised. If the predominant stabilizing force were a collection of long-range, noncovalent interactions (e.g., hydrophobic interactions or H-bonds between nonadjacent segments), cooperative behavior would be expected. In contrast, conformational changes that result from a redistribution of the populations of localized torsional states will gradually become depleted in the helical conformation. Such a process cannot be considered cooperative. This noncooperative behavior is consistent with the lack of observed melting in β-peptides.²⁷⁴ On the basis of these results, it seems that the β-peptide derives its helix-inducing propensity from its torsional potential energy surface.¹⁸⁵

iv. Heterosequences. Heterosequences incorporating both β² and β³ amino acids were also synthesized and with appropriate matching of stereochemistry (i.e., like-configuration) were expected to exhibit the 14-helix. However, their behavior was found to be surprising (Table 5).²⁴⁹ The CD spectra of many oligomer sequences did not show the usual 215/200-nm CD pattern in MeOH, but rather a CD spectrum with an intense single peak at ca. 205 nm was observed (Figure 28). Complicating matters further, this behavior depended somewhat on the terminal protecting groups.²⁴⁹ With *N*-Boc and benzyl ester protecting groups intact, the unusual CD pattern was generally observed, while deprotection mostly gave CD spectra characteristic of the 14-helix. The extreme intensity of the CD signal for the protected forms together with the very long half-lives of the NH/ND exchange rates suggested a new ordered conformation. This was confirmed by detailed ¹H NMR solution-structure analyses which revealed a novel irregular helix consisting of three H-bonded turns: a central 10-membered ring and two 12-membered H-bonded rings (designated 12/10-helix). Molecular dynamics studies have simulated reversible folding into this unique conformation.²⁷⁶

Direct structural evidence for the 10-membered H-bonded ring was found in the crystal structure of a geminally disubstituted tripeptide.²⁷⁷ The *N*-terminal carboxy group and the amide NH of the second amino acid H-bond form a tight turn. This ring is quite similar to the central 10-membered H-bonded ring of the 12/10-helix. Interestingly, even tighter turns could be generated in sequences derived from 1-(aminomethyl)cyclopropanecarboxylic acid.²²⁶ As mentioned above (Figure 26), the conformational constraints in this β-amino acid induce the **S(8)**

Table 5. Role of Sequence Variation and End Groups on the Solution Conformation of β -Peptides

Sequence	Description	End groups	Assigned Structure ^a
	A β^2 -block- β^3 -sequence	R=Boc R'=Bn	12/10-helix
		R=H R'=H ^b	14-helix
	A β^2 -alternating- β^3 sequence	n=1, R=Boc, R'=Bn	12/10-helix
		n=1, R=H, R'=H ^b	12/10-helix ^c
		n=2, R=Boc, R'=Bn	12/10-helix
		n=2, R=H, R'=H ^b	14-helix
	A β^2 - β^3 heterosequence	R=Boc R'=Bn	12/10-helix

^a On the basis of CD spectra in MeOH. ^b Trifluoroacetate salt. ^c Also based on NMR structure determination.

H-bonding pattern between next neighbors. This is an example of residue-controlled or substituent-induced turn formation, and it illustrates how the monomer's torsional potential energy surface can be biased to regulate backbone conformation.

The 12/10 secondary structure was rationalized on the basis of solvophobic interactions.²⁴⁹ Whereas the 14-helix conformation of the β^2 -alternating- β^3 sequence does not provide close interactions between side chains in successive turns, in the 12/10-helix they are directly atop one another. Solvophobic interactions with the terminal protecting groups explained why the protected forms were more prone to adopt the 12/10-helix. In the unprotected form, the dipole moment of the 14-helix may add stability through charge–pole interactions.^{234,249} An alternative rationalization is one that illustrates negative design principles. Whereas many patterns of alkyl substitution disrupt the 14-helix, they only cause mild destabilization of the 12/10-helix pattern.¹⁸⁵ Thus, it is possible to destabilize (i.e., design away) the 14-helix in favor of the 12/10-helix. Regardless of interpretation, in 1997, when Seebach's group communicated their initial findings on the β^2 - β^3 -co-oligomers, it became apparent from this work²⁴⁸ and the related studies by Gellman²³⁸ that the β -peptides are likely to have a high degree of variability in secondary structure type.

v. Water-Soluble β -Peptide Foldamers. Following earlier observations,^{278,279} Seebach's initial paper on β -peptide oligomers showed that this backbone is remarkably resistant to proteolytic digestion and, hence, potentially useful as a candidate for new drugs.²²³ Consequently, there has been considerable activity on the development of β -peptides that are both highly water soluble and conformationally structured in aqueous solution. Several groups have

contributed to the discovery of stable secondary structures from β -peptides in aqueous solution. Some of the oligomers examined for this purpose can be found in Figure 38. To enhance water solubility, β -peptides containing polar serine and lysine side chains were synthesized and studied.^{253,280} While in MeOH these oligomers exhibited the CD profile typical of the 14-helix, in aqueous solution fewer of the oligomers studied maintained this pattern. Those that did exhibit spectral characteristics of the 14-helix in water did so with much reduced intensity. Moreover, in both organic as well as aqueous solvents, the presence of a large number of neighboring cationic side chains destabilizes the secondary structure, consistent with the well-known behavior of poly-(α -homolysine).²¹² It was concluded that oligomers with neutral serine-derived side chains have a smaller helix-disrupting effect in water than the charged lysine derivatives. However, β -peptides that are hydroxylated in the α -position appear to be void of helical secondary structure.²³⁵

To reduce the disruptive consequences of several charged groups, β -peptide sequences having just one polar side chain (either homoglutamate or homolysine) were studied by Gung and Zou (Figure 38).²⁸¹ However, these heptamers were poorly soluble in water. Heptamers bearing two β -HGLu or one β -HGLu and a C-terminal aspartate (D-Asp) were synthesized next and found to be soluble in water up to concentrations from ca. 5 to more than 15 mM (without significant aggregation). However, in going from MeOH to H₂O, the helical content decreased as judged by CD, and no NOE cross-peaks characteristic of the 14-helix were observed in water. It is interesting to note however, that the peptide sequence with the D-Asp C-terminus gave considerably greater CD intensity at 216 nm than the sequence differing by

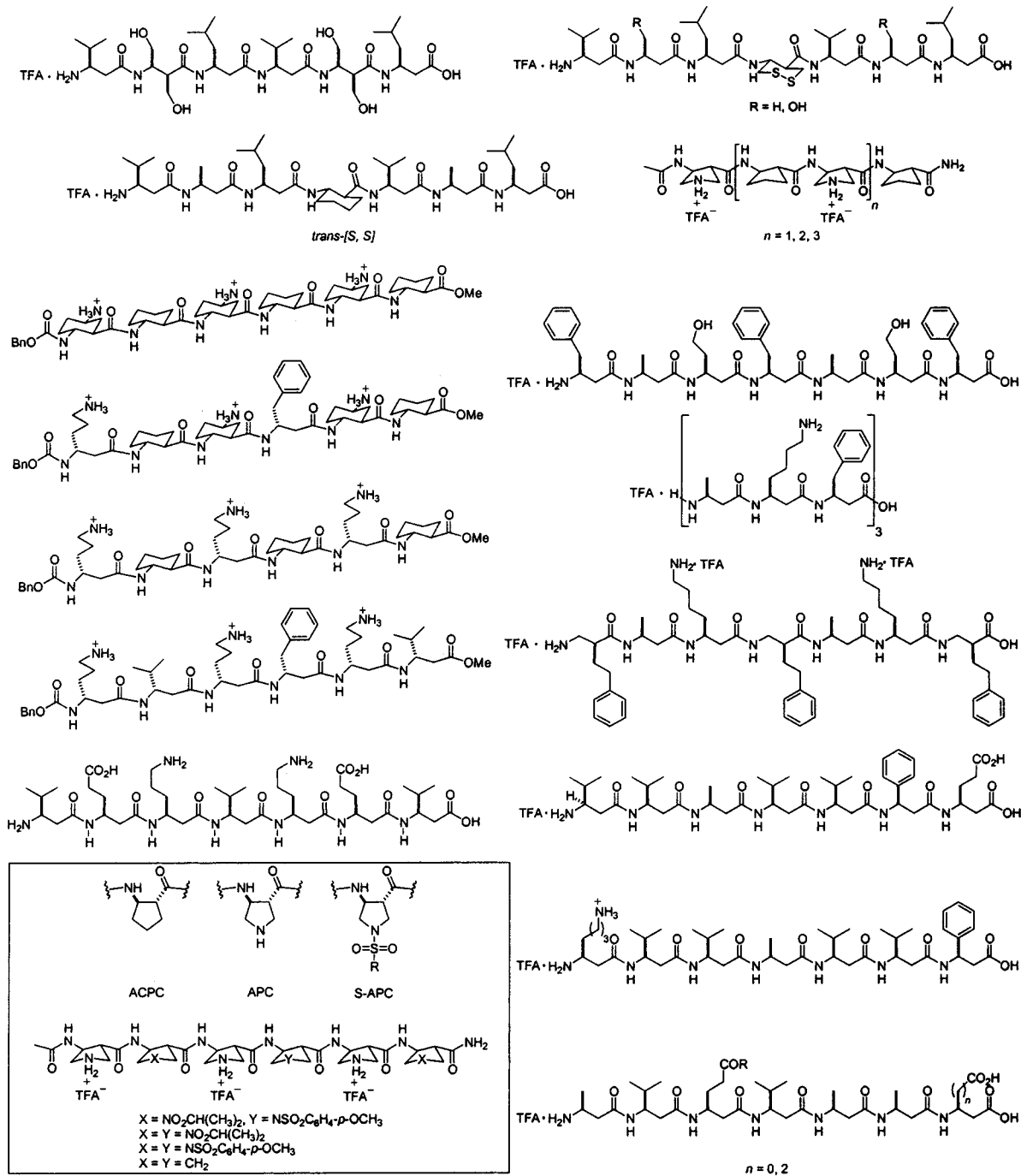


Figure 38. Water-soluble β -peptide oligomers.

only two CH_2 units, suggesting that D-Asp may provide some type of stabilizing C-capping interaction.

Gellman showed that by limiting backbone flexibility it is possible to overcome the poor stability of the 14-helix in aqueous media.²⁸² His group performed systematic studies on oligomers having varying proportions of rigidifying cyclohexyl and acyclic β -amino acid residues (Figure 38). To promote water solubility and reduce aggregation tendencies, an additional amino group was added to the cyclohexane ring of *trans*-2-aminocyclohexanecarboxylic acid (*R,R*-2,5-diaminocyclohexanecarboxylic acid, DCHC).²⁸³ In aqueous solution, all of the DCHC-containing hexameric oligomers displayed a broad CD spectrum with a maximum at 215 nm, characteristic

of the 14-helix. The intensity at 215 nm decreased by ca. 20% upon replacement of two cyclohexyl residues for acyclic residues. 1H NMR studies on this oligomer in water provided NOE data to corroborate the postulated 14-helix. However, with each successive replacement of a cyclic for an acyclic unit, a further decrease in CD intensity was observed, suggesting diminished stability of the 14-helix in H_2O with increasing acyclic content. Similarly, Gellman and co-workers showed that β -peptides containing four to eight pyrrolidine-based residues (APC) provide water-soluble oligomers that acquire the 12-helix conformation in aqueous solution as determined by CD and 1H NMR (Figure 38).²⁸⁴ A recently reported modification of this backbone involves *N*-sulfonylation (S-APC) that enables the modular introduction

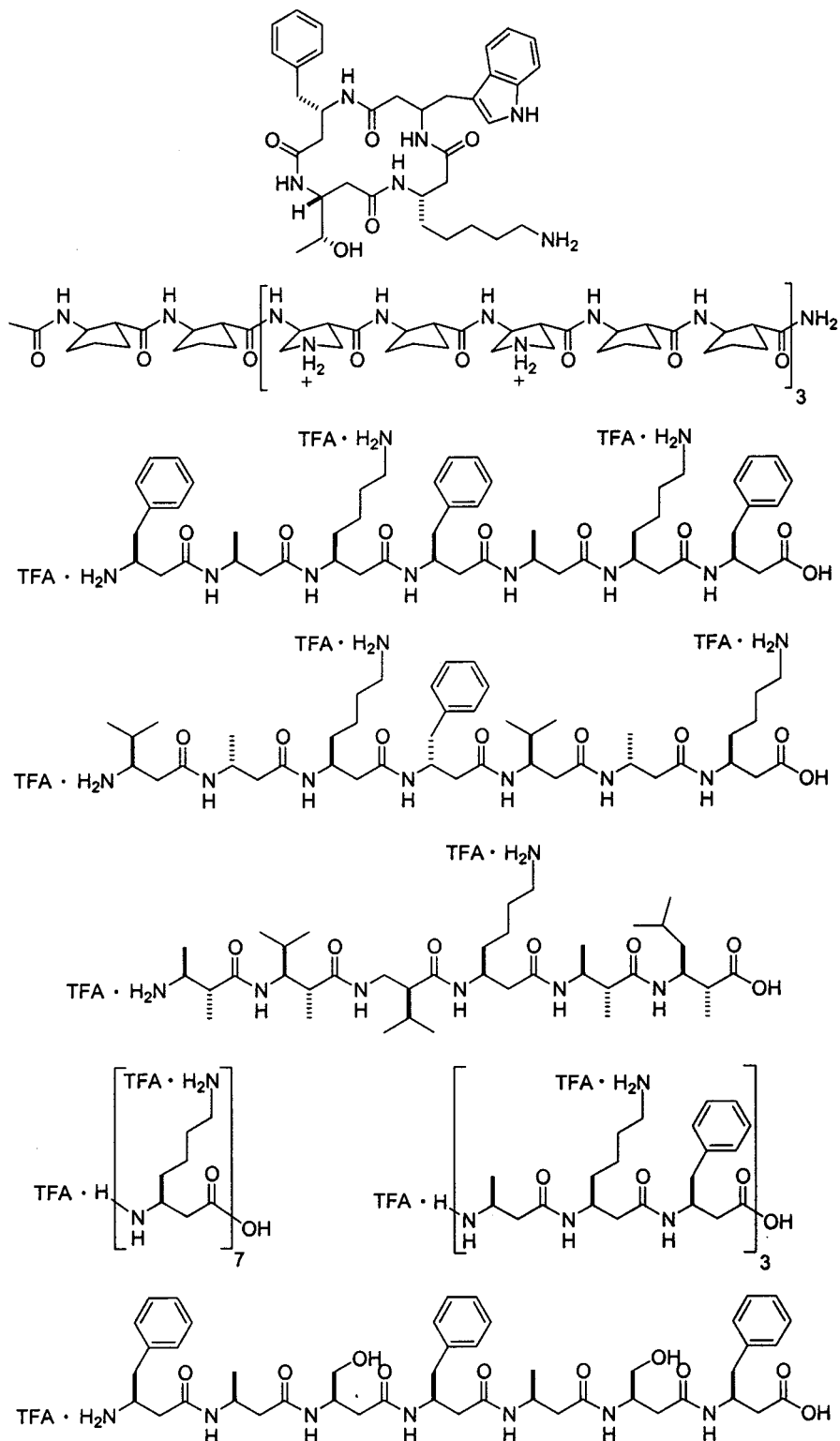


Figure 39. β -Peptide oligomers studied for their biological activity.

of a wide range of side chains onto the APC unit.²⁸⁵ Despite the change in the geometry of the five-membered ring upon sulfonylation, the 12-helix persists, although somewhat more tightly wound.

Seebach further pursued the design of water-soluble helical β -peptides based on sequences having minimal conformational constraints.²⁸⁶ Following on their observation that *like-2,3*-disubstituted β -amino acids increase the stability of the 14-helix conformation, they prepared monomers carrying two serine or

two cysteine side chains and incorporated these into β -hexa- and β -heptapeptides (Figure 38). Ionic side chains were excluded on the basis of their tendency to destabilize the 14-helix conformation. Deprotection of the thiol groups resulted in cyclic disulfide formation in the case of cysteine-containing sequences. To study the CD contribution of the disulfide chromophore, the carbocyclic analogue was also prepared. All of these sequences including the hexapeptide showed a CD spectrum in H_2O characteristic of the

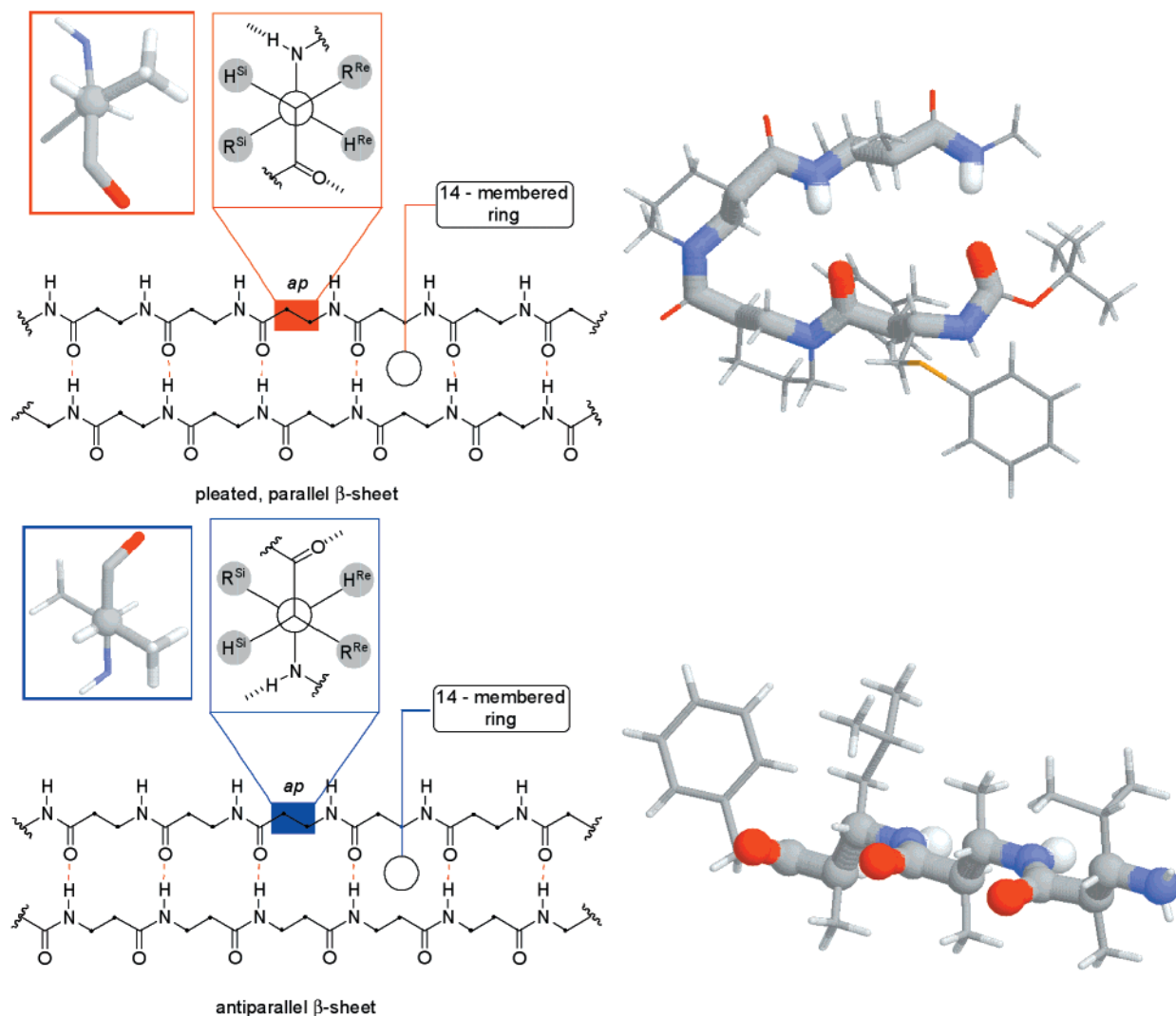


Figure 40. Crystal structures of β -peptide sequences with antiparallel and parallel β -sheetlike structures.²⁰¹ The backbone is rendered in thick cylinders. Newman projections show representative C_{α} – C_{β} dihedral angles in the *ap* conformation.

14-helix. Whereas the hexapeptide without conformational restriction gave no NOE cross-peaks indicating little helical content in water, the heptapeptide containing the cyclic disulfide showed NOEs characteristic of the 14-helix. The low intensity of these cross-peaks suggested that only partially helical conformations, or a mixture of helical and non-helical chains, exist for this sequence under these conditions.

The successful development of water-soluble β -peptides having helical conformations from sequences that do not contain any constrained monomers was achieved using salt-bridge stabilization strategies (Figure 38). This approach was realized independently by Seebach²⁸⁷ and DeGrado.²⁸⁸ Both of these studies showed, by NMR and CD methods, that electrostatic interactions between the side chains of acyclic β -amino acids produce a well-defined 14-helix in aqueous media. Since charged groups resulted from deprotonated acidic and protonated basic residues, the stability of the helical conformation was expected to be pH dependent. Indeed, the CD intensity was shown to reach a maximum at an intermediate value of pH in which the salt bridge would exist. DeGrado showed that the CD intensity depends

markedly on the concentration of added electrolyte. A plot of CD intensity versus the square root of NaCl molality is approximately sigmoidal, with a midpoint near 0.4 M (according to Debye–Hückel theory, the energy of electrostatic interactions between ions scales as the square root of $[\text{NaCl}]$).

vi. Biological Activity of β -Peptide Foldamers. The availability of conformationally structured, water-soluble β -peptide sequences, together with their known stability and resistance to enzymatic degradation,^{289,290} has led to some early observations regarding the biological activity of this oligomer class. Seebach and co-workers designed cyclic β -peptides containing only four residues that bind to the somatostatin receptor with micromolar affinity (Figure 39).²⁹¹ Hexa-, hepta-, and nonameric β -peptides carrying one to seven water-solubilizing groups have also been shown to be inhibitors of small intestinal cholesterol and fat adsorption.²⁹² A correlation was found between the ability of β -peptides to form an amphipathic 14-helix in MeOH and their inhibitory effect. DeGrado^{293,294} and Gellman²⁹⁵ used similar designs in mimicking natural membrane-active peptide toxins and antibiotics. A strong correlation exists among the sequences studied between the helical

content and antibacterial activity. To be therapeutically useful as antibiotics, they must function in the presence of human cells. Interestingly, favorable selectivities have been noted. These studies are clearly in their infancy but point to the likelihood that the β -peptide scaffolding holds much promise as a candidate for the molecular design of bioactive agents.

e. Strands and Turns: Artificial Sheets from β -Peptide Foldamers. There is currently considerable activity in the design and study of peptide sequences that serve as models of β -sheet secondary structures.^{136,156,296} Understanding how the substituent stereochemistry of β -amino acids influences backbone conformation has guided the design of β -peptide sequences with parallel and antiparallel β -sheetlike structures (Figure 40).²⁰¹ The *unlike- $\beta^{2,3}$* residues were predicted to adopt an extended conformation, and indeed, this has now been observed in several cases (Table 4). Although early studies on poly(β -peptides) suggested β -sheet formation from *unlike- $\beta^{2,3}$* residues,¹⁸⁹ the first oligomeric example of a β -strand from β -peptides appeared from Gellman's lab.²⁰⁰ The crystal structure displays the expected antiparallel sheet formation including a β -turn-like conformation stabilized by a 10-membered-ring hydrogen bond. This particular turn unit was based on earlier studies from Gellman's lab on the development of minimal hairpin structures in which it was found that the L-proline-glycolic acid segment functioned effectively.²⁹⁷ In contrast to the *unlike- $\beta^{2,3}$* disubstituted residues, Gellman showed that residues bearing only a single substituent did not lead to a well-ordered solution conformation.²⁰⁰

Whereas Gellman's original artificial β -sheet sequence utilized α -amino acids to fix the turn conformation, he later developed a β -peptide reverse turn that promotes hairpin formation.²⁹⁸ The design was based on nipecotic acid residues but required a heterochiral dipeptide sequence to stabilize antiparallel sheet structures.^{299,300} Seebach showed in 1999 that sequences consisting entirely of β -amino acids could be designed to achieve both turn and strand components.²⁰¹ To enforce an antiparallel pleated sheet arrangement, a turn segment was added between a pair of *unlike- $\beta^{2,3}$* residues. The turn design was based on the sequence that promoted the 12/10-helix. The introduction of the turn motif resulted in significantly enhanced solubility. ¹H NMR structure determination in methanol-*d*₄ showed that this β -peptide adopts both a hairpin arrangement and the expected antiparallel β -sheet. When no turn segment was present, the crystal structure of a tripeptide consisting of *unlike- $\beta^{2,3}$* residues showed 14-membered H-bonded rings in parallel pleated sheets (Figure 40). It can be seen that all of the carbonyl groups are aligned, leading to a polar sheet. Solubility decreased with increasing chain length. Other examples of reverse turns³⁰¹ and β -strands³⁰² from β -amino acids have appeared recently.

2. α -Aminoxy Acids

Another member of the β -peptide family is the α -aminoxy acid repeat, first discussed in the context of peptidomimetics by Yang et al.³⁰³ These authors

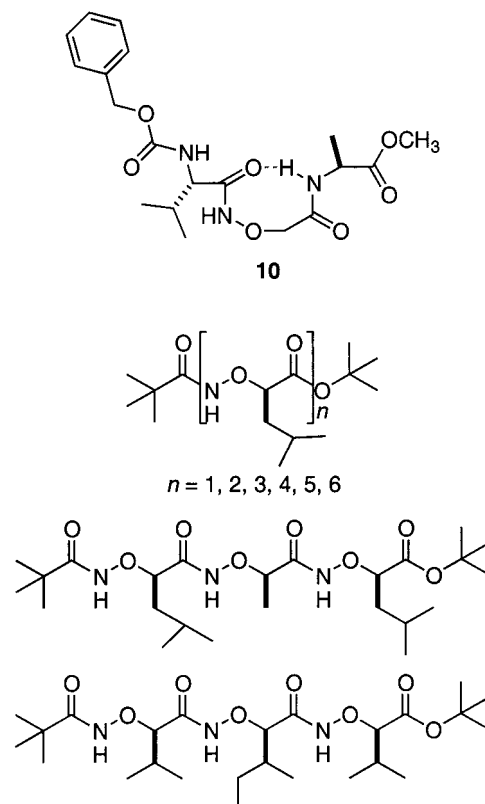


Figure 41. Representative examples of α -aminoxy peptide oligomers.

reasoned that the unusual torsional characteristics of the N–O bond in hydroxylamine resulting from lone-pair electron repulsion would help rigidify the β -peptide backbone. IR and ¹H NMR spectroscopic studies on a series of model compounds showed that an **S(8)** hydrogen bond is favorable, giving rise to a conformation analogous to the γ -turn motif found in proteins. In particular, the O–C bond of N-oxy amides strongly prefers out-of-plane orientations, and the barrier for rotation about the N–O bond is calculated to be about 7 kcal·mol⁻¹. The **S(8)** hydrogen bond between Val–C=O···H–N–Ala was evident in tripeptide **10** (Figure 41), leading to the suggestion that the “N–O turn” can be used as a novel type of backbone fold.

Peptides of α -aminoxy acids, i.e., oxa-peptides, are analogues of β -peptides, with C _{α} replaced by O. Extension of the model studies to higher oligomers from chiral α -aminoxy acid peptides resulted in a helical conformation owing to consecutive, right-handed N–O turns and **S(8)** hydrogen bonds (Figure 41).³⁰⁴ This conformation was supported by a combination of X-ray crystallography, NMR, CD, and computer simulation. Computer simulations predicted a conformation in which each turn consisted of 1.8 units.³⁰⁵ The helical structure was observed in oligomers as short as the trimer and was independent of side chains.

3. Sulfur-Containing β -Peptide Analogues

Several sulfur-containing β -peptide analogues have been generated (Figure 42). Oligomers in which the peptide bond has been replaced by the sulfonamide (i.e., β -sulfonopeptides),^{306–309} sulfonamide (i.e., β -sulfi-

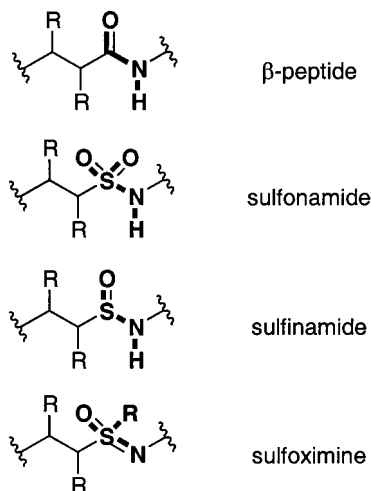


Figure 42. Structural comparison of sulfur-containing β -peptide analogues: oligomers in which the peptide bond has been replaced by sulfonamide (i.e., β -sulfonopeptides),³⁰⁶ sulfinamide (i.e., β -sulfinopeptides),³⁰⁷ or sulfoximine³¹⁰ functional groups.

nopeptides),³⁰⁷ or sulfoximine³¹⁰ moiety have been synthesized and are presently under consideration as possible foldamers. Replacement of the peptide bond with a secondary sulfonamide has two important conformational consequences.^{311,312} First, the barrier to rotation about the S–N bond is much lower than that of the peptide C–N bond. Second, the most favored dihedral angle defined by H–N–S=O is approximately 0° rather than 180° for the H–N–C=O unit.

At this time, relatively little solution characterization work has been performed to show that these oligomers adopt regular secondary structures. Evidence for **S(12)** hydrogen bonding in dipeptides of unsubstituted³⁰⁶ or chiral, β -substituted^{308,313} β -sulfonamides has been found by IR and ^1H NMR spectroscopies. However, in each case, terminal unit

carbamate or amide carbonyl oxygen atoms serve as the H-bond acceptor, owing to the very poor hydrogen-bond acceptor ability of the sulfonamide group.³¹³ It is unclear if these H-bonding interactions will be important in oligomers where the terminal groups play a minor role. To begin to address this issue, Gellman recently evaluated the possibility of two-point hydrogen bonding between a secondary sulfonamide and an α -amino acid residue.³¹⁴ Evidence for intramolecular N–H \cdots O=S and N–H \cdots O=C interactions in chloroform was found from IR and ^1H NMR studies in a molecule containing a sulfonamide linked to a valine by a turn-forming segment.

Very little information is available on the solution conformations of sulfinamide or sulfoximine peptides. These examples clearly show how synthesis can far outpace structural studies in foldamer research, stemming from the difficulties of characterizing solution conformations for each new backbone type.

4. Hydrazino Peptides

Replacing the C_β atom in β -amino acid residues of β -peptides with nitrogen leads to hydrazino peptides.³¹⁵ As a result of this substitution, another H-bond donor and H-bond acceptor are contained within the backbone. Consequently, there is a fairly significant increase in the number of possible secondary structures that could be adopted by this repeat unit including H-bonded rings containing either odd or even numbers of atoms (Figure 43). Several helical and turn motifs were calculated to be stable,³¹⁵ some of which were analogous to their β -peptide counterparts, but there is as of yet no experimental data to support these predictions.

C. The γ -Peptide Family

1. γ -Peptide Foldamers

Like β -peptides, homopolymers of γ -peptides had long been known^{316–319} prior to the search for second-

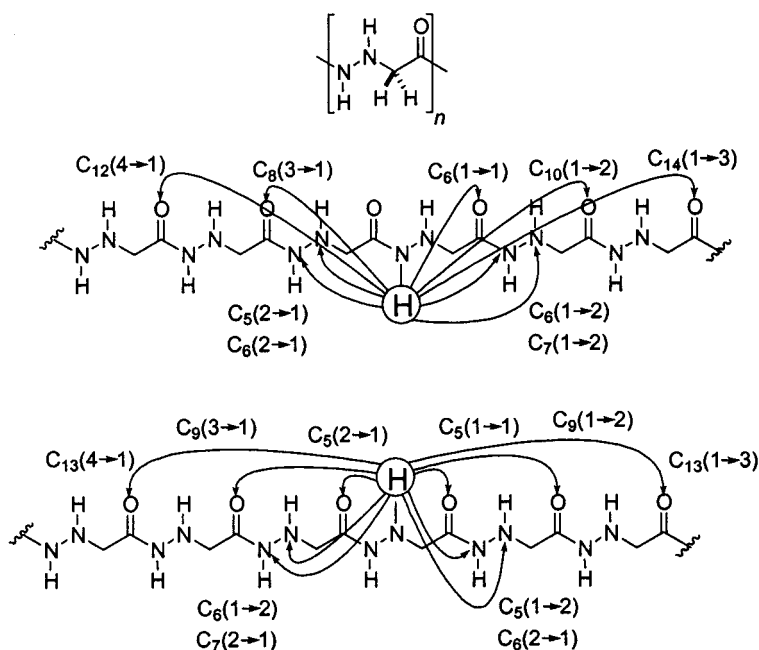


Figure 43. Hydrazino peptide backbones and a diagram showing the many possible intrastrand H-bond interactions in this backbone.

ary structures by systematic studies on discrete oligomers. However, unlike the poly- β -peptides for which helical structures have been clearly established,^{199,202} firm conclusions about the conformational preferences of homopolymers of γ -peptides appear not to have been resolved. From the results of ORD measurements, Rydon suggested a helical structure for the neutral form of poly- γ -D-glutamic acid.³¹⁸ Two left-handed helical models were proposed, both of which invoked three repeats per turn. The models differed as to whether **S(17)** or **S(19)** hydrogen-bonded interactions were involved.³¹⁸ Kajtár and Bruckner synthesized oligo- γ -L-glutamic acids from dimer to heptamer and showed that the ORD signal increases linearly with the chain length, suggesting that the polymer takes on a random conformation.³¹⁶ However, there appears to be no resolution to the question of whether these polymers are helical or conformationally random.^{192,320}

The added torsional degrees of freedom in γ -amino acids^{321,322} might be expected to promote conformationally disordered chains. Yet, just as for β -peptides, this intuitive view does not hold for the γ -peptides either. As stated by Seebach et al., "the surprising difference between the natural α -, and the analogous β - and γ -peptides is that the helix stability increases upon homologation of the residues."²³⁷

The first report demonstrating that chain molecules based on γ -amino acids form regular secondary structure appeared in 1992.³²³ This work targeted the discovery of new classes of protein-like substances with alternative backbones. These oligomers were considered to be vinylogous polypeptides since an (*E*)-ethenyl unit was inserted into each repeat unit to rigidify the backbone. To restrict rotation about the C_{β} - C_{γ} bond and extend the backbone into sheetlike conformations, an α -methyl substituent was initially examined. For this particular substitution pattern, allylic $A^{1,3}$ strain was expected to drive the γ -hydrogen to lie in the plane of the enamide. This conformational preference was borne out in a dipeptide which crystallized into a two-stranded antiparallel sheet; however, longer oligomers failed to form higher order sheetlike structures. Removal of the α -methyl substituent led to vinylogous peptides that organized into long stacks of parallel sheets as revealed by X-ray crystallography. To favor antiparallel alignment, a Pro-Gly dipeptide turn was inserted between a pair of vinylogous amino acids. ¹H NMR data supported the existence of an intramolecular H-bond between the N-H and O=C on the two ends, suggesting the preference of this secondary structure in solution. A peptide sequence which consisted of a vinylogous amino acid, the Pro-Gly turn, and a $\gamma^{2,3}$ -amino acid exhibited a helical conformation that contained 10- and 12-membered H-bond rings.

Two years later, a family of sulfur-containing γ -peptide mimics was reported.^{306,324} This backbone is linked by the sulfonamide group as a replacement for the peptide bond. Being derived from γ -amino- α,β -unsaturated sulfonic acids, these oligomers have come to be known as vinylogous sulfonamidopeptides, closely related to the vinylogous peptides described above. Protein-like side chains added to the γ -carbon gave chiral monomers. The folding patterns of short oligomers ranging from the dimer to the tetramer

have been investigated in solution and the solid state. In chloroform, IR and ¹H NMR studies reveal that the intramolecular H-bond preference is for **S(14)** rings involving the terminal carbamate C=O acceptor. This produces a turn-like motif that is also found in the crystal structures. However, in the solid state a fairly long intramolecular **S(12)** H-bond interaction is formed by utilizing one of the S=O acceptors. Here the carbamate carbonyl is tied up in a much shorter intermolecular H-bond interaction. Although a compact intramolecular H-bond fold is present in solution, the lack of involvement of the S=O bond in all of the oligomers studied calls into question the potential of this backbone to form long-range secondary structures.

In 1998, two reports appeared simultaneously showing that in contrast to this expectation, γ -peptide sequences form remarkably stable helical conformations in solution.^{236,237} The Seebach group described a γ^4 -hexapeptide analogue of the sequence H(-Val-Ala-Leu)₂-OH with L-configuration. Although the CD spectra did not reveal patterns characteristic of secondary structure, conformational analysis by NMR in either pyridine or methanol revealed a right-handed helix with **S(14)** H-bonds from the C=O of residue *i* to the H-N of residue *i*+3 and ca. 2.6 residues per turn. Molecular models of this conformation suggested that the side chains are oriented approximately perpendicular to the helical axis, the H-bonds lie along the helix axis with the dipole moment oriented from the N- to C-terminus, and the C_{α} - C_{β} and C_{β} - C_{γ} bonds adopt (+)-*sc* conformations for this right-handed helix.

Hanessian studied the solution structure of tetra-, hexa-, and octa- γ -peptide analogues of the sequence (-Ala-Val-).²³⁶ All three of these γ^4 -peptides derived from L-amino acids adopted stable right-handed helical conformations in solution. The helical parameters were identical to those found by the Seebach group: 2.6 residues per turn stabilized by **S(14)** H-bonds. Temperature-dependent chemical shifts suggested that these intrastrand interactions are strong. As also noted by Seebach, CD did not reveal a pattern diagnostic of secondary structure. The obvious but important lesson from these reports is that CD cannot be used alone as a means of screening for secondary structure.

Figure 44 compares the 14-helix of the β - and γ -peptides.³²⁵ It is interesting that both backbones prefer H-bond patterns involving 14 atom rings. Obviously these patterns originate differently for the two constitutions. In the case of β -peptides, the **S(14)** H-bond results from the N-H of residue *i*-2 being donated to the carbonyl of residue *i*. In the case of the γ -peptides, the N-H of residue *i* is donated to the carbonyl of residue *i*+3. As a result, with L-amino acids there is a reversal of helix sense, the β -peptide adopting an *M*-helix and the γ -peptide adopting the *P*-helix (as do α -peptides). The direction of the dipole moment is reversed too. Thus, for the β -peptide, the dipole is oriented from the C-terminus to the N-terminus, while for the γ -peptide, it runs from the N-terminus to the C-terminus (as with α -peptides).

Many substituent patterns and stereoisomers are possible for γ -amino acids, but as of yet, these have

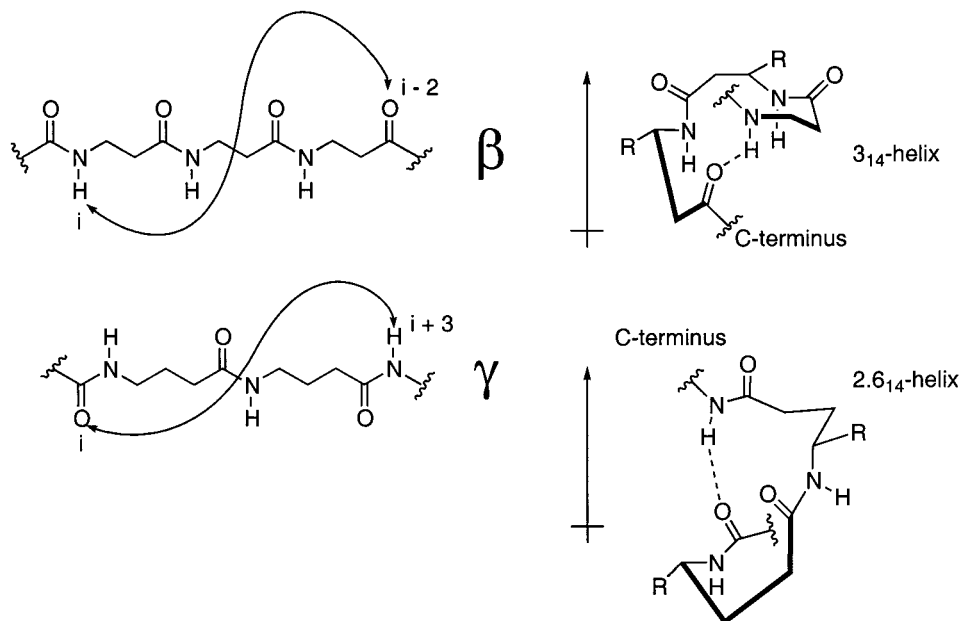


Figure 44. Comparison of helical conformations of β - and γ -peptides.

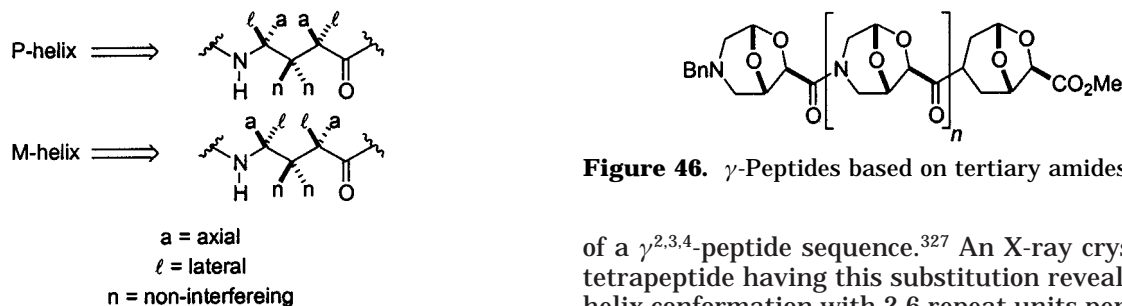


Figure 46. γ -Peptides based on tertiary amides.

Figure 45. Retroanalysis of γ -peptide helices' twist sense.

not been fully characterized. However, Hanessian's initial report²³⁶ included data on $\gamma^{2,4}$ -disubstituted residues. Their observations clearly showed that the addition of an α -substituent can either stabilize or destabilize the helical structure, depending on the relative stereochemistry. Whereas addition of an α -methyl group of *unlike*-configuration stabilized the helical conformation, addition of an α -methyl group having *like*-configuration resulted in the loss of helix formation. They later showed with a different sequence that the $\gamma^{2,4}$ -substitution pattern with L-stereochemistry leads to a reverse turn conformation, stabilized by an **S(14)** H-bond.³²⁶

The Seebach group also investigated substituent effects. On the basis of their helical model, they reasoned that substituents in positions 2 and 4 can occupy either lateral or axial orientations (Figure 45).³²⁵ Axial non-H atoms are projected nearly parallel to the helix axis and severely impinge on the space of the adjacent turn, resulting in helix destabilization. Lateral non-H atoms lie approximately perpendicular to the helix axis and do not experience unfavorable interactions. On position 3, both substituents are tilted with respect to the helix axis and thus oriented in such a way that neither stereochemistry is predicted to interfere with helix formation. These predictions are consistent with Hanessian's observations and are further supported by the study

of a $\gamma^{2,3,4}$ -peptide sequence.³²⁷ An X-ray crystal of a tetrapeptide having this substitution revealed a 14-helix conformation with 2.6 repeat units per turn. A ¹H NMR solution structure in methanol produced a structure nearly superimposed on that obtained by crystallographic analysis. The CD spectrum of this trisubstituted γ -peptide in methanol shows a maximum Cotton effect at 212 nm and zero-point crossing at ca. 196 nm.³²⁵ Other substitution patterns of the γ -peptides have not yet been reported in detail, but preliminary indications suggest that peptide sequences derived from γ^2 - and γ^3 -amino acids do not adopt a preferred secondary structure.³²⁵ However, γ^4 -peptides bearing α - or β -hydroxy groups have been synthesized, and although the structures are still being investigated, CD spectra suggest that these backbones are structured in solution.³²⁵

γ -Peptides that are based on tertiary amides and thus incapable of adopting conformations stabilized by H-bonding interactions have recently been prepared (Figure 46).³²⁸ These oligomers are derived from conformationally rigidified amino acids referred to as BTAA's (bicycles from tartaric acid). As with peptoids,¹⁴⁰ oligomers and polymers of proline,²⁵⁹ and β -peptides based on tertiary amides,^{260,261} complex mixtures of *cis* and *trans* amide rotamers were detected by ¹H NMR spectroscopy and thus hampered solution structure studies. Nonetheless, CD spectra of these oligomers display intense and distinct patterns. On the basis of these data, it was suggested that poly-BTAA's could form secondary structure in solution, although at this time there is no indication of the preferred backbone conformation.

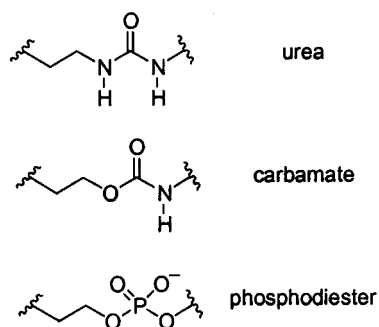


Figure 47. Collection of backbones that can be considered γ -peptide analogues.

2. Other Members of the γ -Peptide Family

Several groups are examining other peptidomimetic backbones, many of which can be classified in the γ -peptide family (Figure 47). Examples include oligoureas,^{329–334} oligocarbamates,^{330,335,336} and phosphodiester.³³⁷ Although at this time the conformational structure of most of these are unknown, it is apparent^{334,338} that they are being considered as foldamer candidates.

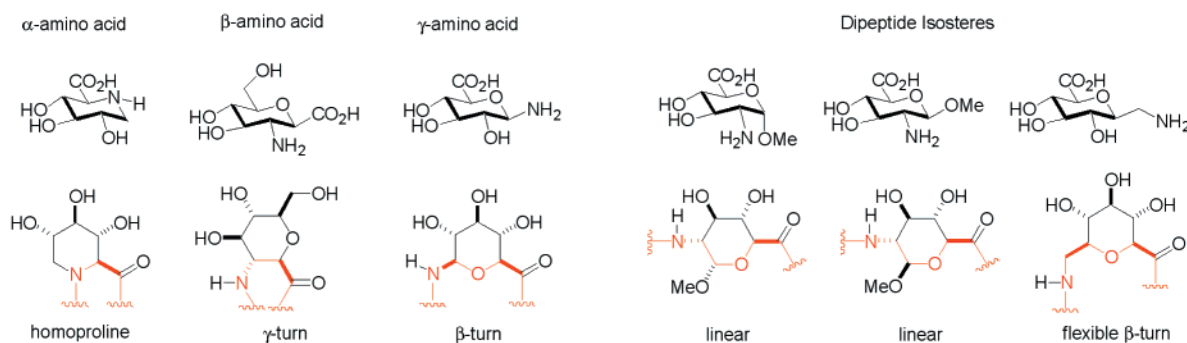


Figure 48. Structures and subunit shapes of sugar amino acids.

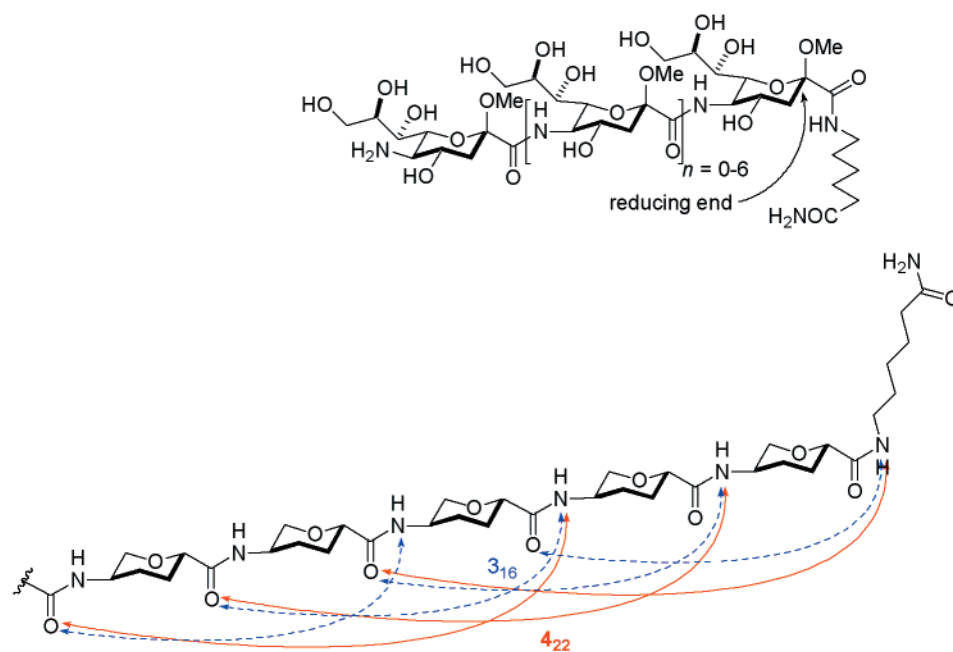


Figure 49. Structures and proposed H-bonding patterns of the 3_{16} and 4_{22} helix for sialooligomers.

D. The δ -Peptide Family

1. Alkene-Based δ -Amino Acids

Members of the δ -peptide family are isosteric replacements of dipeptide units. As such, this is the first member of the peptidomimetics lineage in which a single unit represents two or more α -peptide repeats. The β -turn is a common structural feature of proteins associated with the dipeptide fragment. Thus, it is not surprising that much activity in the δ -peptide family has been aimed at creating β -turn mimics. A long-standing approach has involved δ -amino acids in which the “missing” amide bond is replaced by a *trans*-carbon–carbon double bond.^{339–344} These studies tend to involve the incorporation of a single D-amino acid into a longer α -peptide sequence. Given our focus on peptidomimetic oligomers, the discussion that follows will be on chain sequences based on δ -amino acid repeating units, rather than on β -turn mimetics. Thus far, the chemical literature has mostly involved carbopeptoid backbones.

2. Carbopeptoids

The idea of using carbohydrate amino acids for both³⁴⁵ glyco-^{346–349} and peptidomimetics^{350–352} has

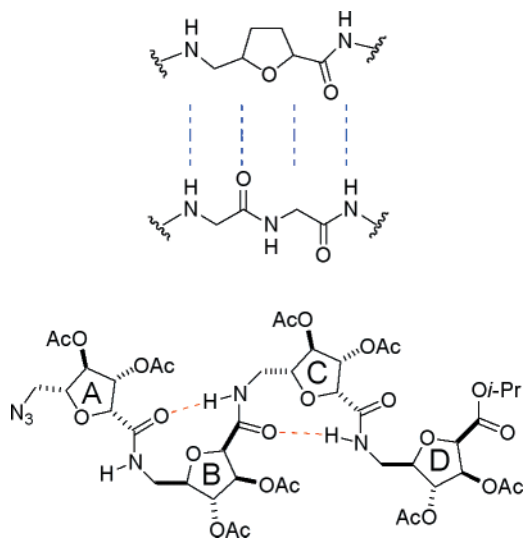


Figure 50. Representation of the solution-phase secondary structure for furanose-based carbopeptoids and a comparison between the α -peptide subunit and the furanose-based subunit as a dipeptide isostere.

gained interest recently. The conformational characteristics of carbohydrate residues incorporated into peptide chains were initially exploited for the rational design of a β -turn mimetic, at which time it was recognized that properly linked sugar amino acids could serve as a dipeptide replacement (Figure 48).³⁵⁰ Carbopeptoids,³⁴⁸ homooligomers of sugar amino acids, have been prepared from both furanose³⁵³ and pyranose³⁵⁴ residues. Additionally, cyclic homooligomers of sugar amino acids have also recently appeared.³⁵⁵

a. Pyranose-Based Carbopeptoid Foldamers.

Motivated by the fact that *O*-glycoside oligomers of sialic acid are helical in solution, Gervay and co-workers reported in 1998 that (1 \rightarrow 5) amide-linked sialooligomers longer than the trimer form ordered secondary structures in water (Figure 49).³⁵⁶ A combination of NMR-determined NH/ND exchange rates (in D₂O/DMSO) and circular dichroism studies (in H₂O) on a series of discrete oligomers showed that a critical length was necessary before evidence of conformational order emerged. However, the conformational features apparently varied with chain length. Thus, while the tetramer, pentamer, and hexamer showed slow exchange of their internal amide protons characteristic of strong intramolecular H-bonds, the heptamer strangely exchanged its protons quickly, suggesting the lack of an ordered structure. The octamer behaved like the pentamer and hexamer. Changes in peak-to-trough intensities as a function of chain length were used to further support the presence of ordered secondary structure in solution.³⁵⁷ In combination with molecular modeling, the hypothesis is that for the shorter oligomers **S(16)** H-bonding interactions stabilize a helix involving three residues per turn while for the octamer **S(22)** hydrogen bonding stabilizes a helix involving four residues per turn.

b. Furanose-Based Carbopeptoid Foldamers.

Shortly after Gervay's report on secondary structure in sialooligomers, Fleet and co-workers announced the observation of secondary structure in furanose

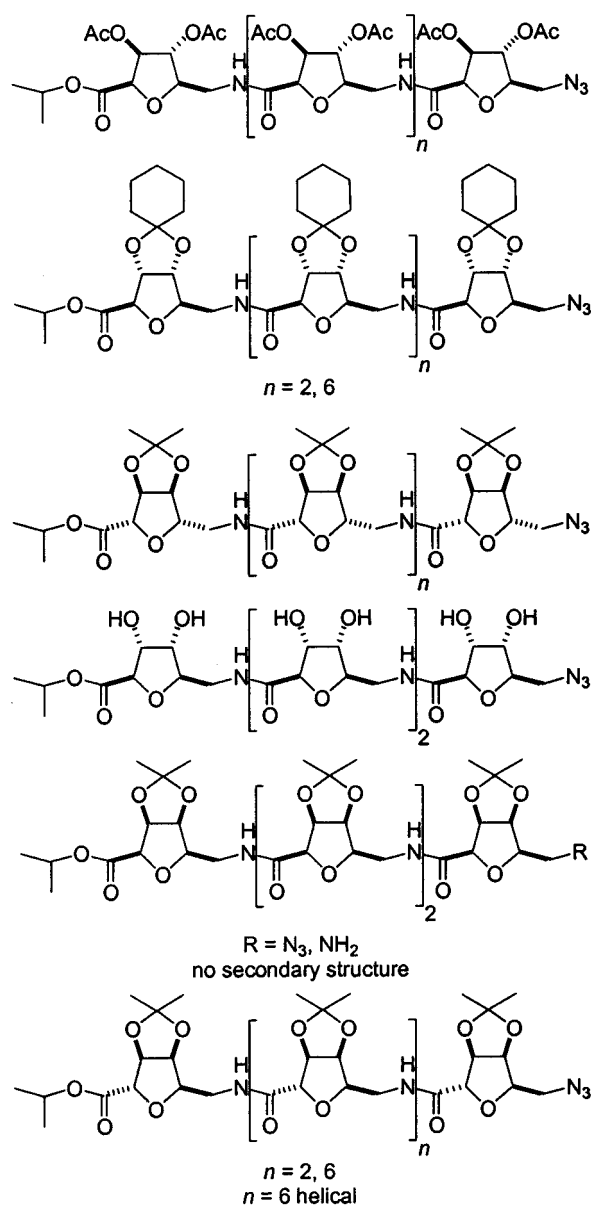


Figure 51. Stereochemical and substituent variations for furanose-based carbopeptoids.

carbopeptoids.³⁵⁸ Their initial finding was based on a β -D-arabino-furanose scaffold, δ -peptides in which each repeat unit can be considered as a dipeptide isostere. On the basis of ¹H NMR NOE data and molecular modeling, a repeating β -turn-type secondary structure was established for the tetramer in CDCl₃ (Figure 50). This structure appears to be stabilized by **S(10)** intramolecular H-bonds between repeat unit *i* and *i*-2.

Subsequent reports by Fleet and co-workers showed that the occurrence and specific type of secondary structure in these furanose-based carbopeptoid foldamers was strongly dependent on both the backbone stereochemistry and the stereochemistry of the ring substituents (Figure 51).^{359–361} Various *cis*-linked furanoses mostly exhibit the repeating β -turn-like conformation mentioned above.^{360,361} However, one of the *cis*-linked stereoisomers displayed no indication of secondary structure.³⁵⁹ This surprising result was rationalized in that one methyl group in the isopropylidene unit of the fused ring is positioned in a way

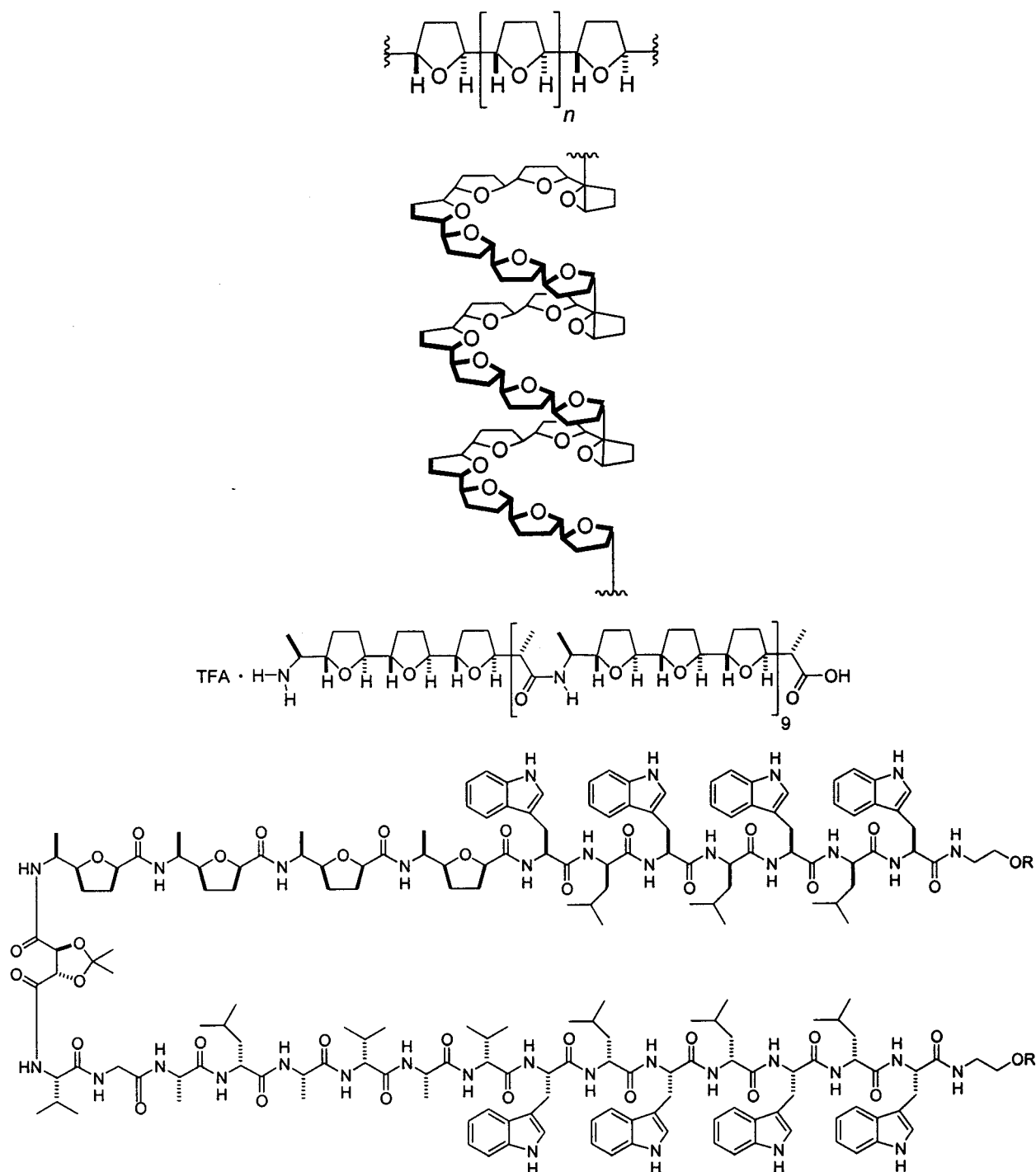


Figure 52. Representative structures of oligotetrahydrofuran amino acid sequences.

that sterically interferes with H-bond formation. In contrast to the β -turns found for the *cis*-linked furanoses, *trans*-linked furanose oligomers give a much different secondary structure. In initial reports that only studied chain lengths up to the tetramer, however, it appeared that no stable secondary structures in the *trans* isomer could be observed.³⁶² ^1H NMR was used to study the solution conformation of a *trans*-linked octamer. At this chain length, it was apparent that a new secondary structure had emerged. In contrast to the backbones derived from *cis*-isomers, long-range NOEs between sugar ring protons were observed. A repeating pattern of NOEs was detected along the backbone, indicating that a regular rela-

tionship exists between adjacent units. Simple modeling suggests a helical structure, stabilized by intrastrand $\text{N}-\text{H}^i \cdots \text{O}=\text{C}^{i-3}$ H-bonds. The conformational preference appeared stronger for octamer than the tetramer since the tetramer has only one stabilizing H-bond. A related octamer in which the protecting groups were removed was studied and found to give a strong Cotton effect at 216 nm in methanol and TFE.³⁶³

Fleet's carbopeptoids are closely related to the oligo tetrahydrofuran amino acid sequence used in the gramicidin-like peptide developed and studied by Koert and co-workers.³⁶⁴ These oligo-THF peptides (Figure 52) were inserted into synthetic lipid bilayer

membranes, and single channel conductance measurements were rationalized by assuming that the oligomers adopt a helical conformation consistent with a cationic channel. Koert's most recent molecular design evolved from his previous studies^{365,366} with 2,5-*trans*-linked THFs as polyether helices. One of his oligomers contained up to 27 furanyl rings and used stereogenic centers bearing methyl groups adjacent to the carbonyl and amino groups to stabilize the helical structure in the region of the peptide bond. The helical conformation was supported on the basis of NMR NOE data and conductance studies of planar lipid bilayers.

V. Single-Stranded Abiotic Foldamers

A. Overview

The peptidomimetic foldamers previously described utilized a top-down design approach; that is, the research involves systematic structural variations of parent chain molecules known to undergo folding reactions. In this section, we describe efforts toward foldamers best classified as employing bottom-up design approaches, involving the identification of novel, abiotic backbones that can fold into secondary structures akin to those found in proteins (helices and sheets). These foldamers often take advantage of rigidity inherent in aromatic units, torsional flexibility of the linkers, and various noncovalent interactions to adopt their discrete folded conformations.³⁶⁷ Since this search has been attempted through a variety of designs, these systems have yet to demonstrate the maturity seen with the peptidomimetics, although a few backbones show great promise and will be described in detail.

While several *polymeric* systems incorporating aromatics into the backbone have been shown to adopt helical conformations, many of these systems will not be described here (although some have previously been included in the literature as foldamers³⁶⁷). In the case of poly(aryl carbonate)s and poly(β -pyrrole)s, solution-phase helical conformations are favorable by atropisomeric bond torsions.^{368,369} Similar bond torsions preset the helical structures of poly(*o*-phenylene)s in the solid state.^{370,371} In contrast, poly(*m*-phenylene)s and poly(ether ketone) PK99, while their conformations are not specified by bond torsion, do not appear to adopt helical structures in solution.^{372,373} Additionally, a poly(*m*-phenylene ethynylene) has been shown to exhibit a reversible hydrogel state in water,³⁷⁴ and sexithiophenes with chiral side chains organize into supramolecular aggregates,^{375,376} but these two examples do not meet the essential criterion of having discrete chain lengths. In general, we have chosen to restrict our treatment of single-stranded foldamers with abiotic backbones according to the definition outlined in the introduction of this article, partitioned by primary folding force and oligomer backbone.

B. Backbones Utilizing Bipyridine Segments

1. Pyridine–Pyrimidines

Polyheterocyclic strands have been used in the spontaneous generation of well-defined secondary

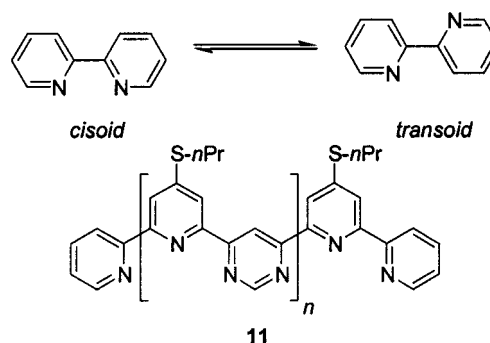


Figure 53. *Cisoid*–*transoid* equilibrium of 2,2'-bipyridine and the structure of oligomer series **11** ($n = 2, 5, 8, 9, 12$).

structures.^{377–380} This system is based on the preference of 2,2'-bipyridine to adopt a *transoid* conformation in solution (Figure 53). The *cisoid* (nonplanar) form of bipyridine has been calculated to be 5.7 kcal·mol⁻¹ less stable than the planar *transoid* conformation. Several other factors are also important for the proper design of a well-defined secondary structure. They include the correct sequence of heterocyclic aromatic rings, the proper linking of the rings at the appropriate positions, and the preference for the *transoid* conformation of the bond which links the aromatic rings. These features were combined in the synthesis and study of several different oligomer lengths **11** ($n = 2, 5, 8, 9, 12$) (Figure 53). The alternating pyridine and pyrimidine rings are connected at the *meta*-position, which provides the proper orientation for the rings to stack into a helical conformation. The helical conformation results from the steric repulsion between the CH groups and the electrostatic interaction stemming from nitrogen atoms on adjacent repeat units.

The sequence-specific, polyheterocyclic oligomers incorporated solubilizing thiopropyl side chains at the C-4 position of the pyridine ring.^{379,380} The characterization of the helical conformation of the oligomers in solution was achieved by a variety of techniques including UV–Vis, fluorescence, and NMR spectroscopy. The shortest oligomer **11** ($n = 2$) gave no indication of a helical conformation regardless of the technique that was employed. Despite the presence of overlapping, terminal pyridine ring, the absence of a helical conformation was attributed to the greater mobility since it can only form one turn. The longer oligomers ($n = 5, 8, 9, 12$) were found to adopt stable, helical conformations in solution (Figure 54). Fluorescence spectroscopy showed that **11** ($n = 5, 8, 9, 12$) in chloroform exhibited an excimer-like emission attributed to intramolecular excited state pyridine dimers. NMR spectroscopy showed that in each case only one folded conformation was observed, indicating the high specificity of the spontaneous helical generation. The assignments of the aromatic signals were made by a combination of COSY and ROESY NMR. In all cases, strong NOE interactions between the expected protons of different aromatic rings were observed in the ROESY NMR. Additional support was offered by a comparison of the chemical shifts of the aromatic protons, which showed progressive upfield shifts with increasing oligomer length,

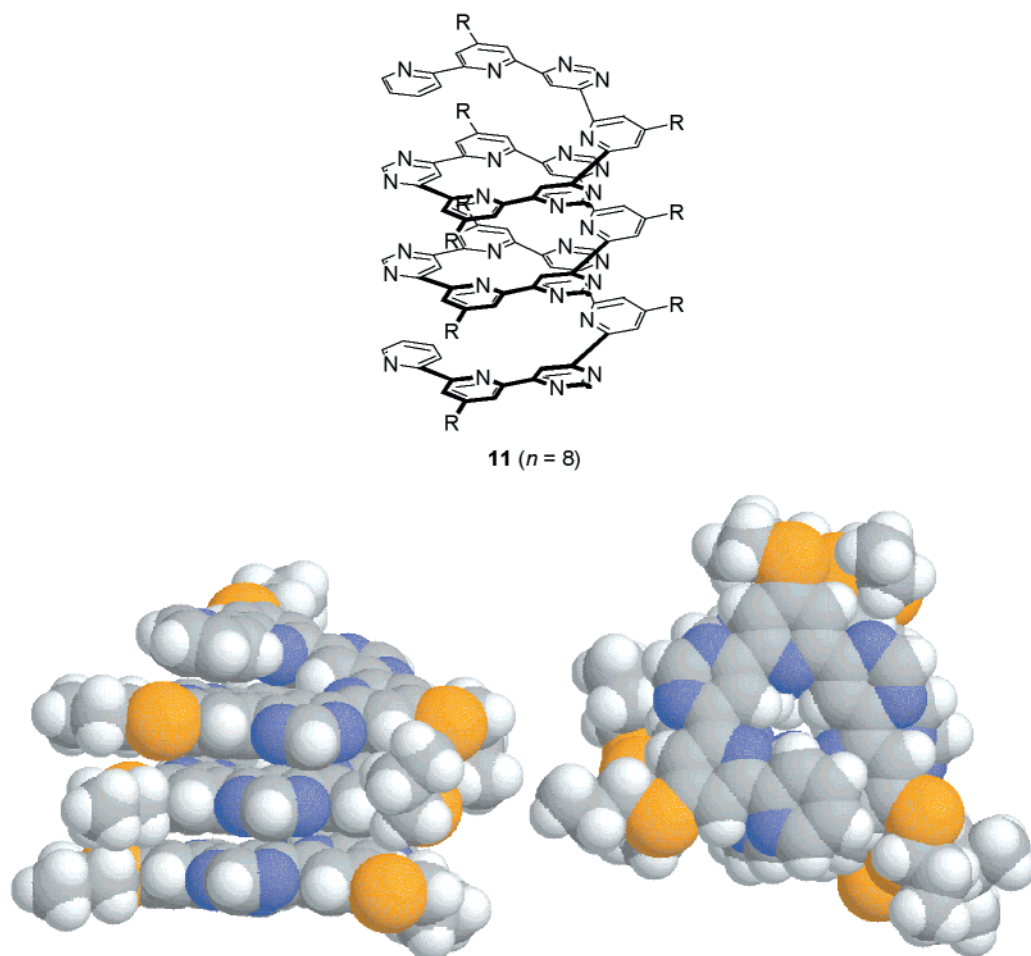


Figure 54. Drawing of the proposed helical conformation of oligomer **11** ($n = 8$), where $R = Sn\text{-}Pr$. Side (bottom left) and top (bottom right) view of the space-filling model of the crystal structure of pyridine–pyrimidine oligomer **11** ($n = 8$) in a helical conformation.

consistent with an increasing number of stacked aromatic rings.

The creation of a chiral, helical structure from polyheterocyclic strands resulted in a racemic mixture of *M* and *P* forms. By using variable temperature NMR and the diastereotopic α -thiomethylene protons, it was possible to determine the barrier to the helical inversion process. A value of $k = 85 \text{ s}^{-1}$ at 251 K and a free energy of activation of $\Delta G^\ddagger = 12.3 \text{ kcal}\cdot\text{mol}^{-1}$ was determined for shorter oligomer **11** ($n = 8$).³⁷⁷ In an analogous fashion, these values were determined for two of the longer oligomers **11** ($n = 5$) ($k = 85 \text{ s}^{-1}$ at 250 K and $\Delta G^\ddagger = 12.4 \text{ kcal}\cdot\text{mol}^{-1}$) and **11** ($n = 12$) ($k = 86 \text{ s}^{-1}$ and $\Delta G^\ddagger = 13.6 \text{ kcal}\cdot\text{mol}^{-1}$).³⁷⁹ The comparable activation free energies led to the proposal that the racemic helical conformation interconverted via a stepwise folding mechanism (Figure 55).³⁷⁹ Interestingly, while this interconversion is certainly dynamic, there is no evidence to indicate that these oligomers undergo the folding reaction (i.e., that they can unfold). The racemization between the *M* and *P* helical conformations was proposed to go through an intermediate, partially unfolded conformation (Figure 55, intermediate B). Furthermore, no spectroscopic evidence was offered to show that the oligomers exist in completely unfolded conformations.

The helical conformation of these oligomers was characterized in the solid state by using X-ray crystallography. Shorter oligomer **11** ($n = 5$) was found to pack in a centrosymmetric cell that contained an enantiomeric pair of oligomers.³⁷⁸ In addition, the helices were found to stack on top of one another creating long channels in the void space of the helix interior. The octamer of **11** was also determined to pack in a helical conformation in the solid-state (Figure 54).³⁷⁹ In this case, a unit cell was found to contain two molecules of only one twist sense, thereby creating a chiral channel from an achiral molecule. Spontaneous chiral resolution occurs concomitantly with crystallization. In both cases a helical pitch of 3.75 Å was determined along with an internal void space from ~ 2.5 to 3 Å. The high degree of solid-state organization led the authors to propose that these systems may have interesting electronic features, when compared to linear molecular wires.

2. Pyridine–Pyrimidines with Hydrazal Linkers

The previous design method has been shown to be highly effective for obtaining well-defined conformations in solution. However, the synthesis of the oligomers described above was challenging. In an attempt to overcome this limitation, Lehn et al. described the synthesis and study of oligomers that

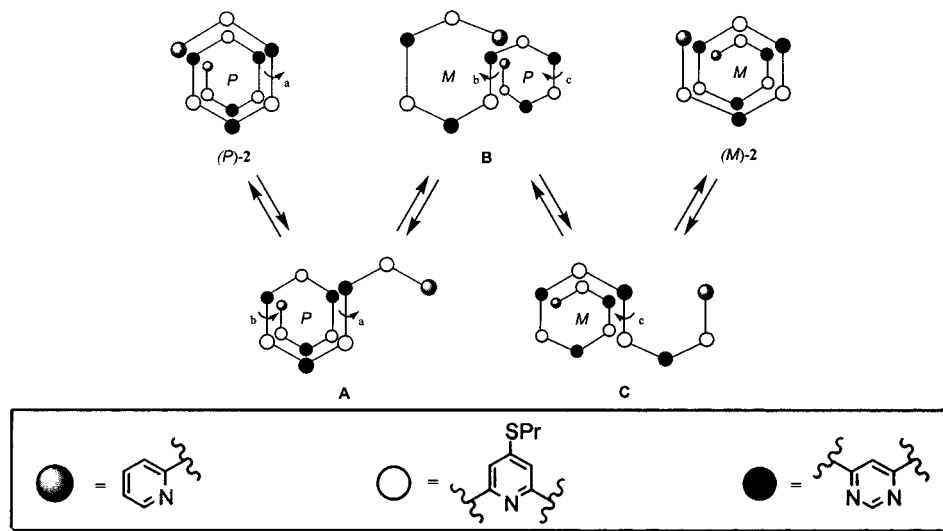


Figure 55. Stepwise mechanism for the helicity inversion of **11** ($n = 5$).

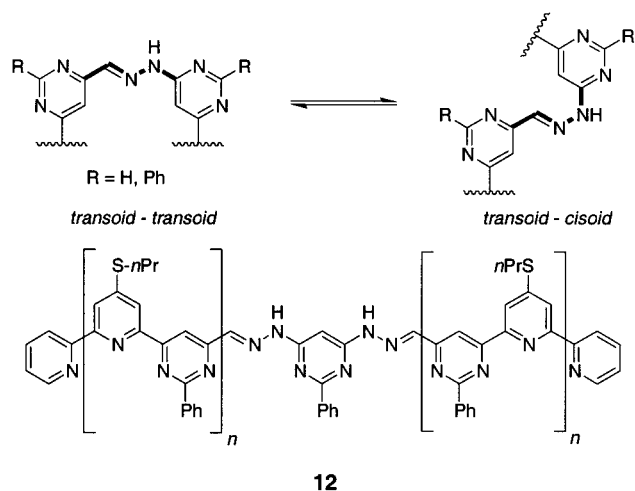


Figure 56. The *transoid*–*transoid* to *transoid*–*cisoid* equilibrium and structure of pyridine–pyrimidine oligomers with hydrazal linkers **12** ($n = 1, 3$).

are more amenable to stepwise synthesis while still taking advantage of selective torsions around adjacent pyridine–pyrimidine bonds.³⁸¹ The system is still based on the preference of 2,2'-bipyridine to adopt a *transoid* conformation in solution (Figure 53). However, the middle portion of the oligomer backbone contains a hydrazal group, which replaces the pyridine fragment of the previously studied oligomers. When α -substituted *N*-heterocycles are used, the *transoid*–*transoid* conformation (Figure 56) is preferred over others (*transoid*–*cisoid* shown for comparison) for several reasons. These include the minimization of secondary steric and electronic interactions, the increased amount of aromatic stacking that occurs when the imine is in the *transoid*–*transoid* conformation, and the conformational rigidity and planarity through conjugation. The synthesis of the desired oligomers **12** ($n = 1, 3$) (Figure 56) remained somewhat difficult but was simplified by having the hydrazal condensation as the final step.

The helical conformation was characterized by NMR spectroscopy and X-ray crystallography. Both oligomers displayed ¹H NMR consistent with a helical conformation as evidenced by the upfield shift of the

aromatic resonances on the terminal pyridine rings. From these data, it was concluded that the shorter oligomer **12** ($n = 1$) adopts a helical conformation of 1.5 turns and the longer oligomer **12** ($n = 3$) adopts a helical conformation containing 2.5 turns. The helical structure of **12** ($n = 1$) was confirmed by X-ray crystallography. The solid-state packing results in an internal cavity of 5.05 Å with the expected aromatic stacking distances of 3.46 Å. These results show that hydrazal condensation is a useful approach for creating longer helical strands and that a pyrimidine–hydrazone subunit is comparable to a pyridine–pyrimidine fragment in polyheterocyclic strands.

3. Pyridine–Pyridazines

Alternative attempts at creating well-defined helical conformations from polyheterocyclic strands have recently been reported by Lehn et al.³⁸² The same design criteria as that used for the previously studied systems was used except that an isomeric pyridine–pyridazine repeat unit was employed (Figure 57). The synthesis of oligomer **13** was accomplished by using a similar procedure to the pyridine–pyrimidine heteronuclear strands.³⁷⁸ It was proposed that **13** would yield a hexagonal, helical structure with 12 rings per turn and a central cavity of ~ 25 Å (determined by molecular modeling). The helical conformation of **13** in solution was characterized by large upfield shifts of the proton resonances for the terminal pyridine rings. The chemical shifts of all aromatic resonances were found to be highly concentration dependent, suggesting that a large amount of intermolecular aggregation was occurring at increased concentrations. Vapor-pressure osmometry measurements showed an apparent molecular weight approximately twice that of the oligomer, indicating a high amount of self-aggregation. Solutions of **13** in dichloromethane and pyridine resulted in gel formation with microstructures that consisted of helical substructures as evidenced by electron microscopy (Figure 58). It was determined that the fibers had an approximate diameter of 80 Å, most likely being composed of two or three bundles of helical stacks. Due to the large size of the cavity, it was proposed that the system

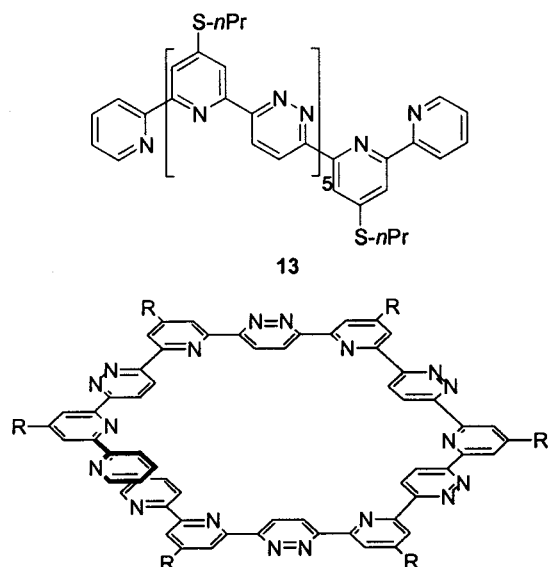


Figure 57. Drawing of the proposed helical conformation of oligomer **13**, where R = *Sn*-Pr.

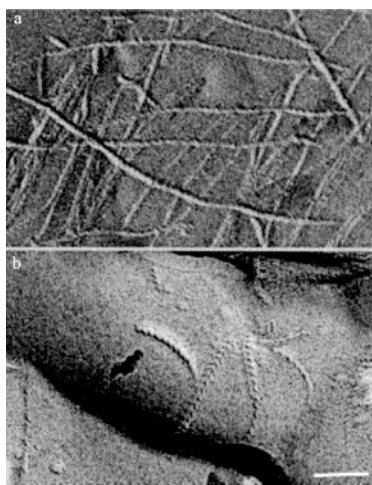


Figure 58. Freeze–fracture electron micrograph of compound **13** in (a) dichloromethane and (b) pyridine showing fiber network formation with helical textures.³⁸² Scale bar represents 100 nm. (Reprinted with permission from ref 382. Copyright 2000 Wiley-VCH.)

self-organized into extended molecular channels with a fairly large opening of ~ 8 Å, potentially useful as functional polymeric materials for ion-active devices requiring internal functionalization with metal-coordinating groups. These oligomers and others in their class have yet to show tolerance for groups present on the inside of the helical cavity. The lack of evidence for an unfolded state makes it unclear whether these oligomers exhibit a folding reaction which may be important when dynamic cavity assembly/disassembly is desired.

C. Backbones Utilizing Solvophobic Interactions

1. Qualification

The preceding section of abiotic, single-stranded oligomers employed aromatic stacking to stabilize the folded conformation. The following backbones utilize solvophobic interactions, and in some of these cases, these stacking contacts occur between adjacent mono-

mer units in their folded states. In these cases, the chain conformations might better be described as a collection of independent units rather than as a cooperative group. Therefore, by the nonadjacency criterion in our definition, we cannot strictly classify the following charged, aedamer, and cyclophane backbones as foldamers. At the same time, the water solubility, intercalating properties, and novel scaffolding of these oligomers, respectively, provide insight toward the future development of analogous backbones as foldamers.

2. Guanidines

Oligo(guanidinium) strands form a stacked arrangement by using a combination of aromatic stacking interactions and the preferred conformation of a charged backbone.^{383–387} These systems are based on the conformational preference of a charged *N,N*-diphenylguanidine group in solution (Figure 59).³⁸³ By using a combination of ¹H NMR spectroscopy and X-ray crystallography, it was determined in a *N,N*-diphenyl-*N,N*-dimethylguanidine model system that the *cisoid–cisoid* conformation is predominant over the alternative conformations in water and other polar, aprotic solvents. The guanidium moiety was incorporated into water-soluble, longer length oligomers (**14–17**) containing three and five aromatic rings linked at both the *meta*- and *para*-positions.

The conformation of the oligomers in solution was characterized by NMR spectroscopy and X-ray crystallography. All four oligomers were found to adopt a helical conformation in both solution and the solid-state (Figure 59). X-ray crystallography showed that the dihedral angle between face-to-face phenyl rings was ca. 30° for the *meta*-substituted oligomers (**14** and **15**) and slightly smaller for the *para*-substituted oligomers (**16** and **17**). These findings were somewhat surprising since the parallel structure had been calculated to be less favorable than other conformations. The *meta*-substituted oligomers pack in a chiral conformation in the solid state with both enantiomeric forms present in a 1:1 ratio. NMR spectroscopy showed that the oligomers exist predominantly as layered structures in both organic solvents and water as evidenced by the upfield shifting of the aromatic protons inside the layers when compared to the terminal phenyl rings. These NOE measurements confirmed the existence of stacked, parallel layers. One possible application of this system is as a polyintercalator targeting the minor groove of DNA.³⁸⁶

3. Aedamers

Another system composed primarily of aromatic rings was reported by Iverson and Lokey.³⁸⁸ These structures take advantage of the stacking propensities of the aromatic electron donor–acceptor interactions (*aedamers*) of covalently linked subunits. For the electron-deficient aromatic rings, 1,4,5,8-naphthalenetetracarboxylic diimide rings were employed and 1,5-dialkoxynaphthalene rings were used for the electron-acceptor rings. Crystal structures of model compounds were used to help determine the location for linking the aromatic rings with the correct length of the tethering unit³⁸⁹ between the rings. A series

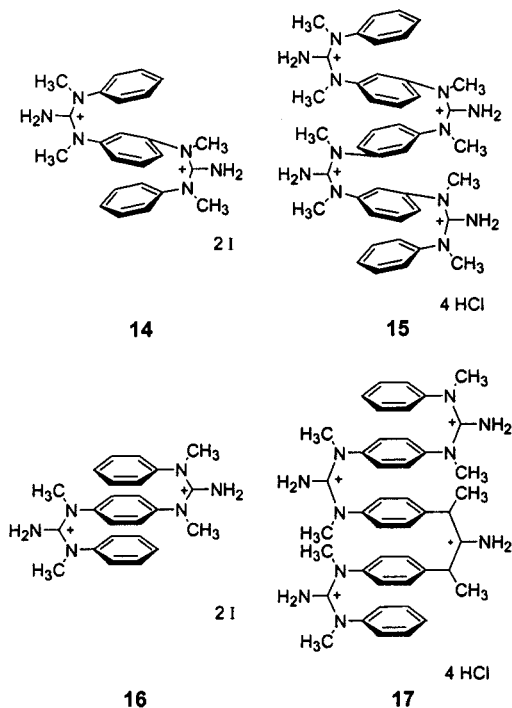
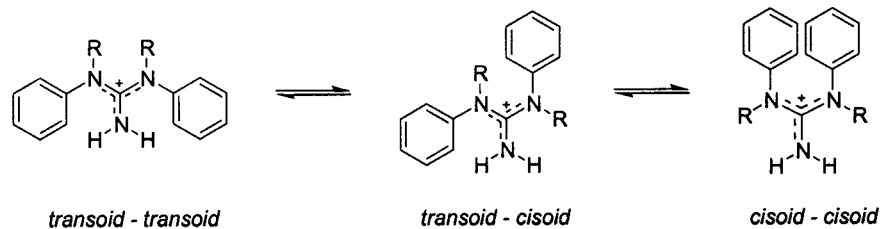


Figure 59. *Transoid-transoid*, *transoid-cisoid*, and *cisoid-cisoid* equilibrium and structure of aromatic oligo-guanidiniums).

of oligomers (**18–20**) was synthesized by solid-phase methods using *L*-aspartic acid as the linker, which helped promote solubility in water and minimized intermolecular aggregation (Figure 60).

In these initial studies, absorption and NMR spectroscopy studies were used to probe the conformation of the oligomers in water. The shorter oligomer **18** ($n = 1$) was found to have to have absorption maxima identical to a solution of the model compounds, indicating the lack of a folded conformation of the aromatic rings. Solutions of the longer oligomers **18** ($n = 2, 3$) showed an 18 nm red shift suggesting that at least two aromatic rings were stacked. NMR studies confirmed the formation of a collapsed conformation as evidenced by diastereotopic methylene hydrogens, presumably resulting from restricted rotation on the NMR time scale, along with the observation of NOE signals between hydrogens on adjacent aromatic rings indicating a stacked conformation. These results showed that oligomers of sufficient length adopt pleated structures in solution (Figure 61) and supported the idea that donor-acceptor interactions alone can be used to create well-defined conformations in an aqueous environment.

One potential application of the aedamer systems is in the area of polyintercalating molecules for DNA.³⁹⁰ For these studies, a new series of oligomers

19 ($n = 1, 2, 3, 4$) was synthesized and studied. These oligomers are comparable to the initially reported system³⁸⁸ except for the linkages between the aromatic rings and the presence of only electron-accepting aromatic rings. In these compounds, a lysine linkage was employed which helped to improve the electrostatic interactions with DNA. A variety of techniques showed that the oligomers are intercalated into the major groove of DNA (based on steric preferences) in a cooperative fashion. While these results do not necessarily involve the study of foldamers, they demonstrate that the conformation of these oligomers in solution can be used to design a better system for application toward more natural, biological systems.

Aedamers have also been shown to have potential applications in the area of molecular sensors.³⁹¹ Aedamer **20** was synthesized in the hope of mimicking the leucine zipper motif found in peptide systems. This was attempted by creating an oligomer that would have one side lined by a hydrophobic unit (leucine) and the other side by a hydrophilic unit (aspartic acid). Instead of adopting the desired leucine zipper, it was determined by UV-Vis, NMR, and dynamic light scattering that **20** intramolecularly folds in solution and undergoes an increase in intermolecular aggregation. Furthermore, it was

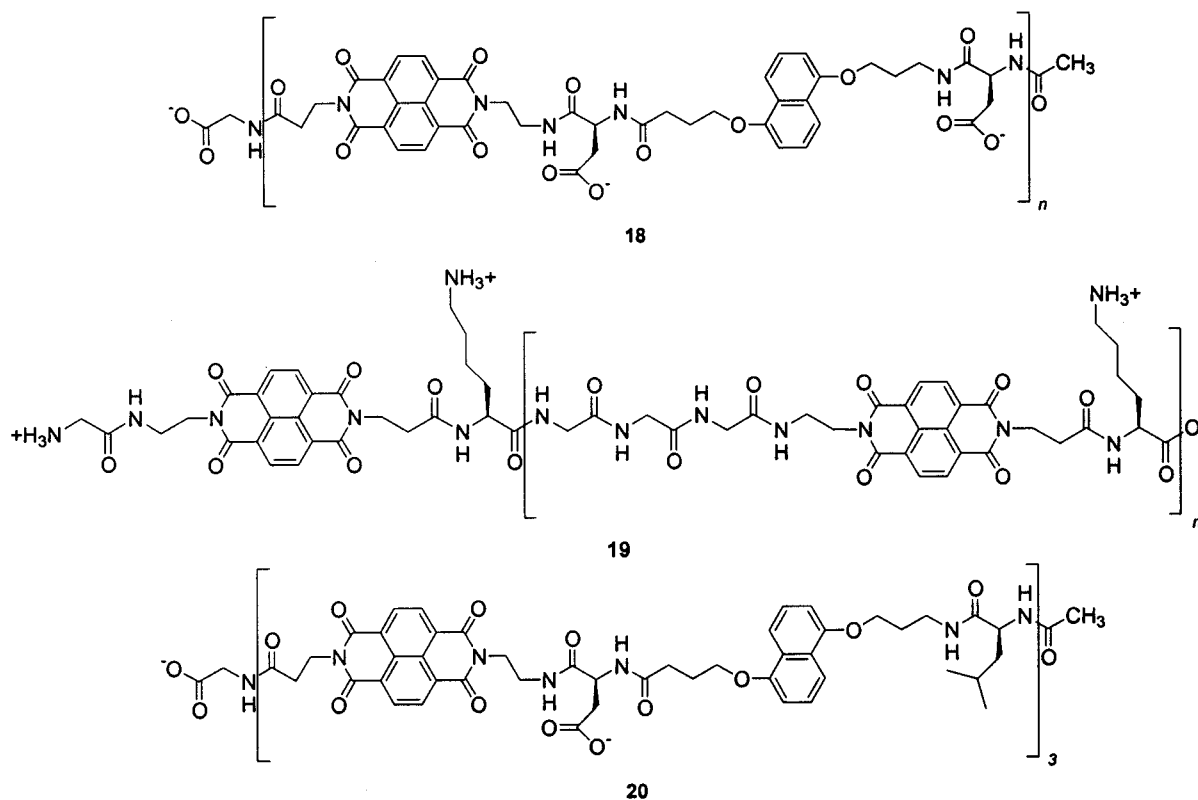


Figure 60. Structures of various aedamers.

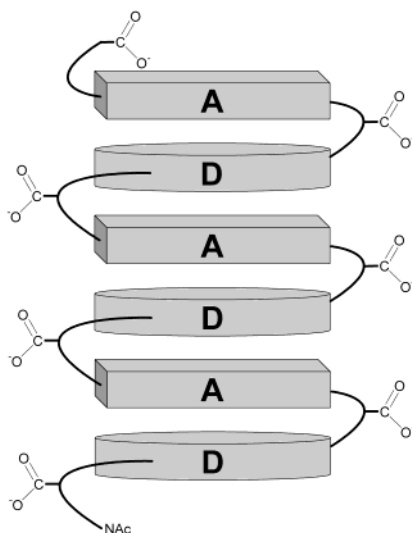


Figure 61. General schematic representation of a secondary structural element based on donor-acceptor interactions.

found that upon heating above 80 °C, 1.5 mM aqueous solutions of **20** undergo an irreversible conformational change (Figure 62). At room temperatures, solutions of **20** are red wine colored. Upon heating, the aedamers begin to unfold and expose the hydrophobic backbones to solution leading to an uncolored, presumably tangled aggregate. It was further found that the transition was induced by the addition of preformed aggregate to solutions of oligomer **20**. This behavior was compared by the authors to the behavior of triple-helix collagen. It was proposed that the color change (red wine to colorless) could therefore be used as a temperature sensor

indicating when a threshold temperature has been reached.

4. Cyclophanes

Differently substituted *N*-benzyl phenylpyridinium cyclophanes have been used as models to probe the solvent effects of face-to-face aromatic stacking (Figure 63).^{392–395} A variety of R groups, both electron-donating and -withdrawing, were explored to measure the aromatic–aromatic stacking interactions. Recently, longer chains with up to five aromatic rings suggest collapsed conformations in aqueous solution, with open conformations in chloroform.³⁹⁶

Investigations into the construction of larger cyclophanes^{397–403} proceeded through the generation of linear oligomers of tetrasubstituted aryl moieties linked through tosylated aminomethyl groups. Through iterative synthesis, chain lengths up to the nonamer⁴⁰¹ were obtained and crystal structures for pentamer **21** revealed stacked, molecular ribbons (Figure 63). Although detailed spectroscopic studies and folding transitions through either solvent or thermal denaturation were not demonstrated, these structures have similar conformations to previously described aedamers. In chloroform, ¹H NMR showed that the S-shaped folded conformation is the preorganized structure before cyclization to the macrocycles.^{398,399} Extensions of this backbone have included the incorporation of *p*-phenylrings,⁴⁰³ pyridines,⁴⁰¹ and biphenyl groups,⁴⁰² as well as the use of thioether linkages.^{397,403}

5. Side Chain–Backbone Interactions

a. Oligo(thiophene)s. Recently, oligothiophenes with chiral *p*-phenyl-oxazoline side chains were

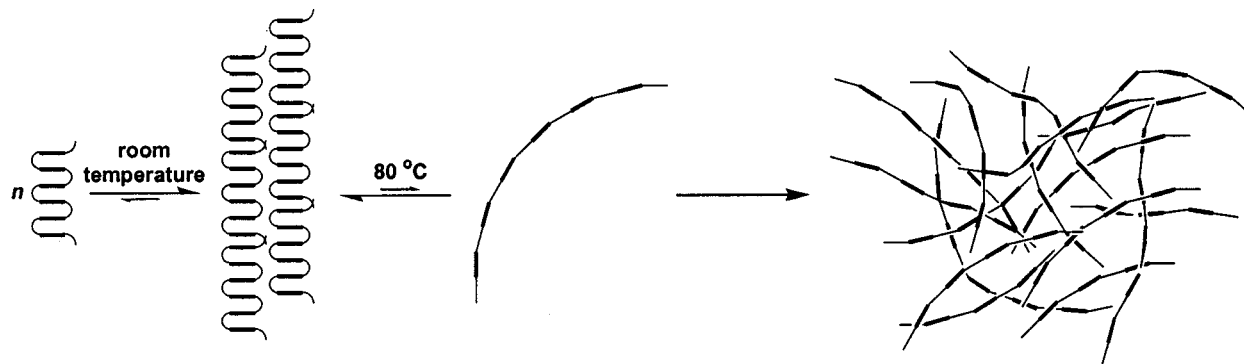


Figure 62. Proposed scheme for the conversion of amphiphilic aedamer **20** to a tangled aggregate state upon heating. (Adapted from ref 391.)

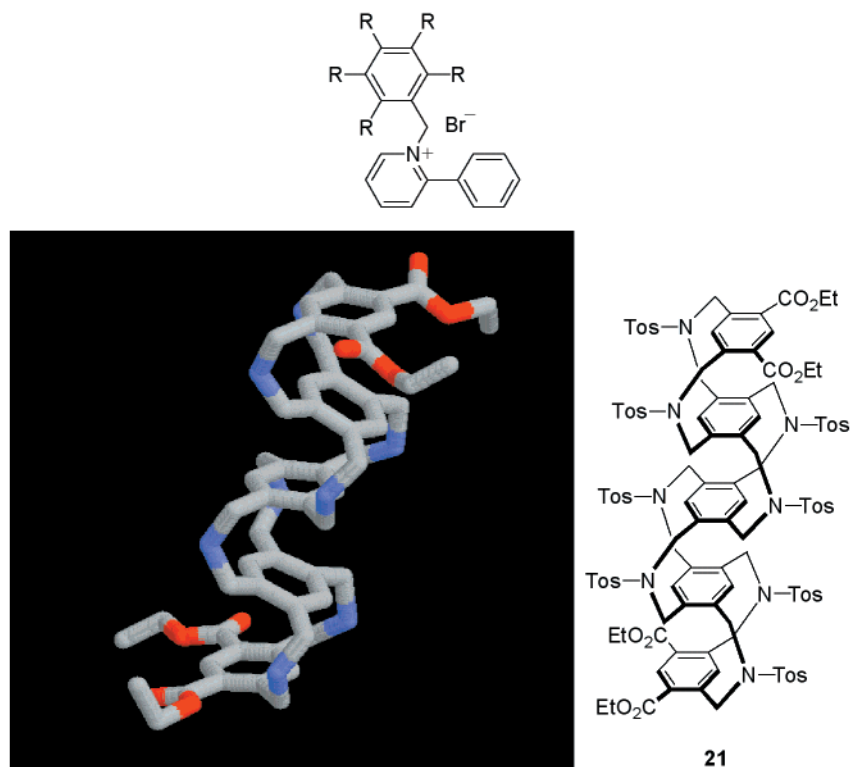


Figure 63. Cyclophanes discussed in the text. (top) Substituted *N*-benzyl phenylpyridinium bromides. (bottom) Part of the crystal structure of the [3.3]*meta*-cyclophane pentamer **21**.³⁹⁹ Side chains have been omitted for clarity.

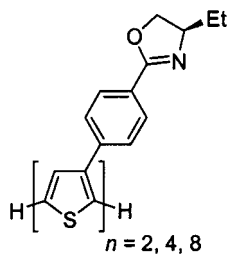


Figure 64. Oligo(thiophene)s bearing chiral *p*-phenyl-oxazoline side chains.

generated by Stille couplings through an iterative divergent/convergent approach (Figure 64).⁴⁰⁴ Though a nonlinear increase in absorptivity was observed in chloroform with increasing chain length, no induced CD was detected. When the octamer was examined in mixtures of chloroform and methanol or acetonitrile, UV red shifts and induced CD signals were seen with increasing amounts of poor solvent; these shifts were not present with the tetramer or hexamer. The

induced CD was independent of the poor solvent used, and the UV and CD showed clear isobestic and isodichroic points, respectively. Both the UV red shifting and the CD signal intensity increased as a function of time, indicating a time dependency for the folding reaction. Although the exact architectural nature of this chain-length-dependent conformational change was not determined, these results are analogous to solvophobic effects seen in the following oligo-(*m*-phenylene ethynylene)s.

b. Oligo(*m*-phenylene ethynylene)s in Solution. A large amount of research has been focused on controlling the secondary structure of nonbiological oligomers through the use of solvophobic interactions. Moore and co-workers synthesized and studied oligomer systems (**22** and **23**) that use nondirectional interactions and local constraints in a covalent backbone to undergo a folding reaction into a helical conformation (Figure 65).⁴⁰⁵ In these systems, the helical preference is controlled by several different

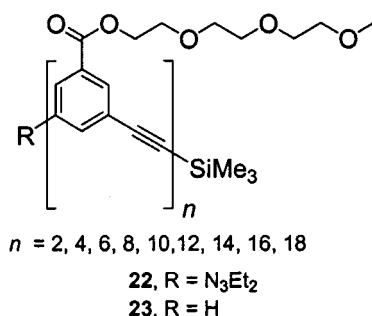


Figure 65. Chemical structures of oligo(*m*-phenylene ethynylene)s.

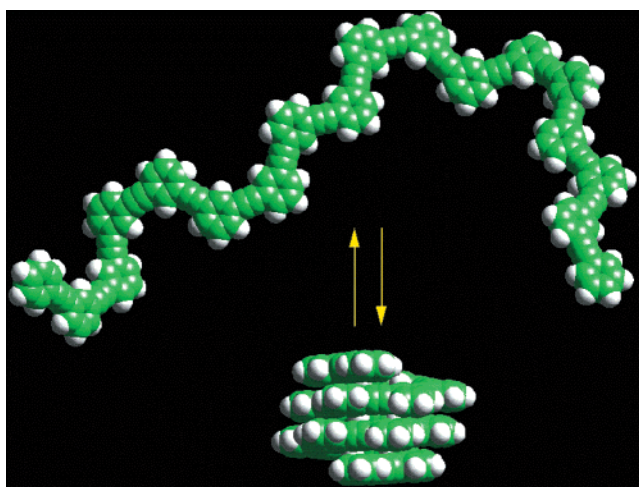


Figure 66. Space-filling model showing the proposed folding reaction for a *m*-phenylene ethynylene oligomer **23** ($n = 18$). Side chains have been omitted for clarity.

factors. These include the *meta*-connectivity of repeat units, which allows the oligomer to fold back upon itself, and the use of polar side chains and a nonpolar backbone. It was postulated that when oligomers of sufficient length are dissolved into a polar solvent, a helical conformation would result since this conformation maximizes the favorable interactions between the polar solvent and polar side chain, maximizes aromatic–aromatic stacking interactions, and minimizes the unfavorable contacts between the hydrocarbon backbone and the polar solvent (Figure 66).

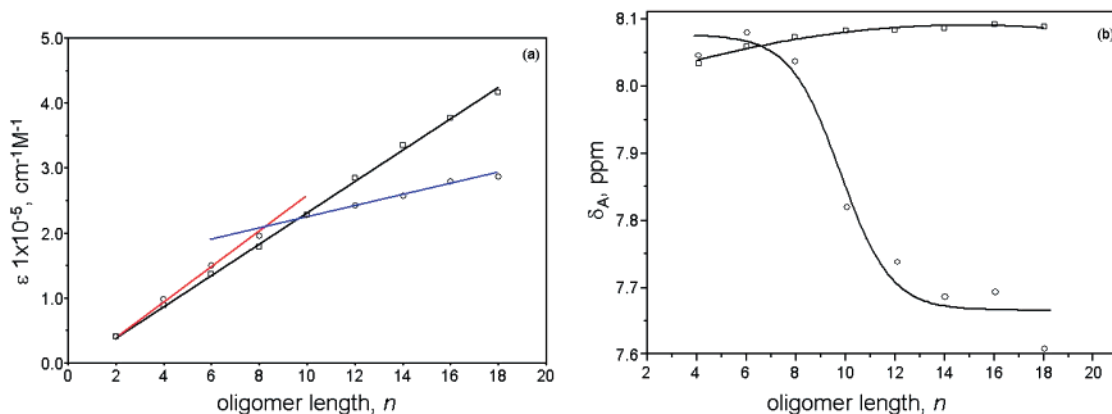


Figure 67. (a) Molar extinction coefficient ϵ (303 nm) versus oligomer length n for oligomer series **22** in chloroform (black, squares) and acetonitrile (red and blue, circles). The lines are linear fits to the data; for acetonitrile, the fits are for $n = 2-8$ (red) and $n = 10-18$ (blue). (b) The average chemical shift δ_A versus chain length n for oligomer series **22** in chloroform (CDCl₃, squares) and acetonitrile (CD₃CN, circles). The curves are drawn only as guides to the eye. All the spectra in chloroform and those of $n = 4, 6, 8$ in acetonitrile did not change upon dilution; the spectra of $n = 10, 12, 14, 16, 18$ in acetonitrile were measured at ca. 10 μM .

The modular nature of phenylene ethynylene oligomers allowed for the synthesis of monodisperse chain lengths and the ability to modify both the pendant groups and backbone in a precise fashion. The syntheses of the oligomers are typically performed using a divergent/convergent growth strategy.^{112,406} The syntheses of the various oligomer series are very similar, differing only by the choice of starting monomer units.

Several different techniques have been used to study the solvophobic driven folding reaction of *m*-phenylene ethynylene oligomers. In the initial studies on oligomer series **22**, a combination of UV–Vis and ¹H NMR spectroscopy was utilized (Figure 67).⁴⁰⁶ Experiments were performed at a concentration where intermolecular interactions are minimized (<10 μM). The lack of aggregation was determined by a combination of vapor-pressure osmometry and dilution experiments. From these studies, it was found that only oligomers with $n > 8$ repeat units were capable of folding into a helical conformation. In a good solvent,⁴⁰⁷ such as chloroform, all oligomers are present in a random conformation since the solvent is able to solvate both the polar side chains and nonpolar backbone. This was confirmed by UV–Vis studies, which indicated a linear dependence of molar absorptivity on oligomer length. ¹H NMR showed little change in the average chemical shift of aromatic resonances indicating no aromatic–aromatic stacking, present in the folded helical conformation. However, in a poor solvent such as acetonitrile, it was observed that oligomers greater than eight units in length exhibit a change in molar absorptivity per repeat unit and an upfield shift of the aromatic resonances. The changes in the UV–Vis spectra were attributed to the increased concentration of a *cisoid* geometry of contiguous aromatic rings typical of the helical confirmation (Figure 68). The changes in the ¹H NMR spectra for the longer oligomer lengths were attributed to the presence of aromatic stacking. In these studies it was also shown that the conformational transition could be controlled by solvent quality and temperature.

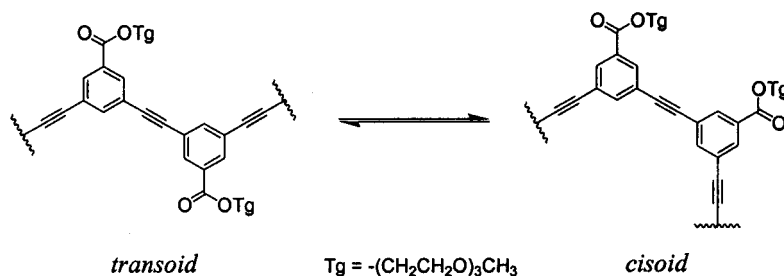


Figure 68. *Transoid*–*cisoid* equilibrium of oligo(*m*-phenylene ethynylene)s.

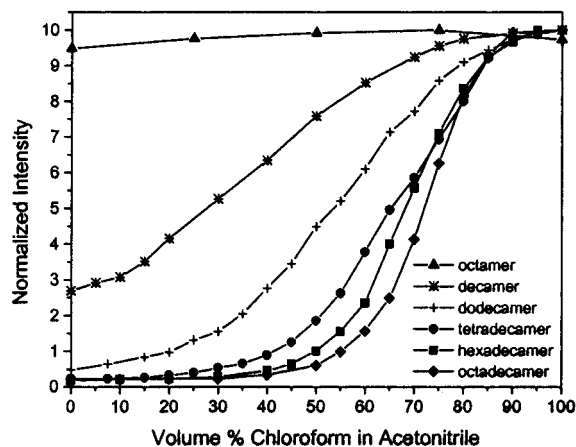


Figure 69. Plot of normalized fluorescence intensity for **23** ($n = 8$) through **23** ($n = 18$) vs the volume percent chloroform in acetonitrile. All spectra were normalized to a constant optical density of 0.1 at 288 nm.

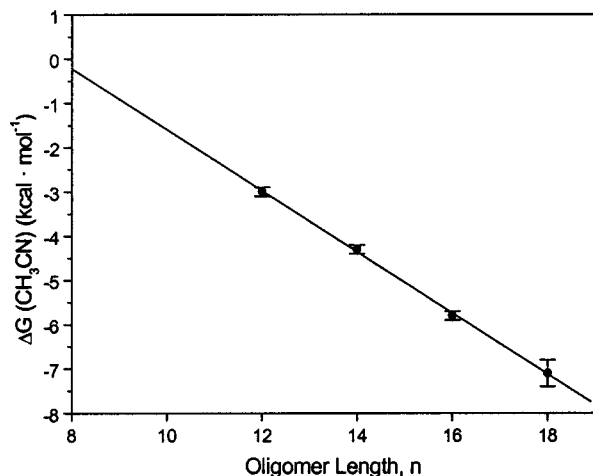


Figure 70. Plot of $\Delta G(\text{CH}_3\text{CN})$ vs oligomer length for **23** ($n = 12$) through **23** ($n = 18$). The linear equation used to fit the data is given by $\Delta G(\text{CH}_3\text{CN}) = 5.1 - 0.68n$ ($\text{kcal} \cdot \text{mol}^{-1}$).

Fluorescence spectroscopy also proved to be a valuable tool in characterizing the folding reaction of *m*-phenylene ethynylene oligomers.¹¹² In these studies, oligomer series **23** was used since the hydrogen end group does not quench fluorescence emission. By monitoring the fluorescence signal⁴⁰⁸ as a function of volume percent chloroform (solvophilic) in acetonitrile (solvophobic) (Figure 69), it was possible to estimate the stability of the folded conformation in pure acetonitrile, $\Delta G(\text{CH}_3\text{CN})$ (Figure 70).⁴⁰⁹ For oligomers greater than eight units in length in CH_3CN , a decrease in the 350 nm fluorescence band and the onset of an excimer-like emission band was

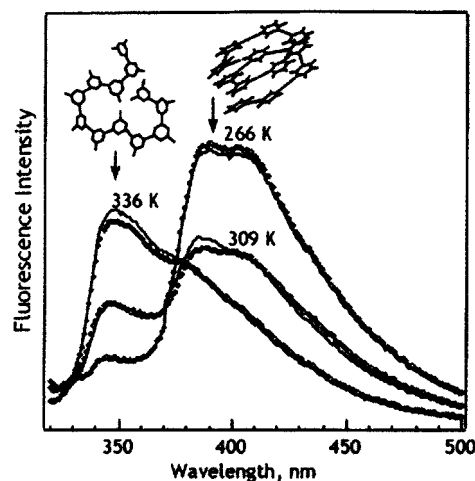


Figure 71. Emission spectra of **23** ($n = 12$) (open diamonds) excited in the broad absorption band peaked at 270–300 nm area diagnostic of its helical content ($\lambda_{\text{ex}} = 288$ nm, $0.5 \mu\text{M}$ **23** [$n = 12$] in 50:50 v/v THF/methanol.) The folded peak at 400 nm decreases at higher T . A spectral/lattice model prediction (solid line) describes the folding transition and equilibrium constant near-quantitatively. Insets show representative unfolded and folded conformations (side chains omitted for clarity).⁴¹⁰

attributed to the presence of aromatic stacking. This coincided with the chain length (i.e., 10-mer) at which upfield shifting and UV hypochromism was noted in previous studies.⁴⁰⁶ It is evident from Figure 70 that a linear relationship exists between oligomer length and conformational stability. An important conclusion is that the stability of the conformationally ordered state was linearly dependent on chain length. This behavior had previously been predicted on the basis of a molecular modeling study.⁴⁰⁶ Solvent denaturation studies suggested that each additional monomer contributed roughly $0.7 \text{ kcal} \cdot \text{mol}^{-1}$ of stability to the folded conformation at 23°C in acetonitrile. Linear extrapolation yielded a free energy value near zero for the octamer, consistent with the absence of folding seen in Figure 69. The observation that each monomer contributes the same increment of stability to the ordered conformation suggested a regularly repeating conformational structure, such as a helix.

The conformational transition of **23** ($n = 12$) was further quantified by monitoring the fluorescence signal using laser T -jump relaxation measurements (Figure 71).⁴¹⁰ These experiments showed that the oligomer folded to a compact structure on a submicrosecond time scale, which is comparable to short helical peptides. However, it was determined that the folding reaction undergoes a transition to nonexpo-



Figure 72. Equilibrium of *P* and *M* helices for oligo(*m*-phenylene ethynylene)s.

nential kinetics at low temperatures. The fluorescence experiments clearly show that solvophobic interactions can be used to collapse the oligomers to a stable, helical conformation in solution and that this transition occurs in a cooperative fashion.

Several design approaches have been used to control the twist sense bias of *m*-phenylene ethynylene oligomers (Figure 72).^{411–413} One approach involved adding a small, chiral perturbation to the oligomer side chain that resulted in a twist sense preference, without disrupting the conformational stability.⁴¹¹ For these studies, a series of *m*-phenylene ethynylene oligomers with chiral side chains (**24**) was generated (Figure 73). This series was analogous to the previously reported achiral series **23**, except for the introduction of a methyl group at the second carbon of each of the side chains. This placed the

stereochemical information in reasonably close proximity to the aromatic backbone. The chiral unit was derived from *L*-ethyl lactate, which is readily available in high enantiomeric purity, using standard synthetic transformations.⁴¹¹ It was found that, within experimental error, the conformational transitions of chiral oligomers **24** displayed the same chain-length and solvent dependence as their achiral counterparts (**23**) as determined by UV-vis and fluorescence spectroscopy (Figure 74). Therefore, the introduction of a methyl group in the side chain did not destabilize the helical state. In chloroform, chiral oligomers **24** showed no optical activity in the backbone chromophore (250–400 nm), regardless of chain length and temperature studied. This is not surprising since in chloroform the oligomers are expected to be in a random conformation; hence, there is little possibility for transferring chiral information from the side chains to the backbone. In CH₃CN, the ellipticity was found to be chain-length dependent and was zero only for oligomers not long enough to adopt a helical conformation ($n < 10$). These results showed that the transfer of chiral information from the side chains

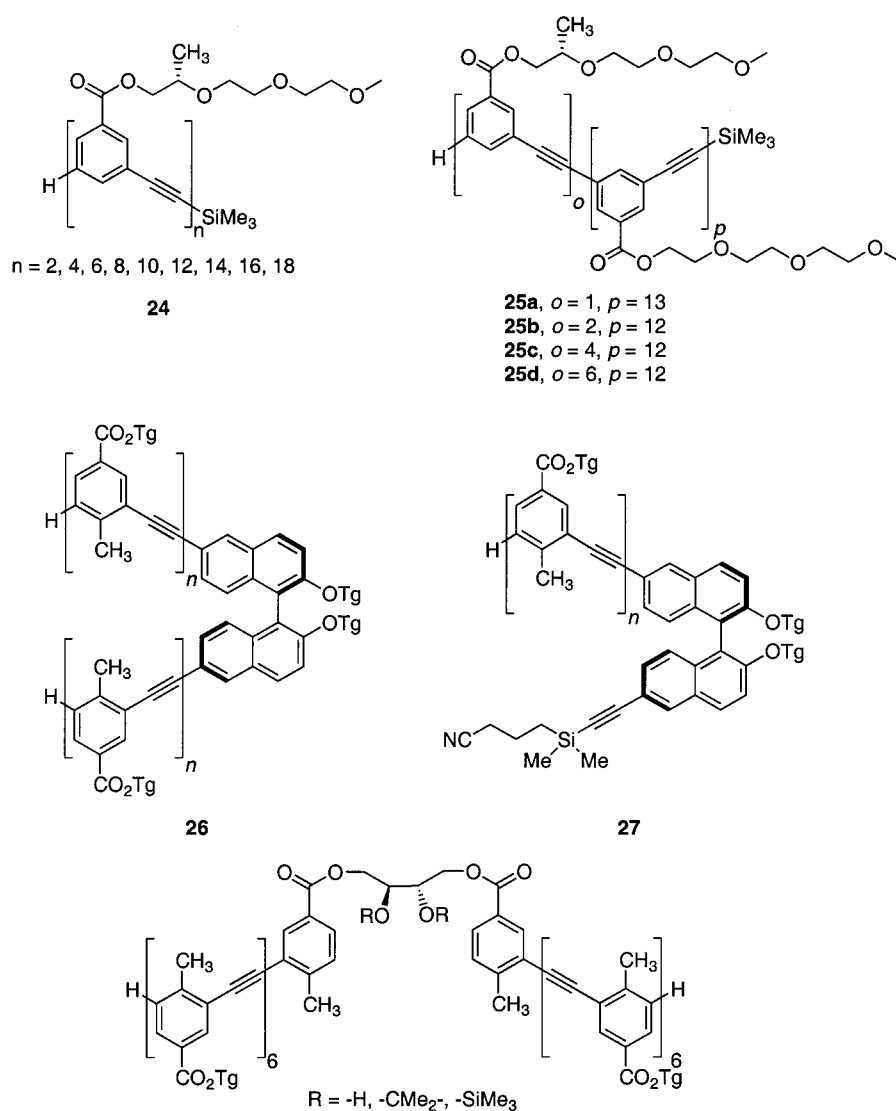


Figure 73. Structures of various oligo(*m*-phenylene ethynylene)s used to bias the twist sense of the helical conformation.

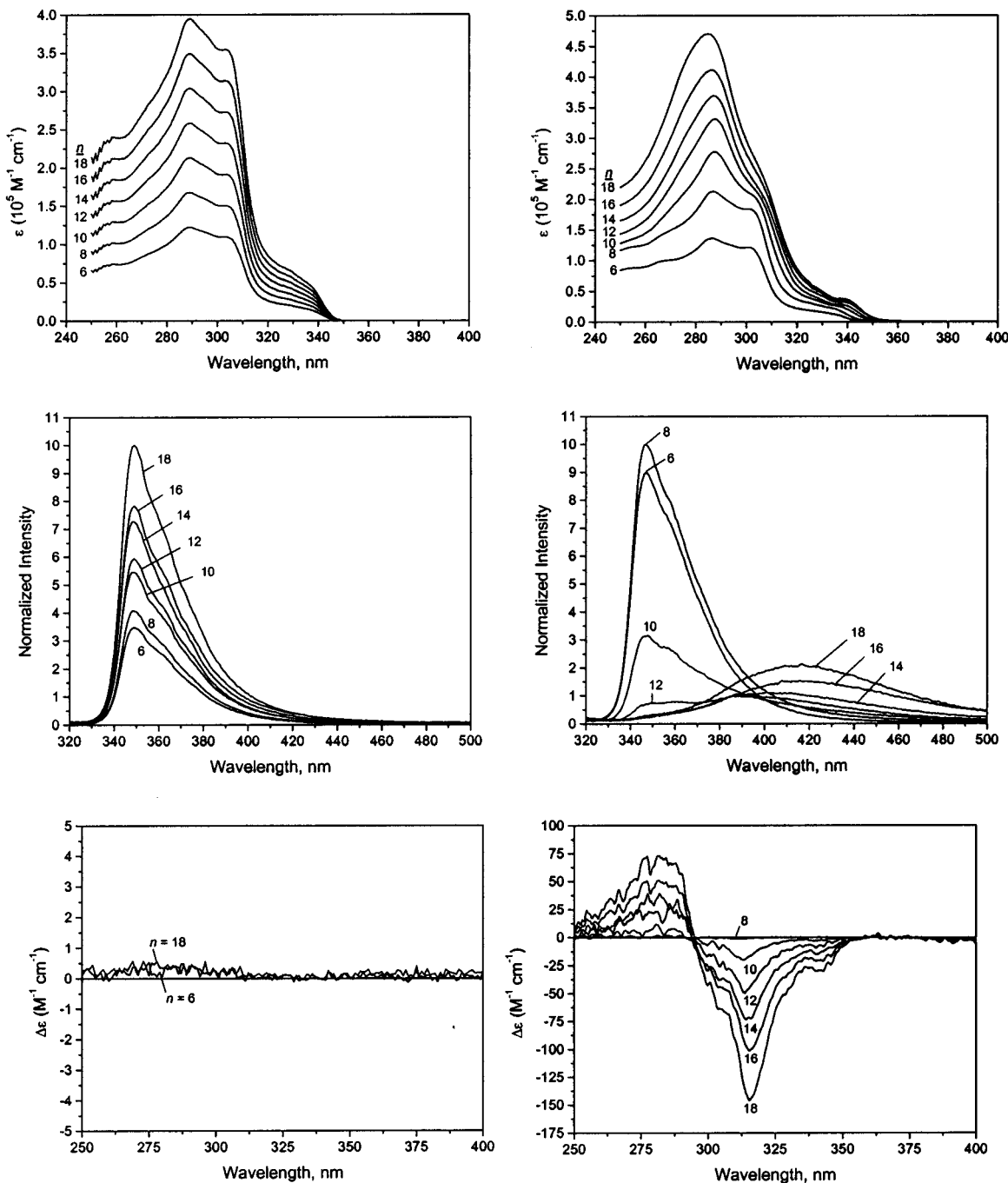


Figure 74. Plots of UV–Vis (top), fluorescence (middle), and circular dichroism spectra (bottom) of oligomers **24** ($n = 6$) through **24** ($n = 18$) in chloroform (left) and acetonitrile (right).

to the main chain could only occur once order is present in the backbone.

By monitoring the CD signal as a function of volume percent chloroform in acetonitrile, it was only at high acetonitrile compositions that a Cotton effect was observed (Figure 75). On the basis of this observation it is plausible that ordering of the solvated side chains, a process that lags behind helix formation, is the mechanism by which chirality is transferred to the backbone. This is analogous to the molten globular state of proteins, a state in which the peptide backbone possesses a native-like conformation while having disordered side chains.^{414,415} An alternative way to explain the observed transition behavior is to consider the dynamics and conforma-

tional uniqueness of the backbone. At high chloroform compositions (but still helical as judged by UV) there are possibly a large number of energetically similar, helical-like backbone conformations that interconvert rapidly. Here, the analogy can also be made to the compact, denatured state of proteins.⁴¹⁶ Regardless of which of these explanations is correct, the transfer of chirality appeared to be a highly cooperative process that required a progression of conformational order beyond the initially formed helical state. These results showed that the side chains played more than just a solubilizing role in these conformationally ordered oligomers.

All members of oligomer series **24** were fully substituted with chiral side chains, not allowing the

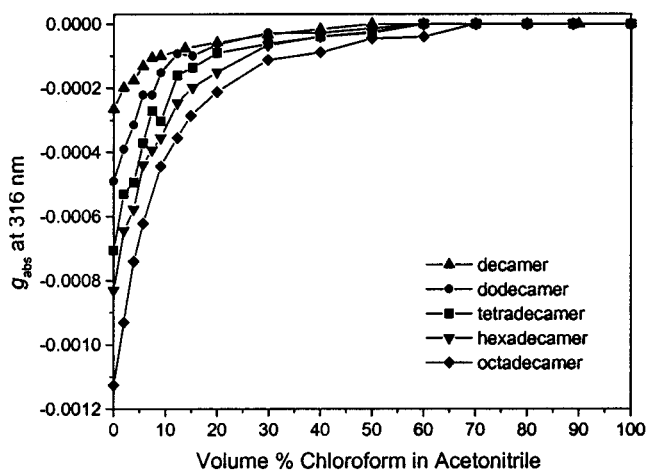


Figure 75. Plot of circular dichroism (g_{abs} at 316 nm, right) for **24** ($n = 10$) through **24** ($n = 18$) vs the volume percent chloroform in acetonitrile.

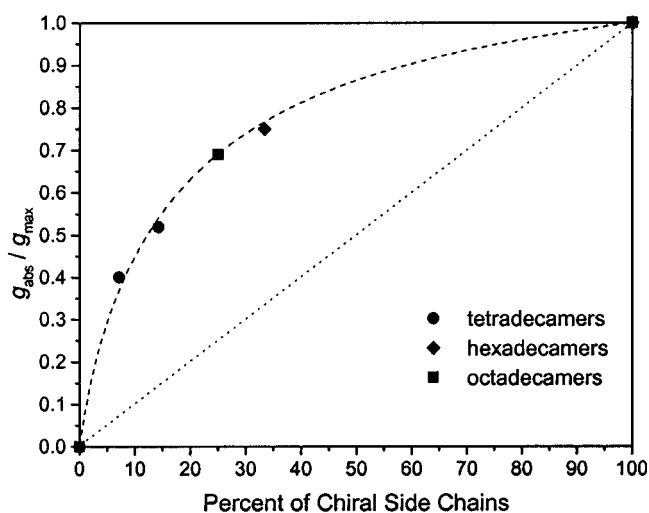


Figure 76. Plot of normalized $g_{\text{abs}}/g_{\text{max}}$ at 315 nm vs percent of chiral side chains for the mixed tetradecamers (**23** ($n = 14$), **25a**, **25b**, and **24** ($n = 14$)), hexadecamers (**23** ($n = 16$), **25c**, and **24** ($n = 16$)), and octadecamers (**23** ($n = 18$), **25d** and **24** ($n = 18$)) in acetonitrile at 20 °C. The dotted lines are meant to guide the eye but do not indicate that an asymptotic value is reached.

cooperativity to be determined. To investigate cooperativity in the folding reaction, oligomers with varying numbers of chiral side chains (**25a–d** in Figure 73) were synthesized and studied.⁴¹⁷ By analogy to the fully chiral (**24**) and achiral (**23**) oligomers, the mixed side-chain oligomers existed in a random conformational state in chloroform and formed a helical conformation in acetonitrile as determined with UV–Vis spectroscopy. Circular dichroism measurements were performed in order to determine the extent of cooperative interactions among the side chains. Shown in Figure 76 is a plot of the normalized Cotton effect ($g_{\text{abs}}/g_{\text{max}}$) vs percent chiral side chains. It can be seen that regardless of overall oligomer length, a positive nonlinear dependence of the optical activity on the percentage of chiral side chain was observed. This positive nonlinear effect strongly supports the cooperative nature of the folding reaction. The results further indicate that the twist sense bias is equally strong for every oligomer length, as

the normalized Cotton effect versus percentage of chiral side chains seems to be independent of chain length.

A CD analysis in aqueous acetonitrile examined the self-assembly of oligomer series **24** into helical columns.⁴¹⁸ The shorter oligomers (**24**, $n = 8, 10, 12$) showed an increase in the stability of the helical conformation with increasing water content. The longer oligomers (**24**, $n = 14, 16, 18$), which have a stable helical conformation in pure acetonitrile, were found to aggregate into multimolecular architectures upon introduction of water. By using the strong intermolecular interactions that exist in aqueous acetonitrile solvent, the intermolecular transfer of chirality was examined for chiral **24** ($n = 18$) and achiral **23** ($n = 18$) octadecamers. In 100% acetonitrile, the CD signal was found to be linearly dependent on the mole percent of chiral octadecamer (Figure 77, top left). These results indicate that if intermolecular aggregation is occurring, there is no transfer of chirality. More importantly, they show that the CD signals observed in 100% acetonitrile can be attributed to a purely intramolecular effect. Examination of solutions in increasing amounts of water showed a positive deviation from linearity; that is, the magnitude of the CD signal was larger than expected for an ideal mixture (Figure 77). Additionally, the observation that the maximum CD signal of certain mixtures of chiral and achiral oligomers was greater than that of the purely chiral octadecamer suggests that more efficient packing is present between achiral molecules than the chiral molecules, since in the former no branching methyl group is present. The transfer of chirality to achiral oligomers appears to be dependent on the presence and intermolecular aggregation of a helical conformation observed for the longer octadecamers. The stacking is promoted by the highly polar aqueous environment, and efficient intermolecular stacking allows for the chirality to be transferred to the achiral helices.

An alternative approach to controlling the twist sense bias involved the use of chiral units in the oligomer backbone (Figure 73).^{412,413} It was determined that a binaphthol unit in the backbone provided a high amount of diastereomeric excess of one twist sense over the other.⁴¹² Circular dichroism spectra of **26** ($n = 2, 4, 6, 12$) in chloroform were independent of chain length, while in acetonitrile a large Cotton effect was observed (Figure 78). The presence of an isodichroic point at 302 nm indicated similar structures of **26** ($n = 2, 4, 6, 12$), and the opposite sign of the signal arising from (*S*)-**26** ($n = 6$) confirmed that the induction of chirality in the backbone was from the binaphthol segment. Furthermore, a continual increase in $\Delta\epsilon$ as the length of the chain increased indicated that the chiral environment persisted along the entire chain length. However, by comparing results on these oligomers to a system containing the binaphthol segment at the chain terminus (**27**), it was determined that the binaphthol in the center causes 3–5 kcal·mol⁻¹ destabilization of the folded, helical conformation.

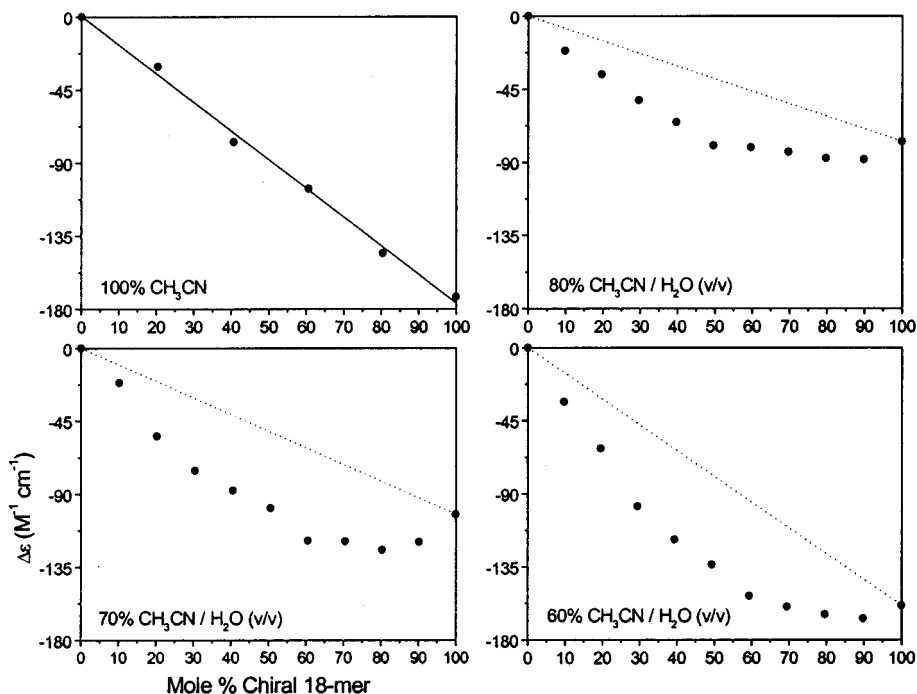


Figure 77. Plot of $\Delta\epsilon_{314}$ vs mole % chiral octadecamer **24** ($n = 18$) for solutions of varying amounts chiral and achiral **23** ($n = 18$) octadecamers in different concentrations of water/acetonitrile (v/v). All spectra were recorded in solutions with a total oligomer concentration of $3.3 \mu\text{M}$. The dotted lines are the expected signals that should arise upon dilution of a sample only containing only chiral octadecamer. The solid line is the least-squares linear fit of the chiral octadecamer dilution data (top left, correlation coefficient = 0.998).

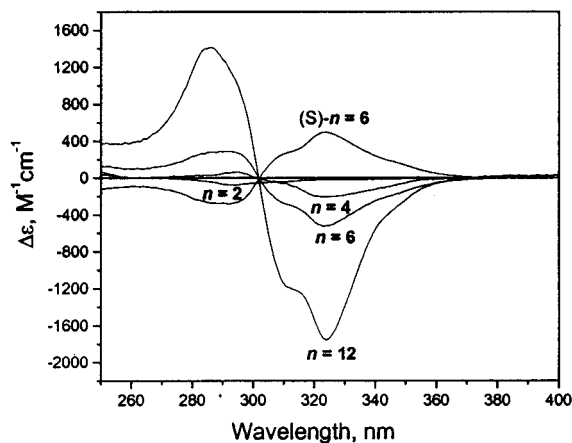


Figure 78. CD spectra of **26** ($n = 2, 4, 6, 12$) in acetonitrile. All samples were prepared with OD ca. 1.0 ($2\text{--}11 \mu\text{M}$ in oligomer), and spectra were recorded at room temperature (23°C).

In another system containing a chiral unit in the backbone, (+)-tartaric acid was used to tether two chains.⁴¹³ It was found that the choice of protecting group on the tartaric acid played an extremely significant role on the magnitude of the twist sense bias **28** ($\text{R} = \text{H}, \text{CMe}_2, \text{SiMe}_3$). The use of a trimethylsilyl ether protecting groups resulted in helices with a very large twist sense bias (Figure 79). Surprisingly, the use of an isopropylidene ketal group or no protecting group was ineffective at helical discrimination and may have possibly inhibited helix formation. At the present time, the exact conformational role of the chiral tether has not been established. Initial molecular modeling experiments indicate that the trimethylsilyl protecting groups may bind within

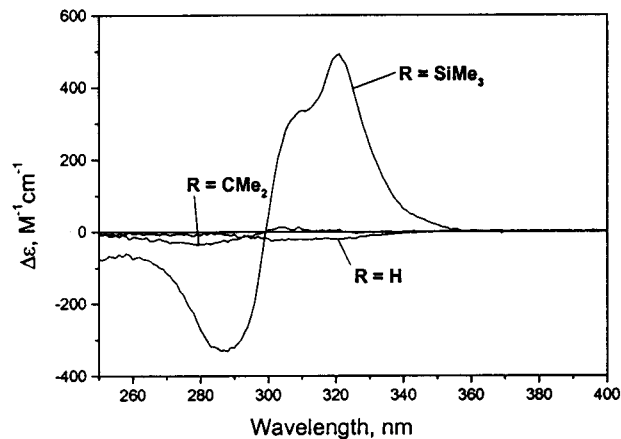


Figure 79. CD spectra of **28** ($\text{R} = \text{H}, \text{CMe}_2, \text{SiMe}_3$) in acetonitrile.

the helical cavity and help in templating helical formation.

Moore and co-workers have also shown that it is possible to control the folding reaction in a nonpolar solvent.⁴¹⁹ For these studies, a series of *m*-phenylene ethynylene oligomers containing nonpolar, (*S*)-3,7-dimethyl-1-octanoxo side chains was synthesized and studied (**29**) (Figure 80). In these oligomers, the addition of apolar side chains rendered the aromatic backbone polar with respect to the side chains. The ability to induce conformational order in such an oligomer was intriguing since both the side chain and backbone are hydrocarbon segments. Structural amphiphilicity in this system is obviously less pronounced, and the promotion of helical order in a lipophilic solvent would bode well for the possibility of forming helical channels in bilayer membranes. UV-Vis and CD measurements indicated that the

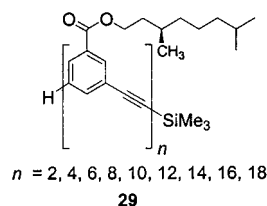


Figure 80. Structure of oligo(*m*-phenylene ethynylene)s **29** with chiral, apolar side chains.

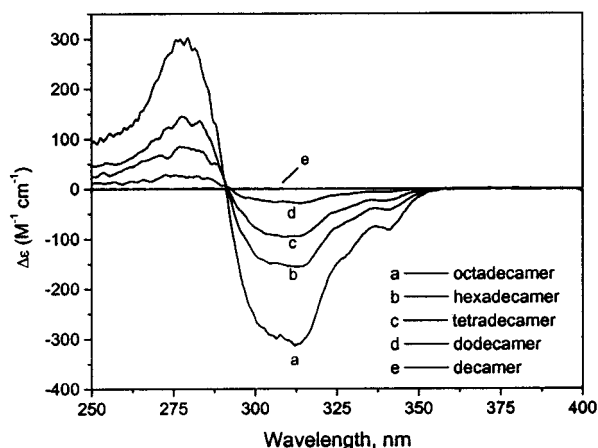


Figure 81. Plots of $\Delta\epsilon$ vs λ for **29** ($n = 10$) through **29** ($n = 18$) in heptane at 20 °C (right). Note the presence of an isodichroic point at 292 nm.

oligomers adopted a random conformation in chloroform as evidenced by a linear dependence of molar absorptivity on chain length and a lack of Cotton effect in the backbone chromophore. In apolar solvents, such as heptane, oligomers of sufficient length ($n > 10$) were found to adopt a helical conformation with a large twist sense bias (Figure 81). In a fashion similar to the chiral polar oligomers **24**, the onset of the twist sense bias occurred abruptly at a solvent composition that was well beyond the conformational transition as monitored by UV spectroscopy. Although the underlying phenomena responsible for this behavior are not well understood, it was apparent that the transfer of chirality was highly coopera-

tive and again required a progression of conformational order beyond the initially formed helical state. It was also noted that for the apolar oligomers **29**, the Cotton effect disappeared at much smaller volume percent chloroform than for the polar, chiral oligomers **24**. This was most likely due to the greater rate at which solvent polarity changes upon addition of chloroform to heptane, in contrast to the smaller change upon addition of chloroform to acetonitrile. It was also shown that the strong twist sense bias was extremely time dependent and could partially be attributed to intermolecular aggregation. These results indicate that nonpolar, solvophobic interactions can be used for controlling the ordering of nonbiological oligomers.

The helical conformation of *m*-phenylene ethynylene oligomers has a tubular cavity, which potentially provides a novel receptor site for catalytic systems. The ordered solution conformation was shown to afford a high-affinity binding site for small molecule guests.⁴²⁰ This was first demonstrated by the diastereoselective complexation of chiral monoterpenes with three different dodecamer length oligomers in polar solvents (Figure 82). The only difference among these oligomers was the addition of methyl groups, which are placed into the tubular cavity upon helical formation, reducing the space available for guest binding. Induced circular dichroism (CD) spectroscopy was used for probing the interaction of small chiral molecules with the achiral oligomers. In the absence of a chiral guest, oligomer **30** exhibited no CD signal as expected for an achiral molecule. However, the addition of enantiomerically pure (–)- α -pinene to a solution of **30** in 40% H₂O/acetonitrile induced a strong Cotton effect in the wavelength range where the oligomer absorbs. The stoichiometry of the complex was strictly 1:1 as determined by the linearity of Benesi–Hildebrand and slope of Hill plots, and the binding affinity constant was found to be ca. 6800 M⁻¹. Molecular models (Figure 83) revealed that the size and shape of α -pinene is complementary to the internal space

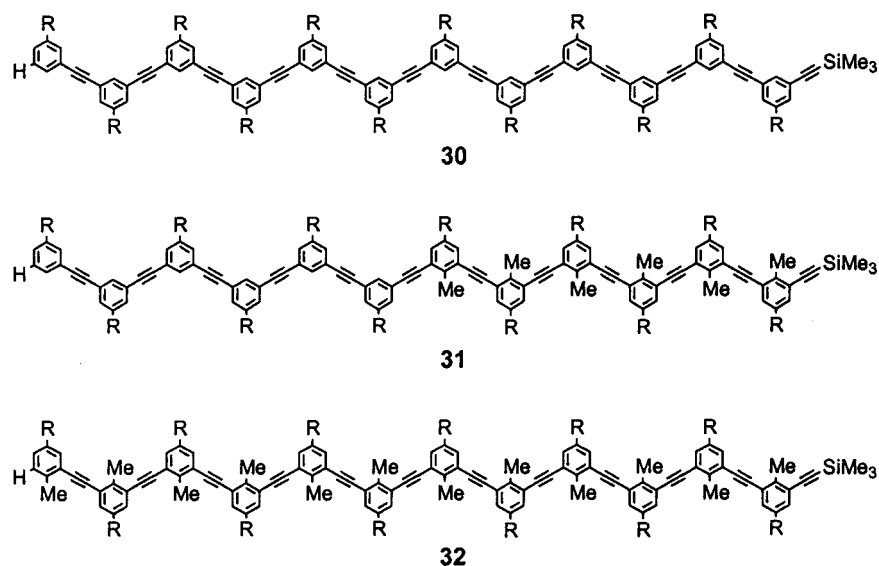


Figure 82. Chemical structures of *m*-phenylene ethynylene oligomeric hosts **30–32** used in binding small molecule guests (R = –CO₂(CH₂CH₂O)₃CH₃).

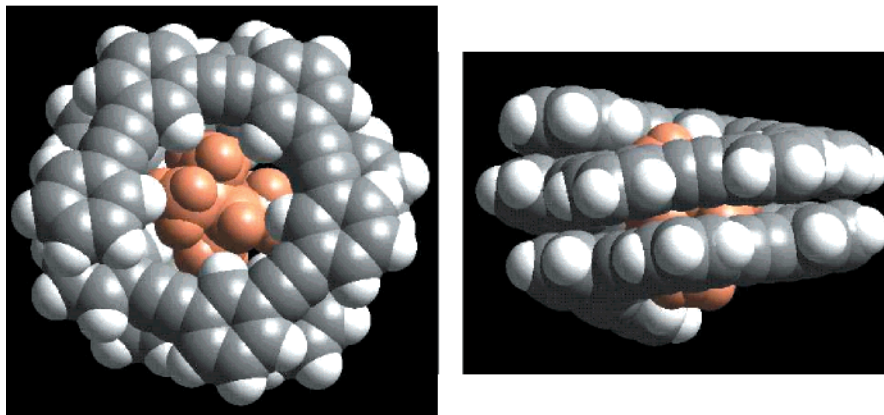


Figure 83. Space-filling model of the 1:1 minimum energy complex of **30** and (-)- α -pinene determined by a Monte Carlo search in which the position and orientation of the helix cavity within the helix cavity was varied. Top and side views are shown.

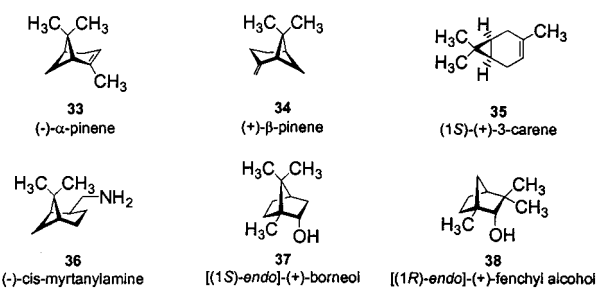


Figure 84. Structures of various terpenes used in the binding study.

Table 6. Association of Oligomer 23 ($n = 12$) with Various Monoterpenes^a

guest	K_{11} (M^{-1})	$-\Delta G^\circ$ ($kcal \cdot mol^{-1}$)	$\Delta \epsilon_\infty$ ($M^{-1} \cdot cm^{-1}$) ^b
33	6830 ^c	5.2	325
34	6000 ^d	5.1	15
35	4450 ^c	5.0	93
36	2970 ^c	4.7	265
37	3920 ^c	4.9	124
38	1790 ^c	4.4	77

^a All measurements were recorded in a mixed solvent of 40% water in acetonitrile (by volume) at 295 K. Abbreviations: K_{11} , association constant; M, molarity; $-\Delta G^\circ$, free energy of complex formation; $\Delta \epsilon_\infty$, saturation value of the CD signal from nonlinear fitting of titration data to a 1:1 binding model. [13 ($n=12$)] = 4.2 μM . ^b CD signal at saturation determined from nonlinear least-squares fitting. ^c Determined from nonlinear least-squares fitting to a 1:1 binding model. ^d Calculated by competition experiments with guest **33**.

of the hydrophobic cavity of the putative helix and interestingly that the molecular volume of α -pinene is roughly 55% of the helix cavity volume, consistent with the criterion suggested by Rebek for molecular encapsulation.⁴²¹ It was also determined that dodecamer **30** forms 1:1 complexes with a variety of monoterpenes **33**–**38** (Figure 84; Table 6). The binding was also found to be a solvophobic driven process, and by extrapolating to pure water, an association constant of 60 000 M^{-1} was estimated.

By performing experiments on modified oligomers (**31** and **32**), it was confirmed that binding was occurring on the interior of the cavity (Figure 85). Each oligomeric host formed a 1:1 complex with (+)- α -pinene, but the association constant dropped by 1 and 2 orders of magnitude for **31** ($K_{11} = 280 M^{-1}$ and $-\Delta G^\circ = 3.3 kcal \cdot mol^{-1}$) and **32** ($K_{11} = 40 M^{-1}$ and

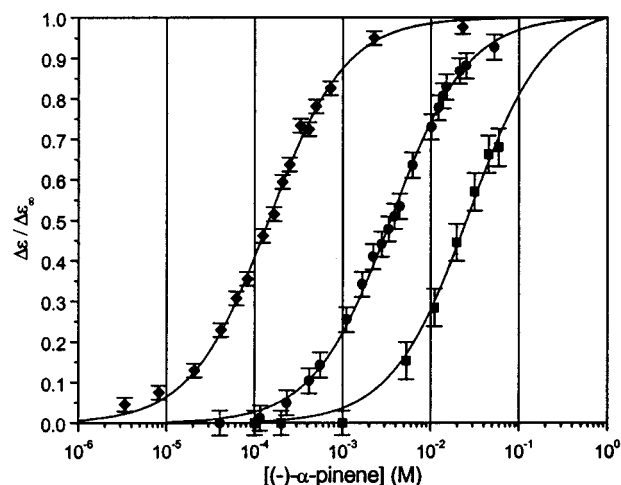


Figure 85. Plot of fractional saturation of the CD signal against (-)- α -pinene concentration for the oligomers: **30** (\blacklozenge); **31** (\bullet); **32** (\blacksquare). The CD signal at saturation, $\Delta \epsilon_\infty$, was obtained from nonlinear least-squares fitting of $\Delta \epsilon$ vs (-)- α -pinene concentration using a 1:1 binding model. The lines are the nonlinear fits of the data to the 1:1 binding model. Error bars are based on the signal-to-noise ratio of the CD spectra. All measurement were recorded in a mixed solvent of 40 volume percent water in acetonitrile (by volume) at 295 K. [oligomer] = 4.2 μM .

$-\Delta G^\circ = 2.1 kcal \cdot mol^{-1}$), respectively. These results indicated that filling the cavity with methyl groups reduced the space for binding. This study shows that conformationally ordered oligomers could serve as a platform for the construction of synthetic receptors. The demonstration that a binding site could be created from a folded chain parallels concepts in biopolymer recognition and suggests a new avenue for supramolecular catalysis. The synthetic modularity of sequence-specific oligomers naturally suggests the use of combinatorial methods in refining the active sites. Molecular adaptation, where binding strength is mediated by conformational changes, is easily imagined from this study.

As an extension of the concept of molecular adaptation, the internal cavity of an oligo(*m*-phenylene ethynylene) helix was also anticipated to be complementary in shape to rodlike chain molecules of appropriate diameter.⁴²² Molecular interactions of this type, while quite unlike those typical of biomacromolecules, were sought to reveal oligomeric

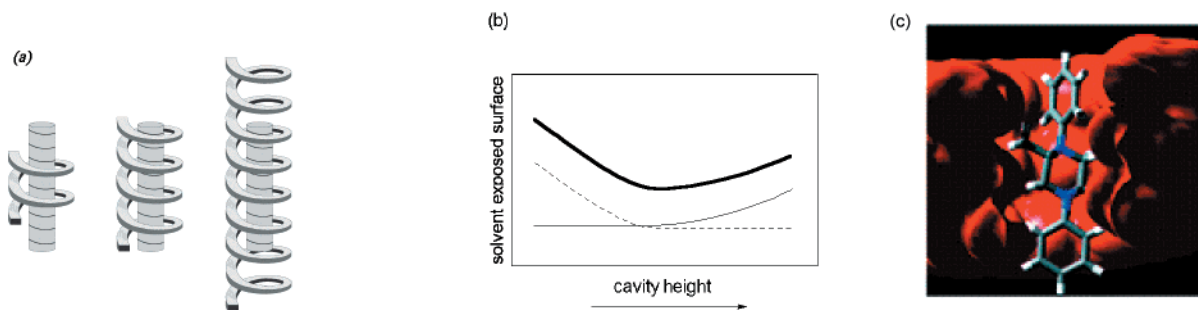


Figure 86. (a) Schematic diagram illustrating the binding of a rodlike guest to helical oligomers of differing lengths. The cavity height is determined by the oligomer length. (b) Solvent-exposed surface of the oligomer cavity (—) and the rodlike guest (---) in a complexed state as a function of cavity height. The total amount of solvent-exposed surface (—) shows a minimum that predicts a cavity length with the highest affinity for the rodlike guest. (c) Minimized structure of **23** ($n = 18$) with **39** determined by a Monte Carlo docking algorithm.

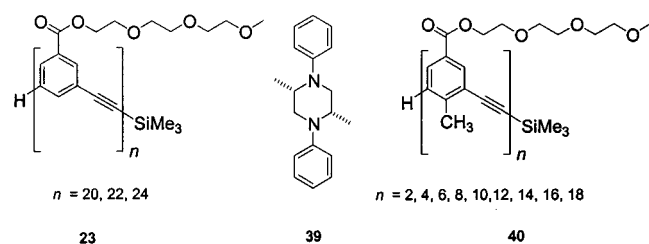


Figure 87. Structures of a rodlike guest and two series of *m*-phenylene ethynylene oligomers.

modularity, both in terms of the helical scaffold and the ligand. Association is based on shape recognition arising from the morphological features of interacting molecular surfaces. These concepts led to the development of rod-shaped chiral guest **39** whose shape is matched to the cylindrical cavity of oligomer series **23** (Figure 86a). The binding affinity of these complexes was postulated to depend on the relative length of the oligomer to its guest, assuming the free energy of binding depends on the area of contact between the interacting molecular surfaces (Figure 86b). Considering the diameter of the cylindrical hydrophobic cavity in helical oligomer series **23**, *cis*-(2*S*,5*S*)-2, 5-dimethyl-*N,N*-diphenylpiperazine **39** was examined as the guest molecule (Figure 87). Compound **39** has a chiral, rodlike structure, and its size and shape are complementary to the cavities of helical **23**, as deduced from molecular modeling studies (Figure 86c).

The binding affinities of **39** with members of oligomer series **23** ($n = 10, 12, 14, 16, 18, 20, 22, 24$) were determined using CD measurements. Induced CD spectra resulting from the interaction of **39** with oligomer series **23** were obtained by subtracting the CD spectrum of **39** from that of the host-guest complex in 40% aqueous acetonitrile. The shape of the induced CD spectra is nearly identical to that obtained when using (–)- α -pinene as the guest molecule.⁴²⁰ CD spectra recorded over a range of guest concentrations showed saturation behavior with an isodichroic point, which is expected for a single stoichiometry relationship between **39** and its oligomeric host. To verify that binding takes place within the helical cavity, solutions of *endo*-methyl-substituted dodecamer **32** with guest **39** as a control were studied. No induced Cotton effect was observed in this case. These results indicate that compound **39** binds to the internal cavity of these oligomers,

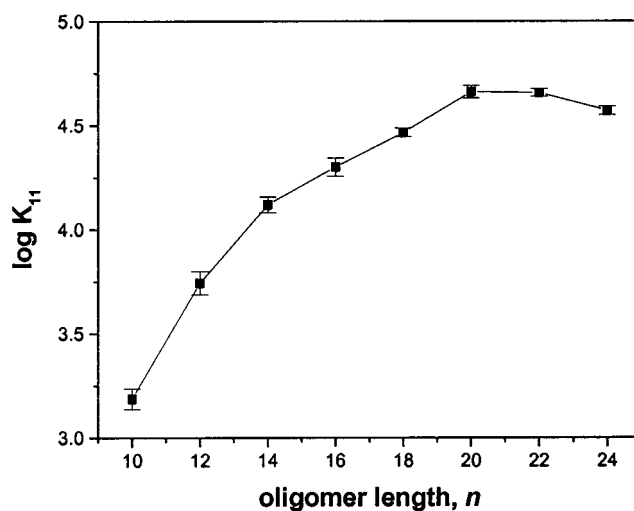


Figure 88. Plot of $\log K_{11}$ versus oligomer length n . The binding affinity of **39** reaches a maximum value with **23** ($n = 20$ and 22). All measurements were recorded in a mixed solvent of 40% H_2O in CH_3CN (by volume) at 294 \pm 1 K. $[\text{39}] = 4.2 \mu\text{M}$.

rather than associating by intercalation. The stoichiometry of the complex of **39** with **23** was determined to be 1:1 by the linearity of Benesi-Hildebrand plots. The association constant (K_{11}), calculated by a nonlinear least-squares fitting method, was found to be $5600 \pm 190 \text{ M}^{-1}$ for the 12-mer of **23**. This value is again similar to that of the complex of (–)- α -pinene and 12-mer of **23**.⁴²⁰ However, a significant dependence of the binding affinities of **39** on the length of the oligomers was observed (Figure 86). In each case, the stoichiometry of the complex was 1:1. The affinity of **39** with the 20-mer and 22-mer of **23** was found to be ca. 30 times larger than that of 10-mer. Interestingly, the K_{11} value of the 24-mer is smaller than that of the 20-mer and 22-mer by an experimentally significant and reproducible margin. The reduction in affinity could be due to destabilization involving a cavity-volume/guest-volume mismatch (Figure 86b).

These results continue to support the hypothesis that all members of oligomer series **23** exist in solution in conformationally well-ordered states with chiral cylindrical cavities capable of binding chiral rodlike guest molecules such as **39**. Co-modularity of host-guest oligomeric pairs such as the system described here raises a number of engaging possibili-

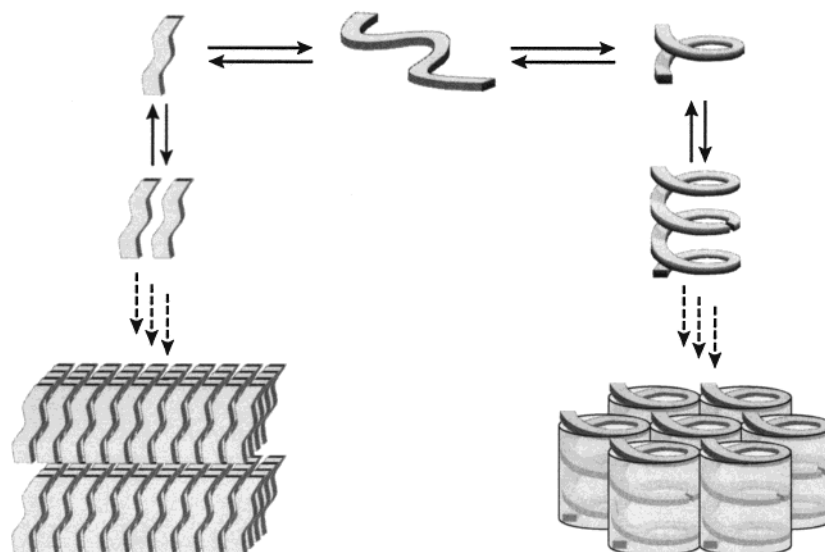


Figure 89. Schematic diagram illustrating the aggregation behavior of *m*-phenylene ethynylene oligomers over a range of concentrations. In dilute solution, the oligomers can exist in a random or helical conformation. At increased concentrations they associate intermolecularly, possibly in an extended lamellar-type fashion or as tubular and hexagonal helical stacks.

ties. It has been presumed that longer rodlike guest molecules will exhibit a maximum affinity to even longer oligomers. For example, the rod lengths of **39** can be easily varied by repeating the aryl–piperazine unit and may possibly be applied to the selective ligation of oligomer fragments to template the growth of chains of a specific length.

c. Oligo(*m*-phenylene ethynylene)s in the Solid State. The solid-state organization of *m*-phenylene ethynylene oligomers has also been investigated.^{423–426} For these studies two different oligomer series were examined (**23** and **40**). Two possible packing models were postulated for the solid-state organization of the oligomers (Figure 89). One possibility is that the oligomers could self-organize into a tubular mesophase.^{427,428} On the other hand, a lamellar organization consisting of extended ribbonlike chains could achieve many of the same local aromatic–aromatic interactions without the costly free volume of the tubular phase. The solid-state conformation was found to be highly dependent on the subtle chemical structure of the backbone.

Oligomer series **23**, which contains a hydrogen-substituted backbone, was found to exhibit a lamellar organization in the solid state. Optical microscopy and differential scanning calorimetry showed that oligomers ($n > 8$) adopt liquid crystalline phases and that they each have a similar mode of solid-state organization. By performing X-ray measurements on samples slowly cooled from the melt⁴²³ or evaporated from solution,⁴²⁵ it was possible to determine that the long-spacing, due to periodic order in the solid state, was directionally proportional to oligomer length (Figure 90). It was also determined that these viscoelastic samples could be mechanically aligned by spreading or rolling the material on flat substrates. This produced macroscopic orientation in the longitudinal direction. It was proposed that the lamellar organization was thermodynamically favored, presumably due to the minimization of free channel void space that would be present in a tubular structure.

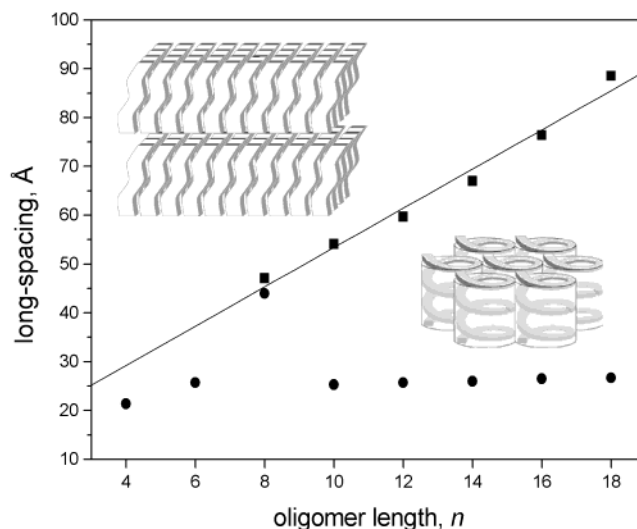


Figure 90. Plot of long-spacings versus oligomer length for two oligo(*m*-phenylene ethynylene) series as observed in SAXD measurements. Series **23** (prepared from the melt) packs in a lamellar arrangement (■, top), and thus, the long-spacings depend linearly on chain length. In contrast, series **40** (prepared from solvent evaporation) exhibits long-spacings that are independent of chain length ($n \geq 10$), suggesting the possibility of helical columns (●, bottom).

Oligomer series **40**, which contains a methyl-substituted backbone, was surprisingly found to adopt a tubular organization in the solid state. Because the melting point of these oligomers exceeds the decomposition point, a new X-ray sample preparation was required. Oligomers were dissolved in a solvent (typically CH_2Cl_2), drawn into a capillary, and left to solidify as evaporation took place. X-ray Bragg spacings were independent of chain length, and each oligomer exhibited a long spacing of 25–26 Å (Figure 90). The small-angle X-ray reflections were indexed to a hexagonal lattice indicating that the oligomers were packing in a tubular arrangement. In addition, it was determined that the oligomers spontaneously acquired a radial macroscopic orientation upon evaporation. These results suggested that the oligomers

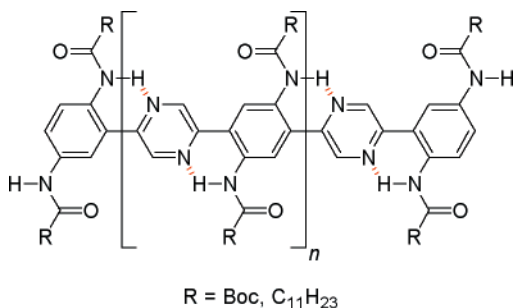


Figure 91. Alternating pyrazine and acylated 1,4-phenylenediamine copolymer that adopts a planarized shape.

that adopt hexagonally packed nanotubes tend to form stable helical conformations in solution (the folded state of oligomer series **40** is more stable than **23** in solution).⁴²⁹ In the case of **40**, the helical stabilization is attributed to the fact that the introduction of methyl groups minimized the costly free space present in series **23**. The tubular structure of this system and others^{377–380,382} could have possible applications as an organic host solid or be used as a template for nano-organization.

D. Backbones Utilizing Hydrogen-Bonding Interactions

1. Aromatic Amide Backbones

Hydrogen bonding is important for creating and stabilizing highly ordered conformations in naturally occurring systems such as α -amino acid peptides and nucleic acids. Recently, H-bonding interactions have been used in combination with the aromatic–aromatic stacking interactions of aromatic rings in oligomer systems. A common motif of this research is the use of aryl amides. It should be mentioned that most of these oligomers make use of interactions between adjacent monomer units only in their H-bonding interactions. Whether these chain conformations behave cooperatively or as a collection of independent units requires experimental verification. Nonetheless, the backbones discussed below are worthy of note in that they each utilize the same repeat unit to achieve various structural ends.

Oligo(acylated 2,2'-bipyridine-3,3'-diamine)s and oligo(2,5-bis[2-aminophenyl]pyrazine)s have shown enhanced planarization and conjugation through intramolecular hydrogen bonding (Figure 91).^{430–432} Dendritic analogues of these oligomers have also been reported.^{433–438}

Hamilton and co-workers reported the generation of a helical conformation based on an oligoanthranilamides (Figure 92).^{439–441} The system is based on the intramolecular H-bonding of two subunits, one being an anthranilamide **41** and the other a 2,6-pyridinedicarboxamide **42**. (Dendritic analogues utilizing anthranilamide and pyridinedicarboxamide subunits have been reported to display solvent-, temperature-, and generation-dependent conformations in solution.^{442–444}) It was proposed that a helical conformation would result from intramolecular H-bonding, the preference of secondary benzamides to adopt a trans conformation in solution, and aromatic–aromatic stacking between the aromatic subunits.

These subunits were combined in the synthesis of several compounds of varying oligomer length (**43**, **44**, **45** R = Me, *n*-Hex).

The helical conformation was characterized by NMR spectroscopy and X-ray crystallography. In chloroform, where H-bonding should be strong, oligomers **43** and **44** exhibited a large downfield shift for the pyridinecarboxamide protons while the terminal NH protons and many of the aromatic protons exhibited a strong upfield shift. These results are indicative of aromatic stacking and H-bonding. The solid-state structure of **43** shows a distinct helical conformation with an aromatic stacking distance of 3.69 Å. The increased bulk of the *N*-oxide unit in **44** resulted in a wider separation of the terminal anthranilamide rings. This resulted in an increased pitch of the helical conformation as evidenced by an increased aromatic stacking distance in the X-ray structure and less significant upfield shifting of the resonances of the terminal aromatic protons.

Intramolecular H-bonding was also used in the creation of systems **45** (R = Me, *n*-Hex) with an extended secondary structure. X-ray crystallography on the less soluble analogue **45** (R = Me) revealed two polymorphs. One contained the desired helical conformation with the expected aromatic stacking distances and two complete turns of the oligomeric backbone. In the solid state, a racemic mixture of right- and left-handed helical conformations is present. Surprisingly, another polymorph contained a left-handed helix for the first portion of the oligomer that reversed to a right-handed helical conformation at the phenylenediamine unit in the center of the strand. The solution conformation showed the expected downfield shifting of H-bonded amide protons and upfield shifting of aromatic resonances due to aromatic stacking. However, the lack of any NOE signals prevented the complete characterization of the solution conformation. Therefore, it was not possible to determine if alternative structures existed. Nonetheless, these results demonstrate that the combination of aromatic stacking interactions and intramolecular H-bonding can be used for the generation of secondary structures in solution. Given the combination of adjacent and nonadjacent noncovalent interactions that contribute to conformational stability, these oligomers do qualify as foldamers.

Additionally, predisposed intramolecular H-bonding has been used for the helical formation of oligo(amide)s (Figure 93).^{445–447} Using a structure akin to one published by Nowick,^{154,155} these systems involve *meta*-connected diaryl amide oligomers (**46**) and the presence of a three-center intramolecular H-bond, which leads to a rigidification of the backbone. Ab initio molecular calculations show a strong preference (>11 kcal·mol⁻¹) for the three-center H-bond over possible alternative conformations. These units were incorporated into oligomer **47** containing six aromatic rings. Upon placing the oligomers in a chloroform solution, an almost complete circle was formed, which represents the first turn of a helical conformation. ¹H NMR NOESY experiments revealed the expected 10 cross-peaks between the amide protons and the protons of the alkoxy α -methylene and methoxy

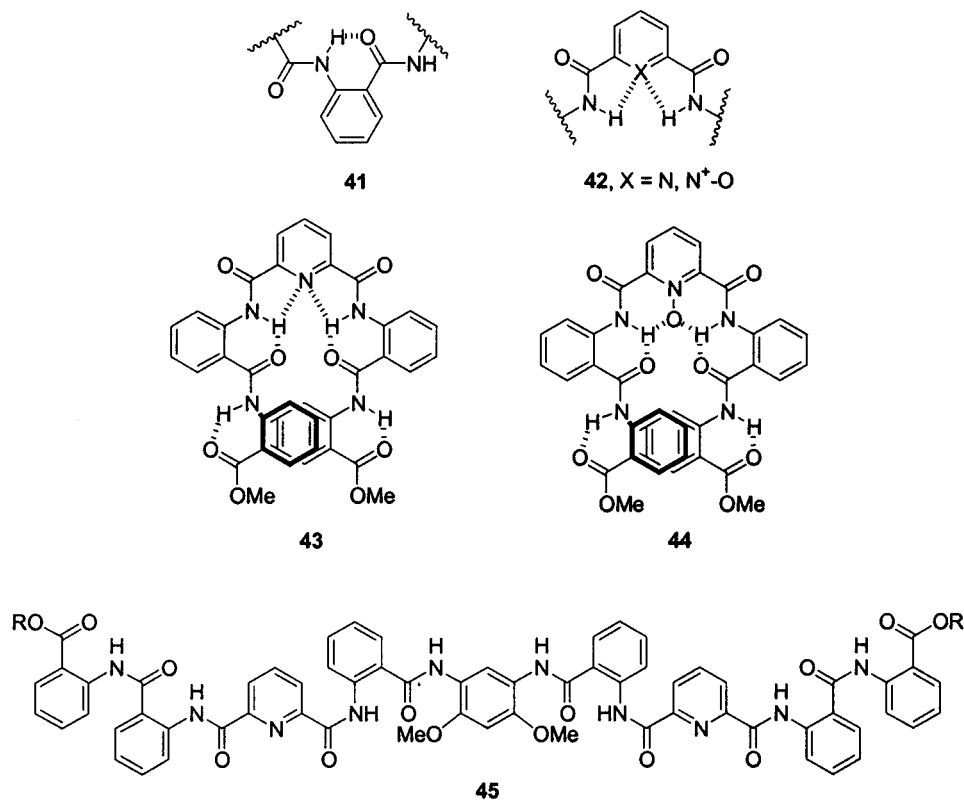


Figure 92. Anthranilamide motifs and derivative oligomers.

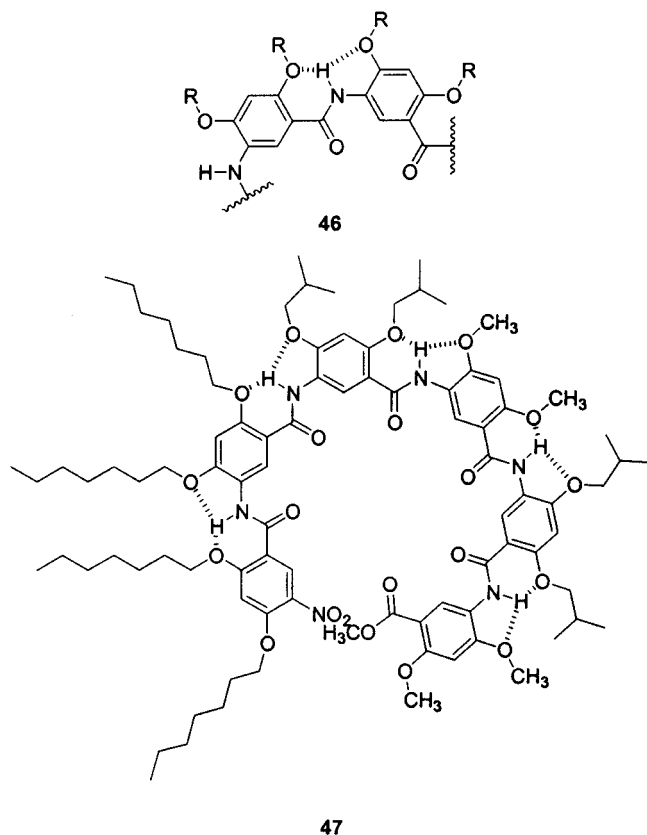


Figure 93. Chemical structure of an oligo(amide) motif and a crescent oligo(amide).

groups, supporting the formation of a curved conformation. On the basis of molecular modeling, this conformation has a ~ 10 Å hydrophobic cavity. At the present time, no oligomers longer than six units have

been synthesized, so it is therefore not known if longer strands would result in a helical conformation. However, if this does occur, it would create a large internal cavity that could possibly be used for the binding of small molecules.

2. Receptor Motif Backbones

a. Diaminopyridine Backbones Templated by Cyanurate.

Molecular recognition mediated by H-bonding between a host diaminopyridine and a guest cyanurate unit (**48**) has also been used for the generation of well-defined foldamers (Figure 94).⁴⁴⁸ An oligomer strand **49** containing four diaminopyridine subunits was synthesized and studied. It was proposed that the interaction of oligomer **49** with 2 equiv of a monosubstituted cyanurate **50** would result in helical conformation **52** (through conformation **51**) stabilized by H-bonding and aromatic stacking interactions. ¹H NMR spectroscopy was used to characterize the interaction of oligomeric host **49** with cyanurate guest **50**. In chloroform and polar, hydrogen bond-competing solvents such as methanol, the spectrum of **49** is broad and poorly resolved, indicating a variety of nonspecific intermolecular interactions. Upon the addition of 2 equiv of cyanurate guest **50**, a sharpening of the signals is observed along with the downfield shift of the amide hydrogens resonances. These results indicated the formation of a well-defined, H-bonding complex whose 2:1 stoichiometry was confirmed by a Job's plot analysis.^{449,450} The binding was determined to be a cooperative process where the binding constant of the second guest was twice that of the first guest. This could be attributed to the preorganization of the strand for the binding of the second guest molecule

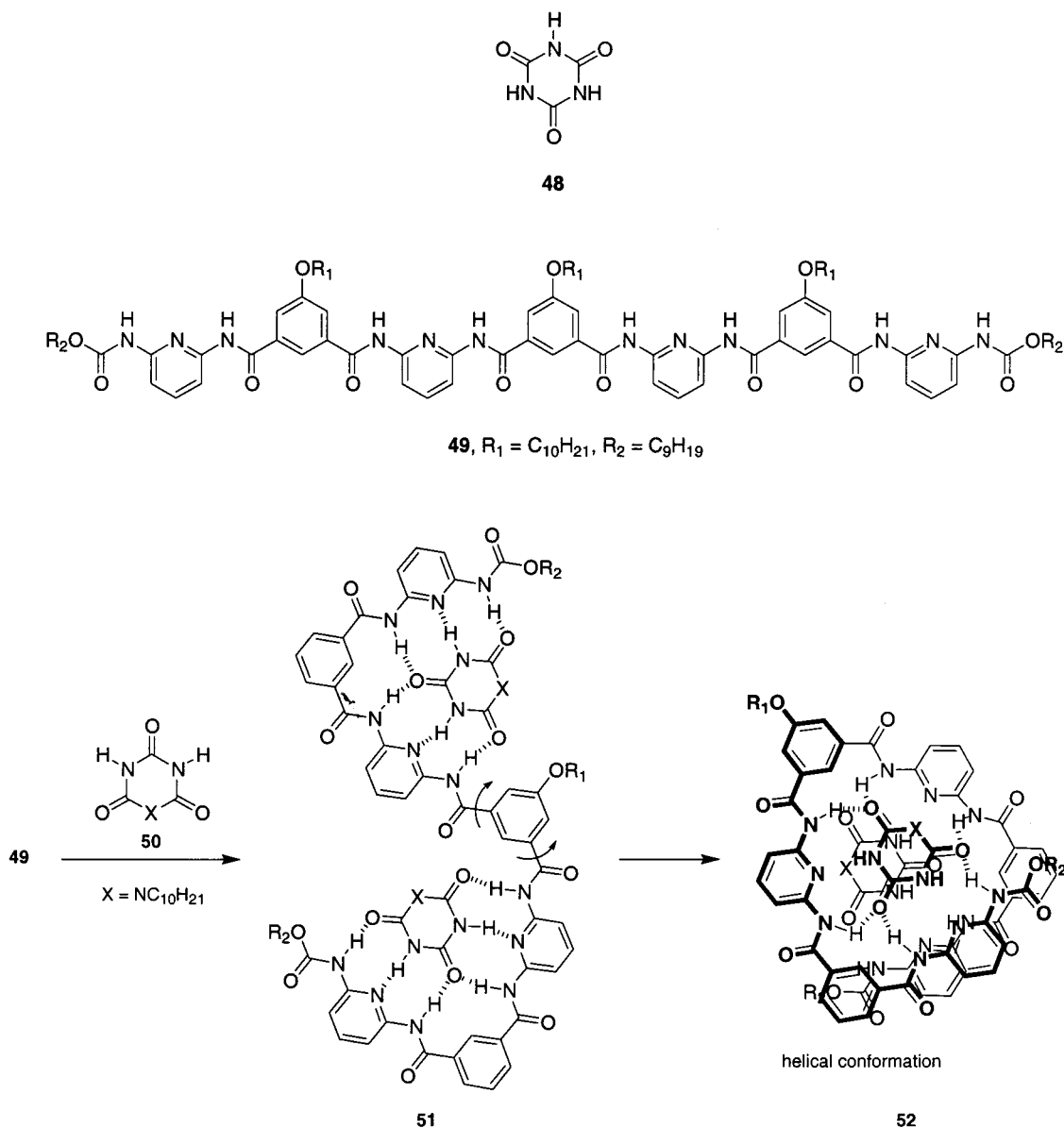


Figure 94. Motifs, oligomers, and helical structure of cyanurate-binding oligo(diaminopyridine)s.⁴⁴⁸

upon binding of the first molecule. An examination of concentrated solutions in hydrocarbon solvents by optical and electron microscopy revealed the presence of entangled fibers. This behavior was attributed to the intermolecular aggregation of the helical conformation **52**, similar to previously described systems.³⁸² These results show that the proper use of intermolecular interactions between a host and guest molecule can template helical conformations and higher ordered structures in solution.

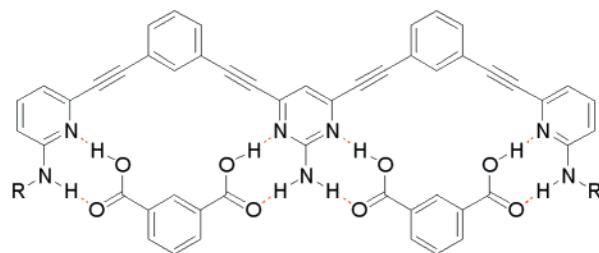
b. Phenylene–Pyridine–Pyrimidine Ethynylene Backbones Templated by Isophthalic Acid. Moore and co-workers reported a phenylene ethynylene-based isophthalic acid receptor that can be extended to a dual-site complex.⁴⁵¹ While this system does not utilize aromatic stacking to adopt a planar conformation, it does employ the rigidity of a phenylacetylene backbone to properly bind its guest via H-bonding. Cocrystallization of the precursor trimer and isophthalic acid gives single crystals of a complex suitable for X-ray structure determination. The resulting complex clearly displays four H-bonds and

packs in 2D sheets. Job's method confirmed the 1:1 stoichiometry of the complex in solution.^{449,450} Pentamer **53**, which can bind 2 equiv of isophthalic acid in solution (stoichiometry determined by Job's method^{449,450}), was also examined by X-ray structural studies. Eight H-bonds were revealed corresponding to the planar configuration of the complex (Figure 95). Overall, these results show that the binding of a guest can modulate the conformation of its respective host and that extending the host backbone can result in multisite foldamer receptors.⁴⁵²

E. Backbones Utilizing Metal Coordination

1. Overview

Up to this point in the review, foldamer structures primarily stabilized by hydrogen bonding and aromatic–aromatic stacking have been considered. At the same time, a significant amount of work has been conducted on chains that fold upon binding ionic species, especially coordination of metal ions, termed *helicates*.⁴⁵³ The folding reaction of these backbones



53

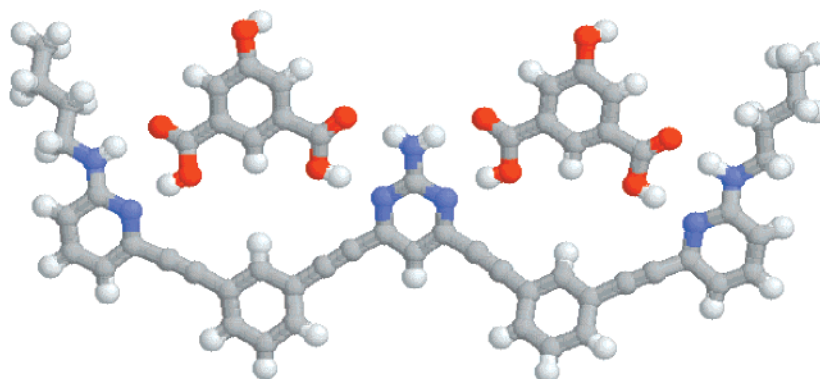


Figure 95. Crystal structure of a trimeric receptor with two molecules of bound isophthalic acid.

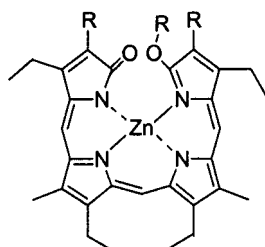


Figure 96. Helical zinc–bilinone complex.

is coupled to the assembly–disassembly process of metal coordination. We are unaware of any reference to helicate structures as foldamers in the literature, although they fulfill the foldamer criteria outlined in this review. Herein, we only consider examples that are chain molecules (at least two repeat units in the backbone) with the stipulation that they must demonstrate an ability to be extended to longer chain lengths. Furthermore, we will not consider infinite helical complexes since they are by their nature polymeric. Thus, the purpose of this section is not an exhaustive review of the helicate literature^{454–457} but an exploration of chain molecules that fold through metal coordination.

2. Metal-Binding Backbones

a. Zinc Bilinones. Acyclic porphyrin derivatives known as bilinones incorporate functionalized pyrroles into a tetrameric backbone such that binding of Zn(II) induces single-stranded helical conformations (Figure 96). Studies aimed at shifting the helical twist sense have involved covalent attachment of chiral moieties to the chain terminus^{458,459} or as tethers⁴⁶⁰ in addition to binding of chiral guests such as amino acids.^{461,462} Using chiral end group modified

bilinones, a recent solvent study demonstrated that solvents of lower polarizability were more efficient at this helical induction since intramolecular van der Waals contacts responsible for the diastereomeric discrimination are more favorable in these solvents.⁴⁵⁹ Although these tetrameric chains adopt folded conformations, it is difficult to envision a homomorphic extension of the chain to longer lengths with retention of these foldamer characteristics. Because of this, discussions of bilinones as foldamers does not seem promising and will not be considered further.

b. Oligopyridines. Although a variety of heteronuclear ligands employing pyridines, imines, and other Lewis basic functionalities have been incorporated into single-stranded helicates, we will focus here primarily on oligopyridines since they are the most common metal-coordinating ligands and have been incorporated into many complex structures.⁴⁵⁶ Oligopyridines are a family of chain molecules that have been thoroughly studied for their ability to bind a variety of metal ions in different stoichiometries and with predictable geometries due to their substitution patterns along the aromatic rings. As the oligomer length increases, *cisoid* and *transoid* conformational states are possible at each interannular torsion along the chain. Quaterpyridines (qtpy) exist as all-*transoid* conformations in the solid-state, with interannular twisting observed in solution,⁴⁶³ while adopting all-*cisoid* planar conformations when complexed (Figure 97) to a variety of transition-metal ions (examples include Co(II),⁴⁶⁴ Co(III),⁴⁶⁵ Cu(II),⁴⁶⁴ Ni(II),⁴⁶³ Pd(II),⁴⁶⁶ Cr(III),⁴⁶⁷ and Y(III)).⁴⁶⁸ Qtpy oligomers are the longest chains of this family that consistently adopt planar conformations within a single-stranded complex. Longer oligopyridine chains,

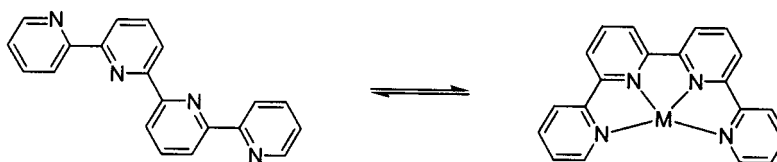


Figure 97. All-*transoid* solution conformation of qtpy, and the all-*cisoid* coordinated form.

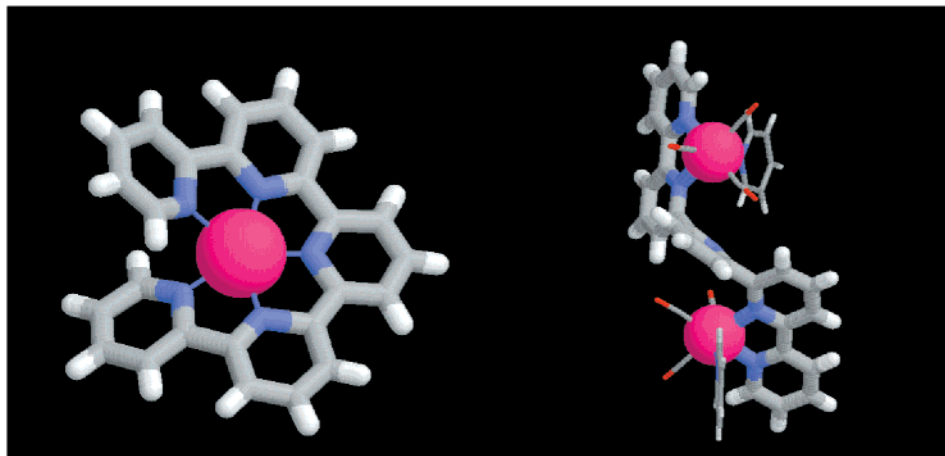
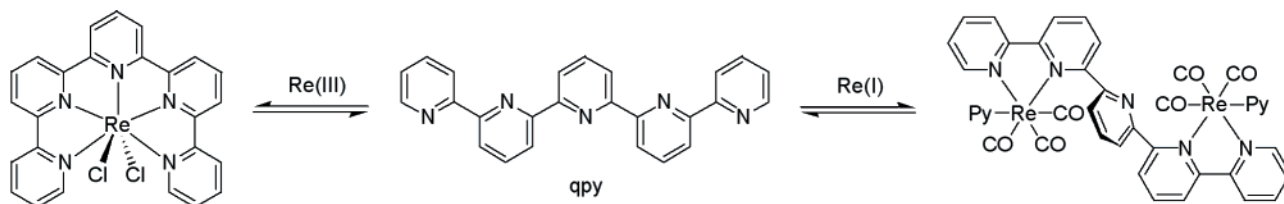


Figure 98. Two different single-stranded qpy helicites in two different Re oxidation states. Crystal structures are shown for each.

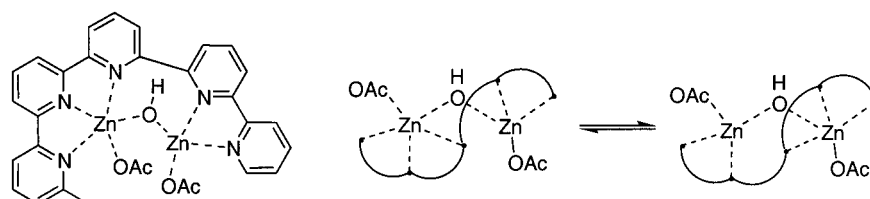


Figure 99. Solution equilibrium of a dinuclear qpy Zn(II) helicate containing a bridging hydroxide.

however, adopt helical conformations upon metal coordination and demonstrate various folded architectures, although becoming increasingly insoluble with longer lengths. Recent approaches that incorporate 4-*tert*-butyl phenyl⁴⁶⁹ and *n*-propylthio side chains⁴⁷⁰ greatly aid in solubilizing these oligomers.

The ability of metal ions to optimize their coordination sphere while minimizing their geometric constraints results in the ability to selectively coordinate to preferred segments within a chain molecule. This is a powerful supramolecular construct for foldamers whose level of architectural control has not been fully exploited. For instance, with Re(III), quinquepyridine (qpy) ($n = 5$) adopts a mononuclear, all-*cisoid* helical complex (also observed in a [Ag(qpy)]-[PF₆]₃ complex⁴⁷¹) (Figure 98). With Re(I), one of two isolated crystals was determined to be the dinuclear helicate where the metal ions partition the oligomer into two bipy segments, leaving the central pyridine uncoordinated.⁴⁷² With Re(III), the helical conformation occurs by interannular twists in the backbone to assuage steric interactions between the termini.

In the Re(I) helicate, the dinuclear coordination mode in the S-shaped conformation is adopted in order to alleviate steric hindrance in alternative complexations (as well as to accommodate the geometric preferences of the CO ligands) with the dihedral angles between the central ring and the bipy fragments opening up to 110° and 112°. ¹H NMR confirmed that the solid-state conformations of both complexes were retained in solution. Similarly, a single-stranded 6,6''-dimethyl-qpy chain binds two Zn(II) ions (bridged by a hydroxyl group) and two acetate species. In the solid state, bipy and tpy oligomer segments bind separately in order to ideally match steric constraints and satisfy the coordination spheres of the Zn(II) ions (Figure 99).⁴⁷³ In solution, the central pyridine coordinates to either of the Zn(II) ions in a dynamic equilibrium as evidenced by ¹H NMR. With sexipyridines (spy), Eu(III) forms a monohelical, 10-coordinate complex through torsional adjustments in the backbone to minimize chain end interactions,⁴⁷⁴ while with Pd(II), spy coordinates to

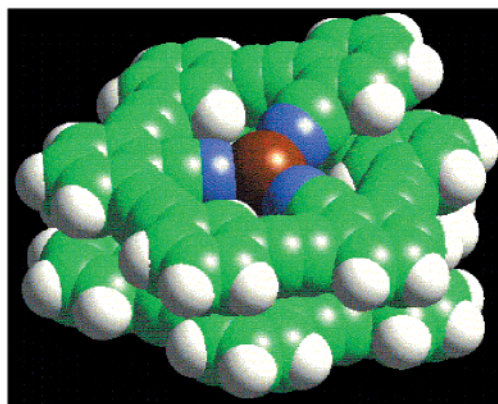
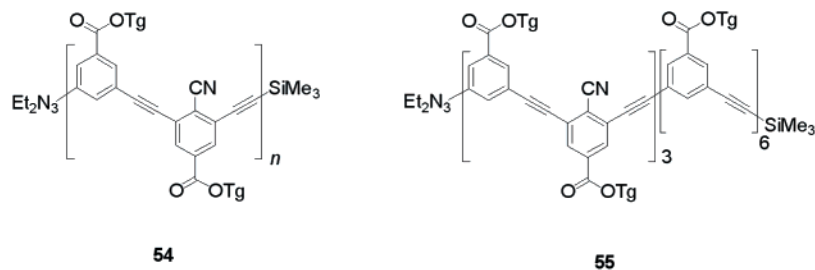


Figure 100. Structures of cyano-substituted oligo(*m*-phenylene ethynylene)s and a space-filling model of **54** coordinated to two Ag^+ ions. Side chains have been omitted for clarity.

two metal ions through two tpy fragments in the chain.⁴⁷⁵

c. Oligo(*m*-phenylene ethynylene)s. A modification of the tubular cavity of oligo(*m*-phenylene ethynylene)s led to the first example of a nonbiological oligomer whose secondary structure could be controlled by both nonspecific (solvophobic) and specific (metal-coordination) interactions.⁴⁷⁶ These features were present in dodecamer **54**, consisting of 12 nonpolar phenylacetylene backbone units, each attached to a polar triethyleneglycol monomethyl ether side chain (Figure 100). Six metal-coordinating cyano groups are located on every other aromatic ring, between the acetylenic linkages. In the helical conformation, this sequence places the six cyano groups into the interior of the tubular cavity creating two approximately trigonal planar coordination sites. Molecular models revealed that each nitrogen atom lies about 2.1 Å from the helical axis, a distance consistent with that needed for metal–nitrile ligation (Figure 100). Both UV–vis and ^1H NMR measurements showed that a helical conformation could be produced by the use of solvophobic interactions alone, indicating that the cyano groups on the interior of the helical cavity did not inhibit the formation of helical structures. All metal-binding experiments were performed in tetrahydrofuran since this solvent does not solvophobically induce helical conformations. Silver triflate (AgO_3SCF_3) was used as the metal source, since it favors a trigonal planar coordination environment. By using a combination of UV–Vis, ^1H NMR, electrospray MS, and isothermal titrational microcalorimetry, it was determined that dodecamer **54** cooperatively bound two moles of AgO_3SCF_3 resulting in a stable, folded conformation. Control experiments on oligomers that did not contain cyano groups (oligomer series **23**) clearly indicated that the

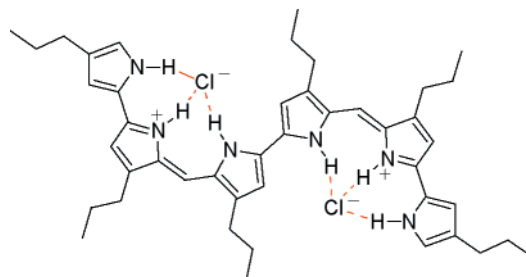


Figure 101. Structure of a hexapyrrin bound to two chloride anions.

conformational changes were a direct result of the interactions between the silver ions and the cyano groups. By performing experiments on a modified oligomer (**55**), it was also possible to determine that solvophobic interactions were playing an important role in the formation and stability of the metal-induced helical formation. The studies showed that oligomer series **22** could be modified to tightly and selectively bind metal ions within the internal cavity of a helical structure. Furthermore, the strength of metal ion binding appeared to be derived from a combination of solvophobic interactions that favored the helical structure along with the more usual metal–ligand interactions.

3. Anionic-Binding Backbones—Hexapyrrins

Compared to their cation-binding analogues, anion-binding foldamers are far less common, purportedly due to the lack of discrete denticity in anion coordination chemistry. However, 5,15,25-tris-nor-hexapyrrins, similar in structure to the bilinones, display a discrete “S”-shaped conformation in solution and in the solid state (Figure 101).⁴⁷⁷ Bilin-derived and respective linear tetrapyrrolic analogues have long been studied as supramolecular building blocks due

to their role as precursors in the generation of natural products such as macrocyclic porphyrins. Sessler and co-workers synthesized fully conjugated hexapyrrin with four *n*-propyl side chains. Crystallization of the dihydrochloric acid salt of this foldamer showed the chain to lie in a completely planar conformation, where one chloride ion rests in each of the two clefts generated in the “S” shape. This configuration allows each of the anions to engage in three hydrogen bonds, where one is ionic in character. The dihydrochloric acid salt was the only analogue generated that packed in this way. Data gained from NOE spectroscopy confirmed that the prevalent solution-phase conformation was also planar. Yet, the presence of an overlapped helix could not be ruled out given that no new cross-peaks could be observed by this method for such a conformation.

VI. Nucleotidomimetic Foldamers

A. Overview

Although the oligomer systems described thus far have involved only single chain folding reactions, the field of foldamers is not limited to this definition. In fact, the scope of foldamers extends to multistrand assemblies where oligomer chains associate and fold through noncovalent *intermolecular interactions between strands*. Within this field, nucleotidomimetics aim at improving the understanding of natural oligonucleotides,⁴⁷⁸ seeking insight on the origins of life,^{479–481} and on the development of antisense (targeting mRNA) and antigene (targeting the major groove of double-stranded DNA) agents.^{482–486} These approaches involve correlating structural modification of the backbone and the nucleobases with conformational changes in the chain and the stability of the generated duplexes. Conformational changes are measured directly by NMR and other structurally determinant techniques or indirectly by thermal denaturation using classic UV melting curves.

To our knowledge, the literature has not completely connected these structures with foldamers since the motivation for research in this area derives primarily from generating stable supramolecular complexes. Because of this, studies of nucleotidomimetic foldamers can best be summarized as “research on foldamers” where the folding reaction is implied but not the central focus as it has been with peptidomimetic and single-stranded abiotic foldamers. From the perspective of the foldamer field, nucleotidomimetics aim to ascertain the interdependence between sugar–backbone conformations and the *strength* of interstrand interactions. That is, given the variety of sequence-dependent pairing motifs and complex-induced conformations possible in natural oligonucleotides, it is of interest to determine how variation of the backbone affects the mode and selectivity of strand association. Examples described herein can afford an expanded conceptualization for the construction of novel foldamer complexes while at the same time approach the field from the point of view of chain folding *and* association. Just as with peptidomimetic foldamers, nucleotidomimetics are approached through a top-down design, and therefore, the success of structural modification is often ascertained by direct comparison to their biological counterparts.

In general, DNA strands adopt unique conformations upon association through interstrand contacts. On the other hand, not only does RNA form duplex structures, but also single chains also commonly fold through intrastrand interactions into complex secondary structures such as hairpins and loops.⁴⁸⁷ Prior to duplex formation, single-stranded oligonucleotides show significant conformational preorganization. This preorganization is a result of phosphates in the backbone linearly extending the oligonucleotide chain through electrostatic repulsion (similar to polyanionic polymer backbones³¹) and base-stacking interactions that align the backbone into an expanded state.⁴⁸⁸ Upon duplex formation, realignment of the oligonucleotide backbone proceeds at an entropic cost in order to maximize the enthalpic gain from intra- and interstrand base interactions within the double helix, thus refining the overall conformation through base pairing. The recognition selectivity is primarily a function of the interstrand base-pairing interactions shown in Figure 102. Exhaustive conformational analysis of the furanose ring in oligonucleotide backbones has revealed several preferred puckered states due to the flexibility of the five-membered ring; these ring conformations are seen in DNA and RNA sequences (Figure 103).^{487,489} In double-stranded (ds) complexes, RNA backbones primarily adopt the 3'-*endo* A-type conformation whereas DNA (d) backbones adopt both the A- and 2'-*endo* B-type conformations (Figure 104). These conformations influence the tilting of the nucleobases; the B-type conformation orients the bases perpendicular to the helical axis, while the bases of the A-type conformation are inclined ca. 14–20° to the axis.⁴⁹⁰ The resulting duplex architectures are stabilized through Watson–Crick (*WC*) base-pairing and have information-rich surfaces both in the major groove, where oligonucleotides can bind through Hoogsteen (*H*) pairing to form triple-helical assemblies, and the minor groove, which contains sites for small molecule interactions.⁴⁸⁷

The successful design of an *oligonucleotide foldamer* will be evaluated in two ways: first, the ability of the foldamer to adopt backbone conformations that promote base interactions, both pairing and stacking, by their intra- or intermolecular stability and, second, the demonstration of attributes such as cooperativity and base selectivity that provide insight into the folding reaction. This survey will primarily focus on backbone modifications of the carbohydrate, linkage, and nucleobases (for reviews, see refs 486 and 491), and to a lesser extent foldamers that bind in the minor groove of oligonucleotide duplexes. On the whole, nucleotidomimetic foldamers are robust. This behavior is perhaps a fundamental property of repeating, polyelectrolyte chain molecules. They can tolerate a variety of modifications within the backbone while retaining their duplex stability primarily due to a well balanced set of supramolecular interactions that, most importantly, includes electrostatic repulsion. It is worth mentioning that thermal denaturation data provided in this discussion is system specific, and therefore, comparisons can only be made to isostructural systems studied under identical conditions.

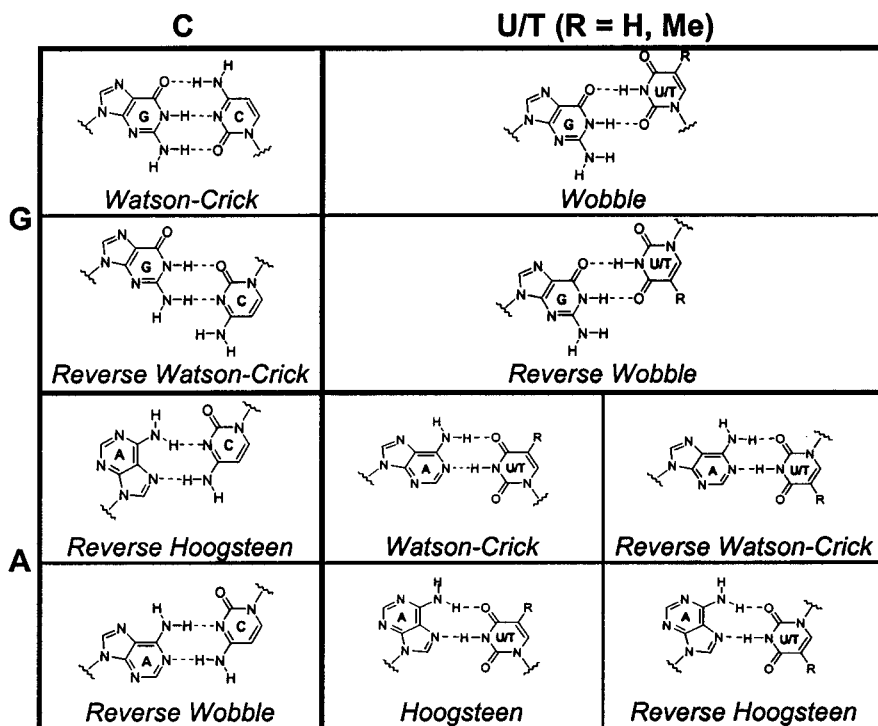


Figure 102. Common nucleotide base-pairing motifs and acronyms used throughout this section.

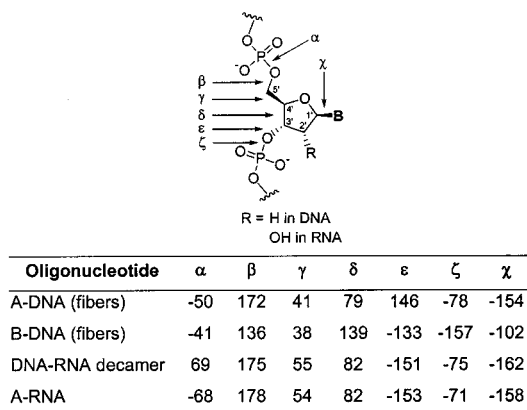


Figure 103. Average torsional angles (in degrees) for the furanose ring in several oligonucleotides from crystal structures.⁴⁸⁹

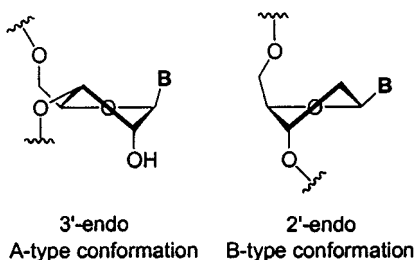


Figure 104. Puckered ring conformations found in the backbones of RNA (A only) and DNA (A and B) duplexes.

B. Isomeric Oligonucleotides

1. Iso-RNA and Iso-DNA

The most straightforward modifications of natural oligonucleotide backbones are constitutional changes involving the 5'→3' phosphodiester linkage. Since 5'→2' oligonucleotides are biologically known but not

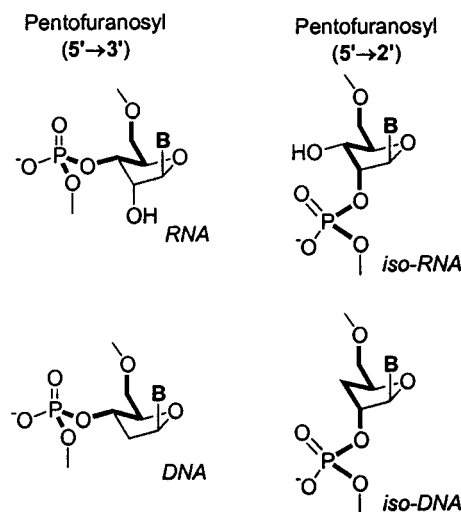


Figure 105. Natural and isomeric furanosyl backbones. **Bold** indicates backbone bonds.

demonstrated to be involved in information transfer,⁴⁹² these isomeric forms of natural RNA and DNA were clear starting points for investigations into alternative backbones (Figure 105). Detailed research on 5'→2' isomeric RNA and DNA (iso-RNA and iso-DNA) duplex formation was reported in three papers in 1992.⁴⁹³⁻⁴⁹⁵ NMR studies on self-complementary iso-RNA⁴⁹⁵ and iso-DNA-CGGCGCCG⁴⁹⁶ indicated antiparallel strand orientation within the *WC* right-handed duplex analogous to the natural duplexes. UV melting studies were conducted on these duplexes where T_m values indicate the temperature at 50% duplex dissociation. The complementary duplex iso-DNA-A₁₂/iso-DNA-U₁₂ was shown to be less stable ($\Delta T_m = 18$ °C) than the corresponding natural DNA duplex, while the self-complementary iso-DNA-(AU)₆ had a higher denaturation temperature ($\Delta T_m = 9.4$

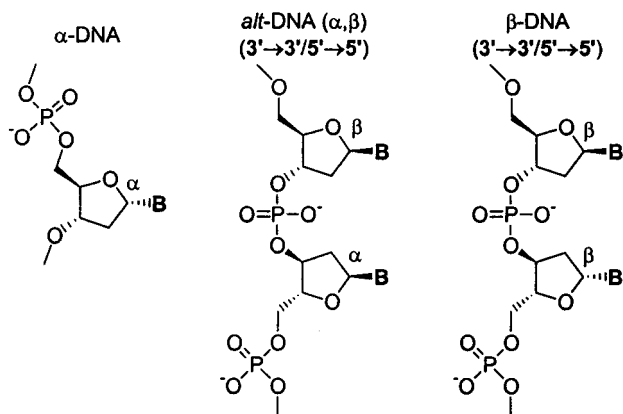


Figure 106. α -, *alt*-, and β -DNA backbones.

°C) but was less cooperative than d(AT)₆.⁴⁹⁴ Iso-DNA-G/C duplexes have one-half the thermodynamic stability as DNA⁴⁹⁷ and have been characterized by ESI-MS.⁴⁹⁸ With heteromeric 16-mers (containing one or two 5'→2' iso-DNA A/T monomers within the 5'→3' backbone), self-complementary strands associate with significantly lower stability than their DNA counterparts.⁴⁹³ Furthermore, iso-RNA-C/U oligomers formed a duplex with its RNA G/A complement but not with DNA⁴⁹⁹ as was found for iso-DNA/RNA duplexes.^{500,501} The order of thermal stability of homo- and heterostranded duplexes for iso-RNA was determined to be as follows: RNA:RNA > DNA:DNA ~ RNA:DNA > RNA:iso-RNA > iso-RNA:iso-RNA ≫ DNA:iso-RNA indicating lower association efficiency for isomeric oligonucleotides.^{502,503} A mixture of iso-DNA-A₁₆ and iso-DNA-T₁₆, which was not able to form complementary duplexes,⁴⁹³ associated into triplexes with reduced thermodynamic stability versus 5'→3' triplex structures,⁵⁰⁴ while iso-RNA-A₇/T₇ and -A₁₀/T₁₀ formed both duplexes and triplexes depending on the oligomer ratio and salt concentration.⁵⁰⁵ Iso-RNA segments linked to DNA hairpins are capable of templating the oligomerization of 2-Me-ImpG (a mononucleotide successfully coupled with DNA templates⁵⁰⁶) although with lower activity than RNA segments.⁵⁰⁷ The research on iso-oligonucleotides highlights the important principle in this field that even subtle backbone modifications can have pronounced effects on interstrand association, reflecting the subtle balance of noncovalent forces at play in oligonucleotide complexes.

2. α -DNA, *alt*-DNA, and L-DNA

Another isomeric modification of deoxyribonucleotides involved the change in the anomeric configuration from the natural β -position to an α -linkage (α -DNA) (Figure 106). NMR studies of α -hexamers duplexed with the natural β -DNA complements established C3'-*endo* and C2'-*endo* furanose conformations for α -T and α -C nucleotides, respectively.⁵⁰⁸ Additionally, α -DNA strands showed enhanced base stacking,⁵⁰⁹ WC antiparallel orientations in ds- α -DNA,⁵⁰⁹ and parallel orientations in α,β -DNA hybrid duplexes in B-type conformations⁵¹⁰ with higher binding to RNA than DNA.⁵¹¹ Initial studies on α,β -T₂₈, a heteromeric sequence of alternating α - and β -deoxynucleotides connected through 3'→3' and

5'→5' linkages (*alt*-DNA), induced less stable hybrid duplexes with both β -d-A₂₈ and poly r-A than either homomeric α - or β -T₂₈ strands.⁵¹² Through the alternating connectivities in α,β -strands, bases are equidistantly aligned since the "flipping" of the nucleotide by the alternating linkages is corrected by the configuration at the base-sugar position. Alternating 3'→3'/5'→5' linkages in β -T₂₈ produced a more significant degree of destabilization than α,β -T₂₈ due to the nonequidistant base arrangement. α,β -DNAs incorporating canonical bases (A, T, C, and G) showed backbone-dependent duplex stabilities and mismatch discrimination with natural DNA and RNA strands.^{513,514} In general, *alt*-DNA has a higher affinity for DNA strands than RNA, adopting B- and A-type conformations, respectively. Although these results are promising for α -DNA as a nucleotidomimetic, some inconsistencies in thermal transitions do exist in that both increased⁵¹⁵ and decreased⁵¹⁶ stabilities are observed, suggesting that certain sequences can lead to conflicting theories about the overall stability induction of the α -backbone. These irregularities in stability trends were also observed in L-DNA A-strands, the enantiomeric form of the natural DNA, where triplexes with poly(U) were stable⁵¹⁷ while L-DNAs with mixed bases did not bind to either RNA or DNA.⁵¹⁸ Other isomeric forms of DNA that have been studied include xylose-DNA,⁵¹⁹ where homostranded duplexes show higher thermal stabilities through multistate transitions, and arabinose-DNA,⁵²⁰ forming stable duplexes with arabinose-A oligomers and poly-U and -T.

C. Carbohydrate Modifications

Modifications of the sugar backbone primarily aim at answering a specific question: why nature chose ribofuranosyl nucleotides rather than some other backbone as the molecular basis for the genetic system of life?^{71,479–481,521,522} The work of Eschenmoser in this area has focused on the search for a chemical etiology of oligonucleotides, approached in a similar vein as peptidomimetic foldamer research, that is, the systematic modification of the backbone to determine relationships between structure and stability. Structural modifications that explore various (CH₂O)_{*n*} aldose-based (*n* = 4, 5, or 6) backbones are depicted in Figure 107.⁵²² Although strides to investigate the constitutional isomers of the furanose nucleotides have been made, the question of how this sugar arose as the "backbone of life" remains a mystery. Due to the extensive work conducted on pyranosyl-RNAs (p-RNAs), they will be explored here in detail as the closest examples to date of foldamer research on nucleotidomimetics.

1. Backbones with C1'-Base Connectivities

a. The Tetrofuranosyl Family. Through the removal of the C5 in the ribopentanosyl backbone, (3'→2')- α -threofuranosyl oligonucleotides (TNA) (Figure 107) were investigated to determine if furanosyl backbones with a "five-bonds-per-backbone" motif (as opposed to six in natural systems) could participate in self- and cross-duplexing with RNA and DNA.⁵²³ In TNAs, WC base-pairing between antiparallel

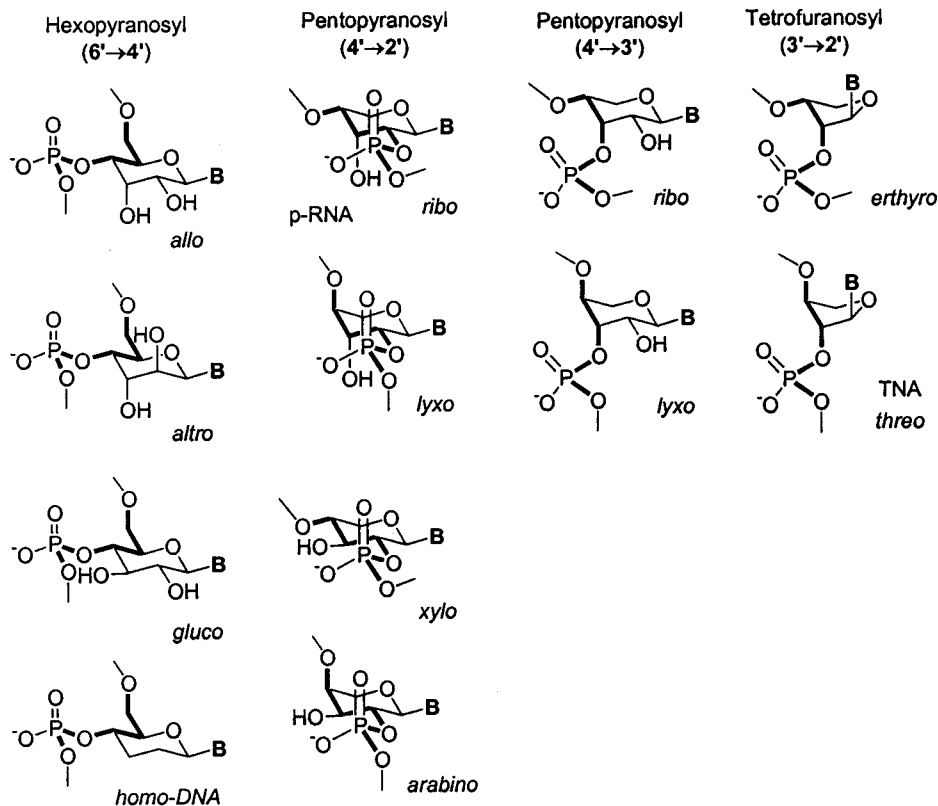


Figure 107. Alternative oligonucleotide backbones investigated with aldohexoses (CH_2O) $_n$ ($n = 4, 5, \text{ or } 6$). **Bold** indicates backbone bonds.

strands is the preferred interaction within the duplex. TNA duplexes show stabilities that are comparable to RNA and DNA duplexes (of the same sequence), are capable of forming hairpins, and form stable cross-paired systems with complementary natural backbones. In particular, much more stable hexadecamer duplexes are formed when the natural backbone is an all-pyrimidine (T) sequence and the TNA is an all-purine (A) sequence, with a T_m decrease of 48 °C for RNA and 32 °C for DNA observed when the base complementarity is switched. By comparing these constitutional analogues to natural oligonucleotides, promising backbones such as TNAs have provided chemical clues about the fitness of DNA and RNA for information storage and transfer.⁵²⁴

b. The Pentopyranosyl Family. *i. p-RNAs.* One of the most thoroughly investigated alternative nucleotide backbones is the 4'→2' *ribopyranosyl* isomer of RNA (p-RNA) with the phosphodiester linkage extending from the C4' to the C2' positions of the hexose (Figure 107). The idealized oligomer conformation reveals an overall linear extension of the chain such that stabilization of the ladder-like duplex formation should occur by *WC* pairing between antiparallel strands with further stabilization provided by *interstrand* base stacking (as opposed to the *intrastrand* stacking known in natural backbones).

Through a variety of 1D- and 2D-NMR methods in D_2O , a self-pairing p-CGAATTCG duplex was determined to exist as a *quasi*-linear conformation with a weak left-handed helical twist in solution,⁵²⁵ which was not predicted from initial modeling (Figure 108). Specifically, two dihedral angles of the ribopyranosyl

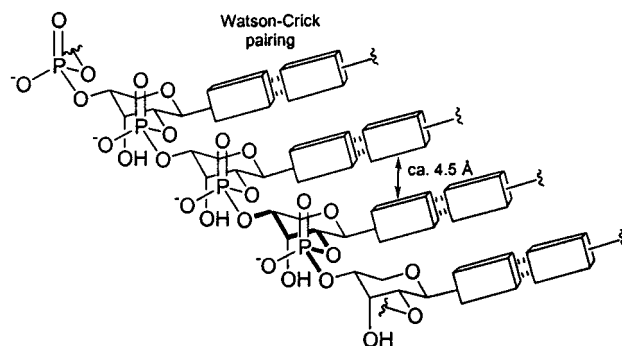
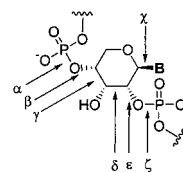


Figure 108. Idealized conformation of a p-RNA duplex (second strand backbone omitted for clarity).



	α	β	γ	δ	ϵ	ζ
p-RNA Idealized	60	180	180	180	-60	180
p-CGAATTCG	70	145	-180	-180	-85	-170

Figure 109. Six dihedral angles of the p-RNA backbone predicted for a linear conformation (actual values determined by NMR and molecular dynamics techniques for the left-handed helix).

backbone were resolved to $\beta = +145 \pm 6^\circ$ and $\epsilon = -85 \pm 5^\circ$, deviating significantly from the idealized angles of $\beta = 180^\circ$ and $\epsilon = -60^\circ$ (Figure 109). The dihedrals γ and δ were estimated to be close to the predicted value of 180° , resulting in an adjustment (calculated from simulations) of α from 60° to ca. 70°

and ζ from 180° to -170° to preserve the proper chair conformation of the ring for pairing interactions (confirmed from UV melting curves of duplexes). This is believed to be a result of minimized steric interactions between the phosphate linkage, the equatorial hydrogens on ribopyranose (distances increase about 1 Å), and increased interstrand stacking through decreased base distances (from over 4 to ca. 3.5 Å). These results suggest that the backbone realignment is a consequence of the intermolecular association. Observed χ values ranged from -120° to -135° within the sequence, while the terminal G residue had a much lower χ value indicating higher conformational lability at this position. Proton exchange experiments and molecular-dynamics simulations supported *WC* pairing throughout the duplex and a rapid opening and closing of the terminal base pairs. Interstrand NOEs confirmed an antiparallel orientation resulting in the inclination of the base pair from the backbone by an angle of 35° and 45° , suggesting that interstrand base interactions should be favorable for purine–purine and purine–pyrimidine stacking but not between two pyrimidines. In addition, an inter-pyranose distance between 3.6 and 4.0 Å was calculated, producing a translational step of 6.5–6.9 Å along the backbone and a pitch of ca. 110 Å, incorporating 18–19 monomers per turn.

Through oligomerization of β -D-ribose phosphoramidite derivatives^{526,527} by automated synthesis and purification by HPLC, adenine (A) and uracil (U) containing p-RNA octamers were initially synthesized and characterized to ascertain the stability of the duplexes formed.⁵²⁸ Although self-pairing A₈ duplexes have formed in other alternative oligonucleotides,⁵²⁹ p-A₈ remains as a single strand under these conditions, indicating that alternative pairing interactions are disfavored due to the topological backbone constraints in this pairing mode, thus enhancing the oligomer's pairing selectivity. The *WC* paired duplex formed from a 1:1 mixture of p-A₈ and p-U₈ revealed concentration-dependent and reversible UV melting curves, temperature-dependent CD spectra, and composition-dependent UV absorptions with a minimum at a 1:1 stoichiometry. The self-complementary octamers, p-A₄U₄, p-U₄A₄, p-(AU)₄, and p-(UA)₄, show duplex formation by self-pairing in an antiparallel orientation.⁵³⁰ Additionally, the higher melting temperature of the p-A₄U₄ duplex in comparison to the natural RNA oligomer indicates an increased stability through stronger base-pairing interactions. This is attributed to the smaller entropic cost of organization necessary to form the p-RNA duplex since the *quasi*-linear rigid chain is preorganized for the proper *WC* pairing orientation. Other nucleobases incorporated into p-RNAs for duplex formation studies include guanine (G), cytosine (C), isoguanine (isoG), 2,6-diaminopurine (Dp), and thymine (T).⁵³¹ In a chain-length study, UV and CD spectra confirmed that p-G_{*n*} (*n* = 6, 8, and 10) exist as single strands at ambient temperature (as do the p-isoG₈ and p-Dp₈ strands). In equimolar mixtures of oligo-p-G_{*n*} and oligo-p-isoG_{*n*} (*n* = 6 and 8), duplex formation proceeds through purine–purine *WC* pairing showing higher thermal stability than DNA sequence analogues.

Duplexes of p-RNA having strands of opposite chirality form through alternative base-pairing modes such as reverse Watson–Crick (*RWC*) pairing.⁵³² The noncanonical bases, isoguanine (isoG) and 5-methylisocytosine (5-Me-isoC), that have the potential to participate in *RWC* pairing with homo-G and -C strands were incorporated into L- and D-p-RNA strands. Both homochiral (D/D) and heterochiral (L/D) duplexes of homomeric strands were compared, in terms of melting curves, to determine the degree of specificity dictated by the backbone stereochemistry. Strands of D-p-isoG_{*n*} and D-p-C_{*n*} (*n* = 6 and 8) did not show any self-pairing or duplex formation under the given conditions, while duplex formation was accomplished using the L-p-isoG_{*n*} with D-p-C_{*n*} (*n* = 6 and 8). The isoG bases promote *RWC* pairing with C in this duplex, allowing for proper co-linear orientation of the strands. Other p-RNA mixtures were shown to form L/D but not D/D duplexes most likely through the *RWC* pairing mode, though pairing assignments in the case of D- and L-p-isoG_{*n*} remain uncertain since mixing curves showed aggregate formation. The p-RNA chains of opposite chirality pair inefficiently as evidenced by the lower melting temperatures of duplexes formed from mixing homochiral D-p-RNAs with complementary L-p-RNAs. This enantioselectivity, as well as the observed pairing selectivity (*WC* only), is believed to be due to the more conformationally restrained p-RNA backbone. It has only four flexible bonds (as opposed to six in DNA) due to the three large substituents occupying equatorial positions. Furthermore, the more constrained phosphodiester linkages connect to secondary carbons on the ring, whereas DNA linkages attach to a primary carbon (5') allowing for greater flexibility. Finally, the alignment of the nucleobases as a consequence of the backbone conformation promotes antiparallel interstrand interactions through *WC* base-pairing only, since *H* and reverse-Hoogsteen (*RH*) pairing disfavor the preferred co-linear chain orientation. This study demonstrates the ability of p-RNAs to form duplexes with the same or opposite sense of chirality backbones, depending on the specific nucleobases used.

In order to mimic RNA architectures and their conformational diversity, a necessary secondary structure is the hairpin turn, a sequence-dependent structure promoted by intramolecular base pairing over interstrand interactions. Investigations of hairpin formation in a series of self-complementary p-RNA base sequences studied at low concentrations (3 μM) with a central p-T₂ segment resulted only in duplex formation while with three T bases competitive duplex formation was observed in melting curves at higher concentrations.⁵³³ Only at the critical length of four T bases did the oligonucleotide show a similar *T_m* at both concentrations, indicating a stabilized hairpin. Furthermore, hairpin p-RNAs synthesized with a noncomplementary base (A or C) at either the 2'- or 4'-end supported the expectation, from modeling of p-RNA duplexes,⁵²⁵ that a dangling base at the 2'-end would stabilize the structure through interstrand stacking of the two terminal bases with purine–purine contacts leading to greater stability than

Table 7. UV Melting Curves for Four Pyranosyl Oligonucleotides

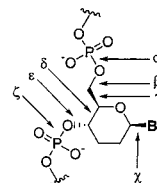
sequence (4'→2')	T_m [°C] ^a					ΔG°_{298} (kcal·mol ⁻¹)				
	pr	pl	px	pa	RNA	pr	pl	px	pa	RNA
A ₈ + T ₈	40.0	47.0	35.4	71.1	16.3 ^b	10.5	-12.3	-8.2	-15.7	-7.3
A ₁₂ + T ₁₂ ^c	60.8	68.0	63.0	95.0	34.9 ^b	-15.4	-19.8	-17.0		-66.3
A ₄ T ₄	27.0	38.2	16.3	61.2	11 ^b	-7.3	-9.4	-6.1	-13.5	-5.6
T ₄ A ₄	40.0	47.0	40.3	69.4	10.8 ^b	-9.8	-11.4	-8.7	-14.5	-5.2
(AT) ₄	38.0	38.3	28.6	60.0		-9.2	-9.5	-6.2		
(TA) ₄	40.0	37.9	33.8	60.8		-9.3	-9.4	-7.6		

^a 0.15 M NaCl. ^b 1.0 M NaCl. ^c Data from ref 535.

pyrimidine–purine stacking. Only dangling bases at the 2'-end led to an increased stability of the p-RNA pairing complex.

ii. α -Lyxo, β -Xylo, and α -Arabinopyranosyls. From the findings on p-RNAs, the question arises, can the properties of p-RNAs be extended to the constitutional isomers of (4'→2') ribopyranosyl: α -lyxo, β -xylo, and α -arabino? A recent study investigated the duplex stability of foldamers with these alternative backbones for comparison to the D- β -ribopyranosyl oligonucleotides.⁵³⁴ Table 7 shows T_m and ΔG values for the complementary and self-complementary AT sequences. Although the β -xylo duplexes are somewhat weaker than D- β -ribo complex, the D- α -arabinopyranosyl duplex has a much higher stability than RNAs or p-RNAs. The stability of the arabinopyranosyls is a consequence of the increased steric constraint induced by the equatorial 3'-hydroxyl in concurrence with the highly constrained pyranose chair from the 4'-axial phosphodiester linkage. Though these backbones show higher stabilities due to stronger base pairing, the tolerance for mismatches is evident from self-pairing of the A₈ and T₈ single strands of the α -lyxo (A and T) and the α -arabino-T₈ backbones. Furthermore, by mixing complementary strands of the four different pyranosyl backbones, duplexes formed with comparable stabilities to homobackbone duplexes, indicating the ability of all four members to adopt similar *WC quasi-linear* conformations as seen in p-RNAs.⁵³⁵ A thorough chain-length and sequence investigation on the (4'→2')- α -L-lyxopyranosyl backbone has recently been reported exploring the self-pairing, complementary pairing, and hairpin formation in this system.⁵³⁶ These results show that with the natural RNA backbone, maximization of base-pairing strength is not realized. In addition, the ability of the pyranosyl family to form stronger duplexes through enhanced base pairing comes at the cost of lower base-matching fidelity.

Extension of the studies on the pyranosyl family involved modification of the phosphodiester linkage from (4'→2') to (4'→3') in the α -ribo and α -lyxo backbones leading to a shortened backbone involving only five instead of the usual six torsions.⁵³⁷ Although the (4'→3') α -ribopyranosyl backbones showed no duplex formation with self-complementary strands, the corresponding α -lyxopyranosyl duplexes showed slightly weaker stabilities from their (4'→2') counterparts. Additionally, this system had the capacity to form intersystem duplexes and triplexes with a complementary strand of either RNA or DNA, believed to be due to the smaller backbone inclination



dd-A ₅ T ₅	α	β	γ	δ	ϵ	ζ	χ (A)	χ (T)
Idealized A	-60	180	60	60	180	-60	-120	-120
Idealized B	180	180	180	60	180	-60	-120	-120
Model A	-56	155	64	49	-137	-68	-75	-101
	to	to	to	to	to	to	to	to
	-72	172	86	67	-178	-80	-91	-139
Model B	165	173	160	50	-154	-59	-108	-78
	to	to	to	to	to	to	to	to
	-167	-136	-174	61	-180	-105	-119	-113

Figure 110. Six hexose dihedral angles of the homo-DNA backbone and the base–hexose torsion as predicted for a linear conformation (actual values determined by NMR and molecular dynamics techniques). For models A and B, values indicate the lower and upper limits of the dihedral angles observed.

and the diaxial phosphodiester orientation of the backbone. These results, as well as the observations with TNAs, suggested that six torsions per repeat unit are not necessary to form stable complexes with natural complements, further revealing the tolerance for structural variation in these polyelectrolyte backbones.

c. The Hexopyranosyl Family. i. Homo-DNAs. Further studies aimed at exploring alternative backbones focused on the introduction of a methylene unit between the C1'- and C2'-positions of furanosyl units of oligonucleotides to generate hexopyranosyl backbones (homo-DNA). Investigations include comparative conformational analysis between natural oligonucleotides and homo-DNA (dd),^{538,539} synthesis and characterization of these oligonucleotides,⁵²⁶ the conformational characterization of a homo-DNA duplex in solution,⁵⁴⁰ and the self-pairing and complementary pairing in the duplex formation.^{529,530,541} Homo-DNA maintains the six-bonds-per-repeat-unit motif of natural systems, having the same configurational orientation of the phosphodiester linkage as in DNA. Idealized models predicted similar conformations to those seen in p-RNAs, where a linear extension of the chain would result in *WC* pairing of bases in an antiparallel fashion with bases adopting anti conformations.⁵³⁸ Dihedral angles for homo-DNA were determined through 1D- and 2D-NMR techniques and molecular dynamics simulations to ascertain the solution structure of a self-complementary dd-A₅T₅ duplex (Figure 110).⁵⁴⁰ The two *quasi-linear* backbone conformations, A and B, are in dynamic equilibrium related by two 120° rotations with all three constitu-

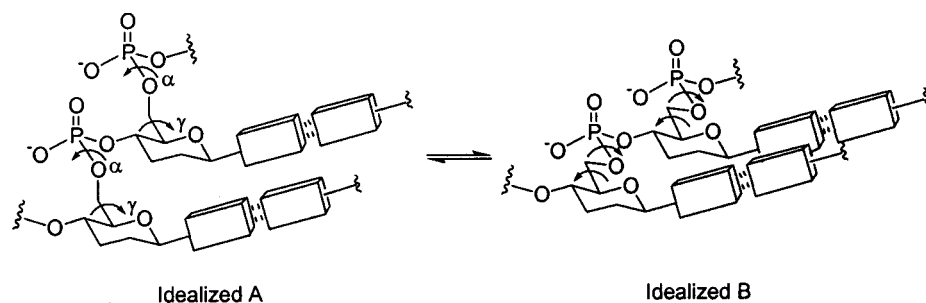


Figure 111. Two idealized conformations of the homo-DNA backbone. Conversion from A to B occurs through a 120° rotation about α and γ of the phosphodiester linkage.

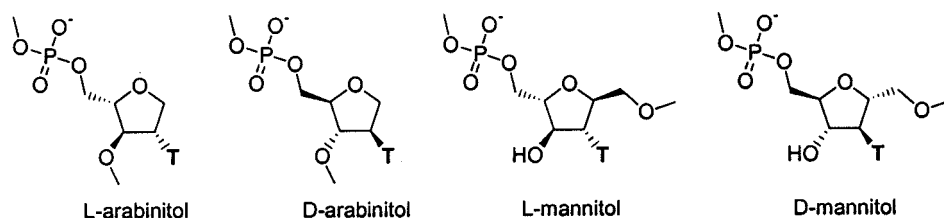


Figure 112. Structures of isonucleotides.

ents of the hexose chair conformation in equatorial positions (Figure 111). A much looser orientation of base pairs was observed through a range of adopted χ torsions in addition to extensive fluctuations in base-pair distances, deviation from coplanarity, and a base-stacking distance of ca. 4.5 Å.

In general, homo-DNA duplexes demonstrate a pairing priority of G–C > A–A ~ G–G > A–T where G–C and A–T pair through the *WC* motif while *RH* pairing occurs in A–A and G–G dd-sequences.⁵²⁹ Through a chain-length study on dd- A_n ($n = 3–6$), self-paired duplexes showed increasing UV melting temperatures with increasing chain length (for $n = 3$, no T_m ; $n = 4$, $T_m < 12$ °C; $n = 5$, $T_m = 32$ °C; $n = 6$, $T_m = 43$ °C) and increasing concentrations (from 4.9 to 92 μ M, $\Delta T_m = 15$ °C), sigmoidal hypochromicity curves (dependent on [NaCl]; where [NaCl] = 15 mM to 1.5 M, $\Delta T_m = 9$ °C), and temperature-dependent CD spectra. Self-complementary dd-(AT) $_n$ ($n = 3–6$) duplexes showed high stability with melting curves ca. 30–40 °C higher than in the corresponding DNA duplexes. Though the self-paired duplex (dd- A_6) $_2$ persisted when mixed with the complementary dd- T_6 , the self-pairing dd- G_6 could be disrupted with dd- C_6 to form the heterostranded complex. Further investigations into the pairing properties of dd-purine sequences revealed *WC* pairing between dd-(G) $_n$ /dd-(isoG) $_n$ and dd-(Dp) $_n$ /dd-(xanthines) $_n$ (X) while dd-(isoG) $_n$ and dd-(Dp) $_n$ oligomers self-pair through *RH* motifs.⁵⁴¹ Overall, sequence discrimination is lower in homo-DNA than DNA due to the linear orientation of the strands, inefficient base-stacking, and the conformational rigidity of the hexose ring which leads to a preorganization of the single strand and decreases the conformational entropic cost of duplex formation.

ii. Other Hexoses. In homo-DNA as in DNA, hydroxyl groups are not present as they are in RNA and the pyranosyl backbones described thus far. Further investigations into hexopyranosyl (6'→4') backbones incorporated 2'- and 3'-hydroxyl groups in β -allo (2'-eq, 3'-ax), β -altro (2'-ax, 3'-ax), and β -gluco

(2'-eq, 3'-eq) (Figure 107).⁵²¹ The presence of these hydroxyls causes intrastrand steric repulsion in the duplex conformation that disrupts *WC* base pairing, encourages purine–purine *RH* self-pairing in allo and altro backbones, and leads to sequence-dependent and lower T_m values than for RNA. For the self-complementary sequence CGCGAARRCGCG (R = U in allo and altro backbones, T in DNA and homo-DNA), no duplex formation was observed for allo and altro backbones at room temperature (though T_m values increased at lower pH) in great contrast to both DNA and homo-DNA. The inclusion of hydroxyls in the hexopyranosyl backbones must induce the backbone to adopt conformations that disfavor the folded state necessary for ideal base pairing in the duplex.

Other variants of hexoses include 2,4- and 3,4-dideoxyhexopyranosyl backbones^{542,543} and have similar connectivities to iso-DNAs but incorporate methylene groups into the ring between the C1–C2 and C2–C3 connections. With one to four multiple-T substitutions of either modified monomer into DNA 13-mers, the 3,4-backbone destabilized the duplex with complementary d- A_{13} to a higher extent than the 2,4-modification, although these heteromeric duplexes retain cooperative transitions. The effect on the duplex with the 3,4-connectivity is similar to the results obtained with homo-DNA. Homomeric 2,4- T_{13} oligomers were unable to form duplexes with the complementary DNA.

2. Backbones with C2'-Base Connectivities

a. Isonucleosides. Another modification of deoxynucleotides involved the repositioning of the base-sugar connection from the C1- to the C2-position to afford 1,4-anhydro-2-deoxy-D- and -L-arabinitol,⁵⁴⁴ dubbed isonucleosides (Figure 112). In 14-mer strands with homo-T bases, D-arabinitol formed slightly less stable duplexes with d- A_{14} ($\Delta T_m = -5.9$ °C) than with d- T_{14} , while L-arabinitol was unable to complex with this complement.⁵⁴⁵ Addition of a methylhydroxyl moiety to the C1'-position of the D-arabinitol gener-

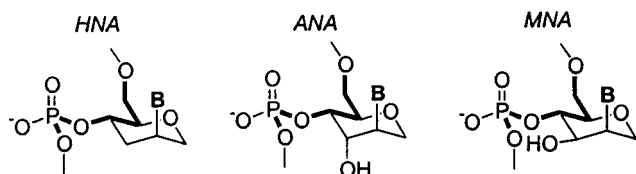


Figure 113. HNA, ANA, and MNA backbones.

ates the D-mannitol monomer, and 14-mers of both D-⁵⁴⁶ and L-mannitol⁵⁴⁵ complexed with d-A₁₄ showed that the methylhydroxyl promotes stability by $\Delta T_m = +1.2$ °C.

b. HNAs. Analogous to investigations into homo-DNA, synthetic insertion of an additional methylene group between the O4' and C1' positions of a furanose generates 1,5-anhydro-D-arabino-hexitol nucleic acids (HNAs),^{547,548} maintaining the natural conformations of the phosphodiester linkage, the axial orientation of C1'-base configuration for intramolecular base-stacking with natural systems, and promoting the 3'-endo, A-type sugar conformation (Figure 113). Initial studies on A and T HNA (h-) 13-mers showed aqueous solubility, self-pairing in the T strand,⁵⁴⁹ stronger WC-paired duplexes than the corresponding DNA duplex ($\Delta T_m = +42.3$ °C), and sequence-dependent stabilities in HNA:DNA duplexes (d-A₁₃:h-T₁₃ $\Delta T_m = +11.4$ °C and h-A₁₃:d-T₁₃ $\Delta T_m = -13.0$ °C).⁵⁴⁹⁻⁵⁵¹ Nucleobases successfully incorporated into HNAs include A, T, C, G, U, D, and Me-C, retaining WC pairing with corresponding complements.⁵⁵² Four different solutions of salts and buffers were explored in order to optimize duplexing and eliminate self-pairing (as indicated by a linear vs sigmoidal increase in absorption with increasing concentration). Furthermore, through a series of HNA mixed sequences complexed with RNA and DNA complements, the higher stability of HNA:RNA over HNA:DNA was demonstrated, as well as a mismatch discrimination in HNA:DNA dodecamer duplexes. ΔT_m changed from -9.0 to -20.3 °C for a single mismatch, indicating a strong sensitivity in base selectivity. CD studies revealed that the HNA:RNA and RNA:RNA duplex have very similar spectra, supporting A-type HNA conformations. Furthermore, NMR studies of an HNA:RNA duplex revealed the HNA strand to have similar conformations as RNA but with a more rigid backbone.⁵⁵³ HNAs containing pyrimidine bases form less stable duplexes than those with purines, and duplex stability in this system follows the stability order of HNA:RNA > RNA:RNA > DNA:RNA. Molecular dynamics simulations revealed that solvation of the minor groove is a critical factor to the higher stability of the HNA:RNA complex over HNA:DNA since the presence of the additional hydrophobic methylene is compensated for by the hydrophilic 2'-OH of RNA.^{554,555} An HNA-GCGCTTTTGC GC strand can form a self-complementary duplex where the T segments form T-T wobble (W) motifs through this pairing mismatch.⁵⁵⁶ Finally, gel electrophoresis studies showed that HNA strands are able to displace an RNA strand of similar length from its homostranded duplex. Overall, the HNA nucleotidomimetic demonstrates the ability of foldamers analogous to natural systems to mimic and even enhance their pairing and selectivity properties through subtle modifications,

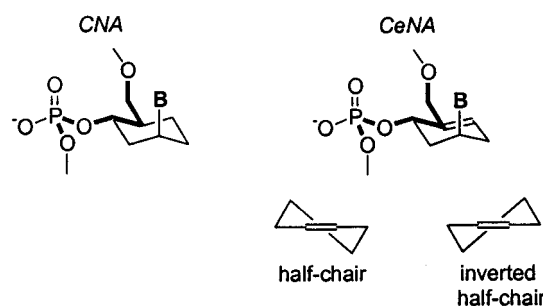


Figure 114. CNA and CeNA backbones with puckered states of CeNAs.

underlying the complexity of parameters responsible for the stability of nucleic acids structures.

c. ANAs. Following the successful design of HNAs, a structural analogue incorporating a C3'-(S)-hydroxyl was synthesized⁵⁵⁷ and has been called ANA (for 1,5-anhydro-D-altritol nucleic acids) (Figure 113). Similar to HNAs, ANAs form A-type WC duplexes stronger with RNA than DNA, but with higher thermal stabilities for homo- and heterostranded duplexes such that the hybrid stability order is ANA:RNA > HNA:RNA > ANA:DNA > HNA:DNA > DNA:RNA.⁵⁵⁸ ANA strands discriminate mismatches to the same degree as DNA and HNA, favoring antiparallel over parallel orientations. The ANA 3'-OH stabilizes hybrid complexes primarily through improved solvation by increasing the polarity of the solvent-accessible surface of the minor groove, as confirmed by molecular dynamics simulations.⁵⁵⁵

d. MNAs. Another member of this series involves inversion of the C3'-OH configuration from (S) in ANAs to (R) in 1,5-anhydro-D-mannitol nucleic acids (MNAs)⁵⁵⁹ (Figure 113). Although NMR studies showed that the MNA monomers preferred the axial base orientation, two AG mixed hexamers did not form duplexes with complementary RNA or DNA at low salt concentrations and formed weak duplexes with HNA. At 1 M NaCl, weak hybridization was observed with RNA. Melting curves of these complexes were very broad indicating multiple transitions over this temperature range. Molecular modeling revealed a more conformationally restrained backbone, through formation of an intramolecular hydrogen bond between the 3'-OH and the 6'-O of the phosphate linkage. This interaction thermodynamically disfavors complexation with RNA.⁵⁵⁵ Hence, even in cases of subtle structural modification, the oligonucleotide backbones can become "too preorganized", illustrating the critical balance between rigidity and flexibility in foldamers.

e. CNAs. With the successful design of HNAs, structural analogues were pursued to determine if hybridization was still operative if the conformationally determinant O of the hexose was replaced by a methylene, resulting in a more flexible carbocyclic ring (Figure 114). These carbohexanyl nucleic acids (CNAs) prefer equatorial base orientations as monomers and therefore were speculated to form quasi-linear chain conformations akin to homo-DNA.⁵⁶⁰ However, CNA oligomers of D-configuration form stable WC antiparallel complexes with both RNA and DNA, while corresponding L-CNA strands do not.⁵⁶¹

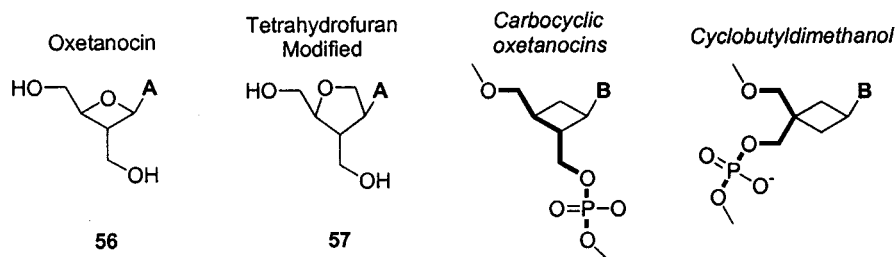


Figure 115. Representative examples of modifications to the sugar backbone.

It is believed that the CNA backbone undergoes a chair inversion to adopt axial base orientations within the duplex to promote base pairing. Homochiral CNA complexes (D/D or L/L) of A₁₃ or T₁₃ are more stable than ds-DNA but show multiple transitions in the melting curve, while heterochiral CNA duplexes (D/L) are much less stable with mixed AT sequences forming only as homochiral complexes. No self-pairing of CNA strands was observed. This study demonstrates that conformational intuition of monomer structures does not easily translate to backbone conformations that favor duplex formation. Thus, CNAs are examples of nucleotidomimetics where a unique backbone conformation is only adopted through the optimization of nonadjacent contacts.

f. CeNAs. The carbocyclic cyclohexene nucleotides (CeNAs) extend CNA research by introducing a 5'-6' alkene within the analogous ring, thereby increasing the flexibility of the backbone such that the energy difference between chair conformations is approximately 0.4 kcal·mol⁻¹ (Figure 114).⁵⁶² When one to three CeNA-A monomers were incorporated into either an RNA or DNA strand and complexed with complementary DNA or RNA, respectively, the thermal stability of the DNA:RNA hybrid was increased up to 5.2 °C with CeNA-DNA and decreased -1.5 °C with CeNA-RNA.⁵⁶³ NMR studies showed that the incorporated CeNAs had little effect on the global structure of the DNA backbone. Although CeNA-A₁₃ associate with complementary DNA and RNA oligomers with comparable and higher stabilities than DNA, triplex formation was also observed. On the basis of CD studies, CeNAs adopt the half-chair conformation in the A-type RNA and the inverted half-chair in the B-type DNA.⁵⁶⁴

g. Other Ring Systems. The discovery of the antibiotic oxetanocin A,⁵⁶⁵ an isomer of deoxyadenosine isolated from *Bacillus megaterium* and containing an oxetanose instead of a furanose ring, led to the incorporation of moiety **56** and a second isomer, involving a C2'-base connectivity **57**, into self-complementary DNA dodecamers. Resulting complexes showed slightly lower *T_m* values (Figure 115).⁵⁶⁶ Extension of this structure to carbocyclic oxetanocin strands led only to triplex formation with RNA hybridization that was stronger than DNA.^{567,568} Similarly, 3,3-bis(hydroxymethyl)cyclobutyl A and T oligomers generated homostranded complexes as well as heterostranded complexes with DNA.^{569,570} Although these nucleic acid variants have not been fully explored as oligomers (a large body of work exists on the properties of similar nucleosides^{571,572}), they demonstrate the tolerance of RNA/DNA pairing motifs toward a variety of structurally related backbones.

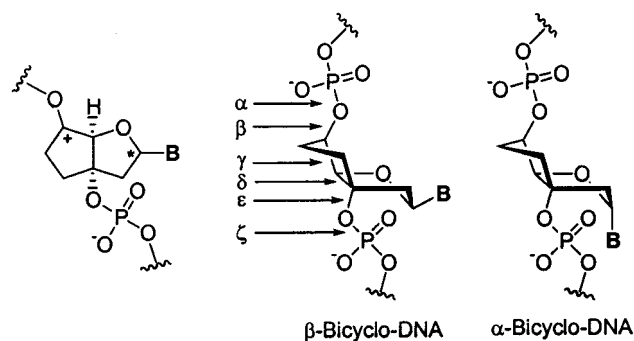


Figure 116. Representative structures of bicyclonucleotides.

3. Torsionally Restricted Oligonucleotides

The incorporation of hexoses into oligonucleotides led to, in certain cases, increased duplex stability through preorganization from the more conformationally restricted six-membered rings versus natural ribose backbones with flexible torsions. This approach has been taken a step further through the use of constrained backbones in which bridging linkages of fused-pyranosyl nucleotides limit the conformational flexibility of the ring.⁵⁷³ This preorganization of the strand then minimizes the entropic cost of organization in duplex formation, and the success of such an approach is often measured by melting temperatures of the heterostranded duplex incorporating the natural, complementary oligonucleotide. Although a variety of fused-oligonucleotides have been investigated, two backbones will be discussed here, dubbed *bicyclic-oligonucleotides* and *locked nucleic acids (LNAs)*, as representative examples of this class of modified ribopyranosyls.

a. Bicyclic-Oligonucleotides. Bicyclicodeoxynucleotides (bicyclo-DNA or bcd) involve an ethylene bridge between the C3' and C5' positions, which constrains the furanose ring into the C2'-endo conformation seen in B-type DNA duplexes through the rotational restriction of the γ and δ torsions (Figure 116).⁵⁷⁴ Adenine decamers of β -bicyclo-DNA form stronger duplexes with RNA and DNA, while bcd-T₁₀ pairs more weakly with comparable base-pairing selectivity, shows increased triplex stability (also demonstrated with bcd-G₆),⁵⁷⁵ and exhibits a higher sensitivity to salt concentration.^{576,577} Through sequential synthesis of various oligomers containing the canonical bases and by determining their pairing properties with complementary bcd, RNA and DNA strands, bicyclo-DNA pairs preferably form through *H* over *WC* motifs and, as a consequence, form parallel (*H* mode) and antiparallel (*RH* mode) orientations due to the torsion angle γ (set to +100°

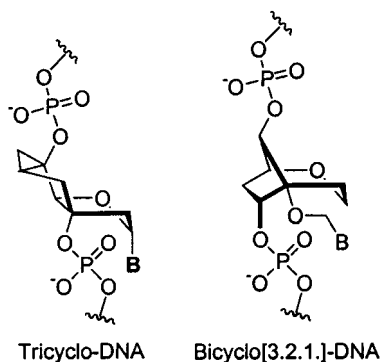


Figure 117. Structures of tricyclo- and bicyclo[3.2.1]-DNA.

relative to DNA).^{578,579} In the *WC* mode, bicyclo-DNA prefers antiparallel orientations as in DNA. The stability of bcd duplexes is dependent on the number of G–C pairs since A–T pairs appeared to be energetically impartial. Furthermore, the rigid bicyclic backbone decreases the entropic cost of intermolecular association while destabilizing the duplex by lowering the enthalpic contribution of complexation. Unexpectedly, hairpin structures were reported⁵⁷⁹ from bcd-CGCGAATTCGCG, a potentially self-complementary sequence. The -AATT- segment forms the hairpin turn, since the A–T pairing does not contribute enthalpically and duplex formation comes at an entropic cost. Overall, the bridging moiety in bicyclo-DNA imparts a number of organizational changes in complex formation, both inter- and intramolecularly, through constraints in the furanose ring that differ considerably from both homo-DNA and p-RNA backbones.

Extensions on the bicyclo-DNA theme have been pursued to explore how similar structural modifications with constrained-ribose backbones affect base-pairing modes and strand orientations. Switching of the base–furanose bond from the β - to the α -position (α -bicyclo-DNA) causes a rearrangement of the pairing properties relative to β -bicyclo-DNA such that parallel hybrid duplexes are favored in AT sequences with comparable stabilities to RNA and DNA.⁵⁷⁵ Reversal of the 5'-OH from (*R*) to (*S*), named 5'-epibicyclo-DNA,^{580,581} eliminates pairing altogether in a decamer T block with complementary RNA, DNA, or bicyclo-DNA. Tricyclo-DNAs extend these examples of covalently constrained rings by incorporating a cyclopropyl ring into the 5'/6'-positions of the carbocyclic ring in bicyclo-DNAs (Figure 117).^{582–584} In duplex studies with itself and DNA, tricyclo-DNA showed enhanced stabilities with the homostranded tricyclo-DNA duplexes having ΔT_m as high as 48 °C over the natural DNA duplex. Again, *H* and *RH* pairing are preferred as in bicyclo-DNA. They have also been shown to stabilize hairpin loops and form triplexes with DNA duplexes. Finally, moieties inducing torsional constraints far removed from the bases have been demonstrated with bicyclo[3.2.1]-DNA in which the base linkage is extended by an oxygen tether (Figure 117).^{585,586} Pyrimidine-based bicyclo[3.2.1]-DNAs are capable of forming *WC* antiparallel duplexes of A-type conformations with complementary DNA. They have slightly lower T_m values, indicating that increased degrees of freedom

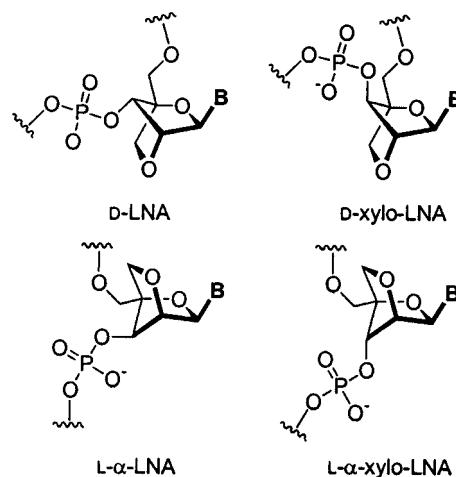


Figure 118. Four of the eight stereoisomers of locked nucleic acids (LNAs).

in the base–backbone linkage can be compensated by more rigid backbones, even modifications far removed than in ribose backbones.

b. LNAs. The pentofuranose backbone can also be restricted to the 3'-*endo* conformation by installing a 2'-*O*,4'-*C*-methylene bridge^{587,588} to generate a class of structures known as locked nucleic acids (LNAs) (Figure 118).^{573,589} When incorporating various nucleobases (A, C, G, T, 5-Me-C, and U) into oligonucleotides or as homooligomeric sequences, LNAs significantly increase T_m values of heterostranded duplexes with RNA (4–8 °C) and DNA (3–5 °C) complements^{588,590,591} without disrupting backbone conformations.⁵⁹² Improved sequence selectivity, aqueous solubility, formation of duplexes only (no triplexes), preorganization of neighboring natural nucleotides, and high binding affinities are traits demonstrated by this system. Stopped-flow kinetics of LNAs revealed that LNA–DNA duplex formation involves a rate-determining association with a subsequent rapid sealing step and that the higher duplex stability with LNAs results from a slower dissociation of the duplexes.⁵⁹³ From the LNA skeleton, eight stereoisomers incorporating T^{594–596} and A⁵⁹⁷ have been generated where β -D/L-ribo-, α -D/L-ribo-, and β -D/L-xylo-LNAs show increased duplex stability with RNA, while no association was observed for α -D/L-xylo-LNAs and RNA.^{594–597} Homooligomeric LNAs, through *WC* antiparallel duplexes with RNA and DNA, adopt the A-type furanose conformation and induce flanking of natural nucleotides into similar conformations, thereby arranging the strand for more efficient base interactions as evidenced by NMR^{598,599} (and consistent with an X-ray analysis⁶⁰⁰). Furthermore, removal of the nucleobase in an incorporated LNA monomer within a DNA strand causes duplex destabilization, confirming that preorganization alone cannot promote stability but instead induces favorable alignment for base stacking.^{601,602} These results indicate LNAs as promising antisense agents in therapeutic applications.⁶⁰³

Bridged nucleic acids, or 2,4'-BNAs, are structurally the same as D-LNA, but research on BNAs has focused on triplex formation with ds-DNA.^{587,588} As observed with D-LNA, 2'-4'-BNA-C and -T incorpo-

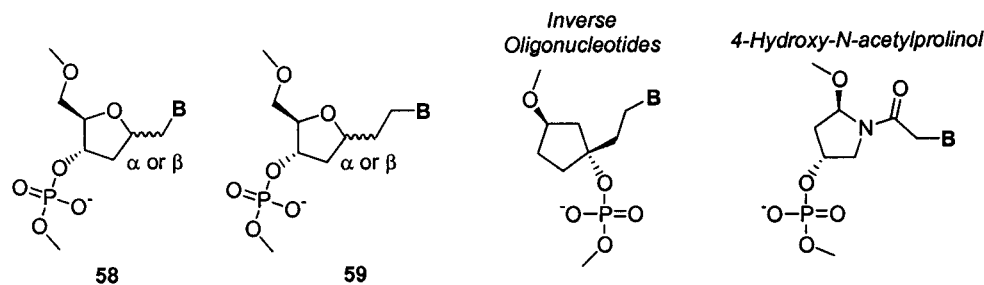


Figure 119. Structures of base–sugar extended oligo(nucleotide)s.

rated in DNA strands promote hybridization of BNA-modified-DNA from 1 to 5 °C and DNA–RNA from 4–6 °C.⁶⁰⁴ Single 2',4'-BNA substitution into DNA strands showed enhanced triplex stabilization and sequence selectivity of ds-DNA at neutral pH. BNA-T incorporation enhances the triplex T_m by 10 °C over DNA-T, while BNA-C increases triplex T_m by 7 °C over DNA-C.⁶⁰⁵ Although these data demonstrate 2',4'-BNA monomers to be potent triplex stabilizers through *H* pairing, homo-BNA strands were not able to form triplexes with ds-DNA presumably due to their rigidity.⁶⁰⁶ Additionally, a 2',4'-BNA incorporating an oxazole nucleobase recognized a C–G pair better than d-T, as evidenced by a triplex T_m increase of 3 °C.⁶⁰⁷ Studies on an isomeric modification of BNA involving bridge attachment from the O3 to C4 (3',4'-BNAs), thereby connecting through 2',5'-linkages,^{608,609} demonstrated that 3',4'-BNA enhanced binding selectivity for RNA over DNA in duplex formation⁶¹⁰ with more stable modified-DNA:RNA duplexes than analogous iso-RNA duplexes.^{499,502}

4. Torsionally Flexible Oligonucleotides

a. Base–Sugar Extensions. An approach to increase the affinity of *alt*-DNA for RNA involved the extension of the base–sugar connection through the insertion of methylene^{611,612} **58** and ethylene⁶¹³ **59** groups into both α - and β -deoxynucleotides (Figure 119). Modeling studies suggested improved base alignment with A-type backbones using these nucleotides since additional conformers are accessible. Single-point 3'→5' substitutions of β -**58** with the canonical bases into DNA strands destabilized a DNA duplex by 9–10 °C,^{612,614} indicating unfavorable steric interactions, while homooligomers of β -**58** were unable to form duplexes with DNA complements. Of the modifications investigated, only the 3'→3' incorporation of α -**58**-T into a DNA strand improved affinity for the complementary RNA strand over DNA.⁶¹⁴ In a similar approach with a carbocyclic ring, single substitutions of *inverse nucleotides*, with ethylene base–sugar connectivities, in d-A₁₃ or d-T₁₃ resulted in a decreased duplex T_m of 4.3 and 11 °C, respectively.⁶¹⁵ Finally, 4-hydroxy-*N*-acetylprolinol nucleotides incorporate amide base–backbone connectivities and T 13-mers duplex with complementary RNA with comparable stability to the natural system.⁶¹⁶

b. Acyclic Backbones. Thus far, the nucleotidomimetics described have focused on modifications of the sugar backbone to investigate intermolecular association through covalent constraint of torsions. In another approach, acyclic glycerol derivatives

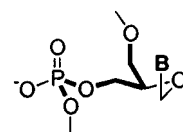


Figure 120. Structure of nucleotides incorporating a glycerol unit in place of the sugar.

incorporating phosphodiester linkages and nucleobases were explored to determine whether increased flexibility promotes duplex formation.⁶¹⁷ Glycerol nucleotides are an isosteric form of the ribose backbone with the C2 removed leading to a more flexible branched chain (Figure 120). One to two glycerol nucleotides were incorporated into central positions in DNA strands and complexed to complementary all-ribose DNA strands. Overall, the melting temperatures of the resulting duplexes were lowered 9–15 °C per glycerol nucleotide due to the increased entropic cost of backbone organization for ideal complexation. This was further confirmed by the absence of duplex formation (<0 °C) when an 11-mer glycerol nucleotide with 5'-d-C and 3'-d-G was mixed with a complementary d-CA₁₁G strand (the natural duplex has a T_m of 55 °C). This system demonstrates that, even with the six bond repeat unit, glycerol nucleotides eliminate the torsional constraints present in natural oligonucleotides that preorganize the strand for ideal association (as seen in another acyclic system, 1,2-*seco*-DNA⁶¹⁸). Similar investigations into acyclic nucleotides incorporated into natural backbones^{619–622} showed, in general, somewhat lower melting temperatures for the resulting duplexes relative to natural systems as well as sequence-dependent heterostrand duplex formation from fully acyclic oligomers with their natural complements.

D. Modifications of the Nucleotide Linkage

The earliest approach to enhancing oligonucleotide duplex stability involved the modification of the phosphodiester linkage, being synthetically accessible and presumed to have minimal deleterious impacts on the puckering states of the furanose ring since they are the most remote functionalities from base interactions. By maintaining the same number of torsions found with phosphodiester backbones with alternative linkages can explore conformational impacts and duplex stability of these structural changes. Even subtle modifications, such as an O→S conversion in phosphorothioates, have been thoroughly explored since their complexation with complemen-

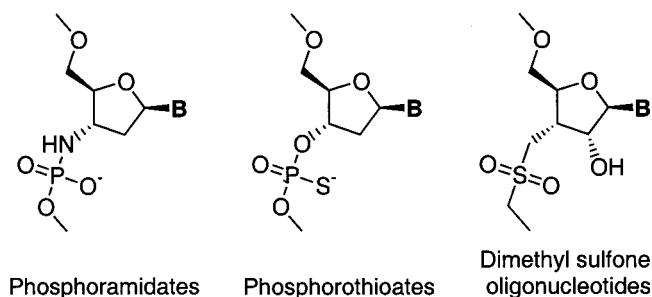


Figure 121. Representative modifications of the phosphate linkage.

tary oligonucleotides^{623–625} and with natural systems has initiated their use as antisense agents.^{626–628} Other linkages that have been used toward these ends include methylphosphonates,^{629,630} amides,^{631–633} sulfonates,⁶³⁴ sulfonamides,⁶³⁵ methyl sulfides,⁶³⁶ methyl sulfoxides,⁶³⁶ phosphorodithioates,⁶³⁷ acetals,⁶³⁸ formacetals,^{639,640} and thioacetals.^{641,642} Though numerous alternative linkages have been investigated to enhance oligonucleotide duplex stability,⁶⁴³ a survey of variants with more foldamer-like research approaches will be discussed herein.

Considerable progress has been accomplished with oligonucleotides where linkages are N3'→P5' phosphoramidates (np-DNA) through substitution of the deoxyribonucleotide O3' to N3' (Figure 121).^{644,645} Initial studies found that this modest modification enhanced *WC* duplex stability of a mixed C/T/A np-DNA 11-mer with complementary DNA by $\Delta T_m = +11.7$ °C and to a much greater extent with RNA ($\Delta T_m = +22.9$ °C).⁶⁴⁴ In addition, self-complementary np-DNAs showed duplex thermal stabilities much higher than ds-DNA or ds-RNA ($\Delta T_m = +26.0$ and $+17.6$ °C, respectively).⁶⁴⁶ Phosphoramidate oligomers also show good water solubility, mismatch discrimination, and enhanced duplex stabilities that were, by and large, found to be base and sequence independent. CD and NMR experiments of duplexes from self-complementary np-DNA strands showed uniform C3'-endo, A-type backbone conformations,^{647,648} while crystal structures revealed that the hydration of the minor groove stabilizes this conformation.⁶⁴⁹ Distamycin, a ds-DNA minor groove binder, was unable to bind with double-stranded np-DNA, supporting the A-type backbone conformations within the duplex.⁶⁴⁶ Triplex formation^{644,646} of 11-mers to a ds-DNA 23-mer was much more stable for np-DNA ($T_m = 45$ °C) than isosequential RNA ($T_m = 26$ °C) or DNA ($T_m < 10$ °C).⁶⁵⁰ Similar results have been obtained with np-RNAs.^{651,652} Finally, recent experiments demonstrated np-DNAs' ability to act as sequence-specific antisense agents through inhibition of protein expression^{653–655} as well as affinity to major groove binding α -helical peptides to the same degree as RNAs.⁶⁵⁶ Interestingly, when the N substitution was made at the O5' rather than the O3', 5'-np-DNA strands were unable to form duplexes with complementary DNA (conversion to the *N*-methyl amidate also disrupted complexation).⁶⁴⁶ Molecular dynamics simulations showed that although the single-stranded 3'- and 5'-amidate-modified DNA strands are solvated to the same degree, the N5' groups are buried in the A-type 5'-np-DNA:RNA duplex while the N3'

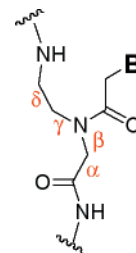


Figure 122. Structure of peptide nucleic acids (PNAs) labeled with dihedral angles.

remains solvent exposed.⁶⁵⁷ The solvent-accessible surface area of the N5' was estimated to be 10 times less than the N3', sufficiently disabling duplex formation altogether.

In an attempt to promote duplex stability through the elimination of interstrand electrostatic repulsion, the neutral, isosteric, and isoelectronic dimethyl sulfone linkage^{658,659} was investigated in RNA backbones. The crystal structure of a GC duplex suggested similar conformations to a *WC* antiparallel ds-RNA,⁶⁶⁰ whereas a UC dimer formed non-*WC* parallel duplexes in *d*-chloroform by NMR.⁶⁶¹ Self-complementary (for antiparallel orientations) dimethyl sulfone linked oligonucleotides showed stronger unimolecular self-pairing than duplexation with RNA or DNA complements.⁶⁵⁹ Furthermore, each oligosulfone has its unique set of properties (solubility, foldability, reactivity), which strongly depend on sequence, varying widely and unpredictably. Chimeric oligomers incorporating one sulfone linkage induced significant decreases in duplex strength when functionalized in the middle of DNA strands.⁶³⁶ In summary, these nonpolar chains behave more like proteins than nucleic acids⁶⁵⁹ in that proteins have variable structure types whereas nucleic acids generally have one universal structure type. Polyanion (repeating charge) seems to be the key to nucleic acid recognition, by modulating the strength of the interaction through electrostatic repulsion. These studies highlight the importance of ionic functionalities in DNA backbones to maintain extended, noncollapsed structures.

1. PNAs

Peptide nucleic acids (PNAs) and structural analogues are the most thoroughly investigated nucleotidomimetic systems studied to date with a number of reviews recently appearing on the subject.^{662–666} PNAs are neutral, δ -peptide backbones with nucleobase extensions from a methylenecarbonyl linker at the β -position (Figure 122). Although progress to date on PNAs has been very promising, the poor water solubility of these oligomers remains a considerable limitation.

Through the successful incorporation of canonical bases to the PNA backbone,^{667–669} PNA oligomers were capable of forming *WC* duplexes with both DNA and RNA in antiparallel and parallel orientations (with the antiparallel orientation defined as the amino terminus of PNA and the 3'-end of the oligonucleotide at the same end). The antiparallel PNA:DNA and PNA:RNA duplexes have T_m s $+13.4$ and $+21.1$ °C, respectively, higher than the parallel form.

Formation proceeds through strand displacement in the oligonucleotide duplex. Kinetic CD studies revealed that PNA complexes form through a rapid base-pairing step, followed by a slow reorganization in the backbone in order to adopt the most thermodynamically stable helical conformation.⁶⁷⁰ Furthermore, ds-PNA duplexes showed increased thermal stabilities⁶⁷⁰ with the duplex stability following the order PNA:PNA > PNA:RNA > PNA:DNA > DNA:DNA.^{668,671} This enhanced stability arises from hydrophobic effects and the absence of interstrand electrostatic repulsion, evidenced by the similarity of PNA:DNA and ds-DNA T_m values in solutions of high ionic strength, where polyanionic backbones are screened by counterions.^{671,672} Chain-length studies on 44 PNA–DNA duplexes revealed an average base-pair binding contribution of 1.6 kcal·mol⁻¹ in lengths from 6- to 20-mers.⁶⁷³ Elucidation of binding sequence-specificity in single-mismatched 9- and 12-mer strands in PNA–DNA duplexes primarily revealed destabilization dependent on the particular base-pair mismatch, its location on the PNA or DNA strand, and its nearest-neighbor environment.⁶⁷³ Single-stranded PNAs terminated with L-lysine (which can induce a helical twist sense of the strand) showed minimal CD intensities indicating the lack of preorganized, helical base stacking⁶⁷⁰ while, within ds-PNA, the CD signal was very intense and resembled ds-DNA.

A crystal structure of a PNA–PNA duplex revealed a widened P-helix relative to DNA–DNA and a large pitch of approximately 18 base pairs, resulting in a deep major groove and a shallow minor one.⁶⁷⁴ Additionally, the polyamide backbone demonstrates “constrained flexibility” in solution such that the PNA strand accommodates the complexed conformation more easily than ribose backbones through greater torsional relaxation. In fact, NMR studies revealed multiple resonances for the uncomplexed PNA backbone, indicating random-coil conformations,⁶⁷⁵ which converge to a singular resonance in an A-type PNA–RNA helix⁶⁷⁶ and a PNA–DNA helix.^{677,678} Although molecular modeling suggested that intrastrand α -helical-type H-bonding in the PNA backbone would result in higher conformational order,^{679–681} NMR studies revealed that this stabilization was not observable in these systems, although this is under debate.⁶⁸² Though PNA folding proceeds via intermolecular complexation, these chain molecules adopt unique conformations through intrastrand *cis*–*trans*-amide isomerization and interstrand noncovalent complementary base pairing, even showing the capacity to form hairpins.⁶⁸³ Though the A-type PNA:RNA duplex shows conformational similarity to ds-RNA, recent molecular dynamics simulations revealed that PNA:DNA duplexes have conformational characteristics of both the A- and B-type as well as a much more flexible PNA backbone than natural oligonucleotides, while retaining torsional preferences.⁶⁸⁴ Crucial to the proper directional sequence selectivity, mixed backbone PNA/DNA chimeras complexed to both RNA and DNA formed exclusively antiparallel duplexes over the parallel orientation.^{665,685}

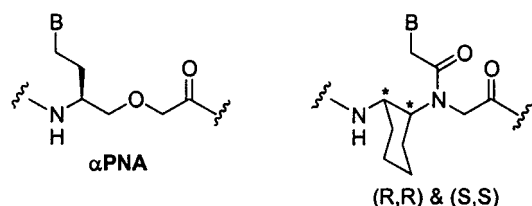


Figure 123. Representative examples of PNA structural modifications.

The potential for PNAs to act as transcription inhibitors has been demonstrated through investigations into effective DNA strand displacement (forming D-loops in PNA–DNA duplexes,^{686,687} PD-loops with bis-PNAs⁶⁸⁸ in (PNA)₂–DNA triplexes,⁶⁸⁹ and other architectures^{690,691} including double duplex strand invasion⁶⁹²) such that both DNA strands form duplexes with the pseudocomplementary PNAs. Triplex PNAs^{663,664} have elucidated a right-handed PNA–PNA–DNA^{668,689,693–696} where a third PNA *H*-pairs to the *WC* PNA strand,⁶⁹⁵ while a chain-length study showed a T_m stabilization of 10 °C per monomer unit⁶⁶⁸ as well as a PNA–PNA–PNA triplex.⁶⁹⁰

Along with inhibitory binding, PNAs can participate in fundamental genetic processes. PNAs facilitate the oligomerization of complementary RNA and vice versa, demonstrating a pathway for information transfer along with providing possible insight into the origin of the RNA world.^{697,698} Furthermore, PNAs can act as primers for DNA polymerases.⁶⁹⁹ Finally, promising antisense and antigene properties⁷⁰⁰ as well as key issues such as improved solubility, stability at physiological conditions, nuclease resistance, and improving cellular uptake of PNA-conjugates are being pursued in efforts to treat disease with PNAs through inhibition of gene expression.^{685,701}

Since a variety of PNA-like oligomers have been synthesized for nucleotide recognition, representative examples of strand modification, both backbone and base linking, are worth mentioning in terms of folding properties (Figure 123). Cyclohexyl-derived PNAs with a more rigid backbone formed stable duplexes with (*S,S*) configurations, while duplexes incorporating the (*R,R*) isomers resulted in decreased stabilities in the right-handed duplex.⁷⁰² Bis-PNAs rapidly form triplex structures due to reduced entropic costs by converting triplex formation into a bimolecular process.^{703,704} PNA chimeras⁶⁶⁵ have been synthesized to form PNA hybrids with DNA⁶⁶⁵ and enhance binding affinities and sequence selection. They also form complexes with peptides⁷⁰⁵ to form conjugates that retain the biological functions of both. A different peptide–PNA conjugate, dubbed α -helical PNAs (α PNAs), incorporates three amino acids into the monomeric backbone unit. α PNAs demonstrate stronger binding to DNA strands (in an all-or-none-type complexation) compared to traditional PNAs, and they have greater water solubility.⁷⁰⁶ A representative PNA–PNA duplex and a PNA₂–DNA triplex are shown in Figure 124. To summarize, the PNA family of nucleotidomimetic foldamers are novel backbones that successfully complex to oligonucleotides even though they are neutral and acyclic. Clearly, the structural rules for ideal complexation of oligonucleotides and neutral, acyclic nucleotido-

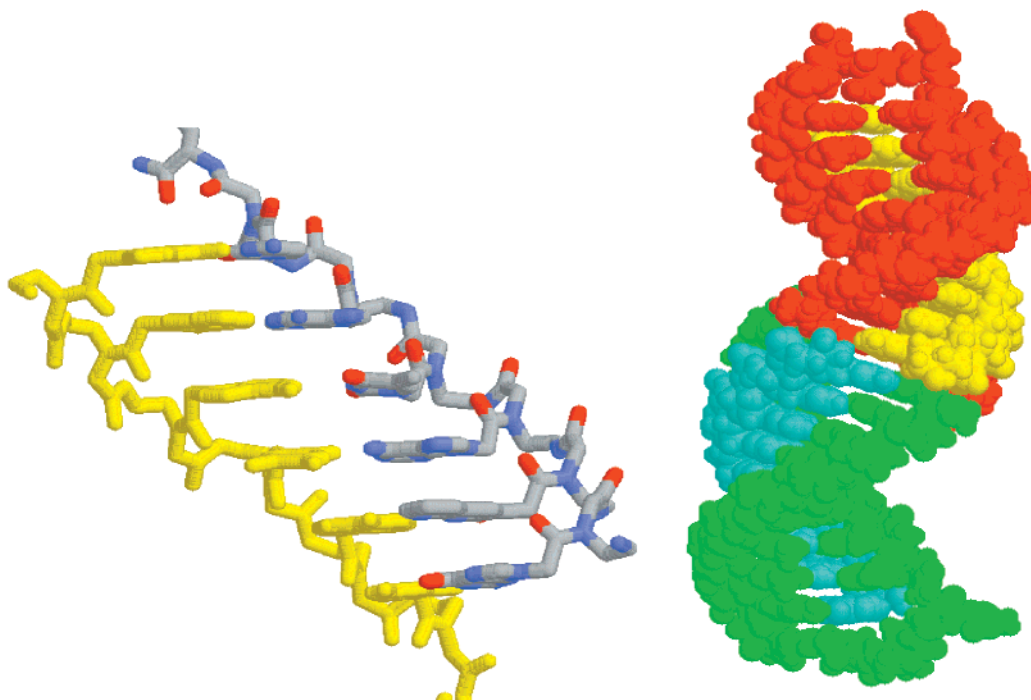


Figure 124. Crystal structure of a peptide nucleic acid duplex (left).⁹⁰¹ For clarity, one strand is colored yellow and the other uses conventional atom colors: PNA₂-DNA triplex (right).⁷¹⁰ Four chains are shown. The DNA chains are colored yellow and blue. The DNA sequence is 5'-(GAAGAAGAG)-3'. The PNA chains are colored red and green. The PNA sequence is H₂N-(CTCTTCTTC-His-Gly-Ser-Ser-Gly-His-CTTCTTCTC)-CO₂H.

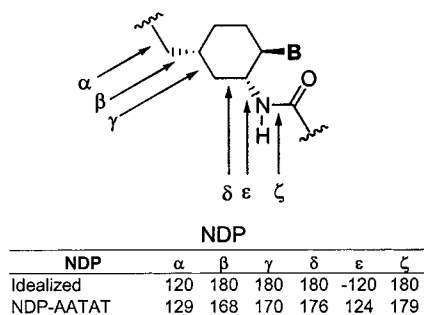


Figure 125. NDPs and their torsion angles.

mimetic chains molecules have yet to be fully determined.

2. NDPs

Nucleo- δ -peptides (NDP) incorporate cyclohexyls linked by carbamoylmethyl groups such that the oligomer is preorganized into an ideal linear conformation analogous to p-RNAs.^{707,708} NDPs map onto α -peptide backbones with three predefined torsions (γ , δ , and ζ) due to the conformation restriction of the cyclohexyl moieties. NMR studies on an NDP-AATAT sequence revealed an antiparallel WC self-paired duplex stabilized by interstrand base stacking. Torsional angles of the backbone are shown in Figure 125, where the dangling A-ends further stabilize the duplex. The global conformation was further refined using molecular dynamics and determined to be a right-handed double helix with a twist of ca. $10 \pm 2^\circ$ and a unit height of $7.5 \pm 0.1 \text{ \AA}$.

3. Fused Sugar-Base Backbones

A recent series of investigations was undertaken to determine if a fusion between the sugar and the

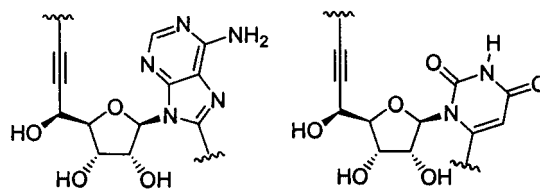


Figure 126. Fused sugar-backbone structures.

nucleobase would provide conformational accessibility to intermolecular complexation. Through the convergent Sonogashira coupling of an iodo-nucleobase to an acetylenic linker, dimers and tetramers of A and U fused bases were generated to explore these chain molecules (Figure 126).⁷⁰⁹⁻⁷¹² UV studies on these single strands did not show any evidence of base interactions, indicating that intrastrand base stacking had been disrupted through this backbone modification. In a related system, phosphodiester-fused A and U bases were single-site incorporated into 14-mer DNA strands and led to duplex formation destabilized by an amount on the order of only one mismatch pair.^{713,714} These examples clearly demonstrate that the double-helix architecture has a strong preference for comblike structures where the backbone adopts conformations that project nucleobases in orthogonal orientations to the helical axis.

4. Cationic Linkages

Oligonucleotide complex stability has also been enhanced with cationic deoxynucleic and ribonucleic guanidine backbones (DNG and RNG) (Figure 127), which are electrostatically attracted to the anionic phosphodiester backbone of natural chains within a complex (substituted guanidinium linkages have also been investigated⁷¹⁵). Through both solution-⁷¹⁶⁻⁷¹⁸ and solid-phase synthesis,⁷¹⁹⁻⁷²² pentameric DNG T

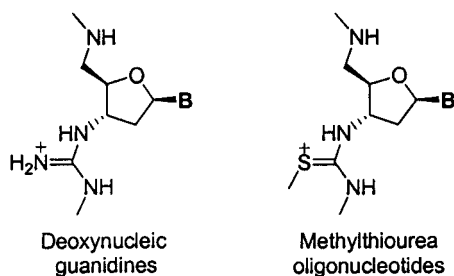


Figure 127. Cationic backbone modifications DNG and DNmt.

strands were generated and formed very stable duplexes and triplexes with poly(rA) and duplexes with poly(dA), remaining intact even near boiling temperatures, while the DNG₂:poly(dA) triplex has a T_m of 85 °C. DNG-T₅ did not bind to poly-(dG), -(dC), and -(dT), showing sequence discrimination.^{718,723} With DNA oligomers, single-point C mismatches lower duplex T_m DNG-T by 4–5 °C at terminal and 15 °C at internal sites.⁷²¹ A thermodynamic and kinetic study of DNG complexation with DNA strands containing G mismatches showed that the electrostatic attraction between the strands overrides base-pairing selectivity in certain cases.^{724,725} Decreased duplex stability is observed at higher ionic strength since the interstrand electrostatic attraction is diminished as a consequence of screening. The major groove width of the DNG:RNA A-type duplex increases while the minor groove width tightens relative to ds-RNA due to the electrostatic contraction of the complex as revealed by molecular modeling⁷²³ and dynamics simulations.⁷²⁶ Similar results were demonstrated in RNG backbones.^{727–729} Hybrid DNG–PNA strands,^{730,731} as well as chimeric DNG–methylthiourea oligonucleotides,⁷³² allow for attenuation of the degree of positive charge embedded in these neutral backbones, enhancement of water solubility of neutral backbones, and minimization of deleterious effects of electrostatic attraction. To increase the hydrophobicity of cationic oligonucleotides, *S*-methylthiourea backbones (DNmt) were generated by solution-^{733,734} and solid-phase synthesis.⁷³⁵ DNmt backbones function similarly to DNG with weaker complex stabilities observed.^{736–738} Overall, these cationic backbones show remarkable stability with their complementary natural oligonucleotides through utilization of electrostatic attraction as a supra-molecular construct, thereby incorporating another stabilizing noncovalent interaction.

E. Alternative Nucleobases

The use of nonbiological nucleobases to enhance oligonucleotide duplex stability is widespread, and an exhaustive exploration of this field is beyond the scope of this review. At the same time, recent studies exist that go beyond this goal with the aim of understanding the function of base interactions in duplex stability and the impact of unusual nucleobases on both conformation and assembly. Herein, we focus on a few of these examples as representatives of the field and to highlight how modifications at nucleobase sites that are “remote” from the backbone can have profound architectural effects on

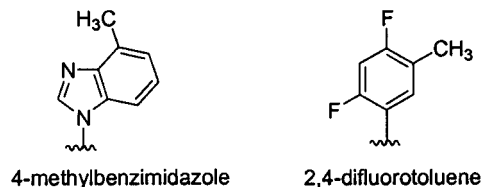


Figure 128. Hydrophobic nucleotide bases.

oligonucleotide complexes. This field has recently been reviewed.⁷³⁹

The role of face-to-face aromatic interactions within duplex DNA and RNA is less evident than base pairing since H-bonding in duplexes can be rationalized through predictable acceptor–donor motifs while the nature and rules of aromatic stacking are less understood. Aromatic–aromatic interactions have been attributed to electrostatics, hydrophobicity, and dispersion forces. To elucidate the factors in nucleobase stacking, the use of nucleotides with alternative nucleobases⁷⁴⁰ at the 5'-termini of DNA strands (dangling ends) to study duplex stabilization was undertaken. Initial studies revealed the overall order of stacking ability to be pyrene > methylindole > phenanthroline ~ naphthalene ≥ difluorotoluene > A > benzene > T, where less polar aromatics of similar size stack stronger than more polar ones.⁷⁴¹ Further investigations with the canonical bases showed the stacking ability to be A > G ≥ T ~ C.⁷⁴² Overall, the best correlation between stacking ability and various properties of the nucleobases was found with the surface area of the aromatic moiety; bases with small overlap, such as pyrrole, stack with the weakest strength and pyrene stacks the strongest. Thus, solvophobic effects were concluded to be the most significant force in the base stacking interactions of this series.

Although the common base-pairing motifs formed through H-bonding interactions in duplexes are well understood, it is unknown whether oligonucleotide complexation can proceed through non-H-bonded pairing. Considerable work has been conducted on alternative H-bonded pairings through isomeric forms of nucleobases, such as iso-C and iso-G,^{743–746} as well as isomorphous nucleobases,^{747–750} aimed at the expansion of the genetic alphabet⁷⁵¹ through enzymatic incorporation. A problem with alternative acceptor–donor systems is the susceptibility of the nucleobases to undergo deleterious tautomeric isomerization.^{745,752,753} To elucidate the necessity of H-bonded pairing in duplex stabilization, single-site substitution in ds-DNA 12-mers with the “complementary” pair of pyrene and hydrogen (an abasic site) nucleotides destabilized the duplex to a smaller extent than expected ($\Delta T_m = 1.6–2.2$ °C relative to an A–T pair) while pyrene oppositely paired to canonical bases reduced the stability to a greater extent ($\Delta T_m = 2.3–4.6$ °C).⁷⁵⁴ Surprisingly, a pyrene–pyrene pair generates a duplex with comparable stability to the unmodified natural duplex. Another non-H-bonded pairing motif, 4-methylbenzimidazole:2,4-difluorotoluene,⁷⁵⁵ destabilized the ds-DNA ($\Delta T_m = 12.1$ °C relative to a central T–A pair) but retained the B-type conformation of the backbone according to NMR and molecular dynamics simulations⁷⁵⁶ (Figure 128). Destabilization in this system is primarily due to cost of solvation of these more hydro-

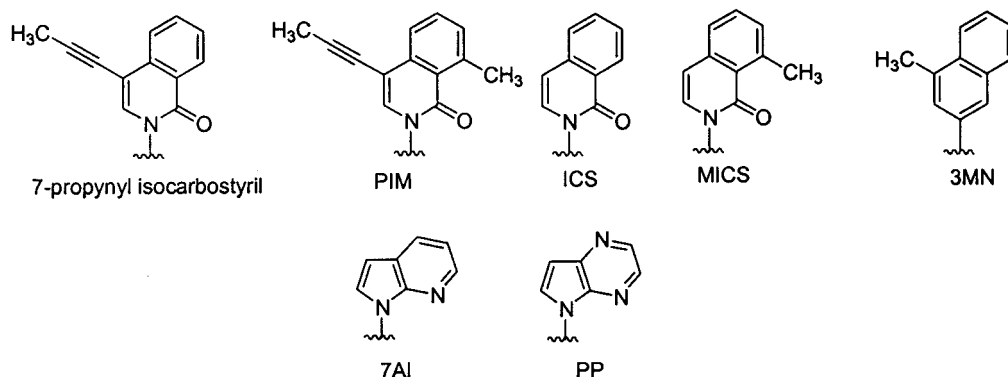


Figure 129. Examples of alternative nucleobases.

phobic bases.⁷³⁹ In similar studies, various aromatic nucleobases have been incorporated into DNA strands for duplex stability as a segue to alternative nucleobase pairing motifs that may be incorporated into DNA strands by polymerases. Of the variety of non-H-bonding aromatic nucleobases investigated,⁷³⁹ promising results for unnatural DNA pairing modes in terms of duplex stability, mismatch discrimination, and incorporation during template-directed polymerase syntheses^{757–759} (see Kool⁷⁶⁰ for a recent review) include 7-propynyl isocarbostyryl:7-propynyl isocarbostyryl,⁷⁵¹ 7AI:ICS,⁷⁶¹ PP:MICS,⁷⁶² PIM:PIM,⁷⁶³ and 3MN:3MN⁷⁶⁴ (Figure 129). Recently, the 7AI:7AI self-pair was not only efficiently incorporated into a growing DNA strand, but also allowed primer extension using mammalian polymerase β , which was not seen using the Klenow fragment of *Escherichia coli* polymerase I.⁷⁶⁵ These nonbiological base-pairing motifs demonstrate the acceptance of the oligonucleotide duplex architecture for non-H-bonding interactions, stressing the importance of base stacking for stability and the potential dispensability of H-bonding interactions at select sites.

Although it is clear that cationic, inorganic species (such as Mg^{2+}) are essential to the structures and stability of the oligonucleotide backbone,⁴⁸⁷ metal–ligand coordination in oligonucleotides has gained increasing attention. Recent studies have utilized the coordination strength of transition metals to incorporate alternative nucleobases into DNA strands as an unconventional interstrand base-pairing motif. After single-site incorporation of pyridine and 2,6-pyridinedicarboxylic methyl diester nucleotides into complementary DNA 15-mers followed by hydrolysis of the methyl diesters, equimolar mixtures of the two strands showed no duplex formation and remained dissociated even at low temperatures (14 °C) (Figure 130).⁷⁶⁶ Upon addition of Cu^{2+} (1, 2, and 5 equiv), duplex formation not only proceeds but comparable thermal stabilities were obtained to the natural ds-DNA ($\Delta T_m = 2.6, 1.7,$ and 1.1 °C lower relative to an A–T pair, respectively). A variety of other transition metals were tested ($Ce^{3+}, Mn^{2+}, Fe^{2+}, Co^{2+}, Ni^{2+}, Zn^{2+}, Pd^{2+},$ and Pt^{2+}) but did not lead to duplex stabilization. Ligand–nucleobase mismatch discrimination was demonstrated with canonical bases where duplexes with mispairs were typically destabilized by ≥ 10 °C. In a related system, 2,2'-bipyridines were attached through a C1'-methylene to the furanose ring (dubbed *ligandosides*) and incorporated at single sites into self-complementary DNA 11-mers.⁷⁶⁷ Upon

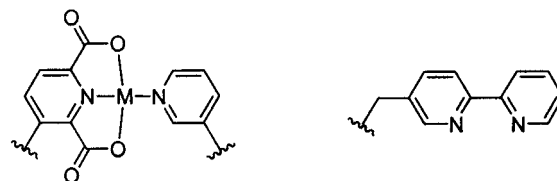


Figure 130. Metal-binding nucleobases.

addition of 1.0 equiv of Cu^{2+} , the T_m of the duplex increased from 56.6 to 64 °C and showed a more cooperative melting transition. Dimeric oligonucleosides have been generated with Cu^{2+} and Ag^+ .⁷⁶⁸ Significantly, these metal-coordinating nucleotides have two potential structural advantages over helicates. First, the ligands are remote from the backbone whereas in helicates the metal-coordinating portions are part of the backbone. Second, the phosphodiester linkages can stabilize the cationic metal center, decreasing any deleterious effects counterions may have in helicates. A recent study has shown that bipyridine ligands can also stabilize DNA duplexes through interstrand base stacking in the *absence* of metal ions.⁷⁶⁹ Efforts toward developing other metal-binding nucleosides include phenylenediamine: Pd(II),⁷⁷⁰ catechol-borates,⁷⁷¹ and 2-aminophenols.⁷⁷² Overall, these systems show great promise for the development of novel nucleotidomimetics incorporating metal coordination as a supramolecular construct in the design of foldamer structures.

VII. Multistranded Abiotic Foldamers

Just as single-stranded abiotic foldamers mimic the secondary structures of proteins through a bottom-up approach, multistranded abiotic foldamers mimic DNA architectures through the assembly and folding of two or more chains through nonadjacent contacts. The following is a survey of the backbones, some very similar to previously described chains in the single-stranded abiotic section, that utilize various non-covalent interactions in adopting their unique conformations.

A. Hydrogen-Bonding-Stabilized Foldamer Multiplexes

Foldamer multiplexes¹¹⁸ incorporating H-bonding motifs have been investigated to generate novel structures that associate through similar motifs as

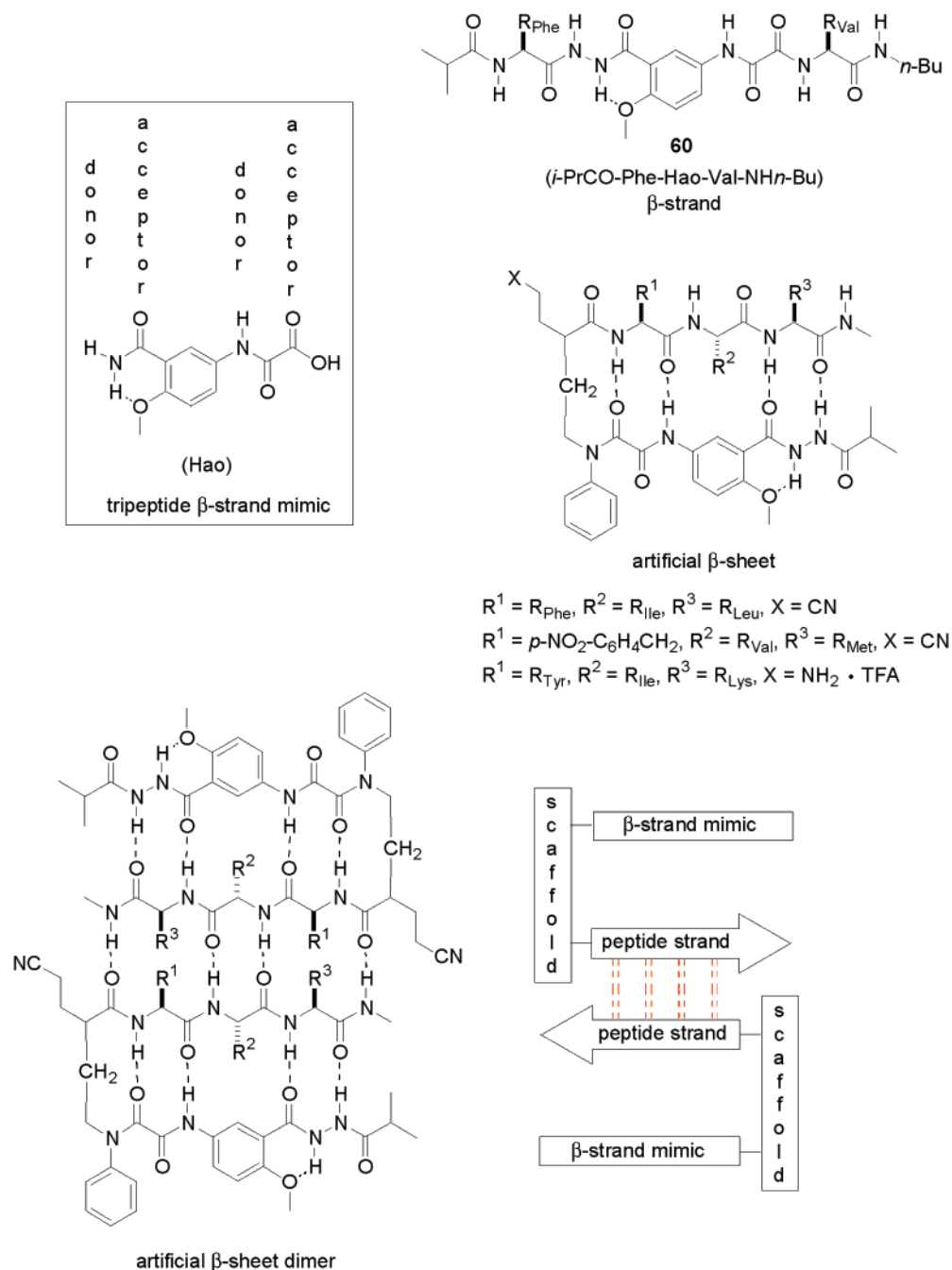


Figure 131. β -Strands and β -sheets incorporating the artificial amino acid Hao.

peptide β -sheet formation and nucleotide base pairing as seen in DNA. The majority of these systems establish a sequence of H-bond donors (D) and acceptors (A) through heterocyclic amide- or urea-linked monomers. Through both theoretical^{774,775} and experimental⁷⁷⁶ work, determination of association constants for triply hydrogen-bonded complementary complexes were shown to be highly dependent on the D/A sequence, with the strongest complexation occurring between all-D and all-A strands, while mixed or alternating D/A sequences showed weaker associations due to repulsive secondary electrostatic interactions. Higher levels of complexity can be achieved in moieties capable of D/A tautomerization and intramolecular H-bonding in addition to intermolecular association.^{777,778} Through these motifs, differentiation between competitive self- versus complementary

dimerization depends on the association strength of the sequence-selective algorithm.

Nowick and co-workers described β -strands and an artificial β -sheet that form strong, H-bonded dimers in CDCl_3 .^{157,773} To prevent indefinite association typical of β -strands, the unnatural amino acid "Hao" was designed to allow H-bonding on only one edge of a β -strand mimic (Figure 131).^{155,157} Hao is an amimo acid based upon hydrazine, 5-amino-2-methoxybenzoic acid, and oxalic acid constituents. This peptidomimetic building block maps onto a tripeptide segment and hence can be considered as an η -peptide. ¹H NMR chemical shift data, NOE studies, and dilution experiments indicated that the peptide derivative **60** strongly dimerized in pure CDCl_3 with an association constant of ca. 10^6 M^{-1} . As expected, the association constant was considerably lower upon

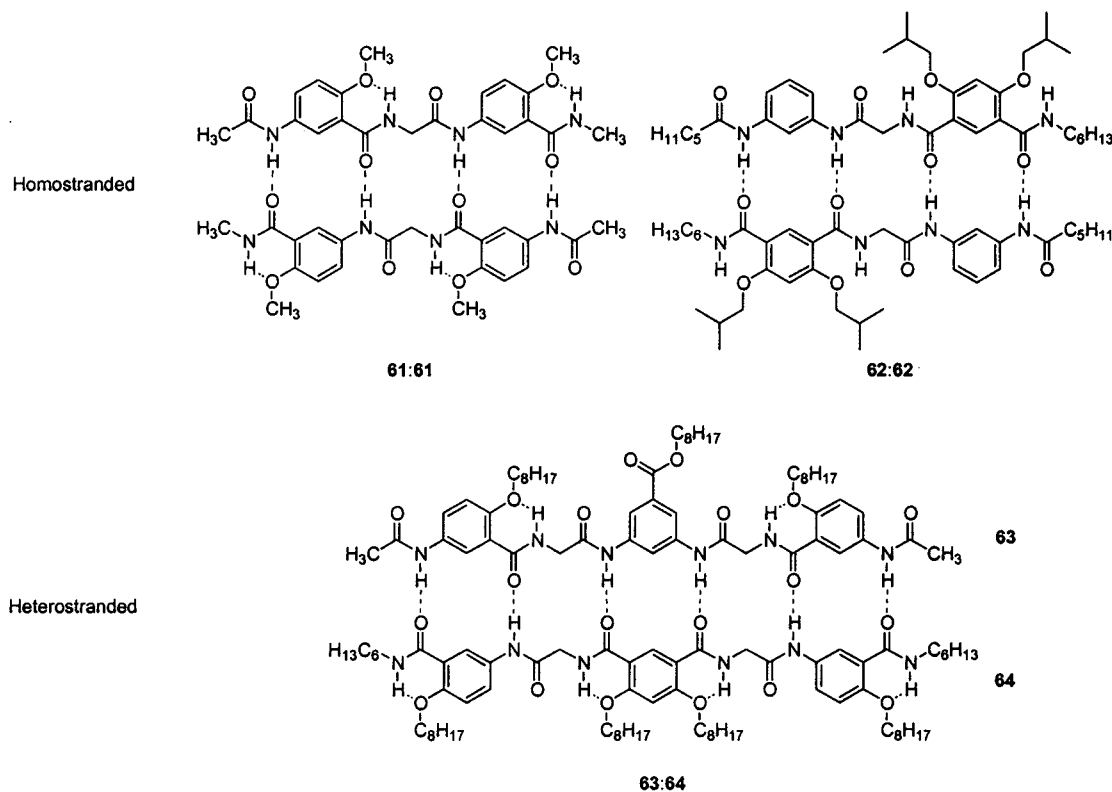


Figure 132. Oligo(arylamide)s complexed through self-complementary ADAD and AADD duplexes and a complementary ADAADA/DADDAD strand.

addition of 10% MeOH. An artificial sheet was constructed in which the Hao unit was attached to one end of Nowick's previously described molecular scaffold while to the other end an α -tripeptide was connected. This structure resulted in an artificial β -sheet that dimerized in solution via the H-bond donors and acceptors on the top edge.⁷⁷³

Arylamide oligomers with various D/A sequences have been recently investigated by Gong et al.^{445,446} Quadruply H-bonded complexes, **61:61** and **62:62**, with D/A sequences DADA and DDAA, respectively, were shown by ¹H NMR and X-ray studies to dimerize through self-complementarity from two dimeric strands (Figure 132). The association constant of **62:62** was determined to be marginally more stable than **61:61** ($6 \times 10^4 \text{ M}^{-1}$ vs $4 \times 10^4 \text{ M}^{-1}$) even though more favorable electrostatic interactions exist with **62**. Although some torsional flexibility exists in both foldamers, these H-bonded duplexes form readily through both intra- and intermolecular H-bonds to adopt planar, β -sheetlike structures. Extension of these preliminary studies to trimeric oligomer lengths enabled the formation of self-complementary planar duplexes stabilized by six H-bonding interactions.⁴⁴⁶ The two symmetric heterotrimers, **63** and **64**, have two and four intramolecular H-bonding interactions and D/A sequences of DADDAD and ADAADA, respectively. Preorganization through intramolecular H-bonding interactions predispose these oligomers to planar, extended conformations, exposing sequence sites for intermolecular association. NOESY experiments under complexing conditions (i.e., CDCl₃) confirmed the close interstrand proximity of the methylene groups. Slight downfield shifting of a NH signal in **64** upon dilution (100 to 10 μm) was

speculated to be a result of decreasing intermolecular stacking interactions. Self-association of both **63** and **64** could produce dimers stabilized by four H-bonding interactions. The self-complexation association constant for **64** was determined to be approximately $4 \times 10^4 \text{ M}^{-1}$ compared to the lower limit **63:64** association constant of $9 \times 10^7 \text{ M}^{-1}$. Recent studies showed that mismatches in the AD sequence lead to a conformational rearrangement of the backbone driven by steric interactions that resulted in >40 times lower duplex stability as evidenced by isothermal titration calorimetry.⁷⁷⁹

A system capable of two-state conformational switching has been produced from two complementary naphthyridinyl urea oligomers (Figure 133).⁷⁸⁰ Both linear molecules **65** and **66** form associated structures through intramolecular H-bonding by rotation about the arylamide bonds. In frame-shifted (relative to **66**) monoaromatic **65**, the folded conformation is observed to intermolecularly associate to produce oligomeric species (of unknown *n*) through noncooperative association at all concentrations. At low concentrations, the bent form of **66** associates to form dimer **67**, while at higher concentrations the extended conformation of **66** dimerizes to **68**. Upon mixing of **66** and **65**, a complementary complex **69** self-assembles with the extended, planar conformations of both molecules at all concentrations. This occurs since the association constant for the formation of **69** is greater than either of the duplexing modes.

Bis-2-ureido-4[1*H*]-pyrimidinones are capable of self-associating into a duplex structure stabilized by eight H-bonding interactions with **70** that are adaptive through a *keto-enol* tautomerization (Figure

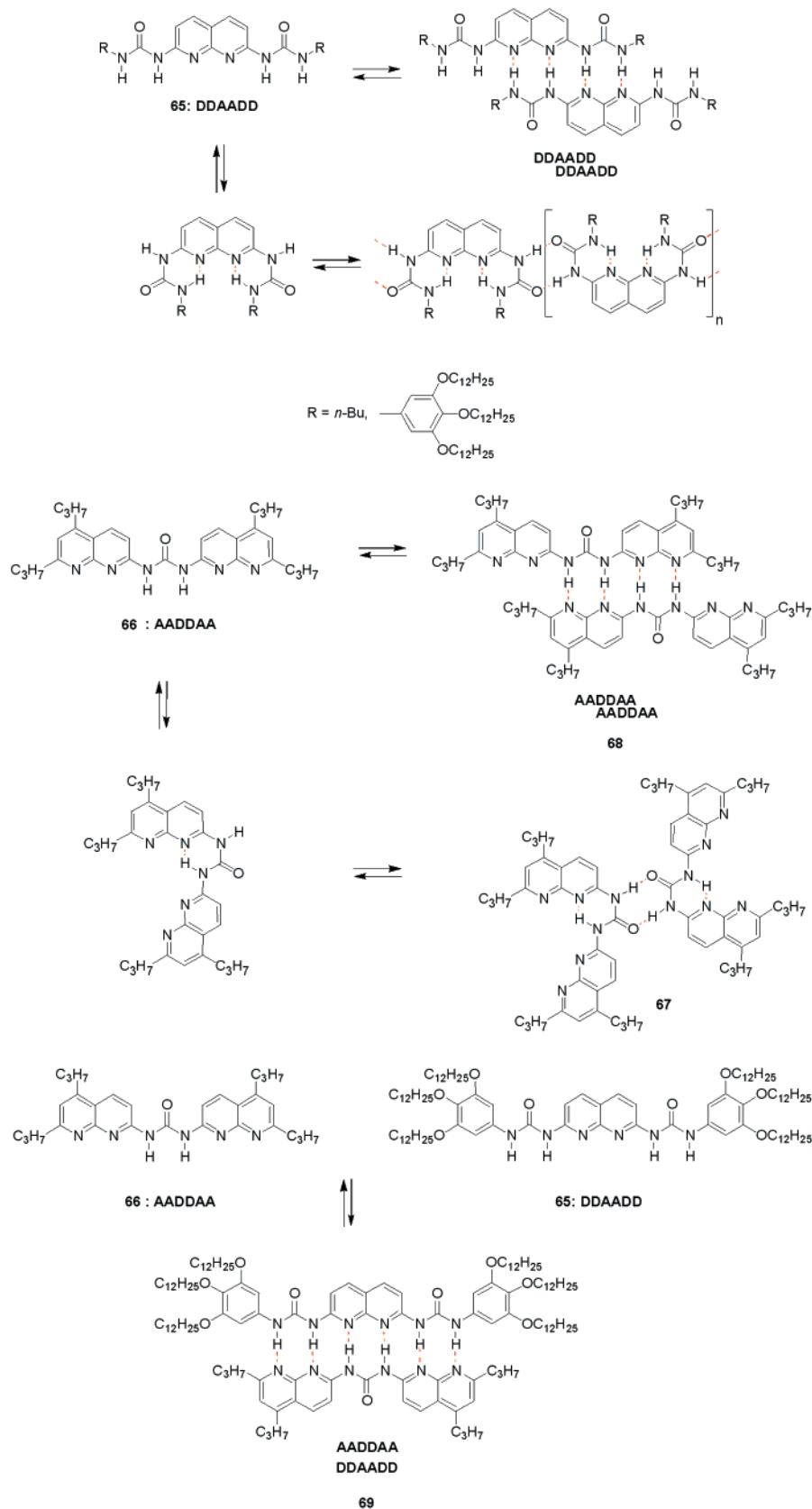


Figure 133. Intra- and intermolecular pairing modes for DDAADD and AADDAA strands.

134).⁷⁸¹ In **70**, two D/A sequences, the *keto* DDAA and the *enol* ADAD, are possible through proton transfer and a switch in the intramolecular H-bonding by a N–C rotation in the urea moiety. X-ray analysis of crystals revealed pyrimidinone aromatic–aromatic

stacking and intermolecular H-bonding where crystals obtained from DMF revealed two possible syn coplanar orientations in the solid-state while crystals grown from CHCl₃ showed anti or helical orientations. NOE and 2D-ROESY experiments revealed

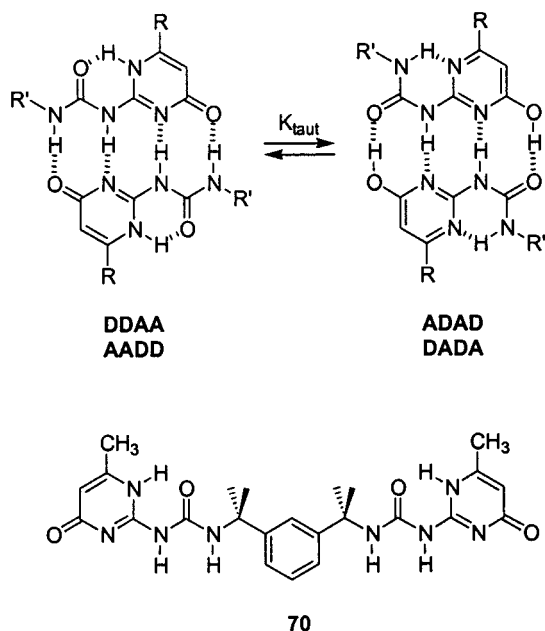


Figure 134. Keto-enol tautomerism in an A/D strand.

cooperative formation and equilibration between the two conformations as well as slow conversion to a third isomer, identified as a *keto-enol* asymmetric duplex with one interstrand pyrimidinone complex and one enolized pyrimidinol pair. At equilibrium, the *syn/anti* ratio to *keto-enol* duplexes exist in an approximately 3:1 ratio.

Recently, an oligomer backbone incorporating aminotriazene repeat units tethered together by methylene groups effectively forms hydrogen-bonded duplexes.⁷⁸² Complexation of the dimeric strands is much stronger in the amine-linked backbone ($X = \text{NH}$) where intrastrand H-bonding preorganizes the dimer for duplexation, whereas the ether-linked backbone ($X = \text{O}$) shows significantly lower association constants (Figure 135).⁴⁵²

B. Duplexes Stabilized by Hydrogen-Bonding and Aromatic-Aromatic Interactions

1. Zipper Duplexes

Hydrogen bonding and aromatic aromatic-aromatic stacking interactions have also been used in the intermolecular organization of complementary

oligomeric strands (Figure 136).⁷⁸³⁻⁷⁸⁸ The system is based on intramolecular H-bonding between an amide carbonyl group and an amide nitrogen. In addition, two aromatic edge to face interactions between an isophthalic acid moiety and a 1,1-bis(4-amino-3,5-dimethylphenyl)cyclohexane group are also important for stabilization. The dimer conformation **72** resulting from the intermolecular H-bonding of two strands of **71** was confirmed by ¹H NMR spectroscopy, which revealed a downfield shift of all amide protons and an upfield shift of the aromatic protons on the isophthaloyl group. These results indicate the presence of H-bonding and aromatic-aromatic stacking interactions.

The symmetry of the initial complexes **72** prevented a definitive confirmation of the structure. To overcome this difficulty, different yet complementary systems were developed (Figure 137). Monomers **73** and **74** are self-complementary and form stable homodimers in solution as homocomplexes as determined by ¹H NMR spectroscopy. However, it was found that the heterocomplex **75** was an order of magnitude more stable than either of the self-complementary strands. NOE experiments revealed several interstrand interactions and indicated contact along the entire length of the complex. Experiments were performed to help probe the possibility of cooperative binding in the recognition process.⁷⁸⁴ The association constants of several heterocomplexes of increasing length were determined by ¹H NMR spectroscopy, showing that as the length of the oligomers increased, the stability of the corresponding complexes increased in a nonlinear fashion indicative of a cooperative binding process. Additionally, significant intermolecular interaction was observed along the entire length of the chain.

2. Pyridylamide Oligomers

Intramolecular H-bonding has been used to create a system that can adopt a single- or double-stranded helical conformation in solution.^{113,789,790} The system is based on 2'-pyridyl-2-pyridinecarboxamide units which are predisposed to form intramolecular H-bonds (Figure 138). H-bonding present in oligomeric strands **76-78** is expected to generate a helical conformation. Dilute solutions of **76** in CDCl₃ (0.5

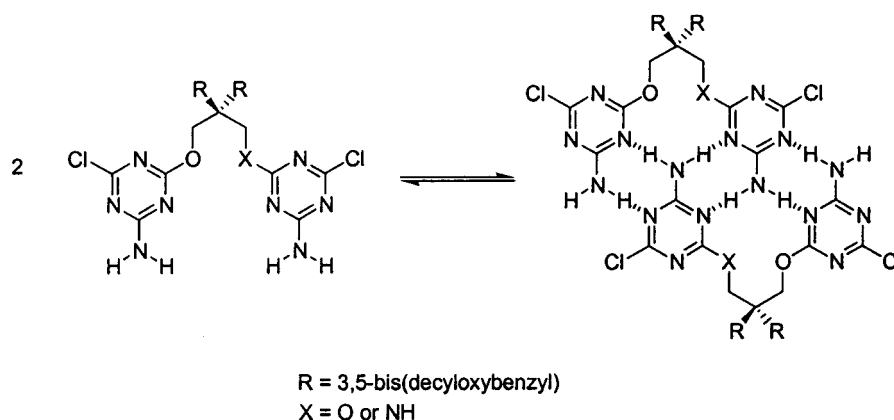


Figure 135. Methylene-bridged triazene dimers and their hydrogen-bonding duplexation.

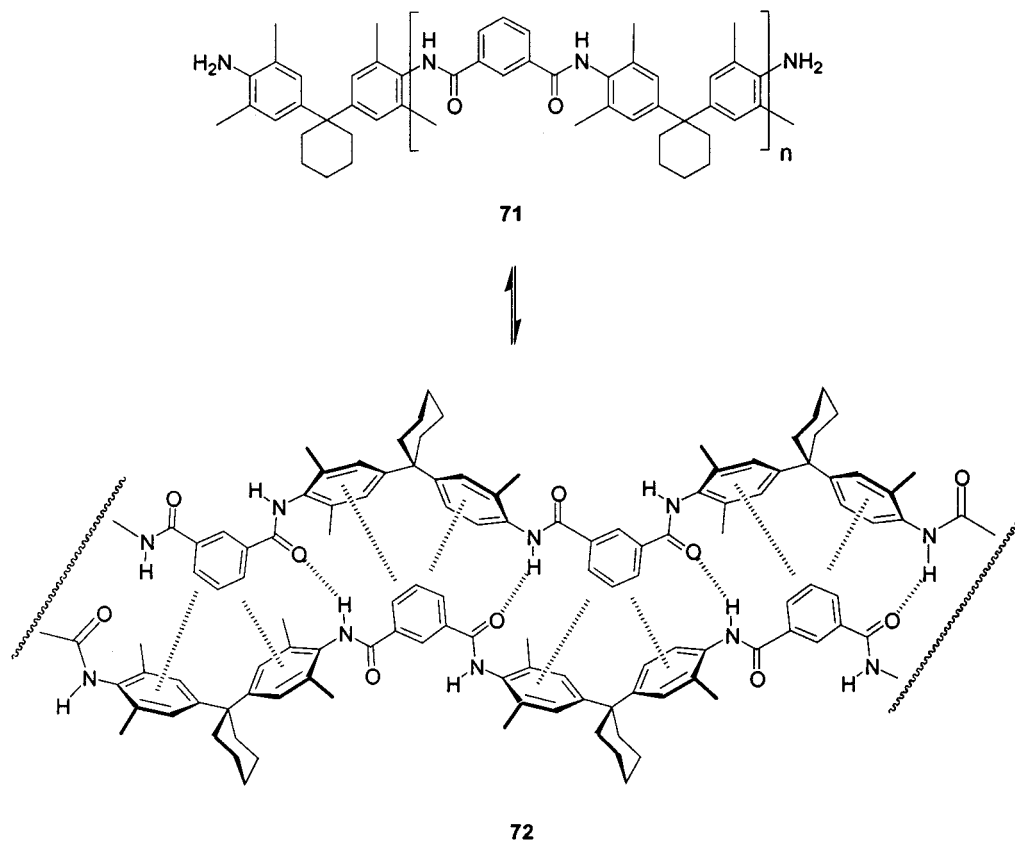


Figure 136. Self-complementary oligomer in a zipper structure. Dotted lines indicate edge–face aromatic–aromatic interactions.

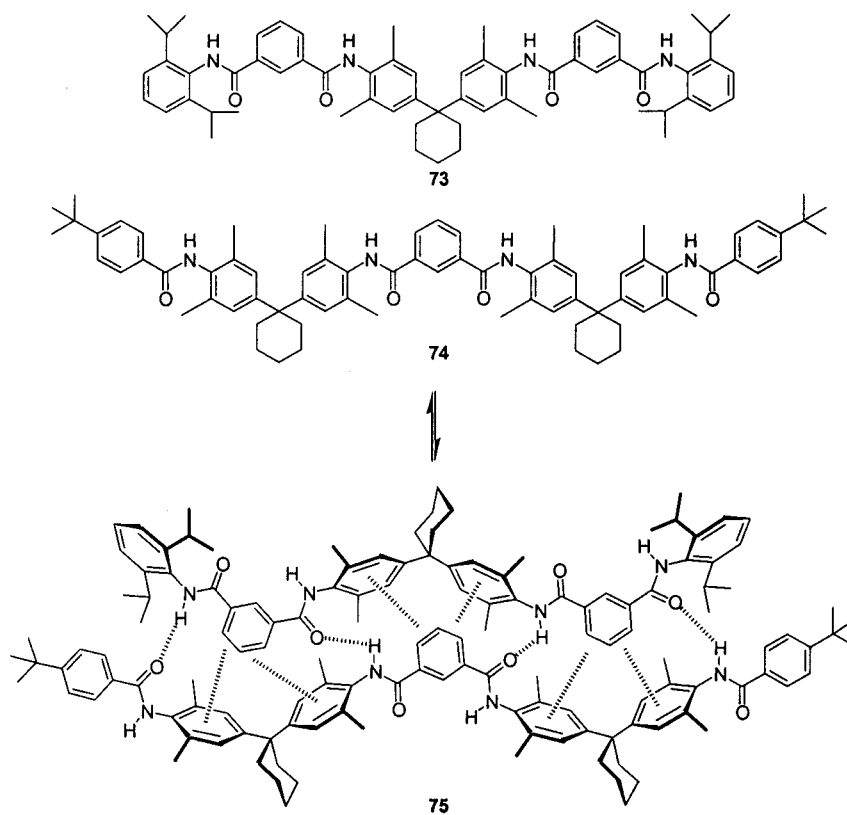


Figure 137. Complementary oligomers in zipper structures.

mM) indicate the presence of a single species as evidenced by a single set of sharp ^1H NMR signals. Aromatic stacking as demonstrated by the upfield

shifting of several of the aromatic signals and an X-ray crystal structure from DMSO/ CH_3CN showed the expected helical conformation.

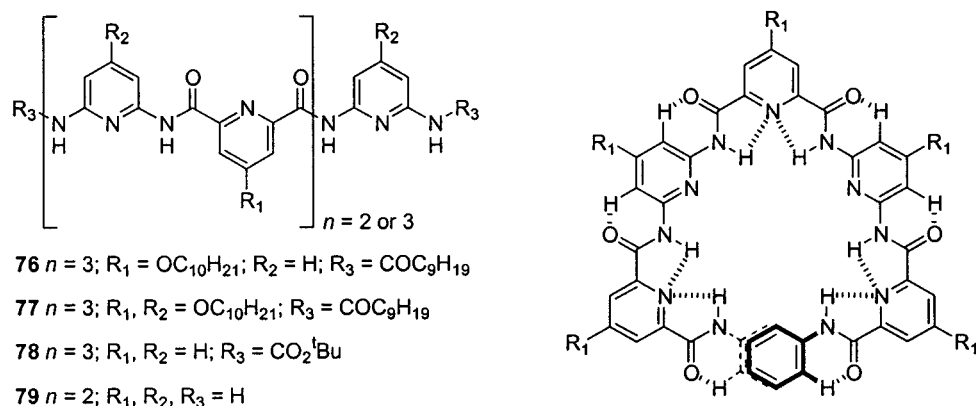


Figure 138. Series of oligo(pyridylamide)s capable of forming single- and double-stranded helices.

Concentration of samples of **76** in chloroform resulted in the generation of a second set of signals proposed to be a double-helical conformation.⁷⁹⁰ An exchange rate between monomer and dimer species was determined to be 8.7 s^{-1} at $25 \text{ }^\circ\text{C}$, and an association constant (K_{dim}) was measured by NMR spectroscopy to be $25\text{--}30 \text{ M}^{-1}$. A crystal structure of less soluble analogue **78** from nitrobenzene/heptane confirmed a double-helical conformation with an average aromatic–aromatic stacking distance of 3.5 \AA . From the X-ray crystal structure, it was concluded that the aromatic stacking between individual strands was responsible for stabilizing the dimer formation since most of the H-bonds were within the same strand and primarily stabilized the helical conformation of the individual chains. This is in contrast to ds-DNA, where aromatic stacking is responsible for intramolecular stabilization and H-bonding is responsible for intrastrand organization. This system was studied in various chlorohydrocarbon solvents, but no correlation existed between solvent polarity and double-helical stability. It was determined that the deleterious presence of water in these solvents competed with intermolecular H-bonding causing destabilization of the complex. The dimerization constant was determined to be $6.5 \times 10^4 \text{ M}^{-1}$. Molecular dynamics simulations revealed a possible folding pathway that involved rearrangement of a loose complex into the double-stranded conformation as well as the stability of the duplex on the time span of the simulation.

C. Helicates: Metal-Coordinating Foldamer Duplexes

1. Oligopyridines

As mentioned earlier in this review, oligopyridines have been thoroughly investigated for their ability to adopt helical conformations upon metal coordination (for reviews on this field, see refs 456, 457, 791, and 792). Thus far, only single-stranded helices from oligopyridines have been described. Yet, the same oligomers may adopt double-stranded helical conformations depending on the coordination metal ion employed. Although quaterpyridine (qtpy) oligomers adopt single-stranded helical conformations with a variety of metal ions, they complex with Cu(I) and Ag(I) in double-helical conformations.⁷⁹³ Double-

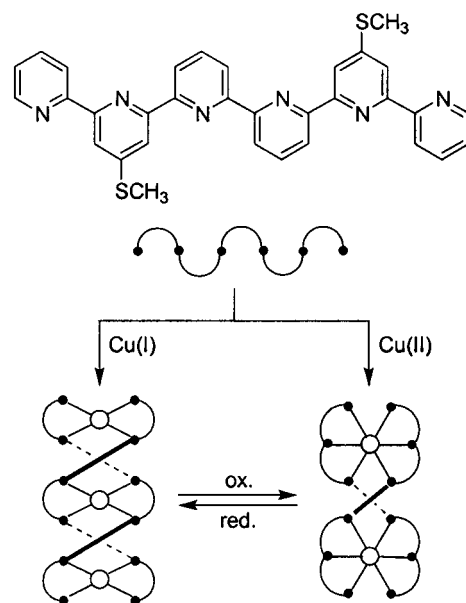


Figure 139. Formation of di- and trinuclear double-stranded helicates from a substituted sexipyridine ligand through supramolecular and electrochemical pathways.

stranded complexation is also possible with quinquipyridines (qpy) when complexed to Pd(II), whereas the shorter qpty associates with two Pd(II) ions in planar, single-stranded conformations.⁴⁶⁶ Crystal structures of sexipyridine complexes revealed a binuclear double-helix with Cd(II)⁴⁶⁶ but a trinuclear double helicate with Cu(II).^{466,475}

A systematic chain-length study of oligopyridines was undertaken using tpy,⁷⁹⁴ qtpy,⁷⁹⁵ qpy,^{795,796} sexipyridines (spy),⁷⁹⁶ septipyridines (septipy),⁴⁷⁰ and oligomers up to the decipyridine ($n = 10$). Alkanethiol side chains on oligomers promote solubility of the longer chains.⁷⁹⁷ Investigations on spy strands and their di- and trinuclear helical complexes were investigated with the goal of forming different metal coordination spheres both synthetically and electrochemically (Figure 139). Both the Cu(I) and Cu(II) helicates were synthesized discretely and converted from one to another by CV as evidenced by spectroelectrochemical analysis.⁷⁹⁶ In these longer oligopyridines, double-helical conformations are a result of the system maximizing coordination bonds and aromatic–aromatic stacking while minimizing the number of components in the assembly. When septipy oligomers are complexed to either Co(II) or Cu(II),

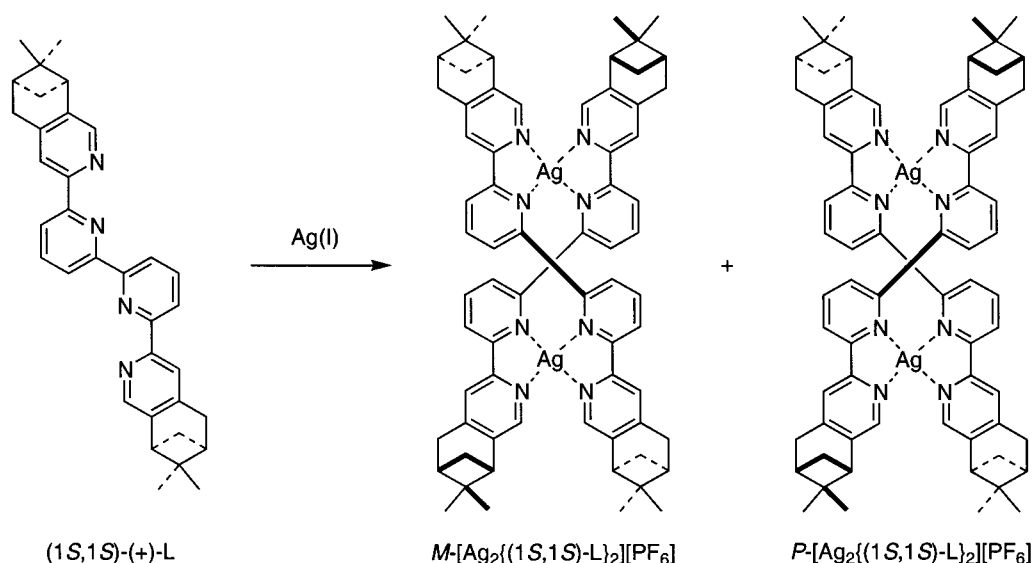


Figure 140. *M* and *P* helical conformations of double helicates from a dimer with a chiral ligand.

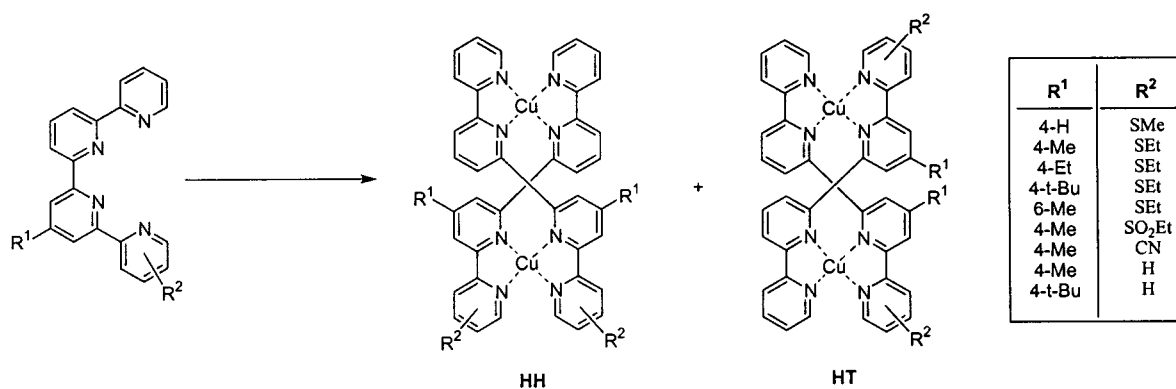


Figure 141. Head-to-head and head-to-tail conformations of double helicates from substituted qtpy ligands.

octahedral coordinations incorporate only six of the seven pyridines in the backbone, leading to strand slipping in solution.⁴⁷⁰ To design out this molecular motion, 1,3-phenylene monomers incapable of coordinating to the metal ions have been used to replace the central positions in qpy,⁷⁹⁸ spy,⁷⁹⁹ and septipy⁸⁰⁰ strands, thereby dividing the chain into localized coordinating segments. Alkynyl linkages have also been incorporated into oligopyridine backbones promoting helicate formation by maintaining the rigidity of the backbone while decreasing interstrand steric interactions.^{801,802}

Helicate duplexes incorporating symmetric oligomers do not possess strand directionality, unlike (3'→5') oligonucleotide duplexes. To enhance architectural control of these assemblies, the covalent attachment of chiral end groups, either through the incorporation of fused moieties or attachment through single bonds to terminal chain ends, has been explored. Qpty strands incorporating fused chiral (1*S*)-(-)- α -pinene end groups formed *M* and *P* helical complexes with Ag(I) (Figure 140).^{803–805} Diastereomeric excess in these complexes can shed light on the effect of interstrand steric interactions on the thermodynamics of helicate formation. It was found in CH₃CN that a 0.024:1.0 ratio (95.3% de) of complexes formed. Upon crystallization, only the major isomer was isolated which was identified as the *P* helix. The

(1*R*,1*R*)-(+)- α -pinene-terminated strand was also synthesized and proved to form the *M* helicate after crystallization. The origin of selectivity arose from interactions of the pinene end groups with the pyridine ligands in the backbone. Additionally, the Cu(I) helicates from this ligand formed in solution with 98.7% de, and after crystallization, again only the *P* helix was isolated. Qpty strands with thioethyl side chains and a methyl end group at the 4'-position were reacted with Cu(I) to produce a 3:2 mixture of the head-to-head (HH) and head-to-tail (HT) configurations, as evidenced by ¹H NMR (Figure 141).⁸⁰⁶ Variation of the side chain and the end group by systematically incorporating bulkier groups at these positions revealed no increased selectivity when groups such as ethyl or *tert*-butyl were employed as the end group while the thioethyl side chain remained.^{807,808} In the absence of a side chain, the *tert*-butyl-terminated quaterpyridine helicate formed the parallel HH configuration exclusively. All other cases resulted in a mixture of HH and HT with the HH configuration preferred. It was speculated that this preference was dependent on the electronic character of the side chain and the resulting helical pitch due to steric interactions between intrastrand substitutions at either the side chain or end group. Constable and co-workers^{809–811} utilized a terpyridine ligand coupled to (1*S*)-(-)-borneol at one terminus to impart

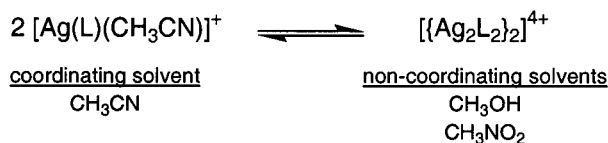
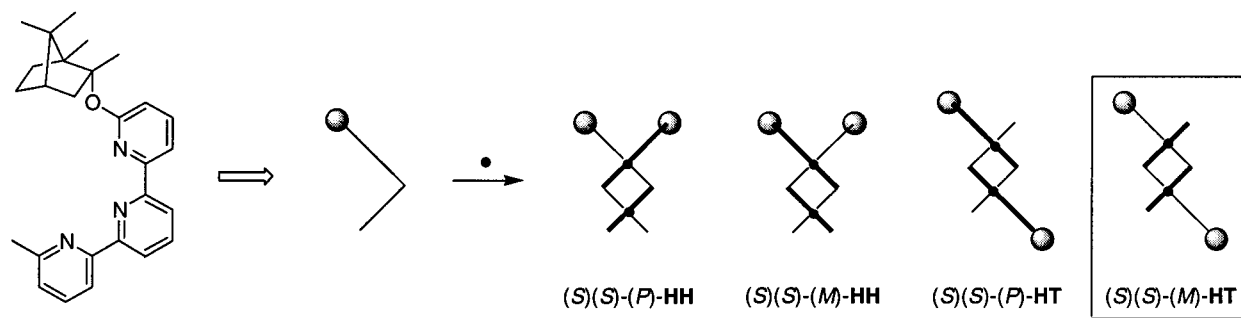


Figure 142. Solvent effects on the formation of helicate structures from a terpy strand. Head-to-tail double-stranded helicates obtained from borneol-terminated terpy ligands.

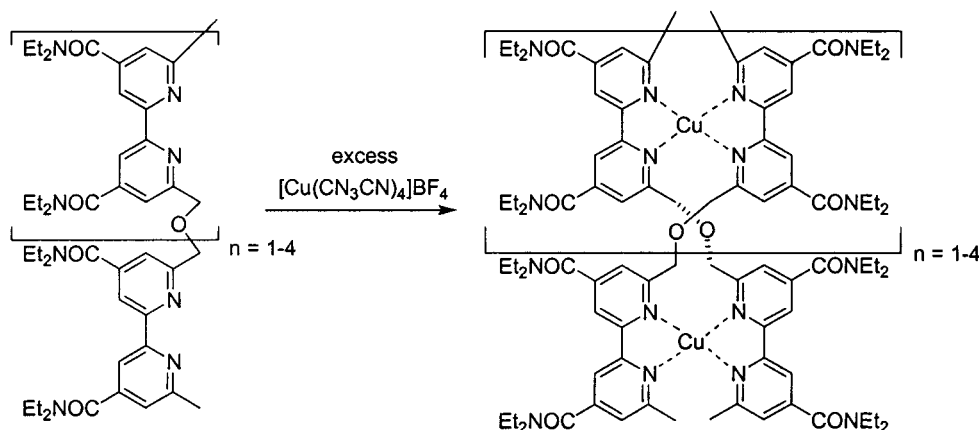


Figure 143. Formation of double-stranded helicates from bipyridine oligomers.

asymmetry in the helicate complex (Figure 142).⁸⁰⁹ Since this strand lacks a C_2 -symmetric axis, four possible helicate isomers may be realized. Molecular modeling studies revealed that the HH isomers are much higher in energy due to steric repulsion of the borneol units. Reaction of the ligands with $[\text{Cu}(\text{MeCN})_4][\text{PF}_6]$ formed a 6.5:1 ratio of two unidentified components in CH_3CN by ^1H NMR, presumably the two diastereomers of the HT configurations. Crystallization of this mixture produced only the major isomer, which was shown to be the $(S)(S)$ - (M) -HT by X-ray analysis. It is unclear why the M helix was favored over the P helix. With $\text{Ag}(\text{I})$, the equilibrium between the mononuclear complex and the dinuclear helicate could be shifted by the choice of solvent.⁸¹⁰ Acetonitrile solutions favored the mononuclear complex through competitive solvent coordination, while less coordinating solvents such as methanol and nitromethane favored the helical duplex, as confirmed by both ^1H NMR and CD.

2. Linked Oligopyridines

a. Ether-Linked Oligopyridines. The incorporation of flexible linkages within the backbone provides

oligopyridine-based chains that can adopt ideal, less constrained coordination geometries within helicate assemblies. One of the most thoroughly investigated systems involves the incorporation of methyl(methoxy) ether linkages between bipy or terpy segments. Initial chain-length studies showed these modified oligomers of varying length ($n = 3-5$) form homostranded helicates with $\text{Cu}(\text{I})$ ⁸¹² (Figure 143) and $\text{Ag}(\text{I})$ ⁸¹³ in CH_3CN .⁸¹⁴ To investigate self-recognition selectivity, a mixture of 2 equiv of the dimer, 1 equiv of the tetramer, and 3 equiv of $\text{Cu}(\text{I})$ produced only the homostranded complexes, demonstrating the preference for homostranded complexation.⁸¹⁵ Furthermore, a mixture of all four oligomers, upon addition of $\text{Cu}(\text{I})$, also formed only the homostranded double-helical structures after reaching equilibrium. Given the lack of heterostranded complexes, this system demonstrates length dependence and multinuclearity matching in the self-recognition process. This example further reveals the sensitivity of the association to alignment mismatches. Self-organization in the assembly of these strands has been shown to be cooperative.^{816,817} The attachment of thymine-nucleoside side chains to these oligopyridine strands produced a double helicate with nucleosides extend-

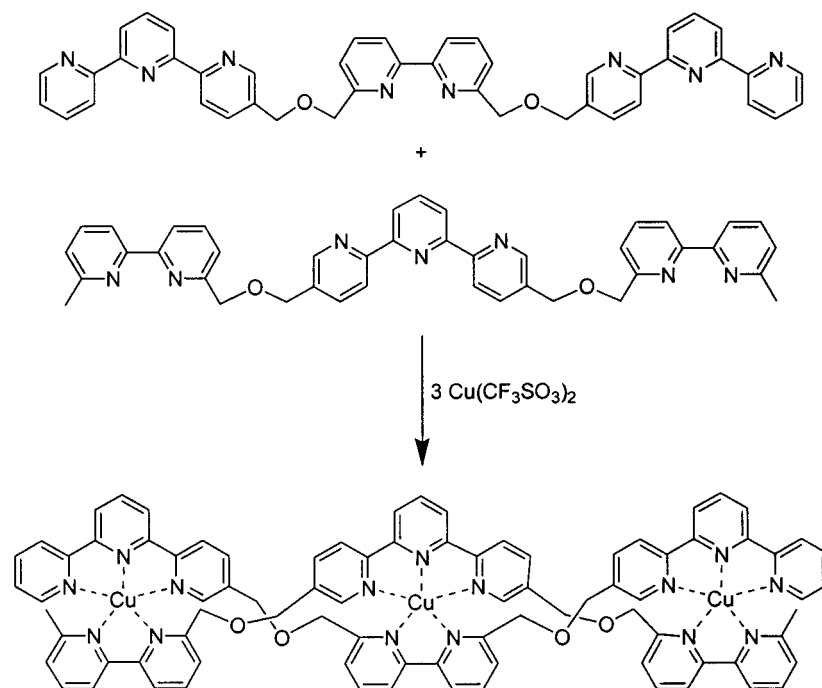


Figure 144. Heterostrand heterotopic double-stranded helicates from tpy-bipy-tpy and bipy-tpy-bipy trimers.

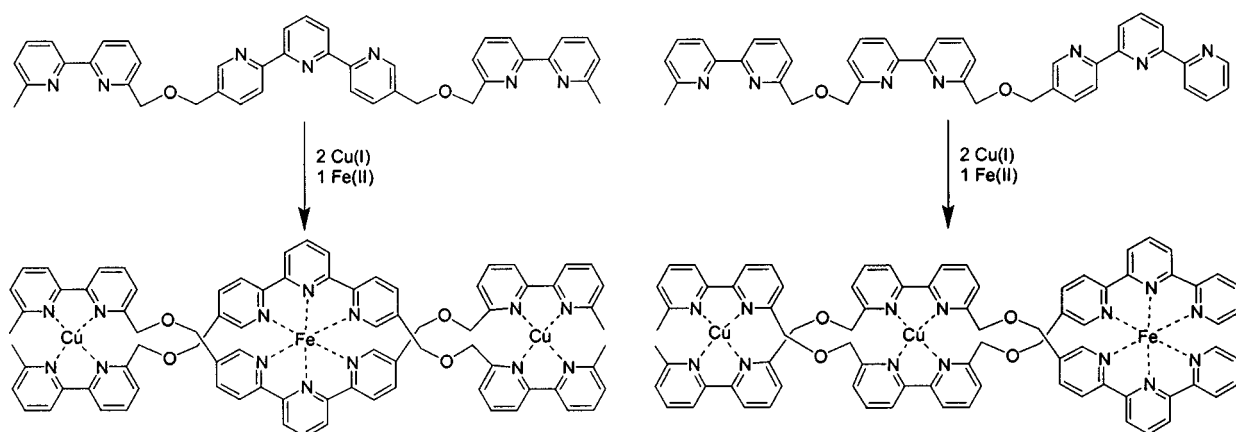


Figure 145. Heteronuclear double-stranded helicates from trimers incorporating bipy and tpy ligands.

ing out from the ionic interior,^{818,819} an architecture similar to one once proposed as the structure of DNA.⁸²⁰

A variety of heteromeric oligopyridine-based strands have been synthesized and complexed into helicates to assess the impact of non-bipy ligands on self-assembly. Two trimeric oligomer strands incorporating a bipy-tpy-bipy and a tpy-bipy-tpy oligomer were generated and complexed with pentacoordinate-preferring Cu(II) ions (Figure 144).⁸²¹ Only the heterotopic, heterostrand helicate was obtained after crystallization. These structures are reminiscent of DNA base matching in that the two separate strands encoded with complementary ligands form into a single complex through segment matching. Upon addition of 2 equiv of Cu(I) and 1 equiv of Fe(II), both bipy-tpy-bipy and bipy-bipy-tpy oligomers formed homostrand, heteronuclear helicates (Figure 145). Phen segments, having similar structure and denticity to bipy but lacking torsional flexibility, have also been incorporated into these oligomers, and double-stranded helicates were formed from Cu(I), Ag(I), and Zn(II) (Figure 146).⁸²² A more

systematic look at bipy/phen mixed trimers involved the synthesis of bipy₃, bipy-phen-bipy, phen-bipy-phen, and phen₃ trimers complexed with Cu(I) and Ag(I) (Figure 147).⁸²³ The homooligomeric phen sequence formed a double-stranded helicate with Cu(I), although a mixture of helicate complexes resulted upon addition of Ag(I). An excess of Ag(I) shifted the equilibrium toward the double-helical complex completely. The heterotopic strand of phen-bipy-phen formed double-stranded helicates with both Cu(I) and Ag(I), indicating that the central unit in the ligand may influence the stability of the helicate through steric interactions.

To probe heterostrand helicate formation, mixtures of these four ligands under helicate-forming conditions were tested (Figure 148). It was found that whether the ligands were mixed prior to ion addition or helicate solutions were mixed together, the heterostrand helicates were thermodynamically favored providing statistical (1:2:1) helicate distributions. Further investigation into the role of the central unit in double-stranded helicates from trimers allowed determination of binding affinity by cyclic voltam-

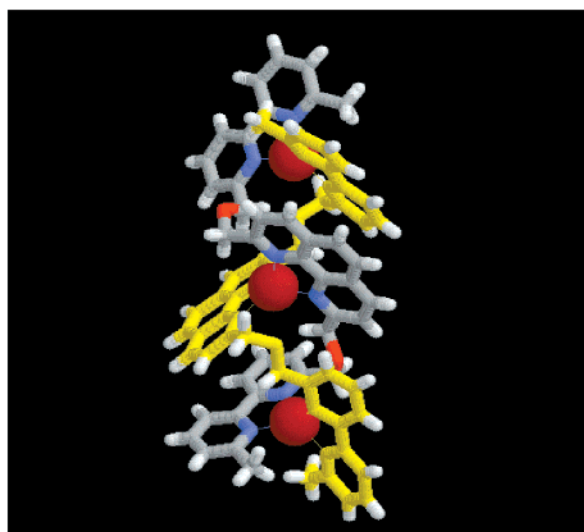
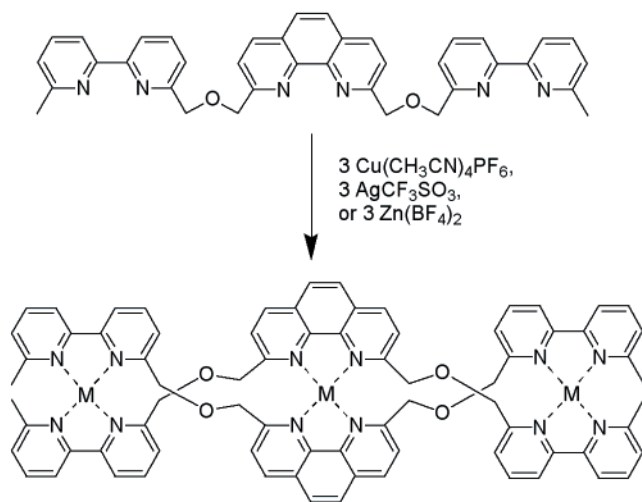


Figure 146. Homotopic helicates from a bipy-phen-bipy trimer. The crystal structure of the Cu(I) complex is shown.⁸²²

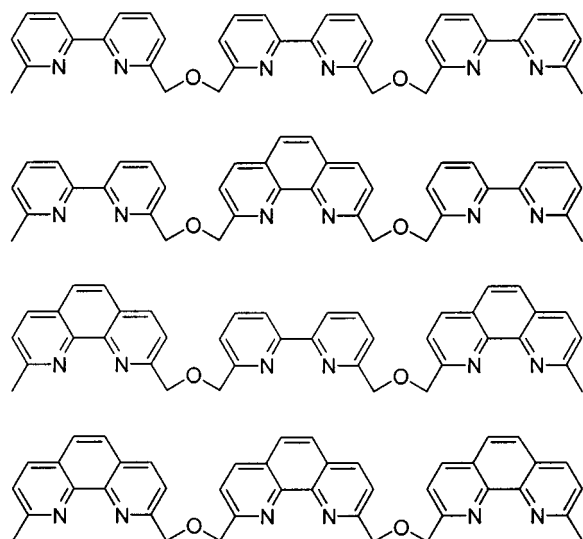


Figure 147. Four trimers consisting of bipy and phen segments.

metry for a series of four different ligands.⁸²⁴ It was found that the central phenanthroline unit in a trimeric ligand binds to Cu(I) 10 times more strongly than a bipy unit and 10^6 times more strongly than a

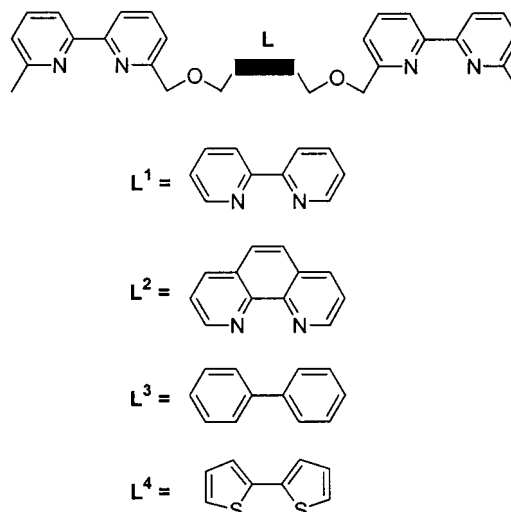


Figure 148. Four trimers consisting of bipy-L-bipy segments.

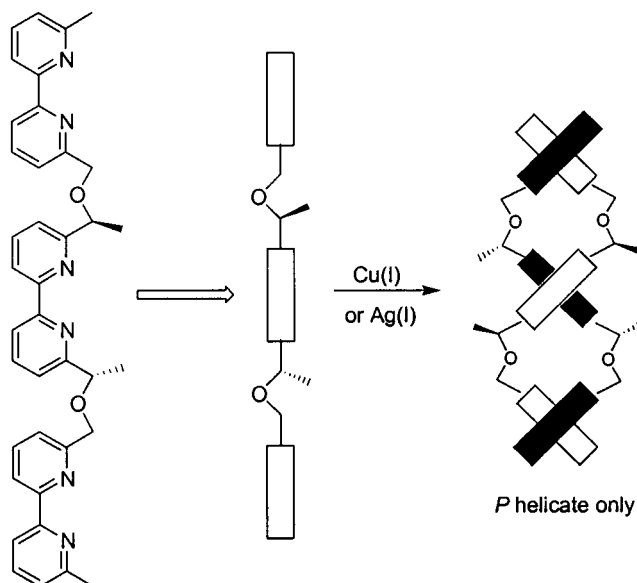


Figure 149. *P* double-stranded helicate from a bipy trimer incorporating stereogenic centers within the linkers.

bithiophene unit. Self-recognition in these ligands was demonstrated by mixing the bipy with either bithiophene- or phen-containing oligomers, where only the homostanded helicates were obtained. However, a mixture of the phen- and the bipy-containing oligomers produced homo- and heterostanded helicates in a statistical 1:2:1 distribution. These results suggest that the Cu(I) ion preferentially binds to two weaker chain segments (bithio) rather than one strong and one weak one. From these investigations, sequence matching in heterotopic helicate formation emerges as an approach to encoding helicates with structural information in recognition processes.

The linked oligopyridine-based foldamers described thus far lack any asymmetric functionalities able to shift the *P* and *M* helical equilibrium. The first report attempting to bias the twist sense of a helicate involved chiral ether linkages to a bipy₃ strand (Figure 149).⁸²⁵ When these oligomers were complexed with 3 equiv of either Cu(I) or Ag(I), only the *P* helicate was obtained. In this conformation, the

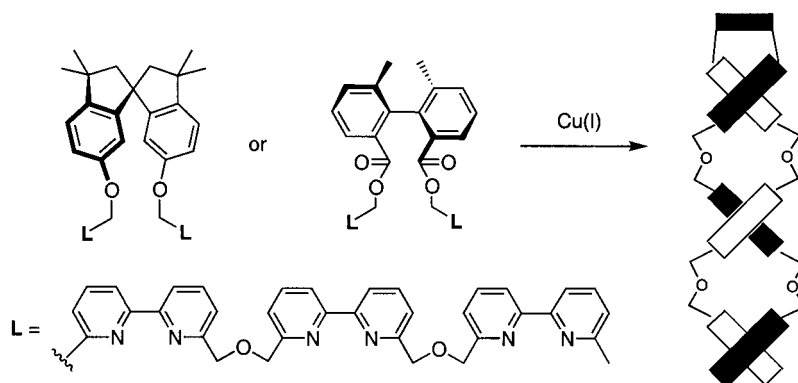


Figure 150. Bipy trimers tethered by chiral bridges.

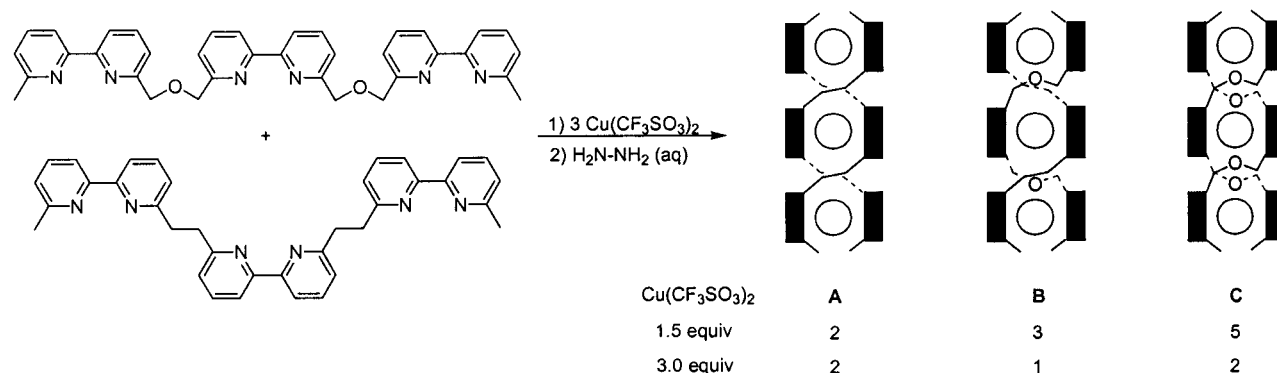


Figure 151. Homo- and heterostranded helicates from two different bipy strands.

methyl groups extend outward to minimize steric repulsions. Rigid, chiral bridges such as spirobisindanol or dimethylbiphenic acid, tethering two bipy₃ oligomers, can effectively bias the twist sense of a Cu(I) helicate by dictating the absolute configuration of the strands through more rigid constraints (Figure 150).^{826,827}

b. Alkyl-Linked Oligopyridines. With the success of the ether-linked bipy helicates, other linkages involving ethyl- and ethylene-linked bipy trimers were explored.⁸²⁸ Oligomers incorporating the alkene spacer did not produce a discrete double-stranded helicate with Cu(I) as evidenced by ¹H NMR, due to the lack of flexibility in the backbone. On the other hand, the ethyl-linked strands were effectively incorporated into the complex. An imine linker has also been utilized to form double-stranded helicates with Cu(I) and Ag(I).⁸²⁹ When the alkyl- and ether-linked oligomers were mixed under helicate-forming conditions to test for recognition, a mixture of homo- and heterostranded complexes was formed in a ratio of 2:2:1 (Figure 151). At equilibrium, the homostranded helicate is favored over the heterostranded helicate, deviating from the statistical distribution, presumably due to the electrostatic attraction between the oxygen and Cu(I) ions and the lower flexibility of the ethyl linker. Furthermore, ethyl-linked bipy₃ strands formed triple-helical complexes with Ni(II),⁸³⁰ while ethyl-linked tpy₃ complexed with Fe(II) produced double-stranded helicates,⁸³¹ where both complexes formed through octahedral coordination geometries. To test the self- vs nonself-recognition selectivity between the ether and alkyl bipy strands, Cu(I) and Ni(II) were added to a mixture of these two oligomers (Figure 152).⁸¹⁵ These trimers self-assembled

into two discrete homostranded helicates: a double-stranded, tetrahedral Cu(I) complex with the ether-linked strand and a triple-stranded, octahedral Ni(II) complex incorporating the alkyl-linked strand. No heterostranded species were observed by ¹H NMR or ESI-MS. Here, the end groups of the strands, as well as the nature and length of the linker group between the ligands endow the oligomer with structural information that directs the self-assembly process. The power of self-recognition processes in the formation of highly organized structures is clear in this case: 11 chemical components of four types (two organic oligomers and two transition-metal ions) combine to form two discrete supramolecular species. At the same time, the ether-linked bipy₃ and the ethyl-linked tpy₃ oligomers formed a heterostranded helicate which was able to form through complexation with Cu(II) (Figure 153).⁸³² Although the Cu(II) ion prefers a pentacoordinate geometry, trigonal bipyramidal and square pyramidal coordination are both possible. In this case, the central copper coordination adopted a trigonal bipyramidal geometry while the terminal ends of the strands coordinate to the terminal copper through square pyramidal orientations as evidenced by X-ray analysis. This occurs since the steric demands at the termini are not as stringent as the central segments.

When the ethyl-linked bipy₃ oligomer was combined with an equimolar quantity of FeCl₂ in ethylene glycol at 170 °C, a pentameric circular helicate was exclusively produced (Figure 154).⁸³³ This complex is believed to form from templation by the Cl⁻ counterion. Further investigations into this system with a variety of counterions revealed a second

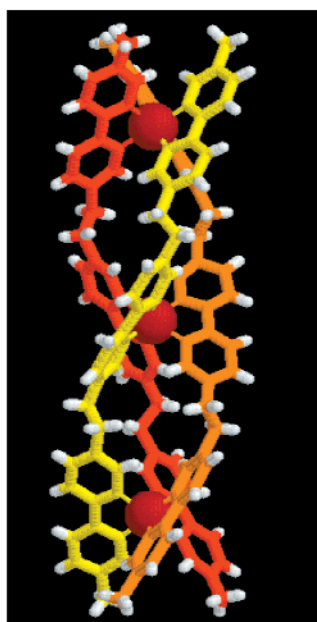
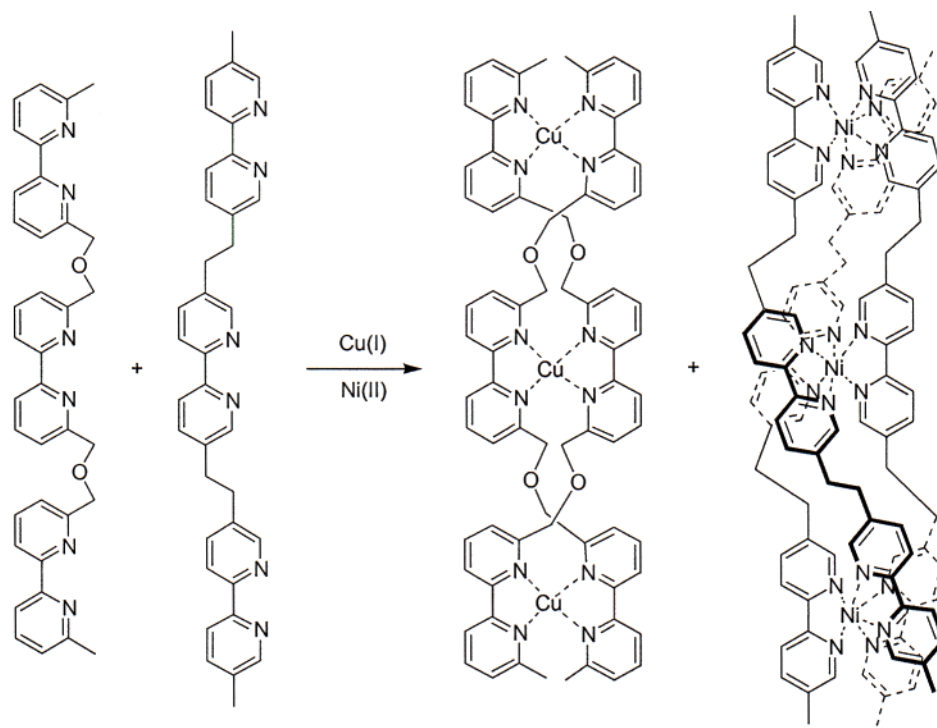


Figure 152. Formation of only homostranded helicates from a mixture of two different bipyridine trimers. Crystal structure of the Ni(II) triple-stranded helicate with the alkyl-linked trimers is shown.⁸⁷⁸

circular helicate, the hexameric complex, in which the counterion is believed to also bind in the central cavity.^{834,835} When a hexanuclear circular helicate prepared using FeSO_4 was heated in the presence of Cl^- , ^1H NMR and ES-MS analysis revealed the shift to the pentameric circular helicate exclusively. This indicates that the Cl^- ion can selectively template the pentameric assembly from the equilibrating mixture of complexes. Investigations into the mechanism of this circular helicate formation revealed that the kinetic product of this reaction is the linear triple-stranded helicate, which over the course of 24 h reassembles into the thermodynamic product, the pentameric circular helicate.⁸³⁶ Similar results were obtained with the use of NiCl_2 under conditions that

accelerated the dissociation of the metal complexes. In this case, a 2:1 ratio of the circular vs the linear Ni(II) species was obtained after a period of 4 days, at which point strand decomposition became a factor. Hence, the additional flexibility of the alkyl linkage within the backbone provides the torsional freedom in the chain necessary to adopt a variety of conformations within the various helicate complexes.

3. Pyridine Analogues

A variety of helicates incorporating pyridine-based analogues have been described in the literature including methylene-linked benzimidazoles⁸³⁷ and their derivatives,^{838–840} bis(phenyloxazoliny)pyridines,^{841,842} bis(pinene-bpy) ligands,⁸⁴³ and bis-imino-

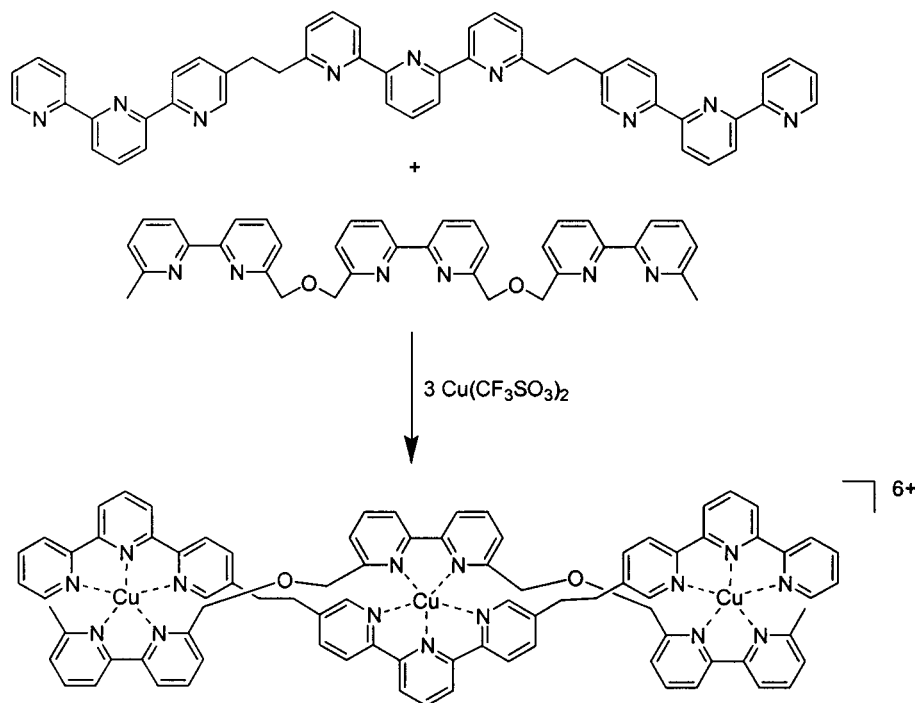


Figure 153. Formation of heterostranded helicates from a bipy trimer and terpy trimer.

quinolines.^{844,845} While these ligands effectively form helicates with a variety of metal ions, we do not consider them as foldamers since it is difficult to envision how their chain lengths may be easily extended, a similar criteria that was used for ruling out many of the receptor systems. Since they do not satisfy our criteria for foldamers, we will not discuss them further (some of these systems have been discussed in recent reviews⁴⁵⁷). However, dipyrromethene oligomers, structurally isomorphous to the phytychromobilins,⁸⁴⁶ have been recently shown to form double-stranded helicates with Zn(II) and Co(II), where a hexameric strand complexes to Zn(II) in a 3:2 ratio (Figure 155).⁸⁴⁷ The oligomers have also been extended to incorporate alkyl spacers of varying length.^{848,849}

4. Catecholates

Catecholates also have the ability to form helicates when complexed to gallium and titanium metal ions.^{455,457} Investigations into the effect of spacer length (and the distance between the metal ions) on self-recognition were conducted with catecholamide ligands.⁸⁵⁰ Ditopic ligands with three different aromatic spacers were synthesized and complexed with Ga(III) to form triple-helical structures (Figure 156). A 1:1:1 mixture of the three ligands with Ga(III) provided only the homostranded helicates as evidenced by ¹H NMR and ESI-MS. The authors argue that the self-recognition process is a combination of effects whereby the helicate structure is favored over polymeric structures due to an entropic driving force disfavoring the polymeric structure, the rigid spacers disfavoring heterostranded helicate formation, and the presence of an energetic drive to fully saturate the coordination sphere of Ga(III). In this mixture, the lack of flexibility in the spacer promotes formation of only the homostranded helicates, since spatial

mismatching could only be compensated by higher order strand incorporation. Variable temperature ¹H NMR studies revealed a dynamic rearrangement involving a twist sense reversal within these triple helicates wherein one or more strands pass through a *meso* state in which the strands adopt a parallel, fully extended conformation.^{851,852} Related dimeric catecholamides form triple-helical complexes with either Ti(III) or Ga(III). Yet, upon the addition of Me_4N^+ , these complexes are interconverted to a tetrahedral cluster in order to provide the necessary cavity space to accommodate the cationic guest (Figure 157).^{853,854}

Self-recognition processes have also been demonstrated to coincide with template-driven helicate formation.⁸⁵⁵ Dimeric catechol-derived strands, previously shown to bind Li^+ ^{856,857} or Na^+ ⁸⁵⁸ within triple-stranded helicates, were synthesized with methylene and ethylene spacers, and the mixtures were coordinated to “Ti(IV)” in the presence of different carbonate bases to form triple-stranded helicates. When the helicate was prepared using Na_2CO_3 , only the homostranded species were observed. Upon addition of Li_2CO_3 , both homostranded species were observed along with a heterostranded species (2 methylene + 1 ethylene strand). When K_2CO_3 was used, the ethylene strands formed dinuclear helicates while the methylene bridged ligands formed indistinguishable higher oligomeric species. Interestingly, when 1:1 mixtures of the bases were utilized, only the homostranded helicates formed. It is worth mentioning that a nonaromatic backbone has also been incorporated into a double-stranded helicate.⁸⁵⁹

D. Multistranded Receptors

Foldamer duplex receptors that assemble through multimodal interactions have been developed in order to generate supramolecular host assemblies for

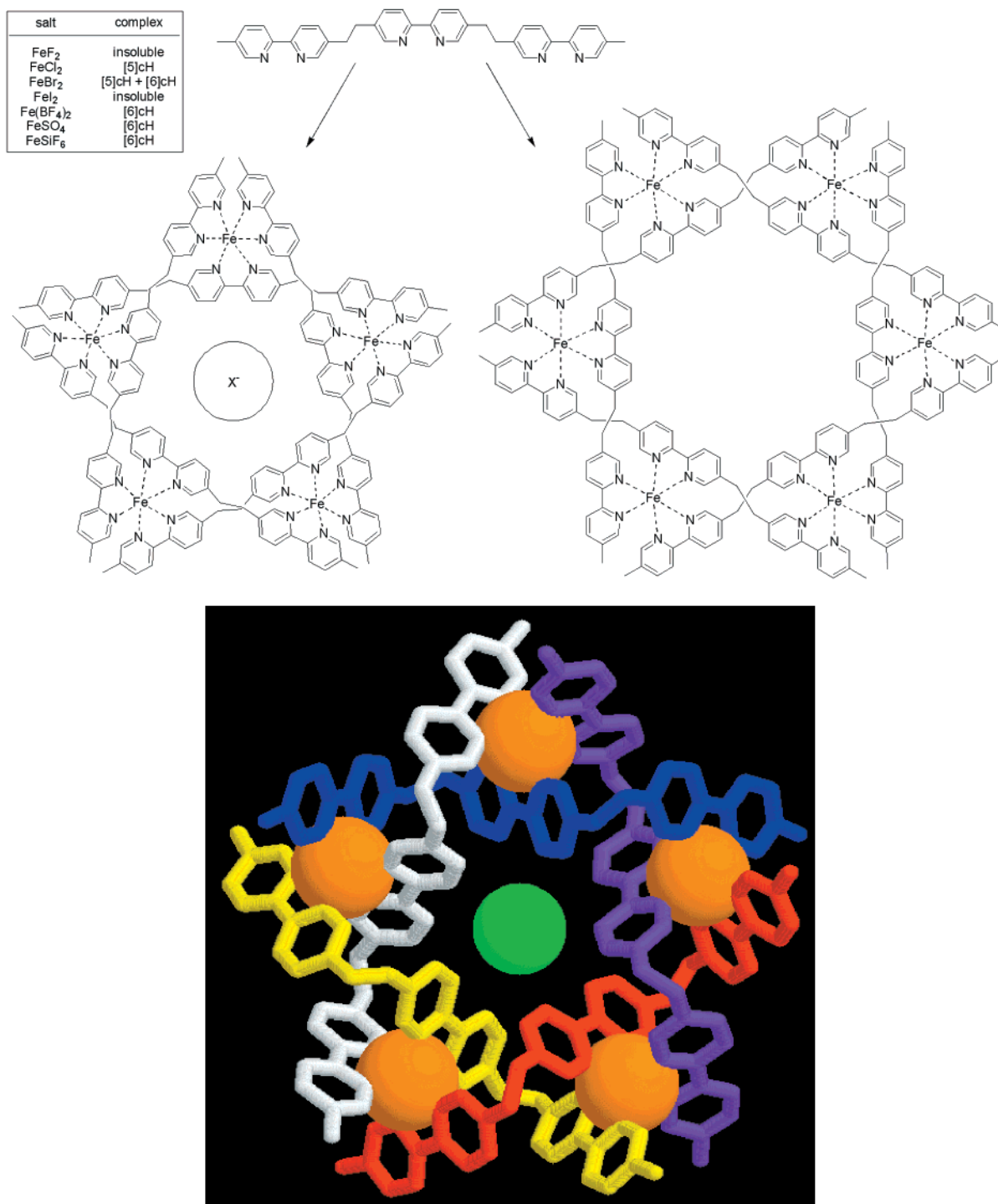


Figure 154. Penta- and hexameric cyclic helicates formed through host–guest templation. The crystal structure of the pentameric complex is shown.

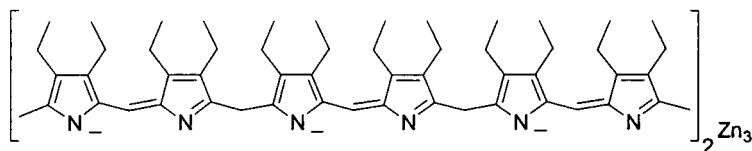


Figure 155. Dipyrromethene double helicates.

molecular recognition of small organic guests.^{114,860} This has been accomplished through the use of heterotopic strands with metal-coordinating ligands and D/A segments such that self-assembly occurs through multiple, noncovalent interactions between

two oligomer chains, a metal ion, and an organic guest. In this way, the metal-coordinating segments are conformationally restricted in the complex while the D/A segments have the torsional flexibility to potentially accommodate structurally diverse guests.

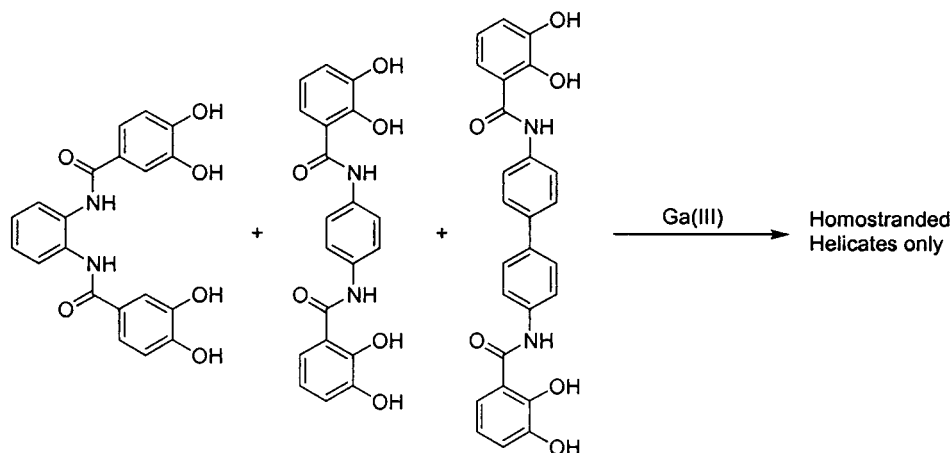


Figure 156. Homostranded helicates from catecholate strands with three different spacers.

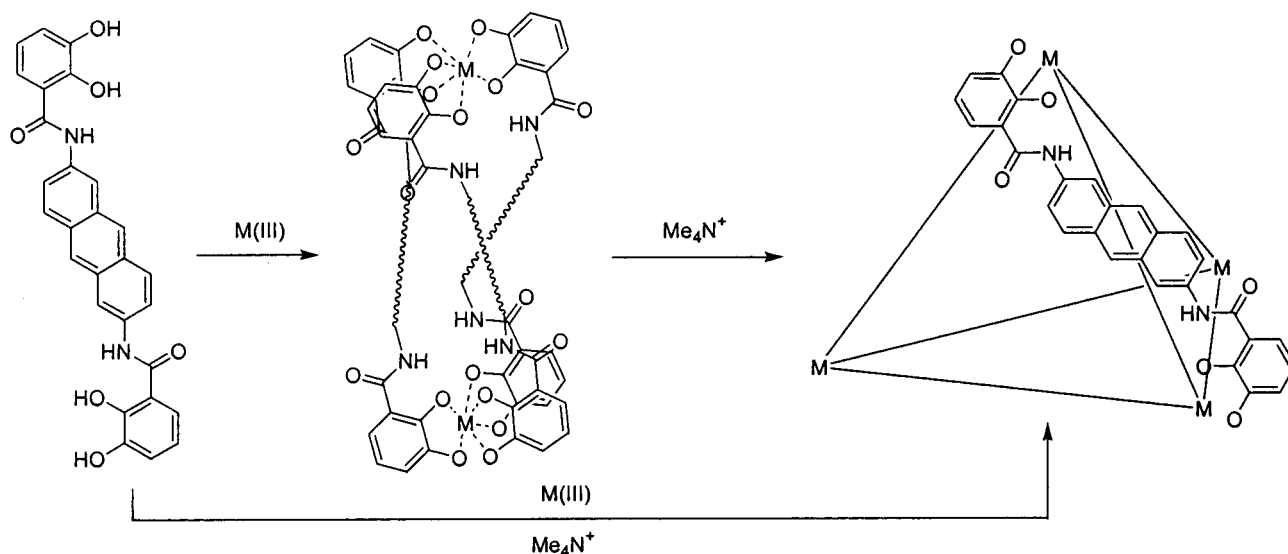


Figure 157. Formation of a triple-stranded helicate and a tetrahedral cluster from catecholate dimers.

These architectures are more commonly referred to as artificial receptors while at the same time fitting under the categorization of foldamer duplexes since they adopt their unique conformations through these noncovalent interactions and form similar architectures as described in the previous two sections on multistranded abiotic foldamers.

In a series of experiments aimed at guest-induced equilibrium shifting of metal-coordinated assemblies, bis(carboxamidobipyridine) ligands with ^tBu **80** (R = Me or H) and with DAD H-bonding caproylpyridyl **81** (R = Me or H) peripheral groups were complexed with Cu(I) and Pd(II) ions to form double-stranded, tetracoordinate complexes (Figure 158).⁸⁶¹ Through the addition of complementary (ADA) guests with varying degrees of flexibility (**82–86**) in the presence of **80** and **81** (both R = Me), a shift in the equilibrium from the **80:80** to the **81:81** complex was promoted through H-bonding in the guest assembly. Guests **82** and **84** are rigid, while **83**, **85**, and **86** have various numbers of single bonds, which increases their torsional flexibility. With 0.5 equiv of Cu(I), **80** (1 equiv) and **81** (1 equiv) formed distorted tetrahedral complexes in chloroform, and by ¹H NMR, the degree of uncomplexed ligand was determined to be 27% of **80** and 73% of **81**. Upon addition of **82**, **83**,

84, or **85**, no shift in the equilibrium was observed though shifts in the NMR indicated H-bonding interactions between **80** and the guests. However, with the addition of **86**, the proportions of the free ligands were shifted to 48% of **80** and 52% of **81** through simultaneous H-bonding between two strands and this bridging guest. When similar Pd(II) complexes formed with **80** and **81** (where R = H) in 5% DMSO in CHCl₃, a square-planar coordination geometry arranges the strands in a coplanar orientation, thereby suggesting a planar, rigid guest could possibly shift the equilibrium toward the host–guest assembly. Binding of the guest shows the ability of each guest to enhance the formation of complexes, as indicated by the proportions of ligands involved in complexes determined by ¹H NMR. Guest **82** is capable of concurrently H-bonding to each strand and stabilizing the **81:81**:Pd(II) complex (even enhancing the shift at lower temperatures).

E. Foldamer–Oligomer Interactions

As the final section of this review, we wish to present more advanced examples of foldamer architectures that lay the foundation for the development of backbones capable of homo- or heterostranded foldamer–foldamer interactions seen with natural

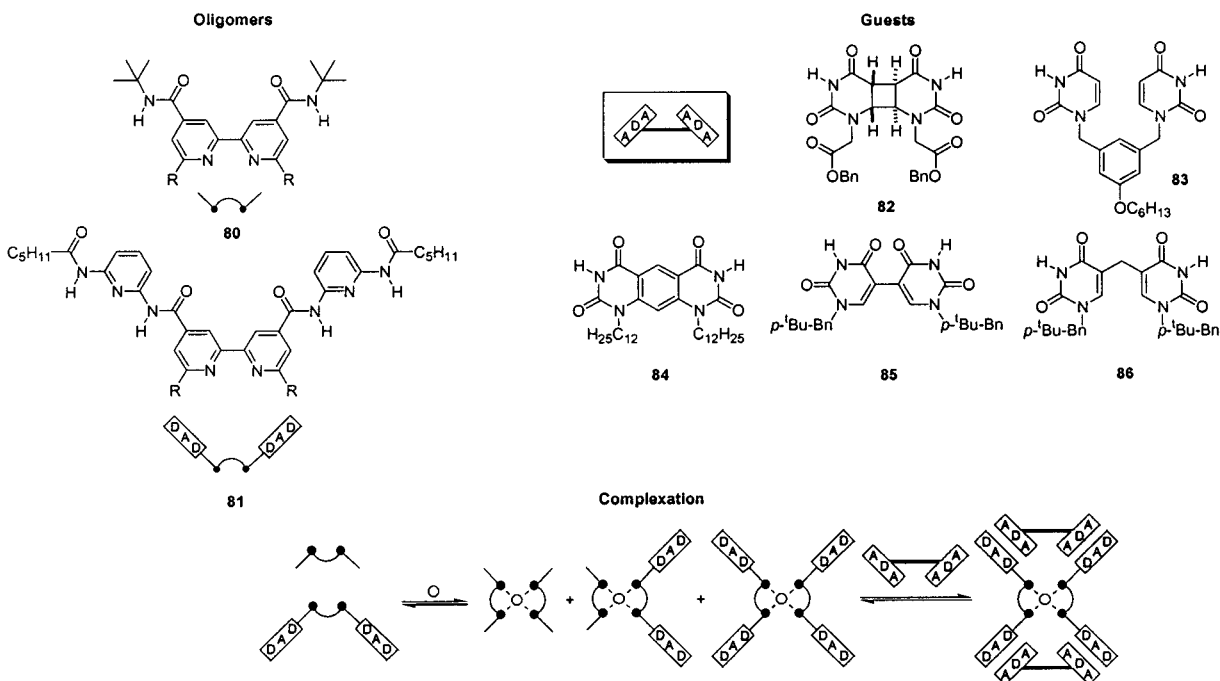


Figure 158. Multistranded receptor formation through H-bonding and metal coordination.

systems (i.e., protein–protein or protein–DNA interactions). This requires two structurally different backbones to associate through recognition processes embedded in the surfaces of their folded conformations. To date, natural systems that adopt secondary structures and *template* the association and folding of small oligomers (or segments of homomorphous backbones) have only been accomplished. These are best described as foldamer–oligomer interactions and provide insight into this next step within the foldamer field.

1. Minor Groove Binding Oligomers

Major groove binding of oligonucleotide variants through triplex formation has been discussed in terms of stability and sequence selectivity. The folding reaction considered here is one in which complexation induces conformational order in an unstructured oligomer. Yet, no nonnucleotidomimetic foldamers have been demonstrated to target the major groove,⁸⁶² suggesting the potential of this unexplored area. However, the minor groove of DNA duplexes offers crucial sites for noncovalent supramolecular recognition, as demonstrated by recent X-ray crystal structures of DNA polymerase:ds-DNA complexes.^{863–865} Although studies aimed at elucidating protein–oligonucleotide interactions are currently being investigated with nucleotidomimetics,^{866–868} we limit our discussion here to members of the lexitropsin and duocarmycin antibiotics, which have shown considerable progress in adapting these systems for more complex sequence recognition.

a. Lexitropsins. The lexitropsin class of natural oligo(*N*-methylpyrrolicarboxamide)s, isolated from *streptomyces* strains,⁸⁶⁹ binds in the minor groove of duplexed DNA through a combination of van der Waals' contacts, H-bonding, hydrophobic, and electrostatic interactions. Distamycin-A is a crescent-shaped, amide-linked *N*-methylpyrrole oligomers with

guanidinium and formyl termini that shows preferential binding to AT-rich sequences in 1:1 and 2:1 stoichiometries with ds-DNA (in antiparallel orientations) (Figure 159). NMR studies have determined that in a distamycin-A:d(CGCGAATTCGCG)₂ complex, two of the pyrroles (Py) remain planar while the third ring rotates to conform to the minor groove twist.⁸⁷⁰ The first chain-length studies ($n = 1–6$) on modified distamycins effectively demonstrated the ability to extend the minor groove sequence recognition of small oligomeric molecules.^{871,872} Through incorporation of imidazoles (Im)⁸⁷³ and hydroxypyrrroles (Hp)⁸⁷⁴ into lexitropsin oligomers, pairing rules for minor groove binding have been ascertained: Py/Im targets C–G, Py/Hp targets A–T, Hp/Py targets T–A, and Im/Py targets G–C.⁸⁷⁵ Since lexitropsin backbones cannot effectively coil around oligonucleotide duplexes at chain lengths higher than five, incorporated β -alanine units add flexibility to the oligomer and also enhance sequence recognition.⁸⁷⁶ Linking of lexitropsin oligomers by γ -butyric acid tethers allow the 2:1 binding mode to become a unimolecular process, thereby enhancing affinity by ca. 100.⁸⁷⁷ A single substitution of imidazole for pyrrole in a lexitropsin hairpin structure showed a decrease in affinity of 2 orders of magnitude, demonstrating the efficient mismatch discrimination in these oligomers.⁸⁷⁸ This field has expanded exponentially, primarily due to the work of the Dervan group, since the development of solid-phase synthetic methodologies.⁸⁷⁹ Since this field has been thoroughly reviewed elsewhere,^{875,880–883} here we only mention the lexitropsins to draw their connection to the field of foldamers; that is, they adopt their unique conformations by undergoing a folding reaction through complexation with the ds-DNA minor groove. Hence, conformational stability is derived by intermolecular noncovalent interactions.

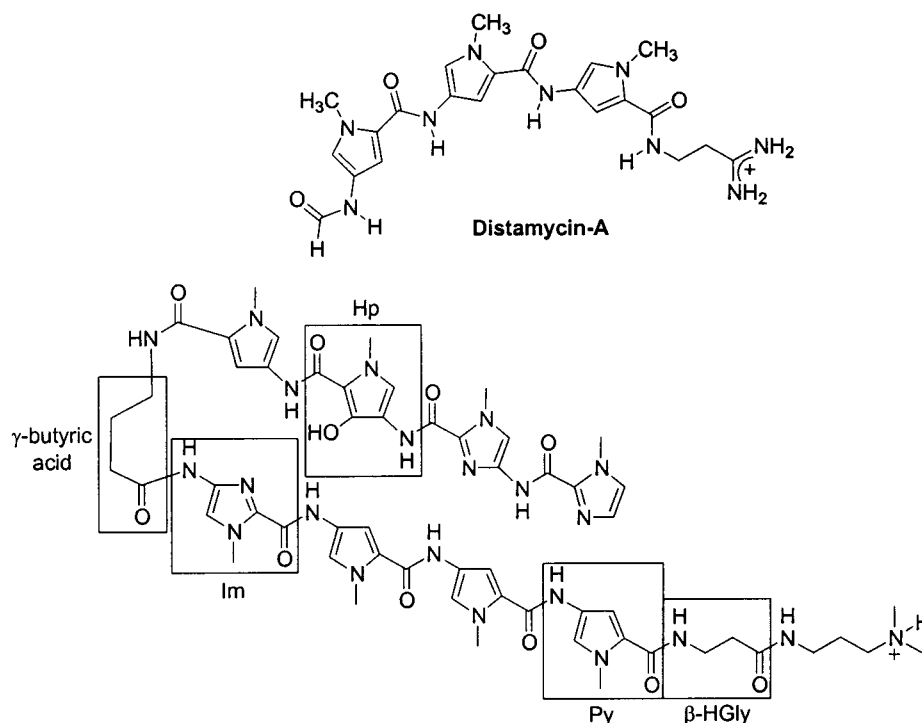


Figure 159. Chemical structure of distamycin-A and an oligomeric analogue.⁸⁷⁵

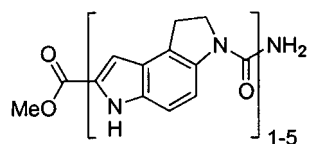


Figure 160. Series of homooligomeric (+)-CC-1065 analogues used to probe the minor groove binding of duocarmycin.

b. Duocarmycins. (+)-CC-1065, isolated from *Streptomyces zelensis*,^{884,885} and the related duocarmycins are a thoroughly investigated class of potent antitumor antibiotics.^{886–889} Their cytotoxic activity occurs from an alkylation of adenine via an adenine-N3 ring-opening S_N2 attack on the cyclopropapyrroloindole (DSA) when bound in the AT-rich nucleotide stretches of the B-DNA minor groove.^{886,887,889} These agents are concave, relatively planar molecules⁸⁹⁰ capable of penetrating the deep and narrow minor groove of an AT-rich complex for alkylation by adopting a conformation that extends along the 5'→3' DNA backbone.^{891,892} Duocarmycin analogues aimed at elucidating the structural origin of the sequence-selectivity and noncovalent binding focused on the generation of homooligomers ($n = 1–5$) to mimic the properties of (+)-CC-1065 (Figure 160).^{893,894} Thermal incubation and denaturation studies of an oligomer series with poly(dA):poly(dT) under approximate physiological conditions revealed increased binding affinity at higher chain lengths, though the kinetic accessibility decreased with increasing length due to the higher entropic costs of organizing longer chains. Initial complexation of the tetramer with ds-DNA associated through a dimeric segment, followed by a much slower rearrangement to the fully complexed conformation, consistent with high-energy rotational barriers predicted by molecular modeling. The most optimal agent for minor groove complexation was the

five base-pair spanning trimer, effectively combining favorable kinetic and thermodynamic properties. This complex is stabilized through hydrophobic and van der Waals interactions, allowing deep penetration into the narrow groove of an AT-rich sequence.

A thorough examination of numerous structural studies aimed at probing the relationship between (+)-CC-1065 minor groove binding and catalytic adenine alkylation revealed a binding-induced conformational change that effectively activates the ligand for nucleophilic attack.⁸⁹⁵ In order for the ligand to bind deep in the AT-rich minor groove to maximize hydrophobic and van der Waals interactions, the ligand is forced to adopt to the intrinsic helical twist of ds-DNA. This is possible only through a torsional rotation between the nitrogen and the carbonyl of the amide, which subsequently destabilizes the ligand ground state by diminishing the vinylogous amide conjugation. Thus, through the noncovalent interactions that promote this unique, folded conformation of (+)-CC-1065 within the complex, the reactivity of the ligand is enhanced.

2. Peptide–Oligomer Complexes

In biological systems, protein–ligand interactions are crucial to molecular recognition and are dominated by noncovalent interactions and conformational matching. Chain molecules capable of interacting with peptides or proteins have targeted their macromolecular surfaces for binding, since active sites of receptors are typically shallow and therefore the extension to longer chains is not possible. Additionally, these exterior surfaces do not typically have repeating functionalities of the same type such that a chain could make regular noncovalent contacts over a long range. These systems have similarity to DNA minor groove binding oligomers where the folding of an oligomer is templated by the folded

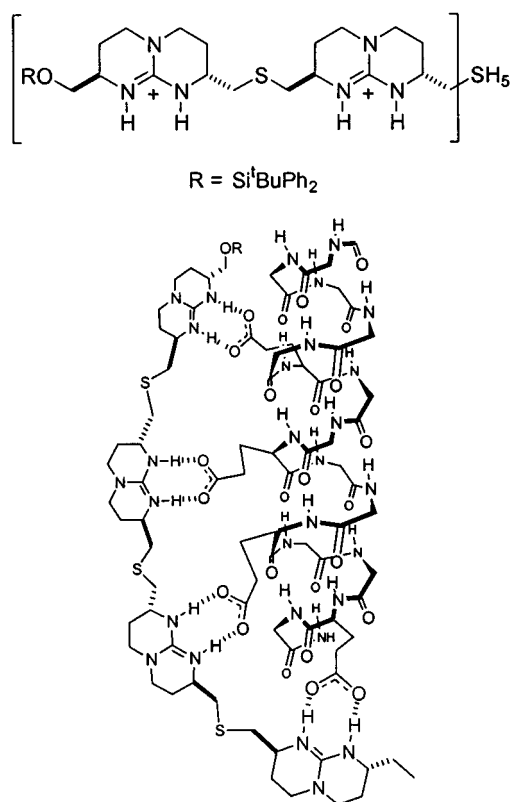


Figure 161. Tetraguanidinium chain bound to aspartate side chains of an α -helical peptide. Charges have been omitted for clarity.

conformation of a completely different backbone. This type of complex hints at foldamer–foldamer interactions that have yet to be demonstrated with two different backbones.

Cationic guanidinium oligomers capable of forming duplexes with peptides containing carboxylate side chains have been developed to interact with the α -helical surface through electrostatic and hydrogen-bonding interactions.^{896–898} When dimeric or tetrameric guanidinium oligomers were mixed with a hexadecameric peptide containing aspartate and asparagine side chains in every third position in 10% H₂O in MeOH, an increase in the CD intensity associated with increased α -helicity was observed. NMR experiments confirmed interstrand interactions as well as the induced α -helical conformation of the peptide (Figure 161).⁸⁹⁶ Further studies revealed that the tetraguanidinium oligomer interacts specifically with the anionic carboxylates extending from the helical peptide.⁸⁹⁷ Increased length of the peptidic side chains from aspartates to glutamates led to lower binding strengths, indicating the importance of a more rigid surface for proper alignment within the guanidinium–peptide complex.⁸⁹⁸

VIII. Conclusion

This review has surveyed the field of foldamers—the study of conformational control in synthetic chain molecules. The products of this field are new oligomeric backbones that adopt a particular type of secondary structure through noncovalent interactions. In this review, we have provided examples of

the secondary structure types schematically represented in Figure 1. When one looks deeper into the chemical details making up these secondary structures, what emerges to date is that only a relatively small number of “good folders” have as of yet been identified. Clearly, there is a long road to travel before “masterpiece sequences” of tylogomers are routinely produced. Yet, even with the limited examples of good folders that are known, one can also conclude that nature is now not alone; at least in terms of structure, we can now point to synthetic chains that begin to approach the order seen in nature’s conformationally structured molecules.

When contemplating new foldamers, it will be instructive to remember the qualities that are common to the good folders. One aspect is the proper balance of flexibility and rigidity within the backbone, defined by the number of torsional degrees of freedom per repeat unit and the torsional potential energy surfaces. Another aspect is the type, strength, location, and number of attractive and repulsive noncovalent interactions that stabilize the desired conformation while destabilizing the energetically accessible but unwanted conformations. In short, the crux of foldamer design and the accompanying folding reaction hinges on the tradeoff between entropy and enthalpy.

Hydrogen bonds and metal coordination bonds have been the mainstay of the supramolecular chemist when it comes to the intentional manipulation of noncovalent interactions. However, nature’s examples teach us the power of using weak, non-directional interactions to stabilize the folded state and deepen the folding funnel. Thus, van der Waals and solvophobic interactions are crucial to foldamer design, although they have been scarcely utilized in synthetic systems. In the simplest sense, such input is realized by incorporating amphiphilic character into the chain.

The long-term future—function through tylogomers—is easy to envision, but plotting a course of action is fraught with difficulty. While oligomeric-sized molecules are relatively easy to generate, the preparation of high molecular weight heteropolymers of a specific sequence represents one of today’s greatest unsolved synthetic challenges. Until this barrier can be overcome, there are certainly valuable properties to be found and fundamental discoveries to be made in the foldamers themselves. At least for today, the oligomer—the chemist’s middle child—comes to the fore.

IX. Acknowledgments

The authors thank members of the Moore group for suggestions and comments as well as J. Gray, D. Loudermilk, and N. Nathan and for their artistic contributions. Work from the authors’ laboratory was supported by grants from the National Science Foundation (NSF CHE 00-91931) and the Department of Energy (DEFG02-91ER45439).

X. References

- (1) Kepler, J. *Mysterium Cosmographicum*; Tuebingen, 1596.
- (2) Bernal, J. D.; Crowfoot, D. *Nature* **1934**, *153*, 794–795.

- (3) The word was coined by Gellman and first published in ref 32.
- (4) Gellman, S. H. *Acc. Chem. Res.* **1998**, *31*, 173–180.
- (5) Deshayes, K.; Broene, R. D.; Chao, I.; Knobler, C. B.; Diederich, F. *J. Org. Chem.* **1991**, *56*, 6787–6795.
- (6) Paruch, K.; Katz, T. J.; Incarvito, C.; Lam, K.-C.; Rhatigan, B.; Rheingold, A. L. *J. Org. Chem.* **2000**, *65*, 7602–7608 and references therein.
- (7) Green, M. M.; Park, J. W.; Sato, T.; Teramoto, A.; Lifson, S.; Selinger, R. L. B.; Selinger, J. V. *Angew. Chem., Int. Ed. Engl.* **1999**, *38*, 3138–3154.
- (8) Lin, L. N.; Brandts, J. F. *Biochemistry* **1980**, *19*, 3055–3059.
- (9) Noe, C. R.; Miculka, C.; Bats, J. W. *Angew. Chem., Int. Ed. Engl.* **1994**, *33*, 1476–1478.
- (10) Nakano, T.; Okamoto, Y.; Hatada, K. *J. Am. Chem. Soc.* **1992**, *114*, 1318–1329.
- (11) Mattice, W. L.; Suter, U. W. *Conformational Theory of Large Molecules*; John Wiley & Sons: New York, 1994.
- (12) Gange, D.; Magnus, P.; Bass, L.; Arnold, E. V.; Clardy, J. *J. Am. Chem. Soc.* **1980**, *102*, 2134–2135.
- (13) Kiupel, B.; Niederalt, C.; Nieger, M.; Grimme, S.; Vögtle, F. *Angew. Chem., Int. Ed. Engl.* **1998**, *37*, 3031–3034.
- (14) Fujii, K.; Furuta, T.; Tanaka, K. *Org. Lett.* **2001**, *3*, 169–171.
- (15) Chan, H. S.; Bromberg, S.; Dill, K. A. *Philos. Trans. R. Soc. London, Ser. B* **1995**, *348*, 61–70.
- (16) Lehn, J.-M. *Supramolecular Chemistry: Concepts and Perspectives*; VCH: Weinheim, Germany, 1995.
- (17) Quinkert, G.; Egert, E.; Griesinger, C. *Aspects of Organic Chemistry*; VCH: Basel, 1996.
- (18) Lightner, D. A.; McDonagh, A. F.; Wijekoon, W. M. D.; Reisinger, M. *Tetrahedron Lett.* **1988**, *29*, 3507–3510.
- (19) Blauer, G. *Isr. J. Chem.* **1983**, *23*, 201–209.
- (20) Chen, Q. Q.; Huggins, M. T.; Lightner, D. A.; Norona, W.; McDonagh, A. F. *J. Am. Chem. Soc.* **1999**, *121*, 9253–9264.
- (21) Kar, A. K.; Tipton, A. K.; Lightner, D. A. *Monatsh. Chem.* **1999**, *130*, 833–843.
- (22) Boiadjiev, S. E.; Lightner, D. A. *J. Heterocycl. Chem.* **1999**, *36*, 969–977.
- (23) Boiadjiev, S. E.; Lightner, D. A. *Tetrahedron: Asymmetry* **1999**, *10*, 2535–2550.
- (24) Tipton, A. K.; Lightner, D. A.; McDonagh, A. F. *J. Org. Chem.* **2001**, *66*, 1832–1838.
- (25) Tucci, F. C.; Rudkevich, D. M.; Rebek, J., Jr. *Chem. Eur. J.* **2000**, *6*, 1007–1016.
- (26) Schmuck, C. *J. Org. Chem.* **2000**, *65*, 2432–2437.
- (27) Galow, T. H.; Ilhan, F.; Cooke, G.; Rotello, V. M. *J. Am. Chem. Soc.* **2000**, *122*, 3595–3598.
- (28) Mena-Osteritz, E.; Meyer, A.; Langeveld-Voss, B. M. W.; Janssen, R. A. J.; Meijer, E. W.; Bauerle, P. *Angew. Chem., Int. Ed.* **2000**, *39*, 2679–2684.
- (29) Crisma, M.; Moretto, A.; Toniolo, C.; Kaczmarek, K.; Zabrocki, J. *Macromolecules* **2001**, *34*, 5048–5052.
- (30) Mirsky, A. E.; Pauling, L. *Proc. Natl. Acad. Sci. U.S.A.* **1936**, *22*, 439–447.
- (31) Flory, P. J. *Principles of Polymer Chemistry*; Cornell University Press: Ithaca, NY, 1953.
- (32) Appella, D. H.; Christianson, L. A.; Karle, I. L.; Powell, D. R.; Gellman, S. H. *J. Am. Chem. Soc.* **1996**, *118*, 13071–13072.
- (33) Moore, J. S. *Curr. Opin. Colloid Interface Sci.* **1999**, *4*, 108–116.
- (34) Baldwin, R. L. *Nat. Struct. Biol.* **1999**, *6*, 814–817.
- (35) Anfinsen, C. B. *Science* **1973**, *181*, 223–230.
- (36) Osguthorpe, D. J. *Curr. Opin. Struct. Biol.* **2000**, *10*, 146–152.
- (37) Shortle, D. *Curr. Biol.* **1999**, *9*, R205–R209.
- (38) Dinner, A. R.; Sali, A.; Smith, L. J.; Dobson, C. M.; Karplus, M. *Trends Biol. Sci.* **2000**, *25*, 331–339.
- (39) Bryngelson, J. D.; Onuchic, J. N.; Socci, N. D.; Wolynes, P. G. *Proteins: Struct., Funct., Genet.* **1995**, *21*, 167–195.
- (40) Kauzmann, W. *Adv. Protein Chem.* **1959**, *14*, 1–63.
- (41) Dill, K. A. *Biochemistry* **1990**, *29*, 7133–7155.
- (42) Eaton, W. A.; Muñoz, V.; Hagen, S. J.; Jas, G. S.; Lapidus, L. J.; Henry, E. R.; Hofrichter, J. *Annu. Rev. Biophys. Biomol. Struct.* **2000**, *29*, 327–359.
- (43) Brawer, S. A. *Relaxation in Viscous Liquids and Glasses*; American Ceramic Society: New York, 1983.
- (44) Jackle, J. *Rep. Prog. Phys.* **1986**, *49*, 171–232.
- (45) Go, N. *Annu. Rev. Biophys. Eng.* **1983**, *12*, 183–210.
- (46) Dill, K. A.; Bromberg, S.; Yue, K.; Fiebig, K. M.; Yee, D. P.; Thomas, P. D.; Chan, H. S. *Protein Sci.* **1995**, *4*, 561–602.
- (47) Jackson, S. E. *Folding Des.* **1998**, *3*, R81–R91.
- (48) Sali, A.; Shakhnovich, E.; Karplus, M. *Nature* **1994**, *369*, 248–251.
- (49) Levinthal, C. *Mossbauer Spectroscopy in Biological Systems*; 1969, pp 22–24.
- (50) Fisher, M. E. *J. Chem. Phys.* **1966**, *44*, 616–622.
- (51) Guttman, A. J. *J. Phys. A* **1987**, *20*, 1839–1854.
- (52) Fisher, M. E.; Hiley, B. J. *J. Chem. Phys.* **1961**, *34*, 1253–1267.
- (53) Camacho, C. J.; Thirumalai, D. *Phys. Rev. Lett.* **1993**, *71*, 2505–2508.
- (54) Jones, C. M.; Henry, E. R.; Hu, Y.; Chan, C. K.; Luck, S. D.; Bhuyan, A.; Roder, H.; Hofrichter, J.; Eaton, W. A. *Proc. Natl. Acad. Sci. U.S.A.* **1993**, *90*, 11860–11864.
- (55) Mattice, W. L. *Annu. Rev. Biophys. Biophys. Chem.* **1989**, *18*, 93–111.
- (56) Muñoz, V.; Henry, E. R.; Hofrichter, J.; Eaton, W. A. *Proc. Natl. Acad. Sci. U.S.A.* **1998**, *95*, 5872–5879.
- (57) Zimm, B. H.; Bragg, J. K. *J. Chem. Phys.* **1959**, *31*, 526–535.
- (58) Poland, D.; Scheraga, H. *Theory of Helix-Coil Transitions in Biopolymers*; Academic Press: New York, 1970.
- (59) Clarke, D. T.; Doig, A. J.; Stapley, B. J.; Gareth, R. J. *Proc. Natl. Acad. Sci. U.S.A.* **1999**, *96*, 7232–7237.
- (60) Eaton, W. A.; Munoz, V.; Thompson, P. A.; Henry, E. R.; Hofrichter, J. *Acc. Chem. Res.* **1998**, *31*, 745–753.
- (61) Elmer, S.; Pande, V. S. *J. Phys. Chem. B* **2001**, *105*, 482–485.
- (62) Yang, W. Y.; Prince, R. B.; Sabelko, J.; Moore, J. S.; Gruebele, M. *J. Am. Chem. Soc.* **2000**, *122*, 3248–3249.
- (63) Daura, X.; van Gunsteren, W. F.; Mark, A. E. *Proteins: Struct., Funct., Genet.* **1999**, *34*, 269–280.
- (64) Riddle, N. S.; Santiago, J. V.; Bray, S. T.; Doshi, N.; Grantcharova, V.; Yi, Q.; Baker, D. *Nat. Struct. Biol.* **1997**, *4*, 805–809.
- (65) Wolynes, P. G. *Nat. Struct. Biol.* **1997**, *4*, 871–874.
- (66) Chan, H. S.; Dill, K. A. *J. Chem. Phys.* **1991**, *95*, 3775–3767.
- (67) White, S. H.; Jacobs, R. E. *J. Mol. Evol.* **1993**, *36*, 79–95.
- (68) Rao, S. P.; Carlstrom, D. E.; Miller, W. G. *Biochemistry* **1974**, *13*, 943–952.
- (69) Chan, H. S.; Dill, K. A. *Macromolecules* **1989**, *22*, 4559–4573.
- (70) Shakhnovich, E.; Farztdinov, G.; Gutin, A. M.; Karplus, M. *Phys. Rev. Lett.* **1991**, *67*, 1665–1668.
- (71) Shakhnovich, E.; Gutin, A. M. *Proc. Natl. Acad. Sci. U.S.A.* **1993**, *90*, 7195–7199.
- (72) Sali, A.; Shakhnovich, E.; Karplus, M. *J. Mol. Biol.* **1994**, *235*, 1614–1636.
- (73) Bryngelson, J. D.; Wolynes, P. G. *Proc. Natl. Acad. Sci. U.S.A.* **1987**, *84*, 7524–7528.
- (74) Derrida, B. *Phys. Rev. B* **1981**, *24*, 2613–2626.
- (75) Bryngelson, J. D.; Onuchic, J. N.; Socci, N. D.; Wolynes, P. G. *Proteins: Struct., Funct., Genet.* **1995**, *21*, 167–195.
- (76) Onuchic, J. N.; Luthey-Schulten, Z.; Wolynes, P. G. *Annu. Rev. Phys. Chem.* **1997**, *48*, 545–600.
- (77) Dinner, A. R.; Sali, A.; Karplus, M.; Shakhnovich, E. *J. Chem. Phys.* **1994**, *101*, 1444–1451.
- (78) Chan, H. S.; Dill, K. A. *J. Chem. Phys.* **1993**, *99*, 2116–2127.
- (79) Gutin, A. M.; Abkevich, V. I.; Shakhnovich, E. I. *Biochemistry* **1995**, *34*, 3066–3076.
- (80) Onuchic, J. N.; Luthey-Schulten, Z.; Wolynes, P. G. *Annu. Rev. Phys. Chem.* **1997**, *48*, 545–600.
- (81) Echt, O.; Sattler, K.; Recknagel, E. *Phys. Rev. Lett.* **1981**, *47*, 1121–1124.
- (82) Berman, A. L.; Kolker, E.; Trifonov, E. N. *Proc. Natl. Acad. Sci. U.S.A.* **1994**, *91*, 4044–4047.
- (83) Lindgård, P. A.; Bohr, H. *Phys. Rev. Lett.* **1996**, *77*, 779–782.
- (84) Wales, D. *Chem. Phys. Lett.* **1998**, *285*, 330–336.
- (85) Kellman, M. E. *J. Chem. Phys.* **1996**, *105*, 2500–2508.
- (86) Yue, K.; Dill, K. A. *Proc. Natl. Acad. Sci. U.S.A.* **1995**, *92*, 146–150.
- (87) Wolynes, P. G. *Simplicity and Complexity in Proteins and Nucleic Acids*; Dahlem University Press: 1999.
- (88) Myers, J. K.; Oas, T. G. *Nat. Struct. Biol.* **2001**, *8*, 552–558.
- (89) Gilis, D.; Rooman, M. *Proteins: Struct., Funct., Genet.* **2001**, *42*, 164–176.
- (90) See ref 86.
- (91) DeGrado, W. F.; Summa, C. M.; Pavone, V.; Nastro, F.; Lombardi, A. *Annu. Rev. Biochem.* **1999**, *68*, 779–819.
- (92) Go, N.; Taketomi, H. *Proc. Natl. Acad. Sci. U.S.A.* **1978**, *75*, 559–563.
- (93) Unger, R.; Moulton, J. *J. Mol. Biol.* **1996**, *259*, 988–994.
- (94) Abkevich, V. I.; Gutin, A. M.; Shakhnovich, E. I. *J. Mol. Biol.* **1995**, *252*, 460–471.
- (95) Fersht, A. R.; Shakhnovich, E. I. *Curr. Biol.* **1998**, *8*, R478–R479.
- (96) Otzen, D. E.; Kristensen, O.; Proctor, M.; Oliveberg, M. *Biochemistry* **1999**, *38*, 6499–6511.
- (97) Chan, H. S.; Dill, K. A. *Proteins: Struct., Funct., Genet.* **1998**, *30*, 2–33.
- (98) Abkevich, V. I.; Gutin, A. M.; Shakhnovich, E. I. *J. Chem. Phys.* **1994**, *101*, 6052–6062.
- (99) Socci, N. D.; Onuchic, J. N. *J. Chem. Phys.* **1994**, *101*, 1519–1528.
- (100) Eastwood, M.; Wolynes, P. *J. Chem. Phys.* **2001**, *114*, 4702–4716.
- (101) Socci, N. D.; Onuchic, J. N. *J. Chem. Phys.* **1995**, *103*, 4732–4744.
- (102) Li, H.; Helling, R.; Tang, C.; Wingreen, N. *Science* **1996**, *273*, 666–669.
- (103) Lipman, D. J.; Wilbur, W. J. *Proc. R. Soc. London, Ser. B* **1991**, *245*, 7–11.

- (104) Govindarajan, S.; Goldstein, R. A. *Biopolymers* **1995**, *36*, 43–51.
- (105) Wang, T.; Miller, J.; Wingreen, N. S.; Tang, C.; Dill, K. A. *J. Chem. Phys.* **2000**, *113*, 8329–8336.
- (106) Martin, R. E.; Diederich, F. *Angew. Chem., Int. Ed.* **1999**, *38*, 1350–1377.
- (107) Tour, J. M. *Chem. Rev.* **1996**, *96*, 537–554.
- (108) Nelson, J. C.; Young, J. K.; Moore, J. S. *J. Org. Chem.* **1996**, *61*, 8160–8168.
- (109) Nelson, J. C. Ph.D. Thesis, University of Illinois, Urbana, IL, 1997.
- (110) Prince, R. B.; Okada, T.; Moore, J. S. *Angew. Chem., Int. Ed.* **1999**, *38*, 233–236.
- (111) Moore, J. S.; Hill, D. J.; Mio, M. J. In *Solid-Phase Synthesis*; Burgess, K., Ed.; Wiley-Interscience: New York, 2000.
- (112) Prince, R. B.; Saven, J. G.; Wolynes, P. G.; Moore, J. S. *J. Am. Chem. Soc.* **1999**, *121*, 3114–3121.
- (113) Berl, V.; Huc, I.; Khoury, R. G.; Krische, M. J.; Lehn, J.-M. *Nature* **2000**, *407*, 720–723.
- (114) Linton, B.; Hamilton, A. *CHEMTECH* **1997**, 34–40.
- (115) Schmidtschen, F. P.; Berger, M. *Chem. Rev.* **1997**, *97*, 1609–1646.
- (116) Davis, A. P.; Wareham, R. S. *Angew. Chem., Int. Ed.* **1999**, *38*, 2978–2996.
- (117) Mazik, M.; Sicking, W. *Chem. Eur. J.* **2001**, *7*, 664–670.
- (118) Archer, E. A.; Gong, H.; Krische, M. J. *Tetrahedron* **2001**, *57*, 1139–1159.
- (119) Beer, P. D.; Gale, P. A. *Angew. Chem., Int. Ed.* **2001**, *40*, 486–516.
- (120) Czarnik, A. W. *Acc. Chem. Res.* **1994**, *27*, 302–308.
- (121) Desilva, A. P.; Gunaratne, H. Q. N.; Gunnlaugsson, T.; Huxley, A. J. M.; McCoy, C. P.; Rademacher, J. T.; Rice, T. E. *Chem. Rev.* **1997**, *97*, 1515–1566.
- (122) Metzger, A.; Anslyn, E. V. *Angew. Chem., Int. Ed. Engl.* **1998**, *37*, 649–652 and references therein.
- (123) Robertson, A.; Shinkai, S. *Coord. Chem. Rev.* **2000**, *205*, 167–199.
- (124) Leininger, S.; Olenyuk, B.; Stang, P. J. *Chem. Rev.* **2000**, *100*, 853–908.
- (125) Baxter, P. N. W.; Lehn, J.-M.; Baum, G.; Fenske, D. *Chem. Eur. J.* **2000**, *6*, 4510–4517.
- (126) Zimmerman, N.; Moore, J. S.; Zimmerman, S. C. *Chem. Ind. (London)* **1998**, 604–610.
- (127) Bosman, A. W.; Janssen, H. M.; Meijer, E. W. *Chem. Rev.* **1999**, *99*, 1665–1688.
- (128) Hirschmann, R. *Angew. Chem., Int. Ed. Engl.* **1991**, *30*, 1278–1301.
- (129) Giannis, A.; Kolter, T. *Angew. Chem., Int. Ed. Engl.* **1993**, *32*, 1244–1267.
- (130) Gante, J. *Angew. Chem., Int. Ed. Engl.* **1994**, *33*, 1699–1720.
- (131) Hruby, V. J.; Li, G.; Haskell-Luevano, C.; Shenderovich, M. *Biopolymers* **1997**, *43*, 219–266.
- (132) Hanessian, S.; McNaughton-Smith, G.; Lombart, H. G.; Lubell, W. D. *Tetrahedron* **1997**, *53*, 12789–12854.
- (133) Ripka, A. S.; Rich, D. H. *Curr. Opin. Chem. Biol.* **1998**, *2*, 441–452.
- (134) Rizo, J.; Gierasch, L. M. *Annu. Rev. Biochem.* **1992**, *61*, 387–418.
- (135) Schneider, J. P.; Kelly, J. W. *Chem. Rev.* **1995**, *95*, 2169–2187.
- (136) Nowick, J. S.; Smith, E. M.; Pairish, M. *Chem. Soc. Rev.* **1996**, *25*, 401–415.
- (137) Soth, M. J.; Nowick, J. S. *Curr. Opin. Chem. Biol.* **1997**, *1*, 120–129.
- (138) Simon, R. J.; Kania, R. S.; Zuckermann, R. N.; Huebner, V. D.; Jewell, D. A.; Banville, S.; Ng, S.; Wang, L.; Rosenberg, S.; Marlowe, C. K.; Spellmeyer, D. C.; Tan, R.; Frankel, A. D.; Santi, D. V.; Cohen, F. E.; Bartlett, P. A. *Proc. Natl. Acad. Sci. U.S.A.* **1992**, *89*, 9367–9371.
- (139) Möhle, K.; Hofmann, H.-J. *Biopolymers* **1996**, *38*, 781–790.
- (140) Kirshenbaum, K.; Barron, A. E.; Goldsmith, R. A.; Armand, P.; Bradley, E. K.; Truong, K. T. V.; Dill, K. A.; Cohen, F. E.; Zuckermann, R. N. *Proc. Natl. Acad. Sci. U.S.A.* **1998**, *95*, 4303–4308.
- (141) Armand, P.; Kirshenbaum, K.; Falicov, A.; Dunbrack, R. L.; Dill, K. A.; Zuckermann, R. N.; Cohen, F. E. *Folding Des.* **1997**, *2*, 369–375.
- (142) Wu, C. W.; Sanborn, T. J.; Zuckermann, R. N.; Barron, A. E. *J. Am. Chem. Soc.* **2001**, *123*, 2958–2963.
- (143) Armand, P.; Kirshenbaum, K.; Goldsmith, R. A.; Farr-Jones, S.; Barron, A. E.; Truong, K. T. V.; Dill, K. A.; Mierke, D. F.; Cohen, F. E.; Zuckermann, R. N.; Bradley, E. K. *Proc. Natl. Acad. Sci. U.S.A.* **1998**, *95*, 4309–4314.
- (144) Wu, C. W.; Sanborn, T. J.; Huang, K.; Zuckermann, R. N.; Barron, A. E. *J. Am. Chem. Soc.* **2001**, *123*, 6778–6784.
- (145) Miller, S. M.; Simon, R. J.; Ng, S.; Zuckermann, R. N.; Kerr, J. M.; Moos, W. H. *Bioorg. Med. Chem. Lett.* **1994**, *4*, 2657–2662.
- (146) Zuckermann, R. N.; Kerr, J. M.; Kent, S. B. H.; Moos, W. H. *J. Am. Chem. Soc.* **1997**, *119*, 10646–10647.
- (147) Murphy, J. E.; Uno, T.; Hamer, J. D.; Cohen, F. E.; Dwarki, V.; Zuckermann, R. N. *Proc. Natl. Acad. Sci. U.S.A.* **1998**, *95*, 1517–1522.
- (148) Nowick, J. S.; Powell, N. A.; Nguyen, T. M.; Noronha, G. *J. Org. Chem.* **1992**, *57*, 3763–3765.
- (149) Etter, M. C. *Acc. Chem. Res.* **1990**, *23*, 120–126.
- (150) Etter, M. C.; MacDonald, J. C.; Bernstein, J. *Acta Crystallogr.* **1990**, *B46*, 256–262.
- (151) Jeffrey, G. A. *An Introduction to Hydrogen Bonding*; Oxford: New York, 1997.
- (152) Nowick, J. S.; Abdi, M.; Bellamo, K. A.; Love, J. A.; Martinez, E. J.; Noronha, G.; Smith, E. M.; Ziller, J. W. *J. Am. Chem. Soc.* **1995**, *117*, 89–99.
- (153) Nowick, J. S.; Mahrus, S.; Smith, E. M.; Ziller, J. W. *J. Am. Chem. Soc.* **1996**, *118*, 1066–1072.
- (154) Nowick, J. S.; Holmes, D. L.; Mackin, G.; Noronha, G.; Shaka, A. J.; Smith, E. M. *J. Am. Chem. Soc.* **1996**, *118*, 2764–2765.
- (155) Nowick, J. S.; Pairish, M.; Lee, I. Q.; Holmes, D. L.; Ziller, J. W. *J. Am. Chem. Soc.* **1997**, *119*, 5413–5424.
- (156) Nowick, J. S. *Acc. Chem. Res.* **1999**, *32*, 287–296.
- (157) Nowick, J. S.; Chung, D. M.; Maitra, K.; Maitra, S.; Stigers, K. D.; Sun, Y. *J. Am. Chem. Soc.* **2000**, *122*, 7654–7661.
- (158) Smith, A. B. I.; Keenan, T. P.; Holcomb, R. C.; Sprengeler, P. A.; Guzman, M. C.; Wood, J. L.; Carroll, P. J.; Hirschmann, R. *J. Am. Chem. Soc.* **1992**, *114*, 10672–10674.
- (159) Smith, A. B. I.; Guzman, M. C.; Sprengeler, P. A.; Keenan, T. P.; Holcomb, R. C.; Wood, J. L.; Carroll, P. J.; Hirschmann, R. *J. Am. Chem. Soc.* **1994**, *116*, 9947–9962.
- (160) Smith, A. B. I.; Favor, D. A.; Sprengeler, P. A.; Guzman, M. C.; Carroll, P. J.; Furst, G. T.; Hirschmann, R. *Bioorg. Med. Chem.* **1999**, *7*, 9–22.
- (161) Smith, A. B. I.; Akaishi, R.; Jones, D. R.; Keenan, T. P.; Guzman, M. C.; Holcomb, R. C.; Sprengeler, P. A.; Wood, J. L.; Hirschmann, R.; Holloway, M. K. *Biopolymers* **1995**, *37*, 29–53.
- (162) Smith, A. B. I.; Benowitz, A. B.; Favor, D. A.; Sprengeler, P. A.; Hirschmann, R. *Tetrahedron Lett.* **1997**, *38*, 3809–3812.
- (163) Meyers, A. I.; Reine, A. H.; Gault, R. *J. Org. Chem.* **1969**, *34*, 698–705.
- (164) Huisgen, R.; Brade, H. *Chem. Ber.* **1957**, *90*, 1432–1436.
- (165) Smith, A. B. I.; Hirschmann, R.; Pasternak, A.; Guzman, M. C.; Yokoyama, A.; Sprengeler, P. A.; Darke, P. L.; Emini, E. A.; Schleif, W. A. *J. Am. Chem. Soc.* **1995**, *117*, 11113–11123.
- (166) Lee, K. H.; Olson, G. L.; Bolin, D. R.; Benowitz, A. B.; Sprengeler, P. A.; Smith, A. B. I.; Hirschmann, R. F.; Wiley, D. C. *J. Am. Chem. Soc.* **2000**, *122*, 8370–8375.
- (167) Lucarini, S.; Tomasini, C. *J. Org. Chem.* **2001**, *66*, 727–732.
- (168) Gante, J. *Synthesis* **1989**, 405–413.
- (169) Han, H.; Janda, K. D. *J. Am. Chem. Soc.* **1996**, *118*, 2539–2544.
- (170) Gante, J.; Krug, M.; Lauterbach, G.; Weitzel, R.; Hiller, W. *J. Pept. Sci.* **1995**, *2*, 201–206.
- (171) Reynolds, C. H.; Hormann, R. E. *J. Am. Chem. Soc.* **1996**, *118*, 9395–9401.
- (172) Perona, J. J.; Craik, C. S. *Protein Sci.* **1995**, *4*, 337–360.
- (173) André, F.; Boussard, D.; Bayeul, D.; Didierjean, C.; Aubry, A.; Marraud, M. *J. Pept. Res.* **1997**, *49*, 556–562.
- (174) Thormann, M.; Hofmann, H.-J. *J. Mol. Struct.* **1999**, *469*, 63–76.
- (175) Ramachandran, G. N.; Sasisekharan, V. In *Advances in Protein Chemistry*; Anfinsen, C. B. J., Anson, M. L., Edsall, J. T., Richards, F. M., Eds.; Academic Press: New York, 1968; Vol. 23.
- (176) Schulz, G. E.; Schirmer, R. H. *Principles of Protein Structure*; Springer-Verlag: New York, 1979.
- (177) Richardson, J. S. In *Advances in Protein Chemistry*; Anfinsen, C. B., Edsall, J. T., Richards, F. M., Eds.; Academic Press: New York, 1981; Vol. 34.
- (178) Branden, C.; Tooze, J. *Introduction to Protein Structure*, 2nd ed.; Garland: New York, 1999.
- (179) Glickson, J. D.; Applequist, J. *J. Am. Chem. Soc.* **1971**, *93*, 3276–3281.
- (180) Narita, M.; Doi, M.; Kudo, K.; Terauchi, Y. *Bull. Chem. Soc. Jpn.* **1986**, *59*, 3553–3557.
- (181) Drey, C. N. C. In *Chemistry and Biochemistry of the Amino Acids*; Barrett, G. C., Ed.; Chapman and Hall: London, 1985.
- (182) Cole, D. C. *Tetrahedron* **1994**, *50*, 9517–9582.
- (183) Möhle, K.; Günther, R.; Thormann, M.; Sewald, N.; Hofmann, H.-J. *Biopolymers* **1999**, *50*, 167–184.
- (184) Wu, Y.-D.; Wang, D.-P. *J. Am. Chem. Soc.* **1998**, *120*, 13485–13493.
- (185) Wu, Y.-D.; Wang, D.-P. *J. Am. Chem. Soc.* **1999**, *121*, 9352–9362.
- (186) Günther, R.; Hofmann, H.-J.; Kuczera, K. *J. Phys. Chem. B* **2001**, *105*, 5559–5567.
- (187) Graf, R.; Lohaus, G.; Börner, K.; Schmidt, E.; Bestian, H. *Angew. Chem., Int. Ed. Engl.* **1962**, *1*, 481–489.
- (188) Kovacs, J.; Ballina, R.; Rodin, R. L.; Balasubramanian, D.; Applequist, J. *J. Am. Chem. Soc.* **1965**, *87*, 119–120.
- (189) Bestian, H. *Angew. Chem., Int. Ed. Engl.* **1968**, *7*, 278–285.
- (190) Schmidt, V. E. *Angew. Makromol. Chem.* **1970**, *14*, 185–202.

- (191) Saudek, V.; Stokrova, S.; Schmidt, P. *Biopolymers* **1982**, *21*, 2195–2203.
- (192) Hardy, P. M.; Haylock, J. C.; Rydon, H. N. *J. Chem. Soc., Perkin Trans. 1* **1972**, 605–611.
- (193) Glickson, J. D.; Applequist, J. *Macromolecules* **1971**, *2*, 628–634.
- (194) Chen, F.; Lepore, G.; Goodman, M. *Macromolecules* **1974**, *7*, 779–783.
- (195) Yuki, H.; Taketani, Y. *Polym. Lett.* **1972**, *10*, 373–378.
- (196) Yuki, H.; Okamoto, Y.; Taketani, Y.; Tsubota, T.; Marubayashi, Y. *J. Polym. Sci., Polym. Chem. Ed.* **1978**, *16*, 2237–2251.
- (197) Kajtár, M.; Hollósi, M.; Riedl, Z. *Acta Chim. Acad. Sci. Hung.* **1976**, *88*, 301–308.
- (198) Yuki, H.; Okamoto, Y.; Doi, Y. *J. Polym. Sci., Polym. Chem. Ed.* **1979**, *17*, 1911–1921.
- (199) Fernández-Santín, J. M.; Aymamí, J.; Rodríguez-Galán, A.; Muñoz-Guerra, S.; Subirana, J. A. *Nature* **1984**, *311*, 53–54.
- (200) Krauthäuser, S.; Christianson, L. A.; Powell, D. R.; Gellman, S. H. *J. Am. Chem. Soc.* **1997**, *119*, 11719–11720.
- (201) Seebach, D.; Abele, S.; Gademann, K.; Jaun, B. *Angew. Chem., Int. Ed.* **1999**, *38*, 1595–1597.
- (202) Fernández-Santín, J. M.; Muñoz-Guerra, S.; Rodríguez-Galán, A.; Aymamí, J.; Lloveras, J.; Subirana, J. A. *Macromolecules* **1987**, *20*, 62–68.
- (203) Doty, P.; Wada, A.; Yang, J. T.; Blout, E. R. *J. Polym. Sci.* **1957**, *23*, 851–861.
- (204) López-Carrasquero, F.; Alemán, C.; Muñoz-Guerra, S. *Biopolymers* **1995**, *36*, 263–271.
- (205) Alemán, C.; Bella, J.; Perez, J. J. *Polymer* **1994**, *1994*, 2596–2599.
- (206) Alemán, C.; Navas, J. J.; Muñoz-Guerra, S. *Biopolymers* **1997**, *41*, 721–729.
- (207) Bella, J.; Alemán, C.; Fernández-Santín, J. M.; Alegre, C.; Subirana, J. A. *Macromolecules* **1992**, *25*, 5225–5230.
- (208) Bode, K. A.; Applequist, J. *Macromolecules* **1997**, *30*, 2144–2150.
- (209) López-Carrasquero, F.; García-Alvarez, M.; Navas, J. J.; Alemán, C.; Muñoz-Guerra, S. *Macromolecules* **1996**, *29*, 8449–8459.
- (210) Martínez de Iarduya, A.; Alemán, C.; García-Alvarez, M.; López-Carrasquero, F.; Muñoz-Guerra, S. *Macromolecules* **1999**, *32*, 3257–3263.
- (211) Cheng, J.; Deming, T. J. *Macromolecules* **2001**, *34*, 5169–5174.
- (212) Fasman, G. D. In *Poly- α -Amino Acids*; Fasman, G. D., Ed.; Marcel Dekker: New York, 1967.
- (213) Karle, I. L. In *The Peptides*; Gross, E., Meienhofer, J., Eds.; Academic Press: New York, 1981; Vol. 4.
- (214) Pavone, V.; Lombardi, A.; Yang, X.; Pedone, C.; Di Blasio, B. *Biopolymers* **1990**, *30*, 189–196.
- (215) Di Blasio, B.; Lombardi, A.; Yang, X.; Pedone, C.; Pavone, V. *Biopolymers* **1991**, *31*, 1181–1188.
- (216) Di Blasio, B.; Lombardi, A.; D'Auria, G.; Saviano, M.; Isernia, C.; Maglio, O.; Paolillo, L.; Pedone, C.; Pavone, V. *Biopolymers* **1993**, *33*, 621–631.
- (217) Pavone, V.; Lombardi, A.; Saviano, M.; Natri, F.; Fattorusso, R.; Maglio, O.; Isernia, C.; Paolillo, L.; Pedone, C. *Biopolymers* **1994**, *34*, 1517–1526.
- (218) Pavone, V.; Lombardi, A.; Saviano, M.; Di Blasio, B.; Natri, F.; Fattorusso, R.; Maglio, O.; Isernia, C. *Biopolymers* **1994**, *34*, 1505–1515.
- (219) For references concerning this hydrogen-bond annotation, see Etter, M. C. *Acc. Chem. Res.* **1990**, *23*, 120–126. Etter, M. C.; MacDonald, J. C.; Bernstein, J. *Acta Crystallogr.* **1990**, *B46*, 256–262.
- (220) Morita, H.; Nagashima, S.; Takeya, K.; Itokawa, H.; Iitaka, Y. *Tetrahedron* **1995**, *51*, 1121–1132.
- (221) Matthews, J. L.; Overhand, M.; Kuhnle, F. N. M.; Ciceri, P. E.; Seebach, D. *Liebigs Ann.* **1997**, 1371–1379.
- (222) Seebach, D.; Matthews, J. L.; Meden, A.; Wessels, T.; Baerlocher, C.; McCusker, L. B. *Helv. Chim. Acta* **1997**, *80*, 173–182.
- (223) Seebach, D.; Overhand, M.; Kuhnle, F. N. M.; Martinoni, B.; Oberer, L.; Hommel, U.; Widmer, H. *Helv. Chim. Acta* **1996**, *79*, 913–941.
- (224) Pavone, V.; Di Blasio, B.; Lombardi, A.; Isernia, C.; Pedone, C.; Benedetti, E.; Valle, G.; Crisma, M.; Toniolo, C.; Kishore, R. *J. Chem. Soc., Perkin Trans. 2* **1992**, 1233–1237.
- (225) Dado, G. P.; Gellman, S. H. *J. Am. Chem. Soc.* **1994**, *116*, 1054–1062.
- (226) Abele, S.; Seiler, P.; Seebach, D. *Helv. Chim. Acta* **1999**, *82*, 1559–1571.
- (227) Quinkert, G.; Egert, E.; Griesinger, C. In *Peptides: Synthesis, Structure, and Applications*; Gutte, B., Ed.; Academic Press: San Diego, 1995.
- (228) Seebach, D.; Matthews, J. L. *Chem. Commun.* **1997**, 2015–2022.
- (229) Seebach, D.; Albert, M.; Arvidsson, P. I.; Rueping, M.; Schreiber, J. V. *Chimia* **2001**, *55*, 345–353.
- (230) Yokouchi, M.; Chatani, Y.; Tadokoro, H.; Teranishi, K.; Tani, H. *Polymer* **1974**, *14*, 267–273.
- (231) Müller, H.-M.; Seebach, D. *Angew. Chem., Int. Ed. Engl.* **1993**, *32*, 477–502.
- (232) Landschulz, W. H.; Johnson, P. F.; McKnight, S. L. *Science* **1988**, *240*, 1759–1764.
- (233) Karle, I. L.; Flippen-Anderson, J. L.; Uma, K.; Sukumar, M.; Balaram, P. *J. Am. Chem. Soc.* **1990**, *112*, 9350–9356.
- (234) Matthews, J. L.; Gademann, K.; Jaun, B.; Seebach, D. *J. Chem. Soc., Perkin Trans. 1* **1998**, 3331–3340.
- (235) Tromp, R. A.; van der Hoeven, M.; Amore, A.; Brussee, J.; Overhand, M.; van der Marel, G. A.; van der Gen, A. *Tetrahedron: Asymmetry* **2001**, *12*, 1109–1112.
- (236) Hanessian, S.; Luo, X.; Schaum, R.; Michnick, S. *J. Am. Chem. Soc.* **1998**, *120*, 8569–8570.
- (237) Hintermann, T.; Gademann, K.; Jaun, B.; Seebach, D. *Helv. Chim. Acta* **1998**, *81*, 983–1002.
- (238) Appella, D. H.; Christianson, L. A.; Klein, D. A.; Powell, D. R.; Huang, X.; Barchi, J. J., Jr.; Gellman, S. H. *Nature* **1997**, *387*, 381–384.
- (239) Appella, D. H.; Christianson, L. A.; Karle, I. L.; Powell, D. R.; Gellman, S. H. *J. Am. Chem. Soc.* **1999**, *121*, 6206–6212.
- (240) Barchi, J. J., Jr.; Huang, X.; Appella, D. H.; Christianson, L. A.; Durrell, S. R.; Gellman, S. H. *J. Am. Chem. Soc.* **2000**, *122*, 2711–2718.
- (241) Appella, D. H.; Christianson, L. A.; Klein, D. A.; Richards, M. A.; Powell, D. R.; Gellman, S. H. *J. Am. Chem. Soc.* **1999**, *121*, 7574–7581.
- (242) Applequist, J.; Bode, K. A.; Appella, D. H.; Christianson, L. A.; Gellman, S. H. *J. Am. Chem. Soc.* **1998**, *120*, 4891–4892.
- (243) Kilpatrick, J. E.; Pitzer, K. S.; Spitzer, R. *J. Am. Chem. Soc.* **1947**, *69*, 2483–2488.
- (244) Schweizer, W. B. In *Structure Correlation*; Bürgi, H.-B., Dunitz, J. D., Eds.; VCH: Weinheim, 1994; Vol. 1.
- (245) Benedetti, E.; Corradini, P.; Pedone, C. *J. Phys. Chem.* **1972**, *76*, 790–797.
- (246) Lifson, S.; Warshel, A. *J. Chem. Phys.* **1968**, *49*, 5116–5129.
- (247) Claridge, T. D. W.; Goodman, J. M.; Moreno, A.; Angus, D.; Barker, S. F.; Taillefumier, C.; Watterson, M. P.; Fleet, G. W. J. *Tetrahedron Lett.* **2001**, *42*, 4251–4255.
- (248) Seebach, D.; Gademann, K.; Schreiber, J. V.; Matthews, J. L.; Hintermann, T.; Jaun, B.; Oberer, L.; Hommel, U.; Widmer, H. *Helv. Chim. Acta* **1997**, *80*, 2033–2038.
- (249) Seebach, D.; Abele, S.; Gademann, K.; Guichard, G.; Hintermann, T.; Jaun, B.; Matthews, J. L.; Schreiber, J. V. *Helv. Chim. Acta* **1998**, *81*, 932–982.
- (250) Watterson, M. P.; Pickering, L.; Smith, M. D.; Hudson, S. J.; Marsh, P. R.; Mordaunt, J. E.; Watkin, D. J.; Newman, C. J.; Fleet, G. W. J. *Tetrahedron: Asymmetry* **1999**, *10*, 1855–1859.
- (251) Suhara, Y.; Hildreth, J. E. K.; Ichikawa, Y. *Tetrahedron Lett.* **1996**, *37*, 1575–1578.
- (252) Seebach, D.; Ciceri, P. E.; Overhand, M.; Jaun, B.; Rigo, D. *Helv. Chim. Acta* **1996**, *79*, 2043–2066.
- (253) Guichard, G.; Abele, S.; Seebach, D. *Helv. Chim. Acta* **1998**, *81*, 187–206.
- (254) Seebach, D.; Sifferlen, T.; Mathieu, P. A.; Häne, A. M.; Krell, C. M.; Bierbaum, D. J.; Abele, S. *Helv. Chim. Acta* **2000**, *83*, 2849–2864.
- (255) Jacobi, A.; Seebach, D. *Helv. Chim. Acta* **1999**, *82*, 1150–1172.
- (256) Rueping, M.; Jaun, B.; Seebach, D. *Chem. Commun.* **2000**, 2267–2268.
- (257) Sifferlen, T.; Rueping, M.; Gademann, K.; Jaun, B.; Seebach, D. *Helv. Chim. Acta* **1999**, *82*, 2067–2093.
- (258) Wu, Y.-D.; Zhao, Y.-L. *J. Am. Chem. Soc.* **2001**, *123*, 5313–5319.
- (259) Rabanal, R.; Ludevid, M. D.; Pons, M.; Giralt, E. *Biopolymers* **1993**, *33*, 1019–1028.
- (260) Huck, B. R.; Langenhan, J. M.; Gellman, S. H. *Org. Lett.* **1999**, *1*, 1717–1720.
- (261) Abele, S.; Vögltli, K.; Seebach, D. *Helv. Chim. Acta* **1999**, *82*, 1539–1558.
- (262) Hintermann, T.; Seebach, D. *Synlett* **1997**, 437–438.
- (263) Gung, B. W.; Zhu, Z. *J. Org. Chem.* **1997**, *62*, 6100–6101.
- (264) DeGrado, W. F.; Schneider, J. P.; Hamuro, Y. *J. Pept. Res.* **1999**, *54*, 206–217.
- (265) Schellman, J. A. *Compt. Rend. Trav. Lab. Carlsberg, Ser. Chim.* **1955**, *29*, 230–259.
- (266) Qian, H.; Schellman, J. A. *J. Phys. Chem.* **1992**, *96*, 3987–3994.
- (267) See ref 57.
- (268) Goodman, M.; Verdini, A. S.; Toniolo, C.; Phillips, W. D.; Bovey, F. A. *Proc. Natl. Acad. Sci. U.S.A.* **1969**, *64*, 444–450.
- (269) Kemp, D. S.; Oslick, S. L.; Allen, T. J. *J. Am. Chem. Soc.* **1996**, *118*, 4249–4255.
- (270) Baldwin, R. L.; Rose, G. D. *Trends Biochem. Sci.* **1999**, *24*, 26–33.
- (271) Baldwin, R. L.; Rose, G. D. *Trends Biochem. Sci.* **1999**, *24*, 77–83.
- (272) Wallimann, P.; Kennedy, R. J.; Kemp, D. S. *Angew. Chem., Int. Ed.* **1999**, *38*, 1290–1292.
- (273) Seebach, D.; Schreiber, J. V.; Abele, S.; Daura, X.; van Gunsteren, W. F. *Helv. Chim. Acta* **2000**, *83*, 34–57.
- (274) Gademann, K.; Jaun, B.; Seebach, D.; Perozzo, R.; Scapozza, L.; Folkers, G. *Helv. Chim. Acta* **1999**, *82*, 1–11.

- (275) Daura, X.; van Gunsteren, W. F.; Mark, A. E. *Proteins: Struct., Funct., Genet.* **1999**, *34*, 269–280.
- (276) Daura, X.; Gademann, K.; Jaun, B.; Seebach, D.; van Gunsteren, W. F.; Mark, A. E. *Angew. Chem., Int. Ed.* **1999**, *38*, 236–240.
- (277) Seebach, D.; Abele, S.; Sifferlen, T.; Hänggi, M.; Gruner, S.; Seiler, P. *Helv. Chim. Acta* **1998**, *81*, 2218–2243.
- (278) Spatola, A. F. In *Chemistry and Biochemistry of Amino Acids, Peptides, and Proteins*; Weinstein, B., Ed.; Marcel Dekker: New York, 1983; Vol. 7.
- (279) Griffith, O. W. In *Annual Review of Biochemistry*; Richardson, C. C., Boyer, P. D., Dawid, I. B., Meister, A., Eds.; Annual Reviews, Inc.: Palo Alto, CA, 1986; Vol. 55.
- (280) Abele, S.; Guichard, G.; Seebach, D. *Helv. Chim. Acta* **1998**, *81*, 2141–2156.
- (281) Gung, B. W.; Zou, D.; Stalcup, A. M.; Cottrell, C. E. *J. Org. Chem.* **1999**, *64*, 2176–2177.
- (282) Appella, D. H.; Barchi, J. J., Jr.; Durell, S. R.; Gellman, S. H. *J. Am. Chem. Soc.* **1999**, *121*, 2309–2310.
- (283) Appella, D. H.; LePlae, P. R.; Raguse, T. L.; Gellman, S. H. *J. Org. Chem.* **2000**, *65*, 4766–4769.
- (284) Wang, X.; Espinosa, J. F.; Gellman, S. H. *J. Am. Chem. Soc.* **2000**, *122*, 4821–4822.
- (285) Lee, H.-S.; Syud, F. A.; Wang, X.; Gellman, S. H. *J. Am. Chem. Soc.* **2001**, *123*, 7721–7722.
- (286) Seebach, D.; Jacobi, A.; Rueping, M.; Gademann, K.; Ernst, M.; Jaun, B. *Helv. Chim. Acta* **2000**, *83*, 2115–2140.
- (287) Arvidsson, P. I.; Rueping, M.; Seebach, D. *Chem. Commun.* **2001**, 649–650.
- (288) Cheng, R. P.; DeGrado, W. F. *J. Am. Chem. Soc.* **2001**, *123*, 5162–5163.
- (289) Hintermann, T.; Seebach, D. *Chimia* **1997**, *51*, 244–247.
- (290) Frackenpohl, J.; Arvidsson, P. I.; Schreiber, J. V.; Seebach, D. *ChemBioChem* **2001**, *2*, 445–455.
- (291) Gademann, K.; Ernst, M.; Hoyer, D.; Seebach, D. *Angew. Chem., Int. Ed.* **1999**, *38*, 1223–1226.
- (292) Werder, M.; Hauser, H.; Abele, S.; Seebach, D. *Helv. Chim. Acta* **1999**, *82*, 1774–1783.
- (293) Hamuro, Y.; Schneider, J. P.; DeGrado, W. F. *J. Am. Chem. Soc.* **1999**, *121*, 12200–12201.
- (294) Liu, D.; DeGrado, W. F. *J. Am. Chem. Soc.* **2001**, *123*, 7553–7559.
- (295) Porter, E. A.; Wang, X.; Lee, H.-S.; Weisblum, B.; Gellman, S. H. *Nature* **2000**, *404*, 565.
- (296) Gellman, S. H. *Curr. Opin. Chem. Biol.* **1998**, *2*, 717–725.
- (297) Haque, T. S.; Little, J. C.; Gellman, S. H. *J. Am. Chem. Soc.* **1996**, *118*, 6975–6985.
- (298) Chung, Y. J.; Christianson, L. A.; Stanger, H. E.; Powell, D. R.; Gellman, S. H. *J. Am. Chem. Soc.* **1998**, *120*, 10555–10556.
- (299) Chung, Y. J.; Huck, B. R.; Christianson, L. A.; Stanger, H. E.; Krauthäuser, S.; Powell, D. R.; Gellman, S. H. *J. Am. Chem. Soc.* **2000**, *122*, 3995–4004.
- (300) Huck, B. R.; Fisk, J. D.; Gellman, S. H. *Org. Lett.* **2000**, *2*, 2607–2610.
- (301) Hanessian, S.; Yang, H. *Tetrahedron Lett.* **1997**, *38*, 3155–3158.
- (302) Motorina, I. A.; Huel, C.; Quiniou, E.; Mispelter, J.; Adjad, E.; Grierson, D. S. *J. Am. Chem. Soc.* **2001**, *123*, 8–17.
- (303) Yang, D.; Ng, F.-F.; Li, Z.-J. *J. Am. Chem. Soc.* **1996**, *118*, 9794–9795.
- (304) Yang, D.; Qu, J.; Li, B.; Ng, F.-F.; Wang, X.-C.; Cheung, K. K.; Wang, D.-P.; Wu, Y.-D. *J. Am. Chem. Soc.* **1999**, *121*, 589–590.
- (305) Wu, Y.-D.; Wang, D.-P.; Chan, K. W. K.; Yang, D. *J. Am. Chem. Soc.* **1999**, *121*, 11189–11196.
- (306) Gennari, C.; Salom, B.; Potenza, D.; Williams, A. *Angew. Chem., Int. Ed. Engl.* **1994**, *33*, 2067–2069.
- (307) Moree, W. J.; van der Marel, G. A.; Liskamp, R. J. *J. Org. Chem.* **1995**, *60*, 5157–5169.
- (308) Gude, M.; Piarilli, U.; Potenza, D.; Salom, B.; Gennari, C. *Tetrahedron Lett.* **1996**, *37*, 8589–8592.
- (309) Monnee, M. C. F.; Marjine, M. F.; Brouwer, A. J.; Liskamp, R. M. J. *Tetrahedron Lett.* **2000**, *41*, 7991–7995.
- (310) Bolm, C.; Moll, G.; Kahmann, J. D. *Chem. Eur. J.* **2001**, *7*, 1118–1128.
- (311) Bindal, R. D.; Golab, J. T.; Katzenellenbogen, J. A. *J. Am. Chem. Soc.* **1990**, *112*, 7861–7868.
- (312) Radkiewicz, J. L.; McAllister, M. A.; Goldstein, E.; Houk, K. N. *J. Org. Chem.* **1998**, *63*, 1419–1428.
- (313) Gennari, C.; Gude, M.; Potenza, D.; Piarulli, U. *Chem. Eur. J.* **1998**, *4*, 1924–1931.
- (314) Langenhan, J. M.; Fisk, J. D.; Gellman, S. H. *Org. Lett.* **2001**, *3*, 2559–2562.
- (315) Günther, R.; Hofmann, H.-J. *J. Am. Chem. Soc.* **2001**, *123*, 247–255.
- (316) Kajtár, M.; Bruckner, V. *Tetrahedron Lett.* **1966**, *7*, 4813–4818.
- (317) Kajtár, M.; Hollósi, M. *Acta Chim. Acad. Sci. Hung.* **1970**, *65*, 403–432.
- (318) Rydon, H. N. *J. Chem. Soc.* **1964**, 1328–1333.
- (319) Watanabe, T.; Ina, T.; Ogawa, K.; Matsumoto, T.; Sawa, S.; Ono, S. *Bull. Chem. Soc. Jpn.* **1970**, *43*, 3939–3940.
- (320) Kajtár, M.; Hollósi, M.; Snatzke, G. *Tetrahedron* **1971**, *27*, 5659–5671.
- (321) Hoffmann, R. W.; Lazaro, M. A.; Caturla, F.; Framery, E. *Tetrahedron Lett.* **1999**, *40*, 5983–5986.
- (322) Hoffmann, M.; Caturla, F.; Lazaro, M. A.; Framery, E.; Bernabeu, M. C.; Valancogne, I.; Montalbetti, C. A. G. N. *New J. Chem.* **2000**, *24*, 187–194.
- (323) Hagihara, M.; Anthony, N. J.; Stout, T. J.; Clardy, J.; Schreiber, S. L. *J. Am. Chem. Soc.* **1992**, *114*, 6568–6570.
- (324) Gennari, C.; Salom, B.; Potenza, D.; Longari, C.; Fioravanzo, E.; Carugo, O.; Sardone, N. *Chem. Eur. J.* **1996**, *2*, 644–655.
- (325) Brenner, M.; Seebach, D. *Helv. Chim. Acta* **2001**, *84*, 1181–1189.
- (326) Hanessian, S.; Luo, X.; Schaum, R. *Tetrahedron Lett.* **1999**, *40*, 4925–4929.
- (327) Seebach, D.; Brenner, M.; Rueping, M.; Schweizer, W. B.; Jaun, B. *Chem. Commun.* **2001**, 207–208.
- (328) Machetti, F.; Ferrali, A.; Menchi, G.; Occhiato, E. G.; Guarna, A. *Org. Lett.* **2000**, *2*, 3987–3990.
- (329) Burgess, K.; Linthicum, D. S.; Shin, H. *Angew. Chem., Int. Ed. Engl.* **1995**, *34*, 907–909.
- (330) Moran, E. J.; Wilson, T. E.; Cho, C. Y.; Cherry, S. R.; Stephans, J. C.; Fodor, S. P. A.; Adams, C. L.; Sundaram, A.; Jacobs, J. W.; Schultz, P. G. *Biopolymers* **1995**, *37*, 213–219.
- (331) Kim, J.-M.; Wilson, T. E.; Norman, T. C.; Schultz, P. G. *Tetrahedron Lett.* **1996**, *37*, 5309–5312.
- (332) Kim, J.-M.; Paikoff, S. J.; Schultz, P. G. *Tetrahedron Lett.* **1996**, *37*, 5305–5308.
- (333) Kruijtzter, J. A. W.; Lefeber, D. J.; Liskamp, R. M. J. *Tetrahedron Lett.* **1997**, *38*, 5335–5338.
- (334) Wilson, M. E.; Nowick, J. S. *Tetrahedron Lett.* **1998**, *39*, 6613–6616.
- (335) Cho, C. Y.; Moran, E. J.; Cherry, S. R.; Stephans, J. C.; Fodor, S. P. A.; Adams, C. L.; Sundaram, A.; Jacobs, J. W.; Schultz, P. G. *Science* **1993**, *261*, 1303–1305.
- (336) Cho, C. Y.; Youngquist, R. S.; Paikoff, S. J.; Beresini, M. H.; Herbert, A. R.; Berleau, L. T.; Liu, C. W.; Wemmer, D. E.; Keough, T.; Schultz, P. G. *J. Am. Chem. Soc.* **1998**, *120*, 7706–7718.
- (337) Lin, P.; Ganesan, A. *Bioorg. Med. Chem. Lett.* **1998**, *8*, 511–514.
- (338) Stigers, K. D.; Soth, M. J.; Nowick, J. S. *Curr. Opin. Chem. Biol.* **1999**, *3*, 714–723.
- (339) Hann, M. M.; Sannes, P. G.; Kennewell, P. D.; Taylor, J. B. *J. Chem. Soc., Chem. Commun.* **1980**, 234–235.
- (340) Cox, M. T.; Heaton, D. W.; Horbury, J. *J. Chem. Soc., Chem. Commun.* **1980**, 799–800.
- (341) Gardner, R. R.; Liang, G.-B.; Gellman, S. H. *J. Am. Chem. Soc.* **1995**, *117*, 3280–3281.
- (342) Gardner, R. R.; Liang, G.-B.; Gellman, S. H. *J. Am. Chem. Soc.* **1999**, *121*, 1806–1816.
- (343) Wipf, P.; Fritch, P. C. *J. Org. Chem.* **1994**, *59*, 4875–4886.
- (344) Wipf, P.; Henninger, T. C.; Geib, S. J. *J. Org. Chem.* **1998**, *63*, 6088–6089.
- (345) Suhara, Y.; Izumi, M.; Ichikawa, M.; Penno, M. B.; Ichikawa, Y. *Tetrahedron Lett.* **1997**, *38*, 7167–7170.
- (346) Fuchs, E.-F.; Lehmann, J. *Carbohydr. Res.* **1976**, *49*, 267–273.
- (347) Wessel, H. P.; Mitchell, C. M.; Lobato, C. M.; Schmid, G. *Angew. Chem., Int. Ed. Engl.* **1995**, *34*, 2712–2713.
- (348) Nicolaou, K. C.; Flörke, H.; Egan, M. G.; Barth, T.; Estevez, V. A. *Tetrahedron Lett.* **1995**, *36*, 1775–1778.
- (349) Suhara, Y.; Ichikawa, M.; Hildreth, J. E. K.; Ichikawa, Y. *Tetrahedron Lett.* **1996**, *37*, 2549–2552.
- (350) Graf von Roedern, E.; Kessler, H. *Angew. Chem., Int. Ed. Engl.* **1994**, *33*, 687–689.
- (351) Graf von Roedern, E.; Lohof, E.; Hessler, G.; Hoffmann, M.; Kessler, H. *J. Am. Chem. Soc.* **1996**, *118*, 10156–10167.
- (352) Chakraborty, T. K.; Ghosh, S.; Jayaprakash, S.; Sharma, J. A. R. P.; Ravikanth, V.; Diwan, P. V.; Nagaraj, R.; Kunwar, A. C. *J. Org. Chem.* **2000**, *65*, 6441–6457.
- (353) Smith, M. D.; Long, D. D.; Marquess, D. G.; Claridge, T. D. W.; Fleet, G. W. J. *Chem. Commun.* **1998**, 2039–2040.
- (354) Gervay, J.; Flaherty, T. M.; Nguyen, C. *Tetrahedron Lett.* **1997**, *38*, 1493–1496.
- (355) Locardi, E.; Stöckle, M.; Gruner, S.; Kessler, H. *J. Am. Chem. Soc.* **2001**, *123*, 8189–8196.
- (356) Szabo, L.; Smith, B. L.; McReynolds, K. D.; Parrill, A. L.; Morris, E. R.; Gervay, J. *J. Org. Chem.* **1998**, *63*, 1074–1078.
- (357) McReynolds, K. D.; Gervay-Hague, J. *Tetrahedron Asymmetry* **2000**, *11*, 337–362.
- (358) Smith, M. D.; Claridge, T. D. W.; Tranter, G. E.; Sansom, M. S. P.; Fleet, G. W. J. *Chem. Commun.* **1998**, 2041–2042.
- (359) Brittain, D. E. A.; Watterson, M. P.; Claridge, T. D. W.; Smith, M. D.; Fleet, G. W. J. *J. Chem. Soc., Perkin Trans. 1* **2000**, 3655–3665.
- (360) Claridge, T. D. W.; Long, D. D.; Hungerford, N. L.; Aplin, R. T.; Smith, M. D.; Marquess, D. G.; Fleet, G. W. J. *Tetrahedron Lett.* **1999**, *40*, 2199–2202.

- (361) Hungerford, N. L.; Claridge, T. D. W.; Watterson, M. P.; Aplin, R. T.; Moreno, A.; Fleet, G. W. J. *J. Chem. Soc., Perkin Trans. 1* **2000**, 3666–3679.
- (362) Smith, M. D.; Long, D. D.; Martin, A.; Marquess, D. G.; Claridge, T. D. W.; Fleet, G. W. J. *Tetrahedron Lett.* **1999**, *40*, 2191–2194.
- (363) Chakraborty, T. K.; Jayaprakash, S.; Srinivasu, P.; Chary, M. G.; Diwan, P. V.; Nagaraj, R.; Sankar, A. R.; Kunwar, A. C. *Tetrahedron Lett.* **2000**, *41*, 8167–8171.
- (364) Schrey, A.; Vescovi, A.; Knoll, A.; Rickert, C.; Koert, U. *Angew. Chem., Int. Ed.* **2000**, *39*, 900–902.
- (365) Koert, U.; Stein, M.; Harms, K. *Angew. Chem., Int. Ed. Engl.* **1994**, *33*, 1180–1182.
- (366) Wagner, H.; Harms, K.; Koert, U.; Meder, S.; Boheim, G. *Angew. Chem., Int. Ed. Engl.* **1996**, *35*, 2643–2646.
- (367) Kirshenbaum, K.; Zuckermann, R. N.; Dill, K. A. *Curr. Opin. Struct. Biol.* **1999**, *9*, 530–535.
- (368) Magnus, P.; Danikiewicz, W.; Katoh, T.; Huffman, J. C.; Folting, K. *J. Am. Chem. Soc.* **1990**, *112*, 2465–2468.
- (369) Takata, T.; Furusho, Y.; Murakawa, K.; Endo, T.; Matsuoka, H.; Hirasa, T.; Matsuo, J.; Sisido, M. *J. Am. Chem. Soc.* **1998**, *120*, 4530–4531.
- (370) Grubbs, R. H.; Kratz, D. *Chem. Ber.* **1993**, *126*, 149–157.
- (371) Blake, A. J.; Cooke, P. A.; Doyle, K. J.; Gair, S.; Simpkins, N. S. *Tetrahedron Lett.* **1998**, *39*, 9093–9096.
- (372) Williams, D. J.; Colquhoun, H. M.; O'Mahoney, C. A. *J. Chem. Soc., Chem. Commun.* **1994**, 1643–1644.
- (373) Baxter, I.; Colquhoun, H. M.; Kohnke, F. H.; Lewis, D. F.; Williams, D. J. *Polymer* **1999**, *40*, 607–612.
- (374) Li, C. J.; Slaven, W. T.; Chen, Y. P.; John, V. T.; Rachakonda, S. H. *Chem. Commun.* **1998**, 1351–1352.
- (375) Kilbinger, A. F. M.; Schenning, A.; Goldoni, F.; Feast, W. J.; Meijer, E. W. *J. Am. Chem. Soc.* **2000**, *122*, 1820–1821.
- (376) Kilbinger, A. F. M.; Cooper, H. J.; McDonnell, L. A.; Feast, W. J.; Derrick, P. J.; Schenning, A.; Meijer, E. W. *Chem. Commun.* **2000**, 383–384.
- (377) Bassani, D. M.; Lehn, J.-M. *Bull. Chem. Soc. Fr.* **1997**, *134*, 897–906.
- (378) Bassani, D. M.; Lehn, J.-M.; Baum, G.; Fenske, D. *Angew. Chem., Int. Ed.* **1997**, 1845–1847.
- (379) Ohkita, M.; Lehn, J.-M.; Baum, G.; Fenske, D. *Chem. Eur. J.* **1999**, *5*, 3471–3481.
- (380) Ohkita, M.; Lehn, J.-M.; Baum, G.; Fenske, D. *Heterocycles* **2000**, *52*, 103–109.
- (381) Gardinier, K. M.; Khoury, R. G.; Lehn, J.-M. *Chem. Eur. J.* **2000**, *6*, 4124–4131.
- (382) Cuccia, L. A.; Lehn, J.-M.; Homo, J.-C.; Schmutz, M. *Angew. Chem., Int. Ed.* **2000**, *39*, 233–237.
- (383) Tanatani, A.; Kagechika, H.; Azumaya, I.; Yamaguchi, K.; Shudo, K. *Chem. Pharm. Bull.* **1996**, *44*, 1135–1137.
- (384) Tanatani, A.; Kagechika, H.; Azumaya, I.; Fukutomi, R.; Ito, Y.; Yamaguchi, K.; Shudo, K. *Tetrahedron Lett.* **1997**, *38*, 4425–4428.
- (385) Tanatani, A.; Yamaguchi, K.; Azumaya, I.; Fukutomi, R.; Shudo, K.; Kagechika, H. *J. Am. Chem. Soc.* **1998**, *120*, 6433–6442.
- (386) Fukutomi, R.; Tanatani, A.; Kakuta, H.; Tomioka, N.; Itai, A.; Hashimoto, Y.; Shudo, K.; Kagechika, H. *Tetrahedron Lett.* **1998**, *39*, 6475–6478.
- (387) Kagechika, H.; Azumaya, I.; Tanatani, A.; Yamaguchi, K.; Shudo, K. *Tetrahedron Lett.* **1999**, *40*, 3423–3426.
- (388) Lokey, R. S.; Iverson, B. L. *Nature* **1995**, *375*, 303–305.
- (389) Zych, A. J.; Iverson, B. L. *J. Am. Chem. Soc.* **2000**, *122*, 8898–8909.
- (390) Lokey, R. S.; Kwok, Y.; Guelev, V.; Pursell, C. J.; Hurley, L. H.; Iverson, B. L. *J. Am. Chem. Soc.* **1997**, *119*, 7202–7210.
- (391) Nguyen, J. Q.; Iverson, B. L. *J. Am. Chem. Soc.* **1999**, *121*, 2639–2640.
- (392) Martin, C. B.; Patrick, B. O.; Cammers-Goodwin, A. *J. Org. Chem.* **1999**, *64*, 7807–7812.
- (393) Martin, C. B.; Mulla, H. R.; Willis, P. G.; Cammers-Goodwin, A. *J. Org. Chem.* **1999**, *64*, 7802–7806.
- (394) Mulla, H. R.; Cammers-Goodwin, A. *J. Am. Chem. Soc.* **2000**, *122*, 738–739.
- (395) Sindkhedkar, M. D.; Mulla, H. R.; Cammers-Goodwin, A. *J. Am. Chem. Soc.* **2000**, *122*, 9271–9277.
- (396) Sindkhedkar, M. D.; Mulla, H. R.; Worth, M. A.; Cammers-Goodwin, A. *Tetrahedron* **2001**, *57*, 2991–2996.
- (397) Josten, W.; Karbach, D.; Nieger, M.; Vögtle, F.; Hägele, K.; Svoboda, M.; Przybylski, M. *Chem. Ber.* **1994**, *127*, 767–777.
- (398) Josten, W.; Neumann, S.; Vögtle, F.; Nieger, M.; Hägele, K.; Przybylski, M.; Beer, F.; Müllen, K. *Chem. Ber.* **1994**, *127*, 2089–2096.
- (399) Breidenbach, S.; Ohren, S.; Nieger, M.; Vögtle, F. *J. Chem. Soc., Chem. Commun.* **1995**, 1237–1238.
- (400) Breidenbach, S.; Ohren, S.; Vögtle, F. *Chem. Eur. J.* **1996**, *2*, 832–837.
- (401) Breidenbach, S.; Ohren, S.; Herbst-Irmer, R.; Kotila, S.; Nieger, M.; Vögtle, F. *Liebigs Ann.* **1996**, 2115–2121.
- (402) Boomgaarden, W.; Vögtle, F.; Nieger, M.; Hupfer, H. *Chem. Eur. J.* **1999**, *5*, 345–355.
- (403) Schwierz, H.; Vögtle, F. *Synthesis* **1999**, *2*, 295–305.
- (404) Sakurai, S.-i.; Goto, H.; Yashima, E. *Org. Lett.* **2001**, *3*, 2379–2382.
- (405) Moore, J. S.; Nelson, J. C.; Prince, R. B. Fourth Francqui Symposium, Brussels, Belgium, 1999; p 263–290.
- (406) Nelson, J. C.; Saven, J. G.; Moore, J. S.; Wolynes, P. G. *Science* **1997**, *277*, 1793–1796.
- (407) Defined according to classic polymer chemistry: see ref 31.
- (408) Monitored at 350 nm in the emission spectra.
- (409) Pace, C. N. In *Methods in Enzymology*; Hirs, C. H. W., Timasheff, S. N., Eds.; Academic Press: New York, 1986; Vol. 131.
- (410) See ref 62.
- (411) Prince, R. B.; Brunsveld, L.; Meijer, E. W.; Moore, J. S. *Angew. Chem., Int. Ed.* **2000**, *39*, 228–230.
- (412) Gin, M. S.; Yokozawa, T.; Prince, R. B.; Moore, J. S. *J. Am. Chem. Soc.* **1999**, *121*, 2643–2644.
- (413) Gin, M. S.; Moore, J. S. *Org. Lett.* **2000**, *2*, 135–138.
- (414) Finkelstein, A. V.; Shakhnovich, E. I. *Biopolymers* **1989**, *28*, 1681–1694.
- (415) Shakhnovich, E. I.; Finkelstein, A. V. *Biopolymers* **1989**, *28*, 1667–1680.
- (416) Dill, K. A.; Stigter, D. *Adv. Protein Chem.* **1995**, *46*, 59–104.
- (417) Prince, R. B.; Moore, J. S.; Brunsveld, L.; Meijer, E. W. *Chem. Eur. J.* **2001**, *7*, 4150–4154.
- (418) Brunsveld, L.; Meijer, E. W.; Prince, R. B.; Moore, J. S. *J. Am. Chem. Soc.* **2001**, *123*, 7978–7984.
- (419) Brunsveld, L.; Prince, R. B.; Meijer, E. W.; Moore, J. S. *Org. Lett.* **2000**, *2*, 1525–1528.
- (420) Prince, R. B.; Barnes, S. A.; Moore, J. S. *J. Am. Chem. Soc.* **2000**, *122*, 2758–2762.
- (421) Mecozzi, S.; Rebek, J., Jr. *Chem. Eur. J.* **1998**, *4*, 1016–1022.
- (422) Tanatani, A.; Mio, M. J.; Moore, J. S. *J. Am. Chem. Soc.* **2001**, *123*, 1792–1793.
- (423) Prest, P.-J.; Prince, R. B.; Moore, J. S. *J. Am. Chem. Soc.* **1999**, *121*, 5933–5939.
- (424) Mio, M. J.; Moore, J. S. *MRS Bull.* **2000**, *25*, 36–41.
- (425) Mio, M. J.; Prince, R. B.; Moore, J. S.; Kuebel, C.; Martin, D. C. *J. Am. Chem. Soc.* **2000**, *122*, 6134–6135.
- (426) Mio, M. J. Ph.D. Thesis, University of Illinois, Urbana, IL, 2001.
- (427) Mindyuk, O. Y.; Stetzer, M. R.; Heiney, P. A.; Nelson, J. C.; Moore, J. S. *Adv. Mater.* **1998**, *10*, 1363–1366.
- (428) Mindyuk, O. Y.; Stetzer, M. R.; Gidalevitz, D.; Heiney, P. A.; Nelson, J. C.; Moore, J. S. *Langmuir* **1999**, *15*, 6897–6900.
- (429) Prince, R. B. Ph.D. Thesis, University of Illinois, Urbana, IL, June 2000.
- (430) Palmans, A. R. A.; Vekemans, J.; Meijer, E. W. *Rec. Trav. Chim. Pays-Bas* **1995**, *114*, 277–284.
- (431) Delnoye, D. A. P.; Sijbesma, R. P.; Vekemans, J.; Meijer, E. W. *J. Am. Chem. Soc.* **1996**, *118*, 8717–8718.
- (432) Pieterse, K.; Vekemans, J.; Kooijman, H.; Spek, A. L.; Meijer, E. W. *Chem. Eur. J.* **2000**, *6*, 4597–4603.
- (433) Palmans, A. R. A.; Vekemans, J. A. J. M.; Fischer, H.; Hikmet, R. A.; Meijer, E. W. *Chem. Eur. J.* **1997**, *3*, 300–307.
- (434) Palmans, A. R. A.; Vekemans, J. A. J. M.; Havinga, E. E.; Meijer, E. W. *Angew. Chem., Int. Ed. Engl.* **1997**, *36*, 2648–2651.
- (435) Palmans, A. R. A.; Vekemans, J. A. J. M.; Hikmet, R. A.; Fischer, H.; Meijer, E. W. *Adv. Mater.* **1998**, *10*, 873–876.
- (436) Brunsveld, L.; Zhang, H.; Glasbeek, M.; Vekemans, J. A. J. M.; Meijer, E. W. *J. Am. Chem. Soc.* **2000**, *122*, 6175–6182.
- (437) Brunsveld, L.; Lohmeijer, B. G. G.; Vekemans, J. A. J. M.; Meijer, E. W. *Chem. Commun.* **2000**, 2305–2306.
- (438) van der Schoot, P.; Michels, M. A. J.; Brunsveld, L.; Sijbesma, R. P.; Ramzi, A. *Langmuir* **2000**, *16*, 10076–10083.
- (439) Hamuro, Y.; Geib, S. J.; Hamilton, A. D. *Angew. Chem., Int. Ed. Engl.* **1994**, 446–448.
- (440) Hamuro, Y.; Geib, S. J.; Hamilton, A. D. *J. Am. Chem. Soc.* **1996**, *118*, 7529–7541.
- (441) Hamuro, Y.; Geib, S. J.; Hamilton, A. D. *J. Am. Chem. Soc.* **1997**, *119*, 10587–10593.
- (442) Recker, J.; Tomcik, D. J.; Parquette, J. R. *J. Am. Chem. Soc.* **2000**, *122*, 10298–10307.
- (443) Huang, B.; Parquette, J. R. *Org. Lett.* **2000**, *2*, 239–242.
- (444) Huang, B.; Parquette, J. R. *J. Am. Chem. Soc.* **2001**, *123*, 2689–2690.
- (445) Gong, B.; Yan, Y. F.; Zeng, H. Q.; Skrzypczak-Jankun, E.; Kim, Y. W.; Zhu, J.; Ickes, H. *J. Am. Chem. Soc.* **1999**, *121*, 5607–5608.
- (446) Zeng, H. Q.; Miller, R. S.; Flowers, R. A.; Gong, B. *J. Am. Chem. Soc.* **2000**, *122*, 2635–2644.
- (447) Zhu, J.; Parra, R. D.; Zeng, H. Q.; Skrzypczak-Jankun, E.; Zeng, X. C.; Gong, B. *J. Am. Chem. Soc.* **2000**, *122*, 4219–4220.
- (448) Berl, V.; Krische, M. J.; Huc, I.; Lehn, J. M.; Schmutz, R. *Chem. Eur. J.* **2000**, *6*, 1938–1946.
- (449) Job, P. *Ann. Chim. (Paris)* **1928**, *9*, 113.
- (450) Ingham, K. C. *Anal. Biochem.* **1975**, *68*, 660–663.
- (451) Bielawski, C.; Chen, Y.-S.; Zhang, P.; Prest, P.-J.; Moore, J. S. *Chem. Commun.* **1998**, 1313–1314.
- (452) Archer, E. A.; Sochia, A. E.; Krische, M. J. *Tetrahedron* **2001**, *57*, 1139–1159.

- (453) Lehn, J.-M.; Rigault, A.; Siegel, J.; Harrowfield, J.; Chevrier, B.; Moras, D. *Proc. Natl. Acad. Sci. U.S.A.* **1987**, *84*, 2565–2569.
- (454) Albrecht, M. *Chem. Soc. Rev.* **1998**, *27*, 281–287.
- (455) Caulder, D. L.; Raymond, K. N. *J. Chem. Soc., Dalton Trans.* **1999**, 1185–1200.
- (456) Constable, E. C. *Tetrahedron* **1992**, *48*, 10013–10059.
- (457) Piguet, C.; Bernardinelli, G.; Hopfgartner, G. *Chem. Rev.* **1997**, *97*, 2005–2062.
- (458) Mizutani, T.; Yagi, S.; Morinaga, T.; Nomura, T.; Takagishi, T.; Kitagawa, S.; Ogoshi, H. *J. Am. Chem. Soc.* **1999**, *121*, 754–759.
- (459) Yagi, S.; Morinaga, T.; Nomura, T.; Takagishi, T.; Mizutani, T.; Kitagawa, S.; Ogoshi, H. *J. Org. Chem.* **2001**, *66*, 3848–3853.
- (460) Yagi, S.; Sakai, N.; Yamada, R.; Takahashi, H.; Mizutani, T.; Takagishi, T.; Kitagawa, S.; Ogoshi, H. *Chem. Commun.* **1999**, 911–912.
- (461) Mizutani, T.; Yagi, S.; Honmaru, A.; Murakami, S.; Furusyo, M.; Takagishi, T.; Ogoshi, H. *J. Org. Chem.* **1998**, *63*, 8769–8784.
- (462) Mizutani, T.; Sakai, N.; Yagi, S.; Takagishi, T.; Kitagawa, S.; Ogoshi, H. *J. Am. Chem. Soc.* **2000**, *122*, 748–749.
- (463) Constable, E. C.; Elder, S. M.; Healey, J.; Tocher, D. A. *J. Chem. Soc., Dalton Trans.* **1990**, 1669–1674.
- (464) Von Henke, W.; Kremer, S.; Reinen, D. *Z. Anorg. Allg. Chem.* **1982**, *491*, 124–136.
- (465) Maslen, E. N.; Raston, C. L.; White, A. H. *J. Chem. Soc., Dalton Trans.* **1975**, 323–326.
- (466) Constable, E. C.; Elder, S. M.; Healy, J.; Ward, M. D.; Tocher, D. A. *J. Am. Chem. Soc.* **1990**, *112*, 4590–4592.
- (467) Constable, E. C.; Elder, S. M.; Tocher, D. A. *Polyhedron* **1992**, *11*, 1337–1342.
- (468) Constable, E. C.; Elder, S. M.; Tocher, D. A. *Polyhedron* **1992**, *11*, 2599–2604.
- (469) Constable, E. C.; Harverson, P.; Smith, D. R.; Whall, L. A. *Tetrahedron* **1994**, *50*, 7799–7806.
- (470) Potts, K. T.; Keshavarz-K, M.; Tham, F. S.; Gheysen, K. A.; Arana, C.; Abuña, H. D. *Inorg. Chem.* **1993**, *32*, 5477–5484.
- (471) Constable, E. C.; Drew, M. G. B.; Forsyth, G.; Ward, M. D. *J. Chem. Soc., Chem. Commun.* **1988**, 1450–1451.
- (472) Ho, P. K.-K.; Cheung, K.-K.; Peng, S.-M.; Che, C.-M. *J. Chem. Soc., Dalton Trans.* **1996**, 1411–1417.
- (473) Fu, Y.-J.; Sun, W.-Y.; Dai, W.-N.; Shu, M.-H.; Xue, F.; Wang, D.-F.; Mak, T. C. W.; Tang, W.-X.; Hu, H.-W. *Inorg. Chim. Acta* **1999**, *290*, 127–132.
- (474) Constable, E. C.; Chotalia, R.; Tocher, D. A. *J. Chem. Soc., Chem. Commun.* **1992**, 771–773.
- (475) Constable, E. C.; Ward, M. D.; Tocher, D. A. *J. Chem. Soc., Dalton Trans.* **1991**, 1675–1683.
- (476) See ref 110.
- (477) Sessler, J. L.; Weghorn, S. J.; Lynch, V.; Fransson, K. *J. Chem. Soc., Chem. Commun.* **1994**, 1289–1290.
- (478) Watson, J. D.; Crick, F. H. C. *Nature* **1953**, *171*, 737–738.
- (479) Eschenmoser, A.; Loewenthal, E. *Chem. Soc. Rev.* **1992**, *21*, 1–16.
- (480) Eschenmoser, A. *Origins Life Evol. Biosphere* **1994**, *24*, 389–423.
- (481) Eschenmoser, A.; Kisakürek, M. V. *Helv. Chim. Acta* **1996**, *79*, 1249–1259.
- (482) Uhlmann, E.; Peyman, A. *Chem. Rev.* **1990**, *90*, 543–584.
- (483) Milligan, J. F.; Matteucci, M. D.; Martin, J. C. *J. Med. Chem.* **1993**, *36*, 1923–1937.
- (484) De Mesmaeker, A.; Häner, R.; Martin, P.; Moser, H. E. *Acc. Chem. Res.* **1995**, *28*, 366–374.
- (485) Egli, M. *Angew. Chem., Int. Ed. Engl.* **1996**, *35*, 1894–1909.
- (486) Herdewijn, P. *Biochim. Biophys. Acta* **1999**, *1489*, 167–179.
- (487) Saenger, W. *Principles of Nucleic Acid Structure*; Springer-Verlag: New York, 1984.
- (488) Vesnaver, G.; Breslauer, K. J. *Proc. Natl. Acad. Sci. U.S.A.* **1991**, *88*, 3569–3573.
- (489) Levitt, M.; Warshel, A. *J. Am. Chem. Soc.* **1978**, *100*, 2607–2613.
- (490) Bush, C. A.; Brahm, J. In *Physico-Chemical Properties of Nucleic Acids*; Duchesne, J., Ed.; Academic Press: London and New York, 1973; Vol. 2.
- (491) Herdewijn, P. *Liebigs Ann.* **1996**, 1337–1348.
- (492) Kerr, I. M.; Brown, R. E. *Proc. Natl. Acad. Sci. U.S.A.* **1978**, *75*, 256–260.
- (493) Dougherty, J. P.; Rizzo, C. J.; Breslow, R. *J. Am. Chem. Soc.* **1992**, *114*, 6254–6255.
- (494) Hashimoto, H.; Switzer, C. *J. Am. Chem. Soc.* **1992**, *114*, 6255–6256.
- (495) Kierzek, R.; He, L.; Turner, D. H. *Nucleic Acids Res.* **1992**, *20*, 1685–1690.
- (496) Robinson, H.; Jung, K.-E.; Switzer, C.; Wang, A. H.-J. *J. Am. Chem. Soc.* **1995**, *117*, 837–838.
- (497) Jung, K.-E.; Switzer, C. *J. Am. Chem. Soc.* **1994**, *116*, 6059–6061.
- (498) Cheng, X.; Gao, Q.; Smith, R. D.; Jung, K.-E.; Switzer, C. *Chem. Commun.* **1996**, 747–748.
- (499) Giannaris, P. A.; Dahma, M. *Nucleic Acids Res.* **1993**, *21*, 4742–4749.
- (500) Sheppard, T. L.; Breslow, R. C. *J. Am. Chem. Soc.* **1996**, *118*, 9810–9811.
- (501) Prakash, T. P.; Jung, K.-E.; Switzer, C. *Chem. Commun.* **1996**, 1793–1794.
- (502) Kandimalla, E. R.; Manning, A.; Zhou, Q.; Shaw, D. R.; Byrn, R. A.; Sasisekharan, V.; Agrawal, S. *Nucleic Acids Res.* **1997**, *25*, 370–378.
- (503) Wasner, M.; Arion, D.; Borkow, G.; Noronha, A.; Uddin, A. H.; Parniak, M. A.; Damha, M. J. *Biochemistry* **1998**, *37*, 7478–7486.
- (504) Jin, R.; Chapman, W. H., Jr.; Srinivasan, A. R.; Olson, W. K.; Breslow, R.; Breslauer, K. J. *Proc. Natl. Acad. Sci. U.S.A.* **1993**, *90*, 10568–10572.
- (505) Sawai, H.; Seki, J.; Ozaki, H. *J. Biomol. Struct. Dyn.* **1996**, *13*, 1043–1051.
- (506) Joyce, G. F.; Visser, G. M.; van Boeckel, C. A. A.; van Boom, J. H.; Orgel, L. E.; van Westrenen, J. *Nature* **1984**, *310*, 602–604.
- (507) Prakash, T. P.; Roberts, C.; Switzer, C. *Angew. Chem., Int. Ed. Engl.* **1997**, *36*, 1522–1523.
- (508) Morvan, F.; Rayner, B.; Imbach, J.-L.; Chang, D.-K.; Lown, J. W. *Nucleic Acids Res.* **1986**, *14*, 5019–5035.
- (509) Morvan, F.; Rayner, B.; Imbach, J.-L.; Chang, D.-K.; Lown, J. W. *Nucleic Acids Res.* **1987**, *15*, 4241–4255.
- (510) Morvan, F.; Rayner, B.; Imbach, J.-L.; Lee, M.; Hartley, J. A.; Chang, D.-K.; Lown, J. W. *Nucleic Acids Res.* **1987**, *15*, 7027–7044.
- (511) Thuong, N.; Asseline, U.; Roig, V.; Takasugi, M.; Hélène, C. *Proc. Natl. Acad. Sci. U.S.A.* **1987**, *84*, 5129–5133.
- (512) Koga, M.; Moore, M. F.; Beaucage, S. L. *J. Org. Chem.* **1991**, *56*, 3757–3759.
- (513) Debart, F.; Tosquellas, G.; Rayner, B.; Imbach, J.-L. *Bioorg. Med. Chem. Lett.* **1994**, *4*, 1041–1046.
- (514) Koga, M.; Wilk, A.; Moore, M. F.; Scremin, C. L.; Zhou, L.; Beaucage, S. L. *J. Org. Chem.* **1995**, *60*, 1520–1530.
- (515) Gagnor, C.; Bertrand, J.-R.; Thenet, S.; Lemaître, M.; Morvan, F.; Rayner, B.; Malvy, C.; Lebleu, B.; Imbach, J.-L.; Paoletti, C. *Nucleic Acids Res.* **1987**, *15*, 10419–10436.
- (516) Paoletti, J.; Bazile, D.; Morvan, F.; Imbach, J.-L.; Paoletti, C. *Nucleic Acids Res.* **1989**, *17*, 2693–2704.
- (517) Fujimori, S.; Shudo, K.; Hashimoto, Y. *J. Am. Chem. Soc.* **1990**, *112*, 7436–7438.
- (518) Garbesi, A.; Capobianco, M. L.; Colonna, F. P.; Tondelli, L.; Arcamone, F.; Manzini, G.; Hilbers, C. W.; Aelen, J. M. E.; Blommers, M. J. *J. Nucleic Acids Res.* **1993**, *21*, 4159–4165.
- (519) Schöppe, A.; Hinz, H.-J.; Rosemeyer, H.; Seela, F. *Eur. J. Biochem.* **1996**, *239*, 33–41.
- (520) Giannaris, P. A.; Dahma, M. J. *Can. J. Chem.* **1994**, *72*, 909–918.
- (521) Eschenmoser, A. *Science* **1999**, *284*, 2118–2124.
- (522) Eschenmoser, A.; Krishnamurthy, R. *Pure Appl. Chem.* **2000**, *72*, 343–345.
- (523) Schöning, K.-U.; Scholz, P.; Guntha, S.; Wu, X.; Krishnamurthy, R.; Eschenmoser, A. *Science* **2000**, *290*, 1347–1351.
- (524) Herdewijn, P. *Angew. Chem., Int. Ed.* **2001**, *40*, 2249–2251.
- (525) Schlönvogt, I.; Pitsch, S.; Lesueur, C.; Eschenmoser, A.; Jaun, B.; Wolf, R. M. *Helv. Chim. Acta* **1996**, *79*, 2316–2345.
- (526) Böhringer, M.; Roth, H.-J.; Hunziker, J.; Göbel, M.; Krishnan, R.; Giger, A.; Schweizer, B.; Schreiber, J.; Leumann, C.; Eschenmoser, A. *Helv. Chim. Acta* **1992**, *75*, 1416–1477.
- (527) Pitsch, S.; Pombo-Villar, E.; Eschenmoser, A. *Helv. Chim. Acta* **1994**, *77*, 2251–2285.
- (528) Pitsch, S.; Wendeborn, S.; Jann, B.; Eschenmoser, A. *Helv. Chim. Acta* **1993**, *76*, 2161–2183.
- (529) Hunziker, J.; Roth, H.-J.; Böhringer, M.; Giger, A.; Diederichsen, U.; Göbel, M.; Krishnan, R.; Jaun, B.; Leumann, C.; Eschenmoser, A. *Helv. Chim. Acta* **1993**, *76*, 259–352.
- (530) Micura, R.; Kudick, R.; Pitsch, S.; Eschenmoser, A. *Angew. Chem., Int. Ed. Engl.* **1999**, *38*, 680–683.
- (531) Pitsch, S.; Krishnamurthy, R.; Bolli, M.; Wendeborn, S.; Holzner, A.; Minton, M.; Lesueur, C.; Schlönvogt, I.; Jaun, B.; Eschenmoser, A. *Helv. Chim. Acta* **1995**, *78*, 1621–1635.
- (532) Krishnamurthy, R.; Pitsch, S.; Minton, M.; Miculka, M.; Windhab, N.; Eschenmoser, A. *Angew. Chem., Int. Ed. Engl.* **1996**, *35*, 1537–1541.
- (533) Micura, R.; Bolli, M.; Windhab, N.; Eschenmoser, A. *Angew. Chem., Int. Ed. Engl.* **1997**, *36*, 870–873.
- (534) Beier, M.; Reck, F.; Wagner, T.; Krishnamurthy, R.; Eschenmoser, A. *Science* **1999**, *283*, 699–703.
- (535) Jungmann, O.; Wippo, H.; Stanek, M.; Huynh, H. K.; Krishnamurthy, R.; Eschenmoser, A. *Org. Lett.* **1999**, *1*, 1527–1530.
- (536) Reck, F.; Wippo, H.; Kudick, R.; Krishnamurthy, R.; Eschenmoser, A. *Helv. Chim. Acta* **2001**, *84*, 1778–1804.
- (537) Reck, F.; Wippo, H.; Kudick, R.; Bolli, M.; Ceulemans, G.; Krishnamurthy, R.; Eschenmoser, A. *Org. Lett.* **1999**, *1*, 1531–1534.
- (538) Eschenmoser, A.; Dobler, M. *Helv. Chim. Acta* **1992**, *75*, 218–259.
- (539) Augustyns, K.; Van Aerschot, A.; Urbanke, C.; Herdewijn, P. *Bull. Soc. Chim. Belg.* **1992**, *101*, 119–130.

- (540) Otting, G.; Billeter, M.; Wüthrich, K.; Roth, H.-J.; Leumann, C.; Eschenmoser, A. *Helv. Chim. Acta* **1993**, *76*, 2701–2756.
- (541) Groebke, K.; Hunziker, J.; Fraser, W.; Peng, L.; Diederichsen, U.; Zimmerman, K.; Holzner, A.; Leumann, C.; Eschenmoser, A. *Helv. Chim. Acta* **1998**, *81*, 375–474.
- (542) Augustyns, K.; Rozenski, J.; Van Aerschot, A.; Janssen, G.; Herdewijn, P. *J. Org. Chem.* **1993**, *58*, 2977–2982.
- (543) Augustyns, K.; Vandendriessche, F.; Van Aerschot, A.; Busson, R.; Urbanke, C.; Herdewijn, P. *Nucleic Acids Res.* **1992**, *20*, 4711–4716.
- (544) Yu, H.-W.; Zhang, L.-R.; Zhou, J.-C.; Ma, L.-T.; Zhang, L.-H. *Bioorg. Med. Chem.* **1996**, *4*, 609–614.
- (545) Yang, Z.-J.; Zhang, H.-Y.; Min, J.-M.; Ma, L.-T.; Zhang, L.-H. *Helv. Chim. Acta* **1999**, *82*, 2037–2043.
- (546) Lei, Z.; Zhang, L.; Zhang, L.-R.; Chen, J.; Min, J.-M.; Zhang, L.-H. *Nucleic Acids Res.* **2001**, *29*, 1470–1475.
- (547) Van Aerschot, A.; Verheggen, I.; Herdewijn, P. *Bioorg. Med. Chem. Lett.* **1993**, *3*, 1013–1018.
- (548) De Bouvere, B.; Kerremans, L.; Rozenski, J.; Janssen, G.; Van Aerschot, A.; Claes, P.; Busson, R.; Herdewijn, P. *Liebigs Ann.* **1997**, 1453–1461.
- (549) Hendrix, C.; Rosemeyer, H.; Verheggen, I.; Seela, F.; Van Aerschot, A.; Herdewijn, P. *Chem. Eur. J.* **1997**, *3*, 110–120.
- (550) Van Aerschot, A.; Verheggen, I.; Hendrix, C.; Herdewijn, P. *Angew. Chem., Int. Ed. Engl.* **1995**, *34*, 1338–1339.
- (551) Hendrix, C.; Rosemeyer, H.; De Bouvere, B.; Van Aerschot, A.; Seela, F.; Herdewijn, P. *Chem. Eur. J.* **1997**, *3*, 1513–1520.
- (552) Boudou, V.; Kerremans, L.; De Bouvere, B.; Lescrinier, E.; Schepers, G.; Busson, R.; Van Aerschot, A.; Herdewijn, P. *Nucleic Acids Res.* **1999**, *27*, 1450–1456.
- (553) Lescrinier, E.; Esnouf, R.; Schraml, J.; Busson, R.; Heus, H. A.; Hilbers, C. W.; Herdewijn, P. *Chem. Biol.* **2000**, *7*, 719–731.
- (554) De Winter, H.; Lescrinier, E.; Van Aerschot, A.; Herdewijn, P. *J. Am. Chem. Soc.* **1998**, *120*, 5381–5394.
- (555) Froeyen, M.; Wroblowski, B.; Esnouf, R.; De Winter, H.; Allart, B.; Lescrinier, E.; Herdewijn, P. *Helv. Chim. Acta* **2000**, *83*, 2153–2182.
- (556) Lescrinier, E.; Esnouf, R.; Schraml, J.; Busson, R.; Herdewijn, P. *Helv. Chim. Acta* **2000**, *83*, 1291–1310.
- (557) Allart, B.; Busson, R.; Rozenski, J.; Van Aerschot, A.; Herdewijn, P. *Tetrahedron* **1999**, *55*, 6527–6546.
- (558) Allart, B.; Khan, K.; Rosemeyer, H.; Schepers, G.; Hendrix, C.; Rothenbacher, K.; Seela, F.; Van Aerschot, A.; Herdewijn, P. *Chem. Eur. J.* **1999**, *5*, 2424–2431.
- (559) Hossain, N.; Wroblowski, B.; Van Aerschot, A.; Rozenski, J.; De Bruyn, A.; Herdewijn, P. *J. Org. Chem.* **1998**, *63*, 1574–1582.
- (560) Maurinsh, Y.; Schraml, J.; De Winter, H.; Blaton, N.; Peeters, O.; Lescrinier, E.; Rozenski, J.; Van Aerschot, A.; De Clercq, E.; Busson, R.; Herdewijn, P. *J. Org. Chem.* **1997**, *62*, 2861–2871.
- (561) Maurinsh, Y.; Rosemeyer, H.; Esnouf, R.; Medvedovici, A.; Wang, J.; Ceulemans, G.; Lescrinier, E.; Hendrix, C.; Busson, R.; Sandra, P.; Seela, F.; Van Aerschot, A.; Herdewijn, P. *Chem. Eur. J.* **1999**, *5*, 2139–2150.
- (562) Wang, J.; Busson, R.; Blaton, N.; Rozenski, J.; Herdewijn, P. *J. Org. Chem.* **1998**, *63*, 3051–3058.
- (563) Wang, J.; Verbeure, B.; Luyten, I.; Lescrinier, E.; Froeyen, M.; Hendrix, C.; Rosemeyer, H.; Seela, F.; Van Aerschot, A.; Herdewijn, P. *J. Am. Chem. Soc.* **2000**, *122*, 8595–8602.
- (564) Herdewijn, P.; De Clercq, E. *Bioorg. Med. Chem. Lett.* **2001**, *11*, 1591–1597.
- (565) Shimada, N.; Hasegawa, S.; Harada, T.; Tomisawa, T.; Fujii, A.; Takita, T. *J. Antibiot.* **1986**, *39*, 1623–1625.
- (566) Kakefuda, A.; Masuda, A.; Ueno, Y.; Ono, A.; Matsuda, A. *Tetrahedron* **1996**, *52*, 2863–2876.
- (567) Katagiri, N.; Morishita, Y.; Oosawa, I.; Yamaguchi, M. *Tetrahedron Lett.* **1999**, *40*, 6835–6840.
- (568) Honzawa, S.; Ohwada, S.; Morishita, Y.; Sato, K.; Katagiri, N.; Yamaguchi, M. *Tetrahedron* **2000**, *56*, 2615–2627.
- (569) Henlin, J.-M.; Rink, H.; Spieser, E.; Baschang, G. *Helv. Chim. Acta* **1992**, *75*, 589–603.
- (570) Henlin, J.-M.; Jaekel, K.; Moser, P.; Rink, H.; Spieser, E.; Baschang, G. *Angew. Chem., Int. Ed. Engl.* **1992**, *31*, 482–484.
- (571) Borthwick, A. D.; Biggadike, K. *Tetrahedron* **1992**, *48*, 571–623.
- (572) Agrofoglio, L.; Suhas, E.; Farese, A.; Condom, R.; Challand, S. R.; Earl, R. A.; Guedj, R. *Tetrahedron* **1994**, *50*, 10611–10670.
- (573) Meldgaard, M.; Wengel, J. *J. Chem. Soc., Perkin Trans. 1* **2000**, 3539–3554.
- (574) Tarköy, M.; Bolli, M.; Schweizer, B.; Leumann, C. *Helv. Chim. Acta* **1993**, *76*, 481–510.
- (575) Bolli, M.; Leumann, C. *Angew. Chem., Int. Ed. Engl.* **1995**, *34*, 694–696.
- (576) Tarköy, M.; Leumann, C. *Angew. Chem., Int. Ed. Engl.* **1993**, *32*, 1432–1434.
- (577) Tarköy, M.; Bolli, M.; Leumann, C. *Helv. Chim. Acta* **1994**, *77*, 716–744.
- (578) Bolli, M.; Litten, J. C.; Schütz, R.; Leumann, C. *J. Chem. Biol.* **1996**, *3*, 197–206.
- (579) Bolli, M.; Trafelet, H. U.; Leumann, C. *Chem. Biol.* **1996**, *24*, 4660–4667.
- (580) Litten, J. C.; Epple, C.; Leumann, C. *J. Bioorg. Med. Chem. Lett.* **1995**, *5*, 1231–1234.
- (581) Litten, J. C.; Leumann, C. *Helv. Chim. Acta* **1996**, *79*, 1129–1146.
- (582) Steffens, R.; Leumann, C. *J. Am. Chem. Soc.* **1997**, *119*, 11548–11549.
- (583) Steffens, R.; Leumann, C. *Helv. Chim. Acta* **1997**, *80*, 2426–2439.
- (584) Steffens, R.; Leumann, C. *J. Am. Chem. Soc.* **1999**, *121*, 3249–3255.
- (585) Epple, C.; Leumann, C. *Chem. Biol.* **1998**, *5*, 209–216.
- (586) Keller, B. M.; Leumann, C. *J. Angew. Chem., Int. Ed.* **2000**, *39*, 2278–2281.
- (587) Obika, S.; Nanbu, D.; Hari, Y.; Morio, K.; In, Y.; Ishida, T.; Imanishi, T. *Tetrahedron Lett.* **1997**, *38*, 8735–8738.
- (588) Singh, S. K.; Nielsen, P.; Koshkin, A. A.; Wengel, J. *Chem. Commun.* **1998**, 455–456.
- (589) Wengel, J. *Acc. Chem. Res.* **1999**, *32*, 301–310.
- (590) Koshkin, A. A.; Singh, S. K.; Nielsen, P.; Rajwanshi, V. K.; Kumar, R.; Meldgaard, M.; Olsen, C. E.; Wengel, J. *Tetrahedron* **1998**, *54*, 3607–3630.
- (591) Singh, S. K.; Wengel, J. *Chem. Commun.* **1998**, 1247–1248.
- (592) Nielsen, C. B.; Singh, S. K.; Wengel, J.; Jacobsen, J. P. *J. Biomol. Struct. Dyn.* **1999**, *17*, 175–191.
- (593) Christensen, U.; Jacobsen, N.; Rajwanshi, V. K.; Wengel, J.; Koch, T. *Biochem. J.* **2001**, *354*, 481–484.
- (594) Rajwanshi, V. K.; Håkansson, A. E.; Dahl, B. M.; Wengel, J. *Chem. Commun.* **1999**, 1395–1396.
- (595) Rajwanshi, V. K.; Håkansson, A. E.; Kumar, R.; Wengel, J. *Chem. Commun.* **1999**, 2073–2074.
- (596) Rajwanshi, V. K.; Håkansson, A. E.; Sørensen, D.; Pitsch, S.; Singh, S. K.; Kumar, R.; Nielsen, P.; Wengel, J. *Angew. Chem., Int. Ed.* **2000**, *39*, 1656–1659.
- (597) Håkansson, A. E.; Wengel, J. *Bioorg. Med. Chem. Lett.* **2001**, *11*, 935–938.
- (598) Petersen, M.; Nielsen, C. B.; Nielsen, K. E.; Jensen, G. A.; Bondensgaard, K.; Singh, S. K.; Rajwanshi, V. K.; Koshkin, A. A.; Dahl, B. M.; Wengel, J.; Jacobsen, J. P. *J. Mol. Recognit.* **2000**, *13*, 44–53.
- (599) Bondensgaard, K.; Petersen, M.; Singh, S. K.; Rajwanshi, V. K.; Kumar, R.; Wengel, J.; Jacobsen, J. P. *Chem. Eur. J.* **2000**, *6*, 2687–2695.
- (600) Egli, M.; Minasov, G.; Teplova, M.; Kumar, R.; Wengel, J. *Chem. Commun.* **2001**, 651–652.
- (601) Kværnø, L.; Wengel, J. *Chem. Commun.* **1999**, 657–658.
- (602) Kværnø, L.; Kumar, R.; Dahl, B. M.; Olsen, C. E.; Wengel, J. *J. Org. Chem.* **2000**, *65*, 5167–5176.
- (603) Wahlestedt, C.; Salmi, P.; Good, L.; Kela, J.; Johnsson, T.; Hökfelt, T.; Broberger, C.; Porreca, F.; Lai, J.; Ren, K.; Ossipov, M.; Koshkin, A.; Jakobsen, N.; Skouv, J.; Oerum, H.; Jacobsen, M. H.; Wengel, J. *Proc. Natl. Acad. Sci. U.S.A.* **2000**, *97*, 5633–5638.
- (604) Obika, S.; Nanbu, D.; Hari, Y.; Andoh, J.-i.; Morio, K.-i.; Doi, T.; Imanishi, T. *Tetrahedron Lett.* **1998**, *39*, 5401–5404.
- (605) Obika, S.; Hari, Y.; Sugimoto, T.; Sekiguchi, M.; Imanishi, T. *Tetrahedron Lett.* **2000**, *40*, 8923–8927.
- (606) Obika, S.; Uneda, T.; Sugimoto, T.; Nanbu, D.; Minami, T.; Doi, T.; Imanishi, T. *Bioorg. Med. Chem.* **2001**, *9*, 1001–1011.
- (607) Obika, S.; Hari, Y.; Morio, K.-i.; Imanishi, T. *Tetrahedron Lett.* **2000**, *40*, 221–224.
- (608) Obika, S.; Morio, K.-i.; Nanbu, D.; Imanishi, T. *Chem. Commun.* **1997**, 1643–1644.
- (609) Obika, S.; Morio, K.-i.; Hari, Y.; Imanishi, T. *Chem. Commun.* **1999**, 2423–2424.
- (610) Obika, S.; Morio, K.-i.; Hari, Y.; Imanishi, T. *Bioorg. Med. Chem. Lett.* **1999**, *9*, 515–518.
- (611) Scremin, C. L.; Boal, K. H.; Wilk, A.; Phillips, L. R.; Beaucage, S. L. *Bioorg. Med. Chem. Lett.* **1996**, *6*, 207–212.
- (612) Hossain, N.; Hendrix, C.; Lescrinier, E.; Van Aerschot, A.; Busson, R.; De Clercq, E.; Herdewijn, P. *Bioorg. Med. Chem. Lett.* **1996**, *6*, 1465–1468.
- (613) Scremin, C. L.; Boal, J. H.; Wilk, A.; Phillips, L. R.; Zhou, L.; Beaucage, S. L. *Tetrahedron Lett.* **1995**, *36*, 8953–8956.
- (614) Boal, J. H.; Wilk, A.; Scremin, C. L.; Gray, G. N.; Phillips, L. R.; Beaucage, S. L. *J. Org. Chem.* **1996**, *61*, 8617–8626.
- (615) Marangoni, M.; Van Aerschot, A.; Augustyns, P.; Rozenski, J.; Herdewijn, P. *Nucleic Acids Res.* **1997**, *25*, 3034–3041.
- (616) Ceulemans, G.; Van Aerschot, A.; Wroblowski, B.; Rozenski, J.; Hendrix, C.; Herdewijn, P. *Chem. Eur. J.* **1997**, *3*, 1997–2010.
- (617) Schneider, K. C.; Benner, S. A. *J. Am. Chem. Soc.* **1990**, *112*, 453–455.
- (618) Peng, L.; Roth, H.-J. *Helv. Chim. Acta* **1997**, *80*, 1494–1512.
- (619) Augustyns, K.; Van Aerschot, A.; Van Schepdael, A.; Urbanke, C.; Herdewijn, P. *Nucleic Acids Res.* **1991**, *19*, 2587–2593.
- (620) Vandendriessche, F.; Augustyns, K.; Van Aerschot, A.; Busson, R.; Hoogmartens, J.; Herdewijn, P. *Tetrahedron* **1993**, *49*, 7223–7238.
- (621) Nielsen, P.; Kirpekar, F.; Wengel, J. *Nucleic Acids Res.* **1994**, *22*, 703–710.

- (622) Nielsen, P.; Dreieø, L. H.; Wengel, J. *Bioorg. Med. Chem.* **1995**, *3*, 19–28.
- (623) Kim, S.-G.; Tsukahara, S.; Yokoyama, S.; Takaku, H. *FEBS Lett.* **1992**, *314*, 29–32.
- (624) Hacia, J. G.; Wold, B. J.; Dervan, P. B. *Biochemistry* **1994**, *33*, 5367–5369.
- (625) Torigoe, H.; Shimizume, R.; Sarai, A.; Shindo, H. *Biochemistry* **1999**, *38*, 14653–14659.
- (626) Stein, C. A.; Cheng, Y.-C. *Science* **1993**, *261*, 1004–1012.
- (627) Alunni-Fabroni, M.; Manioletti, G.; Manzini, G.; Xodo, L. E. *Eur. J. Biochem.* **1994**, *226*, 831–839.
- (628) Xodo, L.; Alunni-Fabroni, M.; Manzini, G.; Quadrioglio, F. *Nucleic Acids Res.* **1994**, *22*, 3322–3330.
- (629) Lesnikowski, Z. J.; Jaworska, M.; Stec, W. J. *Nucleic Acids Res.* **1990**, *18*, 2112–2114.
- (630) Vinogradov, S.; Asseline, U.; Thuong, N. T. *Tetrahedron Lett.* **1993**, *34*, 5899–5902.
- (631) Chur, A.; Holst, B.; Dahl, O.; Valentinhanen, P.; Pedersen, E. B. *Nucleic Acids Res.* **1993**, *21*, 5179–5183.
- (632) Luo, P.; Leitzel, J. C.; Zhan, Z.-Y., J.; Lynn, D. G. *J. Am. Chem. Soc.* **1998**, *120*, 3019–3031.
- (633) Chan, M.-Y.; Fairhurst, R. A.; Collingwood, S. P.; Fisher, J.; Arnold, J. R. P.; Cosstick, R.; O'Neil, I. A. *J. Chem. Soc., Perkin Trans 1* **1999**, 315–320.
- (634) Musicki, B.; Widlanski, T. S. *Tetrahedron Lett.* **1991**, *32*, 1267–1270.
- (635) Perrin, K.; Huang, J.; McElroy, E. B.; Iams, K. P.; Widlanski, T. S. *J. Am. Chem. Soc.* **1994**, *116*, 7427–7428.
- (636) Baeschlin, D. K.; Hyrup, B.; Benner, S. A.; Richert, C. *J. Org. Chem.* **1996**, *61*, 7620–7626.
- (637) Okruszek, A.; Sierzchala, A.; Sochacki, M.; Stec, W. J. *Tetrahedron Lett.* **1992**, *33*, 7585–7588.
- (638) Pudio, J. S.; Cao, X.; Swaminathan, S.; Matteucci, M. D. *Tetrahedron Lett.* **1994**, *35*, 9315–9318.
- (639) Zou, R.; Matteucci, M. D. *Tetrahedron Lett.* **1996**, *37*, 941–944.
- (640) Rozners, E.; Strömberg, R. *J. Org. Chem.* **1997**, *62*, 1846–1850.
- (641) Jones, R. J.; Lin, K. Y.; Milligan, J. F.; Wadwani, S.; Matteucci, M. D. *J. Org. Chem.* **1993**, *58*, 2983–2991.
- (642) Cross, C. W.; Rice, S.; Gao, X. *Biochemistry* **1997**, *36*, 4096–4107.
- (643) Beauceage, S. L.; Iyer, R. P. *Tetrahedron* **1993**, *49*, 6123–6194.
- (644) Gryaznov, S.; Chen, J.-K. *J. Am. Chem. Soc.* **1994**, *116*, 3143–3144.
- (645) Chen, J.-K.; Schultz, R. G.; Lloyd, D. H.; Gryaznov, S. M. *Nucleic Acids Res.* **1995**, *23*, 2661–2668.
- (646) Gryaznov, S. M.; Lloyd, D. H.; Chen, J.-K.; Schultz, R. G.; DeDionisio, L. A.; Rattmeyer, L.; Wilson, W. D. *Proc. Natl. Acad. Sci. U.S.A.* **1995**, *92*, 5798–5802.
- (647) Ding, D.; Gryaznov, S. M.; Lloyd, D. H.; Chandrasekaran, S.; Yao, S.; Rattmeyer, L.; Pan, Y.; Wilson, W. D. *Nucleic Acids Res.* **1996**, *24*, 354–360.
- (648) Ding, D.; Gryaznov, S. M.; Wilson, W. D. *Biochemistry* **1998**, *37*, 12082–12093.
- (649) Tereshko, V.; Gryaznov, S.; Egli, M. *J. Am. Chem. Soc.* **1998**, *120*, 269–283.
- (650) Escudé, C.; Giovannangeli, C.; Sun, J.-S.; Lloyd, D. H.; Chen, J.-K.; Gryaznov, S. M.; Garestier, T.; Hélène, C. *Proc. Natl. Acad. Sci. U.S.A.* **1996**, *93*, 4365–4369.
- (651) Gryaznov, S. M.; Winter, H. *Nucleic Acids Res.* **1998**, *26*, 4160–4167.
- (652) Matray, T. J.; Gryaznov, S. M. *Nucleic Acids Res.* **1999**, *27*, 3976–3985.
- (653) Gryaznov, S.; Skorski, T.; Cucco, C.; Nieboroska-Skorska, M.; Chiu, C. Y.; Lloyd, D.; Chen, J.-K.; Koziolkiewicz, M.; Calabretta, B. *Nucleic Acids Res.* **1996**, *24*, 1508–1514.
- (654) Faria, M.; Wood, C. D.; Perrouault, L.; Nelson, J. S.; Winter, A.; White, M. R. H.; Hélène, C.; Giovannangeli, C. *Proc. Natl. Acad. Sci. U.S.A.* **2000**, *97*, 3862–3867.
- (655) Faria, M.; Spiller, D. G.; Dubertret, C.; Nelson, J. S.; White, M. R. H.; Scherman, D.; Hélène, C.; Giovannangeli, C. *Nat. Biotechnol.* **2001**, *19*, 40–44.
- (656) Rigl, C. T.; Lloyd, D. H.; Tsou, D. S.; Gryaznov, S. M.; Wilson, W. D. *Biochemistry* **1997**, *36*, 650–659.
- (657) Barsky, D.; Corvin, M. E.; Zon, G.; Gryaznov, S. M. *Nucleic Acids Res.* **1997**, *25*, 830–835.
- (658) Huang, Z.; Schneider, K. C.; Benner, S. A. *J. Org. Chem.* **1991**, *56*, 3869–3882.
- (659) Richert, C.; Roughton, A. L.; Benner, S. A. *J. Am. Chem. Soc.* **1996**, *118*, 4518–4531.
- (660) Roughton, A. L.; Portmann, S.; Benner, S. A.; Egli, M. *J. Am. Chem. Soc.* **1995**, *117*, 7249–7250.
- (661) Steinbeck, C.; Richert, C. *J. Am. Chem. Soc.* **1998**, *120*, 11576–11580.
- (662) Nielsen, P. E.; Haaima, G. *Chem. Soc. Rev.* **1997**, 73–78.
- (663) Dueholm, K. L.; Nielsen, P. E. *New J. Chem.* **1997**, *21*, 19–31.
- (664) Uhlmann, E.; Peyman, A.; Breipohl, G.; Will, D. W. *Angew. Chem., Int. Ed. Engl.* **1998**, *37*, 2796–2823.
- (665) Uhlmann, E. *Biol. Chem. Hoppe-Seyler* **1998**, *379*, 1045–1052.
- (666) Nielsen, P. E. *Acc. Chem. Res.* **1999**, *32*, 624–630.
- (667) Nielsen, P. E.; Egholm, M.; Berg, R. H.; Buchardt, O. *Science* **1991**, *254*, 1497–1500.
- (668) Egholm, M.; Buchardt, O.; Nielsen, P. E.; Berg, R. H. *J. Am. Chem. Soc.* **1992**, *114*, 1895–1897.
- (669) Egholm, M.; Behrens, C.; Christensen, L.; Berg, R. H.; Nielsen, P. E.; Buchardt, O. *J. Chem. Soc., Chem. Commun.* **1993**, 800–801.
- (670) Wittung, P.; Nielsen, P. E.; Buchardt, O.; Egholm, M.; Nordén, B. *Nature* **1994**, *368*, 561–563.
- (671) Tomac, S.; Sarkar, M.; Ratilainen, T.; Wittung, P.; Nielsen, P. E.; Nordén, B.; Gräslund, A. *J. Am. Chem. Soc.* **1996**, *118*, 5544–5552.
- (672) Egholm, M.; Buchardt, O.; Christensen, L.; Behrens, C.; Freier, S. M.; Driver, D. A.; Berg, R. H.; Kim, S. K.; Norden, B.; Nielsen, P. E. *Nature* **1993**, *365*, 566–568.
- (673) Ratilainen, T.; Holmén, A.; Tuite, E.; Nielsen, P. E.; Nordén, B. *Biochemistry* **2000**, *39*, 7781–7791.
- (674) Rasmussen, H.; Kastrop, J. S.; Nielsen, J. N.; Nielsen, J. M.; Nielsen, P. E. *Nat. Struct. Biol.* **1997**, *4*, 98–101.
- (675) Ratilainen, T.; Holmén, A.; Tuite, E.; Haaima, G.; Christensen, L.; Nielsen, P. E.; Nordén, B. *Biochemistry* **1998**, *37*, 12331–12342.
- (676) Brown, S. C.; Thomson, S. A.; Veal, J. M.; Davis, D. G. *Science* **1994**, *265*, 777–780.
- (677) Leijon, M.; Gräslund, A.; Nielsen, P. E.; Buchardt, O.; Nordén, B.; Kristensen, S. M.; Eriksson, M. *Biochemistry* **1994**, *33*, 9820–9825.
- (678) Eriksson, M.; Nielsen, P. E. *Nat. Struct. Biol.* **1996**, *3*, 410–413.
- (679) Almarsson, Ö.; Bruice, T. C. *Proc. Natl. Acad. Sci. U.S.A.* **1993**, *90*, 9542–9546.
- (680) Almarsson, Ö.; Bruice, T. C.; Kerr, J.; Zuckermann, R. N. *Proc. Natl. Acad. Sci. U.S.A.* **1993**, *90*, 7518–7522.
- (681) Chen, S.-M.; Mohan, V.; Kiely, J. S.; Griffith, M. C.; Griffey, R. H. *Tetrahedron Lett.* **1994**, *35*, 5105–5108.
- (682) Torres, R. A.; Bruice, T. C. *Proc. Natl. Acad. Sci. U.S.A.* **1996**, *93*, 649–653.
- (683) Armitage, B.; Ly, D.; Koch, T.; Frydenlund, H.; Ørum, H.; Schuster, G. B. *Biochemistry* **1998**, *37*, 9417–9425.
- (684) Soliva, R.; Sherer, E.; Luque, F. J.; Loughton, C. A.; Orozco, M. *J. Am. Chem. Soc.* **2000**, *122*, 5997–6008.
- (685) Uhlmann, E.; Will, D. W.; Breipohl, G.; Langner, D.; Ryte, A. *Angew. Chem., Int. Ed. Engl.* **1996**, *35*, 2632–2635.
- (686) Cherny, D. Y.; Belotserkovskii, B. P.; Frank-Kamenetskii, M. D.; Egholm, M.; Buchardt, O.; berg, R. H.; nielsen, P. E. *Proc. Natl. Acad. Sci. U.S.A.* **1993**, *90*, 1667–1670.
- (687) Peffer, N. J.; Hanvey, J. C.; Bisi, J. E.; Thomson, S. A.; Hassman, C. F.; Noble, S. A.; Babiss, L. E. *Proc. Natl. Acad. Sci. U.S.A.* **1993**, *90*, 10648–10652.
- (688) Bukanov, N. O.; Demidov, V. V.; Nielsen, P. E.; Frank-Kamenetskii, M. D. *Proc. Natl. Acad. Sci. U.S.A.* **1998**, *95*, 5516–5520.
- (689) Nielsen, P. E.; Egholm, M.; Buchardt, O. *J. Mol. Recognit.* **1994**, *7*, 165–170.
- (690) Wittung, P.; Nielsen, P.; Nordén, B. *J. Am. Chem. Soc.* **1997**, *119*, 3189–3190.
- (691) Nielsen, P. E.; Christensen, L. *J. Am. Chem. Soc.* **1996**, *118*, 2287–2288.
- (692) Lohse, J.; Dahl, O.; Nielsen, P. E. *Proc. Natl. Acad. Sci. U.S.A.* **1999**, *96*, 11804–11808.
- (693) Kim, S. K.; Nielsen, P. E.; Egholm, M.; Buchardt, O.; Berg, R. H.; Nordén, B. *J. Am. Chem. Soc.* **1993**, *115*, 6477–6481.
- (694) Demidov, V. V.; Yavnilovich, M. V.; Belotserkovskii, B. P.; Frank-Kamenetskii, M. D.; Nielsen, P. E. *Proc. Natl. Acad. Sci. U.S.A.* **1995**, *92*, 2637–2641.
- (695) Betts, L.; Josey, J. A.; Veal, J. M.; Jordan, S. R. *Science* **1995**, *270*, 1838–1841.
- (696) Kosaganov, Y. N.; Stetsenko, D. A.; Lubyako, E. N.; Kvitko, N. P.; Lazurkin, Y. S.; Nielsen, P. E. *Biochemistry* **2000**, *39*, 11742–11747.
- (697) Böhler, C.; Nielsen, P. E.; Orgel, L. E. *Nature* **1995**, *376*, 578–581.
- (698) Schmidt, J. G.; Nielsen, P. E.; Orgel, L. E. *Nucleic Acids Res.* **1997**, *25*, 4797–4802.
- (699) Lutz, M. J.; Benner, S. A.; Hein, S.; Breipohl, G.; Uhlmann, E. *J. Am. Chem. Soc.* **1997**, *119*, 3177–3178.
- (700) Hanvey, J. C.; Peffer, N. J.; Bisi, J. E.; Thomson, S. A.; Cadilla, R.; Josey, J. A.; Ricca, D. J.; Hassman, C. F.; Bonham, M. A.; Au, K. G.; Carter, S. G.; Bruckenstein, D. A.; Boyd, A. L.; Noble, S. A.; Babiss, L. E. *Science* **1992**, *258*, 1481–1485.
- (701) Ljungström, T.; Knudsen, H.; Nielsen, P. E. *Bioconjugate Chem.* **1999**, *10*, 965–972.
- (702) Lagriffoule, P.; Wittung, P.; Eriksson, M.; Jensen, K. K.; Nordén, B.; Buchardt, O.; Nielsen, P. E. *Chem. Eur. J.* **1997**, *3*, 912–919.
- (703) Egholm, M.; Christensen, L.; Dueholm, K. L.; Buchardt, O.; Coull, J.; Nielsen, P. E. *Nucleic Acids Res.* **1995**, *23*, 217–222.

- (704) Griffith, M. C.; Risen, L. M.; Greig, M. J.; Lesnik, E. A.; Sprankle, K. G.; Griffey, R. H.; Kiely, J. S.; Freier, S. M. *J. Am. Chem. Soc.* **1995**, *117*, 831–832.
- (705) Koch, T.; Naesby, M.; Wittung, P.; Jørgensen, M.; Larsson, C.; Buchardt, O.; Stanley, C. J.; Nordén, B.; Nielsen, P. E.; Ørum, H. *Tetrahedron Lett.* **1995**, *36*, 6933–6936.
- (706) Garner, P.; Dey, S.; Huang, Y. *J. Am. Chem. Soc.* **2000**, *122*, 2405–2406.
- (707) Karig, G.; Fuchs, A.; Büsing, A.; Brandstetter, T.; Scherer, S.; Bats, J. W.; Eschenmoser, A.; Quinkert, G. *Helv. Chim. Acta* **2000**, *83*, 1049–1078.
- (708) Schwalbe, H.; Wermuth, J.; Richter, C.; Szalma, S.; Eschenmoser, A.; Quinkert, G. *Helv. Chim. Acta* **2000**, *83*, 1079–1107.
- (709) Eppacher, S.; Solladie, N.; Bernet, B.; Vasella, A. *Helv. Chim. Acta* **2000**, *83*, 1311–1330.
- (710) Gunji, H.; Vasella, A. *Helv. Chim. Acta* **2000**, *83*, 1331–1345.
- (711) Gunji, H.; Vasella, A. *Helv. Chim. Acta* **2000**, *83*, 2975–2992.
- (712) Gunji, H.; Vasella, A. *Helv. Chim. Acta* **2000**, *83*, 3229–3245.
- (713) Czechtizky, W.; Vasella, A. *Helv. Chim. Acta* **2001**, *84*, 594–612.
- (714) Czechtizky, W.; Vasella, A. *Helv. Chim. Acta* **2001**, *84*, 1000–1016.
- (715) Vandendriessche, F.; Van Aerschot, A.; Voortmans, M.; Janssen, G.; Busson, R.; Van Overbeke, A.; Van den Bossche, W.; Hoogmartens, J.; Herdewijn, P. *J. Chem. Soc., Perkin Trans. 1* **1993**, 1567–1575.
- (716) Dempcy, R. O.; Almarsson, Ö.; Bruice, T. C. *Proc. Natl. Acad. Sci. U.S.A.* **1994**, *91*, 7864–7868.
- (717) Dempcy, R. O.; Browne, K. A.; Bruice, T. C. *J. Am. Chem. Soc.* **1995**, *117*, 6140–6141.
- (718) Dempcy, R. O.; Browne, K. A.; Bruice, T. C. *Proc. Natl. Acad. Sci. U.S.A.* **1995**, *92*, 6097–6101.
- (719) Linkletter, B. A.; Bruice, T. C. *Bioorg. Med. Chem. Lett.* **1998**, *8*, 1285–1290.
- (720) Barawkar, D. A.; Linkletter, B.; Bruice, T. C. *Bioorg. Med. Chem. Lett.* **1998**, *8*, 1517–1520.
- (721) Linkletter, B. A.; Szabo, I. E.; Bruice, T. C. *J. Am. Chem. Soc.* **1999**, *121*, 3888–3896.
- (722) Linkletter, B. A.; Szabo, I. E.; Bruice, T. C. *Nucleic Acids Res.* **2001**, *29*, 2370–2376.
- (723) Browne, K. A.; Dempcy, R. O.; Bruice, T. C. *Proc. Natl. Acad. Sci. U.S.A.* **1995**, *92*, 7051–7055.
- (724) Blaskó, A.; Dempcy, R. O.; Minyat, E. E.; Bruice, T. C. *J. Am. Chem. Soc.* **1996**, *118*, 7892–7899.
- (725) Blaskó, A.; Minyat, E. E.; Dempcy, R. O.; Bruice, T. C. *Biochemistry* **1997**, *36*, 7821–7831.
- (726) Luo, J.; Bruice, T. C. *J. Am. Chem. Soc.* **1998**, *120*, 1115–1123.
- (727) Dempcy, R. O.; Luo, J.; Bruice, T. C. *Proc. Natl. Acad. Sci. U.S.A.* **1996**, *93*, 4326–4330.
- (728) Luo, J.; Bruice, T. C. *J. Am. Chem. Soc.* **1997**, *119*, 6693–6701.
- (729) Kojima, N.; Bruice, T. C. *Org. Lett.* **2000**, *2*, 81–84.
- (730) Barawkar, D. A.; Bruice, T. C. *J. Am. Chem. Soc.* **1999**, *121*, 10418–10419.
- (731) Barawkar, D. A.; Kwok, Y.; Bruice, T. W.; Bruice, T. C. *J. Am. Chem. Soc.* **2000**, *122*, 5244–5250.
- (732) Linkletter, B. A.; Bruice, T. C. *Bioorg. Med. Chem.* **2000**, *8*, 1893–1901.
- (733) Arya, D. P.; Bruice, T. C. *J. Am. Chem. Soc.* **1998**, *120*, 6619–6620.
- (734) Arya, D. P.; Bruice, T. C. *J. Am. Chem. Soc.* **1998**, *120*, 12419–12427.
- (735) Arya, D. P.; Bruice, T. C. *Bioorg. Med. Chem. Lett.* **2000**, *10*, 691–693.
- (736) Arya, D. P.; Bruice, T. C. *Proc. Natl. Acad. Sci. U.S.A.* **1999**, *96*, 4384–4389.
- (737) Arya, D. P.; Bruice, T. C. *J. Am. Chem. Soc.* **1999**, *121*, 10680–10684.
- (738) Luo, J.; Bruice, T. C. *J. Biomol. Struct. Dyn.* **2000**, *17*, 629–643.
- (739) Kool, E. T.; Morales, J. C.; Guckian, K. M. *Angew. Chem., Int. Ed.* **2000**, *39*, 990–1009.
- (740) Ren, R. X.-F.; Chaudhuri, N. C.; Paris, P. L.; Rumney, S., IV; Kool, E. T. *J. Am. Chem. Soc.* **1996**, *118*, 7671–7678.
- (741) Guckian, K. M.; Schweitzer, B. A.; Ren, R. X.-F.; Sheils, C. J.; Paris, P. L.; Tahmassebi, D. C.; Kool, E. T. *J. Am. Chem. Soc.* **1996**, *118*, 8182–8183.
- (742) Guckian, K. M.; Schweitzer, B. A.; Ren, R. X.-F.; Sheils, C. J.; Tahmassebi, D. C.; Kool, E. T. *J. Am. Chem. Soc.* **2000**, *122*, 2213–2222.
- (743) Bain, J. D.; Switzer, C.; Chamberlain, A. R.; Benner, S. A. *Nature* **1992**, *356*, 537–539.
- (744) Switzer, C. Y.; Moroney, S. E.; Benner, S. A. *Biochemistry* **1993**, *32*, 10489–10496.
- (745) Roberts, C.; Bandaru, R.; Switzer, C. *J. Am. Chem. Soc.* **1997**, *119*, 4640–4649.
- (746) Lutz, M. J.; Horlacher, J.; Benner, S. A. *Bioorg. Med. Chem. Lett.* **1998**, *8*, 499–504.
- (747) Piccirilli, J. A.; Krauch, T.; Moroney, S. E.; Benner, S. A. *Nature* **1990**, *343*, 33–37.
- (748) Tor, Y.; Dervan, P. B. *J. Am. Chem. Soc.* **1993**, *115*, 4461–4467.
- (749) Horlacher, J.; Hottiger, M.; Podust, V. N.; Hübscher, U.; Benner, S. A. *Proc. Natl. Acad. Sci. U.S.A.* **1995**, *92*, 6329–6333.
- (750) Lutz, M. J.; Held, H. A.; Hottiger, M.; Hübscher, U.; Benner, S. A. *Nucleic Acids Res.* **1996**, *24*, 1308–1313.
- (751) McMinn, D. L.; Ogawa, A. K.; Wu, Y.; Liu, J.; Schultz, P. G.; Romesberg, F. E. *J. Am. Chem. Soc.* **1999**, *121*, 11585–11586.
- (752) Roberts, C.; Chaput, J. C.; Switzer, C. *Chem. Biol.* **1997**, *4*, 899–908.
- (753) Robinson, H.; Gao, Y.-G.; C., B.; Roberts, C.; Switzer, C.; Wang, A. H.-J. *Biochemistry* **1998**, *37*, 10897–10905.
- (754) Matray, T. J.; Kool, E. T. *J. Am. Chem. Soc.* **1998**, *120*, 6191–6192.
- (755) Guckian, K. M.; Morales, J. C.; Kool, E. T. *J. Org. Chem.* **1998**, *63*, 9652–9656.
- (756) Guckian, K. M.; Krugh, T. R.; Kool, E. T. *J. Am. Chem. Soc.* **2000**, *122*, 6841–6847.
- (757) Morales, J. C.; Kool, E. T. *Nat. Struct. Biol.* **1998**, *5*, 950–954.
- (758) Matray, T. J.; Kool, E. T. *Nature* **1999**, *399*, 704–708.
- (759) Morales, J. C.; Kool, E. T. *J. Am. Chem. Soc.* **2000**, *122*, 1001–1007.
- (760) Kool, E. T. *Curr. Opin. Chem. Biol.* **2000**, *4*, 602–608.
- (761) Ogawa, A. K.; Wu, Y.; McMinn, D. L.; Liu, J.; Schultz, P. G.; Romesberg, F. E. *J. Am. Chem. Soc.* **2000**, *122*, 3274–3287.
- (762) Wu, Y.; Ogawa, A. K.; Berger, M.; McMinn, D. L.; Schultz, P. G.; Romesberg, F. E. *J. Am. Chem. Soc.* **2000**, *122*, 7621–7632.
- (763) Berger, M.; Ogawa, A. K.; McMinn, D. L.; Wu, Y.; Schultz, P. G.; Romesberg, F. E. *Angew. Chem., Int. Ed.* **2000**, *39*, 2940–2942.
- (764) Ogawa, A. K.; Wu, Y.; Berger, M.; Schultz, P. G.; Romesberg, F. E. *J. Am. Chem. Soc.* **2000**, *122*, 8803–8804.
- (765) Tae, E. L.; Wu, Y.; Xia, G.; Schultz, P. G.; Romesberg, F. E. *J. Am. Chem. Soc.* **2001**, *123*, 7439–7440.
- (766) Meggers, E.; Holland, P. L.; Tolman, W. B.; Romesberg, F. E.; Schultz, P. G. *J. Am. Chem. Soc.* **2000**, *122*, 10714–10715.
- (767) Weizman, H.; Tor, Y. *J. Am. Chem. Soc.* **2001**, *123*, 3375–3376.
- (768) Weizman, H.; Tor, Y. *Chem. Commun.* **2001**, 453–454.
- (769) Brotschi, C.; Häberli, A.; Leumann, C. J. *Angew. Chem., Int. Ed.* **2001**, *40*, 3012–3014.
- (770) Tanaka, K.; Shionoya, M. *J. Org. Chem.* **1999**, *64*, 5002–5003.
- (771) Cao, H.; Tanaka, K.; Shionoya, M. *Chem. Pharm. Bull.* **2000**, *48*, 1745–1748.
- (772) Tanaka, K.; Tasaka, M.; Cao, H.; Shionoya, M. *Eur. J. Pharm. Sci.* **2001**, *13*, 77–83.
- (773) Nowick, J. S.; Tsai, J. H.; Bui, Q.-C. D.; Maitra, S. *J. Am. Chem. Soc.* **1999**, *121*, 8409–8410.
- (774) Jørgensen, W. L.; Pranata, J. *J. Am. Chem. Soc.* **1990**, *112*, 2008–2010.
- (775) Pranata, J.; Wierschke, S. G.; Jørgensen, W. L. *J. Am. Chem. Soc.* **1991**, *113*, 2810–2819.
- (776) Murray, T. J.; Zimmerman, S. C. *J. Am. Chem. Soc.* **1992**, *114*, 4010–4011.
- (777) Beijer, F. H.; Sijbesma, R. P.; Kooijman, H.; Spek, A. L.; Meijer, E. W. *J. Am. Chem. Soc.* **1998**, *120*, 6761–6769.
- (778) Söntjens, S. H.; Sijbesma, R. P.; van Genderen, M. H. P.; Meijer, E. W. *J. Am. Chem. Soc.* **2000**, *122*, 7487–7493.
- (779) Zeng, H.; Ickes, H.; Flowers, R. A.; Gong, B. *J. Org. Chem.* **2001**, *66*, 3574–3583.
- (780) Corbin, P. S.; Zimmerman, S. C. *J. Am. Chem. Soc.* **2000**, *122*, 3779–3780.
- (781) Folmer, B. J. B.; Sijbesma, R. P.; Kooijman, H.; Spek, A. L.; Meijer, E. W. *J. Am. Chem. Soc.* **1999**, *121*, 9001–9007.
- (782) Archer, E. A.; Goldberg, N. T.; Lynch, V.; Krische, M. J. *J. Am. Chem. Soc.* **2000**, *122*, 5006–5007.
- (783) Bisson, A. P.; Carver, F. J.; Hunter, C. A.; Waltho, J. P. *J. Am. Chem. Soc.* **1994**, *116*, 10292–10293.
- (784) Bisson, A. P.; Hunter, C. A. *Chem. Commun.* **1996**, 1723–1724.
- (785) Adams, H.; Carver, F. J.; Hunter, C. A.; Osborne, N. J. *Chem. Commun.* **1996**, 2529–2530.
- (786) Adams, H.; Harris, K. D. M.; Hembury, G. A.; Hunter, C. A.; Livingstone, D.; McCabe, J. F. *Chem. Commun.* **1996**, 2531–2532.
- (787) Bisson, A. P.; Hunter, C. A.; Morales, J. C.; Young, K. *Chem. Eur. J.* **1998**, *4*, 845–851.
- (788) Bisson, A. P.; Carver, F. J.; Eggleston, D. S.; Haltiwanger, R. C.; Hunter, C. A.; Livingstone, D. L.; McCabe, J. F.; Rotger, C.; Rowan, A. E. *J. Am. Chem. Soc.* **2000**, *122*, 8856–8868.
- (789) Berl, V.; Huc, I.; Khoury, R. G.; Lehn, J.-M. *Chem. Eur. J.* **2001**, *7*, 2798–2809.
- (790) Berl, V.; Huc, I.; Khoury, R. G.; Lehn, J.-M. *Chem. Eur. J.* **2001**, *7*, 2810–2820.
- (791) Constable, E. C. *Pure Appl. Chem.* **1996**, *68*, 253–260.
- (792) Kaes, C.; Katz, A.; Hosseini, M. W. *Chem. Rev.* **2000**, *100*, 3553–3590.
- (793) Constable, E. C.; Elder, S. M.; Hannon, M. J.; Martin, A.; Raitthy, P. R.; Tocher, D. A. *J. Chem. Soc., Dalton Trans.* **1996**, 2423–2433.
- (794) Potts, K. T.; Keshavarz-K., M.; Tham, F. S.; Abruna, H. D.; Arana, C. *Inorg. Chem.* **1993**, *32*, 4450–4456.

- (795) Potts, K. T.; Keshavarz-K., M.; Tham, F. S.; Abruna, H. D.; Arana, C. *Inorg. Chem.* **1993**, *32*, 4422–4435.
- (796) Potts, K. T.; Keshavarz-K., M.; Tham, F. S.; Abruna, H. D.; Arana, C. *Inorg. Chem.* **1993**, *32*, 4436–4449.
- (797) Potts, K. T.; Raiford, K. A., G.; Keshavarz-K., M. *J. Am. Chem. Soc.* **1993**, *115*, 2793–2807.
- (798) Constable, E. C.; Hannon, M. J.; Tocher, D. A. *J. Chem. Trans., Dalton Trans.* **1993**, 1883–1890.
- (799) Constable, E. C.; Hannon, M. J.; Edwards, A. J.; Raithby, P. R. *J. Chem. Soc., Dalton Trans.* **1994**, 2669–2677.
- (800) Ho, P. K.-K.; Peng, S.-M.; Cheung, K.-K.; Wong, K.-Y.; Che, C.-M. *J. Chem. Soc., Dalton Trans.* **1996**, 1829–1834.
- (801) Potts, K. T.; Horwitz, C. P.; Fessak, A.; Keshavarz-K., M.; Nash, K. E.; Toscano, P. J. *J. Am. Chem. Soc.* **1993**, *115*, 10444–10445.
- (802) Chamchoumis, C. M.; Potvin, P. G. *J. Chem. Soc., Dalton Trans.* **1999**, 1373–1374.
- (803) Baum, G.; Constable, E. C.; Fenske, D.; Kulke, T. *Chem. Commun.* **1997**, 2043–2044.
- (804) Constable, E. C.; Kulke, T.; Neuburger, M.; Zehnder, M. *Chem. Commun.* **1997**, 489–490.
- (805) Baum, G.; Constable, E. C.; Fenske, D.; Housecroft, C. E.; Kulke, T. *Chem. Eur. J.* **1999**, *5*, 1862–1873.
- (806) Constable, E. C.; Heirtzler, F. R.; Neuburger, M.; Zehnder, M. *Supramol. Chem.* **1995**, *5*, 197–200.
- (807) Constable, E. C.; Heirtzler, F. R.; Neuburger, M.; Zehnder, M. *Chem. Commun.* **1996**, 933–934.
- (808) Constable, E. C.; Heirtzler, F.; Neuburger, M.; Zehnder, M. *J. Am. Chem. Soc.* **1997**, *119*, 5606–5617.
- (809) Constable, E. C.; Kulke, T.; Neuburger, M.; Zehnder, M. *Chem. Commun.* **1997**, 489–490.
- (810) Baum, G.; Constable, E. C.; Fenske, D.; Housecroft, C. E.; Kulke, T. *Chem. Commun.* **1998**, 2659–2660.
- (811) Baum, G.; Constable, E. C.; Fenske, D.; Housecroft, C. E.; Kulke, T.; Neuburger, M.; Zehnder, M. *J. Chem. Soc., Dalton Trans.* **2000**, 945–959.
- (812) Lehn, J.-M.; Rigault, A. *Angew. Chem., Int. Ed. Engl.* **1988**, *27*, 1095–1097.
- (813) Garrett, T. M.; Koert, U.; Lehn, J.-M.; Rigault, A.; Meyer, D.; Fischer, J. *J. Chem. Soc., Chem. Commun.* **1990**, 557–558.
- (814) Harding, M. M.; Koert, U.; Lehn, J.-M.; Marquis-Rigault, A.; Piguet, C.; Siegel, J. *Helv. Chim. Acta* **1991**, *74*, 594–610.
- (815) Krämer, R.; Lehn, J.-M.; Marquis-Rigault, A. *Proc. Natl. Acad. Sci. U.S.A.* **1993**, *90*, 5394–5398.
- (816) Garrett, T. M.; Koert, U.; Lehn, J.-M. *J. Phys. Org. Chem.* **1992**, *5*, 529–532.
- (817) Pfeil, A.; Lehn, J.-M. *J. Chem. Soc., Chem. Commun.* **1992**, 838–840.
- (818) Koert, U.; Harding, M. M.; Lehn, J.-M. *Nature* **1990**, *346*, 339–342.
- (819) Schoentjes, B.; Lehn, J.-M. *Helv. Chim. Acta* **1995**, *78*, 1–12.
- (820) Pauling, L.; Corey, R. B. *Nature* **1953**, *171*, 346.
- (821) Smith, V. C. M.; Lehn, J.-M. *Chem. Commun.* **1996**, 2733–2734.
- (822) Greenwald, M.; Wessely, D.; Goldberg, I.; Cohen, Y. *New J. Chem.* **1999**, 337–344.
- (823) Shaul, M.; Cohen, Y. *J. Org. Chem.* **1999**, *64*, 9358–9364.
- (824) Greenwald, M.; Wessely, D. K., E.; Willner, I.; Cohen, Y. *J. Org. Chem.* **2000**, *65*, 1050–1058.
- (825) Zarges, W.; Hall, J.; Lehn, J.-M.; Bolm, C. *Helv. Chim. Acta* **1991**, *74*, 1843–1852.
- (826) Woods, C. R.; Benaglia, M.; Cozzi, F.; Sigel, J. S. *Angew. Chem., Int. Ed. Engl.* **1996**, *35*, 1830–1833.
- (827) Annunziata, R.; Benaglia, M.; Cinquini, M.; Cozzi, F.; Woods, C. R.; Siegel, J. S. *Eur. J. Org. Chem.* **2001**, 173–180.
- (828) Funeriu, D.-P.; He, Y.-B.; Bister, H.-J.; Lehn, J.-M. *Bull. Soc. Chim. Fr.* **1996**, *133*, 673–678.
- (829) Stiller, R.; Lehn, J.-M. *Eur. J. Inorg. Chem.* **1998**, 977–982.
- (830) Krämer, R.; Lehn, J.-M.; De Cian, A.; Fisher, J. *Angew. Chem., Int. Ed. Engl.* **1993**, *32*, 703–706.
- (831) Hasenknopf, B.; Lehn, J.-M. *Helv. Chim. Acta* **1996**, *79*, 1643–1650.
- (832) Hasenknopf, B.; Lehn, J.-M.; Baum, G.; Fenske, D. *Proc. Natl. Acad. Sci. U.S.A.* **1996**, *93*, 1397–1400.
- (833) Hasenknopf, B.; Lehn, J.-M.; Kneisel, B. O.; Baum, G.; Fenske, D. *Angew. Chem., Int. Ed. Engl.* **1996**, *35*, 1838–1840.
- (834) Baxter, P. N. W.; Lehn, J.-M.; Rissanen, K. *Chem. Commun.* **1997**, 1323–1324.
- (835) Hasenknopf, B.; Lehn, J.-M.; Boumediene, N.; Dupont-Gervais, A.; van Dorsselaer, A.; Kneisel, B.; Fenske, D. *J. Am. Chem. Soc.* **1997**, *119*, 10956–10962.
- (836) Hasenknopf, B.; Lehn, J.-M.; Boumediene, N.; Leize, E.; van Dorsselaer, A. *Angew. Chem., Int. Ed. Engl.* **1998**, *37*, 3265–3268.
- (837) Williams, A. F.; Piguet, C.; Bernardinelli, G. *Angew. Chem., Int. Ed. Engl.* **1991**, *30*, 1490–1492.
- (838) Piguet, C.; Hopfgartner, G.; Bocquet, B.; Schaad, O.; Williams, A. F. *J. Am. Chem. Soc.* **1994**, *116*, 9092–9102.
- (839) Petoud, S.; Bunzli, J.-C. G.; Renaud, F.; Piguet, C.; Schenk, K. J.; Hopfgartner, G. *Inorg. Chem.* **1997**, *36*, 5750–5760.
- (840) Charbonniere, L. J.; Williams, A. F.; Piguet, C.; Bernardinelli, G.; Rivara-Minten, E. *Chem. Eur. J.* **1998**, *4*, 485–493.
- (841) Provent, C.; Hewage, S.; Brand, G.; Bernardinelli, G.; Charbonniere, L. J.; Williams, A. F. *Angew. Chem., Int. Ed. Engl.* **1997**, *36*, 1287–1289.
- (842) Provent, C.; Rivara-Minten, E.; Hewage, S.; Brunner, G.; Williams, A. F. *Chem. Eur. J.* **1999**, *5*, 3487–3494.
- (843) von Zelewsky, A.; Mamula, O. *J. Chem. Soc., Dalton Trans.* **2000**, 219–231.
- (844) Amendola, V.; Fabbrizzi, L.; Linati, L.; Mangano, C.; Pallavicini, P.; Pedrazzini, V.; Zema, M. *Chem. Eur. J.* **1999**, *5*, 3679–3688.
- (845) Amendola, V.; Fabbrizzi, L.; Mangano, C.; Pallavicini, P.; Roboli, E.; Zema, M. *Inorg. Chem.* **2000**, *39*, 5803–5806.
- (846) *Photomorphogenesis in Plants*, 2nd ed; Kluwer Academic: Dordrecht, 1994.
- (847) Zhang, Y.; Thompson, A.; Rettig, S. J.; Dolphin, D. *J. Am. Chem. Soc.* **1998**, *120*, 13537–13538.
- (848) Thompson, A.; Dolphin, D. *Org. Lett.* **2000**, *2*, 1315–1318.
- (849) Thompson, A.; Dolphin, D. *J. Org. Chem.* **2000**, *65*, 7870–7877.
- (850) Caulder, D. L.; Raymond, K. N. *Angew. Chem., Int. Ed. Engl.* **1997**, *36*, 1440–1442.
- (851) Kersting, B.; Meyer, M.; Power, R. E.; Raymond, K. N. *J. Am. Chem. Soc.* **1996**, *118*, 7221–7222.
- (852) Meyer, M.; Kersting, B.; Powers, R. E.; Raymond, K. N. *Inorg. Chem.* **1997**, *36*, 5179–5191.
- (853) Schere, M.; Caulder, D. L.; Johnson, D. W.; Raymond, K. N. *Angew. Chem., Int. Ed.* **1999**, *38*, 1588–1592.
- (854) Caulder, D. L.; Powers, R. E.; Parac, T. N.; Raymond, K. N. *Angew. Chem., Int. Ed. Engl.* **1998**, *37*, 1840–1843.
- (855) Albrecht, M.; Schneider, M.; Röttele, H. *Angew. Chem., Int. Ed.* **1999**, *38*, 557–559.
- (856) Albrecht, M. *Chem. Eur. J.* **1997**, *3*, 1466–1471.
- (857) Albrecht, M.; Kotaila, S. *Angew. Chem., Int. Ed. Engl.* **1996**, *35*, 1208–1210.
- (858) Albrecht, M.; Roettele, H.; Burger, P. *Chem. Eur. J.* **1996**, *2*, 1264–1268.
- (859) Airey, A. L.; Swiegers, G. F.; Willis, A. C.; Wild, S. B. *Inorg. Chem.* **1997**, *36*, 1588–1597.
- (860) Linton, B.; Hamilton, A. D. *Chem. Rev.* **1997**, *97*, 1669–1680.
- (861) Huc, I.; Krische, M. J.; Funeriu, D. P.; Lehn, J.-M. *Eur. J. Inorg. Chem.* **1999**, 1415–1420.
- (862) Haq, H.; Ladbury, J. *J. Mol. Recognit.* **2000**, *13*, 188–197.
- (863) Pelletier, H.; Sawaya, M. R.; Kumar, A.; Wilson, S. H.; Kraut, J. *Science* **1994**, *264*, 1891–1903.
- (864) Doublé, S.; Tabor, S.; Long, M. A.; Richardson, C. C.; Ellenberger, T. *Nature* **1998**, *391*, 251–258.
- (865) Kiefer, J. R.; Mao, C.; Braman, J. C.; Beese, L. S. *Nature* **1998**, *391*, 304–307.
- (866) Morales, J. C.; Kool, E. T. *J. Am. Chem. Soc.* **1999**, *121*, 2323–2324.
- (867) Morales, J. C.; Kool, E. T. *Biochemistry* **2000**, *39*, 12979–12988.
- (868) Dzantiev, L.; Alekseyev, Y. O.; Morales, J. C.; Kool, E. T.; Romano, L. J. *Biochemistry* **2001**, *40*, 3215–3221.
- (869) Finlay, A. C.; Hochstein, F. A.; Sobin, B. A.; Murphy, F. X. *J. Am. Chem. Soc.* **1951**, *73*, 341–343.
- (870) Pelton, J. G.; Wemmer, D. E. *Biochemistry* **1988**, *27*, 8088–8096.
- (871) Arcamone, F.; Penco, S.; Delle Monache, F. *Gazz. Chim. Ital.* **1969**, 620–631.
- (872) Arcamone, F.; Nicoletta, V.; Penco, S.; Redaelli, S. *Gazz. Chim. Ital.* **1969**, 632–640.
- (873) Kopka, M. L.; Yoon, C.; Goodsell, D.; Pjura, P.; Dickerson, R. E. *Proc. Natl. Acad. Sci. U.S.A.* **1985**, *82*, 1376–1380.
- (874) White, S.; Szweczyk, J. W.; Turner, J. M.; Baird, E. E.; Dervan, P. B. *Nature* **1998**, *391*, 468–471.
- (875) Dervan, P. B.; Bürli, R. W. *Curr. Opin. Chem. Biol.* **1999**, *3*, 688–693.
- (876) Turner, J. M.; Swalley, S. E.; Baird, E. E.; Dervan, P. B. *J. Am. Chem. Soc.* **1998**, *120*, 6219–6226.
- (877) Mrksich, M.; Parks, M. E.; Dervan, P. B. *J. Am. Chem. Soc.* **1994**, *116*, 7983–7988.
- (878) Traunger, J. W.; Baird, E. E.; Dervan, P. B. *Nature* **1996**, *382*, 559–561.
- (879) Baird, E. E.; Dervan, P. B. *J. Am. Chem. Soc.* **1996**, *118*, 6141–6146.
- (880) Lown, J. W. *J. Mol. Recognit.* **1994**, *7*, 79–88.
- (881) Walker, W. L.; Kopka, M. L.; Goodsell, D. S. *Biopolymers* **1997**, *44*, 323–334.
- (882) Bailly, C. B.; Chaires, J. B. *Bioconjugate Chem.* **1998**, *9*, 513–538.
- (883) Wemmer, D. E. *Annu. Rev. Biophys. Biomol. Struct.* **2000**, *29*, 439–461.
- (884) Hanka, L. J.; Dietz, A.; Gerpheide, S. A.; Kuentzel, S. L.; Martin, D. G. *J. Antibiot.* **1978**, *31*, 1211–1217.
- (885) Martin, D. G.; Biles, C.; Gerpheide, S. A.; Hanka, L. J.; Krueger, W. C.; McGovern, J. P.; Mizsak, S. A.; Neil, G. L.; Stewart, J. C.; Visser, J. *J. Antibiot.* **1981**, *34*, 1119–1125.
- (886) Boger, D. L.; Johnson, D. S. *Proc. Natl. Acad. Sci. U.S.A.* **1995**, *92*, 3642–3649.

- (887) Boger, D. L.; Johnson, D. S. *Angew. Chem., Int. Ed. Engl.* **1996**, *35*, 1438–1474.
- (888) Boger, D. L.; Boyce, C. W.; Garbaccio, R. M.; Goldberg, J. A. *Chem. Rev.* **1997**, *97*, 787–828.
- (889) Boger, D. L.; Garbaccio, R. M. *Acc. Chem. Res.* **1999**, *32*, 1043–1052.
- (890) Chidester, C. G.; Krueger, W. C.; Mizensak, S. A.; Duchamp, D. J.; Martin, D. G. *J. Am. Chem. Soc.* **1981**, *103*, 7629–7236.
- (891) Scahill, T. A.; Jensen, R. M.; Swenson, D. H.; Natzenbuhler, N. T.; Petzold, G.; Wierenga, W.; Brahme, N. D. *Biochemistry* **1990**, *29*, 2852–2860.
- (892) Eis, P. S.; Smith, J. A.; Rydzewski, J. M.; A., C. D.; Boger, D. L.; Chazin, W. J. *J. Mol. Biol.* **1997**, *272*, 237–252.
- (893) Boger, D. L.; Coleman, R. S. *J. Am. Chem. Soc.* **1987**, *109*, 2717–2727.
- (894) Boger, D. L.; Invergo, B. J.; Coleman, R. S.; Zarrinmayer, H.; Kitos, P. A.; Thompson, S. C.; Leong, T.; McLaughlin, L. W. *Chem.-Biol. Interact.* **1990**, *73*, 29–52.
- (895) Boger, D. L.; Garbaccio, R. M. *Bioorg. Med. Chem.* **1997**, *5*, 263–276.
- (896) Pecuh, M. W.; Hamilton, A. D.; Sánchez-Quesada, J.; de Mendoza, J.; Haack, T.; Giralt, E. *J. Am. Chem. Soc.* **1997**, *119*, 9327–9328.
- (897) Haack, T.; Pecuh, M. W.; Salvatella, X.; Sánchez-Quesada, J.; de Mendoza, J.; Hamilton, A. D.; Giralt, E. *J. Am. Chem. Soc.* **1999**, *121*, 11813–11820.
- (898) Salvatella, X.; Pecuh, M. W.; Gairi, M.; Jain, R. K.; Sánchez-Quesada, J.; de Mendoza, J.; Hamilton, A. D.; Giralt, E. *Chem. Commun.* **2000**, 1399–1400.
- (899) IUPAC–IUB *Biochemistry* **1970**, *9*, 3471–3479.
- (900) See ref 241.
- (901) Eldrup, A. B.; Nielsen, B. B.; Haaima, G.; Rasmussen, H.; Kastrup, J. S.; Christensen, C.; Nielsen, P. E. In *The Protein Data Bank*, 2001.
- (902) Johnson, J., W. C. *Methods Biochem. Anal.* **1985**, *31*, 61–163 and references therein
- (903) Lakowicz, J. R. *Principles of Fluorescence*, 2nd ed; Kluwer Academic/Plenum Publishers: New York, 1999.
- (904) Nakanishi, K.; Solomon, P. H. *Infrared Absorption Spectroscopy*; Emerson-Adams Press: New York, 2000.
- (905) Gunther, H. *NMR Spectroscopy*; John Wiley & Sons: New York, 1995.
- (906) Thomas, M. J. K. *Ultraviolet and Visible Spectroscopy*; John Wiley & Sons: New York, 1996.
- (907) Watt, I. M. *The Principle and Practice of Electron Microscopy*; Cambridge University Press: New York, 1996.
- (908) Calvet, E.; Prat, H. *Recent Progress in Microcalorimetry*; Macmillan: New York, 1963.
- (909) Stout, G. H.; Jensen, L. H. *X-ray Structure Determination: A Practical Guide*; John Wiley & Sons: New York, 1989.

CR990120T

Enzymatic Polymerization

Shiro Kobayashi,* Hiroshi Uyama, and Shunsaku Kimura

Department of Materials Chemistry, Graduate School of Engineering, Kyoto University, Kyoto 606-8501, Japan

Received February 8, 2001

Contents

I. Introduction	3793
II. Oxidoreductases	3794
A. Peroxidases	3794
1. Oxidative Polymerization of Phenol Derivatives	3794
2. Oxidative Polymerization of Aniline Derivatives	3798
3. Polymerization of Vinyl Monomers	3798
B. Laccases	3799
C. Other Oxidoreductases	3800
III. Transferases	3800
A. Glycosyltransferases	3800
1. Phosphorylases	3800
2. Glycosyl Transferases	3801
B. Acyltransferases	3802
IV. Hydrolases	3802
A. Glycosidases	3802
1. Natural Glycosidases	3803
2. Mutated Glycosidases	3805
B. Lipases	3806
1. Ring-Opening Polymerization of Cyclic Monomers	3807
2. Polymerization of Diacid Derivatives and Glycols	3810
3. Polycondensation of Oxyacid Derivatives	3812
4. Polymer Modification	3813
C. Proteases	3813
D. Other Hydrolases	3814
VI. Conclusion	3814
VII. Acknowledgments	3814
VIII. References	3814

I. Introduction

There has been an exponential increase in interest in the area of *in vitro* enzyme-catalyzed organic reactions, since many families of enzymes can be utilized for transformation of not only their natural substrates but a wide range of unnatural compounds, yielding a variety of useful materials.¹ Employing enzymes in organic synthesis has several advantages as follows: (i) catalysis under mild reaction conditions with regard to temperature, pressure, and pH, which often lead to remarkable energy efficiency; (ii)

high enantio-, regio-, and chemoselectivities as well as regulation of stereochemistry providing development of new reactions to functional compounds for pharmaceuticals and agrichemicals; (iii) nontoxic natural catalyst with “green” appeal in commercial benefit and ecological requirement.

All naturally occurring polymers are produced *in vivo* by enzymatic catalysis. Recently, *in vitro* synthesis of polymers through enzymatic catalysis (“enzymatic polymerization”) has been extensively developed.² Enzyme catalysis has provided a new synthetic strategy for useful polymers, most of which are otherwise very difficult to produce by conventional chemical catalysts. *In vitro* enzymatic syntheses of polymers via nonbiosynthetic pathways, therefore, are recognized as a new area of precision polymer syntheses.

Furthermore, the enzymatic polymerizations may greatly contribute to global sustainability without depletion of important resources by using nonpetrochemical renewable resources as starting substrates of functional polymeric materials. In the enzymatic polymerizations, the product polymers can be obtained under mild reaction conditions without using toxic reagents. Therefore, the enzymatic polymerization can be regarded as an environmentally friendly synthetic process of polymeric materials, providing a good example to achieve “green polymer chemistry”.³

The present article overviews recent advances in enzymatic polymerizations. We define enzymatic polymerization as chemical polymer synthesis *in vitro* (in test tubes) via nonbiosynthetic (nonmetabolic) pathways catalyzed by an isolated enzyme. Accordingly, polymer syntheses by employing a living system like fermentation and *E. coli* using processes are not included.

More than 100 years ago (1894), Emil Fischer proposed a “Key and Lock” theory as to the specific substrate selectivity by the enzyme, which is presently understood as molecular recognition of the substrate by the enzyme through supramolecular interactions. If the enzymatic reaction takes place *in vivo*, it is always involved to recognize the substrate by the enzyme. This is also true for enzymatic reactions *in vitro*. However, readers will see in this article that the substrate–enzyme relationship is not as strict as the key–lock relationship, but enzymes are dynamic and sometimes very generous in recognizing even unnatural substrates *in vitro*. This situation allows enzymes to catalyze the synthesis of not

* To whom correspondence should be addressed. Phone: +81-75-753-5608. Fax: +81-75-753-4911. E-mail: kobayasi@mat.polym.kyoto-u.ac.jp.



Shiro Kobayashi was born in Himeji, Japan, in 1941. He received his B.S. (1964), M.S. (1966, Professor J. Furukawa), and Ph.D. (1969, Professor T. Saegusa) degrees from Kyoto University. He spent his postdoctoral period (1969–1971, Professor G. A. Olah) at Case Western Reserve University, Cleveland, OH. In 1972, he joined the Department of Synthetic Chemistry, Kyoto University, as Research Associate. In 1986, he was appointed Full Professor at the Department of Applied Chemistry, Tohoku University. He moved to the Department of Materials Chemistry, Kyoto University, in 1997. He has received several awards, such as the Chemical Society of Japan Award for Young Chemists (1976), the Award of the Society of Polymer Science, Japan (1987), the Distinguished Invention Award (1993), the Cellulose Society of Japan Award (1996), the Humboldt Research Award, Germany (1999), the Award of the Chemical Society of Japan (2001), and the Award of the "Hattori-Hokokai" Foundation, Japan (2001). He has been a foreign member of the Northrhine Westfalian Academy of Science, Germany, since 1999. He currently serves as Regional Editor and/or (Executive) Advisory Board Member for 14 international journals including *Macromolecules* and *Biomacromolecules*. His main interests are enzymatic catalysis in polymer synthesis, bio- and biorelated polymers, new polymerizations and reaction mechanisms, and functional and high-performance polymer materials.



Hiroshi Uyama was born in Kobe, Japan, in 1962. He received his B.S. (1985) and M.S. (1987) degrees from Kyoto University. In 1988, he joined the Department of Applied Chemistry, Tohoku University, as Research Associate. He obtained Ph.D. degree under the direction of Professor Shiro Kobayashi in 1991. He moved to the Department of Materials Chemistry, Kyoto University, in 1997. In 2000, he was appointed Associate Professor of the same department. He was honored as the recipient of the Award of the Society of Polymer Science, Japan, for the Outstanding Paper published in the *Polymer Journal* in 1995 and the Chemical Society of Japan Award for Young Chemists in 1997.

only some natural polymers but also a variety of unnatural polymers. Thus, the target macromolecules for the enzymatic polymerization have been polysaccharides, polyesters, polycarbonates, poly(amino acid)s, polyaromatics, vinyl polymers, etc. All the enzymes are generally classified into six groups, and typical polymers produced with catalysis by



Shunsaku Kimura was born in Kyoto, Japan in 1954. He received his B.S. (1976), M.S. (1978), and Ph.D. (1982, Professor Y. Imanishi) degrees from Kyoto University. He joined the Department of Polymer Chemistry, Kyoto University, as Research Associate (1981), Lecturer (1992), and Associate Professor (1993). He moved to the Department of Materials Chemistry, Kyoto University (1996), and in 1999 he was appointed Full Professor. He spent his postdoctoral career (1982–1984, 1986, Professor R. Schwyzer) at ETH-Zurich, Switzerland. He received the Award of the Society of Polymer Science, Japan, in 1999. He currently serves as Associate Editor for *Polymer Journal*. His main interests are polymer supramolecular chemistry, peptide engineering, and optoelectronics devices.

respective enzymes are given in Table 1. Here, enzymatic polymerizations are described according to the nature of catalyst enzymes.

Table 1. Classification of Enzymes and in Vitro Production of Typical Polymers Catalyzed by Respective Enzymes

enzymes	typical polymers
oxidoreductases	polyphenols, polyanilines, vinyl polymers
transferases	polysaccharides, cyclic oligosaccharides, polyesters
hydrolases	polysaccharides, polyesters, polycarbonates, poly(amino acid)s
lyases	
isomerases	
ligases	

II. Oxidoreductases

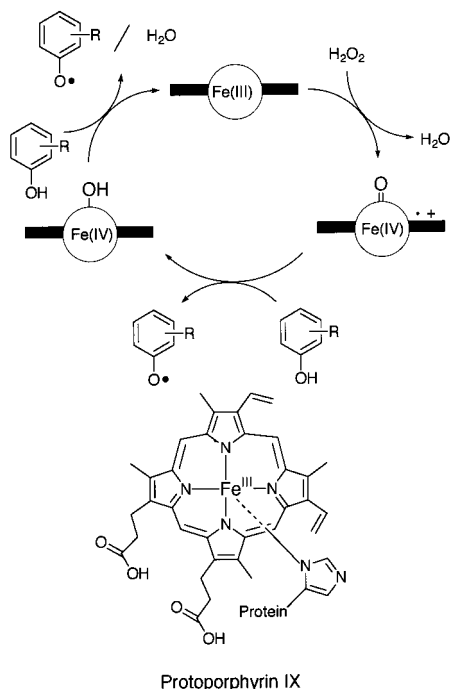
In living cells, various oxidoreductases play an important role in maintaining the metabolism of living systems. Most of oxidoreductases contain low-valent metals as the catalytic center. In vitro enzymatic oxidoreductions have afforded functional organic materials.¹ Recently, some oxidoreductases such as peroxidase, laccase, and bilirubin oxidase have received much attention as catalyst for the oxidative polymerizations of phenol and aniline derivatives to produce novel polyaromatics.

A. Peroxidases

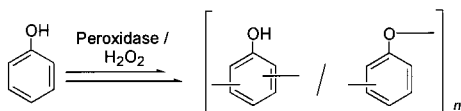
1. Oxidative Polymerization of Phenol Derivatives

Peroxidase catalysis is an oxidation of a donor to an oxidized donor by the action of hydrogen peroxide, liberating two water molecules. Horseradish peroxidase (HRP) is a single-chain β -type hemoprotein that catalyzes the decomposition of hydrogen peroxide at the expense of aromatic proton donors. HRP is a Fe-containing porphyrin-type structure and is well-

Scheme 1



Scheme 2



known to catalyze coupling of a number of phenol and aniline derivatives using hydrogen peroxide as oxidant. The catalytic cycle of HRP for a phenol substrate is shown in Scheme 1. The peroxidase-catalyzed oxidation proceeds fast in aqueous solutions, giving rise to the formation of oligomeric compounds. The resulting oligomers often show low solubility toward the solvent, thereby preventing the further formation of higher molecular weight polymer.

In a mixture of water and water-miscible solvents such as acetone, 1,4-dioxane, and methanol, peroxidase could act as catalyst for oxidative polymerization of various phenol derivatives, yielding a new class of polyaromatics.⁴ The polymerization proceeds at room temperature, and during the polymerization, powdery polymers are often precipitated, which are readily collected after the polymerization.

Phenol, the simplest and most important phenolic compound in industrial fields, is a multifunctional monomer for oxidative polymerization, and hence, conventional polymerization catalysts afford an insoluble product with uncontrolled structure. On the other hand, the peroxidase catalysis induced the polymerization in aqueous organic solvent to give a powdery polymer consisting of phenylene and oxyphenylene units showing relatively high thermal stability (Scheme 2).^{5,6} In the HRP and soybean peroxidase (SBP)-catalyzed polymerization in the aqueous 1,4-dioxane, the resulting polymer showed low solubility; the polymer was partly soluble in *N,N*-dimethylformamide (DMF) and dimethyl sulfoxide and insoluble in other common organic solvents.⁵ On the other hand, the aqueous methanol solvent af-

forded the DMF-soluble polymer with a number-average molecular weight (M_n) of 2100–6000 in good yields.⁶ Furthermore, the unit ratio (regioselectivity) could be controlled by changing the solvent composition to give a polymer with the phenylene unit ranging from 32% to 66%. Molecular weight control of the polyphenol was achieved by the copolymerization with 2,4-dimethylphenol.⁷

The polymerization behaviors and properties of the polyphenols depend on the monomer structure, solvent composition, and enzyme origin. In the HRP-catalyzed polymerization of *p*-*n*-alkylphenols in aqueous 1,4-dioxane, the polymer yield increased as the chain length of the alkyl group increased from 1 to 5.⁸ The molecular weight was on the order of several thousands. HRP catalyzed the oxidative polymerization of all cresol isomers,⁹ whereas among *o*-, *m*-, and *p*-isopropylphenol isomers, only *p*-isopropylphenol was polymerized by HRP catalysis. Poly(*p*-alkylphenol)s obtained in the aqueous 1,4-dioxane often showed low solubility toward organic solvents; however, soluble oligomers with molecular weight less than 1000 were formed from *p*-ethylphenol in aqueous DMF.¹⁰

As for *m*-alkyl-substituted phenols, soluble polyphenols were obtained by HRP or SBP catalyst in aqueous methanol.¹¹ Enzymatically synthesized poly(*m*-cresol) had a glass transition temperature (T_g) higher than 200 °C. The enzyme origin strongly influenced the polymer yield; HRP readily polymerized the monomer having a small substituent, whereas in the case of large substituent monomers, the higher yield was achieved by using SBP as catalyst.

Phenol–formaldehyde resins using prepolymers such as novolaks and resols are widely used in industrial fields. These resins show excellent toughness and temperature-resistant properties.¹² However, the toxic nature of formaldehyde causes problems in their manufacture and practical use. Therefore, the enzymatic processes are highly expected as an alternative for preparation of phenol polymers without using formaldehyde. Advantages for enzymatic synthesis of useful polyphenols are summarized as follows:¹³ (i) the polymerization of phenols proceeds under mild reaction conditions without use of toxic reagents (environmentally benign process); (ii) phenol monomers having various substituents are polymerized to give a new class of functional polyaromatics; (iii) the structure and solubility of the polymer can be controlled by changing the reaction conditions; (iv) the procedures of the polymerization as well as the polymer isolation are very facile.

Numerical and Monte Carlo simulations of the peroxidase-catalyzed polymerization of phenols were demonstrated.¹⁴ The monomer reactivity, molecular weight, and index were simulated for precise control of the polymerization of bisphenol A. In aqueous 1,4-dioxane, aggregates from *p*-phenylphenol were detected by difference UV absorption spectroscopy.¹⁵ Such aggregate formation might elucidate the specific solvent effects in the enzymatic polymerization of phenols.

The mechanistic study of the HRP-catalyzed oxidative polymerization was performed by using in situ

NMR spectroscopy.¹⁶ In the polymerization of 8-hydroxyquinoline-5-sulfonate, the 2-, 4-, and 7-positions were involved in the oxidative coupling with the order of preference being $7 \geq 2 > 4$. The polymerizability of phenols via HRP catalysis was evaluated by the initial reaction rate.¹⁷ Phenols with electron-donating groups were consumed much faster than those with electron-withdrawing groups. The reaction rate of para- or meta-substituted phenols was larger than that of ortho-substituted ones.

A bienzymatic system was developed as catalyst for the oxidative polymerization of phenols.¹⁸ The HRP-catalyzed polymerization of phenol in the presence of glucose oxidase and glucose gave the polymer in a moderate yield, in which hydrogen peroxide was formed in situ by the oxidative reaction of glucose catalyzed by glucose oxidase.

The morphology of the enzymatically synthesized polyphenols was controlled under the selected reaction conditions. HRP-catalyzed dispersion polymerization of phenol in a mixture of 1,4-dioxane and phosphate buffer using poly(vinyl methyl ether) as stabilizer produced monodisperse polyphenol particles in the submicrometer range.¹⁹ *m*-Cresol and *p*-phenylphenol were also converted to the polyphenol particles by the dispersion polymerization. The particle size could be controlled by the stabilizer concentration and solvent composition. Thermal treatment of these particles afforded uniform carbon particles.

The enzymatic synthesis of polyphenols was carried out not only in the monophasic solvents but in interfacial systems such as micelles, reverse micelles, and biphasic and Langmuir trough systems. *p*-Phenylphenol was polymerized in an aqueous surfactant solution to give the polymer with a narrower molecular weight distribution in comparison with that obtained in the aqueous 1,4-dioxane.²⁰

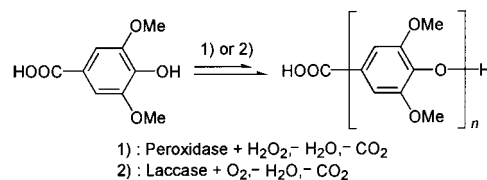
Reverse micellar systems were used for the polymerization of phenol derivatives. HRP-catalyzed polymerization of *p*-ethylphenol in the ternary system composed of a bis(2-ethylhexyl) sodium sulfosuccinate (AOT)–water–isooctane system produced spherical polyphenol particles having 0.1–2 μm diameters quantitatively.²¹ Similar particles were obtained by pouring the solution of enzymatically prepared polyphenol into a nonsolvent containing AOT.²²

The enzymatic polymerization proceeded even in a biphasic system consisting of two mutually immiscible phases (isooctane and water).²³ In the polymerization of *p*-alkylphenols in this system, the molecular weight increased as a function of the carbon number of the alkyl group.

Polyphenol thin films were obtained using Langmuir–Blodgett technique.^{21b,24} A monomeric monolayer was formed from *p*-tetradecyloxyphenol and phenol at the air–water interface in a Langmuir trough, which was polymerized by HRP catalyst in the subphase. The polymerized film could be deposited on silicon wafer with a transfer ratio of 100% for the Y-type film with a thickness of 27.8 Å.

Peroxidase-catalyzed polymerization of phenols has provided a new methodology for functional polymeric materials.

Scheme 3



Poly(oxy-2,6-dimethyl-1,4-phenylene)(poly(phenylene oxide), PPO) is widely used as a high-performance engineering plastic, since the polymer has excellent chemical and physical properties, e.g., a high T_g (ca. 210 °C) and mechanical toughness. PPO was first prepared from 2,6-dimethylphenol monomer using a copper/amine catalyst system.²⁵ The HRP-catalyzed polymerization of 2,6-dimethylphenol gave the polymer consisting of exclusively oxy-1,4-phenylene units.²⁶

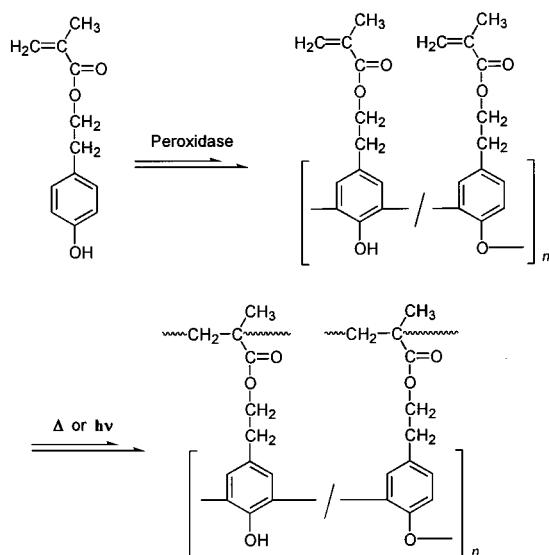
Another PPO derivative was enzymatically obtained from syringic acid (Scheme 3).²⁷ Both HRP and SBP were active for the polymerization involving elimination of carbon dioxide and hydrogen from the monomer to give the polymer with a molecular weight up to 1.3×10^4 . 4-Hydroxy-3,5-dimethylbenzoic acid was also polymerized to give PPO; on the other hand, the polymerization of nonsubstituted 4-hydroxybenzoic acid did not occur under similar reaction conditions. NMR and MALDI-TOF mass analyses showed that the polymer consisted of exclusively 1,4-oxyphenylene units and possessed a phenolic hydroxy group at one terminal end and a benzoic acid group at the other. As one possible application, the polymer from syringic acid was converted to a new PPO derivative, poly(oxy-2,6-dihydroxy-1,4-phenylene), by demethylation with an excess of boron tribromide in dichloromethane.²⁸ The extent of the demethylation was 93%. By utilizing two different terminal functional groups of the polymer, the multiblock copolymer of PPO and aromatic polyester was synthesized by the polycondensation of bisphenol A, isophthalic acid, and the polymer in the presence of triphenylphosphine/hexachloroethane (coupling agent).²⁹

Formation of α -hydroxy- ω -hydroxyoligo(oxy-1,4-phenylene)s was observed in the HRP-catalyzed oxidative polymerization of 4,4'-oxybisphenol in aqueous methanol.³⁰ During the reaction, the redistribution and/or rearrangement of the quinone–ketal intermediate take place, involving the elimination of hydroquinone to give oligo(oxy-1,4-phenylene)s.

Fluorescent naphthol-based polymers were prepared by HRP-catalyzed polymerization of 2-naphthol in AOT/isooctane reverse micelles to give the polymer microspheres.³¹ The precipitated polymer was soluble in a range of polar and nonpolar organic solvents and possessed quinonoid structure. The reverse micellar system induced the peroxidase-catalyzed copolymerization of *p*-hydroxythiophenol and *p*-ethylphenol, yielding the thiol-containing polyphenol particles.³² The attachment of CdS to the particles gave the CdS–polymer nanocomposite showing fluorescence characteristics.

Cross-linkable polyphenols have been enzymatically synthesized. A thermally curable polyphenol

Scheme 4



was synthesized by peroxidase-catalyzed polymerization of bisphenol A.³³ The polymer was cross-linked at 150–200 °C, and the curing improved the thermal stability of the polymer. The reaction with epoxy resin produced the insoluble network polymer. In the HRP-catalyzed polymerization of 4,4'-biphenol, the polymer showing high thermal stability was obtained.³⁴

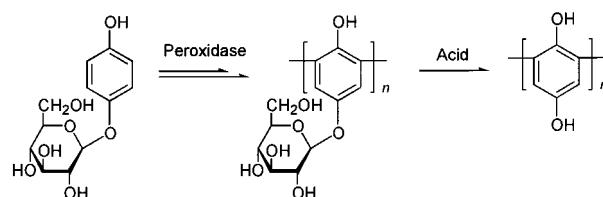
A chemoselective polymerization of a phenol derivative having a methacryloyl group was achieved through HRP catalysis.³⁵ During the polymerization, the methacryloyl group was not involved to give the polymer having the methacryloyl group in the side chain (Scheme 4). The resulting polymer was readily subjected to thermal and photochemical curings.

HRP-catalyzed polymerizations of hydrophobic monomers, *N*-(4-hydroxyphenyl)maleimide, 4'-hydroxymethacrylanilide, and *N*-methacryloyl-11-aminoundecanoyl-4-hydroxyanilide, proceeded even in water in the presence of 2,6-di-*O*-methylated β -cyclodextrin.³⁶ Formation of water-soluble complexes consisting of the hydrophobic monomers as guest molecules and the cyclodextrin derivative as host was detected. The polymerizable moieties in the polymer were not reacted during the polymerization.

m-Ethynylphenol was chemoselectively polymerized to give the polyphenol having the acetylenic group.³⁷ For reference, the copper/amine catalyst system induced the selective oxidative coupling of the acetylene group of the monomer to yield the dimer. Thermal treatment of the resulting polymer produced a carbonized polymer in a much higher yield than enzymatically synthesized poly(*m*-cresol).

Cardanol, the main component obtained by thermal treatment of cashew nut shell liquid (CNSL), is a phenol derivative having the meta substituent of a C15 unsaturated hydrocarbon chain with one to three double bonds as the major component. The SBP-catalyzed polymerization of cardanol in aqueous acetone produced the oily soluble polymer with M_n of several thousands.³⁸ The carbon-carbon unsaturated group in the side chain of cardanol did not change during the polymerization. The curing by

Scheme 5



cobalt naphthenate gave the cross-linked film with a high gloss surface. The hydrogenated cardanol derivative was also oxidatively polymerized by HRP.³⁹

Photo-cross-linkable oligophenols were synthesized by the HRP-catalyzed polymerization of cinnamoyl-hydroquinone-ester and cinnamoyl-4-hydroxyanilide in an aqueous 1,4-dioxane.⁴⁰ UV irradiation of the oligomer films induced the cross-linking by the photochemical [2+2]-cycloaddition of the cinnamoyl function.

A natural phenol, 4-hydroxyphenyl β -D-glucopyranoside (arbutin), was subjected to regioselective oxidative polymerization using peroxidase catalyst in a buffer solution, yielding the water-soluble polymer consisting of a 2,6-phenylene unit (Scheme 5).⁴¹ Acidic deglycosylation of the resulting polymer afforded soluble poly(hydroquinone), which may be an *ortho-ortho* coupling structure. The resulting polymer was applied as a glucose sensor by utilizing its good redox properties.⁴² Chemoenzymatic synthesis of another poly(hydroquinone) was reported; SBP-catalyzed polymerization of 4-hydroxyphenyl benzoate followed by alkaline hydrolysis gave the polymer whose structure was different from that of arbutin.⁴³

A thymidine-containing polyphenol was synthesized by SBP-catalyzed oxidative polymerization of thymidine 5'-*p*-hydroxyphenylacetate.⁴⁴ Amphiphilic esters of tyrosine were polymerized in a micellar solution to give the polymer showing surface activity at the air-water interface.⁴⁵ Polymerization monitoring using a quartz crystal microbalance was reported.

Peroxidase catalyzed the oxidative polymerization of fluorinated phenols to give fluorine-containing polymers.⁴⁶ During the polymerization, elimination of fluorine atom partly took place to give the polymer with a complicated structure. Antioxidant effects of the enzymatically synthesized polyphenols were evaluated.⁴⁷ The autoxidation of tetralin was significantly suppressed in the presence of the polyphenols.

Enzymatically synthesized polyphenol derivatives are expected to have great potential for electronic applications. The surface resistivity of poly(*p*-phenylphenol) doped with nitrosylhexafluorophosphate was around $10^5 \Omega$.^{4a} The iodine-labeled poly(catechol) showed low electrical conductivity in the range from 10^{-6} to 10^{-9} S/cm.⁴⁸ The iodine-doped thin film of poly(phenol-*co*-tetradecyloxyphenol) showed a conductivity of 10^{-2} S/cm, which was much larger than that obtained in aqueous 1,4-dioxane.^{24a} The third-order optical nonlinearity (χ^3) of this film was 10^{-9} esu. An order of magnitude increase in the third-order nonlinear optical properties was observed in comparison with that prepared in the aqueous organic solution.

A novel photoactive azopolymer, poly(4-phenylazophenol), was synthesized using HRP catalyst. The polymer exhibited reversible trans to cis photoisomerization of the azobenzene group with a long relaxation time.⁴⁹ Hydroquinone mono-oligo(ethylene glycol) ether was polymerized by HRP in aqueous 1,4-dioxane. The film prepared from a mixture of the lithiated polyphenol and poly(ethylene glycol) (PEG) showed high ionic conductivities (4×10^{-5} S/cm).⁵⁰ Phenolic copolymers containing fluorophores (fluorescein and calcein) were synthesized using SBP catalyst and used as an array-based metal-ion sensor.⁵¹ Selectivity and sensitivity of metal sensing were controlled by changing the polymer components. A combinatorial approach for screening of specific metal ions was examined.

In vitro synthesis of lignin, a typical phenolic biopolymer, has been attempted by the HRP-catalyzed terpolymerization of *p*-coumaryl alcohol, coniferyl alcohol, and sinapyl alcohol (14:80:6 mol %) in extremely dilute aqueous solutions at pH 5.5.⁵² Dialysis membrane method was applied to the polymerization of coniferyl and sinapyl alcohols, yielding insoluble polymeric materials.⁵³ Coniferyl alcohol was polymerized by HRP in an aqueous acetone to give the insoluble polymer.⁵⁴ In the presence of a small amount of lignin component, the molecular weight distribution became much broader than that in the absence of lignin.⁵⁵ HRP catalyzed the polymerization of soluble oligomeric lignin fragments to yield insoluble polymeric precipitates.⁵⁶

Peroxidase-catalyzed grafting of polyphenols on lignin was performed by HRP-catalyzed polymerization of *p*-cresol with lignin in the aqueous 1,4-dioxane or reverse micellar system.⁵⁷ Phenol moiety in lignin was reacted with *p*-cresol to produce a lignin-phenol copolymer with a branched and/or cross-linked structure. The product was highly insoluble in common organic solvents.

The peroxidase-catalyzed reaction of low-molecular weight coal (molecular weight $\approx 4 \times 10^3$) was performed in a mixture of DMF and buffer.⁵⁸ The resulting product was partly soluble in DMF, and the DMF-soluble part had a larger molecular weight than that of the starting substrate.

Peroxidase catalysis also induced the depolymerization of enzymatically obtained polyphenols.⁵⁹ Formation of HRP compound III intermediate may be related to the onset of the depolymerization. Furthermore, the polyphenols were reported to be subjected to biodegradation, although the degradation proceeded slowly.⁶⁰

HRP was used as catalyst for cross-linking of peptides (soy proteins and wheat gliadin).⁶¹ Tyrosine residues of the proteins were subjected to the enzymatic oxidative coupling, yielding a network of peptide chains. The treatment increased the tensile strength of the materials.

Lignin-degrading manganese(II) peroxidase was used as catalyst for the oxidative polymerization of various phenol derivatives such as guaiacol, *o*-cresol, and 2,6-dimethoxyphenol in the aqueous organic solvents.⁶²

Model complexes of peroxidase were used as catalysts for the oxidative polymerization of phenols. Hematin, a hydroxyferritoporphyrin, catalyzed the polymerization of *p*-ethylphenol in an aqueous DMF.⁶³ Iron-*N,N*-ethylenebis(salicylideneamine) (Fe-salen) showed high catalytic activity for oxidative polymerization of various phenols.⁶⁴ The first synthesis of crystalline fluorinated PPO was achieved by the Fe-salen-catalyzed polymerization of 2,6-difluorophenol. Cardanol was polymerized by Fe-salen to give a cross-linkable polyphenol in high yields.

2. Oxidative Polymerization of Aniline Derivatives

Aniline and its derivatives were oxidatively polymerized by peroxidase catalyst. HRP catalyzed the polymerization of aniline in aqueous organic solvents to produce the polymer with a complicated structure in low yields.⁶⁵ The resulting polymer showed good third-order nonlinear optical properties.⁶⁶

The addition of templates enabled the enzymatic production of conducting polymers with well-defined structure.⁶⁷ In using sulfonated polystyrene (SPS) as a template, the resulting polymer was soluble in water and the conductivity reached 5×10^{-3} S/cm without doping. Besides SPS, a strong acid surfactant (sodium dodecylbenzenesulfonic acid) or poly(vinylphosphonic acid) provided a suitable local template environment leading to the formation of conducting polyaniline.

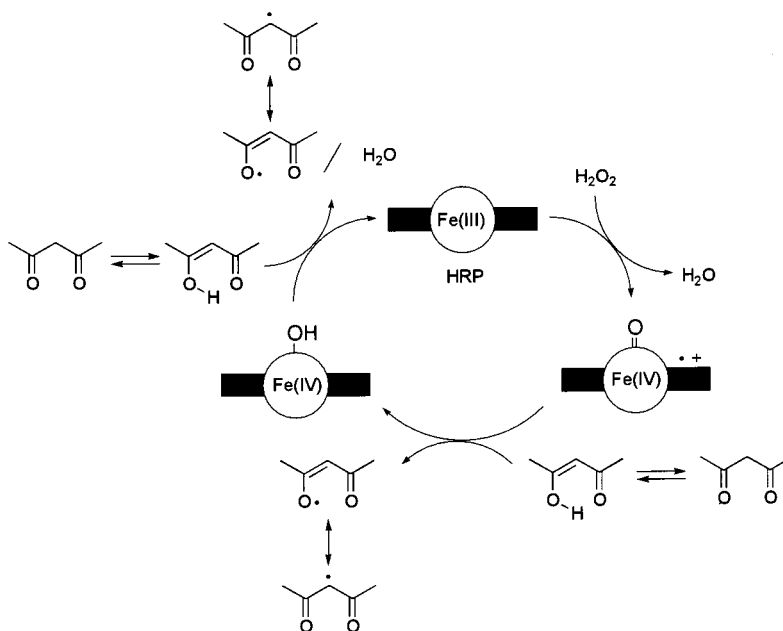
HRP-catalyzed polymerization of *o*-phenylenediamine in an aqueous 1,4-dioxane gave a soluble polymer with a molecular weight of 2×10^4 .⁶⁸ NMR analysis showed the formation of the polymer consisting of an iminophenylene unit. From *p*- and *m*-isomers, the polymer with well-defined structure was not obtained.⁶⁹ HRP-catalyzed polymerization of 4,4'-diaminoazobenzene gave a new photodynamic polyaniline derivative containing an azo group.⁷⁰ Various aniline derivatives, *p*-aminobenzoic acid,⁷¹ *p*-aminophenylmethylcarbitol,⁷² 2,5-diaminobenzene-sulfonate,⁷³ and *p*-aminochalcones,⁷⁴ were polymerized by peroxidase catalyst. Monolayer of aniline/*p*-hexadecylaniline prepared by LB technique at the air-water interface was polymerized through HRP catalysis to give polymeric monolayer.²⁴

A new class of polyaromatics was synthesized by peroxidase-catalyzed oxidative copolymerization of phenol derivatives with anilines. In the case of a combination of phenol and *o*-phenylenediamine, FT-IR analysis showed the formation of the corresponding copolymer.⁷⁵

3. Polymerization of Vinyl Monomers

Some oxidoreductases have been reported to induce polymerization of vinyl monomers. A novel initiating system for vinyl polymerization, HRP/hydrogen peroxide/ β -diketones such as acetylacetone, was demonstrated in which the catalytic action of HRP generates carbon radical, a real initiating species, from hydrogen peroxide and β -diketone through an oxidoreductive pathway (Scheme 6).⁷⁶ Hydrophobic monomers, styrene⁷⁷ and methyl methacrylate (MMA),⁷⁸ were also polymerized by this initiating

Scheme 6



system in a mixture of water and tetrahydrofuran. The polymer from MMA had syndiotactic diad fractions ranging from 0.82 to 0.87.⁷⁸ Manganese peroxidase catalyzed the acrylamide polymerization in the presence of acetylacetone.⁷⁹

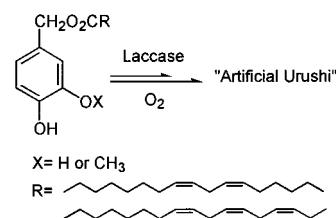
B. Laccases

Laccases having a Cu active site catalyze the oxidative coupling of phenols. Laccases derived from *Pycnoporus coccineus* (PCL) and *Myceliophthora* were active for the polymerization of syringic acid to give PPO with a molecular weight up to 1.8×10^4 (Scheme 2).^{27,80} Enzymatic synthesis of PPO was also achieved from 2,6-dimethylphenol using PCL catalyst.²⁶ The polymerization of 1-naphthol using laccase from *Trametes versicolor* (TVL) proceeded in aqueous acetone to give the polymer with a molecular weight of several thousands.⁸¹

Coniferyl alcohol was polymerized by laccase catalyst. The polymerization behavior depended on the origin of the enzyme. PCL and laccase from *Coriolus versicolor* showed high catalytic activity to give the dehydrogenative insoluble polymer, whereas very low catalytic activity was observed in laccase from *Rhus vernicifera* Stokes.⁵⁴ The increase of the molecular weight was observed in the treatment of soluble lignin using TVL catalyst.⁸²

Urushi is a Japanese traditional coating showing excellent toughness and brilliance for a long period. The main important components of urushi are "urushiols", whose structure is a catechol derivative directly linked to unsaturated hydrocarbon chains consisting of a mixture of monoenes, dienes, and trienes at the 3- or 4-position of catechol.⁸³ Film-forming of urushiols proceeds under air at room temperature without organic solvents; hence, urushi seems to be very desirable for coating materials from an environmental standpoint. In vitro enzymatic hardening reaction of catechol derivatives bearing an unsaturated alkenyl group at the 4-position of the

Scheme 7



catechol ring proceeded using PCL catalyst to give the cross-linked film showing excellent dynamic viscoelasticity.⁸⁴

A novel system of enzymatic polymerization, i.e., a laccase-catalyzed cross-linking reaction of new urushiol analogues for the preparation of "artificial urushi", was demonstrated (Scheme 7).⁸⁵ Single-step synthesis of the urushiol analogues having ester group was achieved by using lipase as catalyst. These compounds were cured in the presence of laccase catalyst under mild reaction conditions without use of organic solvents to produce the cross-linked polymeric film. Properties of the film are comparable to those of natural urushi with a high gloss surface and dynamic viscoelasticity (Figure 1).

Laccase catalyzed the polymerization of acrylamide in water.⁸⁶ The high molecular weight polymer was

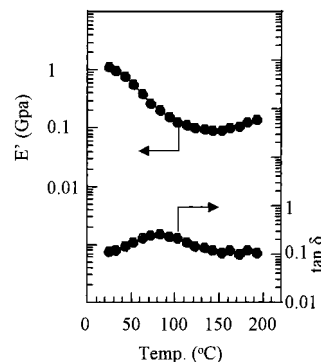


Figure 1. Dynamic viscoelasticity of artificial urushi from urushiol analogue having a linolenic acid group.

obtained using PCL catalyst at 50–80 °C. The polymerization in the presence of acetylacetone proceeded at room temperature. A combination of laccase and organic peroxide initiated the polymerization of acrylamide in the presence of lignin, yielding lignin-graft-polyacrylamide.⁸⁷

C. Other Oxidoreductases

Bilirubin oxidase (BOD), a copper-containing oxidoreductase, catalyzes the oxidative polymerization of aniline and 1,5-dihydroxynaphthalene. The polymerization of aniline in a buffer solution in the presence of BOD-adsorbed solid matrix gave the polyaniline film containing the active enzyme.⁸⁸ The film was electrochemically reversible in its redox properties in acidic aqueous solution. In the BOD-catalyzed polymerization of 1,5-dihydroxynaphthalene in aqueous organic solvents, the insoluble polymer was formed.⁸⁹ The polymer films exhibited a wide band from 300 to 470 nm in their UV spectrum, indicating the formation of a long π -conjugated structure. The polymer treated with HClO₄ showed an electroconductivity of 10⁻³ S/cm.

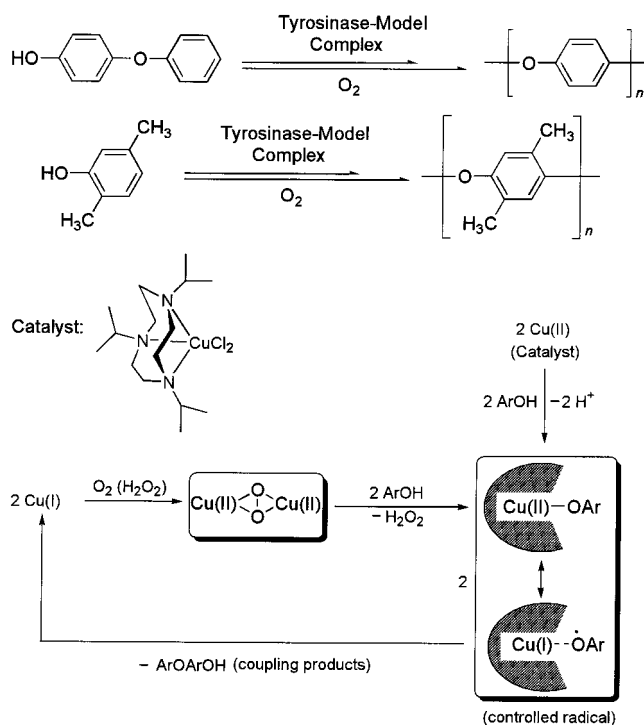
Tyrosinase (polyphenol oxidase, a copper-containing monooxygenase enzyme) was used as catalyst for the modification of natural polymers. Phenol moiety-incorporated chitosan derivatives were subjected to tyrosinase-catalyzed cross-linking, yielding stable and self-sustaining gels.⁹⁰ Tyrosinase also catalyzed the hybrid production between the modified chitosan and proteins.

The enzymatic treatment of chitosan in the presence of tyrosinase and phenol derivatives produced new materials based on chitosan.⁹¹ During the reaction, unstable *o*-quinones were formed, followed by the reaction with the amino group of chitosan to give the modified chitosan. The tyrosinase-catalyzed modification of chitosan with phenols dramatically altered rheological and surface properties of chitosan. The modification with chlorogenic acid onto chitosan conferred the water solubility of chitosan under basic conditions.⁹² A new water-resistant adhesive was developed by the tyrosinase-catalyzed reaction of 3,4-dihydroxyphenethylamine and chitosan.⁹³ Poly(4-hydroxystyrene) was modified with aniline by using tyrosinase catalyst.⁹⁴ The incorporated ratio of aniline into the polymer was very low (1.3%).

Tyrosinase catalyzed the oxidative coupling of soluble lignin fragments to give the insoluble polymer.⁵⁶ Tyrosinase model complexes catalyzed the regioselective oxidative polymerization of phenols, leading to the formation of aromatic polyethers with well-defined structure.^{95–97} The reaction at the unsubstituted ortho positions did not take place, in sharp contrast to the polymerization by a Cu–amine catalyst system.²⁵ From 4-phenoxyphenol⁹⁵ and 2,5-dimethylphenol,⁹⁶ crystalline PPO derivatives were formed (Scheme 8). The polymer from the latter monomer possessed a melting point higher than 300 °C, a class of super engineering plastics.⁹⁶ A “radical-controlled” reaction mechanism is proposed for the high regioselectivity.

Glucose oxidase initiated the vinyl polymerization in the presence of Fe²⁺ and dissolved oxygen.⁹⁸ The

Scheme 8



formation of cross-linked product was observed in the polymerization of acrylamide in the presence of bisacrylamide catalyzed by xanthine oxidase, chloroperoxidase, and alcohol oxidase.⁹⁹

III. Transferases

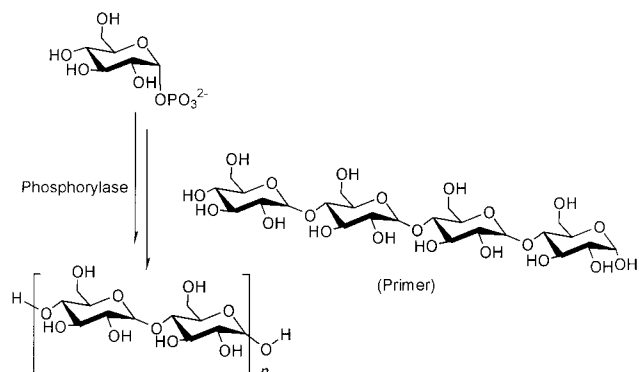
Transferases are enzymes transferring a group from one compound (generally regarded as donor) to another compound (generally regarded as acceptor). For example, a glycosyl group as donor is transferred to an alcohol as acceptor to form a glycosidic bond and an acyl group as donor to an alcohol as acceptor giving rise to an ester bond. Several transferases such as phosphorylases and synthases have been found to be effective for catalyzing *in vitro* synthesis of polysaccharides and polyesters. It is to be noted, however, that some of the *in vitro* reactions below, such as cellulose, chitin, hyaluronic acid, and polyester syntheses, catalyzed by the respective synthases are occurring in a manner similar to biosynthetic pathways *in vivo*. Such reactions are then not in the category of enzymatic polymerization in a strict sense of its definition but are probably instructive to readers.

A. Glycosyltransferases

1. Phosphorylases

A phosphorylase catalyzes *in vitro* production of amylose (poly- α -(1→4)-D-glucopyranose) and its derivatives. Amylose was synthesized from D-glucosyl phosphate as a substrate monomer and malto-oligomers with a minimum length of four glucosyl residues as a primer by using potato phosphorylase (Scheme 9).¹⁰⁰ The reaction proceeded analogously to a living polymerization to form amyloses having relatively uniform chain lengths. Branched polymers

Scheme 9



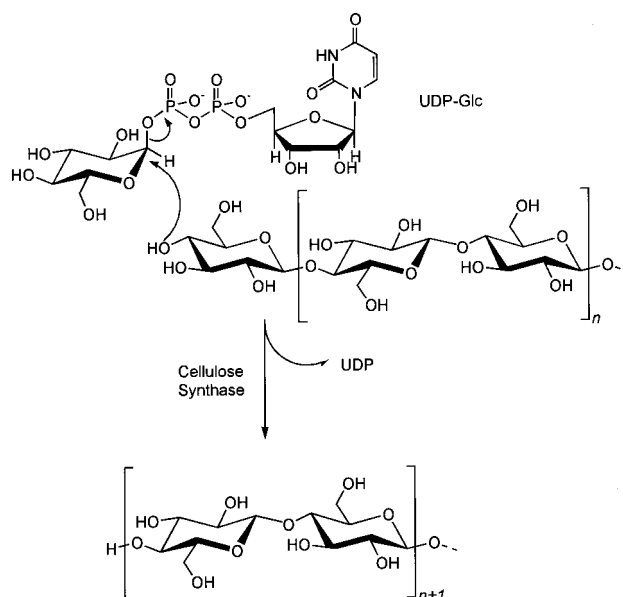
of star and comb shapes carrying amylose chains of uniform length were also obtained by using potato phosphorylase.¹⁰¹ Poly(dimethylsiloxane-*graft*- α (1 \rightarrow 4)-glucopyranose) was synthesized from D-glucosyl phosphate and a polyinitiator based on polysiloxane with statistically distributed maltoheptaamide and maltoheptaoside by using potato phosphorylase.¹⁰² Similarly, this method was extended widely to prepare styryl-type amylose macromonomer,¹⁰³ amylose-*graft*-poly(L-glutamic acid),¹⁰⁴ amylose-*block*-polystyrene,¹⁰⁵ amylose-*block*-poly(ethylene oxide),¹⁰⁶ and amylose-containing silica gel.¹⁰⁷

The synthesis of 2-deoxyamylose derivatives by enzymatic chain elongation of glycogen was reported; only an average of up to 1.5 units of 3- and 4-deoxyglucosyl phosphate were transferred by phosphorylase.¹⁰⁸ On the other hand, an average of 20 units of 2-deoxyglucosyl units were connected to maltotetraose by using potato phosphorylase.¹⁰⁹ One day incubation of D-glucal and the tetrasaccharide with phosphorylase and 0.1 equiv of inorganic phosphate yielded a precipitate of corresponding polysaccharide. The tetrasaccharide is the shortest length as a primer required for the phosphorylase reaction. The polysaccharide became insoluble at a chain length of about 20 and was then released from the enzymatic glycosylation process.

The phosphorolytic synthesis of cello-oligosaccharides by cello-oligosaccharide phosphorylase was carried out by using various cellobiosyl residues as glycosyl acceptors and α -D-glucopyranosyl phosphate as glycosyl donor.¹¹⁰ The crystalline precipitate was obtained, which showed the diffraction diagrams of low molecular weight cellulose II. NMR measurement revealed that an average degree of polymerization of the cello-oligosaccharides was about 8. Cello-oligosaccharides beyond this chain length become insoluble in water. Subsequent chain elongation in the phosphorolytic synthesis may be possible as long as the product is soluble. The product is therefore considered to dissociate completely from the enzyme after each addition of a glucose unit. Various cello-oligosaccharide derivatives substituted at their reducing end were also obtained by the phosphorolytic synthesis in the presence of various primers.

In all cases using phosphorylase as catalyst, it is required to employ a large excess amount of a substrate monomer (glycosyl donor) for a primer in order to shift the reaction equilibrium to the polymer formation.

Scheme 10



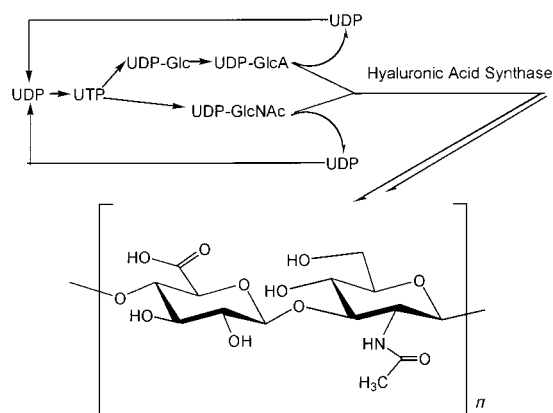
The molecular mechanism of the substrate recognition and phosphorolysis of phosphorylase was presented.¹¹¹ The ternary complex of malto-oligosaccharide phosphorylase, 4-*S*- α -D-glucopyranosyl-4-thio-maltotetraose, and phosphate shows that the phosphate group attacked the glycosidic linkage and promoted the phosphorolysis.

2. Glycosyl Transferases

Biosynthetic mechanisms of cellulose and chitin in living cells have been extensively studied; cellulose and chitin were also formed *in vitro* from the activated monomers, uridine diphosphate glucose (UDP-Glc) and UDP-*N*-acetyl-glucosamine (UDP-GlcNAc), catalyzed by cellulose and chitin synthases, respectively.¹¹² Glycosyltransferases of the Leloir pathway use individual sugar nucleotides as donors, which are activated as glycosyl esters of nucleoside mono- or diphosphates.¹¹³ Scission of the phosphoester bond between uridine diphosphate (UDP) and the monosaccharide will supply the free energy that drives glycosidic linkage formation. A single displacement mechanism with inversion of configuration to yield β -1,4-linkages has been proposed, where the nucleophilic C4-OH at the nonreducing chain end attacks the α -C1-position of UDP-Glc. The reducing chain end points away from the catalytic enzyme (Scheme 10). On the other hand, glycogen synthase forms α -linked products from α -linked donor substrates with retention of anomeric carbon configuration at the reaction center.¹¹⁴ The "retaining" mechanism is most likely due to the formation of a glycosyl enzyme intermediate in the enzymatic process.

Even though the relatively high cost of the glycosyl donors and limited enzyme availability are drawbacks of using glycosyl transferases to saccharide synthesis, the modern recombinant DNA technology enables the increasing availability of glycosyl transferases. Furthermore, the method appears to be effective even for a large-scale stereocontrolled oligosaccharide synthesis when it is combined with *in situ* regeneration of sugar nucleotides.¹¹⁵ This strat-

Scheme 11



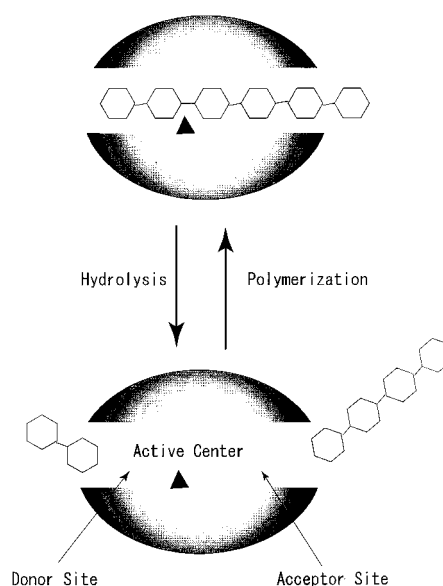
egy also avoids the problem of product inhibition by released nucleoside mono- or diphosphates. Sugar nucleotides are regenerated via sugar nucleotide pyrophosphorylases or sugar nucleotide synthases with a catalytic amount of nucleoside mono- or diphosphate and a stoichiometric amount of the donor monosaccharide. For example, hyaluronic acid with a molecular weight of about 5.5×10^5 has been synthesized from UDP-GlcNAc and UDP-glucuronic acid (UDP-GlcA) using hyaluronic acid synthase coupled with regeneration of the sugar nucleotides (90% yield, Scheme 11).¹¹⁶ For this enzymatic preparation of hyaluronic acid, seven kinds of enzymes, hyaluronic acid synthase, UDP-Glc dehydrogenase, UDP-Glc pyrophosphorylase, UDP-GlcNAc pyrophosphorylase, pyruvate kinase, lactate dehydrogenase, and inorganic pyrophosphatase, were used together in a polymerization solution.

Chitin oligosaccharides were obtained by a bacterial chitin oligosaccharide synthase (NodC) using UDP-GlcNAc as a donor. Elongation of the growing chitin oligosaccharide chain by NodC proceeds by the addition of monosaccharides to C4-OH of the non-reducing terminal GlcNAc residue. Chitin oligosaccharide synthesis by NodC is considered to occur by a processive mechanism because chitin oligosaccharides ranging from chitobiose to chitotetraose could not act as efficient primers for NodC. Therefore, successive addition of saccharide units to a growing chain only proceeds while the product chain remains in contact with the enzyme.¹¹⁷

B. Acyltransferases

Poly(β -hydroxybutyrate) (PHB) is accumulated within the cells of a wide variety of bacteria as an intracellular energy and carbon storage material. Poly(hydroxyalkanoate)s (PHA)s are commercially produced as biodegradable plastics. In the biosynthetic pathways of PHA, the last step is the chain growth polymerization of hydroxyalkanoate CoA esters catalyzed by PHA polymerase (synthase). In the present review, we classified PHA polymerases into transferases by taking them as a family of acyltransferases. PHA polymerase from *Ralstonia eutropha* polymerized the CoA monomers of (*R*)-hydroxyalkanoate in vitro to give the high molecular weight homopolymers and copolymers with well-defined structure.¹¹⁸ The molecular weight of the

Scheme 12



polymers was found to be inversely proportional to the molar ratio of monomer-to-enzyme, and the obtained polymer had a narrow molecular weight distribution, suggesting that the polymerization proceeds in a living fashion. Random copolymers were obtained from the mixture of the two CoA esters in the presence of the polymerase, whereas the sequential copolymerization produced the block copolymers.

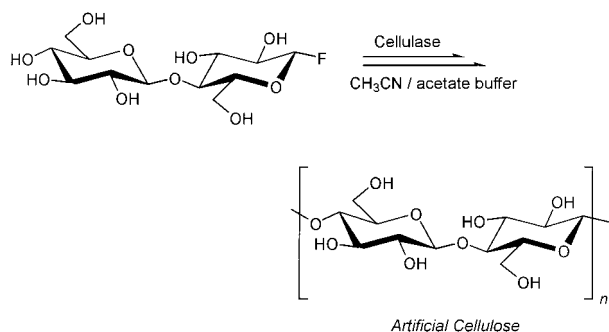
In the combination of recombinant PHA synthase from *Chromatium vinosum* with propionyl-CoA transferase of *Clostridium propionicum*, a two-enzyme in vitro PHB biosynthesis system from (*R*)-hydroxybutyric acid was demonstrated.¹¹⁹ This system required only catalytic amounts of expensive CoA, and hence, PHA could be readily produced in a semipreparative scale.

IV. Hydrolases

It is generally accepted that an enzymatic reaction is virtually reversible, and hence, the equilibrium can be controlled by appropriately selecting the reaction conditions. On the basis of this view, many hydrolases, which are enzymes catalyzing a bond-cleavage reaction by hydrolysis, have been employed as catalysts for the reverse reaction of hydrolysis, leading to polymer production by a bond-forming reaction.

A. Glycosidases

Glycosidases are hydrolysis enzymes to cleave the glycosidic linkage of glycan chains with water. Their catalytic center is normally surrounded by donor and acceptor sites where the reducing and nonreducing sites, respectively, of glycan chains are involved in both reactions of the hydrolysis (bond-cleavage) and the reverse reaction (bond-forming) (Scheme 12). Two major types of glycosidases are known; exo-glycosidases cleaving external glycosidic linkages of polysaccharide chains to liberate mono, di-, or oligo-saccharides from the nonreducing terminal and endo-glycosidases randomly cleaving internal glycosidic linkages of the chains.

Scheme 13**1. Natural Glycosidases**

Glycosidase-catalyzed *in vitro* polymerizations enabled the synthesis of not only various natural polysaccharides, but also some unnatural polysaccharides, when the substrate monomer is appropriately designed in combination with a selected enzyme.

a. Synthesis of Natural Polysaccharides. There are two main approaches for glycosidase-catalyzed synthesis of glycosidic-linked compounds: direct reversal of hydrolysis (equilibrium-controlled synthesis) and promoted formation of a glycosyl enzyme intermediate (kinetically controlled synthesis).¹²⁰ The former synthesis uses a high concentration of mono- or oligo-saccharide as a donor, addition of organic cosolvents, and elevated reaction temperatures to achieve significant transformation. On the other hand, the latter synthesis needs activated starting substrates such as glycosyl fluorides or aryl glycosides as donors. The whole point of the formation of a glycosidic linkage by glycosidases is a rapid formation of an activated glycosyl enzyme intermediate and its rapid reaction with the glycosyl acceptor, which should be much easier than with water.

A typical example of the equilibrium-controlled synthesis is the preparation of hexa-*N*-acetylchitohexaose and hepta-*N*-acetylchitoheptaose from di-*N*-acetylchitobiose under the conditions of high substrate concentration (10 wt %), high ionic strength (30 wt % ammonium sulfate), and high temperature at 70 °C by using egg yolk lysozyme (exo-glycosidase).¹²¹ These products are practically insoluble in

high salt aqueous solution to be selectively precipitated out.¹²²

Cellulase was found to be effective in the synthesis of artificial cellulose in a single-step reaction by polycondensation of β -D-cellobiosyl fluoride (Scheme 13).¹²³ The polymerization is a repetition of the transglycosylation reaction, which became predominant over the hydrolysis reaction when the enzymatic polycondensation was carried out in a mixed solvent of acetonitrile/acetate buffer (5:1, pH 5). This synthesis is therefore kinetically controlled as well as equilibrium controlled. The β configuration of the C1 fluorine atom is necessary to form a reactive intermediate leading to a $\beta(1\rightarrow4)$ product via a “double displacement mechanism”.¹²⁴ Thus, this method provided the first successful *in vitro* synthesis of cellulose, the most abundant biomacromolecules on the earth, the synthesis of which had been unsolved for one-half a century.¹²³

Artificial cellulose showed the cellulose II allomorph, a thermodynamically more stable form with an antiparallel structure, by X-ray diffraction study, when a crude cellulase was employed for the enzymatic polymerization.¹²³ The other allomorph cellulose I is a thermodynamically metastable form with a parallel structure, which living cells normally produce, but was believed impossible to be realized *in vitro*. Interestingly, however, the *in vitro* synthesis of cellulose I was successfully achieved by using a purified cellulase.¹²⁵ The molecular packing of glucan chains in a crystal is affected by the purity of the enzyme as well as the enzymatic polymerization conditions. A novel concept “choro-selectivity” was therefore proposed, which is concerned with the intermolecular relationship in packing of polymers having directionality in their chains.¹²⁶

Furthermore, the enzymatic polymerization provided a novel three-dimensional spherulite composed of artificial cellulose II (Figure 2).¹²⁷ The spherulites consisted of single crystals with the glucan chains oriented perpendicular to the crystalline plane, which is entirely different from those obtained from bacterial cellulose.¹²⁸

Xylan was prepared by enzymatic polycondensation similar to the case of artificial cellulose.¹²⁹ β -Xylo-

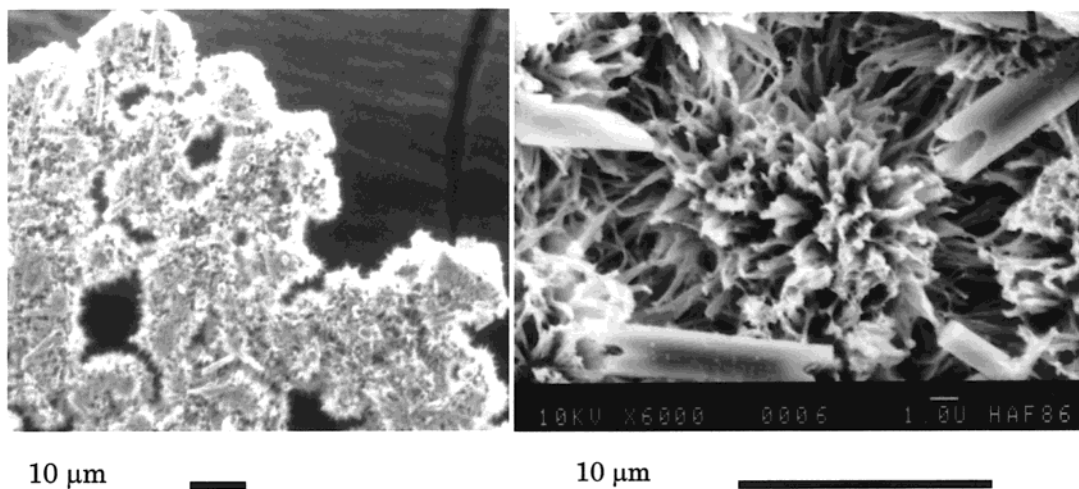
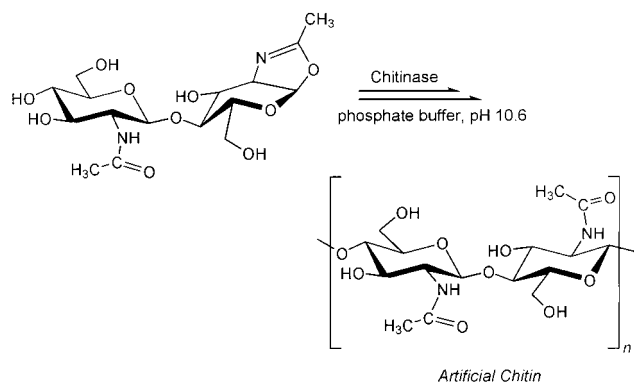


Figure 2. SEM observations of a plate of artificial cellulose spherulites.

Scheme 14

biosyl fluoride was used as a substrate monomer for crude cellulase containing xylanase in a mixed solvent of acetonitrile and acetate buffer. The reaction should proceed through the formation of a glycosyl–enzyme intermediate or a glycosyl oxocarbenium ion intermediate at an active site of the enzyme, followed by the attack of the 4-hydroxy group of an acceptor molecule.

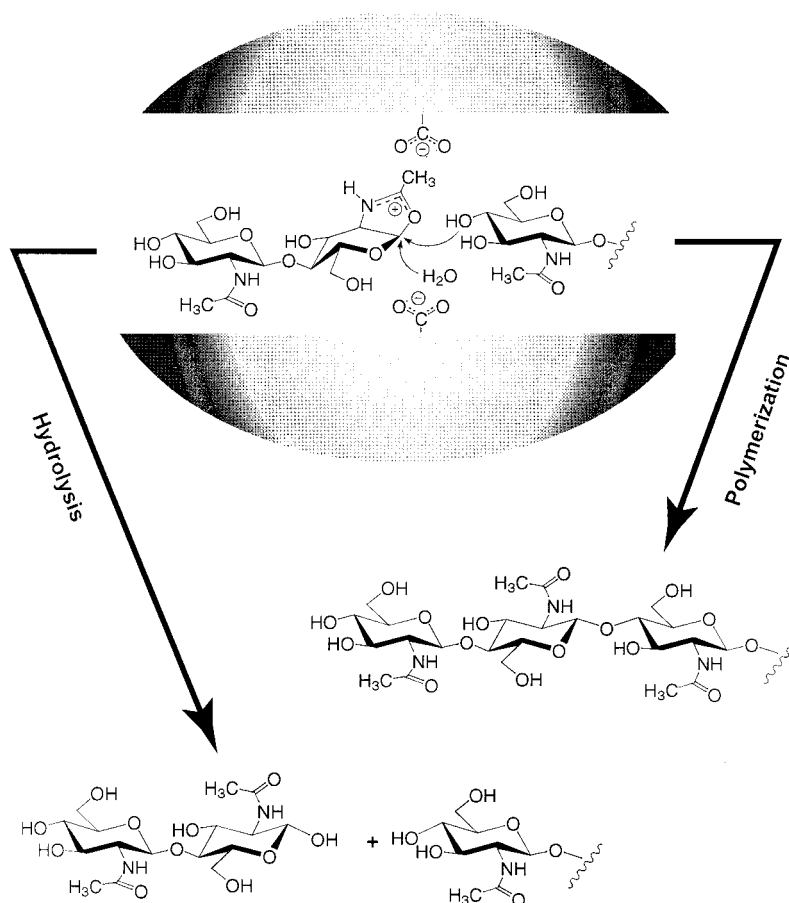
Maltooligosaccharides (artificial amyloses) were prepared by polycondensation of α -D-maltosyl fluoride using α -amylase as the catalyst in a mixed solvent of methanol–phosphate buffer (pH 7).¹³⁰ The yielded maltooligosaccharides contained a mixture from triose to heptaose. The formation of the odd-numbered maltooligosaccharides may be due to enzymatic hydrolysis of the products during the reaction. The

formation of $\alpha(1\rightarrow4)$ -glycosidic linkages is explained by a mechanism involving “double displacement” of the C1 carbon configuration of the monomer.

Chitin is the most abundant biomacromolecule in the animal field, which is found normally in invertebrates as a structural component. This important polysaccharide was synthesized for the first time by the enzymatic polymerization using chitinase and a chitinose oxazoline derivative (Scheme 14).¹³¹ The latter activated monomer has a distorted structure with an α configuration at C1, which resembles a transition-state structure of substrate chitin at the active site during a hydrolysis process (Scheme 15).^{3b,131,132} The ring-opening polyaddition of the chitinose oxazoline derivative was exclusively promoted by chitinase at pH 10.6, where the hydrolytic activity of chitinase was very much lowered.

Upon enzymatic polymerization to produce the artificial chitin, spherulites of 20–50 μm in diameter were also obtained (Figure 3).¹³³ Platelike single crystals were gradually shaped into ribbons, followed by formation of bundlelike assemblies to grow into spherulites in the polymerization solution.

Hyaluronidase is one of the glycosidases catalyzing hydrolysis of glycosidic linkages of hyaluronic acid (HA). It is known that the enzyme also catalyzes the transglycosylation reaction. By utilizing both catalysis functions, reaction between HA (molecular weight $\approx 8 \times 10^5$) as a donor and HA hexasaccharide having glucuronic acid at the nonreducing terminal as an acceptor took place to reconstruct oligomers (up to

Scheme 15

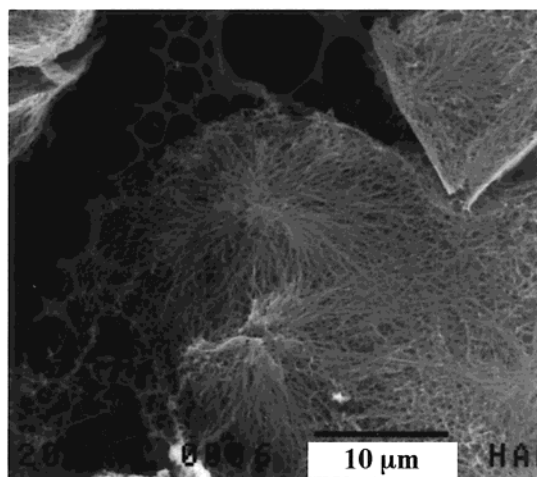
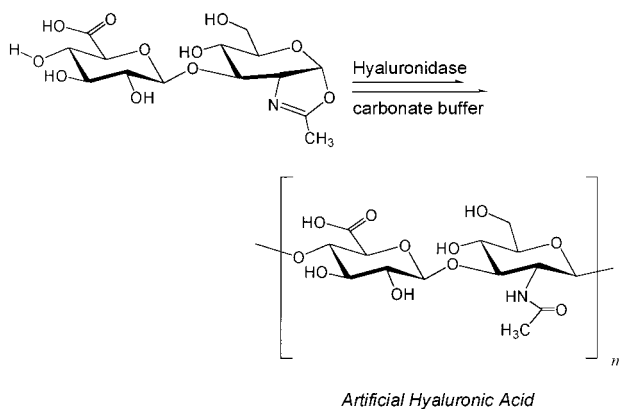


Figure 3. Electron micrograph of artificial chitin spherulite by SEM.

Scheme 16



22mers) of HA. During the reaction, a disaccharide unit was released via hydrolysis from the HA and transferred to the nonreducing terminal of the acceptor.¹³⁴

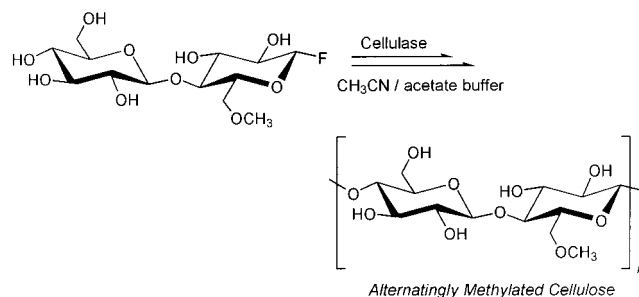
A new enzymatic polymerization has been found to produce artificial HA via ring-opening addition polymerization catalyzed by hyaluronidase (Scheme 16).¹³⁵ The oxazoline part of the starting substrate monomer is a latent *N*-acetyl group of an *N*-acetylglucosamine unit which acts as a donor, adding to 4-OH of glucuronic acid at the acceptor site. This polymerization gave HA having a perfect structure containing GlcNAc β (1 \rightarrow 4)GlcUA β (1 \rightarrow 3) linkages with a molecular weight around 20 000.

b. Synthesis of Unnatural Polysaccharides.

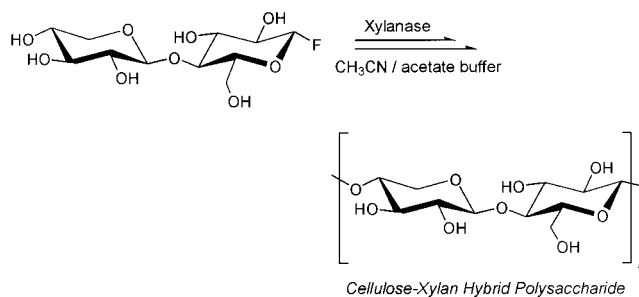
Unnatural polysaccharides were also obtained by the enzymatic polymerization. 6-*O*-Methyl- β -cellobiosyl fluoride was used as a substrate of cellulase, giving rise to an alternately 6-*O*-methylated cellulose derivative (Scheme 17).^{136,137} Another cellobiose derivative, 6'-*O*-methyl- β -cellobiosyl fluoride, gave only a mixture of low molecular weight oligomers.¹³⁷ The difference of reactivity between the two monomers may be explained by easier acceptance of the 6-*O*-methyl glucose unit as the nonreducing terminal at the acceptor site.

The enzymatic polymerization method was extended to use disaccharide monomers composed of different kinds of monosaccharide units to obtain

Scheme 17



Scheme 18



unnatural hybrid polysaccharides. β -Xylopyranosyl-glucopyranosyl fluoride was used as a substrate monomer of xylanase, giving rise to a cellulose-xylan hybrid polymer (Scheme 18).¹³⁸

Thiooligosaccharides can be inhibitors of cellulases and are useful for elucidation of the molecular mechanism of the cellulolytic actions. Hemithiocellobiosaccharides from tetraose to tetradecaose were synthesized by a cellulase mixture using 4-thio- β -cellobiosyl fluoride as an activated donor in a buffer/acetone nitrile solvent system.¹³⁹

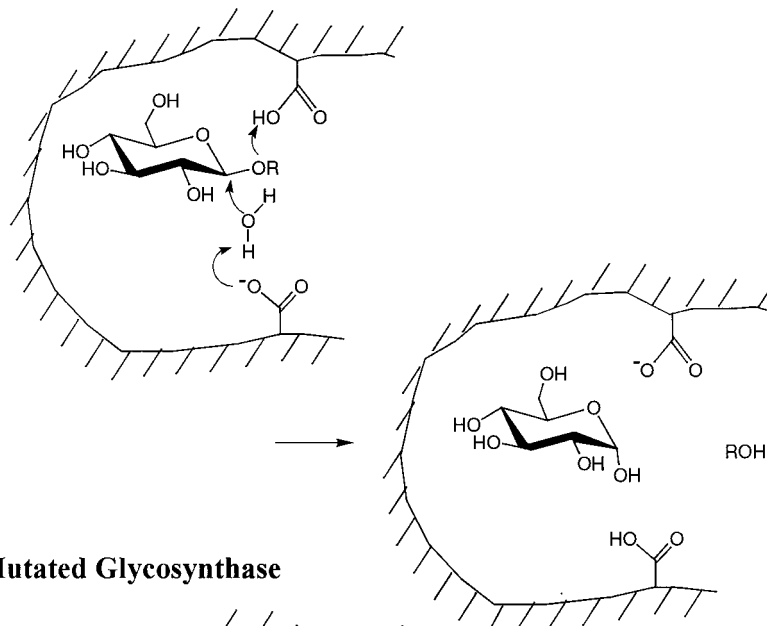
2. Mutated Glycosidases

Novel catalysts by mutating glycosidases to abolish glycosyl hydrolase activity toward unactivated glycosides were developed.¹⁴⁰ The active site of a glycosidase is typically equipped with two residues having a carboxylate side chain to facilitate glycosidic linkage hydrolysis. Conversion of one of the carboxylates to an alanine should make the mutant inactive toward *O*-glycosidic linkages due to the lack of a key catalytic residue. However, the active site may retain the correct steric environment for the formation of a reactive glycosyl donor (Scheme 19). Therefore, this mutated glycosidase may catalyze the ligation of an activated α -glycosyl derivative, bound at the active site in place of the normal glycosyl-enzyme intermediate, to a suitable acceptor sugar bound in the aglycon pocket but does not hydrolyze them.^{140,141} Indeed, the mutated β -glycosidase where Glu358 was replaced with Ala formed a tetrasaccharide from 2 equiv of α -glucosyl fluoride and *p*-nitrophenyl cellobioside in a 64% yield.¹⁴⁰ This mutant was, therefore, named as "glycosynthase".

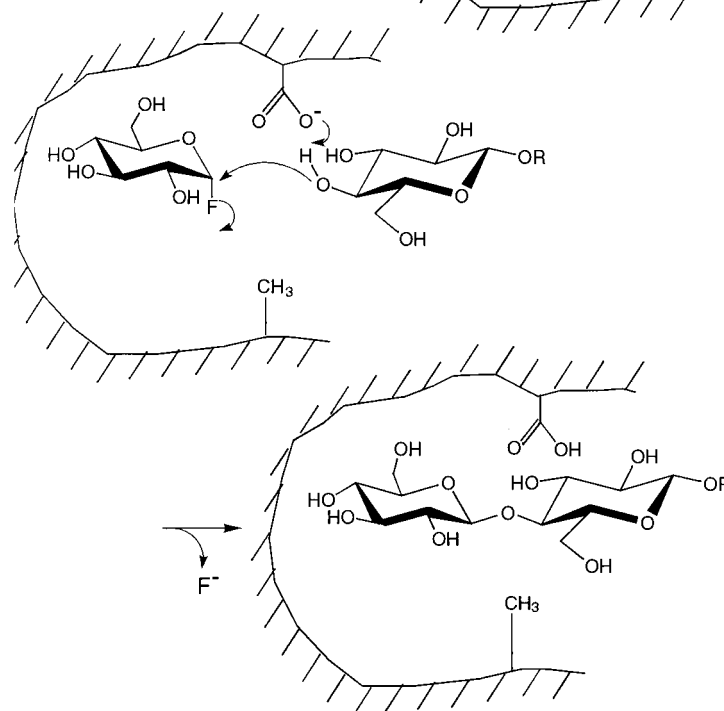
This methodology was applied to the retaining cellulase endoglucanase I (Cel7B).¹⁴² The catalytic nucleophile Glu197 was replaced with Ala to abolish the hydrolytic activity. The mutated endoglucanase catalyzed highly efficient synthesis of β (1 \rightarrow 4)-oligo- and polysaccharides in combination with α -glycobi-

Scheme 19

a) Inverting Glycosidase



b) Mutated Glycosynthase



syl fluorides including 6-substituted derivatives as activated donors. The acceptor subsite of the mutant of Cel7B accommodated various mono- and disaccharides. Notably, the polymerization occurred in a phosphate buffer (pH 7.0).

T4 lysozyme belongs to family 19 chitinases, which show inversion of the anomeric configuration according to the single displacement hydrolysis mechanism.¹⁴³ Thr26 is located at the α side of the substrate and functions as a general acid in cooperation with carboxylic acid nearby. The substitution of Thr26 with His converted the lysozyme from an inverting to a retaining enzyme.¹⁴⁴ This altering can be explained by the nucleophilic property of His to yield a glycosyl enzyme intermediate. Upon point mutation, the mutant showed transglycosylation activity, which

was notably more effective than hydrolysis activity.¹⁴⁵

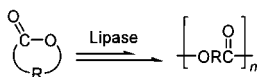
All these instances show the possibility that glycosidases can be converted to glycosynthase by single substitution at the active site, which suppresses the hydrolysis activity of glycosidases. At the same time, however, the nucleophilic attack of aglycon at the acceptor site to the anomer carbon should be significantly promoted in these mutants. This molecular mechanism remains to be solved.

B. Lipases

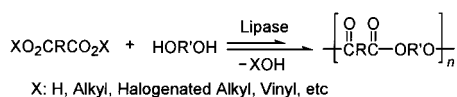
Lipase is an enzyme which catalyzes the hydrolysis of fatty acid esters normally in an aqueous environment in living systems. On the other hand, some lipases are stable in organic solvents and can be used

Scheme 20

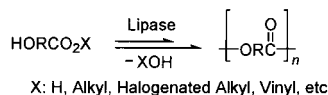
Ring-Opening Polymerization of Lactones



Polycondensation of Dicarboxylic Acids or Their Derivatives with Glycols



Polycondensation of Oxyacids or Their Esters



as catalyst for esterifications and transesterifications.¹⁴⁶ This specific catalysis enabled production of useful polyesters and polycarbonates by various polymerization modes.¹⁴⁷ Typical reaction types of lipase-catalyzed polymerization leading to polyesters are summarized in Scheme 20.

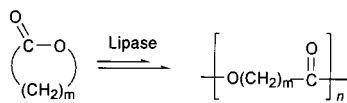
1. Ring-Opening Polymerization of Cyclic Monomers

The first report on an enzymatic ring-opening polymerization appeared in 1993;^{148a,149} ϵ -caprolactone (ϵ -CL, seven-membered lactone) was polymerized using lipase as catalyst. Thereafter, various cyclic compounds were subjected to ring-opening polymerization mainly by lipase catalyst. Figure 4 summarizes cyclic monomers polymerized by enzymes. Among them, the lipase-catalyzed polymerization of lactones has been most extensively investigated.

So far, nonsubstituted lactones with a ring size from 4 to 17 were polymerized by lipase catalyst to give the corresponding polyesters (Scheme 21). *Candida rugosa* lipase (lipase CR) catalyzed the polymerization of β -propiolactone (β -PL, four-membered) to give a polymer with high molecular weight (weight-average molecular weight (M_w) > 5×10^4).¹⁵⁰ The polymerization of β -PL by *Pseudomonas* family lipases produced a mixture of linear and cyclic oligomers with a molecular weight of several hundreds.¹⁵¹

PHB was enzymatically synthesized from β -butyrolactone (β -BL).¹⁵² Even at a high temperature (100 °C), porcine pancreas lipase (PPL) and lipase CR acted as catalyst to give PHB with M_w up to 7300.

Scheme 21



m=2 (4-Membered) : β -PL m=10 (12-Membered) : UDL
 m=3 (5-Membered) : γ -BL m=11 (13-Membered) : DDL
 m=4 (6-Membered) : δ -VL m=14 (16-Membered) : PDL
 m=5 (7-Membered) : ϵ -CL m=15 (17-Membered) : HDL
 m=7 (9-Membered) : OL

The resulting products contained a significant amount of cyclic oligo(β -hydroxybutyrate)s, which were formed by the lipase-catalyzed intramolecular cyclization of PHB.¹⁵³

An enantioselective polymerization of four-membered lactones was demonstrated. Racemic α -methyl- β -propiolactone was stereoselectively polymerized by *Pseudomonas cepacia* lipase (lipase PC) to give an optically active (*S*)-enriched polyester with enantiomeric excess (ee) of 50%.¹⁵⁴ From racemic β -BL, (*R*)-enriched PHB with 20–37% ee was formed by using thermophilic lipase as catalyst.¹⁵⁵

The chemoenzymatic synthesis of biodegradable poly(malic acid) was achieved by the lipase-catalyzed polymerization of benzyl β -malolactonate, followed by the debenzylation.¹⁵⁶ The molecular weight of poly(benzyl β -malolactonate) increased by the copolymerization with a small amount of β -PL using lipase CR catalyst.

Five-membered unsubstituted lactone, γ -butyrolactone (γ -BL), is not polymerized by conventional chemical catalysts. However, oligomer formation from γ -BL was observed by using PPL or *Pseudomonas* sp. lipase as catalyst.^{152a,157} δ -Valerolactone (δ -VL, six-membered) was polymerized by various lipases of different origin to give the polymer with M_n of several thousands.¹⁴⁸ Another six-membered lactone, 1,4-dioxan-2-one, was polymerized by *Candida antarctica* lipase (lipase CA) to give the polymer with M_w higher than 4×10^4 .¹⁵⁸ The resulting polymer is expected as a metal-free polymeric material for medical applications.

As for the enzymatic ring-opening polymerization of ϵ -CL, various commercially available lipases have been tested as a catalyst. Several crude lipases (PPL, lipases CR, PC, and *Pseudomonas fluorescens* lipase (lipase PF)) induced the polymerization; however, a

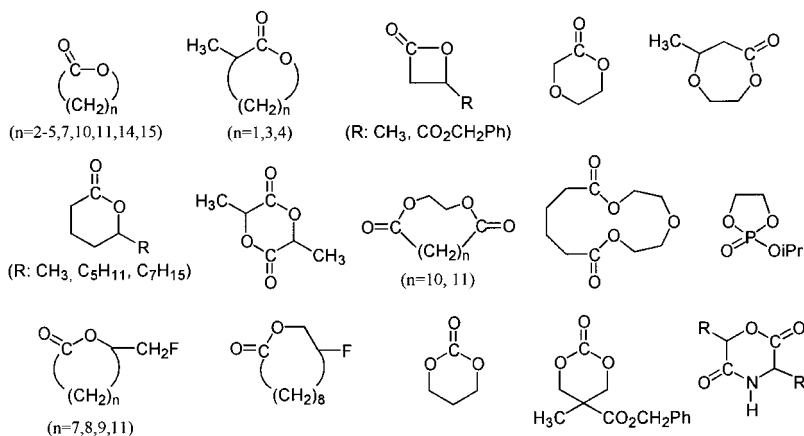


Figure 4. Cyclic monomers polymerized by lipases.

relatively large amount of catalyst (often more than 40 wt % for ϵ -CL) was required for the efficient production of the polymer.^{148,159} On the other hand, lipase CA showed high catalytic activity toward the ϵ -CL polymerization; a very small amount of lipase CA (less than 1 wt % for ϵ -CL) was enough to induce the polymerization.¹⁶⁰ The polymer structure depended on the reaction conditions; the polymerization in bulk produced the linear polymer, whereas the main product obtained in organic solvents was of cyclic structure.¹⁶¹

In the case of polymerization in organic solvents, the solvent hydrophobicity greatly affected the polymerization behaviors. In the lipase CA-catalyzed polymerization, the efficient production of the polymer was achieved in solvents having log P (P = partition coefficient of a given solvent between 1-octanol and water) values from 1.9 to 4.5, whereas solvents with log P from -1.1 to 0.5 showed the low propagation rate.¹⁶² Among the solvents examined, toluene was the best to produce high molecular weight poly(ϵ -CL) efficiently. Variation in the ratio of toluene to ϵ -CL in the reaction at 70°C showed that the monomer conversion and polymer molecular weight were the largest with a ratio of about 2:1. Furthermore, lipase CA could be reused for the polymerization. In the range of five cycles, the catalytic activity hardly changed.^{148b}

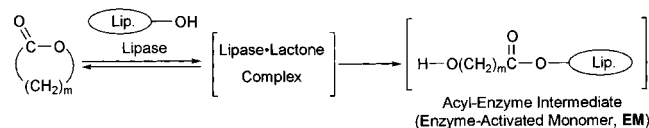
α -Methyl-substituted medium-size lactones, α -methyl- δ -valerolactone (six-membered) and α -methyl- ϵ -caprolactone (seven-membered), were polymerized by lipase CA in bulk to give the corresponding polyesters with M_n of several thousands.¹⁶³ Lipase PC induced the enantioselective polymerization of 3-methyl-4-oxa-6-hexanolide (seven-membered); the apparent initial rate of the (*S*)-isomer was seven times larger than that of the antipode.¹⁶⁴

Lipase-catalyzed ring-opening polymerization of nine-membered lactone, 8-octanolide (OL), has been reported.¹⁶⁵ Lipases CA and PC showed the high catalytic activity for the polymerization. Racemic fluorinated lactones with a ring size from 10 to 14 were enantioselectively polymerized by lipase CA catalyst to give optically active polyesters.¹⁶⁶

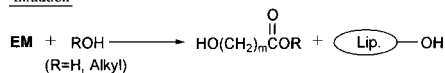
Enzymatic polymerization of macrolides has been extensively studied.¹⁶⁷ So far, four unsubstituted macrolides, 11-undecanolide (12-membered, UDL), 12-dodecanolide (13-membered, DDL), 15-pentadecanolide (16-membered, PDL), and 16-hexadecanolide (17-membered, HDL), were reported to be polymerized by various lipases of different origin. For the polymerization of DDL, the activity order of the catalyst was lipase PC > lipase PF > lipase CC > PPL. High molecular weight polymer with M_n higher than 8×10^4 was synthesized from PDL using lipase CA catalyst in toluene. These macrolides were also polymerized even in an aqueous medium.¹⁶⁸

Immobilized lipase showing high catalytic activity toward the macrolide polymerization was demonstrated.¹⁶⁹ The immobilization of lipase PF on Celite greatly improved the rate of the DDL polymerization. Catalytic activity was further enhanced by the addition of a sugar or poly(ethylene glycol) (PEG) during immobilization. A surfactant-coated enzyme was used

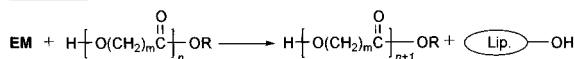
Scheme 22



Initiation



Propagation



as catalyst for the polymerization of PDL.¹⁷⁰ The reaction rate and molecular weight of the resulting polymer using surfactant-coated lipase PC were larger than those by native lipase, suggesting improvement of the catalytic activity by the surfactant coating of lipase.

It is well-known that the catalytic site of lipase is a serine residue and that lipase-catalyzed reactions proceed via an acyl-enzyme intermediate. The enzymatic polymerization of lactones is explained by considering the following reactions as the principal reaction course (Scheme 22).^{167a,171} The key step is the reaction of lactone with lipase involving the ring-opening of the lactone to give an acyl-enzyme intermediate ("enzyme-activated monomer", EM). The initiation is a nucleophilic attack of water, which is contained partly in the enzyme, onto the acyl carbon of the intermediate to produce ω -hydroxycarboxylic acid ($n = 1$), the shortest propagating species. In the propagation stage, the intermediate is nucleophilically attacked by the terminal hydroxyl group of a propagating polymer to produce a one-unit-more elongated polymer chain. This is an "activated monomer mechanism" in contrast to an "active chain-end mechanism", the widely known polymerization mechanism for vinyl monomers.

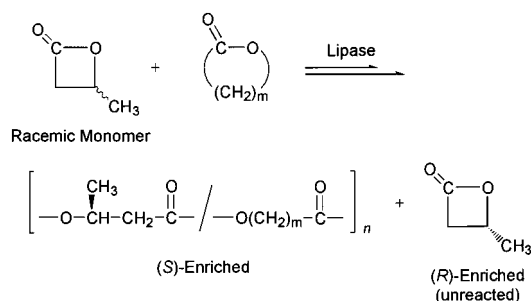
In cyclic compounds, reactivity is generally dependent upon their ring size; the ring strain of small and moderate ring size compounds is larger than that of macrocyclic ones, and hence, they show higher ring-opening reactivity. Table 2 summarizes dipole moment values and reactivities of lactones with different ring size. The dipole moment values of the monomers can be taken as an indication of their ring strain. The values of the macrolides are lower than that of ϵ -CL and close to that of an acyclic fatty acid ester (butyl caproate). The rate constants of the macrolides in alkaline hydrolysis and anionic polymerization are much smaller than those of ϵ -CL. These data imply that the macrolides have much lower ring strain and, hence, show less anionic reactivity and polymerizability than ϵ -CL.

On the other hand, the macrolides showed unusual reactivity toward enzymatic catalysis. Lipase PF-catalyzed polymerization of the macrolides proceeded much faster than that of ϵ -CL. In the evaluation of the enzymatic polymerizability of lactones by Michaelis-Menten kinetics, linearity in the Hanes-Woolf plot was observed for all monomers, indicating that the polymerization followed Michaelis-Menten kinetics.¹⁷² The $V_{\text{max}(\text{lactone})}$ and $V_{\text{max}(\text{lactone})}/K_{\text{m}(\text{lactone})}$ val-

Table 2. Dipole Moments and Reactivities of Unsubstituted Lactones

lactone	dipole moment (Cm)	rate constant		Michaelis–Menten kinetics ^c		
		alkaline hydrolysis ^a ($\times 10^4$, L·mol ⁻¹ ·s ⁻¹)	propagation ^b (10^3 , s ⁻¹)	$K_m(\text{lactone})$ (mol·L ⁻¹)	$V_{\text{max}}(\text{lactone})$ ($\times 10^2$, mol·L ⁻¹ ·h ⁻¹)	$V_{\text{max}}(\text{lactone})/K_m(\text{lactone})$ ($\times 10^2$, h ⁻¹)
δ -VL	4.22	55 000				
ϵ -CL	4.45	2550	120	0.61	0.66	1.1
UDL	1.86	3.3	2.2	0.58	0.78	1.4
DDL	1.86	6.0	15	1.1	2.3	2.1
PDL	1.86	6.5		0.80	6.5	8.1
HDL				0.63	7.2	11
butyl caproate	1.75	8.4				

^a Alkaline: NaOH. Measured in 1,4-dioxane/water (60/40 vol %) at 0 °C. ^b Measured using NaOMe initiator (0.06 mol amount) in THF at 0 °C. ^c Kinetics of the polymerization was carried out using lipase PF (200 mg) as catalyst in the presence of 1-octanol (0.03 mol·L⁻¹) in diisopropyl ether (10 mL) at 60 °C.

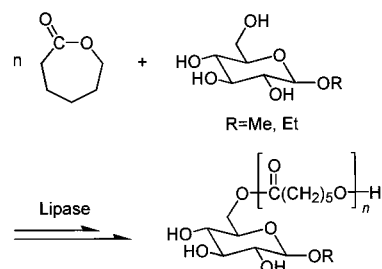
Scheme 23

ues increased with the ring size of lactone, whereas the $K_m(\text{lactone})$ values scarcely changed. These data imply that the enzymatic polymerizability increased as a function of the ring size, and the large enzymatic polymerizability is governed mainly by the reaction rate (V_{max}) but not to the binding abilities, i.e., the reaction process of the lipase–lactone complex to the acyl–enzyme intermediate is the key step of the polymerization.¹⁷¹

The kinetics of the ϵ -CL bulk polymerization by lipase CA showed linear relationships between the monomer conversion and M_n of the polymer; however, the total number of polymer chains was not constant during the polymerization.¹⁷³ The monomer consumption apparently followed a first-order rate law.

The lipase-catalyzed copolymerization of lactones often afforded random copolyesters, despite the different enzymatic polymerizability of lactones in some cases.^{165,167g,174} So far, the random copolymers were enzymatically obtained from combinations of δ -VL- ϵ -CL, ϵ -CL-OL, ϵ -CL-PDL, and OL-DDL. The formation of the random copolymers suggests that the intermolecular transesterifications of the polyesters frequently took place during the copolymerization. By utilizing this specific lipase catalysis, random ester copolymers were synthesized by the lipase-catalyzed polymerization of macrolides in the presence of poly(ϵ -CL).¹⁷⁵

In the lipase-catalyzed polymerization of racemic β -BL, the enantioselectivity was low. The enantioselectivity greatly improved by the copolymerization with ϵ -CL or DDL using lipase CA catalyst, yielding the optically active polyester with ee up to 69% (Scheme 23).¹⁷⁶ It is to be noted that in the case of lipase CA catalyst, the (S)-isomer was preferentially reacted to give the (S)-enriched optically active copolymer. The lipase CA-catalyzed enantioselective

Scheme 24

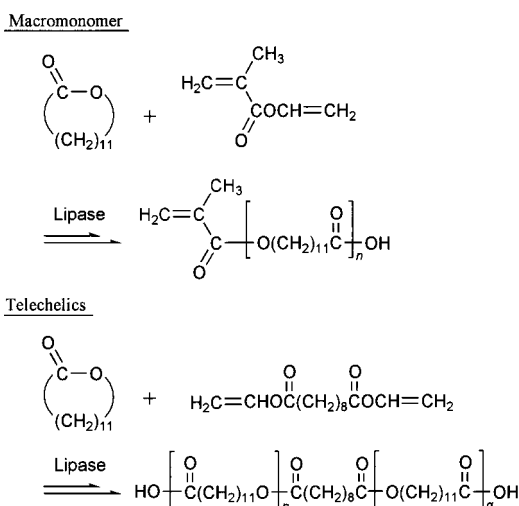
copolymerization of δ -caprolactone (six-membered) with DDL produced the optically active polyester with ee of 76%.

Lipase catalysis provided new methodologies for single-step functionalization of polymer terminal. As shown in Scheme 22, an alcohol acted as an initiating species in the ring-opening polymerization of lactones by lipase CA catalyst to introduce the alcohol moiety at the polymer terminal (“initiator method”).¹⁷⁷ In the polymerization of DDL employing 2-hydroxyethyl methacrylate as initiator under appropriate reaction conditions, the methacryloyl group was quantitatively introduced at the polymer terminal, yielding the methacryl-type polyester macromonomer. This methodology was expanded to synthesis of ω -alkenyl- and alkynyl-type macromonomers by using 5-hexen-1-ol and 5-hexyn-1-ol as initiator.

Polyesters bearing a sugar moiety at the polymer terminal were synthesized by lipase CA-catalyzed polymerization of ϵ -CL in the presence of alkyl glucopyranosides (Scheme 24).¹⁷⁸ In the initiation step, the regioselective acylation at the 6-position of the glucopyranoside took place. Polysaccharides also initiated the lipase-catalyzed polymerization of ϵ -CL.¹⁷⁹ The enzymatic graft polymerization of ϵ -CL on hydroxyethyl cellulose produced cellulose-*graft*-poly(ϵ -CL) with the degree of substitution from 0.10 to 0.32. A poly(ϵ -CL)-monosubstituted first-generation dendrimer was synthesized by using lipase CA, in which the initiator was selectively monoacylated at the initial stage.¹⁸⁰

Polyester macromonomers and telechelics were synthesized by the lipase-catalyzed polymerization of DDL using vinyl esters as terminator (“terminator method”).¹⁸¹ In using vinyl methacrylate and lipase PF as terminator and catalyst, respectively, the quantitative introduction of methacryloyl group at the polymer terminal was achieved to give the

Scheme 25



methacryl-type macromonomer (Scheme 25). By addition of divinyl sebacate, the telechelic polyester having a carboxylic acid group at both ends was obtained.

Lipase-catalyzed ring-opening polymerization of cyclic diesters was investigated. Lactide was polymerized using lipase PC as catalyst at high temperatures (80–130 °C) to produce poly(lactic acid) with M_w higher than 1×10^4 .¹⁸² D,L-Lactide enzymatically gave a polymer with a higher molecular weight than the D,D- and L,L-isomers.

Lipases CA, PC, and PF catalyzed the polymerization of ethylene dodecanoate and ethylene tridecanoate to give the corresponding polyesters.¹⁸³ The polymerization behaviors depended on the lipase origin; in using lipase PC catalyst, these bislactones polymerized faster than ϵ -CL and DDL, whereas the reactivity of these cyclic diesters was in the middle of ϵ -CL and DDL in using lipase CA.

Lipase catalyzed the ring-opening polymerization of cyclic carbonates. Trimethylene carbonate (six-membered, TMC) was polymerized by lipases CA, PC, PF, and PPL to produce the corresponding polycarbonate without involving elimination of carbon dioxide. High molecular weight poly(TMC) ($M_w > 1 \times 10^5$) was obtained by using a small amount of PPL catalyst (0.1 or 0.25 wt % for TMC) at 100 °C.¹⁸⁴ Lipase CA induced the polymerization under milder reaction conditions.¹⁸⁵ The sugar-terminal poly(TMC) was synthesized by the lipase CA-catalyzed polymerization in the presence of methyl glucopyranoside.^{178a}

Chemoenzymatic synthesis of a water-soluble polycarbonate having pendent carboxyl groups on the polymer main chain was achieved by lipase-catalyzed polymerization of 5-methyl-5-benzoyloxycarbonyl-1,3-dioxan-2-one (MBC), followed by debenzoylation.¹⁸⁶ The copolymerization of MBC with TMC using lipase PF catalyst produced the random copolycarbonate.¹⁸⁷

Cyclic dicarbonates, cyclobis(hexamethylene carbonate) and cyclobis(diethylene glycol carbonate), were polymerized by lipase CA.¹⁸⁸ The random ester-carbonate copolymers were enzymatically obtained from DDL-cyclobis(diethylene glycol carbonate) and lactides-TMC.¹⁸⁹

Besides cyclic esters and carbonates, six-membered cyclic depsipeptides and a five-membered cyclic phosphate were subjected to lipase-catalyzed ring-opening polymerizations, yielding poly(ester amide)s¹⁹⁰ and polyphosphate,¹⁹¹ respectively. High temperatures (100–130 °C) were required for the polymerization of the former monomers.

2. Polymerization of Diacid Derivatives and Glycols

So far, biotransformations of various combinations of dicarboxylic acid derivatives and glycols to biodegradable polyesters have been reported. Dicarboxylic acids as well as its derivatives, activated and nonactivated esters, cyclic acid anhydride, and poly-anhydrides, were found to be employed as useful monomers for the enzymatic synthesis of polyesters under mild reaction conditions.

Many dicarboxylic acids and their alkyl esters are commercially available; however, they often showed low reactivity toward lipase catalyst. Thus, development of the reaction apparatus and reaction conditions has been made for efficient production of higher molecular weight polyesters. In the polycondensation of adipic acid and 1,4-butanediol, a horizontal two-chamber reactor was employed to remove the leaving water molecules with use of molecular sieves.¹⁹² A low-dispersity polyester with a degree of polymerization (DP) of ~ 20 was obtained by the two-stage polymerization using *Mucor miehei* lipase (lipase MM).

Enzymatic synthesis of aliphatic polyesters from diacids and glycols in a solvent-free system was carried out.¹⁹³ Lipase CA catalyzed the polymerization under mild reaction conditions to give the polymer with M_n of several thousands, despite the heterogeneous mixture of the monomers and catalyst. The polymerization behaviors strongly depended on the chain length of both monomers. A small amount of adjuvant was effective for the polymer production when both monomers were solid at the reaction temperature. A scale-up experiment produced the polyester from adipic acid and 1,6-hexanediol in a more than 200 kg yield. This solvent-free system claimed a large potential as an environmentally friendly synthetic process of polymeric materials owing to the mild reaction conditions and no use of organic solvents and toxic catalysts.

A dehydration reaction is generally realized in nonaqueous media. Since a product water of the dehydration is in equilibrium with starting materials, a solvent water disfavors the dehydration to proceed in an aqueous medium due to the "law of mass action". However, dehydration polycondensation of dicarboxylic acids and glycols proceeded even in water by using lipase catalyst.¹⁹⁴ Various lipases such as lipases CA, CC, and MM catalyzed the polymerization of sebacic acid and 1,8-octanediol. In the polymerization of α,ω -dicarboxylic acids and glycols, the chain length of the monomers strongly affected the polymer yield and molecular weight; the polymers from 1,12-dodecanedioic acid and 1,10-decanediol were obtained in good yields, whereas no polymer formation was observed in using 1,6-hexanediol.

The polymerization using dialkyl esters also produced the polyesters with relatively low molecular

weight. Lipase CA- or MM-catalyzed polycondensation of dimethyl succinate and 1,6-hexanediol in toluene quickly attained the equilibrium (the conversion of methyl ester moiety was ca. 50%); however, M_n of the product was very low (ca. 300).¹⁹⁵ The equilibrium was shifted by elimination of methanol with nitrogen bubbling, leading to an increase of conversion (>99%) and of the polymer molecular weight ($M_n \approx 3 \times 10^3$). Formation of cyclic oligomers with DP from 2 to 20 as byproduct was observed, and their yield depended on the monomer structure and concentration and reaction temperature. The ring-chain equilibrium was observed, and the molar distribution of the cyclic species obeys the Jacobson–Stockmayer equation.

The molecular weight greatly increased when a vacuum was used in the polymerization using diacids or dialkyl esters as monomer; removal of the formed water or alcohols resulted in a shift of the equilibrium toward the product polymer. In the lipase MM-catalyzed polymerization of sebacic acid or its ethyl ester with 1,4-butanediol in hydrophobic solvents of high boiling points such as diphenyl ether and veratrole under vacuum, M_w of the product polymer reached higher than 4×10^4 , although a long reaction time (>1 week) was required.¹⁹⁶

In lipase-catalyzed esterifications and transesterifications, esters of halogenated alcohols, typically 2-chloroethanol, 2,2,2-trifluoroethanol, and 2,2,2-trichloroethanol, have been used often, owing to an increase of the electrophilicity (reactivity) of the acyl carbonyl and avoiding significant alcoholysis of the products by decreasing the nucleophilicity of the leaving alcohols. The enzymatic synthesis of biodegradable polyesters from the activated diesters was achieved under mild reaction conditions.¹⁹⁷ The polymerization of bis(2,2,2-trichloroethyl) glutarate and 1,4-butanediol at room temperature in diethyl ether gave the polyesters with $M_n \approx 8 \times 10^3$. The polymerization of bis(2,2,2-trichloroethyl) adipate and 1,4-butanediol using PPL catalyst proceeded in a supercritical fluoroform solvent to give the polymer with M_w of several thousands.¹⁹⁸ By changing the pressure, the low-dispersity polymer fractions were separated.

Vacuum technique was applied to shift the equilibrium forward by removal of the activated alcohol formed.^{196,199} In the enzymatic polycondensation of bis(2,2,2-trifluoroethyl) sebacate and aliphatic diols, lipases CR, MM, PC, and PPL produced the polymer with M_w of more than 1×10^4 and lipase MM showed the highest catalytic activity. In the PPL-catalyzed reaction of bis(2,2,2-trifluoroethyl) glutarate with 1,4-butanediol in veratrole or 1,3-dimethoxybenzene, the periodic vacuum method increased the molecular weight ($M_w \approx 4 \times 10^4$).

Enol esters have been shown to be good acylating reagents in lipase-catalyzed reactions, since the leaving unsaturated alcohol irreversibly tautomerizes to an aldehyde or a ketone, leading to the desired product in high yields (see also Scheme 25). Thus, the enzymatic polymerization using divinyl adipate and 1,4-butanediol was first demonstrated in 1994;^{200a} the reaction proceeded in the presence of lipase PF at 45 °C. Under similar reaction conditions, adipic

acid and diethyl adipate did not afford the polymeric materials, indicating the high polymerizability of bis(enol ester) toward lipase catalyst. In the enzymatic polymerization of divinyl adipate or divinyl sebacate with α,ω -glycols with different chain lengths, lipases CA, MM, PC, and PF showed high catalytic activity toward the polymerization.²⁰⁰ A combination of divinyl adipate, 1,4-butanediol, and lipase PC afforded the polymer with $M_n \approx 2 \times 10^4$. The yield of the polymer from divinyl sebacate was higher than that from divinyl adipate, whereas the opposite tendency was observed in the polymer molecular weight. The polyester formation was observed in various organic solvents, and among them, diisopropyl ether gave the best results. The polymerization also proceeded in bulk by using lipase CA as catalyst.

In the case of polyester synthesis from divinyl esters, hydrolysis of the vinyl end group partly took place, resulting in the limitation of the polymer growth.²⁰¹ A mathematical model showing the kinetics of the polymerization predicts the product composition. On the basis of these data, a batch-stirred reactor was designed to minimize temperature and mass-transfer effects.²⁰² The efficient enzymatic production of polyesters was achieved using this reactor; poly(1,4-butylene adipate) with $M_n \approx 2 \times 10^4$ was synthesized in 1 h at 60 °C.

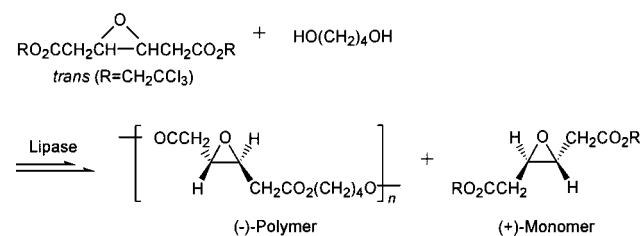
Ester copolymers were synthesized by lipase-catalyzed copolymerization of lactones, divinyl esters, and glycols.²⁰³ Lipases CA and PC showed high catalytic activity for this copolymerization, yielding ester copolymers with M_n higher than 1×10^4 . ¹³C NMR analysis showed that the resulting product was not a mixture of homopolymers but a copolymer derived from the monomers, indicating that two different modes of polymerization, ring-opening polymerization and polycondensation, simultaneously take place through enzyme catalysis in one pot to produce ester copolymers.

Another approach based on the irreversible process was performed by using bis(2,3-butanedione monoxime) alkanedioates as diester substrate.²⁰⁴ Lipase MM efficiently produced the polymer with M_n up to 7.0×10^3 .

Cyclic anhydrides and polyanhydrides were used as starting substrate for enzymatic production of polyesters. A new type of enzymatic polymerization involving lipase-catalyzed ring-opening poly(addition–condensation) of cyclic acid anhydride with glycols was demonstrated.²⁰⁵ The polymerization of succinic anhydride with 1,8-octanediol using lipase PF catalyst proceeded at room temperature to give the polyester. The enzymatic reaction of poly(azelaic anhydride) and glycols using lipase CA catalyst also produced the polyesters in which glycols are apparently inserted into poly(azelaic anhydride).²⁰⁶

Polymerization of oxiranes with succinic anhydride proceeded in the presence of PPL catalyst.²⁰⁷ Under appropriate conditions, M_w reached 1×10^4 . During the polymerization, the enzymatically formed acid group from the anhydride may open the oxirane ring to give a glycol, which is then reacted with the anhydride or acid by lipase catalysis, yielding polyesters.

Scheme 26



Aromatic polyesters were enzymatically synthesized under mild reaction conditions. Divinyl esters of isophthalic acid, terephthalic acid, and *p*-phenylene diacetic acid were polymerized with glycols by lipase CA catalyst to give polyesters containing an aromatic moiety in the main chain.²⁰⁸ In the lipase-catalyzed polymerization of dimethyl isophthalate and 1,6-hexanediol in toluene with nitrogen bubbling, a mixture of linear and cyclic polymers was formed.²⁰⁹ High molecular weight aromatic polyester ($M_w \approx 5.5 \times 10^4$) was synthesized by the lipase CA-catalyzed polymerization of isophthalic acid and 1,6-hexanediol under vacuum.²¹⁰ Enzymatic polymerization of divinyl esters and aromatic diols also afforded the aromatic polyesters.²¹¹

Functional polyesters have been synthesized by utilizing characteristic catalysis of lipase. An optically pure polyester was synthesized by PPL-catalyzed enantioselective polymerization of bis(2,2,2-trichloroethyl) *trans*-3,4-epoxyadipate with 1,4-butanediol in diethyl ether (Scheme 26).²¹² The molar ratio of the diester to the diol was adjusted to 2:1 to produce the (-)-polymer with an enantiomeric purity of >96%. From end group analysis, the molecular weight was calculated to be 5.3×10^3 .

Lipase-catalyzed regioselective polymerization of divinyl esters and polyols to the soluble polymers with relatively high molecular weight was achieved. In the lipase CA-catalyzed polymerization of divinyl sebacate and glycerol at 60 °C, 1,3-diglyceride was the main unit of the formed polymer and a small amount of the branching unit (triglyceride) was contained.²¹³ The regioselectivity of the acylation between primary and secondary hydroxy groups was 74:26. Under the selected reaction conditions, the regioselectivity was perfectly controlled to give a linear polymer consisting exclusively of a 1,3-glyceride unit. The lipase CA-catalyzed polymerization of divinyl esters and sorbitol regioselectively proceeded to produce the sugar-containing polyester with the 1,6-diacylated unit of sorbitol.²¹⁴ Mannitol and *meso*-erythritol were also regioselectively polymerized with divinyl sebacate.

Two-step enzymatic synthesis of polyesters containing a sugar moiety in the main chain was demonstrated.²¹⁵ Sugar diesters were synthesized by lipase CA-catalyzed esterification of sucrose or trehalose with divinyl adipate in acetone, in which the 6- and 6'-positions of the starting sugar were regioselectively acylated. The same enzyme catalyzed the subsequent polycondensation of the isolated diesters with glycols to give the sugar-containing polyesters with M_w up to 2.2×10^4 .

A new class of cross-linkable polyesters having an unsaturated group in the side chain was synthesized

by the lipase CA-catalyzed polymerization of divinyl sebacate and glycerol in the presence of unsaturated higher fatty acids.²¹⁶ The polyester was subjected to hardening by cobalt naphthenate catalyst or thermal treatment, yielding cross-linked transparent film.

All-*trans* unsaturated ester oligomers have been synthesized by lipase-catalyzed polymerization of diesters of fumaric acid and 1,4-butanediol.²¹⁷ No isomerization of the double bond was observed, as opposed to the extensive isomerization found during chemical polycondensations. Crystallinity was found in the enzymatically formed unsaturated oligoesters prepared in acetonitrile, whereas industrial unsaturated polyesters are amorphous.

The lipase CA-catalyzed polymerization of dimethyl maleate and 1,6-hexanediol proceeded using lipase CA catalyst in toluene to produce a mixture of linear and cyclic polymers exhibiting exclusively *cis* structure.²¹⁸ The cyclics were semicrystalline, whereas the linear polymer was amorphous. In the copolymerization of dimethyl maleate and dimethyl fumarate with 1,6-hexanediol by lipase CA catalyst, the content of the cyclization was found to mainly depend on the configuration and concentration of the monomers.²¹⁹

Chemoenzymatic synthesis of alkyds (oil-based polyester resins) was reported.²²⁰ PPL-catalyzed transesterification of triglycerides with an excess of 1,4-cyclohexanedimethanol mainly produced 2-monoglycerides, followed by thermal polymerization with phthalic anhydride to give the alkyd resins with a molecular weight of several thousands. Reaction of the enzymatically obtained alcoholysis product with toluene diisocyanate produced the alkyd-urethanes.

Fluorinated polyesters were synthesized by the enzymatic polymerization of divinyl adipate with fluorinated diols.²²¹ Using 3,3,4,4,5,5,6,6-octafluorooctan-1,8-diol as glycol monomer in the lipase CA-catalyzed polymerization in bulk produced the polymer with the highest molecular weight ($M_n \approx 5 \times 10^3$).

Polycarbonate synthesis by lipase-catalyzed polycondensation was demonstrated. Activated dicarbonate, 1,3-propanediol divinyl dicarbonate, was used as the monomer for enzymatic synthesis of polycarbonates.²²² Lipase CA-catalyzed polymerization with α,ω -alkylene glycols produced the polycarbonates with M_w up to 8.5×10^3 . Aromatic polycarbonates with DP larger than 20 were enzymatically obtained from the activated dicarbonate and xylene glycols in bulk.²¹¹

Higher molecular weight polycarbonate was enzymatically synthesized from diethyl carbonate.²²³ The lipase CA-catalyzed bulk reaction of an excess of diethyl carbonate with 1,3-propanediol or 1,4-butanediol under ambient pressure gave oligomeric products followed by polymerization under vacuum to give aliphatic polycarbonates with M_w higher than 4×10^4 .

3. Polycondensation of Oxyacid Derivatives

Enzymatic polymerizations of oxyacid derivatives have been reported; however, in most cases, only low molecular weight polyesters (molecular weight less or about 1×10^3) were formed.¹⁴⁷ In the PPL-catalyzed polymerization of 12-hydroxydodecanoic

acid at 75 °C for 56 h, M_n reached 2.9×10^3 .²²⁴ Loading a large amount of lipase increased the molecular weight.²²⁵ Use of 10 weight fold lipase CR for 10-hydroxydecanoic or 11-hydroxyundecanoic acid afforded the polyester of relatively high molecular weight (M_w up to 2.2×10^4) in the presence of activated molecular sieves.

PPL catalyzed the polymerization of methyl esters of 5-hydroxypentanoic and 6-hydroxyhexanoic acids.¹⁴⁹ In the polymerization of the latter in hexane at 69 °C for more than 50 days, the polymer with DP up to 100 was formed. Relationships between solvent type and polymerization behaviors were systematically investigated; hydrophobic solvents such as hydrocarbons and diisopropyl ether were suitable for the enzymatic production of high molecular weight polymer. *Pseudomonas* sp. lipase catalyzed the polymerization of ethyl esters of 3- and 4-hydroxybutyric acids, 5- and 6-hydroxyhexanoic acids, 5-hydroxydodecanoic acid, and 15-hydroxypentadecanoic acid.¹⁵⁷ Oxyacid vinyl esters were demonstrated as new monomers for polyester production under mild reaction conditions, yielding the corresponding polyesters with M_n of several thousands.^{27b}

Enzymatic regioselective polymerization of cholic acid was reported. A hydroxy group at the 3-position was regioselectively acylated by lipase CA catalyst to give the oligoester with molecular weight less than 1×10^3 .²²⁶

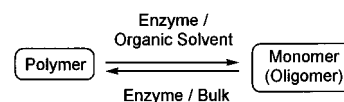
Optically active polyesters were enzymatically obtained from oxyacid derivatives. In the lipase CR-catalyzed polymerization of racemic 10-hydroxyundecanoic acid, the resulting oligomer was enriched in the (*S*)-enantiomer to a level of 60% ee and the residual monomer was recovered with a 33% ee favoring the antipode.²²⁷ Lipase CA catalyzed the polymerization of lactic acid to give the corresponding oligomer with DP up to 9, in which the *R*-enantiomer possessed higher enzymatic reactivity.²²⁸ Optically active oligomers (DP < 6) were also synthesized from racemic ϵ -substituted- ϵ -hydroxy esters using PPL catalyst.²²⁹ The enantioselectivity increased as a function of bulkiness of the monomer substituent. The enzymatic copolymerization of the racemic oxyacid esters with methyl 6-hydroxyhexanoate produced the optically active polyesters with a molecular weight higher than 1×10^3 .

In the polymerization of 12-hydroxydodecanoic acid in the presence of 11-methacryloylaminoundecanoic acid using lipases CA or CR as catalyst, the methacrylamide group was quantitatively introduced at the polymer terminal, yielding a polyester macromonomer.²³⁰

4. Polymer Modification

Lipase catalysts have been used for functionalization of polymers. A terminal hydroxy group of poly(ϵ -CL) was reacted with carboxylic acids using lipase CA catalyst to give end-functionalized polyesters.²³¹ Lipase MM catalyzed the regioselective transesterification of the terminal ester group of oligo(methyl methacrylate) with allyl alcohol.²³² In the PPL-catalyzed reaction of racemic 2,2,2-trichloroethyl 3,4-epoxybutanoate with hydroxy-terminated PEG, the

Scheme 27



(*S*)-isomer of the ester was enantioselectively introduced at the PEG terminal (ee \geq 89%).²³³

Ester copolymers were synthesized by the lipase-catalyzed intermolecular transesterification between two different polyesters, poly(ϵ -CL) and poly(PDL).^{175,234} Under selected conditions, lipase could act as a hydrolytic degradation catalyst of polyesters.²³⁵ A low concentration of poly(ϵ -CL) with a molecular weight $\approx 4 \times 10^4$ in toluene was readily subjected to the degradation in the presence of lipase CA catalyst to give oligomers with molecular weights less than 500. The degradation behavior catalyzed by lipase was quite different than an acid-catalyzed degradation of random bond cleavage of polymer. After the removal of the solvent from the reaction mixture, the residual oligomer was polymerized in the presence of the same catalyst of lipase. These data provide a basic concept that the degradation–polymerization could be controlled by presence or absence of the solvent, providing a new methodology of plastics recycling (Scheme 27). Cyclic dicaprolactone was selectively formed from a very dilute solution of poly(ϵ -CL).

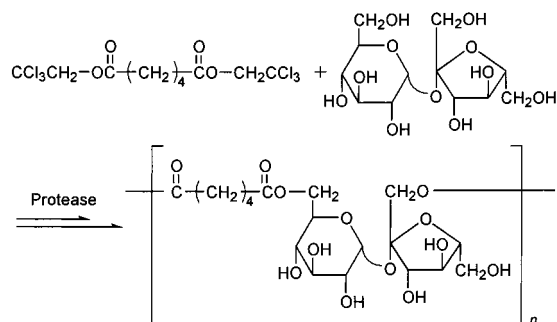
Lipase is known as a catalyst for epoxidation with peroxides. Polybutadiene was subjected to lipase CA-catalyzed oxidation of polybutadiene using hydrogen peroxide as the oxidizing agent in the presence of acetic acid under mild reaction conditions.²³⁶ The epoxide rings formed were opened and esterified.

C. Proteases

As seen for the hydrolysis enzyme, proteases catalyze not only hydrolysis of peptide bonds but also peptide bond formation. The reaction of amino acid esters in the presence of some proteases produces water-insoluble products. Ester hydrochlorides of methionine, phenylalanine, threonine, and tyrosine were polymerized by papain catalyst to give poly(amino acid)s with DP less than 10.²³⁷ In using racemic substrates, only *L*-isomers were stereoselectively polymerized. Papain and α -chymotrypsin induced the polymerization of diethyl *L*-glutamate hydrochloride to give the polymer consisting exclusively of α -peptide linkage.²³⁸ Diethyl *L*-aspartate was polymerized by alkanophilic protease from *Streptomyces* sp. to give the polymer with a mixed structure of α - and β -peptide linkages.²³⁹

Protease mutants were prepared, which showed higher catalytic activity for the enzymatic polymerization of amino acid esters in an aqueous DMF solution. The molecular weight greatly increased by using a subtilisin mutant (subtilisin 8350) derived from BPN' (subtilisin from *Bacillus amyloliquefaciens*) via six site-specific mutants (Met 50 Phe, Gly 169 Ala, Asn 76 Asp, Gln 206 Cys, Tyr 217 Lys, and Asp 218 Ser) in the polymerization of *L*-methionine methyl ester in the aqueous DMF.²⁴⁰ Another mutant (subtilisin 8397), which is the same as 8350 without

Scheme 28



changing Tyr 217, induced the polymerization of single amino acid, dipeptide, and tripeptide methyl esters.²⁴¹

A different type of peptide hydrolase, dipeptide transferase, catalyzed the oligomerization of dipeptide amides. In the case of glycyl-L-tyrosinamide, the corresponding oligomer with DP up to 8 was formed.²⁴²

Some proteases show an esterase activity, especially in their catalytic activity for regioselective acylation of sugars. Protease-catalyzed synthesis of polyester containing a sugar group in the backbone has been achieved.²⁴³ Polycondensation of sucrose with bis(2,2,2-trifluoroethyl)adipate using an alkaline protease from *Bacillus* sp. as catalyst proceeded regioselectively to give an oligoester having ester linkages at the 6- and 1'-positions on the sucrose (Scheme 28). The regioselective catalysis of protease was applied for the modification of polysaccharides.²⁴⁴ Protease (subtilisin Carlsberg) solubilized in isooctane catalyzed the acylation of amylose film with vinyl caprate only at the 6-position of amylose.

D. Other Hydrolases

PHB depolymerases showed catalytic activity for the ring-opening polymerization of cyclic monomers. PHB depolymerase from *Pseudomonas stutzeri* YM1006 polymerized β -BL, and the catalytic activity of the enzyme without substrate-binding domains (SBD) was larger than that with SBD.²⁴⁵ ϵ -CL and TMC were polymerized by PHB depolymerase from *Pseudomonas lemoignei* to give the oligomers with DP of 4 and 12, respectively.²⁴⁶

Epoxide hydrolases, which are contained in crude lipases, induced the ring-opening oligomerization of glycidol in bulk to give a water-soluble oligomer with $M_w \approx 1 \times 10^3$.²⁴⁷ The resulting oligomer was of a branched structure.

VI. Conclusion

The present review describes recent developments on in vitro polymer production using an isolated enzyme as catalyst via nonbiosynthetic pathways (enzymatic polymerization). Beyond the in vivo relationship of the key-and-lock theory, in vitro catalysis of enzymes allowed structural variation of monomers and polymers, leading to not only natural polymers but unnatural polymers including new useful materials. In many cases, enzymes catalyzed highly enantio-, regio-, and chemoselective as well as stereoregulating polymerizations to produce a variety

of functional polymers and structurally complicated polymers, syntheses of which are very difficult to be achieved via conventional chemical routes. Such typical examples may be artificial cellulose, chitin, hyaluronic acid, urushi, etc.

Recently, genetic engineering has been significantly developed to produce tailor-made mutant enzymes (artificial enzymes). Accumulated knowledge of research on catalytic antibodies is also informative for developing new enzyme catalysts.^{3b} Thus, these biocatalysts showing high catalytic activity, reaction selectivity, or stability in organic solvents can eventually be designed and prepared on the basis of relationships between the structure and function of enzymes. These developments will broaden the scope of precision enzymatic syntheses of numerous kinds of polymers. In addition, the enzymatic processes for production of useful polymeric materials are environmentally highly benign, since in most cases biodegradable products are obtained from nontoxic substrates and catalysts under mild reaction conditions. Therefore, in the future, enzymatic polymerizations are expected to provide essential technology in chemical industry.

VII. Acknowledgments

The authors express their thanks for support from various funds, in particular, a Grant-in-Aid for Specially Promoted Research from the Ministry of Education, Science, Sports and Culture, Japan (08102002), and NEDO for the project on the precision polymerizations.

VIII. References

- (a) Jones, J. B. *Tetrahedron* **1986**, *42*, 3351. (b) Klibanov, A. M. *Acc. Chem. Res.* **1990**, *23*, 114. (c) Santaniello, E.; Ferraboschi, P.; Grisenti, P.; Manzocchi, A. *Chem. Rev.* **1992**, *92*, 1071. (d) Wong, C.-H.; Whitesides, G. M. *Enzymes in Synthetic Organic Chemistry*; Pergamon: Oxford, 1994. (e) Seoane, G. *Curr. Org. Chem.* **2000**, *4*, 283.
- (a) Kobayashi, S.; Shoda, S.; Uyama, H. *Adv. Polym. Sci.* **1995**, *121*, 1. (b) Kobayashi, S.; Shoda, S.; Uyama, H. In *The Polymeric Materials Encyclopedia*; Salamone, J. C., Ed.; CRC Press: Boca Raton, 1996; pp 2102–2107. (c) Kobayashi, S.; Shoda, S.; Uyama, H. In *Catalysis in Precision Polymerization*; Kobayashi, S., Ed.; John Wiley & Sons: Chichester, 1997; Chapter 8. (d) Ritter, H. In *Desk Reference of Functional Polymers, Syntheses and Applications*; Arshady, R., Ed.; American Chemical Society: Washington, DC, 1997; pp103–113. (e) *ACS Symposium Series*; Gross, R. A., Kaplan, D. L., Swift, G., Eds.; American Chemical Society: Washington, DC, 1998; Vol. 684. (f) Kobayashi, S.; Uyama, H. In *Materials Science and Technology—Synthesis of Polymers*; Schlüter, A.-D., Ed.; Wiley-VCH: Weinheim, 1998; Chapter 16. (g) Joo, H.; Yoo, Y. J.; Dordick, J. S. *Korean J. Chem. Eng.* **1998**, *15*, 362. (h) Kobayashi, S.; Uyama, H.; Ohmae, M. *Bull. Chem. Soc. Jpn.* **2001**, *74*, 613. (i) Kobayashi, S.; Uyama, H. In *Encyclopedia of Polymer Science and Technology*, 3rd ed.; Kroschwitz, J. I., Ed.; John Wiley & Sons: New York, in press.
- (a) Kobayashi, S. *High Polym. Jpn.* **1999**, *48*, 124. (b) Kobayashi, S. *J. Polym. Sci., Polym. Chem. Ed.* **1999**, *37*, 3041.
- (a) Dordick, J. S.; Marletta, M. A.; Klibanov, A. M. *Biotechnol. Bioeng.* **1987**, *30*, 31. (b) Akkara, J. A.; Senecal, K. J.; Kaplan, D. L. *J. Polym. Sci., Polym. Chem. Ed.* **1991**, *29*, 1561. (c) Akkara, J. A.; Kaplan, D. L.; John, V. T.; Tripathy, S. K. In *The Polymeric Materials Encyclopedia*; Salamone, J. C., Ed.; CRC Press: Boca Raton, 1996; pp 2115–2125. (d) Akkara, J. A.; Ayyagari, M. S. R.; Bruno, F. F. *Trends Biotechnol.* **1999**, *17*, 67. (e) Kobayashi, S.; Uyama, H.; Tonami, H.; Oguchi, T.; Higashimura, H.; Ikeda, R.; Kubota, M. *Macromol. Symp.*, in press.
- (a) Uyama, H.; Kurioka, H.; Kaneko, I.; Kobayashi, S. *Chem. Lett.* **1994**, 423. (b) Uyama, H.; Kurioka, H.; Komatsu, I.; Sugihara, J.; Kobayashi, S. *Macromol. Rep.* **1995**, *A32*, 649. (c)

- Uyama, H.; Kurioka, H.; Sugihara, J.; Kobayashi, S. *Bull. Chem. Soc. Jpn.* **1996**, *69*, 189.
- (6) (a) Oguchi, T.; Tawaki, S.; Uyama, H.; Kobayashi, S. *Macromol. Rapid Commun.* **1999**, *20*, 401. (b) Oguchi, T.; Tawaki, S.; Uyama, H.; Kobayashi, S. *Bull. Chem. Soc. Jpn.* **2000**, *73*, 1389.
- (7) Mita, N.; Tawaki, S.; Uyama, H.; Kobayashi, S. *Polym. J.* **2001**, *33*, 374.
- (8) (a) Kurioka, H.; Komatsu, I.; Uyama, H.; Kobayashi, S. *Macromol. Rapid Commun.* **1994**, *15*, 507. (b) Uyama, H.; Kurioka, H.; Sugihara, J.; Komatsu, I.; Kobayashi, S. *J. Polym. Sci., Polym. Chem. Ed.* **1997**, *35*, 1453.
- (9) Uyama, H.; Kurioka, H.; Sugihara, J.; Komatsu, I.; Kobayashi, S. *Bull. Chem. Soc. Jpn.* **1995**, *68*, 3209.
- (10) Ayyagari, M. S.; Marx, K. A.; Tripathy, S. K.; Akkara, J. A.; Kaplan, D. L. *Macromolecules* **1995**, *28*, 5192.
- (11) Tonami, H.; Uyama, H.; Kobayashi, S.; Kubota, M. *Macromol. Chem. Phys.* **1999**, *200*, 2365.
- (12) Kopf, P. W. In *Encyclopedia of Polymer Science and Engineering*, 2nd ed.; John Wiley & Sons: New York, 1986; Vol. 11, pp 45–95.
- (13) Uyama, H.; Kobayashi, S. *CHEMTECH* **1999**, *29* (10), 22.
- (14) Ryu, K.; MaEldoon, J. P.; Pokora, A. R.; Cyrus, W.; Dordick, J. S. *Biotechnol. Bioeng.* **1993**, *42*, 807.
- (15) Liu, W.; Ma, L.; Wang, J. D.; Jiang, S. M.; Cheng, Y. H.; Li, T. *J. Polym. Sci., Polym. Chem. Ed.* **1995**, *33*, 2339.
- (16) (a) Alva, K. S.; Marx, K. A.; Kumar, J.; Tripathy, S. K. *Macromol. Rapid Commun.* **1997**, *18*, 133. (b) Alva, K. S.; Samuelson, L.; Kumar, J.; Tripathy, S. K.; Cholli, A. L. *J. Appl. Polym. Sci.* **1998**, *70*, 1257.
- (17) Xu, Y.-P.; Huang, G.-L.; Yu, Y.-T. *Biotechnol. Bioeng.* **1995**, *47*, 117.
- (18) Uyama, H.; Kurioka, H.; Kobayashi, S. *Polym. J.* **1997**, *27*, 190.
- (19) (a) Uyama, H.; Kurioka, H.; Kobayashi, S. *Chem. Lett.* **1995**, 795. (b) Kurioka, H.; Uyama, H.; Kobayashi, S. *Polym. J.* **1998**, *30*, 526. (c) Uyama, H.; Kurioka, H.; Kobayashi, S. *Colloids Surfaces A: Physicochem. Eng. Aspects* **1999**, *153*, 189.
- (20) Liu, W.-H.; Wang, J. D.; Ma, L.; Liu, X. H.; Sun, X. D.; Cheng, Y. H.; Li, T. *J. Ann. N. Y. Acad. Sci.* **1995**, *750*, 138.
- (21) (a) Rao, A. M.; John, V. T.; Gonzalez, R. D.; Akkara, J. A.; Kaplan, D. L. *Biotechnol. Bioeng.* **1993**, *41*, 531. (b) Akkara, J. A.; Ayyagari, M. S.; Bruno, F.; Samuelson, L.; John, V. T.; Karayigitoglu, C.; Tripathy, S. K.; Marx, K. A.; Rao, D. V. G. L. N.; Kaplan, D. L. *Biomimetics* **1994**, *2*, 331. (c) Kommareddi, N. S.; Tata, M.; Karayigitoglu, C.; John, V. T.; McPherson, G. L.; Herman, M. F.; O'Connor, C. J.; Lee, Y.-S.; Akkara, J. A.; Kaplan, D. L. *Appl. Biochem. Biotechnol.* **1995**, *51/52*, 241.
- (22) Banerjee, S.; Premchandran, R.; Tata, M.; John, V. T.; McPherson, G. L.; Akkara, J. A.; Kaplan, D. L. *Ind. Eng. Chem. Res.* **1996**, *35*, 3100.
- (23) Ayyagari, M.; Akkara, J. A.; Kaplan, D. L. *Acta Polym.* **1996**, *47*, 193.
- (24) (a) Bruno, F. F.; Akkara, J. A.; Kaplan, D. L.; Sekher, P.; Marx, K. A.; Tripathy, S. K. *Ind. Eng. Chem. Res.* **1995**, *34*, 4009. (b) Bruno, F. F.; Akkara, J. A.; Samuelson, L. A.; Kaplan, D. L.; Mandal, B. K.; Marx, K. A.; Kumar, J.; Tripathy, S. K. *Langmuir* **1995**, *11*, 889.
- (25) (a) Hay, A. S.; Blanchard, H. S.; Endres, G. F.; Eustance, J. W. *J. Am. Chem. Soc.* **1959**, *81*, 6335. (b) Hay, A. S. *J. Polym. Sci., Polym. Chem. Ed.* **1998**, *36*, 505.
- (26) Ikeda, R.; Sugihara, J.; Uyama, H.; Kobayashi, S. *Macromolecules* **1996**, *29*, 8072.
- (27) (a) Ikeda, R.; Sugihara, J.; Uyama, H.; Kobayashi, S. *Polym. Int.* **1998**, *47*, 295. (b) Uyama, H.; Ikeda, R.; Yaguchi, S.; Kobayashi, S. *ACS Symp. Ser.* **2000**, *764*, 113.
- (28) Ikeda, R.; Uyama, H.; Kobayashi, S. *Polym. Bull.* **1997**, *38*, 273.
- (29) Ikeda, R.; Sugihara, H.; Uyama, H.; Kobayashi, S. *Polym. Bull.* **1998**, *40*, 367.
- (30) Fukuoka, T.; Tonami, H.; Maruichi, N.; Uyama, H.; Kobayashi, S.; Higashimura, H. *Macromolecules* **2000**, *33*, 9152.
- (31) Premchandran, R. S.; Banerjee, S.; Wu, X.-K.; John, V. T.; McPherson, G. L.; Akkara, J.; Ayyagari, M.; Kaplan, D. *Macromolecules* **1996**, *29*, 6452.
- (32) Premchandran, R.; Banerjee, S.; John, V. T.; McPherson, G. L.; Akkara, J. A.; Kaplan, D. L. *Chem. Mater.* **1997**, *9*, 1342.
- (33) Kobayashi, S.; Uyama, H.; Ushiwata, T.; Uchiyama, T.; Sugihara, J.; Kurioka, H. *Macromol. Chem. Phys.* **1998**, *199*, 777.
- (34) Kobayashi, S.; Kurioka, H.; Uyama, H. *Macromol. Rapid Commun.* **1996**, *17*, 503.
- (35) Uyama, H.; Lohavisavanpanich, C.; Ikeda, R.; Kobayashi, S. *Macromolecules* **1998**, *31*, 554.
- (36) Reihmann, M. H.; Ritter, H. *Macromol. Chem. Phys.* **2000**, *201*, 798.
- (37) Tonami, H.; Uyama, H.; Kobayashi, S.; Fujita, T.; Taguchi, Y.; Osada, K. *Biomacromolecules* **2000**, *1*, 149.
- (38) Ikeda, R.; Tanaka, H.; Uyama, H.; Kobayashi, S. *Polym. J.* **2000**, *32*, 589.
- (39) Alva, K. S.; Nayak, P. L.; Kumar, J.; Tripathy, S. K. *J. Macromol. Sci., Pure Appl. Chem.* **1997**, *A34*, 665.
- (40) Reihmann, M. H.; Ritter, H. *Macromol. Chem. Phys.* **2000**, *201*, 1593.
- (41) Wang, P.; Martin, D.; Parida, S.; Rethwisch, D. G.; Dordick, J. S. *J. Am. Chem. Soc.* **1995**, *117*, 12885.
- (42) Wang, P.; Amarasinghe, S.; Leddy, J.; Arnold, M.; Dordick, J. S. *Polymer* **1998**, *39*, 123.
- (43) Tonami, H.; Uyama, H.; Kobayashi, S.; Rettig, K.; Ritter, H. *Macromol. Chem. Phys.* **1999**, *200*, 1998.
- (44) Wang, P.; Dordick, J. S. *Macromolecules* **1998**, *31*, 941.
- (45) (a) Sarma, R.; Alva, K. S.; Marx, K. A.; Tripathy, S. K.; Akkara, J. A.; Kaplan, D. L. *Mater. Sci. Eng.* **1996**, *C4*, 189. (b) Marx, K. A.; Zhou, T.; Sarma, R. *Biotechnol. Prog.* **1999**, *15*, 522.
- (46) Ikeda, R.; Maruichi, N.; Tonami, H.; Tanaka, H.; Uyama, H.; Kobayashi, S. *J. Macromol. Sci., Pure Appl. Chem.* **2000**, *A37*, 983.
- (47) Asakura, K.; Shiotani, T.; Honda, E.; Matsumura, S. *J. Jpn. Oil Chem. Soc.* **1993**, *42*, 656.
- (48) Dubey, S.; Singh, D.; Misra, R. A. *Enzymol. Microb. Technol.* **1998**, *23*, 432.
- (49) Liu, W.; Bian, S.; Li, L.; Samuelson, L.; Kumar, J.; Tripathy, S. *Chem. Mater.* **2000**, *12*, 1577.
- (50) Mandal, B. K.; Walsh, C. J.; Sooksimuang, T.; Behroozi, S. *J. Chem. Mater.* **2000**, *12*, 6.
- (51) (a) Kim, J.; Wu, X.; Herman, M. R.; Dordick, J. S. *Anal. Chim. Acta* **1998**, *370*, 251. (b) Wu, X.; Kim, J.; Dordick, J. S. *Biotechnol. Prog.* **2000**, *16*, 513.
- (52) Freudenberg, K. *Science* **1965**, *148*, 595.
- (53) Tanahashi, M.; Higuchi, T. *Wood Res.* **1981**, *67*, 29.
- (54) Okusa, K.; Miyakoshi, T.; Chen, C.-L. *Horzforschung* **1996**, *50*, 15.
- (55) Guan, S.-Y.; Mlynár, J.; Sarkanen, S. *Phytochemistry* **1997**, *45*, 911.
- (56) Guerra, A.; Ferraz, A.; Cotrim, A. R.; da Silva, F. T. *Enzymol. Microb. Technol.* **2000**, *26*, 315.
- (57) (a) Popp, J. L.; Kirk, T. K.; Dordick, J. S. *Enzyme Microb. Technol.* **1991**, *13*, 964. (b) Blinkovsky, A. M.; Dordick, J. S. *J. Polym. Sci., Polym. Chem. Ed.* **1993**, *31*, 1839. (c) Liu, J.; Weiping, Y.; Lo, T. *Electro. J. Biotechnol.* **1999**, *2*, 82.
- (58) Blinkovsky, A. M.; McEldoon, J. P.; Arnold, J. M.; Dordick, J. S. *Appl. Biochem. Biotech.* **1994**, *49*, 153.
- (59) Joo, H.; Chae, H. J.; Yeo, J. S.; Yoo, Y. J. *Process Biochem.* **1997**, *32*, 291.
- (60) Farrell, R.; Ayyagari, M.; Akkara, J.; Kaplan, D. *J. Environ. Polym. Degrad.* **1998**, *6*, 115.
- (61) (a) Stuchell, Y. M.; Krochta, J. M. *J. Food Sci.* **1994**, *59*, 1332. (b) Michon, T.; Wang, W.; Ferrasson, E.; Guéguen, J. *Biotechnol. Bioeng.* **1999**, *63*, 449.
- (62) Iwahara, K.; Honda, Y.; Watanabe, T.; Kuwahara, M. *Appl. Microbiol. Biotechnol.* **2000**, *54*, 104.
- (63) Akkara, J. A.; Wang, J.; Yang, D.-P.; Gonsalves, K. E. *Macromolecules* **2000**, *33*, 2377.
- (64) (a) Tonami, H.; Uyama, H.; Kobayashi, S.; Higashimura, H.; Oguchi, T. *J. Macromol. Sci., Pure Appl. Chem.* **1999**, *A36*, 719. (b) Tonami, H.; Uyama, H.; Higashimura, H.; Oguchi, T.; Kobayashi, S. *Polym. Bull.* **1999**, *42*, 125. (c) Ikeda, R.; Tanaka, H.; Uyama, H.; Kobayashi, S. *Macromol. Rapid Commun.* **2000**, *21*, 496. (d) Tsujimoto, T.; Ikeda, R.; Uyama, H.; Kobayashi, S. *Chem. Lett.* **2000**, 1122. (e) Ikeda, R.; Tanaka, H.; Uyama, H.; Kobayashi, S. *Macromolecules* **2000**, *33*, 6648.
- (65) Akkara, J. A.; Salapu, P.; Kaplan, D. L. *Ind. J. Chem.* **1992**, *31B*, 855.
- (66) Akkara, J. A.; Aranda, F. J.; Rao, D. V. G. L. N.; Kaplan, D. L. In *Frontiers of Polymers and Advanced Materials*; Prasad, P. N., Ed.; Plenum Press: New York, 1994; pp 531–537.
- (67) (a) Samuelson, L. A.; Anagnostopoulos, A.; Alva, K. S.; Kumar, J.; Tripathy, S. K. *Macromolecules* **1998**, *31*, 4376. (b) Liu, W.; Kumar, J.; Tripathy, S.; Senecal, K. J.; Samuelson, L. *J. Am. Chem. Soc.* **1999**, *121*, 71. (c) Liu, W.; Cholli, A. L.; Nagarajan, R.; Kumar, J.; Tripathy, S.; Bruno, F. F.; Samuelson, L. *J. Am. Chem. Soc.* **1999**, *121*, 11345. (d) Nagarajan, R.; Tripathy, S.; Kumar, J.; Bruno, F. F.; Samuelson, L. *Macromolecules* **2000**, *33*, 9542.
- (68) Kobayashi, S.; Kaneko, I.; Uyama, H. *Chem. Lett.* **1992**, 393.
- (69) Ichinose, D.; Muranaka, T.; Sasaki, T.; Kobayashi, M.; Kise, H. *J. Polym. Chem., Polym. Chem. Ed.* **1998**, *36*, 2593.
- (70) Alva, K. S.; Lee, T.-S.; Kumar, J.; Tripathy, S. K. *Chem. Mater.* **1998**, *10*, 1270.
- (71) Alva, K. S.; Marx, K. A.; Kumar, J.; Tripathy, S. K. *Macromol. Rapid Commun.* **1996**, *17*, 859.
- (72) Arias-Marin, E.; Romero, J.; Ledezma-Pérez, A.; Kniajansky, S. *Polym. Bull.* **1996**, *37*, 581.
- (73) Alva, K. S.; Kumar, J.; Marx, K. A.; Tripathy, S. K. *Macromolecules* **1997**, *30*, 4024.
- (74) Goretzki, C.; Ritter, H. *Macromol. Chem. Phys.* **1998**, *199*, 1019.
- (75) Uyama, H.; Kurioka, H.; Kaneko, I.; Kobayashi, S. *Macromol. Reports* **1994**, *A31*, 421.
- (76) (a) Emery, O.; Lalot, T.; Brigodiot, M.; Maréchal, E. *J. Polym. Chem., Polym. Chem. Ed.* **1997**, *35*, 3331. (b) Lalot, T.; Brigodiot,

- M.; Maréchal, E. *Polym. Int.* **1999**, *48*, 288. (c) Teixeira, D.; Lalot, T.; Brigodiot, M.; Maréchal, E. *Macromolecules* **1999**, *32*, 70.
- (77) Singh, A.; Ma, D.; Kaplan, D. L. *Biomacromolecules* **2000**, *1*, 592.
- (78) Kalra, B.; Gross, R. A. *Biomacromolecules* **2000**, *1*, 501.
- (79) Iwahara, K.; Hirata, M.; Honda, Y.; Watanabe, T.; Kuwahara, M. *Biotechnol. Lett.* **2000**, *22*, 1355.
- (80) Ikeda, R.; Uyama, H.; Kobayashi, S. *Macromolecules* **1996**, *29*, 3053.
- (81) Aktas, N.; Kibarar, G.; Tanyolac, A. *J. Chem. Technol. Biotechnol.* **2000**, *75*, 840.
- (82) (a) Milstein, O.; Hüttermann, A.; Majcherczyk, A.; Schulze, K. *J. Biotechnol.* **1993**, *30*, 37. (b) Milstein, O.; Hüttermann, A.; Fründ, R.; Lüdemann, H.-D. *Appl. Microbiol. Biotechnol.* **1994**, *40*, 760.
- (83) (a) Majima, R. *Ber. Dtsch. Chem. Ges.* **1909**, *42B*, 1418. (b) Majima, R. *Ber. Dtsch. Chem. Ges.* **1912**, *45B*, 2727. (c) Majima, R. *Ber. Dtsch. Chem. Ges.* **1922**, *55B*, 191.
- (84) Terada, M.; Oyabu, H.; Aso, Y. *J. Jpn. Soc. Colour Mater.* **1994**, *66*, 681.
- (85) (a) Kobayashi, S.; Ikeda, R.; Oyabu, H.; Tanaka, H.; Kobayashi, S. *Chem. Lett.* **2000**, 1214. (b) Ikeda, R.; Tsujimoto, T.; Tanaka, H.; Oyabu, H.; Uyama, H.; Kobayashi, S. *Proc. Acad. Jpn.* **2000**, *76B*, 155. (c) Ikeda, R.; Tanaka, H.; Oyabu, H.; Uyama, H.; Kobayashi, S. *Bull. Chem. Soc. Jpn.* **2001**, *74*, 1067.
- (86) Ikeda, R.; Tanaka, H.; Uyama, H.; Kobayashi, S. *Macromol. Rapid Commun.* **1998**, *19*, 423.
- (87) (a) Mai, C.; Milstein, O.; Hüttermann, A. *Appl. Microb. Biotechnol.* **1999**, *51*, 527. (b) Mai, C.; Majcherczyk, A.; Hüttermann, A. *Enzyme Microb. Technol.* **2000**, *27*, 167.
- (88) Aizawa, M.; Wang, L.; Shinohara, H.; Ikariyama, Y. *J. Biotechnol.* **1990**, *14*, 301.
- (89) (a) Wang, L.; Kobatake, E.; Ikariyama, Y.; Aizawa, M. *J. Polym. Sci., Polym. Chem. Ed.* **1993**, *31*, 2855. (b) Aizawa, M.; Wang, L. In *The Polymeric Materials Encyclopedia*; Salamone, J. C., Ed.; CRC Press: Boca Raton, 1996; pp 2107–2115.
- (90) Muzzarelli, R. A. A.; Ilari, P.; Xia, W.; Pinotti, M.; Tomasetti, M. *Carbohydr. Polym.* **1994**, *24*, 295.
- (91) (a) Payne, G. F.; Chaubal, M. V.; Barbari, T. A. *Polymer* **1996**, *37*, 4643. (b) Kumar, G.; Bristow, J. F.; Smith, P. J.; Payne, G. F. *Polymer* **2000**, *41*, 2157. (c) Chen, T.; Kumar, G.; Harris, M. T.; Smith, P. J.; Payne, G. F. *Biotechnol. Bioeng.* **2000**, *70*, 564.
- (92) Kumar, G.; Smith, P. J.; Payne, G. F. *Biotechnol. Bioeng.* **1999**, *63*, 154.
- (93) Yamada, K.; Chen, T.; Kumar, G.; Vesnovsky, L.; Timmie Topoleski, L. D.; Pyane, G. F. *Biomacromolecules* **2000**, *1*, 252.
- (94) Shao, L.; Kumar, G.; Lenhart, J. L.; Smith, P. J.; Payne, G. F. *Enzymol. Microb. Technol.* **1999**, *25*, 660.
- (95) (a) Higashimura, H.; Fujisawa, K.; Moro-oka, Y.; Kubota, M.; Shiga, A.; Terahara, A.; Uyama, H.; Kobayashi, S. *J. Am. Chem. Soc.* **1998**, *120*, 8529. (b) Higashimura, H.; Kubota, M.; Shiga, A.; Fujisawa, K.; Moro-oka, Y.; Uyama, H.; Kobayashi, S. *Macromolecules* **2000**, *33*, 1986. (c) Higashimura, H.; Fujisawa, K.; Namekawa, S.; Kubota, M.; Shiga, A.; Moro-oka, Y.; Uyama, H.; Kobayashi, S. *J. Polym. Sci., Polym. Chem. Ed.* **2000**, *38*, 4792. (d) Higashimura, H.; Kubota, M.; Shiga, A.; Koderia, M.; Uyama, H.; Kobayashi, S. *J. Mol. Catal. A* **2000**, *161*, 233.
- (96) Higashimura, H.; Fujisawa, K.; Moro-oka, Y.; Namekawa, S.; Kubota, M.; Shiga, A.; Uyama, H.; Kobayashi, S. *Macromol. Rapid Commun.* **2000**, *21*, 1121.
- (97) (a) Higashimura, H.; Fujisawa, K.; Moro-oka, Y.; Kubota, M.; Shiga, A.; Uyama, H.; Kobayashi, S. *Appl. Catal. A* **2000**, *194*, 195, 427. (b) Higashimura, H.; Fujisawa, K.; Moro-oka, Y.; Kubota, M.; Shiga, A.; Uyama, H.; Kobayashi, S. *J. Mol. Catal. A* **2000**, *155*, 201. (c) Higashimura, H.; Fujisawa, K.; Moro-oka, Y.; Namekawa, S.; Kubota, M.; Shiga, A.; Uyama, H.; Kobayashi, S. *Polym. Adv. Technol.* **2000**, *11*, 733.
- (98) Iwata, H.; Hata, Y.; Matsuda, T.; Ikada, Y. *J. Polym. Chem., Polym. Chem. Ed.* **1991**, *29*, 1217.
- (99) Derango, R. A.; Chiang, L.-C.; Dowbenko, R.; Lasch, J. G. *Biotechnol. Tech.* **1992**, *6*, 523.
- (100) Pfanemueller, B. *Naturwissenschaften* **1975**, *62*, 231.
- (101) Ziegast, G.; Pfanemueller, B. *Carbohydr. Res.* **1987**, *160*, 185.
- (102) Braunmühl, V. v.; Jonas, G.; Stadler, R. *Macromolecules* **1995**, *28*, 17.
- (103) Kobayashi, K.; Kamiya, S.; Enomoto, N. *Macromolecules* **1996**, *29*, 8670.
- (104) Kamiya, S.; Kobayashi, K. *Macromol. Chem. Phys.* **1998**, *199*, 1589.
- (105) Loos, K.; Stadler, R. *Macromolecules* **1997**, *30*, 7641.
- (106) Akiyoshi, K.; Kohara, M.; Ito, K.; Kitamura, S.; Sunamoto, J. *Macromol. Rapid Commun.* **1999**, *20*, 112.
- (107) (a) Enomoto, N.; Furukawa, S.; Ogasawara, Y.; Akano, H.; Kawamura, Y.; Yashima, E.; Okamoto, Y. *Anal. Chem.* **1996**, *68*, 2798. (b) Loos, K.; von Braunmühl, V.; Stadler, R. *Macromol. Rapid Commun.* **1997**, *18*, 927.
- (108) Withers, S. G. *Carbohydr. Res.* **1990**, *197*, 61.
- (109) Evers, B.; Mischnick, P.; Thiem, J. *Carbohydr. Res.* **1994**, *262*, 335.
- (110) Samain, E.; Lancelon-Pin, C.; Ferigo, F.; Moreau, V.; Chanzy, H.; Heyraud, A.; Driguez, H. *Carbohydr. Res.* **1995**, *271*, 217.
- (111) Watson, K. A.; McCleverty, C.; Geremia, S.; Cottaz, S.; Driguez, H.; Johnson, L. N. *EMBO J.* **1999**, *18*, 4619.
- (112) Salmon, S.; Hudson, S. M. *J. Macromol. Sci., Rev. Macromol. Chem. Phys.* **1997**, *C37*, 199.
- (113) Leloir, L. F. *Science* **1971**, *172*, 1299.
- (114) (a) Roach, P. J. *Curr. Top. Cell. Regul.* **1981**, *20*, 45. (b) Kim, S. C.; Singh, A. N.; Raushel, F. M. *J. Biol. Chem.* **1988**, *263*, 10151.
- (115) Wong, C.-H.; Halcomb, R. L.; Ichikawa, Y.; Kajimoto, T. *Angew. Chem., Int. Ed. Engl.* **1995**, *34*, 521.
- (116) Luca, C. D.; Lansing, M.; Martini, I.; Crescenzi, F.; Shen, G.-J.; O'Regan, M.; Wong, C.-H. *J. Am. Chem. Soc.* **1995**, *117*, 5869.
- (117) Kamst, E.; Spaink, P. H. *Trends Glycosci. Glycotechnol.* **1999**, *11*, 187.
- (118) (a) Lenz, R. W.; Farcet, C.; Dijkstra, P. J.; Goodwin, S.; Zhang, S. *Int. J. Biol. Macromol.* **1999**, *25*, 55. (b) Su, L.; Lenz, R. W.; Takagi, Y.; Zhang, S.; Goodwin, S.; Zhong, L.; Martin, D. P. *Macromolecules* **2000**, *33*, 229. (c) Song, J. J.; Zhang, S.; Lenz, R. W.; Goodwin, S. *Biomacromolecules* **2000**, *1*, 433.
- (119) Jossek, R.; Steinbüchel, A. *FEMS Microbiol. Lett.* **1998**, *168*, 319.
- (120) Gijzen, H. J. M.; Qiao, L.; Fitz, W.; Wong, C.-H. *Chem. Rev.* **1996**, *96*, 443.
- (121) Usui, T.; Matsui, H.; Isobe, K. *Carbohydr. Res.* **1990**, *203*, 65.
- (122) Usui, T. *Trends Glycosci. Glycotechnol.* **1992**, *4*, 116.
- (123) Kobayashi, S.; Kashiwa, K.; Kawasaki, T.; Shoda, S. *J. Am. Chem. Soc.* **1991**, *113*, 3079.
- (124) Hehre, E. J. *Adv. Carbohydr. Chem. Biochem.* **2000**, *55*, 265.
- (125) Lee, J. H.; Brown, R. M. Jr.; Kuga, S.; Shoda, S.; Kobayashi, S. *Proc. Natl. Acad. Sci. U.S.A.* **1994**, *91*, 7425.
- (126) Kobayashi, S.; Okamoto, E.; Wen, X.; Shoda, S. *J. Macromol. Sci., Pure Appl. Chem.* **1996**, *A33*, 1375.
- (127) Kobayashi, S.; Hobson, L. J.; Sakamoto, J.; Kimura, S.; Sugiyama, J.; Imai, T.; Itoh, T. *Biomacromolecules* **2000**, *1*, 168, 509.
- (128) Sowden, L. C.; Colvin, J. R. *Can. J. Microbiol.* **1974**, *20*, 509.
- (129) Kobayashi, S.; Wen, X.; Shoda, S. *Macromolecules* **1996**, *29*, 2698.
- (130) Kobayashi, S.; Shimada, J.; Kashiwa, K.; Shoda, S. *Macromolecules* **1992**, *25*, 3237.
- (131) (a) Kiyosada, T.; Shoda, S.; Kobayashi, S. *Polym. Prepr. Jpn.* **1995**, *44*, 660. (b) Kiyosada, T.; Shoda, S.; Kobayashi, S. *Polym. Prepr. Jpn.* **1995**, *44*, 1230. (c) Kobayashi, S.; Kiyosada, T.; Shoda, S. *J. Am. Chem. Soc.* **1996**, *118*, 13113.
- (132) Scheltinga, A. C. T. v.; Armand, S.; Kalk, K. H.; Isogai, A.; Henrissat, B.; Dijkstra, B. W. *Biochemistry* **1995**, *34*, 15619.
- (133) Sakamoto, J.; Sugiyama, J.; Kimura, S.; Imai, T.; Itoh, T.; Watanabe, T.; Kobayashi, S. *Macromolecules* **2000**, *33*, 4155, 4982.
- (134) Saitoh, H.; Takagaki, K.; Majima, M.; Nakamura, T.; Matsuki, A.; Kasai, M.; Narita, H.; Endo, M. *J. Biol. Chem.* **1995**, *270*, 3741.
- (135) Morii, H.; Itoh, R.; Ohmae, M.; Kimura, S.; Kobayashi, S. *79th National Meeting of the Chemical Society of Japan*; Kobe, March, 2001; Abstract 815.
- (136) Shoda, S.; Okamoto, E.; Kiyosada, T.; Kobayashi, S. *Macromol. Rapid Commun.* **1994**, *15*, 751.
- (137) Okamoto, E.; Kiyosada, T.; Shoda, S.; Kobayashi, S. *Cellulose* **1997**, *4*, 161.
- (138) Fujita, M.; Shoda, S.; Kobayashi, S. *J. Am. Chem. Soc.* **1998**, *120*, 6411.
- (139) Moreau, V.; Driguez, H. *J. Chem. Soc., Perkin Trans. 1* **1996**, 525.
- (140) (a) Mackenzie, L. F.; Wang, Q.; Warren, R. A. J.; Withers, S. G. *J. Am. Chem. Soc.* **1998**, *120*, 5583. (b) Withers, S. G. *Can. J. Chem.* **1999**, *77*, 1.
- (141) Ly, H. D.; Withers, S. G. *Annu. Rev. Biochem.* **1999**, *68*, 487.
- (142) Fort, S.; Boyer, V.; Greffe, L.; Davies, G. J.; Moraz, O.; Christiansen, L.; Schuelein, M.; Cottaz, S.; Driguez, H. *J. Am. Chem. Soc.* **2000**, *122*, 5429.
- (143) Brameld, K. A.; Goddard, W. A. G., III. *Proc. Natl. Acad. Sci. U.S.A.* **1998**, *95*, 4276.
- (144) Kuroki, R.; Weaver, L. H.; Matthews, B. W. *Nat. Struct. Biol.* **1995**, *2*, 1007.
- (145) Kuroki, R.; Weaver, L. H.; Matthews, B. W. *Proc. Natl. Acad. Sci. U.S.A.* **1999**, *96*, 8949.
- (146) (a) Xie, Z.-F. *Tetrahedron Asymmetry* **1991**, *2*, 733. (b) Jaeger, K.-E.; Ransac, S.; Dijkstra, B. W.; Colson, C.; van Heuvel, M.; Misset, O. *FEMS Microbiol. Rev.* **1994**, *15*, 29. (c) Theil, F. *Chem. Rev.* **1995**, *95*, 2203. (d) Schmid, R. D.; Verger, R. *Angew. Chem., Int. Ed. Engl.* **1998**, *37*, 1608. (e) Gotor, V. *Bioorg. Med. Chem.* **1999**, *7*, 2189.
- (147) (a) Kobayashi, S.; Uyama, H. In *Biopolyesters*; Babel, W., Steinbüchel, A., Ed.; Springer-Verlag: Heidelberg, 2001; pp 241–262. (b) Kobayashi, S.; Uyama, H. *Curr. Org. Chem.*, in press.
- (148) (a) Uyama, H.; Kobayashi, S. *Chem. Lett.* **1993**, 1149. (b) Kobayashi, S.; Takeya, K.; Suda, S.; Uyama, H. *Macromol. Chem. Phys.* **1998**, *199*, 1729.
- (149) Knani, D.; Gutman, A. L.; Kohn, D. H. *J. Polym. Chem., Polym. Chem. Ed.* **1993**, *31*, 1221.

- (150) Matsumura, S.; Beppu, H.; Tsukada, K.; Toshima, K. *Biotechnol. Lett.* **1996**, *18*, 1041.
- (151) Namekawa, S.; Uyama, H.; Kobayashi, S. *Polym. J.* **1996**, *28*, 730.
- (152) (a) Nobes, G. A. R.; Kazlauskas, R. J.; Marchessault, R. H. *Macromolecules* **1996**, *29*, 4829. (b) Matsumura, S.; Suzuki, Y.; Tsukada, K.; Toshima, K.; Doi, Y.; Kasuya, K. *Macromolecules* **1998**, *31*, 6444.
- (153) Osanai, Y.; Toshima, K.; Matsumura, S. *Chem. Lett.* **2000**, 576.
- (154) Svirkin, Y. Y.; Xu, J.; Gross, R. A.; Kaplan, D. L.; Swift, G. *Macromolecules* **1996**, *29*, 4591.
- (155) Xie, W.; Li, J.; Chen, D.; Wang, P. G. *Macromolecules* **1997**, *30*, 6997.
- (156) (a) Matsumura, S.; Beppu, H.; Nakamura, K.; Osanai, S.; Toshima, K. *Chem. Lett.* **1996**, 795. (b) Matsumura, S.; Beppu, H.; Toshima, K. *Chem. Lett.* **1999**, 249.
- (157) Dong, H.; Wang, H.-D.; Cao, S.-G.; Shen, J.-C. *Biotechnol. Lett.* **1998**, *20*, 905.
- (158) Nishida, H.; Yamashita, M.; Nagashima, M.; Endo, T.; Tokiwa, Y. *J. Polym. Sci., Polym. Chem. Ed.* **2000**, *38*, 1560.
- (159) (a) MacDonald, R. T.; Pulapura, S. K.; Svirkin, Y. Y.; Gross, R. A.; Kaplan, D. L.; Akkara, J.; Swift, G.; Wolk, S. *Macromolecules* **1995**, *28*, 73. (b) Henderson, L. A.; Svirkin, Y. Y.; Gross, R. A.; Kaplan, D. L.; Swift, G. *Macromolecules* **1996**, *29*, 7759.
- (160) Uyama, H.; Suda, S.; Kikuchi, H.; Kobayashi, S. *Chem. Lett.* **1997**, 1109.
- (161) Córdova, A.; Iversen, T.; Hult, K.; Martinelle, M. *Polymer* **1998**, *39*, 6519.
- (162) Kumar, A.; Gross, R. A. *Biomacromolecules* **2000**, *1*, 133.
- (163) Küllmer, K.; Kikuchi, H.; Uyama, H.; Kobayashi, S. *Macromol. Rapid Commun.* **1998**, *19*, 127.
- (164) Kobayashi, S.; Uyama, H.; Namekawa, S. *Polym. Degrad. Stab.* **1998**, *59*, 195.
- (165) Kobayashi, S.; Uyama, H.; Namekawa, S.; Hayakawa, H. *Macromolecules* **1998**, *31*, 5655.
- (166) Runge, M.; O'Hagan, D.; Haufe, G. *J. Polym. Sci., Polym. Chem. Ed.* **2000**, *38*, 2004.
- (167) (a) Uyama, H.; Takeya, K.; Kobayashi, S. *Bull. Chem. Soc. Jpn.* **1995**, *68*, 56. (b) Uyama, H.; Takeya, K.; Hoshi, N.; Kobayashi, S. *Macromolecules* **1995**, *28*, 7046. (c) Uyama, H.; Kikuchi, H.; Takeya, K.; Kobayashi, S. *Acta Polym.* **1996**, *47*, 357. (d) Uyama, H.; Kobayashi, S. In *Biomedical Functions and Biotechnology of Natural and Artificial Polymers*; Yalpani, M., Ed.; ATL Press: Schrewsbury, 1996; pp 5–15. (e) Bisht, K. S.; Henderson, L. A.; Gross, R. A.; Kaplan, D. L.; Swift, G. *Macromolecules* **1997**, *30*, 2705. (f) Namekawa, S.; Uyama, H.; Kobayashi, S. *Proc. Jpn. Acad.* **1998**, *74B*, 65. (g) Kumar, A.; Kalra, B.; Dekhterman, A.; Gross, R. A. *Macromolecules* **2000**, *33*, 6303.
- (168) Namekawa, S.; Uyama, H.; Kobayashi, S. *Polym. J.* **1998**, *30*, 269.
- (169) Uyama, H.; Kikuchi, H.; Takeya, K.; Hoshi, N.; Kobayashi, S. *Chem. Lett.* **1996**, 107.
- (170) Noda, S.; Kamiya, N.; Goto, M.; Nakashio, F. *Biotechnol. Lett.* **1997**, *19*, 307.
- (171) (a) Namekawa, S.; Suda, S.; Uyama, H.; Kobayashi, S. *Int. J. Biol. Macromol.* **1999**, *25*, 145. (b) Kobayashi, S.; Uyama, H. *Macromol. Symp.* **1999**, *144*, 237.
- (172) Uyama, H.; Namekawa, S.; Kobayashi, S. *Polym. J.* **1997**, *29*, 299.
- (173) Deng, F.; Gross, R. A. *Int. J. Biol. Macromol.* **1999**, *25*, 153.
- (174) Uyama, H.; Takeya, K.; Kobayashi, S. *Proc. Jpn. Acad.* **1993**, *69B*, 203.
- (175) Namekawa, S.; Uyama, H.; Kobayashi, S. *Macromol. Chem. Phys.* **2001**, *202*, 801.
- (176) Kikuchi, H.; Uyama, H.; Kobayashi, S. *Macromolecules* **2000**, *33*, 8971.
- (177) Uyama, H.; Suda, S.; Kobayashi, S. *Acta Polym.* **1998**, *49*, 700.
- (178) (a) Bisht, K. S.; Deng, F.; Gross, R. A.; Kaplan, D. L.; Swift, G. *J. Am. Chem. Soc.* **1998**, *120*, 1363. (b) Córdova, A.; Iversen, T.; Hult, K. *Macromolecules* **1998**, *31*, 1040.
- (179) Li, J.; Xie, W.; Cheng, H. N.; Nickol, R. G.; Wang, P. G. *Macromolecules* **1999**, *32*, 2789.
- (180) Córdova, A.; Hult, A.; Hult, K.; Ihre, H.; Iversen, T.; Malmström, E. *J. Am. Chem. Soc.* **1998**, *120*, 13521.
- (181) (a) Uyama, H.; Kikuchi, H.; Kobayashi, S. *Chem. Lett.* **1995**, 1047. (b) Uyama, H.; Kikuchi, H.; Kobayashi, S. *Bull. Chem. Soc. Jpn.* **1997**, *70*, 1691.
- (182) (a) Matsumura, S.; Mabuchi, K.; Toshima, K. *Macromol. Rapid Commun.* **1997**, *18*, 477. (b) Matsumura, S.; Mabuchi, K.; Toshima, K. *Macromol. Symp.* **1998**, *130*, 285.
- (183) Müller, S.; Uyama, H.; Kobayashi, S. *Chem. Lett.* **1999**, 1317.
- (184) Matsumura, S.; Tsukada, K.; Toshima, K. *Macromolecules* **1997**, *30*, 3122.
- (185) (a) Kobayashi, S.; Kikuchi, H.; Uyama, H. *Macromol. Rapid Commun.* **1997**, *18*, 575. (b) Bisht, K. S.; Svirkin, Y. Y.; Henderson, L. A.; Gross, R. A.; Kaplan, D. L.; Swift, G. *Macromolecules* **1997**, *30*, 7735.
- (186) Al-Azemi, T. F.; Bisht, K. S. *Macromolecules* **1999**, *32*, 6536.
- (187) Al-Azemi, T. F.; Bisht, K. S. *Biomacromolecules* **2000**, *1*, 493.
- (188) Namekawa, S.; Uyama, H.; Kobayashi, S.; Kricheldorf, H. R. *Macromol. Chem. Phys.* **2000**, *201*, 261.
- (189) Matsumura, S.; Tsukada, K.; Toshima, K. *Int. J. Biol. Macromol.* **1999**, *25*, 161.
- (190) (a) Feng, Y.; Knüfermann, J.; Klee, D.; Höcker, H. *Macromol. Rapid Commun.* **1999**, *20*, 88. (b) Feng, Y.; Knüfermann, J.; Klee, D.; Höcker, H. *Macromol. Chem. Phys.* **1999**, *200*, 1506. (c) Feng, Y.; Klee, D.; Keul, H.; Höcker, H. *Macromol. Chem. Phys.* **2000**, *201*, 2670.
- (191) Wen, J.; Zhuo, R.-X. *Macromol. Rapid Commun.* **1998**, *19*, 641.
- (192) Binns, F.; Roberts, S. M.; Taylor, A.; Williams, C. F. *J. Chem. Soc., Perkin Trans 1*, **1993**, 899.
- (193) (a) Uyama, H.; Inada, K.; Kobayashi, S. *Chem. Lett.* **1998**, 1285. (b) Binns, F.; Harffey, P.; Roberts, S. M.; Taylor, A. *J. Polym. Sci., Polym. Chem. Ed.* **1998**, *36*, 2069. (c) Binns, F.; Harffey, P.; Roberts, S. M.; Taylor, A. *J. Chem. Soc., Perkin Trans 1* **1999**, 2671. (d) Uyama, H.; Inada, K.; Kobayashi, S. *Polym. J.* **2000**, *32*, 440.
- (194) (a) Kobayashi, S.; Uyama, H.; Suda, S.; Namekawa, S. *Chem. Lett.* **1997**, 105. (b) Suda, S.; Uyama, H.; Kobayashi, S. *Proc. Jpn. Acad.* **1999**, *75B*, 201.
- (195) (a) Mezoul, G.; Lalot, T.; Brigodiot, M.; Maréchal, E. *J. Polym. Sci., Polym. Chem. Ed.* **1995**, *33*, 2691. (b) Berkane, C.; Mezoul, G.; Lalot, T.; Brigodiot, M.; Maréchal, E. *Macromolecules* **1997**, *30*, 7729.
- (196) (a) Linko, Y.-Y.; Wang, Z.-L.; Seppälä, J. *J. Biotechnol.* **1995**, *40*, 133. (b) Wang, Z.-L.; Hiltunen, K.; Orava, P.; Seppälä, J.; Linko, Y.-Y. *J. Macromol. Sci., Pure Appl. Chem.* **1996**, *A33*, 599. (c) Linko, Y.-Y.; Seppälä, J. *CHEMTECH* **1996**, *26* (8), 25.
- (197) Wallace, J. S.; Morrow, C. J. *J. Polym. Sci., Polym. Chem. Ed.* **1989**, *27*, 3271.
- (198) Chaudhary, A. K.; Beckman, E. J.; Russell, A. J. *J. Am. Chem. Soc.* **1995**, *117*, 3728.
- (199) (a) Brazwell, E. M.; Filos, D. Y.; Morrow, C. J. *J. Polym. Sci., Polym. Chem. Ed.* **1995**, *33*, 89. (b) Linko, Y.-Y.; Wang, Z.-L.; Seppälä, J. *Enzyme Microb. Technol.* **1995**, *17*, 506.
- (200) (a) Uyama, H.; Kobayashi, S. *Chem. Lett.* **1994**, 1687. (b) Chaudhary, A. K.; Lopez, J.; Beckman, E. J.; Russell, A. J. *Biotechnol. Prog.* **1997**, *13*, 318. (c) Uyama, H.; Yaguchi, S.; Kobayashi, S. *J. Polym. Sci., Polym. Chem. Ed.* **1999**, *37*, 2737.
- (201) (a) Chaudhary, A. K.; Beckman, E. J.; Russell, A. J. *Biotechnol. Bioeng.* **1997**, *55*, 227. (b) Chaudhary, A. K.; Beckman, E. J.; Russell, A. J. *AIChE J.* **1998**, *44*, 753.
- (202) Kline, B. J.; Lele, S. S.; Lenart, P. J.; Beckman, E. J.; Russell, A. J. *Biotechnol. Bioeng.* **2000**, *67*, 424.
- (203) Namekawa, S.; Uyama, H.; Kobayashi, S. *Biomacromolecules* **2000**, *1*, 335.
- (204) Athawale, V. D.; Gaonkar, S. R. *Biotechnol. Lett.* **1994**, *16*, 149.
- (205) Kobayashi, S.; Uyama, H. *Makromol. Chem., Rapid Commun.* **1993**, *14*, 841.
- (206) Uyama, H.; Wada, S.; Kobayashi, S. *Chem. Lett.* **1999**, 893.
- (207) (a) Matsumura, S.; Okamoto, T.; Tsukada, K.; Toshima, K. *Macromol. Rapid Commun.* **1998**, *19*, 295. (b) Matsumura, S.; Okamoto, T.; Tsukada, K.; Mizutani, N.; Toshima, K. *Macromol. Symp.* **1999**, *144*, 219.
- (208) Uyama, H.; Yaguchi, S.; Kobayashi, S. *Polym. J.* **1999**, *31*, 380.
- (209) Mezoul, G.; Lalot, T.; Brigodiot, M.; Maréchal, E. *Polym. Bull.* **1996**, *36*, 541.
- (210) Wu, X.; Linko, Y.-Y.; Seppälä, J. *Ann. N. Y. Acad. Sci.* **1998**, *864*, 399.
- (211) Rodney, R. L.; Allinson, B. T.; Beckman, E. J.; Russell, A. J. *Biotechnol. Bioeng.* **1999**, *65*, 485.
- (212) Wallace, J. S.; Morrow, C. J. *J. Polym. Sci., Polym. Chem. Ed.* **1989**, *27*, 2553.
- (213) (a) Kline, B. J.; Beckman, E. J.; Russell, A. J. *J. Am. Chem. Soc.* **1998**, *120*, 9475. (b) Uyama, H.; Inada, K.; Kobayashi, S. *Macromol. Rapid Commun.* **1999**, *20*, 171. (c) Uyama, H.; Inada, K.; Kobayashi, S. *Macromol. Biosci.* **2001**, *1*, 40.
- (214) Uyama, H.; Klegraf, E.; Wada, S.; Kobayashi, S. *Chem. Lett.* **2000**, 800.
- (215) Park, O.-J.; Kim, D.-Y.; Dordick, J. S. *J. Polym. Chem., Polym. Chem. Ed.* **2000**, *70*, 208.
- (216) Tsujimoto, T.; Uyama, H.; Kobayashi, S. *Biomacromolecules* **2001**, *2*, 29.
- (217) (a) Geresh, S.; Gilboa, Y. *Biotechnol. Bioeng.* **1990**, *36*, 270. (b) Geresh, S.; Gilboa, Y. *Biotechnol. Bioeng.* **1991**, *37*, 883.
- (218) Mezoul, G.; Lalot, T.; Brigodiot, M.; Maréchal, E. *Macromol. Rapid Commun.* **1995**, *16*, 613.
- (219) Mezoul, G.; Lalot, T.; Brigodiot, M.; Maréchal, E. *Macromol. Chem. Phys.* **1996**, *197*, 3581.
- (220) Kumar, G. S.; Ghogare, A.; Mukesh, D. *J. Appl. Polym. Sci.* **1997**, *63*, 35.
- (221) Mesiano, A. J.; Beckman, E. J.; Russell, A. J. *Biotechnol. Prog.* **2000**, *16*, 64.
- (222) Rodney, R. L.; Stagno, J. L.; Beckman, E. J.; Russell, A. J. *Biotechnol. Bioeng.* **1999**, *62*, 259.
- (223) (a) Matsumura, S.; Harai, S.; Toshima, K. *Proc. Jpn. Acad.* **1999**, *75B*, 117. (b) Matsumura, S.; Harai, S.; Toshima, K. *Macromol. Chem. Phys.* **2000**, *201*, 1632.

- (224) Shuai, X.; Jedlinski, Z.; Kowalczyk, M.; Rydz, J.; Tan, H. *Eur. Polym. J.* **1999**, *35*, 721.
- (225) (a) O'Hagan, D.; Zaidi, N. A. *J. Chem. Soc., Perkin Trans 1* **1993**, 2389. (b) O'Hagan, D.; Zaidi, N. A. *Polymer* **1994**, *35*, 3576.
- (226) Noll, O.; Ritter, H. *Macromol. Rapid Commun.* **1996**, *17*, 553.
- (227) O'Hagan, D.; Parker, A. H. *Polym. Bull.* **1998**, *41*, 519.
- (228) Szakács-Schmidt, A.; Albert, L.; Kelemen-Horváth, I. *Biomed. Chromatogr.* **1999**, *13*, 252.
- (229) Knani, D.; Kohn, D. H. *J. Polym. Sci., Polym. Chem. Ed.* **1993**, *31*, 2887.
- (230) (a) Pavel, K.; Ritter, H. *Makromol. Chem.* **1991**, *192*, 1941. (b) Noll, O.; Ritter, H. *Macromol. Rapid Commun.* **1997**, *18*, 53.
- (231) Córdova, A.; Iversen, T.; Hult, K. *Polymer* **1999**, *40*, 6709.
- (232) Lalot, T.; Brigodiot, M.; Maréchal, E. *Polym. Bull.* **1991**, *26*, 55.
- (233) Wallace, J. S.; Reda, K. B.; Williams, M. E.; Morrow, C. J. *J. Org. Chem.* **1990**, *55*, 3544.
- (234) Kumar, A.; Gross, R. A. *J. Am. Chem. Soc.* **2000**, *122*, 11767.
- (235) (a) Kobayashi, S.; Uyama, H.; Takamoto, T. *Biomacromolecules* **2000**, *1*, 3. (b) Matsumura, S.; Ebata, H.; Toshima, K. *Macromol. Rapid Commun.* **2000**, *21*, 860. (c) Ebata, H.; Toshima, K.; Matsumura, S. *Biomacromolecules* **2000**, *1*, 511.
- (236) Jarvie, A. W. P.; Overton, N.; St Pourcain, C. B. *J. Chem. Soc., Chem. Commun.* **1998**, 177.
- (237) (a) Sluyterman, L. A. E.; Wijdenes, J. *Biochim. Biophys. Acta* **1972**, *289*, 194. (b) Anderson, G.; Luisi, P. L. *Helv. Chim. Acta* **1979**, *62*, 488. (c) Jost, R.; Brambilla, E.; Monti, J. C.; Luisi, P. L. *Helv. Chim. Acta* **1980**, *63*, 375.
- (238) (a) Aso, K.; Uemura, T.; Shiokawa, Y. *Agric. Biol. Chem.* **1988**, *52*, 2443. (b) Uemura, T.; Fujimori, M.; Lee, H.-H.; Ikeda, S.; Aso, K. *Agric. Biol. Chem.* **1990**, *57*, 2277.
- (239) Matsumura, S.; Tsushima, Y.; Otozawa, N.; Murakami, S.; Toshima, K.; Swift, G. *Macromol. Rapid Commun.* **1999**, *20*, 7.
- (240) Wong, C.-H.; Chen, S.-T.; Hennen, W. J.; Bibbs, J. A.; Wang, Y.-F.; Liu, J. L.-C.; Pantoliano, M. W.; Whitlow, M.; Bryan, P. N. *J. Am. Chem. Soc.* **1990**, *112*, 945.
- (241) Zhong, Z.; Liu, J. L.-C.; Dinterman, L. M.; Finkelman, M. A. J.; Mueller, W. T.; Rollence, M. L.; Whitlow, M.; Wong, C.-H. *J. Am. Chem. Soc.* **1991**, *113*, 683.
- (242) Heinrich, C. P.; Fruton, J. S. *Biochemistry* **1968**, *7*, 3556.
- (243) Patil, D. R.; Rethwisch, D. G.; Dordick, J. S. *Biotechnol. Bioeng.* **1991**, *37*, 639.
- (244) Bruno, F. F.; Akkara, J. A.; Ayyagari, M.; Kaplan, D. L.; Gross, R.; Swift, G.; Dordick, J. S. *Macromolecules* **1995**, *28*, 8881.
- (245) Suzuki, Y.; Ohura, T.; Kasuya, K.; Toshima, K.; Doi, Y.; Matsumura, S. *Chem. Lett.* **2000**, 318.
- (246) Kumar, A.; Gross, R. A.; Jendrosseck, D. *J. Org. Chem.* **2000**, *65*, 7800.
- (247) Soeda, Y.; Toshima, K.; Matsumura, S. *Chem. Lett.* **2001**, 76.

CR990121L

The Persistent Radical Effect: A Principle for Selective Radical Reactions and Living Radical Polymerizations

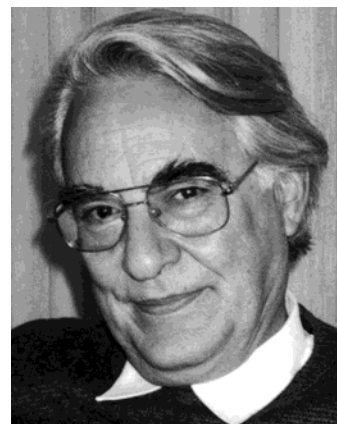
Hanns Fischer*

Physikalisch-Chemisches Institut, Universität Zürich, Winterthurerstrasse 190, CH-8057 Zürich, Switzerland

Received March 23, 2001

Contents

I. Introduction	3581
II. Early References and Basic Kinetics	3583
A. Non-Polymeric Systems	3583
1. Leading Observations	3583
2. Theoretical Description	3584
3. Experimental Verifications	3586
B. Polymer Systems	3587
1. Leading Observations	3587
2. Theoretical Description	3589
3. Experimental Verifications	3592
III. Reactions Exhibiting the Persistent Radical Effect	3594
A. Uncatalyzed and Photochemical Organic and Metal–Organic Reactions	3594
1. Photochemical Reactions Involving NO	3594
2. Thermal Reactions Involving Persistent and Semipersistent Organic Radicals	3594
3. Reactions Involving the Reversible Cleavage of Weak Metal–Carbon Bonds	3596
B. Catalyzed Organic Reactions	3596
1. Catalyzed Kharasch Additions and Related Reactions	3596
2. Photocatalysis	3597
C. Reactions in Polymer Systems	3597
1. Nitroxide-Mediated Systems	3597
2. Mediation by Other Persistent Radicals	3599
3. Organo–Cobalt Complex Mediated Systems	3600
4. Atom Transfer Radical Polymerization	3600
IV. Theoretical Methods and Special Cases of Living Radical Polymerizations	3601
A. The Basic Reaction Mechanism	3601
B. Initial Excess of Persistent Species in Living Radical Polymerizations	3603
C. Decay or Removal of Persistent Species in Living Radical Polymerizations	3605
D. Instantaneous Radical Formation	3606
V. Concluding Remarks	3607
VI. Acknowledgment	3607
VII. References and Notes	3608

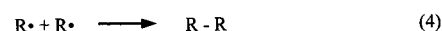
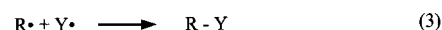


Hanns Fischer, born 1935, started his career at the Technical University Darmstadt, Germany, and obtained his Ph. D. (1963) and Habilitation (1966) working at the Deutsches Kunststoff-Institut mostly on polymer-related transient carbon-centered free radicals with ESR, NMR and CIDNP. After leading a physicochemically oriented division of this Institute, a period at Carnegie-Mellon University, Pittsburgh, and lecturing in Darmstadt, he became Associate (1969) and then full Professor (1971) for Physical Chemistry at the University of Zürich, Switzerland. There, he continued his work on transient organic free radicals, their structure, reaction mechanisms, and reaction kinetics in liquid solutions employing ESR, CIDNP, optical spectroscopy, and muon spin rotation. He has authored about 240 original publications, several reviews, and two books and edits a large series of tables on radical properties and kinetics in Landolt-Börnstein. Honors include the Centenary Medal and Lectureship of the Chemical Society London and the Silver Medal of the International EPR Society. He retires in 2001 but intends further research on the topic of this review.

covered that lead to a highly dominant and unusually selective formation of the cross-reaction products of these radicals. The usual transient radical self-terminations are virtually absent, although chain processes are not involved. This remarkable phenomenon was seldom explained, although it has a quite simple basis.

Consider the mechanism of Scheme 1, where transient R^\bullet and persistent radicals Y^\bullet are formed simultaneously with equal rates from the same or different precursors (1, 2). Then, from the usual radical–radical reactions (3, 4) one obtains $R-Y$ as highly dominant product.

Scheme 1



I. Introduction

From time to time reactions involving both transient and persistent radical intermediates were dis-

* To whom correspondence should be addressed. Phone: +41 1 635 4421. Fax: +41 1 635 6856. E-mail: hfischer@pci.unizh.ch.

Offhand, one may be surprised. Intuitively, one could expect equal concentrations of R^\bullet and Y^\bullet , because the radicals are formed with equal rates, and therefore, the products $R-Y$ and $R-R$ should be formed in the statistical ratio of 2:1. However, this is not the case, except during a very short initial period. The simple cause is that the transient radicals R^\bullet disappear by their self-termination (4) and by the cross-reaction, whereas by definition the persistent radicals Y^\bullet do not self-terminate but disappear only by the cross-reaction.¹ Hence, every self-termination event of R^\bullet (3) causes a buildup of excess Y^\bullet , and this buildup continues as the time goes on. The permanently increasing concentration of Y^\bullet accelerates the cross-reaction at the expense of the self-termination (4). This reaction never stops completely but attains lower and lower levels. Hence, $R-Y$ becomes the main product. In fact, a dynamic equilibrium is reached where the rate of the cross-reaction matches that of the radical generation (1, 2). This leads to the following general conclusions:

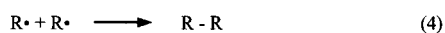
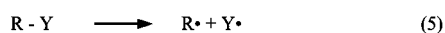
(1) If the transient and persistent radicals are formed with equal rates, one always expects the highly dominant formation of their cross-reaction products, be it $R-Y$ formed by the combination (3), products such as $R(-H)$ and $Y-H$ arising from a disproportionation, or ions such as R^+ and Y^- resulting from a charge-transfer between R^\bullet and Y^\bullet .

(2) If the transient radicals R^\bullet transform rapidly into other transient radicals R'^\bullet , for example by fragmentation, rearrangement, addition to an unsaturated molecule, atom or group transfer, or by any other reaction, then the cross-reaction products between R'^\bullet and Y^\bullet become dominant. The transformation of Y^\bullet to another persistent Y'^\bullet leads to the selective formation of $R-Y'$.

(3) During the reactions, the concentration of the persistent species Y^\bullet increases to a much higher level than the concentrations of the transient radicals R^\bullet or R'^\bullet .

Yet, these statements leave open questions. How persistent must Y^\bullet be to cause this effect, and are equal formation rates really necessary? We answer them later and first consider Scheme 2.

Scheme 2



The two radicals are now produced by the reversible dissociation of a common precursor $R-Y$ but undergo the same reactions as in Scheme 1, otherwise. Now, the above argumentation suggests:

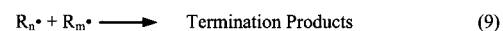
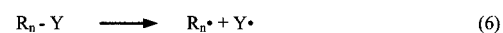
(4) The lifetime of the radical precursor $R-Y$ is markedly prolonged because it is permanently regenerated, and the dynamic equilibrium between the radical generation and the cross-reaction acts like the chemical equilibrium of the reversible decay.

(5) A rapid transformation of R^\bullet into R'^\bullet leads again mainly to $R'-Y$, if the formation of this product is irreversible, and a transformation of Y^\bullet to another persistent Y'^\bullet leads again to $R-Y'$.

However, one may reason now that one will not find a marked lifetime prolongation if the equilibrium constant is above a critical limit. Actually, a too small rate constant of the back-reaction must lead to a fast and complete conversion of $R-Y$ to the final products $R-R$ and Y^\bullet . Also, the self-termination of the transient radicals never ceases completely. Therefore, a true stationary state does not exist, and for the given reaction mechanism, the radical concentrations will always depend on time. Moreover, the apparent equilibrium and the lifetime prolongation of $R-Y$ are only of transient nature, because at sufficiently long times one must always find only self-termination products and persistent radicals.

A technically important situation arises when the transformation of R^\bullet to R'^\bullet occurs by addition to a suitable monomer, M ; the resulting product $R'-Y = R-M-Y$ itself undergoes the fragmentation (5), $R-M^\bullet$ undergoes further monomer addition, and the process continues. This mechanism is displayed in Scheme 3, where $n \geq 0$ denotes the number of monomer units that are contained in the radical and product species.

Scheme 3



Carbon-centered radicals derived from the low molecular compounds $R-Y$ and from the longer chain molecules R_n-Y have similar structures and reactivities, and therefore,

(6) one expects a polymerization without termination,² which is characterized by a transient equilibrium between the dormant polymer R_n-Y and the radicals.

(7) The dormant polymer is living in the sense that it grows until the monomer is depleted, and that it can grow on after additional monomer feed as in an ionic living polymerization.³ The final degree of polymerization is determined by the initial concentrations of the monomer and of the radical precursor R_0-Y , and the formation of block copolymers is possible.

(8) One further obtains a controlled growth of the polymer if the characteristic time for the reversible dissociation is sufficiently short in comparison with monomer conversion, that is, if all chains start to grow practically together.²

However, one may again suspect that this will hold only under favorable kinetic circumstances.

So far, we have introduced the concept of what is now called the "persistent radical effect" without giving specific examples or theoretical proof for its existence. Further, we have indicated that there may be stringent conditions for its occurrence in real chemistry. This review further elucidates the phenomenon, but it is restricted to the most important aspects and to illustrative chemical systems. The next section shows how the main ideas have been developed over the years in order to explain specific

observations, and it reveals the fundamental kinetic conditions for basic reaction schemes. Then, we list a larger variety of examples from organic,⁴ metal-organic, and polymer chemistry and close with an outline of an appropriate theoretical analysis and its application to further cases of practical interest.

Today, the subject is far from being mature. There are probably many more experimental manifestations of the effect than we are aware of, and there may be more kinetic peculiarities and variants. This is the reason we neither present a completely comprehensive description of all pertinent experimental findings nor a complete theory. Moreover, the particular subfield of living radical polymerizations involving the effect has become of practical importance. Hence, in the past few years, a large number of publications and patents have been published on this topic. These are covered in more detail in other parts of this issue, and here, we discuss only those aspects that are important for the operation of the persistent radical effect in living polymerizations.

II. Early References and Basic Kinetics

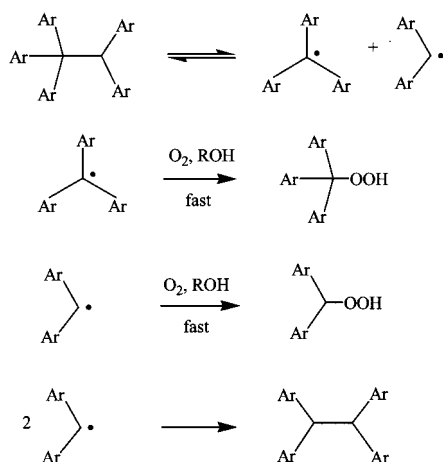
A. Non-Polymeric Systems

1. Leading Observations

To our knowledge, Bachmann et al.⁵ were the first who stated the correct reason for the unusual preference for unsymmetrical coupling reactions in systems involving persistent and transient radicals as early as 1936. They had prepared phenyl- and *p*-biphenyl carrying pentaarylethanes and studied their stability. In oxygenated *o*-dichlorobenzene solutions containing pyrogallol as hydrogen donor, all compounds decomposed quantitatively at 100 °C within a few minutes to triarylmethyl and diarylmethyl hydroperoxides. Various experiments ensured that the primary dissociations to triarylmethyl and diarylmethyl radicals were followed by very fast additions of these radicals to oxygen and by the consecutive very fast hydrogen abstractions of the resulting peroxyradicals from pyrogallol (Scheme 4). Hence, the rates of conversion were equal to the rates of dissociation of the pentaarylethanes.

Surprisingly at first, the pentaarylethanes were much more stable under oxygen-free conditions.

Scheme 4

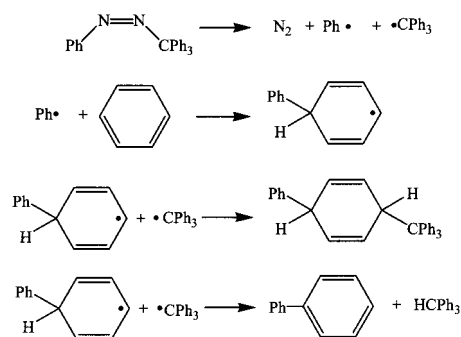


Thus, “penta-*p*-biphenylethane gave only two percent of *s*-tetra-*p*-biphenylethane after being heated for two hours in *o*-dichlorobenzene at 100 °C, the original compound being recovered in 87% yield.” However, the solutions developed the characteristic color of triarylmethyl radicals, and this agreed with the much faster conversion under oxygen. The authors concluded that in the absence of oxygen, “the dissociation of pentaarylethanes is a reversible reaction in which the position of the equilibrium is practically entirely in favor of the pentaarylethane”. They also knew that diarylmethyl radicals but not triarylmethyl radicals dimerize irreversibly under their experimental conditions and, hence, that in these systems diarylmethyl radicals are transient and triarylmethyl radicals are persistent species. Obviously, the cross-coupling between these is strongly favored.

To explain these observations the authors wrote “Now, the irreversible formation of an extremely small amount of *s*-tetraarylethane (by coupling, Scheme 4) results in a corresponding increase in the equilibrium concentration of triarylmethyl radicals; as a result the concentration of diarylmethyl radicals is reduced to such an extent that their association is practically stopped.” Moreover, “The formation of every molecule of *s*-tetraarylethane decreases the rate of formation of the next molecule.” They also clearly noticed the unusual character of the apparent dissociation equilibrium because “the concentration of triarylmethyl radicals is always much greater than the concentration of diarylmethyl radicals,” and “this precluded measurements of the extent of the equilibrium from the color”, that is, the triarylmethyl concentration. Finally, they noted that “it should be borne in mind, however, that a pentaarylethane solution is an unstable system which in infinite time would disproportionate completely into hexaarylethane (“triarylmethyl radicals” would be more appropriate) and *s*-tetraarylethane.” These are the features of a persistent radical effect following Scheme 2.

The second thoughtful description was given by Perkins.⁶ He explained the unusual product distributions of phenylations of aromatic compounds when phenylazotriphenylmethane is used as thermal phenyl radical generator. Scheme 5 provides an example. It had been found⁷ that benzene solutions yield 1,4-dihydro-4-triphenylmethylbiphenyls as major products besides biphenyl and triphenylmethane, and “a particular feature of this scheme is the absence of dimerization and disproportionation of the interme-

Scheme 5

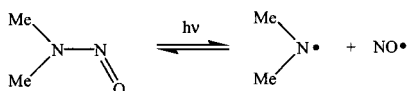


diate phenylcyclohexadienyl radical as both of these processes are known to occur in other systems.”

Perkins cited more so far unexplained examples for the observation of simple product mixtures in reactions where triphenylmethyl radicals from phenylazotriphenylmethane were involved⁸ and Bachmann's work.⁵ Realizing the kinetics expected for Scheme 1, he wrote “The exceptional stability of triphenylmethyl radicals is probably responsible.... This is because any trace occurrence of radical-destroying processes which do not involve triphenylmethyl radicals must give rise to a high concentration of this stable species. The relatively high concentration of triphenylmethyl radicals can subsequently scavenge other radicals which are formed (with the exception of the very short-lived phenyl radical). Under stationary state-conditions triphenylmethyl radicals are being formed at the same rate as that at which they are being converted into products. Hence, the relatively high concentration is maintained, and the scavenging effect continues throughout the reaction.” Thus, Perkins perceived the dynamic equilibrium as expected for Scheme 1. He also considered a variety of other manifestations for what he called “stable radical effects”.⁹

Not being aware of the earlier work, the present author first noticed the phenomenon in 1981. Geiger and Huber¹⁰ had photolyzed dimethylnitrosamine in the gas phase at 1 Torr and under 100 Torr N₂ buffer. This compound fragments from the first excited singlet state into dimethylaminy radicals and nitrous oxide NO with unity quantum yield, but neither photoproducts nor a decrease of the initial compound pressure were observed. Even after 20 h photolysis the back-reaction was complete to more than 99.9% (Scheme 6). This seemed quite puzzling because sterically unhindered aminyl radicals are transient and readily self-terminate by coupling and disproportionation.

Scheme 6



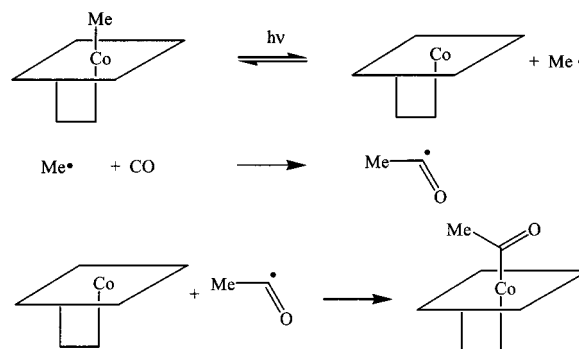
A few years later the author noticed a report by Kraeutler that stated that methylcobalamine is stable under photolysis in aqueous solution in the absence of radical scavengers, but that the presence of CO in moderate concentration (0.03 M) leads to acetylcobalamine in high yield.¹¹ The explanation (Scheme 7) was again unusual in view of the known propensity of methyl and acetyl radicals for rapid coupling reactions.

A discussion of these results led in 1985 to another independent formulation of the correct interpretation by Ingold. Nitrous oxide and the demethylated cobalamine are persistent and will increase in concentration because the transient radicals self-terminate, and the excess persistent species will then scavenge the transient ones.

2. Theoretical Description

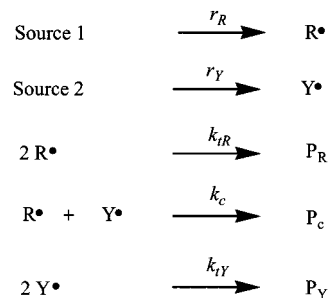
Although the qualitative explanations by Bachmann,⁵ Perkins,⁶ and Ingold are very reasonable, it

Scheme 7



seemed worthwhile to investigate whether the extreme selectivity as, for example, reported by Huber et al.¹⁰ can be rationalized quantitatively. To be more general, the reactions of Scheme 8 were used in our first theoretical analysis. It allowed for unequal rates of generation of the persistent and the transient radicals and for the self-terminations of both radicals.¹² We outline the major results here because they reveal the inner working of the mechanism but now use a simpler formalism.

Scheme 8



The radical concentrations are abbreviated as [R] and [Y], and the notations of Scheme 8 are used for the rates of radical generation (r) and for the rate constants (k) of the bimolecular radical reactions.¹³ The radical concentrations obey the rate equations

$$d[R]/dt = r_R - k_c[R][Y] - k_{tR}[R]^2 \quad (10)$$

and

$$d[Y]/dt = r_Y - k_c[R][Y] - k_{tY}[Y]^2 \quad (11)$$

For the initial conditions [R]₀ = [Y]₀ = 0, both radical concentrations increase at first linearly in time, [R] = $r_R t$, [Y] = $r_Y t$, but at later times the behavior diverges. If all rate parameters are different from zero, a stationary state is found¹² where $d[R]/dt = d[Y]/dt = 0$. From this relation, the conditions on r_R and r_Y emerge for which the selectivity for the formation of the cross-reaction product P_c is a maximum. This selectivity may be defined by the ratio of the rate of the cross-reaction to the sum of the rates of product formation by the self-terminations, that is, by

$$s = \frac{k_c[R][Y]}{k_{tR}[R]^2/2 + k_{tY}[Y]^2/2} = \frac{2(k_c/k_{tR})[Y]/[R]}{1 + (k_{tY}/k_{tR})([Y]/[R])^2} \quad (12)$$

Differentiation with respect to the auxiliary variable $[Y]/[R]$ yields the maximum of s for $[Y]/[R] = (k_{tR}/k_{tY})^{1/2}$. Use of this relation and eqs 10 and 11 for the stationary state and subtraction of the resulting equations 13 and 14 yields $r_R = r_Y$:

$$d[R]/dt = 0 = r_R - k_c(k_{tR}/k_{tY})^{1/2}[R]^2 - k_{tR}[R]^2 \quad (13)$$

and

$$d[Y]/dt = 0 = r_Y - k_c(k_{tR}/k_{tY})^{1/2}[R]^2 - k_{tR}[R]^2 \quad (14)$$

Hence, the maximum selectivity does occur in fact for equal formation rates of the two radicals, as was implied in the discussions of Schemes 1 to 3 and as is valid for the mechanisms of Schemes 4–7. Restricting the further discussion to the case $r_R = r_Y = r$ at the moment and using $[Y]/[R] = (k_{tR}/k_{tY})^{1/2}$ and eq 12 provide

$$s_{\max} = \frac{k_c}{(k_{tR}k_{tY})^{1/2}} \quad (15)$$

Now, if Y^{\bullet} were as transient as R^{\bullet} , one would have approximately $k_{tR} = k_c = k_{tY}$, which gives $s_{\max} = 1$. This leads to the statistical product distribution $[P_R]:[P_C]:[P_Y] = 1:2:1$. However, for a persistent Y^{\bullet} with a small self-termination constant $k_{tY} \ll k_c \approx k_{tR}$ one obtains $s_{\max} \gg 1$.¹⁴ For instance, if the rate constant for the self-termination of Y^{\bullet} were $k_{tY} = 10^3 \text{ M}^{-1} \text{ s}^{-1}$ and the other rate constants diffusion controlled, $k_c = k_{tR} \approx 10^9 \text{ M}^{-1} \text{ s}^{-1}$ in nonviscous liquids, the selectivity would become $s_{\max} \approx 1000$, and this means 99.9% cross-reaction. Hence, the selectivity increases with decreasing self-termination rate constant of the persistent species; however, this species need not be infinitely long-lived. Further, one notes that $[Y]/[R] = (k_{tR}/k_{tY})^{1/2}$ implies $[Y] \gg [R]$ for $k_{tR} \gg k_{tY}$, that is, the large excess of the persistent radical. Moreover, for $k_{tY} \ll k_c \approx k_{tR}$ the self-termination terms on the right-hand sides of eqs 13 and 14 are much smaller than the cross-reaction term. This proves the existence of a dynamic equilibrium

$$k_c[R][Y] = r \quad (16)$$

for which the rate of radical generation is nearly completely balanced by the rate of the cross-reaction.

Our treatment explained the experimental results of Huber et al.¹⁰ and Kraeutler¹¹ quantitatively.¹² However, it is not strictly applicable when Y^{\bullet} does not self-terminate at all because $[Y]/[R]$ and s diverge to infinity for $k_{tY} \rightarrow 0$. Actually, in this case and for equal rates of radical generation, eqs 10 and 11 have no stationary state solution except for infinite time, where $[Y]$ goes to infinity and $[R]$ becomes zero.

Figure 1 shows computed time evolutions of the radical concentrations for $[Y]_0 = [R]_0 = 0$, a common radical generation rate $r = 10^{-6} \text{ M s}^{-1}$, $k_{tR} = k_c = 10^9 \text{ M}^{-1} \text{ s}^{-1}$, and different ratios k_{tY}/k_{tR} in a log–log

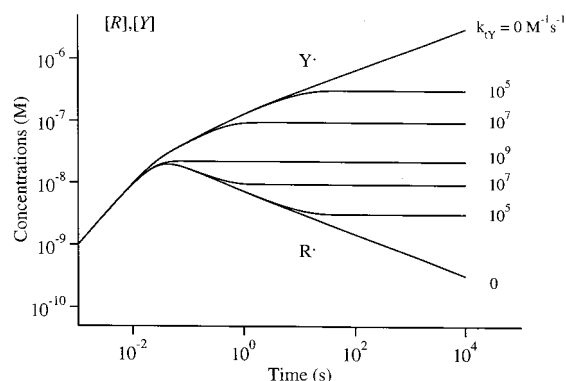


Figure 1. Computed time dependencies of the concentration of the transient (R^{\bullet}) and the persistent radicals (Y^{\bullet}) for $[Y]_0 = [R]_0 = 0$, a common radical generation rate $r = 10^{-6} \text{ M s}^{-1}$, $k_{tR} = k_c = 10^9 \text{ M}^{-1} \text{ s}^{-1}$, and different ratios k_{tY}/k_{tR} in a log–log representation. The log–log representation enhances the visualization of the different time regimes.

representation.¹² Such log–log representations are unusual, but they are needed here and in the following because they allow one to clearly visualize the different time regimes. The interpretation of the time evolution is straightforward. For all ratios of the self-termination constants, both radical concentrations first increase linearly with time, $[R] = [Y] = rt$. When the rate of the terminations become approximately equal to the rate of radical generation, $[R]$ attains a maximum, in times of milliseconds to seconds for usual rate constants. Thereafter, the concentration of the transient radical decreases, and the excess of the persistent species builds up. For nonzero self-termination of the persistent radical, both radical concentrations reach stationary states. For $k_{tY} = 0$, however, $[R]$ continues to decrease and $[Y]$ continues to increase. After the maximum of $[R]$, $\log [R]$ and $\log [Y]$ depend linearly on time. They show slopes of different signs but equal magnitude. For $k_{tY} = 0$, this holds forever, and it is observed also for a nonzero k_{tY} before the stationary states are reached. The magnitudes are smaller than 1, that is, in this regime the time dependencies of both radical concentrations are weak. Empirically, the slopes give $[Y] \sim t^{1/3}$ and $[R] \sim t^{-1/3}$, and such time dependencies are very unusual in chemical kinetics. Furthermore, one finds empirically that the concentrations obey the dynamic equilibrium eq 16.

A rigorous derivation of the unusual time dependencies and of eq 16 for $k_{tY} = 0$ was first found for the reversible radical generation of Scheme 2 with the restriction $k_{tR} = k_c$,¹⁵ which was removed subsequently.^{16,17} The mathematical method will be outlined in section IV. For the mechanism of Scheme 8, with equal radical formation rates and $k_{tY} = 0$, it provides for the radical concentrations at sufficiently long times¹⁸

$$[R] = (r/3k_c k_{tR})^{1/3} t^{-1/3} \quad \text{and} \quad [Y] = (3k_{tR} r^2/k_c^2)^{1/3} t^{1/3} \quad (17)$$

They fulfill the dynamic equilibrium relation (16).

For the reversible radical generation of Scheme 2 and $k_{tY} = 0$, the unusual time dependencies $[Y] \sim t^{1/3}$ and $[R] \sim t^{-1/3}$ and the large excess of $[Y]$ over $[R]$

are also valid. In eqs 17, r must be replaced by $k_d[I]_0$ where k_d is the rate constant of the dissociation of the radical precursor R–Y, and $[I]_0$ is its initial concentration so that^{15–17}

$$[R] = (K[I]_0/3k_{tR})^{1/3} t^{-1/3} \quad \text{and} \\ [Y] = (3K^2k_{tR}[I]_0^2)^{1/3} t^{1/3} \quad (18)$$

where $K = k_d/k_c$. Equation 16 now reads

$$k_c[R][Y] = k_d[I]_0 \quad (19)$$

This is the equilibrium relation for the reversible dissociation with the actual time-dependent concentration of the precursor replaced by its initial value.¹⁹ However, the stoichiometry of the reactions of Scheme 2 requires that the concentration of the persistent radical cannot exceed the initial precursor concentration. This limits the kinetic parameters for which eqs 18 and 19 are valid to

$$K \ll k_c[I]_0/k_{tR}, \quad K \ll [I]_0, \quad \text{and} \quad k_d \leq k_{tR}[I]_0 \quad (20)$$

The first of these conditions is the strongest. They also provide an upper time limit for the operation of the persistent radical effect,¹⁷ but such an upper limit does not exist for the case of continuous radical generation.

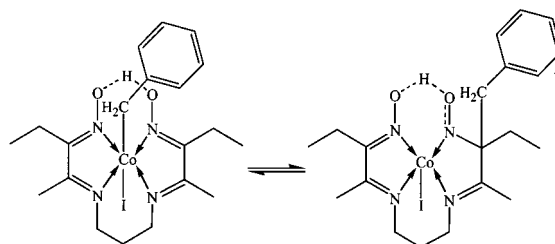
As anticipated in the Introduction, for a system following Scheme 2, the equilibrium constant of the precursor dissociation must not be larger than an upper limiting value. If this holds, one obtains a lifetime of the precursor R–Y that exceeds the natural lifetime $(k_d)^{-1}$ by the factor of $k_c[I]_0/k_{tR}K$, and this may amount to many orders of magnitude.^{15–17}

An insertion of realistic rate parameters shows that the second and the third of the conditions (11) are not critical. For instance, the rate constant k_d for the dissociation of R–Y will normally not exceed $k_d = 1 \text{ s}^{-1}$, because the compound will otherwise be very unstable, even at low temperatures. Experimental rate constants for the reaction of transient with persistent radicals are normally larger than $10^6 \text{ M}^{-1} \text{ s}^{-1}$. Hence, a realistic upper limit of the equilibrium constant is $K = 10^{-6} \text{ M}$. Self-termination constants of transient radicals are normally diffusion-controlled, that is, $10^{10} > k_{tR} > 10^8 \text{ M}^{-1} \text{ s}^{-1}$, and finally, practical aspects set the lower limit of the precursor concentration to $[I]_0 = 10^{-3} \text{ M}$. Hence, the second and the third of the conditions (11) read $K < 10^{-6} \text{ M} \ll [I]_0$ and $k_d/k_{tR} < 10^{-8} \text{ M} \ll [I]_0$ and are always well obeyed. For these numbers, one has $k_c[I]_0/k_{tR} = 10^{-7} \text{ M}$. Obviously, the first condition is not met for the extreme parameters chosen here, but it will be fulfilled for a lower equilibrium constant, a larger initiator concentration, and a larger cross-coupling constant.

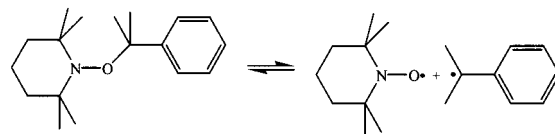
3. Experimental Verifications

The early theoretical conclusions on chemical systems following Scheme 8¹² prompted a first experimental verification.²⁰ Transient *tert*-butyl radicals were generated by photolysis of di-*tert*-butyl ketone in *n*-heptane. Simultaneously and in the same solu-

Scheme 9



Scheme 10



tions, the persistent 2,4,6-tri-*tert*-butylphenoxy radical ($k_{tY} \approx 0$) was generated by hydrogen abstraction from the phenol by photolytically produced *tert*-butoxy radicals, and the rate of generation of *tert*-butyl was varied by changing the ketone concentration. ESR spectra taken during continuous reaction revealed a dramatic decrease of the *tert*-butyl concentration to unobservably low levels when its rate of formation became equal to or lower than that of the persistent species. This is well-described by the appropriate analytic equations. Moreover, time-resolving experiments on the two-radical system showed that the transient radical concentration decayed completely to zero when the radical generation was interrupted. On the other hand, a marked residue of 2,4,6-tri-*tert*-butylphenoxy radicals was leftover even when the transient species was produced in excess, and we will comment on the kinetics in section IV. Use of the semipersistent 2,6-di-*tert*-butyl-4-methylphenoxy radical ($k_{tY} \approx 10^{-8} \text{ M}^{-1} \text{ s}^{-1}$ at room temperature) showed less dramatic effects of the relative rate of radical generation but also supported the theoretical expectations.

A second, and more chemical, verification is due to Finke et al.,²¹ who also invented the descriptive phrase “persistent radical effect” and gave a prototype example to the extreme. The thermal reversible 1,3-benzyl migration in a coenzyme B₁₂ model complex leads to the equilibrium of Scheme 9. Earlier work had shown that the reaction involves freely diffusing benzyl and persistent cobalt macrocycle radicals, but the expected self-termination product bibenzyl of benzyl was missing. Extending the detection limits, the authors found traces of bibenzyl and deduced a selectivity for the formation of the cross-products to the self-termination products of 100 000: 1 or 99.999%. Kinetic modeling further showed that over a time of 1000 years only 0.18% of bibenzyl would be formed, and this stresses the long-time duration of the phenomenon.

More recently, the unusual time-dependence of the radical concentrations (9) was also observed directly.²² Like many other *N*-alkoxyamines (trialkylhydroxylamines), 2-phenyl-2-(2',2',6',6'-tetramethylpiperidine-1'-oxy)propane (cumyl-TEMPO) (Scheme 10) cleaves thermally reversibly into a persistent nitroxide radical (TEMPO) and a transient carbon-

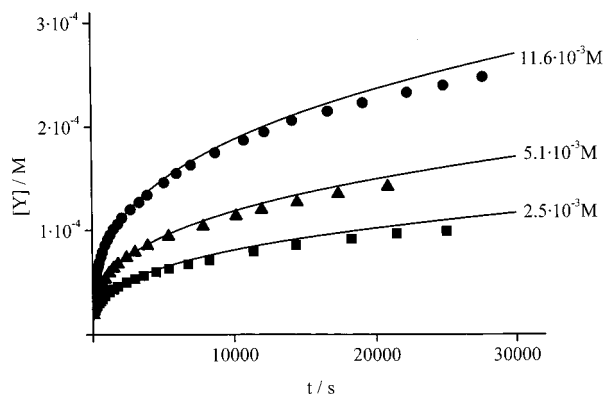


Figure 2. Time dependence of the TEMPO concentration during thermolysis of cumyl-TEMPO in *tert*-butylbenzene for different initial cumyl-TEMPO concentrations at 83 °C. The solid lines confirm the $t^{1/3}$ -dependence (eq 18).

centered radical (cumyl). The time evolution of the nitroxide concentration is easily followed by ESR spectroscopy, and the result is shown in Figure 2. The solid lines correspond to the expected $t^{1/3}$ -dependence (eq 18) with the parameter combination $(3k_{tR}K^2[I]_0^2)^{1/3}$ evaluated at the beginning of the curves. Slight deviations at long times are due to a concurring disproportionation between TEMPO and cumyl, which leads to the hydroxylamine and α -methylstyrene in about a 1% yield.

Variations of the initial alkoxyamine concentration $[I]_0$ and independently measured rate constants k_d , k_c , and k_{tR} nicely confirmed that the system fulfills the conditions (20) and reproduced the value of the parameter combination taken from the experimental data. The same was found for other alkoxyamines.^{16,23} However, it must be mentioned that the observation of such kinetics requires precautions with respect to the purity of chemicals, solvents, and containers. This is necessary because even very minor side reactions may strongly interfere with the many cycles of dissociation and recoupling that are necessary to provide a clear kinetic manifestation of the effect.

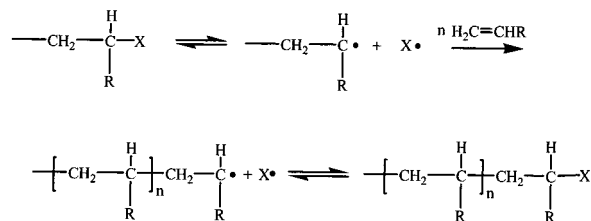
B. Polymer Systems

1. Leading Observations

The development of living and controlled radical polymerizations has been stimulated considerably by early work of Otsu dating back about 20 years ago.²⁴ His concepts center around the reversible reaction of a suitably end-capped polymer chain providing a chain radical that can add to monomer and a persistent species. In 1982 he noted “in order to find a system of living radical polymerization in homogeneous solution, one must try to form propagating polymer chain ends which may dissociate into a polymer with a radical chain end and small radicals which must be stable enough not to initiate a new polymer chain.” He also presented the formal Scheme 11 and mentioned the possibility of a stepwise growth that would lead to molecular weight control.

Otsu knew of the tendency of stable radicals to undergo primary radical cross-termination and was aware of some of the earlier work on triphenylmethyl

Scheme 11

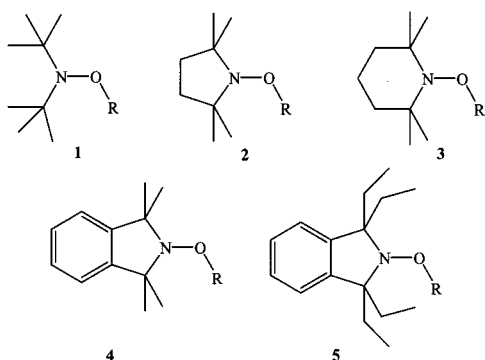


and related persistent radicals. However, he did not mention the excess of the persistent over the transient species or give a reason for the propensity of the cross-reaction. At first, he employed phenylazotriphenylmethane as initiator to polymerize methyl methacrylate at 60 °C. Indeed, the molecular weight increased linearly with the conversion, as is expected for a controlled process.² Livingness was demonstrated by the observation “when the polymer was heated at 80 °C in the presence of the monomer, polymerization was induced and the molecular weight of the polymer increased markedly” and “These findings strongly suggest that the monomer molecules were inserted into the carbon–triphenylmethyl bond, as the result of a radical dissociation.” Otsu also found that in the absence of monomer the polymer was stable in benzene at 80 °C, although there must be dissociation, and this is a clear sign for the lifetime prolongation. In further work, Otsu²⁴ and Braun et al.²⁵ used initiators dissociating into two semipersistent radicals that both can initiate and also tend to cross-terminate. Features of living and controlled polymerizations were again achieved, but the conversions and the molecular weights of the resulting polymers were rather low.

Two further elements of Otsu’s early work are also noteworthy, because they are related to more recent (and more successful) developments: First, he used the reversible halogen atom exchange between low valent metal compounds, in particular Ni(0), and organic halides as initiating and regulating system.²⁶ The polymers obtained from heterogeneous mixtures were partly living and controlled, and this work anticipates the mechanism now called “atom transfer radical polymerization”. Second, he showed²⁴ that the polymerization of methyl methacrylate with phenylazotriphenylmethane is unusually slow but that it is markedly accelerated by the addition of a conventional initiator without loss of polymer livingness.

In 1985, Rizzardo et al.²⁷ filed a patent for the use of alkoxyamines (Scheme 12) as regulating initiators for the living radical polymerization and block copolymerization of vinyl monomers. R is a group that upon dissociation (Scheme 10) forms a radical that adds to the monomer. The mechanism was disclosed shortly thereafter and involves the reversible dissociations shown in Scheme 11, with the nitroxide radical taking the role of X.²⁸ In a later simulation, the group also revealed the reason for the remarkable absence of the usual terminations and rediscovered the principles of the persistent radical effect:²⁹ “As chains undergo termination transient radicals are removed from the system and the concentration of persistent species builds”. Further, the authors noted correctly that, in contrast to normal radical polymer-

Scheme 12

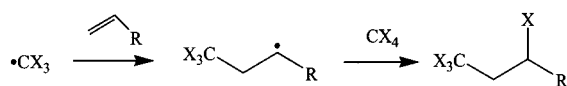


izations with essentially constant radical concentrations, no steady-state approximation is possible.

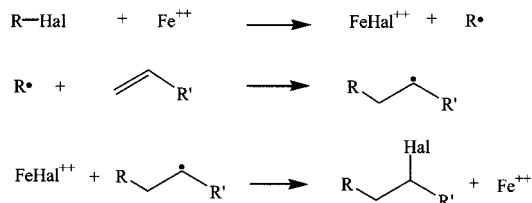
Whereas the patent stressed the controlled formation of oligomers and low molecular weight polymers, Georges et al. showed in 1993 that moderate molecular weight (50 000 au) polystyrenes with low polydispersity indices (1.20) can be obtained by nitroxide-mediated polymerizations at around 120 °C.³⁰ Instead of using alkoxyamines as initiators, they employed a 1.2:1 ratio of the nitroxide radical TEMPO (Scheme 10, and **3** in Scheme 12) and dibenzoyl peroxide in styrene and preheated the reaction mixture to 95 °C for a short time. Under these conditions, benzoyloxy radicals first add to styrene. The coupling of the adduct radicals with TEMPO provides unimeric alkoxyamines that initiate the polymerization at the higher temperature. As expected for a stepwise growth, the degree of polymerization increases fairly linearly with conversion. It was also noticed that a larger initial excess of the persistent species decreased the polydispersity at the expense of a slower polymerization rate. Later work showed, among other results, that the concentration of the persistent nitroxide increases during the polymerization, because of the ongoing termination, that the rate of polymerization can be increased considerably by a slow removal of the excess nitroxide, that these controlled polymerizations display no gel effect, and that they can be extended to aqueous-phase polymerizations and also to the formation of polystyrene–polybutadiene, –polyisoprene and –polyacrylate block copolymers.³¹

The technical potential of the work of Rizzardo et al.^{27–29} and Georges et al.^{30,31} stimulated further research along similar lines by many other groups. We mention here only a few principally important and early results. By an elegant crossover experiment using model polystyrene alkoxyamine derivatives, Hawker et al.³² demonstrated the occurrence of the reversible cleavage. The prolongation of the alkoxyamine lifetime during the reactions became evident from the apparent decay times reported for 1-phenyl-1-(2',2',6',6'-tetramethylpiperidine-1'-oxy)ethane (phenethyl-TEMPO) by Priddy et al.^{33a} of about 150 min in trichlorobenzene at 140 °C and by Hawker et al.^{33b} of about 5 min in styrene at 123 °C. In the latter case, the addition of the 1-phenethyl radical to styrene prevents the regeneration of the parent compound, of course. Further, it was often noticed that the polymerization rates obtained in many

Scheme 13



Scheme 14



nitroxide-mediated processes are inconveniently small, even at temperatures as high as 130 °C, and this is so because the persistent radical effect leads to very low transient radical concentrations.

Using di-*tert*-butylnitroxide (DBNO)-based initiators (**1** in Scheme 12), Catala et al.³⁴ observed that the polymerization rate of styrene is independent of the initiator alkoxyamine concentration. This is unusual in radical polymerizations, and Matyjaszewski et al.^{35a} first pointed out in this case that the styrene polymerization rate is governed by the autoinitiation of the monomer that creates additional propagating species. These authors also published illuminating simulations on the nitroxide-mediated process.^{35b} The autoinitiation of styrene then may have led to the renewed idea³⁶ to add a slowly decomposing conventional initiator to the systems. This had already been realized by Otsu.²⁴ Sparingly applied, it accelerates the polymerizations appreciably without deteriorating the livingness and the control to intolerable extents.³⁶

The facile and reversible dissociation of cobalt–carbon bonds to give a persistent cobalt-derived and a transient alkyl radical was discussed already in connection with Schemes 7 and 9. In 1994, it was first utilized by Wayland et al.³⁷ in living and controlled polymerizations of methyl acrylate. Using (tetramesitylporphyrinato)cobalt neopentyl and variants thereof in benzene solution at 60 °C provided only oligomers for small ratios of monomer to complex, but for ratios of 2500:1, polymers with $M_n = 150\,000$ and about 70% conversion were achieved. The molecular weight increased linearly with conversion, and the polydispersity index was as low as 1.1–1.3. Livingness of the polymer, that is, the fidelity of the porphyrinacetyl end group of the polymer chains, was demonstrated by the formation of block copolymers of methyl and butyl acrylate. Wayland knew of the earlier publications on the persistent radical effect^{12,21} and interpreted his findings in terms of Scheme 3.

The addition of polyhaloalkanes and related halogenated compounds to alkenes can occur via a classical radical chain process (Scheme 13), which is often called the Kharasch reaction.³⁸ In 1961, Minisci et al.³⁹ and Asscher and Vofsi⁴⁰ discovered that this reaction is catalyzed by transition metal ions in their lower valent state such as Cu^+ and Fe^{2+} , and they formulated the mechanism in Scheme 14. The catalysis of the additions by simple metal salts or complexes such as $\text{Cu}(\text{I})$ -2,2'-bipyridyl^{41a} and ruthe-

nium(II) tris(triphenylphosphine) ($\text{RuCl}_2(\text{PPh}_3)_3$)^{41b} found many organic synthetic applications. It was often stated that the intermediacy of freely diffusing carbon-centered radicals is unlikely in these processes, because the normal termination products are absent. However, the transition metal ions and their complexes are persistent, and Scheme 14 involves the simultaneous formation of a persistent species and a transient radical. Hence, the operation of the persistent radical effect is a much more likely cause for the virtual absence of the self-termination reactions.

Monoadditions are usually carried out with about 1:1 ratios of the organic halide and the alkene and very small catalyst concentrations. When lower halide/alkene ratios are used, telomer formation is important. Hence, for small halide concentrations, high polymers may be obtained, and this is supported by Otsu's experiments²⁶ with Ni(0) powders.

The first real success along these lines was achieved in 1995 by Sawamoto et al.,⁴² Matyjaszewski et al.,⁴³ and Percec et al.⁴⁴ The first group used $\text{RuCl}_2(\text{PPh}_3)_3$ as catalyst and CCl_4 as initiating halide in a 1:2 ratio, added methylaluminum bis(2,6-di-*tert*-butylphenoxy) to activate the initiator C–Cl bonds, and employed methyl methacrylate as monomer solvent. Nearly 90% conversion was achieved at 60 °C in about 4 h.⁴² Matyjaszewski employed $\text{Cu}(\text{I})\text{Cl}_2 \cdot 2,2'$ -dipyridyl (1:3) as catalyst and 1-chloro-1-phenylethane (1) as initiator and found 90% conversion of styrene in about 3 h at 130 °C.⁴³ The polymerization of styrene was also addressed by Percec et al.,⁴⁴ who used the same catalyst as Matyjaszewski but diverse aromatic sulfonyl chlorides as initiators. All authors amply demonstrated the livingness of the resulting polymers and the controlled nature of the process with molecular weights increasing with conversion and low polydispersities. In comparison to Otsu's earlier attempt,²⁶ their success is presumably due to the more homogeneous reaction conditions following from the use of metal complexes. Since the addition of haloalkanes to alkenes involves atom transfer steps, Matyjaszewski termed the new method "atom transfer radical polymerization" (ATRP).⁴³ In terms of polymerization rates and generality, ATRP appears to be the most versatile variant of living radical polymerizations based on the persistent radical effect today.

2. Theoretical Description

Before entering the kinetic treatment of living radical polymerizations based on the persistent radical effect, it is necessary to define the terms "living" and "controlled" radical polymerization as used in this review, because a unified terminology has not yet evolved and conflicting views have been expressed.⁴⁵ In the sense of Szwarc,³ we call a polymer "living" that, after formation and isolation, can grow upon further monomer feed and that can be used to build block copolymers. The dormant chains formed in nitroxide and cobalt-complex-mediated polymerizations carry end groups that provide transient radicals upon dissociation to which monomer can add. Hence, these processes are properly "living". In

ATRP, the dormant chains carry halogen atoms as end groups. Alone and freed from the catalyst they will not initiate new polymerizations, but they revive upon addition of the same or another catalyst. Therefore, in a looser sense we will consider these processes also as "living" polymerizations. By "controlled" we mean a polymerization for which the number-average degree of polymerization (X_N) and, hence, the number-average molecular weight of the polymer increase linearly with monomer conversion and for which X_N ideally reaches the ratio of the initial monomer and initiator concentrations at full monomer conversion. These are the characteristics of a polymerization without termination.² If, in addition, all chains start in a time period that is short compared to the overall conversion time, that is, practically at the same time, one obtains a narrow Poisson chain length distribution. Then, the polydispersity index develops as $\text{PDI} = M_w/M_n = X_w/X_n = 1 + 1/X_n$ and decreases with increasing conversion to values close to one.²

"Livingness" and "control" go parallel in many ionic processes, but this need not always be so. Actually, in the radical polymerizations, the dissociation of the dormant chains or the activating halogen transfer may be so slow that considerable conversion occurs before these reactions have occurred at least once. Then, one expects the formation of a polymer with a large "living" fraction but little "control". On the other hand, if the time for appreciable monomer conversion overlaps with the final reaction stage where the termination processes dominate, one may find products with a large degree of "control" but little "livingness".

The theoretical exploration of living radical polymerizations has been approached by numerical simulations of conversion rates and molecular weight distributions. Several methods have been developed.^{15,17,29,35,46,47} Such simulations provide considerable insight into the inner working of the mechanisms and can reproduce the experimental findings. Yet, they are not of general value, because they hold only for the specific kinetic parameters employed in the individual cases. For the analysis of polymerization data, analytical equations are more helpful, and their derivations also reveal the fundamental kinetic aspects. Such derivations address the time dependence of the radical concentrations, of the monomer conversions, and of the evolution of the molecular weight distributions, and they have mainly been worked out by Fukuda et al. and by our group.

Before giving some results, it must be stressed that all equations have been derived and will be valid only for ideal cases, especially only for chain length independent rate constants and in the absence of any reactions besides those considered explicitly. Further, they imply mathematical approximations. Both restrictions can lead to deviations of the experimental data from the theoretical results. Yet, such deviations do not disprove the equations, unless it is demonstrated that the preconditions of the derivations are strictly fulfilled by the chemical systems under study.

In our work,^{15–17} we have mainly concentrated on polymerizations that follow Schemes 3 and 11. Dis-

proportionation was assumed as a general mechanism for the irreversible termination. The latter restriction is not serious, because termination by coupling would simply double the molecular weight of the dead polymer fraction, which should anyway be small.

Since the rate constants, including those of the primary radicals, shall not depend on chain length, the total radical concentrations obey eqs 18, and the equilibrium relation (19) is established if the conditions (20) are fulfilled. The only additional equation is the rate equation for the conversion of the monomer M

$$\frac{d[M]}{dt} = -k_p[R][M] \quad (21)$$

and it does not change the evolution of the concentrations of R[•] and Y[•]. It is easy to show that there will be very little conversion before the equilibrium regime is established.¹⁷ To obtain the conversion in this regime, one inserts eq 18 for [R] into eq 21 and integrates to

$$[M] = [M]_0 e^{-3/2 k_p \left(\frac{K[I]_0}{3k_t} \right)^{1/3} t^{2/3}} \quad \text{or} \\ \ln \frac{[M]_0}{[M]} = \frac{3}{2} k_p \left(\frac{K[I]_0}{3k_t} \right)^{1/3} t^{2/3} \quad (22)$$

(The index R of k_{tR} is dropped here and in the following because k_{tY} is always assumed to be zero).

For a conventional polymerization with a constant rate of initiation r_i and constant radical concentration $[R]_s = (r_i/k_t)^{1/2}$, one has the relation²

$$[M] = [M]_0 e^{-k_p[R]_s t} \quad \text{or} \quad \ln \frac{[M]_0}{[M]} = k_p[R]_s t \quad (23)$$

The difference between eqs 22 and 23 is due to the time dependence of [R] in eq 18.

Polymerization in the equilibrium regime does provide the control of the molecular weight and a narrow molecular weight distribution. The integration of the kinetic equations for the moments of the distribution (see section IV) leads to equations for the number-average degree of polymerization (X_N) and the polydispersity index $PDI = M_w/M_n = X_w/X_n$.

$$X_N = \frac{[M]_0 - [M]}{[I]_0(1 - e^{-k_d t})} \quad (24)$$

$$PDI = 1 - e^{-k_d t} + \frac{1}{X_N} + \frac{[M]_0^2}{([M]_0 - [M])^2} (1 - e^{-k_d t}) \times \\ \left(\frac{\pi k_p^3 [I]_0}{k_d k_c k_t} \right)^{1/2} \operatorname{erf} \left[(3k_p)^{1/2} \left(\frac{K[I]_0}{3k_t} \right)^{1/6} t^{1/3} \right] \quad (25)$$

If the dissociation of the initiator occurs well before the conversion ($k_d t \gg 1$), all chains start to grow practically together at zero time. Then eq 24 provides the desired linear increase of M_n with the conversion and the control by the initial initiator concentration. The PDI decreases with increasing X_N , time, and

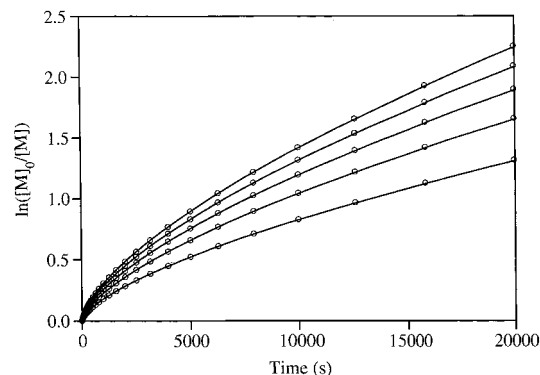


Figure 3. Polymerization index $\ln([M]_0/[M])$ vs time during a polymerization in the equilibrium regime for $k_p = 5000 \text{ M}^{-1} \text{ s}^{-1}$, $k_t = 10^8 \text{ M}^{-1} \text{ s}^{-1}$, $k_d = 0.0045 \text{ s}^{-1}$, $k_c = 2.2 \cdot 10^7 \text{ M}^{-1} \text{ s}^{-1}$, $[M]_0 = 10 \text{ M}$, and $[I]_0 = 0.02, 0.04, 0.06, 0.08,$ and 0.1 M as obtained by numerical integrations and eq 22 (circles).

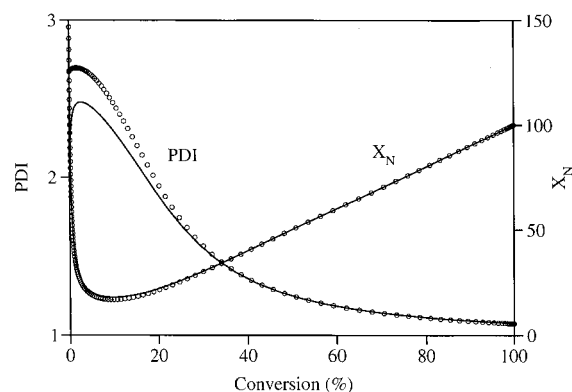


Figure 4. Evolution of the total number-average degree of polymerization X_N and the polydispersity index with conversion during a polymerization in the equilibrium regime for $k_p = 5000 \text{ M}^{-1} \text{ s}^{-1}$, $k_t = 10^8 \text{ M}^{-1} \text{ s}^{-1}$, $k_d = 0.0045 \text{ s}^{-1}$, $k_c = 2.2 \cdot 10^7 \text{ M}^{-1} \text{ s}^{-1}$, $[M]_0 = 10 \text{ M}$, and $[I]_0 = 0.1 \text{ M}$ as obtained by numerical integrations and eqs 24 and 25 (circles).

conversion, and the last term in eq 25 with the error function (erf) reflects the residual influence of the terminations. At short times one has

$$PDI_0 = 1 + \frac{1}{X_N} + \frac{8}{3k_d t} \quad (26)$$

and at infinite time the PDI becomes

$$PDI_\infty = 1 + \frac{[I]_0}{[M]_0} + \left(\frac{\pi k_p^3 [I]_0}{k_d k_c k_t} \right)^{1/2} \quad (27)$$

For properly chosen rate parameters it attains values close to one. Figures 3 and 4 display the behavior of the polymerization index (X_N) and PDI as computed and as predicted by eqs 22, 24, and 25.

The livingness of the polymer is also easily calculated because the number of dead chains is practically equal to the number of the released persistent species, which is known from eq 18. Further, the analytical solutions provide conditions for the rate constants that should allow a successful living and controlled polymerization.¹⁷ First, we may want the concentration fraction of the dead polymer products $[P]/[I]_0$ at the large monomer conversion of 90% to

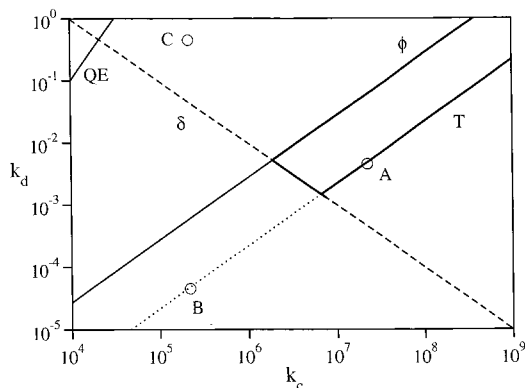


Figure 5. Graphical representation of the kinetic conditions for the existence of the quasiequilibrium (QE, eq 20), a small fraction $\phi < 5\%$ of unreactive polymer, a small residual polydispersity $\delta < 0.2$, and a time $T < 20\,000$ s (5.55 h) for 90% conversion. $k_t = 10^8 \text{ M}^{-1} \text{ s}^{-1}$, $k_p = 5000 \text{ M}^{-1} \text{ s}^{-1}$, and $[I]_0 = 0.1 \text{ M}$. The region where all conditions are obeyed is emphasized by a heavy frame. It should be noticed that the diagram holds only for the absence of initial persistent species and radical generation only from the regulator $I_0 = R_0 - Y$.

be below an allowed upper limit ϕ . From eqs 18 and 22 this requires

$$K = \frac{k_d}{k_c} \leq \frac{k_p [I]_0}{2 \ln(10) k_t} \phi^2 \quad (28)$$

Second, the residual polydispersity index $\text{PDI} - 1 - 1/X_N$ should be smaller than an upper limiting value δ , and hence, from eq 26

$$k_d k_c \geq \frac{\pi k_p^3 [I]_0}{k_t} \frac{1}{\delta^2} \quad (29)$$

Third, the time needed for 90% conversion should not exceed a time T , which is dictated by technical limitations such as working hours. Equation 22 shows this to be the case if

$$K = \frac{k_d}{k_c} \geq \frac{(2 \ln(10))^3 k_t}{9 k_p^3 [I]_0 T^2} \quad (30)$$

Obviously, large equilibrium constants yield short conversion times at the expense of larger dead polymer fractions. This need not conflict with the desired control, however, since the molecular weight and the polydispersity index do not directly depend on K but on k_d (24) and on the product $k_d k_c$ (27).

The optimum values of k_d and k_c depend on the propagation constant (k_p), the termination constant (k_t), and the attempted degree of polymerization through $[I]_0$. For a given set of these latter parameters one finds a range for k_d and k_c in which a living and controlled polymerization should be observed. This is illustrated by the diagram shown in Figure 5, which was constructed with the aid of eqs 28–30. Here, point A corresponds to the rate constants leading to Figure 4, that is, to a process yielding 90% conversion in 5.55 h for a monomer with $k_p = 5000 \text{ M}^{-1} \text{ s}^{-1}$, an average degree of polymerization $X_N = 100$, a polydispersity index of 1.2, and 5% dead

chains. Along a line from point A to point B, K is constant, but k_d and the product $k_d k_c$ decrease. Hence, one obtains in the same time as for case A a polymer with the same small dead fraction, but it shows much less control. On the other hand, along the line from point A to point C, K and k_d increase but the product $k_d k_c$ stays constant. Now, one expects a polymer that is hardly living but shows control for large conversion.¹⁷ Livingness and control do not necessarily imply each other, and discussions of the detailed behavior were given.¹⁷ Diagrams such as that given in Figure 5 should be very useful for predictions or analyses of experimental results. However, it must be stressed that the construction based on eqs 28–30 holds only for ideal cases of a spontaneous evolution of the persistent radical effect without any initial excess of the persistent species and without any additional radical generation, and these are seldom found in practice.

Fukuda et al.^{36b,48,49} covered a situation that is more often encountered in practical polymerizations than the previous scenario. There, transient radicals are generated not only by the dissociation of $R_n - Y$ but also with an additional rate r . These additional radicals are provided by a deliberately added conventional initiator, by impurity derived radical sources such as peroxides, or by the autoinitiation of the monomer. Now, the kinetic equations for the radical concentrations read

$$d[R]/dt = r + k_d([I]_0 - [Y]) - k_c[R][Y] - k_t[R]^2 \quad (31)$$

and

$$d[Y]/dt = k_d([I]_0 - [Y]) - k_c[R][Y] \quad (32)$$

With the ad hoc assumption of the dynamic equilibrium (19) and $d[R]/dt \ll d[Y]/dt$, these equations were solved analytically for constant r .^{36b,48,49} If r is sufficiently small, the radical concentrations are given by eq 18 and the monomer consumption is given by eq 22, as if r were zero. For larger r , the radical concentrations reach the stationary state

$$[R]_s = \left(\frac{r}{k_t}\right)^{1/2} \quad \text{and} \quad [Y]_s = K[I]_0 \left(\frac{k_t}{r}\right)^{1/2} \quad (33)$$

If most of the conversion occurs in this state, the polymerization index becomes

$$\ln \frac{[M]_0}{[M]} = k_p \left(\frac{r}{k_t}\right)^{1/2} t \quad (34)$$

as for a conventional polymerization with a constant initiation rate (23). This is so because the additional radical generation stops the permanent decrease of the transient radical concentration that occurs in its absence (eq 18) and keeps the radical concentration constant at a higher level. Therefore, in comparison to the absence of any additional initiation, the conversion rate is markedly enhanced.

Recently, we explored the effects of the additional initiation in detail, and found that the conditions (20) for the existence of the equilibrium (19) must again

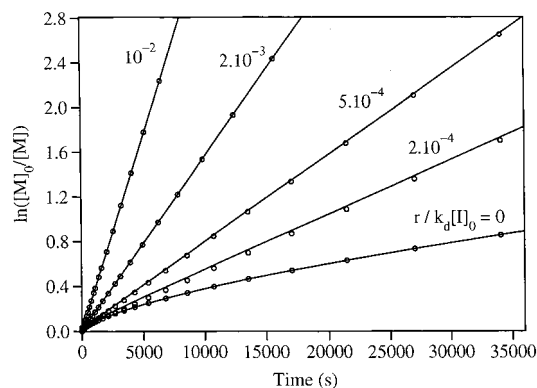


Figure 6. $\ln([M]_0/[M])$ versus time for a polymerization with additional initiation and different ratios $r/k_d[I]_0$. Solid lines are from numerical calculations and circles from the analytical equations. Parameters: $k_d = 3 \times 10^{-3} \text{ s}^{-1}$, $k_c = 5 \times 10^7 \text{ M}^{-1} \text{ s}^{-1}$, $k_t = 10^8 \text{ M}^{-1} \text{ s}^{-1}$, $k_p = 2000 \text{ M}^{-1} \text{ s}^{-1}$, $[I]_0 = 0.1 \text{ M}$, $[M]_0 = 10 \text{ M}$.

be fulfilled.⁵⁰ Equations 33 are valid if $[R]_s = \sqrt{r/k_t} \gg K$, that is, the equilibrium constant must be rather small, because the radical concentrations should normally not exceed 10^{-8} M . Further, a good control and the livingness of the resulting polymer require that the rate of the cross-reaction to dormant chains largely exceeds that of the self-termination to dead products. This provides $r \ll k_d[I]_0$, which means that the rate of the additional initiation must be small compared to the cleavage rate of the dormant species. In practice, a ratio $r/k_d[I]_0 = 0.01$ yields an about 10-fold rate enhancement under retention of most of the livingness and control, but larger initiation rates should not be used if the polymer should be living at high conversion.

Figure 6 shows calculated polymerization rates $\ln([M]_0/[M])$ for various ratios $r/k_d[I]_0$. Even for very small ratios of r and $k_d[I]_0$, rather large rate enhancements are obtained. Moreover, the time dependence of $\ln([M]_0/[M])$ becomes linear. Since some additional initiation by impurities or autoinitiation may always occur, the nonlinear behavior for the ideal case of Figure 3 may be difficult to observe in actual polymerizations, unless $k_d[I]_0$ is sufficiently large.

The expressions for the evolution of the degree of polymerization and the polydispersity index for polymerizations in the stationary state of constant radical concentrations are⁵⁰

$$X_n = \frac{[M]_0 - [M]}{[I]_0(1 - e^{-k_d t}) + rt} \quad (35)$$

$$\text{PDI} = (1 - e^{-k_d t} + rt/[I]_0) \left(1 + \frac{k_p}{k_d} [R]_s \frac{2 - C}{C} \right) + \frac{1}{X_n} \quad (36)$$

Here, C is the fractional monomer conversion. If one has $k_d t \gg 1$ and $rt \ll [I]_0$ at the time of observation, eq 36 reduces to

$$\text{PDI} = 1 + \frac{1}{X_n} + \frac{k_p}{k_d} [R]_s \frac{2 - C}{C} \quad (37)$$

and for small conversions, $C \approx k_p [R]_s t \ll 1$, one

obtains

$$\text{PDI}_0 = 1 + \frac{1}{X_n} + \frac{2}{k_d t} \quad (38)$$

The different numerical factors (eqs 26 and 28) are due to the different time dependencies of the radical concentrations. Equation 38 has also been derived by Fukuda et al.^{36b} by a purely probabilistic method, and it is generally valid for a constant concentration of growing chains.

Theoretical work has also been devoted to examine the influence of reactions that interrupt the often repeated cycles of radical formation (activation) and cross-termination to dormant species (deactivation). For the nitroxide- and the cobalt-mediated systems, such reactions are the formation of $R(-H)$ and YH by a usual radical disproportionation, which competes with the coupling of $R\cdot$ and $Y\cdot$ or by a direct fragmentation of $R-Y$ to the hydroxylamine or a hydridocobalt complex and the alkene.^{22,33a,35,47,51-57} Even rather small fractions of these processes limit the maximum conversion and stop the polymerization prematurely in nearly indistinguishable ways, because they lead to an exponential decay of the dormant species. Before the end of conversion this does not affect the linear dependence of X_n on conversion and causes only minor increases of the polydispersity.⁵⁷ To some extent the deteriorating effect of these reactions can be compensated by the rate enhancement through an additional initiation.⁵⁰

Another aspect⁴⁹ is the initial presence of persistent species in nonzero concentrations $[Y]_0$, and it will be discussed more closely in section IV. In the absence of any additional initiation, the excess $[Y]_0$ at first levels the transient radical concentration to an equilibrium value $[R]_s = K[I]_0/[Y]_0$. This is smaller than that found without the initial excess and lowers both the initial conversion rate and the initially large PDI. Further, it provides a linear time dependence of $\ln([M]_0/[M])$, which is directly proportional to the equilibrium constant. Later in the reaction course, $[Y]$ may exceed $[Y]_0$ because of the self-termination, then $[R]$ is given by eq 18. If there is additional radical generation, the first stages will eventually be replaced by a second stationary state that was described above. Further effects are expected from a decay or an artificial removal of the persistent species that increases the concentration of the transient radicals and the polymerization rate (see section IV). Radical transfer reactions to polymer, monomer, or initiator have not yet been incorporated in the analytical treatments.

ATRP utilizes a bimolecular radical formation reaction (Scheme 14). Apart from this, the rate equations are similar to those holding for the unimolecular cases, and therefore, the theory should be similar. It is not yet far developed, but for equal initial concentrations of catalyst and initiating halide, the equations given above should also hold for ATRP with $k_d[I]_0$ replaced by $k_a[\text{Cat}]_0[\text{RHal}]_0$.¹⁶

3. Experimental Verifications

Stringent quantitative verifications of the analytical equations should confirm the reaction orders with

respect to time and the initial concentrations, and they should even start from the a priori knowledge of the rate constants entering the formulas. Such verifications are emerging now. Thus, several groups measured the expected rather large concentrations of the persistent species [Y] both during nitroxide-mediated polymerizations and ATRP.^{31,49,58,59} Very often, the observed time dependencies of $\ln([M]_0/[M])$ were not curved as in Figure 3 but linear or approximately linear. This points to constant transient radical concentrations that are expected for an extra radical generation, an initial excess of the persistent species, or its decay. The slopes provide $[R]_s$ via eq 34. With $[R]_s$, [Y], and the initial concentrations, the equilibrium constants of the reversible radical formation can then be extracted from the data.

Fukuda et al.⁴⁹ introduced a chromatographic method for the direct determination of rate constants for the radical generation step (activation). For several cases these agree with corresponding values deduced from the time dependence of the polydispersity index (eq 38), and this is also strong support for the underlying theoretical principles. When K is known, the rate constant for radical formation (activation) provides also the rate constant for the cross-reaction (deactivation). All data established for nitroxide-mediated polymerizations so far^{49,59,60,61} are not much different from rate constants for analogous reactions involving small carbon-centered radicals that have been obtained by spectroscopic techniques.^{62,63} The technique has also been applied to ATRP systems.⁶⁴

As indicated earlier, the unusual time dependencies and reaction orders expected in the absence of additional radical generation or of an initial excess of the persistent species are difficult to observe unless special precautions are taken. Moreover, a decrease of the self-termination rate constant k_t with increasing chain length and conversion diminishes the negative curvature of $\ln([M]_0/[M])$ (eq 22),¹⁷ and may lead to a more linear appearance. This was demonstrated first by Matyjaszewski.⁴⁶ To avoid such interferences, experiments designed to prove the unusual polymerization kinetics must be based on systems that exhibit large radical generation (activation) rates, and the conversions should be kept modest. The cleavage rate constants of di-*tert*-butylnitroxide (DBNO, **1** in Scheme 12) based alkoxyamines are known to be rather large. In fact, using a sugar-carrying styrene that does not readily undergo autoinitiation and a benzoyloxy-styryl-DBNO initiator, Fukuda et al. found that the polymerization index increases with time as $t^{2/3}$ and depends on the third root of the initiator concentration.¹⁹ This is as expected from eq 22. Other nitroxides that provide large cleavage rate constants are becoming available now (see below), and with a corresponding alkoxyamine, Lacroix-Desmazes et al. also obtained a clear verification of the theoretical predictions.^{60,65} For ATRP, an example was given by Klumpermann et al.⁶⁶

These measurements provide the equilibrium constant K of the reversible dissociation, if k_t is known. Of course, it would be interesting to obtain both

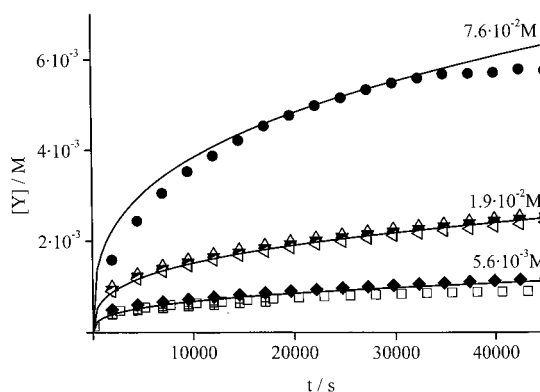


Figure 7. Time evolution of the persistent radical concentration during a polymerization of 0.76 M styrene in *tert*-butylbenzene at 130 °C initiated by the alkoxyamine **6** of Scheme 30 for different alkoxyamine concentrations. The solid lines confirm eq 18.

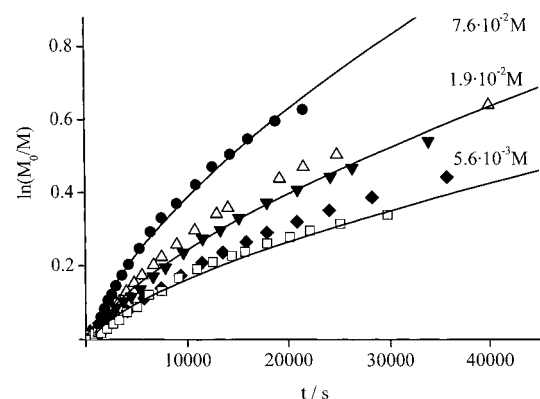


Figure 8. Time evolution of the polymerization index $\ln([M]_0/[M])$ during a polymerization of 0.76 M styrene in *tert*-butylbenzene at 130 °C initiated by the alkoxyamine **6** of Scheme 30 for different alkoxyamine concentrations. The solid lines confirm eq 22.

parameters from the same polymerization, and this is possible by simultaneous measurements of the time dependence of the persistent radical concentration and of the conversion and the combination of eqs 18 and 22.⁵⁹ This was recently achieved on the same sample by combining an ESR spectrometer with a dilatometer and using another new alkoxyamine for the polymerization of styrene. In pure monomer, the autopolymerization still provided a constant nitroxide level and a linear time dependence of $\ln([M]_0/[M])$. However, with styrene diluted by an inert solvent and for conversions below 50%, the results of Figures 7 and 8 were obtained, and they conform to eqs 18 and 22. Moreover, the resulting polymers were living (>90%) and had low polydispersities (1.15–1.30).²³

Before closing this section, it must be mentioned that processes involving the persistent radical effect are not the only way to obtain living and controlled polymerizations. Any reaction scheme that provides an equilibrium between the dormant polymer chains and the transient propagating radicals suffices, if the equilibrium highly favors the dormant chains and is established rapidly and the rate of external radical generation is small. For such other living radical polymerizations, the RAFT process of Rizzardo et al.⁶⁷ and the moderation by degenerative iodine atom transfer⁶⁸ are illuminating examples.

III. Reactions Exhibiting the Persistent Radical Effect

A. Uncatalyzed and Photochemical Organic and Metal–Organic Reactions

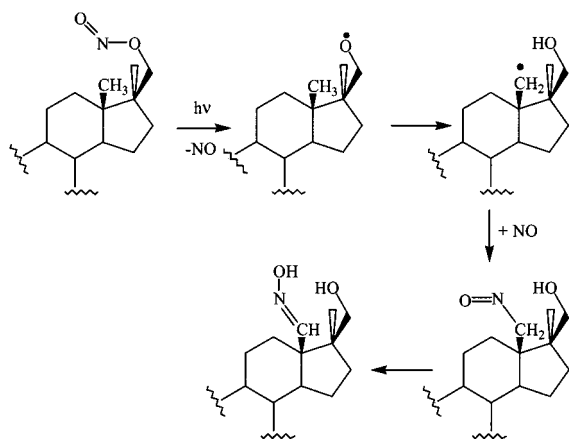
The persistent radical effect must always play a role when transient and persistent radicals are formed with equal or nearly equal rates. It leads to the formation of the mutual reaction products in high yields and to the virtual absence of the self-termination reactions. In the few examples given earlier, the persistent species were radicals and transition metal complexes, but other reaction partners such as molecular ions and even normal molecules may take their place. Furthermore, the phenomenon can also work with other transient species, such as carbenes, nitrenes, and molecules in electronically excited states. A literature search would probably reveal a large variety of diverse reactions that exhibit the effect to some degree, although this went unnoticed, so far. Here, we restrict the survey to evident cases. A few of the reactions have even been designed to exploit the persistent radical effect in synthesis.

1. Photochemical Reactions Involving NO

There are a variety of photochemical reactions involving free nitrous oxide (NO) as persistent radical. Often there is an initial fragmentation, as presented in Scheme 6 for *N,N*-dimethyl-*N*-nitrosamine. One example is the Barton reaction of nitrite esters (Scheme 15). It allows the functionalization of methyl groups in steroids and utilizes an intermediate 1,5-hydrogen atom migration, which converts the initially formed oxygen-centered radical to a carbon-centered species.⁶⁹

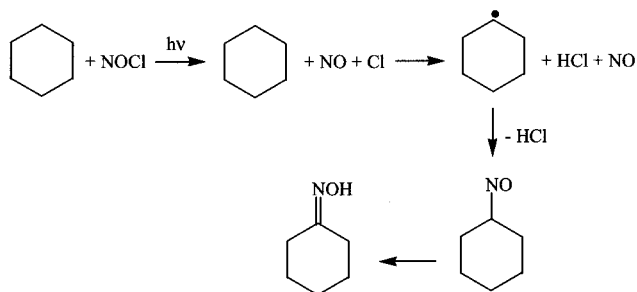
Similar reactions occur with *N*-nitrosoamines R₂NNO and *N*-nitrosoamides RCO(R')NNO.⁷⁰ Apart from the intramolecular hydrogen atom transfer, diverse intramolecular radical additions (cyclizations) and other rearrangements have also been used to obtain cross-reaction products between NO and the radicals resulting from the transformation of the primarily formed R• to another radical R'•.^{69,70} Giving evidence for the persistent radical effect, the yields of the desired products are large and those of the self-termination of the transient intermediates are low,

Scheme 15



although these products have occasionally been observed. The photooxygenation of alkanes with NOCl follows essentially the same course and has industrial importance (Scheme 16).

Scheme 16

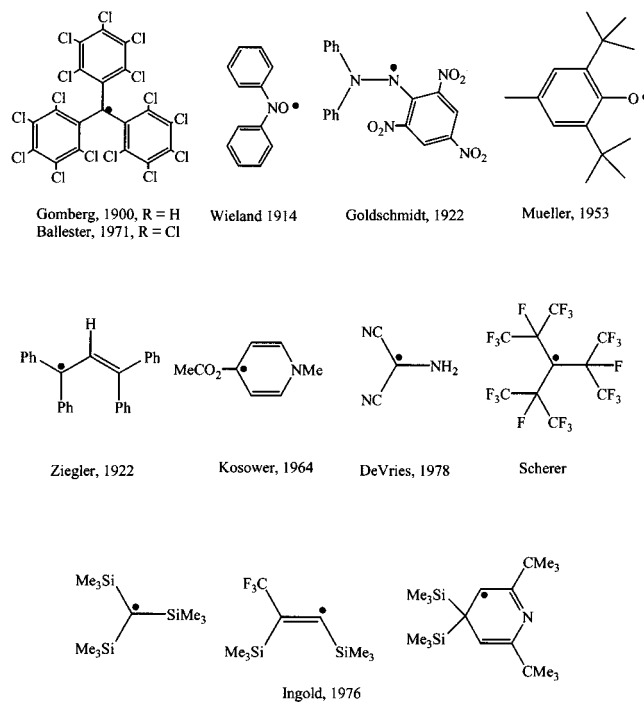


2. Thermal Reactions Involving Persistent and Semipersistent Organic Radicals

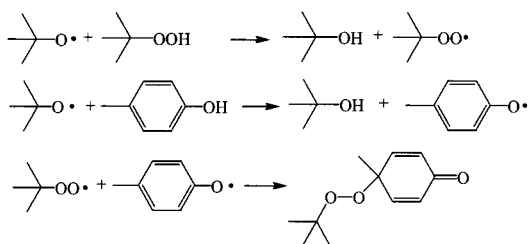
Scheme 17 displays several radicals with lifetimes exceeding about 1 h in oxygen-free liquid solutions and at ambient temperature. Many of them have been isolated in pure form.⁷¹ Their stability has electronic and steric reasons. It is favored by the absence of β -hydrogen atoms, which would facilitate disproportionation. As shown before, the persistent radical effect can also be observed for radicals that are not extremely persistent. Therefore, it is important to notice that the lifetimes of all types of radicals can be adjusted by proper substitution.¹ Comprehensive compilations of the magnetic properties⁷² and of the reactivities⁷³ of radicals are available in the Landolt–Boernstein series. They reveal that a large variety of radicals are persistent enough for eventual synthetic applications using the effect.

The selecting influence of triphenylmethyl radicals on product distributions has already been discussed in earlier sections, and additional examples are found

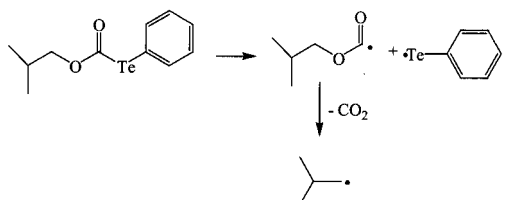
Scheme 17



Scheme 18



Scheme 19



in Perkin's discussion of aromatic substitutions.⁹ Minisci et al.⁷⁴ and Ingold et al.⁷⁵ found that mixed peroxide products dominate in reactions where *tert*-butylperoxy and phenoxyl or carbon-centered radicals are formed simultaneously, and the findings were rationalized in terms of the reactions shown for one example in Scheme 18.

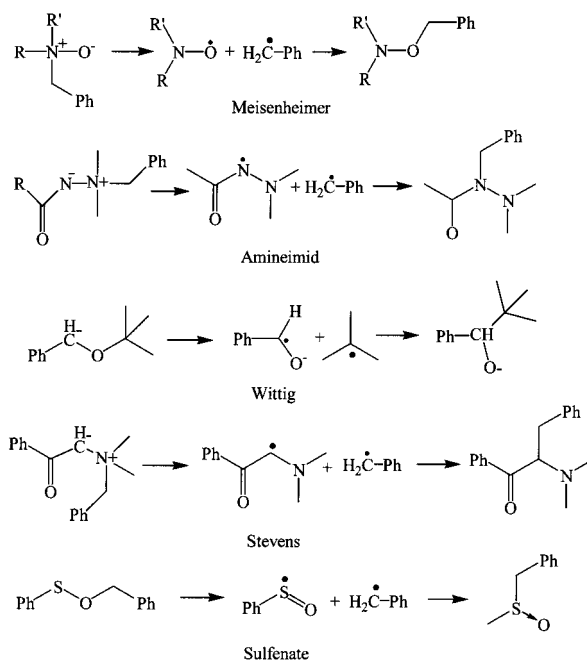
In this case, the *tert*-butylperoxy radicals are the more persistent species. The authors also confirmed that the highest yield of the cross-reaction product is obtained when the cross-reacting radicals are formed with equal rates. Schiesser et al.⁷⁶ introduced phenyl telluroformates as precursors of alkyl radicals (Scheme 19). In the absence of trapping agents, the parent molecules appeared stable, that is, the cross-reaction between the oxyacyl and the tellurium-centered radical is even faster than the decarboxylation of the oxyacyl species, which normally takes only nano- to microseconds. Obviously, the tellurium-centered radical must be rather persistent and builds up in large concentrations.

Other reactions that are very likely subject to the persistent radical effect are molecular rearrangements such as the Meisenheimer, amineimide, Wittig, Stevens, and sulfenate rearrangements of Scheme 20, for which evidence for radical intermediates has been accumulated.⁷⁷

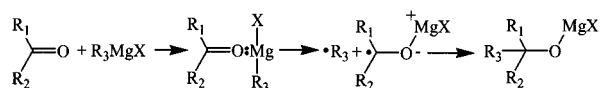
The formation of pinacols, typical radical rearrangements, and the direct observation of ketyl radicals by ESR spectroscopy strongly indicate that Grignard reactions of aryl ketones follow at least in part a single electron-transfer pathway involving transient alkyl and persistent arylketyl radicals (Scheme 21). Walling⁷⁸ analyzed the known product distributions by a kinetic treatment with the ketyl species as being persistent. Most of the experimental findings were explained in terms of usual bulk radical reactions with reasonable rate constants. The operation of the effect should cause rather large concentrations of the ketyl radical species, and these are in fact observed.

Sawaki et al.⁷⁹ recognized that the persistent radical effect properly explains the dominant formation of diphenylmethyl anions when persistent dicyanoanthracene anions and transient diphenylmethyl

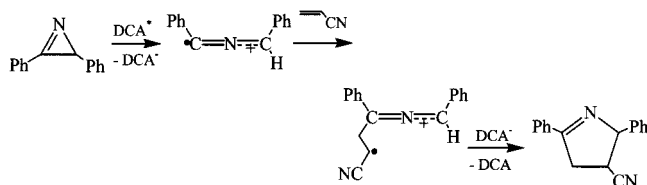
Scheme 20



Scheme 21



Scheme 22

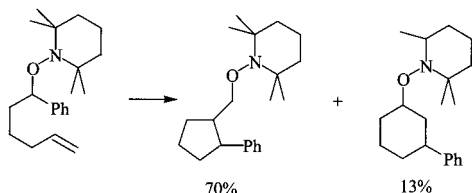


radicals are formed by photochemical means simultaneously, and they noticed the virtual absence of the coupling products of diphenylmethyl. There are a multitude of photochemical reactions involving single-electron transfer to dicyanoanthracene, dicyanonaphthalene, and related sensitizers that yield persistent anions and transient radicals simultaneously. They often lead to selective product formation and may well involve the effect.⁸⁰ Scheme 22 presents an example.^{80a}

The first directed application of the phenomenon toward high-yielding organic synthesis is due to Studer.^{4,81} He employed the reversible dissociation of alkoxyamines for the generation of cyclized derivatives to avoid the usual use of tin-organic compounds in radical cyclizations. One example is shown in Scheme 23.

The straightforward mechanism starts with the cleavage of the parent alkoxyamine to the nitroxide and to the 1-phenylhexen-5-yl radical. This radical undergoes intramolecular 1,5- and 1,6-cyclizations in usual ratios and couples with the nitroxide to the rearranged species. In a large series of experiments, Studer⁸¹ made good use of the rate enhancement of the alkoxyamine cleavage by substituents stabilizing the resulting carbon-centered radicals, by polar sol-

Scheme 23



vents, and by solvents and substituents that undergo hydrogen bonding to the nitroxide group as well as by agents that decrease the retardation by slowly removing the excess nitroxide concentration. Cross-over experiments demonstrated the absence of cage reactions, and several new alkoxyamines were developed that undergo a particularly facile cleavage.^{81,82} It is also noteworthy that Studer often observed considerable amounts of alkenes besides the desired products. This points to the direct elimination of alkenes from the alkoxyamines, which competes with their cleavage into radicals.

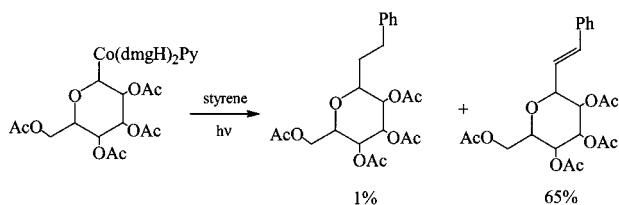
3. Reactions Involving the Reversible Cleavage of Weak Metal–Carbon Bonds

In connection with the work of Kraeutler,¹¹ Finke et al.,²¹ and Wayland et al.³⁷ on reactions involving the homolysis of carbon–cobalt bonds, the operation of the persistent radical effect has already been addressed. There is considerable literature on the synthetic applications of this photochemically and thermally facile process, and we refer to reviews.⁸³

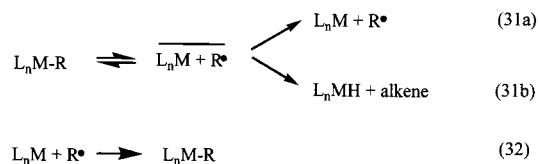
Scheme 24 displays an example designed by Giese et al.⁸⁴ The glycosyl–cobalt complex dissociates and the glycosyl radical adds to styrene. This adduct couples to the cobalt(II) species. The coupling product is not isolated and forms mainly the alkene by a formal “dehydrocobaltation”. The alkane probably stems from a heterolytic cleavage to a radical anion and a cobalt(III) complex, followed by protonation or a direct protonation of the coupling product because this pathway dominates for electron deficient substrates.

Considerable insight into the thermodynamics, kinetics, and mechanisms associated with the reversible cleavage of weak metal–carbon, metal–hydrogen, and metal–metal bonds is due to Halpern.⁸⁵ Scheme 25 shows the major reactions in liquids. The thermal cleavage is believed to produce a caged

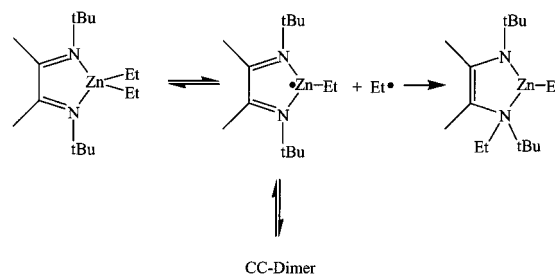
Scheme 24



Scheme 25



Scheme 26



radical pair that undergoes cage return and separation to scavangeable free radicals and forms alkenes by disproportionation. The recombination of the radicals from the bulk is close to diffusion-controlled and does not seem to be accompanied by disproportionation. In usual free radical reactions, disproportionation-to-combination ratios in bulk and cage are often equal. Therefore, the marked difference observed here for the postulated cage return and the bulk process is against the former reaction. In our opinion it is more compatible with an alkene formation by direct elimination from the initial complex. However, this was regarded to be unlikely,⁸⁵ and unusual coordination effects may be involved.

Halpern noticed the relevance of the reactions of Scheme 25 in biological coenzyme B₁₂-mediated rearrangements, and the use of vitamin B₁₂-promoted radical reactions in organic synthesis was pioneered by Scheffold.⁸⁶ The latter reactions are often carried out in electrochemically driven catalytic cycles where the operation of the persistent radical effect is not evident.

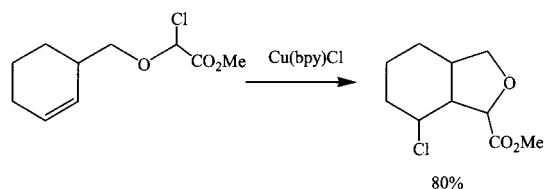
Most of the synthetic literature concerns the utilization of the weak cobalt–alkyl bonds. However, the reversible cleavage into transient radicals and a metal complex residue is also known for many other complexes, for example, those of Ti, V, Cr, Mn, Fe, Ni, Cu, Zn, Zr, Mo, Ru, Rh, W, U, Pb or the lanthanides Sm, Ir, Sc, Hf, Th, etc.^{83c,85,87} Some of them are of synthetic use, and many metal species may be persistent. Hence, the persistent radical effect should be operating. Van Koten⁸⁸ has presented a clear-cut example (Scheme 26). Et₂Zn reacts with di-*tert*-butyl-glyoxaldiimine to a complex that rearranges in nearly quantitative yield by a 1,2-ethyl migration from Zn to nitrogen. The organozinc radical is persistent and forms a weakly CC-bonded dimer. The reaction works at low temperatures, with diversely substituted diimines and α -imino ketones, and with AlEt₃ as inorganic precursor and has been used in synthetic applications.

B. Catalyzed Organic Reactions

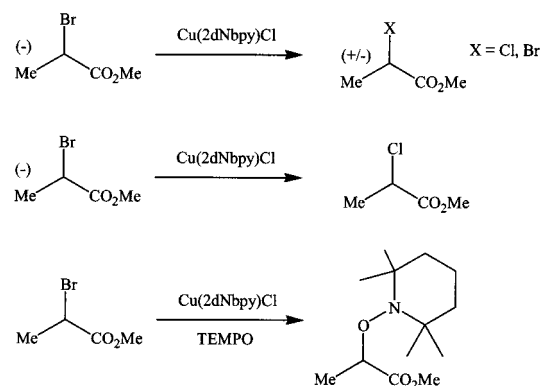
1. Catalyzed Kharasch Additions and Related Reactions

The discovery of Minisci et al.,³⁹ Asscher and Vofsi,⁴⁰ and others⁴¹ of the transition metal catalyzed addition of haloalkanes to alkenes by a redox chain process (Scheme 14) has found vast synthetic applications.^{83c,89} A recent summary has been given by van Koten et al.⁹⁰ Virtually any olefin can serve as the source of reactive unsaturation, and a variety of polyhalogenated compounds such as alkyl halides,

Scheme 27



Scheme 28



perfluoroalkyl iodides, or alkylsulfonyl chlorides can be added across the double bond. The list of the catalytic promoters is extensive. It includes powdered transition metals; their inorganic oxides or halides with the metal in a lower valent state; mono-, di- and trinuclear transition metal complexes with various organic ligands; and metal phosphine compounds such as $\text{RuCl}_2(\text{PPH}_3)_3$. Telomerization is normally avoided by using large ratios of the halogenated compounds to the olefin but has also found synthetic interest.^{89b} More recently, the reaction has been used to obtain radical cyclization products in excellent yields,⁹¹ as for example outlined in Scheme 27.^{91b}

Because of the excellent yields, the intermediacy of freely diffusing carbon-centered radicals in these reactions has often been doubted. However, the identical product distributions of the same cyclizations carried out by transition metal catalysis and by conventional radical reactions point to the opposite.^{91b} Even stronger experimental evidence for normal uncomplexed free radical intermediates has recently been given by Matyjaszewski et al.⁹² This group studied three reactions of methyl 2-bromopropionate with copper(I) chloride complexed by 4,4'-(5-nonyl)-2,2'-bipyridine (dNbpy) under identical conditions. These were (Scheme 28) the racemization of an optically active propionate, the exchange of Br by Cl, and the trapping of the radical intermediate by excess TEMPO. Both the rates and yields of all three reactions were identical. This is only expected if free 1-carboxymethyl-substituted ethyl radicals are the common intermediates, and the rates reflect the rate of radical formation. The observations rule out major contributions by reactions in the metal coordination sphere. In all catalyzed reactions, large concentrations of the persistent metal complexes in the higher valent state should be reached, and these were in fact also observed occasionally.^{58,90}

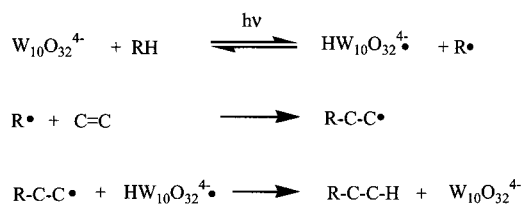
Generally, the reaction rates increase strongly with the decreasing oxidation potential of the complex, and these can be tuned by appropriate ligands. These

ligands also provide the solubility of the complexes and exert additional steric effects. Moreover, the activation of the halide substrate plays an important role. We refer to a collection of relevant references.⁹⁰

2. Photocatalysis

Photochemical reactions of polyoxometalate anions, such as tetrakis(tetra-*n*-butylammonium) decatungstate $(\text{C}_4\text{H}_9\text{N})_4\text{W}_{10}\text{O}_{32}^{4-}$, have been used for the catalytic ethylation, vinylation, carbonylation, and hydroperoxidation of alkanes in liquid solution.⁹³ The simplest mechanism of Scheme 29 involves the reversible formation of a paramagnetic decatungstate species and a transient radical. As proven by optical and EPR spectroscopy, the decatungstate intermediate is persistent.⁹⁴ Moreover, during continuous photoreactions in the presence of a large variety of differently substituted alkanes, the concentration of the decatungstate intermediate exceeded the concentrations of the transient radicals by factors of 100–5000. In pulsed radical generations, the transient species decayed completely after the pulse, whereas residual reduced decatungstate remained. This is experimental proof for the persistent radical effect in these systems and allowed the determination of reaction rate constants.⁹⁴

Scheme 29



C. Reactions in Polymer Systems

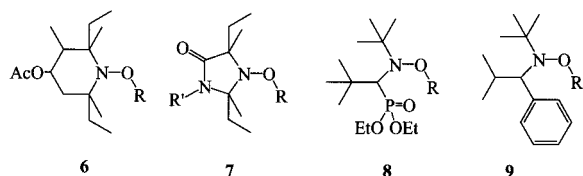
For more complete and practically oriented surveys of living radical polymerizations, we refer to other reviews in this issue⁹⁵ and cover in the following section only some kinetic and mechanistic aspects that are relevant for quantitative treatments.

1. Nitroxide-Mediated Systems

The rate constants of the cleavage of the dormant chains into radicals (activation) and of the reverse coupling (deactivation) influence the degree of livingness and control of the resulting polymer and the monomer conversion rate. To obtain living and well-controlled radical polymerizations, these rate constants must favorably interrelate with the propagation constants k_p and the termination constants k_t of a particular monomer system at a given temperature, as well as with the applied initiator (regulator) concentration $[\text{I}]_0$ and the rate r of an additional radical generation. For systems involving the reversible bond cleavage, we have denoted the activation and deactivation parameters by k_d and k_c (Scheme 8), and their ratio $k_d/k_c = K$ is the equilibrium constant. The knowledge of these quantities and of the factors controlling them allows the preassessment of successful processes.

The alkoxyamines presented in Scheme 12 were used as regulating initiators early on,²⁷ and Scheme

Scheme 30



30 lists a few advanced species.^{60,96–98} Alkoxyamines are usually prepared by the coupling of suitable carbon-centered radicals with the corresponding nitroxides^{60,97,99–101} but can be formed also in situ during polymerizations by the Meisenheimer rearrangement of *N*-oxides¹⁰² (Scheme 20), by sequential radical additions to nitroso compounds and nitrones,¹⁰³ by the coupling of nitroxides with radicals originating directly from conventional initiators, or from the addition of primary initiator radicals to the monomers.^{30,31} Further, polymeric alkoxyamines have been used as initiators.⁴⁹ Since the free nitroxide radicals act as persistent regulating species, it is often believed that they should be fairly stable under polymerization conditions, typically up to temperatures of 130–140 °C. However, this need not be so (see section IV). Except for compounds **1**, **8**, and **9**, the nitroxides indicated in Schemes 12 and 30 are very stable. Di-*tert*-butyl nitroxide **1** slowly decomposes to *tert*-butyl radicals and nitrosobutane. The nitroxides derived from **8** and **9** presumably undergo disproportionation, but the reaction is slow because of steric constraints.⁶²

TEMPO, *p*-substituted TEMPO based alkoxyamines **3**, and compounds such as **4**, **5**, and **7** have been applied successfully for polymerizations of styrene, substituted styrenes, and 4-vinylpyridine, and some copolymerizations and block copolymerizations were reported. However, living and controlled radical polymerization of other monomers, especially acrylates, require the use of the more recently developed structures **6**, **8**, or **9**. These also yield well-controlled and living block copolymers, but methacrylates have so far resisted all efforts to obtain large conversions. Undoubtedly, many failures are due to unfavorable rate constants or side reactions.

As mentioned before, the equilibrium constant *K* can be determined from polymerization data. For polymeric alkoxyamines (macroinitiators) *k_d* has mostly been determined with Fukuda's chromatographic method⁴⁹ or from the early time evolution of the polydispersity (eqs 18 or 22). From *K* and *k_d* one obtains *k_c*. The decay constant *k_d* can also be obtained from the exponential growth of the persistent radical concentration during the cleavage of alkoxyamines under conditions where the transient radicals are completely scavenged, preferably by the irreversible reaction with another persistent radical. This technique has been widely applied to low molecular weight alkoxyamines.^{22,62,104–107} The rate constants of the coupling *k_c* of nitroxides with small carbon-centered radicals are usually measured by laser flash photolysis.^{63,108,109}

Table 1 displays rate data for alkoxyamine-terminated polymers and low molecular model compounds and shows some important trends. At about the same temperature, the dissociation rate constants *k_d* of alkoxyamines (Schemes 12 and 30) with the same leaving radical (polystyryl, 1-phenylethyl) increase in the order **3** (TEMPO) < **6** < **8** (DEPN) < **1** (DBNO) by a factor of about 30. Acrylate radicals dissociate markedly slower than styryl radicals from **1** (DBNO), but there is no appreciable difference for **8** (DEPN). The dependence of *k_d* on the nitroxide structure has been addressed by Moad et al.¹⁰⁴ They found the order five membered ring < six membered ring < open chain nitroxides and pointed out additional steric (compare **3** and **6**) and polar effects.

The activation energies of the cleavage are close to the bond dissociation energies and can be reliably calculated with advanced quantum chemical methods.¹¹⁰ For a large series of low molecular alkoxyamines with different leaving radicals, they decrease linearly with increasing stability of the leaving radical, that is, the R–H bond dissociation energy.^{62,106} Thus, *k_d* increases in the series acrylate < styryl < methacrylate and within one type of radical from primary to secondary and tertiary species. The frequency factors are in the rather narrow range from $3 \times 10^{13} \text{ s}^{-1}$ to $2 \times 10^{15} \text{ s}^{-1}$, and for a larger series of

Table 1. Rate and Equilibrium Constants for the Reversible Dissociation of Polymeric Alkoxyamines and Low Molecular Model Compounds, Frequency Factors, and Activation Energies of Dissociations

alkoxyamine, Schemes 12, 30	T/°C	<i>k_d</i> /s ⁻¹	<i>A_d</i> /s ⁻¹	<i>E_{a,d}</i> /kJ mol ⁻¹	<i>k_c</i> /M ⁻¹ s ⁻¹	<i>K</i> / <i>M</i>	ref		
3 -(TEMPO)-polystyryl	125	0.0016	3×10^{13}	124	7.6×10^7	2.1×10^{-11}	48, 49		
	125	0.00052					$\approx 1 \times 10^8$	$\approx 1 \times 10^{-11}$	31
	120	≈ 0.001							35
3 -1-phenylethyl	120	0.00052	2.5×10^{14}	133	2.5×10^8	2.1×10^{-12}	62, 63		
	120	0.00045	5×10^{13}	128			105		
1 -(DBNO)-polystyryl	120	0.042	3.8×10^{14}	120			48, 49		
1 -phenylethyl	120	0.014	2.2×10^{14}	122			62		
1 -poly- <i>tert</i> -butylacrylate	120	0.001					48, 49		
1 -1- <i>tert</i> -butoxycarbonylethyl	120	0.0011	1.2×10^{14}	128			62		
6 -polystyryl	130	≈ 0.0032			$\approx 6 \times 10^6$	5.2×10^{-10}	23		
6 -1-phenylethyl	120	0.0027			1×10^8	2.7×10^{-11}	62, 63		
8 -(DEPN)-polystyryl	125	0.0034	1×10^{14}	121	5.7×10^5	1.9×10^{-8}	65		
	120	0.011	2×10^{15}	130			6×10^{-9}	59	
	120							48, 49	
8 -1-phenylethyl	120	0.0055	1.9×10^{14}	125	4.6×10^6	1.2×10^{-9}	62, 63		
8 -poly- <i>n</i> -butylacrylate	120	0.0071	1.7×10^{15}	130	4.2×10^7	1.7×10^{-10}	59		
8 -1- <i>tert</i> -butoxycarbonylethyl	120	0.003	3.5×10^{14}	128			62		

model compounds, a clustering around $2 \times 10^{14} \text{ s}^{-1}$ was observed. These frequency factors are remarkably small since for molecular dissociations into fairly large groups values much larger than 10^{15} s^{-1} are usual.¹¹¹ Obviously, nearly the whole bond dissociation energy is needed to reach the transition state of the cleavage while little entropy is gained. Further, we note that the cleavage is favored by polar solvents, external and internal hydrogen bonding, strong steric congestion around the NO group, increasing CNC bond angles, and electron-donating groups on the nitroxide moiety.^{82,104}

The rate constants for the coupling of carbon-centered radicals with nitroxides (Table 1) range from $6 \times 10^5 \text{ M}^{-1} \text{ s}^{-1}$ to about $10^8 \text{ M}^{-1} \text{ s}^{-1}$, and they vary more than the cleavage rate constants. Many studies on small radicals have shown that the rate constants are generally lower than diffusion controlled values and depend very little on temperature.^{63,108,109} In some cases even negative activation energies have been found, whereas the rate constants with small positive activation energies often revealed unusually small frequency factors. This is rationalized by a nearly barrierless cross-coupling reaction, where the location of the transition state is governed by entropy. Support for this explanation is the anticorrelation of the cleavage of alkoxyamines and the coupling rate constants for systems with the same basic structures but different substitutions.⁶³

In total, alkoxyamine systems with large cleavage (activation) rate constants tend to show small coupling (deactivation) rate constants. This provides large equilibrium constants that increase the conversion rates. It must not deteriorate the control since this depends on k_d and the product $k_d k_c$. In comparison, the more recently introduced nitroxides **6**, **8**, and **9** provide larger equilibrium constants than e.g. **3** (TEMPO). For acrylate-derived radicals, the equilibrium constants are usually smaller than for styryl type radicals, and this may, at least in part, explain the failure of TEMPO-regulated acrylate polymerizations. However, judging from model studies,^{62,63} this reason does not apply for methacrylates.

Reactions that convert the alkoxyamines to hydroxylamines and alkenes can strongly limit the monomer conversion. These are either usual radical disproportionations between the nitroxide and the propagating radicals or concerted alkoxyamine decays. Both pathways lead to an exponential decrease of the concentration of the dormant chains with rate constant $k_{\text{dec}} = f_D k_d$, where f_D is the fraction of the side reaction occurring with radical coupling of alkoxyamine decay.⁵⁷ k_{dec} can be measured from the decay of the dormant alkoxyamine chains under non-scavenging conditions, and its relation with k_d provides f_D . From data of Fukuda et al. one can deduce $f_D = 0.4\%$ for a TEMPO-polystyryl compound and $f_D = 1.1\%$ for a di-*tert*-butylnitroxide-poly-*tert*-butylacrylate macroinitiator both at 120°C .^{53,55} Similar small values of f_D hold for TEMPO-cumyl (Scheme 10),²² TEMPO-1-phenylethyl,¹¹² and a better mimetic compound for TEMPO-polystyryl.¹¹³ In these cases, f_D probably represents the usual radical disproportionation. A much larger $f_D \approx 25\%$ holds for TEMPO-

CH(CH₃)CO₂CH₃. It is ascribed to the concerted alkene elimination, which is also known for TEMPO-alkyl compounds.^{81,112} However, for TEMPO-CH(CO₂CH₃)CH₂C(CH₃)₂C₆H₅, the fraction of the side reaction is again low ($f_D \approx 1\%$), so TEMPO-CH(CH₃)CO₂CH₃ is not a good model for TEMPO-terminated acrylates. Nevertheless, one may speculate that side reactions contribute to the difficulties encountered with TEMPO-mediated acrylate polymerizations, because they are virtually absent for DEP_N (**8**) based systems.¹¹² Similarly, the nitroxide **9** exhibits a much better end group fidelity than TEMPO in styrene and acrylate polymerizations.¹¹⁴

The irreversible decay of the dormant alkoxamine chains stops the monomer conversion rather abruptly at the time $t = 1/f_D k_d$. For methyl methacrylate polymerizations this stop has been observed, and it has been demonstrated that it is caused by a considerable fraction of cross-disproportionation between the nitroxide and the propagating radicals.^{51,97,112} Unfortunately, the factors governing disproportionation-to-combination ratios in radical-radical reactions are not well understood up to now, but stereo-electronic effects are certainly very important.¹¹² Hence, one cannot yet predict a nitroxide structure that will allow living methacrylate polymerizations up to large conversions.

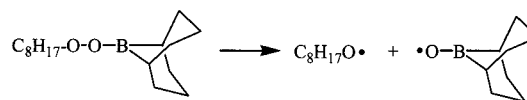
Recently, it has been found that the elimination of the hydroxylamine from a nitroxide-capped polymer occurs particularly facilely upon the controlled monoaddition of maleic anhydride and maleimide derivatives under the creation of a very useful functional end group, that is, the often detrimental side reactions can also be put to good use.¹¹⁵

A complete mechanism of the nitroxide-mediated polymerizations must also take further reactions into account. For the case of TEMPO + styrene, Scaiano et al. showed that the nitroxide radical can add directly to the monomer.¹¹⁶ It can also abstract a hydrogen atom from the Mayo dimer¹¹⁷ and possibly from the polystyryl chains.¹¹⁶ In addition, hydroxylamines can act as hydrogen donors for the propagating radicals and retard the polymerization.¹¹⁸ Quantitative assessments of the importance of these reactions are still missing, but the practical experience with living radical polymerizations points against strong deteriorating influences.

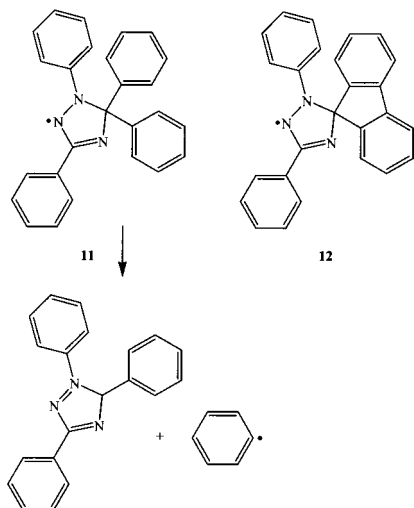
2. Mediation by Other Persistent Radicals

Most of the living radical polymerizations using organic radicals as regulating persistent species involved nitroxides. Exceptions are triphenylmethyl and other carbon-centered radicals in the early work of Otsu and Braun.^{24,25} More recently, Chung showed that borinate radicals **10** formed by the thermal cleavage of in situ generated alkyl boryl peroxides (Scheme 31) can be employed to control methacrylate

Scheme 31



Scheme 32



polymerizations partially.¹¹⁹ Müllen et al.¹²⁰ introduced the triazolynyl radicals **11** and **12** (Scheme 32) for the regulation of styrene, acrylate, methacrylate, and vinyl acetate polymerizations and demonstrated the formation of block copolymers. At least for moderate conversions, they reported more success than obtained with the structurally related verdazyl radicals and with TEMPO.¹²¹ It was also demonstrated that the triazoninyl radicals couple reversibly to the propagating radicals, as is known for nitroxides.

Radical **12** is rather stable under polymerization conditions, but radical **11** decays into a triazole and the phenyl radical, which initiates new chains. Hence, the rate of polymerization is higher with **11** than with **12**, because the decay prevents retarding of the buildup of large persistent radical concentrations such as an additional radical generation. This effect of the radical decay is equivalent to the rate enhancement by partial removal of nitroxides by appropriate additives, which was first applied by Georges et al.³¹ Interestingly, at 95 °C and in toluene solution, the lifetime of **11** is only about 15 min, whereas a reasonable control was found in polymerizations of styrene that lasted many hours at 120–140 °C.¹²⁰ Obviously, the radical moiety **11** is stable while it is coupled to the polymer chain. However, the different time scales raise the question of the upper limit of the conversion rate of the persistent radical to a transient one that can be tolerated in living radical polymerization processes (see section IV.C).

3. Organo–Cobalt Complex Mediated Systems

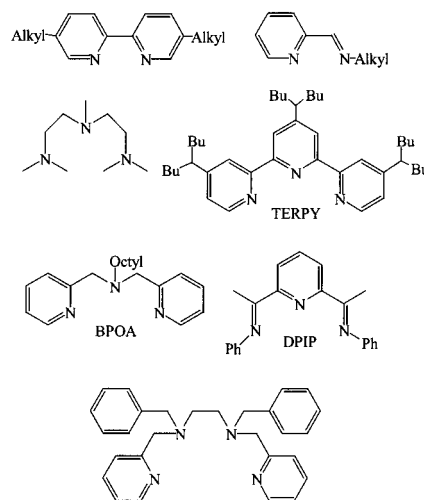
A kinetic study of living radical polymerizations of acrylates initiated by the (tetramesitylporphyrinato)-cobalt(III) organo complexes (TMP)Co–CH(CH₃)CO₂Me and (Br₈TMP)Co–CH(CH₃)CO₂Me has been reported by Wayland et al.¹²² They applied an initial excess of the free cobalt complex and obtained the equilibrium constant for the reversible dissociation of the complex–poly(methyl acrylate) bond as $K = 4.2 \times 10^{-10}$ M for (TMP)Co and $K = 1.3 \times 10^{-8}$ M for (Br₈TMP)Co from the rate of monomer consumption at 50 °C. The temperature dependence led to a bond

dissociation energy of 100 kJ mol⁻¹ for (TMP)Co–poly(methyl acrylate). In comparison with the data given for higher temperatures in Table 1, the equilibrium constants are considerably larger than for the alkoxyamines. The coupling reaction between cobalt complexes and carbon-centered radicals is often diffusion controlled,⁸⁵ and hence, the bond dissociation energy of 100 kJ mol⁻¹ should be close to the cleavage activation energy. For alkoxyamines, the activation energies are larger. Obviously, the cobalt-complex-mediated acrylate polymerization is favored by the weak metal–alkyl bond, and the dissociation constants k_d of the complexes must be on the order of 10⁻²–1 s⁻¹. The frequent “dehydrocobaltation” to a hydridocobalt complex and an olefin⁸⁵ seems to be of minor importance for acrylates, but it may have precluded other cobalt-complex-mediated polymerizations.

4. Atom Transfer Radical Polymerization

In comparison to the nitroxide- and cobalt-mediated processes, atom transfer radical polymerizations are mechanistically more complex. Thus, the catalyst reactivity depends on the ligand, the counterion, the transition metal itself, and the initiating organic halide. Moreover, it is possible that more than one unique catalytic species is involved, and structural investigations are still scarce.¹²³ So far, copper-based systems seem to be the most efficient¹²⁴ when compared to other transition metals such as iron,¹²⁵ nickel,¹²⁶ ruthenium,⁴² rhodium,¹²⁷ or palladium.¹²⁸ The counterions are often chloride and bromide, and bromide normally yields higher rates. As initiators one uses compounds that structurally resemble the chain ends of the dormant chains, that is, for example, α -bromoisobutyrate [(CH₃)₂CBrCO₂Me] for methacrylates, α -bromopropionate (CH₃CHBrCO₂Me) for acrylates, and 1-bromoethylbenzene [C₆H₅CH(CH₃)Br] for styrene, but aromatic sulfonyl chlorides are also quite versatile.^{44,129} A large variety of complexing ligands has been applied,^{130–136} and Scheme 33 lists a few bi-, tri- and tetradentate nitrogen-based systems for the complexation of copper ions. In general, the activity decreases in the order of the ligands alkylamine \approx pyridine > alkyl

Scheme 33



imine \gg aryl imine $>$ arylamine,¹³⁴ and tris(2-(dimethylamino)ethyl)amine seems to be one of the most efficient ligands.¹²⁴

Atom transfer polymerizations are often subject to problems arising from solubility, the initial presence of metal ions in the higher oxidation state, multiple complex equilibria, and a variety of side effects.^{137–139} Quite often, diverse broken reaction orders are observed with respect to catalyst and initiator, and they are difficult to analyze.¹⁴⁰ Nevertheless, with the methods outlined above for nitroxides, some quantitative data for the reversible radical formation steps were obtained.

Table 2 shows results for polymeric and low molecular model systems. If one takes the second-order radical formation into account and assumes 0.1 M concentrations of initiator and catalyst, the atom transfer favors the radical formation (activation) more than the alkoxyamine dissociation. On the other hand, the cross-reaction rate constants k_c and k_{deact} show similar orders of magnitude for both types of reactions. This explains the generally shorter reaction times for the metal-catalyzed systems. In model studies Matyjaszewski et al.¹³⁴ found that the rate constant k_{act} for radical formation from Cu(I) complexes and organobromides increases with decreasing reduction potential of the complex and can be tuned by the choice of the ligand. This is also known in organic synthesis (see above) and it points to an activation-controlled forward reaction. The authors also noticed an anticorrelation between k_{deact} and k_{act} , that is, larger rate constants for the radical formation parallel the smaller rate constants for the reverse reaction. The same holds for the nitroxide-based systems, and it may indicate an entropy-controlled deactivation. If this is generally true, one expects only weak or even negative temperature dependencies of k_{deact} .

IV. Theoretical Methods and Special Cases of Living Radical Polymerizations

A. The Basic Reaction Mechanism

In this section we summarize a method for the quantitative treatment of living radical polymerizations involving the persistent radical effect. It is quite

general and can be applied to many cases. We start with the minimum mechanism given in Scheme 3 and the assumptions stated earlier. The concentrations of the radicals R• and Y• obey

$$d[\text{R}]/dt = k_d[\text{I}] - k_c[\text{R}][\text{Y}] - k_t[\text{R}]^2 \quad (39)$$

$$d[\text{Y}]/dt = k_d[\text{I}] - k_c[\text{R}][\text{Y}] \quad (40)$$

By stoichiometry, they are related by $[\text{I}]_0 - [\text{I}] = [\text{Y}] = [\text{R}] + [\text{P}]$. Hence, $[\text{I}]$ can be expressed by $[\text{Y}]$, and the concentration $[\text{P}]$ of the termination products is practically equal to the concentration of the persistent species $[\text{Y}]$.

According to the rate equations (39 and 40), both radical concentrations increase at first linearly with time as $[\text{R}] = [\text{Y}] = k_d[\text{I}]_0 t$, and they attend a stationary state only at infinite time, where $[\text{Y}]_\infty = [\text{P}]_\infty = [\text{I}]_0$ and $[\text{R}]_\infty = 0$, that is, when the initiator is fully converted to persistent radicals and unreactive products. To find the intermediate behavior and the dynamic equilibrium, we cast the rate equations into simpler forms by using reduced variables and parameters

$$\rho = \frac{[\text{R}]}{[\text{I}]_0} \quad \eta = \frac{[\text{Y}]}{[\text{I}]_0} \quad \tau = k_d t \quad a = \frac{k_c[\text{I}]_0}{k_d} \quad b = \frac{k_t[\text{I}]_0}{k_d} \quad (41)$$

and the definition $\dot{x} = dx/d\tau$. This yields

$$\dot{\rho} = 1 - \eta - a\rho\eta - b\rho^2 \quad (42)$$

$$\dot{\eta} = 1 - \eta - a\rho\eta \quad (43)$$

Obviously, the kinetics are determined by two parameters, a and b , only. It is thus sufficient to solve the differential equations in terms of a and b and then go back to the real concentrations and times via the relations 41.

The parameters a and b depend on $[\text{I}]_0$, and the rate constants and their magnitudes can be estimated. In polymerizations, one often aims at average degrees of polymerization of 100–1000 for an initial monomer concentration of about 10 M (bulk). Hence, one uses $[\text{I}]_0 = 10^{-2}$ – 10^{-1} M. For small radicals R• and low viscosities, the termination constant is

Table 2. Rate and Equilibrium Constants for the Reversible Bromine Atom Transfer Reaction of Polymeric and Low Molecular Model Compounds with Cu-Complexes. For Ligand Structures, See Scheme 33

initiator or dormant chain	catalyst	$T/^\circ\text{C}$	$k_{\text{act}}/\text{M}^{-1} \text{s}^{-1}$	$k_{\text{deact}}/\text{M}^{-1} \text{s}^{-1}$	K	ref
poly(methyl methacrylate)-Br ethylisobutyrate-Br	CuBr/(4,4-di- <i>n</i> -heptyl-2,2-bipyridine) ₂	100			7×10^{-7}	124
	CuBr/TERPY	35	1.5			132
	CuBr/BPOA	35	0.3			132
	CuBr/DPIP	35	0.1			132
polystyryl-Br	CuBr/(4,4-di- <i>n</i> -heptyl-2,2-bipyridine) ₂	110	0.45	1.1×10^7	3.9×10^{-8}	64, 131
		90			2×10^{-8}	64, 131
1-bromoethylbenzene	CuBr/TERPY	35	0.42	4.1×10^5 ^a		132
	CuBr/BPOA	35	0.066	3.3×10^6 ^a		132
	CuBr/DPIP	35	0.014	3.1×10^6 ^a		132
	CuBr/(4,4-di- <i>n</i> -heptyl-2,2-bipyridine) ₂	90			1.2×10^{-9}	131
poly(methyl acrylate)-Br methyl propionate-Br	CuBr/(4,4-di- <i>n</i> -heptyl-2,2-bipyridine) ₂	60	0.065			92
	CuBr/TERPY	35	0.41			132
	CuBr/BPOA	35	0.014			132
	CuBr/DPIP	35	0.011			132

^a 75 °C.

usually $k_t \approx 10^9 \text{ M}^{-1} \text{ s}^{-1}$, and it reduces to 10^7 – $10^8 \text{ M}^{-1} \text{ s}^{-1}$ for long chains. For the special case of alkoxyamines, the cross-coupling rate constants are in the range $k_c = 10^5$ – $10^8 \text{ M}^{-1} \text{ s}^{-1}$, and k_d ranges from 10^{-5} to 1 s^{-1} for reaction temperatures around 120°C (Table 1). This places a between 10^3 and 10^{14} and b between 10^5 and 10^{14} . Hence, a and b are always large compared to 1, and one also expects $a^2/b \gg 1$ for most individual cases.

The system of nonlinear differential equations 42 and 43 has no closed solution. Our analysis starts from an investigation of the possible trajectories of the point $(\rho(\tau), \eta(\tau))$ in the two-dimensional phase plane spanned by the variables ρ and η . These are limited by stoichiometry to values between 0 and 1. Moreover, from eqs 42 and 43 one has

$$\dot{\eta} = \dot{\rho} + b\rho^2 \quad (44)$$

For the given initial conditions this implies that $\eta \geq \rho$ for all times. Hence, all trajectories are in the plane $(0,1) \times (0,1)$, start at the origin $(0,0)$ along the first diagonal and then deviate positively therefrom. Setting $\dot{\eta} = 0$ and $\dot{\rho} = 0$ in eqs 42 and 43 yields the singular point $(0,1)$ at infinite time.

In the intermediate time regime, the evolution of the trajectories follows from the behavior of isoclines, where the time derivatives of the dynamic variables are individually zero, namely isocline $\eta_1(\rho)$, where $\dot{\rho} = 0$, and isocline $\eta_2(\rho)$, where $\dot{\eta} = 0$. From eqs 42 and 43 these are

$$\eta_1(\rho) = \frac{1}{1+a\rho} \quad \text{and} \quad \eta_2(\rho) = \frac{1-b\rho^2}{1+a\rho} \quad (45)$$

The isoclines divide the phase plane into regions of different signs of the time dependencies of ρ and η , as is indicated in Figure 9 in a log–log representation. Consequently, any trajectory can cross the isocline η_1 only horizontally and in the direction of decreasing ρ , and it can cross the isocline η_2 only vertically in the direction of increasing η . Further, η_2 crosses the line $\eta = 0$ at the maximum $\rho = 1/\sqrt{b}$, and both isoclines approach the final point $(0,1)$ with the same slope.

Figure 9 also shows a computed trajectory for the parameters $(a, b) = (10^8, 10^8)$. After the initial

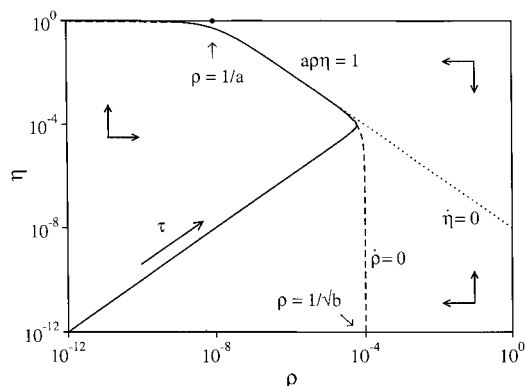


Figure 9. Trajectory of the point (ρ, η) , that is, the reduced concentrations of the radicals R^* and Y^* , and the isoclines $\dot{\rho} = 0$ (dashed) and $\dot{\eta} = 0$ (dotted) in the phase plane and in a log–log representation. Parameters $(a, b) = (10^8, 10^8)$.

increase along the first diagonal, the trajectory bends up and crosses the isocline η_2 vertically. Thereafter, ρ decreases and η continues to increase. The trajectory cannot cross η_2 a second time, since it must do so vertically in the direction of increasing η . It cannot cross the isocline η_1 either, since it must do so horizontally in the direction of decreasing ρ . Therefore, after the first crossing, the trajectory is confined to the region between the two isoclines. This region is very narrow for the chosen parameters. Staying between the isoclines, the trajectory finally approaches the final point. The maximum of ρ is on isocline η_2 . Therefore, ρ is limited to values below $\rho = 1/\sqrt{b}$.

In the log–log representation of the phase diagram, the dynamic equilibrium relation 19 ($k_c[\text{R}][\text{Y}] = k_d[\text{I}]_0$) or $a\rho\eta = 1$ appears as a straight line with slope -1 . It starts at $(\rho, \eta) = (1/a, 1)$, and it is practically identical to η_1 for $\rho > 1/a$. The trajectory must closely follow η_1 , and hence, there is a time range where the equilibrium relation is certainly valid. With increasing $1/a$, the equilibrium line shifts to the right. It will not be reached at all when $1/a$ becomes close to $b^{-1/2}$. Consequently, one condition for the existence of the equilibrium is $a^2/b \gg 1$. Further, because $\rho < 1$, one has $b \geq 1$, and this implies the third condition $a \gg 1$ by combination with the first. With the definitions 41, this yields eqs 20.

In the transition region between the initial and the equilibrium regime, the details of the time evolutions are complicated.¹⁷ However, for the equilibrium regime where $a\rho\eta = 1$, the integration of eq 44 leads to eqs 18.¹⁷ These solutions are obeyed until η approaches 1 and ρ approaches $1/a$, and this happens at the approximate time $t = [\text{I}]_0/3K^2k_t$. For nitroxide-based systems with a large equilibrium constant, $K = 10^{-8} \text{ M}$ (Table 1), a rather small initiator concentration, $[\text{I}]_0 = 10^{-2} \text{ M}$ and $k_t = 10^8 \text{ M}^{-1} \text{ s}^{-1}$, the equilibrium, and that is also the persistent radical effect, lasts for about 90 h, and it is entered at rather short times of at most seconds.¹⁷

Polymerizations are studied typically in time ranges between 100 s and 30 h, that is, in the equilibrium regime. Therefore, for polymerizing systems, one can use eq 20, insert it into the rate equation of the monomer consumption (21), integrate, and obtain eq 22. The further derivation of the control involves the calculation of the moments m_k of the chain length distribution and of their time dependencies.

$$m_k = \sum_{n=1}^{\infty} n^k ([\text{I}_n] + [\text{P}_n] + [\text{R}_n]) \quad k = 0, 1, 2$$

The exclusion of $n = 0$ in the summation ensures that only monomer-containing species are counted, because we start from a monomer-free initiator. If a monomer-containing initiator would be used, the zeroth moment m_0 would be equal to $[\text{I}]_0$, because of the stoichiometry relations. Hence, one has in our case

$$m_0 = [\text{I}]_0 - ([\text{I}_0] + [\text{P}_0] + [\text{R}_0]) \quad (46)$$

where $[\text{I}_0]$, $[\text{P}_0]$, and $[\text{R}_0]$ are the concentrations of the

initiator, the transient radicals, and the products that do not contain monomer units. It seems reasonable to assume and is borne out by numerical calculations that $[I_0]$ decays exponentially because R_0^* immediately adds to the monomer. For the same reason, $[R_0]$ and $[P_0]$ are small compared to $[I_0]$. Thus, one has

$$[I_0] = [I]_0 e^{-k_a t} \quad \text{and} \quad m_0 = [I]_0 (1 - e^{-k_a t}) \quad (47)$$

For the moments m_1 and m_2 , we derived the kinetic equations¹⁶

$$\frac{dm_1}{dt} = -\frac{d[M]}{dt} \quad (48)$$

$$\frac{dm_2}{dt} = -\frac{d[M]}{dt} + 2k_p[M]m_1(R) \quad (49)$$

where $m_1(R) = \sum_{n=1}^{\infty} n[R_n]$. By integration of eq 48 and use of eq 47, one obtains the number-average degree of polymerization $X_N = m_1/m_0$ (24). To calculate m_2 and the polydispersity index $PDI = m_0 m_2 / m_1^2$, one also needs $m_1(R)$. It enters the kinetic equation for the first moment of I.¹⁶

$$\frac{dm_1(I)}{dt} = k_c[Y]m_1(R) - k_d m_1(I) \quad (50)$$

In a controlled process most of the monomer will be incorporated into the dormant chains. This allows one to approximate $m_1(I) = m_1 = [M]_0 - [M]$. Insertion into eq 50, solving for $m_1(R)$, and use of the equilibrium relation (19) cast eq 49 into the form

$$\dot{m}_2 = -\dot{[M]} - 2\dot{[M]}([M]_0 - [M])/[I]_0 + 2k_p^2[M]^2[R]^2/k_d[I]_0 \quad (51)$$

Integration with the aid of eqs 18 and 22 yields m_2 and then the polydispersity index (25).

The phase space analysis visualizes the behavior of the radical concentrations and leads rather directly to the conditions for equilibria, but these can also be derived by other means.^{15,17} It has also been applied to explore the effects of an additional radical generation⁵⁰ and of a direct or indirect decay of the dormant chains.⁵⁷ Examples are discussed below.⁵⁰

B. Initial Excess of Persistent Species in Living Radical Polymerizations

In controlled polymerizations the time needed for radical formation by bond cleavage of the dormant chains or by the activating atom transfer must be much smaller than the total conversion time. Otherwise, one obtains a polymer with a large "living"

fraction but little "control".¹⁷ The latter situation corresponds to parameters close to point B in Figure 5 and has been observed for monomers with large propagation constants k_p . A counterstrategy is to add some persistent species before the reactions, and this has been used both in nitroxide-mediated systems^{59,65,96,141-143} and in ATRP.¹³⁰ Actually, and especially in ATRP, traces of persistent species may always be present as impurities. The initial excess $[Y]_0$ first levels the transient radical concentration to the equilibrium value¹³⁰ $[R]_s = K[I]_0/[Y]_0$, and this is smaller than the radical concentration without the initial excess of the persistent species. Therefore, the conversion rate is lowered, and one obtains a linear time dependence of $\ln([M]_0/[M])$.

In a closer examination,⁵⁰ we cover only radical formation (activation) by bond cleavage and cases for which the conditions (20) for the dynamical equilibrium are fulfilled. The initial presence of the persistent species leads to the stoichiometry relations $[I]_0 - [I] = [Y] - [Y]_0 = [R] + [P]$. A comparison with the earlier relations $[I]_0 - [I] = [Y] = [R] + [P]$ suggests a new time-dependent variable, namely, the persistent radical concentration that arises only from the initiator, $[Y] - [Y]_0$. Consequently, the appropriate new reduced variable $\tilde{\eta}$ is now defined by $\tilde{\eta} = ([Y] - [Y]_0)/[I]_0$, and one has $\eta = \tilde{\eta} + \eta_0$.

The kinetic equations become

$$\dot{\rho} = 1 - \tilde{\eta} - a\rho(\tilde{\eta} + \eta_0) - b\rho^2 \quad (53)$$

$$\dot{\tilde{\eta}} = 1 - \tilde{\eta} - a\rho(\tilde{\eta} + \eta_0) \quad (54)$$

and can again be analyzed with the aid of the phase diagram. The isoclines $\tilde{\eta}_1(\rho)$, where $\dot{\tilde{\eta}} = 0$, and $\tilde{\eta}_2(\rho)$, where $\dot{\rho} = 0$, are

$$\tilde{\eta}_1(\rho) = \frac{1 - a\rho\eta_0}{1 + a\rho} \quad \text{and} \quad \tilde{\eta}_2(\rho) = \frac{1 + a\rho\eta_0 - b\rho^2}{1 + a\rho} \quad (55)$$

Figure 10 shows these isoclines in a log-log representation for different excess concentrations η_0 and for parameters fulfilling the usual equilibrium

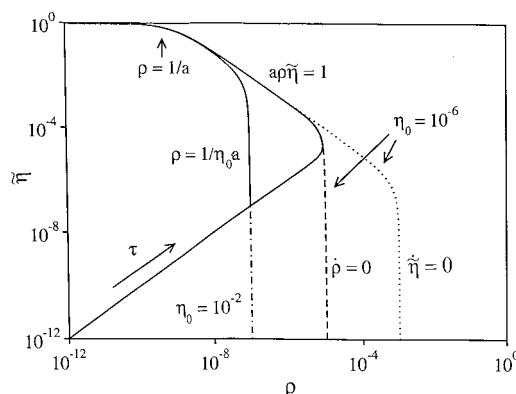


Figure 10. Trajectories of the point $(\rho, \tilde{\eta})$, that is, the reduced concentrations of the radicals R^* and Y^* , and the isoclines $\dot{\rho} = 0$ (dashed) and $\dot{\tilde{\eta}} = 0$ (dotted) in the phase plane and in a log-log representation for different initial concentrations η_0 of the persistent species. Parameters $(a, b) = (10^9, 10^{10})$.

condition $a^2/b \gg 1$. The isoclines intersect the ρ -axis at

$$\rho_1 = 1/a\eta_0 \quad \text{and} \\ \rho_2 = (a\eta_0/2b)(\sqrt{1 + 4b/(a\eta_0)^2} - 1) \quad (56)$$

and these intersections nearly coincide if $\eta_0 \gg \sqrt{b/a}$. For the present parameters this holds for $\eta_0 \gg 10^{-4}$, and is fulfilled for $\eta_0 = 10^{-2}$, as seen in Figure 10. The isoclines are also again superimposed in a region where they satisfy the equilibrium relation $a\tilde{\eta}\rho = 1$.

Figure 10 also displays trajectories. As before, they start along the first diagonal, cross isocline $\tilde{\eta}_2$, and remain confined to the region between $\tilde{\eta}_2$ and $\tilde{\eta}_1$, thereafter. For the small $\eta_0 = 10^{-6}$, the first stage of the time evolution is directly followed by the equilibrium regime $a\tilde{\eta}\rho = 1$, that is, the trajectory is not at all influenced by the initial presence of the persistent species. For $\eta_0 = 10^{-2}$, there is an intermediate region where ρ is constant. Here, one has $a\eta_0\rho = 1$, and $a\tilde{\eta}\rho = 1$ is reached only later. In this case, and more generally for $\eta_0 \gg \sqrt{b/a}$, the two regimes can be combined to $a(\tilde{\eta} + \eta_0)\rho = 1$, that is, the usual equilibrium relation 19.

It is important to notice that for a sufficiently large excess of the persistent species $\eta_0 \gg \sqrt{b/a}$, the intermediate region where ρ is constant and one has $a\eta_0\rho = 1$ does exist even if the dynamic equilibrium 19 does not hold in the absence of the excess $[Y]_0$. Hence, in such unfavorable cases, one can drive the system to equilibrium by a deliberate addition of the persistent radical and, consequently, to control.

Figure 11 shows the radical concentrations $[R]$ and $[Y] - [Y]_0$ versus time in a log-log representation for the same parameters a and b as used for Figure 10 and, specifically, for $k_d = 10^{-3} \text{ s}^{-1}$, $k_c = 10^7 \text{ M}^{-1} \text{ s}^{-1}$, $k_t = 10^8 \text{ M}^{-1} \text{ s}^{-1}$, and $[I]_0 = 0.1 \text{ M}$. A too small initial excess $[Y]_0 = 10^{-7} \text{ M}$ has no effect on the time evolution (compare Figure 1 for $k_{tY} = 0$). For the larger $[Y]_0 = 10^{-3} \text{ M}$, the short time increase of $[Y] - [Y]_0$ and $[R]$ (Figure 10) is followed by a regime where $[R]$ is constant at $[R] = K[I]_0/[Y]_0$. This corresponds to the vertical part of the trajectory in Figure

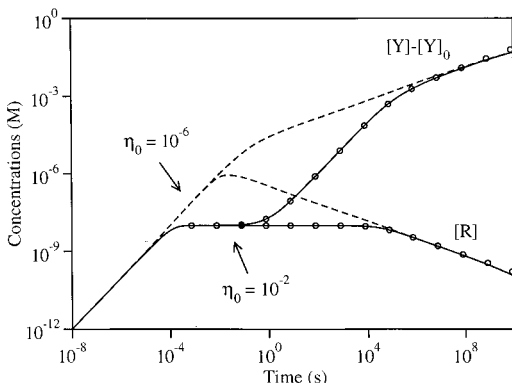


Figure 11. Time dependence of the reduced radical concentrations in a log-log representation for different reduced excess concentrations η_0 of the persistent species. Parameters a and b as used for Figure 10, and specifically $k_d = 10^{-3} \text{ s}^{-1}$, $k_c = 10^7 \text{ M}^{-1} \text{ s}^{-1}$, $k_t = 10^8 \text{ M}^{-1} \text{ s}^{-1}$, and $[I]_0 = 0.1 \text{ M}$. Circles are added according to the analytical equations.

10. It is entered at the time $t_0 = 1/k_c[Y]_0$, where $[R]$ obeys $[R] = k_d[I]_0 t_0 = K[I]_0/[Y]_0$, and this is in the millisecond region. After the long time $t_1 = [Y]_0/3/3K^2 - [I]_0^2 k_t$, eqs 19 hold, then $[R]$ decreases proportionally to $t^{-1/3}$. While $[R]$ is constant, $[Y] - [Y]_0$ takes the same value as $[R]$ at first, then it increases linearly with time. Finally, for $t \gg t_1$, $[Y] - [Y]_0$ increases proportionally to $t^{1/3}$.

Analytical solutions that cover both the intermediate and the final time regimes are also available. Equation 44 is independent of the initial conditions and can be integrated using the combined equilibrium relation $a(\tilde{\eta} + \eta_0)\rho = 1$. As for $\eta_0 = 0$,¹⁶ this yields an implicit equation for the time dependence of η , which leads to the approximate solution

$$[Y] = (3k_t K^2 [I]_0^2 (t - t_0) + [Y]_0^3)^{1/3} + K[I]_0/[Y]_0 \quad (57)$$

Apart from the small last term, it has been given earlier by Fukuda et al.⁴⁹

With $[R]$ given by $[R]_s = K[I]_0/[Y]_0$ before the time t_1 and by eq 18 thereafter, the rate equation for the monomer consumption (21) integrates to

$$\ln \frac{[M]_0}{[M]} = k_p K \frac{[I]_0}{[Y]_0} t \quad \text{for } t < t_1 \quad (58a)$$

and to

$$\ln \frac{[M]_0}{[M]} = k_p K \frac{[I]_0}{[Y]_0} t_1 + \frac{3}{2} k_p \left(\frac{K[I]_0}{3k_t} \right)^{1/3} (t^{2/3} - t_1^{2/3}) \quad \text{for } t > t_1 \quad (58b)$$

These relations reveal that the additional persistent species has no influence on the conversion rate if $[Y]_0 < (3K[I]_0 k_t/k_p)^{1/2}$, whereas 90% conversion occurs before t_1 if $[Y]_0 > (3 \ln(10) K[I]_0 k_t/k_p)^{1/2}$. For a monomer with a large propagation constant of $k_p = 20\,000 \text{ M}^{-1} \text{ s}^{-1}$, and $k_d = 10^{-3} \text{ s}^{-1}$, $k_c = 10^7 \text{ M}^{-1} \text{ s}^{-1}$, $k_t = 10^8 \text{ M}^{-1} \text{ s}^{-1}$, and $[I]_0 = 0.1 \text{ M}$, the first condition holds for $[Y]_0/[I]_0 < 0.004$, that is, 0.4% initial persistent species, and the second for $[Y]_0/[I]_0 > 0.006$, or 0.6%. Since one often applies persistent radical concentrations that are a few percent of the initiator concentration,^{59,65,96,130,141-143} the second situation is met in practice. Then, eq 58a holds, that is, the polymerization index increases linearly with time and depends on the equilibrium constant. Of course, the conversion is retarded. From the previous equations one obtains the ratio between the times for 90% monomer conversion and the ratio of the unreactive products with and without the initial excess of the persistent species as

$$\frac{t_{90}([Y]_0)}{t_{90}([Y]_0 = 0)} = \frac{3}{2} [Y]_0 (k_p/2 \ln(10) K[I]_0 k_t)^{1/2} = \frac{3}{4} \frac{[P]_{90}([Y]_0 = 0)}{[P]_{90}([Y]_0)} \quad (59)$$

For the parameters used above, this yields an about 50-fold reduction of the unreactive products for 1% excess of the persistent species at the expense of an

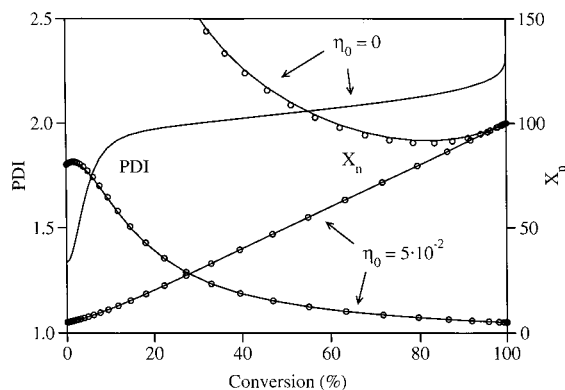


Figure 12. Average degrees of polymerization X_N and polydispersity indices as functions of conversion for a fast propagating monomer in the absence and in the presence of an initial reduced excess concentration η_0 of the persistent species. Parameters as used for Figure 11, and $k_p = 20000 \text{ M}^{-1} \text{ s}^{-1}$, $[M]_0 = 10 \text{ M}$. Circles are added according to the analytical equations.

increase of the conversion time by a factor of 30. In ATRP systems, the effects are less drastic.⁶⁶

In the derivation of the moments one has now to consider the reformation of the initiator I_0 by coupling of R_0 with the excess Y^* , which competes with the addition of R_0^* to the monomer. This leads to a reduction of the effective decay rate constant of I_0 by the probability factor $\beta = k_p[M]_0 / (k_p[M]_0 + k_c[Y]_0)$, so that the zeroth moment is now given by $m_0 = [I]_0(1 - e^{-\beta k_d t})$. The other equations for the moments are not changed by the presence of $[Y]_0$. Therefore, X_N is given by eq 24 with k_d replaced by βk_d .

In most cases, the excess $[Y]_0$ leads to a constant radical concentration $[R]_s = K[I]_0/[Y]_0$ during the polymerization. Insertion into eq 51, integration, and use of the definition provide the polydispersity index

$$\text{PDI} = (1 - e^{-\beta k_d t}) \left(1 + \frac{k_p [I]_0}{k_c [Y]_0} \frac{2 - C}{C} \right) + \frac{1}{X_N} \quad (60)$$

For small conversions but sufficiently long times, this reduces to eq 38.

Figure 12 shows the beneficial effects of 5% excess persistent species on the control of the chain length distribution for a rather fast living polymerization that shows little control without the excess, because the parameters are close to point B in Figure 5. Of course, the much better control is obtained at the expense of a strong retardation of the monomer conversion that amounts to a factor of 150. For fast polymerizations and parameters close to point C in Figure 5, one expects control but little livingness for large conversions, and in this case the improvement requires quite large initial nitroxide concentrations.⁵⁰

C. Decay or Removal of Persistent Species in Living Radical Polymerizations

A strategy to shorten conversion times in slow living radical polymerizations is the reduction of the retarding growth of the persistent radical concentration by their removal through additives or a built-in instability.^{31,118} It is likely that both procedures involve the conversion of the persistent species to a

transient radical that starts a new chain. Hence, the rate increase will cause some loss of control. Here, we explore the effect of the conversion by a first-order process⁵⁰



with rate constant k_Y .

Initially, only the initiator I shall be present. This leads to the stoichiometry relations $[I]_0 - [I] = [Y] + [X] = [R] + [P] - [X]$. Obviously, one needs to consider now three time-dependent variables, and the rate equations are

$$\begin{aligned} d[R]/dt &= k_d([I]_0 - [Y] - [X]) - k_c[R][Y] + k_Y[Y] - k_t[R]^2 \\ d[Y]/dt &= k_d([I]_0 - [Y] - [X]) - k_Y[Y] - k_c[R][Y] \end{aligned}$$

$$d[X]/dt = k_Y[Y]$$

Using the reduced variables (41) and, in addition, $\xi = [X]/[I]_0$ and $d = k_Y/k_d$ yields

$$\rho = 1 - \eta - \xi - a\rho\eta + d\eta - b\rho^2 \quad (62a)$$

$$\eta = 1 - \eta - \xi - a\rho\eta - d\eta \quad (62b)$$

$$\dot{\xi} = d\eta \quad (62c)$$

In the three-dimensional phase space (ρ, η, ξ) the isoclines $\eta_1(\rho)$ and $\eta_2(\rho)$ are now surfaces that intersect at

$$2d\eta = b\rho^2 \quad (63)$$

Figure 13 displays these isoclines for $\xi = 0$ and for the parameters $k_d = k_Y = 3 \times 10^{-3} \text{ s}^{-1}$, $k_c = 5 \cdot 10^7 \text{ M}^{-1} \text{ s}^{-1}$, $k_t = 10^8 \text{ M}^{-1} \text{ s}^{-1}$, and $[I]_0 = 0.1 \text{ M}$, which obey the conditions 20. It also shows the projection of a trajectory onto the plane $(\rho, \eta, 0)$. As before, after crossing η_2 , the trajectory is confined to the space between the isoclines. At first, it behaves like the trajectory in Figure 9. ξ is very small in this regime and can be obtained by integrating eq 62c with η

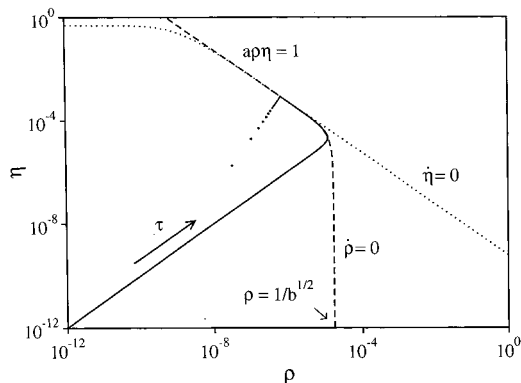


Figure 13. The isoclines $\rho = 0$ (dashed) and $\eta = 0$ (dotted) in the phase plane $(\rho, \eta, 0)$ and a log-log representation, and the trajectory of the point (ρ, η, ξ) , that is, the reduced concentrations of the radicals R^* and Y^* and the fragment X , projected onto the plane $(\rho, \eta, 0)$. Parameters: $k_d = k_Y = 3 \times 10^{-3} \text{ s}^{-1}$, $k_c = 5 \times 10^7 \text{ M}^{-1} \text{ s}^{-1}$, $k_t = 10^8 \text{ M}^{-1} \text{ s}^{-1}$, and $[I]_0 = 0.1 \text{ M}$.

given by eq 18. Then, the trajectory reaches the intersection (63), and the equilibrium equation changes to

$$a\rho\eta = 1 - \xi \quad (64)$$

In this regime, eqs 63 and 64 can be combined to express η by ξ only, and integration of eq 62c yields, with the proper resubstitutions,

$$[X] = [I]_0(1 + (t/t_1 - 1)^3)$$

$t_1 = 3(2[I]_0/K^2k_tk_Y^2)^{1/3}$ is the time where $[X]$ becomes equal to $[I]_0$ and the reactions stop. Knowing $[X]$, one finds the radical concentrations

$$[R] = \left(\frac{2k_YK[I]_0}{k_t} \right)^{1/3} (1 - t/t_1) \quad \text{and} \\ [Y] = \left(\frac{K^2[I]_0^2k_t}{k_Y} \right)^{1/3} (1 - t/t_1)^2 \quad (65)$$

Figure 14 shows the concentrations of all species in a log–log-representation as functions of time for the parameters given above. As qualitatively expected, the decay of Y^* leads to an intermediate stationary state of the radical concentrations. This state is entered at the time $t_0 = 1/6k_Y$, and for $k_Y = 3 \times 10^{-3} \text{ s}^{-1}$, this is at $t_0 = 56 \text{ s}$. It breaks down at the much larger time $t_1 \approx 1.2 \times 10^7 \text{ s} = 3300 \text{ h}$. This may seem surprising, because the natural lifetime of Y^* is only $1/k_Y = 330 \text{ s}$. The explanation is that the unstable persistent species is present in this form only for a small fraction of time and stays essentially incorporated in the dormant chains where it does not decay. This time fraction is approximately equal to $[Y]/[I]_0 = 0.1\%$ for the region where $[Y]$ is constant (Figure 14).

Figure 15 displays the average degrees of polymerization and polydispersities expected without and with the decay of the persistent radical and for the parameters given above. The control remains satisfactory, even for the large decay constant k_Y . On the other hand, the time for 90% conversion is reduced by a factor of about 6. The fraction of unreactive products increases by a factor of 5 but remains small (4%). This confirms the strategy to shorten conver-

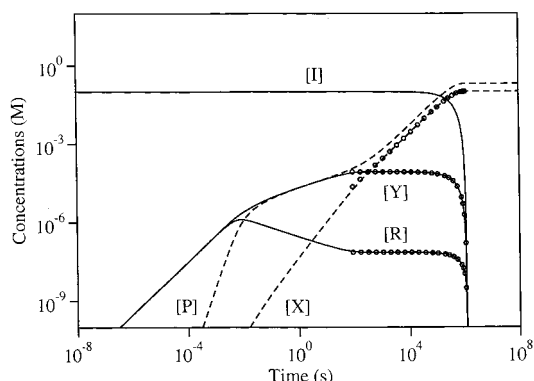


Figure 14. Radical and product concentrations versus time in a log–log representation in the absence and in the presence of a decay of the persistent species. Parameters as used for Figure 13.

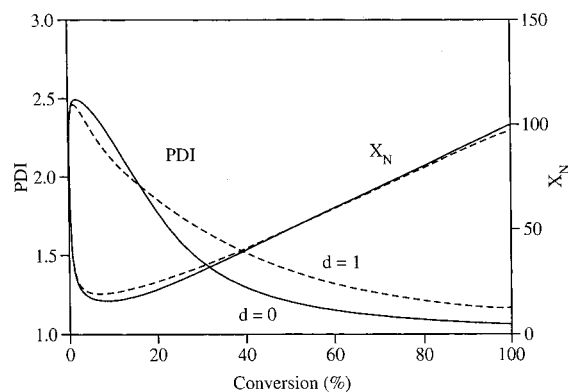


Figure 15. Average degrees of polymerization X_N and polydispersity indices as functions of conversion in the absence and in the presence of a decay of the persistent species. Parameters as used for Figure 11, and $k_p = 5000 \text{ M}^{-1} \text{ s}^{-1}$, $[M]_0 = 10 \text{ M}$.

sion times in slow living radical polymerizations by the removal of these species through additives or a built-in instability.^{31,118}

D. Instantaneous Radical Formation

In all examples discussed so far, the transient and the persistent species were continuously generated. Now, we consider the behavior when both radicals are initially present and then react without further generation by the cross-reaction of R^* with Y^* and by the self-terminations. This initial situation may be created by a pulse photolysis of suitable precursor molecules. The first theoretical treatment was given by O'Shaughnessy et al.,¹⁴⁴ and the resulting equations were later used to determine cross-reaction constants in the photocatalysis reaction of polyoxotungstates (Scheme 29).⁹⁴

In the simplest case, the self-termination of the persistent species is absent, and the rate equations are

$$d[R]/dt = -k_c[R][Y] - k_t[R]^2 \quad (66)$$

$$d[Y]/dt = -k_c[R][Y] \quad (67)$$

with the initial concentrations $[R]_0$ and $[Y]_0$. According to eq 66, the transient species always reach $[R]_\infty = 0$ at infinite time. Insertion into eq 67 does not provide a value for $[Y]_\infty$. However, one can guess that the self-termination of R^* may lead to leftover Y^* and that this will depend on the initial concentrations and the rate constants.

To solve the problem, one combines eqs 66 and 67 to

$$\frac{d[R]}{d[Y]} = 1 + \frac{k_t}{k_c} \frac{[R]}{[Y]} \quad (68)$$

and introduces the auxiliary variable $[Z] = [R]/[Y]$. Differentiation of $[Z]$ with respect to $[Y]$ leads to an equation that is easily integrated. Use of the abbreviations $\rho = [R]/[R]_0$, $\eta = [Y]/[Y]_0$, $\alpha = k_t/k_c$, and $r = [R]_0/[Y]_0$ yields

$$\rho = (r(\alpha - 1))^{-1} \{ (1 + r(\alpha - 1))\eta^{\alpha-1} - 1 \} \cdot \eta \quad (69)$$

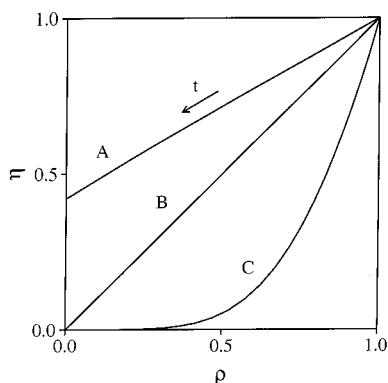


Figure 16. Trajectories of the reduced radical concentrations $\rho = [R]/[R]_0$ and $\eta = [Y]/[Y]_0$ in the phase plane for pulsed radical formation and the parameters $k_c = 5 \times 10^8 \text{ M}^{-1} \text{ s}^{-1}$, $k_t = 0.5k_c$ ($\alpha = 0.5$) and (A) $r^{-1} = 2(1 - \alpha)$, (B) $r^{-1} = \alpha - 1$, and (C) $r^{-1} = (1 - \alpha)/10$.

For infinite time, where $\rho = 0$, eq 69 provides two solutions for η_∞ . The first is

$$\eta_\infty = \frac{1}{(1 + r(\alpha - 1))^{1/(\alpha-1)}} \quad (70a)$$

and it is valid for $\alpha \geq 1$, that is, $k_t \geq k_c$ for all values of $r = [R]_0/[Y]_0$. For $k_t \leq k_c$, it holds if $r^{-1} = [Y]_0/[R]_0 \geq 1 - k_t/k_c$. The second solution is

$$\eta_\infty = 0 \quad (70b)$$

and this is obeyed for $k_t \leq k_c$ if $r^{-1} = [Y]_0/[R]_0 < 1 - k_t/k_c$. Hence, for rate constants leading to the solution (65a), one obtains the surprising result of leftover Y^* , even if very little of this species is produced.¹⁴⁴ In the special case $k_t = k_c$, the final fraction of Y^* is $\eta_\infty = e^{-[R]_0/[Y]_0}$. Moreover, one can show that the curvature of $\eta(\rho)$, that is, of the trajectory in phase space, is negative when eq 70a is reached and positive when there is no leftover. Figure 16 provides an example for the time dependencies of the reduced concentrations.

Equation 70a has been used to extract the ratio of rate constants from the final fraction of Y^* in the reactions of Scheme 29.⁹⁴ The cross-reaction rate constant was found to be considerably smaller than diffusion-controlled values, and it is similar to the rate constants for the coupling of transient radicals with nitroxides (Table 1) or the deactivation step in ATRP (Table 2).

O'Shaughnessy et al.¹⁴⁴ have also considered a slow self-termination of the persistent radicals. The results are similar to those given above, except for a slow decay of Y^* , which sets in when the concentration given by eq 70a is approximately reached. The authors termed the phenomenon of leftover Y^* a kinetic isolation of persistent radicals and suggested applications in diverse polymer–polymer reactions.

V. Concluding Remarks

Whenever in a chemical system transient and persistent radicals are formed with equal or similar rates, be it from the same or different precursors, their cross-reaction products are produced with a surprisingly high selectivity, and the otherwise promi-

nent self-termination products of the transient radicals are virtually absent. This is not because the self-termination reaction does not take place at all. Quite on the contrary, this reaction combined with the reluctance of persistent species to undergo any self-termination causes a buildup of a considerable excess of the persistent over the transient species, and this excess then steers the reaction system toward the cross-reaction channel. Hence, the system orders itself in time, and the self-termination reaction of the transient radicals is important but it causes its own suppression.¹²

This is the basic principle of the persistent radical effect. As shown in this review, there are many variants, because there are additional reversible and irreversible reactions of the transient radicals, but these do not alter the essentials. Although it is quite natural, the principle seems somehow paradoxical, and it is not easily accepted on first sight. It took a long time from its first formulation in 1936⁵ and several reinventions^{6,12} until it is now clearly recognized that it operates in rather diverse branches of chemistry. This review is a first attempt to cover all major aspects and to illustrate them with examples from different fields.

Quite obviously, the often surprisingly high selectivity of the cross-reaction product formation must appeal to synthetic chemists. Whereas most of the examples known today were found accidentally without prior knowledge of the underlying principle, useful and directed new syntheses based on a better understanding are now emerging.^{4,81} Since there are many types of persistent radicals and other intermediates that can take their role, one may envisage a multitude of new developments.

In polymer chemistry, the persistent radical effect can provide living and controlled radical polymerizations as a way to create new materials with very promising properties. First products seem to appear at the horizon. Here again, several rediscoveries were needed until the basics became clear.^{19,29,35} At present, the fundamental and applied research is so active that it becomes difficult to follow, but fortunately, this field is also covered in two other reviews of this issue.

The nonlinear and coupled kinetic equations associated with the phenomenon lead to very surprising and not easily foreseeable rate laws. Their derivation requires mathematical tools that go beyond the usual methods of reaction kinetics, and we expect that the further exploration of reaction variants will reveal additional fascinating kinetic aspects.

Finally, in the past decades of radical chemistry the once active research on the possible types, properties, and structures of persistent radicals and related species was considered boring and unrewarding. Undoubtedly, the new possibilities offered by the persistent radical effect will lead to the rejuvenation of such research.

VI. Acknowledgment

I thank my co-workers G. Ananchenko, T. Kothe, S. Marque, R. Martschke, D. Rueegge, J. Sobek, and M. Souaille for their most important contributions;

A. Studer (Marburg), T. Fukuda (Kyoto), and K. Matyjaszewski (Pittsburgh) for useful correspondence and discussions; and the Swiss National Foundation for Scientific Research for financial support.

VII. References

- Griller, D.; Ingold, K. U. *Acc. Chem. Res.* **1976**, *9*, 13. In the context of this review, radicals are called persistent if their lifetimes in liquid solution exceed those of reactive radical species by many orders of magnitude. They may self-terminate slowly or disappear by other reactions, but these processes do not compete with the cross-coupling with usual transient radicals. Stable radicals can be isolated in pure form. They are included in our definition of persistence.
- Young, R. J.; Lovell, P. A. *Introduction to Polymers*, 2nd ed.; Chapman & Hall: London, 1991. Elias, H.-G. *Macromolecules*, 2nd ed.; Plenum: New York, 1984.
- Szwarc, M. *Nature (London)* **1956**, *198*, 1168. *J. Polym. Sci.* **1998**, *A 36*, ix.
- The operation of the Persistent Radical Effect in organic chemistry has lucidly been described: Studer, A. *Chem. Eur. J.* **2000**, *7*, 1159.
- Bachmann, W. E.; Wiselogle, F. Y. *J. Org. Chem.* **1936**, *1*, 354.
- Perkins, M. J. *J. Chem. Soc.* **1964**, 5932.
- Hey, D. H.; Perkins, M. J.; Williams, *Tetrahedron Lett.* **1963**, 445.
- Russell, G. A.; Bridger, R. F. *Tetrahedron Lett.* **1963**, 737. Bridger, R. F.; Russell, G. A. *J. Am. Chem. Soc.* **1963**, *85*, 3754. Huisgen, R.; Nakaten, H. *Annalen* **1954**, *586*, 70. See also: Grashy, R.; Huisgen, R. *Chem. Ber.* **1959**, *92*, 2641.
- Perkins, M. J. In *Free Radicals*; Kochi, J. K., Ed.; Wiley: New York, 1973; Vol II, p 231 ff. Perkins, M. J. *Radical Chemistry*; Ellis Horwood, London, 1985.
- Geiger, G.; Huber, J. R. *Helv. Chim. Acta* **1981**, *64*, 0989, and private communication.
- Kraeutler, B. *Helv. Chim. Acta* **1984**, *67*, 1053.
- Fischer, H. *J. Am. Chem. Soc.* **1986**, *108*, 3925.
- To avoid the crowding of subsequent formulae by factors of 2, we define the self-termination rates here by, for example, $d[R]/dt = -k_{tr}[R]^2$, deviating from the IUPAC convention.
- An explanation of excess cross-coupling products by different rate constants for the homocoupling reactions has also been given: P. J. Wagner, Wagner, P. J.; Thomas, M. J.; Puchalski, A. E. *J. Am. Chem. Soc.* **1986**, *108*, 7739.
- Fischer, H. *Macromolecules* **1997**, *30*, 5666.
- Fischer, H. *J. Polymer Sci., Part A: Polym. Chem.* **1999**, *37*, 1885.
- Souaille, M.; Fischer, H. *Macromolecules* **2000**, *33*, 7378.
- Depending on the ratio k_t/k_{tr} , other solutions hold in the transition period between the initial linear increase and the behavior given by eqs 8.¹⁷
- An easy derivation of the third root dependence of the radical concentrations with preassumption of the equilibrium was first presented by Fukuda et al.: Ohno, K.; Tsujii, Y.; Miyamoto, T.; Fukuda, T.; Goto, A.; Kobayashi, K.; Akaike, T. *Macromolecules* **1998**, *31*, 1064. These authors also gave an early and clear description of the basic reaction principles: Fukuda, T.; Terauchi, T.; Goto, A.; Ohno, K.; Tsujii, Y.; Miyamoto, T.; Kobatake, S.; Yamada, B. *Macromolecules* **1996**, *29*, 6393.
- Ruegge, D.; Fischer, H. *Int. J. Chem. Kinet.* **1989**, *21*, 703.
- Daikh, B. E.; Finke, R. G. *J. Am. Chem. Soc.* **1992**, *114*, 2938.
- Kothe, T.; Marque, S.; Martschke, R.; Popov, M.; Fischer, H. *J. Chem. Soc. Perkin Trans. 2*, **1998**, 1553.
- Kothe, T. Ph.D. Thesis, Zuerich, **2001**.
- Otsu, T.; Yoshida, M. *Makromol. Chem. Rapid Commun.* **1982**, *3*, 127. Otsu, T.; Yoshida, M. *Makromol. Chem. Rapid Commun.* **1982**, *3*, 133. Otsu, T.; Matsunaga, T.; Kuriyama, A.; Yoshioka, M. *Eur. Polym. J.* **1989**, *25*, 643, and references therein. In a lucid highlight, Prof. Otsu has recently reviewed his work and the iniferter technique. An iniferter is a compound the fragments of which initiate and preferably cross-terminate by primary radical termination and which is subject to chain transfer from the propagating species, although for many of Otsu's examples chain transfer is unlikely. Otsu, T. *J. Polym. Sci., Part A: Polym. Chem.* **2000**, *38*, 2121.
- Bledzki, A.; Braun, D. *Makromol. Chem.* **1981**, *182*, 1047. Braun, D. Skrzek, T.; Steinhauer-Beisser, S. Tretner, H.; Lindner, H. *J. Macromol. Chem. Phys.* **1995**, *196*, 573, and references therein.
- Otsu, T.; Tazaki, T.; Yoshioka, M. *Chem. Express* **1990**, *5*, 801.
- Solomon, D. H.; Rizzardo, E.; Cacioli, P. U.S. Patent 4581429, March 27, 1985.
- Rizzardo, E. *Chem. Aust.* **1987**, *54*, 32.
- Johnson, C. H.; Moad, G.; Solomon, D. H.; Spurling, T. H.; Vearring, D. *J. Aust. J. Chem.* **1990**, *43*, 1215.
- Georges, M. K.; Veregin, R. P. N.; Kazmaier, P. M.; Hamer, G. K. *Macromolecules* **1993**, *26*, 2987.
- Georges, M. K.; Veregin, R. P. N.; Kazmaier, P. M.; Hamer, G. K.; Saban, M. D. *Macromolecules* **1994**, *27*, 7228. Saban, M. D.; Georges, M. K.; Veregin, R. P. N.; Hamer, G. K.; Kazmaier, P. M. *Macromolecules* **1995**, *28*, 7032. Veregin, R. P. N.; Odell, P. G.; Michalak, L. M.; Georges, M. K. *Macromolecules* **1996**, *29*, 2746. Georges, M. K.; Hamer, G. K.; Listigovers, N. A. *Macromolecules* **1998**, *31*, 9087. MacLeod, P. J.; Veregin, R. P. N.; Odell, P. G.; Georges, M. K. *Macromolecules* **1998**, *31*, 530. Moffat, K. A.; Hamer, G. K.; Georges, M. K. *Macromolecules* **1999**, *32*, 1004, and references therein.
- Hawker, C. J.; Barclay, G. G.; Dao, J. *J. Am. Chem. Soc.* **1996**, *118*, 11467.
- (a) Li, I.; Howell, B. A.; Matyjaszewski, K.; Shigemoto, T.; Smith, P. B.; Priddy, D. B. *Macromolecules* **1995**, *28*, 6692. (b) Hawker, C. J.; Barclay, G. G.; Orellana, A.; Dao, J.; Devonport, W. *Macromolecules* **1996**, *29*, 5245.
- Catala, J. M.; Bubel, F.; Oulad Hammouch, S. *Macromolecules* **1995**, *28*, 8841. Oulad Hammouch, S.; Catala, J. M. *Macromol. Rapid Commun.* **1996**, *17*, 8841.
- (a) Greszta, D.; Matyjaszewski, K. *Macromolecules* **1996**, *29*, 5239. (b) Greszta, D.; Matyjaszewski, K. *Macromolecules* **1996**, *29*, 7661.
- (a) Greszta, D.; Matyjaszewski, K. *J. Polym. Sci., Part A: Polym. Chem.* **1997**, *35*, 1857. (b) Goto, A.; Fukuda, T. *Macromolecules* **1997**, *30*, 4272.
- Wayland, B. B.; Pozmik, G.; Mukerjee, S. L. *J. Am. Chem. Soc.* **1994**, *116*, 7943.
- Suess, H.; Pilch, K.; Rudorfer, H. *Z. Phys. Chem.* **1937**, *A179*, 361. Mayo, F. R. *J. Am. Chem. Soc.* **1943**, *65*, 2324. Kharasch, M. S.; Jensen, E. V.; Urry, W. H. *Science* **1945**, *102*, 128.
- Minisci, F.; Pallini, U. *Gazz. Chim. Ital.* **1961**, *91*, 1030. Minisci, F. *Acc. Chem. Res.* **1975**, *8*, 165.
- Asscher, M.; Vofsi, D. *J. Chem. Soc.* **1961**, 22611. Asscher, M.; Vofsi, D. *J. Chem. Soc.* **1963**, 1887, 3921.
- (a) Julia, M.; Le Thuillier, G.; Saussine, L. *J. Organomet. Chem.* **1979**, *177*, 128. (b) Matsumoto, H.; Nakano, T.; Nagai, Y. *Tetrahedron Lett.* **1973**, *51*, 5147.
- Kato, M.; Kamigato, M.; Sawamoto, M.; Higashimura, T. *Macromolecules* **1995**, *28*, 1721.
- Wang, J.-S.; Matyjaszewski, K. *J. Am. Chem. Soc.* **1995**, *117*, 5614.
- Percec, V.; Barboiu, B. *Macromolecules* **1995**, *28*, 7970.
- Darling, T. R.; Davis, T. P.; Fryd, M.; Gridnev, A. A.; Haddleton, D. M.; Ittel, S. D.; Matheson, R. R. Jr.; Moad, G.; Rizzardo, E. *J. Polym. Sci., Part A: Polym. Chem.* **2000**, *38*, 1709, and the following comments.
- Shipp, D. A.; Matyjaszewski, K. *Macromolecules* **1999**, *32*, 2948.
- He, J.; Zhang, H.; Chen, J.; Yang, Y. *Macromolecules* **1997**, *30*, 8010. He, J.; Li, L.; Yang, Y. *Macromolecules* **2000**, *33*, 2286. He, J.; Chen, J.; Li, L.; Pan, J.; Li, C.; Cao, J.; Tao, Y.; Hua, F.; Yang, Y.; McKee, G. E.; Brinkmann, S. *Polymer* **2000**, *41*, 4573, and references therein.
- Fukuda, T.; Goto, A.; Ohno, K. *Macromol. Rapid Commun.* **2000**, *21*, 151.
- Fukuda, T.; Goto, A. *ACS Symp. Ser.* **2000**, *768*, 27. Goto, A.; Fukuda, T. *Macromol. Chem. Phys.* **2000**, *201*, 2138, and references therein.
- Souaille, M.; Fischer, H. *Macromolecules* **2001**, in press.
- Moad, G.; Anderson, A. G.; Ercole, F.; Johnson, C. H. J.; Krstina, J.; Moad, C. L.; Rizzardo, E.; Spurling, T. H.; Thang, S. H. *ACS Symp. Ser.* **1998**, *685*, 332.
- Skene, W. G.; Scaiano, J. C.; Listigovers, N. A.; Kazmaier, P. M.; Georges, M. K. *Macromolecules* **2000**, *33*, 5065.
- Tsujii, T.; Fukuda, T.; Miyamoto, T. *Polymer Preprints* **1997**, *38*, 657. Ohno, K.; Tsujii, Y.; Fukuda, T. *Macromolecules* **1997**, *30*, 2503.
- Goto, A.; Terauchi, T.; Fukuda, T.; Miyamoto, T. *Macromol. Rapid Commun.* **1997**, *18*, 673.
- Goto, A.; Fukuda, T. *Macromolecules* **1999**, *32*, 618.
- Fukuda, T.; Goto, A. *Macromol. Rapid Commun.* **1997**, *18*, 683.
- Souaille, M.; Fischer, H. *Macromolecules* **2001**, *34*, 2830.
- Matyjaszewski, K.; Kajiwarra, A. *Macromolecules* **1998**, *31*, 548. Kajiwarra, A.; Matyjaszewski, K.; Kamachi, M. *ACS Symp. Ser.* **2000**, *768*, 68, and references therein.
- Benoit, D.; Grimaldi, S.; Robin, S.; Finet, J.-P.; Tordo, P.; Gnanou, Y. *J. Am. Chem. Soc.* **2000**, *122*, 5929.
- Le Mercier, C.; Lutz, J.-F.; Marque, S.; Le Moigne, F.; Tordo, P.; Lacroix-Desmazes, P.; Boutevin, B.; Couturier, J.-L.; Guerret, O.; Martschke, R.; Sobek, J.; Fischer, H. *ACS Symp. Ser.* **2000**, *768*, 108, and references therein.
- Lutz, J. F.; Lacroix-Desmazes, P.; Boutevin, B. *Macromol. Chem. Phys.* **2000**, *201*, 662.
- Marque, S.; LeMercier, C.; Tordo, P.; Fischer, H. *Macromolecules* **2000**, *33*, 4403.
- Sobek, J.; Martschke, R.; Fischer, H. *J. Am. Chem. Soc.* **2001**, *123*, 2849, and references therein.

- (64) Ohno, K.; Goto, A.; Fukuda, T.; Xia, J.; Matyjaszewski, K. *Macromolecules* **1998**, *31*, 2699.
- (65) Lutz, J.-F.; Lacroix-Desmazes, P.; Boutevin, B. *Macromol. Rapid Commun.* **2001**, *22*, 189.
- (66) Chambard, G.; Klumpermann, B. *ACS Symp. Ser.* **2000**, *768*, 197. Zhang, H.; Klumperman, B.; Ming, W.; Fischer, H.; van der Linde, R. *Macromolecules*, **2001**, submitted.
- (67) Chiefari, J.; Chong, Y. K.; Ercole, F.; Krstina, J.; Jeffery, J.; Lee, T. P. T.; Mayadunne, R. T. A.; Meijs, G. F.; Moad, C. L.; Moad, G.; Rizzardo, E.; Thang, S. H. *Macromolecules* **1998**, *31*, 5559.
- (68) Matyjaszewski, K.; Gaynor, S.; Wang, J.-S. *Macromolecules* **1995**, *28*, 2093.
- (69) Barton, D. H. R.; Beaton, J. M.; Geller, L. E.; Pechet, M. M. *J. Am. Chem. Soc.* **1960**, *82*, 2640. Akhtar, M. *Adv. Photochem.* **1964**, *2*, 263. Suginome, H.; Osada, A. *J. Chem. Soc. Perkin Trans. 1* **1982**, 1963, and references therein.
- (70) Chow, Y. L. *Acc. Chem. Res.* **1973**, *6*, 354. Flesia, E.; Croatto, A.; Tordo, P.; Surzur, J.-M. *Tetrahedron Lett.* **1972**, 535, and references therein.
- (71) Key references to these radicals include: Gomberg, M. *J. Am. Chem. Soc.* **1900**, *22*, 757. *Chem. Ber.* **1900**, *33*, 3150. Ballester, M.; Riera, J.; Castaner, J.; Badia, C.; Monso, J. M. *J. Am. Chem. Soc.* **1971**, *93*, 2215. Wieland, H.; Offenbaecher, H. *Chem. Ber.* **1914**, *47*, 2111. Goldschmidt, S.; Renn, K. *Chem. Ber.* **1922**, *55*, 628. Mueller, E.; Ley, K. Z. *Naturforsch. B* **1953**, *8*, 694. Ziegler, K. *Chem. Ber.* **1922**, *55*, 2257. Kosower, E. M.; Poziomek, E. J. *J. Am. Chem. Soc.* **1964**, *86*, 5515. de Vries, L. *J. Am. Chem. Soc.* **1978**, *100*, 926, and ref 1.
- (72) *Landolt-Boernstein, New Series, Magnetic Properties of Free Radicals*; Hellwege, K.-H.; Fischer, H., Eds.; Springer: Berlin, 1965–2002; Group II, Vols. 1, 9, 17, 26.
- (73) *Landolt-Boernstein, New Series, Radical Reaction Rates in Liquids*; Springer: Berlin, 1984–1998; Group II, Vols. 13, 18.
- (74) Bravo, A.; Bjorsvik, H.-R.; Fontana, F.; Liguori, L.; Minisci, F. *J. Org. Chem.* **1997**, *62*, 3849.
- (75) MacFaul, P. A.; Arends, I. W. C. E.; Ingold, K.; Wayner, D. D. M. *J. Chem. Soc. Perkin Trans. 2* **1997**, 135.
- (76) Lucas, M. A.; Schiesser, C. H. *J. Org. Chem.* **1996**, *61*, 5754.
- (77) Lepley, A. R. In *Chemically Induced Magnetic Polarization*; Lepley, A. R.; Closs, G. L. Eds.; Wiley: New York, 1973.
- (78) Walling, C. J. *Am. Chem. Soc.* **1988**, *110*, 6846.
- (79) Yokoi, M.; Nakano, T.; Fujita, W.; Ishiguro, K.; Sawaki, Y. *J. Am. Chem. Soc.* **1998**, *120*, 12453.
- (80) (a) Müller, F.; Mattay, J. *Chem. Rev.* **1993**, *93*, 99. (b) Fukuzumi, S.; Itoh, S. *Adv. Photochem.* **1999**, *25*, 107.
- (81) Studer, A. *Angew. Chem. Int. Ed.* **2000**, *39*, 1108.
- (82) Marque, S.; Fischer, H.; Baier, E.; Studer, A. *J. Org. Chem.* **2001**, *66*, 1146.
- (83) (a) Pattenden, G. *Chem. Soc. Rev.* **1988**, *17*, 361. (b) Branchaud, B. P.; Yu, G.-X. *Organometallics* **1993**, *12*, 4262. (c) Iqbal, J.; Bhatia, B.; Nayyar, N. K. *Chem. Rev.* **1994**, *94*, 519, and references therein.
- (84) Ghosez, A.; Göbel, T.; Giese, B. *Chem. Ber.* **1988**, *121*, 1807.
- (85) Halpern, J. *ACS Symp. Ser.* **1990**, *428*, 100, and references therein.
- (86) Scheffold, R.; Abrecht, S.; Orlinski, R.; Ruf, H.-R.; Stamouli, P.; Tinembart, O.; Walder, L.; Weymuth, C. *Pure Appl. Chem.* **1987**, *59*, 363.
- (87) House, D. A. *Adv. Inorg. Chem.* **1997**, *44*, 341, and references therein.
- (88) Van Vliet, M. R. P.; Jastrzebski, J. T. B. H.; van Koten, G.; Vrieze, K.; Spek, A. L. *J. Organometal. Chem.* **1981**, *210*, C49. Wissing, E.; Jstrzebski, J. T. B. H.; Boersma, J.; van Koten, G. *J. Organometal. Chem.* **1993**, *459*, 11, and references therein.
- (89) (a) Bellus, D. *Pure Appl. Chem.* **1985**, *57*, 1827. (b) Boutevin, B. *J. Polym. Sci., Part A: Polym. Chem.* **2000**, *38*, 3235.
- (90) Gossage, R. A.; van de Kuil, L. A.; van Koten, G. *Acc. Chem. Res.* **1998**, *31*, 423.
- (91) (a) Hayes, T. K.; Villani, R.; Weinreb, S. M. *J. Am. Chem. Soc.* **1988**, *110*, 5533. (b) Udding, J. H.; Tuijth, K. C. J. M.; van Zanden, M. N. A.; Hiemstra, H.; Speckamp, W. N. *J. Org. Chem.* **1994**, *59*, 1993.
- (92) Matyjaszewski, K.; Paik, H.; Shipp, D. A.; Isobe, Y.; Okamoto, Y. *Macromolecules* **2001**, *34*, 3127. For related evidence, see: Matyjaszewski, K. *Macromolecules* **1998**, *31*, 4710.
- (93) Jaines, B. S.; Hill, C. L. *J. Am. Chem. Soc.* **1995**, *117*, 4704. Yamase, Y.; Ohtaka, K. *J. Chem. Soc. Dalton Trans.* **1994**, 2599. Ermolenko, L. P.; Delaire, J. A.; Giannotti, C. *J. Chem. Soc. Perkin Trans. 2*, **1997**, 25. Mylonas, A.; Papaconstantinou, E. *J. Photochem. Photobiol.* **1996**, *94*, 77, and references therein.
- (94) Kothe, T.; Martschke, R.; Fischer, H. *J. Chem. Soc. Perkin Trans. 2*, **1998**, 503.
- (95) Hawker, C. *Chem. Rev.* **2001**, *101*, 3661–3688. Sawamoto, M.; Kamigaito, M.; Ando, T. *Chem. Rev.* **2001**, *101*, 3689–3746.
- (96) Benoit, D.; Chaplinski, V.; Braslau, R.; Hawker, C. J. *J. Am. Chem. Soc.* **1999**, *121*, 3904.
- (97) Chong, B. Y. K.; Ercole, F.; Moad, G.; Rizzardo, E.; Anderson, A. G. *Macromolecules* **1999**, *32*, 6896.
- (98) Kramer, A.; Nesvadba, P. 1999, DE Patent 19909767A1, 1999.
- (99) Connolly, T. J.; Baldovi, M. V.; Mohtat, N.; Scaiano, J. C. *Tetrahedron Lett.* **1996**, *37*, 4919.
- (100) Braslau, R.; Burrill, L. C., II; Siano, M.; Naik, N.; Howden, R. K.; Mahal, L. K. *Macromolecules* **1997**, *30*, 6445.
- (101) Matyjaszewski, K.; Woodworth, B. E.; Zhang, X.; Gaynor, S. G.; Metzner, Z. *Macromolecules* **1998**, *31*, 5955.
- (102) Bergbreiter, D. E.; Walchuk, B. *Macromolecules* **1998**, *31*, 6380.
- (103) Zink, M.-O.; Kramer, A.; Nesvadba, P. *Macromolecules* **2000**, *33*, 8106.
- (104) Moad, G.; Rizzardo, E. *Macromolecules* **1995**, *28*, 8722.
- (105) Skene, W. G.; Belt, S. T.; Connolly, T. J.; Hahn, P.; Scaiano, J. C. *Macromolecules* **1998**, *31*, 9103.
- (106) Ciriano, M. V.; Korh, H. G.; van Scheppeningen, W. B.; Mulder, P. *J. Am. Chem. Soc.* **1999**, *121*, 6375.
- (107) Bon, S. A. F.; Chambard, G.; German, A. L. *Macromolecules* **1999**, *32*, 8269.
- (108) Beckwith, A. L. J.; Bowry, V. W.; Ingold, K. U. *J. Am. Chem. Soc.* **1992**, *114*, 4983. Bowry, V. W.; Ingold, K. U. *J. Am. Chem. Soc.* **1992**, *114*, 4992. Chateaufeuf, J.; Luszyk, J.; Ingold, K. U. *J. Org. Chem.* **1988**, *53*, 1629. Beckwith, A. L. J.; Bowry, V. W.; Moad, G. *J. Org. Chem.* **1988**, *53*, 1632.
- (109) Baldovi, M. V.; Mohtat, N.; Scaiano, J. C. *Macromolecules* **1996**, *29*, 5497.
- (110) Marsal, P.; Roche, M.; Tordo, P.; de Sainte Claire, P. *J. Phys. Chem. A* **1999**, *103*, 2899.
- (111) Benson, S. W. *Thermochemical Kinetics*; Wiley: New York, 1968. Rüchardt, C.; Beckhaus, H.-D. *Angew. Chem.* **1980**, *92*, 417.
- (112) Ananchenko, G. S.; Fischer, H. *J. Polym. Sci. Part A: Polym. Chem.* **2001**, in press. Ananchenko, G. S.; Souaille, M.; Fischer, H. *J. Polym. Sci. Part A: Polym. Chem.* In press.
- (113) Skene, W. G.; Scaiano, J. C.; Yap, G. P. A. *Macromolecules* **2000**, *33*, 3536.
- (114) Rodlert, M.; Harth, E.; Rees, I.; Hawker, C. J. *J. Polym. Sci., Part A: Polym. Chem.* **2000**, *38*, 4749.
- (115) Harth, E.; Hawker, C. J.; Fan, W.; Waymouth, R. M. *Macromolecules* **2001**, *34*, 3856.
- (116) Connolly, T. J.; Scaiano, J. C. *Tetrahedron Lett.* **1997**, *38*, 1133.
- (117) Moad, G.; Rizzardo, E.; Solomon, D. H. *Polym. Bull.* **1982**, *6*, 589.
- (118) Gridnev, A. A. *Macromolecules* **1997**, *30*, 7651.
- (119) Chung, T. C.; Janvikul, W.; Lu, H. L. *J. Am. Chem. Soc.* **1996**, *118*, 705.
- (120) Klapper, M.; Brand, T.; Steenbock, M.; Müllen, K. *ACS Symp. Ser.* **2000**, *768*, 152, and references therein.
- (121) Yamada, T.; Nobuka, Y.; Miura, Y. *Polym. Bull.* **1998**, *41*, 1288.
- (122) Wayland, B. B.; Basickes, L.; Mukerjee, S.; Wei, M.; Fryd, M. *Macromolecules* **1997**, *30*, 8105.
- (123) Kickelbick, G.; Reinöhl, U.; Ertel, T. S.; Bertagnolli, H.; Matyjaszewski, K. *ACS Symp. Ser.* **2000**, *768*, 211. Kickelbick, G.; Reinöhl, U.; Ertel, T. S.; Weber, A.; Bertagnolli, H.; Matyjaszewski, K. *Inorg. Chem.* **2001**, *40*, 6. Pintauer, T.; Qiu, J.; Kickelbick, G.; Matyjaszewski, K. *Inorg. Chem.* **2001**, *40*, 2818.
- (124) Queffelec, J.; Gaynor, S. G.; Matyjaszewski, K. *Macromolecules* **2000**, *33*, 8629, and references therein.
- (125) Ando, T.; Kamigaito, M.; Sawamoto, M. *Macromolecules* **1997**, *30*, 4507. Matyjaszewski, K.; Wei, M.; Xia, J.; McDermott, N. E. *Macromolecules* **1997**, *30*, 8161.
- (126) Granel, C.; Dubois, P.; Jerome, R.; Teyssie, P. *Macromolecules* **1996**, *29*, 8576.
- (127) Moineau, G.; Granel, C.; Dubois, P.; Jerome, R.; Teyssie, P. *Macromolecules* **1998**, *31*, 542.
- (128) Lecomte, P.; Drapier, I.; Dubois, P.; Teyssie, P.; Jerome, R. *Macromolecules* **1997**, *30*, 7631.
- (129) Percec, V.; Asandei, A. D.; Asgarzadeh, F.; Barboiu, B.; Holerca, M. N.; Grigoras, C. *J. Polym. Sci. Part A: Polym. Chem.* **2000**, *38*, 4353. Percec, V.; Barboiu, B.; Bera, T. K.; van der Sluis, M.; Grubbs, R. B.; Frechet, J. M. J. *J. Polym. Sci. Part A: Polym. Chem.* **2000**, *38*, 4776.
- (130) Matyjaszewski, K.; Patten, T. E.; Xia, J. *J. Am. Chem. Soc.* **1997**, *119*, 674.
- (131) Davis, K. A.; Paik, H.; Matyjaszewski, K. *Macromolecules* **1999**, *32*, 1767.
- (132) Xia, J.; Matyjaszewski, K. *Macromolecules* **1997**, *30*, 7697.
- (133) Haddleton, D. M.; Perrier, S.; Bon, S. A. F. *Macromolecules* **2000**, *33*, 8246.
- (134) Matyjaszewski, K.; Göbelt, B.; Paik, H.; Horwitz, C. P. *Macromolecules* **2001**, *34*, 430, and references therein.
- (135) Johnson, R. M.; Ng, C.; Samson, C. C. M.; Fraser, C. L. *Macromolecules* **2000**, *33*, 8618.
- (136) Shen, Y.; Zhu, S.; Zeng, F.; Pelton, R. H. *Macromol. Chem. Phys.* **2000**, *201*, 1169.
- (137) Parker, J.; Jones, R. G.; Holder, S. J. *Macromolecules* **2000**, *33*, 9166.
- (138) Acar, A. E.; Yagzi, M. B.; Mathias, L. J. *Macromolecules* **2000**, *33*, 7700.
- (139) Matyjaszewski, K.; Davis, K.; Patten, T. E.; Wei, M. *Tetrahedron* **1997**, *45*, 15321.
- (140) Shipp, D. A.; Matyjaszewski, K. *Macromolecules* **2000**, *33*, 1553.

- (141) Benoit, D.; Hawker, C. J.; Huang, E. E.; Lin, Z.; Russell, T. P. *Macromolecules* **2000**, *33*, 1505. Benoit, D.; Harth, E.; Helms, B.; Vestberg, R.; Rodlert, M.; Hawker, C. J. *ACS Symp. Ser.* **2000**, *768*, 122.
- (142) Lacroix-Desmazes, P.; Lutz, J.-F.; Boutevin, B. *Macromol. Chem. Phys.* **2000**, *210*, 662.
- (143) Bon, A. F.; Bosveld, M.; Klumperman, B.; German, A. L. *Macromolecules* **1997**, *30*, 324.
- (144) Karetakin, E.; O'Shaughnessy, B.; Turro, N. J. *Macromolecules* **1998**, *31*, 4655. *J. Chem. Phys.* **1998**, *108*, 9577.

CR990124Y

Supramolecular Polymers

L. Brunsveld, B. J. B. Folmer, E. W. Meijer,* and R. P. Sijbesma

Laboratory of Macromolecular and Organic Chemistry, Eindhoven University of Technology, P.O. Box 513, 5600 MB Eindhoven, The Netherlands

Received April 23, 2001

Contents

I. Introduction	4071
II. The Term Supramolecular Polymers	4071
III. General Aspects of Supramolecular Polymers	4073
IV. Supramolecular Polymers Based on Hydrogen Bonding	4073
A. Strength of Hydrogen Bonds	4073
B. Hydrogen Bonding Enforced by Liquid Crystallinity	4075
C. Hydrogen Bonding Enforced by Phase Separation	4076
D. Strong Dimerization of Multiple Hydrogen-Bonding Units	4077
E. Ureidopyrimidinone-Based Polymers	4079
V. Supramolecular Polymers Based on Discotic Molecules	4081
A. Arene–Arene Interactions	4082
1. Triphenylenes	4082
2. Phthalocyanines and Porphyrins	4083
3. Helicenes	4084
4. <i>m</i> -Phenylene Ethynylene Oligomers	4084
5. Other Systems	4085
6. Chromonics	4086
B. Hydrogen Bonding	4086
C. Arene–Arene Interactions and Hydrogen Bonding	4087
1. Guanine and Pterine Derivatives	4087
2. Hydrogen-Bonded Pairs	4089
3. Complexation of Tetrazoles with 1,3,5-Tris(4,5-dihydroimidazol-2-yl)benzene	4089
4. C ₃ -Symmetrical Discotic Molecules	4090
VI. Supramolecular Coordination Polymers and Miscellaneous Systems	4091
VII. Conclusions and Outlook	4094
VIII. Acknowledgments	4094
IX. References and Notes	4094

I. Introduction

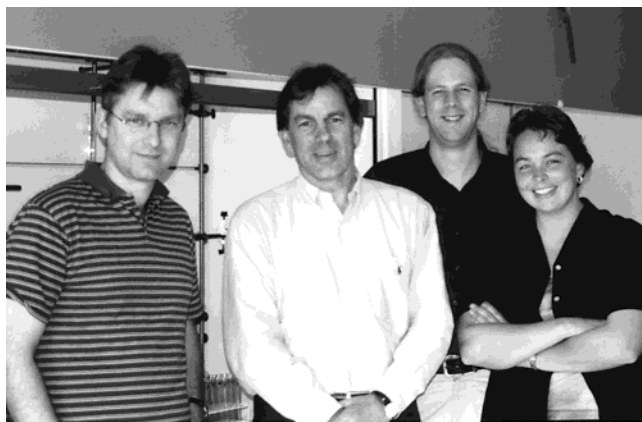
With the introduction of supramolecular polymers, which are polymers based on monomeric units held together with directional and reversible secondary interactions, the playground for polymer scientists has broadened and is not restricted to macromolecular species, in which the repetition of monomeric units is mainly governed by covalent bonding. The importance of supramolecular interactions within polymer science is beyond discussion and dates back to the first synthesis of synthetic polymers; the

materials properties of, e.g., nylons, are mainly the result of cooperative hydrogen bonding. More recently, many exciting examples of programmed structure formation of polymeric architectures based on the combination of a variety of secondary supramolecular interactions have been disclosed.

When the covalent bonds that hold together the monomeric units in a macromolecule are replaced by highly directional noncovalent interactions (Figure 1), supramolecular polymers are obtained. In recent years, a large number of concepts have been disclosed that make use of these noncovalent interactions. Although most of the structures disclosed keep their polymeric properties in solution, it was only after the careful design of multiple-hydrogen-bonded supramolecular polymers that systems were obtained that show true polymer materials properties, both in solution and in the solid state. Polymers based on this concept hold promise as a unique class of novel materials because they combine many of the attractive features of conventional polymers with properties that result from the reversibility of the bonds between monomeric units. Architectural and dynamic parameters that determine polymer properties, such as degree of polymerization, lifetime of the chain, and its conformation, are a function of the strength of the noncovalent interaction, which can reversibly be adjusted. This results in materials that are able to respond to external stimuli in a way that is not possible for traditional macromolecules. These aspects of supramolecular polymers have led to a recent surge in attention for this promising class of compounds^{1–3} and have stimulated us to bring together materials science and supramolecular chemistry.⁴ On the other hand, it is obvious that a large number of important properties of polymers require the covalent and irreversible bonding of the repeating units in the main chain. For applications in which all of these properties are important, supramolecular polymers are not the perfect choice. However, the opportunity to combine macromolecules and concepts derived from supramolecular polymers also has an enormous potential to alter the properties of polymers in a controlled way.

II. The Term Supramolecular Polymers

Interest in supramolecular polymers has been stimulated to a great extent by the impressive progress made in supramolecular chemistry in general,^{5–8} and in the field of synthetic self-assembling molecules in particular. The field in which



Luc Brunsveld (second from right) received his Ph.D. in Supramolecular Chemistry at the Eindhoven University of Technology in 2001 with professor E. W. Meijer. The Ph.D. research was focused on supramolecular architectures in water and a small part of that has been performed in the group of professor J. S. Moore at the University of Illinois, Urbana-Champaign. He did his undergraduate research in the group of professor E. W. Meijer on supramolecular hydrogen-bonded polymers. His research interests are in the field of supramolecular architectures and chirality. Currently he is working as a postdoctoral fellow in the group of professor Waldmann at the MPI in Dortmund, Germany.

Brigitte J. B. Folmer (right) received her B.A. degree in chemistry from the University of Nijmegen in 1996, where she did her graduation work on host-guest chemistry in the group of professor R. J. M. Nolte. In 2000 she received her Ph.D. degree from the University of Technology in Eindhoven with professor E. W. Meijer. Her thesis was focused on the properties of supramolecular polymers based on hydrogen bonding. Currently she is working at Organon N. V. (AkzoNobel) in Oss, The Netherlands. Her research interests include organic synthesis and supramolecular chemistry and particularly the role of noncovalent interactions in receptor-ligand complexes and supramolecular materials.

E. W. "Bert" Meijer (second from left) is professor of Macromolecular and Organic Chemistry at the Eindhoven University of Technology, The Netherlands. He received his Ph.D. in Organic Chemistry at the University of Groningen in 1982 with professor Hans Wynberg. He was research scientist in the area of optoelectronic materials at Philips Research Laboratories from 1982 to 1989 and group leader of new polymeric materials at DSM Research from 1989 to 1992. Since 1992 he has been a full professor in Eindhoven, and since 1995 he is also adjunct professor at the University of Nijmegen. His research interests are in dendrimers, supramolecular systems, and organic materials for electronics. For correspondence, he can be reached by e-mail at E. W. Meijer@tue.nl or by fax at 31-40-2451036. For further information consult the www.tue.chem.nl/toc website of the laboratory of Macromolecular and Organic Chemistry.

Rint P. Sijbesma (left) did his graduate research with professor Roeland Nolte at the University of Nijmegen; the focus was on synthetic receptor molecules. From 1992 to 1993 he worked as a postdoctoral research assistant with professor Fred Wudl (University of California, Santa Barbara) on the synthesis of water-soluble C_{60} -derivatives. In 1993 he took his present position as assistant professor in the laboratories of professor E. W. Meijer, where he is working in the field of supramolecular polymer chemistry.

supramolecular chemistry and polymer science meet has developed into a vast area of research, ranging from the study of interacting biomacromolecules, such as DNA and proteins, to the self-assembly of large synthetic molecules into well-defined architectures. Examples of the latter include the formation of PMMA stereocomplexes, highly organized block-copolymer architectures, and self-assembled polymer architectures inspired by the structure of tobacco mosaic virus (TMV).⁹ Noncovalent interactions have also been employed to fold macromolecules (aptly

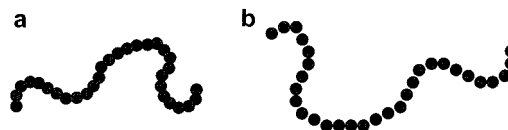


Figure 1. Schematic representation of a covalent polymer (a); and a supramolecular polymer (b).

named "foldamers")¹⁰ into well-defined conformations. These examples of using secondary interactions in and between synthetic macromolecules typify the potential of a supramolecular approach to highly organized, functional materials.

Partly influenced by our own research interests, the focus in this review is on the role of specific, noncovalent interactions such as hydrogen bonding, metal coordination, and π - π (or arene-arene) interactions to form so-called supramolecular polymers. The high directionality of these interactions inherently stresses the one-dimensional nature of these polymers. It is instructive to notice that from this point of view, supramolecular polymers and crystalline compounds are at opposite ends of the spectrum of molecular materials. In molecular crystals, it is difficult to define a dominant direction of the interactions – crystals are fundamentally 3-dimensional – and even when interactions are stronger in one direction than in others, all specific aggregation is lost when these materials are heated or dissolved. Supramolecular polymers, on the other hand, are 1-dimensional in nature, and in melts or (dilute) solutions of these materials distinguishable polymeric entities continue to exist. A fascinating intermediate class of materials consists of compounds that form polymers in the liquid crystalline state. Here, cooperativity between a relatively weak secondary interaction and excluded volume interactions (which are entropic in nature) leads to a significant degree of polymerization.¹¹ However, in the isotropic melt or in solution, most of the polymeric properties are lost. Because hydrogen-bonded liquid crystals have played an important role in developing the concept of supramolecular polymers, they will be covered in some detail in this review. Polymers that are held together by topological constraints, such as polycatenanes and polyrotaxanes, will not be treated in this review.¹²

Taking everything into account, we like to propose the following definition for supramolecular polymers: *Supramolecular polymers are defined as polymeric arrays of monomeric units that are brought together by reversible and highly directional secondary interactions, resulting in polymeric properties in dilute and concentrated solutions, as well as in the bulk. The monomeric units of the supramolecular polymers themselves do not possess a repetition of chemical fragments. The directionality and strength of the supramolecular bonding are important features of systems that can be regarded as polymers and that behave according to well-established theories of polymer physics.* In the past the term "living polymers" has been used for this type of polymers. However, to exclude confusion with the important field of living polymerizations, we prefer to use the term supramolecular polymers. With this definition, the term supramolecular polymer is rather restricted and not

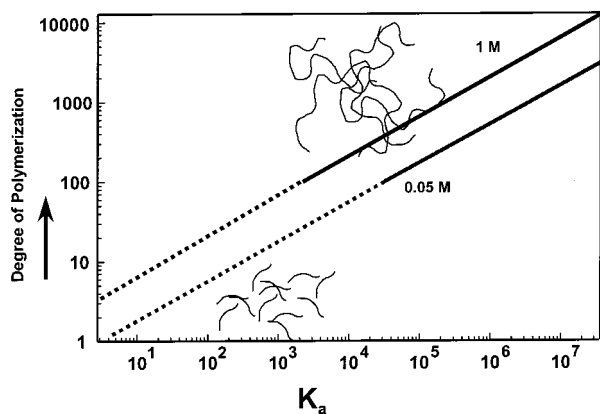


Figure 2. Theoretical relationship between the association constant K_a and DP, using a simple isodesmic association function, or “multistage open association” model.

used for telechelic macromolecules reversibly bound together by specific supramolecular interactions. However, modified telechelics are included in this review because many issues in the field are important for associating telechelics as well.

III. General Aspects of Supramolecular Polymers

It is useful to review some of the general aspects of the supramolecular approach, taking into account the limitations of our definition of supramolecular polymers. Using a directional complementary couple (A–B) or a self-complementary unit (A–A), it is possible to form all known structures of polymers, including linear homo- and copolymers, cross-linked networks, and even (hyper)branched structures in the case of complementary couples.¹³ In supramolecular polymers, which are formed by the reversible association of bifunctional monomers, the average degree of polymerization (DP) is determined by the strength of the end group interaction.¹⁴ The degree of polymerization is obviously dependent on the concentration of the solution and the association constant, and a theoretical relationship is given in Figure 2.

To obtain polymers with a high molecular weight, a high association constant between the repeating units is a prerequisite. In analogy with covalent condensation polymers, the chain length of supramolecular polymers can be tuned by the addition of monofunctional “chain stoppers”.¹⁵ This also implies that impurities will have a strong influence on the maximal DP, because it is easy to have a small fraction of monofunctional impurity in the synthesis of the bifunctional monomer. Hence, as in traditional polymer synthesis, the purification of the monomers is extremely important to obtain high molecular weights.

In another approach, supramolecular polymers can be formed by planar structures that have the possibility to assemble on both sides of the plane. Here, one structural element is responsible for the formation of the polymer, and chain stoppers are difficult to design. Hence, the DP is completely governed by the association constant and the concentration. As a result of the structural motive, these supramolecular polymers are rather stiff and resemble rodlike poly-

mers, with interesting architectural properties but without significant materials properties in the bulk.

In a third approach, supramolecular polymers are based on the reversibility of metal-coordination bonding. These polymers are the closest analogues to conventional macromolecules, because most of the polymers disclosed make use of strong bonding,¹⁶ in which the reversibility can be tuned by chemical means only. However, appropriate choice of the metal ion can give rise to bonding that resembles that of the other two approaches. The DP of the polymers in the case of the coordination polymers is similar to that of the condensation polymers, and achieving exact stoichiometry is of distinct importance here.

True supramolecular polymers are reversible aggregates that can break and recombine on experimental time scales. It is this feature that has been investigated in detail by Cates in a physical model, predicting stress relaxation and other viscoelastic properties of entangled “living polymers” as a function of the interaction strength of the monomer end groups.^{17–19} Although this model was made for cylindrical micelles, it is shown by the work on ureidopyrimidone-based supramolecular polymers that the model also describes in detail the viscosity behavior of reversible supramolecular polymers. Many of the materials properties of supramolecular polymers are those well-known for traditional polymers, although the reversibility will lead to an unconventional temperature dependence of the materials' properties.

IV. Supramolecular Polymers Based on Hydrogen Bonding

Although hydrogen bonds between neutral organic molecules are not among the strongest noncovalent interactions, they hold a prominent place in supramolecular chemistry because of their directionality and versatility.^{20–22} The relationship between the degree of polymerization and the strength of the noncovalent interaction between monomers in a supramolecular polymer (see Figure 2) implies that cooperativity is required to obtain significant degrees of polymerization. Hence, either multiple-hydrogen bonds must be used or hydrogen bonds should be supported by additional forces, like excluded volume interactions. Examples of both approaches to hydrogen-bonded supramolecular polymers will be discussed.²³

A. Strength of Hydrogen Bonds

Combining several hydrogen bonds in a functional unit is a valuable tool for increasing the strength of this interaction, and employing a particular arrangement of the hydrogen bonding sites enhances its specificity. The strength of single hydrogen bonds basically depends on the nature of donor and acceptor, although it is influenced to a large extent by the solvent. Association strength between multiple hydrogen-bonding units obviously depends on the same factors, as well as on the number of hydrogen bonds. It has also been shown that the particular arrange-

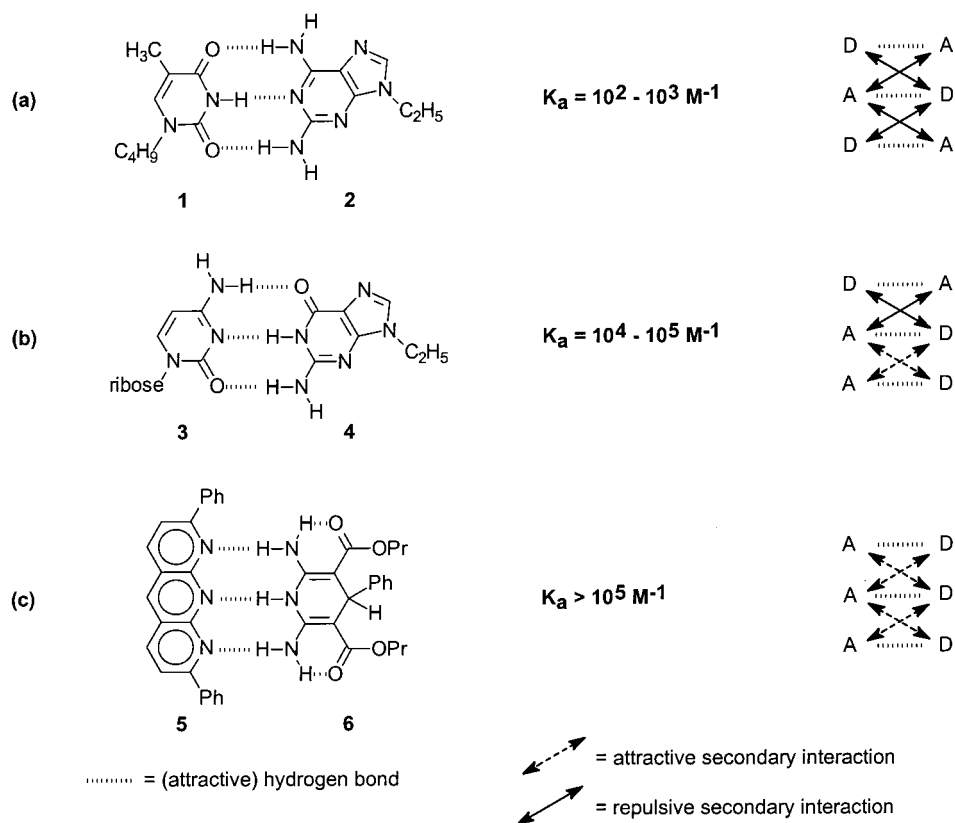


Figure 3. Stability of complexes with different hydrogen-bonding motifs.

ment of neighboring donor and acceptor sites is an additional factor which significantly affects the strength of the complexation. This phenomenon was first recognized for the association of linear arrays of 3 hydrogen-bonding sites (Figure 3); whereas complexes between the common ADA–DAD (1–2) motif exhibit an association constant of around 10^2 M^{-1} in chloroform, this value is around 10^4 M^{-1} in complexes with a DAA–DDA (3–4) motif, while AAA and DDD arrays (5–6) exhibit association constants exceeding 10^5 M^{-1} . Detailed calculations by Jorgenson^{24,25} showed that this effect is due to differences in secondary interactions between these motifs. In the complexes, diagonally opposed sites repel each other electrostatically when they are of the same kind (both donor or both acceptor), whereas disparate sites attract each other. In the DDD–AAA motif the number of attractive secondary interactions is maximized, and in the ADA–DAD motif the number of repulsive interactions is at its largest.

Very stable complexes can be obtained when quadruple hydrogen-bonding units are employed.^{26–30} Aspects of multiple hydrogen-bonding units that are of special importance with respect to application in supramolecular polymers are the self-complementarity of DADA and DDAA arrays and the possibility of tautomerism. The latter may lead to loss of complexation when complementarity is lost, or when a DDAA array tautomerizes to a DADA array with a higher number of repulsive secondary interactions. We have reported on self-complementary quadruple H-bonding units based on mono-ureido derivatives of diamino-triazines²⁹ (DADA-array) with a dimerization constant of $K_{\text{dim}} = 2 \times 10^4 \text{ M}^{-1}$ and hydrogen-

bonding units based on 2-ureido-4[1H]-pyrimidinones (DDAA), which dimerize in chloroform with an association constant of $K_{\text{dim}} = 6 \times 10^7 \text{ M}^{-1}$.^{30,31} The supramolecular polymers that were developed using these hydrogen-bonding units will be discussed in detail below. Zimmermann and co-workers have reported a very stable self-complementary quadruple hydrogen-bonding unit (7), depicted in Figure 4, in which all tautomers can dimerize via quadruple hydrogen bonds.

There is ample opportunity for developing new multiple hydrogen-bonding units for use in supramolecular polymers with novel, attractive features, such as ease of synthesis, insensitivity to tautomerization,²⁸ and stronger association by using arrays of 6 bonds³² or 8 hydrogen bonds.³³ The use of heteroaromatic compounds as multiple hydrogen-bonding units for self-assembly has recently been reviewed.³⁴

Application of hydrogen-bonding units as associating end-groups in difunctional or multifunctional molecules results in the formation of supramolecular polymers with varying degrees of polymerization (DP). The early examples of hydrogen-bonded supramolecular polymers rely on units, which associate using single, double, or triple hydrogen bonds that all have association constants below 10^3 M^{-1} . In isotropic solution, the DP of these polymers is expected to be low. In the liquid crystalline state, however, the interactions are stabilized by excluded volume interactions, and the DP is much higher. Examples of linear supramolecular polymers based on weak hydrogen-bonding interactions assisted by liquid crystallinity or phase separation will be treated below, followed by a discussion of supramolecular

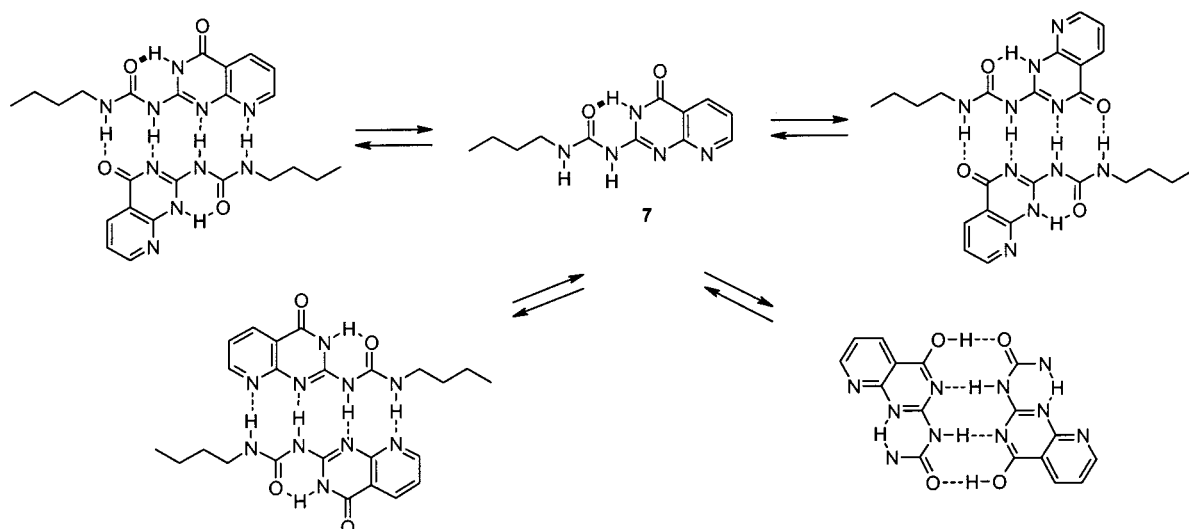


Figure 4. Hydrogen-bonding unit **7** that dimerizes via quadruple hydrogen bonding without regard to tautomeric form.

polymers based on strong hydrogen-bond interactions that persist in the isotropic state (melt or solution).

B. Hydrogen Bonding Enforced by Liquid Crystallinity

The first hydrogen-bonded supramolecular polymers all showed liquid crystallinity, although the separate components making up these polymers displayed a narrow liquid crystalline regime or no liquid crystallinity at all. The liquid crystalline phase in the supramolecular polymer is stabilized by the increased aspect ratio of aggregates compared to the constituent molecules. There is a strong cooperativity between association and the induction of the liquid crystalline phase, because anisotropy in the liquid crystal strongly enhances the degree of polymerization of the hydrogen-bonded molecules.³⁵ Liquid crystalline supramolecular polymers are unique in the respect that they combine the potential to exhibit the electrooptical properties associated with low-molar-mass liquid crystals with the benefit of the good mechanical properties of conventional polymers.³⁶ Odijk,^{37,38} van der Schoot,³⁹ and Ciferri⁴⁰ developed a theoretical basis for the relation between chain growth and orientation in supramolecular liquid crystals.

The group of Lehn is recognized to be the first to develop a supramolecular main-chain polymer. By triple hydrogen bonding between difunctional diaminiopyridines (**8**) and difunctional uracil (**9**) derivatives (Figure 5) supramolecular polymer chains were formed (**10**).^{41,42} The 1:1 mixture of **8** and **9** exhibits liquid crystallinity over a broad temperature window, whereas, in contrast, the pure compounds are solids which melt in an isotropic liquid without displaying a liquid crystalline phase. Because of the chirality of the tartaric acid spacer used, the fibers observed by electron microscopy showed biased helicity.⁴³ Lehn and co-workers expanded the scope of supramolecular polymers by the development of rigid rod polymers (**11**, Figure 5).^{44,45} In these polymers, a rigid 9,10-dialkoxyanthracene core connects the hydrogen-

bonded groups via an imide group. Because of the increased molecular rigidity, the system is not thermotropic liquid crystalline, but a lyotropic liquid crystalline phase is observed in apolar solvents, that is birefringent and highly viscous.

A number of supramolecular liquid crystalline polymers based on a single hydrogen bond have been reported. Incorporation of single hydrogen-bonding units is synthetically more straightforward than those with triple hydrogen bonds, and, particularly, the single hydrogen bond between a pyridyl unit and carboxylic acids has been utilized frequently in supramolecular liquid crystalline polymers (LCP's).^{46–50} The complexation between a pyridyl unit and a carboxylic acid is stronger than carboxylic acid dimerization; a K_a value of approximately 500 M^{-1} was estimated for the pyridyl/carboxylic acid complex.⁴⁷ Kato and Fréchet have described a variety of self-assembled side-chain liquid crystalline polymers (SLCPs), with various backbones.^{48,49} Polyacrylates and polysiloxanes functionalized with pendant benzoic acids display stable mesophases upon self-assembly with stilbazoles. The reverse principle has been employed for the formation of supramolecular liquid crystalline polyurethanes.⁵⁰ Furthermore, the stability of the induced mesophase has been enlarged by employing the double hydrogen bond between benzoic acids in the polymer main-chain and 2-(acylamino)pyridines.^{51,52}

Utilization of the single hydrogen bond between pyridine and benzoic acids in SLCP's has been a source of inspiration for other groups in the development of main-chain supramolecular polymers based on diacids and dipyridines.^{53–56} Supramolecular rod-coil polymers have been developed by assembly of 4,4'-bipyridines and telechelic polypropylene oxide with benzoic acid end-groups, which show highly ordered liquid crystalline phases.⁵⁷ The use of tartaric acid derivatives in combination with bipyridine units resulted in the formation of hydrogen-bonded, chiral main-chain LCP's, as has been shown by circular dichroism measurements, optical microscopy, and X-ray data.^{58,59}

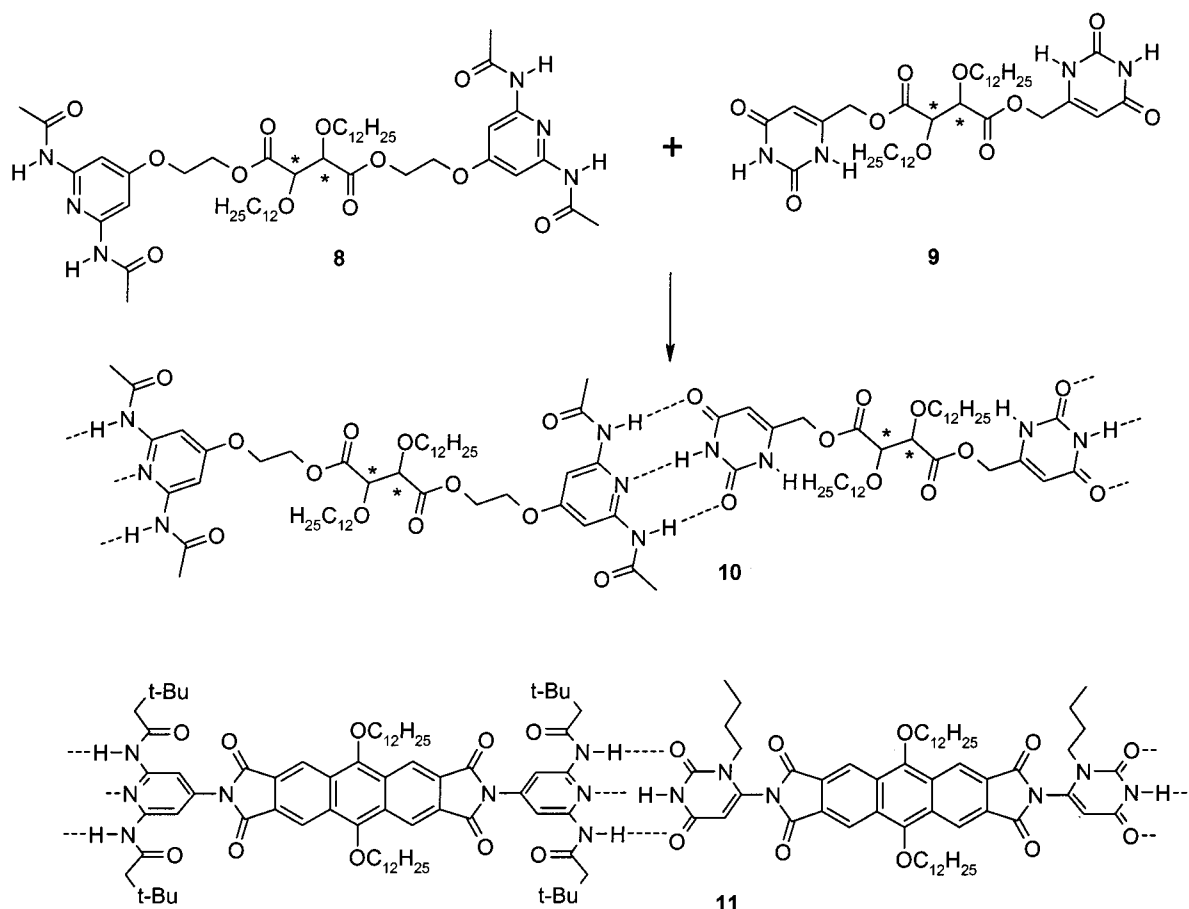


Figure 5. Liquid crystalline supramolecular polymers developed by Lehn, based on triple hydrogen bonds: from chiral, tartaric acid based monomers (**10**) and from rigid monomers (**11**).

A columnar mesophase has been used by the group of Percec for the creation of hydrogen-bonded supramolecular polymers.^{60,61} The phase separation of the apolar side groups of substituted benzamides with the core of the molecule accounts for the self-assembly into a cylindrical structure in which hydrogen bonding acting along the columnar axis occurs and stabilizes the column.

Next to side-chain LCPs and main-chain LCPs, supramolecular networks were obtained by complexation of bipyridines with polyacrylates containing pendant benzoic acid groups. In a related approach, Kato and Fréchet have studied supramolecular networks based on low-molecular-weight components, in which a trifunctional benzoic acid derivative was combined with a difunctional pyridine derivative.⁶² The hierarchy of the LC-phase that was formed turned out to be dependent on the flexibility of the trifunctional compound used.

Although chain extension based on single hydrogen bonding is observed, supramolecular materials based on this interaction, in most aspects, resemble small molecules more than they resemble polymers. Only the triple hydrogen-bonded supramolecular polymers reported by Lehn show some typical polymer properties, such as the ability to draw fibers from the melt. By using multifunctional low-molecular-weight building blocks, Griffin was able to obtain materials that exhibited polymer-like properties.⁶³

Hydrogen bonding between pyridine units in a tetrafunctional compound (**12**) and benzoic acid units in difunctional compounds (**13**, Figure 6), resulted in the formation of reversible ladder-like polymers (**14**) or networks (**15**). These materials are liquid crystalline, and the large drop in material properties above the isotropisation temperature demonstrates that, also here, the interplay between association and liquid crystallinity is instrumental in the process of polymerization.⁶³ DSC studies on these networks reveal a memory effect, resulting in a consistent decrease of crystallinity as the time the material is in the isotropic state increases.⁶⁴

C. Hydrogen Bonding Enforced by Phase Separation

The methodology of increasing the strength of a relatively weak hydrogen-bond interaction by (crystalline) domain formation is frequently encountered in chain extension of conventional polymers, and is in principle analogous to the enforcement of association in the liquid crystalline phase. Lillya et al. has shown that by end-capping of poly-THF with benzoic acid functionalities, the material properties improve significantly due to the formation of large crystalline domains of the hydrogen-bonded units.⁶⁵ Furthermore, end capping of poly(dimethylsiloxane)s with benzoic acid groups has been reported to result in a change in polymer properties upon functionalization. However, the change in properties seems to be less

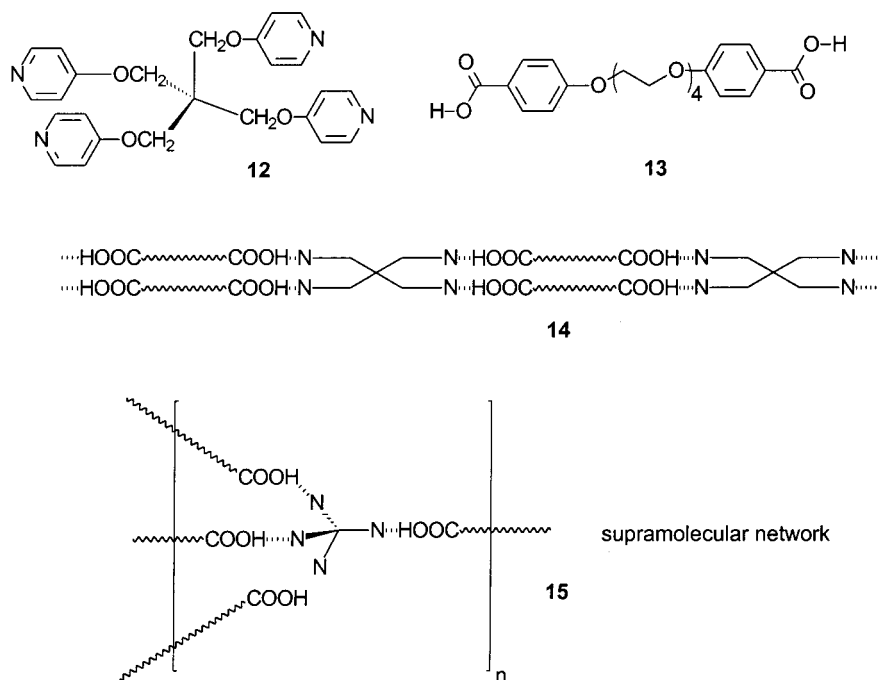


Figure 6. Formation of a linear ladder-type supramolecular polymer (**14**) or a hydrogen-bonded network (**15**) based on the single hydrogen bond between a pyridine unit and a benzoic acid unit.

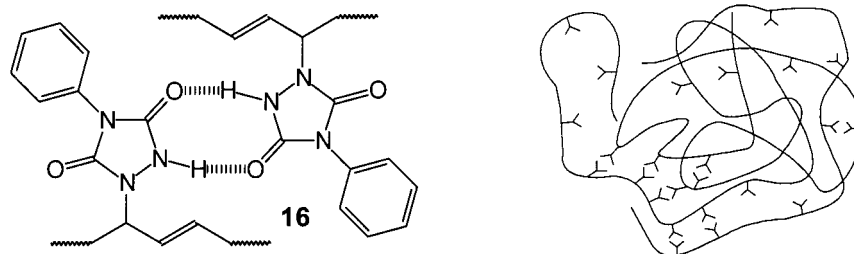


Figure 7. Formation of a supramolecular network by hydrogen bonding between phenylurazole units and subsequent formation of ordered clusters.

remarkable than the results obtained with poly-THF.⁶⁶ On the basis of detailed FTIR spectroscopy and viscosimetry studies, a quantitative model for the chain length and weight distribution of the functionalized polysiloxane in solution was described by Bouteiller et al.⁶⁷ These associative polymers with hydrogen-bonded groups, either telechelic or in the side-chains, are of considerable interest for numerous applications, such as rheology modifiers, adhesives, adsorbents, coatings, surfactants, and stabilizers, because of the reversibility of interactions in the chain and between chains.⁶⁸ Particularly, Stadler made an impressive contribution to this field by studying the properties of polybutadienes functionalized with hydrogen-bonded phenylurazole units (**16**, Figure 7).^{69–87}

Because of their reversible chain extension and the subsequent formation of small crystalline domains, the functionalized polymers exhibit properties typical for thermoplastic elastomers. At low temperatures the hydrogen-bond interaction contributes to the properties comparable to covalent interactions, whereas at high temperatures these interactions disappear and the materials exhibit flow behavior typical for a low-molecular-weight polymer. DSC,^{72,73} light and X-ray scattering,^{71,74} dynamical mechanical analy-

ses,^{75–81} dielectric spectroscopy^{82,83}, deuterium-NMR,⁸⁴ and IR spectroscopy^{85–87} were used to analyze the properties of these materials.

Although the strength of association between units, which assemble by only a single or double hydrogen bond, is low, chain extension by these synthetically accessible units is a versatile tool for gaining a significant improvement in material properties. A modest degree of polymerization in combination with physical interchain interactions by means of domain formation results in high-molecular-weight assemblies with improved material properties. Without domain formation, or when low-molecular-weight building blocks are used, a very high degree of polymerization, and consequently a high association constant, is required, as will be discussed in the following section.

D. Strong Dimerization of Multiple Hydrogen-Bonding Units

The number of supramolecular polymers based on very strong multiple hydrogen-bonded units is relatively small because of the increased synthetic efforts required for the synthesis of the monomers. Intriguing architectures such as nanotubes⁸⁸ are obtained

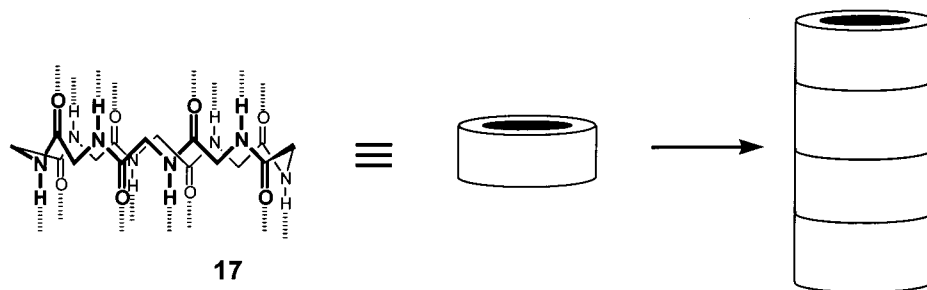


Figure 8. Formation of nanotubes based on hydrogen bonding between cyclic peptides.

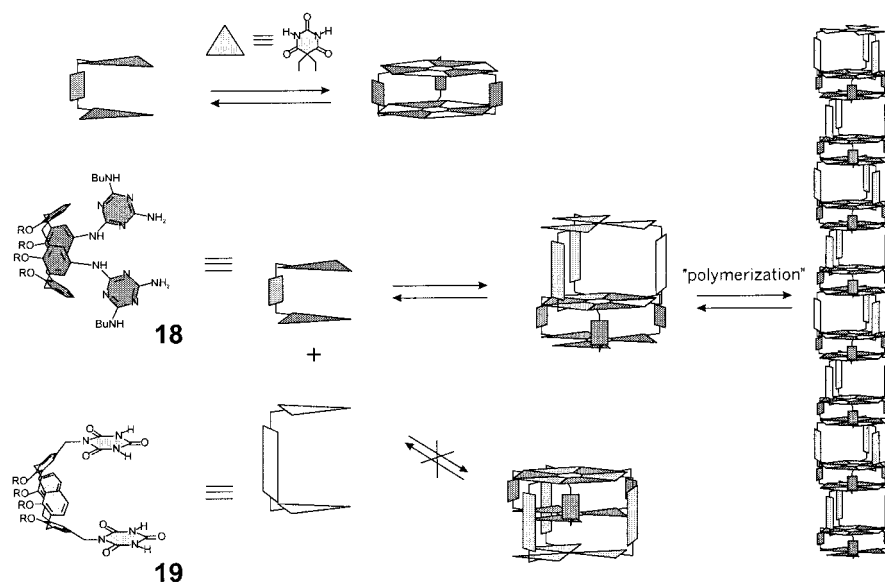


Figure 9. Nanorods based on the cyclic hydrogen-bonding motif of cyanuric acid and melamine in bifunctional calixarene derivatives **18** and **19**. (Reprinted with permission from ref 106. Copyright 1999 American Chemical Society.)

when bifunctional compounds with cyclic arrays of hydrogen-bonding sites are used. Ghadiri has studied nanotubes that self-assemble from cyclic peptides (**17**). These tubes can be considered reversible polymers because of their multiple-hydrogen bonding. On the basis of earlier work by De Santis⁸⁹ and Tomasic,⁹⁰ cyclic peptides were designed, composed of an even number of alternating d- and l-amino acids, which assemble into extended linear stacks through hydrogen bonding between the flat ring-shaped peptides (Figure 8).^{91–102}

These nanotubes were found to be very robust and turned out to be stable to a wide range of pH and solvents, as well as to physical stress.⁹⁴ From variable temperature studies in chloroform, Ghadiri and co-workers concluded that the dimeric form was favored over the monomer by 23 kJ mol⁻¹, and they postulated that this gain in stabilization energy would be additive as the number of assembled rings increased.⁹⁵ The association constant is dependent on the peptide residue used and is around 2500 M⁻¹. By selective backbone *N*-methylation the self-assembly of the peptides is limited to the formation of dimers.^{96,97} Subsequently linking of two of the *N*-methylated peptides by a short spacer results again in the formation of linear reversible polymers, this time with the direction of chain growth perpendicular to the direction of hydrogen bonding. A clever combination of this approach with the photoisomerization

of an azobenzene unit, resulted in a system that can be switched between intramolecular dimerization and linear polymer formation by UV light.^{98,99} The cyclic peptides were shown to self-assemble in membranes to form trans-membrane ion channels,¹⁰⁰ whose orientation in the membrane has been studied in detail with different IR techniques.¹⁰¹ The nanotubes have been used in size-selective ion-sensing on self-assembled monolayers.¹⁰² Tubular assemblies based on hydrogen bonding between cyclic β -peptides, have been reported by Seebach,¹⁰³ and by Ghadiri who showed that these related structures also self-assemble to form membrane-spanning ion channels.¹⁰⁴ Stable peptide nanotubes have been obtained by using the hydrogen-bond formation between urea groups in cysteine based macrocycles.¹⁰⁵

The groups of Reinhoudt¹⁰⁶ and of Whitesides¹⁰⁷ have reported independently on the formation of supramolecular “nanorods” based on the well-known cyanuric acid–melamine motif. These hydrogen-bonded polymeric rods are composed of parallel cyanuric acid–melamine rosettes (Figure 9).

Both groups employed the same rationale: the self-assembly of dimelamine derivative with a dicyanurate derivative in which the spatial distance between the two cyanurate units is different from the distance between the two melamine units. It was anticipated that this mismatch prevented the formation of a closed disklike assembly and induced the formation

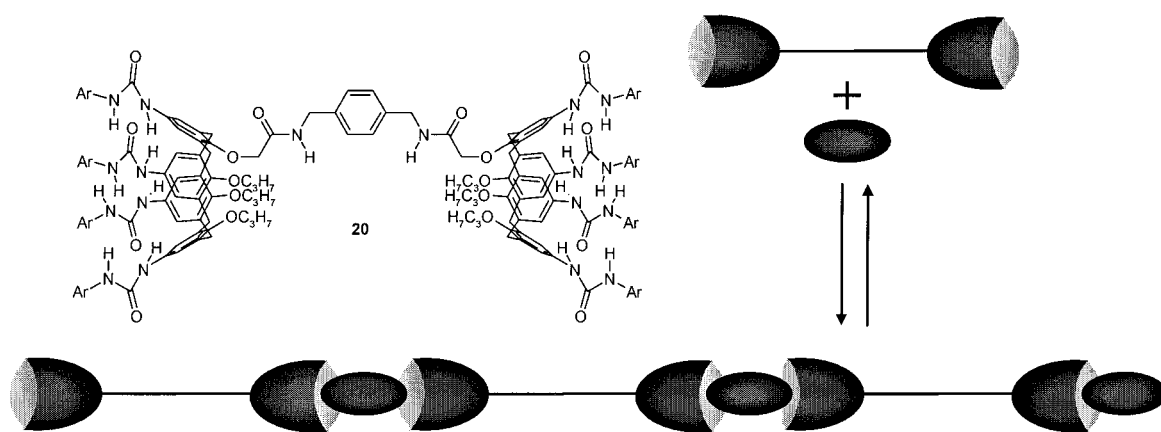


Figure 10. Bifunctional calixarene derivative **20** and a cartoon-like representation of its polymerization induced by small molecules.

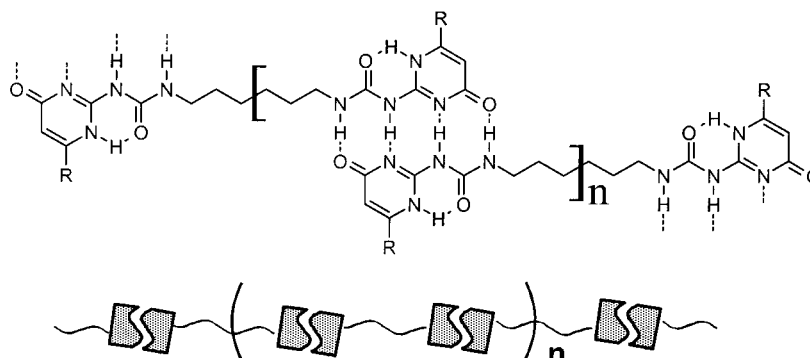


Figure 11. Polymeric assembly of a bifunctional ureidopyrimidinone derivative.

of polymeric entities. A 1:1 mixture of dimelamine (**18**) and dicyanurate (**19**) resulted in a viscous solution, indicating that high-molecular-weight aggregates were formed. The nature of the aggregates was further investigated by NMR spectroscopy, gel permeation chromatography (GPC), and transmission electron microscopy (TEM).

The group of Rebek Jr. has developed an ingenious way to form supramolecular polymers by utilizing the hydrogen bonding between urea functionalized calixarenes (Figure 10).^{108–112} These calixarenes had been shown to form very stable dimeric capsules which bind a solvent molecule inside their cavity. Association of bifunctional molecules consisting of two covalently connected calixarene moieties (**20**) results in the formation of “polycaps”. The association between the monomers is based upon hydrogen bonding in cooperation with complexation of a small guest; the polymerization of the assembly is driven by encapsulation of small guests such as benzene. Solutions of these molecules in *o*-dichlorobenzene show polymer-like rheological behavior, with a strong concentration-dependent viscosity.¹¹¹ The physical integrity of the noncovalent assemblies under shear was demonstrated by the observation of strong normal forces in rheometry experiments. The “polycaps” can be drawn into fibers with a tensile strength in the order of 10^8 Pa.¹⁰⁹ Networks from tetrafunctional molecules in solution display a stronger elastic component in their rheological behavior, and they have complicated time dependent properties such as shear thickening. When the “polycaps” are fitted with

long alkyl chains, chloroform solutions develop liquid crystallinity.¹¹²

Although these supramolecular polymers possess intriguing new properties, synthetic barriers hamper extensive study of the mechanical properties of these materials. The supramolecular polymers discussed above are the products of multistep synthesis, and it is a daunting task to prepare sufficient amounts of material for evaluations such as melt–rheological experiments and tensile testing. The development of the ureidopyrimidinone functionality, a synthetic very accessible quadruple hydrogen-bonding unit with a very high association constant, has helped enormously to open the way to complete exploration of all aspects of supramolecular polymers.

E. Ureidopyrimidinone-Based Polymers

The ureidopyrimidinone unit can be made in a one-step procedure from commercially available compounds,^{29,31} and it dimerizes with an association constant of 6×10^7 M⁻¹ in CDCl₃. Difunctional compounds (**21**), possessing two of these ureidopyrimidinone units, form very stable and long polymer chains in solution as well as in the bulk (Figure 11).^{113,114}

Dissolving a small amount of this low-molecular-weight compound (**21**) in chloroform results in a solution with a high viscosity. It can be calculated that polymers with chain lengths of the order of 10^6 Da can be formed when highly purified monomers are used. The presence of monofunctional impurities

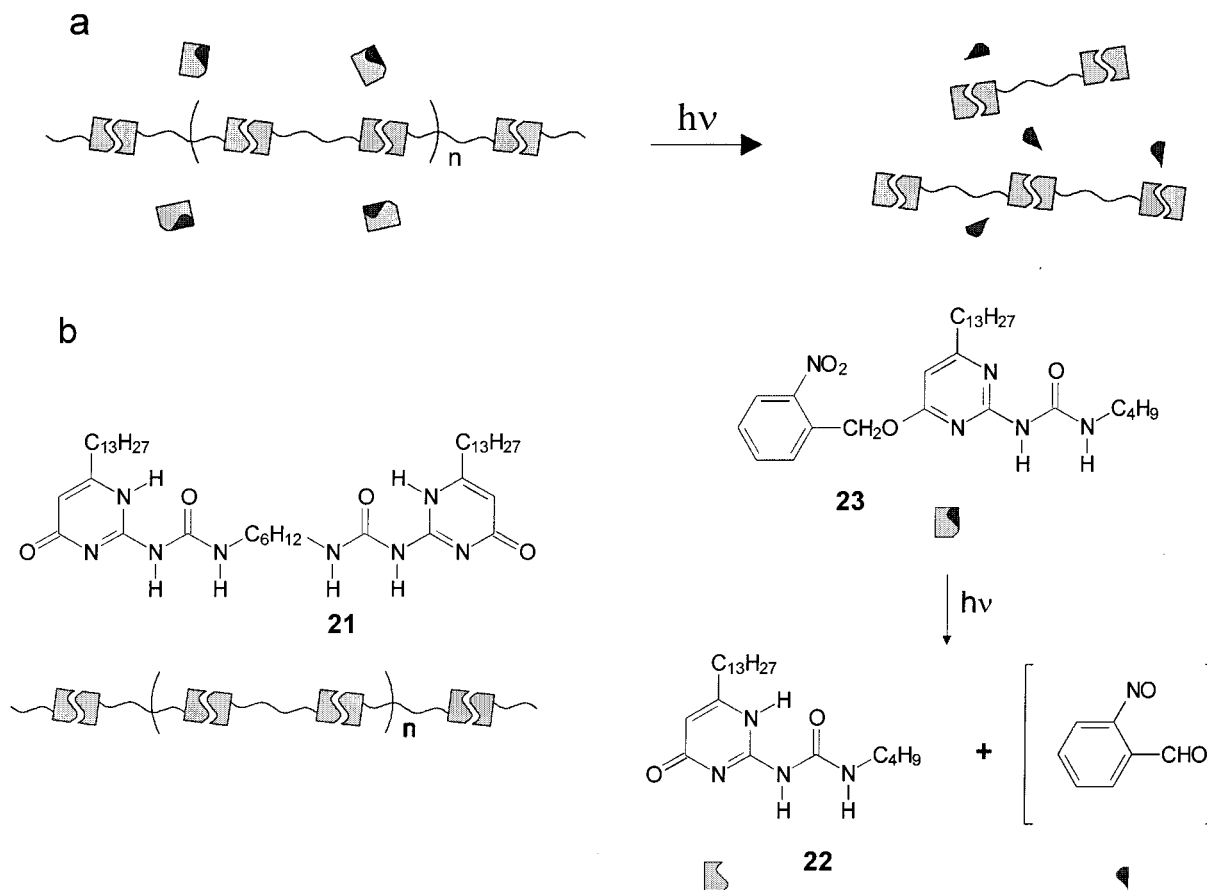


Figure 12. Light-induced depolymerization of UPy-based supramolecular polymers. Concept (a); and compounds used (b).

is expected to lead to a dramatic reduction in DP, because they will act as “chain stoppers”. In fact, deliberate addition of small amounts of monofunctional compounds (**22**) results in a sharp drop in viscosity, proving the reversibility and unidirectionality of association. The reversibility of the linkages between the building blocks is instrumental in the development of materials that change their properties in response to environmental changes, so-called ‘smart materials’. Application of a light-sensitive monofunctional compound (**23**) yielded a material from which the degree of polymerization in solution could be tuned by UV irradiation (Figure 12).¹¹⁵

Although the supramolecular polymers based on bifunctional ureidopyrimidinone derivatives in many ways behave like conventional polymers, the strong temperature dependence of their mechanical properties really sets them apart from macromolecular polymers. At room temperature, the supramolecular polymers show polymer-like viscoelastic behavior in bulk and solution, whereas at elevated temperatures liquid-like properties are observed. These changes are due to a 3-fold effect of temperature on the reversible polymer chain. Because of the temperature dependence of the K_a value of UPy association, the average DP of the chains is drastically reduced at elevated temperatures. Simultaneously, faster dynamics of the scission–recombination process leads to faster stress relaxation in an entangled system. These two effects occur in addition to the temperature-dependent stress relaxation processes that are also operative in melts

or solutions of conventional polymers. Similar to the behavior in the melt, solution viscosities of UPy-based supramolecular polymers are also strongly temperature-dependent. Recently a very surprising inversion of the normal temperature-dependence of the solution viscosity was observed in solutions of preorganized difunctional compounds (**24**), which form a mixture of linear polymer chains and cyclic dimers (Figure 13).¹¹⁶ The thermodynamic parameters of this equilibrium are such that polymerization is favored at higher temperatures. As a result, the viscosity of a 145 mM chloroform solution of the compound was observed to increase by a factor of 3.9 when the temperature was increased from 255 to 323 K. Entropy-driven polymerizations are rare, and the unexpected effect in this system is the first time it was observed in a reversible synthetic system.

The quadruple hydrogen-bonded unit has been further employed in the chain extension of telechelic polysiloxanes,¹¹⁷ poly(ethylene/butylenes), polyethers, polyesters, and polycarbonates.¹¹⁸ In these compounds, the material properties were shown to improve dramatically upon functionalization, and materials were obtained that combine many of the mechanical properties of conventional macromolecules with the low melt viscosity of organic compounds. This strategy can be seen as closing the gap between polymers and oligomers by taking the best of both worlds. Especially in the field of conjugated polymers for plastic electronic devices, expectations for future applications of this strategy are high.¹¹⁹

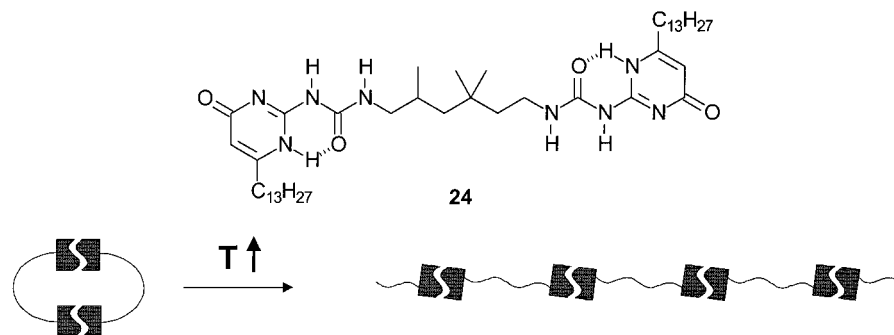


Figure 13. Entropy-driven ring-opening polymerization of the cyclic dimer of **24**.

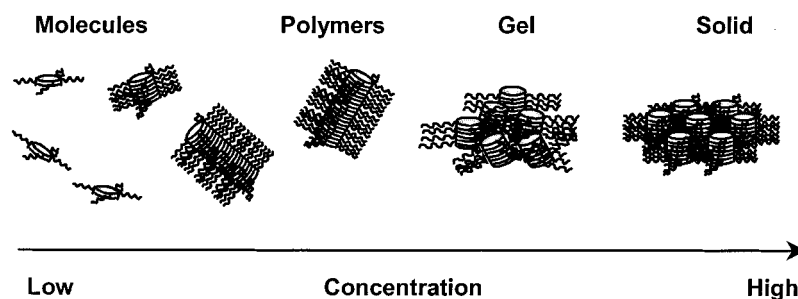


Figure 14. Self-assembly of discotic molecules with the different aggregates given as a function of concentration.

Very recently, Coates et al. used a vinyl-substituted Urypic unit to be part of an olefin polymerization using the Brookhart catalyst. With small amounts of Urypic units incorporated, the polyolefins showed thermo-plastic elastomeric properties.¹²⁰

The reversibility of supramolecular polymers adds new aspects to many of the principles that are known from condensation polymerizations. A mixture of different supramolecular monomers, for example, will yield copolymers, but it is extremely simple to adjust the copolymer composition instantaneously by adding an additional monomer. Moreover, the use of monomers with a functionality of three or more, will give rise to a network formation. However, in contrast to condensation networks, the “self-healing” supramolecular network can reassemble to form the thermodynamically most favorable state, thus forming denser networks.¹²¹

Although the “virtual” molecular weight and lifetime of supramolecular polymers and networks based on strong hydrogen-bonding functionalities is extremely high, low creep resistance is an intrinsic property of these materials that may limit future applications. Strong interchain interactions, especially in crystalline domains, may be employed to tackle this problem and may lead to thermoplastic elastomers with enhanced processability. With the facile synthetic accessibility of these self-complementary Urypic units at hand it is expected that many novel materials properties can be obtained, and multiple hydrogen bonding between repeating units offers an ideal motive for supramolecular polymers, both in solution and in the solid state.

V. Supramolecular Polymers Based on Discotic Molecules

Discotic molecules are ditopic structures with a disc-shaped core and a periphery of a number of

flexible side-chains. The core generally consists of a planar aromatic system, whereas the side-chains are usually flexible alkyl chains.¹²² This anisotropy generates thermotropic liquid crystalline mesophases, as was first discovered in 1977. The structural properties make discotic molecules highly suitable for the formation of supramolecular polymers in solution. The strong π - π (or arene-arene) interactions of their cores make discotics prone to aggregate in either polar or apolar solvents, forming rodlike or wormlike polymers. Because of the polarizability and good intermolecular contact of the planar aromatic system attractive intermolecular stacking interactions occur. In polar or in very apolar solvents the π - π stacking may be strengthened significantly by solvophobic interactions. In this section we will use the general term arene-arene interactions, but it should be noted that solvophobic effects are generally stronger than π - π stacking.

Actually, discotic liquid crystals are the only type of liquid crystals able to form linear architectures, i.e., supramolecular polymers, in dilute solution by means of these stacking interactions. Other types of liquid crystals have ordering interactions of the same order of magnitude in at least two dimensions. This gives rise to gels at appreciable concentration, i.e., uncontrolled growth of the aggregates, whereas at lower concentrations the intermolecular interactions are generally too weak to generate polymeric architectures.

In discotics, the interdisk stacking interaction is several orders of magnitude stronger than the inter-columnar interactions, because of the phase separation induced by the side-chains whose van der Waals interactions are much weaker. Generally, long polymers are obtained via discotics that have strong and specific intermolecular interactions, either via a large aromatic core or via additional specific intermolecular

interactions such as hydrogen bonding. Moreover, the combination of two or more interactions accounts for the formation of highly ordered columns. Only at higher concentrations, the intercolumnar interactions become prominent, and superstructure formation or gelation occurs followed by the liquid crystalline phase in the bulk. An illustrative picture displaying the self-assembly of discotic molecules into supramolecular polymers is given in Figure 14.

In this section we will discuss those discotic molecules that have been shown to form supramolecular polymers. For information concerning discotic liquid crystals in general, their synthesis, behavior, and applications the reader is referred to review the literature.¹²² The mechanical properties of the supramolecular polymers from discotic liquid crystalline molecules are not particularly interesting and have not been studied in detail, therefore, these properties will not be covered here. It should be noted, however, that because of the strong intermolecular interactions, the thermotropic mesophases of discotics generally show much better mechanical properties than those of calamitics, illustrating the beneficial properties of strong unidirectional interactions. Because the specific interactions between the disks in the rigid-rod supramolecular polymers often gives rise to well-defined architectures, we will discuss the architectures of these supramolecular polymers in more detail.

This section is divided into three parts. The first part, section A, deals with rodlike polymers formed by the arene–arene interactions. In the second part (B) discotics will be discussed for which unidirectional hydrogen bonding is the driving force for supramolecular polymerization. Finally, section C will deal with supramolecular polymers formed by a combination of arene–arene interactions and hydrogen bonding.

A. Arene–Arene Interactions

1. Triphenylenes

Alkoxy substituted triphenylenes (**25a–e**) were among the first discotic molecules shown to be liquid crystalline.^{123,124} A large variety of different triphenylenes has been synthesized and their thermotropic mesomorphism has been studied in great detail.¹²² The aromatic core of triphenylenes is relatively small; nevertheless, polymerization of triphenylenes (**25a–c**) does occur in deuterated hexadecane as shown with small angle neutron scattering (SANS).¹²⁵ At low concentrations the DP is small, but at higher concentrations (10^{-3} M) rodlike polymers are observed. The intercore distance was determined to be ~ 6 Å, a value significantly larger than the stacking distance of ~ 3.5 Å in the liquid crystalline state. This result indicates that the molecules are loosely stacked, most probably due to the absence of specific intermolecular interactions. Furthermore, the triphenylenes are highly mobile and undergo both lateral and rotational translation, similar to that in the liquid crystalline state.¹²⁶ The supramolecular polymerization of triphenylenes was also visualized using optical techniques. Increase of the concentration of a solution of

triphenylene **25d** resulted in a broadening of the UV–Vis spectrum and an increase of the absorbance.¹²⁷

Ringsdorf and co-workers have shown that triphenylenes can form alternating donor–acceptor supramolecular polymers in solution by doping them with equimolar amounts of electron acceptors.^{128,129} Supramolecular polymers formed in this manner allow for electron transfer perpendicular to the molecular planes upon excitation of the chromophores, i.e., unidirectional charge-transport through the column.¹³⁰ The formation of these donor–acceptor pairs is favored in apolar solvents. In more polar solvents the triphenylenes alone do not polymerize and consequently donor–acceptor polymers with low DP are formed.

The “loose” way of stacking of the triphenylenes was shown by the absence of a Cotton effect in circular dichroism (CD) experiments for chiral triphenylene **25e** in heptane.¹³¹ Even though this chiral molecule does form a supramolecular polymer, the side-chain chirality is not expressed in the column: a phenomenon typical for molecules arranged in an unordered assembly. Mixing of achiral alkoxytriphenylene **25d** with a bulky chiral electron acceptor derived from (–)-menthol 3,5-dinitrobenzoate (**26**) did introduce supramolecular chirality in the columns.¹²⁷ The sterically demanding “bulky” menthol group intercalates in the alkyl side-chains of the triphenylene and induces a noncooperative helical twist into the columns (Figure 15), resulting in an induced CD effect in the chromophore of the triphenylene.

Triphenylenes provided with nonionic di(ethylene oxide) side-chains (**25f**)^{132–134} or with ionic alkyl chains (**25g**)¹³⁵ form supramolecular polymers in water.¹³⁶ The arene–arene interactions of the aromatic cores allow for the formation of columnar “micelles”. At low concentrations the columns are relatively short, and the solutions are isotropic. At higher concentrations the longer columns interact and lyotropic mesophases are formed.¹³³ Computer simulations showed that in the isotropic solution the polymerization of the discotics is driven by solute–solute attraction and follows the theory of isodesmic linear aggregation; the association constants for dimerization, trimerization, and etc., are equal and the DP of the column thus can easily be tuned by concentration and temperature.^{137,138} At higher concentrations the sizes of the columns are influenced by their neighbors, the columns align, and the DP rises rapidly.

Fluorescence studies have shown that the radiative lifetime of **25f** increases upon increasing DP, suggesting that the mobile excitons move through the supramolecular polymers and relax at their ends.¹³⁹ Insertion of electron acceptors between the triphenylenes accounts for the formation of longer polymers and increases the order within the column. An X-ray diffraction ring with a diffraction spacing of 3.5 Å indicates a short intermolecular distance, a feature not present for undoped samples.¹⁴⁰ A chiral electron acceptor resulted in the formation of a cholesteric mesophase.

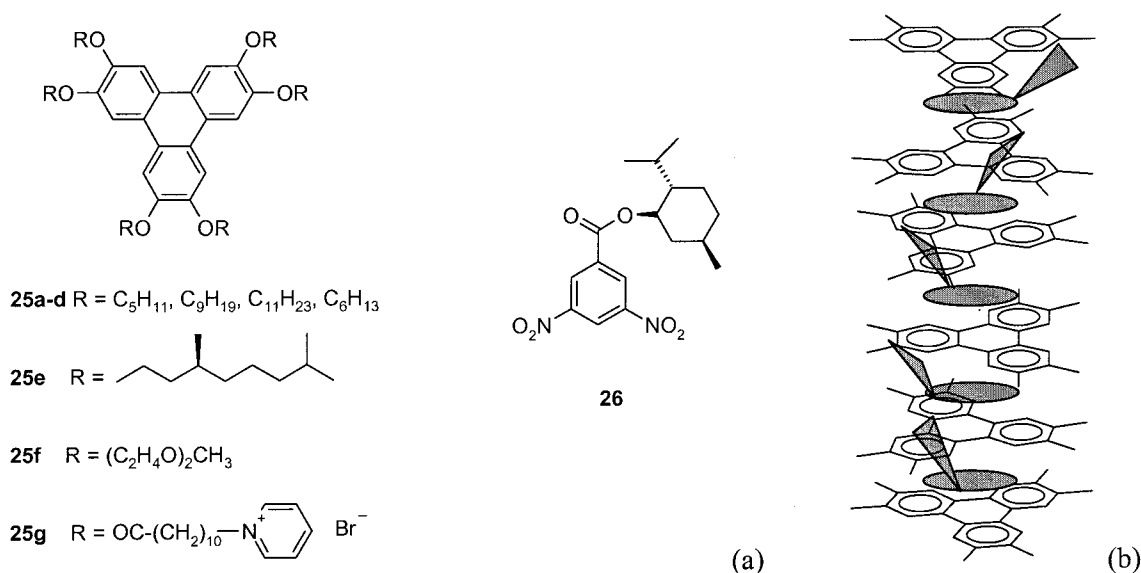


Figure 15. (a) Apolar (**25a–e**) and polar (**25f–g**) triphenylenes and electron acceptor (–)-menthol 3,5-dinitrobenzoate (**26**). (b) Helical columns based on the donor–acceptor system as studied by Schuster.

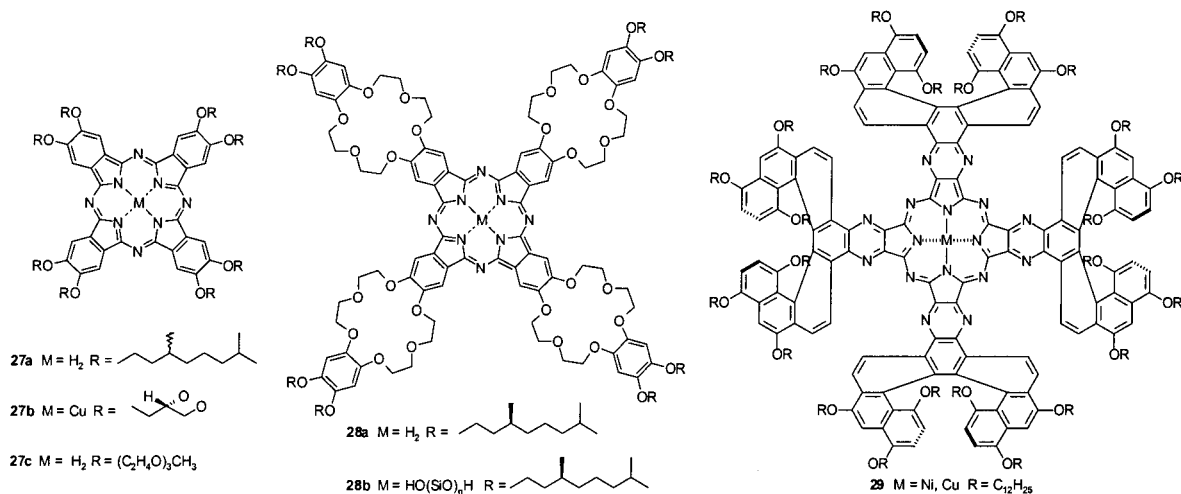


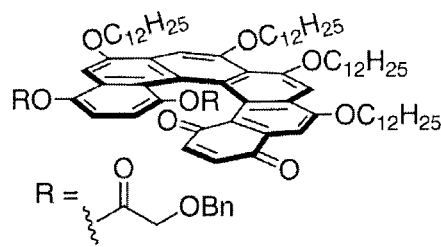
Figure 16. Extended-core phthalocyanine discotics **27–29**.

2. Phthalocyanines and Porphyrins

With respect to triphenylenes, phthalocyanines have a significantly larger core, in principle generating stronger intermolecular arene–arene interactions.¹⁴¹ Moreover, their optical and electrical properties can be easily tuned by incorporation of a metal in the core. The aggregation of nonliquid crystalline phthalocyanines in both water^{142,143} and in organic solvents^{144,145} has been studied intensively in the past; and more recently the formation of Langmuir–Blodgett^{146,147} films and the aggregation of liquid crystalline compounds also have been investigated.^{148–150} In contrast to the isodesmic aggregation of triphenylenes, phthalocyanines show a nonisodesmic behavior as they preferably dimerize and do not form oligomers until much higher concentrations.^{151–156} Experiments on Langmuir–Blodgett films of phthalocyanine **27a** have indicated that large columnar aggregates are present (Figure 16), but that they consist of repeating oligomers built up from two to six molecules.¹⁵¹ Apparently, dimerization significantly lowers the intermolecular affinity of phthalocyanines,

and only in phase-separated systems such as gels, or in the solid, are long supramolecular polymers formed.¹⁵⁷

Interestingly, it has been possible to obtain helical phthalocyanine polymers. By locking the position of phthalocyanines, rotation is prevented. Amphiphilic, chiral metallophthalocyanine **27b** dissolves molecularly in DMSO, but addition of water results in the formation of a helical dimer.¹⁵⁸ In the twisted helical stacks, rotation is no longer possible because of intermolecular hydrogen bonding. At higher concentrations polymeric fibrous assemblies are formed. For apolar analogues in apolar solvents similar chiral dimers and higher aggregates have been obtained.¹⁵⁹ By providing the phthalocyanine with a periphery of crown ethers^{160,161} and chiral alkoxy side-chains (**28a**), self-assembly in helical aggregates occurs, as was deduced from the emergence of a Cotton effect and large helices observed with electron microscopy at higher concentrations.¹⁶² The side-chains induce a twist in the aggregate because of steric interactions since the aggregates formed by their achiral coun-



30

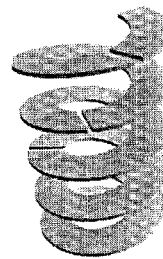


Figure 17. Liquid crystalline disc-shaped helicene **30** and its mode of association into helical columns. (Reprinted with permission from ref 189. Copyright 2000 John Wiley & Sons, Inc.)

terparts are not helical.¹⁶³ The helicity of this aggregate could be “turned off” by the addition of potassium salt, overruling the twist imposed by the chiral side-chains, with the ion–dipole coordination of potassium ions to two crown ether rings of two different phthalocyanines. The unwinding of the helical aggregate results in a nonassociating achiral dimer. In contrast, the supramolecular chirality of covalent polymer **28b** remains present upon the addition of potassium ions, illustrating the ease of tuning the properties of supramolecular polymers via external stimuli.¹⁶⁴

Providing phthalocyanines with chiral bulky helicenes at the periphery (**29**) also results in helical aggregates.¹⁶⁵ Aggregation in chloroform occurs upon addition of ethanol as was observed with UV–Vis spectroscopy, while CD spectroscopy revealed the helical nature of the columnar aggregates. Calculations have indicated that two phthalocyanines need to be rotated to allow a favorable intermolecular distance of 3.4 Å, because of the bulky helicenes. As such, phthalocyanines provided with racemic helicenes cannot stack in such a defined manner, because of the steric hindrance of the racemic side groups. Aggregation of a smaller analogue of **29**, a triphenylene-based porphyrazine, has been shown to occur as well.¹⁶⁶

Polymerization of phthalocyanines in water occurs for derivatives substituted with oligo(ethylene oxide) side-chains (**27c**).^{167,168} In the lyotropic mesophases in water supramolecular polymers are present, and a comparative aggregation study between tetraphenylporphyrins and phthalocyanines proved the polymerization of the phthalocyanines to be stronger.¹⁶⁸ The strong arene–arene interactions and the flatness of the aromatic core in the phthalocyanines causes them to aggregate more strongly, also mediated by the additional hydrophobic effect.

Porphyrins are close analogues to the phthalocyanines, and ionic porphyrins can be considered to fall into the class of the chromonics (vide infra), however, nonionic porphyrins also have been shown to aggregate.¹⁶⁸ Also, porphyrins are mainly forming dimers in solution,^{169,170} although aggregation into larger aggregates such as fibers has been shown.¹⁷¹ Within the aggregates the molecules are rotating freely, but use of additional interactions such as intermolecular hydrogen bonding hinders the rotation and generates chiral aggregates.¹⁷¹

3. Helicenes

Nonracemic helicene **30** has been shown to form supramolecular polymers, and the helical shape of

their rigid cores renders these columns helical (Figure 17).¹⁷² The high DP at high concentrations in dodecane results in an increase of the viscosity and an increase of the Cotton effect as observed with CD spectroscopy. The helical supramolecular polymer gives rise to a stronger expression of chirality, because the intrinsic shape of the helicenes generates a tight “intertwined” fit. More detailed measurements have been performed on columns formed by a non-liquid crystalline helicene.^{173–175} These supramolecular polymers have been proven to be extremely promising systems for second-order nonlinear optics. They form highly organized Langmuir–Blodgett films in which the chiral polymeric organization makes the second-order NLO susceptibility approximately 30 times larger for the nonracemic material than for the racemic material with the same chemical structure.¹⁷⁶

4. *m*-Phenylene Ethynylene Oligomers

Whereas helicene **30** studied by Katz¹⁷² is helical under all conditions, the *m*-phenylene ethynylene oligomers studied by Moore are flexible and can reversibly fold into helices. Depending on the substitution pattern, the oligomers fold either into lamellae (**31a**)¹⁷⁷ or into column-forming helices (**31b**)¹⁷⁸ in the liquid crystalline state (Figure 18). In solution the oligomers can be directed to fold from a random coil into a helix.^{179,180} Increasing the polarity by addition of water (a nonsolvent for the backbone) results in the polymerization of the helices in helical columns.¹⁸¹ The polymerization of the oligomers is a cooperative process: a chiral oligomer **31c** creates a homochiral platform for an achiral oligomer **31a** to stack and thus amplifies its chirality to the achiral oligomer. Also, apolar *m*-phenylene ethynylene oligomers **31d** fold into helices.¹⁸² Because of the strongly favored arene–arene interactions in apolar solvents, the helical folding coincides with stabilizing stacking of the oligomers into helical columnar polymers, giving a strong and time-dependent enhancement of the Cotton effect.

Cyclic *m*-phenylene ethynylene oligomers **32** adopt a completely flat conformation (Figure 19) and form highly stable thermotropic mesophases due to strong π – π stacking of the cores.¹⁸³ These arene–arene interactions also induce polymerization in solution.¹⁸⁴ The DP depends heavily on the nature of the substituents on the macrocycle.¹⁸⁵ Planarity is a strict requirement for polymerization as the DP is strongly suppressed for nonplanar macrocycle **33**.¹⁸⁶ Butadiyne bridged macrocycles with benzenes (**34**) or with pyridines (**35**), the larger analogues of the *m*-phen-

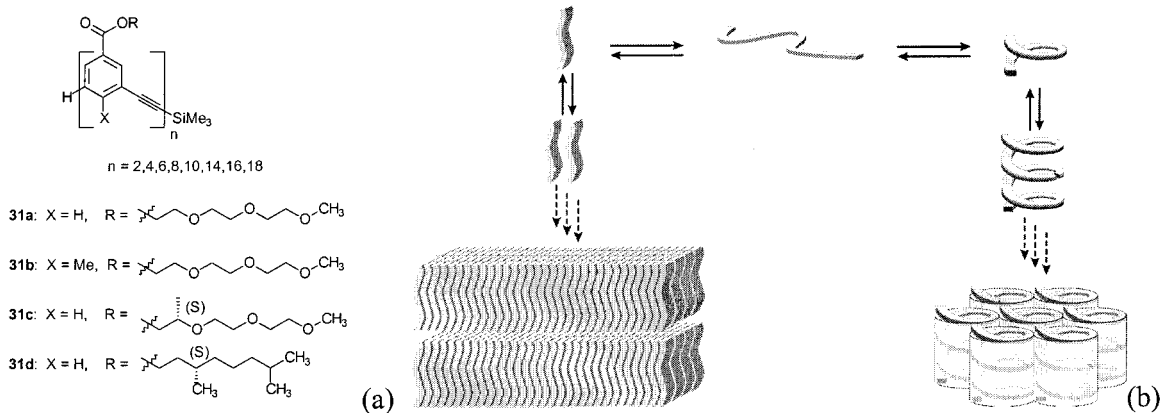


Figure 18. *m*-Phenylene ethynylene oligomers as studied by Moore (a), that fold from a random coil in good solvents into helices and columns in poor solvents and into lamellae or hexagonally packed columns in the solid state (b). (Reprinted with permission from ref 178. Copyright 2000 American Chemical Society.)

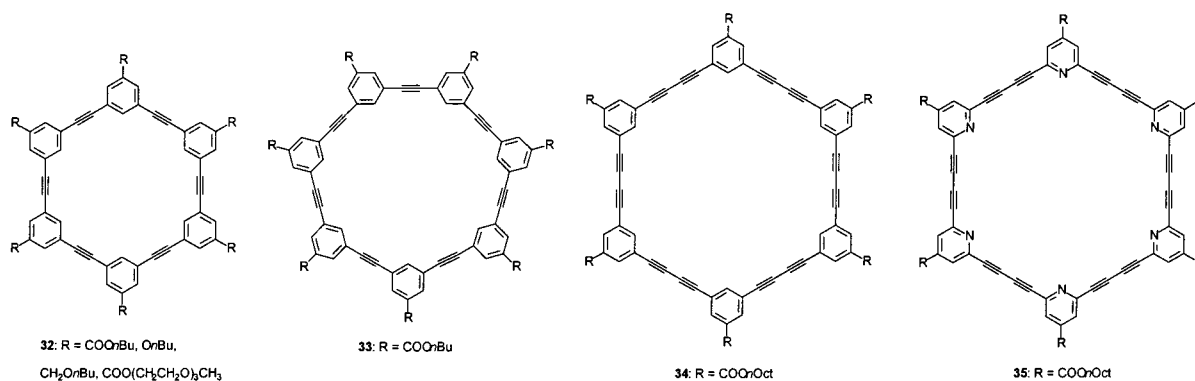


Figure 19. Extended-core *m*-phenylene ethynylene cycles **32**–**35**.

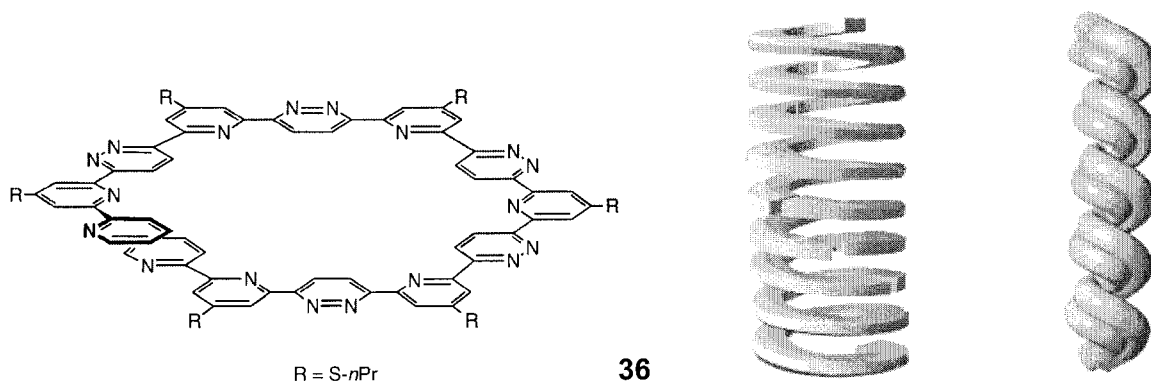


Figure 20. Pyridine–pyridazine oligomer **36** studied by Lehn and its proposed mode of aggregation into columns and superstructures. (Reprinted with permission from ref 190. Copyright 2000 John Wiley & Sons, Inc.)

ylene ethynylene macrocycles, have been shown to form columnar polymers as well.^{187,188}

5. Other Systems

Folding into helices¹⁸⁹ and subsequent polymerization of the helices into columns and larger architectures (Figure 20) is observed for pyridine–pyridazine oligomers (**36**).¹⁹⁰ Similar to the *m*-phenylene ethynylene oligomers **31**, these flexible oligomers adopt a helical conformation because of programmed intramolecular interactions. At higher concentration the polymers self-assemble to give helical fibers, which were visualized with electron microscopy. Upon binding of cyanuric acid, oligo-isophthalamides fold to a helical disk, and these disks

also subsequently self-assemble to form fibers at higher concentrations.¹⁹¹ The controlled use of external stimuli and programmed intermolecular interactions illustrates the power to generate and direct supramolecular polymers.

Ringsdorf showed a nice example of confinement of supramolecular polymers.¹⁹² In cyclohexane, hexacinnamoyl azacrown **37** self-assembles to form supramolecular columnar polymers. The periphery of photopolymerizable groups forms cross-links via photocycloaddition and allows the pre-assembled supramolecular polymer to be transferred into a rodlike covalent polymer (Figure 21). Performing the reaction on molecularly dissolved molecules gives rise to a randomly cross-linked polymer with a lower DP.

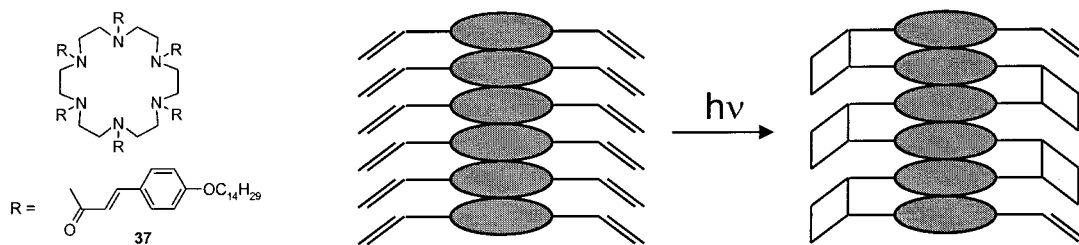


Figure 21. Hexa-cinnamoyl azacrown with polymerizable side-chains **37** as studied by Ringsdorf, and the photopolymerization into covalent columns in solution.

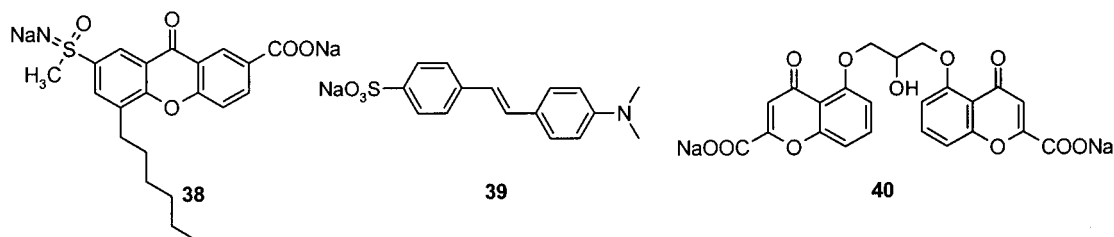


Figure 22. Examples of drug and dye molecules forming chromonic mesophases in water.

As early as 1986, the aggregation in solution of an alkyl modified 2,6,2',6'-tetraphenyl-[4,4']-bipyranilidene was shown, and the self-assembly was related to its thermotropic mesomorphism.¹⁹³ The addition of the more polar solvent methanol to methylene chloride induces aggregation into J aggregates. As the nonliquid crystalline compound without the side-chains does not aggregate, it might be concluded that the self-assembly is, in this case, not dominated by the aggregation of the aromatic core. Self-assembly via aggregation of the side-chains occurs, which is fundamentally different from the previously discussed polymers, and generally leads to 3-dimensional growth.

A variety of smaller discotic molecules have been shown to form lyotropic mesophases in either alkane solvents or water. These discotics range from alkyl-oxydibenzopyrenes¹⁹⁴ and hexaesters of hexahydroxybenzene and -cyclohexane¹⁹⁵ to metallo-discogens.¹⁹⁶

6. Chromonics

Discotic molecules provided with oligo(ethylene oxide) side-chains form supramolecular polymers in water. If the discotics are provided with ionic groups the compounds are known as chromonics (for examples see **38–40**, Figure 22).^{197,198} Even though chromonics are crystalline and do not form supramolecular polymers in the solid state, we mention them briefly here because of their practical importance and widespread occurrence. A large body of work, dating back to the early part of the 20th century, has been performed on these compounds, and the reader is referred to review articles for detailed information.^{197,198} The most common chromonics are drugs and dyes, which explains the early recognition of their aggregation. Their self-assembly in water makes them a highly important type of lyotropic liquid crystal, as it influences their performance. The molecules first self-assemble, isodesmic, into supramolecular rodlike polymers, followed by the formation of lyotropic mesophases. The rodlike polymers

induce a strong increase in the viscosity of the solution, and the dynamic properties of these aggregates leads to rheological behavior typical for entanglement networks.¹⁹⁹ The observations have indicated that chromonics are suited as simple model systems for a broader and deeper insight into the principles of flow.

B. Hydrogen Bonding

Section V–A has dealt with the formation of supramolecular polymers by nonspecific arene–arene stacking, which generally results in irregular or “loose” stacking. The use of additional steric interactions in these structures allowed for a control over supramolecular order or helicity. In this section we will discuss columnar supramolecular polymers formed by the more specific intermolecular hydrogen bonds.

The main body of work on columnar hydrogen-bonded architectures has been performed on 1,3,5-benzene triamides (**41**), which are C_3 -symmetric molecules consisting of a single benzene ring and 3 side-chains connected via amide bonds.^{200,201} The molecules arrange themselves in columns via 3-fold intermolecular hydrogen bonding as proven by X-ray diffraction²⁰² and infrared spectroscopy. The weak arene–arene interactions of the single central benzene group are subordinate to the strong 3-fold hydrogen bonding. For packing reasons, the intermolecular hydrogen bonds rotate out of the plane, thus inducing helicity in the columns. Achiral compounds **41a–d** form an equimolar mixture of left- and right-handed helical columns, but the homochiral side-chains of chiral discotic compound **41e** introduce an energy difference between left and right-handed columns and bias the helicity.²⁰³ Figure 23 shows the formation of the helical columnar polymers by the polymerization of **41d** in a cartoon-like presentation.²⁰²

The helical rigid-rod polymers have a high DP even in very dilute solution (10^{-6} M in hexane), due to their large association constant ($5 \cdot 10^8$ L/mol). When

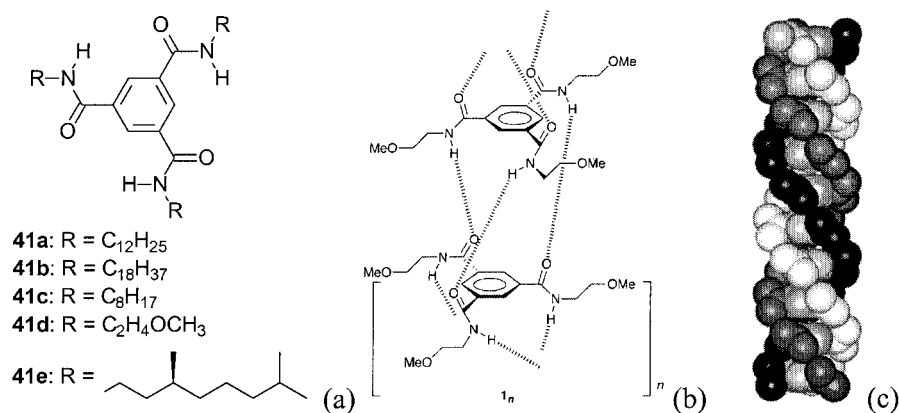


Figure 23. (a) 1,3,5-Benzene trisamides that form columns in apolar solvents via 3-fold intermolecular hydrogen bonding; (b) solid state arrangement of the helical columns; (c) graphical representation of the helical hydrogen-bonded columns. (Reprinted with permission from ref 202. Copyright 1999 Royal Society of Chemistry.)

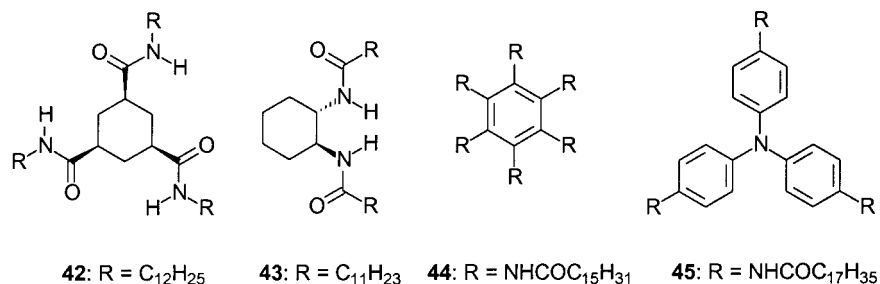


Figure 24. Small discotics that form columnar polymers via intermolecular hydrogen bonding.

chiral (**41e**) and achiral (**41c**) molecules are blended mixed columns are formed, and, surprisingly, only one chiral disk (on average) on every 200 achiral disks is enough to bias the helicity of a complete columnar polymer for one helicity. These results are analogous to those obtained in chiral polymers with covalent bonds in the main chain²⁰⁴ and are explained by a strong intracolumnar cooperative effect via directional hydrogen bonding in polymers with a very high DP. At higher concentrations, the long columns gelate the solvent via lateral intercolumnar interactions,^{200,201} reminiscent of the behavior of rigid-rod covalent polymers such as polyaramides and poly(γ -benzyl-L-glutamate).²⁰⁵

Cis-1,3,5-cyclohexanetricarboxamides (**42**) are another example of discotic molecules assembling in columns via intermolecular hydrogen bonding (Figure 24).²⁰⁶ Because of the cis arrangement of the amides, all three can participate in the uni-directional hydrogen bonding. Depending on the type of solvent, the compound either gels the solvent or forms a transparent viscoelastic fluid. No mention is made of the presence of helicity in the columnar aggregates or at a microscopic level, in contrast to the trans-1,2-diaminocyclohexane derived gelators (**43**), which form chiral supercoiled structures observable with electron microscopy.²⁰⁷

Aggregation via hydrogen bonding and formation of columns and lyotropic liquid crystals and gels has also been described for benzenehexamine derivatives **44**²⁰⁸ that assemble via 6-fold intermolecular hydrogen bonding, and for tris(stearoylamino)triphenylamine **45**²⁰⁹ that assembles via 3-fold intermolecular hydrogen bonding.

C. Arene–Arene Interactions and Hydrogen Bonding

Although hydrogen bonds can be employed for the creation of highly ordered columns (section V–B), their use is highly limited to apolar solvents. In contrast, arene–arene interactions allow for supramolecular polymer formation in a large variety of solvents, but without positional control (section V–A). Thus, the combination of arene–arene interactions and hydrogen-bonding should allow for formation of highly ordered supramolecular polymers with high DP in solvents as desired. In this section we discuss such supramolecular polymers. Hydrogen bonding has been utilized both for the formation of the discotic entity itself and as a tool to control the order within the columns. Furthermore, the occurrence of hydrogen bonds allows for a controlled hierarchical growth of the well-defined columns, and subtle tuning of the interactions can be achieved by selection of solvent type.

1. Guanine and Pterine Derivatives

The most impressive work on self-assembling chiral discotics has been performed on guanine- and pterine-related molecules by Gottarelli, Spada, and co-workers.²¹⁰ These molecules organize in lamellae in the solid state,^{211,212} but form disc-shaped tetramers in solution via intermolecular hydrogen bonding. The subsequent stacking of the disks into helical columns has been most elaborately studied. The system is of interest because of its strong similarities to DNA and other biopolymers.^{213,214}

Oligomeric deoxyguanosines **46** all assemble into columns in water.²¹⁵ Using SANS, the average length

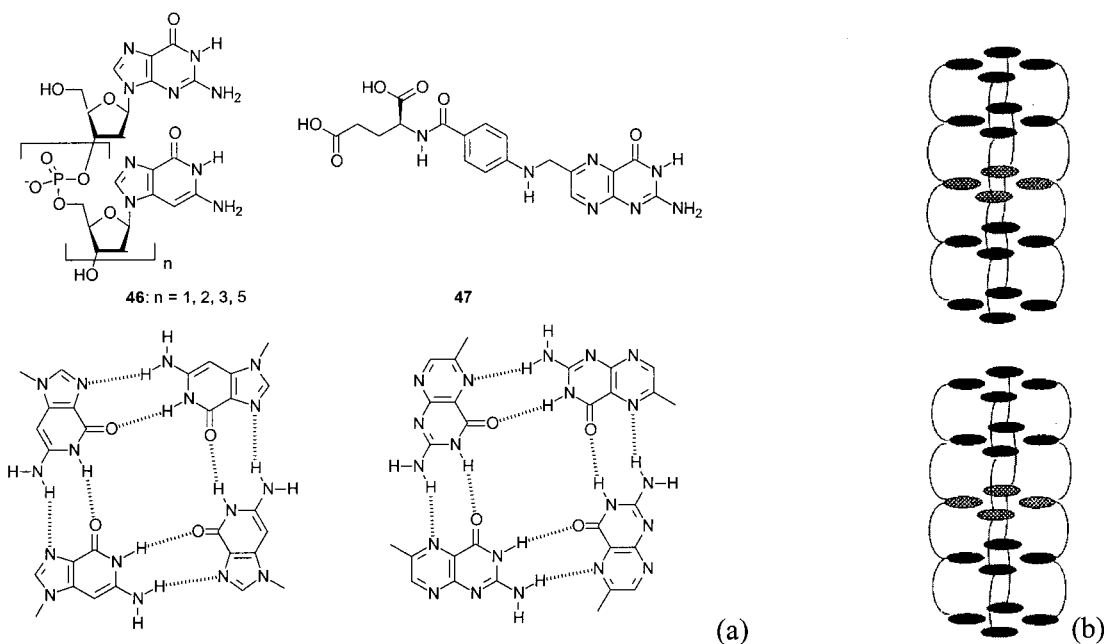


Figure 25. (a) Deoxyguanosine oligomers **46** and folic acid **47** and their mode of self-assembly in tetramers; (b) mode of aggregation of eight d(GpGpApGpG) molecules. First, self-assembly in “barrels” occurs, followed by stacking of these “barrels” in columns. (Reprinted with permission from ref 222. Copyright 1995 Royal Society of Chemistry.)

of the columns (DP) of freshly prepared samples was determined to be around 6 nm at a concentration of 1% in D₂O.²¹⁰ Increase of the temperature resulted in loss of the cylindrical aggregates. When the sodium salt is used, subsequent cooling does not result in the re-formation of the cylindrical polymers. In contrast, use of the potassium salt does allow for reversible self-assembly. The addition of extra potassium salt even increases the DP; it binds to the inner carbonyls of the G-tetramer and stabilizes the tetramer.²¹⁶

The formation of lyotropic liquid crystalline mesophases by a deoxyguanosine derivative in water was reported in 1988,²¹⁷ after which this behavior was found for other monomers and oligomers of deoxyguanosine phosphate.²¹⁸ The microscopic textures observed show the presence of cholesteric and hexagonal phases at lower and higher concentrations, respectively. The polymeric columns are formed in a hierarchical manner: first a well-defined “barrel” is formed by the assembly of four oligodeoxyguanosine oligomers, and then these “barrels” stack on top of one another to give the columns (Figure 25 b).^{210,215} This stepwise self-assembly process was elucidated using CD experiments, which revealed two melting transitions. Furthermore, it was shown that formation of the liquid crystalline phase depends on the amount of electrostatic repulsive interactions from the phosphate groups and the hydrophilic/hydrophobic balance.

Not only guanosine, but also pterine derivatives, give rise to supramolecular polymers in water.²¹⁹ Similar to the guanosines, folic acid **47** assembles in disc-shaped tetramers in water. Addition of sodium or potassium salts aids the tetramerization and induces the aggregation into columns.²²⁰ At the relatively high concentration of 4%, w/w, these columns have an average DP of 9 disks. Melting experiments performed in water and upon the addition of salt showed very interesting results. The

intensity of the Cotton effect was followed as a function of temperature, indicating the amount of chirality present in the columns. In water a single melting transition was detected, whereas in the presence of salt two melting transitions were visible, indicating hierarchical assembly.²²¹

Gottarelli, Davis, and co-workers have prepared apolar guanosine derivatives **48a** and **b** for study in organic solvents. In dilute solution in the presence of potassium ions, disc-shaped structures are formed.²²² In chloroform compound **48b** is molecularly dissolved, but upon contact of the organic layer with an aqueous layer containing potassium salts, **48b** extracts the potassium into the organic layer. An octameric potassium complex is formed, consisting of two stacked G-quartets between which a potassium ion is sandwiched via interactions with the carbonyls of the guanines (Figure 26).^{223,224} Upon the addition of more salt the octamers polymerize into a columnar architecture. In this polymer potassium ions and G-quartets alternate in the stacking.²²⁵ The Cotton effect observed for the polymer indicates a helical columnar nature. Apart from the formation of octamers, the formation of decamers has also been observed.²²⁶

Compound **48b** was shown to display enantioselectivity in the extraction of chiral potassium salts from water into the organic phase.²²⁷ The supramolecular polymer possesses a homochiral helical architecture onto which one of the anionic enantiomers preferentially binds. Intriguingly, for some of the anions the octamer and polymer show opposite selectivity, illustrating the difference in supramolecular chirality of the two. Furthermore, the polymer is capable of inducing a Cotton effect in the achiral potassium *N*-(2,4-dinitrophenyl)glycinate. The use of these polymers as artificial ion channels is currently under investigation, as the apolar side-chains would allow incorporation into a membrane.^{224,228} Also,

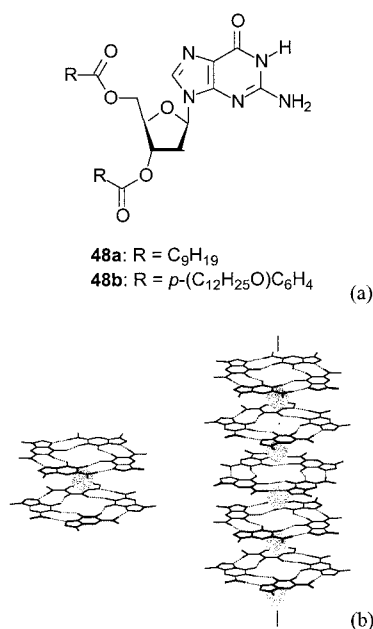


Figure 26. (a) Apolar modified deoxyguanosines, soluble in organic solvents; (b) self-assembly of apolar deoxyguanosines in octamers and polymers upon the addition of potassium ions. (Reprinted with permission from ref 225. Copyright 2001 John Wiley & Sons, Inc.)

these helical columns are ideal supramolecular polymeric architectures for the creation of functional arrays. By providing the guanosines with apolar porphyrins, self-assembly into columns with a periphery of porphyrins was achieved in chloroform by the addition of potassium salt.²²⁹ The formation of such functional polymers using external stimuli offers a unique approach for the creation of bio-inspired self-assembled polymers.

2. Hydrogen-Bonded Pairs

Similar to the guanosine and pterine derivatives, intermolecular hydrogen bonding generates discotics based on molecules **49**. Two molecules **49** dimerize via quadruple intermolecular hydrogen bonding resulting in an extended-core discotic liquid crystal that stacks in apolar solvents and forms columnar supramolecular polymers.²³⁰ Within these columns the discotics are rotating freely. When two hydrogen-bonding units are connected via a short spacer, a bifunctional molecule is generated (**50**), capable of forming hydrogen-bonded, supramolecular polymers

in chloroform similar to the bifunctional ureidopyrimidinones **21** discussed in section IV-E.¹¹³ The disks are in an alternating array of disks and spacers, and they stack in apolar solvents forming a columnar polymer. The columns are helical, in contrast to those formed by monofunctional molecules **49** (Figure 27). The presence of a covalent linkage between consecutive layers of the column prevents rotation of the disks. A comparison might be made here to the function of the sugar–phosphate backbone in DNA.

The intrinsic helicity of the columns formed by bifunctional **50** allows chiral side-chains to control for a preferred handedness (**50b**). The supramolecular polymeric backbone also accounts for a higher DP with respect to monofunctional **49**, as could be observed with SANS and an increased thermostability of the lyotropic mesophase in dodecane. The induction of chirality in the helical columns of **50b** by the chiral side is a cooperative process via the backbone: the helicity of a racemic mixture of helical columns of achiral **50a** is biased when end-capped with monofunctional chiral **49b**.

Helical columns of bifunctional ureidotriazines could also be created in water.²³⁰ In water the aromatic cores of compound **52** stack and create a hydrophobic environment that favors the formation of intermolecular hydrogen bonds. The chiral side-chains can express their chirality within the columnar polymer because of the backbone-generated helicity. In contrast, for monofunctional **51** water interferes with the hydrogen bonding and **51** does not dimerize nor polymerize until it reaches highly elevated concentrations. The bifunctional nature of **52** allows for a high local concentration of stacking units. A comparison might be made here to the individual DNA bases that also do not dimerize and stack in water, unless they are connected to a polymer backbone.

3. Complexation of Tetrazoles with 1,3,5-Tris(4,5-dihydroimidazol-2-yl)benzene

Another example of supramolecular columnar polymers formed by the combined use of hydrogen bonding and arene–arene interactions are the complexes of tetrazoles and 1,3,5-tris(4,5-dihydroimidazol-2-yl)benzene (**53**, Figure 28).²³¹ Four molecules self-assemble to give a supramolecular disc-shaped molecule, which subsequently polymerizes into columns when in nonpolar solvents. Upon formation of a

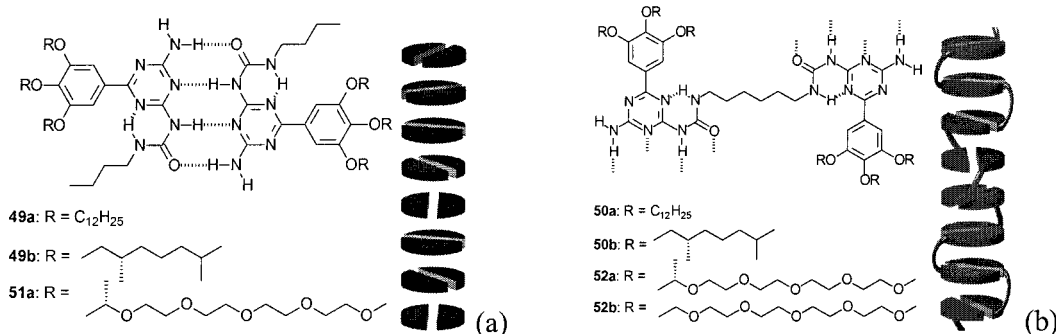


Figure 27. (a) Monofunctional ureidotriazines **49** and **51** and the mode of association of **49** via quadruple hydrogen bonding in a disk and stacking of the disks in columns lacking positional order; (b) bifunctional ureidotriazines **50** and **52** and the helical columns formed by these molecules in which the disks are positionally ordered.

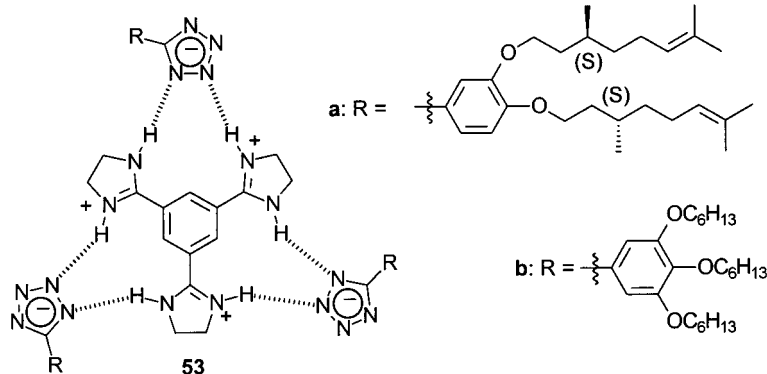


Figure 28. Extended -core discotic **53** built up via intermolecular hydrogen bonding.

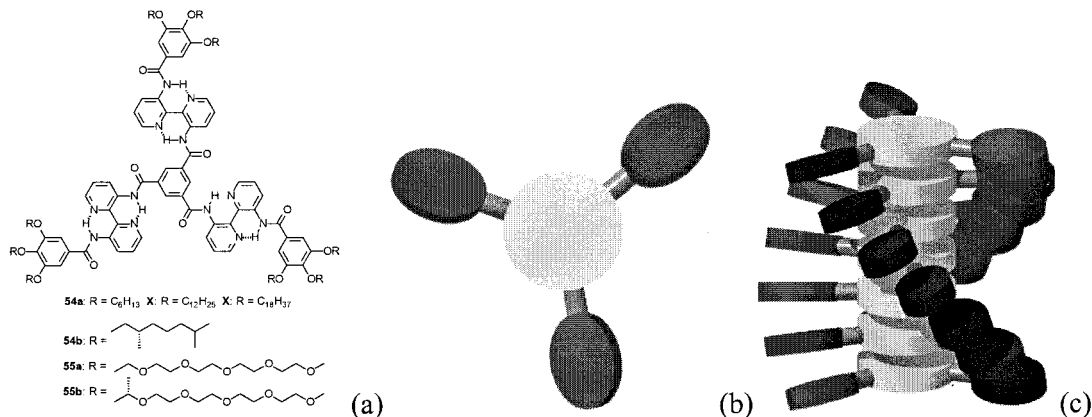


Figure 29. (a) C₃-symmetrical disc-shaped molecules **54** and **55** with achiral and chiral side-chains; (b) a cartoon representation of the propeller-like conformation attained by the C₃-symmetrical molecular; and (c) formation of helical columns by the propellers. (Reprinted with permission from ref 237. Copyright 2000 American Chemical Society.)

columnar aggregate of the chiral disks **53a**, the chirality of the side-chains induces a bias in the helicity of the supramolecular assembly. “Sergeant and soldiers” measurements²⁰⁴ were performed and showed that there is no amplification of chirality from **53a** to **53b**; the induction of helicity in columns of **53** is a noncooperative process.

4. C₃-Symmetrical Discotic Molecules

Molecules that have the best potential for a high degree of polymerization and for the creation of a well-defined architecture in all solvent types need to have a large aromatic core, as well as structuring intermolecular hydrogen-bonding interactions. Disc-shaped molecules **54** and **55** feature these requirements. Discotic molecules **54**²³² form polymeric structures with a rigid-rod character and large DP in very dilute solution (10⁻⁶ M in hexane), due to their large (10⁸ L/mol) association constant.²³³ The aggregation of the disks is a cooperative process; the molecules attain a chiral, propeller-like conformation (Figure 29) and the conformation of subsequent monomers is biased toward a propeller with the same handedness. The optimized stacking interactions result in a helical column. The chirality placed in the side-chains of **54b** accounts for the formation of homo-chiral columns via the transfer of the side-chain chirality into the supramolecular helical polymer. Using “sergeant and soldiers” experiments²⁰⁴ for mixtures of **54a** and **54b**, the presence of only one disk with chiral side-chains per 80 achiral disks is

enough to obtain helical polymers of one helicity exclusively. This experiment shows that there is a high energetic penalty for helix reversal within the polymer. Lateral interactions between the supramolecular polymers arise at higher concentrations and result in the formation of a lyotropic liquid crystalline gel.²³⁴ Because of the chiral propeller-like conformation of the molecules, the columns have a dipole moment along their axes, which allows alignment and switching of the columns in the gel by an electric field.

Polar, water-soluble analogues **55** of these C₃-symmetrical molecules have also been studied, and they have been shown to form helical columns in a variety of polar solvents.^{235,236} A stepwise association process is observed when alcohol solutions of **55** are cooled. The molecules first polymerize into achiral columns with a small DP governed by their generic arene–arene interactions. Subsequently, these achiral columns become helical via a phase transition (Figure 30) and a strong growth spurt of the DP occurs, rendering a DP > 1000.²³⁷ During this transition, specific intermolecular hydrogen-bonding interactions occur that order the molecules in a helical fashion in addition to the arene–arene stacking. In water, the helicity of the columns is similarly lost at higher temperatures, but polymerization is maintained. Because of the increased strength of the arene–arene interactions and lower critical solution temperature (LCST) of the side-chains in water at higher temperature, long columns remain even at 90

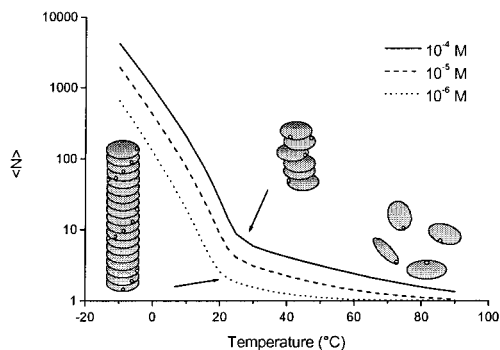


Figure 30. Average number of molecules **55**, $\langle N \rangle$, participating in one column in *n*-butanol at three different concentrations is given as a function of temperature. Arrows mark the transition from achiral to helical aggregates.

°C as proven by SANS. This stepwise growth of the columns shows great similarity to the self-assembly of the tobacco mosaic virus without the ribonucleic acid strand and will undoubtedly aid in the understanding of biopolymer self-assembly.²³⁸

In *n*-butanol the average distance between helix reversals in columns containing both **55a** and **55b** was found to exceed 400 molecules via “sergeant and soldiers”²⁰⁴ experiments. The high persistence length of the helicity results in strong (400-fold) amplification of chirality. In water, the helix inversions were found to occur after, on the average, every 12 disks, indicating that the helical order within the columns is highly solvent-dependent.²³⁶ In water, the solvent interferes with interactions accounting for helical order at all temperatures, resulting in a lower energy barrier for helix inversions.

VI. Supramolecular Coordination Polymers and Miscellaneous Systems

Metal coordination has been used to prepare a wide range of supramolecular complexes with geometries varying in complexity from simple cyclic dimers to catenanes, helicates, and cages with intricate geometries.²³⁹ In view of the apparent ease of construction of these well-defined assemblies, the number of 1-dimensional coordination polymers that has been characterized in solution is surprisingly small. There is extensive literature about coordination polymers in the solid state; this is outside the scope of the present review because these polymers do not exist outside the confinement of their crystal lattice. Most soluble coordination polymers, be they linear^{240–248} or hyperbranched,^{249,250} are held together by kinetically stable metal–ligand interactions and do not show the dynamic reversibility that is observed in true supramolecular polymers. Kinetically labile coordination complexes of metal ions such as Cu(I) and Ag(I) are required to form such aggregates. The first report of dynamic oligomers using these metals dates from 1992,²⁵¹ and it describes stereoregular coordination polymers using peptide-based polydentate ligand **56** containing thienyl, imidazolyl, and thioether donor sites (Figure 31).

The solid-state structure of the complex with silver triflate was determined with X-ray diffraction. On the

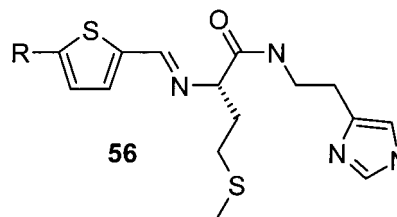


Figure 31. Peptide-based ligand **56** which forms reversible coordination polymers with Ag(I).

basis of a combination of vapor pressure osmometry and conductivity measurements in methanol, the average DP at 0.14 M concentration was estimated to be approximately 11. The reversibility of association was evident from the concentration dependence of the DP; at low concentrations only a monomeric complex was observed. Coordination complexes of Cu(I) and Ag(I) with phenanthroline ligands **57** have been used to prepare the first constitutionally well-defined coordination polymers from kinetically labile complexes in 1996.²⁵² It was demonstrated that high-molecular-mass polymers can be obtained from rigid bis(phenanthroline)ligand and Cu(I), if the solvent used cannot act as a competitive ligand for the metal (Figure 32).

The authors showed that ligand exchange takes place instantaneously in a mixture of Cu(I) and Ag(I) model complexes in coordinating solvents such as acetonitrile, whereas in 1,1,2,2-tetrachloroethane no evidence of ligand exchange was observed after several hours. The strategy to obtain the polymer was based on using the latter solvent, in which ligand exchange is slowed as much as possible. Upon titrating a solution of the monomer with $[\text{Cu}(\text{MeCN})_4]\text{PF}_6$, ¹H NMR spectra showed that end groups were present when less than 1 equiv copper salt had been added, and that at a 1:1 stoichiometry, only broad polymer resonances remained.²⁵³ The resulting solutions displayed high viscosities, indicating high molecular masses. Upon further addition of metal salt, the viscosity decreased again. From this experiment, it can be concluded that exchange between free and coordinated Cu(I) ions continues to occur, even in a noncoordinating solvent. When the polymer was precipitated and redissolved, no signs of degradation of the polymer were observed.

A different approach to coordination polymers has been taken by Terech and co-workers, who studied the aggregation of a Cu(II) tetraoctanoate (**58**, Figure 33). Using neutron scattering, it was shown that in apolar solvents the complex molecules assemble in a linear fashion to form threads with a cross section containing approximately 1 binuclear copper complex.²⁵⁴ Studies in Decalin²⁵⁵ have shown that under certain conditions, the rheological behavior of this system can be described by the theory of living polymers that has been developed by Cates and co-workers.^{256,257} It was suggested that, below a given transition temperature, physical junctions between chains act both as chain extenders and as efficient physical cross-links, resulting in rheological behavior that matches Cates’ predictions of reversible polymers in the semidilute (entangled) regime. Above

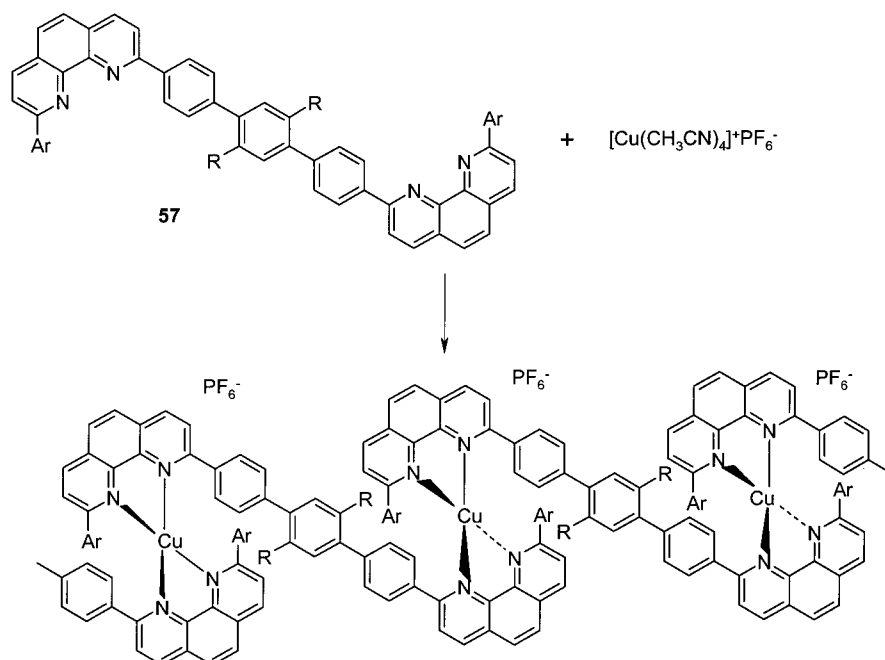


Figure 32. Bifunctional metal complexing **57** and its mode of polymerization upon addition of Cu^+ .

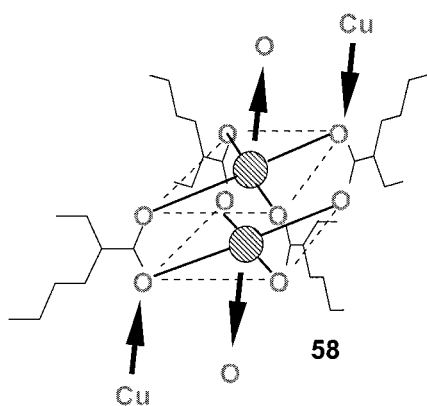


Figure 33. Mode of aggregation of Cu(II) tetraoctanoate **58** into linear polymers. (Reprinted with permission from ref 254. Copyright 1992 American Chemical Society.)

T_{trans} , these physical junctions melt, and the relatively short chains are no longer entangled.

Hunter and co-workers recently reported soluble, high-molecular-weight coordination polymers based on porphyrins.²⁵⁸ A porphyrin was provided with two pendant pyridine groups and a cobalt atom (which has six coordination sites) in the center. The bifunctional molecule **59** was anticipated to form coordination polymers in the fashion depicted in Figure 34. It was shown by ^1H NMR diffusion studies that polymeric aggregates were indeed obtained, and aggregation was confirmed by size exclusion chromatography, which showed that **59** forms aggregates which are significantly larger than those of **60**, which cannot associate beyond the dimeric state. Moreover, the size of the aggregate was shown to be dependent on the concentration of the solution. SEC was also used to show that the size of the aggregates could be tuned by addition of increasing amounts of monofunctional compound, incidentally demonstrating the reversibility of the aggregation process. Using the oligomer peaks in SEC that were observed upon

mixing **59** and **60** as calibration, the authors calculated that the aggregates in a 7 mM solution of **59** have an average molecular mass of 136 kDa, corresponding to a DP of about 100. These experiments nicely demonstrate the balance between kinetic stability (required for successful separation by SEC) and the reversibility needed for tuning the DP with monofunctional molecules.

Usually, ion–dipole interactions are insufficiently directional for the formation of linear supramolecular polymers because the functional groups providing the interaction tend to form clusters in such a system. Recently, Gibson and co-workers have shown that the combination of crown ethers and secondary ammonium ions can successfully be employed for this purpose.²⁵⁹ They designed a system based on Stoddart's finding that 24-dibenzocrown-8 and dibenzylammonium hexafluorophosphate associate strongly ($K_a = 2.7 \times 10^4$ in CDCl_3).²⁶⁰ Association of bifunctional molecules **61** and **62** was investigated by Gibson, and was shown to lead to chain extended aggregates (Figure 35), as was evident from the strong concentration dependence of the viscosity of 1:1 solutions of these compounds in $\text{CHCl}_3/\text{acetone}$. On the basis of end group analysis by NMR, the molecular weight of the aggregates was estimated to be 22 kDa for a 2 M solution, whereas at low concentrations the spectrum was dominated by signals of a cyclic dimer. Flexible films and fibers were obtained from concentrated equimolar solutions of **61** and **62**, from which it was inferred that entangled linear aggregates are present in the solid material. The same interaction between secondary ammonium groups and crown ether moieties has been used in dendritic self-assembly.²⁶¹

Li and McGown used the well-studied inclusion behavior of cyclodextrins to obtain nanotube aggregates of cyclodextrins (**63**) and diphenylhexatriene (**64**) (DPH).²⁶² These reversible, polymer-like aggregates can be formed because two phenyl "head-

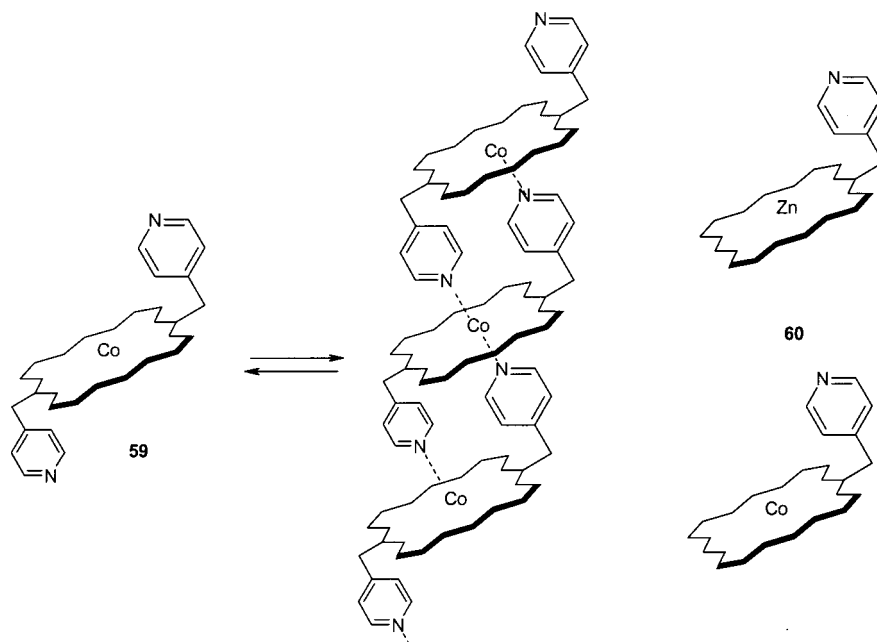


Figure 34. Formation of coordination polymers from porphyrin **59** and two chain stoppers **60**.

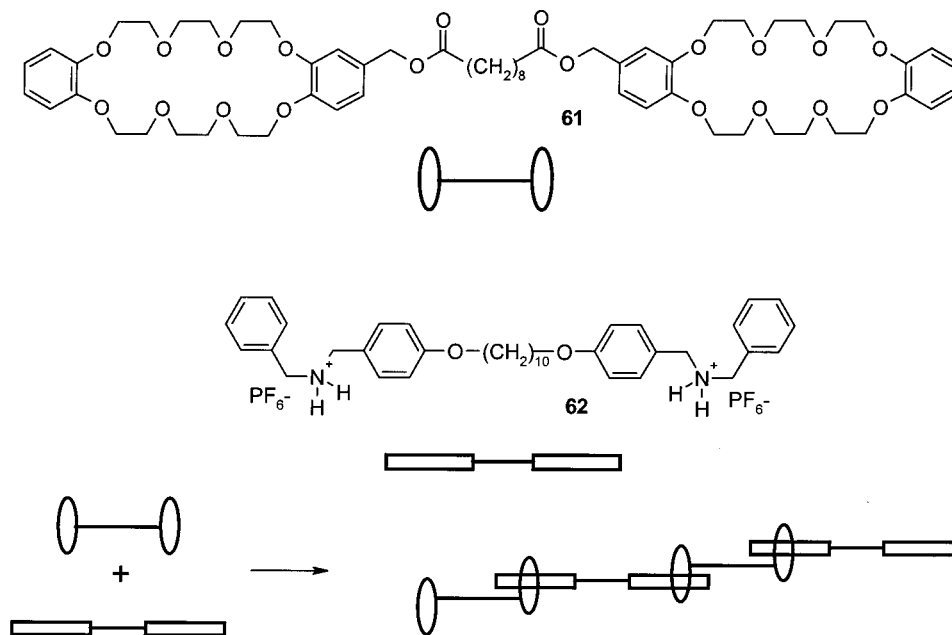


Figure 35. Polymerization via interactions between bifunctional ammonium compounds and bifunctional crown ether derivatives.

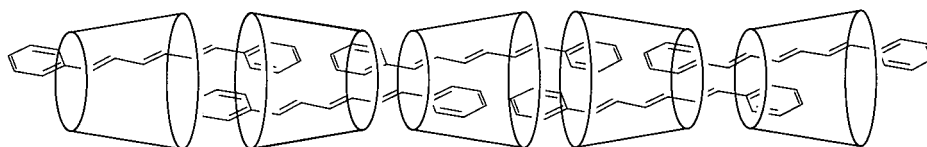


Figure 36. Supramolecular polymer consisting of β -cyclodextrin **63** and DPH **64**.

groups" of DPH fit into the cavity of β -cyclodextrin, and the cavity of γ -cyclodextrin can accommodate three phenyl groups. Binding of the phenyl groups of one DPH molecule in two different cyclodextrin cavities (Figure 36), results in polymeric aggregates with an estimated length of 20 β -cyclodextrins, or 20–35 γ -cyclodextrins, based on light scattering results. Scanning tunneling microscopy of the ag-

gregates on graphite confirmed their nanotube architecture.

The specific inclusion of adamantyl groups in β -cyclodextrin in aqueous environments has been used as binding interaction between adamantyl end-capped poly(ethylene oxide)^{263,264} or polyester and a cyclodextrin polymer. Even though the formation of linear chain extended structures was not specifically

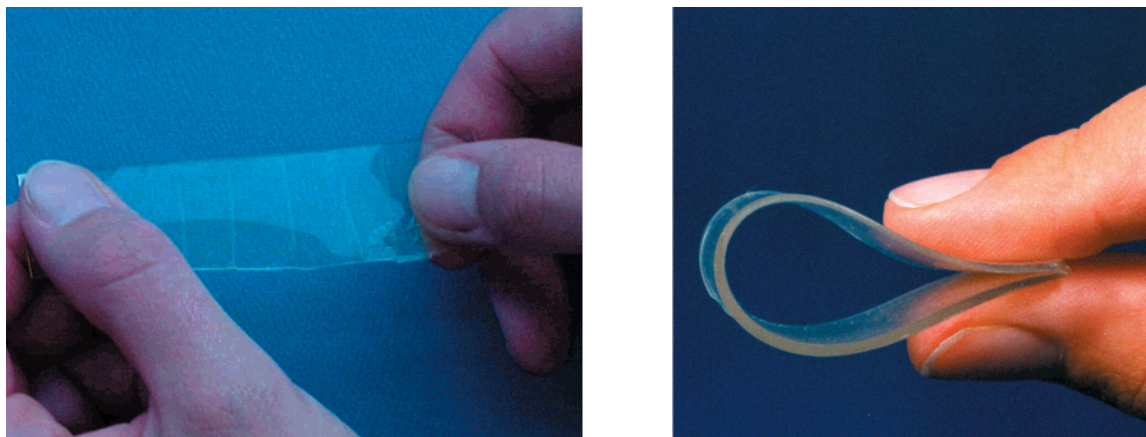


Figure 37. Supramolecular polymer materials created with the ureidopyrimidone unit. (Reprinted with permission from ref 118. Copyright 2000 John Wiley & Sons, Inc.)

studied – polyfunctionality of the cyclodextrin polymer gives rise to network architectures – the highly defined 1:1 stoichiometry of the interaction and its reversibility make this an interesting system. Interaction between the two polymers has been demonstrated through dynamic light scattering and viscosity measurements. The limiting value of the relaxation time in light scattering measurements (230 ms) was suggested to be related to the lifetime of the inclusion of adamantyl groups in the cyclodextrin cavity.

VII. Conclusions and Outlook

Roughly fifteen years after the first experiments toward supramolecular polymers (monomeric units held together by specific directional secondary interactions), it can be concluded that a new research area is added to the field of polymer science. The progress in supramolecular chemistry has paved the way to assembling small molecules into polymer arrays: structures that possess many of the well-known properties of “traditional” macromolecules. Because of the reversibility in the bonding, these supramolecular polymers are under thermodynamic equilibrium, and their properties can be adjusted by external stimuli. In this review we have analyzed three different classes of supramolecular polymers, in which hydrogen-bonded systems have been shown to be technologically relevant, having surpassed the state of being merely scientific curiosities. A large variety of applications is foreseen to be feasible, especially as this approach can also be used for the modification of telechelic oligomers or to modify existing polymers. But also, the possibility to tune the properties by simple copolymer formation due to just mixing monomers seems very attractive, whereas hybrids between blocks of macromolecules and supramolecular polymers are easy to prepare. Therefore, novel thermoplastic elastomers, superglues, hotmelts, and tunable polymeric materials are within reach (Figure 37).

Discotic molecules are of interest for their solution properties and their intriguing supramolecular architectures, in which a level of control in two-dimensional structures can be reached, that shows them to be of particular interest as models for natural systems. Their relatively poor mechanical properties,

such as low strength of the supramolecular gels and their phase transitions, gives them a low added-value with respect to covalent polymers as construction materials. However, their strong π - π interactions within a column lead to high electronic mobilities, a property that is essential in the development of plastic transistors and photovoltaics.^{265,266} Coordination polymers and a number of other approaches show the versatility of the supramolecular polymer approach.

Finally, an important conclusion that arises after discussing the literature on supramolecular polymers relates to the fact that these polymers are also interesting systems to be used by polymer theorists to verify a number of polymer theories. The thermodynamic nature of the supramolecular polymers enables the study of these systems without the kinetic constraints that are normally involved in the study of macromolecules. The future, however, will show the scope and limitations of this new field of supramolecular polymers. We foresee a bright future, and it is now clear that the status of supramolecular polymers has grown from scientific curiosities into systems with technological relevance.

VIII. Acknowledgments

We acknowledge the many contributions of and discussions with our colleagues Jef Vekemans, Anja Palmans, Felix Beijer, Ronald Lange, and Ky Hirschberg. The research presented has been supported by the Eindhoven University of Technology, DSM Research, and The Netherlands Organization for Chemical Research (CW), with financial aid from The Netherlands Organization for Scientific Research (NWO), the National Research School Combination Catalysis (NSRC-C), and the Dutch Polymer Institute.

IX. References

- (1) *Supramolecular Polymers*; Ciferri, A., Ed.; Marcel Dekker: New York, 2000.
- (2) Moore, J. S. *Curr. Opin. Colloid Interface Sci.* **1999**, *4*, 108–116.
- (3) Zimmerman, N.; Moore, J. S.; Zimmerman, S. C. *Chem. Ind.* **1998**, 604.
- (4) Brunsveld, L.; Folmer, B. J. B.; Meijer, E. W. *MRS Bull.* **2000**, *25*, 49.

- (5) Cram, D. J.; Cram, J. M. *Science* **1974**, *183*, 803.
- (6) Pedersen, C. J. *J. Am. Chem. Soc.* **1967**, *89*, 7017.
- (7) Pedersen, C. J. *Angew. Chem., Int. Ed. Engl.* **1988**, *27*, 1053.
- (8) Lehn, J.-M. *Makromol. Chem., Macromol. Symp.* **1993**, *69*, 1.
- (9) Percec, V. *J. Macromol. Sci., Pure Appl. Chem.* **1996**, *A33*, 1479–1496.
- (10) Gellman, S. H. *Acc. Chem. Res.* **1998**, *31*, 173–180.
- (11) Ciferri, A. *Liq. Cryst.* **1999**, *26*, 489–494.
- (12) For a recent review of interlocked molecules see: Raymo, F. M.; Stoddart, J. F. *Chem. Rev.* **1999**, *99*, 1643–1663.
- (13) Lehn, J.-M. In *Supramolecular Polymers*; Ciferri, A., Ed.; Marcel Dekker: New York, 2000.
- (14) Bruce Martin, R. *Chem. Rev.* **1996**, *96*, 3043–3064.
- (15) Flory, P. J. *Principles of Polymer Chemistry*; Cornell University Press: Ithaca, NY, 1953.
- (16) Archer, R. D. *Coord. Chem. Rev.* **1993**, *128*, 49–68.
- (17) Cates, M. E. *Macromolecules* **1987**, *20*, 2289–2296.
- (18) Cates, M. E. *J. Phys. Chem.* **1990**, *94*, 371–375.
- (19) Graneek, R.; Cates, M. E. *J. Chem. Phys.* **1992**, *96*, 4758–4767.
- (20) Krische, M. J.; Lehn, J.-M. *Struct. Bonding (Berlin)* **2000**, *96*, 3–29.
- (21) Sijbesma, R. P.; Meijer, E. W. *Curr. Opin. Colloid Interface Sci.* **1999**, *4*, 24–32.
- (22) Fredericks, J. R.; Hamilton, A. D. *Comprehensive Supramolecular Chemistry*; Lehn, J.-M., Ed.; Pergamon: New York, 1996; Chapter 16.
- (23) For an interesting recent review focused on the self-assembly in synthetic macromolecular systems via multiple hydrogen bonding see: Sherrington, D. C.; Taskinen, K. A. *Chem. Soc. Rev.* **2001**, *30*, 83–93.
- (24) Jorgenson, W. L.; Pranata, J. *J. Am. Chem. Soc.* **1990**, *112*, 2008–2010.
- (25) Pranata, J.; Wierschke, S. G.; Jorgenson, W. L. *J. Am. Chem. Soc.* **1991**, *113*, 2810–2819.
- (26) Sessler, J. L.; Wang, R. *Angew. Chem., Int. Ed. Engl.* **1998**, *37*, 1726–1729.
- (27) Kolotuchin, S. V.; Zimmerman, S. C. *J. Am. Chem. Soc.* **1998**, *120*, 9092–9093.
- (28) Corbin, P. S.; Zimmerman, S. C. *J. Am. Chem. Soc.* **1998**, *120*, 9710–9711.
- (29) Beijer, F. H.; Sijbesma, R. P.; Kooijman, H.; Spek, A. L.; Meijer, E. W. *J. Am. Chem. Soc.* **1998**, *120*, 6761–6769.
- (30) Beijer, F. H.; Kooijman, H.; Spek, A. L.; Sijbesma, R. P.; Meijer, E. W. *Angew. Chem., Int. Ed. Engl.* **1998**, *37*, 75–78.
- (31) Söntjens, S. H. M.; Sijbesma, R. P.; van Genderen, M. H. P.; Meijer, E. W. *J. Am. Chem. Soc.* **2000**, *122*, 7487–7493.
- (32) Zeng, H.; Miller, R. S.; Flowers, R. A.; Gong, B. *J. Am. Chem. Soc.* **2000**, *122*, 2635–2644.
- (33) Folmer, B. J. B.; Sijbesma, R. P.; Kooijman, H.; Spek, A. L.; Meijer, E. W. *J. Am. Chem. Soc.* **1999**, *121*, 2001–2007.
- (34) Zimmerman, S. C.; Corbin, P. S. *Struct. Bonding (Berlin)* **2000**, *96*, 63–94.
- (35) Ciferri, A. *Liq. Cryst.* **1999**, *26*, 489–494.
- (36) Imrie, C. T. *Trends Polym. Sci.* **1995**, *3*, 22–29.
- (37) Odijk, T. *J. Phys. (Paris)* **1987**, *48*, 125–129.
- (38) Odijk, T. *Curr. Opin. Colloid Interface Sci.* **1996**, *1*, 337–340.
- (39) Van der Schoot, P. *J. Phys. II* **1995**, *5*, 243–248.
- (40) Ciferri, A. *Liq. Cryst.* **1999**, *26*, 489–494.
- (41) Fouquey, C.; Lehn, J.-M.; Levelut, A.-M. *Adv. Mater.* **1990**, *2*, 254–257.
- (42) Lehn, J.-M. *Makromol. Chem., Macromol. Symp.* **1993**, *69*, 1–17.
- (43) Gulik-Krczywicki, T.; Fouquey, C.; Lehn, J.-M. *Proc. Natl. Acad. Sci. U.S.A.* **1993**, *90*, 163–167.
- (44) Kotera, M.; Lehn, J.-M.; Vigneron, J.-P. *J. Chem. Soc. Chem. Commun.* **1994**, 197–199.
- (45) Kotera, M.; Lehn, J.-M.; Vigneron, J.-P. *Tetrahedron* **1995**, *51*, 1953–72.
- (46) Aoki, K.-I.; Nakagawa, M.; Ichimura, K. *Chem. Lett.* **1999**, *11*, 1205–1206.
- (47) Lee, J. Y.; Painter, P. C.; Coleman, M. M. *Macromolecules* **1988**, *21*, 954–960.
- (48) Kumar, U.; Kato, T.; Fréchet, J. M. J. *J. Am. Chem. Soc.* **1992**, *114*, 6630–6639.
- (49) Kato, T.; Kihara, H.; Kumar, U.; Uryu, T.; Fréchet, J. M. J. *Angew. Chem., Int. Ed. Engl.* **1994**, *33*, 1644–1645.
- (50) Ambrozic, G.; Zigon, M. *Macromol. Rapid Commun.* **2000**, *21*, 53–56.
- (51) Kato, T. *Supramol. Sci.* **1996**, *3*, 53–59.
- (52) Kato, T.; Nakano, M.; Moteki, T.; Uryu, T.; Ujiie, S. *Macromolecules* **1995**, *28*, 8875–8876.
- (53) Lee, C.-M.; Jariwala, C. P.; Griffin, A. C. *Polymer* **1994**, *35*, 4550–4554.
- (54) Lee, C.-M.; Griffin, A. C. *Macromol. Symp.* **1997**, *117*, 281–290.
- (55) Alexander, C.; Jariwala, C. P.; Lee, C. M.; Griffin, A. C. *Macromol. Symp.* **1994**, *77*, 283–294.
- (56) He, C.; Donald, A. M.; Griffin, A. C.; Waigh, T.; Windle, A. H. *J. Polym. Sci. B* **1998**, *36*, 1617–1624.
- (57) Lee, M.; Cho, B.-K.; Kang, Y.-S.; Zin, W.-C. *Macromolecules* **1999**, *32*, 8531–8537.
- (58) Singh, A.; Lvov, Y.; Qadri, S. B. *Chem. Mater.* **1999**, *11*, 3196–3200.
- (59) He, C.; Lee, C.-M.; Griffin, A. C.; Bouteiller, L.; Lacoudre, N.; Boileau, S.; Fouquey, C.; Lehn, J.-M. *Mol. Cryst. Liq. Cryst. Sci. Technol., Sec. A* **1999**, *332*, 251–258.
- (60) Ungar, G.; Abramic, D.; Percec, V.; Heck, J. A. *Liq. Cryst.* **1996**, *21*, 73–86.
- (61) Percec, V.; Ahn, C.-H.; Bera, T. K.; Ungar, G.; Yeardley, D. J. P. *Chem. Eur. J.* **1999**, *5*, 1070–1083.
- (62) Kihara, H.; Kato, T.; Uryu, T.; Fréchet, J. M. J. *Chem. Mater.* **1996**, *8*, 961–968.
- (63) Pourcain, C. B. St.; Griffin, A. C. *Macromolecules* **1995**, *28*, 4116–4121.
- (64) Wiegel, K. N.; Griffin, A. C. *Polym. Prepr.* **1999**, *40*, 1136–1137.
- (65) Lillya, C. P.; Baker, R. J.; Hütte, S.; Winter, H. H.; Lin, Y.-G.; Shi, J.; Dickinson, L. C.; Chien, J. C. W. *Macromolecules* **1992**, *25*, 2076–2080.
- (66) Abed, S.; Boileau, S.; Bouteiller, L.; Lacoudre, N. *Polym. Bull.* **1997**, *39*, 317–324.
- (67) Abed, S.; Boileau, S.; Bouteiller, L. *Macromolecules* **2000**, *33*, 8479–8487.
- (68) Rubinstein, M.; Dobrynin, A. V. *Curr. Opin. Colloid Interface Sci.* **1999**, *4*, 83–87.
- (69) Stadler, R.; De Lucca Freitas, L. *Makromol. Chem., Macromol. Symp.* **1989**, *26*, 451–457.
- (70) Müller, M.; Dardin, A.; Seidel, U.; Balsamo, V.; Iván, B.; Spiess, H. W.; Stadler, R. *Macromolecules* **1996**, *29*, 2577–2583.
- (71) Schirle, M.; Hoffmann, I.; Pieper, T.; Kilian, H.-G.; Stadler, R. *Polym. Bull.* **1996**, *36*, 95–102.
- (72) Stadler, R.; Burgert, J. *Makromol. Chem.* **1986**, *187*, 1681–1690.
- (73) Hilger, C.; Stadler, R. *Makromol. Chem.* **1991**, *192*, 805–817.
- (74) Bica, C. I. D.; Burchard, W.; Stadler, R. *Macromol. Chem. Phys.* **1996**, *197*, 3407–3426.
- (75) Stadler, R.; De Lucca Freitas, L. *Colloid Polym. Sci.* **1986**, *264*, 773–778.
- (76) De Lucca Freitas, L.; Burgert, J.; Stadler, R. *Polym. Bull. (Berlin)* **1987**, *17*, 431–438.
- (77) De Lucca Freitas, L.; Stadler, R. *Macromolecules* **1987**, *20*, 2478–85.
- (78) De Lucca Freitas, L.; Stadler, R. *Colloid Polym. Sci.* **1988**, *266*, 1095–1101.
- (79) Hilger, C.; Stadler, R.; De Lucca Freitas, L. *Polymer* **1990**, *31*, 818–823.
- (80) Hilger, C.; Stadler, R. *Polymer* **1991**, *32*, 3244–3249.
- (81) Mueller, M.; Seidel, U.; Stadler, R. *Polymer* **1995**, *36*, 3143–50.
- (82) Müller, M.; Stadler, R.; Kremer, F.; Williams, G. *Macromolecules* **1995**, *28*, 6942–6949.
- (83) Müller, M.; Kremer, F.; Stadler, R.; Fischer, E. W.; Seidel, U. *Colloid Polym. Sci.* **1995**, *273*, 38–46.
- (84) Dardin, A.; Stadler, R.; Boeffel, C.; Spiess, H. W. *Makromol. Chem.* **1993**, *194*, 3467–3477.
- (85) Stadler, R.; De Lucca Freitas, L. *Polym. Bull. (Berlin)* **1986**, *15*, 173–179.
- (86) Seidel, U.; Stadler, R.; Fuller, G. G. *Macromolecules* **1994**, *27*, 2066–2072.
- (87) Seidel, U.; Stadler, R.; Fuller, G. G. *Macromolecules* **1995**, *28*, 3739–3740.
- (88) For a recent review of self-assembled organic nanotubes, see: Bong, D. T.; Clark, T. D.; Granja, J. R.; Ghadiri, M. R. *Angew. Chem., Int. Ed.* **2001**, *40*, 988–1011.
- (89) De Santis, P.; Morosetti, S.; Ricco, R. *Macromolecules* **1974**, *7*, 52–58.
- (90) Tomasic, L.; Lorenzi, G. P. *Helv. Chim. Acta* **1987**, *70*, 1012–1016.
- (91) Ghadiri, M. R.; Granja, J. R.; Milligan, R. A.; McRee, D. E.; Khazanovich, N. *Nature* **1993**, *366*, 324–327.
- (92) Khazanovich, N.; Granja, J. R.; McRee, D. E.; Milligan, R. A.; Ghadiri, M. R. *J. Am. Chem. Soc.* **1994**, *116*, 6011–6012.
- (93) Hartgerink, J. D.; Clark, T. D.; Ghadiri, M. R. *Chem.–Eur. J.* **1998**, *4*, 1367–1372.
- (94) Hartgerink, J. D.; Ghadiri, M. R. *New Macromolecular Architecture and Functions*; Kamachi, M., Nakamura, A., Eds.; Springer-Verlag: Berlin, 1996.
- (95) Lee, D. H.; Ghadiri, M. R. *Comprehensive Supramolecular Chemistry*; Lehn, J.-M., Ed.; Pergamon: New York, 1996; Chapter 12.
- (96) Clark, T. D.; Buriak, J. M.; Kobayashi, K.; Isler, M. P.; McRee, D. E.; Ghadiri, M. R. *J. Am. Chem. Soc.* **1998**, *120*, 8949–8962.
- (97) Ghadiri, M. R.; Kobayashi, K.; Granja, J. R.; Chadha, R. K.; McRee, D. E. *Angew. Chem., Int. Ed. Engl.* **1995**, *34*, 93–95.
- (98) Vollmer, M. S.; Clark, T. D.; Steinem, C.; Ghadiri, M. R. *Angew. Chem., Int. Ed.* **1999**, *38*, 1598–1601.
- (99) Steinem, C.; Janshoff, A.; Vollmer, M. S.; Ghadiri, M. R. *Langmuir* **1999**, *15*, 3956–3964.
- (100) Ghadiri, M. R.; Granja, J. R.; Buehler, L. K. *Nature* **1994**, *369*, 301–304.
- (101) Kim, H. S.; Hartgerink, J. D.; Ghadiri, M. R. *J. Am. Chem. Soc.* **1998**, *120*, 4417–4424.

- (102) Motesharei, K.; Ghadiri, M. R. *J. Am. Chem. Soc.* **1997**, *119*, 11306–11312.
- (103) Seebach, D.; Matthews, J. L.; Meden, A.; Wessels, T.; Baerlocher, C.; McCusker, L. B. *Helv. Chim. Acta* **1997**, *80*, 173–182.
- (104) Clark, T. D.; Buehler, L. K.; Ghadiri, M. R. *J. Am. Chem. Soc.* **1998**, *120*, 651–656.
- (105) Ranganathan, D.; Lakshmi, C.; Karle, I. L. *J. Am. Chem. Soc.* **1999**, *121*, 6103–6107.
- (106) Klok, H. A.; Joliffe, K. A.; Schauer, C. L.; Prins, L. J.; Spatz, J. P.; Möller, M.; Timmerman, P.; Reinhoudt, D. N. *J. Am. Chem. Soc.* **1999**, *121*, 7154–7155.
- (107) Choi, I. S.; Li, X.; Simanek, E. E.; Akaba, R.; Whitesides, G. M. *Chem. Mater.* **1999**, *11*, 684–690.
- (108) Castellano, R. K.; Rudkevich, D. M.; Rebek, J., Jr. *Proc. Natl. Acad. Sci. U.S.A.* **1997**, *94*, 7132–7137.
- (109) Castellano, R. K.; Nuckolls, C.; Eichhorn, S. H.; Wood, M. R.; Lovinger, A. J.; Rebek, J., Jr. *J. Am. Chem. Soc.* **1996**, *118*, 2603–2606.
- (110) Castellano, R. K.; Rebek, J., Jr. *J. Am. Chem. Soc.* **1998**, *120*, 3657–3663.
- (111) Castellano, R. K.; Clark, R.; Craig, S. L.; Nuckolls, C.; Rebek, J., Jr. *Proc. Natl. Acad. Sci. U.S.A.* **2000**, *97*, 12418–12421.
- (112) Castellano, R. K.; Nuckolls, C.; Eichhorn, S. H.; Wood, M. R.; Lovinger, A. J.; Rebek, J., Jr. *Angew. Chem., Int. Ed.* **1999**, *38*, 2603–2606.
- (113) Sijbesma, R. P.; Beijer, F. H.; Brunsveld, L.; Folmer, B. J. B.; Hirschberg, J. H. K. K.; Lange, R. F. M.; Lowe, J. K. L.; Meijer, E. W. *Science* **1997**, *278*, 1601–1604.
- (114) Folmer, B. J. B.; Sijbesma, R. P.; Meijer, E. W. *Polym. Mater. Sci. Eng.* **1999**, *217*, 39.
- (115) Folmer, B. J. B.; Cavini, E.; Sijbesma, R. P.; Meijer, E. W. *Chem. Commun.* **1998**, 1847–1848.
- (116) Folmer, B. J. B.; Sijbesma, R. P.; Meijer, E. W. *J. Am. Chem. Soc.* **2001**, *123*, 2093–2094.
- (117) Hirschberg, J. H. K. K.; Beijer, F. H.; van Aert, H. A.; Magusin, P. C. M. M.; Sijbesma, R. P.; Meijer, E. W. *Macromolecules* **1999**, *32*, 2696–2705.
- (118) Folmer, B. J. B.; Sijbesma, R. P.; Versteegen, R. M.; van der Rijt, J. A. J.; Meijer, E. W. *Adv. Mater. (Weinheim, Ger.)* **2000**, *12*, 874–878.
- (119) El-Ghayoury, A.; Peeters, E.; Schenning, A. P. H. J.; Meijer, E. W. *Chem. Commun.* **2000**, 1969–1970.
- (120) Rieth, L. R.; Eaton, R. F.; Coates, G. W. *Angew. Chem., Int. Ed.* **2001**, *40*, 2153–2156.
- (121) Lange, R. F. M.; van Gorp, M.; Meijer, E. W. *J. Polym. Sci. A* **1999**, *37*, 3657–3670.
- (122) *Handbook of Liquid Crystals*. Demus, D., Goodby, J., Gray, G. W., Spiess, H. W., Vill, V., Eds.; Wiley-VCH Verlag: Weinheim, 1998; Vol. 2B.
- (123) Billard, J.; Dubois, J. C.; Tinh, N. H.; Zann, A. *Nouv. J. Chim.* **1978**, *2*, 535–540.
- (124) Destrade, C.; Mondon, M. C.; Malthete, J. *J. Phys. (Paris)* **1979**, *3*, 17–21.
- (125) Sheu, E. Y.; Liang, K. S.; Chiang, L. Y. *J. Phys. (Paris)* **1989**, *50*, 1279–1295.
- (126) Vallerien, S. U.; Werth, M.; Kremer, F.; Spiess, H. W. *Liq. Cryst.* **1990**, *8*, 889–893.
- (127) Gallivan, J. P.; Schuster, G. B. *J. Org. Chem.* **1995**, *60*, 2423–2429.
- (128) Markovitsi, D.; Bengs, H.; Ringsdorf, H. *J. Chem. Soc., Faraday Trans.* **1992**, *88*, 1275–1279.
- (129) Markovitsi, D.; Bengs, H.; Pfeffer, N.; Charra, F.; Nunzi, J.-M.; Ringsdorf, H. *J. Chem. Soc., Faraday Trans.* **1993**, *89*, 37–42.
- (130) Boden, N.; Bushby, R. J.; Clements, J.; Movaghar, B.; Donovan, K. J.; Kreozis, T. *Phys. Rev. B: Condens. Matter Mater. Phys.* **1995**, *52*, 13274–13280.
- (131) Brunsveld, L.; Palmans, A. R. A.; Meijer, E. W. Unpublished results.
- (132) Boden, N.; Bushby, R. J.; Hardy, C. *J. Phys., Lett.* **1985**, *46*, 325–328.
- (133) Boden, N.; Bushby, R. J.; Hardy, C.; Sixl, F. *Chem. Phys. Lett.* **1986**, *123*, 359–364.
- (134) Zimmermann, H.; Poupko, R.; Luz, Z.; Billard, J. *Liq. Cryst.* **1989**, *6*, 151–166.
- (135) Keller-Griffith, R.; Ringsdorf, H.; Vierengel, A. *Colloid Polym. Sci.* **1986**, *264*, 924–935.
- (136) For an interesting review concerning the assembly of triphenylenes and other liquid crystals in water, see: Ringsdorf, H.; Schlarb, B.; Venzmer, J. *Angew. Chem.* **1988**, *100*, 117–162.
- (137) Edwards, R. G.; Henderson, J. R.; Pinning, R. L. *Mol. Phys.* **1995**, *86*, 567–598.
- (138) Henderson, J. R. *J. Chem. Phys.* **2000**, *113*, 5965–5970.
- (139) Hughes, R.; Smith, A.; Bushby, R.; Movaghar, B.; Boden, N. *Mol. Cryst. Liq. Cryst. Technol., Sect. A* **1999**, *332*, 547–557.
- (140) Boden, N.; Bushby, R. J.; Hubbard, J. F. *Mol. Cryst. Liq. Cryst. Sci. Technol., Sect. A* **1997**, *304*, 195–200.
- (141) van Nostrum, C. F.; Nolte, R. J. M. *Chem. Commun.* **1996**, 2385–2392.
- (142) Kratky, O.; Oelschlaeger, H. *J. Colloid Interface Sci.* **1969**, *31*, 490–502.
- (143) Farina, R. D.; Halko, D. J.; Swinehart, J. H. *J. Phys. Chem.* **1972**, *76*, 2343–2348.
- (144) Monahan, A. R.; Brado, J. A.; DeLuca, A. F. *J. Phys. Chem.* **1972**, *76*, 446–449.
- (145) Piechocki, C.; Simon, J. *Nouv. J. Chim.* **1985**, *9*, 159–166.
- (146) Osburn, E. J.; Chau, L.-K.; Chen, S.-Y.; Collins, N.; O'Brien, D. F.; Armstrong, N. R. *Langmuir* **1996**, *12*, 4784–4796.
- (147) Nicolau, M.; Rojo, G.; Torres, T.; Agulló-López, F. *J. Porphyrins Phthalocyanines* **1999**, *3*, 703–711.
- (148) van der Pol, J. F.; Neeleman, E.; Nolte, R. J. M.; Zwikker, J. W.; Drenth, W. *Makromol. Chem.* **1989**, *190*, 2727–2745.
- (149) van der Pol, J. F.; Neeleman, E.; van Miltenburg, J. C.; Zwikker, J. W.; Nolte, R. J. M.; Drenth, W. *Macromolecules* **1990**, *23*, 155–162.
- (150) Duro, J. A.; Torres, T. *Chem. Ber.* **1993**, *126*, 269–271.
- (151) Schutte, W. J.; Sluyters-Rehbach, M.; Sluyters, J. H. *J. Phys. Chem.* **1993**, *97*, 6069–6073.
- (152) Terekhov, D. S.; Nolan, K. J. M.; McArthur, C. R.; Leznoff, C. C. *J. Org. Chem.* **1996**, *61*, 3034–3040.
- (153) Law, W.-F.; Lui, K. M.; Ng, D. K. P. *J. Mater. Chem.* **1997**, *7*, 2063–2067.
- (154) Kobayashi, N.; Ojima, F.; Osa, T.; Vigh, S.; Leznoff, C. C. *Bull. Chem. Soc. Jpn.* **1989**, *62*, 3469–3474.
- (155) George, R. D.; Snow, A. W.; Shirk, J. A.; Barger, W. R. *J. Porphyrins Phthalocyanines* **1998**, *2*, 1–7.
- (156) Shankar, R.; Jha, N. K.; Vasudevan, P. *Indian J. Chem., Sect. A* **1993**, *32*, 1029–1033.
- (157) Osburn, E. J.; Schmidt, A.; Chau, L.-K.; Chen, S. Y.; Smolenyak, P.; Armstrong, N. R.; O'Brien, D. F. *Adv. Mater.* **1996**, *8*, 926–928.
- (158) Kimura, M.; Muto, T.; Takimoto, H.; Wada, K.; Ohta, K.; Hanabusa, K.; Shirai, H.; Kobayashi, N. *Langmuir* **2000**, *16*, 2078–2082.
- (159) Duro, J. A.; de la Torre, G.; Torres, T. *Tetrahedron Lett.* **1995**, *36*, 8079–8082.
- (160) Sielcken, O. E.; van Tilborg, M. M.; Roks, M. F. M.; Hendriks, R.; Drenth, W.; Nolte, R. J. M. *J. Am. Chem. Soc.* **1987**, *109*, 4261–4265.
- (161) Kobayashi, N.; Lever, A. B. P. *J. Am. Chem. Soc.* **1987**, *109*, 7433–7441.
- (162) Engelkamp, H.; Middelbeek, S.; Nolte, R. J. M. *Science* **1999**, *284*, 785–788.
- (163) van Nostrum, C. F.; Picken, S. J.; Nolte, R. J. M. *Angew. Chem., Int. Ed. Engl.* **1994**, *33*, 2173–2175.
- (164) Engelkamp, H.; van Nostrum, C. F.; Picken, S. J.; Nolte, R. J. M. *Chem. Commun.* **1998**, 979–980.
- (165) Fox, J. M.; Katz, T. J.; van Elshocht, S.; Verbiest, T.; Kauranen, M.; Persoons, A.; Thongpanchang, T.; Krauss, T.; Brus, L. *J. Am. Chem. Soc.* **1999**, *121*, 3453–3459.
- (166) Mohr, B.; Wegner, G.; Ohta, K. *J. Chem. Soc., Chem. Commun.* **1995**, *24*, 995–996.
- (167) McKeown, N. B.; Painter, J. *J. Mater. Chem.* **1994**, *4*, 1153–1156.
- (168) Kroon, J. M.; Koehorst, R. B. M.; van Dijk, M.; Sanders, G. M.; Sudhölter, E. J. R. *J. Mater. Chem.* **1997**, *7*, 615–624.
- (169) Kano, K.; Minamizono, H.; Kitae, T.; Negi, S. *J. Phys. Chem. A* **1997**, *101*, 6118–6124.
- (170) Ruhlmann, L.; Nakamura, A.; Vos, J. G.; Fuhrhop, J.-H. *Inorg. Chem.* **1998**, *37*, 6052–6059.
- (171) Fuhrhop, J.-H.; Demoulin, C.; Boettcher, C.; Köning, J.; Siggel, U. *J. Am. Chem. Soc.* **1992**, *114*, 4159–4165.
- (172) Nuckolls, C.; Katz, T. J. *J. Am. Chem. Soc.* **1998**, *120*, 9541–9544.
- (173) Nuckolls, C.; Katz, T. J.; Castellanos, L. *J. Am. Chem. Soc.* **1996**, *118*, 3767–3768.
- (174) Lovinger, A. J.; Nuckolls, C.; Katz, T. J. *J. Am. Chem. Soc.* **1998**, *120*, 264–268.
- (175) Nuckolls, C.; Katz, T. J.; Katz, G.; Collings, P. J.; Castellanos, L. *J. Am. Chem. Soc.* **1999**, *121*, 79–88.
- (176) Verbiest, T.; Van Elshocht, S.; Kauranen, M.; Heliemans, L.; Snauwaert, J.; Nuckolls, C.; Katz, T. J.; Persoons, A. *Science* **1998**, *282*, 913–915.
- (177) Prest, P. J.; Prince, R. B.; Moore, J. S. *J. Am. Chem. Soc.* **1999**, *121*, 5933–5939.
- (178) Mio, M. J.; Prince, R. B.; Moore, J. S.; Kuebel, C.; Martin, D. C. *J. Am. Chem. Soc.* **2000**, *122*, 6134–6135.
- (179) Nelson, J. C.; Saven, J. G.; Moore, J. S.; Wolynes, P. G. *Science* **1997**, *277*, 1793–1796.
- (180) Prince, R. B.; Saven, J. G.; Wolynes, P. G.; Moore, J. S. *J. Am. Chem. Soc.* **1999**, *121*, 3114–3121.
- (181) Brunsveld, L.; Meijer, E. W.; Prince, R. B.; Moore, J. S. *J. Am. Chem. Soc.* **2001**, *123*, 7978–7984.
- (182) Brunsveld, L.; Prince, R. B.; Meijer, E. W.; Moore, J. S. *Org. Lett.* **2000**, *2*, 1525–1528.
- (183) Zhang, J.; Moore, J. S. *J. Am. Chem. Soc.* **1994**, *116*, 2655–2656.
- (184) Moore, J. S. *Acc. Chem. Res.* **1997**, *30*, 402–413.

- (185) Lahiri, S.; Thompson, J. L.; Moore, J. S. *J. Am. Chem. Soc.* **2000**, *122*, 11315–11319.
- (186) Shetty, A. S.; Zhang, J.; Moore, J. S. *J. Am. Chem. Soc.* **1996**, *118*, 1019–1027.
- (187) Tobe, Y.; Utsumi, N.; Nagano, A.; Naemura, K. *Angew. Chem.* **1998**, *110*, 1347–1349.
- (188) Tobe, Y.; Nagano, A.; Kawabata, K.; Sonoda, M.; Naemura, K. *Org. Lett.* **2000**, *2*, 3265–3268.
- (189) For a short review of aggregating helices, see: Katz, T. J. *Angew. Chem., Int. Ed.* **2000**, *39*, 1921–1923.
- (190) Cuccia, L. A.; Lehn, J.-M.; Homo, J.-C.; Schmutz, M. *Angew. Chem., Int. Ed.* **2000**, *39*, 233–237.
- (191) Berl, V.; Krische, M. J.; Huc, I.; Lehn, J.-M.; Schmutz, M. *Chem. Eur. J.* **2000**, *6*, 1938–1946.
- (192) Mertesdorf, C.; Ringsdorf, H.; Stumpe, J. *Liq. Cryst.* **1991**, *9*, 337–357.
- (193) Saeva, F. D.; Reynolds, G. A. *Mol. Cryst. Liq. Cryst.* **1986**, *132*, 29–34.
- (194) Zamir, S.; Singer, D.; Spielberg, N.; Wachtel, E. J.; Zimmermann, H.; Poupko, R.; Luz, Z. *Liq. Cryst.* **1996**, *21*, 39–50.
- (195) Usol'tseva, N.; Praefcke, K.; Smirnova, A.; Blunk, D. *Liq. Cryst.* **1999**, *26*, 1723–1734.
- (196) Usol'tseva, N.; Praefcke, K.; Singer, D.; Gündogan, B. *Liq. Cryst.* **1994**, *16*, 617–623.
- (197) Lydon, J. *Curr. Opin. Colloid Interface Sci.* **1998**, *3*, 458–466.
- (198) Vasilevskaya, A. S.; Generalova, E. V.; Sonin, A. S. *Russ. Chem. Rev.* **1989**, *58*, 904–916.
- (199) Rehage, H. In *Structure and Flow in Surfactant Solutions*; Herb, C. A., Prud'homme, R. K., Eds.; ACS Symposium Series 578; American Chemical Society: Washington, DC, 1994; pp 63–84.
- (200) Yasuda, Y.; Iishi, E.; Inada, H.; Shirota, Y. *Chem. Lett.* **1996**, 575–576.
- (201) Hanabusa, K.; Koto, C.; Kimura, M.; Shirai, H.; Kakehi, A. *Chem. Lett.* **1997**, 429–430.
- (202) Lightfoot, M. P.; Mair, F. S.; Pritchard, R. G.; Warren, J. E. *Chem. Commun.* **1999**, 1945–1946.
- (203) Brunsveld, L.; Schenning, A. P. H. J.; Broeren, M. A. C.; Janssen, H. M.; Vekemans, J. A. J. M.; Meijer, E. W. *Chem. Lett.* **2000**, 292–293.
- (204) Green, M. M.; Peterson, N. C.; Sato, T.; Teramoto, A.; Lifson, S. *Science* **1995**, *268*, 1860–1866.
- (205) *Encyclopedia of Polymer Science and Engineering*; Wiley: New York, 1987; Vol 9.
- (206) Hanabusa, K.; Kawakami, A.; Kimura, M.; Shirai, H. *Chem. Lett.* **1997**, 191–192.
- (207) Hanabusa, K.; Yamada, M.; Kimura, M.; Shirai, H. *Angew. Chem.* **1996**, *108*, 2086–2088.
- (208) Kohne, B.; Praefcke, K.; Derz, T.; Hoffmann, H.; Schwandner, B. *Chimia* **1986**, *40*, 171–172.
- (209) Yasuda, Y.; Takebe, Y.; Fukumoto, M.; Inada, H.; Shirota, Y. *Adv. Mater.* **1996**, *8*, 740–741.
- (210) For a review on guanosine and pterine self-assembly until 1996, see: Gottarelli, G.; Spada, G. P.; Garbesi, A. In *Comprehensive Supramolecular Chemistry*; Lehn, J.-M., Ed.; Pergamon Press: Oxford, UK, 1996; Vol. 9, pp 483–506.
- (211) Kanie, K.; Yasuda, T.; Ujiie, S.; Kato, T. *Chem. Commun.* **2000**, 1899–1900.
- (212) Gottarelli, G.; Masiero, S.; Mezzina, E.; Pieraccini, S.; Rabe, J. P.; Samori, P.; Spada, G. P. *Chem. Eur. J.* **2000**, *6*, 3242–3248.
- (213) de Groot, F. M. H.; Gottarelli, G.; Masiero, S.; Proni, G.; Spada, G. P.; Dolci, N. *Angew. Chem., Int. Ed. Engl.* **1997**, *36*, 954–955.
- (214) Proni, G.; Gottarelli, G.; Mariani, P.; Spada, G. P. *Chem. Eur. J.* **2000**, *6*, 3249–3253.
- (215) Bonazzi, S.; Capobianco, M.; DeMorais, M. M.; Garbesi, A.; Gottarelli, G.; Mariani, P.; Ponzi Bossi, M. G.; Spada, G. P.; Tondelli, L. *J. Am. Chem. Soc.* **1991**, *113*, 5809–5816.
- (216) Proni, G.; Spada, G. P.; Gottarelli, G.; Ciuchi, F.; Mariani, P. *Chirality* **1998**, *10*, 734–741.
- (217) Spada, G. P.; Carcuro, A.; Colonna, F. P.; Garbesi, A.; Gottarelli, G. *Liq. Cryst.* **1988**, *3*, 651–654.
- (218) Mariani, P.; Mazabard, C.; Garbesi, A.; Spada, G. P. *J. Am. Chem. Soc.* **1989**, *111*, 6369–6373.
- (219) Bonazzi, S.; DeMorais, M. M.; Gottarelli, G.; Mariani, P.; Spada, G. P. *Angew. Chem., Int. Ed. Engl.* **1993**, *32*, 248–250.
- (220) Ciuchi, F.; Di Nicola, G.; Franz, H.; Gottarelli, G.; Mariani, P.; Ponzi Bossi, M. G. Spada, G. P. *J. Am. Chem. Soc.* **1994**, *116*, 7064–7071.
- (221) Gottarelli, G.; Mezzina, E.; Spada, G. P.; Carsughi, F.; Di Nicola, G.; Mariani, P.; Sabatucci, A.; Bonazzi, S. *Helv. Chim. Acta* **1996**, *79*, 220–234.
- (222) Gottarelli, G.; Masiero, S.; Spada, G. P. *J. Chem. Soc., Chem. Commun.* **1995**, 2555–2557.
- (223) Marlow, A. L.; Mezzina, E.; Spada, G. P.; Masiero, S.; Davis, J. T.; Gottarelli, G. *J. Org. Chem.* **1999**, *64*, 5116–5123.
- (224) Forman, S. L.; Fettingner, J. C.; Pieraccini, S.; Gottarelli, G.; Davis, J. T. *J. Am. Chem. Soc.* **2000**, *122*, 4060–4067.
- (225) Mezzina, E.; Mariani, P.; Itri, R.; Masiero, S.; Pieraccini, S.; Spada, G. P.; Spinozzi, F.; Davis, J. T.; Gottarelli, G. *Chem. Eur. J.* **2001**, *7*, 388–395.
- (226) Cai, M.; Sidorov, V.; Lam, Y.-F.; Flowers, R. A., II; Davis, J. T. *Org. Lett.* **2000**, *2*, 1665–1668.
- (227) Andrisano, V.; Gottarelli, G.; Masiero, S.; Heijne, E. H.; Pieraccini, S.; Spada, G. P. *Angew. Chem., Int. Ed.* **1999**, *38*, 2386–2388.
- (228) Sidorov, V.; Kotch, F. W.; El-Kouedi, M.; Davis, J. T. *Chem. Commun.* **2000**, 2369–2370.
- (229) Masiero, S.; Gottarelli, G.; Pieraccini, S. *Chem. Commun.* **2000**, 1995–1996.
- (230) Hirschberg, J. H. K. K.; Brunsveld, L.; Ramzi, A.; Vekemans, J. A. J. M.; Sijbesma, R. P.; Meijer, E. W. *Nature* **2000**, *407*, 167–170.
- (231) Kraft, A.; Osterod, F.; Fröhlich, R. *J. Org. Chem.* **1999**, *64*, 6425–6433.
- (232) Palmans, A. R. A.; Vekemans, J. A. J. M.; Fischer, H.; Hikmet, R. A. M.; Meijer, E. W. *Chem. Eur. J.* **1997**, *3*, 300–307.
- (233) Palmans, A. R. A.; Vekemans, J. A. J. M.; Havinga, E. E.; Meijer, E. W. *Angew. Chem., Int. Ed. Engl.* **1997**, *36*, 2648–2651.
- (234) Palmans, A. R. A.; Vekemans, J. A. J. M.; Hikmet, R. A.; Fischer, H.; Meijer, E. W. *Adv. Mater.* **1998**, *10*, 873–876.
- (235) Brunsveld, L.; Zhang, H.; Glasbeek, M.; Vekemans, J. A. J. M.; Meijer, E. W. *J. Am. Chem. Soc.* **2000**, *122*, 6175–6182.
- (236) Brunsveld, L.; Lohmeijer, B. G. G.; Vekemans, J. A. J. M.; Meijer, E. W. *Chem. Commun.* **2000**, 2305–2306.
- (237) van der Schoot, P.; Michels, M. A. J.; Brunsveld, L.; Sijbesma, R. P.; Ramzi, A. *Langmuir* **2000**, *16*, 10076–10083.
- (238) Klug, A. *Angew. Chem.* **1983**, *95*, 579–596.
- (239) Swiegers, G. F.; Malefetse, T. J. *Chem. Rev.* **2000**, *100*, 3483–3537.
- (240) For soluble main-chain coordination polymers see refs 240–247.
- (241) *Macromolecule–Metal Complexes*; Ciardelli, F., Tsuchida, E., Woehrle, D., Eds.; Springer: Berlin, 1996.
- (242) Constable, E. C.; Harverson, P. *Chem. Commun.* **1996**, 1821–1822.
- (243) Knapp, R.; Schott, A.; Rehahn, M. *Macromolecules* **1996**, *29*, 478–480.
- (244) Schubert, E. W.; Eschbaumer, C. *Macromol. Symp.* **2001**, *163*, 177–187.
- (245) Chen, H.; Cronin, J. A.; Archer, R. D. *Inorg. Chem.* **1995**, *34*, 2306–2315.
- (246) Chen, H.; Cronin, J. A.; Archer, R. D. *Macromolecules* **1994**, *27*, 2174–2180.
- (247) Sauvage, J.-P. *Chem. Rev.* **1994**, *94*, 993–1019.
- (248) For a review of earlier main-chain coordination polymers, see ref 16.
- (249) Gorman, C. *Adv. Mater.* **1998**, *10*, 295–309.
- (250) Venturi, M.; Serroni, S.; Juris, A.; Campagna, S.; Balzani, V. *Top. Curr. Chem.* **1998**, *197*, 193–228.
- (251) Modder, J. F.; Vrieze, K.; Spek, A. L.; Challa, G.; van Koten, G. *Inorg. Chem.* **1992**, *31*, 1238–1247.
- (252) Velten, U.; Rehahn, M. *Chem. Commun.* **1996**, 2639–2640.
- (253) Velten, U.; Lahn, B.; Rehahn, M. *Macromol. Chem. Phys.* **1997**, *198*, 2789–2816.
- (254) Terech, P.; Schaffhauser, V.; Maldivi, P.; Guenet, J. M. *Langmuir* **1992**, *8*, 2104–2106.
- (255) Dammer, C.; Maldivi, P.; Terech, P.; Guenet, J. M. *Langmuir* **1995**, *11*, 1500–1506.
- (256) Cates, M. E. *Macromolecules* **1987**, *20*, 2289–2296.
- (257) Cates, M. E.; Candau, S. J. *J. Phys. Condens. Matter* **1990**, *2*, 6869–6892.
- (258) Michelsen, U.; Hunter, C. A. *Angew. Chem., Int. Ed.* **2000**, *29*, 764–767.
- (259) Yamaguchi, N.; Gibson, H. W. *Angew. Chem., Int. Ed.* **1999**, *38*, 143–147.
- (260) Ashton, P. R.; Campbell, P. J.; Chrystal, E. J. T.; Glink, P. T.; Menzer, S.; Philp, D.; Spencer, N.; Stoddart, J. F.; Tasker, P. A.; Williams, D. J. *Angew. Chem., Int. Ed. Engl.* **1995**, *34*, 1865–1869.
- (261) Yamaguchi, N.; Hamilton, L. M.; Gibson, H. W. *Angew. Chem., Int. Ed.* **1998**, *37*, 3275–3279.
- (262) Li, G.; McGown, L. B. *Science* **1994**, *264*, 249–251.
- (263) Sandier, A.; Brown, W.; Mays, H.; Amiel, C. *Langmuir* **2000**, *16*, 1634–1642.
- (264) Amiel, C.; Seville, B. *Adv. Colloid Interface Sci.* **1999**, *79*, 105–122.
- (265) Adam, D.; Schumacher, P.; Simmerer, J.; Häussling, L.; Siemensmeyer, K.; Etbach, K. H.; Ringsdorf, H.; Haarer, D. *Nature* **1994**, *371*, 141–143.
- (266) van de Craats, A. M.; Warman, J. M.; Fechtenkötter, A.; Brand, J. D.; Harbison, M. A.; Müllen, K. *Adv. Mater.* **1999**, *11*, 1469–1472.

Chiral Architectures from Macromolecular Building Blocks

Jeroen J. L. M. Cornelissen,[†] Alan E. Rowan,[†] Roeland J. M. Nolte,^{†,‡} and Nico A. J. M. Sommerdijk^{*,‡}

Department of Organic Chemistry, University of Nijmegen, Nijmegen, The Netherlands, and Laboratory of Macromolecular and Organic Chemistry, Eindhoven University of Technology, P.O. Box 513, 5600 MB Eindhoven, The Netherlands

Received March 1, 2001

Contents

I. Introduction	4039
II. Chiral Architectures from Low-Molecular-Weight Compounds	4039
III. Chiral Macromolecules: Secondary Structure	4045
A. Helical Polymers Having Low Helix Inversion Barriers	4046
B. Helical Polymers Having High Helix Inversion Barriers	4053
IV. Chiral Macromolecular Architectures: Tertiary Structure	4062
V. Conclusions and Outlook	4066
VI. Acknowledgments	4066
VII. References	4066

I. Introduction

In the course of evolution, Nature has developed a multitude of biomacromolecules tailored to deal with complicated tasks such as information storage, support of tissue, transport, and the performance of localized chemical transformations. Although large numbers of researchers in the fields of chemistry and physics have been, and still are, pursuing the same goals using synthetic systems, nucleic acids and proteins still outclass man-made materials. This has made an increasing number of scientists over the past decades turn their eye to Nature to design and synthesize increasingly precise nanoscopic and even mesoscopic structures using polymeric materials.

For the structuring of matter, Nature uses the self-assembly of both low- and high-molecular-weight compounds as a tool. Many biological architectures, the dimensions of which may range over several orders of magnitude, for their robustness rely on two structural components: the α -helix and β -sheet structures of peptides. It is the secondary structure of these two components which, in a delicate interplay among steric, hydrophobic, electrostatic, and hydrogen-bonding interactions, gives rise to the tertiary structure of Nature's main building blocks, the proteins. To achieve the high levels of organization, information must be built into the smallest building blocks, i.e., the amino acids. Indeed these building units do contain this information in the form of chirality,

hydrogen-bonding capacity, steric demands, electrostatic properties, hydrophilic or hydrophobic character, or metal ion binding capability. Supramolecular chemistry since its early days has been inspired by biological assembly methods and has already delivered a large number of architectures of macromolecular size based on these secondary interactions.^{1,2}

In our view, the same principles, when applied to polymer chemistry, allow the construction of large and complex, but precise, macromolecular architectures. In this review, focus will be on chiral polymers with a defined secondary structure in solution (section III) and on chiral macromolecular architectures arising from the aggregation of polymers (section IV).³ Some examples from supramolecular chemistry relevant to the design of chiral self-organizing polymers will be given in the following section. In this section we will also discuss the different approaches for the construction of chiral oligomeric structures (foldamers).⁴

II. Chiral Architectures from Low-Molecular-Weight Compounds

1. Supramolecular Chirality. By building-in structural information, researchers have designed and synthesized self-assembling low-molecular-weight surfactants preprogrammed to form chiral superstructures such as "cigars", twisted ribbons, helices, tubes, braids, boomerangs, and superhelices in aqueous media.^{5–11} Comparable structures were generated by aggregation of other low-molecular-weight compounds in organic solvents.^{12,13} The sensitivity to molecular geometry is highlighted by dramatic differences in the aggregation behavior of two regioisomeric phospholipid analogues, **1** and **2**, both having the (*R*) configuration (Figure 1). Phospholipid **1** forms platelike aggregates, whereas **2**, which has a more linear shape, is able to pack in such a way that its molecular chirality is expressed on the supramolecular level, leading to the formation of helices, all with a diameter of 22 nm and a regular pitch of 92 nm.

One other important principle to be learned from Nature is that when the structural dimensions of the architectures enter the multi-micrometer domain, different levels of organization are involved, e.g., as in collagen, which consists of polypeptide strands that are organized in triple helices (tropocollagen) that assemble to form fibrils and ultimately generate the

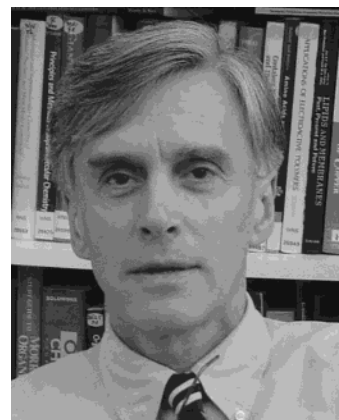
* To whom correspondence should be addressed. Phone: +31 40 247 5870. Fax: +31 40245 1036. E-mail: N.Sommerdijk@tue.nl.

[†] University of Nijmegen.

[‡] Eindhoven University of Technology.



Jeroen J. L. M. Cornelissen started to study chemistry in 1992 at the University of Nijmegen, from which he graduated in 1996 after working on conducting polymers (in the group of E. W. Meijer, Eindhoven University of Technology) and substrate-selective catalysis (in the group of Roeland J. M. Nolte). In the latter group, he subsequently performed his Ph.D. research on chiral architectures from polymers and block copolymers of isocyanopeptides. Since June 2001 he has been working as a postdoctoral fellow at the IBM Almaden Research Center in San Jose, CA.



Roeland J. M. Nolte received his Ph.D. in physical organic chemistry from the University of Utrecht (1973), where he stayed and became Assistant Professor and then Associate Professor. In 1981, he was a visiting scientist at UCLA in the group of Donald J. Cram. In 1987, he moved to the University of Nijmegen and became Professor of Organic Chemistry, and since 1994 he has also been Professor of Supramolecular Chemistry at the Eindhoven University of Technology. His principal research interest is supramolecular chemistry, focusing on the design of catalysts and polymeric materials.



Alan E. Rowan completed his Ph.D. in physical organic chemistry in 1991 at the University of Liverpool, England. After a period of postdoctoral research at the University of Otago, New Zealand, he returned to Europe and became Assistant Professor at the University of Nijmegen in 1996. His scientific interests are in the design and construction of supramolecular assemblages possessing catalytic and electronic properties.

collagen fibers.¹⁴ Several accounts of similar hierarchical order have also been reported for aggregates of synthetic low-molecular-weight compounds.¹⁵ The possibility to organize matter by hierarchical self-assembly is exemplified by the aggregation behavior of the imidazole-modified amphiphilic gluconamide **3** in an aqueous medium in the presence of copper(II) ions (Figure 2).^{13a} The molecules of **3** form 4:1 complexes with Cu^{2+} which subsequently organize into double-layered sheets. These sheets roll-up into left-handed helical tubes, which cluster to form fibrils with a thickness of 150 nm. These fibrils further organize to form the supermolecular braids as is shown in Figure 2.

Another important lesson from Nature teaches us that the way chirality is expressed depends not only on the chiral information encoded in the molecules, or on the level of organization. It may also be triggered or altered by changes in the local environment of the aggregate, such as polarity, the presence of specific ions, pH, or temperature. The supercoiling



Nico A. J. M. Sommerdijk obtained his Ph.D. (Cum Laude) in 1995 at the University of Nijmegen for his study of the synthesis and aggregation behavior of chiral surfactant molecules. After this, he did postdoctoral work with John D. Wright at the University of Kent (U.K.) on sol-gel-based sensor materials and with Brigid R. Heywood at Keele University (U.K.) on the influence of self-assembling surfactants on the crystallization of inorganic materials. In 1997, he returned to Nijmegen to work on supramolecular assemblies of surfactants and polymeric materials. After this, he moved to the Eindhoven University of Technology in 1999, where he became Assistant Professor of Biomimetic Materials Chemistry. His key research interests are the fabrication of organic-inorganic composite materials and the construction of polymer-enzyme hybrid systems using the tools from supramolecular and macromolecular chemistry.

of DNA is such a process that is influenced by small changes in the local ionic strength which can cause the reversal of the helical twist in the DNA coils.¹⁶ Similar phenomena have been reported for surfactant aggregates,¹⁷ first exemplified by the self-assembly behavior of compound **2**, which organizes into left-handed helices that may either cluster to form ropes with the same handedness or aggregate to form right-handed superhelices with widths of 350 nm, a pitch of 250 nm, and lengths exceeding 10 μm (Figure 1).^{3e}

These examples demonstrate how low-molecular-weight chemistry may be a guideline on how to use chirality as a tool in the construction of highly ordered polymeric materials since it will give a bias

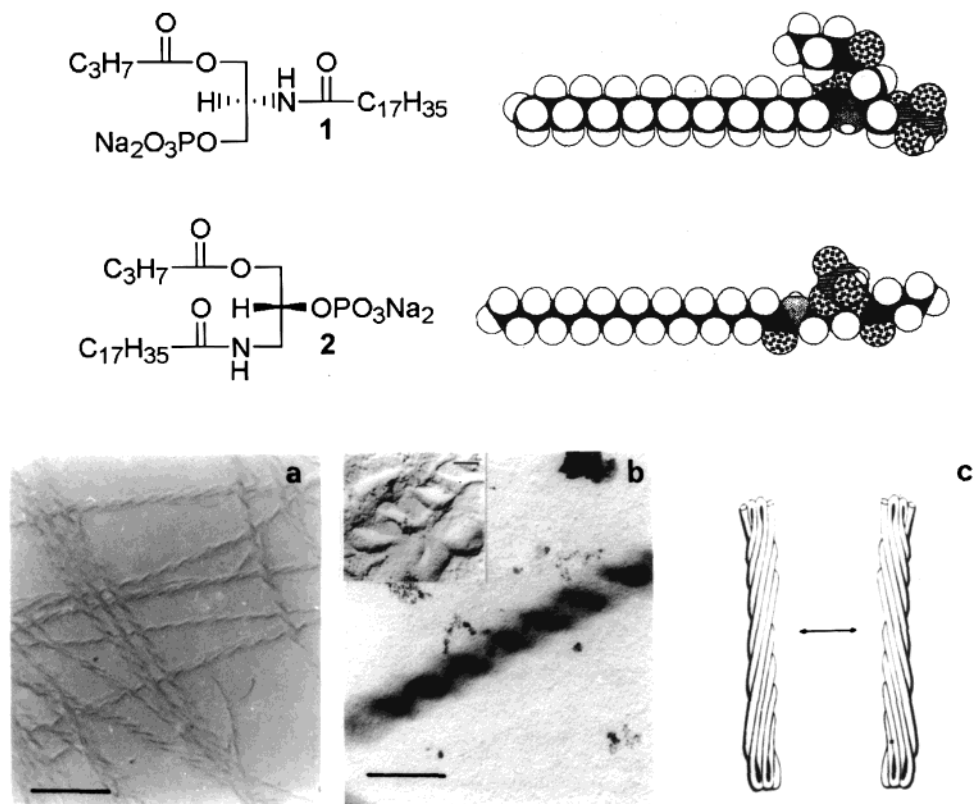


Figure 1. Top: Structures and CPK models of regioisomeric phospholipid analogues. Bottom: (a, b) TEM micrographs of aggregates of **2**. (a) Right-handed helices. (b) Superhelices formed by further assembly of the helices shown in (a). Inset: freeze-fractured replica of the superhelix. (c) Schematic representation of the superhelical winding.

as to how building blocks at the monomeric level will be built into the polymer chains. Together with other molecular information embedded in the monomers, it will dictate how polymer chains will fold and, ultimately, interact with neighboring chains to form well-defined polymeric architectures.

The aggregation of small chiral molecules can be used not only as a guideline for the construction of chiral polymer structures; the following examples show that it may also be directly applied to generate polymer architectures, e.g., by serving as a template for the organization of macromolecules into larger structures, to organize amphiphilic monomers, or even to form polymeric strands based on strong supramolecular interactions.

Lipid molecules with specific ligands or binding sites for selected protein templates have been demonstrated to direct the organization of these proteins into tubular structures with an outer shell consisting of a crystalline layer of biomacromolecules packed in a perfect helical arrangement.¹⁸ Helical polymer architectures can also be obtained from chiral lipids and surfactants carrying polymerizable groups which can be fixed by photopolymerization as has been reviewed by O'Brian et al.¹⁹ Already in 1985, Yager, Schoen, and co-workers reported on polymerized lipid tubes comprising helically folded bilayer sheets.²⁰ More recently Percec et al. demonstrated the control over the backbone conformation of different polymers through the programmed self-assembly of monomers (Figure 3a).²¹ The polymerization of styrenes and methacrylates equipped with tapered gallic acid-derived monodendrons induces a helical conformation

in the backbones of the resulting cylindrical polymer architectures above a critical degree of polymerization (>20 for styrene, >15 for methacrylate).^{22,23}

The double helix of DNA exemplifies Nature's ability to construct complex chiral structures in an aqueous medium by making use of both hydrogen-bonding and hydrophobic interactions. Inspired by this phenomenon, Sijbesma and Meijer used dimeric building blocks equipped with 4-fold hydrogen-bonding units to obtain true polymeric structures in solution based on supramolecular interactions. By the interplay between the stacking of the aromatic hydrogen-bonding units and the incorporated enantiomerically pure solubilizing side chains, they were able to generate helical self-assembled polymeric architectures in organic solvents as well as in aqueous media (Figure 3b,c).²⁴

2. Foldamers: Oligomers with a Preferred Helical Conformation. With the design of polymers with well-defined secondary and tertiary structures as the ultimate goal, researchers have taken up the task of identifying and synthesizing new structural elements that contain the information required for the programmed folding of molecular chains. This has led to the development of a class of compounds generally referred to as "foldamers" and defined by Gellman as polymers "with a strong tendency to adopt a specific compact conformation".²⁵ Essential in the design of foldamers is the identification of new backbones with well-defined structural preferences, and foldamers are thus further defined as oligomers of modest length that in solution display such a specific conformational preference. As the two most

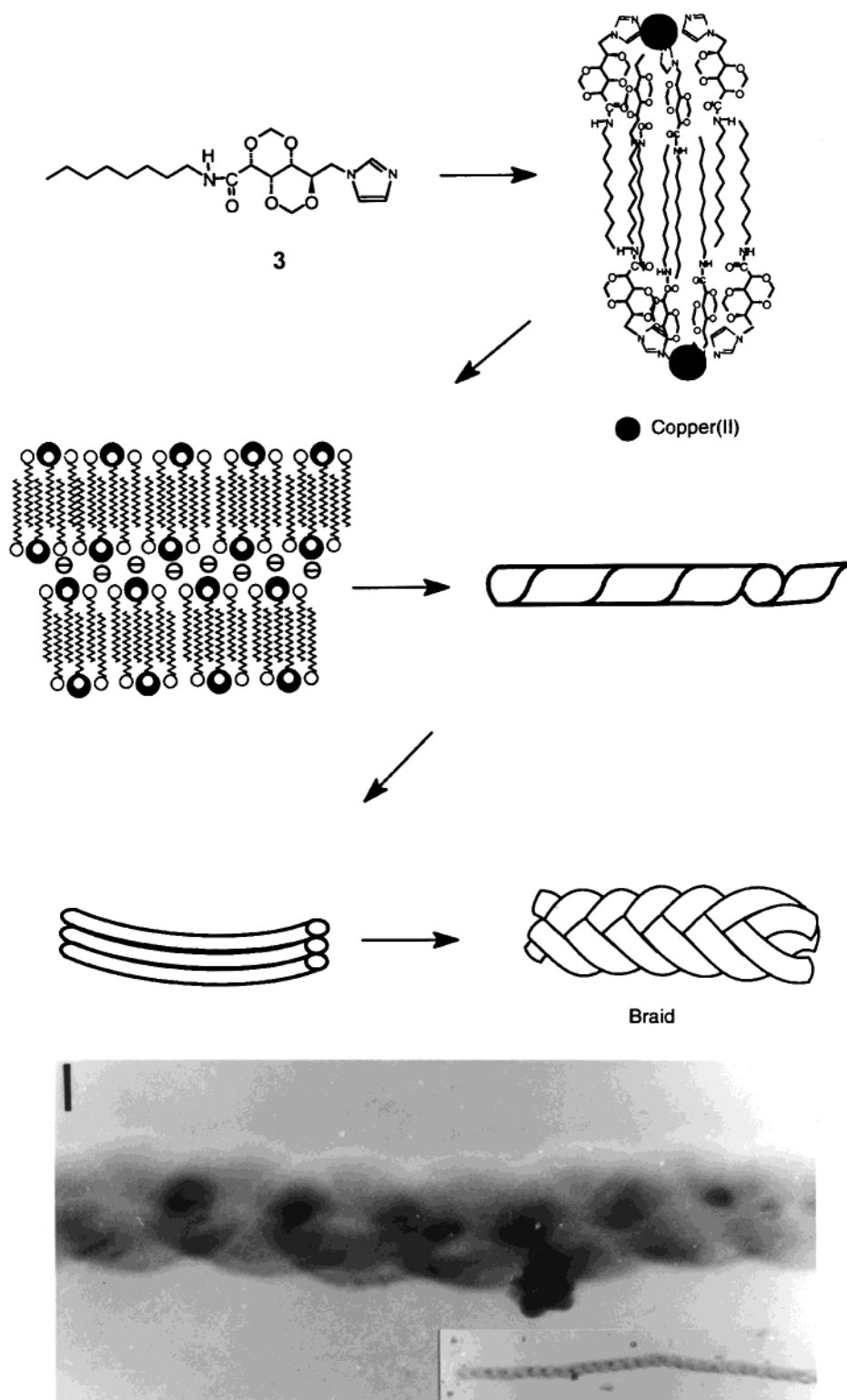


Figure 2. Hierarchical organization in the aggregation of an amphoteric imidazole-containing gluconamide in the presence of copper(II) ions.

common structural elements found in Nature are helices and β -sheets, the realization of their synthetic equivalents has been adopted as a research target by a large number of scientists.²⁶ In this review, we will limit ourselves to examples in which the research has concentrated on systems with homogeneity in the backbone since a polymer approach may be applied to these materials and we will not go into the fields of polypeptide synthesis and peptidomimetics. Poly-

(amino acid)s probably are the most simple example of how structural information in the polymer backbone can dictate the folding of the molecules in a predefined manner. Some of these polymers, e.g., poly(benzyl glutamate), have now been synthesized in a true polymer approach by the ring-opening reaction of *N*-carboxyanhydride monomers (see also section III.A).²⁷ The preference of these poly(α -amino acid)s **4** (Chart 1) for the α -helix and the 3/10-helical

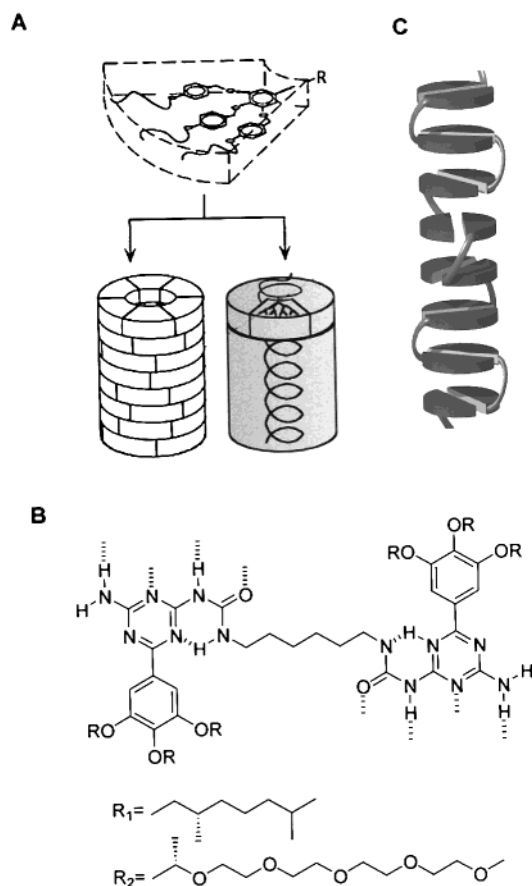


Figure 3. (a) Formation of helical macromolecular structures through the polymerization of preorganized monomers bearing tapered side groups. (b) Structure of dimeric hydrogen-bonding units able to form helical self-assembled polymers in organic (R_1) or aqueous (R_2) solution. (c) Schematic representation of a right-hand helical self-assembled polymer.

structure has been extrapolated to the design of other helical structures based on oligomers of β -peptides **5**. The groups of Gellman and Seebach have provided methodologies and guidelines for the construction of defined helical architectures from these compounds.

Gellman's efforts have concentrated on conformationally rigidified monomers, aiming at the realization of helical structures with long-term stability.²⁸ Molecular modeling calculations predicted that oligomers of *trans*-2-aminocyclohexanecarboxylic acid (**6**) and of *trans*-2-aminocyclopentanecarboxylic acid (**7**) (Chart 1) have particular preferences for the formation of a 14-helix and a 12-helix, respectively. The crystal structure of oligomers **6** (based on the former monomer) indeed revealed a perfect 14-helix, but although strong indications for the presence of a similar structure in solution were obtained, no definitive solution data have been presented yet.²⁹ For a hexamer (**7a**) and an octamer (**7b**) of the cyclopentane-derived β -peptide, the solution structure was determined using NMR. This supported the existence of the 12-helix structure which was also found in the solid state.³⁰ More recently also X-ray data on the packing of these helices in the solid state have become available, which may help to design tertiary structures based on these foldamers.³¹

Seebach and co-workers have developed hetero-hexa- β -peptides, e.g., **8** (Chart 1), which form helical structures in water as well as in organic solvents.³² They demonstrated that the conformational restrictions in the backbone imposed by the use of cyclic monomers were not a prerequisite for the formation of these helical structures. Gellman's group later showed, however, that the incorporation of cyclic β -amino acids in the sequence *does* have a positive effect on the stabilization of the helix.³³ Exploring the possibilities of these types of monomers, Seebach and co-workers demonstrated that also β -sheets and turns can be realized,³⁴ and that the 14-helix can also be attained through the use of γ -amino acids.³⁵

Other foldamers that have been reported are the vinyllogous amino acids **9**,³⁶ the β -sulfonopeptides **10**,³⁷ and the vinyllogous sulfonopeptides **11** (Chart 1).³⁸ Related to this work are also the investigations carried out on peptide nucleic acids (PNAs) which have recently been reviewed by Nielsen.³⁹ PNAs are a new class of flexible oligomeric DNA analogues in which the base pairs are carried by a peptide backbone. When this backbone consists of cyclohexyl-derived amino acids, the molecules adopt a more rigid conformation and are able to also form a double-helical structure.⁴⁰

Hamilton and co-workers have prepared oligomers from anthranillic acid and pyridine-2,6-dicarboxylic acid moieties which use hydrogen bonds between nearest-neighbor groups to rigidify their structure and maintain a helical conformation.⁴¹ Lehn's group has published a similar approach using oligoisophthalamides which can fold into helical aggregates through the formation of hydrogen bonds. In this work, cyanuric acid is used as a template around which the oligomer folds into a helix, forming hydrogen bonds to the guest molecule.⁴² The helices aggregate, thereby generating fibers, which in turn cluster to form bundles of lengths up to several micrometers. A templating agent is not required for the folding of oligo(pyridinecarboxamide)s **12** (Chart 2). These molecules fold by the formation of intramolecular hydrogen bonds into double helices that reversibly dissociate into single-helical strands upon heating.⁴³

Rather than relying on hydrogen bonding to achieve the appropriate folding of oligomeric compounds, Lokey and Iverson used attractive aromatic electron donor-acceptor (AEDA) interactions between dialkoxynaphthalene and naphthalenetetracarboxylic diimide. Oligomers **13** (Chart 2) containing these groups were termed "aedamers" and were shown to give pleated structures in solution, yielding a distinct "plum color" due to broad charge-transfer absorption bands in the visible region.⁴⁴ By using different amino acids as the linkers between the donor and acceptor units, solubility could be tuned; Nguyen and Iverson used hydrophilic and hydrophobic residues, alternatingly, as linkers between the aromatic units, yielding amphiphilic stacks which aggregated in aqueous media.⁴⁵

The folding of oligo(*m*-phenyleneethynylene)s (Figure 4) into helical stacks driven by solvophobic effects was reported by Moore and co-workers.⁴⁶ These

Chart 1

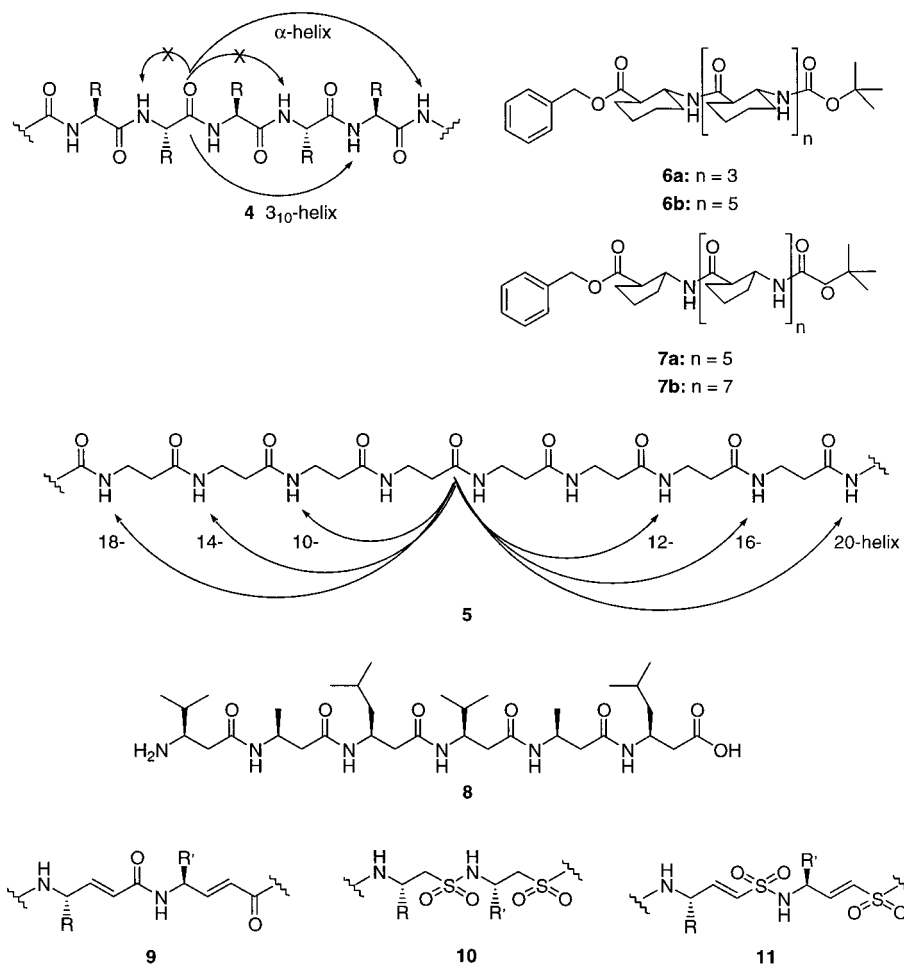
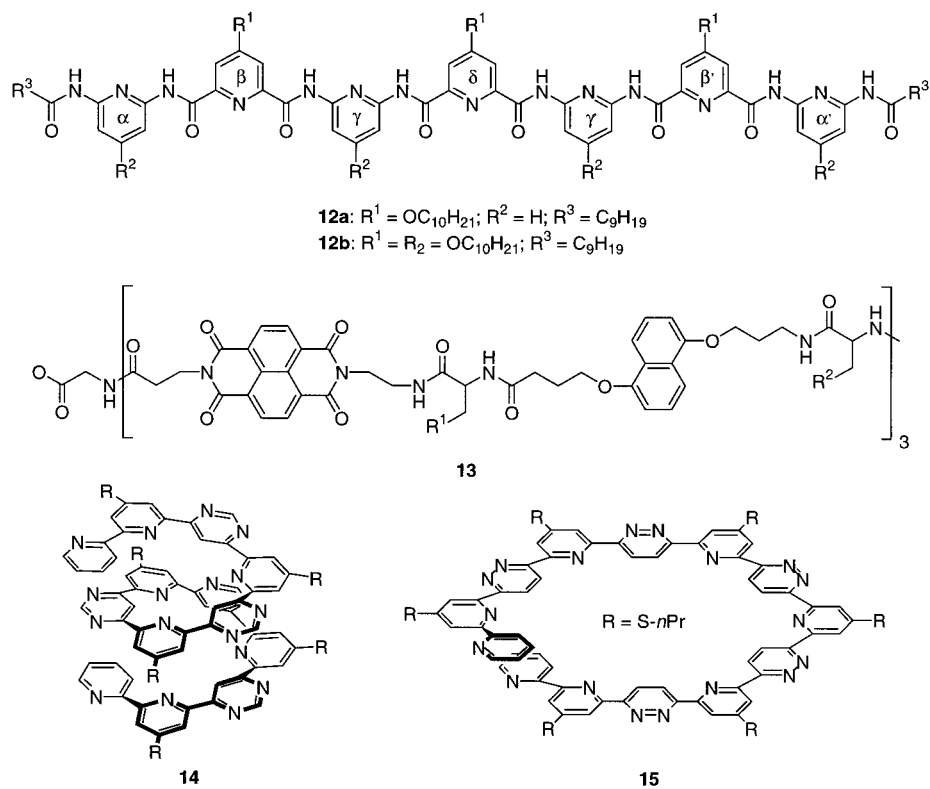


Chart 2



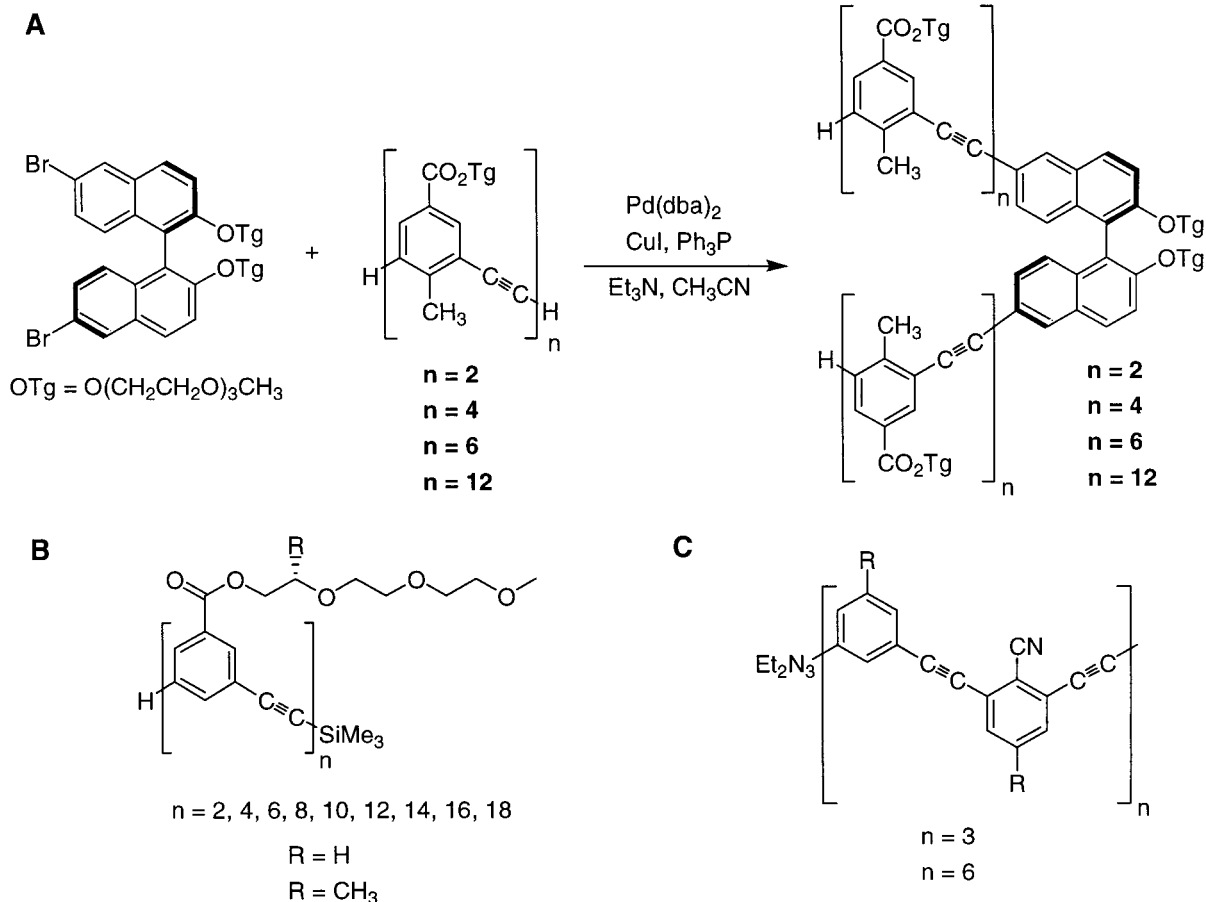


Figure 4. (a) Synthesis of oligo(*m*-phenyleneethynylene)s containing a chiral binaphthyl group. (b) Structure of oligo(*m*-phenyleneethynylene)s with optically active ethylene oxide side chains. (c) Same as (b) but with cyano groups that allow the binding of metal ions.

molecules exhibit a large degree of conformational flexibility due to the fact that rotation is possible around the ethynylene linkers, which allows switching between the transoid and cisoid states, the latter of which leads to a helical conformation. The aromatic backbone bears pendant oligo(ethylene oxide) chains to ensure solubility in a large variety of solvents, and oligomers consisting of up to 18 repeat units were prepared. To obtain a helical bias, initially binaphthyl groups were incorporated into the backbone of the oligomers;⁴⁷ later chiral side chains were used.⁴⁸ By equipping every second phenylene group with a cyano group on the free meta position, silver ions could be bound into the interior of these foldamers, which aided the stability of the helices⁴⁹ (Figure 4).

Metal ion complexation has been used to direct the helical folding of many oligomeric compounds. The resulting complexes are known as helicates and have been reviewed by Williams,⁵⁰ and by Piguët et al.⁵¹

The group of Lehn has demonstrated how by careful design oligomeric strands **14** (Chart 2) of alternating pyridine and pyrimidine can fold into helical structures using the geometry of the molecules, without the further need of specific directing forces or agents.⁵² In their design, they used the fact that when these aromatic building blocks are linked at the appropriate positions the preference for a transoid conformation automatically leads to a helical structure. When pyridazines **15** (Chart 2) are used instead of pyrimidine groups, the helices organize

themselves into a long tubular structure with an internal diameter of 8 Å. These fibers display a helical twist and stretch out over several micrometers.⁵³

III. Chiral Macromolecules: Secondary Structure

A chiral organization *within* a macromolecule in most cases is present as a helical conformation of the polymeric backbone. In the 1950s, it was first recognized that the polymerization of substituted olefins could lead to the formation of macromolecules with a helical conformation.⁵⁴ Experimental evidence for the existence of such a structure *in solution* was first reported in 1960 by Pino and Lorenzi⁵⁵ and later also by others.^{56,57} The properties of these helical macromolecules are highly dependent on the helix inversion barrier. The screw sense of one particular strand is stable at room temperature when this helical inversion barrier is high ($\geq \sim 85$ kJ·mol⁻¹), whereas the two screw senses may be in equilibrium when the inversion barrier is lower.⁵⁸ In the case of nonchiral side chains, the left- and right-handed helices are enantiomers, having equal free energies. When the polymer contains chiral side chains, the helices are diastereomers and consequently have different free energies (Figure 5). Polymers with low helix inversion barriers have dynamic properties which can be used to build chiral architectures that respond to interactions with small molecules, light, or subtle changes in monomer composition or temperature as will be

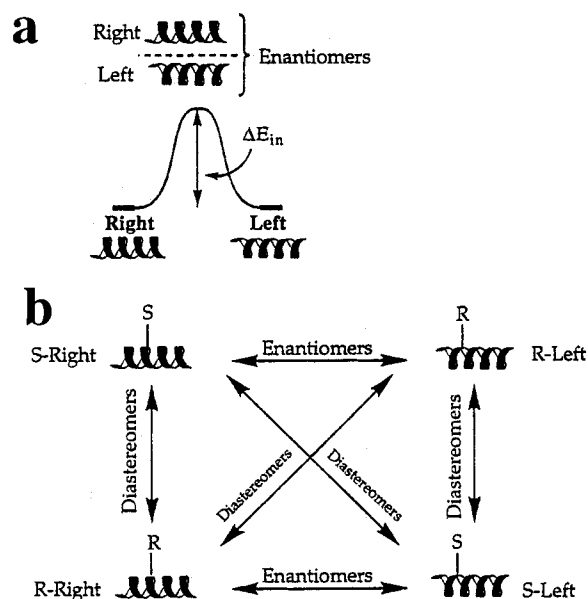


Figure 5. (a) Energy relationships between helical polymers from achiral monomers. (b) Relational diagram between helical polymers from chiral monomers. (Modified from ref 58.)

discussed in the following section. When the helix inversion barrier of the polymer is high, the helical conformation is formed under kinetic conditions. This implies that upon incorporation into the growing chain each monomer contributes to the helix, and is sterically locked into its conformation. These types of polymers will be discussed in part B of this section.

A. Helical Polymers Having Low Helix Inversion Barriers

1. Polyisocyanates. Polyisocyanates (Nylon 1) are stiff helical polymers, which have been extensively investigated in the last 20 years in particular due to the pioneering work of Goodman and Chen⁵⁹ and more recently the elegant studies of Green.⁶⁰ Their stiffness is a result of the partial double-bond character of the backbone amide bonds. The polymer backbone is helical due to steric constraints, which prevent the amide bonds from being planar whether they are in a *cis* or *trans* conformation (Figure 6).

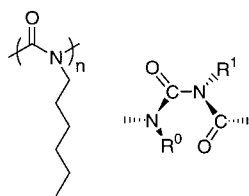


Figure 6. Structure of poly(*n*-hexyl isocyanate) and a generalized polyisocyanate structure indicating the steric restrictions in these polymers.

The helical nature of these polymers was confirmed by analysis of the X-ray crystal structure of poly(butyl isocyanate) in the late 1960s, which revealed a 3/8-helix, in which the monomeric units are translated along the helical axis by 1.94 Å per monomer and rotated by 135° per monomer.⁶¹ This helical conformation is also adopted in solution for both poly(alkyl isocyanates) and poly(aryl isocyanates) although the

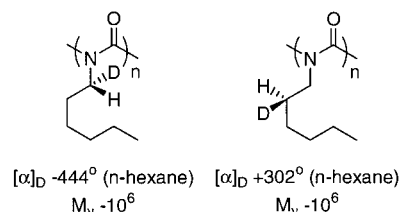


Figure 7. Introduction of optical activity in polyisocyanates by H/D substitution.

latter are less well defined than the former. When an achiral monomer is polymerized, left- and right-handed helices are formed, which are distributed throughout the polymer chains and are dynamically interconverting. Empirical force field studies on poly(alkyl isocyanates) predict a barrier of 52 kJ·mol⁻¹ for the *cis*–*trans* isomerization of the conjugated, partial double bonds in the polymer backbones, which agrees closely with the observed experimental data.⁶²

The helical sense of the polymer can be controlled by a variety of means, such as inclusion of a chiral monomer, the use of a chiral solvent, or the use of a chiral initiator for the polymerization. The group of Green has elegantly demonstrated that the helical sense of poly(alkyl isocyanate)s is extremely sensitive to even slight chiral biases in the monomer. They showed that substitution of a proton for a deuterium (Figure 7) is sufficient to induce a preferential helical sense in the resulting polymers.^{60,63} It is remarkable that this substitution induces such an effect, especially since in hexane at 25 °C this isotopic effect would favor a *P*-helix over the *M*-helix by only 3.1 J·mol⁻¹, implying that the *P*-helix would exist in excess of the *M*-helix by only 0.12%. However, for a long polymer chain ($n = 2000$), this minute excess is amplified by a cooperative mechanism to give a ratio of 67:33 (*P*-helix:*M*-helix). The same research group further highlighted the cooperative nature within the polymeric helices by investigating the helical preference of copolymers of chiral and achiral polyisocyanates. They discovered that the presence of even a minor amount of chiral monomer induced a helical preference upon polymerization of the achiral monomer. Somewhat surprisingly it was also discovered that a polyisocyanate constructed from a random copolymerization of monomers containing nearly equal numbers of mirror image units exhibits the same CD spectrum as a polyisocyanate obtained from the homopolymerization of the enantiopure monomers (Figure 8). The ability of the majority unit to impose itself upon the minority (majority rules concept) becomes more prominent as the helical reversal becomes more difficult to attain.

The observed cooperativity arises from infrequent helical reversals, which separate long blocks of opposing helical senses, forcing many units of the chain to take the same helical sense. In this way, the chiral bias of each unit of the chain is amplified. In the case of the helical preference induced by the isotope effect, the helix reversal was found to cost 6.3 kJ·mol⁻¹ and to occur on average only once in every 762 units. This long persistence length, which in turn is the result of the infrequent helical reversals, accounts for the chiral amplification in these polymer systems. More

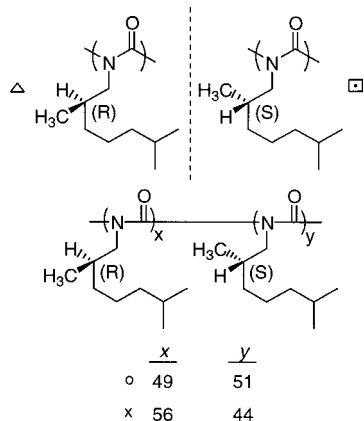
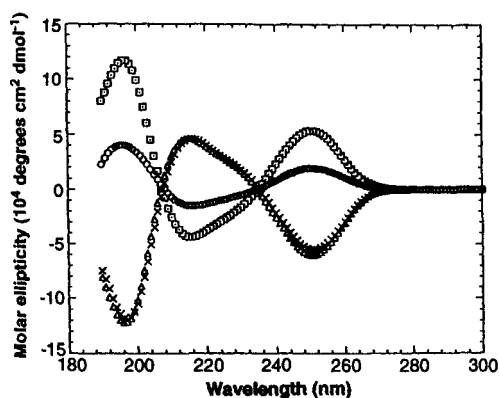
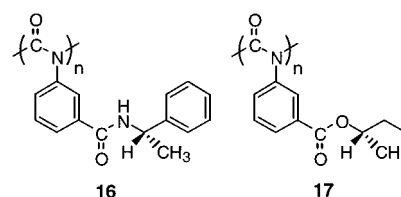


Figure 8. Majority rules effect in polyisocyanates: (left) CD spectra of homo- and copolymers; (right) structure and composition of the polymers. (Reprinted with permission from ref 60. Copyright 1995 American Association for the Advancement of Science.)

recently the mixed copolymer experiments have been extended to include a *diluting* achiral component. The highly disproportionate relationship which arises from the majority rule effect, as was demonstrated for the mixed (*R*)- and (*S*)-copolymers,⁶⁴ was found to be unaffected by the overwhelming presence of achiral units randomly distributed along the chain.⁶⁵ Experimental results were fitted to a one-dimensional random-field Ising model, which showed that the dilution of the chiral units with achiral units increases the helical domain size in a manner that compensates for the dilution.

The sensitivity of the helical preference of polyisocyanates to small chiral influences is also observed in chiral solvents. Poly(*n*-hexyl isocyanate) was found experimentally to have a persistence length of 20–40 nm depending on the solvent in which the measurements were carried out.⁶⁶ It was hypothesized that in more polar solvents a local interaction of the solvent would give rise to larger torsional oscillations around the backbone bonds. It was indeed observed that dissolution of poly(*n*-hexyl isocyanate) in non-racemic chiral solvents, e.g., (*S*)-1-chloro-2-methylbutane, changed the persistence length and in addition also resulted in an excess of one helical sense.⁶⁷ The chiral bias favoring one helical sense by itself is miniscule, but due to the cooperativity, a chiral preference is observed. More recently it was noted that the circular dichroism of these polymers decreases upon the addition of an achiral or racemic

Chart 3

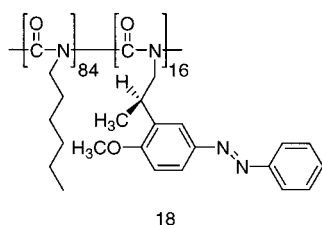


cosolvent, which can be quantitatively interpreted as reflecting the composition of the solvent mixture in contact with the helical backbone of the polymer.⁶⁸

Poly(aryl isocyanate)s possessing a phenyl group directly connected to the polymer main chain have until recently been considered to adopt a random-coil conformation in solution due to the lack of stiffness of the polymer main chain.⁶⁹ The group of Okamoto, however, has demonstrated that when an optically active anionic initiator is used in the polymerization reaction, chiral polymers are obtained, which have a one-handed helical structure dictated by the initiator. The polymer main chains are stiff enough to maintain this helical conformation in solution.⁷⁰ The same group more recently reported that chiral aromatic isocyanates can be polymerized to give well-defined polymers with a helical preference. (*S*)-**16** (Chart 3) showed a very large negative optical rotation, $[\alpha]_{365}^{25} = -1969^\circ$, which was found to be temperature independent, implying that (*S*)-**16** (Chart 3) adopts a perfect helical conformation in solution even at room temperature. Polymerization of achiral monomers in the presence of chiral monomers gave helices that exhibited cooperative effects similar to the ones seen for their alkyl equivalents.⁷¹ Optically active (*S*)-**17** (Chart 3) was found to display an unusual conformational change accompanied by inversion of the helical structure when the temperature was changed. At -45°C in THF, **17** possessed a predominantly one-handed helical conformation with a helical sense opposite to that at 25°C .⁷²

Switching the helical sense of polyisocyanates is a research topic that is receiving increasing attention. This is due to the result of the extreme sensitivity of the helices to slight chiral influences arising from the large cooperativity present in these polymers. In 1996, the group of Zentel polymerized optically active isocyanates containing azo chromophores to give polymers with a preferred helical twist and photo-switchable functions.⁷³ Their preliminary studies revealed that upon photoswitching the chromophore from the *trans* to the *cis* state, the percentage of right-handed (*P*) helical segments increases and the observed CD effect for the polymer reverses. Films consisting of a copolymer of photochromic isocyanate and *n*-hexyl isocyanate (**18**) (Chart 4) embedded in poly(methyl methacrylate) (PMMA) exhibited stable photochromic switching, whereas upon irradiation the preferential helical sense of the polymer was reversed. Upon thermal relaxation of the chromophore, the photoinduced helical preference was retained. The inclusion of the polymer within the PMMA matrix increases the barrier to helix reversal, thereby fixing the polymer.⁷⁴ In a similar approach, the group of Green demonstrated that achiral polymers containing racemic photoresolvable ketones (**19**)

Chart 4



can be switched from one helical preference to another upon photoexcitation of the chromophore (Figure 9).⁷⁵ A small enantiomeric excess produced by irradiation, even diluted by a large proportion of achiral pendants, is capable of enforcing an excess of one helical sense in the polymer. An elegant approach to the manipulation of the helical sense of polyisocyanates is the polymers synthesized by Green, which possess two different nonracemic chiral molecules that are in competition with each other to control the polymer sense.⁷⁶ The competition leads to thermal switching of the helical sense at a compensation point that depends continuously and predictably on the composition of the polymers.

Stiff, rodlike polymers are known to aggregate to form lyotropic nematic liquid crystals⁷⁷ and to self-assemble to form gels.⁷⁸ The helical nature of the polyisocyanates is transferred into the properties of the aggregates. When the polymer contains monomers bearing chiral side groups, the liquid crystalline superstructure is no longer nematic but cholesteric. This switching of the liquid crystalline phase can also be attained by doping with small chiral molecules, mimicking the chiral solvation effect seen for the polymers in solution.⁶⁷ The number of helical reversals per polymer changes upon aggregation to a gel. Molecular modeling predicts that at the reversal point the polymer has a kink of 150°. It was observed by recording optical activity that a reduction in the number of helical reversals (and hence an increase in persistence length) in the polymer chains occurs due to close parallel packing of the polymer rods.

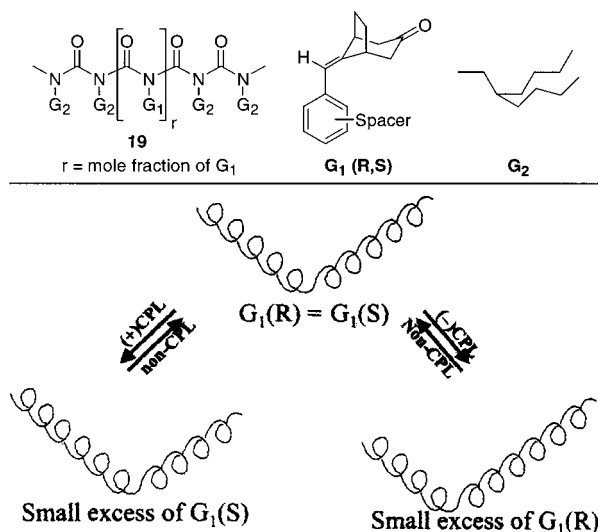


Figure 9. Switching of photosensitive polyisocyanates between two helical preferences by irradiation with circularly polarized light (CPL). (Reprinted with permission from ref 75. Copyright 2000 American Chemical Society.)

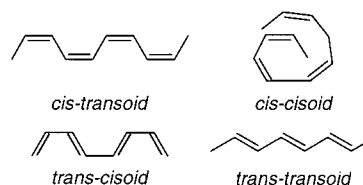
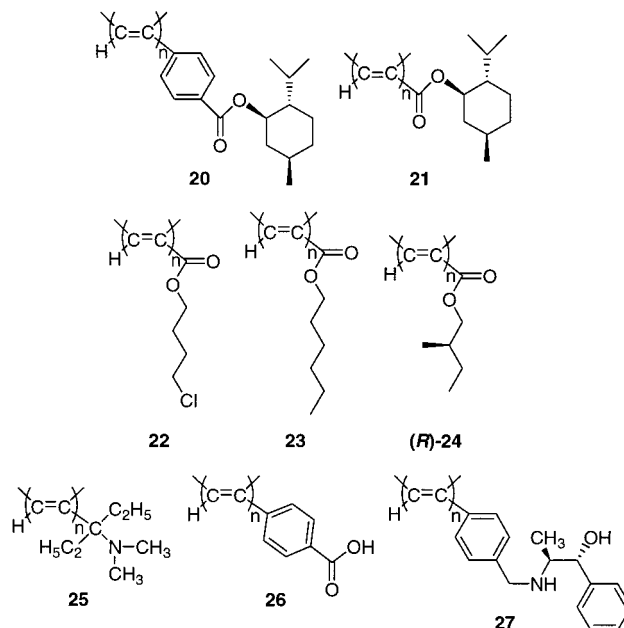


Figure 10. Possible configurations of polyacetylene.

Chart 5



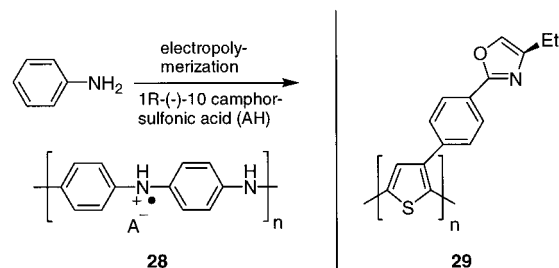
2. Chiral π -Conjugated Polymers. Polyacetylenes can exist in four different conformations: the cis-cisoid, cis-transoid, trans-cisoid, and trans-transoid conformations (Figure 10).⁷⁹ Although this type of conjugated polymer has interesting electronic properties (e.g., *trans*-polyacetylene has a low-energy $\pi-\pi^*$ electronic absorption of 1.8 eV⁸⁰) and substituted *trans*-polyacetylenes have been investigated extensively, studies on substituted polyacetylenes with a predominantly cis configuration are limited. A helical geometry was proposed for the cis-cisoid and cis-transoid polyacetylenes on the basis of the findings of Simonescu et al., who for the first time prepared and identified all four stereoisomers of poly(phenylacetylene).⁸¹ This structure was later confirmed for other polyacetylenes using experimental and computational methods.^{79,82} Characteristic for these helices is the very short persistence length of the helical domain, exemplified by the high population of helix reversal points present along the polymeric backbone of poly(phenylacetylene).⁸³ Already in 1967 Ciardelli and co-workers synthesized the first chiral polyacetylene by polymerizing (*S*)-4-methyl-1-hexyne.⁸⁴ Polyacetylenes equipped with chiral appendages may be prepared by ring-opening metathesis polymerization,⁸⁵ but the most widely applied route is the addition polymerization using $[\text{Rh}(\text{nbd})\text{Cl}]_2$ (nbd = norbadiene) complex as a catalyst, leading to highly regioregular cis-transoidal polyacetylenes.^{86,87}

With the aim of preparing membranes for optical resolution, acetylene polymers **20** (Chart 5) were synthesized for which, on the basis of the high optical

activity, a helical conformation was proposed.⁸⁸ The optical rotation and ellipticity of the related polymer **21** (Chart 5) prepared using the $[\text{Rh}(\text{nbd})\text{Cl}]_2$ catalyst were much higher than those prepared by a $\text{MoOCl}_4\text{-Bu}_4\text{Sn}$ catalyst, which produces a much more irregular macromolecular chain.⁸⁹ In a more extended investigation, a similar comparison was made for a variety of poly(propionic ester)s with other chiral substituents.⁹⁰ It was concluded that the appearance of intense CD effects, originating from a helical backbone conformation, corresponded with a large band gap energy (ca. 3.2 eV). Furthermore, the introduction of bulky substituents into the polymers was found to enhance the persistence length of the single-handed helix, leading to an increase in the magnitude of the Cotton effects and optical rotations. Conformational studies in solution were undertaken to elucidate the helical structure of poly(propionic ester)s.⁹¹ The chiroptical properties of copolymers of **21** and **22** (Chart 5) were found to be strongly related to the enantiomeric excess of the monomer of **21**, which suggested that these polymers had a long helical persistence length. In contrast, the copolymer of **23** and **24** had random-coil character when the (*R*)-**24** (Chart 5) content was 60%.

A number of optically inactive polyacetylenes were prepared by Yashima and others to study the induction of helicity upon their complexation of an optically active compound in organic solvents, in thin films, and in water.⁹² In the case of aliphatic polyacetylene derivatives, a helical conformation was only induced in **25** (Chart 5) when this polymer was complexed with mandelic acid.⁹³ Poly(arylacetylene)s substituted with optically active pendant groups adopt a helical backbone conformation.^{94–96} Using optically inactive poly[(4-carboxyphenyl)acetylene] (**26**) (Chart 5), a CD spectrum could be induced upon complexation of chiral amines⁹⁷ and amino alcohols in DMSO solutions and in films.⁹⁸ Interestingly, the sign and shape of the induced CD effect was found to depend on the stereochemistry, bulkiness, degree of substitution (primary, secondary, or tertiary), and absolute configuration of the amines. Nonlinear correlations were found between the enantiomeric purity of the complexing agents and the observed ellipticity, and between the concentration of the chiral amines and the amount of helicity induced in the macromolecules. Poly[(4-dihydroxyborophenyl)acetylene]⁹⁹ and poly(arylacetylene)s bearing an amine group¹⁰⁰ have been used in the chirality assignment of carbohydrates and steroids, and carboxylic acids, respectively. Polymer **27** (Chart 5) in DMSO solution exists as a right-handed helix, but it reverses handedness upon the addition of mandelic acid.¹⁰¹ For **26**, the induced helicity can be “memorized” when the optically active amine is replaced by various achiral amines. Although this helicity is self-repairing, small structural changes in the achiral component strongly influence the efficiency of helix retention.¹⁰² Furthermore, helical polyacetylenes with pendant lactose side groups have been applied for the molecular recognition of lectin,¹⁰³ and derivatives bearing (*R*)-(1-phenylethyl)carbamoyl groups have been used as a chiral stationary phase for HPLC.¹⁰⁴

Scheme 1. (Left) Synthesis of Polyaniline by Electropolymerization in the Presence of an Optically Active Acid and (Right) Structure of Oxazoline-Containing Polythiophene 29



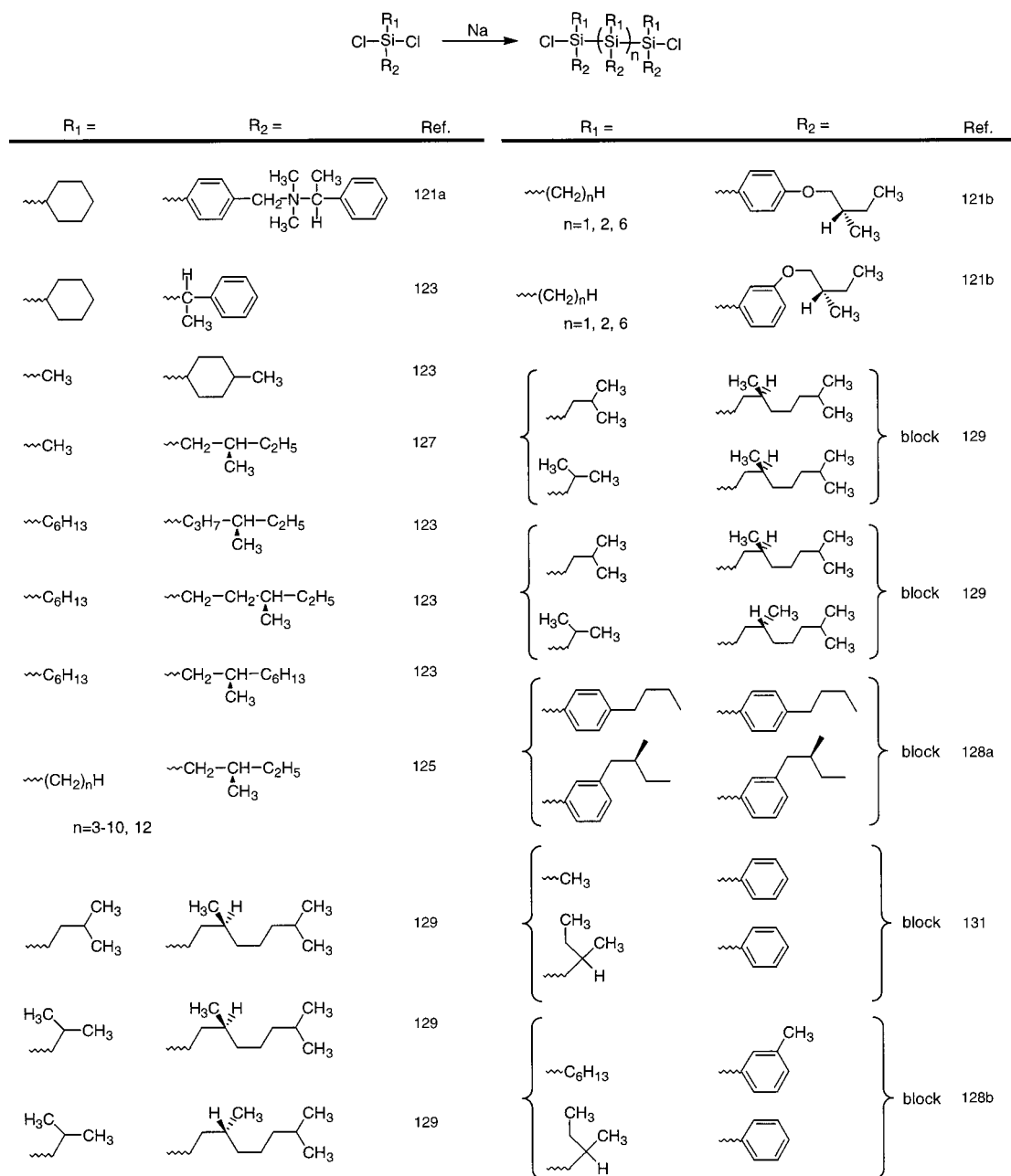
Many papers have appeared on the synthesis and characterization of other chiral-conjugated polymers for possible applications in, among others, membrane resolution of racemates,¹⁰⁵ enantioselective HPLC,¹⁰⁶ and asymmetric catalysis.¹⁰⁷ Remarkably, only for a relatively small number of these chiral π -conjugated polymers, which have been reviewed by Pu,¹⁰⁸ the strong optical activity in the π - π^* transition is ascribed to the presence of a secondary structure, i.e., to a helical conformation of the polymer backbone in solution. Most of them only display helicity in an aggregated form. In fact, apart from the polyacetylenes, the aforementioned foldamers, and “binaphthyl-based polymers” (see section B), only a few examples of conjugated polymers with a helical main chain exist. Main chain helicity has been reported for one substituted poly(phenylenevinylene),¹⁰⁹ for an oligo(β -pyrole),¹¹⁰ for a cyclophane analogue of poly(*p*-phenylene), and for polyanilines.^{111,112}

A special feature of the polyanilines (**28**) is the fact that they are prepared by electrochemical polymerization in the presence of a chiral dopant (Scheme 1). Polymers prepared in the presence of enantiomeric counterions give rise to CD spectra with completely different signs. These signals are lost completely upon deprotonation of the polymer. This suggests that the helicity is maintained by hydrogen-bonding and/or electrostatic interactions with the counterions.

Another very interesting class of chiral conjugated polymers, which has been explored by Swager and co-workers,¹¹³ comprises macromolecules in which the monomeric units are equipped with receptor groups. Binding of analyte molecules leads to changes in the folding of the polymers and consequently to changes in their electrooptical properties, allowing them to act as effective sensors for a variety of different analytes. Surprisingly, only one example has been reported in which the binding of the guest leads to a change in the helical conformation of the reporter polymer. The regioregular polythiophene **29** (see also section IV) bearing chiral oxazoline-derived side groups only gives rise to a CD effect in poor solvents such as alcohols. However, exposure to copper(II) ions in a good solvent such as chloroform gives rise to a strong Cotton effect in the CD spectrum of the polymer which was attributed to the induction of a helical conformation in the polythiophene backbone.¹¹⁴

3. Polysilanes. Polysilanes are linear polymers of silicon in which the σ -electrons in the polymer

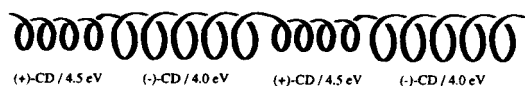
Scheme 2. Wurtz Coupling of Enantiopure Dichlorosilanes and the Structure of the Resulting Chiral Polymers



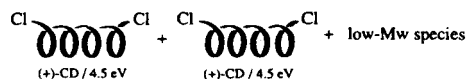
backbone are delocalized. This σ -conjugation gives rise to electronic properties that allow for possible applications as electroluminescent, nonlinear optical, lithographic, and semiconductor materials.¹¹⁵ Since polysilanes are electroactive main chain polymers, the properties of these macromolecules are strongly related to the substituents on silicon. Not only the direct electronic effects of substitution but also its indirect effect on the conformation of the polymer backbone, along which conjugation occurs, affects the optoelectronic properties of these polymers.¹¹⁶

The parent polysilane chain is extremely flexible, and for tetrasilane, the energy barriers between the gauche-gauche and gauche-anti rotation were calculated to be only 6.3 ± 0.8 and $2.9 + 0.4$ kJ·mol⁻¹, respectively.¹¹⁷ For permethylated silanes, still no distinct conformational preferences could be determined; however, for the more bulky *n*-hexyl substitu-

ents, a preference for a dihedral angle of 150° was found which corresponds to a 7/3-helix, a structure which is remarkably similar to the one proposed for the solid-state structure of poly(*di-n*-butylsilane) and poly(*di-n*-pentylsilane).¹¹⁸⁻¹²⁰ By the introduction of enantiopure substituents in the dialkyldichlorosilane monomers, polysilanes can be prepared displaying a preferred handedness of the helical backbone (Scheme 2).^{121,123-127} This backbone chirality can also be induced by using terminal chiral substituents as was demonstrated for oligosilanes with isopropyl side groups.¹²² In a detailed study by Fujiki, it was demonstrated that the optoelectronic properties of such helical polymers are directly related to their conformational properties, since the folding of the all-silicon backbone affects the effective conjugation length.¹²³ Fujiki synthesized a large number of chiral polysilanes using the Würtz synthesis (Scheme 2) and



• Formation of *P*-Screw-Sense Telomers with Si-Cl terminals.



• Recondensation of *P*-Screw-Sense Telomers with Na in Toluene.



Figure 11. Screw-sense-selective photolytic cleavage of the M-helical segments in poly[methyl(2-methylbutyl)silane] and subsequent Würtz coupling of P-helical segments. (Reprinted with permission from ref 127. Copyright 1994 American Chemical Society.)

found that the lowest excitonic Si(σ)–Si(σ^*) absorption band and the bandwidth at half-height of a large number of fractionated chiral polysilanes have a logarithmic relation with the viscosity index of these polymers, which relates to their helical segment length. Poly[alkyl(2-methylbutyl)silane]s have a helical-rod structure and can be regarded as a model for a 5 Å wide quantum wire.¹²⁴ For poly[*n*-decyl((*S*)-2-methylbutyl)silane], the rigidity was even high enough that the polymer chain could be visualized by AFM.¹²⁵ It was demonstrated by Fujiki and co-workers that the properties of such polymers can be regulated by varying the temperature and the solvent.¹²⁶ For poly[*((S)*-2-methylbutyl)(6,9,12-trioxytetradecyl)silane], the predominantly left-handed (M) helical segments were found to tighten and increase in length upon cooling, and also an increase in the number of helix inversions was found. Upon addition of a poor solvent, the number of kinks in the polymer backbone increased

as may be expected upon aggregation of the polymer strands.

Fujiki further showed that poly[methyl(2-methylbutyl)silane] chains in solution consist of diastereomeric segments with opposite handedness.¹²⁷ A special feature of this polymer was that the M-helical segments were more tightly wound than the P-helical ones. Consequently, the absorption and CD bands of the former were blue shifted with respect to those of the latter ones. This allowed the screw-sense-selective photolytic cleavage of the M-helical segments in CCl₄, leaving only the P-helices which became substituted with terminal chloride atoms (Figure 11). Recondensation of these segments using a Würtz-type coupling with sodium in toluene resulted in single-handed P-helical polymers.

Reversible control over the helix sense in polysilanes was achieved in the case of poly(diarylsilanes)¹²⁸ as well as in (co)polymers of ((*S*)-3,7-dimethyloctyl)(3-methylbutyl)silane,¹²⁹ which both showed helix reversal upon heating. For the latter polymer (Figure 12a), it was calculated that the potential curve has a double-well (“W”) shape (Figure 12b) with a slight preference for the M-helix over the P-helix. CD spectroscopy indeed revealed that above the transition temperature the ordered (low-entropy) M-helical conformation becomes less stable than the entropically more favored P-helical state (Figure 12c,d).

The optically inactive poly(methylphenylsilane) (PMPS) was considered for many years to exist in an all-trans conformation. However, although calculations had indicated that PMPS could possibly exist as a loosely wound 15₇-helix,¹³⁰ it was only very recently that it was experimentally demonstrated that this polymer indeed adopts a helical backbone

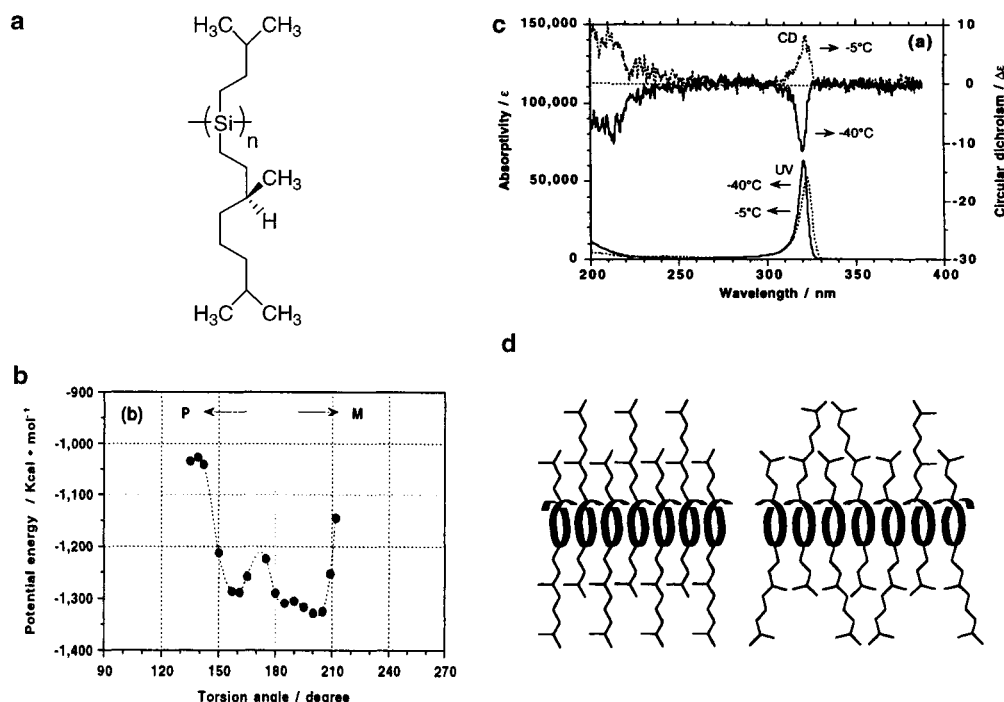


Figure 12. (a) Structure of poly[*((S)*-3,7-dimethyloctyl)(3-methylbutyl)silane]. (b) Energy diagram showing the double-well shape. (c) CD and UV spectra of both screw senses. (d) Schematic representation of the two helical forms. (Reprinted with permission from ref 129. Copyright 2000 American Chemical Society.)

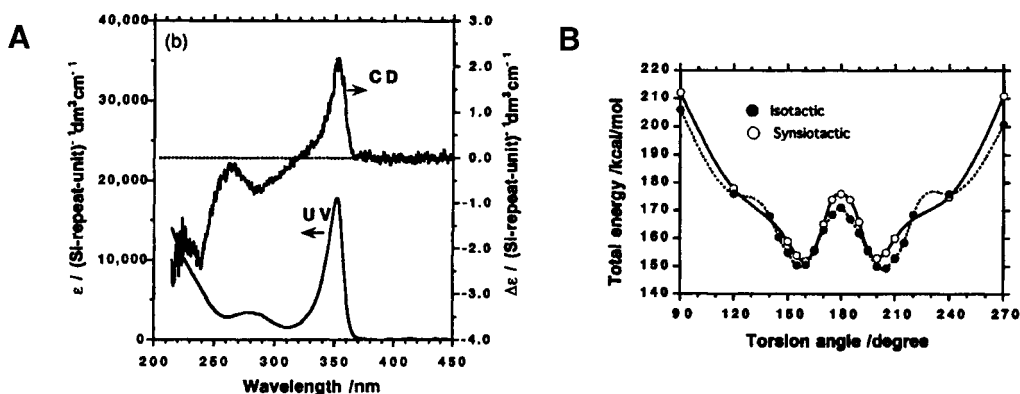
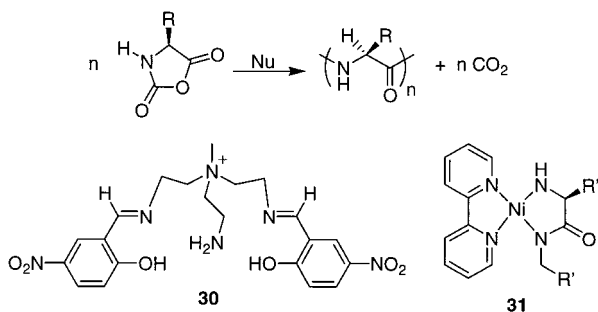


Figure 13. (a) CD and UV/vis spectra of optically active doped poly(methylphenylsilane). (b) Calculated energy diagram of this polymer. (Reprinted with permission from ref 131b. Copyright 2000 American Chemical Society.)

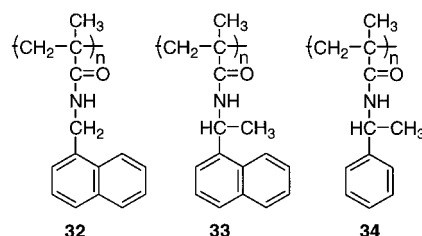
Scheme 3. Polymerization of Amino Acid *N*-Carboxyanhydrides Resulting in Poly(amino acids)



conformation (with an equal distribution of left- and right-handed helical conformations).¹³¹ In these experiments, which showed similar results for poly(*n*-hexyl-*m*-tolylsilane), the PMPS was doped with a chiral monomer [(*S*)-2-methylbutyl]phenylsilane]. The resulting (atactic) copolymers showed a cooperative preferential helical ordering, giving rise to a distinct CD effect (Figure 13a). Molecular modeling indeed indicated the preference of both syndiotactic and isotactic polymers for a helical structure with torsion angles that deviate approximately 25° from the all-trans conformation (Figure 13b).¹³² The helical order in PMPS can be expressed on a supramolecular level in helical aggregates of PMPS-*co*-poly(ethylene oxide) block copolymer as will be discussed in section IV.¹³³

4. Miscellaneous. The combined set of secondary interactions, ultimately resulting in the well-defined folding of peptides, can be divided into separate contributions as was concluded from a detailed study on poly(amino acids). Polymers can be prepared from amino acids with an inherent propensity for adopting a given secondary structure (e.g., helices, sheets, turns), using chemical (opposite to biological) synthesis, which also allows the incorporation of D-amino acids as well as artificial amino acids.^{134,135} Poly(amino acid)s have been prepared in the past from the corresponding *N*-carboxyanhydrides (NCAs) using amines or transition metals as initiators (Scheme 3). This procedure, for example, was used for growing polymers from a surface.^{136,137} It results, however, in polymers with ill-defined lengths. A major advancement in controlling the degree of polymerization was achieved by Deming. Using a Ni(II) based on ligand

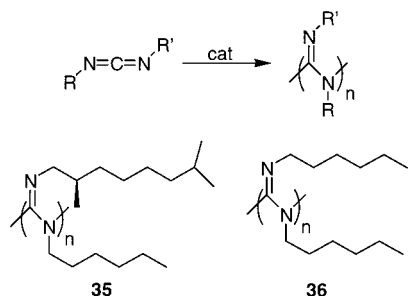
Chart 6



30 catalyst, control over the molecular weight was achieved in the polymerization of Glu-NCA.¹³⁸ Later the procedure was improved by using catalyst **31**,¹³⁹ and it was found that next to nickel also cobalt and iron initiators could be employed.²⁷ Using this approach, it was possible to prepare di- or triblock copolymers by subsequent polymerization of different NCAs. This allows the synthesis of polymers consisting of α -helical or random-coil blocks, as well as polymers with differently charged regions. This method clearly is suited to provide control over the parameters that are important for the organization of these macromolecules into more highly organized (tertiary) structures.²⁷

Nakahari and co-workers prepared polymethacrylamides **32–34** (Chart 6) to study the effect of intramolecular hydrogen bonding between the amide functionalities in the side chains on the conformation of the polymers. Without stabilizing effects (e.g., without sterically demanding substituents), these types of polymers had very low helix inversion barriers and no organized secondary (helical) macromolecular structure could be observed at room temperature. From ¹H NMR and IR studies, it was concluded that the amount of hydrogen bonding was substantially higher for isotactic **32** and **33** than for the atactic derivatives of these polymers, although a monomolecular reference compound showed intermolecular hydrogen bonds in the same solvent even at lower concentrations.¹⁴⁰ More detailed studies on optically active polymers **33** and **34** led to the conclusion that more stable intramolecular hydrogen bonds are formed in the former polymer than in the latter. It was proposed that these polymers have at least a partial helical secondary structure since they maintain their structure in dioxane, a hydrogen-bond-accepting solvent. The organization in these macromolecules was disrupted by the addition of

Scheme 4. Synthesis of Polyguanidines via the Polymerization of Carbodiimines

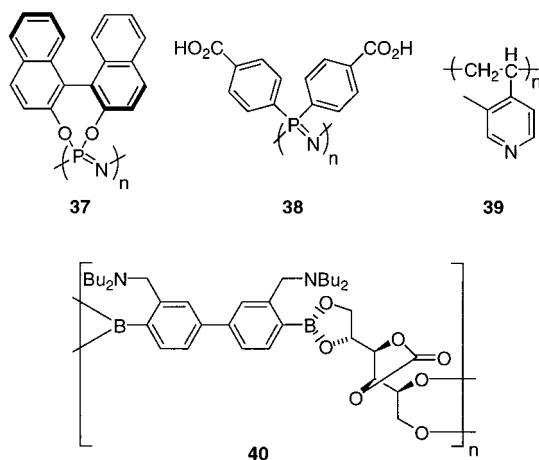


TFA.¹⁴¹ Remarkably, the hydrogen bonds in **33** and **34** are weaker in thin films than in solution, although XRD measurements pointed to a hexagonal arrangement of the macromolecules, suggesting that also in this case they possess a rodlike structure.¹⁴²

An interesting class of rigid helical polymers is obtained by the polymerization of carbodiimides (Scheme 4). These polymers, referred to as polyguanidines, can be prepared by using titanium(IV) complexes¹⁴³ and both copper(I) and copper(II) amidinate complexes¹⁴⁴ as catalysts. The chiroptical properties of polyguanidines have been investigated using **35** and **36** as examples, the former, in contrast to the latter, being optically active. Surprisingly, the optical rotation of **35** directly after polymerization was comparable to that of the monomer, but changed sign and increased significantly upon annealing at elevated temperatures. It was found that a kinetically controlled structure is formed during polymerization, which changes to the thermodynamically controlled helical one upon annealing (for this process $E_a = 26.8 \pm 1.3 \text{ kJ}\cdot\text{mol}^{-1}$). This process was catalyzed by acid, and addition of optically active camphorsulfonic acid to **37** (Chart 7) resulted in an excess of one helical sense from an initially racemic mixture of macromolecular helices.¹⁴⁵

Studies performed by Carriedo et al. indicated that the spirocyclic phosphazene polymer **37** can adopt a helical conformation in solution.¹⁴⁶ Yashima et al. subsequently investigated the chiroptical response of **38** (Chart 7) upon complexation with (*R*)- α -phenylethylamine in DMSO.¹⁴⁷ The resulting optical rotation and its response to changes in temperature

Chart 7



suggest that a helical conformation can also be induced in this polyphosphazene.

Isotactic vinyl polymers often possess a helical conformation in the solid state; however, without bulky substituents present (vide infra) in solution at room temperature, helix–helix reversal takes place fast and no optical activity is observed. Ortiz and Kahn reported a borderline case in which a non-bonded interaction between the monomers leads to the formation of isotactic **39** (Chart 7) by anionic polymerization at $-78 \text{ }^\circ\text{C}$. Optically active polymers can be isolated, but in solution the proposed one-handed helicity is lost in less than 1 h.¹⁴⁸ An intriguing class of polymers formed by polycondensation of diboric acid and chiral tetraalcohols has been studied by Mikami and Shinkai and is exemplified by polymer **40** (Chart 7). In this *D*-mannitol-based polymer, the noncovalent intramolecular interaction between the amines and the boron atoms imposed a sp^3 -hybridization on boron, which, according to calculations, results in a helical conformation of the macromolecule.¹⁴⁹

B. Helical Polymers Having High Helix Inversion Barriers

1. Sterically Restricted Poly(methacrylate ester)s.

It was recognized by Okamoto and co-workers¹⁵⁰ that the anionic polymerization of triphenylmethyl methacrylate (TrMA, **41**) (Chart 8) at low temperature in the presence of an optically active initiator results in the formation of an isotactic, optically active polymer. The helical conformation of the backbone in these macromolecules is the result of steric interactions between the bulky trityl groups, as was shown by the loss of optical activity upon their conversion to methyl ester groups. This class of bulky

Chart 8

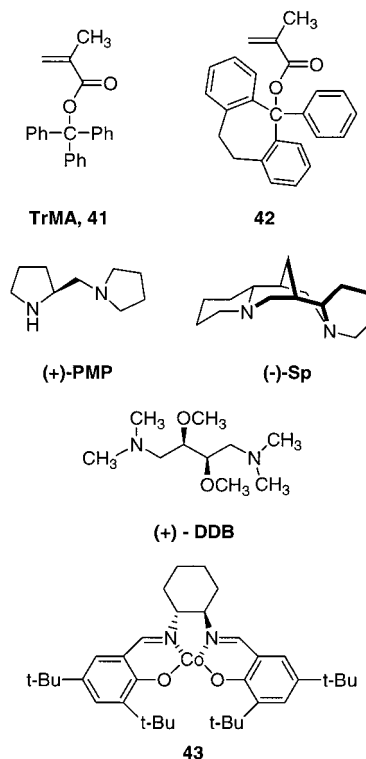


Table 1. Asymmetric Polymerization of TrMA with (-)-Sp, (+)-DDB, and (+)-PMP–FiLi Complexes in Toluene at -78 °C^a

initiator	time (h)	yield ^c (%)	B/H ^b -insoluble part					tacticity ^g (%), mm	
			yield (%)	[α] ²⁵ _D ^d (deg)	[θ] ^e × 10 ⁻⁴ (235 nm)	[θ] ^e × 10 ⁻⁵ (210 nm)	DP ^f		M _w /M _n ^f
(i)-Sp–FiLi	24	99	82	+383	+9.42	+2.32	60	1.31	>99 ^h
(+)-DDB–FiLi	24	100	93	+344	+8.45	+1.86	47	1.10	>99 ^h
(+)-PMP–FiLi	3	100	94	+334	+7.78	+1.76	39	1.12	>99 ^h

^a Reprinted with permission from ref 153. Copyright 1992 American Chemical Society. Conditions: TrMA, 1.0 g; toluene, 20 mL; [TrMA]/[Li] = 20. ^b A mixture of benzene and hexane (1:2, v/v). ^c CH₃OH = insoluble part. ^d *c* = 0.5 (tetrahydrofuran). ^e The CD spectrum was measured in tetrahydrofuran at ca. 25 °C. Units: cm² dmol⁻¹. ^f Determined by GPC of poly(MMA) derived from poly(TrMA). ^g Determined by ¹H NMR of poly(MMA) derived from poly(TrMA). ^h The signals due to the racemo sequence were found only in the termination end.

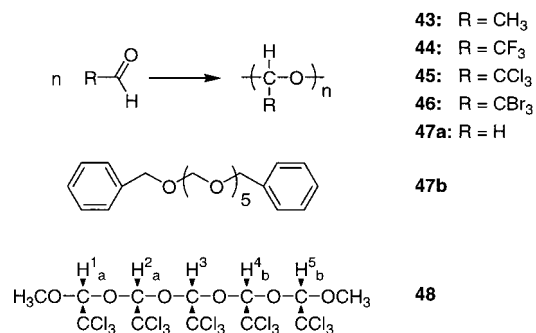
poly(methacrylate ester)s has been extensively explored and reviewed by Okamoto and his group,^{151,152} and only a brief outline is given here.

Different chiral auxiliary ligands (Chart 8) can be used in the polymerization of **41** with organolithium compounds, resulting in polymers with high optical activities and an almost perfect isotactic configuration of the polymer backbone.¹⁵³ Some of the results of this asymmetric polymerization reaction are summarized in Table 1. It appears that the optical activity of the resulting macromolecules increases with the length of the polymer chain and that apart from the highly optically active polymer also a small amount of oligomers with low optical activity is formed. On the basis of these observations, it has been assumed that growing chains with a specific favorable stereoconfiguration propagate relatively fast, while others having the other, unfavorable stereochemistry do not grow beyond the oligomer stage. This kinetic control over the helicity has been confirmed by helix-induced asymmetric polymerization experiments.¹⁵⁴ Using the aforementioned approach, a helical TrMA prepolymer was synthesized, the living chain end of which could be used to subsequently polymerize bulky methacrylate esters in an asymmetric manner.

Screening of an impressive series of polymers derived from different bulky methacrylate esters, e.g., **42** (Chart 8), and using a variety of chiral ligands has revealed the scope of the process of forming helical poly(methacrylate ester)s and their applicability in, for example, the separation of chiral compounds.¹⁵¹ These polymers were prepared not only by anionic polymerization, but also by cationic, free-radical, and Ziegler–Natta techniques. Recently, Nakano and Okamoto reported the use of a cobalt(II)–salophen complex (**43**) in the polymerization of methacrylate ester **41**.¹⁵⁵ The free-radical polymerization in the presence of this optically active metal complex resulted in the formation of an almost completely isotactic polymer with an excess of one helical sense.

2. Phthalocyaninatopolysiloxane. Engelkamp et al. have demonstrated that dihydroxyphthalocyanatosilicon modified with eight (*S*)-citronellol side groups can be polymerized using procedures developed for the related *n*-alkyl derivatives.¹⁵⁶ The resulting material had an estimated degree of polymerization of 27 and was found to be strongly CD active. The CD effects were attributed to a rotational offset

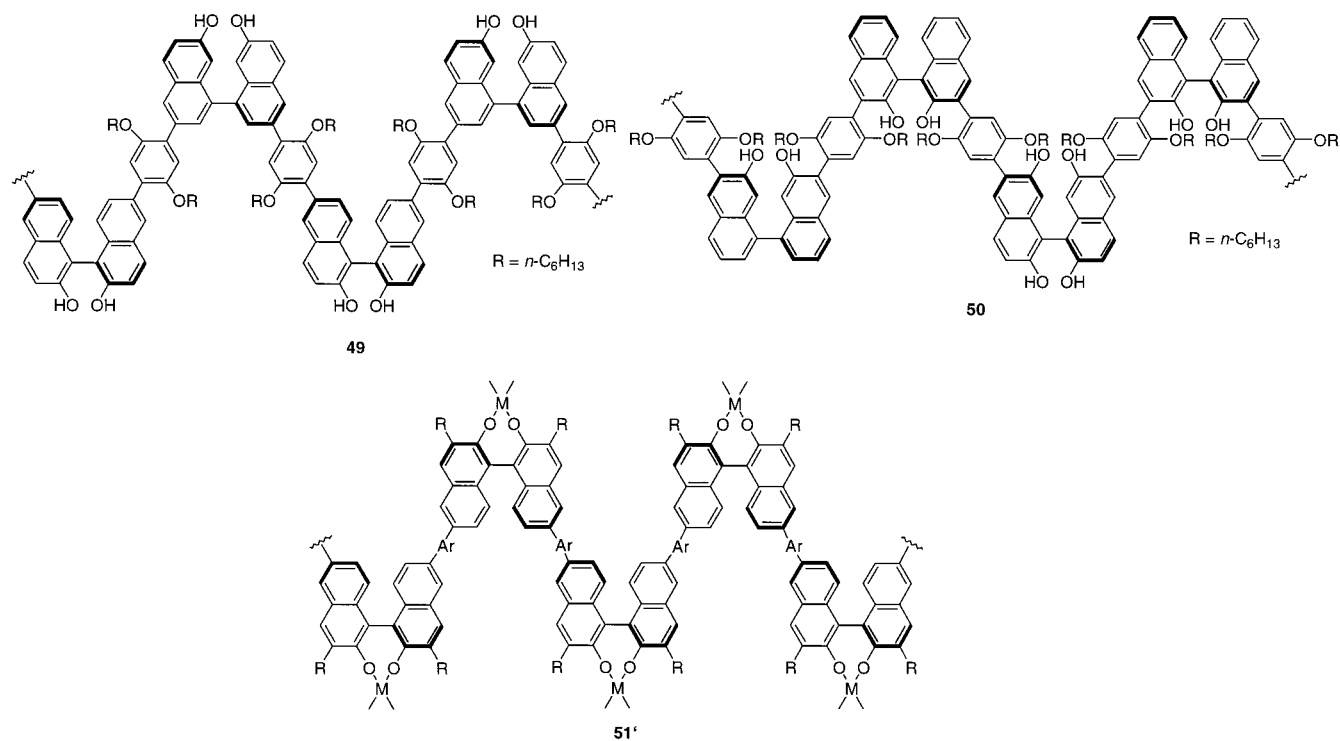
Scheme 5. Synthesis of Polyaldehydes



of the neighboring monomers, leading to a helical organization in the polymer chain. This arrangement was shown to be different in gel-assembled stacks of the corresponding metal-free crown ether phthalocyanines and is possibly imposed by the fixed intermonomer distances. These helices do not show any sign of helix reversal up to temperatures of 120 °C as was concluded from VT NMR experiments.

3. Polyaldehydes. Polyaldehydes are characterized by an oxymethylene repeat unit (Scheme 5), and depending on the substituents present on the carbon atoms, a helical conformation can be present. Research activities related to these compounds have recently been reviewed by Vogl.^{157–159} The all-gauche and hence helical organization of oligoformaldehyde **47** in the solid state was demonstrated by a single-crystal X-ray study.¹⁶⁰ Polymerization of higher aldehydes generally takes place in the gel phase, a condition which appears to contribute significantly to the stereoregularity of the resulting polymers. The most intensively studied polyaldehyde is poly(trichloroacetaldehyde) (polychloral, **45**). Isotactic polychloral is prepared by anionic polymerization and is insoluble in organic solvents. By using optically active lithium alkoxides as initiators, polymers are obtained which display high optical activities in films. For polychloral, a 4/1-helical conformation with a helical pitch of 0.51 nm was found using X-ray diffraction analysis. Due to the insolubility of these materials, no conformational studies have been performed in solution; however, molecular mechanics calculations and NMR spectroscopic and crystallographic studies indicated similar helical characteristics for well-defined oligomers. Although pentamer **48** is symmetric, nonequivalent signals were found for all protons in the solution NMR spectra at 30 °C and attributed to a helical conformation. From VT NMR

Chart 9



experiments, the activation energy (E_a) and the rate of transition from one helical conformation to the other one were determined to be 68.6 kJ·mol⁻¹ and 3.9 s⁻¹ at 20 °C, respectively.¹⁶¹

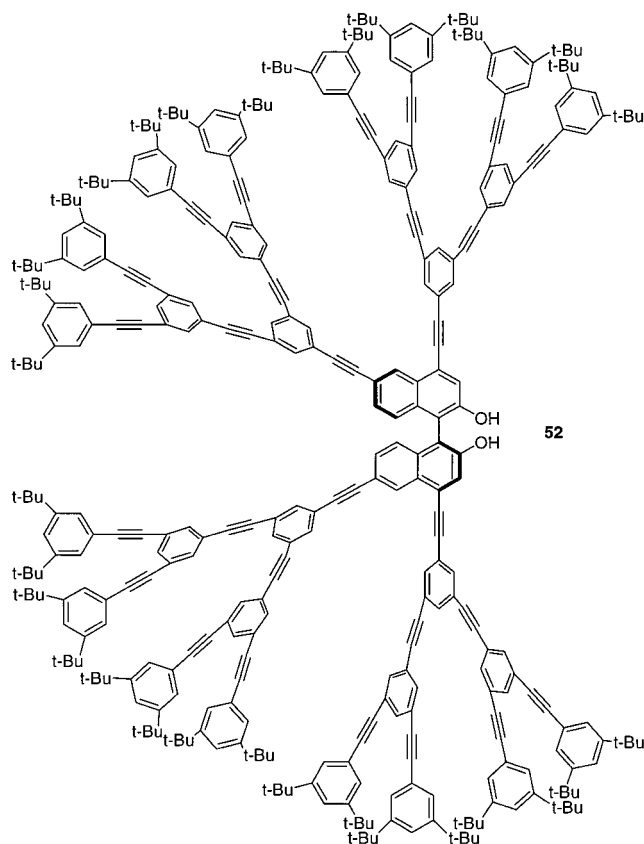
4. Binaphthyl-Based Polymers. Molecules that derive their chirality from their molecular geometry, e.g., helicenes, can be used to construct architectures in which the chirality of the individual molecules is amplified and perpetuates over long distances (see also section II).¹⁶² Katz et al. have prepared oligomers with more than one helical turn based on bis(salicylaldimine).¹⁶³ The helical conformation of these molecules has a marked effect on their optical properties; i.e., very intense absorption bands and CD effects were observed compared to those of the low-molecular-weight parent compounds. Extending this concept further, higher-molecular-weight materials have been obtained via the linking of conjugated segments with optically active 1,1'-binaphthyl groups as was reported and recently reviewed by Pu.¹⁰⁸ Pu et al. have used binaphthyl linkers to connect a large variety of conjugated molecules such as aryleneethynylenes, phenylenevinylens, polythiophenes, oligophenylenes, and oligoethynylenes (e.g., **49**) (Chart 9). In the cases where the linkers contain phenyl groups, meta as well as para substitution has been used. In the former case, this leads to the introduction of an extra turn in the polymer backbone, whereas, in the latter case, the turns are exclusively due to the binaphthyl groups. The resulting materials have a rigid helical conformation and can be applied to anchor catalytic complexes based on Al(III) and Zn(II) via the hydroxy groups on their naphthyl units.¹⁶⁴ The twist in the backbone of the polymer molecules can be tuned by connecting the conjugated segments either via the 3,3'-positions or via the 6,6'-positions (**50**) (Chart 9). Connection at the 3,3'-positions provides better control over the conforma-

tion of the catalytic center, and also allows interaction of substituents on the conjugated segments with the metal. These modifications allow tuning of the catalytic properties and have led to the finding of good chemical yields and excellent enantioselectivities in, e.g., the asymmetric reduction of aldehydes and the epoxidation of α,β -unsaturated ketones. By synthesizing copolymers containing alternating BINOL and BINAP groups, a mixed Ru(III)–Zn(II) catalyst was prepared (**51**). This catalyst was able to perform an asymmetric tandem reaction involving a diethylzinc addition to acetylbenzaldehyde and the subsequent catalytic hydrogenation of the product to form the corresponding diol in chemical yields larger than 99% and with diastereoselectivities of 75–87%.

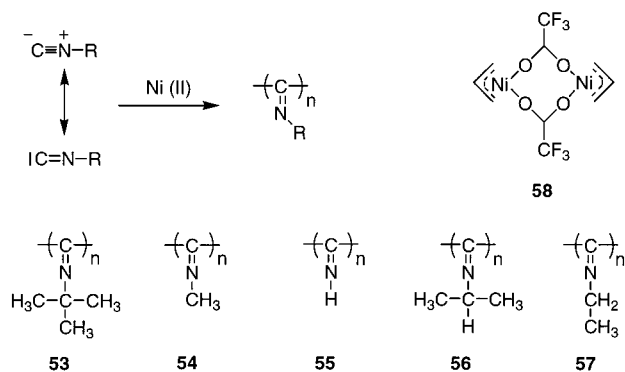
On the basis of the same principles, Pu et al. have synthesized a chiral dendritic compound (**52**) (Chart 10) which shows fluorescence quenching upon binding of amino alcohols. An enantioselective response was observed on addition of a number of amino alcohols; the most significant effect was obtained with phenylalaninol.¹⁶⁵

5. Polyisocyanides. Polymers of isocyanides have the exceptional feature that every carbon atom in the main chain is provided with a substituent (Scheme 6). It was already proposed by Millich¹⁶⁶ that these macromolecules would have a helical conformation as the result of a restricted rotation around the single bonds constituting the polymeric backbone. Until Nolte's report on the applicability of Ni(II) as a catalyst for the polymerization of isocyanides, routes toward polyisocyanides were limited.¹⁶⁷ This transition-metal catalyst allowed the polymerization of the sterically demanding poly(*tert*-butyl isocyanide) (**53**), which subsequently could be resolved by chromatography into the left- and the right-handed helical forms using poly[(*S*)-*sec*-butyl isocyanide] as the stationary phase.¹⁶⁸ These experiments confirmed the

Chart 10



Scheme 6. Nickel(II)-Catalyzed Polymerization of Isocyanides



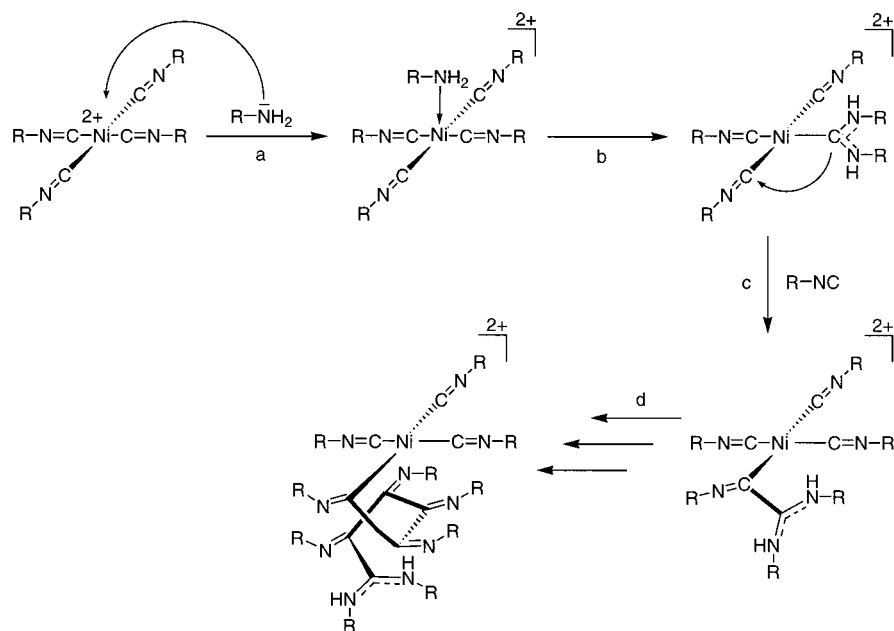
structural proposition of Millich and provided the first example of an optically active polymer solely based on the stable helical conformation of the backbone.¹⁶⁸

The nickel(II)-catalyzed polymerization of isocyanides proceeds relatively fast, a remarkable observation given the steric crowding that is introduced upon formation of the polymer chain. The driving force for the reaction is the conversion of a formally divalent carbon in the monomer into a tetravalent carbon in the polymer, yielding a heat of polymerization of $81.4 \text{ kJ}\cdot\text{mol}^{-1}$.¹⁶⁹ For this polymerization reaction, a *merry-go-round mechanism* has been proposed. Upon mixing of the isocyanides with the Ni(II) catalyst, a square-planar complex is formed (Scheme 7), which in some occasions can be isolated when bulky isocyanides are used. Subsequent attack by a nucleophile on one of the isocyanide ligands is

the initiation step of the polymerization reaction. Via coordination to the nickel (step a), this nucleophile migrates to the isocyanide and a carbene-like intermediate is observed (step b). In the presence of a chiral bias (introduced in the monomer or in the nucleophile), there is a preference for reacting with specifically one of the two neighboring isocyanide monomers on the nickel. After this step, the free coordination position is occupied by an isocyanide from solution (step c), the reaction sequence continues in the direction of the initial step (i.e., one particular helical sense is formed), and each rotation around the nickel adds one turn to the helix (step d). In the absence of a chiral bias, there is an equal probability of attack of the carbene-like carbon atom on both neighboring ligands, leading to a racemic mixture of helical polymers. The easy formation of the tightly coiled helix is explained by the pre-organizing effect of the nickel center: only a slight rearrangement of bonds is required to form the polymer molecule.

The merry-go-round mechanism of isocyanide polymerization can be used to explain and predict a number of the properties of polyisocyanides.¹⁶⁹ However, work by Deming and Novak indicated that some aspects of the mechanism are more complex and involve the reduction of Ni(II) to Ni(I) during the polymerization reaction. Using ESR, cyclic voltammetry, and magnetic susceptibility measurements, it was shown that when an excess (10 equiv) of *tert*-butyl isocyanide is added to NiCl₂, the isocyanide acts as a reductant and an inactive nickel(I) catalyst is formed. Under atmospheric conditions, this reduced catalyst is reoxidized by oxygen to the more active nickel(II) species. The optimum oxygen concentration appears to be at 1 atm of air. At high oxygen contents, no polymerization occurs; instead, the nickel catalyzes the oxidation of the isocyanide to the isocyanate.¹⁷⁰ Taking into account these observations, Deming and Novak investigated the electron-deficient η^3 -allylnickel trifluoroacetate (**58**) as a polymerization catalyst. They found it to be a highly active system (Table 2) which, in a noncoordinating solvent, displayed living chain growth behavior.¹⁷¹

Detailed kinetic and mechanistic investigations have been carried out by Deming and Novak employing this type of Ni catalyst. In toluene, a linear relation was found between the monomer conversion and the degree of polymerization as well as between the catalyst-to-monomer ratio and the molecular weight, for a system consisting of **58** and α -methylbenzyl isocyanide (for racemic as well as for pure enantiomers).¹⁷¹ It also appeared possible to copolymerize a second isocyanide monomer (e.g., **53**) after complete consumption of the first one. Different kinetic behavior was observed under a N₂ atmosphere compared to an O₂-rich environment. Under N₂, the polymerization was found to be first order in monomer, obeying the rate expression $v_p = k_{\text{obsd}}[\text{catalyst}][\text{monomer}]$, with $k_{\text{obsd}}(298 \text{ K}) = 3.7(1) \times 10^{-2} \text{ L}\cdot\text{mol}^{-1}\cdot\text{s}^{-1}$. Under O₂, the rate was found to be zero order in monomer ($v_p = k_{\text{obsd}}[\text{catalyst}]$, with $k_{\text{obsd}}(298 \text{ K}) = 5.1(1) \times 10^{-2} \text{ s}^{-1}$).¹⁷² Although these rate constants are comparable, in such cases, a zero-order

Scheme 7. Merry-go-Round Mechanism in Ni(II)-Catalyzed Isocyanide Polymerization**Table 2. Molecular Weight Characteristics of Selected Polymers^a**

monomer	catalyst	conditions	yield (%)	M_n	M_w/M_n
<i>tert</i> -C ₄ H ₉ NC	58	N ₂ , neat	100	2200	1.03
C ₆ H ₅ CH(CH ₃)NC	NiCl ₂	N ₂ , H ₂ O	75	13220	1.45
C ₆ H ₅ CH(CH ₃)NC	NiCl ₂	air, H ₂ O	100	7420	1.64
C ₆ H ₅ CH(CH ₃)NC	58	N ₂ , toluene	100	24000	1.15

^a Reprinted with permission from ref 171. Copyright 1992 American Chemical Society.

reaction will appear faster than a first-order reaction, due to the lack of rate dependence on monomer concentration. The differences in transition state were examined by determination of thermodynamic activation parameters by performing an Eyring analysis of the rate constants.¹⁷³ More kinetic data have been reported by Deming and Novak investigating substituent effects on the monomer¹⁷⁴ and by Hong and Fox using functional isocyanides.¹⁷⁵ An in-depth discussion of the mechanistic parameters based on these results is beyond the scope of this review, and for this we refer to the work cited.¹⁷⁶

The conformation of polyisocyanides has been the subject of several computational studies. Using the extended Hückel theory, Kollmar and Hoffmann showed that repulsion between the lone pairs of the imino groups in a polyisocyanide chain favors a departure from a planar structure.¹⁷⁷ Similar repulsive effects are known to be operative in polyketones as was reported by Cui and Kertesz, who found a new type of helical Peierls-like distortion for polyketone and polyisocyanide. They suggested that as a result of the existence of partially filled crossing bands a helical structure is formed.¹⁷⁸ Calculations by Kollmar and Hoffman on the series of polymers **53**–**55** indicated that steric effects are more important than electronic effects in determining the polymer structure. For the hypothetical polymer **55**, a broad range of helical conformations was predicted, in contrast to **53** for which the authors proposed a rigid 4/1-helix.

According to this theoretical analysis, polymer **54**, which only is moderately sterically restricted, may adopt two helical structures with different dihedral angles.

Huige and Hezemans^{179,180} have performed extensive molecular mechanics calculations using the consistent force-field method on various oligo- and polyisocyanides. The hexadecamer of *tert*-butyl isocyanide was calculated to have a helical middle section and disordered ends. The dihedral angle N=C–C=N in the middle section was found to be 78.6°, and the number of repeat units per helical turn was 3.75. The latter number is in agreement with circular dichroism calculations using Tinoco's exciton theory (3.6–4.6) and De Voe's polarizability theory (3.81). The molecular mechanics calculations further predicted that the less bulky polymers **56** and **57** form helical polymers as well, whereas a disordered structure was calculated for poly(methyl isocyanide) (**55**).

Clericuzio et al. recently published ab initio and molecular mechanics studies on octameric oligoisocyanides. These calculations, in contrast to the aforementioned ones, showed the so-called syndio conformation to be the minimum-energy geometry although the 4/1 conformation was recognized as a local minimum (Figure 14).¹⁸¹ The obtained set of data was used to tentatively explain some of the features in the UV/vis, CD, and ¹³C NMR spectra of compounds prepared by Salvadori's¹⁸² and Green's groups.¹⁸³ Regarding properties such as optical absorptions at long wavelengths, low intensity of the CD bands, and the chemical shift dispersion of backbone carbon atom resonances, the calculations were found to fit the experimental results. Nevertheless, the outcome of the calculations is the thermodynamic minimum conformation of the polymer backbone, whereas the polymerization is kinetically controlled, possibly leading to a different conformation. However, if the helix inversion barrier is not too high, the 4/1-helix imposed during the polymer-

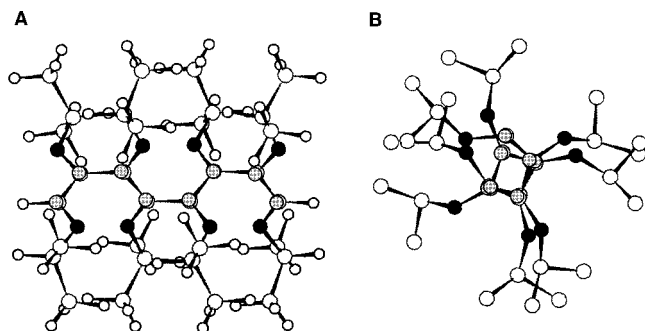


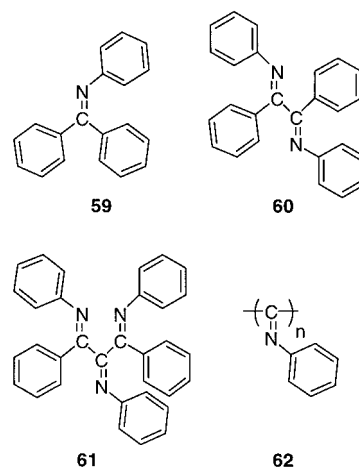
Figure 14. Models of the (a) syndio conformation and (b) 4/1-helical conformation of poly(isopropyl isocyanide) (**56**). (Reprinted with permission from ref 181. Copyright 1997 American Chemical Society.)

ization reaction may unfold to give the proposed syndio conformation.

In-depth studies of the absolute conformations of polyisocyanides are limited. Green and co-workers found,¹⁸³ using ¹³C NMR and light scattering experiments, a limited persistence length (~3 nm) for polyisocyanides without bulky substituents. By means of NMR techniques, Spencer et al.^{184,185} studied oligoimine compounds **59–61** as model compounds for polymer **62** (Chart 11). In particular for the triimine **61**, the conformational analysis is in line with the model of Clericuzio et al.¹⁸¹ (vide infra). In the case of polymer **62**, a combination of GPC, light scattering, and X-ray diffraction showed that the native polyisocyanide has rigid-rod character, but slowly precipitates from solution as a random coil. Using UV/vis spectroscopy, the Arrhenius activation energies for this rod-to-coil transition were determined in different solvents; $E_a(\text{CCl}_4) = 44 \text{ kJ}\cdot\text{mol}^{-1}$, $E_a(\text{THF}) = 51 \text{ kJ}\cdot\text{mol}^{-1}$, and $E_a(\text{CH}_2\text{Cl}_2) = 70 \text{ kJ}\cdot\text{mol}^{-1}$.¹⁸⁶ These data indeed suggest that the helix inversion barrier for **62** is not sufficiently high to have a stable helical conformation at room temperature, but that as a result of the merry-go-round mechanism initially the 4/1-helix is formed as the kinetic product. Helical poly(*tert*-butyl isocyanide) (**53**), obtained by chiral resolution,¹⁶⁸ retains its optical activity even at elevated temperatures.¹⁸⁷ This enabled the use of this polyisocyanide as a chiral absorbent in liquid column chromatography although a different procedure was used for preparing it in the optically active form.¹⁸⁸

Several procedures have been established in the past for the helix-sense-selective polymerization of isocyanides.¹⁶⁹ For the introduction of a chiral bias, required for the discrimination of the otherwise enantiomeric helical senses, three distinct approaches can be applied. One is the use of a chiral monomer, which makes the left- and right-handed helices diastereotopic, and as a result one of the two will be energetically favorable (Figure 5). A second approach involves the use of a chiral catalyst or a chiral initiator, in which case during the initiation of the polymerization there will be a preference for the formation of one particular helical sense that will be retained upon propagation due to the helix inversion barrier. The former approach has been employed in numerous cases (vide infra); the accounts of the use of optically active Ni catalysts are limited.^{189–192} The

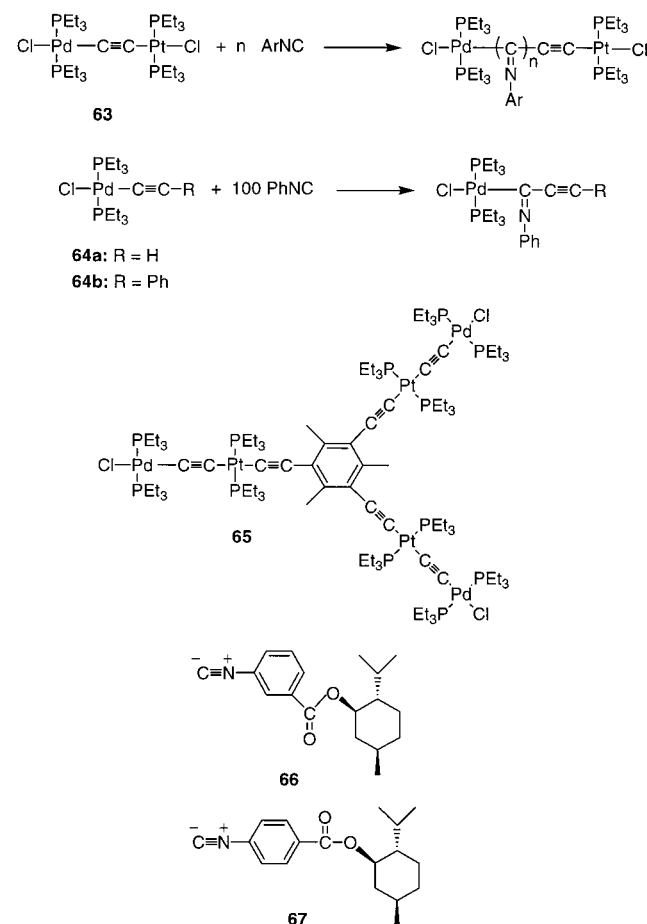
Chart 11



third approach is the selective restraining of the growth of one particular helix by addition of a sterically encumbered optically active comonomer to an achiral one. Polymerization of a fast propagating isocyanide of the latter type (e.g., phenyl isocyanide, 4-methoxyphenyl isocyanide) in the presence of the slowly polymerizing (*S*)-isocyanoisovaleric acid leads to the formation of P-helical high-molecular-weight homopolymers of the former isocyanide and M-helical copolymers with a substantially lower degree of copolymerization. Upon copolymerization, the bulky chiral monomer prefers to be included into M-type helices and slows their propagation, while the P-helices continue to grow fast and consequently consume the majority of the achiral monomer.¹⁹³

An alternative to the nickel-catalyzed synthesis of polyisocyanides has been developed by Takahashi and co-workers.¹⁹⁴ They found that the dinuclear palladium–platinum μ -ethynediyl complex **63**¹⁹⁵ is active in the polymerization of aryl isocyanides (Scheme 8),¹⁹⁶ but not with alkyl isocyanides. The isocyanides exclusively insert into the Pd–C bond, but not into the Pt–C bond.¹⁹⁷ The importance of the Pt–C bond, however, is highlighted by the fact that only one isocyanide monomer is inserted into complex **64** although a 100-fold excess was used. The living nature of the catalyst was shown by the formation of block copolymers, which was possible since the active Pd end groups remained connected to the polymer when all monomers were consumed. Using this feature, it proved to be possible to polymerize an achiral isocyanide with an oligomer prepared from an optically active isocyanide.¹⁹⁸ This procedure, however, was only applicable for initiating complexes in which the oligomer exceeds a critical degree of polymerization, and the optical activity is only retained in the case of sterically demanding achiral isocyanides. Initiators may carry multiple palladium–platinum μ -ethynediyl units as was demonstrated by preparation of polyisocyanides from **65**.¹⁹⁹ A detailed study on the helix-sense-selective polymerization using chiral oligomer complexes derived from isocyanides **66** and **67** gave some interesting results.²⁰⁰ First, the optical activity of the polymers, expressed in their optical rotation and CD effects, drastically increased in going from the meta-substituted aryl isocyanides **66** to the para-substituted ones **67**.

Scheme 8. Polymerization of Isocyanides by a Dinuclear Palladium–Platinum μ -Ethyne-diyl Complex



Second, the rate constants for propagation were virtually identical no matter whether the monomer that was incorporated had the same or the opposite chirality as the one constituting the initiating oligomer. This suggests thermodynamic rather than kinetic control over the helical sense, which contradicts the high helix inversion barrier previously proposed for helical polyisocyanides. However, the observation of a nonlinear relation between the optical purity of the isocyanide and the induced helical sense in the polymer²⁰¹ (majority rules concept) confirms this suggestion. These observations indicate that factors other than steric interactions may be operative during the synthesis of these particular polyisocyanides.

Nonsteric helix-stabilizing effects have recently been reported for peptide-derived polyisocyanides. Polymers built from di- and tripeptide-based isocyanides containing different functional groups have been synthesized as protease mimics (Chart 12; **68**–**70**).^{202–204} More recently compounds **71** and **72** (Chart 12) were synthesized to investigate the effect of this hydrogen bonding between side chains on the conformational properties of the polymer backbone.^{205–207} IR and ¹H NMR studies in which the amide NH characteristic bands and signals of the monomer were compared with those of the polymer showed the involvement of the side-chain amide groups in well-defined arrays of hydrogen bonds along the polymeric backbone. In these studies the single-crystal X-ray

Chart 12

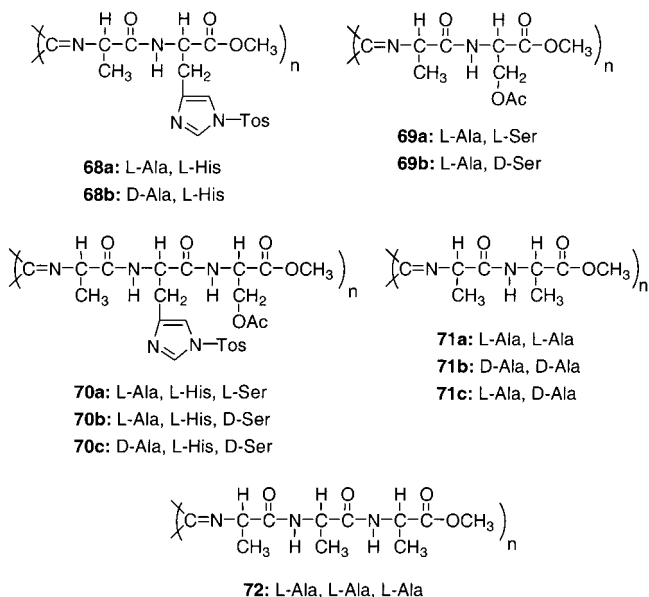


Table 3. Selected Infrared and ¹H NMR Data of Isocyanopeptides and their Polymers²⁰⁷

	isocyanopeptide			peptide polymer		
	ν_{NH}^a (KBr)	ν_{NH}^a (CDCl ₃)	δ_{NH}^b (CDCl ₃)	ν_{NH}^a (KBr)	ν_{NH}^a (CDCl ₃)	δ_{NH}^b (CDCl ₃)
71a	3279	3430 ^c	6.91	3276	3265	9.18 ^c
71c	3304	3416	6.97	3280	3252	9.42
72	3315	3420 ^d	7.04	3300	3290	9.50
	3285		6.38	3267	3260	7.81

^a In cm⁻¹. ^b In ppm. ^c Split signals; average values are given. ^d In a non-hydrogen-bonded state, only one signal is observed for both N–H vibrations. All measurements were performed at room temperature.

structure of the monomer of **71a** served as a reference point (Table 3).

The hydrogen bonds are formed between the amide carbonyl groups in side chains n and the amide NH groups in side chains $n + 4$ (Figure 15). In the case of the tripeptide-derived polyisocyanide **72**, a similar β -sheet-like hydrogen-bonding arrangement was found. This chiral architecture, based on secondary interactions, represents a mimic of the naturally occurring β -helices, which are recently discovered structural motifs in proteins.²⁰⁸ The additional interactions between the side chains stabilize the helical conformation of these polymers, leading to an enhanced rigidity. This rigidity was reflected, for

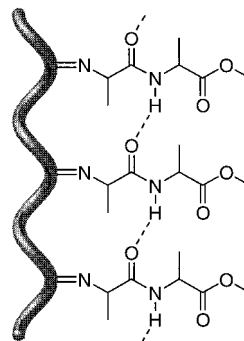
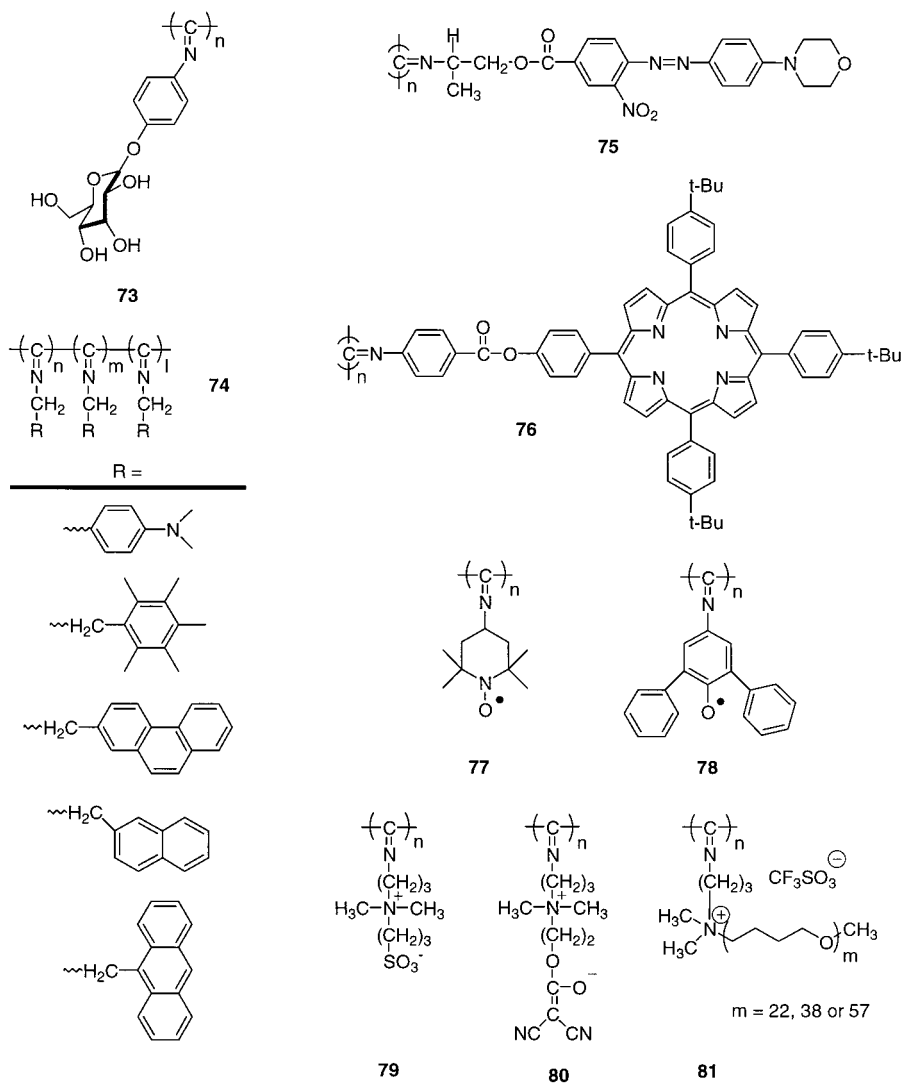


Figure 15. Schematic representation of the hydrogen-bonding array in peptide-derived polyisocyanide **71b**.

Chart 13

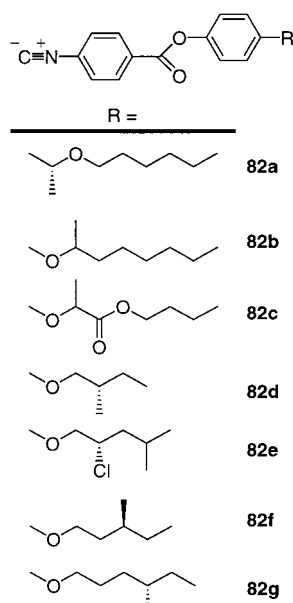


example, in the well-defined hexagonal organization of the molecules in the solid state as well as in the formation of a lyotropic liquid crystalline phase in concentrated CHCl_3 solution. Similar to the unfolding of proteins, the disruption of the hydrogen bonds in the polymers proceeds in a cooperative fashion as could be monitored by CD spectroscopy.²⁰² Although not recognized at that time, some of the intriguing physical properties of polyisocyanides **68**–**70** synthesized in the early 1980s, e.g., $\text{p}K_a$ values which strongly deviate from those of amino acids and very intense Cotton effects, can now be explained by the presence of an intramolecular chain of hydrogen bonds between the peptide side groups.

Hasegawa et al. reported on glycosylated poly-(phenyl isocyanide)s primarily to study the recognition of lectins by these polymers,²⁰⁹ as well as the adsorption and self-organizing properties of these polymers (in particular **73**) (Chart 13) on a hydrophilic surface.²¹⁰ Molecular dynamics calculations indicated that also in this case additional stabilization of the helical backbone by hydrogen bonding between side-chain residues takes place. Due to the high saccharide density along the rigid polyisocyanide backbone, the binding affinity of lectins was approximately 100 times lower than for flexible

glycoproteins. Hong and Fox¹⁷⁵ synthesized block copolymer **74** (Chart 13) with a rigid backbone to spatially organize chromophores and quencher groups to study directional electron transfer and energy migration.²¹¹ Excimer formation, which is a complication observed in flexible polymeric systems, is depressed, and long-living charge-separated states are observed. Both features are in line with the rigid character of the polymer, despite the absence of limiting steric interactions close to the backbone imine groups. Extensive nonlinear optical studies have been performed by Persoons and co-workers^{212,213} on **75** (Chart 13) and related compounds.^{214–216} Second-harmonic light was generated by Langmuir–Blodgett films of these polyisocyanides but not by spin-coated or -cast films. This NLO activity probably results from a side-chain orientation realized at the air–water interface. In solution the orientational correlation between the side-chain chromophores led to unexpectedly high first hyperpolarizabilities (exceeding 5000×10^{-30} eu). The breaking of centrosymmetry, which is required for a second-order nonlinear response, could be attributed to the consistent angle of $\sim 60^\circ$ these chromophores make with the axis of the helical backbone, rather than to the helical organization itself.

Chart 14



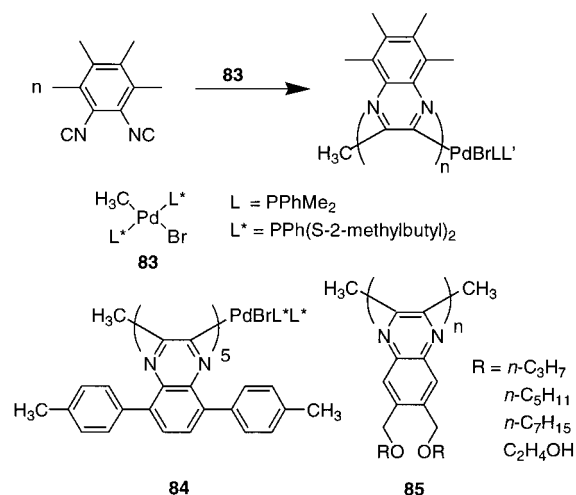
Recently, isocyanides containing a porphyrin group have been polymerized using the palladium–platinum μ -ethynediyl catalyst discussed above (e.g., **76**) (Chart 13).²¹⁷ Longer polymers (DP > 30) show a distinct splitting of the Soret band, indicating stacking of the porphyrins connected to the helical backbone. Other investigations toward polyisocyanides with potential applications as functional devices or specialty materials comprise the polymers **77** and **78** (Chart 13), designed as macromolecular ferromagnets; however, no paramagnetic bulk behavior was found.^{218–220}

Galín and co-workers have synthesized the zwitterionic polymers **79** and **80** (Chart 13) as potential lyotropic liquid crystals and as complexing agents for alkali-metal salts.²²¹ Although only local ordering phenomena were found, the persistence length of the polyisocyanides was increased by a factor of 2, compared to poly(dizwitterionic methacrylate)s. The same group also prepared the “superhairy” polymer **81** (Chart 13), which behaved as a cationic polyamphiphile.²²² Further applications for these polymers, e.g., as lyotropic or thermotropic polymeric materials, may be foreseen.

Polyisocyanides with cholesterol-containing pendant groups have been reported to display thermotropic liquid crystalline properties.²²³

It was demonstrated that a stereocenter positioned far away from the reactive isocyanide group as in monomer **82b** (Chart 14) can still induce chirality in the main chain of polyisocyanides, resulting in the formation of an excess of one particular helix.^{224–226} Kinetic control over the helix sense in the polymerization of **82b** was confirmed by the noncooperative transfer of chirality from the monomer to the macromolecule; e.g., a linear relation was found between the ee present in the isocyanide and the optical activity in the polymers formed.²²⁷ The kinetic inhibition of the growth of one particular handedness using (*S*)-2-isocyanovaleic acid¹⁸⁴ (vide supra) is used to force **82b** and **82c** into a macromolecular helicity with a screw sense opposite that of the one preferred

Scheme 9. Palladium(II)-Catalyzed Polymerization of 1,2-Diisocynoarenes to Polyquinoxalines



by homopolymers of these isocyanides. Using this procedure, it is possible to create diastereomeric helices that include monomeric building blocks of identical absolute configuration but have opposite helical secondary structures.

The palladium-catalyzed polymerization of 1,2-diisocynoarenes has been reported to result in the formation of a different type of helical polyisocyanide (Scheme 9), referred to as a poly(2,3-quinoxaline).²²⁸ Using Pd complexes **83** with chiral phosphine ligands (e.g., bis(*S*)-2-methylbutyl)phenylphosphine) as catalysts in the polymerization of 1,2-diisocyno-3,6-di-*p*-tolylbenzene did not lead to polymers with a large excess of one handedness, but it was possible to separate the optically pure pentamers **84**. Because these oligomers still contained the Pd(II) center, it was possible to subsequently use these compounds as initiators for the helix-sense-selective polymerization of other 1,2-diisocynoarenes.²²⁹ The chiral selectivity is caused by the helical oligomer and not by the phosphine substituent as was demonstrated by ligand exchange experiments.²³⁰ When a chiral Pd catalyst was derived from an optically active binaphthyl compound, the X-ray structure of a stable and rigid helical structure of the growing oligo-(quinoxaliny)palladium(II) complex could be solved.²³¹ The helical conformation of poly(2,3-quinoxaline)s was confirmed through empirical calculations. Two minimal energy conformations were determined, from which the theoretical CD spectra based on the exciton theory were calculated. It was found that the experimental CD spectrum for (+)-poly(2,3-quinoxaline) was in agreement with the spectrum calculated for a right-handed helix with a dihedral angle between the planes of adjacent quinoxalines of 135°. ²³²

Homopolymers and block copolymers of poly(2,3-quinoxaline)s containing functional side chains (**85**) have been prepared employing the Pd(II)-catalyzed helix-sense-selective polymerization.^{233–235} Recently it was reported that side chains can be modified without the quenching of the living site of the polymer.^{236,237} The helical induction by the 1,1'-binaphth-2-ylpalladium(II) complexes has been investigated in detail, mainly using NMR techniques.

It was found that the choice of substituents on the binaphthyl groups strongly affected the diastereomeric formation of oligomeric intermediates, the screw sense of which was maintained in the further helix-sense-selective propagation steps.²³⁸

IV. Chiral Macromolecular Architectures: Tertiary Structure

The interaction between chiral molecules may lead to superb properties and well-defined function as is exemplified in Nature by the high tensile strength in the α -helical coiled-coil superstructure in myosin and the storage of genetic information in the double helix of DNA. The design and synthesis of chiral superstructures in synthetic macromolecular systems is currently being studied by various groups. In the generation of such tertiary structures, i.e., structures with order beyond the constituting elements, two distinct categories may be distinguished, which will be discussed in the following sections: (1) the self-assembly of chiral polymers that do not have a secondary structure in solution, leading to the formation of aggregates with induced chirality, and (2) the self-assembly of helical macromolecules in solution, leading to chiral hierarchical structures. The discussion will be limited to macromolecular assemblages in solution; thin films and bulk materials formed by these polymers will only be mentioned as examples to illustrate interesting phenomena.

1. Chiral Architectures from Nonhelical Polymers. Association of stereoregular polymers belongs to this category since for a number of these so-called stereo complexes a helical superstructure is found.²³⁹ The formation of such macromolecular complexes can be achieved using different secondary interactions of varying strength,²⁴⁵ although van der Waals forces are the most frequently observed. In particular, the complexation between isotactic (*it*-PMMA) and syndiotactic (*st*-PMMA) PMMA has been investigated in great detail.²⁴⁰ Despite the intense efforts of several research groups in this area,^{241,242} the exact mechanism of stereo complex formation is still under debate.²⁴³ The same type of stereo complex is formed independent of the method of preparation and the initial *it/st* ratio.²⁴⁴ This complex comprises a double-stranded 9/1-helix with an asymmetric unit consisting of one *it*-PMMA unit and two *st*-PMMA units (Figure 16).^{245,246}

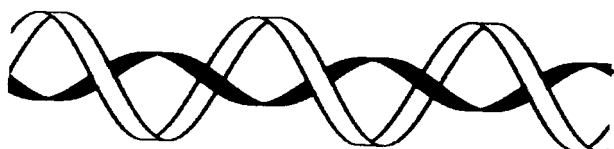


Figure 16. Schematic representation of the stereo complex of *it*-PMMA (black ribbon) surrounded by *st*-PMMA.

Another type of stereo complex, i.e., a tightly wound 3/1-helix, is formed when polymers of L-lactic acid (PLLA) and D-lactic acid (PDLA) are mixed in the blend.^{247,248} Also in solution aggregation of block copolymers containing PLA segments has been found;^{249,250} however, no studies toward the morphology of the aggregates have been conducted.

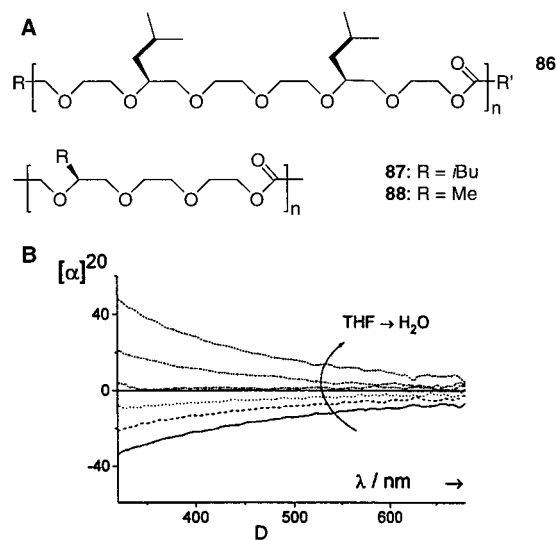


Figure 17. (a) Structures of optically active poly(ethylene oxide) derivatives. (b) ORD spectra of **88** in THF upon increasing the water content. (Reprinted with permission from ref 253. Copyright 1997 American Chemical Society.)

Meijer and co-workers²⁵¹ have reported the aggregation of ribbon-type amphiphilic polymers, based on chiral, substituted poly(ethylene oxide)s (PEOs), as synthetic analogues of coiled-coil-forming peptides (Figure 17). Polymers **86–88** were prepared by ring-opening polymerization of 2-oxo(crown ether) monomers or by polycondensation of the corresponding ω -hydroxycarboxylic acids.²⁵² The amphiphilic nature of these poly(ethylene oxide)s modified with hydrophobic side chains was confirmed by fluorescence studies, giving critical aggregation constants (*cac*'s) covering a wide range (from 0.002 mg·mL⁻¹ for **86** to 0.15 mg·mL⁻¹ for **88**), depending on the size and repetition frequency of the hydrophobic segments in the polymer chain. The conformation of these macromolecules in solutions comprising different water:THF ratios was studied using ORD spectroscopy.²⁵³ Increasing the water content led to a less negative optical rotation, and in the case of **88**, an inversion of the optical rotation was observed (Figure 17b). On the basis of reference studies in which KSCN was complexed with similar ethylene oxide derivatives, the authors concluded that helical superstructures were formed from **86–88** upon increasing the water content.²⁵¹ TEM studies revealed the formation of large well-defined aggregates; however, details of the hierarchical order in the aggregates could not be unveiled.

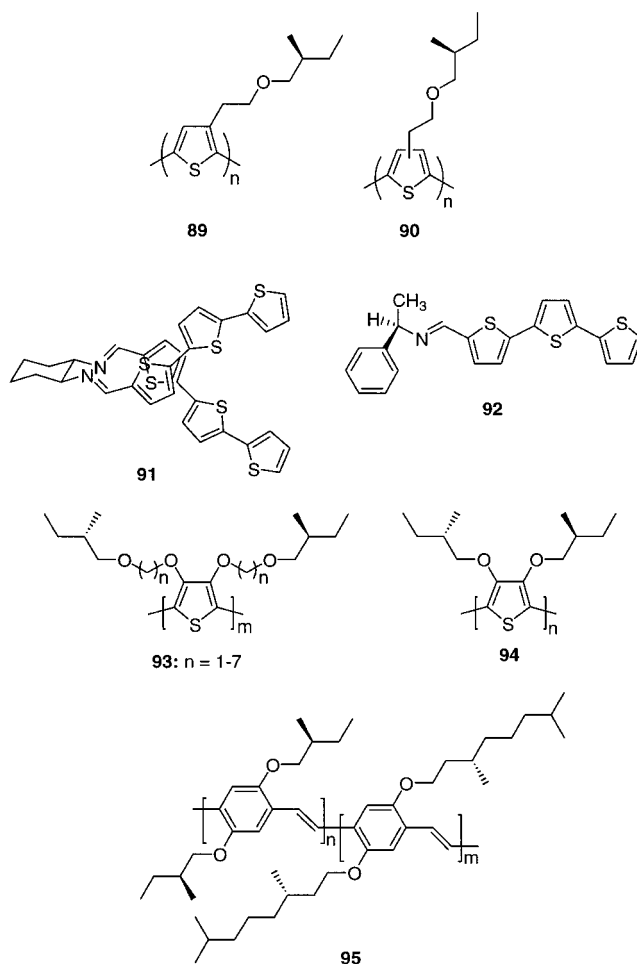
In section III.A, it was already discussed that there is a considerable interest in polymers having a π -conjugated backbone, and a number of applications have been recognized for these materials.²⁵⁴ Interesting, especially with respect to interchain interactions, are the reports on chiral conjugated polymers which display only optical activity in the π - π^* transition of the conjugated backbone when they are aggregated, i.e., in poor solvents and in thin films. The interaction between different polymer chains in the aggregates (microcrystallites) leads to the splitting of the excited state, i.e., exciton coupling. Introducing

dissymmetry into this interchain organization, by optically active auxiliaries, allows the study of these interactions by chiroptical techniques. These aggregation-induced chiroptical effects have been most extensively studied for polythiophenes bearing enantiomerically pure chiral pendant groups as will be discussed below. Aggregation-induced CD effects have also been reported for chiral polydiacetylenes,²⁵⁵ poly(*p*-phenylenevinylene),²⁵⁶ poly(*p*-phenylene)s,²⁵⁷ polypyrroles,²⁵⁸ poly(*p*-phenyleneethynylene)s,²⁵⁹ poly-(3,3'-dialkylterthiophene),²⁶⁰ poly[(dialkylthiothienylene)vinylene],²⁶¹ poly[(2',3'-dialkylthiothienylene)vinylene],²⁶¹ and poly(thienylenevinylene).²⁶² For all these polymers, the chiroptical properties are associated with exciton coupling between different conjugated chromophores and are attributed to the result of a helical packing of the polymer chains in aggregated phases. In this review, we will discuss only the organization and chiroptical properties of these polymers in aggregates since these may be considered as the tertiary structure of these materials as imposed by chirality, steric interactions, and solvophobic effects.

Polythiophenes are an important class of chemically and thermally stable conducting polymers. Unsubstituted polythiophene is an intractable material; however, many processable, both mono- and disubstituted, polythiophenes have become available.²⁶³ Monosubstitution leads to asymmetry in the monomer, and consequently may lead to the formation of regioirregular materials featuring head–tail, tail–tail, or head–head linkages. Since 1992, however, procedures have been known for the preparation of poly(3-substituted thiophenes) containing head–tail couplings, exclusively.²⁶⁴ With these better defined polymers, the construction of chiral architectures became feasible, and in the initial publications on regioirregular polythiophenes substituted with enantiomerically pure chiral pendant groups, strong bisignate CD effects²⁶⁵ and high specific optical rotations^{265,266} were reported.²⁶⁷ Bouman and others showed by studying the solvatochromic and thermochromic behavior of regioregular **89** and regiorandom **90** (Chart 15) that these polymers only displayed optical activity in the π – π^* transition when aggregated as microcrystallites in solution or thin films.²⁶⁸ The formation of ordered crystalline domains in the aggregated phases results in an intermolecular chiral orientation of the rigid polymer chains. The enhanced crystallinity of regioregular polythiophene derivative **89** results in significantly larger chiroptical effects, when compared to those of regiorandom polymer **90**; e.g., $[\alpha]_{513} = 140000^\circ$ for **89**, and $[\alpha]_{513} = 5000^\circ$ for **90**. These observations are in agreement with the assumption that the induced optical activity in the π – π^* transition has an intermolecular origin.

A cholesteric organization of the rigid oligothiophene chains in the aggregates has been proposed for **91** and **92** (Chart 15) on the basis of theoretical and experimental work, which is in line with the observed bisignate CD spectra.^{269,270} In aggregated phases, the sign of the induced optical activity in the π – π^* transition alternates with the parity of the

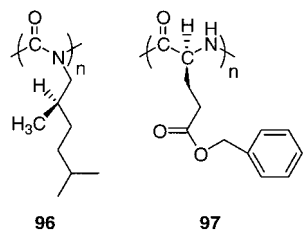
Chart 15



number of atoms in the spacer of polymers **93** (Chart 15), as was reported by Ramos et al.²⁷¹ Stereomutation of the aggregated phase of chiral substituted polythiophenes, i.e., inversion of the chirality as judged from the sign of the CD effect, has been observed upon altering the solvent conditions.^{272,273} Another investigation showing the sensitivity and complexity of the ordering and conformational phenomena in π -conjugated polymer chains has been conducted by Langeveld-Vos et al.²⁷⁴ They reported that the “majority rules” principle applies for a copolymer of thiophenes equipped with (*R*) and (*S*) chiral side chains, and the “sergeants and soldiers” rule for aggregates consisting of chiral and achiral substituted polythiophene chains. The latter example can be regarded as an interchain effect; intrachain cooperativity has been reported for a chiral poly(*p*-phenylene).²⁷⁵ Only a small percentage of the substituents in the polymer were chiral, but significant optical activity was observed in the aggregated state of the macromolecule.

For all these polymers, the chiroptical properties are associated with exciton coupling phenomena between different conjugated chromophores and are thought to result from a helical packing of the polymer chains in aggregated phases. Effects similar to those resulting from the intermolecular packing of polymeric chains have been found in connection with the intramolecular chain folding of oligo(phenylacetylene)s (see section III).⁴⁶

Chart 16

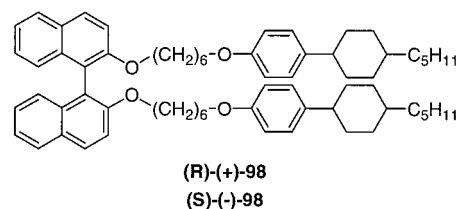


In a paper on the chiroptical properties of optically active poly[3,4-bis((*S*)-2-methylbutoxy)thiophene] (**94**) (Chart 15), it was demonstrated for the first time that the photoluminescence of chiral polythiophene is circularly polarized when the polymer chains are aggregated in solution.²⁷⁶ The degree of crystallinity was high inside the aggregates as was evidenced by the occurrence of vibronic bands in both the UV/vis and CD spectra.²⁷⁷ The observed circular polarization of the luminescence when the polymers are aggregated proves that the chiral packing of the chains is not destroyed upon photoexcitation and only a small structural reorganization takes place in the excited state, consistent with the observed small Stokes shift. By applying this phenomenon to light-emitting diode technology, circularly polarized electroluminescence was obtained from a film prepared by spin coating of **95** (Chart 15).²⁷⁸

2. Hierarchical Structures from Helical Polymers. The formation of a nematic liquid crystalline phase, characterized by orientational but not positional molecular order, is often observed for stiff helical macromolecules in solution.²⁷⁹ Parameters important in describing these structures are the pitch, the radius, and the handedness of the helices. In a liquid crystalline state, the aggregation of the helices is in some cases accompanied by the formation of a cholesteric phase. The rodlike molecules in this case are no longer oriented parallel, but are twisted with respect to their nearest neighbors. Among others, poly[(*R*)-2,6-dimethylheptyl isocyanate] (**96**),^{280,60} poly-(γ -benzyl α ,L-glutamate) (PBLG, **97**),^{281,282} and schizophylan²⁸³ (a triple-helical polysaccharide rod) were found to display cholesteric liquid crystalline mesophases in concentrated solutions (Chart 16). The major models describing the transfer of the helical chirality to the cholesteric phase are the *straight-rod*²⁸⁰ and the *threaded EFJC*^{77a} models. Both models approach the macromolecular helix as a screw-threaded cylinder, which implies that the aggregation of two such helices is mainly dependent on the ratio pitch/diameter. The models predict that at a critical value inversion of the helicity of the resulting super-helix will take place.

The straight-rod model predicts a right-handed cholesteric helix for **96** and a left-handed one for PBLG and schizophylan, which is in agreement with experimental results.²⁸⁰ In the threaded EFJC model, the flexibility of the macromolecular helix can be freely chosen. The handedness of the cholesteric phase is based on entropic "hard core" repulsion phenomena between the helices and an enthalpic chiral dispersion force. Right-handed mesophases were predicted for solutions of **96**, **97**, and schizophylan. However, only for **96** this was in agreement

Chart 17



with the experimentally determined handedness; a direct explanation for this discrepancy was not given.

An astonishing helical architecture was prepared recently by Akagi et al.²⁸⁴ They polymerized acetylene in a chiral nematic reaction field. To this end, the Ziegler–Natta catalyst $\text{Ti}(\text{O}-n\text{-Bu})_4\text{-Et}_3\text{Al}$ was dissolved in the stable chiral nematic mesophase obtained by mixing 5–14 wt % (*R*)- or (*S*)-**98** (Chart 17) with a known nematic liquid crystal, and this medium was subsequently used for the preparation of polyacetylene films. It was found that polymers prepared in the (*R*) chiral nematic liquid crystals had counterclockwise (*M*) helical fibrillar morphologies and those prepared in the (*S*) phase clockwise (*P*) morphologies (Figure 18). CD spectra of these films showed a positive Cotton effect for the *M*-helical fibrils and a negative Cotton effect for the *P*-type ones, in the $\pi\text{-}\pi^*$ transition region of the polyacetylene chain. Since the helical pitch of a chiral nematic phase can be controlled by the optical purity or the type of chiral dopant, and the liquid crystalline phase templates the helicity, it was also possible to produce fibrils with a different helical pitch. An interesting hierarchical transfer of chirality was observed in this case, i.e., going from the chiral twist in **98** to the helical polymer and ultimately to the spiral morphology in the microscopic regime.

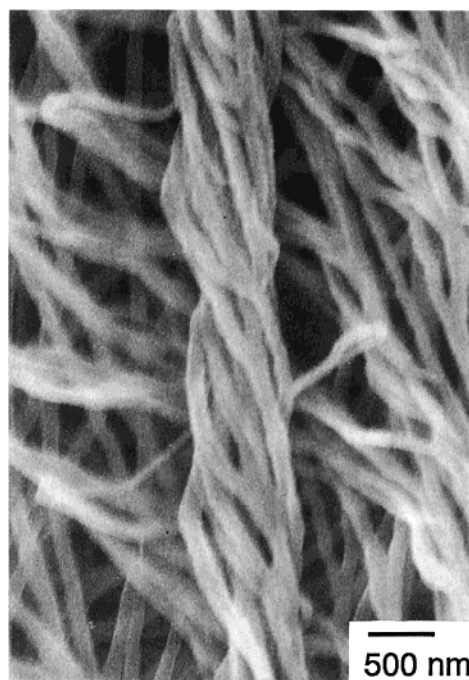


Figure 18. Scanning electron micrograph of a left-handed helical morphology formed by polyacetylene polymerized in a chiral nematic reaction field. (Reprinted with permission from ref 284. Copyright 1998 American Association for the Advancement of Science.)

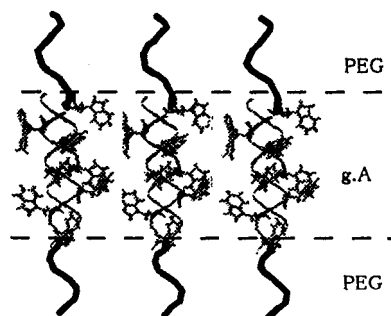
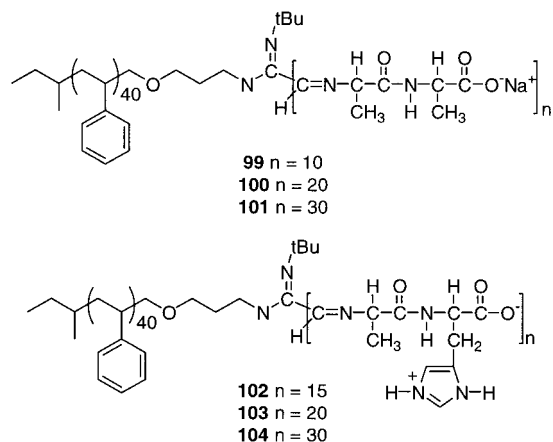


Figure 19. Proposed organization in bilayers formed by a gramicidin A–poly(ethylene oxide) hybrid. (Reprinted with permission from ref 285. Copyright 1999 American Chemical Society.)

Chart 18



Hybridization of gramicidin A, a hydrophobic 15-mer peptide, with a hydrophilic PEO chain resulted in the formation of an amphiphilic compound as was reported by Kimura et al.²⁸⁵ Upon dispersion in water, these hybrid polymers, in which the degree of polymerization of the PEO segment was 13, gave vesicles with an average diameter of 85 nm. An illustration of the proposed organization of the molecules in the vesicle bilayer is given in Figure 19. Inclusion experiments confirmed the vesicular nature of the aggregates, while CD measurements supported the presence of the proposed antiparallel double-stranded helix conformation.

The formation of dissymmetric, helical superstructures from polymeric building blocks was first reported by Cornelissen et al.²⁸⁶ An amine-end-capped polystyrene was used as the initiator for the polymerization of dipeptide-derived isocyanides (see also section III.B) which resulted in a series of amphiphilic block copolymers (**99**–**104**) (Chart 18), consisting of a hydrophobic polystyrene segment and a rigid hydrophilic helical polyisocyanide block. CD data revealed that the helical screw pitch was right-handed in the case of **99**–**101**, and left-handed in the case of **102**–**104**. The effect of a changing ratio between the hydrophilic and hydrophobic blocks on the aggregate morphology in an aqueous environment with optimized pH (pH 5.6) was investigated by TEM. For **101** and **104**, no distinct morphologies were obtained, whereas for both **100** and **103** the generation of micellar fibers was observed. Interestingly, the flexibility of the fibers formed by **103** could

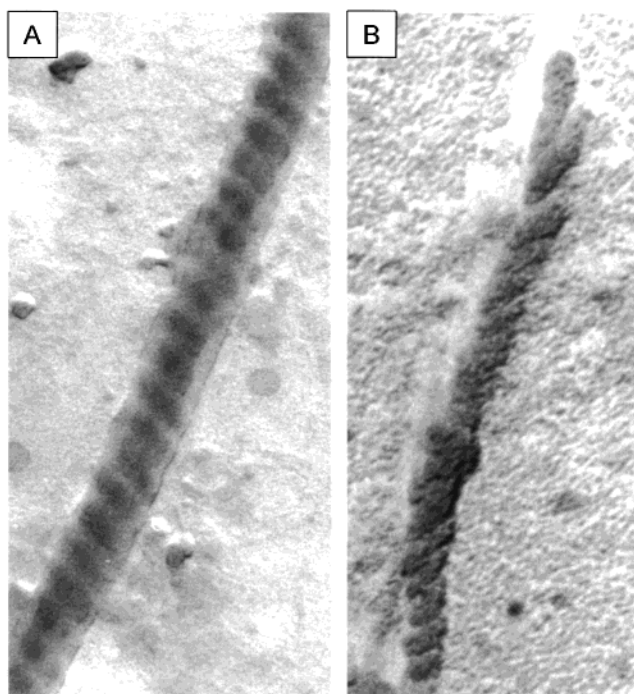
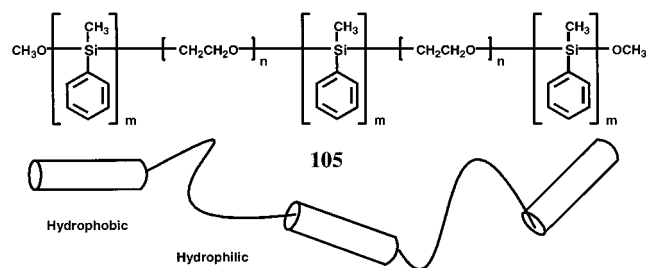


Figure 20. Transmission electron micrographs of the (a) right-handed and (b) left-handed helical superstructures obtained from assembled polystyrene–polyisocyanopeptide block copolymers **99** and **102**, respectively.

Chart 19



be tuned by varying the anion: the flexibility was found to increase on going from a mono- to a di- and then to a tricarboxylate (i.e., from acetate to tartrate to citrate) counterion. Further reduction of the helical polyisocyanide part (**99** and **102**) resulted in the formation of bilayer-type structures. In addition to collapsed vesicles and bilayer fragments, helical superstructures were observed: for **99**, a left-handed helix was found, whereas **102** gave a right-handed one (Figure 20). Remarkably, in both cases, the handedness of the superhelices had been reversed with respect to that of the polyisocyanide helices in the constituting block copolymers.

Although the precise mechanism of formation of these superstructures is still unclear, a hierarchical organization is evident, since transfer of chirality takes place from the amino acid in the monomer to the secondary helical structure of the polyisocyanide blocks and, ultimately upon assembly, to the helical superstructure.

The chiral structures discussed above are formed by relatively well-defined macromolecules. Interestingly, superhelical structures can also be obtained from rather polydisperse multiblock copolymers, viz., of PEO and PMPS (**105**; PDI = 1.6) (Chart 19). In a

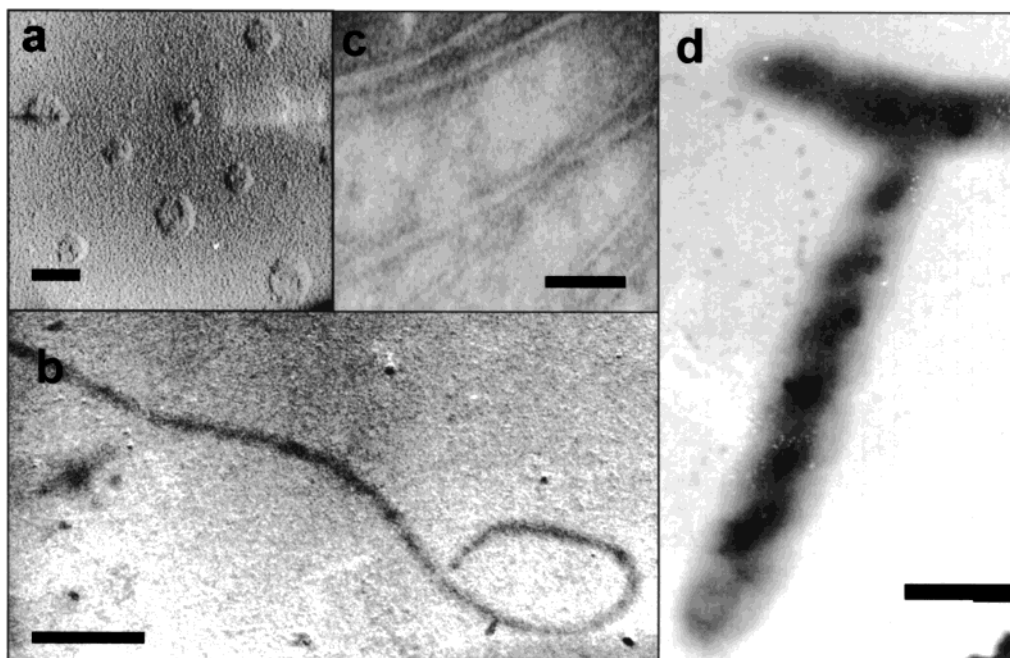


Figure 21. Transmission electron micrographs showing the formation of (a) vesicles, (b, c), micellar fibers, and (d) superhelices from a PEO-PMPS block copolymer (**105**).

preliminary communication, the formation of vesicles was reported in pure water (Figure 21a).²⁸⁷ In a later paper,¹³³ it was described that the aggregation behavior of this amphiphilic polymer can be tuned by dispersing it in water-THF mixtures of varying composition. Below water concentrations of 40% (v/v) no aggregates were found. Electron microscopy demonstrated the presence of micellar rods in mixtures containing 40–80% (v/v) water (Figure 21b,c). In solvent mixtures containing more than 80% water, helices (Figure 21d)¹³³ with both left- and right-handed screw pitch were observed. Given the multi-block nature of the polymer and the polydispersity of the PMPS blocks, it is unlikely that the helical superstructures arise from preferential aggregation of PMPS segments with identical screw senses. A cooperative process was assumed to occur in which the handedness of the initial PMPS segment(s) determine(s) the handedness of the subsequent PMPS segments assembling in the same aggregate, such that a chiral architecture is formed by hierarchical assembly of these dynamic helical macromolecules.

V. Conclusions and Outlook

On the way from molecular to macromolecular and supramolecular chemistry, researchers have realized increasingly complex functional materials; however, these still lag behind compared to highly sophisticated macroscopic architectures with precise and predefined structure that are encountered in biological systems. In this review, we have summarized the first steps chemists have taken toward the construction of macromolecular architectures with defined three-dimensional structures. In the past decade, polymers with defined secondary structure mimicking one or more aspects from biological systems have been prepared. Issues important for the programmed organization of synthetic macromolecules that have

been addressed include the conformational dynamics of the helicity and their effect on the (photo)physical properties of the polymers, the induction of helicity in the polymer chain, the influence of kinetics on the macromolecular secondary structure, and the use of multiple interactions in the hierarchical organization of macromolecules to well-defined supramolecular assemblies.

It is evident that mastering the organization of macromolecules is essential for the generation of materials with sophisticated properties. Since polymers with a permanent and precisely defined helical structure allow the generation of well-defined chiral superstructures, it is our contention that this class of macromolecules provides the route toward a better understanding of the principles underlying the generation of functional polymeric materials with tertiary structure from synthetic building blocks with a known secondary structure. In the future, these principles may be extrapolated to understand and ultimately predict also the assembly processes taking place between macromolecules with a more dynamic backbone conformation, ultimately allowing their application for the construction of advanced polymeric materials and devices.

VI. Acknowledgments

We thank The Netherlands Organization for Scientific Research (NWO) for financial support of J.J.L.M.C.

VII. References

- (1) Rowan, A. E.; Nolte, R. J. M. *Angew. Chem., Int. Ed.* **1998**, *37*, 63–68.
- (2) Feiters, M. C.; Nolte, R. J. M. In *Advances in Supramolecular Chemistry. Vol. 6. Chiral Self-assembled Structures of Biomolecules and Synthetic Analogues*; Gokel, G. W., Ed.; JAI Press Inc.: Stamford, CT; Vol. 6, pp 41–156.
- (3) As chiral dendrimers do not possess a secondary or tertiary structure, they will not be included in this review. For an

- excellent overview on these intriguing macromolecular architectures see: Peerlings, H. W. I.; Meijer, E. W. *Chem.-Eur. J.* **1997**, *3*, 1563.
- (4) Foldamers are discussed in detail in another review in this issue; see: Hill, D. J.; Mio, M. J.; Prince, R. B.; Hughes, T. S.; Moore, J. S. *Chem. Rev.* **2001**, *101*, 3893–4012.
- (5) (a) Sommerdijk, N. A. J. M.; Buynsters, P. J. J. A.; Pistorius, A. M. A.; Wang, M.; Feiters, M. C.; Nolte, R. J. M.; Zwanenburg, B. *J. Chem. Soc., Chem. Commun.* **1994**, 1941. (b) *J. Chem. Soc., Chem. Commun.* **1994**, 2739. (c) Sommerdijk, N. A. J. M.; Lambermon, M. H. L.; Feiters, M. C.; Nolte, R. J. M.; Zwanenburg, B. *Chem. Commun.* **1997**, 455. (d) Sommerdijk, N. A. J. M.; Lambermon, M. H. L.; Feiters, M. C.; Nolte, R. J. M.; Zwanenburg, B. *Chem. Commun.* **1997**, 1423. (e) Sommerdijk, N. A. J. M.; Buynsters, P. J. J. A.; Akdemir, H.; Geurts, D. G.; Pistorius, A. M. A.; Feiters, M. C.; Nolte, R. J. M.; Zwanenburg, B. *Chem.-Eur. J.* **1998**, *4*, 127. (f) Buynsters, P. J. J. A.; Feiters, M. C.; Nolte, R. J. M.; Sommerdijk, N. A. J. M.; Zwanenburg, B. *Chem. Commun.* **2001**, 269–270. (g) Buynsters, P. J. J. A.; Feiters, de Gelder, R.; Ten Holte, P.; M. C.; Nolte, R. J. M.; Pistorius, A. M. A.; Sommerdijk, N. A. J. M.; VerHaegen, A. A. C.; Zwanenburg, B. *J. Mater. Chem.* **2001**, *11*, 269–277.
- (6) Hafkamp, J. H.; Feiters, M. C.; Nolte, R. J. M. *Angew. Chem.* **1994**, *106*, 1054–1055.
- (7) Schnur, J. M. *Science* **1993**, *262*, 1669–1676.
- (8) Nakashima, N.; Asakuma, S.; Kunitake, T. *J. Am. Chem. Soc.* **1985**, *116*, 10057–10069.
- (9) Frankel, D. A.; O'Brian, D. F. *J. Am. Chem. Soc.* **1994**, *107*, 509–510.
- (10) Fuhrhop, J.-H.; Helfrich, W. *Chem. Rev.* **1993**, *93*, 5–1582.
- (11) Yanagawa, H.; Ogawa, Y.; Furuta, H.; Tsuno, K. *J. Am. Chem. Soc.* **1989**, *111*, 4567–4570.
- (12) (a) Engelkamp, H.; Middelbeek, S.; Nolte, R. J. M. *Science* **1999**, *284*, 785–788. (b) Palmans, A. R. A.; Vekemans, J. A. J. M.; Havinga, E. E.; Meijer, E. W. *Angew. Chem., Int. Ed. Engl.* **1997**, *36*, 2648–2651. (c) Gulik-Krzywicki, T.; Fouquey, C.; Lehn, J.-M. *Proc. Natl. Acad. Sci. U.S.A.* **1993**, *90*, 163–167. (d) Tachibana, T.; Kambara, H. *J. Am. Chem. Soc.* **1965**, *87*, 3015–3016.
- (13) (a) Hafkamp, R. J. H.; Kokke, B. P. A.; Danke, I. M.; Geurts, H. P. M.; Rowan, A. E.; Feiters, M. C.; Nolte, R. J. M. *Chem. Commun.* **1997**, 545–546. (b) Hanabusa, K.; Yamada, M.; Kimura, M.; Shirai, H. *Angew. Chem., Int. Ed. Engl.* **1996**, *35*, 1949–1951. (c) De Loos, M.; van Esch, J.; Stokroos, I.; Kellogg, R. M.; Feringa, B. M. *J. Am. Chem. Soc.* **1997**, *119*, 12675–12676. (d) Van Esch, J. H.; Feringa, B. L. *Angew. Chem., Int. Ed.* **2000**, *39*, 2263–2266.
- (14) Stryer, L. *Biochemistry*, 4th ed.; Freeman: New York, 1975.
- (15) (a) Engelkamp, H.; Middelbeek, S.; Nolte, R. J. M. *Science* **1999**, *284*, 785–788. (b) Yang, W.; Chai, X.; Chi, L.; Liu, X.; Cao, J.; Lu, R.; Jiang, Y.; Tang, X.; Fuchs, H.; Li, T. *Chem.-Eur. J.* **1999**, *5*, 1144–1149.
- (16) Reich, Z.; Zaidmann, L.; Gutman, S. B.; Arad, T.; Minski, A. *Biochemistry* **1994**, *33*, 14177–14184.
- (17) (a) Oda, R.; Huc, I.; Candua, S. J. *Angew. Chem., Int. Ed.* **1998**, *37*, 2689–2691. (b) Oda, R.; Huc, I.; Schmutz, M.; Candua, S. J.; MacKintosh, F. C. *Nature* **1999**, *399*, 566–569.
- (18) (a) Wilson-Kubalek, E. M.; Brown, R. E.; Celia, H. Milligan, R. A. *Proc. Natl. Acad. Sci. U.S.A.* **1998**, *95*, 8040–8045. (b) Ringler, P.; Müller, W.; Ringsdorf, H.; Brisson, A. *Chem.-Eur. J.* **1997**, *3*, 620–625.
- (19) O'Brian, D. F.; Armitage, B.; Benedicto, A.; Benett, D. E.; Lamparski, H. G.; Lee, Y.-S.; Srisiri, W.; Sisson, T. M. *Acc. Chem. Res.* **1998**, *31*, 861–868.
- (20) Yager, P.; Schoen, P. E.; Davies, C.; Price, R.; Singh, A. *Biophys. J.* **1985**, *48*, 899–906.
- (21) (a) Percec, V.; Ahn, C.-H.; Ungar, G.; Yearley, D. J. P.; Möller, M.; Sheiko, S. S. *Nature* **1998**, *391*, 161. (b) Percec, V.; Ahn, C.-H.; Cho, W.-D.; Jamieson, A. M.; Kim, T. Möller, M.; Prokhorva, S. A.; Sheiko, S. S.; Cheng, S. Z. D.; Zhang, A.; Ungar, G.; Yearley, D. J. P. *J. Am. Chem. Soc.* **1998**, *120*, 8619. (c) Chvalun, S. N.; Blackwell, J.; Cho, W.-D.; Kwon, Y. K.; Percec, V.; Heck, J. A. *Polymer* **1998**, *39*, 4415.
- (22) Kwon, Y. K.; Chvalun, S. N.; Blackwell, J.; Percec, V.; Heck, J. A. *Macromolecules* **1995**, *28*, 1552.
- (23) A similar organization was achieved by connecting the dendritic groups to *N*-phenylmaleimide and 7-oxabicyclo[2.2.1]hept-2-ene. In this case, the resulting polymers were more rigid and already at low degrees of polymerization displayed helicity in their backbones; see: Percec, V.; Schleuter, Ronda, J. C.; Johansson, G.; Ungar, G.; Zhou, J. P. *Macromolecules* **1996**, *29*, 1464.
- (24) Hirschberg, J. H. K. K.; Brunsveld, L.; Ramzi, A.; Vekemans, J. A. J. M.; Sijbesma, R. P.; Meijer, E. W. *Nature* **2000**, *407*, 167–170.
- (25) Gellman, S. H. *Acc. Chem. Res.* **1998**, *31*, 173–180.
- (26) Kirshenbaum, K.; Zuckermann, R.; Dill, K. A. *Curr. Struct. Biol.* **1999**, *9*, 530.
- (27) Deming, T. J. *Nature* **1997**, *390*, 386.
- (28) Dado, G. P.; Gellman, S. H. *J. Am. Chem. Soc.* **1994**, *116*, 1054.
- (29) Appella, D. H.; Christianson, L.; Karle, I. L.; Powell, D. R.; Gellman, S. H. *J. Am. Chem. Soc.* **1996**, *118*, 13071.
- (30) Appella, D. H.; Christianson, L. A.; Klein, D. A.; Powell, D. R.; Huang, X.; Barchi, J. J.; Gellman, S. H. *Nature* **1997**, *387*, 381.
- (31) Appella, D. H.; Christianson, L. A.; Klein, D. A.; Richards, M. R.; Powell, D. R.; Gellman, S. H. *J. Am. Chem. Soc.* **1999**, *121*, 7574–7581.
- (32) Hintermann, T.; Seebach, D. *Chimia* **1997**, *51*, 224–248.
- (33) Appella, D. H.; Barchi, J. J.; Durell, S. R.; Gellman, S. H. *J. Am. Chem. Soc.* **1999**, *121*, 2309–2310.
- (34) (a) Seebach, D.; Abele, S.; Gademann, K.; Jaun, B. *Angew. Chem., Int. Ed.* **1999**, *38*, 1595–1597. (b) Seebach, D.; Sifferlen, T.; Mathieu, P. A.; Häne, A. M.; Krell, C. M.; Bierbaum, D. J.; Abele, S. *Helv. Chim. Acta* **2000**, *83*, 2849–2864.
- (35) Seebach, D.; Brenner, M.; Schweizer, B.; Jaun, B. *Chem. Commun.* **2001**, 207–208.
- (36) Hagihara, M.; Anthony, N. J.; Stout, T. J.; Clardy, J.; Schreiber, S. L. *J. Am. Chem. Soc.* **1992**, *114*, 6568.
- (37) Gude, M.; Piarulli, U.; Potenza, D.; Salom, B.; Gennari, C. *Tetrahedron Lett.* **1996**, *37*, 8589.
- (38) (a) Gennari, C.; Salom, B.; Potenza, D.; Williams, A. *Angew. Chem.* **1994**, *33*, 446. (b) Gennari, C.; Salom, B.; Potenza, D.; Longari, C.; Fioravanzo, E.; Carugo, O.; Sardone, N. *Chem.-Eur. J.* **1996**, *2*, 664.
- (39) Nielsen, P. E. *Acc. Chem. Res.* **1999**, *32*, 624–630.
- (40) Lagriffoule, P.; Wittung, P.; Erikson, M.; Jensen, K. K.; Nördén, B.; Buchart, O.; Nielsen, P. E. *Chem.-Eur. J.* **1997**, *3*, 912–919.
- (41) (a) Hamuro, Y.; Geib, S. J.; Hamilton, A. H. *Angew. Chem.* **1994**, *33*, 446. (b) Hamuro, Y.; Geib, S. J.; Hamilton, A. H. *J. Am. Chem. Soc.* **1996**, *118*, 7529.
- (42) Berl, V.; Krische, M. J.; Huc, I.; Lehn, J.-M. Schutz, M. *Chem.-Eur. J.* **2000**, *6*, 1938–1947.
- (43) Berl, V.; Huc, I.; Khoury, R. G.; Krische, M. J.; Lehn, J.-M. *Nature* **2000**, *407*, 720–723.
- (44) Lokey, R. S.; Iverson, B. L. *Nature* **1995**, *375*, 303–305.
- (45) Guyen, J. Q.; Iverson, B. L. *J. Am. Chem. Soc.* **1999**, *121*, 2639–2640.
- (46) Nelson, J. C.; Saven, J. G.; Moore, J. S.; Wolynes, P. *Science* **1997**, *227*, 1793.
- (47) Gin, M. S.; Yokazawa, T.; Prince, R. B.; Moore, J. S. *J. Am. Chem. Soc.* **1999**, *121*, 2643–2644.
- (48) Prince, R. B.; Brunsveld, L.; Meijer, E. W.; Moore, J. S. *Angew. Chem., Int. Ed.* **2000**, *39*, 228–230.
- (49) Prince, R. B.; Okada, T.; Moore, J. S. *Angew. Chem., Int. Ed.* **1999**, *38*, 233–236.
- (50) Williams, A. *Chem.-Eur. J.* **1997**, *3*, 15.
- (51) Piguet, C.; Bernadinelli, G.; Hopfgartner, G. *Chem. Rev.* **1997**, *97*, 2005–2062.
- (52) (a) Hanan, G. S.; Lehn, J.-M. Kyritsakas, N.; Fischer, J. *J. Chem. Soc., Chem. Commun.* **1995**, 765–766. (b) Hanan, G. S.; Schubert, U. S.; Volkmer, D.; Riviere, E.; Lehn, J.-M. *Can. J. Chem.* **1997**, *75*, 169–182. (c) Bassani, D. M.; Lehn, J.-M.; Baum, G.; Fenske, D. *Angew. Chem., Int. Ed. Engl.* **1997**, *36*, 1845–1847. (d) Bassani, D. M.; Lehn, J.-M. *Bull. Soc. Chim. Fr.* **1997**, *134*, 897–906. (e) Ohkita, M.; Lehn, J.-M.; Baum, G.; Fenske, D. *Chem.-Eur. J.* **1999**, *12*, 3471–3481. (f) Gardinier, K. M.; Khoury, R. G.; Lehn, J.-M. *Chem. Eur. J.* **2000**, *6*, 4124–4131.
- (53) Cuccia, L. A.; Lehn, J.-M.; Homo, J.-C.; Schmutz, M. *Angew. Chem., Int. Ed.* **2000**, *39*, 233–237.
- (54) Natta, G.; Corradini. *Nuovo Cimento* **1960**, *10* (Suppl. 15), 9.
- (55) Pino, P.; Lorenzi, G. P. *J. Am. Chem. Soc.* **1960**, *82*, 4745.
- (56) (a) Pino, P.; Chirardelli, G. P.; Lorenzi, G. P.; Natta, G. *J. Am. Chem. Soc.* **1962**, *84*, 1487. (b) Pino, P.; Chirardelli, G. P.; Lorenzi, G. P. *J. Am. Chem. Soc.* **1963**, *85*, 3888. (c) Pino, P. *Adv. Polym. Sci.* **1965**, *4*, 393. (d) Pino, P.; Salvadori, P.; Chiellini, E.; Luisi, P. L. *Pure Appl. Chem.* **1968**, *16*, 469.
- (57) (a) Farima, M.; Peraldo, M.; Natta, G. *Angew. Chem.* **1965**, *77*, 149. (b) Schultz, R. C.; Kaiser, E. *Adv. Polym. Sci.* **1965**, *4*, 236.
- (58) Novak, B. M.; Goodwin, A. A.; Schlitzer, D.; Patten, T. E.; Deming, T. J. *Polym. Prepr. (Am. Chem. Soc., Div. Polym. Chem.)* **1996**, *37*, 446.
- (59) (a) Goodman, M.; Chen S. *Macromolecules* **1970**, *3*, 398. (b) Goodman, M.; Chen S. *Macromolecules* **1971**, *4*, 625.
- (60) Green, M. M.; Peterson, N. C.; Sato, T.; Teramoto, A.; Cook, R.; Lifson, S. *Science* **1995**, *268*, 1861.
- (61) Shmueli, U.; Traub, W.; Rosenheck, J. *Polym. Sci.* **1969**, *7*, 515.
- (62) Lifson, S.; Felder, C. E.; Green, M. M. *Macromolecules* **1992**, *25*, 4142.
- (63) Gu, H.; Nakamura, Y.; Sato, T.; Teramoto, A.; Green, M. M.; Andreola, C.; Peterson, N. C.; Lifson, S. *Macromolecules* **1995**, *28*, 1016.
- (64) Selinger, J. V.; Selinger, R. L. B. *Mol. Cryst. Liq. Cryst.* **1996**, *288*, 33.
- (65) Jha, S. K.; Cheon, K.-S.; Green, M. M.; Selinger, J. V. *J. Am. Chem. Soc.* **1999**, *121*, 1665.
- (66) Cook, R.; Johnson, R. D.; Wade, C. G.; O'Leary, D. J.; Munoz, B.; Green, M. M. *Macromolecules* **1990**, *23*, 3454.

- (67) Green, M. M.; Khatri, C.; Peterson, N. C. *J. Am. Chem. Soc.* **1993**, *115*, 4941.
- (68) Khatri, C. A.; Pavlova, Y.; Green, M. M.; Morawetz, H. *J. Am. Chem. Soc.* **1997**, *119*, 6991.
- (69) Bur, A. J.; Fetters, L. J. *Chem. Rev.* **1976**, *76*, 727.
- (70) Okamoto, Y.; Matsuda, M.; Nakano, T.; Yashima, E. *Polym. J.* **1993**, *25*, 391.
- (71) Maeda, K.; Okamoto, Y. *Macromolecules* **1998**, *31*, 1046.
- (72) Maeda, K.; Okamoto, Y. *Macromolecules* **1998**, *31*, 5164.
- (73) Muller, M.; Zentel, R. *Macromolecules* **1996**, *29*, 1609. Mayer, S.; Maxein, G.; Zentel, R. *Macromolecules* **1998**, *31*, 8522.
- (74) Mayer, S.; Zentel, R. *Macromol. Rapid Commun.* **2000**, *21*, 927.
- (75) Li, J.; Schuster, B.; Cheon, K.-S.; Green, M. M.; Selinger, J. V. *J. Am. Chem. Soc.* **2000**, *122*, 2603.
- (76) Cheon, K.-S.; Selinger, J. V.; Green, M. M. *Angew. Chem., Int. Ed.* **2000**, *39*, 1483.
- (77) (a) Sato, T.; Nakamura, J.; Teramoto, A.; Green, M. M. *Macromolecules* **1998**, *31*, 1398. (b) Green, M. M.; Zanella, S.; Gu, H.; Sato, T.; Gottarelli, G.; Jha, S. K.; Spada, G. P.; Schoevaars, A. M.; Feringa, B.; Teramoto, A. *J. Am. Chem. Soc.* **1998**, *120*, 9810. (c) Maxein, G.; Keller, H.; Novak, B. M.; Zentel, R. *Adv. Mater.* **1998**, *3*, 341.
- (78) (a) Geunet, J. M.; Jeon, H. S.; Khatri, C.; Jha, S. K.; Palsara, N. P.; Green, M. M.; Brület, A.; Thierry, A. *Macromolecules* **1997**, *30*, 4590. (b) Green, M. M.; Khatri, C.; Reidy, M. P.; Levon, K. *Macromolecules* **1993**, *26*, 4723.
- (79) Simionescu, C. I.; Percec, V. *Prog. Polym. Sci.* **1982**, *8*, 133.
- (80) Patil, A.; Heeger, A. J.; Wudl, F. *Chem. Rev.* **1988**, *88*, 183.
- (81) Simionescu, C. I.; Percec, V.; Dumitrscu, J. *Polym. Sci., Polym. Chem. Ed.* **1977**, *15*, 2497.
- (82) Nishide, H.; Kaneko, T.; Igarashi, M.; Tsuchida, E.; Yoshioka, N.; Lahti, P. M. *Macromolecules* **1994**, *27*, 3082.
- (83) Yashima, E.; Huang, S.; Matsushima, T.; Okamoto, Y. *Macromolecules* **1995**, *28*, 4184.
- (84) Ciardelli, F.; Lanzillo, S.; Pieroni, O. *Makromol. Chem.* **1967**, *103*, 1.
- (85) Moore, J. S.; Gorman, C. B.; Grubbs, R. H. *J. Am. Chem. Soc.* **1991**, *113*, 1704.
- (86) Masudas, T. In *Catalysis in Precision Polymerization*; Kobayashi, S., Ed.; Wiley: Chichester, U.K., 1997; Chapter 2.
- (87) Tabata, M.; Inaba, Y.; Yokota, K.; Nozaki, Y. *J. Macromol. Sci., Pure Appl. Chem.* **1994**, *A31*, 465.
- (88) Aoki, T.; Kokai, M.; Shinohara, K.; Oikawa, E. *Chem. Lett.* **1993**, 2009.
- (89) Nakako, H.; Nomura, R.; Tabata, M.; Masuda, T. *Macromolecules* **1999**, *32*, 2861.
- (90) Nakako, H.; Mayahara, Y.; Nomura, R.; Tabata, M.; Masuda, T. *Macromolecules* **2000**, *33*, 3978.
- (91) Nomura, R.; Fukushima, Y.; Nakako, H.; Masuda, T. *J. Am. Chem. Soc.* **2000**, *122*, 8830.
- (92) Saito, M. A.; Maeda, K.; Onouchi, H.; Yashima, E. *Macromolecules* **2000**, *33*, 4616.
- (93) Yashima, E.; Goto, H.; Okamoto, Y. *Polym. J.* **1998**, *30*, 69.
- (94) Yamaguchi, M.; Omata, K.; Hirama, M. *Chem. Lett.* **1992**, 2261.
- (95) Kishimoto, Y.; Itou, M.; Miyataka, T.; Ikariya, T.; Noyori, R. *Macromolecules* **1995**, *28*, 6662.
- (96) In this context, also the introduction of bulky substituents was studied: Yashima, E.; Huang, S.; Matsushima, T.; Okamoto, Y. *Macromolecules* **1995**, *28*, 4184.
- (97) Yashima, E.; Matsushima, T.; Okamoto, Y. *J. Am. Chem. Soc.* **1995**, *117*, 11596.
- (98) Yashima, E.; Matsushima, T.; Okamoto, Y. *J. Am. Chem. Soc.* **1997**, *119*, 6345.
- (99) Yashima, E.; Nimura, T.; Matsushima, T.; Okamoto, Y. *J. Am. Chem. Soc.* **1996**, *118*, 9800.
- (100) Yashima, E.; Maeda, Y.; Matsushima, T.; Okamoto, Y. *Chirality* **1997**, *9*, 593.
- (101) Yashima, E.; Maeda, Y.; Okamoto, Y. *J. Am. Chem. Soc.* **1998**, *120*, 8895.
- (102) Yashima, E.; Maeda, Y.; Okamoto, Y. *Nature* **1999**, *399*, 449.
- (103) Matsuura, K.; Furuno, S.; Kobayashi, K. *Chem. Lett.* **1998**, 847.
- (104) Yashima, E.; Huang, S.; Okamoto, Y. *J. Chem. Soc., Chem. Commun.* **1994**, 1811.
- (105) Aoki, T.; Shinohara, K.-I.; Kaneko, T.; Oikawa, E. *Macromolecules* **1996**, *29*, 4192.
- (106) Yashima, E.; Huang, S.; Okamoto, Y. *J. Chem. Soc., Chem. Commun.* **1994**, 1811.
- (107) Pu, L. *Chem.—Eur. J.* **1999**, *5*, 2227.
- (108) (a) Pu, L. *Acta Polym.* **1997**, *48*, 116–141. (b) Pu, L. *Chem. Rev.* **1998**, *98*, 2405.
- (109) Harlev, E.; Wudl, F. Synthesis and Optical properties of Chiral Poly [2,5-bis (3,7-dimethyl-6-octenoxy)-1,4-phenylenevinylene]. In *Conjugated Polymers and Related materials, The Connection of Chemical and Electronic Structure*, Proceedings of the 81st Nobel Symposium; Salaneck, W. R., Lundström, I., Rånby, B., Eds.; Oxford University Press: Oxford, U.K., 1993; p 139.
- (110) Magnus, P.; Danikiewicz, W.; Katoh, T.; Huffman, J. C.; Folting, K. *J. Am. Chem. Soc.* **1990**, *112*, 2465.
- (111) (a) Majidi, M. R.; Kane-Maguire, L. A. P.; Wallace, G. G. *Polymer* **1994**, *35*, 3113. (b) Majidi, M. R.; Kane-Maguire, L. A. P.; Wallace, G. G. *Polymer* **1995**, *36*, 3597. (c) Majidi, M. R.; Kane-Maguire, L. A. P.; Norris, I. D.; Wallace, G. G. *Polymer* **1996**, *37*, 359. (d) Majidi, M. R.; Ashraf, S. A.; Kane-Maguire, L. A. P.; Wallace, G. G. *Synth. Met.* **1997**, *84*, 115.
- (112) Havinga, E. E.; Bouman, M. M.; Meijer, E. W.; Pomp, A.; Simenon, M. M. *J. Synth. Met.* **1994**, *66*, 93.
- (113) McQuade, D. T.; Pullen, A. E.; Swager, T. M. *Chem. Rev.* **2000**, *100*, 2537–2574.
- (114) Yashima, E.; Goto, H.; Okamoto, Y. *Macromolecules* **1999**, *32*, 7942–7945.
- (115) (a) Miller, R. D.; Michl, J. *Chem. Rev.* **1989**, *89*, 1359–1410. (b) *Inorganic Polymers*; Mark, J. E., Allock, H. R., West, R., Eds.; Prentice Hall: Upper Saddle River, NJ, 1992. (c) West, R. Organopolysilanes. In *Comprehensive Organometallic Chemistry*; Abel, E. W., Stone, F. G. A., Wilkinson, G., Eds.; Pergamon: New York, 1994. (d) Jones, R. G.; Holder, S. J. In *Silicon-containing Polymers. The Science and Technology of Their Synthesis and Applications*; Jones, R. G., Ando, W., Chojnowski, J., Eds.; Kluwer: Norwell, MA, 2000; pp 353–373.
- (116) Teramae, H.; Takeda, K. *J. Am. Chem. Soc.* **1989**, *111*, 1281.
- (117) (a) Pfeifer, M.; Spangenberg, H. *J. Z. Phys. Chem.* **1966**, *232*, 47. (b) Cox, A. P.; Varma, R. *J. Chem. Phys.* **1967**, *46*, 2007.
- (118) (a) Schilling, F. C.; Bovey, F. A.; Lovinger, A. J.; Zeigler, J. M., *Macromolecules* **1989**, *22*, 3655–3063. (b) Schilling, F. C.; Lovinger, A. J.; Zeigler, J. M.; Davis, D.; Bovey, F. A. *Macromolecules* **1989**, *22*, 4645–4650.
- (119) Miller, R. D.; Farmer, B. L.; Flemming, W.; Sooriyakumaran, R.; Rabolt, J. F. *J. Am. Chem. Soc.* **1987**, *109*, 2509–2510.
- (120) Furukawa, S. *Thin Solid Films* **1998**, *331*, 222–228.
- (121) (a) Terunuma, D.; Nagumo, K.; Kamata, N.; Matsuoka, K.; Kuzuhara, H., *Chem. Lett.* **1998**, 681–682. (b) Nakashima, H.; Fujiki, M.; Koe, J. R. *Macromolecules* **1999**, *32*, 7707–7709.
- (122) Obata, K.; Kabuto, C.; Kira, M. *J. Am. Chem. Soc.* **1997**, *119*, 11345–11346. (b) Obata, K.; Kira, M. *Macromolecules* **1998**, *31*, 4666.
- (123) Fujiki, M. *J. Am. Chem. Soc.* **1996**, *118*, 11345–11346.
- (124) Fujiki, M. *Appl. Phys. Lett.* **1994**, *65*, 3251–3253.
- (125) (a) Ebihara, K.; Koshihara, S.-Y.; Yoshimoto, M.; Maeda, T.; Ohnishi, T.; Koinuma, H.; Fujiki, M. *Jpn. J. Appl. Phys.* **1997**, *36*, L1211–L1213. (b) Furukawa, K.; Ebata, K.; Fujiki, M. *Adv. Mater.* **2000**, *12*, 1033.
- (126) Fujiki, M.; Toyoda, S.; Yuan, C.-H.; Takigawa, H. *Chirality* **1998**, *10*, 667–675.
- (127) (a) Fujiki, M. *J. Am. Chem. Soc.* **1994**, *116*, 6017–6018. (b) Fujiki, M. *J. Am. Chem. Soc.* **1994**, *116*, 11976–11981.
- (128) (a) Koe, J. R.; Fujiki, M.; Motonaga, M.; Nakashima, H. *Chem. Commun.* **2000**, 389–390. (b) Koe, J. R.; Fujiki, M.; Motonaga, M.; Nakashima, H. *Macromolecules* **2001**, *34*, 1082–1089.
- (129) Fujiki, M. *J. Am. Chem. Soc.* **2000**, *122*, 3336–3343.
- (130) Sundararajan, P. R. *Macromolecules* **1988**, *21*, 1256–1261.
- (131) (a) Toyoda, S.; Fujiki, M. *Chem. Lett.* **1999**, 699–700 (b) Toyoda, S.; Fujiki, M. *Macromolecules* **2000**, *34*, 640–644.
- (132) It should be noted that in ref 131 Toyoda and Fujiki do not comment on the tacticity of the prepared polymers.
- (133) Sommerdijk, N. A. J. M.; Holder, S. J.; Hiorns, R. C.; Jones, R. G.; Nolte, R. J. M. *Macromolecules* **2000**, *33*, 8289.
- (134) Deming, T. J. *Adv. Mater.* **1997**, *9*, 299.
- (135) The formation of a defined secondary structure from poly(amino acids) is beyond the scope of this review. See: Schneider, J. P.; Kelly, J. W. *Chem. Rev.* **1995**, *95*, 2169.
- (136) Whitesell, J. K.; Chang, H. K. *Science* **1993**, *261*, 73.
- (137) Jaworek, T.; Neher, D.; Wegner, G.; Wieringa, R. H.; Schouten, A. *J. Science* **1998**, *279*, 57.
- (138) Deming, T. J. *J. Am. Chem. Soc.* **1997**, *119*, 2759.
- (139) Deming, T. J. *J. Am. Chem. Soc.* **1998**, *120*, 4240.
- (140) Nakahira, T.; Lin, F.; Boon, C. T.; Karato, T.; Annaka, M.; Yoshikuni, M.; Iwabuchi, S. *Polym. J.* **1997**, *29*, 701.
- (141) Nakahira, T.; Fan, L.; Boon, C. T.; Fukada, T.; Karato, T.; Annaka, M.; Yoshikuni, M. *Polym. J.* **1998**, *30*, 910.
- (142) Fan, L.; Fukada, T.; Annaka, M.; Yoshikuni, M.; Nakahira, T. *Polym. J.* **1999**, *31*, 364.
- (143) Goodwin, A.; Novak, B. M. *Macromolecules* **1994**, *27*, 5520.
- (144) Shibayama, K.; Seidel, S. W.; Novak, B. M. *Macromolecules* **1997**, *30*, 3159.
- (145) Schlitzer, D. S.; Novak, B. M. *J. Am. Chem. Soc.* **1998**, *120*, 2196.
- (146) Carriedo, G. A.; Garcia Alonso, F. J.; Gonzalez, P.; Garcia-Alvarez, J. L. *Macromolecules* **1998**, *31*, 3189.
- (147) Yashima, E.; Maeda, K.; Yamanaka, T. *J. Am. Chem. Soc.* **2000**, *122*, 7813.
- (148) Ortiz, L. J.; Khan, I. M. *Macromolecules* **1998**, *31*, 5927.
- (149) Mikami, M.; Shinkai, S. *Chem. Lett.* **1995**, 603.
- (150) Okamoto, Y.; Suzuki, K.; Ohta, K.; Hatada, K.; Yuki, H. *J. Am. Chem. Soc.* **1979**, *101*, 4763.
- (151) Okamoto, Y.; Nakano, T. *Chem. Rev.* **1994**, *94*, 349.
- (152) Okamoto, Y.; Yashima, E. *Prog. Polym. Sci.* **1990**, 263.
- (153) Nakano, T.; Okamoto, Y.; Hatada, K. *J. Am. Chem. Soc.* **1992**, *114*, 1318.

- (154) Yu, B.; Ding, M.-X.; Wang, Y.-C.; Hu, H.-Z.; Wang, F.-S. *Makromol. Chem., Macromol. Symp.* **1992**, *63*, 279.
- (155) Nakano, T.; Okamoto, Y. *Macromolecules* **1999**, *32*, 2391.
- (156) Engelkamp, H.; van Nostrum, C. F.; Picken, S. J.; Nolte, R. J. M. *Chem. Commun.* **1998**, 979.
- (157) Sikorski, P.; Cooper, S. J.; Atkins, E. D. T.; Jaycox, G. D.; Vogl, O. *J. Polym. Sci., Part A: Polym. Chem.* **1998**, *36*, 1855.
- (158) Hatada, K.; Jaycox, G. D.; Vogl, O. In *Macromolecular Design of Polymeric Materials. Series: Plastics Engineering*; Hatada, K., Jaycox, G. D., Vogl, O., Eds.; Marcel Dekker: New York, 1997; Chapter 11, p 181.
- (159) Vogl, O. *J. Polym. Sci., Part A: Polym. Chem.* **2000**, *38*, 2293.
- (160) Noe, C. R.; Miculka, C.; Bats, J. W. *Angew. Chem.* **1994**, *106*, 1559.
- (161) Ute, K.; Hirose, K.; Kashimoto, H.; Hatada, K.; Vogl, O. *J. Am. Chem. Soc.* **1991**, *113*, 6305.
- (162) Katz, T. J. *Angew. Chem.* **2000**, *39*, 1921–1923.
- (163) (a) Dai, Y.; Katz, T. J.; Nichols, D. A. *Angew. Chem., Int. Ed. Engl.* **1996**, *35*, 2109–2111. (b) Dai, Y.; Katz, T. J. *J. Org. Chem.* **1997**, *62*, 1274–1285.
- (164) Yu, H.-B.; Hu, Q.-S.; Pu, L. *J. Am. Chem. Soc.* **2000**, *122*, 6500–6501.
- (165) Puch, V. J.; Hu, Q.-S.; Pu, L. *Angew. Chem., Int. Ed.* **2000**, *39*, 3638–3641.
- (166) Millich, F. *Chem. Rev.* **1972**, *72*, 101.
- (167) Nolte, R. J. M.; Drenth, W. In *New Methods for Polymer Synthesis*; Mijs, W. J., Ed.; Plenum Press: New York, 1992; Chapter 9, p 273.
- (168) Nolte, R. J. M.; van Beijen, A. J. M.; Drenth, W. *J. Am. Chem. Soc.* **1972**, *96*, 5932.
- (169) Nolte, R. J. M. *Chem. Soc. Rev.* **1994**, *23*, 11.
- (170) Deming, T. J.; Novak, B. M. *Macromolecules* **1991**, *24*, 326.
- (171) Deming, T. J.; Novak, B. M. *Macromolecules* **1991**, *24*, 6043.
- (172) Deming, T. J.; Novak, B. M. *J. Am. Chem. Soc.* **1993**, *115*, 9101.
- (173) Nolte, R. J. M.; Drenth, W. *Recl. Trav. Chim. Pays-Bas* **1973**, *92*, 788.
- (174) Deming, T. J.; Novak, B. M. *Macromolecules* **1993**, *26*, 7092.
- (175) Hong, B.; Fox, M. A. *Macromolecules* **1994**, *27*, 5311.
- (176) An intermediate isolated from the polymerization of phenyl isocyanide using NiCl₂ had an intriguing structure but did not give conclusive directions toward the mechanism of polymerization: Euler, W. B.; Huang, J.-T.; Kim, M.; Spencer, L.; Rosen, W. *Chem. Commun.* **1997**, 257.
- (177) Kollmar, C.; Hoffmann, R. *J. Am. Chem. Soc.* **1990**, *112*, 8230.
- (178) Cui, C. X.; Kertesz, M. *Chem. Phys. Lett.* **1990**, *169*, 445.
- (179) Huige, C. J. M. Ph.D. Thesis, University of Utrecht, The Netherlands, 1985.
- (180) Huige, C. J. M.; Hezemans, A. M. F.; Nolte, R. J. M.; Drenth, W. *Recl. Trav. Chim. Pays-Bas* **1993**, *112*, 33.
- (181) Clericuzio, M.; Alagona, G.; Ghio, C.; Salvadori, P. *J. Am. Chem. Soc.* **1997**, *119*, 1059.
- (182) Pini, D.; Iuliano, A.; Salvadori, P. *Macromolecules* **1992**, *25*, 6059.
- (183) Green, M. M.; Gross, R. A.; Schilling, F.; Zero, K.; Crosby, C., III. *Macromolecules* **1988**, *21*, 1839.
- (184) Spencer, L.; Kim, M.; Euler, W. B.; Rosen, W. *J. Am. Chem. Soc.* **1997**, *119*, 8129.
- (185) Spencer, L.; Euler, W. B.; Traficante, D. D.; Kim, M.; Rosen, W. *Magn. Reson. Chem.* **1998**, *36*, 398.
- (186) Huang, J.-T.; Sun, J.; Euler, W. B.; Rosen, W. *J. Polym. Sci., Part A: Polym. Chem.* **1997**, *35*, 439.
- (187) Van Beijen, A. J. M.; Nolte, R. J. M.; Drenth, W. *Recl. Trav. Chim. Pays-Bas* **1980**, *99*, 121–123.
- (188) Yamagashi, A.; Tanaka, I.; Tanigushi, M.; Takahashi, M. *J. Chem. Soc., Chem. Commun.* **1994**, 1113.
- (189) Kamer, P. C. J.; Nolte, R. J. M.; Drenth, W. *J. Chem. Soc., Chem. Commun.* **1986**, 1789.
- (190) Kamer, P. C. J.; Nolte, R. J. M.; Drenth, W. *J. Am. Chem. Soc.* **1988**, *110*, 6818.
- (191) Deming, T. J.; Novak, B. M. *J. Am. Chem. Soc.* **1992**, *114*, 4400.
- (192) Deming, T. J.; Novak, B. M. *J. Am. Chem. Soc.* **1992**, *114*, 7926.
- (193) Kamer, P. C. J.; Cleij, M. C.; Nolte, R. J. M.; Harada, T.; Hezemans, A. M. F.; Drenth, W. *J. Am. Chem. Soc.* **1988**, *110*, 1581.
- (194) Onitsuka, K.; Joh, T.; Takahashi, S. *Angew. Chem.* **1992**, *104*, 893.
- (195) Onitsuka, K.; Yanai, F.; Joh, T.; Takahashi, S. *Organometallics* **1994**, *13*, 3862.
- (196) Recently also the isocyanide polymerizations using an alkynylnickel complex has been reported: Takei, F.; Tung, S.; Yanai, K.; Onitsuka, K.; Takahashi, S. *J. Organomet. Chem.* **1998**, *559*, 91.
- (197) The reversible insertion of aryl isocyanides in a palladium–sulfur bond leading to oligoisocyanides has been reported: Kuniyasu, H.; Sugoh, K.; Su, M. S.; Kurosawa, H. *J. Am. Chem. Soc.* **1997**, *119*, 4669.
- (198) Takai, F.; Yanai, K.; Onitsuka, K.; Takahashi, S. *Angew. Chem., Int. Ed. Engl.* **1996**, *35*, 1554.
- (199) Ohshiro, N.; Shimizu, A.; Okumura, R.; Takei, F.; Onitsuka, K.; Takahashi, S. *Chem. Lett.* **2000**, 786.
- (200) Takei, F.; Yanai, K.; Onitsuka, K.; Takahashi, S. *Chem.–Eur. J.* **2000**, *6*, 983.
- (201) Takei, F.; Onitsuka, K.; Takahashi, S. *Polym. J.* **1999**, *31*, 1029.
- (202) Van der Eijk, J. M.; Nolte, R. J. M.; Drenth, W.; Hezemans, A. M. F. *Macromolecules* **1980**, *13*, 1391.
- (203) Visser, H. G. J.; Nolte, R. J. M.; Zwikker, J. W.; Drenth, W. *J. Org. Chem.* **1985**, *50*, 3133.
- (204) Visser, H. G. J.; Nolte, R. J. M.; Zwikker, J. W.; Drenth, W. *J. Org. Chem.* **1985**, *50*, 3138.
- (205) (a) Cornelissen, J. J. L. M.; Graswinckel, W. S.; Sommerdijk, N. A. J. M.; Nolte, R. J. M. *Polym. Prepr. (Am. Chem. Soc., Div. Polym. Chem.)* **1999**, *40*, 548. (b) Cornelissen, J. J. L. M.; Graswinckel, W. S.; Rowan, A. E.; de Gelder, R.; Sommerdijk, N. A. J. M.; Nolte, R. J. M. *Polym. Prepr. (Am. Chem. Soc., Div. Polym. Chem.)* **2000**, *41*, 953.
- (206) Cornelissen, J. J. L. M.; Graswinckel, W. S.; Adams, P. J. H. M.; Nachttegaal, G. M.; Kentgens, A. P. M.; Sommerdijk, N. A. J. M.; Nolte, R. J. M. *J. Polym. Sci., Part A: Polym. Chem.* **2001**, *39*, 4255.
- (207) Cornelissen, J. J. L. M.; Donners, J. J. J. M.; de Gelder, R.; Graswinckel, W. S.; Rowan, A. E.; Sommerdijk, N. A. J. M.; Nolte, R. J. M. *Science* **2001**, *293*, 676.
- (208) Branden, C.; Tooz, J. *Introduction to Protein Structure*; Garland Publishing Inc.: New York, 1999.
- (209) Hasegawa, T.; Kondoh, S.; Matsuura, K. Kobayashi, K. *Macromolecules* **1999**, *32*, 6595.
- (210) Hasegawa, T.; Matsuura, K.; Ariga, K.; Kobayashi, K. *Macromolecules* **2000**, *33*, 2772.
- (211) Hong, B.; Fox, M. A. *Can. J. Chem.* **1995**, *73*, 2101.
- (212) Kauranen, M.; Verbiest, T.; Boutton, C.; Teerenstra, M. N.; Clays, K.; Schouten, A. J.; Nolte, R. J. M.; Persoons, A. *Science* **1995**, *270*, 966.
- (213) Kauranen, M.; Verbiest, T.; Meijer, E. W.; Havinga, E. E.; Teerenstra, M. N.; Schouten, A. J.; Nolte, R. J. M.; Persoons, A. *Adv. Mater.* **1995**, *7*, 641.
- (214) Teerenstra, M. N.; Hagting, Oostergetel, G. T.; Schouten, A. J.; Devillers, M. A. C.; Nolte, R. J. M. *Thin Solid Films* **1994**, *248*, 110.
- (215) Teerenstra, M. N.; Klap, R. D.; Bijl, M. J.; Schouten, A. J.; Nolte, R. J. M.; Verbiest, T.; Persoons, A. *Macromolecules* **1996**, *29*, 4871.
- (216) Teerenstra, M. N.; Hagting, J. G.; Schouten, A. J.; Nolte, R. J. M.; Kauranen, M.; Verbiest, T.; Persoons, A. *Macromolecules* **1996**, *29*, 4876.
- (217) Takei, F.; Onitsuka, K.; Kobayashi, N.; Takahashi, S. *Chem. Lett.* **2000**, 914.
- (218) Bosch, J.; Rovira, C.; Veciana, J.; Castro, C.; Palacio, F. *Synth. Met.* **1993**, *55*, 1141.
- (219) Vlietstra, E. J.; Nolte, R. J. M.; Zwikker, J. W.; Drenth, W.; Meijer, E. W. *Macromolecules* **1990**, *23*, 946.
- (220) Abdelkader, M.; Drenth, W.; Meijer, E. W. *Chem. Mater.* **1990**, *3*, 598.
- (221) Bieglé, A.; Mathis, A.; Galin, J. C. *Macromol. Chem. Phys.* **2000**, *201*, 113.
- (222) Grassi, B.; Rempp, S.; Galin, J. C. *Macromol. Chem. Phys.* **1998**, *199*, 239.
- (223) Van Walree, C. A.; van der Pol, C. A.; Zwikker, J. W. *Recl. Trav. Chim. Pays-Bas* **1990**, *109*, 561.
- (224) Amabilino, D. B.; Ramos, E.; Serrano, J. L.; Sierra, T.; Veciana, J. *J. Am. Chem. Soc.* **1998**, *120*, 9126.
- (225) Ramos, E.; Bosch, J.; Serrano, J. L.; Sierra, T.; Veciana, J. *J. Am. Chem. Soc.* **1996**, *118*, 4703.
- (226) Similar long-distance chirality transfer has been reported for the polymerization of helicene-derived isocyanides: Chen, J. P.; Gao, J. P.; Wang, Z. Y. *Polym. Int.* **1997**, *44*, 83.
- (227) Amabilino, D. B.; Ramos, E.; Serrano, J. L.; Veciana, J. *Adv. Mater.* **1998**, *10*, 1001.
- (228) Ito, Y.; Ihara, E.; Murakami, M. *J. Am. Chem. Soc.* **1990**, *112*, 6446.
- (229) Ito, Y.; Ihara, E.; Murakami, M. *Angew. Chem.* **1992**, *104*, 1508.
- (230) Ito, Y.; Kojima, Y.; Murakami, M. *Tetrahedron Lett.* **1993**, *34*, 8279.
- (231) Ito, Y.; Ohara, T.; Shima, R.; Suginome, M. *J. Am. Chem. Soc.* **1996**, *118*, 9188.
- (232) Ito, Y.; Ihara, E.; Murakami, M.; Sisido, M. *Macromolecules* **1992**, *25*, 6810.
- (233) Ito, Y.; Kojima, Y.; Suginome, M.; Murakami, M. *Heterocycles* **1996**, *42*, 597.
- (234) Ito, Y.; Ihara, E.; Uesaka, T.; Murakami, M. *Macromolecules* **1992**, *25*, 6711.
- (235) Ito, Y.; Miyake, T.; Ohara, T.; Suginome, M. *Macromolecules* **1998**, *31*, 1697.
- (236) Ito, Y.; Miyake, T.; Suginome, M. *Macromolecules* **2000**, *33*, 4034.
- (237) Ito, Y.; Kojima, Y.; Murakami, M.; Suginome, M. *Bull. Chem. Soc. Jpn.* **1997**, *70*, 2801.
- (238) Ito, Y.; Miyake, T.; Hatano, S.; Shima, R.; Ohara, T.; Suginome, M. *J. Am. Chem. Soc.* **1998**, *120*, 11880.
- (239) Liquori, A. M.; Anzuino, G.; Coiro, V. M.; D'Alagni, M.; de Santis, P.; Savino, M. *Nature* **1965**, *206*, 358.

- (240) An overview is given in Mizumoto, T.; Sugimura, N.; Moritani, M.; Sato, Y.; Masuoka. *Macromolecules* **2000**, *33*, 6757.
- (241) Spevacek, J. *Makromol. Chem., Macromol. Symp.* **1990**, *39*, 71.
- (242) Hatada, K.; Kitayama, T.; Ute, K.; Nishiura, T. *Macromol. Symp.* **1998**, *132*, 221.
- (243) te Nijenhuis, K. *Adv. Polym. Sci.* **1997**, *130*, 76–81.
- (244) Vorenkamp, E. J.; Bosscher, F.; Challa, G. *Polymer* **1979**, *20*, 59.
- (245) Schomaker, E. Ph.D. Thesis, State University Groningen, The Netherlands, 1988.
- (246) Challa, G. In *Integration of Fundamental Polymer Science and Technology—5*; Lemstra, P. J., Kleintjes, L. A., Eds.; Elsevier Applied Science: London, 1991; Vol. 5, p 85.
- (247) For a recent overview see: Spassky, N.; Pluta, C.; Simic, V.; Thiam, M.; Wisniewski, M. *Macromol. Symp.* **1998**, *128*, 39.
- (248) Spinu, M.; Gardener, K. H. *Polym. Mater. Sci. Eng.* **1994**, *74*, 19.
- (249) Stevels, W. M.; Ankone, M. J. K.; Dijkstra, P. J.; Feijen, J. *Macromol. Chem. Phys.* **1995**, *196*, 3687.
- (250) de Jong, S. J.; de Smedt, S. C.; Wahls, M. W. C.; Demeester J.; Kettenes-van den Bosch J. J.; Hennink, W. E. *Macromolecules* **2000**, *33*, 3680.
- (251) Janssen, H. M.; Peeters, E.; van Zundert, M. F.; van Genderen, M. H. P. G.; Meijer, E. W. *Angew. Chem., Int. Ed. Engl.* **1997**, *36*, 122.
- (252) Janssen, H. M.; Peeters, E.; van Zundert, M. F.; van Genderen, M. H. P.; Meijer, E. W. *Macromolecules* **1997**, *30*, 8113.
- (253) Janssen, H. M.; Meijer, E. W. *Macromolecules* **1997**, *30*, 8129.
- (254) Peeters, E. Ph.D. Thesis, Eindhoven University of Technology, The Netherlands, 2000.
- (255) Drake, A. F.; Udvarhelyi, P.; Ando, D. J.; Bloor, D.; Obhi, J. S.; Mann, S. *Polymer* **1989**, *30*, 1063.
- (256) Harlev, E.; Wudl, F. In *Conjugated Polymers and Related Materials. The Interconnection of Chemical and Electronic Structure*, Proceedings of the 81st Nobel Symposium; Salaneck, W. R., Lundström, L., Rånby, B., Eds.; Oxford University Press: Oxford, U.K., 1993; p 139.
- (257) (a) Fiesel, R.; Scherf, U. *Acta Polym.* **1998**, *49*, 445. (b) Fiesel, R.; Neher, D.; Scherf, U. *Synth. Met.* **1999**, *102*, 1457.
- (258) (a) Delabouglise, D.; Garnier, F. *Synth. Met.* **1990**, *39*, 117. (b) Mouter, J.-C.; Saint-Aman, E.; Tran-Van, F.; Angibeaud, P.; Utille, J.-P. *Adv. Mater.* **1992**, *4*, 511.
- (259) (a) Fiesel, R.; Scherf, U. *Macromol. Rapid Commun.* **1998**, *19*, 427. (b) Fiesel, R.; Halkyard, C. E.; Rampey, M. E.; Kloppenburg, L.; Studer-Martinez, S. L.; Scherf, U.; Bunz, U. H. F. *Macromol. Rapid Commun.* **1999**, *20*, 107.
- (260) Andreani, F.; Angiolini, L.; Caretta, D.; Salatelli, E. *J. Mater. Chem.* **1998**, *8*, 1109.
- (261) Goldoni, F.; Janssen, R. A. J.; Meijer, E. W. *J. Polym., Sci. Part A: Polym. Chem.* **1999**, *37*, 4629.
- (262) Cornelissen, J. J. L. M.; Peeters, E.; Janssen, R. A. J.; Meijer, E. W. *Acta Polym.* **1998**, *49*, 471.
- (263) For a recent review see: McCullough, R. D. *Adv. Mater.* **1998**, *10*, 93.
- (264) (a) McCullough, R. D.; Lowe, R. D. *J. Chem. Soc., Chem. Commun.* **1992**, 70–71. (b) McCullough, R. D.; Lowe, R. D.; Jayaramam, M.; Anderson, D. L. *Org. Chem.* **1993**, *58*, 903. (c) Chen, T. A.; Wu, X.; Rieke, R. D. *J. Am. Chem. Soc.* **1995**, *117*, 233.
- (265) Andersson, M.; Ekeblad, P. O.; Hjertberg, T.; Wennerström, O.; Inganäs, O. *Polym. Commun.* **1991**, *32*, 546.
- (266) Lemaire, M.; Delabouglise, D.; Garreau, R.; Guy, A.; Roncali, J. *J. Chem. Soc., Chem. Commun.* **1988**, 658.
- (267) Other early reports on chiral polythiophenes include the following: (a) Elsenbaumer, R. L.; Eckhardt, H.; Iqbal, Z.; Toth, J.; Baughman, R. H. *Mol. Cryst. Liq. Cryst.* **1985**, *118*, 111. (b) Lemaire, M.; Delabouglise, D.; Garreau, R.; Roncali, J. In *Recent Advances in Electroorganic Synthesis*; Torii, S., Ed.; Elsevier Science Publisher: Amsterdam, 1987; p 385. (c) Kotkar, D.; Joshi, V.; Ghosh, P. K. *J. Chem. Soc., Chem. Commun.* **1988**, 917. (d) Roncali, J.; Garreau, R.; Delabouglise, D.; Garnier, F.; Lemaire, M. *Makromol. Chem., Macromol. Symp.* **1988**, *20/21*, 601. (e) Roncali, J.; Garreau, R.; Delabouglise, D.; Garnier, F.; Lemaire, M. *Synth. Met.* **1989**, *28*, C341.
- (268) Bouman, M. M.; Havinga, E. E.; Janssen, R. A. J.; Meijer, E. W. *Mol. Cryst. Liq. Cryst.* **1994**, *256*, 439.
- (269) Langeveld-Voss, B. M. W.; Beljonne, D.; Shuai, Z.; Janssen, R. A. J.; Meskers, S. C. J.; Meijer, E. W.; Brédas, J. L. *Adv. Mater.* **1998**, *10*, 1343.
- (270) Gray, G. W.; McDonnel, D. G. *Mol. Cryst. Liq. Cryst.* **1977**, *34*, 211.
- (271) Ramos-Lermo, E.; Langeveld-Voss, B. M. W.; Janssen, R. A. J.; Meijer, E. W. *Chem. Commun.* **1999**, 791.
- (272) Langeveld-Voss, B. M. W.; Christiaans, M. P. T.; Janssen, R. A. J.; Meijer, E. W. *Macromolecules* **1998**, *31*, 6702.
- (273) Bidan, G.; Guillerez, S.; Sorokin, V. *Adv. Mater.* **1996**, *8*, 157.
- (274) Langeveld-Vos, B. M. W.; Waterval, R. J. M.; Janssen, R. A. J.; Meijer, E. W. *Macromolecules* **1999**, *32*, 227.
- (275) Fiesel, R.; Scherf, U. *Acta Polym.* **1998**, *49*, 445.
- (276) Langeveld-Voss, B. M. W.; Janssen, R. A. J.; Christiaans, M. P. T.; Meskers, S. C. J.; Dekkers, H. P. J. M.; Meijer, E. W. *J. Am. Chem. Soc.* **1996**, *118*, 4908.
- (277) Langeveld-Voss, B. M. W.; Peeters, E.; Janssen, R. A. J.; Meijer, E. W. *Synth. Met.* **1997**, *84*, 611.
- (278) Peeters, E.; Christiaans, M. P. T.; Janssen, R. A. J.; Schoo, H. F. M.; Dekkers, H. P. J. M.; Meijer, E. W. *J. Am. Chem. Soc.* **1997**, *119*, 9909.
- (279) Papkov, S. P. *Adv. Polym. Sci.* **1984**, *59*, 75.
- (280) Sato, T.; Sato, Y.; Umemura, Y.; Teramoto, A.; Nagamura, Y.; Wagner, J.; Weng, D.; Okamoto, Y.; Hatada, K.; Green, M. M. *Macromolecules* **1993**, *26*, 4551.
- (281) Lyotropic liquid crystalline behavior of rodlike peptides was reported for the first time by Robinson, C.; Ward, J. C. *Nature* **1957**, *180*, 1183.
- (282) The phase behavior of PBLG has been investigated thoroughly: Wee, E. L.; Miller, W. G. *Nature* **1990**, *346*, 44.
- (283) Itou, T.; Van, K.; Teramoto, A. *J. Appl. Polym. Sci., Appl. Polym. Symp.* **1985**, *41*, 35.
- (284) Akagi, K.; Piao, G.; Kaneko, S.; Sakamaki, K.; Shirakawa, H.; Kyotani, M. *Science* **1998**, *282*, 1683.
- (285) Kimura, S.; Kim, D.-H.; Sugiyama, J.; Imanishi, Y. *Langmuir* **1999**, *15*, 4461.
- (286) Cornelissen, J. J. L. M.; Fischer, M.; Sommerdijk, N. A. J. M.; Nolte, R. J. M. *Science* **1998**, *280*, 1427.
- (287) Holder, S. J.; Hiorns, R. C.; Sommerdijk, N. A. J. M.; Williams, S. J.; Jones, R. G.; Nolte, R. J. M. *Chem. Commun.* **1998**, 1443.

CR990126I

Visualization of Macromolecules—A First Step to Manipulation and Controlled Response

Sergei S. Sheiko* and Martin Möller*

Laboratory of Organic and Macromolecular Chemistry, University of Ulm, D-89069 Ulm, Germany

Received July 12, 2001

Contents

1. Introduction	4099
2. Structure of Individual Molecules at Interfaces	4100
2.1. Conformation of 2D Confined Macromolecules	4100
2.2. Structural Effects by Specific Interactions with the Substrate	4103
2.3. Metastable Tertiary Structures by Local Contraction and Twisting	4107
2.4. Microscopic Structure of Adsorbed Macromolecules	4108
3. Manipulated Conformational Transitions of Adsorbed Macromolecules	4113
4. Motility of Molecules	4115
4.1. Dragged Motion of λ -DNA	4117
4.2. Brownian Motion of Adsorbed λ -Phage DNA	4117
4.3. Stimulated Motion of Monodendron-Jacketed Polymers	4117
5. Synopsis	4120
6. Acknowledgment	4121
7. References	4121

1. Introduction

The size and complexity of the structure of macromolecules allows the combination of different, in some cases even antagonistic, properties, e.g., in solubility, in flexibility, or electronic properties. The control of the connectivity of the molecular subunits can be used to transform short-range interactions into complex long-range structural organization. The examples of biomacromolecules demonstrate how single polymer molecules and their ensembles can serve as functional nanoobjects. While functional properties such as catalytic activity, directed motion, and the energy transport are well established in the case of biomolecules,^{1–7} our ability to develop synthetic molecular devices is in its infancy. Significant efforts are directed toward shape control and directed motion.^{8–14}

A major basis for the advancement in macromolecular functionality is our improving ability to control the macromolecular and supramolecular structures in great detail. Dense and cascade-type branching provided access to three-dimensional molecules, which do not interpenetrate but interact via their surfaces. Recent synthetic developments include microgels,^{15–17} dendrimers,^{18–26} and arborescent graft

polymers.^{27–31} Polymerization of substituted monomers as well as graft polymerization from a linear chain can yield cylindrically shaped macromolecules such as “hairy rods”,^{32,33} wormlike brushes,^{34–40} and monodendron-jacketed chains.^{41–46} The advancement in the control of the primary molecular structure and the manipulation techniques of the molecular conformation of such hyperbranched molecules make them intriguing building units for nanoscopic devices, biochemical sensors, molecular containers, templates for nanolithography, energy transfer funnels, and polyfunctional initiators and catalysts.^{47–63}

Shape control and the development of shape-responsive molecules relies also on the availability of analytical tools that provide spatial resolution down to subnanometer scale, strong contrast with respect to the chemical composition and physical properties, sensitivity to molecular forces in the pN range, and in-situ monitoring of molecular motion and conformation with a time resolution down to and even below milliseconds.

Molecular probes, such as optical or magnetic tweezers,^{64–71} micropipets,⁷² and microfibers,^{73,74} have been developed to manipulate single molecules and to measure their response to mechanical actions such as stretching, torsion, and compression. A force resolution down to 0.1 pN enabled quantitative measurement of the molecular forces and provided novel information on the basic principles of folding, motion, and interactions of individual molecules. Complementary to the local mechanical probes, actions of external fields were monitored on individual polymer molecules.^{75–77}

Scanning probe microscopy, SPM, enables both visualization of single molecules^{78–84} and probing of their properties.^{85–94} In contrast to scanning tunneling microscopy (STM) that is limited to imaging of conductive materials,⁹⁵ scanning force microscopy (SFM) became a versatile method for characterization of the microstructure of polymeric materials at the nanometer scale.⁹⁶ In addition to the topological resolution, SFM can distinguish surface areas differing in local mechanical properties and composition, respectively.^{101–103} Mechanical properties, such as viscoelasticity, friction, and adhesion, as well as long-range electrostatic and steric forces can be characterized on the scale of a few nanometers.^{104–109}

SFM does not require any sample treatment like etching and metal sputtering but can visualize the native structure of the sample.^{97–100} SFM is, however,



Sergei S. Sheiko was born in Moscow, Russia, in 1963. He received his B.A. degree in Physics from the Moscow Physico-Technical Institute in 1986 and his Ph.D. degree in Physical Sciences with Eduard Oleynik from the Institute of Chemical Physics of the Russian Academy of Sciences in 1990. From 1991 to 2000, he was working with Martin Möller at the University of Twente, Netherlands, and later at the University of Ulm, Germany. In 2001, he completed his Habilitation in Macromolecular Chemistry and joined the Department of Chemistry of the University of North Carolina at Chapel Hill. His main research interests include wetting and ordering phenomena in thin polymer films and functional properties of individual macromolecules.



Martin Möller studied chemistry at the University of Hamburg and Freiburg and then completed his Ph.D. degree at the Institute of Macromolecular Chemistry under the direction of Hans-Joachim Cantow on the microstructure of amorphous and semicrystalline polymers. He then worked with Robert Lenz at the University of Massachusetts on ionic block-copolymers. In 1982 he returned to Freiburg, where he studied the structure and dynamics of crystalline and columnar flexible polymers by high-resolution-solid-state NMR techniques. In 1989 he moved to the University of Twente in the Netherlands, where he became professor of macromolecular materials and polymer technology. Then in 1993 he joined the University of Ulm as Professor of organic and macromolecular chemistry. His current interests regard the synthesis and structure–property relationships in branched and hyperbranched polymers, blockcopolymers, surface modification, self-organization of polymers in the bulk and in thin films, and the formation of functional nanostructures.

a contact method, and therefore, deformation of molecules due to contact with the probe is inevitable. Imaging of molecular details requires a sufficient fixation of the molecules so they do not get moved during scanning. Thus, SFM can provide a superior resolution and visualization of the molecular shape in the range below 100 nm at ambient conditions, however, with the handicap that the molecules are constrained to a 2D conformation by the necessary fixation on the support.

Biological macromolecules such as DNA represent prominent examples for SFM studies on single molecules.^{79,110–118} Different techniques and deposition protocols have been reported to attach DNA molecules to a solid substrate and thus enable their imaging under water as well as in air. Strong electrostatic binding to the surface allowed DNA molecules to be scanned for long periods of time without damage and displacement. Imaging possibilities have been enhanced significantly with the introduction of the intermittent contact modes, since lateral forces were removed and perpendicular forces were reduced considerably due to higher sensitivity of the amplitude to the force variations.^{108,109,119–121} At present, the local sensitivity of intermittent contact SFM to surface interactions and mechanical properties, in combination with a sharp tip, controlled humidity, and strong attachment to the substrate, enables stable and reliable imaging of the microstructure and the chemical composition of single molecules with a resolution down to 1 nm. Here, SFM is complementary to fluorescent microscopy, which allows observation of single biomolecules that are labeled with a fluorophore in a bulk solution but with a resolution larger than 100 nm.^{123–130}

Recently, single chains of synthetic polymers have been visualized and examined regarding their conformation.^{79–81,131–133} Mostly these were molecules with a well defined rather invariant shape like fullerenes, carbon nanotubes, and some polymer molecules. In this review we will focus on less rigid or even soft hyperbranched polymer molecules (Figure 1): (i) their visualization followed by analysis of the conformation and motion and (ii) probing of their properties such as specific interactions and mechanical properties. For comparison, some relevant examples from biomacromolecules are discussed.

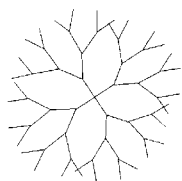
2. Structure of Individual Molecules at Interfaces

2.1. Conformation of 2D Confined Macromolecules

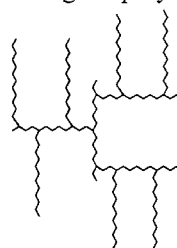
So far, high-resolution microscopy can depict the contour of a macromolecule but does not resolve the individual atoms of a macromolecule. The information on the molecular structure obtainable from such an image includes the contour length, the curvature, and the end-to-end distance. This enables quantitative analysis both of the local properties (chain configuration and flexibility) and of the overall conformation (excluded volume effects and random-walk statistics). For polymer chains with a rodlike backbone or polymer molecules whose secondary structure is straightened by hydrogen bonds between the constituting monomers, e.g., DNA and proteins, the observed length L is directly related to its degree of polymerization, N , or its molecular mass M by the length per monomer unit $l_m = L/N$, and the linear density $\lambda = M/L$, respectively.

Figure 2 shows an SFM image of poly(isocyno-L-Alanine L-Alanine-OMe) (L,L-PIAA), that adopts a rigid-rod-like helix conformation stabilized by β -sheet-like hydrogen bonding between the alanine side chains.¹³¹ Comparison of the number-average molec-

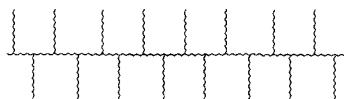
a: Dendrimers



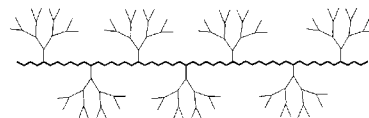
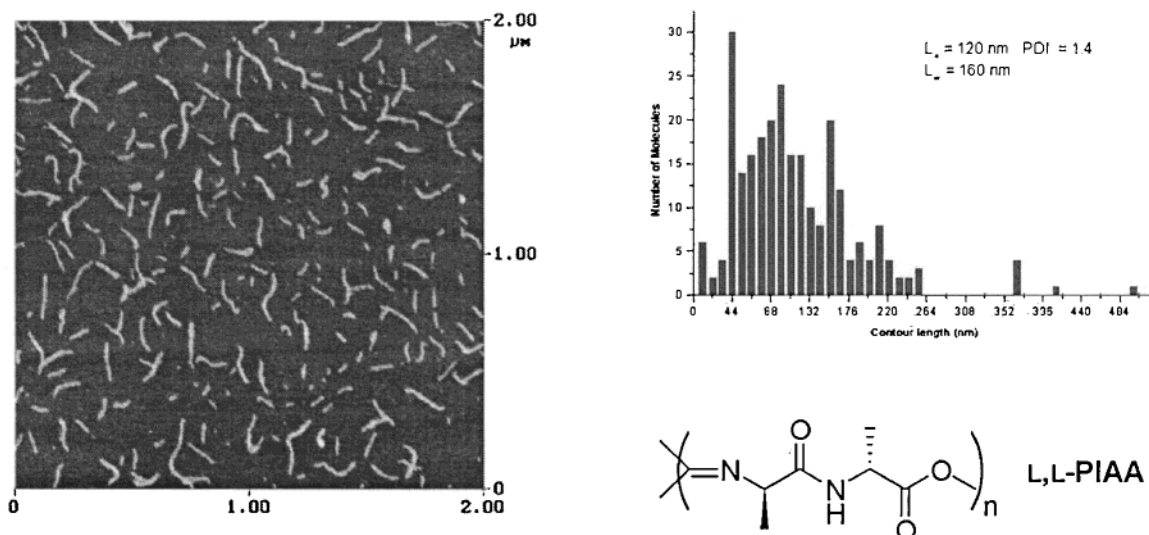
b: Arborescent-graft polymers



c: Molecular brushes



d: Monodendron-jacketed chains

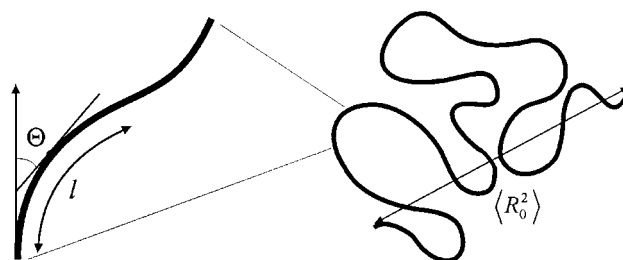
**Figure 1.** Hyperbranched molecular architectures.**Figure 2.** Height image of L,L-PIAA molecules on mica as measured by tapping mode SFM. The histogram shows distribution of the apparent lengths of the adsorbed molecules.

ular weight $M_n = 150$ kg/mol ($M_w/M_n = 1.4$) and the observed length of the molecules yields a length per monomer unit of $l_m \sim 0.1$ nm, which is consistent with the helical structure.

The local curvature, ρ , and the end-to-end distance, $\langle R_0^2 \rangle$, of disordered macromolecules reflect the chain flexibility and the long-range interactions, which on the other hand control macroscopic properties such as the viscosity of a polymer solution and melts. The description of the corresponding interdependences is usually done by means of scaling relations, the analysis of a polymer property as a power of polymer length, i.e., Property $\sim L^k$.¹³⁴ Figure 3 depicts a schematic drawing of a wormlike molecule confined to a flat surface. The molecular flexibility, i.e., resistance to in-plane bending, can be characterized by the persistence length.¹³⁵ In an unperturbed state, the persistence length of a 2D-confined polymer chain should be 2 times longer than in a 3D system, i.e., in bulk or solution at the Θ temperature.^{135–137}

Experimentally, one can use two complementary ways to evaluate the persistence length from the images of the chains. The bond-correlation function

$$\langle \cos(\Theta) \rangle = e^{-l/l_p} \quad (1)$$

**Figure 3.** Molecular parameters which became accessible upon visualization of single molecules, i.e., contour length L , the end-to-end distance $\langle R_0^2 \rangle$, and the local curvature $\rho = d\Theta/dl$.

gives the average cosine angle between the tangents along the brush molecule separated by distance l . The characteristic length l_p corresponds to the persistence length. Since the method evaluates the local curvature, it can be applied to molecules of either length. The second method is based on the Kratky–Porod formula,¹³⁸ which depicts the dependence between the end-to-end distance $\langle R_0^2 \rangle$, the contour length L , and

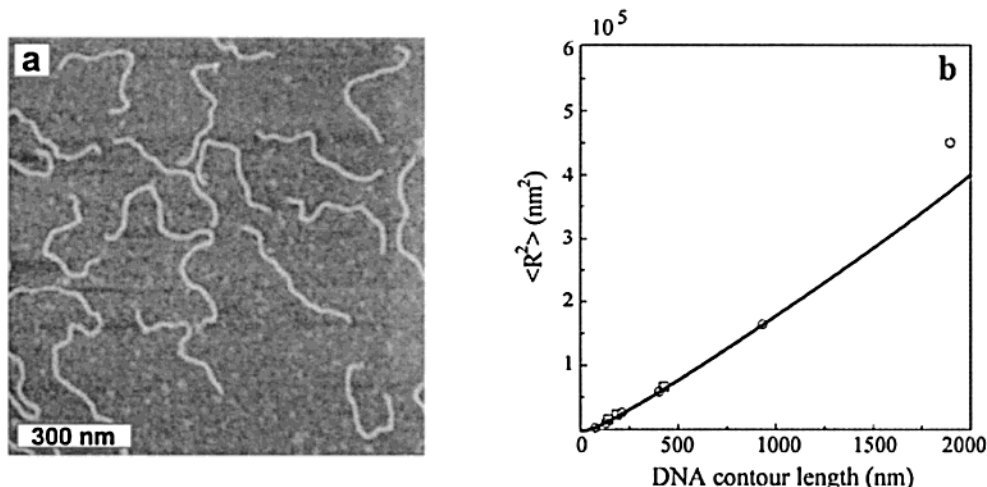


Figure 4. (a) SF micrograph of DNA molecules deposited on mica from a physiological solution. (b) Mean-square end-to-end distance, $\langle R^2 \rangle$, as a function of the DNA contour length measured in different buffer solutions. The continuous line represents the $\langle R^2 \rangle$ evaluated from eq 2 for a DNA persistent length of 53 nm.⁷⁹

the persistent length as

$$\langle R_0^2 \rangle = 2l_p L \left[1 - \frac{l_p}{L} (1 - e^{-L/l_p}) \right] \quad (2)$$

The Kratky–Porod formula may be not applicable for long molecules with $L \gg l_p$, for which excluded volume interactions should be taken into account. Intramolecular excluded volume effects result from repulsion between segments within the same molecule, which can cause an increase of the end-to-end distance. These effects are particularly strong for 2D systems, which demonstrate an increased density of segments and do not permit the chain crossings. Both methods require complete visualization of a statistical ensemble of single molecules in order to determine the length L , the angle Θ , and the end-to-end distance $\langle R_0^2 \rangle$. In addition, they assume the observation of molecules in their natural state, in which molecules are not constrained and freely fluctuate around their equilibrium conformation.

The concurrent effects of adsorption, solvent evaporation, and capillary forces can, however, lead to kinetically trapped conformations (see below). The question arises whether and under what conditions an equilibrium 2D conformation can be achieved.

Optimum conditions were reported for DNA molecules deposited on mica.⁷⁸ In water, mica is negatively charged; and therefore, mica repels negatively charged DNA molecules. When divalent cations, such as Mg^{2+} , Mn^{2+} , Co^{2+} , and Ca^{2+} , are adsorbed, the surface charge is inverted. Thus, DNA adhesion can be promoted if deposition is done from a buffer solution containing divalent cations.¹⁰⁸ Because the divalent cations and thus the adhesion sites can diffuse along the surface, the deposition process was assumed to allow equilibration rather than being dominated by kinetic trapping effects. A typical example is a 0.5 nM DNA solution in a pH 7.4 buffer with NaCl (10 mM) and $MgCl_2$ (2 mM). In this case, the adsorption of DNA molecules from solution is controlled by diffusion. A diffusion coefficient of $D = 5.5 \times 10^{-8} \text{ cm}^2/\text{s}$ was found using the formula n_s/n_0

$= \sqrt{4D/\pi} \sqrt{t}$, where n_s is the surface concentration of the adsorbed molecules and n_0 the concentration of the molecules in solution.

At low concentrations from 0.5 to 2 nM, the molecules are adsorbed onto mica as single species as shown in Figure 4a. Figure 4b shows a plot of $\langle R_0^2 \rangle$ as a function of the contour length L . Both parameters were measured directly from the SFM micrographs. Assuming that the molecular conformation was not perturbed by excluded volume interactions between molecular segments as well as by interactions between the segments and the substrate, Rivetti et al. used the Kratky–Porod formula to determine a persistence length of 53 nm.⁷⁹ The data were in good agreement with those obtained by electron microscopy and gel electrophoresis.¹³⁹ For the molecules adsorbed on mica, the crossover of the perturbed and unperturbed regimes was found at contour lengths of about 1000 nm (ca. 20 times the persistence length). Therefore, evaluation by the Kratky–Porod formula (eq 2) is limited to DNA molecules whose length is shorter than 1000 nm.

The effect of excluded volume repulsion on the molecular conformation was investigated for long DNA molecules in an aqueous environment by fluorescence optical microscopy. Figure 5a shows fluorescence images of λ -phage DNA fragments bound to a glass-supported cationic lipid membrane in 10 mM HEPES buffer. Since the observed molecules were much longer than the persistence length, the excluded volume effects resulted in the coil expansion. Figure 5b depicts the log–log representation of the radius of gyration as a function of the number of base pairs for a set of molecules that consist of 880, 6141, 14 953, and 26 528 base pairs.¹⁴⁰ The scaling exponent for the 2D-confined molecules was found to be $\nu = 0.79 \pm 0.04$. This experimental value is in good agreement with the theoretical prediction $\nu = 3/4$ for self-avoiding statistical chains in two dimensions¹⁴¹ and consistent with a persistence length l_p of 50 nm. For individual DNA molecules in solution, the scaling exponent was determined to $\nu = 3/5$.¹⁴²

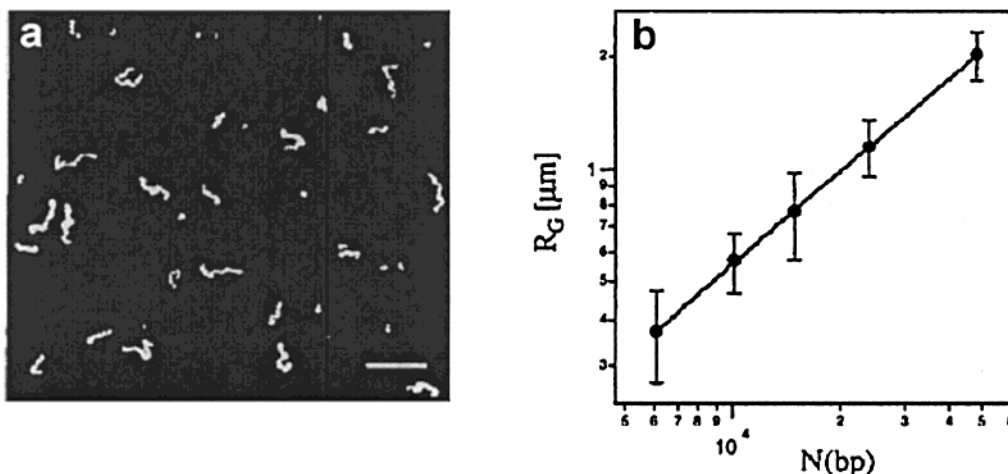


Figure 5. Static scaling analysis of single DNA molecules. (a) Fluorescence micrograph of λ -phage DNA cut by the restriction enzyme BbrPI. (b) The log–log plot of the averaged radius of gyration of DNA fragments as a function of fragment length in number of base pairs N (bp). The straight line fits the scaling $R_g \propto N^\nu$, with $\nu = 0.79 \pm 0.04$.¹⁴⁰

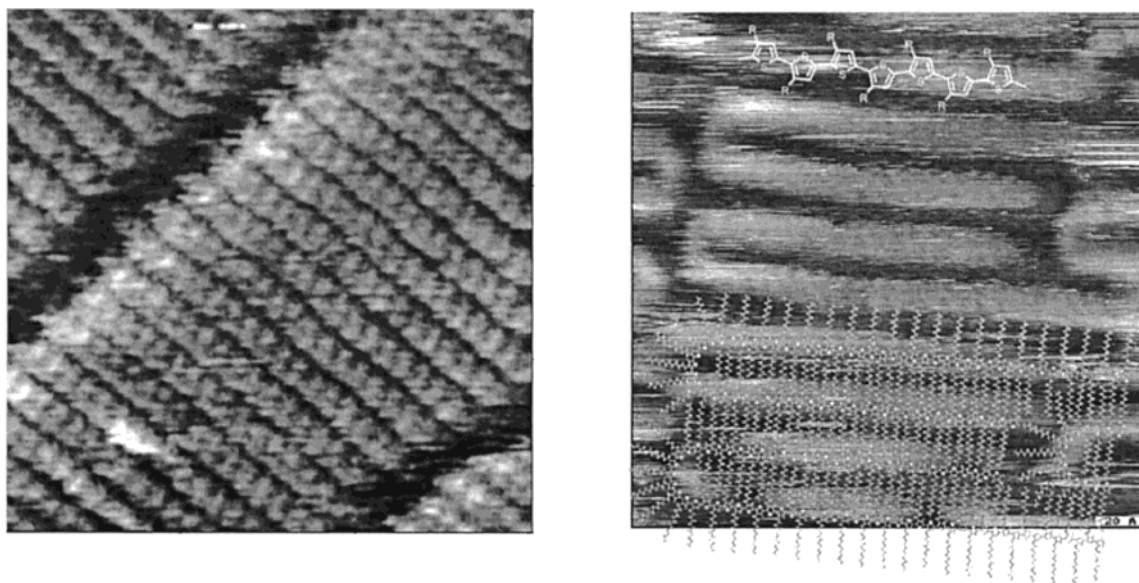


Figure 6. (a) STM image of C36H74 alkane on graphite.¹⁴³ (b) Head-to-tail-coupled poly(3-dodecylthiophene) in the HOPG/liquid (1,2,4-trichlorobenzene) interface 20×20 nm.¹⁴⁵

2.2. Structural Effects by Specific Interactions with the Substrate

Absence of surface interactions that effect the conformation of the macromolecules is, however, not the rule. Below we will discuss examples of how the molecular conformation can be effected by specific interaction with the substrate. Obviously, one cannot regard the apparent persistence length of the adsorbed molecules as a characteristic value for the chain flexibility.

Spectacular pictures of adsorbed chain molecules have been obtained for n -alkanes on graphite where the carbon chains were oriented according to the 3-fold symmetry of the graphite (Figure 6a). The orientation of the main chain has been explained by the close matching between the repeat length $l_c = 2.54$ Å of a $-(\text{CH}_2-\text{CH}_2)-$ sequence in all-trans planar zigzag conformation and the crystallographic spacing $a = 2.46$ Å of the graphite surface.^{143,144}

Also, interactions of the side chains with the substrate can cause alignment of adsorbed molecules.

Figure 6b shows the ordering of polythiophene molecules with alkyl side chains along the crystallographic axes of the graphite.¹⁴⁵ Formation of highly ordered monolayers follows from the epitaxial-like orientation of the hydrocarbon chains with respect to the graphite lattice.

Also, relatively long polymer molecules can be extended and aligned by specific adsorption of the side groups with the substrate. Detailed studies of the molecular conformation affected by adsorption on a solid substrate have been possible with so-called monodendron-jacketed polymers.^{41,146–148} Scheme 1 depicts two examples of monodendron-jacketed macromolecules: 14-ABG-PS carries three monoalkoxybenzyl ether groups per monomer unit, whereas the stronger branched 3,4,5-t-3,4,5-PS monomer is substituted by three trisalkoxybenzyl ether groups and has a 2 times larger molecular mass.¹⁴⁹

Figure 7 shows an SF micrograph of 14-ABG-PS on graphite together with a cartoon of the molecular structure.¹⁴⁷ The macromolecules are arranged in

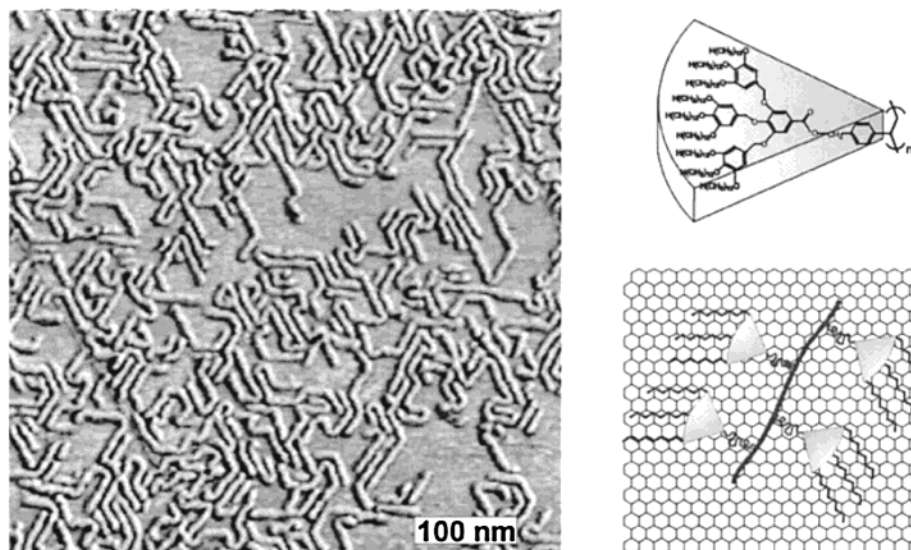
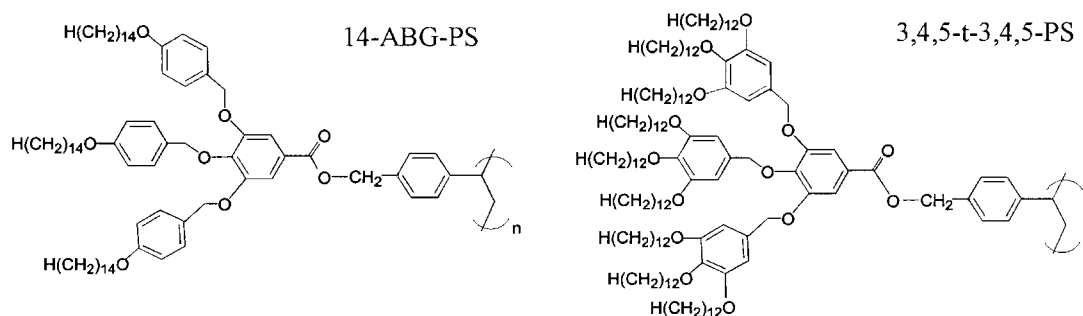


Figure 7. SFM micrograph of 14-ABG-PS molecules on HOPG prepared by spin casting of a solution in cyclopentane ($c = 0.1$ mg/mL). Individual molecules aligned parallel to the substrate and bent at characteristic angles of 60° and 120° to follow the 6-fold symmetry of graphite.¹⁴⁷

Scheme 1



straight segments with bends of a characteristic angle of 60° and 120° . Also, in this case the ordering of the macromolecules is explained by an epitaxial adsorption of the alkyl tails of the monodendron side groups on highly oriented pyrolytic graphite, HOPG. Specific interaction of the side chains with the substrate has been verified by STM studies on monolayers of the monodendrons.¹⁴⁸

It has also been possible to observe how the chains adsorb originally in a coiled conformation and how they expand subsequently to the ordered pattern. Figure 8 shows a series of SFM images of a polyox-norbornene substituted by the same dendron groups as in the case of 14-ABG-PS after different times for adsorption.¹⁴⁸ Besides the increase in surface coverage, one observes the relaxation within minutes.

On mica, the 14-ABG-PS polymer did not show any particular order (Figure 9). Only a short-range orientational order of densely packed cylinders was observed.

The dense arrangement of the chains points to the action of other forces that can control the molecular conformation of adsorbed macromolecules in addition to the interaction with the substrate. Capillary forces and dewetting during evaporation of the solvent can cause condensation and dense packing of the molecules in monolayer patches,^{147,148,150} For large molecules with a diameter of ca. 5 nm, capillary forces are in the range of a few nN, which is sufficient to

move the molecules or molecular parts along the substrate and to cause aggregation of individual molecules into monolayers.

Another example for wormlike synthetic macromolecules is depicted in Figure 10. The SFM images show poly(methyl methacrylate) brush molecules that adsorbed as extended threats on a flat mica surface. The backbone consists of methacrylate units, each of which is grafted by a methyl methacrylate side chain.¹⁵¹ The molecular properties are summarized in Table 1.

Neglecting the interaction with the substrate, the overall conformation of the brush molecule is controlled by the repulsion and excluded volume of the densely grafted side chains. Thus, the spatial demand of the side chains results in bending rigidity and prevents the collapse of a brush molecule to a dense globule. Yet, in contrast to DNA, where the segmental conformation, i.e., the rotational angles of the bonds in the backbone, is fixed to a large extent, the brush molecules possess a flexible backbone. Thus, the brush acquires rigidity on the length scale of its thickness or larger, but the conformation within short segments of the backbone can be disordered similar to that in a coil molecule. The monodendron-jacketed polymers depicted in Figures 7–9 can be regarded as an intermediate case, where the rigidity of the backbone conformation is caused not only by the bulkiness but also by self-assembly of the side chains

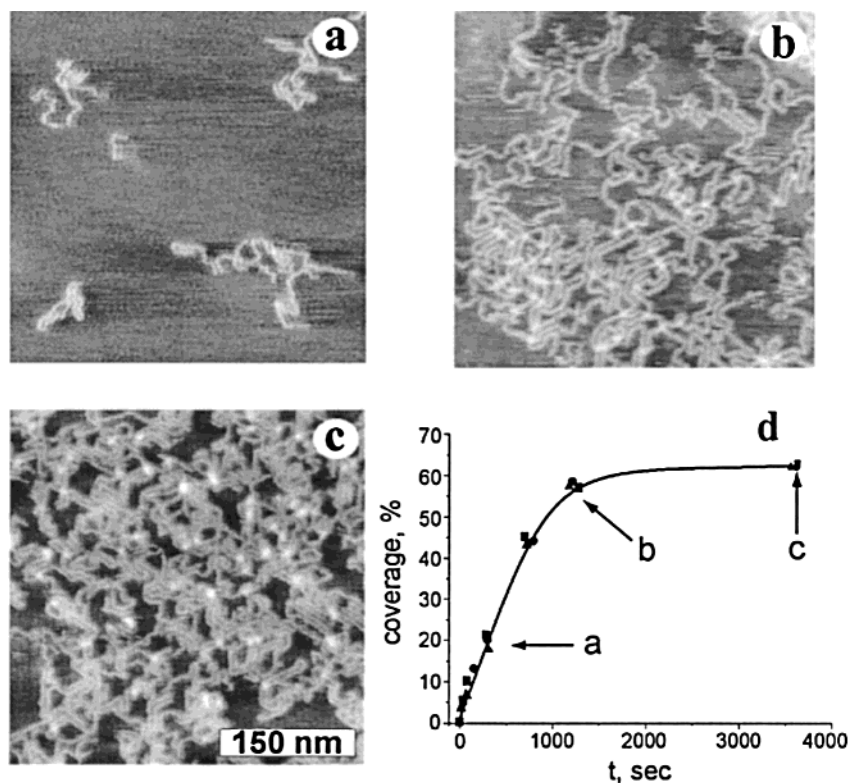


Figure 8. (a–c) A series of SFM micrographs was measured after adsorption of polyoxanorbornene DP100 from THF solution with concentration 0.001 mg/mL on mica during different times. The adsorption time is indicated by arrows in d, representing dependence of the coverage on the time for different polyoxanorbornenes (■) DP 100, (●) DP 200, (▲) DP 400.¹⁴⁸

Table 1. Molecular Characterization of the PMMA Brushes Depicted in Figure 5¹⁵¹

length of side chains ^a	total molecular weight ^b	contour length (SFM) ^c	L_w/L_n	length/monomer (SFM)
2410 g/mol	1.08×10^7 g/mol	367 nm	1.3	0.07 ± 0.1 nm

^a MALDI-TOF. ^b Small angle light scattering. ^c $L_w = (\sum n_i L_i^2) / (\sum n_i L_i)$.

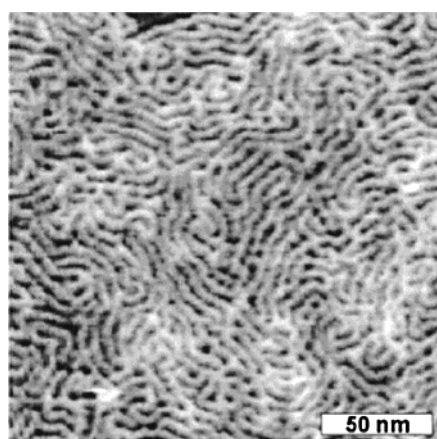


Figure 9. SFM micrographs of 14-ABG-PS molecules on mica deposited from a CHCl_3 solution ($c = 0.1$ mg/mL). Molecules are densely packed because of the action of capillary forces during evaporation of the solvent.¹⁴⁷

with their π -stacking of the aromatic units. Yet, also in this case, the self-assembly to column structures does not prevent some randomness in the rotational isomeric states.^{146,149} Because of this flexibility of the main chain, the brush and also dendron-jacketed molecules can experience an axial contraction com-

pared to the maximum contour length given for an all-trans planar zigzag conformation (2/1 helix).

A reduced length per monomer unit, i.e., of the effective grafting distance h , has been demonstrated for the PMMA brush molecules depicted in Figure 10. Comparison of the degree of polymerization of the PMMA brushes with their length determined by a detailed evaluation of a set of SFM images yielded a length per monomer unit of $h = 0.07 \pm 0.01$ nm. The value is 3 times shorter than the monomer length in a completely stretched backbone ($h_{\text{all-trans}} = 0.25$ nm).

Evaluation of the cross section of the brush molecules in Figure 10 (including correction for tip indentation¹⁵² convolution of the surface profile with the shape of the tip apex and comparison with electron microscopy images) demonstrated that the molecules adopt a hemicircular cross section of 11 ± 1 nm width and a height of 4.2 ± 0.5 nm. These values are consistent with $h = 0.07 \pm 0.01$ nm for the length per repeat unit of the backbone, i.e., with the molecular weight of the side chains and the bulk density of PMMA, a length of 0.07 nm corresponds to a cylinder with a cross section of 45 nm^2 , comparable to the cross section of 38 nm of a hemicircular profile with 11 nm width and 4.2 nm height.

Light scattering studies allowed a complementary characterization of the size and conformation of the

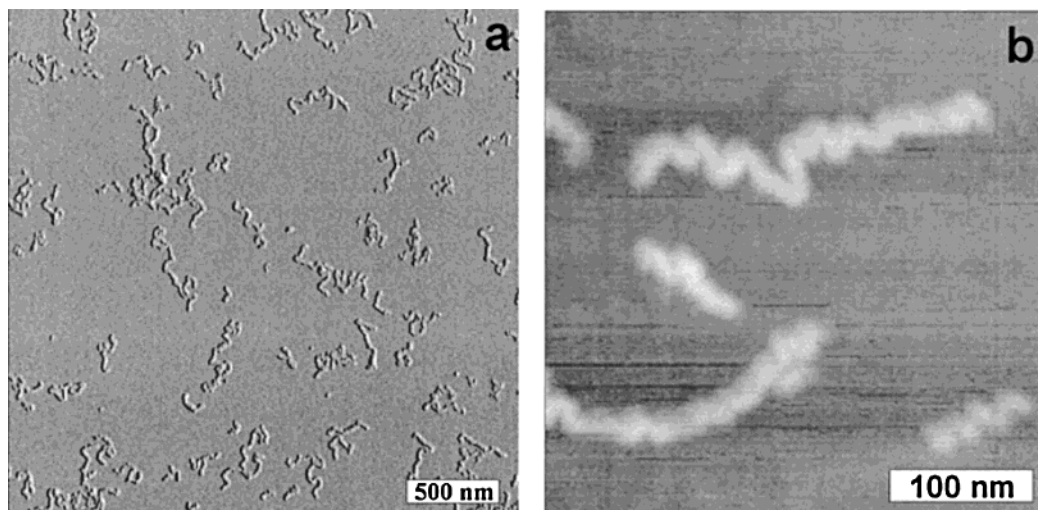


Figure 10. (a) Molecular brushes with poly(methyl methacrylate) side chains were adsorbed on mica and annealed above the glass transition temperature $T = 105\text{ }^{\circ}\text{C}$ for 24 h. (b) The undulated structures in higher magnification images demonstrate the tendency of the brush molecules to contraction via the buckling mechanism. The height of the molecules was determined to be 2 nm and the width 16 ± 2 nm.

PMMA brush molecules in THF solution.¹⁵¹ Also, in this case, the monomer length $h = 0.081 \pm 0.008$ nm indicated an axial contraction compared to the fully stretched all-trans conformation. The coincidence of the experimentally determined values for h in dilute solution and for the dry adsorbed molecules might be regarded as an indication that the axial contraction of a densely grafted brush molecule does not depend strongly on the quality of the solvent. It must, however, be noted that adsorption of the side chains, i.e., their confinement to a 2D conformation, can cause significant stretching compared to the unconfined brush (see below). Thus, an axial contraction caused by decreasing solvent quality or in a dry brush might well be compensated by stretching due to partial adsorption of the side chains. That this is in fact the case is indicated by the remarkable buckling of the brush conformation observed in Figure 10b. Buckling can be explained by a transformation where the molecules first contract as the solvent evaporates and then expand axially as the side chains start to adsorb tightly. Buckling is typical for confined anisotropic systems when the strain cannot be released completely, such as thin films, microtubuli, and nanotubes.^{153–155}

The driving force for the axial contraction was elucidated by O. Borisov by scaling analysis of a linear brush molecule.¹⁵⁶ Because of the dense substitution, the side chains get stretched. Stretching of the side chains with respect to the Gaussian dimension leads to conformational entropy loss. Thus, if the grafting density h^{-1} is fixed, the cylindrical brush experiences an extensional axial force of entropic origin. In a bad solvent or in air when the brush is collapsed, a negative contribution to the axial force has to be taken into account due to the excess interfacial energy of the brush. The interfacial energy per unit area is proportional to τ^2 , where τ describes the quality of the solvent given by the relative deviation from the Θ point, $\tau = (T - \Theta)/\Theta$. The free energy per side chain, F , in a collapsed brush comprises the elastic penalty for extension of a side chain, the excess free energy of the interface, and the

free energy of excluded volume interaction.^{156–159}

$$\frac{F(R, h)}{k_B T} = \frac{R^2}{N} + |\tau|^2 R h - |\tau|^2 N \quad (3)$$

Here N is the number of monomer units in the side chains and R is their end-to-end distance. In a uniformly collapsed brush below the Θ point, the binary interactions are attractive and the polymer density $\propto |\tau|$. The thickness of the collapsed brush scales as $R \propto (N/h|\tau|)^{1/2}$. The axial tension is given by

$$f k_B T = - \frac{dF/k_B T}{dh} \cong (|\tau| h^2)^{-1} - |\tau|^{3/2} (N/h)^{1/2} \quad (4)$$

The degree of stretching of the side chains and the extensional force on the backbone decreases with decreasing grafting density and decreasing solvent quality τ (i.e., increasing $|\tau|$).

If the backbone is not stiff but flexible, an eventually resulting negative axial tension can be partly released by contraction, i.e., variation of the effective grafting density h . Moreover, under the condition of a fixed monomer density $N/(R^2 h) \cong |\tau|$, minimization of the total elastic free energy of the collapsed brush has been shown to result to¹⁵⁶

$$\begin{aligned} h(\tau) &\cong h(\tau_{\Theta} (|\tau|/|\tau_{\Theta}|)^{-1/3}) \\ R(\tau) &\cong R(\tau_{\Theta} (|\tau|/|\tau_{\Theta}|)^{-1/3}) \end{aligned} \quad (5)$$

with τ_{Θ} corresponding to the onset of the side chain collapse.

The detailed analysis¹⁵⁶ demonstrated that the onset of the side chain collapse is shifted toward the range of poorer solvent conditions compared to that in an individual chain of length N . Both the side chains and the backbone remain extended at $\tau \leq \tau_{\Theta}$ with respect to the Gaussian dimensions for densely grafted brushes, and the length of a dense brush is

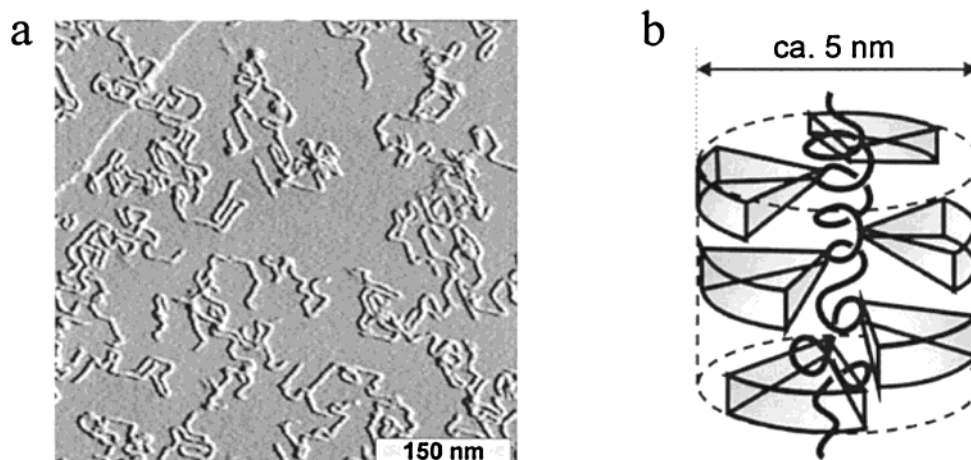


Figure 11. (a) SFM micrograph of single 14-ABG-PS molecules on HOPG, and (b) suggested conformation of monodendron-jacketed linear chains.¹⁴⁶

Table 2. Molecular Dimensions and Length Per Monomer Unit of 14-ABG-PS, 3,4,5-t-3,4-PS, and 3,4,5-t-3,4,5-PS from SFM Micrographs and SEC and SLS Data^{146,147}

	polymers		
	14-ABG-PS	3,4,5-t-3,4-PS	3,4,5-t-3,4,5-PS
M_n^a , g/mol	1194	1612	2140
M_w^b , 10^6 g/mol	1.1	1.2	2.0
M_w/M_n	2.6	2.6	2.2
a , \AA	52.1	41.4	47.7
l_{XDR} , \AA	0.8	1.8	2.0
l_{SFM} , \AA	1.2	1.9	2.3

^a Molecular weight of the monomer unit. ^b Molecular weight of the polymers determined by size exclusion chromatography in tetrahydrofuran using a light scattering detector. ^c Column diameter determined by X-ray diffraction measurement in the columnar mesophase. ^d X-ray spacing along the column axis per repeat unit of the main chain as determined for the columnar mesophase in bulk. ^e Length of the cylindrical molecules per repeat unit of the main chain determined from the SFM micrographs as $l_{\text{SFM}} = M \cdot L_n / M_n$.

predicted to depend only weakly on the solvent conditions within the regime of a poor solvent.

Also, in the case of the monodendron-jacketed macromolecules, the chain length-per-repeat unit $l_{\text{SFM}} = L_n / DP_n$ could be evaluated from the molecular length in comparison with the independently determined degree of polymerization DP_n . Figure 11 depicts an SFM image of single 14-ABG-PS molecules deposited on the surface of highly oriented pyrolytic graphite.^{146,147} The 5 nm thick molecular threads are aligned parallel to the substrate plane. Table 2 summarizes the molecular dimensions and the values of the length per monomer unit, l_{SFM} , for three monodendron-jacketed polystyrenes with three, six, and nine terminal alkyl chains per dendron, respectively.

The value of $l_{\text{SFM}} = 1.2 \text{ \AA}$ for 14-ABG-PS is in good agreement with the stacking period in the columnar hexagonal mesophase that was obtained from the macroscopic density and the X-ray periodicity of the columnar packing. This value is almost 2 times less than the length $l_0 = 2.5 \text{ \AA}$ expected for a fully extended main chain in an all-trans planar zigzag conformation. In contrast, 3,4,5-t-3,4,5-PS with the sterically more demanding side groups demonstrated

almost complete stretching of the backbone with $l_{\text{SFM}} = 2.3 \text{ \AA}$.

Clearly, also the monodendron-jacketed polystyrenes are contracted in length compared to the full contour length. For 14-ABG-PS it must be noted, however, that the coincidence of the length per monomer unit in the adsorbed and the hexagonal columnar mesophase has to be considered to occur by chance. As discussed for Figure 7, the molecular conformation of 14-ABG-PS is significantly affected by the interaction with the substrate.^{146–148} Certainly such an interaction with the substrate will be a factor that changes the segmental conformation and does not only align the molecular segments in a straight line. In this case, the length per monomer unit results from the interplay between the interfacial and intramolecular interactions. Constraint of the tightly adsorbed side chains to the surface plane causes extension of the backbone, while aggregation of desorbed side chains favors contraction.

2.3. Metastable Tertiary Structures by Local Contraction and Twisting

It is obvious that the conformation of adsorbed molecules can be far from equilibrium if the adsorption process has been fast and irreversible. In this case, the molecules do not have time to sample the whole assembly of thermodynamic states and get trapped kinetically at the contact sites. Yet, there are distinct kinetic pathways that give rise to the formation of peculiar tertiary structures in connection with the axial contraction and local twisting. An example discussed above is the buckling of the PMMA brushes in Figure 10. Another example is demonstrated in Figure 12. Here 14-ABG-PS molecules are depicted that were deposited by fast spin coating on mica.¹⁴⁷ The molecules were adsorbed randomly without interfacial ordering effects, and quick evaporation of the solvent caused underwinding or overwinding of the molecules, i.e., significant torsional strain is evidenced by the observation of supercoils, so-called plectonemes (from the Greek meaning “braided string”).¹⁶¹

The drawing of a monodendron-jacketed chain in Figure 11 indicates that axial contraction is enabled

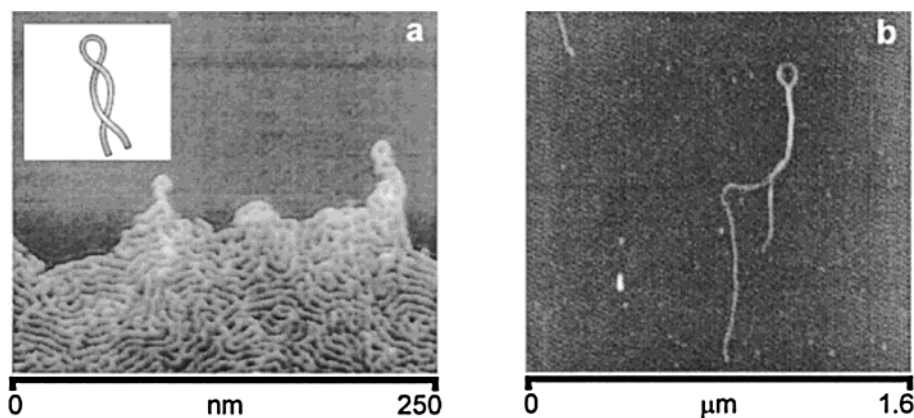


Figure 12. SFM micrographs of (a) 14-ABG-PS on mica¹⁴⁷ and (b) twisted ribbon structure of polypeptide β -sheets.¹⁶⁴ The plectoneme conformation is caused by the backward folding of the torsionally stressed molecules. Insert in a depicts a plectoneme supercoil.

by local winding up of the backbone. Regular helix formation is highly unlikely because of the atactic stereostructure and was also not observed in the mesophase state.¹⁶⁰ However, axial contraction must clearly be linked to local twisting. Thus, the observed supercoiling is a way of releasing torsional stress.^{162,163} To the best of our knowledge, the supercoil formation of the monodendron-jacketed polystyrene is one of the first observations of a defined tertiary structure in synthetic polymers. While in biomolecules the tertiary structures are typically stabilized by specific interactions between side groups, the supercoil of the monodendron-jacketed polymers is metastable. Eventually, annealing offered a path for the stress relaxation and led to vanishing of the supercoil conformation.¹⁴⁷ Figure 12b shows a similar conformation observed for a polypeptide.¹⁶⁴

2.4. Microscopic Structure of Adsorbed Macromolecules

How adsorption of the side chains to a flat substrate affects the backbone conformation has been observed in further microscopic detail for brush molecules with a methacrylate backbone and poly(*n*-butyl acrylate) side chains. These poly(*n*-butyl acrylate) brushes were prepared by living radical grafting from a multifunctional macromolecular initiator.³⁸ The synthetic approach allowed observation of the same batch of molecules without (macroinitiator) and with poly(*n*-butyl acrylate) side chains (brush).

After adsorption on mica, the SFM length of the brush molecules corresponded to an almost fully extended backbone approaching the trans zigzag conformation (Figure 13b). In contrast, the apparent length of the macroinitiator, which was scanned by SFM prior to grafting, was 2 times shorter than the contour length of the main chain (Figure 13a).

The extension of brush molecules is caused by excluded volume repulsion of the 2D-adsorbed side chains. Therefore, the length of adsorbed brushes should also depend on the grafting density. Copolymer brushes with a random sequence of methyl methacrylate and poly(*n*-butyl acrylate)-substituted methacrylate units were prepared with different compositions, i.e., grafting densities. Table 3 com-

pares the lengths of *p*nBuA brushes with different numbers of nongrafted MMA monomers. One can see that less densely grafted brushes undergo stronger axial contraction of the main chain. When the average length of the MMA sequences became larger than four monomeric units, the observed length per monomer unit decreased significantly. This value is remarkably similar to the length $l_k \sim 12 \text{ \AA}$ of the statistical (Kuhn) segment of PMMA.

In addition to the visualization of the molecular contour, topographic and phase contrast SFM enabled clear resolution of the fine molecular structure. Figure 14 shows SFM micrographs of single brush molecules, where one can easily distinguish both the backbone and the tightly adsorbed side chains. For example, white contours in the height micrograph (Figure 14b) correspond to the backbone wrapped by nonadsorbed side chains, while the grayish areas between the white threads demonstrate the hairy structure of the adsorbed segments of the side chains. The molecules in Figure 14a,b differ in the degree of polymerization of the side chains as $DP_n = 52 \pm 10$ and $DP_n = 10 \pm 2$, respectively. This difference was readily detected by SFM. The brushes in Figure 14a show a thicker corona of side chains around the backbone compared to the brush in Figure 14b.

The distance between the backbones in densely packed monolayers, like the one shown in Figure 14b, increases linearly with the number-average degree of polymerization of the side chains, $D \sim DP_n$. The distance is, however, significantly larger than the number-average length of a fully extended side chain, $l_0 = DP_n \times 2.5 \text{ \AA}$. These observations suggest that the absolute distance between adsorbed brushes is not determined by the number-average length of the side chains but it is controlled by a small fraction of longer side chains.

Extension and stiffening of the backbone because of the tight adsorption of the side chains are connected with a significant loss of entropy. A certain decrease in the entropy by bending of the backbone without changing the degree of adsorption of the side chains can, however, be enabled by an uneven distribution of the side chains between the two sides of the backbone. On the concave side of the bend, the space available per side chain is increased compared

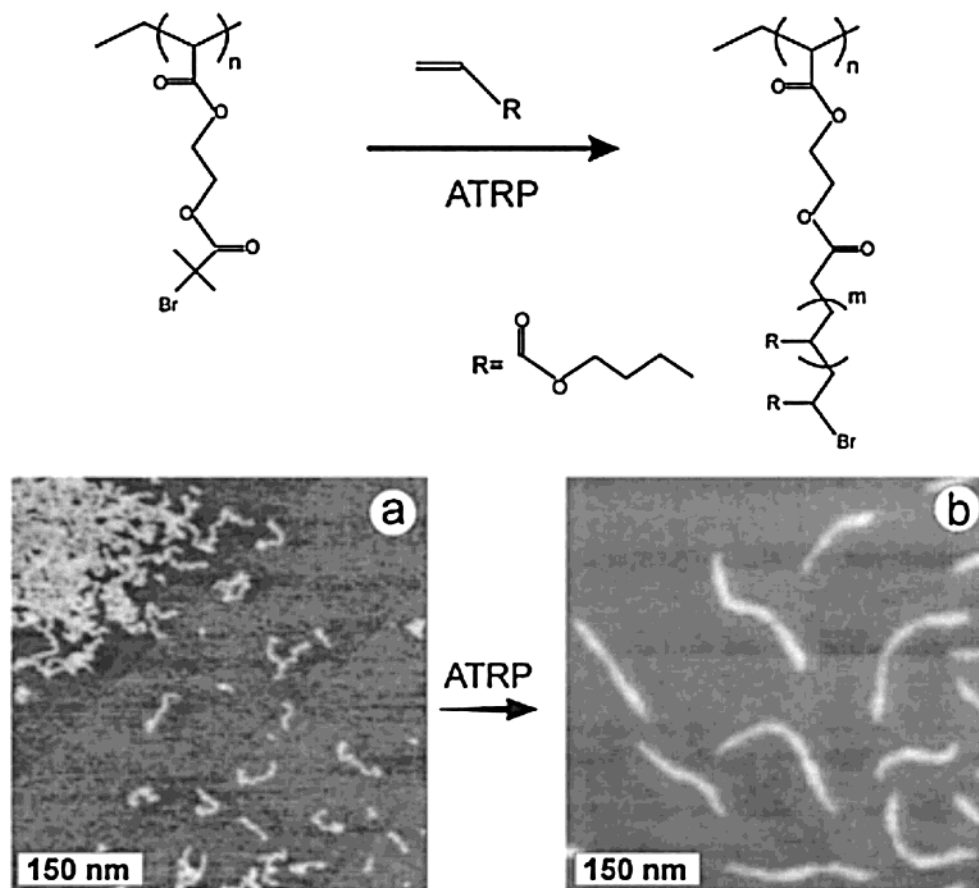


Figure 13. (Top) Preparation of PBA brushes by grafting from the macroinitiator using ATRP.³⁸ (Bottom) Single molecules of the macroinitiator (a) and PBA brushes (b) adsorbed on mica were visualized by tapping-mode SFM. Clearly, the grafting of long side chains led to almost full extension of the backbone approaching the contour length $L = N \cdot l_0$, where $l_0 = 0.25$ nm is the monomer length of a hydrocarbon chain in the all-trans conformation.

Table 3. Axial Contraction of *p*nBuA brushes as a Function of the Grafting Density

polymer	MMA, %	DP _n , side chains	DP _n , backbone	L _n , nm	l _m = L _n /DP _n , nm
homopolymer	0	35	567	123	0.22 ± 0.2
copolymer 1	35	58	477	120	0.25 ± 0.2
copolymer 2	56	42	637	127	0.2 ± 0.2
copolymer 3	77	32	710	116	0.16 ± 0.2

to the straight conformation. Thus, for these chains and the backbone, bending yields an increased configurational entropy.

Computer simulations demonstrated that such an uneven distribution of the side chains leads to bending.¹⁶⁵ Scaling analysis showed that the uneven side chain distribution and bending is favorable in particular for long side chains and lower grafting densities (Figure 15). In the case of an isolated single chain, bending can furthermore reduce the line tension, in the optimum case by formation of a spiral structure.^{166,167}

Indeed, bending and even spiral conformations were observed for PMMA brush molecules that were deposited from a solution in THF.^{165,167} This is shown by the SFM micrograph in Figure 16. Nevertheless, the situation in Figure 16 is a snapshot of a situation that emerged upon evaporation of the solvent and does not represent an equilibrium conformation.

Clear experimental evidence that the coiling of brushes on solid substrates is thermodynamically

favored could be obtained in the case of the brushes with poly(*n*-butylacrylate), PBA, side chains. The low glass transition temperature of PBA ($T_g = -54$ °C) favors fast equilibration upon thermal annealing. The sample in Figure 17a was prepared by spreading a dilute solution of the PBA brush molecules in CHCl₃ on water (Langmuir trough). The surface pressure was increased to obtain a condensed film that was then transferred onto a mica substrate. Similar to Figure 13, the backbones were predominantly extended. This indicates a rather even distribution of the side chains to the one and the other side as it might be expected for fast adsorption at the substrate surface. When the film on mica was, however, annealed for 48 h at 120 °C, considerable coiling of the molecules occurred as shown in Figure 17b.

Summarizing the evidence from Figures 13–15 and 17, it results that the backbone conformation of the brush molecule is strongly affected by the adsorption and side distribution of the grafts. The most important contribution is the repulsion between the ad-

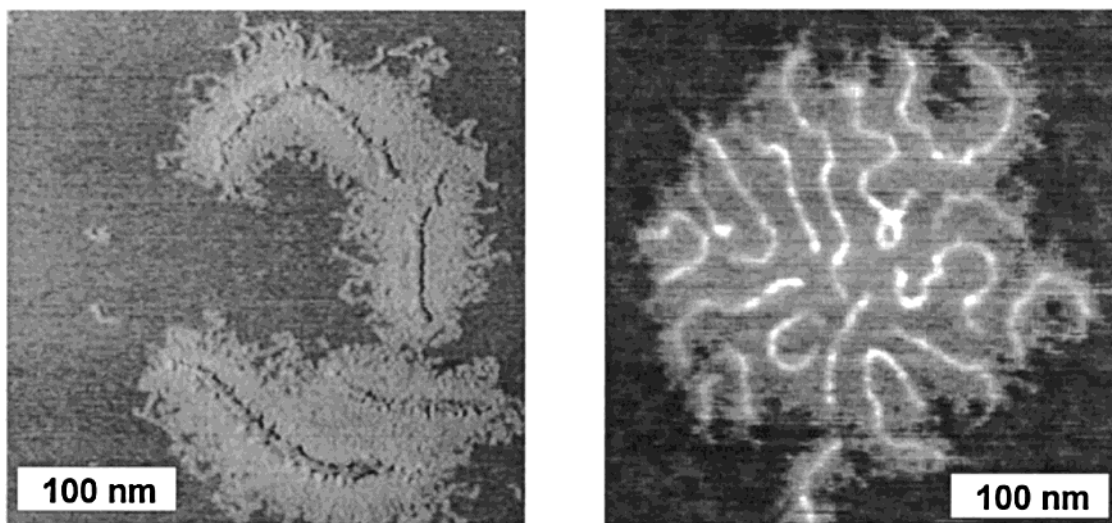


Figure 14. Molecular brushes with poly(*n*-butyl acrylate) side chains of different degrees of polymerization: (a) $n = 52$ and (b) $n = 10$.

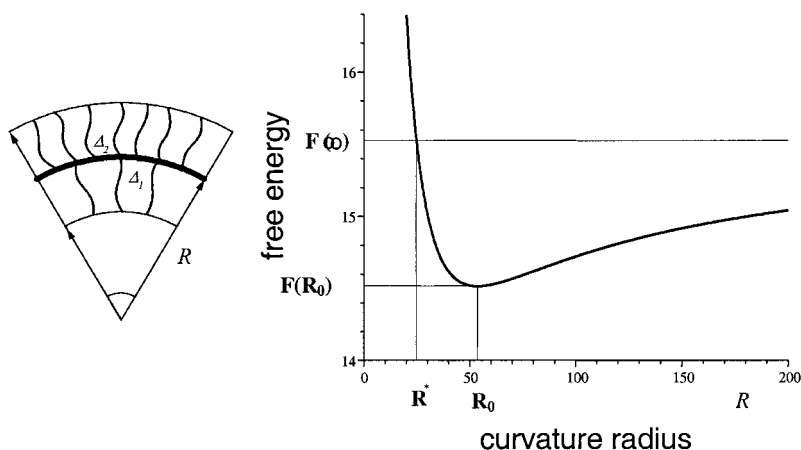


Figure 15. Calculation of the free energy of a brush molecule with asymmetrically distributed side chains as a function of the bending curvature ($DP_{\text{side chains}} = 100$, $\Delta_1 = 4$, $\Delta_2 = 8$, one side chain per two backbone units).

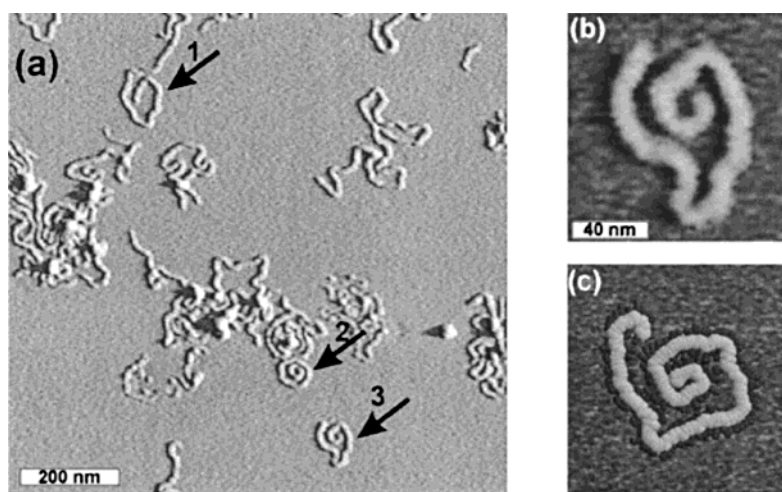


Figure 16. (a) SFM micrograph of PMMA brushes lying flat on the mica surface. The arrows show one of the typically observed conformations—2D helices of tightly wound cylindrical brushes. (b) Zoomed image of molecule 3 in part a. (c) Typical snapshot of the simulated 2d bottle-brush structure consisting of the 128-segment main chain and the 4-segment side chains grafted at $\sigma = 1$ and $\varphi = 0.1$.

sorbed side chains that leads to the extension of the whole brush molecule. Hence, the conformation and

the persistence length must depend on the grafting density and the fractions of the adsorbed and de-

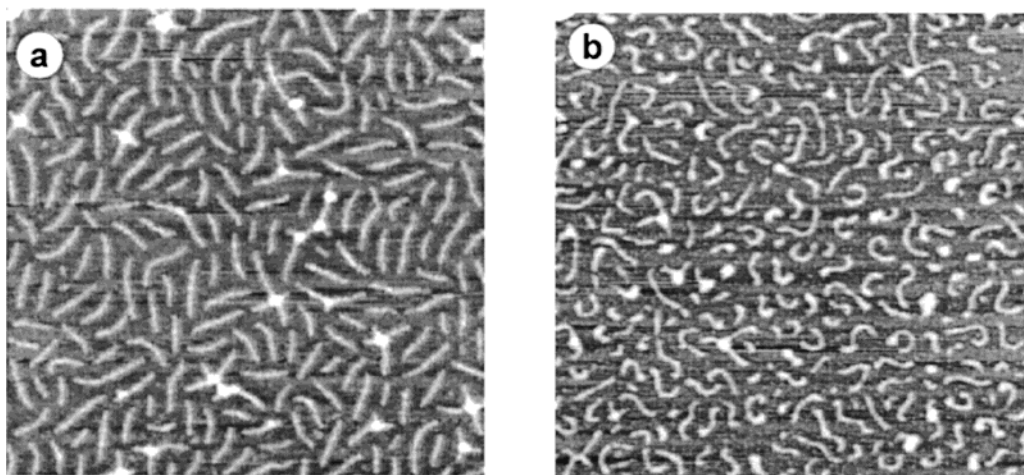


Figure 17. SF micrograph of a condensed film of poly(*n*-butylacrylate) brushes, DP_{side chain} = 60: (a) transferred from water onto mica and (b) after annealing at 120 °C for 48 h.

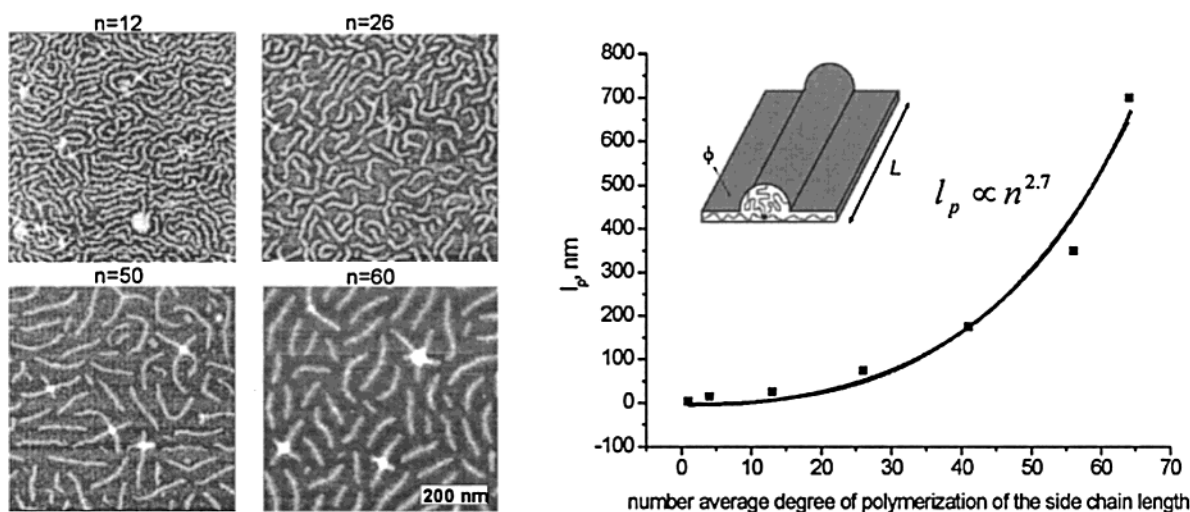


Figure 18. (Left) SFM images of poly(*n*-butylacrylate) brushes with varying degree of polymerization, *n*, of the poly(*n*-butylacrylate) side chains on mica (spin cast samples). (Right) Persistence length of a molecular brush as a function of the side chain length *n*. The continuous line describes the power function $l_p \propto n^{2.7}$ and the points experimental values from SFM.¹⁶⁷

sorbed side chains. While tightly adsorbed side chains favor extension of the backbone, desorbed side chains favor the coiling process.

The dependence of the persistence length l_p on the fraction of the adsorbed side chains Θ has been derived from scaling analysis¹⁶⁸

$$l_p \cong \left(\frac{\phi}{x}\right)^5 n^3 + \left(\frac{1-\phi}{x}\right)^3 n \quad (6)$$

where $x = L/(a \cdot N)$ denotes the degree of longitudinal contraction which denotes the effective grafting density.

The degree of contraction was evaluated by minimization of the free energy of the adsorbed brush. Three contributions were considered: the elastic energy of the main and side chains, the interfacial energy, and the mixing entropy between adsorbed and desorbed chains.¹⁶⁸ The persistence length varies with the side chain length with a cubic power dependence $l_p \cong n^3$ in the strong adsorption regime ($\phi, x \approx 1$) and with a square dependence $l_p \cong n^2$ in the weak adsorption regime ($\phi \approx 0, x \cong n^{-1/3}$). The

dependence of l_p on the length of the side chains can be described by a power function n^α with α varying between 2 and 3 (see Figure 18, right).

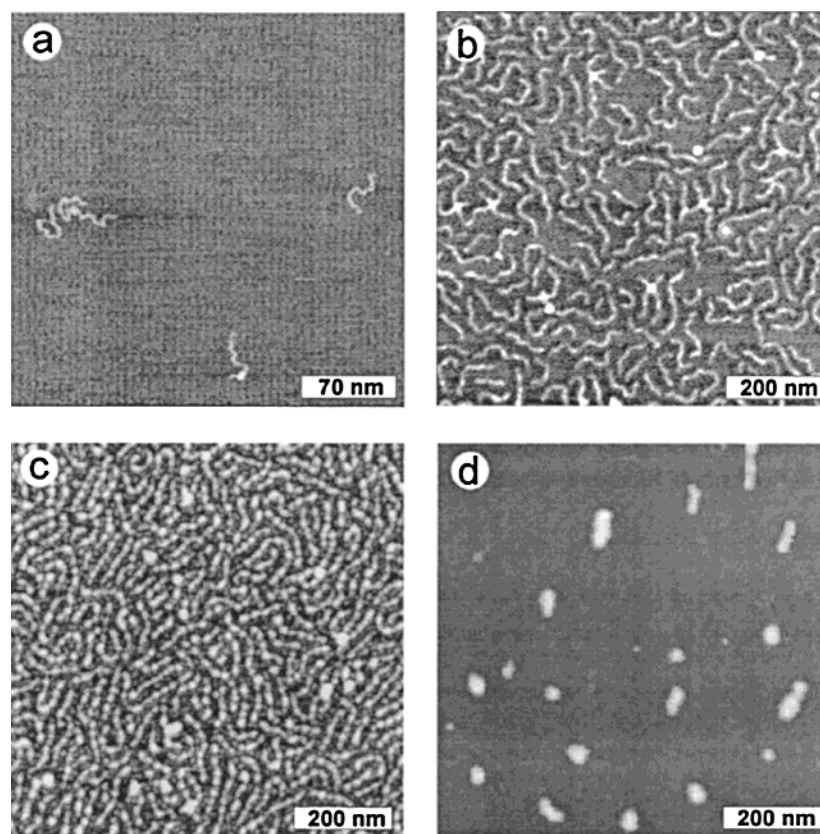
The theoretical analysis has been verified experimentally. The SFM images in Figure 18 depict the contour of four poly(*n*-butylacrylate) brushes differing in the degree of polymerization of the poly(*n*-butylacrylate) side chains. All four molecules were prepared by grafting from the same macroinitiator sample. Clearly, the extension and straightening of the molecules improved with the side chain length. The diagram in Figure 18 (right) gives a fit of the n^α dependency to experimental values. The resulting exponent $\alpha = 2.7 \pm 0.2$ is indicative of a relatively large fraction of adsorbed side chains as expected for strong interaction between the polar acrylates and the polar mica surface.

Because the adsorption of the side chains is such a strong factor in controlling the macromolecular conformation, not only the length of side chains but also their composition is of great importance. This can be demonstrated by comparing the structures for the brush molecules with poly(*n*-butylacrylate) side

Table 4. Molecular Characterization of Brush Molecules with Poly(styrene)-*block*-poly(*n*-butylacrylate) Side Chains Prepared by ATRP¹⁶⁹

polymer	$M_w/10^6$ ^a	M_w/M_n	DP _{backb} ^b	DP _{core} /DP _{shell} ^c	I_m ^d
pBPfEM	0.14	1.16	514		
pBPfEM- <i>g</i> -p <i>n</i> BuA	1.18	1.22	514	15	0.22 ± 0.01
pBPfEM- <i>g</i> -(p <i>n</i> BuA- <i>b</i> -pS)	1.85	1.24	514	15/9	0.20 ± 0.01
pBPfEM- <i>g</i> -(pS- <i>b</i> -p <i>n</i> BuA)	2.49	1.26	514	27/9	0.16

^a THF, MALLS-detector. ^b Degree of polymerization of the backbone. ^c Degree of polymerization of the side chain blocks. ^d Monomer length was calculated as $I_m = L_n/DP_n$, where DP_n = 514 is the number-average degree of polymerization of the main chain.

**Figure 19.** AFM micrographs of four different polymers adsorbed on mica: (a) single molecules of macroinitiator pBPfEM, (b) monolayer of homopolymer pBPfEM-*g*-p*n*BuA brush, (c) monolayer of pBPfEM-*g*-(p*n*BuA-*block*-pS) brush, and (d) single molecules of pBPfEM-*g*-(pS-*block*-p*n*BuA) brush.¹⁶⁹

chains and poly(styrene)-*block*-poly(*n*-butylacrylate) side chains, respectively. While the *n*-butylacrylate units interact strongly with a polar substrate like mica, there is a much weaker adsorption of the styrene units and correspondingly of a polystyrene brush.¹⁶⁹ Diblock side chains offer the possibility to distinguish between adsorption effects of the inner polymer segment, adjacent to the backbone, and the outer side chain tail.

Brushes with diblock side chains have been prepared by the same concept as illustrated in Figure 13. In this case either a polystyrene block or a poly(*n*-butylacrylate) block was grafted first by atom transfer polymerization, ATRP, on a poly(2-bromopropanoyl ethyl methacrylate), pBPfEM, on which in a second step the other monomer was polymerized as the second block.¹⁶⁹ Table 4 summarizes the molecular structure of the corresponding polymers, i.e., (i) the macroinitiator or mere backbone molecule (pBPfEM) from which (ii) a brush with *p**n*BuA homopolymer side chains (pBPfEM-*g*-p*n*BuA), (iii) a

brush with an inner *p**n*BuA and an outer polystyrene block (pBPfEM-*g*-(p*n*BuA-*b*-PS)), and (iv) the inverse structure with an inner polystyrene and an outer *p**n*BuA block (pBPfEM-*g*-(pS-*b*-p*n*BuA)) have been prepared. Because all molecules have been prepared from the same macroinitiator, they have the same length, DP_{backbone} = 514. Due to the consequential addition of the blocks, the side chains vary in length.

Figure 19 shows SFM images of the four polymers that have been deposited by spin casting from THF solution on freshly cleaved mica. In each case, single molecules are resolved lying flat on the substrate. One clearly recognizes distinct differences in the 2D conformation, which can be attributed to the different adsorption behavior of the side chains. The images allowed one to measure the length of the macro-molecules and to evaluate the contraction of the backbone relative to the contour length of the fully extended main chain.

The length of the brush molecules per monomer unit of the backbone, I_m , was evaluated from the

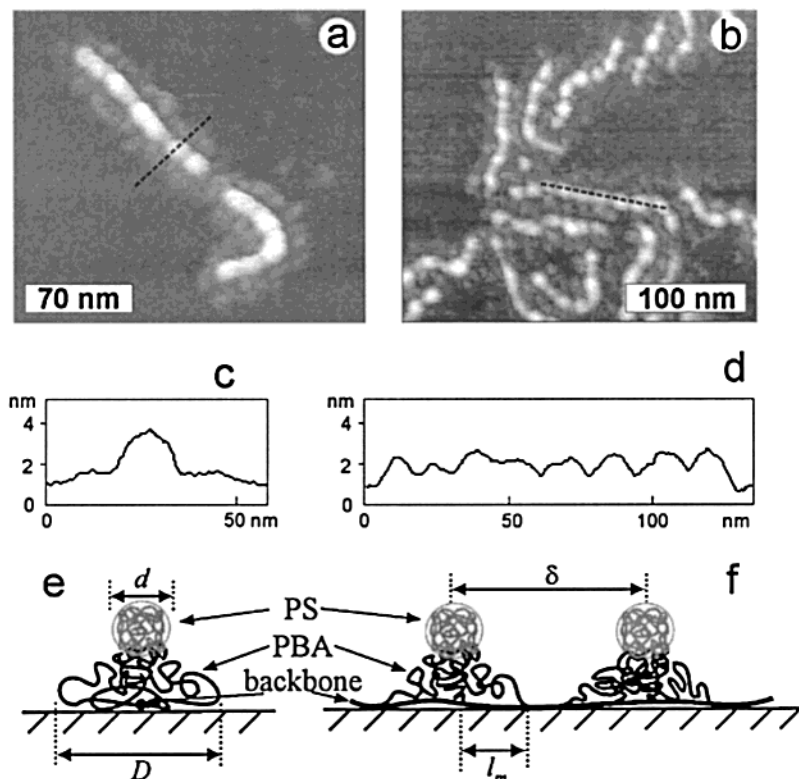


Figure 20. SFM micrographs of single molecules of pBPEM-*graft*-(*pnBuA*-*block*-pS) brushes. The cross sectional profiles (c and d) were drawn perpendicular and parallel to the molecular contour along the dotted lines in a and b, respectively. The scheme explains the necklace morphology upon looking at the molecule from the edge (e) and from the side (f).

images and compared to $l_{\max} = 0.25$ nm for all-trans conformation of an aliphatic chain (Table 4). For the *pnBuA* brush, the length $l_m = 0.22$ nm indicates almost complete stretching of the backbone as shown before (Figure 14, Table 3). The *pnBuA*-*b*-pS brushes with a *pnBuA* core and a pS shell demonstrated similar extension to $l_m = 0.20$ nm. In contrast, a significantly shorter monomer length $l_m = 0.16$ nm, was determined for the inverted structure, i.e., pS-*b*-*pnBuA* with a pS core and a *pnBuA* shell. The axial contraction is consistent with the more globular conformation of the coiled up molecule morphology of the brush molecules in Figure 19d compared to those in Figure 19b,c. As might be expected, the stretching and straightening of the brush molecules are predominantly controlled by the adsorption of the side chain segments near the backbone.

The extended block-copolymer brush in Figure 19c exhibited well defined periodic undulations in thickness. This is seen in further detail in the enlarged images in Figure 20a,b. A thin corona of the tightly adsorbed chain segments is depicted surrounding the undulated backbone of the single molecule of *pnBuA*-*b*-pS in Figure 20a. The cross-sectional profiles in Figure 20d,c were recorded along the molecular backbone and perpendicular to it, respectively. After correction for the radius ($R \sim 8$ nm), the diameter of the globuli forming the necklace-like string and their separation was determined from the image to be $d = 5 \pm 1$ nm and $\delta = 15 \pm 2$ nm, respectively.

A tentative interpretation of the undulations is presented in Figure 20e,f: In contrast to the *pnBA* chains that adsorb flatly, the pS tails in the block-copolymer brushes tend to aggregate to clusters. The

driving force might be found in entropically favorable coiling and in reduced unfavorable contacts between the pS and *pnBuA* blocks as well as between pS and air. While the PS segments form clusters, the *pnBuA* chain fragments remain tightly adsorbed on the substrate. This interpretation is consistent with the intermolecular distances D measured in Figure 20b,c.

3. Manipulated Conformational Transitions of Adsorbed Macromolecules

Conformational transitions and the corresponding stimuli response of macromolecules provide fundamental means for the molecular assembly and function of biological systems.¹⁻⁷ Establishing a likewise control factor in the field of synthetic macromolecules is recognized as a major challenge in nanotechnology.

According to theoretical considerations, the transition between the state of an expanded coil and a compact globule can be discrete, depending on the nature of the interaction and the chain flexibility.¹⁷⁰ Equilibrium coexistence of two conformations of single macromolecules as an unambiguous criterion for a first-order transition¹⁷¹⁻¹⁷⁴ has been clearly observed only in the case of relatively large DNA molecules.¹⁷⁴ However, the peculiar branching topology in dendrimers, block-copolymer micelles, and cylindrical brushes provides a unique means to introduce the competitive interactions necessary for a conformational transition.^{168,175-177} In the following it will be shown that coexistence between an extended and a globular conformation can occur in the case of poly(*n*-butyl acrylate) brush molecules¹⁶⁸ and be visualized in detailed resolution on a significantly smaller length scale than possible in the case of DNA.

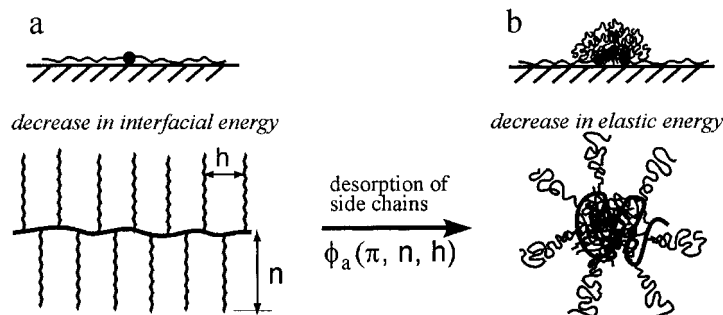


Figure 21. Conformations of cylindrical brushes upon adsorption on a surface: (a) extended chain, (b) globule.

Table 5. Molecular Characterization of the PBPEM Macroinitiators and the Corresponding PBA Brushes by Multiangle Laser Light Scattering Size Exclusion Chromatography (MALLS-SEC) and Static Light Scattering (SLS)¹⁶⁸

polymer	macroinitiator			brush		
	M_w , ^a g/mol	M_w/M_n	N ^b	M_w , ^c g/mol	M_w/M_n ^d	n_{LS} ^e
A	2.2×10^5	1.3	641	4.6×10^6	1.1	46
B	1.6×10^5	1.3	453	1.6×10^6	1.2	20
C	1.8×10^5	1.4	490	1.4×10^6	1.3	15

^a By MALLS-SEC using $dn/dc=0.084$ (error bar 5%). ^b Number-average degree of polymerization calculated as $N = M_w/M_0$, where $M_0 = 265$ g/mol – molecular weight of the monomer unit of pBPPEM. ^c By SLS using the refractive-index increment $dn/dc = 0.068$. ^d Polydispersity from MALLS-SEC. ^e The number-average degree of polymerization of the side chains was determined as $n_{LS} = (M_n - M_0)/m$, where $m = 128$ g/mol – molecular weight of BA and M_n = number-average molecular weight of the PBA brush measured by MALLS-SEC and SLS.

As discussed above, the conformation of molecular brushes at an interface is determined by the interaction of the side chains with the substrate and entropic flexibility of both the side chain and the flexible backbone. The stretched backbone conformation of pnBA brushes depicted in Figures 13, 14, 17, and 18 is enabled by a large number of energetically favorable surface contacts. One can envision a transition to a globular conformation if the interaction strength is reduced and coiling becomes entropically favored at the expense of the surface contacts. Since the energy and the entropy contribution vary differently with respect to contact area and interaction strength, the brushes can undergo a transition at a critical interaction strength at which the free energies of the stretched and collapsed state become equal. Such a transition may occur upon changing thermodynamic variables, e.g. solvent quality and temperature, or under the effect of an external field. Thus, instead of variation of the interfacial energies, the number of surface contacts available per molecule or side chain can be altered by reducing or expanding the surface area per molecule as done experimentally on a Langmuir trough. In this case the free energies of the extended and collapsed state become equal at a critical surface pressure, at which point the brushes can undergo a transition. The concept is schematically depicted in Figure 21 and has been realized in experiment with pnBA brush molecules.¹⁶⁸

Table 5 lists the molecular structure parameters of three different pnBA brush molecules basically differing in the length of the side chains, which were

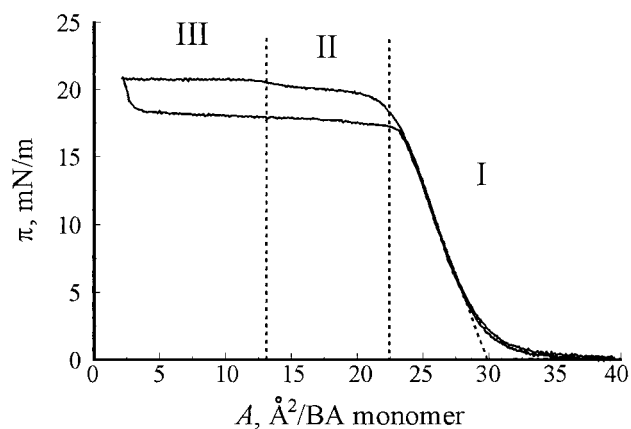


Figure 22. Langmuir isotherm for the compression of a monolayer of poly(*n*-butyl acrylate) brush molecules with the degree of polymerization of the side chains $n = 46$.¹⁶⁸

determined by size exclusion chromatography and light scattering in dilute solution.

Owing to the amphiphilic nature of *n*-butyl acrylate groups, the pnBA brushes spread on a water surface. Figure 22 shows a π - A isotherm (surface pressure versus monolayer area per BA residue) for polymer A with the longest side chains. Corresponding to the low glass transition temperature, $T_g = -54$ °C, compression of the PBA brushes was fully reversible as expected for equilibrium spreading. The pressure onset occurred at about 35 \AA^2 and rose until a critical area of 22 \AA^2 , at which the pressure leveled off at 19.5 mN/m . The plateau between 22 and 13 \AA^2 was followed by a second plateau with a distinct increase in pressure from 19.5 to 21 mN/m . The linear extrapolation of the isotherm to zero pressure gave the area $a_0 = 28 \pm 1 \text{ \AA}^2$, which is consistent with the monomer area of 29.3 \AA^2 measured for linear PBA. The values indicate that practically all BA monomer units are in contact with the water surface, whereby the butyl tails are oriented toward air perpendicular to the surface. The plateau between 22 and 13 \AA^2 is remarkable and indicates a structural transition within the monofilm.

The molecular structures at the different stages of compression were visualized by SFM on samples that were transferred onto a mica substrate while the pressure was kept constant. Figure 23 shows such a series of SFM micrographs obtained at different compression.

In each micrograph, the brush molecules were clearly resolved individually. At areas above 22 \AA^2

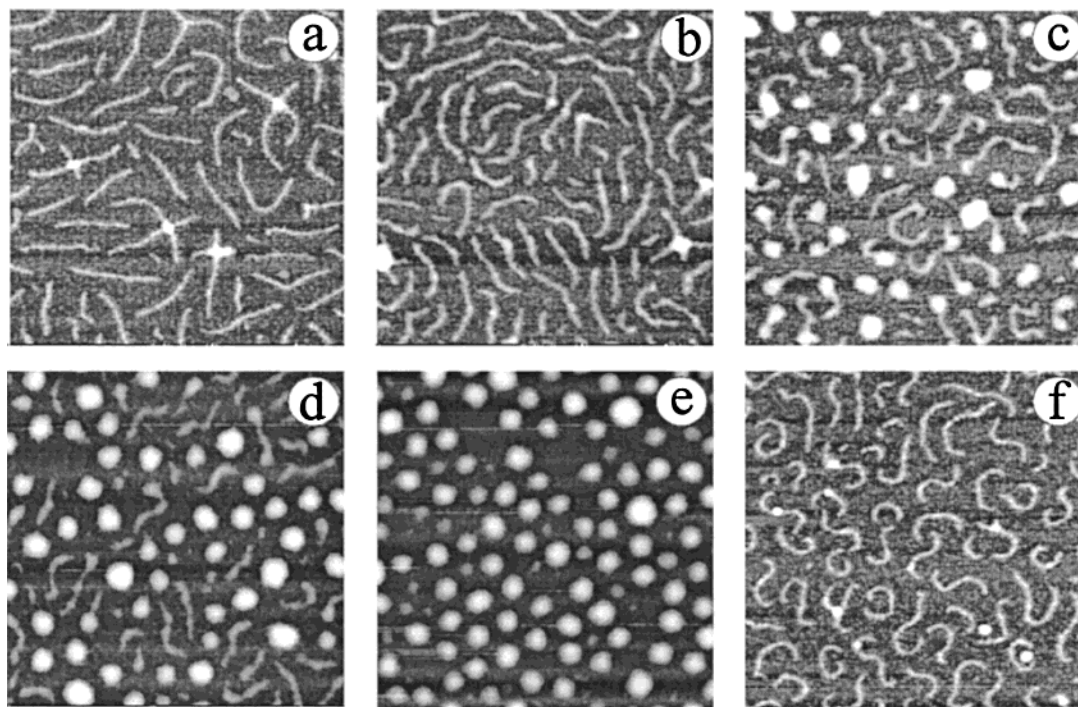


Figure 23. SFM micrographs of monolayers of pnBA brushes (sample A in Table 5) transferred on mica at different degrees of compression: (a) 30 \AA^2 , (b) 23 \AA^2 , (c) 21 \AA^2 , (d) 17 \AA^2 , (e) 13 \AA^2 , (f) 30 \AA^2 (after expansion).¹⁶⁸

the molecular cylinders retained their stretched conformation but became packed increasingly dense. The wormlike entities in Figure 23a, b mark the contour of the backbone and represent the extended brush molecules as depicted in Figure 21a. The space between is occupied by the fraction of the side chains which are tightly adsorbed. The fundamental collapse of the wormlike structure predicted above was observed in the transition zone between 22 and 13 \AA^2 . The SFM images in Figure 23c–e demonstrate that the molecules became more flexible and coiled, while at the same time a significant decrease in length is observed. The round spots in Figure 23c–e are assigned to single molecules which collapsed to a pancake-like or nearly globular structure as illustrated in Figure 21b. As the number of chains in Figure 23a and number of globuli in Figure 23e was fairly equal, it was concluded that the molecular collapse is accompanied by desorption of the side chains from the water surface and is occurring in first as an intramolecular collapse and only in a later stage by intermolecular aggregation as the collapsed molecules get piled up.

The observed conformational transition was analyzed theoretically assuming partial desorption of the side chains under compression, i.e., upon variation of the spreading parameter.¹⁶⁸ The total free energy $F = F_{\text{el}}^{2D} + F_{\text{el}}^{8D} + F_s + F_{\text{mix}}$ (F_{el} = elastic contribution to the free energy, F_s = surface energy of the brush, F_{mix} = mixing entropy of the side chains) was minimized with respect to two independent variables: the fraction of adsorbed 2D chains, ϕ_a , and the relative contour length of the brush, L/aN . Above a critical length of the side chains, the free energy has two minima, i.e., (i) the extended brush with a large fraction of adsorbed side chains and (ii) the collapsed globuli with a smaller fraction of adsorbed side

chains. Since the free energies of these two conformations depend in an opposite way on the interaction strength, the variation of either the area available per molecule A or the spreading parameter $S = \gamma_1 - \gamma_{12} - \gamma_2$ can cause a discontinuous first-order transition from one state to the other. The results of the evaluation are summarized in Figure 24, where the fraction of adsorbed side chain units is plotted against the surface pressure and the critical surface pressure S_c is plotted against the inverse length of the side chains $1/n$.

Switching between two distinct conformations has been observed also for spherical branched particles such as block copolymer micelles. Block copolymers of poly(styrene) and poly(*N*-alkyl-4-vinylpyridinium iodide) were aggregated to micelles with a polystyrene core and a poly(*N*-alkylpyridinium iodide) corona. These micelles could be spread on water from a solution in CHCl_3 and compressed to a monofilm¹⁷⁰ (Figure 25b). Due to the amphiphilicity of the *N*-alkylpyridinium iodides, the poly(pyridinium iodide) block gets adsorbed in a 2D conformation with the *n*-alkyl groups pointing to the air. Upon lateral compression of the condensed monofilm of surface micelles, also in this case, a distinct phase transition was observed upon lateral compression as the corona chains got desorbed from the water/air interface (Figure 25a). The transition was particularly pronounced in the case of longer chains, i.e., *n*-octyl pyridinium groups. The cooperative desorption/collapse is consistent with recent X-ray reflectivity data.¹⁷⁸

4. Motility of Molecules

So far we have encountered two particular features of the conformation of brush molecules adsorbed on

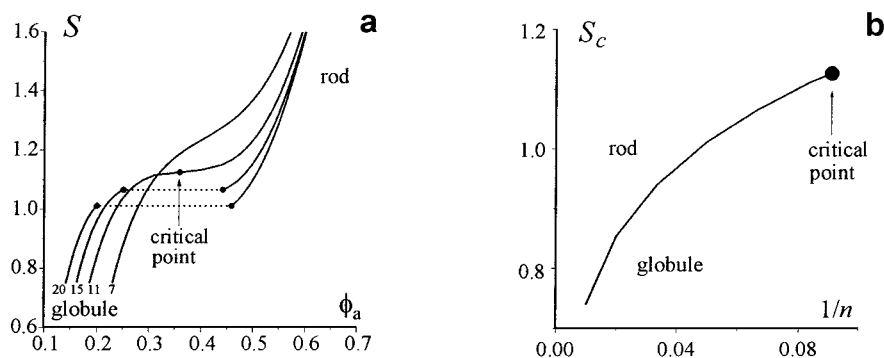


Figure 24. Phase transition from the extended coil to a globule state as found by scaling analysis. The transition is caused by lowering the surface pressure below a certain critical value S_c at which the fraction of adsorbed monomers $\phi_a = N_{2D}/N$ undergoes discrete changes (a). Hereby, the S_c depends critically on the side chain length (b).¹⁶⁸

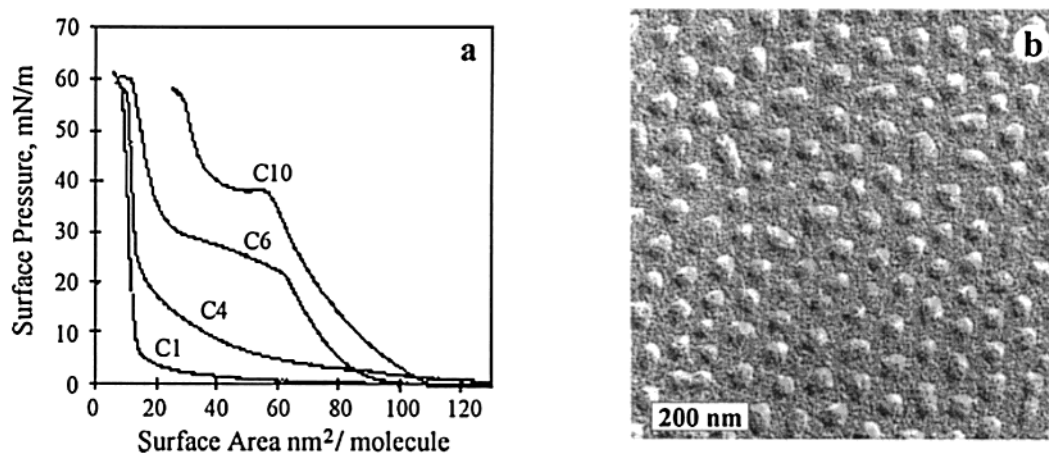


Figure 25. Surface pressure–area/molecule isotherms of Langmuir films (a) of $(PS)_{260}(RPVP^+I^-)_{240}$, where the P4VP block was quaternized with different n -alkyl iodides $R = C_1, C_4, C_6, C_{10}$. Metal-shadowed TEM micrographs (b) of the LB films of $P(S_{260}-b-VP_{71}/C_{10}I)$ deposited on a carbon-coated surface at 2 mN/m from a pure water surface.¹⁷⁸

a flat surface. These are (i) the observation that the brush gets stretched as the side chains get confined to a 2D layer upon adsorption and (ii) the observation that the 2D brush winds up if the side chains get distributed unevenly between the two faces of the backbone. Both effects provide an intriguing access to stimulated molecular action. For example, if we assume a tightly adsorbed brush molecule with two different side chains whose mutual interaction parameter can be switched from attractive to repulsive by an external field, such a molecule can undergo a stimulated transition from an extended (even distribution of side chains) to a curled conformation (uneven distribution of the side chains). Yet, we cannot propose a realistic concept for such a system. However, a molecular rod–coil actuator appears to be much more feasible based on the experiments summarized in Figures 21–25. Besides the variation of the surface pressure used in the experiment in Figure 22, stimulated adsorption/desorption of a brush molecule can, in principle, be achieved by a number of means, e.g., photoisomerization of suitable groups in the side chains, by mechanical interaction with the tip of a scanning probe microscope, or by changes of the temperature. The latter means have the advantage that isolated molecules can be addressed also in contrast to the isothermal compression of a monofilm.

Ultimately, a stimulated molecular action like the stretch–coiling transition can form a basis for mo-

lecular motility and the development of molecular motors. Complex protein molecules such as kinesin, myosin, and dynein are examples of molecular motors from biology. These molecules can undergo directed movement along cytoskeletal filaments based on coordinated conformational changes which lead to periodic adsorption and detachment of molecular fragments on the filament surface.^{179–183} The movement occurs via a sequence of elementary steps which are driven by ATP hydrolysis,¹⁸⁴ but the steps can take place stochastically and some of them are directed backward.¹⁸⁵ Respectively, two models have been proposed to explain the motion of motor proteins: single-step directed motion and the biased Brownian ratchet model.^{184,185} In the latter case an anisotropic ratchet potential is turned off and on. This way the Brownian motion of a particle can be transformed into a directed motion.¹⁸⁶

In the following we want to discuss, first, experiments on the motility of brush molecules based on stimulated desorption/adsorption. The stimulation is effected by the tip of a scanning force microscope as the molecules are probed. Essential questions are whether this can cause mobility different from Brownian motion but also different from dragging of the molecules. For comparison, we summarize results on the dragged motion of a λ -phage DNA through an entangled solution and the Brownian motion of DNA molecules adsorbed on a fluid lipid membrane.

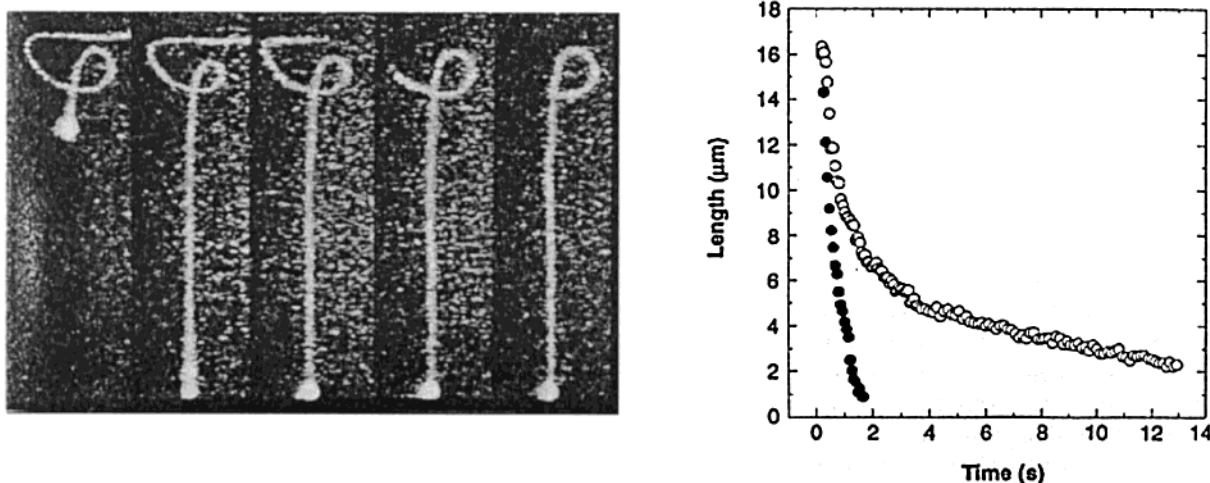


Figure 26. (a) Tiled series of images showing tube deformation and stress recovery in a concentrated polymer solution. The times for images are 0, 0.3, 1.6, 2.3, 3.0 s. (b) Comparison of the relaxation of a 17 nm molecule linearly stretched to full extension at 80 mm/s in (○) concentrated polymer solution and in (●) pure solvent.⁶⁵

4.1. Dragged Motion of λ -DNA

Recent developments of optical trapping and fluorescent labeling techniques allowed detection and probing of single molecules.^{65,142} To test the dragged motion and relaxation of a single macromolecule, the end of a fluorescently labeled λ -phage DNA was chemically linked to a latex bead and dragged by means of optical tweezers through an entangled solution of nonlabeled molecules at velocities from 5 to 100 $\mu\text{m/s}$. As the test chain was pulled or relaxed through the concentrated polymer solution, it closely followed the path of the bead (Figure 26a). The motion through the entanglement network was shown to be much different from the motion in a viscous Newtonian fluid, where the chain moved in a direction perpendicular to its contour. As the bead was rapidly moved away from the loop, tension in the chain increased and the loop was pulled tight. When the bead stopped, the loop recovered to the original size.

4.2. Brownian Motion of Adsorbed λ -Phage DNA

As discussed before for the example in Figure 5, DNA chains are confined to two dimensions but are free to diffuse laterally if they get adsorbed to a fluid lipid membrane. The microscopy experiments of the fluorescence-labeled molecules also allowed direct analysis of the chain dynamics, self-diffusion of the molecules, and conformational relaxation as a function of the chain length.¹⁴⁰ With the exception of a number of molecules that showed anomalous diffusion attributed to surface defects, the overall motion was described by the mean-square displacement linear in time: $\langle |R_{\text{cm}}(t) - R_{\text{cm}}(0)|^2 \rangle = 4Dt$. The diffusion coefficient D_{cm} (center of mass) decreases inversely proportional to the length of the polymer as predicted for the dynamical scaling of the Rouse model, $D_{\text{Rouse}} \sim N^{-1}$, in the absence of hydrodynamic interaction.^{187,188} Fitting of the experimental data yielded $D_{\text{cm}} \sim N^{0.95 \pm 0.06}$ (Figure 27b). Hence, the 2D diffusion is substantially different from DNA three-dimensional self-diffusion in bulk, where long-ranged hydrodynamic interaction plays a dominant role.^{142,189}

One can also analyze the rotational relaxation of the adsorbed molecules.¹⁴⁰ Figure 27a shows a time sequence of a single molecule with an overlay of the unit vector $u(t)$ defined as the direction of the longer principal axis of the gyration tensor. An instantaneous polymer configuration may be described by an ellipse, and therefore, the simplest conformational change is the rotational motion of an ellipse. The time correlation function of $u(t)$ decays exponentially where τ_r denotes the rotational relaxation time, $\langle u(t)u(0) \rangle \propto \exp(-t/\tau_r)$.

As shown in Figure 27c, the rotational relaxation time varies as a power of length, $\tau_r \propto N^\mu$ with $\mu = 2.6 \pm 0.4$. The experimental result is in remarkable agreement with the scaling behavior of the rotational relaxation $\tau_r \propto N^{1+2\nu}$ with $\mu_{\text{theory}} = 2.5$, which follows from the Rouse model and the Flory exponent $\nu = 3/4$.¹⁸⁹

4.3. Stimulated Motion of Monodendron-Jacketed Polymers

The observation that a macromolecular brush gets stretched as the side chains get adsorbed on a flat surface provides a means to stimulate molecular motility by desorption of the brush molecule or a segment of it. If the molecule is in a subsequent period allowed to relax to the adsorbed stretched state it will eventually do a step forward. This is depicted schematically in Figure 28 as a sort of a creep motion. Here, the desorbed state might be characterized as an excited state whose formation requires input of energy. In the case that the structure of the surface and of the molecule favor relaxation into a distinct direction, i.e., in the case of an asymmetric potential, the motion of the molecule can be become directed.

The examples shown in Figures 7, 8, and 11 of the monodendron-jacketed polymers adsorbed on HOPG demonstrated that these macromolecules orient along the main axes of graphite. Thus, relaxation by adsorption according to the scheme in Figure 28 will be directed along these axes, either forward or backward. In particular, if the desorption effects only

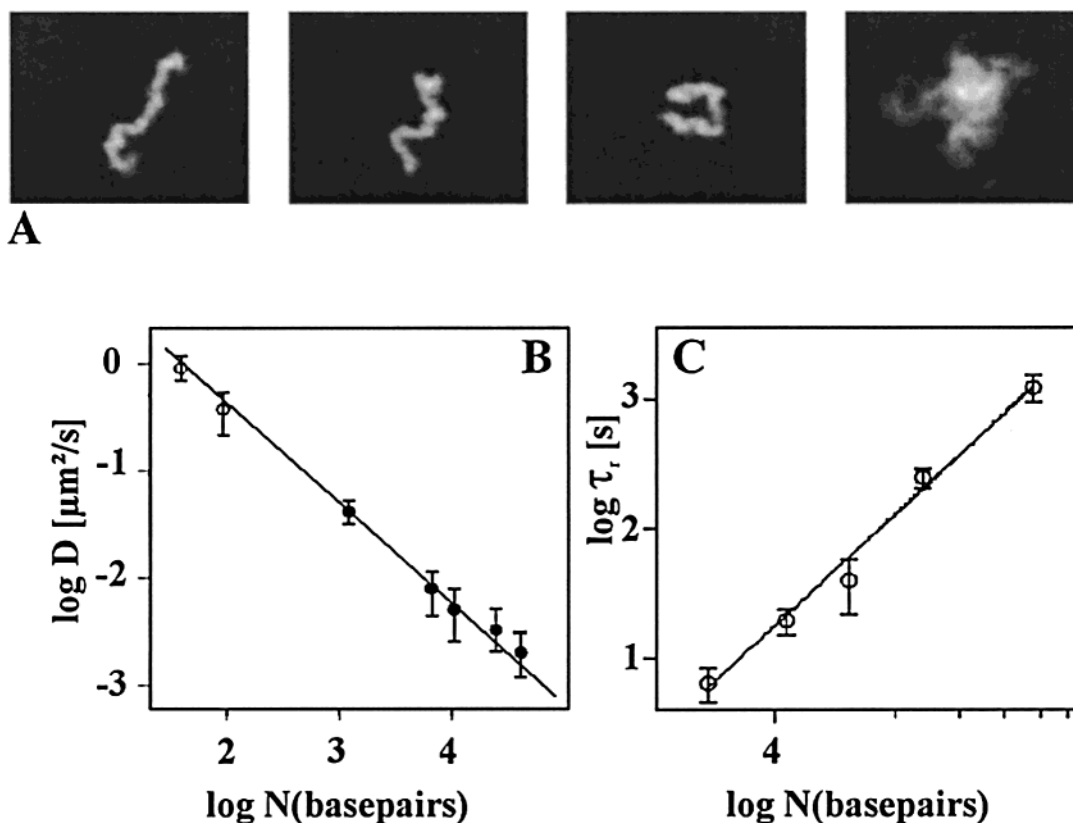


Figure 27. Dynamical scaling of DNA confined to the surface of a supported lipid membrane. (a) Time sequence ($\Delta t = 30$ s) of a DNA molecule diffusing on a cationic lipid membrane. The image on the right depicts an overlay of 16 images: time average yields a smeared fluorescence distribution. (b) Scaling behavior of the self-diffusion coefficient of the center of mass D with the number of base pairs. (c) Scaling behavior of the rotational relaxation time τ_r with the number of base pairs.¹⁴⁰

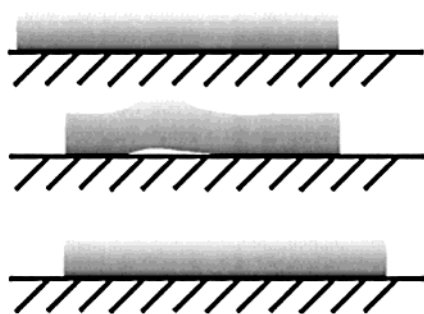


Figure 28. Creep motion by contraction upon desorption and subsequent stretching upon adsorption of an abstract molecular object.

a segment of the molecule as depicted in Figure 28, it will keep some memory of its original orientation toward the substrate and eventually follow this line. The examples of the pnBA brushes in Figures 14 and 23 have demonstrated that the transition between the stretched and the coiled conformation is particularly pronounced for comb or brush molecules with long side chains that adsorb tightly. Combination of both structural features might, thus, be expected to allow a creeping step in a preferred direction.

Figure 29 depicts the molecular structure of a polymethacrylate where each monomer unit has been substituted by a tris(*p*-undecyloxybenzyloxy)benzoate unit via a tetraethylenglycol spacer. From the molecules, which we have been able to study so far, this is the structure that suits the model best. For the bulk structure a transition from a low-temperature

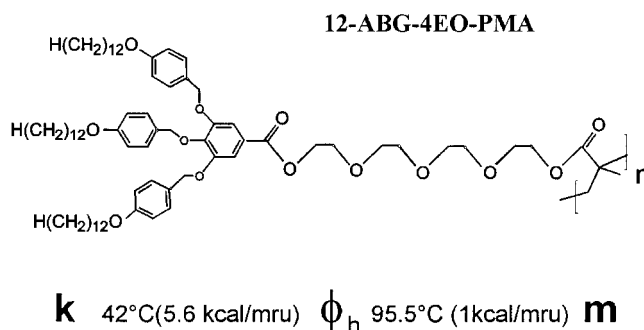


Figure 29. Chemical structure and phase transitions of 12-ABG-4EO-PMA.

crystal phase to a hexagonal columnar state ϕ_h has been found at 42 °C. Axial extension by ca. 7% has been found by X-ray upon transition from the crystalline to the hexagonal phase.¹⁶⁰

Similar to the other monodendron-jacketed polymers discussed above, also 12-ABG-4EO-PMA orders along the main axes of HOPG upon adsorption. Figure 30 shows on the right side a scanning force micrograph with a number of single molecules that have been deposited from dilute solution on HOPG.

A scanning force microscope equipped with a temperature cell enabled in-situ monitoring of the motion of the single molecules and small molecular clusters at elevated temperature.¹⁹⁰ The diagram on the left side of Figure 30 depicts the traces of the molecules that were recorded by imaging the sample within intervals of 4 h 20 min over a period of 12 h at 35

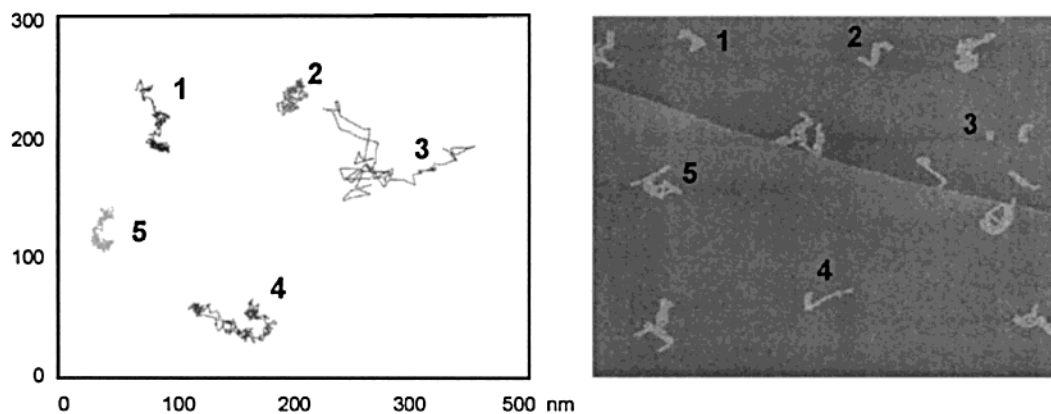


Figure 30. Random walk of single molecules as observed in situ by tapping-mode SFM at 35 °C.

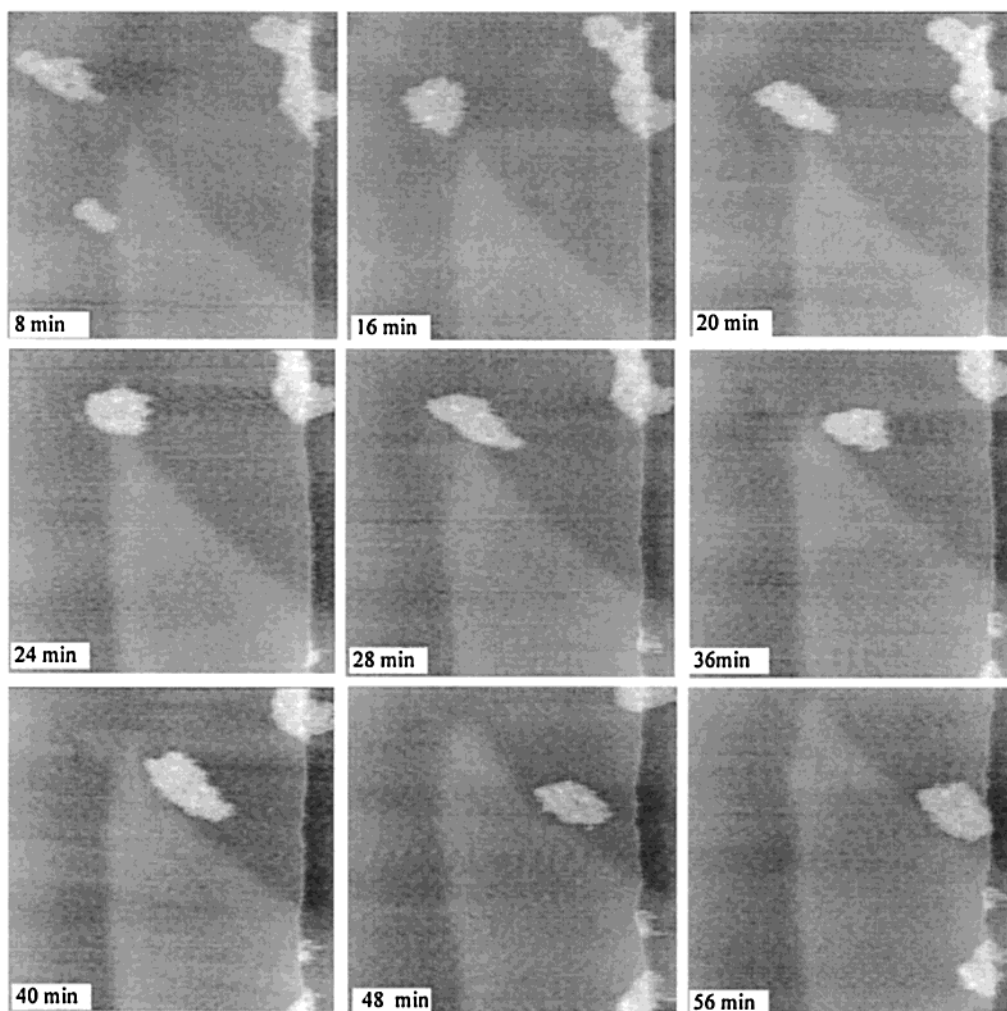


Figure 31. Persistent motion of a small cluster of five 14ABG-4EO-PMA molecules along the terrace of HOPG at 40 °C. The width of each image corresponds to 486 nm.

°C. The motion patterns are consistent with a random walk, i.e., a mean square displacement linear in time, $\langle \Delta R^2 \rangle = 4Dt$. Evaluation of the time dependencies yielded diffusion coefficients for each molecule, e.g., for the five molecules/clusters marked by the numbers in Figure 30, the following diffusion coefficients were obtained: $D(1) = 0.01 \text{ nm}^2/\text{s}$; $D(2) = 0.09 \text{ nm}^2/\text{s}$; $D(3) = 1.7 \text{ nm}^2/\text{s}$; $D(4) = 0.04 \text{ nm}^2/\text{s}$; $D(5) = 0.06 \text{ nm}^2/\text{s}$. Within the accuracy of the evaluation procedure ($\pm 0.02 \text{ nm}^2/\text{s}$) the following trends could be deduced from the observation of more than 100 mol-

ecules: (i) The diffusion becomes faster upon raising the temperature; (ii) smaller molecules or clusters of a few molecules exhibit a higher mobility than larger ones, (iii) within certain time intervals the molecules appear to be tight to yet unknown obstacles on the substrate, so that they can only sway around, (iv) some molecules move along a distinct line that is probably a defect in the surface structure of HOPG, e.g., a grain boundary, (v) molecules can show an increased mobility characterized by a diffusion coefficient that is 10–20 times larger than the average

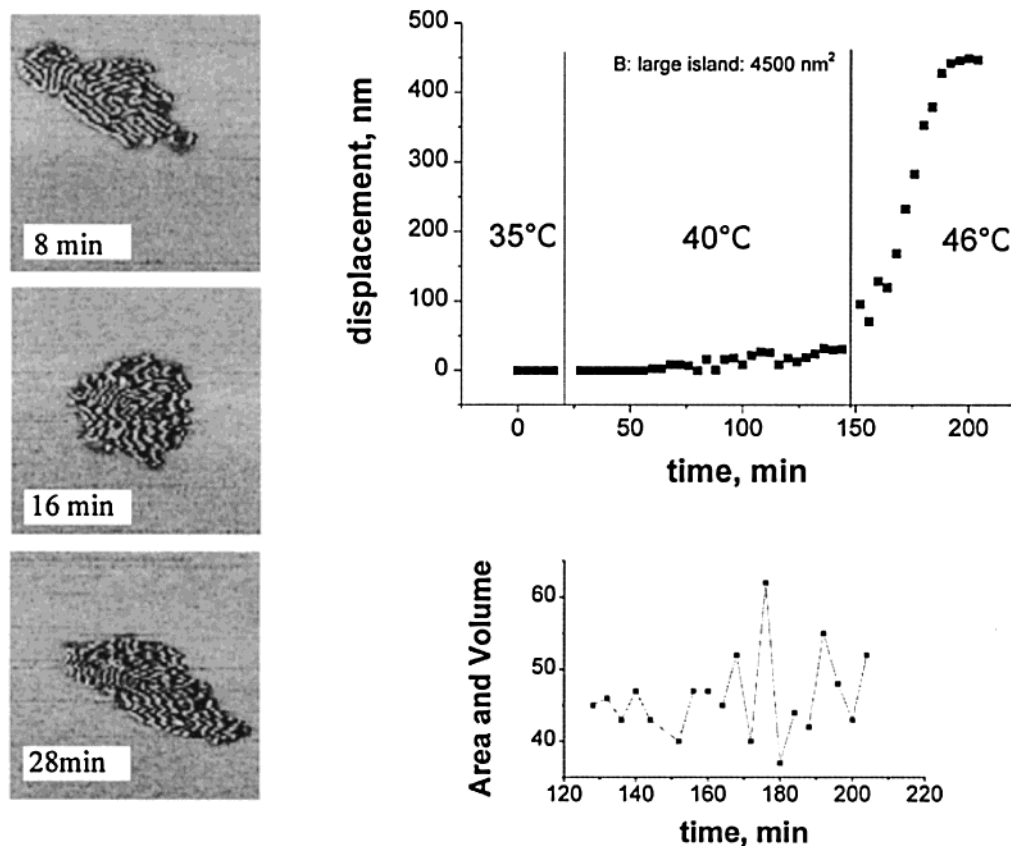


Figure 32. Time variation of (a) the displacement and (b) cluster size during its motion on HOPG at 46 °C. The in-situ-measured SFM micrographs depict momentary shape and inner structure of the cluster including packing of the molecules at different intervals after the motion started—8, 16, and 28 min.

value (see 3 in Figure 30). The two latter observations can be seen as an indication that the motion can be guided by the substrate and eventually switch for some time to a higher “gear”. This, however, will require a mechanism other than Brownian motion.

That the motion can, indeed, change significantly was observed for larger clusters of a number of molecules at further elevated temperature. Figure 31 shows a series of six micrographs captured during a time period of 1 h at a temperature of 46 °C. One can clearly see that a small cluster consisting of ca. five molecules moves steadily along the terrace of the HOPG substrate. The motion started at 46 °C and continued for 60 min until the cluster got trapped in the gusset formed by two terraces on the HOPG surface.

Besides the remarkable directionality of the motion, the images demonstrate also a periodic variation of the cluster from an elongated to a circular shape. The diagrams in Figure 32 depict the time dependence of the displacement and the cluster size. Until the cluster was finally trapped, the speed remained fairly constant, as can be seen from the constant slope in Figure 32a. The oscillatory variation of the cluster area and shape is shown in the graph in Figure 32b.

The motion can be explained according to the coarse model depicted in Figure 28. Although the actual cause of the motility remains unknown, local perturbations of the molecular structure are believed to be caused by the mechanical contact with the scanning tip.¹⁹⁰ Clearly, the SFM images shown in Figure 32 demonstrate an alternation from a more-

ordered to a less-ordered structure and vice versa. Systematic variation of the tapping parameters have demonstrated further that the well-ordered structure formed after relaxation can be disordered by the interaction with the probing tip. This occurs without direct displacement of the cluster of molecules. A quantitative and more detailed study of this phenomenon is still in progress.

5. Synopsis

The examples discussed above demonstrate that the complex architecture of hyperbranched and brush-like macromolecules can lead to properties and characteristics in the molecular conformation that are not known for linear macromolecules. Competing effects at different length scales result in very peculiar ordering and transformations. The not yet proven model of a molecular motion demonstrates how the interplay of the different interactions and elastic forces might be exploited for creating a molecular walker. While on one hand the adsorption of the molecules on a flat surface is necessary to perform SFM studies on macromolecules with molecular resolution, the surface interaction also causes, on the other hand, a perturbation that can be manipulated in very specific ways. Here we proposed that the localized interaction of the probing tip of a scanning probe microscope can be exploited to stimulate macromolecules to move according to their particular relaxation modes. Other means to apply an external field can be considered such as photo-

chemical transformations or varying electrical or magnetic fields. This way it will be possible to develop more perfected approaches to design sophisticated functional systems based on hyperbranched molecules.

6. Acknowledgment

The authors are indebted to Profs. Oleg Borisov, Alexei R. Khokhlov, Krzysztof Matyjaszewski, Aziz Muzafarov, Virgil Percec, Igor Potemkin, and Manfred Schmidt for a long-standing fruitful cooperation. We also acknowledge the experimental help of Ahmed Mourran, Svetlana Prokhorova, David Shirvanians, and Bernd Tartsch. Financial support was provided by the Deutsche Forschungsgemeinschaft (SH 46/2-1; GRK-328: "Molecular organization and dynamics on surfaces and interfaces", SFB 569 "Hierarchic Structure Formation and Functions of Organic-Inorganic Nanosystems").

7. References

- Stayton, P. S.; Shimoboji, T.; Long, C.; Chilkoti, A.; Chen, G.; Harris, J. M.; Hoffman, A. S. *Nature* **1995**, *378*, 472.
- Mao, C.; Sun, W.; Shen, Z.; Seeman, N. *Nature* **1999**, *397*, 144.
- Montemagno, C.; Bachand, G.; Stelick, S.; Bachand, M. *Nanotechnology* **1999**, *19*, 225.
- Noji, H.; Yashuda, R.; Yoshida, M.; Kinosita, K., Jr. *Nature* **1997**, *386*, 299.
- Dennis, J. R.; Howard, J.; Vogel, V. *Nanotechnology* **1999**, *19*, 232.
- Lu, H.; Schulten, K. *Biophys. J.* **2000**, *79*, 51.
- Jelezko, F.; Tietz, C.; Gerke, U.; Bittl, R.; Wrachtrup, J. *Single Mol.* **2000**, *1*, 184.
- Holerca, M. N.; Percec, V. *Biomacromolecules* **2000**, *1*, 6.
- Stapert, H. R.; Nishiyama, N.; Jiang, D.-L.; Aida, T.; Kataoka, K. *Langmuir* **2000**, *16*, 8182.
- Davis, A. P. *Nature* **1999**, *401*, 120.
- Kelly, T. R.; de Silva, H.; Silva, R. A. *Nature* **1999**, *401*, 150.
- Koumura, N.; Zijlstra, R. W.; van Delden, R. A.; Harada, N.; Feringa, B. L. *Nature* **1999**, *401*, 152.
- Collier, C. P.; Wong, E. W.; Belohradský, M.; Raymo, F. M.; Stoddart, J. F.; Kuekes, P. J.; Williams, R. S.; Heath, J. R. *Science* **1999**, *285*, 391.
- Kwon, I. C.; Bae, Y. H.; Kim, S. W. *Nature* **1991**, *354*, 291.
- Antonietti, M.; Basten, R.; Lohmann, S. *Macromol. Chem. Phys.* **1995**, *196*, 441.
- Baumann, F.; Deubzer, B.; Geck, M.; Dauth, J.; Sheiko, S. S.; Schmidt, M. *Adv. Mater.* **1997**, *9*, 955.
- Senff, H.; Richtering, W.; Norhausen, Ch.; Weiss, A.; Ballauff, M. *Langmuir* **1999**, *15*, 102.
- Dvornic, P. R.; Tomalia, D. A. *Curr. Opin. Colloid Interface Sci.* **1996**, *1*, 221.
- Fréchet, J. M. J.; Henmi, M.; Gitzov, I.; Aoshima, S.; Leduc, M. R.; Grubbs, R. B. *Science* **1995**, *269*, 1080.
- Newkome, G. R.; He, E.; Moorefield, C. N. *Chem. Rev.* **1999**, *99*, 1689.
- Fischer, M.; Vögtle, F. *Angew. Chem., Int. Ed. Engl.* **1999**, *38*, 884.
- Hawker, C. J. *Adv. Polym. Sci.* **1999**, *147*, 113.
- Zeng, F.; Zimmerman, S. C. *Chem. Rev.* **1997**, *97*, 1681.
- Ignat'eva, G. M.; Rebrov, E. A.; Myakushev, V. D.; Chenskaya, T. B.; Muzafarov, A. M. *J. Polym. Sci., Part A* **1997**, *39*, 843.
- Majoral, J. P.; Caminade, A. M. *Top. Curr. Chem.* **1998**, *197*, 79.
- Bosman, A. W.; Jansen, H. M.; Meijer, E. W. *Chem. Rev.* **1999**, *99*, 1665.
- Gauthier, M.; Möller, M. *Macromolecules* **1991**, *24*, 4548.
- Tomaila, D. A.; Hedstrand, D. H.; Ferrito, M. S. *Macromolecules* **1991**, *24*, 1435.
- Jean-Luc, S.; Gnanou, Y. *Macromol. Symp.* **1995**, *95*, 137.
- Gauthier, M.; Tichagwa, L.; Downey, J. S.; Gao, S. *Macromolecules* **1996**, *29*, 519.
- Taton, D.; Cloutet, E.; Gnanou, Y. *Macromol. Chem. Phys.* **1998**, *199*, 2501.
- Wu, J.; Lieser, G.; Wegner, G. *Adv. Mater.* **1996**, *8*, 151.
- Cao, Y.; Smith, P. *Polymer* **1993**, *34*, 3139.
- Ito, K.; Kawaguchi, S. *Adv. Polym. Sci.* **1999**, *142*, 129.
- Tsukahara, Y.; Tsutsumi, K.; Yamashita, Y.; Shimada, S. *Macromolecules* **1990**, *23*, 5201.
- Wintermantel, M.; Gerle, M.; Fischer, K.; Schmidt, M.; Wataoka, I.; Urakawa, H.; Kajiwarra, K.; Tsukahara, Y. *Macromolecules* **1996**, *29*, 978.
- Ruokolainen, J.; Torkkeli, M.; Serimaa, R.; Vahvaselkä, S.; Saariaho, M.; ten Brinke, G. *Macromolecules* **1996**, *29*, 6621.
- Beers, K. L.; Gaynor, S. G.; Matyjaszewski, K.; Sheiko, S. S.; Möller, M. *Macromolecules* **1998**, *31*, 9413.
- Schappacher, M.; Deffieux, A. *Macromolecules* **2000**, *33*, 7371.
- O'Donnell, P. M.; Brzezinska, K.; Wagener, K. B. *Polym. Prepr. (Am. Chem. Soc., Div. Polym. Chem)* **1999**, *40*(2), 138.
- Percec, V.; Ahn, C.-H.; Ungar, G.; Yeardeley, D. J. P.; Möller, M.; Sheiko, S. S. *Nature* **1998**, *161*, 391.
- Percec, V.; Ahn, C.-H.; Cho, W.-D.; Jamieson, A. M.; Kim, J.; Leman, T.; Schmidt, M.; Gerle, M.; Möller, M.; Prokhorova, S. A.; Sheiko, S. S.; Cheng, S. Z. D.; Zhang, A.; Ungar, G.; Yeardeley, D. J. P. *J. Am. Chem. Soc.* **1998**, *120*, 8619.
- Holerca, M. N.; Percec, V. *Biomacromolecules* **2000**, *1*, 6.
- Bo, Z.; Zhang, C.; Severin, I.; Rabe, J. P.; Schlüter, A. D. *Macromolecules* **2000**, *33*, 2688.
- Yin, R.; Zhu, Y.; Tomalia, D. A. *J. Am. Chem. Soc.* **1998**, *120*, 2678.
- Jahromi, S.; Coussens, B.; Meijerink, N.; Braam, A. W. M. *J. Am. Chem. Soc.* **1998**, *120*, 9753.
- Wang, P. W.; Liu, Y. J.; Devadoss, C.; Bharathi, P.; Moore, J. S. *Adv. Mater.* **1996**, *8*, 237.
- Zhao, M.; Crooks, R. M. *Adv. Mater.* **1996**, *11*, 217.
- Albrecht, M.; van Koten, G. *Adv. Mater.* **1996**, *11*, 171.
- Vasilenko, N. G.; Rebrov, E. A.; Muzafarov, A. M.; Esswein, B.; Striegel, B.; Möller, M. *Macromol. Chem. Phys.* **1998**, *199*, 889.
- Leduc, M. R.; Hawker, C. J.; Dao, J.; Frechet, J. M. J. *J. Am. Chem. Soc.* **1996**, *118*, 11111.
- Zimmerman, S. C. *Curr. Opin. Colloid Interface Sci.* **1997**, *2*, 89.
- Cooper, A. J.; Londono, J. D.; Wignall, G.; McClain, J. B.; Samulski, E. T.; Lin, J. S.; Dobrynin, A.; Rubinstein, M.; Burke, A. L. C.; Frechet, J. M. J. *Nature* **1997**, *389*, 368.
- Jansen, J. F. G. A.; de Brabander-van der Berg, E. M. M.; Meijer, E. W. *Science* **1994**, *266*, 1226. Jansen, J. F. G. A.; de Brabander-van der Berg, E. M. M.; Meijer, E. W. *J. Am. Chem. Soc.* **1995**, *117*, 4417. Jansen, J. F. G. A.; de Brabander-van der Berg, E. M. M.; Meijer, E. W. *J. Am. Chem. Soc.* **1996**, *118*, 7398.
- Armut, A.; Vögtle, F.; Decola, L.; Azzellini, G. C.; Balzani, V.; Ramanujam P. S.; Berg R. H. *Chem. Eur. J.* **1996**, *4*, 699.
- Goimo, M.; Esumi, K. *J. Colloid Interface Sci.* **1998**, *203*, 214.
- Esumi, K.; Suzuki, A.; Aihara, N.; Usui K.; Torigoe, K. *Langmuir* **1998**, *14*, 3157.
- Jiang, D.-L.; Aida, T. *Nature* **1997**, *388*, 454.
- Junge, D. M.; McGrath, D. V. *J. Am. Chem. Soc.* **1999**, *121*, 4912.
- Larre, C.; Donnadieu, B.; Caminade, A. M.; Majoral, J. P. *Chem. Eur. J.* **1998**, *4*, 2031.
- Lorenz, K.; Hölter, D.; Stühn, B.; Mülhaupt, R.; Frey, H. *Adv. Mater.* **1996**, *8*, 414.
- Richardson, R. M.; Ponomarenko, S. A.; Boiko, N. I.; Shibaev, V. P. *Liq. Cryst.* **1999**, *26*, 101.
- van Hest, J. C. M.; Delnoye, D. A. P.; Baars, M. W. P. L.; van Genderen, M. H. P.; Meijer, E. W. *Science* **1999**, *268*, 1592.
- Peerlings, H. W. I.; Meijer, E. W. *Chem. Eur. J.* **1997**, *3*, 1563.
- Bao, Z.; Amundson, K. R.; Lovinger, A. J. *Macromolecules* **1998**, *31*, 8647.
- Smith, S. B.; Finzi, L.; Bustamante, C. *Science* **1992**, *258*, 1122.
- Perkins, T. T.; Quake, S. R.; Smith, D. E.; Chu, S. *Science* **1994**, *264*, 822.
- Wang, M. D.; Yin, H.; Landick, R.; Gelles, J.; Block, S. M. *Biophys. J.* **1997**, *72*, 1335.
- Baumann, C. G.; Smith, S. B.; Bloomfield, V. A.; Bustamante, C. *Proc. Natl. Acad. Sci.* **1997**, *94*, 6185.
- Maier, B.; Strick, T. R.; Croquette, V.; Bensimon, D. *Single Mol.* **2000**, *1*, 145.
- Wirtz, D. *Phys. Rev. Lett.* **1995**, *75*, 2436.
- Ziemann, F.; Rädler, J.; Sackmann, E. *Biophys. J.* **1994**, *66*, 2210.
- Furst, E. M.; Gast, A. P. *Phys. Rev. Lett.* **1999**, *82*, 4130.
- Merkel, R.; Nassoy, P.; Leung, A.; Ritchie, K.; Evans, E. *Nature* **1999**, *397*, 50.
- Cluzel, P.; Lebrun, A.; Heller, C.; Lavery, R.; Viovy, J.-L.; Chatenay, D.; Caron, F. *Science* **1996**, *271*, 792.
- Ishijima, A.; Kojima, H.; Higuchi, H.; Harada, Y.; Funatsu, T.; Yanagida, T. *Biophys. J.* **1996**, *70*, 383.
- Perkins, T. T.; Smith, D. E.; Larson, R. G.; Chu, S. *Science* **1995**, *268*, 83.
- Schurr, J. M.; Smith, S. B. *Macromolecules* **1990**, *29*, 1161.
- Long, D.; Viovy, J.-L.; Ajdari, A. *Biopolymers* **1996**, *39*, 755.
- Kumaki, J.; Nishikawa, Y.; Hashimoto, T. *J. Am. Chem. Soc.* **1996**, *118*, 3321.
- Rivetti, C.; Guthold, M.; Bustamante, C. *J. Mol. Biol.* **1996**, *264*, 919.
- Sheiko, S. S. *Adv. Polym. Sci.* **1999**, *151*, 61.
- Rabe, J. P. *Curr. Opin. Colloid Interface Sci.* **1998**, *3*, 27.

- (82) Anselmetti, D.; Fritz, J.; Smith, B.; Fernandez-Busquets, X. *Single Mol.* **2000**, *1*, 53.
- (83) Han, W.; Lindsay, S. M. *Nature* **1997**, *386*, 563.
- (84) Hansma, H. G.; Vesenska, J.; Siegerist, C.; Kelderman, G.; Morrett, H.; Sinsheimer, R. L.; Elings, V.; Bustamante, C.; Hansma, P. K. *Science* **1992**, *256*, 1180.
- (85) Rief, M.; Gautel, M.; Oesterhelt, F.; Fernandez, J. M.; Gaub, H. E. *Science* **1997**, *276*, 1109.
- (86) Aimé, J. P.; Gauthier, S. In *Scanning Probe Microscopy of Polymers*; Ratner, B. D., Tsukruk, V. V., Eds.; ACS Symposium Series 694; American Chemical Society: Washington, DC, 1998.
- (87) Leuba, S. H.; Zlatanova, J.; Karymov, M. A.; Bash, R.; Liu, Y.-Z.; Lohr, D.; Harrington, R. E.; Lindsay, S. M. *Single Mol.* **2000**, *1*, 185.
- (88) De Paris, R.; Strunz, T.; Oroszlan, K.; Güntherodt, H.-J.; Hegner, M. *Single Mol.* **2000**, *1*, 285.
- (89) Yamamoto, S.; Tsujii, Y.; Fukuda, T. *Macromolecules* **2000**, *33*, 5995.
- (90) Hadziioannou, G.; Ortiz, C. *Macromolecules* **1999**, *32*, 780.
- (91) Kudera, M.; Gaub, H. E. *Langmuir* **2000**, *16*, 4305.
- (92) Furukawa, K.; Ebata, K.; Matsumoto, N. *Appl. Phys. Lett.* **1999**, *75*, 781.
- (93) Lee, G. U.; Chrisey, L. A.; Colton, R. J. *Science* **1994**, *266*, 771.
- (94) Chatellier, X.; Senden, T. J.; Joanny, J.-F.; di Meglio, J.-M. *Europhys. Lett.* **1998**, *41*, 303.
- (95) Binnig, G.; Rohrer, H.; Gerber, Ch.; Weibel, E. *Phys. Rev. Lett.* **1982**, *49*, 57.
- (96) Binnig, G.; Quate, C. F.; Gerber, Ch. *Phys. Rev. Lett.* **1986**, *56*, 930.
- (97) *Procedures in scanning probe microscopies*; Colton, R. J., Engel, A., Frommer, J. E., Gaub, H. E., Gewirth, A. A., Guckenberger, R., Rabe, J., Heckl, W. M., Parkinson, B., Eds.; John Wiley & Sons: Chichester, 1998.
- (98) Magonov, S. N.; Whangbo, M.-H. *Surface analysis with STM and AFM*; VCH Publishers: Weinheim, 1996.
- (99) Tsukruk, V. V. *Rubber Chem. Technol.* **1997**, *70*, 430.
- (100) Kajiyama, T.; Tanaka, K.; Ge, S.-R.; Takahara, A. T. *Prog. Surf. Sci.* **1996**, *52*, 1.
- (101) Akari, S.; Horn, D.; Keller, W.; Schrepp, W. *Adv. Mater.* **1995**, *7*, 549.
- (102) Noy, A.; Sanders, C. H.; Vezenov, D. V.; Wong, S. S.; Lieber, C. M. *Langmuir* **1998**, *14*, 1508.
- (103) Thomas, R. C.; Tangyungyoung, P.; Houston, J. E.; Michalske, T. A.; Crooks, R. M. *J. Phys. Chem.* **1994**, *98*, 4493.
- (104) Overney, R. M.; Meyer, E.; Frommer, J. E.; Brodbeck, D.; Lüthi, R.; Howald, L.; Güntherodt, H.-J.; Fujihira, M.; Takano, H.; Gotoh, Y. *Nature* **1992**, *359*, 133.
- (105) Manne, S.; Gaub, H. E. *Curr. Opin. Colloid Interface Sci.* **1997**, *2*, 145.
- (106) Wahl, K. J.; Stepnowski, S. V.; Unertl, W. N. *Tribol. Lett.* **1998**, *5*, 103.
- (107) Overney, R. M. *Trends Polym. Sci.* **1995**, *3*, 359.
- (108) Burnham, N. A.; Kulik, A. J.; Gremaud, G.; Gallo, P.-J.; Oulevey, F. *J. Vac. Sci. Technol. B* **1996**, *14*, 794.
- (109) Rosa, A.; Weilandt, E.; Hild, S.; Marti, O. *Meas. Sci. Technol.* **1997**, *8*, 1.
- (110) Bustamante, C.; Rivetti, C. *Annu. Rev. Biophys. Struct.* **1996**, *25*, 395.
- (111) Bustamante, C.; Keller, D.; Yang, G. *Curr. Opin. Struct. Biol.* **1993**, *3*, 363.
- (112) Lyubchenko, Y. L.; Oden, P. I.; Lampner, D.; Lindsay, S. M.; Dunker, K. A. *Nucleic Acids Res.* **1993**, *21*, 1117.
- (113) Schaper, A.; Starink, J. P.; Jovin, T. M. *FEBS Lett.* **1994**, *355*, 91.
- (114) Hansma, H. G.; Bezanilla, M.; Zenhausern, F.; Adrian, M.; Sinsheimer, R. L. *Nucleic Acids Res.* **1993**, *21*, 505.
- (115) Zenhausern, F.; Adrian, M.; ten Heggeler-Bordier, B.; Eng, L. M.; Descouts, P. *Scanning* **1992**, *14*, 212.
- (116) Hansma, H. G.; Vesenska, J.; Siegerist, C.; Kelderman, G.; Morrett, H.; Sinsheimer, R. L.; Elings, V.; Bustamante, C.; Hansma, P. K. *Science* **1992**, *256*, 1180.
- (117) Yang, G.; Vesenska, J. P.; Bustamante, C. J. *Scanning* **1996**, *18*, 344.
- (118) Hansma, H. G.; Sinsheimer, R. L.; Groppe, J.; Bruice, T. C.; Elings, V.; Gurley, G.; Bezanilla, M.; Mastrangelo, I. A.; Hough, P. V. C.; Hansma, P. K. *Scanning* **1993**, *15*, 296.
- (119) Zhong, Q.; Innis, D.; Kjoller, K.; Elings, V. B. *Surf. Sci. Lett.* **1993**, *290*, L688.
- (120) Leuba, S.; Yang, G.; Robert, C.; Samori, B.; van Holde, K.; Zlatanova, J.; Bustamante, C. *Proc. Natl. Acad. Sci. U.S.A.* **1994**, *91*, 11621.
- (121) Han, W.; Lindsay, S. M. *Nature* **1997**, *386*, 563.
- (122) Hallett; P.; Tskhovrebova, L.; Trinick, J.; Offer, G.; Miles, M. J. *J. Vac. Sci. Technol. B* **1996**, *14*, 1444.
- (123) Chu, S. *Science* **1991**, *253*, 861.
- (124) Perkins, T. T.; Smith, D. E.; Larson, R. G.; Chu, S. *Science* **1995**, *268*, 83.
- (125) Käs, J.; Strey, H.; Sackmann, E. *Nature* **1994**, *268*, 226.
- (126) Bustamante, C. *Annu. Rev. Biophys. Biochem.* **1991**, *20*, 415.
- (127) Tinnefeld, P.; Buschmann, V.; Herten, D.-P.; Han, K.-T.; Sauer, M. *Single Mol.* **2000**, *1*, 215.
- (128) Trautman, J. K.; Macklin, J. J.; Brus, M. E.; Bezig, E. *Nature* **1994**, *380*, 451.
- (129) Funatsu, T.; Harada, Y.; Tokunaga, M.; Yanagida, T. *Nature* **1995**, *374*, 555.
- (130) Schäfer, B.; Gemeinhardt, H.; Uhl, V.; Greulich, K. O. *Single Mol.* **2000**, *1*, 33.
- (131) Cornelissen, J. J. L. M.; Graswinckel, W. S.; Rowan, A. E.; Sommerdijk, N. A. J. M.; Nolte, R. J. M. *Polym. Prepr.* **2000**, *41* (1), 953.
- (132) Falvo, M. R.; Clary, G. J.; Taylor, R. M., II; Chi, V.; Brooks, F. P., Jr.; Washburn, S.; Superfine, R. *Nature* **1997**, *389*, 582.
- (133) Ponomarenko, S. A.; Boiko, N. T.; Zhu, X. M.; Agina, E. V.; Shibaev, V. P.; Magonov, S. N. *J. Polym. Sci., Part A* **2001**, *43*, 247.
- (134) de Gennes, P. G. *Scaling Concepts in Polymer Physics*; Cornell University Press: Ithaca, NY, 1979.
- (135) Landau, L. D.; Lifshitz, E. M. *Statistical Physics, Part 1*, 3rd ed.; Pergamon Press: Oxford, New York, 1980.
- (136) Schellman, J. A. *Biopolymers* **1974**, *13*, 217.
- (137) Grosberg, A. Y.; Khokhlov, A. R. *Statistical Physics of Macromolecules*; API Press: Woodbury, NY, 1994.
- (138) Kratky, O.; Porod, G. *Recueil* **1949**, *68*, 1106.
- (139) Vasquez, C.; Kleinschmidt, A. K. *J. Mol. Biol.* **1968**, *34*, 137.
- (140) Maier, B.; Rädler, J. O. *Macromolecules* **2000**, *33*, 7185.
- (141) Edwards, S. F. *Proc. Phys. Soc. London* **1965**, *85*, 613.
- (142) Smith, D. E.; Perkins, T. T.; Chu, S. *Macromolecules* **1996**, *29*, 1372.
- (143) Rabe, J. P.; Buchholz, S. *Phys. Rev. Lett.* **1991**, *66*, 2096.
- (144) Wavkushevskij, A.; Cantow, H.-J.; Magonov, S. N.; Möller, M.; Liany, W.; Whanbo, M.-H. *Adv. Mater.* **1995**, *5*, 821.
- (145) Mena-Osteritz, E.; Bäuerle, P. *Angew. Chem., Int. Ed.* **2000**, *39*, 2679.
- (146) Prokhorova, S. A.; Sheiko, S. S.; Möller, M.; Ahn, C.-H.; Percec, V. *Macromol. Rapid Commun.* **1998**, *19*, 359.
- (147) Prokhorova, S. A.; Sheiko, S. S.; Möller, M.; Ahn, C.-H.; Percec, V. *Macromolecules* **1998**, *32*, 2653.
- (148) Prokhorova, S. A.; Sheiko, S. S.; Mourran, A.; Semenov, A. E.; Möller, M.; Beginn, U.; Zipp, G.; Ahn, C.-H.; Percec, V. *Langmuir* **2000**, *16*, 6862.
- (149) Balagurusamy, V. S. K.; Ungar, G.; Percec, V.; Johansson, G. *J. Am. Chem. Soc.* **1997**, *119*, 1539.
- (150) Kralchevsky, P. A.; Nagayama, K. *Langmuir* **1994**, *10*, 023.
- (151) Gerle, M.; Fischer, K.; Schmidt, M.; Roos, S.; Müller, A. H. E.; Sheiko, S. S.; Prokhorova, S. A.; Möller, M. *Macromolecules* **1999**, *32*, 2629.
- (152) Sheiko, S. S.; Möller, M.; Reuvekamp, E. M. C. M.; Zandbergen, H. W. *Ultramicroscopy* **1994**, *53*, 371. Neves, B. R. A.; Vilela, J. M. C.; Russell, P. E. *Ultramicroscopy* **1999**, *76*, 61.
- (153) Elbaum, M.; Fyngenson, D. K.; Libchaber, A. *Phys. Rev. Lett.* **1996**, *76*, 4078.
- (154) Lourie, O.; Cox, D. M.; Wagner, H. D. *Phys. Rev. Lett.* **1998**, *81*, 1638.
- (155) Huck, W. T. S.; Bowden, N.; Onck, P.; Pardo, T.; Hutchinson, J. W.; Whitesides, G. M. *Langmuir* **2000**, *16*, 3497.
- (156) Sheiko, S. S.; Borisov, O. V.; Prokhorova, S. A.; Schmidt, U.; Möller, M.; Schmidt, M. Manuscript in preparation.
- (157) Birshtein, T. M.; Borisov, O. V.; Zhulina, E. B.; Khokhlov, A. R.; Yurasova, T. A. *Polym. Sci. USSR* **1987**, *29*, 1293.
- (158) Rouault, Y.; Borisov, O. V. *Macromolecules* **1996**, *29*, 2605.
- (159) Williams, D. R. M. *Macromolecules* **1993**, *26*, 6667.
- (160) Kwon, Y. K.; Chvalun, S. N.; Schneider, A. I.; Blackwell, J.; Percec, V.; Heck, J. A. *Macromolecules* **1994**, *27*, 6129.
- (161) Strick, T. R.; Allemand, J.-F.; Bensimon, D.; Croquette, V. *Biophys. J.* **1998**, *74*, 2016.
- (162) Marko, J. F.; Siggia, E. D. *Science* **1994**, *265*, 506.
- (163) Marko, J. F.; Siggia, E. D. *Phys. Rev. E* **1995**, *52*, 2912.
- (164) McLeish, T. *Science* **1997**, *278*, 1577.
- (165) Khalatur, P. G.; Khokhlov, A. R.; Prokhorova, S. A.; Sheiko, S. S.; Möller, M.; Reineker, P.; Shirvanyanz, D. G.; Starovoitova, N. *Eur. Phys. J.* **2000**, *1*, 99.
- (166) Potemkin, I. I.; Khokhlov, A. R.; Reineker, P. *Eur. Phys. J.* **2001**, *4*, 93.
- (167) Potemkin, I. I.; Sheiko, S. S.; Khokhlov, A. R.; Möller, M. Manuscript in preparation.
- (168) Sheiko, S. S.; Prokhorova, S. A.; Beers, K. L.; Matyjaszewski, K.; Potemkin, I. I.; Khokhlov, A. R.; Möller, M. *Macromolecules* **2001**, *34*, 8354.
- (169) Börner, H. G.; Beers, K.; Matyjaszewski, K.; Sheiko, S. S.; Möller, M. *Macromolecules* **2001**, *34*, 4375.
- (170) Lifshitz, I. M.; Grosberg, A. Yu.; Khokhlov, A. R. *Rev. Mod. Phys.* **1978**, *50*, 683.
- (171) Swislow, G.; Sun, S.-T.; Nishio, I.; Tanaka, T. *Phys. Rev. Lett.* **1980**, *44*, 796.
- (172) Rark, I. M.; Wang, Q.-W.; Chu, B. *Macromolecules* **1987**, *20*, 1965.
- (173) Ueda, M.; Yoshikawa, K. *Phys. Rev. Lett.* **1996**, *77*, 2133.

- (174) Yoshikawa, K.; Takahashi, M.; Vasilevskaya, V. V.; Khokhlov, A. R. *Phys. Rev. Lett.* **1996**, *76*, 3029.
- (175) Tokuhiya, H.; Zhao, M.; Baker, L. A.; Phan, V. T.; Dermody, D. L.; Garcoa, M. E.; Peez, R. F.; Crooks, R. M.; Mayer, T. M. *J. Am. Chem. Soc.* **1998**, *120*, 4492.
- (176) Sheiko, S. S.; Buzin, A. I.; Muzafarov, A. M.; Rebrov, E. A.; Getmanova, E. V. *Langmuir* **1998**, *14*, 7468.
- (177) Li, S.; Hanley, S.; Khan, I.; Varshney, S. K.; Eisenberg, A.; Lennox, R. B. *Langmuir* **1997**, *9*, 2243.
- (178) Li, Z.; Zhao, W.; Rafailovich, M. H.; Sokolov, J.; Lennox, R. B.; Eisenberg, A.; Wu, X. Z.; Kim, M. W.; Sinha, S. K.; Tolan, M. *Langmuir* **1995**, *11*, 4785.
- (179) Bloom, G. S.; Endow, S. A. *Protein Profile* **1995**, *2*, 1105.
- (180) Barton, N. R.; Goldstein, L. S. *Proc. Natl. Acad. Sci.* **1996**, *93*, 1735.
- (181) Mooseker, M. S.; Cheney, R. E. *Annu. Rev. Cell Dev. Biol.* **1995**, *11*, 633.
- (182) Sellers, J. R.; Goodson, H. V. *Protein Profile* **1995**, *2*, 1323.
- (183) Gibbons, B. H.; Asaj, D. J.; Tang, W.-J. Y.; Hays, T. S.; Gibbons, I. R. *Mol. Biol. Cell.* **1994**, *5*, 57.
- (184) Spudich, J. A. *Nature* **1994**, *372*, 515.
- (185) Kitamura, K.; Tokunaga, M.; Iwane, A. H.; Yanagida, T. A. *Nature* **1999**, *397*, 129.
- (186) Adjari, A.; Prost, J. *C. R. Acad. Sci. Paris* **1993**, *II* 315, 1635.
- (187) Muthukumar, M. *J. Chem. Phys.* **1985**, *82*, 5696.
- (188) Komura, S.; Seki, K. *J. Phys. II* **1995**, *5*, 5.
- (189) Doi, M.; Edwards, S. *The Theory of Polymer Dynamics*; Clarendon: Oxford 1986; p 100.
- (190) Tartsch, B.; Prokhorova, S.; Sheiko, S. S.; Holcera, M. N.; Percec, V., Möller, M. Manuscript in preparation.

CR990129V

Learning Polymer Crystallization with the Aid of Linear, Branched and Cyclic Model Compounds

Goran Ungar^{*,†,‡} and Xiang-bing Zeng[†]

Department of Engineering Materials, University of Sheffield, Sheffield S1 3JD, U.K., and Venture Business Laboratory, University of Hiroshima, Higashi-Hiroshima, Japan

Received July 30, 2001

Contents

I. Introduction	4157
II. Lamellar Structure and Chain Conformation	4158
A. Early Studies	4158
B. Integer Folded (IF) Forms	4159
C. Noninteger Folded (NIF) Form	4160
D. Fold- and End-Surface	4163
E. Chain Tilt	4166
F. Cyclic Oligomers	4168
G. Oligomers with Specific Endgroups	4169
H. Monodisperse Block Copolymers	4170
I. Branched Oligomers	4171
J. Binary Mixtures	4173
III. Crystallization Process and Morphology	4175
A. Stepwise Growth Rate vs Temperature Gradient	4175
B. Crystallization Rate Minima and Negative Order Kinetics	4175
C. Crystallization and Morphology	4178
D. Lamellar Thickening	4181
E. Implications for Polymer Crystallization Theory	4182
IV. Conclusions	4185
V. List of Symbols and Abbreviations	4186
VI. Acknowledgments	4186
VII. References	4186

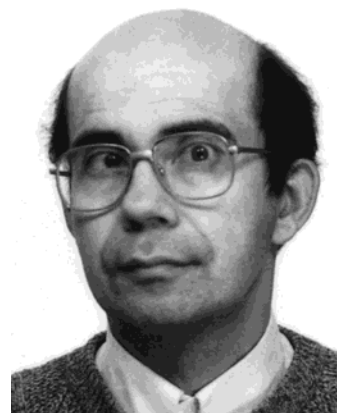
1. Introduction

It is now universally accepted that polymers with reasonably flexible chains crystallize as thin lamellae with chain folding (see schematic drawing in Figure 1). A crystalline lamella is the basic morphological unit which, in the case of melt-crystallized polymers, is the building block of larger structures such as spherulites, row-structures, transcrystalline layers, etc. The reason that polymer crystals are thin is entirely kinetic; a thin crystal grows faster than a thick one, as the addition of short straight stretches of flexible chains presents a lower entropic barrier than the addition of long extended chains. Folding is a necessary accompaniment to lamellar morphol-

* To whom correspondence should be addressed. Phone: (44) 114 222 5457. Fax: (44) 114 222 5943. E-mails: g.ungar@sheffield.ac.uk.

† Department of Engineering Materials.

‡ Venture Business Laboratory.



Goran Ungar obtained his first degree and masters degree from the University of Zagreb, Croatia. In 1979, he obtained his Ph.D. from University of Bristol, England. His thesis was on radiation effects in polymers, under the supervision of Professor Keller. After spending several years at Ruđer Bošković Institute in Zagreb and at University of Bristol, he moved in 1989 to University of Sheffield where he now holds the post of Reader in the Department of Engineering Materials. His research interests are crystalline polymers, structure, and physical properties of liquid crystal polymers, liquid crystals, and supramolecular assemblies.



Xiangbing Zeng was born in 1971, P. R. China. He graduated in 1992 from the University of Science and Technology of China. He received his M. S. degree in condensed matter physics in 1995 at the Institute of Physics, Chinese Academy of Sciences. He received his Ph.D. degree in 2001 at the University of Sheffield. He studied lamellar structures in pure and mixed long chain *n*-alkanes and derivatives under the supervision of Dr. G. Ungar. He is working as a Research Assistant in the Department of Engineering Materials, University of Sheffield. His main research interests are polymer crystal structure, scattering methods, polymer crystallization and polymer physics.

ogy. Thus, it is kinetics driven, unlike the folding in proteins, which is thought to be thermodynamically

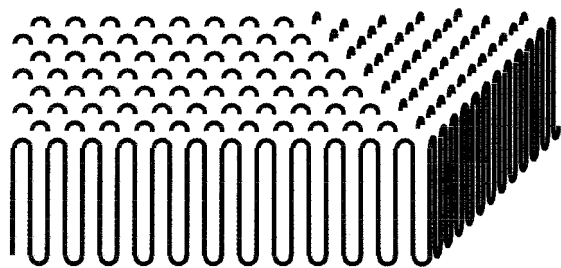


Figure 1. Schematic drawing of a chain-folded polymer crystal.

stable. The order in the schematic structure of the lamella in Figure 1 is certainly idealized, but the exact nature of the fold surface is still unresolved and is a topic of continuing controversy, as are some fundamental aspects of the theory of polymer crystallization. There are a number of reviews and books on the subject.^{1,2,3,4}

Polydispersity has been a greater hindrance to fundamental studies on crystallization and crystal morphology than in most other areas of polymer science. The reason is that, while most polymer properties depend on some power of chain length L , in folded-chain crystals of fold length l it is the length $L - ml$ remaining after m folds that matters in crystallization. If all chains were the same length, nearly 100% crystallinity could be achieved by l adjusting to $l = L/m$, with m being an integer; thus, all chains could end exactly at the crystal surface. However, if a chain is several units shorter than the others, the final incomplete traverse through the crystal layer may leave too large a void; thus, the length $L - ml$ would remain uncrystallized. Polydispersity, which would normally be considered low, may still mean large nonuniformity in $L - ml$. This, in turn, causes the loss of a preferred l -value, reduction in crystallinity, masking of the crystal surface for surface analysis, etc. Furthermore, partial fractionation that occurs on crystallization of polydisperse material makes it difficult to obtain accurately such essential information as crystal growth rate dependence on supercooling and thus find decisive experimental evidence to distinguish between competing crystallization theories. One can approximate monodisperse polymers by using narrow molecular weight fractions. However, the way to achieve truly monodisperse material is to use classical methods of synthetic chemistry rather than polymerization. In the case of polypeptides, it is also possible to resort to biosynthesis using genetically modified bacteria. Monodisperse oligomers with a few tens of chain atoms have been synthesized chemically and studied for many years, most notably n -alkanes, the oligomers of polyethylene (see Sections II.A and II.J), and more recently short oligomers of a number of aromatic polymers.^{5,6} Single-crystal X-ray structures of such oligomers have, e.g., helped in structure determination of their polymer analogues, since polymer single crystals are in general far too small for such analysis.

To be of maximum benefit in studies of crystallization and morphology, monodisperse compounds with chains long enough to fold must be synthesized. Thus

far, this has been achieved with alkanes, alkane-oxyethylene block copolymers, nylon oligomers, and a few sequential oligopeptides. This review will concentrate on studies of monodisperse systems where such exist. Research on narrow molecular weight fractions of polymers will also be covered where data on monodisperse analogues are scarce or absent, notably poly(ethylene oxide). Studies of the crystalline or semicrystalline state of large cyclic oligomers, long-chain branched model compounds, and end-group modified chains are reviewed in addition to those on simple linear chains. Crystallizable di- and tri-block copolymers are covered only partially, to the extent that they impinge on other topics in this article and bear on the general subject of polymer crystallization. The article covers a considerable time span in view of the fact that no review of this kind has been presented in the past. The exception is an early review by Keller in proceedings of a conference which, to the authors' knowledge, have never been published.⁷

II. Lamellar Structure and Chain Conformation

A. Early Studies

Crystalline n -alkanes have been studied for many years as model chain molecules, and their crystal structure,^{8,9,10} crystal growth and morphology,¹¹ melting temperature,^{12,13} chain mobility,¹⁴ conformational defects,^{15,16} self-diffusion,^{17,18} and other properties were extrapolated to represent the crystalline phase of polyethylene. An early comprehensive review of structural and thermodynamic data was presented by Broadhurst.¹⁹ The extrapolation is valid as the orthorhombic subcell of most crystalline n -alkanes is the same as the unit cell of polyethylene. The similarity extends even to the mesomorphic hexagonal high-pressure phase of polyethylene,²⁰ which has its counterpart in the rotator phase in alkanes with up to 40 carbons.^{21,22} Already in 1952, crystals of n -alkanes as long as a hundred C atoms were studied.¹¹ However, the chain length of the alkanes available until 1985 remained insufficient for chain-folding, which limited their usefulness as model polymers.

The first oligomers prepared systematically with increasing molecular weight that crossed the boundary between extended- and folded-chain crystallization were aliphatic oligoamides^{23,24} and oligourethanes.²⁵ Both had large monomer repeat units and could therefore be obtained with comparatively high homologue purity (e.g., 95%). Their lamellar periodicity l , as measured by small-angle X-ray scattering (SAXS), was proportional to the average length of extended chains. However, above a certain molecular weight, l remained constant, which was attributed to the onset of chain folding. This is illustrated in Figure 2. The folding was clearly of the noninteger type (see Section II.C) and the model of molecules following each other as in Figure 3⁷ has been proposed. Similar behavior was also found in a series of polydisperse low molecular weight poly(ethylene oxides) (PEO) samples,²⁶ in contrast to the observations on sharp fractions of this polymer, described next.

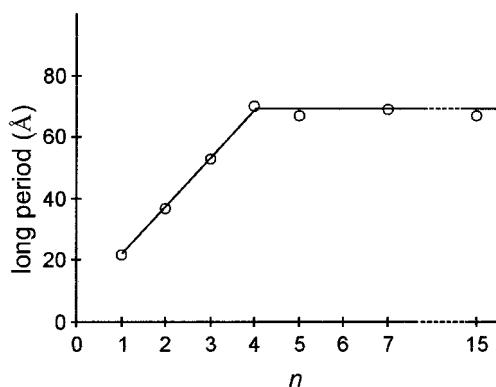


Figure 2. SAXS long period vs number of monomer units n in oligourethane $\text{HO}(\text{CH}_2)_2\text{O}(\text{CH}_2)_2[\text{OCONH}(\text{CH}_2)_6\text{NHCOO}(\text{CH}_2)_2\text{O}(\text{CH}_2)_2]_n\text{OH}$ (after ref 25).

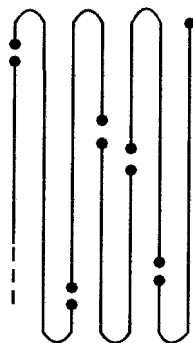


Figure 3. Model proposed to explain the constant l_{SAXS} value for oligourethanes with $\text{DP} > 4$ (after ref 7).

As PEO oligomers could be obtained with narrow molecular weight distribution, their solid state and crystallization kinetics have been studied extensively since early on. Skoulios and co-workers²⁷ found that by crystallizing a fraction with $M_n = 24\,000$ at decreasing crystallization temperatures T_c , the SAXS lamellar periodicity l assumed discrete values corresponding closely to integer fractions of the average chain length L , i.e., $l = L, L/2, L/3$, or $L/4$. Such behavior indicates that the preferred crystallization modes were those which place the chain ends at the surface of the crystalline lamellae. This is in contrast to the situation in polydisperse polymers where l decreases continuously with decreasing T_c , l being proportional to $1/\Delta T$, where $\Delta T = T_m - T_c$, is the supercooling and T_m the melting point.

Many of the important findings from the now classic series of studies by Kovacs and co-workers on narrow PEO fractions have been summarized in refs 28 and 29. Molecular weight fractions were crystallized from the melt in a wide range of supercooling ΔT . Single crystals, large by polymer standards, were grown from the melt at low and moderate ΔT , and revealing experiments were carried out by optical microscopy. They confirmed the quantization of lamellar thickness, a phenomenon which received further support from the observation that melting temperatures also varied in discrete steps. An opinion has existed at the time that integer folding in PEO fractions may be due to the specific nature of the OH end groups and their hydrogen-bonding tendency. We shall return to specific aspects of these studies in subsequent sections.

Chain conform.	E	F2	F3	F4	F5
Paraffin		∩	∩∩	∩∩∩	∩∩∩∩
C102	+				
C150	+	+			
C198	+	+	+		
C246	+	+	+	+	
C294	+	+	+	+	
C390	+	+	+	+	+

Figure 4. Integer folded (IF) forms observed in long n -alkanes $\text{C}_{102}\text{H}_{206}$ through $\text{C}_{390}\text{H}_{782}$. For a given alkane more folds per molecule are obtained with increasing supercooling ΔT (after ref 40).

B. Integer Folded (IF) Forms

The first monodisperse oligomers showing chain folding were long normal alkanes synthesized in 1985 independently by Bidd and Whiting³⁰ and by Lee and Wegner.³¹ Whiting et al. used Wittig coupling in a sequence of chain-doubling steps. Since at each step the product and reactants had a molecular weight ratio of 2:1, it was possible to separate them cleanly and avoid homologue impurities. The method has subsequently been perfected and extended to long alkane derivatives.³²

Crystallization experiments on long alkanes have been performed both from solution and from melt. Many orders of small-angle X-ray diffraction were present due to the high regularity of lamellar stacking. This allowed accurate measurement of lamellar spacing. At the same time the length of straight chain segments was determined by low-frequency Raman spectroscopy using the longitudinal acoustic mode (LAM). While alkane $n\text{-C}_{102}\text{H}_{206}$ could only be obtained in extended-chain form, $n\text{-C}_{150}\text{H}_{302}$ could also be crystallized with chains folded in two (F2, once-folded) from solution or by quenching from melt. With increasing chain length, the maximum number of folds per chain increased, and the longest alkane, $\text{C}_{390}\text{H}_{782}$, could be obtained with $m = 4$ folds, i.e., with chains folded in five ($l = L/5$).³³ The different chain conformations achieved by crystallizing Whiting's alkanes are shown in Figure 4.

In mature crystals the strong preference for integer folding (IF) was indeed confirmed. In solution-grown crystals the relationship $l = L/(m + 1)$, with m an integer, was strictly observed for l measured by both SAXS and LAM. The agreement for l_{SAXS} was to 0.1 nm. For melt-crystallized alkanes, l_{SAXS} had to be corrected for the 35° chain tilt with respect to the layer normal (see Section II.E). These results on alkanes have shown that the preference for integer folding is inherent in monodisperse oligomers and is not due to the specific nature of the end-groups as might have been argued in the case of PEO. In fact it was found subsequently that fractions of methoxy-terminated PEO also exhibit a preference for integer folding.³⁴

The fact that the length of a straight chain segment traversing the crystal (stem length, l_s) is known precisely in IF of a monodisperse oligomer has been used for the calibration of analytical techniques such as Raman LAM spectroscopy and for determining

fundamental polymer parameters such as equilibrium melting point and ultimate elastic modulus of a polymer.

Raman spectra of certain crystalline polymers and their oligomers show a series of identifiable LAM bands in the low-frequency region, corresponding to symmetrical longitudinal backbone vibration modes. In the simplest approach, the stem is considered as a continuous elastic rod, the frequency of the vibration being³⁵

$$\nu_j = \frac{j}{2l_s} \left(\frac{E}{\rho} \right)^{1/2} \quad (1)$$

where E is Young's modulus of the chain, ρ the density, and j the vibration order (only odd orders are Raman active). The fact that LAM frequency is inversely proportional to the straight stem length l_s makes this a valuable technique for studying polymer morphology. Extended chain monodisperse oligomers are ideal for testing eq 1,^{36–38} and finding the value of E , since $l_s = L$. Although eq 1 has been commonly used in the past, weak interlamellar forces result in an upward shift of ν . Thus according to Strobl et al.,³⁹ who studied alkanes C_nH_{2n+2} with $33 \leq n \leq 94$,

$$\nu_j = \frac{2236j}{n-1.6} + \frac{2.2}{j} \quad (2)$$

The associated elastic modulus of polyethylene is $E = 290$ GPa. However, the critical test of eq 2 is in the $l_s \rightarrow \infty$ region. The results for long extended-chain alkanes up to $C_{294}H_{590}$ were at variance with eq 2 and obeyed the simple $\nu_1 \rightarrow \infty 1/n$ law, with $\nu \rightarrow 0$ as $l_s \rightarrow \infty$ and with $E = 350$ GPa.^{40,41} Recent experiments point to end-surface disorder as a possible cause of the discrepancy. In the longest pure alkanes, very slow crystallization from the melt is needed in order to create a highly ordered end-surface; this was found to result in higher ν than the more rapid crystallization.⁴² Furthermore, alkane mixtures give lower ν than pure alkanes. The above discrepancy is thus possibly due to the lack of surface order in the longest alkanes used in previous studies. That surface disorder has a noticeable effect is also borne by the observation by Khoury et al.⁴³ that the LAM frequency of n - $C_{36}H_{74}$ and n - $C_{94}H_{190}$ is affected by end group packing; the effect was attributed to differences in methyl end group interaction.

While the interlamellar forces in n -alkanes are weak and their contribution to the LAM frequencies is small, in systems with strongly interacting chain ends the effect can be very pronounced.⁴⁴ For example, while in n -alkanes, the ratio ν_3/ν_1 is around 2.8, quite close to 3 as expected from eq 1, ν_3/ν_1 is only 2.1–2.3 for monodisperse oligo(oxyethylenes) and PEO fractions.^{45,46} In PEO fractions, this effect makes it difficult to distinguish between LAM-3 of the extended chain conformation and LAM-1 of the once folded chain, and peak assignment must be made with caution. The helical conformation of PEO accounts for its low elastic modulus (25 GPa), as obtained from LAM frequencies.⁴⁷

Linear oligomers have been used extensively in the determination of polymer melting points. The equi-

librium melting temperature of an ideal polymer crystal, though fundamentally important in crystallization, cannot be determined directly. Instead, it is often obtained by extrapolation to infinite chain length of melting points of a series of extended-chain oligomers. Early extrapolations were based on the presumption that both the enthalpy and entropy of fusion were linear in the number of repeat units n per chain.^{48,19} However, in their analysis of melting points of alkanes $C_{11}H_{23}$ to $C_{100}H_{202}$, Flory and Vrij¹² suggested that a nonlinear term $R \ln n$ be included in the entropy of fusion to account for the "unpairing" of chain ends upon melting of the crystal. Their extrapolation leads to a 4 K increase in the equilibrium melting point of polyethylene (from 414.5 to 418.5 K), but the quality of fit was hardly improved compared with previous equations¹⁹ as pointed out by Wunderlich.¹³ The validity of the term $R \ln n$ is supported by studies on PEO fractions,⁴⁹ while evidence for it is not clear in long-chain ketones.⁵⁰

The melting points of long alkanes with $150 < n < 390$ were found to be consistently lower than predicted by Flory's theory.^{31,33} This has been discussed in terms of the premelting effect.⁵¹ Assuming a constant entropy change due to premelting, Carlier et al. found a linear relationship between the melting points T_m of oligomers and the value $(\ln n + C)/n$ where C is a constant.⁵² These authors have carried out extrapolations for polyethylene ($11 < n < 390$), poly(tetrafluoroethylene) ($5 < n < 24$), poly(methyl-eneoxide) ($4 < n < 22$), poly(ethylene oxide), poly(etheretherketones) (PEEK, $1 < n < 4$), and poly(phenylene sulfide) (PPS, $1 < n < 7$). Studies of melting points of folded-chain PEO fractions have shown that, for a given fold length l , the melting point increases with increasing total chain length L , i.e., with increasing number of folds per chain.⁵³ End- and fold-surface free energies for PEO were derived. These parameters were also derived for polyethylene,^{54,55} using melting point data for different IF forms of n -alkanes.³³ Melting points of monodisperse linear and cyclic oligo(oxyethylenes) were found to be in general agreement with the Flory-Vrij expression, provided "segment" and "repeat unit" were appropriately defined.¹²⁶

C. Noninteger Folded (NIF) Form

While mature alkane crystals show a strong tendency for integer folding, when melt crystallization was monitored in real time by SAXS using synchrotron radiation, it was found that below the extended-chain growth temperature region the initial lamellar periodicity l was a noninteger fraction of L , even after correcting for tilt.⁵⁶ It corresponded to a fold length between L and $L/2$ and was dependent on crystallization temperature T_c and time. These "noninteger folded" (NIF) lamellae subsequently transformed isothermally by thickening to extended-chain or, at lower T_c , by "thinning" to once-folded (F2) chain lamellae with hairpin chain conformation. In Figure 5a the real-time SAXS recording of isothermal crystallization of $C_{246}H_{494}$ shows the rapid emergence of NIF marked by the strong first-order peak. This is followed by its demise and concurrent replacement

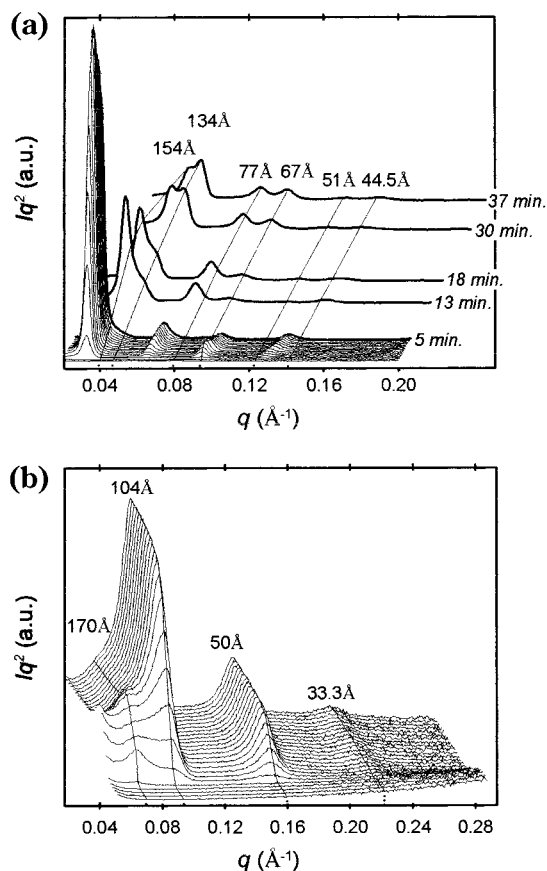


Figure 5. Time evolution of SAXS during isothermal crystallization of (a) *n*-alkane $C_{246}H_{494}$ at $T_c = 111$ °C and (b) branched alkane $C_{96}H_{193}CH(CH_3)C_{94}H_{189}$ at $T_c = 110$ °C from the melt. Abscissa scale is marked in q (in \AA^{-1}) and $d = 2\pi/q$ (in \AA). In panel a, the spectra were recorded sporadically after the first 5 min. Time t is counted from the moment of reaching T_c . In panel b, time frames of 12 s begin from the start of cooling and T_c is reached in frame 4. In panel a, the first-order NIF peak is initially by far the strongest, while in panel b, centered at 170 \AA , it is weak and short-lived (from 59 with permission of American Chemical Society).

by the once-folded form. Subsequently, NIF and its transformation to IF forms were also found in PEO fractions.^{57,58}

The nature of the NIF form, at least in alkanes, has only been understood after electron density profiles normal to the lamellae had been reconstructed using SAXS intensities of a number of diffraction orders.⁵⁹ It turns out that NIF is up to one-third amorphous, with some chains integrally folded in two and others not folded at all but traversing the crystalline layer only once (see Figure 6b). These latter chains are only half-crystalline, with their protruding ends, or cilia, forming the amorphous layer. From the crystalline layer thickness l_c , determined from the electron density profile, and from $l_{\text{LAM}} = l_c/2$, determined from time-resolved Raman spectroscopy,⁶¹ it was established that the chains are tilted at 35° to the normal in the crystalline layers.

Compared to the integer F2 form, NIF allows crystals to grow faster since not all chains need attach “correctly”, i.e., with their ends flush with the crystal surface (Figure 6a). However, if the lamella is to grow, nearly half the chains do need to be placed

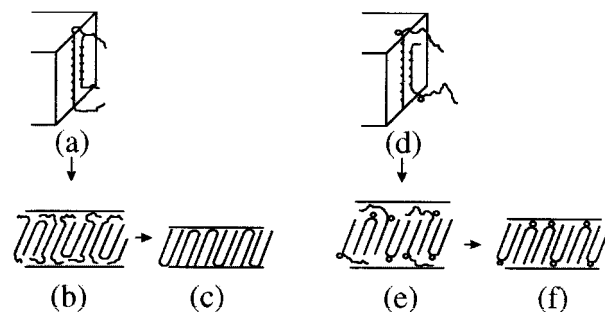


Figure 6. Schematic representation of molecular deposition on the crystal growth face (a, d), the NIF form (b, e), and the F2 form (c, f) for a linear alkane (a–c) and the branched alkane $C_{96}H_{193}CH(CH_3)C_{94}H_{189}$ (d–f). (From 59 with permission of American Chemical Society).

“correctly” and crystallize fully with a fold in the middle. Otherwise the overcrowding at the crystal–amorphous interface, caused by the doubling in cross-section of chains emanating from the crystal,⁶⁰ would build up unsustainably. It is because of this overcrowding effect that lamellar crystals of flexible polymers cannot grow laterally without chain folding. More information on the surface overcrowding effect is provided by studies of alkane mixtures (see Section II.J).

The growth of semicrystalline NIF in preference to that of the highly crystalline F2 form is a typical example of crystallization kinetics controlling polymer morphology. The best known example is, of course, the very fact that thin folded-chain crystals form in preference to the more stable extended-chain crystals.

It is interesting to compare crystallization of a linear alkane with one having a methyl branch in the middle, $C_{96}H_{193}CH(CH_3)C_{94}H_{189}$. There is a strong tendency for methyl branches to be rejected to the lamellar surface and $C_{96}H_{193}CH(CH_3)C_{94}H_{189}$ persistently gives F2 crystals (for more on branched oligomers see Section II.I). Figure 5b shows the evolution of SAXS during isothermal crystallization of the branched alkane. The appearance of the small NIF diffraction peak at $l = 170$ \AA is succeeded immediately by the emergence of the comparatively strong 104 \AA peak and its higher orders attributed to the once-folded form. The rapid NIF \rightarrow F2 transformation can be explained by the fact that here the only successful deposition mode of the first stem (first half) of the molecule is one which places the branch at one lamellar basal surface and the chain end at the other (see Figure 6d). This leaves the molecule with an uncrystallized cilium at one end only, its length being precisely half the chain. Such a cilium is ideally suited to complete a second traverse of the crystal. Thus, although some cilia remain uncrystallized during primary formation of the lamellae, giving rise to the NIF form (Figure 6e), when they subsequently enter the crystal, it is relatively easy for the F2 conformation to be achieved (Figure 6f). In contrast, for a linear alkane in the NIF form, a half-crystallized molecule generally has a cilium at each end; neither of them is long enough to complete a second traverse without rearrangements involving the whole molecule. In the sequence melt \rightarrow NIF \rightarrow

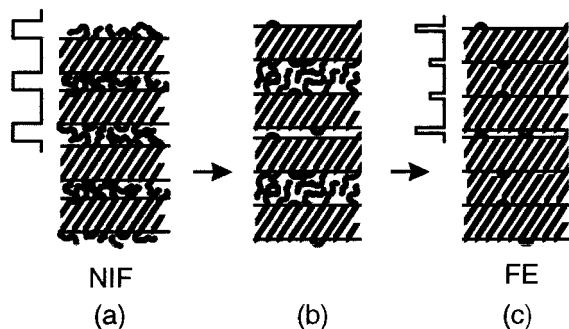


Figure 7. Schematic representation of the transformation from (a) NIF (four layers shown) to (c) mixed folded-extended (FE) forms (two triple layers shown) in long-chain *n*-alkanes with around 200 C atoms. The intermediate stage in panel b should not be taken literally, as the cilia are likely to crystallize simultaneously with their coalescence in the middle layer (from ref 61, by permission of Elsevier Science Publishers).

F2, the melt \rightarrow NIF step is fast but the NIF \rightarrow F2 step (“lamellar thinning”) is slow in linear alkanes. The reverse is true for the branched alkane.

As described, the process of “lamellar thinning”, after NIF formation, consists for most alkanes of the uncrystallized cilia finding their way into the crystal layer (Figure 6, panels b, c, e, f); the overall long period l is reduced gradually while the crystalline thickness l_c remains constant. Recently, however, another more efficient mechanism of NIF transformation has been discovered for *n*-alkanes in the length range of 200 carbons.⁶¹ Instead of folding back into the crystal, the half-crystallized NIF chains translate cooperatively down and up in alternative layers. All cilia emanating from two adjacent crystal layers thus converge in the space between them (see Figure 7b) and crystallize. This results in a triple-layer crystalline superlattice in which once-folded and extended chains are mixed in the outer two sublayers, while the middle layer contains only interdigitated portions of unfolded chains (Figure 7c). The “mixed integer” character of this form has been confirmed by Raman LAM spectroscopy. Similar examples of cooperative lamellar transformations and complex superlattice formation have recently been found in Y-shaped branched alkanes and long alkane mixtures (see Sections II.I and II.J).

Even though the NIF form in PEO fractions behaves in a similar way to that in long alkanes, it is not clear at this stage if it has the same structure. The fact that the oligomers are not monodisperse is partly responsible for this uncertainty. While NIF density profiles have not been reported for PEO, published time-resolved SAXS curves can provide a qualitative clue. Whereas the model of NIF in Figure 7 gives rise to high SAXS intensity which diminishes with the decrease in the amorphous fraction l_a/l , there would be no significant change in intensity upon the NIF \rightarrow IF conversion in the case of the model in Figure 3. This can be seen from the simple general expression for the total small-angle scattering intensity Q for a two-phase lamellar system:⁶²

$$Q = \frac{l_a}{l} \left(1 - \frac{l_a}{l} \right) (\Delta\eta)^2 \quad (3)$$

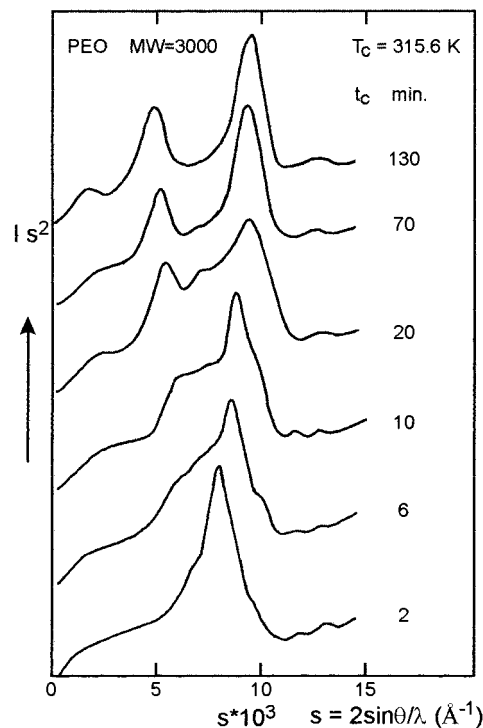


Figure 8. SAXS curves recorded during isothermal crystallization of PEO fraction $M_n = 3000$ at 43 °C. The initial NIF peak (first order) at $t_c = 2$ min gives way to extended and F2 peaks at approximately 5×10^{-3} and $10 \times 10^{-3} \text{ \AA}^{-1}$, respectively (from ref 58 by permission of John Wiley & Sons).

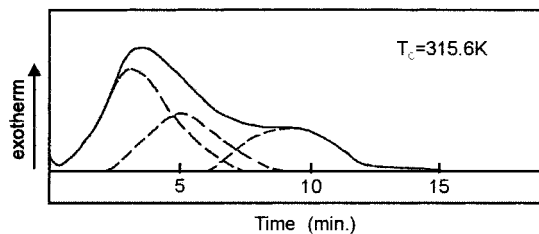


Figure 9. DSC crystallization exotherm for PEO fraction $M_n = 3000$ at 43 °C. Compare with Figure 8 (from ref 58 by permission of John Wiley & Sons).

where $\Delta\eta$ is the crystalline-amorphous electron density difference. Figure 8 shows a series of SAXS traces recorded during isothermal crystallization of a $M_n = 3000$ fraction of PEO at 43 °C, while Figure 9 shows the corresponding DSC exotherm. The overall SAXS intensity does not appear to change much from the first frame (2 min), dominated by the NIF peak, through to the end of the experiment when only the extended and the F2 forms are left. However, at $t = 2$ min crystallization had only just started (Figure 9), while it is complete at $t = 15$ min. This indicates that the initial NIF form scatters considerably more strongly than the IF forms, which would support the two-phase NIF model in Figure 6 and Figure 7. A hybrid model of NIF in PEO has been suggested in the drawing in Figure 10.⁶³ This modifies the model in Figure 3, having chains trail each other through the crystal layer of noninteger thickness, with added loops rather than cilia forming the noncrystalline phase responsible for high SAXS intensity. Electron density reconstruction may help

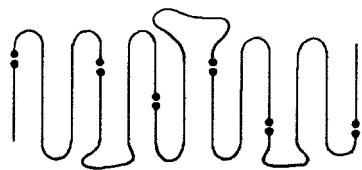


Figure 10. A proposed model of the structure of NIF form in PEO fractions. The black dots represent OH groups (after ref 63).

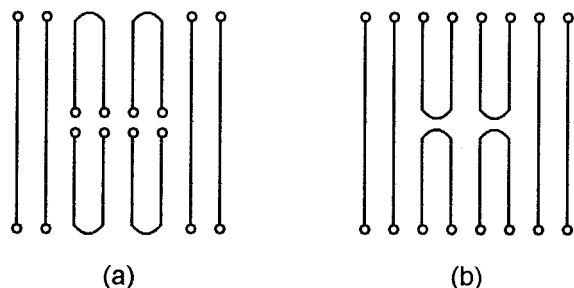


Figure 11. Schematic models of E + F2 crystals of PEO fractions: (a) with internal, (b) with external H-bonds. The models were proposed on the basis of LAM spectra. Model b was preferred (from ref 38 by permission of American Chemical Society).

resolve this structure by establishing the crystalline thickness l_c .

The model of NIF in Figure 6 and Figure 7, as well as that in Figure 10, also appears to be consistent with the "self-decoration" effect observed in PEO fractions,^{28,64} whereby growing chain-folded crystals become decorated by dense overgrowth on their fold surface after quenching. Surface nucleation by cilia, i.e., NIF, is most likely to be responsible, since extended-chain crystals show no such decoration (see Figure 39 and Figure 46).

Raman LAM studies on PEO fractions crystallizing below the F2 melting point consistently show a NIF band with frequency intermediate between those of extended and once-folded chains.^{38,57} This contravenes both the LAM and electron density evidence for the alkanes according to which the length of the straight stem in NIF is always half the chain length. It was found that the noninteger LAM band in PEO transforms with time into F2 and E bands, but no amount of annealing could remove the F2 band completely.⁵⁷ The origin of the discrepancy between the observations on NIF forms in alkanes and PEO is unclear and the structure of NIF in PEO fractions remains essentially unresolved. It ought to be mentioned that LAM in PEO is much more sensitive to end-effects (end-group type, see Section II.G, interlamellar interaction) and intracrystalline packing as compared to alkanes.^{44,65}

The persistence of the F2 LAM band on annealing, without the presence of a SAXS or a DSC melting peak corresponding to F2 lamellae, has led Kim and Krimm³⁸ to propose a tentative model of once-folded chains embedded into an extended-chain lamella (see Figure 11b). A similar structure, proposed in a preceding study³⁶ (Figure 11a) was dismissed on grounds that it would transform easily to the extended chain form.

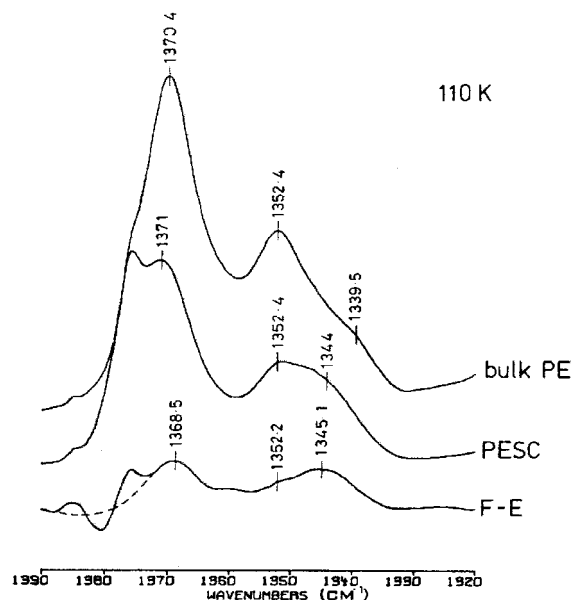


Figure 12. (F-E) Characteristic FTIR spectrum of {110} chain folds in solution-grown single crystals of *n*-alkane $C_{198}H_{398}$ (spectrum of extended-chain crystals subtracted from that of once-folded crystals); (PESC) solution-grown single crystals of polyethylene; (bulk PE); melt-crystallized linear polyethylene. All bands are CH_2 wagging defect modes except the CH_3 band at 1378 cm^{-1} . Spectra recorded at 110 K (from ref 68 by permission of Elsevier Science Publ.)

D. Fold- and End-Surface

The nature of the fold surface of polymer crystals has been a controversial issue for several decades. Models have ranged from the highly ordered, with tight adjacently re-entrant folds (idealized in Figure 1),² to the random re-entry "switchboard" model with loose loops.⁶⁶ One of the reasons for the controversy is the lack of a suitable conformation-sensitive surface technique. However, perhaps a more important reason is the fact that even in solution-grown single crystals an amorphous layer of cilia and probably adsorbed chains covers the fold surface.⁶⁷ Monodisperse long alkane crystals grown from solution in an integer folded form have the advantage of not containing cilia and thus having the fold surface uncovered. This was taken advantage of in recording the IR spectrum of chain folds in crystals of alkane $n-C_{198}H_{398}$.⁶⁸ It was ascertained first by electron microscopy of surface-decorated⁶⁹ crystals used that the folds were predominantly in the {110} planes. The spectrum of extended-chain crystals was subtracted in order to obtain the spectrum of pure folds. In the methylene wagging range, sensitive to conformational defects, the fold spectrum at room temperature was almost indistinguishable from that of amorphous polyethylene, indicating that a range of fold conformations were present. However, at low temperature, the fold spectrum differed considerably from that of bulk polyethylene (see Figure 12). It was dominated by bands at 1368 and 1345 cm^{-1} , the former being due to *gtg* defects and the latter appearing to be specific to regular {110} folds. Significantly, the prominent *gg* band at 1352 cm^{-1} almost vanished at low temperature. The 1345 cm^{-1} band

Table 1. Parameters of Inter-crystalline Layer for Extended (E) and Once-Folded (F2) Chain Long Alkanes Derived from SAXS

sample	form	temp (°C)	electron deficiency per unit area of interlayer, κ (electron \AA^{-2}) ^a	width of interlayer from κ assuming noncrystalline density = 0.85 g cm^{-3} (\AA) ^a	integral width of interlayer (I_a) (from Fourier synthesis) (\AA)
C ₁₉₄ H ₃₉₀ or C ₁₉₈ H ₃₉₈ melt-crystallized	E	rt 120	0.66	13	15 ^b 26 ^b
	F2	rt	0.40	8	17 ^c
C ₂₄₆ H ₄₉₄ melt-crystallized	E	rt 122	0.66	13	26 ^b 32 ^b
	F2	rt	0.73	14.5	18 ^c
linear polyethylene melt-crystallized		rt	2.4	48	

^a Using absolute intensity SAXS data.⁷⁶ ^b From ref 75. ^c From ref 77.

also appears as a shoulder in the low-temperature spectrum of polyethylene single crystals, but not in that of bulk polyethylene. A band at 1345 cm^{-1} has been suggested to represent tight folds by previous studies of polyethylene using curve deconvolution.^{70,71}

The observed high conformational uniformity, i.e., "tight" folds, could not have been attained at low-temperature had the folds not been connecting adjacent stems in the first instance. A switchboard-type fold surface would not have produced the spectrum at the bottom of Figure 12, but rather one like that at the top of the figure.

A band of moderate intensity has been observed at 1080 cm^{-1} in the Raman spectrum of once-folded solution-crystallized *n*-alkane C₁₆₈H₃₃₈.⁷² This spectral region is associated with C–C stretching vibrations of methylene sequences containing gauche bonds. Extended-chain shorter alkanes (*n*-C₄₈H₉₈, *n*-C₇₂H₁₄₆) did not show this band. The 1080 cm^{-1} band is also observed in semicrystalline polyethylene.⁷³ Low-temperature spectra were not reported.

Information on the density profile across the intercrystalline chain-fold or chain-end layer can be obtained from SAXS intensities.^{74,75} Table 1 gives experimental data describing the state of the lamellar surface layer in E and F2 forms of two long alkanes.^{75,76,77} The electron density profile normal to the layer surface is proportional to the mass density profile in the case of alkanes. This has a minimum as one crosses the inter-crystalline gap. The integral of that minimum (κ) and its integral width (I_a) are listed. As can be seen, solution-grown crystals have the smallest inter-crystalline gap (κ), although it is spread over a width of 17 \AA (I_a), hence the gap is shallow. Melt-crystallized alkanes have a similar I_a , but the gap is deeper. The gaps for E and F2 forms are similar, but the relative contribution of the interlayer is of course twice as large in the F2 form. In comparison, κ for polydisperse polyethylene is much greater.

As mentioned earlier, in addition to *n*-alkanes, pure monodisperse nylon 6⁷⁸ and nylon 6,6⁷⁹ oligomers have also been successfully synthesized with sufficient length to form chain-folded crystals. Once-folded chain crystals of nylon 6 nonamer and decamer,^{80,81} and twice-folded crystals of nylon 6 17-mer⁸² have been obtained from solution and studied by means of X-ray and electron microscopy and diffrac-

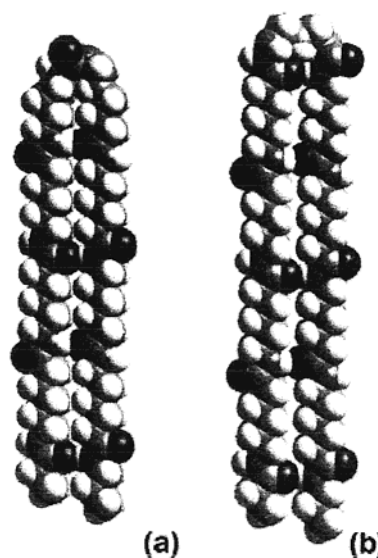


Figure 13. A once-folded conformation of nylon 6 nonamer with an amide fold (a) and of decamer with an alkane fold (b). (After ref 80).

tion. Nylon 6 oligomers were found capable of forming alkane folds or amide folds, although it was thought previously that amide folds could only be found in nylon 4⁸³ and nylon 4,6.⁸⁴ Symmetrical once-folded conformations of 9-mer and 10-mer, consistent with the measured SAXS long spacings, have different fold types (Figure 13). The crystal subcell is that of nylon 6 α -structure with hydrogen-bonded sheets. On the basis of molecular mechanics calculation aided by simulation, it was concluded that the folds were in the plane of the sheets. In 12-amide and 16-amide nylon 6,6, only once-folded crystals have been obtained.⁸⁵ Temperature-induced structural changes in crystals of monodisperse nylon 6 and nylon 6,6, such as unfolding, intersheet shear, and orthorhombic-pseudohexagonal transition, have also been studied.⁸⁵

Several monodisperse model proteins with repeating sequences of amino acids have been biosynthesized by the recombinant DNA technique and have had their structure studied.⁸⁶ Multigram quantities were produced in pilot fermentators. Thus, poly(L-alanyl-glycine), poly(AG), with alternating alanyl and glycy units, was prepared with two different chain lengths: (AG)₆₄ and (AG)₂₄₀.⁸⁷ Structural studies were

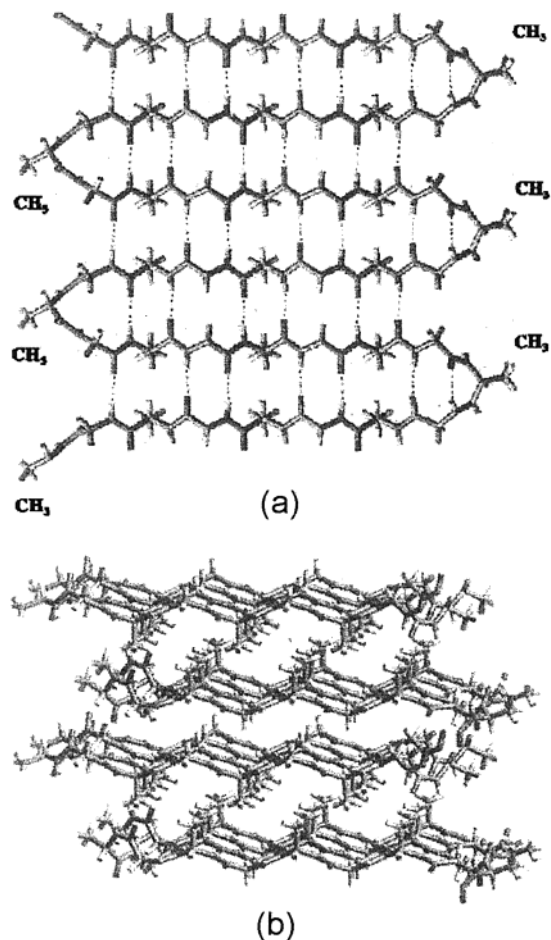


Figure 14. (a) Top view of a single antiparallel β -sheet of biosynthesized monodisperse poly(alanyl-glycine). Fold length is commensurate with the octapeptide periodicity. Vertical dotted lines indicate H-bonds. (b) Arrangement of β -sheets into 3-D crystal. Sheets lie horizontally. Energy-minimized model refined using X-ray data (from ref 87, by permission of the American Chemical Society).

carried out on pressed partially oriented crystal mats. The structure was found to be similar, but not identical to that found previously in oriented films of synthetic poly(AG) and fibers of corresponding silk fibroin.^{88,89} The structure was that of antiparallel β -sheets, i.e., layers of internally hydrogen-bonded chains in the 2_1 zigzag conformation, with adjacent chains oriented in opposite directions. In silk II, extended antiparallel chains form stacked strands of β -sheets. In biosynthesized (AG)₆₄, the chains are folded. The antiparallel arrangement is compatible with adjacently re-entrant chain folding. In poly(AG) a fold occurs after every 8 amino acids, as determined from the observed X-ray spacing of 32 Å. The 32-Å-wide β -sheets were stacked to form a 3-D crystal, as suggested in the computer model in Figure 14. Note that the individual β -sheets are polar as the methyl groups not involved in the folds are all either above or below the plane of the sheet.

The following polypeptides of the type [(AG)_xEG]_n (*E* = glutamic acid) have also been prepared by biosynthesis: *x* = 3, *n* = 36; *x* = 4, *n* = 28; *x* = 5, *n* = 20; and *x* = 6, *n* = 14.^{86b,90} Structural studies were carried out on [(AG)₃EG]₃₆. The basic pattern of antiparallel β -sheets of folded chains forming 3-D

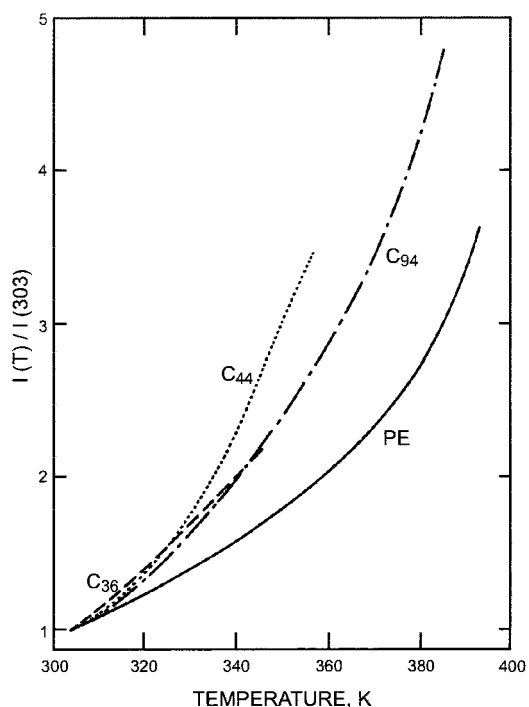


Figure 15. Temperature dependence of relative intensities of the first order (001) small-angle X-ray diffraction for *n*-alkanes C₃₆H₇₄, C₄₄H₉₀, C₉₄H₁₉₀, and linear polyethylene (from ref 93 by permission of National Institute of Standards and Technology).

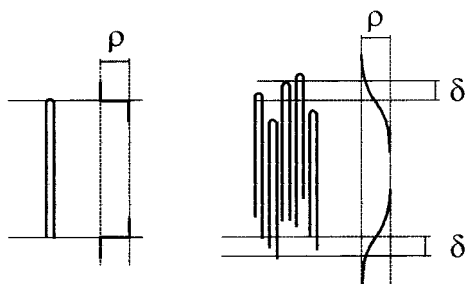
crystals was present here too. The measured fold length of 32 Å was found to be commensurate with the length of the chemical repeat of eight amino acids. The fold occurred at the glutamic acid position, so that the layers had carboxylic groups on their surface.^{91a} A similar structure was also found in a related polypeptide which had the alternative tri-(alanyl-glycyl) segments reversed, i.e., [(AG)₃EG-(GA)₃EG]₁₀.^{91b} In both cases, the X-ray data were compatible with molecular models containing the so-called γ -fold. A γ -fold encompasses two planar amide groups, whereas a β -fold contains only one amide group. Most globular proteins contain γ -folds. Since γ -folds are found in both poly[(AG)₃EG] and poly[(AG)₃EG-(GA)₃EG], it was concluded that interaction between sheets is not the primary factor determining the fold type.

Returning to long *n*-alkanes, it was found that when the once-folded crystalline C₁₉₈H₃₉₈ is heated from 110 K to room temperature, the IR spectrum of chain folds changes from that in Figure 12 (bottom) to one that is not very different from that of amorphous polyethylene.⁶⁸ This indicates reversible conformational disordering with increasing temperature. While remaining adjacently re-entrant, the loops become looser. Reversible thermal disordering of the fold-surface in long alkanes is particularly pronounced close to the melting point.^{40,92}

A similar reversible thermal disordering of the surface layer has also been observed in extended-chain alkanes, starting from the early work on *n*-C₉₄H₁₉₀,⁹³ where the effect has been compared to the premelting phenomenon in polymers.⁹⁴ This is illustrated in Figure 15 where the temperature-

Table 2. Relative Intensities of the "Crystalline" Signal in the Magic-Angle Spinning ^{13}C NMR Spectra of Alkane $n\text{-C}_{168}\text{H}_{338}$ (ref 95)

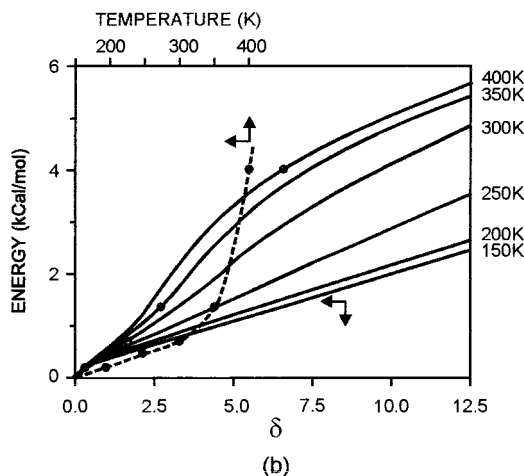
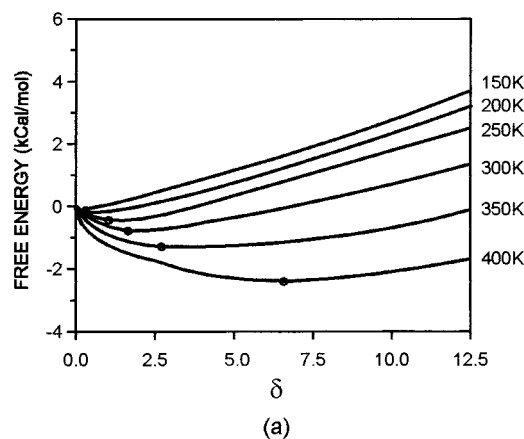
T ($^{\circ}\text{C}$)	internal CH_2	$\alpha\text{-CH}_2$	CH_3
27	0.96 ± 0.05	0.87 ± 0.05	0.79 ± 0.1
87	0.92 ± 0.05	0.63 ± 0.1	0.42 ± 0.1

**Figure 16.** Model used to calculate equilibrium surface disorder in once-folded chain crystals of n -alkanes. Left: complete order. ρ = density (after ref 40).

induced increase in SAXS intensity for extended-chain alkanes and polyethylene are compared. The close relationship between the "noncrystalline fraction" l_a/l and SAXS intensity is evident from eq 3. While in relative terms the intensity increase for polyethylene is the smallest, in absolute terms it is in fact the largest. Table 1 shows the increase in the interlayer widths between room temperature and close to the melting point for extended-chain $\text{C}_{194}\text{H}_{390}$ and $\text{C}_{246}\text{H}_{494}$.

Solid-state ^{13}C NMR experiments on extended-chain $n\text{-C}_{168}\text{H}_{338}$ have shown the strong reversible thermal disordering of chain ends very clearly.⁹⁵ The methyl and α -methylene signals are clearly distinguished from those of inner methylenes; the respective "crystalline" (all-trans) signals are at 16.1, 25.7, and 33.6 ppm, while their "amorphous" (conformationally averaged) counterparts are at 15.5, 24.2, and 31.5 ppm. The relative intensities of the "crystalline" component are shown in Table 2 for 27 and 87 $^{\circ}\text{C}$.

The problem of smooth vs rough surface in a crystal of once-folded alkane has been treated quantitatively.⁴⁰ The method is similar and somewhat simpler for extended chains. The calculation was based on the model in Figure 16. In the figure on the left, l is exactly equal to $L/2$. This allows only two configurations of the molecule: hairpin up and hairpin down (only one is shown in Figure 16). However, if the surface is allowed to be rough, many more configurations become available, as shown on the right. A self-consistent mean field approach was adopted where the interaction potential profile ψ was iteratively matched against the density profile ρ . ψ takes the form of the error function whose width is defined by the standard deviation δ (step function with $\delta = 0$ in the extreme case on the left). Protruding ends were allowed rotational isomeric freedom while the folds were kept tight in this simple model. Standard thermodynamic parameters for polyethylene were used and the resulting free energies vs δ are plotted in Figure 17a. Smooth surface ($\delta = 0$) is favored only below ca. 200 K, the minimum in free energy moving to larger δ (increased roughness) with increasing

**Figure 17.** Molecular free energies (a) and internal energies (b) vs surface roughness parameter δ at different temperatures for once-folded alkane crystal, using the model in Figure 16. Circles mark the free energy minima. The dashed line shows the temperature dependence of equilibrium energy (after ref 40).

temperature. The corresponding energies are shown in Figure 17b, the dashed curve delineating the temperature dependence of the equilibrium state energy. The premelting, or surface roughening, is evident. The dashed curve in Figure 17b should be compared to the temperature dependence of SAXS intensity (Figure 15 and ref 92) and of enthalpy (see Figure 5a in ref 92).

More about the fold surface can be learned from studies of cyclic compounds (see Section II.F).

E. Chain Tilt

Closely associated with lamellar surface disorder is the phenomenon of chain tilt. In many crystalline polymers, chains are often tilted relative to the layer normal. In polyethylene, this leads, e.g., to the "hollow pyramid" shape of solution-grown single crystals.¹ Further, chain tilt is believed to be responsible for lamellar twist in melt-crystallized spherulites.^{96,97} The development of tilt is associated with crystallization or annealing at high temperatures. Thus, e.g., perpendicular-chain lamellar morphology in rolled polyethylene transforms into "parquet-floor" morphology on annealing.⁹⁸ Crystal lamellae with tilted chains are obtained at high T_c from the

melt.^{99,100} In solution-grown crystals of long alkanes, whether folded or extended, the chains are perpendicular, while in those grown from melt, chains are tilted.^{33,93} As in polyethylene, the difference has been associated with T_c being lower in the former case. In polyethylene and long alkanes the tilt is usually 35 degrees, which means that the basal plane is {201} instead of {001} as in the case of perpendicular chains. The {201} tilt arises when each consecutive chain along the a -axis is shifted by one lattice period in the chain direction. Such tilt allows chain ends and folds an increased surface area, by a factor of $1/(\cos 35^\circ)$, while maintaining the crystallographic packing of the rest of the chain intact.¹⁰¹

In apparent agreement with the behavior of polyethylene, shorter n -alkanes crystallize with perpendicular chains as long as T_c is below ca. 60–70 °C.⁸ This is true for odd-numbered alkanes; even-numbered ones display a more complex behavior due to molecular symmetry.¹⁹ At higher temperatures in alkanes such as $C_{33}H_{68}$, a {h01} tilted form is brought about through one or several discrete transitions.¹⁰ In this case, tilt is associated with equilibrium surface disorder, and the absence of tilt with high end-group order. When perpendicular-chain solution-crystallized n -alkanes with more than ca. 50 carbons are heated, chain tilt is introduced gradually. Up to $C_{94}H_{190}$ crystals melt before a tilt of 35° is reached,^{93,102} whereas for alkanes $C_{198}H_{398}$ and longer, the 35° tilt angle is attained, remaining constant until the melting point.¹⁰³ The change is mostly irreversible, i.e., the tilt remains on cooling, which is also often the case with shorter alkanes.

While the lack of tilt in alkanes such as $C_{33}H_{68}$ is identified with high surface order, in polyethylene, it was attributed to a rough disordered surface.^{97,104} Experiments with a recently synthesized¹⁰⁵ end-deuterated long alkane, $C_{12}D_{25}C_{192}H_{384}C_{12}D_{25}$, have provided direct proof that the latter is indeed the case for long chains.¹⁰³ As expected, solution-grown extended-chain crystals have perpendicular chains which gradually tilt to 35° with increasing temperature, as determined by SAXS. However, parallel IR spectroscopy experiments reveal that, instead of increasing in disorder, the crystal surface becomes more ordered at higher temperatures. At all times, crystal interior is more ordered than the surface, but internal order improves only marginally on annealing. The above assertions are evident from the temperature dependence of CH_2 and CD_2 bending modes, shown respectively in panels a and b of Figure 18. In ordered orthorhombic crystals of pure H or D species, these bands are well-resolved doublets due to crystal field (Davydov) splitting. The reduced CD_2 splitting indicates positional or orientational disorder of the deuterated surface layer. Since isolated or amorphous chains show no splitting, the singlet component around 1089 cm^{-1} in the unannealed (25 °C) sample is attributed to excursions of the $C_{12}D_{25}$ group outside the crystal or inside the hydrogenous layer. With increasing temperature, these excursions disappear (Figure 18b).

The above evidence suggests that low-temperature solution crystallization produces a high degree of

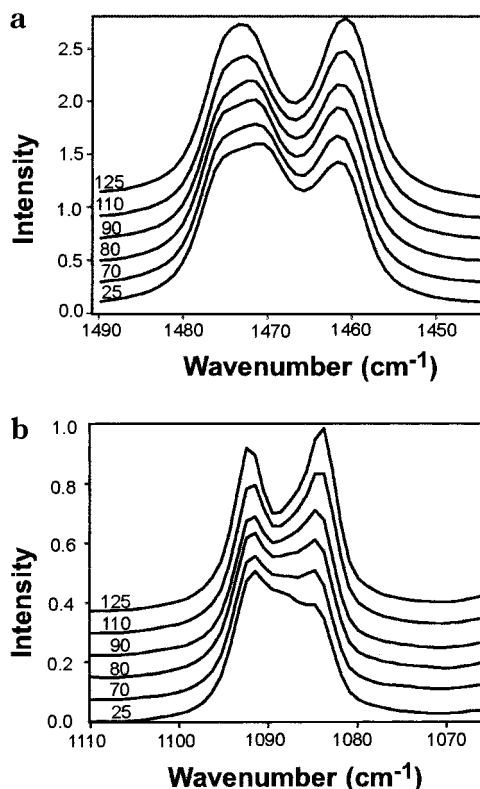


Figure 18. (a) CH_2 and (b) CD_2 deformation bands in the IR spectrum of extended-chain solution-grown crystals of end-labeled n -alkane $C_{12}D_{25}C_{192}H_{384}C_{12}D_{25}$. The sample was annealed at the temperatures indicated (in °C) and the spectra recorded at 110 K (from ref 103).

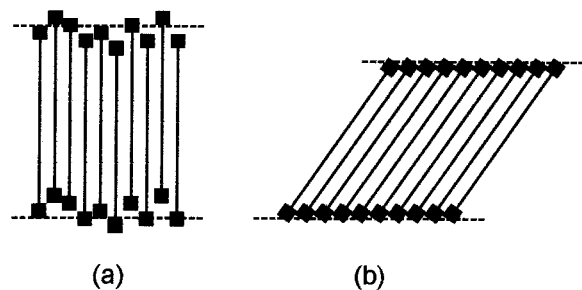


Figure 19. Schematic representation of deuterium end-labeled chains in a crystal as-grown from solution (a) and after annealing (b). The end-group disorder in panel a causes the reduction in CD band splitting in Figure 18b (from ref 103).

translational disorder with randomly staggered chain ends (see Figure 19a). With increasing temperature and mobility, this frozen-in disorder is reduced as uniform stagger with chain tilt replaces the random stagger (Figure 19b). Further support is provided by recent experiments which show that, where it was possible to melt-crystallize extended-chain long alkanes at a high supercooling, perpendicular chains were obtained; these would tilt on subsequent annealing.¹⁰⁶ In light of the above evidence, the model of “buried folds”, i.e., randomly staggered folds, which has been invoked in the past as a possible solution to the surface overcrowding problem,¹⁰⁷ merits attention in the case of crystals grown from melt or solution at low temperatures. The experiments on $C_{12}D_{25}C_{192}H_{384}C_{12}D_{25}$ show that, once annealed, the crystals retain tilted chains, with subsequent heating

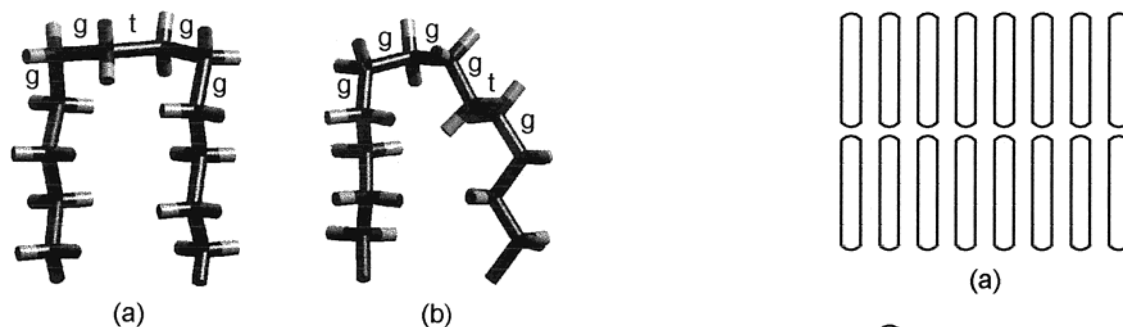


Figure 20. (a) Structure of the chain fold in crystalline monoclinic cycloalkane $c\text{-(CH}_2\text{)}_{34}$, representative of the $\{100\}$ fold in polyethylene (after ref 109); (b) calculated minimum energy conformation of a $\{110\}$ chain fold in orthorhombic polyethylene (after ref 116).

and cooling causing only reversible changes in surface disorder, in agreement with the ideas discussed in the preceding section.

The observation that in polyethylene crystals lateral faces with perpendicular chains grow faster than those with tilted chains^{96,97} is in agreement with the above link between orthogonality and high kinetically induced surface disorder. A parallel situation exists in shorter even-numbered n -alkanes with 28 or more carbons, where a form with perpendicular chains and comparatively rough surface results from rapid melt crystallization, despite the stable structure having smooth $\{011\}$ tilted basal planes.¹⁹ Thus, the only case where orthogonality is due to a highly ordered surface appears to be that of odd-numbered shorter alkanes.^{8,10}

A new crystal structure with tilted chains has recently been found in pentamer of nylon-6 and nylon-8, termed λ -phase.¹⁰⁸ Molecules are in the all-trans conformation and hydrogen bond to antiparallel neighbors to form the usual nylon 6 hydrogen-bonded sheets. However, in this structure, the sheets stack with progressive c -axis shear, and consequently, the molecular layer thickness is noticeably reduced.

F. Cyclic Oligomers

Large cyclic alkanes crystallize as collapsed rings consisting of two straight stems linked by two folds,^{109–111} (cf. Figure 21a). For this reason they have been studied as model folded polyethylene chains. Cycloalkanes up to $(\text{CH}_2)_{96}$ were synthesized by Schill et al.¹¹² and up to $c\text{-(CH}_2\text{)}_{288}$ by Lee and Wegner.³¹ It has been reported that cycloalkanes up to $c\text{-(CH}_2\text{)}_{48}$ are monoclinic, while $c\text{-(CH}_2\text{)}_{72}$ and $c\text{-(CH}_2\text{)}_{96}$ show a mixture of monoclinic and orthorhombic modifications, depending on crystallization conditions.^{72,111} The large ring $c\text{-(CH}_2\text{)}_{144}$ was always orthorhombic, irrespective of crystallization conditions.⁷² Orthorhombic refers here to the subcell, involving only four CH_2 groups; this cell is the same as that in long linear alkanes and polyethylene.

In monoclinic cycloalkanes, unlike in the orthorhombic ones, the zigzag planes of the two stems are parallel to each other (see Figure 20a). The folds in monoclinic cycloalkanes may therefore be representative of polyethylene folds lying in the $\{100\}$ plane,

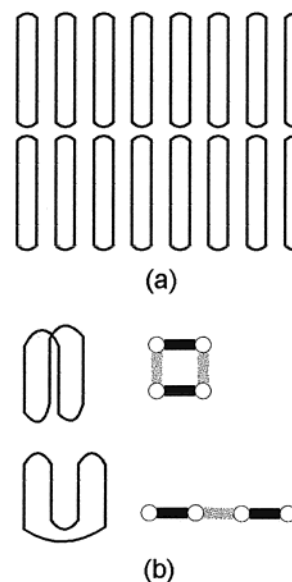


Figure 21. (a) Packing of collapsed rings into crystalline layers; (b) Side and top view of two proposed possible conformations of the folded large cyclic PEO $M_n = 10\,000$ (schematic, from ref 122 by permission of American Chemical Society).

i.e., connecting adjacent stems along the crystallographic b -axis. Such folds are expected primarily in melt-grown polyethylene crystals, where $\{100\}$ growth face is dominant, but not in the rhombic solution-grown crystals where $\{110\}$ folds prevail.¹¹³ In the orthorhombic form, the zigzag planes of the two cycloalkane stems are nearly perpendicular to each other, rather than parallel, and the folds in orthorhombic cycloalkanes may therefore be representative of $\{110\}$ folds in polyethylene (Figure 20b).

Using atomic force microscopy (AFM), lamellar surface of normal and cyclic alkanes $\text{C}_{33}\text{H}_{68}$, $\text{C}_{36}\text{H}_{74}$, $(\text{CH}_2)_{48}$, and $(\text{CH}_2)_{72}$ was examined to atomic scale.¹¹⁴ In the cycloalkanes, the observed images are consistent with adjacent re-entry $\{100\}$ folds in a monoclinic crystal structure.

Room-temperature IR spectra of monoclinic cycloalkanes $(\text{CH}_2)_n$ with $30 < n < 96$ show three bands whose intensity increases as $1/n$, associating them in some ways with the fold.¹¹⁵ These are the 1344 cm^{-1} CH wagging band, already discussed in Section II.D, as well as bands at 1442 and 700 cm^{-1} , presumably CH bending and CH rocking. In melt-crystallized $c\text{-(CH}_2\text{)}_{72}$ and $c\text{-(CH}_2\text{)}_{96}$, which contain an orthorhombic fraction, bands at 1368 cm^{-1} and around 1300 cm^{-1} are also seen, which signifies the presence of gtg defects; the gg band at 1352 cm^{-1} is also present. These results can be rationalized by considering the minimum energy tight fold models: a $ggtgg$ conformation for a $\{100\}$ fold (monoclinic cycloalkanes) and possibly a $gtggg^*g^*$ for a $\{110\}$ fold [orthorhombic cycloalkanes (see Figure 20b)].¹¹⁶ The observed spectra could be understood assuming (a) that the $1342\text{--}1344\text{ cm}^{-1}$ band represents strained gg sequences [monoclinic cycloalkanes and once-folded orthorhombic n -alkanes at low-temperatures (see Section II.D)], and (b) that the 1352 cm^{-1} band represents relaxed gg sequences (orthorhombic once-

folded *n*-alkanes and cycloalkanes at room temperature). Low-temperature spectra of cycloalkanes have not been reported. The calculated energy of a model {110} fold (20.4 kJ/mol) is somewhat higher than that of a {100} fold (16.3 kJ/mol).¹¹⁵ This is consistent with the smaller rings being monoclinic and larger rings orthorhombic. It would appear that stem packing favors the orthorhombic form while folds favor the monoclinic form.

A detailed solid-state ¹³C NMR study on *c*-(CH₂)₁₂, *c*-(CH₂)₂₄, and *c*-(CH₂)₃₆ has been carried out resulting in the assignment of chemical shifts for a number of rotational isomeric sequences in alkanes.¹¹⁷ Chemical shifts for carbons at the center of sequences *gtgg*, *gttg*, *ggtt*, *tggt*, *gttt*, and *tttt* were identified. The assignments were based on low temperature spectra, since at higher temperatures the cycloalkanes investigated transform into highly conformationally disordered crystals with a pseudo-hexagonal structure.^{118,119} In terms of enthalpy and entropy, as well as number of nonplanar conformers, this “mesophase” is closer to the melt than to the ordered crystal. It has therefore been compared to the high-pressure hexagonal mesophase in polyethylene, rather than to the “rotator” phase in linear alkanes with $n \leq 40$.¹²⁰

Even in the largest cyclic alkane synthesized, *c*-(CH₂)₂₈₈, only the “extended” ring conformation has been observed, i.e., the two stems constituting the collapsed ring did not fold further.³¹

Cyclic PEO has been prepared in two ways: (a) with narrow PEO fractions as starting material, using ring closure Williamson reaction^{121,122} and (b) as monodisperse rings, effectively large unsubstituted crown ethers.^{123–126} The largest monodisperse ring prepared and used in crystallization studies was *c*-E₂₇ (E = CH₂CH₂O), or 81-crown-27. In the latter case, the two stems of the collapsed ring were found to have the same helical *tgt* conformation and the same monoclinic subcell as linear PEO chains.¹²⁵ In contrast, smaller rings show a different crystal structure.¹²⁴ The boundary was found to lie between *c*-E₁₆ and *c*-E₁₈.¹²⁶ The melting points of the ring compounds were significantly higher than those of their linear analogues, an effect attributed to a decreased melting entropy.

Rings prepared from commercial PEO fractions had M_n up to 10000 (equivalent to *c*-E₂₂₇).¹²² SAXS and Raman LAM measurements showed that for $M_n = 6000$ such cyclic polymers crystallize as collapsed rings forming layers, as in the case of the large crown ethers and cycloalkanes (see Figure 21a). However, the cyclic polymer of $M_n = 10\,000$ crystallized in a folded conformation when cooled from its melt at moderate rates. That is to say, each stem of the collapsed ring was folded again in two (see Figure 21b). When the $M_n = 10\,000$ sample was crystallized slowly at a high temperature, the conformation of the extended collapsed ring (Figure 21a) was obtained.

A Raman study has shown that LAM-1 frequencies of cyclic PEOs in the range $1000 < M_n < 3000$ are only 1.8 times higher than those of their linear counterparts.¹²⁷ This is in contrast with cycloalkanes, where the LAM-1 frequency of *c*-(CH₂)_{*n*} is nearly exactly twice that of linear C_{*n*}H_{2*n*+2}.¹²⁸

Small ring oligomers of several other polymers have been synthesized, and their crystal structures determined. Thus, relevant to the industrially important cyclic impurities in poly(ethylene terephthalate) (PET), the structures of the low-temperature¹²⁹ and the high-temperature¹³⁰ modifications of cyclic PET trimer have been determined. The structure of cyclic dimer of poly(butylene terephthalate) (PBT) has also been determined¹³¹ in order to help understand a mechanically induced polymorphic transition in the parent polymer. Limited crystallization work has been done on the otherwise extensively studied cyclic oligosiloxanes;¹³² the object was “cold crystallization” near the glass transition temperature.

Cyclic main-chain liquid crystal oligomers have been shown to display a number of crystalline polymorphs in addition to smectic and nematic phases.¹³³ These collapsed rings have rigid mesogens in their “stems” while folds form selectively in the flexible spacer. Significant difference between even and odd-membered rings are seen, particularly where the flexible spacer is short.

G. Oligomers with Specific Endgroups

Prior to the synthesis of long *n*-alkanes in 1985, the narrowest molecular weight distribution achieved in paraffinoid chain systems in the 100–400 C-atom range was α,ω -dicarboxylic acids produced by selective oxidation of solution-grown polyethylene single crystals. Nitric acid or ozone treatments¹³⁴ were applied to remove the fold layer, and the length of the remaining alkanoid diacid was determined by the thickness of the original crystalline layer; this, in turn, could be controlled by the choice of crystallization or annealing temperature. The carboxylic end groups have also been reduced, resulting first in α,ω -dibromoalkanes and, finally, alkanes. While crystallization studies on alkanes thus produced have not been reported, both the long diacids and dibromides showed only continuous change of long spacing with crystallization temperature.¹³⁴

Most linear oligomers can be regarded as having “special” end-groups, and as stated at the beginning, one of the reasons for synthesising long alkanes was the similarity of end groups with the bulk of the chain. In a number of studies of PEO fractions, which are normally OH-terminated, methoxy-terminated equivalents (MPEO) were also examined for comparison. Thus, it was found that crystallization is more rapid in MPEO compared to that in PEO and that the same is true for subsequent transformation of NIF into IF forms.³⁴ OH groups show a degree of hydrogen bonding, as evidenced by IR spectroscopy. The self-diffusion coefficient of MPEO in the melt was found by spin-echo NMR measurements to be higher, by a factor of 1.17, than that of PEO, although the activation energies were the same.

There has been some evidence from TEM¹³⁵ and Raman⁴⁵ that hydroxy-terminated PEO fractions form double-layer crystals, but doubts have been expressed subsequently.³⁸ End-group interaction in low-molecular weight PEO fractions certainly has a pronounced effect on LAM frequency. The following two linear relationships were found between the

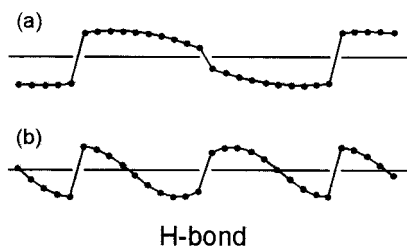


Figure 22. Schematic representation of the vibrational displacement describing the first (a) and the second (b) LAM modes for a molecular dimer in α -methyl- ω -hydroxy-[oligo(oxyethylenes)]. Longitudinal displacement is presented as transverse (from ref 47 by permission of American Chemical Society).

frequency of LAM-1 mode (in cm^{-1}) and reciprocal chain length (in \AA^{-1}):³⁸

$$\text{PEO: } \nu_1 = 1161.1 L^{-1}$$

$$\text{MPEO: } \nu_1 = 1094.7 L^{-1}$$

The case for double layer formation in PEO-type oligomers has been made in a series of monodisperse α -methyl- ω -hydroxy[oligo(oxyethylenes)], or $\text{C}_1\text{E}_p\text{OH}$, where p is the number of oxyethylene units.⁴⁷ The authors have applied the dynamic model by Minoni and Zerbi⁴⁴ to describe the two strongest LAM peaks observed in Raman spectra. These correspond to what can be described as first and second modes of a dimer (see Figure 22).

When a series of OH-terminated monodisperse oligo(oxyethylenes) and PEO fractions were compared, it was found that in the former case H-bonding has a considerably stronger effect in increasing the LAM-1 frequency relative to methoxy terminated chains.¹²¹ This stronger H-bonding was attributed to the regularity of the end-surface in monodisperse compounds.

Short-chain fatty acids are well-known to crystallize as double layers due to dimerization by hydrogen bonding.¹³⁶ Recently, however, bilayer crystallization has been demonstrated in a very long-chain n -alkanoic acid, $\text{C}_{191}\text{H}_{393}\text{COOH}$.¹³⁷ Figure 23 shows a series of SAXS curves recorded during slow cooling of the acid from the melt. The traces in the front represent the bilayer phase crystallized at the highest temperature. Odd diffraction orders of the 410 \AA periodicity are dominant, which is compatible with the electron density profile in Figure 24a, with carboxylic layer maxima and methyl layer minima. Below 129 $^\circ\text{C}$, crystallization switches to producing 205- \AA -thick monolayers, as indicated by the apparent intensification of even-order reflections. In the monolayer form, carboxylic groups are evenly distributed between either surface of the crystal layer (see Figure 24b). IR spectra show that most carboxylic groups are H-bonded both below and above the melting point.¹³⁸ $\text{C}_{191}\text{H}_{393}\text{COOH}$ dimers thus act as supramolecular chains of twice their molecular length. Crystallized in bilayers and monolayers, they can be considered, respectively, as extended and once-folded supramolecules. The two corresponding melting points differ by 2 $^\circ\text{C}$, compared to a difference of 3 $^\circ\text{C}$

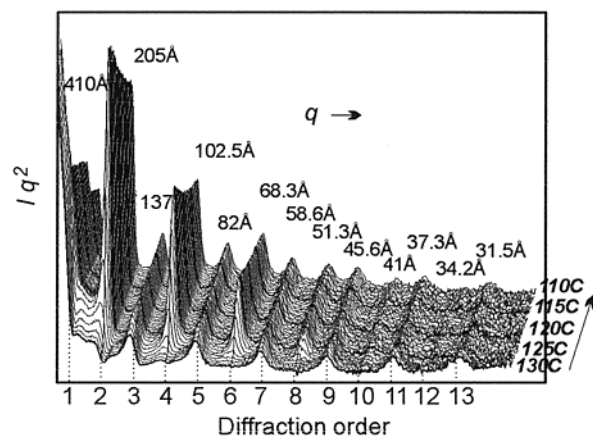


Figure 23. SAXS traces (Lorentz corrected intensities vs q) of n - $\text{C}_{191}\text{H}_{385}\text{COOH}$ recorded during cooling of an already partially crystallized sample at 0.3 $^\circ\text{C}/\text{min}$ from 132 to 112 $^\circ\text{C}$. Bragg spacings corresponding to the observed peak positions, recording temperatures and diffraction orders of the bilayer phase are marked (from ref 137 by permission of American Chemical Society).

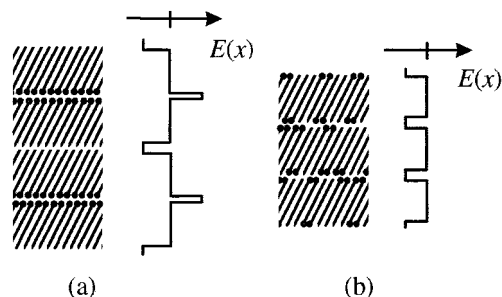


Figure 24. Schematic sketches of the double layer (a) and monolayer (b) structure of n - $\text{C}_{191}\text{H}_{385}\text{COOH}$. Circles represent carboxylic groups. Electron density profiles, $E(x)$, are shown schematically on the right (from ref 137 by permission of American Chemical Society).

between the melting points of extended and once-folded alkane $\text{C}_{390}\text{H}_{782}$ (see Table 3).

A comparative study has been performed on PEO fractions with molecular weights 3000 and 7100 having the following end-groups: hydroxy (HPEO), methoxy (MPEO), t -butoxy (TPEO), and phenoxy (PPEO).¹³⁹ Initial NIF long period l_{SAXS} obeyed the $c/(\Delta T)$ dependence, with the constant c decreasing in the series MPEO, HPEO, TPEO, PPEO. A similar descending series MPEO, TPEO, HPEO, PPEO was found in NMR diffusion coefficients. The differences are generally more pronounced for the 3000 fraction. The NIF \rightarrow IF transformation was also found to be retarded in the less mobile oligomers. Since the bulky end-groups tended to promote NIF rather than disfavor it, the results seem to support a model of NIF in which chain ends remain outside the crystal layer.

H. Monodisperse Block Copolymers

Although many block copolymers have a narrow molecular weight distribution, they will not be reviewed here as they present a broad subject of their own. Short uniform di-block chain compounds have been prepared and extensively studied in cases such

Table 3. Comparison of Melting Points of the Two Lamellar Forms of *n*-Alkanoic Acid C₁₉₁H₃₉₃COOH with Those of Integer Forms of Alkanes C₁₉₄H₃₉₀ and C₃₉₀H₇₈₂ (ref 138)

compd	form	T _m (°C)	form	T _m (°C)
C ₁₉₄ H ₃₉₀	extended	126.2 ± 0.3		
C ₁₉₁ H ₃₉₃ COOH	monolayer	130.0 ± 0.5	bilayer	131.9 ± 0.3
C ₃₉₀ H ₇₈₂	once-folded	129.0 ± 0.3	extended	132.0 ± 0.3

as alkyl-perfluoroalkyl diblocks^{140,141} and alkyl-oligo-(oxyethylene) and similar nonionic surfactants. The current review is limited to long, truly monodisperse di-block and tri-block chain molecules. By doubling and tripling monodisperse ethylene glycol oligomers, such as pentadeca(ethylene glycol), Booth and co-workers prepared several series of C_nE_pC_n triblock copolymers, where E_p denotes *p*-mer of ethylene oxide and C_n a normal alkyl end-group C_nH_{2n+1}. For *p* ≤ 25, the E segment was crystalline (helical conformation) and extended, with the alkyl chain ends either amorphous (small *n*) or in a disordered crystalline state similar to the rotator phase (intermediate *n*). For *n* > 26 and at lower temperatures, the structure is dictated by the alkyls forming ordered crystalline layers. Here the E blocks are noncrystalline although in the predominantly planar zigzag conformation which better matches the cross-sectional area of the alkyl groups. From SAXS measurements it was concluded that for smaller *p* the E blocks are essentially extended, but for *p* = 15 and 25 they are once-folded. Only for *p* ≥ 45¹⁴² can both blocks be nearly completely crystalline. Extended, once-folded and noninteger forms are observed; the NIF converts to one of the IF forms at a higher temperature through melting and recrystallization.

Monodisperse diblock oligo(ethylene oxide) mono-*n*-alkyl ethers have also been prepared and studied.¹⁴³ Oligomers with hydroxy-ended E-blocks formed bilayer crystals (cf. Section II.G and Figure 22), and the methoxy-ended oligomers formed monolayer crystals. The helical oxyethylene blocks were perpendicular to the layer plane, while the alkyl blocks were generally tilted at 30° to the layer normal. Monodisperse triblock oligomers with a central methylene block and outer oxyethylene blocks were also studied subsequently¹⁴⁴ and both fully crystalline and partly crystalline structures were found, with chains in wholly trans-planar and mixed trans-planar/helical conformations.

An AFM study was carried out on thin crystalline films of a diblock and a triblock poly(oxyethylene)/poly(oxybutylene) (E/B) copolymer deposited on silicon.¹⁴⁵ At room-temperature E blocks are crystalline and B blocks are amorphous. The crystal thickness determined from AFM was compared to the bulk layer spacing determined by SAXS. It was shown that E₄₁B₂₂E₄₁ largely crystallizes in a monolayer form with unfolded E blocks at the substrate and folded B blocks at the polymer–air interface and with the E blocks tilted at an angle of ca. 40° to the substrate normal. Multiple layers with a common step height were observed for the diblock E₂₇B₆ crystallites, which were largely comprised of unfolded chains, also with E block tilted at an angle of ca. 40°.

I. Branched Oligomers

Cheng and co-workers have studied 2-, 3-, and 4-arm branched oligomer fractions where the PEO arms are connected via a benzene ring. Symmetrical two-arm PEO oligomers were prepared by coupling two chains of a PEO fraction with 1,4-benzene dicarbonyl dichloride.¹⁴⁶ In the material with the arm's molecular weight *M_n^a* = 2200, NIF crystals form initially, followed by apparent thinning during subsequent annealing. The lamellar spacing of NIF is longer than the extended chain length of one arm but shorter than that of the two-arm PEO. The long spacing of the final crystal, as well as its melting point, are similar to those of linear PEO with the length of a single arm. Similar but more complex behavior was observed in the two-arm PEO with *M_n^a* = 5500, where individual arms have the ability to fold.

Three two-arm PEOs with the same arm length (*M_n^a* = 2200) but coupled via different substitutions (1,2-, 1,3-, and 1,4-) of the benzene rings were further studied.^{147,148} The broad melting peak for samples crystallized at low supercoolings was regarded as composed of two overlapping components, and so was the first-order SAXS peak. It was postulated that the SAXS peak with shorter spacing corresponded to the extended chain conformation of the two-arm PEO, whereby one layer of benzene rings exists between two neighboring lamellae, while once-folded two-arm PEOs would have two phenylene layers lying between neighboring PEO lamellae and thus have a longer spacing. It was found further that by changing the coupling angle of the arms, i.e., changing from 1,4- (180°) to 1,2-substitution (60°), the extended conformation became increasingly difficult to achieve.

In the case of three- and four-arm PEOs, it was found that at low supercoolings the initial NIF lamellae undergo continuous thinning.¹⁴⁹ However, the final system has a 10–15% lower crystallinity (after weight correction for the coupling agent) compared to that of the equivalent linear PEO, suggesting that uncrystallized PEO arms exist between the crystalline layers. At high supercoolings, the long period remained constant. On subsequent heating the crystallinity decreases by about 10% (partial melting) and only increased slightly (by 1–2%) upon prolonged annealing. The underlying mechanism remains unclear.

Melt- or solution-crystallization of alkanes C₉₆H₁₉₃-CH(CH₃)C₉₄H₁₈₉ and C₉₆H₁₉₃CH(C₄H₉)C₉₄H₁₈, which contain a short branch in the center of an otherwise linear chain, always produced the once-folded (F2) conformation (see Figure 6f). In melt-crystallization, this is formed via a very short-lived NIF intermediary stage, see Figure 5b and Figure 6e. As described in Section II.C, the rapid NIF → F2 transition is

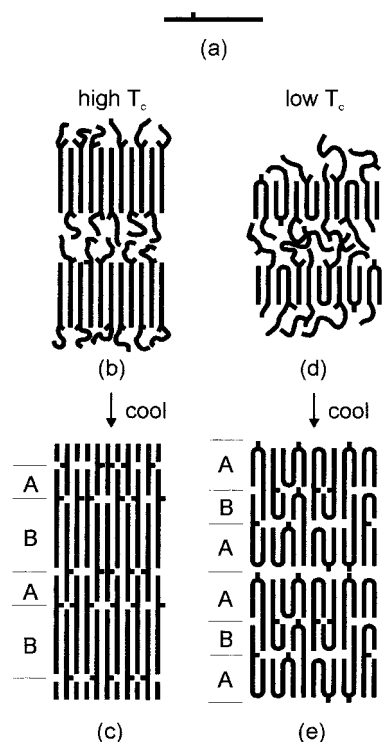


Figure 25. Schematic drawing of different lamellar structures observed in asymmetric methyl-branched alkane $C_{191}H_{383}CH(CH_3)C_{99}H_{199}$ (a); (b) semicrystalline form obtained at high T_c ; (c) double layer crystalline form obtained from panel b on cooling; (d) semicrystalline form obtained at low T_c ; (e) triple layer crystalline form obtained from panel d on cooling. Chain tilt is neglected in this and Figure 26, for simplicity (from ref 151).

believed to be due to the initial preference for “correct” chain attachment dictated by the exclusion of the branch to the lamellar surface.

The above butyl-branched alkane was studied by solid-state ^{13}C NMR, alongside its linear analogue $C_{198}H_{398}$, to establish the solid-state diffusion coefficient.¹⁵⁰ Both alkanes were in the once-folded form. The progressive saturation experiments have shown that the longitudinal relaxation of magnetization is consistent with a solid state chain diffusion process. Reptation and one-dimensional diffusion models were demonstrated to satisfactorily represent the data. The addition of the branch to the alkane chain was shown to result in a decrease in the diffusion coefficient, which ranged from $0.0918 \text{ nm}^2 \text{ s}^{-1}$ for the linear chain to $0.016 \text{ nm}^2 \text{ s}^{-1}$ for the branched chain. These diffusion coefficients are consistent with those of polyethylene.

Asymmetrically methyl-branched alkane $C_{191}H_{383}CH(CH_3)C_{99}H_{199}$ (Figure 25a), synthesized recently,¹⁰⁵ has been studied by real-time SAXS.¹⁵¹ The compound can be crystallized in two different semicrystalline forms, depending on crystallization temperature T_c . Electron density reconstruction has shown that in each case the structure consists of alternating crystalline and amorphous layers with respective thicknesses l_c and l_a ($l_c + l_a = l$). In the first form, obtainable only at high T_c , the longer arm of the alkane crystallizes as extended chain, while the shorter arm remains as a *cilium*, contributing to the

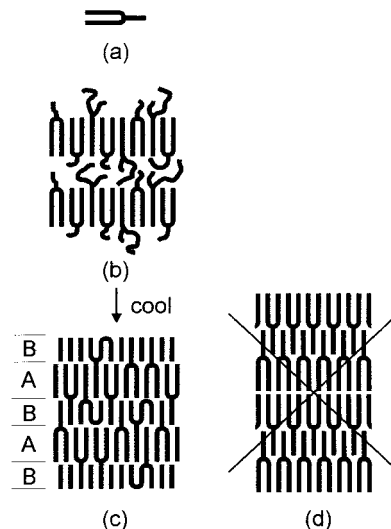


Figure 26. Schematic drawing of lamellar structures in Y-shaped alkane $C_{120}H_{241}CH(C_{61}H_{123})C_{119}H_{239}$ (a); (b) high-temperature semicrystalline form; (c) low temperature double layer crystalline form; (d) the hypothetical energy favored but kinetically unattainable structure (from ref 151).

amorphous layer (Figure 25b). At low T_c , another semicrystalline form is obtained. Here l_c is smaller and is determined by the length of the shorter arm. As shown in Figure 25d, the extended shorter arm and part of the longer arm may contribute to the crystalline layer, with the remainder of the long arm staying in the amorphous layer.

When either of the semicrystalline forms of the asymmetric alkane are cooled, they transform to a double-layer and a triple-layer crystalline structure, respectively. These 1-d superlattices are described as ABAB... and ABAABA... stacks of crystalline layers as depicted in Figure 25, panels c and e. Note that the structure in Figure 25e is related to the mixed integer “folded-extended” structure in some pure n -alkanes (Figure 7c) and in binary mixtures of long n -alkanes (Section II.J, Figure 30b).

Y-shaped alkane $C_{120}H_{241}CH(C_{61}H_{123})C_{119}H_{239}$, which has two long and one shorter arm (Figure 26a), has also been prepared¹⁰⁵ and investigated.¹⁵¹ A semicrystalline structure was found in the high-temperature region, with the crystalline layer thickness being determined by the length of the long arms. From the thickness of the amorphous layer l_a it was concluded that some molecules have both their long arms crystallized, but others have only one crystallized, the other two remaining in the amorphous layer (see Figure 26b). A double layer crystalline superstructure is formed in a transition on subsequent cooling, with one layer containing only long arms of the molecules and the other layer containing both extended short arms and folded long arms (see Figure 26c).

From the observations on branched PEO and alkanes more general conclusions can be drawn about the overcrowding problem at the crystalline–amorphous interface in polymers and about the mechanism of chain deposition during crystal growth. Thus, e.g., although for the Y-shaped alkane the energeti-

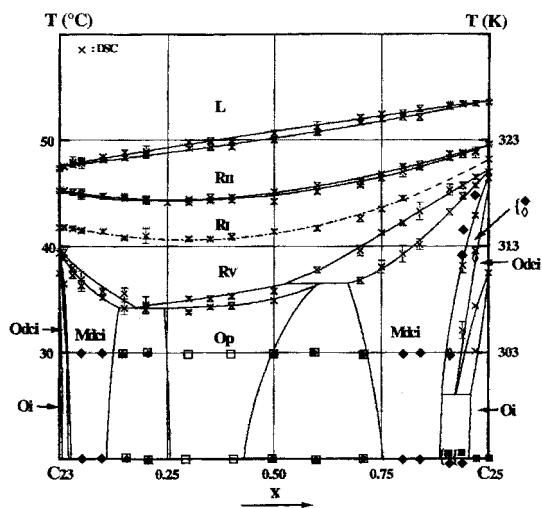


Figure 27. Binary phase diagram of the *n*-alkane system $C_{23}H_{48}$ – $C_{25}H_{52}$. Phases denoted with capital letters R, O, and M refer, respectively, to rotator, orthorhombic and monoclinic (from ref 157 by permission of Materials Research Society).

cally most stable state is that in Figure 26d, this state has proven to be kinetically unattainable. Further, by measuring the thickness of the amorphous layer l_a as a function of time and T_c one can obtain detailed experimental information on the number of chains crossing the crystal–amorphous boundary, giving valuable insight into the equilibrium and kinetic overcrowding effects, fold adjacency etc.

J. Binary Mixtures

A number of early studies have focused on phase diagrams of various binary *n*-alkane systems.^{152–154} General conditions for solid solution were set out by Kitaigorodskii¹⁵⁵ in terms of molecular size and symmetry. The maximum allowed difference in the number of C atoms has been stated empirically as¹⁵⁶

$$n_{\text{long}} = 1.224n_{\text{short}} - 0.411 \quad (4)$$

Binary phase diagrams of these shorter *n*-alkanes have turned out recently to be rather complex and subtle, even if the chain length difference is minimal and even in the case of two odd alkanes, where previously it was thought that miscibility is complete. Figure 27 illustrates this on the example of $C_{23}H_{48}$ – $C_{25}H_{52}$.¹⁵⁷ In the case of even alkanes, although the stable phases of the individual even component may be triclinic or monoclinic, the most prevalent crystal structures of the mixture is orthorhombic at low temperatures and rotator (usually pseudohexagonal) at higher temperatures.^{158–163} The orientationally disordered rotator phase allows improved miscibility close to the melting point, but with increasing chain length it is destabilized; it has not been seen to play a role in mixtures of long alkanes.

Because the length difference of the two miscible components is small, the disorder is considered mainly in terms of site occupancies close to the lamellar surface.^{159,163} Thus, alkane solid solutions provide good models of surface disorder, which has been studied by infrared and Raman spectroscopy.

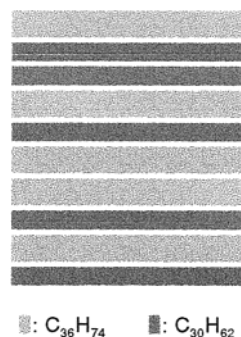


Figure 28. Proposed structural model of the $C_{30}H_{62}$ – $C_{36}H_{74}$ binary mixture. The $C_{30}H_{62}$ and $C_{36}H_{74}$ species are separated in individual layers, which stack randomly (after ref 163).

copy.^{16,164,165} Alkane mixtures have also helped understand the nature of the rotator phase,^{21,160,166} as well as chain defects and molecular motion in general.¹⁶⁷ Phase change induced by mixing has been utilized in monitoring interdiffusion after crystals of different alkanes are put in mechanical contact.^{17,18,168}

Beside true solid solutions in which disparate molecules are intimately mixed, various modulated lamellar structures were observed in mixtures $C_{30}H_{62}$ + $C_{36}H_{74}$,¹⁶⁹ $C_{30}H_{62}$ + $C_{40}H_{82}$,¹⁷⁰ and $C_{28}H_{58}$ + $C_{36}H_{74}$.¹⁷¹ The structural models proposed were mostly based on random or nonrandom stacking of lamellae which were essentially composed of pure components¹⁶³ (Figure 28). Recent structural studies have been extended to multicomponent mixtures.¹⁷²

Crystallization theory and equilibrium thermodynamics of mixed alkanes have been discussed by Lauritzen, Passaglia, and DiMarzio¹⁷³ (LPD) and Asbach and Kilian.¹⁷⁴ In the LPD theory, the excess end-surface energy comes from exposed side surface due to nonuniformity in chain length. In contrast, Asbach et al. treat the enthalpy of mixing in more general terms. LPD theory has been applied to melting and the solid-state transition of binary mixtures of *n*-alkanes.¹⁷⁵

In contrast to the shorter alkanes, long *n*-alkanes were recently found to form solid solutions in a wide range of compositions, even if the chain lengths of the components differed by more than 100 C-atoms. Binary mixtures of long alkanes with the chain length ratio between 1.3 and 2 have been found to form predominantly two mixed phases, a high-temperature and a low-temperature one, separated by a reversible transition.¹⁷⁶ Figure 29 shows SAXS traces of the high-temperature form of four 1:1 w:w mixtures of $C_{162}H_{326}$ with a longer alkane of increasing length, including pure $C_{162}H_{326}$. The inset shows the corresponding best-fit electron density profiles perpendicular to the lamellae. The central high-density crystalline layer retains the same thickness l_c for all mixtures; however, the thickness of the low-density amorphous layer l_a increases in proportion with the surplus length of the longer alkane. Accordingly, the structural model in Figure 30a was proposed: while the shorter alkane is fully crystalline and confined to the crystal layer, the longer alkane chains traverse the crystal layer and the surplus length, the *cilia*,

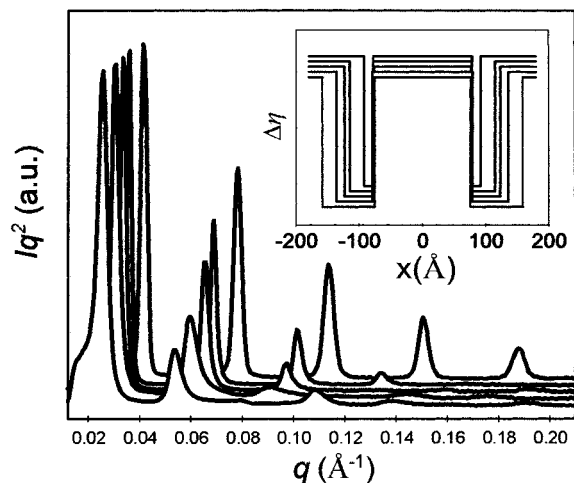


Figure 29. Small-angle diffractograms of $C_{162}H_{326}$ and of the high-temperature phase of 1:1 w:w binary mixtures of $C_{162}H_{326}$ with, from top to bottom, $C_{194}H_{390}$, $C_{210}H_{422}$, $C_{246}H_{494}$, and $C_{258}H_{518}$. The inset shows the corresponding best-fitting electron density model profiles (from ref 176 with permission of the American Physical Society).

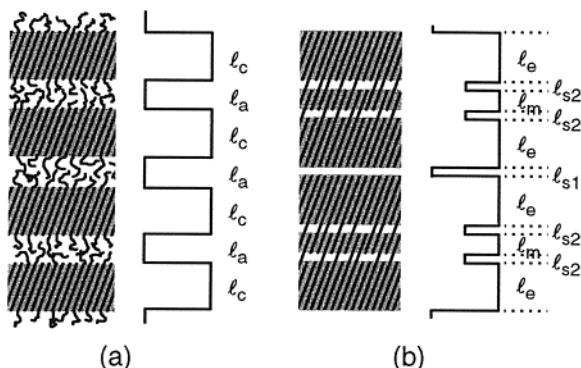


Figure 30. Schematic structures of (a) the high-temperature semicrystalline phase, and (b) the low-temperature triple-layer superlattice in binary long alkanes. Model electron density profiles are shown on the right, with density increasing from left to right (from ref 176 with permission of the American Physical Society).

form the amorphous layer. This “semicrystalline form” (SCF) is related to the NIF form in pure alkanes (Section II.C), where the role of the shorter alkane is taken by folded chains. In contrast to the NIF form, the SCF in binary alkanes is the thermodynamically stable form within a given range of temperatures and compositions.^{176,177} SCF is also related to the high-temperature forms of branched long alkanes (Figure 25b,d and Figure 26b), some of which are also stable.

Below the phase transition temperature, the SAXS pattern of the binary mixtures becomes complex, but curve resolution and Fourier synthesis revealed a superlattice structure based on a triple-layer repeat unit as shown in Figure 30b.¹⁷⁶ The two outer layers l_e contain extended chains of the shorter alkane (e.g., $C_{162}H_{326}$) as well as the major portion of the longer chain molecules (e.g., $C_{246}H_{494}$). The middle layer l_m contains only the surplus length of the longer molecules protruding from the two end-layers. All three layers are crystalline, although there is evidence from WAXS, calorimetry and Raman LAM spectroscopy

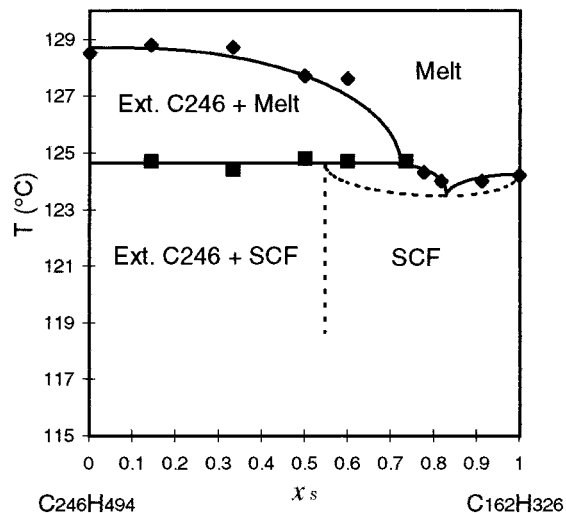


Figure 31. Equilibrium phase diagram of the $C_{162}H_{326}$ – $C_{246}H_{494}$ binary system. x_s = molar fraction of $C_{162}H_{326}$, Ext. C246 = extended-chain $C_{246}H_{494}$, SCF = semicrystalline form (from ref 177a with permission of the American Chemical Society).

that crystal perfection of the middle layer is poor. The transition between the SCF and the triple-layer superlattice is thought to occur through a cooperative process with pairs of SCF layers acting in tandem.

The equilibrium phase diagram of the $C_{162}H_{326}$ – $C_{246}H_{494}$ binary system (high-temperature range) is shown in Figure 31. The most important feature is the phase boundary of the semicrystalline phase. At temperatures below the triple point the single phase SCF was found to be stable in the range $0.56 \pm 0.04 < x_s < 1$, where x_s is the molar fraction of the shorter alkane $C_{162}H_{326}$. The reason that a SCF phase with $x_s < 0.56$ is unstable is believed to be due to steric overcrowding at the crystalline–amorphous interface. In the case of polyethylene it has been recognized that the cross-section area required by an amorphous chain is at least twice that required by a straight crystalline chain.^{178–180} In polymers, the overcrowding problem is resolved partly by chain tilt (see Section II.E), but for the greater part by adjacently re-entrant chain-folding. In the case of a mixed alkanes with high x_s , the overcrowding problem is resolved by the shorter chains ending at the crystal surface. However, for $x_s < 0.56$ the problem becomes insoluble and the excess longer component phase separates. Since the chains in SCF are tilted by 35° , it follows that the effective cross-section area of a chain crossing the crystalline–amorphous interface increases by a factor of $(0.44 \cos 35^\circ)^{-1} = 2.8$.

Studying shorter n -alkanes, Bonsor and Bloor¹⁷⁵ have suggested the possibility of two short chains substituting for one longer chain in a solid solution of molecules with a length ratio 1:2. Their experimental results on the binary system $C_{19}H_{40}$ – $C_{44}H_{90}$ were inconclusive. In contrast, in binary long n -alkanes such as $C_{122}H_{246}$ – $C_{246}H_{494}$, crystalline solid solutions were indeed shown to form readily; however, in this case the long chains ($C_{246}H_{494}$) are either folded or extended, while the short chains are extended.¹⁸¹ The resulting structure is a triple-layer superlattice, similar to that in Figure 7c, and the

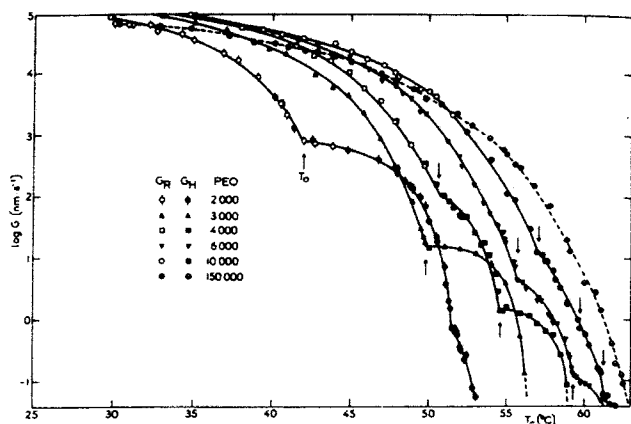


Figure 32. Temperature dependence of growth rate G_H of $\{010\}$ faces of single crystals and G_R of spherulites for five low molecular weight fractions and a polymer of PEO (from ref 28 by permission of John Wiley & Sons.).

thickness of the basic layer unit is determined by the length of the shorter $C_{122}H_{246}$ chain.⁶¹

III. Crystallization Process and Morphology

A. Stepwise Growth Rate vs Temperature Gradient

Studies on PEO fractions in the molecular weight range between 1500 and 12 000 have shown²⁸ that the slope of the increasing crystal growth rate with supercooling $dG/d(\Delta T)$ increases sharply at a series of specific crystallization temperatures T_c^m ($m = 1, 2, 3, \dots$). These mark the transitions between the growth of crystals with $m-1$ and m folds per chain. Figure 32 shows the temperature dependence of the growth rate from the melt normal to the $\{010\}$ lateral face for five low molecular weight fractions and a polymer (note the log rate scale). The breaks in the slope at T_c^m are particularly pronounced in low molecular weight fractions and are completely lost in the polymer. The existence of such sharp increases in $dG/d(\Delta T)$ is, at least qualitatively, entirely predictable by the secondary nucleation theory once quantization of lamellar thickness is accepted.¹⁸ The supercoolings at which growth transitions occur, relative to the melting point of extended chains, are given by

$$\Delta T_c^m = \frac{2\sigma_{e(\infty)}T_m}{\Delta h_f} \left(\frac{m}{m+1} \right) \left[\left(\frac{L}{m+1} \right) - \delta \right] \quad (5)$$

Here $\sigma_{e(\infty)}$ is the fold-surface free energy for $L = \infty$, and Δh_f is heat of fusion. δ is a small constant, reflecting the fact that some finite supercooling is required for crystal growth (see Section III.E). Equation 5 can be used for the determination of accurate $\sigma_{e(\infty)}$ for the parent polymer.

According to the secondary nucleation theory, polymer crystals grow by deposition of layers of stems on the side surface of the lamella¹⁸³ (see Figure 33). Each new layer needs to be nucleated ("secondary" or surface nucleation), after which it spreads comparatively rapidly. The main barrier to secondary nucleation is the excess side surface free energy $2b\sigma$

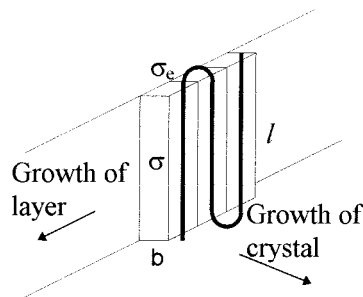


Figure 33. Chain deposition on the side surface of a polymer crystal. σ and σ_e are side-surface and end (fold-) surface free energies, b is the width of the chain (after ref 183).

for the creation of the two new surfaces either side of the single-stem nucleus; here b is the chain width and σ the side surface free energy. For polymer crystals of fixed fold length l , the slope $dG/d(\Delta T)$ should be constant within the limited temperature interval that is accessible for studying.¹⁸⁴ Indeed, when plotted on a linear scale, the growth rates G vs ΔT dependence in Figure 32 does not deviate much from linearity for a given m .¹⁸⁵ However, linear G vs ΔT is also consistent with the alternative polymer crystallization theory, the so-called "roughness-pinning theory" of Sadler.^{185,186} According to this theory, the difference between nucleation and growth of molecular layers on the growth face is negligible and the growth surface is rough rather than smooth (see Section III.E).

On closer scrutiny the crystal growth data for PEO fractions deviated somewhat from those expected from secondary nucleation theory; there were departures from linearity of G vs ΔT near the T_c^m transition temperatures,¹⁸⁵⁻¹⁸⁸ and the value of σ derived from the kinetics was unrealistically low.¹⁸⁷

B. Crystallization Rate Minima and Negative Order Kinetics

Crystallization rate experiments on monodisperse n -alkanes have shown a rather different picture. Not only is there a sharp increase in $dG/d(\Delta T)$ at the transition between extended and once-folded (or NIF) crystallization mode ($T_c^{m=1}$) but the $dG/d(\Delta T)$ gradient actually becomes *negative* as $T_c^{m=1}$ is approached from above.¹⁸ This was found to occur both in crystallization from melt¹⁸⁹ and from solution,¹⁹⁰ and it applies both to crystal growth and primary nucleation.¹⁹¹ Figure 34 shows the way G passes through a maximum and reaches a sharp minimum at the transition from extended to once-folded chain crystal growth of $C_{198}H_{398}$ from solution for two different concentrations.¹⁹² The rate minimum at $T_c^{m=1}$ has been observed in a number of alkanes from $C_{162}H_{326}$ to $C_{294}H_{590}$.¹⁹³⁻¹⁹⁶ In alkane $C_{294}H_{590}$, where crystallization rate from solution is sufficiently low for $T_c^{m=2}$ to be accessible, a crystallization rate minimum has been observed between the once-folded and twice-folded growth intervals.¹⁹⁷ A weak minimum at $T_c^{m=1}$ has also been reported in melt-crystallization of a methyl-terminated PEO fraction.¹⁹⁸

The negative $dG/d(\Delta T)$ observed in alkanes has been attributed to an effect termed "self-poisoning".¹⁸⁹

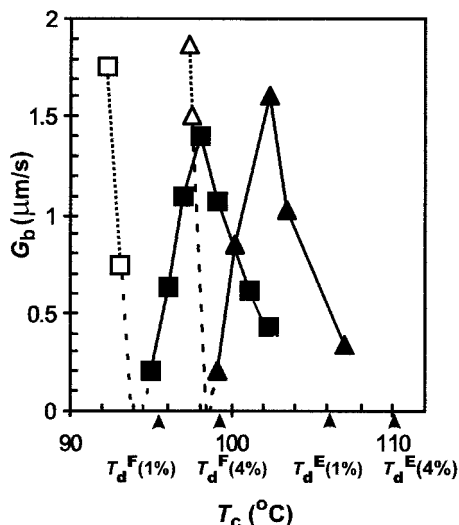


Figure 34. Initial crystal growth rate (G_b along [010]) vs crystallization temperature from 1.1 wt % (■, □) and 4.2 wt % solutions (▲, △) of $C_{198}H_{398}$ in 1-phenyldecane. (■, ▲) extended chain, (□, △) once-folded chain crystals. T_d^E and T_d^F are the dissolution temperatures of extended-chain and once-folded-chain crystals. The retardation in growth around T_d^F is caused by “self-poisoning” (from ref 192 by permission of American Physical Society).

This proposed mechanism recognizes the fact, highlighted by the roughness-pinning crystallization theory of Sadler, that chains wrongly attached to the crystal surface may hinder further growth. This blocking, or “pinning”, may be overlooked in polymers, but in monodisperse oligomers, it becomes very pronounced as, e.g., the folded-chain melting point T_m^F is approached from above. Although only extended-chain depositions are stable, close to T_m^F , the lifetime of folded-chain depositions becomes significant. As extended chains cannot grow on a folded-chain substrate,²⁸ growth is temporarily blocked until the folded-chain overgrowth detaches. At T_m^F itself the detachment rate of folded chains drops to the level of the attachment rate and the entire surface is blocked for extended chains.

The growth rate minima cannot be explained by the secondary nucleation theory in its present form because the competing attachments to the growth face are ignored and the deposition of a whole stem is treated as a single event.¹⁹⁹ However, the minimum in G is well reproduced, at least qualitatively, with even the simplest departure from the classical approach, i.e., by splitting the stem, or the alkane chain, into two segments and allowing the second segment the choice of aligning coaxially with the first segment (extended chain) or alongside it (folded chain) (see Figure 35).²⁰⁰ The forbidden step is attachment of an extended chain onto a folded chain. A Monte Carlo simulation study, where these same selection rules were applied, has also reproduced the kinetics of the self-poisoning minimum and has provided some additional insight into the crystal shape.²⁰⁰

Another manifestation of the self-poisoning effect is the anomalous negative order kinetics of crystallization from solution. In long alkanes, there is a supersaturation range in which crystal growth rate

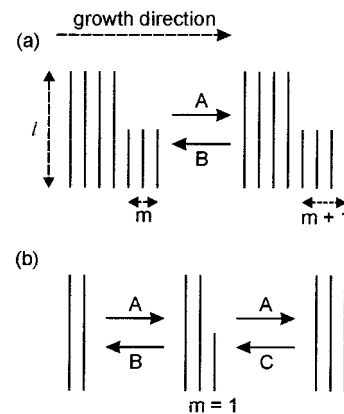


Figure 35. The model of elementary steps as used in the rate equation and Monte Carlo simulation treatments that reproduced the self-poisoning minimum. A cross-section (row of stems) normal to the growth face is shown. There are three elementary steps differing in their barrier and driving force: attachment (rate A) and detachment (rate B) of segments equal to half the chain length, and partial detachment of an extended chain (rate C). The key self-poisoning condition is that attachment of the second half of an extended chain is allowed only if $m = 1$, i.e., an extended chain cannot deposit onto a folded chain (from ref 200 by permission of the American Institute of Physics).

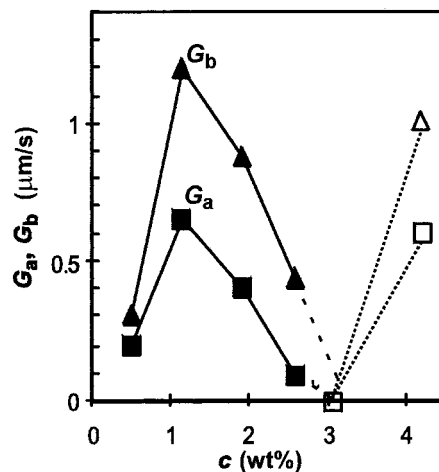


Figure 36. Initial crystal growth rate G_a (along [100]) and G_b (along [010]) of $C_{198}H_{398}$ vs solution concentration at 98.0 °C. (■, ▲) Extended chain, (□, △) once-folded chain crystals. Note the negative dG/dc gradient for $1\% < c < 3\%$ (from ref 192 by permission of American Physical Society).

actually *decreases* with increasing concentration c .¹⁹² For n - $C_{198}H_{398}$, this range is from 1 to 3% (see Figure 36). The two-segment-stem rate equation model of ref 200 has been adapted to include solution concentration, and again, both the G vs c and G vs T minima were reproduced well (see Figure 37, panels a and b). The calculated *temperature* dependence of G (Figure 37b) should be compared with the experimental data in Figure 34. The unusual retardation in crystal growth with increasing *concentration* in Figure 37a should be compared with Figure 36. This effect can be explained as follows. For $c < 3\%$, the attachment rate A is lower than the folded-chain detachment rate B^F , so only extended chains can grow. However, as $c = 3\%$ is approached, A becomes comparable to B^F and an increasing fraction of the growth face equal to A/B^F is covered by folded chains

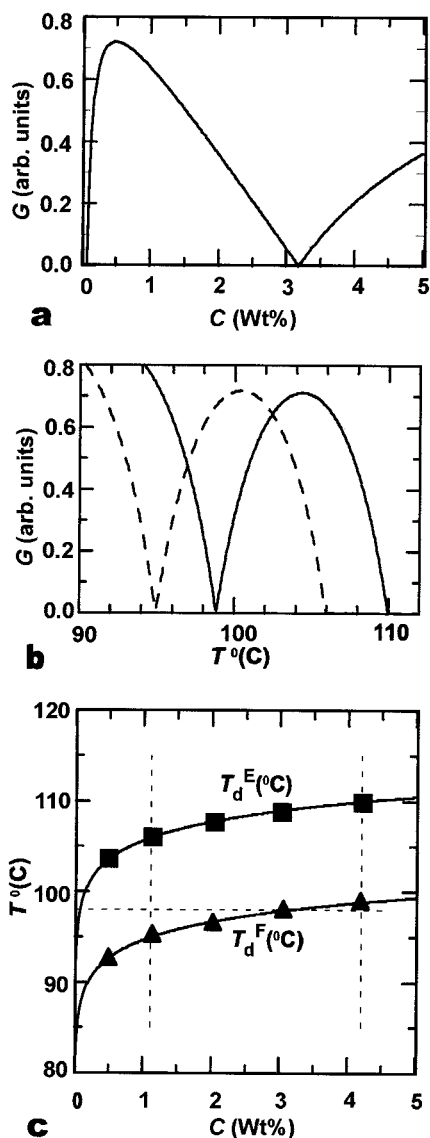


Figure 37. (a) Crystal growth rate G of n -C₁₉₈H₃₉₈ calculated as a function of concentration at $T_c = 98.0$ °C, cf. Figure 36. (b) G calculated as a function of T_c for $c = 1.1\%$ (dashed) and $c = 4.2\%$ (full), cf. Figure 34 (c). Binary phase diagram C₁₉₈H₃₉₈ – phenyldecane. Equilibrium liquidus curve $T_d^E(c)$ for extended chain crystals and non-equilibrium curve $T_d^F(c)$ for once-folded chain crystals were calculated, matched to the experimental dissolution temperatures (■, ▲) using three fitting parameters. Experimental $T_d^E(c)$ and $T_d^F(c)$ values were determined in situ at near zero heating rate (from ref 192 by permission of American Physical Society).

at any time. Hence the extended-chain crystal growth rate is

$$G^E = (1 - A/B^F)(A - B^E) \quad (6)$$

and as $c \rightarrow 3\%$ and $A \rightarrow B^F$, so $G^E \rightarrow 0$.

Figure 37c shows the alkane–solvent phase diagram calculated by equating $A = B^E$ (top curve: equilibrium liquidus) and $A = B^F$ (bottom curve: metastable liquidus). Imagining that crystal growth rate G is plotted on the z -axis, and bearing in mind that on either of the liquidus lines G is zero, the c and T dependencies of G in Figure 37a and b can be

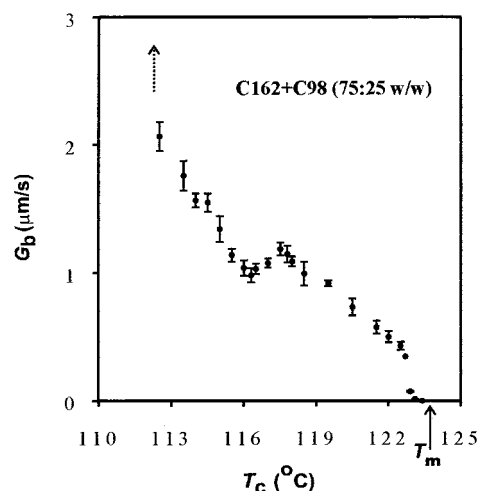


Figure 38. Crystal growth rate G_b vs temperature for a 75:25 w:w mixture of C₁₆₂H₃₂₆ and C₉₈H₁₉₈. The “poisoning” minimum at the melting point of C₉₈H₁₉₈ (116 °C) is seen. The steep increase in G below 112.5 °C (out of scale) is due to the transition to once-folded C₁₆₂H₃₂₆ growth (from ref 203).

visualized, respectively, as horizontal and vertical cuts through the phase diagram.

If the initial solution concentration c is higher than that corresponding to the maximum in G , then G will initially increase during the crystal growth as c decreases. This auto-accelerated crystallization gives rise to a further phenomenon, described as “dilution wave”.¹⁹² Thus, e.g., crystallization from an initially 4.2% phenyldecane solution of C₁₉₈H₃₉₈ at $T_c = 97.4$ °C results in folded-chain crystals which soon cease to grow as the metastable equilibrium is reached between folded-chain crystals and the pseudo-saturated solution (lower liquidus in Figure 37c). As both nucleation and growth of extended-chain crystals are highly suppressed under these conditions, no visible change occurs for some considerable time, after which rather suddenly the folded-chain crystals are replaced by needle-shaped extended-chain crystals. The transformation sweeps through the suspension. As the first extended-chain crystal forms successfully, it depletes the surrounding solution and thus triggers the growth of other extended-chain crystals in the vicinity. A “dilution wave” is thus generated easing the inhibitory effect of high concentration on extended-chain growth. The reaction diffusion equation describing the dilution wave has been found²⁰¹ to coincide with that used in genetics to describe the spread of an advantageous gene.²⁰² The wave spreading rate is determined by the polymer diffusion constant and the crystal growth rate G^E .

Recently, a new type of growth rate minimum has been induced above $T_c^{m=1}$ in melt-crystallization of several n -alkanes by the admixture of a shorter alkane with the melting point between those of the extended and once-folded-chain crystals of the host.²⁰³ Figure 38 illustrates this on the example of a 75:25 w:w mixture of C₁₆₂H₃₂₆ and C₉₈H₁₉₈. A relatively small but reproducible minimum is observed at 116 °C, in the middle of the extended-chain growth range of C₁₆₂H₃₂₆; this temperature coincides with the melting point of C₉₈H₁₉₈. Here the retardation and

the negative $dG/d(\Delta T)$ slope above 116 °C are not due to “self-poisoning” but rather to “poisoning” by the $C_{98}H_{198}$ chain attachments which are nearly stable and are thus blocking the growth face of the host crystals. Below the temperature of the minimum there is no drastic increase in $dG/d(\Delta T)$ since (a) $C_{98}H_{198}$ cannot grow rapidly as a minority component and (b) the growth is retarded by folded-chain $C_{162}H_{326}$ depositions due to the vicinity of $T_c^{m=1}$. Indeed, below $T_c^{m=1} = 112.5$ °C, there is a very steep increase in G as chain-folded crystallization of $C_{162}H_{326}$ takes over, incorporating the guest $C_{98}H_{198}$ chains in a semicrystalline NIF-type structure described in Section II.C.

Lower crystal growth rates in alkane $C_{162}H_{326}$ were also reported when a fraction of a shorter ($C_{122}H_{246}$) or a longer alkane ($C_{246}H_{494}$) was added.²⁰⁴ The addition of $C_{122}H_{246}$ had a somewhat larger retarding effect.

C. Crystallization and Morphology

The shapes of melt-grown single crystals of narrow PEO fractions have been studied in great detail by Kovacs and co-workers.^{28,29,64} Particular attention was paid to the narrow temperature range of the extended to folded-chain growth transition. Careful investigation revealed that there are in fact three close transition temperatures, one for each of the three $\{hk0\}$ growth face types. These differences, combined with the thickening process, resulted in “pathological” crystals, to be discussed briefly in the next section. A more general observation is that more or less faceted crystals grow at most temperatures, except just above the transition temperature range $T_c^{m=1}$, where crystals are rounded and sometimes indeed circular. This has been confirmed by subsequent studies, as illustrated in Figure 39.¹⁹⁸

The discovery of rounded polymer crystal edges^{99,205} has motivated Sadler to propose the rough-surface theory of crystal growth.¹⁸⁶ However, it was shown subsequently^{206–208} that the curvature of $\{100\}$ faces in polyethylene can be explained quantitatively by applying Frank’s model of initiation and movement of steps.²⁰⁹ Curvature occurs when the average step propagation distance is no larger than several stem widths, which places this type of crystal growth at the borderline between nucleated and rough-surface type. Thus, the increase in curvature of PEO crystal faces immediately above $T_c^{m=1}$ (Figure 39) means a reduction in the ratio v/i , where i is the initiation rate and v the propagation rate of new layers of stems. A connection has been made between the rounding of PEO crystals and a conspicuous downward deviation from linearity of measured G vs ΔT just above $T_c^{m=1}$.¹⁸⁵ In the past, the effect had been attributed to impurities,¹⁸⁸ but, subsequently, it was suggested to have been caused by self-poisoning.²¹⁰ Since $G = b \sqrt{2iv}$, the retardation in G combined with the reduction in v/i was taken to mean that the propagation rate of new surface layers v is more obstructed than their nucleation i . The blocking of niches retarding v and leading to a rounded face is schematically drawn in Figure 40.

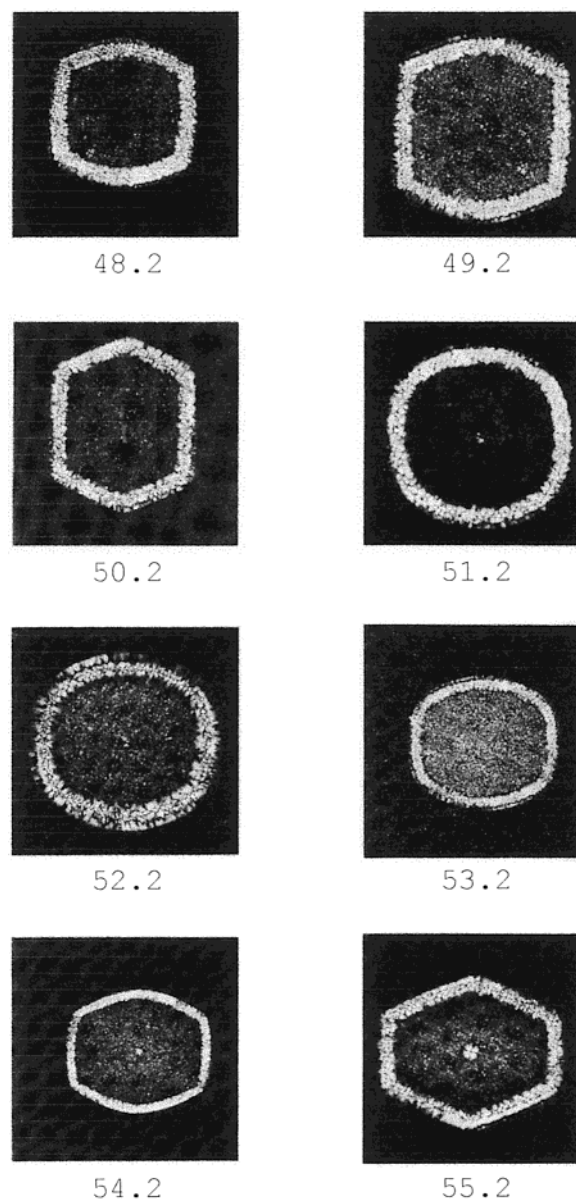


Figure 39. Optical micrographs of PEO single crystals (fraction $M_n = 3000$) grown from the melt as a function of crystallization temperature (°C). The extended-folded chain growth transition $T_c^{m=1}$ is between 51.2 and 50.2 °C (adapted from ref 198).

Whereas melt-grown single crystals of PEO fractions become rounded near the extended- to folded-chain growth transition, crystals of long alkanes show a whole range of morphologies within the temperature interval of extended-chain growth, both from melt and from solution.^{191,192,211} Figure 41 shows how the crystal habit in solution-grown $C_{198}H_{398}$ changes with decreasing T_c from perfect rhombic lozenges with $\{110\}$ lateral facets (a), through nearly hexagonal “truncated lozenges” ($\{110\}$ and $\{100\}$ faces) (b), through leaf-shaped (“lenticular”) crystals with curved $\{100\}$ faces (c, d), finally ending with needlelike crystals bounded by practically straight $\{100\}$ faces just above the growth rate minimum (e). On lowering T_c , further chain-folded crystallization takes over and the habit reverts to that of truncated lozenges (f). At still lower T_c (not shown), the shape changes to

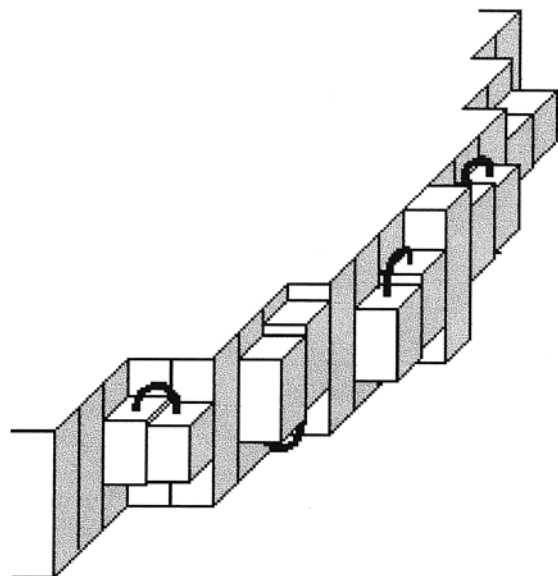


Figure 40. Schematic representation of a growth face of an extended-chain crystal with step propagation hindered by transient folded-chain depositions (from ref 210, by permission of Kluwer Academic Publishers).

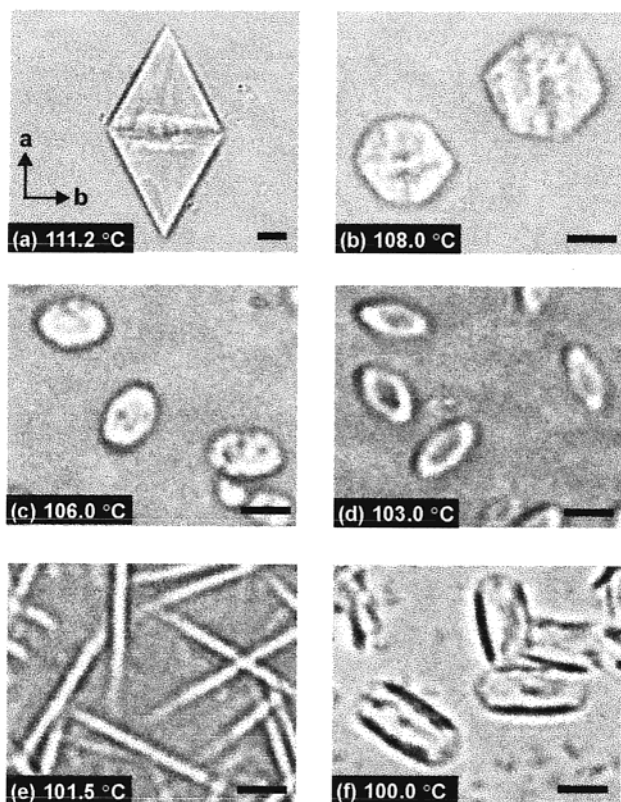


Figure 41. Series of in situ optical micrographs (interference contrast) of $n\text{-C}_{198}\text{H}_{398}$ lamellar single crystals grown from octacosane (initially 2%) at the temperatures indicated. (a–e) extended chain, (f) once-folded chain. Bar length represents 10 μm (from ref 214).

lenticular and the cycle is repeated. The remarkable feature is that the T_c dependence of crystal habit within one such cycle is the exact reversal of that in solution-crystallized polyethylene. In polyethylene rhombic {110}, lozenges grow at low T_c and with increasing temperature the habit changing gradually

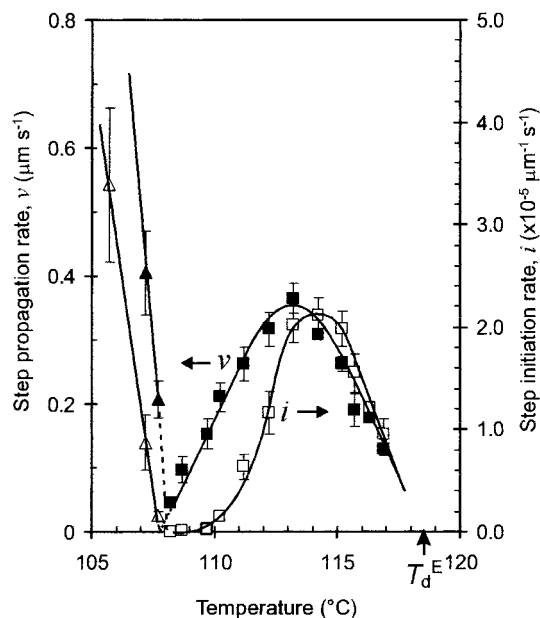


Figure 42. Initiation rate i (empty symbols) and propagation rate v (full symbols) of new steps on the {100} growth face of $n\text{-C}_{246}\text{H}_{494}$ crystals in 5% octacosane solution as a function of crystallization temperature. (■, □) Extended chain, (▲, △) once-folded chain (from ref 214).

toward elongated lenticular crystals which grow at the highest T_c from either solution or from melt.^{207,212}

The morphological changes described and exemplified in Figure 41 are determined, essentially, by the temperature dependence of only two parameters: (a) the ratio of growth rates normal to {110} and {100} faces, G_{110}/G_{100} and (b) the ratio v/i for {100} growth. Thus rhombic lozenges bounded by {110} lateral faces will be seen for any $G_{110}/G_{100} \leq \cos(\varphi/2)$, where $\varphi/2 = \tan^{-1}(a/b)$ and a, b are unit cell parameters. As T_c is reduced and the growth minimum is approached, G_{110}/G_{100} increases beyond the value of $\cos(\varphi/2)$, and the lozenges become truncated by {100} faces. The temperature dependencies of G_{100} and G_{110} are different, and for all alkanes, the growth normal to {100} faces is more retarded by self-poisoning than the growth normal to {110} faces. This applies both to solution²¹¹ and to melt crystallization.²⁰³ On the other hand, the curvature of the {100} faces is determined by the ratio of step propagation and step initiation rates v/i on these faces.

The profiles of the curved “{100}” faces in solution- and melt-crystallized alkanes were fitted to those calculated according to Mansfield,²⁰⁶ taking account of the centered rectangular lattice representative of polyethylene and alkanes.²¹³ As an example, i and v values thus obtained are plotted against T_c for $\text{C}_{246}\text{H}_{494}$ (5% in octacosane) in Figure 42.²¹⁴ While both the nucleation rate and propagation rate of steps on {100} faces pass through a maximum and a minimum as a function of T_c , and then increase steeply in the chain-folded temperature region, there is a significant difference in the shape of the two graphs near the growth rate minimum. In this and other examples of solution crystallization, initiation (i) is considerably more suppressed by self-poisoning than propagation (v), and the slope $d i/d(\Delta T)$ turns

negative further away from the minimum, (i.e., at a higher temperature) than the corresponding slope $dv/d(\Delta T)$. At the minimum, the $\{100\}$ faces are straight (see needlelike crystals in Figure 41e), this time not because layer completion is uninhibited, but rather because i is extremely low.

Comparing the morphological changes in melt-grown crystals of PEO fractions (see above, Figure 39 and Figure 40) and solution-grown crystals of long alkanes, we find that v is more affected by self-poisoning in PEO while i is more affected in the alkanes. Furthermore, the case of melt-crystallization of n -alkanes is closer to that of solution-crystallized alkanes.²⁰³ The difference between PEO and alkanes is not yet understood.

The cause of the changes in crystal habit with changing T_c in polyethylene, or in any other polymer for that matter, is unknown. These changes have a profound effect on morphology of industrial polymers. Thus, in melt-solidified polyethylene crystals grow along the crystallographic b -axis with lenticular morphology similar to that formed from polyethylene solutions at the highest T_c ^{99,100} or from long alkanes at the lowest T_c within the extended-chain regime (Figure 41, panels d and e). Hoffman and Miller²¹⁵ proposed that the retardation in v , leading to curved crystal edges, comes from lattice strain imposed by the bulky chain folds in the depositing chains; this results in strain surface energy σ_s which acts by slowing down the substrate completion process. To be consistent with the observed morphology in polyethylene, σ_s would have to be higher on $\{100\}$ faces than on $\{110\}$ faces. However, it is difficult to see how this argument would apply to crystallization of extended-chain n -alkanes with no chain folds.

Since the morphological trend with increasing T_c in polyethylene is the exact opposite of that observed in alkanes, and since the latter seems to be clearly associated with self-poisoning, it is tempting to interpret the changes in polyethylene as being due to an increasing effect of self-poisoning with increasing T_c . Self-poisoning in polydisperse polymers, if present, would be difficult to detect from crystallization kinetics, since lamellar thickness l changes continuously with T_c , and thus, no rate minima can be expected. However, self-poisoning is envisaged to affect crystal growth in the following manner. At any T_c , there is a minimum fold length l_{\min} below which attachments are more likely to melt than be built into the crystal. However, chain segments which are only slightly shorter than l_{\min} will have a reasonably long lifetime as well as a higher attachment rate because of the lower barrier $E^* = 2bl\sigma$. This would cause self-poisoning at any T_c . A snapshot of a cut normal to the surface of a growing crystal might thus look as in Figure 43. This situation corresponds to the "kinetic roughness" in the roughness-pinning model of Sadler¹⁸⁶ (see Section III.E). The reason for self-poisoning in polyethylene being more pronounced at higher T_c , as suggested by morphology, is one of a number of open questions.

While extended-chain crystals of $C_{162}H_{326}$ and $C_{198}H_{398}$ grown from octacosane at the smallest supercooling are faceted rhombic lozenges (see Figure

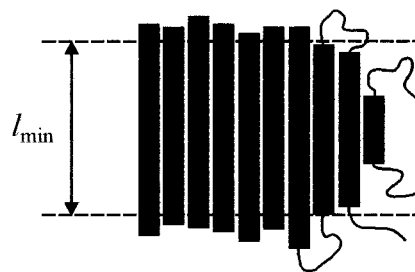


Figure 43. A possible instantaneous configuration of a row of stems perpendicular to the crystal surface schematically illustrating self-poisoning in a polydisperse polymer. The same picture could apply to a layer of stems depositing onto the crystal surface and parallel to it; in that case it would illustrate the retarding effect on layer spreading rate v (see also Section III.E).

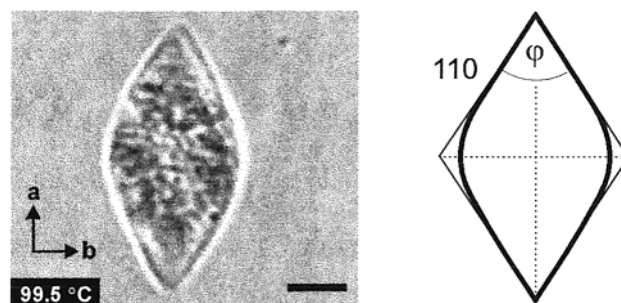


Figure 44. (Left) An "a-axis lenticular" crystals of $C_{162}H_{326}$ in 1-phenyldecane grown from an initially 1.0% solution at 99.5 °C. Interference optical micrograph. Bar length 10 μm . (Right) Schematic outline of the crystal, indicating the four $\{110\}$ sectors (from ref 211 with permission of the American Chemical Society).

41a), those grown under similar conditions from 1-phenyldecane have an unusual habit shown in Figure 44.²¹¹ This habit has not been seen in polyethylene and it has been termed "a-axis lenticular" because, unlike the more common lenticular (lens-like) polyethylene crystals, its long axis is parallel to the crystal a -axis. In fact, the habit can be best described as being bounded by curved $\{110\}$ faces. The interesting feature is the asymmetry of the curvature; while the faces are curved at the obtuse apex, they are straight at the acute apex. This has been attributed to the propagation rates of steps on the $\{110\}$ face being different in the two directions; the rate v_s , directed toward the acute apex, is higher than the rate v_b directed toward the obtuse apex. Similar asymmetry may be expected in other polymers where the growth face lacks a bisecting mirror plane normal to the lamella.

Crystallization of alkanes from dilute solutions (typically 0.01% or less) in good solvents such as toluene results invariably in faceted crystals, as shown already very early on $C_{94}H_{190}$ ²¹⁶ and subsequently on longer alkanes.⁶⁸

Morphology of long alkanes is also being studied in order to evaluate the role of cilia in lamellar splay, a key factor in the formation of polymer spherulites.^{204,217} The hypothesis is that cilia exert an entropic repulsive force when crystalline lamellae approach each other closely. Earlier results seemed to have indicated that in long alkanes spherulites are

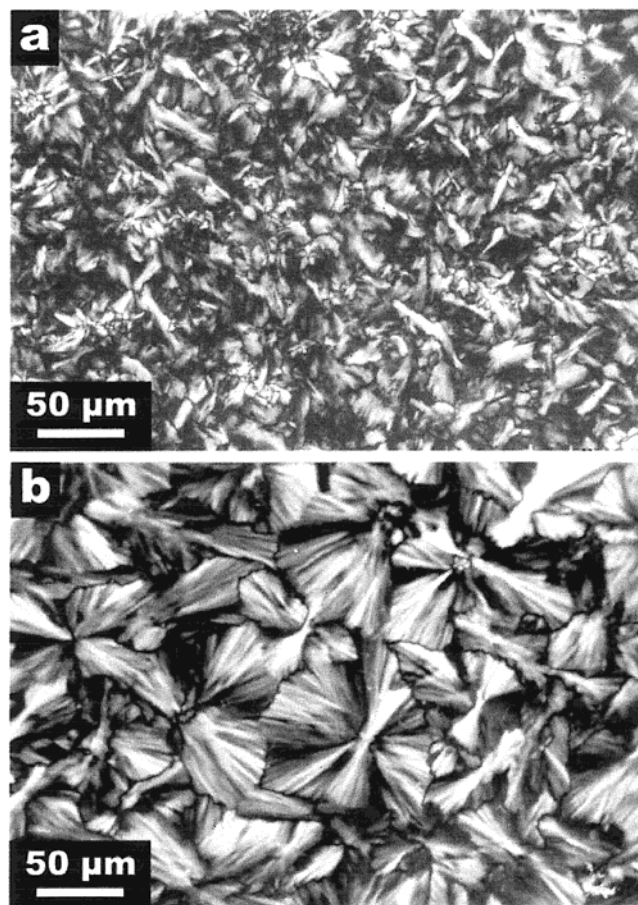


Figure 45. Optical micrographs, between crossed polarizers, of alkane $C_{162}H_{326}$ to which 10 wt % was added of (a) $C_{122}H_{246}$, and (b) $C_{246}H_{494}$. $T_c = 120$ °C. The mixture with the longer-chain guest molecules (b) shows a texture resembling that of polymer spherulites (from ref 204 by permission of American Chemical Society).

indeed formed in the folded-chain crystallization region, but not in the extended-chain region. This would lend support to the cilia hypothesis, in view of the NIF structure. Subsequent work has shown, however, that even extended-chain lamellae splay and diverge, and the angle of divergence increases with increasing degree of supercooling. The idea of transient ciliation has therefore been suggested; the initial crystalline stem length would thus depend on supercooling even within the extended-chain growth regime, the cilium length increasing with increasing supercooling. It must be recognized, however, that the transient cilia would have to be confined to a narrow growth front of the lamellae, since otherwise, without chain-folding, the overcrowding effect would prevent further growth (see Sections II.C and II.J).

Supporting evidence for cilia being responsible for lamellar divergence and the consequent tendency for spherulite formation comes from the morphology of alkane mixtures.²⁰⁴ In Figure 45, optical textures are shown of two mixtures with $C_{162}H_{326}$ the majority component. The sample in Figure 45a has 10 wt % $C_{122}H_{246}$ added, while the sample in Figure 45b has the same amount of added $C_{246}H_{494}$. The morphology in Figure 45b has recognizable features of polymer spherulites, while that in Figure 45a has not. This

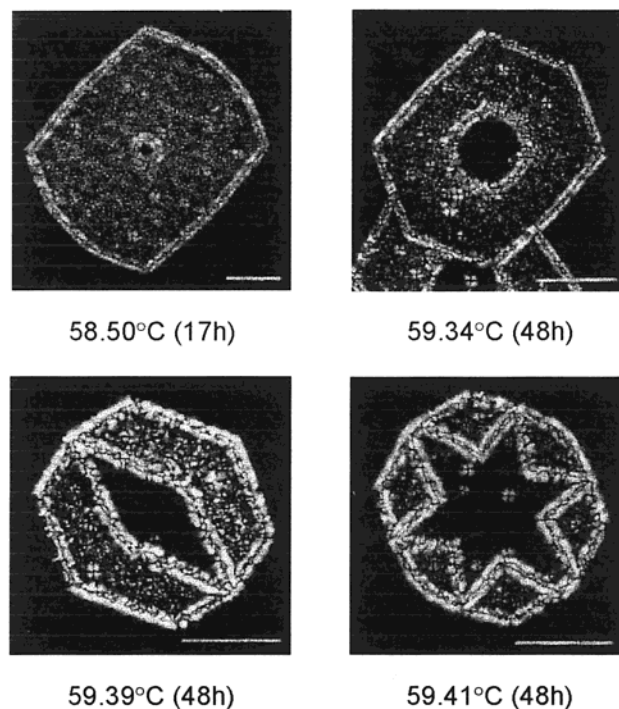


Figure 46. Crystals of PEO fraction $M_n = 6000$ grown from the melt at temperatures indicated, and then quenched to achieve surface decoration by small spherulites. The black undecorated areas are extended chain (from ref 28 by permission of John Wiley & Sons).

is attributed to permanent cilia existing in the semicrystalline form (SCF) of the $C_{162}H_{326}$ - $C_{246}H_{494}$ blend.

D. Lamellar Thickening

Since the thin lamellar crystals of polymers are metastable and owe their shape to criteria of kinetics rather than equilibrium thermodynamics, at elevated temperatures aided by increased mobility, they often thicken. The thickening is normally continuous and logarithmic in time.²¹⁸ However, already the earliest SAXS studies of PEO fractions have shown lamellar thickness to increase in a stepwise manner.²¹⁹ Each step corresponded to one integer folded (IF) form. The quantized nature of lamellar thickening has proven highly advantageous in visualizing the thickening process using different microscopy techniques. Below are three examples illustrating the use of optical, electron, and atomic force microscopy.

Figure 46 shows four crystals of PEO fraction $M_n = 9000$ grown from the melt at the temperatures indicated.²⁸ As in Figure 39, the crystals were “self-decorated” by quenching. Crystallization temperature of 58.50 °C is in the region of once-folded-chain growth, but the other three temperatures are in the transition region between folded and extended chain growth. The folded-chain crystals were grown from a small extended-chain seed. As the octagonal and hexagonal folded-chain crystals in the top row of Figure 46 were growing, the central extended-chain portion was spreading radially at a slower rate, maintaining a circular envelope. Here thickening also involves incorporation of new molecules from the

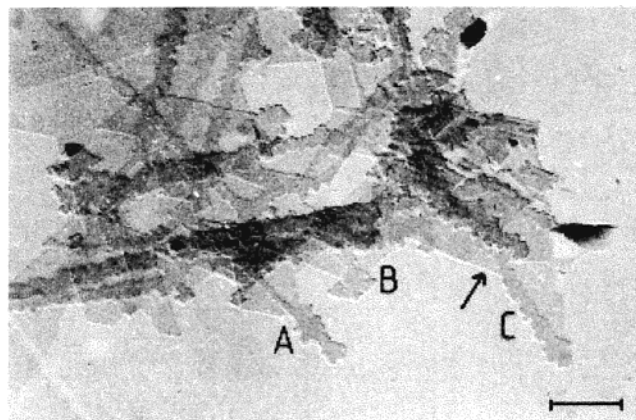


Figure 47. Lozenge-shaped crystals of once-folded alkane $C_{198}H_{398}$ grown from a 0.02% solution in toluene and partially thickened isothermally during annealing at $T_c = 73\text{ }^\circ\text{C}$ for $t = 5\text{ h}$. Marker = 1 micron (from ref 220b by permission of John Wiley & Sons).

surrounding melt. At $T_c = 59.39\text{ }^\circ\text{C}$, the black extended-chain portion is rhombus-shaped and directed along the a -axis. At this temperature, the folded-chain growth in the $[100]$ direction is already slower than the extended-chain growth, hence an extended-chain tip progresses ahead of the folded-chain layer. At $59.41\text{ }^\circ\text{C}$, the folded-chain rate in the $[140]$ direction also drops below the extended-chain rate, hence the four additional arms to the extended-chain star in the pathological crystal in Figure 46d.

Thickening of once-folded and twice-folded n -alkane crystals in solution has been studied by DSC and transmission electron microscopy.^{220,221} Figure 47 shows a group of initially lozenge-shaped once-folded-chain crystals of $C_{198}H_{398}$ (cf. Figure 41a) partially thickened isothermally at T_c while freely suspended in solution.^{220b} Thickening was found to invariably start at an apex followed by rapid spreading of a strip along the sector boundary, i.e., either along the $[100]$ or the $[010]$ direction. At the end of the process a network of crosshatched extended-chain strips is all that remains. Figure 47 contains a number of details illustrative of the progress of thickening. The extended-chain strip, which traverses the crystal, widens with time, consuming the adjacent folded-chain layer (see, e.g., areas marked A and B). It has been proposed that material is transported to the thickened strip by slippage along the $\{110\}$ lattice planes. Such slippage leaves behind smooth $\{110\}$ lamellar edges, as in crystal A. Surface decoration has indeed shown that the fold regularity becomes severely disrupted in those areas that had undergone slippage.

The slippage within a crystal can be seriously impeded either by multilayer crystals or where a portion of the unthickened crystal is bounded on two or more sides by thickened strips. An example of how an overlaying layer inhibits slippage is provided by the crystal marked C in Figure 47. Here it is the left-hand side which had mainly been consumed in the widening of the extended-chain strip. It seems that the slippage of the right-hand side of the crystal had been prevented by the complex overgrowth on that side. In fact, the slippage of the left-hand half had

also ceased when the (110) slip plane reached the overlying second layer nearby. Thus, the portion of the folded-chain layer marked with an arrow could not easily be pulled in by thickening.

Isothermal thickening from F4 to F3 and F3 to F2-folded forms of $C_{294}H_{590}$ crystals in toluene solution shows a rather different pattern.²²¹ Transformation from chains folded in three to chains folded in two ($F3 \rightarrow F2$) destroys any recognizable crystal shape and results in an irregular crystal habit with narrow (20–30 nm) strips of thickened material. Transport of mass required for solid-state thickening is clearly more impeded than in the case of $F2 \rightarrow E$ transformation in $C_{198}H_{398}$. The $F4 \rightarrow F3$ conversion in $C_{294}H_{590}$ crystals did not proceed at all by solid state diffusion, judging by the resulting “picture-frame” F3 crystals. This latter morphology implies that “thickening” occurs through dissolution of the F4 crystal interior and simultaneous F3 precipitation at crystal edges. It should be noted that in polyethylene, thickening does not normally take place at T_c in solution crystallization; if temperature is raised subsequently to about $T_c + 10\text{ }^\circ\text{C}$, picture-frame crystals may appear.²²²

If single layer polymer crystals are deposited on a substrate and annealed, thickening is accompanied by the creation of holes, as pulling in of material from the side to feed the thickened regions is severely restricted.²²³ However, holes can develop on annealing even in multilayer crystals.²²³ Such “Swiss cheese” morphology has also been observed using AFM of annealed once-folded solution-grown crystals of $C_{162}H_{326}$ deposited on mica.²²⁴ The thickening process could in this case also be studied in real time. Figure 48 shows two out of a series of AFM height-contrast images taken at different annealing times. A thickened extended-chain strip is seen to develop and propagate along the edge of the crystal.

Thickening is facilitated considerably when crystal lamellae are stacked on top of one another, reducing the need for large scale transport of matter. Figure 49 shows the changing SAXS curve during continuous heating of a mat of stacked solution-grown crystals of alkane $n\text{-}C_{390}H_{782}$ with the chains initially folded in five (F5).²²⁵ The first and second-order SAXS peaks are seen to move to lower angles in a stepwise fashion, the crystals passing through integer forms $F5 \rightarrow F4 \rightarrow F3 \rightarrow F2$.

E. Implications for Polymer Crystallization Theory

To discuss the implications of the observed crystal growth behavior of model chains, certain issues in polymer crystallization theory need summarizing. The secondary nucleation theory has been the dominant theory for several decades and has undergone numerous modifications since its original establishment by Frank and Tosi²²⁶ and Lauritzen and Hoffman (LH).²²⁷ As mentioned in Section III.A, it assumes that the lateral growth of a crystal lamella of thickness l proceeds by deposition of layer upon layer of stems (straight chain segments) of length l , each layer being nucleated by the deposition of the first stem (see Figure 33). Deposition of the first stem

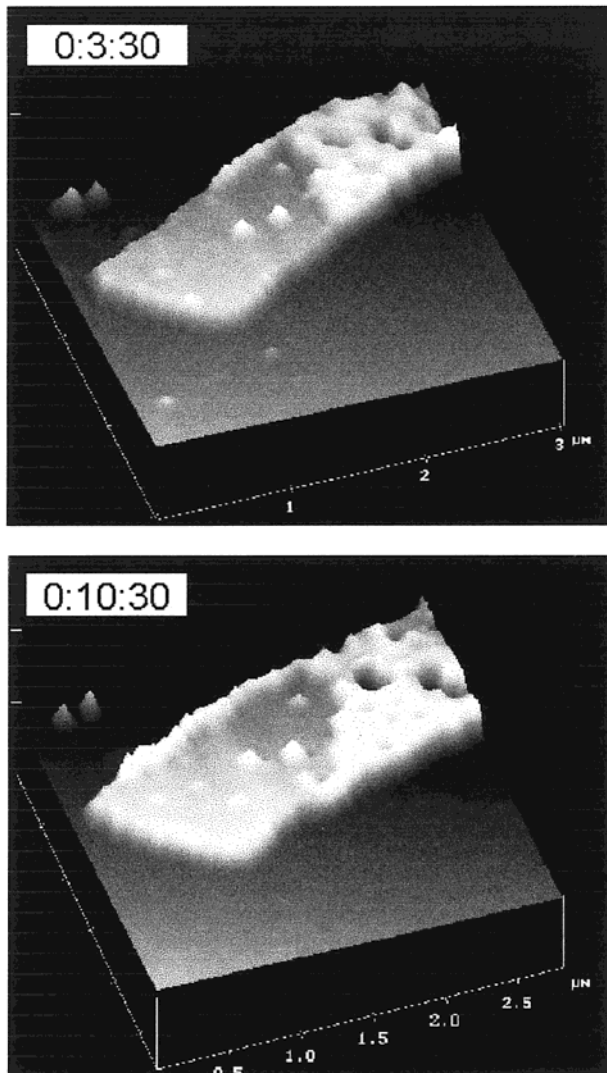


Figure 48. Two out of a sequence of height AFM images of a crystal of $n\text{-C}_{162}\text{H}_{326}$, initially once-folded, recorded during annealing at 100 °C. The extended-chain form propagates along the edge of the crystal (from ref 224 by permission of Elsevier Science).

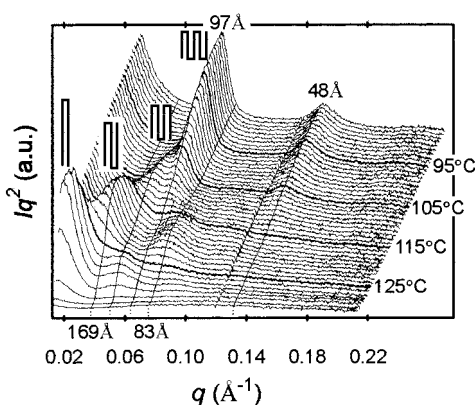


Figure 49. Series of SAXS intensity functions recorded during heating of solution-crystallized $n\text{-C}_{390}\text{H}_{782}$ at 2 deg C/min. The integer forms that the crystals pass through are marked by the corresponding symbols of their molecular conformation (from ref 225).

raises the net free energy by $2bl\sigma - \psi abl\Delta\phi$, where σ is the side-surface free energy, $\Delta\phi$ the bulk free energy of crystallization per unit volume, and ψ is

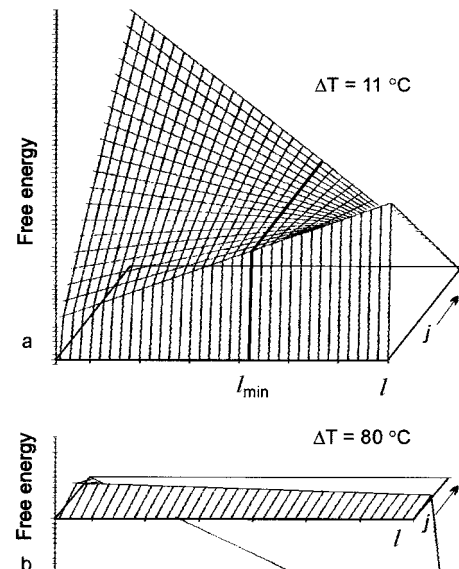


Figure 50. Free energy of a new layer of stems on the lateral growth face of a polymer crystal as a function of stem length l and the number of stems in the layer, j . Calculated according to the Lauritzen-Hoffman theory, with $\psi = 1$. (a) $\Delta T = 11$ °C, (b) $\Delta T = 80$ °C. Standard data for polyethylene were used. Case a predicts $l = l_{\min} + \delta l$ with a small δl , while (b) predicts $l \rightarrow \infty$.

the “apportioning factor” determining what fraction of the crystallization energy had been released at the peak of the barrier during the attachment of a stem.¹⁸³ Deposition of subsequent stems (“substrate completion”) is then fast, since the barrier for each new stem is only $2ab\sigma_e - \psi abl\Delta\phi$ (σ_e is the end-surface energy). According to this surface-energy-based theory, the barrier for deposition of the first stem is highest of all due to the large surface area bl . Provided l is larger than the minimum thickness l_{\min} of crystals stable at a given T_c , attachment of each subsequent stem reduces the free energy of the new layer. This is illustrated in Figure 50a, where the free energy is shown as a function of l and j , j being the number of stems in the layer. For simplicity, Figure 50 shows the situation for $\psi = 1$; for $0 < \psi < 1$, there would be an additional maximum between each j and $j+1$.

The elementary steps in the LH theory are the deposition of the first stem (rate constant A_0), deposition of subsequent stems (A), and removal of a stem (B). The individual rate constants are of the form $\beta \exp[-(\text{barrier})/kT]$, where β contains the viscosity factor etc. Hence,

$$A_0 = \beta \exp[-(2bl\sigma - \psi abl\Delta\phi)/kT] \quad (7a)$$

$$A = \beta \exp[-(2ab\sigma_e - \psi abl\Delta\phi)/kT] \quad (7b)$$

$$B = \beta \exp[-(1 - \psi)abl\Delta\phi/kT] \quad (7c)$$

The whole process is treated as a series of consecutive reactions and the steady-state solution gives the net flux S_l for a given crystal thickness l as

$$S_l = N_0 A_0 \left(1 - \frac{B}{A}\right) \quad (8)$$

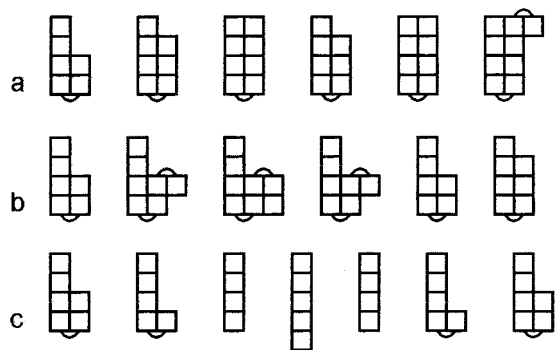


Figure 51. A series of fluctuations at the crystal growth face. The squares represent crystallized chain segments. (a) Steps allowed in the Frank-Tosi model,²²⁶ (b and c) some other possible steps (after ref 4).

N_0 is the total number of stems. Substituting eq 7 into eq 8, we get

$$S_l = \beta N_0 \{ \exp[(-2bl\sigma + \psi abl\Delta\phi)/kT] \{ 1 - \exp[(-abl\Delta\phi + 2ab\sigma_e)/kT] \} \} \quad (9)$$

The second factor in eq 9 (“driving force factor”) increases with increasing l , and for $l > l_{\min} = 2\sigma_e/(\Delta\phi)$, it is positive. At small and moderate ΔT , the first factor (“barrier factor”) decreases with increasing l . Hence $S(l)$ has a maximum. The l -value of the maximum, as well as the average value of l , is somewhat larger than l_{\min} . Thus,

$$\langle l \rangle = l_{\min} + \delta l \quad (9)$$

The secondary nucleation theory is “coarse grain” and makes a serious simplification by treating the stem deposition as a single event. The most conspicuous consequence of this in the application to polymers is the erroneous prediction of δl increasing and diverging at large ΔT , the so-called δl catastrophe.¹⁸³ The increase in l would happen because the large increase in crystallization free energy $\Delta\phi \approx \Delta T\Delta s_f$ (s_f = entropy of fusion) would cause the energy barrier to decrease rather than increase with l , as illustrated in Figure 50b. Setting $\psi < 1$ would reduce but not eliminate the problem; it would in fact only shift the δl upturn to lower temperatures.

Frank and Tosi²²⁶ considered the sequential deposition of stem segments, allowing forward and backward fluctuations, but did not allow folding back until the stem reached l_{\min} , see Figure 51a. Thus, their approach does not eliminate the δl catastrophe. However, Point²²⁸ did consider the multitude of pathways in the deposition of the first (nucleus) stem of a new layer. The stem was allowed to fold after each deposited segment (see Figure 51, panels b and c). The elementary steps in the deposition of the stem were addition and removal of segments, with rate constants A and B , and the net forward rate of folding, C_f . The solution of the steady-state equation gave then the value of $\langle l \rangle$, which was somewhat larger than l_{\min} . This removed the δl catastrophe as it changed the nature of the free energy barrier from energetic to probabilistic (entropic). Forming a long extended stem in a flexible polymer will always be

less probable and thus slower than forming a shorter stem, irrespective of ΔT . Point did not, however, extend this treatment to the deposition of subsequent stems, i.e., layer completion was handled as attachment of complete stems.

The most radical departure from LH theory was that by Sadler,^{185,186,199} whose theory was intended to describe crystallization at higher temperatures, where lateral crystal faces are above their roughening transition temperature T_R . High equilibrium roughness removes the necessity of surface nucleation as there is no surplus free energy associated with a step. The model is fine grain, and each stem is made up of individual segments. In a simple cubic crystal, the roughening transition on a $\{100\}$ surface should occur at $kT\epsilon \approx 0.6$,⁴ where ϵ is the pairwise nearest neighbor attraction energy. If whole stems are treated as nondivisible units on a polymer crystal surface, then ϵ is so large that the surface at equilibrium is always smooth and flat. However, a simple estimate shows that, if polyethylene stems were broken down into segments of no more than six CH_2 units, the surface would be thermodynamically rough. This crude estimate does not take account of connectivity between segments, and there are numerous problems in estimating T_R of such complex systems as polymer crystals. However, Sadler argued that the fact that the $\{100\}$ faces in polyethylene become curved at high temperatures indicates the roughening transition. In contrast, $\{110\}$ faces with somewhat denser packing of surface chains and hence a higher ϵ would have a higher T_R , hence the $\{110\}$ faces remain faceted.

To solve the problem analytically, Sadler studied a simplified model containing a row of stems, i.e., a cut through the crystal normal to the side surface. Monte Carlo simulation was also done in parallel. Surface configurations were allowed to evolve naturally and beyond those in Figure 51b and c. On average there were multiple temporary attachments of stems with $l < l_{\min}$, the outermost stems having the smallest l . The theory could explain most observations in polymer crystallization, such as the temperature dependencies of crystal growth rate and lamellar thickness. The model, like that of Point, avoids the δl catastrophe. Sadler’s model is often referred to as the “roughness-pinning” model. Roughness refers to equilibrium and kinetic surface roughness, resulting from splitting stems into segments and negating the need for nucleation. “Pinning” refers to the adopted rule that a “buried” segment cannot move unless the stems that cover it detach. Thus, a stem is immobilized, or pinned down, even if covered by only temporary unstable attachments with $l < l_{\min}$. The free energy barrier for crystal growth is thus entropic rather than enthalpic, but in contrast to the model by Point, a significant contribution comes from “pinning”.²²⁹

Most experimental observations on polymer crystallization can be interpreted reasonably well by a number of crystallization theories, some of which differ fundamentally in their starting premises. Apart from the δl catastrophe, the experimental ΔT dependencies of crystal thickness and growth rate can

be explained by most theories. Thus, e.g., the free energy barrier is roughly linear in l in both LH theory ($=2lbo$), as well as in the fine-grain theories of Point and Sadler ($-sT = kT \ln(w)^{-1}$, where $w \cong p^n$, p being the number of conformers per segments and n the number of segments in a stem; hence $-sT \propto n \propto l$).

Experimental results on monodisperse model polymers therefore provide much needed further tests for the theories. The self-poisoning minimum in particular can be regarded as one of the key probes, alongside the δl catastrophe and the curved crystal faces. As it happens, in the course of their rate equation analysis Sadler and Gilmer included in their investigation a model with certain energetically preferred stem lengths and indeed observed minima in growth rate vs ΔT .¹⁹⁹ Since no such effect had been observed at the time, the work remained unpublished until the experimental results on alkane $C_{246}H_{494}$ became available.¹⁸⁹ The subsequent theoretical and simulation analysis of the ΔT ²⁰⁰ and concentration¹⁹² dependencies of alkane growth rate was based on Sadler's model. In our opinion, only fine grain theories can describe the minimum. An attempt to interpret it in terms of the coarse-grain LH theory²³⁰ had to resort to highly unusual Arrhenius-type terms and could be disputed on other grounds.²¹⁰ The chances are that Point's model might also predict the minimum if applied to monodisperse chains; up to now, this has not been tested. However, it is almost certain that neither the roughness-pinning theory nor Point's model would predict crystal shapes correctly, the former because it fails to distinguish between nucleation and growth. On the other hand, Point's original fine-grain treatment would not be able to explain the minimum in v , such as that in Figure 42, because it only applies to nucleation and not to growth of new layers.

As mentioned in Section III.C, the fact that the temperature dependence of crystal habits in polyethylene is an almost exact reversal of that in alkanes approaching the rate minimum is an indication that self-poisoning is present in crystallization of the polymer and that it is more pronounced at higher temperatures. Figure 43 tentatively describes the row of stems normal to a self-poisoned surface in a polymer crystal. The situation is the same as that envisaged by Sadler. However, Figure 43 could equally apply to a layer of stems parallel to the surface, in which case it would describe retardation in v , a case not considered by Sadler. Paradoxically, it is the exact shape of rounded crystals of alkanes and polyethylene that point indirectly to poisoning of polymer crystal faces and the similarity with Sadler's model. However, we now know that this model was conceived by mistakenly associating the rounding with nonnucleated growth. At this juncture, it would appear that a synthesis of Sadler's model and the nucleation theory could come close to explaining most experimental observations in polymers as well as in monodisperse model compounds. A similar outcome may potentially be expected from Point's theory, extended to include fine-grain treatment of layer completion.

Several significant developments in polymer crystallization theory have been made more recently, e.g., the two-dimensional nucleation and sliding diffusion theory of Hikosaka,²³¹ the two-stage crystallization model by Strobl,²³² and a number of simulation studies have been carried out and are in progress. Past and future experiments on model compounds will undoubtedly benefit these developments.

IV. Conclusions

Research on model compounds and sharp oligomer fractions has already had a profound effect on our understanding of polymer crystallization and morphology. The availability of monodisperse polymers removes the dependence of this field of science on essentially impure multicomponent experimental systems. It also helps close the gap between polymer science and mainstream chemistry and physics.

The list of achievements made possible with the aid of model compounds includes (1) discovery of integer folding, stepwise lamellar thickening, crystal growth rate transitions, separation of the effects of temperature and crystal thickness in crystallization kinetics; (2) visualization and elucidation of the topology of lamellar thickening, taking advantage of the enhanced quantized thickness contrast; (3) observation and structural characterization of transient noninteger folding and of the subsequent transformations, new insights into primary chain deposition, ciliation, and subsequent rearrangements, of relevance to secondary crystallization in polymers; (4) new 1-D superlattices in mixed long chains, unexpected stability of semicrystalline structures, and experimental determination of the extent of overcrowding at the crystal-amorphous surface; (5) the role of cilia in pure and binary systems, the effect on lamellar branching and spherulite growth; (6) the discovery of self-poisoning and its unusual consequences for crystallization kinetics, the resolution of the effect on the deposition of the first and subsequent stems, discovery of poisoning by shorter chains, the likely effect of self-poisoning on crystallization and morphology of polymers; (7) elucidation of the nature of the fold surface and end surface, determination of the spectral bands due to folds (IR, Raman, NMR), and new insights into chain tilt and surface disorder; (8) improved understanding of the effect of chain length and lamellar thickness on melting point and Raman LAM frequency, derivation of improved values for equilibrium melting point and Young's modulus of polymer chains; (9) better understanding of end-group effects and bilayer formation; and (10) of the effect of specific chemical defects and short and long branches on the crystallization process and the resulting structure.

There is ample scope for future research. For example, new monodisperse oligomers are currently being contemplated, notably aromatic and model biopolymers. Deuterium-labeled long alkanes are being studied by neutron scattering and NMR. Fold surfaces of IF crystals, devoid of amorphous overlayer, may be amenable to studies by different

surface techniques. Primary nucleation and high-pressure studies are underway.

V. List of Symbols and Abbreviations

AFM	atomic force microscopy
b	width of a molecular chain
E	extended chain
E	Young's modulus
F2, F3, ..., $F(m+1)$	chains folded in two, three etc.
Δf	bulk free energy of crystallization
G	crystal growth rate
IF	integer folded
i	rate of initiation (secondary nucleation) of a new row of stems on crystal growth face
j	order of the longitudinal acoustic mode (LAM); number of stems in a layer
L	chain length
l	long period (l_{SAXS} or l_{LAM})
l_c	thickness of the crystalline layer
l_a	thickness of the amorphous or disordered layer
l_s	length of straight chain segment traversing the crystal (stem length)
LAM	longitudinal acoustic mode
m	number of folds per molecular chain
M_n	number average molecular mass
M_n^a	number average molecular mass of an arm in a branched oligomer
n	number of monomer repeat units per chain (e.g. number of carbons in an alkane)
NIF	noninteger folded
ν	Raman frequency
p	number of monomer units in the alternative block in a diblock or tri-block chain
PEO	poly(ethylene oxide)
PET	poly(ethylene terephthalate)
ψ	free energy barrier apportioning parameter
q	modulus of the wavevector, $q = 4\pi(\sin\theta)/\lambda$, where θ is half the scattering angle and λ is radiation wavelength
SAXS	small-angle X-ray scattering
SCF	semicrystalline form
σ	side-surface free energy
σ_e	end- or fold-surface free energy
T_c	crystallization temperature
T_c^m	growth transition temperature between $m-1$ and m folds per molecule
T_m	melting temperature
T_R	roughening transition temperature
$\Delta T = T_m - T_c$	supercooling
TEM	transmission electron microscopy
v	rate of step propagation on a crystal growth face

VI. Acknowledgments

This work was supported by Engineering and Physical Research Council and the Petroleum Research Fund, administered by the American Chemical Society. GU also acknowledges a grant from VBL, University of Hiroshima, during his sabbatical leave.

VII. References

- (1) (a) Wunderlich, B. *Macromolecular physics, Vol. 1: Crystal structure, morphology, defects*; Academic Press: New York, 1973. (b) *Macromolecular physics, Vol. 2: Crystal nucleation, growth, annealing*; Academic Press: New York, 1976.
- (2) Keller, A. In *Sir Charles Frank: An Eightieth Birthday Tribute*; Chambers, R. G.; Enderby, J. E.; Keller, A.; Lang, A. R.; Steeds, J. W., Eds.; Adam Hilger: Bristol, 1991.
- (3) Gedde, U. W. *Polymer Physics*; Chapman and Hall, 1995.
- (4) For a review of polymer crystallization theory, see Armitstead, K.; Golbeck-Wood, G. *Adv. Polym. Sci.* **1992**, *100*, 219.
- (5) Jonas, A.; Legras, R.; Scherrenberg, R.; Reynaers, H. *Macromolecules* **1993**, *26*, 526; Dupont, O.; Jonas, A. M.; Nysten, B.; Legras, R.; Adriaensens, P.; Gelan, J. *Macromolecules* **2000**, *33*, 562.
- (6) Rueda, D. R.; Zolotukhin, M. G.; Nequiqueo, G.; Garcia, C.; De La Campa, J. G.; De Abajo, J. *Macromol. Chem. Phys.* **2000**, *201*, 427.
- (7) Keller, A. Lecture presented at Symposium "La Vie", Société de la Vie, Palais de Versailles, June 1977.
- (8) Smith, A. E. *J. Chem. Phys.* **1953**, *21*, 2229.
- (9) Shearer, H. M. M.; Vand, V. *Acta Crystallogr.* **1956**, *9*, 379.
- (10) Pieszek, W.; Strobl, G. R.; Makahn, K. *Acta Crystallogr., Sect. B* **1974**, *30*, 1278.
- (11) Dawson, I. M. *Proc. R. Soc. (London)* **1952**, *A214*, 72.
- (12) Flory, P. J.; Vrij, A. *J. Am. Chem. Soc.* **1963**, *85*, 3548.
- (13) Wunderlich, B.; Czornyj, G. *Macromolecules* **1977**, *10*, 906.
- (14) Yamanobe, T.; Sorita, T.; Komoto, T.; Ando, I.; Sato, H. *J. Mol. Struct.* **1985**, *131*, 267.
- (15) Zerbi, G.; Magni, R.; Gussoni, M.; Moritz, K. H.; Bigotto, A.; Dirlikov, S. *J. Chem. Phys.* **1981**, *75*, 3175.
- (16) Maroncelli, M.; Qi, S. P.; Strauss, H. L.; Snyder, R. G. *J. Am. Chem. Soc.* **1982**, *104*, 6237.
- (17) Ungar, G.; Keller, A. *Colloid Polym. Sci.* **1979**, *257*, 90.
- (18) Zerbi, G.; Piazza, R.; Holland-Moritz, K. *Polymer* **1982**, *23*, 1921.
- (19) Broadhurst, M. G. *J. Res. Natl. Bur. Stand., Sect. A* **1962**, *66*, 241.
- (20) Bassett, D. C.; Block, S.; Piermarini, G. *J. Appl. Phys.* **1974**, *45*, 4146.
- (21) Ungar, G. *Macromolecules* **1986**, *19*, 1317.
- (22) Sirota, E. B.; King, H. E., Jr.; Singer, D. M.; Shao, H. H. *J. Chem. Phys.* **1993**, *98*, 5809.
- (23) Zahn, H.; Pieper, W. *Angew. Chem.* **1961**, *73*, 246.
- (24) Balta-Calleja, F. J.; Keller, A. *J. Polym. Sci. A2* **1963**, *2*, 2151.
- (25) Kern, W.; Davidovits, J.; Rautekus, K. J.; Schmidt, G. F. *Makromol. Chem.* **1961**, *43*, 106.
- (26) Balta-Calleja, F. J.; Keller, A. *J. Polym. Sci. A* **1964**, *2*, 2171.
- (27) Arlie, J. P.; Spegt, P.; Skoulios, A. *C. R. Acad. Sci. Paris* **1965**, *260*, 5774.
- (28) Kovacs, A. J.; Gonthier, A.; Straupe, C. *J. Polym. Sci., Polym. Symp.* **1975**, *50*, 283.
- (29) Buckley, C. P.; Kovacs, A. J. In *Structure of Crystalline Polymers*; Hall, I. H., Ed.; Elsevier-Applied Science: London, 1984; pp 261–307.
- (30) Bidd, I.; Whiting, M. C. *J. Chem. Soc., Chem. Commun.* **1985**, 543; Bidd, I.; Holdup, D. W.; Whiting, M. C. *J. Chem. Soc., Perkin Trans. 1* **1987**, 2455.
- (31) Lee, K. S.; Wegner, G. *Makromol. Chem.-Rapid Commun.* **1985**, *6*, 203.
- (32) Brooke, G. M.; Burnett, S.; Mohammed, S.; Proctor, D.; Whiting, M. C.; *J. Chem. Soc., Perkin Trans. 1* **1996**, 1635.
- (33) Ungar, G.; Stejny, J.; Keller, A.; Bidd, I.; Whiting, M. C. *Science* **1985**, *229*, 386.
- (34) Cheng, S. Z. D.; Chen, J. H.; Zhang, A. Q.; Heberer, D. P. *J. Polym. Sci., Part B: Polym. Phys.* **1991**, *29*, 299.
- (35) Mizushima, S.-I.; Shimanouchi, T. *J. Am. Chem. Soc.* **1949**, *71*, 1320.
- (36) Palmö, K.; Krimm, S. *J. Polym. Sci., Polym. Phys. Ed.* **1996**, *34*, 37.
- (37) Hartley, A.; Leung, Y. K.; Booth, C.; Shepherd, I. W. *Polymer* **1976**, *17*, 355.
- (38) Kim, I.; Krimm, S. *Macromolecules* **1996**, *29*, 7186.
- (39) Strobl, G. R.; Eckel, R. *J. Polym. Sci., Polym. Phys. Ed.* **1976**, *14*, 913.
- (40) Ungar, G. In *Integration of Fundamental Polymer Science and Technology, Vol. 2*; Lemstra, P. J.; Kleintjens, L. A., Ed.; Elsevier Applied Sci.: London, 1988; pp 342–362.
- (41) Snyder, R. G.; Strauss, H. L.; Alamo, R.; Mandelkern, L. *J. Chem. Phys.* **1994**, *100*, 5422.
- (42) Zeng, X. B.; Ungar, G. Unpublished material.
- (43) Khoury, F.; Fanconi, B.; Barnes, J. D.; Bolz, L. H. *J. Chem. Phys.* **1973**, *59*, 5849.
- (44) Minoni, G.; Zerbi, G. *J. Phys. Chem.* **1982**, *86*, 4791.
- (45) Song, K.; Krimm, S. *Macromolecules* **1990**, *23*, 1946.
- (46) Viras, K.; Teo, H. H.; Marshall, A.; Domszy, R. C.; King, T. A.; Booth, C. *J. Polym. Sci., Polym. Phys. Ed.* **1983**, *21*, 919.
- (47) Campbell, C.; Viras, K.; Masters, A. J.; Craven, J. R.; Hao, Z.; Yeates, S. G.; Booth, C. *J. Phys. Chem.* **1991**, *95*, 4647.
- (48) Garner, W. E.; Van Bibber, K.; King, A. M. *J. Chem. Soc.* **1931**, 1533.
- (49) Buckley, C. P.; Kovacs, A. J. *Prog. Colloid Polym. Sci.* **1975**, *58*, 44.
- (50) Nakasone, K.; Urabe, Y.; Takamizawa, K. *Thermochim. Acta* **1996**, *286*, 161.

- (51) Mandelkern, L.; Prasad, A.; Alamo, R. G. *Macromolecules* **1990**, *23*, 3696.
- (52) Carlier, V.; Devaux, J.; Legras, R.; Blundell, D. J. *J. Polym. Sci., Polym. Phys.* **1998**, *36*, 2563.
- (53) Buckley, C. P.; Kovacs, A. J. *Colloid Polym. Sci.* **1976**, *254*, 695.
- (54) Hoffman, J. D. *Polym. Commun.* **1986**, *27*, 39.
- (55) Hoffman, J. D.; Miller, R. L. *Polymer* **1997**, *38*, 3151.
- (56) Ungar, G.; Keller, A. *Polymer* **1986**, *27*, 1835.
- (57) Song, K.; Krimm, S. *Macromolecules* **1989**, *22*, 1504.
- (58) Cheng, S. Z. D.; Zhang, A. Q.; Chen, J. H.; Heberer, D. P. *J. Polym. Sci., Part B: Polym. Phys.* **1991**, *29*, 287.
- (59) Ungar, G.; Zeng, X. B.; Brooke, G. M.; Mohammed, S.; *Macromolecules* **1998**, *31*, 1875.
- (60) Guttman, C. M.; DiMarzio, E. A.; Hoffman, J. D. *Polymer* **1981**, *22*, 1466.
- (61) Zeng, X. B.; Ungar, G.; Spells, S. J. *Polymer* **2000**, *41*, 8775.
- (62) Glatter, O.; Kratky, O. *Small Angle X-ray Scattering*; Academic Press: London, 1982.
- (63) Cheng, S. Z. D.; Chen, J. H.; Zhang, A. Q.; Barley, J. S.; Habenschuss A.; Schack, P. R.; *Polymer* **1992**, *33*, 1140.
- (64) Kovacs, A. J.; Gonthier, A. *Kolloid Z. Z. Polym.* **1972**, *250*, 530.
- (65) Campbell, C.; Viras, K.; Booth, C. *J. Polym. Sci., Part B: Polym. Phys.* **1991**, *29*, 1613.
- (66) Yoon, D. Y.; Flory, P. J. *Faraday Discuss. Chem. Soc.* **1979**, *68*, 288.
- (67) Hoffman, J. D.; Davis, G. T. In *Polymer Surfaces*; Clark, D. T.; Feast, W. J., Ed.; John Wiley & Sons: Chichester 1978; pp 259–268.
- (68) Ungar, G.; Organ, S. J. *Polym. Commun.* **1987**, *28*, 232.
- (69) Wittmann, J. C.; Lotz, B. *J. Polym. Sci., Polym. Phys. Ed.* **1985**, *25*, 205.
- (70) Painter, R. C.; Havens, J.; Hart, W. W.; Koenig, J. L. *J. Polym. Sci., Polym. Phys. Ed.* **1977**, *15*, 1223.
- (71) Spells, S. J.; Organ, S. J.; Keller, A.; Zerbi, G. *Polymer* **1987**, *28*, 697.
- (72) Lee, K.-S.; Wegner, G.; Hsu, S. L. *Polymer* **1987**, *28*, 889.
- (73) Strobl, G. R.; Hagedorn, W. *J. Polym. Sci., Polym. Phys. Ed.* **1978**, *16*, 1181.
- (74) Strobl, G. R. *Kolloid Z. Z. Polym.* **1970**, *250*, 1039.
- (75) Zeng, X. B.; Ungar, G. *Polymer* **1998**, *39*, 4523.
- (76) Ungar, G. In *Characterization of solid polymers*; Spells, S. J., Ed.; Chapman and Hall: London, 1994; pp 56–121.
- (77) Zeng, X. B.; Ungar, G. Unpublished work.
- (78) Brooke, G. M.; Mohammed, S.; Whiting, M. C. *J. Chem. Soc., Perkin Trans. 1* **1997**, *22*, 3371.
- (79) Brooke, G. M.; Mohammed, S.; Whiting, M. C. *Polymer* **1999**, *49*, 773.
- (80) Atkins, E. D. T.; Hill, M. J.; Jones, N. A.; Sikorski, P. *J. Mater. Sci.* **2000**, *35*, 5179.
- (81) Jones, N. A.; Sikorski, P.; Atkins, E. D. T.; Hill, M. J. *Macromolecules* **2000**, *3*, 4146.
- (82) Cooper, S. J.; Atkins, E. D. T.; Hill, M. J. *Macromolecules* **1998**, *31*, 5032.
- (83) Bellinger, M. A.; Waddon, A. J.; Atkins, E. D. T.; MacKnight, W. J. *Macromolecules* **1994**, *27*, 2130.
- (84) Atkins, E. D. T.; Hill, M. J.; Hong, S. K.; Keller, A.; Organ, S. J. *Macromolecules* **1992**, *25*, 917.
- (85) Cooper, S. J.; Atkins, E. D. T.; Hill, M. J. *Macromolecules* **1998**, *31*, 1, 8947.
- (86) (a) McGrath, K. P.; Fournier, M. J.; Mason, T. L.; Tirrell, D. A. *J. Am. Chem. Soc.* **1992**, *114*, 727. (b) Krejchi, M. T.; Atkins, E. D. T.; Waddon, A. J.; Fournier, M. J.; Mason, T. L.; Tirrell, D. A. *Science* **1994**, *265*, 1427.
- (87) Panitch, A.; Matsuki, K.; Cantor, E. J.; Cooper, S. J.; Atkins, E. D. T.; Fournier, M. J.; Mason, T. L.; Tirrell, D. A. *Macromolecules* **1997**, *30*, 42.
- (88) Fraser, R. D. B.; MacRae, T. P.; Stewart, F. H. C.; Suzuki, E. *J. Mol. Biol.* **1965**, *11*, 706.
- (89) Lotz, B.; Keith, H. D. *J. Mol. Biol.* **1971**, *61*, 201.
- (90) Deguchi, Y.; Fournier, M. J.; Mason, T. L.; Tirrell, D. A. *J. Macromol. Sci., Pure Appl. Chem.* **1994**, *A31*, 1691.
- (91) (a) Krejchi, M. T.; Cooper, S. J.; Deguchi, Y.; Atkins, E. D. T.; Fournier, M. J.; Mason, T. L.; Tirrell, D. A. *Macromolecules* **1997**, *30*, 5012. (b) Parkhe, A. D.; Cooper, S. J.; Atkins, E. D. T.; Fournier, M. J.; Mason, T. L.; Tirrell, D. A. *Int. J. Biol. Macromol.* **1998**, *23*, 251.
- (92) Ungar, G. *Am. Chem. Soc. Polym. Prepts.* **1990**, *31* (2), 108.
- (93) Sullivan, P. K.; Weeks, J. J. *J. Res. Natl. Bur. Stand., Sect. A* **1970**, *74*, 203.
- (94) Nukushina, Y.; Itoh, Y.; Fischer, E. W. *J. Polym. Sci., Polym. Lett.* **1965**, *3*, 383.
- (95) Möller, M.; Cantow, H. J.; Drotloff, H.; Emeis, D. *Makromol. Chem.* **1986**, *187*, 1237.
- (96) Keith, H. D.; Padden, F. J. *Macromolecules* **1996**, *29*, 7776.
- (97) Abo el Maaty, M. I.; Bassett, D. C. *Polymer* **2001**, *42*, 4957.
- (98) Hay, I. L.; Keller, A. *J. Mater. Sci.* **1966**, *1*, 41; Hay, I. L.; Keller, A. *J. Mater. Sci.* **1967**, *2*, 538; Hay, I. L.; Keller, A. *J. Mater. Sci.* **1968**, *3*, 646.
- (99) Khoury, F. *Faraday Discuss. Chem. Soc.* **1979**, *68*, 404.
- (100) Bassett, D. C.; Hodge, A. M. *Proc. R. Soc. London A* **1981**, *377*, 25.
- (101) Gautam, S.; Balijepalli, S.; Rutledge, G. C. *Macromolecules* **2000**, *33*, 9136.
- (102) Takamizawa, K.; Ogawa, Y.; Oyama, T. *Polym. J.* **1982**, *14*, 441.
- (103) de Silva, D. S. M.; Gorce, J. P.; Boda, E.; Zeng, X. B.; Ungar, G.; Spells, S. J. Manuscript in preparation.
- (104) Hoffman, J. D.; Weeks, J. J. *J. Chem. Phys.* **1965**, *42*, 4301.
- (105) Brooke, G. M.; Farren, C.; Harden, A.; Whiting, M. C. *Polymer* **2001**, *42*, 2777.
- (106) Zeng, X. B.; Ungar, G. Unpublished material.
- (107) Sadler, D. M. *Faraday Discuss. Chem. Soc.* **1979**, *68*, 106.
- (108) Sikorski, P.; Atkins, E. D. T. *Macromolecules* **2001**, *34*, 4788.
- (109) Kay, H. F.; Newman, B. A. *Acta Crystallogr., Sect. B* **1968**, *B24*, 615.
- (110) Groth, P. *Acta Chem. Scand., Ser. A* **1979**, *A33*, 199.
- (111) Trzebiatowski, T.; Dräger, M.; Strobl, G. R. *Makromol. Chem.* **1982**, *183*, 731.
- (112) Schill, G.; Logemann, E.; Fritz, H. *Chem. Ber.* **1976**, *109*, 497.
- (113) Spells, S. J.; Keller, A.; Sadler, D. M. *Polymer* **1984**, *25*, 749.
- (114) Stocker, W.; Bar, G.; Kunz, M.; Moller, M.; Magonov, S. N.; Cantow, H.-J. *Polym. Bull.* **1991**, *26*, 215.
- (115) Grossmann, H. P.; Arnold, R.; Bürkle, K. R. *Polym. Bull.* **1980**, *3*, 135.
- (116) Petraccone, V.; Corradini, P.; Allegra, L. *J. Polym. Sci., Part C: Polym. Symp.* **1972**, *38*, 419.
- (117) Möller, M.; Gronski, W.; Cantow, H. J.; Höcker, H. *J. Am. Chem. Soc.* **1984**, *106*, 5093.
- (118) Grossmann, H. P. *Polym. Bull.* **1981**, *5*, 137.
- (119) Kögler, G.; Drotloff, H.; Möller, M. *Mol. Cryst. Liq. Cryst.* **1987**, *153*, 179.
- (120) Vaughan, A. S.; Ungar, G.; Bassett, D. C.; Keller, A. *Polymer* **1985**, *26*, 726.
- (121) Yan, Z. G.; Yang, Z.; Price, C.; Booth, C. *Makromol. Chem., Rapid Commun.* **1993**, *14*, 725.
- (122) Cooke, J.; Viras, K.; Yu, G. E.; Sun, T.; Yonemitsu, T.; Ryan, A. J.; Price, C.; Booth, C. *Macromolecules* **1998**, *31*, 3030.
- (123) Chenevert, R.; D'Astous, L. *J. Heterocycl. Chem.* **1986**, *23*, 1785.
- (124) Gibson, H. W., et al. *J. Org. Chem.* **1994**, *59*, 2186.
- (125) Yang, Z.; Yu, G. E.; Cooke, J.; AliAdib, Z.; Viras, K.; Matsuura, H.; Ryan, A. J.; Booth, C. *J. Chem. Soc., Faraday Trans.* **1996**, *92*, 3173.
- (126) Yang, Z.; Cooke, J.; Viras, K.; Gorry, P. A.; Ryan, A. J.; Booth, C. *J. Chem. Soc., Faraday Trans.* **1997**, *93*, 4033.
- (127) Viras, K.; Yan, Z. G.; Price, C.; Booth, C.; Ryan, A. J. *Macromolecules* **1995**, *28*, 104.
- (128) Grossmann, H. P.; Böstler, H. *Polym. Bull.* **1981**, *5*, 175.
- (129) Hasek, J.; Jecny, J.; Langer, V.; Huml, K.; Sedlacek, P. *Acta Crystallogr., Sect. B* **1982**, *38*, 2710.
- (130) Kitano, Y.; Ashida, T. *Polym. J.* **1992**, *24*, 1099.
- (131) Kitano, Y.; Ishitani, A.; Ashida, T. *Polym. J.* **1991**, *23*, 949.
- (132) Clarson, S. J.; Dodgson, K.; Semlyen, J. A. *Polymer* **1985**, *26*, 930.
- (133) Percec, V.; Asandei, A. D.; Chu, P. *Macromolecules* **1996**, *29*, 3736.
- (134) Keller, A.; Udagawa, Y. *J. Polym. Sci., Pt. A-2* **1970**, *8*, 19.
- (135) Barnes, W. J.; Price, F. *Polymer* **1964**, *5*, 283.
- (136) Abrahamson, S.; v. Sydow, E. *Acta Crystallogr.* **1954**, *7*, 591.
- (137) Ungar, G.; Zeng, X. B. *Macromolecules* **1999**, *32*, 3543.
- (138) Zeng, X. B.; Ungar, G. Manuscript to be published.
- (139) Cheng, S. Z. D.; Wu, S. S.; Chen, J. H.; Zhuo, Q. H.; Quirk, R. P.; Von Meerwall, E. D.; Hsiao, B. S.; Habenschuss, A.; Zsack, P. R. *Macromolecules* **1993**, *26*, 5105.
- (140) Hopken, J.; Moller, M. *Macromolecules* **1992**, *25*, 2482.
- (141) Twieg, R.; Rabolt, J.; Russell, T.; Farmer, B. *Abstr. Pap. Am. Chem. Soc.* **1984**, *187*, (Apr.) 17-Poly.
- (142) Yeates, S. G.; Booth, C. *Makromol. Chem.-Macromol. Chem. Phys.* **1985**, *186*, 2663.
- (143) Craven, J. R.; Hao, Z.; Booth, C. *J. Chem. Soc., Faraday Trans.* **1991**, *87*, 1183.
- (144) Campbell, C.; Viras, K.; Richardson, M. J.; Masters, A. J.; Booth, C. *Makromol. Chem., Macromol. Chem. Phys.* **1993**, *194*, 799.
- (145) Hamley, I. W.; Wallwork, M. L.; Smith, D. A.; Fairclough, J. P. A.; Ryan, A. J.; Mai, S. M.; Yang, Y. W.; Booth, C. *Polymer* **1998**, *39*, 3321.
- (146) Lee, S.-W.; Chen, E.-Q.; Zhang, A.; Yoon, Y.; Moon, B.-S.; Lee, S.; Harris, F. W.; Cheng, S. Z. D.; von Meerwall, E. D.; Hsiao, B. S.; Verma, R.; Lando, J. B. *Macromolecules* **1996**, *29*, 8816.
- (147) Chen, E.-Q.; Lee, S.-W.; Zhang, A.; Moon, B.-S.; Honigfort, P. S.; Mann, I.; Lin, H.-M.; Harris, F. W.; Cheng, S. Z. D.; Hsiao, B. S.; Yeh, F. *Polymer* **1999**, *40*, 4543.
- (148) Chen, E.-Q.; Lee, S.-W.; Zhang, A.; Moon, B.-S.; Mann, I.; Harris, F. W.; Cheng, S. Z. D.; Hsiao, B. S.; Yeh, F.; von Meerwall, E. D. In *Scattering from Polymers*, ACS series **2000**, *739*, 118.
- (149) Chen, E.-Q.; Lee, S.-W.; Zhang, A.; Moon, B.-S.; Mann, I.; Harris, F. W.; Cheng, S. Z. D.; Hsiao, B. S.; Yeh, F.; von Meerwall, E. D.; Grubb, D. T. *Macromolecules* **1999**, *32*, 4784.
- (150) Driver, M. A. N.; Klein, P. G. *Macromol. Symp.* **1999**, *141*, 263.
- (151) Zeng, X. B.; Ungar, G. Manuscript in preparation.

- (152) Mazee, W. M. *Anal. Chim. Acta* **1957**, *17*, 97.
- (153) Nechitailo, N. A.; Topchiev, A. V.; Rozenberg, L. M.; Terenteva, E. M. *Russian Journal of Physical Chemistry (English translation)* **1960**, *34* (12), 1268.
- (154) Mnyukh, Yu. V. *J. Struct. Chem. (English translation)* **1960**, *1* (3), 346.
- (155) Kitaigorodskii, A. *Organic Chemical Crystallography*; Consultants Bureau: New York, 1961.
- (156) Matheson, R. R., Jr.; Smith, P. *Polymer* **1985**, *26*, 288.
- (157) Rajabalee, F.; Metivaud, V.; Mondieig, D.; Haget, Y.; Cuevas-Diarte, M. A. *J. Mater. Res.* **1999**, *14*, 2644.
- (158) Luth, H.; Nyburg, S. C.; Robinson, P. M.; Scott, H. G. *Mol. Cryst. Liq. Cryst.* **1974**, *27*, 337.
- (159) Gerson, A. R.; Nyburg, S. C. *Acta Crystallogr., Sect. B* **1994**, *50*, 252.
- (160) Ungar, G.; Masic, N. *J. Phys. Chem.* **1985**, *89*, 1036.
- (161) Doucet, J.; Denicolo, I.; Craievich, A. F.; Collet, A. *J. Chem. Phys.* **1981**, *75*, 5125.
- (162) Denicolo, I.; Craievich, A. F.; Doucet, J. *J. Chem. Phys.* **1984**, *80*, 6200.
- (163) Dorset, D. L. *Macromolecules* **1985**, *18*, 2158; Dorset, D. L. *Macromolecules* **1986**, *19*, 2965; Dorset, D. L. *Macromolecules* **1987**, *20*, 2782; Dorset, D. L. *Macromolecules* **1990**, *23*, 623.
- (164) Kim, Y.; Strauss, H. L.; Snyder, R. G. *J. Phys. Chem.* **1989**, *93*, 3 (1), 485.
- (165) Clavell-Grunbaum, D.; Strauss, H. L.; Snyder, R. G. *J. Phys. Chem. B* **1997**, *101* (3), 335.
- (166) Sirota, E. B.; King, H. E., Jr.; Shao, H. H.; Singer, D. M. *J. Phys. Chem.* **1995**, *99*, 798.
- (167) Basson, I.; Reynhardt, E. C. *J. Chem. Phys.* **1991**, *95* (2), 1215.
- (168) Yamamoto, T.; Nozaki, K. *Polymers* **1994**, *35*, 3340; Yamamoto, T.; Nozaki, K. *Polymers* **1995**, *36*, 2505; Yamamoto, T.; Nozaki, K. *Polymers* **1997**, *38*, 2643.
- (169) Dorset, D. L.; Snyder, R. G. *J. Phys. Chem.* **1996**, *100*, 9848.
- (170) Dorset, D. L. *J. Phys. Chem. B* **1997**, *101*, 4970.
- (171) Gilbert, E. P. *J. Phys. Chem. Chem. Phys.* **1999**, *1*, 5209.
- (172) Chevallier, V.; Provost, E.; Bourdet, J. B.; Bouroukba, M.; Ptitjean, D.; Dirand, M. *Polymer* **1999**, *40*, 2121, 2129.
- (173) Lauritzen, J. I., Jr.; Passaglia, E.; DiMazio, E. A. *J. Res. Natl. Bur. Stand., Sect. A* **1967**, *71* (4), 245.
- (174) Asbach, G. I.; Kilian, H.-G.; Starcke, Fr. *Colloid Polym. Sci.* **1982**, *260*, 151.
- (175) Bonsor, D. H.; Bloor, D. *J. Mater. Sci.* **1977**, *12*, 1559.
- (176) Zeng, X. B.; Ungar, G. *Phys. Rev. Lett.* **2001**, *86*, 4875.
- (177) (a) Zeng, X. B.; Ungar, G. *Macromolecules* **2001**, *34*, 6945. (b) Zeng, X. B.; Ungar, G. *Polymer* **2002** (in press).
- (178) DiMarzio, E. A.; Guttman, C. M. *Polymer* **1980**, *21*, 733.
- (179) Mansfield, M. L. *Macromolecules* **1988**, *21*, 126.
- (180) Balijepalli, S.; Rutledge, G. C. *J. Chem. Phys.* **1998**, *109*, 6523; *Macromol. Symp.* **1998**, *133*, 71.
- (181) Boda, E.; Zeng, X. B.; Ungar, G. Manuscript in preparation.
- (182) Hoffman, J. D. *Macromolecules* **1986**, *19*, 1124.
- (183) Hoffman, J. D.; Davis, G. T.; Lauritzen, J. I., Jr. In *Treatise on Solid State Chemistry*; Hannay, N. B., Ed.; Plenum Press: New York, 1976; Vol. 3, Chapter 7, pp 497–614.
- (184) Hoffman, J. D. *Macromolecules* **1985**, *18*, 772.
- (185) Sadler, D. M. *J. Polym. Sci., Polym. Phys. Ed.* **1985**, *23*, 1533.
- (186) Sadler, D. M. *Polymer* **1983**, *24*, 1401.
- (187) Point, J. J.; Kovacs, A. J. *Macromolecules* **1980**, *13*, 399.
- (188) Toda, A. *J. Phys. Soc. Jpn.* **1986**, *55*, 3419.
- (189) Ungar, G.; Keller, A. *Polymer* **1987**, *28*, 1899.
- (190) Organ, S. J.; Ungar, G.; Keller, A. *Macromolecules* **1989**, *22*, 1995.
- (191) Organ, S. J.; Keller, A.; Hikosaka, M.; Ungar, G. *Polymer* **1996**, *37*, 2517.
- (192) Ungar, G.; Mandal, P.; Higgs, P. G.; de Silva, D. S. M.; Boda, E.; Chen, C. M. *Phys. Rev. Lett.* **2000**, *85*, 4397.
- (193) Boda, E.; Ungar, G.; Brooke, G. M.; Burnett, S.; Mohammed, S.; Proctor, D.; Whiting, M. C. *Macromolecules* **1997**, *30*, 4674.
- (194) Organ, S. J.; Barham, P. J.; Hill, M. J.; Keller, A.; Morgan, R. L. *J. Polym. Sci., Pt. B: Polym. Phys.* **1997**, *35*, 775.
- (195) Sutton, S. J.; Vaughan, A. S.; Bassett, D. C. *Polymer* **1996**, *37*, 5735.
- (196) Hobbs, J. K.; Hill, M. J.; Barham, P. J. *Polymer* **2001**, *42*, 2167.
- (197) Morgan, R. L.; Barham, P. J.; Hill, M. J.; Keller, A.; Organ, S. J. *J. Macromol. Sci., Phys. B* **1998**, *37*, 319.
- (198) Cheng, S. Z. D.; Chen, J. H. *J. Polym. Sci.; Part B: Polym. Phys.* **1991**, *29*, 311.
- (199) Sadler, D. M.; Gilmer, G. H. *Polym. Commun.* **1987**, *28*, 243.
- (200) Higgs, P. G.; Ungar, G. *J. Chem. Phys.* **1994**, *100*, 640.
- (201) Higgs, P. G.; Ungar, G. *J. Chem. Phys.* **2001**, *114*, 6958.
- (202) Fisher, R. A. *Ann. Eugenics* **1937**, *7*, 355.
- (203) de Silva, D. S. M.; Ungar, G.; Zeng, X. B. Manuscript in preparation.
- (204) Hosier, I. L.; Bassett, D. C.; Vaughan, A. S. *Macromolecules* **2000**, *33*, 8781.
- (205) Keith, H. D. *J. Appl. Phys.* **1964**, *35*, 3115.
- (206) Mansfield, M. L. *Polymer* **1988**, *29*, 1755.
- (207) Toda, A. *Polymer* **1991**, *32*, 771.
- (208) Point, J. J.; Villers, D. *J. Cryst. Growth* **1991**, *114*, 228.
- (209) Frank, F. C. *J. Cryst. Growth* **1974**, *22*, 233.
- (210) Ungar, G. In *Polymer Crystallization*; Dosiere, M., Ed.; NATO ASI Series; Kluwer: Dordrecht, 1993; pp 63–72.
- (211) Ungar, G.; Putra, E. G. R. *Macromolecules* **2001**, *34*, 5180.
- (212) Organ, S. J.; Keller, A. *J. Mater. Sci.* **1985**, *20*, 1571.
- (213) Toda, A. *Faraday Discuss.* **1993**, *95*, 129.
- (214) Putra, E. G. R.; Ungar, G. Submitted for publication.
- (215) Hoffman, J. D.; Miller, R. L. *Macromolecules* **1989**, *22*, 3038, 3502; Hoffman, J. D.; Miller, R. L. *Polymer* **1991**, *32*, 963.
- (216) Khoury, F. *J. Appl. Phys.* **1963**, *34*, 73.
- (217) Hosier, I. L.; Bassett, D. C. *Polymer* **2000**, *41*, 8801.
- (218) Fischer, E. W.; Schmidt, G. F. *Angew. Chem.* **1962**, *74*, 551.
- (219) Spegt, P. *Makromol. Chem.* **1970**, *139*, 139.
- (220) (a) Ungar, G.; Organ, S. J. *J. Polym. Sci., Part B: Polym. Phys. Ed.* **1990**, *28*, 2353. (b) Organ, S. J.; Ungar, G.; Keller, A. *J. Polym. Sci., Part B: Polym. Phys. Ed.* **1990**, *28*, 2365.
- (221) Hobbs, J. K.; Hill, M. J.; Barham, P. J. *Polymer* **2000**, *41*, 8761.
- (222) Holland, V. F. *J. Appl. Phys.* **1964**, *35*, 59; Blackadder, D. A.; Schleinitz, H. M. *Polymer* **1986**, *7*, 603.
- (223) Geil, P. H. *Polymer Single Crystals*; Wiley: New York, 1963; Chapter 5.
- (224) Winkel, A. K.; Hobbs, J. K.; Miles, M. J. *Polymer* **2000**, *41*, 8791.
- (225) Boda, E.; Ungar, G.; Zeng, X. B. Manuscript in preparation.
- (226) Frank, F. C.; Tosi, M. *Proc. R. Soc. (London)* **1961**, *A263*, 323.
- (227) Lauritzen, J. I., Jr.; Hoffman, J. D. *J. Res. Natl. Bur. Stand., Sect. A* **1960**, *64*, 73; Hoffman, J. D.; Lauritzen, J. I., Jr. *J. Res. Natl. Bur. Stand., Sect. A* **1961**, *65*, 73.
- (228) Point, J. J. *Macromolecules* **1979**, *12*, 770; Point, J. J. *Discuss. Faraday Soc.* **1979**, *68*, 167.
- (229) Sadler, D. M. *Nature* **1987**, *326*, 174.
- (230) Hoffman, J. D. *Polymer* **1992**, *32*, 2828.
- (231) Hikosaka, M. *Polymer* **1990**, *31*, 458.
- (232) Heck, B.; Hugel, T.; Iijima, M.; Strobl, G. *Polymer* **2000**, *41*, 8839.

CR990130U

Advanced Solid-State NMR Methods for the Elucidation of Structure and Dynamics of Molecular, Macromolecular, and Supramolecular Systems

Steven P. Brown[†] and Hans Wolfgang Spiess^{*}

Max-Planck-Institut für Polymerforschung, Postfach 3148, D-55021 Mainz, Germany

Received February 5, 2001

Contents

I. Introduction	4125
II. Improving the Resolution in ¹ H Solid-State NMR	4127
A. Magic-Angle Spinning	4128
B. Homonuclear ¹ H Decoupling Methods	4129
III. Homonuclear 2D Double-Quantum NMR Spectroscopy	4132
A. The Excitation of Homonuclear DQC	4132
B. Rotor-Synchronized 2D DQ MAS Spectra	4133
C. ¹ H- ¹ H DQ MAS Spinning-Sideband Patterns	4134
IV. Heteronuclear 2D NMR Methods	4137
A. Heteronuclear Correlation Spectroscopy	4137
B. The Quantitative Determination of Heteronuclear Dipolar Couplings	4139
V. Structural Determination by Solid-State NMR	4140
VI. Hydrogen-Bonded Systems	4140
A. Rotor-Synchronized ¹ H DQ MAS NMR Spectroscopy	4141
B. ¹ H DQ MAS NMR Spinning-Sideband Patterns	4142
VII. Aromatic π - π Interactions and Ring-Current Effects	4144
A. Aggregation Shifts	4145
B. Hexabenzocoronone Derivatives	4145
C. A Molecular Tweezer Host-Guest Complex	4147
VIII. The Investigation of Dynamic Processes	4149
A. A Molecular Tweezer Host-Guest Complex	4149
B. The Making and Breaking of Hydrogen Bonds in a HBC Derivative	4149
C. The Order Parameter in Columnar Discotic Mesophases	4151
IX. Conclusions	4153
X. Acknowledgment	4154
XI. References	4154

I. Introduction

In polymer science today, much interest is focused on the controlled design of well-ordered superstructures based on the self-assembly of carefully chosen building blocks. Of particular importance in

this respect are noncovalent interactions,¹ e.g., hydrogen bonding and aromatic π - π interactions. For example, Sijbesma et al have shown that linear polymers and reversible networks are formed from the self-assembly of monomers incorporating two and three 2-ureido-4-pyrimidone units, respectively, on account of the propensity of these units to dimerize strongly in a self-complementary array of four cooperative hydrogen bonds.² However, such specific interactions are not a prerequisite for a well-controlled self-assembly: e.g., as demonstrated by Percec and co-workers, the self-assembly in the bulk of dendritic building blocks into spherical, cylindrical, and other supramolecular architectures occurs as a consequence of both shape complementarity and the demixing of aliphatic and aromatic segments.^{3,4}

Despite the presence of considerable order on different length scales, single crystals suitable for diffraction studies, and hence full crystal structures, are not available for such self-assembled supramolecular structures. If the mechanisms governing self-assembly are to be better understood, analytical methods capable of probing the structure and dynamics of these partially ordered systems are essential. In recent years, the field of solid-state NMR has enjoyed rapid technological and methodological development, and we will show, in this review, that advanced solid-state NMR methods are well placed to meet the challenges provided by modern polymer chemistry. In particular, much insight can be achieved for small amounts (10–20 mg) of as-synthesized samples.

The great utility of NMR lies in its unique selectivity, which is due to the differentiation of chemically distinct sites on the basis of the chemical shift. Indeed, solution-state NMR spectroscopy has developed into an indispensable method for characterizing organic molecules:^{5,6} currently, one can even determine the complete three-dimensional structure of proteins of molecular masses approaching 50 kD.⁷ In the solid state, however, the fast isotropic molecular tumbling that leads to the observation of inherently high-resolution solution-state spectra is absent, and anisotropic interactions, e.g., the chemical shift anisotropy (CSA), and the dipolar and quadrupolar couplings, lead to a broadening of the resonances.^{8–10} These anisotropic interactions, on one hand, have the significant disadvantage of hindering the resolution of distinct sites but, on the other hand, contain valuable structural and dynamic information.

^{*} To whom correspondence should be addressed. Tel: 00 49 6131 379120; Fax: 00 49 6131 379320; Email: spiess@mpip-mainz.mpg.de.

[†] Present Address: Laboratoire de Stéréochimie et des Interactions Moléculaires, UMR-5532 CNRS/ENS, Ecole Normale Supérieure de Lyon, 69364 Lyon, France.



Steven P. Brown was born in Coventry, England in 1972. He obtained a B. A. in Chemistry from Oxford University, England, in 1994. At Oxford, first as a Part II undergraduate student and subsequently for his D. Phil, which he received in 1997, he carried out research in the laboratory of Dr. S. Wimperis into NMR of half-integer quadrupolar nuclei, in particular the solid-state multiple-quantum (MQ) magic-angle spinning (MAS) experiment. From 1998 until 2000, he carried out postdoctoral research at the Max Planck Institute for Polymer Research, Mainz, Germany. Working in the group of Professor H. W. Spiess, he applied solid-state NMR methods, in particular, the combination of very-fast MAS with ^1H double-quantum (DQ) spectroscopy, to the investigation of structural and dynamic questions in supramolecular systems. He is currently a Marie Curie Fellow in the group of Professor L. Emsley at the Ecole Normale Supérieure, Lyon, France.



Hans Wolfgang Spiess received his Ph.D. in physical chemistry at the University of Frankfurt, Germany, with H. Hartmann in 1968. After a two year's postdoctoral stay at Florida State University with R. K. Sheline, he returned to Germany and joined the staff of the Max-Planck-Institute, Department of Molecular Physics at Heidelberg, under the direction of K. H. Hausser. In 1975, he changed to the Chemistry Department of the University at Mainz, where he became a Professor in 1978. After professorships at the Universities of Münster (1981–82) and Bayreuth (1983–84), he was appointed as a director at the newly founded Max-Planck-Institute for Polymer Research in Mainz. His main research interests are development of solid-state NMR and pulsed ESR techniques for the study of structure and dynamics of synthetic polymers and supramolecular systems.

One way by means of which the structural and dynamic information inherent to the anisotropic interactions can be probed in a site-selective fashion involves the investigation of samples where specific isotopic labels, e.g., ^2H , ^{13}C , ^{15}N , are introduced. ^2H is a spin $I = 1$ nucleus, and the quadrupolar interaction dominates ^2H NMR. By an analysis of one-dimensional line shapes, fast dynamic processes (10^{-4} to 10^{-7} s) can be quantitatively probed, while two-dimensional exchange experiments allow the inves-

tigation of slower motions (up to 1 s).⁹ The dipolar coupling between two nuclei has an inverse cubed dependence on the internuclear separation, and, thus, solid-state NMR experiments which provide access to this interaction can be used to determine specific distance constraints. Indeed, the last 10 years have seen much interest focused on solid-state NMR experiments applicable to samples incorporating spin $I = 1/2$ isotopic labels, usually ^{13}C or ^{15}N , such that only particular dipolar-coupled spin pairs are present.^{11,12} In particular, the rotational-echo double-resonance (REDOR)^{13–15} technique has become very popular for determining distances between two heteronuclei, while other methods further allow the determination of torsional angles.^{16,17} Although all these methods provide much valuable information, the synthetically demanding requirement for specific isotopic labeling is restrictive. Indeed, the purpose of this review is to demonstrate that much information can be obtained for as-synthesized samples, i.e., without resorting to isotopic labeling.

One of the most important recent advances in solid-state NMR has been the development of magic-angle spinning (MAS) probes capable of supporting ever greater rotation frequencies, ν_R .¹⁸ Today, a ν_R of 25–30 kHz is routinely achievable, with an ν_R of 50 kHz even having been reported.¹⁹ A particularly promising application for this new technology is ^1H solid-state NMR, where the line narrowing won by very-fast MAS alone is sufficient to allow some ^1H resonances due to particular chemically distinct protons to be resolved in ^1H MAS NMR spectra of small to moderately sized organic solids.^{20–30}

The importance of solution-state NMR today owes much to the extension of the experiment to a second (and higher) dimension.⁵ Multidimensional NMR spectroscopy is also of much significance in solid-state NMR: in particular, since spectral resolution is always a pertinent problem, an important motivation for performing a multidimensional experiment is the resulting increase in resolution. Indeed, a number of groups have recently developed new approaches for obtaining high-resolution two-dimensional (2D) ^1H - ^{13}C correlation experiments.^{31–33} Such experiments allow the better resolution and assignment of the ^1H resonances, by taking advantage of, first, the much greater resolution in the ^{13}C dimension on account of the larger chemical shift range and inherently narrower line widths, and, second, the relative insensitivity of ^{13}C chemical shifts (as compared to the case of ^1H chemical shifts) to through-space influences.

Multidimensional NMR experiments also provide additional information that is unavailable from one-dimensional (1D) spectra even in the limit of high-resolution. For example, 2D ^2H exchange experiments, which identify a particular change in molecular orientation between two evolution periods, have already been mentioned above.⁹ For dipolar-coupled nuclei, the combination of fast MAS with 2D multiple-quantum (MQ) spectroscopy achieves high resolution, while allowing the structural and dynamic information inherent to the dipolar couplings to be accessed. Specifically, using the homonuclear ^1H - ^1H double-

quantum (DQ) MAS experiment,³⁴ it has recently been demonstrated that the semiquantitative information about specific proton–proton proximities yielded by rotor-synchronized 2D spectra allows the differentiation between distinct hydrogen-bonding structures²¹ as well as the identification of particular aromatic π – π packing arrangements.^{22,24} Moreover, it has further been shown that an analysis of rotor-encoded ¹H DQ MAS spinning-sideband patterns^{35,36} enables the quantitative determination of the internuclear distance for a well-isolated pair of aromatic protons in a hexabenzocoronene derivative in the solid phase as well as the order parameter of the liquid-crystalline (LC) phase.²² In addition, attention has focused on the development of methods suitable for the measurements of heteronuclear dipolar couplings between protons and other spin $I = 1/2$ nuclei (i.e., ¹H–¹³C and ¹H–¹⁵N).^{37–40}

As indicated by the opening paragraphs, the emphasis of this review is on advanced solid-state NMR experiments suitable for providing insight into the mechanisms of self-assembly which are of much relevance in modern polymer science. As such, we restrict our attention to the spin $I = 1/2$ nuclei found in organic solids, in particular, ¹H and ¹³C, and focus on recently developed, i.e., within the last 10 years, solid-state NMR methods that probe the structural and dynamic information inherent to the dipolar coupling. Importantly, we will show that ¹H NMR of rigid solids is now feasible.

We note that the considerable progress made in solid-state NMR of half-integer quadrupolar nuclei, e.g., ²³Na, ²⁷Al, and ¹⁷O, as a consequence of the introduction of the MQMAS experiment by Frydman and Harwood in 1995,⁴¹ falls outside the scope of this review. In addition, it is to be remembered that the NMR experiments we describe are equally applicable to biological molecules; indeed, much of the recent development of solid-state NMR methodology, e.g., the experiments for determining torsional angles,^{16,17} has been stimulated by the considerable interest in biological systems. Reviewing the biological applications is, however, not an aim of this review, although a few relevant examples will be mentioned. To further specify the scope of this article, as far as the probing of dynamics is concerned, we will only consider methods suitable for probing fast processes. Thus, recently developed methods, such as one-dimensional exchange spectroscopy by sideband alternation (ODESSA),⁴² time-reverse ODESSA,⁴³ and centerband-only detection of exchange (CODEX),^{44,45} which are capable of probing slower dynamics (time scales ranging from milliseconds to seconds), will not be discussed.

To give an outline of the structure of the review, the main body is divided into two parts: first (in sections II–IV), the NMR experiments will be introduced, and, second (in sections V–VIII), specific applications will be described, which illustrate what structural and dynamic insight can be provided. These specific applications can be considered to be case studies, which illustrate how a particular system can be approached experimentally, with the methodology being extendable to other organic systems.

As has been stressed above, an important aspect of this review is to highlight the importance of ¹H solid-state NMR—this is reflected in the chosen applications, which illustrate the valuable structural information gained on account of the marked sensitivity of the ¹H chemical shift to hydrogen-bonding and aromatic π – π effects. In addition, the ability to probe dynamic events, such as the making and breaking of hydrogen bonds as well as guest mobility in a supramolecular complex, is demonstrated.

II. Improving the Resolution in ¹H Solid-State NMR

Table 1 lists the NMR-active nuclei (i.e., those with $I > 0$) of most relevance for organic solids, together

Table 1. Properties of the NMR-Active Nuclei of Most Relevance for Organic Solids

nucleus	I	$\gamma/10^7 \text{ rad T}^{-1} \text{ s}^{-1}$	natural abundance/%
¹ H	1/2	26.8	99.99
² H	1	4.1	0.02
¹³ C	1/2	6.7	1.10
¹⁴ N	1	1.9	99.63
¹⁵ N	1/2	–2.7	0.37
¹⁷ O	5/2	–3.6	0.04
¹⁹ F	1/2	25.2	100.00
²⁹ Si	1/2	–5.3	4.67
³¹ P	1/2	10.8	100.00

with their nuclear spin quantum numbers, their magnetogyric ratios (γ), and natural abundances.⁴⁶ The low natural abundance of the nuclei ²H, ¹³C, ¹⁵N explains why selective isotopic labeling is successful in these cases. Moreover, the central importance of protons in solution-state NMR is evident from Table 1: a near 100% natural abundance is combined with the highest magnetogyric ratio (and hence best sensitivity) of all naturally occurring nuclei. It is, however, exactly this combination that makes solid-state ¹H NMR problematic.

The dipolar coupling constant, D , defining the dipolar coupling between two nuclei is given by

$$D = \frac{(\mu_0/4\pi)\hbar\gamma_1\gamma_2}{r^3} \quad (1)$$

where r denotes the internuclear separation. The dependence of D on the product of the magnetogyric ratios of the two nuclei means that the dipolar coupling constant for two ¹H nuclei is a factor of approximately 16 times larger than that for a pair of ¹³C nuclei at the same separation. As an example, the ¹H–¹H D in a CH₂ group (assuming $r = 0.18 \text{ nm}$) is 20 kHz, which is about twice the typically encountered chemical shift range (15 ppm) at today's largest solid-state NMR magnets (corresponding to ¹H Larmor frequencies of 700–800 MHz), and is much larger than the through-bond J couplings which characterize solution-state spectra.

A major difference between the *through-space* dipolar and *through-bond* J couplings is that the former is an *anisotropic* rather than an *isotropic* interaction. This means that the dipolar coupling between a pair of nuclei depends on the orientation

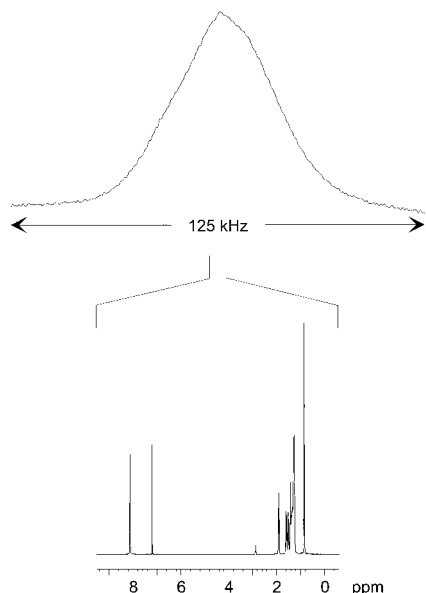


Figure 1. A comparison of the static solid-state and solution-state ^1H NMR spectra of a typical organic compound.

of the internuclear vector with respect to the direction of the static magnetic field, B_0 . Specifically, the dipolar coupling is proportional to $(3 \cos^2\theta - 1)$, where θ is the angle between the internuclear vector and the B_0 direction. For a powdered sample, there is a uniform distribution of orientations, and thus the NMR spectrum consists of a superposition of many lines, corresponding to the different dipolar couplings—such a powder spectrum is referred to as being anisotropically broadened.^{8–10}

In organic solids, protons are ubiquitous, and an extensive network of dipolar-coupled protons exists—in so-called spin-counting experiments, clusters of over 100 dipolar-coupled protons can be identified.^{47,48} As shown in Figure 1, the static ^1H NMR spectrum of a typical organic solid is simply a broad featureless hump. The striking difference to the corresponding ^1H solution-state NMR spectrum is evident. It should be stressed that the problem in the former case is not a lack of information, but rather there is essentially an overload, such that the net effect is the virtual loss of all information. The challenge facing the solid-state NMR spectroscopist is then how can experiments be designed that combine high-resolution, i.e., a recovery of the chemical shift resolution, with the preservation of the valuable information inherent to the anisotropic interactions, i.e., for ^1H NMR, the structural and dynamic information inherent to the dipolar coupling.

A. Magic-Angle Spinning

On account of its angular dependence, molecular motion leads to an averaging of the dipolar coupling; as will be shown later, determining the reduction in the dipolar coupling allows the identification of particular dynamic processes. The extreme case is found in solution, where fast isotropic tumbling of the molecules leads to the averaging to zero of the line broadening due to the dipolar couplings as well

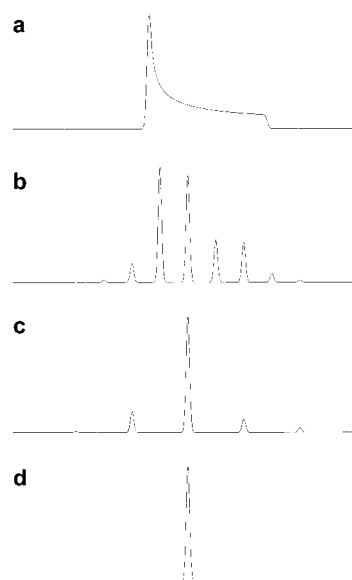


Figure 2. Simulated spectra showing the effect of MAS on the anisotropic line shape due to a CSA interaction. In (a), the sample is static, while the spectra (b) to (d) correspond to an increase in the MAS frequency, ν_R .

as the other anisotropic interactions. To achieve high resolution, the solid-state NMR spectroscopist would like to mimic this averaging process. First, we note that anisotropic interactions such as the dipolar coupling between a pair of nuclei, the CSA, and the first-order quadrupolar interaction all have an orientation dependence that can be represented by a second-rank tensor.^{8–10} For such interactions, rather than requiring an isotropic motion, a physical rotation of the sample around an axis inclined at an angle of $\arctan(\sqrt{2}) = 54.7^\circ$, the so-called magic angle, to the external magnetic field suffices.^{49,50} That this is so can be understood by considering that sample rotation around a single axis leads to the components perpendicular to the rotation axis being zero on average, and only the component parallel to the rotation axis remains nonzero on average. Thus, in a powdered sample, for any orientation of, e.g., the internuclear vector for a pair of dipolar-coupled spins, rotation around an axis yields an “average orientation” parallel to the axis of rotation. Under MAS, this parallel component has an anisotropic frequency equal to zero for all cases, and the anisotropic broadening is averaged to zero for all crystallite orientations.

A familiar example of the application of MAS is ^{13}C NMR, where the combination of ^1H - ^{13}C cross-polarization (CP)^{51,52} with MAS, CP MAS NMR⁵³, is routinely used to investigate a wide range of systems. Under the application of high-power proton decoupling, the dominant anisotropic broadening is the CSA; in this case, as illustrated by the simulated spectra in Figure 2, the static line shape breaks up into a centerband and spinning sidebands, whose line widths are narrow and independent of ν_R . A full mathematical treatment of MAS and anisotropic interactions can be found in, e.g., refs 8, 9, 54, and 55.

The effect of MAS on a dipolar-coupled multiproton network is quite different. Figure 3 shows the effect

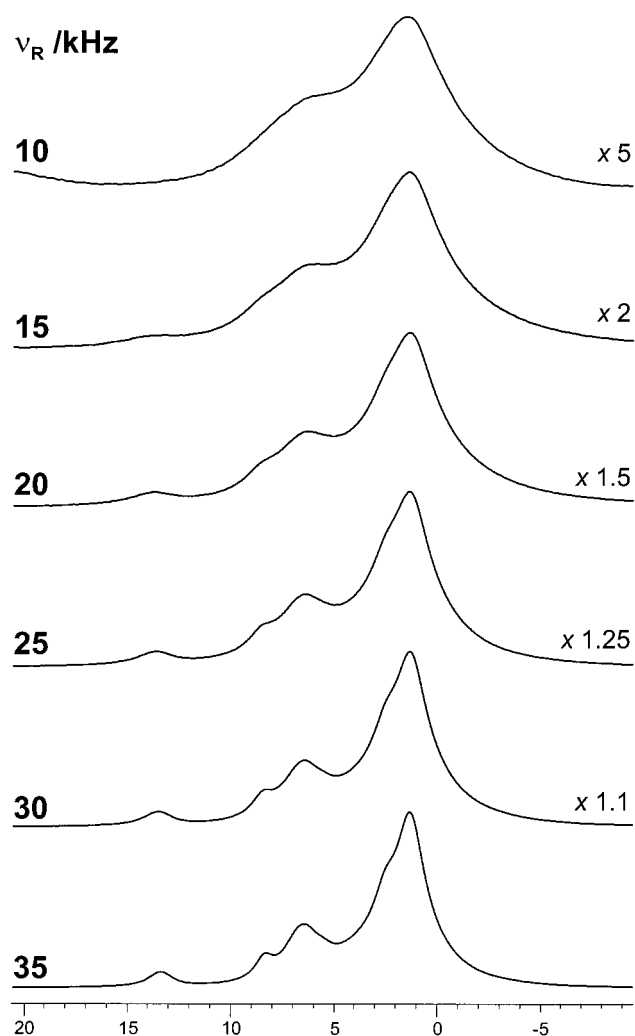


Figure 3. The effect of increasing the MAS frequency, ν_R , on the centerband of a ^1H MAS spectrum of a typical organic compound. (Reproduced with permission from ref 21. Copyright 1998 American Chemical Society.)

of increasing ν_R upon the centerband in the ^1H MAS NMR spectrum of a typical organic solid. It is apparent that the line width is not independent of ν_R , with a line narrowing being observed upon increasing ν_R —although, even at 35 kHz, the line widths are much larger than those observed in ^{13}C MAS spectra. The difference between the two cases is explained in a classic paper by Maricq and Waugh:⁵⁴ The CSA is an example of an interaction where the anisotropic broadening is refocused at the end of each rotor period, τ_R , i.e., the corresponding Hamiltonian commutes with itself at all times. By comparison, when there are three or more dipolar-coupled protons, the perturbing influence of the other dipolar-coupled protons upon a particular dipolar-coupled pair means that the dipolar Hamiltonian no longer commutes with itself at all times, and the evolution under the dipolar coupling of a particular pair is no longer refocused at the end of each τ_R .

By decreasing the rotor diameter, MAS probes capable of supporting a much faster ν_R have become available; e.g., 1997 saw the delivery of the first commercial probes designed for rotors with an outer and inner diameter of 2.5 and 1.2 mm, respectively. Such a rotor, which, when full, contains 10 mg of

sample, can be spun to a ν_R of up to 35 kHz. We note that rotors with even smaller diameters, and thus smaller sample volumes, have been produced, which allow an even faster ν_R (up to 50 kHz).¹⁹

The enhanced line narrowing achieved by a ν_R of 30+ kHz, as compared to that obtained at a ν_R of 15 kHz (the maximum achievable with a conventional 4 mm MAS rotor), is evident in Figure 3. This line-narrowing effect, upon increasing ν_R , of MAS on the ^1H NMR spectrum of a dipolar-coupled proton network can be understood as being due to an increase in the spin-pair character of the interaction (the homonuclear dipolar coupling between an isolated pair of nuclei is refocusable, as in the case of the CSA).⁵⁶ As a concluding remark, we note that very-fast MAS has also been applied by Scheler to ^{19}F NMR of fluoropolymers such as PTFE; in this case, as well as achieving a line narrowing due to the reduction in the residual dipolar broadening, an additional advantage is the spectral simplification achieved by the reduction in the number of spinning sidebands (^{19}F CSAs are much bigger than ^1H CSAs).⁵⁷

B. Homonuclear ^1H Decoupling Methods

As will be shown later, the resolution provided by the combination of very-fast MAS ($\nu_R \geq 30$ kHz) and high magnetic fields (^1H Larmor frequency ≥ 500 MHz) is sufficient to allow specific proton–proton proximities to be identified on the basis of the observation of particular peaks in ^1H 2D DQ MAS spectra. The line narrowing achieved by MAS alone at a ν_R equal to 35 kHz is, however, still far from the limiting case, where all residual dipolar broadening has been removed.

Brute-force fast MAS is not the only means by which line narrowing can be achieved in ^1H solid-state NMR. A particularly ingenious alternative approach, first presented over 30 years ago, involves the removal of the dipolar broadening by specific multiple-pulse techniques, where radio frequency (rf) pulses achieve rotations in spin space.^{58,59} By combining these multiple-pulse experiments with MAS—combined rotation and multiple-pulse spectroscopy (CRAMPS)^{60–62}—well-resolved ^1H spectra have been obtained.⁶³ The very time-consuming nature of the necessary setup for the CRAMPS experiment has, however, discouraged the widespread take-up of the approach. Nevertheless, recently, Hohwy et al have shown that ^1H CSAs can be fully determined by a CRAMPS approach employing MSHOT-3 homonuclear multiple-pulse decoupling.⁶⁴

An important consideration in a CRAMPS experiment is the interference between the two averaging processes, i.e., does the physical rotation of the sample by MAS impair the performance of the multiple-pulse sequence, the latter having originally been designed for static samples. Indeed, a low ν_R , i.e., less than 3 kHz, is used in a conventional CRAMPS experiment, such that, to a first approximation, the sample can be considered to be static during each cycle of the multiple-pulse sequence. In this so-called “quasi-static” limit, the multiple-pulse sequence can be considered to take care of the

homogeneous dipolar broadening, with MAS being required to deal with the CSA.

Recently, Hafner and Spiess have shown that CRAMPS experiments employing a basic multiple-pulse sequence (WHH-4 or variants thereof)⁵⁸ at a moderately fast ν_R (10–15 kHz) can deliver a line narrowing corresponding to that achievable by the conventional CRAMPS approach, with a particular advantage being that the method is comparatively insensitive to experimental imperfections.^{65–67} As reflected in the naming of this approach as multiple-pulse assisted MAS, such experiments represent a shift in philosophy in that both MAS and the multiple-pulse sequence “attack” the dipolar broadening; the latter can be considered to “clean up” the residual dipolar broadening, which remains as a consequence of the insufficiency of the used ν_R .

The success of the multiple-pulse assisted MAS approach requires some thought concerning the synchronization of the duration of each cycle of the multiple-pulse sequence, τ_C , with the rotor period: For the CH₃ group in L-alanine, the smallest line width (full-width at half-maximum height, fwhmh) of about 250 Hz (for comparison, the fwhmh under MAS at 35 kHz is 750 Hz)²⁰ is obtained for a plateau of τ_C/τ_R values between 0.2 and 0.3.⁶⁸ It has been shown that, using zero-order average Hamiltonian theory,^{59,69} favorable synchronization conditions can be identified by a straightforward graphical approach.⁶⁷ The quasi-static regime is not a prerequisite for the success of multiple-pulse assisted MAS; for example, a marked line narrowing has been observed for a benzoxazine dimer using WHH-4 at 35 kHz, where τ_C/τ_R equals 1.5.²¹ It is to be noted that a homonuclear decoupling method does not only remove the dipolar broadening, it also scales the isotropic chemical shift scale; all fwhmh's quoted here are those measured in a “corrected” spectrum where the normal ppm values of the different resonances have been restored.

An alternative means by which homonuclear ¹H decoupling can be achieved is the Lee-Goldburg experiment, in which the offset of the ¹H *rf* irradiation is set equal to $\omega_1/\sqrt{2}$, where ω_1 is the inherent nutation frequency of the pulse ($|\omega_1| = |\gamma B_1|$, where B_1 is the *rf* field strength), such that, in the vector model picture of NMR, the spins rotate around an effective field tilted away from the static magnetic field direction by the magic angle.⁷⁰ In this way, the zero-order average dipolar Hamiltonian vanishes. The decoupling performance is significantly enhanced in the frequency-switched Lee-Goldburg (FSLG) experiment, which involves breaking up the continuous *rf* irradiation into a series of 2π rotations of the proton magnetization about the effective field, with a switch between the two LG conditions $\pm\omega_1/\sqrt{2}$ accompanied by a simultaneous shift in the phase by π at the end of each segment.^{71–73} The better performance of the FSLG method is a consequence of the setting to zero of all odd-order terms in the dipolar average Hamiltonian on account of the introduced symmetry. The FSLG method has been found to function well for a ν_R between 10 and 16 kHz,⁷⁴ with a further marked improvement being possible if the

sample volume is restricted by the application of a static magnetic field gradient and a selective pulse.⁷⁵

In the first applications of the FSLG technique, homonuclear ¹H decoupling was employed to remove the perturbing effects of the dipolar-coupled proton network such that, for example, the spinning-sideband patterns in a ¹³C MAS spectrum directly reflect the heteronuclear ¹³C-¹H dipolar couplings.^{71,72} In addition, Levitt et al. presented a modified FSLG sequence, which, by the incorporation of acquisition windows, allowed the direct recording of high-resolution ¹H spectra.⁷³ Of more importance, however, has been the subsequent incorporation of the method into a number of experiments that achieve high-resolution in an indirect ¹H dimension, i.e., in cases where the FSLG irradiation does not need to be combined with direct acquisition (in this respect, the FSLG method can be termed a windowless decoupling method). For example, FSLG decoupling is an integral part of the ¹H-¹³C correlation experiments presented by de Groot and co-workers³¹ and Emsley and co-workers,³² which will be described later.

Recently, Vega and co-workers have presented a phase-modulated Lee-Goldburg experiment (PMLG) experiment, in which only the phase of a series of adjacent pulses is changed, i.e., ω_1 remains constant.^{76,77} In an ingenious reinterpretation of the LG concept, the zero-order term in the average Hamiltonian can be shown to vanish when the modulation of the pulse phase described by

$$\phi(t) = \omega_{\text{PMLG}} t \quad (2)$$

satisfies the condition:

$$|\omega_{\text{PMLG}}| = \omega_1/\sqrt{2}. \quad (3)$$

An LG irradiation unit has a duration corresponding to a 2π rotation of the proton magnetization about the effective field, i.e.,

$$\tau_{\text{LG}} = \sqrt{(2/3)}(2\pi/\omega_1). \quad (4)$$

Thus, the angle through which the *rf* precesses in each LG unit is given by

$$\alpha_{\text{LG}} = |\omega_{\text{PMLG}}|\tau_{\text{LG}} = 207.8^\circ \quad (5)$$

If the sign of ω_{PMLG} is negated between alternate LG units, the symmetrization required to ensure the removal of odd-order terms in the dipolar average Hamiltonian is achieved. To demonstrate the feasibility of the PMLG sequence, Vinogradov et al employed a 2D experiment in which a high-resolution ¹H dimension, incorporating PMLG decoupling, is correlated with ¹H acquisition, with only moderate MAS (10–15 kHz) providing line narrowing in the direct dimension. The resulting resolution obtained for a sample of malonic acid is illustrated in Figure 4.⁷⁶

Using Lee-Goldburg based decoupling methods, a fwhmh of 150–170 Hz has been reported for the aliphatic ¹H resonances in L-alanine⁷⁸—this is demonstrated in part c of Figure 5, where, for comparison, the (a) static and (b) MAS ($\nu_R = 30$ kHz) spectra are also shown. The spectrum in Figure 5c was recorded

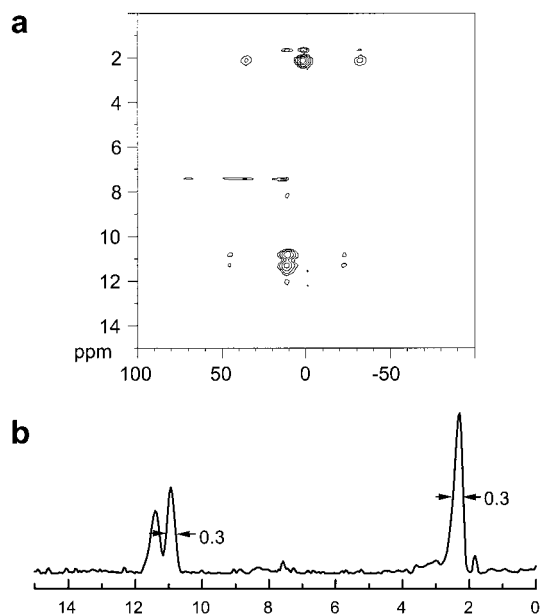


Figure 4. (a) A ^1H 2D PMLG spectrum of malonic acid ($(\text{COOH})_2\text{CH}_2$). The high-resolution (F_1) projection is shown in (b), with the achieved line widths (fwhmh in ppm) being indicated. (Reproduced with permission from Figures 3a and 4a of ref 76. Copyright 1999 Elsevier.)

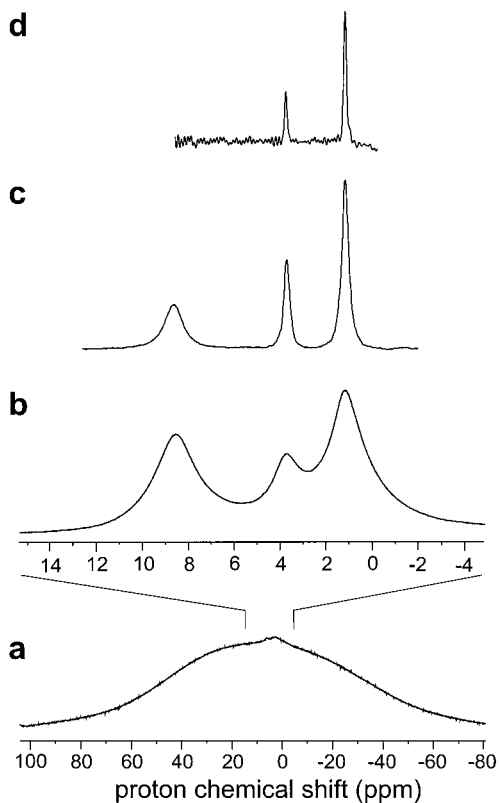


Figure 5. ^1H (500 MHz) NMR spectra of natural abundance powdered L-alanine, recorded with (a and b) a one-pulse experiment for (a) a static sample and (b) under MAS at a $\nu_R = 30$ kHz, (c) the 2D FSLG ($\nu_R = 12.5$ kHz) experiment in Figure 6a, and (d) the CT-CRAMPS ($\nu_R = 12.5$ kHz) experiment in Figure 6b using FSLG decoupling. (Reproduced with permission from ref 78. Copyright 2001 American Chemical Society.)

using a modified version of the 2D method proposed by Vinogradov et al.⁷⁶; as shown in the pulse sequence and coherence transfer pathway diagram^{79,80} in Fig-

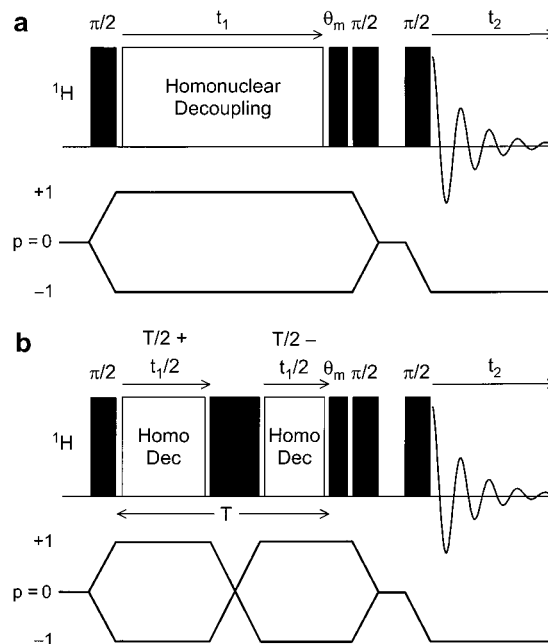


Figure 6. Pulse sequences and coherence transfer pathway diagrams for (a) a 2D CRAMPS experiment incorporating a z-filter to ensure that pure absorption-mode line shapes are obtained and (b) a 2D constant-time CRAMPS experiment. The relative performance of the two experiments with respect to yielding high-resolution ^1H NMR spectra in the indirect (F_1) dimension is illustrated by Figure 5c,d and is discussed in the text. (Adapted with permission from Figure 2 of ref 78. Copyright 2001 American Chemical Society.)

ure 6a, the incorporation of a z-filter⁸¹ (the final two $\pi/2$ pulses) ensures that pure absorption-mode line shapes are obtained.^{5,80} Lesage et al. have further shown that the frontiers of high-resolution ^1H solid-state NMR can be pushed back yet further: using the constant-time (CT) CRAMPS experiment shown in Figure 6b, a fwhmh as low as 60 Hz can be obtained for the aliphatic resonances in L-alanine; the achieved line-narrowing, as demonstrated in Figure 5d, is striking.⁷⁸ The success of this constant-time approach is based on the fact that the evolution of the proton magnetization in t_1 is only modulated by antisymmetric interactions, i.e., those interactions that change sign under a π rotation in spin space and are hence refocusable by a 180° pulse. The resolution enhancement over the experiment in Figure 6a is hence achieved by removing the broadening due to the symmetric interactions (those which are invariant to a π rotation); the symmetric interactions instead lead to an attenuation of the signal intensity by a factor of $\exp\{-t|\mathbf{H}^{(s)}|\}$.

To conclude this section, it is evident that much progress has recently been made with respect to obtaining high-resolution ^1H solid-state NMR spectra. Indeed, the field is an area of ongoing active research, e.g., Sakellariou et al. have recently employed a computer optimization approach to develop a new homonuclear decoupling sequence, termed DUMBO-1,⁸² and it is to be expected that further advances will be made in the coming years. Concerning polymer chemistry, the point is not far from being reached where the routinely achievable resolution in ^1H solid-state NMR is limited not by residual dipolar

broadening but rather by the inherent range of chemical shifts associated with a sample, which is not perfectly crystalline.

III. Homonuclear 2D Double-Quantum NMR Spectroscopy

The previous section has been devoted to methods that seek to achieve line narrowing in solid-state ^1H NMR by reducing the homogeneous broadening due to the extended homonuclear proton–proton dipolar coupling network. Such line narrowing is obviously essential to allow the resolution of distinct resonances. However, this is achieved at the expense of the loss of the valuable structural and dynamic information inherent to the dipolar coupling. A method is, therefore, required which, in addition to achieving high resolution, allows the accessing of the information inherent to the dipolar coupling. One such method is two-dimensional ^1H - ^1H DQ MAS spectroscopy,^{34,83} with the key to the DQ approach lying in the fact that the creation of a DQ coherence (DQC) relies on the existence of a dipolar coupling between two protons.

In solution-state NMR, many important experiments incorporate the creation and evolution of MQ coherence (MQC).^{5,6,84–86} Since MQC cannot be directly detected, experiments that follow the evolution of a MQC are inherently at least two-dimensional. This is the case with ^1H - ^1H DQ MAS spectroscopy. Figure 7 shows a corresponding pulse sequence and coherence transfer pathway diagram: first, a DQC is excited, which subsequently evolves during an incremented time period t_1 ; the DQC is then converted into observable single-quantum (SQ) coherence (SQC), which is detected in the acquisition period, t_2 . To select the desired coherence transfer pathways, e.g., only DQC during t_1 , a phase cycling scheme is employed.^{79,80} Pure absorption-mode two-dimensional line shapes are ensured by the selection of symmetric pathways such that the time-domain

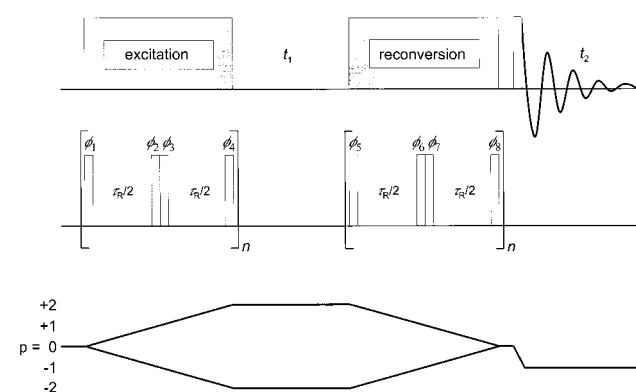


Figure 7. Pulse sequence and coherence transfer pathway diagram for a ^1H DQ MAS experiment using the BABA recoupling sequence for the excitation and reconversion of DQCs. The rectangular blocks represent pulses of flip angle 90° , with the choice of the phases being described in, e.g., ref 25. If the t_1 increment is set equal to a rotor period, a rotor-synchronized two-dimensional spectrum is obtained, while reducing t_1 , and hence increasing the DQ spectral width, leads to the observation of a DQ MAS spinning-sideband pattern.

signal is amplitude modulated in t_1 .^{5,80} Sign discrimination can be restored in the F_1 dimension by the TPPI⁸⁷ or States-TPPI⁸⁸ method, which for the evolution of DQC in t_1 , in both cases, involves incrementing the phases of all excitation pulses by 45° after recording each t_1 point.

A. The Excitation of Homonuclear DQC

In the solid state, the first ^1H MQ experiments were performed on static samples by Baum et al.,^{47,48} as mentioned above, these elegant experiments allow the determination of the size of spin clusters by monitoring the time development of MQC, with average Hamiltonian theory having been used to specially design the excitation and reconversion sequences. In contrast to the homonuclear decoupling methods discussed in the previous section where it was necessary to ensure that the dipolar terms in the average Hamiltonian vanish, in this case the aim is the generation of a DQ Hamiltonian, $\mathbf{H}_{XX} - \mathbf{H}_{YY}$. In a MQ experiment, it is not enough to simply excite the MQC, attention must be paid to the careful reconversion of the MQC back to the initial state, usually longitudinal magnetization, from which directly observable transverse magnetization can be created by a single 90° r_f pulse. For the spin-counting experiments due to Baum et al.,^{47,48} a reconversion sequence which is the apparent time reversal of that used for excitation was employed, such that the destructive interference of the many MQCs is prevented.

For the excitation of DQC under MAS, the interference with the sample rotation must be considered, as was the case for the CPMAS experiment discussed in the previous section. In particular, if a sequence designed for a static MQ experiment is used without modification, the excitation (and reconversion) time is limited to $\tau_R/2$, since the rotor modulation causes the action of the pulse sequence in the second half of the rotor period to be the time reversal of that which occurred in the first half of the rotor period. Starting with the suggestion of Meier and Earl,^{89,90} who simply proposed the phase switching of the static sequences used by Baum et al.,^{47,48} every half rotor period to prevent the process of self-time-reversal, many different approaches have been presented that allow excitation (and reconversion) times of one or more rotor periods. Such pulse sequences that counteract the effect of MAS are referred to as *recoupling* methods,^{11,12} examples that have been used in homonuclear DQ MAS NMR spectroscopy include BABA,⁹¹ C7,⁹² DRAMA,⁹³ DRAWS,⁹⁴ and HORROR.⁹⁵ We note that Levitt and co-workers have recently introduced a very helpful classification system, based on symmetry principles, which covers such sequences.^{96,97}

Much of the considerable effort that has been devoted to the optimization of recoupling sequences for the excitation and reconversion of homonuclear DQC has been motivated by the desire to probe weak dipolar couplings, e.g., between two specific ^{13}C labels. For ^1H DQ MAS NMR of rigid solids, where the dipolar couplings under consideration are usually

quite large, the demands imposed on the recoupling sequence are less severe. Moreover, to enable a ν_R of 30+ kHz to be used to obtain a sufficient line narrowing, it is important that the method is robust. In this respect, in our laboratory, we find that the BABA sequence, although it does not deliver the maximum amount of DQC, is a good candidate. As shown in Figure 7, BABA, which derives its name from the presence of back-to-back pulses, consists of segments of duration half a rotor period, where an evolution period is bracketed by two 90° pulses, with the phases of the pulses in adjacent segments being shifted by 90° . This shifting of the phases achieves a negation of the spin-part of the DQ Hamiltonian, which exactly compensates the negation of the spatial part caused by MAS. Modified two- and four- τ_R versions of the BABA sequence have also been presented, which provide compensation with respect to offset and pulse imperfections.⁹⁸ A fuller account of the operation of BABA and other recoupling sequences is found in, e.g., refs 67 and 83.

B. Rotor-Synchronized 2D DQ MAS Spectra

The two-dimensional DQ MAS experiment can be performed in two distinct ways. We consider first spectra recorded in a rotor-synchronized fashion in t_1 , i.e., the t_1 increment is set equal to one rotor period, τ_R . In this way, all spinning sidebands in F_1 can be considered to fold back onto the centerband position. The appearance of a rotor-synchronized 2D ^1H DQ MAS spectrum is illustrated in Figure 8. Since the DQ frequency corresponding to a given DQC is simply the sum of the two SQ frequencies, DQCs between like (AA) and unlike (AB) spins can, in general, be distinguished in that, in the former case, a single peak at $(2\nu_A, \nu_A)$ is observed, while, in the latter case, two peaks at $(\nu_A + \nu_B, \nu_A)$ and $(\nu_A + \nu_B, \nu_B)$ are observed. [The notation (ν_1, ν_2) refers to a DQ peak centered at ν_1 and ν_2 in the F_1 and F_2 dimensions, respectively.]

To a first approximation, which is fully valid in the limit of short recoupling times and for an isolated

spin pair, it can be shown that the efficiency of DQC excitation is directly proportional to the dipolar coupling constant, D .^{83,99} (In this respect, a short recoupling time, τ_{repl} , corresponds to the case where $\sin(D\tau_{\text{repl}}) = D\tau_{\text{repl}}$.) Since the reconversion to SQC efficiency has the same dependence, the integrated intensity of the DQ peaks due to a given DQC, in this limiting case, is proportional to D^2 . The inverse cubed dependence of D on the internuclear distance, r , between the two nuclei means that the DQ peak intensity is inversely proportional to r^6 . Therefore, by a simple inspection of which peaks are present in a rotor-synchronized ^1H DQ MAS spectrum, and, often more importantly, which are absent, much insight is obtained into proton–proton proximities. For example, in Figure 8a, only two of the six possible types of DQ peaks (see Figure 8b) are observed, which is consistent with the structural arrangement shown in Figure 8c. (As discussed in section VIIB, in this particular case, the inequivalence of the aromatic protons A, B, and C is a consequence of intermolecular ring current effects.) The reliability of such a semiquantitative approach has been clearly demonstrated for cases where an X-ray single-crystal structure is available to corroborate the proton–proton proximity information provided by ^1H DQ MAS spectra.^{21,24,29} It should be noted that an advantage of the DQ approach over a spin diffusion experiment^{9,100} in which a mixing time is inserted between two SQ evolution periods is that an auto (i.e., AA) peak is only observed if there is a close proximity of two protons; in the spin diffusion experiment, strong auto peaks are seen for all resonances regardless of whether there is a close proximity.

Later in this review, examples will be presented where rotor-synchronized ^1H DQ MAS spectra provide both structural and dynamic insight. The method is, however, not restricted to ^1H NMR, for example, ^{31}P - ^{31}P DQ MAS spectra of inorganic phosphates and glasses have also been presented.^{101–105} In addition, Nielsen et al. have presented a ^{13}C - ^{13}C DQ MAS experiment,¹⁰⁶ using which C–C connectivities of the alkyl backbone can be established, thus, allowing the

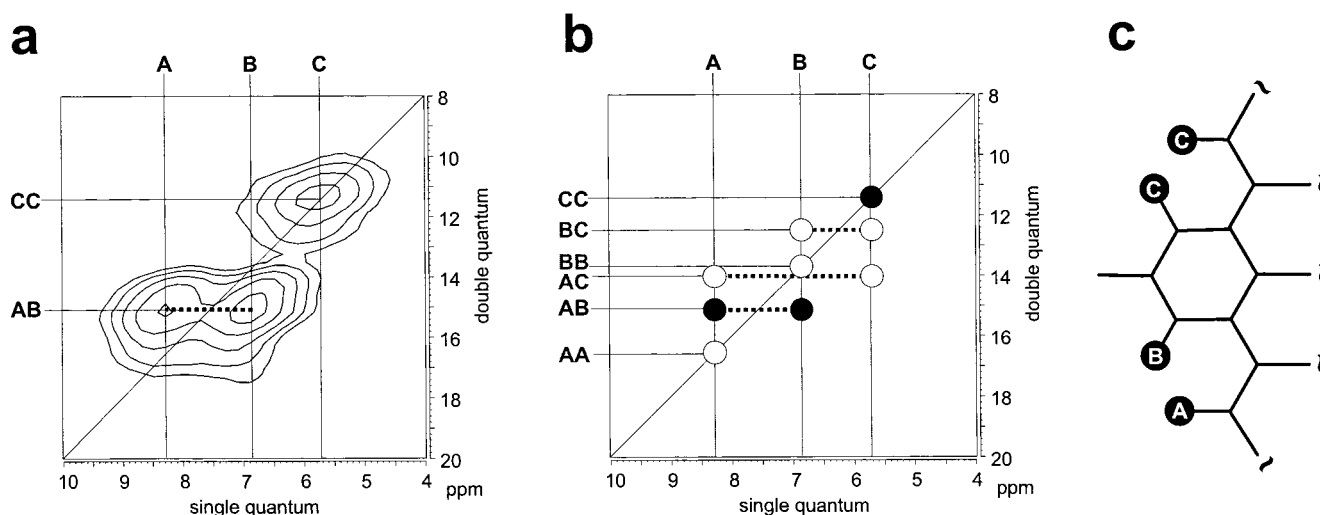


Figure 8. (a) A representative rotor-synchronized ^1H DQ MAS spectrum. (b) A schematic representation showing the positions of the six possible DQ peaks; the observed AB and CC peaks (filled circles) imply the proton–proton proximities indicated in (c). As discussed in section VIIB, in this particular case, the inequivalence of the aromatic protons A, B, and C is a consequence of intermolecular ring current effects. (Reproduced with permission from ref 24. Copyright 2000 Elsevier.)

assignment of the ^{13}C resonances.^{87,96} In ref 107, Hong refers to the technique as the INADEQUATE experiment, which reflects the fact that the original solution-state INADEQUATE experiment due to Bax et al. creates DQC between two J -coupled nuclei.¹⁰⁸ However, an important difference between the dipolar-mediated solid-state DQ MAS experiment and the INADEQUATE experiment is that, in the latter, the use of isotropic J couplings for the creation of DQC means that auto peaks between spins with the same chemical shift are not observed. With regard to the information provided about through-space proximities, the DQ MAS experiment is, in fact, more similar to the solution-state NOESY experiment, the latter being heavily exploited in the structural elucidation of biopolymers.¹⁰⁹ Indeed, it is important to add that Emsley and co-workers have recently shown that the INADEQUATE experiment can be applied under MAS to rigid solids, with the resulting 2D spectrum identifying J -coupled, and hence only through-bond, correlations.^{110,111}

Finally, we note that Schmidt-Rohr and co-workers have elegantly demonstrated that 2D ^{13}C - ^{13}C DQ spectra recorded for static samples can identify the chain conformation statistics for ^{13}C -labeled polymer samples.¹¹² Remembering that the frequency of a given ^{13}C resonance depends on the orientation of the CSA tensor, the method relies on the fact that the adoption of a particular torsional angle along the chain results in DQ peaks for only specific pairs of ^{13}C frequencies. In particular, it was shown that trans and gauche conformations lead to very different 2D DQ powder spectra, and it was thus possible to quantitatively determine the conformation statistics for a sample of amorphous poly(ethylene terephthalate) (PET).

C. ^1H - ^1H DQ MAS Spinning-Sideband Patterns

Rotor-synchronized ^1H DQ MAS spectra can only deliver information about relative proton-proton proximities (except for cases where the DQ peak(s) due to a known internal or external standard are well resolved).⁸³ The DQ MAS experiment (see Figure 7) can, however, be performed in an alternative fashion: if the t_1 increment is reduced, which corresponds to an increase in the DQ spectral width, a DQ MAS spinning-sideband pattern is observed^{35,36} (provided that a recoupling sequence which has an amplitude dependence on the rotor phase, e.g., BABA⁹¹ or DRAMA⁹³, is used).

The origin of such patterns is of interest, since for an isolated spin pair there is no anisotropic evolution of the DQCs during t_1 (the neglecting of the ^1H CSA implicit to this statement will be discussed later). Thus, DQ spinning sidebands cannot arise by the normal single-quantum mechanism, whereby the observed sideband pattern can be considered to map out the anisotropy of the spin interaction which is active during the evolution period. Instead, it has been shown that the origin of such spinning sidebands lies in the t_1 -dependent change in the Hamiltonian active during the reconversion period relative to that active during the excitation of DQC.^{35,36} This

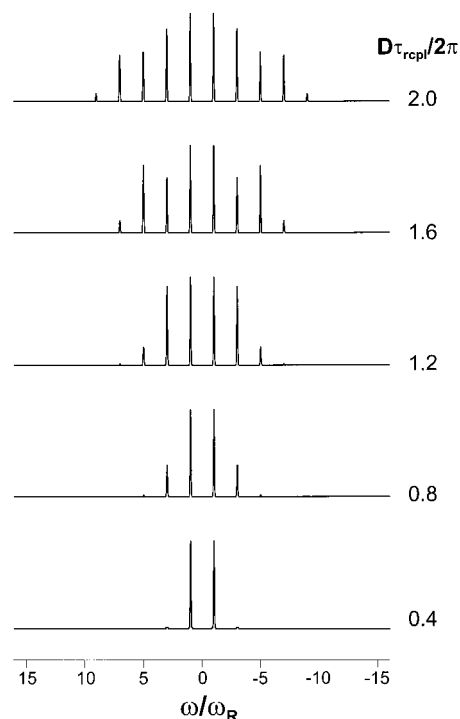


Figure 9. Simulated homonuclear DQ MAS spinning-sideband patterns generated in the time domain using eq 6, with the powder average being performed numerically, for different values of the product of D and τ_{rcpl} .

mechanism has subsequently been termed reconversion rotor encoding (RRE).¹¹³

For an isolated spin pair and using $N\tau_{\text{R}}$ of the BABA recoupling method for both the excitation and reconversion of DQCs, the DQ time-domain signal is given by:⁹⁹

$$s(t_1, t_2 = 0) = \langle \sin[3/(\pi\sqrt{2})D \sin(2\beta) \cos(\gamma + 2\pi\nu_{\text{R}}t_1) N\tau_{\text{R}}] \times \sin[3/(\pi\sqrt{2})D \sin(2\beta) \cos(\gamma)N\tau_{\text{R}}] \rangle \quad (6)$$

where β and γ are Euler angles relating the principal axes system of the dipolar-coupling tensor to the rotor-fixed reference frame; the $\langle \rangle$ brackets denote a powder average. Simulated DQ MAS spinning-sideband patterns generated in the time domain using eq 6, with the powder average being performed numerically, for different values of the product of D and τ_{rcpl} are shown in Figure 9. A particularly striking feature is that only odd-order spinning sidebands are observed; there is no intensity at the centerband and even-order sideband positions. In addition, the observed patterns are very sensitive to the product of D and τ_{rcpl} , with an increase in this product leading to the appearance of higher-order spinning sidebands. Importantly, since τ_{rcpl} is known, the absolute value of D can be extracted to a high degree of accuracy by an analysis of DQ MAS spinning-sideband patterns; in this way, as will be illustrated later, proton-proton distances as well as dynamic processes can be quantitatively determined.

In organic solids, protons rarely exist as well-isolated spin pairs. An important question that must then be asked is, what is the effect upon the observed

^1H DQ MAS spinning-sideband patterns of dipolar couplings to protons external to the spin pair under consideration. To answer this question, consider a model isosceles triangle three-spin system, where the distances between spins A & B, A & C, and B & C are 0.198, 0.238, and 0.238 nm, respectively, corresponding to $(D/2\pi)$ s of 15.5, 8.9, and 8.9 kHz. Spins A and B, which participate in the strongest dipolar coupling, are on resonance, while spin C is 4 kHz off resonance, such that the sideband patterns due to the distinct DQCs can be resolved. Using these parameters, three-spin explicit density matrix simulations were performed, further assuming that all radio frequency pulses are infinitely short.

In Figure 10 a–c, ^1H DQ MAS spinning-sideband patterns for uncompensated BABA recoupling sequences of duration one, two, and four rotor periods at MAS frequencies of 15, 30, and 60 kHz in panels a, b, and c, respectively, are presented. The sideband patterns are detected at spin B; in this way, for each sideband order, the left- and right-hand peaks correspond to DQCs between spins B & C and A & B, respectively. The same line broadening (2 kHz) was applied in each case, and the narrowing of the lines is a consequence of the fact that the displayed spectral width (in kHz) doubles on going from (a) to (b), and from (b) to (c). Some phase distortions are observed for the sidebands due to the BC DQC on account of the off-resonance excitation. For comparison, Figure 10d,e presents spectra generated for a BABA recoupling sequence of duration two rotor periods at a MAS frequency of 30 kHz using the analytical time-domain formula for an isolated spin pair in eq 6, with $(D/2\pi)$ s of (d) 8.9 and (e) 15.5 kHz, i.e., corresponding to the perturbing (BC) and dominant (AB) couplings in the model system.

For the three-spin simulation at a MAS frequency of 15 kHz (Figure 10a), significant intensity at the centerband and even-order spinning-sideband positions is observed. The presence of these peaks arises from the evolution during t_1 of a DQC, due to a particular two spins, under dipolar couplings to other spins; this mechanism, by means of which spinning sidebands are, in fact, most commonly generated, may be termed evolution rotor modulation.¹¹³ On increasing the MAS frequency from 15 to 30 to 60 kHz, the intensity of the centerband and even-order spinning-sideband peaks is observed to decrease. During t_1 , no recoupling pulse sequence is applied, and the averaging of the dipolar couplings to zero becomes ever more efficient upon increasing the MAS frequency, such that there is a virtual absence of centerband and even-order sideband intensity in Figure 10c.

During the excitation and reconversion of DQCs, the BABA recoupling sequence is applied, which acts against the averaging to zero of the dipolar couplings by MAS. Since the origin of the RRE mechanism is the t_1 -dependent change in the Hamiltonian active during the DQ reconversion period relative to the excitation period,¹¹³ it is to be expected that the observed odd-order sideband pattern is dependent on the perturbing dipolar couplings in a multispin

system. Comparing the isolated spin-pair analytical spectra (Figure 10d,e) to the two sideband patterns in Figure 10c, it is apparent that, while the patterns for the DQC with the weaker dipolar coupling constant are quite different, i.e., the third-order sidebands are much higher for the three-spin system, the pattern for the dominant coupling in the three-spin system is only slightly different from that for the isolated spin pair. It is also important to note that the odd-order sideband pattern is virtually unchanged on doubling the MAS frequency from 30 to 60 kHz; the only change is the loss of the slight asymmetry in the first-order sidebands due to the perturbing coupling in Figure 10c. Therefore, a MAS frequency of 30 kHz suffices, as far as the determination of the limiting ^1H DQ MAS sideband pattern is concerned; a higher MAS frequency, though, would lead to better resolution, provided that the line broadening is due to residual dipolar couplings rather than an inherent distribution of chemical shifts.

To repeat the main conclusion, which can be reached from a consideration of the simulated DQ MAS spinning-sideband patterns in Figure 10, it is possible, for a multispin system, to determine the dominant D_{IS} , and hence the shortest proton–proton distance, to a high degree of accuracy, while the uncertainty associated with the determination of the weaker perturbing dipolar couplings is much greater. This observation is in agreement with the findings of Hodgkinson and Emsley, who concluded that the measurements of medium- to long-range C–C distances in fully labeled ^{13}C systems, i.e., the determination of a small perturbing D in the presence of a dominant D between two directly bonded ^{13}C nuclei, using homonuclear recoupling methods is prone to large errors.¹¹⁴ However, unlike this ^{13}C case, where the C–C bond distance is usually not of interest, the determination of the closest proton–proton distance is often of much importance; an example concerning a complex hydrogen-bonded arrangement will be described later.

In the above discussion, the CSA has been neglected. However, at a ^1H Larmor frequency of 700 MHz, the CSA anisotropy parameter for hydrogen-bonded protons is nonnegligible, being approximately 10 kHz. Indeed, Tekeley et al. have shown that the CSA is responsible for distortions in the ^1H (300.1 MHz) DQ MAS spinning-sideband spectra obtained for barium chlorate monohydrate, $\text{BaClO}_3 \cdot \text{H}_2\text{O}$, with an excitation time of $\tau_{\text{R}}/2$.¹¹⁵ However, these distortions manifest themselves mostly only in terms of a marked asymmetry of the lower-order sideband intensities, with the ratios of the average sideband intensities (e.g., first:third) being virtually unchanged. Furthermore, De Paul et al. have shown that including the CSA has only a minor effect on sideband patterns simulated for related rotor-encoded longitudinal magnetization (RELM) experiments, which also use BABA recoupling.¹¹⁶ Thus, unless a very high degree of accuracy is required, the CSA can be safely neglected in an analysis of ^1H DQ MAS spinning-sideband patterns. However, for cases where the CSA is significantly bigger than the dipolar coupling, the situation is very different, e.g., as shown

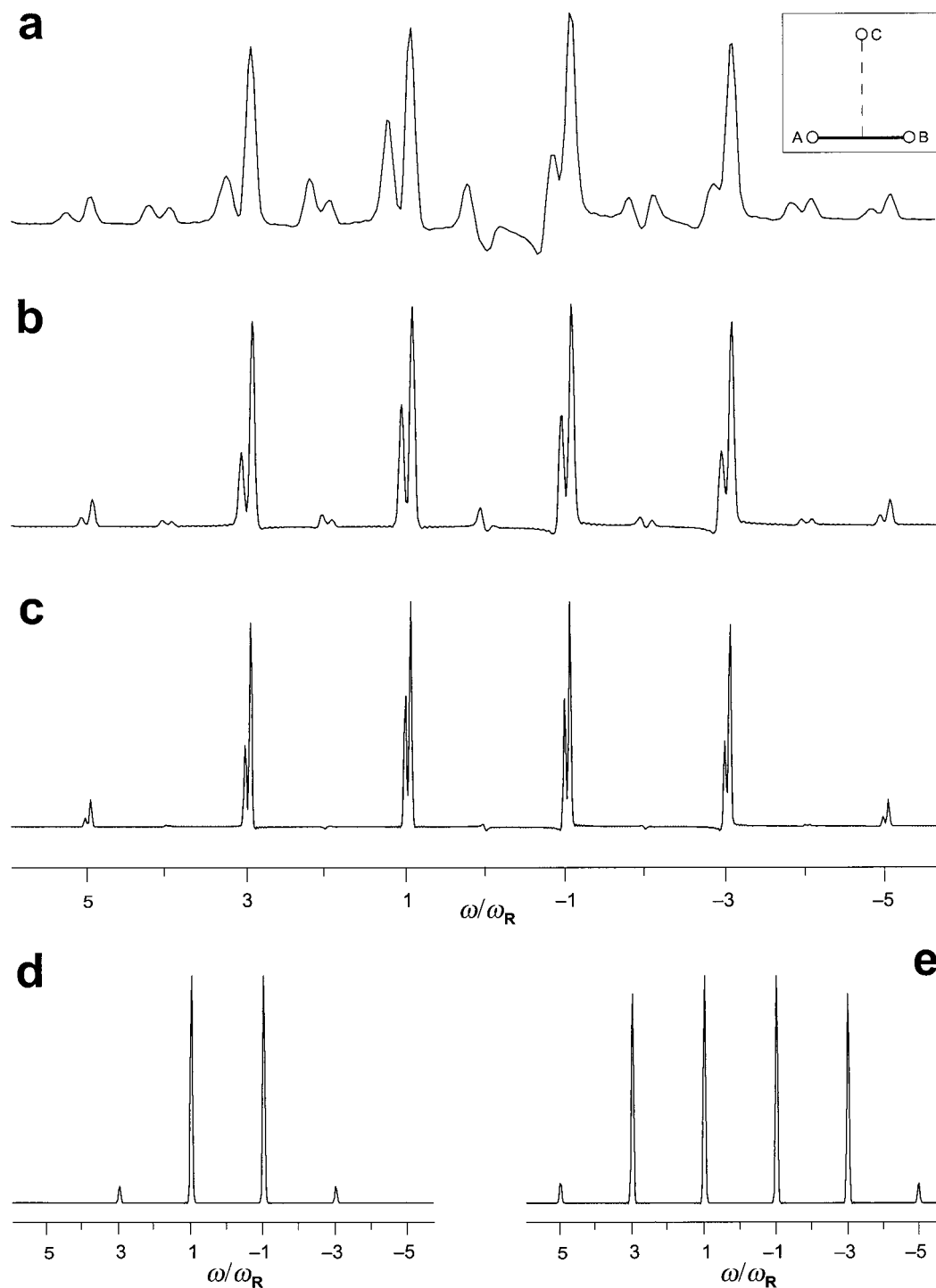


Figure 10. (a–c) Simulated ^1H DQ MAS spinning-sideband patterns for an isosceles triangle arrangement of three spins, where the $(D/2\pi)$ s for spins A & B, A & C, and B & C are 15.5, 8.9, and 8.9 kHz (corresponding to distances of 0.198, 0.238, and 0.238 nm), respectively. Spins A & B are on resonance, while spin C is 4 kHz off resonance. The sideband patterns are detected at spin B; in this way, for each sideband order, the left- and right-hand peaks correspond to DQCs between spins B & C and A & B, respectively. Numerical density matrix simulations, assuming infinitely short radio frequency pulses, were performed for uncompensated BABA recoupling sequences of duration one, two, and four rotor periods at MAS frequencies of 15, 30, and 60 kHz in (a), (b), and (c), respectively. (d) and (e) Spectra generated using the analytical time-domain formula for an isolated spin pair, eq 6, with $(D/2\pi)$ s of (d) 8.9 and (e) 15.5 kHz, for a BABA recoupling sequence of duration two rotor periods at a MAS frequency of 30 kHz. The same Gaussian line-broadening was applied for all spectra. (Reproduced with permission from ref 30. Copyright 2001 American Chemical Society.)

by De Paul et al., ^{31}P DQ MAS spinning-sideband patterns are dominated by the CSA, such that it is not possible to extract information about phosphorus–phosphorus proximities.¹¹⁶ In addition, we note that

Gregory et al. were able to determine the relative orientation of ^{13}C CSA tensors from an analysis of ^{13}C DQ MAS spinning-sideband patterns obtained using the DRAWS recoupling method.¹¹⁷

IV. Heteronuclear 2D NMR Methods

A. Heteronuclear Correlation Spectroscopy

When analyzing a new sample, after obtaining a rotor-synchronized ^1H DQ MAS spectrum, which typically only takes 1 h to record on account of the excellent sensitivity of ^1H NMR, one of the most important next steps is to acquire a ^1H - ^{13}C heteronuclear correlation (HETCOR) spectrum. Such experiments allow the better resolution and assignment of the ^1H resonances, by taking advantage of, first, the much greater resolution in the ^{13}C dimension on account of the larger chemical shift range and inherently narrower line widths, and, second, the comparative insensitivity of ^{13}C chemical shifts to through-space influences. The enhanced sensitivity does come at a price, namely, the poorer sensitivity of ^{13}C NMR, especially at natural abundance. Nevertheless, three different methods have recently been presented, with which ^1H - ^{13}C HETCOR spectra can be obtained in typically 8–12 h with 10–20 mg of sample at natural abundance.^{31–33}

It should be emphasized that solid-state HETCOR spectroscopy is not new: as early as 1982, Caravatti et al. presented an experiment that employed a multiple-pulse sequence at a low ν_R (as in the conventional CRAMPS approach) to achieve homonuclear decoupling in t_1 .^{118,119} The use of this approach to obtain HETCOR spectra of range of organic solids including isotactic polypropylene and lignite,¹²⁰ as well as to investigate hydrogen bonding in amino acids and peptides¹²¹ has been described. Moreover, the CP–WISE (wide-line separation) technique which uses the ^{13}C resolution to distinguish different mobilities as identified by the ^1H line width has gained popularity in polymer science.^{9,122} In addition, correlation experiments are, of course, not restricted to only ^{13}C and ^1H ; for example, Mirau et al have used ^1H - ^{29}Si correlation experiments, namely, both an experiment incorporating ^1H homonuclear decoupling and a WISE experiment, to study the structure and dynamics of polymers and the water interface in porous glass composites.¹²³ We note that it is not our intention to give a full account of the development of solid-state HETCOR spectroscopy in this review. Indeed, our focus is on the recently developed methods, which employ fast or very-fast MAS. In this way, problems with ^{13}C CSAs, which scale linearly with the magnetic field strength, are much reduced.

The pulse sequences and coherence transfer pathway diagrams for the ^1H - ^{13}C HETCOR experiments due to van Rossum et al. (FSLG-decoupled CP correlation),³¹ Lesage et al. (MAS- J -HMQC),^{32,124} and Saalwächter et al. (REPT-HSQC)^{33,125} are shown in Figures 11, 12, and 13, respectively. The methods differ, first, in the means by which coherence transfer is achieved. The first and last approaches both make use of the heteronuclear dipolar couplings, although the use of REDOR recoupling^{13–15} allows a more controlled transfer—the method is termed recoupled polarization transfer (REPT)—in the latter case as compared to the ramped CP¹²⁶ step employed by Van Rossum et al. By comparison, the method in Figure 12 developed by Emsley and co-workers utilizes the

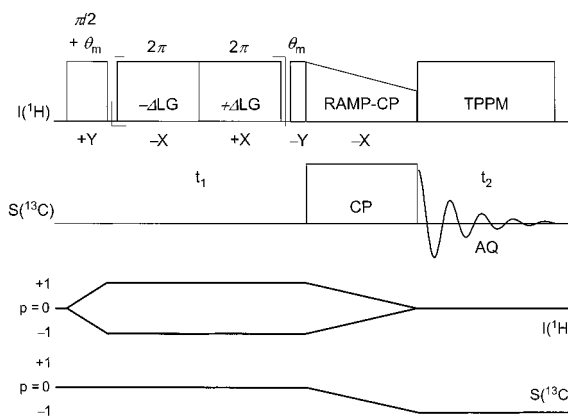


Figure 11. Pulse sequence and coherence transfer pathway diagram for the FSLG-decoupled CP HETCOR experiment, as presented in ref 31.

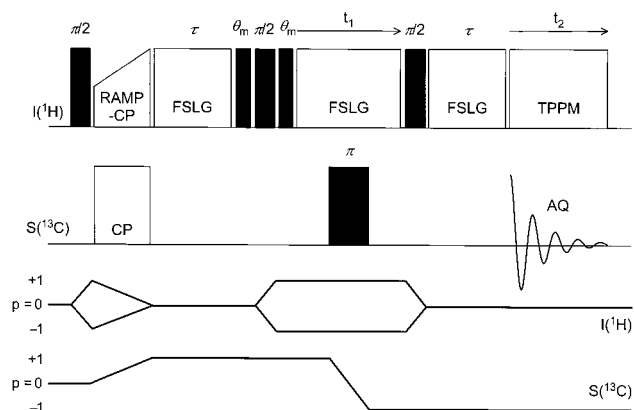


Figure 12. Pulse sequence and coherence transfer pathway diagram for the MAS- J -HMQC experiment, as presented in refs 32 and 124.

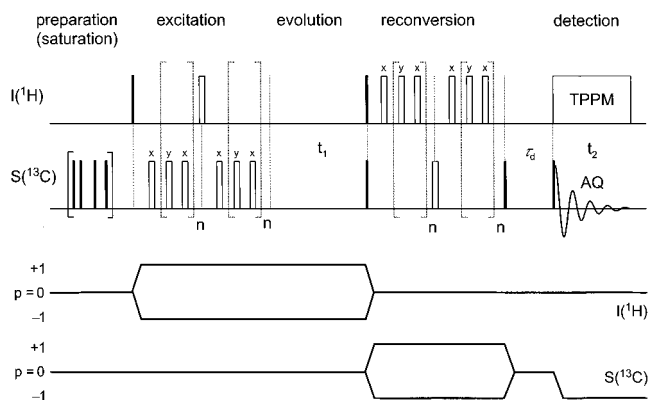


Figure 13. Pulse sequence and coherence transfer pathway diagram for the REPT-HSQC heteronuclear (^1H - ^{13}C) experiment. Dark- and light-shaded rectangular blocks represent r_f pulses of flip angle 90° and 180° , respectively. For more details, see ref 125.

isotropic through-bond J coupling. Moreover, while the methods in Figures 11 and 12 use a homonuclear dipolar coupling scheme, namely, FSLG, at a moderate ν_R , to achieve narrow ^1H line widths, the method due to Saalwächter et al. simply makes use of brute-force very-fast MAS. As noted in section IIB, a homonuclear decoupling method causes a scaling of the isotropic chemical shift scale, which must be corrected for. For FSLG decoupling, the theoretical

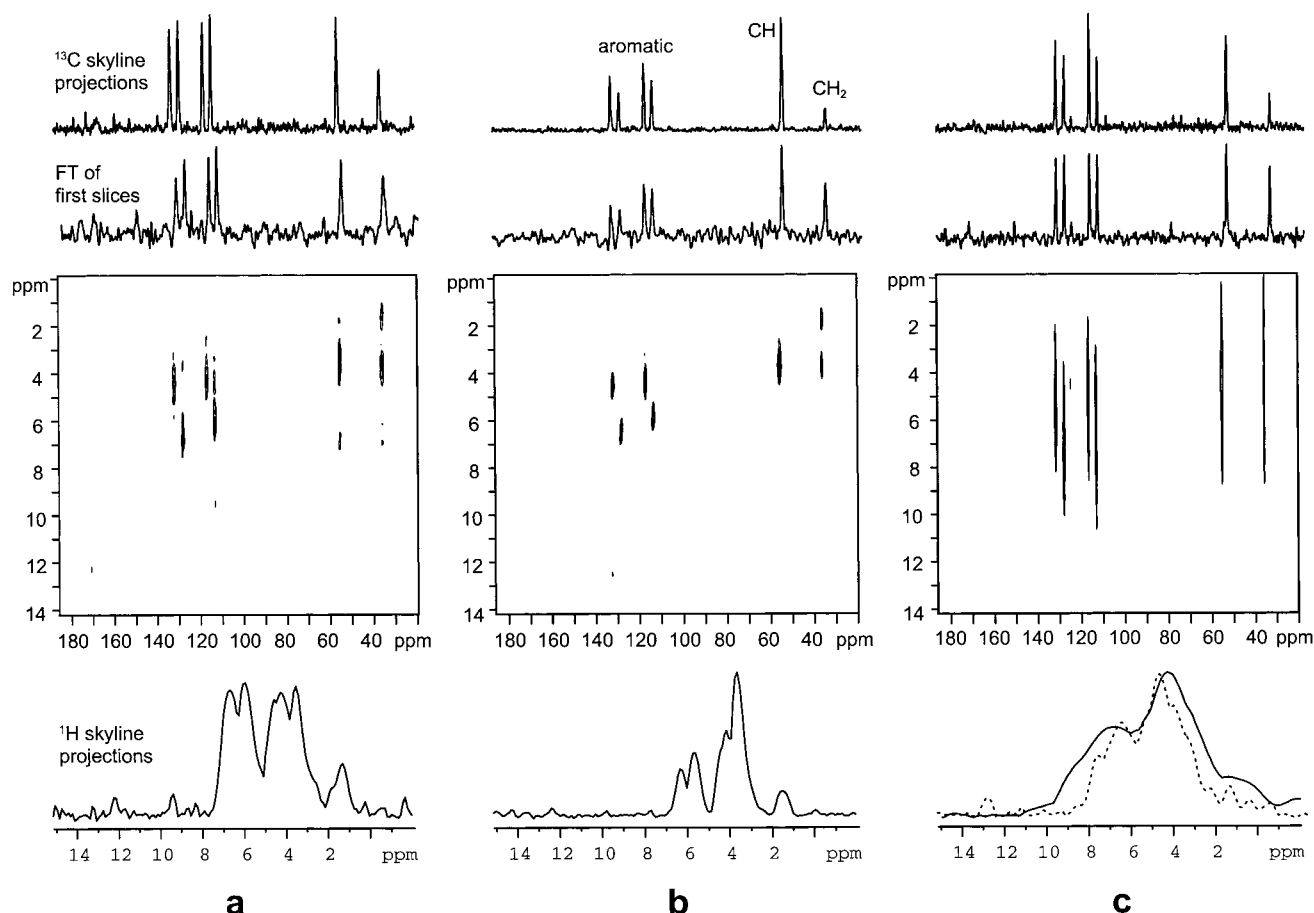


Figure 14. A comparison of three HETCOR spectra of naturally abundant L-tyrosine·HCl recorded under as far as possible equivalent conditions using (a) the FSLG-decoupled CP (Figure 11), (b) the MAS-*J*-HMQC (Figure 12), and (c) the REPT-HSQC (Figure 13) experiments. Above each spectrum, the ^{13}C skyline projection as well as the Fourier transformation of the first slice ($t_1 = 0$) of the 2D data set is shown, while below each spectrum the ^1H skyline projections are shown. The spectra were recorded at a ^1H Larmor frequency of 500 MHz; the improvement in resolution at a Larmor frequency of 700 MHz for the REPT-HSQC experiment is shown as a dashed line. (Reproduced with permission from ref 125. Copyright 2001 Academic Press.)

scaling factor is $1/\sqrt{3} = 0.58$, although, experimentally the precise scaling factor must be calibrated.

The experiments also differ with respect to the type of coherence that evolves during t_1 : in Figure 11, normal ^1H transverse magnetization is present, while in the other two cases, heteronuclear spin modes are created, namely, heteronuclear MQC and heteronuclear SQC for the techniques in Figures 12 and 13, respectively. The analogy to the well-known solution-state heteronuclear single-quantum correlation (HSQC)¹²⁷ and heteronuclear multiple-quantum correlation (HMQC)¹²⁸ experiments (dilute-spin, e.g., ^{13}C , detected) is to be noted. We will return to the differences between the heteronuclear spin modes later. In all experiments, TPPM ^1H decoupling¹²⁹ is applied during ^{13}C acquisition; the better performance of TPPM over conventional continuous wave decoupling under fast MAS has been explained recently in terms of the requirement to reintroduce the homonuclear ^1H dipolar network to suppress the broadening due to the cross term between the heteronuclear dipolar coupling and the ^1H CSA.^{97,130}

^1H - ^{13}C HETCOR spectra obtained for a sample of L-tyrosine·HCl at a ^1H Larmor frequency of 500 MHz using the FSLG-decoupled CP (Figure 11), the MAS-*J*-HMQC (Figure 12), and the REPT-HSQC (Figure

13) experiments are presented in Figure 14 panels a, b, and c, respectively. The ^1H line widths (fwhmh) for the FSLG-decoupled spectra are approximately 1 ppm as compared to over 3 ppm for the REPT-HSQC experiment (this does reduce to about 2 ppm at a ^1H Larmor frequency of 700 MHz). Moreover, Lesage and Emsley have recently shown that a fwhmh of only 150 Hz (0.3 ppm) can be obtained in a HETCOR spectrum of a sample of L-alanine recorded at a ^1H Larmor frequency of 500 MHz using a MAS-*J*-HSQC experiment.¹³¹ In this respect, the experiments with homonuclear ^1H decoupling are superior. However, in using only very-fast MAS, it has been argued that the REPT-HSQC experiment is more robust.

The principal motivation in recording a ^1H - ^{13}C HETCOR experiment is the determination and identification of the ^1H chemical shifts of the protons bound to particular carbons. For the relatively small organic molecules of relevance in modern polymer chemistry, most of the ^{13}C chemical shifts can usually be assigned by reference to the solution-state spectrum. (This is, of course, to be contrasted with the larger systems of importance in biology. A discussion of the various assignment approaches available for such systems, e.g., the ^{13}C - ^{13}C correlation experi-

ments discussed at the end of section IIIB, is beyond the scope of this review.) For correlation methods based on the dipolar coupling, it is necessary to ensure that the observed peaks are then not due to close through-space proximities. In this respect, the REPT method is better than CP, although it is to be noted that van Rossum et al. have recently presented a HETCOR experiment employing LG-CP (see discussion in the following subsection).⁴⁰ This problem is obviously avoided by utilizing through-bond J couplings. It could be expected that the necessity for relatively long excitation periods on account of the small size of the J couplings would cause significant sensitivity losses. However, for the examples presented, the observed signal-to-noise is impressive; for example, the successful recording of a ^1H - ^{15}N MAS- J -HMQC spectrum with ^{15}N at natural abundance has even been presented.¹²⁴ Finally, we note that the existence of methods based on both dipolar and J couplings opens up the possibility for distinguishing through-bond connectivities and through-space proximities on a medium- to long-range, such that insight into intermolecular packing arrangements is provided. In this way, the two approaches are complementary in a similar way to the case of the COSY and NOESY^{5,6} solution-state NMR experiments.

B. The Quantitative Determination of Heteronuclear Dipolar Couplings

A major advantage of solid-state NMR is that localized molecular motions can be quantitatively probed by the measurement of site-specific anisotropic NMR coupling parameters.^{9,132} In particular, the determination of the ^1H - ^{13}C dipolar coupling for directly bonded C-H pairs can provide much insight into, e.g., aromatic ring flips. The development of very-fast MAS and new homonuclear ^1H decoupling methods has led to a recent resurgence of interest in methods seeking to probe dynamics by the determination of heteronuclear one-bond dipolar couplings.

Figure 15 presents the pulse sequence for a general separated local field (SLF) experiment.¹³³⁻¹³⁶ The basic principle of the SLF technique is that a spinning-sideband pattern, from which the heteronuclear dipolar coupling can be extracted, is obtained in the indirect dimension for each resolved resonance in the direct dimension, i.e., the dipolar interaction is separated from the chemical shift interaction. In the original SLF papers, a homonuclear decoupling method is applied in t_1 , but recently McElheny et al.

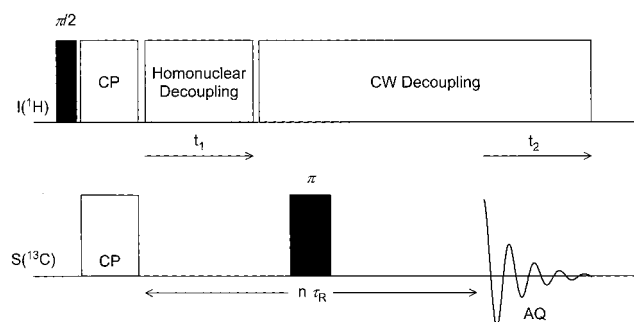


Figure 15. Pulse sequence for a conventional separated local field (SLF) heteronuclear experiment.

have shown that fast MAS alone at a ν_R of at least 12 kHz provides sufficient proton dipolar decoupling such that relatively reliable ^1H - ^{13}C dipolar couplings can be extracted. Very-fast MAS should be avoided since the higher-order spinning-sidebands become too weak to allow a reliable fitting.³⁹

Alternatively, in a modification of the original SLF method, Hohwy et al. have presented a sophisticated experiment in which a pulse sequence is applied during t_1 which actively recouples the weak heteronuclear dipolar coupling while decoupling the homonuclear ^1H - ^1H dipolar coupling.³⁸ Instead of giving a spinning-sideband pattern, a powder line shape is obtained in the indirect dimension. It is shown that this experimental approach allows the accurate determination of both N-H distances as well as the H-N-H bond angle in a NH_2 group. Another state-of-the-art method that has recently been proposed involves performing CP from ^1H to ^{13}C with the rf pulse on the ^1H channel fulfilling the Lee-Goldburg condition discussed earlier.⁴⁰ The suppression of the homonuclear ^1H dipolar couplings means that a LG-CP signal builds up in an oscillatory manner, reflecting coherent heteronuclear transfer. The Fourier transformation of such build-up curves yields powder spectra with marked singularities from the separation of which the heteronuclear dipolar coupling can be determined.

In direct analogy to the homonuclear DQ MAS experiment, if the t_1 increment in the REPT pulse sequences is not set equal to τ_R , a spinning-sideband pattern rotor-encoded by the heteronuclear dipolar coupling is obtained.^{33,37,125} In Figures 13 and 16, two alternative implementations of the REPT experiment are presented, which can be seen to differ as to where, with respect to t_1 , the second and third 90° pulses are applied. In both cases, the evolution of transverse ^1H magnetization, $-I_y$, under the heteronuclear dipolar coupling gives at the end of the first REDOR recoupling period a heteronuclear SQC, $2I_xS_z$. In the REPT-HSQC experiment in Figure 13, there are no pulses before the start of the t_1 period; as illustrated in the previous subsection, this variant is suitable for a HETCOR experiment, since only ^1H transverse magnetization evolves during t_1 .

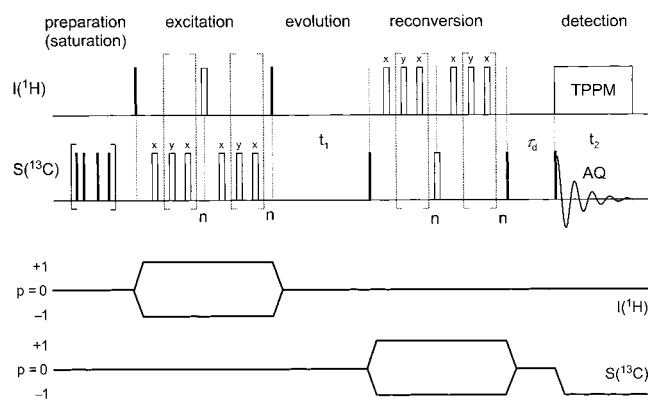


Figure 16. Pulse sequence and coherence transfer pathway diagram for the REPT-HDOR heteronuclear (^1H - ^{13}C) experiment, which is suitable for recording rotor-encoded spinning-sideband patterns. Dark- and light-shaded rectangular blocks represent rf pulses of flip angle 90° and 180° , respectively. For more details, see ref 125.

In Figure 16, a ^1H 90° pulse is applied before t_1 to give a state of heteronuclear dipolar order, $2I_zS_z$, which does not evolve under either the ^1H or ^{13}C chemical shift during t_1 . This experiment is suitable for recording rotor-encoded spinning-sideband patterns without any distortions from chemical shift evolution. It is referred to as REPT-HDOR (heteronuclear dipolar order rotor encoding). In most cases, the loss of chemical shift information in the ^1H dimension is not a problem. An advantage of the REPT-HDOR approach is that it is only necessary to record the t_1 signal for one τ_R ; the acquired signal can then be catenated and multiplied by a weighting function to introduce an artificial line broadening before Fourier transformation. The heteronuclear REPT spinning-sideband patterns for a heteronuclear spin pair are identical to those shown in Figure 9 for DQ MAS of a homonuclear spin pair except for a factor of 1.5 which reflects the difference in the homonuclear and heteronuclear dipolar Hamiltonians.

If a ^{13}C 90° pulse is applied before t_1 a heteronuclear MQC, $2I_xS_x$, is obtained. Indeed, this REPT-HMQC experiment is described in the original paper.³³ The disadvantage in this case is that, to record a HETCOR experiment, a 180° pulse must be applied in the center of t_1 to refocus the ^{13}C chemical shift evolution. Note the presence of such a pulse in the MAS-J-HMQC experiment in Figure 12. The inclusion of this 180° pulse leads to a timing problem;¹²⁵ however, Lesage and Emsley have recently shown that the insertion of a 180° pulse in the center of t_1 leads to a better resolution in a HSQC experiment on account of the refocusing of the heteronuclear J and residual dipolar couplings.¹³¹ Finally, it should be mentioned that a related set of experiments, termed dipolar heteronuclear multiple-spin correlation (DIP-HMSC), have recently been described, which also incorporate REDOR recoupling but begin with ^{13}C transverse magnetization created by a CP step.¹³⁷

V. Structural Determination by Solid-State NMR

In polymer science, an understanding of the relationship between microscopic structure and macroscopic properties is essential for an intelligent design of new improved materials. In this section, we present some case studies that illustrate the role which solid-state NMR can play with regard to the determination of the microscopic structure. It is first necessary to consider how solid-state NMR relates to other methods for structural determination, in particular the established scattering methods. For solids, for which a single crystal of suitable size can be obtained, the ability of X-ray or neutron diffraction methods to determine the complete three-dimensional structure with atomic resolution cannot be matched.

The proven power of the single-crystal diffraction techniques does not, however, make solid-state NMR irrelevant. In materials science, most samples do not possess long-range translational order, and it is not possible to prepare single crystals. Such samples are, however, usually well-ordered on a local scale. The solid-state NMR methods introduced in the previous

sections are all designed for application to powdered samples, i.e., there is no requirement for a single crystal. The ability of solid-state NMR to provide structural information about partially ordered samples will be demonstrated in this section. In this respect, we note that the analysis of solid-state NMR spectra obtained for samples where it was not possible to prepare a single crystal suitable for X-ray diffraction is greatly aided by the existence of X-ray or neutron single-crystal structures of related systems.

Solid-state NMR is also not redundant for the case where it is possible to prepare a single-crystal suitable for an X-ray analysis, since structure determination by single-crystal X-ray diffraction methods, being based on the diffraction of X-rays by electrons, is not well suited to the localization of lighter atoms. This is of particular relevance with regard to the localization of hydrogen-bonded protons, in which case a neutron diffraction study is to be preferred.¹³⁸ It should be noted, though, that neutron diffraction is not the perfect solution: as well as the requirement for both larger crystals and very expensive facilities, the investigation of protons is complicated by their large incoherent cross section, such that deuteration, which may cause a change in the hydrogen-bonding arrangement, is often required. Thus, solid-state NMR methods that can provide interproton and proton-heteroatom distance constraints, by means of which the localization of the important protons in the single-crystal structure can be refined, are of much value.

In addition, solid-state NMR is well-suited to an investigation of polymorphism. In this respect, it is to be remembered that, when selecting single crystals suitable for a diffraction study, it could happen that minor crystalline forms, which may less readily form single crystals, are missed. For example, using a modified version^{139,140} of the magic-angle turning (MAT)¹⁴¹ experiment, which allows the separation of ^{13}C CSA tensor spinning-sideband patterns, Harper and Grant were able to assign the observed ^{13}C resonances to different polymorphic forms of the terpene verbenol.¹⁴² In this case, single crystals suitable for an X-ray diffraction analysis could only be obtained for the major crystalline form.

To summarize: solid-state NMR should not be considered as a replacement for the established scattering methods. Instead, the two methods should be thought of as being complementary, since they have much to offer each other.

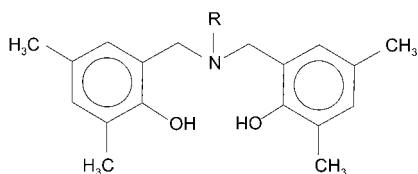
VI. Hydrogen-Bonded Systems

To investigate hydrogen bonding by solid-state NMR, the obvious nuclei to investigate are either ^1H or ^2H . Considering ^1H NMR, the components of the ^1H CSA tensors of the hydrogen bonded protons in a number of compounds, in particular carboxylic acids, have been determined for static single crystals using multiple-pulse dipolar decoupling methods. For a general hydrogen bond $\text{O}-\text{H}\cdots\text{O}$, a clear correlation between the ^1H isotropic chemical shift and the hydrogen-bond strength as given by the $\text{O}\cdots\text{H}$ and $\text{O}\cdots\text{O}$ distances determined by single-crystal diffraction studies has been established.¹⁴³⁻¹⁴⁵ These studies

also established a corresponding correlation with the ^2H quadrupolar coupling constant, as determined from the powder line shapes obtained for deuterated samples. In this section, we show that the advanced ^1H solid-state NMR methods available today yield much structural information about complex hydrogen-bonding arrangements, without requiring either a single crystal or isotopic labeling. In particular, the shifting of hydrogen-bonded resonances well away from the aliphatic peaks means that solid-state ^1H NMR methods are ideally suited to the investigation of what is often the most interesting part of the structure.

A. Rotor-Synchronized ^1H DQ MAS NMR Spectroscopy

As a first example, we show how rotor-synchronized ^1H DQ MAS spectra can distinguish between the solid-state hydrogen-bonded structures adopted by two different alkyl-substituted benzoxazine dimers [*N,N*-bis(3,5-dimethyl-2-hydroxybenzyl) "R" amine, where "R" = methyl or ethyl], **1**, in the solid state.²¹



1

These dimers are of interest because they serve as model compounds for a new class of phenolic materials, the polybenzoxazines, whose synthesis and characterization has been described by Ishida and co-workers.^{146–149} These polybenzoxazine resins were found to have a number of unusual, but commercially favorable, properties, in particular a near-zero shrinkage or volumetric expansion upon curing (polymerization) as well as low water absorption. In addition, the resins have high glass-transition temperatures even though they have been shown to have low cross-link densities. Explanations for these properties have been hypothesized in terms of favorable hydrogen-bonding interactions.¹⁵⁰

In Figure 17a, the 1D ^1H (500.1 MHz) MAS ($\nu_R = 35$ kHz) spectra of the methyl (solid line) and ethyl (dashed line) dimers are superimposed. Note that the spectra demonstrating the resolution enhancement effect of increasing the ν_R in Figure 3 were for this ethyl benzoxazine dimer. Of most importance are the clear differences between the two spectra in the low-field region, which corresponds to the hydrogen-bonded protons. For the ethyl dimer, in addition to the peaks due to the aliphatic and aromatic protons, two resonances at 13.2 and 8.2 ppm can be identified. By comparison, for the methyl dimer, a single peak at 11.2 ppm, together with a shoulder at 7.2 ppm (this peak is better resolved in the ^1H 2D DQ MAS spectrum – see below), is observed. The change of a single substituent from methyl to ethyl would not be expected to change the affinity of the amine nitrogen

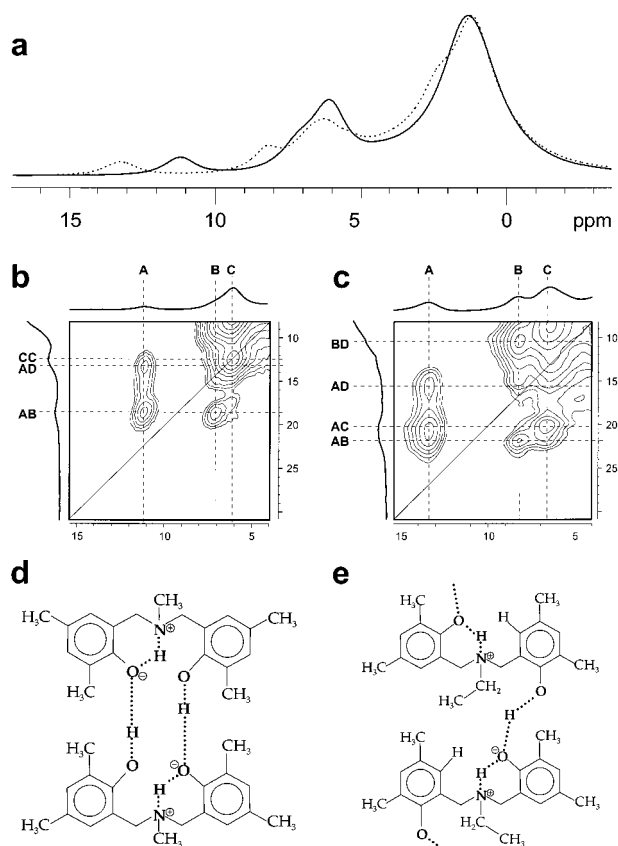


Figure 17. (a) The ^1H (500.1 MHz) MAS ($\nu_R = 35$ kHz) spectra of the methyl (solid line) and ethyl (dashed line) benzoxazine dimers, **1**. (b, c) The low-field regions of rotor-synchronized ^1H DQ MAS spectra of (b) the methyl and (c) the ethyl dimers. (d, e) Schematic representations of the proposed arrangement of (d) the methyl dimers into pairs, and (e) the ethyl dimers into a chainlike structure. (Adapted with permission from Figures 1, 5, 6, 8, and 9 of ref 21, Copyright 1998 American Chemical Society.)

to protons to the extent that would be necessary to explain a 2 ppm low-field shift of the most low-field resonance. Instead, lengthening the *N*-alkyl chain seems to induce a more profound change in the arrangement of the hydrogen bonds.

Figure 17b,c shows the low-field regions of rotor-synchronized ^1H 2D DQ MAS NMR spectra recorded for the methyl and ethyl dimers, respectively. The labels A & B, C, and D refer to the SQ resonances of the hydrogen-bonded, aromatic, and aliphatic protons, respectively. For the methyl dimer, an X-ray single-crystal structure exists,¹⁵¹ which indicates that the dimers form themselves into pairs. This X-ray study was, however, not able to locate the positions of the vital hydrogen-bonded protons. Figure 17d presents a schematic representation of a pair of methyl dimers linked by an extended hydrogen-bonded arrangement, the latter having been proposed on the basis of molecular modeling results.

The validity of the structural model in Figure 17d is proven by the ^1H DQ MAS spectrum in Figure 17b. First, the observation of two hydrogen-bonded resonances is explained: A and B correspond to the O–H \cdots N and O–H \cdots O protons, respectively (this assignment is on the basis of CRAMPS spectra and also results subsequently obtained for a ^{15}N labeled sample). Remembering that a DQ peak is only

observed if the two protons have a close through-space proximity, the observation of a strong AB cross-peak and the absence of an AA auto peak is consistent with the extended hydrogen-bonded arrangement in Figure 17d. The presence of a strong CC auto peak is interesting: for an isolated pair of dimers, there are no two nearby aromatic protons that are close enough to explain this observation; rather, the crystal structure indicates a close approach of aromatic protons belonging to different pairs of dimers.

Although the ^1H DQ MAS spectrum of the ethyl dimer in Figure 17c is similar to that of the methyl dimer in Figure 17b, for example, a clear AB cross-peak between the $\text{O}-\text{H}\cdots\text{N}$ and $\text{O}-\text{H}\cdots\text{O}$ protons can be identified, so providing evidence for the same type of extended $\text{N}\cdots\text{H}-\text{O}\cdots\text{H}-\text{O}$ hydrogen-bonded link in both samples, there exist some profound differences. The most striking differences between the methyl- and ethyl-dimer spectra are, while for the methyl dimer, there is a strong aromatic auto peak (CC) and only weak intensity corresponding to a DQC between a $\text{O}-\text{H}\cdots\text{N}$ and an aromatic proton (AC), the situation is reversed for the ethyl dimer. As discussed above, the strong aromatic auto peak in the methyl dimer is due to the close proximity of two aromatic protons of two different hydrogen-bonded dimer pairs, and the clear difference in the ethyl spectrum therefore indicates an alternative packing arrangement.

A consideration of the basic structure of the benzoxazine dimer reveals that the observation of both the strong AC peak and the absence of the CC peak for the ethyl dimer can be explained if one of the aromatic rings is flipped such that instead of pairs of hydrogen-bonded dimers there exist hydrogen-bonded chains as shown in Figure 17e. In addition, this alternative packing arrangement gives rise to a close proximity of the $\text{O}-\text{H}\cdots\text{O}$ proton and the *N*-ethyl chain. The resulting cross-peak between the $\text{O}-\text{H}\cdots\text{O}$ proton and the ethyl-chain CH_2 protons (BD) is, indeed, clearly seen in the DQ MAS spectrum of the ethyl dimer (Figure 17c).

A further example of the utility of rotor-synchronized ^1H DQ MAS NMR spectra is the investigation of the change in the quadruple hydrogen-bonding arrangement formed by dimers of 2-ureido-4-pyrimidone units upon a keto to enol tautomerism.^{83,152} The ability of monomers incorporating two and three of these units to self-assemble into linear polymers and reversible networks, respectively, was noted in the Introduction.² In an additional related example focusing on ionic intermolecular interactions, Rodriguez et al. have presented 2D rotor-synchronized ^1H DQ MAS spectra that prove the intimate contact of the two polymers, poly(sulfonated styrene) (PSS) and poly(diallyldimethylammonium chloride) (PDADMAC), in both a polyelectrolyte complex and thin self-assembled PSS/PDADMAC multilayers on silica colloids.²⁶

B. ^1H DQ MAS NMR Spinning-Sideband Patterns

The rotor-synchronized ^1H DQ MAS experiment can be considered to be a workhorse method; valuable semiquantitative insight is provided by the straight-

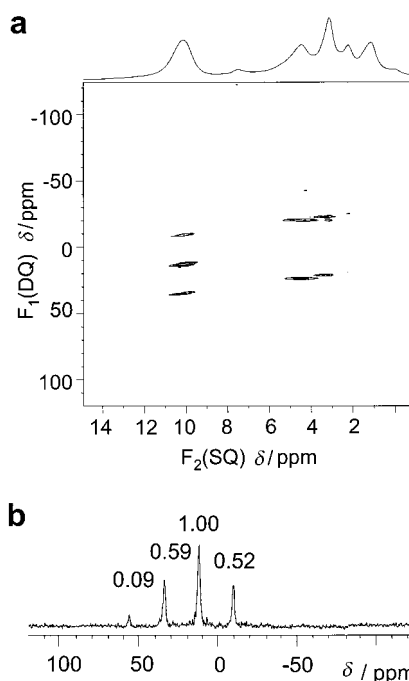


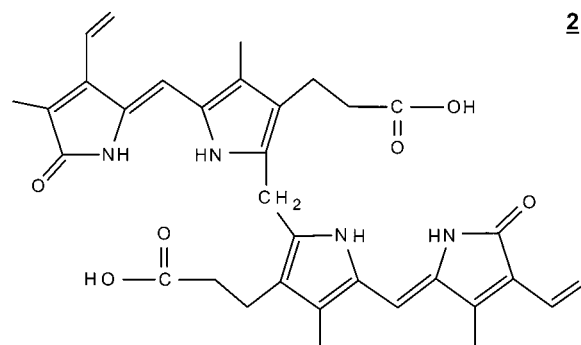
Figure 18. (a) A 2D ^1H (500.1 MHz) DQ MAS spectrum of an all-silica ZSM-12 zeolite. The spectrum on top is the ^1H MAS spectrum. (b) The ^1H DQ MAS spinning-sideband pattern for the SQ resonance at 10 ppm, corresponding to the hydrogen-bonded protons. (Reproduced with permission from Figures 4 and 5 of ref 153. Copyright 2000 American Chemical Society.)

forward interpretation of spectra that typically require less than 1 h of measuring time. The recording of ^1H DQ MAS spinning sideband patterns usually requires a significantly longer measuring time (8–12 h). However, as illustrated by the following examples, the extra investment is often rewarded by important structural information.

As noted above, the presence of centerband and even-order sideband intensity in a ^1H DQ MAS spectrum arises from the evolution during t_1 of a DQC, due to a particular two spins, under dipolar couplings to other spins. In an elegant use of this phenomenon, Shantz et al have shown how the observation of an intense centerband in the ^1H DQ MAS spinning-sideband pattern for the SQ resonance at 10 ppm—see Figure 18—proves that at least three silanol protons are engaged in hydrogen bonding within the defect sites in an all-silica ZSM-12 zeolite.¹⁵³

The simulated spinning-sideband patterns for a model three-spin system presented in Figure 10 demonstrated that at a very-fast ν_R , i.e., 30+ kHz, the evolution during t_1 of a DQC under perturbing dipolar couplings to other spins is suppressed, such that the intensity of the centerband and even-order sidebands is usually weak. In addition, Figure 10 showed that the effect of a perturbing dipolar coupling on the odd-order spinning-sideband pattern generated by the RRE mechanism for the DQC corresponding to the dominant D is small, such that it is possible, for a multispin system, to determine the dominant D , and hence the shortest proton–proton distance, to a high degree of accuracy. As an explicit example of this, consider the hydrogen-

bonded arrangement in bilirubin IX α (henceforth referred to simply as bilirubin), **2**.³⁰



Bilirubin is an unsymmetrically substituted tetrapyrrole dicarboxylic acid, which is found in the body as a product of the metabolism of hemoglobin from red blood cells.¹⁵⁴ Bilirubin itself is intrinsically unexcretable, and its removal from the body requires it first to be conjugated enzymatically with glucuronic acid in the liver. An insufficient elimination of the yellow-orange pigment, bilirubin, results in hyperbilirubinemia, which manifests itself as jaundice; such a condition is usually associated with a pathologic liver disease, e.g., hepatitis, or an insufficiency of the bilirubin glucuronyl transferase enzyme, the latter being commonly the case in newly born infants.¹⁵⁵

On account of its medical importance, much effort has been devoted to the investigation of the structure of bilirubin. X-ray single-crystal studies have demonstrated that bilirubin crystallizes in the solid-state with the ridge-tile-shaped conformation illustrated in Figure 19: the two halves of the molecule can be considered to be planar tiles, aligned at an angle of approximately 100° with respect to each other.^{156,157} The crystal structure indicates that the carboxylic acid group of one dipyrinone unit adopts an ideal geometry for intramolecular hydrogen bonding with the lactam and pyrrole moieties of the other dipyrinone unit. The involvement of the carboxylic acid groups in strong intramolecular hydrogen bonding renders bilirubin effectively insoluble in aqueous solution.

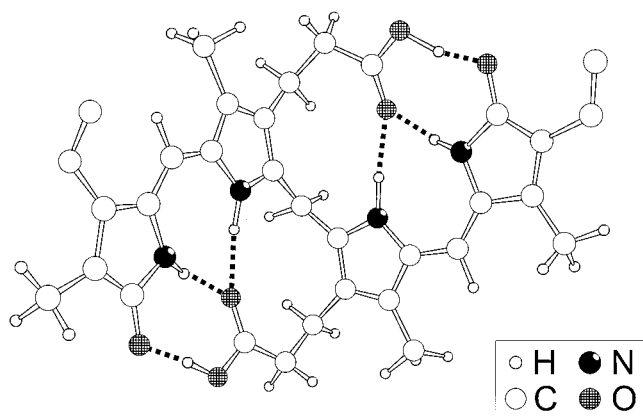


Figure 19. The structure adopted by bilirubin, **2**, in the solid state, as determined by an X-ray single-crystal diffraction study.¹⁵⁷ The intramolecular hydrogen-bonding arrangement is indicated. (Reproduced with permission from ref 30. Copyright 2001 American Chemical Society.)

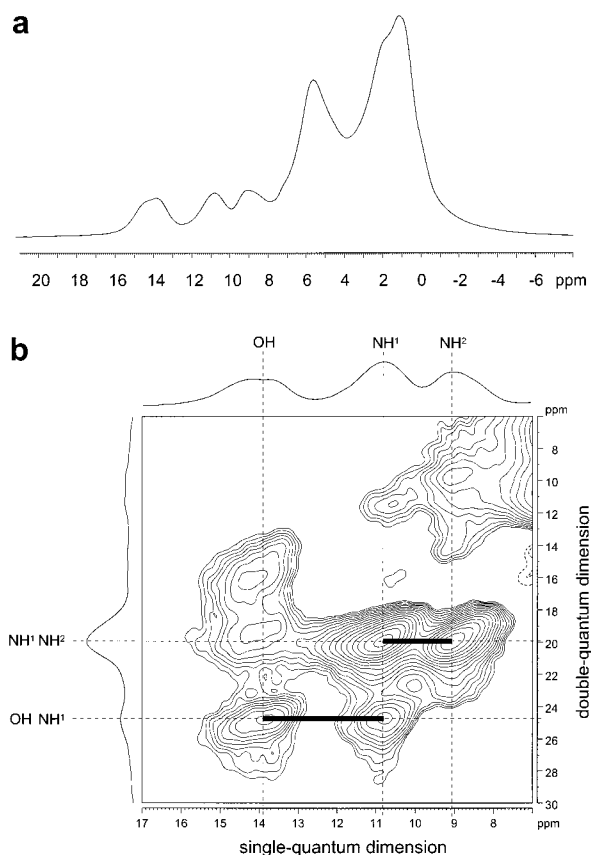


Figure 20. (a) ^1H (700.1 MHz) MAS ($\nu_R = 30$ kHz) NMR spectrum of bilirubin, **2**. (b) The part corresponding to the hydrogen-bonded resonances of a rotor-synchronized ^1H DQ MAS NMR spectrum, together with skyline SQ and DQ projections, of bilirubin, **2**. (Reproduced with permission from ref 30. Copyright 2001 American Chemical Society.)

As stated above, the exact localization of protons by X-ray scattering is very difficult. Indeed, in the first X-ray single-crystal study,¹⁵⁶ the positions of the vital hydrogen-bonded protons were very poorly defined. Furthermore, although Le Bas et al. went to considerable trouble to obtain a single crystal of suitable quality to allow the location of the hydrogen-bonded protons, they were still forced to artificially calculate the position of one of the three hydrogen-bonded protons in each half of the bilirubin molecule.¹⁵⁷ There is, therefore, likely to be a significant uncertainty in the proton–proton distances derived from the X-ray structure.

Figure 20a presents the 1D ^1H MAS spectrum of bilirubin, recorded at a ^1H Larmor frequency of 700.1 MHz and a MAS frequency of 30 kHz. Three low-field resonances can clearly be resolved. In Figure 20b, the part of a 2D rotor-synchronized ^1H DQ MAS spectrum corresponding to these hydrogen-bonded resonances is shown. Only the proton corresponding to the middle hydrogen-bonded peak at 10.8 ppm can then be seen to be in close proximity to both the other two hydrogen-bonded protons. By reference to the intramolecular hydrogen-bonded arrangement known from the single-crystal X-ray investigation (see Figure 19), the peak at 10.8 ppm can then be assigned to the lactam NH proton. The solid-state ^1H chemical shifts are very similar to the solution-state values obtained using chloroform as a solvent, where there

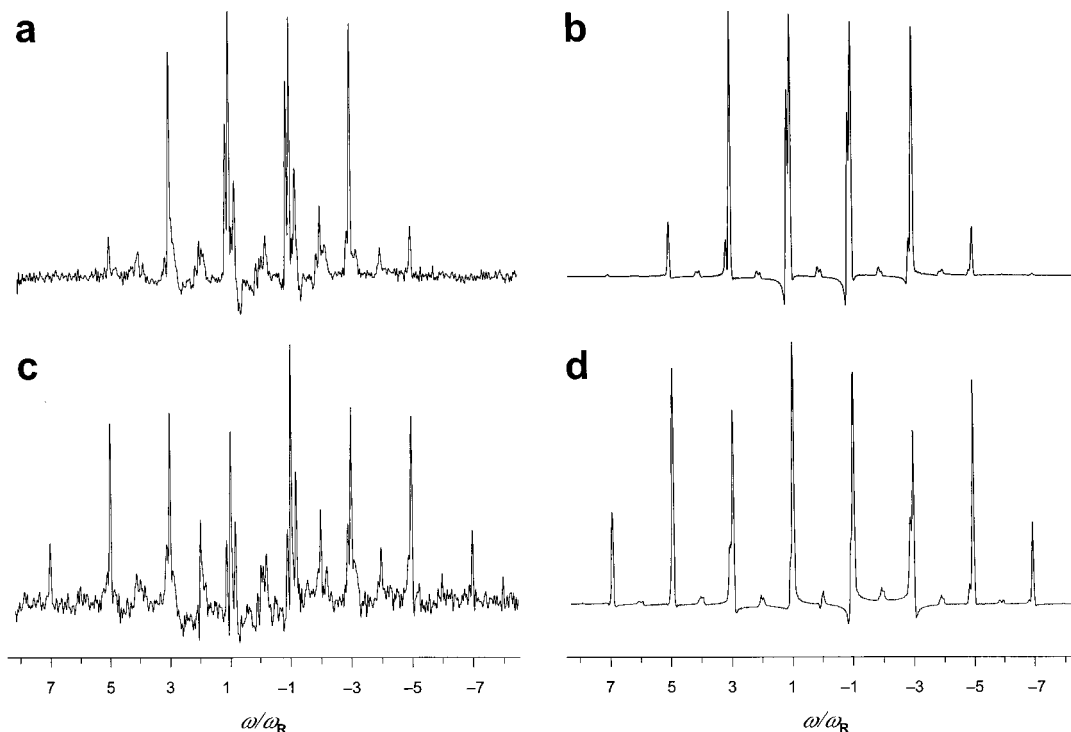


Figure 21. (a, c) ^1H (700.1 MHz) DQ MAS NMR spinning-sideband patterns obtained for the NH^1 hydrogen-bonded resonances of bilirubin, **2**, (see Figure 20b) at a MAS frequency of 30 kHz. BABA recoupling sequences of duration (a) two or (c) three τ_{R} were used for the excitation and reconversion of DQCs. The corresponding best-fit simulated three-spin ^1H DQ MAS spinning-sideband patterns are presented in (b) and (d). (Reproduced with permission from ref 30. Copyright 2001 American Chemical Society.)

is strong evidence that the intramolecular hydrogen-bonding arrangement shown in Figure 19 persists. On this basis and considering the intensities of the respective DQ peaks, the SQ resonances at 9.1 and 13.9 ppm can be assigned to the pyrrole NH and carboxylic acid OH protons, respectively.

In Figure 21 a and c, ^1H (700.1 MHz) DQ MAS spinning-sideband patterns obtained for the lactam (at 10.8 ppm) NH resonances of bilirubin, with τ_{rcpl} equal to (a) two and (c) three rotor periods at a $\nu_{\text{R}} = 30$ kHz are shown. In the rotor-synchronized ^1H DQ MAS spectrum in Figure 20b, in addition to the intense NH–NH DQ peaks, weaker DQ peaks due to DQCs involving the OH and aliphatic protons are observed. An inspection of the spectra in Figure 21 reveals the existence of spinning sidebands due to all these different DQCs; note that the DQ peak for the NH–NH pair is at the second-to-left position.

In ref 30, a protocol is presented whereby the dominant D , and hence the shortest proton–proton distance, can be determined by finding the best fit simulated three-spin spectra on the basis of a comparison of the extracted integrated experimental sideband intensities with those in the simulated spectra. In this way, the distance between the lactam and pyrrole NH protons in bilirubin is determined to be 0.186 ± 0.002 nm (corresponding to a dominant D of 18.5 ± 0.5 kHz), proving an exceptionally close approach of two protons being noncovalently bonded to the same atom. The accuracy is better than what can be reliably expected from a standard X-ray structural analysis. We note that, at this degree of accuracy, the different effects of vibrational averaging should be considered, when comparing distances

extracted by solid-state NMR to those determined by neutron diffraction studies.^{136,158} The corresponding best-fit simulated three-spin spinning-sideband patterns are shown in Figure 21b,d. The analysis also yields a distance between the lactam NH and carboxylic acid OH protons of 0.230 ± 0.008 nm (corresponding to a perturbing D of 9.9 ± 1.0 kHz) and an H–H–H angle of $122 \pm 4^\circ$ —note that the precision of these values is less than for the case of the shortest proton–proton distance.

VII. Aromatic π – π Interactions and Ring-Current Effects

In addition to hydrogen-bonding effects, the ^1H chemical shift is very sensitive to the ring currents associated with aromatic moieties.¹⁵⁹ In comparison to the solution state, where isotropic molecular tumbling means that such effects are only seen for unusual intramolecular geometries,¹⁶⁰ in the solid state, the protons are exposed to the ring currents due to other nearby through-space aromatic moieties, be they intra- or intermolecular. However, it is only with the renewed interest in methods offering high resolution ^1H solid-state spectra that the widespread importance of ring current effects in the solid-state is being appreciated. It should be noted that ring current effects are not restricted to ^1H NMR—it will be shown below that shifts of the order of 1 ppm are also observed in the ^{13}C dimension. However, the effects are much more pronounced in ^1H NMR on account of the small chemical shift range and the usual location of the protons in “exposed” parts of the molecule.

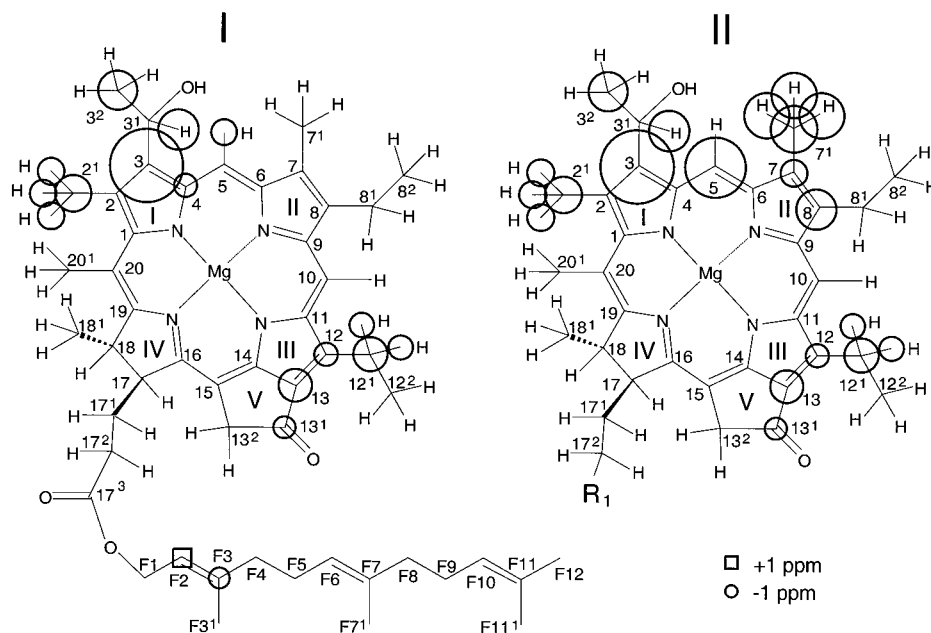


Figure 22. A representation of the aggregation shifts, i.e., the difference between the chemical shift in the aggregate (i.e., the solid state) and in the monomer (i.e., in solution), as determined for the ^1H and ^{13}C nuclei in a uniformly ^{13}C enriched bacteriochlorophyll (BChl) *c* in intact chlorosomes of *Chlorobium tepidum*, using 2D ^1H - ^{13}C and 3D ^1H - ^{13}C - ^{13}C dipolar correlation spectroscopy at a magnetic field of 14.1 T. Circles correspond to upfield changes upon aggregation with the size of the circle indicating the magnitude of the change. The different representations in I and II correspond to the experimental observation of two separate components. (Reproduced with permission from ref 162. Copyright 2001 American Chemical Society.)

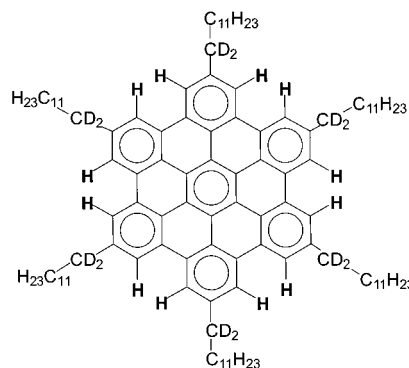
A. Aggregation Shifts

Probably the first clear example of the importance of ring current effects in ^1H solid-state NMR was presented by van Rossum et al.,¹⁶¹ who were able to determine and assign the ^1H and ^{13}C chemical shifts in a uniformly ^{13}C enriched bacteriochlorophyll (BChl) *c* in intact chlorosomes of *Chlorobium tepidum*, using 2D ^1H - ^{13}C and 3D ^1H - ^{13}C - ^{13}C dipolar correlation spectroscopy at a magnetic field of 14.1 T. As shown in Figure 22, what the authors refer to as “aggregation shifts”, which are defined as the difference between the chemical shift in the aggregate (i.e., the solid state) and in the monomer (i.e., in solution), are observed for particular ^1H and ^{13}C nuclei. Note that in Figure 22, circles correspond to upfield changes upon aggregation with the size of the circle indicating the magnitude of the change. Making the assumption that these aggregation shifts are predominantly due to the ring currents arising from the aromatic moieties of nearby through-space molecules, the authors proposed a stacking arrangement that ensures overlap between only those aromatic moieties where the aggregation shifts are observed. Moreover, by combining the information provided by the NMR spectra with the results of modeling studies and electron microscopy, it was possible to propose a novel 3D suprastructure, namely, a bilayer tube, for the chlorosome antenna, which is of much interest on account of its role as a supramolecular light harvesting device.¹⁶²

B. Hexabenzocoronone Derivatives

A striking example of the importance of ring-current effects in solid-state ^1H NMR is provided by the polycyclic aromatic molecule,¹⁶³ hexa-*n*-dodecyl-

hexa-*peri*-hexabenzocoronone (henceforth referred to as HBC- C_{12}), **3**.²² Note that, in the following, spectra



3

are presented for a sample in which the α -carbons of the alkyl side chains were deuterated (87%), this sample having been synthesized to carry out ^2H NMR. Figure 23a presents ^1H (500.1 MHz) MAS NMR spectra of the solid phase of **3**, recorded at a ν_R of 35 kHz. The 6-fold symmetry of the individual molecules means that only one distinct aromatic proton resonance is expected, as is indeed found to be the case in the solution-state spectrum (not shown). However, in Figure 23a, three aromatic resonances are clearly identified.

In principle, the observed ^1H MAS spectrum in Figure 23a can be ascribed to two different scenarios: either there exist three different types of HBC crystallographic environment, where the 6-fold symmetry of each individual molecule is maintained, with the three environments then becoming equivalent in the LC phase, or there is a reduction of the 6-fold

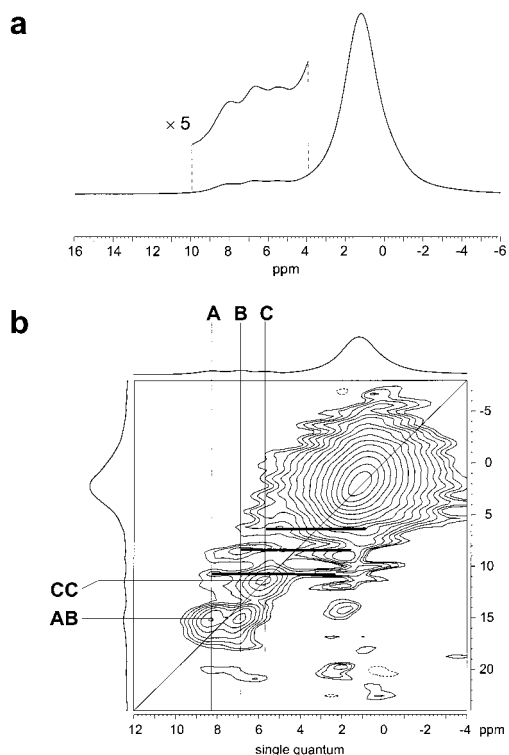


Figure 23. (a) ^1H (500.1 MHz) MAS ($\nu_R = 35$ kHz) spectrum and (b) rotor-synchronized ^1H DQ MAS NMR spectrum, together with skyline SQ and DQ projections, of HBC-C_{12} , **3**. (Reproduced with permission from ref 22. Copyright 1999 American Chemical Society.)

symmetry of each molecule due to the packing arrangement in the crystal, leading to inequivalent aromatic proton sites within each HBC disk. These scenarios can be distinguished by DQ MAS NMR.

Information about the relative proximities of the three resolved aromatic protons is provided by the rotor-synchronized ^1H DQ MAS 2D spectrum of α -deuterated HBC-C_{12} in Figure 23b. Here, we focus on the peaks in the bottom left-hand corner of the spectrum, due to DQCs involving only aromatic protons—this spectral region is actually that which was shown in Figure 8a. As is evident from the molecular structure of HBC-C_{12} , the 12 aromatic protons are grouped in pairs of “bay protons” with a H–H distance of approximately 0.20 nm, while the closest distance to another aromatic proton is 0.41 nm. Therefore, the aromatic region of the DQ MAS spectrum will be dominated, for the short excitation period used here, by the dipole–dipole couplings within the three pairs. In Figure 23b, it is apparent that the extension to a second frequency dimension has yielded a significant resolution improvement over the one-dimensional spectrum (Figure 23a), and three separate resonances can be clearly distinguished. Strong CC auto and AB cross-peaks are observed, which imply the presence of only two types of pairs of aromatic protons, $\text{H}_A\text{-H}_B$ and $\text{H}_C\text{-H}_C$, in a ratio, as determined from the peak intensities, of 2:1.

For unsubstituted HBC, an X-ray single-crystal study¹⁶⁴ showed that the molecules pack in the so-called herringbone pattern, which optimizes the π – π interactions between adjacent disks. In ref 22, it was hypothesized that HBC-C_{12} adopts the same colum-

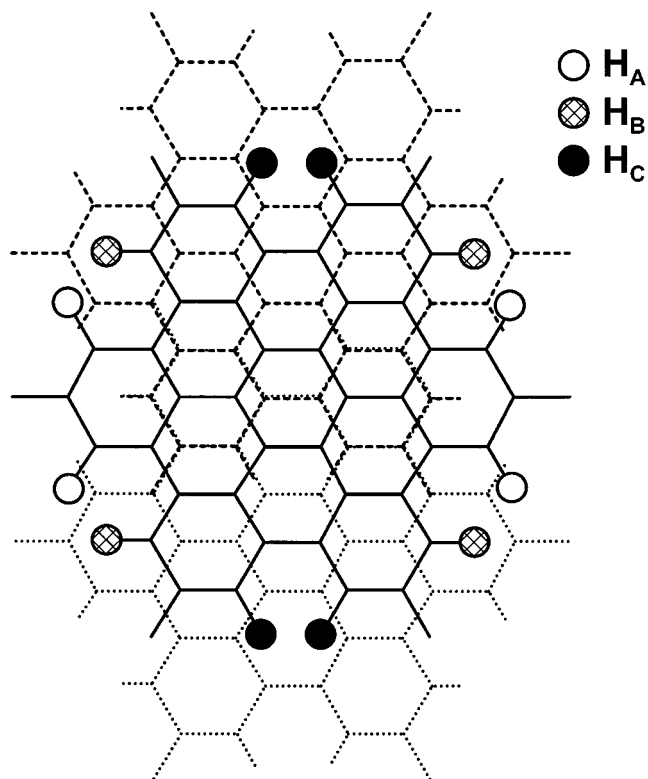


Figure 24. A representation of the proposed stacking of the aromatic cores in HBC-C_{12} , based on the structure of unsubstituted HBC, which is known, from a X-ray single-crystal study,¹⁶⁴ to crystallize in the so-called herringbone pattern. Three HBC-C_{12} molecules are shown; the molecules above and below the central HBC-C_{12} molecule are indicated by dashed and dotted lines, respectively. (Reproduced with permission from ref 22. Copyright 1999 American Chemical Society.)

nar packing of the aromatic cores as in unsubstituted HBC, with the presence of the long alkyl chains now meaning that the individual columns of aromatic cores are much more separated from each other. Figure 24 shows qualitatively how such a stacking of the HBC cores leads to three different aromatic proton environments. Three aromatic cores are shown; the molecules above and below the central aromatic core are indicated by dashed and dotted lines, respectively, with the aromatic protons of the central layer highlighted.

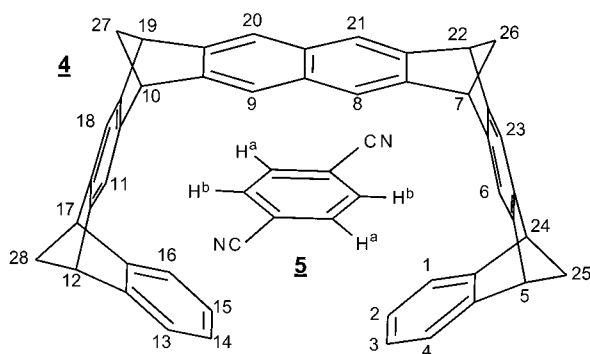
The interplanar distance in unsubstituted HBC is 0.342 nm,¹⁶⁴ and thus the aromatic protons of one layer will experience the ring currents of the extended π -electron systems of adjacent layers. In HBC-C_{12} , three different aromatic proton environments can thus be identified with respect to the degree to which the proton experiences the ring current of the adjacent layers. The unshaded circles represent protons that lie neither above nor below the π orbitals of an adjacent layer, and therefore correspond to the least shielded resonance (highest ppm). Fully shaded and hatched circles then represent protons that lie over or below an inner and outer part, respectively, of an adjacent ring system; the fully shaded protons would be expected to be the most shielded. Assigning the unshaded, hatched, and fully shaded protons to the A, B, and C resonances in Figure 23b, respectively, the observed presence of

only AB and CC pairs in the ratio 2:1, with the C resonance having the smallest chemical shift value (most shielded), is then explained. Thus, it is the second of the two scenarios, i.e., the reduction of the 6-fold to a 2-fold symmetry for each individual molecule, identified above which is borne out by experiment.

The advances in computing power as well as the development of methodology means that the use of quantum chemical calculations of NMR parameters in the interpretation of experimental results is becoming ever more popular.^{165–167} As an example of the utility of such a combined experimental and theoretical approach, it has recently been shown that the ab initio calculation of ^1H chemical shifts for model HBC oligomers allows the quantitative assignment of the experimental observation of three aromatic resonances in HBC- C_{12} (see Figure 23) to a specific packing arrangement, with the qualitative hypothesis of the adoption of the structure of unsubstituted HBC (see Figure 24) being proved.¹⁶⁸ Moreover, these calculations showed that the ring currents effects are quite long-range, with an aromatic ring still exerting an influence at a distance of 0.7 nm, i.e., the next nearest HBC neighbor must be considered. We note that the further use of rotor-synchronized ^1H DQ MAS spectroscopy and ab initio quantum chemical calculations to investigate two other HBC derivatives is described in refs 24 and 169.

C. A Molecular Tweezer Host–Guest Complex

As the final example in this section, we show how an investigation of the changes in ^1H chemical shifts caused by aromatic ring currents provides insight into the nature of the supramolecular host–guest complex, **4@5**.²⁹ The receptor **4** belongs to a family



of molecules termed molecular tweezers due to their concave–convex topology and propensity to selectively form complexes with electron-deficient aromatic and aliphatic compounds as well as organic cations.^{170,171} This and other molecular tweezer host–guest complexes have been studied by ^1H solution-state NMR, exploiting the large upfield shifts of the substrate resonances upon complexation caused by host aromatic ring currents. For the specific complex studied here between the naphthalene-spaced tweezer **4** and 1,4-dicyanobenzene **5**, complex formation and dissociation in CDCl_3 at room temperature is fast with respect to the NMR time scale, as evidenced by a single guest ^1H resonance shifted by 4.35 ppm

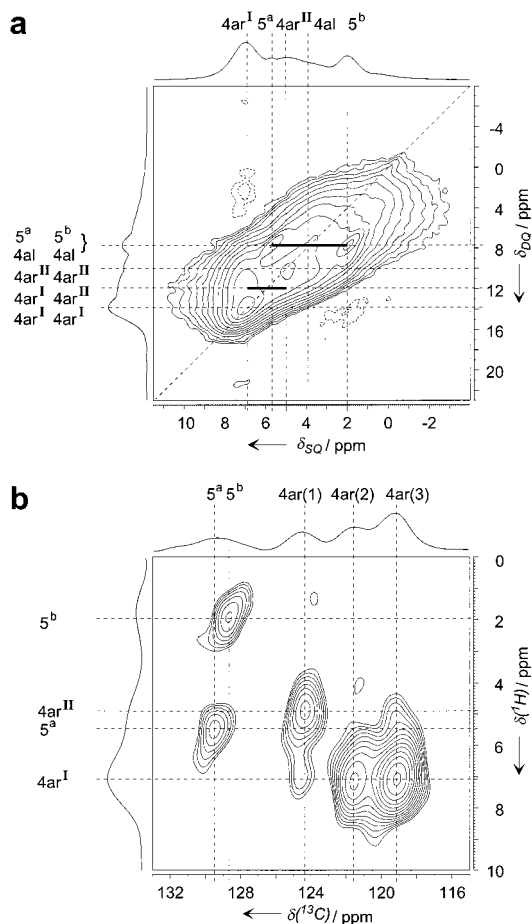


Figure 25. (a) Rotor-synchronized ^1H (700.1 MHz) DQ MAS NMR spectrum, together with skyline projections, of **4@5**. (b) The aromatic region of a ^1H - ^{13}C REPT-HSQC NMR correlation spectrum, together with sum projections, of **4@5**. Both spectra were recorded under MAS at 30 kHz. The recoupling time equalled one rotor period, such that predominantly only one-bond correlations are selected. The notations **4ar** and **4al** refer to host aromatic and alkyl protons, respectively, while **5^a** and **5^b** refer to the two distinct guest aromatic protons. (Reproduced with permission from ref 29. Copyright 2001 Wiley.)

relative to that observed for **5** alone. A solid-state investigation has the advantage that the guest remains complexed on the time scale of the NMR experiment, and thus the structure and dynamics of the host–guest complex can be probed directly. It should be noted that an X-ray single-crystal structure is available for **4@5**;¹⁷¹ therefore, this study offers the opportunity to check the reliability of the described approach and to demonstrate that additional complementary insight can be provided.

Figure 25a presents a rotor-synchronized ^1H (700 MHz) DQ MAS NMR spectrum of **4@5**. The assignment of the resolved ^1H DQ peaks is aided by reference to Figure 25b, where the aromatic region of a ^1H - ^{13}C heteronuclear correlation spectrum of **4@5**, recorded with the REPT-HSQC experiment shown in Figure 13, is presented. A short excitation time was used such that predominantly only one-bond C–H correlations are observed. In solution, the aromatic CH resonances of **4** and **5** are found between 116.5 and 124.1 and at 131.0 ppm, respectively. The relative insensitivity of ^{13}C chemical shifts to ring

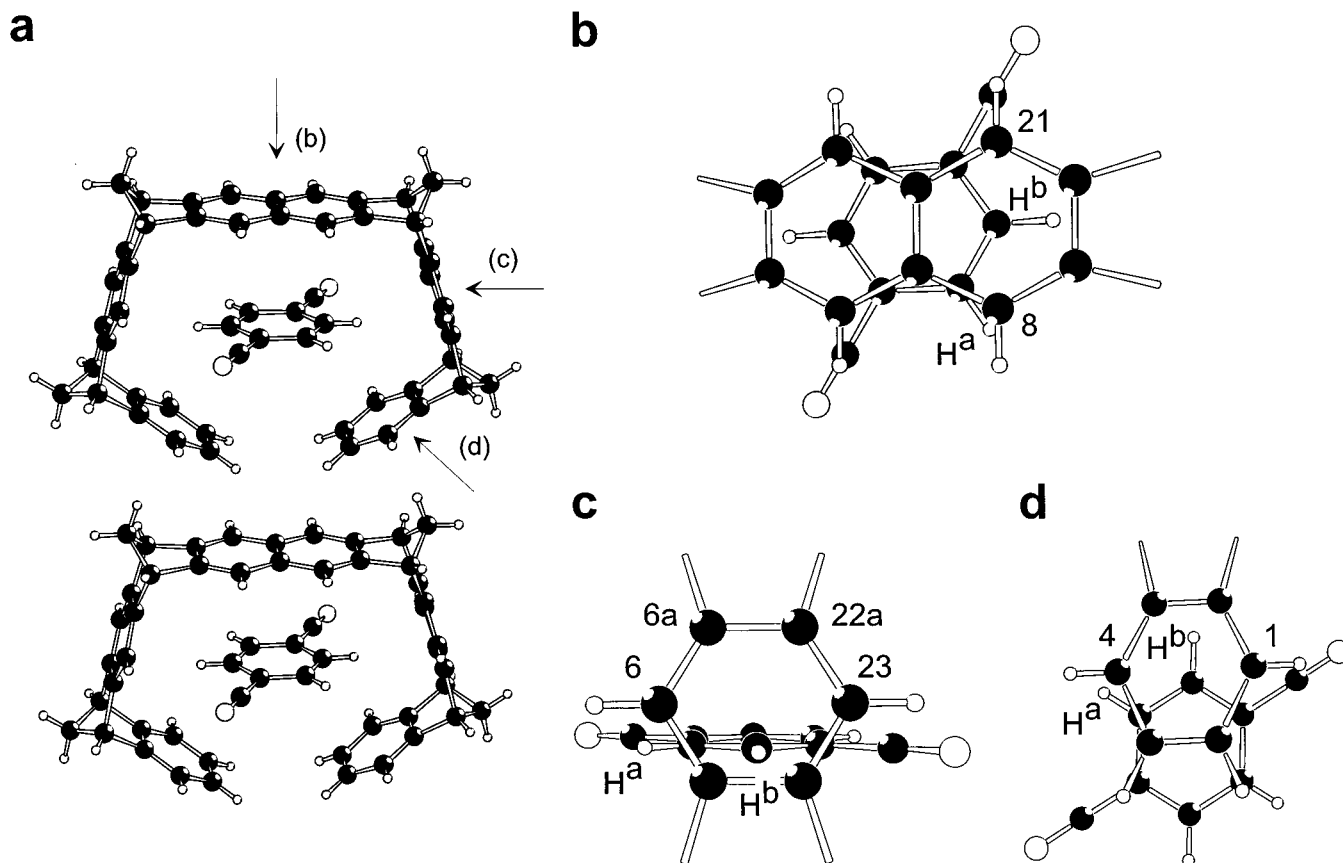


Figure 26. The solid-state packing arrangement of $4@5$, as determined by an X-ray single-crystal investigation.¹⁷¹ Large white, large black, and small white circles represent nitrogen, carbon, and hydrogen atoms, respectively. In (b), (c) and (d), views through the naphthalene, inner benzene and outer benzene rings, respectively, are shown. The distance from H^b to the center of the inner benzene ring is 260 pm (view (c)) as opposed to 404 pm to the middle of the naphthalene unit (view (b)) and 314 pm to the center of the outer benzene ring (view (d)). Specific carbon and hydrogen atoms are labeled according to the above chemical structure. (The notation xa refers to the quaternary carbon between carbons x and x+1.) (Reproduced with permission from ref 29. Copyright 2001 Wiley.)

current effects then allows the clear assignment of the two separate peaks at ^{13}C chemical shifts of 129.6 and 128.7 ppm in Figure 25b to the guest CHs (labeled 5a and 5b), with the corresponding ^1H chemical shifts being 5.6 and 2.0 ppm, respectively.

The pair of cross-peaks at a DQ frequency of 7.6 ppm in Figure 25a can thus be identified as being due to two neighboring guest CH protons. It is further interesting to note that two distinct host aromatic ^1H resonances can be resolved in both the ^1H DQ MAS and ^1H - ^{13}C REPT-HSQC spectra: the ^{13}C peak at 124.4 ppm (4ar^{I}) can be assigned to the meta pair of carbons of the outer benzene ring (2, 3, 14, and 15), with the corresponding ^1H chemical shift being 4.9 ppm (4ar^{II}). From Figure 25b, the other aromatic protons have, within the experimental resolution, the same chemical shift of 7.1 ppm (4ar^{I}). In this way, the observation of diagonal ^1H DQ peaks at 13.8 and 10.0 ppm, as well as shoulders corresponding to DQ cross-peaks at 12.0 ppm can be explained.

The observed experimental features can be qualitatively understood by reference to the structure of $4@5$, which is known from an X-ray single-crystal analysis.¹⁷¹ In Figure 26a, the side-by-side arrangement of two $4@5$ complexes is displayed, while Figures 26b, 26c, and 26d show views through the different host aromatic moieties. It is apparent that

Table 2. Comparison of the ^1H Chemical Shifts (in ppm) for $4@5$ Determined by NMR Experiments and ab Initio Calculations²⁹

	solution-state NMR	solid-state NMR	ab initio (monomer)	ab initio (dimer)
H^a (guest)	3.5	5.6	5.5	5.2
H^b (guest)	3.5	2.0	2.5	2.1
H2,3,14,15	6.4	4.9	6.6	5.5–5.6
other arom	7.0–7.2	7.1–7.2	7.2–8.0	6.9–7.7
$H_{\text{bridgehead}}$	4.1	3.8 ^a	3.9–4.2	3.3–4.0
H25,28 ^b	2.4	2.0–3.8 ^a	2.2	2.1
H26,27 ^b	2.5	0.6–2.3 ^a	2.0–2.1	0.4–1.0

^a These ^1H chemical shifts were determined from the alkyl region of the ^1H - ^{13}C correlation spectrum (not shown). ^b Note that the two protons in each CH_2 group are inequivalent.

the two guest aromatic protons experience the ring currents due to the host to different degrees. Moreover, from Figure 26a, the end pair of aromatic protons can be seen to be directed into the ring current due to the naphthalene unit of the next host, explaining the 4ar^{II} resonance.

As was the case with the HBC- C_{12} example discussed above, ab initio quantum chemical calculations were carried out, thus providing a fully quantitative interpretation of the experimental results. Table 2 presents the experimental solution- and solid-state ^1H chemical shifts obtained by quantum chemical calculations (for details, see ref 29) for a single

4@5 complex and a pair of **4@5** complexes in the arrangement shown in Figure 26a (denoted as monomer and dimer, respectively). The good agreement between the monomer calculation and the experimental solid-state *guest* ^1H chemical shifts reveals that these values are largely determined by *intra*-complex effects. In contrast, the marked difference between the solid- and solution-state ^1H chemical shifts of the end pair of host aromatic protons (H2,3,14,15) can only be explained by considering a *dimer*.

By calculating the ^1H chemical shifts of the guest protons due to the three host aromatic moieties, namely, the central naphthalene unit (Figure 26b), and the inner (Figure 26c) and outer benzene ring (Figure 26d), the quantum chemical calculations were further able to elucidate the role of the different chemical units. First, it was found that the guest ^1H chemical shifts derived by summing the changes due to the separate aromatic moieties are in good agreement with the values calculated for the whole system. It can thus be concluded that the only influence of the linking units is to determine the positioning of the host aromatic moieties. Second, the difference between the guest ^1H chemical shifts is mainly due to the arrangement of the guest with respect to the inner benzene ring (Figure 26c).

VIII. The Investigation of Dynamic Processes

A unique strength of solid-state NMR is its ability to probe molecular dynamics with site selectivity.^{9,132} In this section, we present some specific examples that illustrate the considerable insight into dynamic processes provided by advanced solid-state NMR experiments applicable to as-synthesized samples, i.e., without the requirement for isotopic labeling. These examples focus on well-defined processes that are fast as compared to the time scale of the ^1H DQ MAS experiment, this being on the order of 10^{-6} to 10^{-4} s. In addition, it should be noted that the extraction of dipolar couplings by following the build-up of DQC in a ^1H DQ MAS experiment has been shown to provide insight into the complex dynamic processes in polymer melts,¹⁷² block copolymers,¹⁷³ and elastomers.¹⁷⁴

A. A Molecular Tweezer Host–Guest Complex

Figure 27 presents slices at a DQ frequency of 7.6 ppm taken from ^1H DQ MAS spectra of **4@5** (discussed in section VII C) recorded at different temperatures.²⁹ It is to be noted that the heating due to friction at a very-fast ν_R is significant, and in the examples presented in this section, the correction term relative to the bearing gas temperature was calibrated using the ^{119}Sn resonance of $\text{Sm}_2\text{Sn}_2\text{O}_7$ as a chemical shift thermometer.¹⁷⁵ The peaks due to the guest protons, H^a (5.6 ppm) and H^b (2.0 ppm), disappear upon heating, indicating dynamic processes, (see Figure 27) where the two types of guest protons are exchanged by either (A) a 180° flip about the long axis of the guest, or (B) a rotation between two equivalent sites in the complex. A quantitative analysis is hampered by the peak at 3.9 ppm due to

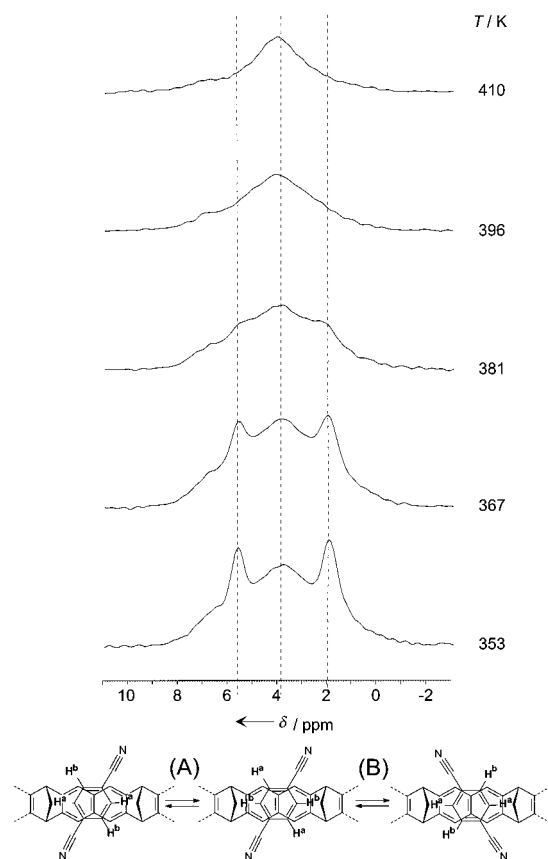


Figure 27. The effect of temperature, T , on slices at a DQ frequency of 7.6 ppm taken from ^1H (700.1 MHz) DQ MAS NMR spectra of **4@5**. At the bottom, the dynamic processes consistent with the observed NMR results are shown. The two processes, (A) and (B), cannot be distinguished by current NMR experiments. (Reproduced with permission from ref 29. Copyright 2001 Wiley.)

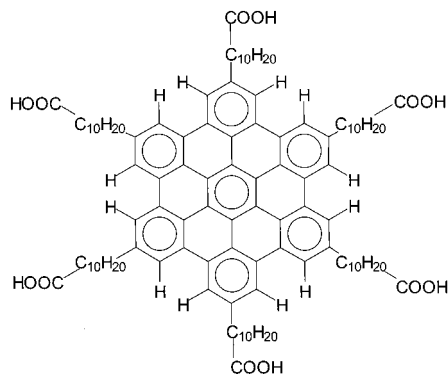
host alkyl protons—the fast exchange peak would be expected to appear at exactly this position. It was noted, though, that no peak was observed in a slice corresponding to the guest ^{13}C CH resonance in a ^1H - ^{13}C correlation spectrum recorded at 410 K (spectrum not shown). Thus, it can be concluded that, at this temperature, the exchange process is in the intermediate regime, i.e., coalescence. From the difference in the chemical shifts of the guest protons H^a and H^b ($\Delta\delta = 3.8$ ppm), the rate constant for the exchange process at 410 K can be estimated to be 5600 s^{-1} , corresponding to a Gibbs free enthalpy of activation, ΔG^\ddagger , of 72 kJ mol^{-1} .¹⁷⁶

B. The Making and Breaking of Hydrogen Bonds in a HBC Derivative

The established importance of hydrogen bonds in biological systems as well as the recognized potential for their incorporation into synthetic systems lies in the relative ease with which they can be broken and then reformed. It is thus essential that methods exist by which hydrogen bond dynamics can be investigated. Using ^2H solid-state NMR, hydrogen exchange by proton tunneling between the two tautomeric forms of a carboxylic acid dimer has been probed,¹⁷⁷ while intramolecular hydrogen-bond exchange dynamics have been extensively investigated by Limbach and co-workers using ^{15}N solid-state NMR, e.g.,

in *N,N*-bisarylformamidines¹⁷⁸ or a phenylenediamine.¹⁷⁹ In this subsection, we will show that the resolution routinely achievable in ¹H solid-state NMR methods allows the making and breaking of hydrogen bonds to be directly probed.

Consider the hexabenzocoronene (HBC) derivative, 2, 5, 8, 11, 14, 17-hexa[10-carboxydecyl]hexa-*peri*-hexabenzocoronene, **6**, (henceforth referred to as



6

HBC-C₁₀COOH), where all six alkyl chains have been capped by a carboxylic acid group.²⁵ In the solid phase at $T = 320$ K, the presence of hydrogen-bonded COOH dimers is demonstrated by the observation of an auto COOH peak in the ¹H DQ MAS NMR two-dimensional spectrum; see Figure 28. Considering the COOH peak in the one-dimensional ¹H MAS spectra, as shown in Figure 29a, both a shift to high field of the peak position as well as an initial increase followed by a subsequent decrease in the line width are observed upon heating. These effects are represented graphically in Figure 30a,b. These observations are interpreted in terms of a chemical exchange process involving the making and breaking of hydrogen bonds, with the coalescence point corresponding to $T = 362$ K.

The equilibrium constant at a given temperature can be calculated from the observed chemical shift

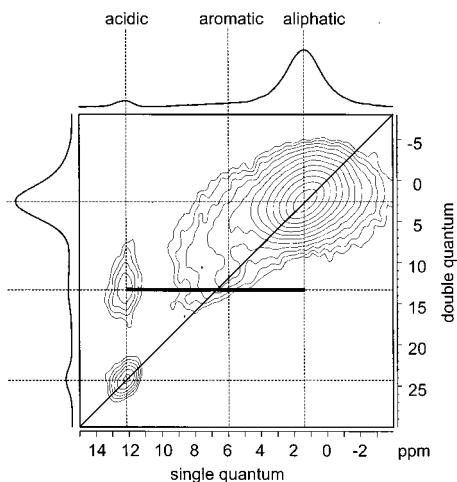


Figure 28. Rotor-synchronized ¹H (500.1 MHz) DQ MAS ($\nu_R = 30$ kHz) NMR spectrum, together with skyline SQ and DQ projections, of the room-temperature phase of as-synthesized HBC-C₁₀COOH, **6**. (Reproduced with permission from ref 25. Copyright 2000 The PCCP Owner Societies.)

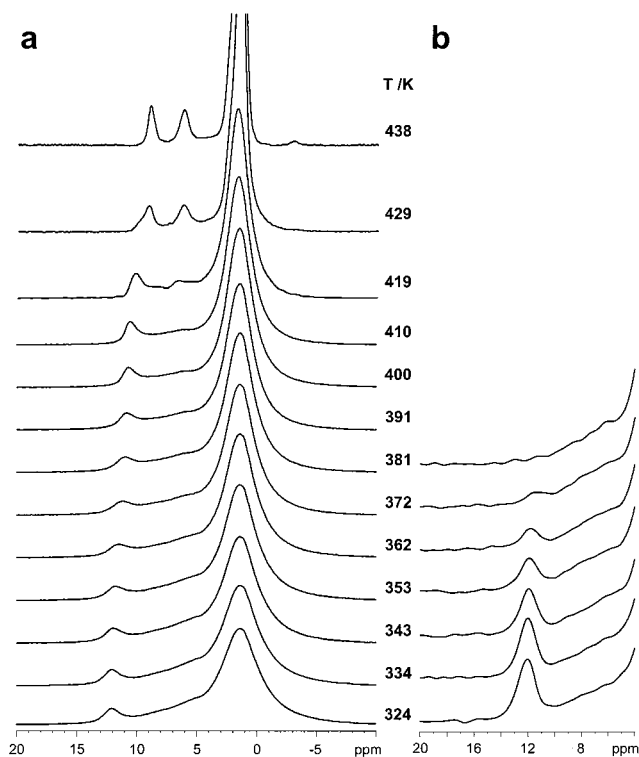


Figure 29. The effect of temperature on (a) ¹H (500.1 MHz) MAS ($\nu_R = 30$ kHz) and (b) ¹H DQF MAS NMR spectra of as-synthesized HBC-C₁₀COOH, **6**. (Reproduced with permission from ref 25. Copyright 2000 The PCCP Owner Societies.)

provided that the ¹H chemical shifts of the hydrogen-bonded and free states are known. Only the COOH protons in hydrogen-bonded dimers can give rise to a COOH auto peak in the ¹H DQ MAS spectrum (Figure 28), and thus the chemical shift of the hydrogen-bonded protons can be determined to be 12.1 ppm. The chemical shift of the free COOH protons cannot be so easily identified; however, the initially observed chemical shift of 9.0 ppm for the COOH protons on heating into the LC phase is strikingly low, and it is thus assumed that the chemical shift of the free state can be assigned to this value. A thermodynamic analysis yields for the opening of the hydrogen-bonded dimers: $\Delta H = 45 \pm 4$ kJ mol⁻¹ and $\Delta S = 113 \pm 11$ J K⁻¹ mol⁻¹.

In ¹H DQ-filtered (DQF) MAS spectra of HBC-C₁₀COOH (see Figure 29b), the intensity of the COOH peak is observed, upon heating, to reduce faster than expected from thermodynamic factors alone, and above $T = 380$ K, no signal is detected, see Figure 30c, where the experimentally observed DQ signal intensities for the COOH protons, relative to the intensity of the $T = 324$ K spectrum, are shown as crosses, while circles represent the expected reduction, again relative to the $T = 324$ K case, due solely to the combined temperature dependence of the equilibrium constant and the bulk magnetization. At $T = 381$ K, where the COOH peak intensity disappears below the noise level in Figure 29b, the number of hydrogen-bonded and free COOH protons are known, on the basis of the thermodynamic analysis described above, to be in the ratio $\sim 3:2$; thus, the loss of signal cannot be due to the absence of pairs of COOH protons in close proximity.

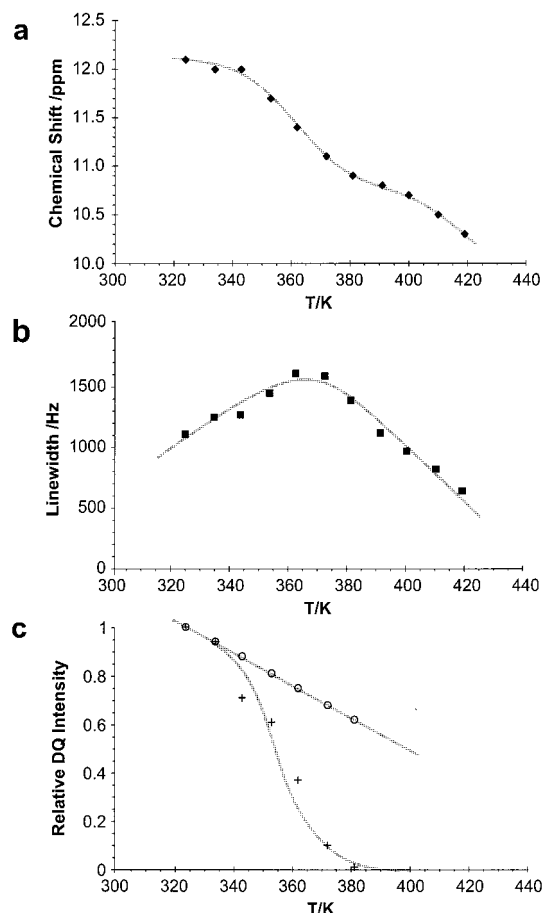


Figure 30. The effect of temperature on (a) the observed chemical shift and (b) the line width (fwhmh) in ^1H MAS spectra (Figure 28a), and (c) the intensity in ^1H DQF MAS spectra (Figure 28b) of the COOH resonance for a sample of as-synthesized HBC- C_{10}COOH , **6**. In (c), in addition to the crosses, which represent the experimental DQF intensities, the intensities that are expected on account of solely the combined temperature dependence of the equilibrium constant and the NMR bulk magnetization are shown as circles. Both the experimental and thermodynamically expected intensities are normalized relative to the $T = 324$ K case. In all plots, best-fit lines are included as a guide for the eye. (Reproduced with permission from ref 25. Copyright 2000 The PCCP Owner Societies.)

To observe a signal in a DQF experiment, the hydrogen-bonded form must exist for the duration of the DQ filter part of the NMR experiment, i.e., $133 \mu\text{s}$ for the spectra in Figure 29b. It is then apparent that the fall off in the DQ intensity with increasing temperature can be explained by a decrease in the proportion of hydrogen-bonded dimers having lifetimes over $133 \mu\text{s}$, until at $T = 381$ K, the concentration is less than that required to observe an NMR signal. In this way, an analysis of the DQF data yields the temperature dependence of the dimer lifetimes, and hence the kinetics of the exchange process could be determined: the activation energy and Arrhenius parameter equal $89 \pm 10 \text{ kJ mol}^{-1}$ and $4.2 \times 10^{16} \text{ s}^{-1}$, respectively.

C. The Order Parameter in Columnar Discotic Mesophases

The HBC derivatives introduced in the previous sections represent a relatively new family of discotic

aromatic mesogen, which have a number of favorable properties as compared to the more established triphenylenes; for example, the mesophases are stable over a very wide temperature range¹⁸⁰ and exhibit an exceptionally high one-dimensional charge carrier mobility.¹⁸¹ In this section, we will show that the recording of homo- and heteronuclear MQ spinning-sideband patterns allows the order parameter of the LC phases to be quantitatively determined.

Figure 31 presents experimental ^1H DQ MAS spinning sideband patterns for the aromatic protons in (a) the crystalline and (b) the LC phases of α -deuterated HBC- C_{12} .²² The MAS frequency was 35 and 10 kHz in (a) and (b), respectively, with two rotor periods being used for excitation/reconversion in both cases, such that τ_{rcpl} equals 57 and $200 \mu\text{s}$ in the two cases. The dotted lines represent best fit spectra simulated using the analytical time-domain expression for an isolated spin pair in eq 6. As noted in section VIIB, the aromatic protons exist as well isolated pairs of bay protons, and, thus, an analysis based on the spin-pair approximation is appropriate here. As is evident from the insets on the right of Figure 31, the DQ MAS spinning sideband patterns are very sensitive to the product of the D and τ_{rcpl} . The best-fit spectra for the solid and LC phases then correspond to $D/(2\pi)$ s equal to 15.0 ± 0.9 and $6.0 \pm 0.5 \text{ kHz}$, respectively.

Comparing the evaluated D values for the crystalline and LC phases, a reduction of D by a factor of 0.40 ± 0.04 is observed, corresponding to an order parameter¹⁸² of 0.80 ± 0.08 . In the LC phase, fast axial rotation of the molecule about an axis perpendicular to the ring (passing through the center of symmetry) is expected.¹⁸² For a molecule undergoing such a motion, the dipolar coupling constant is reduced by a factor of $1/2(1 - 3\cos^2\theta)$, where θ is the angle between the principal axes system (here the internuclear vector) and the molecular rotation axis.¹⁸³ (Note that this dynamic averaging term is not included in the earlier definition of D in eq 1.) Thus, for the case where the internuclear vector is perpendicular to the rotation axis ($\theta = 90^\circ$), a reduction by a factor of 0.5 is expected. The value of 0.40 can be explained by postulating the presence of out-of-plane motion in addition to the axial rotation. The ability to probe such motion is of much importance, since it is likely to impair efficient charge carrier mobility.

As a complementary alternative to using the change in a H-H dipolar coupling to probe a dynamic process, methods that determine heteronuclear ^1H - ^{13}C dipolar couplings offer much promise. Figure 32 presents, on the left-hand side, ^1H - ^{13}C spinning-sideband patterns obtained at the aromatic C-H ^{13}C resonance for the solid and LC phases of HBC- C_{12} , using the REPT-HMQC experiment discussed in section IVB.³⁷ In addition, the dotted lines represent simulated spectra, obtained using the best-fit D for the CH groups, namely, 20.9 ± 0.5 and $8.2 \pm 0.9 \text{ kHz}$ for the solid and LC phases, respectively. The order parameter is hence determined to be 0.78 ± 0.09 . This value, thus, agrees with that determined from the analysis of ^1H DQ MAS spinning-sideband patterns discussed above. In addition, these values are

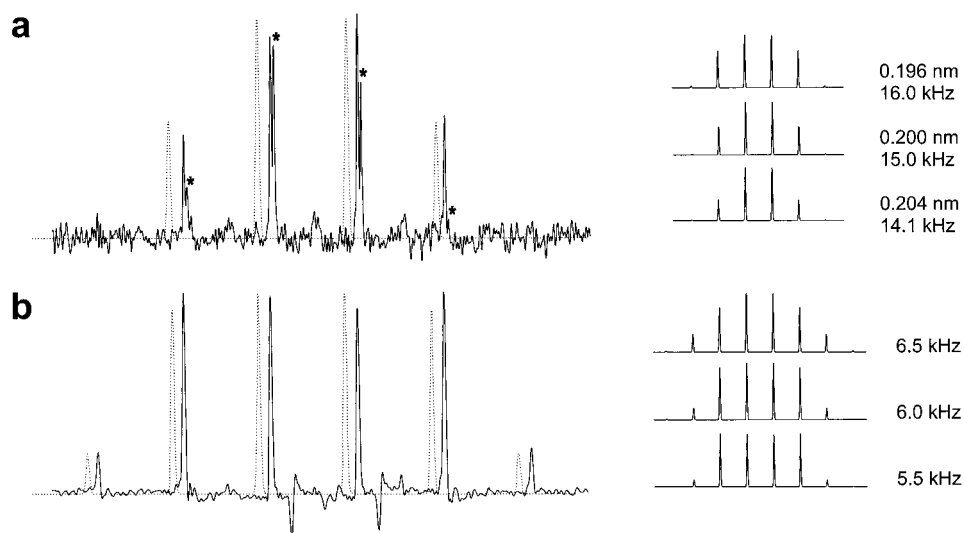


Figure 31. Extracted columns from ^1H (500.1 MHz) DQ MAS spectra of HBC- C_{12} , **3**, showing the DQ spinning sideband patterns for (a) the aromatic protons at 8.3 ppm in the solid phase ($T = 333$ K), and (b) the aromatic protons at 6.2 ppm in the LC phase ($T = 386$ K). In each case, best-fit spectra, generated according to the spin-pair expression in eq 6, are shown (shifted to the left to allow a better comparison) as dotted lines. A spinning frequency, ν_R , equal to 35 and 10 kHz was used for the solid and LC phases, respectively, with the two rotor-period compensated BABA recoupling sequence being used for the excitation and reconversion of DQCs in both cases. In (a), additional peaks corresponding to DQCs between aromatic and residual undeuterated α -carbon protons are marked by *. The insets to the right of the experimental spectra show the sensitivity of the spinning-sideband patterns to the product $D\tau_{\text{rcpl}}$. (Reproduced with permission from ref 22. Copyright 1999 American Chemical Society.)

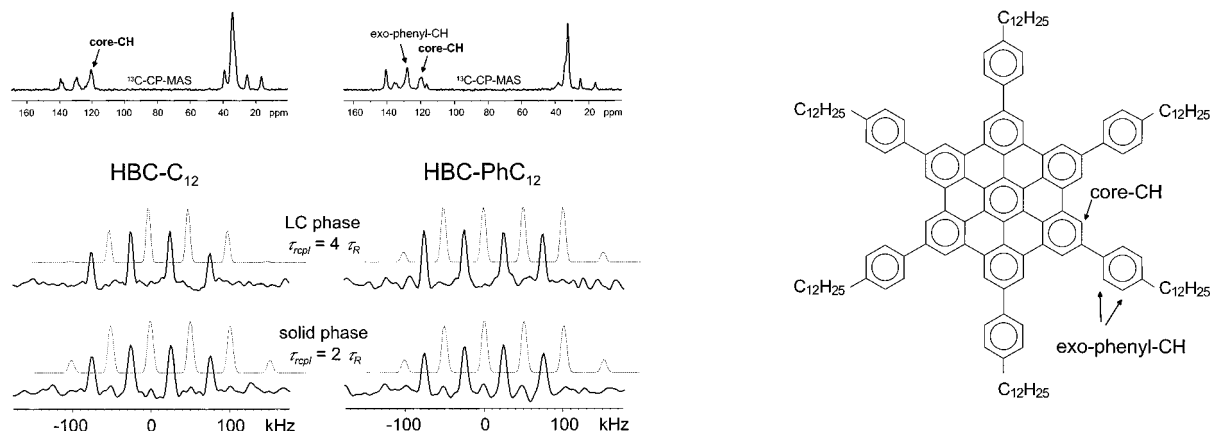


Figure 32. ^1H - ^{13}C heteronuclear MQ MAS spinning-sideband patterns, obtained at a $\nu_R = 25$ kHz, using the REPT-HMQC experiment. The patterns correspond to the sum projections over the ^{13}C resonance due to the aromatic core CH in the 2D spectra of HBC- C_{12} , **3**, and HBC- PhC_{12} , **7**. The spectra for the room temperature (solid) and high-temperature LC phases were recorded at 35 and 120 $^\circ\text{C}$, respectively. The dotted traces represent simulated spectra, obtained by taking into account the best-fit D s for the CH groups. At the top, ^{13}C CP-MAS ($\nu_R = 15$ kHz) spectra are presented, with the signal positions of the aromatic CH resonances being identified. (Reproduced with permission from ref 37. Copyright 1999 Wiley.)

in agreement with a value of 0.84 obtained from an analysis of ^2H 1D NMR line shapes.¹⁸⁰

An advantage of the heteronuclear ^1H - ^{13}C approach is that it benefits from the better resolution in a ^{13}C SQ dimension. An example of this is provided by the hexa(*para-n*-dodecylphenyl)-substituted HBC (henceforth referred to as HBC- PhC_{12}), **7**.³⁷ In this case, ^1H solid-state NMR is unable to distinguish the core and exo-phenyl protons. By comparison, as shown in the ^{13}C CP MAS spectrum at the top right of Figure

32, the corresponding ^{13}C resonances are well resolved. It is thus possible to use the heteronuclear approach to probe separately the dynamics of the core and the outer phenyl rings. For example, the right-hand-side of Figure 32 presents ^1H - ^{13}C spinning-sideband patterns obtained at the core aromatic CH ^{13}C resonance for the solid and LC phases of HBC- PhC_{12} , using the REPT-HMQC experiment.

A comparison of the spinning-sideband patterns obtained for the LC phases of HBC- C_{12} and HBC- PhC_{12} reveals that the third-order spinning sidebands are significantly higher in the latter case; they are of the same height as the first-order spinning sidebands for HBC- PhC_{12} . Since the same experimental conditions were used in both cases, this result immediately indicates a larger dipolar coupling and, hence, a larger order parameter for HBC- PhC_{12} . Indeed, the order parameter is determined to be 0.93 ± 0.09 , indicating less out-of-plane mesogen mobility. It is interesting that this NMR result is correlated with an improved intra- and intercolumnar packing as evidenced by powder X-ray diffraction patterns.³⁷

Finally, we note that an analysis of ^1H - ^{13}C spinning-sideband patterns obtained using the REPT-HDOR experiment (see Figure 16) has also been used to provide evidence of restricted dynamics in a shape-persistent polyphenylene dendrimer.¹⁸⁴

IX. Conclusions

In this review, we have demonstrated that the advanced solid-state NMR methods existing today are well placed to provide answers to the structural and dynamic questions of relevance in modern polymer chemistry. In particular, the further development of high-resolution ^1H solid-state NMR methods has opened up the possibility of routinely directly probing hydrogen-bonding and aromatic π - π interactions. It is to be emphasized that only 10–20 mg of a powdered as-synthesized sample is required, i.e., there is no need for synthetically demanding selective isotopic labeling or a single crystal. Moreover, the potential applications of solid-state NMR are not restricted to the many examples given in the previous sections: in our laboratory, for example, preliminary results have been obtained that provide insight into proton conduction in imidazole-based materials as well as the local order and dynamics in the cylindrical macromolecules synthesized by Percec and co-workers, which were mentioned in the introduction.

Solid-state NMR spectroscopy should certainly not be used in isolation. For example, when a new sample is to be investigated, we insist, in our laboratory, on receiving assigned ^1H and ^{13}C solution-state NMR spectra (except, of course, for cases where the sample is insoluble). An example of the importance of this is provided by the ^1H - ^{13}C correlation spectrum of the host-guest complex in Figure 25b, where the assignment of the guest resonances is based on the known solution-state ^{13}C chemical shifts and the comparative insensitivity of ^{13}C chemical shifts to through-space aromatic ring currents.

In addition, if dynamic processes are to be investigated, it is very useful if differential scanning calorimetry (DSC) curves can be first obtained, so that the temperatures at which phase transitions occur are known in advance. Moreover, when carrying out variable temperature studies of organic solid, it is important to be aware of the fact that the observed behavior, in terms of, e.g., phase transition temperatures and NMR spectra, can differ significantly depending on whether the solid phase formed from solution or from a LC phase or melt. It is, therefore, necessary to see both the first and subsequent DSC heating curves; a clear example of this phenomenon is described in ref 25. Furthermore, we note that, in our experience, different batches of a material, synthesized by the same procedure, can give slightly different solid state ^1H NMR spectra, even though the purity of the material as determined by standard methods, e.g., solution-state NMR, is judged to be the same. This is particularly the case for hydrogen-bonded systems, and thus it seems that solid-state NMR is able to distinguish subtly different packing arrangements, suggesting potential quality-control applications.

As stated in section V, solid-state NMR should not be considered as a replacement for the established diffraction methods. Instead, the two methods should be thought of as being complementary, since they have much to offer each other. For example, as discussed in section VIIB, the existence of a single-crystal X-ray structure for unsubstituted HBC allowed a qualitative interpretation of the observed ^1H DQ MAS spectrum of HBC- C_{12} , where it was not possible to obtain a single-crystal suitable for an X-ray analysis. The symbiosis between ^1H solid-state NMR and X-ray single-crystal methods was further well illustrated by the case of bilirubin in section VIB, where an X-ray single-crystal structure exists. On one hand, the reliable establishing of the heteroatom positions facilitated the assignment of the observed peaks in the ^1H DQ MAS spectrum. On the other hand, it was shown that an analysis of ^1H DQ MAS spinning-sideband patterns allowed the determination of the distance between two hydrogen-bonded protons to a precision of ± 0.002 nm; since structure determination by single-crystal X-ray diffraction methods, being based on the diffraction of X-rays by electrons, is not well suited to the localization of lighter atoms, the ability of solid-state NMR to provide distance constraints, which can be used in the optimization of a crystal structure, in particular, the very relevant hydrogen-bonded part, is of much importance.

In section VII, the value of a combined experimental and theoretical approach, incorporating the *ab initio* calculation of ^1H chemical shifts, was illustrated. First, in section VIIB, it was stated that the calculation of ^1H chemical shifts for model HBC oligomers allowed the quantitative assignment of the experimental observation of three aromatic resonances in HBC- C_{12} to a specific packing arrangement. Moreover, in section VIIC, the ability to identify the importance of intra- and intercomplex interactions as well as the role of the separate aromatic moieties was discussed. The advances in computing power as well as the development of methodology means that the use of quantum chemical calculations of NMR parameters in the interpretation of experimental results will become ever more popular.

It should not be forgotten that the development of advanced solid-state NMR methodology is an area of ongoing active research. For example, as evidenced by section II, various groups are pursuing the goal of reducing the ^1H solid-state NMR line width ever further. Moreover, the utility of the ^1H DQ MAS method would be much enhanced if homonuclear decoupling methods, which, as illustrated by Figure 5, yield a striking improvement in the ^1H line width as compared to very-fast MAS, could be incorporated in a robust and artifact-free manner. It is to be hoped that the problems of significant spectral artifacts encountered in an earlier attempt to combine ^1H DQ MAS spectroscopy with the multiple-pulse assisted MAS approach²⁰ can be overcome. To conclude, it is envisaged that solid-state NMR can become as highly valuable to the chemist as solution-state NMR is today.

X. Acknowledgment

We thank Prof. Lyndon Emsley, Dr. Robert Graf, Dr. Kay Saalwächter, and Dr. Ingo Schnell for helpful comments on the manuscript. We are also very grateful to Prof. Huub de Groot and Prof. Lyndon Emsley for providing preprints of unpublished articles.

XI. References

- Prins, L. J.; Reinhoudt, D. N.; Timmerman, P. *Angew. Chem., Int. Ed. Engl.* **2001**, *40*, 2382.
- Sijbesma, R. P.; Beijer, F. H.; Brunsveld, L.; Folmer, B. J. B.; Hirschberg, J. H. K. K.; Lange, R. F. M.; Lowe, J. K. L.; Meijer, E. W. *Science* **1997**, *278*, 1601.
- Hudson, S. D.; Jung, H.-T.; Percec, V.; Cho, W.-D.; Johansson, G.; Ungar, G.; Balagurusamy, V. S. K. *Science* **1997**, *278*, 449.
- Percec, V.; Cho, W.-D.; Ungar, G. *J. Am. Chem. Soc.* **2000**, *122*, 10273.
- Ernst, R. R.; Bodenhausen, G.; Wokaun, A. *Principles of Nuclear Magnetic Resonance in One and Two Dimensions*; Clarendon: Oxford, 1987.
- Claridge, T. D. W. *High-Resolution NMR Techniques in Organic Chemistry*; Pergamon: Amsterdam, 1999.
- Sattler, M.; Schleucher, J.; Griesinger, C. *Prog. NMR Spectrosc.* **1999**, *34*, 93.
- Mehring, M. *Principles of High-Resolution NMR in Solids*; Springer: Berlin, 1983.
- Schmidt-Rohr, K.; Spiess, H. W. *Multidimensional Solid State NMR and Polymers*; Academic Press: New York, 1994.
- Emsley, L.; Laws, D. D.; Pines, A. *Lectures on Pulsed NMR (3rd ed.) In The Proceedings of the International School of Physics "Enrico Fermi"*, Course CXXXIX; Maraviglia, B., Ed.; IOS Press: Amsterdam, 1999; p 45.
- Bennett, A. E.; Griffin, R. G.; Vega, S. In *NMR Basic Principles and Progress*; Springer-Verlag: Berlin, 1994; Vol. 33, p 1.
- Dusold, S.; Sebald, A. *Ann. Rep. NMR Spectrosc.* **2000**, *41*, 185.
- Gullion, T.; Schaefer, J. *J. Magn. Reson.* **1989**, *81*, 196.
- Gullion, T.; Schaefer, J. *Adv. Magn. Reson.* **1989**, *13*, 57.
- Gullion, T. *Concepts Magn. Reson.* **1998**, *10*, 277.
- Feng, X.; Lee, Y. K.; Sandström, D.; Edén, M.; Maisel, H.; Sebald, A.; Levitt, M. H. *Chem. Phys. Lett.* **1996**, *257*, 314.
- Hong, M.; Gross, J. D.; Griffin, R. G. *J. Phys. Chem. B* **1997**, *101*, 5869.
- Jakobsen, H. J. *Encyclopedia of Nuclear Magnetic Resonance*; Grant, D. M., Harris, R. K., Eds.; Wiley: Chichester, 1996; Vol. 1, p 398.
- Samoson, A.; Tuhem, T. *The Alpine Conference on Solid-State NMR*; Chamonix, France, 1999.
- Schnell, I.; Lupulescu, A.; Hafner, S.; Demco, D. E.; Spiess, H. W. *J. Magn. Reson.* **1998**, *133*, 61.
- Schnell, I.; Brown, S. P.; Low, H. Y.; Ishida, H.; Spiess, H. W. *J. Am. Chem. Soc.* **1998**, *120*, 11784.
- Brown, S. P.; Schnell, I.; Brand, J. D.; Müllen, K.; Spiess, H. W. *J. Am. Chem. Soc.* **1999**, *121*, 6712.
- Gil, A. M.; Lopes, M. H.; Neto, C. P.; Rocha, J. *Solid State Nucl. Magn. Reson.* **1999**, *15*, 59.
- Brown, S. P.; Schnell, I.; Brand, J. D.; Müllen, K.; Spiess, H. W. *J. Mol. Struct.* **2000**, *521*, 179.
- Brown, S. P.; Schnell, I.; Brand, J. D.; Müllen, K.; Spiess, H. W. *Phys. Chem. Chem. Phys.* **2000**, *2*, 1735.
- Rodriguez, L. N. J.; De Paul, S. M.; Barrett, C. J.; Reven, L.; Spiess, H. W. *Adv. Mater.* **2000**, *12*, 1934.
- Ishii, Y.; Tycko, R. *J. Magn. Reson.* **2000**, *142*, 199.
- Yamauchi, K.; Kuroki, S.; Fujii, K.; Ando, I. *Chem. Phys. Lett.* **2000**, *324*, 435.
- Brown, S. P.; Schaller, T.; Seelbach, U. P.; Koziol, F.; Ochsenfeld, C.; Klärner, F.-G.; Spiess, H. W. *Angew. Chem., Int. Ed. Engl.* **2001**, *40*, 717.
- Brown, S. P.; Zhu, X. X.; Saalwächter, K.; Spiess, H. W. *J. Am. Chem. Soc.* **2001**, *123*, 4275.
- Van Rossum, B.-J.; Förster, H.; De Groot, H. J. M. *J. Magn. Reson.* **1997**, *124*, 516.
- Lesage, A.; Sakellariou, D.; Steuernagel, S.; Emsley, L. *J. Am. Chem. Soc.* **1998**, *120*, 13194.
- Saalwächter, K.; Graf, R.; Spiess, H. W. *J. Magn. Reson.* **1999**, *140*, 471.
- Geen, H.; Titman, J. J.; Gottwald, J.; Spiess, H. W. *Chem. Phys. Lett.* **1994**, *227*, 79.
- Geen, H.; Titman, J. J.; Gottwald, J.; Spiess, H. W. *J. Magn. Reson.* **1995**, *A 114*, 264.
- Gottwald, J.; Demco, D. E.; Graf, R.; Spiess, H. W. *Chem. Phys. Lett.* **1995**, *243*, 314.
- Fechtenkötter, A.; Saalwächter, K.; Harbison, M. A.; Müllen, K.; Spiess, H. W. *Angew. Chem., Int. Ed. Engl.* **1999**, *38*, 3039.
- Hohwy, M.; Jaroniec, C. P.; Reif, B.; Rienstra, C. M.; Griffin, R. G. *J. Am. Chem. Soc.* **2000**, *122*, 3218.
- McElheny, D.; DeVita, E.; Frydman, L. *J. Magn. Reson.* **2000**, *143*, 321.
- van Rossum, B.-J.; de Groot, C. P.; Ladizhansky, V.; Vega, S.; de Groot, H. J. M. *J. Am. Chem. Soc.* **2000**, *122*, 3465.
- Frydman, L.; Harwood, J. S. *J. Am. Chem. Soc.* **1995**, *117*, 5367.
- Gérardy-Montouillout, V.; Malveau, C.; Tekeley, P.; Olender, Z.; Luz, Z. *J. Magn. Reson. A* **1996**, *123*, 7.
- Reichert, D.; Zimmermann, H.; Tekeley, P.; Poupko, R.; Luz, Z. *J. Magn. Reson.* **1997**, *125*, 245.
- deAzevedo, E. R.; Hu, W.-G.; Bonagamba, T. J.; Schmidt-Rohr, K. *J. Am. Chem. Soc.* **1999**, *121*, 8411.
- deAzevedo, E. R.; Hu, W.-G.; Bonagamba, T. J.; Schmidt-Rohr, K. *J. Chem. Phys.* **2000**, *112*, 8988.
- Harris, R. K. *Encyclopedia of Nuclear Magnetic Resonance*; Grant, D. M., Harris, R. K., Eds.; Wiley: Chichester, 1996; Vol. 5, p 3301.
- Baum, J.; Munowitz, M.; Garroway, A. N.; Pines, A. *J. Chem. Phys.* **1985**, *83*, 2105.
- Baum, J.; Pines, A. *J. Am. Chem. Soc.* **1986**, *108*, 7447.
- Andrew, E. R.; Bradbury, A.; Eades, R. G. *Nature* **1958**, *182*, 1659.
- Lowe, I. *Phys. Rev. Lett.* **1959**, *2*, 285.
- Hartmann, S. R.; Hahn, E. L. *Phys. Rev.* **1962**, *128*, 2042.
- Pines, A.; Gibby, M. G.; Waugh, J. S. *J. Chem. Phys.* **1972**, *56*, 1776.
- Schaefer, J.; Stejskal, E. O. *J. Am. Chem. Soc.* **1976**, *98*, 1031.
- Maricq, M. M.; Waugh, J. S. *J. Chem. Phys.* **1979**, *70*, 3300.
- Herzfeld, J.; Berger, A. E. *J. Chem. Phys.* **1980**, *73*, 6021.
- Filip, C.; Hafner, S.; Schnell, I.; Demco, D. E.; Spiess, H. W. *J. Chem. Phys.* **1999**, *110*, 423.
- Scheler, U. *Solid State Nucl. Magn. Reson.* **1998**, *12*, 9.
- Waugh, J. S.; Huber, L. M.; Haeberlen, U. *Phys. Rev. Lett.* **1968**, *20*, 180.
- Haeberlen, U.; Waugh, J. S. *Phys. Rev.* **1968**, *175*, 453.
- Gerstein, B. C.; Pembleton, R. G.; Wilson, R. C.; Ryan, L. M. *J. Chem. Phys.* **1977**, *66*, 361.
- Scheler, G.; Haubenreisser, U.; Rosenberger, H. *J. Magn. Reson.* **1981**, *44*, 134.
- Maciel, G. E.; Bronnimann, C. E.; Hawkins, B. *Adv. Magn. Reson.* **1990**, *14*, 125.
- Dec, S. F.; Bronnimann, C. E.; Wind, R. A.; Maciel, G. E. *J. Magn. Reson.* **1989**, *82*, 454.
- Hohwy, M.; Rasmussen, J. T.; Bower, P. V.; Jakobsen, H. J.; Nielsen, N. C. *J. Magn. Reson.* **1998**, *133*, 374.
- Hafner, S.; Spiess, H. W. *J. Magn. Reson. A* **1996**, *121*, 160.
- Hafner, S.; Spiess, H. W. *Solid State Nucl. Magn. Reson.* **1997**, *8*, 17.
- Hafner, S.; Spiess, H. W. *Concepts in Magn. Reson.* **1998**, *10*, 99.
- Filip, C.; Hafner, S. *J. Magn. Reson.* **2000**, *147*, 250.
- Haeberlen, U. *Adv. Magn. Reson. Suppl. I*; Academic Press: San Diego, 1976.
- Lee, M.; Goldberg, W. I. *Phys. Rev. A* **1965**, *140*, 1261.
- Bielecki, A.; Kolbert, A. C.; Levitt, M. H. *Chem. Phys. Lett.* **1989**, *155*, 341.
- Bielecki, A.; Kolbert, A. C.; de Groot, H. J. M.; Griffin, R. G.; Levitt, M. H. *Adv. Magn. Reson.* **1990**, *14*, 111.
- Levitt, M. H.; Kolbert, A. C.; Bielecki, A.; Ruben, D. J. *Solid State Nucl. Magn. Reson.* **1993**, *2*, 151.
- Lesage, A.; Steuernagel, S.; Emsley, L. *J. Am. Chem. Soc.* **1998**, *120*, 7095.
- Charmont, P.; Lesage, A.; Steuernagel, S.; Engelke, F.; Emsley, L. *J. Magn. Reson.* **2000**, *145*, 334.
- Vinogradov, E.; Madhu, P. K.; Vega, S. *Chem. Phys. Lett.* **1999**, *314*, 443.
- Vinogradov, E.; Madhu, P. K.; Vega, S. *Chem. Phys. Lett.* **2000**, *329*, 207.
- Lesage, A.; Duma, L.; Sakellariou, D.; Emsley, L. *J. Am. Chem. Soc.* **2001**, *123*, 5747.
- Bodenhausen, G.; Kogler, H.; Ernst, R. R. *J. Magn. Reson.* **1984**, *58*, 370.
- Hore, P. J.; Jones, J. A.; Wimperis, S. *NMR: The Toolkit*; Oxford University Press: Oxford, 2000.
- Sørensen, O. W.; Rance, M.; Ernst, R. R. *J. Magn. Reson.* **1984**, *56*, 527.
- Sakellariou, D.; Lesage, A.; Hodgkinson, P.; Emsley, L. *Chem. Phys. Lett.* **2000**, *319*, 253.
- Schnell, I.; Spiess, H. W. *J. Magn. Reson.* **2001**, *151*, 153.
- Bodenhausen, G. *Prog. NMR Spectrosc.* **1981**, *14*, 137.
- Weitekamp, D. P. *Adv. Magn. Reson.* **1983**, *11*, 111.
- Norwood, T. J. *Prog. NMR Spectrosc.* **1992**, *24*, 295.
- Marion, D.; Wüthrich, K. *Biochem. Biophys. Res. Commun.* **1983**, *113*, 967.
- Marion, D.; Ikura, M.; Tschudin, R.; Bax, A. *J. Magn. Reson.* **1989**, *85*, 393.

- (89) Meier, B. H.; Earl, W. L. *J. Chem. Phys.* **1986**, *85*, 4905.
- (90) Meier, B. H.; Earl, W. L. *J. Am. Chem. Soc.* **1987**, *109*, 7937.
- (91) Sommer, W.; Gottwald, J.; Demco, D. E.; Spiess, H. W. *J. Magn. Reson.* **1995**, *A 113*, 131.
- (92) Lee, Y. K.; Kurur, N. D.; Helmle, M.; Johannessen, O. G.; Nielsen, N. C.; Levitt, M. H. *Chem. Phys. Lett.* **1995**, *242*, 304.
- (93) Tycko, R.; Dabbagh, G. *J. Am. Chem. Soc.* **1991**, *113*, 9444.
- (94) Gregory, D. M.; Wolfe, G.; Jarvie, T.; Shiels, J. C.; Drobny, G. P. *Mol. Phys.* **1996**, *89*, 1835.
- (95) Nielsen, N. C.; Bildsøe, H.; Jakobsen, H. J.; Levitt, M. H. *J. Chem. Phys.* **1994**, *101*, 1805.
- (96) Brinkmann, A.; Edén, M.; Levitt, M. H. *J. Chem. Phys.* **2000**, *112*, 8539.
- (97) Carravetta, M.; Edén, M.; Zhao, X.; Brinkmann, A.; Levitt, M. H. *Chem. Phys. Lett.* **2000**, *321*, 205.
- (98) Feike, M.; Demco, D. E.; Graf, R.; Gottwald, J.; Hafner, S.; Spiess, H. W. *J. Magn. Reson.* **1996**, *A 122*, 214.
- (99) Graf, R.; Demco, D. E.; Gottwald, J.; Hafner, S.; Spiess, H. W. *J. Chem. Phys.* **1997**, *106*, 885.
- (100) Caravetti, P.; Neuenschwander, P.; Ernst, R. R. *Macromolecules* **1985**, *18*, 119.
- (101) Feike, M.; Graf, R.; Schnell, I.; Jäger, C.; Spiess, H. W. *J. Am. Chem. Soc.* **1996**, *118*, 9631.
- (102) Dollase, W. A.; Feike, M.; Förster, H.; Schaller, T.; Schnell, I.; Sebald, A. *Steuernagel, S. J. Am. Chem. Soc.* **1997**, *119*, 3807.
- (103) Geen, H.; Gottwald, J.; Graf, R.; Schnell, I.; Spiess, H. W.; Titman, J. J. *J. Magn. Reson.* **1997**, *125*, 224.
- (104) Witter, R.; Hartmann, P.; Vogel, J.; Jäger, C. *Solid State Nucl. Magn. Reson.* **1998**, *13*, 189.
- (105) Schemdt auf der Günne, J.; Eckert, H. *Chem. Eur. J.* **1998**, *4*, 1762.
- (106) Nielsen, N. C.; Creuzet, F.; Griffin, R. G.; Levitt, M. H. *J. Chem. Phys.* **1992**, *96*, 5668.
- (107) Hong, M. *J. Magn. Reson.* **1999**, *136*, 86.
- (108) Bax, A.; Freeman, R.; Frenkiel, T. A. *J. Am. Chem. Soc.* **1981**, *103*, 2102.
- (109) Wüthrich, K. *NMR of Proteins and Nucleic Acids*; Wiley: New York, 1986.
- (110) Lesage, A.; Auger, C.; Caldarelli, S.; Emsley, L. *J. Am. Chem. Soc.* **1997**, *119*, 7867.
- (111) Lesage, A.; Bardet, M.; Emsley, L. *J. Am. Chem. Soc.* **1999**, *121*, 10987.
- (112) Schmidt-Rohr, K.; Hu, W.; Zumbulyadis, N. *Science* **1998**, *280*, 714.
- (113) Friedrich, U.; Schnell, I.; Brown, S. P.; Lupulescu, A.; Demco, D. E.; Spiess, H. W. *Mol. Phys.* **1998**, *95*, 1209.
- (114) Hodgkinson, P.; Emsley, L. *J. Magn. Reson.* **1999**, *139*, 46.
- (115) Tekeley, P.; Demco, D. E.; Canet, D.; Malveau, C. *Chem. Phys. Lett.* **1999**, *309*, 101.
- (116) De Paul, S. M.; Saalwächter, K.; Graf, R.; Spiess, H. W. *J. Magn. Reson.* **2000**, *146*, 140.
- (117) Gregory, D. M.; Metha, M. A.; Shiels, J. C.; Drobny, G. P. *J. Chem. Phys.* **1997**, *107*, 28.
- (118) Caravatti, P.; Bodenhausen, G.; Ernst, R. R. *Chem. Phys. Lett.* **1982**, *89*, 363.
- (119) Caravatti, P.; Braunschweiler, L.; Ernst, R. R. *Chem. Phys. Lett.* **1983**, *100*, 305.
- (120) Bronnimann, C. E.; Ridenour, C. F.; Kinney, D. R.; Maciel, G. E. *J. Magn. Reson.* **1992**, *97*, 522.
- (121) Gu, Z.; Ridenour, C. F.; Bronnimann, C. E.; Iwashita, T.; McDermott, A. *J. Am. Chem. Soc.* **1996**, *118*, 822.
- (122) Schmidt-Rohr, K.; Clauss, J.; Spiess, H. W. *Macromolecules* **1992**, *25*, 3273.
- (123) Mirau, P. A.; Heffner, S. A.; Schilling, M. *Solid State Nucl. Magn. Reson.* **2000**, *16*, 47.
- (124) Lesage, A.; Charmont, P.; Steuernagel, S.; Emsley, L. *J. Am. Chem. Soc.* **2000**, *122*, 9739.
- (125) Saalwächter, K.; Graf, R.; Spiess, H. W. *J. Magn. Reson.* **2001**, *148*, 398.
- (126) Metz, G.; Wu, X.; Smith, S. O. *J. Magn. Reson. A* **1994**, *110*, 219.
- (127) Bodenhausen, G.; Ruben, D. J. *Chem. Phys. Lett.* **1980**, *69*, 185.
- (128) Müller, L. *J. Am. Chem. Soc.* **1979**, *101*, 4481.
- (129) Bennett, A. E.; Rienstra, C. M.; Auger, M.; Lakshmi, K. V.; Griffin, R. G. *J. Chem. Phys.* **1995**, *103*, 6951.
- (130) Ernst, M.; Zimmermann, H.; Meier, B. H. *Chem. Phys. Lett.* **2000**, *317*, 581.
- (131) Lesage, A.; Emsley, L. *J. Magn. Reson.* **2001**, *148*, 449.
- (132) Spiess, H. W. *Chem. Rev.* **1991**, *91*, 1321.
- (133) Hester, R. K.; Ackerman, J. L.; Neff, B. L.; Waugh, J. S. *Phys. Rev. Lett.* **1976**, *36*, 1081.
- (134) Munowitz, M. G.; Griffin, R. G.; Bodenhausen, G.; Huang, T. H. *J. Am. Chem. Soc.* **1981**, *103*, 2529.
- (135) Munowitz, M. G.; Griffin, R. G. *J. Chem. Phys.* **1982**, *76*, 2848.
- (136) Roberts, J. E.; Harbison, G. S.; Munowitz, M. G.; Herzfeld, J.; Griffin, R. G. *J. Am. Chem. Soc.* **1987**, *109*, 4163.
- (137) Saalwächter, K.; Spiess, H. W. *J. Chem. Phys.* **2001**, *114*, 5707.
- (138) Jeffrey, G. A.; Saenger, W. *Hydrogen Bonding in Biological Structures*; Springer-Verlag: New York, 1991.
- (139) Gann, S. L.; Baltisberger, J. H.; Pines, A. *Chem. Phys. Lett.* **1994**, *210*, 405.
- (140) Alderman, D. W.; McGeorge, G.; Hu, J. Z.; Pugmire, R. J.; Grant, D. M. *Mol. Phys.* **1998**, *95*, 1113.
- (141) Gan, Z. *J. Am. Chem. Soc.* **1992**, *114*, 8307.
- (142) Harper, J. K.; Grant, D. M. *J. Am. Chem. Soc.* **2000**, *122*, 3708.
- (143) Berglund, B.; Vaughan, R. W. *J. Chem. Phys.* **1980**, *73*, 2037.
- (144) Jeffrey, G. A.; Yeon, Y. *Acta Crystallogr.* **1986**, *B42*, 410.
- (145) Harris, R. K.; Jackson, P.; Merwin, L. H.; Say, B. J.; Hagele, G. *J. Chem. Soc., Faraday Trans.* **1988**, *84*, 3649.
- (146) Ning, X.; Ishida, H. *J. Polym. Sci. Chem. Ed.* **1994**, *32*, 1121.
- (147) Ishida, H.; Allen, D. J. *J. Polym. Sci. Phys. Ed.* **1996**, *34*, 1019.
- (148) Shen, S. B.; Ishida, H. *Polym. Composites* **1996**, *17*, 710.
- (149) Ishida, H.; Low, H. Y. *Macromolecules* **1997**, *30*, 1099.
- (150) Wirasate, S.; Dhumrongvaraporn, S.; Allen, D. J.; Ishida, H. *J. Appl. Polym. Sci.* **1998**, *70*, 1299.
- (151) Dunkers, J.; Zarate, E. A.; Ishida, H. *J. Phys. Chem.* **1996**, *100*, 13514.
- (152) Schnell, I.; Langer, B.; Söntjens, S. H. M.; van Genderen, M. H. P.; Sijbesma, R. P.; Spiess, H. W. *J. Magn. Reson.* **2001**, *150*, 57.
- (153) Shantz, D. F.; Schmedt auf der Günne, J.; Koller, H.; Lobo, R. F. *J. Am. Chem. Soc.* **2000**, *122*, 6659.
- (154) McDonagh, A. F. *Bile Pigments: Bilatrienes and 5, 15-Biladienes*. In *The Porphyrins*; Dolphin, D., Ed.; Academic Press: New York, 1979; Vol. VI, Chapter 6.
- (155) Chowdhury, J. R.; Wolkoff, A. S.; Chowdhury, N. R.; Arias, I. M. In *The Metabolic and Molecular Bases of Inherited Diseases*; Scriver, C. R., Beaudet, A. L., Sly, W. S., Valle, D., Eds.; McGraw-Hill: New York, 1995; Vol. II, pp 2161–2208.
- (156) Bonnett, R.; Davies, J. E.; Hursthouse, M. B. *Nature* **1976**, *262*, 326.
- (157) Le Bas, G.; Allegret, A.; Mauguén, Y.; de Rango, C.; Bailly, M. *Acta Crystallogr.* **1980**, *B36*, 3007.
- (158) Henry, E. R.; Szabo, A. *J. Chem. Phys.* **1985**, *82*, 4753.
- (159) Lazzaretto, P. *Prog. NMR Spectrosc.* **2000**, *36*, 1.
- (160) Waugh, J. S.; Fessenden, R. W. *J. Am. Chem. Soc.* **1956**, *79*, 846.
- (161) van Rossum, B.-J.; Boender, G. J.; Mulder, F. M.; Raap, J.; Balaban, T. S.; Holzwarth, A.; Schaffner, K.; Prytulla, S.; Oshkinat, H.; de Groot, H. J. M. *Spectrochim. Acta* **1998**, *A54*, 1167.
- (162) van Rossum, B.-J.; Steensgaard, D. B.; Mulder, F. M.; Boender, G. J.; Schaffner, K.; Holzwarth, A. R.; de Groot, H. J. M. *Biochemistry* **2001**, *40*, 1587.
- (163) Watson, M. D.; Fechtenkötter, A.; Müllen, K. *Chem. Rev.* **2001**, *101*, 1267.
- (164) Goddard, R.; Haenel, M. W.; Herndon, W. C.; Krüger, C.; Zander, M. *J. Am. Chem. Soc.* **1995**, *117*, 30.
- (165) Gauss, J. *Ber. Bunsen-Ges. Phys. Chem.* **1995**, *99*, 1001.
- (166) de Dios, A. C. *Prog. NMR Spectrosc.* **1996**, *29*, 229.
- (167) Bühl, M. *Structural Applications of NMR Chemical Shift Computations* In *Encyclopedia of Computational Chemistry*; von Ragué Schleyer, P., Allinger, N. L., Clark, T., Gastgeiger, J., Kollman, P. A., Schaefer, H. F., III, Schreiner, P. R., Eds.; Wiley: Chichester, 1998; p 1835.
- (168) Ochsenfeld, C.; Brown, S. P.; Schnell, I.; Gauss, J.; Spiess, H. W. *J. Am. Chem. Soc.* **2001**, *123*, 2597.
- (169) Ochsenfeld, C. *Phys. Chem. Chem. Phys.* **2000**, *2*, 2153.
- (170) Klärner, F.-G.; Benkhoff, J.; Boese, R.; Burkert, U.; Kamieth, M.; Naatz, U. *Angew. Chem., Int. Ed. Engl.* **1996**, *35*, 1130.
- (171) Klärner, F.-G.; Burkert, U.; Kamieth, M.; Boese, R.; Benet-Buchholz, J. *Chem. Eur. J.* **1999**, *5*, 1700.
- (172) Graf, R.; Heuer, A.; Spiess, H. W. *Phys. Rev. Lett.* **1998**, *80*, 5738.
- (173) Dollase, T.; Graf, R.; Heuer, A.; Spiess, H. W. *Macromolecules* **2001**, *34*, 298.
- (174) Graf, R.; Demco, D. E.; Hafner, S.; Spiess, H. W. *Solid State Nucl. Magn. Reson.* **1998**, *12*, 139.
- (175) Langer, B.; Schnell, I.; Spiess, H. W.; Grimmer, A.-R. *J. Magn. Reson.* **1999**, *138*, 182.
- (176) Günther, H. *NMR-Spektroskopie*; Thieme Verlag: Stuttgart, 1992; p. 310 (eqs 9.11 and 9.12).
- (177) Stöckli, A.; Meier, B. H.; Kreis, R.; Meyer, R.; Ernst, R. R. *J. Chem. Phys.* **1990**, *93*, 1502.
- (178) Anulewicz, R.; Wawer, I.; Krygowski, T. M.; Männle, F.; Limbach, H.-H. *J. Am. Chem. Soc.* **1997**, *119*, 12223.
- (179) Takeda, S.; Inabe, T.; Benedict, C.; Langer, U.; Limbach, H.-H. *Ber. Bunsen-Ges. Phys. Chem.* **1998**, *102*, 1358.
- (180) Herwig, P.; Kayser, C. W.; Müllen, K.; Spiess, H. W. *Adv. Mater.* **1996**, *8*, 510.
- (181) van de Craats, A. M.; Warman, J. M.; Fechtenkötter, A.; Brand, J. D.; Harbison, M. A.; Müllen, K. *Adv. Mater.* **1999**, *11*, 1469.
- (182) Demus, D.; Goodby, J. W.; Gray, G. W.; Spiess, H. W.; Vill, V., Eds. *Handbook of Liquid Crystals*; Wiley-VCH: Weinheim, 1998.
- (183) Abragam, A. *The Principles of Nuclear Magnetism*; Clarendon: Oxford, 1961.
- (184) Wind, M.; Wiesler, U.-M.; Saalwächter, K.; Müllen, K.; Spiess, H. W. *Adv. Mater.* **2001**, *13*, 752.

Metal-Catalyzed Living Radical Polymerization

Masami Kamigaito, Tsuyoshi Ando, and Mitsuo Sawamoto*

Department of Polymer Chemistry, Graduate School of Engineering, Kyoto University, Kyoto 606-8501, Japan

Received July 14, 2001

Contents

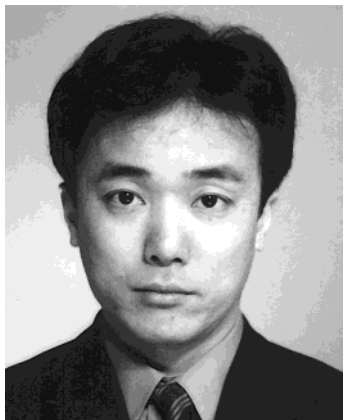
I. Introduction	3689	F. Mechanisms	3712
A. Background: Precision and Living Polymerization	3689	1. Radical Scavengers	3712
B. Living Radical Polymerization	3691	2. Stereochemical Structures	3712
C. Overview of Metal-Catalyzed Living Radical Polymerization	3692	3. Copolymerizations	3712
II. Design of the Initiating Systems	3693	4. EPR	3713
A. Transition-Metal Catalysts	3693	5. NMR	3713
1. Ruthenium	3693	6. MS	3713
2. Iron	3695	7. CV	3714
3. Copper	3695	8. Kinetics	3714
4. Nickel	3698	9. Other Mechanistic Analyses	3714
5. Palladium	3699	III. Precision Polymer Synthesis	3715
6. Rhodium	3699	A. Pendant-Functionalized Polymers	3715
7. Rhenium	3699	B. End-Functionalized Polymers	3716
8. Molybdenum	3700	1. α -End-Functionalized Polymers	3716
9. Immobilized Catalysts	3700	2. ω -End-Functionalized Polymers	3719
B. Initiators	3700	C. Block Copolymers	3721
1. Haloalkanes	3701	1. Block Copolymers via Sequential Metal-Catalyzed Living Radical Polymerization	3721
2. Allyl Halides	3702	2. Block Copolymers via Combination of Other (Living) Polymerizations	3724
3. (Haloalkyl)benzenes	3702	D. Random Copolymers	3728
4. Haloketones	3702	E. Alternating Copolymers	3730
5. Haloesters	3703	F. Gradient Copolymers	3730
6. Haloamides	3703	G. Telechelic and Star Polymers	3730
7. Halonitriles	3704	1. Telechelic Polymers with Bifunctional Initiators	3730
8. Sulfonyl Halides	3704	2. Star Polymers with Multifunctional Initiators	3732
9. Conventional Radical Initiators	3704	3. Star Polymers by Linking Reaction	3734
C. Monomers	3705	H. Comb and Graft Copolymers	3734
1. Methacrylates	3705	1. Comb Polymers	3734
2. Acrylates	3706	2. Graft Polymers	3735
3. Styrenes	3706	I. Hyperbranched Polymers	3737
4. Vinylpyridines	3707	J. Polymer Brushes	3737
5. Acrylonitrile	3707	1. Silicon Wafer	3738
6. Acrylamides	3707	2. Gold	3738
7. Other Monomers	3707	3. Silica Particle and Bead	3739
D. Additives	3708	4. Silica Gel and Silica Capillary	3739
E. Solvents	3709	5. Polymer Latex	3739
1. Aprotic Polar Solvents	3709	IV. Conclusions	3739
2. Protic Polar Solvents	3710	V. References	3739
3. Water	3710		
4. Suspension, Dispersion, and Emulsion Polymerizations in Water (Heterogeneous System)	3710		
5. Other Special Solvents	3711		

* To whom correspondence should be addressed. Phone: +81-75-753-5603. Fax: +81-75-753-5623. E-mail: sawamoto@star.polym.kyoto-u.ac.jp.

I. Introduction

A. Background: Precision and Living Polymerization

Rivaling polyolefin production, radical polymerization is most widely employed in industrial- and

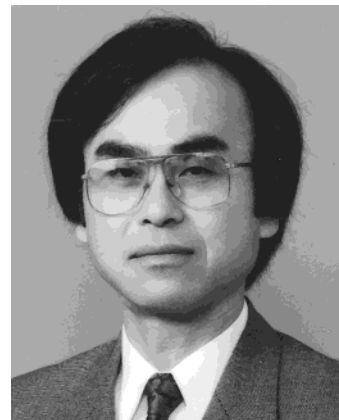


Masami Kamigaito was born in 1965 in Nagoya, Japan. He received his B.S. and M.S. degrees and Ph.D. degree in polymer chemistry from Kyoto University in 1993 under the direction of Professor Toshinobu Higashimura. After postdoctoral research with Professor Mitsuo Sawamoto, he joined the faculty at Kyoto University in 1995, where he is now Associate Professor of Polymer Chemistry. In 1997–1998, he was a visiting scientist under Professor Robert M. Waymouth at Stanford University. He is the recipient of the 1999 Award for the Encouragement of Research in Polymer Science of the Society of Polymer Science, Japan, and the 2001 Arthur K. Doolittle Award of the ACS PMSE Division. His research interests include metal catalysis for precision polymer synthesis, particularly living cationic and radical polymerization.



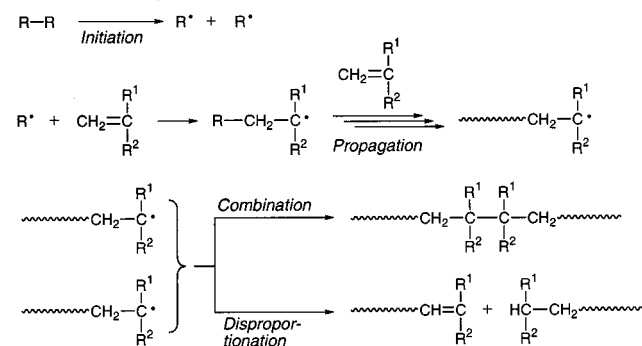
Tsuyoshi Ando received his bachelor degree in 1995, master degree in 1997, and Ph.D. degree in 2000 from Kyoto University. His doctoral study was on the development of transition-metal-catalyzed living radical polymerization systems under the direction of Professor Mitsuo Sawamoto, where he received a Research Fellowship for Young Scientists of the Japan Society for the Promotion of Scientists (1998–2000). He joined the Kyoto University faculty, Department of Polymer Chemistry, Faculty of Engineering, as a research instructor in 2000. His research activity is focused on controlled reactions, including precision polymerization, catalyzed by metal compounds.

laboratory-scale processes for polymer synthesis, because of its tolerance to protic compounds such as water, a high reaction rate, a polymerization temperature usually higher than ambient, and other advantages.¹ Unlike ionic reaction intermediates, however, the growing radical species therein usually suffers from bimolecular termination reactions such as radical recombination and disproportionation (Scheme 1). Radical polymerization had thus been considered unsuitable for precision polymer synthesis, in contrast to the ionic counterparts where the growing species are inherently repulsive to each other.



Mitsuo Sawamoto, born in Kyoto, Japan (1951), received his B.S. (1974), M.S. (1976), and Ph.D. (1979) degrees in polymer chemistry from Kyoto University under the direction of Toshinobu Higashimura. After postdoctoral research with Joseph P. Kennedy at the Institute of Polymer Science, The University of Akron, Akron, OH (1980–81), he joined the faculty of the Department of Polymer Chemistry, Kyoto University, in 1981 as a research instructor. He was promoted to Lecturer (1991), to Associate Professor (1993), and to Professor (1994), his current position, of the same department. Sawamoto also serves as one of the three Editors of the *Journal of Polymer Science, Part A: Polymer Chemistry* (1995–present) and as an Editorial Advisory Board member of *Macromolecular Chemistry and Physics*, the *Journal of Macromolecular Science, Chemistry*, and *e-Polymers*, and is the recipient of the 1991 Award of the Society of Polymer Science, Japan, the 1998 Divisional Award of the Chemical Society of Japan, the 2001 Aggarwal Lectureship in Polymer Science, Cornell University, and the 2001 Arthur K. Doolittle Award of the ACS PMSE Division. With more than 250 articles and reviews, his research interest covers living radical and cationic polymerizations, precision polymer synthesis, and the chemistry of radical and carbocationic reaction intermediates.

Scheme 1. Elementary Reactions for Conventional Radical Polymerization



One of the most effective methods for precision polymer synthesis is “living” polymerization, the first example of which was discovered in the anionic polymerization of styrene with sodium naphthalenide in 1956.² Living polymerization is free from side reactions such as termination and chain transfer and can thus generate polymers of well-defined architectures and molecular weights, i.e., one polymer chain per molecule of initiator. When the initiation is faster than, or at least comparable in rate to, propagation, the obtained polymers have narrow molecular weight distributions (MWDs) where the ratio of weight-average to number-average molecular weight (M_w/M_n) is around 1.1. In general, however, living anionic polymerization was limited to nonpolar hydrocarbon monomers such as styrenes and 1,3-dienes at first, but has now been developed to polar monomers such

as (meth)acrylates and other functional derivatives.^{3–6} Similar proliferation has recently occurred in other polymerizations, including cationic,^{7–9} coordination,¹⁰ ring-opening,¹¹ and ring-opening metathesis,¹² for which precise reaction control had been considered difficult for some time. In this regard, living radical polymerization has been among the most challenging frontiers in precision polymer synthesis and polymer chemistry.

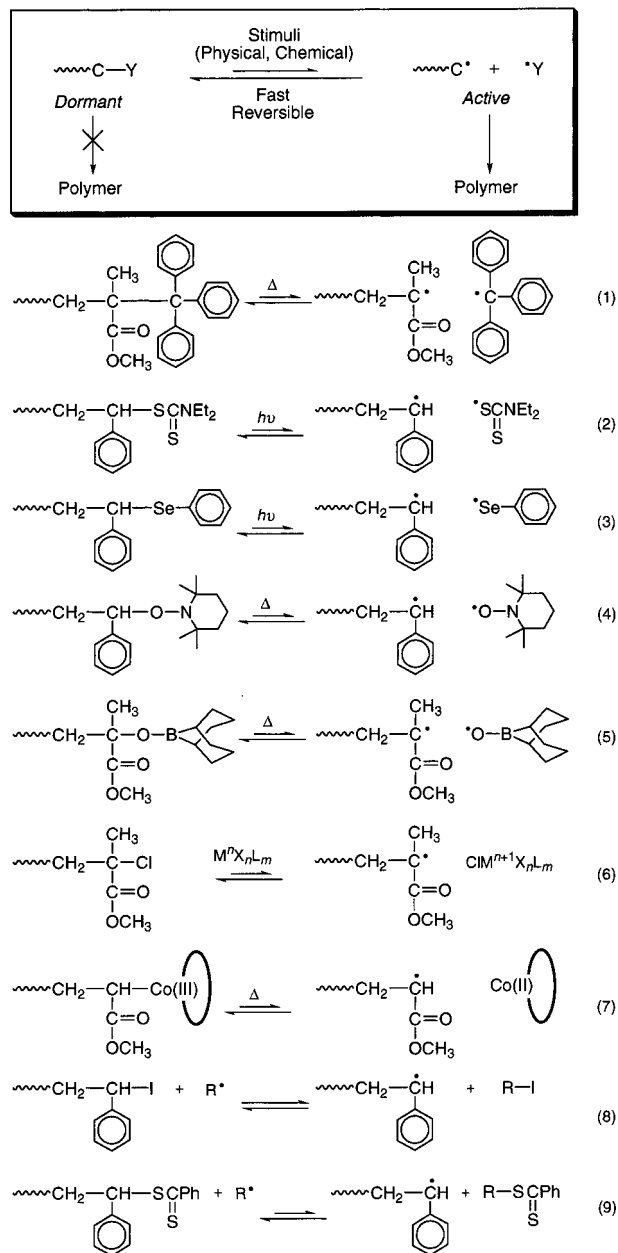
B. Living Radical Polymerization

Given this rapid progress in precision polymerization, living radical polymerization had been one of the most difficult subjects. The difficulty primarily stems from the inherent and “built-in” bimolecular termination of the growing radicals, and the prevailing consensus was (or still is) that it might not be suppressed, though not impossible. Starting with the pioneering works by Otsu et al. in the 1980s,^{13,14} however, the number of studies on living radical polymerizations started to mushroom, especially in the 1990s. There are now numerous systems and proposed methodologies for controlling radical polymerizations, even in comparison to some of the “classical” anionic living polymerizations. Typical examples of these systems are summarized in eqs 1–9.

At first glance, the examples vary clearly in mechanism or in chemicals to be employed, but importantly, the concept or the strategy for controlling radical polymerization appears to be common, namely, to lower the (instantaneous) concentration of a growing radical species by introducing a covalent dormant species that exists predominantly over, and in fast equilibrium with, the growth-active radical species. Such a dynamic and rapid equilibrium not only minimizes the extent or probability of the radical bimolecular termination but also gives an equal opportunity of propagation to all polymer (or dormant) terminals via the frequent interconversion between the active and the dormant species. These features thus lead to nearly uniform chain length (molecular weight) determined by the molar ratio of monomers to the dormant species (or the initiator). Another factor for consideration is the so-called “persistent radical”,¹⁵ a relatively stable radical that does not react with its own kind but does combine with the growing end. Its importance has been pointed out to be necessary for the control, as reviewed by Fischer in this issue.

The covalent bonds for dormant species include C–C (eq 1),^{16,17} C–S (eqs 2 and 9),^{13,14,18} C–Se (eq 3),¹⁹ C–O (eqs 4 and 5),^{20–25} C–halogen (eqs 6 and 8),^{26–28} and C–metal (eq 7),²⁹ all of which can reversibly and homolytically be activated into the growing radical species by physical stimuli such as heat or light or by chemical stimuli such as a metal catalyst or another radical species. Although the controllability, applicability, and reaction conditions depend on which systems are employed, a wide variety of vinyl monomers such as styrenes, methacrylates, acrylates, dienes, and vinyl acetate can be polymerized in a controlled fashion with the use of these or similar systems. Among these, nitroxide-mediated (eq 4)^{20–24} and metal-catalyzed^{27,28} systems

(eq 6) have most extensively been studied, probably due to the high controllability, the wide applicability, and the relatively easy access to the catalysts and other components to be employed.

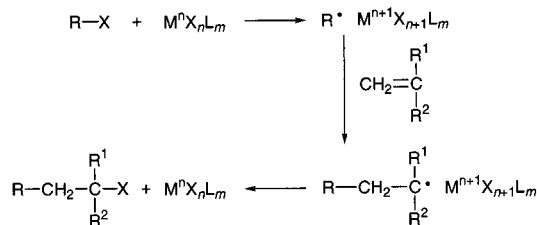


This review primarily covers the metal-catalyzed living radical polymerizations. As will be discussed, their advantages include dual control of the growing end by the terminal halogen and the metal complex, relatively low temperatures needed (60–100 °C), and commercially available compounds used; among others, the nitroxide-mediated living radical polymerization is reviewed in this issue by Hawker. Another metal-mediated living radical polymerization is based on carbon–metal bonds such as carbon–cobalt (eq 7)²⁹ and others, which fall outside the scope of this review, because the metals therein do not serve as the catalysts. Some reviews on this topic are available,^{30,31} and it is closely related to catalytic chain transfer³² reviewed by Gridnev and Ittel in a separate paper herein.

C. Overview of Metal-Catalyzed Living Radical Polymerization

Metal-catalyzed living radical polymerization can be traced back to metal-catalyzed radical addition reactions to alkenes, sometimes collectively called Kharasch or atom-transfer radical addition (ATRA) reactions in organic chemistry (Scheme 2).³³ Thus, a

Scheme 2. Metal-Catalyzed Radical Addition Reaction (Kharasch Addition Reaction)

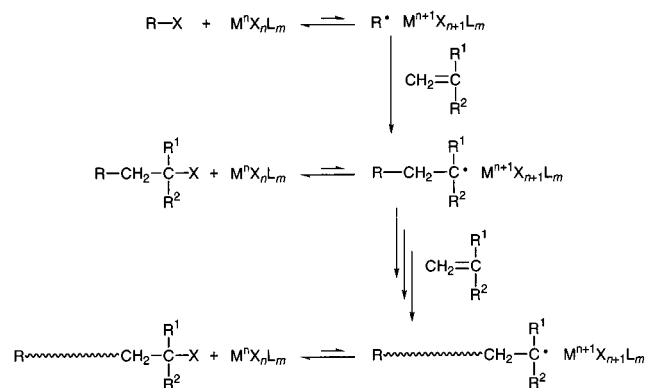


radical species generated from an organic halide (R-X, X = halogen) or a related compound in the presence of a metal catalyst attacks an unsaturated compound (e.g., CH₂=CHR') to form an adduct (R-CH₂-CHR'-X) with a carbon-halogen bond. The metal catalyst thus undergoes a reversible one-electron redox reaction via abstraction of the halogen from the reactant R-X, followed by a one-electron reduction, i.e., release of the halogen now attached to the oxidized metal back to the resulting radical species (R•). The reaction therefore proceeds catalytically and in a chain reaction mechanism, with a high chemo- and regioselectivity, to give the adduct in a high and often quantitative yield, in sharp contrast to other addition reactions via radical intermediates. This is due to the controlled formation of the radical intermediates via metal catalysis, although it is not clear whether free radicals, metal-complexed radicals, or organometallic intermediates are involved. In any case, these features would lead to the following hypothesis: i.e., if the carbon-halogen bond in the adduct is successively activated by the metal complex, a controlled radical polymerization will similarly proceed via the metal-assisted repetitive activation and formation of the carbon-halogen bond (dormant species) at the polymer chain end.

This idea was indeed realized around 1994, which is when we reported the first example, i.e., the living polymerization of methyl methacrylate catalyzed by a ruthenium(II) complex coupled with carbon tetrachloride as the initiator.²⁷ Shortly after this, an independent report was published for a similar system with styrene and a copper catalyst, which was coined atom-transfer radical polymerization (ATRP) after the predecessor in organic chemistry.²⁸ In these examples, however reminiscent to classical free radical polymerizations they might be, the number-average molecular weights of the polymers increase in direct proportion to monomer conversion and agree well with the calculated values assuming that one molecule of the halide initiator generates one polymer chain. The molecular weight distributions (MWDs) are as narrow as with the polydispersity (M_w/M_n) below or close to 1.1, comparable to those in living anionic polymerizations.

The metal-catalyzed living radical polymerization thus proceeds (or at least is mostly considered to proceed) via reversible activation of carbon-halogen terminals by the metal complex, where the metal center undergoes redox reactions via interaction with the halogens at the polymer terminal, as shown in Scheme 3. The reaction is usually initiated by the

Scheme 3. Metal-Catalyzed Living Radical Polymerization



activation (homolytic cleavage) of the carbon-halogen bond in an appropriate organic halide (R-X) via one-electron oxidation of the metal center ($\text{M}^n\text{X}_n\text{L}_m$) to form an initiating radical species (R•) and an oxidized metal compound ($\text{M}^{n+1}\text{X}_{n+1}\text{L}_m$). The R• reacts with the halogen on the oxidized metal to regenerate R-X or adds to the monomer to generate a radical species [R-CH₂-C(R¹)(R²)•]. It is sooner or later transformed into the adduct [R-CH₂-C(R¹)(R²)-X] of R-X and the monomer via abstraction of a halogen atom from $\text{M}^{n+1}\text{X}_{n+1}\text{L}_m$. The carbon-halogen bond of the adduct is subsequently activated by the metal complex, similarly to R-X, to result in a similar carbon-halogen bond at the polymer terminal via a repetitive set of the reactions. The key factors for these reactions are the low concentration of the radical intermediates at a given time and their fast but reversible transformation into the dormant species before undergoing successive addition to monomers.

In this reaction, one polymer chain forms per molecule of the organic halide (*initiator*), while the metal complex serves as a *catalyst* or as an *activator*, which catalytically activates, or homolytically cleaves, the carbon-halogen terminal. Therefore, the initiating systems for the metal-catalyzed living radical polymerization consist of an initiator and a metal catalyst. The effective metal complexes include various late transition metals such as ruthenium, copper, iron, nickel, etc., while the initiators are haloesters, (haloalkyl)benzenes, sulfonyl halides, etc. (see below). They can control the polymerizations of various monomers including methacrylates, acrylates, styrenes, etc., most of which are radically polymerizable conjugated monomers. More detailed discussion will be found in the following sections of this paper for the scope and criteria of these components (initiators, metal catalysts, monomers, etc.).

The metal-catalyzed living or controlled radical polymerizations can apparently be distinguished

from the conventional radical polymerization that involves a metal-assisted formation of the initiating radical species via irreversible redox processes, although the initiating system for the latter also consists of two components, a metal complex and an organic halide.^{34,35} In these examples, except for a few,^{36,37} the control of molecular weights and MWDs is generally difficult. The use of effective telomers can also make the control of molecular weights better in low molecular weight regions. However, the controllability is much better for the recently developed systems with reversible activation. A few reviews dealing with comparison between the new and the old metal-catalyzed systems are also available.^{30,38}

This review covers mainly the scientific literature that has appeared in relevant journals until early 2001 concerning the metal-catalyzed (or atom-transfer) living radical polymerization. The word "living" employed here simply refers to polymerizations that provide control over the molecular weights, the molecular weight distributions, and the chain end reactivity as do other living polymerizations. Its definition and use criteria, along with the word "controlled", are still under discussion and have recently been discussed elsewhere.³⁹ Thus, the discussion on the difference between these words is not to be treated here.

The review roughly consists of two parts, the scope and design of initiating systems followed by precision polymer synthesis. The former will treat the scope of metal catalysts, initiators, and monomers along with polymerization mechanisms. The latter will focus on the precision synthesis of various polymers with controlled structures and interesting properties or functions, such as block, end-functionalized, star, and other architecturally well-defined polymers. Other reviews are also available, comprehensive,^{31,40–44} and relatively short,^{45–52} dealing with the recent developments of the field.

II. Design of the Initiating Systems

The initiating systems for the metal-catalyzed living radical polymerizations consist of a metal complex (or catalyst) and an initiator; the former allows the generation of radical species from the latter or the dormant polymer terminal. The choice of the metals and the initiators according to the monomer structures is crucial for controlling radical polymerizations. The rate and control of the polymerization can also be increased by the addition of other compounds or by changing solvents. This first part will deal with the design of the initiating systems from the viewpoint of various components, i.e., metal complex catalysts, initiators, monomers, additives, and solvents, as well as the relevant reaction mechanisms.

A. Transition-Metal Catalysts

One of the most important components in the metal-catalyzed living radical polymerization is the transition-metal complex. As a catalyst, the complex induces reversible activation (homolytic cleavage) of

a dormant carbon–halogen bond at a polymer terminal via a one-electron redox reaction of the metal center. In this process, the metal center attacks the halogen at the chain end and is oxidized via a single electron transfer followed by halogen abstraction, thus generating a growing radical species. Sooner or later, the oxidized metal center donates the halogen therein back to the radical growing species, along with reduction of the metal center, before or after the propagation reaction between the radical and monomer. The lower oxidation state of the metal center [e.g., Ru(II)] should be more stable than its higher counterpart [e.g., Ru(III)] so as to establish an extremely low concentration of the radical species as well as a fast reversible reaction with the halogen.

This set of reactions, i.e., the activation/cleavage of a carbon–halogen bond, the formation of a radical species, the repetitive addition (propagation) of the radical species to the monomer, and the regeneration of the carbon–halogen bond, are called the Kharasch or ATRA reactions. There are various metal complexes active for these reactions, as have been utilized in organic synthesis. Indeed, some of the metal complexes active for living radical polymerization were originally developed for the small-molecule reactions, but along with the recent advances in polymerization, new and more active complexes have emerged, too. Although there are still no consistent rules for designing catalysts, there have been several papers dealing with the relationships between the metal center, catalyst structure, or ligand and their catalytic activities.^{53,54} In general, it is suggested that the catalytic activity increases with increasing electron density of the metal center or with decreasing redox potential of the complex, because, upon the onset of radical generation, the catalyst should give one electron to the halide terminal. The following sections will focus on the transition-metal catalysts employed for living radical polymerization.

1. Ruthenium

This group 8 transition metal was one of the first whose complexes [RuCl₂(PPh₃)₃ etc., Ph = C₆H₅] were demonstrated to induce living radical polymerization.²⁷ Among the various oxidation states of ruthenium complexes (–2 to +6), the divalent form with phosphine ligands has effectively been employed for the metal-catalyzed living radical polymerization as well as Kharasch addition reactions (Figure 1). The dichloride RuCl₂(PPh₃)₃ (Ru-1) was the first complex employed for the metal-catalyzed living radical polymerization of methyl methacrylate (MMA) in conjunction with CCl₄ as an initiator in the presence of a metal alkoxide such as MeAl(ODBP)₂ (ODBP = 2,6-di-*tert*-butylphenoxy) as an additive.²⁷ In toluene at 60 °C, the polymerization proceeded homogeneously to give polymers with molecular weights that were controlled by the feed ratio of monomer to initiator and relatively narrow MWDs ($M_w/M_n \approx 1.3$). The radical nature of the polymerization was suggested by inhibition of the polymerization on addition of a radical scavenger or inhibitor such as galvinoxyl and 2,2,6,6-tetramethyl-1-piperidinyloxy (TEMPO).^{27,55} The tacticity of the polymers was similar to that prepared in conventional radical systems.²⁷

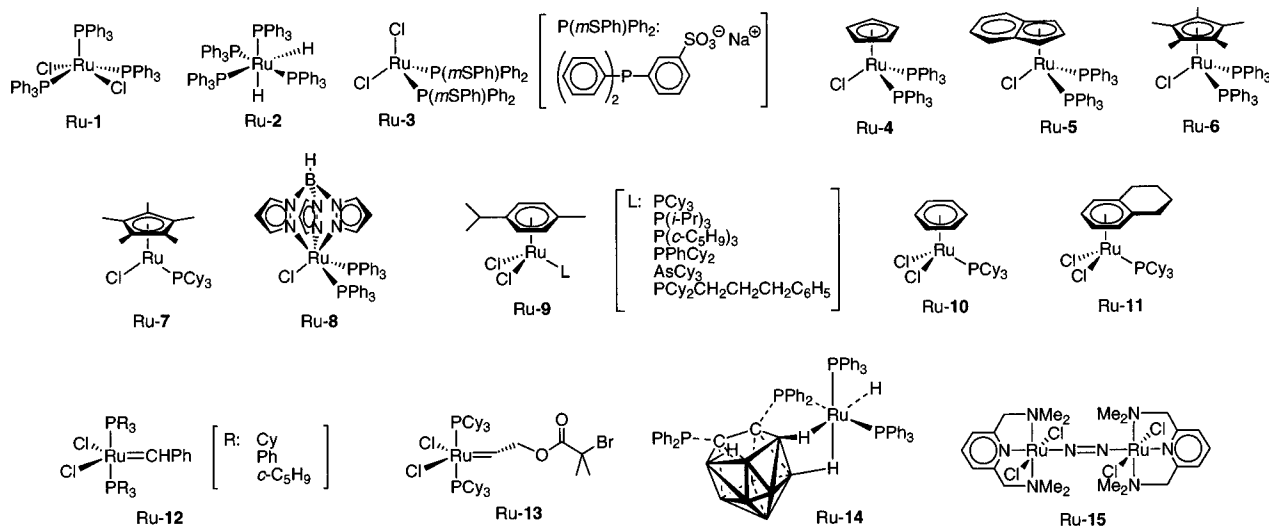


Figure 1. Ruthenium catalysts.

The ruthenium-catalyzed polymerization was further improved by using CHCl_2COPh and $\text{Al}(\text{O}-i\text{-Pr})_3$ in place of CCl_4 and $\text{MeAl}(\text{ODBP})_2$, respectively, resulting in very narrow MWDs ($M_w/M_n = 1.1$) of poly(MMA).⁵⁶ This complex can also be applicable for styrene polymerization in conjunction with an iodo initiator to give relatively narrow MWDs ($M_w/M_n \approx 1.2$).⁵⁷ A similar PPh_3 -based ruthenium(II) hydride (Ru-2) is more active than the chloride Ru-1, thus inducing faster polymerizations.⁵⁸ The hydride complex is still active at 30 °C to give polymers with narrow MWDs ($M_w/M_n \approx 1.2$). A ruthenium complex with an ionic phosphine ligand (Ru-3), which is soluble in water or methanol, catalyzes homogeneous living radical polymerization of 2-hydroxyethyl methacrylate (HEMA) in methanol;⁵⁹ no protection of the hydroxyl group is required for HEMA.

Among a series of the 18-electron half-metallocene-type ruthenium complexes (Ru-4, Ru-5, and Ru-6), the indenyl derivative Ru-5 led to the fastest living radical polymerization of MMA.⁶⁰ In this case, additives such as aluminum alkoxides are not necessary for controlled polymerization. However, addition of an amine such as *n*- Bu_2NH dramatically increased the rate to complete the polymerization in 5 h at 100 °C without broadening the MWDs.⁶¹

Though less active, the Cp^* complex Ru-6 is a versatile catalyst, which enables living radical polymerizations of three different types of monomers, i.e., MMA, styrene, and methyl acrylate (MA), in conjunction with a chloride initiator and $\text{Al}(\text{O}-i\text{-Pr})_3$. The initiating system with Ru-6 gives controlled molecular weights and narrow MWDs ($M_w/M_n = 1.1\text{--}1.2$) for all the monomers in toluene at 80 °C without changing the initiator and reaction conditions according to the monomers.⁶² The catalytic activity of these half-metallocene-type complexes increased in the order Ru-4 < Ru-5 < Ru-6; namely, the lower the redox potential of the complex, the faster the polymerization.⁵³ Another half-metallocene-type ruthenium complex with 16-electrons (Ru-7) is more active than Ru-6, because the former has a vacant site that can interact with a halogen at the polymer terminal without release of phosphine ligand.⁶² A trispyrazolyl

borate-based complex (Ru-8), isoelectronic to 18-electron half-metallocene-type complexes, also induced living radical polymerization of MMA either with or without additives, where the rates and molecular weights were not changed on addition of $\text{Al}(\text{O}-i\text{-Pr})_3$.⁵³

A series of *p*-cymene-based ruthenium dichloride complexes (Ru-9) with various phosphines and related two-electron-donor ligands was synthesized and used for the radical polymerizations of several monomers as well as Kharasch addition reactions.^{63,64} Controlled polymerizations were achieved with basic and bulky phosphine or arsenic ligands ($L = \text{PCy}_3$, $\text{P}(i\text{-Pr})_3$, $\text{P}(c\text{-C}_5\text{H}_9)_3$, PPhCy_2 , AsCy_3 , $\text{PCy}_2\text{CH}_2\text{CH}_2\text{CH}_2\text{C}_6\text{H}_5$). Among them, the tricyclohexylphosphine complex ($L = \text{PCy}_3$) is most active and efficient in giving well-controlled molecular weights and narrow MWDs ($M_w/M_n \approx 1.1$) for methacrylates.⁶³ In contrast, less basic or less bulky phosphine-, pyridine-, isocyanide-, and antimony-based ligands led to less efficient and/or less controlled polymerizations. Similar complexes carrying benzene (Ru-10) or tetralin (Ru-11) can also be employed; the activity decreased in the order *p*-cymene > benzene > tetralin.⁶⁵

A complex with a bridged ligand with arene and phosphine can be obtained via release of the *p*-cymene ligand from Ru-9 ($L = \text{PCy}_2\text{CH}_2\text{CH}_2\text{CH}_2\text{C}_6\text{H}_5$) on heating to 120 °C, but it was significantly less active than the precursor Ru-9 ($L = \text{PCy}_2\text{CH}_2\text{CH}_2\text{CH}_2\text{C}_6\text{H}_5$), which induces efficient living radical polymerization.⁶⁵ The activation process of these arene-based 18-electron complexes is thus release of arene ligands, which results in active and coordinately unsaturated 12-electron complexes.

A series of so-called Grubbs ruthenium-carbene complexes (Ru-12) can mediate living radical polymerization of MMA and styrene to afford controlled polymers with narrow MWDs ($M_w/M_n \approx 1.2$).^{63,66} The polymerization apparently proceeds via a radical mechanism, as suggested by the inhibition with galvinoxyl. For example, a novel ruthenium-carbene complex (Ru-13) carries a bromoisobutyrate group and can thus not only initiate but also catalyze living radical polymerization of MMA without an initiator.⁶⁷

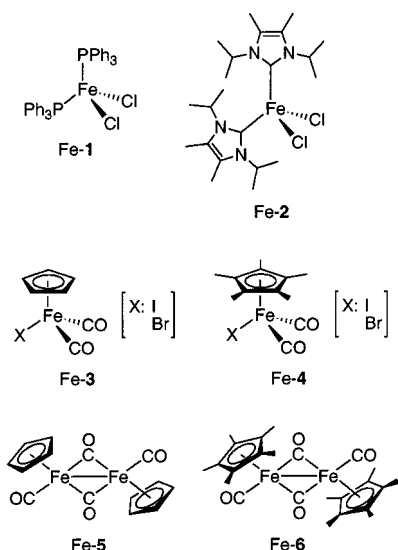


Figure 2. Iron catalysts.

The complex is also active in ring-opening metathesis polymerization of 1,5-cyclooctadiene (COD), where the ruthenium–carbene bond is now the initiating point. Therefore, a mixture of MMA and COD undergoes a dual or tandem living polymerization of both monomers to generate block copolymers of COD and MMA, which can be converted into ethylene-*block*-MMA copolymers on subsequent hydrogenation, also catalyzed by the complex.

Ruthenium–carborane 14-electron complexes were investigated as catalysts for the radical reactions, and among them, a hydride complex (Ru-14) proved effective in giving narrow MWDs ($M_w/M_n \approx 1.2$) and controlled molecular weights without additives in the MMA polymerizations.⁶⁸ A binuclear azo-bridged complex with nitrogen ligands (Ru-15) can be employed for MMA polymerization with CCl_4 as an initiator to give polymers with relatively narrow MWDs ($M_w/M_n = 1.4\text{--}1.6$).⁶⁹

2. Iron

As with ruthenium, iron belongs to the group 8 series of elements and can similarly take various oxidation states (-2 to $+4$), among which Fe(II), Fe(I), and Fe(0) species have been reported to be active in Kharasch addition reactions.³³ For metal-catalyzed living radical polymerizations, several Fe(II) and Fe(I) complexes have thus far been employed and proved more active than the Ru(II) counterparts in most cases (Figure 2). The iron-based systems are attractive due to the low price and the nontoxic nature of iron.

$\text{FeCl}_2(\text{PPh}_3)_2$ (Fe-1) was first employed for the metal-catalyzed living radical polymerization of MMA in conjunction with a chloride or a bromide initiator, and the rate of the polymerization is faster than with $\text{RuCl}_2(\text{PPh}_3)_3$.⁷⁰ The polymerization with Fe-1 catalyst was best controlled when coupled with $\text{CH}_3\text{C}(\text{CO}_2\text{C}_2\text{H}_5)_2\text{Br}$ as an initiator without additives in toluene at 80°C ($M_w/M_n = 1.1\text{--}1.3$). A similar fast living polymerization of styrene and MMA can be achieved with an iron complex and a higher electron-donating ligand such as imidazolone (Fe-2) in

conjunction with a bromide initiator to result in narrow MWDs ($M_w/M_n = 1.1\text{--}1.3$).⁷¹ Addition of FeCl_3 slowed the polymerization but narrowed the MWDs further ($M_w/M_n = 1.1$).

The use of Cp or Cp*-based ligands is also beneficial for the iron-based systems in controlling radical polymerization. For instance, $\text{FeCpI}(\text{CO})_2$ (Fe-3, X = I) induced a living radical polymerization of styrene in conjunction with an iodide initiator [$(\text{CH}_3)_2\text{C}(\text{CO}_2\text{C}_2\text{H}_5)\text{I}$] in the presence of $\text{Ti}(\text{O}-i\text{Pr})_4$ to give very narrow MWDs ($M_w/M_n = 1.1$) and controlled molecular weights.⁷² The rate was increased with the use of the corresponding bromide, while the MWD was narrowed by replacement of Cp with Cp*.⁷³ A faster and controlled polymerization was possible with dinuclear Fe(I) complexes (Fe-5 and Fe-6) in the absence of metal alkoxides.

Mixtures of iron(II) halides (FeBr_2 and FeCl_2) and ligands were also employed for living radical polymerization. Similar controlled radical polymerizations of MMA and styrene were achieved with FeBr_2 and nitrogen- and phosphine-based ligands such as *n*- Bu_3N , *n*- Bu_3P , and 4,4'-bis(5-nonyl)-2,2'-bipyridine.⁷⁴ Halide anions derived from ammonium or phosphonium salts [*n*- Bu_4NX (X = Cl, Br, I) and *n*- Bu_4PBr] were also available as ligands for FeBr_2 to mediate controlled polymerizations of styrene, MMA, and MA, although the systems were heterogeneous.⁷⁵ In search of less toxic ligands, dicarboxylic acids [$\text{NH}(\text{CO}_2\text{H})_2$, $\text{C}_6\text{H}_4\text{-1,3-(CO}_2\text{H)}_2$, and $\text{HO}_2\text{CCH}_2\text{-CH}_2\text{CO}_2\text{H}$]^{76–79} and acetic acid⁷⁸ were used for FeCl_2 , and the resulting complexes induced controlled polymerizations of MMA and styrene to give relatively broad MWDs ($M_w/M_n = 1.3\text{--}1.8$).

Fe(III) species can also be employed in a so-called reverse or alternative atom-transfer radical polymerization (section II.B.9). A mixture of FeCl_3 and PPh_3 can mediate a controlled polymerization of MMA in the presence of AIBN to give similarly narrow MWDs ($M_w/M_n = 1.1\text{--}1.3$).⁸⁰ An ammonium halide such as *n*- Bu_4NBr can be employed in place of PPh_3 as a ligand for FeBr_3 in the AIBN-initiated radical polymerization.⁷⁴

3. Copper

Copper catalysts have been extensively employed for the metal-catalyzed living or controlled radical polymerizations. Most of the polymerizations are conducted by a mixture of copper(I) bromide or chloride and a nitrogen-based ligand (Figure 3), and in select examples by isolated complexes (Figure 4). A wide variety of nitrogen ligands have been searched and employed (Figure 3), and they can be classified into bidentate (L-1 to L-17, e.g., bipyridines, pyridinimines, diamines), tridentate (L-18 to L-26), quadridentate (L-27 to L-33), and formally hexadentate (L-34). An overview of some of these ligands has been described in recent papers.^{54,81} The following gives specific examples of these ligands, though no systematic relationship has been established between their activity or utility and structures. However, quite recent papers deal with the relationships between the structure and the activity for several ligands.^{82,83}

The Cu(I)-based initiating system was first reported for styrene polymerization by Wang and

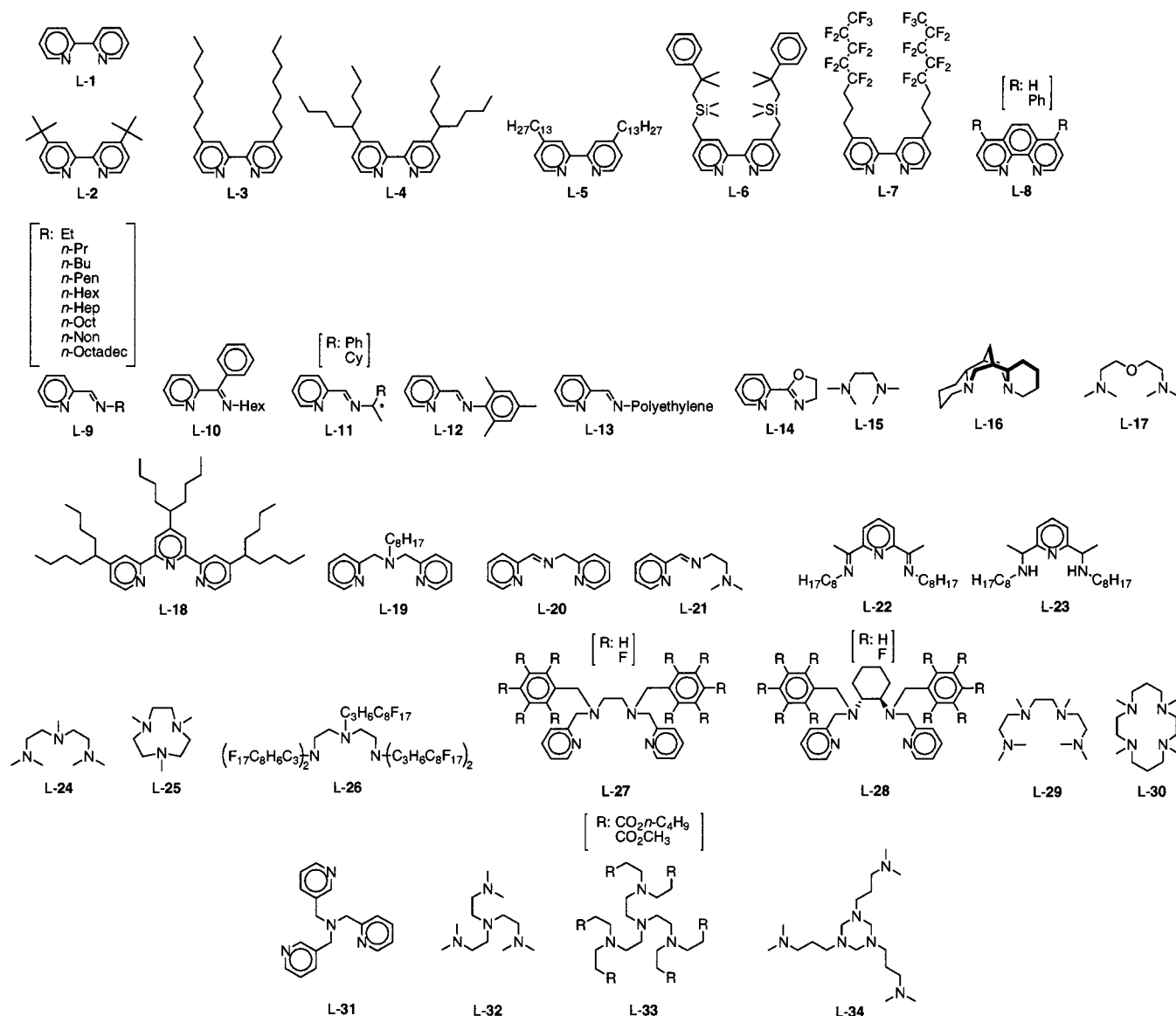


Figure 3. Ligands for copper catalysts.

Matyjaszewski and has subsequently been applied to a wide range of monomers. The first system consists of CuCl and 2,2'-bipyridine (L-1) ligand, coupled with 1-phenylethyl chloride as an initiator.²⁸ Though a heterogeneous system, the polymers had controlled M_n , in direct proportion to monomer conversion up to 100000 amu, and narrow MWDs ($M_w/M_n < 1.5$). The Cu(I)/L-1 system also proved effective for other monomers such as MA. The use of CuBr and a bromide initiator narrows the MWDs of polystyrene and poly(MA) ($M_w/M_n \approx 1.1$), while broader MWDs ($M_w/M_n \approx 1.4$) were obtained for poly(MMA).⁸⁴

In an effort to solubilize the catalyst, long-chain alkyl groups on the 4,4'-positions of bipyridine were introduced. Typical ligands in this line include L-2, L-3, and L-4. Homogeneous polymerizations have been achieved with L-3⁸⁵ and L-4⁸⁶ independently and almost simultaneously by two research groups. The polymerizations proceeded faster than the heterogeneous ones to give polystyrene of very narrow MWDs ($M_w/M_n = 1.05$). A longer alkyl chain substituent (L-5) is similarly efficient.⁸⁷ Alternatively, homogeneous polymerization of styrene can be achieved even with

the CuBr/L-1 system by adding 10% DMF, while the MWDs were relatively broad ($M_w/M_n = 1.4-1.8$).⁸⁸

A difficulty in isolation and clarification of the active Cu(I)-bipyridine complexes was overcome with the use of a silyl-containing bipyridyl ligand (L-6), which generates an ionic complex (Cu-1) on mixing with an equimolar amount of CuBr.^{89,90} The complex as well as an equimolar mixture of CuBr and L-6 showed levels of control similar those with L-3 and CuBr. An active Cu(I) species with bipyridine-type ligands presumably has a tetrahedral 18-electron species, as suggested for the similar complexes isolated after the polymerization of MA with L-4.^{91,92}

A Cu(II) complex with a bipyridine-type ligand (Cu-4) is effective in the controlled polymerization of styrene and acrylates in the presence of Al(O-*i*Pr)₃, which most probably serves as a reducing agent of Cu(II) into Cu(I).^{93,94} A fluoroalkyl-substituted bipyridine ligand (L-7) was also employed in supercritical carbon dioxide for the polymerization of fluorinated acrylates and methacrylates.⁹⁵ Similar pyridine-based bidentate ligands, 1,10-phenanthroline and its

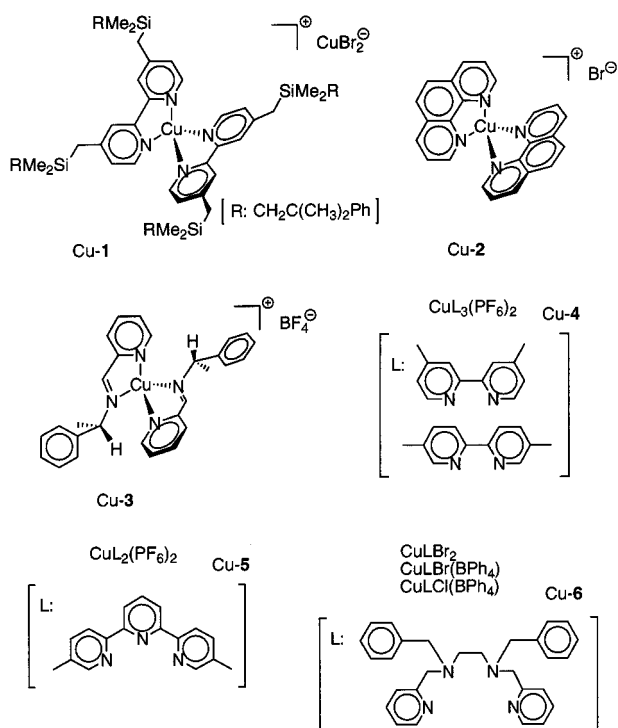


Figure 4. Isolated copper catalysts.

derivatives (L-8, R = H, Ph), were also used for CuCl,^{96,97} CuBr,⁹⁸ and Cu(0)⁹⁹ in controlled polymerizations of styrene and MMA. A homogeneous polymerization of styrene proceeds with the diphenyl-substituted ligand (L-8, R = Ph) with CuCl in 1,2-dimethoxybenzene to afford better controlled polymers than L-4 does under the same conditions.⁹⁶ A preformed and isolated complex (Cu-2) induced a similar controlled polymerization of styrene although the mixture was heterogeneous with the unsubstituted phenanthroline.⁹⁸

A series of Schiff-base or pyridinimine-type bidentate ligands (L-9) has been efficiently used for the homogeneous living radical polymerization of methacrylates ($M_w/M_n = 1.1-1.2$) with CuBr and a bromide initiator in nonpolar solvents such as toluene and *p*-xylene.¹⁰⁰⁻¹⁰² These ligands can therefore clearly differ from bipyridines, which need some special solvent such as ethers for controlling polymerizations of methacrylates (section II.E.1). However, an active Cu(I) species has a similar tetrahedral structure, as suggested by an isolated Cu(I) complex with tetrafluoroborate anion.¹⁰¹ The solubility depends on the alkyl substituents (R), and homogeneity can be achieved with alkyl chains longer than *n*-Bu at 90 °C. The rate increases on going from R = Et to R = *n*-Pr; however, no increase was observed with longer alkyl chains. Slower and less controlled polymerizations occurred when branching was introduced into the α -position of the side chain (L-10).¹⁰² A similar ligand, diazabutadiene or diimine, which has no pyridine moiety, does not induce controlled polymerization most probably due to the high stability of Cu(I) complexes with regard to oxidation.¹⁰² The catalysts prepared in situ by the addition of ligands L-9 to CuBr prior to the polymerizations are similarly effective.¹⁰¹

Possible control of stereochemistry was investigated with the use of chiral Schiff bases L-11 (R = Ph, Cy) as ligands or their recrystallized catalyst Cu-3 in the polymerizations of MMA with a bromide initiator in xylene at 90 °C.¹⁰³ Unfortunately, the tacticity of the polymers is not different from that in conventional polymerizations, while control of molecular weights was achieved.

Styrene polymerization was investigated with some pyridinimine ligands. Homogeneous living polymerizations can be achieved with L-9 (R = *n*-Oct) in xylene¹⁰⁴ and with L-12 in the bulk,¹⁰⁵ both with a bromide initiator and CuBr, where the former gave narrower MWDs than the latter ($M_w/M_n = 1.2$ and 1.5-1.8, respectively). L-9 (R = *n*-Oct) is also applicable for MA polymerization to give relatively narrow MWDs.⁸¹

Catalyst removal is efficient with the use of a polyethylene-segmented pyridinimine ligand (L-13) in the polymerization of MMA with CuBr.¹⁰⁶ A similar ligand, 2-(2'-pyridyl)-4,5-dihydroxyloxazole (L-14), is employed for CuCl-mediated polymerizations of methacrylates.¹⁰⁷

Diamine compounds such as L-15 coordinate to copper species, but their use for MA, MMA, and styrene results in slower polymerizations and broader MWDs ($M_w/M_n = 1.3-2.5$) than those with bipyridine-based bidentate ligands.^{81,108} An increase of the number of amine linkages and bulkier substituents further broadened the MWDs.⁸¹ Sparteine (L-16), a bicyclic diamine, was found to be an efficient ligand for homogeneous living radical polymerization of styrene and MMA with CuBr and CuCl, respectively, to give better-controlled polymers ($M_w/M_n = 1.1-1.3$).¹⁰⁹ A diamine with an ether moiety (L-17) was also employed in a CuCl-based system.¹¹⁰

Tridentate nitrogen ligands form 1:1 uncharged complexes with copper, in contrast to bidentate ligands that form tetrahedral ionic complexes.⁸¹ Well-controlled polymers of styrene and MA are obtained with a substituted terpyridine (L-18), whereas the unsubstituted derivative induced a heterogeneous and uncontrolled polymerization.¹¹¹ A similar controlled polymerization of styrene was reported for a substituted terpyridine-based complex of Cu(II) (Cu-5) coupled with Al(O-*i*-Pr)₃.¹¹² A tridentate ligand with two pyridines and one amine (L-19) gave narrow MWDs for styrene, MA, and MMA ($M_w/M_n = 1.1-1.4$), although the M_n values for PMMA were slightly higher than the calculated values.¹¹³ Another tridentate ligand (L-20) with two pyridines and one imine was effective for styrene and MA.⁸¹ A ligand (L-21) with one pyridine moiety gave narrow MWDs of styrene.⁸¹ Diiminopyridine L-22 can be employed for controlled radical polymerizations of MMA ($M_w/M_n < 1.3$), while diaminopyridine L-23 is effective for MA and styrene ($M_w/M_n < 1.3$).¹¹⁴

A substituted linear triamine (L-24) is effective for three types of monomers, styrene, MA, and MMA, to give relatively narrow MWDs ($M_w/M_n = 1.1-1.4$), where the polymerizations of styrene and MA are faster than those with L-1.¹⁰⁸ A cyclic triamine (L-25) with ethylene linkers is similarly effective.⁸¹ A perfluoroalkyl-substituted triamine (L-26) is useful

Cu(I)	Cu(0)
CuCl	Cu
CuBr	
Cu(OTf) [Cu(OTf) ₂ + Cu]	
CuPF ₆	Cu(II)
Cu(OAc)	CuS
Cu(2-thiophenecarboxylate)	CuSe
CuSCN	CuCl ₂
Cu ₂ O	CuBr ₂
Cu ₂ S	
Cu ₂ Se	
Cu ₂ Te	
CuSPh	
CuSBu	
CuC≡CPh	

Figure 5. Copper catalysts.

in living radical polymerization of MMA under fluorous biphasic conditions, where the reaction mixtures were homogeneous under the reaction conditions but were heterogeneous under the workup conditions.¹¹⁵ The obtained polymers had narrow MWDs, and the catalysts can be reused at least twice without a significant loss of activity.

Ligands with four nitrogen-based coordinating sites were also studied by several researchers. A series of ligands with two pyridine and two amine parts (L-27 and L-28) were employed for MMA in conjunction with CuBr and a bromide initiator to lead to controlled polymerization ($M_w/M_n = 1.1-1.4$) in the presence of Cu(0).¹¹⁶ Slower polymerizations occurred with fluorinated derivatives. Some isolated Cu(II) complexes (Cu-6) were effective in the presence of Cu(0), similar to the Cu(I) catalysts preformed in situ. No changes in tacticity were observed even with the use of chiral ligands (L-28). A linear quadridentate amine (L-29) was effective similarly to a tridentate amine (L-24) to induce fast controlled polymerizations of styrene, MA, and MMA.¹⁰⁸ A cyclic quadridentate amine (L-30) afforded broad MWDs but induced fast and quantitative polymerizations of *N,N*-dimethylacrylamide.¹¹⁷ Controlled polymerizations of styrene and acrylates are achieved with tripodal ligands such as L-31¹¹³ and L-32,^{118,119} where very fast living polymerizations of acrylates proceeded to reach 80% conversion within 3 h even at 22 °C with L-32. A tripodal ligand with ester substituents (L-33) was effectively employed for 2-(dimethylamino)ethyl methacrylate.¹²⁰ A multidentate ligand with six possible coordination sites (L-34) was reported for MMA in THF or in γ -butyrolactone.¹²¹

Copper(I) salts other than bromides and chlorides were also employed as catalysts coupled with nitrogen-based ligands (Figure 5). These salts seem to accelerate polymerization due to the formation of unbridged monomeric and highly active Cu(I) species, whereas copper(I) halides generally form bridged dimeric complexes in organic solution. However, in most cases, broadening of the MWDs originates from the rate of polymerization being faster than generation of dormant species (deactivation of the radical species), as well as irreversible termination via transfer of halogens from a polymer terminal to the complex, i.e., the formation of copper halides. Copper(I) triflate [Cu(OTf), Tf = CF₃SO₂], generated from Cu(OTf)₂ and Cu(0) in situ, induced faster polymerizations of MA and styrene in the presence of L-24.¹²² A much faster polymerization of MA was attained with CuPF₆/L-4, where the apparent polymerization rate constant is

40 times greater than that with CuBr, to give controlled molecular weights but broader MWDs ($M_w/M_n = 1.4-1.6$).¹²³ Copper(I) carboxylates such as Cu(OAc) and Cu(2-thiophenecarboxylate) with L-4 also led to faster polymerizations of styrene but broader MWDs.¹²⁴ Addition of copper(I) or copper(II) halide was effective in improving the controllability for M_n and MWDs without deceleration. With a sulfonyl chloride as initiator, CuSCN leads to a polymerization of MMA faster than copper halides do; however, the less active C-SCN terminal accumulates via a ligand exchange reaction.¹²⁵

Dicopper chalcogens induced controlled polymerizations of MMA and *n*-butyl methacrylate (nBMA), where the rate increased in the order Cu₂O < Cu₂S < Cu₂Se < (CuCl <) Cu₂Te, in the presence of L-1 or L-4 with a sulfonyl chloride initiator. The polymers had controlled molecular weights and MWDs ($M_w/M_n = 1.1-1.2$) at high conversions (>80%).^{126,127} There was an induction period, which decreased in the order Cu₂O > Cu₂S > Cu₂Se > Cu₂Te. These copper salts are converted presumably into reactive and soluble CuCl complexes via the reaction with the chlorine in the initiator during the induction period, although the mechanism has not been established yet. Organocopper species such as CuSPh are also effective in the controlled polymerizations of MMA in the presence of L-1 and a sulfonyl chloride, where the rate increased in the order CuC≡CPh < CuSPh < (CuCl <) CuSBu.¹²⁸ Similar ligand exchange reactions occur with these systems to form CuCl and result in low initiation efficiency especially at the high concentrations of organocoppers employed.

Metallic copper, Cu(0), can also be employed for controlled radical polymerization in the absence or presence of copper(II) or copper(I) halides.^{126,129} Cu(0) is most probably converted in situ into an active Cu(I) species via abstraction of halogen from the initiator and the polymer terminal or from added copper(II) or copper(I) halides. The use of Cu(0) as an accelerator or reducing agent of Cu(II) species will be discussed later (section II.D).

Cu(II) species such as CuS and CuSe can induce controlled polymerizations, the rate of which is decreased when compared with their Cu(I) counterparts (Cu₂S and Cu₂Se).¹²⁷ These Cu(II) species are presumably converted into copper(I) halides via a ligand exchange reaction with the initiator or polymer chain end similarly to Cu₂S and Cu₂Se. Copper(II) halides such as CuCl₂ and CuBr₂ per se are not active but can be converted into active copper(I) halides by combination with a conventional radical initiator such as AIBN.^{130,131} This system is sometimes called a reverse or alternative atom-transfer radical polymerization, which will also be discussed later (section II.B.9).

4. Nickel

Among the various oxidation states of nickel (0-IV), Ni(II) and Ni(0) are the most stable. There have been only a limited number of examples of nickel-catalyzed Kharasch addition reactions, in contrast to those of ruthenium, iron, and copper, probably be-

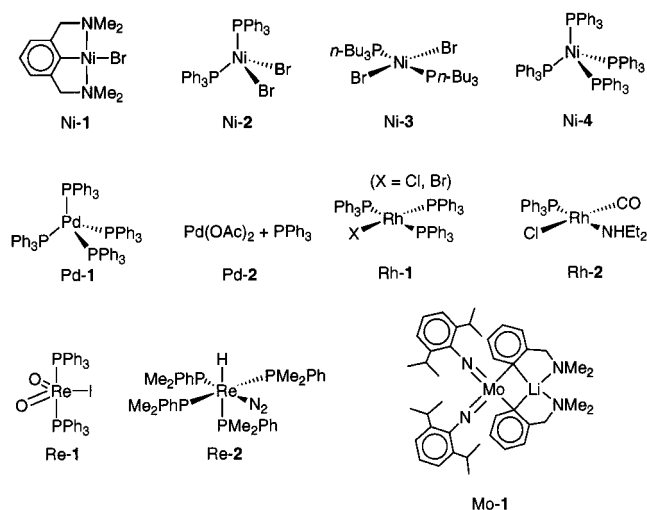


Figure 6. Other metal catalysts.

cause nickel easily undergoes oxidative addition and reductive elimination, which accompanies a two-valence change in its oxidation state rather than the one-electron redox cycle as required in the radical addition processes. However, several Ni(II) and Ni(0) complexes with selected ligands can act as efficient catalysts for living radical polymerizations via a one-electron redox cycle, especially when coupled with bromide initiators (Figure 6). The activity of nickel complexes thus far developed is relatively mild in contrast to that of more active Ru(II) and Cu(I) complexes.

A Ni(II) complex with a bis-ortho-chelating nitrogen ligand (Ni-1) was successfully employed for the living radical polymerization of methacrylates with CCl_4 or $(\text{CH}_3)_2\text{C}(\text{CO}_2\text{C}_2\text{H}_5)\text{Br}$ as an initiator.¹³² The polymerization proceeded homogeneously and reached 80% conversion in about 1 day at 80 °C to give polymers with narrow MWDs ($M_w/M_n = 1.1\text{--}1.2$), although the initiation efficiency was lower ($I_{\text{eff}} = 0.8$). The radical nature of the polymerizations was suggested by the effects of radical inhibitors such as galvinoxyl and also by the tacticity of the polymers.

A phosphine-based nickel(II) bromide complex (Ni-2) also induces living radical polymerization of MMA specifically when coupled with a bromide initiator in the presence of $\text{Al}(\text{O}-i\text{Pr})_3$ as an additive in toluene at 60 and 80 °C.¹³³ The reaction rates and the effects of radical inhibitors are similar to those with Ni-1, whereas chloride initiators are not effective in reaction control. Additives are not necessary when the polymerization is carried out in the bulk or at high concentrations of monomer, either methacrylate or *n*-butyl acrylate (nBA).¹³⁴ An alkylphosphine complex (Ni-3) is thermally more stable and can be employed for MMA, MA, and nBA in a wide range of temperatures (60–120 °C) without additives.¹³⁵ A fast polymerization proceeds at 120 °C to reach 90% conversion in 2.5 h. A zerovalent nickel complex (Ni-4) is another class of catalyst for living radical polymerization of MMA in conjunction with a bromide initiator and $\text{Al}(\text{O}-i\text{Pr})_3$ to afford polymers with narrow MWDs ($M_w/M_n = 1.2\text{--}1.4$) and controlled molecular weights.¹³⁶ The Ni(0) activity is similar to that of Ni(II) complexes whereas the controllability

is inferior. Mechanistically, the role of the zerovalent complex apparently needs further clarification.

5. Palladium

Palladium belongs to the group 10 elements, and as with nickel, it forms stable Pd(0) and Pd(II) complexes. The use of such complexes (Pd-1 and Pd-2) has been reported for the polymerization of MMA with CCl_4 initiator in toluene at 70 °C.¹³⁷ The activity is moderate (conversion 70–80% in 24 h), similar to that of the nickel complexes. The M_n increased in direct proportion to monomer conversion, while the MWD was broader ($M_w/M_n \approx 1.8$). In contrast, polymerizations of styrene and acrylates were not controlled with Pd catalysts.

6. Rhodium

Among possible oxidation states of rhodium ranging from +4 to –3, the most common are +1 and +3. One of the most famous Rh(I) complexes (Rh-1), the so-called Wilkinson catalyst, widely used for hydrogenation, was investigated for living radical polymerization by several researchers. The chloride complex Rh-1 ($X = \text{Cl}$) was first examined for styrene in the bulk at 130 °C coupled with sulfonyl chloride as an initiator.⁸⁶ The obtained polymers had broader MWDs ($M_w/M_n = 1.7$) than those with the ruthenium or copper catalysts. In contrast, it induced faster polymerizations of MMA in the presence of CCl_4 or CHCl_2COPh in THF or in a mixture of THF and water at 60 °C, where conversion reached 90% in 4 h in the latter medium to give PMMA with a slight reduction in the MWDs ($M_w/M_n = 1.3\text{--}1.7$).¹³⁸ The effects of galvinoxyl and the tacticity of PMMA are again in agreement with the radical nature of the polymerization. A bromide complex (Rh-1, $X = \text{Br}$) in conjunction with a bromide initiator afforded PMMA with narrower MWDs ($M_w/M_n = 1.3$).¹³⁹

In another example, the novel Rh(I) complex Rh-2 was employed with CCl_4 for MMA and styrene bulk polymerizations at 60 °C, which reached 90% conversion in 14 h.¹⁴⁰ The MWD of PMMA was narrower than that of polystyrene ($M_w/M_n = 1.43$ vs 2.08), while the initiation efficiency was very low in both cases.

7. Rhenium

Rhenium belongs to the group 7 elements, which, in general, display the characteristics of early and late transition metals. It can take a wide range of oxidation states and give stable high-valent complexes as do group 8–10 metals. A rhenium(V) iodide complex (Re-1) induced efficient living radical polymerizations of styrene coupled with an iodide initiator and $\text{Al}(\text{O}-i\text{Pr})_3$ over a wide range of temperatures between 30 and 100 °C.¹⁴¹ Conversion reached 90% within 6 h at 100 °C, and its catalytic activity for styrene is higher than that of Ru-1. The MWDs became narrower with decreasing temperature ($M_w/M_n = 1.2\text{--}1.5$). The radical nature of the polymerization was suggested by inhibition of the polymerization by TEMPO. However, the terminal iodide group was not converted into the nitroxyl group, most probably due to a low concentration of radical species

as well as deactivation of the Re(V) complex via interaction with TEMPO. The system can equally be employed for acrylate polymerizations, although the MWDs are broader ($M_w/M_n = 1.6\text{--}1.8$).¹⁴²

There is also a report on the use of a Re(I) complex (Re-2) in 1,2-dichloroethane at 50 °C, where the increase of molecular weights with conversion was observed in the MMA polymerization.¹⁴³ Due to the absence of initiator, the solvent presumably serves as a supplier of the initiating radical species. The radical nature of the polymerization was suggested from the copolymerization behavior of MMA and styrene.

8. Molybdenum

A group 6 metal complex can be a candidate as a catalyst for radical polymerization because of its variable oxidation states, despite its sensitivity to air and protic compounds. A lithium molybdate(V) complex (Mo-1) can polymerize styrene in conjunction with benzyl chloride in toluene at 80 °C to yield polystyrene with relatively broad MWDs ($M_w/M_n = 1.5\text{--}1.7$).¹⁴⁴ The initiation efficiency was low (~10%), and decomposition of the complex was observed.

9. Immobilized Catalysts

Immobilized catalysts have been studied in metal-catalyzed living radical polymerization for, in part, easy removal of the catalysts from the products. In most examples, the catalytic metal centers are attached to solid supports, such as silica gel and polystyrene beads, via spacers and/or coordinating ligands (Figure 7). The central metals thus far employed include copper and ruthenium.

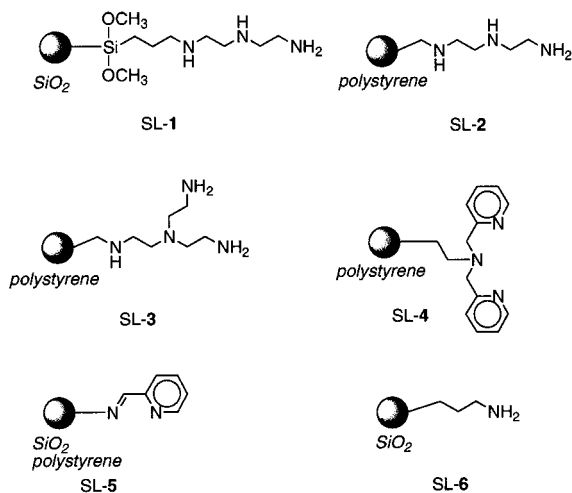


Figure 7. Ligands for immobilized catalysts.

Several silica-based materials such as silica gels, silica powder, and fumed silica (Aerosil) were employed as supports for CuBr by modification of their surface as in SL-1.¹⁴⁵ Thus, for instance, bulk polymerization of styrene was investigated but resulted in polymers of uncontrolled molecular weights and broad MWDs ($M_w/M_n = 2\text{--}10$) due to the slow deactivation or initiation of the growing radical species relative to propagation. Organic polymer-supported ligands on a cross-linked polystyrene

(Merrifield resin) such as SL-2 and SL-3 also resulted in uncontrolled polymerizations of acrylates, methacrylates, and styrene. A better control can be achieved with the use of SL-4 for a mixture of CuBr₂ and CuBr in the polymerization of MA, where the molecular weights became closer to the calculated values, and the MWDs became narrower ($M_w/M_n = 1.6\text{--}2.0$).¹⁴⁵ The residual copper in the reaction mixture was estimated about 3% of the initial amount, which indicates that the metal was effectively bound to the resin.

The use of another supported ligand such as SL-5 on silica gels and polystyrene resins induced controlled radical polymerization of MMA, resulting in narrower MWDs ($M_w/M_n = 1.5\text{--}1.6$), although the molecular weights were higher than the calculated values.^{146,147} Block copolymerization and the reuse of the catalysts have also been achieved. Physically adsorbed catalysts obtained by mixing silica gels or amino-functionalized silica gels with CuBr in the presence of free ligands gave narrower MWDs ($M_w/M_n = 1.3\text{--}1.4$) but resulted in coloring of the solution due to free copper complexes.

A ruthenium complex (Ru-1) can also be supported on a silica gel such as SL-6.¹⁴⁸ The ruthenium-catalyzed MMA polymerization gave controlled molecular weights, closer to the calculated values, and narrow MWDs ($M_w/M_n = 1.5\text{--}1.7$). Block copolymerization as well as the reuse of the catalysts is possible. The polymerization was faster in the presence of SL-6 than in the absence, most probably due to the effects of amines as additives as will be discussed below (section II.D). The residual ruthenium in the reaction mixture was estimated to be about 10% of the initial feed.

A similar, physically bound CuBr catalyst on a silica gel support (L-29) was also employed for MMA polymerization.¹⁴⁹ The polymers had narrow MWDs ($M_w/M_n \approx 1.3$), but the molecular weights were higher than the calculated values. The recycled catalysts have a lower activity but lead to better control of molecular weights; i.e., the M_n agreed well with the calculated values, and the MWDs were narrower ($M_w/M_n \approx 1.2$). The physically supported catalysts were further employed for the synthesis of end-functionalized polymers.¹⁵⁰ When physically supported silica gel catalysts are packed into a continuous column reactor, a controlled polymerization is possible.¹⁵¹

In contrast, unsupported catalysts can be removed by precipitation of polymers,¹⁵² passing through an alumina column,¹⁵² or using an absorbant,²⁷ but complete removal is difficult. The use of ion-exchange resins was investigated and seems more practical.¹⁵³ Another efficient method for catalyst removal is to use special ligands or catalysts such as L-26¹¹⁵ and Ru-3,⁵⁹ which can be removed with the use of fluoro solvents and water, respectively. Ionic liquid can also be employed for catalyst removal (section II.E.5).

B. Initiators

The role of the initiator in metal-catalyzed living radical polymerization is to form an initiating radical species via homolytic cleavage of its labile bond such as C–halogen by the metal catalysts. In most cases,

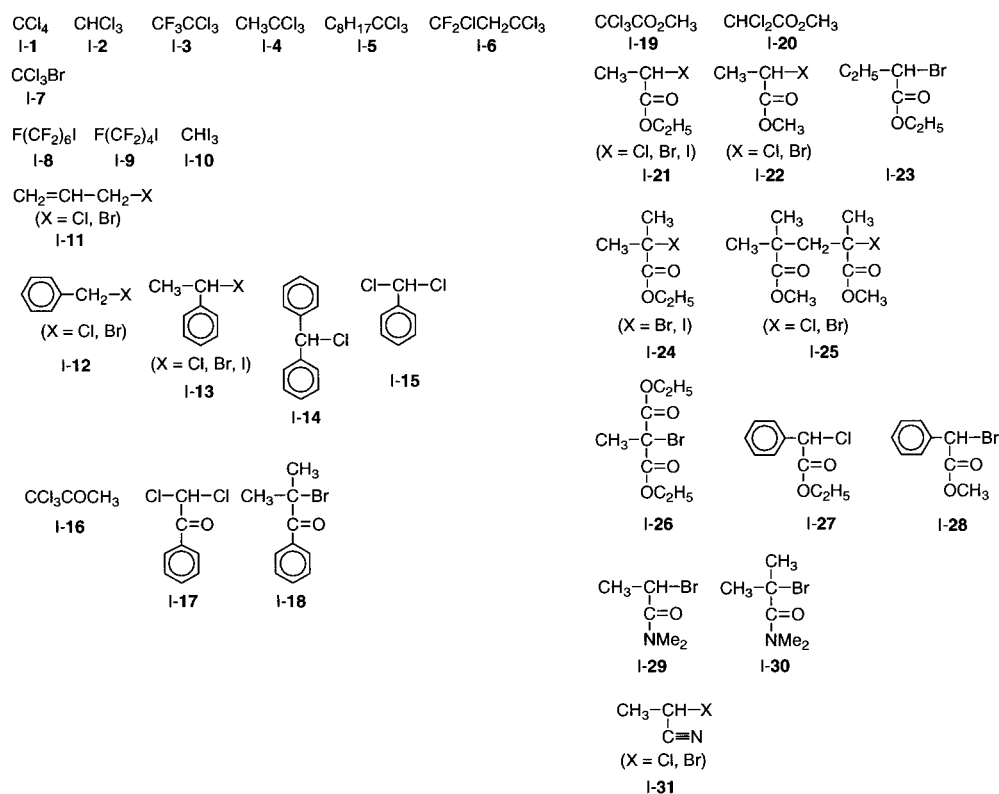


Figure 8. Organic halide initiators.

the dissociated halogen or its equivalent is subsequently reattached to the propagating radical chain end to give a dormant species. The initiator is thus chosen so that the initiation occurs fast and is quantitative, with the dormant polymer chain end being stable during the polymerization. This means that the initiator should be carefully selected in accordance with the structure and reactivity of the monomers and metal complexes.

Most of the initiators thus far successfully employed are organic halides with a potentially active carbon–halogen bond, which can easily generate a radical species through electronic and steric effects of their substituents (Figure 8). These organic halides therefore possess surplus halogens or conjugated substituents such as allyl, aryl, carbonyl, and cyano groups for stabilization of the generated radical species by the inductive and/or resonance effects. However, in some cases, an extensive stabilization of the initiating radical may disturb its addition to the monomer and thus result in slow initiation, which causes uncontrolled molecular weights and/or broad MWDs. An organic halide, the structure of which is similar to that of the dormant chain end of the polymer, is preferentially used so that the activity of the carbon–halogen bond in the initiator is similar to that of the dormant polymer terminal.

Halogen (*X*) in the initiators (*R–X*) include chlorine, bromine, and iodine, where the reactivity of the C–*X* bond increases in the order Cl < Br < I, but the stability of the C–*X* bond decreases vice versa. Chlorides and bromides have thus been widely employed.

The following summarizes various initiators in terms of their structures, focusing on available

monomers and metal complexes. There have been some papers discussing various halide initiators in the metal-catalyzed living polymerization.^{154,155}

1. Haloalkanes

Carbon tetrachloride (I-1) was the first initiator employed for the metal-catalyzed living radical polymerization of MMA in conjunction with Ru-1.²⁷ The M_n values increase with conversion and are controlled by the molar ratio of monomer to initiator. They agree with the calculated values assuming that one molecule of CCl₄ generates one living polymer chain, but become smaller at the later stages of the polymerizations. Despite CCl₄ being a chain-transfer agent or a telomer in free radical polymerization, no evidence is found to suggest such reactivity in the metal-mediated processes; the initiator is quantitatively consumed during the early stages. A similar result was also obtained in the Cu(I)-catalyzed MMA polymerizations.^{156,157}

Another possible problem is that such polyhalogen compounds may act as multifunctional initiators to give telechelic or star polymers. The initiating moiety thus involved midchain (---CCl₂---) may also induce side reactions, and in fact the lower M_n at the latter stages of the polymerizations of MMA is due to the generation of new polymer chains via chain transfer.¹⁵⁶ CCl₄ can be also employed for other metal complexes such as Fe,⁷⁰ Ni,¹³² Pd,¹³⁷ and Rh^{138,140} as well as other monomers such as styrene⁸⁴ to give well-controlled molecular weights and relatively narrow MWDs ($M_w/M_n = 1.3$).

A series of 1,1,1-trichloroalkanes (I-2 to I-6) were examined as initiators for the Cu(I)-catalyzed polymerizations of styrene,¹⁵⁸ MMA,¹⁵⁶ and MA.¹⁵⁶ These

polychloroalkanes are efficient initiators to give controlled molecular weights and narrow MWDs ($M_w/M_n = 1.1-1.7$; narrowness depending on the initiators and monomers), with most of them serving as bifunctional initiators. In contrast, CHCl_3 (**I-2**) is not a good initiator in the Ru-**1**-based system probably due to the low activity or the high redox potential of the ruthenium complex relative to the copper catalyst.¹⁵⁴ 1,1-Dichloroalkanes such as CH_2Cl_2 and $\text{CH}_3\text{-CCl}_2\text{CH}_3$ and monochloroalkanes such as $\text{C}_4\text{H}_9\text{Cl}$ are totally inactive with Cu(I) and Ru(II) complexes.^{84,154,156}

A haloalkane with mixed halogens (**I-7**) led to living polymerization of methacrylates, acrylates, and acrylamides when coupled with ruthenium and nickel complexes.^{133,135,159,160} The weak C-Br bond is preferentially activated, while multifunctional initiation is possible. However, CCl_3Br is the initiator of choice if obtaining narrow MWDs is desired without paying attention to monomer structures.

The use of perfluoroalkyl iodides **I-8** and **I-9** and iodoform (**I-10**) was also studied in the Ru(II)- and Cu(I)-based systems for styrene and MA.^{57,142} Fine control of molecular weights and MWDs was attained for the former monomer, although an iodine-transfer mechanism could not be totally ruled out.

2. Allyl Halides

Allyl radical is relatively stable due to the conjugation of a vinyl group with the carbon-centered radical. Allyl chloride and bromide (**I-11**, X = Cl, Br) were thus employed as initiators for controlled radical polymerization of styrene in conjunction with CuCl/L-**1** and CuBr/L-**1**, respectively.¹⁶¹ The molecular weights agreed well with the calculated values assuming the formation of one living polymer chain per initiator and increased in direct proportion to monomer conversion. The MWDs were narrower with bromide than with chloride ($M_w/M_n \approx 1.2$ vs 1.3).

3. (Haloalkyl)benzenes

A series of (haloalkyl)benzenes (**I-12** to **I-15**) were extensively examined and proved effective specifically for polymerizations of styrene and its derivatives, due to the benzyl radical being similar to the growing radical chain ends therein. Among them, benzyl chloride (**I-12**, X = Cl), which forms a primary radical, has the strongest carbon-halogen bond, but induces the controlled radical polymerization of styrene with CuCl/L-**1** in the bulk at 130 °C.⁸⁴ The MWD is slightly broader than that obtained with CCl_4 under similar conditions, due to the slow initiation ($M_w/M_n = 1.45$ vs 1.30). A similar slow initiation was observed for benzyl bromide (**I-12**, X = Br) in the polymerization of styrene with CuBr/L-**4**, while the MWDs were quite narrow ($M_w/M_n = 1.2$).¹⁶² This initiator can also be employed with the CuCl/L-**4** pair for MMA to give relatively narrow MWDs ($M_w/M_n \approx 1.3$); note that this system involves halogen exchange between the initiator/dormant end and the metal catalyst (section II.F.5).

1-Phenylethyl halides (**I-13**, X = Cl, Br, I), adducts of styrene and the corresponding hydrogen halide, can be considered as a unimer of the dormant C-X terminal of polystyrene, and thus they are particu-

larly suited for controlling polymerizations of styrenes. The first example of the controlled radical polymerization of styrene indeed involves **I-13** (X = Cl) and CuCl/L-**1**, where the M_n increased in direct proportion to monomer conversion and agreed well with the calculated values in a molecular weight range from 4000 to 100000.²⁸ The relatively broad MWDs with the chloride **I-13** (X = Cl) are improved by using the bromide counterpart **I-13** (X = Br) for CuBr/L-**4** ($M_w/M_n \approx 1.5$ vs 1.1).^{84,85}

The activity of the carbon-halogen bonds of **I-13** (X = Cl, Br) as well as **I-12** (X = Br) in the Cu(I)/L-**3** system was examined by monitoring the capping of the generated radical species by TEMPO in toluene-*d*₈.¹⁶³ The activation energy of the C-X bonds decreased in the order **I-13** (X = Cl) > **I-12** (X = Br) > **I-13** (X = Br), which would reflect the rate of initiation and thereby the MWDs of the produced polymers. The bromo initiator **I-13** (X = Br) can be also employed with iron complexes such as Fe-**2**⁷¹ and a mixture of FeBr₂ and a nitrogen- or phosphine-based ligand⁷⁴ to give polystyrene with narrow MWDs ($M_w/M_n = 1.1-1.2$). The chloride **I-13** (X = Cl) and the bromide **I-13** (X = Br) are not suited for the styrene polymerization with ruthenium (Ru-**1**), giving broader MWDs [$M_w/M_n > 2$ (X = Cl), ≈ 1.9 (X = Br)] while the molecular weights were controlled with the latter.⁵⁷ However, the iodide **I-13** (X = I) gives controlled molecular weights and narrower MWDs ($M_w/M_n \approx 1.5$) in conjunction with Ru-**1**. The use of an iodide complex such as Re-**1** is preferred with such an iodide initiator to avoid halogen-exchange reactions, and polystyrenes with narrower MWDs ($M_w/M_n \approx 1.2$) are produced.¹⁴¹

Radical species can be generated more easily from benzhydryl chloride (**I-14**), carrying two phenyl groups. This compound induced the radical polymerization of MMA catalyzed by CuCl/L-**4** to give narrow MWDs ($M_w/M_n = 1.1-1.2$),¹⁶⁴ although it should be added slowly into the mixture to suppress bimolecular termination of the initiating radical species.¹⁵⁵ Introduction of an additional chlorine at the α -position, as in **I-15**, is effective in narrowing MWDs in the Cu(I)-catalyzed polymerization of styrene and MMA.¹⁶⁵ It serves as a bifunctional initiator for the former and a monofunctional initiator for the latter.

4. Haloketones

As described above, radical formation is favored by introducing an electron-withdrawing and conjugating substituent in the α -position relative to the C-halogen bonds. A series of haloketones (**I-16** to **I-18**) proved effective especially in Ru(II)- and Ni(II)-mediated living radical polymerizations of MMA. The PMMA obtained with trichloro- (**I-16**) and dichloroketones (**I-17**) in the presence of Ru-**1** had controlled M_n in direct proportion to monomer conversion, in good agreement with the calculated values, and narrow MWDs ($M_w/M_n = 1.1-1.2$).⁵⁶ A similar living polymerization is possible with more active Ru(II) complexes such as Ru-**2**⁵⁸ and Ru-**5**.⁶⁰ The controllability of polymerizations with **I-17** is superior to that with CCl_4 when coupled with Ru-**1**, while it serves as a bifunctional initiator.¹⁵⁴ A monofunc-

tional bromoketone (**I-18**) is specifically effective in nickel-catalyzed living radical polymerizations of MMA.^{132,135,136} However, haloketones are generally too reactive for the copper-catalyzed homogeneous systems and result in uncontrolled polymerizations probably due to the reduction of the electrophilic radical species into anions by the highly active Cu(I) catalysts.¹⁵⁵

5. Haloesters

Relative to haloketones, haloesters have been successfully employed with a wider range of metal complexes, including Ru, Fe, Cu, Ni, etc. A less electron-withdrawing ester group can moderately activate the carbon–halogen bond and does not make the resulting radical too electrophilic. This type of initiator can be more versatile for various monomers including styrenes, methacrylates, acrylates, etc. by careful design of their structures. Some specific examples follow.

Trichloroacetate **I-19** and dichloroacetate **I-20** can be employed for the Ru-**1**-mediated living radical polymerization of MMA to give narrow MWDs ($M_w/M_n \approx 1.2$), where the latter seems to be monofunctional.^{56,154}

A series of α -halopropionates (**I-21** and **I-22**, X = Cl, Br), model compounds of the dormant polymer terminal of acrylates, are suitable for not only acrylates but also styrenes and acrylamides. Ethyl 2-chloropropionate (**I-21**, X = Cl) was employed for the controlled radical polymerizations of MA and styrene catalyzed by CuCl/L-**1** to afford relatively narrow MWDs ($M_w/M_n \approx 1.5$).⁸⁴ A better controlled polymerization of MA is achieved with the bromides **I-21** and **I-22** (X = Br) in conjunction with CuBr/L-**1** to give narrower MWDs ($M_w/M_n \approx 1.2$).⁸⁴ A similar result was obtained with the combination of **I-23** and CuBr/L-**1** for the polymerization of styrene.¹⁶⁶ A nickel-based system with Ni-**2** and **I-21** (X = Br) gave another controlled polymerization of nBA.¹³⁴ The iodide compound **I-21** (X = I) is specifically effective in conjunction with an iodide complex such as Re-**1** to induce controlled polymerization of styrene.¹⁴¹

α -Halopropionates are generally less suitable for MMA polymerization due to the low reactivity of their C–X bonds compared with that of the dormant methacrylate terminal, due to the difference in the reactivity of secondary and tertiary halides.¹⁵⁴ However, the use of a halogen-exchange method for **I-21** (X = Br) and CuCl/L-**1** improves MMA polymerization to give controlled molecular weights and narrow MWDs ($M_w/M_n = 1.2$ – 1.4), where a less reactive chlorine-capped dormant species is generated after the initiation.¹⁶⁷ Controlled polymerization of *N,N*-dimethylacrylamide has been achieved with **I-22** (X = Cl) in conjunction with CuCl in toluene at 20 °C.¹⁶⁸

2-Bromoisobutyrate **I-24** (X = Br), a unimer model of poly(methacrylate) with a dormant C–Br terminal, is more versatile for various monomers such as methacrylates, acrylates, and styrenes; various metal complexes including Ru, Fe, Cu, and Ni can be employed in this case. Living or controlled radical polymerization of MMA was successfully done with **I-24** (X = Br) coupled with ruthenium,⁵⁶ iron,^{70,71}

copper,^{84,100} and nickel^{132–136} complexes to give well-controlled molecular weights and narrow MWDs ($M_w/M_n = 1.1$ – 1.5). Similarly, **I-24** (X = Br) is suitable for styrene and acrylates with ruthenium,⁶⁰ iron,⁷³ copper,⁸⁴ and nickel catalysts.¹³⁵ An iodoester (**I-24**, X = I) was specifically employed with iodo complexes of Re and Fe to initiate living radical polymerization of styrenes and acrylates, where it performs as a better initiator than other iodides such as **I-13** (X = I) and **I-21** (X = I).^{72,73,141,142,169} In contrast, the chloride versions such as $(\text{CH}_3)_2\text{C}(\text{CO}_2\text{CH}_3)\text{Cl}$ are poor initiators for MMA, although they can be regarded as a unimer of PMMA with a C–Cl dormant terminal.¹⁷⁰ The problem with the chloride initiators can be overcome with a dimer type of initiator, i.e., MMA dimers capped with chlorine (**I-25**, X = Cl), which achieves fast initiation catalyzed by Ru-**1** to give well-controlled molecular weights and narrower MWDs ($M_w/M_n \approx 1.3$). This is most probably due to electronic and/or steric effects. The former is related to the electron-deficient α -carbon atom, which is suggested by the lower-field ¹³C NMR chemical shifts relative to that in the unimer **I-24**, while the latter factor is related to the so-called back strain effect, which makes the dissociation of the C–Cl bond easier during the rehybridization of the α -carbon from sp^3 to sp^2 , thus relieving steric hindrance. When coupled with Ru-**6**, the dimer initiator is highly versatile and can be employed for not only MMA but also styrene and MA to give narrow MWDs under the same conditions ($M_w/M_n = 1.1$ – 1.2) as describe above.⁶² A similarly higher reactivity of the dimer-type compound was observed for the bromide version **I-25** (X = Br), which can be employed for MMA with Ru-**1**¹⁷⁰ and Ni-**3**.^{60,135}

The malonate-type initiator **I-26** can generate a stabilized initiating radical rapidly and can be employed for the living radical polymerization of MMA with Ru-**1**¹⁵⁴ and Fe-**1**⁷⁰ to afford narrow MWDs ($M_w/M_n \approx 1.2$) but slightly higher M_n values than the calculated values. Control of molecular weights for PMMA is achieved with the **I-26**/CuBr/L-**4** system, while no polymerizations occurred with $\text{CH}(\text{CO}_2\text{Et})_2\text{Br}$.¹⁵⁵

A compound such as **I-27**, which possesses one ester and one phenyl group adjacent to the chlorine atom, induces controlled polymerization of both MMA and styrene in the presence of CuBr/L-**1**.¹⁷¹ The initiation occurs faster than with **I-21** (X = Cl) and $\text{CH}_2\text{ClCO}_2\text{C}_2\text{H}_5$, both of which have no phenyl substituent. A bromide (**I-28**) with a similar structure proved effective in the CuBr/L-**24**-mediated polymerization of MMA.¹⁴⁹

6. Haloamides

Bromides with *N,N*-alkylamide groups (**I-29** and **I-30**) can be good initiators for acrylamides. They were employed for the Ru-catalyzed polymerization of *N,N*-dimethylacrylamide (DMAA) to give controlled molecular weights and broad MWDs ($M_w/M_n \approx 1.6$).¹⁶⁰ In contrast, the chloride version $\text{CH}_3\text{CH}(\text{CONMe}_2)\text{Cl}$ failed to give controlled molecular weights,¹⁶⁰ and similar halides without alkyl substituents on the amide nitrogens, such as CH_3CH -

(CONH₂)X (X = Cl, Br), do not lead to controlled polymerization of DMAA.¹⁷²

7. Halonitriles

Halonitriles I-31 (X = Cl, Br), unimer models of halogen-capped dormant poly(acrylonitrile), are specifically employed for the polymerization of acrylonitrile with copper halides. Controlled molecular weights and narrow MWDs ($M_w/M_n = 1.1-1.4$) are achieved.^{173,174} The strong electron-withdrawing cyano group facilitates the formation of the initiating radical, and may thus be employed for other monomers such as MMA with Fe catalysts⁷⁴ and styrene with CuCl/L-1.⁸⁴

8. Sulfonyl Halides

Sulfonyl halides, particularly arenesulfonyl halides, can afford radical species much faster than carbon halides by the assistance of a metal complex and efficiently add to olefins with little dimerization of sulfonyl radicals in comparison to carbon-centered radicals. Another feature of the compounds is that there is little effect of the substituents on the rate of addition to an olefin. These properties make sulfonyl halides an efficient and "universal" series of initiators for the metal-catalyzed living radical polymerizations of various monomers including methacrylates, acrylates, and styrenes (Figure 9).^{152,175-177}

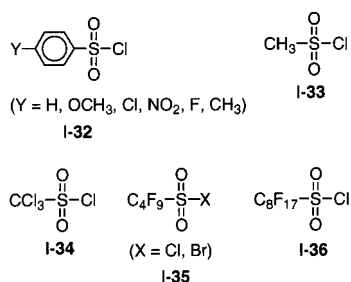


Figure 9. Sulfonyl halide initiators.

Arenesulfonyl halides I-32 were first employed for the CuCl/L-1-catalyzed polymerization of styrene in the bulk at 130 °C to give polymers with controlled molecular weights and relatively narrow MWDs ($M_w/M_n = 1.4-1.8$).¹⁵² No significant effects were observed with different ring substituents.

The polymers possess one sulfonyl group per chain, which can be utilized as end-functional polymers as discussed later (section III.B.1). Narrower MWDs ($M_w/M_n = 1.2-1.4$) were obtained in MMA polymerization with I-32 as well as I-33 and I-34 in conjunction with CuCl/L-1 in *p*-xylene at 90 °C.¹⁷⁵ In a homogeneous system with CuCl/L-4, I-32 can afford narrow MWDs ($M_w/M_n = 1.1-1.3$) for styrene, MMA, and nBA.¹⁷⁶ The fast addition of the sulfonyl radical to these monomers was evidenced by ¹H NMR analysis of the reactions, where the apparent rate constants of initiation are 4 (for styrene and MMA), 3 (nBA), and 2 (MA) orders of magnitude higher than those of propagation. A similar controlled and homogeneous polymerization of MMA with I-32 (X = CH₃)/CuBr/L-4 was reported in diphenyl ether at 90 °C.¹⁷⁸ A better control of molecular weights and MWDs with I-32 (X = CH₃)/CuBr/L-9 in diphenyl ether was also

observed when compared with that of bromoisobutyrate [I-24 (X = Br)]/CuBr/L-9 in *p*-xylene.¹⁷⁹

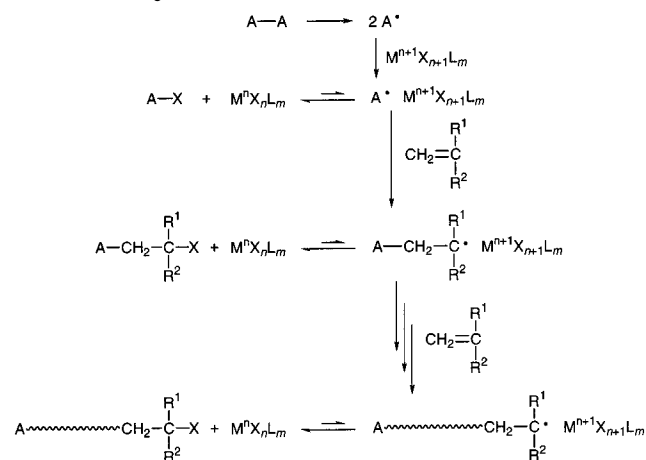
Perfluoroalkanesulfonyl halides I-35 and I-36 induced controlled polymerization of styrene and MMA in the presence of copper catalysts, although the initiation efficiency is lower.¹⁷⁷ With the alkanesulfonyl halides I-35 and I-36, decomposition by loss of SO₂ from the initial sulfonyl radical occurs to give a perfluoroalkyl radical, which then adds to the monomer to initiate the polymerization.

The use of arenesulfonyl halides was also investigated for the ruthenium-catalyzed polymerization of MMA.¹⁸⁰ Living polymers are indeed attained, where the α -end group ($F_n \approx 1.0$) and the MWDs are controlled ($M_w/M_n = 1.2-1.5$), whereas the M_n values were higher than the calculated values due to low initiation efficiency ($I_{\text{eff}} \approx 0.4$).

9. Conventional Radical Initiators

Another route to the metal-catalyzed living or controlled radical polymerization is through initiation by a conventional radical initiator (A-A) such as AIBN in conjunction with a metal complex [$M^{n+1}X_{n+1}L_m$] at a higher oxidation state, for example, CuCl₂/L-1 (Scheme 4). This system is sometimes

Scheme 4. Reverse-Type Metal-Catalyzed Living Radical Polymerization



called a "reverse (or alternative)" atom-transfer radical polymerization.^{80,130} The difference between the normal route with R-X/ $M^nX_nL_m$ and the reverse route lies in the initiation mechanism. The latter is initiated by the formation of radical species A• via homolytic cleavage, while the former by the formation of radical species from R-X assisted by $M^nX_nL_m$. The radical species thus generated (A•) gives an adduct (A-X) by abstraction of halogen from $M^{n+1}X_{n+1}L_m$, leaving a metal complex at a lower oxidation state [$M^nX_nL_m$]. Alternatively, A• adds to the monomer to form an initiating radical species [A-CH₂-C(R¹)-(R²)•] or a propagating species, which is also converted into a similar covalent species with a C-X bond accompanying reduction of $M^{n+1}X_{n+1}L_m$. After formation of the dormant C-X species and the metal catalyst at a lower oxidation state, the polymerization proceeds similarly to the normal-type metal-catalyzed processes already discussed. Figure 10 summarizes

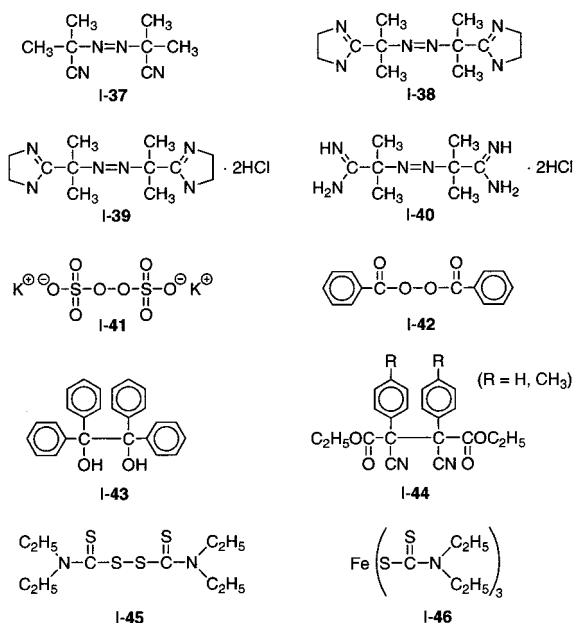


Figure 10. Conventional radical initiators employed for metal-catalyzed polymerizations.

the initiators thus far employed in such reverse-type polymerizations.

This type of polymerizations was first reported for the bulk polymerization of styrene with AIBN (I-37)/CuCl₂/L-1 at 130 °C.¹³⁰ The M_n increased in direct proportion to monomer conversion and agreed well with the calculated values assuming that one AIBN molecule forms two polymer chains. The MWDs were narrow ($M_w/M_n = 1.3-1.6$). However, the heterogeneous system with L-1 is not applicable for other monomers such as methacrylates and acrylates. This can be overcome with the use of the homogeneous CuBr₂/L-4 system for MA and MMA polymerization¹³¹ or by lowering the initiation temperature to 65–70 °C followed by polymerization at 100 °C for MA even in the heterogeneous system.¹⁸¹

Iron(III) chloride (FeCl₃) with PPh₃ ligands can be similarly employed with AIBN for MMA⁸⁰ and styrene,¹⁸² while the AIBN/FeBr₃/*n*-Bu₄PBr system is effective in MMA and MA polymerization.⁷⁵

An azo compound with an imidazoline group (I-38) is applicable to MMA coupled with FeCl₃ and PPh₃.¹⁸³ Water-soluble azo compounds such as I-39 and I-40 with CuBr₂ and L-4 induced emulsion living radical polymerization of nBMA ($M_w/M_n = 1.2-1.6$), though the initiation efficiency is rather low.¹⁸⁴ A similar emulsion polymerization was conducted with I-41.¹⁸⁴

A conventional peroxide initiator such as BPO (I-42) does not work in a manner similar to that of azo initiators in the homogeneous system for styrene with CuBr₂ and L-4.¹⁸⁵ In this polymerization, the Cu(I) species is generated via reduction of Cu(II) species by a styryl radical and further acts as an accelerator in the decomposition of BPO. It then reacts with the remaining BPO to form the benzoyloxy radical and inactive copper(II) benzoate salts again. Thus, no polymerization occurs. However, the use of a heterogeneous system and low-temperature initiation at 70 °C followed by the polymerization at 110 °C in fact induces styrene polymerization. The polymers had

narrow MWDs ($M_w/M_n = 1.2-1.4$) and controlled M_n values, which agreed well with the calculated values assuming the formation of one polymer chain per BPO molecule.¹⁸⁶ The polymerizations of styrene and MMA with BPO can be controlled with copper(I) halide.^{185,187}

There were also several reports on the use of other radical generators such as I-43^{188,189} and I-44¹⁹⁰⁻¹⁹² in conjunction with FeCl₃/PPh₃ or with CuCl₂/L-1 for MMA and styrene. Polymers obtained with I-43 have a methyl group at the α -end because a hydrogen radical is the initiator. Low temperatures are enough for I-44 (75 °C for R = H, 85 °C for R = CH₃) to afford PMMA with narrow MWDs ($M_w/M_n = 1.2-1.3$), although the M_n values were lower than the calculated values.

In situ heating of a mixture of I-45 and FeCl₃ with PPh₃ results in the formation of dithiocarbamate-iron complexes that decompose into Et₂NC(S)S-Cl and FeCl₂/PPh₃, and finally initiates the polymerization via activation of the S-Cl bond by FeCl₂.¹⁹³ The bulk MMA polymerization at 100 °C reaches 80% in 8 min to give controlled molecular weights and narrow MWDs ($M_w/M_n \approx 1.1$). A similar polymerization of MMA can also be done with an iron(III) complex system (I-46/FeCl₃/PPh₃).¹⁹⁴ Air could be a radical source for methacrylate polymerization with CuCl₂/L-29 and results in polymers with high molecular weights up to 700000 and narrow MWDs ($M_w/M_n \approx 1.1$).¹⁹⁵

In addition to the wide variety and number of initiators shown in Figures 8–10, various “functionalized” initiators have been designed and examined, as will be separately treated later (cf. Figure 13).

C. Monomers

The rapid progress and proliferation of metal-catalyzed living radical polymerization has allowed a variety of vinyl monomers to be polymerized into well-defined polymers of controlled molecular weights and narrow MWDs. Most of them are conjugated monomers such as methacrylates, acrylates, styrenes, acrylonitrile, acrylamides, etc., except dienes, which possess not only alkyl substituents but also aprotic and protic functional groups. This fact attests to the versatility and flexibility of metal catalysis for precision polymerization.

However, less conjugated monomers such as vinyl acetate, vinyl chloride, and ethylene are still difficult to polymerize in a controlled way by metal-catalyzed polymerizations. This is most probably due to the difficulty in activation of their less reactive carbon-halogen bonds. The following sections will discuss these aspects from the viewpoint of the monomers listed in Figure 11. Functional monomers will be discussed later in another section, Precision Polymer Synthesis.

1. Methacrylates

Living radical polymerization of methacrylates has been achieved by the use of various complexes including ruthenium, iron, copper, nickel, palladium, and rhodium. Among them, the most precisely con-

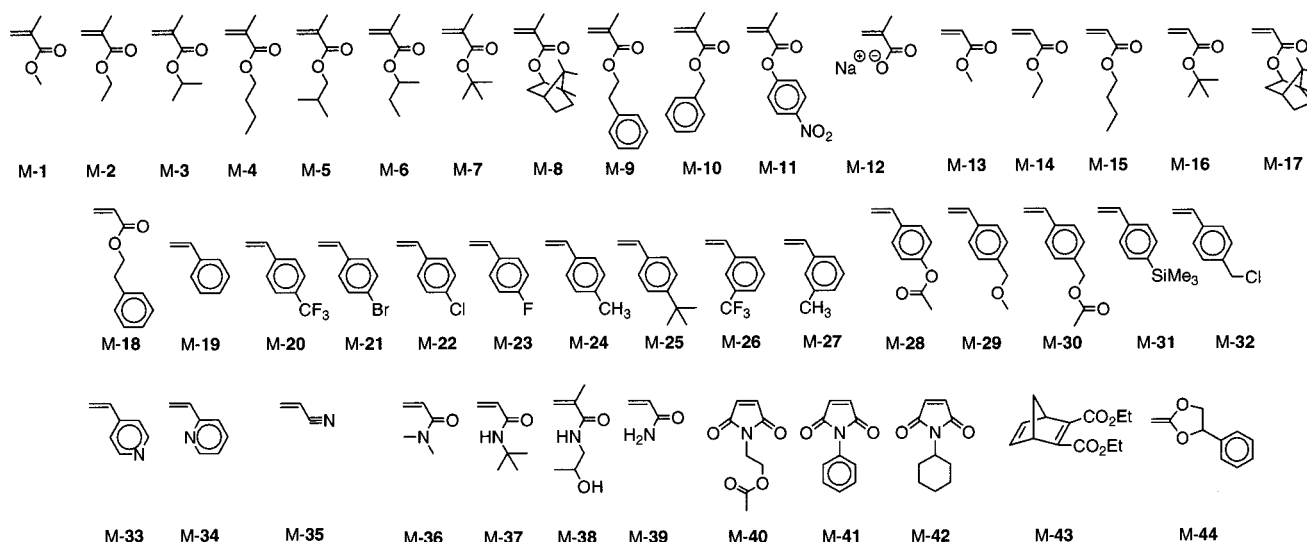


Figure 11. Monomers.

trolled polymerizations ($M_w/M_n = 1.1-1.2$) were reported with the R-Cl/Ru,⁵⁶ R-Br/Ni,¹³³ R-Br/Cu,¹⁰⁰ and RSO₂Cl/Cu¹⁷⁶ systems, where R-X means an initiator with a particular halogen (X). The carbon-halogen bonds derived from methacrylates are highly reactive, in contrast to those from other monomers due to the two substituents, methyl and ester groups, which stabilize the relevant radical species. This may in turn require relatively mild metal complexes such as ruthenium and nickel, whereas some special issues, such as use of polar solvents⁸⁴ or a halogen-exchange reaction,¹⁹⁶ should be considered for the copper/bipyridine-based systems.

Recommended initiators for methacrylate polymerizations are I-24 (X = Br) and I-25 (X = Cl), both of which are unimer and dimer models of poly(methacrylate) dormant terminals, respectively. For example, PMMA with precisely controlled molecular weights, very narrow MWDs ($M_w/M_n = 1.1$), and nearly perfect end-capping with halogen was obtained with the I-25 (X = Cl)/Ru-5/Al(O-*i*-Pr)₃ initiating system.^{60,197} Alternatively, arenesulfonyl chlorides can lead to well-controlled poly(methacrylate)s with narrow MWDs ($M_w/M_n = 1.1-1.2$) in combination with copper catalysts.^{126,176}

The alkyl substituents of methacrylates are varied as methyl (M-1),^{27,84,100,132,133,176} ethyl (M-2),^{102,198} isopropyl (M-3),¹⁹⁹ *n*-butyl (M-4),^{102,132,176,198} isobutyl (M-5),¹⁰² *sec*-butyl (M-6),¹⁰² *tert*-butyl (M-7),^{63,102} isobornyl (M-8),⁶³ 2-phenylethyl (M-9),¹⁹⁵ benzyl (M-10),¹⁹⁹ and 4-nitrophenyl (M-11)¹⁶⁶ methacrylates were also polymerized in a controlled way, and the polymer from M-11 can be converted easily into poly(methacrylic acid) via deprotection of the nitrophenyl group. Sodium methacrylate (M-12), an ionic monomer, can be polymerized directly into poly(methacrylic acid) sodium salt with controlled molecular weights and narrow MWDs ($M_w/M_n = 1.2-1.3$) with a water-soluble bromide initiator and CuBr/L-1 in water under alkaline conditions (pH 8-9) at 90 °C, although the polymerization stopped around 70-80%.²⁰⁰

2. Acrylates

Acrylates generate highly reactive radical species but give less reactive carbon-halogen bonds than those of methacrylates. These differences from the methacrylate counterparts thus call for active catalysts with lower redox potentials. Copper-based systems have most extensively been studied and are best suited in controlling the MWDs ($M_w/M_n = 1.1-1.2$)^{84,85,176} of poly(acrylate)s, but ruthenium,⁶² iron,²⁰¹ nickel,^{134,135} and rhenium¹⁴² catalysts are often effective too. In the Cu(I) catalysis, chloride and bromide initiators may be coupled with CuBr and CuCl in conjunction with various nitrogen-based ligands. For example, CuBr with I-31 (X = Br) and L-3 afforded poly(MA) with very narrow MWDs ($M_w/M_n = 1.1$) in the bulk at 110 °C.⁸⁵ In contrast, bromide and iodide initiators are preferably used with other metals such as Ru(II)⁶² to increase the reactivity of the dormant C-X bonds. Among the most suitable initiators are unimer models of poly(acrylate)s such as I-21.

Similarly to methacrylates, various alkyl groups are available as substituents including methyl (M-13),^{62,84,85,135,142,176,201} ethyl (M-14),⁹⁴ *n*-butyl (M-15),^{84,134,142,176,201} *tert*-butyl (M-16),²⁰¹⁻²⁰³ isobornyl (M-17),²⁰⁴ and 2-phenylethyl (M-18).¹⁹⁵

3. Styrenes

A large number of styrenic monomers have been investigated in metal-catalyzed radical polymerizations. Polymerization of styrene (M-19) can be controlled with copper,^{28,84,85,152,176} ruthenium,^{57,60,62,66,86,205} iron,⁷¹⁻⁷⁵ rhodium,^{86,140} rhenium,¹⁴¹ and molybdenum catalysts.¹⁴⁴ The polymerizations have actively been studied with the copper-based systems, among which precisely controlled molecular weights and very narrow MWDs ($M_w/M_n = 1.1$) were obtained in a homogeneous system consisting of I-13 (X = Br), CuBr, and L-3 in the bulk at 130 °C.⁸⁵ Similar well-controlled polymerizations are feasible with several ruthenium (Ru-5)⁶⁰ and iron (Fe-2,⁷² Fe-3,⁷³ and Fe-4⁷¹) complexes in conjunction with a bromide or iodide initiator. Even a chloride initiator (I-25, X = Cl) can afford narrow MWDs ($M_w/M_n = 1.1$) when coupled

with the Ru(II)–Cp* complex (Ru-6) in the presence of Al(O-*i*-Pr)₃ in toluene at 80 °C.⁶²

A series of substituted styrenes (M-19 to M-27) were polymerized with the I-13 (X = Br)/CuBr/L-1 system in diphenyl ether at 110 °C to give controlled M_n that increased in direct proportion to monomer conversion.²⁰⁶ The polymerization rate was faster with more electron-withdrawing substituents due to the increase of monomer reactivity and the carbon–halogen bond in the dormant species. The MWDs of the polymers with electron-donating substituents (M-24 and M-25) were relatively broad ($M_w/M_n = 1.4–1.7$). Introduction of a strongly electron-donating substituent such as a methoxy group gave only oligomers, probably because of the formation of cationic propagating species via the heterolysis of the dormant C–Br.

Though not in the late-transition-metal family, a rhenium complex is applicable for both electron-donating (M-24) and -withdrawing (M-22) groups to give well-controlled molecular weights and narrow MWDs ($M_w/M_n = 1.2–1.3$).¹⁶⁹ Living radical polymerization of 4-acetoxystyrene (M-28) was reported with the use of a copper-²⁰⁷ or iron-based¹⁶⁹ system. The acetoxy groups in the polymers can be removed after the polymerization to form poly(*p*-vinylphenol) with controlled molecular weights.²⁰⁸ Copolymerizations of M-29 or M-30 with styrene were studied with the copper-based systems to give well-controlled copolymers.²⁰⁹ Rhenium (Re-1) and iron (Fe-5) complexes induced polymerization of M-30 in conjunction with I-24 (X = I) to give controlled molecular weights but relatively broader MWDs ($M_w/M_n \approx 1.8$) due to side reaction of its benzyl group.¹⁶⁹ Controlled polymerization of a silyl-substituted styrene (M-31) was also achievable.²¹⁰ 4-(Chloromethyl)styrene (M-32), which has a reactive C–Cl bond in the unit, is polymerized with the copper-based systems to produce a hyperbranched or linear polymer depending on the conditions.^{211–213} This will be discussed later in Precision Polymer Synthesis (section III.I).

4. Vinylpyridines

Metal-catalyzed living radical polymerizations of vinylpyridines were investigated with the copper-based systems. One of the difficulties in the polymerization is a decrease of catalytic activity imposed by the coordination of the monomers by the metal complex. Controlled radical polymerization of 4-vinylpyridine (M-33) was achieved by an initiating system consisting of a strong binding ligand such as L-32 and a chloride-based system [I-13 (X = Cl)/CuCl] in 2-propanol at 40 °C.²¹⁴ The M_n increased in direct proportion to monomer conversion, and the MWDs were narrow ($M_w/M_n = 1.1–1.2$). In contrast, 2-vinylpyridine (M-34) can be polymerized in a controlled way with chlorine-capped polystyrene as an initiator and the CuCl/L-1 pair in *p*-xylene at 140 °C.²¹⁵ Block copolymers with narrow MWDs ($M_w/M_n = 1.1–1.2$) were obtained therein.

5. Acrylonitrile

A good control of molecular weights and MWDs was accomplished for this monomer (M-35) with a

copper-based system, consisting of I-31 (X = Cl, Br), CuX (X = Cl, Br), and L-1 in ethylene carbonate at 45–65 °C.^{173,174} The M_n is controlled up to 30000, keeping relatively narrow MWDs ($M_w/M_n < 1.5$). The end-group analysis showed some loss of the terminal halogen most probably due to the reduction of the growing radical by CuX to form the corresponding polymer anion that subsequently deactivates quickly.

6. Acrylamides

Polymerizations of acrylamides were investigated with several systems based on copper and ruthenium. The system with Ru-1 and a bromide initiator such as I-29 in the presence of Al(O-*i*-Pr)₃ induced quantitative polymerizations of M-36 in toluene at 60–80 °C to give polymers of controlled molecular weights and relatively broad MWDs ($M_w/M_n \approx 1.6$).¹⁶⁰ In contrast, molecular weight control is difficult with a chloride initiator. The copper-based systems are applicable, but the polymerization strongly depends on the initiators, copper halides, ligands, temperatures, and solvents. Namely, in some cases the polymerizations were not quantitative due to side reactions such as cyclization and loss of terminal halogens.^{117,168,172} Among them, I-22 (X = Cl)/CuCl/L-32 induced the best controlled polymerization in toluene at 20 °C to give narrow MWDs ($M_w/M_n = 1.1–1.2$), though limited to 80% conversion.¹⁶⁸ Similar controlled polymerizations were also feasible for M-37 and M-38 with the same initiating system.¹⁶⁸ Unsubstituted acrylamide (M-39) was polymerized with CuCl/L-1 in conjunction with benzyl chloride I-12 (X = Cl) or with a surface-confined initiator in DMF at 130 °C.^{216–218} The polymers obtained with I-12 were analyzed by matrix-assisted laser desorption–ionization time-of-flight mass spectrometry (MALDI-TOF-MS), which showed monomodal MWDs, but there was no detailed analysis of the polymer. The polymer obtained by the surface initiation had narrow MWDs ($M_w/M_n = 1.1–1.3$).

7. Other Monomers

Via metal catalysis, cyclic monomers such as *N*-substituted maleimides M-40, M-41, and M-42 do not homopolymerize but can copolymerize with vinyl monomers, among which alternating copolymers can be obtained with styrene via a radical mechanism. The I-13 (X = Br)/CuBr/L-1 system induced alternating copolymerizations with styrene to give controlled molecular weights and narrow MWDs ($M_w/M_n = 1.1–1.4$) in the bulk or anisole at 80–110 °C.^{219–222}

A bicyclic monomer containing a maleate ester unit (M-43) undergoes a very slow 2,6-addition polymerization with I-12 (X = Cl)/CuCl/L-1 in the bulk at 130 °C to afford narrow MWDs ($M_w/M_n \approx 1.2$) (11% conversion in 2 weeks).²²³ Enchainment of this monomer to the chlorine-terminated polystyrene increases the decomposition temperature of the polymer.

Ring-opening living radical polymerization was also reported for M-44, where the I-23/CuBr/L-1 system gave polymers with controlled molecular weights and narrow MWDs in the bulk at 120 °C.²²⁴ However, unlike in conventional radical polymerization, the content of the ring-opened units is not 100% but

varies from 38% to 67% depending on the conditions. Cationic polymerizations concurrently occur, which can be suppressed by the addition of pyridine.

As pointed out, living radical polymerization of less conjugated monomers such as vinyl acetate has not been achieved yet. However, irreversible activation of the carbon–halogen bond in CCl_4 with $\text{Fe}(\text{OAc})_2/\text{L-24}$ generates trichloromethyl radical to induce radical polymerization of vinyl acetate via the radical telomerization mechanism.²²⁵ The molecular weights can be controlled by the molar ratio of monomer to CCl_4 although the MWDs were broad in the usual radical telomerization ($M_w/M_n \approx 1.8$).

Polymerization of ethylene is one of the most important unsolved problems in metal-catalyzed living radical polymerization. This is due to the difficulty of the activation of the primary carbon–halogen bond. The unpolymerizable nature of ethylene can be utilized for the end-functionalization of PMMA with a terminal $\text{CH}_2\text{CH}_2\text{Br}$ group (section III.B.2).²²⁶

D. Additives

Metal-catalyzed living or controlled radical polymerizations can generally be achieved with initiating systems consisting of an organic halide as an initiator and a metal complex as a catalyst or an activator as described above. However, these polymerizations are slow in most cases due to low concentration of the radical species, as required by the general principle, the dormant-active species equilibria, for living radical polymerization (see the Introduction).

A promising solution for this inherent problem is the use of additives. Some additives are needed for acceleration and/or better control of the polymerizations. These additives most probably can effectively reduce the metal species in higher oxidation states or form more efficient catalysts via coordination.

Metal alkoxides such as $\text{Al}(\text{O-}i\text{-Pr})_3$ are employed for the ruthenium-, iron-, nickel-, rhenium-, and copper-catalyzed polymerizations and are effective in increasing the polymerization rate as well as narrowing the MWDs of the produced polymers. In fact, the use of such additives can be found in the first examples of metal-catalyzed living radical polymerization. Thus, for the mild catalyst Ru-1, $\text{MeAl}(\text{ODBP})_2$ was added to achieve a faster and quantitative polymerization of MMA with CCl_4 in toluene at 60 °C.²⁷ A trialkoxide [$\text{Al}(\text{O-}i\text{-Pr})_3$] is less active as an additive but more effective in controlling the molecular weights and MWDs than $\text{MeAl}(\text{ODBP})_2$.^{56,198} Other metal alkoxides such as $\text{Ti}(\text{O-}i\text{-Pr})_4$ and $\text{Sn}(\text{O-}i\text{-Pr})_4$ induce faster polymerizations of MMA with Ru-1 than $\text{Al}(\text{O-}i\text{-Pr})_3$, while the controllability is lower.²²⁷ Aluminum acetylacetonate [$\text{Al}(\text{acac})_3$] is an alternative mild additive that does not induce an ester-exchange reaction between the ester group and the monomer or monomer units in the polymer chain, which might occur with aluminum alkoxides.²²⁸ These metal alkoxides are also effective for other complexes such as Fe-3,⁷² Ni-2,¹³³ Re-1,¹⁴¹ and CuBr/L-1.²²⁹ $\text{Al}(\text{O-}i\text{-Pr})_3$ can even make the Cu(II) species active, where the controlled polymerizations of styrene,

MMA, and EA were possible with an organic bromide and CuBr_2 in the presence of $\text{Al}(\text{O-}i\text{-Pr})_3$.^{93,94}

The addition of aluminum compounds was initially intended to increase the monomer reactivity via coordination to its carbonyl group or to increase the reactivity of the terminal group via the coordination of the terminal carbonyl group.²⁷ However, this possibility proved less probable, because strong Lewis acids such as SnCl_4 were not effective in a similar acceleration.²²⁷ There was no increase in the halogen-exchange rate in the model reaction between I-24 ($X = \text{Br}$) and Ru-1 on addition of $\text{Al}(\text{O-}i\text{-Pr})_3$, while under similar conditions the polymerization rate was clearly increased relative to that of the additive-free system.¹⁷⁰ Possible interactions between the added $\text{Al}(\text{O-}i\text{-Pr})_3$ and monomer, terminal group, and ruthenium complex were investigated with the use of kinetics, NMR, and cyclic voltammetry.²²⁷ These studies suggest that the added metal compounds most probably interact with the metal catalysts in their higher oxidation states, or increase the concentrations of radical species out of the coordination spheres, resulting in smooth redox reactions. Further studies are required to clarify these interesting features of metal-mediated radical processes.

Zerovalent metals such as Cu(0) and Fe(0) can effectively reduce CuBr_2 and FeBr_3 into active CuBr and FeBr_2 , respectively, to dramatically increase the polymerization rate.¹²⁹ For example, addition of Cu(0) to the polymerization mixture of MA with I-22 ($X = \text{Br}$)/CuBr/L-4 in the bulk at 90 °C increased the rate by about 10 times; i.e., the reaction reached 97% conversion in 570 min without additives, whereas 96% in 55 min in the presence of Cu(0). This is attributed to the removal of a small amount of Cu(II) species generated via irreversible termination of the growing or the initiating radical species. A similar fast polymerization is possible with CuBr_2 in the presence of Cu(0). This allows the controlled radical polymerization even in the presence of oxygen or without purification of the monomer, where Cu(0) and Fe(0) can reduce the generated Cu(II) and Fe(III) species into active Cu(I) and Fe(II), respectively.²³⁰ The I-13 ($X = \text{Br}$)/CuBr₂/Cu(0)/L-4 system induced a fast polymerization of unpurified styrene at 110 °C to reach 90% conversion within 2 h. Controlled molecular weights and narrow MWDs are available even when the polymerization is performed in ampules sealed in air. However, no polymerization occurred open to air.

Phenols usually serve as radical inhibitors in conventional radical polymerization but can enhance the polymerizations of MMA with I-21 ($X = \text{Br}$)/CuBr/L-9 ($R = n\text{-Pen}$).²³¹ For example, on addition of 10 equiv of 2,6-di-*tert*-butyl-4-methylphenol with respect to initiator ($[\text{I-21}]:[\text{CuBr}]:[\text{L-9}]:[\text{phenol}] = 1:3:1:10$), the conversion increased from 55% to 75% in 4 h in xylene at 90 °C without any changes in the MWDs. Similar effects were observed for 4-methoxyphenol, phenol, and 2,6-di-*tert*-butylphenol.^{231–233} No inhibition but enhancement of the polymerization by the addition of phenols may suggest that the growing species is different from that in conventional radical polymerization. However, phenols do not act as

inhibitors even for some conventional free radical (meth)acrylate polymerizations as suggested elsewhere.¹⁵⁵ An explanation is that the added phenols substitute nitrogen-based ligands on copper catalysts to increase the catalytic activity, which is suggested by the isolation of methanol-coordinated catalysts²³⁴ and NMR analysis of the mixture of catalysts and phenols.²³³

Benzoic acid also increases the polymerization rate with copper catalysts, most probably via displacement of the nitrogen ligand and creation of a coordination site on the metal.²³⁵ Similarly, carboxylate salts such as sodium benzoate and acetate have remarkable effects on rate enhancement.¹⁰⁷ Addition of sodium benzoate, 4 equiv with respect to CuCl, to I-32 (Y = OCH₃)/CuCl/L-1 enhances the polymerization rate of nBMA 2.4 times in diphenyl ether at 120 °C, where the reaction reaches 90% conversion in 1 h. The MWDs were still narrow. A similar rate enhancement was observed with a mixture of para-substituted benzoic acids and metal carbonates M₂-CO₃ (M = Cs, K, Na, Li). These are due to in situ formation of cuprous carboxylate that has higher activity as described above (section II.A.3).

The ruthenium-catalyzed living radical polymerizations provide good cases for considerable acceleration by the addition of alkylamines.^{61,236} For example, on addition of *n*-butylamines to the polymerization of MMA with I-25 (X = Cl)/Ru-1 in toluene at 80 °C, the rate was increased dramatically. Time for 75% conversion: 269 h (no additive) > 29 h [Al(*i*-Pr)₃] > 17 h (*n*-Bu₃N) > 9 h (*n*-Bu₂NH) > 4 h (*n*-BuNH₂). *n*-Bu₃N and *n*-Bu₂NH gave narrow MWDs ($M_w/M_n = 1.2$) and controlled molecular weights, similarly to Al(*i*-Pr)₃, but broad MWDs were obtained with *n*-BuNH₂ ($M_w/M_n \approx 1.8$). These added amines most probably coordinate to the ruthenium complex to produce more active complexes, as suggested by NMR analysis of amine/Ru(II) catalyst mixtures. An increased catalytic activity was also observed on addition of silica gel supported amine ligands.¹⁴⁸

In the heterogeneous systems based on Cu₂O/L-1 and Cu(0)/L-1, phase-transfer catalysts such as C(CH₂-OCOPh)₄ and poly(ethylene glycol) can increase the rate and control the polymerization more precisely.¹⁰⁷

Rate enhancement can also be achieved by irradiation of visible light.²³⁷ The polymerization of MMA with I-17/CuCl/L-1 in toluene at 80 °C in the dark ceased around 40% conversion, but under irradiation of visible light, the polymerization became quantitative. This is due to a photochemical effect on the inner-sphere complex between the catalyst and the dormant alkyl chloride.

E. Solvents

Metal-catalyzed living radical polymerizations may be carried out either in solution or in the bulk. Importantly, unlike conventional free radical polymerization, the Trommsdorff or gel effect is absent in these living processes in the bulk.²³⁸ For the solution processes, nonpolar or less polar solvents are employed, such as toluene, xylene, and benzene. Polar solvents are sometimes employed for not only solubilizing the monomers, the produced polymers, and

the catalysts but also acceleration and better control of the polymerization. Due to the radical nature of the polymerizations, even protic solvents such as alcohol and water can be employed. Some of these solvents, e.g., toluene, are known as chain-transfer agents, but the effects of potential chain-transfer agents have not yet been examined well in metal-catalyzed living radical polymerizations.

1. Aprotic Polar Solvents

Aprotic polar solvents thus far employed in metal-catalyzed polymerizations include dimethoxybenzene (DMB), diphenyl ether (DPE), ethylene carbonate, acetonitrile, *N,N*-dimethylformamide (DMF), and acetone, among others. Most of them are employed for copper catalysts because of their low solubility. For well-solubilized Ru(II), Ni(II), and Fe(II) complexes with phosphine or other ligands, such an additional precaution is not necessary, and toluene or other relatively nonpolar solvents have mostly been used.

Unsubstituted 2,2'-bipyridine (L-1) cannot completely solubilize copper halide in the bulk or nonpolar solvents, and thus the polymerization systems are heterogeneous as described above. Various solvents were thus investigated in the polymerization of nBA with I-22 (X = Br)/CuBr/L-1, and ethylene carbonate proved effective in fast and homogeneous living polymerizations.²³⁹ Relative to the heterogeneous systems, these reactions give polymers of narrower MWDs. This is due to the increased solubility of the copper complex and/or to the change in the structure of the copper species (known to form a dimeric species in organic media) into a monomeric form. Similar effects were observed for DMF and acetone in *tert*-butyl acrylate (tBA) polymerizations with I-22 (X = Br)/CuBr/L-24.²⁰² Styrene polymerization with I-13 (X = Cl)/CuCl/L-1 at 130 °C became homogeneous in the presence of a limited amount of DMF (~10% v/v) to give polymers with well-controlled molecular weight up to 40000.⁸⁸ Copper-based systems with bipyridines, such as R-Cl/CuCl/L-4, are not suited for controlling methacrylate polymerization in the bulk or in nonpolar solvents, but are effective in DPE solvent, where monomeric copper species may form.^{107,126,164,178,240} Acetonitrile is another choice of solvent in some Cu-catalyzed polymerizations.^{93,112,167,241}

In the homogeneous MMA polymerization with I-32 (Y = CH₃)/CuBr/L-9 (R = *n*-Pen), the rate increased in the order xylene < DMB < DPE,¹⁷⁹ probably due to the differences in the dielectric constant and coordination ability of the solvents. With the homogeneous Ru-1 catalyst, the polymerization of MMA was faster in a polar solvent such as CH₂Cl₂ than in toluene.¹⁵⁹ A more detailed analysis on solvent effects was carried out by end-capping a polymer radical with hydroxyl-TEMPO, where the radical intermediate was generated from bromide macroinitiators via CuBr/L-4 catalyst.²⁴² A polar solvent such as butyl acetate increases the radical-generation rate from poly(acrylate)s but not from polystyrene. On the other hand, no rate increase was found for both macroinitiators in DMF, which is

considered not only a polar solvent but also a coordinating ligand.

2. Protic Polar Solvents

Protic polar solvents such as alcohols are necessary to solubilize polar functional monomers and their polymers. Due to the robust nature of several catalysts to hydroxyl groups, alcohols can be employed in the metal-catalyzed living or controlled radical polymerization.

Ruthenium complexes such as Ru-1 are stable in alcohol and can induce living radical polymerization of MMA in toluene/methanol mixtures or in methanol, isobutanol, and *tert*-amyl alcohol to give polymers with controlled molecular weights and narrow MWDs ($M_w/M_n \approx 1.2$).^{55,159} The polymerization proceeds faster in methanol than in toluene.

Methanol is a good solvent for HEMA and its polymer, and thus can be employed for its homogeneous living radical polymerization with Ru-3, which is also highly soluble in methanol.⁵⁹ Copper-based systems also give homogeneous living radical polymerizations of HEMA in a mixture of methyl ethyl ketone and 1-propanol,²⁴³ of acrylamides in methanol,^{117,172} and of 4-vinylpyridine (M-33) in 2-propanol.²¹⁴

3. Water

In homogeneous free radical polymerization, water is often employed as solvent for water-soluble monomers and polymers with more polar functional substituents such as hydroxyl, amino, oxyethylene, ammonium, and carboxylate groups, along with emulsion, suspension, and dispersion processes. This is also the case for metal-catalyzed living radical polymerization.

2-Hydroxyethyl acrylate (HEA) can be polymerized homogeneously in water at 90 °C with the I-22 (X = Br)/CuBr/L-1 initiating system to give polymers with relatively narrow MWDs ($M_w/M_n = 1.34$), although the polymerization was slower, and the MWDs were broader than in the bulk ($M_w/M_n < 1.2$).²⁴⁴ A similar controlled polymerization of an amino-functionalized methacrylate 2-(dimethylamino)ethyl methacrylate was achieved with the same initiating system in water.²⁴⁵ Monomethoxy-capped oligo(ethylene oxide) methacrylate, a highly hydrophilic monomer, can be polymerized very fast with I-21 (X = Br)/CuCl/L-1 in water at 20 °C.²⁴⁶ The polymerization reached 90% within 30 min to give narrow MWDs ($M_w/M_n < 1.2$). The fast reaction is attributed to the formation of mononuclear copper(I) species.

Water is the solvent of choice for ionic monomers such as sodium methacrylate, where a direct radical polymerization (i.e., with the nonprotected form of the monomer) is carried out with the copper-based systems in aqueous media (pH 8–9) at 90 °C to afford controlled molecular weights and narrow MWDs.²⁰⁰ Another ionic monomer, sodium 4-vinylbenzoate, is polymerized very fast in aqueous media (pH 11) at 20 °C.²⁴⁷ An ammonium salt monomer, [2-(methacryloxy)ethyl]trimethylammonium chloride (FM-6; Figure 12), was polymerized in water with CuBr/L-1 in conjunction with a surface-confined initiator, while

the polymerization was heterogeneous due to the hydrophobicity of the initiator.²⁴⁸

4. Suspension, Dispersion, and Emulsion Polymerizations in Water (Heterogeneous System)

In industrial processes, radical polymerization is usually performed under heterogeneous conditions such as suspension, dispersion, or emulsion. The metal-catalyzed radical polymerization also proceeds under such aqueous/organic biphasic conditions but often suffers from difficulties in controlling the molecular weights and MWDs of the products and in keeping particles or latexes from coagulation. The former problem stems from the partitioning of the metal species into the aqueous phase while the growing polymer terminal exists in the organic phase. The latter is caused by some undesirable interactions among metal catalysts, ligands, and additives such as dispersants or surfactants. However, these problems can be overcome by careful choices of initiators, catalysts, dispersants or surfactants, temperatures, and concentrations according to the monomers as summarized in a review for the copper-catalyzed systems.²⁴⁹

Another problem involves the classification of these metal-based heterogeneous systems into suspension, dispersion, and emulsion polymerizations similarly to conventional systems. This is due to not only a lack of detailed analysis of reaction mechanisms and particle sizes but also fundamental differences in several aspects such as the locus of initiation and the molecular weight of polymers in comparison with the conventional counterparts. The terms suspension and emulsion will be used in the following sections for simple classification but are not based on the strict definition for conventional free radical systems.

Various metal complexes of Ru, Fe, Cu, Ni, and Pd are active in the radical polymerizations of hydrophobic methacrylates, acrylates, and styrenes under aqueous heterogeneous conditions to yield polymers with controlled molecular weights and relatively narrow MWDs. Importantly, a variety of these organometallic catalysts are tolerant to water, despite the fact that many similar complexes often lose their catalytic activity in the presence of water or even moisture.

A ruthenium-based system with Ru-1 and organic halides (initiators) induces living radical polymerization of MMA in mixtures of toluene and water, where the M_n increased in direct proportion to monomer conversion up to 10⁵, and the MWDs were as narrow as those obtained in toluene ($M_w/M_n \approx 1.2$).^{55,159} The polymerization proceeded in a suspension system under vigorous stirring irrespective of the absence of suspension stabilizers (dispersants). The controlled polymerization can also be achieved even in the absence of toluene (i.e., bulk monomer containing a catalyst system is dispersed in water), though the MWDs became broader ($M_w/M_n \approx 1.4$) due to the low solubility of the complex in the monomer and/or the high viscosity of the organic particles. A rate increase was observed by the addition of water to the ruthenium-based system in organic media, and similarly, faster living polymerizations proceed in these dispersed systems with Ru catalysts.

A similar effect of water was observed in the iron-catalyzed polymerization of styrene.^{76,250} An iron complex is less stable in water than ruthenium and thus considered difficult to use as an active catalyst in such an aqueous suspension system. For example, $\text{FeBr}_2(\text{PPh}_3)_2$ (Fe-1, X = Br; Figure 2) rapidly decomposes upon exposure to water. However, a Cp-based iron complex (Fe-3; Figure 2) proved effective in living radical suspension polymerizations of acrylates and styrene to give narrow MWDs ($M_w/M_n = 1.1-1.2$).²⁵⁰ These polymerizations are also clearly faster than those in organic media under otherwise similar conditions.

Nickel (Ni-1) and palladium (Pd-2) complexes were employed for suspension polymerization of MMA in the presence of a small amount (1–5 wt %) of sorbitane monooleate poly(ethylene glycol) (20) (Tween 80) as a surfactant.^{132,137} The obtained polymer had controlled molecular weights and moderate MWDs ($M_w/M_n = 1.4-1.7$) similarly to those obtained in toluene, although there was no detailed analysis on the size of the particles.

Detailed studies were performed on the copper-catalyzed suspension or emulsion polymerizations.²⁴⁹ Living or controlled emulsion radical polymerization of nBMA can be achieved in the presence of nonionic poly(oxyethylene)-based surfactants such as Brij 97, Brij 98, and Tween 20 with the I-21 (X = Br)/CuBr/L-3 or L-4 system.^{249,251,252} The M_n increased in direct proportion to monomer conversion up to 5×10^4 ($M_w/M_n = 1.1-1.2$). The particle sizes are around 1000–4000 nm, suggesting a suspension, but can be reduced to about 300 nm with the use of hexadecane as a cosurfactant along with ultrasonication.^{249,252}

Surfactants largely affect the polymerizations. Anionic surfactants such as sodium dodecyl sulfate adversely affect the control of molecular weights and MWDs, whereas poly(ethylene glycol) facilitates molecular weight control but leads to coagulation.²⁵¹ Water-soluble or more hydrophilic ligands such as L-1, L-24, L-32, and L-9 (R = $\text{CH}_2\text{CH}_2\text{CHPh}_2$) are detrimental to the control of molecular weights due to unfavorable partitioning of the Cu(II) species into water.^{249,251,253} Other monomers such as MMA, nBA, and styrene can also be polymerized with the copper-based systems in emulsion to give polymers with controlled molecular weights and MWDs.^{249,251,253}

Random and block copolymerizations of these monomers were also investigated with ruthenium, iron, and copper catalysts and gave successful results depending on the conditions.^{110,250,254}

The so-called reverse atom-transfer radical polymerization is feasible in aqueous emulsion too. This system enables the formation of initiating radical species in the water phase with the use of water-soluble initiators such as I-39, I-40, and I-41 as in conventional emulsion radical polymerization.^{184,249,252,255} The copper-catalyzed emulsion radical polymerization of nBMA afforded polymers with narrow MWDs ($M_w/M_n = 1.1-1.4$), but the M_n values were much higher than the calculated values due to the termination between the initiating radicals in the aqueous phase.^{184,255} The emulsions are relatively stable and their particle sizes are around 100–300

nm even without sonication.^{184,255} There were no effects of the size and number of particles on the polymerization rate.²⁵² It is suggested that the nucleation mechanism in the reverse atom-transfer emulsion radical polymerization is different from that in the conventional processes, because of the lack of formation of high molecular weight polymers during the early stages.²⁵⁵

Another aqueous heterogeneous polymerization was recently reported for the precipitation polymerization of MMA and styrene complexed with methylated β -cyclodextrin.²⁵⁶ The polymerization was carried out in water with I-21 (X = Br)/CuBr/L-4 to give polymers with controlled molecular weights and relatively narrow MWDs ($M_w/M_n = 1.3-1.8$). Initially, the reaction mixture was homogeneous with the hydrophilic cyclodextrin-complexed MMA, but sooner or later it became heterogeneous due to the formation of water-insoluble polymers.

5. Other Special Solvents

Apart from water, supercritical carbon dioxide (scCO_2) is an environmentally friendly solvent and currently attracts much attention as a medium for organic reactions and polymerizations. The solvent was also employed for the copper-catalyzed radical polymerizations of fluorinated (meth)acrylates with the I-22 (X = Br)/CuCl initiating system in the presence of Cu(0) and bipyridine-based ligands such as L-1, L-4, and L-7.⁹⁵ A fluorinated ligand (L-7) induced a homogeneous polymerization without any visible precipitation to give polymers with controlled molecular weights. This system is equally applicable for random and block copolymerizations between the fluorinated monomers and MMA. Dispersion polymerization of MMA was also conducted in scCO_2 with poly(perfluorinated acrylate)s as dispersants to form PMMA with controlled molecular weights and relatively narrow MWDs ($M_w/M_n = 1.4$).

The use of fluorous solvents or ligands leads to so-called fluorous biphasic conditions, where at an ambient temperature two phases separate, the phases becoming miscible at a higher temperature. This permits the homogeneous polymerization at high temperatures, and the facile separation of products from the catalysts under ambient conditions. A fluorous biphasic system consisting of I-24 (X = Br), CuBr, and L-26 was employed for polymerizations of MMA in an equivolume mixture of (perfluoromethyl)cyclohexane and toluene.¹¹⁵ The polymerization proceeded most likely in a homogeneous phase to give polymers with controlled molecular weights and narrow MWDs ($M_w/M_n = 1.2-1.3$). They are easily isolated from the organic phase as a colorless glassy solid with a minimum contamination of copper. It is also reported that the catalysts, largely remaining in the fluorous phase, can be recycled for second and third polymerizations without loss of catalytic activity.

Another special class of solvent, ionic liquids such as 1-butyl-3-methylimidazolium hexafluorophosphate, was used for the polymerization of MMA with I-24 (X = Br)/CuBr/L-9 (R = *n*-Pr), which proceeded even at 30 °C, reached 90% conversion within 5 h,

and gave polymers with narrow MWDs ($M_w/M_n = 1.3-1.4$).²⁵⁷ The products are easily removed by washing with toluene, while the catalyst is highly soluble in the ionic liquid and can be reused.

F. Mechanisms

The metal-catalyzed living polymerizations most probably proceed via a carbon-centered radical species reversibly generated from a carbon-halogen terminal (dormant species) and a metal catalyst. The radical nature of the polymerizations has been suggested by several facts and observations, some of which were already discussed above. This part deals with the analysis of the polymerizations based on various methods and apparatuses for mechanistic investigation. Short overviews on the mechanistic studies are also available.²⁵⁸⁻²⁶²

1. Radical Scavengers

One of the most useful methods to determine a polymerization mechanism is to examine the effects of additives or potential terminating agents (scavengers or quenchers). Since the beginning of development of metal-catalyzed living radical polymerization, therefore, terminating experiments have been carried out extensively, and they were particularly important at that time, because combinations of haloalkanes and transition-metal catalysts do not automatically warrant radical-growth mechanisms. As potential terminators, two classes of compounds have primarily been employed: protic compounds such as water and alcohols, and radical scavengers such as galvinoxyl, 1,1-diphenyl-2-picrylhydrazyl (DPPH), and TEMPO. Namely, there are well-known terminators for anionic and radical growing species, respectively, and their use was based on the fact that the monomers employed in the early-phase development were primarily MMA and styrene, which polymerize by both mechanisms.

It was soon realized that almost all of the metal-catalyzed living processes are not quenched by the protic compounds but clearly by the radical scavengers, and this phenomenon was the case for such metal catalysts as ruthenium,^{29,55,56,58,63,66} copper,²⁸ nickel,^{132,133,135} rhodium,¹³⁸ and rhenium.¹⁴¹ The carbon-centered radical most probably reacts with these scavengers (Y) to produce a dead polymer chain end with inactive covalent C-Y or C-H bond or unsaturated carbon-carbon double bond.

The first set of quenching experiments has been reported for the Ru-mediated polymerization of MMA,^{27,55} and the Kyoto group observed the reaction is immune to methanol and alcohol but is quantitatively terminated with galvinoxyl, DPPH, and TEMPO added in 5-10-fold molar excess over the initiator. End-group analysis on the quenched products revealed that the terminating moieties are not attached to the growing end; rather *exo*-olefins result via hydrogen abstraction from the MMA's α -methyl group.

On the other hand, the formation of C-Y bonds was observed in the copper-catalyzed model reactions between the isolated polymers or model compounds such as I-13 and TEMPO or hydroxy-TEMPO.^{163,242}

However, TEMPO may also deactivate the metal complexes to form inactive metal species in higher oxidation states instead of giving the C-TEMPO terminal.¹⁴¹ A similar inhibition by these compounds was also observed for living anionic polymerizations and group-transfer polymerizations of MMA, both of which proceed via an anionic mechanism.²⁶³ Alternatively, some of the phenols, which are scavengers in conventional radical polymerizations of styrene, can increase the polymerization rate as mentioned above (section II.D).²³¹ Though these inhibition effects cannot completely prove radical-growth mechanisms for the metal-catalyzed living polymerizations, they are at least consistent with the proposed pathways.

2. Stereochemical Structures

The stereochemistry of polymers, in general, provides useful information about the polymerization mechanism by which they are formed. More specifically in the metal-catalyzed living radical polymerization, it has been anticipated that the proposed mechanism via metal-assisted reversible radical generation (cf. Scheme 3) might induce different and/or better stereochemical control than in the classical radical counterpart, in which the growing end is a really "free" radical. The anticipation originates from the fact that the oxidized metal catalyst, with the halogen from the dormant species, might reside in close vicinity to the resulting radical end, inducing a situation reminiscent of ion pair growing species in ionic polymerizations where the counterions exert a strong influence on the stereochemistry of propagation.

Surprisingly or not, the tacticity of PMMA obtained with various metals including Ru,^{27,56,58,63} Cu,^{28,84,97,100,102,103,116,232,263} Fe,^{70,80} Ni,^{132,133} Pd,¹³⁷ and Rh¹³⁸ was almost the same (almost atactic, slightly syndiotactic) as the tacticity of those obtained with conventional radical initiators such as AIBN under similar conditions. The triad ratio of *rr:mr:mm* as determined by ¹³C NMR is usually 58:38:4 and does not change even with the use of chiral and/or bulky ligands.^{103,116} These results may exclude a coordination mechanism and suggest a radical nature. However, the stereochemical structure alone is not strong evidence for the radical polymerization because, for example, group-transfer polymerization, basically via an anionic mechanism, results in a stereo structure of PMMA similar to those for free radical processes.²⁶³

3. Copolymerizations

Monomer reactivity ratios in copolymerization and copolymer structures can also give insight into the mechanism of the polymerizations. As observed with ruthenium²⁰⁵ and copper,^{264,265} MMA-styrene and related copolymerizations turned out to be "living" if initiated with the metal catalysts effective for the corresponding homopolymerizations. Besides these synthetic aspects to be covered later in this review (section III.D), the results also give some insight into the reaction mechanisms. With a ruthenium catalyst (Ru-1), MMA and styrene were copolymerized at varying monomer feed ratios.²⁰⁵ The products were true copolymers, as evidenced by single MWD profiles

by size-exclusion chromatography (SEC) and a set of hetero- and homochain NMR signals, among others. The MWDs were fairly narrow, clearly narrower than those from the corresponding AIBN-initiated samples, and the M_n was directly proportional to the total weight (overall conversion) of the consumed monomers. All these findings demonstrate that the copolymers are living.

Equally important, the two comonomers were polymerized in parallel, with MMA consumption slightly faster, and the copolymer composition curve shows a shallow S-shaped profile, similar but not identical to those for the textbook examples of free radical MMA/styrene copolymerization. Thus, once again, the observation is consistent with some radical growth in the metal catalysis, and their difference from a conventional radical copolymerization is not deniable but not conclusive.

Kinetic analyses were done for several copper-catalyzed copolymerizations of MMA/nBMA,²⁶³ nBA/styrene,^{264,266} and nBA/MMA.²⁶⁷ All these studies show that there were no significant differences in reactivity ratio as well as in monomer sequence between the copper-catalyzed and conventional radical polymerizations. Only a difference was observed in the copolymerizations between MMA and ω -methacryloyl-PMMA macromonomers where the reactivity of the latter is higher in the metal-catalyzed polymerizations.²⁶⁷ However, this can be ascribed not to the different nature of the propagating species but to the difference in the time scale of monomer addition or other factors. Simulation has also been applied for the copolymerization study.²⁶⁸

4. EPR

One of the most effective and direct ways to prove a radical mechanism is to detect the radical intermediate by electron paramagnetic resonance (EPR), but this approach has not been fruitful yet for the detection due to the low concentrations of the radical species or other factors.

EPR was indeed applied to the copper-catalyzed radical polymerization of styrene, MA, and MMA.^{162,269–271} Invariably, it was difficult to detect any radical growing species because of the low concentrations of the radical species, but just specifically for copper, the accumulated paramagnetic Cu(II) species was generated via radical termination. This indicates that 3–6% of the initially added Cu(I) catalyst is converted into the Cu(II) counterpart during the polymerization (especially its initial stage).

5. NMR

In the mechanistic study of metal-catalyzed living polymerization, this method has thus far been utilized primarily for analysis of model reactions to uncover the interaction between a metal catalyst and a carbon–halogen dormant end.^{170,176} Typical models for the dormant end include α -haloesters, such as alkyl haloisobutyrate and MMA dimer halides I-25 (Figure 8) (for methacrylate), alkyl 2-halopropionate (for acrylate), and α -phenylethyl halide (for styrene).

NMR analysis of model reactions for the polymerizations and polymer terminal groups revealed that

the halogens at a dormant polymer terminal exchange with those in a metal catalyst.^{154,155,170,196,272,273} According to the proposed homolytic cleavage mechanism (Scheme 3), the halogen-exchange reaction proceeds via abstraction of (one of) the terminal halogens by the metal catalyst followed by return of one of the halogens on the metal species onto the growing radical center; thus, the process presumably occurs via a radical intermediate.

In a typical example, the MMA dimers I-25 were employed as authentic terminal models for PMMA.¹⁷⁰ NMR readily distinguishes chlorine replacement at the bromine ends in I-25. Taking this advantage, the Kyoto group examined the halogen-exchange reactions by treating I-25 (X = Br) and Ru-1 in NMR sample tubes, mimicking the radical-generation process of their Ru(II)-mediated living polymerizations. Almost immediately after mixing the two components followed by heating to the polymerization temperature, the chloride version of I-25 (X = Cl) was clearly detected by NMR, and it increasingly predominated, demonstrating that the bromine end is rapidly replaced (exchanged) by the chlorine in the metal catalyst.

Another interesting aspect of the model reactions has been reported for copper-mediated processes.²⁷³ Thus, optically active methyl 2-bromopropionate was mixed with a CuCl catalyst, and the reaction was followed by NMR and polarimetry. The latter analysis showed, as in solvolysis, that the model quickly undergoes racemization; i.e., the halogen on the chiral carbon dissociates and recouples.

The degrees of the exchange reactions depend on several factors, the central metals, the ligands, the structures of the terminal groups, and the reaction conditions. The absence of carbon–metal species, which would form via oxidative addition of the metal complexes into the carbon–halogen bonds, also excludes the coordination mechanism.

6. MS

The polymers and their terminal groups (α and ω) in metal-mediated living radical polymerizations have been analyzed by modern mass spectrometry, particularly MALDI-TOF-MS,^{100,125,173,174,197,239,244,274–277} time-of-flight static secondary ion mass spectrometry (TOF-SSIMS),^{278,279} and electrospray ionization mass spectrometry (ESIMS).^{172,277,280} All these analyses support the existence of fairly stable carbon–halogen terminals.

The MALDI-TOF-MS spectra of the obtained polymers basically show only one series of peaks separated exactly by the mass of each monomer. The observed mass of each peak agrees well with the theoretical one, which possesses one initiator fragment at the α -end and one halogen terminal group at the ω -end in each polymer chain (with a single degree of polymerization) (Scheme 3). The observed isotopic distribution was in excellent agreement with the simulated profile based on the neutral abundance of ^2H , ^{13}C , etc.¹⁹⁷ In some cases, laser irradiation of the samples leads to partial or complete loss of the terminal halogens during the analysis depending on the polymer structures and analytical conditions.^{197,239,244,276} In other cases, MS analysis in turn

reveals that some polymers suffer from halogen loss during polymerizations.^{172,174,275}

7. CV

The correlation between the physical parameters of the catalysts and their catalytic activity will clarify polymerization mechanisms. The redox potential of the metal complexes is certainly among these parameters, because metal-assisted living radical polymerization is triggered by oxidation of the metal complex; i.e., a single electron is transferred from the metal to a dormant carbon–halogen terminal. The redox potential was thus measured for ruthenium,^{53,227} iron,⁷³ and copper⁵⁴ complexes by cyclic voltammetry (CV). These studies basically indicate that a complex with a lower redox potential induces a faster reversible cleavage (activation) of a carbon–halogen terminal and, in turn, generates more radical species. For example, among half-metallocene–ruthenium complexes (Ru-4, -5, and -6 in Figure 1) the redox potential decreases in the order Ru-4 > Ru-5 > Ru-6, and the halogen exchange rate follows the same order (Ru-6 gives the fastest).⁵³

However, there is no definite correlation between the polymerization rate and the redox potential, partly because a higher concentration of the radical species may lead to a higher probability of bimolecular termination and a higher concentration of persistent radical species.^{54,261} Another possibility of side reaction is due to the reduction of the radical into an anion with metal complexes with extremely low redox potential. An appropriate range for the redox potential of the metal catalysts was suggested between -0.3 and $+0.6$ V (versus NHE) for living radical polymerization.⁵⁴

8. Kinetics

Kinetic analysis of metal-catalyzed radical polymerization was extensively performed for homogeneous copper-based systems.^{123,164,176,281} Almost invariably, the polymerization follows a first-order kinetics with respect to the monomer, initiator, and copper(I) halide as expected from the proposed mechanism; i.e., the reaction between the monomer and the radical species, which is generated via the Cu(I)-catalyzed activation of the carbon–halogen terminal, originated from the initiator. Addition of Cu(II) species retards the polymerization by shifting the equilibrium between the covalent and radical species. However, the polymerization kinetics were not simple inverse first order with respect to the initial copper(II) halide concentration due to the persistent radical effect, which resulted in an increase in Cu(II) concentration during the initial stages of the polymerization.^{123,164,281} This also indicates the presence of irreversible bimolecular termination reactions, prone to the radical polymerizations. The equilibrium constants for the activation/radical dissociation process are calculated on the assumption that the absolute propagation rate constant in the metal-catalyzed polymerization is the same as that in the conventional free radical processes, and the values vary with the monomers from 10^{-9} to 10^{-7} and increase in the order acrylates < styrene < methacrylates.^{123,176} The concentration of

the radical species is thus estimated to be very low, between 10^{-8} and 10^{-7} mol/L, which may minimize bimolecular termination.

The kinetic parameter for the radical dissociation of a carbon–halogen terminal was obtained with the use of an isolated polystyrene with a terminal C–Br bond in the presence of a copper catalyst and a conventional radical initiator with a long half-life.^{282,283} The result was compared with that of low molecular weight compounds of similar carbon–halogen bonds.¹⁶³ The second-order rate constant of the model compound I-13 (X = Br), an effective initiator for styrene, is comparable to that of the polymer terminal. Alternatively, rate constants can be obtained by using a combination of nitroxide-exchange reactions and HPLC analysis.²⁴²

Computer simulations were also done for these polymerizations although the details are omitted in this review.^{284–287}

9. Other Mechanistic Analyses

While the radical nature of the metal-catalyzed polymerizations seems to be generally accepted, there still remains a question whether the propagating radical species therein is the same in nature as the “free radicals” in the conventional systems. The metal-assisted radical formation most probably proceeds through an inner-sphere electron transfer from the metal to the carbon–halogen terminal as reported in Kharasch addition reactions.^{288,289} The resulting radical species may temporarily be confined in the coordination sphere of the complex in a higher oxidation state. The confined situation or environment might exert some effects on the polymerization such as suppression of bimolecular termination. Although this possibility was suggested for some systems around the time when the metal-catalyzed systems were discovered,^{27,100,132} there is still no strong supporting evidence.²⁹⁰ In this aspect, the lack of stereoregulation (see above) is particularly frustrating.

If similar radical species are involved in both living and conventional polymerizations, it follows that the metal-assisted growing species may suffer from side reactions prone to free radical systems, however well suppressed in the living systems. This then determines the lifetime of the growing end as well as the maximum molecular weights to be achieved therein. The highest molecular weights are still below 10^6 with all the reported living systems.

Side reactions such as termination and transfer were investigated in the polymerizations of styrene,²⁹¹ acrylates,²⁹² and methacrylates.²⁹³ The occurrence of thermally initiated radical polymerizations was observed in the copper-catalyzed styrene polymerization, while the resulting polymer chain can be converted into the dormant polymer terminal via abstraction of halogens from the persistent metal radical in higher oxidation states.²⁹⁴

The effects of chain-transfer agents such as octanethiol on copper-catalyzed polymerizations are similar to those on conventional radical polymerizations.²⁹⁵ These may also mean little difference among the growing species generated from the carbon–halo-

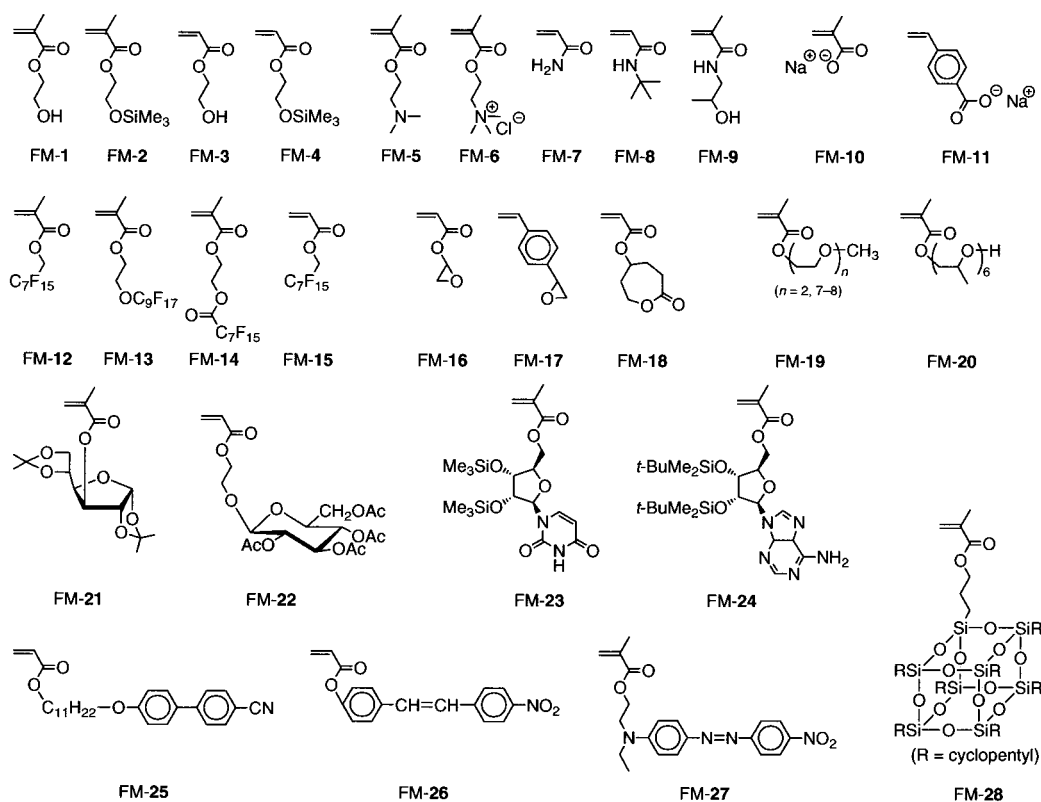


Figure 12. Functional monomers.

gen terminals and in conventional radical systems. Another interesting observation is that a simultaneous metal-catalyzed and nitroxide-mediated living radical polymerization of styrene is possible via fast scrambling of terminal halogen and TEMPO groups to form a single type of polymer chains.²⁹⁶

These suggest, in part, that a key to metal-catalyzed radical polymerizations might be the persistent radical effect,^{15,297,298} as pointed out for nitroxide-mediated systems. More detailed mechanistic studies are required.

III. Precision Polymer Synthesis

One of the most distinguishable characteristics of the metal-catalyzed living radical polymerization is that it affords polymers with controlled molecular weights and narrow MWDs from a wide variety of monomers under mild conditions even in the presence of a protic compound such as water. This permits the synthesis of a vast number of polymers with controlled structures such as end-functionalized polymers, block copolymers, star polymers, etc., where they are widely varied in comparison with those obtained by other living polymerizations. This is primarily due to the tolerance to various functional groups and the polymerizability/controllability of various vinyl monomers as mentioned above.

This section is thus directed to precision polymer synthesis with the use of metal-catalyzed living radical polymerizations. In this synthetic aspect, numerous reviews are available already.^{219,265,299–310}

A. Pendant-Functionalized Polymers

Radical polymerization, in general, is more tolerant of polar functionality than its ionic counterpart, and

as we have already seen in this review, this advantage is apparently passed on to the metal-catalyzed living polymerizations. This in turn leads to direct polymerization of functionalized monomers and the synthesis of pendant functionalized polymers of well-defined structure and molecular weights without tedious protection and deprotection processes. These functional groups include not only hydroxyl, amino, and amido groups but also ionic and other special groups, which are, in most cases, introduced directly into methacrylates, acrylates, and styrenes as substituents. Figure 12 is a nearly complete inventory of functionalized monomers for which metal-mediated living radical polymerizations have been reported.

A hydroxyl-functional monomer, HEMA (FM-1), can be polymerized in a controlled way with several transition-metal complexes including ruthenium,⁵⁹ copper,^{241,243} and nickel³¹¹ in the bulk and in alcohols. In view of the relatively broad MWDs of the products ($M_w/M_n = 1.3–1.8$), further optimization of the reaction conditions is needed, although the catalyst and the growing terminal keep the activity during the polymerizations. Better-controlled polymerizations of a protected form of HEMA with a trimethylsilyl group (FM-2) were also conducted with ruthenium, copper, and nickel.^{243,312} 2-Hydroxyethyl acrylate (FM-3), an acrylate with a hydroxyl group, can be polymerized with the I-22 (X = Br)/CuBr/L-1 system in the bulk and in water to give narrow MWDs ($M_w/M_n = 1.2–1.3$) where the polymerization is faster and better controlled in the bulk.²⁴⁴ Its protected version (FM-4) was polymerized with I-22 (X = Br)/CuBr/L-24 in the bulk to give similarly narrow MWDs ($M_w/M_n \approx 1.2$).³¹³ Soluble in organic media, these silyloxy-protected monomers (FM-2 and FM-4) can be effec-

tively employed for block or random copolymerizations with aliphatic methacrylates.^{243,312,313}

Amino- and amido-functionalized monomers can also be polymerized directly with metal catalysts. Living radical polymerization of 2-(dimethylamino)ethyl methacrylate (FM-5) was achieved with I-31 (X = Br)/CuBr/L-29 in dichlorobenzene at 50 °C.³¹⁴ Its ammonium salt (FM-6) was polymerized from the surface of a cross-linked polystyrene latex with CuBr/L-1 in water at 80 °C to generate hydrophilic shells, although there were no data for polymer molecular weight.²⁴⁸ As described above (section II.C.6), (meth)acrylamides with at least their amido protons unprotected (FM-7, FM-8, and FM-9) can be polymerized with copper-based systems,^{117,168,217,218} but a further optimization seems to be necessary.

Ionic monomers carrying a carboxylate salt, such as FM-10²⁰⁰ and FM-11,²⁴⁷ can be polymerized with a water-soluble bromide initiator in conjunction with CuBr and L-1 in aqueous media to give moderately controlled molecular weights and MWDs ($M_w/M_n = 1.2-1.3$). The reaction media should be kept under alkaline conditions (pH 8–11) to avoid loss of the catalytic activity; seemingly free acid functions in the monomers and/or polymers are detrimental.

Perfluoroalkyl (meth)acrylates FM-12 and FM-15 have been polymerized homogeneously in scCO₂ with copper catalysts/fluorinated ligand systems, but the MWDs of the products are not reported due to the lack of appropriate analytical methods.⁹⁵ Other fluorinated monomers (FM-13 and FM-14) were used for block copolymerization with styrene and acrylates with CuBr/L-1 in the bulk under heterogeneous conditions.³¹⁵

Epoxy and lactone groups seem to remain intact under the conditions for metal-catalyzed living radical polymerization. Therefore, glycidyl acrylate (FM-16) can be exclusively polymerized via the vinyl moiety with I-22 (X = Br)/CuBr/L-4 in the bulk at 90 °C to high conversion ($M_w/M_n \approx 1.2$).³¹⁶ Statistical copolymers of styrene and FM-17, an epoxy-functionalized styrene, with controlled molecular weights were obtained with a CuBr-based system at 100 °C, whereas a similar reaction with TEMPO gave products of bimodal MWDs that might come from the high reaction temperature (124 °C).³¹⁷ An acrylate with ϵ -caprolactone can be polymerized with I-21 (X = Br)/Ni-2 in the bulk at 90 °C to result in polymers with controlled molecular weights ($M_w/M_n = 1.1-1.3$).³¹⁸

Methacrylates with pendant oxyethylene units (FM-19) were polymerized in a controlled way with metal catalysts in the bulk or in water. The catalytic systems include a bromide initiator coupled with Ni-2 for $n = 2$ (bulk, 80 °C)³¹⁹ and CuCl for $n = 7-8$.^{246,320} The latter polymerization proceeded very fast in aqueous media at 20 °C to reach 95% conversion in 30 min and gave very narrow MWDs ($M_w/M_n = 1.1-1.3$). The fast reaction is attributed to the formation of a highly active, monomeric copper species complexed by the oxyethylene units. A statistical copolymerization of FM-19 ($n = 7-8$) and FM-20, a methacrylate with a oligo(propylene oxide) pendant group, led to hydrophilic/hydrophobic copolymers with narrow MWDs ($M_w/M_n = 1.2$).³²⁰

Polymers containing sugar moieties, so-called glycopolymers, have been attracting attention as biocompatible materials. Some of them have been obtained by the polymerization of FM-21³²¹ and FM-22³²² with CuBr-based initiating systems. Their block copolymerizations with styrene are also feasible as described below (section III.C.1).

Metal-catalyzed living radical polymerization can be further extended to multifunctional nucleoside-containing monomers. Examples are silyl-protected monomers with uridine (FM-23) or adenosine (FM-24) groups, both of which can be polymerized with a combination of a bromide initiator, CuBr, and L-9 (R = *n*-Pen) or L-32 homogeneously in toluene ($M_w/M_n = 1.1-1.4$).³²³

Side-chain liquid-crystalline polymers with controlled molecular weights have been obtained by the polymerization of FM-25 with I-22 (X = Br)/CuBr/L-3 in the bulk at 100 °C, to examine the thermotropic transition as a function of the MWD.³²⁴ Second-order nonlinear optical materials with branched structure were prepared by the copper-catalyzed radical polymerization of FM-26 and FM-27 using hyperbranched poly[4-(chloromethyl)styrene] as a multifunctional initiator.³²⁵

A methacrylic monomer with polyhedral oligomeric silsesquioxanes (FM-28) as a pendant group can be polymerized with I-24 (X = Br)/CuBr/L-32 in toluene ($M_w/M_n = 1.14$).³²⁶ Block and star copolymers of this partially inorganic monomer with MA and nBA are expected to function as new hybrid materials.

B. End-Functionalized Polymers

As in other living polymerizations, metal-catalyzed living radical processes can be employed for the synthesis of end-functionalized polymers. To this end, there are two general methods, i.e., a functional initiator method and an end-capping method, and both are indeed applicable therein. In the former, living radical polymerization is initiated with a functionalized organic halide initiator coupled with a metal catalyst to form polymers with an α -end (head) functionality. In the latter, a metal-catalyzed living radical polymerization is terminated with a functionalized quencher that in turn introduces an ω -end (tail) functionality. An alternative method for ω -end functionalization is to transform a stable carbon-halogen ω -terminal via polymer reactions. Examples of these approaches will be discussed below.

1. α -End-Functionalized Polymers

Taking advantage of the tolerance of living radical polymerization for functional groups, a variety of functionalized initiators have been designed. A general way is to attach a functional group to a halogen compound such as a haloester, (haloalkyl)benzene, haloalkane, or sulfonyl halide. Most of the functional groups therein are insulated from the initiation moiety via a spacer to avoid possible side reactions, as shown in Figure 13, where entries are grouped in terms of the intended α -functionalities.

For instance, hydroxyl-functionalized initiators (FI-1 to FI-6) were employed for living radical polymerization of MMA,^{134,139,156,157,274,327} MA,²⁸⁰ nBA,¹³⁴

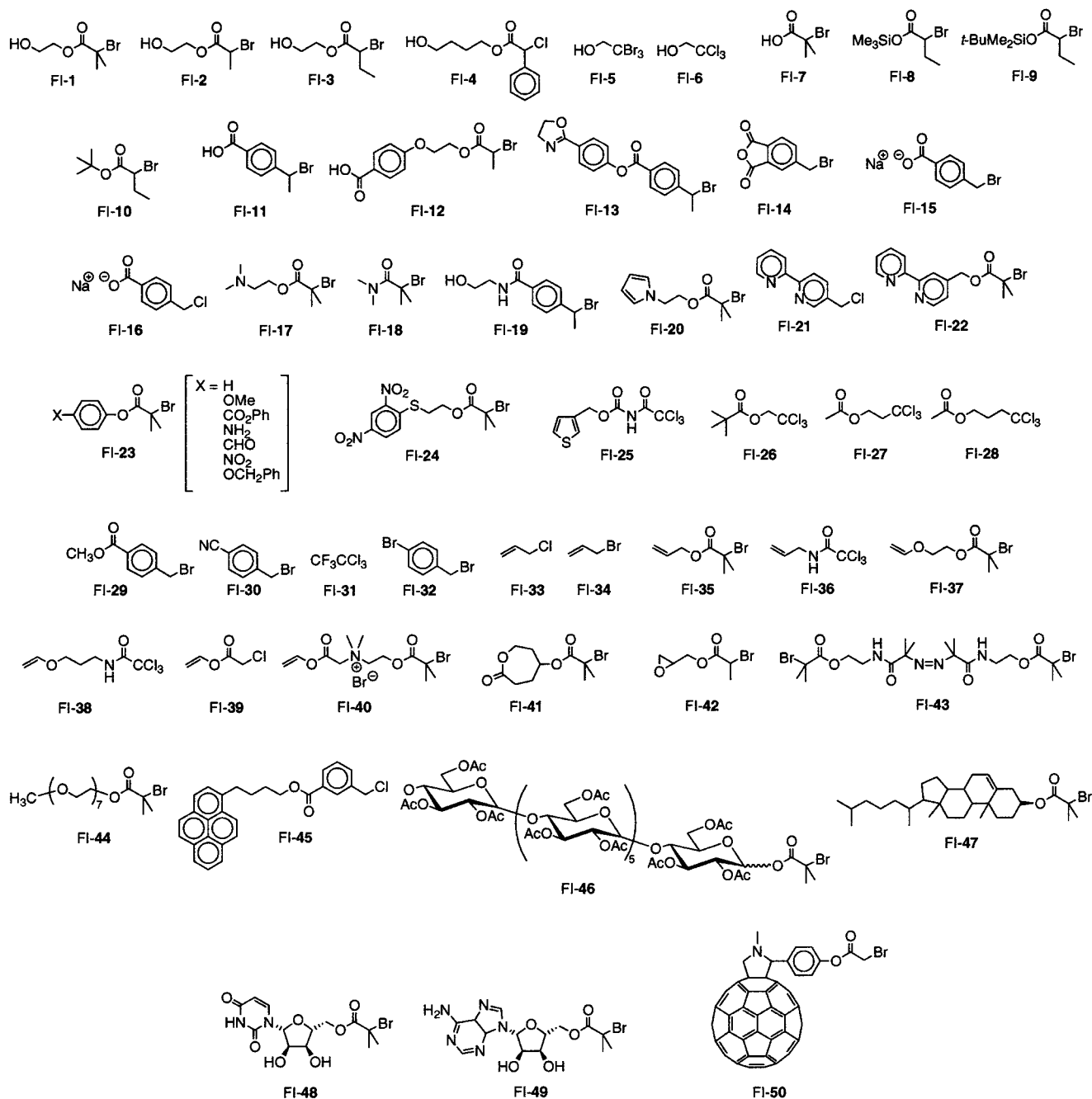


Figure 13. Organic halide functional initiators.

tBA,³²⁸ styrene,^{280,329} and sodium methacrylate.²⁰⁰ Note that for these no protection of the protic function is required, in sharp contrast to similar initiators for ionic living polymerizations. Initiator FI-1 generates an HEMA radical and thus is applied to MMA with CuBr/L-9 (R = *n*-Pr) in xylene at 90 °C; near complete attachment of the α -end function has been shown by MALDI-TOF-MS.²⁷⁴ This initiator can also be employed for sodium methacrylate²⁰⁰ and tBA.³²⁸ An acrylate version FI-2 is for MA with CuBr/L-4, but the initiation efficiency for styrene is reported to be lower ($I_{\text{eff}} \approx 0.7$) due to side reactions upon initiation.²⁸⁰ In contrast, a nearly quantitative initiation was achieved with FI-3 in the styrene polymerization with CuBr/L-1.³²⁹ A chloride FI-4 is another interesting initiator that can generate a radical doubly stabilized by a carbonyl and a phenyl substituent and

has been employed for MMA/CuBr/L-1.³²⁷ Simpler initiators such as FI-5^{134,139} and FI-6^{156,157} are commercially available and applied to MMA, nBA, and styrene with CuBr/L-1 or L-4 as well as Ni-2, although the plural carbon-halogen bonds therein might cause multiple initiations.

Carboxyl groups were also introduced at the α -end of poly(methacrylate)s^{134,235,320} and polystyrene^{330,331} by using unprotected and protected initiators. 2-Bromoisobutyric acid (FI-7) was employed for MMA coupled with CuBr/L-9 (R = *n*-Pen)²³⁵ and with Ni-2¹³⁴ to give narrow MWDs ($M_w/M_n = 1.1-1.3$) but M_n values higher than the calculated values. This unprotected initiator, on the other hand, has poor efficiency ($I_{\text{eff}} = 0.10$) for styrene, probably because of the intramolecular cyclization into a γ -butyrolactone after addition of one styrene unit.³³⁰ Protection

of the acid function by trimethylsilyl (FI-8), *tert*-butyldimethylsilyl (FI-9), or *tert*-butyl (FI-10) groups leads to improved initiation efficiencies (ca. 0.6, 0.8, and 1.0, respectively). Benzoic acid initiators with a well-separated halogen (FI-11 and FI-12) afforded well-defined polystyrenes with narrow MWDs at relatively high initiation efficiencies ($I_{\text{eff}} \approx 0.7$); thus, rigid aromatic spacers may help.³³⁰ Similar results were obtained with protected initiators such as FI-13 and FI-14.³³¹ Salt-type initiators FI-15 and FI-16 are specifically employed for the aqueous-phase polymerization of hydrophilic monomers such as FM-19 (Figure 12).³²⁰

Nitrogen-containing groups such as amine, aniline, amide, pyrrole, and pyridine are also available for the functional initiator method. A bromoester with a dimethylamino group (FI-17) was used in aqueous media for oligo(ethylene glycol) methacrylate (FM-19) ($M_w/M_n \approx 1.4$).^{246,320} Poly(tBA)³²⁸ and polystyrene³³¹ with terminal amide functions were prepared with FI-18 and FI-19, respectively. The pyrrole-containing initiator FI-20 induced living radical polymerization of methacrylates, acrylates, and styrene with Ni-2 or CuBr/L-1, giving macromonomers for electrochemical polymerization.³¹⁹ The 2,2'-bipyridine unit in FI-21 and FI-22 is to attach binding sites onto polystyrene³³² and poly(MMA),³³³ respectively, for macroligand chelation with Ru and other metal cations. A series of 4-substituted-phenyl 2-bromoisobutylates (FI-23) with amino, nitro, and aldehyde groups, etc. were successfully employed for MMA with CuBr/L-9 ($R = n\text{-Oct}$) ($M_w/M_n = 1.1\text{--}1.2$; $I_{\text{eff}} = 0.8\text{--}1.0$).¹⁹⁹

Thiols also provide good binding points toward a metal surface such as gold for the synthesis of polymer brushes, etc. A protected initiator (FI-24) gave thiol-functionalized PMMA with Ni-2 as a catalyst.³³⁴ The thiophene-capped PMMA from FI-25 can be employed as a macromonomer for electrochemical copolymerization with pyrrole,³³⁵ as with those from FI-20 (see above).

A series of poly(chloroalkyl ester)s (FI-26 to FI-28) can be employed for styrene polymerization with CuCl/L-1 to give polymers with ester groups at the α -end.¹⁵⁸ Benzyl bromides FI-29³¹⁷ and FI-30³²⁸ are another possibility for α -end functionalization.

Multiple halogen compounds FI-31¹⁵⁸ and FI-32³²⁸ seem interesting to attest the chemoselectivity of transition-metal catalysis, and the CF_3 - and the aromatic bromide therein, respectively, remain intact during the living polymerizations to afford α -end functions, though their utility might be limited.

End-functionalized polymers with polymerizable groups such as double bonds and heterocycles of course provide macromonomers; allyl, vinyl ester, vinyl ether, lactone, and epoxy are examples of such a category whose α -ends are not susceptible or have little susceptibility to metal-catalyzed radical polymerization. As discussed above, for example, allyl chloride and bromide (FI-33 and FI-34) are effective initiators to be used for styrene with CuCl and CuBr catalysts,¹⁶¹ while allyl compounds with remote halogens such as FI-35 and FI-36 allow the polymerization of methacrylates with high initiation effi-

ciency.^{120,150} Vinyl ether derivatives FI-37 and FI-38 can initiate living polymerizations of styrene, methacrylates, and acrylates with copper catalysts from their halogen moiety, though carefully selected reaction conditions are required.^{150,336} Thus, the vinyl ether double bonds are susceptible to radical addition at higher conversions to result in bimodal MWDs and termination. Interestingly, vinyl acetate groups can be introduced at the α -end of polystyrenes and poly(methacrylate)s by using FI-39³³⁷ and FI-40,^{246,247,320} because they only poorly copolymerize with styrene and methacrylates even under radical conditions. Macromonomers for ring-opening polymerizations can be obtained from FI-41³²⁸ and FI-42³¹² for tBA and MMA.

An azo bromoester bifunctional compound FI-43 induces a living polymerization of nBA with a highly active catalytic system (CuBr/L-32) at 30 °C from the latter function alone.³³⁸ The low temperature allows the azo group to elude concurrent thermal dissociation (<0.5%). The obtained polymers of narrow MWDs were employed for block copolymerization with vinyl acetate at 90 °C.

End-functionalized polymers with relatively long hydrophilic segments can be prepared from an initiator (FI-44) with oligo(oxyethylene glycol) units.^{200,246,247,320} Initiators FI-45 to FI-50 are for other functionalities of special interest. For example, the pyrenyl group in FI-45 can become a tag for distinguishing the end-functionalized polymers from nonfunctionalized byproducts and was used in simultaneous metal-catalyzed and nitroxide-mediated living radical polymerizations of styrene.²⁹⁶ Biologically related functions such as oligosaccharide,³³⁹ cholesterol,^{340,341} and nucleosides³²³ are incorporated in FI-46 to FI-49 for CuBr/L-9 ($R = n\text{-Pen}$ or $n\text{-Oct}$), whereas FI-50 (with CuBr/L-1) is to introduce a C_{60} or fullerene terminal.³⁴²

In addition to the carbon-centered radical initiators, arenesulfonyl halides are simple and efficient functionalized initiators by introducing a variety of functional termini; conjugation between the aryl and the sulfonyl groups is absent (FI-51 to FI-58; Figure 14).¹⁷⁵ Typically, a series of monosubstituted derivatives (FI-51) are commercially available and afford hydroxyl, carboxyl, nitro, and halo groups in living

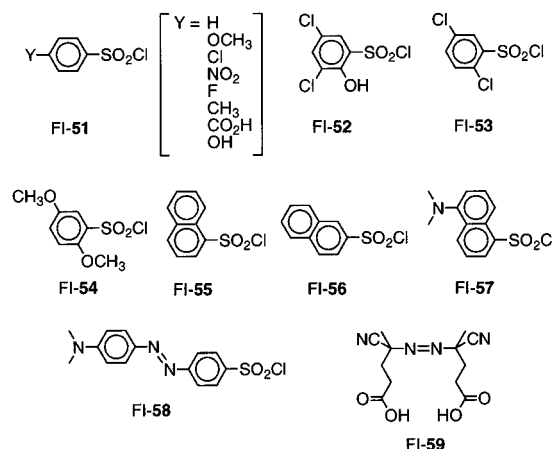


Figure 14. Sulfonyl halide and conventional radical functional initiators.

radical polymerization of styrene, MMA, and nBMA with the copper^{152,175} or ruthenium¹⁸⁰ catalysts (end functionality $F_n \approx 1.0$). Other sulfonyl chlorides (FI-52 to FI-58) are similarly applicable.^{126,175,343}

An alternative and perhaps simpler way to synthesize α -end-functionalized polymers is to use a functional azo initiator (FI-59) in the presence of transition metals in a higher oxidation state such as FeCl₃ with PPh₃ as a ligand.⁸⁰ This method is a variant of the reverse atom-transfer polymerization and gives polystyrenecarboxylic acid with narrow MWDs ($M_w/M_n = 1.14$).

2. ω -End-Functionalized Polymers

In contrast to the frequent use of the initiator method and the wide variety of available functional initiators, the end-capping method is not as frequently employed, primarily because of the difficulty in selective and quantitative quenching radical polymerization, particularly in the metal-catalyzed living systems involving dormant halogen species. This stems from several factors: the extremely low concentration of the radical species relative to the dormant species, the highly stable dormant carbon-halogen bond, and the limited availability, thus far, of suitable quenchers that can add to the growing carbon radical without deteriorating the metal complex catalyst. However, with the use of selected compounds, the halogen terminal can be converted into functional groups via metal-catalyzed radical reactions or other reactions.

Metal-catalyzed end-capping via a radical mechanism can be carried out either by in situ quenching of the polymerization or by the reaction of isolated halogen-capped polymers. Mostly the same quencher may be used for both methods. Despite the less frequent applications, however, a wide variety of quenching end-capping agents have been reported (EC-1 to EC-15) (Figure 15). Most of these compounds have a vinyl group that can add to a polymer terminal under metal-catalyzed conditions to form much less reactive carbon-halogen bonds or unsaturated groups via release of low molecular weight halogen compounds.

The first of these are silyl enol ethers EC-1 with a phenyl group or α -(silyloxy)styrenes. They can effectively quench the ruthenium-catalyzed living radical polymerization of MMA to give the ω -end-functionalized PMMA with a ketone group with high end functionality ($F_n \approx 1.0$).^{293,344} The method is also useful to attach an aromatic ω -end group not only for end-functionalization (via the substituent on the ring) but also for end-group analysis (via the aromatic protons). The quenching reaction is considered to proceed via addition of the growing radical to the vinyl group of EC-1 to generate another radical terminal that is stabilized by the α -phenyl group, followed by elimination of the trimethylsilyl group with the chlorine at the polymer terminal (or on the metal center) due to their high affinity toward halogens (Scheme 5). The quenching is quantitative and selective, and proceeds faster with an electron-donating substituent (X; OCH₃ > H > F > Cl) on the phenyl group of EC-1 and at its higher concentration.

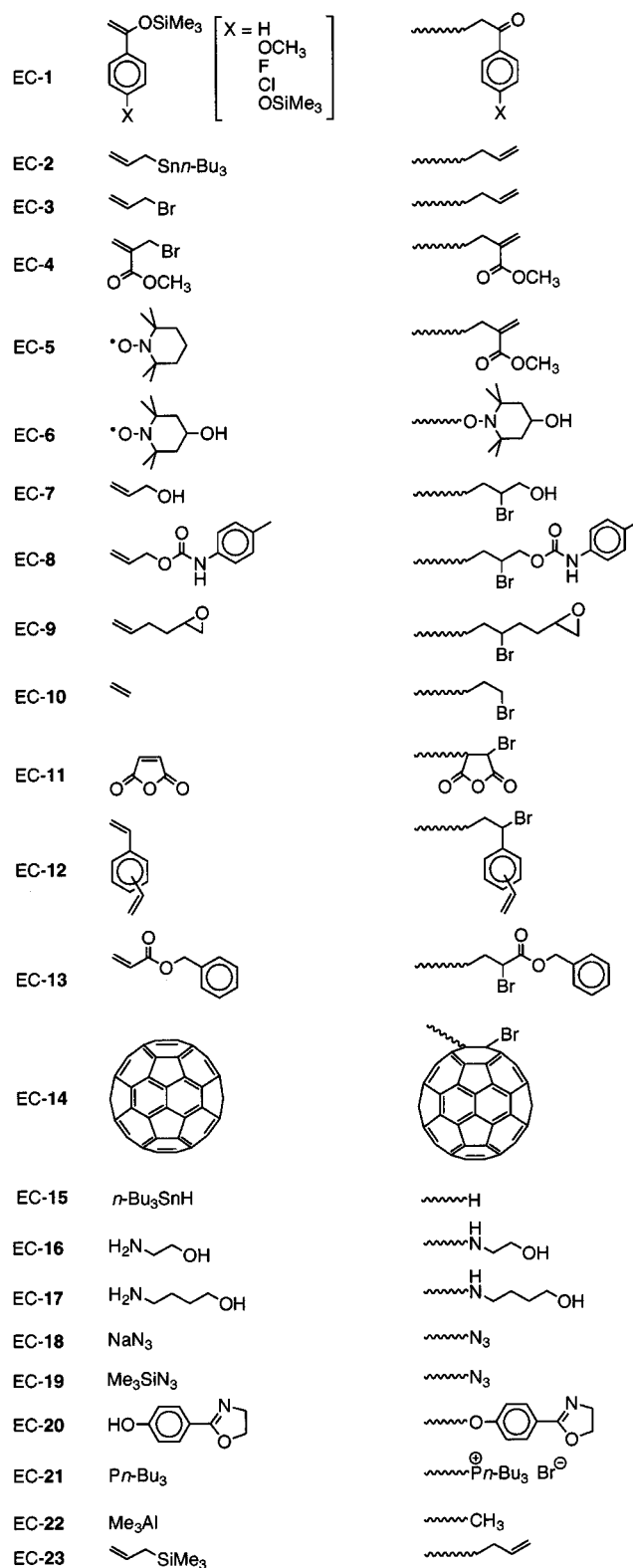
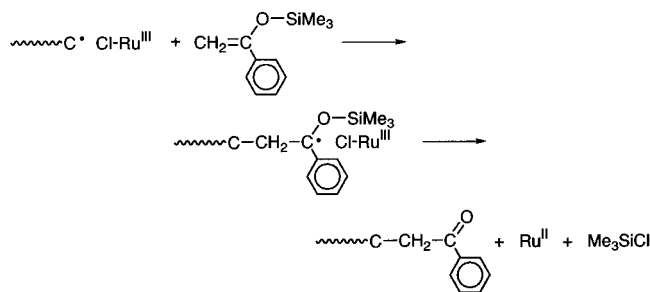


Figure 15. End functionalization of carbon-halogen terminals.

In contrast, silyl enol ethers with an α -alkyl group (α -silyloxy vinyl ethers) proved less efficient, indicating the stability of the resultant silyloxy radicals is among the critical factors in designing good quenchers of this class. These are due to the degree of the affinity of the PMMA radical toward the vinyl groups in the quenchers. This silyl enol ether capping is applicable for copper-catalyzed polymerizations [with

Scheme 5. Quenching of Metal-Catalyzed Living Radical Polymerization with Silyl Enol Ethers



EC-1 ($X = \text{OSiMe}_3$), in the reported examples, carried out on isolated PMMA. The quenching has been carried out, not in situ, but on isolated PMMA samples.²²⁶ The trimethylsilyloxy group at the 4-position can be also converted into the phenol function.

An interesting application of the silyl enolate capping reaction has been developed by Percec, who coined the capping agents "TERMINI" (irreversible terminator multifunctional initiator).³⁴⁵ This refers to a "protected multifunctional compound able to quantitatively terminate a living polymerization and, after deprotection, to quantitatively reinitiate the same or a different living polymerization in more than one direction". Typical TERMINI agents are designed to possess one silyl enolate function for quenching (as in Scheme 5) and two or more protected sulfonyl chlorides for subsequent multiple initiation of metal-catalyzed living radical polymerization. Obviously from this design the TERMINI method is applicable for the efficient and well-defined synthesis of dendrimers and their libraries, along with other polymers of complex and multibranch architectures.

The silyl enolate quenching process (Scheme 5) is, in principle, similar to addition fragmentation reactions as well as the more recent reversible addition fragmentation chain transfer (RAFT; see also eq 9),¹⁸ in that all three involve an initial addition of the growing radical across a reactive vinyl group that carries both a radical-stabilizing group (a phenyl and an ester) and a good (radical) leaving group. The difference among them is whether the released radical via fragmentation is capable of reinitiating radical polymerization (e.g., capable in RAFT, incapable in the silyl enolate capping).

Allyltri-*n*-butylstannane (EC-2) similarly terminates the copper-catalyzed polymerization of MA to give allyl-functionalized polymers via elimination of the stannyl group accompanying the bromine originated from the dormant polymer terminal.³⁴⁶ Allyl ω -end PMMA was obtained also by the copper-catalyzed reaction between allyl bromide (EC-3) and the isolated bromine-capped PMMA, although the functionalization was 57%.²²⁶ Another allyl derivative (EC-4) similarly leads to methacrylate-based macromonomers quantitatively in the presence of Cu(0).³⁴⁷

The same poly(methacrylate)-based macromonomer can be obtained via the TEMPO (EC-5)-promoted elimination of hydrogen and bromine from the isolated bromine-ended PMMA in the presence of CuBr/L-9 ($R = n\text{-Pr}$), though the functionality was 78%.²²⁶ In contrast, the carbon-bromine bond in the poly-

styrene and poly(*n*BA), which have no α -methyl substituent, can be displaced into the carbon-TEMPO terminal via the copper-catalyzed reaction with EC-6.²⁴²

Allyl compounds ($\text{CH}_2=\text{CH}-\text{CH}_2\text{R}$) without good radical leaving groups react with the growing radical in the metal-catalyzed polymerizations to result in an inactive carbon-halogen terminal ($---\text{CH}_2-\text{CHX}-\text{CH}_2\text{R}$). Thus, the reaction is, formally, an addition of alkyl halide (the halogen-capped growing end) across an olefin. For example, copper-catalyzed radical polymerizations of MA²⁸⁰ and MMA³²⁷ were quenched with allyl alcohol (EC-7) to generate a β -bromo alcohol terminal. A similar reaction was reported with EC-8³²⁷ and EC-9.³⁴⁶ Ethylene (EC-10) cannot polymerize with the metal-based radical systems but can react with the terminal carbon of isolated halogen-capped PMMA in the presence of CuBr and L-9 ($R = n\text{-Oct}$) to yield a primary bromide end quantitatively.²²⁶ Similarly, a single unit of maleic anhydride (EC-11) can be introduced to polystyrene and PMMA.^{226,348} Even one unit of divinylbenzene (EC-12) can be attached quantitatively at a low temperature (25 °C), where the homopolymerizations are suppressed.²²⁶ However, the end-capping yield with benzyl acrylate (EC-13), a more reactive monomer, cannot exceed 62%.²²⁶ An interesting application of these one-step olefin additions is found with EC-14 to attach a C_{60} end (35% yield).³⁴⁹

Almost all metal-catalyzed living polymerizations give polymers capped with halogens that are stable after the usual workup. These terminal halogens would be undesirable, because they may lower the polymer's thermal stability. Dehalogenation by tributyltin hydride (EC-15) is of importance in this respect and effectively works for the bromide terminals in polystyrene, PMMA, and poly(MA) in the presence of copper catalysts.²⁷⁷

An alternative method for ω -end functionalization is to transform the terminal halide by ionic reactions. Thus, nucleophilic substitution was examined with compounds EC-16 to EC-23. For example, an amino alcohol (EC-16) in DMSO at room temperature gives polystyrene with hydroxyl groups.^{280,350} However, an amino alcohol with a longer spacer (EC-17) should be employed for poly(MA) to avoid multiple alcohol functionalities.²⁸⁰

Transformation into azide groups was achieved for polystyrene, poly(MA), and poly(*n*BA) with the use of sodium azide (EC-18)³⁵¹⁻³⁵³ or trimethylsilyl azide (EC-19)^{161,351,354} in the presence of tetrabutylammonium fluoride. The azide groups can be further converted into amino ($-\text{NH}_2$) groups by treatment with $\text{PPh}_3/\text{H}_2\text{O}$ ³⁵¹ or LiAlH_4 .³⁵⁴ The reaction between the azide end group in polystyrene and C_{60} was also examined.³⁵³

Nucleophilic substitution with the phenolate anion derived from EC-20 and K_2CO_3 induced 30% substitution, along with elimination of hydrogen bromide.³³¹ Phosphonium groups can be introduced at the polystyrene and poly(MA) terminal via reaction with EC-21,³⁵⁵ and methyl groups with Me_3Al (EC-22).³⁵⁶ An allyl terminal is obtained also via an ionic pathway, where the polystyryl carbocation generated

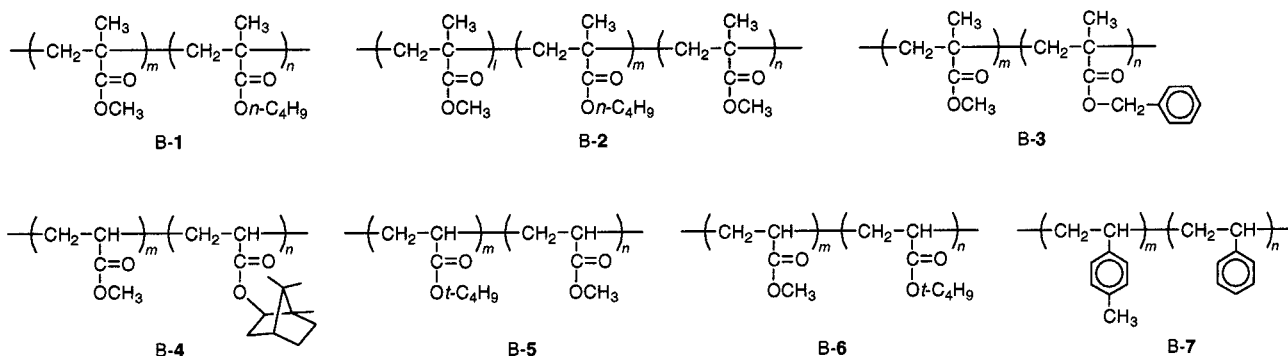


Figure 16. Block copolymers between the same family of monomers.

from the chlorine terminal polystyrene in the presence of TiCl_4 reacts with allyltrimethylsilane (EC-23).³⁵⁶ The allyl terminal was further transformed into epoxy and alcohol.

C. Block Copolymers

One of the most important applications of living polymerization is obviously block copolymerization. Block copolymers are usually obtained via sequential living polymerization of a monomer followed by another. This is also true for the metal-catalyzed living radical polymerization, which permits synthesis of a wide variety of block copolymers and apparently is more versatile than other living polymerizations. Another way is the use of isolated halogen-capped polymers as macroinitiators, taking advantage of the stability of the dormant carbon–halogen terminal even toward air and moisture. The procedure for the former method is apparently simpler than the latter because the reaction can be done in one pot. However, the problem therein is contamination of the first monomer's unit(s) in the second segments, because the second monomer is often added before the complete consumption of the first monomer to avoid side reactions at high conversion.

The synthetic strategy for a wider variety of block copolymers is to combine the metal-catalyzed living radical and other living polymerizations. This can be accomplished by the introduction of a potentially active carbon–halogen bond into the polymers obtained commercially or by some living processes.

This section discusses the block copolymer syntheses by these two approaches, and Figures 16–25 give comprehensive lists of reported block copolymers.

1. Block Copolymers via Sequential Metal-Catalyzed Living Radical Polymerization

A wide variety of block copolymers can be obtained by the metal-catalyzed living radical polymerizations, which are now applicable to numerous monomers. Most of them are block copolymers prepared from methacrylates, acrylates, and styrenes; combinations are therefore within the same family or between different families.

Block Copolymers between the Same Family of Monomers. Block copolymers derived from the same family of monomers (Figure 16) are obtained relatively easily, because the two monomers can normally be polymerized with common initiating systems and under similar reaction conditions.

Block copolymers between alkyl or related methacrylates (B-1,^{132,198,357} B-2,¹⁹⁸ and B-3^{115,146,148}) were prepared via the ruthenium-, copper-, and nickel-catalyzed living radical polymerizations. These block copolymers can be synthesized both via sequential living radical polymerizations and via the living radical polymerization initiated from isolated polymers. For example, the ruthenium-catalyzed sequential living radical polymerization of MMA followed by nBMA affords AB block copolymers B-1 with narrow MWDs ($M_w/M_n = 1.2$), which can be extended further into ABA block copolymers B-2 with similarly narrow MWDs ($M_w/M_n = 1.2$).¹⁹⁸ Star block copolymers with B-1 as arm chains were similarly synthesized but with multifunctional initiators.³⁵⁷

Block copolymers between alkyl acrylates such as B-4,³⁵⁸ B-5,^{202,203} and B-6,²⁰³ on the other hand, have been synthesized by the macroinitiator methods mostly with copper catalysts. Star block copolymers with a soft poly(MA) core and a hard poly(isobornyl acrylate) shell were synthesized by using multifunctional initiators.³⁵⁸ Poly(tBA) segments in B-5 and B-6 can be converted into hydrophilic poly(acrylic acid).²⁰³ Block copolymers between *p*-methylstyrene and styrene (B-7) were also prepared by the rhenium-catalyzed living radical polymerization in conjunction with an alkyl iodide initiator.¹⁶⁹

Block Copolymers between Different Families of Monomers. Block copolymers among different families of monomers (e.g., methacrylate/acrylate) can be efficiently prepared by metal-catalyzed radical polymerizations (Figure 17). Though widely feasible, the synthesis often calls for specific care, and in particular the initiating systems including terminal halogens, metals, and ligands should be carefully selected so that they are effective for both monomers in different families. For the macroinitiator method, in contrast, the catalysts for the first and the second polymerizations should not be necessarily the same.

Most of the block copolymers consisting of methacrylates and acrylates (B-8 to B-12) have been prepared via macroinitiator methods. AB- and BA-type block copolymers of MMA and MA (B-8^{76,135,359} and B-9³⁵⁹) were prepared with nickel, copper, and iron catalysts. Due to the higher activity of the carbon–halogen terminals in poly(methacrylate)s than in poly(acrylate)s, block copolymerization from PMMA is successfully performed via both sequential and macroinitiator methods, where the controllability seems better in the copper-based system. Similar

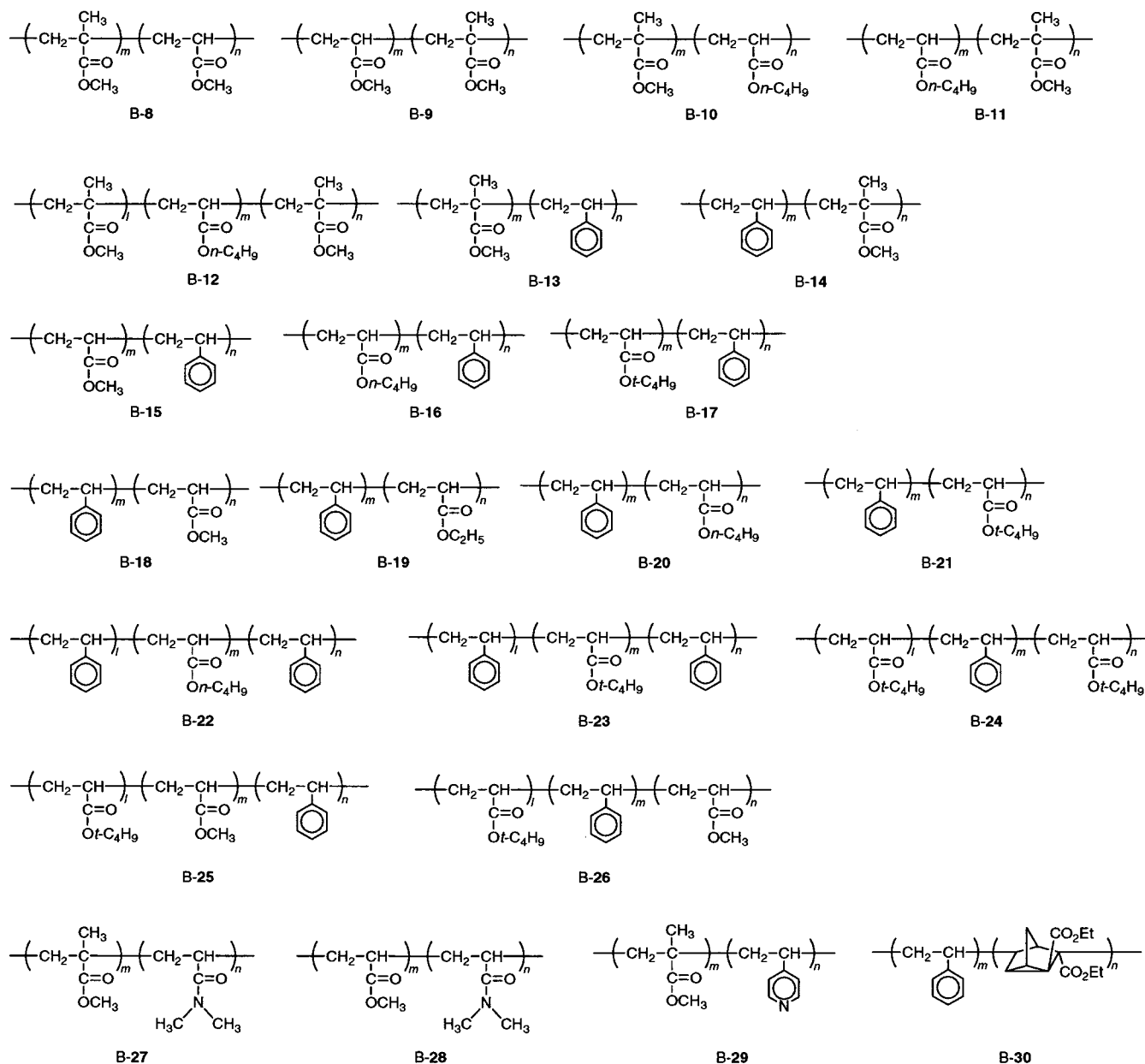


Figure 17. Block copolymers between different families of monomers.

results were also obtained for B-10.^{135,138,359} In contrast, for BA-type block copolymers from MA, halogen-exchange reactions from C–Br into C–Cl terminals (see above) should be employed so that the initiation from the less active dormant terminal of acrylates can be quantitative and faster.³⁵⁹ This method gave B-9 with fairly narrow MWDs ($M_w/M_n = 1.15$) without contamination of homopoly(MA). A similar block copolymer with nBA and MMA (B-11) can be prepared by the same method.³⁶⁰

ABA-type block copolymers B-12 with a hard PMMA as the outer segment (A) and a soft poly(nBA) as the inner segment (B) are expected as all-acrylic thermoplastic elastomers. Examples of B-12 have been prepared with copper and nickel catalysts via bifunctional initiation.^{359–364} Unfortunately, the copolymers by R–Br/Ni-2 via the macroinitiator method were reported to be inferior as thermoplastic elastomers to those by living anionic polymerizations. A possible reason is the presence of short PMMA seg-

ments caused by the lower activity of the C–Br terminal of poly(nBA).³⁶³ The use of halogen-exchange methods with the copper-based systems can narrow the MWDs of the ABA block copolymers.^{359,360,364}

The MMA/styrene block copolymers of both AB and BA types (B-13 and B-14) were synthesized with copper and iron catalysts, although the MWDs were slightly broader ($M_w/M_n = 1.4–1.5$) than those of the other block copolymers.^{76,94,241,365}

A wider range of acrylate/styrene block copolymers have been prepared by copper catalysts, partially because the homopolymerizations of both monomers can be controlled with common initiating systems. Both AB- (B-15 to B-17)^{202,230,254,366,367} and BA-type (B-18 to B-21)^{28,112,169,230,366,368,369} block copolymers were obtained from macroinitiators prepared by the copper-based systems. The block copolymerizations can also be conducted under air²³⁰ and under emulsion conditions with water.²⁵⁴ Combination of the Re- and Ru-mediated living radical polymerizations in

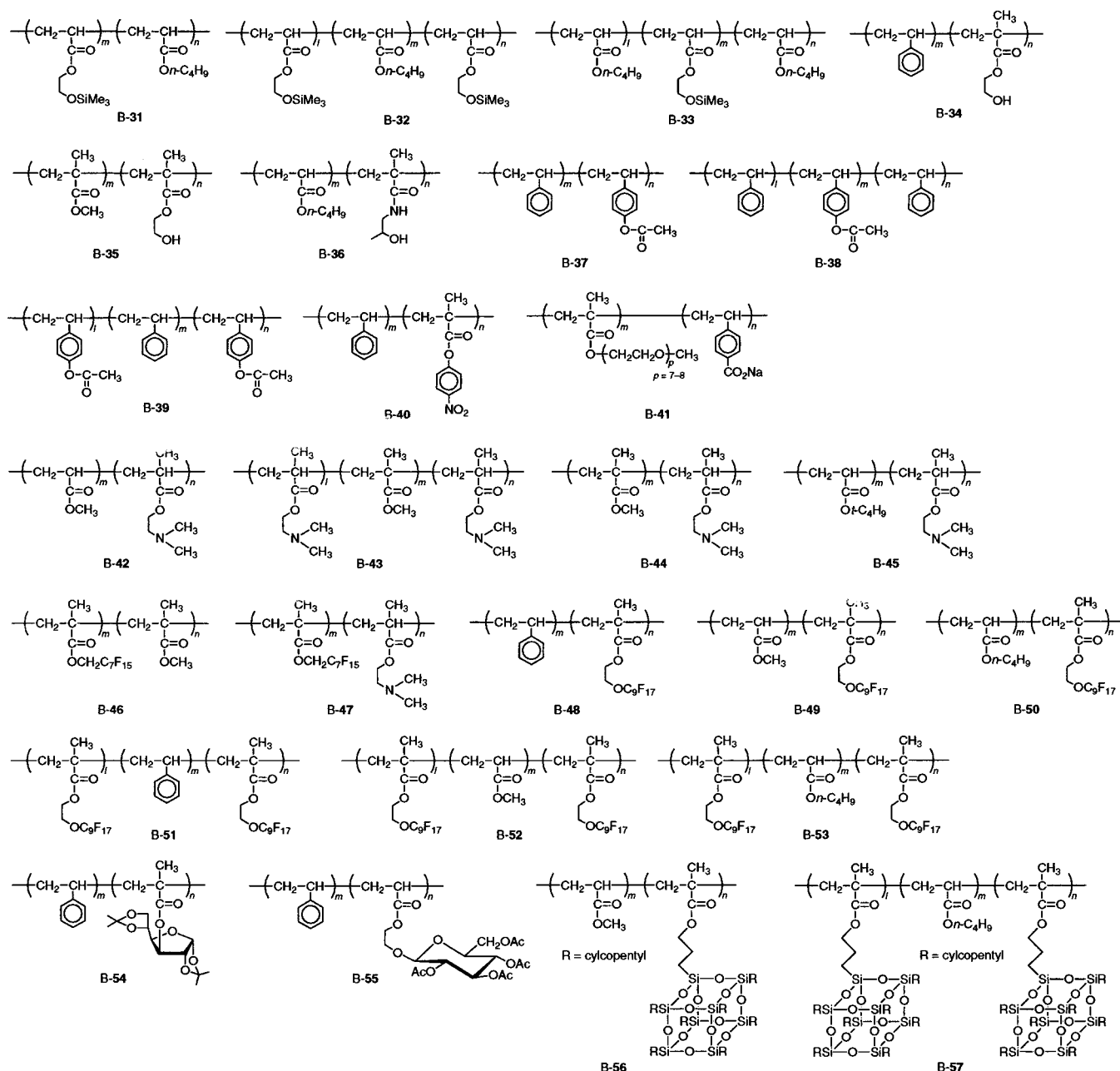


Figure 18. Block copolymers with functional segments.

the macroinitiator method is effective for the synthesis of B-18.¹⁶⁹

A series of ABA- and BAB-type triblock copolymers (B-22 to B-24) were obtained by two-step block copolymerization with bifunctional initiators²⁰² or by three-step block copolymerization with monofunctional initiators.^{202,366,368} ABC-type block copolymers B-25²⁰³ and B-26²⁰² consisting of styrene, MA, and tBA can be obtained by the latter method; the tBA segment may be hydrolyzed to give amphiphilic triblock copolymers.

Acrylamide-based block copolymers B-27³⁷⁰ and B-28¹¹⁷ were prepared by the ruthenium- and copper-based systems, respectively. The vinylpyridine (B-29)^{214,371} segment can be introduced into the block copolymers with MMA. The polystyrene-based block copolymers B-30 with short segments of a bicyclic monomer had a higher decomposition temperature than the homopolystyrene with C-Br terminals.²²³

Block Copolymers with Functional Segments.

Various block copolymers with functional groups can be prepared by direct block copolymerization of functional monomers or by sequential polymerizations of their protected forms, followed by deprotection (Figure 18).

Block copolymers with hydroxyl segments were prepared by various ways: An example utilizes the copper-catalyzed sequential copolymerizations of nBA and 2-[(trimethylsilyl)oxy]ethyl acrylate by the macroinitiator method into B-31 to B-33. The copolymers were then hydrolyzed into amphiphilic forms by deprotection of the silyl groups.³¹³ A direct chain-extension reaction of polystyrene and PMMA with HEMA also afforded similar block copolymers with hydroxyl segments (B-34 and B-35).^{241,243} In block polymer B-36, a hydroxy-functionalized acrylamide provides a hydrophilic segment.¹¹⁷ Block copolymers of styrene and *p*-acetoxystyrene (B-37 to B-39), prepared by iron

and copper catalysts, were precursors of amphiphilic block copolymers with hydroxy groups.^{169,208,372}

Carboxyl groups may be introduced into block copolymers via direct polymerizations of free-acid monomers or protection–deprotection procedures. Block copolymers of styrene and nitrophenyl methacrylate (B-40) are used for the latter method, where the activated ester pendant is effectively converted into methacrylic acid or acrylamide under mild conditions.¹⁶⁶ A homogeneous aqueous system with copper catalysts gives block copolymers with benzoate groups (B-41) via sequential block copolymerization of the two water-soluble monomers.²⁴⁷

Block copolymers with pendant amino groups can be obtained by the block copolymerization of (meth)acrylates and 2-(dimethylamino)ethyl methacrylate catalyzed by copper to afford B-42 to B-45.^{243,373}

Perfluoroalkyl groups are also introduced into block copolymers with methacrylates, acrylates, and styrene (B-46 to B-53), which can be synthesized in *scCO*₂ or in the bulk.^{95,315} Amphiphilic block copolymers based on glycopolymer segments (B-54 and B-55) are synthesized by copper-catalyzed polymerizations.^{321,322} Comonomers with a polyhedral oligomeric silsesquioxane unit afforded hybrid polymers between organic and inorganic components (B-56 and B-57).³²⁶

2. Block Copolymers via Combination of Other (Living) Polymerizations

Block copolymers can be prepared by combination of metal-catalyzed living radical polymerization and other polymerizations. Namely, polymers with carbon–halogen terminals may be synthesized by some living polymerization, and the product is further used to initiate living radical polymerization in the presence of transition-metal catalysts. Therefore, this method is essentially a variant of the macroinitiator method discussed above. Such carbon–halogen terminals can be obtained by transformation of the polymer terminal with some reagents or by use of halogenated initiators for the first-step living polymerization. In some cases, there is no need for the transformation since the first-step polymerization also proceeds via similar carbon–halogen chain ends as in living cationic polymerization (see below). Reviews on block copolymer synthesis based on mechanism transformation are available elsewhere.^{301,302}

Another method is based on initiation of other polymerizations from the polymers prepared by living radical polymerization as macroinitiators. The following sections give specific examples.

Anionic Vinyl Polymerization. The carbanionic terminals in living anionic polymerization can be transformed into carbon–halogen bonds suited for radical generation. The backbones utilized thus far for this approach include polystyrene (B-58 to B-62)^{215,374} and polyisoprene (B-63 and B-64),^{374,375} although the former segment can also be prepared by the living radical polymerization (Figure 19).

For B-58 to B-60 and B-62, the polystyryllithium terminal was converted into a bromide by the reaction with styrene oxide followed by treatment with 2-bromoisobutyryl bromide.³⁷⁴ The same method is

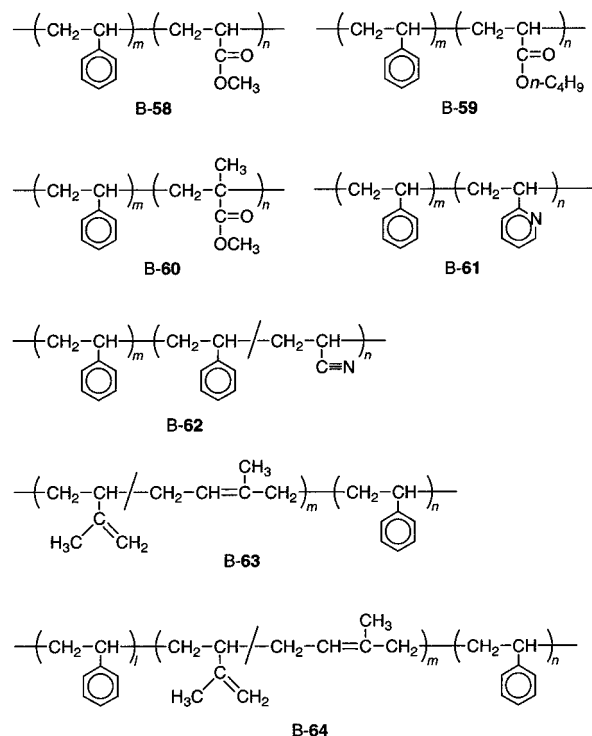


Figure 19. Block copolymers prepared via living anionic polymerization.

utilized for isoprene as in B-64.³⁷⁴ Such macroinitiators induced living radical polymerization of methacrylates, acrylates, and styrene in the presence of the copper catalysts to give block copolymers with narrow MWDs ($M_w/M_n = 1.1–1.2$). The use of ethylene oxide for quenching the living anionic polymerization of styrene followed by treatment with SOCl_2 resulted in a carbon–chlorine terminal for a subsequent polymerization of 2-vinylpyridine (B-61).²¹⁵

A transformation method can introduce some functional groups at the junction as in B-63, which bear a fluorescent dye between the polyisoprene and polystyrene segments.³⁷⁵ The preparation is based on quenching the living anionic polymerization of isoprene with 1-(9-phenanthryl)-1-phenylethylene followed by addition of excess α, α' -dibromo-*p*-xylene, which affords a C–Br terminal effective for the copper-catalyzed radical polymerization of styrene.

Cationic Vinyl Polymerization. Living cationic polymerizations, in general, are based on the reversible activation and heterolytic dissociation of carbon–halogen terminals by a Lewis acid.^{7–9} Despite the difference in the activation processes, some of the carbon–halogen bonds obtained in living cationic polymerization can be used as an initiating site for metal-catalyzed living radical polymerization without any modification. Figure 20 shows block copolymers obtained in this way.

The polystyrene obtained by living cationic polymerization with R–Cl/Lewis acid possesses a carbon–chlorine terminal that is subsequently used for the living radical polymerizations of acrylates and methacrylates to give block copolymers such as B-65 to B-67.^{376–378}

Chlorine-capped polyisobutylene, prepared via cationic polymerization, was also used as a macroinitiator for the copper-catalyzed radical polymeriza-

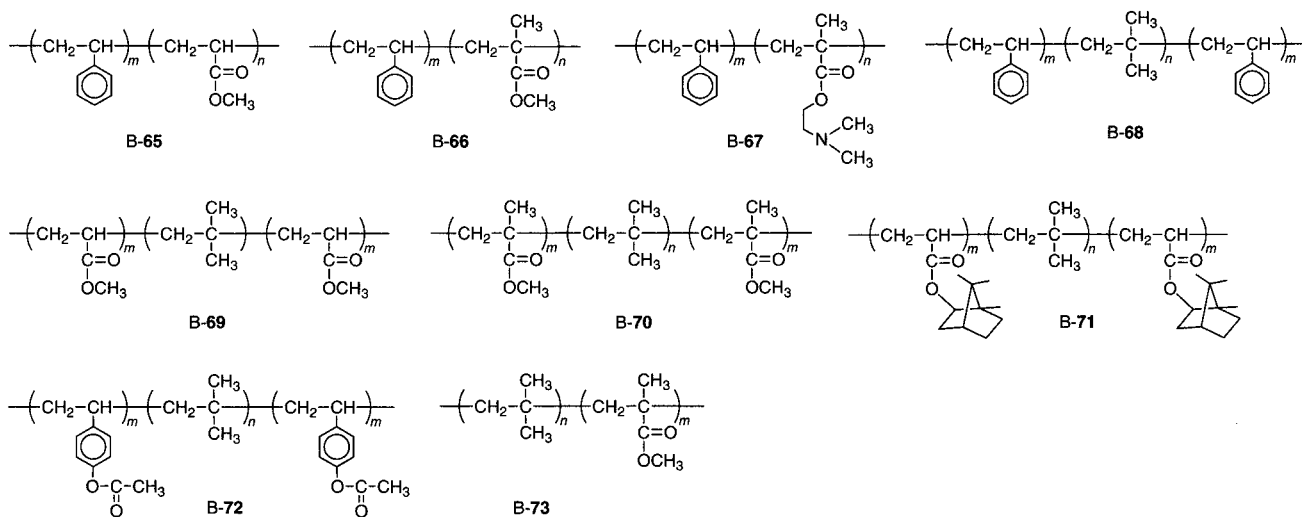


Figure 20. Block copolymers prepared via living cationic polymerization.

tions of acrylates, methacrylates, and styrenes as in B-68 to B-73.^{204,379–381} The C–Cl terminal of the polyisobutylene cannot initiate the living radical polymerization due to its lower activity for redox reactions, but it can be modified into an active form by inserting several units of styrene. Polymers B-68 to B-72 were prepared in this way from bifunctional initiators.^{204,380} Another method is based on transformation of the chloride terminal into hydroxyl functions followed by esterification with 2-bromopropionyl³⁷⁹ and 2-bromoisobutyryl halides³⁸¹ as employed in the preparation of B-68 and B-73, respectively.

Radical Vinyl Polymerization. Conventional radical polymerization and telomerization can also be beneficial for block copolymer synthesis, because in some cases they polymerize monomers inactive for metal catalysts, although side reactions often render the block copolymers in low yield and with ill control of molecular weights. However, a combination with conventional radical polymerizations affords novel block copolymers in higher yields than before (Figure 21).

Halogen compounds such as chloroform and carbon tetrachloride are well-known telomers in conventional radical polymerizations. They give oligomers or polymers with a CCl₃ terminal, which can act as an initiating group for metal-catalyzed radical polymerization. This method was employed for vinyl acetate to prepare AB block copolymers with styrene (B-74)^{338,382} or with nBA (B-75).^{330,338} The block copolymers based on vinylidene fluoride (B-76 to B-80) were similarly prepared with CHCl₃,^{157,383} perfluoroalkyl iodides,³⁸⁴ and bromides³⁸⁵ as telomers followed by the copper-catalyzed radical polymerizations.

Another route to block copolymers in conjunction with conventional radical systems is to use azo initiators bearing reactive carbon–halogen bonds such as (chloromethyl)benzyl, 2-bromoisobutyryl, and trichloromethyl groups.^{338,386} This method can afford diblock (B-74 and B-75) and triblock (B-81) copolymers, depending on the mode of termination reactions in the conventional radical polymerizations with the azo compounds. In these cases, the order of

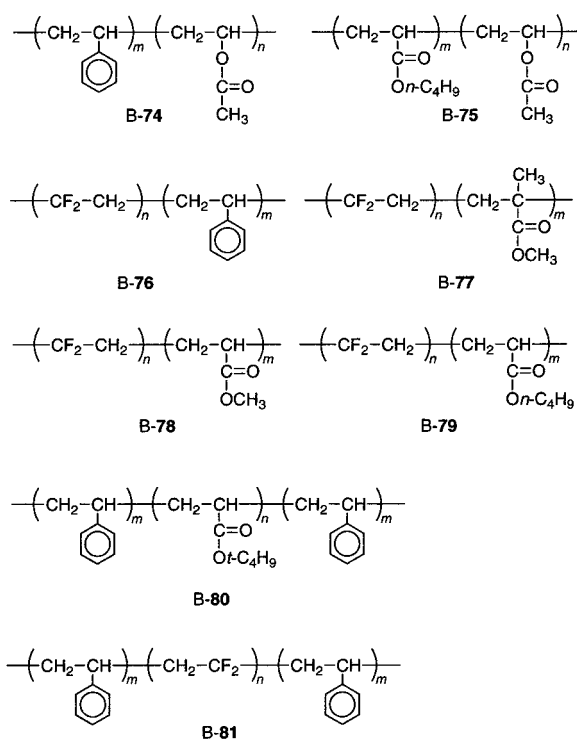


Figure 21. Block copolymers prepared via conventional radical polymerization.

the two polymerizations can be reversed, where conventional radical polymerization is initiated by the azo macroinitiators prepared by a metal-catalyzed radical polymerization.³³⁸

Ionic Ring-Opening Polymerization. Living ionic ring-opening polymerization of cyclic ethers, esters, and siloxanes gives polymers with controlled molecular weights and defined terminal structures and is thus applied to the synthesis of block copolymers coupled with the metal-catalyzed living radical polymerizations (Figure 22).

Transformation of cationic ring-opening polymerization of THF into the copper-catalyzed radical polymerizations of styrene, acrylates, and methacrylates leads to various block copolymers (B-82 to B-88).^{387,388} Diblock (B-82 to B-84) and ABC-type triblock (B-85) copolymers were prepared via the

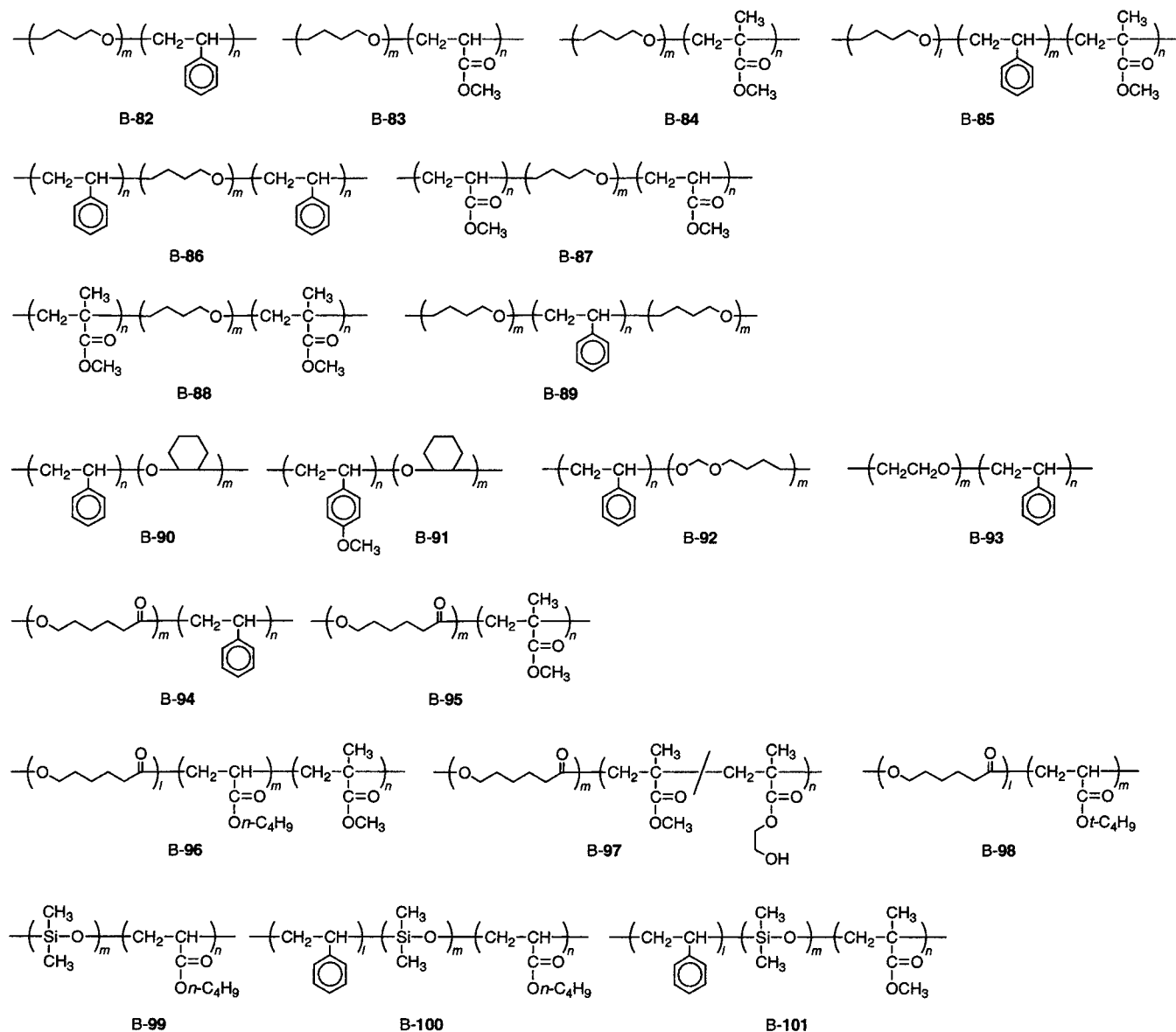


Figure 22. Block copolymers prepared via ionic ring-opening polymerization.

copper-catalyzed radical polymerizations from poly-(THF) macroinitiators obtained with 2-bromopropionyl bromide and silver triflate.³⁸⁷

The ABA-type block copolymers **B-86** to **B-88** were synthesized via termination of telechelic living poly-(THF) with sodium 2-bromoisopropionate followed by the copper-catalyzed radical polymerizations.³⁸⁷ A similar method has also been utilized for the synthesis of 4-arm star block polymers (arm **B-82**), where the transformation is done with β -bromoacetyl chloride and the hydroxyl terminal of poly(THF).³⁸⁸ The BAB-type block copolymers where polystyrene is the midsegment were prepared by copper-catalyzed radical polymerization of styrene from bifunctional initiators, followed by the transformation of the halogen terminal into a cationic species with silver perchlorate; the resulting cation was for living cationic polymerization of THF.³⁸⁹ A similar transformation with $\text{Ph}_2\text{I}^+\text{PF}_6^-$ was carried out for halogen-capped polystyrene and poly(*p*-methoxystyrene), and the resultant cationic species subsequently initiated cationic polymerization of cyclohexene oxide to produce

B-90 and **B-91**, respectively.³⁹⁰ Another route coupled with cationic ring-opening polymerizations is accomplished for polymer **B-92** with the use of a hydroxyl-functionalized initiator with a C–Br terminal, where the OH group initiates the cationic polymerizations of 1,3-dioxepane in the presence of triflic acid.³²⁹ Poly(ethylene oxide)-based block copolymers **B-93** are obtained by living anionic polymerization of ethylene oxide and the subsequent transformation of the hydroxyl terminal into a reactive C–Br terminal with 2-bromopropionyl bromide, followed by the copper-catalyzed radical polymerization of styrene.³⁹¹

Living ring-opening polymerization of ϵ -caprolactone with aluminum alkoxide or alkylaluminum can be combined with nickel-catalyzed living radical polymerization for the synthesis of linear and dendrimer-like star block copolymers **B-94** to **B-98**.^{139,392–394} Such block copolymers were first synthesized via living radical polymerization with $\text{CBr}_3\text{CH}_2\text{OH}$, where the C–Br bond is a radical initiating site and the hydroxyl group is for the subsequent ring-opening

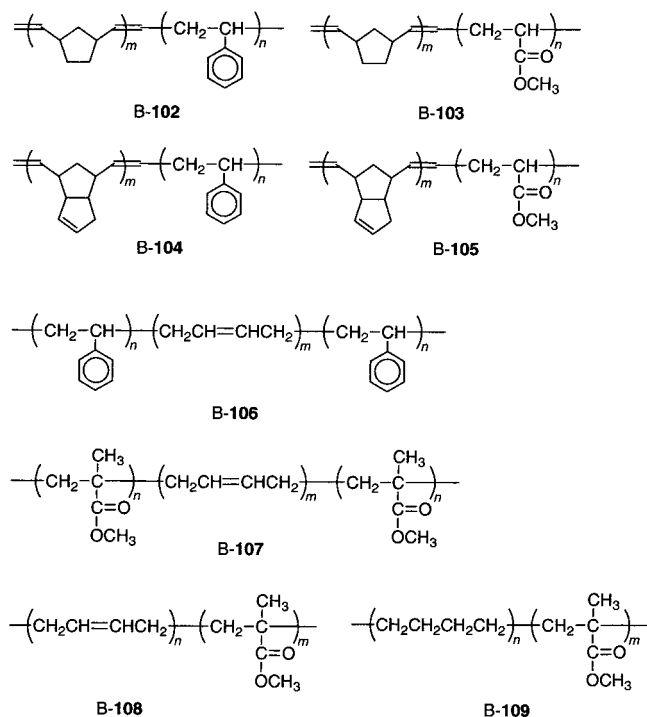


Figure 23. Block copolymers prepared via ring-opening metathesis polymerization.

polymerization. The reverse order of the two processes is also possible.¹³⁹ More interestingly, the two living polymerizations can be performed simultaneously; namely, MMA and ϵ -caprolactone undergo parallel growth initiated by the $\text{CBr}_3\text{CH}_2\text{OH}/\text{Ni-2}/\text{Al}(\text{O-}i\text{-Pr})_3$ system.³⁹² The aluminum compound might have a dual function, one as a catalyst for anionic ring-opening polymerization and the other as an additive for Ni-2 to facilitate the living radical process.¹³³

Poly(dimethylsiloxane) segments can also be introduced into the block copolymers as in B-99 to B-101, where the silane terminal of poly(dimethyl-

siloxane) or block copolymers of styrene and dimethylsiloxane are converted into the C-Br terminal by hydrosilylation of 3-butenyl 2-bromoisobutyrate.³⁹⁵

Ring-Opening Metathesis Polymerization. When coupled with living radical systems, living ring-opening metathesis polymerization (ROMP) also permits the synthesis of other types of block copolymers (Figure 23) such as B-102 to B-108.^{67,396,397} A molybdenum carbene or ROMP intermediate is converted into a benzyl bromide-type terminal by quenching the ROMP with *p*-(bromomethyl)benzaldehyde by a retro-Wittig reaction.³⁹⁶ The macroinitiator thus obtained induced living radical polymerizations of styrene and MA with copper catalysts to afford B-102 to B-105.

Poly(1,4-butadiene) segments prepared by the ruthenium-mediated ROMP of 1,5-cyclooctadiene can be incorporated into the ABA-type block copolymers with styrene (B-106) and MMA (B-107).³⁹⁷ The synthetic method is based on the copper-catalyzed radical polymerizations of styrene and MMA from the telechelic poly(butadiene) obtained by a bifunctional chain-transfer agent such as bis(allyl chloride) or bis-(2-bromopropionate) during the ROMP process. A more direct route to similar block copolymers is based on the use of a ruthenium carbene complex with a C-Br bond such as Ru-13 as described above.⁶⁷ The complex induced simultaneous or tandem block copolymerizations of MMA and 1,5-cyclooctadiene to give B-108, which can be hydrogenated into B-109, in one pot, catalyzed by the ruthenium residue from Ru-13.

Condensation Polymerization. Condensation polymerization generally affords telechelic polymers with functional terminals, which thus can be transformed into reactive carbon-halogen bonds for the metal-catalyzed radical polymerizations (Figure 24).

Polysulfones obtained from bisphenol A and bis(4-fluorophenyl) sulfone were converted into telechelic macroinitiators by the reaction with 2-bromopropio-

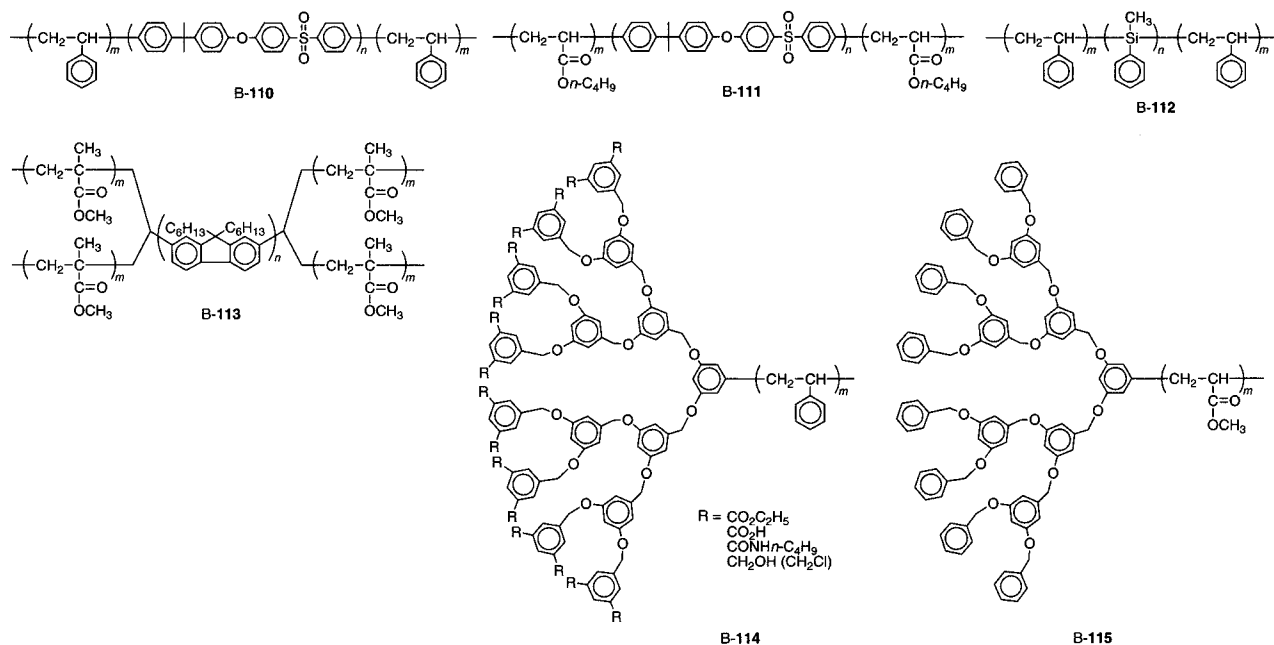


Figure 24. Block copolymers prepared via condensation polymerization.

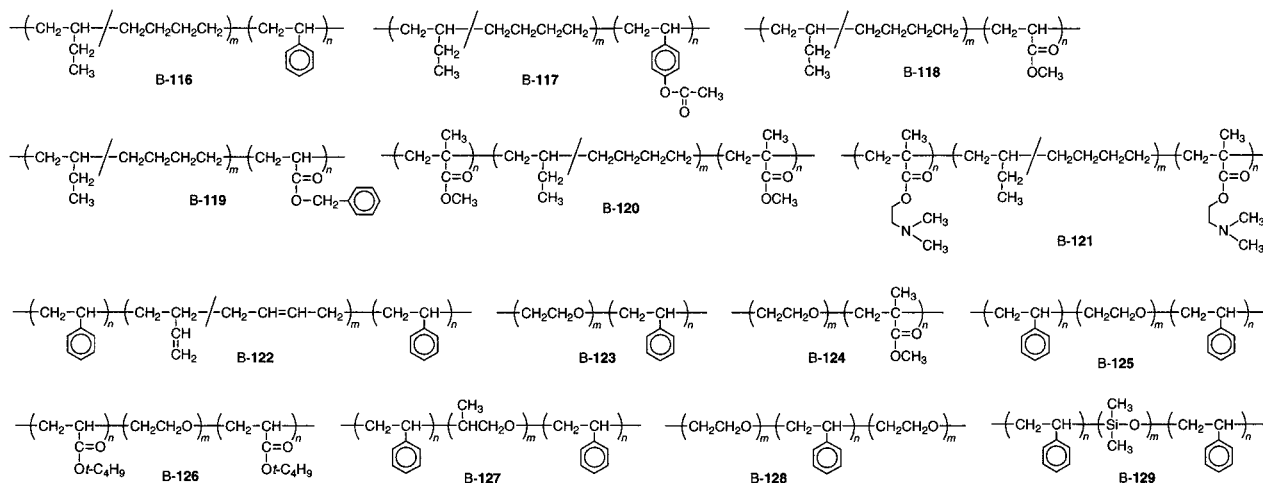


Figure 25. Block copolymers prepared from commercially available polymers.

nyl bromide. The telechelic bisbromide was subsequently employed for the copper-catalyzed block polymerization of styrene or nBA to give B-110 and B-111, respectively.³⁹⁸ A polysilylene-based block copolymer (B-112) was synthesized similarly from a telechelic polysilane macroinitiator with benzyl chloride terminals.³⁹⁹ Another block copolymer (B-113) consisting of a fluorene unit in the midsegment was obtained by two-step polymerizations, the Ni(0)-mediated condensation polymerization of 2,7-dibromo-9,9-dihexylfluorene and the Ni(II)-mediated living radical polymerization of MMA after the transformation of the telechelic terminals.⁴⁰⁰

Polystyrene B-114⁴⁰¹ and poly(acrylate) B-115⁴⁰² are connected to a dendrimer at its focal core. These are prepared with dendrimer-type macroinitiators with a benzyl bromide at the focal point, from which are initiated the copper-catalyzed living radical polymerizations of styrene and acrylates, respectively. For B-114, various functional groups (R) were introduced into the periphery.

Commercially Available Polymers. Modification of terminal groups for block copolymer synthesis can be applied to commercially available end-functionalized polymers although most of them are produced by living anionic polymerization. Thus, some of the block copolymers shown in Figure 25 were already described above.

Hydroxyl-capped poly(ethylene-*co*-butylene), a so-called Kraton, was converted into a macroinitiator via esterification with 2-bromopropionyl chloride, and then employed for the block copolymerizations of styrene and *p*-acetoxystyrene (B-116 and B-117).⁴⁰³ A similar method is utilized for B-118 to B-121 where the esterification is with 2-bromoisobutyryl bromide.³⁴¹ A commercially available polybutadiene is also employed for B-122 via a similar transformation into the chloroacetyl group.⁴⁰⁴

Poly(oxyethylene) units can be introduced by using commercially available poly(ethylene oxide)s and poly(ethylene glycol)s via esterification of the terminal hydroxyl groups with appropriate acyl halides. Various AB- (B-123 and B-124) and ABA-type (B-125 and B-126) block copolymers were thus prepared,^{171,327,405–408} along with a poly(propylene oxide)-based version (B-127).⁴⁰⁴ The polymer coupling be-

tween a telechelic polystyrene with terminal maleic anhydride units and a commercially available poly(ethylene glycol methyl ether) gave B-128.³⁴⁸

Polysiloxane-based ABA-type block copolymers B-129 can be prepared from commercially available poly(dimethylsiloxane) as a starting material followed by functionalization and the subsequent copper-catalyzed radical polymerization of styrene.⁴⁰⁹

D. Random Copolymers

A distinctive advantage of radical polymerization is that a variety of monomer pairs can readily be copolymerized into true random/statistical copolymers.

A mixture of two monomers that can be homopolymerized by a metal catalyst can be copolymerized as in conventional radical systems. In fact, various pairs of methacrylates, acrylates, and styrenes have been copolymerized by the metal catalysts in random or statistical fashion, and the copolymerizations appear to also have the characteristics of a living process. The monomer reactivity ratio and sequence distributions of the comonomer units, as discussed already, seem very similar to those in the conventional free radical systems, although the detailed analysis should be awaited as described above. Apart from the mechanistic study (section II.F.3), the metal-catalyzed systems afford random or statistical copolymers of controlled molecular weights and sharp MWDs, where, because of the living nature, there are almost no differences in composition distribution in each copolymer chain in a single sample, in sharp contrast to conventional random copolymers, in which there is a considerable compositional distribution from chain to chain. Figure 26 shows the random copolymers thus prepared by the metal-catalyzed living radical polymerizations.

There are several examples of random copolymers of methacrylates (R-1 to R-3). MMA/nBMA copolymerization was carried out with a copper catalyst, but the products were of low molecular weight because this study was directed to mechanistic studies.²⁶³ Random copolymers of MMA and nBMA (R-1) were also obtained in emulsion ($M_w/M_n = 1.2–1.3$).²⁵⁴ Two monomers were consumed almost simultaneously to give a random or statistical distribution of repeat units along the chains. Copolymerization of MMA

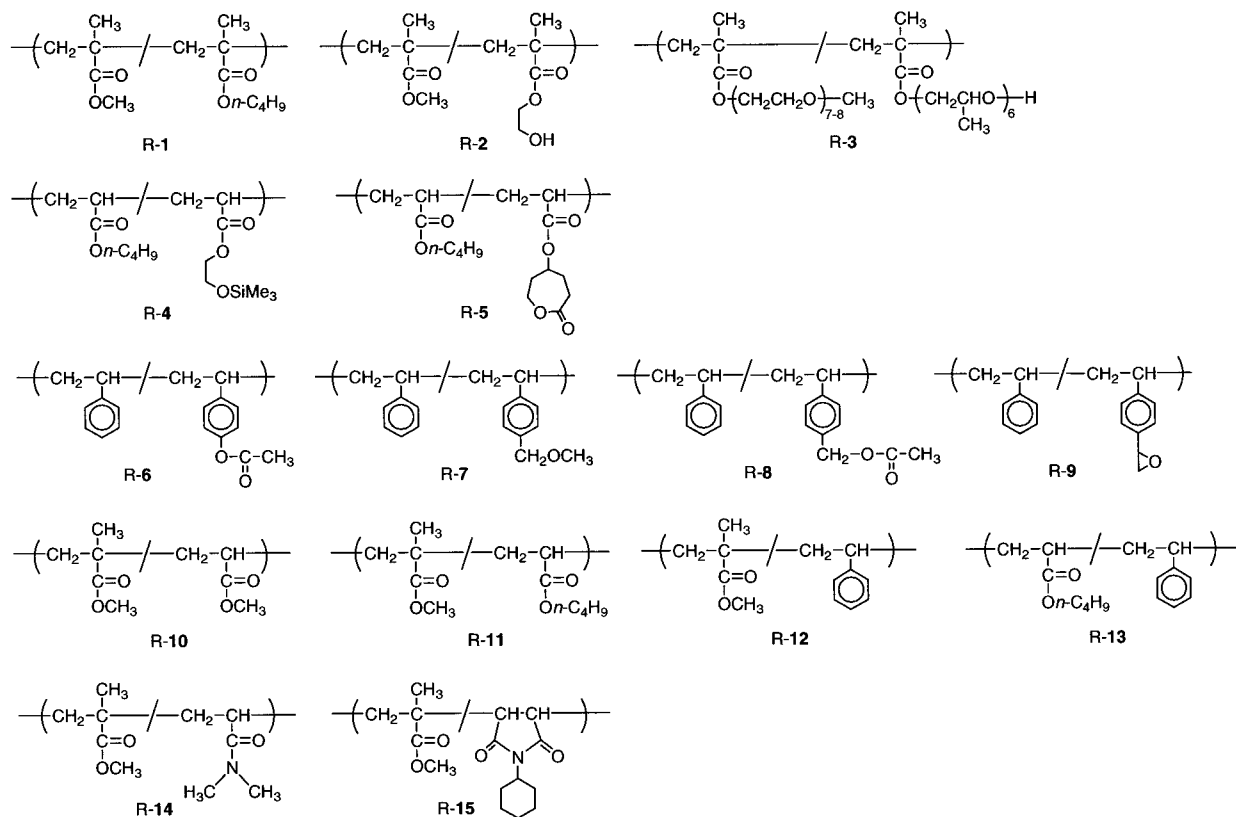


Figure 26. Random copolymers.

and HEMA was investigated by ruthenium and rhodium catalysts to give random copolymers **R-2** which possess hydroxyl functions randomly distributed along the chains.^{59,138} Random copolymers between hydrophilic and hydrophobic segments (**R-3**) were also synthesized by the copper catalysts in water.³²⁰

Random copolymers between acrylates (**R-4** and **R-5**) were prepared by the copper and nickel catalysts. The former one has random distribution of the hydroxyl groups along with the chains similarly to **R-2** and shows different behavior in water in comparison to the block copolymers.³¹³ In copolymer **R-5**, the ϵ -caprolactone units are distributed randomly and can function as linking agents in the subsequent copolymerizations with ϵ -caprolactone.³¹⁸

For styrene-based random copolymers, functional groups can be introduced into the polymer chains via copolymerization with functional styrene derivatives, because the electronic effects of the substituents are small in the metal-catalyzed polymerizations in comparison to the ionic counterparts. Random copolymer **R-6** is of this category, synthesized from styrene and *p*-acetoxystyrene.³⁷² It can be transformed into styrene/*p*-vinylphenol copolymers by hydrolysis.³⁸⁰ The benzyl acetate and the benzyl ether groups randomly distributed in **R-7** and **R-8** were transformed into benzyl bromide, which can initiate the controlled radical polymerizations of styrene in the presence of copper catalysts to give graft copolymers.²⁰⁹ Epoxy groups can be introduced, as in **R-9**, by the copper-catalyzed copolymerizations without loss of epoxy functions, while the nitroxide-mediated systems suffer from side reactions due to the high-temperature reaction.³¹⁷

Metal-catalyzed radical polymerization enables the controlled random copolymerization of the monomers that belong to different families such as methacrylates, acrylates, and styrenes, in contrast to the fact that the living anionic counterparts give their block copolymers in most cases. However, some of the metal-catalyzed systems may suffer from slight broadening of the MWDs due to the difference in the cross-propagation processes and in reactivity of the dormant carbon-halogen terminals depending on which monomer pair is employed. Another problem is that, at least thus far, the available metal catalysts are more or less "monomer-specific" and few of them are universally applicable to different families of monomers such as methacrylates and styrenes.

Copolymerizations of an equimolar mixture of MMA and MA (**R-10**) or nBA (**R-11**) with the nickel catalysts led to simultaneous consumption of the two monomers and gave their random copolymers with controlled molecular weights and relatively narrow MWDs ($M_w/M_n \approx 1.5$).¹³⁵ The copper-catalyzed systems also induced controlled random copolymerizations of MMA and nBA in organic solvents and in emulsion ($M_w/M_n \approx 1.2$).^{254,267} However, methacrylate/acrylate copolymerization may result in gradient structures rather than random structures (section III.F).

The styrene-based random copolymers **R-12** and **R-13** were prepared by ruthenium and copper catalysts, respectively. For the former copolymer (**R-12**), the copolymerizations were investigated with various compositions of the two monomers, which revealed that the composition curve is similar to that of conventional radical copolymerizations.²⁰⁵ The latter copolymers (**R-13**) obtained with R-Br/CuBr have

narrow MWDs ($M_w/M_n = 1.1-1.2$) because the systems are effective in controlling homopolymerizations of both styrene and nBA.²⁶⁴ The R-Cl/CuCl system also gave R-13 although the MWDs became slightly broader ($M_w/M_n = 1.3-1.4$).³⁶⁶

Other methacrylate-based copolymers are also possible with acrylamide (R-14)³⁷⁰ and maleimide (R-15),⁴¹⁰ which can be prepared by ruthenium and copper catalysts, respectively. Both copolymers have amide groups randomly distributed in the PMMA chains.

E. Alternating Copolymers

Alternating copolymers can be obtained from the monomers that cannot homopolymerize alone but can copolymerize in conjunction with the appropriate monomers. As described above, *N*-substituted maleimides copolymerize with styrene in this fashion in the presence of copper catalysts to give alternating copolymers with controlled molecular weights ($M_w/M_n = 1.1-1.2$). The substituents in the maleimides include 2-acetoxyethyl, phenyl, and cyclohexyl groups.²¹⁹⁻²²²

F. Gradient Copolymers

Another type of copolymer with controlled composition or sequence distribution is a gradient copolymer, in which the repeat-unit composition (sequence) changes along a backbone; i.e., "A" units are predominant, for example, near the α -end, and their abundance continuously decreases, while "B" units increasingly predominate near the ω -end. Such polymers can be prepared by metal-catalyzed radical polymerization; two methods are known so far: One method is based on the automatic formation of a gradient composition due to an inherent monomer reactivity difference, and the other is based on continuous addition of a second monomer at a controlled rate into a polymerizing solution of the first monomer. The former is exemplified in the copolymers obtained of MMA and nBA.⁴¹¹ Although they are considered random copolymers, detailed analysis indicates that there is a gradient structure therein. The latter method was applied for pairs of styrene/nBA and styrene/acrylonitrile. The physical properties of the copolymers were studied in comparison to those of other copolymers.

Another copolymer with compositional change along the chains is an ABC-type block/random copolymer that consists of three segments, each of which is a copolymer of the two monomers with a different composition. A mixture of styrene/MMA (3:1 molar ratio) was polymerized with the ruthenium-based systems, and two portions of MMA were sequentially added at varying styrene conversions.²⁰⁵ The styrene/MMA sequential compositions from the α - to the ω -end in the final products with relatively narrow MWDs ($M_w/M_n \approx 1.5$) are about (3:1)-(1:1)-(1:4). These interesting experiments show not only that the Ru-catalyzed MMA/styrene copolymerization is in fact living irrespective of the initial monomer composition, but also that the reaction might lead to new copolymers differing from statistical or gradient derivatives.

G. Telechelic and Star Polymers

Telechelic and star polymers can be obtained by a so-called multifunctional initiator method where metal-catalyzed living radical polymerizations are initiated from halogen compounds with plural reactive carbon-halogen bonds. This method can give multiarmed or star polymers with a predetermined number of arms that corresponds to the number of the carbon-halogen bonds in the initiator. Numerous polyhalogen compounds are accessible and synthesized from various polyfunctional compounds as summarized in Figures 27 and 28, where the arm numbers may be varied between 2 and 12.

Another route to synthesizing star polymers by living polymerization involves the use of multifunctional end-capping agents, but this method is not suited for metal-catalyzed radical polymerizations, at least so far, due to the lack of universal and convenient terminating agents, as described above (section III.B.2).

The third method is based on a polymer-linking reaction where the linear polymers are obtained by the living radical polymerization with divinyl compounds. This can afford star polymers with a relatively large number of arms, up to several hundred per molecule, while the number of arms by definition involves a statistical distribution in a single sample.

1. Telechelic Polymers with Bifunctional Initiators

Halogen compounds with two reactive carbon-halogen bonds can be bifunctional initiators for metal-catalyzed living radical polymerizations to give telechelic polymers. The effective bifunctional initiators include MI-1 to MI-26 with various spacers between the initiating sites.

α,α' -Dichloro-*p*-xylene (MI-1, X = Cl) is a bifunctional initiator for the copper-catalyzed living radical polymerization of styrene to give telechelic polymers with controlled molecular weights and narrow MWDs ($M_w/M_n = 1.45$).⁸⁴ The bromide version of MI-1 (X = Br) is more versatile and gives telechelic polymers of styrene,^{84,315,348} MA,^{84,315} nBA,³¹⁵ and *p*-acetoxystryrene²⁰⁷ with narrow MWDs ($M_w/M_n = 1.1-1.3$). The telechelics are further employed as macroinitiators for ABA-type block copolymers. The copper-catalyzed radical polymerization of MMA with MI-2 gave polymers with narrow MWDs ($M_w/M_n = 1.2$) but in low initiation efficiency ($I_{\text{eff}} = 0.13$).⁴¹² The obtained PMMA possesses one anthracene unit in the middle of the polymer backbone. α,α' -Dichlorotoluene (MI-3) serves as a bifunctional initiator for the copper-catalyzed radical polymerization of styrene, while it works as a monofunctional version for MMA polymerization due to the low reactivity of the second C-Cl bond after the initiation.¹⁶⁵ A halo ketone, dichloroacetophenone (MI-4), induces living radical polymerization of MMA in the presence of ruthenium catalysts to give polymers with extremely narrow MWDs ($M_w/M_n \approx 1.1$).⁵⁶ As it turned out, both of the carbon-chlorine bonds in the initiator initiate living polymerization.¹⁵⁴

Ester-type bifunctional initiators can readily be prepared by a reaction of dialcohols or diphenols with β -haloacyl halides. For example, bis(dichloroacetate)s

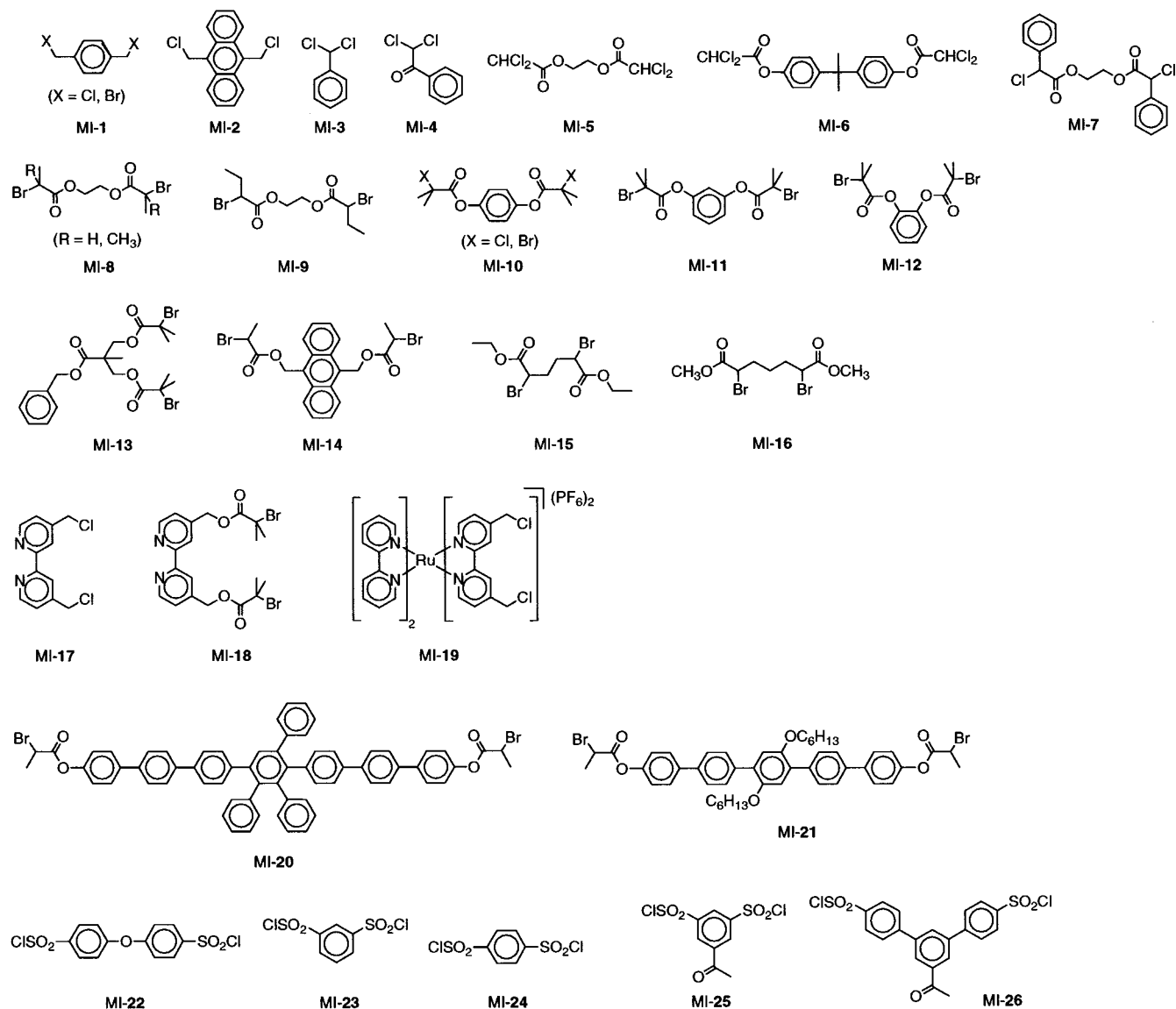


Figure 27. Bifunctional initiators.

such as MI-5 and MI-6 serve as a bifunctional initiator for MMA in the presence of Ru-1 and Al(acac)₃ to give telechelic PMMA with controlled molecular weights and narrow MWDs ($M_w/M_n = 1.3-1.4$). In contrast to dichloroacetophenone (see above), one dichloroacetate unit serves as a monofunctional initiator in the ruthenium catalysis (Ru-1).²²⁸ Another chloride-type bifunctional initiator (MI-7) affords telechelic polystyrene in the presence of copper catalysts.¹⁷¹ Bromoesters MI-8 and MI-9 derived from ethylene glycol were employed for acrylate and styrene with copper catalysts.^{313,326,358,359,368,389,413} These telechelic polymers can further be employed as bifunctional macroinitiators for ABA block copolymers.^{313,326,359,368,389} The obtained telechelic polystyrenes can produce polymer network gels by a copper-mediated linking reaction with divinylbenzene.⁴¹³ A series of bromoesters (MI-10 to MI-12), derived from diphenols and 2-bromoisobutyryl bromide, are effective in the copper-mediated living radical polymerizations of various acrylates and styrene ($M_w/M_n \approx 1.1$).²⁶³ A chloroester (MI-10, X = Cl) gave similar polymers with slightly broader MWDs ($M_w/M_n \approx 1.2$).

Telechelic PMMA can be obtained from MI-13 with Ni-2 as a catalyst.⁴¹⁴ Anthracene-labeled polystyrene can be synthesized with the copper-catalyzed polymerizations initiated with MI-14; the aromatic tag or probe is located near the midpoint of a polymer chain.⁴¹⁵ Dibromoacetates MI-15 and MI-16 are commercially available and effective for methacrylates, acrylates, and styrene with nickel and copper catalysts.^{134,256,360-362} The resultant telechelic polymers have been subsequently employed for the synthesis of various ABA triblock copolymers.

Functional groups can also be introduced in the spacer units. Bifunctional initiators with bipyridine units such as MI-17 and MI-18 induced the living radical polymerizations of styrene and MMA, respectively, with copper catalysts to give polymers that carry a coordination site at the middle of the chain.^{87,333} These polymers can be connected together into star polymers with a ruthenium cation at the core, where the arm numbers are varied among three, four, five, and six in combination with the polymers obtained from the monofunctional initiator with a bipyridine unit (FI-21 and FI-22; Figure 13).⁴¹⁶ A

modified method for the coupling reaction with the metal center can also afford heteroarm star polymers consisting of polystyrene and PMMA chains.⁴¹⁷ The bifunctional initiator complexed with ruthenium prior to the polymerization (MI-19) is also effective in the copper-catalyzed polymerization.^{87,333}

Bifunctional initiators with oligophenylenes as a rigid spacer unit (MI-20 and MI-21) generate rigid/flexible triblock copolymers of styrene.⁴¹⁸

Disulfonyl halides such as MI-22 to MI-26 are effective bifunctional initiators for various monomers including methacrylates, acrylates, and styrenes, because the sulfonyl halide part, as pointed out for their monofunctional versions, can induce fast initiation without a bimolecular termination reaction between the sulfonyl radicals.^{240,343}

2. Star Polymers with Multifunctional Initiators

Halogen compounds with more than two reactive carbon-halogen bonds afford star polymers, the arm number of which is defined by the number of the initiating sites, whereas the arm length therein is determined simply from the initial molar ratio of monomer to initiator. The multifunctional initiator method gave various star polymers with 3 (MI-27 to MI-33), 4 (MI-34 to MI-42), 5 (MI-43), 6 (MI-44 to MI-50), 8 (MI-51 and MI-52), and 12 arms (MI-53 and MI-54).

A benzyl bromide-type initiator (MI-27) was utilized for the copper-catalyzed synthesis of 3-armed poly(acrylate)s with mesogen units as side-chain groups.³²⁴ The effect of molecular architecture on the thermotropic behavior was compared with the corresponding linear polymers in both living and conventional polymerizations.

Haloester-type trifunctional initiators are obtained from triols by a method similar to those for bifunctional haloesters. 3-arm star polymers of MMA are obtained with dichloroacetates MI-28 and MI-29, for which Ru-1 and Al(acac)₃ are employed.²²⁸ The polymers have controlled molecular weights and narrow MWDs. Similarly, MI-30 and MI-31 with copper catalysts gave 3-arm star polymers of styrene, acrylates, and methacrylates; suitable copper catalysts vary with each monomer.^{199,326,358,368} The obtained star polymers can be further transformed into star block copolymers comprised of hydrophilic/hydrophobic³⁶⁸ or organic/inorganic³²⁶ segments by block copolymerizations of other monomers.

Trisulfonyl chlorides MI-32 and MI-33 are also efficient in the copper-catalyzed radical polymerization of methacrylates and styrene ($M_w/M_n = 1.1-1.4$).³⁴³ The polystyrene arms can be cleaved from the core with a base, giving polymers (arms) whose molecular weights are about 1/3 of the original.

Tetra(bromomethyl)benzene (MI-34) was employed for alternating radical copolymerization of styrene and *N*-cyclohexylmaleimide to give controlled molecular weights and narrow MWDs ($M_w/M_n = 1.2-1.4$).²²¹ Another benzyl halide initiator (MI-37) with a cyclosiloxane core induced styrene polymerization ($M_w/M_n = 1.16$).³⁵⁸ An ester-type initiator (MI-35) is effective in the copper-catalyzed radical polymerization of nBA.³⁵⁸ A tetrafunctional sulfonyl chloride

(MI-38) from the same tetraol can be employed for methacrylates and styrene polymerization.³⁴³

Another tetrafunctional ester (MI-36) is the smallest number of a series of dendrimer-type initiators such as MI-46 and MI-53 for 6- and 12-arm star polymers, respectively.^{414,419,420} These initiators induce the living radical polymerizations of MMA with Ni-2 to give the corresponding multiarmed polymers with controlled molecular weights although the arm number with MI-53 is slightly lower than 12 due to incomplete initiation from all the carbon-bromine bonds.

A series of calixarene-core-type initiators (MI-40, MI-47, and MI-51) were prepared and employed for the radical polymerizations of MMA, styrene, and tBA. Ruthenium catalysts³⁵⁷ were first employed, and copper catalysts are equally effective.^{421,422} PMMA obtained with the dichloroacetate version of MI-40 had narrow MWDs ($M_w/M_n = 1.1-1.2$) and controlled numbers of arms, which were ascertained by the scission of arms from the cores after the polymerizations.³⁵⁷

The star polymers obtained with the bromoester-type calixarene-based initiators were analyzed by SEC equipped with a multiangle laser light scattering (MALLS) detector. The arm numbers were well controlled (close to the initiator's functionality), although the octafunctional initiator MI-51 induced star-star coupling in the styrene-polymerization at conversions higher than 20%.⁴²¹ A similar series of tetra-, hexa-, and octafunctionalized initiators with calixarene cores were synthesized for sulfonyl chloride versions (MI-41, MI-48, and MI-52) and employed for copper-catalyzed MMA polymerizations.³⁴³

Carbosilane-based dendritic bromoesters MI-39 and MI-54 are also effective as multifunctional initiators for 4- and 12-arm star PMMA with narrow MWDs ($M_w/M_n = 1.1-1.2$).⁴²³ However, star-star coupling was observed with the use of MI-54.

A pentafunctionalized initiator can be obtained from esterification of β -D-glucose, and star PMMA with 5 arms are obtained.³⁴⁰ Inorganic cores, other than silicon, can also be employed such as the cyclotriphosphazene (MI-44 and MI-45), which gives 6-arm polymers from styrene, acrylates, and methacrylates.^{303,358} Tetra- (MI-42)^{87,332} and hexafunctionalized initiators (MI-49^{87,332} and MI-50⁴²⁴) with a ruthenium center can be also employed for the radical polymerizations of styrene and MMA in the presence of appropriate catalysts such as copper, ruthenium, and nickel.

Other multifunctional initiators include star polymers prepared from initiators via living radical or other living polymerizations. In particular, all of the star polymers via metal-catalyzed living polymerization, by definition, carry a halogen initiating site at the end of each arm, and thus they are potentially all initiators. Thus, star-block copolymers with three polyisobutylene-*block*-PMMA arms and four poly(THF)-*block*-polystyrene or poly(THF)-*block*-polystyrene-*block*-PMMA were synthesized via combination of living cationic and copper-catalyzed living radical polymerizations.^{381,388} Anionically synthesized star polymers of ϵ -caprolactone and ethylene oxide have

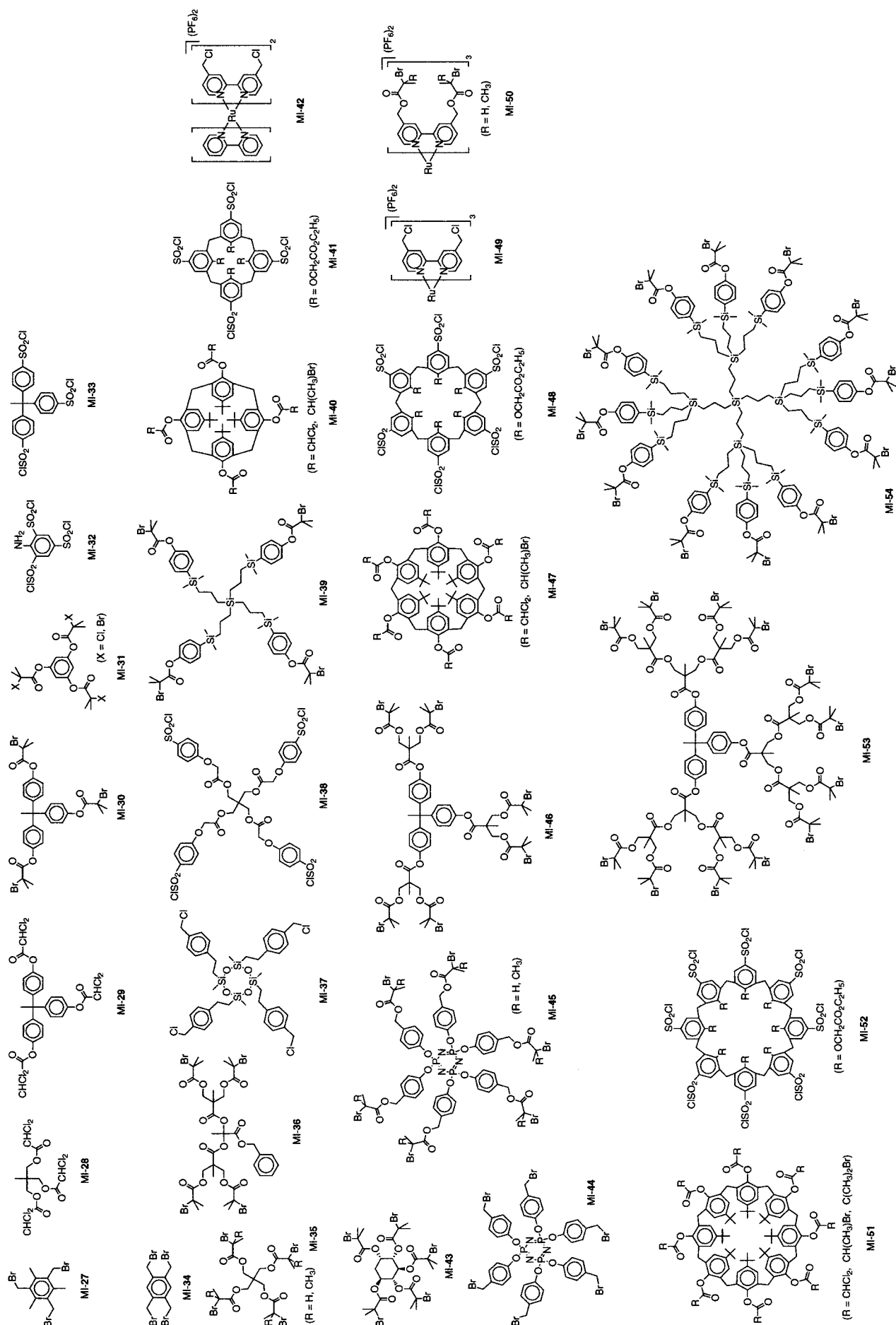


Figure 28. Multifunctional initiators.

hydroxy groups at their terminal, which can be transformed into C–Br bonds. The functionality of C–Br bonds to be introduced thereby can be either mono-, bi-, or tetrafunctional, and thus one can increase the initiating sites on the transformation. With the use of this method, the arm numbers of PMMA chains can be increased up to 24 arms.³⁹³ This method can also afford miktoarmed PEO-*block*-(polystyrene)₂ and (polystyrene)₂-*block*-PEO-*block*-(polystyrene)₂ H-type copolymers.³⁹¹

3. Star Polymers by Linking Reaction

As is known in anionic and other living polymerizations, star polymers with a large number of arms (>10) can be prepared conveniently by a linking reaction of linear polymers with divinyl compounds. Similar to the synthesis of block copolymers (section III.C.1), there are two ways for the synthesis by metal-catalyzed radical polymerizations, where the linking reaction is done via sequential addition of the divinyl compounds into the polymerization mixture after the almost completion of the vinyl monomers, or via isolation of halogen-capped monofunctional linear polymers followed by linking reaction in the presence of the metal catalysts and the divinyl compounds. The former method may involve incorporation of the first vinyl monomer units (remaining at the first stage) in the cores while the latter is free from such contamination though more cumbersome than the first. Also, the former one can be carried out in a one-pot reactor.

The sequential-addition method was systematically employed for the ruthenium-catalyzed living radical polymerization of MMA followed by in situ linking reaction with various dimethacrylates and related bifunctional monomers.⁴²⁵ The yields of star polymers depend on several factors such as halogens at the polymer terminal and the spacer-unit structure (length and rigidity) in the linking agents, where chloride terminals and a soft aliphatic or a rigid long aromatic spacer are favorable. The best yield reached 93%. The arm number of the star-polymers was also determined from the molecular weights measured by static light scattering or by SEC coupled with MALLS. In an example, about 20 arms of PMMA chains were linked together into one star polymer. Divinyl compounds with amide and alcohol groups form core-functionalized star polymers with 20–640 PMMA arms in the ruthenium-catalyzed living radical polymerization of MMA.⁴²⁶ In particular, bisacrylamides are good linking agents, and they give interesting star polymers in the core of which a large number of amide functions are embedded.

The copper-based system gave star polymers consisting of polystyrene and poly(tBA) arms by the linking reaction of isolated linear polymers.^{328,427} The linking reaction of Br-terminated polystyrenes was examined with three divinyl compounds, divinylbenzene, 1,4-butanediol diacrylate, and ethylene glycol dimethacrylate with CuBr/L-1 catalyst.⁴²⁷ The first agent gave soluble star polymers, while the acrylate and methacrylate versions resulted in insoluble gels, attributed to star-star coupling. The formation of star polymers with divinylbenzene can be accelerated with

L-24 as a ligand, up to 85–90% yield. The linking reaction of a poly(tBA) with a bromide terminal was also possible with divinylbenzene, whereas the other two divinyl compounds led to side reactions.³²⁸ The yield of star polymers can be increased up to 95% with the use of additives. The α -end-functionalized linear polymers afford surface-functionalized star polymers with various functional groups such as alcohols, amines, epoxides, and nitriles.

H. Comb and Graft Copolymers

Comb and graft copolymers were also prepared by metal-catalyzed living radical polymerizations. There are two methods available for the synthesis, one of which is via the metal-catalyzed radical polymerization of macromonomers in the absence or the presence of comonomers (“grafting through” method), and the other is via graft polymerization from the reactive carbon–halogen bonds attached to the main chains (“grafting from” method). In contrast to ionic living polymerizations, there have been no reports on the use of “grafting onto” method, partly due to the lack of efficient ω -end capping agents as described above (section III.B.2).

1. Comb Polymers

Comb or densely grafted polymers are defined as polymers that have at least one polymeric chains per monomer unit of the main chain, and Figure 29 shows examples obtained by metal-catalyzed living radical polymerization. Comb polymers possess physical properties similar to those of star polymers in solution.

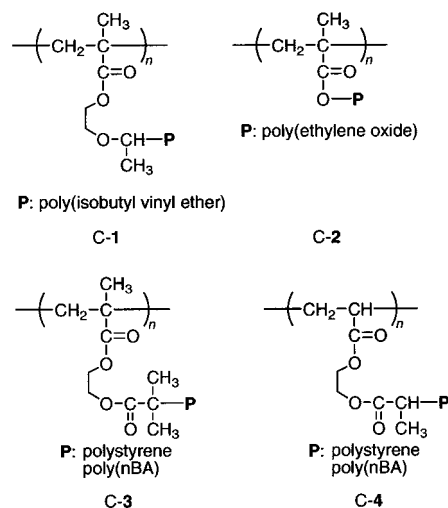


Figure 29. Comb polymers.

Combination of a living ionic polymerization and a metal-catalyzed radical polymerization also leads to comb polymers, where both the molecular weights of the arm and main-chain polymers are well controlled. PMMA with poly(vinyl ether) arm polymers of controlled molecular weights (C-1) were prepared by the copper-catalyzed radical polymerization of methacrylate-capped macromonomers carrying a poly-(isobutyl vinyl ether), which were obtained by living cationic vinyl polymerization with a methacryloxy-capped end-functionalized initiator.⁴²⁸ Comb polymers with

poly(oxyethylene glycol) with varying molecular weights between 400 and 2000 were also obtained by the copper-catalyzed radical polymerizations of the corresponding macromonomers.^{319,320,429} However, this method is not always suitable for high molecular weight macromonomers because the polymerization suffers from incomplete conversion and limits the degree of polymerization of the main-chain units.

Another method is based on the metal-catalyzed polymerization from carbon–halogen bonds in the main-chain units, which was applied for the synthesis of C-3 and C-4.⁴³⁰ For C-3, the main chain polymers with controlled molecular weights were prepared via the copper-catalyzed radical polymerization of trimethylsilyl-protected HEMA followed by the transformation of the silyloxy group into 2-bromoisobutyrate. The pendant C–Br bonds were subsequently activated by the copper catalysts to polymerize styrene and nBA. A more direct way is employed for C-4; i.e., via conventional radical polymerization of 2-[(2-bromopropionyl)oxy]ethyl acrylate followed by the copper-catalyzed graft polymerization of styrene and nBA from the C–Br substituent.

2. Graft Polymers

Various graft copolymers were synthesized by metal-catalyzed radical polymerizations, as detailed in Figure 30. Most of them were from random copolymerization of a macromonomer with a low molecular weight comonomer.

In a study, copper-catalyzed radical copolymerization of nBA and methacryloxy-capped poly(MMA) was compared with conventional radical copolymerization.^{267,431} The graft copolymers G-1 obtained with copper catalysts are more homogeneous in terms of MWD ($M_w/M_n \approx 1.6$ vs 3) and the number of side chains. This is attributed to diffusion control being less important in the metal-catalyzed radical polymerization, where the growing radical species is rapidly converted into the dormant covalent species.

There are several examples of graft copolymers obtained from macromonomer prepared by the metal-catalyzed polymerizations. Conventional radical copolymerization of *N*-vinylpyrrolidone and vinyl acetate-capped polystyrene synthesized with copper catalysts gave graft copolymers G-2, which formed hydrogels in water.³³⁷ Electrochemical copolymerization of pyrrole and thiophene-capped poly(MMA) affords G-3.³³⁵

A graft copolymer consisting of poly(ϵ -caprolactone) as main chain and PMMA as branches was also synthesized by ring-opening copolymerization of ϵ -caprolactone and ϵ -caprolactone-capped PMMA macromonomer; the macromonomer was prepared by a nickel catalyst.³¹² The obtained graft copolymers have relatively narrow MWDs ($M_w/M_n = 1.3$ – 1.4) because both the polymerizations are living. There are two other ways for the preparation; one is graft polymerization of MMA from the C–Br moiety in the pendant groups of poly(ϵ -caprolactone), and the other is simultaneous or dual living polymerization of MMA and ϵ -caprolactone in the presence of a functionalized ϵ -caprolactone with C–Br bond (FI-41). Both the methods afford similar products with narrow MWDs.

Another dual living polymerization of MMA and ϵ -caprolactone in the presence of HEMA gave graft copolymers with poly(ϵ -caprolactone) as branches (G-5) because the hydroxyl group in HEMA serves as an initiating site for ϵ -caprolactone.³⁹² A similar graft structure is obtained in graft polymerization of ethylene oxide from the hydroxyl group.³⁹³

The metal-catalyzed copolymerization from carbon–halogen bonds in the main chain can be employed widely for graft polymer synthesis. A combination of nitroxide-mediated and copper-catalyzed living radical polymerizations, for example, gives graft copolymers G-6, where the main chain is prepared by the former.⁴³² The chlorobenzyl unit in the copolymer is not active during the polymerization but, upon copper catalysis, it can initiate living radical polymerizations of styrene and methacrylates.

A similar well-defined graft copolymer consisting of polystyrene main chain and branches (G-7) can be prepared simply via repetition of copper-catalyzed living radical polymerizations.²⁰⁹ Thus, the synthesis starts with the copolymerization of styrene and *p*-(acetoxymethyl)styrene or *p*-(methoxymethyl)styrene, followed by bromination of the substituent into the benzyl bromide moiety, which then initiates the copper-catalyzed radical polymerization of styrene to give graft polymers with 8–14 branches.

A combination of metallocene-catalyzed syndiospecific styrene polymerization and the metal-catalyzed radical polymerization affords various graft copolymers consisting of syndiotactic polystyrene main chains (G-8).⁴³³ The reactive C–Br bonds (7–22% content) were generated by bromination of the polystyrene main chain with *N*-bromosuccinimide in the presence of AIBN.

Another graft copolymer with polystyrene segments in main chain is derived from the triblock copolymers of polyisobutylene and poly(*p*-methylstyrene) prepared by living cationic copolymerizations (G-9).⁴³⁴ The grafting point was generated by the bromination of the *p*-methyl groups into benzyl bromide, which are then employed for the copper-catalyzed polymerization of styrene and *p*-acetoxy-styrene. A similar graft copolymer (G-10) can be obtained from a commercially available polymer (EXXPRO) consisting of isobutylene, *p*-methylstyrene, and *p*-(bromomethyl)styrene units.^{265,435} The mechanical properties of the graft copolymers were also investigated. Another commercial product, poly(styrene-*block*-ethylene-*co*-propylene) (Kraton 147) with 29.0 wt % styrene units, is also used as a backbone.⁴³⁶ About 6.4 mol % chloromethylated styrene units are first introduced by chloromethylation, which then initiates graft polymerization of ethyl methacrylate to give the products G-11.

A polyolefin-based graft copolymer such as G-12 is prepared from a commercially available EPDM rubber (Vistollon 2727).⁴³⁷ The allyl group is partially converted into allyl bromide moiety, and living radical polymerization of MMA initiated therefrom with copper catalysts. Graft copolymers of polyethylene (G-13) were synthesized from commercially available poly(ethylene-*co*-glycidyl methacrylate) as a starting material, the epoxy groups of which were esterified

content of nBA. A more direct and simple way for poly(vinyl chloride)-based graft copolymers is to use the allyl chloride and tertiary chloride units as structural defects in the base polymers for the initiating moiety in the metal-catalyzed living radical polymerization.⁴⁴⁰ This method can afford various graft copolymers G-15, which was characterized by SEC, NMR, DSC, and film preparation.

Hybrid graft copolymers having silicon-based polymer backbones were also prepared by the metal-mediated radical polymerizations of styrene. The phenyl groups of poly[(methylphenyl)silylene] were bromomethylated and then employed as the grafting points of polystyrene (G-16).^{294,441} Polysiloxane can be employed also as a backbone (G-17) by introduction of benzyl chloride units into the pendant vinyl-functionalized poly(dimethylsiloxane).⁴⁰⁹

I. Hyperbranched Polymers

In vinyl polymerization, hyperbranched polymers can be obtained from the monomers that have an initiating group along with a vinyl group (Figure 31).

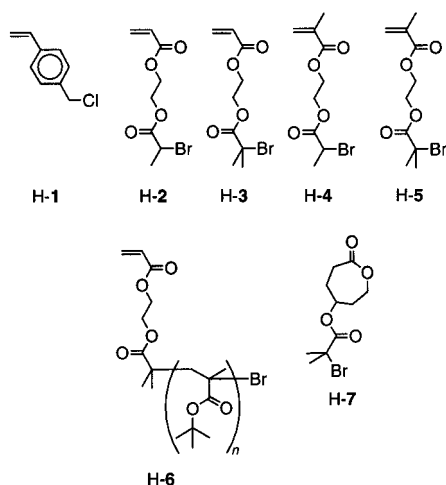


Figure 31. Monomers for hyperbranched polymers.

The self-condensing vinyl polymerization, which was initially developed for living cationic polymerization,⁴⁴² is also applicable for metal-catalyzed living radical polymerizations.

For example, *p*-(chloromethyl)styrene (H-1) was employed for copper-catalyzed self-condensing vinyl polymerizations.²¹¹ The hyperbranched structure was supported by the fact that the molecular weight measured by SEC was lower than those by viscosity and light scattering. The average number of branches per polymer chain was estimated to be 25. In contrast, another paper reported that the reaction conditions should be changed for the synthesis of hyperbranched structure.²¹³ A high catalyst-to-monomer ratio around 0.1–0.3 should be employed to minimize the formation of linear polymers due to the difference in reactivity between the primary and the secondary benzylic halide sites. The residual carbon–halogen bonds were transformed into functional groups such as cyano, ester, thioether, and imide to generate multifunctionalized hyperbranched polymers.

Acrylic hyperbranched polymers are obtained by the copper-catalyzed radical polymerizations of H-2,

where addition of CuBr₂ is needed to decrease the concentrations of the radical species generated from the monomers.⁴⁴³ Under appropriate conditions, nearly ideal self-condensing vinyl polymerizations proceed. The obtained polymer was a viscous solid with a subambient *T*_g (–11 °C). Detailed kinetic and mechanistic studies were carried out to determine the difference in reactivity among the C–Br bonds in terminals and side chains.^{212,444,445} Similar meth-(acrylic) hyperbranched polymers were prepared from H-3 and H-5 while the products with H-4 were most likely linear polymers.⁴⁴⁶

The self-condensing copper-catalyzed polymerization of macromonomer of poly(tBA) with a reactive C–Br bond (H-6) affords hyperbranched or highly branched poly(tBA).⁴⁴⁷ Copolymerization of H-1 and *N*-cyclohexylmaleimide induced alternating and self-condensing vinyl polymerization.⁴⁴⁸ The residual C–Cl bond was further employed for the copper-catalyzed radical homopolymerization of styrene to give star polymers with hyperbranched structures. Hyperbranched polymers of H-1 further serve as a complex multifunctionalized macroinitiator for the copper-catalyzed polymerization of a functional monomer with polar chromophores to yield possible second-order nonlinear optical materials.³²⁵

The graft copolymers with poly(H-1) arms have multiple carbon–halogen bonds that can initiate copper-catalyzed radical polymerization to give highly branched dendrigraft polymers.⁴³² The products with styrene or nBMA had relatively narrow MWDs because each chain was prepared by living polymerization.

A combination of other polymerization pathways also results in some hyperbranched structures. Multifunctional hydroxyl groups in polyglycerol with hyperbranched structure, prepared by anionic polymerization of glycidol, were esterified with 2-bromoisobutyryl bromide and then employed as a hyperbranched multifunctional macroinitiator for the copper-catalyzed radical polymerization of MA to give products with 45–55 poly(MA) arms.⁴⁴⁹

Another method for hyperbranched polymers is based on a simultaneous or dual living polymerization such as metal-catalyzed radical and ring-opening ionic polymerizations.³¹¹ In this method, copolymerizations of HEMA and H-7 are carried out in the presence of Ni-2 and Sn(Oct)₂, where the C–Br bond in H-7 serves as an initiating point for the nickel-catalyzed radical polymerization of HEMA and the OH group in HEMA for the tin-catalyzed ring-opening polymerization of H-7. The products had hyperbranched structures, similarly to those obtained in self-condensing vinyl polymerizations. Addition of MMA and/or ϵ -caprolactone into the system gave looser hyperbranched structures.

J. Polymer Brushes

Polymer brushes can be obtained by metal-mediated living radical polymerization from the initiator moiety confined to the surface of a substrate via spacers. The surface-initiated living polymerization can control the thickness and the density of brushes; the former is regulated by brush's chain length and

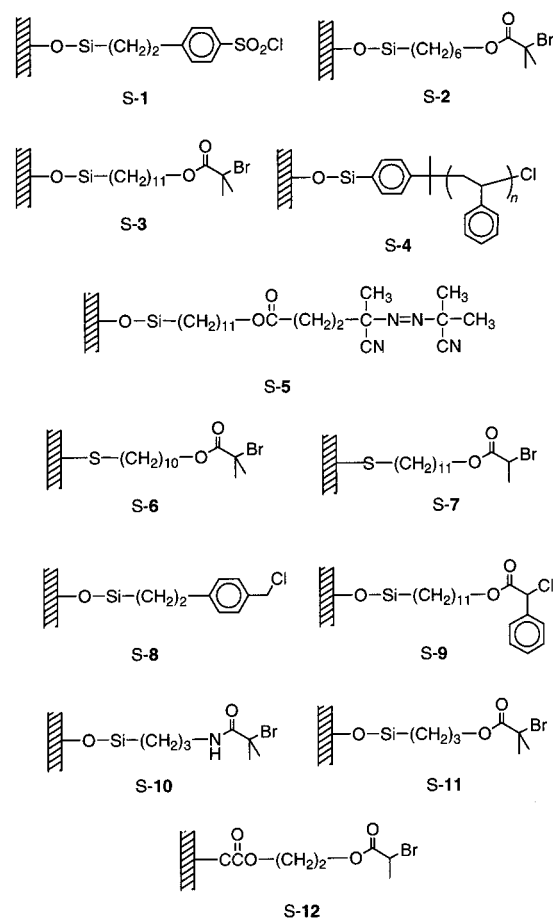


Figure 32. Initiating moiety for polymer brushes.

the latter by the density of the attached initiator. The substrate for these polymer brushes include silicon wafer, silica bead, silica nanoparticle, porous silica gel, silica capillary, polymer latex, and gold, and the attachment of polymer brushes alter the chemical properties of their surface for various applications. Figure 32 summarizes the initiating moiety employed for such surface modification.

1. Silicon Wafer

The control of the molecular weights, MWDs, and surface density of graft chains was achieved by the copper-catalyzed radical polymerization of MMA from sulfonyl chloride initiators attached to silicon wafer (S-1) by the Langmuir–Blodgett technique.⁴⁵⁰ The surface-initiated polymerization is better controlled on addition of free or unconfined initiators such as *p*-toluenesulfonyl chloride, because uncontrolled molecular weights and broad MWDs were obtained in the absence. This may be attributed to a low concentration of Cu(II) species, which convert the radical species into the dormant, originating from the low concentration of the initiator moiety confined on the surface. The thickness of the polymer layer increased up to 70 nm in direct proportion to the molecular weights of free polymers produced in solution, although the molecular weights of the graft polymers were unknown. The graft density can be varied in a wide range between 0.07 and 0.7 chains/nm² by photodecomposing the surface-fixed initiator, where the highest value is at least 10 times larger than

those of the polymer brushes prepared by the adsorption of block copolymers on surface.^{451,452} Glycopolymers and block copolymers of MMA and 4-vinylpyridine were grown from the surface by the same technique.^{371,453} A similar PMMA layer was also obtained in the nickel-catalyzed surface-initiated polymerization from S-2 in the presence of ethyl 2-bromoisobutyrate as a free initiator, where the thickness increased up to 50 nm.⁴⁵⁴

Such a controlled radical polymerization can be performed even in the absence of free initiators, where larger amounts of Cu(II) species are added in the system.³⁶⁹ The polystyrene layer obtained from S-3 in the presence of 5 mol % Cu(II) relative to Cu(I) increased up to 20 nm in thickness, in direct proportion to the M_n of the polymers prepared in the other experiments with ethyl 2-bromopropionate but without surface-confined initiator under similar conditions. For MA, the layer thickness increases up to 60 nm. Block copolymer layers were also prepared by block copolymerization of MA or tBA from the polystyrene. Modification of the hydrophilicity of a surface layer was achieved by the hydrolysis of the poly(styrene-*block*-tBA) to poly(styrene-*block*-acrylic acid) and confirmed by a decrease in water contact angle from 86° to 18°.

Block copolymer surface was also prepared by the copper-catalyzed radical polymerization of MMA from a surface-confined macroinitiator of polystyrene (S-4) obtained by living cationic polymerization although the blocking efficiency was unknown.³⁷⁸ The block copolymerization increased the film thickness by 9 nm and changed the water contact angles. Other monomers such as MA and 2-(*N,N*-dimethylamino)-ethyl methacrylate were also polymerized from S-4.³⁷⁷ The changes in contact angles were observed by treatment of the surface with several solvents and air.

An azo-type initiator (S-5) can also be attached to the silicon wafer and induces the controlled radical polymerization of styrene in the presence of CuBr₂.³⁶⁵ The block copolymerization of MMA from the surface-confined polystyrene macroinitiator was also conducted.

2. Gold

Polymer brushes can be grown from gold surface in a similarly controlled manner by the metal-catalyzed surface-initiated radical polymerization. The attachment of the initiator moiety can be attained via the thiol group as in S-6⁴⁵⁵ and S-7.⁴⁵⁶

Several monomers such as tBA, MMA, isobornyl methacrylate, 2-(*N,N*-dimethylamino)ethyl methacrylate, and HEMA were polymerized from S-6 with copper catalysts to form layers ranging from 5 to 48 nm with varying contact angles depending on the polymers. The brushes of PMMA grow from the surface with a high graft density as indicated by the low value of the area per PMMA chain (200 Å²/chain). However, a grafting efficiency is estimated around 10% from the surface confined initiators. The initiator can be attached also on the patterned area by microprinting method. The hydrophobic polymers as brushes are resistant to etchants, which permits the selective etching of gold surface.

Another example is the copper-catalyzed surface-initiated radical polymerization of MMA from S-7 at room temperature without addition of free initiator. The molecular weights and MWDs of the polymers were directly measured after removing the brushes from the surface. For example, the surface with 40 nm thickness had M_n of 68900 and MWDs of 1.45. A high graft density ($180 \text{ \AA}^2/\text{chain}$) and decreased surface roughness (0.54 nm) were observed. This method is free from solution and thermal polymerizations due to the absence of free initiators and a low polymerization temperature, which permits a simple washing step without Soxhlet extraction.

3. Silica Particle and Bead

Surface-initiated living radical polymerization is also applied for spherical surfaces such as silica nanoparticles and beads.

Spherical silica nanoparticles, with an average diameter of 70 nm, modified with the initiator moiety (S-8) were employed for the copper-mediated radical polymerization of styrene.⁴⁵⁷ The diameter of the particles and the molecular weights of the obtained polymers increased with conversion. For example, the average diameter of the particles obtained at 58.8% monomer conversion was increased to 188 nm, where the M_n and MWDs of the arm polymers were 26500 and 1.33, respectively. Given a narrow size distribution (<10%), the nanoparticles within the film domains were observed to pack into hexagonal arrays. A smaller silica nanoparticle with 14 nm was employed also for the copper-catalyzed radical polymerization of styrene initiated with S-9.⁴⁵⁸

Silica microspheres ($\sim 3 \mu\text{m}$) with initiating moiety (S-8) induced the copper-catalyzed radical polymerization of benzyl methacrylate to form polymer layers on the surface.⁴⁵⁹ The thickness of polymer shell can be increased to 550–600 nm, where the M_n and MWDs of the arm polymers were 26500 and 1.26, respectively. Removal of the core silica by chemical etching gave uniform hollow polymer microspheres.

4. Silica Gel and Silica Capillary

Organic polymer layer on the surface of silica gels or porous silica can modify the surface to increase the resistance of the silica surface to basic compounds.

The first example of the surface-initiated metal-catalyzed radical polymerization was reported for acrylamide from the initiator moiety S-8 attached to porous silica gels.²¹⁶ A silica gel with an average pore size of 860 Å gave polyacrylamide with film thickness of 100 Å after the polymerization, where polymer molecular weights were around 13000–15000.²¹⁸ The silica gels coated with polyacrylamide can even separate a basic protein without significant damages of silica gels by size-exclusion mode. The same technique was also employed for the silica capillaries and results in polymer coating without clogging of narrow capillaries.²¹⁷

Functionalized methacrylates with pendent nucleosides such as uridine and adenosine (FM-23 and FM-24) were also polymerized from the surface of silica gels in the presence of the copper catalysts.⁴⁶⁰ For

the polymerizations, bromide-type initiator fragments S-10 and S-11 were attached to the surface and initiated the homopolymerization or copolymerizations. A higher loading of the polymers was observed with S-11 than S-10.

5. Polymer Latex

Organic compounds such as polystyrene latexes were also used as substrates for the surface-initiated radical polymerization.²⁴⁸ Reactive C–Br bonds (S-12) were introduced at the surface via radical emulsion copolymerization of styrene and 2-(2-bromopropionyloxy) ethyl methacrylate in the presence of divinylbenzene under selected conditions. The surface-initiated polymerization of hydrophilic monomers such as FM-3 and FM-6 resulted in hydrophilic shell and hydrophobic core latexes.

IV. Conclusions

This paper has provided, we believe, a comprehensive, up-to-date, critical, and objective review on the discovery and the subsequent fast development of living radical polymerizations catalyzed by transition-metal complexes in the period from 1994 to early 2001. These metal-catalyzed living radical polymerizations have rapidly been developing since their discovery in 1994, and the scope of applicable monomers, metal catalysts, and initiators has been expanding. Their advantages include versatility toward a variety of monomers, feasibility in a wide range of reaction conditions, and relatively easy access to the materials. This permits many researchers to use the systems for the precision synthesis of various polymers with controlled architectures.

As in many other fields of science, however, these extensive developments have also elicited a number of interesting and challenging problems that are still waiting for solutions and answers. These may include the kinetics and mechanism of the polymerizations, the nature of the true growing intermediates that are considered to associate with the metal catalyst (e.g., are they really radicals identical or similar to those in classical “free” radical polymerizations?), the guiding principles for designing metal catalysts, and the “novel” polymers that can be synthesized by the metal-based systems but cannot be by other (living) radical polymerizations. In addition to these problems, future research efforts will therefore be directed toward the development of more efficient and versatile catalyst systems for various monomers including nonconjugated vinyl monomers, as well as the synthesis of specific polymers with special architectures and the application to industry processes.

V. References

- (1) For a review on radical polymerization, see: Moad, G.; Solomon D. H. *The Chemistry of Free Radical Polymerization*; Elsevier Science: Oxford, U.K., 1995.
- (2) (a) Szwarc, M. *Nature* **1956**, *178*, 1168–1169. (b) Szwarc, M.; Levy, M. Milkovich, R. *J. Am. Chem. Soc.* **1956**, *78*, 2656–2657.
- (3) Eastmond, G. C.; Webster, O. W. In *New Methods of Polymer Synthesis*; Ebdon, J. R., Ed.; Blackie: Glasgow, U.K., 1991; pp 22–75.
- (4) Aida, T. *Prog. Polym. Sci.* **1994**, *19*, 469–528.
- (5) Sugimoto, H.; Inoue, S. *Adv. Polym. Sci.* **1999**, *146*, 39–119.
- (6) Hirao, A.; Nakahama, S. *Acta Polym.* **1998**, *49*, 133–144.

- (7) (a) Higashimura, T.; Sawamoto, M. *Adv. Polym. Sci.* **1984**, *62*, 49–94. (b) Sawamoto, M. *Prog. Polym. Sci.* **1991**, *16*, 111–172. (c) Sawamoto, M.; Kamigaito, M. In *New Methods of Polymer Science*; Ebdon, J. R., Eastmond, G. C., Eds.; Blackie: Glasgow, U.K., 1995; Vol. 2, pp 37–68.
- (8) Kennedy, J. P.; Iván, B. *Designed Polymers by Carbocationic Macromolecular Engineering: Theory and Practice*; Hanser: Munich, Germany, 1992.
- (9) *Cationic Polymerizations*; Matyjaszewski, K., Ed.; Marcel Dekker: New York, 1996.
- (10) Yasuda, H. *Prog. Polym. Sci.* **2000**, *25*, 573–626.
- (11) Mecerreyes, D.; Jérôme, R.; Dubois, Ph. *Adv. Polym. Sci.* **1999**, *147*, 1–59.
- (12) Grubbs, R.; Khosravi, E. In *Synthesis of Polymers*; Schlüter, A.-D., Ed.; Materials Science and Technology Series; Wiley-VCH: Weinheim, Germany, 1999; pp 65–104.
- (13) Otsu, T.; Yoshida, M. *Makromol. Chem., Rapid Commun.* **1982**, *3*, 127–132.
- (14) Otsu, T. *J. Polym. Sci., Part A: Polym. Chem.* **2000**, *38*, 2121–2136.
- (15) Fischer, H. *J. Polym. Sci., Part A: Polym. Chem.* **1999**, *37*, 1885–1901.
- (16) Borsig, E.; Lazar, M.; Căpla, M.; Florián, Š. *Angew. Makromol. Chem.* **1969**, *9*, 89–95.
- (17) Otsu, T.; Yoshida, M.; Tazaki, T. *Makromol. Chem., Rapid Commun.* **1982**, *3*, 133–140.
- (18) Chiefari, J.; Chong, Y. K.; Ercole, F.; Krstina, J. Jeffery, K.; Tam, P. T. Le.; Mayadunne, R. T. A.; Meijs, G. F.; Moad, C. L.; Moad, G.; Rizzardo, E.; Thang, S. H. *Macromolecules* **1998**, *31*, 5559–5562.
- (19) Kwon, T. S.; Kumazawa, S.; Yokoi, T.; Kondo, S.; Kunisada, H. Yuki, Y. *J. Macromol. Sci., Pure Appl. Chem.* **1997**, *A34*, 1553–1567.
- (20) Solomon, D. H.; Rizzardo, E.; Cacioli, P. U.S. Patent 4,581,429, Apr 8, 1986.
- (21) Georges, M. K.; Veregin, R. P. N.; Kazmaier, P. M.; Hamer, G. K. *Macromolecules* **1993**, *26*, 2987–2988.
- (22) Georges, M. K.; Veregin, R. P. N.; Kazmaier, P. M.; Hamer, G. K. *Trends Polym. Sci.* **1994**, *2*, 66–72.
- (23) Hawker, C. J. *J. Am. Chem. Soc.* **1994**, *116*, 11185–11186.
- (24) (a) Hawker, C. J. *Acc. Chem. Res.* **1997**, *30*, 373–382. (b) Malmström, E. E.; Hawker, C. J. *Macromol. Chem. Phys.* **1998**, *199*, 923–935.
- (25) Chung, T. C.; Janvikul, W.; Lu, H. L. *J. Am. Chem. Soc.* **1996**, *118*, 705–706.
- (26) Oka, M.; Tatemoto, M. In *Contemporary Topics in Polymer Science*; Bailey, W. J.; Tsuruta, T., Eds.; Plenum: New York, 1984; pp 763–777.
- (27) (a) Kato, M.; Kamigaito, M.; Sawamoto, M.; Higashimura, T. *Polym. Prepr. Jpn.* **1994**, *43*, 1792–1793. (b) Kato, M.; Kamigaito, M.; Sawamoto, M.; Higashimura, T. *Macromolecules* **1995**, *28*, 1721–1723.
- (28) Wang, J.-S.; Matyjaszewski, K. *J. Am. Chem. Soc.* **1995**, *117*, 5614–5615.
- (29) Wayland, B. B.; Poszmik, G.; Mukerjee, S. L. *J. Am. Chem. Soc.* **1994**, *116*, 7943–7944.
- (30) Qiu, J.; Matyjaszewski, K. *Acta Polym.* **1997**, *48*, 169–180.
- (31) Sawamoto, M.; Kamigaito, M. In *Synthesis of Polymers*; Schlüter, A.-D., Ed.; Materials Science and Technology Series; Wiley-VCH: Weinheim, Germany, 1999; Chapter 6, pp 163–194.
- (32) Gridnev, A. *J. Polym. Sci., Part A: Polym. Chem.* **2000**, *38*, 1753–1766.
- (33) For reviews on radical addition reactions, see: (a) Curran, D. P. In *Comprehensive Organic Synthesis*; Trost, B. M., Fleming, I., Eds.; Pergamon: Oxford, U.K., 1991; Vol. 4, pp 715–777. (b) Iqbal, J.; Bhatia, B.; Nayyar, N. K. *Chem. Rev.* **1994**, *94*, 519–554.
- (34) (a) Bamford, C. H.; Eastmond, G. C.; Hargreaves, K. *Trans. Faraday Soc.* **1968**, *64*, 175–184. (b) Bamford, C. H.; Sakamoto, I. *J. Chem. Soc., Faraday Trans. 1* **1974**, *70*, 330–343. (c) Bamford, C. H.; Sakamoto, I. *J. Chem. Soc., Faraday Trans. 1* **1974**, *70*, 344–354.
- (35) Kameda, N.; Itagaki, N. *Bull. Chem. Soc. Jpn.* **1973**, *46*, 2597–2598.
- (36) Otsu, T.; Tazaki, T.; Yoshioka, M. *Chem. Express* **1990**, *10*, 801–804.
- (37) Niwa, M.; Katsurada, N.; Matsumoto, T.; Okamoto, M. *J. Macromol. Sci., Chem.* **1988**, *A25*, 445–466.
- (38) Boutevin, B. *J. Polym. Sci., Part A: Polym. Chem.* **2000**, *38*, 3235–3243.
- (39) Darling, T. R.; Davis, T. P.; Fryd, M.; Gridnev, A. A.; Haddleton, D. M.; Ittel, S. D.; Matheson Jr., R. R.; Moad, G.; Rizzardo, E. *J. Polym. Sci., Part A: Polym. Chem.* **2000**, *38*, 1706–1709. See also the comments included in the same series issue: *J. Polym. Sci., Part A: Polym. Chem.* **2000**, *38*, 1710–1752.
- (40) Sawamoto, M.; Kamigaito, M. *CHEMTECH* **1999**, *29* (6), 30–38.
- (41) Sawamoto, M.; Kamigaito, M. *Polym. News* **2000**, *25*, 149–155.
- (42) Patten, T. E.; Matyjaszewski, K. *Acc. Chem. Res.* **1999**, *32*, 895–903.
- (43) Matyjaszewski, K. *Chem.—Eur. J.* **1999**, *5*, 3095–3102.
- (44) Patten, T. E.; Matyjaszewski, K. *Adv. Mater.* **1998**, *10*, 901–915.
- (45) Sawamoto, M.; Kamigaito, M. In *New Macromolecular Architecture and Functions*; Kamachi, M., Nakamura, A., Eds.; Springer-Verlag: Berlin, Germany, 1996; pp 11–20.
- (46) Gaynor, S. G.; Greszta, D.; Wang, J.-S.; Matyjaszewski, K. In *New Macromolecular Architecture and Functions*; Kamachi, M., Nakamura, A., Eds.; Springer-Verlag: Berlin, Germany, 1996; pp 1–9.
- (47) Sawamoto, M.; Kamigaito, M. *J. Macromol. Sci., Pure Appl. Chem.* **1997**, *A34*, 1803–1814.
- (48) Matyjaszewski, K. *J. Macromol. Sci., Pure Appl. Chem.* **1997**, *A34*, 1785–1801.
- (49) Sawamoto, M.; Kamigaito, M. In *Controlled Radical Polymerization*; Matyjaszewski, K., Ed.; ACS Symposium Series 685; American Chemical Society: Washington, DC, 1998; Chapter 18, pp 296–304.
- (50) Matyjaszewski, K. *Macromol. Symp.* **1999**, *143*, 257–268.
- (51) Sawamoto, M.; Kamigaito, M. *Macromol. Symp.* **2000**, *161*, 11–18.
- (52) Matyjaszewski, K. *Macromol. Symp.* **2000**, *152*, 29–42.
- (53) Ando, T.; Kamigaito, M.; Sawamoto, M. *Macromolecules* **2000**, *33*, 5825–5829.
- (54) Qiu, J.; Matyjaszewski, K.; Thouin, L.; Amatore, C. *Macromol. Chem. Phys.* **2000**, *201*, 1625–1631.
- (55) Nishikawa, T.; Ando, T.; Kamigaito, M.; Sawamoto, M. *Macromolecules* **1997**, *30*, 2244–2248.
- (56) Ando, T.; Kato, M.; Kamigaito, M.; Sawamoto, M. *Macromolecules* **1996**, *29*, 1070–1072.
- (57) Kotani, Y.; Kamigaito, M.; Sawamoto, M. In *Controlled/Living Radical Polymerization*; Matyjaszewski, K., Ed.; ACS Symposium Series 768; American Chemical Society: Washington, DC, 2000; Chapter 12, pp 168–181.
- (58) Takahashi, H.; Ando, T.; Kamigaito, M.; Sawamoto, M. *Macromolecules* **1999**, *32*, 6461–6465.
- (59) Fujii, Y.; Ando, T.; Kamigaito, M.; Sawamoto, M. *Polym. Prepr. Jpn.* **1999**, *48*, 1123–1124; *Macromolecules*, submitted for publication.
- (60) Takahashi, H.; Ando, T.; Kamigaito, M.; Sawamoto, M. *Macromolecules* **1999**, *32*, 3820–3823.
- (61) Hamasaki, S.; Sawauchi, C.; Kamigaito, M.; Sawamoto, M. *J. Polym. Sci., Part A: Polym. Chem.*, submitted for publication.
- (62) Watanabe, Y.; Ando, T.; Kamigaito, M.; Sawamoto, M. *Macromolecules* **2001**, *34*, 4370–4374.
- (63) Simal, F.; Demonceau, A.; Noels, A. F. *Angew. Chem., Int. Ed.* **1999**, *38*, 538–540.
- (64) Simal, F.; Sebille, S.; Hallet, L.; Demonceau, A.; Noels, A. F. *Macromol. Symp.* **2000**, *161*, 73–85.
- (65) Simal, F.; Jan, D.; Demonceau, A.; Noels, A. F. In *Controlled/Living Radical Polymerization*; Matyjaszewski, K., Ed.; ACS Symposium Series 768; American Chemical Society: Washington, DC, 2000; Chapter 16, pp 223–233.
- (66) Simal, F.; Demonceau, A.; Noels, A. F. *Tetrahedron Lett.* **1999**, *40*, 5689–5693.
- (67) Bielawski, C. W.; Louie, J.; Grubbs, R. H. *J. Am. Chem. Soc.* **2000**, *122*, 12872–12873.
- (68) Simal, F.; Sebille, S.; Demonceau, A.; Noels, A. F.; Nuñez, R.; Abad, M.; Teixidor, F.; Viñas, C. *Tetrahedron Lett.* **2000**, *41*, 5347–5351.
- (69) del Río, I.; van Koten, G.; Lutz, M.; Spek, A. L. *Organometallics* **2000**, *19*, 361–364.
- (70) Ando, T.; Kamigaito, M.; Sawamoto, M. *Macromolecules* **1997**, *30*, 4507–4510.
- (71) Louie, J.; Grubbs, R. H. *Chem. Commun.* **2000**, 1479–1480.
- (72) Kotani, Y.; Kamigaito, M.; Sawamoto, M. *Macromolecules* **1999**, *32*, 6877–6880.
- (73) Kotani, Y.; Kamigaito, M.; Sawamoto, M. *Macromolecules* **2000**, *33*, 3543–3549.
- (74) Matyjaszewski, K.; Wei, M.; Xia, J.; McDermott, N. E. *Macromolecules* **1997**, *30*, 8161–8164.
- (75) Teodorescu, M.; Gaynor, S. G.; Matyjaszewski, K. *Macromolecules* **2000**, *33*, 2335–2339.
- (76) Zhu, S.; Yan, D. *J. Polym. Sci., Part A: Polym. Chem.* **2000**, *38*, 4308–4314.
- (77) Zhu, S.; Yan, D. *Macromolecules* **2000**, *33*, 8233–8238.
- (78) Zhu, S.; Yan, D. *Macromol. Rapid Commun.* **2000**, *21*, 1209–1213.
- (79) Zhu, S.; Yan, D.; Zhang, G.; Li, M. *Macromol. Chem. Phys.* **2000**, *201*, 2666–2669.
- (80) Moineau, G.; Dubois, Ph.; Jérôme, R.; Senninger, T.; Teyssié, Ph. *Macromolecules* **1998**, *31*, 545–547.
- (81) Xia, J.; Zhang, X.; Matyjaszewski, K. In *Transition Metal Catalysis in Macromolecular Design*; Boffa, L. S., Novak, B. M., Eds.; ACS Symposium Series 760; American Chemical Society: Washington, DC, 2000; Chapter 13, pp 207–223.

- (82) Matyjaszewski, K.; Göbelt, B.; Paik, H.-j.; Horwitz, C. P. *Macromolecules* **2001**, *34*, 430–440.
- (83) Matyjaszewski, K.; Paik, H.-j.; Zhou, P.; Diamanti, S. J. *Macromolecules* **2001**, *34*, 5125–5131.
- (84) Wang, J.-S.; Matyjaszewski, K. *Macromolecules* **1995**, *28*, 7901–7910.
- (85) Patten, T. E.; Xia, J.; Abernathy, T.; Matyjaszewski, K. *Science* **1996**, *272*, 866–868.
- (86) Percec, V.; Barboiu, B.; Neumann, A.; Ronda, J. C.; Zhao, M. *Macromolecules* **1996**, *29*, 3665–3668.
- (87) Collins, J. E.; Fraser, C. L. *Macromolecules* **1998**, *31*, 6715–6717.
- (88) Pascual, S.; Coutin, B.; Tardi, M.; Polton, A.; Varion, J.-P. *Macromolecules* **1999**, *32*, 1432–1437.
- (89) Levy, A. T.; Olmstead, M. M.; Patten, T. E. *Inorg. Chem.* **2000**, *39*, 1628–1634.
- (90) Levy, A. T.; Patten, T. E. In *Transition Metal Catalysis in Macromolecular Design*; Boffa, L. S., Novak, B. M., Eds.; ACS Symposium Series 760; American Chemical Society: Washington, DC, 2000; Chapter 14, pp 224–235.
- (91) Kickelbick, G.; Reinöhl, U.; Ertel, T. S.; Bertagnolli, H.; Matyjaszewski, K. In *Controlled/Living Radical Polymerization*; Matyjaszewski, K., Ed.; ACS Symposium Series 768; American Chemical Society: Washington, DC, 2000; Chapter 15, pp 211–222.
- (92) Pintauer, T.; Jasieczek, C. B.; Matyjaszewski, K. *J. Mass Spectrom.* **2000**, *35*, 1295–1299.
- (93) Schubert, U. S.; Hochwimmer, G.; Spindler, C. E.; Nuyken, O. *Macromol. Rapid Commun.* **1999**, *20*, 351–355.
- (94) Schubert, U. S.; Hochwimmer, G.; Spindler, C. E.; Nuyken, O. *Polym. Bull.* **1999**, *43*, 319–326.
- (95) Xia, J.; Johnson, T.; Gaynor, S. G.; Matyjaszewski, K.; DeSimone, J. *Macromolecules* **1999**, *32*, 4802–4805.
- (96) Destarac, M.; Bessière, J.-M.; Boutevin, B. *Macromol. Rapid Commun.* **1997**, *18*, 967–974.
- (97) Cheng, G.-L.; Hu, C.-P.; Ying, S.-K. *Polymer* **1999**, *40*, 2167–2169.
- (98) Cheng, G.-L.; Hu, C.-P.; Ying, S.-K. *Macromol. Rapid Commun.* **1999**, *20*, 303–307.
- (99) Cheng, G.-L.; Hu, C.-P.; Ying, S.-K. *J. Mol. Catal. A: Chem.* **1999**, *144*, 357–362.
- (100) Haddleton, D. M.; Jasieczek, C. B.; Hannon, M. J.; Shooter, A. J. *Macromolecules* **1997**, *30*, 2190–2193.
- (101) Haddleton, D. M.; Duncalf, D. J.; Kukulj, D.; Crossman, M. C.; Jackson, S. G.; Bon, S. A. F.; Clark, A. J.; Shooter, A. J. *Eur. J. Inorg. Chem.* **1998**, 1799–1806.
- (102) Haddleton, D. M.; Crossman, M. C.; Dana, B. H.; Duncalf, D. J.; Heming, A. M.; Kukulj, D.; Shooter, A. J. *Macromolecules* **1999**, *32*, 2110–2119.
- (103) Haddleton, D. M.; Duncalf, D. J.; Kukulj, D.; Heming, A. M.; Shooter, A. J.; Clark, A. J. *J. Mater. Chem.* **1998**, *8*, 1525–1532.
- (104) Amass, A. J.; Wyres, C. A.; Colclough, E.; Marcia Hohn, I. *Polymer* **2000**, *41*, 1697–1702.
- (105) DiRenzo, G. M.; Messerschmidt, M.; Mülhaupt, R. *Macromol. Rapid Commun.* **1998**, *19*, 381–384.
- (106) Liou, S.; Rademacher, J. T.; Malaba, D.; Pallack, M. E.; Brittain, W. J. *Macromolecules* **2000**, *33*, 4295–4296.
- (107) van der Sluis, M.; Barboiu, B.; Pesa, N.; Percec, V. *Macromolecules* **1998**, *31*, 9409–9412.
- (108) Xia, J.; Matyjaszewski, K. *Macromolecules* **1997**, *30*, 7697–7700.
- (109) Yu, B.; Ruckenstein, E. *J. Polym. Sci., Part A: Polym. Chem.* **1999**, *37*, 4191–4197.
- (110) Wan, X.; Ying, S. J. *Appl. Polym. Sci.* **2000**, *75*, 802–807.
- (111) Kickelbick, G.; Matyjaszewski, K. *Macromol. Rapid Commun.* **1999**, *20*, 341–346.
- (112) Schubert, U. S.; Hochwimmer, G.; Spindler, C. E.; Nuyken, O. In *Controlled/Living Radical Polymerization*; Matyjaszewski, K., Ed.; ACS Symposium Series 768; American Chemical Society: Washington, DC, 2000; Chapter 18, pp 248–262.
- (113) Xia, J.; Matyjaszewski, K. *Macromolecules* **1999**, *32*, 2434–2437.
- (114) Göbelt, B.; Matyjaszewski, K. *Macromol. Chem. Phys.* **2000**, *201*, 1619–1624.
- (115) Haddleton, D. M.; Jackson, S. G.; Bon, S. A. F. *J. Am. Chem. Soc.* **2000**, *122*, 1542–1543.
- (116) Johnson, R. M.; Ng, C.; Samson, C. C. M.; Fraser, C. L. *Macromolecules* **2000**, *33*, 8618–8628.
- (117) Teodorescu, M.; Matyjaszewski, K. *Macromolecules* **1999**, *32*, 4826–4831.
- (118) Xia, J.; Gaynor, S. G.; Matyjaszewski, K. *Macromolecules* **1998**, *31*, 5958–5959.
- (119) Queffelec, J.; Gaynor, S. G.; Matyjaszewski, K. *Macromolecules* **2000**, *33*, 8629–8639.
- (120) Zeng, F.; Shen, Y.; Zhu, S.; Pelton, R. *Macromolecules* **2000**, *33*, 1628–1635.
- (121) Shen, Y.; Zhu, S.; Zeng, F.; Pelton, R. H. *Macromol. Chem. Phys.* **2000**, *201*, 1169–1175.
- (122) Woodworth, B. E.; Metzner, Z.; Matyjaszewski, K. *Macromolecules* **1998**, *31*, 7999–8004.
- (123) Davis, K. A.; Paik, H.-j.; Matyjaszewski, K. *Macromolecules* **1999**, *32*, 1767–1776.
- (124) Matyjaszewski, K.; Wei, M.; Xia, J.; Gaynor, S. G. *Macromol. Chem. Phys.* **1998**, *199*, 2289–2292.
- (125) Singha, N. K.; Klumperman, B. *Macromol. Rapid Commun.* **2000**, *21*, 1116–1120.
- (126) Percec, V.; Barboiu, B.; van der Sluis, M. *Macromolecules* **1998**, *31*, 4053–4056.
- (127) Percec, V.; Asandei, A. D.; Asgarzadeh, F.; Bera, T. K.; Barboiu, B. *J. Polym. Sci., Part A: Polym. Chem.* **2000**, *38*, 3839–3843.
- (128) Percec, V.; Asandei, A. D.; Asgarzadeh, F.; Barboiu, B.; Holerca, M. N.; Grigoras, C. *J. Polym. Sci., Part A: Polym. Chem.* **2000**, *38*, 4353–4361.
- (129) Matyjaszewski, K.; Coca, S.; Gaynor, S. G.; Wei, M.; Woodworth, B. E. *Macromolecules* **1997**, *30*, 7348–7350.
- (130) Wang, J.-S.; Matyjaszewski, K. *Macromolecules* **1995**, *28*, 7572–7573.
- (131) Xia, J.; Matyjaszewski, K. *Macromolecules* **1997**, *30*, 7692–7696.
- (132) Granel, C.; Dubois, Ph.; Jérôme, R.; Teyssié, Ph. *Macromolecules* **1996**, *29*, 8576–8582.
- (133) Uegaki, H.; Kotani, Y.; Kamigaito, M.; Sawamoto, M. *Macromolecules* **1997**, *30*, 2249–2253.
- (134) Moineau, G.; Minet, M.; Dubois, Ph.; Teyssié, Ph.; Senninger, T.; Jérôme, R. *Macromolecules* **1999**, *32*, 27–35.
- (135) Uegaki, H.; Kotani, Y.; Kamigaito, M.; Sawamoto, M. *Macromolecules* **1998**, *31*, 6756–6761.
- (136) Uegaki, H.; Kamigaito, M.; Sawamoto, M. *J. Polym. Sci., Part A: Polym. Chem.* **1999**, *37*, 3003–3009.
- (137) Lecomte, Ph.; Drapier, I.; Dubois, Ph.; Teyssié, Ph.; Jérôme, R. *Macromolecules* **1997**, *30*, 7631–7633.
- (138) Moineau, G.; Granel, C.; Dubois, Ph.; Jérôme, R.; Teyssié, Ph. *Macromolecules* **1998**, *31*, 542–544.
- (139) Hawker, C. J.; Hedrick, J. L.; Malmström, E. E.; Trollsås, M.; Mecerreyes, D.; Moineau, G.; Dubois, Ph.; Jérôme, R. *Macromolecules* **1998**, *31*, 213–219.
- (140) Petrucci, M. G. L.; Lebus, A.-M.; Kakkar, A. K. *Organometallics* **1998**, *17*, 4966–4975.
- (141) Kotani, Y.; Kamigaito, M.; Sawamoto, M. *Macromolecules* **1999**, *32*, 2420–2424.
- (142) Uegaki, H.; Kotani, Y.; Kamigaito, M.; Sawamoto, M. In *Transition Metal Catalysis in Macromolecular Design*; Boffa, L. S., Novak, B. M., Eds.; ACS Symposium Series 760; American Chemical Society: Washington, DC, 2000; Chapter 12, pp 196–206.
- (143) Komiya, S.; Chigira, T.; Suzuki, T.; Hirano, M. *Chem. Lett.* **1999**, 347–348.
- (144) Brandts, J. A. M.; van de Geijn, P.; van Faassen, E. E.; Boersma, J.; van Koten, G. *J. Organomet. Chem.* **1999**, *584*, 246–253.
- (145) Kickelbick, G.; Paik, H.-j.; Matyjaszewski, K. *Macromolecules* **1999**, *32*, 2941–2947.
- (146) Haddleton, D. M.; Kukulj, D.; Radigue, A. P. *Chem. Commun.* **1999**, 99–100.
- (147) Haddleton, D. M.; Radigue, A.; Kukulj, D.; Duncalf, D. J. In *Transition Metal Catalysis in Macromolecular Design*; Boffa, L. S., Novak, B. M., Eds.; ACS Symposium Series 760; American Chemical Society: Washington, DC, 2000; Chapter 15, pp 236–253.
- (148) Haddleton, D. M.; Duncalf, D. J.; Kukulj, D.; Radigue, A. P. *Macromolecules* **1999**, *32*, 4769–4775.
- (149) Shen, Y.; Zhu, S.; Zeng, F.; Pelton, R. H. *Macromolecules* **2000**, *33*, 5427–5431.
- (150) Shen, Y.; Zhu, S.; Zeng, F.; Pelton, R. *Macromol. Chem. Phys.* **2000**, *201*, 1387–1394.
- (151) Shen, Y.; Zhu, S.; Pelton, R. *Macromol. Rapid Commun.* **2000**, *21*, 956–959.
- (152) Percec, V.; Barboiu, B. *Macromolecules* **1995**, *28*, 7970–7972.
- (153) Matyjaszewski, K.; Pintauer, T.; Gaynor, S. *Macromolecules* **2000**, *33*, 1476–1478.
- (154) Ando, T.; Kamigaito, M.; Sawamoto, M. *Tetrahedron* **1997**, *53*, 15445–15457.
- (155) Matyjaszewski, K.; Wang, J.-L.; Grimaud, T.; Shipp, D. A. *Macromolecules* **1998**, *31*, 1527–1534.
- (156) Destarac, M.; Matyjaszewski, K.; Boutevin, B. *Macromol. Chem. Phys.* **2000**, *201*, 265–272.
- (157) Destarac, M.; Boutevin, B.; Matyjaszewski, K. In *Controlled/Living Radical Polymerization*; Matyjaszewski, K., Ed.; ACS Symposium Series 768; American Chemical Society: Washington, DC, 2000; Chapter 17, pp 234–247.
- (158) Destarac, M.; Bessiere, J.-M.; Boutevin, B. *J. Polym. Sci., Part A: Polym. Chem.* **1998**, *36*, 2933–2947.
- (159) Nishikawa, T.; Kamigaito, M.; Sawamoto, M. *Macromolecules* **1999**, *32*, 2204–2209.
- (160) Senoo, M.; Kotani, Y.; Kamigaito, M.; Sawamoto, M. *Macromolecules* **1999**, *32*, 8005–8009.
- (161) Nakagawa, Y.; Matyjaszewski, K. *Polym. J.* **1998**, *30*, 138–141.
- (162) Kajiwara, A.; Matyjaszewski, K.; Kamachi, M. *Macromolecules* **1998**, *31*, 5695–5701.
- (163) Goto, A.; Fukuda, T. *Macromol. Rapid Commun.* **1999**, *20*, 633–636.

- (164) Wang, J.-L.; Grimaud, T.; Matyjaszewski, K. *Macromolecules* **1997**, *30*, 6507–6512.
- (165) Neumann, A.; Keul, H.; Höcker, H. *Macromol. Chem. Phys.* **2000**, *201*, 980–984.
- (166) Liu, Y.; Wang, L.; Pan, C. *Macromolecules* **1999**, *32*, 8301–8305.
- (167) Wang, X.-S.; Luo, N.; Ying, S.-K. *J. Polym. Sci., Part A: Polym. Chem.* **1999**, *37*, 1255–1263.
- (168) Teodorescu, M.; Matyjaszewski, K. *Macromol. Rapid Commun.* **2000**, *21*, 190–194.
- (169) Kotani, Y.; Kamigaito, M.; Sawamoto, M. *Macromolecules* **2000**, *33*, 6746–6751.
- (170) Ando, T.; Kamigaito, M.; Sawamoto, M. *Macromolecules* **2000**, *33*, 2819–2824.
- (171) Reining, B.; Keul, H.; Höcker, H. *Polymer* **1999**, *40*, 3555–3563.
- (172) Rademacher, J. T.; Baum, M.; Pallack, M. E.; Brittain, W. J.; Simonsick, Jr., W. J. *Macromolecules* **2000**, *33*, 284–288.
- (173) Matyjaszewski, K.; Jo, S. M.; Paik, H.-j.; Gaynor, S. G. *Macromolecules* **1997**, *30*, 6398–6400.
- (174) Matyjaszewski, K.; Jo, S. M.; Paik, H.-j.; Shipp, D. A. *Macromolecules* **1999**, *32*, 6431–6438.
- (175) Percec, V.; Kim, H.-J.; Barboiu, B. *Macromolecules* **1997**, *30*, 8526–8528.
- (176) Percec, V.; Barboiu, B.; Kim, H.-J. *J. Am. Chem. Soc.* **1998**, *120*, 305–316.
- (177) Feiring, A. E.; Wonchoba, E. R.; Davidson, F.; Percec, V.; Barboiu, B. *J. Polym. Sci., Part A: Polym. Chem.* **2000**, *38*, 3313–3335.
- (178) Grimaud, T.; Matyjaszewski, K. *Macromolecules* **1997**, *30*, 2216–2218.
- (179) Destarac, M.; Alric, J.; Boutevin, B. *Macromol. Rapid Commun.* **2000**, *21*, 1337–1341.
- (180) Matsuyama, M.; Kamigaito, M.; Sawamoto, M. *J. Polym. Sci., Part A: Polym. Chem.* **1996**, *34*, 3585–3589.
- (181) Wang, W.; Dong, Z.; Xia, P.; Yan, D.; Zhang, Q. *Macromol. Rapid Commun.* **1998**, *19*, 647–649.
- (182) Chen, X.-P.; Qiu, K.-Y. *Polym. Int.* **2000**, *49*, 1529–1533.
- (183) Zilg, C.; Thomann, R.; Baumert, M.; Finter, J.; Mülhaupt, R. *Macromol. Rapid Commun.* **2000**, *21*, 1214–1219.
- (184) Qiu, J.; Gaynor, S. G.; Matyjaszewski, K. *Macromolecules* **1999**, *32*, 2872–2875.
- (185) Xia, J.; Matyjaszewski, K. *Macromolecules* **1999**, *32*, 5199–5202.
- (186) Zhu, S.; Wang, W.; Tu, W.; Yan, D. *Acta Polym.* **1999**, *50*, 267–269.
- (187) Wang, W.; Yan, D. In *Controlled/Living Radical Polymerization*; Matyjaszewski, K., Ed.; ACS Symposium Series 768; American Chemical Society: Washington, DC, 2000; Chapter 19, pp 263–275.
- (188) Chen, X.-P.; Qiu, K.-Y. *Macromolecules* **1999**, *32*, 8711–8715.
- (189) Chen, X.-P.; Qiu, K.-Y. *J. Appl. Polym. Sci.* **2000**, *77*, 1607–1613.
- (190) Qin, D.-Q.; Qin, S.-H.; Qiu, K.-Y. *J. Polym. Sci., Part A: Polym. Chem.* **2000**, *38*, 101–107.
- (191) Qin, D.-Q.; Qin, S.-H.; Chen, X.-P.; Qiu, K.-Y. *Polymer* **2000**, *41*, 7347–7353.
- (192) Qin, D.-Q.; Qin, S.-H.; Qiu, K.-Y. *Macromolecules* **2000**, *33*, 6987–6992.
- (193) Chen, X.-P.; Qiu, K.-Y. *Chem. Commun.* **2000**, 233–234.
- (194) Chen, X.-P.; Qiu, K.-Y. *Chem. Commun.* **2000**, 1403–1404.
- (195) Acar, A. E.; Yağci, M. B.; Mathias, L. J. *Macromolecules* **2000**, *33*, 7700–7706.
- (196) Matyjaszewski, K.; Shipp, D. A.; Wang, J.-L.; Grimaud, T.; Patten, T. E. *Macromolecules* **1998**, *31*, 6836–6840.
- (197) Nonaka, H.; Ouchi, M.; Kamigaito, M.; Sawamoto, M. *Macromolecules* **2001**, *34*, 2083–2088.
- (198) Kotani, Y.; Kato, M.; Kamigaito, M.; Sawamoto, M. *Macromolecules* **1996**, *29*, 6979–6982.
- (199) Haddleton, D. M.; Waterson, C. *Macromolecules* **1999**, *32*, 8732–8739.
- (200) Ashford, E. J.; Naldi, V.; O'Dell, R.; Billingham, N. C.; Armes, S. P. *Chem. Commun.* **1999**, 1285–1286.
- (201) Onishi, I.; Baek, K.-Y.; Kotani, Y.; Kamigaito, M.; Sawamoto, M. *Polym. Prepr. Jpn.* **1999**, *48*, 136; *J. Polym. Sci., Part A: Polym. Chem.*, submitted for publication.
- (202) Davis, K. A.; Matyjaszewski, K. *Macromolecules* **2000**, *33*, 4039–4047.
- (203) Ma, Q.; Wooley, K. L. *J. Polym. Sci., Part A: Polym. Chem.* **2000**, *38*, 4805–4820.
- (204) Coca, S.; Matyjaszewski, K. *J. Polym. Sci., Part A: Polym. Chem.* **1997**, *35*, 3595–3601.
- (205) Kotani, Y.; Kamigaito, M.; Sawamoto, M. *Macromolecules* **1998**, *31*, 5582–5587.
- (206) Qiu, J.; Matyjaszewski, K. *Macromolecules* **1997**, *30*, 5643–5648.
- (207) Gao, B.; Chen, X.; Iván, B.; Kops, J.; Batsberg, W. *Macromol. Rapid Commun.* **1997**, *18*, 1095–1100.
- (208) Chen, X.; Jankova, K.; Kops, J.; Batsberg, W. *J. Polym. Sci., Part A: Polym. Chem.* **1999**, *37*, 627–633.
- (209) Doerfler, E. M.; Patten, T. E. *Macromolecules* **2000**, *33*, 8911–8914.
- (210) McQuillan, B. W.; Paugio, S. *Fusion Technol.* **2000**, *38*, 108–109.
- (211) Gaynor, S. G.; Edelman, S.; Matyjaszewski, K. *Macromolecules* **1996**, *29*, 1079–1081.
- (212) Matyjaszewski, K.; Gaynor, S. G. *Macromolecules* **1997**, *30*, 7042–7049.
- (213) Weimer, M. W.; Fréchet, J. M. J.; Gitsov, I. *J. Polym. Sci., Part A: Polym. Chem.* **1998**, *36*, 955–970.
- (214) Xia, J.; Zhang, X.; Matyjaszewski, K. *Macromolecules* **1999**, *32*, 3531–3533.
- (215) Ramakrishnan, A.; Dhamodharan, R. *J. Macromol. Sci., Pure Appl. Chem.* **2000**, *A37*, 621–631.
- (216) Huang, X.; Wirth, M. J. *Anal. Chem.* **1997**, *69*, 4577–4580.
- (217) Huang, X.; Doneski, L. J.; Wirth, M. J. *Anal. Chem.* **1998**, *70*, 4023–4029.
- (218) Huang, X.; Wirth, M. J. *Macromolecules* **1999**, *32*, 1694–1696.
- (219) Matyjaszewski, K.; Coessens, V.; Nakagawa, Y.; Xia, J.; Qiu, J.; Gaynor, S.; Coca, S.; Jasieczek, C. In *Functional Polymers*; Patil, A. M.; Schulz, D. N.; Novak, B. M., Eds.; ACS Symposium Series 704; American Chemical Society: Washington, DC, 1998; Chapter 2, pp 16–27.
- (220) Chen, G.-Q.; Wu, Z.-Q.; Wu, J.-R.; Li, Z.-C.; Li, F.-M. *Macromolecules* **2000**, *33*, 232–234.
- (221) Jiang, X.; Xia, P.; Liu, W.; Yan, D. *J. Polym. Sci., Part A: Polym. Chem.* **2000**, *38*, 1203–1209.
- (222) Li, F.-M.; Chen, G.-Q.; Zhu, M.-Q.; Zhou, P.; Du, F.-S.; Li, Z.-C. In *Controlled/Living Radical Polymerization*; Matyjaszewski, K., Ed.; ACS Symposium Series 768; American Chemical Society: Washington, DC, 2000; Chapter 27, pp 384–393.
- (223) Ellzey, K. A.; Novak, B. M. *Macromolecules* **1998**, *31*, 2391–2393.
- (224) Pan, C.-Y.; Lou, X.-D. *Macromol. Chem. Phys.* **2000**, *201*, 1115–1120.
- (225) Xia, J.; Paik, H.-j.; Matyjaszewski, K. *Macromolecules* **1999**, *32*, 8310–8314.
- (226) Bon, S. A. F.; Steward, A. G.; Haddleton, D. M. *J. Polym. Sci., Part A: Polym. Chem.* **2000**, *38*, 2678–2686.
- (227) Ando, T.; Kamigaito, M.; Sawamoto, M. *Macromolecules* **2000**, *33*, 6732–6737.
- (228) Ueda, J.; Matsuyama, M.; Kamigaito, M.; Sawamoto, M. *Macromolecules* **1998**, *31*, 557–562.
- (229) Guo, J.; Han, Z.; Wu, P. *J. Mol. Catal. A: Chem.* **2000**, *159*, 77–83.
- (230) Matyjaszewski, K.; Coca, S.; Gaynor, S. G.; Wei, M.; Woodworth, B. E. *Macromolecules* **1998**, *31*, 5967–5969.
- (231) Haddleton, D. M.; Clark, A. J.; Crossman, M. C.; Duncalf, D. J.; Heming, A. M.; Morsley, S. R.; Shooter, A. J. *Chem. Commun.* **1997**, 1173–1174.
- (232) Haddleton, D. M.; Kukulj, D.; Duncalf, D. J.; Heming, A. M.; Shooter, A. J. *Macromolecules* **1998**, *31*, 5201–5205.
- (233) Haddleton, D. M.; Shooter, A. J.; Heming, A. M.; Crossman, M. C.; Duncalf, D. J.; Morsley, S. R. In *Controlled Radical Polymerization*; Matyjaszewski, K., Ed.; ACS Symposium Series 685; American Chemical Society: Washington, DC, 1998; Chapter 17, pp 284–295.
- (234) Haddleton, D. M.; Clark, A. J.; Duncalf, D. J.; Heming, A. M.; Kukulj, D.; Shooter, A. J. *J. Chem. Soc., Dalton Trans.* **1998**, 381–385.
- (235) Haddleton, D. M.; Heming, A. M.; Kukulj, D.; Duncalf, D. J.; Shooter, A. J. *Macromolecules* **1998**, *31*, 2016–2018.
- (236) Hamasaki, S.; Kamigaito, M.; Sawamoto, M. *Polym. Prepr. Jpn.* **1999**, *48*, 1117–1118; *Macromolecules*, submitted for publication.
- (237) Guan, Z.; Smart, B. *Macromolecules* **2000**, *33*, 6904–6906.
- (238) Matyjaszewski, K. In *Solvent-Free Polymerizations and Processes*; Long, T. E., Hunt, M. O., Eds.; ACS Symposium Series 713; American Chemical Society: Washington, DC, 1998; Chapter 6, pp 96–112.
- (239) Matyjaszewski, K.; Nakagawa, Y.; Jasieczek, C. B. *Macromolecules* **1998**, *31*, 1535–1541.
- (240) Percec, V.; Kim, H.-J.; Barboiu, B. *Macromolecules* **1997**, *30*, 6702–6705.
- (241) Wang, X.-S.; Luo, N.; Ying, S.-K. *Polymer* **1999**, *40*, 4157–4161.
- (242) Chambard, G.; Klumperman, B.; German, A. L. *Macromolecules* **2000**, *33*, 4417–4421.
- (243) Beers, K. L.; Boo, S.; Gaynor, S. G.; Matyjaszewski, K. *Macromolecules* **1999**, *32*, 5772–5776.
- (244) Coca, S.; Jasieczek, C. B.; Beers, K. L.; Matyjaszewski, K. *J. Polym. Sci., Part A: Polym. Chem.* **1998**, *36*, 1417–1424.
- (245) Zeng, F.; Shen, Y.; Zhu, S.; Pelton, R. *J. Polym. Sci., Part A: Polym. Chem.* **2000**, *38*, 3821–3827.
- (246) Wang, X.-S.; Lascelles, S. F.; Jackson, R. A.; Armes, S. P. *Chem. Commun.* **1999**, 1817–1818.
- (247) Wang, X.-S.; Jackson, R. A.; Armes, S. P. *Macromolecules* **2000**, *33*, 255–257.
- (248) Guerrini, M. M.; Charleux, B.; Vairon, J.-P. *Macromol. Rapid Commun.* **2000**, *21*, 669–674.
- (249) Matyjaszewski, K.; Qiu, J.; Shipp, D. A.; Gaynor, S. G. *Macromol. Symp.* **2000**, *155*, 15–29.
- (250) Fujii, Y.; Ando, T.; Kamigaito, M.; Sawamoto, M. *Polym. Prepr. Jpn.* **2001**, *50*, 106; *Macromolecules*, submitted for publication.

- (251) Gaynor, S. G.; Qiu, J.; Matyjaszewski, K. *Macromolecules* **1998**, *31*, 5951–5954.
- (252) Matyjaszewski, K.; Qiu, J.; Tsarevsky, N. V.; Charleux, B. *J. Polym. Sci., Part A: Polym. Chem.* **2000**, *38*, 4724–4734.
- (253) Chambard, G.; de Man, P.; Klumperman, B. *Macromol. Symp.* **2000**, *150*, 45–51.
- (254) Matyjaszewski, K.; Shipp, D. A.; Qiu, J.; Gaynor, S. G. *Macromolecules* **2000**, *33*, 2296–2298.
- (255) Qiu, J.; Pintauer, T.; Gaynor, S. G.; Matyjaszewski, K.; Charleux, B.; Varion, J.-P. *Macromolecules* **2000**, *33*, 7310–7320.
- (256) Storsberg, J.; Hartenstein, M.; Müller, A. H. E.; Ritter, H. *Macromol. Rapid Commun.* **2000**, *21*, 1342–1346.
- (257) Carmichael, A. J.; Haddleton, D. M.; Bon, S. A. F.; Seddon, K. R. *Chem. Commun.* **2000**, 1237–1238.
- (258) Matyjaszewski, K. *Macromolecules* **1998**, *31*, 4710–4717.
- (259) Matyjaszewski, K. *Macromolecules* **1999**, *32*, 9051–9053.
- (260) Matyjaszewski, K. *Macromol. Symp.* **1996**, *111*, 47–61.
- (261) Matyjaszewski, K. In *Controlled Radical Polymerization*; Matyjaszewski, K., Ed.; ACS Symposium Series 685; American Chemical Society: Washington, DC, 1998; Chapter 16, pp 258–283.
- (262) Matyjaszewski, K. *Macromol. Symp.* **2000**, *161*, 1–9.
- (263) Haddleton, D. M.; Crossman, M. C.; Hunt, K. H.; Topping, C.; Waterson, C.; Suddaby, K. G. *Macromolecules* **1997**, *30*, 3992–3998.
- (264) Arehart, S. V.; Matyjaszewski, K. *Macromolecules* **1999**, *32*, 2221–2231.
- (265) Gaynor, S. G.; Matyjaszewski, K. In *Controlled Radical Polymerization*; Matyjaszewski, K., Ed.; ACS Symposium Series 685; American Chemical Society: Washington, DC, 1998; Chapter 24, pp 396–417.
- (266) Chambard, G.; Klumperman, B. In *Controlled/Living Radical Polymerization*; Matyjaszewski, K., Ed.; ACS Symposium Series 768; American Chemical Society: Washington, DC, 2000; Chapter 14, pp 197–210.
- (267) Roos, S. G.; Müller, A. H. E.; Matyjaszewski, K. *Macromolecules* **1999**, *32*, 8331–8335.
- (268) Heuts, J. P. A.; Davis, T. P. *Macromol. Rapid Commun.* **1998**, *19*, 371–375.
- (269) Matyjaszewski, K.; Kajiwara, A. *Macromolecules* **1998**, *31*, 548–550.
- (270) Kajiwara, A.; Matyjaszewski, K. *Macromol. Rapid Commun.* **1998**, *19*, 319–321.
- (271) Kajiwara, A.; Matyjaszewski, K. *Polym. J.* **1999**, *31*, 70–75.
- (272) Haddleton, D. M.; Heming, A. M.; Kukulj, D.; Jackson, S. G. *Chem. Commun.* **1998**, 1719–1720.
- (273) Matyjaszewski, K.; Paik, H.-j.; Shipp, D. A.; Isobe, Y.; Okamoto, Y. *Macromolecules* **2001**, *34*, 3127–3129.
- (274) Haddleton, D. M.; Waterson, C.; Derrick, P. J.; Jasieczek, C. B.; Shooter, A. J. *Chem. Commun.* **1997**, 683–684.
- (275) Bednarek, M.; Biedroń, T.; Kubisa, P. *Macromol. Chem. Phys.* **2000**, *201*, 58–66.
- (276) Borman, C. D.; Jackson, A. T.; Bunn, A.; Cutter, A. L.; Irvine, D. J. *Polymer* **2000**, *41*, 6015–6020.
- (277) Coessens, V.; Matyjaszewski, K. *Macromol. Rapid Commun.* **1999**, *20*, 66–70.
- (278) Eynde, X. V.; Matyjaszewski, K.; Bertrand, P. *Surf. Interface Anal.* **1998**, *26*, 569–578.
- (279) Eynde, X. V.; Bertrand, P. *Surf. Interface Anal.* **1998**, *26*, 579–589.
- (280) Coessens, V.; Matyjaszewski, K. *Macromol. Rapid Commun.* **1999**, *20*, 127–134.
- (281) Matyjaszewski, K.; Patten, T. E.; Xia, J. *J. Am. Chem. Soc.* **1997**, *119*, 9, 674–680.
- (282) Ohno, K.; Goto, A.; Fukuda, T.; Xia, J.; Matyjaszewski, K. *Macromolecules* **1998**, *31*, 2699–2701.
- (283) Fukuda, T.; Goto, A.; Ohno, K. *Macromol. Rapid Commun.* **2000**, *21*, 151–165.
- (284) Shipp, D. A.; Matyjaszewski, K. *Macromolecules* **1999**, *32*, 2948–2955.
- (285) Shipp, D. A.; Matyjaszewski, K. *Macromolecules* **2000**, *33*, 1553–1559.
- (286) Butté, A.; Storti, G.; Morbidelli, M. *Chem. Eng. Sci.* **1999**, *54*, 3225–3231.
- (287) Zhu, S. *Macromol. Theory Simul.* **1999**, *8*, 29–37.
- (288) van de Kuil, L. A.; Grove, D. M.; Gossage, R. A.; Zwikker, J. W.; Jenneskens, L. W.; Drenth, W.; van Koten, G. *Organometallics* **1997**, *16*, 4985–4994.
- (289) Gossage, R. A.; van de Kuil, L. A.; van Koten, G. *Acc. Chem. Res.* **1998**, *31*, 423–431.
- (290) Matyjaszewski, K.; Woodworth, B. E. *Macromolecules* **1998**, *31*, 4718–4723.
- (291) Matyjaszewski, K.; Davis, K.; Patten, T. E.; Wei, M. *Tetrahedron* **1997**, *53*, 15321–15329.
- (292) Roos, S. G.; Müller, A. H. E. *Macromol. Rapid Commun.* **2000**, *21*, 864–867.
- (293) Tokuchi, K.; Ando, T.; Kamigaito, M.; Sawamoto, M. *J. Polym. Sci., Part A: Polym. Chem.* **2000**, *38*, 4735–4748.
- (294) Parker, J.; Jones, R. G.; Holder, S. J. *Macromolecules* **2000**, *33*, 9166–9168.
- (295) Heuts, J. P. A.; Mallesch, R.; Davis, T. P. *Macromol. Chem. Phys.* **1999**, *200*, 1380–1385.
- (296) Korn, M. R.; Gagné, M. R. *Chem. Commun.* **2000**, 1711–1712.
- (297) Fischer, H. *Macromolecules* **1997**, *30*, 5666–5672.
- (298) Souaille, M.; Fischer, H. *Macromolecules* **2000**, *33*, 7378–7394.
- (299) Gaynor, S. G.; Matyjaszewski, K. In *Controlled/Living Radical Polymerization*; Matyjaszewski, K., Ed.; ACS Symposium Series 768; American Chemical Society: Washington, DC, 2000; Chapter 24, pp 347–360.
- (300) Haddleton, D. M.; Heming, A. M.; Jarvis, A. P.; Khan, A.; Marsh, A.; Perrier, S.; Bon, S. A. F.; Jackson, S. G.; Edmonds, R.; Kelly, E.; Kukulj, D.; Waterson, C. *Macromol. Symp.* **2000**, *157*, 201–208.
- (301) Matyjaszewski, K. *Macromol. Symp.* **1998**, *132*, 85–101.
- (302) Matyjaszewski, K.; Teodorescu, M.; Acar, M. H.; Beers, K. L.; Coca, S.; Gaynor, S. G.; Miller, P. J.; Paik, H.-j. *Macromol. Symp.* **2000**, *157*, 183–192.
- (303) Matyjaszewski, K.; Miller, P. J.; Fossum, E.; Nakagawa, Y. *Appl. Organomet. Chem.* **1998**, *12*, 667–673.
- (304) Ambade, A. V.; Kumar, A. *Prog. Polym. Sci.* **2000**, *25*, 1141–1170.
- (305) Wooley, K. L. *J. Polym. Sci., Part A: Polym. Chem.* **2000**, *38*, 1397–1407.
- (306) Voit, B. *J. Polym. Sci., Part A: Polym. Chem.* **2000**, *38*, 2505–2525.
- (307) Améduri, B.; Boutevin, B.; Gramain, Ph. *Adv. Polym. Sci.* **1997**, *127*, 87–142.
- (308) Huang, X.; Doneski, L. J.; Wirth, M. J. *CHEMTECH* **1998**, *28* (12), 19–24.
- (309) Zhao, B.; Brittain, W. J. *Prog. Polym. Sci.* **2000**, *25*, 677–710.
- (310) Coessens, V.; Pintauer, T.; Matyjaszewski, K. *Prog. Polym. Sci.* **2001**, *26*, 337–377.
- (311) Mecerreyes, D.; Trollsås, M.; Hedrick, J. L. *Macromolecules* **1999**, *32*, 8753–8759.
- (312) Mecerreyes, D.; Atthoff, B.; Boduch, K. A.; Trollsås, M.; Hedrick, J. L. *Macromolecules* **1999**, *32*, 5175–5182.
- (313) Mühlebach, A.; Gaynor, S. G.; Matyjaszewski, K. *Macromolecules* **1998**, *31*, 6046–6052.
- (314) Zhang, X.; Xia, J.; Matyjaszewski, K. *Macromolecules* **1998**, *31*, 5167–5169.
- (315) Zhang, Z.-B.; Ying, S.-K.; Shi, Z.-Q. *Polymer* **1999**, *40*, 5439–5444.
- (316) Matyjaszewski, K.; Coca, S.; Jasieczek, C. B. *Macromol. Chem. Phys.* **1997**, *198*, 4011–4017.
- (317) Jones, R. G.; Yoon, S.; Nagasaki, Y. *Polymer* **1999**, *40*, 2411–2418.
- (318) Mecerreyes, D.; Humes, J.; Miller, R. D.; Hedrick, J. L.; Detrembleur, C.; Lecomte, P.; Jérôme, R.; Roman, J. S. *Macromol. Rapid Commun.* **2000**, *21*, 779–784.
- (319) Mecerreyes, D.; Pomposo, J. A.; Bengoetxea, M.; Grande, H. *Macromolecules* **2000**, *33*, 5846–5849.
- (320) Wang, X.-S.; Armes, S. P. *Macromolecules* **2000**, *33*, 6640–6647.
- (321) Ohno, K.; Tsujii, Y.; Fukuda, T. *J. Polym. Sci., Part A: Polym. Chem.* **1998**, *36*, 2473–2481.
- (322) Li, Z.-C.; Liang, Y.-Z.; Chen, G.-Q.; Li, F.-M. *Macromol. Rapid Commun.* **2000**, *21*, 375–380.
- (323) Marsh, A.; Khan, A.; Haddleton, D. M.; Hannon, M. J. *Macromolecules* **1999**, *32*, 8725–8731.
- (324) Kasko, A. M.; Heintz, A. M.; Pugh, C. *Macromolecules* **1998**, *31*, 256–271.
- (325) Zhang, X.; Wang, P.; Zhu, P.; Ye, C.; Xi, F. *Macromol. Chem. Phys.* **2000**, *201*, 1853–1857.
- (326) Pyun, J.; Matyjaszewski, K. *Macromolecules* **2000**, *33*, 217–220.
- (327) Keul, H.; Neumann, A.; Reining, B.; Höcker, H. *Macromol. Symp.* **2000**, *161*, 63–73.
- (328) Zhang, X.; Xia, J.; Matyjaszewski, K. *Macromolecules* **2000**, *33*, 2340–2345.
- (329) Xu, Y.; Pan, C.; Tao, L. *J. Polym. Sci., Part A: Polym. Chem.* **2000**, *38*, 436–443.
- (330) Zhang, X.; Matyjaszewski, K. *Macromolecules* **1999**, *32*, 7349–7353.
- (331) Malz, H.; Komber, H.; Voigt, D.; Hopfe, I.; Pionteck, J. *Macromol. Chem. Phys.* **1999**, *200*, 642–651.
- (332) Wu, X.; Fraser, C. L. *Macromolecules* **2000**, *33*, 4053–4060.
- (333) Fraser, C. L.; Smith, A. P. *J. Polym. Sci., Part A: Polym. Chem.* **2000**, *38*, 4704–4716.
- (334) Carrot, G.; Hilborn, J.; Hedrick, J. L.; Trollsås, M. *Macromolecules* **1999**, *32*, 5171–5173.
- (335) Alkan, S.; Toppare, L.; Hepuzer, Y.; Yagci, Y. *J. Polym. Sci., Part A: Polym. Chem.* **1999**, *37*, 4218–4225.
- (336) Shen, Y.; Zhu, S.; Zeng, F.; Pelton, R. *Macromolecules* **2000**, *33*, 5399–5404.
- (337) Matyjaszewski, K.; Beers, K. L.; Kern, A.; Gaynor, S. G. *J. Polym. Sci., Part A: Polym. Chem.* **1998**, *36*, 823–830.
- (338) Paik, H.-j.; Teodorescu, M.; Xia, J.; Matyjaszewski, K. *Macromolecules* **1999**, *32*, 7023–7031.

- (339) Haddleton, D. M.; Ohno, K. *Biomacromolecules* **2000**, *1*, 152–156.
- (340) Haddleton, D. M.; Edmonds, R.; Heming, A. M.; Kelly, E. J.; Kukulj, D. *New J. Chem.* **1999**, *23*, 477–479.
- (341) Haddleton, D. M.; Jarvis, A. P.; Waterson, C.; Bon, S. A. F.; Heming, A. M. In *Controlled/Living Radical Polymerization*; Matyjaszewski, K., Ed.; ACS Symposium Series 768; American Chemical Society: Washington, DC, 2000; Chapter 13, pp 182–196.
- (342) Zhou, P.; Chen, G.-Q.; Li, C.-Z.; Du, F.-S.; Li, Z.-C.; Li, F.-M. *Chem. Commun.* **2000**, 797–798.
- (343) Percec, V.; Barboiu, B.; Bera, T. K.; van der Sluis, M.; Grubbs, R. B.; Fréchet, J. M. J. *J. Polym. Sci., Part A: Polym. Chem.* **2000**, *38*, 4776–4791.
- (344) Ando, T.; Kamigaito, M.; Sawamoto, M. *Macromolecules* **1998**, *31*, 6708–6711.
- (345) Percec, V.; Barboiu, B.; Bera, T. K.; Kim, H.-J.; Fréchet, J. M. J.; Grubbs, R. H. *Preprints of the IUPAC International Symposium on Ionic Polymerization*, Kyoto, 1999; p 37.
- (346) Coessens, V.; Pyun, J.; Miller, P. J.; Gaynor, S. G.; Matyjaszewski, K. *Macromol. Rapid Commun.* **2000**, *21*, 103–109.
- (347) Bon, S. A. F.; Morsley, S. R.; Waterson, C.; Haddleton, D. M. *Macromolecules* **2000**, *33*, 5819–5824.
- (348) Koulouri, E. G.; Kallitsis, J. K.; Hadziioannou, G. *Macromolecules* **1999**, *32*, 6242–6248.
- (349) Shen, X.; He, X.; Chen, G.; Zhou, P.; Huang, L. *Macromol. Rapid Commun.* **2000**, *21*, 1162–1165.
- (350) Coessens, V.; Matyjaszewski, K. *J. Macromol. Sci., Pure Appl. Chem.* **1999**, *A36*, 811–826.
- (351) Coessens, V.; Nakagawa, Y.; Matyjaszewski, K. *Polym. Bull.* **1998**, *40*, 135–142.
- (352) Coessens, V.; Matyjaszewski, K. *J. Macromol. Sci., Pure Appl. Chem.* **1999**, *A36*, 667–679.
- (353) Li, L.; Wang, C.; Long, Z.; Fu, S. *J. Polym. Sci., Part A: Polym. Chem.* **2000**, *38*, 4519–4523.
- (354) Matyjaszewski, K.; Nakagawa, Y.; Gaynor, S. G. *Macromol. Rapid Commun.* **1997**, *18*, 1057–1066.
- (355) Coessens, V.; Matyjaszewski, K. *J. Macromol. Sci., Pure Appl. Chem.* **1999**, *A36*, 653–666.
- (356) Iván, B.; Fónagy, T. In *Controlled/Living Radical Polymerization*; Matyjaszewski, K., Ed.; ACS Symposium Series 768; American Chemical Society: Washington, DC, 2000; Chapter 26, pp 372–383.
- (357) Ueda, J.; Kamigaito, M.; Sawamoto, M. *Macromolecules* **1998**, *31*, 6762–6768.
- (358) Matyjaszewski, K.; Miller, P. J.; Pyun, J.; Kickelbick, G.; Diamanti, S. *Macromolecules* **1999**, *32*, 6526–6535.
- (359) Shipp, D. A.; Wang, J.-L.; Matyjaszewski, K. *Macromolecules* **1998**, *31*, 8005–8008.
- (360) Matyjaszewski, K.; Shipp, D. A.; McMurtry, G. P.; Gaynor, S. G.; Pakula, T. *J. Polym. Sci., Part A: Polym. Chem.* **2000**, *38*, 2023–2031.
- (361) Moineau, C.; Minet, M.; Teyssié, Ph.; Jérôme, R. *Macromolecules* **1999**, *32*, 8277–8282.
- (362) Leclère, Ph.; Moineau, G.; Minet, M.; Dubois, Ph.; Jérôme, R.; Brédas, J. L.; Lazzaroni, R. *Langmuir* **1999**, *15*, 3915–3919.
- (363) Tong, J. D.; Moineau, G.; Leclère, Ph.; Brédas, J. L.; Lazzaroni, R.; Jérôme, R. *Macromolecules* **2000**, *33*, 470–479.
- (364) Moineau, G.; Minet, M.; Teyssié, Ph.; Jérôme, R. *Macromol. Chem. Phys.* **2000**, *201*, 1108–1114.
- (365) Sedjo, R. A.; Mirous, B. K.; Brittain, W. J. *Macromolecules* **2000**, *33*, 1492–1493.
- (366) Cassebras, M.; Pascual, S.; Polton, A.; Tardi, M.; Vairon, J.-P. *Macromol. Rapid Commun.* **1999**, *20*, 261–264.
- (367) Burguière, C.; Pascual, S.; Coutin, B.; Polton, A.; Tardi, M.; Charleux, B.; Matyjaszewski, K.; Vairon, J.-P. *Macromol. Symp.* **2000**, *150*, 39–44.
- (368) Davis, K. A.; Charleux, B.; Matyjaszewski, K. *J. Polym. Sci., Part A: Polym. Chem.* **2000**, *38*, 2274–2283.
- (369) Matyjaszewski, K.; Miller, P. J.; Shukla, N.; Immaraporn, B.; Gelman, A.; Luokala, B. B.; Siclován, T. M.; Kickelbick, G.; Vallant, T.; Hoffmann, H.; Pakula, T. *Macromolecules* **1999**, *32*, 8716–8724.
- (370) Senoo, M.; Kotani, Y.; Kamigaito, M.; Sawamoto, M. *Macromol. Symp.* **2000**, *157*, 193–200.
- (371) Yamamoto, S.; Tsujii, Y.; Fukuda, T. *Macromolecules* **2000**, *33*, 5995–5998.
- (372) Gao, B.; Chen, X.; Iván, B.; Kops, J.; Batsberg, W. *Polym. Bull.* **1997**, *39*, 559–565.
- (373) Zhang, X.; Matyjaszewski, K. *Macromolecules* **1999**, *32*, 1763–1766.
- (374) Acar, M. H.; Matyjaszewski, K. *Macromol. Chem. Phys.* **1999**, *200*, 1094–1100.
- (375) Tong, J.-D.; Ni, S.; Winnik, M. A. *Macromolecules* **2000**, *33*, 1482–1486.
- (376) Coca, S.; Matyjaszewski, K. *Macromolecules* **1997**, *30*, 2808–2810.
- (377) Zhao, B.; Brittain, W. J. *Macromolecules* **2000**, *33*, 8813–8820.
- (378) Zhao, B.; Brittain, W. J. *J. Am. Chem. Soc.* **1999**, *121*, 3557–3558.
- (379) Jankova, K.; Kops, J.; Chen, X.; Gao, B.; Batsberg, W. *Polym. Bull.* **1998**, *41*, 639–644.
- (380) Chen, X.; Iván, B.; Kops, J.; Batsberg, W. *Macromol. Rapid Commun.* **1998**, *19*, 585–589.
- (381) Keszler, B.; Fenyvesi, G.Y.; Kennedy, J. P. *J. Polym. Sci., Part A: Polym. Chem.* **2000**, *38*, 706–714.
- (382) Destarac, M.; Pees, B.; Boutevin, B. *Macromol. Rapid Commun.* **2000**, *201*, 1189–1199.
- (383) Destarac, M.; Matyjaszewski, K.; Silverman, E. *Macromolecules* **2000**, *33*, 4613–4615.
- (384) Jo, S.-M.; Lee, W.-S.; Ahn, B.-S.; Park, K.-Y.; Kim, K.-A.; Paeng, I.-S. R. *Polym. Bull.* **2000**, *44*, 1–8.
- (385) Zhang, Z.-B.; Ying, S.-K.; Shi, Z. *Polymer* **1999**, *40*, 1341–1345.
- (386) Destarac, M.; Boutevin, B. *Macromol. Rapid Commun.* **1999**, *20*, 641–645.
- (387) Kajiwara, A.; Matyjaszewski, K. *Macromolecules* **1998**, *31*, 3489–3493.
- (388) Xu, Y.; Pan, C. *Macromolecules* **2000**, *33*, 4750–4756.
- (389) Xu, Y.; Pan, C. *J. Polym. Sci., Part A: Polym. Chem.* **2000**, *38*, 337–344.
- (390) Başkan Düz, A.; Yağci, Y. *Eur. Polym. J.* **1999**, *35*, 2031–2038.
- (391) Angot, S.; Taton, D.; Gnanou, Y. *Macromolecules* **2000**, *33*, 5418–5426.
- (392) Mecerreyes, D.; Moineau, G.; Dubois, Ph.; Jérôme, R.; Hedrick, J. L.; Hawker, C. J.; Malmström, E. E.; Trollsås, M. *Angew. Chem., Int. Ed.* **1998**, *37*, 1274–1276.
- (393) Hedrick, J. L.; Trollsås, M.; Hawker, C. J.; Atthoff, B.; Claesson, H.; Heise, A.; Miller, R. D.; Mecerreyes, D.; Jérôme, R.; Dubois, Ph. *Macromolecules* **1998**, *31*, 8691–8705.
- (394) Zhang, Q.; Remsen, E. E.; Wooley, K. L. *J. Am. Chem. Soc.* **2000**, *122*, 3642–3651.
- (395) Miller, P. J.; Matyjaszewski, K. *Macromolecules* **1999**, *32*, 8760–8767.
- (396) Coca, S.; Paik, H.-j.; Matyjaszewski, K. *Macromolecules* **1997**, *30*, 6513–6516.
- (397) Bielawski, C. W.; Morita, T.; Grubbs, R. H. *Macromolecules* **2000**, *33*, 678–680.
- (398) Gaynor, S. G.; Matyjaszewski, K. *Macromolecules* **1997**, *30*, 4241–4245.
- (399) Lutsen, L.; Gordina, G. P.-G.; Jones, R. G.; Schué, F. *Eur. Polym. J.* **1998**, *34*, 1829–1837.
- (400) Klaerner, G.; Trollsås, M.; Heise, A.; Husemann, M.; Atthoff, B.; Hawker, C. J.; Hedrick, J. L.; Miller, R. D. *Macromolecules* **1999**, *32*, 8227–8229.
- (401) Leduc, M. R.; Hayes, W.; Fréchet, J. M. J. *J. Polym. Sci., Part A: Polym. Chem.* **1998**, *36*, 1–10.
- (402) Zhu, L.; Tong, X.; Li, M.; Wang, E. *J. Polym. Sci., Part A: Polym. Chem.* **2000**, *38*, 4282–4288.
- (403) Jankova, K.; Kops, J.; Chen, X.; Batsberg, W. *Macromol. Rapid Commun.* **1999**, *20*, 219–223.
- (404) Wang, X.-s.; Luo, N.; Ying, S.-k.; Liu, Q. *Eur. Polym. J.* **2000**, *36*, 149–156.
- (405) Jankova, K.; Truelsen, J. H.; Chen, X.; Kops, J.; Batsberg, W. *Polym. Bull.* **1999**, *42*, 153–158.
- (406) Jankova, K.; Chen, X.; Kops, J.; Batsberg, W. *Macromolecules* **1998**, *31*, 538–541.
- (407) Cheng, S.; Xu, Z.; Yuan, J.; Ji, P.; Xu, J.; Ye, M.; Shi, L. *J. Appl. Polym. Sci.* **2000**, *77*, 2882–2888.
- (408) Bednarek, M.; Biedron, T.; Kubisa, P. *Macromol. Rapid Commun.* **1999**, *20*, 59–65.
- (409) Nakagawa, Y.; Miller, P. J.; Matyjaszewski, K. *Polymer* **1998**, *39*, 5163–5170.
- (410) Jiang, X.; Yan, D.; Zhong, Y.; Liu, W.; Chen, Q. *Polym. Int.* **2000**, *49*, 893–897.
- (411) Matyjaszewski, K.; Ziegler, M. J.; Arehart, S. V.; Greszta, D.; Pakula, T. *J. Phys. Org. Chem.* **2000**, *13*, 775–786.
- (412) Kim, C. S.; Oh, S. M.; Kim, S.; Cho, C. G. *Macromol. Rapid Commun.* **1998**, *19*, 191–196.
- (413) Asgarzadeh, F.; Ourdouillie, P.; Beyou, E.; Chaumont, Ph. *Macromolecules* **1999**, *32*, 6996–7002.
- (414) Heise, A.; Nguyen, C.; Malek, R.; Hedrick, J. L.; Frank, C. W.; Miller, R. D. *Macromolecules* **2000**, *33*, 2346–2354.
- (415) Ohno, K.; Fujimoto, K.; Tsujii, Y.; Fukuda, T. *Polymer* **1999**, *40*, 759–763.
- (416) Wu, X.; Fraser, C. L. *Macromolecules* **2000**, *33*, 7776–7785.
- (417) Fraser, C. L.; Smith, A. P.; Wu, X. *J. Am. Chem. Soc.* **2000**, *122*, 9026–9027.
- (418) Tsolakis, P. K.; Koulouri, E. G.; Kallitsis, J. K. *Macromolecules* **1999**, *32*, 9054–9058.
- (419) Heise, A.; Hedrick, J. L.; Trollsås, M.; Miller, R. D.; Frank, C. W. *Macromolecules* **1999**, *32*, 231–234.
- (420) Heise, A.; Hedrick, J. L.; Frank, C. W.; Miller, R. D. *J. Am. Chem. Soc.* **1999**, *121*, 8647–8648.
- (421) Angot, S.; Murthy, K. S.; Taton, D.; Gnanou, Y. *Macromolecules* **1998**, *31*, 7218–7225.
- (422) Angot, S.; Murthy, K. S.; Taton, D.; Gnanou, Y. *Macromolecules* **2000**, *33*, 7261–7274.

- (423) Hovestad, N. J.; van Koten, G.; Bon, S. A. F.; Haddleton, D. M. *Macromolecules* **2000**, *33*, 4048–4052.
- (424) Johnson, R. M.; Corbin, P. S.; Ng, C.; Fraser, C. L. *Macromolecules* **2000**, *33*, 7404–7412.
- (425) Baek, K.-Y.; Kamigaito, M.; Sawamoto, M. *Macromolecules* **2001**, *34*, 215–221.
- (426) Baek, K.-Y.; Kamigaito, M.; Sawamoto, M. *Macromolecules* **2001**, *34*, 7629–7635.
- (427) Xia, J.; Zhang, X.; Matyjaszewski, K. *Macromolecules* **1999**, *32*, 4482–4484.
- (428) Yamada, K.; Miyazaki, M.; Ohno, K.; Fukuda, T.; Minoda, M. *Macromolecules* **1999**, *32*, 290–293.
- (429) Haddleton, D. M.; Perrier, S.; Bon, S. A. F. *Macromolecules* **2000**, *33*, 8246–8251.
- (430) Beers, K. L.; Gaynor, S. G.; Matyjaszewski, K. *Macromolecules* **1998**, *31*, 9413–9415.
- (431) Ross, S. G.; Müller, A. H. E.; Matyjaszewski, K. In *Controlled/Living Radical Polymerization*; Matyjaszewski, K., Ed.; ACS Symposium Series 768; American Chemical Society: Washington, DC, 2000; Chapter 25, pp 361–371.
- (432) Grubbs, R. B.; Hawker, C. J.; Dao, J.; Fréchet, J. M. J. *Angew. Chem., Int. Ed. Engl.* **1997**, *36*, 270–272.
- (433) Liu, S.; Sen, A. *Macromolecules* **2000**, *33*, 5106–5110.
- (434) Truelsen, J. H.; Kops, J.; Batsberg, W. *Macromol. Rapid Commun.* **2000**, *21*, 98–102.
- (435) Fónagy, T.; Iván, B.; Szesztay, M. *Macromol. Rapid Commun.* **1998**, *19*, 479–483.
- (436) Pan, Q.; Liu, S.; Xie, J.; Jiang, M. *J. Polym. Sci., Part A: Polym. Chem.* **1999**, *37*, 2699–2702.
- (437) Wang, X.-S.; Luo, N.; Ying, S.-K. *Polymer* **1999**, *40*, 4515–4520.
- (438) Matyjaszewski, K.; Teodorescu, M.; Miller, P. J.; Peterson, M. L. *J. Polym. Sci., Part A: Polym. Chem.* **2000**, *38*, 2440–2448.
- (439) Paik, H.-j.; Gaynor, S. G.; Matyjaszewski, K. *Macromol. Rapid Commun.* **1998**, *19*, 47–52.
- (440) Percec, V.; Asgarzadeh, F. *J. Polym. Sci., Part A: Polym. Chem.* **2001**, *39*, 1120–1135.
- (441) Jones, R. G.; Holder, S. J. *Macromol. Chem. Phys.* **1997**, *198*, 3571–3579.
- (442) Fréchet, J. M. J.; Henmi, M.; Gitsov, I.; Aoshima, S.; Leduc, M. R.; Grubbs, R. B. *Science* **1995**, *269*, 1080–1083.
- (443) Matyjaszewski, K.; Gaynor, S. G.; Kulfan, A.; Podwika, M. *Macromolecules* **1997**, *30*, 5192–5194.
- (444) Matyjaszewski, K.; Gaynor, S. G.; Müller, A. H. E. *Macromolecules* **1997**, *30*, 7034–7041.
- (445) Yan, D.; Müller, A. H. E.; Matyjaszewski, K. *Macromolecules* **1997**, *30*, 7024–7033.
- (446) Matyjaszewski, K.; Pyun, J.; Gaynor, S. G. *Macromol. Rapid Commun.* **1998**, *19*, 665–670.
- (447) Cheng, G.; Simon, P. F. W.; Hartenstein, M.; Müller, A. H. E. *Macromol. Rapid Commun.* **2000**, *21*, 846–852.
- (448) Jiang, X.; Zhong, Y.; Yan, D.; Yu, H.; Zhang, D. *J. Appl. Polym. Sci.* **2000**, *78*, 1992–1997.
- (449) Maier, S.; Sunder, A.; Frey, H.; Mülhaupt, R. *Macromol. Rapid Commun.* **2000**, *21*, 226–230.
- (450) Ejaz, M.; Yamamoto, S.; Ohno, K.; Tsujii, Y.; Fukuda, T. *Macromolecules* **1998**, *31*, 5934–5936.
- (451) Yamamoto, S.; Ejaz, M.; Tsujii, Y.; Matsumoto, M.; Fukuda, T. *Macromolecules* **2000**, *33*, 5602–5607.
- (452) Yamamoto, S.; Ejaz, M.; Tsujii, Y.; Fukuda, T. *Macromolecules* **2000**, *33*, 5608–5612.
- (453) Ejaz, M.; Ohno, K.; Tsujii, Y.; Fukuda, T. *Macromolecules* **2000**, *33*, 2870–2874.
- (454) Husseman, M.; Malmström, E. E.; McNamara, M.; Mate, M.; Mecerreyes, D.; Benoit, D. G.; Hedrick, J. L.; Mansky, P.; Huang, E.; Russell, T. P.; Hawker, C. J. *Macromolecules* **1999**, *32*, 1424–1431.
- (455) Shah, R. R.; Merrezeys, D.; Husemann, M.; Rees, I.; Abbott, N. L.; Hawker, C. J.; Hedrick, J. L. *Macromolecules* **2000**, *33*, 597–605.
- (456) Kim, J.-B.; Bruening, M. L.; Baker, G. L. *J. Am. Chem. Soc.* **2000**, *122*, 7616–7617.
- (457) von Werne, T.; Patten, T. E. *J. Am. Chem. Soc.* **1999**, *121*, 7409–7410.
- (458) Böttcher, H.; Hallensleben, M. L.; Nuß, S.; Wurm, H. *Polym. Bull.* **2000**, *44*, 223–229.
- (459) Mandal, T. K.; Fleming, M. S.; Walt, D. R. *Chem. Mater.* **2000**, *12*, 3481–3487.
- (460) Marsh, A.; Khan, A.; Garcia, M.; Haddleton, D. M. *Chem. Commun.* **2000**, 2083–2084.

CR9901182

Catalytic Chain Transfer in Free-Radical Polymerizations

Alexei A. Gridnev*

DuPont Performance Coatings, 2401 Grays Ferry Avenue, Philadelphia, Pennsylvania 19146

Steven D. Ittel*

DuPont Central Research and Development, Experimental Station, Wilmington, Delaware 19880-0328

Received February 12, 2001

Contents

1. General Features of Catalytic Chain Transfer	3611
1.1. Free-Radical Polymerization	3611
1.2. Catalytic Chain Transfer	3612
2. Catalysts	3617
2.1. Catalyst Screening	3617
2.2. Cobalt Catalyst Activities	3618
2.3. Non-Cobalt CCT Catalysts	3623
3. Mechanism	3623
3.1. Reaction Schemes	3623
3.2. Hydrogen Atom Abstraction and Catalyst Structure	3625
3.3. Hydrogen Atom Addition	3626
3.4. Alternative Mechanisms for Olefin Reactions with Co ^{III} -H	3628
3.5. Living Radical Polymerizations	3630
3.6. Catalytic Inhibition of Polymerization	3632
3.7. Catalyst Poisons and Other Adverse Reactions	3633
4. Monomers for CCT	3636
4.1. Methacrylates	3636
4.1.1. Di- and Trimethacrylates	3636
4.1.2. Emulsion Polymerization	3637
4.2. Methacrylonitrile	3638
4.3. α -Methyl Styrene	3638
4.4. Styrene	3638
4.5. Acrylates	3639
4.6. Acrylonitrile	3640
4.7. Dienes	3641
4.8. Macromonomer Reinitiation and Nonpolymerizable Monomers	3641
4.9. Isomerizational CCT	3642
4.10. Copolymerizations	3643
5. Applications of CCT Products	3645
5.1. Reduction of MW	3646
5.2. Macromonomers for Graft Copolymers	3648
5.3. RAFT	3648
5.4. Copolymerization (Graft-Copolymers)	3649
5.5. Hyperbranched and Cross-Linked Materials	3649
6. Conclusions	3649
7. Glossary	3650
8. References	3650

1. General Features of Catalytic Chain Transfer

1.1. Free-Radical Polymerization

While free-radical chain reactions were known shortly after the turn of the 20th century, it was not until the mid-1930s that free-radical polymerization was recognized. Today, free-radical polymerization finds application in the synthesis of many important classes of polymers including those based upon methacrylates, styrene, chloroprene, acrylonitrile, ethylene, and the many copolymers of these vinyl monomers. Many good reviews and books on this subject are available.^{1,2}

Free-radical polymerizations are subject to the many complications one might expect of radical chemistry, but the simple underlying mechanism is composed of three primary processes—*initiation*, *propagation*, and *termination*. Generally, the *initiation* takes place by cleavage of an azo or peroxide compound (the “initiator”) to yield the “primary radical”. In this paper, the chemistry will be limited to azo initiators because peroxides interfere with subsequent chemistry (see section 3.7). The *propagation* or growth reaction occurs when monomers add to the primary radical or to the radical at the end of the growing polymer chain. *Termination* occurs primarily by the bimolecular reaction of two growing polymer radicals. The two primary mechanisms observed are radical–radical combination and disproportionation in which one radical abstracts a hydrogen atom from another radical resulting in one saturated chain end and one olefinic chain end. In addition to these primary reactions, there are a variety of other reactions that occur. There may be very low levels of *chain transfer* to monomer, a reaction that leads to termination of one chain with simultaneous initiation of another new chain so that there is no change in the number of radical species present.

The propagation reaction in free-radical polymerizations is rapid.¹ One important feature of the polymerization is that high molecular weight polymer is formed even at very low levels of monomer conversion. Thus, each propagating radical or its progeny lives for well under a minute. To control molecular weights in these polymerizations, the use of chain



Alexei Gridnev graduated with his Masters degree from Moscow University of Fine Chemical Technology, Russia, in 1979 with majors in synthesis and technology of biologically active compounds. The same year he was employed by the Semenov Institute of Chemical Physics of the Russian Academy of Sciences, where he studied catalysis of chain transfer to monomer. In 1984 he received his Doctorate degree in Polymer Science. In 1986 Dr. Gridnev was transferred to the Institute of Physico-Technical Research of the Russian Academy of Sciences as a senior research chemist to work on several projects including the synthesis of model compounds for biochemical research. In 1992 he moved to the University of Pennsylvania in the laboratory of Professor Brad Wayland, where he continued the study of hydrogen transfer in reactions of free radicals with cobalt chelates as a senior research associate. In 1994 he began work for E.I. DuPont de Nemours and Co., first in CR&D in Wilmington, DE, and later at Marshall Laboratory in Philadelphia, PA. Alexei Gridnev is the author of more than 50 articles and patents, predominantly in the area of catalysis of free-radical processes.



Steve Ittel was born in Hamilton, OH (1946), and received his B.S. degree in Chemistry from Miami University in 1968. After two years of studying photochemical smog in the greater New York City area for the USPHS, he attended Northwestern University, where he received his Ph.D. degree in Inorganic Chemistry in 1974 with Jim Ibers. Joining DuPont's Central Research, he was involved in the elucidation of fluxional processes in five- and seven-coordinate inorganic complexes. After work on C-H activation, diamagnetic and paramagnetic agostic M-H-C interactions, and cyclohexane oxidation, he moved to research management. Never straying far from the scientific edge, he has been involved in small molecule catalysis including hydrocarbon oxidation, fluoro-organometallic chemistry, and olefin hydrocyanation. The molecules started getting larger as his interests turned toward elastomeric polypropylene, catalytic chain transfer in free-radical polymerizations, and most recently ethylene polymerization with polar comonomers. He has over 100 publications and patents and a book to his credit. Another interest, having both technical and aesthetic aspects, is the nurture and styling of a collection of about 100 bonsai.

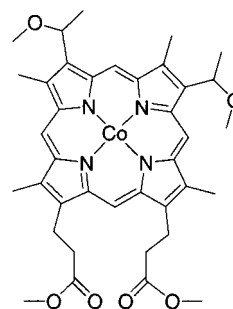
terminators is often employed.³ Thus, compounds such as thiols will react with a growing polymer chain to yield a thiol-terminated species.^{4,5} In this instance, there would be only one polymer chain per

initiating radical and each polymer chain would be terminated stoichiometrically by one thiol. This approach is acceptable for moderate molecular weights but becomes problematic for the synthesis of very low molecular weight species.

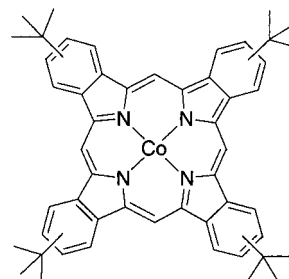
In general, radical reactions are not selective. The polymerizations allow only a limited degree of control. For instance, tacticity of the polymerization may be controlled by the addition of Lewis acids.⁶ The reactivity ratios of monomers and rates of polymerization can also be controlled by the addition of Lewis acids.⁷⁻⁹

1.2. Catalytic Chain Transfer

In 1975, Boris Smirnov and Alexander Marchenko discovered a method in which they could control the molecular weight in a methacrylate polymerization by introducing catalysts that could greatly enhance the process of chain transfer to monomer.¹⁰ They found that substituted cobalt porphyrins, **1**, or benzoporphyrins, **2**, provided dramatic reductions in the molecular weight of the methacrylate polymers during radical polymerization with little to no reduction in overall yield of polymer.¹¹⁻¹⁵



1, cobalt tetramethoxy hematoporphyrin-IX



2, cobalt tetra-(*tert*-butylbenzo)porphyrin

The catalytic chain-transfer (CCT) process displays all of the features characteristic of typical, uncatalyzed chain transfer other than taking place at a rate competitive with chain propagation. Thus, the rate of polymerization at low conversions is independent of the concentration of the cobalt porphyrin (Figure 1) while the molecular weight, \bar{M}_n , decreases linearly by over 2 orders of magnitude with increasing concentration of cobalt catalyst (Figure 2). As expected for a typical polymerization, the rate of polymerization increases linearly with the square root of the concentration of the azo initiator and no polymerization occurs in the absence of the initiator.

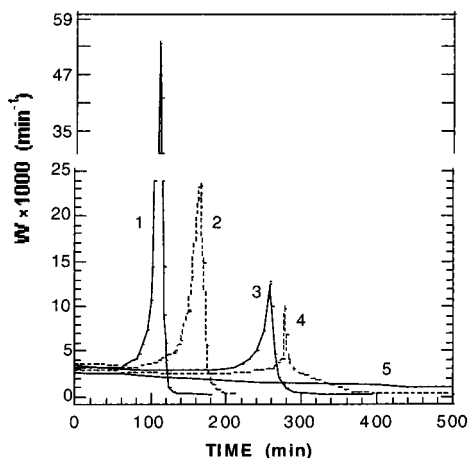


Figure 1. Temporal dependence of the rate of polymerization of bulk MMA under CCT conditions.

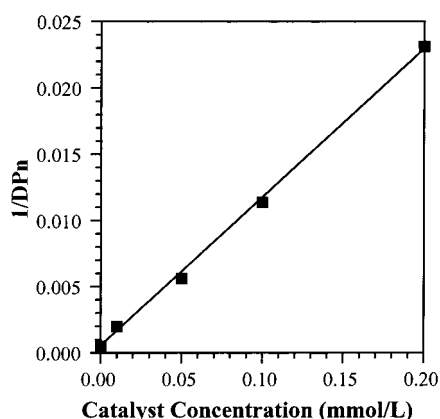


Figure 2. Dependence of $(DP_n)^{-1}$ on the concentration of Co^{II} -mesoporphyrin-II.

Free-radical polymerizations of bulk monomers are subject to the gel effect or Trommsdorff effect.¹⁶ Figure 1 also indicates that CCT suppresses the gel effect. Because the resulting product is lower in molecular weight, the viscosity of the polymerizing medium is not as high at a given degree of conversion. Thus, the observed sharp maxima in the rates of polymerization at time τ can be used as a quantitative measure of the chain-transfer constant of CCT.¹⁷ At 60 °C in a bulk polymerization of MMA initiated with 0.04 mol/L AIBN, the following empirical equation relates the chain-transfer constant of CCT, k_C , to the concentration of cobalt catalyst, $[LCo]$, in mol/L and the time of maximum polymerization rate, τ , in minutes¹⁸

$$\frac{400}{\tau} = 3.6 - \lg(k_C[LCo]) \quad (1)$$

The linearity of this relationship is demonstrated in Figure 3. Any deviation from linearity from eq 1 indicates complications in the course of the polymerization. The complications are typically catalyst poisoning or polymerization retardation (see section 3.6).

The cobalt porphyrin, $PorCo$, was recovered from the product by flash chromatography and reused several times without any detectable change in molecular structure, clearly indicating the catalytic

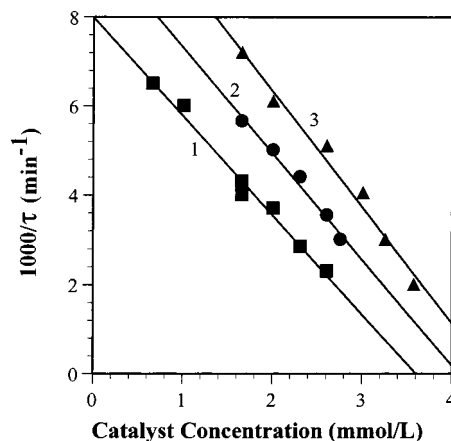
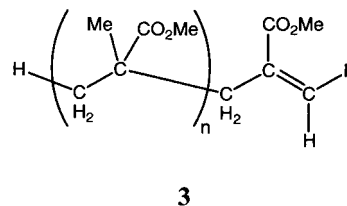


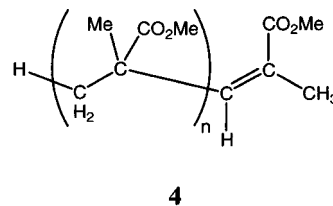
Figure 3. Dependence of reciprocal time of the maximum polymerization rate on the concentration of catalyst for Co^{II} -mesoporphyrin-II (1), Co^{III} (pyridine)bis(dimethylglyoximate) iodide (2), and Co^{II} tetra-*tert*-butylbenzporphyrin (3).

character of the process of molecular weight reduction.

NMR analysis of the resulting oligomers,^{19–22} supported by IR spectroscopy²³ and labeling experiments,¹⁹ indicated that the product of methyl methacrylate polymerizations is **3**.

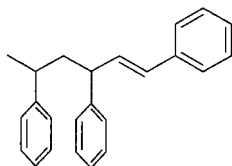


The same species has been observed in the spontaneous polymerization of MMA, but its yield is limited to at most 50% because it arises from disproportionation of two radical chains.²⁴ In low productivity polymerizations, some product derived from the initiating radical could be observed, but in high conversion polymerizations, it appeared that virtually all of the product molecules were initiated with a hydrogen atom and terminated with an olefinic end group. This polymeric product can be formed in the presence of cobalt porphyrin only by hydrogen transfer from the α -methyl group of methacrylate end unit of the propagating radical to monomer. The turn-over number of this reaction was calculated to be at least 10^6 , while selectivity is virtually quantitative.^{2,25,26} It is the quantitative nature of the double bond formation that makes this new product useful in a number of applications. It is interesting that the isomeric compound, **4**, is not observed in the reaction mixture even though it is more stable thermodynamically.²⁷



The kinetic preference for **3** could be attributed to steric screening of the internal methylene protons near the tertiary carbon center through their interaction with the large planar porphyrin molecule.

Styrene lacks a methyl group on the propagating radical, so chain termination must lead to a different type of product. A thorough analysis has led to the conclusion that the product is terminated exclusively by a trans substituted olefinic group.²⁸ For example, the trimer is **5**.

**5**

One of the most striking features of CCT is the exceptionally fast rate at which it takes place. The molecular weight of a polymer can be reduced from tens of thousands to several hundred utilizing concentrations of cobalt catalyst as low as 100–300 ppm or $\sim 10^{-3}$ mol/L. The efficiency of catalysis can be measured as the ratio between the chain-transfer coefficients of the catalyzed reaction versus the uncatalyzed reaction. The chain-transfer constant to monomer, C_M , in MMA polymerization is believed to be approximately 2×10^{-5} .²⁹ The chain-transfer constant to catalyst, C_C , is as high as 10^3 for porphyrins and 10^4 for cobaloximes. Hence, improved efficiency of the catalyzed relative to the uncatalyzed reaction, C_C/C_M , is $10^4/10^{-5}$ or 10^9 . This value for the catalyst efficiency is comparable to many enzymatically catalyzed reactions whose efficiencies are in the range of 10^9 – 10^{11} .¹⁸ The rate of hydrogen atom transfer for cobaloximes, the most active class of CCT catalysts to date, is so high that it is considered to be controlled by diffusion.^{5,30–32} Indeed, k_C in this case is comparable to the termination rate constant.³³

The very high rates of catalytic chain transfer finally made it practical to prepare low molecular weight oligomers by free-radical polymerization. The chemistry of low molecular weight oligomers was relatively unexplored for several reasons. Previous routes to oligomers involved complicated and unpleasant chemistry or were very expensive. Thiol chain termination required high levels of chain-transfer agents, leaving high levels of toxic or malodorous residues. It is also possible to obtain low molecular weight species by utilizing high levels of initiator, but in addition to being expensive, high levels of azo initiators can lead to toxic cross-coupling products. Living polymerizations required high levels of initiator or catalysts because each initiator leads to only one macromonomer, making them commercially unattractive when low molecular weights are required. A further reason was that the main objective of polymer science had generally been the synthesis of high molecular and even ultrahigh molecular weight species, primarily to improve mechanical properties. Recent changes in industrial requirements have brought lower molecular weight

species into focus. For example, the lower solvent content required to meet low VOC constraints for paints³⁴ brings renewed interest in low-viscosity oligomers that can be cured during or shortly after application.^{35,36} Highly structured pigment dispersants for paints and other applications are often based upon block copolymers³⁷ accessible through macromonomers, and ink-jet printers require sophisticated polymer formulations to achieve the very rigorous set of demands placed upon those systems.³⁸

The Mayo equation is often used to determine chain-transfer constants.³⁹ C_s is determined from measurements of DP_n over a range of $[S]/[M]$ with the provision that DP_n^0 remains constant throughout the range evaluated.^{40,41} A plot of $1/DP_n$ versus $[S]/[M]$ yields a straight line with a slope of C_s and intercept of DP_n^0 . Catalytic chain transfer obeys the Mayo equation well for DP_n of 20 and higher. When DP_n is less than 20, there is an apparent deviation from linearity for DP_n versus the concentration of the cobalt catalyst. This phenomenon was observed for methacrylate.¹⁴ It appears that at low molecular weights or high catalyst concentrations, the catalyst is losing activity (Figure 4).

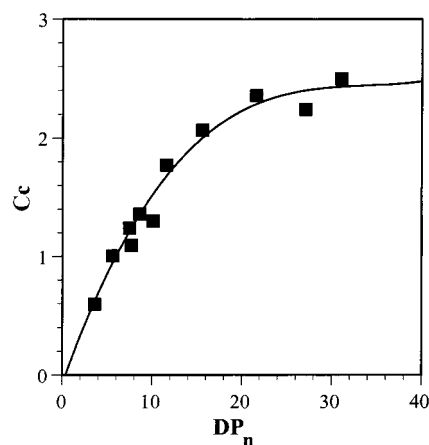


Figure 4. Dependence of the average chain-transfer constant on the number-average degree of polymerization. Data are taken from ref 14.

This unusual behavior was detected for measurements of polydispersity as well. While polydispersity is close to 2 for $DP_n > 20$ as expected for free-radical polymerizations in which there is a high level of chain transfer,^{40,42} the polydispersity index decreases to values approaching 1.1–1.2 for $DP_n < 10$. To explain this unusual behavior for C_c , low MMA oligomers were separated into fractions by HPLC⁴³ and C_c was calculated for each individual radical, $C_{C(n)}$. The resulting dependence of $C_{C(n)}$ on DP is shown in Figure 5.

$C_{C(n)}$ stays unchanged for DP values down to 6, and then it starts to diminish rapidly. C_c by definition is an “average” term, and as a result, it does not change as rapidly with decreasing degree of polymerization as does $C_{C(n)}$. Having determined $C_{C(n)}$ for each “ n ”, one can now plot the calculated dependence of C_c against DP_n . The calculated dependence does not correlate well with the earlier results.¹⁴ In fact, evidence that indicates that C_c decreases with increasing chain length has been reported.^{44,45} A viable

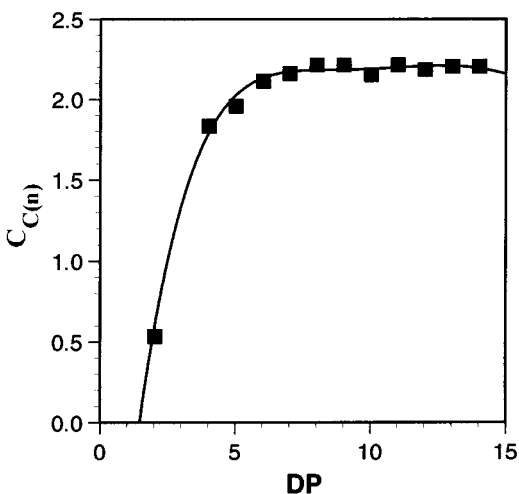


Figure 5. Dependence of $C_{C(n)}$ on DP.

explanation for the ambiguity at these low molecular weights was not recognized until later.^{46,47}

As mentioned above, free-radical oligomerizations of acrylates to DP of less than 10 were little explored at the time that CCT was discovered. Methods of polymer characterization developed for high molecular weight polymers begin to fail at these low oligomers, though new methods are being developed.^{48,49} End groups are generally not important in the chromatography of high polymers. With the decrease of molecular weights down to several hundred, the physical effects of end groups become more important. They can change fundamental parameters such as refractive indexes and UV absorptions. Because UV absorption and refractive index, primary tools for detection in chromatographic techniques, were dependent on DP_n , quantification of analyses was made more difficult.^{46,47} Figure 6 shows that

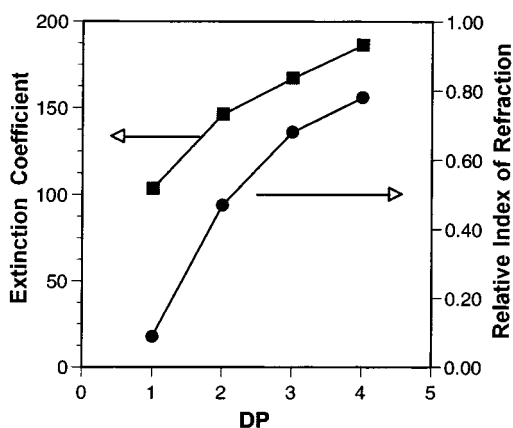


Figure 6. Dependence of the extinction coefficient and relative index of refraction of low MMA oligomers on the degree of polymerization.

these parameters for MMA dimers differ from those of high polymer by over 50% with smaller differences for higher oligomers. For example, if a solvent with a refractive index close to that of MMA dimer is used in the analysis, errors can be substantial. In an extreme example, the use of toluene for the analysis would give inverse peaks for all of the low oligomers while high polymer would give a positive peak. Some moderate oligomers would be invisible to the analy-

sis. Failure to consider the change in physical properties of low oligomers may result in substantial differences between the calculated and observed dependence of C_C on DP_n . Molecular weights for higher polymers may be transformed via the known Mark-Houwink-Sakurada (MHS) constants for poly(methyl acrylate).⁵⁰ The MHS constants should be used only for a specified molecular weight range because at low molecular weights the MHS constants are a function of chain length.⁵¹ A similar effect has been quantified in styrene oligomers, and the effect is detectable out to hexamers.²⁸

The terminal double bond becomes an issue in the thermodynamic calculation of conversion as well. Polymerization of olefinic molecules can generally be described as the conversion of double bonds into two single bonds. While not an issue for high polymers, any double bonds remaining in the final product decrease the thermodynamic parameters associated with this process. Thus, the heat of polymerization in the CCT process decreases according to eq 2⁵²

$$\frac{\Delta H_n}{\Delta H_\infty} = \frac{DP_n - 1}{DP_n} \quad (2)$$

where ΔH_n is the heat of polymerization when the degree of polymerization equals n and ΔH_∞ is the heat of polymerization for high polymer. For $DP_n > 8$, the resulting error would be less than 10%, but with MW reduction below this number, the effect of the chain end becomes more pronounced. Other parameters, like the volume reduction during polymerization, should follow the same pattern. The reduction in the heat of polymerization could be one of the reasons for the reported¹² minor (<20%) reduction of initial catalyst activity when concentrations of active catalysts are greater than 0.005 mol/L. Another reason for reduction of catalyst activity at the beginning of polymerization is the formation of $LCo-R_n$ (section 3.2).

A full understanding of polymerizations resulting in $DP_n < 8$ requires additional theoretical consideration and reevaluation of many of the well-known and widely used equations and relationships. The Mayo equation (eq 3) provides a good example of a relationship established for high polymer that fails when extended to oligomers.

$$\frac{1}{DP_n} = \frac{1}{DP_{n0}} + \frac{k_c[LCo]}{k_p[M]} \quad (3)$$

M is monomer, and DP_n and DP_{n0} are the number-average degree of polymerization corresponding to those obtained with and without chain-transfer agent. In an extreme, at elevated levels of an active catalyst (for example $k_c = 10^7$ L/mol·s and $[LCo] = 0.01$ mol), the calculated DP_n can be less than 1, clearly an impossible situation. Hence, the Mayo equation in its standard form is not applicable for many cases of CCT when low oligomers are being prepared. Rede-termination of the dependence of the number-average degree of polymerization on the concentrations of

monomer and CCT catalyst concentration in the short-chain approximation gives eq 4⁵²

$$\frac{1}{DP_n - 2} = \frac{1}{DP_{n0}} + \frac{k_c[\text{LCo}]}{k_p[\text{M}]} \quad (4)$$

For high polymer, eq 4 is indistinguishable from eq 3. For the case of intensive CCT, when the MW of the resulting product is low, eq 4 can be reduced to eq 5

$$DP_n = 2 + \frac{k_p[\text{M}]}{k_c[\text{LCo}]} \quad (5)$$

There also arises an interesting semantic issue. Equation 5 indicates that product lower than the dimer cannot be obtained by CCT. Clearly, the actual degree of polymerization is quantized in units of one and DP_1 is called “starting material”. Nonetheless, at high levels of an active catalyst, starting monomer is frequently converted to radical and then back to “monomeric product” before addition of a second monomer can occur. At $DP_n < 12-15$, deviation from the linear dependence of DP_n on the concentration of catalytic chain-transfer agent are observed as expected.¹⁴ At the same time, the polydispersity (if this is a meaningful term) narrows and becomes dependent upon DP_n according to eq 6

$$\frac{DP_w}{DP_n} = 2 - \frac{3}{DP_n} + \frac{2}{(DP_n)^2} \quad (6)$$

This expression also differs from the text book definition. Hence, the observed narrowing of polydispersity and reduction of observed catalytic activity in CCT under high concentrations of an active catalyst has, at least in part, kinetic origins.

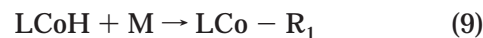
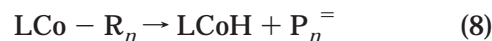
To understand the distribution of products in the low-MW region, it is important to realize that for low molecular weight polymeric radicals, the many different chain-transfer constants may depend on DP_n . The length dependence of chain-transfer constants for short radicals can be significant. Thus, k_p of the dimeric radicals of MMA and MAN are about 20 times higher than those of high polymeric radicals, but the difference diminishes rapidly with growth of the radical. Pulsed-laser methods have been utilized extensively for the determination of free-radical polymerization kinetics and have been the subject of a review.⁵⁰ The technique allows the investigation of chain length dependence not only for chain propagation but also for chain termination.⁵³⁻⁵⁶ Care must be taken in doing the experiments and utilizing the results.⁵⁷ Other techniques involving nitroxides⁵⁸ and computational chemistry⁵⁹ have been suggested. Nonetheless, the pulsed laser technique remains the IUPAC-recommended approach.⁶⁰

The difference in propagation rate constants of the low molecular weight species was also demonstrated using a technique based upon CCT. At high rates of CCT, only small radicals are present in the system. This makes it possible to measure the rates of propagation and chain transfer separately by gradual changes in the concentration of chain-transfer cata-

lyst.⁶¹ Discussion of the absolute propagation rate constants of small radicals is not related directly to the purpose of this review, but there are two points worth making.

First, the chain-transfer coefficient, k_c , is almost independent of radical lengths despite the array of claims in the literature.⁴⁴⁻⁴⁷ Thus, k_c of the meso-tetraphenyl derivative of Co-porphyrin with the dimeric MMA radical is 2.8×10^6 L/mol·s versus 2.4×10^6 L/mol·s for high polymer. As a result, C_c decreases with DP_n because $C_c = k_c/k_p$. The reason that k_c is independent of the size of the radical is not clear. CCT seems to be diffusion controlled, and the large size and required orientation of the porphyrin molecule may be controlling. It cannot be excluded that the rate of CCT is determined by the rate of formation of intermediate species such as a caged radical pair. In the latter case with low molecular weight species, one might observe length dependence of the k_c for highly active CCT catalyst, like cobaloximes.

The second significant point is that propagation in the presence of the cobalt catalyst occurs by a free-radical mechanism, not by a coordination polymerization mechanism described by eqs 7-9 as suggested in some publications.^{2,62-64}



The main evidence is that the values of k_c for the small radicals obtained with the CCT-based method are very close to those obtained by other methods.^{55,65} This is not to say that formation of a Co-C bond does not occur; it is simply not an important step on the catalytic cycle.⁶⁶ It does, however, remove catalyst from the catalytic cycle.

To conclude the introduction, all of the phenomena of CCT are fully explained by normal free-radical polymerization once a short-chain approximation has been applied. Experimental data indicates that the short-chain approximation becomes important for $DP_n < 15$ and $DP < 6$. Equations 4-6 were obtained with the simplifying assumptions that chain-transfer constants do not depend on the degree of polymerization, though this is known to be incorrect. Nonetheless, they provide a closer description of reality than do the descriptions formulated for high polymer. The exact dependence of DP_n and DP_w requires knowledge of all rate constants for each radical.

Theoretical investigations have been used to model coenzyme B₁₂. While important conclusions may be drawn, the work has not been extended with CCT in mind. Due to computational limitations, the initial work was limited to the triaminomethylcobalt^{III}-amide system.⁶⁷ Force fields specifically designed to do molecular mechanical calculations on cobalamins⁶⁸ and cobaloximes⁶⁹ are relevant for conformational studies but cannot elucidate the mechanisms of cobaloxime reactions because they do not account for electronic effects. Computational investigation of

Table 1. Effect of Substituents on MMA CCT Activity for Cobaloximes 6^a, 7^b and 8

compound	X ₁	X ₂	A or E	E (base)	C _c	ref
6a	Me	Me	Me	H ₂ O	<50	77
6b		-(CH ₂) ₄ -	Et	H ₂ O	<50	77
6c	Me	Me	CN	Py	<50	77
6d	Me	Me	NO ₂	Py	<50	77
6e	Ph	Ph	CN	Py	<50	77
6f	Ph	Ph	Et	H ₂ O	<50	77
6g	Me	Me	Cl	Py	5 000	77
6h	Me	Me	I	Py	1 000	77
6i	Me	Me	CNS	Py	4 000	77
6j	Me	Me	sec-Bu	H ₂ O	13 000	77
6k	Ph	Ph	CNS	Py	25 000	77
6l	Me	COOEt	Cl	Py	12 000	77
6m	Me	COMe	Cl	Py	25 000	77
6n		-(CH ₂) ₄ -	Cl	Py	4 000	77
6o	α-furyl	α-furyl	Cl	Py	100 000	77
6p	Ph	Ph	Cl	H ₂ O	25 000	77
6q	Ph	Ph	Cl	Py	30 000	77
6r	Ph	Ph	Cl	P(Ph) ₃	100 000	77
6s	Me	Me	Py	Py	2 100	78
6s ^e	Me	Me	Py	Py	700	79
6t	Me	Me	NEt ₃	NEt ₃	1 600	78
6u	Me	Me	PPh ₃	PPh ₃	4 100	78
6u	Me	Me	PPh ₃	PPh ₃	20 000	44
7a			Cl		11 000	77
7b			ClO ₄		<50	77
7c			NO ₃		<50	77
8a ^c	Me	Me			11 000	77
8b ^d	Ph	Ph			66 000	77

^a Run in bulk MMA at 60 °C. ^b Measured in MMA:methanol = 7:3 v/v at 60 °C. ^c MMA:methanol = 7:3 v/v. ^d MMA:methanol = 7:3 v/v + 1% Py. ^e MMA:methanol = 1:1 v/v.

relative bond-breaking energetics requires quantum mechanics, and until recently, few calculations have been attempted because of their large size. Semiempirical models have been important in the discussion of the balance between steric and electronic effects in B₁₂ reactions,⁷⁰ but they are not effective for the determination of equilibrium structures. DFT calculations are expected to provide higher accuracy. Calculation of nuclear quadrupole couplings of simple coenzyme B₁₂ models without a planar framework proved to be reasonable.⁷¹ The B3LYP method has been used to evaluate the equilibrium structures of corrin models with different axial alkyl groups.⁷² The equilibrium structures of methyl B₁₂ and adenosyl B₁₂ have a different electronic structure for the two Co–C bonds. The HOMO energy is higher in AdoB₁₂ than in MeB₁₂, favoring homolytic cleavage because of the 5'-deoxyadenosyl group that induces more electron density on cobalt. This may explain part of the homolysis heterolysis dichotomy. Comparison of the computational geometries with experimental results⁷³ suggests two very different reaction coordinates for the two coenzymes related to competitive heterolysis or homolysis of the two respective Co–C bonds.⁷⁴ Unfortunately, these studies invoke chemical and structural differences that are not available to the catalysts in CCT.

2. Catalysts

2.1. Catalyst Screening

Testing new compounds for catalytic chain-transfer activity in free-radical polymerizations is an interest-

Table 2. Influence of Cobaloximes 6 Substituents on CCT Activity in Styrene^{a,77}

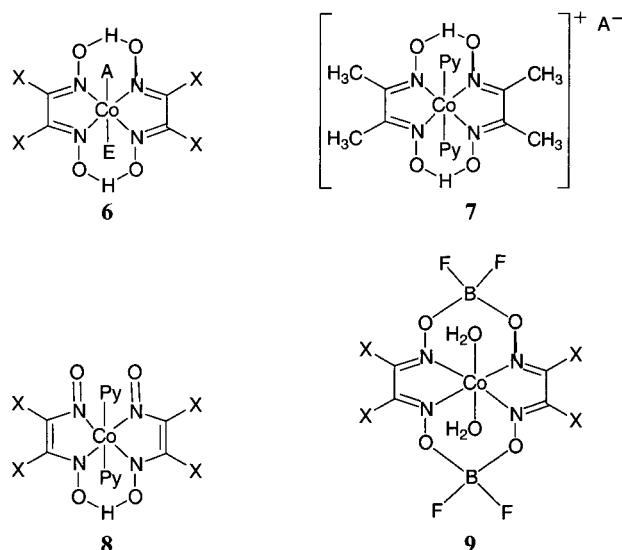
compound	X ₁	X ₂	A	E (base)	C _c
6a	Me	Me	Me	H ₂ O	<4
6d	Me	Me	NO ₂	Py	<4
6e	Ph	Ph	CN	Py	<4
6g	Me	Me	Cl	Py	450
6n		-(CH ₂) ₄ -	Cl	Py	300
6q	Ph	Ph	Cl	Py	350
6r	Ph	Ph	Cl	P(Ph) ₃	500

^a Bulk styrene, 60 °C.

ing science and art. Choosing the optimal testing conditions is crucial for getting reliable results. Side reactions can both mask and mimic CCT so that considerable judgment is required. The results of polymerization in the presence of cobalt chelates depend on temperature, solvent, pH, the sterics and electronics of the chelating ligand, the presence of additional ligands, and the monomer chosen. Minute concentrations of impurities, particularly oxygen,^{75,76} in the reaction media or even in the tested complex may corrupt the results. The issue of polymerization conditions will be discussed later in section 3.7 and to a lesser extent in other sections. Redox or other reactions in the polymerization media, changes in the rate constants due to presence of solvents, and other phenomena can lead to reduction of MW in the absence of CCT. One generally expects a profound effect, so when C_c < 50, the presence of CCT can be questionable. This is not to say that cobalt chelates with C_c < 50 are not CCT catalysts, but confirmation requires additional investigation.

Unless otherwise mentioned in the text, all scouting for CCT reported here was carried out at 60 °C in MMA or in a methanol solution of MMA if LCo was not directly soluble in monomer. AIBN was used as the azo initiator because peroxides often decompose or poison the cobalt complexes.

The best known CCT catalysts are cobaloximes having the general structures 6, 7, 8, and 9.^{77–81} Data on their catalytic activities in MMA and styrene polymerizations are presented in Tables 1 and 2, respectively.



As a result of the ready availability of required starting material and smooth, well-developed syntheses,⁸² the cobaloximes **6–8** served as convenient models for understanding how axial ligands and substituents on the macrocyclic ligand affected the catalytic behavior of these Co^{II} species.⁸³ There are some advantages to using the Co^{III}–alkyl versions of these catalysts.⁸⁴ The macrocyclic ligand in cobaloximes is an almost perfectly planar structure carrying a formal double negative charge. The hydrogen bonding between the two monoanionic covalent halves of the equatorial ligand is sufficient to confer considerable structural rigidity and chemical stability.^{85–88} The complexes are able to withstand strong acids^{89,90} and even Grignard reagents.⁹¹ In deuterium oxide solutions, replacement of the bridging hydrogen atom with deuterium is slow even in the presence of bases or acids.^{92,93} This stability allows the catalysts to be employed in aqueous systems as well as organic media.⁹⁴

The axial ligands can be divided into two groups. Group A comprises monoanionic ligands that result in an oxidation state of three in cobalt. These may be the anions resulting from acido ligand (for instance chloride) or may be alkyls. The hydride ligand would also fall into this category and plays an important role in the catalytic chemistry, but in general, they have not been observed directly. Electron-donating ligands, E, are neutral, Lewis base ligands which are coordinatively bound and are not involved in the oxidation state of the cobalt. From a practical point of view, E ligands, particularly water, are often present in the catalysts employed for CCT, but they are often unspecified.

2.2. Cobalt Catalyst Activities

As shown in the Table 1, the activities of cobaloximes **6** can vary by more than 3 orders of magnitude.^{77–81,95,96} Ligands of class A showed no catalytic activity when A = primarily alkyl, CN, or NO₂ (entries **6a** through **6f**). When A is halogen, pseudohalogen, or secondary alkyl (entries **6g–6k**), the resulting cobaloximes are potent chain-transfer catalysts. Variation of substituents on the dioximate moieties (entries **6L–6o**) changes the CCT chain-transfer constants severalfold. The presence of ligands of the E type (entries **6p–6r**) also cause variations of severalfold, and it seems at first glance that C_C increases with the strength of their ligand field.

For charged cobaloximes such as **7**, the choice of the A ligand is crucial (Table 1). Differences in this catalytic activities of these cobaloximes with chloride and other acido ligands range over 3 orders of magnitude. Cobalt^{III} oximes **8** with no A ligands are among the most active. These observations are consistent for both MMA and styrene as monomer (Table 2).

Cobaloximes with structure **9** have a BF₂ bridge rather than the more usual hydrogen atom bridge between the two dioxime moieties. Such a modification leads to better stability of the cobalt^{II} oximes toward oxidation by oxygen by air. While of little consequence in an academic laboratory, it is impor-

tant on a commercial scale that the compounds can be stored and handled by chemical operators without special precautions.^{97–100}

It is difficult to compare the activities of the H-bridged cobalt^{II} oximes with their BF₂-bridged counterparts because of their increased sensitivity to oxygen. The in situ preparation of cobalt^{II} oximes in radical polymerization of MMA has been described.⁷⁹ Making such cobaloximes in situ requires methanol, pyridine, or other solvents to dissolve the starting materials, and as a result, the concentrations of the monomers are 70% or less in the final solution. In one example, the data indicate $C_C \approx 700$ for Py-(dmgH)₂Co^{II},⁷⁹ which is substantially less than that of the cobalt^{III} oximes shown in Table 1. A second approach for in situ synthesis is to use starting materials such as cobalt 2-ethylhexanoate that are soluble in MMA, thereby making additional solvent unnecessary.¹⁰¹

Traditional methods of handling air-sensitive materials¹⁰² are generally appropriate for making cobalt^{II} dioximes because cobaloximes of the type E(dmgH)₂Co^{II} tend to dimerize and precipitate from methanol solutions. Thus, (PPh₃)(dmgH)₂Co^{II}–Co^{II}-(dmgH)₂(PPh₃) was synthesized and tested in bulk MMA to give a relatively unusual result. The catalytic activity of such LCo depends on the concentration and ranges from $C_C = 800$ to $C_C = 20\,000$.⁴⁴ The reasons for such a distribution of C_C values will be detailed later. At this point it is sufficient to indicate that the catalytic activities of cobaloximes **6–8** depend very much on axial ligands of the A type and much less on substituents in the equatorial ligand and ligand of the E type. The latter two may change the chain-transfer constant 2- to 4-fold, while ligands of the A type may reduce C_C by orders of magnitude. The A ligands giving the highest activities are halides, especially chloride. E type ligands tend to increase C_C with increasing ligand strength as one may see in Table 1 (phosphines > py > H₂O).⁷⁸ The same results were observed in porphyrins, although the effect is smaller than in cobaloximes perhaps due to a larger “electron pool”.

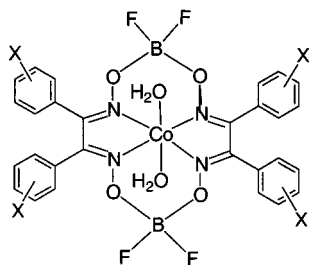
When cobaloximes, **9**, with a BF₂-bridging ligand,^{103,104} were first reported as CCT catalysts,^{105,106} they quickly became the CCT catalysts of choice.^{44,107–117} They are often introduced into the reaction mixture as either Co^{II} or Co^{III}–alkyl species. It is presumed that the Co^{III}–alkyl species are quickly and quantitatively reduced to Co^{II} in situ.^{77,118} Data on their activity are reported in Table 3. Substituents in the cobaloximes **9** have a slight effect on the catalytic activity but more surprising is the dependence of C_C on solvents employed for the polymerizations (see Tables 2 and 3). In one case the dependence of C_C on solvent was traced to impurities, presumably acids, in butanone.¹¹⁵ Freshly distilled butanone does not reduce the CCT chain-transfer constant. In another case C_C was found to be dependent upon impurities in the initiator.⁷⁶ Regardless of the origin of the solvent effect, the existence of such an effect makes it difficult to extrapolate observations

Table 3. Catalytic Activity of Cobaloximes, 9,^a in MMA CCT^{105,112,115–120}

entry	X	X	C_C				
			THF	butanone	methanol	toluene	bulk
9a	Me	Me		27 000	11 000–20000		41 000
9b	2-C ₄ H ₃ O			7 200			
9c	C ₆ H ₅	C ₆ H ₅		20 500		23 000	18 000–20 000
9d		-(CH ₂) ₄ -					14 000
9e	4-MeC ₆ H ₄	4-MeC ₆ H ₄	25 000				
9f	4-EtC ₆ H ₄	4-EtC ₆ H ₄	27 000				
9g	4- ⁱ PrC ₆ H ₄	4- ⁱ PrC ₆ H ₄	25 000				
9h	4-tBuC ₆ H ₄	4-tBuC ₆ H ₄	21 000				
9i	4-BrC ₆ H ₄	4-BrC ₆ H ₄		4 500			
9j	4-MeOC ₆ H ₄	4-MeOC ₆ H ₄	15 000				7 000
9k	4-NO ₂ C ₆ H ₄	4-NO ₂ C ₆ H ₄	5 000	5 000			
9l	4-BrC ₆ H ₄	4-SO ₃ NaC ₆ H ₄			7 300		
9m	3-MeC ₆ H ₄	3-MeC ₆ H ₄	28 000				
9n	2-MeC ₆ H ₄	2-MeC ₆ H ₄	16 000				

^a Monomer is MMA, 60 °C.

made in solution polymerizations in the presence of **9** or the subset of complexes



to emulsion or suspension polymerizations reported in Table 3.¹¹⁹

In cobaloximes **6–8** it could be concluded that electron-withdrawing groups (EWG) increase C_C . Compare, for example, entries **6g**, **6L–o**, **8a**, and **8b** in Table 1. Table 3 does not afford the same conclusion.

For cobaloxime **9a**, chain-transfer constants obtained using the new CLD techniques of rate constant calculations^{40,122} were $C_C = 25\,000$ for MMA and $C_C = 660$ for styrene polymerization at 60 °C.^{123,124} In other cobaloximes, a reverse trend was observed, with electron-donating substituents (entries **9e–h** in Table 3) increasing activity while EWG (entries **9i–L** in Table 3) led to a decrease relative to hydrogen (**9c**, Table 3). The data of Table 3 can be explained by the presence of the strong EWG, BF₂, in cobaloximes **9**.⁹⁷ The electron-withdrawing group reduces electron density on cobalt to the extent that the lone electron on Co^{II} behaves less like a free radical. Electron-donating substituents in the equatorial ligands of **9** help to restore the free-radical properties of the cobalt atom, while additional EWG in the equatorial ligand exacerbate the electron density problem on cobalt. This explanation leads to the conclusion that some value of electron density on the cobalt atom is required for optimal hydrogen atom abstraction during CCT.

The effect of solvents on the properties of BF₂-bridged cobaloximes in methacrylate CCT carries over to polymerization of styrene. Thus, for cobaloximes **9** in the polymerization of styrene, $C_C = 500$ in butanone¹²⁰ while $C_C = 1400$ in bulk.¹¹⁵ Cobaloxime **9c** showed $C_C = 700$ in bulk styrene

polymerization,¹¹⁵ a value 20–30 less than C_C in polymerization of methacrylates. This is similar to that observed for cobaloximes, **6** (Table 1), and for cobalt porphyrins, although in the last case the kinetic picture is more complex. Interestingly, the rate of CCT in styrene polymerization has been shown to be light dependent.¹²⁵ The rate was found to be less than 100 in the dark but increases to a maximum value of $C_C = 5000$ under UV irradiation. The value of C_C was also found to be dependent upon the initiator concentration, decreasing with higher initiator levels. Apparently, UV irradiation homolyzes the Co^{III}–C bond formed by addition of styrene radical to the Co^{II}.

Viscosity of the medium can also play a role in the kinetics due to the importance of diffusion in the observed rate constants. In the bulk radical polymerization of 2-phenoxyethyl methacrylate, thiol chain-transfer reagents operate at rates close to those observed for MMA while the rate of CCT catalyzed by **9a** is an order of magnitude slower (2×10^3 at 60 °C) than that of MMA.⁵ The thiol reactions involve a chemically controlled hydrogen transfer event, whereas the reaction of methacrylate radicals with cobalt are diffusion controlled. The higher bulk viscosity of the 2-phenoxyethyl methacrylate has a significant influence on the transfer rate.

The chain-transfer reaction is essentially unchanged in going from bulk polymerization to toluene solution.³⁰ In the low-viscosity medium, supercritical CO₂, chain transfer was found to be significantly enhanced by an order of magnitude (10^8 L mol⁻¹ s⁻¹) compared with toluene or bulk MMA as a medium. Again, the results are consistent with a diffusion-controlled rate-determining step.³⁰ However, another report indicates no enhancement of chain transfer in supercritical CO₂.¹²⁶ This discrepancy may be the result of the necessity of using different catalysts in the two media.

While on the subject of polymerization media, there is also a report of CCT in ionic liquids.¹²⁷ 1-Butyl-3-methylimidazolium hexafluorophosphate is a room-temperature ionic liquid. Although such liquids have been found to be excellent solvents for a number of chemical transformations, there are few reports of polymerizations.¹²⁸ Nonetheless, Co^{II}-mediated cata-

Table 4. Values of C_c in MMA Polymerizations for a Variety of Cobalt Complexes^a

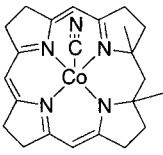
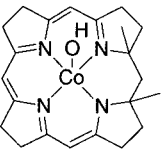
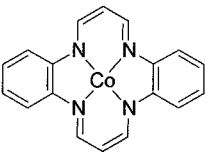
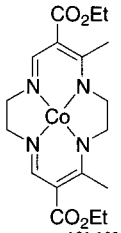
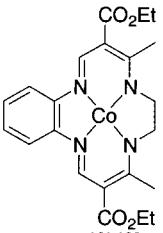
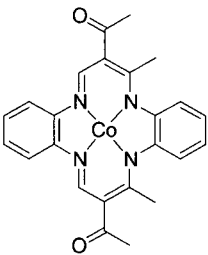
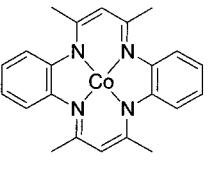
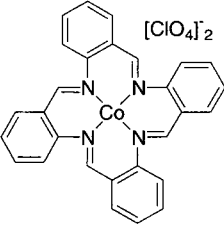
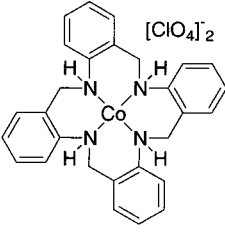
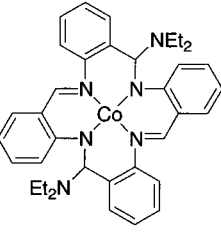
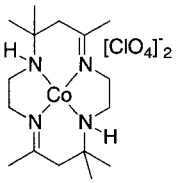
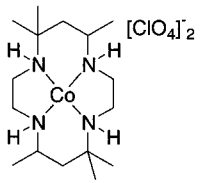
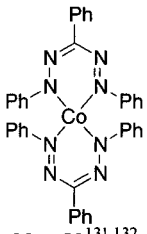
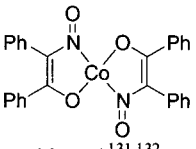
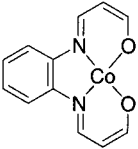
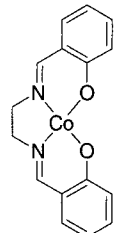
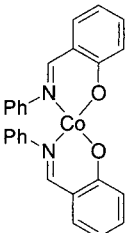
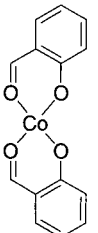
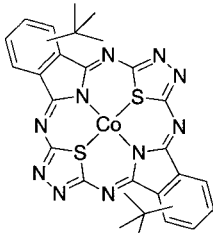
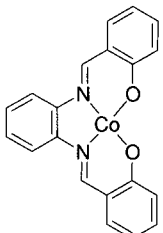
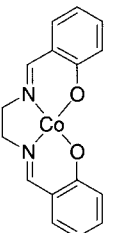
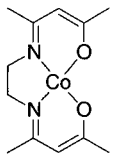
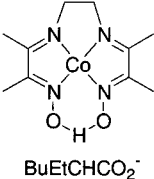
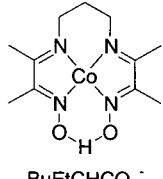
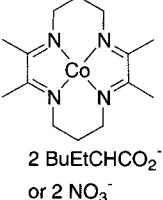
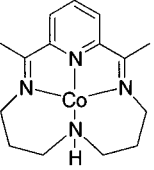
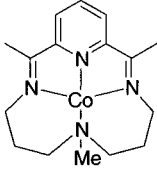
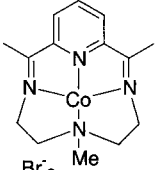
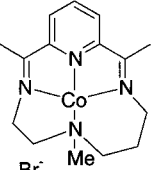
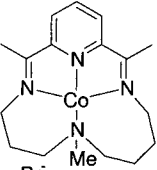
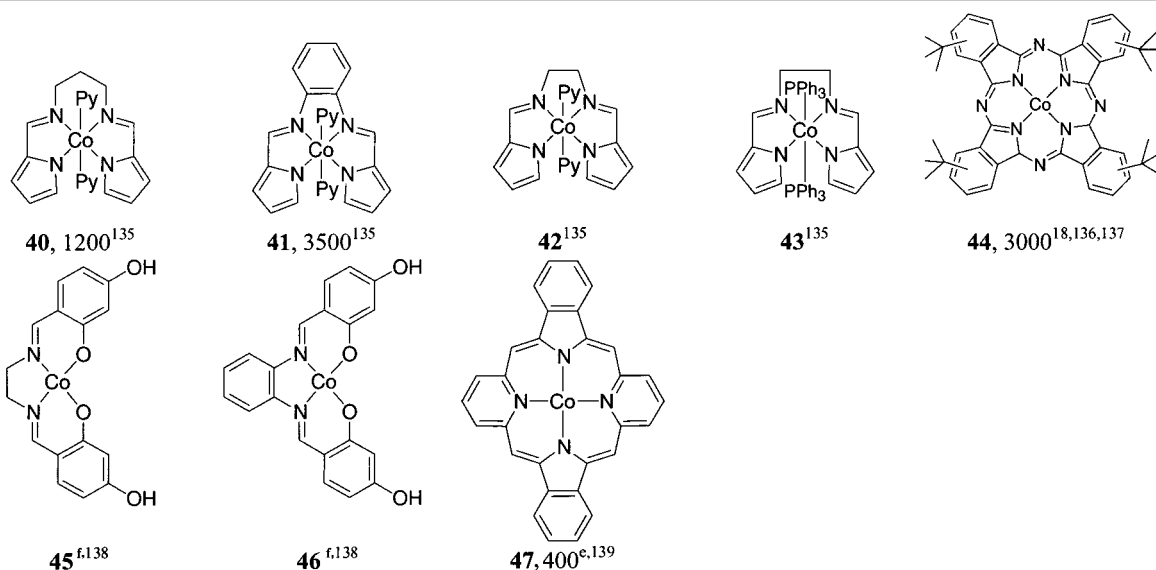
				
10 ^b , <50 ^{131,132}	11 ^b , 400 ^{131,132}	12, 400 ^{131,132}	13, <50 ^{131,132}	14, 750 ^{131,132}
				
15, 250 ^{131,132}	16 ^c , 1100 ^{131,132}	17, <50 ^{131,132}	18, <50 ^{131,132}	19, <50 ^{131,132}
				
20, <50 ^{131,132}	21, <50 ^{131,132}	22, <50 ^{131,132}	23, <50 ^{131,132}	24, <50 ^{131,132}
				
25, <50 ^{131,132}	26, 0 ¹⁰⁹	27, 0 ¹⁰⁹	28, <50 ^{131,132}	29 ^d , 15 ⁶²
				
30, 150 ¹⁰¹	31, 7 ¹⁰¹	32, 600 ¹⁰¹	33, 500 ¹⁰¹	34, 170 ^{101, 134}
				
X ₂ 35 ¹³³ Br, 650 OAc, 670 CNS, 900	Br ₂ 36, 130 ¹³³	Br ₂ 37, <10 ¹³³	Br ₂ 38, <120 ¹³³	Br ₂ 39, 120 ¹³³

Table 4. (Continued)

^a In many instances, there were unspecified axial ligands present. ^B Cobalamin substituents not shown. ^c Catalytic inhibition in L/mol·sec. ^d Irradiated with sunlamp. Temperature is unknown. ^e In MMA/DMF = 9:1 at 60 °C. ^f LRP initiators.

lytic chain transfer has been observed in the radical polymerization of MMA.

Polymerization of MMA both thermally and photochemically in the ordered media, cholesteryl oleyl carbonate and cholesteryl 2-ethylhexyl carbonate, were studied in the presence and absence of cobalt tetraphenylporphyrin. The percentage conversion and molecular weight were lowered in the presence of CoTPP for thermal polymerizations. In photopolymerizations, the percentage conversion was high and the molecular weights were low.¹²⁹

In the photodecomposition of polystyrene-bound cobaloximes, the polymer chain decreases the mobility of bis(dimethylglyoximato)pyridinecobalt(L) and increases the probability of recombination of L and a radical fixed on the polymer chain. Retardation of the dissociation resulted in a larger equilibrium constant for the polymeric system than that for the analogous monomeric system.¹³⁰

Table 4 presents C_C for a variety of catalysts other than cobaloximes that have been tested in MMA radical polymerizations.^{101,109,131–136} In addition, the following values have been reported: MMA, C_C = from 3×10^5 to 2.4×10^5 (from 40 to 70 °C, **9a**);³¹ and $C_C = 1.9 \times 10^4$, $k_{Co} = 1.6 \times 10^6 \text{ M}^{-1} \text{ s}^{-1}$ (60 °C, **9c**).⁵ Where data at several temperatures are available, C_C is relatively independent of temperature because k_P and k_{Co} change at approximately the same rate.

It is clear that cobalt catalysts **10–44** are much less active than cobaloximes, generally by 2 orders of magnitude. It is concluded that the hydrogen transfer reaction is not diffusion controlled in their case. This difference in reactivity also suggests that some of the trends found for cobaloximes may not work for other cobalt chelates. Unfortunately, there have been few studies to this end. Most of the values of C_C in Table 4 were calculated having only one or two points on the Mayo dependence. For cases when $C_C < 50$, it is usually necessary to carry out ad-

ditional experiments to confirm that the reduction in molecular weight is actually due to CCT rather than other reactions including noncatalytic chain transfer. As a reasonable indication of the accuracy of the chain-transfer constant measurements, the C_C of compound **30** (salcomine) was found to range from <50 to 150.

It is clear that a core of four nitrogen atoms in the coordination center is crucial for active CCT. Replacement of two nitrogen atoms with oxygen (**23–26**, **29–31**) or sulfur (**28**) essentially shuts down the ability of LCo to abstract hydrogen from free radicals. Compound **28** is particularly interesting because of the similarity of molecular structure of this chelate to cobalt phthalocyanines, which are known to be good CCT catalysts.

The influence of axial ligands on cobalt dimethylglyoxime complexes holds for these other ligands. Axial ligands that preclude CCT by cobaloximes (e.g., CN) also interfere with the ability of cobalamin **10** to react with radicals. When hydroxyl is the A ligand on cobalamin (**11**), it does not interfere with hydrogen transfer. Halogen, pseudohalogen, and carboxylic acids are "good" ligands. Somewhat surprisingly, in **34**, NO_3^- is also "good" for CCT while in cobaloximes such ligands resulted in the absence of catalytic activity.

The presence of four nitrogen atoms coordinated in the equatorial plane in LCo does not guarantee noticeable catalytic properties. It would be of interest to determine the factors that control activity. One explanation suggests that only low-spin LCo can be CCT catalysts.¹⁰⁹ Thorough investigation indicated, however, that this could be a necessary but is not a sufficient condition. For example, CCT catalysts such as cobalt^{II} oximes bearing either H or BF_2 bridges have the same magnetic moment, $\mu = 1.8\text{--}2.1$, as noncatalysts **16**, **19**, **20**, and **23**.^{140,141} An empirical observation ascribes catalytic properties to all LCo that have four nitrogen atoms coordinated in the

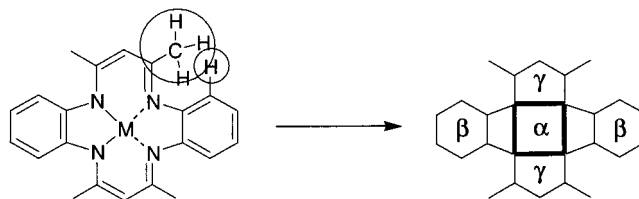
equatorial coordination plane which are incorporated into an extended system of conjugated π -bonds. The equatorial plane may be either open C-shaped or closed O-shaped. Planarity of the macrocycle is important.^{131,132} Cobalamin **10** represents such a structure. It has four nitrogen atoms in an O-shaped π -conjugated system.

The active LCo complexes indicated above can be used to test this theory. Porphyrins and phthalocyanines have an O-shaped system which has a more extended π -system than that in cobalamins, but it does not provide a substantial increase in reactivity. It should be noted that the hydrogen bonds of the cobaloxime catalysts are essentially as effective as π -bonds in continuing the effects of delocalization around the macrocyclic ring. This effect has been noted elsewhere.¹⁴² Catalyst **11** comprises an O-shaped π -system. Replacement of one π -bond with a σ -bond in the analogue **13** significantly affects the catalytic properties since both complexes retain their O-shape with π -conjugation. Additional replacement of π -bonds with σ -bonds leads to a complete loss of catalytic properties as chelates **13**, **20**, or **21** indicate. Chelate **22**, cannot be a CCT catalyst because of the absence of interaction between the two π -systems. Chelate **34** is an exception; its molecular structure is similar to **21** and **13**, but it catalyzes chain transfer with a measurable rate. A possible explanation of this phenomenon will be provided in section 3.7.

As with cobaloximes, substituents on the equatorial ligand have only a moderate effect on the value of C_C for the complexes in Table 3. The same is true for substituents on cobalt porphyrins, **1** and **45–51** (Table 4). For tetrakis(pentafluoroethylphenyl)porphyrin–Co^{II} the substituent effect is not clear. The fluorinated porphyrin works moderately for the polymerization of MMA in supercritical CO₂ with chain-transfer constant $C_C = 550$ at 60 °C.¹²⁶ Unfortunately, no data on the chain-transfer constant in bulk polymerization are available, so that it is not clear whether this reduced value of C_C is the result of solvent or the presence of a strong EWG such as pentafluorophenyl in the porphyrin macrocycle. Similar experiments with **9c** (Table 2) led to $C_C = 378\,000$, which is 20 times higher than in bulk MMA or in organic solvents.³⁰ We may conclude at this point that additional experiments are required with different catalysts to allow us to make reliable conclusions.

Complexes **13–15** provide interesting additional information on the influence of substituents. Catalytic activity gradually decreases with increasing steric interference between the protons of the methyl groups and the benzylic ring. This steric interference is so high that complex **16** is substantially twisted so that the macrocycle is not planar but rather is "saddle-shaped". According to the crystal structure, cobalt and the four nitrogen atoms are laying in an approximate plane (α), while the aromatic rings (β) are above the coordination plane, and the wings γ are twisted below this plane (Scheme 1). The dihedral angle between the planes β and γ is 43°.^{147,148} As a result of the substantial nonplanarity of the molecule, chelate **16** behaves differently from its planar analogues.^{149–152}

Scheme 1. Atomic Planes of 15 from Crystallographic Data, Showing the Four-Membered α -Plane, the Aromatic Six-Membered β -Planes, and the Five-Membered γ -Planes



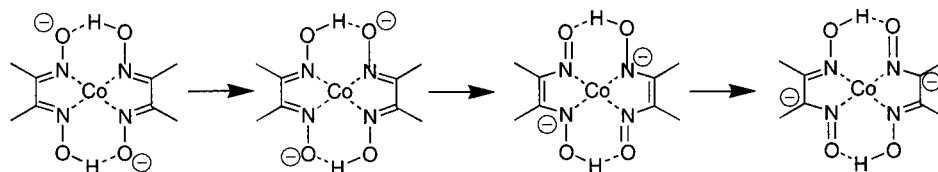
In radically polymerized MMA, LCo **16** does not catalyze hydrogen transfer to monomer but instead catalyzes a termination reaction. This conclusion was reached by comparison of DP_n versus the decrease in rate of polymerization. As mentioned in the Introduction, CCT catalysts do not change the rate of polymerization. In the case of **16**, the rate of polymerization and DP_n decrease linearly with concentration of **16** with a stoichiometric coefficient of inhibition >4 . The steric encumbrance of chelate **15** represents an intermediate case between **14** and **16** since it has only two methyl groups instead of four in **16**. Since these methyl groups may twist, only one benzene ring twists slightly from the γ -planes, and complex **16** generally retains the C-shape of the π -conjugation. As a result, **16** shows the properties of a CCT catalyst but its C_C is lower than that of **14** or **34**.

Complexes **35–39** also support this conclusion. Catalyst **35** has a planar, C-shaped system of π -conjugation. The three-carbon bridges between the NH and other coordinated nitrogens provide adequate flexibility in coordination so that the entire equatorial ligand is planar. Chelates based on [14]-annulenes are known to exist as strictly planar structures, while bigger/longer ligands, like chelate **39**, can exist in different conformations. Chelates **37** and **38** are not effective catalysts for CTC due to the shortening of the bridge between the two nitrogen atoms from three carbon atoms to two. The two neighboring five-membered rings do not support a planar structure, so that the cobalt and the coordinated nitrogen atoms in these chelates cannot form a perfect plane. A planer molecule cannot be formed at all in the case of **37** with only 12 atoms in the macrocyclic ligand. The observed structures of **37**, **38**, and **39** are reflected in their chain-transfer constants: catalytic activity decreases with increasing nonplanarity of the structure in the series **35** $>$ **39** $>$ **38** \gg **37**.

Additional understanding of the role of π -conjugation is provided by cobaloximes **6–8** and other CCT catalysts with hydrogen bonds which complete the macrocycle (i.e., **32** and **33**). The common feature shared by a π -bond and these hydrogen-bonded systems is their ability to delocalize their electron density.^{131,132} Resonance isomers with different bonding of the H or BF₂ bridges to the oxygen atoms allow the electrons to delocalize around the equatorial plane as shown in Scheme 2.

A necessity for a delocalized ring current in CCT catalysts explains the requirement that the equatorial ligand be flat. Chelate **17** would have been a good

Scheme 2. Delocalized Nature of Cobaloximes



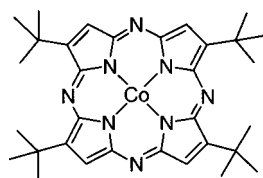
test of this conclusion. It has a 16-member macrocycle that is antiaromatic, and as a result, the equatorial macrocycle is slightly twisted. Hence, it cannot provide ring effective delocalization unless doubly charged to fit the $(4n + 2)$ Huckel requirement. Unfortunately, **17** was tested as the perchlorate salt which makes the results ambiguous.

A phenomenological approach does not explain how the structural features of the CCT catalysts affect the catalytic process. It is obvious that redox properties are involved here. A systematic study of redox potentials and CCT is reflected in Table 5. The higher

Table 5. MMA CCT Chain-Transfer Constants, C_C , and Selected Polarographic Half-Wave Potentials for the Reduction of Co^{II} to Co^{I} ,^a $E_{1/2}$, for Cobalt Porphyrins¹⁴³

entry	ligand on Co^{II}	$E_{1/2}$ (V)	C_C	ref
48	tetra(<i>o</i> -bromophenyl)porphyrin		1300	139
1	tetramethyl hematoporphyrin IX	-1.06	2400	143
49	mesoporphyrin IX dimethyl ester	-0.98	1800	143
50	tetrakis(<i>p</i> -methoxyphenyl)porphine	-0.91	1500	143
51	tetramethyl coproporphyrin IX	-0.90	1500	143
52	tetraphenylporphine	-0.82	1400	143
53	etioporphyrin	-0.79	1100	143
54	protoporphyrin IX dimethyl ester	-0.71	1000	143
2	tetra(<i>tert</i> -butylbenzo)porphyrin	-0.70	900	143
55	tetra(pentafluorophenyl)porphine		550	126
56	tetra- <i>tert</i> -butyltetraazaporphine		2500	144
57	tetramesitylporphyrin		1500	145
58	tetra(4-sulfonatophenyl)porphyrin		~1000	146
59	tetra(2,4,6-trimethyl-3,5-disulfonatophenyl)porphyrin		~5000	146

^a See also, refs 13, 15, and 17.



56

the reduction potential for LCo^{2+} to LCo^+ , the higher the catalyst activity. While the trend is reasonable, it is important to note the higher values for C_C for the same LCo in this reference. Thus, tetra-*tert*-butylbenzoporphyrin-Co, **2**, has $C_C = 900$ in Table 5 while in another reference $C_C = 300$.¹⁵ Tetraphenylporphyrin-Co, **52**, has $C_C = 1400$ in Table 5 while $C_C = 4000$ elsewhere.¹²

2.3. Non-Cobalt CCT Catalysts

CCT is not limited to macrocyclic complexes of cobalt^{II}. Nonetheless, early experiments with porphyrin complexes of Fe, Ni, V, Sn, Cu, Zn, Mg, Cr, Pd, Pt, and Mn demonstrated no activity.^{13,25} Likewise, dioximates of Ni and Cu were found to be inert

Table 6. Chain-Transfer Activity of Organometallic Catalysts in MMA Polymerizations

$[(\text{C}_5\text{H}_5)\text{Cr}(\text{CO})_3]_2$ 60 , 100 ¹⁵³ 160(Sty)	$[(\text{C}_5\text{H}_5)\text{Cr}(\text{CO})_3]_2$ 61 , 1000 ¹⁵⁴
$(\text{C}_5\text{H}_5)\text{Cr}(\text{CO})_3(\text{C}_5\text{H}_5)\text{Mo}(\text{CO})_3$ 62 , 162 ¹⁵³	$[(\text{C}_5\text{H}_5)\text{Cr}(\text{CO})_2(\text{PPh}_3)]_2$ 63 , 60 ¹⁵³
$[(\text{C}_5\text{H}_5)\text{Mo}(\text{CO})_3]_2$ 64 , 2 ¹⁵³	$[(\text{C}_5\text{H}_5)\text{W}(\text{CO})_3]_2$ 65 , 1 ¹⁵³
$[(\text{C}_5\text{H}_5)\text{Fe}(\text{CO})_2]_2$ 66 , 0.5 ¹⁵³	$[(\text{C}_5\text{Me}_5)\text{Fe}(\text{CO})_2]_2$ 67 , 9 ¹⁵³
$[(\text{C}_5\text{H}_5)\text{Ru}(\text{CO})_2]_2$ 68 , <1 ¹⁵³	$[(\text{C}_5\text{Me}_5)\text{Os}(\text{CO})_2]_2$ 69 , <1 ¹⁵³

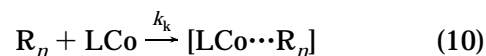
in radical polymerizations.¹⁸ It would be expected that many metal complexes could be catalysts if they are radical-like and have an easily accessible one-electron oxidation. The additional requirement is that they be kinetically labile, because the free-radical polymerization sequence is so rapid that a kinetically inert complex might catalyze one or fewer transfers over the lifetime of a single polymerization chain reaction. Experience with non-cobalt systems is relatively limited. The effects of a series of organometallic complexes were explored in radical polymerizations, and the data is presented in Table 6.¹⁵³⁻¹⁵⁵ Most of the MMA polymerizations were carried out in refluxing butanone (80 °C).

Among complexes **60**–**69** only the chromium complexes, **60**–**63**, showed a significant ability to reduce MW. The catalytic process relies upon the dissociation of the dimeric precursors to paramagnetic monomeric organometallic radicals, and the sterically hindered complex, [(pentaphenylcyclopentadienyl)Cr(CO)₃]₂, **61**, a derivative of **60**, was more active ($C_C = 1000$ at 100 °C for MMA) than its unsubstituted analogue. The greater steric bulk of the phenyl-substituted **61** increases the dissociation, thereby making the active paramagnetic components more available for the catalytic process.¹⁵⁶ Pentacyanocobaltate, [(CN)₅Co]K₃, **70**, has very little activity in the reduction of MW, with $C_C \approx 6$.¹⁵⁷

3. Mechanism

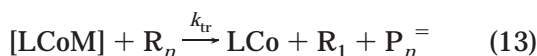
3.1. Reaction Schemes

Three possible reaction mechanisms for CCT have been proposed. The first two involve metal activation of a substrate to attack by another reactive species, while the third involves sequential reaction of two different species with the metal center. The first was based upon formation of an intermediate complex of the cobalt catalyst with the propagating radical^{11,14}



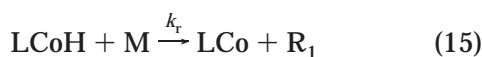
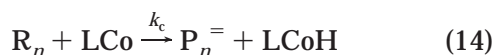
R_n and R_1 correspond to the polymeric and monomeric radicals respectively, M is monomer, LCo is a cobalt^{II} chelate, $[LCo \cdots R_n]$ is an intermediate complex, and $P_n^=$ is oligomer or polymer with a terminal double bond. Although eq 10 has been observed on numerous occasions, catalyst regeneration (eq 11) is more problematic. It is unlikely that a monomer like methacrylate would abstract a hydrogen atom from a coordinated metal alkyl. It would be expected that hydrogen atom abstraction could be from the α -position, but rearrangement to a coordinated olefin that could be dissociated is possible.¹⁵⁸ This mechanism, deemed to be unlikely, has been explicitly tested and found lacking.¹²⁴

A second proposed mechanism of the CCT was based upon a Michaelis–Menton-type mechanism.¹² This mechanism is typical of enzymatic catalysis,¹⁵⁹ and the rates of CCT have been compared to those of enzymes. It requires the formation of a complex between the catalyst and the monomer (eq 12). The propagating radical then reacts with the complex (eq 13) to transfer a hydrogen atom to the monomer.



There is little support for the mechanism expressed by eqs 12 and 13. MMA is able to form a π -complex with cobalt porphyrins,¹⁶⁰ but the chain-transfer constant for its formation (1.8 L/mol s) is not high and is much smaller than the observed CCT chain-transfer constants. If the mechanism of eqs 12 and 13 is correct, then reduced concentrations of monomer should disfavor formation of $LCoM$, resulting in a decrease in the rate of CCT. The chain-transfer constant of the chain transfer is independent of the concentration of monomer.^{14,52} The mechanism expressed by eqs 12 and 13 will not be considered further.

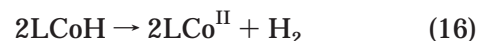
A third reaction scheme (eq 14 and 15) encompasses what is the currently accepted mechanism. This scheme was suggested simultaneously with eqs 10 and 12 and calls for the formation of the cobalt hydride, $LCoH$, as an intermediate species.^{161,162}



Since no change in the spectrum of $PorCo^{II}$ was observed during the catalysis, it was assumed that the concentration of $PorCoH$ was very low due to its high reactivity.

Hydrides of cobalt chelates are well documented in inorganic chemistry,^{89,163} and cobaloximes received particular attention in the 1960–70s because their chemical behavior was somewhat similar to that of vitamin B₁₂.^{85,86,164–171} Although the hydrides of cobaloximes are very reactive, two instances in which $(DH)_2CoH$ was isolated have been reported.^{88,172} It is believed that in the absence of radicals or monomer, the main mode of decomposition of $(DH)_2CoH$

is the bimolecular disproportionation reaction, eq 16.^{173–178}

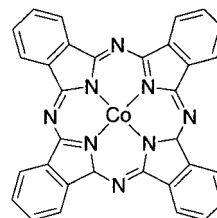


The chain-transfer constant of about 10^5 L/mol s^{172,175} makes it difficult to study the properties of $(DH)_2CoH$. Equation 16 is reversible, and under basic conditions the equilibrium is shifted to the left. $LCoH$ complexes are weakly acidic and are dissociated easily according to eq 17.

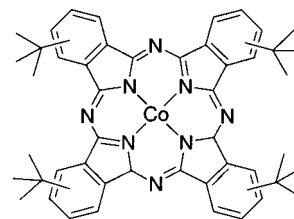


Equations 16 and 17 are known not only for cobaloximes, but also for other cobalt chelates as well. Thus, the addition of bases stabilizes $LCoH$ in its anionic form, slowing the disproportionation reaction in eq 16. The anion which is formally LCo^{I-} behaves as a supernucleophile in S_N2 reactions, reacting with a wide variety of substrates such as acetylenes, olefins, alkyl chlorides, or alkyl bromides.^{181,182} The high reactivity of the LCo^{I-} complex together with eq 16 at times makes it difficult to distinguish whether $LCoH$ or LCo^I is the species responsible for a particular reaction. In many cases both LCo^I and $LCoH$ are present in the reaction media simultaneously.

Very stable Co^I chelate complexes are obtained from phthalocyanine ligands (for example, **44** and **71**).



71, Co^{II} phthalocyanine



44, Soluble Co^{II} (tetra-*t*-butylphthalocyanine)

Cobalt phthalocyanines, $PhtCo$, can be readily reduced either with hydrazine,¹⁸³ with sodium borohydride,¹⁸⁴ or electrochemically.^{185,186} In the latter case, $PhtCo$ can undergo five sequential reductions to the pentaanion. All of the negatively charged species have distinct visible spectra. The visible spectrum of $PhtCo^I$ is independent of counterion or solvent. When radical polymerization of methacrylate is conducted in the presence of amides such as dimethylformamide, hexamethylphosphorus tri-

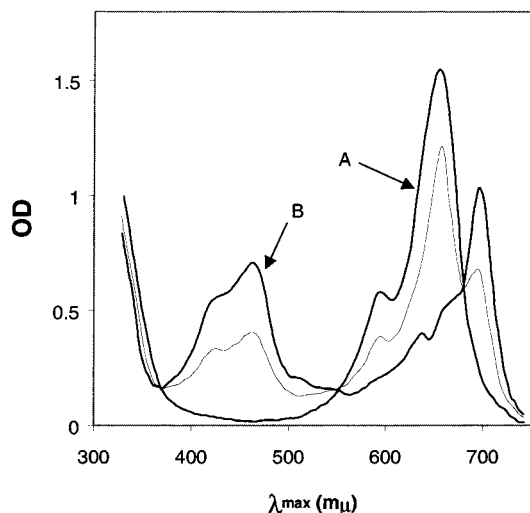


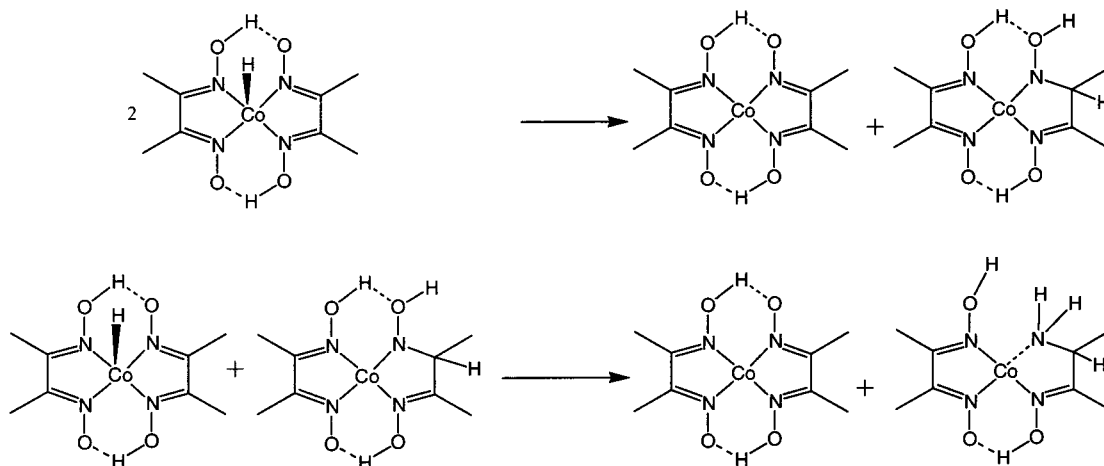
Figure 7. Visible spectra of cobalt phthalocyanine under CCT conditions in HMPA demonstrating the reduction to Co^{I} .¹⁸⁷ A and B are before and after polymerization.

mide, or tetramethylurea, the starting PhtCo^{II} is converted into PhtCo^{I} .¹⁸⁷ It is presumed that the tertiary radical reacts with the phthalocyanine to yield the Co^{III} hydride which then dissociates in the presence of base to give $\text{Co}^{\text{I-}}$.¹⁸⁸ DMSO also promotes dissociation but is less effective than amides. Since the visible spectra are independent of the method of reduction, UV-vis spectroscopy is an easy and a reliable method to monitor reduction of cobalt phthalocyanine. The three isosbestic points (see Figure 7) indicate that no side reactions occur during the reduction of cobalt phthalocyanine with tertiary radicals.

If a radical polymerization is conducted in bulk methacrylate in the absence of a base, PhtCo^{I} is not formed in detectable quantities. The methacrylate is not responsible for converting PhtCo^{II} into PhtCo^{I} . An azo initiator causes reduction even if the methacrylate is replaced with ethyl acetate. Hence, it is the tertiary radicals which convert PhtCo^{II} into PhtCo^{I} .

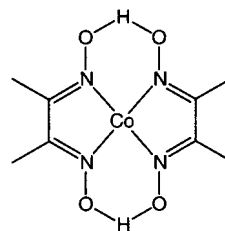
In the case of porphyrins, reduction of Co^{II} to Co^{I} is more difficult. No conditions under which tertiary free radicals would reduce PorCo^{II} into PorCo^{I} at spectroscopically detectable levels were identified.

Scheme 3. Autohydrogenation of the Dimethylglyoxime Ligand



The reduction can be performed electrochemically,^{162,189} by treatment of PorCo^{II} with sodium amalgam at room temperature,^{190,191} or with borohydride¹⁹²⁻¹⁹⁴ at elevated temperatures.¹⁹⁵ In each case, the PorCo^{I} is labile and tends to decompose back to PorCo^{II} and related products when the reducing agent is removed.

Cobaloxime complexes of cobalt, $(\text{DMG})\text{Co}^{\text{II}}$ **72**, give Co^{I} -cobaloximes $(\text{DMG})\text{Co}^{\text{I}}$ in the presence of amides by reaction with tertiary free radicals. This



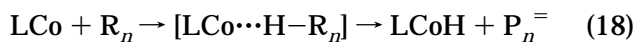
72

makes them similar to phthalocyanines in initial reactivity, but the resulting $(\text{DMG})\text{Co}^{\text{I}}$ decomposes slowly with irreversible changes in the equatorial ligand. The rate of $(\text{DMG})\text{Co}^{\text{I}}$ decomposition depends on both the equatorial and the axial ligands and ranges from 2 to $0.06\% \text{ min}^{-1}$.¹⁸⁷ Among the decomposition products is 3-amino-2-oximinobutane by autoreduction of the dimethylglyoxime ligand.¹⁷⁵⁻¹⁷⁷ Autohydrogenation is very slow in the presence of substrates such as olefin or alkyl halides, indicating that the autohydrogenation is bimolecular as in Scheme 3.

3.2. Hydrogen Atom Abstraction and Catalyst Structure

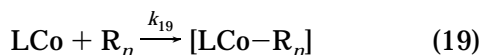
The process of hydrogen abstraction (eq 14) by LCo from a propagating radical is usually the rate-determining step in CCT. It occurs at diffusion-controlled or close to diffusion-controlled rates indicating that the activation energy for the process must be extremely low. The activation energy of eq 14 depends on the catalyst structure and resulting electronics. For systems such as the less active PorCo with MMA,¹⁹⁶ a significant isotope effect $k_{\text{H}}/k_{\text{D}}$ of about 3.5 was observed.¹⁹⁷ This value of the $k_{\text{H}}/k_{\text{D}}$

effect is similar to the range (1.9–3.3) of kinetic isotope effects observed for hydrogen atom abstraction from a variety of substrates by different metallo-radicals.^{198–201} It seems reasonable to conclude that hydrogen atom abstraction in CCT occurs by the three-centered intermediate illustrated in eq 18



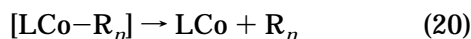
The kinetic isotope effect would be expected to be smaller or zero if the rate-limiting step involved a concerted β -hydride elimination.²⁰²

Another reaction of radicals with Co^{II} chelates known to occur at diffusion rates is recombination (eq 19).



In the case of vitamin B₁₂, eq 19 is well investigated and its rate constant $k_{19} = 4 \times 10^9$ L/mol·s for primary radicals.²⁰³ Comparison of this value with the rate constant for methyl radical dimerization of $\sim 10^{10}$ L/mol·s¹⁹¹ indicates that eq 19 proceeds at diffusion-controlled rates. Newer approaches may provide greater accuracy in the measurement of rates of recombination of free radicals, providing a better understanding of hydrogen atom abstraction (eq 18).²⁰⁵

The ratio between the rates of parallel eqs 18 and 19 is an issue of practical importance. Cobalt chelates may be good capping agents in living radical polymerization, LRP.^{206,207} This requires that eq 19 be reversible and the forward and backward (eq 20) rates be approximately equal.



These conditions have been met in a number of systems yielding living radical polymerizations at moderate temperatures.^{207–213} For successful LRP, eq 18 should not occur at all and eq 19 is required. For the CCT technologies of this review, the rate of eq 18 should be more than competitive with eq 19, though a low equilibrium level of formation of $\text{LCo}-\text{R}$ is not detrimental. In addition to choice of proper temperature, solvent, and monomer, the molecular structure of LCo has proven to be the most important factor in achieving effective LRP or CCT. Those LCo that are not effective for CCT should be screened for LRP, though there are many means by which both reactions can fail.

3.3. Hydrogen Atom Addition

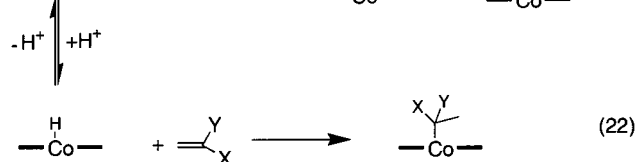
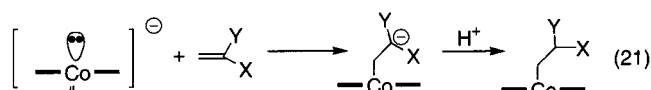
Hydrogen atom transfer from the hydride form of the catalyst to monomer (eq 15) is relatively unexplored in comparison with the initial reaction in the catalytic cycle, hydrogen atom abstraction from the growing radical. This is despite the fact that the two reactions are essentially the microscopic reverse, because the substituents on the organic fragment are relatively removed from the metal center. Early investigations of CCT were frustrated by the fact that concentrations of LCoH were below detection lim-

its.¹⁶¹ The failure to observe LCoH called into question its role as an intermediate species in CCT.

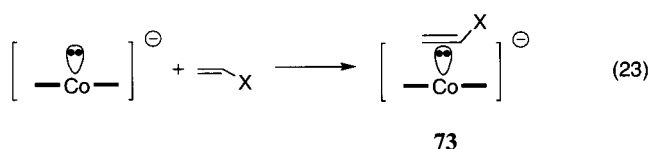
The addition of LCoH to olefinic double bonds is well documented in the chemistry of cobaloximes. Because LCoH has the ability to dissociate to H^+ and LCo^{I} , both the hydride and Co^{I} form of the cobalt chelate must be considered in any system where LCoH can be obtained.

The anionic chelates LCo^{I} are highly reactive nucleophiles, in some cases called supernucleophiles for their reactivity.²¹⁴ They readily replace halogen atoms in alkylhalides,^{214,215} transalkylate phosphates,²¹⁶ add to aldehydes,²¹⁷ and add to double bonds.²¹⁸ The fragmentation of haloalkylurethanes in the presence of LCo^{I} was proposed to go through π -olefinic intermediates, but radical chemistry is more likely.²¹⁹ The large body of Co^{I} -chelate chemistry has been reviewed elsewhere, and we refer the reader to available surveys.^{43,163,220–225}

For the purposes of this review, it is important to recognize the dual nature of cobalt macrocycle complexes. Both species, $\text{LCo}^{\text{III}}\text{H}$ and LCo^{I} , can add to double and triple bonds forming alkyl and alkenyl cobalt chelates but the products are different. The Co^{III} hydride reaction occurs in a Markovnikov addition while LCo^{I} provide anti-Markovnikov products. It is believed that eqs 21 and 22 explain the difference.

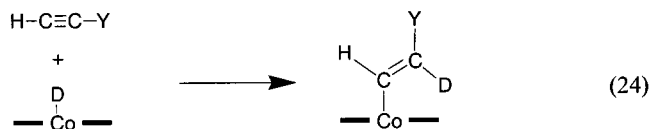


Substituents X and Y are electron-withdrawing groups. For olefins with strong EWG like CN, the formation of π -complexes (**73**) was observed.²²⁶



Strong bases ($\text{p}K_{\text{a}} > 11$) also convert alkyl cobaloximes and alkyl cobalamins into π -complexes such as **73**. This is usually followed by further decomposition to olefins and alkanes. The stability of complexes such as **73** depends very much upon X and the nature of the axial ligand in the cobalt chelate.^{98,218,227–230} Strong nucleophiles such as RS^{\ominus} or CN^{\ominus} can cause decomposition of $\text{LCo}-\text{R}$ as well.^{98,231} Under the normal conditions of radical polymerization, Markovnikov organocobaloxime should form whenever the hydride, LCoH , appears in the polymerization mixture. If 1,2-vinylidene monomers are being polymerized, then thermally unstable *tert*-alkyl-cobaloximes are obtained. These species are expected to undergo homolytic Co–C cleavage to yield tertiary radicals.

An alternative mechanism calls for hydrogen atom transfer by the reverse of eq 14 with no organometallic intermediates. Attempts to distinguish between these two possible pathways of hydrogen addition employed deuterium labeling. Stereoselectivity in the addition of LCoH to double and triple bonds was observed. Early work indicated Co–D cis addition to olefins and acetylenes.²³² Later experiments showed

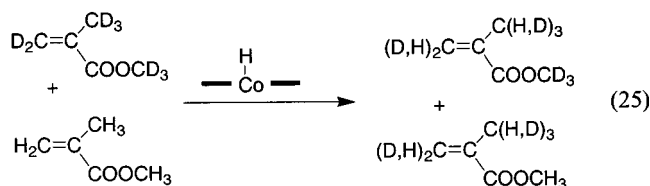


a maximum of ~70% cis addition.²³³ Cis addition falls to ~60% when octaethylporphyrin–CoD reacts with phenylacetylene.²³⁴

It is important to carefully control reaction conditions during experiments with LCoH and LCoD, particularly the availability of exchangeable hydrogen atoms. LCoD can be prepared using NaBD₄. Borohydrides are known to change the acidity of the reaction medium during the course of the reduction reaction, and this can have a direct effect on the outcome of the reaction. An alternative approach to Co–D complexes is through the decomposition of deuterated alkylcobaloximes. D/H exchange with CH₃OD is negligible, but the synthesis of the deuterated organometallic precursor is itself a problem.

Steady-state, free-radical methods of LCoD generation were developed.¹⁹⁷ The methods are versatile and work for LCo like cobalt porphyrins that are not readily reduced by borohydrides. The use of tributyltin hydride has also been reported.²³⁵ The initial approach employed AIBN-*d*₁₂. Using this deuterated radical source, cis addition of the resulting LCoD was demonstrated to be the predominant mode of reaction for maleic anhydride and other cyclic olefins such as cyclohexene and 2,5-dihydrofuran. Selectivity depended upon temperature, and this important feature will be discussed below. Unfortunately, AIBN has a limited thermal operating window of 50–70 °C. Lower or higher temperatures would require the nontrivial synthesis of different deuterated azo initiators. To circumvent this problem, a second steady-state free-radical approach was developed.

When perdeutero-MMA was copolymerized with perhydro-MMA in the presence of AIBN and a CCT catalyst under conditions that favor formation of MMA-dimer, it was observed that the product had undergone hydrogen/deuterium scrambling. Unreacted monomers in the reaction mixture were also scrambled.



It was clear that rapid hydrogen/deuterium exchange was occurring in a radical cage²³⁶ involving LCoH/LCoD and MMA before the monomeric radical

escaped the cage to propagate polymerization in solution. The suggestion was confirmed by employing perhydro azo initiator and MMA-*d*₈. The unsaturated molecule 2,5-dihydrofuran was added to trap the intermediate. As expected, the isolated tetrahydrofuran cobalt complex was deuterated in the *cis*-vinyl position. Unexpectedly, MMA-*d*₈ was discovered to be a highly efficient deuterium donor. A 2-fold excess of MMA relative to LCo was enough to convert LCoH into a LCoD before reaction with dihydrofuran. Using these methods, the results shown in Figure 8

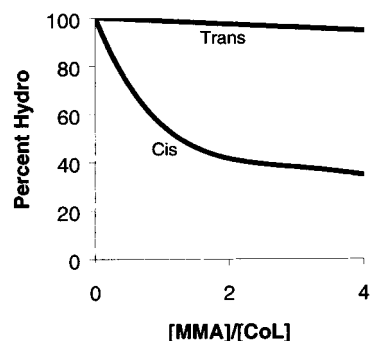
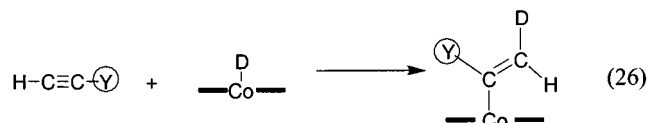


Figure 8. Hydrogen/deuterium dependence at the β -carbon atom of (TAP)Co–(3-tetrahydrofuranyl) on the concentration of MMA-*d*₈ relative to cobalt.¹⁹⁷

were obtained. Thus, to obtain LCoD, the azo initiator appropriate for the desired temperature is combined with a small portion of MMA-*d*₈.

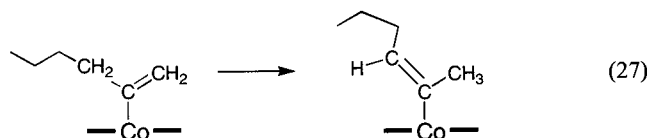
Stereoselectivity of the addition of LCoD to olefins is very dependent upon the temperature. The most probable reason for diminished selectivity is the thermal lability of the Co–C bond at temperatures above 50 °C for all olefins studied to date. In the case of maleic anhydride, the initial product is LCo–succinyl anhydride. Under more forcing conditions in the presence of excess AIBN, formation of a new organometallic species, LCo–succinyl anhydride–C(CN)(CH₃)₂ was detected. Formation of the new adduct almost certainly resulted from Co–C bond cleavage, and this same cleavage would lead to stereochemical inversion. At temperatures less than 50 °C, additions are somewhat more stereoselective. Nonetheless, maleic anhydride was the only olefin to give quantitative cis addition at lower temperatures. Other olefins displayed some trans addition even at these temperatures. Thermal isomerization results in loss of selectivity at longer reaction times, but even the product initially formed displays some trans isomer, and thermal instability of the Co–C bond cannot explain this observation. There must be some inherent lack of selectivity.

In contrast to olefins, the addition of acetylenes to LCoD shows clear trans addition as in eq 26.



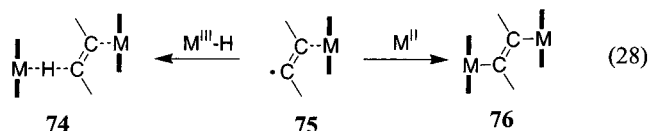
The reaction proceeds well even in the presence of a 100-fold excess of MMA-*d*₈ to generate the label. The addition of the cobalt deuteride to 1-hexyne or

5-hexynenitrile displays Markovnikov regioselectivity and *trans* (*anti*) stereoselectivity. The high conversion of the Co^{II} to vinyl cobalt $^{\text{III}}$ porphyrins allowed labeling using AIBN- d_{12} as a source of (TAP)CoD. Unexpectedly, the incorporation of deuterium into the axial vinyl substituent on cobalt was dependent upon the concentration of the acetylene, with only 40 atom-% *trans*-vinylic deuterium addition at 0.04 M 1-hexyne increasing systematically to 90 atom-% at 1 M. The deuterium content of the product increased during the course of a reaction at fixed acetylene concentration with no deuterium incorporation at the *cis*-vinylic site occurring during these experiments. The unaccounted deuterium was lost to an unknown side reaction. The presence of a large excess of exchangeable MMA- d_8 overcame the unknown reaction and provided a high level of deuterium incorporation in the *trans*-vinyl position. In some cases, isomerization (eq 27) of the initial product was observed.



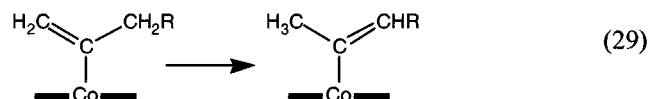
The source of *trans* stereoselectivity for Co-H addition reactions to acetylenes while olefins are generally *cis* is unclear. *Cis*²³⁷ and *trans*²³⁸ additions of acetylenes are known in platinum chemistry, and radical intermediates are thought to play a role in some insertions.²³⁹ *Cis* additions indicate concerted insertion reactions, while *trans* additions are indicative of radical pathways. Sterically demanding acetylenes can lead to a reversal of regio- and stereochemistry.²⁰⁸

Species such as **74** and **75** could be intermediates in the *trans* addition of cobalt hydride to acetylene.



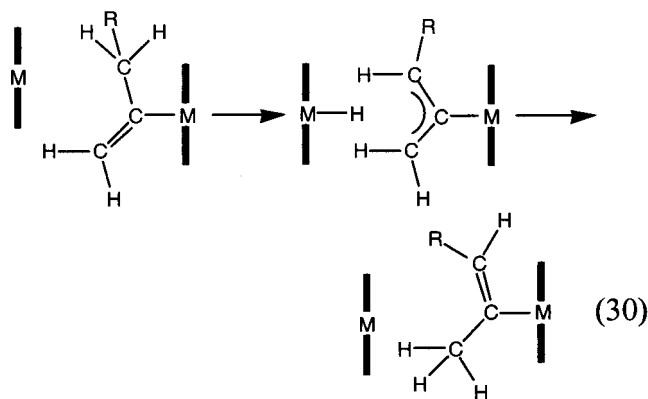
Bridged species such as **76** are well documented in rhodium porphyrin chemistry.^{240,241} An acetylene bonded to one metal-centered radical is presumed to be trapped by addition of a second metal-centered radical. Lower bond dissociation energies of cobalt relative to rhodium would disfavor species such as **76** and facilitate the reaction with metal-hydride intermediates to form a *trans* product.

Involvement of a second porphyrin in the reaction of CoH with acetylenes was inferred from the inverse relationship between the rate of eq 29 and the steric bulk of the porphyrin molecule.^{5b}



Unimolecular isomerization could occur by a Co-C bond cleavage to yield radical intermediates that isomerize. The rate of isomerization of the coordi-

nated vinyl would be expected to be higher for sterically hindered porphyrins that favor homolytic dissociation, but this does not fit the observations. An alternative unimolecular mechanism would involve a concerted 1,3-hydrogen shift, but it is difficult to explain why a relatively remote terminal group of the axial ligand would have an effect on the rate of isomerization as observed. The decrease in the rate of isomerization for a coordinating nitrile substituent versus a noncoordinating methyl substituent is explained by a bimolecular catalyzed reaction as in eq 30.



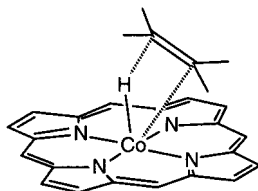
The reactive, unsaturated site of an incoming porphyrin molecule would be filled by the nitrile substituent preventing interaction with the α - or β -sites of the vinylcobalt porphyrin molecule. The methyl group would have no such interaction, allowing the porphyrin to approach in an active state. Such a Co^{II} -catalyzed isomerization of an allylcobalt $^{\text{III}}$ is preceded by cobaloxime chemistry.²⁴² Kinetic investigation of the isomerization indicates that the rate of isomerization of the primary acetylene adduct to the secondary product early in the reaction is several times the rate late in the reaction when Co^{II} would be depleted, supporting the intermediacy of a species such as **74**.

3.4. Alternative Mechanisms for Olefin Reactions with $\text{Co}^{\text{III}}\text{-H}$

The chemistry of vitamin B₁₂-catalyzed rearrangements has been a subject of intensive investigation.²⁴³ Although there is much to support the free-radical nature of such rearrangements, there is a growing body of evidence which favors nonradical mechanisms under at least some conditions.²⁴⁴⁻²⁴⁶ Polar effects are known to play an important role in the addition of free radicals to double bonds.²⁴⁷ Radicals can form relatively stable adducts with a variety of salts,²⁴⁸ phosphines,²⁴⁹ and conjugated double bonds.²⁵⁰ Additionally, radical species can undergo one-electron oxidation/reduction when reacted with metals or olefins,²⁵¹ and these one-electron transfers can be quite reversible.²⁵² For these reasons, radical, ionic, or electron-transfer mechanisms cannot be ruled out. A given metal complex may be able to convert radical species into ionic intermediates and back. Because of this complication, the origin of some selectivities may be based on the limiting step of a multistep process.

Experiments with model compounds demonstrated the exceptional importance of the π -system in molecules involved in chain-transfer catalysts. Cobalt chelates without planar, extended conjugated π -systems are not active in chain-transfer catalysis.¹³² One possible explanation of this could be the necessity of hydrogen atom migration from cobalt to ligand during the catalysis. Disruption of the conjugation by the hydrogen atom migration should be less in an extended π -system.

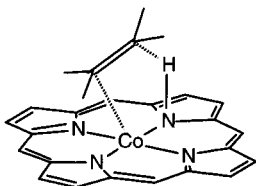
Concerted insertion of an olefin into a CoH bond or its microscopic reverse, β -hydride elimination, involves the intermediate species **77**.



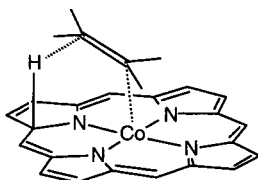
77

The availability of only one coordination site due to the large rigid equatorial ligand of the cobalt porphyrin macrocycle would appear to make such an intermediate unlikely. Viewed as a transition state with a large component of C–H bond formation, the Co–C bond formation would occur later in the process. In the extreme of complete C–H bond formation prior to Co–C formation, the intermediate is indistinguishable from a radical mechanism.

The cobalt–hydride intermediate has not been isolated and is virtually undetected. Cobalt hydride reaction with an olefin by first migrating the hydrogen atom from cobalt to a porphyrin nitrogen atom (**78**) or carbon atom (**79**) is preceded by the isomerization of a benzylcobalt chelate. In that case, the benzyl migrates reversibly from the cobalt to the carbon atom of the equatorial ligand.²⁵³



78



79

It is also reported that alkyl groups in N-substituted Ni and Pd corroles can migrate from pyrrolic nitrogen to the β -carbon atom of the pyrrolic ring.²⁵⁴ The intermediate is also preceded by complexes bearing partially hydrogenated cobaloxime ligands produced by exposure of the complexes to molecular hydrogen.¹⁷⁷ Migration of organic substituent from metal to nitrogen and addition of acetylenic substrate to both metal and macroligand have been reported in several dozen publications.^{255,256} Support for a possible role for hydrogen atom migration from the metal atom to a macrocyclic ligand is provided by the coexistence of a normal rhodium phthalocyanine

hydride and its isomeric form in which the hydrogen atom is located on one of the ligand nitrogen atoms.²⁵⁷ Hydrides of cobalt chelates are known to be less stable than those of rhodium, so it is likely that a hydrogen atom would undergo migration from cobalt to ligand at rates faster than those in rhodium phthalocyanine. Mechanisms based upon these intermediates or transition states are plausible alternatives to the caged radical pair, though the intermediates would have to be very short-lived because the rates of the catalytic chain transfer are so high. Rapid, reversible migration of the hydrogen atom between cobalt and ligand could be responsible for the poor stereoselectivity of cobalt hydride addition to the double bond of cyclopentene at low temperatures when thermal isomerization of the Co–C adduct is known to be negligible.²⁰⁸ If a Co–H transfer is not stereoselective and a ligand hydrogen atom transfer is stereoselectively cis, then the overall stereoselectivity of cyclopentene addition to LCo^{III}H would reflect the ratio between the concentrations the isomers, CoH, and LH.

An important feature of the LH form of the hydride is that it contains a Co^{III} bearing a very open coordination site for reaction with nucleophiles. There are several publications on the unusual reaction of “naked” cobalt^{III} in porphyrins with acetylenes and olefins.^{256h–j,258} This could also explain the trans addition of the hydrides to acetylenes. A charge-transfer intermediate in the reaction of the LH isomer with an acetylene or alkene could explain the difference in behavior of substituted versus unsubstituted olefins. If the above explanation is correct, then it would require essential equality between the energies of the Co–H and L–H complexes. Parameters such as solvent properties could shift the equilibrium concentrations of the two isomers of the hydrides, leading to apparently different results in the same reaction and explain poor reproducibility in stereoselectivities.^{232,233}

The role of protic intermediates was recognized in the very earliest work on hydridocobalt^{III} chelate reactions.²⁵⁹ In basic solutions, H/D exchange was relatively fast, while neutral or acidic conditions reduced the rate significantly.^{230,260} The chemistry is associated with hydridocobalt^{III} and the deprotonated anionic complex which is formally cobalt^I. Under basic conditions, the regiochemistry is reversed with acrylonitrile giving the primary alkyl, Co^{III}CH₂CH₂CN.

Caution is required in extrapolating the conclusions from one particular set of reactants and conditions to other closely related systems. The chimeric nature of CoH, reacting as a free-radical or an ionic species, can depend both on the nature of the equatorial ligand and on the trans substituents, particularly if migration of the hydrogen atom over the surface of the equatorial ligand plays a role in the insertion reaction. In this case, the structure of the equatorial ligand rather than the redox potential of the metal center may control the course of the reaction.

The addition of double bonds to hydridocobalt^{III} chelates is clearly dependent on the structure of organic substrate. Generally, electron-withdrawing

substituents promote cis addition while electron-donating substituents lead to loss of selectivity in the reaction. It is likely that olefins and acetylenes react with CoH by different mechanisms and parallel reactions may occur.²⁶¹

3.5. Living Radical Polymerizations

The phenomenon of living polymerization is observed whenever propagation and reversible termination are significantly faster than any process for irreversible termination. The primary route of termination in free-radical polymerizations is bimolecular in nature. If the persistent radical effect can be employed to reduce the instantaneous concentration of active radicals in solution at a given time, then bimolecular termination can be greatly reduced. This is done by establishing an equilibrium between active and dormant radicals. The resulting polymerization is living in that M_n increases in direct proportion to the conversion of monomer. The molecular weight distribution in resulting living radical polymerization (LRP) is narrow, and it is possible to prepare a number of desirable polymer architectures such as block copolymers and end-functional polymers.

Under certain conditions, some poor CCT catalysts are potentially good candidates for living radical polymerizations, LRP, if the factor limiting the CCT is formation of a stable metal alkyl species, $\text{LCo}^{\text{III}}\text{-R}$, which removes active cobalt^{II} from the reaction.^{262–264} This stable species is not an intermediate in the CCT reaction but rather represents a side reaction.¹²³ This has been observed for a variety of olefins, actually allowing isolation of the $\text{Co}^{\text{III}}\text{-alkyls}$ ²⁶² and determination of the Co–C bond strengths and kinetics of Co–C bond homolysis of several of these species.^{265–269} The strong ring currents of porphyrins and phthalocyanines²⁷⁰ make the use of NMR spectroscopy particularly advantageous. In many cases involving catalysts **48–59**, retardation of polymerization was observed, thereby complicating the overall mechanistic picture. Retardation has also been reported for porphyrin complexes of metals other than cobalt, with the retardation increasing in the order $\text{Zn} \approx \text{Ni} < \text{Pd} < \text{Cu} \approx \text{Mn} \approx \text{Cr}$.¹⁷ This retardation indicates that these porphyrin complexes may participate in other reactions with the propagating radical including LRP since retardation is an inherent feature of LRP,²⁷¹ but additional experiments are required to discover the origin of the retardation. This effect may sometimes be referred to as the “persistent radical effect”.^{272–276}

In selected cases, it is possible to convert effective CCT catalysts to species suitable for LRP by incorporating special substituents into the design of the equatorial ligand. Above, we demonstrated that substituents usually have little effect on CCT chain-transfer constants. These limited effects are generally deemed to be electronic in nature. There are several special instances of ortho-substituted phenyl substituents having a substantial influence on C_c . Ortho-substitution on phenyls can play a significant role by preventing the phenyl rings from being coplanar with the macrocycle through steric interactions such as those discussed above with chelate **16** as an

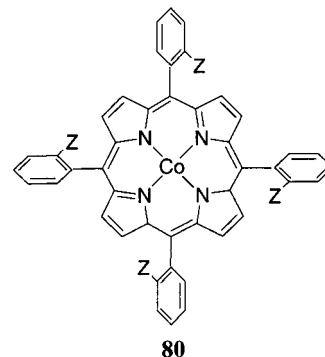
Table 7. CCT in Polymerization^a of Bulk Styrene Catalyzed by Porphyrins **80¹⁴⁴**

entry	substituent, Z	C_c	phenyl–Z bond length (nm)
80a (50) ^b	H	2150	0.108
80b	OMe	1530	0.135
80c	Me	1000	0.152
80d	Cl	610	0.170
80e	Br	550	0.185

^a Bulk MMA, 60 °C. ^b 4-Anisyl.

example. The difference between **16**, where π -delocalization was interrupted, and ortho-substituted phenyls in the macrocycle is that they force the phenyl to be perpendicular to the macrocycle plane, positioning the ortho-substituents directly above or below the plane of the macrocycle. This creates a steric obstruction to the propagating radical as reaction with the cobalt center takes place.

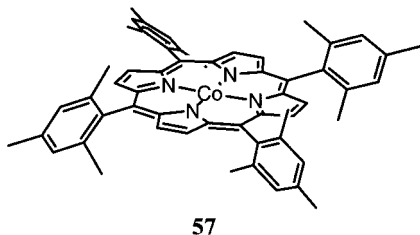
Porphyrin molecules provide a good example of this effect.¹⁴⁴ In Table 7, a clear connection between the size of the ortho substituents and the chain-transfer constant, C_c , is observed. The electronic effects of the substituents are less important because methyl and chloro have similar C_c but significantly different electronic effects. According to X-ray data, porphyrins such as **80** are so restricted in rotation of the phenyl rings that four atropo-isomers can be easily separated by preparative chromatography.



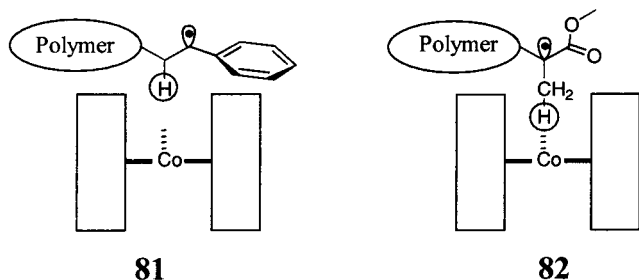
The substituents, Z, can be located both below and above the plane. Both sides of the porphyrin plane are equivalent, so the purely statistical ratio between concentrations of the atropo-isomers (above the plane/below the plane)—(0/4):(1/3):(2/2)—is 1:4:3. About 12% of all the porphyrin molecules will have one completely unsubstituted side (the other side being tetrasubstituted) having the same steric exposure as an unsubstituted porphyrin. Experimentally, the methoxy-substituted porphyrin displayed 8% of the (0/4) atropo-isomer, which is very close to the expected value based upon populations of active species alone.²⁷⁷ Hence, it would be expected that at most 10% of the ortho-substituted phenyl porphyrins **80** could provide full activity regardless of the size of the Z-substituents. The concentration of atropo-isomers (1/3) and (2/2) are approximately equal, so if the (2/2) isomer completely blocks radical approach, then C_c should be about one-half of that of the unsubstituted porphyrins. From Table 7, one may conclude that having one methyl or one methoxy group is not enough to block the cobalt reaction with the propa-

gating radical while one bromo substituent is. Even taking tetrakis(*p*-methoxyphenyl)porphyrin–Co ($C_C = 2200^{144}$) as an electronically corrected, ortho-unsubstituted reference catalyst, one may draw the same conclusion.

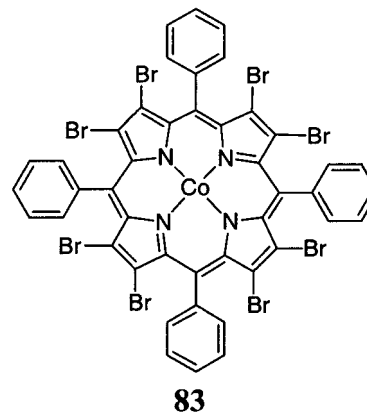
The cobalt complex of tetrakis(mesityl)porphyrin, **57**, is one of the most commonly utilized sterically hindered porphyrins because there are no atropo issues, with each side of the macrocycle having four ortho-substituents.



In the polymerization of MMA, **57** is one-half as effective as its unsubstituted analogue, tetraphenyl porphyrin cobalt, with their respective C_C being 1500 and 4000.¹⁴⁵ In contrast, **57** was found to be completely inactive in styrene polymerizations, with $C_C < 1$, while **80c**, a mono-ortho-unsubstituted analogue, has $C_C = 1000$ (Table 7). This is an unusual result because the polystyrenic radical is a secondary radical while the polyMMA radical is tertiary and more sterically hindered. The ortho-methyl substituents in **57** create a fence around cobalt so that the cobalt atom is sitting at the bottom of a pocket. It is difficult to explain how a tertiary polyMMA radical reacts with such a deeply hidden cobalt while the polystyrenic radical cannot. The nature of the resulting product suggests the answer. The secondary styrenic radical is too bulky to insert its β -hydrogen atom into the pocket of **81**.¹⁴⁵ In contrast, free radicals having a β -methyl group, like the PMMA propagating radical, can extend the methyl group into the "pocket" of porphyrin **77**, allowing hydrogen atom transfer to cobalt as shown in **82**.

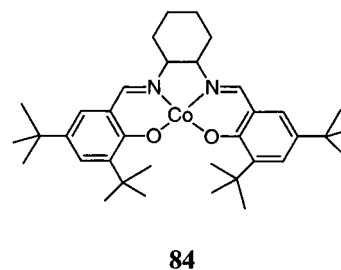


Careful tuning of steric and electronic effects can lead to the elimination of CCT, allowing living radical polymerization to dominate.^{207,278} Acrylates can be polymerized by the LRP mechanism using **57** as a capping agent, and there is no hydrogen atom abstraction leading to catalytic chain transfer. Another reported successful cobalt porphyrin as a capping agent for LRP in polymerization of acrylates is when the octabromotetraphenylporphyrin Co derivative, **83**, is employed; the temperature for active LRP is reduced from 80 to 30 °C.^{279,280}



Porphyrin **83** is substantially twisted due to unfavorable steric interactions between bromine atoms and the hydrogen atoms of the phenyl substituents.^{281–283} Like complex **16**, **83** is saddle-shaped. The nonplanarity of the LCo structure reduces the hydrogen atom abstraction capability of **83**, making it very good for capping propagating radicals without side reactions.

Chelate **84** exemplifies another approach in the construction of cobalt chelates suitable for LRP.



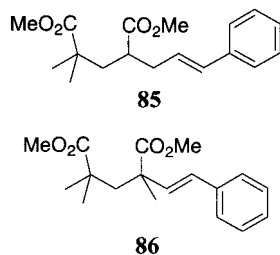
The replacement of one or more of the equatorial chelating nitrogen atoms with atoms of other elements reduces the π -conjugation to the extent that CCT does not occur. The attempted use of **84** for LRP led to side reactions, but it is not obvious that the side reaction was hydrogen transfer.²⁸⁴

One additional example of LRP in the presence of LCo will be discussed below (see section 4.5 on acrylates).

The photochemistry of cobalt–carbon bonds is well established^{285–288} and can be utilized to initiate a living radical polymerization in systems where the monomer leads to stable Co^{III} alkyl species.^{289,290} Photolysis of the Co–C bond liberates an active radical species which adds monomer before being retrapped by the cobalt center. Another photon is required after each trapping event. Useful end group functionality (–OH, –COOH, –COOR, –halogen, or –CN) is introduced through the choice of starting cobalt complex. The molecular weight of the polymer increased with conversion, and products with narrow molecular weight distributions were obtained as expected for a living system. Polymers with block, star, and radical–block architectures are possible. Similar results can be obtained with rhodium^{III}–alkyl porphyrin complexes. It is possible to start with Rh^{II} and obtain an alkyl-bridged rhodium dimer when employing acrylates. When the sterics are undemanding, the bridge consists of two carbon atoms, but

when steric demands are increased, a four-carbon bridge is obtained through head-to-head dimerization of the acrylate.²⁹¹

Photochemical reactivation of methacrylate oligomers has been observed.²⁹² For instance, MMA dimer was metalated with a cobaloxime. The preformed methylene-bound product was photolyzed in the presence of styrene yielding **85** rather than the expected **86**. The poor yield of **85** is not unexpected, considering the high reactivity of the methylene-based radical species that would be generated.



It would be expected that the highly reactive methylene-radical intermediate would react quickly with any available styrene.

In concluding this section, the criteria described above for the identification of good CCT catalysts are also useful in the identification of good capping agents for LRP. The extended, planar, π -conjugated system of good CCT agents should be reduced for good LRP agents. Substitution of two of the four nitrogen atoms in the equatorial chelate in good CCT catalysts leads to good LRP catalysts. Of course, in the search for good LRP capping agents, it is important that the properties of the metalloradical be tuned to the properties of the propagating radical. More reactive propagating radicals should be paired with less stabilized metalloradicals, i.e., in going from methacrylates to acrylates, the LRP end-capping metalloradical should have fewer nitrogen atoms in the coordination plane and a less extended π -system.

3.6. Catalytic Inhibition of Polymerization

Catalytic inhibition, CI, of polymerization was discovered almost simultaneously with CCT.¹³ In searching for the best CCT catalyst, the solubility of the catalyst is one of the important issues. Cobalt chelates with large planar ligands are poorly soluble in the desired monomers and common organic solvents such as acetone and dichloroethane. The solubility can be improved by incorporating more substituents into the equatorial ligands of the complexes, but this approach requires substantial synthetic effort. The easier approach is to use amides and DMSO as solvents because these solvents will dissolve most of the complexes both as their electroneutral forms and as salts.

The testing of cobalt phthalocyanine in radical polymerization was first conducted in quinoline solution because it was known to be inert for radical polymerization. Surprisingly, instead of CCT, catalytic inhibition was observed.¹⁴ Inhibition is generally considered to be an undesirable event in polymerization. In those few cases when inhibition of polymerization is required (for instance, monomer stabili-

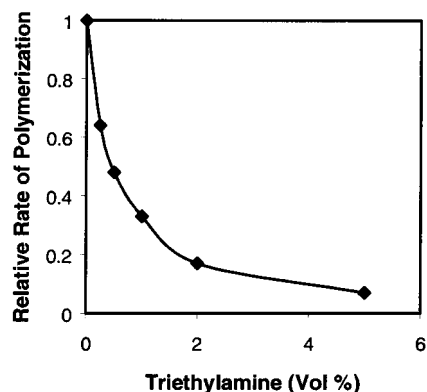


Figure 9. Dependence of CI on added triethylamine.

zation), less expensive noncatalytic inhibitors worked well. As a result, the phenomenon of CI did not attract much attention.

Subsequently, CI was observed in polymerization of MMA with high concentrations of cobaloximes,^{77,293} phthalocyanines,^{14,136,294,295} and porphyrins.²⁹⁵ CI is observed only when the cobaloxime was in the 2+ oxidation state and can catalyze chain transfer.²⁹⁶ Thus, CI is a phenomenon that is closely connected to CCT. The first explanation involved a "hydride" (as in eq 31), where P_n is a polymer obtained from the propagating radical which has been terminated by hydrogen atom donation by $\text{Co}^{\text{III}}\text{-H}$.¹⁶¹

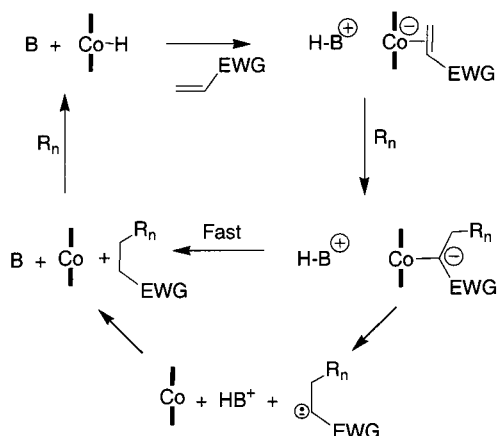


The second explanation of CI was that the polymerization rate constants are dependent upon the radical DP for $\text{DP} < 8$, so that retardation occurs due to the higher value of k_t for small radicals.⁴⁴ As indicated above, the propagation rate constants actually increase at lower molecular weights. There are two additional reasons to believe that k_t cannot be responsible for the CI.

First, low oligomers of the same DP can be obtained with different catalysts, but the observed decrease in the rate of polymerization is different. For cobaloximes the decrease is substantial, while cobalt porphyrins do not reduce the rate of polymerization¹³ except in the very initial stages when some adduct between the propagating radical and cobalt porphyrin forms.⁵² Retardation should be independent of the type of the catalyst if it were dependent upon k_t .

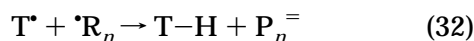
Second, for cobalt phthalocyanines, CCT and CI are dependent upon the addition of quinoline.^{136,294} Addition of low concentrations (0.1–0.001 M) of quinoline reduces the rate of CCT by cobalt phthalocyanines. Higher concentrations of quinoline increased CI and slowed CCT, converting CCT catalysts into CI catalysts. These observations were interpreted in favor of eq 31.

In copolymerization of acrylonitrile and styrene, 1–5% of added nitrogen base may promote MW reduction.²⁹⁷ Several bases including pyridine, triethylamine, and DABCO convert CCT catalysts into CI catalysts in the polymerization of MMA,²⁹⁸ suggesting that the bases are proton acceptors converting LCo-H or LCo-R_n into a π -complex of LCo^{I} with monomer. Figure 9 shows the dependence of the

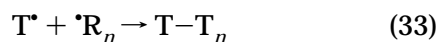
Scheme 4. Effect of Base in Catalytic Termination

inhibition on added triethylamine in an MMA polymerization at 60 °C with tetra(anisyl)porphyrin (2×10^{-4} M).¹³⁹ Interestingly, the noncoordinating molecule DABCO behaves the same as triethylamine, indicating that coordination as a ligand is not important. The resulting complex may trap the next radical by converting it into an anion, as in Scheme 4. Triphenylphosphine behaves similarly to the amines. At amounts equimolar to the cobalt, it may increase the rate of CCT, while higher concentrations decrease CCT by facilitating CI.^{78,298} Whether phosphines are basic enough to participate in Scheme 4 remains an open question.

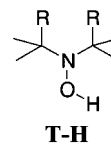
In addition to cobalt complexes, other compounds are potentially able to catalyze the termination of growing radical chains. As a result of their free-radical nature, nitroxides (T^{\bullet}) and other capping agents in LRP are potentially able to abstract hydrogen atoms from propagating radicals through eq 32



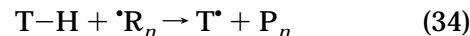
The ability of nitroxides to abstract hydrogen atoms from various organic substrates has been known since the initial discovery of nitroxides.²⁹⁹ Since the coupling eq 33 is much faster reaction than eq 32, eq 32 may seem to be of little consequence under the conditions of LRP.



Nonetheless, the probability of termination eq 32 may be important in two circumstances. First, during LRP, the probability of eq 32 increases with each forward and reverse reaction, eq 33, leading to the accumulation of polymer with unsaturated ends with time. Second, low MW free radicals may be more prone to eq 32 than higher MW radicals because of the dependence of reactivity on molecular weight. Nitroxide may react with the propagating radicals of styrene by eq 32 at significant rates.³⁰⁰ Thus, at 90 °C, $k_{32}/k_{33} = 0.1-0.3$. As a result of hydrogen atom transfer, hydroxylamines, **T-H**, are formed.



These hydroxylamines terminate propagating radicals by eq 34.



The reaction rate constants can be 15–35 L/mol·s depending upon the molecular structure of the nitroxide. The combination of eqs 32 and 34 constitutes a catalytic cycle of CI by hydrogen atom transfer.

3.7. Catalyst Poisons and Other Adverse Reactions

An understanding of side reactions is an important part of any commercial process. The level of understanding is an indicator of the maturity of the process. In the first excitement of a new discovery, side reactions are far from the researcher's mind, but practical implementation of a technology generally uncovers everything that can go wrong. Transition-metal complexes involved in free-radical polymerization may be attacked by the highly reactive free radicals. Free radicals can add to double bonds of porphyrins.³⁰¹ Metal-free porphyrins readily react with secondary propagating radicals (Scheme 5) such as those of acrylates yielding the chlorin, **89**. Further addition yields the bacteriochlorin structure, **90**.

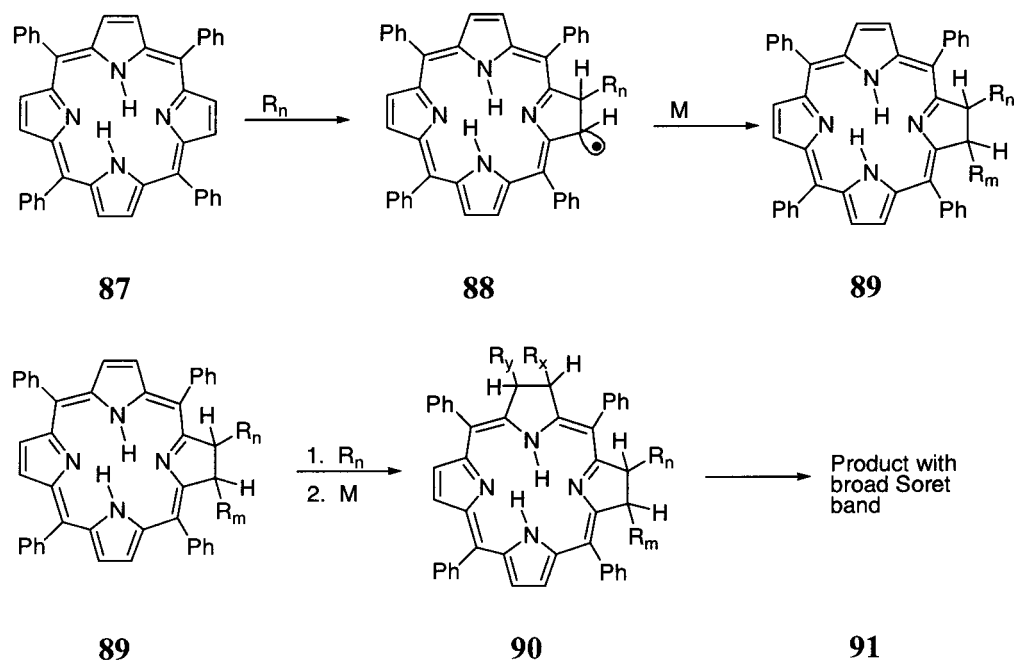
The rates of radical addition to the double bonds decrease from **87** to **90**, allowing the process to be observed stepwise. Under extreme conditions, it is possible to obtain species where the cyclic π -conjugation is completely destroyed in some final uncharacterized product **91**.

In Scheme 5, the radicals derived from acrylates and vinylpyrrolidone (VP) give products that are spectroscopically similar. VP is the more interesting monomer because it provides a polymer with solubility different from that of the porphyrin. Porphyrins are generally insoluble in water and methanol, but after "copolymerization" with VP, they become soluble in water and most organic solvents. The high conversion polymerization of VP with porphyrin results in a cross-linked material from which porphyrin does not leach into solution, indicating that the macrocyclic radical **88** actually propagates polymerization rather than trapping the excess of propagating radicals.³⁰²

Metalloporphyrins behave differently, and the mechanism is dependent upon the nature of the metal.³⁰¹ In addition to the formation of M-C adducts, there are other unspecified reactions with metalloporphyrins which have not been characterized spectroscopically. It is presumed that Scheme 5 may be included in the processes that affect CCT in the case of vinylic monomers that yield a secondary propagating radical.

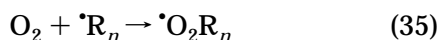
In the chemistry of cobaloximes, the addition of radicals to the double bonds of the equatorial ligand

Scheme 5. Radical Attack on Tetraphenylporphyrin

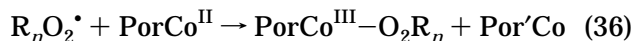


was reported.²⁵³ The benzyl radical is involved in an equilibrium between cobalt and carbon-centered adducts.

Oxygen may substantially reduce the catalytic activity of porphyrin CCT catalyst.⁷⁵ First, the peroxy radical, $R_nO_2^\bullet$ forms as in eq 32.



The peroxy radical then oxidizes the cobalt porphyrin with the formation of several products with a rate constant of $7000 \text{ M}^{-1} \text{ s}^{-1}$, typical for peroxy radicals in their reaction with cobalt^{II} complexes. In addition to the alkylperoxyCo^{III}–porphyrin, **92**, in eq 36, there is concomitant formation of a Por'Co species in which the porphyrin ligand has been modified.



Reaction of the porphyrin ligand leads to degradation of the Soret band and reduction of ring current in NMR spectra after prolonged polymerization in the presence of air.⁷⁵ The concentration of Por'Co species increases with time during a polymerization, possibly because of multiple reactions of peroxy radicals with the porphyrin macrocycle.

The BF_2 -bridged cobaloximes probably behave similarly to cobalt porphyrins, but detailed studies are not available. The H-bridged cobaloximes are more reactive toward oxidation than cobalt porphyrins or phthalocyanines; their Co^{II} complexes are oxidized immediately by dioxygen upon contact. The increased oxygen stability of Co^{III} BF_2 -bridged complexes explains why they are preferred for industrial applications. The alkyl–Co^{III}–cobaloximes, where the alkyl radical is more stable than methyl, decompose at elevated temperatures to yield the active Co^{II} derivatives. Studies indicate that the oxidized Co^{III} species are reduced by propagating PMMA radicals.^{77,188,303,304} When the monoanionic ligand, A, is halogen in a

Table 8. MMA Chain-Transfer Constants^a of Reaction 37 for Different Cobaloximes²⁹⁶

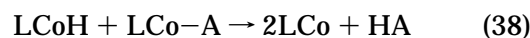
catalyst	substituents	axial ligands	K	E	($\text{M}^{-1} \text{ s}^{-1}$)
6h	CH ₃	CH ₃	I	Py	120
6g	CH ₃	CH ₃	Cl	Py	200
6i	CH ₃	CH ₃	CNS	Py	200
6n		–(CH ₂) ₄ –	Cl	Py	280
6p	Ph	Ph	Cl	H ₂ O	520
6q	Ph	Ph	Cl	Py	700
6r	Ph	Ph	Cl	P(Ph) ₃	2800
6o	α -furyl	α -furyl	Cl	Py	1200
6m	CH ₃	COCH ₃	Cl	Py	800
6l	CH ₃	COOC ₂ H ₅	Cl	Py	1300

^a Bulk MMA, 60 °C, [AIBN] = 0.04 M.

Co^{III}–cobaloxime (eq 37), a carbon-centered free radical is required for reduction.¹⁸⁷



The reduction can be effected by either MMA-propagating radicals or other tertiary radicals such as those provided by the decomposition of azo initiators. The reduction in eq 34 is autoaccelerated, indicating involvement of LCoH, most likely through eq 38.³⁰⁴



Unaccelerated rate constants of the reduction in eq 37 are several orders of magnitude less than k_{Co} (see Table 8).

The Co^{II} complexes obtained by eq 38 may interact with other products of the reaction such as HCl. While cobalt porphyrins are generally unaffected by counterions and byproducts, cobaloximes show complicated patterns of reactivity. When Co^{III}–Cl cobaloxime catalysts are re-isolated after catalysis, stoichiometric chloride is obtained despite the conclusion that the catalysts had passed through a Co^{II}, halide-free state. For Co^{III}–Cl cobaloxime catalysts, there is an induction period defined stoichiometrically

lyst decomposition. Cobalt porphyrins and cobalt phthalocyanines are much more stable under basic pH and in the presence of free radicals than cobaloximes. Thus, the Co^I phthalocyanine that forms by reduction by free radicals in amides is very stable, being stored in a sealed glass ampule for 1 year without any change of its characteristic blue-green color. The more rapid decomposition of dioximates of Co^I is on a time frame comparable with polymerizations (0.06–2% min⁻¹).¹⁸⁸

In conclusion, there are a variety of processes that can affect CCT by increasing or, more often, reducing the rate of the chain transfer by affecting the catalyst. Some of them are more pronounced at the beginning of polymerization, while others are become more significant at the end. The most common is the reversible or irreversible poisoning of CCT catalysts by peroxides because it is difficult to reduce the concentration of peroxides in the monomer to commonly used levels of catalyst (100 ppm or less). This is why erratic results on catalytic activity of cobalt chelates in CCT are not uncommon. Employment of low-conversion reactions (like 2–4%) makes testing results especially vulnerable. These side reaction can often be recognized by deviation from linearity of eq 1, but such careful investigation is not the norm.

4. Monomers for CCT

4.1. Methacrylates

Methacrylates are the monomers most commonly utilized in CCT, and MMA seems to be the monomer against which all comparisons are made. It was discussed extensively in the section on catalysts. In addition to the methyl ester, many other methacrylate esters are mention in the literature. Table 9 lists

Table 9. CCT Chain-Transfer Constants^a for Different Methacrylates^{5,126,313–317}

ester group	C _c	catalyst	ref
PhOC ₂ H ₄ –	2000	9c	5
(MeO) ₃ SiC ₃ H ₆ –	27000 ± 1200	9a	313
[Me ₃ SiO] ₃ SiC ₃ H ₆ –	7500 ± 1400	9a	313
lauryl	20000 ± 1400	9a	313
3-(<i>N</i> -triazolyl)-4-hydroxyphenyl-	4000 ± 200	9a	313
Me ₂ NC ₂ H ₄ –	4400 ± 600	9a^b	314
(<i>N</i> -phthalimidoyl) ₂ C ₂ H ₄ –	500	9a^c	315
methyl	1300	52^d	126
methyl	34000	9c	316
ethyl	26000	9c	316
butyl	16000	9c	316
methyl	2400	1	317
butyl	670	1	317
hexyl	430	1	317
heptyl	250	1	317
octyl	250	1	317
nonyl	150	1	317
decyl	110	1	317
hexadecyl	130	1	317
hydroxyethyl	1120	9a^e	312
glycerol monomethyl	958	9a^e	312
methacrylic acid	1058	9a^e	312

^a Polymerization conducted at 60 °C in neat monomer unless otherwise indicated. ^b 70 °C in neat monomer. Catalytic termination is observed. ^c Chain-transfer constant calculated on the basis of the article data. 80 °C; 30% in toluene. Catalytic termination is observed. ^d 50% monomer in supercritical CO₂. ^e In water.

a variety of monomer for which chain-transfer constants are available or could be calculated. In keeping with patent strategies, many additional monomers are mentioned in patents but are not exemplified. Nonetheless, the monomers that have been studied³¹¹ range from simple alkyl methacrylates to highly reactive species such as glycidyl methacrylates, 2-isocyanatoethyl methacrylates, or methacrylic acid⁸⁰ and to biologically derived materials such as 2-methacryloxyethyl phosphoryl choline, glycerol monomethyl methacrylate, or 3-*O*-methacryloyl-1,2:5,6-di-*O*-isopropylidene-D-glucofuranose.³¹²

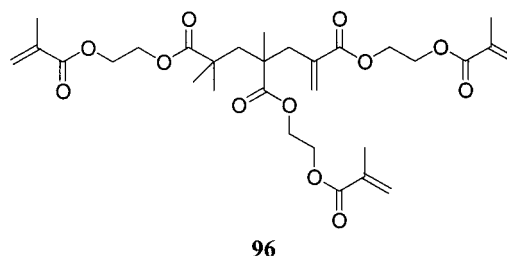
Several CCT catalysts are soluble in MMA but insoluble in the resulting polymer.³¹⁸ Interestingly, when these CCT catalysts are added to frontal polymerizations, they are carried in the polymerization front, decreasing the molecular weight throughout the resulting polymer.

In addition to standard methacrylates, it has been possible to extend CCT to carbohydrate-based systems.³¹⁹

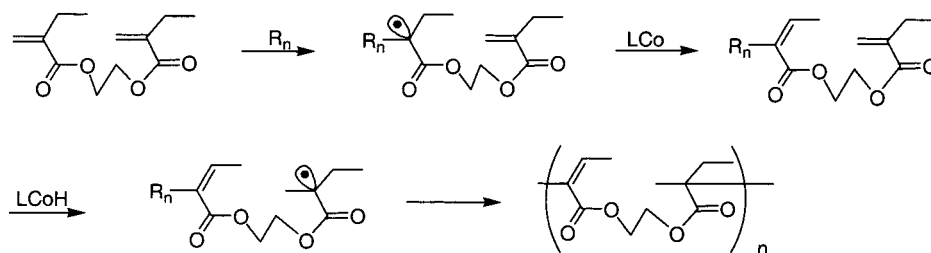
4.1.1. Di- and Trimethacrylates

Dimethacrylate monomers and polymethacrylate monomers must be discussed separately from other methacrylates because of their ability to cross-link under normal free-radical polymerization conditions. Even at very low conversion, less than 1%, they produce completely cross-linked polymers that cannot be solvent-swollen and are insoluble. CCT agents reduce molecular weight and thereby move the gelation point to a much higher degree of conversion, though CCT cannot prevent gelation completely.³²⁰

Hyperbranched polymers were synthesized by direct free-radical polymerization of ethylene glycol dimethacrylate monomer in the presence of a CCT catalyst. The free-radical homopolymerization of divinyl monomers is thought to selectively yield trimer **96**,^{321,322} though previous work on oligomer distributions would indicate that this is unlikely.

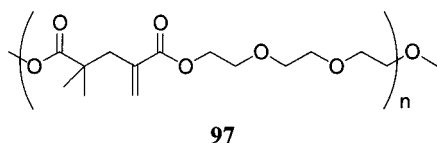


Polymerization of the trimers then leads to cascade branching, ultimately yielding soluble hyperbranched polymers instead of the insoluble networks obtained in the absence of the CCT catalyst. Terminating polymerization at moderate conversion provides highly reactive hyperbranched methacrylate. As mentioned above, there is some similarity between living radical polymerization and polymerizations carried out with high levels of CCT catalyst. Both processes preclude rapid chain growth by periodically interrupting chain growth. As a result, molecular weight tracks monomer conversion to a greater extent than it would in the absence of CCT. The oligomerization results in polymers with very low intrinsic viscosity.^{323–325} The

Scheme 8. Oligomerization of Ethylene Glycol Diethacrylate

molecular weight and intrinsic viscosity of the hyperbranched polymers indicated that the average molecular weight ranged from a few thousand to more than 40 000. The reaction provides an alternative to the complex, multistep, routes to dendritic and starlike polymers. The superior physicochemical and molecular properties of star and dendrimer polymers³²⁶ are believed to justify their very complex technology, but the cascading polymerization provides polymers that meet the requirements for many commercial applications where such perfection is not required.^{36,327–329}

In a similar report utilizing triethylene glycol dimethacrylate, the polymer was described as a linear polyester.³³⁰ Again, this description is probably incomplete, though it is possible at high catalyst loadings to prepare methacrylic dimers. Under ideal conditions, this would lead to the linear, unsaturated polymer **97**.



This was a single example with minimal characterization. A more direct approach to the polyester involves transesterification of the dimer with neopentyl glycol to oligomers and chain extension with diacids and glycols.³³¹ These species are effective pigment binders in paints.

Oligomerization of ethyleneglycol diethacrylate, EGEtA, provided polyester by radical polymerization according to Scheme 8.³³² Bis(dimethylglyoximato)-Co^{III}(benzil)(Py) as a CCT catalyst reduced the molecular weight of the resulting polymer. No rate constants were determined. The authors surprisingly observed that the yield of the oligomer increases with the concentration of the CCT catalyst. A similar dependence was found in AMS oligomerization and was attributed to minimization of bimolecular termination by rapid capture of the dimer radicals by CCT catalysts.³³³ Related branched macromonomers were also prepared by copolymerization of methyl methacrylate with 1,6-hexanediol dimethacrylate in the presence of α -methylstyrene dimer as a molecular weight control (see section 5.1).³³⁴

Branched polymers can also be obtained by copolymerization of MMA with dimethacrylates based upon the condensation product of hexamethylenediisocyanate with two hydroxyethyl methacrylates.³³⁵

This product is then further grafted with glycidyl methacrylate.

4.1.2. Emulsion Polymerization

The kinetics of solution polymerizations involving CCT are not substantially different from bulk polymerizations. An initial report that toluene as a solvent led to reduced catalysis rate³³⁶ seems to be unfounded.¹²⁴

Emulsion polymerization is an attractive route for making polymer compositions without solvent or with minimal amount of organic solvent.^{32,94,337–340} CCT in emulsion polymerization may provide narrower polydispersity relative to noncatalytic chain-transfer agents.³³⁹

Starved-feed emulsion polymerization can be conducted without emulsifiers if suitable comonomers and procedures are utilized.³⁴¹ Polymerization of a water-soluble methacrylate like HEMA in the presence of a CCT agent is carried out initially. The resulting HEMA oligomer is further copolymerized with hydrophobic monomers so that the resulting diblock copolymer serves as a surfactant (see, for instance, sections 5.3 and 5.4). During the cross-linking process, all of this surfactant is incorporated into the polymer backbone and is thus immobilized, overcoming the problem of residual surfactant in the final product.

In contrast to solution polymerization, emulsion polymerization is more complex.¹¹⁹ Monomer feeding can be crucial in obtaining the desired molecular weight.³⁴² The partitioning coefficient of the CCT agent between phases is another key factor.^{343,344} The solubility of the cobaloxime catalysts can be regulated by the size of substituents on the equatorial ligand. The distribution coefficient for water/MMA drops sharply from 0.4 to 0.05 when the substituents in the equatorial ligand change from methyl to ethyl in **9**. Further increase of the substituent alkyl group does not change this ratio substantially.¹²⁰

Generally, efficiency of CCT catalysis drops in emulsion polymerization. The following values of CCT chain-transfer constants may be compared with solution and bulk polymerization: $C_C^{\text{MMA}} = 1100 \text{ M}^{-1} \text{ s}^{-1}$, $C_C^{\text{EMA}} = 640 \text{ M}^{-1} \text{ s}^{-1}$, $C_C^{\text{n-BMA}} = 520 \text{ M}^{-1} \text{ s}^{-1}$, $C_C^{2\text{-EHMA}} = 400 \text{ M}^{-1} \text{ s}^{-1}$ (75 °C, water, **9a**).³⁴² In miniemulsion polymerization, the choice of catalyst depends on the choice of initiator (see Table 10).³⁴⁵

Azo initiators provide good catalyst activity in both solution and miniemulsion polymerizations, while the peroxide initiator $\text{K}_2\text{S}_2\text{O}_8$ substantially decreases the efficiency of molecular weight reduction by **9a**. The results in Table 10 may be explained by the ability

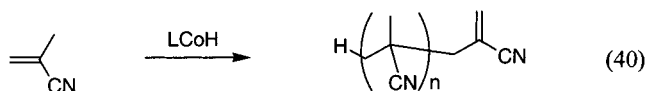
Table 10. Comparison of Miniemulsion (65 °C) and Bulk (60 °C) Polymerization³⁴⁵

initiator	catalyst	C_c	
		miniemulsion	bulk
AIBN	9a	21 000	24 000
AIBN	9c	11 000	14 000
K ₂ S ₂ O ₈	9	830	
K ₂ S ₂ O ₈	9c	12 000	

of potassium dipersulfate to oxidize the CCT catalyst when it is in the water phase. Since the **9c** catalyst is less soluble in water than **9a** catalyst, it is less susceptible to oxidation poisoning. In the case of **9c**, the peroxy radicals react with monomer rather than with the catalyst. More details on oxidative catalyst poisoning were given in section 3.7.

4.2. Methacrylonitrile

Methacrylonitrile is a slow polymerizing monomer under conditions of CCT, and it yields oligomer with a double-bond end group similar to methacrylates (eq 40). The resulting oligomeric products have a stronger tendency to copolymerize with additional monomer and thus be incorporated into subsequent polymer chains than do MMA oligomers.¹³⁹



This tendency is presumably the result of the smaller size of the nitrile group relative to the ester group, so that reaction of LCoH with MAN oligomer is more competitive with that of the monomer. The chain-transfer constant C_c is not known for the polymeric MAN radical, but for the MAN dimer radical, the rate coefficient for CCT k_c is $8 \times 10^5 \text{ M}^{-1} \text{ s}^{-1}$ (at 60 °C with TAPCo^{II}).³⁴⁶

4.3. α -Methyl Styrene

A major limitation of α -methylstyrene in free-radical polymerizations is its very low ceiling temperature of 61 °C.³⁴⁷ As a result, AMS is utilized commercially only in radical copolymerization. Nonetheless, it is among the most active CCT monomers with $C_c = 9 \times 10^5$ at 50 °C for **9a** as CCT catalyst.³⁴⁸ This value is relatively unchanged at 40 °C. This high value reflects the low $k_p = 1.7 \text{ M}^{-1} \text{ s}^{-1}$ so that $k_c = 5 \times 10^5 \text{ M}^{-1} \text{ s}^{-1}$.

AMS dimer, AMSd (**98**), is useful as a radical addition–fragmentation–chain-transfer radical (RAFT) agent,^{349–352} which is covered later. In the polymerization of styrene, AMSd is as active as methacrylate trimers and tetramers with a chain-

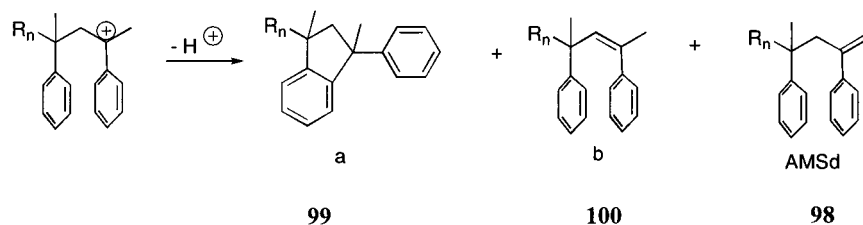
transfer constant C_{AMSd} of 0.29 at 110 °C.³⁵³ Although AMSd has been known to be a good molecular weight control agent for decades, commercially feasible methods for its manufacture have become available only recently. Most are based upon cationic polymerization. The major objective is to avoid internal Freidel–Crafts substitution to give the indane product **a** in Scheme 9. This reaction is the major reason cationic polymerization is not used for commercial polymerization of styrene or its derivatives.

To minimize the indane, **99**, formation, dimerization was conducted in two-phase systems containing toluenesulfonic acid,³⁵⁴ sulfuric acid,^{355,356} electrophilic transition-metal complexes,³⁵⁷ the polymeric solid-state acid Nafion,^{358,359} metal oxide solid-state catalysts such as tungstophosphoric acid,³⁶⁰ various zeolites,^{361,362} mixed oxides,³⁶³ and montmorillonite clay in the presence of organic solvents.^{364,365} The major limitation of the cationic approach, however, is the unavoidable formation of internal isomer **100**. Since isomer **100** is inert in radical polymerization, the lower the content of isomer **100**, the higher the activity of the **98** mixture. Even in the very best cases, its presence is never less than 5–15%.

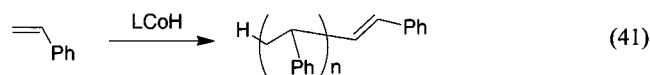
CCT also can be employed to synthesize **98**.³⁶⁶ Temperatures over 150 °C facilitate the process. A process yielding undetectable levels (probably, <0.2%) of isomer **99** in the final AMSd, **98**, provides a high-quality process for AMS dimerization.³⁶⁷ Apparently, the “ceiling temperature” of the dimer of AMS is much higher than that of AMS polymer. The monomeric radical obtained in reaction with LCoH is capable of adding one or two monomeric units but then sterics reduce the value of the propagation rate constant, thereby preventing further radical growth. The decrease in propagation rate constant improves the efficiency of any chain-terminating reactions. As emphasized earlier,⁶¹ low MW polymer chemistry is significantly different from that of high polymer. Many concepts and equations well established for conventional polymer science may encounter serious limitations when used to describe oligomers with $\text{DP} < 6$.

4.4. Styrene

While there is a considerable body of research on CCT polymerizations of styrene itself, there are no reports of CCT in polymerizations of substituted styrenes. In the case of styrene as well as in the case of other vinylic monomers bearing no methyl group adjacent to the propagating radical, CCT always provides oligomers with an exclusively trans configuration of the double bond.^{28,368} Because there is no abstractable methyl hydrogen atom, the only site for

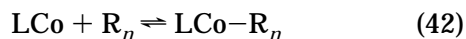
Scheme 9. Cationic Oligomerization of α -Methylstyrene

hydrogen atom abstraction is the methylene group (eq 41). In proton NMR spectra, the vinylic protons of the styrene end group appear as a singlet due to a strong AB-type interaction. However, this singlet can be observed as two peaks at 6.40 and 6.43 ppm by high-field NMR.



The chain-transfer constants for styrene polymerization with porphyrinic CCT catalysts are given in Table 4. In addition, the following values can be found in the literature: $k_C = 1.4 \times 10^5 \text{ M}^{-1} \text{ s}^{-1}$ (40–70 °C, **9a**),³¹⁴ and $k_{CC} = 6.4 \times 10^4 \text{ M}^{-1} \text{ s}^{-1}$, $C_S = 400$ (40 °C, **9c**).⁴⁰ The low C_S in styrene systems can be partly attributed to the formation of Co–C bonds, reducing the concentration of active Co^{II} catalyst. The experimental observation that the molecular weight distribution of the polymer formed in CCT remains constant with conversion is not explained.³⁶⁹

Styrene is capable of forming moderately stable Co–C bonds.³⁷⁰ The formation and decomposition of adducts between the CCT catalysts and the propagating radicals results in “reversible inhibition”.^{123,271} In this case, an induction period is observed at the beginning of polymerization. This induction period is characterized by the steady growth of the rate of polymerization similar to the classic kinetics of a polymerization inhibited by a weak inhibitor. Depending upon conditions, the time required to reach steady-state polymerization kinetics (eq 42) may require tens of minutes.



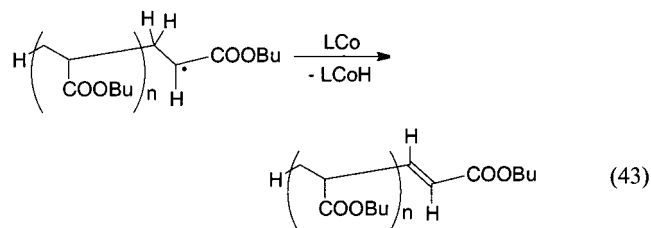
This period of time may be comparable with the experimental frequency of sampling the reaction mixture, thereby confounding the reduction of molecular weight attributable to formation and dissociation of the corresponding organometallic species with the reduction of molecular weight due to CCT.³⁷¹ Moreover, continuous decomposition of the CCT catalyst during polymerization has been observed.³⁷² As a result, some values of the apparent chain-transfer constants of CCT for styrene and other vinylic monomers would be time dependent. Molecular weight distributions at moderate and high conversions can be bimodal.¹²³ These styrene polymerizations are in contrast to MMA polymerization at high conversion that follow kinetic model predictions with only a slight accumulation of lower MW products due to reduction of monomer concentration toward the end of polymerization.¹¹⁸ Consistent with the formation of an equilibrium concentration of Co^{III}–alkyl, C_C was found to be less than 100 in the dark but increases to a maximum value of 5000 under UV irradiation. Previous work has demonstrated the photolysis of the Co–R bond.^{285–288} The value of C_C was also found to be dependent upon the initiator concentration, decreasing with higher initiator levels.¹²⁵ Both of these observations are consistent with the formation of a large equilibrium concentration of Co^{III}–R that can be converted back to Co^{II} photochemically.

4.5. Acrylates

Catalytic chain transfer in acrylate polymerizations is problematic due to the propensity of acrylates to form stable Co–C bonds between the CCT agent and the propagating radical of both the monomer and its oligomers.^{268,269,373} It has even been possible to observe a growing polymer chain terminated with a Co–C bond directly by MALDI.³⁷⁴ This bond is stronger than that in the case of styrene. These complications have a direct impact on the use of CCT in acrylic polymerizations.

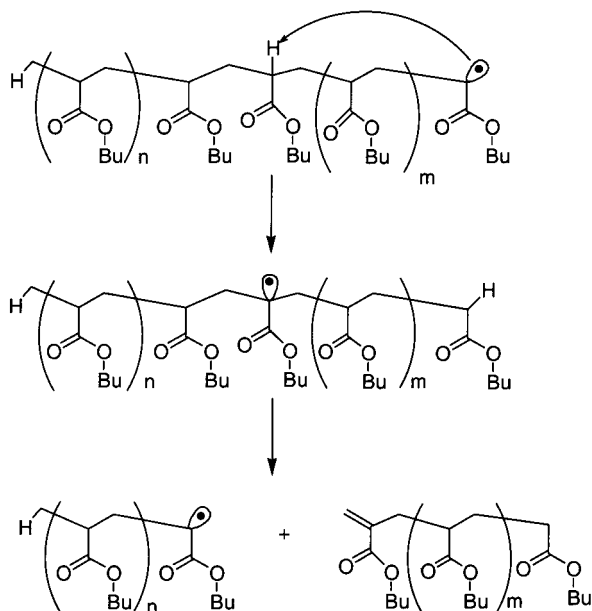
Starting with a Co^{II} CCT catalyst, the initial radicals formed will react with the Co^{II} forming Co^{III}–R, thereby effectively removing much of the Co^{II} from the reaction mixture. This reaction was originally described as “reversible inhibition”.³⁷⁵ This has the effect of trapping all of the initiating radicals and causing an induction period in the polymerization until the Co^{II} is essentially consumed. Once a stoichiometric number of initiating radicals have been produced, polymerization starts but the product is relatively high in molecular weight. The catalyst appears to be relatively ineffective because the concentration of Co^{II} is low. Nonetheless, there is a finite equilibrium concentration of Co^{II} that is low relative to the quantity of catalyst charged but still high relative to the concentration of propagating radicals. There is also a slow reversible reaction of Co^{III}–R liberating radicals to reinitiate polymerization.^{376–378} Similar phenomena have been observed with other reversible capping agents for the propagating radical chains.^{379,380} The suggestion to change the term “reversible inhibition” to “deactivation”³⁸¹ is not an improvement because in addition to reversible inhibition there are other reactions that can deactivate capping agents in living radical polymerizations.

The accepted approach to overcoming this limitation is to increase the temperature of the process.^{382,383} This observation is additional evidence that the intermediate state in CCT, hydrogen atom abstraction from the propagating radical (eq 43), involves a caged radical pair rather than an adduct of the propagating radical with the cobalt chelate.



A characteristic feature of acrylate polymerization is the reaction of “radical back-biting”.^{384–387} Due to the high activity of the acrylic propagating radical and the presence of substantial numbers of tertiary hydrogen atoms in the polyacrylate backbone, a propagating radical can abstract a hydrogen atom from itself or from another polyacrylate molecule. According to the proposed mechanism shown in Scheme 10, the newly formed radical may undergo

Scheme 10. Back-Biting in Growing Acrylate Chains

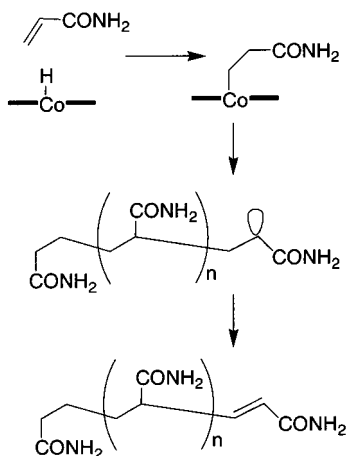


fragmentation. The net result of the back-biting is the formation of oligomer with a terminal double bond of a "methacrylate moiety" with vinylic proton resonances at 6.2 and 5.5 ppm.³⁸³ When the polymerization of acrylic acid is conducted at temperatures above 225 °C, the resulting oligomers have a DP below 50.³⁸⁸ The products are useful as detergent additives and for subsequent polymerization.

Originally the reaction in Scheme 10 was discovered at temperatures approaching 240 °C,³⁸⁸ which are close to the ceiling temperature of acrylates. More recently it was demonstrated that this process is relatively independent of temperature and can be observed as low as 90 °C. Thus, the polymerization of acrylates in the presence of CCT may result in a mixture of vinyl-terminated products.

Another "side reaction" in the polymerization of acrylates could be the anti-Markovnikov addition of Co–H to the olefinic double bond. This reaction shown in Scheme 11 was suggested to explain the absence of any methyl group in the polymer backbone of acrylamide radically polymerized in the presence

Scheme 11. Proposed Mechanism to Explain Poly(acrylamide) Structure

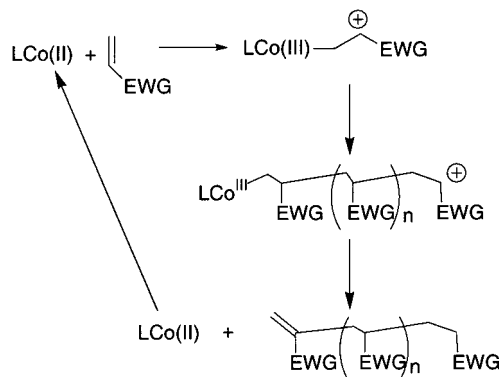


of a CCT catalyst.³⁸⁹ The Markovnikov hydrogen atom addition normally observed in CCT requires that one methyl group should start each polymer molecule and each should be terminated by one vinylic end. In the case of acrylamide, the theoretical number of vinylic hydrogen atoms was observed but expected resonances attributable to CH₃–CH at the head of the chain were absent.

It cannot be excluded that the back-biting depicted in Scheme 10 could be responsible for the observed absence of methyl proton.³⁸⁹ Scheme 10 would leave most of the dead polymer molecules without methyl end groups. The chemical shifts of the vinylic protons in the resulting oligo-acrylamides are at 5.75 and 6.25 ppm, which is similar to the methacrylate end group of polyBA which has been terminated by back-biting. In oligo-acrylates produced by CCT, the vinylic protons have resonances at 6.8 and 5.85 ppm.³⁸³ The mechanism of Scheme 11 in acrylate polymerization requires additional study.

There is a cationic analogue of Scheme 11 when *N*-vinyl carbazole polymerization was induced by poly(vinyl chloride)-bound dimethylglyoxime complexes of Co^{II}, Ni^{II}, and even Cu^{II} (Scheme 12).³⁹⁰

Scheme 12. Cationic Route to Macromonomers



The polymerization shown in Scheme 12 was observed at room temperature and explains the stoichiometric formation of vinylidene end groups. This reaction seems to be a cationic polymerization rather than an example of CCT.

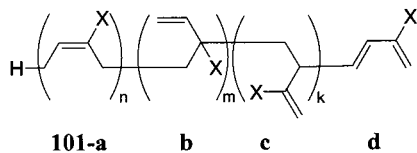
Finally, Scheme 10 is a good example that interesting chemistry remains to be found even in well-studied polymerization systems. In addition to acrylates, substantial back-biting occurs even in radically polymerized styrene.³⁸³ Despite the long-standing utilization of acrylates in radical polymerization, the reaction shown in Scheme 10 was overlooked.

4.6. Acrylonitrile

Investigation of CCT homopolymerization of acrylonitrile is difficult as a result of the insolubility of polyAN even at low molecular weight. Copolymerization with styrene was reported.^{297,371} Addition of minor quantities of amines (about 3%) was shown to have a positive synergetic effect on CCT at 60 °C (bis(diphenylglyoximato)Co^{II}(Py)Cl, AIBN). The role of amines is possibly to stabilize the Co–C bond with formation of a π -complex instead.

4.7. Dienes

Polymerizations involving CCT of this interesting class of monomers has been described in only one reference.³⁹¹ The polymerization of dienes in the presence of CCT catalysts provides oligomers, **101**, with a terminal pair of conjugated double bonds, **101d**.



Diene monomers can be considered to be difunctional monomers. In addition to “normal” 1,4-polymerization that produces polymer with 2,3-vinylidene double bonds **101a**, 1,2-polymerization leads to pendant vinyl groups **101b** and **101c** as well.³⁹² (For simplicity, not all possible isomers are being considered.) These pendant vinyl groups are able to propagate in further radical polymerization, thereby complicating the polymerization, but they also provide functionality for further chemical cross-linking in the final product. In this respect polymerization of diene monomers is somewhat similar to polymerization of dimethacrylates described above, but there are two important differences. First, the groups **101c** and especially **101b** are much less reactive in radical polymerization than the double bonds in methacrylates. Second, the number of pendant vinyl groups **101b** and **101c** per chain in polydienes is substantially less than the number of pendant groups in dimethacrylates. In polychloroprene, for example, the combined vinyl groups account for about 10% of all double bonds.³⁹³

CCT suppresses the gel effect in radical polymerization of chloroprene. The polydispersity stays low, <2, up to 80% conversion. Then, because of cross-linking through pendant vinyl group, both the polydispersity and the molecular weight start to grow exponentially. Table 11 summarizes the use of CCT

Table 11. CCT in Radical Polymerization of Different Diene Monomers³⁹¹

	isoprene	chloroprene	2,3-dichlorobutadiene
C_C^a	190	30	<14
k_C ($M^{-1}s^{-1}$)	75 000	50 000	N/A
k_P ($M^{-1}s^{-1}$)	~400 ^b	1700 ^c	N/A

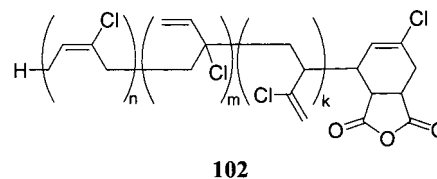
^a Solution polymerization of 67% v/v diene in 1,2-dichloroethane, 70 °C, $(dmgBF_2)_2Co^{II}(MeOH)_2$, $[AIBN] = 8$ g/L, 30% conversion. ^b Estimate from ref 394. ^c From ref 395.

in polymerization of several commercially significant dienes.

The presence of electron-withdrawing substituents such as halogen on dienes substantially increases their propagation rate constants and reduces termination rate constants. As shown in Table 11, k_C does not increase from isoprene to chloroprene so that C_C decreases. The trend continues for 2,3-dichlorobutadiene. Although the propagation rate constant for 1,2-dichlorobutadiene is not known, its C_C is less than

that of chloroprene by a factor of 2 or more, which could be attributed to higher steric constraint around the radical center created by the two chlorine substituents. The paucity of information on propagation rate constants of diene monomers in free-radical polymerization limits further physical studies in this area. The only other reported value of k_P for isoprene is 2 orders of magnitude smaller.³⁹⁶

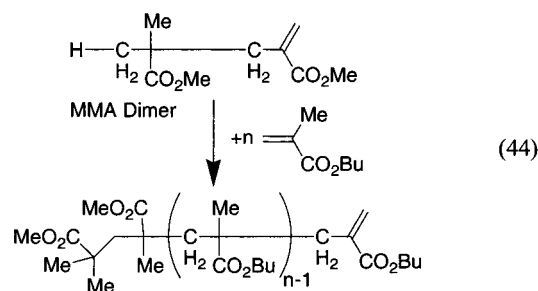
The reactivity of conjugated double bonds is significantly different from that of isolated double bonds in the polymer backbone of polydienes. This difference can be used for selective chemical modification of the dienes with reactions such as the Diels–Alder reaction. With maleic anhydride as an enophile, selective addition to the terminal pair of conjugated double bonds in a chloroprene oligomer is complete in a few hours to give **102**.³⁹¹



According to MALDI-TOF, only one MAn molecule per one chloroprene oligomer is added.

4.8. Macromonomer Reinitiation and Nonpolymerizable Monomers

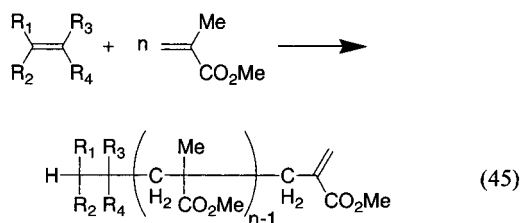
It had been demonstrated that MMA macromonomers do not copolymerize with methacrylates under normal polymerization conditions, and it had also been stated that they do not copolymerize under CCT conditions.¹¹⁰ While this is true, experiments involving cobalt-catalyzed deuterium exchange between MMA dimer and MMA-*d*₈ made it clear that the Co–H or Co–D was adding to the double bond of the dimer to give radical, suggesting that the dimer was being converted to dimer radical. Distilled MMA dimer was exposed to butyl methacrylate under normal CCT polymerization conditions. It was observed that in addition to the expected BMA oligomers and starting MMA dimer, there were species involving MMA dimer coupled with BMA as in eq 44.^{397,398}



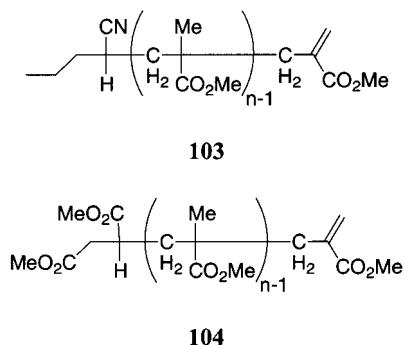
It was already known that MMA dimer was not incorporated into BMA polymer under normal free-radical conditions, though it would act as a chain-transfer agent (see RAFT, section 5.3). It is thus possible to reinitiate seemingly dead polymer chains by addition of a hydrogen atom.

This reinitiation is of commercial interest in a number of circumstances. In preparation of low oligomers by CCT, large quantities of dimer are formed, but dimer is often less attractive than the other oligomers for reasons of activity and volatility. Dimer could be distilled out of the higher oligomers and combined with additional monomer in the oligomerization process to be converted to higher molecular weight species. An extruder-based process for synthesis of lower macromonomers would involve recycle of monomer.¹⁰⁷ In addition, it is possible to react the dimers or oligomers of one monomer with a second monomer, thereby forming block copolymers. The resulting polymers would be a complex mixture with homopolymer of the new monomers, but there are some applications where this would not be a complication.

Extension of macromonomer reinitiation led to copolymerizations with "nonpolymerizable monomers".^{399–401} Methacrylate oligomers cannot be homopolymerized due to the steric bulk of the substituents at what would be the radical center. Thus, they are subject only to reinitiation under CCT conditions. There are many other olefinically unsaturated species which do not undergo homopolymerization or copolymerization with normal free-radical monomers.⁴⁰² These can be represented by the tetrasubstituted olefin in eq 45, though more often the desired olefin is 1,2-disubstituted.



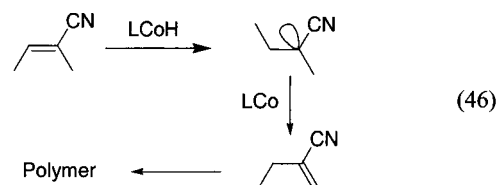
For instance, 2-pentenitrile with MMA gave **103** and dimethyl maleate gave **104**, but both contained MMA homooligomers.



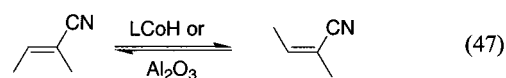
Other examples of nonpolymerizable monomers included 2-cyano-2-butene, crotonaldehyde, ethyl crotonate, and cyclopentene-1-one. The reactions are most productive if carried out with very high concentrations of the nonpolymerizable monomer relative to the conventional monomer. Where possible, the nonpolymerizable monomer is the solvent for the reaction and the conventional monomer would be

added under starved-feed conditions. Such an approach would minimize the percentage of chains initiated with the conventional monomer.

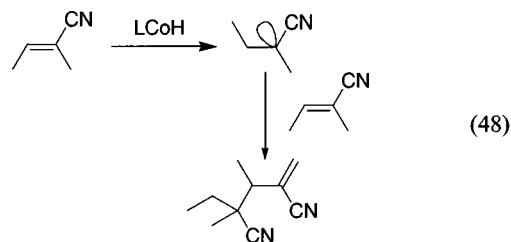
An attempt to polymerize 2-methyl-2-butenenitrile, MBN, by first isomerizing to methylenebuteronitrile (eq 46) led to isomerization instead (eq 47).



Heating an *E/Z* = 1:2 mixture of MBN isomers in the presence of AIBN and a cobalt catalyst results in the reverse composition of *E* and *Z* isomers, 2:1, in 2 h.



Without cobalt chelate and azo initiator there was no change. Oligomerization (eq 48) also occurs, but the rate is several orders of magnitude slower.



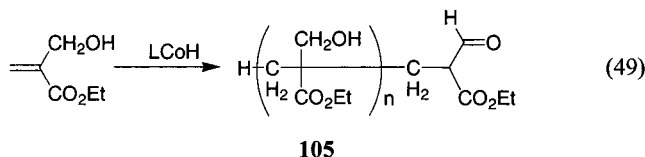
For reasons not understood, heating the isomer mixture with basic alumina causes the reverse transformation, restoring the original 1:2 ratio between MBN isomers. Formation of radical species from MBN was confirmed by observation of copolymer with MMA when minor quantities of MMA were added into a reaction mixture of MBN, cobalt porphyrin, and AIBN.¹³⁹ Therefore, we may draw the conclusion that H-abstraction from the methyl group from the propagating radical of methacrylates is governed by bulk substituents in the propagating radical and the large planar structure of CCT catalyst.

4.9. Isomerizational CCT

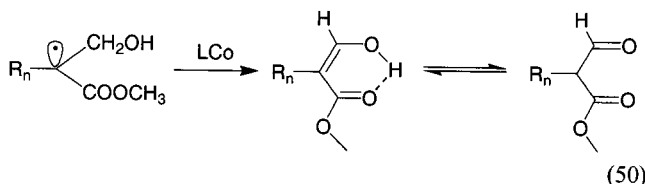
Vitamin B₁₂ is known for its ability to catalyze molecular rearrangements. A variety of cobalt chelates are logical models for vitamin B₁₂, and their stoichiometric and catalytic activities in a variety of reactions,⁴⁰³ particularly olefin isomerizations, were studied intensively.^{404–411} Noncatalytic isomerization reactions based upon the synthesis of alkylcobalt chelates as model intermediates were favored. A variety of catalytic oxidations of substrates such as hydroquinone, azo compounds, phosphines, and olefins were also investigated.^{412–415} Copolymerization of α -methylstyrene and other monomers with oxygen in the presence of CoTPP led to alternating polyperoxides.^{416–418} Cobaloximes were found to catalyze

the alkylation of alkenes and aldehydes by organozinc compounds.^{419,420} Catalytic hydrogenation of olefinic double bonds is a well-known reaction.^{180,421–423} It is therefore interesting that within the limits of detection (<1%), hydrogenation of double bonds was never observed in CCT.

Polymerization of monomers containing α -hydroxymethyl groups results in oligomers terminated with an aldehyde group.^{424–427} For instance, eq 49 shows the reaction for conversion of ethyl α -hydroxymethylacrylate, EHMA, to **105**.

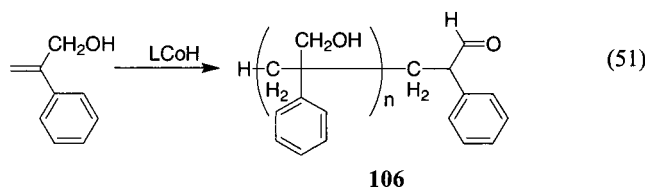


Apparently, the cobalt catalyst abstracts a hydrogen atom from the α -methylene group. The resulting enol is stabilized by isomerization to an aldehyde and formation of a quasi-aromatic ring through a hydrogen bond (eq 50).



The ratio between enol and aldehyde isomers is about 1.4. The chain-transfer constant in eq 49 ($C_C = 700$) is an order of magnitude less than that of MMA. One may conclude that this value reflects steric obstruction of the methylene group by the OH group and that there is no significant enthalpy gain in the enol structure shown in eq 50 relative to a PMMA terminal double bond.

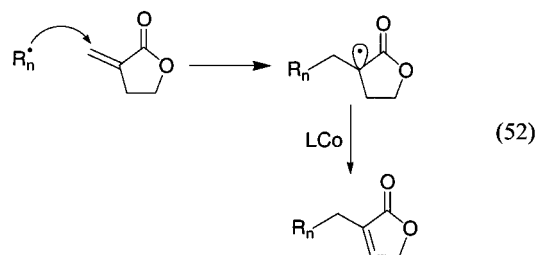
The reaction is even more efficient for 2-phenylallyl alcohol (eq 51) and particularly its copolymers, yielding the oligomer with a terminal aldehyde, **106**.



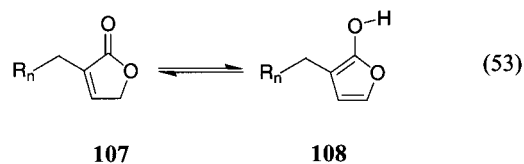
To ensure uniform end-group functionality, careful selection of the comonomers is necessary, but the approach is described.

Attempts to use other hydroxymethyl monomers such as allyl alcohol, 2-methylallyl alcohol, and 2-chloroallyl alcohol for isomerizational copolymerizations with methyl acrylate gave mixed results due to the poor copolymerization rate constants of these olefins and the ability of acrylic radicals to abstract hydrogen atoms from allyl alcohols.

Another example of iCCT comes from polymerization of α -methylnebutyrolactone (MBL).⁴²⁸ CCT from the radical derived from this monomer leads to the unsaturated lactone shown in eq 52.



Usually, monomers without methyl groups in the position α to the double bond are several times less active than those with an α -methyl group. For instance, the polymerization of EHMA above is a good example. MBL was expected to be active in CCT, but the activity observed was unexpected. Its C_C was 8×10^4 , while C_C for MMA is 4×10^4 . The keto–enol tautomerization (eq 53) is responsible for the high CCT rates because the product of the tautomerism is further stabilized by aromaticity.



Such tautomerism is not possible in MBL monomer but becomes possible after hydrogen atom abstraction by CCT. The enol form (**108**) of the lactone (**107**) is a substituted hydroxyfuran.

Isomerizational CCT is an additional tool to produce end groups with chemical functionality different from that of normal CCT. Both EHMA and MBL provide end groups that are quite reactive toward electrophiles. For successful application in iCCT, the monomers should allow a significant thermodynamic driving force by addition of a free radical followed by hydrogen atom abstraction and isomerization.

4.10. Copolymerizations

A combination of variables controls the outcome of the copolymerization of two or more unsaturated monomers by CCT free-radical polymerization.³⁸² Of course, all of the features that control the outcome of a normal free-radical polymerization come into effect.^{40,426,429} These include the molar ratio of monomers, their relative reactivity ratios and their normal chain-transfer constants, the polymerization temperature, and the conversion. In the presence of a CCT catalyst, the important variables also include their relative CCT chain-transfer constants and the concentration of the Co chain-transfer agent. The combination of all of these features controls the molecular weight of the polymer and the nature of the vinyl end group. In addition, they can also control the degree of branching of the product.

In a typical copolymerization involving monomers that are considered to be good for CCT³¹¹ in combination with those that are less effective,⁴³⁰ it is typical that the chain-transfer constant of a given catalyst diminishes.¹³⁵ It is also observed that there is a period of inhibition of polymerization which is dependent upon the concentration of catalyst and the ratio and

Table 12. Copolymerization Chain-Transfer Constants, C_c , for Selected Catalysts

composition			catalyst		
MMA	BA	St	39b	39c	5s
10	0	0	1200	3500	630
9	1	0	1000	560	184
8	1	1	700	500	200
5	5	0	440	130	31

Calculated from ref 135.

nature of monomers.⁴³¹ The catalysts in Table 12 were prepared in situ rather than under optimized conditions, making the results a questionable combination of solubilities, formation rate constants, and chain-transfer constants. Nonetheless, the effects in copolymerizations presented in Table 12 are typical. Addition of butyl acrylate or styrene lowers the effective C_c , and the reduction can be significant.

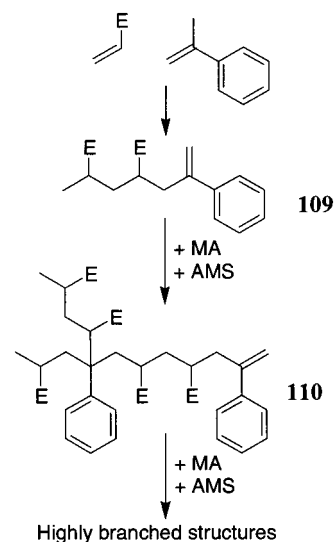
In a copolymerization of styrene and methyl methacrylate under CCT conditions, the fraction of unsaturated styrene end groups is proportional to the fraction of styrene in the monomer feed.³⁶⁸ Due to the stability of styrene radicals, the relative fraction of propagating styrene radicals is large over the whole range of monomer feed compositions.^{432,433} This feature complicates the determination of radical reactivity ratios but may be compensated for by measuring the average transfer rate coefficient as a function of monomer feed composition.

Measurement of reactivity ratios under normal free-radical and CCT polymerization conditions indicates that CCT is a modified free-radical polymerization as expected.⁴³⁴ The reactivity ratios for MMA and butyl methacrylate were used as a mechanistic probe. Reactivity ratios were 1.04 and 0.81 for classical anionic polymerization, 1.10 and 0.72 for alkylaluminum/trialkylaluminum initiated polymerization, 1.76 and 0.67 for group transfer polymerization, 0.98 and 1.26 for atom transfer radical polymerization, 0.75 and 0.98 for CCT, and 0.93 and 1.22 for classical free-radical polymerization. These ratios suggest that ATRP and CCT proceed via radical propagation.

The composition of CCT copolymerization products has been explored in a more complete manner utilizing matrix-assisted laser desorption/ionization time-of-flight (MALDI-TOF) mass spectrometry.⁴³⁵ The bivariate distributions of monomer composition and chain length were determined for a series of copolymers of MMA and butyl methacrylate (BMA) produced by CCT. The relationship between the distributions of copolymers and the kinetics of the copolymerization reactions was derived using the terminal copolymerization model.^{436,437} The reactivity ratios, CCT coefficients, and initiator selectivities were $r^{\text{MMA}} = 1.09$ and $r^{\text{BMA}} = 0.77$, $C_c^{\text{MMA}} = 17\,900$ and $C_c^{\text{BMA}} = 6150$, and $S^{\text{MMA}} = 0.535$, respectively. The reactivity ratios for these polymerizations by ¹H NMR ($r^{\text{MMA}} = 0.75$ and $r^{\text{BMA}} = 0.98$) were in general agreement.

Monomers that form tertiary radicals bearing methyl substituents are generally considered to be good CCT monomers. These include MMA, AMS, and methacrylonitrile.³¹¹ In addition, dienes can be good

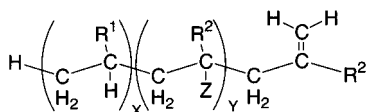
CCT monomers. Monomers that form secondary radicals or do not possess methyl substituents are generally considered to be poor CCT monomers.⁴³⁰ These include MA, styrene, acrylonitrile, and vinyl acetate. Copolymerization of the good CCT monomers with poor CCT monomers in the presence of a CCT catalyst leads initially to oligomers terminated after the incorporation of a good CCT monomer. Thus, in general, the mixed oligomers will contain a terminal methylene unit. For example, copolymerization of methyl acrylate with α -methylstyrene mixture in the presence of a CCT catalyst leads initially to oligomers with a terminal double bond.³⁷⁴ As shown in Scheme 13, the most frequent product will be oligomers of

Scheme 13. Illustrative Products in Methyl Acrylate Copolymerization with α -Methylstyrene: E = CO₂Me

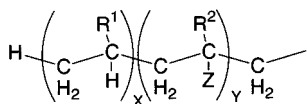
methyl acrylate terminated with an α -methylstyrene moiety, **109**. The methyl acrylate radical is highly reactive but spends much of its time coordinated to the cobalt catalyst.

Insertion of a single AMS leads to a relatively stable radical with an appreciable lifetime. Because AMS is an effective CCT monomer, generating a growing radical with an available methyl C–H bond, CCT occurs with high probability, producing structure **109** that has a terminal double bond that is reactive toward poor CCT monomers. The unsaturated species, **109**, is a copolymerizable monomer that can be incorporated into an additional growing polymer chain forming a branch point. Incorporation of **109** again leads to a relatively stable radical species, but unlike AMS incorporation, it does not provide a readily accessible methyl at the radical center, so continued propagation is the most likely outcome. Early in the polymerization this is an unlikely event, but as the other monomers are depleted, the relative molar concentration of **109** increases, leading ultimately to a substantial portion of branched product, **110**. At high conversion, the concentrations of AMS, MA, **109**, and **110** become similar and a complicated dendritic structure emerges. The ultimate product has been described by structure **111**, where the R¹ and R² substituents are typically

carboalkoxy, phenyl, or cyano and where Z is typically methyl.



111



112

In addition, Z can be described by **112**. When Z is methyl, structure **111** would be a simple random copolymer of the poor monomer bearing only R¹, terminated by the good comonomer bearing a methyl and R². Interestingly, Z can be a single branch **112** when it contains only methyl as Z, but **112** can also contain additional branches again defined by **112**, building into a highly branched system.

The entire process relies upon elevated temperatures to destabilize any Co^{III}-alkyls and high catalyst concentrations such that ample Co^{II} is available. This also leads to relatively low molecular weights for the initial products. It also helps that the susceptibilities of the two monomers to CCT are significantly different and that the concentration of the good CCT monomer is high. Unbranched structures are favored by low conversion, while high conversion favors reinsertion and high branching. The low molecular weight and resulting higher concentration of oligomers favors reincorporation and branching.

Scheme 13 may be generalized by describing A-type monomers³¹¹ and B-type monomers.⁴³⁰ A-type monomers provide chain termination and branching. The A monomers would stay mostly in the branching point. Because B-type monomers are not nearly as effective for CCT, they are generally not the ultimate group in resulting macromonomers. Nonetheless, they are capable of copolymerizing both with the A monomers and with the olefinically terminated macromonomers. Thus, they incorporate oligomers and monomers into higher polymer. In Scheme 13 one can understand how the structure of the final product depends on the relative concentration of oligomers, A monomers, B monomers, and cobalt catalyst. In Table 13, the results of butyl acrylate copolymeriza-

Table 13. Batch Polymerization of BA:MMA (4 v/v mixture at 90 °C)^a

time (h)	1.5	3	7	22
percent conversion	12	24	55	93
M_n	540	640	890	2300
PDI	2.08	2.08	7	2.8

^a A 50% solution in 1,2-dichloroethane, [VAZO-88] = 2 g/L; [cobaloxime 8] = 0.25 g/L.

tion with 20% MMA are presented.

Because MMA is incorporated into polymer chains more rapidly, the concentration of MMA decreases steadily relative to BA during the course of the

polymerization while the concentration of terminally unsaturated macromonomers is steadily increasing. These varying concentrations favor the formation of highly branched polymer at high conversion.

The product may be of more complex structure if more than two monomers are utilized. For example, if nonhomopolymerizable monomers as described above⁴⁰² are included at the beginning of the polymerization, the final product would have them on the periphery of the branched structure. Feeding the polymerization with different monomers would provide additional flexibility to this "arms-first" approach of making hyperbranched polymers.

Batch polymerizations of styrene, MMA, and 2-hydroxyethyl methacrylate carried out in the presence of either dodecanethiol or **9c** indicate that the overall rates of polymerization do not differ significantly in the two systems.⁴³⁸ The molecular weight distribution of the polymer formed in the presence of the thiol becomes increasingly broad, whereas the **9c**-mediated polymerization produces a relatively uniform product during the course of the reaction. The polymer product formed with **9c** was found to be slightly less stable thermally than the product formed by the thiol, presumably a result of the unsaturated end groups.

To prepare water-soluble polymers employing CCT, it is necessary to modify the polymerization conditions.^{312,439} Use of a standard batch reaction leads to hydrolysis of catalyst, changing the catalyst level over the course of the polymerization, yielding a mixture of products and poor control of the reaction. A feed or starved-feed process that adds catalyst over the course of the reaction maintains a constant catalyst level and high conversion. The approach can be applied to a range of monomers such as methacrylic acid, 2-aminoethyl methacrylate hydrochloride, 2-hydroxyethyl methacrylate, 2-methacryloxyethyl phosphoryl choline, glycerol monomethyl methacrylate, and 3-*O*-methacryloyl-1,2:5,6-di-*O*-isopropylidene-D-glucufuranose.

5. Applications of CCT Products

In general, the products of CCT are utilized in further chemistry, but there are some applications where they are employed directly. For instance, CCT catalysts may be used directly in the preparation of emulsions for electrophotographic toners.³⁴⁰ The resulting emulsions are more stable than those obtained with thiol chain-transfer reagents. They may be combined directly with suspensions of black or colored pigments and precipitated to yield toners of narrow particle size. Apparently there may be occasions where highly bimodal molecular weight distributions are desired for toner applications, and then the CCT catalyst is added partway through the polymerization.^{440,441} Alternatively, the CCT catalysts may be employed directly in the casting composition for thermoformable sheet compositions, lowering viscosities and improving toughness of the final sheet goods.⁴⁴²

For some application sensitive to color, it may be necessary to decolorize some macromonomers. The process used is dependent on the properties of the

macromonomer and the catalyst used in its preparation.^{443,444} While most polymerizations are carried out in batch reactions or starved-feed reactions, continuous reactors can also be employed.⁴⁴⁵

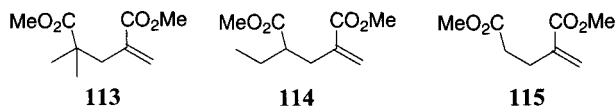
Ethylene–vinyl alcohol copolymers are important oxygen barrier resins for the food packaging industry, and aesthetics of the packaging films are important. The role of α -methylstyrene dimer added to ethylene–vinyl acetate copolymers after polymerization but before saponification is difficult to understand. Nonetheless, the resulting polymers have the advantages of good melt extrusion stability and drawdown resistance resulting in films without streaking.⁴⁴⁶ In addition, they have good interlayer adhesiveness and gas barrier properties.

5.1. Reduction of MW

Federal requirements to produce increasingly lower VOC paints³⁴ have been a significant driver of CCT technology.⁴⁴⁷ Telechelic polymers and other functional systems are used as low-viscosity reactive cross-linkers,³⁵ and pigment dispersants.³⁷

A good example of cross-linking utilizing low molecular weight oligomers involves poly(ortho esters) and isocyanates.⁴⁴⁸ Oligomers of hydroxyethyl methacrylate provide multiple hydroxyl groups for reaction of trimethyl orthoformate and hexamethylene diisocyanate trimer, in the presence of a sulfonate catalyst, to give a product with flowability for application but which cures to give good weatherability and adhesion. Similar systems are useful for the electrodeposited underlayer used for corrosion resistance in automotive finishes.⁴⁴⁹

The MMA dimer, **113**, readily prepared by CCT, is not homopolymerizable; this is attributed to the steric constraints imposed by the steric bulk appended to the α -position.⁴⁵⁰ Interestingly, the isomeric olefin **114** can be polymerized to low molecular weight,⁴⁵¹ and the less hindered species **115** is readily polymerized to higher molecular weight,⁴⁵² though in both cases fragmentation chain transfer is observed. In copolymerization with MMA, **114** acts as a chain-transfer agent.

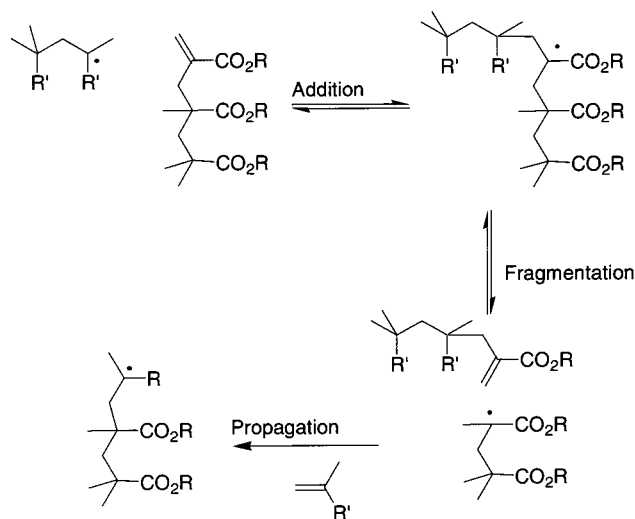


All three species are copolymerizable with styrene. The three species were prepared in interesting solid-state dimerizations involving their salts and mixed salts.^{453–455}

Attempted copolymerizations of MMA oligomers with MMA were relatively unsuccessful. Rather, the MMA oligomers served as chain-transfer agents. The chain-transfer activities of a series of MMA oligomers were evaluated in MMA polymerizations over the temperature range 45–100 °C.⁴⁵⁶ The transfer constants were determined by analysis of the chain length distributions of the resulting polymers as a function of macromonomer concentration. The MMA dimer was substantially less effective as a chain-transfer agent than the MMA trimer or the higher macromonomers. At 60 °C, the constants were 0.013

for dimer, 0.19 for trimer, 0.31 for tetramer, and 0.21 for mixed higher oligomers with an average DP of 24. The transfer constants demonstrated only a small temperature dependence and no variation with conversion. There was no discernible retardation in the rate of polymerization. A reduced yield of polymer was observed. In bulk polymerizations with conversions greater than 10%, the reduced yield was attributed to the absence of the gel (Trommsdorff) effect. The results are interpreted in terms of the addition–fragmentation mechanism for chain transfer shown in Scheme 14.⁴⁵⁷

Scheme 14. Mechanism of Addition–Fragmentation Chain Transfer



Thermal degradation of the oligomers as a model for the transfer process indicates that the process is homolytic bond cleavage and not a retro-ene reaction.⁴⁵⁸

MMA oligomers are effective chain-transfer agents in a variety of copolymerizations.^{337,459–461} If the dimer of hydroxyethyl methacrylate is employed as a chain-transfer agent in MMA polymerization, the resulting product is an α,ω -telechelic polymer.⁴⁶² It was noted that the chain-transfer constant was dependent upon the concentration of the dimer. Emulsion copolymerization of MMA oligomer which was essentially trimer with butyl methacrylate, 2-ethylhexyl methacrylate, hydroxyethyl methacrylate, methacrylamide, and methacrylic acid gave a latex with average particle diameter of over 100 nm and a molecular weight reduced significantly from that which would have been obtained without the trimer.³³⁷ The dimer of methacrylic acid is useful for control of molecular weight in emulsion polymerizations.⁴⁶³

Other dimers that have been employed are those of methacrylic acid and its anhydride,⁴⁶⁴ ethyl methacrylate, methacrylonitrile, and α -methylstyrene.^{465,466} The cross dimers of these monomers with each other as well as with MMA were also found to be effective, with those species containing α -methylstyrene being particularly effective.

The dimer of α -methylstyrene is useful in controlling molecular weight in polystyrene manufacture.^{467,468} The control of molecular weight with

malodorous sulfur compounds is particularly important in room-temperature-curable hand lay-up molding and spray-up molding applications.⁴⁶⁹ In dental adhesives which are cured by UV irradiation, the presence of α -methylstyrene dimer controls hardening time and the heat of polymerization.⁴⁷⁰

Polymers incorporating AMS dimer are utilized in a number of aspects of paper making. It is desirable to maintain as much of the fiber from the paper pulp as possible in the paper rather than in the wastewater. These polymers must demonstrate thickening at low shear ratio and good flowability at high shear ratio. A copolymer of Et acrylate, methacrylic acid, and poly(ethylene glycol) acrylate palmityl ether prepared utilizing AMS dimer in a chain-transfer polymerization performed well as a fiber retention agent.⁴⁷¹ To enhance the surfactant properties of these polymers, other useful monomers include sulfonates of vinyl-terminated polyalkyleneglycols and vinyl-terminated alkylpolyalkylene glycols. Surface properties of the paper are particularly important in printing, and the molecular weight of latex polymers containing acrylamide, acrylic acid, acrylonitrile, butadiene, itaconic acid, MMA, and styrene are controlled with AMS dimer.⁴⁷²

After the paper making process is complete, latexes that are useful as binders for the application of clays or CaCO_3 to paper for printing paper may be prepared using the dimer of AMS. In a typical formulation, styrene, butadiene, Me methacrylate, and acrylonitrile were emulsion polymerized in the presence of AMS dimer to obtain a copolymer latex.⁴⁷³ Surprisingly, the AMS dimer was used in combination with *tert*-dodecylmercaptan, so there may have been some residual odor. Unsaturated carboxylic acids, such as acrylic acid, or sulfonic acids, such as 2-ethylsulfonyl acrylate, or unsaturated amides, such as acrylamide, are also useful, providing the polarity necessary in these applications.⁴⁷⁴

The dimer of AMS is used in the preparation of waterborne coatings.⁴⁷⁵ When used to control molecular weight in copolymerizations of diacetone acrylamide, acrylic acid, MMA, MA, and BA with a Na vinylsulfonate copolymer ammonia salt, the resulting waterborne coating shows good gloss and excellent resistance against water, salt-spray, and blistering. Similar systems are utilized for can coatings.⁴⁷⁶ When the polymers are going to be used in food applications, it is particularly important that they be low odor. Therefore, it is useful to replace mercaptans with AMS dimer.⁴⁷⁷

Polymerization of *N,N*-dimethylaminopropylacrylamide with AMS dimer gave a polymer useful in the preparation dispersant polymers for black pigmented inks for ink-jet applications.^{478–481} In one, the polymerization was initiated with 2,2'-azobis(2-methylpropioamide) dihydrochloride in a water–2-propanol mixture, and it is likely that the spent catalyst was extracted into the aqueous phase.⁴⁷⁸ The inks demonstrate good storage stability. Imide and urea functionalities are also incorporated into polymers for dispersants utilizing CCT technology.⁴⁸²

Powder coatings are an important step toward the lowering of volatile emissions from painting opera-

tions. Polymers for automotive finishes typically contain methyl methacrylate, butyl methacrylate, and glycidyl methacrylate. Incorporation of AMS dimer into one of these polymerizations yields polymers of the proper molecular weight which are free from the odor problems associated with thiol chain-transfer agents.^{483,484} Formulation into a powder coating gave a product with little yellowing.

Formulation of poly(vinyl chloride) into sheet goods is often beset with color problems. The kneading process takes place in the presence of dibutyltin maleate to initiate cross-linking reactions. The presence of AMS dimer in the kneading process leads to less yellowing and better thermal stability for the PVC sheet.⁴⁸⁵

AMS dimer was used to prepare a macromonomer of 2-ethylhexyl methacrylate. Copolymerization of the resulting macromonomer with butyl acrylate and acrylic acid gave a polymer backbone with T_g less than 10 °C that is useful in adhesive applications.⁴⁸⁶ The adhesive is better than the same composition made without the intermediacy of the macromonomer.

Control of molecular weight and branching can also be an issue in the preparation of ABS (acrylonitrile, butadiene, styrene) rubbers. AMSd is employed to lower molecular weight, and the functional end groups may be reincorporated into the polymer to yield branching.⁴⁸⁷

In the copolymerization of difunctional acrylics to prepare cross-linked amorphous glasses for lenses, it is useful to control molecular weight utilizing the AMS dimer. For instance, copolymerization of diallyl isophthalate, dibutyl maleate, and diethyleneglycol bis(allyl carbonate) in the presence of AMSd in a mold gave a lens showing good refractive index, transparency, and impact resistance.⁴⁸⁸ Similar results are obtained for metal-containing optical coatings based upon neodymium in di(2-methacryloyloxyethyl)phosphate, mono(2-methacryloyloxyethyl)phosphate, methacrylic acid, and phenoxyethyl acrylate. The resulting antiglare coatings are very moisture resistant.⁴⁸⁹

The compound 3,9-divinyl-2,4,8,10-tetraoxaspiro[5.5]undecane together with a peroxide is utilized in the cross-linking or curing of polyethylene for wire and cable applications. Addition of 2,4-diphenyl-4-methyl-1-pentene (AMSd) inhibits scorch or premature cross-linking of the polymer, presumably through interception of the radicals.⁴⁹⁰

Apparently, AMSd is also useful in the reduction of the molecular weight of waste polymer.⁴⁹¹ Heating polystyrene foam pieces recycled from food packaging materials at 160 °C for 1 h in the presence of AMSd reduced the M_n from approximately 70 000 to 10 000. The mode of action is unknown, but it is presumed that AMS radicals are generated and abstract hydrogen atoms from the polystyrene backbone, resulting in chain cleavage.

In a more esoteric application, the dimers are useful in the study of free-radical chemistry through trapping experiments.^{351,352}

5.2. Macromonomers for Graft Copolymers

In some instances, the macromonomers synthesized by CCT can be copolymerized with acrylics to form comb copolymers. While β -scission predominates in copolymerizations with methacrylates, acrylates and styrene give both incorporation to yield comb copolymers and β -scission.⁴⁹² Products of this type have been thoroughly characterized by a variety of spectroscopic techniques. When high levels of CCT macromonomers are employed, it is possible to go beyond the comb structure and obtain more highly branched polymers.⁴⁹³

In a more specific example, macromonomer composed of *n*-butyl methacrylate and methacrylic acid prepared by CCT was copolymerized with *n*-butyl acrylate containing a small portion of methyl methacrylate.³⁴¹ Comparison to the equivalent copolymer made with a macromonomer prepared with a thiol chain-transfer agent demonstrated that the CCT macromonomer formed a copolymer while the thiol macromonomer did not. When these compositions were cured using trifunctional isocyanates, they were useful as both clear and pigmented automotive finishes.

Dispersions of organic or inorganic particles that are insoluble in the liquid vehicle are stabilized by polymeric dispersants. These dispersants are usually structured polymeric systems (random, block, or graft) having at least one segment that is soluble in the vehicle and at least one segment that is insoluble in the vehicle and having an affinity for the particle. They have improved stability when the insoluble segment contains cross-linkable groups. One or both segments can be prepared by CCT.^{494–495}

Core-shell microgels can be prepared utilizing CCT macromonomers⁴⁹⁶ and self-stabilized cross-linked latexes.^{497–501}

Methyl methacrylate macromonomers were copolymerized to provide a hydrophobic graft on an otherwise hydrophilic polymer.^{502,503} Such systems are useful in the preparation of soft contact lenses. Hydrophobic methyl methacrylate macromonomers were synthesized by CCT and subsequently copolymerized with any of the hydrophilic monomers *N,N*-dimethylacrylamide, 2-hydroxyethyl acrylate, or *N*-vinyl-2-pyrrolidone by γ -radiation to yield xerogels. The copolymerization was confirmed by NMR analyses and by subsequent aqueous extraction of the resultant copolymers. On swelling in deionized water, hydrogels were formed that had significantly higher Young's moduli than hydrogels based on random copolymers of equivalent composition

Polar polyacrylamide with well-defined nonpolar polystyrene grafts (PAM-*g*-PSt) was synthesized via macromonomer technique.⁵⁰⁴ The resulting amphiphilic polymers exhibit good emulsifying properties. Interestingly, when PAM-*g*-PSt was blended with PMAA grafted with PMMA, an intermolecular complex membrane was formed. The permeability of the membrane is controlled reversibly by changing the pH value, making it a chemical valve.

Oligomers of acrylic acid having a DP below 50 are useful as detergent additives and boosters.³⁸⁸ When employed in subsequent polymerizations, the result-

ing multiblock copolymers can be neutralized to form ionomeric networks.

Graft acrylic polyols for two-component polyurethane coatings can be prepared by free-radical copolymerization of MMA, BMA, BA, acrylic acid, HEMA, and PMMA macromonomers.⁵⁰⁵ The polymers offer an advantage over conventional resins with respect to the application/appearance of coatings as well as the final film properties. Some of these advantages were higher solids and a better control of the coating rheology, an increase in the cross-linking reactivity of the polyols with polyisocyanate, and improvement in film toughness. The change in the morphological structure of the films under tensile stress was of particular interest.

In an alternative approach, chloride-containing polymers such as styrene-*co*-chloromethylstyrene were grafted with MMA by initiating from the chloro groups with chlorocobaloxime.^{506,507} Similar reaction had been noted under photochemical conditions, but the reactions can also be run thermally. The mechanism is unclear, but improved polymerization in the presence of zinc as a reducing agent suggests that Co^I may have been involved. Polymerization was also initiated from halide donors such as chloroform or trichloroethane without the reducing agent.

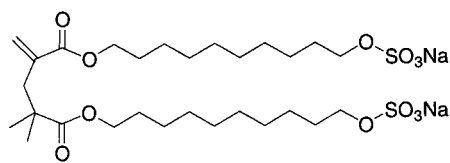
5.3. RAFT

RAFT (reversible addition-fragmentation transfer) polymerization is gaining popularity as an alternative to living polymerizations for the synthesis of narrow molecular weight or structured polymers.^{508–514} Early work in the area demonstrated that the methacrylate oligomers synthesized by CCT can be employed in the RAFT process,^{512,515} as can dimers of α -methylstyrene prepared cationically.³⁵⁰ Today, RAFT technology is dominated by the use of thiocarbonylthio compounds and the term RAFT has come to imply the use of these compounds. The RAFT process, very similar to that shown in Scheme 14, involves a series of reversible addition-fragmentation steps.^{508,509} Addition of a propagating radical to an MMA oligomer gives an adduct radical which can fragment to form terminated polymeric chain and a new radical. The reaction of the new radical with a monomer (M) results in a new propagating radical. Subsequent addition-fragmentation steps allow a dynamic equilibrium to be established between the active propagating radicals and dormant polymer such that there is an equal probability of growth for all chains, resulting in an apparent living polymerization and a narrow molecular weight distribution.

CCT of benzyl methacrylate leads to a mixture of poly(benzyl methacrylate) macromonomers from which the dimer macromonomer could be isolated.⁵¹⁶ When the benzyl dimer is used as a RAFT chain-transfer agent, PMMA with α - and ω -terminal benzyl methacrylate units is obtained. Catalytic hydrogenation of the α,ω -benzyl terminal methyl methacrylate polymer results in the evolution of toluene and formation of α,ω -dicarboxyl functional telechelic PMMA.

When it is important that surfactants utilized in free-radical emulsion polymerization not be free to

migrate through the polymer in the final application, it is possible to incorporate species such as **116** into the polymerization through RAFT.⁵¹⁷

**116**

An MMA dimer obtained by CCT was hydrolyzed and then re-esterified with 1,10-decanediol. The resulting diester was allowed to react with chlorosulfonic acid to produce the methacrylate dimer surfactant, 2,4-bis(sodium 10-sulfate decanoxycarbonyl)-4-methylpent-1-ene. At the beginning of a polymerization, the molecule acts as a surfactant and subsequent incorporation of the dimer in the polymerization yields a surfactant-functionalized polymer. Thus, additional surfactants are not required.

5.4. Copolymerization (Graft-Copolymers)

Branched acrylic polymers based upon the copolymerization of acrylates and related monomers with methacrylate macromonomers are particularly useful in waterborne coatings. A macromonomer based upon isobutyl methacrylate, 2-ethylhexyl methacrylate, and 2-hydroxyethyl methacrylate was copolymerized with butyl acrylate, 2-hydroxyethyl acrylate, methacrylic acid, methyl methacrylate, and styrene.⁵¹⁸ After neutralization with dimethylethanolamine or inorganic bases, the polymer could be cross-linked with melamine resin on a metal surface. These systems may be used for either pigmented layers or clear coats.

5.5. Hyperbranched and Cross-Linked Materials

Much of the material in this section was already covered under polymerizations of di- and triacrylates in section 4.1.1.

Copolymerization of di- and trimethacrylates with functionalized monomers, like glycidyl methacrylate, leads to low-viscosity oligomers capable of nonradical cross-linking. This process promises substantial value for industrial applications. Star polymers useful in coatings were prepared by copolymerizing methacrylate macromonomers with diacrylates.⁵¹⁹ For instance, a star polymer was synthesized by copolymerization of a 2-ethylhexyl methacrylate/isobutyl methacrylate/hydroxyethyl methacrylate macromonomer with butanediol diacrylate.

6. Conclusions

Catalytic chain transfer is a versatile tool that complements other means of polymerization. It allows the synthesis of the large variety of structured polymers shown in Figure 11. The primary outlet for CCT is to control molecular weight in free-radical polymerizations without the use of stoichiometric chain terminators (sections 1–3). All of the products can be considered to be monofunctional in that they are all terminated by unsaturation. The unsaturation

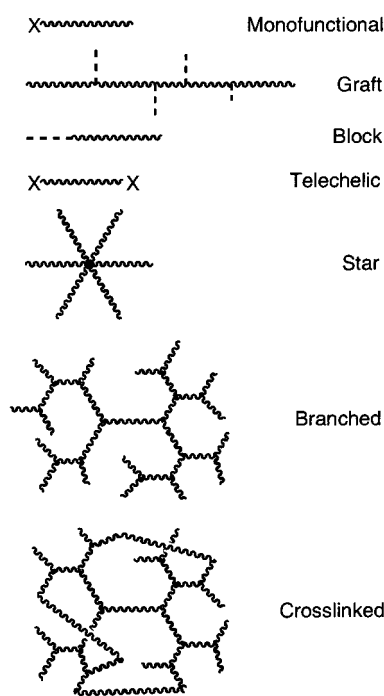


Figure 11. Polymer structures available through CCT.

is largely olefinic in nature but can also be aromatic or aldehydic through isomerizational CCT (section 4.9). In what would appear to be a homeopathic application, the products of CCT themselves, free of cobalt CCT catalyst, can be used to control molecular weight through RAFT (section 5.1).

If functionalized macromonomers are utilized in RAFT with nonfunctionalized monomers, the resulting polymers may be telechelic in other polymerizations (section 5.3).

It is interesting that the bulk of products prepared by CCT go into applications where aesthetics are important. The most widely practiced application for CCT polymers is in automotive and other higher technology finishes. In these applications, polyfunctional polymers are cross-linked to provide tough, impermeable finishes with good aesthetics (section 4.1). Copolymerization of the olefinically unsaturated macromonomers with smaller monomers such as acrylates leads to graft copolymers (section 5.4). If the large macromonomers are copolymerized with a minimal amount of comonomer, the resulting polymer is more like a star, but incorporation of macromonomers into macromonomers leads to branched and hyperbranched systems (sections 4.10 and 5.5). CCT polymers find utility in paper and printing technologies only in the higher end applications—making paper where high quality is demanded or making inks and pigments for high-quality printing.

Only complexes having an unpaired electron can operate as CCT catalysts with the low activation energies or high rates required for this process because only they have essentially zero activation energies for reactions with the growing radical chains.

The abstraction of a hydrogen atom from a growing radical chain by a paramagnetic metal center is analogous to the disproportionation reaction between two radical chains in a normal free-radical polymer-

- Mahabadi, H. K.; O'Driscoll, K. F. *J. Polym. Sci., Polym. Chem. Ed.* **1979**, *17*, 1891.
- (17) Golikov, I. V.; Mironicev, V. E.; Golubchikov, O. A.; Smirnov, B. R. *Izv. Vyssh. Uchebn. Zaved., Khim. Khim. Tekhnol.* **1983**, *26*, 1118 (Russian); *Chem. Abstr.* **1984**, *100*, 68782v.
- (18) Gridnev, A. A. Ph.D. Thesis, Institute of Chemical Physics, 1983.
- (19) Smirnov, B. R.; Morozova, I. S.; Marchenko, A. P.; Markevich, M. M.; Puschaeva L. M.; Enikolopyan, N. S. *Dokl. Chem.* **1980**, *253*, 383. Smirnov, B. R.; Morozova, I. S.; Marchenko, A. P.; Markevich, M. A.; Pushchaeva, L. M.; Enikolopyan, N. S. *Dokl. Akad. Nauk SSSR* **1980**, *253* (4), 891 [Chem.] (Russian); *Chem. Abstr.* **1981**, *94*, 16161.
- (20) McCord, E. F.; Anton, W. L.; Wilczek, L.; Ittel, S. D.; Nelson, L. T. J.; Raffell, K. D. *Macromol. Symp.* **1994**, *86*, 47.
- (21) Cacioli, P.; Moad, G.; Rizzardo, E.; Serelis, A. K.; Solomon, D. H. *Polym. Bull.* **1984**, *11*, 325.
- (22) Cacioli, P.; Hawthorne, D. G.; Johns, S. R.; Solomon, D. H.; Rizzardo, E.; Willing, R. I. *J. Chem. Soc., Chem. Commun.* **1985**, 1355.
- (23) Ozerkovskii, B. V.; Roschupkin, V. P. *Dokl. Chem.* **1980**, *254*, 731; *Dokl. Akad. Nauk SSSR* **1980**, *254* (1), 157 [Phys. Chem.] (Russian); *Chem. Abstr.* **1981**, *94*, 31186.
- (24) Lingnau, J.; Stickler, M.; Meyerhoff, G. *Eur. Polym. J.* **1980**, *16* (8), 785.
- (25) Karmilova, L. V.; Ponomarev, G. V.; Smirnov, B. R.; Bel'govskii, I. M. *Russ. Chem. Rev.* **1984**, *53*, 132.
- (26) Parshall, G. W.; Ittel, S. D. *Homogeneous Catalysis*; Wiley: New York, 1992; p 85.
- (27) McCord, E. F.; Anton, W. L.; Wilczek, L.; Ittel, S. D.; Nelson, L. T. J.; Raffell, K. D.; Hansen, J. E.; Berge, C. *Macromol. Symp.* **1994**, *86* (Advances in NMR Studies of Polymeric Materials), 47.
- (28) Gridnev, A. A.; Cotts, P. M.; Roe, C.; Barth, H. *J. Polym. Sci., Part A: Polym. Chem.* **2001**, *39*, 1099.
- (29) *Polymer Handbook*, 2nd ed.; Brandrup I., Immergut, E. H., Eds.; Interscience: New York, 1975; p II-60.
- (30) Forster, D. J.; Heuts, J. P. A.; Lucien, F.; Davis, T. P. *Macromolecules* **1999**, *32* (17), 5514.
- (31) Kukulj, D.; Davis, T. P. *Macromol. Chem. Phys.* **1998**, *199* (8), 1697.
- (32) Bon, S. A. F.; Morsley, D. R.; Waterson, J.; Haddleton, D. M.; Lees, M. R.; Horne, T. *Macromol. Symp.* **2001**, *165* (Developments in Polymer Synthesis and Characterization), 29.
- (33) *Polymer Handbook*, 2nd ed.; Brandrup I., Immergut, E. H., Eds.; Interscience: New York, 1975; p II-48.
- (34) See, for instance: (a) Liebscher, H. *FATIPEC Congr.* **1998**, 24th (Vol. A), A/345. (b) Mestach, D. *PPCJ, Polym. Paint Colour J.* **2000**, *190* (4431), 28. (c) Dobson, I. *Pigm. Resin Technol.* **1999**, *28* (2), 89. (d) Kershaw, Y. *Eur. Coat. J.* **1998**, (4), 230, 234. (e) Marrion, A. R. *Chem. Phys. Coat.* **1994**, 8.
- (35) See, for instance: (a) Bloembergen, S.; McLennan, I. J.; Cassar, S. E.; Narayan, R. *Adhes. Age* **1998**, *41* (2), 20. (b) Kennan, L. D.; Lo, P. Y. K.; Saxena, A. K.; Suzuki, To. U.S. Patent 5731379 March 24, 1998. (c) Ito, Y.; Kojima, S. (Toa Gosei Kk, Japan) Jpn. Pat. Appl. 08319310, Priority date Dec 3, 1996. (d) Jenkins, R. D. (Union Carbide Chemicals and Plastics Technology Corp., USA) Eur. Pat. Appl. EP 729989 A2 19960904, Priority date Feb 28, 1995. (e) Kuwano, K.; Nagata, K.; Nagasawa, M.; Hibino, H. *Kobunshi Ronbunshu* **1996**, *53* (3), 165 (Japanese); *Chem. Abstr.* **1996**, *124*, 263436.
- (36) Adamsons, K.; Blackman, G.; Gregorovich, B.; Lin, L.; Matheson, R. *Prog. Org. Coat.* **1998**, *34* (1-4), 64.
- (37) For examples of polymers as solids dispersants, see: (a) McIntyre, P. F.; King, J. G.; Spinelli, H. J.; Jakubauskas, H. G. (E.I. DuPont de Nemours and Co.) U.S. Patent 5859113, Jan 12, 1999. (b) Ishibashi, H. *Techno-Cosmos* **1997**, *12*, 45. (c) Whalen-Shaw, M. U.S. Patent 5320672, June 14, 1994. (d) Weingart, F.; Brodt, G.; Lehner, A.; Tanakai, T. *Shikizai Kyokaiishi* **1996**, *69* (1), 19. (e) Kawanishi, W. (Kyoeisha Chemical Co., Ltd., Japan) Eur. Pat. Appl. EP 732346 A1 19960918, Priority date March 16, 1995.
- (38) For examples of ink jet polymers, see: (a) Reardon, J. E. (E.I. DuPont de Nemours and Co.) Eur. Pat. Appl. EP 928821 A1 19990714, Priority date Jan 12, 1998. (b) Hesler, C. M.; Simon, E. S. (Rohm and Haas Co.) U.S. Patent 5821283, Oct 13, 1998. (c) Grezzo, P. L. A.; Bednarek, M. B.; Ma, Z.; Prasad, K. A. (E.I. DuPont de Nemours and Co., USA) U.S. Patent 5713993, Feb 3, 1998.
- (39) Mayo, F. R. *J. Am. Chem. Soc.* **1943**, *65*, 2324.
- (40) For example, see: Heuts, J. P. A.; Kukulj, D.; Foster, D. J.; Davis, T. P. *Macromolecules* **1998**, *31* (9), 2894.
- (41) For example, see: Moad, G.; Moad, C. L. *Macromolecules* **1996**, *29* (24), 7727.
- (42) Olaj, O. F.; Zifferer, G.; Gleixner, G.; Stickler, M. *Eur. Polym. J.* **1986**, *22* (7), 585.
- (43) Smirnov, B. R.; Marchenko, A. P.; Plotnikov, V. D.; Kuzayev, A. I.; Enikolopyan, N. S. *Polym. Sci.* **1981**, *A23*, 1169. *Vysokomol. Soedin., Ser. A* **1981**, *23* (5), 1051 (Russian); *Chem. Abstr.* **1981**, *95*, 81600.
- (44) Burczyk, A. F.; O'Driscoll, K. F.; Rempel, G. L. *J. Polym. Sci., Chem. Ed.* **1984**, *22*, 3255.
- (45) Sanayei, R. A.; O'Driscoll, K. F. *J. Macromol. Sci., Chem.* **1989**, *A26* (8), 1137.
- (46) Ittel, S. D.; Gridnev, A. A.; Wayland, B. B.; Fryd, M. *Polym. Prepr. (Am. Chem. Soc., Div. Polym. Chem.)* **1994**, *35* (1), 704.
- (47) Gridnev, A. A.; Ittel, S. D.; Fryd, M. *J. Polym. Sci., Part A: Polym. Chem.* **1995**, *33* (7), 1185.
- (48) Simonsick, W. J., Jr.; Aaserud, D. J.; Grady, M. C. *Polym. Prepr. (Am. Chem. Soc., Div. Polym. Chem.)* **1997**, *38* (1), 483.
- (49) Simonsick, W. J., Jr.; Aaserud, D. J.; Grady, M. C.; Prokai, L. *Book of Abstracts*, 213th National Meeting of the American Chemical Society, San Francisco, CA, April 13-17, 1997; American Chemical Society: Washington, DC, 1997; POLY-208.
- (50) Hutchinson, R. A.; Paquet, D. A., Jr.; McMinn, J. H.; Beuermann, S.; Fuller, R. E.; Jackson, C. *DECHEMA Monogr.* **1995**, *131* (5th International Workshop on Polymer Reaction Engineering, 1995), 467.
- (51) Kurata, M.; Tsunashima, Y. In *Polymer Handbook*, 4th ed.; Brandrup, J., Immergut, E. H., Grulke, E. A., Eds.; Wiley-Interscience: New York, 1999.
- (52) Gridnev, A. A.; Bel'govskii, I. M.; Enikolopyan, N. S. *Vysokomol. Soedin., Ser. B (Polym. Sci.)* **1986**, *B28* (2), 85 (Russian); *Chem. Abstr.* **1986**, *105*, 6846.
- (53) Hutchinson, R. A.; Paquet, D. A., Jr.; McMinn, J. H. *Macromolecules* **1995**, *28* (16), 5655.
- (54) Deady, M.; Mau, A. W. H.; Moad, G.; Spurling, T. H. *Makromol. Chem.* **1993**, *194* (6), 1691.
- (55) Krstina, J.; Moad, G.; Willing, R. I.; Danek, S. K.; Kelly, D. P.; Jones, S. L.; Solomon, D. H. *Eur. Polym. J.* **1993**, *29* (2,3), 379.
- (56) Buback, M.; Busch, M.; Kowollik, C. *Macromol. Theory Simul.* **2000**, *9* (8), 442.
- (57) Olaj, O. F.; Vana, P.; Zoder, M.; Kornherr, A.; Zifferer, G. *Macromol. Rapid Commun.* **2000**, *21* (13), 913.
- (58) Moad, G.; Rizzardo, E.; Solomon, D. H.; Beckwith, A. L. *J. Polym. Bull. (Berlin)* **1992**, *29* (6), 647.
- (59) Heuts, J. P. A.; Gilbert, R. G.; Radom, L. *Macromolecules* **1995**, *28* (26), 8771.
- (60) Beuermann, S. E.; Buback, M.; Davis, T. P.; Gilbert, R. G.; Hutchinson, R. A.; Kajiwarra, A.; Klumperman, B.; Russell, G. T. *Macromol. Chem. Phys.* **2000**, *201* (12), 1355.
- (61) Gridnev, A. A.; Ittel, S. D. *Macromolecules* **1996**, *29* (18), 5864.
- (62) Bandaranayake, W. M.; Pattenden, G. *J. Chem. Soc., Chem. Commun.* **1988**, (17), 1179.
- (63) Kijima, M.; Miyamori, K.; Sato, T. *J. Org. Chem.* **1987**, *52* (4), 706.
- (64) Pattenden, G. *Chem. Soc. Rev.* **1988**, *17* (4), 361.
- (65) Moad, G.; Rizzardo, E.; Solomon, D. H.; Beckwith, A. L. *J. Polym. Bull. (Berlin)* **1992**, *29* (6), 647.
- (66) Gridnev, A. A.; Ittel, S. D.; Fryd, M.; Wayland, B. B. *Organometallics* **1996**, *15* (1), 222.
- (67) Christianson, D. W.; Lipscomb, W. N. *J. Am. Chem. Soc.* **1985**, *107*, 2682.
- (68) (a) Marques, H. M.; Brown, K. L. *J. Mol. Struct. (THEOCHEM)* **1995**, *340*, 97. (b) Marques, H. M.; Brown, K. L. *Inorg. Chem.* **1995**, *34*, 3733.
- (69) (a) Marques, H. M.; Warden, C.; Monye, M.; Shongwe, M. S.; Brown, K. L. *Inorg. Chem.* **1964**, *37*, 2578. (b) Marques, H. M.; Brown, K. L. *Coord. Chem. Rev.* **1999**, *190-192*, 127.
- (70) (a) Hansen, L. M.; Pavan Kumar, P. N. V.; Marynick, D. S. *Inorg. Chem.* **1994**, *33*, 728. (b) Hansen, L. M.; Derecskei-Kovacs, A.; Marynick, D. S. *J. Mol. Struct. (THEOCHEM)* **1998**, *431*, 53. (c) Zhu, L.; Kostic, N. M. *Inorg. Chem.* **1987**, *26*, 4194.
- (71) (a) Torrent, M.; Musaev, D. G.; Morokuma, K.; Ke, S.-C.; Warncke, K. *J. Phys. Chem. B* **1999**, *103* (40), 8618. (b) Ke, S.-C.; Torrent, M.; Musaev, D. G.; Morokuma, K.; Warncke, K. *Biochemistry* **1999**, *38* (39), 12681.
- (72) Jensen, K. P.; Sauer, S. P. A.; Liljefors, T.; Norrby, P.-O. *Organometallics* **2001**, *20* (3), 550.
- (73) (a) Becke, A. D. *J. Chem. Phys.* **1993**, *98* (7), 5648. (b) Scott, A. P.; Radom, L. *J. Phys. Chem.* **1996**, *100* (41), 16502. (c) Jensen, F. *Introduction to Computational Chemistry*; John Wiley & Sons Ltd.: Chichester, 1999.
- (74) (a) Walker, L. A., II; Jarrett, J. T.; Anderson, N. A.; Pullen, S. H.; Matthews, R. G.; Sension, R. J. *J. Am. Chem. Soc.* **1998**, *120* (15), 3597. (b) Walker, L. A., II; Shiang, J. J.; Anderson, N. A.; Pullen, S. H.; Sension, R. J. *J. Am. Chem. Soc.* **1980**, *102* (29), 7286.
- (75) Pliss, E. M.; Machtin, V. A.; Smirnov, B. R.; Mogilevich, M. M.; Rzhetskaya, N. N.; Mironychev, V. E. *Vysokomol. Soedin., Ser. B* **1983**, *25* (4), 260; *Chem. Abstr.* **1982**, *98*, 216087.
- (76) Vollmerhaus, R.; Pierik, S.; Van Herk, A. M. *Macromol. Symp.* **2001**, *165* (Developments in Polymer Synthesis and Characterization), 123.
- (77) Gridnev, A. A. *Polym. Sci.* **1989**, *31*, 2369; *Vysokomol. Soedin., Ser. A* **1989**, *31* (10), 2153 (Russian); *Chem. Abstr.* **1990**, *112*, 199160.
- (78) Janowicz, A. H. (DuPont de Nemours and Co.) U.S. Patent 4886861, Dec 12, 1989; *Chem. Abstr.* **1990**, *113*, 41529.

- (79) Carlson, G. M.; Abbey, K. J. (SCM Corp.) U.S. Patent 4526945, 1985; *Chem. Abstr.* **1985**, 103, 142530.
- (80) Carlson, G. M. (SCM Corp.) U.S. Patent 4547323, Oct 15, 1985; *Chem. Abstr.* **1986**, 104, 89184.
- (81) Abbey, K. J.; Carlson, G. M.; Masola, M. J.; Trumbo, D. *Polym. Mater. Sci. Eng.* **1986**, 55, 235.
- (82) (a) Brown, T. M.; Dronfield, A. T.; Cooksey, C. J.; Crich, D. *J. Chem. Educ.* **1990**, 67 (11), 973. (b) Schrauzer, G. N. *Inorg. Synth.* **1968**, 11, 61.
- (83) Brown, T. M.; Cooksey, C. J. *Educ. Chem.* **1987**, 24 (3), 77.
- (84) Hawthorne, D. G. (Commonwealth Scientific and Industrial Research Organization, Australia) PCT Int. Appl. WO 8703605 A1 19870618, Priority date Dec 3, 1986; *Chem. Abstr.* **1987**, 107, 237504.
- (85) Bresciani-Pahor, N.; Forcolin, M.; Marzilli, L. G.; Randaccio, L.; Summers, M. F.; Toscano, P. *J. Coord. Chem. Rev.* **1985**, 63 1.
- (86) Schrauzer, G. N. *Acc. Chem. Res.* **1968**, 1 (4), 97.
- (87) Peshkova, V. M.; Savostina, V. M.; Ivanova, E. K. *The Oximes*; Nauka: Moscow, 1977 (Russian).
- (88) Schrauzer, G. N. *Angew. Chem.* **1976**, 88 (14), 465.
- (89) *The Porphyrins*; Dolphin, D., Ed.; Wiley: New York, 1978; Vol. V.
- (90) Fergusson, S. B.; Baird, M. C. *Inorg. Chim. Acta* **1982**, 63 (1), 41.
- (91) Ingraham, L. L. *Ann. N. Y. Acad. Sci.* **1964**, 112 (2), 713.
- (92) Schrauzer, G. N.; Windgassen, R. J. *J. Am. Chem. Soc.* **1966**, 88 (16), 3738.
- (93) Asaro, F.; Liguori, L.; Pellizer, G. *Angew. Chem., Int. Ed.* **2000**, 39 (11), 1932.
- (94) Moad, G.; Moad, C. L.; Krstina, J.; Rizzardo, E.; Thang, S. H.; Fryd, M. (E.I. DuPont de Nemours and Co., USA, and Commonwealth Scientific and Industrial Research Organization) PCT Int. Appl. WO 9615158 A1 19960523, Priority date Nov 9, 1994.
- (95) Hussain, M. S. *Book of Abstracts*, 216th National Meeting of the American Chemical Society, Boston, Aug 23–27, 1998; American Chemical Society: Washington, DC, 1988; INOR-144.
- (96) Enikolopov, N. S.; Bel'govskii, I. M.; Gridnev, A. A.; Marchenko, A. P.; Smirnov, B. R. (Institute of Chemical Physics, Chernogolovka, USSR) Soviet Pat. SU 940487 A1 19870323, March 23, 1987 (Russian); *Chem. Abstr.* **1987**, 107, 154922.
- (97) Nonaka, Y.; Hamada, K. *Bull. Chem. Soc. Jpn.* **1981**, 54 (10), 3185.
- (98) Bakac, A.; Espenson, J. H. *J. Am. Chem. Soc.* **1984**, 106 (18), 5197.
- (99) Drago, R. S.; Gaul, J. H. *Inorg. Chem.* **1979**, 18 (7), 2019.
- (100) Tovrog, B. S.; Kitko, D. J.; Drago, R. S. *J. Am. Chem. Soc.* **1976**, 98 (17), 5144.
- (101) Janowicz, A. H. (DuPont) U.S. Patent 4680352, July 14, 1987.
- (102) Shriver, D. F. *Manipulation of Air-Sensitive Compounds*; Krieger Publishing: Malabar, FL, 1982.
- (103) Nonaka, Y.; Hamada, K. *Bull. Chem. Soc. Jpn.* **1981**, 54 (10), 3185.
- (104) Lawson, E. E.; Edwards, H. G. M.; Johnson, A. F. *Spectrochim. Acta, Part A* **1994**, 50 (11), 1899.
- (105) (a) Janowicz, A. H. (DuPont) U.S. Patent 4694054, July 2, 1991. (b) Janowicz, A. H. (E.I. DuPont de Nemours and Co.) Eur. Pat. Appl. EP 261942 A2 19880330, Priority date Sept 23, 1986; *Chem. Abstr.* **1988**, 109, 111104.
- (106) Melby, L. R.; Janowicz, A. H.; Ittel, S. D. (E.I. DuPont de Nemours and Co.) Eur. Pat. Appl. EP 199436 A1 19861029, Priority date March 1, 1985; *Chem. Abstr.* **1987**, 106, 157018.
- (107) Suddaby, K. G.; Sanayei, R. A.; Rudin, A.; O'Driscoll, K. F. *J. Appl. Polym. Sci.* **1991**, 43 (8), 1565.
- (108) Davis, T. P.; Kukulj, D.; Maxwell, I. A. *Macromol. Theory Simul.* **1995**, 4 (1), 195.
- (109) Davis, T. P.; Kukulj, D.; Haddleton, D. M.; Maloney, D. R. *Trends Polym. Sci.* **1995**, 3 (11), 365.
- (110) Haddleton, D. M.; Maloney, D. R.; Suddaby, K. G. *Proc. Am. Chem. Soc., Div. Polym. Mater. Sci. Eng.* **1995**, 73, 420.
- (111) Haddleton, D. M.; Muir, A. V. G. (Zeneca Ltd., UK) PCT Int. Pat. Appl. WO 9504759 A1 19950216, Priority date Aug 9, 1993; *Chem. Abstr.* **1995**, 123, 229300.
- (112) Haddleton, D. M.; Muir, A. V. G.; Leeming, S. W. (Zeneca Ltd., UK) PCT Int. Pat. Appl. WO 9517435 A1 19950629, Priority date Dec 20, 1993; *Chem. Abstr.* **1995**, 123, 314835.
- (113) Muir, A. V. G.; Lawson, J. R.; Haddleton, D. M. (Zeneca Ltd., UK) PCT Int. Pat. Appl. WO 9527737 A1 19951019, Priority date April 11, 1994; *Chem. Abstr.* **1995**, 124, 88185.
- (114) Maloney, D. R.; Hunt, K. H.; Lloyd, P. M.; Muir, A. V. G.; Richards, S. N.; Derrick, P. J.; Haddleton, D. M. *J. Chem. Soc., Chem. Commun.* **1995**, (5) 561.
- (115) Haddleton, D. M.; Maloney D. R.; Suddaby, K. G.; Muir, A. V. G.; Richards, S. N. *Macromol. Symp.* **1996**, 111, 37.
- (116) Arvanitopoulos, L. D. University Microfilms Int., Order No.: DA9528470, 1995. From *Diss. Abstr. Int., B* **1995**, 56 (4), 2048; *Chem. Abstr.* **1995**, 123, 341092.
- (117) Haddleton, D. M.; Maloney, D. R.; Suddaby, K. G. *Macromolecules* **1996**, 29 (1), 481.
- (118) Kowollik, C.; Davis, T. P. *J. Polym. Sci., Part A: Polym. Chem.* **2000**, 38 (18), 3303.
- (119) Suddaby, K. G.; Haddleton, D. M.; Maloney, D. R.; Hastings, J. J.; Richards, S. N.; O'Donnell, J. P. *Macromolecules* **1996**, 29 (25), 8083.
- (120) (a) Waterson, J. L.; Haddleton, D. M.; Harrison, R. J.; Richards, S. N. *Polym. Prepr. (Am. Chem. Soc., Div. Polym. Chem.)* **1998**, 39 (2), 457. (b) Waterson, J. L.; Haddleton, D. M.; Harrison, R. J.; Richards, S. N. *Book of Abstracts*, 216th National Meeting of the American Chemical Society, Boston, MA, Aug 23–27, 1998, American Chemical Society: Washington, DC, 1998; POLY-097.
- (121) Haddleton, D. M.; Muir, A. V. G.; Leeming, S. W.; O'Donnell, J. P.; Richards, S. N. (Zeneca Limited, UK) PCT Int. Pat. Appl. WO 9613527 A1 19960509, Priority date Oct 28, 1994; *Chem. Abstr.* **1996**, 125, 87506.
- (122) Christie, D. I.; Gilbert, R. G. *Macromol. Chem. Phys.* **1996**, 197 (1), 403.
- (123) Heuts, J. P. A.; Forster, D. J.; Davis, T. P.; Yamada, B.; Yamazoe, H.; Azukizawa, M. *Macromolecules* **1999**, 32 (8), 2511.
- (124) Heuts, J. P. A.; Forster, D. J.; Davis, T. P. *Macromol. Rapid Commun.* **1999**, 20 (6), 299.
- (125) Pierik, B.; Masclee, D.; Vollmerhaus, R.; van Herk, A.; German, A. L. In *Free Radical Polymerization. Kinetics and Mechanism. Macromolecular Symposia Series*; Buback, M., Ed.; Wiley-VCH: Weinheim, 3rd IUPAC-Sponsored International Symposium on Free Radical Polymerization: Kinetics And Mechanism, Il Chiocho/Lucca, Italy, June 3–8, 2001.
- (126) Mang, S. A.; Dokolas, P.; Holmes, A. B. *Org. Lett.* **1999**, 1 (1), 125.
- (127) Haddleton, D. M.; Carmichael, A. J.; Leigh, D. A. *Abstr. Pap.-Am. Chem. Soc.* **2001**, IEC-164. *Chem. Abstr.* Accession No. AN 2001:200830.
- (128) Proulx, G. (E.I. DuPont de Nemours and Co.) U.S. Patent 6037442, March 14, 2000; *Chem. Abstr.* **2000**, 132, 208286.
- (129) Deshpande, D. D.; Aravindakshan, P. *Polym. Photochem.* **1984**, 4 (4), 295.
- (130) Nishikawa, H.; Terada, E.; Tsuchida, E.; Kurimura, Y. *J. Polym. Sci., Polym. Chem. Ed.* **1978**, 16 (10), 2453.
- (131) Gridnev, A. A.; Lampeka, Ya. D.; Smirnov, B. R.; Yatsimirskii, K. B. *Theor. Exp. Chem. (Teor. Eksp. Khim.)* **1987**, 23, 293; *Chem. Abstr.* **1987**, 107, 218111.
- (132) Goncharov, A. V.; Gridnev, A. A.; Lampeka, Ya. D.; Gavrish, S. P. *Theor. Exp. Chem.* **1989**, 25, 642. *Teor. Eksp. Khim.* **1989**, 25 (6), 698 (Russian); *Chem. Abstr.* **1990**, 113, 6846.
- (133) Haddleton, D. M.; Muir, A. V. G. (Zeneca Ltd., UK) U.S. Patent 5602220, Feb 11, 1997. PCT Int. Pat. Appl. WO 9504759 A1 19950216, Priority date Aug 9, 1993; *Chem. Abstr.* **1995**, 123, 229300.
- (134) Melby, L. R.; Janowicz, A. H.; Ittel, S. D. Eur. Pat. Appl. EP 196783 A1 19861008, Priority date March 1, 1985; *Chem. Abstr.* **1987**, 106, 67837.
- (135) Lin, J. C.; Abbey, K. J. (Glidden Co.) U.S. Patent 4680354, July 14, 1987; *Chem. Abstr.* **1987**, 107, 218231.
- (136) Smirnov, B. R.; Pushchaeva, L. M.; Plotnikov, V. D. *Polym. Sci., Part A* **1989**, 31 (11), 2607; *Vysokomol. Soedin., Ser. A* **1989**, 31 (11), 2378 (Russian); *Chem. Abstr.* **1990**, 112, 159007.
- (137) This paper refers to the use of phthalocyanine despite its vanishingly low solubility. The compound actually utilized was tetra-*tert*-butylphthalocyanine.
- (138) Christie, D. I.; Claverie, J.; Kanagasabapathy, S. (BASF A.-G.) PCT Int. Appl. WO 0059954, Priority date April 1, 1999; *Chem. Abstr.* **2000**, 133, 282215.
- (139) Gridnev, A. A. Unpublished results.
- (140) Farmery, K.; Kildhal, N. K.; Busch, D. H. *J. Coord. Chem.* **1980**, 10 (1,2), 85.
- (141) Bakac, A.; Brynildson, M. E.; Espenson, J. H. *Inorg. Chem.* **1986**, 25 (23), 4108.
- (142) (a) Claramunt, R. M.; Elguero, J.; Katritzky, A. R. *Adv. Heterocycl. Chem.* **2000**, 77, 1. (b) Claramunt, R. M.; Sanz, D.; Alarcón, S. H.; Torralba, M. P.; Elguero, J.; Foces-Foces, C.; Pietrzak, M.; Langer, U.; Limback, H.-H. *Angew. Chem., Int. Ed.* **2001**, 40 (2), 420.
- (143) (a) Smirnov, B. R.; Mairanovskii, V. G.; Muratov, I. M.; Enikolopyan, N. S. *Bull. Russ. Acad. Sci. (Chem.)* **1988**, 1439; *Izv. Akad. Nauk SSSR, Ser. Khim.* **1988**, (6), 1439 (Russian); *Chem. Abstr.* **1988**, 109, 100728. (b) Morozova, I. S.; Mairanovskii, V. G.; Smirnov, B. R.; Pushchaeva, L. M.; Enikolopyan, N. S. *Dokl. Akad. Nauk SSSR* **1981**, 258 (4), 895 (Russian); *Chem. Abstr.* **1981**, 95, 204500.
- (144) Nokol, A. Yu.; Gridnev, A. A.; Semeikin, A. S.; Mironov, A. F. *Izv. Vissch. Uchebn. Zaved., Khim. Tekh.* **1988**, 31 (10), 52 (Russian); *Chem. Abstr.* **1989**, 110, 173808.
- (145) Gridnev, A. A.; Semeikin, A. S.; Koifman, O. I. *Theor. Exp. Chem.* **1990**, 26, 118; *Teor. Eksp. Khim.* **1990**, 26 (1), 129 (Russian); *Chem. Abstr.* **1990**, 113, 6862.
- (146) Basicakes, L.; Parks, G. F.; Wayland, B. B. *Polym. Prepr. (Am. Chem. Soc., Div. Polym. Chem.)* **2000**, 41 (2), 1886.
- (147) Soriana-Garsia, M.; Toscano, P. A.; Gomez-Lara, J.; Lopez-Morales, M. E. *Acta Crystallogr., Sect. C* **1985**, 41, 1024.

- (148) Weiss, M. C.; Bursten, B.; Peng, S. M.; Goedken, V. L. *J. Am. Chem. Soc.* **1976**, *98* (25), 8021.
- (149) Weiss, M. C.; Gordon, G. C.; Goedken, V. L. *J. Am. Chem. Soc.* **1979**, *101* (4), 857.
- (150) Gruenig, G.; Jaeger, E. G.; Moeller, U.; Wiesener, K. *Z. Phys. Chem. (Leipzig)* **1986**, *267* (5), 994.
- (151) Weiss, M. C.; Goedken, V. L. *J. Am. Chem. Soc.* **1976**, *98* (11), 3389.
- (152) Dzugan, S. J.; Busch, D. H. *Inorg. Chem.* **1990**, *29* (13), 2528.
- (153) Janowicz, A. H. (DuPont) U.S. Patent 4746713, May 24, 1988. (b) Janowicz, A. H. (E.I. DuPont de Nemours and Co., USA) Eur. Pat. Appl. EP 222619 A2 19870520, Priority date Nov 13, 1985.
- (154) (a) Abramo, G. P.; Norton, J. R. *Macromolecules* **2000**, *33* (8), 2790. (b) Abramo, G. P.; Norton, J. R. *Book of Abstracts*, 216th ACS National Meeting of the American Chemical Society, Boston, MA, Aug 23–27, 1998; American Chemical Society: Washington, DC, 1998; INOR-423. (c) Abramo, G. P.; Norton, J. R. *Book of Abstracts*, 216th ACS National Meeting of the American Chemical Society, Boston, MA, Aug 23–27, 1998; American Chemical Society: Washington, DC, 1998; INOR-423. (d) Norton, J. R.; Abramo, G. P. *Abstr. Pap.-Am. Chem. Soc.* **2000**, INOR-313.
- (155) Abramo, G. P. Dissertation, Columbia University, 2000. Available from UMI, Order No. DA9985849. From *Diss. Abstr. Int., B* **2001**, *61* (9), 4710. *Chem. Abstr.* Accession No. AN 2001:439216.
- (156) Woska, D. C.; Ni, Y.; Wayland, B. B. *Inorg. Chem.* **1999**, *38* (18), 4135.
- (157) Janowicz, A. H. (DuPont) U.S. Patent 4722984, Feb 2, 1988. (b) Janowicz, A. H. Eur. Pat. Appl. EP 229481 A2 19870722 to DuPont, Priority date Dec 3, 1985; *Chem. Abstr.* **1987**, *107*, 237502.
- (158) Brookhart, M.; Tucker, J. R.; Husk, G. R. *J. Am. Chem. Soc.* **1983**, *105* (2), 258.
- (159) For reviews, see: (a) Humphrey, A. E. *Adv. Chem. Ser.* **1972**, *109* (Chem. React. Eng., Int. Symp. 1st), 630. (b) *Enzymes*, 3rd ed.; Boyer, P. D., Ed.; Academic Press: New York, 1970. (c) Holt, A. *Neuromethods* **1999**, *33* (Cell Neurobiology Techniques), 131. (d) *Contemporary Enzyme Kinetics and Mechanism*, 2nd ed.; Purich, D. L., Ed.; Academic: San Diego, CA, 1996 (e) *Fundamentals of Enzyme Kinetics*; Cornish-Bowden, A., Ed.; Portland Press: London, U.K., 1995.
- (160) Shapiro, Yu. E.; Dozorova, H. P.; Golikov, I. V.; Smirnov, B. R. *Koord. Khim.* **1982**, *8* (4), 509.
- (161) Smirnov, B. R.; Morozova, I. S.; Puschaeva, L. M.; Marchenko, A. P.; Enikolopyan, N. S. *Dokl. Chem.* **1980**, *255*, 542. Smirnov, B. R.; Morozova, I. S.; Puschaeva, L. M.; Marchenko, A. P.; Enikolopyan, N. S. *Dokl. Akad. Nauk SSSR* **1980**, *255* (3), 609 (Russian); *Chem. Abstr.* **1981**, *94*, 122035.
- (162) Morozova, I. S.; Mairanovskii, V. G.; Smirnov, B. R.; Puschaeva, L. M.; Enikolopyan, N. S. *Dokl. Akad. Nauk SSSR* **1981**, *258* (4), 895 (Russian); *Chem. Abstr.* **1981**, *95*, 204500.
- (163) *B₁₂*; Dolphin, D., Ed.; Wiley: New York, 1982; Vols. 1 and 2.
- (164) Schrauzer, G. N.; Holland, R. J.; Seck, J. A. *J. Am. Chem. Soc.* **1971**, *93* (6), 1503.
- (165) (a) Schrauzer, G. N.; Holland, R. J. *J. Am. Chem. Soc.* **1971**, *93* (6), 1505. (b) Schrauzer, G. N.; Holland, R. J. *J. Am. Chem. Soc.* **1971**, *93* (16), 4060.
- (166) Schrauzer, G. N.; Windgassen, R. J. *J. Am. Chem. Soc.* **1967**, *89* (9), 1999.
- (167) Naumberg, M.; Duong, K. N. V.; Gaudemer, A. *J. Organomet. Chem.* **1970**, *25*, 231.
- (168) Schrauzer, G. N.; Windgassen, R. J.; Kohnle, J. *Chem. Ber.* **1965**, *98* (10), 3324.
- (169) (a) Halpern, J. *ACS Symp. Ser.* **1990**, *428* (Bonding Energ. Organomet. Compd), 100; *Chem. Abstr.* **1990**, *113*, 152516. (b) Halpern, J. *NATO ASI Ser., Ser. C* **1989**, *257* (Paramagn. Organomet. Species Act./Sel., Catal.), 423; *Chem. Abstr.* **1990**, *112*, 35020. (c) Ng, F. T. T.; Rempel, G. L.; Halpern, J. *Inorg. Chim. Acta* **1983**, *77* (5), L165.
- (170) Dodd, D.; Johnson, M. D. *J. Organomet. Chem.* **1973**, *52* (1), 1.
- (171) Schrauzer, G. N. *Ann. N. Y. Acad. Sci.* **1969**, *158* (2), 526.
- (172) Chao, T.; Espenson, I. H. *J. Am. Chem. Soc.* **1978**, *100*, 123.
- (173) Halpern, J.; Ng, F. T. T.; Rempel, G. L. *J. Am. Chem. Soc.* **1979**, *101* (23), 7124.
- (174) Ng, F. T. T.; Rempel, G. L. *J. Am. Chem. Soc.* **1982**, *104* (4), 621.
- (175) Simandi, L. I.; Budo-Zahonyi, E.; Nagy, F. *Katal. Reakts. Zhidk. Faze* **1972**, *284*. From *Zh. Khim.* **1973**, Abstr. No. 5B950 (Russian); *Chem. Abstr.* **1973**, *79*, 104548.
- (176) Szeverenyi, Z.; Budo-Zahonyi, E.; Simandi, L. I. *J. Coord. Chem.* **1980**, *10* (1,2), 41.
- (177) Simandi, L. I.; Budo-Zahonyi, E.; Szeverenyi, Z.; Nemeth, S. *J. Chem. Soc. (Dalton)* **1980**, (2), 276.
- (178) Branchaud, B.; Yu, G. X. *Organometallics* **1993**, *12*, 4262.
- (179) Shanthalakshmy, P.; Vancheesan, S.; Tajaram, J.; Kuriaacose, J. C. *Indian J. Chem.* **1980**, *19A* (9), 901.
- (180) Simandi, L. I.; Szeverenyi, Z.; Budo-Zahonyi, E. *Inorg. Nucl. Chem. Lett.* **1975**, *11* (11), 773.
- (181) Schneider, P. W.; Phelan, P. F.; Halpern, J. *J. Am. Chem. Soc.* **1969**, *91* (1), 77.
- (182) Schrauzer, G. N.; Kratel, G. *Chem. Ber.* **1969**, *102* (7), 2392.
- (183) Day, P.; Hill, H. A. O.; Prince, M. G. *J. Chem. Soc. A* **1968**, (1), 90.
- (184) Stillman, M. J.; Thomson, A. J. *J. Chem. Soc., Faraday Trans. 2* **1974**, *70* (5), 790.
- (185) Clack, D. W.; Yandle, J. R. *Inorg. Chem.* **1972**, *11* (8), 1738.
- (186) Rollman, L. D.; Iwamoto, R. T. *J. Am. Chem. Soc.* **1968**, *90* (6), 1455.
- (187) Gridnev, A. A.; Bel'govskii, I. M.; Enikolopyan, N. S. *Dokl. Phys. Chem.* **1986**, *289* (6), 1408 [Phys. Chem.]; *Chem. Abstr.* **1987**, *106*, 120253.
- (188) Gridnev, A. A.; Bel'govskii, I. M.; Enikolopyan, N. S. *Dokl. Chem.* **1986**, *289* (3), 281 [Chem.] (Russian); *Chem. Abstr.* **1987**, *105*, 202139.
- (189) Perree-Fauvet, M.; Gaudemer, A.; Boucly, P.; Devynck, J. *J. Organomet. Chem.* **1976**, *120* (3), 439.
- (190) Ogoshi, H.; Watanabe, E.; Koketsu, N.; Yoshida, Z. *Bull. Chem. Soc. Jpn.* **1976**, *49* (9), 2529.
- (191) Clarke, D. A.; Dolphin, D.; Grigg, R.; Johnson, A. W.; Pinnock, H. A. *J. Chem. Soc. (C)* **1968**, (7), 881.
- (192) Whitlock, H. W.; Bower, B. K. *Tetrahedron Lett.* **1965**, (52), 4827.
- (193) Mikolański, W.; Baum, G.; Massa, W.; Hoffman, R. W. *J. Organomet. Chem.* **1989**, *376* (2–3), 397.
- (194) Setsune, J.; Ishimaru, Y.; Moryama, T.; Kitao, T. *J. Chem. Soc., Chem. Commun.* **1991**, (8), 555.
- (195) A. Gridnev's unpublished attempt to use NBu₄BH₄ gave only partial conversion of PorCo^{II} into PorCo^I and only at temperatures >70 °C.
- (196) Wayland, B. B.; Gridnev, A. A.; Woska, D. C. *Book of Abstracts*, 214th National Meeting of the American Chemical Society, Las Vegas, NV, Sept 7–11, 1997; American Chemical Society: Washington, DC, 1997; INOR-170.
- (197) Gridnev, A. A.; Ittel, S. D.; Wayland, B. B.; Fryd, M. *Organometallics* **1996**, *15* (24), 5116.
- (198) Huston, P.; Espenson, J. H.; Bakac, A. *Organometallics* **1992**, *11* (10), 3165.
- (199) McBride, J. M. *J. Am. Chem. Soc.* **1971**, *93* (23), 6302.
- (200) Gibian, M. J.; Corley, R. C. *J. Am. Chem. Soc.* **1972**, *94* (12), 4178.
- (201) Derenne, S.; Gaudemer, A.; Johnson, M. D. *J. Organomet. Chem.* **1987**, *322* (2), 239.
- (202) *Isotopes in Organic Chemistry*; Buncl, E., Lee, C. C., Eds.; Elsevier: Amsterdam, 1987.
- (203) Endicott, J. F.; Netzel, T. L. *J. Am. Chem. Soc.* **1979**, *101* (14), 4000.
- (204) Endicott, J. F.; Ferraudi, G. J. *J. Am. Chem. Soc.* **1977**, *99* (17), 243.
- (205) Gridnev, A. A.; Ittel, S. D. *Macromolecules* **1996**, *29* (18), 5864.
- (206) Kamigaito, M.; Ando, T.; Sawamoto, M. *Chem. Rev.* **2001**, *101* (12), 3689–3746.
- (207) Wayland, B. B.; Poszmik, G.; Mukerjee, S. L.; Fryd, M. *J. Am. Chem. Soc.* **1994**, *116* (17), 7943.
- (208) Gridnev, A. A.; Ittel, S. D.; Fryd, M.; Wayland, B. B. *Organometallics* **1993**, *12* (12), 4871.
- (209) Arvanitopoulos, L. D.; Greuel, M. P.; King, B. M.; Shim, A. K.; Harwood, H. J. *ACS Symp. Ser.* **1998**, *685* (Controlled Radical Polymerization), 316.
- (210) Arvanitopoulos, L. D.; Greuel, M. P.; Harwood, H. J. *Polym. Prepr. (Am. Chem. Soc., Div. Polym. Chem.)* **1994**, *35*, 549.
- (211) Fryd, M.; Wayland, B. B.; Poszmik, G.; Mukerjee, S. L. (E.I. DuPont de Nemours and Co. and University of Pennsylvania) PCT Int. Pat. Appl. WO 9525765, Priority date March 15, 1994; *Chem. Abstr.* **1996**, *124*, 57038.
- (212) Wayland, B. B.; Mukerjee, S.; Poszmik, G.; Woska, D. C.; Basickes, L.; Gridnev, A. A.; Fryd, M.; Ittel, S. D. *ACS Symp. Ser.* **1998**, *685*, 305.
- (213) Wayland, B. B.; Basickes, L.; Mukerjee, S.; Mingli, W.; Fryd, M. *Macromolecules* **1997**, *30* (26), 8109.
- (214) Schrauzer, G. N.; Deutsch, E. *J. Am. Chem. Soc.* **1969**, *91* (12), 3341.
- (215) Eckert, H.; Ugi, I. *Angew. Chem.* **1975**, *87* (23), 847.
- (216) Haglund, J.; Rafiq, A.; Ehrenberg, L.; Golding, B. T.; Toernqvist, M. *Chem. Res. Toxicol.* **2000**, *13* (4), 253.
- (217) Schrauzer, G. N.; Windgassen, R. J. *Nature (London)* **1967**, *214* (5087), 492.
- (218) Schrauzer, G. N.; Weber, J. H.; Beckham, T. M. *J. Am. Chem. Soc.* **1970**, *92*, 7078.
- (219) Eckert, H.; Ugi, I. *J. Organomet. Chem.* **1976**, *118* (2), C55.
- (220) Pratt, J. M. *Inorganic Chemistry of Vitamin B₁₂*; Academic Press: New York, 1972.
- (221) Schneider, Z.; Stroinski, A. *Comprehensive B₁₂ Chemistry: Biochemistry: Nutrition: Ecology: Medicine*; de Gruyter, Berlin, Fed. Rep. Ger. 1987.
- (222) *Chemistry and Biochemistry of B₁₂*; Banerjee, R., Ed.; Wiley: New York, 1999.
- (223) Ridge, B. *Organomet. Chem.* **1985**, *13*, 381; *Organomet. Chem.* **1983**, *11*, 387.

- (224) Gupta, B. D.; Roy, S. *Inorg. Chim. Acta* **1988**, *146* (2), 209.
- (225) Madeja, K. Z. *Chem.* **1988**, *28* (11), 396.
- (226) Ramasami, T.; Espenson, J. H. *Inorg. Chem.* **1980**, *19* (6), 1523.
- (227) Brown, K. L.; Hessly, R. K. *Inorg. Chim. Acta* **1981**, *53* (2), L115.
- (228) Misono, A.; Uchida, Y.; Hidai, M.; Kanai, H. *Bull. Chem. Soc. Jpn.* **1967**, *40*, 2089.
- (229) Espenson, J. H.; Wang, D. M. *Inorg. Chem.* **1979**, *18* (10), 2853.
- (230) Charland, J. P.; Attia, W. M.; Randaccio, L.; Marzilli, L. G. *Organometallics* **1990**, *9* (5), 1367.
- (231) Stadlbauer, E. A.; Holland, R. J.; Lamm, F. P.; Schrauzer, G. N. *Bioinorg. Chem.* **1974**, *4* (1), 67.
- (232) Naumberg, M.; N-V-Duong, K.; Gaudemer, A. *J. Organomet. Chem.* **1970**, *25* (1), 231.
- (233) Derenne, S.; Gaudemer, A.; Johnson, M. *J. Organomet. Chem.* **1987**, *322* (2), 239.
- (234) Setsune, J.; Ishimaru, Y.; Moriyama, T.; Kitao, T. *J. Chem. Soc., Chem. Commun.* **1991**, (8), 555.
- (235) Fukuzumi, S.; Noura, S. *J. Porphyrins Phthalocyanines* **1997**, *1* (3), 251.
- (236) (a) Koenig, T. W.; Hay, B. P.; Finke, R. G. *Polyhedron* **1988**, *7* (16,17), 1499. (b) Koenig, T.; Finke, R. G. *J. Am. Chem. Soc.* **1988**, *110* (8), 2657.
- (237) Clark, H. C.; Wong, C. S. *J. Organomet. Chem.* **1975**, *92* (2), C31.
- (238) Clark, H. C.; Hine, K. E. *J. Organomet. Chem.* **1976**, *105* (2), C32.
- (239) Appleton, T. G.; Chisholm, M. H.; Clark, H. C. *J. Am. Chem. Soc.* **1972**, *94* (25), 8912.
- (240) (a) Wei, M.; Wayland, B. B. *Organometallics* **1996**, *15* (22), 4681. (b) Bunn, A. G.; Wayland, B. B. *J. Am. Chem. Soc.* **1992**, *114* (17), 6917.
- (241) Ogoshi, H.; Setsune, J.; Yoshida, Z. *J. Am. Chem. Soc.* **1977**, *99* (11), 3869.
- (242) Cooksey, C. J.; Dodd, D.; Johnson, M. D.; Lockman, B. L. *J. Chem. Soc., Dalton Trans.* **1978**, (12), 1814.
- (243) See, for instance: (a) *B₁₂*, Dolphin, D., Ed.; Wiley-Interscience: New York, 1982; Vols. 1 and 2. (b) Stubbe, J. *J. Biol. Chem.* **1990**, *265*, 5329. (c) Halpern, J. *Science (Washington, D.C.)* **1985**, *227*, 869. (d) Fleming, P. E.; Daikh, B. E.; Finke, R. G. *J. Inorg. Biochem.* **1998**, *69* (1,2), 45. (e) Finke, R. G. In *Vitamin B₁₂, B₁₂-Proteins, 4th Lect. European Symposium*; Kraeutler, B., Arigoni, D., Golding, B. T., Eds.; Meeting Date 1996, Wiley-VCH Verlag GmbH: Weinheim, Germany, 1996; Vol. 383. (f) Vendrova, O. E.; Yurkevich, A. M. *Khim.-Farm. Zh.* **1987**, *21* (3), 335; *Chem. Abstr.* **1988**, *108*, 221422 (g) Darbieu, M. H. *Rev. Roum. Chim.* **1986**, *31* (11,12), 1031; *Chem. Abstr.* **1987**, *107*, 115904.
- (244) Choi, G.; Choi, S. C.; Galan, A.; Wilk, B.; Dowd, P. *Proc. Natl. Acad. Sci. U.S.A.* **1990**, *87*, 3174.
- (245) Pratt, J. M. *Chem. Soc. Rev.* **1985**, *14*, 161.
- (246) He, M.; Dowd, P. *J. Am. Chem. Soc.* **1996**, *118*, 711;
- (247) Giese, B. *Angew. Chem., Int. Ed. Engl.* **1983**, *22*, 753. Behari, K.; Bevington, J. C.; Huckberby, T. N. *Makromol. Chem.* **1987**, *188*, 2441. Diart, V.; Roberts, B. P. *J. Chem. Soc., Perkin Trans. 2* **1992**, 1761. Golubev, V. B.; Mun, G. A.; Zubov, V. P. *Vest. Moskovsk. Univ. Khim. (Engl. Transl.)* **1987**, *42*, 592. Giese, B.; Lachein, S. *Angew. Chem., Int. Ed. Engl.* **1981**, *20*, 967. Tedder, J. M. *Angew. Chem., Int. Ed. Engl.* **1982**, *21*, 401. Giese, B.; Meixner, J. *Chem. Ber.* **1981**, *114*, 2138. Giese, B.; Kretzschmar, G.; Meixner, J. *Chem. Ber.* **1980**, *113*, 2787. Moad, G.; Rizzardo, E.; Solomon, D. H. *Macromolecules* **1982**, *15*, 909. Moad, G.; Rizzardo, E.; Solomon, D. H. *J. Macromol. Sci.-Chem.* **1982**, *A17*, 51. Moad, G.; Rizzardo, E.; Solomon, D. H. *Aust. J. Chem.* **1983**, *36*, 1573. Tedder, J. M. In *Reactivity, Mechanism and Structure in Polymer Chemistry*; Jenkins, A. D., Ledwith A., Eds.; Wiley: London, 1974; p 31. James, D. G. L.; Ogawa, T. *Can. J. Chem.* **1965**, *43*, 640. Giese, B.; Meister, J. *Chem. Ber.* **1977**, *110*, 2558. ElSoueni, A.; Tedder, J. M.; Walton, J. C. *J. Chem. Soc., Faraday Trans. Soc. 1* **1981**, *89*, Owen, G. E.; Pearson, J. M.; Szwarc, M. *J. Chem. Soc., Faraday Trans. Soc.* **1965**, *61*, 1722. Vertommen, L. L. T.; Tedder, J. M.; Walton, J. C. *J. Chem. Res. (S)* **1977**, 18. Citterio, A.; Arnoldi, A.; Minisci, F. *J. Org. Chem.* **1979**, *44*, 2674. Citterio, A.; Minisci, F.; Arnoldi, A.; Pagano, R.; Parravivini, A.; Porta, O. *J. Chem. Soc., Faraday Trans. Soc. 2* **1978**, *519*. Giese, B.; He, J.; Mehl, W. *Chem. Ber.* **1988**, *121*, 2063. Ghodoussi, V.; Gleicher, G. J.; Kravetz, M. *J. Org. Chem.* **1986**, *51*, 5007. Giese, B.; Meister, J. *Angew. Chem.* **1977**, *89*, 178. Szwarc, M. *J. Polym. Sci.* **1955**, *16*, 367. Mayo, F. R.; Lewis, F. M.; Walling, C. *J. Am. Chem. Soc.* **1948**, *70*, 1529. Viehe, H. G.; Merenyi, R.; Stella, L.; Janovsek, Z. *Angew. Chem.* **1979**, *91*, 982. Giese, B.; Lachein, S. *Angew. Chem.* **1981**, *93*, 1016.
- (248) Tanaka, H. *Prog. Polym. Sci.* **1992**, *17*, 1107.
- (249) Ogawa, T.; Gallegos, J.; Inoue, M. *Eur. Polym. J.* **1978**, *14*, 825.
- (250) Canizal, G.; Burillo, G.; Munoz, E.; Gleason, R.; Ogawa, T. *J. Polym. Sci., Part A: Polym. Chem.* **1994**, *32*, 3147. Burillo, G.; Ogawa, T.; Hwang, J. S. *J. Polym. Sci.; Part A: Polym. Chem.* **1992**, *30*, 2159.
- (251) Baciocchi, E.; Floris, B.; Muraglia, E. *J. Org. Chem.* **1993**, *58*, 2013. Santi, R.; Bergamini, F.; Citterio, A.; Sebastiano, R.; Nicolini, M. *J. Org. Chem.* **1992**, *57*, 4250.
- (252) Simandi, L.; Barna, T.; Argay, G.; Simandi, T. *Inorg. Chem.* **1995**, *34*, 6337. Jung, O. S.; Pierpont, C. G. *Inorg. Chem.* **1994**, *33*, 2227. Pierpont, C. G.; Lange, C. W. In *Progress in Inorganic Chemistry*; Karlin, K. D., Ed.; Wiley: New York, 1994; Vol. 41, p 331.
- (253) (a) Daikh, B. E.; Hutchinson, J. E.; Gray, N. E.; Smith, B. L.; Weakley, T. J. R.; Finke, R. G. *J. Am. Chem. Soc.* **1990**, *112*, 7830. (b) Daikh, B. E.; Finke, R. G. *J. Am. Chem. Soc.* **1991**, *113*, 4160. (c) Daikh, B. E.; Weakley, T. J. R.; Finke, R. G. *Inorg. Chem.* **1992**, *31*, 137. (d) Giannotti, C.; Merle, G. *J. Organomet. Chem.* **1975**, *99*, 145.
- (254) (a) Grigg, R.; Johnson, A. W.; Shelton, G. *Justus Liebigs Ann. Chem.* **1971**, *746*, 32. (b) Broadhurst, M. J.; Grigg, R.; Shelton, G.; Johnson, A. W. *J. Chem. Soc., Chem. Commun.* **1970**, 231.
- (255) For reviews, see: (a) *Cytochrome P-450: Structure, Mechanism, and Biochemistry*; Ortiz de Montellano, P. R., Ed.; Plenum Press: New York, 1986. (b) Lavalle, D. K. *The Chemistry and Biochemistry of N-Substituted Porphyrins*; VCH Publishers: New York, 1987.
- (256) Some of the most recent examples: (a) Artaud, I.; Gregoire, N.; Battoni, J. P.; Dupre, D.; Mansuy, D. *J. Am. Chem. Soc.* **1988**, *110*, 8714. (b) Callot, H. J.; Cromer, R.; Louati, A.; Metz, B.; Chevrier, B. *J. Am. Chem. Soc.* **1987**, *109*, 2946. (c) Collmann, J. P.; Hampton, P. D.; Brauman, J. I. *J. Am. Chem. Soc.* **1990**, *112*, 2986. (d) Komives, E. A.; Tew, D.; Olmstead, M. M.; Ortiz de Montellano, P. R. *Inorg. Chem.* **1988**, *27*, 3112. (e) Setsune, J.; Iida, T.; Kitao, T. *Tetrahedron Lett.* **1988**, *29*, 5677. (f) Setsune, J.; Iida, T.; Kitao, T. *Chem. Lett.* **1989**, 885. (g) Setsune, J.; Fukunara, K.; Ishimaru, Y.; Kitao, T. *Chem. Express* **1990**, *5*, 403. (h) Setsune, J.; Ikeda, M.; Kishimoto, Y.; Ishimaru, Y.; Fukunara, K.; Kitao, T. *Organometallics* **1991**, *10*, 1099. (i) Setsune, J.; Saito, Y.; Ishimaru, Y.; Ikeda, M.; Kitao, T. *Bull. Chem. Soc. Jpn.* **1992**, *65*, 639.
- (257) Chen, M. J.; Nunez, L.; Rathke, J. W.; Rogers, R. D. *Organometallics* **1996**, *15* (9), 2338.
- (258) Silverman, R. B.; Dolphin, D. *J. Am. Chem. Soc.* **1974**, *98* (15), 4626.
- (259) (a) Collat, J. W.; Abbot, J. C. *J. Am. Chem. Soc.* **1964**, *86* (11), 2308. (b) Das, P. K.; Hill, H. A. O.; Pratt, J. M.; Williams, R. J. P. *Biochim. Biophys. Acta* **1967**, *141* (3), 644.
- (260) Chao, T.-H.; Espenson, J. H. *J. Am. Chem. Soc.* **1978**, *100* (1), 129.
- (261) Gjerde, H. B.; Espenson, J. H. *Organometallics* **1982**, *1* (3), 435.
- (262) Gridnev, A. A.; Ittel, S. D.; Fryd, M.; Wayland, B. B. *J. Chem. Soc., Chem. Commun.* **1993**, (12), 1010.
- (263) Davis, T.; Heuts, H.; Moad, G.; Rizzardo, E. *Chem. Aust.* **1998**, *65* (10), 12.
- (264) Okamoto, Y.; Nakano, T. (Daicel Chemical Industries, Ltd., Japan Heisei) *Jpn. Kokai Tokkyo Koho JP 09132610 A2* 19970520, Priority date Nov 7, 1995; *Chem. Abstr.* **1997**, *127*, 66325.
- (265) Kim, S. H.; Chen, H. L.; Feilchenfeld, N.; Halpern, J. *J. Am. Chem. Soc.* **1988**, *110* (10), 3120.
- (266) Gjerde, H. B.; Espenson, J. H. *Organometallics* **1982**, *1* (3), 435.
- (267) Woska, D. C.; Wayland, B. B. *Inorg. Chim. Acta* **1998**, *270* (1,2), 197.
- (268) (a) Wayland, B. B.; Gridnev, A. A.; Ittel, S. D.; Fryd, M. *Inorg. Chem.* **1994**, *33* (17), 3830. (b) Gridnev, A. A.; Ittel, S. D. *Book of Abstracts*, 213th National Meeting of the American Chemical Society, San Francisco, CA, April 13–17, 1997; American Chemical Society: Washington, DC, 1997; POLY-294.
- (269) (a) Woska, D. C.; Xie, Z. D.; Gridnev, A. A.; Ittel, S. D.; Fryd, M.; Wayland, B. B. *J. Am. Chem. Soc.* **1996**, *118* (38), 9102. (b) Woska, D. C.; Gridnev, A. A.; Wayland, B. B. *Book of Abstracts*, 211th National Meeting of the American Chemical Society, New Orleans, LA, March 24–28, 1996; American Chemical Society: Washington, DC, 1996; INOR-486. (c) Xie, Z. D.; Wayland, B. B. *Book of Abstracts*, 210th National Meeting of the American Chemical Society, Chicago, IL, Aug 20–24, 1995; American Chemical Society: Washington, DC, 1995; Pt. 1, INOR-567.
- (270) Abraham, R. J.; Medforth, C. J. *Magn. Reson. Chem.* **1988**, *26* (9), 803.
- (271) Smirnov, B. R. *Polym. Sci.* **1990**, *A32*, 583. Smirnov, B. R. *Vysokomol. Soedin., Ser. A* **1990**, *32* (3), 583 (Russian); *Chem. Abstr.* **1990**, *113*, 6866.
- (272) Fischer, H. *Chem. Rev.* **2001**, *101* (12), 3581–3610.
- (273) Fischer, H. *J. Am. Chem. Soc.* **1986**, *108* (14), 3925.
- (274) (a) Fischer, H. *Macromolecules* **1997**, *30* (19), 5666. (b) Kothe, T.; Marque, S.; Martschke, R.; Popov, M.; Fischer, H. *J. Chem. Soc., Perkin Trans. 2* **1998**, (7), 1553. (c) Fischer, H. *J. Polym. Sci., Part A: Polym. Chem.* **1999**, *37* (13), 1885.
- (275) Daikh, B. E.; Finke, R. G. *J. Am. Chem. Soc.* **1992**, *114* (8), 2938.
- (276) Branchaud, B. P.; Yu, G. X. *Organometallics* **1993**, *12* (11), 4262.
- (277) Dirks, J. W.; Underwood, G.; Matheson, J. C.; Gust, D. *J. Org. Chem.* **1979**, *44* (14), 2551.
- (278) (a) Wayland, B. B.; Mukerjee, S.; Poszmiak, G.; Woska, D. C.; Fryd, M. *Polym. Prepr. (Am. Chem. Soc., Div. Polym. Chem.)* **1997**, *38* (1), 742. (b) Wayland, B. B.; Fryd, M. *Book of Abstracts*, 213th National Meeting of the American Chemical Society, San

- Francisco, CA, April 13–17, 1997; American Chemical Society: Washington, DC, 1997; POLY-504. (c) Fryd, M.; Wayland, B. B.; Poszmick, G.; Mukerjee, S. L. (DuPont de Nemours and University of Pennsylvania) PCT Int. Pat. Appl. WO 9525765 A2 19950928, Priority date March 15, 1994; *Chem. Abstr.* **1996**, 124, 57038 (d) Wayland, B. B.; Fryd, M.; Mukerjee, S.; Poszmick, G. *Book of Abstracts*, 210th National Meeting of the American Chemical Society, Chicago, IL, Aug 20–24, 1995; American Chemical Society: Washington, DC, 1995; Pt. 2, PMSE–230.
- (279) Wei, M.; Wayland, B. B.; Fryd, M. *Polym. Prepr. (Am. Chem. Soc., Div. Polym. Chem.)* **1997**, 38 (1), 681.
- (280) Wayland, B. B.; Basickes, L.; Mukerjee, S.; Wei, M.; Fryd, M. *Macromolecules* **1997**, 30, 8109.
- (281) Lindsey, J. S.; Wagner, R. W. *J. Org. Chem.* **1989**, 54 (4), 828.
- (282) Bhyrappa, P.; Nethaji, M.; Krishnan, V. *Chem. Lett.* **1993**, (5), 869.
- (283) Hoffman, P.; Robert, A.; Meunier, B. *Bull. Soc. Chim. Fr.* **1992**, 129 (1), 85.
- (284) Nakano, T.; Okamoto, Y. *ACS Symp. Ser.* **1998**, 685, 451.
- (285) Schrauzer, G. N.; Lee, L.-P.; Sibert, J. W. *J. Am. Chem. Soc.* **1970**, 92 (10), 2997.
- (286) Arcos, T.; de Castro, B.; Ferreira, M. J.; Rangel, M.; Raynor, J. B. *J. Chem. Soc., Dalton Trans.* **1994**, (3), 369.
- (287) Sakaguchi, Y.; Hayashi, H.; I'Haya, Y. *J. Phys. Chem.* **1990**, 94 (1), 291.
- (288) Loginov, A. V.; Yakovlev, V. A.; Shagisultanova, G. A. *Koord. Khim.* **1989**, 15 (7), 942 (Russian); *Chem. Abstr.* **1989**, 111, 183932
- (289) (a) Arvanitopoulos, L. D.; Greuel, M. P.; Harwood, H. J. *Polym. Prepr. (Am. Chem. Soc., Div. Polym. Chem.)* **1994**, 35 (2), 549. (b) Arvanitopoulos, L. D. University Microfilms Int., Order No. DA9528470. 1995. From *Diss. Abstr. Int., B* **1995**, 56 (4), 2048; *Chem. Abstr.* **1995**, 123, 341092. (c) Arvanitopoulos, L. D.; King, B. M.; Huang, C.-Y.; Harwood, H. J. *Polym. Prepr. (Am. Chem. Soc., Div. Polym. Chem.)* **1997**, 38 (1), 752.
- (290) Bhandal, H.; Pattenden, G. *J. Chem. Soc., Chem. Commun.* **1988**, (16), 1110.
- (291) Wayland, B. B.; Poszmick, G.; Fryd, M. *Organometallics* **1992**, 11 (11), 3534.
- (292) Bandaranayake, W. M.; Pattenden, G. *J. Chem. Soc., Chem. Commun.* **1988**, (17), 1179.
- (293) Suddaby, K. G.; O'Driscoll, K. F.; Rudin, A. *J. Polym. Sci., Part A: Polym. Chem.* **1992**, 30 (4), 643.
- (294) Plotnikov, V. D. *Vysokomol. Soedin., Ser. A Ser. B* **1995**, 37 (11), 1823 (Russian); *Chem. Abstr.* **1996**, 125, 168717.
- (295) Enikolopyan, N. S.; Smirnov, B. R.; Askarov, K. A. *Khim. Fiz.* **1984**, 3 (1), 86 (Russian); *Chem. Abstr.* **1984**, 100, 103957.
- (296) Gridnev, A. A. *Polym. J. (Tokyo)* **1992**, 24 (7), 613.
- (297) Gridnev, A. A.; Goncharov, A. V. *Kinet. Catal.* **1989**, 30, 675; *Kinet. Katal.* **1989**, 30 (3), 767 (Russian); *Chem. Abstr.* **1990**, 112, 56748.
- (298) Gridnev, A. A.; Melnikov, V. P. Unpublished results.
- (299) Rozantsev, E. G. *Free Nitroxyl Radicals*; Plenum Press: New York, 1970.
- (300) Gridnev, A. A. *Macromolecules* **1997**, 30 (25), 7651. Anderson, A.; Gridnev, A. A.; Moad, G.; Rizzardo, E.; Thang, S. (DuPont) U.S. Pat. 6,271,340, Aug 7, 2001.
- (301) Gridnev, A. A.; Nechvolodova, E. M. *Theor. Exp. Chem.* **1989**, 25, 670. Gridnev, A. A.; Nechvolodova, E. M. *Teor. Eksp. Khim.* **1989**, 25 (6), 727 (Russian); *Chem. Abstr.* **1990**, 112, 217578.
- (302) Nechvolodova, E. M.; Gridnev, A. A.; Rish, I. G.; Bel'govskii, I. M.; Enikolopov, N. S. U.S.S.R. Patent SU 1392071 A1 19880430 (Russian), Priority date Jan 28, 1985; *Chem. Abstr.* **1988**, 109, 111111.
- (303) (a) Muratore, L. M.; Heuts, J. P. A.; Davis, T. P. *Macromol. Chem. Phys.* **2000**, 201 (9), 985. (b) Correction: Muratore, L. M.; Heuts, J. P. A.; Davis, T. P. *Macromol. Chem. Phys.* **2000**, 201 (12), 1386.
- (304) Buts, A. V.; Bel'govskii, I. M.; Gridnev, A. A.; Smirnov, A. A. *Polym. Sci.* **1993**, B35, 1376; *Vysokomol. Soedin., Ser. B* **1993**, 35 (8), 1376 (Russian); *Chem. Abstr.* **1994**, 120, 55078.
- (305) Tolman, C. A.; Druliner, J. D.; Krusic, P. J.; Nappa, M. J.; Seidel, W. C.; Williams, I. D.; Ittel, S. D. *J. Mol. Catal.* **1988**, 48 (1), 129.
- (306) Tolman, C. A.; Druliner, J. D.; Nappa, M. J.; Herron, N. In *Activation and Functionalization of Alkanes*; Hill, C. L., Ed.; Wiley: New York, 1989; p 303
- (307) Magnuson, R. H.; Halpern, J.; Levitin, I. Ya.; Vol'pin, M. E. *J. Chem. Soc., Chem. Commun.* **1978**, (2), 44.
- (308) Vol'pin, M. E.; Levitin, I. Ya.; Sigán, A. I.; Nikitaev, A. T. *J. Organomet. Chem.* **1985**, 279 (1,2), 263.
- (309) Marchaj, A.; Bakac, A.; Espenson, J. H. *Inorg. Chem.* **1992**, 31 (23), 4860.
- (310) Bakac, A.; Espenson, J. H. *J. Am. Chem. Soc.* **1984**, 106 (18), 5197.
- (311) Specifically mentioned monomers include methyl methacrylate, ethyl methacrylate, propyl methacrylates (all isomers), butyl methacrylates (all isomers), 2-ethylhexyl methacrylate, isobornyl methacrylate, methacrylic acid, benzyl methacrylate, phenyl methacrylate, cyclohexyl methacrylate, 2-hydroxyethyl methacrylate, 2-hydroxypropyl methacrylate, 2-isocyanatoethyl methacrylate, methacrylonitrile, alpha methyl styrene, trimethoxysilylpropyl methacrylate, triethoxysilylpropyl methacrylate, tributoxysilylpropyl methacrylate, dimethoxymethylsilylpropyl methacrylate, diethoxymethyl-silylpropyl methacrylate, dibutoxymethylsilylpropyl methacrylate, diisopropoxymethylsilylpropyl methacrylate, dimethoxysilylpropyl methacrylate, diethoxysilylpropyl methacrylate, dibutoxysilylpropyl methacrylate, diisopropoxysilylpropyl methacrylate, glycidyl methacrylate, isopropenyl butyrate, isopropenyl acetate, isopropenyl benzoate, isopropenyl chloride, isopropenyl fluoride, isopropenyl bromide, itaconic, aciditaconic anhydride, dimethyl itaconate, methyl itaconate, *N-tert*-butyl methacrylamide, *N-n*-butyl methacrylamide, *N*-methylol methacrylamide, *N*-ethylol methacrylamide, isopropenylbenzoic acids (all isomers), diethylamino α -methylstyrenes (all isomers), methyl- α -methylstyrenes (all isomers), diisopropenylbenzenes (all isomers), isopropenylbenzene sulfonic acids (all isomers), methyl 2-hydroxymethylacrylate, ethyl 2-hydroxymethylacrylate, propyl 2-hydroxymethylacrylates (all isomers), butyl 2-hydroxymethylacrylates (all isomers), 2-ethylhexyl 2-hydroxymethylacrylate, isobornyl 2-hydroxymethylacrylate, methyl 2-chloromethylacrylate, ethyl 2-chloromethylacrylate, propyl 2-chloromethylacrylates (all isomers), butyl 2-chloromethylacrylates (all isomers), 2-ethylhexyl 2-chloromethylacrylate, isobornyl 2-chloromethylacrylate, chloroprene, vinylpyrrolidone, 2-phenylallyl alcohol and substituted 2-phenylallyl alcohols, *N*-isopropenylpyrrolidinone, 3-isopropenyl- α,α -dimethyl isocyanate, isopropenylanilines, isopropenyl chloroformate, 2-aminoethyl methacrylate hydrochloride, 2-methacryloxyethyl phosphoryl choline, glycerol monomethyl methacrylate, and 3-*O*-methacryloyl-1,2:5,6-di-*O*-isopropylidene-D-glucofuranose.
- (312) Haddleton, D. M.; Depaquis, E.; Kelly, E. J.; Kukulj, D.; Morsley, S. R.; Bon, S. A. F.; Eason, M. D.; Steward, A. G. *J. Polym. Sci., Part A: Polym. Chem.* **2001**, 39 (14), 2378.
- (313) Steward, A. G.; Haddleton, D. M.; Muir, A. V. G.; Willis, S. L. *Polym. Prepr. (Am. Chem. Soc., Div. Polym. Chem.)* **1998**, 39 (2), 459.
- (314) Eason, M. D.; Haddleton, D. M.; Khoshdel, E. *Polym. Prepr. (Am. Chem. Soc., Div. Polym. Chem.)* **1998**, 39 (2), 455.
- (315) Kelly, E. J.; Haddleton, D. M.; Khoshdel, E. *Polym. Prepr. (Am. Chem. Soc., Div. Polym. Chem.)* **1998**, 39 (2), 453.
- (316) Heuts, J. P. A.; Forster, D. J.; Davis, T. P. *Macromolecules* **1999**, 32 (12), 3907.
- (317) Mironychev, V. Y.; Mogilevich, M. M.; Smirnov, B. R.; Shapiro, Y. Y.; Golikov, I. V. *Polym. Sci.* **1986**, A28, 2103; *Vysokomol. Soedin., Ser. A* **1986**, 28 (9), 1891; *Chem. Abstr.* **1987**, 106, 120255.
- (318) Ivanov, V. V.; Stegno, E. V.; Pushchaeva, L. M. *Khim. Fiz.* **1997**, 16 (5), 140 (Russian); *Chem. Abstr.* **1997**, 127, 162163.
- (319) Haddleton, D. M.; Ohno, K.; Wong, B.; Depaquis, E.; Angot, S.; Steward, A. J. *Abstr. Pap.-Am. Chem. Soc.* **2001**, PMSE–207. *Chem. Abstr.* Accession No. AN 2001:203906.
- (320) Golikov I. V.; Semiannikov, V. A.; Mogilevich, M. M. *Polym. Sci.* **1985**, B27, 304; *Vysokomol. Soedin., Ser. B* **1985**, 27 (4), 304 (Russian); *Chem. Abstr.* **1985**, 103, 71735.
- (321) Guan, Z. (E.I. DuPont de Nemours and Co., USA) U.S. Patent 5767211, June 16, 1998; *Chem. Abstr.* **1998**, 129, 82088.
- (322) Guan, Z.; Jackson, C. *Polym. Mater. Sci. Eng.* **1998**, 79, 7.
- (323) Guan, Z. *Polym. Mater. Sci. Eng.* **1999**, 80, 50.
- (324) Guan, Z.; Jackson, C. *Book of Abstracts*, 216th National Meeting of the American Chemical Society, Boston, MA, Aug 23–27, 1998; American Chemical Society: Washington, DC, 1998; PMSE–004.
- (325) Guan, Z. *Book of Abstracts*, 217th National Meeting of the American Chemical Society, Anaheim, CA, March 21–25, 1999; American Chemical Society: Washington, DC, 1999; PMSE–097.
- (326) Grayson, S. M.; Fréchet, J. M. J. *Chem. Rev.* **2001**, 101 (12), 3819–3868.
- (327) Sunder, A.; Mülhaupt, R. (Bayer Aktiengesellschaft, Germany) PCT Int. Pat. Appl. WO 200037532 A2 20000629 (German), Priority date Dec 22, 1998; *Chem. Abstr.* **2000**, 133, 74520.
- (328) (a) Sunder, A.; Kramer, M.; Hanselmann, R.; Mülhaupt, R.; Frey, H. *Angew. Chem., Int. Ed. Engl.* **1999**, 38 (23), 3552. (b) Frey, H.; Mülhaupt, R.; Sunder, A. *Book of Abstracts*, 219th National Meeting of the American Chemical Society, San Francisco, CA, March 26–30, 2000, American Chemical Society: Washington, DC, 2000; MACR-034. *Chem. Abstr.* Accession No. AN 2000: 331583.
- (329) Sunder, A.; Hanselmann, R.; Frey, H.; Muelhaupt, R. *Macromolecules* **1999**, 32 (13), 4240.
- (330) Abbey, K. J. (SCM Corp.) U.S. Patent 4,608,423, Aug 26, 1986; *Chem. Abstr.* **1986**, 105, 228619.
- (331) (a) Lin, J. C.; Carlson, G. M.; Abbey, K. J.; Trumbo, D. L. *J. Appl. Polym. Sci.* **1993**, 48 (9), 1549. (b) Lin, J. C.; Carlson, G. M.; Abbey, K. J. (SCM Corp., USA) U.S. Patent 4621131, Feb 6, 1986; *Chem. Abstr.* **1987**, 106, 68831.
- (332) Yamada, B.; Toda, K.; Aoki, S. *Polym. Bull.* **1995**, 35, 245.

- (333) Gridnev, A. A. *J. Polym. Sci.*, submitted for publication.
- (334) Ogawa, T.; Fujii, T.; Seko, K. (Kansai Paint Co., Ltd., Japan) Jpn. Kokai Tokkyo Koho JP 2000239334 A2 20000905, Priority date Feb 23, 1999 (Japanese); *Chem. Abstr.* **2000**, 133, 193636.
- (335) Ogawa, T.; Fujii, T.; Seko, K. (Kansai Paint Co., Ltd., Japan) Jpn. Kokai Tokkyo Koho JP 2000191734 A2 20000711, Priority date Oct 20, 1998; *Chem. Abstr.* **2000**, 133, 89956.
- (336) Suddaby, K. G.; Maloney, D. R.; Haddleton, D. M. *Macromolecules* **1997**, 30 (4), 702.
- (337) Antonelli, J. A.; Berge, C. T.; Darmon, M. J.; Murphy, C. E. (E.I. DuPont de Nemours and Co., USA) U.S. Patent 5773534, June 30, 1998; *Chem. Abstr.* **1998**, 129, 109433.
- (338) Haddleton, D. M.; Padgett, J. C.; Overbeek, G. C. (Zeneca Ltd., UK.; Zeneca Resins B.V.) PCT Int. Pat. Appl. WO 9504767 A1 19950216, Priority date Aug 5, 1993; *Chem. Abstr.* **1995**, 123, 199712.
- (339) Huybrechts, J. (E.I. DuPont de Nemours and Co., USA Designated States) PCT Int. Pat. Appl. WO 9942505 A1 19990826, Priority date Feb 19, 1998; *Chem. Abstr.* **1999**, 131, 171643.
- (340) Cheng, C.-M.; Tshudy, D. J. (Xerox Corp., USA) U.S. Patent 5928829, Jul, 7, 1999; *Chem. Abstr.* **1999**, 131, 108894.
- (341) Huybrechts, J.; Fryd, M.; Bruylants, P.; Stranimajer, K. (E.I. DuPont de Nemours and Co.) PCT Int. Pat. Appl. WO 9532229 A1 19951130, Priority date May 19, 1994; *Chem. Abstr.* **1996**, 124, 205085.
- (342) Haddleton, D. M.; Morsley, D. R.; O'Donnell, J. P.; Richards, S. N. *J. Polym. Sci., Part A: Polym. Chem.* **1999**, 37 (18), 3549.
- (343) Kukulj, D.; Davis, T. P.; Suddaby, K. G.; Haddleton, D. M.; Gilbert, R. G. *J. Polym. Sci., Part A: Polym. Chem.* **1997**, 35 (5), 859.
- (344) Davis, T.; Gilbert, R.; Kukulj, D. (Unisearch Ltd., Australia) PCT Int. Pat. Appl. WO 9850436 A1 19981112, Priority date May 8, 1997; *Chem. Abstr.* **1999**, 130, 4196.
- (345) Kukulj, D.; Davis, T. P.; Gilbert, R. G. *Macromolecules* **1997**, 30 (25), 7661.
- (346) Calculation made using results in ref 61.
- (347) McCormick, H. W. *J. Polym. Sci.* **1957**, 25, 488.
- (348) Kukulj, D.; Heuts, J. P. A.; Davis, D. P. *Macromolecules* **1998**, 31, 6034.
- (349) Suyama, S.; Ishigaki, H.; Watanabe, Y.; Nakamura, Y. *Polym. J.* **1995**, 27, 503.
- (350) Watanabe, Y.; Ishigaki, H.; Okada, H.; Suyama, S. *Chem. Lett.* **1993**, (7) 1089.
- (351) Watanabe, Y.; Ishigaki, H.; Okada, H.; Suyama, S. *Polym. J. (Tokyo)* **1997**, 29 (4), 366.
- (352) Watanabe, Y.; Ishigaki, H.; Okada, H.; Suyama, S. *Polym. J. (Tokyo)* **1998**, 30 (3), 192.
- (353) Fischer, J. P.; Luders, W. *Makromol. Chem.* **1972**, 155, 239.
- (354) Nishizawa, H.; Saito, T.; Itoh, T.; Mashita, K. (GOI Chemical Co. Ltd., Japan) Eur. Pat. Appl. EP 641756 A1 19950308, Priority date Sept 6, 1993; *Chem. Abstr.* **1995**, 123, 144853.
- (355) Chaudhuri, B.; Sharma, M. M. *Ind. Eng. Chem. Res.* **1989**, 28 (12), 1757.
- (356) Chaudhuri, B. *Org. Process Res. Dev.* **1999**, 3 (3), 220.
- (357) Jiang, Z.; Sen, A. *Organometallics* **1993**, 12 (4), 1406.
- (358) Sun, Q.; Harmer, M. A.; Farneth, W. E. *Chem. Commun. (Cambridge)* **1996**, (10), 1201.
- (359) Heidekum, A.; Harmer, M.; Holderich, W. F. *Catal. Lett.* **1997**, 47 (3,4), 243.
- (360) Sakata, Y.; Nishi, K. (Cosmo Sogo Kenkyusho Kk, Japan; Cosmo Oil Co Ltd.) Jpn. Pat. Appl. JP 08012601 A2 19960116, Priority date July 1, 1994; *Chem. Abstr.* **1996**, 124, 316720.
- (361) Talzi, V. P.; Doronin, V. P.; Sorokina, T. P.; Ignashin, S. V. *Zh. Prikl. Khim. (St. Petersburg)* **2000**, 73 (5), 787 (Russian); *Chem. Abstr.* **2000**, 133, 322203.
- (362) Issakov, J.; Litvin, E.; Minachev, Ch.; Ohlmann, G.; Scharf, V.; Thome, R.; Tissler, A.; Unger, B. *Stud. Surf. Sci. Catal.* **1994**, 84, 2005.
- (363) Ito, Y.; Nomura, Y. (Mitsui Petrochemical Industry, Japan) Jpn. Pat. Appl. JP 08281104 A2 19961029, Priority date April 10, 1995; *Chem. Abstr.* **1997**, 126, 61848.
- (364) Pillai, M.; Wali, A.; Satish, S. *React. Kinet. Catal. Lett.* **1995**, 55 (2), 251.
- (365) Kuwayama, J.; Masamoto, T. (Nissei Kagaku Kogyo Kk, Japan) Jpn. Pat. Appl. JP 08295641 A2 19961112, Priority date April 28, 1995; *Chem. Abstr.* **1997**, 126, 74542.
- (366) (a) Himori, S.; Inui, Y. Jpn. Pat. Appl. JP 08027043 A2 19960130 Priority date July 18, 1994; *Chem. Abstr.* **1996**, 124, 316723. (b) Himori, S. (Mitsubishi Chemical Corp., Japan) Jpn. Pat. Appl. JP 08217703 A2 19960827, Priority date Feb 17, 1995; *Chem. Abstr.* **1996**, 125, 300599 (c) Himori, S. (Mitsubishi Chemical Corp., Japan) Jpn. Pat. Appl. JP 08217702 A2 19960827, Priority date Feb 15, 1995; *Chem. Abstr.* **1996**, 125, 300598.
- (367) Gridnev, A. A. (E.I. DuPont de Nemours and Co.) PCT Int. Pat. Appl. WO 9941218 A1 19990819, Priority date Feb 11, 1998; *Chem. Abstr.* **1999**, 131, 144963.
- (368) Greuel, M. P.; Harwood, H. J. *Polym. Prepr. (Am. Chem. Soc., Div. Polym. Chem.)* **1991**, 32 (1), 545.
- (369) Heuts, J. P. A.; Forster, D. J.; Davis, T. P. *ACS Symp. Ser.* **2000**, 760 (Transition Metal Catalysis in Macromolecular Design), 254.
- (370) Nokel, A. Yu.; Gridnev, A. A.; Semeikin, A. S.; Mironov, A. F. *Izv. Vyssh. Uchebn. Zaved., Khim. Khim. Tekhnol.* **1988**, 31 (10), 52 (Russian); *Chem. Abstr.* **1989**, 110, 173808.
- (371) Nokel, A. Yu.; Gridnev, A. A.; Mironov, A. F. *Izv. Vyssh. Uchebn. Zaved., Khim. Khim. Tekh.* **1990**, 33 (2), 57. (Russian); *Chem. Abstr.* **1990**, 113, 132875.
- (372) Smirnov, B. R.; Plotnikov, V. D.; Ozerkovskii, B. V.; Roshchupkin, V. P.; Enikolopyan, N. S. *Polym. Sci.* 1981, A23, 2588; *Vysokomol. Soedin., Ser. A* **1981**, 23 (11), 2588 (Russian); *Chem. Abstr.* **1982**, 96, 104826.
- (373) Heuts, J. P. A.; Forster, D. J.; Davis, T. P. *Polym. Mater. Sci. Eng.* **1999**, 80, 431.
- (374) Roberts, G. E.; Heuts, J. P. A.; Davis, T. P. *Macromolecules* **2000**, 33, 7765.
- (375) Oganova, A. G.; Smirnov, B. R.; Ioffe, N. T.; Enikolopyan, N. S. *Dokl. Akad. Nauk SSSR* **1983**, 268 (4), 917 [Phys. Chem.] (Russian); *Chem. Abstr.* **1983**, 98, 216029.
- (376) Morozova, I. S.; Oganova, A. G.; Nosova, V. S.; Novikov, D. D.; Smirnov, B. R. *Izv. Akad. Nauk SSSR, Ser. Khim.* **1987**, (12), 2830 (Russian); *Chem. Abstr.* **1988**, 108, 75929.
- (377) Oganova, A. G.; Smirnov, B. R.; Ioffe, N. T.; Kim, I. P. *Izv. Akad. Nauk SSSR, Ser. Khim.* **1984**, (6), 1258 (Russian); *Chem. Abstr.* **1984**, 101, 111447.
- (378) Oganova, A. G.; Smirnov, B. R.; Ioffe, N. T.; Enikolopyan, N. S. *Izv. Akad. Nauk SSSR, Ser. Khim.* **1983**, (9), 2036 (Russian); *Chem. Abstr.* **1984**, 100, 7211.
- (379) Otsu, T.; Yoshida, M.; Tazaki, T. *Makromol. Chem., Rapid Commun.* **1982**, 3 (2), 133.
- (380) Bledzki, A.; Braun, D.; Titzschkau, K. *Makromol. Chem.* **1983**, 184 (4), 745.
- (381) Penczek, S.; Biela, T.; Duda, A. *Macromol. Rapid Commun.* **2000**, 21 (17), 1276.
- (382) Moad, G.; Rizzardo, E.; Moad, C. L.; Ittel, S. D.; Wilczek, L.; Gridnev, A. A. (E.I. DuPont de Nemours and Co., USA, and Commonwealth Scientific & Industrial Research Organization, Australia) PCT Int. Pat. Appl. WO 9731030 A1 19970828, Priority date Feb 23, 1996; *Chem. Abstr.* **1997**, 127, 234752.
- (383) Chiefari, J.; Jeffery, J.; Mayadunne, R. T. A.; Moad, G.; Rizzardo, E.; Tang, S. H. *Macromolecules* **1999**, 32, 7700.
- (384) Chiefari, J.; Moad, G.; Rizzardo, E.; Gridnev, A. A. (E.I. DuPont de Nemours and Co., USA, and Commonwealth Scientific and Industrial Research Organization) PCT Int. Pat. Appl. WO 9847927 A1 19981029, Priority date April 23, 1997; *Chem. Abstr.* **1998**, 129, 331174.
- (385) McCord, E. F.; Shaw, W. H., Jr.; Hutchinson, R. A. *Macromolecules* **1997**, 30 (2), 246.
- (386) (a) Plessis, C.; Arzamendi, G.; Leiza, J. R.; Schoonbrood, H. A. S.; Charmot, D.; Asua, J. M. *Macromolecules* **2000**, 33 (1), 4. (b) Plessis, C.; Arzamendi, G.; Leiza, J. R.; Schoonbrood, H. A. S.; Charmot, D.; Asua, J. M. *Macromolecules* **2000**, 33 (14), 5041.
- (387) Chiefari, J.; Jeffery, J.; Mayadunne, R. T. A.; Moad, G.; Rizzardo, E.; Tang, S. H. *ACS Symp. Ser.* **2000**, 768 (Controlled/Living Radical Polymerization), 297.
- (388) Freeman, M. B.; Larson, G. R.; Merritt, R. F.; Paik, Y. H.; Shulman, J. E.; Swift, G.; Wilczynski, R. (Rohm and Haas Co.) Eur. Pat. Appl. EP 687690 A1 19951220, Priority date June 13, 1994; *Chem. Abstr.* **1996**, 124, 177243.
- (389) Martchenko, A.; Bremner, T.; O'Driscoll, K. F. *Eur. Polym. J.* **1997**, 33, 713.
- (390) Moitra, S.; Biswas, M.; Uryu, T. *Polym. Commun.* **1989**, 30 (7), 225.
- (391) Gridnev, A. A.; Ittel, S. D. (E.I. DuPont de Nemours and Co.) U.S. Patent 5,847,060, Dec 8, 1998; *Chem. Abstr.* **1999**, 130, 52826.
- (392) (a) Johnson, P. R. *Rubber Chem. Technol.* **1976**, 49 (3), 650. (b) Johnson, P. R. In *Kirk-Othmer Encyclopedia of Chemical Technology*, 3rd ed.; Grayson, M., Eckroth, D., Eds.; Wiley: New York, 1979; Vol. 5, p 773; *Chem. Abstr.* **1979**, 90, 138819.
- (393) Stewart, C. A.; Takeshita, T.; Coleman, M. L. *Chloroprene Polymers in Encyclopedia of Polymer Science and Engineering*, Wiley: New York, 1985; Vol. 3, p 441.
- (394) Kamachi, M.; Kajiwarra, A. *Macromolecules* **1996**, 29, 2378.
- (395) Hutchinson, R. A.; Aronson, M. T.; Richards, J. R. *Macromolecules* **1993**, 26, 6410.
- (396) Morton, M.; Salatiello, M. P.; Landfield, H. J. *Polym. Sci.* **1952**, 8, 279.
- (397) Gridnev, A. A.; Ittel, S. D. (E.I. DuPont de Nemours and Co., USA) PCT Int. Pat. Appl. WO 9633224 A1 19961024, Priority date April 21, 1996; *Chem. Abstr.* **1997**, 126, 8825.
- (398) Gridnev, A. A.; Ittel, S. D. *Book of Abstracts*, 218th National Meeting of the American Chemical Society, New Orleans, Aug 22-26, 1999; American Chemical Society: Washington, DC, 1999; POLY-452.
- (399) Ittel, S. D.; Gridnev, A. A. (E.I. DuPont de Nemours and Co.) U.S. Patent 5,883,206, March 16, 1999 and U.S. Patent 6,177,958, Sept 12, 2000, *Chem. Abstr.* **1997**, 127, 278600.

- (400) Gridnev, A. A.; Simonsick, W. J., Jr.; Ittel, S. D. *J. Polym. Sci., Part A: Polym. Chem.* **2000**, *38* (10), 1911.
- (401) Gridnev, A.; Ittel, S. D. *Polym. Prepr. (Am. Chem. Soc., Div. Polym. Chem.)* **1999**, *40* (2), 185.
- (402) Specifically mentioned olefinically unsaturated organic molecules are butenenitrile (all isomers), pentenenitrile (all isomers), methyl butenecarboxylate (all isomers), ethyl butenecarboxylate (all isomers), propyl butenecarboxylate (all isomers), butyl butenecarboxylate (all isomers), 2-ethylhexyl butenecarboxylate (all isomers), methyl pentenecarboxylate (all isomers), ethyl pentenecarboxylate (all isomers), perfluoropropylvinyl ether, methyl cinnamate, ethyl cinnamate, propyl cinnamate (all isomers), cinnamionitrile, methylmaleic anhydride, cyclopenten-1-one, cyclohexen-1-one, cyclohepten-1-one, dimethyl fumarate, dimethyl fumarate, diethyl maleate, methyl crotonate, ethyl crotonate, crotonaldehyde, crotononitrile, methylfumarionitrile, diphenylethylene (all isomers), triphenylethylene, methyl octadecen-2-oate, ethyl octadecen-2-oate, methyl hexadecen-2-oate, ethyl hexadecen-2-oate, coumarin, methyl coumarin-3-carboxylate, and methylitronic anhydride.
- (403) Madeja, K. Z. *Chem.* **1988**, *28* (11), 396; *Chem. Abstr.* **1989**, *111*, 22741.
- (404) Coveney, D. J.; Patel, V. F.; Pattenden, G. M.; Thompson, D. M. *J. Chem. Soc., Perkin Trans. 1* **1990**, (10), 2721.
- (405) Bhandal, H.; Howell, A. R.; Patel, V. F.; Pattenden, G. M. *J. Chem. Soc., Perkin Trans. 1* **1990**, (10), 2709.
- (406) Bhandal, H.; Patel, V. F.; Pattenden, G. M.; Russll, J. J. *J. Chem. Soc., Perkin Trans. 1* **1990**, (10), 2691.
- (407) Silverman, R. B.; Dolphin, D. *J. Am. Chem. Soc.* **1973**, *95* (5), 1686.
- (408) Gaudemer, F.; Gaudemer, A. *Tetrahedron Lett.* **1980**, *21* (15), 1445.
- (409) McHatton, R. C.; Espenson, J. H.; Bakac, A. *J. Am. Chem. Soc.* **1986**, *108* (19), 5885.
- (410) Cooksey, C. J.; Dodd, D.; Gatford, C.; Johnson, M. D.; Lewis, G. J.; Titchmarsh, D. M. *J. Chem. Soc., Perkin Trans. 2* **1972**, (5), 655.
- (411) Nishikubo, Y.; Branchaud, B. P. *J. Am. Chem. Soc.* **1999**, *121* (47), 10924.
- (412) Nemeth, S.; Szeverenyi, Z.; Simandi, L. I. *Inorg. Chim. Acta* **1980**, *44* (3), L107.
- (413) Omura, Y.; Nakamura, M.; Oka, M.; Fujiwara, Y.; Itoi, K. (Showa Kuraray Co.) Japanese. Pat. Appl. JP 49127937 19741207, Priority date April 19, 1973, CA82: 170383.
- (414) Bied-Charreton, C.; Gaudemer, A. *J. Organomet. Chem.* **1977**, *124* (3), 299.
- (415) Howell, A. R.; Pattenden, G. M. *J. Chem. Soc., Chem. Commun.* **1990**, (2), 103.
- (416) Jayaseharan, J.; Kishore, K. *J. Am. Chem. Soc.* **1998**, *120* (4), 825.
- (417) Nanda, A. K.; Kishore, K. *Polymer* **2000**, *42* (6), 2365.
- (418) Nanda, A. K.; Kishore, K. *Macromolecules* **2001**, *34* (6), 1600.
- (419) Hu, C. M.; Qiu, Y. L. *J. Org. Chem.* **1992**, *57* (12), 3339.
- (420) Oguni, N.; Omi, T.; Yamamoto, Y.; Nakamura, A. *Chem. Lett.* **1983**, (6), 841.
- (421) Shanthalakshmy, P.; Vancheesan, S.; Rajaram, J.; Kuriacose, J. C. *Indian J. Chem.* **1980**, *19A*, 901.
- (422) Takeuchi, S.; Ohgo, Y.; Yoshimura, J. *Bull. Chem. Soc. Jpn.* **1974**, *47* (2), 463.
- (423) Ohgo, Y.; Takeuchi, S.; Yoshimura, J. *Bull. Chem. Soc. Jpn.* **1971**, *44* (1), 283.
- (424) Heuts, J. P. A.; Morrisson, D. M.; Davis, T. P. *Book of Abstracts*, 218th National Meeting of the American Chemical Society, New Orleans, Aug 22–26, 1999; American Chemical Society: Washington, DC, 1999; POLY-318.
- (425) Davis, T. P.; Zammit, M. D.; Heuts, J. P. A.; Moody, K. *Chem. Commun. (Cambridge)* **1998**, (21), 2383.
- (426) Heuts, J. P. A.; Morrison, D. A.; Davis, T. P. In *Controlled/Living Radical Polymerization: Progress in ATRP, NMP and RAFT*; Matyjaszewski, K., Ed.; ACS Symposium Series 768; American Chemical Society: Washington, DC, 2000; p 313.
- (427) Heuts, J. P. A.; Morrisson, D. M.; Davis, T. P. *Polym. Prepr. (Am. Chem. Soc., Div. Polym. Chem.)* **1999**, *40* (2), 346.
- (428) Gridnev, A. A.; Ittel, S. D. (E.I. DuPont de Nemours and Co.) PCT Int. Pat. Appl. WO 0035960 A2 20000622, Priority date Dec 16, 1998; *Chem. Abstr.* **2000**, *133*, 59233.
- (429) Heuts, J. P. A.; Cooté, M. L.; Davis, T. P.; Johnston, L. P. M. In *Controlled Radical Polymerization*; Matyjaszewski, K., Ed.; ACS Symposium Series 685; American Chemical Society: Washington, DC, 1998; p 120.
- (430) Specifically mentioned monomers include methyl acrylate, ethyl acrylate, propyl acrylate (all isomers), butyl acrylates (all isomers), 2-ethylhexyl acrylate, isobornyl acrylate, acrylic acid, benzyl acrylate, phenyl acrylate, acrylonitrile, glycidyl acrylate, 2-hydroxyethyl acrylate, hydroxypropyl acrylates (all isomers), hydroxybutyl acrylates (all isomers), diethylaminoethyl acrylate, triethyleneglycol acrylate, *N-tert*-butyl acrylamide, *N-n*-butyl acrylamide, *N*-methyl-ol acrylamide, *N*-ethyl-ol acrylamide, *N,N*-dimethylacrylamide, trimethoxysilylpropyl acrylate, triethoxysilylpropyl acrylate, tributoxysilylpropyl acrylate, dimethoxymethylsilylpropyl acrylate, diethoxymethylsilylpropyl acrylate, dibutoxymethylsilylpropyl acrylate, diisopropoxymethylsilylpropyl acrylate, dimethoxysilylpropyl acrylate, diethoxysilylpropyl acrylate, dibutoxysilylpropyl acrylate, diisopropoxysilylpropyl acrylate, vinyl acetate, vinyl propionate, vinyl butyrate, vinyl benzoate, vinyl chloride, vinyl fluoride, vinyl bromide, vinylbenzoic acids (all isomers), diethylaminostyrenes (all isomers), methylstyrenes (all isomers), divinylbenzenes (all isomers), and vinylbenzene sulfonic acids (all isomers), *N*-vinylpyrrolidinone. For this application, styrene and substituted styrenes would be included.
- (431) Pierik, B.; Masclee, D.; Van Herk, A. *Macromol. Symp.* **2001**, *165* (Developments in Polymer Synthesis and Characterization), 19.
- (432) Heuts, J. P. A.; Kukulj, D.; Forster, D. J.; Davis, T. P. *Polym. Prepr. (Am. Chem. Soc., Div. Polym. Chem.)* **1997**, *38* (1), 647.
- (433) Heuts, J. P. A.; Kukulj, D.; Forster, D. J.; Davis, T. P. *Book of Abstracts*, 213th National Meeting of the American Chemical Society, San Francisco, CA, April 13–17, 1997; American Chemical Society, Washington, DC, 1997; POLY-284. *Chem. Abstr.* Accession No. AN 1997:164209.
- (434) Haddleton, D. M.; Crossman, M. C.; Hunt, K. H.; Topping, C.; Waterson, C.; Suddaby, K. G. *Macromolecules* **1997**, *30* (14), 3992.
- (435) Suddaby, K. G.; Hunt, K. H.; Haddleton, D. M. *Macromolecules* **1996**, *29* (27), 8642.
- (436) Rudin, A. *The Elements of Polymer Science and Engineering*; Academic Press: New York, 1982.
- (437) Odian, G. *Principles of Polymerization*, 2nd ed.; John Wiley & Sons: New York, 1981.
- (438) Heuts, J. P. A.; Muratore, L. M.; Davis, T. P. *Macromol. Chem. Phys.* **2000**, *201* (18), 2780.
- (439) Haddleton, D. M.; Kelly, E. J.; Kukulj, D.; Morsley, S. M.; Steward, A. G. *Book of Abstracts*, 217th National Meeting of the American Chemical Society, Anaheim, CA, March 21–25, 1999; American Chemical Society: Washington, DC, 1999; POLY-024. *Chem. Abstr.* Accession No. AN 1999:146060.
- (440) Yeates, S. G.; De La Motte, A. M. (Zeneca Limited, UK) PCT Int. Pat. Appl. WO 9634018 A1 19961031, Priority date April 28, 1995; *Chem. Abstr.* **1997**, *126*, 8811.
- (441) Nakamura, J.; Inagaki, G.; Sugiura, S.; Harada, Y. (Mitsubishi Rayon Co., Ltd., Japan) Jpn. Kokai Tokkyo Koho JP 2000231220 A2 20000822, Priority date Feb 9, 1999 (Japanese); *Chem. Abstr.* **2000**, *133*: 170230.
- (442) Lynch, J. P.; Irvine, D. J.; Beverly, G. M. (Imperial Chemical Industries PLC, UK) PCT Int. Pat. Appl. WO 9804603 A1 19980205, Priority date July 7, 1996; *Chem. Abstr.* **1998**, *128*, 128715.
- (443) Gridnev, A. A. (E.I. DuPont de Nemours and Co.) U.S. Patent 5750772, May 12, 1998; *Chem. Abstr.* **1998**, *129*, 5243.
- (444) Gridnev, A. A. (E.I. DuPont de Nemours and Co.) U.S. Patent 5726263, March 10, 1998; *Chem. Abstr.* **1998**, *128*, 205254.
- (445) Cunningham, M. F.; O'Driscoll, K. F.; Mahabadi, H. K. *Polym. React. Eng.* **1993**, *1* (2), 229.
- (446) Yoshimi, K.; Kazeto, O.; Katayama, M. (Kuraray Co., Ltd., Japan) Eur. Pat. Appl. EP 1101773 A1 20010523, Priority date Nov 18, 1999; *Chem. Abstr.* **2001**, *134*, 367699.
- (447) See, for example: Paul, S. *Surface Coatings*; John Wiley & Sons: Chichester, 1985.
- (448) Ogawa, T.; Fujii, T.; Isaka, H. (Kansai Paint Co., Ltd., Japan) Jpn. Kokai Tokkyo Koho JP 2001163922 A2 20010619; Priority date Dec 3, 1999 (Japanese). *Chem. Abstr.* **2001**, *135*, 47688.
- (449) Sawada, E.; Shimazaki, A. (Kansai Paint Co., Ltd., Japan) Jpn. Kokai Tokkyo Koho JP 2001131472 A2 20010515, Priority date Nov. 1, 1999; *Chem. Abstr.* **2001**, *134*, 354611.
- (450) Kudoh, M.; Akutsu, F.; Odagawa, Y.; Naruchi, K.; Miura, M. *Macromol. Chem. Phys.* **1994**, *195* (1), 385.
- (451) Otsu, T.; Yamada, B.; Fujita, M.; Okuo, M. *J. Polym. Sci., Part A: Polym. Chem.* **1991**, *29* (6), 837.
- (452) Kobatake, S.; Yamada, B. *J. Polym. Sci., Part A: Polym. Chem.* **1996**, *34* (1), 95.
- (453) Kudoh, M.; Naruchi, K.; Akutsu, F.; Miura, M. *J. Chem. Soc., Chem. Commun.* **1992**, (2), 105.
- (454) Naruchi, K.; Maruo, T.; Tanaka, S.; Kanekiyo, T.; Yamada, K. *Nippon Kagaku Kaishi* **1981**, (8), 1345 (Japanese); *Chem. Abstr.* **1981**, *95*, 151203.
- (455) Naruchi, K.; Tanaka, S.; Miura, M. *Nippon Kagaku Kaishi* **1979**, (7), 931 (Japanese); *Chem. Abstr.* **1979**, *91*, 157216.
- (456) Moad, C. L.; Moad, G.; Rizzardo, E.; Thang, S. H. *Macromolecules* **1996**, *29* (24), 7717.
- (457) Tanaka, H.; Kawai, H.; Sato, T.; Ota, T. *J. Polym. Sci., Part A: Polym. Chem.* **1989**, *27* (5), 1741.
- (458) Morrow, G. R.; Rae, I. D. *Aust. J. Chem.* **1987**, *40* (8), 1477.
- (459) Abbey, K. J.; Trumbo, D. L.; Carlson, G. M.; Masola, M. J.; Zander, R. A. *J. Polym. Sci., Part A: Polym. Chem.* **1993**, *31* (13), 3417.

- (460) Suyama, S.; Ishigaki, H. (Nippon Oils & Fats Co. Ltd., Japan) Jpn. Pat. Appl. JP 07126311 A2 19950516, Priority date Nov 2, 1993; *Chem. Abstr.* **1995**, 123, 287218.
- (461) Tanaka, H.; Kawai, H.; Sato, T.; Ota, T. *J. Polym. Sci., Part A: Polym. Chem.* **1989**, 27 (5), 1741.
- (462) Haddleton, D. M.; Topping, C.; Hastings, J. J.; Suddaby, K. G. *Macromol. Chem. Phys.* **1996**, 197 (9), 3027.
- (463) Ishigaki, H.; Suyama, S. (Nippon Oils & Fats Co. Ltd., Japan) Jpn. Pat. Appl. JP 06279512 A2 19941004, Priority date March 29, 1993; *Chem. Abstr.* **1995**, 122, 217008.
- (464) Trumbo, D. L.; Abbey, K. J.; Carlson, G. M. *J. Polym. Sci., Part C: Polym. Lett.* **1987**, 25 (5), 229.
- (465) Yamada, B.; Tagashira, S.; Aoki, S. *J. Polym. Sci., Part A: Polym. Chem.* **1994**, 32 (14), 2745.
- (466) Suyama, S.; Ishigaki, H.; Watanabe, T.; Okada, H. (Nippon Oils & Fats Co. Ltd., Japan) Jpn. Pat. Appl. JP 06322009 A2 19941122, Priority date March 2, 1993; *Chem. Abstr.* **1995**, 122, 214864.
- (467) (a) Ishigaki, H.; Okada, H.; Suyama, S. (Nippon Oils & Fats Co. Ltd., Japan) Jpn. Pat. Appl. JP 03212402 A2 19910918, Priority date Jan 18, 1990; *Chem. Abstr.* **1992**, 116, 60239. (b) Suyama, S.; Ishigaki, H.; Okada, H. Jpn. Pat. Appl. JP 03111405 A2 19910513, Priority date Sept 9, 1989; *Chem. Abstr.* **1991**, 115, 184183.
- (468) Ostrovskaya, A. I.; Kravchenko, B. V.; Yankovskij, N. J. A.; Aleshina, A. B.; Polokha, A. M.; Kunchij, L. K.; Ilchenko, V. N.; Radchenko, A. A.; Titov, V. N. (Gorlovskij Arendnyj Kontsern "Stirol", Ukraine) Russ. Pat. RU 2050368 C1 19951220, Priority date Jan 22, 1992; *Chem. Abstr.* **1996**, 125, 115498.
- (469) Horikoshi, K.; Ohtani, K.; Yamamoto, T. (Showa Highpolymer Co., Ltd.) Jpn. Pat. Appl. JP 2000327729 A2 20001128, Priority date May 24, 1999 (Japanese); *Chem. Abstr.* **2000**, 133, 363436.
- (470) Nagashima, M.; Kazama, H. (Tokuyama K. K., Japan) Jpn. Pat. Appl. JP 11071220 A2 19990316, Priority date July 4, 1997; *Chem. Abstr.* **1999**, 130, 272048.
- (471) (a) Shinike, H.; Takeda, K.; Sakuraba, N. (Daiichi Kogyo Seiyaku Co., Ltd., Japan) Jpn. Pat. Appl. JP 11124791 A2 19990511, Priority date Oct 17, 1997; *Chem. Abstr.* **1999**, 130, 353852. (b) Shinichi, H.; Okamura, H.; Sakuraba, N. (Daiichi Kogyo Seiyaku Co., Ltd., Japan) Jpn. Pat. Appl. JP 10226988 A2 19980825, Priority date Dec 9, 1996; *Chem. Abstr.* **1998**, 129, 231161.
- (472) Nishioka, T.; Miwata, H.; Fujiwara, W. (Nippon A and L Co., Ltd., Japan) Jpn. Kokai Tokkyo Koho JP 2001011244 A2 20010116 (Japanese); *Chem. Abstr.* **2001**, 134, 102325.
- (473) Kaneko, T.; Muroi, T.; Tsurumi, M. (Asahi Chemical Industry Co., Ltd., Japan) Jpn. Pat. Appl. JP 04239502 A2 19920827, Priority date Jan 22, 1991; *Chem. Abstr.* **1993**, 118, 23989.
- (474) Wang, Y.; Lin, M.; Lin, Q.; Lin, Z.; Huang, J. (Jiulian Chemical Industrial Co., Ltd., Peoples Republic of China) Chinese Pat. Appl. CN 1128765 A 19960814, Priority date Feb 9, 1995; *Chem. Abstr.* **1999**, 131, 186440.
- (475) Kato, N. (BASF Dispersion K. K., Japan) Jpn. Pat. Appl. JP 2000264927 A2 20000926 (Japanese); *Chem. Abstr.* **2000**, 133, 253959.
- (476) Shima, T.; Yamada, K.; Fujikake, M. (Sanyo Chemical Industries, Ltd., Japan) Jpn. Pat. Appl. JP 2000313848 A2 20001114 (Japanese); *Chem. Abstr.* **2000**, 133, 336608. (b) Shima, T.; Fujikake, M.; Yamada, K. Jpn. Pat. Appl. JP 2001002981 A2 20010109 (Japanese); *Chem. Abstr.* **2001**, 134, 72996.
- (477) (a) Ando, T.; Aoki, M.; Totani, H. (Denki Kagaku Kogyo K. K., Japan) Jpn. Pat. Appl. JP 2001031046 A2 20010206 (Japanese). AN2001: 89549. (b) Ando, T.; Aoki, M.; Totani, H. Jpn. Pat. Appl. JP 2001026619 A2 20010130 (Japanese). *Chem. Abstr.* **2001**, 134, 132648.
- (478) Ito, N.; Ito, Y.; Uotani, N. (Showa Denko K. K., Japan) Jpn. Pat. Appl. JP 11049994 A2 19990223, Priority date July 31, 1997; *Chem. Abstr.* **1999**, 130, 224437.
- (479) Ma, S.-H.; Fryd, M. (E.I. DuPont de Nemours and Co., USA) Eur. Pat. Appl. EP 826751 A2 19980304, Priority Aug 30, 1996; *Chem. Abstr.* **1998**, 128, 193780.
- (480) Ma, S.-H.; Anton, W. L. (E.I. DuPont de Nemours and Co., USA) Eur. Pat. Appl. EP 851014 A2 1998070, Priority date Dec 72, 1996; *Chem. Abstr.* **1998**, 129, 110253.
- (481) Ma, S.-H.; Fryd, M.; Berge, C. T. (E.I. DuPont de Nemours and Co., USA) Jpn. Pat. Appl. JP 11269418 A2 19991005, Priority date Dec 29, 1998; *Chem. Abstr.* **1999**, 131, 259021.
- (482) Huybrechts, J. (E.I. DuPont de Nemours and Co., USA) U.S. Patent 5852123, Dec 22, 1998; *Chem. Abstr.* **1999**, 130, 82921.
- (483) Harada, Y.; Inagaki, M.; Sugiura, S.; Nakamura, J. (Mitsubishi Rayon Co., Ltd., Japan) Jpn. Kokai Tokkyo Koho JP 2001115064 A2 20010424, Priority date Oct 20, 1999. Japanese; *Chem. Abstr.* **2001**, 134, 312531.
- (484) Harada, Y.; Inagaki, G.; Shimizu, K. (Mitsubishi Rayon Co., Ltd., Japan) Jpn. Pat. Appl. JP 11035879 A2 19990209, Priority date July 17, 1997; *Chem. Abstr.* **1999**, 130, 210850.
- (485) Ishigaki, H.; Watanabe, Y.; Isokura, K. (Nippon Oil and Fats Co., Ltd., Japan) Jpn. Pat. Appl. JP 09302181 A2 19971125, Priority date May 20, 1996; *Chem. Abstr.* **1998**, 128, 35502.
- (486) Charmot, Do.; Dorget, M.; Oger, N.; Schoonbrood, H. (Rhodia Chimie, France) PCT Int. Pat. Appl. WO 9957167 A1 19991111, Priority date April 26, 1999 (French); *Chem. Abstr.* **1999**, 131, 337539.
- (487) Kobayashi, K.; Teramoto, K. (Denki Kagaku Kogyo K. K., Japan) Jpn. Kokai Tokkyo Koho JP 2001064464 A2 20010313, Priority date Aug 27, 1999 (Japanese); *Chem. Abstr.* **2001**, 134, 223482.
- (488) Yokoyama, K. (Daiso Co., Ltd.) Jpn. Kokai Tokkyo Koho JP 2001040044 A2 20010213, Priority date Aug 2, 1999 (Japanese); *Chem. Abstr.* **2001**, 134, 148363.
- (489) Machida, K.; Watabe, S.; Kamitono, H.; Shoji, M. (Kureha Chemical Industry Co., Ltd., Japan) Jpn. Kokai Tokkyo Koho JP 2001122923 A2 20010508, Priority date Sept 26, 1999 (Japanese); *Chem. Abstr.* **2001**, 134, 312235.
- (490) Keogh, M. J. (Union Carbide Chemicals and Plastics Technology Corp.) Eur. Pat. Appl. EP 1041583 A1 20001004, Priority date March 31, 1999; *Chem. Abstr.* **2000**, 133, 282691.
- (491) Kimura, T.; Inui, Y.; Nakajima, N.; Kashiwazaki, M. Jpn. Kokai Tokkyo Koho JP 2001055467 A2 20010227. Priority date Aug 18, 1999. Japanese; *Chem. Abstr.* **2001**, 134, 194313.
- (492) (a) Wilczek, L.; McCord, E. F.; Hansen, J.; Raffell, K. D.; Fuller, R. E.; Jackson, C.; Harrison, D.; Rizzardo, E. *Book of Abstracts*, 210th National Meeting of the American Chemical Society, Chicago, IL, Aug 20–24, 1995; American Chemical Society: Washington, DC, 1995; Pt. 2, POLY-197. (b) Wilczek, L.; McCord, E. F.; Hansen, J.; Raffell, K. D.; Fuller, R. E.; Jackson, C.; Harrison, D.; Rizzardo, E. *Polym. Prepr. (Am. Chem. Soc., Div. Polym. Chem.)* **1995**, 36 (2), 106–7.
- (493) Wilczek, L.; Mccord, E. F. (E.I. DuPont de Nemours and Co., USA, and Commonwealth Scientific and Industrial Research Organization) PCT Int. Pat. Appl. WO 9731031 A1 19970828, Priority date Feb 23, 1996; *Chem. Abstr.* **1997**, 127, 221147.
- (494) (a) Fryd, M.; Visscher, K. B. (E.I. DuPont de Nemours and Co.) PCT Int. Pat. Appl. WO 0020520 A1 20000413, Priority date Oct 6, 1998; *Chem. Abstr.* **2000**, 132, 265914. (b) Fryd, M.; Visscher, K. B. U.S. Patent 6262152 B1, July 17, 2001.
- (495) Chu, I.-C.; Fryd, M.; Lynch, L. E. (E.I. DuPont de Nemours and Co.) PCT Int. Pat. Appl. WO 9421701 A1 19940929, Priority date March 3, 1993; *Chem. Abstr.* **1995**, 123, 199706.
- (496) Berge, C. T.; Fryd, M.; Johnson, J. W.; Moad, G.; Rizzardo, E.; Scopazzi, C.; Thang, S. H. (E.I. DuPont de Nemours and Co., USA, and Commonwealth Scientific & Industrial Research Organization) PCT Int. Pat. Appl. WO 0002939 A1 20000120, Priority date July 10, 1998; *Chem. Abstr.* **1999**, 132, 93843.
- (497) Chang, D. C. K.; Fryd, M. (E.I. DuPont de Nemours and Co., USA) PCT Int. Pat. Appl. WO 9903937 A1 19990128, Priority date July 17, 1997; *Chem. Abstr.* **1999**, 130, 140556.
- (498) Huybrechts, J.; Fryd, M.; Berge, C. T.; White, D. A., Jr. (E.I. DuPont de Nemours and Co.) Can. Pat. Appl. CA 2149399 AA 19951120, Priority date May 5, 1994; *Chem. Abstr.* **1996**, 124, 292435.
- (499) Huybrechts, J.; Fryd, M.; Bruylants, P. (E.I. DuPont de Nemours and Co.) PCT Int. Pat. Appl. WO 9532255 A1 19951130, Priority date May 19, 1994; *Chem. Abstr.* **1996**, 124, 148842.
- (500) Huybrechts, J.; Bruylants, P.; Stranimaier, K.; Fryd, M. (E.I. DuPont de Nemours and Co.) PCT Int. Pat. Appl. WO 9532228 A1 19951130, Priority date May 19, 1994; *Chem. Abstr.* **1990**, 124, 205086.
- (501) Huybrechts, J.; Fryd, M.; Bruylants, P.; Stranimaier, K. (E.I. DuPont de Nemours and Co.) PCT Int. Pat. Appl. WO 9532229 A1 19951130, Priority date May 19, 1994; *Chem. Abstr.* **1996**, 124, 205085.
- (502) Muratore, L. M.; Steinhoff, K.; Davis, T. P. *Polym. Prepr. (Am. Chem. Soc., Div. Polym. Chem.)* **1999**, 40 (2), 175.
- (503) Muratore, L. M.; Steinhoff, K.; Davis, T. P. *J. Mater. Chem.* **1999**, 9 (8), 1687.
- (504) Guo, J.-s.; Wu, X.-d.; Xie, H.-q. *Shiyou Huagong* **2000**, 29 (7), 486 (Chinese); *Chem. Abstr.* **2000**, 133, 238684.
- (505) Matsuno, Y.; Adachi, T.; Numa, N. *Prog. Org. Coat.* **1999**, 35 (1–4), 117.
- (506) Shim, A. K.; Harwood, H. J. *Polym. Prepr. (Am. Chem. Soc., Div. Polym. Chem.)* **1999**, 40 (2), 132.
- (507) Harwood, H. J.; Shim, A. K. (University of Akron) PCT Intl. Pat. Appl. WO 2000050467 A 20001102, Priority date Feb 26, 1999; *Chem. Abstr.* **2000**, 133, 193673.
- (508) Rizzardo, E.; Chiefari, J.; Chong, B. Y. K.; Ercole, F.; Krstina, J.; Jeffery, J.; Le, T. P. T.; Mayadunne, R. T. A.; Meijs, G. F.; Moad, C. L.; Moad, G.; Thang, S. H. *Macromol. Symp.* **1999**, 143 (World Polymer Congress, 37th International Symposium on Macromolecules, 1998), 291.
- (509) Riizzardo, E.; Meijs, G. F.; Thang, S. H. *Macromol. Symp.* **1995**, 98 (35th IUPAC International Symposium on Macromolecules, 1995), 101.
- (510) Rizzardo, E.; Chong, Y. K.; Evans, R. A.; Moad, G.; Thang, S. H. *Macromol. Symp.* **1996**, 111, 1.
- (511) Haddleton, D. M.; Maloney, D. R.; Suddaby, K. G.; Clarke, A.; Richards, S. N. *Polymer* **1997**, 38 (25), 6207.
- (512) Krstina, J.; Moad, C. L.; Moad, G.; Rizzardo, E.; Berge, C. T.; Fryd, M. *Macromol. Symp.* **1996**, 111 13.

- (513) Haddleton, D. M.; Topping, C.; Kukulj, D.; Irvine, D. *Polymer* **1998**, *39* (14), 3119.
- (514) Devlin, B. P.; Darling, T. R.; Berge, C. T.; Darmon, M. J.; Grady, M. C.; Hansen, J. E.; Simonsick, W. J.; Matheson, R. R.; Litty, L. L.; Paquet, D. A.; Wilczek, L.; Gridnev, A. A. *Polym. Prepr. (Am. Chem. Soc., Div. Polym. Chem.)* **1997**, *38* (1), 458.
- (515) Krstina, J.; Moad, G.; Rizzardo, E.; Winzor, C. L.; Berge, C. T.; Fryd, M. *Macromolecules* **1995**, *28* (15), 5381–5.
- (516) Haddleton, D. M.; Topping, C.; Kukulj, D.; Irvine, D. *Polymer* **1998**, *39* (14), 3119.
- (517) Wilkinson, T. S.; Boonstra, A.; Montoya-Goni, A.; van Es, S.; Monteiro, M. J.; German, A. L. *J. Colloid Interface Sci.* **2001**, *237* (1), 21.
- (518) Antonelli, J. A.; Barsotti, R. J.; Becton, L. E. A.; Scopazzi, C. (E.I. DuPont de Nemours and Co.) U.S. Patent 6107392, Aug 22, 2000; *Chem. Abstr.* **2000**, *133*, 178988.
- (519) Antonelli, J. A.; Scopazzi, C. (E.I. DuPont de Nemours) U.S. Patent 5310807, May 10, 1994; *Chem. Abstr.* **1994**, *121*, 206292.

CR9901236

Polymers with Complex Architecture by Living Anionic Polymerization

Nikos Hadjichristidis,* Marinos Pitsikalis, Stergios Pispas, and Hermis Iatrou

Department of Chemistry, University of Athens, Panepistimiopolis Zografou, 15771 Athens, Greece

Received January 31, 2001

Contents

I. Introduction	3747
II. Star Polymers	3747
A. General Methods for the Synthesis of Star Polymers	3747
1. Multifunctional Initiators.	3749
2. Multifunctional Linking Agents	3751
3. Use of Difunctional Monomers	3754
B. Star–Block Copolymers	3754
C. Functionalized Stars	3755
1. Functionalized Initiators	3755
2. Functionalized Terminating Agents	3756
D. Asymmetric Stars	3757
1. Molecular Weight Asymmetry	3757
2. Functional Group Asymmetry	3760
3. Topological Asymmetry	3761
E. Miktoarm Star Polymers	3761
1. Chlorosilane Method	3761
2. Divinylbenzene Method	3766
3. Diphenylethylene Derivative Method	3766
4. Synthesis of Miktoarm Stars by Other Methods	3770
III. Comb-Shaped Polymers	3771
A. "Grafting Onto"	3771
B. "Grafting From"	3773
C. "Grafting Through"	3774
IV. Block–Graft Copolymers	3775
V. α,ω -Branched Architectures	3776
VI. Cyclic Polymers	3778
A. Cyclic Homopolymers from Precursors with Homodifunctional Groups	3780
1. Cyclic Homopolymers	3780
2. Cyclic Block Copolymers	3782
3. Tadpole and Bicyclic Polymers	3784
B. Cyclic Homopolymers from Precursors with Heterodifunctional Groups	3786
C. Catenanes	3786
VII. Hyperbranched Architectures	3787
VIII. Concluding Remarks	3790
IX. List of Symbols and Abbreviations	3790
X. References	3790

I. Introduction

Immediately after the discovery of the living character¹ of anionic polymerization,² polymer chemists started synthesizing well-defined linear homopolymers and diblock copolymers with low molecular

weight and compositional polydispersity. Later star homopolymers and block copolymers, the simplest complex architectures, were prepared. Polymer physical chemists and physicists started studying the solution³ and the bulk properties of these materials.⁴ The results obtained forced the polymer theoreticians either to refine existing theories⁵ or to create new ones.⁶ Over the past few years, polymeric materials having more complex architectures have been synthesized. The methods leading to the following complex architectures will be presented in this review:

(1) star polymers and mainly asymmetric and miktoarm stars; (2) comb and α,ω -branched polymers; (3) cyclic polymers and combinations of cyclic polymers with linear chains; and (4) hyperbranched polymers.

Emphasis has been placed on chemistry leading to well-defined and well-characterized polymeric materials. Complex architectures obtained by combination of anionic polymerization with other polymerization methods are not the subject of this review.

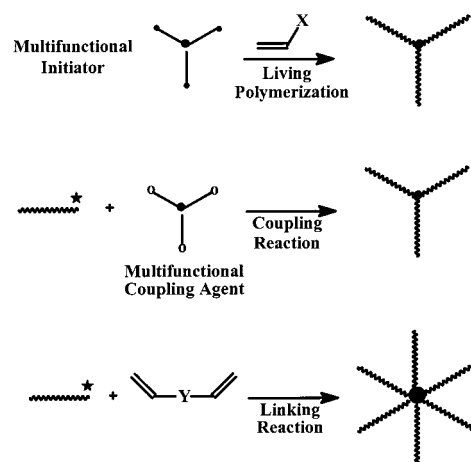
II. Star Polymers

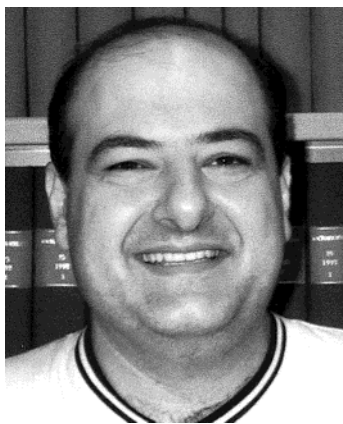
Star polymers are branched polymers consisting of several linear chains linked to a central core. The synthesis of star polymers has been the subject of numerous studies since the discovery of living anionic polymerization.^{7–10}

A. General Methods for the Synthesis of Star Polymers

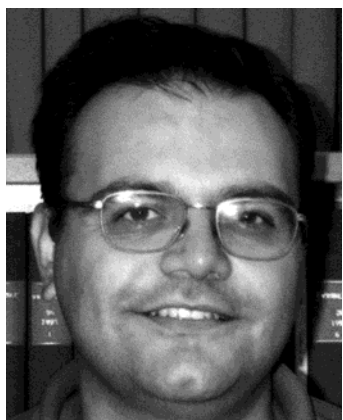
Three general synthetic methods have been developed, as outlined in Scheme 1:

Scheme 1





Marinos Pitsikalis received his B.Sc. and Ph.D. from the University of Athens, Greece in 1989 and 1994, respectively. His postdoctoral research was done at the University of Alabama at Birmingham, with Prof. J. W. Mays (1995–1996). Since 1998, he has been a Lecturer at the Industrial Chemistry Laboratory, Department of Chemistry, University of Athens. He has been a Visiting Scientist at the University of Milano, Italy (March 1991); University of Alabama at Birmingham (September–October 1993); Max Plank Institute for Polymer Science, Germany (August 1994); National Institute for Standards and Technology (December 1995); and IBM Almaden Research Center (February 1995). He has published 35 papers in refereed scientific journals and made 30 announcements at international scientific conferences.

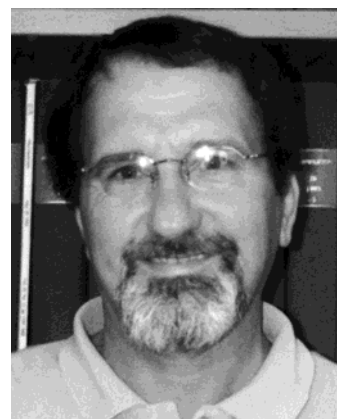


Stergios Pispas received his B.Sc. and Ph.D. from the University of Athens, Greece, in 1989 and 1994, respectively. He did postdoctoral research at the University of Alabama at Birmingham, with Prof. J. W. Mays (1994–1995). He has been a Research Associate at the University of Athens since 1997 and a Visiting Researcher at the National Hellenic Research Foundation of Greece since 2001. He has enjoyed being a Visiting Scientist at the following facilities: Foundation for Research and Technology, Greece (November 1990); University of Alabama at Birmingham (August–September 1992 and September–October 1993); Max Plank Institute for Polymer Science, Germany (February 1994); University of Massachusetts at Amherst (July–September 1995); IBM Almaden Research Center (October 1995); Foundation for Research and Technology, Greece (July 1998); and Institut de Chimie des Surfaces et Interfaces-CNRS, France (November 2000). In 1995, he received the American Institute of Chemists Foundation Award for Distinguished Postdoctoral Research. He has published 48 papers in refereed scientific journals and made 33 announcements at international scientific conferences.

Use of Multifunctional Initiators. In this method, multifunctional organometallic compounds that are capable of simultaneously initiating the polymerization of several branches are used in order to form a star polymer. There are several requirements that a multifunctional initiator has to fulfill in order to produce star polymers with uniform arms, low molecular weight distribution, and controllable molecular weights. All the initiation sites must be



Hermis Iatrou received his B.Sc. and Ph.D. from the University of Athens, Greece, in 1989 and 1993, respectively. He did postdoctoral research at the Institute of Material Science in the Center of Nuclear Science in Juelich, Germany, with Prof. Dr. Dieter Richter (1994–1995), and University of Alabama at Birmingham, with Prof. Jimmy Mays (August 1997–February 1998). He has been a Research Associate at the University of Athens since 1998. He has published 30 papers in refereed scientific journals and made 27 announcements at international scientific conferences.



Nikos Hadjichristidis received his B.Sc. from the University of Athens, Greece, in 1966, his Ph.D. from the University of Liège, Belgium, in 1971, and his D.Sc. from the University of Athens, Greece in 1978. He did postdoctoral research at the University of Liège with Professor V. Desreux (1971–1972) and National Research Council of Canada with Dr. J. Roovers (1972–1973). His career at the University of Athens has included being Lecturer (1973), Assistant Professor (1982), Associate Professor (1985), Full Professor (1988), Director of Industrial Chemistry Laboratory (since 1994), and Chairman of the Chemistry Department (1991–1995 and since 1999). His travels include the following: Visiting Scientist, University of Liège (Summers 1974, 1975); Visiting Research Officer, NRC of Canada (Summer 1976); Visiting Scientist, University of Akron, at Dr. L. Fetters' Laboratory (Summers 1977 through 1982); Distinguished Visiting Scientist, NRC of Canada (1983); Visiting Professor, Exxon Research and Engineering Co., NJ (since 1984, every year for 1–2 months). His further accomplishments include being President of the European Polymer Federation (1995–1996), a member of the National Advisory Research Council (since 1994), President of the State Highest Chemical Board (since 1995), and Director of the Institute of "Organic and Pharmaceutical Chemistry" of the National Hellenic Research Foundation (2000–2001). He has received the Academy of Athens Award for Chemistry (1989), the Empirikion Award for Sciences (1994), and the Greek Chemists Association Award (2000). He has published more than 220 papers in refereed scientific journals.

equally reactive and have the same rate of initiation. Furthermore, the initiation rate must be higher than the propagation rate. Only a few multifunctional initiators satisfy these requirements, and consequently, this method is not very successful. Complications often arise from the insolubility of these

initiators, due to the strong aggregation effects. The steric hindrance effects, caused by the high segment density, causes excluded volume effects.

Use of Multifunctional Linking Agents. This method involves the synthesis of living macroanionic chains and their subsequent reaction with a multifunctional electrophile, which acts as the linking agent. It is the most efficient way to synthesize well-defined star polymers, because there can be absolute control in all the synthetic steps. The functionality of the linking agent determines the number of the branches of the star polymer, provided that the linking reaction is quantitative. The living arms can be isolated and characterized independently along with the final star product. Consequently, the functionality of the star can be measured directly and with accuracy. Disadvantages of the method can be considered the sometimes long time required for the linking reaction and the need to perform fractionation in order to obtain the pure star polymer, since in almost all cases a small excess of the living arm is used in order to ensure complete linking.

Use of Difunctional Monomers. In this method a living polymer precursor is used as initiator for the polymerization of a small amount of a suitable difunctional monomer, such as divinylbenzene (DVB) or ethyleneglycol dimethacrylate (EGDM).^{3,11,12} Microgel nodules of tightly cross-linked polymer are formed upon the polymerization. These nodules serve as the branch point from which the arms emanate. The functionality of the stars prepared by this method can be determined by molecular weight measurements on the arms and the star product, but it is very difficult to predict and control the number of arms. The number of branches incorporated in the star structure is influenced by many parameters. The most important is the molar ratio of the difunctional monomer over the living polymer. The functionality of the star increases by increasing this ratio. Other parameters that influence the number of branches are the chemical nature (polystyrene, polydiene etc.), the concentration and the molecular weight of the living polymer chain, the temperature and the time of the reaction, the rate of stirring, the composition of the isomers in the case of DVB (ratio of *m*, *o*, and *p* isomers), etc. Another disadvantage of this procedure is that the final products are characterized by a distribution in the number of the arms incorporated into the star structure. Consequently, the number of the arms determined experimentally by molecular weight measurements is an average value. It is obvious that although this method is technologically very important and can be applied on an industrial scale, it is less suitable for the preparation of well-defined stars.

Recent advances in all three methodologies developed for the synthesis of star polymers will be presented in the following sections.

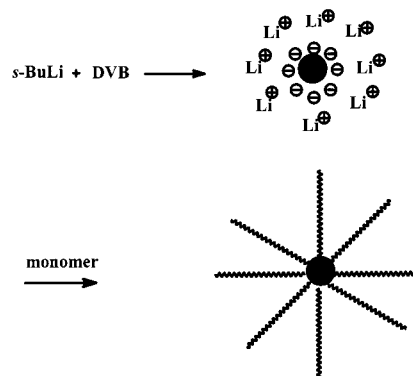
1. Multifunctional Initiators.

The use of DVB as a multifunctional initiator was initially demonstrated by Burchard et al.^{13,14} and was later developed by Rempp and his collaborators.^{15,16} DVB was polymerized by butyllithium in benzene at

high dilution to obtain a stable microgel suspension. These microgels, which were covered by living anionic sites, were subsequently used as multifunctional initiators to polymerize styrene, isoprene, or butadiene. A slight variation was adopted by Funke.^{17,18} The polymerization of DVB was initiated by living poly(*tert*-butylstyryl)lithium chains having low molecular weights in order to avoid the solubility problems arising from the strong association of the carbon–lithium functions in the nonpolar solvent.

Rempp et al. synthesized poly(*tert*-butyl acrylate)¹⁶ (PtBuA) and poly(ethylene oxide)¹⁹ (PEO) stars, according to Scheme 2.

Scheme 2

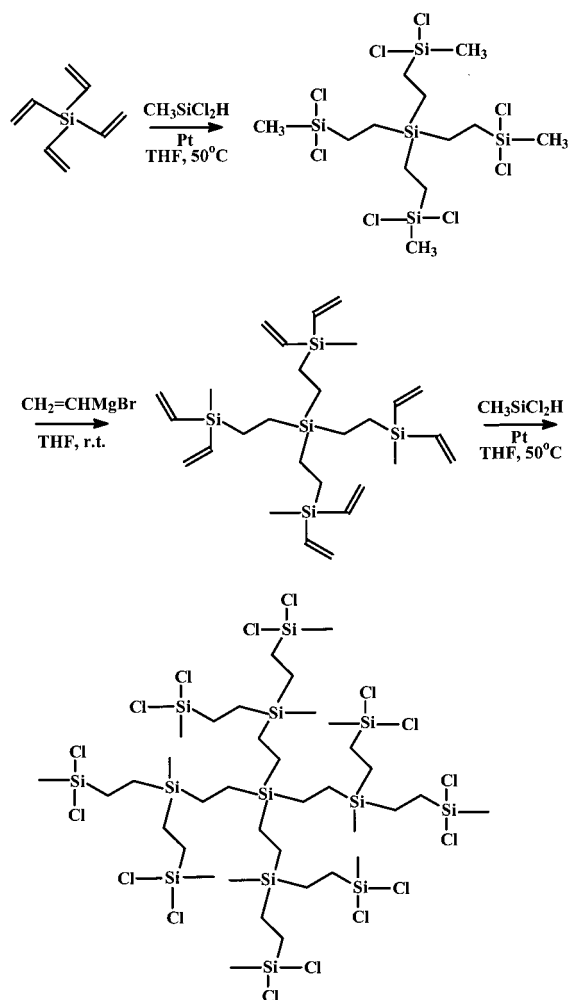


The synthesis of the PtBuA stars was performed in the polar solvent tetrahydrofuran (THF) to minimize the strong association effects, using naphthalene lithium to polymerize the DVB. DVB polymerization was initiated by electron-transfer instead of by addition. The polymerization of the tBuA was carried out at $-55\text{ }^{\circ}\text{C}$ in the presence of LiCl and after the active centers have been reacted with a suitable amount of 1,1-diphenylethylene (DPE) to reduce their nucleophilicity. It was found that the mole ratio [DVB]:[Li⁺] should vary between 1.5 and 2.5 to obtain a stable microgel suspension. The molecular weight of the branch cannot be measured directly but can be calculated from the ratio of the monomer consumed during the polymerization over the total Li concentration. The products were characterized by size exclusion chromatography (SEC) and light scattering (LS). The results showed the existence of broad molecular weight distributions and even multimodal peaks. The formation of a rather small amount of aggregates was obtained in most cases. It was removed by filtration or centrifugation. The molecular characteristics of the final products and the calculated molecular weight of the branches revealed the existence of large numbers of arms, ranging from 22 to 1300.

For the synthesis of the PEO stars, potassium naphthalene was used to generate the multifunctional initiator. The molar ratio [DVB]:[K⁺] was less than 3 in all cases. The functionalities of the stars, as determined by LS measurements, were also rather large, ranging from 5 to 219.

Alternatively, PEO stars were synthesized using cumylpotassium to polymerize DVB and thus prepare the polyfunctional initiator.²⁰ The products exhibited

Scheme 3



a large distribution of functionalities and molecular weights.

The polyfunctional initiator method provides the possibility to prepare end-functionalized stars by deactivating the living branches by suitable electrophilic terminating agents. Polystyrene (PS) and PEO stars having end hydroxyl groups were prepared by this method.^{15,19}

Another approach was proposed by Lutz et al.^{21,22} *m*-Diisopropenylbenzene (DIB) was polymerized anionically under such conditions that the second double bond remained unaffected. Linear polymers having molecular weights between 3000 and 10 000 and pendent double bonds were prepared. The remaining double bonds were reacted with cumylpotassium to create active sites along the PDIB chain. The polymerization of ethylene oxide was initiated from these active sites to produce PEO stars.

PEO stars having 4, 8, and 16 arms were prepared using hydroxy-functionalized carbosilane dendrimers of several generations.²³ The dendrimers were prepared starting with tetravinylsilane and using two reactions, the hydrosilylation of the vinylsilane groups with dichloromethylsilane and the nucleophilic replacement of silicon chloride by vinylmagnesium bromide, as shown in Scheme 3. The end groups were converted to hydroxy groups and were activated using potassium naphthalene. The polymerization of

ethylene oxide was initiated by these active sites. The final products had narrow molecular weight distributions and were characterized by SEC, viscometry, NMR spectroscopy, static light scattering (SLS), and dynamic light scattering (DLS). The results of these methods confirmed the preparation of well-defined star polymers. The tedious preparation of the dendrimer core molecules is the only drawback of this method.

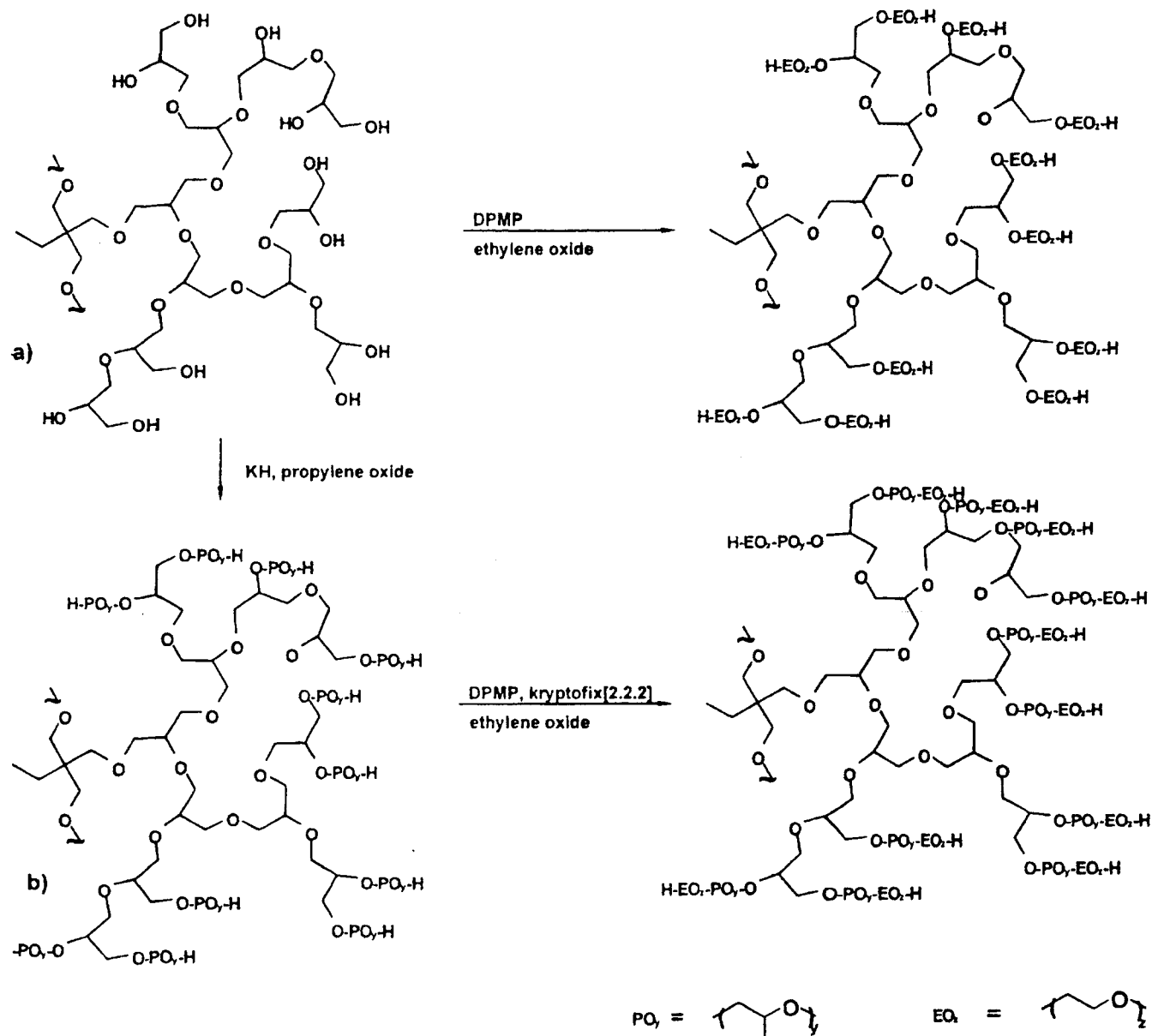
Hyperbranched polyglycerol and polyglycerol modified with short poly(propylene oxide) chains, activated with diphenylmethylpotassium (DPMP), were employed as multifunctional initiators for the synthesis of PEO stars,²⁴ as depicted in Scheme 4. Hyperbranched polyglycerol was found to be an unsuitable initiator due to the strong association effects caused by its highly polar groups. The incorporation of the poly(propylene oxide) chains (degree of polymerization, 23–52) was crucial for the synthesis of the PEO stars. These products were characterized by SEC coupled to a multiangle laser light scattering detector, as well as by NMR spectroscopy and differential scanning calorimetry. Moderate to large molecular weight distributions were obtained ranging from 1.4 up to 2.2. The functionalities of these stars were calculated to vary between 26 and 55.

A novel hydrocarbon-soluble trifunctional initiator was proposed by Quirk et al.²⁵ It was prepared by the reaction of 3 mol of *sec*-butyllithium (*s*-BuLi) with 1,3,5-tris(1-phenylethenyl)benzene (tri-DPE), as presented in Scheme 5. This initiator was found to be efficient for the polymerization of styrene only when THF was also added in the reaction mixture ([THF]:[*s*-BuLi] = 20). The polymerization reaction was monitored by UV-vis spectroscopy. The limitations of the method include the extreme care that should be exercised over the stoichiometry of the reaction between *s*-BuLi and tri-DPE and the fact that a minimum arm molecular weight around 6×10^3 is required for a successful synthesis. For arm molecular weights lower than this limit, incomplete initiation was observed. If these requirements are fulfilled, well-defined three-arm polystyrene stars can be prepared.

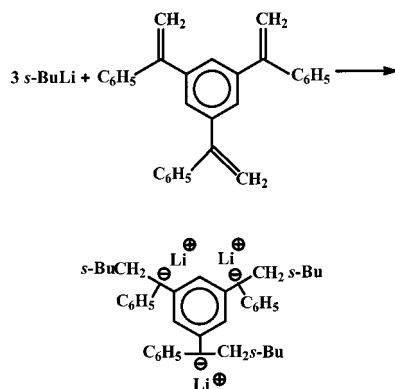
The same initiator was also used to produce a three-arm PBd star.²⁶ Complete monomer consumption was observed, but SEC analysis showed a bimodal distribution. This behavior was attributed to the strong association effects of the trifunctional initiator in a nonpolar solvent. The problem was overcome when *s*-BuOLi was added in the reaction mixture in a ratio [*s*-BuLi]:[*s*-BuOLi] = 2. *s*-BuOLi was shown to be capable of disrupting the initiator association without affecting appreciably the microstructure of the PBd chains. Therefore, a well-defined star polymer with low molecular weight distribution was obtained.

Polyolithiated carbosilane dendrimers were also employed as multifunctional initiators for the polymerization of styrene, ethylene oxide, and hexamethylcyclotrisiloxane (D₃),²⁷ according to Scheme 6. The dendrimers had 16 or 32 allyl groups at their periphery. A hydrosilylation route was performed to

Scheme 4



Scheme 5



react half of these terminal allyl groups with di-decylmethylsilane. The remaining allyl groups were lithiated by the addition of *s*-BuLi, to produce the multifunctional initiators. These initiators carrying theoretically 8 or 16 carbanionic sites were soluble in hydrocarbon solvents and were subsequently used

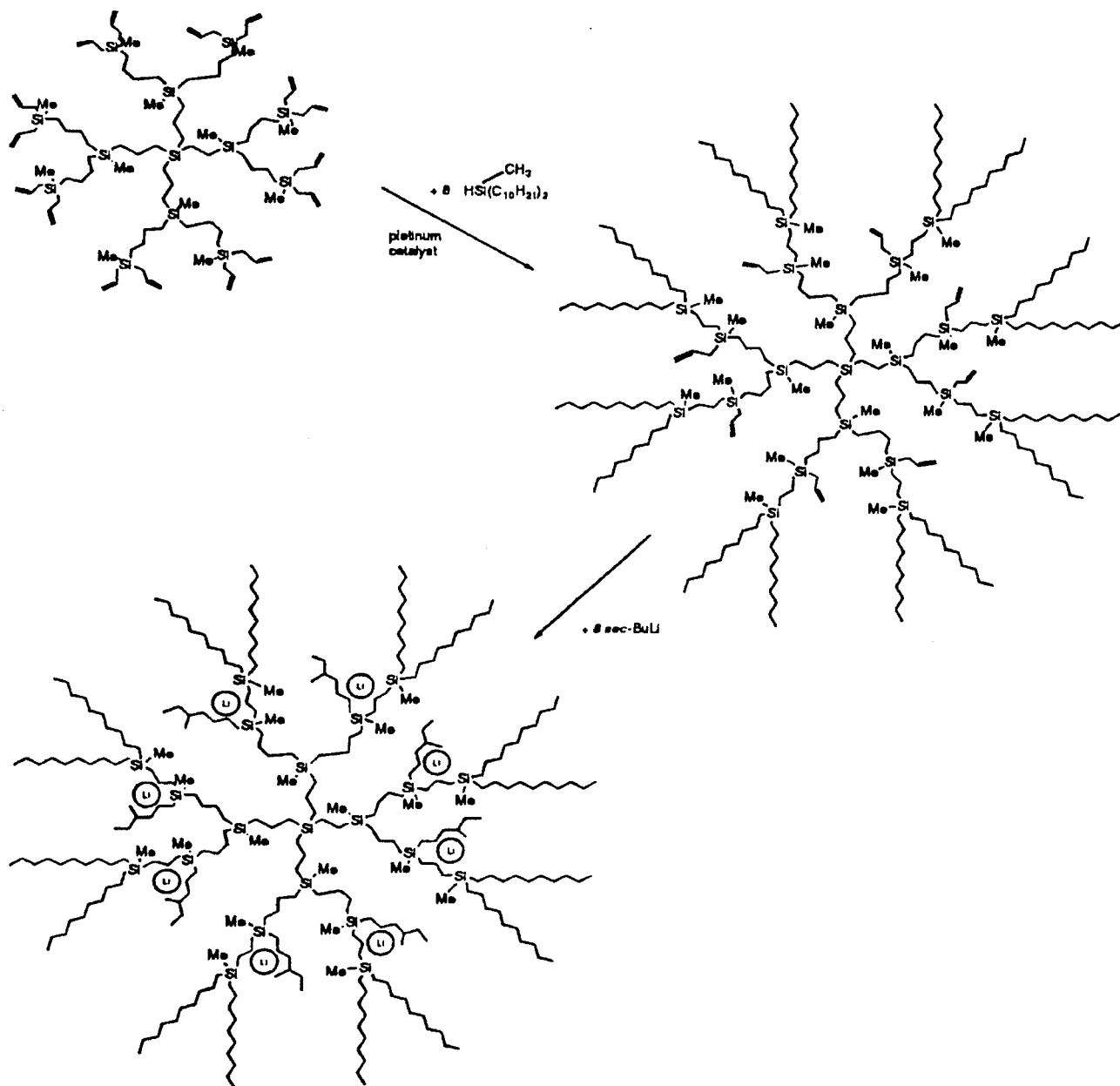
for the polymerization of St, EO, and D₃ under suitable conditions. SEC analysis showed the existence of monomodal peaks. However, molecular characterization data were not provided in this study and the number of branches for these stars was not determined, thus leaving uncertain the formation of the desired structures.

2. Multifunctional Linking Agents

The most general and useful method for the synthesis of star polymers by anionic polymerization is the linking reaction of the living polymers with a suitable electrophilic reagent. Several linking agents have been used for the synthesis of star polymers.⁷ The most important of those are the chlorosilanes²⁸ and the chloromethyl or bromomethyl benzene derivatives.^{29,30}

The linking reactions of living polymers with the chlorosilanes proceed without any side reactions. However, the efficiency of the linking reaction de-

Scheme 6



depends on the steric requirements of the linking agent and the living macromolecular chain end. The linking efficiency can be improved by separating the Si–Cl groups by spacers, such as methylene groups, and/or by end-capping the living chains with a few units of butadiene in order to reduce the steric hindrance and facilitate the linking reaction. Under these conditions, well-defined stars have been prepared with functionalities ranging from 3 up to 18.^{31–37} Recent advances in the synthesis of pure carborane dendrimers led to the preparation of linking agents with functionalities as high as 128.³⁸ These dendrimers were successfully used for the synthesis of PBd stars having 32, 64, and 128 branches.^{39,40} The products were characterized by SEC, membrane osmometry (MO), vapor pressure osmometry (VPO), and LS, and their dilute solution properties were extensively studied in the framework of several theoretical models. Low molecular weight distribution polymers having functionalities close to the

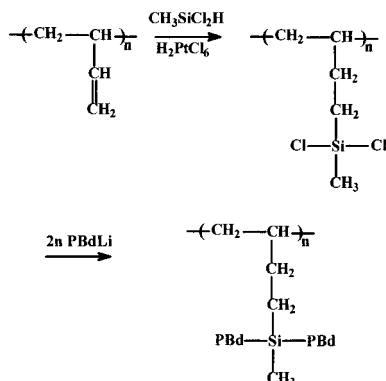
theoretical value were obtained in all cases. However, extended periods of time were needed for complete linking reactions, and fractionation was required to eliminate excess arm (purposely added) and low molecular weight impurities.

The validity of the chlorosilane linking agents for the synthesis of star polymers was reevaluated recently using NMR⁴¹ and matrix-assisted laser desorption/ionization time-of-flight mass spectrometry (MALDI-TOF MS)⁴² techniques. Polyisoprene (PI) and polybutadiene (PBd) stars having low arm molecular weights ($M \sim 10^3$) and functionalities ranging between 3 and 64 were prepared. It was observed that for stars having 16 or less arms, the structural quality with respect to the polydispersity and the functionality agrees very well with the theoretical values. For stars having theoretically 32 and 64 arms, the average functionalities of the chlorosilane linking agent was found to be 31 and 60, respectively, whereas the number of arms of the

stars were 29 and 54, respectively. Both the linking agents and the star products had narrow molecular weight distributions. These results clearly demonstrate the steric requirements of this linking reaction.

This method was extended to the synthesis of PBd stars having more than 200 arms.⁴³ Low molecular weight linear and star poly(1,2-butadiene) with 18 arms was extensively hydrosilylated with methylchlorosilane and used as linking agents to prepare multiarm PBd stars, as shown in Scheme 7. The

Scheme 7

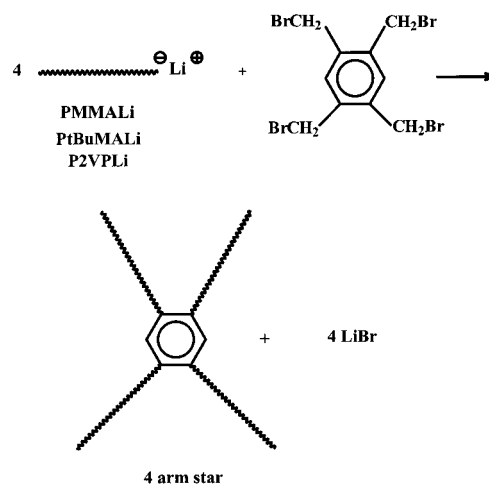


synthesis is similar to the one used for the preparation of graft polymers, but the low backbone molecular weight makes them behave as starlike structures. Star polymers having 270 and 200 arms were finally prepared from the linear and the 18-arm star poly(1,2-butadiene), respectively. These products are characterized by a distribution in the number of arms, due to the lack of absolute control over the hydrosilylation reaction. However, this arm number distribution was rather low, as was found by SEC-LALLS measurements.

Another important class of linking agents are the chloromethyl and bromomethyl benzene derivatives.^{29,30} The major drawbacks are that the use of these compounds is accompanied by side reactions such as lithium-halogen exchange, and linking agents with functionalities only up to 6 have been used.⁷ Nevertheless, these compounds are valuable for the synthesis of poly(meth)acrylates and poly(2-vinylpyridine) (P2VP) stars, since they can be used efficiently at $-78\text{ }^{\circ}\text{C}$, where the polymerization of these polar monomers takes place. The chlorosilanes cannot be used because the linking reaction either does not proceed at these low temperatures or leads to unstable products.

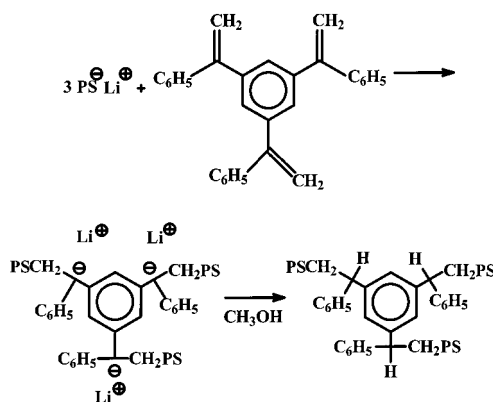
Hogen-Esch and Toreki reported the synthesis of three-arm P2VP stars using 1,3,5-tri(chloromethyl)benzene.⁴⁴ Only SEC and viscometry data were provided in this study. Mays et al. extended this work with the synthesis of four-arm stars having poly(*tert*-butyl methacrylate) (PtBuMA), poly(methyl methacrylate) (PMMA), and P2VP branches⁴⁵ (Scheme 8). 1,2,4,5-Tetra(bromomethyl)benzene was used as the linking agent. Combined characterization results by SEC and MO revealed the formation of well-defined star polymers. The use of bromo derivatives and the low temperatures under which the linking was conducted prevented the formation of byproducts.

Scheme 8

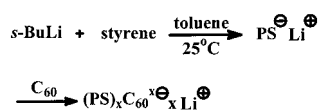


1,3,5-Tris(1-phenylethenyl)benzene was used by Quirk and Tsai as a linking agent for the synthesis of a three-arm PS star,²⁵ as shown in Scheme 9. SEC, MO, and LS results showed that a well-defined star was prepared by this procedure. Despite the fact that the arm molecular weight used was rather low ($M_n = 8.5 \times 10^3$), it can be concluded that there is no steric limitation for the synthesis of three-arm PS stars using this coupling agent. Previous efforts to use methyltrichlorosilane as a linking agent for the synthesis of three-arm PS stars were not successful, due to incomplete coupling (steric hindrance effects).²⁸

Scheme 9

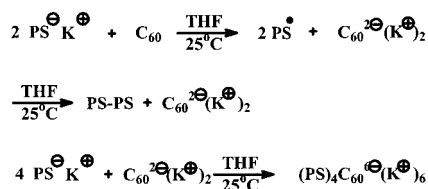


Soon after the discovery of fullerenes, efforts were made to use C_{60} as a coupling agent for the preparation of star polymers. Samulski et al.⁴⁶ reported the reaction of living polystyryllithium with C_{60} , and later Ederle and Mathis extended this work, providing mechanistic aspects on this reaction in different solvents.⁴⁷ In the nonpolar solvent toluene, it was found that by using an excess of living PSLi chains over the C_{60} a six-arm star can be prepared by addition of the carbanions onto the double bonds of the fullerene (Scheme 10). A similar behavior was observed when living polyisoprenyllithium was used for the coupling reaction. However, when the living PS chains were end-capped with one unit of DPE, only the three-arm star was produced, showing that the functionality of the product can be adjusted by

Scheme 10

changing the steric hindrance of the living chain end. The functionality could be also controlled by the stoichiometry of the reaction between the living polymers and the C₆₀. However, it was impossible to selectively incorporate one or two chains per C₆₀ molecule.

In polar solvents, such as THF a different situation was observed. During the reaction of a living polystyrylpotassium with C₆₀ in THF, a two-electron transfer was initially observed followed by the addition of four chains, according to Scheme 11. When the living PS chain was end-capped with 2-vinylpyridyl or 1,1-diphenylethyl groups, the number of the linked chains was reduced to 3 and 0, respectively, showing that both the reactivity and the bulkiness of the end group play an important role in this reaction.

Scheme 11**3. Use of Difunctional Monomers**

Several star polymers have been prepared by reacting living polymers with DVB. The method has been applied in the past for the synthesis of PS^{48,49} and polydiene⁵⁰ stars. Rather narrow molecular weight distribution PS stars were obtained when the [DVB]:[PSLi] ratio was varied from 5.5 to 30 and the corresponding functionality was between 13 and 39. Similar behavior was obtained for polydiene stars when the [DVB]:[PDLi] ratio was from 5 to 6.5 and the functionality of the star was varied between 9 and 13. In other cases, broad distributions were observed, caused by the large distribution of the functionalities of the stars prepared by this method.

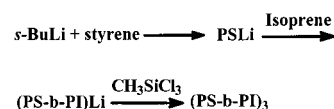
More recently, PMMA stars were prepared by reacting living PMMA chains with ethylene glycol dimethacrylate (EGDM).⁵¹ The polymers were characterized by SEC, LS, and viscometry. It was found that well-defined polymers can be prepared when the arm molecular weight was rather high (e.g. $M_w = 40\,000$). It seems that this high molecular weight is necessary to prevent intercore and gelation reactions from taking place.

EGDM was also reacted with isotactic living PMMA chains obtained using *tert*-butylmagnesium bromide as initiator in the presence of 1,8-diazabicyclo[5.4.0]undec-7-ene.⁵² A star polymer with a number of arms estimated between 20 and 30 was synthesized. SEC connected with LS and viscometry detectors was used to characterize the sample. Similar reaction using syndiotactic living PMMA chains, obtained with the initiator system *t*-BuLi/R₃Al, failed to give star

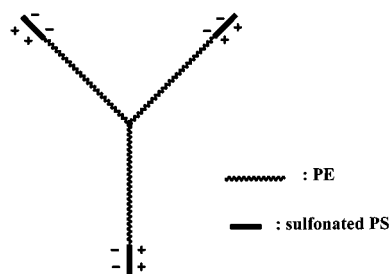
polymers. However, when EGDM was replaced by the butane-1,4-diol dimethacrylate, a PMMA star was obtained having 50–120 arms.

B. Star-Block Copolymers

Star-block copolymers are star polymers in which each arm is a diblock (or a triblock) copolymer. They can be prepared by all the methods reported earlier. The best way involves the linking reaction of a living diblock copolymer, prepared by sequential anionic polymerization of the two monomers, with a suitable linking agent. Using this method and chlorosilane linking agents, Fetters and collaborators synthesized star-block copolymers (PS-*b*-PI)_{*n*}, where *n* = 4, 8, 12, 18.^{53,54} An example is given in Scheme 12. Well-defined structures of low polydispersities were obtained.

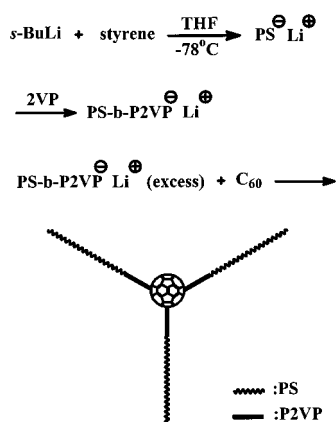
Scheme 12

Using the same method Storey et al. prepared ionic star-block copolymers.^{55,56} Styrene was oligomerized followed by the polymerization of butadiene. The living diblock copolymer was subsequently linked with methyltrichlorosilane to provide a three-arm star-block copolymer of styrene and butadiene. Hydrogenation of the diene blocks and sulfonation of the styrene blocks produced the desired ionic star-block structure having ionic outer blocks and hydrophobic inner blocks, as depicted in Scheme 13.

Scheme 13

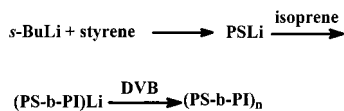
C₆₀ was also employed for the synthesis of star-block copolymers.⁴⁷ Living PS-*b*-P2VP diblocks, having short P2VP chains, were prepared by sequential anionic polymerization in THF. These living diblocks were reacted with a suspension of C₆₀ in THF, leading to the formation of a three-arm star-block copolymer (Scheme 14). The corresponding reaction with the living PS homopolymer results in the formation of a four-arm star. The lower reactivity of the 2VP anion seems responsible for this behavior. The SEC analysis showed that the product had a broad molecular weight distribution, indicating that a mixture of stars with different functionalities was obtained.

DVB was used to prepare a multifunctional initiator from which the polymerization of styrene was initiated, followed by the polymerization of ethylene oxide. Quite broad polydispersities were reported for these star-block copolymers, due to the random

Scheme 14

distribution of core sizes and functionalities.⁵⁷ Lithium naphthalene in the presence of lithium chloride was employed to form the multifunctional DVB cores. These cores initiated the polymerization of styrene at -40°C to produce the living PS stars. The living arms were end-capped with DPE to reduce their nucleophilicity and then were used to initiate the polymerization of tBuA at -55°C . Finally, methanol was added to deactivate the living diblock branches.¹⁶ The functionality of the stars was reported to range from 190 to 320. The molecular weight distributions were broad and sometimes multimodal. (PS-*b*-P2VP)_{*n*} star block copolymers, having P2VP interior blocks, were also prepared by the same method.⁵⁸

Living PS-*b*-PI diblock anions were reacted with a small amount of DVB in benzene to form star-block copolymers⁵⁹ (Scheme 15). The molar ratio of DVB

Scheme 15

to diblock anions ranged from 3.6 to 15.4, resulting in star functionalities ranging from 15.6 to 91.5. Narrow molecular weight distributions were obtained except in one case, where the distribution was bimodal.

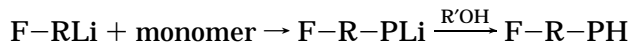
Star-block copolymers were also prepared by Teyssié et al.⁶⁰ from the reaction of living diblock copolymers with EGDM. (PS-*b*-PtBuA)_{*n*} and (PMMA-*b*-PtBuA)_{*n*} were synthesized by this method. The polydispersity of the stars was rather narrow but slightly increased compared to the parent diblocks, meaning that a distribution of functionalities existed in the final products. Only SEC was used to characterize the polymers.

C. Functionalized Stars

The introduction of functional groups at the end(s) or along the polymer chain can produce new materials that can be used as models to study and manipulate fundamental phenomena in polymer science, such as association, adsorption, chain dynamics, and block copolymer morphology.^{61–65} The synthesis of end-functionalized polymers remains a challenging problem in polymer chemistry. Among the different

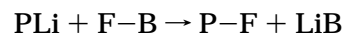
methods developed for the introduction of end-functional groups, anionic polymerization has been found to be a most valuable tool, since it proceeds without chain termination or chain transfer reactions.⁶⁶ There are two primary approaches to incorporate functional end groups:

Use of Functionalized Initiators.⁶⁷ This method can be described by the following reactions:



where F is the functional group and P the polymer chain. This procedure ensures complete functionalization, provided that the functional initiator produces narrow molecular weight distribution polymers with predictable molecular weights. The functional group should have low Lewis base character in order to maintain a low vinyl content in the polydiene. Another important parameter is that the functionalized initiator should be soluble in hydrocarbon solvents, in order to produce polydienes with low vinyl contents.

Use of Functionalized Terminating Agents.^{66,68} The living polymer is terminated with a functionalized electrophilic reagent, according to the reaction:



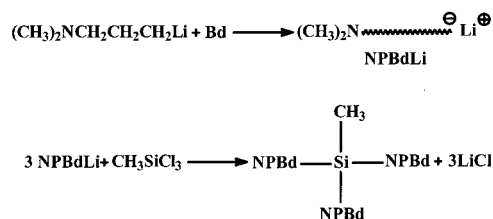
Care should be taken in the choice of the suitable terminating agent, since this reaction can be subject to several side reactions, leading to incomplete functionalization.

The synthesis of functional polymers is not always a straightforward procedure, because of the competition or antagonism of functional groups with the active living ends. Therefore, several protective groups have been used to mask reactive functionality.⁶⁸

These methods have also been employed for the synthesis of functionalized star polymers. Recent applications will be presented in the following sections.

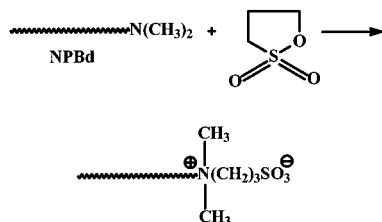
1. Functionalized Initiators

The polymerization of a monomer with a functionalized initiator followed by the reaction of the living chains with a suitable linking agent results in the formation of well-defined star polymers. Fetters et al.⁶⁹ prepared 3- and 12-arm star polyisoprenes (3N-PI and 12N-PI), end-functionalized with dimethylamine end groups, by reacting living PI chains, produced with 3-dimethylaminopropyl lithium (DMAPLi) and the appropriate chlorosilane linking agent. The same initiator was later employed for the synthesis of three-arm PBd stars (3N-PBd)⁷⁰ according to Scheme 16. The initiator is soluble in benzene and

Scheme 16

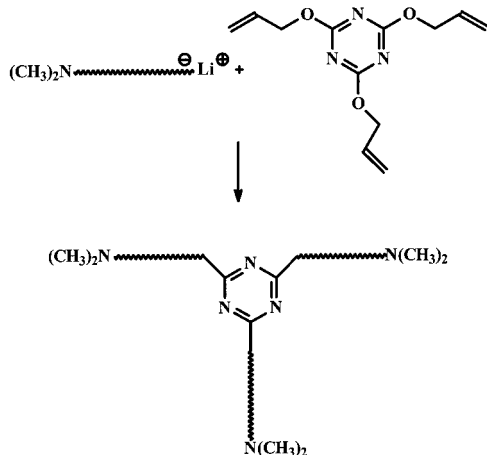
produces polydienes with low vinyl contents. It is also an efficient initiator for the polymerization of dienes, meaning that the rate of initiation is faster than the rate of propagation and the initiator is totally consumed during the initiation step.⁷¹ Polydienes with predictable molecular weights and narrow molecular weight distributions were prepared using this initiator. SEC, MO, and LS results showed that well-defined structures were obtained. The dimethylamine end groups were later transformed to sulfobetaine groups by reaction with 1,3-cyclopropane sultone (Scheme 17).

Scheme 17



DMAPLi was also used by Burchard to synthesize three-arm PS stars (3N-PS) having dimethylamine end groups.⁷² In this case 1,3,5-triallyloxy-2,4,6-triazine was the linking agent, as shown in Scheme 18.

Scheme 18

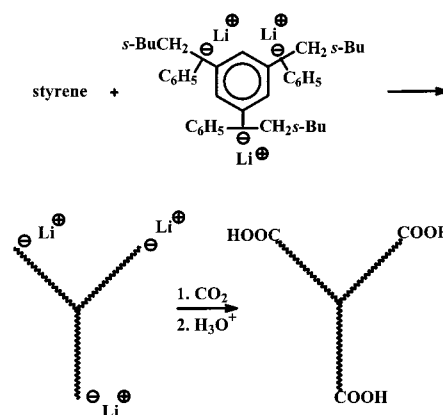


An acetal-protected lithium initiator was used to polymerize styrene followed by linking with 1,3,5-triallyloxy-2,4,6-triazine to produce three-arm star polystyrenes.⁷³ The protective acetal group was cleaved by weak acidic treatment in THF to give star polymers with terminal OH groups. These functional groups were coupled with toluene-2,4-diisocyanate to give randomly cross-linked products. Unfortunately, few characterization data were provided in this study.

2. Functionalized Terminating Agents

This functionalization method can be applied for the synthesis of star polymers only when a multifunctional initiator is used. The living branches emanate from the core and therefore can be subjected to several terminating reactions with suitable electrophilic reagents.

Scheme 19

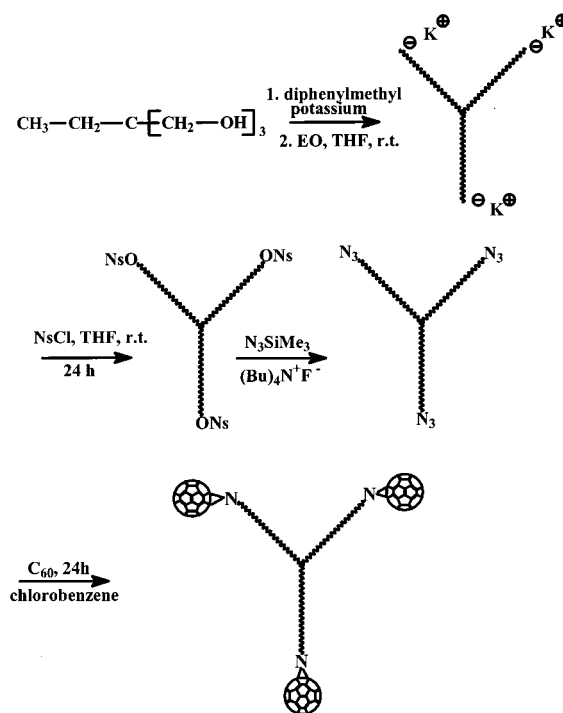


Multifunctional DVB initiators were used to polymerize styrene, and the living arms were subsequently reacted with ethylene oxide to produce PS chains with terminal hydroxyl groups.⁵⁷

The trifunctional initiator produced by the reaction of 3 mol of *s*-BuLi with 1,3,5-tris(1-phenylethenyl)benzene was also employed for the synthesis of an end-functionalized polystyrene star.²⁵ After the polymerization was completed, the living star polymer was carboxylated by the introduction of gaseous carbon dioxide (Scheme 19). End-group titration indicated that the star had 2.8 functional groups per molecule. However, SEC analysis revealed the existence of an appreciable amount of side high molecular weight products. The situation was not improved, even after end-capping the living branches with DPE units prior to the carboxylation reaction. It was shown that it is more successful to perform the carboxylation reaction with the freeze-dried living polymer solution. In this case the amount of byproducts was lower than 2%.

Three-arm PEO stars having terminal C_{60} groups⁷⁴ were prepared by the procedure given in Scheme 20.

Scheme 20



1,1,1-Tris(hydroxymethyl)propane treated with diphenylmethyl potassium (DPMP) was employed as a trifunctional initiator to produce a living three-arm PEO star. The living arms were reacted with 4-nitrobenzenesulfonyl chloride to transform the alkoxides to nosylate functionalities. The success of this procedure was evaluated by IR and NMR spectroscopies. The nosylated (Ns) PEO star was subjected to an azidation reaction using tetrabutylammonium fluoride and trimethylsilyl azide. The triazide PEO was then allowed to react with C₆₀ to produce the final functionalized star. IR, NMR, and SEC analysis revealed the formation of well-defined functionalized stars.

D. Asymmetric Stars

Asymmetric stars are a special class of stars that is characterized by an asymmetry factor compared to the classical symmetric structures described previously. The following parameters have been considered as asymmetry factors:

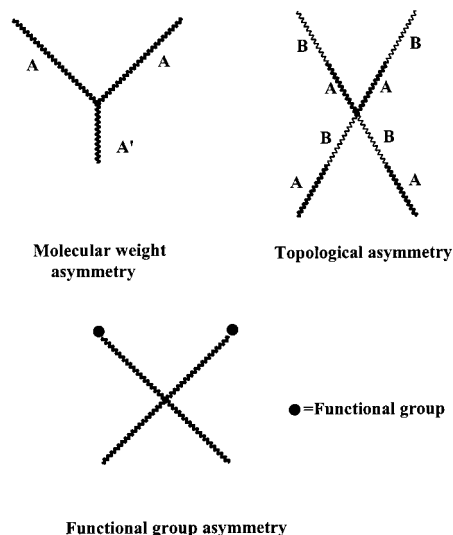
Molecular Weight Asymmetry. All the arms of the star are identical in chemical nature, but they have different molecular weights.

Functional Group Asymmetry. The arms are of the same chemical nature and have the same molecular weight, but they have different end groups.

Topological Asymmetry. The arms of the star are block copolymers that may have the same molecular weight and composition but differ with respect to the polymeric block that is covalently attached to the core of the star.

These structures are schematically shown in Scheme 21. The synthesis of asymmetric stars can be accomplished by the same general methods reported for the symmetric stars but in such way that a controlled incorporation of the arms, differing in molecular weight, end functional groups, or topology is achieved. Efficient methods for the synthesis of asymmetric star polymers were developed only recently.

Scheme 21



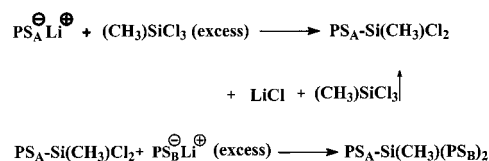
1. Molecular Weight Asymmetry

i. Chlorosilane Method. The chlorosilane method was initially reported by Fetters⁷⁵ and was later

developed by Hadjichristidis, Mays, and collaborators.^{88–91} Chlorosilanes are used as linking agents for the stepwise replacement of the chlorine atoms by the polymer chains. This procedure can be achieved taking into account the different reactivity of the living polymer ends toward the Si–Cl bond, as this is determined by the steric hindrance effects, the charge localization on the terminal carbon atom,⁷ and the excluded volume of the living chain that is affected by the reaction solvent. The reactivity of the living chain end decreases by charge delocalization and by increasing the steric hindrance. The latter can be affected by both structures, that of the living chain end and the chlorosilane linking agent. The steric hindrance concerning the living end increases in the order $\text{BdLi} < \text{IsLi} < \text{SLi} < \text{DPELi}$. The closer the Si–Cl groups in the linking agent, the more sterically hindered is the reaction with the living chains. For example, overall SiCl_4 is less reactive than $\text{Cl}_2\text{Si}-\text{CH}_2-\text{CH}_2-\text{SiCl}_2$. The reactivity is also influenced by other parameters such as the molecular weight of the living chain, the polarity of the solvent, where the reaction takes place, and the temperature. When all these factors are optimized, well-defined products are produced. However, the disadvantage of this method is that it is time-consuming and requires elaborate high-vacuum techniques to be performed.

The method was first applied to the synthesis of asymmetric PS stars having two arms of equal molecular weights (PS_B) and a third one (PS_A) having molecular weight either half or twice that of the identical arms.⁷⁵ The procedure, given in Scheme 22,

Scheme 22



involves the reaction of the living arm PS_ALi with a 10-fold excess of methyltrichlorosilane for the preparation of the methylchlorosilane end-capped PS_A . This is the crucial step of the synthesis, keeping in mind that there is a possibility to form the coupled byproduct, i.e., the two-arm star with only one remaining Si–Cl group. This is avoided by using a large excess of the linking agent, adding the linking agent solution to a dilute living polymer solution under vigorous stirring and performing the linking reaction at low temperatures (5 °C). Under these conditions, no coupled byproduct is observed.

After freeze-drying the end-capped PS_A branch, the excess silane was removed under high vacuum by heating the resulting porous material at 50 °C for at least 3 days. After the silane was removed the end-capped polymer was dissolved in benzene, which was introduced directly by distillation from the vacuum line.

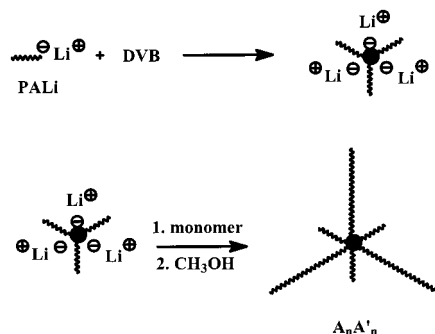
The two remaining Si–Cl bonds of the methylchlorosilane end-capped PS_A arm were then reacted with a small excess of living PS_BLi chains. The PS_BLi chains were end-capped with a few units of butadiene to facilitate the completion of the linking reaction.

The excess of the PS_B arm was removed by fractionation. Detailed characterization results by SEC, MO, and LS revealed that well-defined structures were obtained.

The method was also applied in the synthesis of asymmetric PBd^{75} and PI^{76} stars. When the molecular weight of the PI chain that was reacted with the excess silane was less than 5.5×10^3 , the formation of the coupled byproduct could not be avoided, due to the low steric hindrance of the living PI chain end. The byproduct was removed by fractionation. The stars were characterized by SEC, MO, and LS, showing that the desired structures having low polydispersities were efficiently prepared.

ii. Divinylbenzene Method. As already discussed, when appropriate living polymer chains react with a small amount of DVB, a star polymer is formed consisting of a highly cross-linked polydivinylbenzene core from which the arms emanate. This is actually a living star since the core carries anionic centers. The number of these active sites is theoretically equal to the number of the arms of the star. Subsequent addition of a new monomer results in the growth of new arms from the core and therefore the formation of an asymmetric star of the type $A_nA'_n$ can be achieved, if the molecular weight of the original chains is different than that obtained by the chains formed in the second step. This general procedure is depicted in Scheme 23.

Scheme 23



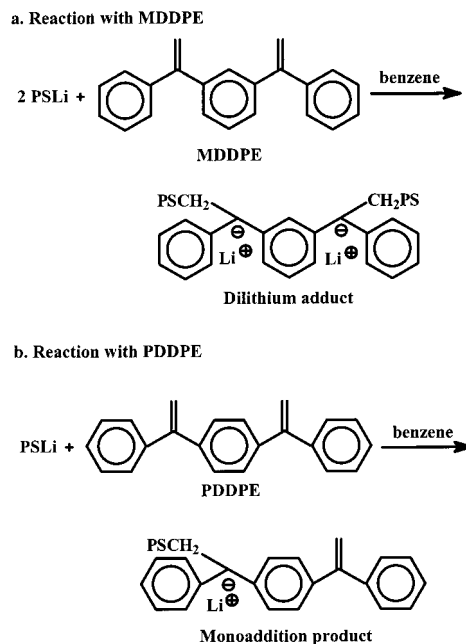
The drawbacks associated with this method have been already mentioned. Probably the most important is the architectural limitation, i.e., only asymmetric stars of the type $A_nA'_n$ can be prepared by this method. However, even these structures are not unambiguously characterized. A fraction of the living arms A is not incorporated in the star structure, probably due to steric hindrance effects. These living chains may act as initiators for the polymerization of the monomer that is added for the preparation of the asymmetric star. Another problem is that the active sites of the living A_n star are not equally accessible to the newly added A' monomers, due to steric hindrance effects. Furthermore, the rate of initiation is not the same for these active sites. For all these reasons, it is obvious that the final products are structurally ill-defined with a rather great dispersity of the n values and are characterized by broad molecular weight distributions. Nevertheless, this method is technically important, since it can be applied on an industrial scale and also provides the

possibility of preparing end-functionalized asymmetric stars after reaction of the growing living branches A' with suitable electrophilic compounds.

Using this method asymmetric stars of the type $(PS_A)_n(PS_B)_n$ were prepared.⁷⁷ Living PS chains were obtained by *s*-BuLi initiation and reacted with a small amount of DVB to give a living star polymer. The anionic sites of the star core were subsequently used to initiate the polymerization of a new quantity of styrene. This initiation step was accelerated by the addition of a small quantity of THF. It was revealed by SEC analysis that high molecular weight species were also present, probably due to the formation of linked stars. These structures can be obtained when living anionic branches of one star react with the residual double bonds of the DVB-linked core of another star.

iii. Diphenylethylene Derivative Method. The method is based on the use of 1,1-diphenylethylene derivatives that are nonhomopolymerizable monomers. Rich chemistry was developed, leading to the formation of several types of asymmetric stars. Quirk reacted living PS chains with either 1,3-bis(1-phenylethenyl)benzene, (MDDPE) or 1,4-bis(1-phenylethenyl)benzene (PDDPE), according to Scheme 24.

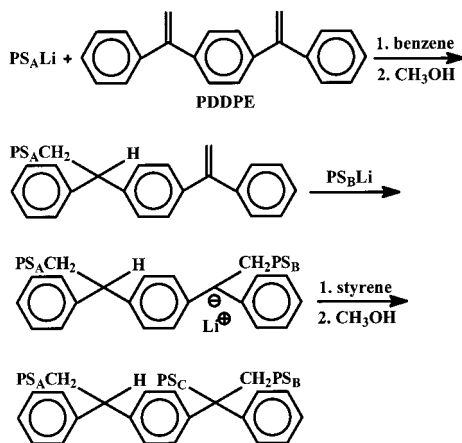
Scheme 24



It was shown that 2 mol of the living polymer reacts rapidly with the DPE derivatives to form the dilithium adduct in hydrocarbon solvents, whereas in THF monoaddition is reported.^{7,26,78–80} This reaction was monitored by UV–visible spectroscopy. The analysis revealed that the stoichiometric addition of PSLi was quantitative. However, PDDPE exhibited less tendency to form the diadduct both in polar and nonpolar solvents. This behavior can be attributed to the better delocalization of the negative charge in the para than in the meta isomer. Mainly, low molecular weight polystyrenes have been used for these studies.

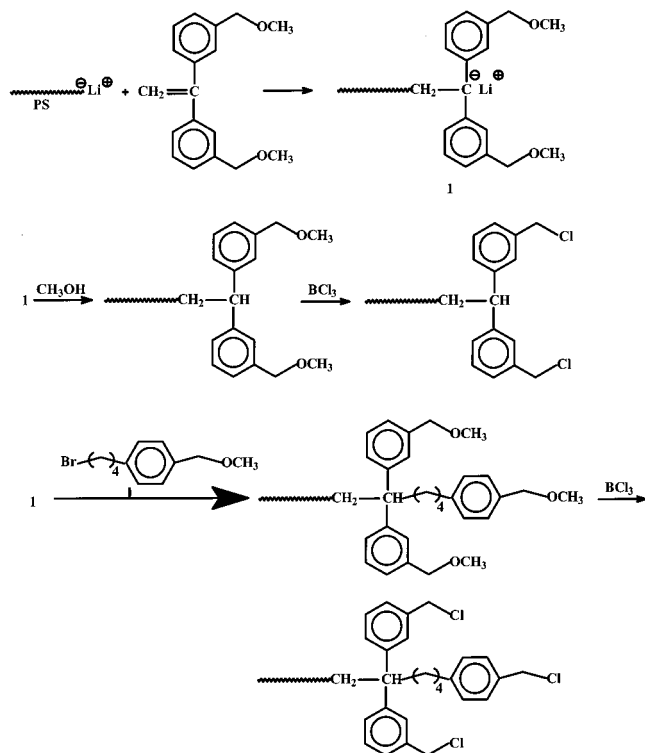
Taking into account the above observation, a three-arm asymmetric PS star was successfully prepared⁸¹

Scheme 25

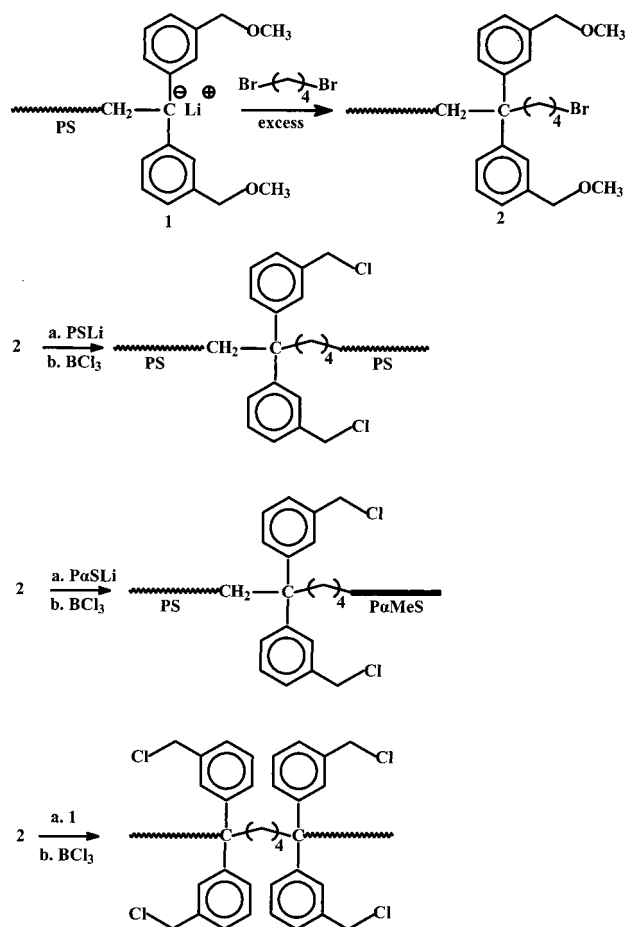


(Scheme 25). The monoadduct product was reacted with a second polystyryllithium chain, having different molecular weight, to form the coupled product. The efficiency of this coupling reaction depends on the control of the stoichiometry between the reactants. Under optimum conditions the efficiency of the coupling reaction can be higher than 96%. Finally, the addition of styrene leads to the formation of the product. The polymerization took place in the presence of THF to accelerate the crossover reaction. The SEC analysis showed the existence of a small quantity of the PS homopolymer product and the second arm of the monoadduct, due to incomplete linking reactions. The weak points of the method are the great care that should be exercised over the stoichiometry of the reactions and the inability to isolate and consequently characterize the third arm. However, the method is valuable, since it provides the possibility to functionalize the third arm by reaction with a suitable electrophilic agent.

Scheme 26



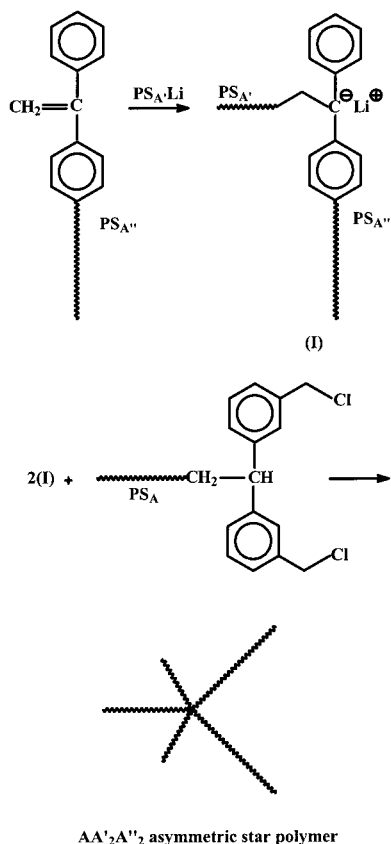
Scheme 27



More recently Hirao developed a general method employing DPE derivatives carrying protected chloromethyl groups.^{82–86} PS asymmetric stars of the types AA'₂, AA'₂A''₂, AA'₃, AA'₄, AA'A''₂, and AA'₄A''₄ were prepared by this method. The whole procedure is based on the reaction sequence shown in Scheme 26. Living PS was reacted with 1,1-bis(3-methoxymethylphenyl)ethylene followed by transformation of the methoxymethyl groups to chloromethyl groups using BCl₃ in CH₂Cl₂ at 0 °C for 10–30 min. Prior to the reaction with the BCl₃, the living end-functionalized PS is able to react with other compounds such as 1-(4'-bromobutyl)-4-methoxymethylbenzene as shown in Scheme 26. Despite the difficult multistep procedure of this method, it was shown that polystyrenes with predictable molecular weights, narrow molecular weight distributions, and almost nearly quantitative degrees of functionalization can be synthesized. Small amounts (<5%) of coupled PS byproducts can be produced during the transformation reaction, due to a Friedel–Crafts side reaction among the polymer chains.

More complicated in-chain functionalized structures with two or four chloromethyl groups were prepared according to Scheme 27.⁸² The living end-functionalized PS with two methoxymethyl groups was reacted with a 10-fold excess of 1,4-dibromobutane to introduce a bromobutyl end group. The terminal bromobutyl group was subsequently coupled with living PS to afford a linear PS chain having two in-chain methoxymethylphenyl groups. These groups

Scheme 28

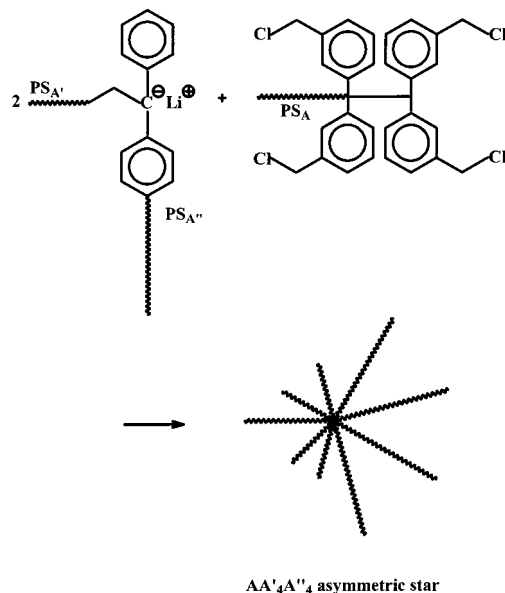


were transformed to chloromethyl groups. Alternatively, the terminal bromobutyl group can be reacted with another living end-functionalized PS with two methoxymethyl moieties, resulting in the synthesis of a linear PS chain having anywhere across the chain four functional chloromethyl groups, after performing the transformation reaction. If the four functions are required at the middle of the polymer chain, it is easier to couple a small excess of the living end-functionalized PS having two methoxymethyl moieties with 1,3-dibromobutane. Unreacted polymer from the coupling reactions was removed by HPLC fractionation.

These functionalized PS derivatives were used for the synthesis of complicated asymmetric star structures of the general type AA'₂, AA'₃, AA'₄, AA'A''₂, A₂A'₂, and AA'A''₄, where all the arms are polystyrenes having different molecular weights. The coupling reactions with living PS chains were not always complete, resulting in the formation of considerable amounts (up to 10%) of stars with lower functionalities. It was reported that side reactions such as Li-Cl exchange and single-electron transfer reactions take place to a certain extent. The formation of the byproducts was suppressed by end-capping the living PSLi chains with DPE. No steric hindrance problems were reported for these linking reactions. However, only low molecular weight arms were used for the synthesis of these asymmetric stars. It remains a question whether the use of high molecular weight arms will lead to the same success.

DPE-functionalized macromonomers were also used for linking reactions with living polymeric anions,

Scheme 29

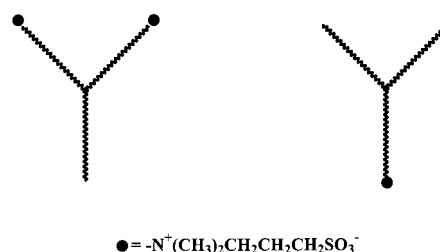


followed by the coupling with chloromethyl groups. Characteristic examples for the synthesis of AA'₂A''₂ and AA'₄A''₄ asymmetric star polymers are given in Schemes 28 and 29, respectively. Well-defined star polymers with rather low molecular weight branches were obtained with this method.

2. Functional Group Asymmetry

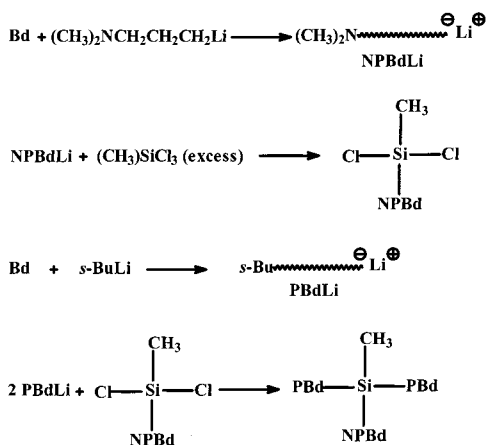
Several methods can be potentially used for the synthesis of functionalized symmetric stars. The chlorosilane method has been applied for the synthesis of three-arm PBd stars carrying one or two end-functional groups,⁷⁰ as shown in Scheme 30. The dimethylamino end groups were later transformed to sulfozwitterions by reaction with 1,3-propane sultone.

Scheme 30



The synthesis of three-arm stars with one end-standing dimethylamino group is given in Scheme 31. The functional initiator dimethylaminopropyllithium (DMAPLi) is used to polymerize butadiene. The living end-functionalized polymer is then reacted with a large excess of methyltrichlorosilane ([Si-Cl]:[C-Li] = 100) to produce the methyltrichlorosilane end-capped amine-functionalized PBd. The excess silane was removed on the vacuum line by continuous pumping for a few days, after the polymer was redissolved in benzene. Purified benzene was then introduced to dissolve the silane-capped arm. Finally, a slight excess of PBd living chains prepared by the nonfunctionalized initiator *s*-BuLi were reacted with

Scheme 31



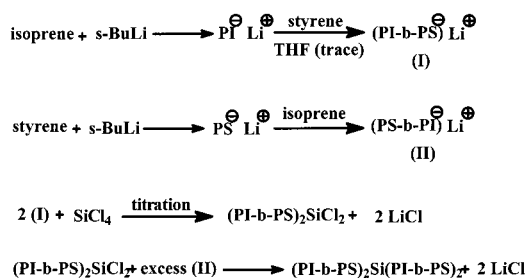
the macromolecular linking agent, giving the functionalized PBd star with one dimethylamine end group.

A similar procedure was followed for the synthesis of three-arm stars carrying two functional groups. The only difference is that the nonfunctionalized arm was prepared first and reacted with the excess methyltrichlorosilane followed, after the removal of the excess silane, with the addition of a small excess of the living functionalized arms. When the molecular weight of the living PBd arm was lower than 10 000, a considerable amount (10%) of coupling was observed during the reaction with the methyltrichlorosilane, due to the low steric hindrance of the living chain end. This amount was drastically suppressed when the arm was end-capped with a unit of DPE in the presence of THF to accelerate the crossover reaction. Well-defined products were obtained, as was evidenced by SEC, MO, and LS data.

3. Topological Asymmetry

A new star-block copolymer architecture, the inverse star-block copolymer, was recently reported.⁸⁷ These polymers are stars having four poly(styrene-*b*-isoprene) copolymers as arms. Two of these arms are connected to the star center by the polystyrene block, whereas the other two are connected through the polyisoprene block. The synthetic procedure is given in Scheme 32. The living diblocks (I) were prepared by anionic polymerization and sequential addition of monomers. A small quantity of THF was used to accelerate the initiation of the polymerization of styrene. The living diblock copolymer (I) was slowly added to a solution of SiCl_4 . The reaction was monitored by SEC on samples with-

Scheme 32



drawn from the reactor during the synthesis. The bulkiness of the living styryllithium chain end slows the incorporation of a third arm considerably. Only a minor quantity ($\sim 1\%$) of trimer was evidenced by SEC. The difunctional linking agent thus prepared was then reacted with a small excess of the living diblock copolymer (II) to produce the desired product. These living diblocks were end-capped with three or four units of butadiene to facilitate the linking reaction. Detailed characterization results by SEC, MO, LS, differential refractometry, and NMR spectroscopy revealed the formation of well-defined products.

E. Miktoarm Star Polymers

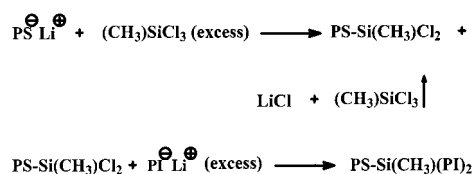
The term miktoarm (from the greek word $\mu\kappa\tau\acute{o}\varsigma$, meaning mixed), or heteroarm star polymers, refers to stars consisting of chemically different arms. In the past decade considerable effort has been made toward the synthesis of miktoarm stars, when it was realized that these structures exhibit very interesting properties.⁸⁸⁻⁹⁰ The synthesis of the miktoarm star polymers can be accomplished by methods similar to those reported for the synthesis of asymmetric stars. The chlorosilane, DVB, and DPE derivative methods have been successfully employed in this case. Furthermore, several other individual methods have appeared in the literature. The most common examples of miktoarm stars are the A_2B , A_3B , A_2B_2 , A_nB_n ($n > 2$) and ABC types. Other less common structures, like the ABCD, AB_5 , and AB_2C_2 are now also available.

1. Chlorosilane Method

i. A_2B Miktoarm Star Copolymers. A near monodisperse miktoarm star copolymer of the A_2B type was first reported by Mays,⁹¹ A being PI and B PS. The synthetic method adopted was similar to the one applied by Fetters for the synthesis of the asymmetric PS and PBd stars. The living PS chains were reacted with an excess of methyltrichlorosilane to produce the monosubstituted macromolecular linking agent. The steric hindrance of the living polystyryllithium and the excess of the silane led to the absence of any coupled byproduct. The excess silane was removed and then a slight excess of the living PI chains was added to produce the miktoarm star $\text{PS}(\text{PI})_2$. Excess PI was then removed by fractionation. The reaction sequence, given in Scheme 33 was monitored by SEC, and the molecular characterization of the arms and the final product was performed by MO.

This method was later extended by Iatrou and Hadjichristidis⁹² to the synthesis of the A_2B stars, where A and B were all possible combinations of PS, PI, and PBd. In this case a more sophisticated high-

Scheme 33

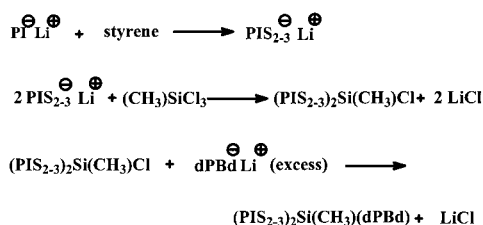


vacuum technique was employed to ensure the formation of products that are characterized by high degrees of chemical and compositional homogeneity. This was tested using several techniques such as SEC, MO, LS, differential refractometry, and NMR spectroscopy.

In a more recent study, a series of (d-PS)(PI)₂ stars, where d-PS is deuterated PS, was prepared by the same technique.⁹³ No difference was observed by using the deuterated arm compared to the PS(PI)₂ stars. A similar study concerning the synthesis of (d-PBd)-(PBd)₂ stars containing a deuterated PBd arm was also reported.⁹⁴ Both kinds of arms have almost the same molecular weight, and consequently, the only difference was that one of them was labeled with deuterium.

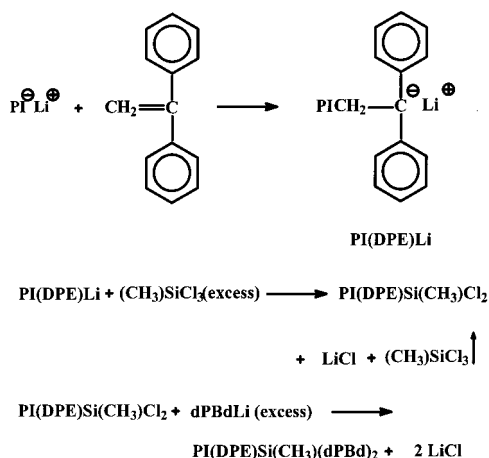
Miktoarm stars of the type (d-PBd)(PI)₂ and PI(d-PBd)₂ were synthesized according to the reaction Schemes 34 and 35, respectively.⁹⁵ A different ap-

Scheme 34



proach was adopted for the synthesis of the (d-PBd)-(PI)₂ star. Instead of incorporating the different arm first (d-PBd in this case), the two living PI chains were reacted with methyltrichlorosilane in a stoichiometric ratio of 2:1. To avoid the formation of the three-arm PI star, the living PI chains were end-capped with a few units of styrene to increase the steric hindrance of the living end. In the case of the PI(d-PBd)₂ star, the more common procedure was adopted. The living PI arm was reacted first with the linking agent. Due to the low molecular weight of the PI chain and the reduced steric hindrance of its living end, the polymer was end-capped with one unit of DPE. This method proved to be efficient to avoid the formation of coupled byproducts. Well-defined stars were obtained in both cases, as revealed by extensive molecular characterization results. In the final step

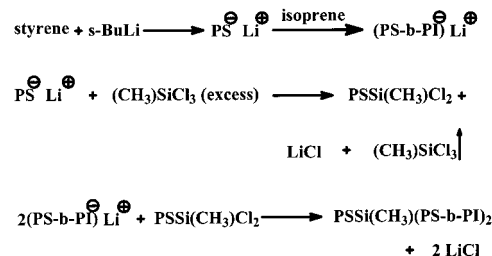
Scheme 35



the polymers were hydrogenated, transforming the PI branches to poly(ethylene-*alt*-propylene) and the d-PBd to partially deuterated polyethylene.

Miktoarm stars of the general type B(A-*b*-B)₂, where A is PI and B is PS, were prepared,⁹⁶ according to Scheme 36. The living PI arm was reacted with

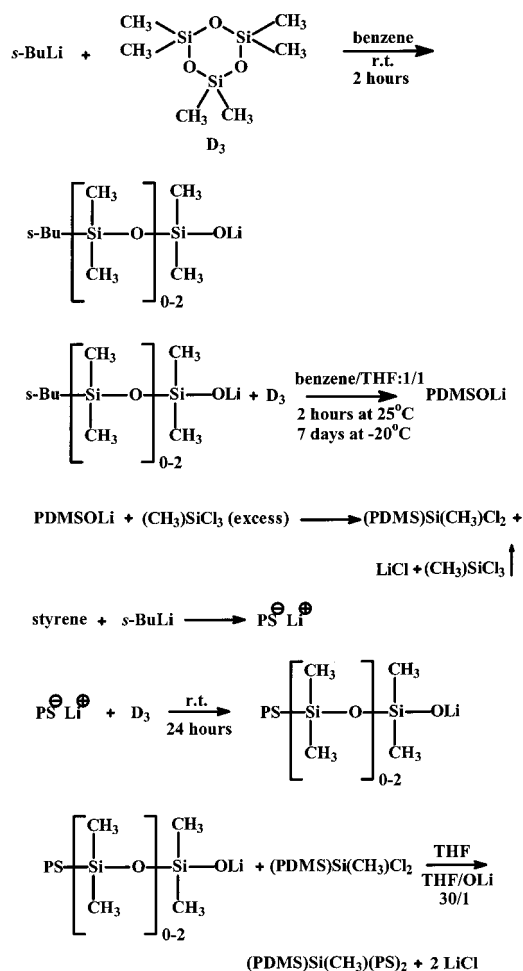
Scheme 36



an excess of the linking agent to give the dichloro end-capped macromolecular linking agent followed, after the removal of the excess silane, by the addition of the living diblock copolymer PS-*b*-PILi. The characterization data showed that polymers of high chemical and compositional homogeneity were formed.

Very recently the development of the controlled anionic polymerization of hexamethylcyclotrisiloxane (D₃) led to the synthesis of a PDMS(PS)₂ miktoarm star,⁹⁷ according to Scheme 37. A benzene:THF (50:50 v/v) solution of the living PDMS arm was added

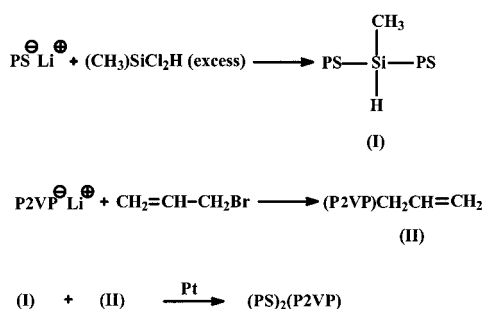
Scheme 37



slowly into a large excess of methyltrichlorosilane, leading to the formation of the monoadduct product. The macromolecular linking reagent thus formed was then reacted with living PS chains that were previously end-capped with D_3 . This capping reaction was necessary to avoid the backbiting side reactions of the very reactive PSLi anion to the PDMS arm and to facilitate the linking. THF was also added to accelerate the linking reaction.

A different approach was adopted by Eisenberg et al.⁹⁸ for the synthesis of P2VP(PS)₂ miktoarm stars, where P2VP is poly(2-vinylpyridine). Methylchlorosilane (CH₃SiCl₂H) was used as linking agent to produce the two-arm PS star. Living P2VP was reacted with allyl bromide to give an end-functionalized polymer carrying a terminal vinyl group. In the last step a hydrosilylation reaction of the Si-H group of the two-arm star with the end-double bond of the P2VP chain produced the desired structure (Scheme 38). Rather high molecular weight distribu-

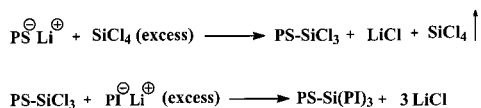
Scheme 38



tions ($M_w/M_n = 1.33-1.50$) were obtained, probably due to incomplete hydrosilylation reaction. High molecular weight P2VP, end-capped with vinyl groups (macromonomer), were used to avoid the steric hindrance effects and facilitate the hydrosilylation reaction. Consequently, the method suffers limitations and cannot be used in general for the synthesis of miktoarm stars.

ii. A₃B Miktoarm Star Copolymers. The method employed for the synthesis of the A₂B miktoarm stars can be expanded to the synthesis of A₃B structures using silicon tetrachloride (SiCl₄) instead of methyltrichlorosilane as the linking agent. Living PS chains were reacted with an excess of SiCl₄ to produce the trichlorosilane end-capped PS. After evaporation of the excess silane, the macromolecular linking agent was added to a solution containing a small excess of living PI chains to give the desired PSPI₃ star.⁹⁹ The reaction sequence, shown in Scheme 39, was monitored by SEC. Well-defined polymers with narrow molecular weight distribution were obtained.

Scheme 39



The same procedure was recently applied for the synthesis of four-arm PBd stars, where all the arms had the same molecular weight but one of them was

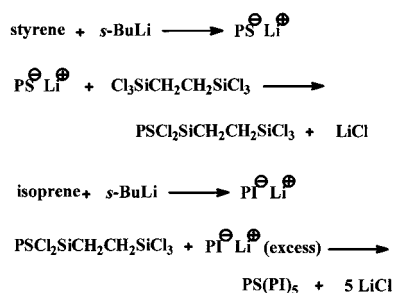
deuterated [(d-PBd)(PBd)₃].⁹⁴ The product was studied by SEC, MO, and LS.

As in the case of the B(A-*b*-B)₂ stars, the B(A-*b*-B)₃ structures were also prepared, A being PI and B being PS.⁹⁶ SiCl₄ was the linking agent in that case, and well-defined polymers were also obtained.

A different strategy was applied by Tsiang for the synthesis of (A-*b*-B)₃ stars, where A is PS and B is PBd.¹⁰⁰ The living chains B were reacted with the SiCl₄ in a molar ratio 3:1, followed by the addition of the living A-*b*-B chains. However, the control of the first step was rather limited, since not only the desired B₃SiCl but also the byproducts B₂SiCl₄ and B₄Si were formed. This behavior was observed due to the absence of steric hindrance of the living PBd chain end. It is obvious that this method is very demanding regarding the stoichiometric control of the reagents. It seems more appropriate in this case to incorporate the living A-*b*-B arm first and then to add the other three arms.

iii. A_nB (*n* > 3) Miktoarm Star Copolymers. The synthesis of PSPI₅ miktoarm stars¹⁰¹ was accomplished by the reaction sequence outlined in Scheme 40. Living PS was reacted with the hexafunc-

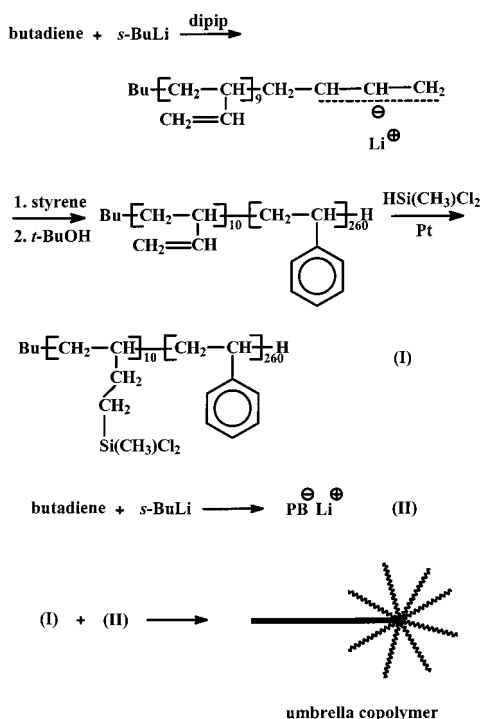
Scheme 40



tional chlorosilane 1,2-bis(trichlorosilyl)ethane in a ratio [C-Li]:[Si-Cl] = 1:6. Dropwise addition of the living polymer solution into the vigorously stirred solution of the linking agent was performed to link only one PS arm per chlorosilane molecule. However, even with these precautions the local excesses of the living polymer could not be completely avoided, leading to the formation of the coupled byproduct (~10% by SEC analysis). The macromolecular pentachlorosilane linking agent was then reacted with a small excess of the living PI chains to produce the final structure. Careful fractionation was performed to remove the excess PI and the (PS)₂(PI)₄ byproduct formed during the synthesis. The stoichiometric reaction between the living PS chains and the linking agent was chosen instead of an excess of the silane, since this high molecular weight chlorosilane is not volatile (mp ~26 °C) and its excess can only be removed by fractional precipitation, a process that is difficult to perform under vacuum. Despite these difficulties, narrow molecular weight distribution products characterized by compositional and chemical homogeneity were obtained.

More complicated structures of the general type AB_{*n*}, called umbrella copolymers, were synthesized by Roovers et al.^{102,103} using the procedure shown in Scheme 41. This name was given due to the relatively high molecular weight of the A compared to the B

Scheme 41

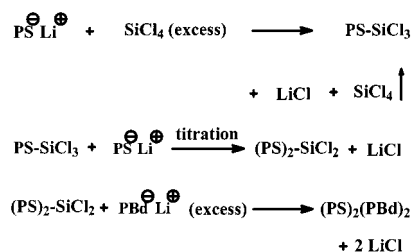


arms. Butadiene was oligomerized in the presence of dipiperidinoethane, followed by the polymerization of styrene. A block copolymer having a PS block and a short 1,2-PBd tail was thus prepared. The side double bonds of the 1,2-PBd units were hydrosilylated using $\text{HSi}(\text{CH}_3)_2\text{Cl}$ or $\text{HSi}(\text{CH}_3)\text{Cl}_2$ in the presence of a suitable platinum catalyst. Subsequent addition of living 1,4-PBdLi or P2VPK chains led to the formation of the umbrella stars. It is obvious that the number of the B branches is actually an average value and cannot be predicted by this method, since there is no absolute control over the hydrosilylation reaction and the short 1,2 PBd ends have a wider molecular weight distribution. However, this procedure offers the possibility to prepare complicated structures having interesting properties.

iv. A_nB_n ($n \geq 2$) Miktoarm Star Copolymers.

The most common type of polymers in this category is the A_2B_2 type of miktoarm star copolymers. The synthesis of the PS_2PBd_2 stars was accomplished by Iatrou and Hadjichristidis¹⁰⁴ using the reaction sequence outlined in Scheme 42. The living PS chains reacted with a large excess of SiCl_4 , which is the linking agent to produce the trichlorosilane end-capped PS. The excess silane was evaporated on the vacuum line as described earlier. The second living PS arm was incorporated to the macromolecular

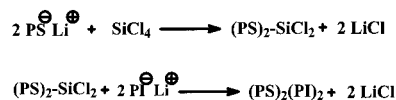
Scheme 42



linking agent PSSiCl_3 by a slow stoichiometric addition, called titration, to produce the dimer, PS_2SiCl_2 . This step was the most crucial of the synthesis and was monitored by SEC on samples withdrawn from the reactor. Finally, a small excess of living PBd chains was introduced to give the desired PS_2PBd_2 product. This method provides the best control over the steps of linking the various arms, but it is time-consuming and extreme care should be exercised, especially in the titration step.

PS_2PI_2 stars were prepared by Young et al.¹⁰⁵ using a different approach, shown in Scheme 43. Living PS

Scheme 43



chains were reacted with SiCl_4 in a molar ratio 2:1 for the formation of the two-arm product. The formation of the three-arm product is avoided by the increased steric hindrance of the living PS chain end. Subsequent addition of the living PI chains resulted in the formation of the desired miktoarm star. The control over the addition of the first two arms is not as absolute as in the previous method, but the procedure is faster and may lead to the formation of well-defined products.

The synthesis of the $(\text{PI})_2(\text{PBd})_2$ stars¹⁰⁶ was accomplished using the two different approaches presented above. The difficulty in this case is that both living PI and PBd chain ends are not sterically hindered, making the control of the incorporation of the first two arms more ambiguous. The problem was resolved by extending the living PI chains with a few units of styrene and then incorporating the PI chains in two consecutive steps (reaction with excess silane and then titration) and finally linking the two living PBd chains. A small quantity of THF was added to accelerate the capping reaction with styrene and ensure that all the PI chains are end-capped with styrene units. According to the second approach, the reactivity of the living PI chain ends was reduced by performing the linking stoichiometric reaction with the silane at -40°C for 3 days, followed by the addition of the living PBd arms at room temperature. Both approaches produced well-defined structures, as was evidenced by the extensive molecular weight characterization of the arms, the intermediate, and the final products.

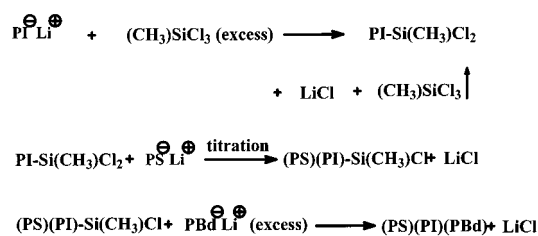
$(\text{PI})_2(\text{dPBd})_2$ stars were also prepared by the method developed by Iatrou and Hadjichristidis,⁹⁵ using deuterated butadiene. The final products were then hydrogenated, the PI arms being transformed to poly(ethylene-*alt*-propylene) and the dPBd arms to partially deuterated polyethylene.

The synthesis of the PS_8PI_8 miktoarm stars, also called Vergina star copolymers, was also reported.¹⁰⁷ A silane carrying eight Si-Cl₂ groups [$\text{Si}[\text{CH}_2\text{CH}_2\text{-Si}(\text{CH}_3)(\text{CH}_2\text{CH}_2\text{Si}(\text{CH}_3)\text{Cl}_2)_2]_4$] was used in this case as linking agent. The living PS chains were reacted with the linking agent in a molar ratio 8:1 for the synthesis of the eight-arm intermediate. The steric hindrance of the living PS chain ends prevents the

incorporation of more than one arm per SiCl₂ group, even if a 5% excess of PSLi is used. The characterization data of the purified PS₈(Si-Cl)₈ intermediate showed that the number of the PS arms was very close to the theoretical number. Subsequent addition of the living PI chains led to the formation of the PS₈PI₈ miktoarm star.

v. ABC Miktoarm Star Terpolymers. The synthesis of the (PS)(PI)(PBd) star terpolymer was accomplished by a method similar to the one developed for the synthesis of the PS₂PI₂ stars. Living PI chains reacted with a large excess of methyltrichlorosilane to produce the dichlorosilane end-capped polyisoprene. After the evaporation of the excess silane, the living PS arm was incorporated by a slow stoichiometric addition (titration). Samples were taken during the addition and were analyzed by SEC to monitor the progress of the reaction and determine the end point of the titration. When the formation of the intermediate product (PS)(PI)Si(CH₃)Cl was completed, a small excess of the living PBd chains was added to give the final product.¹⁰⁸ The reaction sequence is outlined in Scheme 44.

Scheme 44



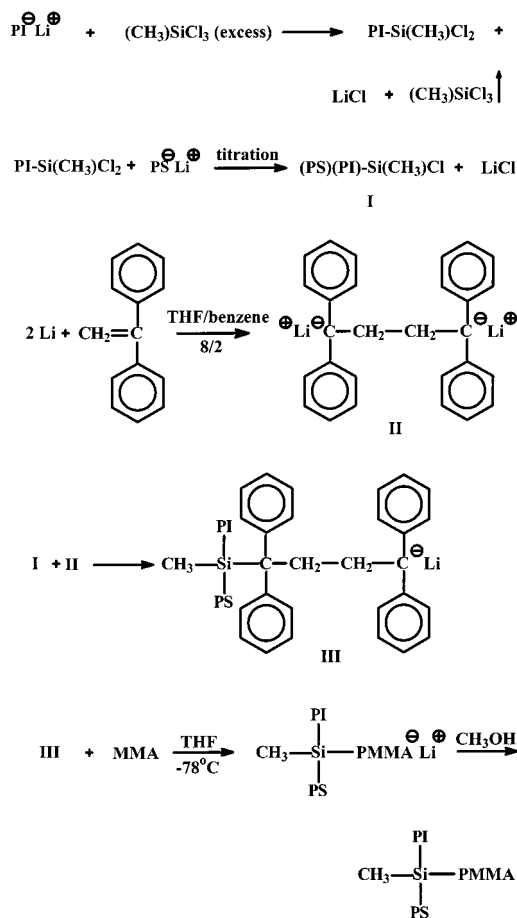
The order of linking of the various arms to the linking agent is crucial for the success of the synthesis. The less sterically hindered chain end, namely the PBdLi, has to be incorporated last, whereas the most sterically hindered, namely the PSLi, at the titration step. Extensive characterization data for the arms, the intermediate, and the final product confirmed that the ABC star was characterized by high structural and compositional homogeneity.

The same methodology was adopted for the synthesis of the (PS)(PI)(P2VP) miktoarm star terpolymer.¹⁰⁹ The monofunctional linking agent (PI)(PS)-Si(CH₃)Cl was synthesized in benzene solution. Benzene was then evaporated and the linking agent was dissolved in THF, followed by the addition of the living P2VPLi chains, prepared in THF at -78 °C. The linking was conducted at -78 °C to avoid side reactions with the living P2VP chains. Well-defined stars were prepared as shown by the extensive molecular weight characterization data given in this study.

A (PI)(PS)(PDMS) miktoarm star terpolymer was synthesized by the same method.⁹⁷ The (PI)(PS)Si(CH₃)Cl macromolecular linking agent was prepared as previously mentioned, followed by the addition of the living PDMSLi chains to give the desired product. Also in this case a well-defined polymer with narrow molecular weight distribution was obtained.

The same route was adopted for the synthesis of asymmetric AA'B star polymers.¹¹⁰ The two A arms were PIs having different molecular weights, and B

Scheme 45



was deuterated polystyrene (dPS). The higher molecular weight PI branch was introduced first, followed by the slow stoichiometric addition (titration) of the living dPS chains. The lower molecular weight PI branch was incorporated at the end of the procedure.

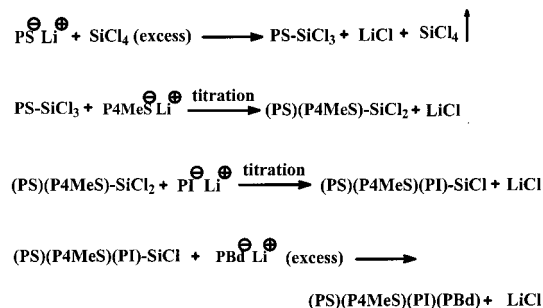
A different approach was employed for the synthesis of (PI)(PS)(PMMA) miktoarm star terpolymers,^{111,112} as outlined in Scheme 45. It is well-known that the reaction between living PMMA chains with Si-Cl bonds fails to give the linked product. Therefore, after the monofunctional macromolecular linking agent (PI)(PS)Si(CH₃)Cl was formed, it was reacted with a dilute solution containing a stoichiometric amount of a difunctional initiator, synthesized by the reaction between DPE and Li. According to this procedure, one of the active centers of the difunctional initiator was linked to the remaining Si-Cl bond, whereas the other one was used to initiate the polymerization of MMA, resulting in the formation of the desired product. It is obvious that the PMMA branches cannot be isolated and characterized independently. This method is very demanding, and extreme care has to be taken for the control of the different reaction steps. It was found that during the synthesis of the difunctional initiator a large amount of the monofunctional byproduct (as high as ~30%) was also obtained. This byproduct does not interfere with the synthesis of the ABC star, since it reacts with the macromolecular linking agent (PI)(PS)Si(CH₃)Cl to give the terminated PS-*b*-PI diblock,

which can be removed by fractionation. Nevertheless, it reduces the yield of the desired product and makes the control of its composition more difficult. Despite these difficulties, well-defined structures were obtained.

vi. ABCD Miktoarm Star Quaterpolymers.

Only one example of the synthesis of ABCD miktoarm star quaterpolymers is reported in the literature.¹⁰⁴ It consists of four different arms, PS, PI, PBd, and poly(4-methylstyrene) (P4MeS). A step by step incorporation of the branches was adopted in this case, as shown in Scheme 46. The synthetic proce-

Scheme 46



cedure involved two titration steps. Therefore, the order of linking of the different branches plays an essential role in controlling the reaction sequence. PS was chosen to react first with an excess of SiCl₄, followed after the evaporation of the excess silane by the slow stoichiometric addition of the living P4MeS chains in order to form the difunctional linking agent (PS)-(P4MeS)SiCl₂. A second titration step was then performed with the addition of the living PI chains to form the monofunctional linking agent (PS)-(P4MeS)(PI)SiCl. The fourth arm, namely PBdLi, was added in the last step to give the desired product. Complete linking was observed in all the reaction steps by SEC. Combined characterization results from several methods revealed that a well-defined star was produced.

2. Divinylbenzene Method

The DVB method can be applied for the synthesis of miktoarm stars of the type A_nB_n in a similar manner as in the case of the asymmetric A_nA'_n stars. It is a three-step procedure starting from the synthesis of the living chains A. These living chains initiate the polymerization of a small quantity of DVB, leading to the formation of a living star polymer carrying within its core a number of active sites equal to the number of arms that have contributed to its formation. During the third step, these active sites are used to polymerize the monomer B, thus producing the miktoarm star A_nB_n.

This method for the synthesis of miktoarm stars was first reported by Funke^{17,18} and then extended and improved by Rempp et al.¹⁰ In all cases published in the literature, the A arms are PS chains, whereas a variety of B chains has been used such as PtBuMA, PtBuA, PEO, P2VP, and PEMA^{58,113–115}. Special care was given to the synthesis of amphiphilic stars carrying both hydrophobic and either cationic or anionic branches. The polymerization of the sty-

rene was initiated with *s*-BuLi, except in the case of the PS_nPEO_n stars, where cumyl potassium was used. After the formation of the living PS star the SEC analysis showed that a considerable part (as high as 15%) of the PS chains was not incorporated in the star structure, mainly due to accidental deactivation. When the second monomer was a (meth)acrylate, the active sites were first capped with one unit of DPE to reduce their nucleophilicity. The final stars usually had *n* values between 4 and 20.

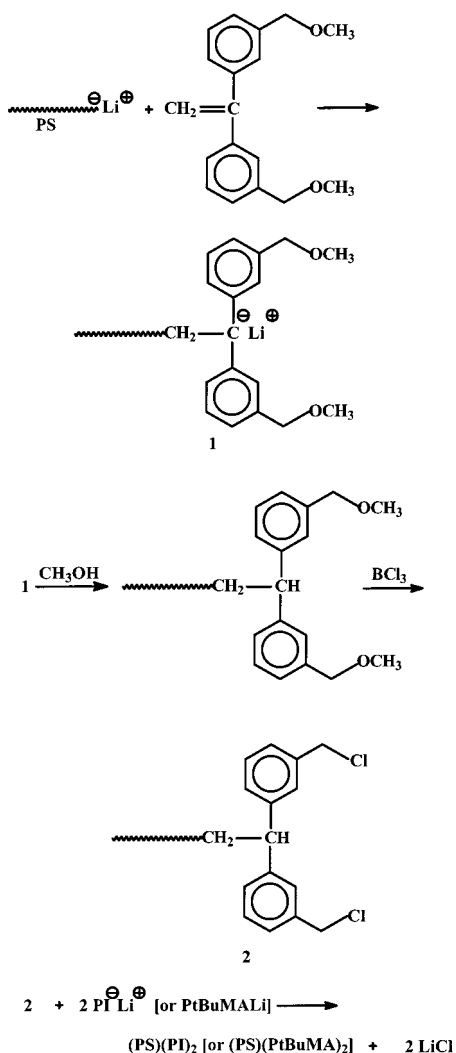
An important feature of this method is that the second-generation branches growing from the living core are living and therefore are susceptible to end-functionalization reactions or can be potentially used to initiate the polymerization of another monomer, leading to the formation of a A_n(B-*b*-C)_n structure. All the drawbacks of the method reported earlier in the discussion concerning the asymmetric stars and the use of DVB as a multifunctional initiator apply in this case as well. The poor control over the structural parameters (*n* values, composition, molecular weights of the B chains), the inability to independently characterize the B arms, and the existence of a distribution in the number of arms within the same sample indicate that the products have rather poor molecular and compositional homogeneity.

3. Diphenylethylene Derivative Method

The DPE derivative methods are based on the procedures developed by Quirk and Hirao, as was previously reported in the case of the asymmetric stars. The first procedure relies on the use of either 1,3-bis(1-phenylethenyl)benzene (MDDPE) or 1,4-bis(1-phenylethenyl)benzene (PDDPE), whereas the second relies on the formation of macromonomers carrying DPE end groups with methoxymethyl moieties that can be transformed to chloromethyl groups. Other specific methods have also been developed utilizing DPE derivatives for the synthesis of miktoarm stars. The discussion given in the case of the asymmetric stars concerning the advantages and limitations of the methods apply here as well. The recent achievements using this methodology will be presented in the following paragraphs.

i. A₂B Miktoarm Star Copolymers. A₂B miktoarm stars, where A is PS and B is PI or PtBuMA, were synthesized by Hirao et al.^{116,117} according to the reaction in Scheme 47. Living PS chains were reacted with a 1.2-fold excess of 1,1-[bis(3-methoxymethylphenyl)]ethylene in THF at -78 °C for 1 h. Only the monoadduct product was obtained under these conditions. The end-methoxymethyl groups were then transformed to chloromethyl moieties by reaction with BCl₃ in CH₂Cl₂ at 0 °C for 2 h. NMR studies showed that this transformation reaction goes to completion. The macromolecular linking agent was then carefully purified by repeated precipitation and freeze-drying from benzene solution and then reacted with living PILi or PtBuMALi chains to give the desired products. A small amount (5%) of the dimeric product was observed by SEC analysis. It was proposed that this byproduct is obtained by the Li-Cl exchange and/or electron transfer reactions. SEC and NMR methods have been only used for the

Scheme 47



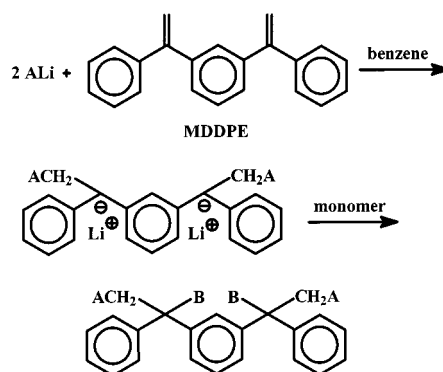
molecular characterization of these structures. Low molecular weight arms were employed to facilitate the NMR analysis.

ii. A₂B₂ Miktoarm Star Copolymers. The use of MDDPE for the synthesis of A₂B₂ type of miktoarm stars has been extensively investigated.²⁶ The method involves the reaction of the living A arms with MDDPE in a molar ratio 2:1, leading to the formation of the living dianionic coupled product. The active sites are subsequently used as initiator of another monomer to give the A₂B₂ structure, as shown in Scheme 48.

The coupling reaction of the living A chains can be monitored by UV-vis spectroscopy and SEC. This step can be very efficient, although careful control over the stoichiometry is needed. The efficiency of the coupling reaction is reduced on increasing the molecular weight of the arm. Only living PS chains have been successfully used for this coupling reaction. It was found that the poly(dienyl)lithium compounds are not reactive enough and the presence of Lewis bases is required in order to accelerate the coupling reaction. However, in this case the subsequent addition of another diene for further polymerization leads to polydienes exhibiting high vinyl contents.

The crossover reaction used to initiate the polymerization of the B monomers has to proceed in such

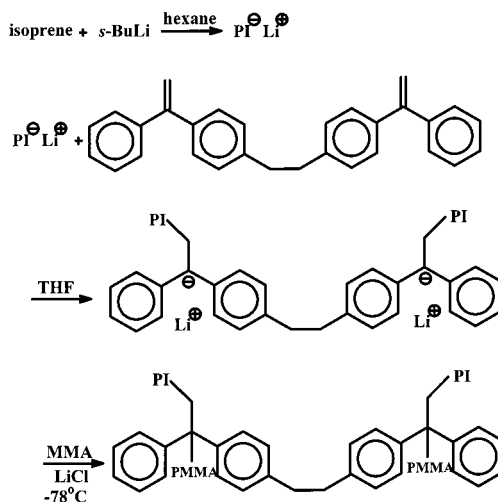
Scheme 48



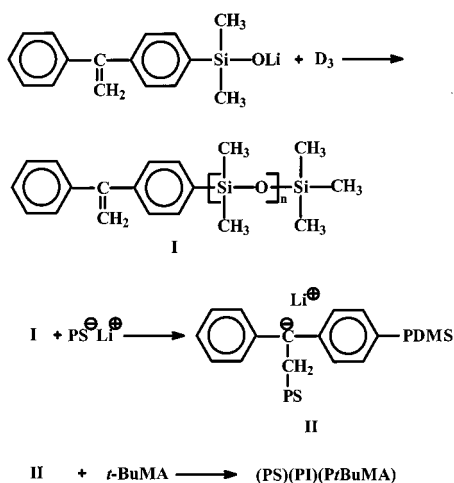
a way that the rate constants of the two active centers should be similar. Only in this way is the formation of uniform chains obtained. This result can only be achieved when a polar compound is added prior to the crossover reaction. It was found that among the different polar additives *s*-BuOLi does not appreciably affect the polydiene's microstructure. The growing B arms cannot be isolated and characterized independently. Miktoarm stars PS₂PI₂ and PS₂PbD₂ were prepared by this method.^{80,118} An advantage of this procedure is that the growing B chains are living, thus leaving the opportunity to introduce end-functional groups by reaction with a suitable electrophile or to continue the polymerization with the addition of another monomer. Taking advantage of this fact, the synthesis of the miktoarm star PS₂(PS-*b*-PbD)₂ was reported.¹¹⁹

A similar method was employed for the synthesis of PI₂PMMA₂ miktoarm stars,¹²⁰ shown in Scheme 49. 1,1-(1,2-Ethanediy)bis[4-(1-phenylethenyl)benzene] (EPEB) was used as the linking agent in this case. A solution of EPEB was slowly added to the solution of the living PI chains, leading to the formation of the coupled product. LiCl was then added and the polymerization of MMA was initiated at -78 °C to give the desired product. Unreacted PI chains formed by accidental deactivation during the coupling reaction were removed by fractionation. Molecular characterization data showed that well-defined stars were prepared by this method.

Scheme 49



Scheme 50

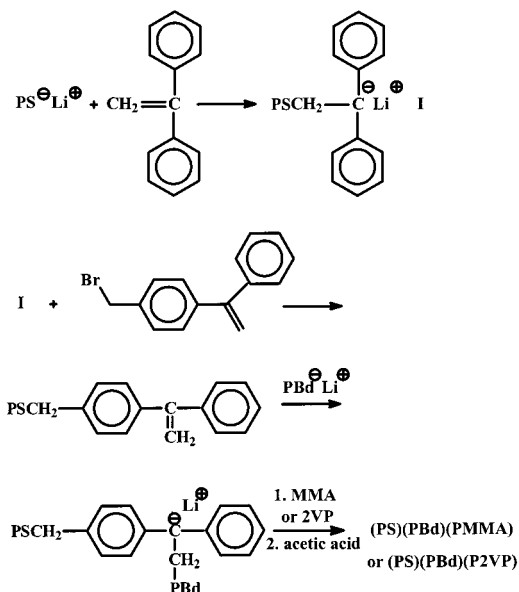


iii. ABC Miktoarm Star Terpolymers. Several approaches have been developed for the synthesis of ABC miktoarm star terpolymers. A (PS)(PDMS)-(PtBuMA) star was prepared¹²¹ according to the method shown in Scheme 50. The lithium salt of the *p*-(dimethylhydroxy)silyl- α -phenylstyrene was prepared and consequently used as initiator for the polymerization of hexamethylcyclotrisiloxane (D₃). Living PS chains were then reacted with the double bond of the end-reactive PDMS, leading to the formation of the living coupled product. The active sites were used for the polymerization of *t*BuMA for the synthesis of the final star.

The molecular weight distribution of the original PDMS was rather broad ($M_w/M_n = 1.3\text{--}1.4$). Therefore, fractionation was performed in order to reduce the polydispersity of the product before conducting the subsequent steps of the synthesis. Despite the fact that the living PS chains were reported to attack the PDMS chains, no side reactions were detected in this study.

A similar synthetic route was adopted by Stadler et al. for the synthesis of the (PS)(PBd)(PMMA)¹²²

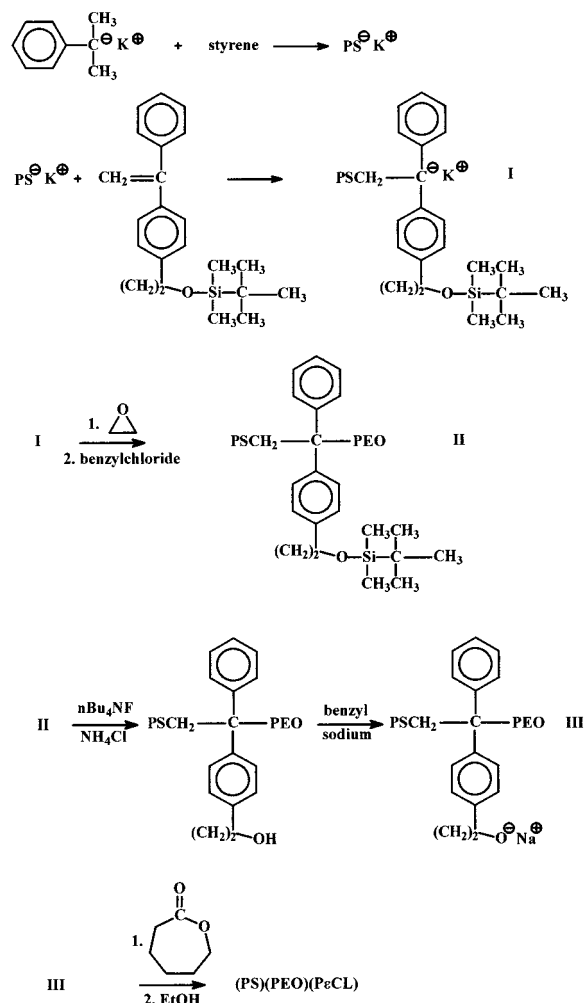
Scheme 51



and (PS)(PBd)(P2VP)¹²³ stars (Scheme 51). Living PS chains were reacted with 1-(4-bromomethylphenyl)-1-phenylethylene to produce DPE end-functionalized PS. The living PS chains were first end-capped with a DPE unit to reduce their reactivity and increase the steric hindrance of the living chain end. Under these conditions, the addition of the PSLi chains to the DPE derivative and the halogen–lithium exchange reactions are minimized. The functionalization of the PS was reported to be quantitative, as judged by UV spectroscopic analysis. The next step involved the linking of living PBdLi chains, prepared in THF at $-10\text{ }^\circ\text{C}$, to the double bond of the end-reactive PS. A living diblock copolymer was thus prepared. The active site was finally used to polymerize MMA or 2VP to produce the miktoarm star terpolymer. A multippeak product, especially in the case of the (PS)(PBd)(PMMA) star, was revealed by SEC analysis. The pure product was obtained after fractionation.

Dumas et al.^{124,125} have developed a procedure for the synthesis of ABC miktoarm star terpolymers containing amphiphilic branches. Styrene was polymerized in THF at $-78\text{ }^\circ\text{C}$ using cumylpotassium as initiator. The living chains were then reacted with 1-[4-(2-*tert*-butyldimethylsiloxy)ethyl]phenyl-1-phenylethylene, as illustrated in Scheme 52. The living center was then used to initiate the polymerization

Scheme 52

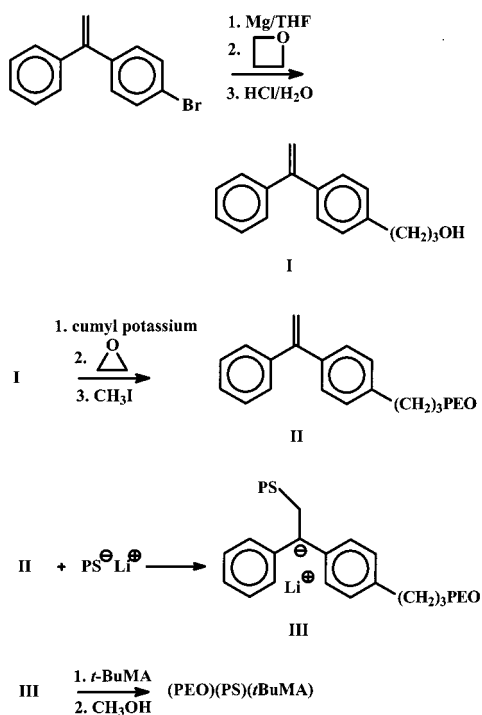


of ethylene oxide. After removal of the protecting group with tetrabutylammonium fluoride, the corresponding alcoholate was formed in the presence of diphenylmethylsodium and used for the polymerization of ϵ -caprolactone (ϵ -CL). Rather broad molecular weight distributions were obtained ($M_w/M_n = 1.2-1.4$). Only SEC and NMR analysis have been reported.

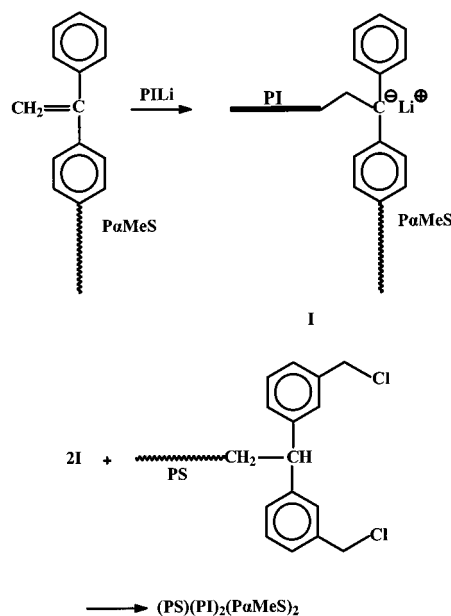
The alcoholate was alternatively reacted with tin octoate to initiate the polymerization of L-lactide (LL) and produce (PS)(PEO)(PLL) star terpolymer. In another application of the method, the 1,1-diphenylalkylpotassium intermediate (I) was used to initiate the polymerization of MMA at -78°C . After deprotecting and activating the hydroxyl group, the polymerization of ethylene oxide was initiated, leading to the formation of the (PS)(PMMA)(PEO) star terpolymer. If ϵ -CL is polymerized instead of EO, then (PS)(PMMA)(P ϵ -CL) stars are produced. Limited characterization data were given for these stars. In all cases two of the arms grow from the star center and thus cannot be isolated and characterized. However, interesting amphiphilic structures were obtained.

The potassium salt of 1-(4-hydroxypropylphenyl)-1-phenylethylene was used to initiate the polymerization of ethylene oxide, leading to the formation of a PEO chain having an end-DPE group.²⁶ The macromonomer was then quantitatively reacted with PSLi to form the living diblock copolymer. The active site was used to polymerize tBuMA after the temperature was reduced to 5°C (Scheme 53). Only SEC and NMR spectroscopy were employed for the characterization of the star structure. This technique has not been used for the synthesis of stars having high molecular weights, raising questions about the efficiency of the method in this case.

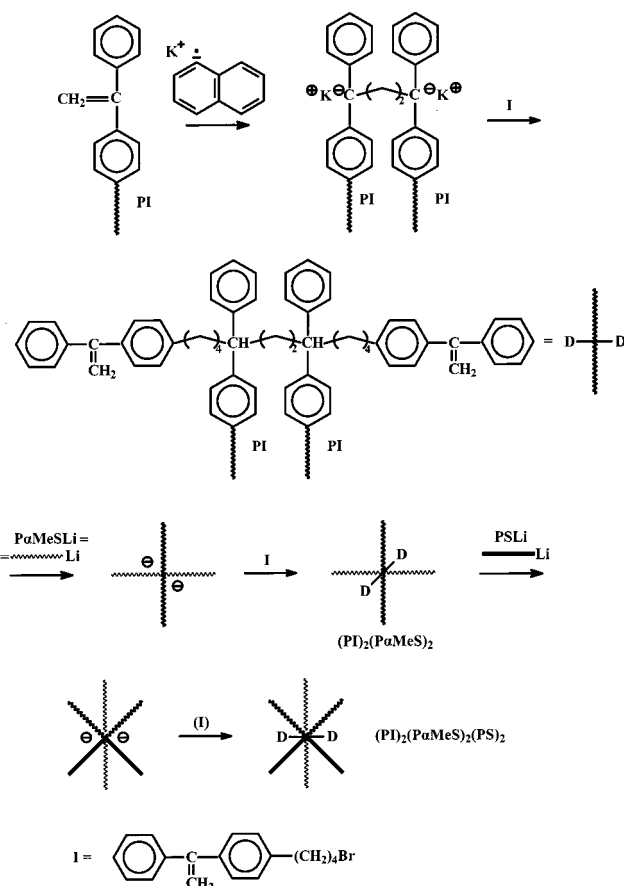
Scheme 53



Scheme 54



Scheme 55



iv. More Complex Architectures. A new methodology that permits the synthesis of a variety of miktoarm stars was developed by Hirao as described in the case of the asymmetric stars. In a series of papers the synthesis of the following structures has been reported: AB_3 , AB_4 , A_2B_4 , A_2B_{12} , ABC_2 , ABC_4 , AB_2C_2 , and $A_2B_2C_2$, where A is PS, B is PI, and C is poly(α -methyl styrene) (P α MeS).^{82-86,116,117} Characteristic examples are given in Schemes 54 and 55. It

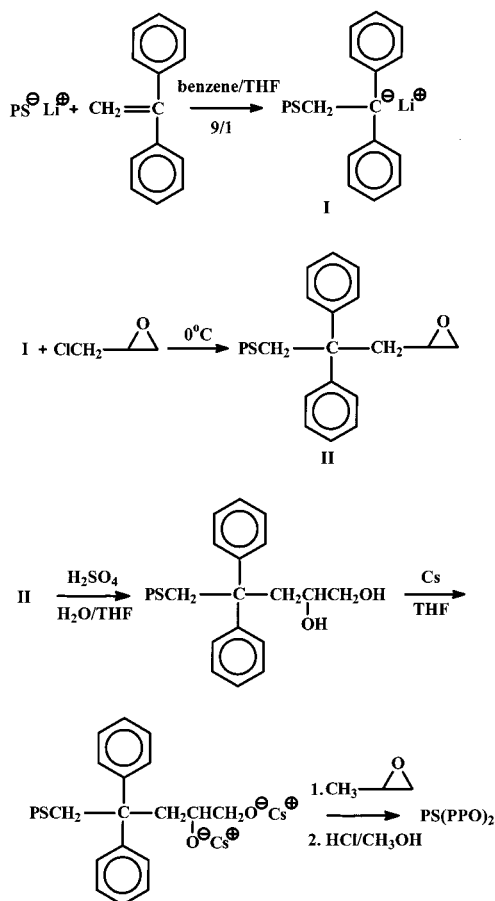
was shown that this methodology is very powerful with respect to the variety of structures that can be obtained, and it offers the possibility to prepare even more complex products. However, this multistep procedure is time-consuming and extra care is needed to avoid the presence of side reactions. The formation of byproducts was minimized by the choice of reaction conditions, leading to the formation of well-defined products. The exclusive use of low molecular weight arms poses questions about the efficiency of the method when higher molecular weight arms, having more sterically hindered chain ends, are used.

4. Synthesis of Miktoarm Stars by Other Methods

Several other specific methods have been reported in the literature for the synthesis of miktoarm stars. Usually they do not have general applicability, but most of them lead to products that cannot easily be obtained by the more general methods described earlier. Therefore, these techniques are valuable tools in polymer synthesis.

A miktoarm star copolymer carrying one PS arm and two poly(propylene oxide) arms¹²⁶ was prepared by the method given in Scheme 56. Living PS chains were end-capped with one unit of DPE, to reduce the reactivity of the chain end, followed by the addition of epichlorohydrin to produce the epoxide functionalized polymer. It was shown by SEC analysis and chemical titration that the epoxide content of the final product was 95 wt %. The desired functionalized

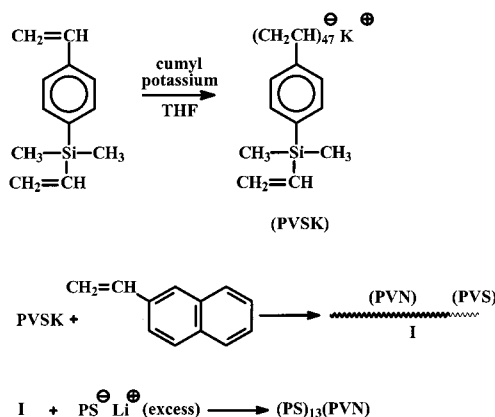
Scheme 56



product was isolated by silica gel thin-layer chromatography. The epoxide group was then hydrolyzed under acidic conditions to give the ω -dihydroxyl-functionalized PS. The pure product was obtained by silica gel chromatography. The hydroxyl groups were reacted with cesium metal in THF at room temperature for 5 h to give the cesium alkoxides, which were subsequently used as initiators for the polymerization of propylene oxide. The crude product contained 36 wt % of the desired PS(PPO)₂ star and 64 wt % of PPO homopolymer, as a result of chain transfer to the PPO monomer. The homopolymer was removed by fractionation in a methanol/water mixture. Only SEC and ¹H NMR analysis were given, making it difficult to prove that the final product contains two equal PPO arms.

Star polymers carrying one poly(2-vinylnaphthalene) (PVN) and several PS arms were prepared by Takano et al.¹²⁷ according to Scheme 57. (4-Vinyl-

Scheme 57

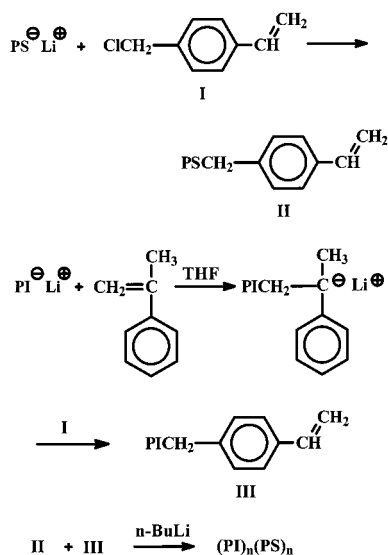


phenyl)dimethylvinylsilane (VS) was oligomerized using cumyl potassium as initiator, followed by the polymerization of vinylnaphthalene. The vinylsilyl double bonds of the monomer remained unaffected during the polymerization of VS. This was accomplished by carrying out the reaction in THF and using short polymerization times. These double bonds were subsequently used as linking agents with living PSLi chains. The characterization results showed that on average 13 PS arms were incorporated into the star structure. This method does not provide the best control over the number of PS arms since, probably for steric hindrance reasons, only one out of 3.6 silylvinyl groups was used for the PS arms.

A macromonomer technique was employed by Ishizu and Kuwahara to prepare miktoarm star copolymers of the (PS)_n(PI)_m type.¹²⁸ PS and PI macromonomers were prepared by coupling the living chains with *p*-chloromethylstyrene. The PS and PI macromonomers (vinyl end-capped chains) were copolymerized anionically in benzene using *n*-BuLi as initiator. The products are comb-shaped copolymers, but they behave as miktoarm stars of the type A_nB_m. The reaction sequence is given in Scheme 58.

Miktoarm stars containing PS and PMMA branches were synthesized using C₆₀ as the linking agent.¹²⁹ Living PSLi chains were added to C₆₀ to form the

Scheme 58



living star with six arms. Subsequent addition of MMA resulted in the grow of PMMA branches. The sample was characterized only by SEC. The chromatogram was bimodal, indicating that a mixture of products was obtained. Judging from the SEC data, it was concluded that six PS and at least two PMMA branches were incorporated in the star structure. It is obvious that this method does not produce well-defined polymers, and more efforts are needed to understand the linking chemistry of living carbanionic species with C_{60} .

A similar synthetic route was adopted for the synthesis of $(PS)_6(PI)$ miktoarm stars, also reported as palm tree structures.¹³⁰ The living star carrying six PS branches was formed by the reaction of living PS chains with C_{60} . Isoprene was subsequently added. It was claimed that only one PI arm can grow from the core, although six C-Li species are available. A considerable increase in the molecular weight distribution was observed during the formation of the PS_6 star ($M_w/M_n = 1.07-1.14$ compared to values of 1.04 for the PS arm) and the miktoarm star ($M_w/M_n = 1.2-1.3$). Slow initiation was blamed for the broad molecular weight distribution of the final structure. However, the existence of a mixture of stars containing more than one PI arm cannot be ruled out.

III. Comb-Shaped Polymers

Graft polymers consist of a main polymer chain, the backbone, with one or more side chains attached to it through covalent bonds, the branches. Graft copolymers are comb-shaped polymers where the chemical nature of the backbone and the branches differs. The chemical nature and composition of the backbone and the branches differ in most cases. Branches are usually distributed randomly along the backbone, although recently advances in synthetic methods allowed the preparation of better defined structures.^{88,90}

Randomly branched comb-shaped polymers can be prepared by three general synthetic methods: the "grafting onto", the "grafting from", and the "grafting through" or macromonomer method.⁸⁸

A. "Grafting Onto"

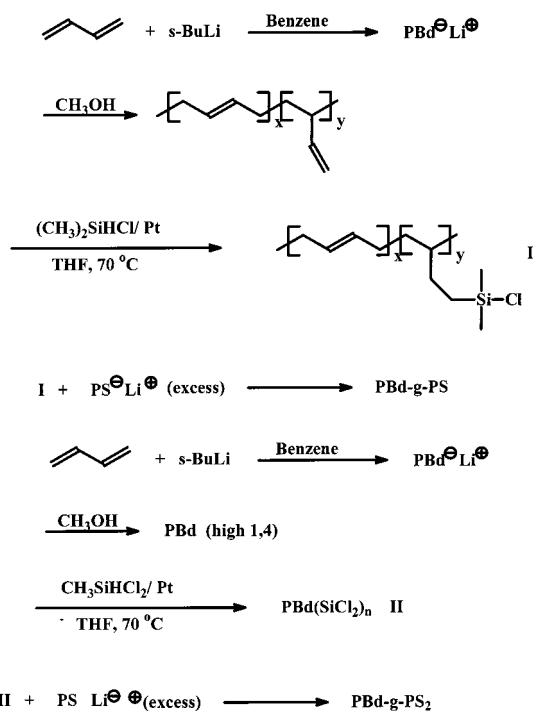
In the "grafting onto" method the backbone and the arms are prepared separately by a living polymerization mechanism. The backbone bears functional groups distributed along the chain that can react with the living branches. Upon mixing the backbone and the branches in the desired proportion and under the appropriate experimental conditions, a coupling reaction takes place resulting in the final comb-shaped polymers.

By the use of an anionic polymerization mechanism, the molecular weight, molecular weight polydispersity, and the chemical composition of the backbone and branches can be controlled. Additionally, both backbone and branches can be isolated and characterized separately. The average number of branches can be controlled primarily by the number of the functional groups (branching sites) present in the backbone and sometimes by the ratio of the functional groups to the active chain end concentration of the branches used in the coupling reaction.

The branching sites can be introduced onto the backbone either by postpolymerization reactions or by copolymerization of the main backbone monomer(s) with a suitable comonomer, with the desired functional group (unprotected or in a protected form if this functional group interferes with the polymerization reaction). Branches of comb-shaped polymers are commonly prepared by anionic polymerization, and backbones with electrophilic functionalities such as anhydrides, esters, pyridine, or benzylic halide groups are employed.⁸⁸ The actual average number of branches in the final copolymer can be found by the determination of the overall molecular weight of the copolymer and the known molecular weights of the backbone and the branches.

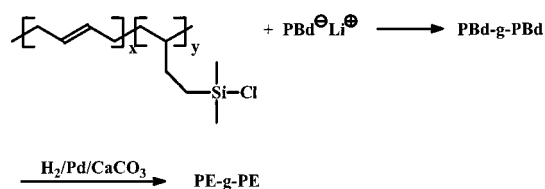
A representative example is the preparation of poly(butadiene-*g*-styrene) graft copolymers¹³¹ (Scheme

Scheme 59



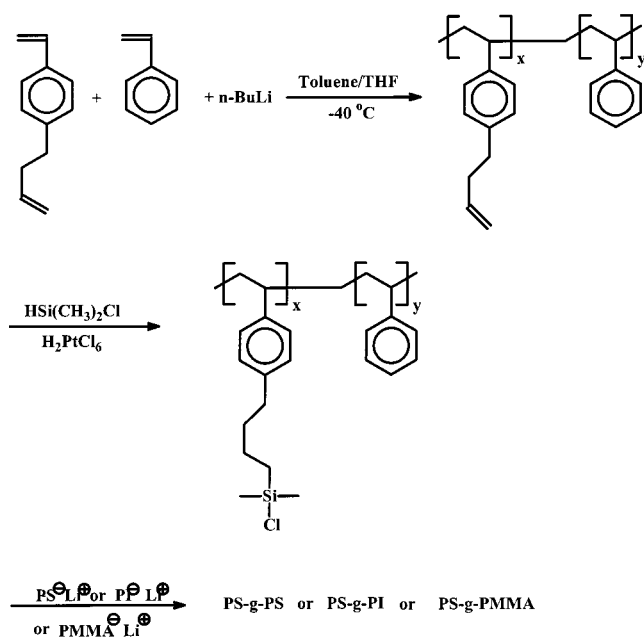
59). The PBd backbones were synthesized by anionic polymerization in benzene, resulting in PBds with high 1,4-addition (1,2-addition was lower than 10%). Postpolymerization catalytic hydrosilylation using $(\text{CH}_3)_2\text{SiHCl}$ was used for introduction of chlorosilane groups, preferentially at the 1,2-double bonds. Finally, a linking reaction between living polystyrene anions and the Si-Cl groups of the PBd backbone gave poly(Bd-*g*-S) graft copolymers with randomly placed single PS branches. When $\text{HSiCl}_2\text{CH}_3$ was used in the hydrosilylation step, difunctional branching sites were introduced in the backbone. Subsequent reaction with excess PSLi afforded graft copolymers with randomly distributed double PS branches (PBd-*g*-PS₂). Characterization of the final products showed that they possessed a high degree of molecular weight and compositional homogeneity. By the same synthetic scheme, PBd comb polymers were prepared, and after catalytic hydrogenation, well-defined graft polyethylenes were obtained¹³² (Scheme 60).

Scheme 60



Ruckenstein and Zhang reported that the anionic copolymerization of 4-(vinylphenyl)-1-butene with styrene in toluene/THF at -40°C gives well-defined polymers,¹³³ since under these experimental conditions the vinylic double bond is selectively polymerized. The copolymers were subjected to hydrosilylation for the introduction of Si-Cl groups at the olefinic double bonds. These groups were used as grafting sites for the linking of PSLi, PILi, and PMMALi living chains in order to synthesize PS-*g*-

Scheme 61

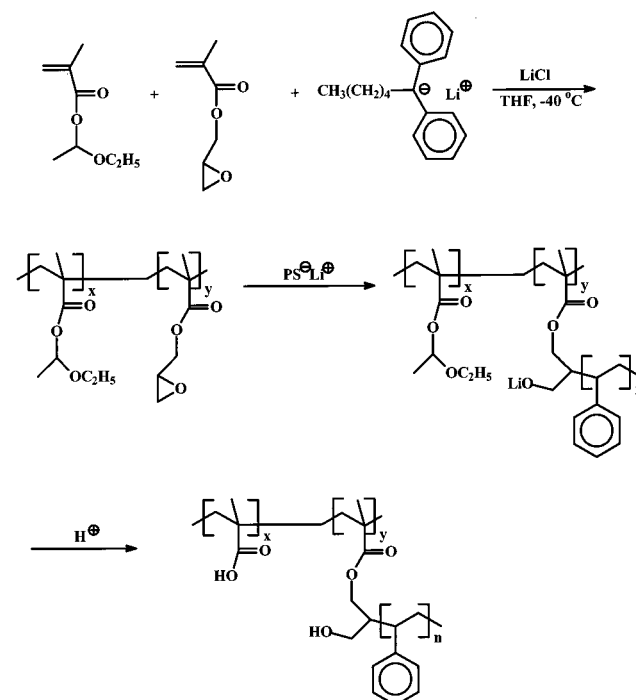


PS, PS-*g*-PI, and PS-*g*-PMMA comb-shaped polymers with well-defined molecular characteristics (Scheme 61). The PS-*g*-PMMA graft copolymers were found to decompose in proton-containing media, while they were stable in organic solvents.

Anionically prepared and subsequently hydrosilylated PBds were also used for the formation of PBd-*g*-poly(sodium methacrylate) graft copolymers.¹³⁴ The precursors were PBd-*g*-poly(*tert*-butyl methacrylate) graft copolymers. These were prepared by reaction of the hydrosilylated PBd backbone with living PtBuMA anions end capped with *tert*-butyl 4-vinylbenzoate. This modification of the living end proved to be necessary, since in this way the expected C-silylation stable product is obtained instead of the O-silylated one, when uncapped living PtBuMA is used. Hydrolysis of the graft copolymers followed by neutralization with sodium hydroxide yielded the amphiphilic analogues.

Ruckenstein and Zhang presented the synthesis of amphiphilic graft copolymers with poly(methacrylic acid) hydrophilic backbones and hydrophobic PS side chains.¹³⁵ The precursors of the backbones were random copolymers of 1-(ethoxy)ethyl methacrylate (EEMA) and glycidyl methacrylate (GMA) prepared by anionic copolymerization of the two monomers. These copolymers had narrow molecular weight and composition polydispersities as well as predetermined molecular weights and compositions. The amount of GMA in the copolymers determines the number of grafting sites in the backbone, and it was kept low in all cases. In the next step a predetermined amount of a solution of living PSLi was added to the solution of the living backbone, resulting in a rapid reaction between PSLi active chain ends and the epoxy groups of GMA in the backbone. Unreacted epoxy groups were neutralized by 1,1-diphenylhexyllithium. The final graft copolymers had relatively narrow molec-

Scheme 62

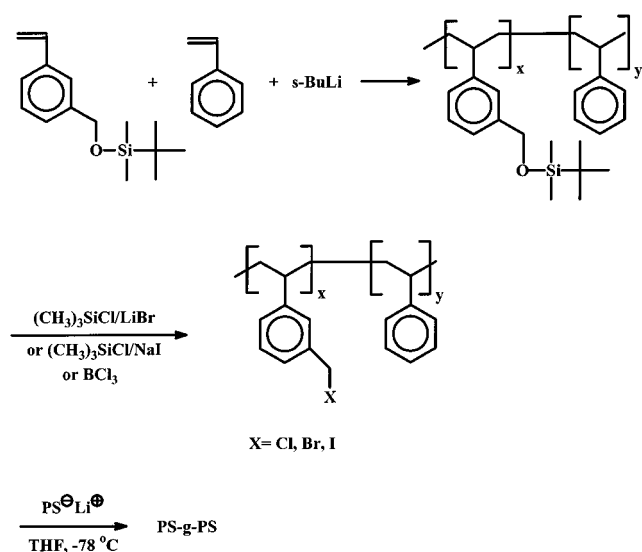


ular weight distributions. The EEMA units were then subjected to hydrolysis, and the desired amphiphilic comblike copolymers were obtained (Scheme 62). It is characteristic that no excess of PSLi was used in this work, introducing another way of controlling the number of grafted chains per backbone through control of the stoichiometry between potential grafting sites and number of living side chains.

Using the same methodology, PMMA-*g*-PS and poly(allyl methacrylate)-*g*-PS graft copolymers were prepared.¹³⁶ In all cases GMA was anionically copolymerized with the appropriate methacrylic monomer in order to produce the backbone of the graft. In the case of poly(allyl methacrylate)-*g*-PS, the allylic groups of allyl methacrylate were converted to hydroxyl groups by hydroboration-oxidation reaction, giving amphiphilic graft copolymers with hydrophilic backbones and hydrophobic branches. Reaction of GMA homopolymers with a PSLi, PILi, and PSLi/PILi mixture resulted in the formation of PGMA-*g*-PS, PGMA-*g*-PI, and PGMA-*g*-(PS,PI) graft copolymers.¹³⁷

Hirao and Ryu synthesized PS graft copolymers with one side chain in almost every monomeric unit.¹³⁸ They used anionically synthesized poly(*m*-*tert*-butyldimethylsilyloxy)styrene)s as precursors for the preparation of *m*-halomethylstyrenes by reaction with BCl₃, (CH₃)₂SiCl/LiBr, and (CH₃)₂SiCl/NaI for the introduction of Cl, Br, and I, respectively. The transformation reactions were quantitative. The halomethylstyrenes, having well-defined molecular weights and low molecular weight polydispersities, were subsequently used as backbones for the preparation of comb-shaped polymers. Reaction of the highly reactive benzyl halides with living PSLi chains in THF gave the aforementioned PS combs (Scheme 63). The final products, isolated after fractionation, were similar in respect to their molecular characteristics with the polymer obtained when living PSLi was coupled with poly(*m*-chloromethylstyrene) at -78 °C or diphenylethylene-capped PSLi at -40 °C. Reaction times were shorter in the former case, due to the higher reactivity of PSLi. PS combs were also pre-

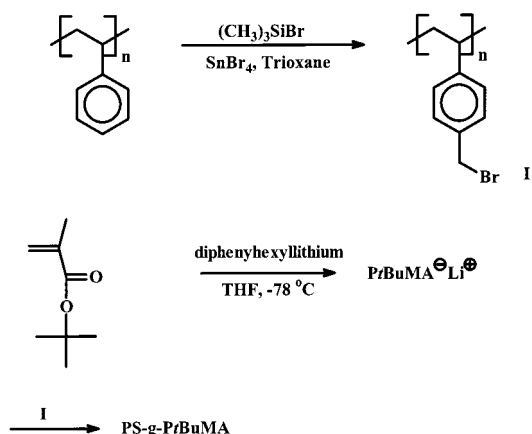
Scheme 63



pared by reaction of poly(*m*-bromomethylstyrene) with PSLi end-capped with DPE.

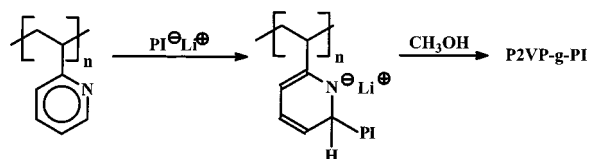
Partially chloromethylated or bromomethylated anionically prepared polystyrenes have been used for the preparation of several graft copolymers containing PS backbones and PI,⁴³ P2VP,^{45,139} P4VP,¹⁴⁰ PtBuMA,⁴⁵ and PEO^{141,142} branches. Some of these copolymers are precursors for amphiphilic graft copolymers (Scheme 64).

Scheme 64



Watanabe et al. reported the synthesis of P2VP-*g*-PS and P2VP-*g*-PI copolymers.¹⁴³ The P2VPs used as the backbones were prepared by anionic polymerization. After thorough purification for complete removal of terminating impurities, these homopolymers were directly reacted with living PILi and PILi to give the desired graft copolymers (Scheme 65). The final products had narrow molecular weight distributions. No grafting was observed when the side chains were end-capped with DPE.

Scheme 65



B. "Grafting From"

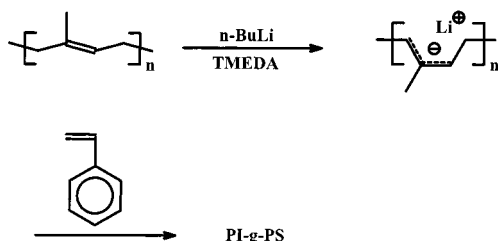
In the "grafting from" method, after the preparation of the backbone, active sites are produced along the main chain that are able to initiate the polymerization of the second monomer(s). Polymerization of the second monomer results in the formation of branches and the final graft copolymer. The number of branches can be controlled by the number of active sites generated along the backbone, assuming that each one of them initiates the formation of one branch. Obviously, the isolation and characterization of each part of the graft copolymer in this case is almost always impossible. Knowledge of precursor molecular characteristics is limited to the backbone. Isolation of the branches can be achieved only in some cases and usually involves selective chemical decomposition of the backbone, e.g., ozonolysis of polydiene backbone in poly(diene-*g*-styrene) graft copolymers.¹³³ Following this methodology, several

graft copolymers were synthesized by the use of anionic polymerization.

Anionic active sites can be generated by metalation of allylic, benzylic, or aromatic C–H bonds, present in the backbone, by organometallic compounds, such as *s*-BuLi, in the presence of strong chelating agents that facilitate the reaction. The metalation of polydienes with *s*-BuLi in the presence of *N,N,N',N'*-tetramethylethylenediamine (TMEDA) presents a representative example.^{144–146}

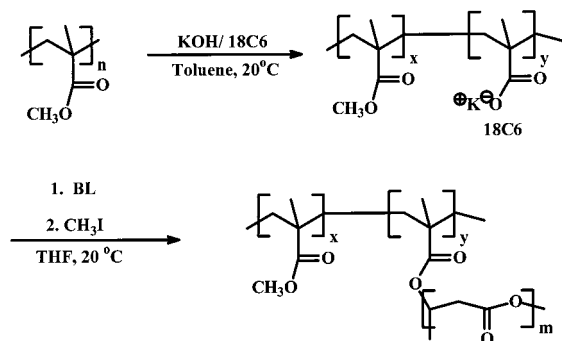
Metalation of PI and PBd by this procedure and subsequent polymerization of styrene led to the formation of PI-*g*-PS and PBd-*g*-PS copolymers with well-defined molecular characteristics^{144–148} (Scheme 66).

Scheme 66



In another approach, PMMA-*g*-poly(β -butyrolactone) copolymers were synthesized using the “grafting from” technique.¹⁴⁹ Anionically polymerized PMMA was treated with the 18-crown-6 complex of potassium hydroxide in toluene, resulting in a macromolecular initiator (Scheme 67). The average number

Scheme 67



of grafting sites per macroinitiator was determined by reaction of the modified PMMA with benzyl bromide and subsequent characterization of the copolymer. The carboxylate active groups formed were used as initiating sites for the anionic polymerization of β -butyrolactone in THF at room temperature. The grafting process was followed by ¹H NMR and the final copolymers, obtained after termination with methyl iodide, were characterized by SEC, VPO, and NMR. The grafting efficiency was determined to be high and the density of the grafting sites could be controlled easily.

C. “Grafting Through”

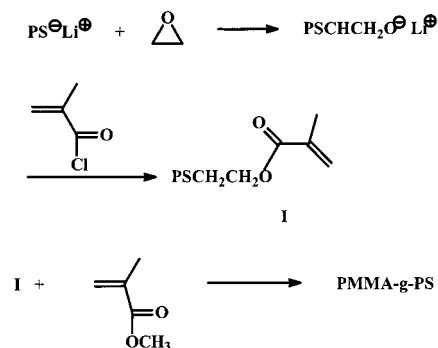
In the grafting through method, preformed macromonomers are copolymerized with another monomer in order to produce the graft copolymer. Macromono-

mers are oligomeric or polymeric chains that have a polymerizable end group. In this case, the macromonomer comprises the branch of the copolymer and the backbone is formed in situ. The number of branches per backbone can be generally controlled by the ratio of the molar concentrations of the macromonomer and the comonomer. Several other factors have to be considered. Among them the most important one is the copolymerization behavior of the macromonomer and the comonomer forming the backbone. Depending on the reactivity ratios, r_1 and r_2 , of the reacting species, different degree of randomness can be achieved, with respect to the placement of the branches. Since macromonomer and comonomer incorporation in the graft copolymer can vary in the course of the copolymerization reaction due to changes in the concentration of the two compounds in the mixture, different kinds of graft copolymers are formed as a function of time. Phase separation can also occur in these systems, due to the formation of the copolymers, leading to increased compositional and molecular weight heterogeneity of the final product.

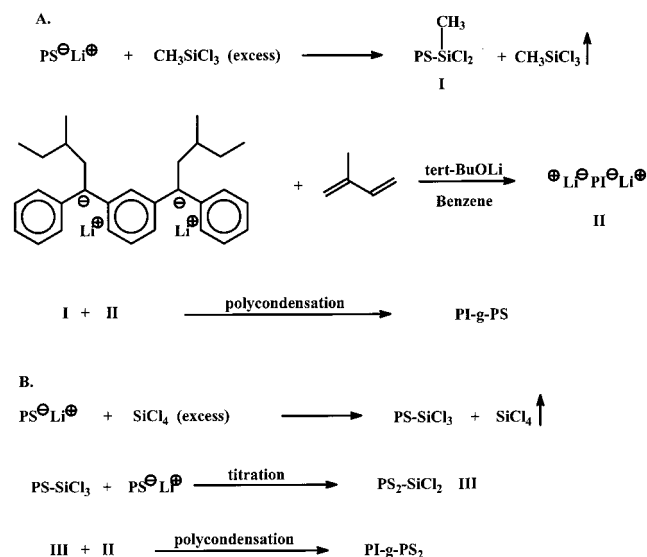
PS macromonomer formation by anionic polymerization has been described in several cases.^{150–153} In one of them styrene was polymerized by *s*-BuLi, and once the monomer has been consumed completely, a slight excess of ethylene oxide was added.¹⁵⁰ The oxirane end-capped living polymer is then reacted with methacryloyl chloride to give a PS macromonomer with a methacrylate type polymerizable end unit. If the oxirane end-capped living polymer is reacted with benzyl bromide (or chloride), PS macromonomer with a styrenic polymerizable end unit is produced. Alternatively, living PS was end-capped with 1,1-diphenylethylene and then reacted with vinyl benzyl bromide (chloride). In a similar way, living PMMALi anions can be end-capped with methacryloyl chloride or vinyl benzyl bromide (chloride) by direct reaction. These macromonomers were used, after complete removal of protonic impurities, in subsequent anionic copolymerization with MMA or styrene to give the corresponding PMMA-*g*-PMMA, PMMA-*g*-PS, and PS-*g*-PS comb-shaped polymers (Scheme 68). Direct polymerization of the macromonomers results in the formation of polymacromonomers, i.e., graft copolymers with a side chain on every backbone monomer.¹⁵⁴

Graft copolymers of St and Is, with trifunctional or tetrafunctional branching points, situated equi-

Scheme 68



Scheme 69

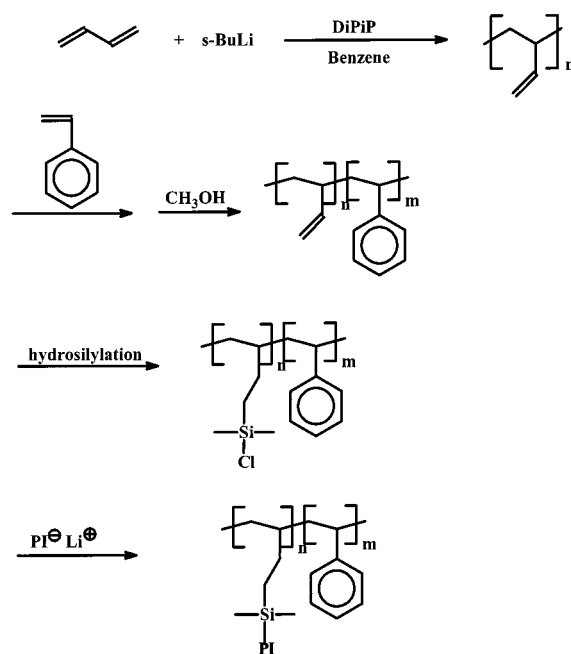


distantly on the backbone, were synthesized by a combination of living anionic and condensation polymerization methodologies¹⁵⁵ (Scheme 69). In the case of graft copolymers with the trifunctional branching points, a living PSLi was reacted with excess MeSiCl₃ to give a macromolecule with two terminal SiCl bonds. This was reacted, after removal of excess silane, with a difunctional PI produced by the difunctional initiator derived from MDDPE and *s*-BuLi, following a polycondensation reaction scheme, giving a well-defined graft copolymer with PI backbone and PS branches. In this way, the length of the branches and the distance between them on the backbone could be controlled. Some control over the average number of branches could also be exercised by the molar ratio of the difunctional macromonomers. In the case of the grafts with tetrafunctional branching points, the PS branch was reacted with SiCl₄ in a controllable way to give (PS)₂SiCl₂ (Scheme 69). The first branch was introduced by reaction with excess SiCl₄, which was subsequently removed, and the second PS was introduced via a titration procedure in order to avoid substitution of the third Cl. The macromolecular linking agent was reacted with a predetermined amount of a difunctional PI to give the desired graft copolymer. In both cases, crude reaction products had relatively wide molecular weight distributions as a result of the condensation mechanism of the second synthetic step, but after fractionation, narrow molecular weight distribution products were obtained.

IV. Block-Graft Copolymers

Block-graft copolymers, having a PS–PB diblock as a backbone and PS, PI, PB and PS-*b*-PI branches, were prepared by anionic polymerization and hydrosilylation reactions.¹⁵⁶ The diblock copolymer backbone was prepared by sequential addition of styrene and butadiene. The polymerization of butadiene took place in the presence of dipiperidinoethane, resulting in high 1,2-content. The backbone was then subjected to hydrosilylation in order to incorporate the desired amount of SiCl groups on the PB block. These groups were then used as branching sites, where PSLi, PILi,

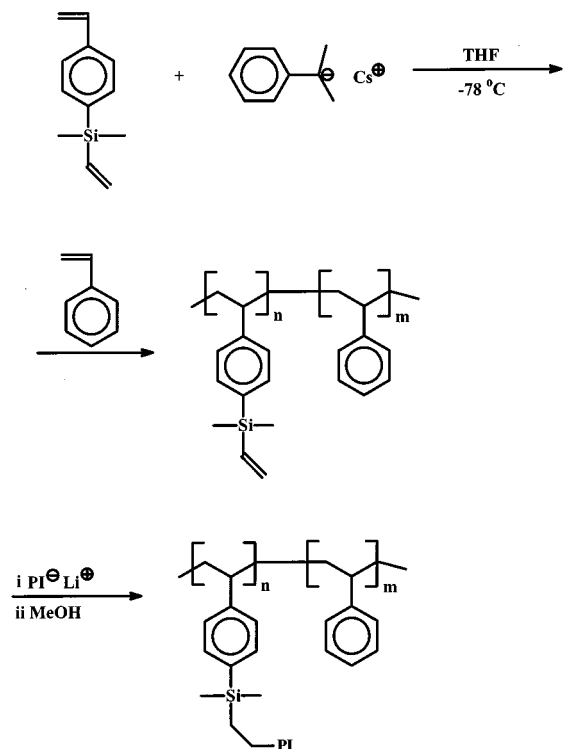
Scheme 70



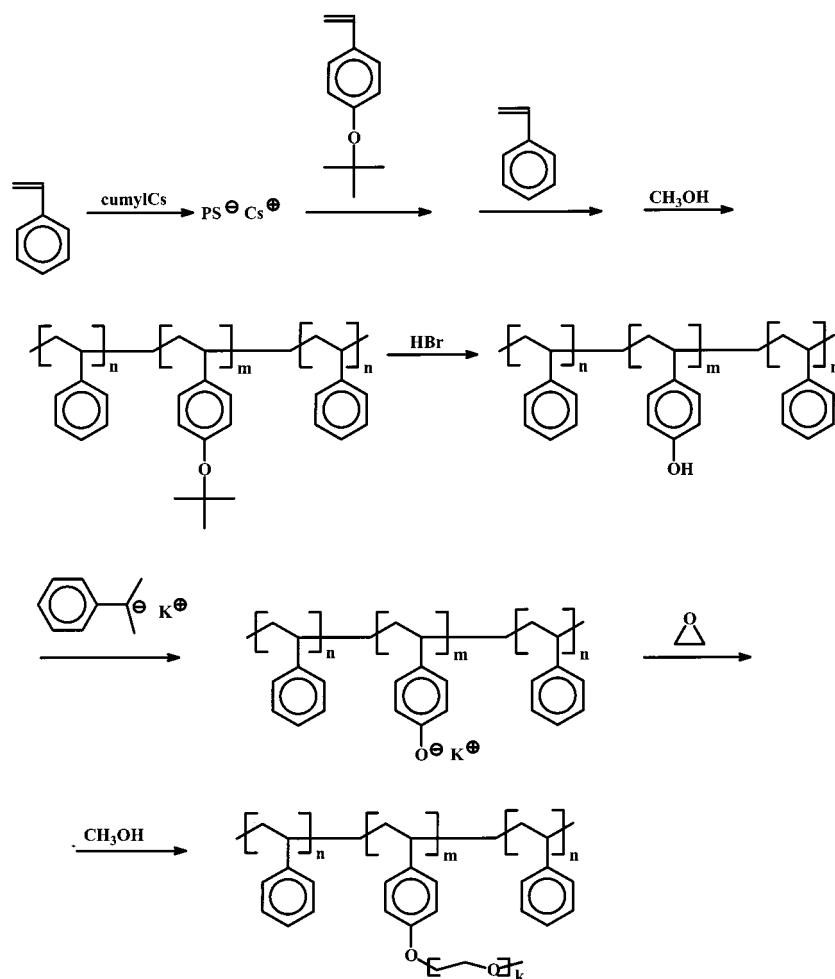
PBLi, and PSPILi living chains were linked (Scheme 70). The use of MeSiHCl₂ instead of Me₂SiHCl in the hydrosilylation step produced difunctional branching sites along the PB part of the backbone, leading to the formation of block-graft copolymers with two chains grafted on each branching point.

Se et al. presented the synthesis of poly[(*VS-g-I-b-S*)] block-graft copolymers.¹⁵⁷ The backbone, a diblock copolymer of 4-(vinyl dimethylsilyl)styrene (VS) and styrene, was prepared first by anionic polymerization. The VS monomer was polymerized selectively through the styryl double bond at low

Scheme 71



Scheme 72



temperature in THF using cumylcesium as initiator followed by the addition of styrene. Living PILi was then allowed to react with the vinylsilyl groups of the VS block, giving the final graft copolymer (Scheme 71). Detailed characterization of the polymers obtained by SEC, osmometry, and ultracentrifugation techniques proved their high molecular weight and compositional homogeneity, as well as their desired architecture.

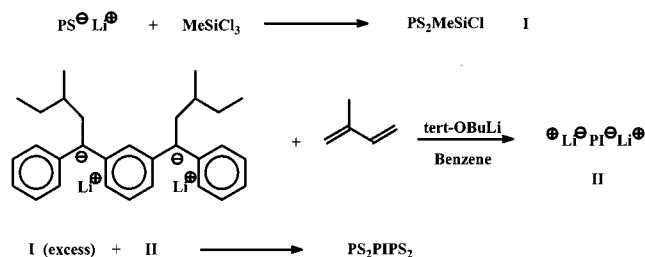
The synthesis of block-graft copolymer containing styrene, hydroxystyrene, and ethylene oxide of the types PS-*b*-(PHS-*g*-PEO) and PS-*b*-(PHS-*g*-PEO)-*b*-PS, where PHS is poly(*p*-hydroxystyrene), has been reported.¹⁵⁸ The ABA triblock copolymer comprising the backbone was synthesized by a three-step sequential addition of monomers i.e., styrene and *p*-*tert*-butoxystyrene (the precursor to hydroxystyrene). The PBS blocks were converted to poly(*p*-hydroxystyrene), by reaction with hydrogen bromide. The OH groups thus formed were transformed to potassium alkoxide groups by reaction with cumyl potassium or 1,1-diphenylethylene potassium. The resulting macromolecular initiators were used for the polymerization of EO, forming the branches of the block-graft-block copolymers (Scheme 72). Molecular characterization of the products by SEC and osmometry indicated that they possessed narrow molecular weight distributions and predictable molecular weights and compositions.

Ruckenstein et al. reported the preparation of PMMA-*b*-(PGMA-*g*-PS) and PMMA-*b*-(PGMA-*g*-PI) block-graft copolymers, where PGMA is poly(glycidyl methacrylate).¹³⁷ The PMMA-*b*-PGMA diblock was obtained first by anionic polymerization through sequential addition of monomers. Then living PSLi and PILi chains were linked to the diblock backbone by reaction with the glycidyl groups of the GMA block. Molecular characterization of the final products confirmed the intended architecture and relatively narrow molecular weight distributions.

V. α,ω -Branched Architectures

By the use of anionic polymerization and controlled chlorosilane chemistry, the exact placement of the side chains along the backbone is possible. Using this combination, H- and super-H-shaped copolymers were synthesized. In the case of H-shaped copolymers,¹⁵⁹ living PSLi and MeSiCl₃ were reacted in a ratio SiCl:Li = 3:2.1. Due to the sterically hindered PSLi anion, only two Cl atoms were substituted, resulting in a PS dimer having an active Si-Cl bond at the center. The macromolecular linking agent was reacted with a difunctional PI chain (the connector), synthesized using the difunctional initiator derived from MDDPE and *s*-BuLi in benzene solution and in the presence of lithium-*tert*-butoxide, giving the

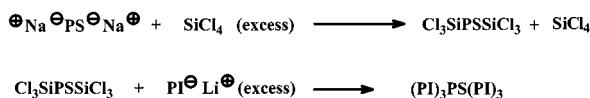
Scheme 73



H-copolymer as shown in Scheme 73. This synthetic scheme is an extension of the one used for the preparation of H-shaped polystyrene homopolymers.¹⁶⁰

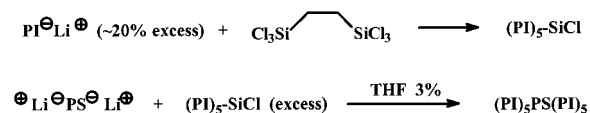
For the synthesis of the $(\text{PI})_3\text{PS}(\text{PI})_3$ super-H copolymers,¹⁶¹ a difunctional PS chain, derived from the polymerization of isoprene in THF using sodium naphthalene as initiator, was reacted with a large excess of SiCl_4 , giving a PS chain with three Si-Cl active bonds at each end. After elimination of excess SiCl_4 and the addition of excess P ILi living arms, the $(\text{PI})_3\text{PS}(\text{PI})_3$ super-H shaped copolymer was isolated (Scheme 74). Using the same synthetic strategy, $(\text{PS}-\text{PI})_3\text{PS}(\text{PI}-\text{PS})_3$ block copolymers were also synthesized.¹⁶²

Scheme 74



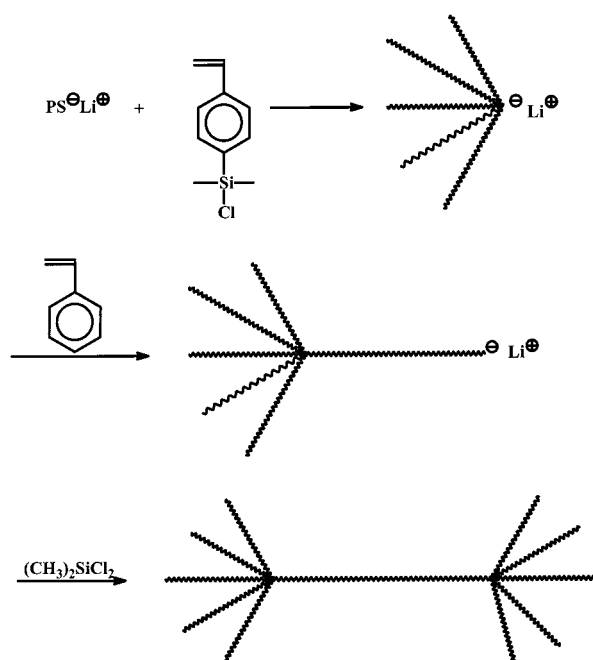
$(\text{PI})_5\text{PS}(\text{PI})_5$ copolymers (pom-pom shaped) were synthesized in a way similar to the preparation of H-shaped copolymers¹⁰¹ (Scheme 75). A hexafunctional silane was reacted with P ILi in a ratio $\text{SiCl}:\text{Li} = 6:5$, giving the five-arm star having a SiCl group at the central point. These functional stars were reacted in a second step with a difunctional PS, giving the desired pom-pom copolymers.

Scheme 75



$(\text{PS})_n\text{PS}(\text{PS})_n$ homopolymers were prepared by a synthetic scheme involving anionic polymerization of styrene followed by addition of 4-(chlorodimethylsilyl)styrene (CDMSS) in the first step.¹⁶³ By controlling the amount of CDMSS added to the solution of the living PS relative to the amount of the initial chain ends, the extent of coupling (number of arms, n) can be controlled. The star PS thus formed contains one living chain end that can be used for the polymerization of additional styrene in the second step. Coupling of the living stars with $(\text{CH}_3)_2\text{SiCl}_2$ in the third step results in the formation of $(\text{PS})_n\text{PS}(\text{PS})_n$ pom-pom polymers (Scheme 76). Due to the statistical nature of the first step, there is a distribution in the number of arms connected to the ends of the main PS chain.

Scheme 76

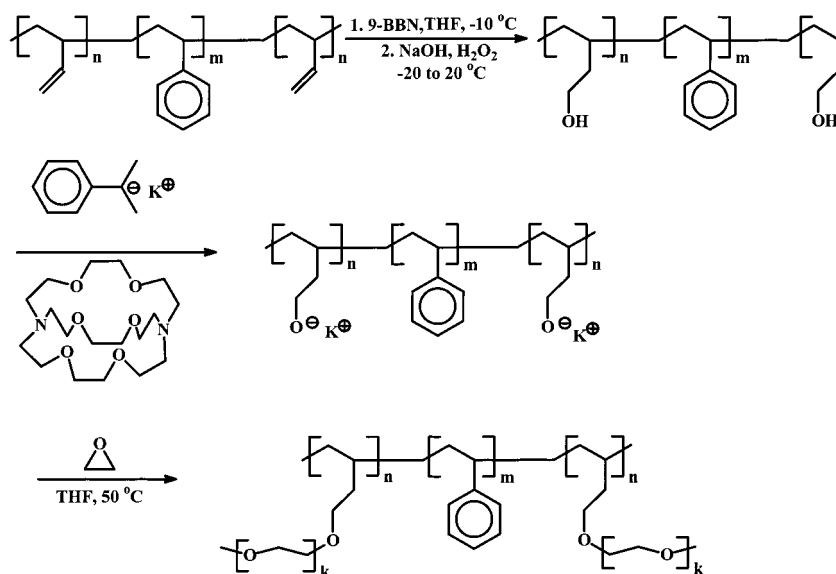


Pom-pom or dumbbell copolymers with a high functionality of the end-grafted chains were synthesized by first preparing a P Bd -1,2-PS-P Bd -1,2 triblock copolymer having short P Bd blocks by anionic polymerization, using naphthalene potassium as difunctional initiator.¹⁶⁴ The pendant double bonds in the P Bd blocks were subjected to hydroboration-oxidation, producing OH groups. These groups were transformed to alkoxides, by reaction with cumylpotassium in the presence of cryptant(kryptofix-[2.2.2]). In this way, precipitation of the polyfunctional initiator was avoided. The alkoxide groups were subsequently used as initiating sites for the polymerization of ethylene oxide. The dumbbell-shaped $(\text{PEO})_n\text{PS}(\text{PEO})_n$ copolymer was prepared in this way (Scheme 77). Characterization of the obtained polymers indicated a low degree of molecular weight and compositional heterogeneity.

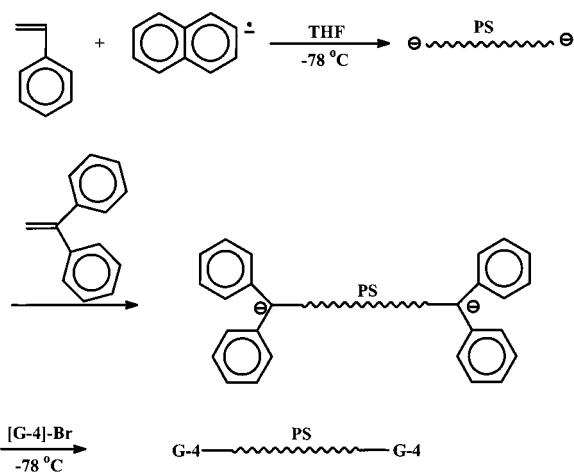
Dumbbell copolymers were also synthesized by Frechet et al.¹⁶⁵ A difunctional PS living chain, prepared in THF using potassium naphthalenide as initiator, was end-capped with DPE and subsequently reacted with a fourth-generation dendrimer having a bromomethyl group at its converging point (Scheme 78).

π -Shaped graft copolymers, i.e., graft copolymers with a PI backbone and two identical PS branches, were synthesized by anionic polymerization.¹⁵⁹ P ILi was reacted with excess MeSiCl_3 in order to produce the macromolecular linking agent P ISiCl_2 . P SLi was slowly added to P ISiCl_2 in order to replace the second Cl atom. The course of the reaction was followed by SEC. The junction point functionalized $(\text{PS})(\text{PI})\text{SiCl}$ diblock was subsequently reacted with a difunctional living PI in a 2.1:1 ratio to give the π -shaped copolymer after fractionation (Scheme 79). In this case the length of the PS branches of the connecting part of the backbone, the length of the two backbone parts between the branching points, and the ends of

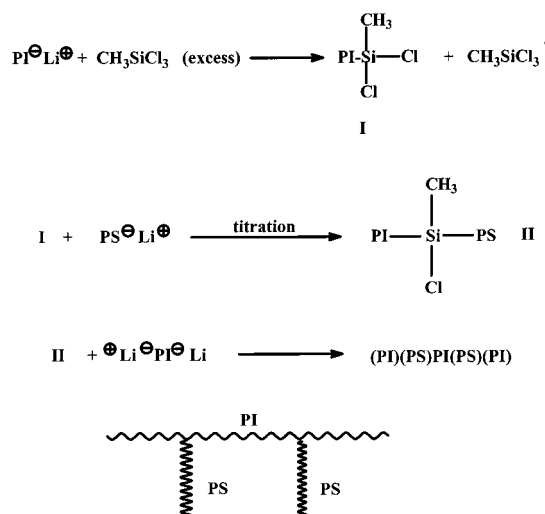
Scheme 77



Scheme 78



Scheme 79



the main chain could be controlled, leading to a well-defined graft architecture.

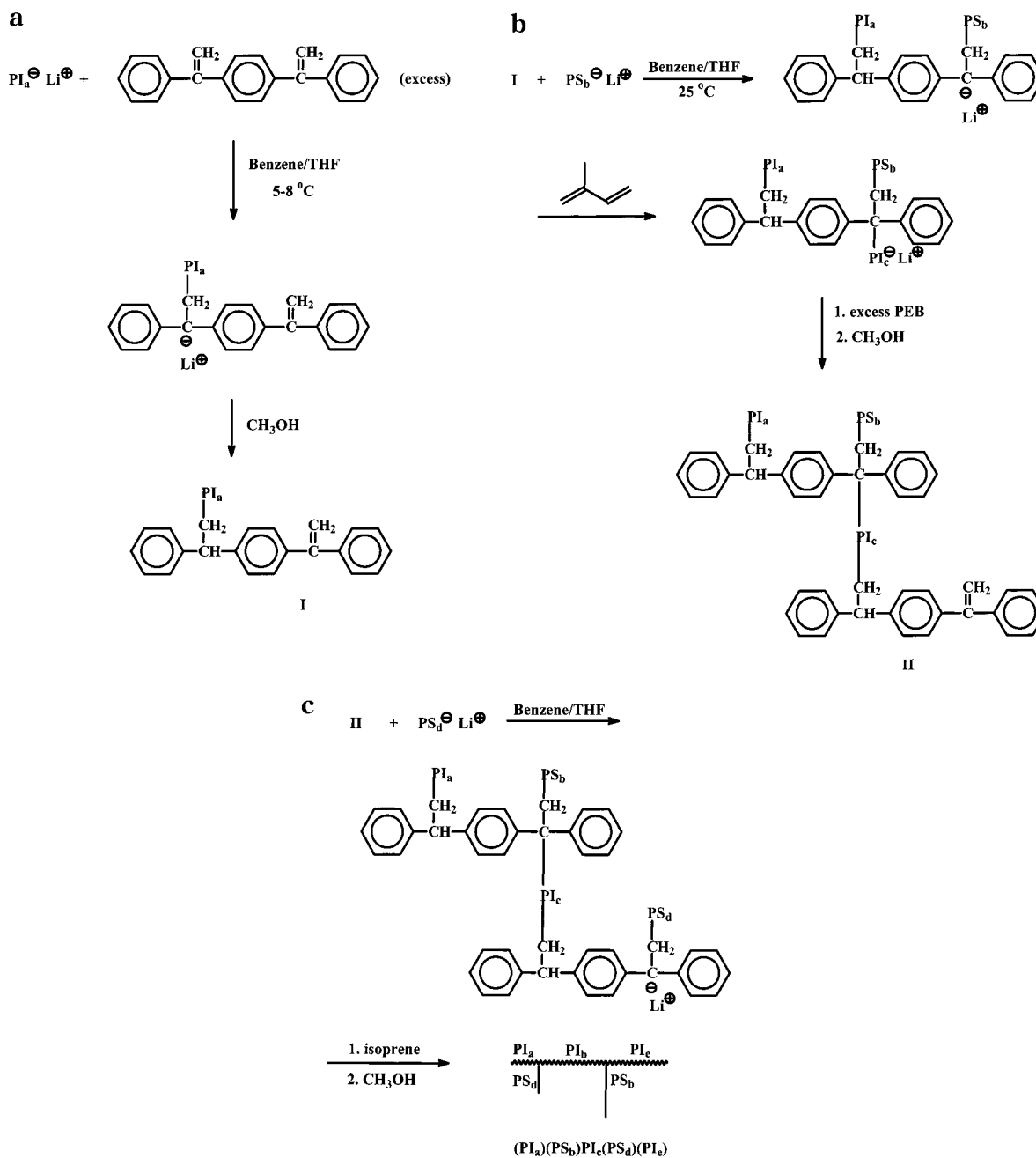
Exact graft copolymers¹⁶⁶ with a PI backbone and two PS branches, where the position of the branching points along the backbone and the length of each branch could be controlled exactly, were synthesized using anionic polymerization methodology and non-polymerizable DPE derivatives for branching point formation (Scheme 80). Living PILi is produced and reacted with PDDPE in the presence of a small amount of THF. By taking advantage of the differences in the reactivity of the two double bonds and the appropriate stoichiometry, monitored by titration, only one chain is introduced on PDDPE. The product is isolated and purified. Then it is reacted with living PSLi in order to introduce the second part of the molecule. After complete reaction, the living centers on PDDPE are used to polymerize Is in the presence of THF. The resulting ABB' star has an anionic active center on the end of the B' branch, which can react with PDDPE again, giving a star-shaped, double-bond-functionalized polymer. After isolation and thorough purification of the intermediate, another PS branch is introduced by reaction with the remaining

double bond. The active site is used for the formation of the last part of the molecule by polymerization of Is. Despite the numerous reaction steps and the demanding purification of the intermediate products, the method allows control over almost all molecular characteristics of the final graft copolymer and can be extended to the preparation of grafts with a higher number of branches.

VI. Cyclic Polymers

The first attempts to synthesize cyclic polymers involved a ring-open chain equilibrium based on backbiting reactions of poly(dimethylsiloxanes).¹⁶⁷ However, this method was limited to low molecular weight and polydisperse cyclic polymers and was characterized by the inability to isolate the corresponding linear precursor in order to prove the cyclic structure by comparing the properties. Now a days living polymerization processes leading to narrow molecular weight distribution polymers are generally preferred. The linear precursor of the cyclic polymer

Scheme 80

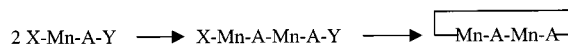
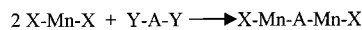
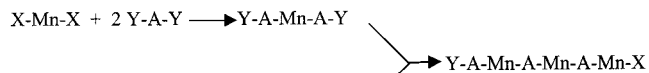


has either two identical or two different functional groups capable of reacting with each other. In the first case, an α,ω -homodifunctional macromolecule was synthesized first, followed by the reaction with an appropriate difunctional linking agent. In the second case, an α,ω -heterodifunctional macromolecule was prepared by using functional protected initiator and by neutralizing the living anion with the appropriate linking agent containing another protected group. The cyclic structure is formed by the coupling reaction of the two reactive groups.

The first case is shown below schematically:

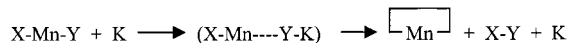


Besides the intramolecular reaction, several intermolecular reactions can occur:



These reactions lead to undesirable, high molecular weight polycondensates, which are either linear or cyclic and should be removed from the low molecular weight desirable cyclic product.

In the second case, the cyclization requires an activation step:



This synthetic approach presents several advantages, such as an exact stoichiometry of addition of the two reagents is not required, since the two reactive groups are in the same molecule and only a catalytic amount of the activator K is needed. In both cases, the possibility of intramolecular versus intermolecular reaction depends on their effective concentration. The probability of intramolecular reaction, i.e., of finding the ω -end of a chain within a small reaction volume v_e close to the α -end is given by

$$P_i = (3/2\pi)^{3/2} v_e / \langle r^2 \rangle^{3/2}$$

where $\langle r^2 \rangle$ is the mean square end-to-end distance of the chain in the reaction medium. The probability of the intermolecular reaction, i.e., of finding the chain end of another molecule is given by

$$P_e = (N_A c / M) v_e$$

where N_A is Avogadro's number, c the concentration of the polymer, and M the molecular weight. The concentration at which the intra- and intermolecular reaction are equally likely is given by

$$c_{\text{equal}} = [(3/2\pi) / \langle r^2 \rangle]^{3/2} M / N_A$$

This equation shows that (a) the more dilute the polymer solution, the more probable the cyclization over the polycondensation is, and (b) at the same molecular weight, double the concentration (higher yield) can be used for heterodifunctional than for homodifunctional polymers. The practical strategies used for the preparation of cyclic copolymers will be presented below.

A. Cyclic Homopolymers from Precursors with Homodifunctional Groups

Many different linking agents and functional groups have been proposed for the synthesis of cyclic polymers using homodifunctional groups. However, the general strategy followed by most authors is similar and can be outlined as follows:

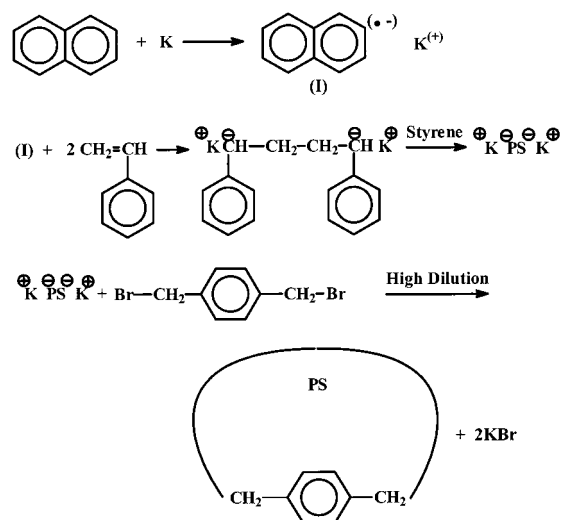
- preparation of a monodisperse α, ω -homodifunctional living polymer,
- reaction of the living polymer with a homodifunctional linking agent,
- and (c) fractionation for purification of the cyclic polymer.

In all cases a high dilution of the linking reaction was used in order to increase the yield of cyclization.

1. Cyclic Homopolymers

Hild et al.¹⁶⁸ prepared ring polystyrenes under argon atmosphere by reacting α, ω -dipotassium polystyrene, synthesized by potassium naphthalenide, with dibromo-*p*-xylene in a mixture of THF:benzene or cyclohexane in a ratio 1:1 (v/v) (Scheme 81). The addition of the reagents was made by using two dropping funnels. After fractional precipitation, the yield of the synthetic procedure was between 30% and 46%. The apparent molecular weight obtained by SEC was about 20% lower than that obtained by

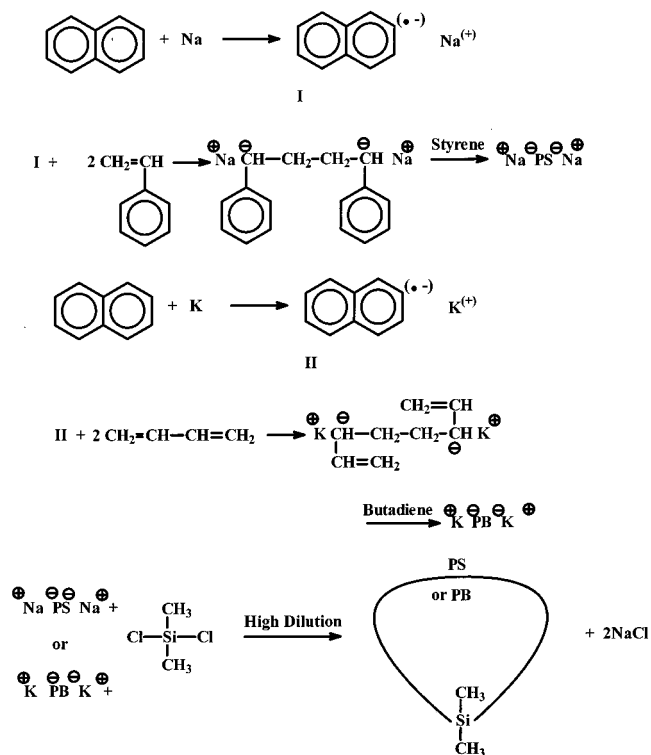
Scheme 81



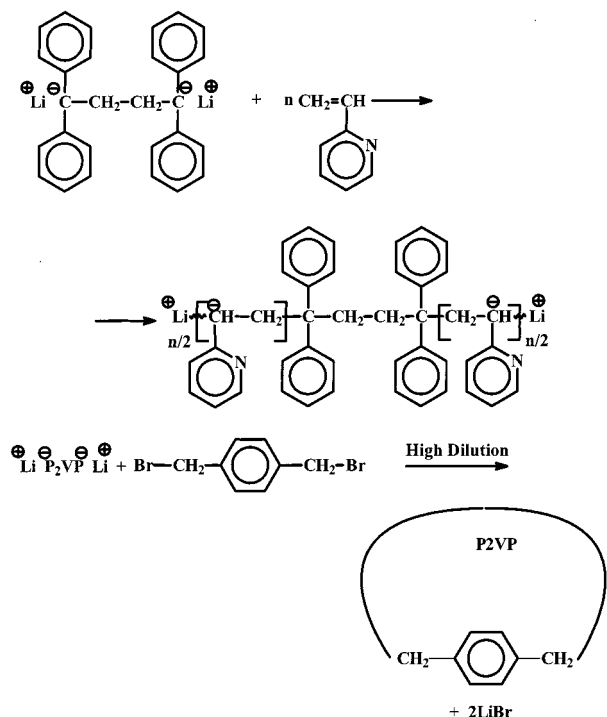
light scattering, and this was attributed to the lower hydrodynamic volume that is expected for a cyclic polymer when compared to the corresponding linear material.

Roovers et al.¹⁶⁹ synthesized cyclic PS under high-vacuum conditions by using naphthalene sodium as a difunctional initiator. The polymerization solvent was a mixture of THF:benzene in a ratio of 1:1 (v/v). The linking agent was dichlorodimethylsilane, and the linking reaction was performed in cyclohexane at room temperature, which is close to θ conditions for PS (Scheme 82). Although the procedure has been questioned by some authors due to the higher possibility of forming permanent "knots", no clear evidence of this conjecture has been forthcoming. Roovers synthesized a series of cyclic PSs having molecular weights $(2.0-55) \times 10^4$ g/mol. The separation of the

Scheme 82



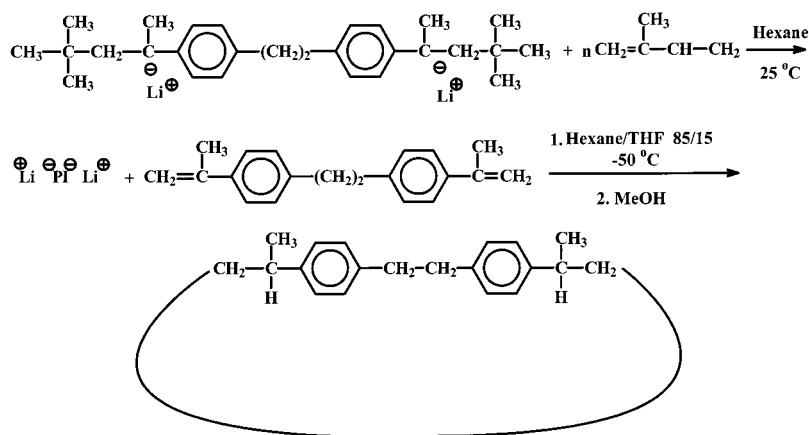
Scheme 83



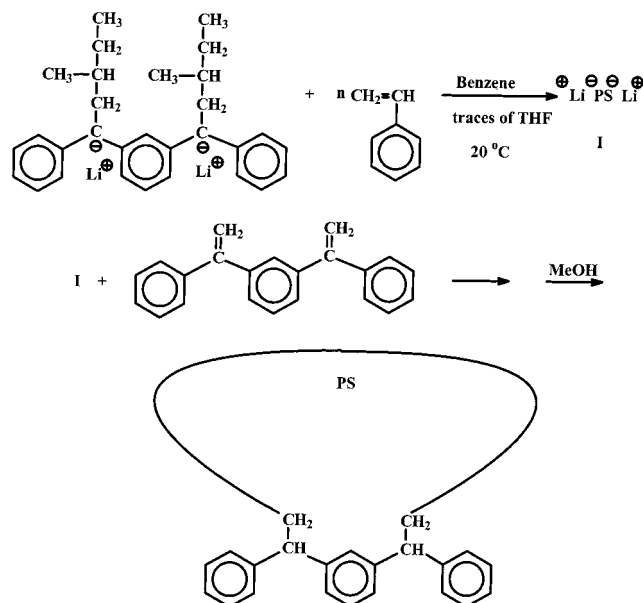
cyclic from the linear precursor was achieved by ultracentrifugation. The $g' = [\eta]_r/[\eta]_l$ values, where $[\eta]_r$ and $[\eta]_l$ are the intrinsic viscosities of the cyclic and the corresponding linear polymer, respectively, varied from 0.58 to 0.68, which is in good agreement with the theoretically and experimentally reported values.

A few years later, by using the same experimental procedures, the same scientists prepared cyclic polybutadienes¹⁷⁰ (Scheme 82). THF was the polymerization solvent, which results in a 60% 1,2-content. From the g' values was concluded that some of the cyclic polybutadienes (PBd) were contaminated by their linear precursors. A high-resolution column set was used in order to separate the linear from the cyclic polymer. In this work the characterization analysis was the most comprehensive presented so far. Recently, these cyclic PSs were analyzed by high-pressure liquid chromatography under critical conditions, which is a method that can separate linear and cyclic macromolecules according to their archi-

Scheme 84



Scheme 85



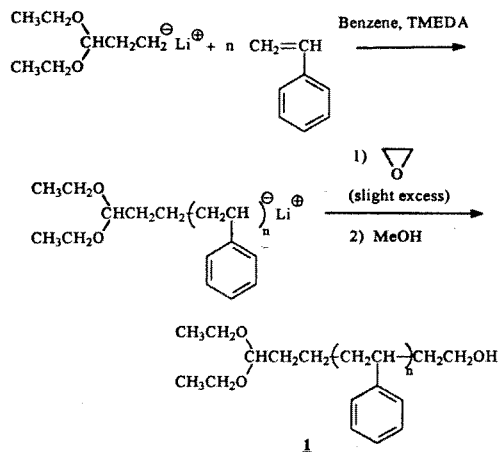
itecture and not according to their hydrodynamic volume, and verified the low degree of contamination.¹⁷¹

Hogen-Esch et al.¹⁷² synthesized α,ω -dilithium poly(2-vinylpyridine) by anionic polymerization of 2-vinylpyridine with 1,4-dilithio-1,1,4,4-tetraphenylbutane, in THF at -78 °C under inert atmosphere. The cyclization reaction was performed in high dilution by adding 1,4-bis(bromomethyl)benzene (Scheme 83). The main indication for the formation of the cyclic polymers was the significant difference in the T_g value between the cyclic and the linear precursor.

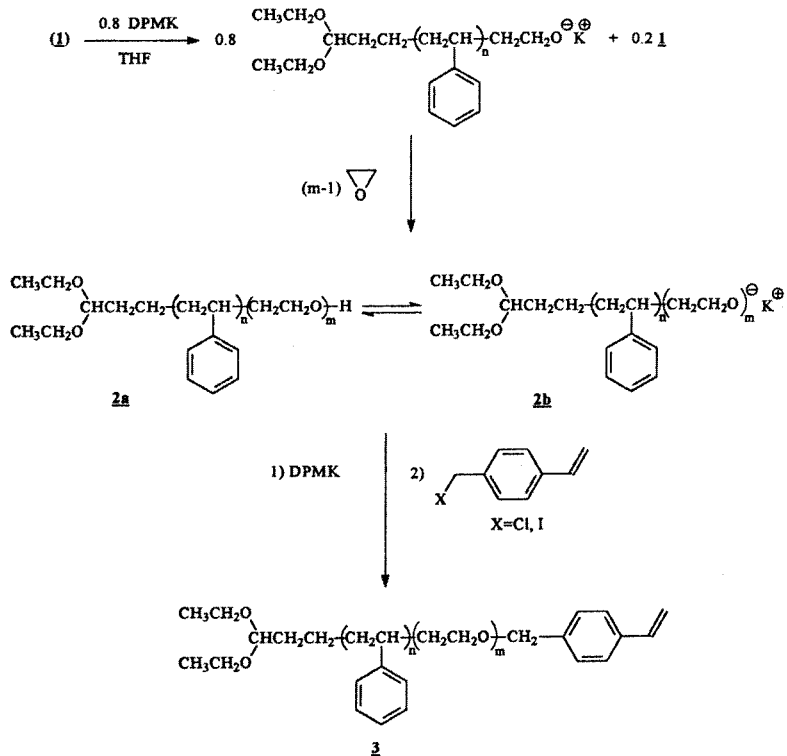
A few years later the synthesis of cyclic polyisoprenes with high 1,4-content was presented by Madani et al.¹⁷³ They used hexane as polymerization solvent at -40 °C, and a difunctional initiator formed by the reaction of 1,2-bis(4-isopropenylphenyl)ethane with 2 mol of *t*-BuLi. This initiator was soluble in organic solvents. The linking agent was a nonconjugated diene, 1,2-bis(isopropenyl-4-phenyl)ethane. The cyclization was performed in the presence of 15% THF at -50 °C (Scheme 84). Under the same conditions they tried to synthesize bicyclic and tadpole molecules. They found a high yield of cyclization by using only SEC analysis. The high yield was attributed to

Scheme 90

Part a

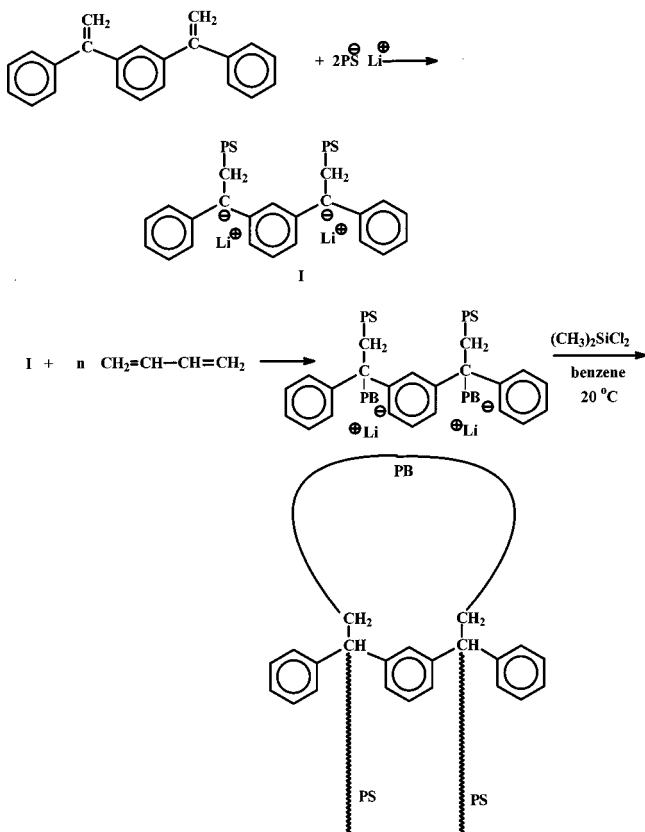


Part b



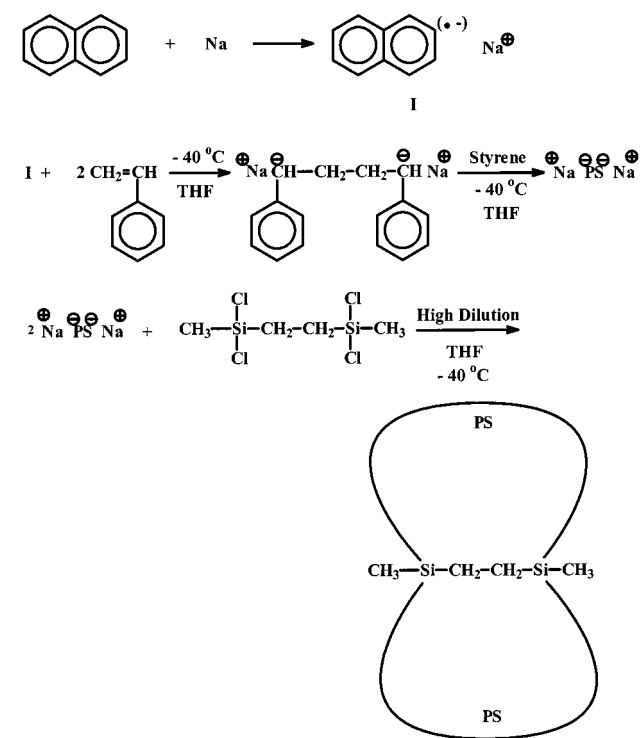
al.^{175,176} Styrene was polymerized by lithium naphthalenide initiator at -78°C in THF, followed by the polymerization of hexamethylcyclotrisiloxane (D_3). The resulting α,ω -living triblock PDMS-PS-PDMS was cyclized with dichlorodimethylsilane at $5-10^\circ\text{C}$

Scheme 91



under high dilution conditions (Scheme 86). The purity of the cyclic copolymers was investigated by ^1H NMR, ^{29}Si NMR, and FTIR. The lack of SiOH or SiCl groups in the final copolymers was a direct indication of the high purity of the cyclics. However, due to the backbiting reaction of the living PDMS under the conditions used for the cyclization reaction, the quality of the cyclics is questionable. In the same

Scheme 92



study the synthesis of a linear CBABC and the corresponding cyclic ABCB is described, where A is PS, B is 2,2,5,5-tetramethyl-2,5-disila-1-oxacyclopentane, and C is PDMS.

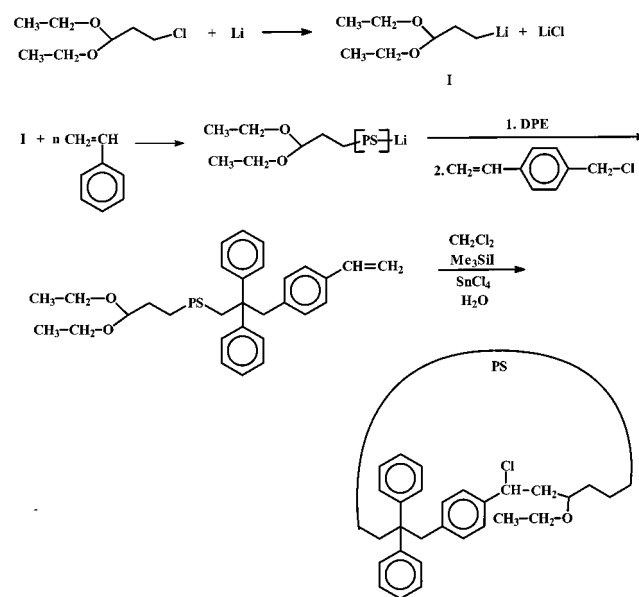
Ma et al.¹⁷⁷ synthesized α,ω -dilithium poly(styrene-*b*-butadiene-*b*-styrene)s (PS-*b*-PBd-*b*-PS) by using 1,3-bis(1-phenylethenyl)benzene activated with 2 mol of *s*-BuLi as initiator for the sequential polymerization of butadiene and styrene in the presence of *s*-BuOLi in benzene. The cyclization reaction was performed under high dilution in cyclohexane with either dichlorodimethylsilane or MDPPE (Scheme 87). The cyclic copolymer was isolated by fractional precipitation. The only indication of the formation of this architecture was the lower intrinsic viscosity.

Ishizu et al.^{178,179} synthesized poly(I-*b*-S-*b*-I) triblock copolymer by the sequential polymerization of styrene and isoprene, using lithium naphthalenide as initiator in a mixture of THF:benzene equal to 8:2 (v/v) at -78°C . The α,ω -living triblock was reacted first with 1,1-diphenylethylene followed by a reaction with a large excess of 1,3-dibromopropane. The cyclization reaction was performed by reacting the α,ω -dibromofunctional triblock copolymer with 1,6-diaminohexane (Scheme 88) in a mixture of dimethylformamide (DMF)/1,1,2-trichloroethylene/water (interfacial condensation). The cyclics were characterized only by SEC. The morphology study has shown that the cyclic copolymers exhibited smaller domain spacings compared to the corresponding linear copolymers.

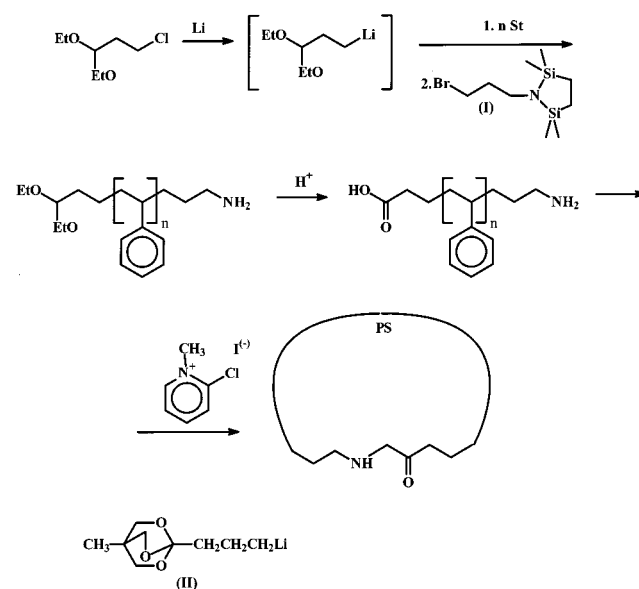
Yu et al.¹⁸⁰ have synthesized cyclic diblock copolymers of ethylene oxide and propylene oxide. They polymerized sequentially propylene oxide and ethylene oxide by using the difunctional initiator (I) shown in Scheme 89. The cyclization reaction of the α,ω -hydroxyl-ended diblock macromolecules was carried out under Williamson conditions. A solution of the triblock precursor in a mixture of dichloromethane and hexane 65:35 (v/v) was added to a stirred suspension of powdered KOH (85% w/v) in the same dichloromethane/hexane mixture (Scheme 89). After separation and evaporation of the organic phase, the cyclic diblocks were isolated by fractional precipitation. The dilute solution properties of the cyclics and the corresponding linear triblock and diblock copolymers with the same composition and total molecular weight were compared. By examining the micellar behavior in water they found that the aggregation numbers were on the order $N_T < N_C < N_D$, where N_T , N_C , and N_D , are the aggregation numbers of the triblocks, cyclic, and diblocks, respectively.

Recently, the group of Deffieux¹⁸¹ presented the synthesis and solution properties of macrocyclic poly(styrene-*b*-ethylene oxide). The synthetic route involved the preparation of a linear α -diethylacetal- ω -styrenyl poly(styrene-*b*-ethylene oxide) precursor and cyclization by cationic activation with SnCl_4 catalyst. The α -diethylacetal- ω -styrenyl poly(styrene-*b*-ethylene oxide) precursor was synthesized by using α -diethylacetalpropyllithium as initiator of styrene. The functional living PS was end-capped with ethylene oxide, and the resulted ω -hydroxyl group was reacted with diphenylmethylpotassium. The potassium alkox-

Scheme 93



Scheme 94

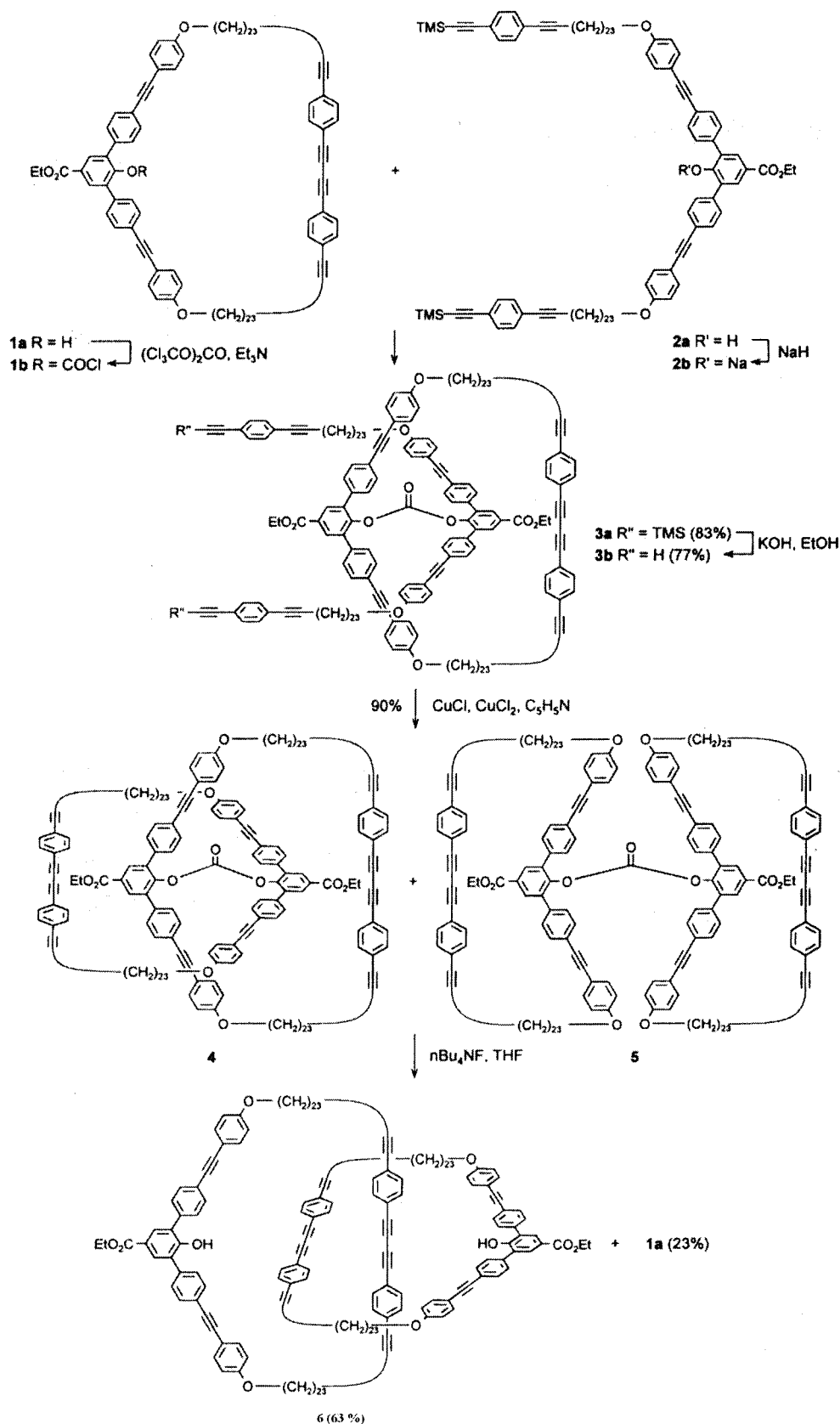


ide was used to initiate the polymerization of ethylene oxide. Finally, the potassium alkoxide group was reacted with *p*-chloromethyl styrene to anchor a styrenyl group at the ω -end of the copolymer chains (Scheme 90b). The cyclization procedure was performed under high dilution conditions.

3. Tadpole and Bicyclic Polymers

Tadpole polymers are polymers consisting of one cyclic chain and one or more linear chains. Quirk and Ma¹⁸² prepared a tadpole copolymer consisting of a cyclic PBd and two linear PS chains. First they reacted PDPPE with two monofunctional living PS chains. The resulting difunctional PS was used to initiate the polymerization of butadiene. The living PBd chains were then cyclized with dichlorodimethylsilane in benzene as shown in Scheme 91. The separation of the tadpole copolymer from the polycondensates was achieved by fractional precipitation.

Scheme 95



The smaller the ring fraction in the copolymer, the more difficult the separation. Insufficient characterization results were given.

Antonietti et al.¹⁸³ synthesized bicyclic PS homopolymers. They prepared difunctional PS initiated by sodium naphthalene in THF at -40°C . The cycliza-

tion reaction was performed in a 0.5% solution of linear precursor by using 1,2-bis(methyldichlorosilyl)ethane (Scheme 92). Although the final product was proved to have double the molecular weight, sufficient characterization results to prove the architectures claimed were not presented.

Along the same lines, Mandani et al.¹⁷³ reacted a difunctional polyisoprene with silicon tetrachloride, to prepare bicyclic polyisoprenes. The only indication for the formation of the bicyclic homopolymer was the lower hydrodynamic volume obtained by SEC. However, the final polymer was not isolated for further characterization.

B. Cyclic Homopolymers from Precursors with Heterodifunctional Groups

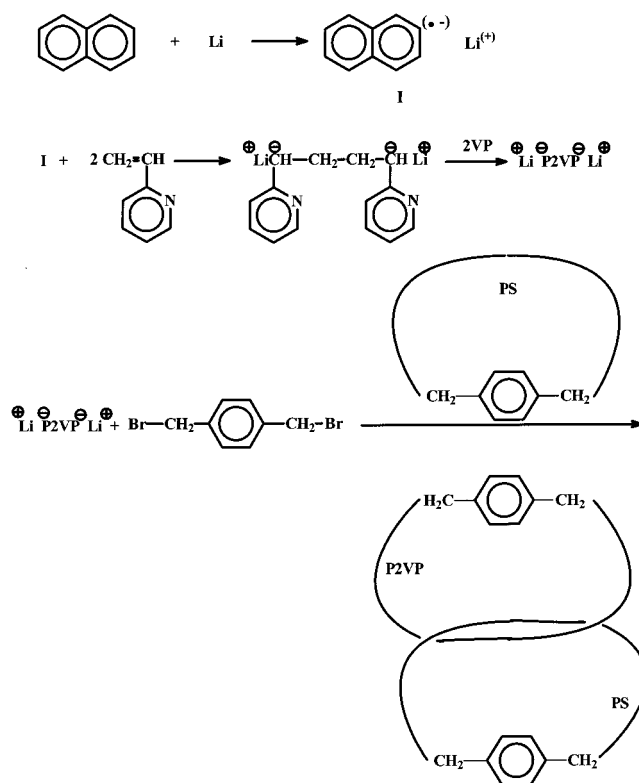
Deffieux was one of the first to use precursors with α,ω -heterodifunctional reactive groups. With his collaborators¹⁸⁴ he synthesized α -acetal-functionalized linear PS by using 3-lithiopropionaldehyde diethylacetal as initiator. After polymerization, the living anion was reacted first with 1,1-diphenylethylene and then with *p*-chloromethylstyrene. The acetal group of the initiator was converted into the α -iodo ether group with trimethylsilyliodide. The cyclization was performed as shown in Scheme 93. The yield was between 80% and 85%. The molecular weight range of the cyclics prepared was between 2000 and 6700. The presence of 10% linear precursor in the final product was detected by NMR spectroscopy. More recently, Pasch et al.¹⁸⁵ analyzed the cyclic PS with liquid chromatography under critical conditions. They found that the higher the molecular weight of the polymer, the higher the contamination with linear precursor. The cyclic structure was also confirmed by MALDI-TOF MS experiments.

Kubo et al.¹⁸⁶ prepared cyclic PS from α -carboxyl- ω -amino bifunctional linear PS. The linear precursor was synthesized by using 3-lithiopropionaldehyde diethylacetal as the carboxyl-protected functional initiator and 2,2,5,5-tetramethyl-1-(3-bromopropyl)-1-aza-2,5-disila-cyclopentane (Scheme 94 (I)) as the amino-protected terminating agent of the living anions. The preparation of the linear polymer for the cyclization involved five steps in order to deprotect the reactive groups and four purifications on silica gel to give the α -carboxyl- ω -amino bifunctional linear PS. The cyclization was performed under high dilution conditions by intramolecular amidation with an overall yield of 30–35% (Scheme 94). More recently, another approach for the preparation of α -carboxyl- ω -amino bifunctional linear PS was presented by Kubo et al.¹⁸⁷ 1-(3-Lithiopropyl)-4-methyl-2,6,7-trioxabicyclo[2.2.2]octane was used as initiator (Scheme 94 (II)) and 2,2,5,5-tetramethyl-1-(3-bromopropyl)-1-aza-2,5-disilacyclopentane (I) for neutralization of the living ends. The former is a carboxyl-protected initiator, while the latter is an amino-protected linking agent. After deprotection of the functional groups, the cyclization was performed under the same conditions presented above. The molecular weight of the samples prepared was between 1700 and 2700. The overall yield of their approach was 81%. The authors performed NMR spectroscopy and MALDI-TOF analysis of the cyclics in order to determine their purity.

C. Catenanes

Catenanes consist of two or more chemically independent cyclic molecules that penetrate each other

Scheme 96

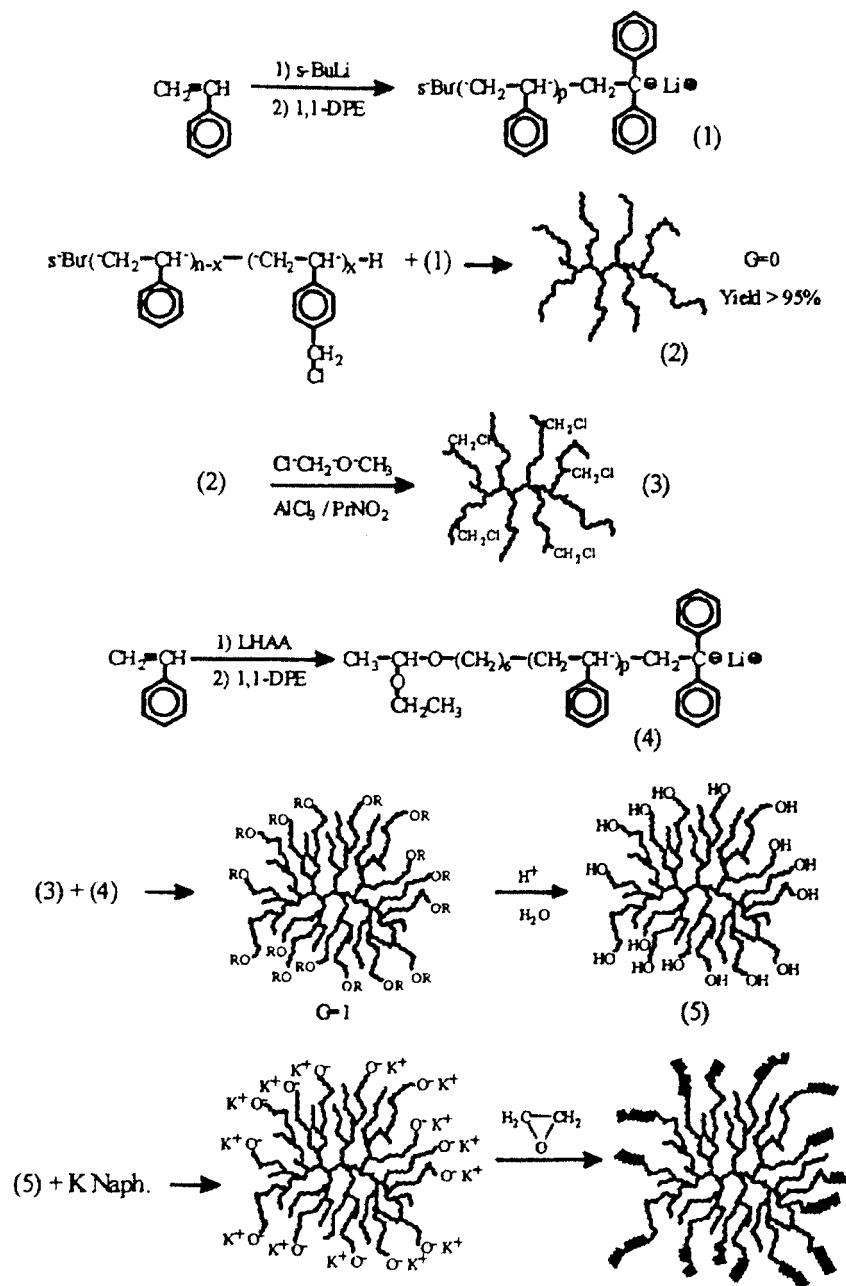


and therefore are not covalently but only topologically linked. The ring molecules are allowed to rotate independently of each other.

Unsal et al.^{188,189} synthesized a catenane consisting of two interpenetrating rings. They used a cyclic oligomer of polyethylene that contains one 4-hydroxybenzoate group that carries toluene units in the 3- and 5-positions (Scheme 95). The polyethylene chains are connected with this group through ether bonds. The linear precursor of the next cycle that will be connected to the first was a similar molecule containing the latter group and polyethylene oligomers prepared by anionic polymerization and hydrogenation, and in the chain ends were acetylene units (**2a**, Scheme 95). The cyclic compound was transformed into the chloroformate **1b** by reaction with triphosgene in the presence of triethylamine. The cycle precursor was deprotonated with sodium hydride and reacted with **1b** to form **3a**, which was purified by column chromatography and desilylated to give product **3b**, followed by cyclization by oxidative acetylene dimerization under high dilution conditions. Treatment of **4** with *n*-Bu₄NF in THF gave the catenane **6**. The SEC analysis showed that low molecular weight products that were identical to the cyclic compound **1a** were also formed. From this it was concluded that on cyclization of **3b**, the dumbbell-shaped carbonate **5** was formed in addition to the intended catenane precursor **4**. The intermediate products were characterized by NMR spectroscopy. The catenanes were characterized only by SEC and NMR spectroscopy.

Gan et al.¹⁹⁰ synthesized catenated copolymers containing one cyclic PS and one cyclic poly(2-vinylpyridine) (P2VP). The preparation involved the cyclization of a difunctional P2VP polymeric chain in

Scheme 97



the presence of cyclic PS. The polymerization of 2-vinylpyridine was performed in THF by using lithium naphthalenide as initiator. The cyclization reaction was performed at room temperature at relatively high concentration of cyclic PS in order to increase the possibility of the formation of catenanes (Scheme 96). The catenanes were isolated from the side products and cyclic PS homopolymer by treating the crude product with cyclohexane, which is a poor solvent for P2VP, and methanol, which is poor solvent for PS. Indications for the formation of the catenanes were obtained only by NMR spectroscopy.

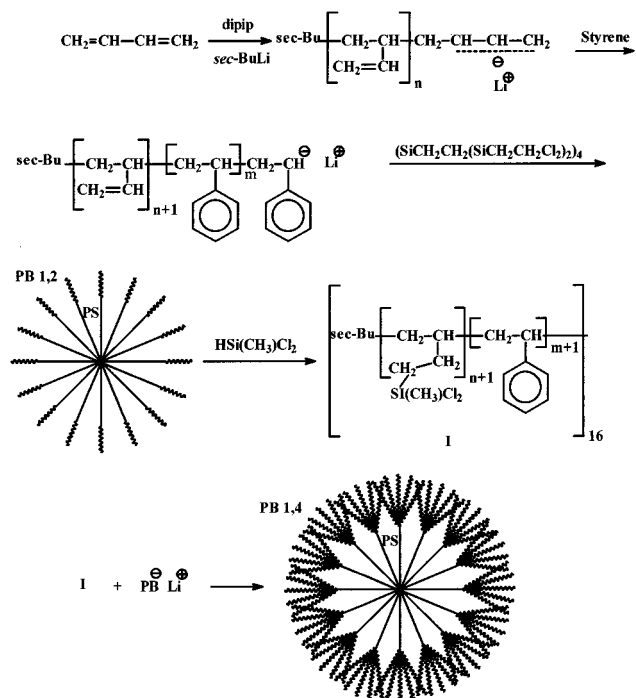
VII. Hyperbranched Architectures

Branched polymers have physical properties distinct from their linear analogues, both in solution and in the melt. However, the more complicated the structure, the more difficult the development of

techniques for synthesizing polymers with well-defined molecular characteristics and the more difficult to characterize them. Many synthetic approaches have been presented for the preparation of hyperbranched polymers, mainly by polycondensation reactions.^{191,192} In most cases the resulting polymers exhibited high molecular and compositional polydispersity, and their molecular architectures could not be exactly defined. Even so, their properties were very interesting, and therefore these polymers can be used in many technological applications. Here several synthetic approaches to the synthesis of hyperbranched polymers by anionic polymerization will be presented.

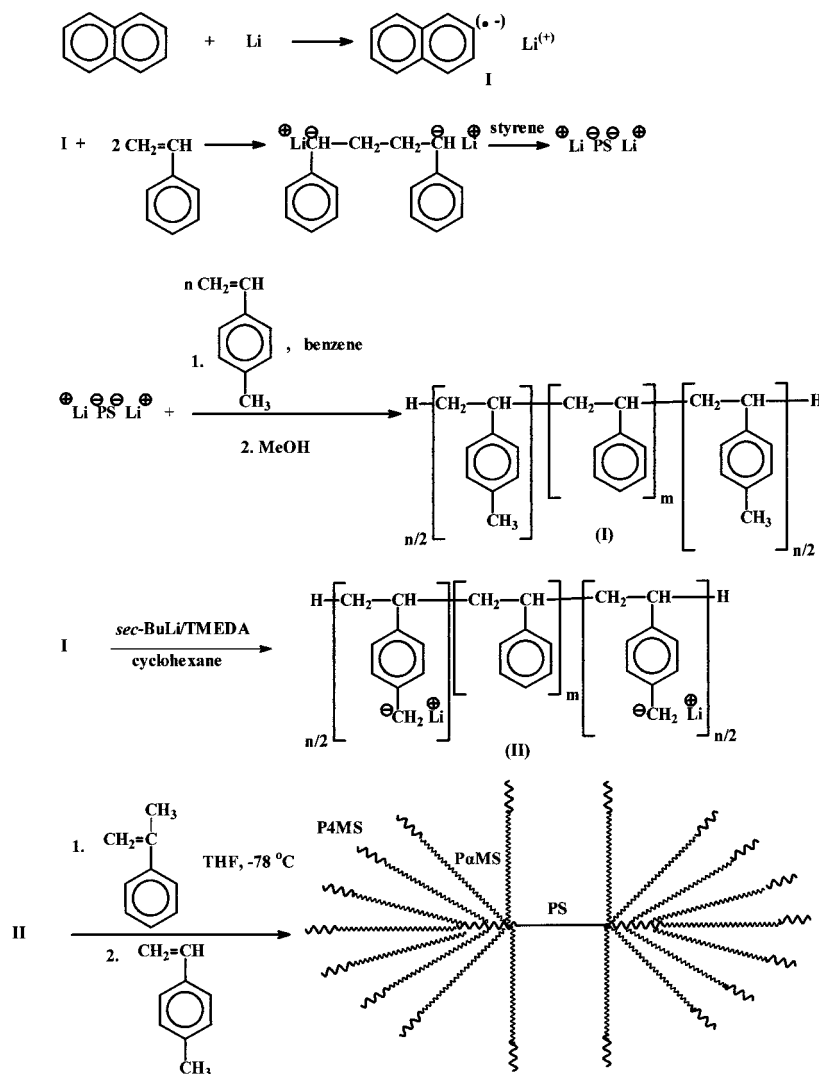
Gauthier et al.¹⁹³ prepared highly branched arborescent graft copolymers of PS and poly(ethylene oxide). Their synthetic approach involved the reaction of living PS end-capped with DPE with chlorometh-

Scheme 98

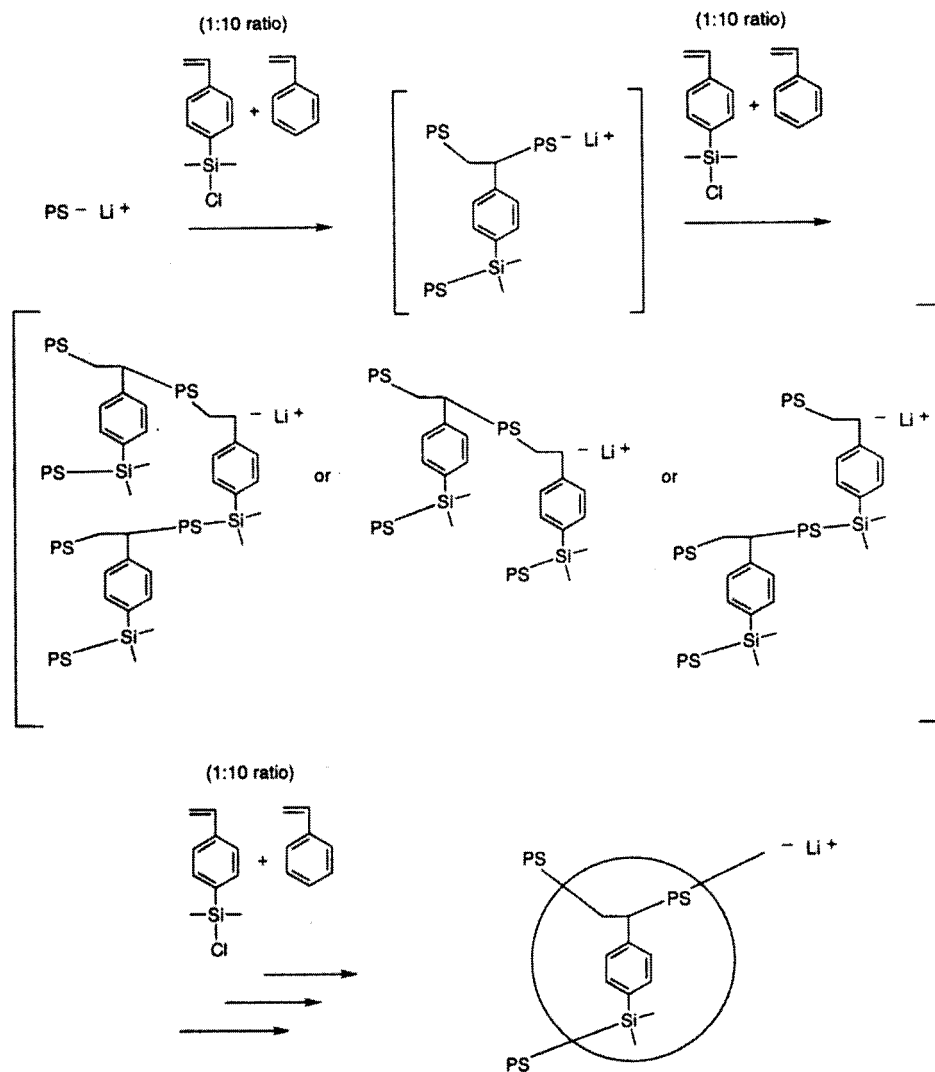


ylated linear polystyrene. The produced graft polymer was further chloromethylated and was reacted with living PS end-capped with DPE that contains a hydroxyl-protected group. The hydroxyl groups of the resulting graft polymer were deprotected and titrated by potassium naphthalenide in order to transform the hydroxyl to $-\text{O}^{\ominus}\text{K}^{\oplus}$ groups. These anions are capable of polymerizing ethylene oxide. The resulted copolymer exhibits a PS core and long arms (shell) of poly(ethylene oxide). The hyperbranched materials were isolated by fractional precipitation. The composition analysis of the copolymers were performed by FTIR and NMR spectroscopies. SEC was used for the evaluation of the polydispersities of the final products. Dynamic light scattering experiments of the intermediate PS core and the final copolymer were performed in order to demonstrate the incorporation of the poly(ethylene oxide) chains. Roovers et al.^{102,103} prepared umbrella star copolymers of PS and PBd or P2VP. The structure of these copolymers can be described as a multiarm star in which each arm, instead of a free end, connects to another star molecule. The core of the umbrella polymers was PS chains, while the shell was either PBd or P2VP. The synthesis of these copolymers involved the preparation of 1,2-PBd-*b*-PS polymeric chains in which the

Scheme 99



Scheme 100



1,2-PBd block is short, followed by coupling with an appropriate chlorosilane linking agent, depending on the desired number of arms. After isolation of the star by fractional precipitation, the double bonds of the 1,2-PBd were hydrosilylated in order to incorporate $-Si(CH_3)Cl_2$ or $-Si(CH_3)Cl$, followed by reaction with living PBd or P2VP chains (Scheme 98).

Ishizu et al.¹⁹⁴ synthesized hyperbranched macromolecules that resemble dendrimers. The synthetic approach involved the preparation of poly(4-methylstyrene-*b*-PS-*b*-poly(4-methylstyrene) triblock copolymer by using naphthalene lithium as difunctional initiator. The 4-methyl groups of the terminal blocks were metalated with *s*-BuLi/tetramethylethylenediamine (TMEDA) complex in a molar ratio of 1:2. After removal of the excess *s*-BuLi by repeated precipitation of the living polymer and transfer of supernatant solution to another flask under high vacuum conditions, the polymer was dissolved in THF and was used as the initiator of α -methylstyrene at $-78^\circ C$. After the polymerization of α -methylstyrene, a small amount of 4-methylstyrene was added. The procedure of metalation of the α -methyl groups and polymerization of α -methylstyrene can be repeated many times to form a dendritic type hyperbranched polymer (Scheme 99). The characterization of the inter-

mediate polymers was performed by SEC and static light scattering. It was found that an average number of 29 arms of poly(α -methylstyrene) was attached to each initial poly(4-methylstyrene) block. The intrinsic viscosity of the hyperbranched copolymers was measured, and the g' values were calculated.

Recently Hasan et al.¹⁹⁵ synthesized hyperbranched copolymers by using a dendritic type initiator. Low molecular weight living PS chains were reacted with a mixture of vinylbenzyl chloride or 4-(chlorodimethylsilyl)styrene and styrene in a molar ratio 1:10. The living ends of polystyrene chains can polymerize the styrene monomer and at the same time can react with the $-SiCl$ or $-CH_2Cl$ group of the or 4-(chlorodimethylsilyl)styrene or vinylbenzyl chloride, as shown in Scheme 100. A dendritic type initiator is obtained for polymerization of either styrene or isoprene. The weak point of this approach is that the positions of the grafting points of the macromolecular initiator are randomly distributed along the PS chains. Moreover, the number of the linear PS or PI chains cannot be controlled. The molecular weight of the resulting polymer was characterized by SEC coupled with multiangle laser light scattering. In the case of the copolymers, the composition was determined by 1H NMR.

VIII. Concluding Remarks

Anionic polymerization has proven to be a very powerful tool for the synthesis of well-defined macromolecules with complex architectures. Although, until now, only a relatively limited number of such structures with two or three different components (star block, miktoarm star, graft, α,ω -branched, cyclic, hyperbranched, etc. (co)polymers) have been synthesized, the potential of anionic polymerization is unlimited. Fantasy, nature, and other disciplines (i.e., polymer physics, materials science, molecular biology) will direct polymer chemists to novel structures, which will help polymer science to achieve its ultimate goal: to design and synthesize polymeric materials with predetermined properties.

Furthermore, anionic polymerization will lead to well-defined multicomponent multiblock copolymers. A plethora of novel multiphase morphologies will be hopefully discovered. The potentiality of these multicomponent multiblock copolymers to be used as multifunctional smart materials is enormous.

Finally, combination of anionic with other polymerization methods (cationic, living radical, ROMP, metallocenes, etc.) will open new horizons for the synthesis of more complex and more fascinating macromolecular structures.

In the years to come there will be a new thrust in polymer synthesis like the one in the early 1960s, on the condition that characterization techniques for complex architectures will be also advanced.

IX. List of Symbols and Abbreviations

$[\eta]_l$	intrinsic viscosity of a linear polymer
$[\eta]_r$	intrinsic viscosity of a ring polymer
$\langle r^2 \rangle$	mean square end-to-end distance
c	polymer concentration
CDMSS	4-(chlorodimethylsilyl)styrene
c_{equal}	polymer concentration at which intra- and intermolecular reactions of α,ω -difunctional polymers are equally likely
D_3	hexamethylcyclotrisiloxane
DIB	<i>m</i> -disopropenylbenzene
DLS	dynamic light scattering
DMAPLi	3-dimethylaminopropyllithium
DMF	dimethylformamide
d-PBd	deuterated polybutadiene
DPE	1,1-diphenylethylene
DPMP	diphenylmethylpotassium
d-PS	deuterated polystyrene
DVB	divinylbenzene
EEMA	1-(ethoxy)ethyl methacrylate
EGDM	ethylene glycol dimethacrylate
EPEB	1,1-(1,2-ethanediyl)bis[4-(1-phenylethenyl)-benzene]
FTIR	Fourier transform infrared spectroscopy
g'	the ratio $[\eta]_r/[\eta]_l$
GMA	glycidyl methacrylate
HPLC	high performance liquid chromatography
Is	isoprene
LALLS	low angle laser light scattering
LL	poly(L-lactide)
LS	light scattering
MALDI-TOF-MS	matrix-assisted laser desorption/ionization time-of-flight mass spectroscopy
MDDPE	1,3-bis(1-phenylethenyl)benzene
M_n	number-average molecular weight

MO	membrane osmometry
M_w	weight-average molecular weight
M_w/M_n	molecular weight distribution
N_A	Avogadro's number
NMR	nuclear magnetic resonance
Ns	nosyl group
P ϵ -CL	poly(ϵ -caprolactone)
P2VP	poly(2-vinylpyridine)
P2VPK	poly(2-vinylpyridinyl) potassium
P4MeS	poly(4-methylstyrene)
P4VP	poly(4-vinylpyridine)
PBd	polybutadiene
PBdLi	polybutadienyllithium
PBS	poly(<i>p</i> - <i>tert</i> -butoxystyrene)
PDDPE	1,4-bis(1-phenylethenyl)benzene
PDMS	poly(dimethylsiloxane)
PDMSLi	poly(dimethylsiloxanyl) lithium
P_e	probability of intermolecular reaction of α,ω -difunctional chains leading to the formation of polycondensates
PEMA	poly(ethyl methacrylate)
PEO	poly(ethylene oxide)
PHS	poly(<i>p</i> -hydroxystyrene)
PI	polyisoprene
P_i	probability of intramolecular reaction of an α,ω -difunctional chain leading to the formation of a cyclic polymer
PILi	polyisoprenyllithium
PMMA	poly(methyl methacrylate)
PMMALi	poly(methyl methacrylyl) lithium
PPO	poly(propylene oxide)
PS	polystyrene
PS- <i>b</i> -PILi	polystyrene- <i>block</i> -polyisoprenyllithium
PSLi	polystyryllithium
<i>Pt</i> BuA	poly(<i>tert</i> -butyl acrylate)
<i>Pt</i> BuMA	poly(<i>tert</i> -butyl methacrylate)
<i>Pt</i> BuMALi	poly(<i>tert</i> -butyl methacrylyl) lithium
PVN	poly(2-vinylnaphthalene)
r_1, r_2	copolymerization reactivity ratios
<i>s</i> -BuLi	<i>sec</i> -butyllithium
<i>s</i> -BuOLi	lithium <i>sec</i> -butoxide
SEC	size exclusion chromatography
SLS	static light scattering
St	styrene
<i>t</i> -BuLi	<i>tert</i> -butyllithium
THF	tetrahydrofuran
TMEDA	<i>N,N,N,N</i> -tetramethylethylenediamine
tri-DPE	1,3,5-tris(1-phenylethenyl)benzene
v_e	reaction volume of an end-functionalized group
VPO	vapor pressure osmometry
VS	(4-vinylphenyl)dimethylvinylsilane

X. References

- Ziegler, K.; Jacov, L.; Wollthan, H.; Wenz, A. *Ann. Chem.* **1934**, *511*, 64.
- Szwarc, M. *Nature* **1956**, *178*, 1168.
- Bauer, B. J.; Fetters, L. J. *Rubber Chem. Technol.* **1978**, *51*, 406.
- Graessley, W. W. *Acc. Chem. Res.* **1977**, *10*, 332.
- Grest, G. S.; Fetters, L. J.; Huang, J. S. *Adv. Chem. Phys.* **1996**, *44*, 67.
- Milner, S. T. *Macromolecules* **1994**, *27*, 2333.
- Hsieh, H. L.; Quirk, R. P. *Anionic Polymerization. Principles and Practical Applications*; Marcel Dekker: New York, 1996.
- Mishra, M. K.; Kobayashi, S. Ed. *Star and Hyperbranched Polymers*; Marcel Dekker: 1999.
- Hatada, K.; Kitayama, T.; Vogl, O. *Macromolecular Design of Polymeric Materials*; Marcel Dekker: 1997.
- Rempp, P.; Franta, E.; Herz, J.-E. *Adv. Polym. Sci.* **1988**, *86*, 145.
- Bywater, S. *Adv. Polym. Sci.* **1979**, *30*, 90.
- Worsfold, D. J. *Macromolecules* **1970**, *3*, 514.
- Eschwey, H.; Hallensleben, M. L.; Burchard, W. *Makromol. Chem.* **1973**, *173*, 235.

- (14) Burchard, W.; Eschwey, H. *Polymer* **1975**, *16*, 180.
- (15) Lutz, P.; Rempp, P. *Makromol. Chem.* **1988**, *189*, 1051.
- (16) Tsitsilianis, C.; Lutz, P.; Graff, S.; Lamps, J.-P.; Rempp, P. *Macromolecules* **1991**, *24*, 5897.
- (17) Okay, O.; Funke, W. *Makromol. Chem. Rapid Commun.* **1990**, *11*, 583.
- (18) Funke, W.; Okay, O. *Macromolecules* **1991**, *24*, 2623.
- (19) Gnanou, Y.; Lutz, P.; Rempp, P. *Makromol. Chem.* **1988**, *189*, 2885.
- (20) Rein, D.; Lamps, J. P.; Rempp, P.; Lutz, P.; Papanagopoulos, D.; Tsitsilianis, C. *Acta Polym.* **1993**, *44*, 225.
- (21) Naraghi, K.; Ederle, Y.; Haristoy, D.; Lutz, P. *J. Polym. Prepr.* **1997**, *38(1)*, 599.
- (22) Naraghi, K.S.; Plentz Menegheti S.; Lutz, P. *J. Macromol. Rapid Commun.* **1999**, *20*, 122.
- (23) Comanita, B.; Noren, B.; Roovers, J. *Macromolecules* **1999**, *32*, 1069.
- (24) Knischka, R.; Lutz, P. J.; Sunder, A.; Mulhaupt, R.; Frey, H. *Macromolecules* **2000**, *33*, 315.
- (25) Quirk, R. P.; Tsai, Y. *Macromolecules* **1998**, *31*, 8016.
- (26) Quirk, R. P.; Yoo, T.; Lee, Y.; Kim, J.; Lee, B. *Adv. Polym. Sci.* **2000**, *153*, 67.
- (27) Vasilenko, N. G.; Rebrov, E. A.; Muzafarov, A. M.; Ebwein, B.; Striegel, B.; Moller, M. *Macromol. Chem. Phys.* **1998**, *199*, 889.
- (28) Morton, M.; Helminiak, T. E.; Gadkary, S. D.; Bueche, F. *J. Polym. Sci.* **1962**, *57*, 471.
- (29) Orofino, T.; Wenger, F. *J. Phys. Chem.* **1963**, *67*, 566.
- (30) Mayer, R. *Polymer* **1974**, *15*, 137.
- (31) Zelinski, R. P.; Wofford, C. F. *J. Polym. Sci. Part A* **1965**, *3*, 93.
- (32) Roovers, J.; Bywater S. *Macromolecules* **1972**, *5*, 384.
- (33) Roovers, J.; Bywater S. *Macromolecules* **1974**, *7*, 443.
- (34) Hadjichristidis, N.; Roovers, J. *J. Polym. Sci. Polym. Phys. Ed.* **1974**, *12*, 2521.
- (35) Hadjichristidis, N.; Guyot, A.; Fetters, L. J. *Macromolecules* **1978**, *11*, 668.
- (36) Hadjichristidis, N.; Fetters, L. J. *Macromolecules* **1980**, *13*, 191.
- (37) Roovers, J.; Hadjichristidis, N.; Fetters, L. J. *Macromolecules* **1983**, *16*, 214.
- (38) Zhou, L.-L.; Roovers, J. *Macromolecules* **1993**, *26*, 963.
- (39) Zhou, L.-L.; Hadjichristidis, N.; Toporowski, P. M.; Roovers, J. *Rubber Chem. Technol.* **1992**, *65*, 303.
- (40) Roovers, J.; Zhou, L.-L.; Toporowski, P. M.; van der Zwan, M.; Iatrou, H.; Hadjichristidis, N. *Macromolecules* **1993**, *26*, 4324.
- (41) Pitsikalis, M.; Hadjichristidis, N.; Di Silvestro, G.; Sozzani, P. *Macromol. Chem. Phys.* **1995**, *196*, 2767.
- (42) Allgaier, J.; Martin, K.; Rader, H. J.; Mullen, K. *Macromolecules* **1999**, *32*, 3190.
- (43) Roovers, J.; Toporowski, P.; Martin, J. *Macromolecules* **1989**, *22*, 1897.
- (44) Hogen-Esch, T. E.; Toreki, W. *Polym. Prepr.* **1989**, *30(1)*, 129.
- (45) Pitsikalis, M.; Sioula, S.; Pispas, S.; Hadjichristidis, N.; Cook, D. C.; Li, J.; Mays, J. W. *J. Polym. Sci.: Part A: Polym. Chem.* **1999**, *37*, 4337.
- (46) Samulski, E. T.; Desimone, J. M.; Hunt, M. O.; Menciloglu, Y.; Jarnagin, R. C.; York, G. A.; Wang, H. *Chem. Mater.* **1992**, *4*, 1153.
- (47) Ederle, Y.; Mathis, C. *Macromolecules* **1997**, *30*, 2546.
- (48) (a) Mays, J. W.; Hadjichristidis, N.; Fetters, L. J. *Polymer* **1988**, *29*, 680. (b) Worsfold, D. J.; Zilliox, J. G.; Rempp, P. *Can. J. Chem.* **1969**, *47*, 3379.
- (49) Tsitsilianis, C. Graff, S.; Rempp, P. *Eur. Polym. J.* **1991**, *27*, 243.
- (50) Bi, L.-K.; Fetters, L. J. *Macromolecules* **1976**, *9*, 732.
- (51) Efstratiadis, V.; Tselikas, Y.; Hadjichristidis, N.; Li, J.; Yunan, W.; Mays, J. W. *Polym. Int.* **1994**, *33*, 171.
- (52) Hatada, K.; Kitayama, T. Vogl, O. *Macromolecular Design of Polymeric Materials*; Marcel Dekker: 1997; p.154.
- (53) Nguyen, A. B.; Hadjichristidis, N.; Fetters, L. J. *Macromolecules* **1986**, *19*, 768.
- (54) Alward, D. B.; Kinning, D. J.; Thomas, E. L.; Fetters, L. J. *Macromolecules* **1986**, *19*, 215.
- (55) Storey, R. F.; George, S. E. *Polym. Mater. Sci. Eng.* **1988**, *58*, 985.
- (56) Storey, R. F.; George, S. E.; Nelson, M. E. *Macromolecules* **1991**, *24*, 2920.
- (57) Rein, D.; Rempp, P.; Lutz, P. *J. Makromol. Chem., Macromol. Symp.* **1993**, *67*, 237.
- (58) Tsitsilianis, C.; Voulgaris, D. *Macromol. Chem. Phys.* **1997**, *198*, 997.
- (59) Ishizu, K.; Uchida, S. *Polymer* **1994**, *35*, 4712.
- (60) Teyssie, P.; Fayt, R.; Jacobs, C.; Jerome, R.; Varshney, S. K. *Polym. Prepr.* **1991**, *32(1)*, 299.
- (61) Hara, M.; Wu J. *Multiphase Polymers: Blends and Ionomers*; Utracki, L. A., Weiss R. A., Eds.; ACS Symposium Series 395; American Chemical Society: Washington, DC, 1988; Chapter 19.
- (62) Nagata, N.; Kobatake, T.; Watanabe, H.; Veda, A.; Yoshioka, A. *Rubber Chem. Technol.* **1987**, *60*, 837.
- (63) Fitzgerald, J. J.; Weiss, R. A. *J. Macromol. Sci., Rev. Macromol. Chem. Phys.* **1988**, *C28*, 1.
- (64) Mauritz, K. A. *Macromol. Sci., Rev. Macromol. Chem. Phys.* **1988**, *C28*, 65.
- (65) Hadjichristidis, N.; Pispas, S.; Pitsikalis, M. *Prog. Polym. Sci.* **1999**, *24*, 875.
- (66) Young, R. N.; Quirk, R. P.; Fetters, L. J. *Adv. Polym. Sci.* **1984**, *56*, 1.
- (67) Schulz, D. N.; Sanda, J. C.; Willoughby, B. G. *Anionic Polymerization: Kinetics, Mechanisms and Synthesis*; McGrath, J. E., Ed.; ACS Symposium Series No 166; American Chemical Society: Washington, D C, 1981.
- (68) (a) Quirk, R. P.; Yin, J.; Guo, S.-H.; Xu, X.-W.; Summers, G.; Kim, J.; Zhu, L.-F.; Schock, L. E. *Makromol. Chem. Makromol. Symp.* **1990**, *32*, 47. (b) Schulz, D. N.; Datta, S.; Waymouth, R. M. *Functional Polymers: Modern Synthetic Methods and Novel Structures*; Patil, A. O.; Schulz, D. N.; Novak, B. M. Eds.; ACS Symposium Series No 704; Am. Chem. Soc. Washington, DC, 1998.
- (69) Davidson, N. S.; Fetters, L. J.; Funk, W. G.; Graessley, W. W.; Hadjichristidis, N. *Macromolecules* **1988**, *21*, 112.
- (70) Pitsikalis, M.; Hadjichristidis, N. *Macromolecules* **1995**, *28*, 3904.
- (71) Pispas, S.; Pitsikalis, M.; Hadjichristidis, N.; Dardani, P.; Morandi, F. *Polymer* **1995**, *36*, 3005.
- (72) Burchard, W.; Merkle, G. *J. Phys. Chem.* **1992**, *96*, 3915.
- (73) Weissmuller, M.; Burchard, W. *Polym. Int.* **1997**, *44*, 380.
- (74) Taton, D.; Angot, S.; Gnanou, Y.; Wolert, E.; Setz, S.; Duran, R. *Macromolecules* **1998**, *31*, 6030.
- (75) Pennisi, R. W.; Fetters, L. J. *Macromolecules* **1988**, *21*, 1094.
- (76) Gell, C. B.; Graessley, W. W.; Efstratiadis, V.; Pitsikalis, M.; Hadjichristidis, N. *J. Polym. Sci.: Part B: Polym. Phys. Ed.* **1997**, *35*, 1943.
- (77) Frater, D. J.; Mays, J. W.; Jackson, C. *J. Polym. Sci. Polym. Phys. Ed.* **1997**, *35*, 141.
- (78) Tung, L. H.; Lo, G. Y. S. *Macromolecules* **1994**, *27*, 2219.
- (79) Tung, L. H.; Lo, G. Y. S. *Macromolecules* **1994**, *27*, 1680.
- (80) Quirk, R. P.; Lee, B.; Schock, L. E. *Makromol. Chem., Macromol. Symp.* **1992**, *53*, 201.
- (81) Quirk, R. P.; Yoo, T. *Polym. Bull.* **1993**, *29*.
- (82) Hirao, A.; Hayashi, M.; Haraguchi, N. *Macromol. Chem. Phys.* **2000**, *21*, 1171.
- (83) Hayashi, M.; Hirao, A. *Kobunshi Ronbunshu* **2000**, *57(12)*, 781.
- (84) Hirao, A.; Hayashi, M. *Macromolecules* **1999**, *32*, 6450.
- (85) Hirao, A.; Hayashi, M. *Acta Polym.* **1999**, *50*, 219.
- (86) Hayashi, M.; Kojima, K.; Nakahama, S.; Hirao, A. *Polym. Prepr.* **1998**, *39(2)*, 478.
- (87) Tselikas, Y.; Hadjichristidis, N.; Lescanec, R. L.; Honeker, C. C.; Wohlgemuth, M.; Thomas, E. L. *Macromolecules* **1996**, *29*, 3390.
- (88) Pitsikalis, M.; Pispas, S.; Mays, J. W.; Hadjichristidis, N. *Adv. Polym. Sci.* **1998**, *135*, 1.
- (89) Hadjichristidis, N.; Pispas, S.; Pitsikalis, M.; Iatrou, H.; Vlahos, C. *Adv. Polym. Sci.* **1999**, *142*, 71.
- (90) Hadjichristidis, N. *J. Polym. Sci.: Part A: Polym. Chem.* **1999**, *37*, 857.
- (91) Mays, J. W. *Polym. Bull.* **1990**, *23*, 247.
- (92) Iatrou, H.; Siakali-Kioulafa, E.; Hadjichristidis, N.; Roovers, J.; Mays, J. W. *J. Polym. Sci. Polym. Phys. Ed.* **1995**, *33*, 1925.
- (93) Pochan, D. J.; Gido, S. P.; Pispas, S.; Mays, J. W.; Ryan, A. J.; Fairclough, J. P. A.; Hamley, I. W.; Terrill, N. J. *Macromolecules* **1996**, *29*, 5091.
- (94) Hutchings, L. R.; Richards, R. W. *Polym. Bull.* **1998**, *283*.
- (95) Ramzi, A.; Prager, M.; Richter, D.; Efstratiadis, V.; Hadjichristidis, N.; Young, R. N.; Allgaier, J. *Macromolecules* **1997**, *30*, 7171.
- (96) Avgeropoulos, A.; Hadjichristidis, N. *J. Polym. Sci. Polym. Chem. Ed.* **1997**, *35*, 813.
- (97) Bellas, V.; Iatrou, H.; Hadjichristidis, N. *Macromolecules* **2000**, *33*, 6993.
- (98) Khan, I. M.; Gao, Z.; Khougaz, K.; Eisenberg, A. *Macromolecules* **1992**, *25*, 3002.
- (99) Tselikas, Y.; Hadjichristidis, N.; Iatrou, H.; Liang, K. S.; Lohse, D. J. *J. Chem. Phys.* **1996**, *105*, 2456.
- (100) Tsiang, R. C. C. *Macromolecules* **1994**, *27*, 4399.
- (101) Velis, G.; Hadjichristidis, N. *Macromolecules* **1999**, *32*, 534.
- (102) Wang, F.; Roovers, J.; Toporowski, P. M. *Macromol. Symp.* **1995**, *95*, 205.
- (103) Wang, F.; Roovers, J.; Toporowski, P. M. *Macromol. Rep.* **1995**, *A32 (Suppl 5 and 6)*, 951.
- (104) Iatrou, H.; Hadjichristidis, N. *Macromolecules* **1993**, *26*, 2479.
- (105) Wright, S. J.; Young, R. N.; Croucher, T. G. *Polym. Int.* **1994**, *33*, 123.
- (106) Allgaier, J.; Young, R. N.; Efstratiadis, V.; Hadjichristidis, N. *Macromolecules* **1996**, *29*, 1794.
- (107) Avgeropoulos, A.; Poulos, Y.; Hadjichristidis, N.; Roovers, J. *Macromolecules* **1996**, *29*, 6076.
- (108) Iatrou, H.; Hadjichristidis, N. *Macromolecules* **1992**, *25*, 4649.
- (109) Zioga, A.; Sioula, S.; Hadjichristidis, N. *Macromol. Symp.* **2000**, *157*, 239.

- (110) Lee, C.; Gido, S. P.; Pitsikalis, M.; Mays, J. W.; Beck, Tan N.; Trevino, S. F.; Hadjichristidis, N. *Macromolecules* **1997**, *30*, 3738.
- (111) Sioula, S.; Tselikas, Y.; Hadjichristidis, N. *Macromol. Symp.* **1997**, *117*, 167.
- (112) Sioula, S.; Tselikas, Y.; Hadjichristidis, N. *Macromolecules* **1997**, *30*, 1518.
- (113) Tsitsilianis, C.; Papanagopoulos, D.; Lutz, P. *Polymer* **1995**, *36*, 3745.
- (114) Tsitsilianis, C.; Boulgaris, D. *Macromol. Rep.* **1995**, *A32 (Suppl. 5 and 6)*, 569.
- (115) Tsitsilianis, C.; Boulgaris, D. *Polymer* **2000**, *41*, 1607.
- (116) Hayashi, M.; Negishi, Y.; Hirao, A. *Proc. Jpn. Acad., Ser. B* **1999**, *75B*, 93.
- (117) Hayashi, M.; Kojima, K.; Hirao, A. *Macromolecules* **1999**, *32*, 2425.
- (118) Quirk, R. P.; Yoo, T.; Lee, B. *J. M. Sci.-Pure Appl. Chem.* **1994**, *A31*, 911.
- (119) Quirk, R. P.; Lee, B. *Polym. Prepr.* **1991**, *32(3)*, 607.
- (120) Fernyhough, C. M.; Young, R. N.; Tack, R. D. *Macromolecules* **1999**, *32*, 5760.
- (121) Fujimoto, T.; Zhang, H.; Kazama, T.; Isono, Y.; Hasegawa, H.; Hashimoto, T. *Polymer* **1992**, *33*, 2208.
- (122) Huckstadt, H.; Abetz, V.; Stadler, R. *Macromol. Rapid Commun.* **1996**, *17*, 599.
- (123) Huckstadt, H.; Gopfert, A.; Abetz, V. *Macromol. Chem. Phys.* **2000**, *201*, 296.
- (124) Lambert, O.; Dumas, P.; Hurtrez, G.; Riess, G. *Macromol. Rapid Commun.* **1997**, *18*, 343.
- (125) Lambert, O.; Reutenauer, S.; Hurtrez, G.; Riess, G.; Dumas, P. *Polym. Bull.* **1998**, *40*, 143.
- (126) Quirk, R. P.; Zhuo, Q. *Polym. Prepr.* **1996**, *37(2)*, 641.
- (127) Takano, A.; Okada, M.; Nose, T.; Fujimoto, T. *Macromolecules* **1992**, *25*, 3596.
- (128) Ishizu, K.; Kuwahara, K. *Polymer* **1994**, *35*, 4907.
- (129) Ederle, Y.; Mathis, C. *Macromolecules* **1997**, *30*, 4262.
- (130) Ederle, Y.; Mathis, C. *Macromolecules* **1999**, *32*, 554.
- (131) Xenidou, M.; Hadjichristidis, N. *Macromolecules* **1998**, *31*, 5690.
- (132) Hadjichristidis, N.; Xenidou, M.; Iatrou, H.; Pitsikalis, M.; Poulos, Y.; Avgeropoulos, A.; Sioula, S.; Paraskeva, S.; Velis, G.; Lohse, D. J.; Schultz, D. N.; Fetters, L. J.; Wright, P. J.; Mendelson, R. A.; Garcia-Franco, C. A.; Sun, T.; Ruff, C. J. *Macromolecules* **2000**, *33*, 2424.
- (133) Ruckenstein, E.; Zhang, H. *Macromolecules* **1999**, *32*, 6082.
- (134) Gohy, J.-F.; Charlier, C.; Zhang, J.-X.; Dubois, P.; Jerome, R. *Macromol. Chem. Phys.* **1999**, *200*, 1630.
- (135) Zhang, H. J.; Ruckenstein, E. *Macromolecules* **2000**, *33*, 814.
- (136) Ruckenstein, E.; Zhang, H. *J. Polym. Sci. Part A Polym. Chem.* **2000**, *38*, 1195.
- (137) Zhang, H.; Ruckenstein, E. *Macromolecules* **1998**, *31*, 4753.
- (138) Ryu, S. W.; Hirao, A. *Macromolecules* **2000**, *33*, 4765.
- (139) Selb, J.; Gallot, Y. *Polymer* **1979**, *20*, 1259.
- (140) Selb, J.; Gallot, Y. *Polymer* **1979**, *20*, 1273.
- (141) George, M. H.; Majid, M. A.; Barrie, J. A.; Rezaian, I. *Polymer* **1987**, *28*, 1287.
- (142) Candau, F.; Afchar-Taromi, F.; Rempp, P. *Polymer* **1977**, *18*, 1253.
- (143) Watanabe, H.; Amemiya, T.; Shimura, T.; Kotaka, T. *Macromolecules* **1994**, *27*, 2336.
- (144) Falk, J.; Schlott, R.; Hoeg, D. J. *Macromol. Sci. Chem.* **1973**, *7(8)*, 1647.
- (145) Falk, J.; Hoeg, D. J.; Schlott, R.; Pendelton, J. F. *Macromol. Sci. Chem.* **1973**, *7(8)*, 1669.
- (146) Falk, J.; Hoeg, D. J.; Schlott, R.; Pendelton, J. F. *Rubber Chem. Technol.* **1973**, *46*, 1044.
- (147) Hadjichristidis, N.; Roovers, J. *J. Polym. Sci. Part A Polym. Chem.* **1978**, *16*, 851.
- (148) Al-Jarrah, M. M. F.; Al-Kafaji, J. K. H.; Apikian, R. L. *Br. Polym. J.* **1986**, *18*, 256.
- (149) Kowalczyk, M.; Adamus, G.; Jedlinski, Z. *Macromolecules* **1994**, *27*, 572.
- (150) Rempp, P.; Franta, E. In *Recenet Advances in Anionic Polymerization*; Hogen-Esch, T. E., Smid, J., Eds.; Elsevier: New York, 1987; p 353.
- (151) Norton, R. L.; McCarthy, T. J. *Polym. Prepr.* **1987**, *28(1)*, 174.
- (152) Feast, W. J.; Gibson, V. C.; Johnson, A. F.; Khosravi, E.; Moshin, M. A. *Polymer* **1994**, *35*, 3542.
- (153) Tanaka, S.; Uno, M.; Teramachi, S.; Tsukahara, Y. *Polymer* **1995**, *36*, 2219.
- (154) Ederle, Y.; Isel, F.; Grutke, S.; Lutz, P. J. *Macromol. Symp.* **1998**, *132*, 197.
- (155) Iatrou, H.; Mays, J. W.; Hadjichristidis, N. *Macromolecules* **1998**, *31*, 6697.
- (156) Velis, G.; Hadjichristidis, N. *J. Polym. Sci. Part A Polym. Chem.* **2000**, *38*, 1136.
- (157) Se, K.; Yamazaki, H.; Shibamoto, T.; Takano, A.; Fujimoto, T. *Macromolecules* **1997**, *30*, 1570.
- (158) Se, K.; Miyawaki, K.; Hirahara, K.; Takano, A.; Fujimoto, T. *J. Polym. Sci. Part A Polym. Chem.* **1998**, *36*, 3021.
- (159) Gido, S. P.; Lee, C.; Pochan, D. J.; Pispas, S.; Mays, J. W.; Hadjichristidis, N. *Macromolecules* **1996**, *29*, 7022.
- (160) Roovers, J.; Toporowski, P. M. *Macromolecules* **1981**, *14*, 1174.
- (161) Iatrou, H.; Avgeropoulos, A.; Hadjichristidis, N. *Macromolecules* **1994**, *27*, 6232.
- (162) Avgeropoulos, A.; Hadjichristidis, N. *J. Polym. Sci. Part A Polym. Chem.* **1997**, *35*, 813.
- (163) Knauss, D. M.; Huang, T. *Polym. Prepr.* **2000**, *41(2)*, 1332.
- (164) Bayer, U.; Stadler, R. *Macromol. Chem. Phys.* **1994**, *195*, 2709.
- (165) Gitsov, I.; Frechet, J. M. J. *Macromolecules* **1994**, *27*, 7309.
- (166) Paraskeva, S.; Hadjichristidis, N. *J. Polym. Sci.* **2000**, *38*, 931.
- (167) Longi, P.; Greco, F.; Rossi, U. *Makromol. Chem.* **1968**, *116*, 113.
- (168) Hild, G.; Kohler, A.; Rempp, P. *Eur. Polym. J.* **1983**, *16*, 843.
- (169) Roovers, J.; Toporowski, P. *Macromolecules* **1983**, *16*, 843.
- (170) Roovers, J.; Toporowski, P. *J. Polym. Sci.: Part B: Polym. Phys.* **1988**, *26*, 1251.
- (171) Lee, C.; Lee, H.; Lee, W.; Chang, T.; Roovers, J. *Macromolecules* **2000**, *33*, 8119.
- (172) Hogen-Esch, T. E.; Sundararajan, J.; Toreki, W. *Makromol. Chem. Macromol. Symp.* **1991**, *47*, 23.
- (173) Madani, E.; Favier, P.; Hemery, P.; Sigwalt, P. *Polym. Int.* **1992**, *27*, 353.
- (174) Lepoittevin, B.; Dourges, M.; Masure, M.; Hemery, P.; Baran, K.; Cramali, H. *Macromolecules* **2000**, *33*, 8218.
- (175) Yin, R.; Hogen-Esch, T. E. *Macromolecules* **1993**, *26*, 6952.
- (176) Yin, R.; Amis, E.; Hogen-Esch, T. E. *Macromol. Symp.* **1994**, *85*, 217.
- (177) Ma, J. *Macromol. Symp.* **1995**, *91*, 41.
- (178) Ishizu, K.; Ichimura, A. *Polymer* **1998**, *39*, 6555.
- (179) Ishizu, K.; Kanno, H. *Polymer* **1996**, *37*, 1487.
- (180) Yu, G.; Garrett, C.; Mai, S.; Altinok, H.; Attwood, D.; Price, C.; Booth, C. *Langmuir* **1998**, *14*, 2278.
- (181) Cramail, S.; Schappacher, M.; Deffieux, A. *Macromol. Chem. Phys.* **2000**, *201*, 2328.
- (182) Quirk, R. P.; Ma, J. *Polym. Prepr.* **1988**, *29(2)*, 10.
- (183) Antonietti, M.; Folsch, K. *Macromol. Chem., Rapid Commun.* **1988**, *9*, 423.
- (184) Lurbert, R.; Schappacher, M.; Deffieux, A. *Polymer* **1994**, *35*, 4562.
- (185) Pasch, H.; Deffieux, A.; Henze, I.; Schappacher, M.; Lurbert, R. *Macromolecules* **1996**, *29*, 8776.
- (186) Kubo, M.; Hayashi, T.; Kobayashi, H.; Tsuboi, K.; Itoh, T. *Macromolecules* **1997**, *30*, 2805.
- (187) Kubo, M.; Takeuchi, H.; Ohara, T.; Itoh, T.; Nagahata, R. *J. Polym. Sci., Part A: Polym. Chem.* **1999**, *37*, 2027.
- (188) Ünsal, O.; Godt, A. *Chem. Eur. J.* **1999**, *6*, 1728.
- (189) Ünsal, O.; Godt, A.; Song, D. *Polym. Prepr.* **2000**, *41(1)*, 187.
- (190) Gan, Y.; Dong, D.; Hogen-Esch, T. *Polym. Prepr.* **1995**, *36(1)*, 408.
- (191) Tomalia, D. A.; Naylor, R.; Goddard, W.; III *Angew. Chem., Int. Ed. Engl.* **1990**, *29*, 138.
- (192) Fréchet, J.; Hawker, C.; Wooley, L. *Macromol. Sci. Pure Appl. Chem.* **1994**, *A31*, 1627.
- (193) Gauthier, M.; Tichagwa, L.; Downey, J.; Gao, S. *Macromolecules* **1996**, *29*, 519.
- (194) Ishizu, K.; Takahashi, D.; Takeda, H. *Macromol. Rapid Commun.* **2000**, *21*, 660.
- (195) Hasan, A.; Muallem, A.; Knauss, D. *J. Polym. Sci.: Part A: Pol. Chem.* **2001**, *39*, 152.

CR9901337